PERIÓDICO TCHÊ QUÍMICA

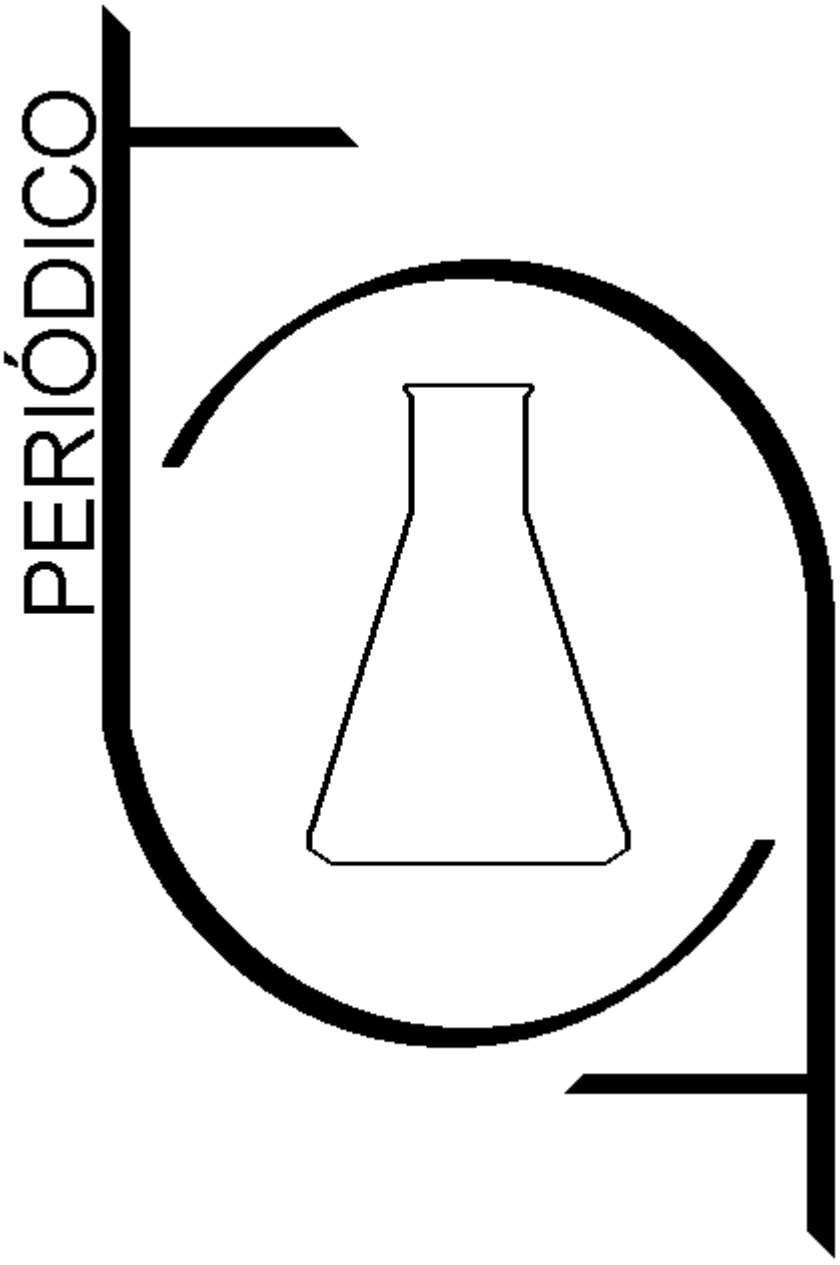

Volume 16 - Número 33 - 2019 ISSN 2179-0302

Órgão de divulgação científica e informativa

www.periodico.tchequimica.com

PERIÓDICO TCHÊ QUÍMICA

ISSN - 1806-0374 (Impresso) - ISSN - 1806-9827 (CD-ROM) - ISSN - 2179-0302 (Online)

Volume 16 **Número 33 – 2019** **ISSN 2179 - 0302**

Órgão de divulgação científica e informativa.

Dados Internacionais de Catalogação na Publicação (CIP)

Periódico Tchê Química: órgão de divulgação científica e informativa [recurso eletrônico] / Grupo Tchê Química – Vol. 1, n. 1 (Jan. 2004)- . – Porto Alegre: Grupo Tchê Química, 2005 - Semestral.
Sistema requerido: Adobe Acrobat Reader.
Modo de acesso: World Wide Web:
<http://www.tchequimica.com>

Descrição baseada em: Vol. 14, n. 28 (ago. 2017).
ISSN 1806-0374
ISSN 2179-0302
1. Química. I. Grupo Tchê Química.

CDD 540

Bibliotecário Responsável
Ednei de Freitas Silveira
CRB 10/1262

Periódico Tchê Química. ISSN 2179-0302. (2019); vol.16 (n°33)
Downloaded from www.periodico.tchequimica.com

PERIÓDICO TCHÊ QUÍMICA

Volume 16 Número 33 – 2019 ISSN 2179 - 0302

Órgão de divulgação científica e informativa.

Comissão Editorial

Editores-chefe

- Dr. Luis Alcides Brandini De Boni, deboni@tchequimica.com
- Dr. Eduardo Goldani, goldani@tchequimica.com

Editores técnicos

- Ednei de Freitas Silveira – *Bibliotecário Responsável*
- Dr. Francisco José Santos Lima, lima@tchequimica.com , Brasil, UFRN.
- Dr. Carlos Eduardo Cardoso, cardoso@tchequimica.com, Brasil, USS.
- Dr. Sérgio Machado Corrêa, correa@tchequimica.com, Brasil, UERJ.

Corpo Editorial

Membros

- Teresa M. Roseiro Maria Estronca, Dr., roseiro@tchequimica.com, Portugal, UC.
- Monica Regina da Costa Marques, Dr., aguiar@tchequimica.com, Brasil, UERJ.
- Ketevan Kupatadze, Dr., kupatadze@tchequimica.com , Geórgia, ISU.
- Márcio von Mühlen, Dr., vonmuhlen@tchequimica.com, EUA, MIT.
- Élcio Jeronimo de Oliveira, Dr., elcio@tchequimica.com, Brasil, CTA.
- José Carlos Oliveira Santos, Dr., zecarlosufcg@tchequimica.com, Brasil, UFCG.
- Alcides Wagner Serpa Guarino, Dr., guarino@tchequimica.com, Brasil, UNIRIO.
- Roseli Fernandes Gennari, Dr., gennari@tchequimica.com, Brasil, USP.
- Rafael Rodrigues de Oliveira, Dr., oliveira@tchequimica.com, Brasil, Brava Biosciences.
- Lívio César Cunha Nunes, Dr., nunes@tchequimica.com, Brasil, UFPI.
- João Guilherme Casagrande Jr, Dr., casagrande@tchequimica.com, Brasil, EMBRAPA.
- Denise Alves Fungaro, Dr., fungaro@tchequimica.com, Brasil, IPEN.
- Murilo Sérgio da Silva Julião, Dr., juliao@tchequimica.com, Brasil, UVA.
- Amit Chaudhry, Dr., chaudhry@tchequimica.com, India, Panjab University.
- Hugo David Chirinos Collantes, Dr., chirinos@tchequimica.com, Peru, UNI.
- Carlos E. de Medeiros J., Dr. jeronimo@tchequimica.com, Brasil, PETROBRAS.
- Walter José Peláez, Dr., pelaez@tchequimica.com, Argentina, UNC.
- Rodrigo Brambilla, Dr., brambilla@tchequimica.com, Brasil, UFRGS.
- Joan Josep Solaz-Portolés, Dr., solaz@tchequimica.com, Espanha, UV.
- José Euzébio Simões Neto, Dr. simoes@tchequimica.com, Brasil, UFRP.
- Aline Maria dos Santos Teixeira, Dr., santos@tchequimica.com, Brasil, UFRJ.

- César Luiz da Silva Guimarães, Me., guimaraes@tchequimica.com, Brasil, IBAMA.
- Daniel Ricardo Arsand, Dr., arsand@tchequimica.com, Brasil, IFSul.
- Paulo Sergio Souza, Dr., souza@tchequimica.com, Brasil, Fundação Osorio.
- Moisés Rômolos Cesário, Dr., romolos@tchequimica.com, França, ULCO.
- Andrian Saputra, Dr., saputra@tchequimica.com, Universidade de Lampung, Indonésia.
- Vanessa Barbieri Xavier, Dr., xavier@tchequimica.com, Brasil, PUCRS.
- Danyelle Medeiros de Araújo Moura, Dr., moura@tchequimica.com, Brasil, UFRN.
- Gabriel Rubensam, Me., grubensam@tchequimica.com, Brasil, UFRGS.
- Masurquede de Azevedo Coimbra, Me., coimbra@tchequimica.com, Brasil, Sec. de Saúde do Estado - RS.
- Oana-Maria Popa, Me., popa@tchequimica.com, IPN, Romênia.

Periódico Tchê Química

ISSN - 1806-0374 (Print)
ISSN - 2179-0302 (Online)

LCCN: 2010240735

Divulgação *on-line* em
http://www.periodico.tchequimica.com
http://www.journal.tchequimica.com
http://www.tchequimica.com

Esta revista é indexada e resumida pelo CAS, EBSCO,Latindex, Sumários, Index Copernicus, Scopus, OAIJ, CAB Abstracts e Reaxys.

* CAS (*Chemical Abstracts Service, a division of the American Chemical Society*.)
* OAIJ (*Open Academic Journals Index*)

Missão

O Periódico Tchê Química (PTQ) publica artigos de pesquisa originais, artigos de revisão, notas curtas (publicações científicas), revisões de livros, artigos de fórum, editoriais e entrevistas. Pesquisadores de todos os países são convidados a publicar nas páginas do PTQ.

A responsabilidade sobre os artigos é de exclusividade dos autores.

Correspondências
Rua Anita Garibaldi, 359/603.
Bairro Mon't Serrat. CEP: 90450-001
Porto Alegre – RS. Brasil.
Skype: tchequimica
www.periodico.tchequimica.com
tchequimica@tchequimica.com

Downloaded from www.periodico.tchequimica.com

Índice

Downloaded from www.periodico.tchequimica.com

Downloaded from www.periodico.tchequimica.com

15- Artigo / Article

PEREIRA, Francisco Claudece; LIMA, Francisco José Santos

BRASIL

NOVO MÉTODO PARA A ESTIMATIVA DAS CONSTANTES DE ESTABILIDADE DE COMPLEXOS COM O EDTA

A NEW METHOD FOR CONSTANT ESTIMATE STABILITY OF COMPLEX WITH EDTA

Página – 148

16- Artigo / Article

GLOTOVA, Irina Anatolievna; GALOCHKINA, Nadezhda Alekseevna; SELEMENEV, Vladimir Fedorovich; PEREGONCHAYA, Olga Vladimirovna; SOKOLOVA , Svetlana Anatol'evna

RÚSSIA

ESTUDO DE ESPECTROSCÓPIA-IV DA IMOBILIZAÇÃO DE COMPOSTOS DE SELÊNIO EM COLÁGENO BIOMODIFICADO

IR-SPECTROSCOPIC STUDY OF IMMOBILIZATION OF SELENIUM COMPOUNDS ON BIOMODIFIED COLLAGEN

Página – 159

17- Artigo / Article

FERREIRA, ANA PAULA MOTA; TEIXEIRA, ERICO JUNE NEVES; OLIVEIRA, IOLANDA MIRANDA DE; PINHEIRO, HELILMA DE ANDRÉA; MARQUES, ALDALÉA LOPES BRANDES

BRASIL

NOVO MÉTODO VOLTAMÉTRICO PARA DETERMINAÇÃO DE FENANTRENO EM ÁGUA SUBTERRÂNEA

NEW VOLTAMMETRIC METHOD FOR DETERMINATION OF PHENANTHRENE IN GROUNDWATER

Página – 169

18 - Artigo / Article

MIKUSEV, GLEB I.; BAIKEEV, RUSTEM F.; MAGOMEDOV, RUSLAN O.; MIKUSEV, IVAN E.; MISHAKIN, TIMUR S.

RÚSSIA

TECNOLOGIAS PARA PREVISÃO DA CONDIÇÃO FUNCIONAL DA MÃO APÓS O TRATAMENTO CIRÚRGICO DA DOENÇA (CONTRATURA) DE DUPUYTREN

TECHNOLOGY FOR PROGNOSIS OF THE FUNCTIONAL STATUS OF HAND AFTER SURGICAL TREATMENT OF DUPUYTREN'S DISEASE (CONTRACTURE)

Página – 178

19- Artigo / Article

BYTSENKO, OKSANA A.; SHATILOV, ALEKSEY V.; DANEKO, ALEKSANDR I.; FILONOVA, ELENA V.; MARKOV, ALEXEY B.

RÚSSIA.

EFEITO DA IRRADIAÇÃO DE VIGA ELETRÔNICA DE ALTA CORRENTE NA RESISTÊNCIA À CORROSÃO DE ÓXIDO DE SULFETO DE REVESTIMENTOS DE NI-CR-AL-Y-PLASMA

EFFECT OF HIGH-CURRENT ELECTRON BEAM IRRADIATION ON RESISTANCE OF SULFIDE-OXIDE CORROSION OF NI-CR-AL-Y ION-PLASMA COATINGS

Página – 198

20- Artigo / Article

SHESTAKOVA, KSENIIA MIKHAILOVNA; SAVCHUK, SERGEY ALEXANDROVICH; MESONZHNIK, NATALIA VLADIMIROVNA; KUHARENKO, ALEXEY VLADIMIROVICH; APPOLONOVA, SVETLANA ALEXANDROVNA

RÚSSIA

DESENVOLVIMENTO E APLICAÇÃO DE UM MÉTODO DE TRIAGEM RÁPIDA PARA DETERMINAÇÃO DE NOVAS SUBSTÂNCIAS PSICOCATIVAS E SEUS METABOLITOS EM URINA

DEVELOPMENT AND APPLICATION OF A RAPID SCREENING METHOD FOR DETERMINATION OF NEW PSYCHOACTIVE SUBSTANCES AND THEIR METABOLITES IN URINE

Página – 206

21- Artigo / Article

PRAZDNOVA, EVGENIYA V.; GOROVTSOV, ANDREY V.; CHISTYAKOV, VLADIMIR A.; VASILCHENKO, NIKITA G.; KUKHARENKO, LIDIYA E.;

RÚSSIA

INFLUÊNCIA DO TIPO DE SOLO E DA CULTURA ANTERIOR NA SUPRESSÃO DO FUSÁRIO POR BACTÉRIAS FORMADORAS DE ESPOROS LOCAIS

THE INFLUENCE OF SOIL TYPE AND PRECEDING CROP ON THE SUPPRESSION OF FUSARIUM BY INDIGENOUS SPORE-FORMING BACTERIA

Página – 225

22- Artigo / Article

DIKHANBAYEVA FATIMA; ZHAKSYLYKOVA GULSHAT; SYZDYKOVA LAILA; SMAILOVA ZHULDYZ; TASTURGANOVA ELMIRA

CAZAQUISTÃO

PRODUÇÃO DE LATICÍNIOS À BASE DE LEITE DE CAMELO PARA FINS ESPECIAIS

PRODUCTION OF A DAIRY PRODUCT BASED ON CAMEL MILK FOR SPECIAL PURPOSES

Página – 241

Downloaded from www.periodico.tchequimica.com

Downloaded from www.periodico.tchequimica.com

Downloaded from www.periodico.tchequimica.com

Downloaded from www.periodico.tchequimica.com

Downloaded from www.periodico.tchequimica.com

Downloaded from www.periodico.tchequimica.com

Downloaded from www.periodico.tchequimica.com

Downloaded from www.periodico.tchequimica.com

Downloaded from www.periodico.tchequimica.com

PERIÓDICO TCHÊ QUÍMICA
ARTIGO de REVISÃO

CRISINA: UMA REVISÃO SOBRE SUAS APLICAÇÕES TERAPÊUTICAS

CHRISIN: A REVIEW OF ITS THERAPEUTIC APPLICATIONS

KULTZ, Thiellen Wrobel[1*]; ROZISCA, Erica Aparecida[2]; CAMARGO, Luciana Erzinger Alves[3].

[1] Universidade Estadual do Centro-Oeste, Programa de Pós-Graduação em Química

[2] Universidade Estadual do Centro-Oeste, Programa de Pós-Graduação em Ciências Farmacêuticas

[3]Coordenação de Farmácia Faculdade Guairacá

** Autor correspondente*
e-mail: thyta_kultz@hotmail.com

Received 21 May 2019; received in revised form 26 August 2019; accepted 28 August 2019

RESUMO

A crisina, flavonoide encontrado naturalmente em plantas e produtos apícolas, tem despertado o interesse entre pesquisadores de todo o mundo, devido à grande gama de propriedades terapêuticas, como atividade anti-inflamatória e atividade antioxidante e sua potencial atividade antitumoral. O objetivo desse trabalho foi investigar as diversas aplicações terapêuticas da crisina, relacionando ensaios *in vitro* e *in vivo*, bem como suas aplicações na área da nanotecnologia. Devido a isso, este artigo foi desenvolvido com pesquisas relacionando as palavras-chave em sites de busca científica, como o PubMed, Scielo, Google Acadêmico, etc. Reunindo grande parte da literatura recente, pôde-se perceber que as propriedades biológicas da crisina, tais como a atividade anti-inflamatória, atividade antitumoral e atividade antioxidante, podem ser verificadas usando extratos de plantas devidamente tratados e purificados, ou em aplicações usando a nanotecnologia como sendo alternativa para uma aplicação direcionada e precisa dessas atividades. Dessa forma, foram verificadas aplicações contra o câncer de mama, contra o câncer na tireoide, contra o câncer de cólon de útero. Conclui-se que a crisina apresenta inúmeras atividades e propriedades terapêuticas testadas por ensaios *in vitro* e *in vivo*, além de todo a sua potencial aplicação nanotecnológica. Esses resultados mostram e justificam a importância de seu estudo tanto para a sociedade quanto para o âmbito científico. O diferencial deste trabalho é a reunião de informações sobre a nanotecnologia e as atividades terapêuticas relacionadas à crisina, o que contribuem para futuros trabalhos aliando-se os temas.

Palavras-chave: crisina, artigo de revisão, nanotecnologia, aplicações terapêuticas, ensaios.

ABSTRACT

The chrysin, flavonoid mainly encountered in plants and beekeeping products, has awakened the interest between researchers from all over the world, due the wide range of therapeutic properties, like anti inflammatory and antioxidant activities and also your potent antitumor effect. The goal of this task was investigate the various therapeutic applications of chrysin, relating in vitro and in vivo assays, as well as your applications in nanotecnology field. Because of that, this article has been developed with researches relating keywords in scientific search sites, like PubMed, Scielo, Google Scholar, etc. Gathering great part of recent literature, it could be seen that the biological properties of chrysin, such as anti inflamatory, antioxidant and antitumoral activities, can be verified by using plants extracts properly treated and purified, or in applications using nanotecnology as being an alternative for a directly and precise use of these activities. Thus, it has been verified the uses against breast cancer, thyroid cancer and uterine colon cancer. Therefore, concludes that chrysin features numerous activities and therapeutic properties tested by in vitro and in vivo assays, in addition to all its nanoapplication potential. These results show and justify the importance of this research for society and for the scientific scope. The differential of this article is the combination of nanotechnology studies and the therapeutic properties of chrysin, which contributes to future research on the topics.

Keywords: chrysin, review article, nanotechnology, therapeutic applications, trials.

Downloaded from www.periodico.tchequimica.com

1. INTRODUÇÃO

A crisina, também chamada de 5,7-di-hidroxiflavona, é um composto natural amplamente encontrado em diversas espécies vegetais, entre eles frutas, cogumelos e também principais produtos apícolas, como o mel e a própolis (Samarghandian, 2011; Jayakumar, 2009). Ela pertence à classe dos flavonoides, a qual engloba compostos polifenólicos de baixa massa molecular (Mani, 2014).

A crisina, na forma molecular, contém em sua estrutura três anéis aromáticos com estruturas ressonantes. Além disso, contém dois grupos fenol, um grupo aceto e um grupo éter presentes no segundo anel aromático, os quais possibilitam a captura de íons livres, bem como a quelação de íons metálicos (Silva, 2015; Hussein, 2018). Essa estrutura característica de flavonoides permite a realização de reações tanto núcleofílicas quanto eletrofílicas de substituição e eliminação (Borges Filho, 2014; Walle, 1999).

A crisina foi isolada como substância, no ano de 1990, utilizando várias etapas de extração e fracionamento por Cromatografia Líquida de Alta Eficiência (CLAE) (Borges Filho, 2014). Desde então, vem sendo amplamente estudada demonstrando inúmeros benefícios a saúde através de seu amplo espectro de propriedades biológicas, como atividades antioxidante, antitumoral, anticonvulsionante, anti-inflamatória e anti-hipertensiva. Além disso, a crisina apresenta efeitos terapêuticos contra doenças como o mal de Parkinson, carcinomas na glândula da tireoide, diabetes, entre outras (Rani, 2016; Woo, 2004; Medina, 1990).

Uma tecnologia que vem se destacando para a aplicação em compostos bioativos como a crisina é a nanoencapsulação de materiais, a qual utiliza polímeros, sendo eles naturais ou sintéticos, para o aprisionamento de compostos em nanopartículas. Desta maneira, torna-se interessante reunir as informações, pesquisas e todo o tipo de referencial, bem como os estudos e as análises realizadas utilizando a molécula crisina como princípio ativo. Portanto, este artigo contempla uma revisão bibliográfica que tem por objetivo dissertar sobre os aspectos científicos, tecnológicos e físico-químicos das formulações de nanopartículas contendo crisina, juntamente com sua potencial aplicação em análises *in vitro* ou *in vivo*.

2. FLAVONOIDES, CRISINA

Flavonoides são um grupo de compostos naturais pertencente à classe dos polifenóis, compreendendo estruturas que contém hidroxilas ligadas a anéis aromáticos. Os flavonoides são encontrados em frutas, verduras, plantas, chás e vinhos sendo responsáveis pela coloração desses alimentos. Há inúmeros flavonoides que são amplamente estudados, tais como o resveratrol, a quercitina, a rutina, o kaempferol, a hespiridina, a tangeretina entre outros (Hussein, 2018; Bagul, 2018; Zhang, 2015; Kilic, 2017).

Em produtos apícolas, os quais derivam do funcionamento do metabolismo de espécies de abelhas, é muito comum encontrar o flavonoide de cor amarela, crisina. A crisina é encontrada também em diversas plantas, como a *Passiflora coreulea*, também conhecida como maracujá do mato e *Hypericum afrum* A distribuição dessa planta é ampla na América do Sul, sendo muito encontrada nas regiões do leste do Brasil até o sul da Bolívia (Zheng, 2003).

A crisina possui na sua estrutura funções orgânicas como dois grupos fenol, um grupo cetona e um grupo éter. Esses grupos funcionais estão implicados em promover alterações significativas na molécula da crisina, tornando-a mais reativa e disponível para reações. Eles são responsáveis por algumas reações importantes como acilações e carboxilações com o grupo fenol, bem como hidratações e oxidações com o grupo cetona. Essas reações alteraram a estrutura da molécula, gerando metabólitos intermediários da 'molécula-mãe'.

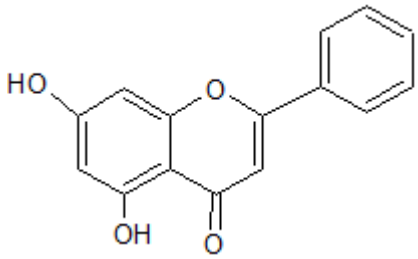

Figura 1. Fórmula estrutural do composto Crisina (5,7-di-hidroxiflavona)

Na literatura são encontrados vários mecanismos evidenciando que as reações de nitração, desidratação, halogenação e substituição modificam a estrutura da molécula de crisina, deixando-a mais ativa no combate a duas linhagens de células tumorais específicas, linhagem HT-29 e linhagem SGC-7901 (Zheng, 2003).

Downloaded from www.periodico.tchequimica.com

2.1 MÉTODOS DE OBTENÇÃO E PURIFICAÇÃO DA CRISINA

Para a obtenção e purificação de compostos da classe dos flavonoides, existem vários e diferentes métodos, que são dependentes da matriz de cada amostra. *Hypericum afrum* é um planta procedente principalmente em regiões da Tunísia e da Argélia, sendo categorizada como quase ameaçada de extinção, devido ao declínio de seu habitat (Larit, 2017). Essa planta é uma das onde a crisina é encontrada, sendo que, com o objetivo de extraí-la da planta, juntamente com outros três flavonoides (quercitina, miricetina e genisteína), foi utilizado o método de extração sólido-líquido, tendo como solvente uma mistura de álcool etílico e água, na proporção de 80:20 (v/v). Os extratos foram retirados com essa mistura pelo tempo de 24 horas, sendo o extrato final filtrado e evaporado a 40°C. Nesse trabalho testaram-se partições de solventes diferentes, como clorofórmio, acetato de etila e n-butanol, obtendo-se como fração com maior inibição das enzimas MAO contra MAO A e B, a fração composta por acetato de etila (Larit, 2017).

Scutellaria discolor é uma espécie de arbusto, que contém a molécula crisina em sua composição (Laishram, 2015). Utilizando o método de extração denominado imersão, pôde-se extrair a crisina, fazendo uso da acetona como solvente de imersão. Nesse trabalho, após extração, o extrato foi filtrado, com o auxílio de um rota-evaporador e também liofilizado. As frações desse extrato foram submetidas a cromatografia em sílica gel, após isso uma etapa de cristalização, seguida de caracterização por análise espectrofotométrica (Laishram, 2015).

Uma outra espécie de erva, a qual contem crisina entre outros flavonoides, como a icarrina, é *Epidemium elatum*, encontrada principalmente na região do Paquistão. Para elaborar um extrato que contenha esses flavonoides, foi necessário uma extração sólido-líquido utilizando-se metanol como solvente extrator. Após isso, relata-se que o solvente foi evaporado, utilizando um rota-evaporador, e o extrato metanólico bruto da erva foi obtido. Além dessa etapa, o extrato passou por uma etapa de separação, através de uma coluna de cromatografia contendo sílica gel, e isolamento através do equipamento de cromatografia líquida com espectrômetro de massas (LC-MS), além de outras técnicas de determinação e identificação para os compostos isolados a partir do extrato como espectrômetro de Ressonância Magnética Nuclear (RMN), espectroscopia de infra-vermelho com transformada de Fourier (IV-TF), foram utilizadas técnicas cromatográficas diferentes, como a cromatografia flash, cromatografia em coluna de fase normal, utilizando a detecção UV. Para tal, foi utilizado um cromatógrafo da marca Agilent 1200, contento bomba quaternária, amostrador automático, desgaseificador, detector UV e forno de coluna controlado por EZ, usando também coluna cromatográfica C-18, (4,6X250mm), com temperatura de forno de 70°C, eluição isocrática com fase móvel composta de acetonitrila:água (25:75 v/v) e fluxo de 0,5 mL/min. Os volumes de injeção foram variados de 2 a 5 µL, conforme a análise realizada. Com o auxílio dessas várias etapas cromatográficas, os flavonoides foram isolados e identificados (naseer, 2015).

Em outro procedimento de extração relatado, contendo algumas mudanças dos acima citados, uma erva rizomatosa, planta que contém raízes com gemas, possui alguns derivados de crisina. Esta erva foi preparada através da extração utilizando o álcool etílico como solvente extrator em um sistema de refluxo. O extrato obtido foi fracionado através de sistemas cromatográficos, como cromatografia em sílica gel e cromatografia em camada delgada, além de ser purificado utilizando a coluna Sephadex originando os compostos crisina-7-O-β-D-glucuronato de butila e crisina-7-O-β-D-glucuronato de metila (Han, 2018).

Isolando alguns compostos bioativos da casca de *Oroxilum indicum*, Nagasaka e colaboradores (2018), utilizaram uma extração com metanol para comprovar que a crisina, isolada através de frações de acetato de etila e hexano, foi responsável pela ativação de p53, um gene com a função de suprimir as células cancerosas.

Outro interessante estudo abordando a extração de crisina é o de Yasir e colaboradores (2017), o qual utiliza a extração de metóxi-crisina em plantas da família *Solanaceae*, fazendo a extração em fase sólida em um cartucho SPE (extração em fase sólida) contendo coluna C-18, usando eluição com metanol e água destilada na proporção de 50%/50% (v/v). A identificação dos compostos isolados foi realizada através do equipamento CL-ESI-MS/MS (cromatografia líquida com ionização por eletrospray acoplado a espectroscopia de massas).

Downloaded from www.periodico.tchequimica.com

2.2 CRISINA E ESTUDOS *in vitro*

Os flavonoides em geral, incluindo a crisina, são fontes de estudos para a descoberta e desenvolvimento de novos medicamentos. A literatura relata que a crisina possui diversas propriedades biológicas, entre elas antiflamatórias (Shin, 2009; Bae, 2011), antioxidantes (Veerappan, 2015; Souza, 2015), anticâncer (Khoo, 2010; Zhu, 2016), neuroprotetora (Mehri, 2014), que são relatados em diversos trabalhos científicos.

Muitos estudos *in vitro* confirmam essas ações, como Park e colaboradores (2018), que identificaram a atividade inibitória da crisina sobre células de coriocarcinoma humano, tumor que possui capacidade rápida de metástase e também difícil cura. Nesse estudo, a crisina interrompeu a homeostase intracelular, a produção de espécies reativas de oxigênio e a peroxidação lipídica, o que alterou o potencial das mitocôndrias e os níveis de Ca^{2+}, ocasionando a morte das células de coriocarcinoma.

Em células de câncer de tireoide, a crisina inibiu o crescimento celular através da ativação intracelular da proteína NOTCH1, relacionada ao crescimento de tumores na tireoide. O ensaio *in vitro* também foi confirmado por testes *in vivo* (Yu, 2012). A crisina induziu apoptose em linhas celulares de leucemia MOLT-4 e JVM-13 e B-CLL. Os resultados demonstraram que a exposição das linhagens celulares à crisina diminuiu a viabilidade das células, e os mesmos sugerem que a crisina induziu seletivamente a apoptose de linfócitos do sangue periférico isolados de pacientes com leucemia linfocítica crônica humana por via mitocondrial *in vitro* (Zaric, 2015).

Em células de câncer de mama metastáticas, a crisina suprimiu a migração e invasão dessas células através da inibição da via do sinal Akt, e assim regulando a modulação da metaloproteinase de matriz-10 e a transcrição epitelial-mesenquimal, indicando que a crisina exerce atividades antimetastáticas em células de câncer de mama avançado ou metastático (Yang, 2018, B).

Fu e colaboradores (2007) investigaram o efeito da crisina em células humanas de câncer de próstata. Nesse estudo, o flavonoide crisina inibiu a expressão do fator HIF-1α e do fator de crescimento endotelial vascular DU145, sendo que a inibição deste último foi confirmado através de ensaios *in vivo.*

Choi e Yun (Choi, 2016) mostraram através de marcadores e técnicas de PCR e immunoblot que a crisina desempenha um papel modulador duplo na forma de induzir o escurecimento dos adipócitos 3T3-L1, bem como aumentar o metabolismo lipídico, o que pode ser um estudo promissor para a prevenção da obesidade.

Em relação à prevenção de cataratas, Sundararajan e colaboradores (Sundararajan, 2016) testaram a eficácia da crisina aplicada no cristalino de ratos Wistar cultivados *in vitro*, onde verificaram o acúmulo de cálcio. O trabalho revelou que em cristalinos não tratados a opacificação dos mesmos foi densa, enquanto os tratados não apresentaram tal opacificação, e assim concluíram que a crisina diminuiu o acúmulo de cálcio no cristalino, e subsequente prevenção da catarata.

Também foi avaliado o efeito da crisina sobre as lesões causadas por *Staphylococcus aureus*. Nesse estudo, foram realizados ensaios de hemólise, de *Western blot* e de RT-PCR a fim de avaliar o efeito da crisina na secreção de α-hemolisina por *Staphylococcus. aureus*. Sendo assim, ensaios realizados resultaram na inibição causada pelo flavonoide, o que conferiu um grau significativo de proteção contra a pneumonia causada por *Staphylococcus aureus* (Wang, 2011).

2.3 CRISINA E ESTUDOS *in vivo*

Além de testes *in vitro*, a literatura aborda muitos trabalhos em modelos animais (*in vivo*), onde foram testadas as diversas ações farmacológicas da crisina. Um interessante trabalho que investigou os efeitos protetores da crisina na lesão pulmonar em ratos, mostrou que a mesma foi capaz de inibir a infiltração de neutrófilos, o que atenuou a lesão nos tecidos pulmonares, e diminuiu os níveis de marcadores PMNs, bem como o estresse oxidativo dos pulmões dos ratos (Yang, 2018, B).

Bahadori et al. (2016) investigaram o efeito da crisina em câncer de cólon do útero CT26, revelando assim que a crisina obteve um efeito citotóxico dose-dependente, também demonstrando uma redução do tamanho do tumor nos ratos tratados em comparação com o de ratos não tratados. Os marcadores confirmaram que o tamanho dos tumores diminuíram pela regulação negativa do Sall4 e positiva do Bax.. No câncer bucal induzido por 7,12-dimetilbenzantraceno (DMBA) em hamsters, a crisina promoveu a prevenção através dos

Downloaded from www.periodico.tchequimica.com

seus efeitos antioxidantes, onde o grupo tratado com a crisina obteve uma inibição na formação tumoral e redução do tamanho do tumor bucal (Karthikeyan, 2013).

A crisina também apresentou efeito anticancerígeno em melanoma, a qual apresentou atividades biológicas sob células B16F10 em camundongos BALB. O estudo revelou que em 14 dias de tratamento, a crisina reduziu em 60% o tamanho do tumor e que em 21 dias, o tumor foi reduzido em 71% por meio de apoptose e paragem do ciclo celular na fase G2. Além disso, o tratamento com crisina aumentou a atividade citotóxica de NK, CTL e macrófagos (Sassi, 2018).

No trabalho *in vitro/vivo* de Guo e colaboradores (2016), a crisina apresentou um efeito protetor dos neurônios granulares primários devido à sua atividade antioxidante. No modelo *in vivo* de doença de Parkinson, a crisina recuperou a perda de neurônios dopaminérgicos e aumentou o nível de dopamina, além de exercer diversos efeitos contra a doença de Parkinson por meio de vários mecanismos.

Outro estudo realizado verificou a ação da crisina na superacumulação de matriz extracelular na fibrose de fígado em camundongos induzida por tetracloreto de carbono. Os fígados com fibrose tiveram um aumento na expressão de colágeno, inibidores teciduais e modulação de metaloproteinases de matriz. O tratamento com a crisina reduziu as alterações estruturais no órgão, as quais não foram observadas no grupo de regressão espontânea (Balta, 2018). Já Rehman e colaboradores (2014) verificaram o efeito da crisina na lesão hepática em ratos tratados com cisplatina, e concluíram que a mesma protegeu contra o dano hepático através da atenuação do estresse oxidativo e resposta inflamatória causada pela toxicidade da cisplatina no fígado.

Na fibrose miocárdica após infarto, a crisina agiu como protetora do miocárdio lesado através da supressão do estresse oxidativo e da inflamação. Após 4 semanas de tratamento, a acocardiografia monstrou que a função cardíaca foi significativamente melhorada após o tratamento com crisina, além de obter um efeito cardioprotetor antifibrótico na zona periférica do miocárdio após o infarto (Yang, 2018, A).

Além das atividades da crisina descritas acima, a mesma foi analisada em outros estudos pré-clínicos, alguns apresentados na Tabela 1, em anexo.

2.4 CRISINA E NANOTECNOLOGIA

Nos últimos anos muitos relatos demonstram que a crisina possui um grande potencial para aplicações terapêuticas, porém seu uso é limitado devido às suas propriedades físico-químicas, como baixa estabilidade, baixa solubilidade em água, rápido metabolismo e baixa captação celular, atrapalhando seus efeitos benéficos (Mohammandian, 2017; Eatemadi, 2016). Diante dos inúmeros obstáculos apresentados, o uso da nanotecnologia vem sendo investigada para melhorar o fornecimento do composto ao organismo, permitindo assim uma lenta liberação, aumento da biodisponibilidade e redução da degradação da crisina no organismo (Anari, 2015).

Visando a baixa biodisponibilidade da crisina no organismo, Dong e colaboradores (2017) prepararam nanoemulsões com diferentes carregadores, além de avaliarem a farmacocinética dos mesmos em ratos. Concluíram que as nanoemulsões de oleato de sódio melhoraram a absorção oral da crisina, além de apresentarem um tamanho esférico de 83 nm e eficiência de encapsulação de 89% do composto (Balta, 2018).

Kim e colaboradores (2017) desenvolveram nanopartículas injetáveis de MPEG/PCL para incorporar a crisina. Suas propriedades físico-químicas foram avaliadas e os efeitos anticancerígenos investigados em células A549 e *in vivo*. As nanopartículas apresentaram tamanho de 77 nm, potencial zeta de -2,22mV e eficiência de encapsulação de 46,96%. O efeito anticâncer foi confirmado, apresentando um atraso significativo no crescimento do tumor.

Também foi relatado o uso de nanofibras de PCL/PEG como carregadoras de crisina. Os resultados mostraram que as nanofibras apresentaram atividades antioxidante, citoprotetora e antiflamatória para aplicação e auxilio na cicatrização de feridas. As nanofibras demonstraram-se citocompatíveis, as quais exibiram atividade antioxidante e assim protegeram células fibroblásticas do estresse oxidativo. Em relação à capacidade antiinflamatória das nanofibras carregadas com crisina, as mesmas apresentaram uma menor produção de interleucinas nos macrófagos (2017).

Relacionando a nanotecnologia, crisina e inflamação, Firouzi-Amandi et al. (2018) desenvolveram nanopartículas de PLGA-PEG

Downloaded from www.periodico.tchequimica.com

contendo crisina, onde investigaram sua eficiência na modulação da polaridade de macrófagos de marcadores e citocinas pró-inflamatórios, bem como marcadores anti-inflamatórios. Os resultados demonstraram que as nanopartículas obtiveram um tamanho de 235 nm, e quando comparadas com a crisina livre apresentaram-se menos tóxicas aos macrófagos. Além disso as nanopartículas contendo crisina reduziram os marcadores pró-inflamatórios e os níveis de citocinas, aumentando paralelamente os marcadores anti-inflamação.

Outra formulação utilizando PLGA-PEG como polímero, provocou o aumento da solubilidade da crisina e a diminuição de seus efeitos tóxicos. Além disso, no estudo, foram testados os nanocristais em células T47D de câncer de mama *in vitro*. Concluiu-se que os nanocristais de PLGA-PEG e crisina aumentaram a citotoxidade em células cancerígenas e não danificaram células normais do organismo, o que seria promissor na terapia de câncer de mama (Anari, 2015).

Vedagiri, Surekha e Sumathi (2015) formularam nanopartículas lipídicas contendo crisina, e os resultados da caracterização evidenciaram o tamanho médio de 240 nm, a encapsulação de mais de 86% do composto, o potencial zeta de -40,4mV e a liberação controlada da crisina. Testes *in vivo* das nanopartículas preparadas foram realizados em outro estudo, o qual confirmou que as mesmas obtiveram efeito terapêutico em lesões neuronais em ratos. Portanto concluíram que as nanopartículas lipídicas contendo crisina poderiam ser usadas como um potencial terapêutico para combater a doença de Alzheimer (Vedagari, 2015).

Um recente trabalho utilizou a albumina bovina como polímero para o carreamento da crisina. Essa formulação apresentou nanopartículas esféricas com diâmetro médio de 1328 nm, potencial zeta de -10mV e eficiência de encapsulação entre 44 e 84%. Apesar dos resultados da caracterização físico-química não estarem dentro dos resultados comumente relatados na literatura, o uso da albumina como carregador para crisina é uma grande inovação (2018).

Kaur, Malik & Kaur (2015) obtiveram nanocristais de crisina, os quais foram avaliados para estudos de dissolução *in vitro* e atividade anti-inflamatória *in vivo*. A solubilidade dos nanocristais aumentou quando comparados com a crisina livre (1,12 µg e 0,04 µg/ml), a sua dissolução foi de 95%, e uma maior atividade sequestradora de radicais livres foi evidenciada (70%). A inibição do edema na pata de rato foi maior quando os nanocristais foram usados. Diante de todas as referências encontradas, a aplicação da nanotecnologia para melhorar as características da crisina é fundamental para a potencialização de suas ações terapêuticas.

3. CONCLUSÕES

A crisina tem se tornado uma promissora molécula com atividades variadas, as quais tem sido alvo de grande interesse por parte dos pesquisadores, e evidenciadas na literatura através de ensaios *in vitro* e/ou *in vivo* utilizando seus vários efeitos terapêuticos. Sua potencial atividade anticâncer necessita ser cada vez mais explorada, bem como seus demais efeitos terapêuticos, atividade antioxidante, anti-inflamatória, entre outras. Com base em todas as informações obtidas para o desenvolvimento deste artigo de revisão, verificou-se uma potencial aplicabilidade da crisina em diversas patologias, e a união desses efeitos com a nanotecnologia pode solucionar eventuais limitações de suas propriedades físico-químicas e potencializar as aplicações de maior interesse da crisina.

4. AGRADECIMENTOS

Agradecemos ao nosso orientador Najeh Khalil, por todo o incentivo e apoio nesse artigo. Agradecemos também aos órgãos de fomento CAPES e CNPQ, pelas bolsas concedidas.

5. REFERÊNCIAS:

1. Anandhi, R.; Thomes, P.A.; Geraldine, P. Mol Cell Biochem, **2014**, 385, 1-2.
2. Anari, e.; Akbarzadeh, A.; Arghami, N. Artificial Cells, Nanomedicine, and Biotechnology, **2015**, 44, 6.
3. Bae, Y.; Lee, S.; Kim, S.H. Toxicol Appl Pharmacol, **2011**, 254, 1.
4. Bagul, P.K., Katare, P.B., Bugga, P., Dinda, A.K., Banerjee, S.K. Cell, **2018**, 7, 12.
5. Bahadori, M.; Baharara, J.; Amini, E. Iran J Biotechnol, **2016**, 14, 3.
6. Balta, C.; Ciceu, A.; Herman, H.; Rosu, M.; Boldura, O.M.; Hermenean, A. Dose

Downloaded from www.periodico.tchequimica.com

Response, **2018**, 16, 3.

7. Borges Filho, C. Avaliação da bioatividade do flavonoide crisina em camundongos submetidos ao estresse crônico moderado e imprevisível. **2014**. 113f. Dissertação (Mestrado em Bioquímica). Universidade Federal do Pampa. Itaqui, RS, 2014.
8. Choi, J.H.; Yun, J.W. Nutrition, **2016**, 32, 9.
9. Deldar, Y.; Pilehvar-Soltanahmadi, Y.; Dadashpour, M.; Saheb, S.M.; Rahmati-Yamchi, M.; Zarghami, N. Artificial Cells, Nanomedicine, and Biotechnology, **2017**, 46, 4.
10. Dong, D.; Quan, E.; Yuan, X.; Xie, Q.; Li, Z.; Wu, B. Mol. Pharmaceutics, **2017**, 14, 9.
11. Dou, W.; Zhang, J.; Zhang, E.; Sun, A.; Ding, L.; Chou, G.; Wang, Z.; Mani, S. J Pharmacol Exp Ther, **2013**, 345, 3.
12. Eatemadi, A.; Daraee, H.; Aiylabegan, H.T.; Negahdari, B.; Rajeian, B.; Zarghami, N. Biomed Pharmacother, **2016**, 84.
13. Feng, X.; Qin, H.; Shi, Q.; Zhang, Y.; Zhou, F. Wu, H.; Ding, S.; Niu, Z.; Lu, Y.; Shen, P. Biochem Pharmacol, **2014**, 89, 4.
14. Ferrado, J.B.; Perez, A.A.; Visentini, F.F.; Islan, G.A.; Castro, G.R.; Santiago, L.G. Colloids Surf B Biointerfaces, **2018**, 21, 173.
15. Filho, C.B.; Jesse, C.R; Donato F.; Giacomeli R.; Del Fabbro L.; da Silva Antunes M.; de Gomes M.G.; Goes A.T.; Boeira S.P.; Prigol M.; Souza L.C.; Neuroscience, **2015**, 19, 289.
16. Firouzi-Amandi, A.; Dadashpour, M.; Nouri, M.; Zarghami N.; Serati-Nouri H.; Jafari-Gharabaghlou D.; Karzar B. H.; Mellatyar H.; Aghebati-Maleki L.; Babaloo Z.; Pilehvar-Soltanahmadi Y. Biomed Pharmacother, **2018**, 105.
17. Fu, B.; Xue, J.; Li, Z. Shi, X.; Jiang, B.H.; Fang, J. Mol Cancer Ther, **2007**, 6, 17.
18. Guo, B.; Zheng, C.; Cai, W.; Cheng, J.; Wang, H.; Li, H.; Sun, Y.; Cui, W.; Wang, Y.; Han, Y.; Lee, S.M.; Zhang, Z. J. Agric. Food Chem, **2016**, 64.
19. Han, Q.T., Xiao, K., Xiang, K.L., Li, G.S., Dai, S.J. Chemistry and Biodiversity, **2018**, 15, 7.
20. Hussein, R.M., Mohamed, W.R., Omar, H.A. Pesticide Biochemistry and Physiology, **2018**, 152.
21. Jayakumar, T., Thomas, P. A., & Geraldine, P. Innov. Food. Sc.i Emerg. Techno., **2009**, 10(2), 228–234.
22. Kang, M.K. et al. Nutrients, **2018**, 10, 8.
23. Karthikeyan, S.; Srinivasan, S.; Wani, S.A. International Journal of Nutrition, Pharmacology, Neurological Diseases, **2013**, 3, 1.
24. Kaur, H., Malik, D.S., Kaur, G. Pharmaceutical Nanotechmology, **2015**, 3, 3.
25. Khoo, B.Y.; Chua, S.L.; Balaram, P. Int J Mol Sci, **2010**, 11.
26. Kilic, K., Sakat, M.S., Yildirim, S., Kandemir, F.M., Gozeler, M.S., Dortbudak, M.B., Kucukler, S. **2018**.
27. Kim, K.M.; Lim, H.K.; Shim, S.H.; Jung, J. International Journal of Nanomedicine Dovepress, **2017**, 12.
28. Laishram, S., Moirangthem, D.S., Borah, J.C., Pal, B.C., Suman, P., Gupta, S.K., Kalita, M.C., Talikdar, N.C. Life Sciense, **2015**, 143.
29. Larit, F., Elokely, K.M., Chaurasiya, N.D., Benyahia, S., Nael, M.A., León, F., Abu-Darwish, M.S., Efferth, T., Wang, Y., Belouahem-Abed, D., Benayache, S., Tekwani, B.L., Cutler, S.J. Phytomedicine, **2017**, 40.
30. Lee, E.J.; Kang, M.K.; Kim, D.Y.; Kim, Y.H.; Oh, H.; Kang, Y.H. Nutrients, **2018**, 10, 7.
31. Mani, V. M., Asha, S., Sadig, A. M. M. Biomed & Aging Pathol, **2014**, 4, 1.
32. Medina, J.H., Paladini, A.C., Wolfman, C., Stein, M.L., Calvo, D., Diaz, L.E., Pena, C. Biochemical Pharmacology, **1990**, 40, 10.
33. Mehri, S.; Karami, H.V.; Hassani, F.V.; Hosseinzadeh, H. Iran Biomed J, **2014**, 18, 2.
34. Mohammadian, F.; Pilehvar, Y.; Zarghami, F. et al. Artificial Cells Nanomed Biotechnol, **2017**, 45, 6.
35. Nagazaka, M., Hashimoto, R., Inoue, Y.,

Downloaded from www.periodico.tchequimica.com

Ishiuchi, K., Matsuno, M., Itoh, Y., Hayashi, H. Molecules, **2018**, 23, 6.

36. Naseer, S., Lone, SH., Lone, J.A., Khuroo, M.A., Bhat, K.A. Journal of Chromatography B, **2015**, 989.
37. Park, W.; Park, S.; Lim, W.; Song, G. Biochem Biophys Res Commun, **2018**, 503, 4.
38. Rani, N., Bharti, S., Bhatia, J., Nag, T.C., Ray, R., Arya, D.S. Chemico-Biolical Interactions, **2016**, 250.
39. Ravisshankar, D. Salamah, M.; Attina A.; Pothi R.; Vallance, T.M.; Javed, M.; Williams, H.F.; Alzahrani, S.E.M.; Kabova, E.; Vaiyapuri, R.; Shankland, K.; Gibbins, J.; Strohfeldt, K.; Greco, F.; Osborn, H.M.I.; Vaiyapuri, S. Sci Rep, **2017**, 7, 1.
40. Rehman, M.U.; Ali, N.; Rashid, S.; Jain, T.; Nafees, S.; Tahir, M.; Khan, A.Q.; Lateef, A.; Khan, R.; Hamiza, O.O.; Kazim, S.; Qamar, W.; Sultana S. Pharmacol Rep, **2014**, 66, 6.
41. Roy, S.; Sil, A.; Chakraborty. Journal Cellular Physiology, **2018**.
42. Samarghandian, S.; Afshari, J.T.; Davoodi, S. Clinics, **2011**, 66, 6.
43. Sangeetha, K.S.S., Umamaheswari, S., Reddy, C.U.M., Kalkura, S.N. International Journal of Pharmaceutical Sciences and Research, **2017**, 8, 3.
44. Sassi, A.; Maatouk, M.; El Gueder, D.; Bzéouich, I.M.; Abdelkefi-Ben Hatira, S.; Jemni-Yacoub, S.; Ghedira, K.; Chekir-Ghedira, L.; Chemico Biological Interact, **2018**, 283.
45. Shin, E.K.; Kwon, H.S.; Kim, Y.H.; Shin, H.K.; Kim, J.K. Biochem Biophys Res Commun, **2009**, 381, 4.
46. Silva, L.R., Vale, L.M., Calou, I.B.F., Deus, M.S.M., Ferreira, P.M.P., Peron, A.P. Acta Toxicol Argent, **2015**, 23, 1.
47. Souza, L.C.; Antunes, M.S., Filho, C.B.; Del Fabbro, L.; de Gomes, M.G.; Goes, A.T.; Donato, F.; Prigol, M.; Boeira, S. P.; Jesse, C.R.; Pharmacol Biochem Behav, **2015**, 134.
48. Sundararajan, M.; Thomas, P.A.; Teresa, P.A.; Anbukkarasi, M.; Geraldine, P. Molecular Vision, **2016**, 22.
49. Vedagari, A. & Thangarajan, S. Neuropeptides, **2015**.
50. Vedagari, A.; Surekha, R.; Sumathi, T. International Journal of Pharma and Bio Sciences, **2015**, 6, 1.
51. Veerappan, R. & Senthilkumar, R. International Journal of Nutrition, **2015**, 5, 1.
52. Walle, U.K., Galijatovic, A., Walle, T. Biochemical Pharmacology, **1999**, 58.
53. Wang, J.; Qiu, J.; Dong, J.; Li, H.; Luo, M.; Dai, X.; Zhang, Y.; Leng, B.; Niu, X.; Zhao, S.; Deng, X. J Appl Microbiol, **2011**, 111, 6.
54. Woo, K.J., Jeong, Y.J., Park, J.W., Kwon, T.K. Biochemical and Biophysical Research Communications, **2004**, 325.
55. Yang, B.; Huang, J.; Xiang, T.; Yin, X.; Luo, X.; Huang, J.; Luo, F.; Li, H.; Li, H.; Ren, G. J Appl Toxicol, **2013**, 34, 1.
56. Yang, M.; Xiong, J.; Zou, Q.; Wang, D.D.; Huang, C.X. J Mol Histol, **2018, A**.
57. Yang, Z.; Guan, Y.; Li, J.; Li, L.; Li, Z. Eur J Pharmacol, **2018, B**, 836.
58. Yasir, M., Sultana, B., Anwar, F. Journal of.Food Science and Technology, **2017**, 55, 7.
59. Yu, X.M.; Phan, T.; Patel, P.N.; Jaskula-Sztul, R.; Chen, H. Cancer, **2012**, 119, 4.
60. Yumnam, S., Raha, S., Kim, S.M., Venkatamare Gowda Saralamma, V., Lee, H.J., Há, S.E., Heo, J.D., Lee, S.J., Kim, E.H., Lee, W.S., Kim, J.A., Kim, G.S. Oncology Reports, **2018**, 40, 6.
61. Zaric, M.; Mitrovic, M.; Nokolic, I.; Baskic; D.; Popovic, S.; Djurdjevic, P.; Milosavljevic, Z.; Zelen, I. Anticancer Agents Med Chem, **2015**, 15, 2.
62. Zhang, X., Cai, Y., Zhang, W., Chen, X. Biochemistry and Cell Biology, **2018**, 25.
63. Zhang, Z., Li, G., Szeto, S.S.W., Chong, C.M., Quan, Q., Huang, C., Cui, W., Guo, B., Wang, Y., Han, Y., Siu, K.W.M., Lee, S.M.Y., Chu, I.K. Free Radical Biology and Medicine, **2015**, 84.
64. Zheng, X. Meng, W.D., Xu, Y.Y., Cao, J.G., Qing F.L. Bioorg. Med. Chem. Lett, **2003**, 13, 5.
65. Zhu, Z.Y.; Chen, L.; Liu, F.; Chen, L.J.; Meng, M.; Sun, H.Q.; Zhang, Y.M. Arch Pharm Res, **2016**, 39, 10.

Downloaded from www.periodico.tchequimica.com

Tabela 1: Demais trabalhos com avaliações *in vitro* e *in vivo* envolvendo a crisina.

Patologia	Artigo	Ano	Autores
Câncer de mama	Potentiating apoptosis and modulation of p53, Bcl2, and Bax by a novel chrysin ruthenium complex for effective chemotherapeutic efficacy against breast cancer.	Set/2018	Roy, 2018
Depressão	Chronic unpredictable mild stress decreases BDNF and NGF levels and Na^+,K^+ ATPase activity in the hippocampus and prefrontal cortex of mice: antidepressant effect of chrysin	Mar/2015	Filho, 2015
Retinopatia diabética	Chrysin ameliorates malfunction of retinoid visual cycle through blocking activation of AGE-RAGE-ER stress in glucose-stimulated retinal pigment epithelial cells and diabetic eyes	Ago/2018	Kang, 2018
Nefropatia diabética	Chrysin inhibits advanced glycation end products-induced kidney fibrosis in renal mesangial cells and diabetic kidneys.	Jul/2018	Lee, 2018
Colite	Chrysin ameliorates chemically induced colitis in the mouse through modulation of a PXR/NF-κB signaling pathway.	Jun/2013	Dou, 2013
Função plaquetária	Ruthenium-conjugated chrysin analogues modulate platelet activity, thrombus formation and haemostasis with enhanced efficacy.	Jul/2018	Ravisshankar, 2017
Aterosclerose	Evaluation of the anti-atherogenic potential of chrysin in Wistar rats.	Jan/2014	Anandhi, 2014
Inflamação	Chrysin attenuates inflammation by regulating M1/M2 status via activating PPARγ.	Jun/2014	Feng, 2014

Downloaded from www.periodico.tchequimica.com

PERIÓDICO TCHÊ QUÍMICA
ARTIGO ORIGINAL

DESENVOLVIMENTO E VALIDAÇÃO DE MÉTODOS HPLC DE DETERMINAÇÃO QUANTITATIVA DOS ANTIBIÓTICOS DE FLUOROQUINOLONA - HIDROCLORETO DE MOXIFLOXACINA E NORFLOXACINA EM APOIO AO ESTUDO DE ADSORÇÃO EM ZEOLITOS NATURAIS

DEVELOPMENT AND VALIDATION OF QUANTITATIVE DETERMINATION HPLC METHODS OF THE FLUOROQUINOLONE ANTIBIOTICS - MOXIFLOXACIN HYDROCHLORIDE AND NORFLOXACIN IN SUPPORT OF ADSORPTION STUDY ON NATURAL ZEOLITES

ბუნებრივ ცეოლითებზე ადსორბციის შესწავლისათვის ფტორქინოლონური ანტიბიოტიკების - მოქსიფლოქსაცინის ჰიდროქლორიდისა და ნორფლოქსაცინის მესქ მეთოდების შემუშავება და ვალიდაცია

RUBASHVILI, Imeda[1]*; ZAUTASHVILI, Marine[1]; KORDZAKHIA, Teimuraz[1]; EPRIKASHVILI, Luba[1];

[1]Ivane Javakhishvili Tbilisi State University, Petre Melikishvili Institute of Physical and Organic Chemistry

** Correspondence author*
e-mail: rubashvili@yahoo.fr

Received 20 July 2019; received in revised form 10 November 2019; accepted 11 November 2019

RESUMO

Os antibióticos da fluoroquinolona têm sido amplamente utilizados na medicina humana e animal. A poluição residual por antibióticos se tornou um dos mais graves problemas ambientais e de saúde humana atualmente. Portanto, tem sido uma grande exigência desenvolver métodos e tecnologias de tratamento eficientes e econômicos para a remoção de antibióticos da água industrial e doméstica contaminada. Existe a técnica mais utilizada - adsorção para o tratamento de águas residuais. Devido à alta capacidade de troca catiônica, bem como às propriedades das peneiras moleculares, as zeólitas naturais podem ser utilizadas como adsorventes para remoção dos antibióticos mencionados acima das águas residuais e no processo de purificação. A presente pesquisa refere-se ao desenvolvimento e validação de novos métodos de HPLC seletivos, sensíveis e rápidos para a determinação quantitativa dos antibióticos fluoroquinolonas mais frequentemente utilizados - cloridrato de moxifloxacina e norfloxacina em soluções aquosas para medir sua adsorção nas zeólitas naturais e para análises de rotina de águas residuais. Os métodos de HPLC propostos foram validados com relação à robustez (estudo de estabilidade da solução padrão, teste de compatibilidade do filtro de membrana, estudo de efeitos de fatores críticos usando o projeto de experimentos - DoE), teste de adequação do sistema, especificidade, faixa de linearidade (acima da faixa de concentração de 0,05 a 2000 µg/mL para ambos os antibióticos), precisão, exatidão, limites de detecção (LOD) e quantificação (LOQ). O LOD e LOQ foram 0,01 e 0,05 µg/mL para cloridrato de moxifloxacina e 0,008 e 0,05 µg/mL para norfloxacina, respectivamente. O experimento de adsorção por zeólitas naturais, em condições estáticas e dinâmicas, foram usadas para a preparação da amostra de ambos os antibióticos de fluoroquinolona.

Palavras-chave: *Cloridrato de moxifloxacina, Norfloxacina, HPLC, Validação e zeólita natural.*

ABSTRACT

The fluoroquinolone antibiotics have been widely used in human and animal medicine. Residual antibiotics pollution has become one of the most serious environmental and human health problems today. Therefore, it has been a great exigency to develop some efficient and cost-effective treatment methods and technologies for antibiotics removal from industrial and household contaminated water. There is the most used technique - adsorption for the treatment of wastewaters. Due to high cation-exchange ability as well as to the molecular sieve properties, natural zeolites can be used as adsorbents for removal of the above-mentioned antibiotics from wastewaters and in the purification process. The present research concerns the development and validation of new, selective, sensitive and rapid HPLC methods for the quantitative determination of the most frequently used fluoroquinolone antibiotics – moxifloxacin hydrochloride and norfloxacin in aqueous

Downloaded from www.periodico.tchequimica.com

solutions to measure their adsorption on the natural zeolites and for routine analysis of wastewaters. The proposed HPLC methods were validated with respect to robustness (standard solution stability study, membrane filter compatibility test, critical factors effect study using design of experiments - DoE), system suitability test, specificity, linearity-range (over the concentration range of 0.05 to 2000 µg/mL for both antibiotics), precision, accuracy, limits of detection (LOD) and quantitation (LOQ). The LOD and LOQ were 0.01 and 0.05 µg/mL for moxifloxacin hydrochloride and 0.008 and 0.05 µg/mL for norfloxacin, respectively. Adsorption experiment by natural zeolites in static and dynamic conditions was used for sample preparation of both test fluoroquinolone antibiotics.

Keywords: *Moxifloxacin hydrochloride, Norfloxacin, HPLC, Validation, and Natural zeolite.*

რეზიუმე

ფტორქინოლონური ანტიბიოტიკები ფართო გამოყენებას ჰპოვებს ადამიანისა და ცხოველების სამედიცინო პრაქტიკაში. დღეისათვის, ანტიბიოტიკების ნარჩენებით დაბინძურება ერთ-ერთ ყველაზე სერიოზულ პრობლემას წარმოადგენს გარემოსთვის და ადამიანის ჯანმრთელობისთვის. ამიტომ განსაკუთრებულად მნიშვნელოვანია შემუშავდეს ეფექტური და ნაკლები დანახარჯების მქონე საყოფაცხოვრებო და სამრეწველო ჩამდინარე დაბინძურებული წყლებიდან ანტიბიოტიკების მოცილების მეთოდები და ტექნოლოგიები. ადსორბცია ჩამდინარე წყლების გაწმენდისათვის ხშირად გამოყენებად ტექნიკას წარმოადგენს. ბუნებრივი ცეოლითები, რომლებიც ხასიათდებიან მაღალი იონ-მიმოცვლისა და მოლეკულურ-საცრული თვისებებით, შესაძლებელია გამოყენებული იქნას ჩამდინარე წყლებიდან ზემოთხსენებული ანტიბიოტიკების მოცილებისა და გაწმენდის პროცესში. წარმოდგენილი კვლევა ეხება წყალხსნარებში ბუნებრივ ცეოლითებზე ადსორბციის შესწავლისა და ჩამდინარე წყლების რუტინული ანალიზებისთვის ხშირად გამოყენებადი ფტორქინოლონური ანტიბიოტიკების - მოქსიფლოქსაცინის ჰიდროქლორიდისა და ნორფლოქსაცინის რაოდენობრივი განსაზღვრის ახალი, სელექტური, მგრძნობიარე და სწრაფი მაღალეფექტური სითხური ქრომატოგრაფული მეთოდების შემუშავებასა და ვალიდაციას. შემოთავაზებული მესქ მეთოდები ვალიდირებული იქნა შემდეგი პარამეტრების - მდგრადობის (სტანდარტული ხსნარების სტაბილურობის შესწავლა, მემბრანული ფილტრის შესაბამისობის შემოწმება, კრიტიკული ფაქტორების გავლენის შესწავლა ექსპერიმენტის დიზაინის გამოყენებით), სისტემის ვარგისობის შემოწმების, სპეციფიკურობის, სწორხაზოვნება-დიაპაზონის (0.05-დან 2000 მკგ/მლ კონცენტრაციის დიაპაზონში ორივე ანტიბიოტიკისთვის), სიზუსტის, სისწორის, აღმოჩენის ქვედა და რაოდენობრივი განსაზღვრის ზღვრების გამოყენებით. აღმოჩენისა და რაოდენობრივი განსაზღვრის ზღვრებია შესაბამისად 0.01 და 0.05 მკგ/მლ მოქსიფლოქსაცინის ჰიდროქლორიდისათვის, ნორფლოქსაცინისათვის - 0.008 და 0.05 მკგ/მლ. ორივე ფტორქინილონური ანტიბიოტიკისათვის ნიმუშების მომზადებისთვის გამოყენებული იქნა ბუნებრივ ცეოლითებზე ადსორბციის ექსპერიმენტი სტატიკურ და დინამიკურ პირობებში.

საკვანძო სიტყვები: მოქსიფლოქსაცინის ჰიდროქლორიდი, ნორფლოქსაცინი, მესქ, ვალიდაცია და ბუნებრივი ცეოლითები.

1. INTRODUCTION

Today, one of the most serious environmental and human health problems is residual antibiotics pollution. Therefore, it has been a great exigency to develop some efficient and cost-effective treatment technologies for removal of antibiotics residues from industrial and household contaminated waters. One of the most used, cost-effective, and modern technique for wastewaters treatment is adsorption method. Natural zeolite with high cation-exchange abilities and molecular sieve properties has been widely used as an adsorbent in purification processes, for removal of various toxic inorganic and organic compounds from aquatic environments. To conduct adsorption study in order to give information about various solid adsorptive materials for removal antibiotics residues from contaminated water, there are two main separate activities: first of these activities is to develop a method for adsorption study including the investigation of the main factors affected on adsorption process and calculation of the uptake adsorbate and the adsorption capacity. Second is to develop a selective, precise, and a sensitive analytical method for quantitative determination of each adsorbate (contaminant) in sample solution.

Quinolone antibiotics are synthetic

Downloaded from www.periodico.tchequimica.com

antibacterial drugs with the 4-quinolone basic structure. The most commonly used quinolones are fluoroquinolone (FQ) antibiotics. The presence of fluorine atoms is a critical factor for high pharmacological activity. FQs can inhibit the proliferation of many Gram-negative and Gram-positive bacteria [1], so, they have been widely used in human and animal medicine. However, as a result of antibiotic overuse, public concern about FQs has been greatly increasing in the past decades. The environmental concern of FQ residues in the aquatic environments is not only on their potential to increase antibiotic resistance but also on their unfavorable ecotoxicity profile [2]. Moxifloxacin (MOX) and norfloxacin (NOR) belong to the fluoroquinolone antibiotics family. These active pharmaceutical ingredients (API) are frequently used in medical and veterinary practice. The presence of the above-mentioned FQ residues in effluents from households, hospitals, and pharmaceutical industries is a major cause of acute and chronic toxicity, as well as the emergence of resistant bacteria. Consequently, the removal of the FQ residues from aquatic environments, wastewaters is a crucial issue [3]. The structure, main physical-chemical properties, and the content in surface waters [4-6] are shown in Table 1.

Various HPLC methods for the quantitative determination of moxifloxacin [7-13] and norfloxacin [14-17] have been reported in several papers and pharmacopeias [4,5]. A literature review revealed that no adequate and suitable HPLC methods with method validation data for the quantitative determination of MOX and NOR residues at a very low concentration level in aqueous solutions for adsorption study on natural zeolites are to be found. introduction must clearly state the problem, the reason for doing the work, the hypotheses or theoretical predictions under consideration and the essential background. It should not contain equations or mathematical notation. A brief survey of the relevant literature so that a non-specialist reader could understand the significance of the presented results.

The present research concerns the development and validation of new, selective, sensitive and rapid high performance liquid chromatographic (HPLC) methods for the quantitative determination of the most frequently used fluoroquinolone antibiotics – moxifloxacin HCl and norfloxacin in aqueous solutions to measure their adsorption on the natural zeolites namely clinoptilolite, mordenite, and their modified forms.

2. MATERIALS AND METHODS:

2.1. Reagents and chemicals

The certified analytical standards of moxifloxacin hydrochloride and norfloxacin, HPLC grade acetonitrile (ACN), trifluoroacetic acid, orthophosphoric acid, trimethylamine, sodium hydroxide, and hydrochloric acid were purchased from Merk (Germany).

2.2. Instrumentation and materials

HPLC grade purified water was obtained using Milli Q Adventage A10 purification system (France). The chromatographic analysis was performed using LC-20AD Prominence Shimadzu HPLC System (Japan). Analytical balance ALX-210 (USA) and Hanna Instruments HI 2211 pH-meter (USA), also Durapore polyvinylidene difluoride (PVDF) membrane syringe filters were used for standard and sample preparation. All the measuring equipment was appropriately calibrated. The experiment was carried out in climate parameters controlled laboratory area (temperature, t=22±3^{0}C, relative humidity, RH=45±15%). For sample preparation, local natural zeolites – clinoptilolite and mordenite (particle sizes of 0.5-1.0 mm; canal sizes of 0.39 x 0.54 nm) obtained from the regions of Georgia were used as adsorbents which were prepared and treated previously for the method development and validation using the laboratory standard procedure [18].

2.3. Chromatographic system conditions

HPLC analytical methods for the quantitative determination of MOX HCL and NOR in sample aqueous solutions were developed using HPLC column - Agilent SB-C18 4.6 x 250 mm, 5 µm (USA). For MOX HCl determination a mixture of buffer pH 2.5 and ACN 60:40 v/v was used as a mobile phase (MP) with isocratic elution, and for NOR determination - a mixture of buffer - orthophosphoric acid solution (1:1000) and ACN 85:15 v/v; The flow rate of MP was 1.0 mL/min; Detector wavelengths were 293 nm and 275 nm, and Injected volumes were 10 µL and 20 µL for methods of MOX HCl and NOR determination, respectively; The column temperature was maintained at 40°C. The MP was used as a diluent in both analytical procedures. The run time was 5 min for MOX HCl and 11 min for NOR.

Downloaded from www.periodico.tchequimica.com

2.4. Standard and sample preparation

20 mg of the analytical standard of each FQ antibiotic - MOX HCl/NOR was weighed and transferred to 20 mL volumetric flask, dissolved in 15 mL of diluent and then diluted to volume with the same diluent, mixed well (standard stock solution – 1 mg/mL). The obtained solution was filtered through 0.45 µm PVDF membrane syringe filter and transferred 1 mL of this solution to 10 mL volumetric flask, diluted to volume with diluent, mixed well (0.1 mg/mL).

The sample stock solutions (adsorbate influent solution) were prepared the following procedure: MOX HCl and NOR analytical standards were diluted in HPLC grade purified water in order to obtain the concentration of 1.0 mg/mL.

For adsorption process study by static method, 0.2 g of zeolitic adsorbent was transferred to 50 mL Erlenmeyer flask and added 20 mL of each FQ antibiotic sample stock solution. Initially, zeolite sample with adsorbate FQ antibiotic solution was left on an orbital shaker at 150 rpm for 15 min, then statically for the determined time interval. Then the adsorbent sample was centrifuged at 3000 rpm for 5 min. 1 mL of the obtained supernatant was used, transferred 10 mL of volumetric flask and diluted to volume with diluent, mix well.

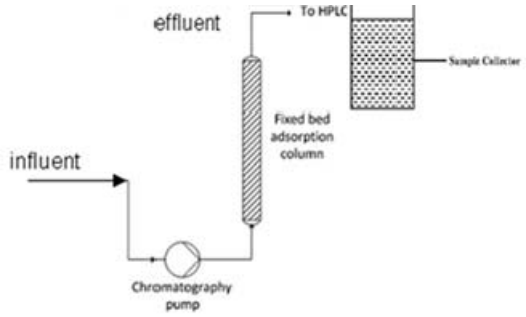

Figure 1. *The laboratory dynamic type equipment for adsorption study.*

For adsorption process study by dynamic method using the specially constructed laboratory dynamic type equipment with fixed bed adsorption glass column (internal diameter - 1.0 cm and length - 8 cm) packed with 9 g of the selected natural zeolite adsorbent and chromatography pump (Figure 1). MOX HCl and NOW influent solutions were added to a glass beaker and pumped with two different flow rates of the influent stream - 1.5 and 5.0 mL/min into the adsorption column. The effluent samples were collected initially, at different time intervals and the end of the adsorption experiment after the saturation state occurred. The obtained solutions were filtered through 0.45 µm PVDF membrane syringe filter, and 1 mL of these solutions were diluted to 10 mL with diluent, mix well. The initial pH value of adsorbate effluent sample solution was adjusted by adding 0.1 M NaOH and HCl solution.

2.5. Analytical method validation

The developed HPLC methods were validated with respect to robustness (standard solution stability, PVDF membrane filter compatibility test, critical factors effect study using design of experiments - DoE) system suitability test (SST), specificity, linearity-range, precision, limits of detection (LOD) and quantitation (LOQ) according to methodologies [19-21] and ICH Q2 guideline requirements [22]. Microsoft Excel was used for statistical assessment and graphical analysis.

2.6. Design of experiments

For the robustness parameter of method validation, the qualitative critical factors were considered and selected, which are given with their levels summarized in table 2. The SST parameters - column efficiency (theoretical plates – N), tailing factor (USP symmetry - As), relative standard deviation (RSD) of peak areas (RSD_A) and RSD of retention times (RSD_{RT}) (n=6) and peak purity (PP) obtained from standard solution chromatograms were used as the response variable for analytical HPLC method. The experiment was conducted in 2^{5-2}=8 runs for five two-level factors.

2.7. Calculation of the content moxifloxacin HCl and norfloxacin in the sample solution

The concentration of each FQ antibiotic – C_u in an effluent sample solution, mg/mL was calculated by the following formula:

$$C_u=A_u\times W\times D_1\times P/A_s\times D_2\times 100 \qquad \text{(Eq. 1)}$$

Where, A_u – The peak area of each FQ obtained with influent/effluent sample solution; A_s – The peak area of each FQ obtained with standard solution; W – The weight of FQ standard, mg; D_1 – The dilution factor of sample solution; D_2 – The dilution factor of standard solution; P – The purity of standard, %.

Downloaded from www.periodico.tchequimica.com

3. RESULTS AND DISCUSSION:

3.1. Robustness study

The final chromatographic conditions were determined by optimizing the system operational parameters: the wavelength for detection, the composition of the mobile phase, the flow rate, the nature of stationary phase and checking the system suitability test parameters: theoretical plates, tailing factor, peak purity, etc. The calibration curve showed very good linearity for a wide concentration range at 293 and 275 nm for MOX and NOR, respectively. Five critical factors were selected, and small variations (low and high levels) were induced in the nominal values of both methods. 8-run design experiment was performed to assess the effect of each factor on the SST results. Table 3 shows the DoE results of the robustness test for the developed HPLC methods. The variability of the checked STT parameters is within the acceptance criteria, and the results show that these analytical procedures are robust.

The stability of the standard solution was studied initially, after 24 hours, 3, 5, 7, 9 days stored at room temperature against a freshly prepared standard solution. The stability was checked using two standard solutions by calculating the percentage difference between peak areas of standard solutions stored and freshly prepared which should not be more than 5.0 % and the bias in terms of peak area between two standard solutions should be within 0.98-1.02 (acceptance criteria). The percentage differences between peak areas obtained with standard solution stored at room temperature for 9 days and freshly prepared one are 4.4 % and 3.9 % for MOX HCl and NOR, respectively. This gives the confidence that FQ antibiotics residues are stable within 9 days, and the concentration does not change in sample solutions during the experiment of adsorption study.

The PVDF membrane syringe filter compatibility was checked using standard solution and by calculating the percentage difference between peak areas of standard solutions filtered and non-filtered, which should not be more than 0.5 % (acceptance criteria). The percentage difference between peak areas of standard solutions filtered and non-filtered is 0.14 % and 0.32 % for MOX HCl and NOR, respectively, which gives the confidence that adsorption of each analyte does not occur on the used membrane syringe filter.

3.2. Specificity

The specificity parameter was checked by injecting standard solution and the background control (without FQ antibiotic) sample solution - blank. The results show that there is no interference from blank and diluent at the retention time of analyte (adsorbate) peak. The MOX and NOR peaks were pure. Purity factor (975 for MOX and 980 for NOR) was more than purity threshold (950). Figure 2, 3 shows the 3D spectra and the chromatogram obtained from the standard solution of MOX HCl and NOR, respectively.

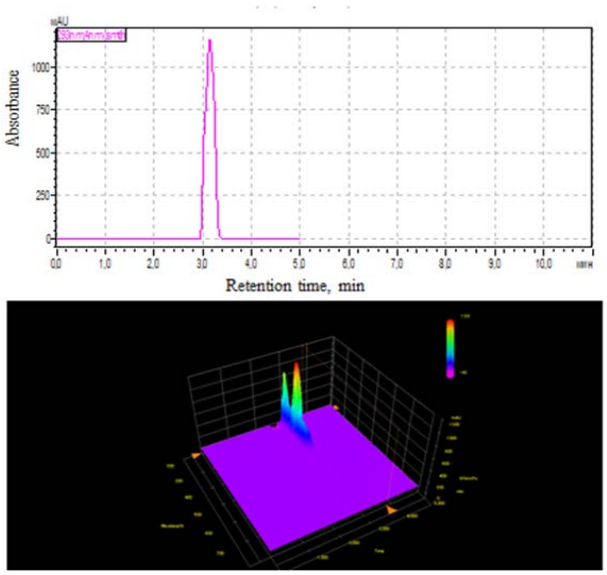

Figure 2. *The chromatogram and the 3D spectra of MOX HCl peak obtained from standard solution with 0.1 mg/mL concentration*

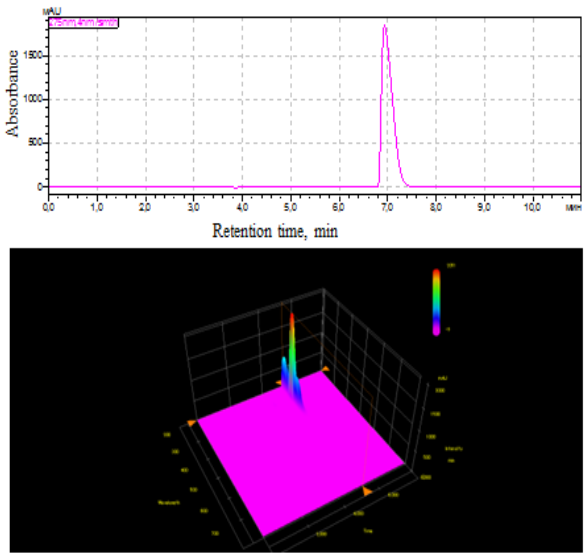

Figure 3. *The chromatogram and the 3D spectra of NOR peak obtained from standard solution with 0.1 mg/mL concentration*

Downloaded from www.periodico.tchequimica.com

Figure 4, 5 shows the chromatogram obtained from the blank solution of MOX HCl and NOR, respectively.

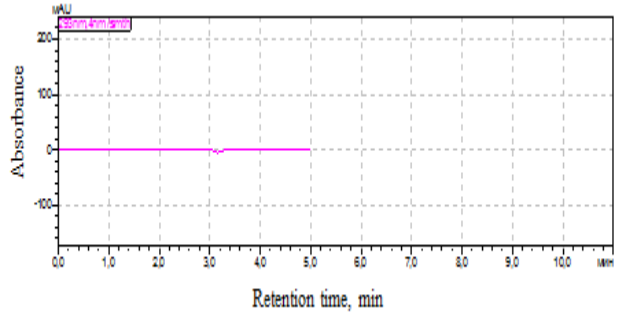

Figure 4. *The chromatogram of blank solution for MOX HCl*

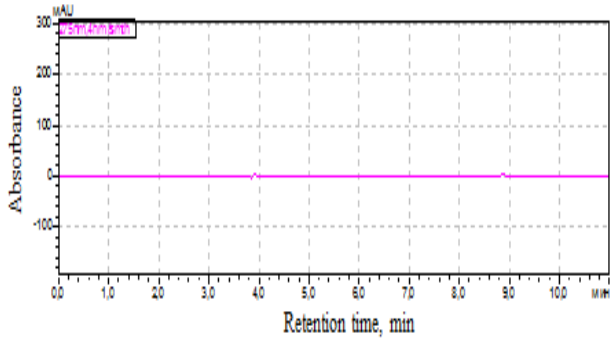

Figure 5. *The chromatogram of the blank solution for NOR*

3.3. Linearity and range; Limits of quantitation (LOQ) and detection (LOD)

The standard working solutions were prepared at six different concentration levels ranging from 0.00005 mg/mL to 2.0 mg/mL from the standard stock solution of both FQ antibiotics - MOX HCl and NOR. Six replicate injections (n=6) were carried out for each concentration level. The linearity over the given range was checked by the square of correlation coefficient - R^2 (acceptance criteria: >0.998), RSD of peak areas - RSD_A (acceptance criteria: <2.0 % for >1.0 mg/mL concentration levels and RSD_A<5.0 % for >0.00005 mg/mL concentration levels and for the last concentration <10 %), RSD of retention times - RSD_{RT} (acceptance criteria: <1.0 %).

The calibration curves (linearity graph) were constructed by plotting the peak area versus the corresponding concentration of the injected working standard solution. The value of the square of the correlation coefficient indicates very good linearity (R2>0.9996 for MOX HCl and R2>0.9999 for NOR). Figure 6, 7 shows the linearity graph for MOX HCl and NOR, respectively.

The limits of quantitation (LOQ) and detection (LOD) were established by injecting a series of stepwise diluted working solutions. The LOQ was estimated by calculating RSD of peak areas - RSD_A for six replicate injections which should be <10 % and the signal-to-noise ratio - S/N - >10 (acceptance criteria). The LOD was estimated to be three times and more of s/N ratio (acceptance criteria). The determined LOQ and LOD for MOX HCl and NOR are presented in Table 4.

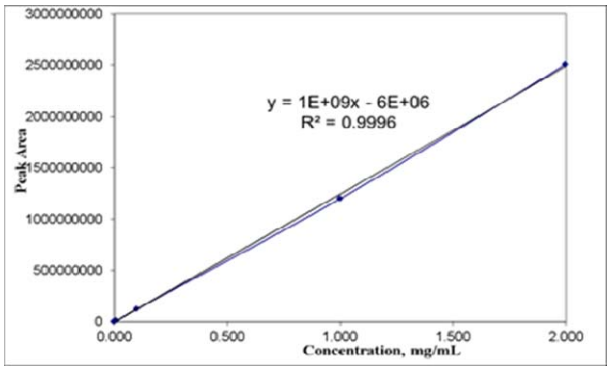

Figure 6. *The calibration curve for MOX HCl over the concentration range 0.00005-2.0 mg/mL*

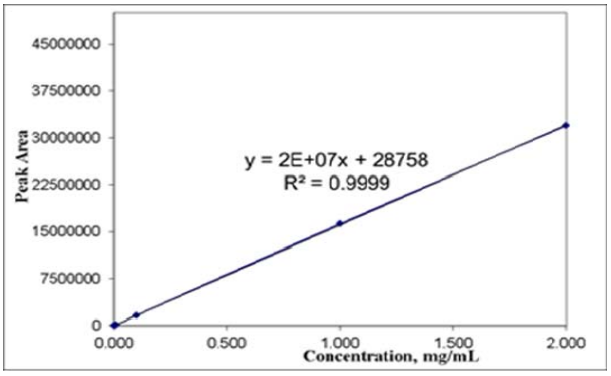

Figure 7. *The calibration curve for NOR over the concentration range 0.00005-2.0 mg/mL*

3.4. System suitability test parameters

The SST parameters were measured in order to check the chromatographic system performance. This test was carried out by six replicate injections (n=6) of the standard solution of each FQ antibiotic. The main SST parameters including RSD of peak areas - RSD_A, RSD of the retention times - RSD_{RT}, peak tailing factor - A_s

Downloaded from www.periodico.tchequimica.com

(USPcoefficient of the peak symmetry $S=W_{0.05}/2f$) and column efficiency - the number of theoretical plates was measured. The results are summarized in Table 5.

3.5. Accuracy

The accuracy was expressed as the percentage of each FQ antibiotic recovered from a spiked sample solution (effluent sample solution + added standard solution) with the corresponding RSD. The average recovery should be within 95.0–105.0 % and RSD of the percentage recoveries should be <3.0 % for each concentration level of spiked solution (acceptance criteria). The recovery - Rec, % was calculated by the following formula:

$$Rec,\%=(C_1-C_2)\times 100/C_s \qquad \text{(Eq. 2)}$$

Where, C_1 – the concentration of each FQ antibiotic obtained with the spiked sample solution, mg/mL, C_2 - the concentration of each FQ antibiotic obtained with the effluent sample solution, mg/mL and C_s – the concentration of each FQ antibiotic obtained with a standard solution, mg/mL [19-21]. The results of the recovery are given in Table 6 which is well within the usually accepted limits indicating the accuracy of both methods.

3.6. Precision

The precision of the developed analytical methods was estimated by measuring repeatability (intra-day) on six replicate injections of standard solution and on six individual determinations of MOX HCl, and NOR in sample solution obtained using adsorption static method. For sample preparation, 0.2-0.2 g of zeolite adsorbent samples were transferred separately to six 50 mL Erlenmeyer flasks and added 20 mL of each FQ antibiotic standard stock solutions at 1.0 mg/mL concentration. Initially, zeolite samples with adsorbate FQ antibiotic solutions were left on an orbital shaker at 150 rpm for 15 min, then statically for 3 hours. After that zeolite samples were centrifuged at 3000 rpm for 5 min and 1-1 mL of the obtained supernatants were used and diluted to 10 mL with diluent, mix well. The precision was checked by calculating RSD of the concentration of each FQ antibiotic, mg mL-1 and retention times of MOX and NOR for six individual determinations which should not be more than 5.0 % and 1.0 %, respectively. The results are shown in Table 7. Figure 8, 9 shows chromatograms obtained from sample solutions. The results were within than acceptance criteria which indicate that this method has good precision.

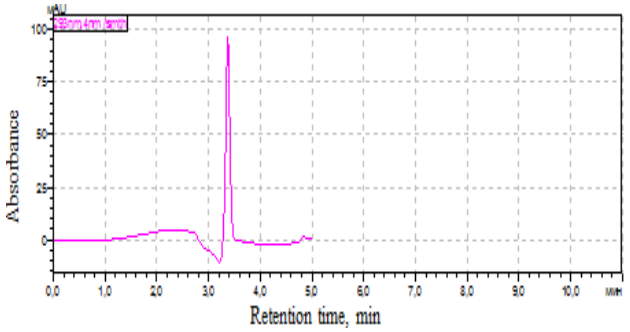

Figure 8. *The chromatogram of effluent sample solution of MOX HCl*

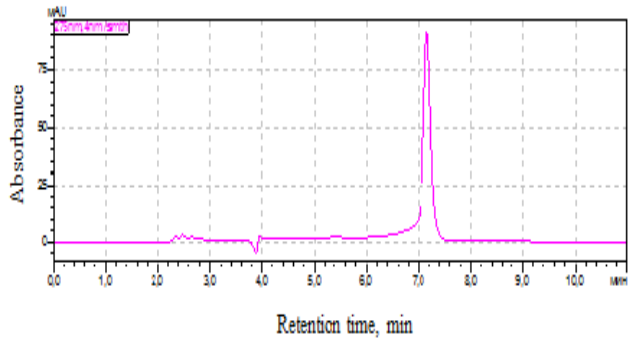

Figure 9. *The chromatogram of effluent sample solution of NOR*

4. CONCLUSIONS:

Analytical procedures were developed and validated for the quantitative determination of moxifloxacin HCl, and norfloxacin in aqueous solutions was found to be robust, precise, linear and accurate. No interferences from blank solution were observed. Hence, the proposed and validated HPLC methods can be successfully used to measure adsorption of moxifloxacin HCl and norfloxacin on the natural zeolites and their modified forms; also, they can be applied by other laboratories for routine analysis of wastewaters and pharmaceutical formulations containing the above-mentioned APIs.

5. ACKNOWLEDGMENTS:

The research was financially supported by the Shota Rustaveli National Science Foundation within the framework of project #217138.

Downloaded from www.periodico.tchequimica.com

6. REFERENCES:

1. Bryan, L.E.; Bedard, J.; Wong, S.; Chamberland, S. *Clin. Invest. Med.* **1989**, 12 (1), 14.
2. Golet, E.M.; Alder, A.C.; Giger, W. *Environ. Sci. Technol.* **2002**, 36, 3645. http://dx.doi.org/10.1021/es0256212.
3. Prutthiwanasan, B.; Phechkrajang, C.; Suntornsuk, L. *Talanta.* **2016,** 159, 74. http://dx.doi.org/10.1016/j.talanta.2016.05.080.
4. US Pharmacopeia National Formulary USP 41-NF-36, Moxifloxacin, The United States Pharmacopeial Convention. United Book Press, Inc: Baltimore, 2018.
5. US Pharmacopeia National Formulary USP 41-NF-36, Norfloxacin, The United States Pharmacopeial Convention. United Book Press, Inc: Baltimore, 2018.
6. Suzuki S.; Phuong Hoa P.T. *Front. Microbiol.* **2012**, 3. http://dx.doi.org/10.3389/fmicb.2012.00067.
7. Wang, N.; Zhu, L.; Zhao, X.; Yang, W.; Sun. H. *Int. Sch. Res. Notices Pharmacol.* **2013**, 7. http://dx.doi.org/10.1155/2013/462918.
8. Xu, H.; Xin, D.; Yu, Y.; Li, Z.; Lu, J. *J. Chromatogr. B.* **2010,** 878 (32), 3437. http://dx.doi.org/10.1016/j.jchromb.2010.10.024.
9. Ashour, S.; Kattan, N. *SOJ Pharm. Pharm. Sci.* **2016**, 3 (3), 1. http://dx.doi.org/10.15226/2374-6866/3/3/00145.
10. Abdelaziz, A.A; Elbanna, T.E.; Gamaleldeen, N.M. Braz. *J. Microbiol.* **2012,** 43 (4), 1291. http://dx.doi.org/10.1590/S1517-83822012000400008.
11. Razzaq, S.N.; Khan, I.U.; Mariam, I.; Razzaq, S.S. *Chem. Cent. J.* **2012,** 6 (1), 1. http://dx.doi.org/10.1186/1752-153X-6-94).
12. Motwani, S.K.; Khar, R.K.; Ahmad, F.J.; Chopra, S.; Kohli, K.; Talegaonkar S. *Anal. Chim. Acta***. 2007,** 582 (1) 75. http://dx.doi.org/10.1016/j.aca.2006.08.053.
13. Razzaq, S.N.; Ashfaq, M.; Khan, I.U., Mariam, I., Razzaq, S.S.; Azeem, W. *Arab. J. Chem.* 2017, 10 (3), 321. http://dx.doi.org/10.1016/j.arabjc.2014.11.016.
14. Chierentin, L.; Nunes Salgado, H.R. *J. Chromatogr. Sep. Tech.* **2013,** 4 (171). http://dx.doi.org/10.4172/2157-7064.1000171.
15. Khan, F.U.; Iqbal, Z.; Khan, I.; Shahbaz, N.; Hassan, M.; Ullah, F. *J. Chromatogr. B.* **2016,** 1017–1018, 120. http://dx.doi.org/10.1016/j.jchromb.2016.03.002).
16. Negeswara-Rao R.; Nagaraju V. *J. Pharm. Biomed. Anal.* **2004,** 34 (5), 1049-1056. http://dx.doi.org/10.1016/j.jpba.2003.11.009.
17. Oliveira, P.R.; Bernardi, L.S.; Mendes, C.; Cardoso, S.G.; Sangoi, M.A.; Silva, M.R. *J. Chromatogr. Sci.* 2009, 47 (9), 739. http://dx.doi.org/10.1093/chromsci/47.9.739.
18. Rubashvili, I.; Eprikashvili, L.; Kordzakhia, T.; Zautashvili, M.; Pirtskhalava, N.; Dzagania M. *Mediterr. J. Chem.* **2019**, 9 (2), 142.
19. Rubashvili, I.; Tsitsagi, M.; Ebralidze, K.; Tsitsishvili, V.; Eprikashvili, L.; Chkhaidze, M.; Zautashvili, M. *Eurasian J. Anal. Chem.* **2018,** 13 (2), em06. http://dx.doi.org/10.29333/ejac/82931.
20. Rubashvili, I.; Karukhnishvili, N.; Makharadze, M. *Rev. Roum. Chim.* **2018,** 63 (3), 205.
21. Rubashvili, I.; Tsitsagi, M; Tsitsishvili, V.; Kordzakhia, V.; Ebralidze, K.; Buzariashvili, M.; Khachidze, M. *The Chemist.* **2019,** 91 (2), 33.
22. International Conference on Harmonization, Harmonized Tripartite guideline, Validation of analytical procedures, text and methodology Q2 (R1). Brussels, Belgium, 2005.

Downloaded from www.periodico.tchequimica.com

Table 1. *The structure, main physical-chemical properties and the content in surface water of MOX and NOR*

Parameter	**FQ antibiotics**	
	MOX	**NOR**
Molecular formula	$C_{21}H_{24}FN_3O_4$	$C_{16}H_{18}FN_3O_3$
CAS number	354812-41-2	70458-96-7
Molecular structure	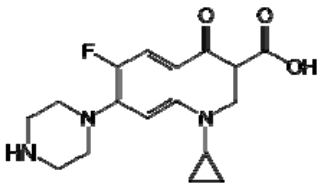	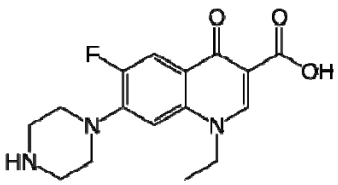
Molecular weight, g/mol	401.438	319.331
The acid dissociation constants, pKa	pKa1=6.43; pKa2=10.63	pKa1=0.16; pKa2=8.68
Chemical name	(4aS-cis)-1-Cyclopropyl-6-fluoro-1,4-dihydro-8-methoxy-7-(octahydro-6H-pyrrolol[3,4-b]pyridin-6-yl)-4-oxo-3-quinolinecarboxylic acid	1,4-Dihydro-1-ethyl-6-fluoro-4-oxo-7-(1-piperazinyl)-3-quinolinecarboxylic acid
Water solubility, mg/mL at 25^0C and pH 5-7.5	1.15-5	0.45-161
Concentration in surface water, μg/L	0.006-0.017	0.0023-0.12
Toxicity, oral LD50 (rat), g/kg	1.32	4

Table 2. *Robustness factors and design of experiment*

#	**Factor (Xi)**	**Unit**	**Low Level (-)**	**Nominal Level (0)**	**High Level (+)**
1	Flow rate of MP (X1)	mL/min	0.9	1.0	1.1
2	MOX/NOR standard stock solution (X2)	pH	4.0	7.0	-
3	ACN percentage in MP for MOX/NOR (X3)	%	35 10	40 15	45 20
4	Column temperature (X4)	°C	35	40	45
5	DAD wavelength for MOX/NOR (X5)	nm	291 273	293 275	295 277

Downloaded from www.periodico.tchequimica.com

Table 3. *The results of the robustness parameter (critical factors effect study)*

#	Factors					Parameters							
						N		A_s		RSD_A, %		RSD_{RT}, %	
	X1	X2	X3	X4	X5	MOX	NOR	MOX	NOR	MOX	NOR	MOX	NOR
1	+	+	+	+	+	2865	3895	1.22	0.96	1.362	0.736	0.698	0.365
2	+	+	-	+	+	2563	3645	1.35	0.93	1.568	0.987	0.745	0.498
3	+	-	+	-	+	3256	3712	1.27	0.91	1.032	0.898	0.125	0.245
4	+	-	-	-	-	2463	3100	1.18	0.89	1.500	1.456	0.632	0364
5	-	+	+	-	-	3125	3564	1.23	0.93	1.952	1.365	0.455	0.522
6	-	+	-	-	+	3145	3666	1.09	0.86	1.300	1.112	0.245	0.601
7	-	-	+	+	-	2699	3056	1.11	0.87	0.856	1.354	0.112	0.471
8	-	-	-	+	+	2491	3444	1.13	0.89	1.505	1.866	0.733	0.326
Acceptance criteria						>2000		<2.0		<2.0		<1.0	

Table 4. *The LOQ and LOD of MOX HCl and NOR methods*

Parameter	**Value**	
	MOX HCl	**NOR**
LOQ, mg/mL	0.00005	0.00005
LOD, mg/mL	0.00001	0.000008
RSD of peak areas for LOQ (n=6)	3.561	2.956
RSD of retention times for LOQ (n=6)	0.671	0.583
s/N for LOQ	25	21
s/N for LOD	4	7

Table 5. *The system suitability parameters results*

Parameter	**MOX HCl**	**NOR**	**Acceptance criteria**
N	3166	4532	>2000
RSD_A (n=6), %	1.796	1.629	<2.0
RSD_{RT} (n=6), %	0.762	0.866	<1.0
A_s	1.12	0.93	<2.0

Downloaded from www.periodico.tchequimica.com

Table 6. *The results of the accuracy study*

Added standard solution, mg/mL	Average concentration of spiked sample solution, mg/mL (n=3)	Concentration of effluent sample solution, mg/mL	Acceptance criteria
MOX HCl			
0.0788	0.1319	0.05650	97.5
0.0985	0.1527		98.5
0.1182	0.1750		100.2
Average recovery - Rec, %			98.7
RSD, % of the percentage recoveries			1.383
NOR			
0.0797	0.1654	0.0862	99.7
0.0996	0.0961		96.5
0.1195	0.1222		102.3
Average recovery - Rec, %			99.5
RSD, % of the percentage recoveries			2.920

Table 7. *The results of the precision study*

The number of sample solution	MOX HCL		NOR	
	Concentration, mg/mL	Retention time, min	Concentration, mg/mL	Retention time, min
1	0.0351	3.326	0.0401	7.674
2	0.0385	3.388	0.0421	7.537
3	0.0355	3.390	0.0435	7.578
4	0.0341	3.347	0.0445	7.495
5	0.0377	3.345	0.0412	7.529
6	0.0366	3.352	0.043	7.480
Average	0.0363	3.358	0.0424	7.549
SD	0.002	0.026	0.002	0.070
RSD	4.582	0.762	3.774	0.931

Downloaded from www.periodico.tchequimica.com

PERIÓDICO TCHÊ QUÍMICA
ARTIGO ORIGINAL

INFLUÊNCIA DO USO DO ÓLEO DA *CARAPA GUIANENSIS* (ÓLEO DA ANDIROBA) COMPARADO COM FLUIDO DE CORTE COMERCIAL NO PROCESSO DE TORNEAMENTO DO AÇO ABNT 1045

INFLUENCE OF THE USE OF *CARAPA GUIANENSIS* OIL (ANDIROBA OIL) COMPARED WITH COMMERCIAL CUTTING FLUID IN THE TURNING PROCESS OF THE ABNT 1045 STEEL GRADES

BOTELHO, Tamires Isabela Mesquita[1*]; FIGUEIREDO, Gleidson Silva[1]; PRAXEDES Fernanda Malato[2]; TEIXEIRA, Jean Valdir Uchôa[2]; MONTEIRO, Elane Botelho[3];

[1] Universidade Federal do Pará, Faculdade de Engenharia Mecânica, Campus Belém, Belém – PA, Brasil

[2] Instituto Federal do Pará, Faculdade de Engenharia Materiais, Campus Belém, Belém – PA, Brasil

[3] Universidade do Vale do Taquari (UNIVATES), Programa de Pós-Graduação em Sistemas Ambientais Sustentáveis, Lajeado/RS – Brasil

* Autor correspondente
e-mail: tamiresisabela@yahoo.com.br

Received 19 July 2019; received in revised form 15 October 2019; accepted 13 November 2019

RESUMO

Os crescentes avanços tecnológicos obtidos tanto no desenvolvimento de novos materiais como de máquinas ferramenta aumentaram a demanda pelos processos de usinagem e aliado a isto o uso de fluidos de corte aumentou. Entretanto é necessário que os fluídos de corte possuam características que não agridam o ambiente ou o operador. Nos processos de usinagem os fluidos de corte, quando escolhidos e aplicados apropriadamente, podem refletir em benefícios durante o processo de fabricação. Este trabalho avaliou o desempenho de um fluido de corte comercial comparando-o com óleo vegetal extraído da carapa guianensis no processo de torneamento do aço abnt 1045. Manteve-se a velocidade de corte (vc), avanço da ferramenta (f) e a profundidade de corte (ap) e verificou-se a influência do uso de ambos a quais exerciam sobre o metal com as seguintes variáveis: análise do cavaco, acabamento superficial, temperatura de corte e desgaste da ferramenta. Foi observado que com a utilização do com óleo da andiroba gerou-se melhor cavaco para a segurança do operador, maiores temperaturas de corte na peça, maior desgaste da ferramenta e melhor acabamento superficial com diferença de 23%, comparado com fluido de corte comercial. Sendo assim o fluido à base da andiroba pela aplicação convencional comparado com o fluido de corte comercial demonstrou uma alternativa viável no processo de torneamento do aço abnt 1045, pelo fato de ser biodegradável e redução dos fluidos de corte derivados do petróleo.

Palavras-chave: *fluido de corte comercial, óleos vegetais, carapa guianensis, temperatura da peça, desgaste da ferramenta.*

ABSTRACT

The increasing technological advances obtained both in the development of new materials and of machine tools increased the demand for the machining processes and in addition, the use of increased cutting fluids. However, it's necessary to have characteristics that don't harm the environment and the operator. In machining processes, cutting fluids, when properly chosen and applied, may reflect benefits during the manufacturing process. This work evaluated the performance of a commercial cutting fluid by comparing it with vegetable oil extracted from carapa guianensis in the abnt 1045 steel turning process. The cutting speed (vc), tool feed (f) and depth (ap) and the influence of the use of both of them on the metal was verified with the following variables: chip analysis, surface finish, cutting temperature and tool wear. It was observed that with the use of andiroba oil, better chip was generated for the safety of the operator, higher cutting temperatures in the piece, higher tool wear and better surface finish with a difference of 23% compared to commercial cutting fluid. Thus, the fluid from andiroba based on the conventional application demonstrated a viable alternative in the turning process of abnt 1045 steel, because it's biodegradable and reduces petroleum-based cutting fluids.

Downloaded from www.periodico.tchequimica.com

Keywords: *commercial cutting fluid, vegetable oils, carapa guianensis, temperature of the part, tool wear.*

1. INTRODUÇÃO

A usinagem está presente na confecção dos mais variados produtos de diferentes ramos setoriais. É um processo de fabricação por remoção de cavacos. Sendo assim, todo processo em que há uma peça bruta que, após ser removido material em forma de cavaco de seu interior e exterior, formando uma peça com superfícies desejadas, detalhadas e acabadas de forma que satisfaça plenamente ao cliente, é considerado um processo de usinagem (Santos e Dias, 2010). Durante os processos de usinagem as ferramentas aquecem e sofrem altos desgastes que exigem trocas constantes de suas arestas de corte. Além disto, há o aquecimento das peças usinadas, o que pode provocar dois efeitos indesejáveis: alterações nas dimensões pretendidas e geração de tensões internas que podem comprometer a utilização das mesmas. Para minimizar os desgastes das ferramentas e o aquecimento das peças, vários recursos podem ser utilizados, entre os quais o emprego de um fluido de corte.

Com o aumento das atividades industriais e a evolução dos processos de usinagem, houve um acréscimo no consumo dos fluidos de corte, e também a necessidade dos fluidos serem mais eficientes. Surgiram então os fluidos de corte de extrema pressão (E.P.) que são óleos emulsionáveis, usados quando a lubrificação é um fator importante, isto é, em velocidades reduzidas de corte (onde o coeficiente de atrito é grande) e para usinagem de materiais mais duros. Nos dias de hoje, após constantes desenvolvimentos, surgiram óleos contendo cloro, associações de cloro e enxofre, fósforo enxofre e cloro (Diniz e Scandiffio, 2001).

O emprego de fluidos de corte melhora a eficiência dos processos de usinagem proporcionando: aumento da vida da ferramenta de corte, maior controle de tolerâncias dimensionais, melhoria no acabamento superficial da peça usinada, promove a redução nas forças de usinagem e amenização de vibrações (Rodrigues, 2005; Stemmer, 2005). O efeito do uso de fluidos de corte depende não somente das propriedades do fluido, mas também das condições de usinagem, ou seja, da ferramenta de corte, material peça e parâmetros de corte.

No entanto, apesar de todos os benefícios dos fluidos de corte, pesquisas ressaltam que sua aplicação cria severos impactos ambientais, como a poluição ou contaminação da água, do solo, e do ar, além de problemas para a saúde dos operadores. Neste cenário, tendências tecnológicas e de aplicação visam à redução, substituição ou à eliminação do uso dos fluidos de corte nos processos de usinagem (Vacaro, 2009; Souza, 2011; Lawal *et al*; 2012). Dentre os diversos tipos de fluidos de corte existentes, os fluidos de corte emulsionáveis, principalmente aqueles de base mineral, ainda são os mais utilizados nas indústrias metal-mecânica devido ao custo-benefício. Esses fluidos, dependendo da sua concentração, apresentam alto poder refrigerar a peça-ferramenta, fundamental para usinagem com altas rotações. Estudos realizados comparam fluidos sintéticos, semi-sintético, emulsionáveis e concluem que aqueles que utilizam emulsão são mais favoráveis que os demais para a propagação de microrganismos (Moore *et al.*, 2000; Veillete *et al.*, 2004).

Atualmente existe um crescente desenvolvimento de fluidos de corte com base em diversos óleos vegetais, por serem biodegradáveis e ambientalmente amigáveis. Alguns trabalhos como os óleos de milho, mamona, soja e recentemente a andiroba (Botelho *et al.,* 2019 e Grosse *et al.*, 2016). Com isso existe uma utilização e potencial como fluido de corte, nos processos de usinagem, no entanto segundo Gonçalves (2013) poucas pesquisas relatam estudos sobre a reologia e tribologia de óleos vegetais.

O aço ABNT 1045 é muito utilizado no setor metal-mecânica, possui características de boa usinabilidade, boa resistência mecânica, média soldabilidade e alta forjabilidade, sendo aplicado na fabricação de eixos e peças para indústria agrícola, automobilística, de máquinas e equipamentos em geral (Araújo, *et al*., 2015).

O objetivo deste trabalho é investigar a temperatura de corte, acabamento superficial, desgaste da ferramenta e análise do cavaco resultante em operação de torneamento do aço ABNT 1045, com velocidade de corte (vc), avanço da ferramenta (f) e a profundidade de corte (ap) iguais, comparando a influência do fluido de corte comercial com óleo vegetal extraído da *Carapa Guianensis*.

Downloaded from www.periodico.tchequimica.com

2. MATERIAIS E METÓDOS

2.1. Materiais

Para a realização da usinagem dos metais, foi utilizado um torno mecânico convencional, modelo Nardini NZ VS (figura 1). Foram utilizadas ferramentas bits de aço rápido 3/8 x 3” 12, com ângulos αo= 02°; $\gamma 0$ = 46°.

Figura 1. *Torno mecânico convencional*

Os materiais utilizados para a confecção dos corpos-de-prova foram 2 (duas) barras cilíndricas (tarugos) de 38mm de comprimento x 23mm de diâmetro de aço ABNT 1045 (Figura 2). Não foi feita nenhum tratamento térmico, sendo ensaiados em estado bruto, com dureza apresentada na Tabela 1. O fluido de corte utilizado foi o óleo emulsionável, fluido biodegradável elaborado a partir de aditivos de extrema pressão, aditivos (anti-ferruginosos), bactericidas, anti-espumantes e corantes, o fabricante recomenda a utilização pura ou diluída em água sendo a cada 1 litro para 19 litros de água.

O sistema utilizado para aplicação do fluido foi de forma convencional, métodos como este encontram-se na literatura (Biscione, 2010; Magri, 2015) que proporcionou uma vazão em torno de 757,23 mL/s. O fluido aplicado não foi diluído em água, pois segundo Muniz (2008), a estabilidade das emulsões de um fluido de corte pode ser afetada pela qualidade da água; esta deve ser isenta de impurezas, microorganismos e excesso de cloro. A dureza da água é uma propriedade de grande importância no preparo das emulsões.

Figura 2. *Corpo-de-prova do aço ABNT 1045.*

Tabela 1. *Dureza do aço ABNT 1045*

Aço ABNT	HB
1045	174 ± 0,5

2.1. Métodos

O fluido de corte, óleo da *carapa guianensis*, foi coletado de forma artesanal no município de Igarapé-Mirim (PA), sendo este material rejeito do processo de fabricação artesanal da região. O fluido foi aplicado na zona de corte via a técnica convencional por inundação (vazão de 630,93 ml/s) e na direção (sobrecabeça, como ilustrado na Figura 3).

A análise do pH foi realizada com pHmetro portátil digital da marca HI221. A viscosidade dinâmica da carapa guianensis utilizou-se um viscosímetro do fabricante Hake à temperatura de 40°C, uma vez que abaixo de 25°C o óleo permanece solidificado. Esta temperatura foi mantida constante durante o experimento utilizando um cilindro coaxial modelo VT-550, segundo a norma ASTM D 2770-4.

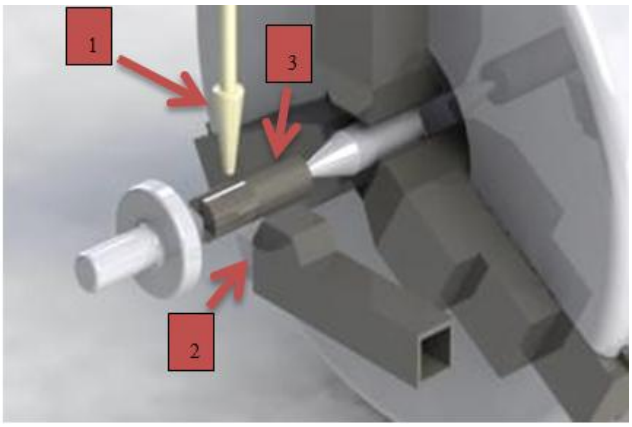

Figura 3. *Detalhe da montagem do sistema ferramenta-peça, com a seta 1 indicando o bocal, seta 2 a ferramenta de corte e a seta 3 a disposição da peça entre ponta.*

Downloaded from www.periodico.tchequimica.com

Foram definidos os seguintes parâmetros de corte como variáveis de entrada: velocidade de corte (Vc), avanço (f) e profundidade (ap), sendo obtida a Vc através da Equação (1).

$$Vc = \frac{\pi.d.n}{1000} \quad \text{(Eq. 1)}$$

Aplicada as condições de d = 23 mm e "n" igual à velocidade de rotação (m/mim), idênticas ás todas as operações de usinagem, tem-se, conforme Tabela 2.

Tabela 2. *Parâmetros de corte como variáveis de entrada.*

Vc (m/min)	f (mm/volta)	ap (mm/volta)
298	0,053	0,5

No processo de torneamento, após o primeiro e o último passe da usinagem de cada corpo-de-prova, foram coletados os cavacos resultantes, que foram analisados de acordo com a norma ISO 3685 para todas as amostras. Uma técnica de medição encontrada na literatura (Silva, Konno, *et.al.*, 2015) foi seguida. O termômetro infravermelho digital foi colocado de maneira que os pontos de corte sempre estivessem direcionados na zona do corte conforme mostra a Figura 4.a.

As aquisições dos dados foram possíveis através da interface do computador com o software de dados térmicos da termocâmera FLIR Tool®. Antes e após os processos de torneamento foi feita a captura das imagens para a identificação e análise visual do desgaste da ferramenta de corte. Para esta análise, utilizou-se o Microscópio Cooling Tech U200X (figura 4.b), com a ampliação do local especifico da ponta da ferramenta nas vistas superior e lateral (figura 4.c).

Por fim, após a usinagem dos corpos-de-prova foi realizada a análise do acabamento superficial de cada amostra em todas as condições citadas anteriormente, através do rugosímetro portátil digital modelo TR200 (figura 4.d). O parâmetro utilizado foi o desvio aritmético médio (Ra), cujo valor representa a média dos valores absolutos das coordenadas em relação á linha média no comprimento de amostragem (NBR ISO 4287, 2002).

3. RESULTADOS E DISCUSSÃO:

3.1. Viscosidade Dinâmica a 40°C e pH

O fluido de corte comercial utilizado no procedimento experimental possui a viscosidade cinemática de 2,2 Pa.s na temperatura de 20°. O valor de viscosidade dinâmica do óleo da *Carapa Guianesis* a 40°C, foi de 0,11 Pa.s (110 cP). Utilizando valores de densidade da literaturade 0,87 kg/m³ (Maia et al., 2014), estima-se que a viscosidade cinemática seja de 12,64 cSt.

Segundo Souza (2009), a viscosidade deve ser satisfatoriamente baixa para permitir uma boa movimentação do fluido e alta o suficiente para que ocorra uma boa aderência do fluido às superfícies da ferramenta, comportamento observado no óleo da andiroba. Ao satisfazer estes aspectos, o óleo de andiroba atua como lubrificante, reduzindo o atrito na interface peça-ferramenta. Como consequência, pode ocorrer uma redução das forças de corte e da rugosidade, este último analisado posteriormente. A elevada precisão de lubrificação torna-se uma vantagem do uso de fluidos de corte de base vegetal em relação os fluidos de cortes solúveis, independentes da condição de corte empregada (Gonçalves, 2013). Contudo, segundo Silva (2000), quanto menos viscoso for o fluido de corte melhor será a operação de usinagem.

O pH (potencial hidrogeniônico) é um indicativo da ação de microrganismos no fluido de corte devido a produção de subprodutos ácidos em seu metabolismo, além do consumo de emulgadores e agentes anticorrosivos. Como efeito, ocorre a redução do pH da emulsão e da proteção anticorrosiva (Boufleuer, 2004). O fluido de corte comercial utilizado possui pH 10,0, sendo este um valor ótimo de trabalho (Grub apud Runge e Duarte, 2013).

A análise de pH do óleo de andiroba revelou uma média de 2,3. Este valor se encontra abaixo dos valores encontrados na literatura. Melo da Silva et al. (2014) avaliaram parâmetros físico-químicos dos óleos de andiroba comercializados em 3 localidades, onde as médias de pH foram de 4,95 (supermercado), 5,80 (Bragança) e 5,83 (Ver-O-Peso). O pH encontrado para óleo de andiroba é significativamente mais ácido que o recomendado para os fluidos comerciais. Contudo, o pH ácido não é favorável ao crescimento de bactérias, os quais preferem

Downloaded from www.periodico.tchequimica.com

ambientes de neutralidade (6,5-7,5) (Grub apud Tortora, 2013), de forma que o crescimento de bactérias pode não ser favorecido. Deve-se ressaltar, no entanto, que elevada acidez não é desejável, pois contribui para os processos corrosivos (Maia *et al*., 2015).

3.2. Análises do Cavaco

A análise realizada nos cavacos resultantes no processo de usinagem do aço ABNT 1045 com aplicação do fluido de corte comercial e óleo da andiroba é mostrada na Tabela 2. Sua obtenção foi no decorrer de cada torneamento correspondente a cada condição e conforme a norma ISO 3685.

Observa-se que na condição com fluido de corte comercial o cavaco obtido é contínuo e helicoidal tipo arruela longo, isso acontece na usinagem de materiais dúcteis como aços, o metal cisalha na zona primária de cisalhamento com grandes deformações e permanece homogêneo, sem fragmentação mesmo de forma de fita externa não é possível observa nenhuma evidência clara de fratura ou trinca, esses fenômenos ocorrem para que uma nova superfície seja formada. Com o óleo da andiroba comportou-se como tubular emaranhada longo é um processo diferente do cavaco contínuo devido à diminuição da resistência mecânica do metal pelo aumento da temperatura (Machado, 2011).

3.3. Rugosidade

Na Figura 5 são mostrados os valores parâmetro Ra (μm), obtidos dos corpos de prova para as condições com o óleo da andiroba e com fluido de corte comercial do aço ABNT 1045.

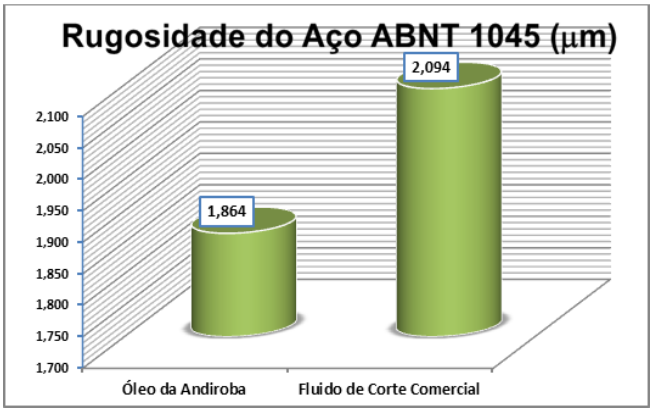

Figura 5. *Rugosidade da peça.*

Quanto aos valores de rugosidade, da Figura 5 observa-se que houve um melhor acabamento superficial com o uso do óleo da *Carapa Guinanesis* diminui 23% em relação ao fluido de corte comercial. A redução da rugosidade corrobora o bom desempenho do óleo de andiroba como lubrificante na viscosidade de trabalho encontrada.

Pesquisas vêm sendo realizadas para maior otimização dos processos de usinagem, para que se tenha uma melhor peça acabada, desta forma, irá agir de maneira direta ao desgaste da ferramenta. Botelho (2019) comparou a análise de acabamento superficial em aços ABNT 1020 e 1045 e apresentou comportamento semelhante com o uso do óleo da andiroba.

O desempenho do óleo do coco babaçu usado na técnica mínima quantidade de fluido – MQF, com diferentes vazões, durante o processo de usinagem o fresamento, apresentou menores resultados, ou seja, melhor acabamento superficial, comparado com o fluido de corte comercial, devido o atrito na interface cavaco-ferramenta (Araújo *et al*., 2013).

Um estudo da minimização do custo-benefício de usinagem por torneamento de aço ABNT 52100, aplica-se o método de superfície de resposta foi realizado por Mendes *et al*. (2007), considerando a vida da ferramenta e o acabamento superficial da peça. Seus resultados indicam que a diminuição do custo é obtida com as maiores rotações, ou seja, velocidades de corte utilizadas no seu experimento, com maiores taxas de remoção de material da peça usinada.

3.4. Temperatura da Peça

A temperatura de corte é um resultado da união dos seguintes parâmetros: Processo de torneamento, máquina ferramenta, ferramenta de corte, material e os diferentes fluídos de corte. A Figura 6 mostra a comparação das curvas de temperatura em função do tempo para as condições com o óleo da andiroba e com fluido de corte comercial.

Downloaded from www.periodico.tchequimica.com

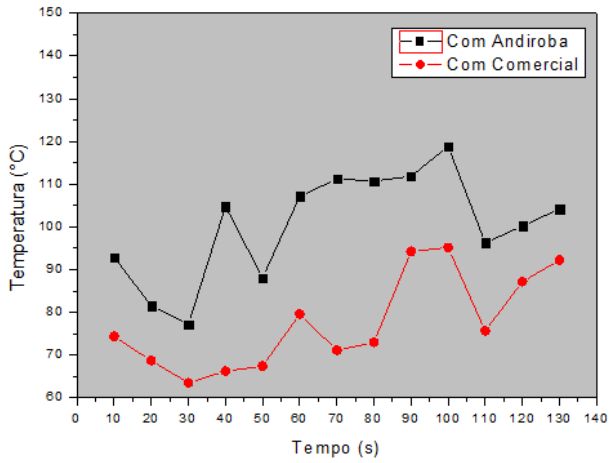

Figura 6. *Temperatura pelo tempo do aço ABNT 1045 com óleo da andiroba e com fluido de corte comercial.*

Segundo Diniz (2013) O aumento da temperatura está diretamente ligada com a velocidade de corte e consequentemente o conjunto ferramenta/peça, com a elevação da temperatura haverá alteração nas propriedades mecânica da ferramenta que diminuirá sua vida útil e reduzirá de maneira drástica sua produtividade, elevando o custo e tempo.

A redução da temperatura para o caso do uso de fluido de corte comercial é devido o fluido reduzir a área de contato na interface cavaco-ferramenta, diminuindo, dessa forma, a zona de aderência na superfície de saída do cavaco (Machado *et al*., 2009). Fluido de corte emusionável possui em sua composição aditivos de extrema pressão, aditivos (anti-ferruginosos), bactericidas, anti-espumantes e corantes, o que contribui para a diminuição da temperatura de corte no processo de torneamento. E a inconstância na curva de temperatura de corte no caso de utilização do fluido provavelmente deve-se ao sistema de aplicação utilizado (convencional).

Neste caso, devido à velocidade de corte estipulada e com o uso da *Carapa Guianesis*, houve um aumento na velocidade de escoamento do cavaco que conseqüentemente, ocasionou um aumento significativo da temperatura sobre a superfície de saída da ferramenta, fato também observado por Nouari *et al*. (2005) e Botelho *et al*. (2019).

Suarez *et al.* (2009) estudaram as temperaturas de usinagem que influencia no controle dimensional no processo de fabricação e no rugosidade final das peça. O aumento da temperatura somou-se ainda para diminuir as forças e a potência de usinagem. Sabe-se que a interface de contato entre a ferramenta-peça trabalho no processo de usinagem na superfície de flanco está sujeita a pressões elevadas e consequentemente a altas temperaturas (Tönshoff, 2004). Durante o processo de torneamento, observou-se que houve várias oscilações de temperatura para todas as condições. Tais resultados já são conhecidos da literatura (Guimarães, 2014; Haddag e Nouari, 2013).

3.5. Desgaste da Ferramenta

A seguir são apresentadas as imagens laterais e de topo, com seus respectivos desgastes e $VB_{Máx}$ das ferramentas utilizadas no processo experimental (figura 7).

O calor gerado durante a usinagem desses materiais é concentrado na região de corte, resultando em elevadas temperaturas nessa região, que aumentam os desgastes da ferramenta de corte por processo termicamente induzido, como difusão e a reação química entre a ferramenta e o material da peça (Shokrani *et al*. 2012). A usinagem com o óleo da andiroba apresenta maior desgaste da ferramenta de corte, para os parâmetros de corte definidos nesta pesquisa, isso se deve pela falta de aditivos, por ser um óleo vegetal puro comparado com o fluido de corte que obteve menor desgaste da ferramenta, ou seja, maior vida útil. Consequentemente, esses parâmetros irão refletir na baixa qualidade e alto custo de fabricação da peça (Korkut *et al.* 2003).

4. CONCLUSÕES:

Os resultados obtidos dos testes de torneamento, nas condições impostas pela metodologia do presente trabalho, possibilitaram as seguintes conclusões:

• O óleo da *carapa guianensis* apresentou valores para a análise da viscosidade dinâmica a 40°C de 0,11 Pa.s e o fluido de corte comercial a 20°C de 2,2 Pa.s. Para a análise de pH o resultado adquirido foi de 2,3 e 10, respectivamente para a andiroba e fluido comercial;

• Em relação ao estudo do cavaco, a condição com óleo da andiroba gera melhor segurança ao operador;

• Os valores de rugosidade média, Ra, a diferença de 23%, para o óleo da andiroba que obteve melhor acabamento superficial;

• A aplicação da andiroba proporcionou maiores temperaturas de corte na peça.

Downloaded from www.periodico.tchequimica.com

• Por fim, relacionado ao desgaste da ferramenta de corte, com o óleo da andiroba obteve maior VBmáx.

5. AGRADECIMENTOS:

Agradecemos a Base Naval de Val-de- Cans (BNVC), pelo espaço experimental, ao Instituto Federal Pará (IFPA), pelas análises e ao Conselho Nacional de Desenvolvimento Científico e Tecnológico (CNPq).

6. REFERÊNCIAS

1. ASTM D (**2004**), 2770-04: *Standard practice for calculating viscosity index from kinematic Viscosity at 40 and 100*. Annual Book of ASTM Standards, ASTM International, West Con-shohocken.
2. Araujo, A. S., Machado, A. R., Neves, T. E. S., Paiva, A. E., Rodrigues, J. R. P.; Esforços de usinagem e acabamento superficial no fresamento frontal do aço abnt 1045 com aplicação mqf do óleo refinado vegetal de coco babaçu. 7º Congresso brasileiro de engenharia de fabricação, Penedo, Rio de Janeiro, Brasil, 20-24 de maio de **2013**.
3. Araujo, A. S., Farias, F. P, Morais, L. O. Anais do 8º Congresso Brasileiro de Engenharia de Fabricação, **2015**.
4. Biscione, R. P. B. Dissertação (Mestrado) - Universidade Estadual Paulista, Faculdade de Bauru, **2010**.
5. Botelho, T. I. M, Monteiro Junior, P. L., DA Silva, M. A. S., Da Silva, R. B., Saldanha, A. Periódico Tchê Química, v. 31, p. 12, **2019**.
6. Boufleuer, N. T. Dissertação (mestrado) - Universidade Federal do Acre, Rio Branco, AC, Brasil, **2004**.
7. Diniz, A. E., Scandiffio, I. Anais do 1º Congresso Brasileiro de Engenharia de Fabricação, **2001**.
8. Diniz, A. E., Coppini, N. L. Tecnologia da Usinagem dos Materiais. 8 ed. Janeiro **2013**, p. 26.
9. Gonçalves, J.F.S. Proposição de método de desenvolvimento de fluido de corte de base vegetal. Tese de Doutorado, Instituto Tecnológico da Aeronáutica, São José dos Campos, São Paulo, Brasil, **2013**.
10. Grosse, T., Winter, M., Baron, S., Hoffmeister, H., Herrmann, C., Droder, K. CIRP Journal of Manufacturing Science and Technology. p. 89-98, **2016**.
11. Guimarães, C. B. Dissertação (mestrado), Universidade Federal do Pará, Pará, Brasil, **2014**.
12. Haddag, B., Nouari, M. Wear. 302, 1158–1170, **2013**.
13. Korkut, I; Kasap, M.;Ciftci, I; Seker, U. *Materials and Desing*. Turkey, v.25, p.303-305, out. **2003**.
14. Grub, A. M. Dissertação de Mestrado. Universidade Federal de Uberlândia, Uberlândia, MG. Brasil, **2013.**
15. ISO (**1993**) 3685: *Tool Life Testing with Single-Point Turning Tools*. ISO - International Organization for Standardization.
16. Lawal, S.A., Choudhudhury, I.A., Nukman, Y. J. Clean. Prod. 41, 210 e 221. **2013.**
17. Magri, A. XIX Colóquio de Usinagem, Anais em CD Rom, Artigo: 12. **2010.**
18. Machado, Á. R., Abrão, A. M., Coelho, R. T.; Da Silva, M. B. Teoria da Usinagem dos Materiais. 2.ed. São Paulo - SP: Editora Edgard Blucher, **2011**. 397p.
19. Machado, A.R.; Da Silva, M.B.; Coelho, R. T; Abrão, A. M. Teoria da Usinagem dos Materiais. 1ªed. São Paulo: Editora Blucher, **2009**.
20. Maia, D. J., Segre, N., Scatigno, A. G., Stella, M. B. Experimentação no Ensino de Química. P. 71-75, **2015**.
21. Melo da Silva, P. M, Da Silva, D. P, De Souza, E. C, Dos Silva, A. S, Muller, R. C. S. 54° Congresso Brasileiro de Quimica. Natal, Rio Grande o Norte, Brasil, 3 – 7 de outubro de **2014**.
22. Mendes, R. R. A, Paiva, A. P, Ferreira, J. R., 4º Congresso Brasileiro de Engenharia de Fabricação. Águas de São Pedro, SP, Brasil, 15-18 de abril de **2007**.
23. Moore, J.S., Christensen, M., Wilson, R.W., Wallace Jr.,R.J., Zhang, Y., Nash, D.R., Shelton, B. AIHAJ. USA, v. 61, n°2, p. 205-13, abr. **2000**
24. Muniz, C.A.S. Tese de Doutorado. Universidade federal do Rio Grande do Norte, RN, Natal, Brasil, **2008**.

Downloaded from www.periodico.tchequimica.com

25. NBR ISO (**2002**) 4287: Especificações geométricas do produto (GPS) - Rugosidade: Metódo do perfil - Termos, definições e parâmetros da rugosidade. NBR - Norma Brasileira. Interna-tional. ISO - Organization for Standardization
26. Nouari M., List G., Gehin D., Gomez B., Manaud J. *Wear behaviour of cemented carbide tools in dry machining of aluminum alloy*. França, **2005**.
27. Rodrigues, J. R. P. Revista Maquinas e Metais, v.476, pp.42-53, **2005**.
28. Santos, L. K; Dias, S. Estudo da viabilidade de modernização de um setor de usinagem de uma metalúrgica. <https://www.trabalhosfeitos.com/ensaios/Usinagem/43891630.html> Acessado em 01 de maio de 2016.
29. Shokrani, A.;Dhokia, V.; Newman, S.T.. International Journal of Machine Tools and Manufacture. United Kingdom, v.57, p. 83-101, Fev. **2012**.
30. Souza, A. J. de. Processos de fabricação por usinagem < http://en.lccv.ufal.br/wpcontent/uploads/sites/17/2015/04/ApostilaUsinagem_Parte1.pdf >. Acessado em 29 dez. 2015.
31. Souza, J. Dissertação (mestrado) - Instituto Tecnológico da Aeronáutica, São Paulo, SP, Brasil, **2009.**
32. Stemmer, C.E. Ferramentas de Corte I. Editora da UFSC, 6ª Edição, Florianópolis, **2005**.
33. Suarez, M. P., Costa, E.S., Machado, A.R., Abrão, A.M., V Congresso Brasileiro de Engenharia de Fabricação, Belo Horizonte, MG, Anais em CD Rom, Artigo: 011072262, 14-17 de Abril de **2009**.
34. Tönshoff, T., Ben Amor, R., Pereira, A. A., Boehs L. III Congresso Nacional de Engenharia Mecânica, Belém, PA, Brasil, 10-13 de agosto de **2004**.
35. VACARO, Tiago. Redução da utilização de fluidos de corte: uma abordagem ecológica na gestão de processos de usinagem.<https://www.ucs.br/ucs/pesquisa/jovenspesquisadores2009/trabalhos/poster/e_TiagoVacaro.pdf>. Acessado em 24 julho 2016.
36. Veillete, M., Thorne, P.S., Gordon, T.;Duchaine, C. *Six Month Tracking of Microbial Ghowth in a Metalworking Fluid After Sytem Cleaning and Recharging. Ann Occup Hyg*. Canadá, v. 48, n° 6, p. 541-546, Agosto. **2004**

Downloaded from www.periodico.tchequimica.com

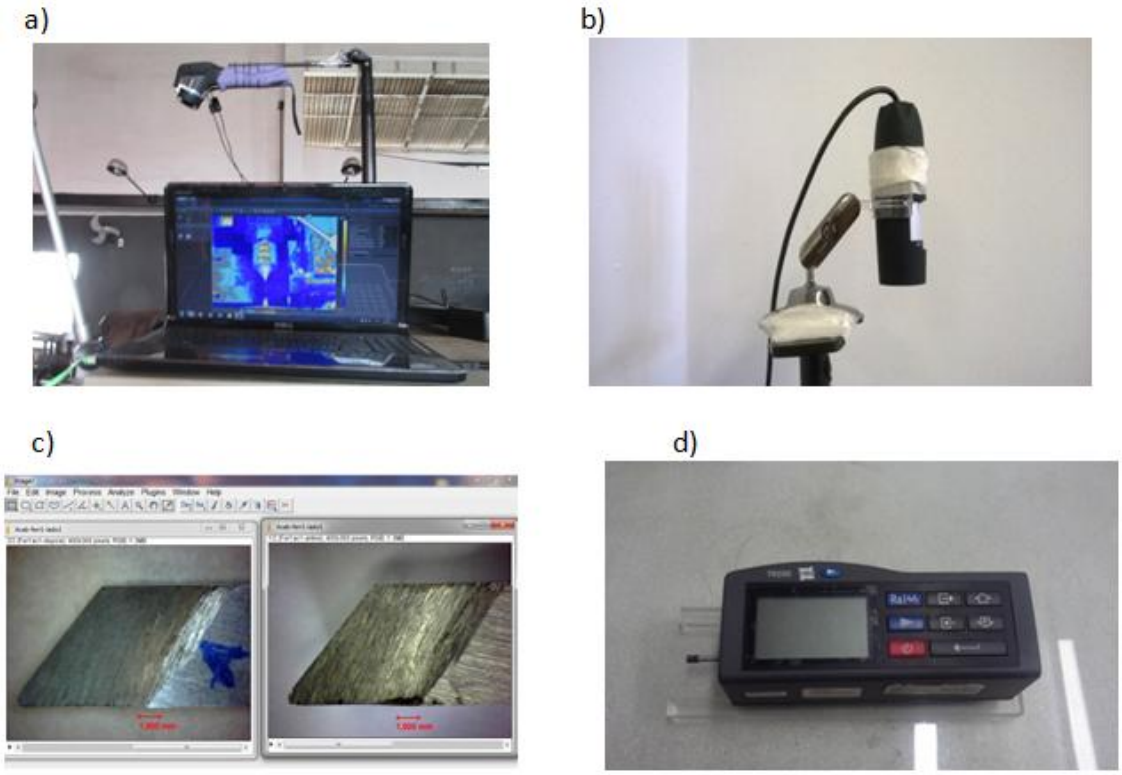

Figura 4. *a) Disposição do termômetro infravermelho em relação ao torno; b) microscópio cooling tech; c)vistas superior da ponta da ferramenta; d)rugosimetro digital.*

Tabela 2. *Cavaco gerado no torneamento, com fluido de corte comercial e óleo da andiroba.*

Fluido de Corte Comercial	Óleo da Andiroba
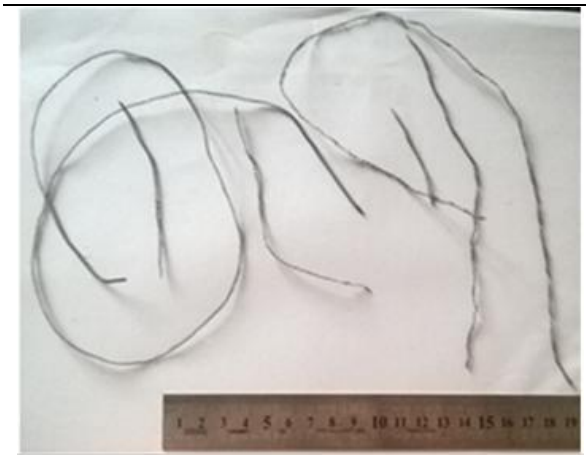	

Downloaded from www.periodico.tchequimica.com

PERIÓDICO TCHÊ QUÍMICA
ARTIGO ORIGINAL

ESTUDO DAS PROPRIEDADES TERMOFÍSICAS E FÍSICO-MECÂNICAS DE FERRO FUNDIDO DE ALTA LIGA DE ALUMÍNIO CHYU22SH

STUDY OF THE THERMOPHYSICAL AND PHYSICAL - MECHANICAL PROPERTIES OF HIGH-ALLOYED ALUMINUM CAST IRON CHYU22SH

ИССЛЕДОВАНИЕ ТЕПЛОФИЗИЧЕСКИХ И ФИЗИКО-МЕХАНИЧЕСКИХ СВОЙСТВ ВЫСОКОЛЕГИРОВАННОГО АЛЮМИНИЕВОГО ЧУГУНА ЧЮ22Ш

ZHUMADILOVA, Zhanar O.[1]; KALDYBAYEVA, Saule T.[2]; NURULDAEVA, Gulzhan Zh.[3]; KUMAR, Dauren B.[4]

[1,3] Kazakh National Research Technical University named after K. I. Satpayev (Satbayev University), Institute of Architecture and Civil Engineering, 22 Satpayev Str., zip code 050013, Almaty – Republic of Kazakhstan (phone: +77771388677)

[2,4] Al-Farabi Kazakh National University, 71 Al-Farabi Avenue, zip code 050040, Almaty Republic of Kazakhstan

** Corresponding author*
e-mail: zhanar_85@mail.ru

Received 26 June 2019; received in revised form 05 November 2019; accepted 16 November 2019

RESUMO

Ligas de alta liga, nas quais cromo e níquel são elementos de liga, são amplamente utilizados como materiais resistentes ao calor. Seu conteúdo total em ligas resistentes ao calor atinge 30% ou mais. No entanto, a vida útil das peças de trabalho feitas de ligas resistentes ao calor é limitada. Além disso, quanto maior a temperatura de operação, menor é a vida útil. Isso leva ao aumento de custos para manter as unidades em condições de trabalho. Exemplos dessas peças são a grade de máquinas de aglomeração, detalhes de plantas de caldeiras, fornos de torrefação, aquecimento e fusão de vidro, moldes de fundição, coletores de exaustão de motores forçados de automóveis, entre outros exemplos. A esse respeito, reduzir o custo de produtos resistentes ao calor, mantendo suas características operacionais e vida útil, torna-se uma necessidade. Uma das opções promissoras para resolvê-lo é fabricar essas peças de ferro fundido de alumínio resistente a altas temperaturas CHYU22SH (CHYU22SH - ferro fundido padrão). As peças fundidas de ferro fundido CHYU22SH diferem, em primeiro lugar, pela resistência ao calor a altas temperaturas no ar (até 1100 ° C) e em meios contendo enxofre, dióxido de enxofre, óxidos de vanádio e vapor de água. Além disso, elas podem operar funcionalmente como um produto resistente ao desgaste, com alta resistência a temperaturas normais e elevadas. O trabalho apresenta as propriedades térmicas e mecânicas da fundição, bem como os resultados da análise microestrutural de ferros fundidos de alta liga de alumínio. Os resultados de análises e testes mostram que a liga de ferro fundido CHYU22SH pode ser obtida por fundição com paredes longas com uma espessura de 4 mm, sem defeitos externos e internos. Ao fazê-lo, as peças fundidas têm uma estrutura uniforme, propriedades mecânicas altas e estáveis, além de serem inferiores em ~ 17-24% em peso do que um ferro fundido semelhante. Os resultados de estudos laboratoriais experimentais - industriais de laboratório confirmam a influência das condições de solidificação nos parâmetros da estrutura do ferro fundido CHYU22SH.

Palavras-chave: *análise microestrutural, teste tecnológico, teste em escala piloto, peça fundida, capacidade de aquecimento.*

ABSTRACT

Highly alloyed alloys, in which expensive chromium and nickel are alloying elements, are widely used as heat-resistant materials. Their total content in heat-resistant alloys reaches 30% or more. However, the life of working parts made of heat-resistant alloys is limited. Moreover, the higher the operating temperature, the shorter it is. This leads to increased costs for maintaining the units in working condition. Examples of such parts are the grate of agglomeration machines, details of boiler plants, roasting, heating, and glass melting furnaces,

Downloaded from www.periodico.tchequimica.com

casting molds, exhaust manifolds of forced automobile engines, etc. In this regard, reducing the cost of heat-resistant products, while maintaining their operating characteristics and life, becomes very actuality. One of the promising options to solve it is to manufacture these parts made of high-alloyed heat-resistant aluminum cast iron CHYU22SH (CHYU22SH - standard cast iron). Castings made of cast iron CHYU22SH differ, first of all, by being heat resistance at high temperatures in air (up to 1100 °C) and in media containing sulfur, sulfur dioxide, oxides of vanadium, and water vapor. In addition, they can functionally operate as a wear-resistant product having high strength at normal and elevated temperatures. The paper presents the thermal and mechanical properties of casting, as well as the results of microstructure analysis of aluminum cast irons. The results of analyses and tests show that cast iron CHYU22SH can be obtained by casting with long walls of a thickness of 4 mm without external and internal defects. By doing so the castings have a uniform structure, high and stable mechanical properties, as well as lower by ~17-24% weight than similar cast of gray iron. The results of experimental - industrial testing laboratory studies confirm the influence of solidification conditions on the parameters of the structure of cast iron CHYU22SH.

Keywords: *microstructural analysis, technological test, pilot-scale testing, cast part, heat capacity.*

АБСТРАКТ

В качестве жаростойких материалов широко применяют в основном высоколегированные сплавы, в которых легирующими элементами являются дорогостоящие хром и никель. Общее содержание их в жаростойких сплавах достигает 30 % и более. Тем не менее, срок жизни рабочих деталей из жаростойких сплавов ограничен. Причем, чем выше рабочие температуры, тем он короче. Это обусловливает повышенные затраты на поддержание агрегатов в рабочем состоянии. Примерами таких деталей являются колосники агломерационных машин, детали котельных установок, обжиговых, нагревательных и стекловаренных печей, формы для литья, выхлопные коллекторы форсированных автомобильных двигателей и др. В связи с этим, снижение затрат на жаростойкие изделия при сохранении их рабочих характеристик, в том числе и срока службы, становится весьма актуальной задачей. Одним из перспективных вариантов ее решения является изготовление таких деталей из высоколегированного алюминиевого жаростойкого чугуна ЧЮ22Ш (ЧЮ22Ш-стандартный чугун). Отливки из чугуна ЧЮ22Ш отличаются, прежде всего, жаростойкостью при высоких температурах как в воздушной среде (до 1100° С) так и в средах, содержащих серу, сернистый газ, окислы ванадия и пары воды. Кроме того, они функционально могут работать и как износостойкие изделия, имеющие высокую прочность при нормальной и повышенной температурах. В работе представлены теплофизические, литейные и механические свойства, а также результаты микроструктурного анализа алюминиевых чугунов. Результаты анализов и лабораторных испытаний свидетельствуют о том, что из чугуна ЧЮ22Ш могут быть получены отливки с протяженными стенками толщиной 4 мм без наружных и внутренних дефектов. При этом они имеют однородную структуру, высокие и стабильные показатели механических свойств, а также меньшую на ~ 17 - 24 % массу, чем аналогичная отливка из серого чугуна. Результаты опытно – промышленного опробования подтверждают данные лабораторных исследований о влиянии условий затвердевания отливок на параметры структуры чугуна ЧЮ22Ш.

Ключевые слова: *микроструктурный анализ, технологическая проба, опытно–промышленные опробования, литая деталь, теплоемкость.*

INTRODUCTION

Design technology in modern foundries uses a variety of commonly used software packages for modeling of mold filling, solidification, and cooling of castings. Using these programs help to solve many technological problems. One of the stages of modeling in such programs (LVMFlow, ProCAST, Polygon) is the choice of the alloy from the database. Unfortunately, iron CHYU22SH is not present in any of the databases of the above-mentioned programs. Accordingly, casting simulation in the production of castings from this alloy is not possible. In the database for jobs of preparing a new alloy, it is necessary to know some of its properties, including its thermophysical properties.

Heat-resistant materials are widely used in most high alloys, which are expensive alloying elements chromium and nickel. The total content of heat-resistant alloys then reaches 30% or more. However, the life of the working parts of the heat-resistant alloys is limited. Moreover, the higher its operating temperatures, the shorter its life. This results in a higher cost to maintain the units in working condition. Examples of such devices are grate sintering machines, parts of boilers, kilns, glass furnaces and heaters, molds,

Downloaded from www.periodico.tchequimica.com

exhaust manifold-boosted automobile engines.

MATERIALS AND METHODS

2.1 Thermophysical properties

Thermophysical properties of cast iron are needed for computer simulation of melt filling of the cavity mold, solidification, and cooling of the castings in order to select the best technology option of obtaining them without having casting defects. However, such information on cast iron CHYU22SH is virtually non-existent. In (Kovalevich, 1991, Zhuravlev, 1981) writing indicates that the specific heat of aluminum cast-iron type CHYU22SH at normal temperature is lower than that of gray and ductile cast irons, with increasing temperature as the thermal conductivity of aluminum iron increases at a time when the undoped iron is reduced (Ten, 2015). Therefore, at high temperatures (900 – 1000 °C) a superior thermal conductivity CHYU22SH GCI (gray cast iron) and HCING (high-strength cast iron with nodular graphite) are produced (Kumanin, 1976).

It was measured the specific heat, thermal conductivity, and thermal diffusivity of CHYU22SH iron in the temperature range 500 - 1000 °C. Experiments were conducted in the laboratory of Satbayev University on the devices NETZSCH DSC 404 C Pegasus (to determine the heat capacity) and the NETZSCH LFA 457 Micro-Flash® (for the determination of heat and thermal diffusivity). Tests were conducted on specimens made of strong cast samples and had a density of 5909 kg/m^3. Sample sizes had a diameter of 12.700 mm and a thickness of 3.1580 mm (Tanski, 2016; Jiang, 2016, Lagunov, 1980). The results are shown in Table 1 as the mean values of five measurements.

According to our data the specific heat of cast iron CHYU22SH increases with increasing temperature to 536 J/kg K at 500 °C and 585 J/kg K at 1000 °C, which is comparable with that of the undoped cast iron with spheroidal graphite (nodural cast iron with nodular graphite, 570 - 592 in 500 °C and 595-649 at 1000 °C).

Thermal conductivity of cast iron CHYU22SH increases with increasing temperature and is more significant than the heat - from 12.64 W/m·K at 500 °C to 15.53 W/m·K at 1000 °C. The obtained values are much smaller than given in (Kaldybayeva, 2011): 16.28 W/m K at 200 °C and 26.75 W/m·K at 500 °C. At the (Kaldybayeva, 2011) same temperature (500 °C) values, differ by more than double. It is assumed that in the figures more reliable heat, as obtained on modern equipment, is shown with each value measured five times and performed in a wide range of temperatures. On this basis, (Kaldybayeva, 2011) can assume that the aluminum cast iron CHYU22SH has a thermal conductivity approximately 3 times lower than the undoped iron CING (cast iron with nodular graphite) with ferritic metal matrix, which at 400 °C has a thermal conductivity of 38 W/(m·K). Since the thermal conductivity in undoped iron decreases with increasing temperature, while the cast iron CHYU22SH is on the rise at the operating temperature of 1000 - 1100 °C, this difference should be much reduced (Utepov, 2014; Ten, 2016; Safronov, 2017, Kerzhentsev, 1971).

Thermal diffusivity in iron CHYU22SH increases monotonically with $4 \cdot 10^{-6}$ m^2/s to $4.5 \cdot 10^{-6}$ m^2/s with increasing temperature from 500 to 1000 °C. The (Kaldybayeva, 2011) lack of published data does not allow comparing the obtained values. In undoped cast iron CING (cast iron with nodular graphite) the indicator is $(5.5\text{-}6.5) \cdot 10^{-6}$ m^2/s at 600 °C and $(5.0\text{-}5.6) \cdot 10^{-6}$ m^2/s at 800 °C. Comparison of the data shows that the iron CHYU22SH at 600 and 800 °C has a thermal conductivity at 33 and 20% lower, respectively, but at higher temperatures and thermal irons CHYU22SH and CING can be slightly different (Kaldybayeva, 2011; Stefanescu, 2017; Utepov, 2017; Prasad, 2018; Martin, 2016, Sitko, 2017).

To assess the possibility of obtaining a particular set of alloy castings its casting properties such as fluidity, shrinkage, the mechanical effect of the distance, and the distance of the profits are needed to be known.

2.2. Casting properties

To assess the possibility of obtaining a particular set of alloy castings, we need to know its casting properties such as fluidity, shrinkage, the mechanical effect of the distance, and the distance of the profits.

The results of determining the parameters of fluidity and shrinkage of cast iron CHYU22SH are shown in Table 2.

As can be seen, the spiral fluidity test values that are measured are comparable with published data; however, free casting shrinkage is less than 1.5 times when compared with the data (Tanski, 2016). In (Utepov, 2014; Zhang, 2018; Paul, 2018) with increasing carbon content in the

Downloaded from www.periodico.tchequimica.com

aluminum cast iron above 2%, a decrease of fluidity occurs as a result of the graphite in the melt.

Preshrinkage expansion of high-alloyed aluminum cast iron CHYU22SH is much smaller compared with that of the undoped cast iron (0.07%) (Galdin, 1992).

2.2.1. Power options castings

There is a need for supply of castings devoid of the formation of these defects in the form of shrinkage cavities and shrinkage porosity. The latter is a consequence of the formation in the inner sections of the casting of closed areas in which the solidification of the alloy occurs under conditions of full or partial nutritional deficiency (Kurdyumov, 1996; Galdin, 1992).

Casting alloys are characterized by varying propensity for the formation of shrinkage defects. The share of volume shrinkage, which is found in the form of shrinkage cavity and porosity shrinkage, mainly depends on the interval of crystallization of the alloy and the casting cooling intensity. Alloys that have a small range of crystallization shrinkage of its volume mainly found in the form of shrinkage cavities are required. Alloys with a wide range of crystallization of a large or a significant portion of the volumetric shrinkage found in the form of shrinkage porosity are also required. At the same time with increasing intensity of the cooling sections of the casting a high temperature gradient is formed, due to the width of the two-phase solid-liquid region at the final stage of solidification, which is narrow and, consequently, reduces the proportion of volume shrinkage that is found in the form of shrinkage porosity (Galdin, 1992; Vasiliev, 1976; Kavalevich, 1991). All other things being the same, the tendency of the alloy for forming shrinkage defects in the form of shrinkage cavities and shrinkage porosity increases with an increase in its volumetric shrinkage (Table 3).

In most cases, high volumetric shrinkage results in the formation of shrinkage in the castings because of unacceptable defects in the form of internal shrinkage cavities and shrinkage porosity. It is necessary to provide good quality castings to eliminate them. This is achieved by setting profits in the right place, required quantity, and sufficient size. At the same time directional solidification condition in which the solidification front moves sequentially from the end parts (peripheral areas) to the inside, from thin to thick walls, and the latter to the profits must necessarily be provided. The number and size of the profits should be necessarily minimum. This minimizes the consumption of metal in the profit and complexity of their subsequent separation from the castings.

To solve such a complex task requires knowledge of the power setting of castings, that is, the distance (radius) L_{dp} of the food arrived, the distance of the mechanical effect of $L_{me,}$ and the total area of effective supply $L_{\Sigma} = L_{dp} + L_{me}$. These parameters are estimated as multiples of the casting thickness t or the reduced-thickness R = V/S, where V and S, are, respectively, the amount fed host (casting) and surface cooling. These strongly depend on the type of alloy (Table 4).

Regarding the influence of the thickness of the casting on these parameters, we have only a few observations. For high-alloy cast iron, aluminum CHYU22SH data on the parameters of supply castings are completely absent. However, this iron has a high volumetric shrinkage (3.2-7.0% according to (Kovalevich, 1991) 4.5-8%, according to (Stefanescu, 2017; Jiang, 2016; Shayakhmetov, 2014)) and because of the casting during solidification, it will become malnourished. But without knowing the parameters of supply castings from this alloy, we cannot properly organize the directional solidification.

Therefore, we require a detailed study of the power settings of cast iron CHYU22SH casting. To do this, we developed a 2-, 3-, and 4-lobed squared test. Figure 1 gives an example of a 2-blade test. The sample consists of a riser - a profit 1, profit platform (base) 2, and immediately squared tests 3.

Profit for the samples was calculated by the method of Namur – Shklennik (Equation 1):

$$V_p = m \cdot \xi \cdot R_{TU}{}^3 \cdot (1+\beta)^3 \cdot y \cdot z + 3 \cdot \beta \cdot V_f \quad \text{(Eq.1)}$$

where: m - is the coefficient of non-identity of the metal in the casting temperature and profit by the end of fill or a dimensionless coefficient depending on the distance between the profit and the place of supply of metal to the casting:

ξ - dimensionless coefficient configuration profits (Equation 2):

$$\xi = \frac{S_{ef}{}^3}{V_p{}^2} \quad \text{(Eq.2)}$$

where S_{ef} - is the surface area of the profits, in contact with the form;

Downloaded from www.periodico.tchequimica.com

V_p - is the amount of profit;

R_{TU} - is the effective reduced thickness of the thermal unit (Equation 3):

$$R_{TU} = \frac{V_{TU}}{S_{TU.ef}} \qquad \text{(Eq.3)}$$

V_{TU} - is the amount of thermal unit;

$S_{TU.ef}$ - is the effective surface area of the thermal unit;

β - is the volumetric shrinkage of cast iron;

y - is the coefficient of a non-identity configuration of the casting and profits - a dimensionless coefficient that takes into account the relative length of time of solidification thermal unit and profits, depending on their configuration (Equation 4):

$$y = \frac{m_{sol.TU}}{\tau_{sol.profit}} \qquad \text{(Eq.4)}$$

z - is the coefficient of the cooling cooling conditions are not identical to the profit and and metal casting (Equation 5):

$$z = \frac{b_{f.p.}}{b_{f.TU}} \qquad \text{(Eq.5)}$$

where $b_{f.p}$ and $b_{f.TU}$ are thermal storage capacity of the form in contact with a profit and thermal unit;

V_f - is the amount of form or the part for which the calculated profit.

The thickness of the bars t was 6, 12, 24, 30, 36, 42, and 48 mm with a width of 100 mm. The length of the bars ℓ is selected from the principle of sufficiency. At the same time, we believe that the high-alloyed aluminum ductile iron CHYU22SH power distance is approximately the same as that of ductile iron ($L\Sigma \approx 6 \cdot t$). Based on this, it is taken (with a small margin) $\ell = 7 \cdot t$. These samples were cast in sand - clay raw form.

Of the cast samples obtained template, we customize the individual. To do this, blocks were cut in half along the longitudinal plane. Milling was done to the plane of the section for the identified areas of porosity on the plate (Figure-2).

To do this, we have tried various methods, including visual, ultrasonic, and hardness measurement methods. The ultrasonic method for determination of shrinkage defects did not give stable results, probably due to the presence of graphite inclusions and the presence of oxide prisoner. The visual method can detect only the surface porosity that is manifested, which is not always, and the hidden porosity remains unaccounted for. The adequate results were obtained using the method of measuring the Rockwell hardness (HRC). The hardness was measured on the centre line of the plate at distances that were multiples of the petal thickness t (Figure-3).

The distance of the mechanical effect L_{TU} and the distance from the feed arrived L_{dp}, and their sum is the total distance of the effective power $L_{\Sigma} = L_{dp} + L_{me}$ measured by the length of the dense metal part and the end, respectively.

Cast iron CHYU22SH (Table 5) was smelted in an induction crucible furnace HFICF - frequency - 0.06 with the main lining (HFICF - high-frequency induction crucible furnace).

Following the modification of cast iron was poured into molds heated to 800 °C, with a melt temperature ranging 1420 - 1450 °C.

After solidification, it was cooled in a form completely. Then to relieve stress, reduce hardness, and improve the workability, it was subjected to annealing, and after heat treatment produced crop gating system and finishing operations (Tanski, 2016, Saburov, 1967).

The molded piece "exhaust manifold" thus made is presented in Figure 4.

Visual inspection revealed no visible external defects in the casting foundry. A plate control, cut from the castings showed their lack of these and internal defects.

We evaluate the mechanical properties of cast iron with cast collector bars (Figure-5).

Before machining the bars were subjected to heat treatment. Then cylindrical samples were produced for mechanical testing having a diameter of 8 mm and a gauge length of 50 mm.

Tensile tests were performed on the instrument Zwick/Roell Z250. The hardness of iron was measured on the instrument Wolpert Hardness Taster 930, at a load of 187 kg. The results are shown in Table 6.

The results of the mechanical tests show that the resulting iron CHYU22SH has a tensile strength of ~390 MPa, which is 30% above the lower margin in accordance with GOST 7769-02 (Government standard). The hardness of iron (~ 270 HB) is within the regulated values, but closer to the lower limit. In this case, the yield stress of iron is ~340 MPa, elongation 0.6%, and modulus of normal elasticity ~160 GPa. The results obtained show that the tensile strength of

Downloaded from www.periodico.tchequimica.com

aluminum-smelted iron corresponds to the ultimate strength VCH35 – VCH40 (standard cast iron), yield strength, respectively, CVH50 exists and corresponds to the hardness of VCH100 (standard cast iron) (G. Nuruldaeva, 2019; Zhang, 2018).

For the structure of cast iron were performed on a microscope Neophot 21 firms ZEISS JENA at different magnifications. It consists of a metal matrix and uniformly distributed in its compact form of graphite inclusions (Figure-6a).

The metal matrix is doped with aluminum ferrite - *α* phase, which is uniformly distributed in the iron - aluminum carbide ε phase (Figure-6, *b,* and *c*).

Graphite inclusions (in accordance with GOST 3443-01) mainly take the form of NGf5 and only partially NGf4 (NGf - nodular graphite form). The size of graphite inclusions should be in the range of 30-60 microns.

3. RESULTS AND DISCUSSION

The results of analyses and tests show that cast iron CHYU22SH can be obtained by casting with long walls of a thickness of 4 mm without external and internal defects. By doing so, the castings have a uniform structure, high and stable mechanical properties, as well as lower by 17-24% weight than similar cast of gray iron.

4. CONCLUSIONS

1. Thus, a combination of innovative and traditional casting technology allows for a short time to develop manufacturing technology options and assess the quality indicators of the castings of various alloys, including decreased fluidity, high linear and volumetric shrinkage, as well as susceptibility to saturation of the gases and dust production. This integrated approach allows us not only to speed up technological preparation for the production of castings but also reduce costs for manufacturing and finishing of expensive mold tools. An example of such an approach is to develop practical applications for future technology for high-quality cast iron CHYU22SH cast parts "exhaust manifold" with increased operational and consumer properties.

2. Thus, the results of experimental - industrial testing laboratory studies confirm the influence of solidification conditions on the parameters of the structure of cast iron CHYU22SH. Application of the developed technology allows obtaining high-quality recommendations casting a thin (4 mm) and thick, without shrinkage defects in origin, are guaranteed to have the required degree of spheroidization of graphite inclusions, high and stable mechanical properties, as well as a smaller mass.

5. ACKNOWLEDGMENTS:

The authors are grateful to the leadership of the Kazakh National Research Technical University named after K. I. Satpayev (Satbayev University) for creating the conditions for carrying out this work.

6. REFERENCES:

1. Ten, E. B., Bazlova, T. A., Likholobov, E. Y. Effect of Out-of-Furnace Treatment on the Structure and Mechanical Properties of Steel 110G13l // Metal Science and Heat Treatment. – Volume 57. Issue 3-4. 146-150 p.p. 1 July 2015.
2. Kumanin I. B. Reviews of casting processes. 216 p. Mechanical Engineering, Moscow. 1976.
3. Kaldybayeva S. Research of Crystallization of Aluminum cast iron. Journals of Minerals & Materials Characterization & Engineering., Vol.10, No.13 -2011. pp. 1197-1203.
4. Kurdyumov A. V. Pikunov M. V., Chursin V. M., Bibikov E. L. Casting of non-ferrous alloys. 504 p. Moscow Inst.Steel&Alloys, Moscow, 1996.
5. Galdin N. M., Chistyakov V. V., Shatulsky A. A. Gating system and profit for shaped castings. 256 p. Mechanical Engineering, Moscow, 1992.
6. Vasiliev E. A. Castings of ductile cast iron. 239 p. Mechanical Engineering, Russia, 1976.
7. Kavalevich E. V. Aluminum cast iron. Handbook. Editor A. D. Sherman and A. A. Zhukov. 576 p. Moscow: Metallurgy, Russia, 1991.
8. Stefanescu D. M., Alonso G., Larranaga P. Reexamination of crystal growth theory of graphite in iron-carbon alloys// Acta Materialia, vol. 139 - 2017.- pp.109-121.
9. Utepov E. B., Ten E. B., Zhumadilova Z.O., Smailova G. A., Shevtsova V.S. Damping Metallic materials with a nanostructured Coating // Metallurgist. – Volume 60. – Issue 9-10, 1. – January 2017. – pp. 961-966.
10. Tanski T, Labisz K, Krupinska B. Analysis of crystallization kinetics of cast aluminum-silicon alloy// Journal of thermal analysis and

Downloaded from www.periodico.tchequimica.com

calorimetry, vol. 123 - 2016. - pp. 63-74.
11. Utepov E. B., Madizhanova A. T., Malgazhdarova M. K., Egemova Sh. B. Research of acoustic properties of alloyed steels. Metallurgist. 2014. Volume 8. pp. 92-95.
12. Ten, E. B., Kol, O. A. Action of protective coatings on surface carbonizing of steel castings // Chernye Metally. – Issue 5. – 1 May 2016. – pp. 35-39.
13. Safronov N. N., Kharisov L. R., Safronov G. N. Aluminum cast iron with compacted inclusions of graphite from dispersed production waste// published in Tekhnologiya Metallov, 2017, No. 4, pp. 2–5.
14. Shayakhmetov B. K., Kimanov B. M., Ten E. B., Isagulov A. Z., Zholdubaeva Z. D., Isagulova D. A. Gravimetric and Dilatometric research of elements action on three dimensional filter by thermal effects // Metalurgija. – vol. 53. – No, 1. – 2014. – pp. 44-46.
15. Zhang J, Xia S, Ye S. Experimental investigation on the noise reduction of an axial piston pump using free-layer damping material treatment// published in Applied Acoustics– vol. 139 – 2018- pp. 1-7.
16. Paul P, Raja P, Aruldhas P. Effectiveness of particle and mass impact damping on tool vibration during hard turning process// Proceedings of the institution of mechanical engineers part b-journal of engineering manufacture, vol. 232 –2018- pp. 776-786.
17. Prasad D, Radha P, Shoba Ch. Optimizing of Wire EDM Parameters for Damping Capacity of Aluminum Alloy // Materials today proceedings, vol. 5 - 2018- pp. 168-169.
18. Zhuravlev V. N., Nikolaev O. I. Mechanical steels. Directory. - M.: Mechanical Engineering, 1981. - 391 p.
19. Kerzhentsev V. V., Dedenko L. G. Mathematical processing and registration of the results of the experiment. - M.: MSU, 1971. - 10 p.
20. Saburov V. P. Effect of the modification on the properties of cast iron casting, aluminum-doped. Casting properties of metals and alloys. Proceedings of the Eleventh 11th Conference on the Theory of casting processes. Edited by B.B. Gulyaev. 267p. Moscow: Publishing House "Science" (1967).
21. G. Nuruldaeva, Zh. Zhumadilova, S. Kaldybayeva, D. Kumar. Dissipative properties of the high alloy aluminum cast iron CHYU22SH. The scientific and technical journal "INDUSTRY OF KAZAKHSTAN". No.2 (106) 2019. International code ISSN 1608-8425. P.59. Almaty, RSE "National Center for the Integrated Processing of Mineral Resources of the Republic of Kazakhstan".
22. Martin P, Micheal R. Piezoelectric shunt damping of a circular saw blade with autonomous power supply for noise and vibration reduction// Journal of sound and vibration, vol. 361 -2016- pp. 20- 31.
23. Jiang J, Yue M, Fu H. Phase diagram calculation and experimental research on Fe-12Cr-B-Al alloys// Materrial wissenschaft und werkstoftechnik, vol. 47 - 2016.- pp. 808-814.
24. Lagunov L. F., Osipov G. L. Anti-noise measures in mechanical engineering. - M.: Mechanical Engineering, 1980. - 150 p.
25. Sitko Ye. A., Sukurov B. M., Ospanov Ye., Medvedev O. S. The effect of thermal treatment of converter slags from Balkhash Copper-Smelting plant on their structure and phase composition./ News of the academy of science of the Republic of Kazakhstan. Series of Geology and Technical series. 3 (423), 2017, № 3, p. 175-184.

Downloaded from www.periodico.tchequimica.com

Table 1. *Thermophysical properties of cast iron CHYU22SH*

Name of property	**Temperature, °C**					
	500	600	700	800	900	1000
Specific heat capacity $C_{c.i}$, J /(kg·K)	536 ± 0.001	549 ± 0.001	559 ± 0.001	565 ± 0.001	573 ± 0.001	585 ± 0.001
Thermal conductivity $\lambda_{c.i}$, W/(m·K)	12.64 ± 0.028	13.11 ± 0.068	13.64 ± 0.048	14.19 ± 0.136	14,93 ± 0.157	15.53 ± 0.141
Thermal diffusivity $a_{c.i}$, 10^{-6} m^2/s	3.99 ± 0.009	4.04 ± 0.021	4.13 ± 0.014	4.25 ± 0.041	4.41 ± 0.047	4.49 ± 0.041

Table 2. *Fluidity and casting shrinkage of cast iron CHYU22SH (*Ten*, 2016; Safronov, 2017; Shayakhmetov, 2014)*

Fluidity, mm	**Casting shrinkage, %**		**Preshrinkage expension, %**
	Free	**Difficult**	
(525 - 775)/(590-830)	(1.42 – 1.52)/(2.2-2.5) /(2.5-2.8)	(1.26 – 1.47)	0.01/ (0.15-0.35)

Table 3. *Volume shrinkage of casting alloys (%) (Kurdyumov, 1996; Galdin, 1992; Vasiliev, 1976)*

Casting alloys						
Steels	**Cast irons (standard cast irons)**			**Non-ferrous metals**		
	Malleable cast iron	Gray cast iron	HCING (high-strength cast iron with nodular graphite)	Copper	Aluminium	Magnesium
4.1 - 7.0	4.0 - 6.0	1.5 - 3.0	2.0 - 6.0	4.0 - 7.5	3.0 - 6.0	3.4 – 5.0

Downloaded from www.periodico.tchequimica.com

Table 4. *Power supply castings for different groups of alloys*

Alloys	Area of dense metal expressed in thickness		
	Profit zone	**Mechanical zone**	**Sum**
Carbon steel	(2.0)·t	(2.5)·t	(4.5)t
Copper alloys	(2.0-4.5)t	(3.6-5.8)t	(5.6-10.3)t
Aluminium alloys	(2.5-4.0)t	(4.0-4.5)·t	(6.5-8.5)t
Gray cast iron	-	-	Very large
Cast iron with nodular	-	-	6.0-6.5t
Cast iron CHYU22SH	+	+	+

Table 5. *The chemical compound of the experimental melting of cast iron CHYU22SH (Stefanescu, 2017)*

Element	C	Si	Mn	Al	S	P
Mass, %	1.6 - 2.0	1.3 - 1.5	0.45 - 0.50	21.5 - 3.7	0.01 - 0.02	0.10 - 0.12

Table 6. *Results of mechanical testing of tensile specimens at room temperature*

Number of tests	Ultimate strength σ_B,	Yield strength $\sigma_{o,2}$, MPa	Elongation ε, %	Elastic modulus	Hardness, HB
The requirements of GOST 7769-02	290 least	-	-	-	241 - 364
1	381	334	0.5	148	268.5 *
2	402	347	0.6	176	264.5 *
3	394	342	0.5	161	274.0 *
4	378	328	0.7	151	276.5 *
Averages	389 ± 11	338 ± 8	0.6 ± 0.1	159 ± 13	270.9 ± 14.5

* Mean values of four measurements.
GOST – Government standard.

Downloaded from www.periodico.tchequimica.com

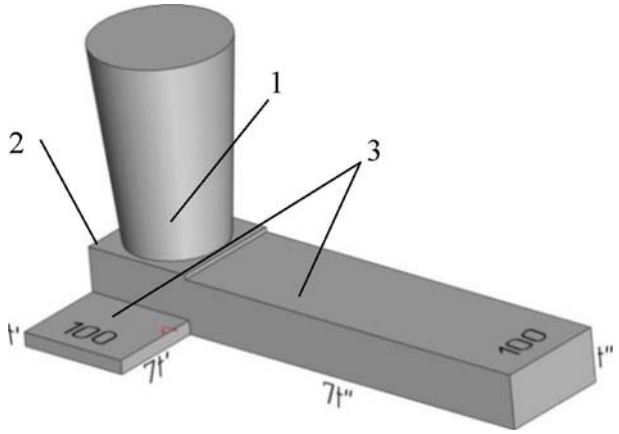

Figure 1. *2^x blade test: 1 - strut-profit, 2 - base, 3 - part of the investigated samples*

Figure 2. *Flow test and preparation for the testing template*

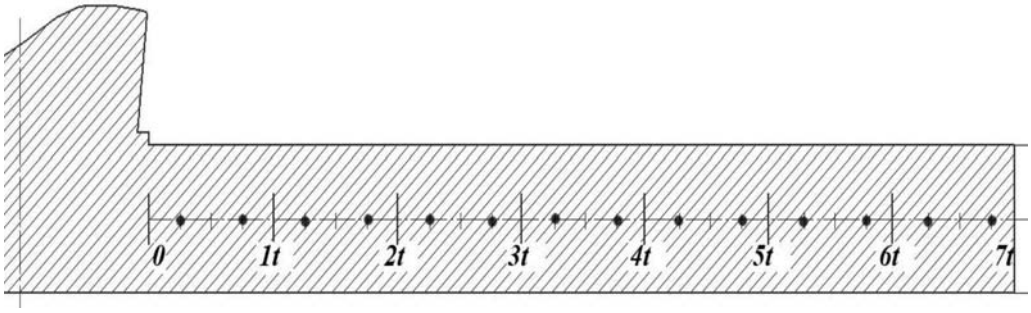

Figure 3. *The scheme of measurement of hardness to determine the parameters of the casting supplies, • - the point of measurement of hardness*

Downloaded from www.periodico.tchequimica.com

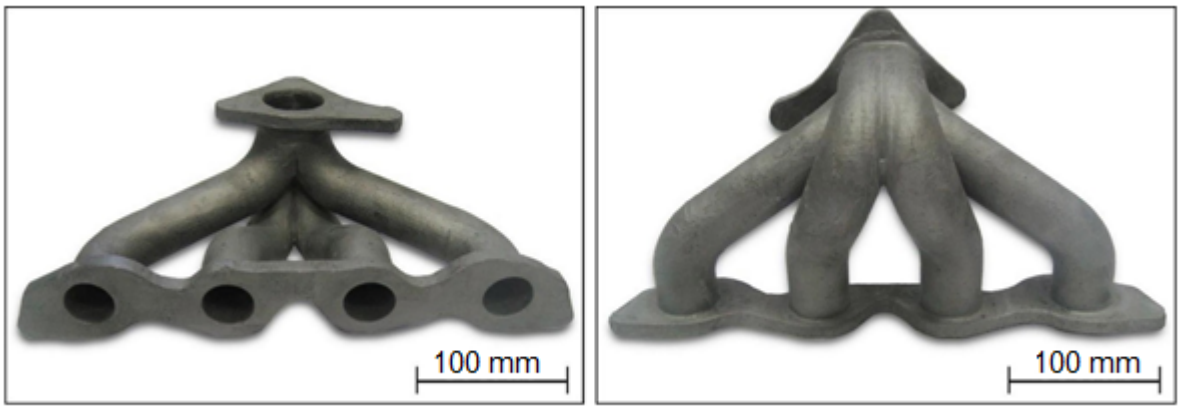

Figure 4. *Cast item "exhaust manifold" of cast iron CHYU22SH*

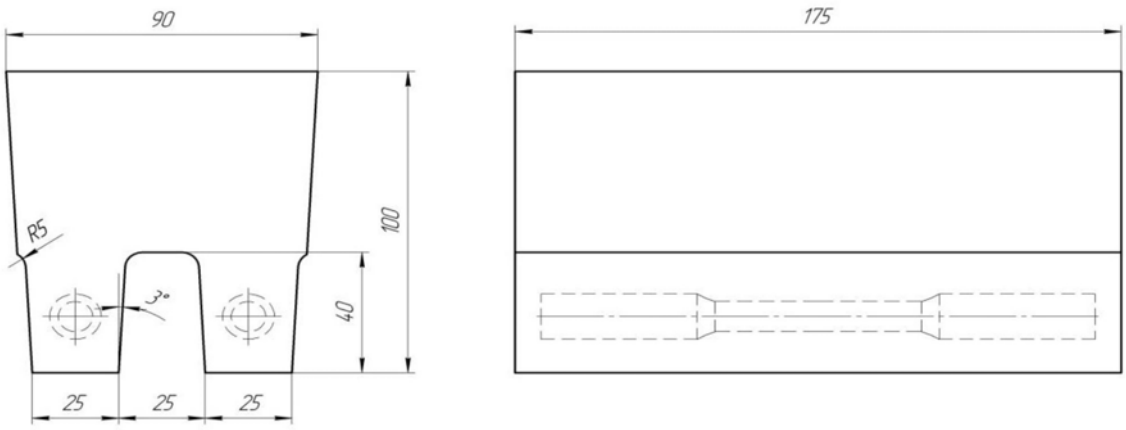

Figure 5. *Cast iron bars to test the mechanical properties*

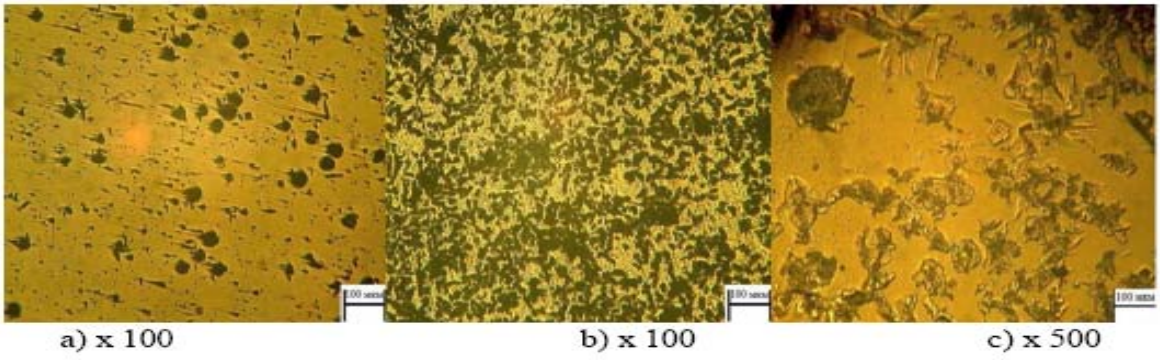

Figure 6. *Structure of the iron CHYU22SH in the samples breaking (a) is not etched; (b) and (c) after etching*

Downloaded from www.periodico.tchequimica.com

PERIÓDICO TCHÊ QUÍMICA
ARTIGO ORGINAL

POSSIBILIDADE DE AUMENTAR O PODER DE ENSAIO DO QUI-QUADRADO EM PEQUENAS AMOSTRAS POR MEIOS DE TRANSIÇÃO PARA A ANÁLISE DO SEU ESPECTRO DISCRETO

POSSIBILITY TO INCREASE THE CHI-SQUARE TEST POWER ON SMALL SAMPLES BY MEANS OF TRANSITION TOWARDS ANALYZING OF IT'S DISCRETE SPECTRUM

ВОЗМОЖНОСТЬ УСИЛЕНИЯ МОЩНОСТИ ХИ-КВАДРАТ КРИТЕРИЯ НА МАЛЫХ ВЫБОРКАХ ЗА СЧЕТ ПЕРЕХОДА К АНАЛИЗУ ЕГО ДИСКРЕТНОГО СПЕКТРА

VOLCHIKHIN, Vladimir[1]; IVANOV, Alexander[2]; GAZIN, Alexei[3*]

[1,2,3] Lipetsk State Pedagogical P. Semenov-Tyan-Shansky University, Lipetsk, Russian Federation

** Correspondence author*
e-mail: professor-gazin@yandex.ru

Received 20 June 2019; received in revised form 06 November 2019; accepted 23 November 2019

RESUMO

O objetivo do trabalho é aumentar a potência do teste qui-quadrado, analisando o espectro dos estados de saída dessa forma discreta de teste. A recusa de uma hipótese de continuidade do espectro dos estados de saída de uma molécula qui-quadrado permite observar 22 linhas espectrais de diferentes amplitudes de probabilidade em uma amostra de 11 experimentos. Propõe-se obter um modo de suporte para a superposição quântica dos estados de saída da molécula qui-quadrado através da seleção aleatória de 11 experimentos da população geral de 21 experimentos. Isso torna possível obter cerca de 200.000 estados diferentes da molécula, o que é suficiente para estimar os estados de 8 níveis da amplitude de probabilidade de 22 linhas espectrais de saída. No caso do histograma com 6 intervalos, a hipótese de um espectro contínuo do teste do qui-quadrado para uma amostra de 11 experimentos não nos permite distinguir entre leis normais e uniformes de distribuição de dados com uma probabilidade de confiança aceitável para a prática. A situação muda drasticamente se levarmos em conta a natureza discreta do espectro dos estados da molécula qui-quadrado. É possível obter retratos digitais significativamente diferentes da distribuição de dados normal e uniforme. Suas diferenças são de cerca de 40 bits conforme a distância de Hamming. A molécula qui-quadrado pode ser interpretada como um certo neurônio quadrado com uma estrutura Gammerstein. A simulação das equações de Schrödinger em um computador comum possui complexidade computacional exponencial em relação ao número de elétrons (graus de liberdade ou experimentos). Por esse motivo, a reprodução de cálculos quânticos em 22 qubits e mais dentro da estrutura da mecânica quântica em um computador comum é tecnicamente difícil de executar. Uma situação completamente diferente surge com o apoio da superposição quântica da molécula qui-quadrado. O suporte da superposição quântica da molécula qui-quadrado possui complexidade computacional linear. Como conseqüência, é possível implementar cálculos quânticos de 22 qubit, 222 qubit, 2222 qubits e superiores em um computador comum.

Palavras-chave: *teste qui-quadrado, amostras pequenas, espectro discreto de estados do teste qui-quadrado para amostras pequenas*.

ABSTRACT

The purpose of the work is to increase the chi-square test power by analyzing the spectrum of output states of this test discrete form. The refusal from a hypothesis of a spectrum continuity of a chi-square molecule output states allows you to observe 22 spectral lines of different probability amplitudes on a sample of 11 experiments. It is proposed to obtain a mode of support for the quantum superposition of the output states of the chi-square molecule through the random selection of 11 experiments from the general population of 21 experiments. This makes it possible to obtain about 200,000 different states of the molecule, which is quite sufficient to estimate the 8-level states of the probability amplitude of 22 output spectral lines. In the case of the histogram with 6 intervals, the hypothesis of a continuous spectrum of the chi-square test for a sample of 11 experiments does not allow us to distinguish between normal and uniform laws of data distribution with a confidence probability acceptable for practice. The situation changes dramatically if the spectrum discrete nature of the chi-square molecule states is taken into account. It is possible to obtain significantly different digital

Downloaded from www.periodico.tchequimica.com

portraits of the normal and uniform data distribution. Their differences are about 40 bits as per the Hamming distance. The chi-square molecule can be interpreted as a certain square neuron with a Gammerstein structure. Simulation of Schrödinger equations on an ordinary computer has exponential computational complexity in relation to the number of electrons (degrees of freedom or experiments). For this reason, the reproduction of quantum computations on 22 qubits and more within the framework of quantum mechanics on an ordinary computer is technically difficult to perform. A completely different situation arises with the support of quantum superposition of the chi-square molecule. The support of quantum superposition of the chi-square molecule has linear computational complexity. As a consequence, it is possible to implement 22-qubit, 222-qubit, 2222-qubits, and higher quantum computations on an ordinary computer.

Keywords: *chi-square test, small samples, discrete spectrum of states of the chi-square test for small samples.*

АННОТАЦИЯ

Целью работы является повышение мощности хи-квадрат критерия за счет анализа спектра выходных состояний дискретной формы этого критерия. Отказ от гипотезы непрерывности спектра выходных состояний хи-квадрат молекулы позволяет на выборке из 11 опытов наблюдать 22 спектральных линии разной амплитуды вероятности. Предложено получать режим поддержки квантовой суперпозиции выходных состояний хи-квадрат молекулы за счет случайного выбора 11 опытов из генеральной совокупности в 21 опыт. Это позволяет получать порядка 200 000 разных состояний молекулы, что вполне достаточно для оценки 8-ми уровневых состояний амплитуды вероятности 22 выходных спектральных линий. Гистограммы с 6 интервалами гипотеза непрерывного спектра хи-квадрат критерия при выборке в 11 опытов не позволяет различать нормальный и равномерный законы распределения данных приемлемой для практики доверительной вероятностью. Ситуация кардинально меняется, если учитывать дискретный характер спектра состояний хи-квадрат молекулы. Удается получать значительно различающиеся цифровые портреты нормального и равномерного распределений данных. Их отличия составляют порядка 40 бит по расстоянию Хэмминга. Хи-квадрат молекулу можно интерпретировать как некоторый квадратичный нейрон со структурой Гаммерштейна. Моделирование уравнений Шредингера на обычном компьютере имеет экспоненциальную вычислительную сложность по отношению к числу электронов (степеней свободы или опытов). По этой причине воспроизведение квантовых вычислений на 22 кубит и более в рамках квантовой механики на обычном компьютере технически трудно выполнимо. Совершенно иная ситуация возникает при поддержке квантовой суперпозиции хи-квадрат молекул. Поддержка квантовой суперпозиции хи-квадрат молекулы имеет линейную вычислительную сложность. Как следствие на обычном компьютере можно реализовать квантовые вычисления на 22 кубита, 222 кубита, 2222 кубита и выше.

Ключевые слова: *хи-квадрат критерий, малые выборки, дискретный спектр состояний хи-квадрат критерия при малых выборках.*

---

1. INTRODUCTION

The algorithm given in (GOST R 52633.5-2011) requires about 20 examples of the “Own” image for automatic training of neural network converters “biometrics – access code”. If the examples are “good”, their distribution on each of the biometric parameters is close to the normal distribution law. If the data is “bad”, their distribution is close to the uniform law. In order to check the normality of the distribution law of values, the classical chi-square test can be used (Kobzar, 2006; GOST R 50.1.037-2002). Unfortunately, it is possible to apply the chi-square test with a confidence probability acceptable for practice only on very large samples from 200 to 400 experiments (GOST R 50.1.037-2002).

Thus, if a sample of 11 experiments is used, it is possible to distinguish between normal and uniform distribution laws of values by the chi-square test under the conditions of equal error probabilities of the first and second kinds P1xP2xPEEx0.484. If the sample size is increased up to 21 experiments, the values of equiprobable errors decrease to the value of P1xP2xPEEx0.352. It turns out that in the case of such small sample sizes, the confidence probability of decision making on the Pearson's chi-squared test is in the range from 0.516 to 0.848, which is not enough for practical needs. The power of the classical statistical chi-square test is low on the small sample. It is necessary to take measures which can reduce the probabilities of errors of the first and second kinds and in doing so to increase the power of the applied statistical functional on small samples.

It should be noted that one of such

Downloaded from www.periodico.tchequimica.com

methods is parallel use of several statistical tests when processing one small sample. In such a way, the application of three different statistical tests (Ivanov, 2019a; Ivanov, 2019b) allows you to reduce the probabilities of errors of the first and second kinds by about 20%. The increase of the number of tests to be united up to 12 allows you to reduce the probabilities of errors of the first and second kinds by about 93% (Ivanov, 2019b). If to generalize about 60 statistical tests, then statistical estimates on small samples should have the probabilities of errors of the first and second kinds about 0.01 and less (Ivanov, 2019b), which is quite acceptable for practice.

Another direction to increase the power of statistical estimates is the transition from the practice of continuous output data analysis of the conventional chi-square test towards analyzing the spectral lines of the discrete variant of the chi-square test. The first discrete variant of the chi-square test was discovered in 1973 (Dahiya and Gurland, 1973). The authors of this discovery did not understand what to do with their new, unexpected result. It is for this reason that the title of the article (Dahiya and Gurland, 1973) was formulated with a question mark. The problem was that the mechanical and mathematical thought in 1973 was not ready for quantum calculations, qubits, quantum superposition, and quantum entanglement. All this was formulated later in the works of Yuri Manin (1980), Richard Feyman (1981), Paul Benioff (1982) and Stephen Wisner (1983). As a consequence, the fact that the chi-square test has a “promising” discrete form, which can be considered as a certain chi-square mathematical molecule, was forgotten for 50 years. Only in 2015, the forgotten fact was discovered again (Akhmetov *et al*., 2015a; Akhmetov *et al*., 2015b). Under the new conditions of the XXI century, a different situation arose, because quantum-mechanical mathematics of a large number of qubits, quantum physics, and quantum chemistry had already been well studied.

It is quite possible to be on the threshold of appearing another branch of scientific understanding of reality that is the precision quantum statistics of small samples (Kulagin *et al*., 2016; Volchikhin *et al*., 2017a; Ivanov, 2016; Volchikhin, 2017b; Volchikhin, 2017c). Presumably, their discrete analogues can be constructed for a set of usual traditionally continuous statistical tests and for a set of usual traditionally continuous statistical moments, having spectral lines of output states as in the case of a hydrogen molecule or molecules of other substances (Yelashev, 2015; Yelashev, 2018). Moreover, there are initially discrete classical statistical tests (Kobzar, 2006) such as

- Wilcoxon test;
- Attila-Kersinga-Tsukini test;
- Bracheya-Gastvayda-Wright test;
- Boosa test;
- Gupta test;
- Fraser test;
- Symbolic symmetry test.

These tests initially have discrete (linear) spectra of output states. However, this fact has never been used for transition to qubits and for support of the quantum superposition for extraction of additional information from the ratio of spectral lines (probability amplitudes of quantum states occurrence of statistical molecules).

Much depends on the subjective interpretation of the experimental data. It is known that in physics, electrons can be considered both as waves and particles (the postulate of Louis de Broglie); everything depends on the position of the observer and his educational and subjective preferences. Approximately the same is observed in the statistics of small samples. It is possible to consider the values of correlation coefficients of two statistical parameters as a continuous value, however, if the observer wishes, these values turn out to be discrete. Therefore, they can be considered as states of correlational molecules (Volchikhin *et al*., 2017d; Serikov and Kachalin, 2019) with a finite number of output spectral lines for small samples.

2. MATERIALS AND METHODS

2.1. The transition from ordinary molecules of chemistry and physics towards mathematical chi-square molecules

It is known from physics that the planetary model of a hydrogen molecule generates a series of Lyman, Balmer, Pashen and Bracket spectral lines. Each of the series is generated by electron jumps from one orbit to another, as shown in Figure 1.

Assumed that for some molecule at some temperature the most probable is to find the largest number of electrons in the fourth orbit, a chi-square molecule with a discrete spectrum of

Downloaded from www.periodico.tchequimica.com

states as in the hydrogen molecule will be obtained. In this case, six orbits can be interpreted as six histogram intervals, as shown in Figure 1.

In order to move from the usual chi-square test with the usual continuous spectrum to the chi-square molecule with the discrete output spectrum, it is necessary that the mathematical expectation of the analyzed sample should always be on the boundary of the third and fourth intervals (Dahiya and Gurland, 1973; Akhmetov *et al*., 2015a; Akhmetov *et al*., 2015b; Kulagin *et al*., 2016) for the histogram of 6 intervals. Calculation of the values of the chi-square molecule for the sample of 11 experiments should be performed by Eq. 1:

$$\chi^2 = 11 \cdot \sum_{i=1}^{6} \frac{\left(\frac{n_i}{11} - P_i\right)^2}{P_i} \quad \text{(Eq. 1)}$$

Where n_i is the number of experiments included in the i-th interval of the histogram; P_i is the probability of hitting into the i-th interval of the histogram of the theoretical (verifiable) value distribution.

In this case, the spectrum of states in Eq. 1 is always finite; it has 21 lines of a significant level of probability amplitudes on the range of values of the chi-square test from 0 to 10. This is shown in Figure 2.

The height of the spectral lines of the chi-square molecule $\psi(\chi^2)$ corresponds to the probability amplitude of occurrence of one or another discrete chi-square state. The sum of all probability amplitudes of all spectral lines over the entire range of states is singular:

$$\Psi = \int_0^{\infty} \psi(\chi^2) \cdot d(\chi^2) = 1 \quad \text{(Eq. 2)}$$

Since the spectrum of states of the considered chi-square molecules is discrete and finite, the continuous integral (Eq. 2) can always be replaced by some finite sum (Eq. 3):

$$\Psi = \int_0^{\infty} \psi(\chi^2) \cdot d(\chi^2) = 1 = \sum_{i=1}^{N} \psi_i(\chi^2) \quad \text{(Eq. 3)}$$

where N is the number of spectral lines in the finite range from 0 to $\max(\chi^2)$.

Note that the number of spectral lines N for the chi-square molecules depends on the number of experiments in the sample and the number of intervals in the histogram. So, if the number of experiments in the sample is increased from 11 to 21, the number of significant spectral lines increases from 21 to 159, as it is shown in Figure 5.

The transition from continuous spectra to discrete spectra is a cardinal change that leads to a huge increase in the sensitivity of statistical methods of data processing. Thus, in the analysis of continuous spectra the sensitivity of the method (relative error) is quite achievable at the level of 0.1%, and the transition to the analysis of discrete spectrum lines (Yelashev, 2015; Yelashev, 2018) allows you to detect extremely small values at the level of 0.0000001% of the weight composition of impurities. In this way, forensic scientists detect gold microinclusions on the balance pan, where previously criminal gold was weighed. All you have to do is to wipe the balance pan with cotton-wool and alcohol. Then you should burn the cotton-wool, and split up the light of the flame by a prism, seeing the lines of the flame spectrum. Gold microinclusions are detected because the spectral lines of gold heated by the flame become visible, and they are between the spectral lines of burning organics (alcohol and cotton-wool).

Similar statistical relations are obtained by multivariate neural network analysis of biometric data. A neural network converter “Biometrics – Access Code” can be considered as a neural network molecule (Volchikhin *et al*., 2017c) generating a discrete spectrum of amplitudes of the output code state probabilities. Probability estimation of errors of the second kind (the erroneous omission of “Alien” as “Own”), estimated in accordance with GOST R 52633.3, reaches values less than 0.000000001.

Approximately the same error probabilities of the first and second kinds should be achieved by statistical calculations based on a deep statistical analysis of the spectral lines of chi-square molecules. In this case, the structure of the chi-square molecule can be considered as a chi-square neuron. The structure of such a neuron is shown in Figure 4.

Downloaded from www.periodico.tchequimica.com

2.2. Maintaining the neurodynamic mode of one chi-square neuron (one chi-square molecule)

It should be noted that the model of the hydrogen molecule (Figure 3) is a dynamic structure described by the Schroedinger differential equation given in (Yelashev, 2015; Yelashev, 2018; Buravlev, 2000). The equation of the chi-square molecule (Eq. 1) is static, i.e., to realize the potential advantages of discrete spectral analysis (Akhmetov *et al*., 2015a; Akhmetov *et al*., 2015b; Kulagin *et al*., 2016) it is necessary to drive the static chi-square molecule (Eq. 1) into the dynamic mode of the continuous data conversion. One of the methods of organizing the dynamics for the chi-square molecule is the random extraction of many small sub-samples of 11 experiments from the general sample of 21 experiments. This method is illustrated in Figure 5.

If repetitive small sub-samples are not used, it is possible to get

$$C_{21}^{11} = \frac{21!}{11!(21-11)!} = 352716 \qquad \text{(Eq. 4)}$$

a series of 11 experiments (Eq. 4). Such a large number of series of 11 experiments can be successively fed to the comparators of the chi-square neuron, providing a mode of chaotic neurodynamics, in its turn generating the appearance of spectral lines. Obviously, it is possible to feed to the input of the chi-square neuron both data with the normal distribution law of values and data with a uniform distribution of values. As a result, different spectra will be obtained, and it is possible to compare these spectra, maintaining a quantum superposition in neurodynamics.

2.3. Calculations performed in the quantum superposition support mode

One of the methods of processing the chi-square molecule spectra is the separation of the 22 most significant lines in terms of the probability amplitude by condition (Eq. 5):

$$\frac{\psi_{норм}(\chi^2) + \psi_{равн}(\chi^2)}{2} \geq 0.01 \qquad \text{(Eq. 5)}$$

At least one of the probability amplitudes of normal or uniform distributions should be significant, as shown in Figure 6.

In this situation, 22 spectral lines of the chi-square molecules with a normal nuclear and a uniform nuclear will be described by the table of states 1.

The data will be processed by comparing the probability amplitudes of the chi-square molecule spectra with 8 levels of comparators corresponding to the vector of reference values {0.01, 0.02, 0.03, ..., 0.08}. During quantization, the value “0” will be assigned if the detected probability amplitude is below the threshold. If the probability amplitude is above the threshold, the code state “1” is assigned.

This transformation results in obtaining digital portraits of the chi-square molecule states in the form of 176 bits. Figure 7 shows two digital portraits of the chi-square molecule upon its excitation by data with normal and uniform laws of value distribution.

It should be noted that only significant spectral lines were taken into account in the formation of digital portraits. As a consequence, the total probability of all considered states is less than one (Eq. 6):

$$\begin{cases} \Psi_{норм} = \sum_{i=1}^{22} \psi_i(\chi^2) = 0.899 \\ \Psi_{равн} = \sum_{i=1}^{22} \psi_i(\chi^2) = 0.912 \end{cases} \qquad \text{(Eq. 6)}$$

3. RESULTS AND DISCUSSION:

Remaining in the traditional continuous models about the distribution of chi-square test values for the sampling of 21 experiments there is only one decision with an error probability of the first and second kinds P1≈P2≈PEE≈0.352. In case of moving over to discrete representations of data for many sub-samples of 11 experiments, there is the opportunity to make 22 decisions. There is the opportunity to make our own decision on each of the most significant probability amplitudes of 22 spectral lines.

In this case, equal error probabilities of the first and second kinds are described in the first approximation by the following ratio (Eq. 7):

$$P_{EE,i} \approx 1 - \frac{h_i}{s_i + h_i} \qquad \text{(Eq. 7)}$$

where i is the number of the spectral line on

Downloaded from www.periodico.tchequimica.com

which the decision is made; hi is the number of states "*" in the Hamming portrait (Figure 7) for the i-th spectral line, si is the number of states "1" in the Hamming portrait (Figure 7) for the i-th spectral line.

Estimates of error probabilities in decisions made according to one spectral line are given in Table 1.

As can be seen from Table 1, approximately half of the spectral lines give worse decisions than the decisions made within the framework of the "continuous" spectrum of chi-square test states. These decisions are marked by background fill. The second half of the spectral lines gives the decisions with very good separability of the normal distribution hypothesis and the uniform distribution hypothesis in the study sample. Moreover, analysis of the spectral lines with the numbers 3, 11, 12, 13, 21, 22 should lead to almost error-free decision-making. The probabilities of detecting different spectral lines are given in Table 2.

4. CONCLUSIONS:

It should be highlighted that all the above mentioned leads to a significant complication of calculations performed in comparison with classical calculations. Formally, it is possible to consider that instead of one chi-square test calculation for a sample of 21 experiments, it will be necessary to perform about 10,000 calculations for samples in 11 experiments. Taking into account the 22 most significant spectral lines, the states of the neural network molecule, arising with a probability of 0.912 (obtained by solving simultaneous Eq. 6), are taken into account. A sample of 10,000 calculations is quite sufficient for a reliable estimation of the probability amplitude of each of the 22 spectral lines.

At the beginning of the 20th century, at the time of Pearson, a 10,000-fold complication of calculations was impossible. Today, at the beginning of the 21st century, calculations of such complexity are easily performed on ordinary desktop computers. Calculation of one Pearson's chi-squared test takes about 0.01 seconds, so the calculation of 10,000 such tests takes about 3 minutes of machine time. The costs are quite acceptable for many practical cases of statistical data processing of biometrics, biology, medicine, pharmacology, and economics

It seems that the brightest applications may be pharmaceutical applications. The development of new drugs takes several years and costs dozens of millions of dollars. Market launch of a new drug is possible only after its sufficiently complete statistical testing, which is carried out on several hundred patients with the necessary pathology. Such testing can take several years, which increases the cost of a new drug (the payback period increases as well). Reduction of the required number of patients, on which a new drug is tested, by several times, should finally lead to a significant reduction in its cost while reducing the payback period of the new drug.

The fundamentally important point is that the computational costs of solving Schrödinger equations grow exponentially as the number of degrees of freedom or electrons in the simulated molecule grows. For the very reason, it is inexpediently to model Schrödinger equations using software methods on conventional computers. A completely different situation arises for the chi-square molecule, for which the quantum superposition of the output states is supported in a programmatic manner. Equations of mathematical molecules (chi-square molecules, correlation molecules, and excess molecules) have linear computational complexity. That is, the problem of analyzing the ratio of 22 spectral lines (22 quantum states or 22 qubits), which is considered in this article, will become 2-fold more complicated and will take about 6 minutes of machine time to analyze 44 spectral lines (44 quantum states).

The fundamental results obtained at the end of the last century for quantum-mechanical computing devices are quite applicable in practice for chi-square molecules, excess molecules, and correlation molecules. There is no sense in waiting for the appearance of full-fledged quantum computers for solving statistical problems because the results quite suitable for practical use can be obtained by software methods of quantum superposition support on ordinary desktop computers. Our article was meant to be a description of one simplest example of a similar approach implementation.

5. REFERENCES:

1. Akhmetov, B. B., Ivanov, A. I., Serikova, N. I., Funtikova Yu.V. Discrete nature of the distribution law of chi-square test for small test samples. *Bulletin of the*

Downloaded from www.periodico.tchequimica.com

National Academy of Sciences of the Republic of Kazakhstan, **2015a**, *1*, 17-25.
2. Akhmetov, B., Ivanov, A., Gilmutdinov, A., Bezyaev A., Funtikova Y. The Family of Chi-Square Molecules Pearson: Software-Continuum Quantum Accelerators of High-Dimensional Calculations. *International Conference on New Directions in Multidisciplinary Research & Practice (NDMRP-15-265).* April 22, Istanbul, Turkey. **2015b**.
3. Dahiya, R. C., Gurland J. How many classes in the Pearson chi-square test? *Journal of the American Statistical Association,* **1973**, *68*(343), 707-712.
4. GOST R 50.1.037-2002. 2001. *Applied statistics. Rules of check of experimental and theoretical distribution of the consent. Part I. Tests of χ2 type.* Gosstandart of Russia.
5. GOST R 52633.3-2011. *Information protection. Information protection technology. The high reliability biometric protection means endurance testing from matching attacks.* Gosstandart of Russia. **2011**.
6. GOST R 52633.5-2011 (The state standard of the Russian Federation 52633.5-2011). **2011**. *Information protection. Information protection technology. The neural net biometrics-code converter automatic training.* Gosstandart of Russia.
7. Ivanov, A. I., Bannykh, A. G., Kupriyanov, E. N., Lukin, V. S., Perfilov, K. A., Savinov, K. N.Collection of Artificial Neurons Equivalent to Statistical Tests for Their Joint Use in Testing the Hypothesis of Normality of Small Samples of Biometric Data. *Proceedings of the All-Russian Scientific and Technical Conference "Information Technologies Security"*, April 24; Penza, Russia, **2019a**,156-164.
8. Ivanov, A. I., Kupriyanov, E. N., Tureev, S. V. Neural network generalization of the classical statistical tests for processing the small samples of the biometric data. *Reliability,* **2019b**, *2*, 22-27.
9. Ivanov, A.I. Multivariate neural network processing of biometric data with program reproduction of quantum superposition effects. *Penza Electrical Engineering Institute Publishing House.* **2016**.
10. Kobzar, A. I., ed. *Applied Mathematical Statistics. For Engineers and Scientists.* Fizmatlit. **2006**.
11. Kulagin, V. P., Ivanov, A. I., Gazin, A. I., Akhmetov, B. B. Cyclical continuum-quantum calculations: increase of the chi-square test power on small samples. *Analytics,* **2016**, *5*(30), 22-29.
12. Serikov, A. V., Kachalin, S. B. Correlation Molecule with Elliptical Quantizers for Calculations on Small Training Samples. *Proceedings of the 1-st All-Russian Scientific and Technical Conference*, April 24; Penza, Russia, **2019**, 123-129.
13. Volchikhin, V. I., Ivanov, A. I. Neural network molecule: solution of the inverse biometric problem through the software support of the quantum superposition at the outputs of the artificial neuron network. *Mordovia University Bulletin,* **2017a**, *27*(4), 518-523.
14. Volchikhin, V. I., Ivanov, A. I., Bezyaev, A. V., Kupriyanov E.N. Neural network analysis of small samples of biometric data using the chi-square test and the Anderson-Darling test. *Engineering technologies and systems,* **2019**, *29*(2), 2005-2017.
15. Volchikhin, V. I., Ivanov, A. I., Gazin, A. I., Bannih, A. G. Conditions of obtaining the discrete kurtosis spectrum of statistical distributions of biometric data for small samples. *Journal of Computational and Engineering Mathematics,* **2017b**, *4*(4), 53-63.
16. Volchikhin, V. I., Ivanov, A. I., Pashchenko, D. V., Akhmetov, B. B., Vyatchanin, S. E. Opportunities of creating a cyclic continuum-quantum chi-square machine for testing statistical hypotheses on small samples of biometric and other nature data. *Bulletin of higher education institutions. Volga region. Technical sciences*. *Penza State University,* **2017c**, *1*, 5-15.
17. Volchikhin, V. I., Ivanov, A. I., Serikov, A. V., Serikova, Y. I. Quantum superposition of the states discrete spectrum of the mathematical correlation molecule for small samples of biometric data. *Mordovia University Bulletin,* **2017d**, *27*(2), 230-243.
18. Yelashev, M. A. Atomic and Molecular Spectroscopy. Atomic Spectroscopy, *Editorial URSS*, **2018**.
19. Yelashev, M. A. Atomic and Molecular Spectroscopy. Molecular Spectroscopy, *Editorial URSS,* **2015**.
20. Buravlev Yu. M. Atomic-emission Spectrometry of Metals and Alloys. *Donetsk: DonSU*, **2000**.

Downloaded from www.periodico.tchequimica.com

Table 1. *Estimates of error probabilities in decisions made according to one spectral line*

i	PEE
1	0.5
2	0.5
3	0.0
4	0.25
5	0.75
6	0.20
7	1.0
8	0.2
9	0.25
10	0.8
11	0.0
12	0.0
13	0.0
14	0.43
15	0.8
16	0.725
17	0.8
18	0.6
19	0.8
20	0.25
21	0.0
22	0.0

Table 2. *The probability amplitudes of the spectrum No. 2 lines*

Spectrum data of the chi-square molecular for 11 experiments, 6 histogram intervals, normal value distribution law of the program pseudo-random number generator

D	1	2	3	4	5	6	7	8	9	10	11	12	13	14	15	16	17	18	19	20	21	22
x^2	3.19	3.47	4.23	4.33	4.54	4.60	4.78	4.85	5.03	5.06	5.65	5.82	6.16	6.40	6.62	6.92	7.20	8.48	8.54	9.28	9.58	10.96
Ψ	0.0269	0.0233	0.0136	0.0403	0.0335	0.0557	0.1977	0.0423	0.0320	0.0920	0.0255	0.0452	0.0069	0.0372	0.0483	0.0749	0.0299	0.0257	0.0163	0.0267	0.0035	0.0017

Spectrum data of the chi-square molecular for 11 experiments, 6 histogram intervals, uniform value distribution law of the program pseudo-random number generator

D	1	2	3	4	5	6	7	8	9	10	11	12	13	14	15	16	17	18	19	20	21	22
x^2	3.19	3.47	4.23	4.33	4.54	4.60	4.78	4.85	5.03	5.06	5.65	5.82	6.16	6.40	6.62	6.92	7.20	8.48	8.54	9.28	9.58	10.96
Ψ	0.0104	0.0085	0.0076	0.0108	0.0239	0.0110	0.2071	0.0107	0.0137	0.0650	0.0062	0.0429	0.0094	0.0742	0.0359	0.1563	0.0454	0.0514	0.0604	0.0398	0.0108	0.0103

Downloaded from www.periodico.tchequimica.com

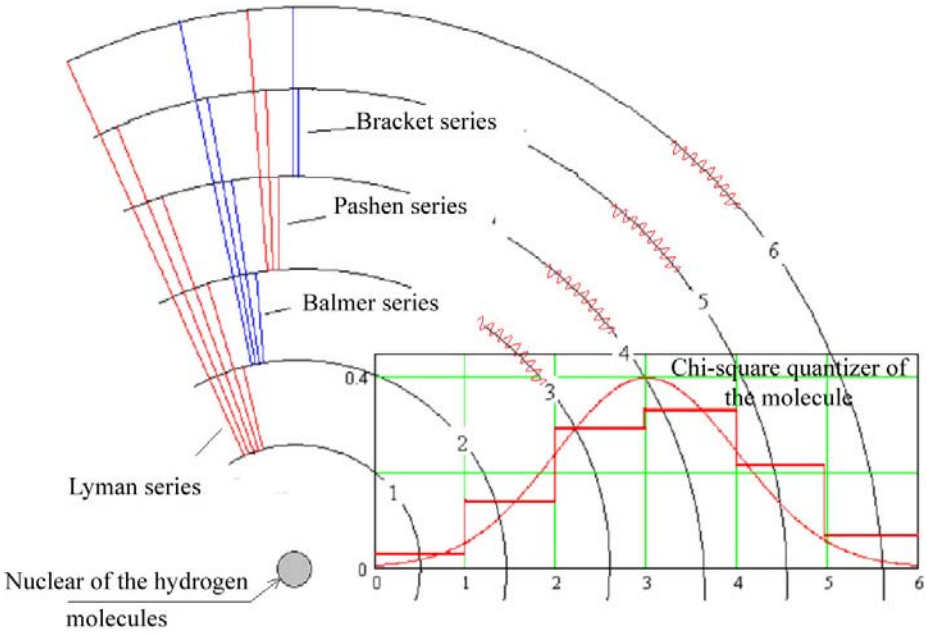

Figure 1. *The planetary model of a hydrogen molecule generating a series of spectrum lines*

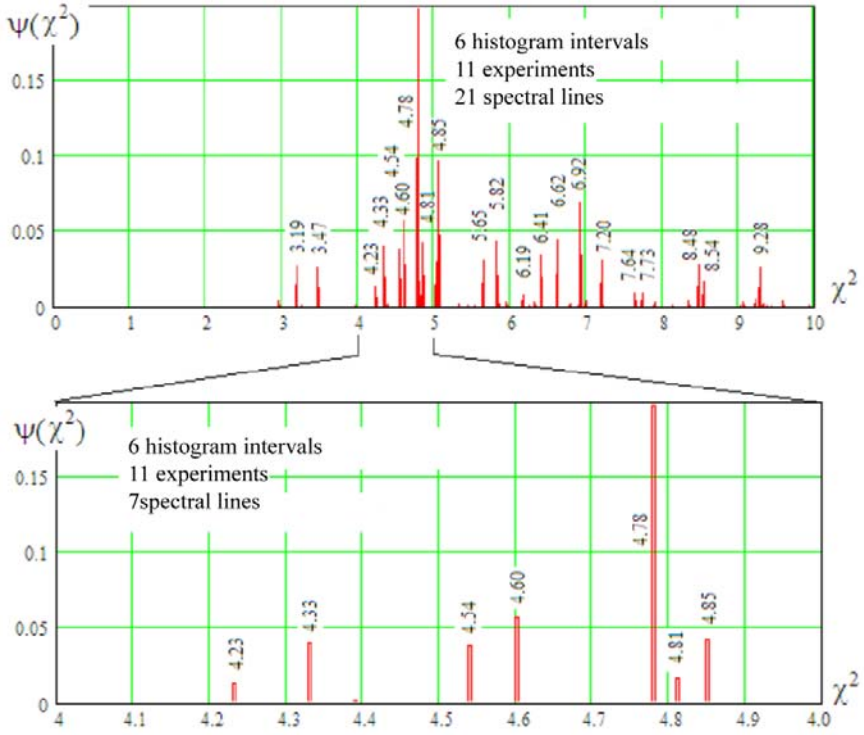

Figure 2. *Position of spectral lines of the chi-square molecule in 11 experiments and 6 histogram intervals for normal data distribution*

Downloaded from www.periodico.tchequimica.com

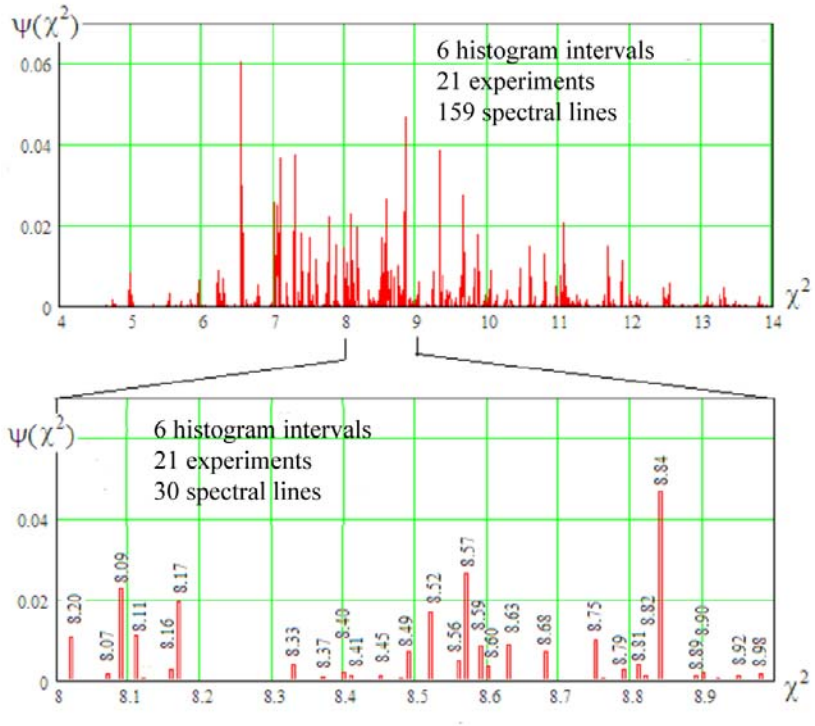

Figure 3. *Position of spectral lines of the chi-square molecule in 21 experiments and 6 histogram intervals for normal data distribution*

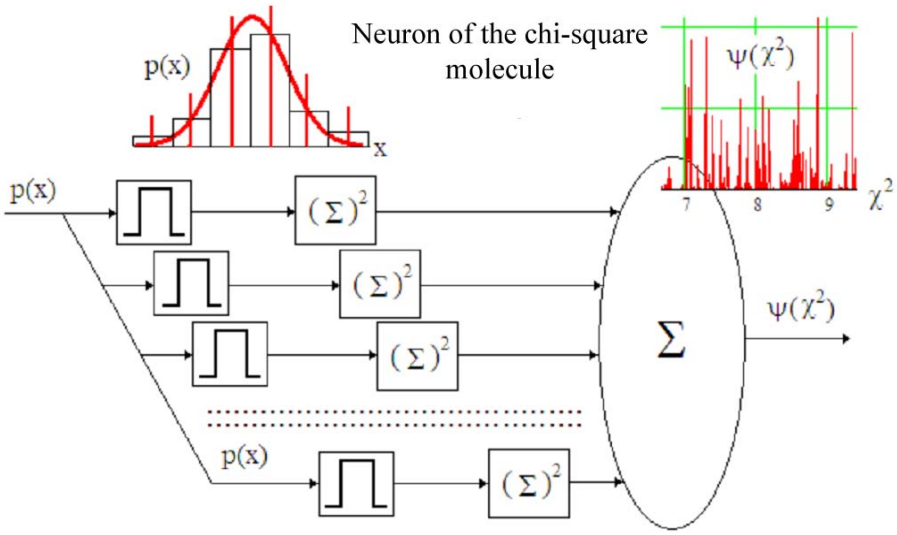

Figure 4. *The structure of the chi-square neuron with input quantization of data by comparators of the histogram interval separation*

Downloaded from www.periodico.tchequimica.com

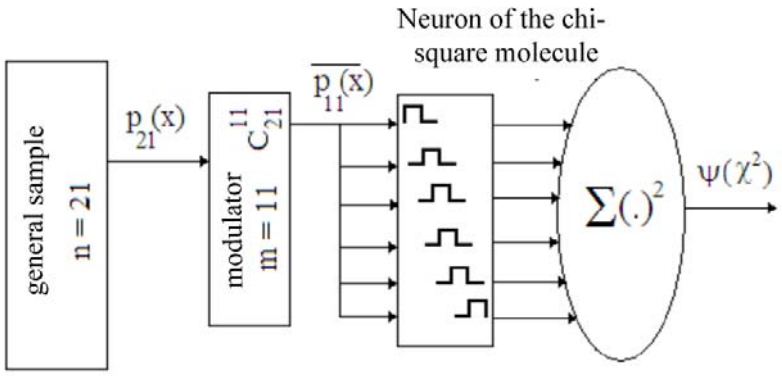

Figure 5. *Creating a set of small sub-samples by random extraction of 11 experiments from a large general sample of 21 experiments (neurodynamics)*

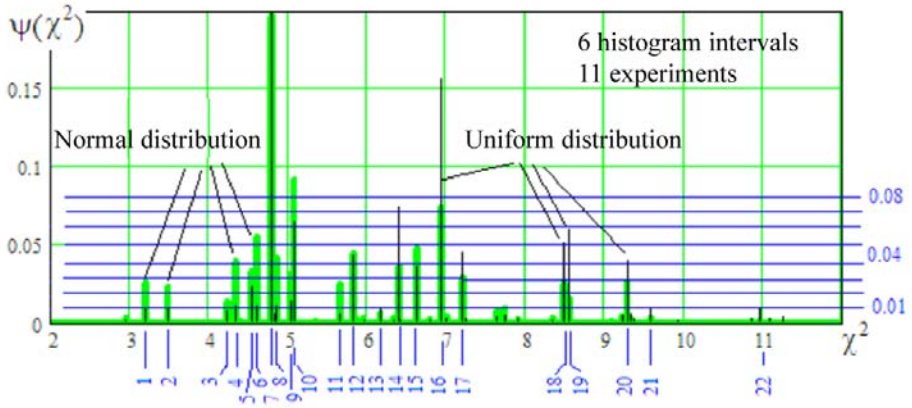

Figure 6. *Eight levels quantizing the amplitude of the spectral line of the chi-square molecule normal and uniform spectra*

Downloaded from www.periodico.tchequimica.com

Digital portrait of normal data distribution

	1	2	3	4	5	6	7	8	9	10	11	12	13	14	15	16	17	18	19	20	21	22
0.08	"0"	"0"	"0"	"0"	"0"	"0"	"1"	"0"	"0"	"1"	"0"	"0"	"0"	"0"	"0"	"0"	"0"	"0"	"0"	"0"	"0"	"0"
0.07	"0"	"0"	"0"	"0"	"0"	"0"	"1"	"0"	"0"	"1"	"0"	"0"	"0"	"0"	"0"	"1"	"0"	"0"	"0"	"0"	"0"	"0"
0.06	"0"	"0"	"0"	"0"	"0"	"0"	"1"	"0"	"0"	"1"	"0"	"0"	"0"	"0"	"0"	"1"	"0"	"0"	"0"	"0"	"0"	"0"
0.05	"0"	"0"	"0"	"0"	"0"	"1"	"1"	"0"	"0"	"1"	"0"	"0"	"0"	"0"	"0"	"1"	"0"	"0"	"0"	"0"	"0"	"0"
0.04	"0"	"0"	"0"	"1"	"0"	"1"	"1"	"1"	"0"	"1"	"0"	"0"	"0"	"1"	"1"	"1"	"0"	"0"	"0"	"0"	"0"	"0"
0.03	"0"	"0"	"0"	"1"	"1"	"1"	"1"	"1"	"1"	"1"	"0"	"0"	"0"	"1"	"1"	"1"	"1"	"0"	"0"	"0"	"0"	"0"
0.02	"1"	"1"	"0"	"1"	"1"	"1"	"1"	"1"	"1"	"1"	"1"	"0"	"0"	"1"	"1"	"1"	"1"	"1"	"0"	"0"	"0"	"0"
0.01	"1"	"1"	"1"	"1"	"1"	"1"	"1"	"1"	"1"	"1"	"1"	"0"	"0"	"1"	"1"	"1"	"1"	"1"	"1"	"0"	"0"	"0"

Digital portrait of uniform data distribution

	1	2	3	4	5	6	7	8	9	10	11	12	13	14	15	16	17	18	19	20	21	22
0.08	"0"	"0"	"0"	"0"	"0"	"0"	"1"	"0"	"0"	"0"	"0"	"0"	"0"	"0"	"0"	"1"	"0"	"0"	"0"	"0"	"0"	"0"
0.07	"0"	"0"	"0"	"0"	"0"	"0"	"1"	"0"	"0"	"0"	"0"	"0"	"0"	"1"	"0"	"1"	"0"	"0"	"0"	"0"	"0"	"0"
0.06	"0"	"0"	"0"	"0"	"0"	"0"	"1"	"0"	"0"	"1"	"0"	"0"	"0"	"1"	"0"	"1"	"0"	"0"	"0"	"0"	"0"	"0"
0.05	"0"	"0"	"0"	"0"	"0"	"0"	"1"	"0"	"0"	"1"	"0"	"0"	"0"	"1"	"0"	"1"	"0"	"1"	"1"	"0"	"0"	"0"
0.04	"0"	"0"	"0"	"0"	"0"	"0"	"1"	"0"	"0"	"1"	"0"	"1"	"0"	"1"	"0"	"1"	"1"	"1"	"1"	"1"	"0"	"0"
0.03	"0"	"0"	"0"	"0"	"0"	"0"	"1"	"0"	"0"	"1"	"0"	"1"	"0"	"1"	"1"	"1"	"1"	"1"	"1"	"1"	"0"	"0"
0.02	"0"	"0"	"0"	"0"	"1"	"0"	"1"	"0"	"0"	"1"	"0"	"1"	"0"	"1"	"1"	"1"	"1"	"1"	"1"	"1"	"0"	"0"
0.01	"1"	"1"	"0"	"1"	"1"	"1"	"1"	"1"	"1"	"1"	"0"	"1"	"1"	"1"	"1"	"1"	"1"	"1"	"1"	"1"	"1"	"1"

Portrait of Hamming distances between normal and uniform distribution

	1	2	3	4	5	6	7	8	9	10	11	12	13	14	15	16	17	18	19	20	21	22
0.08	"0"	"0"	"0"	"0"	"0"	"0"	"1"	"0"	"0"	"0"	"0"	"0"	"0"	"0"	"0"	"0"	"0"	"0"	"0"	"0"	"0"	"0"
0.07	"0"	"0"	"0"	"0"	"0"	"0"	"1"	"0"	"0"	"0"	"0"	"0"	"0"	"0"	"0"	"1"	"0"	"0"	"0"	"0"	"0"	"0"
0.06	"0"	"0"	"0"	"0"	"0"	"0"	"1"	"0"	"0"	"1"	"0"	"0"	"0"	"0"	"0"	"1"	"0"	"0"	"0"	"0"	"0"	"0"
0.05	"0"	"0"	"0"	"0"	"0"	"0"	"1"	"0"	"0"	"1"	"0"	"0"	"0"	"0"	"0"	"1"	"0"	"0"	"0"	"0"	"0"	"0"
0.04	"0"	"0"	"0"	"0"	"0"	"0"	"1"	"0"	"0"	"1"	"0"	"0"	"0"	"0"	"0"	"1"	"0"	"0"	"0"	"0"	"0"	"0"
0.03	"0"	"0"	"0"	"0"	"0"	"0"	"1"	"0"	"0"	"1"	"0"	"0"	"0"	"0"	"0"	"1"	"0"	"0"	"0"	"0"	"0"	"0"
0.02	"0"	"0"	"0"	"0"	"1"	"0"	"1"	"0"	"0"	"1"	"0"	"0"	"0"	"0"	"0"	"1"	"0"	"0"	"0"	"0"	"0"	"0"
0.01	"1"	"1"	"0"	"1"	"1"	"1"	"1"	"1"	"1"	"1"	"0"	"0"	"0"	"1"	"1"	"1"	"1"	"1"	"1"	"1"	"0"	"0"

Figure 7. *Digital portraits of the chi-square molecule upon its excitation by data with normal and uniform distribution of values*

Downloaded from www.periodico.tchequimica.com

PERIÓDICO TCHÊ QUÍMICA
ARTIGO ORIGINAL

ANÁLISE DOS RESULTADOS DE MICROSCOPIA ELETRÔNICA BASEADOS NA COMBINAÇÃO DO MÉTODO DE INFILTRAÇÃO COM DIFERENTES TECNOLOGIAS DE RESTAURAÇÃO E NA INVESTIGAÇÃO *IN VITRO* DO TRATAMENTO DA DESMINERALIZAÇÃO FOCAL DO ESMALTE EM ESTADO DEFEITUOSO

ANALYSIS OF ELECTRONIC MICROSCOPY RESULTS BASED ON COMBINING THE INFILTRATION METHOD WITH DIFFERENT RESTORATION TECHNOLOGIES AND *IN VITRO* INVESTIGATION OF ENAMEL FOCAL DEMINERALIZATION TREATMENT AT THE DEFECT STAGE

АНАЛИЗ РЕЗУЛЬТАТОВ ЭЛЕКТРОННОЙ МИКРОСКОПИИ ПРИ СОЧЕТАНИИ МЕТОДА ИНФИЛЬТРАЦИИ С РАЗЛИЧНЫМИ РЕСТАВРАЦИОННЫМИ ТЕХНОЛОГИЯМИ ПО РЕЗУЛЬТАТАМ ИССЛЕДОВАНИЯ IN VITRO ДЛЯ ЛЕЧЕНИЯ ОЧАГОВОЙ ДЕМИНЕРАЛИЗАЦИИ ЭМАЛИ В СТАДИИ ДЕФЕКТА

SEVBITOV, Andrei*; DAVIDYANTS, Alla; KUZNETSOVA, Maria; DOROFEEV, Aleksei; MIRONOV, Sergei

Department of Propaedeutic of Dental Diseases
of I. M. Sechenov First Moscow State Medical University (Sechenov University)

** Correspondence author*
e-mail: avsevbitov@mail.ru

Received 12 July 2019; received in revised form 16 November 2019; accepted 24 November 2019

RESUMO

Atualmente, um grande número de métodos para prevenção e tratamento de cárie foi desenvolvido e implementado. No entanto, os problemas com a extensão e o desenvolvimento desse processo são redobrados a cada ano. Nesse contexto, é urgente o desenvolvimento de métodos que impeçam o desenvolvimento dessa patologia. Até o momento, foram obtidos resultados a longo prazo do tratamento de cárie no estágio de coloração por infiltração. Essa técnica permite interromper o desenvolvimento do processo carioso no estágio local impregnando tecidos patologicamente alterados com um medicamento à base de metacrilato, que estabiliza o desenvolvimento de cárie e cria condições para a restauração de áreas danificadas. Mas a questão do uso do Icon no tratamento da desmineralização focal do esmalte no estágio do defeito ainda é relevante. O objetivo desta pesquisa foi estudar a eficácia do tratamento de desmineralização focal do esmalte com base na aplicação do método de infiltração em combinação com várias tecnologias de restauração. A pesquisa foi realizada em 30 dentes selecionados, que foram removidos por várias razões e não haviam sido tratados previamente por via endodôntica. Após a limpeza mecânica da superfície dentária da placa na superfície vestibular de todas as amostras, foi criada a desmineralização artificial do esmalte no estágio do defeito. Um defeito pontual foi criado na superfície vestibular de todas as amostras dentro da zona de desmineralização usando boro esférico. A infiltração com Icon (DMG) foi realizada de acordo com as instruções do fabricante e os dentes foram divididos em 6 grupos de 5 amostras cada. O estudo revelou uma dependência entre a escolha do material de enchimento e o tamanho da cavidade preparada. Nos casos em que a cavidade é extensa, é preferível o uso de materiais compósitos com consistência e compômeros tradicionais. Se a cavidade for pequena, materiais fluidos (compósitos ou compômeros) podem ser usados para restaurar o defeito, porque esses materiais se espalham uniformemente pela cavidade dentária devido à sua consistência líquida. No modelo experimental, foi possível estabelecer a eficácia da combinação do método de infiltração com a preparação e restauração de Icon com materiais de preenchimento fotopolimerizáveis.

Palavras-chave: *desmineralização focal do esmalte, tratamento, método de infiltração, defeito, tecnologias de restauração.*

ABSTRACT

Currently, a large number of methods for caries prevention and treatment have been developed and implemented. However, the problems with the extension and development of this process are redoubling every year. Against this background, it is urgent to develop methods that prevent the development of this pathology.

Downloaded from www.periodico.tchequimica.com

To date, long-term results of treatment of caries in the staining stage by infiltration have been obtained. This technique makes it possible to stop the development of the carious process at the spot stage by impregnating pathologically altered tissues with a methacrylate-based drug, which stabilizes the development of caries and creates conditions for the restoration of damaged areas. But the question of using Icon for the treatment of focal demineralization of enamel in the defect stage is still relevant. The purpose of this research is to study the effectiveness of enamel focal demineralization treatment based on the application of the infiltration method in combination with various restoration technologies. The research was conducted on 30 selected teeth, which were removed for various reasons and had not been previously treated endodontically. After mechanical cleaning of the tooth surface from the plaque on the vestibular surface of all samples was created artificial demineralization of enamel in the defect stage. A point defect was created on the vestibular surface of all samples within the demineralization zone using spherical boron. Then the infiltration with Icon (DMG) was carried out according to the manufacturer's instructions, and the teeth were divided into 6 groups of 5 samples each. The study revealed a dependence between the choice of filling material and the size of the prepared cavity. In cases in which the cavity is extensive, using composite materials with traditional consistency and compomers is preferable. If the cavity is small, then fluid materials (composites or compomers) can be used to restore the defect because these materials spread evenly throughout the tooth cavity due to their liquid consistency.On the experimental model, it was possible to establish the effectiveness of the combination of the infiltration method with Icon preparation and restoration with light curing filling materials.

Keywords: enamel focal demineralization, treatment, infiltration method, defect, restoration technologies.

АННОТАЦИЯ

В настоящее время разработано и внедрено большое количество методик профилактики и лечения кариеса. Но проблема распространенности и развития данного процесса с каждым годом все сильнее усугубляется. На этом фоне имеет актуальность разработка методов препятствующих развитию данной патологии. На сегодняшний день получены долгосрочные результаты лечения кариеса в стадии пятна методом инфильтрации. Данная методика дает возможность остановить развитие кариозного процесса на стадии пятна за счет пропитывания патологически измененных тканей препаратом на основе метакрилата, что стабилизирует развитие кариеса и создает условия для восстановления поврежденных участков. Но вопрос применения препарата Icon для лечения очаговой деминерализации эмали в стадии дефекта по-прежнему остается актуальным. Целью настоящего исследования явилось изучение эффективности лечения очаговой деминерализации эмали путем применения метода инфильтрации в сочетании с различными реставрационными технологиями. Исследование проводилось на удаленных зубах, было отобрано 30 зубов, удаленных по различным показаниям, ранее эндодонтически не леченых. После механической очистки поверхности зубов от налета на вестибулярной поверхности всех образцов была создана искусственная деминерализация эмали в стадии дефекта. На вестибулярной поверхности всех образцов, в пределах зоны деминерализации, с помощью шаровидного бора, был создан точечный дефект. Затем провели инфильтрацию препаратом Icon (DMG) согласно инструкции производителя и разделили зубы на 6 групп по 5 образцов в каждой. Выявлена зависимость выбора пломбировочного материала от размера отпрепарированной полости. В том случае, когда полость обширная, более предпочтительнее использование композитных материалов традиционной консистении и компомеров. Если полость небольшая, то возможно применение текучих материалов (композитов, компомеров) для восстановления дефекта, так как этот материал, благодаря своей жидкой консистенции равномерно распространяется по всей полости зуба. На экспериментальной модели удалось установить эффективность сочетания метода инфильтрации препаратом Icon с реставрацией пломбировочными материалами светового отверждения.

Ключевые слова: *очаговая деминерализация эмали, лечение, метод инфильтрации, дефект, реставрационные технологии*.

1. INTRODUCTION

Currently, a large number of methods for caries prevention and treatment have been developed and implemented [1-3]. However, the problems associated with the extension and development of this process are redoubling every year. Therefore, methods are needed to prevent the development of this pathology. For many years, medicine has been focused on stopping the hard tooth tissue destruction process. Many invasive and non-invasive methods are used for this purpose [3-8]. Attempts have been made both to preserve tissues with the help of

Downloaded from www.periodico.tchequimica.com

remineralizing therapy and to excise the affected areas by means of preparation. These methods are widely used worldwide, but the development process is still underway [8-10].

To date, long-term results of caries treatment in the stain stage have been obtained using the infiltration method. This technique makes it possible to stop the development of the carious process at the stain stage due to impregnation of pathologically changed tissues with a drug based on methacrylate, which stabilizes the development of caries and creates conditions for the restoration of damaged areas. However, the question of whether the “Icon” drug can be used for the treatment of enamel focal demineralization in the defect stage remains relevant. Currently, laboratory [11-19] and clinical [20-25] investigations are being actively conducted worldwide to confirm the potential for the use of the infiltration method for the treatment of caries in the stain stage. In fact, the immediate and long-term results of enamel focal demineralization treatment in the defect stage can be improved by applying the infiltration method in combination with various restoration technologies [25-28]

The purpose of this research is to study the effectiveness of enamel focal demineralization treatment based on the application of the infiltration method in combination with various restoration technologies.

2. MATERIALS AND METHODS

The research was conducted on 30 selected teeth, which were removed for various reasons and had not been previously treated endodontically. After mechanical cleaning of dental plaque from the tooth surface (Figure. 1), artificial demineralization of the enamel in the defect stage was created on the vestibular surface of all patterns.

For this purpose, we isolated the entire tooth surface except for the light-cured composite material under investigation. This procedure was necessary to prevent direct penetration of the substance used. The teeth were immersed in hydrochloric acid (HCL) with a regular decrease in the percentage from large to small for 4 weeks (Figure. 2).

After a preset time, the patterns were removed, rinsed with water, and cleaned of filling material. A point defect was created on the vestibular surface of all patterns within the demineralization zone using a spherical dental cutter (Figure. 3).

Then, the patterns were infiltrated with “Icon” (DMG) according to the manufacturer's instructions, and the teeth were divided into 6 groups of 5 patterns each. The first group was the control group because the effectiveness of the infiltration method needed to be evaluated within the limits of the solution of continuity of the enamel. The artificially created enamel focal demineralization in the defect stage was treated with Icon (DMG) without subsequent filling (Figure. 4).

In the second group, the defect was restored with EcuSphere Shine (DMG) using light-cured composite material in combination with the 5th generation adhesive system. In the third group, the defect was restored with the same EcuSphere Shine composite (DMG) with the 6th generation adhesive system (Figure. 5).

Thus, we not only evaluated the efficiency of applying the light-cured composite in combination with the infiltration method but also compared the adhesive force of the filling material to the tooth tissues through the use of two systems of different generations that are widely used globally. In the fourth group, the restoration was performed using Ketac Molar (3M ESPE) glass-ionomer cement. The cavities of the patterns of the fifth group were restored with the fluid composite EcuSphere Flow (DMG). In the last sixth group, the cavities were restored with the fluid compomer PrimaFlow (DMG) (Figure. 6).

Figure 1. *Appearance of the extracted teeth included in the study (a) and sample preparation (b)*

Figure 2. *Sample preparation (a) and immersion in hydrochloric acid (b)*

Downloaded from www.periodico.tchequimica.com

Figure 3. *Purification of samples (a) and artificial creation of the defect with a bore (b)*

Figure 4. *Infiltration of all teeth with Icon according to the instructions and preparation of the control group*

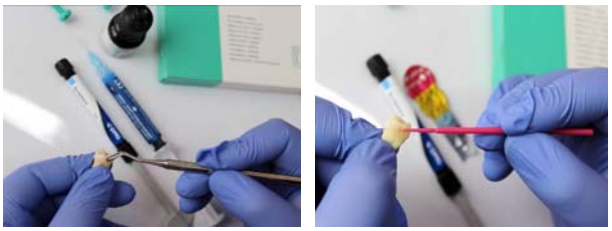

Figure 5. *Restoration with the EcuSphere Shine composite in combination with the 5th generation adhesive system (a) and EcuSphere Shine composite in combination with the 6th generation adhesive system (b)*

After the restoration of the defects, all teeth were prepared in the experimental cell pathology laboratory by immersing the patterns in nitric acid (7.5% HNO_3), followed by daily replacement of the solution with a smaller percentage ratio for 20 days. Then, the teeth were kept in alcohol (C_2H_5OH) of different percentages for 7 days with a daily change from 70% to 99%, followed by one hour in chloroform. Finally, the teeth were filled with paraffin for 24 hours for the subsequent manufacture of slices with a sledge microtome (HM 450).

After preparation of thin slices, microscopic examination of the patterns was carried out using scanning electron microscopy (SEM). The enamel surface and deep layers of the tooth hard tissues were evaluated using a low-vacuum scanning electron microscope (model JEOL JSM-6380LV, Japan). The tooth microrelief was examined in the secondary electron emission mode with an accelerating voltage of 10–15 kV and a magnification ranging from 400 to 1300 times. A conductive coating — carbon or gold — was applied to chips of the extracted teeth to prevent electronic charging and thermal damage. The deposition of carbon or gold on a tooth with a thickness of 10–20 nm was carried out by thermal evaporation in a vacuum at 1.3×10^{-3} Pa. This protective coating has a low X-ray absorption coefficient and sufficient electrical conductivity, which is the basis for its use and significantly improves the image quality. The prepared object (tooth) was fastened to the holder and placed in the chamber of the scanning electron microscope.

3. RESULTS AND DISCUSSION:

The microscopic examination revealed significant differences among the patterns. Effective application of the infiltration method in combination with the light-cured composite EcuSphere Shine and the 5th and 6th generation adhesive system was achieved (Figure. 7).

The boundaries of the filling material transition in the tooth tissue are solid and have no macro and micro damages. During the examination of the tooth slices in the enamel focal demineralization zone, the presence of infiltration in the damaged area was clearly visible as a shinier and lighter area. In photomicrographs, these areas appear to be covered with frost in contrast to the more matte, healthy enamel. A microscopic examination of the control group patterns showed uniform impregnation of the tooth tissues with infiltration throughout the entire depth of the defect. The picture shows the presence of infiltration on the cavity paries of the tooth (Figure. 8).

Figure 6. *Restoration with Ketac Molar glass ionomer cement, EcuSphere Flow fluid composite, and PrimaFlow fluid compomer*

Downloaded from www.periodico.tchequimica.com

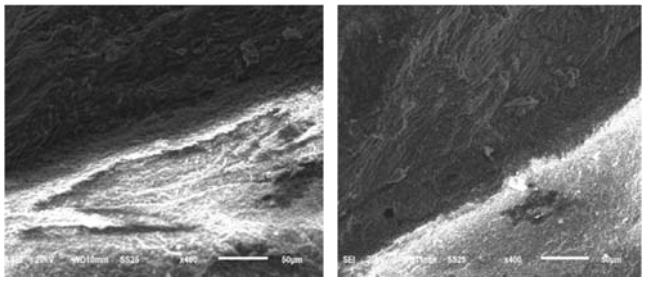

Figure 7. *Microscopic examination of light-cured composite material-sealed EcuSphere Shine samples in combination with the 5th (a) and 6th (b) generation adhesive systems*

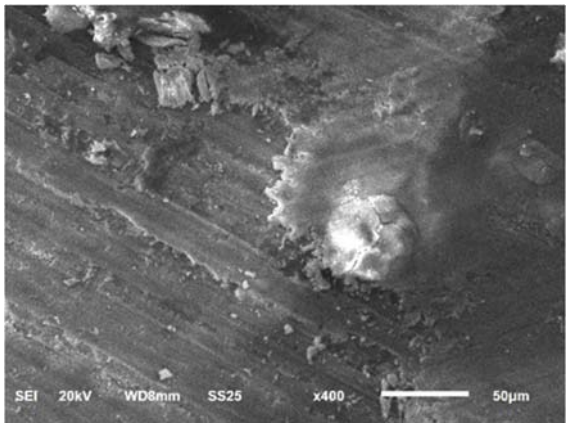

Figure 8. *Microscopic examination of the control group*

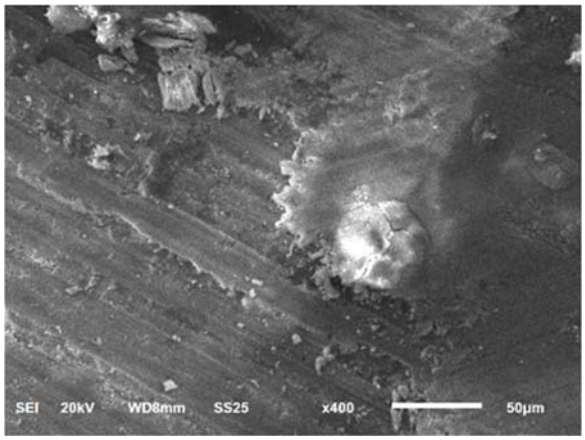

Figure 9. *Microscopic examination of samples recovered with the glass ionomer cement Ketac Molar*

Visually, the presence of a filling material in the cavity of the tooth was distinctly noticeable on the slices and during microscopic examination of the patterns restored by the glass-ionomer cement Ketac Molar (Figure. 9). A partial detachment of the filling material from the cavity paries was observed, which indicated a lack of adhesion to the tooth tissues or its complete absence.

A detailed examination of the recovered defects using the fluid compomer PrimaFlow and the composite EcuSphere Flow determined the penetration of the infiltration into the tooth tissues along the entire length of the defect (Figure. 10).

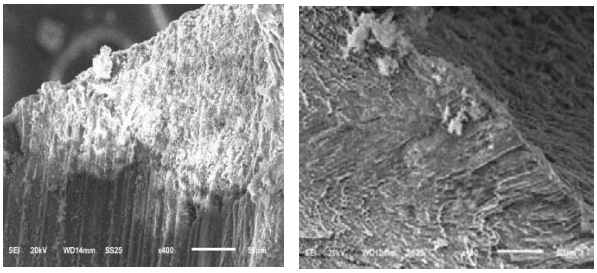

Figure 10. *Microscopic examination of the samples sealed with the fluid compomer PrimaFlow (a) and the fluid composite EcuSphere Flow (b)*

In areas impregnated with infiltration, the penetration of the drug into the initial dentinal layers was confirmed. This finding is of very important clinical relevance since the probability of recurrence of the carious process becomes higher in cases of incomplete infiltration of the entire volume of the damaged tissues. Although in the in vitro study, we investigated drug infiltration on dry patterns, dentin fluid is present in the vital dentin and can become an insurmountable obstacle for the penetration of hydrophobic infiltration. During the course of the research, we obtained satisfactory results for the application of this method in combination with the light-cured composite EcuSphere Shine and the 5th or 6th generation adhesive system.

4. CONCLUSIONS:

The experimental model allowed to establish the effectiveness of the combination of the infiltration method with the “Icon” drug and the restoration of light-cured filling materials, such as the composite EcuSphere Flow, EcuSphere Shine, and compomer PrimaFlow. The obtained electron microscopic examination clearly show close contact of the filling material with the tooth tissues, which indicates high adhesion between them. The use of a combination of methods on the enamel surface did not result in damage, which confirmed the safety of using the presented treatment regimen in practice.

Downloaded from www.periodico.tchequimica.com

5. ACKNOWLEDGMENTS:

This work was done at Sechenov University with supported by the "Russian Academic Excellence Project 5-100".

6. REFERENCES:

1. Paris S., Meyer-Lueckel H., Kielbassa A.M. Resin infiltration of natural caries lesions. *J Dent Res*. **2007**; 86: 7: 662-666.
2. Paris S., Chatzidakis A.J., Meyer-Lueckel H. Influence of application time on caries infiltration in primary teeth. *Int J Paediat Dentist*. **2009**; 19(S1): 9.
3. Mueller J., Meyer-Lueckel H., Paris S. et al. Inhibition of lesion progression by the penetration of resins in vitro: influence of the application procedure. *Oper Dent*. **2006**; 313: 338-45.
4. Sevbitov A.V., Dorofeev A.E., Davidyants A.A., Ershov K.A., Timoshin A.V. Assessment of pain perception of elderly patients with different levels of dentophobia during surgical dental appointment. *Asian Journal of Pharmaceutics.* **2018**; 12 (S3): 1012-1016.
5. Sevbitov A.V., Brago A.S., Enina Yu.I., Dorofeev A.E., Mironov S.N. Experience in the application of hybrid ceramic restorations in the cervical region. *Asian Journal of Pharmaceutics*. **2018**; 12(S3): 1106-1109.
6. Yumashev A. V., Utyuzh A. S., Mikhailova M.V., Samusenkov V.O., Volchkova I.R. Selecting clinical and laboratory methods of manufacture of orthopaedic titanium alloy structures using a biopotentiometer. *Current Science (India)*. **2018**; 114(4): 891-896.
7. Sevbitov A.V., Enina Yu.I., Derevyanchenko S.P., Dorofeev A.E. Comparative evaluation of effectiveness of restorations in cervical teeth region by direct and indirect method. *International Journal of Civil Engineering and Technology*. **2019**; 10(3): 3099-3105.
8. Enina Yu.I., Sevbitov A.V., Dorofeev A.E., Pustokhina I.G. Experimental substantiation of the choice of the restoration method in the cervical area of teeth with abfraction defects. International *Journal of Mechanical Engineering and Technology*. **2019**; 10(5): 41-47.
9. Álvaro Furtado, Gisela-Crippa Furtado, Ossam El Haje, Henrique-Damian Rosário, Ademir Franco, Irina Makeeva, Luiz-Renato Paranhos. Soft-tissue cone-beam computed tomography (ST-CBCT) technique for the analysis of skeletal, dental and periodontal effects of orthopedic rapid maxillary expansion. *J Clin Exp Dent*. **2018**; 10(9): e883-90.
10. Kuznetsova M.Yu., Nevdakh A.S., Platonova V.V., Sevbitov A.V., Dorofeev A.E. Evaluation of effectiveness of a preparation on the basis of phytoecdysteroids for treatment of traumatic injuries of oral mucosa in orthodontic patients. *International Journal of Green Pharmacy.* **2018**; 12(S1): 297-300.
11. Doméjean S, Ducamp R, Léger S, Holmgren C. Resin infiltration of non-cavitated caries lesions: a systematic review. *Med Princ Pract*. **2015**; 24(3): 216-21.
12. Meyer-Lueckel H, Balbach A, Schikowsky C, Bitter K, Paris S. Pragmatic RCT on the Efficacy of Proximal Caries Infiltration. *J Dent Res*. **2016**; 95(5): 531-6.
13. Kielbassa AM, Ulrich I, Werth VD, Schüller C, Frank W, Schmidl R. External and internal resin infiltration of natural proximal subsurface caries lesions: A valuable enhancement of the internal tunnel restoration. *Quintessence Int*. **2017**; 48(5): 357-368.
14. Liang Y, Deng Z, Dai X, Tian J, Zhao W. Micro-invasive interventions for managing non-cavitated proximal caries of different depths: a systematic review and meta-analysis. *Clin Oral Investig*. **2018**; 22(8): 2675-2684.
15. Altarabulsi MB, Alkilzy M, Petrou MA, Splieth C. Clinical safety, quality and effect of resin infiltration for proximal caries. *Eur J Paediatr Dent*. **2014**; 15(1): 39-44.
16. Wright JT, Tampi MP, Graham L, Estrich C, Crall JJ, Fontana M, Gillette EJ, Nový BB, Dhar V, Donly K, et al. Sealants for preventing and arresting pit-and-fissure occlusal caries in primary and permanent molars: A systematic review of randomized controlled trials-a report of the American Dental Association and the American Academy of Pediatric Dentistry. *J Am Dent Assoc*. **2016**; 147(8): 631-645.
17. Ammari MM, Soviero VM, da Silva Fidalgo TK, Lenzi M, Ferreira DM, Mattos CT, de Souza IP, Maia LC. Is non-cavitated proximal lesion sealing an effective method for caries control in primary and permanent teeth? A systematic review and meta-analysis. *J Dent.* **2014**; 42(10): 1217-27.
18. Meyer-Lueckel H, Bitter K, Paris S. Randomized controlled clinical trial on proximal caries infiltration: three-year follow-up. *Caries Res*. **2012**; 46(6): 544-8.
19. Paris S, Hopfenmuller W, Meyer-Lueckel H. Resin infiltration of caries lesions: an efficacy randomized trial. *J Dent Res. 2010*; 89(8): 823-6.

Downloaded from www.periodico.tchequimica.com

20. Ammari MM, Jorge RC, Souza IPR, Soviero VM. Efficacy of resin infiltration of proximal caries in primary molars: 1-year follow-up of a split-mouth randomized controlled clinical trial. *Clin Oral Investig*. **2018**. 22(3):1355-1362.
21. Bille J, Carstens K. Approximal caries progression in 13- to 15-year-old Danish children. *Acta Odontol Scand*. **1989**. 47(6): 347-54.
22. Phark JH, Duarte S Jr, Meyer-Lueckel H, Paris S. Caries infiltration with resins: a novel treatment option for interproximal caries. *Compend Contin Educ Dent*. **2009**; 30(3):13-7.
23. Lausch J, Askar H, Paris S, Meyer-Lueckel H. Micro-filled resin infiltration of fissure caries lesions in vitro. *J Dent*. **2017**; 57: 73-76.
24. Paris S, Lausch J, Selje T, Dörfer CE, Meyer-Lueckel H. Comparison of sealant and infiltrant penetration into pit and fissure caries lesions in vitro. *J Dent*. **2014**; 42(4): 432-8.
25. Paris S, Lausch J, Selje T, Dörfer CE, Meyer-Lueckel H. Comparison of sealant and infiltrant penetration into pit and fissure caries lesions in vitro. *J Dent*. **2014**; 42(4): 432-8.
26. Paris S, Lausch J, Selje T, Dörfer CE, Meyer-Lueckel H. Comparison of sealant and infiltrant penetration into pit and fissure caries lesions in vitro. *J Dent*. **2014**; 42(4):432-8. Epub 2014 Jan 18.
27. Manoharan V, Arun Kumar S, Arumugam SB, Anand V, Krishnamoorthy S, Methippara JJ. Is Resin Infiltration a Microinvasive Approach to White Lesions of Calcified Tooth Structures?: A Systemic Review. *Int J Clin Pediatr Dent*. **2019**; 12(1): 53-58.
28. Arslan S, Kaplan MH. The Effect of Resin Infiltration on the Progression of Proximal Caries Lesions: A Randomized Clinical Trial. *Med Princ Pract*. **2019**; 3.

Downloaded from www.periodico.tchequimica.com

PERIÓDICO TCHÊ QUÍMICA
ARTIGO ORIGINAL

ADESÃO DE PATÓGENOS PERIODONTAIS A MATERIAIS UTILIZADOS PARA COROAS TEMPORÁRIAS DE LONGO PRAZO

ADHESION OF PERIODONTAL PATHOGENS TO MATERIALS USED FOR LONG-TERM TEMPORARY CROWNS

АДГЕЗИЯ ПАРАДОНТАЛЬНЫХ ПАТОГЕНОВ К МАТЕРИАЛАМ, ИСПОЛЬЗУЕМЫХ ДЛЯ ДОЛГОСРОЧНЫХ ВРЕМЕННЫХ КОРОНОК

UTYUZH, Anatolij[1]; NIKOLENKO, Denis[2]; YUMASHEV, Alexey[3*]; VOLCHKOVA, Ilona[4]; SAMUSENKOV, Vadim[5];

[1,2, 3, 4, 5] Department of Prosthetic Dentistry, I. M. Sechenov First Moscow State Medical University (Sechenov University), Moscow, Russian Federation

** Correspondence author*
e-mail: yumashev031996@mail.ru

Received 26 July 2019; received in revised form 10 November 2019; accepted 24 November 2019

RESUMO

As coroas provisórias são amplamente utilizadas no tratamento protético em odontologia e surgiram novos materiais para coroas temporárias, incluindo a poliéterétercetona, que têm requisitos de alta qualidade para uso em próteses temporárias de longo prazo. De particular importância na prótese são as características da adesão da microflora oral patogênica às estruturas ortodônticas. Este estudo avaliou a adesão da flora bacteriana periodontal cariogênica e patogênica das espécies de Candida a polieterétercetona Dentokeep não polida e polida (PEEK), material de polimetilmetacrilato polido (PMMA) polido (Re-Fine Acrylic) e plástico acrílico de cura a quente - um líquido em pó tipo, em que o pó é um copolímero contendo enxofre em suspensão e o líquido é uma mistura de monômeros acrílicos e oligômeros─ (Sinma-M) recomendados para a fabricação de coroas temporárias de longo prazo. Estudou-se o efeito de polir ou remover o polimento do material de estudo na adesão de vários microrganismos. O polimento do Dentokeep PEEK influenciou significativamente a adesão primária. A adesão microbiana aos materiais da amostra foi estudada usando cavitação ultrassônica. A adesão de microrganismos a cada material foi classificada como baixa (0-0,27), moderada (0,28-0,69) ou alta (0,70-1). *Streptococcus sanguinis*, Prevotella intermedia e *Candida albicans* aderiram moderadamente ao Dentokeep PEEK não polido, enquanto *Porphyromonas gingivalis* e *Candida krusei* foram altamente aderentes. As espécies de Candida e a linhagem periodontal patogênica de P. intermedia aderiram moderadamente ao Dentokeep PEEK polido, enquanto S. *sanguinis* e P. *gingivalis* foram altamente aderentes. As coroas temporárias requerem medidas higiênicas adicionais para erradicar a microbiota cariogênica (acidogênica), periodontal patogênica e fungica e manter a composição qualitativa e quantitativa normal da microbiocenose oral durante o tratamento protodôntico. Em conclusão, PEEK é um material promissor para a fabricação de coroas temporárias de longo prazo.

Palavras-chave: *Odontologia, Polieterétercetona, Restaurações temporárias, Coroas provisórias, Compatibilidade.*

ABSTRACT

Provisional crowns are widely used in prosthodontic treatment in dentistry, and new materials for temporary crowns, including polyetheretherketone, have emerged, which have high-quality requirements for use in long-term temporary prosthetics. Of particular importance in prosthetics are the features of adhesion of pathogenic oral microflora to orthodontic structures. This study evaluated the adhesion of cariogenic and pathogenic periodontal bacterial flora and *Candida* species to unpolished and polished Dentokeep polyetheretherketone (PEEK), polished polymethyl methacrylate (PMMA) material (Re-Fine Acrylic), and hot-curing acrylic plastic ─ a powder-liquid type, where the powder is a suspension graft fluorine-containing copolymer, and the liquid is a mixture of acrylic monomers, and oligomers─(Sinma-M) recommended for manufacturing long-term temporary crowns. The effect of polishing or un-polishing the study material on the adhesion of various microorganisms was studied. Polishing of Dentokeep PEEK significantly influenced primary

Downloaded from www.periodico.tchequimica.com

adhesion. Microbial adhesion to sample materials was studied using ultrasonic cavitation. Adhesion of microorganisms to each material was categorized as low (0–0.27), moderate (0.28–0.69), or high (0.70–1). *Streptococcus sanguinis*, *Prevotella intermedia*, and *Candida albicans* adhered moderately to unpolished Dentokeep PEEK, whereas *Porphyromonas gingivalis* and *Candida krusei* were highly adherent. *Candida* species and *P. intermedia* pathogenic periodontal strain moderately adhered to polished Dentokeep PEEK, whereas *S. sanguinis* and *P. gingivalis* were highly adherent. Temporary crowns require additional hygienic measures to eradicate cariogenic (acidogenic), pathogenic periodontal, and fungal microbiota and maintain the normal qualitative and quantitative composition of oral microbiocenosis during prosthodontic treatment. In conclusion, PEEK is a promising material for the manufacture of long-term temporary crowns.

Keywords: *Dentistry, Polyetheretherketone, Temporary restorations, Provisional crowns, Biocompatibility*.

АННОТАЦИЯ

Временные коронки широко используются для протезирования зубов в стоматологии, появились новые материалы для временных коронок, включая полиэфирэфиркетон, которые удовлетворяют высоким требованиям к качеству для долгосрочного временного протезирования. Особое значение в протезировании имеют особенности адгезии патогенной микрофлоры полости рта к ортодонтическим структурам. В этом исследовании оценивали адгезию кариесогенной и патогенной пародонтальной бактериальной флоры и грибов рода *Candida* к неполированному и полированному полиэфирэфиркетону Dentokeep (PEEK), полированному полиметилметакрилату (PMMA) (Re-Fine Acrylic) и акриловой пластмассы горячего отверждения – типа порошок-жидкость, где порошок представляет собой суспензионный привитой фторсодержащий сополимер, а жидкость представляет собой смесь акриловых мономеров и олигомеров (Sinma-M), рекомендованных для изготовления долгосрочных временных коронок. Было изучено влияние полированного или не полированного материала на адгезию различных микроорганизмов. Полировка Dentokeep PEEK значительно повлияла на первичную адгезию. Микробную адгезию к материалам образцов изучали с помощью ультразвуковой кавитации. Адгезия микроорганизмов к каждому материалу была классифицирована как низкая (0–0,27), умеренная (0,28–0,69) или высокая (0,70–1). *Streptococcus sanguinis*, *Prevotella intermedia* и *Candida albicans* обладали умеренной адгезией к нешлифованному Dentokeep PEEK, тогда как *Porphyromonas gingivalis* и *Candida krusei* – высокой адгезивностью. Грибы рода *Candida* и пародонтопатогенный штамм *P. intermedia* обладали умеренной адгезией к полированному Dentokeep PEEK, тогда как *S. sanguinis* и *P. gingivalis* отличались высокой адгезией. Временные коронки требуют дополнительных гигиенических мер для устранения кариесогенной (ацидогенной), пародонтопатогенной и грибковой микробиоты и поддержания нормального качественного и количественного состава микробиоценоза полости рта во время протезирования. В заключение следует отметить, что PEEK является перспективным материалом для изготовления долгосрочных временных коронок.

Ключевые слова: стоматология, полиэфирэфиркетон, временное протезирование, провизорные коронки, биосовместимость.

1. INTRODUCTION

Currently, temporary crowns are manufactured for most patients during prosthodontic treatment (Abdullah *et al.*, 2018; Kasim *et al.*, 2018; Klur *et al.*, 2019). The positive features of temporary restorations are well known to dentists and include protecting the tooth stump from external influences after tooth preparation for prosthodontic structure and providing patients with psychological comfort associated with the ability to communicate fully with family and the society during the prosthodontic treatment (Arutjunov *et al.*, 2012; Afanas'eva *et al.*, 2015; Timoshin *et al.*, 2018). Deadlines for the manufacture of permanent orthodontic structures (bridge-like prosthetic dentures, single crowns, veneers, and dental inserts) are from 5 to 30 days (Utjuzh *et al.*, 2016), and provisional crowns are retained in patients' oral cavity during this time (Goncharov *et al.*, 2016; Ibragimov *et al.*, 2011; Utjuzh *et al.*, 2017). Recently, numerous polymers have emerged in the market as dental materials for the production of provisional crowns using a direct method (Abdullah *et al.*, 2016; Taylor *et al.*, 2016).

Dentokeep polyetheretherketone (Dentokeep Peek, PEEK) is a new polymeric material for provisional crowns that have not yet been sufficiently characterized and studied in terms of clinical efficacy and influence on oral microbiocenosis (Bathala *et al.*, 2019; Najeeb *et*

Downloaded from www.periodico.tchequimica.com

al., 2016).

Currently, in dentistry, the materials recommended for the manufacture of provisional crowns are polished polymethyl methacrylate (PMMA) material (Re-Fine Acrylic) and hot-curing acrylic plastic─a powder-liquid type, where the powder is a suspension graft fluorine-containing copolymer, and the liquid is a mixture of acrylic monomers and oligomers─(Sinma-M) (Davydova *et al.*, 2013; Makeeva *et al.*, 2016).

A variety of microorganisms are present in the oral cavity of an individual, raising concerns regarding the use of temporary recovery materials (Zhimova *et al.*, 2015; Sampaio-Maia, 2016). A specific class of acidogenic streptococci plays the role of stabilizing species that support the normal quantitative and qualitative composition of the microbial flora of the oral cavity (Deo *et al.*, 2019). However, their excessive colonization of the tooth surface and congestion on temporary restorations (crowns) have negative effects as cariogenic factors (Chen *et al.*, 2019; Conrads and About, 2018). A group of periodontal anaerobic bacteria has recently been classified as pathogenic species that can destroy the organic base of the tooth cement, particularly the collagenous periodontal base in root caries, and cause periodontitis. Fungi of the genus *Candida* play a role in the pathology of the oral mucosa and periodontium in individuals with a genetic predisposition and certain immune system defects (Makeeva *et al.*, 2016; Tsarev *et al.*, 2014).

Some clinical situations are known to require longer use of temporary bridge-like prosthetic dentures or individual crowns (up to 12 months). However, along with the performance of certain functions (protective, chewing, aesthetic, and communicative), the presence of temporary restorative devices in the oral cavity could cause complications, leading to the failure of orthopaedic treatment, and contribute to the development or aggravation of chronic periodontitis. This is because the materials from which temporary restorations are made have higher adherence to microbial colonization than the tooth enamel or the materials used to manufacture permanent, fixed orthodontic structures under the conditions of a dental laboratory (Afanas'eva *et al.*, 2015; Tsarev *et al.*, 2014; Yumashev *et al.*, 2016).

The degree of adhesion of microorganisms, in turn, determines the features of subsequent microbial colonization of both temporary structures and permanent prosthetic dentures, which is subsequently established and affects the entire oral microbiocenosis (Tsarev *et al.*, 2011).

The purpose of this study was to investigate the adhesion of cariogenic (or acidogenic) and pathogenic periodontal bacterial flora and fungi of the *Candida* genus to unpolished and polished PEEK, PMMA, and Sinma-M materials. In clinical dentistry, there is a practice of using polished and unpolished materials for restorations. The choice of material depends on each clinical case, and sometimes, this choice is made by doctors based on their experience. This study comparatively assessed indices of the primary adhesion of representative pathogenic periodontal and acidogenic microbial flora, and *Candida* species to samples of the materials under investigation.

2. MATERIALS AND METHODS

PEEK was the test substance in this study, while the following materials recommended for the manufacture of provisional crowns, Re-Fine Acrylic, and Sinma-M were used for the comparison. All samples were manufactured using the same disc-shaped pattern. The PEEK and Re-fine samples were milled using computer-aided design/computer-aided manufacturing (CAD/CAM) technology, whereas the Sinma M samples were made using a thermal polymerization method. Next, the samples were polished to a mirror shine according to the instructions (Goncharov *et al.*, 2016; Ibragimov *et al.*, 2011). The group included 30 samples each of polished PEEK, unpolished PEEK, polished Re-Fine Acrylic, and unpolished Sinma-M materials, totaling 120 samples. For each group of microorganisms, six samples of each material were prepared. For the experimental studies, the strains of microorganisms used were in accordance with existing recommendations, (Goncharov *et al.*, 2016; Ibragimov *et al.*, 2011) and belonged to the following groups (Goncharov *et al.*, 2016; Ibragimov *et al.*, 2011):

1. **Cariogenic (acidogenic) streptococci**: *Streptococcus sanguinis* – gram-positive, microaerophilic cocci;

2. **Pathogenic periodontal species**: *Porphyromonas gingivalis* and *Prevotella intermedia* – gram-negative, strictly anaerobic rods;

3. **Yeast**: *Candida albicans* and *Candida krusei*.

Downloaded from www.periodico.tchequimica.com

As control strains of microorganisms, the densities of the bacterial and fungal suspensions were 10^9 CFU/ml and -10^{7-8} CFU/ml, respectively. Samples of materials with test strains were incubated in a thermostat-controlled environment for 2 h at 37°C. To remove the non-adherent bacteria or yeast, the samples were first washed three times with 10 mL sterile isotonic sodium chloride solution.

Then, each sample was placed in a separate plastic chamber containing 1 mL sterile isotonic sodium chloride solution and sonicated in an Ultra-Est-M ultrasound bath (GeoSoft Research and Production Company, Russia) at a frequency of 60 kHz for 10 min to collect microbial cells that adhered primarily to the surface of the dental material. To assess the primary adhesiveness of the organisms, identical disc-shaped samples were prepared (0.5 cm in diameter). These were UV-sterilized and then placed in a Petri dish. Then, 100 µL each of 1-day-old bacterial culture suspensions of the test strains was applied to the surface (Table/Fig 1). The technique of setting the primary adhesion test was consistent with the protocol described in the manual by Tsarev (Tsarev *et al.*, 2014). The resulting flushing from the samples was inoculated at the amount of 100 µL on 5% Columbia blood agar using an automatic micropipette. The material was distributed on the nutrient medium surface using a sterile plastic loop.

A dense Saburo medium was used to study the yeast adhesion. The obtained colonies were counted and examined using a research stereomicroscope (Nikon, Japan). Based on the determined decimal logarithm, the primary adhesion index was calculated for each sample of the material/test strains using the Equation 1 proposed by Tsarev (Tsarev *et al.*, 2014):

$$Ia = lgA/lgN \quad \text{(Eq. 1)}$$

where Ia is the index of primary adhesion; A is the number of bacteria deposited on the sample; N is the number of bacteria in the washout from the sample (Tsarev *et al.*, 2014). All samples were tested once.

3. STATISTICAL ANALYSIS

All the experimental data were processed using the Statistica 6.0 statistical software package for Windows. The statistical significance of differences between the compared groups was determined using the Kruskal-Wallis statistical test. Differences between the groups were considered statistically significant at $p < 0.05$. The average values are expressed as the means ± the standard deviation (SEM).

4. RESULTS AND DISCUSSION:

Based on the obtained values of the primary adhesion index, the degree of adhesion of the representative oral microbiota was evaluated (Table/Fig 2) as low (< 0.27), moderate (0.28–0.69), and high (> 0.70) (Timoshin *et al.*, 2018). The *S. sanguinis* acidogenic species was characterized by a high adhesion index for Re-Fine Acrylic (0.74 ± 0.64) and polished PEEK (0.70 ± 1.10) and moderate adhesion indices for Sinma M (0.58 ± 0.70) and unpolished PEEK (0.60 ± 0.68) (Table 1). The analysis of the representative bacterial pathogenic periodontal flora showed the following results. *P. gingivalis* showed the highest adhesion to all materials studied, including both polished and unpolished PEEK (0.77 ± 0.80) (Table 2). Another pathogenic periodontal species *P. intermedia* was characterized by moderate adhesion to the investigated materials, while the polished and unpolished PEEK did not differ in adhesion indices **(**0.51 ± 1.04**)** (Table 3)**.**

The adhesion index of *C. albicans* for the investigated materials was moderate for all the materials studied and did not depend on the PEEK polishing degree (0.61 ± 0.70 and 0.59 ± 1.10, for polished and unpolished, respectively) (Table/Fig 3D). In contrast, the less common *C. krusei* strain was highly adherent to Re-Fine Acrylic (0.75 ± 1.10) and unpolished PEEK (0.80 ± 1.12), while polished PEEK showed a moderate level of adhesion (0.63 ± 0.70) (Table 3 and 5). The results of primary adhesion index determination of the microorganisms on the investigated sample materials are given in Table 4, Figure 3.

The representative pathogenic periodontal species of bacteria differed in their degree of adhesion to the studied materials – the most unfavorable indicators (with an extremely high degree of adhesion) were characteristic for the *P. gingivalis* strain, while the other frequently encountered periodontal pathogen, *P. intermedia*, showed moderate adhesion. The adhesion of *C. albicans* could be defined as moderate for all the investigated materials, and it did not depend on PEEK polishing. Contrastingly, the less common *C. krusei* strain was highly adherent to Re-Fine

Downloaded from www.periodico.tchequimica.com

Acrylic and unpolished PEEK.

Polishing the PEEK material had a significant effect on the mechanisms of primary adhesion, and, in bacteria and fungi, this effect was manifested in different ways. A study of polished and unpolished materials, which was conducted using PEEK, showed that with regard to cariogenic microflora, polishing did not significantly affect the degree of adhesion, whereas, in *C. krusei*, it was significantly reduced. Evaluation of the primary adhesion of the acidogenic *S. sanguinis* strain to the material samples revealed that the polished PEEK was characterized by a higher adhesion index than the unpolished sample. Thus, the findings showed that the adhesion of the test microorganisms *S. sanguinis, P. intermedia,* and *Candida albicans* to the new material for manufacturing temporary crowns, i.e., unpolished PEEK, was moderate, whereas that of *P. gingivalis* and *C. krusei* was high. Furthermore, the fungal *Candida* species and pathogenic periodontal strain *P. intermedia* showed moderate adhesion to polished PEEK, whereas *S. sanguinis* and *P. gingivalis* showed a high adhesion. We proved that there are statistically significant differences between the materials in the context of the adhesion of the microorganisms. In this context, unpolished PEEK was better than PMMA in preventing the adhesion of *S. sanguinis*, and polished PEEK was better than PMMA in preventing the adhesion of *C. krusei*. PEEK had no advantage over Sinma M.

The obtained results also suggested that the mechanisms of adhesion to polished and unpolished materials differed in streptococci and fungi. The streptococci seemed to interact through receptors and material molecules, which were not affected or may have been strengthened by polishing, whereas fungi, particularly *C. krusei*, likely had the main mechanism of attachment associated with surface roughness. Therefore, the polishing process likely reduced the degree of adhesion, which corresponds to the literature data based on scanning electron and atomic force microscopy (Kasim *et al.*, 2018; Utjuzh *et al.*, 2017; Abdullah *et al.*, 2016).

According to studies by Tsarev *et al.* (2014), who previously investigated various materials for the manufacture of temporary restorative, prosthetic dentures, representative pathogenic periodontal flora showed the highest degree of adhesion to composite photopolymerizable materials (Filtek, 3M ESPE); the degree of adhesion of *S. sanguinis* was 0.63-0.90, and that of *C. albicans* was 0.75-0.85. Similar data were obtained by Goncharov *et al.* (2016) who studied newly imported materials for provisional crowns—acrylic self-hardening plastic (Tempron, GC Corporation) and bis-acrylic composite with a new generation of fillers (Protemp, 3M ESP)—and domestic material—polymeric composite material based on multifunctional methacrylates (Tempocor, VladMiVa)—in polished, lacquered, and uncoated states. It was found that the domestic material showed a lower level of adhesion for pathogenic periodontal microbes than other organisms, but streptococci and *Porphyromonas* differed significantly in the level of adhesion on lacquer, which raises concerns of the need to improve the antiadhesive characteristics of the lacquers used (Goncharov *et al.,* 2016). For the Tempocor material without and with lacquers, the degree of adhesion of *S. sanguinis* was 0.45 and 0.88, that of *P. gingivalis* was 0.60 and 0.60, that of *C. albicans* was 0.50 and 0.50, and that of *C. krusei* was 0.75 and 0.78, respectively. For the Tempron material, the degree of adhesion of *S. sanguinis* was 0.67, *P. gingivalis* was 0.80, *C. albicans* was 0.58, and *C. krusei* was 0.71, which are significantly worse than the PEEK values. PEEK also had the advantage of being used to assess the degree of adhesion over the Protemp material with respect to *C. albicans* and *C. krusei*, for which the adhesion indices were 0.60 and 0.75, respectively (Goncharov *et al.,* 2016). In conclusion, the results of this study indicate that PEEK is a promising material for the manufacture of long-term temporary crowns. The disadvantages of temporary acrylic crowns have long been known, which further underscores the potential benefits and justifies undertaking clinical studies on the effectiveness of PEEK-based long-term temporary crowns.

5. CONCLUSIONS:

In the study had assessed indices of the primary adhesion of representative pathogenic periodontal and acidogenic microbial flora and Candida species to samples of the materials under investigation.

The study concluded that the primary adhesion depends on the type and polishing of the material. To establish this fact, the degree of adhesion of microorganisms to PEEK, Re-Fine Acrylic and Sinma-M were determined.

Installed features indices of the primary

Downloaded from www.periodico.tchequimica.com

adhesion of mouth microflora allowed us to conclude about the most preferred materials for use in restorative dentistry. With the best side of themselves showed PEEK, while other materials had a higher degree of adhesion.

The results of the study can help dentists to choose the most optimal material for the patient in prosthodontic treatment in dentistry.

It is rational to continue the study of the adhesion of microorganisms to other materials for prosthetics in order to expand knowledge about their pro-adhesiveness.

Manufacturers' Details

Dentokeep Peek material: HT-Trading GmbH & Co. KG, Germany

Re-Fine Acrylic: Yamahachi Dental MFG, Co, Japan

Sinma M: Stoma JSC, Ukraine

Ultra-Est-M ultrasound bath: GeoSoft Research and Production Company, Russia

Research stereomicroscope: Nikon, Japan

6. REFERENCES:

1. Abdullah, A. O., Pollington, S., Liu, Y. Comparison between direct chairside and digitally fabricated temporary crowns. *Dent Mater J.*, **2018**, *37*(6), 957-963.
2. Abdullah, A. O., Tsitrou, E. A., Pollington, S. Comparative in vitro evaluation of CAD/CAM vs conventional provisional crowns. *J Appl Oral Sci.*, **2016**, *24*(3), 258-263.
3. Afanas'eva, V. V., Arutjunov, D. S., Deev, M. S., Ippolitov, E. V., Careva, T. V. Clinical and microbiological aspects of the microbial biofilm formation on structural materials used for fixing and relining removable dentures. *Russian Journal of Dentistry*, **2015**, *19*, 44-46.
4. Arutjunov, S. D., Carjov, V. N., Ippolitov, E. V., Apresjan, S. V., Trefilov, A. G. Formation of a biofilm on temporary dentures: the ratio of primary microbial adhesion, coaggregation and colonization. *Stomatology*, **2012**, *5*, 5-10.
5. Bathala, L., Majeti, V., Rachuri, N., Singh, N., Gedela, S. The Role of Polyether Ether Ketone (Peek) in Dentistry - A Review. *J Med Life.*, **2019**, *12*(1), 5-9.
6. Chen, Y., Li, Y., Zou, J. Intrageneric and Intergeneric Interactions Developed by Oral Streptococci: Pivotal Role in the Pathogenesis of Oral Diseases. *Curr Issues Mol Biol.*, **2019**, *32*, 377-434.
7. Conrads, G., About, I. Pathophysiology of Dental Caries. *Monogr Oral Sci.*, **2018**, *27*, 1-.10.
8. Davydova, M. M., Plakhtij, L. J., Tsarev, V. N. Methods of microbiological research used in dentistry. In Tsarev, V. N., editor. Microbiology, virology and immunology of the oral cavity. Moscow: GEOTAR-MEDIA, **2013**, 223-268.
9. Deo, P. N., Deshmukh, R. Oral microbiome: Unveiling the fundamentals. *J Oral Maxillofac Pathol.*, **2019**, *23*(1), 122-128.
10. Goncharov, N. A., Leshcheva, E. A., Trefilova, Y. A., Tsareva, E. V., Trefilov, A. G. Reasons for use of pharmaceutical crowns in tooth preparation taking into account microbial adhesion on the surface of orthpaedical material. *Clinical Dentistry*, **2016**, 1, 52-55.
11. Ibragimov, T. I., Trefilov, A. G., Gorelova, L. A. The experience of studying the adhesion of representatives of the microflora of the oral cavity to the materials used for relining of removable dentures by a direct method. *Dental Practitioner*, **2011**, *9*, 35-38.
12. Kasim, S. A. V., G, N. A., Krishnaswamy, N. R. A windowed temporary crown for a peg-shaped latera incisor. *J Clin Orthod.*, **2018**, *52*(10), 561-562.
13. Klur, T., Hasan, I., Ottersbach, K., Stark, H., Fichte, M., Dirk, C., Bourauel, C. PEKK-made indirect temporary crowns and bridges: a clinical pilot study. *Clin Oral Investig.*, **2019**, *23*(2), 771-777.
14. Kraneveld, E. A., Buijs, M. J., Bonder, M. J., Visser, M., Keijser, B. J., Crielaard, W., Zaura, E. The relation between oral Candida load and bacterial microbiome profiles in Dutch older adults. *PLoS One*, **2012**, *7*(8), e42770.
15. Makeeva, I. M., Daurova, F. J., Bjakova, S. F., *et al.* Sensitivity of microbial associations of exudate of periodontal pocket and odontogenic focus to antibacterial drugs. *Stomatology*, **2016**, *95*, 26-30.
16. Najeeb, S., Zafar, M. S., Khurshid, Z., Siddiqui, F. Applications of polyetheretherketone (PEEK) in oral implantology and prosthodontics. *J Prosthodont Res.*, **2016**, *60*(1), 12-19.
17. Sampaio-Maia, B., Caldas, I. M., Pereira,

Downloaded from www.periodico.tchequimica.com

M. L., Pérez-Mongiovi, D., Araujo, R. The Oral Microbiome in Health and Its Implication in Oral and Systemic Diseases. *Adv Appl Microbiol.*, **2016**, *97*, 171-210.
18. Taylor, P. D., Georgakis, G., Niggli, J. An Investigation Into the Integrity of Fit of Provisional Crowns Using Current Proprietary Temporary Crown Materials. *Eur J Prosthodont Restor Dent.*, **2016**, *24*(2), 50-57.
19. Timoshin, A. V., Sevbitov, A. V., Ergesheva, E. V., Boichuk, A. V., Sevbitova, M. A. Experience of treating aphthous lesions of oral mucosa by preparations on the basis of collagen and digestase. *Asian J. Pharm.*, **2018**, *12*, 284-287.
20. Tsarev, V. N., Ippolitov, E. V., Trefilov, A. G., Arutjunov, S. D., Pivovarov, A. A. Features of adhesion of anaerobic parodontopathogenic bacteria and *Candida albicans* fungi to experimental samples of basic dental plastics depending on the surface roughness and polishing method. *Microbiol. Epidemiol. Immunol. J.*, **2014**, *6*, 21-27.
21. Tsarev, V. N., Trefilov, A. G., Klejmenova, G. N., Ljovkin, A. V. Spatio-temporal model of the oral cavity biofilm formation: the relationship between the processes of primary adhesion and microbial colonization. *Dent. Forum.*, **2011**, *5*, 126-131.
22. Utjuzh, A. S., Jumashev, A. V., Admakin, O. I., Lushkov, R. M. The use of the irrigator in patients with orthopedic structures, based on dental implants. *Clin. Dent.*, **2017**, *2*, 47-49.
23. Utjuzh, A. S., Jumashev, A. V., Lushkov, R. M. Clinical example of orthopedic treatment of a patient after mandible resection caused by sarcoma with the use of dental implants. *Clin. Dent.*, **2016**, *4*, 56-58.
24. Yumashev, A. V., Utyuzh, A. S., Volchkova, I. R., Mikhailova, M. V., Kristal, E. A. The influence of mesodiencephalic modulation on the course of postoperative period and osseointegration quality in case of intraosseus dental implantation. *Indian J. Sci. Technol.*, **2016**, *9*, 104307.
25. Zhirnova, A. I., Shcherbakov, A. S., Chervinets, I. V. Oral microbiocenosis features of diabetic patients after orthopedic treatment with various types of crowns. *Stomatologiia*, **2015**, *94*(1), 45-49.

Downloaded from www.periodico.tchequimica.com

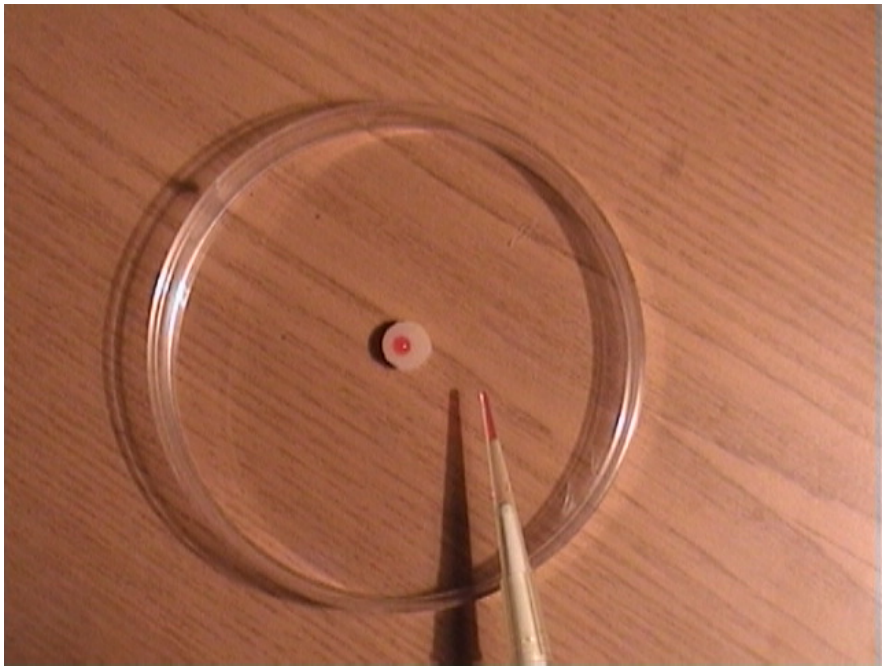

Figure 1. *Application of the test strain suspension on samples of dental polymers used to manufacture provisional crowns*

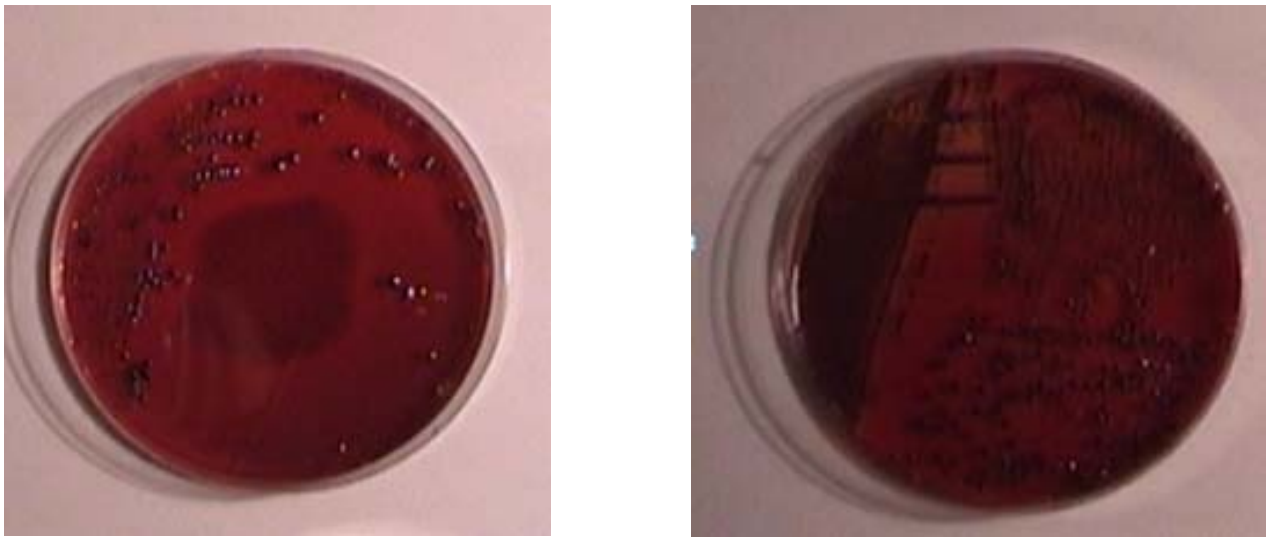

A *B*

Figure 2. *The evaluation results of Prevotella intermedia strain adhesion to the Dentokeep polyetheretherketone (PEEK) material used to manufacture provisional crowns (A – low index, B – high index)*

Downloaded from www.periodico.tchequimica.com

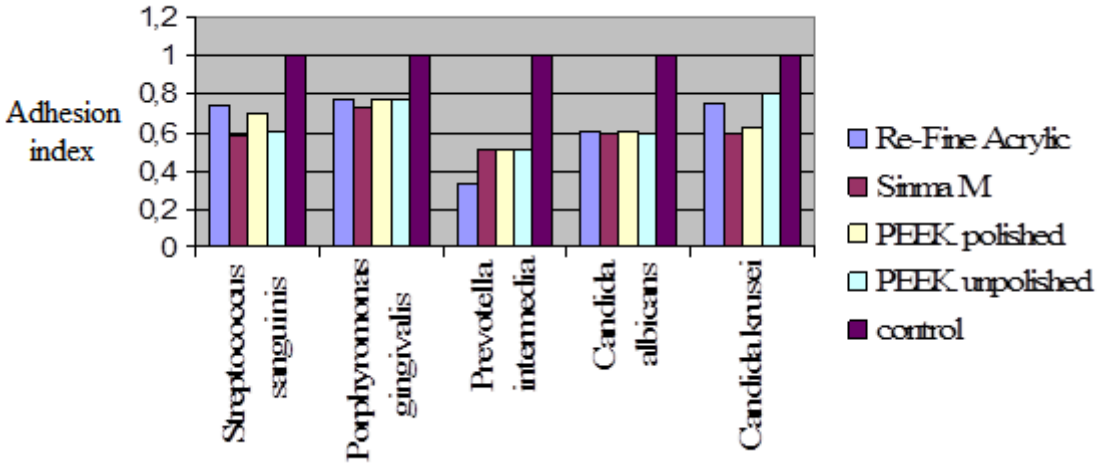

Figure 3. *The results of in vitro adhesion of oral microbiota representatives to materials used for provisional crowns*

Table 1. *Comparative evaluation results of in vitro adhesion of oral Streptococcus sanguinis to materials used for provisional crowns, (mean ± SEM, n = 6)*

	Material	***CFU count***	***CFU Lg***	***Adhesion index***
1	Re-Fine Acrylic	5×10^6	6.7	0.74 ± 0.64**
2	Sinma M	2×10^5	5.3	0.58 ± 0.70*
3	PEEK polished	10^6	6	0.70 ± 1.10*/ **
4	PEEK unpolished	4×10^5	5.6	0.60 ±0.68*/ **
	control	10^9	9	1

*Note: *p < 0.05 compared to Re-Fine Acrylic*
***p < 0.05 compared to Sinma M*

Table 2. *Comparative evaluation results of in vitro adhesion of oral Porphyromonas gingivalis to materials used for provisional crowns, (mean ± SEM, n = 6)*

	Material	***CFU count***	***CFU Lg***	***Adhesion index***
1	Re-Fine Acrylic	10^7	7	0.77 ± 1.35**
2	Sinma M	4×10^6	6.6	0.73 ± 1.15*
3	PEEK polished	10^7	7	0.77 ± 0.50**
4	PEEK unpolished	10^7	7	0.77 ± 0.80**
	control	10^9	9	1

*Note: *p < 0.05 compared to Re-Fine Acrylic*
***p < 0.05 compared to Sinma M*

Downloaded from www.periodico.tchequimica.com

Table 3. *Comparative evaluation results of in vitro adhesion of oral Prevotella intermedia to materials used for provisional crowns (mean ± SEM, n = 6)*

	Material	CFU count	CFU Lg	Adhesion index
1	Re-Fine Acrylic	10^3	3	0.33 ± 1.21**
2	Sinma M	4×10^4	4.6	0.51 ± 0.70*
3	PEEK polished	4×10^4	4.6	0.51 ± 0.70*
4	PEEK unpolished	4×10^4	4.6	0.51 ± 1.04*
	control	10^9	9	1

*Note: *p < 0.05 compared to Re-Fine Acrylic*
***p < 0.05 compared to Sinma M*

Table 4. *Comparative evaluation results of in vitro adhesion of oral Candida albicans to materials used for provisional crowns (mean ± SEM, n = 6)*

	Material	CFU count	CFU Lg	Adhesion index
1	Re-Fine Acrylic	8×10^4	4.90	0.61±1.04
2	Sinma M	6×10^4	4.78	0.59±1.10
3	PEEK polished	8×10^4	4.90	0.61±0.70
4	PEEK unpolished	6×10^4	4.78	0.59±1.10
	Control	10^8	8	1

*Note: *p < 0.05 compared to Re-Fine Acrylic*
***p < 0.05 compared to Sinma M*

Table 5. *Comparative evaluation results of in vitro adhesion of oral Candida krusei to materials used for provisional crowns, (mean ± SEM, n = 6)*

	Material	CFU count	CFU Lg	Adhesion index
1	Re-Fine Acrylic	10^6	6	0.75 ± 1.10**
2	Sinma M	6×10^4	4.78	0.59 ± 1.06*
3	PEEK polished	10^5	5	0.63+0.70*/ **
4	PEEK unpolished	3×10^6	6.4	0.80 ± 1.12*/ **
	Control	10^8	8	1

*Note: *p < 0.05 compared to Re-Fine Acrylic*
***p < 0.05 compared to Sinma M*

Downloaded from www.periodico.tchequimica.com

PERIÓDICO TCHÊ QUÍMICA
ARTIGO ORIGINAL

ESTUDO DA ADSORÇÃO DOS CORANTES VIOLETA CRISTAL E VERDE MALAQUITA EM MATERIAL ZEOLÍTICO

ADSORPTION STUDY OF CRYSTAL VIOLET AND MALACHITE GREEN DYES IN ZEOLITIC MATERIAL

KLUNK, Marcos Antônio[1]*; DASGUPTA, Sudipta[2]; DAS, Mohuli[2]; WANDER, Paulo Roberto[1]; SHAH, Zeban[3]

[1] Department of Mechanical Engineering, University of Vale do Rio dos Sinos, São Leopoldo, RS, Brazil

[2] Department of Earth Sciences, Indian Institute of Technology Bombay, Powai, Mumbai 400076, India

[3] Department of Chemistry, Federal University of Rio Grande do Sul, Porto Alegre, RS, Brazil

** Autor correspondente*
e-mail: marcosak@edu.unisinos.br

Received 14 July 2019; received in revised form 06 September 2019; accepted 26 September 2019

RESUMO

Violeta cristal e verde malaquita são corantes utilizados na indústria têxtil. Estes compostos orgânicos são agentes tóxicos capaz de poluir recursos hídricos, bem como destruir a biota existente neste local. A descoloração de efluentes têxteis sempre foi um problema mundial, mas tem sido acentuada ao longo do tempo com a crescente operação em grande escala e mudanças na origem do uso de corantes. A descoloração das águas residuais pode ser conseguida removendo fisicamente o corante da água ou destruindo o seu grupo cromóforo. A adsorção é referida como um dos métodos mais eficientes e viáveis para descolorir um efluente. As peneiras moleculares (zeólitas) tem se mostrado uma alternativa eficiente na descoloração dos efluentes têxteis quando comparados a outros processos na indústria. A sodalita é uma zeólita que apresentar a capacidade de adsorver os grupos funcionais azo, relacionados a cor. O foco principal deste trabalho é utilizar a sodalita no processo de descoloração de uma solução sintética de violeta cristal e verde malaquita. Os experimentos foram realizados variando-se os tempos de contato entre o material zeolítico e as soluções sintética dos corantes. Os resultados nos revelaram que ambos os corantes sofreram um processo de descoloração. Conforme as análises, tempos maiores de contato (12, 24, 48 e 72 horas) com a sodalita mostra-se mais eficiente na remoção da cor. Um fator decisivo neste processo é a maior razão Si/Al (2.5) de sodalita que potencializa o processo e eficiência dos experimentos.

Palavras-chave: *Indústria Têxtil, Impactos Ambientais, Sodalita, Descoloração, Grupo Cromóforo*

ABSTRACT

Violet crystal and malachite green are dyes used in the textile industry. These organic compounds are toxic agents capable of polluting water resources as well as destroying the existing biota in this location. The decolorization of textile effluents has always been a global problem, but it has accentuated over time with increasing scale operation and changes in the origin of the dyes used. Decolorization of wastewater achieved by physically removing the dye from the water or by destroying its chromophore group. Adsorption is referred to as one of the most efficient and feasible methods for discoloring an effluent. Molecular sieves (zeolites) showed to be an efficient alternative in the discoloration of textile effluents when compared to other processes in the industry. Sodalite is a zeolite that has the ability to adsorb the azo functional groups related to color. The focus of this work is to use sodalite in the process of discoloration of a synthetic solution of crystal violet and malachite green. The experiments performed by varying the contact times between the zeolitic material and the synthetic solutions of the dyes. The results revealed that both dyes had a decolorization process. According to analyzes, greater times of contact (12, 24, 48, and 72 hours) with sodalite is more efficient in the removal color. A decisive factor in this process is the higher Si/Al ratio (2.5) of sodalite that potentiates the process and efficiency of the experiments.

Keywords: *Textile Industry, Environmental Impacts, Sodalite, Decolorization, Chromophore Group*.

Downloaded from www.periodico.tchequimica.com

1. INTRODUCTION

Pollution in aquatic systems is caused by industrial activity (Klunk *et al.,* 2017). The chemical contaminants present in the water resources are textile dyes, surfactants, and heavy metals (Klunk *et al.,* 2019a; Kumar *et al.,* 2017). These toxic agents cause the destruction of biota and changes in natural landscapes, as well as the destruction of water for human consumption (Humelnicu *et al.,* 2017). The great cause of pollution in water the textile dyes (Klunk *et al.,* 2019b). The main route of entry of the dyes into the environment is through the release of waste water. About 10 to 15 % of all dyes are directly discarded as wastewater in the dyeing process (Francis *et al.,* 2017). The first effect to be detected after illegal dumping is its aesthetic nature. At the concentration of 1 mg/L of dye, it is already enough to give color to the water resource (Chawla *et al.,* 2017). This situation makes it impossible to use water for recreational purposes and affects the natural balance of plants and other living things in the environment (Kooli *et al.,* 2015).

According to with "Ecological and Toxicological Association of Dyes and Organic Pigment Manufacturers", the majority of dyes (98 %) present lethal concentration values (LC50) in fish larger than 1 mg/L (Forgacs *et al.,* 2004). The decolorization of textile effluents has always been a global problem, but it has been accentuated over time with increasing scale operation and changes in the origin of the dyes used (Abdulrahman, 2014). As consumers become more demanding with the product (brightness, color, resistance to washing and light), the colorants become less receptive to degradation and resistant to moderate oxidation conditions (Koshy and Singh, 2016). Decolorization of wastewater can be achieved by physically removing the dye from the water or by destroying its chromophore group. Adsorption is referred to as one of the most efficient and feasible methods for discoloring an effluent (Ali, 2012; Al-Anber and Al-Anber, 2008). It is advantageous in terms of the possibility of re-use of process water, initial cost, ease of operation and insensitivity to toxic substances (Fraga *et al.,* 2014; Klunk *et al.,* 2012; Ali *et al.,* 2012; Atun *et al.,* 2011). The present work has the objective of studying the adsorption of the dye crystal violet (CV) and malachite green (MG) using molecular sieves (zeolites) as adsorbent material. For this study, standard solutions of the dyes (50 mg/L) were prepared which were contacted with the zeolitic material in the periods of 1 - 72 hours. Sodalite (zeolite) was used as adsorbent material in four Si/Al ratios (1.0, 1.5, 2.0, and 2.5). These ratios allow identifying the best adsorption condition of the dyes under study. At the end of the experiments, the products of decolorization system were analyzed by Ultraviolet - Visible Spectroscopy (UV-VIS), Fourier Transform Infrared Spectroscopy (FTIR) e High Performance Liquid Chromatography (HPLC), to verify the efficiency of the adsorbent in the removal of the color from the textile effluent.

2. MATERIALS AND METHODS

2.1. Molecular Sieves

Molecular sieves, also called zeolites, are hydrated aluminosilicates mineral of alkali metals and alkaline earths (mainly sodium, potassium, and magnesium) (Ali, 2012; Ali and Gupta, 2007). According to the International Association of Mineralogy, a zeolitic mineral is a crystalline substance with a structure characterized by structures in continuous three-dimensional crystalline networks of tetrahedral composed of four atoms of oxygen around a cation (SiO_4, AlO_4), so that each oxygen is cut between two tetrahedral (Atun *et al.,* 2011). The zeolites, in general, have structures in continuous three-dimensional crystalline networks, composed of tetrahedral of type MO_4 (being, M = Si, Al, Be, Ge, Fe, P, Co) (Belviso *et al.,* 2013). Due to its properties, such as the cation exchange capacity, its high surface area, its acid centers, the size of its channels and cavities and its selectivity of form 40, the natural zeolites are of great interest for the study (Koshy and Singh, 2016; Zhou *et al.,* 2014; Xie *et al.,* 2014). It should be noted that the low cost of natural zeolites has provided and stimulated the development of cheaper treatment systems (Chang and Shih, 2000; Blanchard *et al.,* 1984).

Despite having a very varied chemical composition, zeolites are usually classified according to their structure. For this study, the sodalite zeolite was synthesized and used as adsorbent material of textile dyes. Sodalite (SOD) ($Na_8Al_6Si_6O_{24}Cl_2$) was first discovered by Thomson in 1811, and after a few years in 1930, its structure was clarified by Paulling (Smith *et al.,* 2008; Smith, 2000). From this discovery, different synthesis processes were carried out to produce sodalite with the most varied compositions. The arrangement of this mineral is entirely formed by uniform truncated octahedral polyhedral, called sodalite or β-cage (Ding *et al.,* 2010; Nakano and Nozue, 2007; Bibb and Dale, 1985). Then, the α cages (supercages) with the inside diameter of

Downloaded from www.periodico.tchequimica.com

~11 Å are formed among the β cages. The α cages are connected by the sharing of the 8-membered ring with each other and also arrayed in a simple cubic structure. The lattice constant is 12.3 Å (Nakano and Nozue, 2007; Bibb and Dale, 1985).

2.2. Textile Dyes

Dyes are classified as anionic (acid dyes, direct and reactive), cationic (basic dyes) and nonionic (dispersive dyes) (Humelnicu *et al.,* 2017). The cationic dyes (referring to this work) present a characteristic behavior according to their concentration in solution (Almasian *et al.,* 2015). The dye molecules can bind to form molecular dimers, or even higher trimers and aggregates of the dyes (Alver *et al.,* 2012; Liu and Chiou, 2005).

In the experiments, were used the aqueous solutions of the CV and MG. The properties of the CV is cationic classification, with molecular formula $C_{25}H_{30}N_3Cl$, molecular weight 407.99 g/mol, and visible region exhibit the main peak with a maximum absorbance at λ_{max} at 591 nm. The retention time in HPLC is 10.2 min (Al-Kadhemy and Abaas, 2012; Alsharuee, 2012). Therefore, for the dye MG, also follows in the same classification of cationic, with molecular formula $C_{23}H_{25}N_2Cl$, molecular weight 364.91 g/mol and visible region exhibit the main peak with a maximum absorbance at λ_{max} at 620 nm. The retention time in HPLC is 4.3 min (Sartape *et al.,* 2017; Hameed and El-Khaiary, 2008).

2.3. Synthesis of the zeolitic material

The synthesis of zeolitic material (sodalite) was developed according to the studies of Henmi (1987). Sodium hydroxide solution was prepared by dissolving 80 g of NaOH in 1 L of distilled water. In order to obtain the zeolites with Si/Al ratio 1.0, 1.5, 2.0, and 2.5 was used as an aluminum solution, by dissolving the metakaolin ($Al_2O_3.2SiO_2$). For the Si source, biomass residue from pyrolysis experiments was used (Klunk *et al.,* 2017b; Klunk *et al.,* 2018a; Ruoso *et al.,* 2019; Cataluña *et al.,* 2018; Caetano *et al.,* 2018; Caetano *et al.,* 2015a; Caetano *et al.,* 2015b). The gel was then oven-dried at 90 °C for 24 hours. In this process, sodalite acts as an ionic adsorbent agent enable of decolorization from textile industry effluents (Klunk *et al.,* 2019c).

In environmental terms, the use of biomass contributes to the low emissions of carbon dioxide (CO_2) (Klunk *et al.,* 2018b; Cataluña *et al.,* 2017; Caetano *et al.,* 2015c; Caetano *et al.,* 2017). These low carbon dioxide emissions can be predicted by geochemical modeling (Klunk *et al.,* 2015; Klunk *et al.,* 2018c; Klunk *et al.,* 2019d; Ponomarev *et al.,* 2017).

2.4. Synthesis of the zeolitic material

In order to simulate dye contaminated effluent, was used as an aqueous solution of CV and MG (MERCK™) (Cooper, 1993). Dyes concentrations were determined by UV-visible spectrophotometry at wavelengths of 591 and 620 nm. An amount of 100 mg of adsorbent (sodalite) was placed in contact with 25 ml of a solution of adsorbate (CV and MG) at a concentration of 50 mg/L under constant stirring at 150 rpm for 24 hours (De Gisi *et al.,* 2016). After the contact time, the suspensions were centrifuged for 30 minutes at 2000 rpm, and an aliquot of the supernatant was extracted for determination of the final concentration of the dyes (Qu *et al.,* 2013).

In order to determination CV and MG color removal, 10 mL aliquots of the dyes were sampled at different periods (1, 2, 3, 4, 5, 6, 12, 24, 48 and 72 h) with 50 g of the zeolitic material (Sodalite) in different ratio Si/Al (1.0; 1.5; 2.0 and 2.5) (Klunk *et al.,* 2019c). The aqueous solution was examined by UV-Visible spectrophotometry (Ultra-Fast Scan UV-1900 - SHIMADZU™), FTIR (IRAffinity-1S - SHIMADZU™) and HPLC (LC-20A Prominence - SHIMADZU™).

3. RESULTS AND DISCUSSION

3.1. Response adsorption of CV and MG dyes in zeolitic material

In the present study, in order to follow the molecular sieve dye decolorization process, were used some analytical techniques such as UV-Vis spectroscopy, HPLC, and FTIR spectroscopy.

3.1.1. Ultraviolet - Visible Spectroscopy (UV-VIS)

UV–Vis spectroscopy is the primary technique to determine dye decolorization (Sartape *et al.,* 2017). In Figure 1, the spectra of CV and MG at a concentration of 50 mg/L in visible region exhibit the main peak with a maximum absorbance at λ_{max} at 591 nm and 620 nm

Downloaded from www.periodico.tchequimica.com

respectively (De Gisi *et al.,* 2016; Qu *et al.,* 2013). The results of the UV-Visible spectra showed that peaks at λ_{max} reached at 0 h (FZ – free zeolite) decreased significantly until 72 h. The most efficient sodalite ratio for dye discoloration is 2.5 for both CV and MG. For the Si/Al ratio 1.0, the decolorization became less useful for the samples that remained for 72 hours in contact with the adsorbent.

3.1.2. High Performance Liquid Chromatography (HPLC)

After adsorption with molecular sieve for 1, 2, 3, 4, 5, 6, 12, 24, 48 and 72 hours, the intermediates in the aqueous CV and MG solutions were extracted and analyzed via HPLC. In Figure 2, the peak at the retention time of 10.2 and 4.3 min was identified as CV and MG respectively (Cao *et al.,* 2019; Yang *et al.,* 2016; Xie *et al.,* 2013; Ayed *et al.,* 2009; Andersen *et al.,* 2009). The extracted sample after adsorption shows that decolorization is increasing according to the ratios of Si/Al increase. These values agree when comparing the results of UV-Vis spectroscopy.

3.1.3. Fourier Transform Infrared Spectroscopy (FTIR)

FTIR has widely used as a proper technique for investigation of dyes decolorizations experiments. In dyes decolorization studies, FTIR spectrum enables the determination of type interactions that occur within azo dyes containing different functional groups. Taking this into account, the FTIR spectroscopy used the region of 4500-500 cm^{-1} to investigate the decolorization process, and the results were shown in Figure 3 and Figure 4 to CV and MG respectively. According to the FTIR spectra, the assignments of the primary infrared bands obtained with each dye at free zeolite (FZ) and 72 h in contact with the adsorbent material in two different Si/Al ratios (1.0 and 2.5). The FTIR spectroscopy from CV have peaks at 3413 – 2921 cm^{-1} indicates C-H asymmetric stretching and free $-NH_2$ group showed amide antisymmetric stretching vibration (Bevilacqua and Busca, 2002). Also, the peak at 2344 cm^{-1} corresponding to a symmetric and asymmetric stretching of the tertiary amine salt. The results showed remarkable variations in ranged from 1591 - 520 cm^{-1} to CV and 1650 – 545 cm^{-1} to MG (Ayed *et al.,* 2009). In 1591 cm^{-1} corresponding to the C=C stretching of the benzene ring. The intensity variations of 1483 cm^{-1} are to six-member ring carbon-carbon vibrations and indicate a sideways ring stretch absorbs $=CH_2$. In 1361 cm^{-1} peak for the C–N stretch of aromatic tertiary amine (Akyuz and Akyuz, 2006). At 1172 cm^{-1} corresponds to the C–N stretching vibrations (Al-Kadhemy *et al.,* 2013). The peaks at 941, 831, 722 cm^{-1} correspond to symmetric out of plane bending of the ring hydrogens. The bands at 520 cm^{-1} are due to Si–O–Al (octahedral) from zeolitc material (Tyagi *et al.,* 2006).

The FTIR spectroscopy from MG have peaks at 3435 cm^{-1} indicates $-NH_2$ group showed amide antisymmetric stretching vibration (Barapatre *et al.,* 2017; Vijayalakshmidevi and Muthukumar, 2013; Nishioka, 1976). The peaks at 1650 – 1400 cm^{-1} is C=C aromatic ring and C–N stretch aromatic tertiary amine. Also, the peaks at 1190 and 1125 cm^{-1} are for aromatic C–N stretching vibrations of aliphatic amine (Saravanakumar and Kathiresan, 2014). Eventually, the peak at 620 cm^{-1} indicates aromatic amines. Bands at 545 cm^{-1} were related to the internal asymmetric stretching vibration of Si-O-Si or Si-O-Al were characteristic of Sodalite structure (Cheriaa *et al.,* 2012). Among them, the band at 545 cm^{-1} is related to a structure of the double five-membered rings of the pintails zeolites (Coates, 2000).

The changes in intensity variations for the dyes decolorization experiments are related to the adsorption capacity of the zeolitic as molecular sieves. According to the FTIR spectra, there was the formation of new functional groups when compared to the sample without zeolite (free zeolite). What occurred was a decrease in the intensity of the peaks. Again, the results can be compared with the other techniques used in this study, showing the same behavior.

4. CONCLUSIONS

The sodalite can be efficiently utilized as adsorbent for the removal of dyes (CV and MG) from aqueous solutions. In this context, the Si/Al ratios are responsible for the efficiency of the process. It was possible to identify that in the 2.5 ratios, the molecular sieve shows to be more active to adsorb both dyes (CV and MG). Soon for a reason 1.0, the process did not show us very efficiently. This discrepancy lies in the cation exchange capacity of the dyes. Thus, a low Si/Al ratio makes the molecular sieve less susceptible to the azo groups in the dye molecules. It is evident that for the three techniques used in this

Downloaded from www.periodico.tchequimica.com

process of decolorization of textile dyes, the behavior of the adsorbate has the ability to retain the color related functional groups.

The zeolite used to removal the color of a textile effluent can be more efficient in the ratio Si/Al 2.5. Nevertheless, the concentration of the synthetic solution of an effluent containing CV and MG has its importance, since often the industries do a process of dilution, being able to impact in the capacity of retention of the molecular sieve.

5. ACKNOWLEDGMENTS

The authors acknowledge the Brazilian agencies CNPq (National Council of Technological and Scientific Development – Brasília, DF, Brazil), CAPES (Coordination for the Improvement of Higher Education Personnel) for the research funding, and the generous assistance of all the people from the company who granted us access to their database and perception information.

6. REFERENCES

1. Klunk, M. A., Ponomarev, A. A., Dasgupta, S., Das, M. Arsenic Speciation in Groundwater using the Softwares PHREEQC, GWB, and GEODELING. *Southern Brazilian Journal of Chemistry*. **2017a**, 25, 30-35.
2. Klunk, M. A., Dasgupta, S., Das, M., Wander, P. R. Computer Codes of Geochemical Modeling used to Water-Rock Interaction Simple and Complex Systems. *Periódico Tchê Química*. **2019a**, 16(32), 108-118.
3. Kumar, M. A., Harthy, D. K., Kumar, V. V., Balashri, K. G., Seenuvasan, M., Anuradha, D., Sivanesand, S. Detoxification of a triphenylmethane textile colorant using acclimated cells of Bacillus mannanilyticus strain AVS. *Environmental Progress & Sustainable Energy.* **2017**, 36(2), 394–403.
4. Humelnicu, I., Băiceanu, A., Ignat, M. -E., Dulman, V. The removal of Basic Blue 41 textile dye from aqueous solution by adsorption onto natural zeolitic tuff: Kinetics and thermodynamics. *Process Safety and Environmental Protection.* **2017**, 105, 274–287.
5. Klunk, M. A., Shah, Z., Wander, P. R. Use of Montmorillonite Clay for Adsorption Malachite Green Dye. *Periódico Tchê Química.* **2019b**, 16(32), 279-286.
6. Francis, S., Joseph, S., Koshy, E. P., Mathew, B. Green synthesis and characterization of gold and silver nanoparticles using Mussaenda glabrata leaf extract and their environmental applications to dye degradation. *Environmental Science and Pollution Research.* **2017**, 24(21), 17347–17357.
7. Chawla, S., Uppal, H., Yadav, M., Bahadur, N., Singh, N. Zinc peroxide nanomaterial as an adsorbent for removal of Congo red dye from waste water. *Ecotoxicology and Environmental Safety.* **2017**, 135, 68–74.
8. Kooli, F., Liu, Y., Al-Faze, R., Al Suhaimi, A. Effect of acid activation of Saudi local clay mineral on removal properties of basic blue 41 from an aqueous solution. *Applied Clay Science.* **2015**, 116-117, 23–30.
9. Forgacs, E., Cserháti, T., Oros, G. Removal of synthetic dyes from wastewaters: a review. *Environment International.* **2004**, 30(7), 953–971.
10. Abdulrahman G. Adsorption of Acid Dyes from Wastewater on Saudi Bentonite Clay. *Trends in Applied Sciences Research.* **2014**, 9, 557-573.
11. Koshy, N., Singh, D. N. Fly ash zeolites for water treatment applications. *Journal of Environmental Chemical Engineering.* **2016**, 4(2), 1460–1472.
12. Ali, I. New Generation Adsorbents for Water Treatment. *Chemical Reviews.* **2012**, 112(10), 5073–5091.
13. Al-Anber, M., Al-Anber, Z. A. Utilization of natural zeolite as ion-exchange and sorbent material in the removal of iron. *Desalination.* **2008**, 225(1-3), 70–81.
14. Fraga, A., Klunk, M. A., Oliveira, A., Furtado, G., Knornschild, G. H., Dick, L. F. P. Soil corrosion of the AISI1020 steel buried near electrical power transmission line towers. *Materials Research-Ibero-american Journal of Materials.* **2014**, 17, 1637-1643.
15. Klunk, M. A., Oliveira, A., Furtado, G., Knornschild, G. H., Dick, L. F. P. Study of the Corrosion of Buried Steel Grids of Electrical Power Transmission Towers. *ECS Transactions.* **2012**, 43, 23-27.
16. Ali, I., Asim, M., Khan, T. A. Low cost adsorbents for the removal of organic pollutants from wastewater. *Journal of Environmental Management.* **2012**, 113, 170–183.
17. Atun, G., Hisarlı, G., Kurtoğlu, A. E., Ayar,

Downloaded from www.periodico.tchequimica.com

N. A comparison of basic dye adsorption onto zeolitic materials synthesized from fly ash. *Journal of Hazardous Materials.* **2011**, 187(1-3), 562–573.
18. Ali, I., Gupta, V. K. Advances in water treatment by adsorption technology. *Nature Protocols.* **2007**, 1(6), 2661–2667.
19. Belviso, C., Cavalcante, F., Fiore, S. Ultrasonic waves induce rapid zeolite synthesis in a seawater solution. *Ultrasonics Sonochemistry.* **2013**, 20(1), 32–36.
20. Zhou, L., Chen, Y. -L., Zhang, X. -H., Tian, F. -M., Zu, Z. -N. Zeolites developed from mixed alkali modified coal fly ash for adsorption of volatile organic compounds. *Materials Letters.* **2014**, 119, 140–142.
21. Xie, J., Wang, Z., Wu, D., Kong, H. Synthesis and properties of zeolite/hydrated iron oxide composite from coal fly ash as an efficient adsorbent to simultaneously retain cationic and anionic pollutants from water. *Fuel.* **2014**, 116, 71–76.
22. Chang, H. -L., Shih, W. -H. Synthesis of Zeolites A and X from Fly Ashes and Their Ion-Exchange Behavior with Cobalt Ions. *Industrial & Engineering Chemistry Research.* **2000**, 39(11), 4185–4191.
23. Blanchard, G., Maunaye, M., Martin, G. Removal of heavy metals from waters by means of natural zeolites. *Water Research.* **1984**, 18(12), 1501–1507.
24. Smith, P., Wingate, C., Silva, L. Mobility of included soda in sodalite. In: Proceedings of the 8th International Alumina Quality Workshop, **2008**.
25. Smith, J. V. Microporous and other Framework Materials with Zeolite-type Structures, Springer, New York, **2000**.
26. Ding L., Yang H., Rahimi P., Omotoso O., Friesen W., Fairbridge C., Shi Y., Siauw, Ng. Solid transformation of zeolite NaA to sodalite. M*icroporous and Mesoporous Materials.* **2010**, 130, 303–308.
27. Nakano, T., Nozue, Y. Orbital degeneracy and magnetic properties of potassium clusters incorporated into nanoporous crystals of zeolite A. *Journal of Computational Methods in Sciences and Engineering.* **2007**, 443–462.
28. Bibby, D. M., Dale, M. P. Synthesis of silica-sodalite from non-aqueous systems. *Nature.* **1985**, 317, 157-158.
29. Almasian, A., Parvinzadeh Gashti, M., Olya, M. E., Chizari Fard, G. Poly(acrylic acid)-zeolite nanocomposites for dye removal from single and binary systems. *Desalination and Water Treatment.* **2015**, 1-19.
30. Alver, E., Metin, A.Ü. Anionic dye removal from aqueous solutions using modified zeolite: Adsorption kinetics and isotherm studies. *Chemical Engineering Journal.* **2012**, 200-202, 59–67.
31. Liu, H. -L., Chiou, Y. -R. Optimal decolorization efficiency of Reactive Red 239 by UV/TiO_2 photocatalytic process coupled with response surface methodology. *Chemical Engineering Journal.* **2005**, 112(1-3), 173–179.
32. Al-Kadhemy M. F. H., Abaas W.H. Absorption spectrum of Crystal Violet in Chloroform solution and doped PMMA thin films. *Atti Della Fondazione Giorgio Ronchi.* **2012,** 3, 359-367.
33. Alsharuee I. F. Theoretical model to study the effect of concentration on the absorption spectrum of crystal violet in methanol using asymmetric double sigmoid. *Atti Della Fondazione Giorgio Ronchi.* **2012**, 1, 5-14.
34. Hameed, B. H., El-Khaiary, M. I. Malachite green adsorption by rattan sawdust: Isotherm, kinetic, and mechanism modeling. *Journal of Hazardous Materials.* **2008**, 159(2-3), 574–579.
35. Henmi, T. Synthesis of hydroxy-sodalite ("zeolite") from waste coal ash. *Soil Science and Plant Nutrition.* **1987**, 33(3), 517-521.
36. Klunk, M. A., Dasgupta, S., Das, M. Influence of Fast Pyrolysis with Temperature on Gas, Char and Bio-oil Production. *Southern Brazilian Journal of Chemistry.* **2017b**, 25, 1-11.
37. Klunk, M. A., Dasgupta, S., Das, M. Slow Pyrolysis of Rice Straw: Analysis of Biochar, Bio-Oil, and Gas. *Southern Brazilian Journal of Chemistry.* **2018a**, 26, 17-25.
38. Ruoso, F. S., Bittencourt, L. C., Sudati, L. U., Klunk, M. A., Caetano, N. R. New Parameters for the Forest Biomass Waste Ecofirewood Manufacturing Process Optimization. *Periódico Tchê Química.* **2019**, 16(32), 560-571.
39. Klunk, M. A., Dasgupta, S., Nunes, B. V. G., Wander, P. R. Synthesis of Sodalite Zeolite to Treatment of Textile Effluents. *Periódico Tchê Química.* **2019c**, 16, 778-783.
40. Klunk, M. A., Dasgupta, S., Das, M., Shah, Z. System of Adsorption of CO_2 in

Downloaded from www.periodico.tchequimica.com

Coalbed. *Southern Brazilian Journal of Chemistry.* **2018b**, 26, 2-9.
41. Cataluña, R., Shah, Z., Venturi, V., Caetano, N. R., Da Silva, B. P., Azevedo, C. M. N., Da Silva, R., Suarez, P. A. Z., Oliveira, L. P. Production process of di-amyl ether and its use as an additive in the formulation of aviation fuels. *Fuel.* **2018**, 228, 226-233.
42. Caetano, N. R., Venturini, M. S., Centeno, F. R., Lemmertz, C. K., Kyprianidis, K. G. Assessment of mathematical models for prediction of thermal radiation heat loss from laminar and turbulent jet non-premixed flames. *Thermal Science and Engineering Progress.* **2018**, 7, 241–247.
43. Caetano, N. R., Stapasolla, T. Z., Peng, F. B., Schneider, P. S., Pereira, F. M., Vielmo, H. A. Diffusion Flame Stability of Low Calorific Fuels. *Defect and Diffusion Forum.* **2015a**, 362, 29-37.
44. Caetano, N. R., Cataluña, R., Vielmo, H. A. Analysis of the Effect on the Mechanical Injection Engine Using Doped Diesel Fuel by Ethanol and Bio-Oil. *International Review of Mechanical Engineering.* **2015b**, 9(2), 124-128.
45. Cataluña, R., Shah, Z., Pelisson, L., Caetano, N. R., Da Silva, R., Azevedo, C., Biodiesel Glycerides from the Soybean Ethylic Route Incomplete Conversion on the Diesel Engines Combustion Process. *Journal of the Brazilian Chemical Society.* **2017**, 00, 1-8.
46. Caetano, N. R., Soares, D., Nunes, R. P., Pereira, F. M., Schneider, P. S., Vielmo, H. A., van der Laan, F. T. A comparison of experimental results of soot production in laminar premixed flames. *Open Engineering.* **2015c**, 5, 213–219.
47. Caetano, N. R.; Silva, B. P. Technical and Economic Viability for the Briquettes Manufacture. *Defect and Diffusion Forum.* **2017**, 380, 218-226.
48. Klunk, M. A., Damiani, L. H., Feller, G., Rey, M. F., Conceiçao, R. V., Abel, M., De Ros, L. F. Geochemical modeling of diagenetic reactions in Snorre Field reservoir sandstones: a comparative study of computer codes. *Brazilian Journal of Geology.* **2015**, 45, 29-40.
49. Klunk, M. A., Dasgupta, S., Conceiçao, R. V. Computerized geochemical modeling of burial diagenesis of the Eocene turbidite reservoir elements: Urucutuca Formation, Espírito Santo Basin, southeastern Brazil passive margin. *Journal of Palaeogeography.* **2018c**, 7, 12-26.
50. Klunk, M. A., Dasgupta, S., Schropfer, S. B., Nunes, B. V. G., Wander, P. R. Comparative Study of Geochemical Speciation Modeling Using GEODELING Software. *Periódico Tchê Química.* **2019d**, 16(31), 816-822.
51. Ponomarev, A. A., Bubnova, A. V., Klunk, M. A. The Use of X-Ray Microtomography to Assess Changes in the Voids Structure of Rocks. *Southern Brazilian Journal of Chemistry.* **2017**, 25, 12-16.
52. Cooper, P., Removing colour from dye house wastewater – a critical review of technology available. *Journal of the Society of Dyers and Colourists.* **1993**, 109, 97-100.
53. De Gisi, S., Lofrano, G., Grassi, M., Notarnicola, M. Characteristics and adsorption capacities of low-cost sorbents for wastewater treatment: A review. *Sustainable Materials and Technologies.* **2016**, 9, 10-40.
54. Qu, X., Alvarez, P. J., and Li, Q. Applications of nanotechnology in water and wastewater treatment. *Water Research.* **2013**, 47, 3931-3946.
55. Sartape, A. S., Mandhare, A. M., Jadhav, V. V., Raut, P. D., Anuse, M. A., Kolekar, S. S. Removal of malachite green dye from aqueous solution with adsorption technique using Limonia acidissima (wood apple) shell as low cost adsorbent. *Arabian Journal of Chemistry.* **2017**, 10, S3229–S3238.
56. Cao, D. -J., Wang, J. -J., Zhang, Q., Wen, Y. -Z., Dong, B., Liu, R. -J., Geng, G. Biodegradation of triphenylmethane dye crystal violet by Cedecea davisae. *Spectrochimica Acta Part A: Molecular and Biomolecular Spectroscopy*. **2019**, 210, 9-13.
57. Yang, X., Zheng, J., Lu, Y., Jia, R. Degradation and detoxification of the triphenylmethane dye malachite green catalyzed by crude manganese peroxidase from Irpex lacteus F17. *Environmental Science and Pollution Research.* **2016**, 23(10), 9585–9597.
58. Xie, J., Peng, T., Chen, D. -D., Zhang, Q. -J., Wang, G. -M., Wang, X., Deng, J. Determination of malachite green, crystal violet and their leuco-metabolites in fish by HPLC–VIS detection after immunoaffinity column clean-up. *Journal of Chromatography B.* **2013**, 913-914, 123–128.

Downloaded from www.periodico.tchequimica.com

59. Ayed, L., Cheriaa, J., Laadhari, N., Cheref, A., Bakhrouf, A. Biodegradation of crystal violet by an isolatedBacillus sp. *Annals of Microbiology.* **2009**, 59(2), 267–272.
60. Andersen, W. C., Turnipseed, S. B., Karbiwnyk, C. M., Lee, R. H., Clark, S. B., Rowe, W. D., Miller, K. E. Multiresidue method for the triphenylmethane dyes in fish: Malachite green, crystal (gentian) violet, and brilliant green. *Analytica Chimica Acta.* **2009**, 637(1-2), 279–289.
61. Bevilacqua M., Busca G. A study of the localization and accessibility of Brønsted and Lewis acid sites of H-mordenite through the FT-IR spectroscopy of adsorbed branched nitriles. *Catalysis Communications.* **2002**, 3, 497-502.
62. Akyuz S., Akyuz T. FT-IR spectroscopic investigations of adsorption of 2-, 3- and 4-pyridinecarboxamide on montmorillonite and saponite from Anatolia. *Vibrational Spectroscopy.* **2006**, 42, 387-391.
63. Al-Kadhemy, M. F. H., Abaas, W. H., Fakher, I. The Effect of Gamma Radiation on the FTIR Spectrum of Crystal Violet Doped Polystyrene Films. *Caspian Journal of Applied Sciences Research.* **2013**, 2(7), 11-17.
64. Tyagi B., Chudasama C., Jasra D. R. V. Determination of structural modification in acid activated montmorillonite clay by FT-IR spectroscopy. *Spectrochimica Acta A.* **2006**, 64, 273–278.
65. Barapatre, A., Aadil, K. R., Jha, H. Biodegradation of Malachite Green by the Ligninolytic FungusAspergillus flavus. *CLEAN - Soil, Air, Water.* **2017**, 45(4), 1600045, 1-12.
66. Vijayalakshmidevi, S. R., Muthukumar, K. Biodegradation of malachite green by Ochrobactrum sp. *World Journal of Microbiology and Biotechnology.* **2013**, 30(2), 429–437.
67. Nishioka, N. S. Thesis, University of California, Berkeley, CA, **1976**.
68. Saravanakumar, K., Kathiresan, K. Bioremoval of the synthetic dye malachite green by marine Trichoderma sp. *SpringerPlus.* **2014**, 3(1), 631.
69. Cheriaa, J., Khaireddine, M., Rouabhia, M., Bakhrouf, A. Removal of Triphenylmethane Dyes by Bacterial Consortium. *The Scientific World Journal.* **2012**, 1–9.
70. Coates, J. Interpretation of infrared spectra. A practical approch. In Encyclopedia of Analytical Chemistry. Meyers, R.A. Ed., pp. 10815–10837, John Wiley & Sons, Chichester, UK, **2000**.

Downloaded from www.periodico.tchequimica.com

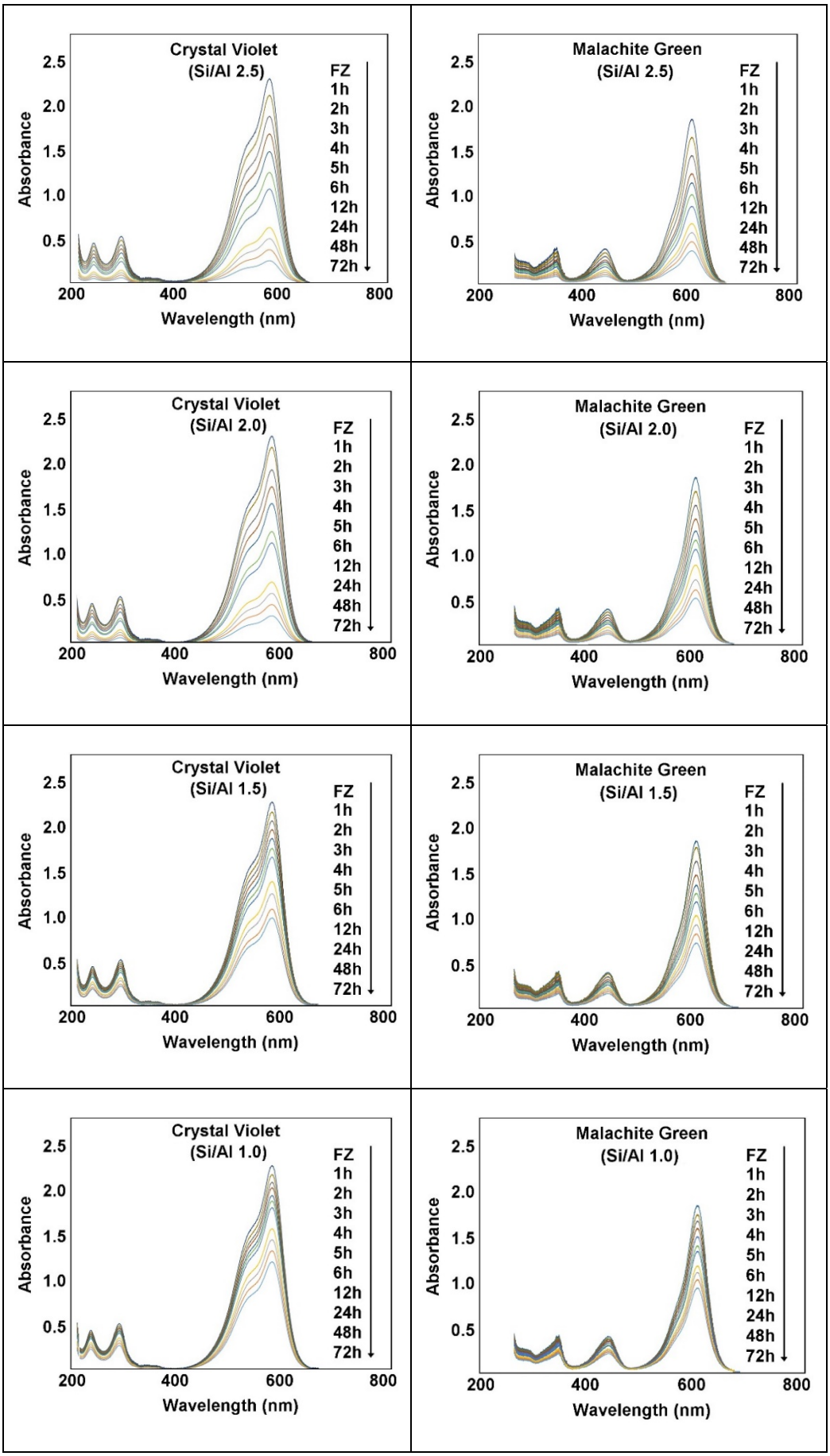

Figure 1: *UV-vis spectrum of CV and MG. *FZ: Free-Zeolite*

Downloaded from www.periodico.tchequimica.com

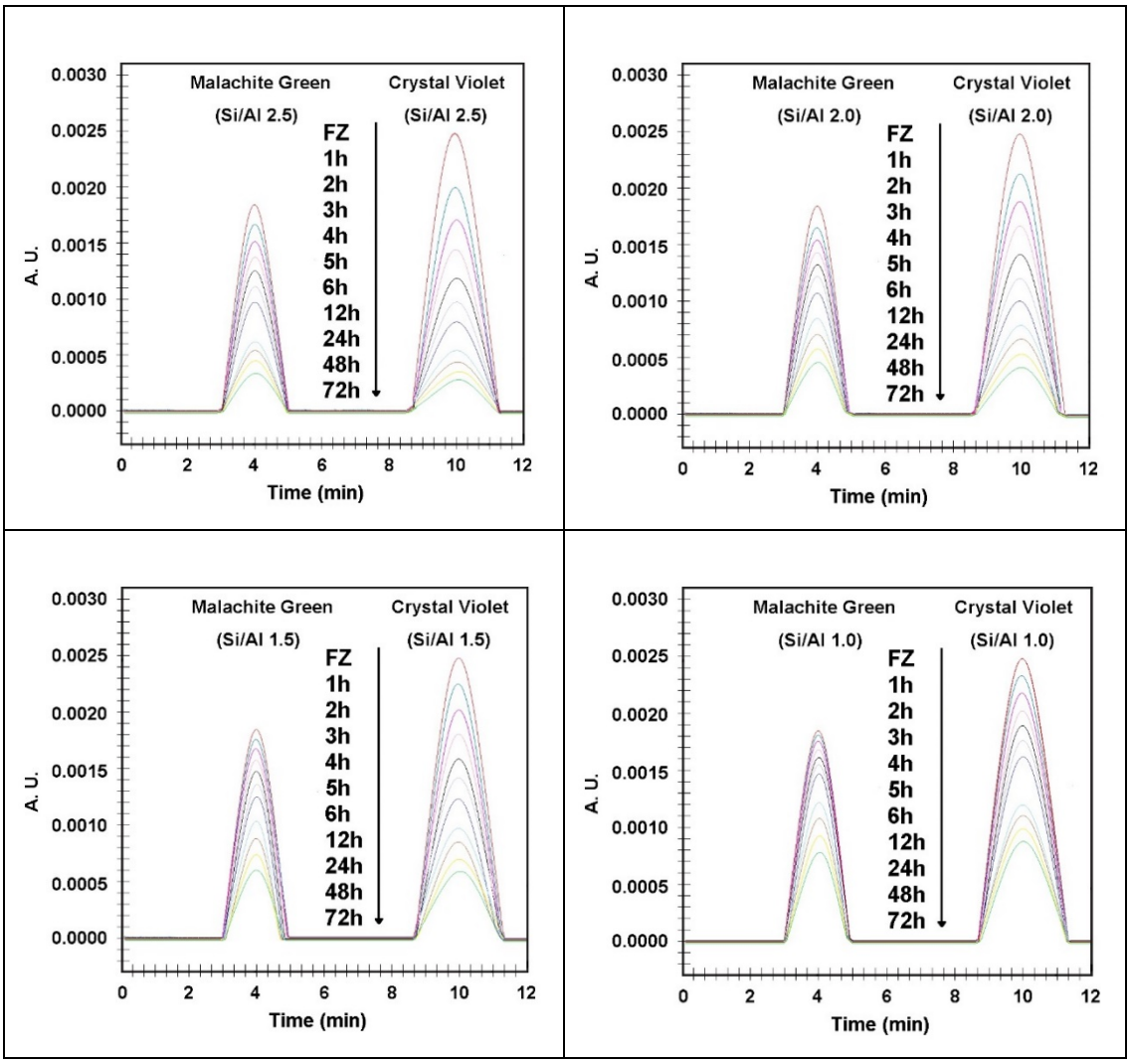

Figure 2: *Chromatogram of the CV and MG of decolorization analyzed by HPLC. *FZ: Free-Zeolite*

Downloaded from www.periodico.tchequimica.com

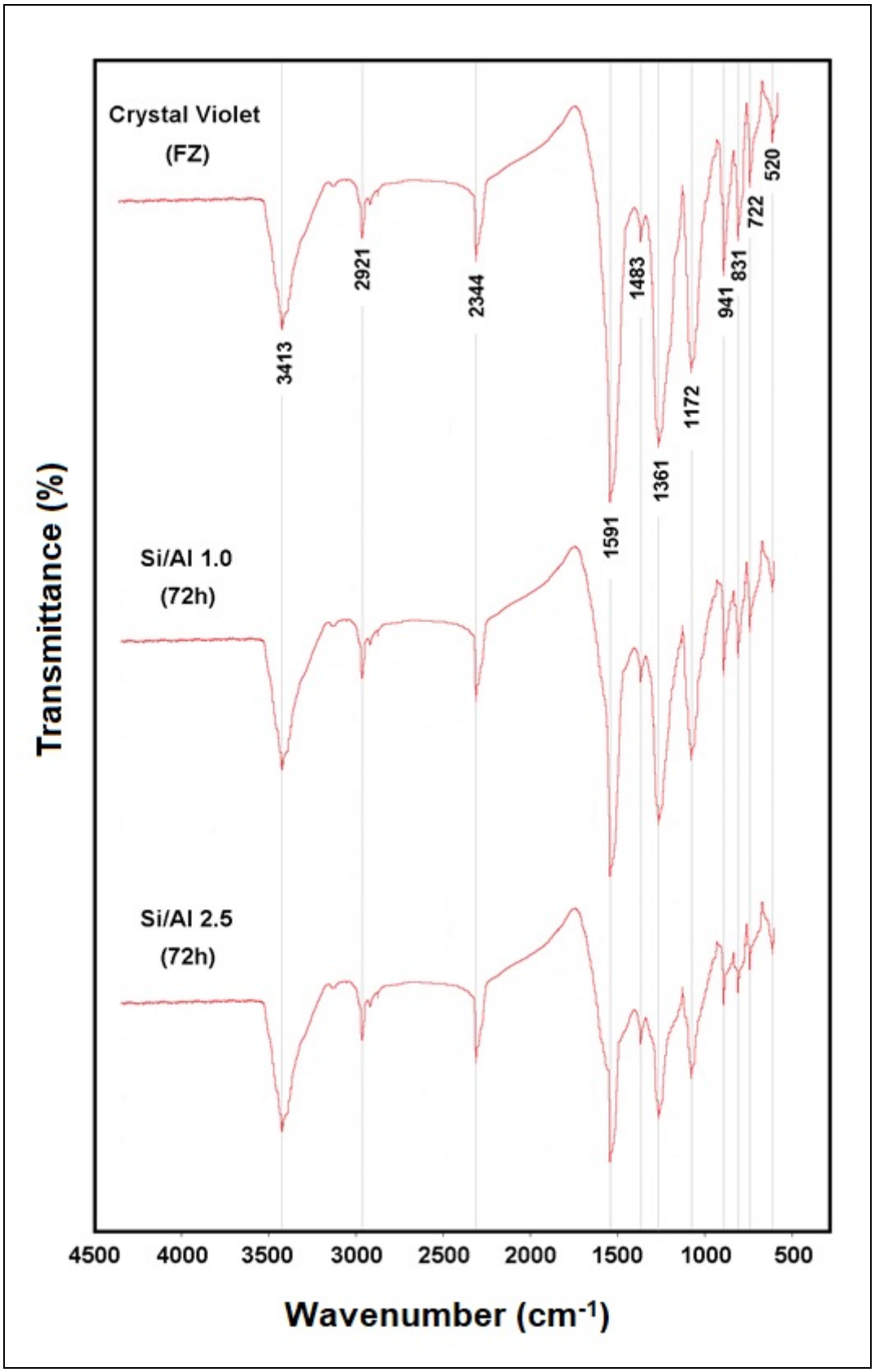

Figure 3: *FTIR spectra of CV. *FZ: Free-Zeolite*

Downloaded from www.periodico.tchequimica.com

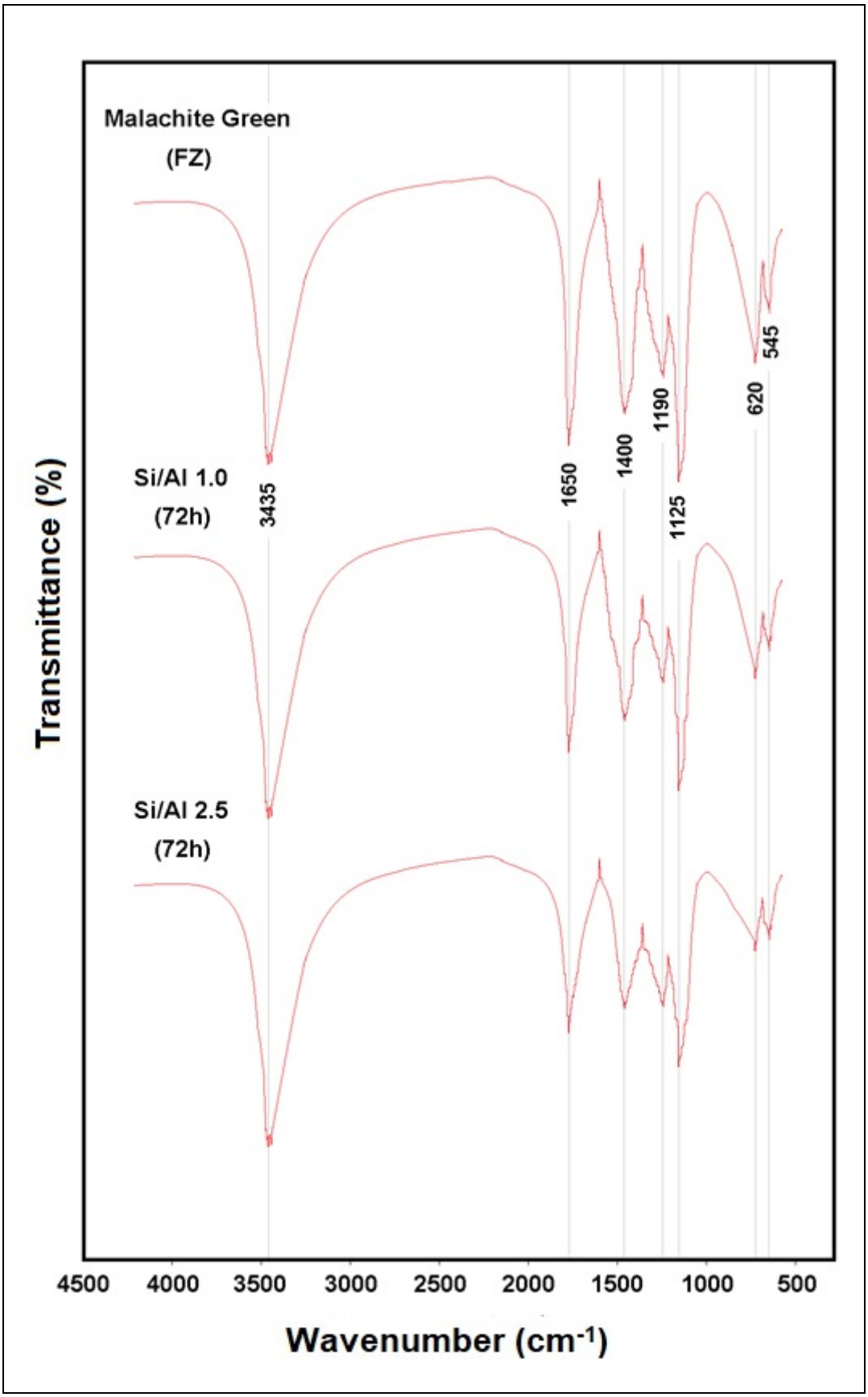

Figure 4: *FTIR spectra of MG. *FZ: Free-Zeolite*

PERIÓDICO TCHÊ QUÍMICA
ARTIGO ORIGINAL

APLICAÇÃO TERAPÊUTICA E PROFILÁTICA DA MODULAÇÃO MESODIENCEFÁLICA DURANTE IMPLANTES DENTÀRIOS EM PACIENTES COM DIABETES MELLITUS DO TIPO 2

THERAPEUTIC AND PROPHYLACTIC APPLICATION OF MESODIENCEPHALIC MODULATION DURING DENTAL IMPLANTATION IN PATIENTS WITH TYPE 2 DIABETES MELLITUS

ТЕРАПЕВТИЧЕСКОЕ И ПРОФИЛАКТИЧЕСКОЕ ПРИМЕНЕНИЕ МЕЗОДИЭНЦЕФАЛЬНОЙ МОДУЛЯЦИИ ПРИ ЗУБНОЙ ИМПЛАТНАЦИИ У ПАЦИЕНТОВ С САХАРНЫМ ДИАБЕТОМ 2-ГО ТИПА

YUMASHEV, Alexey[1*]; MATVEEVA, Elena[2]; TAMBOVTSEVA, Nataliia[3]; LI, Jiaqi[4]; YANG, Bowen [5];

[1,2, 3, 4, 5] Department of Prosthetic Dentistry, I. M. Sechenov First Moscow State Medical University (Sechenov University), Moscow, Russian Federation

** Correspondence author*
e-mail: yumashev031996@mail.ru

Received 12 June 2019; received in revised form 26 September 2019; accepted 03 October 2019

RESUMO

O implante dentário é estressante e pode aumentar os níveis de açúcar no sangue, colocando em risco pacientes com diabetes mellitus. Há necessidade de tratamentos alternativos que possam prevenir manifestações de estresse mental e somático durante o implante dentário nesses pacientes. Examinamos a eficácia terapêutica e profilática da modulação mesodientefálica (MDM) em pacientes com diabetes mellitus tipo 2 leve que foram submetidos a implante dentário. Este estudo clínico randomizado controlado incluiu 67 pacientes com diabetes mellitus tipo 2 leve e uma patologia dentária compreendendo um único defeito em uma arcada dentária. O grupo G-1 (n = 22) recebeu implantes dentários e terapia MDM durante o período pós-implantação inicial. O grupo TG-2 (n = 22) recebeu implantes dentários e terapia MDM durante os períodos pré-implantação e pós-implantação precoce. O grupo RG (n = 23) recebeu implantes dentários sem terapia com MDM. Os níveis de glicose no sangue, frequência cardíaca e estado emocional dos pacientes nos períodos pré e pós-implantação foram comparados. Em todos os grupos, os níveis de açúcar no sangue e a freqüência cardíaca atingiram o pico 5 minutos após a conclusão do procedimento odontológico. O aumento de 5 minutos antes do início para 5 minutos após a conclusão dos procedimentos odontológicos foi significativo nos grupos TG-1 e RG, mas não no grupo TG-2. Após 10 dias do procedimento, a qualidade de vida foi significativamente maior nos dois grupos de tratamento do que no grupo RG. O MDM tem valor terapêutico e profilático para pacientes com diabetes mellitus tipo 2 submetidos a implante dentário durante os períodos pré e pós-implante, bem como sobre a qualidade de vida no período de recuperação pós-operatória precoce

Palavras-chave: *Gliicose no sangue; implantação dentária; modulação mesodiencefálica; profilaxia; diabetes mellitus tipo 2*.

ABSTRACT

Dental implantation is stressful and can increase blood sugar levels, placing patients with diabetes mellitus at risk. There is a need for alternative treatments that can prevent mental and somatic stress manifestations during dental implantation in such patients. We investigated the therapeutic and prophylactic efficacy of mesodiencephalic modulation (MDM) in patients with mild type 2 diabetes mellitus who underwent dental implantation. This clinical randomized controlled study included 67 patients with mild type 2 diabetes mellitus and a dental pathology comprising a single defect in a dental arch. Group G-1 (n = 22) received dental implants and MDM therapy during the early post-implantation period. Group TG-2 (n = 22) received dental implants and MDM therapy during pre-implantation and early post-implantation periods. Group RG (n = 23) received dental implants without MDM therapy. Patients' blood glucose levels, heart rate, and emotional state in

Downloaded from www.periodico.tchequimica.com

pre-and post-implantation periods were compared. In all groups, blood sugar levels and heart rate peaked at 5 minutes after dental procedure completion. An increase from 5 minutes before starting to 5 minutes after completing the dental procedures was significant in TG-1 and RG groups but not in the TG-2 group. Quality of life was significantly higher in both the treatment groups than in the RG group at 10 days after the procedure. MDM has therapeutic and prophylactic value for patients with mild type 2 diabetes mellitus undergoing dental implantation during pre- and post-implantation periods as well as on the quality of life in the early post-surgery recovery period.

Keywords: *blood glucose; dental implantation; mesodiencephalic modulation; prophylaxis; type 2 diabetes* mellitus

АННОТАЦИЯ

Имплантация зубов вызывает стресс и может повышать уровень сахара в крови, подвергая риску больных сахарным диабетом. Существует потребность в альтернативных методах лечения, которые помогут предотвратить проявления психического и соматического стресса во время имплантации зубов у таких пациентов. Мы исследовали терапевтическую и профилактическую эффективность мезодиэнцефальной модуляции (МДМ) у пациентов с легкой формой сахарного диабета 2-го типа, которые перенесли имплантацию зубов. Данная работа представляет собой клиническое контролируемое исследование методом случайной выборки и охватывает 67 пациентов с легкой формой сахарного диабета 2-го типа. У всех пациентов наблюдалась стоматологическая патология, включающая единственный дефект зубного ряда. Группа G-1 (n = 22) получала зубные имплантаты и МДМ-терапию в раннем постимплантационном периоде. Группа TG-2 (n = 22) получала зубные имплантаты и МДМ-терапию во время предимплантационного и раннего постимплантационного периодов. Группа RG (n = 23) получала зубные имплантаты без МДМ-терапии. У пациентов сравнивали уровень глюкозы в крови, частоту сердечных сокращений и эмоциональное состояние в период до и после имплантации. Во всех группах уровень сахара в крови и частота сердечных сокращений достигли пика через 5 минут после завершения стоматологической процедуры. Увеличение от 5 минут до начала до 5 минут после завершения стоматологических процедур было значительным в группах TG-1 и RG, но не в группе TG-2. Качество жизни было значительно выше в обеих группах лечения, чем в группе RG, через 10 дней после процедуры. МДМ имеет терапевтическое и профилактическое значение для пациентов с легким сахарным диабетом 2 типа, перенесших дентальную имплантацию в период до и после имплантации, а также для качества жизни в раннем послеоперационном периоде восстановления.

Ключевые слова: глюкоза; имплантация зубов; мезодиэнцефальная модуляция; профилактика; сахарный диабет 2-го типа

1. INTRODUCTION

Dental procedures, particularly invasive interventions like dental implantation, are stressful for patients (Bracha *et al*., 2006; Kvale *et al*., 2004; Enkling *et al*., 2013; Lalabonova, 2015). In patients with type 2 diabetes mellitus, stress may trigger hyperglycemia (Chang *et al*., 2018; Kampling *et al*., 2018; Davis *et al*., 2017; Moradi *et al*., 2015; Renna *et al*., 2016). Since type 2 diabetes mellitus is related to endocrine diseases, which have a psychosomatic component, stress resistance in this patient population is already reduced, and dental treatment in these patients may lead to a sharp increase in blood glucose levels (Rau *et al*., 2017; Whitworth, 2016; van Dooren *et al*., 2016). Dentists thus often face the challenge of planning safe invasive interventions in patients with type 2 diabetes mellitus. In patients with type 2 diabetes, blood glucose levels can increase above acceptable values during dental procedures, creating an adverse complication for both dental care and type 2 diabetes mellitus. In addition, hyperglycemia may negatively affect the patient's local dental status after dental implantation surgery, impacting the regenerative ability of the weakened tissues. These difficulties may lead to a prolonged post-surgery recovery period and post-implantation complications that reduce the patient's quality of life and negatively affect the survival and stability of the implant (Lacigova *et al*., 2013; Jumashev *et al*., 2016a, Jumashev *et al*., 2016b). Therefore, there is a need for the development of techniques that can address the problem of increased blood glucose levels in patients with type 2 diabetes mellitus who require dental prosthesis involving dental implants (Ershov *et al*., 2018; Timoshin *et al*., 2018).

Patients with mild type 2 diabetes mellitus

Downloaded from www.periodico.tchequimica.com

are often treated exclusively with diet therapy and graduated physical exercises; it would be inappropriate to administer hypoglycemic medicinal products to this patient group prophylactically before commencing invasive dental procedures (Lalabonova, 2015). Other prophylactic approaches are required for moderating increases in blood glucose levels caused by invasive dental procedures. Physiotherapy offers a promising solution.

Among the available physiotherapeutic methods (such as low-level laser therapy, photodynamic therapy, ultrasonic decontamination, and photobiomodulation), mesodiencephalic modulation (MDM) therapy most closely meets the needs of dental patients with type 2 diabetes mellitus (Torkzaban *et al*., 2018; Alasqah *et al*., 2019; Stein *et al*., 2007; Tang and Arany, 2013). MDM therapy has been proven to reduce stress, increase insulin secretion, and reduce insulin resistance (Lacigova *et al*., 2013; Jumashev *et al*., 2016a; Jumashev *et al*., 2016b). MDM therapy focuses on impulse currents on the mesencephalic structures of the brain through electrodes that are attached using the fronto-occipital technique (Karev, 2005). MDM therapy activates and normalizes the body's anti-stress system complex, and its effects are clinically reflected at both general and local levels (Karev, 2005).

The purpose of this study was to evaluate the efficacy of MDM therapy as a prophylactic and therapeutic treatment in patients with type 2 diabetes mellitus receiving prosthetic dental implants.

2. MATERIALS AND METHODS

The study was approved by the Commission on Bioethics I. M. Sechenov First Moscow State Medical University. This clinical randomized controlled study was conducted at the Prosthetic Dentistry Department of I. M. Sechenov First Moscow State Medical University and included 67 patients who were diagnosed with mild type 2 diabetes mellitus (E11 according to the International Classification of Diseases-10 code (ISCDRHP, 2016) and a dental pathology comprising a single defect of the dental arch (in either the upper or lower jaw). The included patients were scheduled to receive intraosseous screw dental implants (Astra Tech Dental Implants System, Dentsply Sirona, Mölndal, Sweden).

The mean age in the study group was 53.82 ± 0.69 years. The time from diagnosis of type 2 diabetes mellitus to the beginning of the study was 6.21 ± 0.54 years. The following inclusion criteria were applied: treatment of type 2 diabetes mellitus exclusively with diet therapy and graduated physical exercises, no use of hypoglycemic medicinal products, and presence of appropriate bone architecture (D2–D3) for implant placement. The following exclusion criteria were applied: the presence of micro- or macrovascular complications of type 2 diabetes mellitus, tumor, epilepsy, tuberculosis, HIV, endogenous mental pathologies, diseases associated with impaired blood clotting, acute and chronic infectious diseases, active forms of periodontal pathologies, and skin diseases in the location of electrode application. All patients gave informed consent to participate in the study. The patients were randomized to the groups using a random number table.

All study patients received standard oral cavity prophylaxis before implant placement and concomitant anesthesia during the placement of the dental implant, according to standard protocols. Patients in all the groups were recommended to refrain from taking food for 2 hours before and for 4 hours after the dental procedures. All the patients were subjected to classical two-stage intraosseous implantation without bone augmentation by using the Astra Tech Implant System (Figure 1).

The patients were randomly divided into three groups based on the type of treatment to be administered. The first treatment group (TG-1) comprised 22 patients who received dental implants in conjunction with MDM therapy during the early post-implantation period, according to an in-house developed algorithm. The second treatment group (TG-2) comprised 22 patients who received dental implants in conjunction with MDM therapy during the pre-implantation and the early post-implantation periods, according to an in-house developed algorithm. The reference group (RG) comprised 23 patients who received dental implants without MDM therapy. MDM therapy is a modification of the physiotherapeutic method of transcranial stimulation, which is a targeted effect of calibrated electric currents on the median cerebral structures. MDM therapy was performed using an MDM-2000/1 device (ZAT ad, Czech Republic), designed for pulsed exposure to currents on the subcortical-stem (mesodiencephalic) region of the brain (Figure 2). During the MDM therapy session, the patient sits. Two nickel-plated copper electrodes were fixed on the patient's head: the anode - in the middle of

Downloaded from www.periodico.tchequimica.com

the forehead, the cathode - in the middle of the nape (Figure 3).

To achieve clinical effects with MDM therapy, impulse currents had a carrier frequency of 10,000 Hz and were modulated from 20 to 100 Hz, and the patients were prepared accordin to Figure 1. The power of the current applied during an MDM therapy session varied from 0.5 to 4 mA and was set individually, depending on the patient's subjective sensations (Yur'evna *et al.*, 2018). In the pre-implantation period, TG-2 patients received five MDM therapy sessions in total per day, with the last session. Patients received one MDM therapy session per day. The last session of MDM therapy in the pre-implantation period was carried out one day before the dental procedures. In the post-implantation period, TG-1 and TG-2 patients received 10 MDM therapy sessions in all, one MDM therapy session per day, from the first day of the post-implantation period. The first MDM therapy was performed 30 minutes after the procedure of dental implant placement. The duration of each MDM therapy session was 30 minutes.

Blood glucose levels were measured in all patients by using One Touch blood glucose meter (LifeScan, Wayne, PA, USA) four times, i.e., during the first consultation (usually 1 week before the prosthetic procedure), 5 minutes before the start of dental procedures, and 5 minutes and 1 hour after the termination of dental procedures. Concomitantly with the blood glucose level measurement, the pulse rate was measured using a Contec K-80B pulsometer. Immediately before dental procedures and 5 minutes and 1 hour thereafter, the patients self-identified their own psycho-emotional state. They rated their emotional discomfort level (fear, anxiety, and emotional tension) on a four-point score, where 0 means no symptoms, 1 means weak symptoms, 2 means moderate symptoms, and 3 means severe symptoms. Fear, anxiety, and emotional tension were quantified separately (Yumashev, 2017; Utyuzh, 2018).

In order to determine the treatment efficacy and rehabilitation of patients, the MOS 36-Item Short-Form Health Survey (MOS SF-36, https://www.rand.org/health-care/surveys_tools/mos/36-item-short-form.html) was used to evaluate the quality of life of patients. Scores for each of the eight indicators addressed in the questionnaire vary between 0 and 100 points, where 0 points mean complete lack of well-being and 100 points mean complete well-being in the context of the indicator under consideration. Patients were evaluated with the MOS SF-36 10 days after dental implant placement.

For statistical analysis, descriptive and mathematical statistics were used. These include calculation of the arithmetic mean values and standard deviations, standard error of the mean. The student's t-test was used for pair-wise comparison of values between groups. P-values < 0.05 were considered to be significant.

3. RESULTS

We developed an algorithm for MDM therapy sessions for treatment of patients who required dental implants but who had also had a long-term diagnosis of type 2 diabetes mellitus.

During the first consultation, the mean blood glucose level and heart rate values did not differ significantly across the three groups (Table 1). Five minutes before the start of dental procedures, patients in all groups showed a significant increase in blood glucose level compared to their first measurements (tEmp = 13.7; 6.0, and 15.3, $p < 0.01$, respectively). Wherein the blood glucose levels did not significantly differ between TG-1 and RG, whereas the blood glucose levels and heart rate in TG-2 patients were significantly lower than those in the other groups who did not receive MDM therapy during the pre-implantation period (tEmp = 13.7 and 7.7, $p < 0.01$, respectively).

All the patients demonstrated peak blood glucose levels 5 minutes after terminating the dental procedures. In TG-2, blood glucose level at 5 minutes after completing the dental procedures was 2.8 mmol/L less than that in TG-1. This trend continued until 1 hour after completing the dental procedures. Although blood glucose level 5 minutes before starting and 5 minutes after completing the dental procedures did not differ significantly from that in RG, the blood glucose level in TG-1 1 hour after completing the dental procedures was 1.6 mmol/L less than that in RG (Table 1, Figure 4). Blood glucose levels in the post-implantation period (5 minutes after the dental procedures) showed a significant increase in TG-1 (9.2 ± 0.21 mmol/L) and RG (9.3 ± 0.25 mmol/L) compared to the values obtained 5 minutes before starting the dental procedures (tEmp = 7.4 and 8.1, $p < 0.01$, respectively). However, at 1 hour after completing the dental procedures, there was a significant decrease in blood glucose level in TG-1 (7.6 ± 0.12 mmol/L) and TG-2 (5.8 ± 0.22

Downloaded from www.periodico.tchequimica.com

mmol/L) compared to levels taken at 5 minutes after completing the dental procedures (tEmp = 7.8 and 6.1, $p < 0.01$, respectively). These values were significantly different from those in RG, where blood glucose levels remained at the level of the previous measurement (tEmp = 7.2 and 12.1, $p < 0.01$, respectively) (Table 1, Figure 4).

For heart rate, dynamics similar to those for blood glucose was noted (Table 2, Figure 5). There were significant differences in heart rate values in TG-2 patients, who received MDM therapy sessions in the pre-implantation period, compared to the values in TG-1 and RG. Namely, the heart rate at 1 hour after completing the dental procedure in all groups was significantly reduced compared to the previous measurement and was similar to that in the first measurement. The latter two groups showed a pronounced increase in heart rate from 5 minutes before the start to 5 minutes after the completion of dental procedures, while there was no marked difference between these second and the third measurements in TG-2 (Table 2, Figure 5).

The psycho-emotional state at all stages of the survey was significantly better in TG-2 than in TG-1 and RG (Table 3). Five minutes before commencing the dental procedures, indicators in TG-2 of a stressed state were lower than those in TG-1 (fear reduced by 1.7 points, anxiety reduced by 1.8 points, and emotional stress reduced by 1.7 points). At 5 minutes after completing the dental procedures, the fear indicators were reduced by 0.2 points, anxiety by 0.5 points, and emotional stress by 1.2 points compared to those in TG-1. At 1 hour after the dental manipulations in TG-2, there were no indications of fear and anxiety, as in TG-1. Additionally, in TG-2, the indicators of emotional stress were minimal, and there were no significant differences between TG-1 and TG-2. There was no significant difference between TG-1 and RG in any of the psycho-emotional indicators at 5 minutes before starting or at 5 minutes after completing the dental procedures; however, there were significant differences at 1 hour after completing the dental procedures in terms of anxiety and emotional stress, with anxiety being 0.3 points less and emotional stress being 3.2 points less in TG-1 than in RG (Table 3).

In terms of quality of life at 10 days after dental implantation, quality of life was significantly higher for patients in both treatment groups than in RG patients (Table 4). TG-1 and TG-2 indices were not significantly different, but TG-1 and TG-2 patients faired significantly better than RG patients. The most significant differences in TG-1 and TG-2 compared with RG patients were in terms of physical functioning (by 16 and 17 points respectively, tEmp = 7.8 and 9,5, $p < 0.01$, respectively), pain (by 26.4 and 27.2 points respectively, tEmp = 26.5 and 28.2, $p < 0.01$, respectively), general health (by 20.3 and 21.1 points respectively, tEmp = 19.8 and 20.7, $p < 0.01$, respectively), emotional functioning (by 24.4 and 24.4 points respectively, tEmp = 24.2 and 24.3, $p < 0.01$, respectively), and mental health (by 23.3 and 23.4 points respectively, tEmp = 21.3 and 21.8, $p < 0.01$, respectively) (Table 4).

4. DISCUSSION:

The results of our study allowed us to prove the effectiveness of MDM therapy in treating patients with type 2 diabetes mellitus who require dental implantation. MDM therapy improved the psycho-emotional state of patients and reduced their blood sugar levels and heart rate. These effects of MDM therapy make it a method of choice for the treatment of patients with type 2 diabetes mellitus who need to undergo dental implantation.

It is important to improve the efficacy of treating patients who require dental implant procedures, given the side effects of such procedures in these patients, which are partly due to the stressful nature of this dental procedure. Since stress is associated with increased blood sugar, patients with diabetes are at increased risk. Physiotherapeutic methods may be a useful adjunctive technique to correct blood sugar levels in patients (in addition to the main methods of treatment for type 2 diabetes mellitus). Our results demonstrate the advisability of using MDM therapy during both pre- and post-implantation periods in patients with type 2 diabetes mellitus to prevent an increase in blood glucose levels immediately before and during invasive medical procedures, to normalize blood glucose levels after invasive procedures, to improve the quality of life of patients in the early post-surgical period by promoting faster pain neutralization and function recovery, and to stabilize their psycho-emotional state.

It was found that 5 minutes before starting the dental procedures in patients, blood glucose levels rose, which can be explained by the development of psycho-emotional stress while awaiting the start of invasive dental procedures. These findings were confirmed by the increase in heart rate in patients compared to the initial

Downloaded from www.periodico.tchequimica.com

measurement as well as by patients' self-identification of their emotional discomfort level. Our study demonstrated the efficacy of MDM therapy in preventing this increase in blood glucose levels during dental implantation in patients with type 2 diabetes mellitus due to psycho-emotional and somatic stress. The increase in blood glucose levels caused by the situation could be decreased in patients who received MDM therapy after the first session. Our study results indicate an increase in resistance to stress factors in patients with type 2 diabetes mellitus due to MDM therapy. In particular, MDM therapy sessions contributed to preventing the development of pronounced anxiety, fear, and emotional stress while patients waited for the invasive dental procedures to start, as evidenced by the results of patients' self-assessment of their emotional discomfort level. In most cases, the abovementioned emotional phenomena were evaluated by the patients in TG-2 as being only weakly present, whereas the patients in TG-1 and RG evaluated these symptoms as being present to a moderate or severe degree.

Unlike awaiting the start of invasive dental procedures, which involves pure psycho-emotional stress, dental implantation involves two pathogenic types of stress: psycho-emotional and somatic stresses. The third measurement values (5 minutes after terminating the dental procedures) in TG-2 demonstrated the efficacy of MDM therapy in preventing the development of distress associated with both the pathogenic aspects of stress during dental implantation. The dynamics of emotional experiences in all groups was interesting. Before the dental procedures, the patients in all the groups showed equal dominance of such emotional phenomena as fear, anxiety, and emotional stress, whereas 5 minutes after completing the dental procedures, fear and anxiety were neutralized, while emotional stress values remained elevated. One hour after the completion of the dental procedures in TG-1 and TG-2 (after a session of MDM therapy), the emotional state of patients was stabilized, according to their self-identification of neutralization of fear, anxiety, and emotional stress, while in RG, the level of emotional discomfort remained elevated and demonstrated no significant differences from the previous measurement, which was correlated with blood glucose levels.

Use of MDM therapy demonstrated a significant improvement in the quality of life of patients with type 2 diabetes mellitus in the early post-implantation period as compared to patients who had not received MDM therapy as an adjunctive therapy and prophylaxis. High quality of life in patients in both the treatment groups was achieved mainly due to higher values (compared to RG) of physical functioning; reduced pain, swelling, and inflammation at the site of implantation; normalization of emotional and mental health; and improved general well-being. A direct relationship was noted between blood glucose levels, heart rate, and emotional discomfort in patients with type 2 diabetes mellitus, which may be evidence of a shared etiopathological factor of these conditions. We did not notice the limitations and side effects when MDM therapy is used in patients with diabetes mellitus.

There are indications that dental phobia may be a contraindication for dental procedures. Therefore, to eliminate anxiety in patients who require dental treatment, various techniques have been developed, such as adequate psychological and dental pretreatment (Enkling *et al*., 2013). This technique initially reduces patients' anxiety levels; however, anxiety recurs subsequently (Enkling *et al*., 2013). In our study, we demonstrated the effectiveness of MDM therapy, physiotherapy, for improving the quality of life and reducing blood glucose levels during dental implantation in patients with type 2 diabetes mellitus. The program developed by us makes it possible to achieve the normalization of the psycho-emotional state for a longer period (we used an observation period of 10 days). Thus, MDM therapy may be considered as an appropriate method for the prevention and relief of manifestations of psycho-emotional and somatic stress during dental implantation, which may be particularly useful in patients with type 2 diabetes mellitus. We think that it is rational to continue research on the use of MDM therapy in patients receiving dental treatment not only in diabetic patients but also in other diseases, the genesis of which is associated with psycho-emotional dysfunction and physiological dysfunction.

5. CONCLUSIONS:

Improving the provision of dental care for patients with type 2 diabetes mellitus is an urgent task of modern dentistry, and it is important that dentists should consider the impact of type 2 diabetes mellitus on the recovery period after dental interventions. This study sets out the experience of providing dental care to patients

Downloaded from www.periodico.tchequimica.com

with type 2 diabetes mellitus using MDM therapy. It was proved that the use of MDM therapy in a complex of procedures for dental implantation reduces blood glucose levels and heart rate after implantation, as well as improves the emotional state of patients.

In conclusion, MDM therapy can be considered as an additional component of the provision of dental care to patients with type 2 diabetes mellitus in order to improve the condition of patients.

6. REFERENCES:

1. Alasqah, M. N. Antimicrobial efficacy of photodynamic therapy on dental implant surfaces: a systematic review of in vitro studies. *Photodiagnosis Photodyn Ther*, **2019**, S1572-1000(18)30465-4.
2. Bracha, H. S., Vega, E. M., Vega, C. B. Posttraumatic dental-care anxiety (PTDA): is "dental phobia" a misnomer? *Hawaii Dental J*, **2006**, *37*, 17-19.
3. Chang, M. W., Huang, C. Y., Liu, H. T., Chen, Y. C., Hsieh, C. H. Stress-induced and diabetic hyperglycemia associated with higher mortality among intensive care unit trauma patients: a cross-sectional analysis of the propensity score-matched population. *Int J Environ Res Public Health,* **2018**, *15*, E992.
4. Davis, G., Fayfman, M., Reyes-Umpierrez, D., Hafeez S., Pasquel F. J., Vellanki P., Haw, J. S., Peng, L., Jacobs, S., Umpierrez G. E. Stress hyperglycemia in general surgery: why should we care? *J Diabetes Complications,* **2017**, *1056-8727*, 31341-31347.
5. Enkling, N., Hardt, K., Katsoulis, J., Ramseier, C. A., Colombo, A., Jöhren, P., Mericske-Stern, R. Dental phobia is no contraindication for oral implant therapy. *Quintessence Int*, **2013**, *44*, 363-371.
6. Ershov, K. A., Sevbitov, A. V., Dorofeev, A. E., Pustokhina, I. G. Evaluation of elderly patients' adaptation to removable dentures. *Indo Am J Pharmaceut Sci,* **2018**, *5*, 1638-1641.
7. International Statistical Classification of Diseases and Related Health Problems 10th Revision (ICD-10), **2016**. https://icd.who.int/browse10/2016/en#/E11
8. Yumashev, A. V., Gorobets, T. N., Admakin, O. I., Kuzminov, G. G., Nefedova, I. V. Key aspects of adaptation syndrome development and anti-stress effect of mesodiencephalic modulation. *Indian J Sci Technol,* **2016**, *9*, № 19, 93911.
9. Yumashev, A. V., Utyuzh, A. S., Volchkova, I. R., Mikhailova, M. V., Kristal, E. A. The influence of mesodiencephalic modulation on the course of postoperative period and osseointegration quality in case of intraosseous dental implantation. *Indian J Sci Technol,* **2016**, *9*, № 42, 104307.
10. Kampling, H., Mittag, O., Herpertz, S., Baumeister, H., Kulzer, B., Petrak, F. Can trajectories of glycemic control be predicted by depression, anxiety, or diabetes-related distress in a prospective cohort of adults with newly diagnosed type 1 diabetes? Results of a five-year follow-up from the German multicenter diabetes cohort study (GMDC-Study). *Diabetes Res Clin Pract,* **2018**, *141*, 106-117.
11. Karev, V. A. *Mesodiencephalic modulation*. Moscow. **2005**.
12. Kvale, G., Berggren, U., Milgrom, P. Dental fear in adults: a meta-analysis of behavioral interventions. *Community Dent Oral Epidemiol*, **2004**, *32*, 250-264.
13. Lacigova, S., Tomesova, J., Gruberova, J., Rusavy, Z., Rokyta, R. "Mesodiencephalic" modulation in the treatment of diabetic neuropathy. *Neuro Endocrinology Letter,* **2013**, *34,* 135-142.
14. Lalabonova, C. K. Impact of dental anxiety on the decision to have implant treatment. *Folia Med*, **2015**, *57*, 116-121.
15. Moradi, S., Keshavarzi, A., Tabatabaee, S. M. Is stress hyperglycemia a predicting factor of developing diabetes in future? *Exp Clin Endocrinol Diabetes,* **2015**, 614-616.
16. Rau, C. S., Wu, S. C., Chen, Y. C., Chien, P. C, Hsieh, H. Y, Kuo, P. J., Hsieh, C. H. Stress-induced hyperglycemia in diabetes: a cross-sectional analysis to explore the definition based on the trauma registry data. *Int J Environ Res Public Health,* **2017**, *14*, E1527.
17. Renna, C. P., Boyer, B. A., Prout, M. F., Scheiner, G. Posttraumatic stress related to hyperglycemia: prevalence in adults with type I diabetes. *J Clin Psychol Med Settings,* **2016**, *23*, 269-284.
18. Stein, J. M., Hammächer, C., Michael, S. S. Combination of ultrasonic decontamination, soft tissue curettage,

Downloaded from www.periodico.tchequimica.com

and submucosal air polishing with povidone-iodine application for non-surgical therapy of peri-implantitis: 12 month clinical outcomes. *J Periodontol*, **2007**.
19. Tang, E., Arany, P. Photobiomodulation and implants: implications for dentistry. *J Periodontal Implant Sci*, **2013**, *43*, 262-268.
20. Timoshin, A. V., Sevbitov, A. V., Ergesheva, E. V., Boichuk, A. V., Sevbitova, M. A. Experience of treatment of aphthous lesions of oral mucosa by preparations on the basis of collagen and digestase. *Asian J Pharm,* **2018**, *12*(1), 284-287.
21. Torkzaban, P., Kasraei, S., Torabi, S., Farhadian, M. Low-level laser therapy with 940 nm diode laser on stability of dental implants: a randomized controlled clinical trial. *Lasers Med Sci,* **2018**, *33*, 287-293.
22. Utyuzh, A. S., Yumashev, A. V., Lang, H. W., Zekiy, A. O., Lushkov, R. M. Comprehensive treatment and rehabilitation of patients with osteosarcoma of the mandible. *Implant Dent*, **2018**, *3*, 332-341.
23. van Dooren, F. E., Denollet, J., Verhey, F. R., Stehouwer, C. D., Sep S. J., Henry, R. M., Kremers, S. P., Dagnelie, P. C., Schaper, N. C., van der Kallen, C. J., Koster, A., Pouwer, F., Schram, M. T. Psychological and personality factors in type 2 diabetes mellitus, presenting the rationale and exploratory results from The Maastricht Study, a population-based cohort study. *BMC Psychiatry*, **2016**, 16:17.
24. Whitworth, S. R., Bruce, D. G., Starkstein, S. E., Davis, W. A., Davis, T. M., Bucks, R. S. Lifetime depression and anxiety increase prevalent psychological symptoms and worsen glycemic control in type 2 diabetes: the Fremantle Diabetes Study Phase II. *Diabetes Res Clin Pract,* **2016**, *122*, 190-197.
25. Yumashev, A. V., Utyuzh, A. S., Admakin, O. I., Zakharov, A. N., Nefedova, I. V. Mesodiencephalic modulationsverfahren bei der korrektur von belastungsstorngen. *Int J Appli Fund Res*, **2017**, *1*, 1-14.
26. Kuznetsova M.Yu., Nevdakh A. S., Platonova V.V., Sevbitov A. V., Dorofeev A. E. Evaluation of effectiveness of a preparation on the basis of phytoecdysteroids for treatment of traumatic injuries of oral mucosa in orthodontic patients. *Int J Green Pharm*, 2018, *12*, 297-300.

Table 1. *Mean blood glucose levels at different treatment stages*

Mean blood glucose levels (mmol/L)	Groups		
	TG-1	TG-2	RG
	(n = 20)	(n = 22)	(n = 23)
During the first consultation	5.5 ± 0.09	5.5 ± 0.08	5.5 ± 0.07
5 minutes before start of dental procedures	7.4 ± 0.11	6.1 ± 0.11	7.4 ± 0.11
5 minutes after completing dental procedures	9.2 ± 0.21	6.4 ± 0.09	9.3 ± 0.25
One hour after completing dental procedures	7.6 ± 0.12	5.8 ± 0.22	9.2 ± 0.25
p (t)	< 0.01	< 0.01	< 0.01

Table 2. *Mean heart rate values in the different groups at different treatment stages*

Mean heart rate (beats/minute)	Group		
	TG-1	TG-2	RG
	(n = 20)	(n = 22)	(n = 23)
During the first consultation	66.9 ± 0.81	66.7 ± 0.90	66.8 ± 0.76
5 minutes before start of dental procedures	76.1 ± 0.80	68.2 ± 0.82	75.9 ± 0.89
5 minutes after completing dental procedures	85.2 ± 0.45	70.1 ± 0.37	85.4 ± 0.39
One hour after completing dental procedures	67.5 ± 0.72	65.5 ± 0.80	68.2 ± 0.76
p (t)	< 0.01	< 0.01	< 0.01

Downloaded from www.periodico.tchequimica.com

Table 3. *Mean emotional discomfort values at different treatment stages on the four-point scale of emotional discomfort level (fear, anxiety, emotional tension) self-reported by patients*

Measurement	Index	Group			Comparisons		
		TG-1	TG-2	RG	TG-1 vs TG-2	TG-1 vs RG	TG-2 vs RG
		points	points	points	p(t)	p(t)	p(t)
5 minutes before starting dental procedures	fear	2.9 ± 0.16	1.2 ± 0.18	2.8 ± 0.12	< 0.01	> 0.05	< 0.01
	anxiety	2.7 ± 0.09	0.9 ± 0.18	2.8 ± 0.10	< 0.01	> 0.05	< 0.01
	emotional stress	2.8 ± 0.09	1.1 ± 0.06	2.8 ± 0.08	< 0.01	> 0.05	< 0.01
5 minutes after completing dental procedures	fear	0.2 ± 0.08	0.0 ± 0.00	0.2 ± 0.11	< 0.01	> 0.05	> 0.05
	anxiety	0.6 ± 0.18	0.1 ± 0.05	0.6 ± 0.18	< 0.05	> 0.05	< 0.05
	emotional stress	2.8 ± 0.13	1.6 ± 0.11	2.8 ± 0.12	< 0.01	> 0.05	< 0.01
One hour after completing dental procedures	fear	0.0 ± 0.00	0.0 ± 0.00	0.0 ± 0.00	> 0.05	> 0.05	> 0.05
	anxiety	0.0 ± 0.00	0.0 ± 0.00	0.3 ± 0.12	> 0.05	< 0.05	< 0.05
	emotional stress	0.3 ± 0.10	0.2 ± 0.06	3.5 ± 0.12	> 0.05	< 0.01	< 0.01

Table 4. *Quality of life assessment in the different patient groups at 10 days after dental implant placement, based on the MOS SF-36 score*

Indicator	Group			Comparisons	
	TG-1	TG-2	RG	TG-1 vs RG	TG-2 vs RG
	points	points	points	p(t)	p(t)
Physical functioning	89.6 ± 0.68	90.6 ± 1.05	73.6 ± 1.12	< 0.01	< 0.01
Role functioning	88.3 ± 1.18	88.4 ± 1.14	88.0 ± 1.25	> 0.05	> 0.05
Pain	99.0 ± 1.02	99.8 ± 1.25	72.6 ± 1.72	< 0.01	< 0.01
General health	94.6 ± 1.30	95.4 ± 1.42	74.3 ± 1.65	< 0.01	< 0.01
Vitality	85.0 ± 1.25	85.6 ± 1.04	85.0 ± 1.14	> 0.05	> 0.05
Social functioning	83.4 ± 1.50	83.6 ± 1.49	83.401 ± 1.48	> 0.05	> 0.05
Role emotional functioning	99.0 ± 0.78	99.0 ± 1.01	74.6 ± 1.48	< 0.01	< 0.01
Mental health	98.9 ± 0.82	99. ± 1.54	75.6 ± 1.62	< 0.01	< 0.01

Downloaded from www.periodico.tchequimica.com

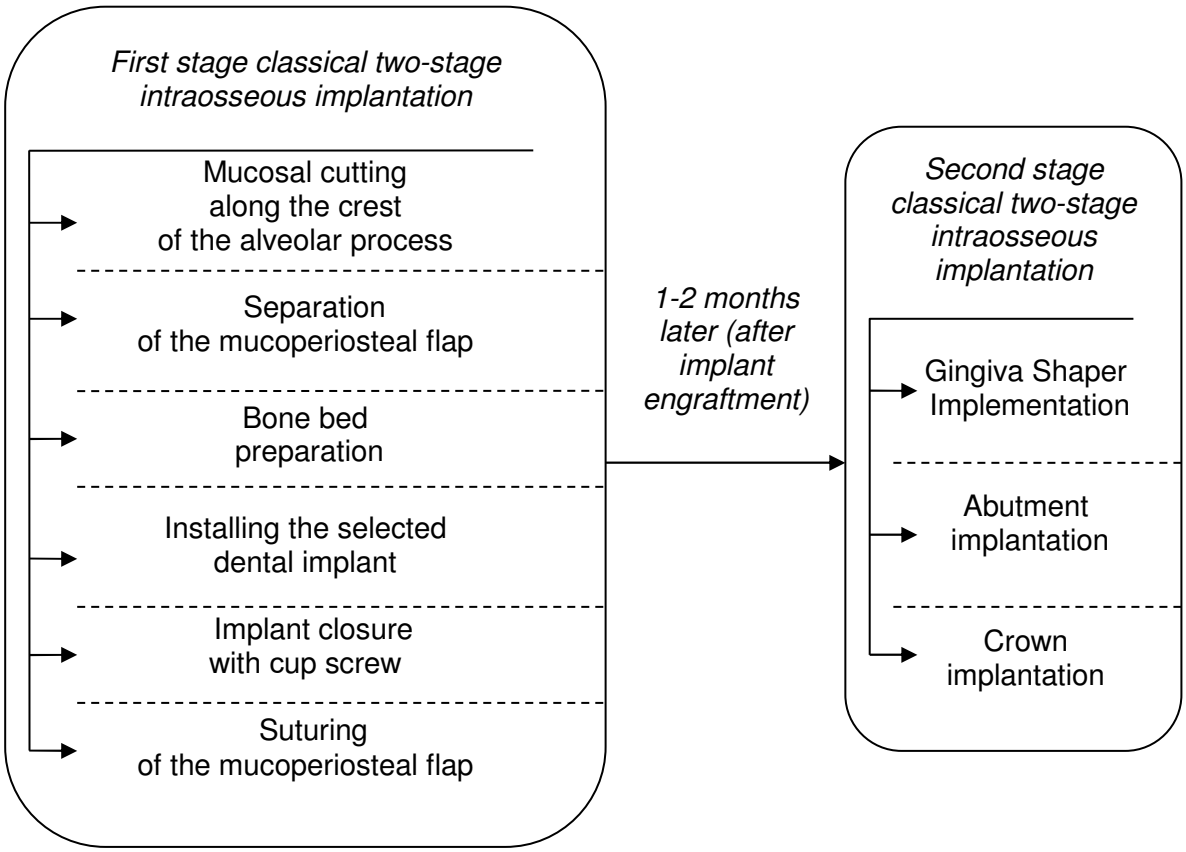

Figure 1. *Content of stage of the classical two-stage intraosseous implantation*

Figure 2. *The device "MDM-2000/1" for mesodiencephalic therapy*

Downloaded from www.periodico.tchequimica.com

Figure 3. *The MDM Therapy Procedure*

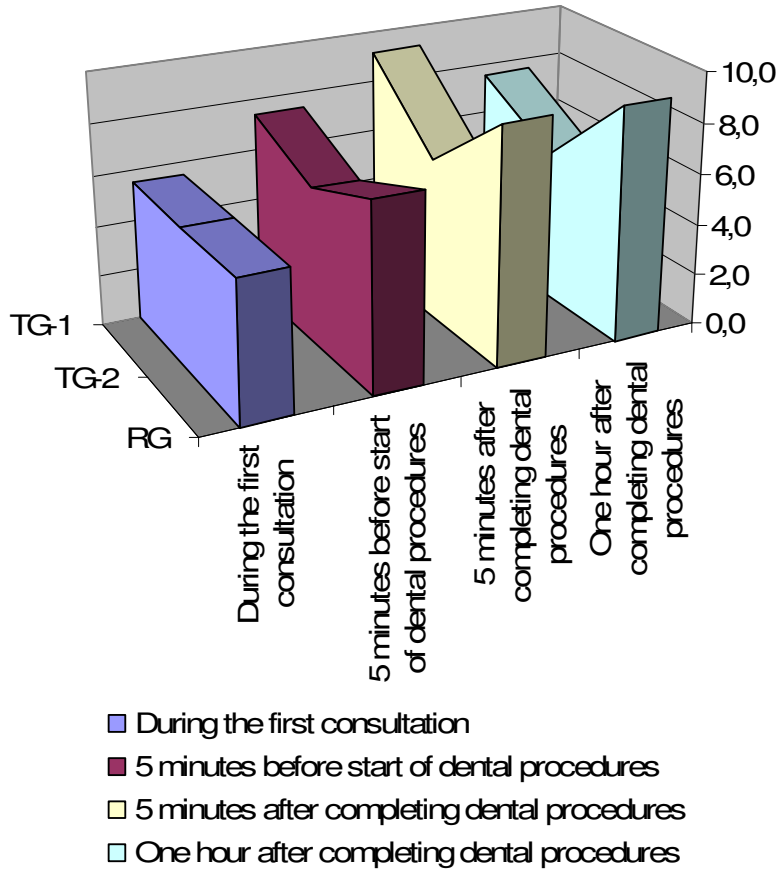

Figure 4. *Mean blood glucose levels at different treatment stages*

Downloaded from www.periodico.tchequimica.com

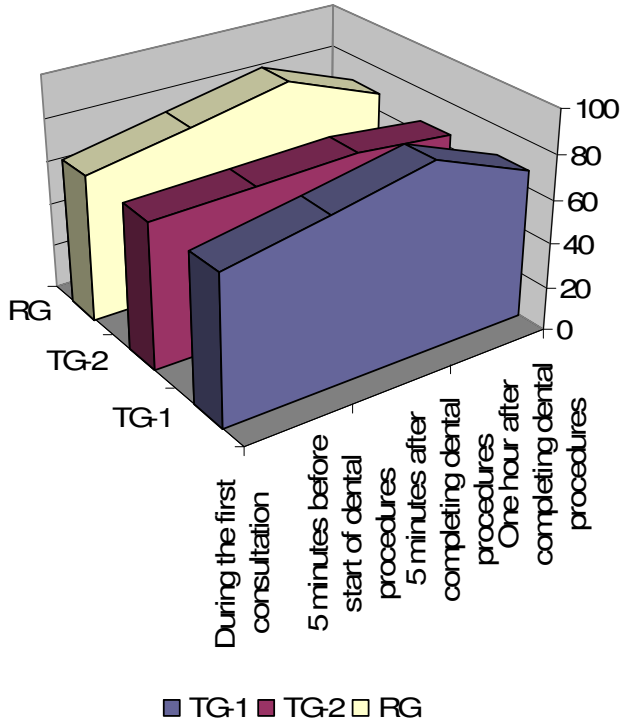

Figure 5. *Mean heart rate values in the different groups at different treatment stages*

Downloaded from www.periodico.tchequimica.com

PERIÓDICO TCHÊ QUÍMICA
ARTIGO ORIGINAL

CARACTERÍSTICAS COMPARATIVAS DO CRISTALOGRAMA DO FLUIDO ORAL EM PACIENTES USUÁRIOS DE HEROÍNA E METADADONA

COMPARATIVE CHARACTERISTICS OF THE CRYSTALLOGRAM OF THE ORAL FLUID IN PATIENTS WHO USE HEROIN AND METHADONE

СРАВНИТЕЛЬНАЯ ХАРАКТЕРИСТИКА КРИСТАЛЛОГРАММ РОТОВОЙ ЖИДКОСТИ У ПАЦИЕНТОВ, УПОТРЕБЛЯЮЩИХ ГЕРОИН И МЕТАДОН

SEVBITOV, Andrei*; DOROFEEV, Aleksei; KUZNETSOVA, Maria; TIMOSHIN, Anton; ERSHOV, Kirill

Department of Propaedeutic of Dental Diseases
of I. M. Sechenov First Moscow State Medical University (Sechenov University)

** Correspondence author*
e-mail: avsevbitov@mail.ru

Received 12 August 2019; received in revised form 19 November 2019; accepted 24 November 2019

RESUMO

Atualmente, o problema da toxicodependência é um dos principais problemas, não apenas na área da saúde, mas também na sociedade como um todo, pois representa uma séria ameaça à vida e à saúde da parte saudável da população. As pessoas que sofrem de dependência de drogas são caracterizadas não apenas por distúrbios graves do sistema nervoso central, órgãos internos, mas também por alterações patológicas na membrana mucosa da cavidade oral. Os resultados dos estudos indicam que pessoas que sofrem de dependência de opiáceos (principalmente a dependência de heroína) e que consomem metadona (uma droga sintética do grupo de opioides usados em alguns países como terapia de substituição no tratamento da dependência de drogas), juntamente com os efeitos tóxicos gerais no corpo, há mudanças significativas no estado da dentição. O objetivo do trabalho foi analisar os resultados de cristalogramas dos fluidos orais em pacientes consumidores de heroína e metadona e identificar as características morfologicas dos cristais, dependendo da substância utilizada. Pela primeira vez, foram detectadas alterações na morfologia do cristal em pacientes que consumiam heroína e metadona. O artigo apresenta os resultados de análises de cristalogramas do fluido oral de pacientes em uso de heroína e metadona, características de sua morfologia, características distintas de qualidade, incluindo a falta de crescimento de cristais e ruptura de sua estrutura. Observe-se que tais alterações morfológicas na cristalização do fluido oral de pacientes dependentes de drogas identificadas pela primeira vez e podem ser usadas para fins de diagnóstico em odontologia para identificar pacientes que consomem heroína ou metadona. A análise dos resultados desses cristalogramas nas categorias de pacientes estudadas permitiu diferenciá-los dependendo da substância utilizada (heroína, metadona), que pode ser utilizado na prática clínica.

Palavras-chave: *cristalograma, toxicodependência, heroína, metadona*

ABSTRACT

Currently, the problem of drug addiction is one of the main not only in healthcare but also in society, because it poses a serious threat to the life and health of the working-age population. Persons suffering from drug addiction, are characterized not only by severe disorders of the Central nervous system, internal organs, but also pathological changes in the mucous membrane of the oral cavity. The results of studies indicate that persons suffering from drug dependence on opiates (mainly from heroin addiction) and taking methadone (a synthetic drug from the group of opioids used in some countries as substitution therapy in the treatment of drug dependence), along with the general toxic effects on the body, there are significant changes in the state of the dentition.The aim of the work is to analyze the results of oral fluid crystallograms in patients using heroin and methadone and to identify the features of crystal morphology depending on the substance used. For the first time, changes in crystal morphology were detected in patients taking heroin and methadone. The article presents the results of the analysis of crystallograms of oral fluid of patients using heroin and methadone, the features of their morphology, distinctive quality features, including the lack of crystal growth and rupture of its structure. It is noted that these morphological changes in the crystallization of oral fluid of drug-dependent

Downloaded from www.periodico.tchequimica.com

patients identified for the first time and can be used for diagnostic purposes in dentistry to identify patients who use heroin or methadone. Analysis of the results of these crystallograms in the studied categories of patients allows to differentiate them depending on the substance used (heroin, methadone), which can be used in clinical practice.

Keywords: *crystallogram, drug addiction, heroin, methadone*.

АННОТАЦИЯ

В настоящее время проблема наркомании является одной из главных не только в здравоохранении, но и в обществе в целом, поскольку представляет серьезную угрозу жизни и здоровья трудоспособной части населения. Для лиц, страдающих наркотической зависимостью, характерны не только тяжелые расстройства ЦНС, поражения внутренних органов, но и патологические изменения слизистой оболочки полости рта. Результаты исследований свидетельствуют о том, что у лиц, страдающих наркотической зависимостью от опиатов (в основном, от героиновой зависимости) и принимающих метадон (синтетический препарат из группы опиоидов, применяемый в некоторых странах в качестве заместительной терапии при лечении наркотической зависимости), наряду с общим токсическим воздействием на организм, происходят существенные изменения состояния зубочелюстной системы. Цель работы состоит в анализе результатов кристаллограмм ротовой жидкости у пациентов, употребляющих героин и метадон, и выявлении особенностей морфологии кристаллов в зависимости от употребляемого вещества. Впервые обнаружены изменения в морфологии кристаллов у пациентов, принимающих героин и метадон. В статье приведены результаты анализа кристаллограмм пациентов, употребляющих героин и метадон, выявлены особенности их морфологии, отличительные качественные признаки, среди которых отсутствие роста кристалла и разрыв его структуры. Отмечено, что данные морфологические изменения кристаллизации ротовой жидкости у наркозависимых пациентов выявлены впервые и могут быть использованы с диагностической целью в стоматологии для выявления пациентов, употребляющих героин или метадон. Анализ результатов данных кристаллограмм у исследуемых категорий пациентов позволяет дифференцировать их в зависимости от употребляемого вещества (героина, метадона), что может быть использовано в клинической практике.

Ключевые слова: *кристаллограмма, наркомания, героин, метадон*.

1. INTRODUCTION

A direct threat to the nation today is drug addiction, which is becoming an epidemic. 52 million people (1% of the World's population) who systematically abuse drugs are registered in the world. The share of drug addicts coming to the Russian Federation, according to the research Institute of narcology is about 5 million people. Opium addiction is recognized as the most malignant, accounting for 82.9% of the total number of drug addictions (Evstratenko *et al.,* 2018; Martusevich *et al.,* 2014; Mazzeoet *et al.,* 2013; Simonova *et al.,* 2014; Timoshin *et al.,* 2018; Vaijayanthimala *et al.,* 2015; Voloshina *et al.,* 2018; Dos Silva *et al.,* 2019). The results of studies indicate that persons suffering from drug dependence on opiates (mainly from heroin addiction) and taking methadone (synthetic drug from the group of opioids used in some countries as a replacement therapy in the treatment of drug dependence), along with the general toxic effects on the body, there are significant changes in the state of the dental system. Drug addicts are characterized by a lack of motivation for a healthy lifestyle, disregard for basic hygiene standards (daily oral hygiene, a timely visit to the dentist) (Dos Silva, Santos *et al.,* 2019; Gigena *et al.,* 2015; Walter *et al.,* 2015; Yang *et al.,* 2015; Gupta *et al.,* 2012; Mateos-Moreno *et al.,* 2013; Protrka *et al.,* 2013). All this, combined with the General harmful effects of drugs on the state of the body leads to early manifestations of oral diseases (periodontal disease) and more severe course of existing pathologies (caries and its complications) (Du M., et al., 2001; Dukić W, et al., 2013, Vehkalahti M, Nikula-Sarakorpi E and Paunio I., 1996).

Currently, in clinical dentistry, the method of crystallography is used, which consists of the analysis of crystallization figures that are formed when saliva is dried. Among the main morphological features of the crystalline aggregates of mixed saliva are qualitative and quantitative (Du M *et al.,* 2001; Dukić *et al.,* 2013; Vehkalahti *et al.,* 1996; Girardin *et al.,* 2019; Di Fazio *et al.,* 2018; Fiorentin *et al.,* 2018; Cone *et al.,* 2012). The quantitative characteristics include the length of the crystal, the angle of branching, the number of generations of branches of the 1st, 2nd order, the width of the

Downloaded from www.periodico.tchequimica.com

crystal, the number of microprongs along the length of the crystal. Among the qualitative features, great importance is given to the unevenness of thickness throughout one figure, the asymmetry of branching, the presence of the curvature of the main" trunk" of the crystal, the appearance of crystals with blurred contours, the shape of crystals, the change in the deforming and destructive nature (Kunkel *et al.,* 2015; Grabenauer *et al.,* 2018; Pesce *et al.,* 2012).

Depending on the different pathology of the crystalline structure of the oral fluid is capable of changing orientation (as a result of a breach morphology), which is primarily manifested in the lack of structure (from partial to complete). According to the literature data, studies to determine the structure of crystals in mixed saliva in drug-dependent patients have not been conducted before. In this regard, the study of the features of the crystallography of the oral fluid of drug-addicted patients who use heroin and methadone is very interesting (Rook; 2005).

The aim of the work is to analyze the results of crystallograms of oral fluid of patients using heroin and methadone and to identify the features of crystal morphology depending on the substance used.

2. MATERIALS AND METHODS

All research methods under this article have been conducted in accordance with the relevant guidelines and regulations. All experimental protocols were approved by the Local Ethics Committee of I. M. Sechenov First Moscow State Medical University (Sechenov University). Prior to the study, informed consent was obtained from all patients for the upcoming study.

All patients (110 people: 75 men and 35 women aged 20 to 50 years) in the rehabilitation period of treatment were divided into 2 groups: the first and second main groups. The first major group consisted of 58 heroin users (40 men and 18 women). The mean age of patients was 29.41±1.46 years. The second main group consisted of 52 people (35 men and 17 women) taking methadone as replacement therapy. The mean age of patients was 31.27±1.56 years.

Determination of dental status showed that all patients of the first and second main groups are in dire need of various types of dental care. The control group (35 people: 20 men and 15 women aged 20 to 50 years) consisted of healthy patients who had never used drugs and methadone. The average age of patients made up 32.81±1.64 years. The study used mixed saliva to study the crystal structures of oral fluid. The material was collected before meals, on an empty stomach. Unstimulated saliva was used. The patient was not recommend smoking, brushing the teeth, drinking heavily, or rinsing the mouth before taking the material for the study. The obtained samples were deposited on the surface of the substrate (the surface for drying the biofluid) with a drop of 0.1 mm. Strictly in a horizontal position, dried at a temperature of 18-25 ºC. After drying, the structure of the saliva was examined using a Leica DM-LS optical microscope (Germany) with a Sony DC30P video camera. The resulting image was transmitted to the monitor screen. With a small magnification, an image of the entire surface of the dried drop was scanned, then with a larger magnification, some parts of its surface were examined. The selected areas of the crystallogram were recorded on a computer as a graphic file, AdodePhotoshop 6.0 and PhotoDraw 2000 were used for image processing. The obtained data were entered into an Excel 2000 spreadsheet from Microsoft Office 2000 SR-1 and analyzed with regard to the statistical packages Statistica-5.0 and StatgraphicsPlus 5. To evaluate the null hypothesis, the Student's t-test was used. The results were considered reliable at $p \leq 0.05$.

3. RESULTS AND DISCUSSION:

Comparative characteristics of the qualitative characteristics of crystallogram aggregates of mixed saliva in patients of the control group (%) are presented in Figure 1.

It is noted that these qualitative signs may occur in the morphological structure of mixed saliva of practically healthy patients in different proportions (crystallization of the oral fluid is not strictly the same). The variability in the formation of crystal aggregates of patients of the control group may be due to gender characteristics (the influence of female sex hormones) and mucin heterogeneity. A comparative characteristic of the frequency of detection of qualitative signs of crystallograms of oral fluid aggregates of patients (as a percentage) of the first and second main groups is shown in Figure 2.

According to the presented data, for the patients of the first main group, the following signs prevailed: lack of crystal growth, lack of apex of a crystal, one-sided branching, and uneven thickness throughout one crystal figure ($p < 0.01$). At the same time, in most cases - in 56

Downloaded from www.periodico.tchequimica.com

people (96.6%), the absence of crystal growth was noted (Figure 3).

In the patients of the second main group in 98% (in 51 people), a break in the crystal structure was observed ($p < 0.01$) (Fig. 4). In 40.4% and 38.5% of cases, branch asymmetry, and the presence of processes of the first generation from the top of the crystal were recorded.

The intake of narcotic substances (heroin) and methadone as a synthetic drug from the group of opioids is having a negative impact not only on the general state of the immune status, the work of the Central nervous system, internal organs and state of homeostasis of the salivary glands, causing gross violations of the morphology of the crystals of the oral fluid (Wasels *et al.,* 1994).

In patients taking heroin, the main morphological feature of crystallograms is the lack of growth. For drug-dependent patients who use methadone, a characteristic feature is the rupture of the crystal structure.

Analysis of the results of these crystallograms in the studied categories of patients allows to differentiate them depending on the substance used (heroin, methadone), which can be used in clinical practice (Presley *et al.,* 2003; Sordi *et al.,* 2017).

4. CONCLUSIONS:

For the first time, changes in crystal morphology were found in patients taking heroin and methadone.

2. For patients who use heroin, according to crystallography, a characteristic feature is the lack of crystal growth; for patients who use methadone – a rupture of the crystal structure.

3. This crystallography technique can be used in clinical practice for the purpose of differential diagnosis in patients using heroin and methadone.

5. ACKNOWLEDGMENTS:

This work was done at Sechenov University with supported by the "Russian Academic Excellence Project 5-100".

6. REFERENCES:

1. Evstratenko, V. V., Sevbitov, A. V., Platonova, V. V., Selifanova, E. I., Dorofeev, A. E. The characteristics of crystallization of mixed saliva in patients using heroin and methadone. *Klinichescheskaya Laboratornaya Diagnostika*, **2018**, 63(4), 223-227.
2. Martusevich, A. K., Yanchenko, V. A., Zhdanova, O. B., Artese, F., Napisanova, L. A., Virbalene, R. Crystallization characteristics of biological fluids of patients with postoperative alveococcosis. *Sovremennye Tehnologii v Medicine*, **2014**, 6(2), 38-42.
3. Mazzeo, M. A., Linares, J. A., López, M. M., Bachmeier, E., Wietz, F. M., Galván, V., Valentinuzzi, M. C., Riveros, J. A., Finkelberg, A. Analysis of saliva samples from oncological patients treated with 5-fluorouracil and leucovorin calcium by scanning electron microscopy with energy dispersive system. *Journal of Oral Pathology and Medicine*, **2013**, 42(10), 788-792.
4. Simonova, Z. G., Martusevich, A. K., Shubina, O. I., Emanuel, V.L. Structuring characteristics of biological fluids of patients with combined cardiovascular and gastrointestinal pathology. *Sovremennye Tehnologii v Medicine*, **2014**, 6(3), 64-70.
5. Timoshin, A. V., Dorofeev, A. E., Davidyants, A. A., Ershov, K. A., Pustokhina, I. G., Danshina, S. D. Features of the dental status of patients taking narcotic smoking mixtures. *Indo American Journal of Pharmaceutical Sciences*. **2018**, 5(9), 9114-9117.
6. Vaijayanthimala, V., Lee, D. K., Kim, S. V., Yen, A., Tsai, N., Ho, D., Chang, H.-C., Shenderova, O. Nanodiamond-mediated drug delivery, and imaging: Challenges and opportunities. *Expert Opinion on Drug Delivery*. **2015**. 12(5), 735-749.
7. Voloshina, I. M., Borisov, V. V., Sevbitov, A.V., Davidyants, A.A., Mironov, S. N., Kuznetsova, M. Yu., Ergesheva, E. V. Distinctive features of microcrystallization of mixed saliva in children with different levels of activity of carious process. *Asian Journal of Pharmaceutics*, **2018**, 12(S3), 1017-1020.
8. Dos Silva, D. S., De Yamaguchi, K. K. L. Drug chemistry, and self-medication

Downloaded from www.periodico.tchequimica.com

awareness as a tool in teaching organic functions. *Periodico Tche Quimica*, **2019**, 16(31), 223-234
9. Silva, P. D. C., Santos, B. L. C. D., Soares, G.L., Oliveira, W.A.D Anti-Candida albicans activity of the association of citronelal with anfotericin B or with cetoconazole. *Periodico Tche Quimica*, **2019**, 16(31), 223-234
10. Gigena, P. C., Cornejo, L. S., Lescano-de-Ferrer, A. Oral health in drug addict adolescents and non psychoactive substance users. *Acta Odontol Latinoam*, **2015**, 28(1), 48-57.
11. Walter M., Bentz D., Schicktanz N., Milnik A., Aerni A., Gerhards C., Schwegler K., Vogel M., Blum J., Schmid O., Roozendaal B., Lang UE, Borgwardt S., de Quervain D. Effects of cortisol administration on craving in heroin addicts. *Transl Psychiatry*. **2015**, 28(5), 610.
12. Yang T., Guo X., Wang H., Fu S., Wen Y., Yang H. Magnetically optimized SERS assay for rapid detection of trace drug-related biomarkers in saliva and fingerprints. *Biosens Bioelectron*. **2015**, 15(68), 350-357.
13. Gupta T., Shah N., Mathur V. P., Dhawan A. Oral health status of a group of illicit drug users in Delhi, India. *Community Dent Health*, **2012**, 29(1), 49-54.
14. Mateos-Moreno M. V., Del-Río-Highsmith J., Riobóo-García R., Solá-Ruiz M. F., Celemín-Viñuela A. Dental profile of a community of recovering drug addicts: Biomedical aspects. Retrospective cohort study. Med Oral Patol Oral Cir Bucal. 2013 Jul 1;18(4):e671-9
15. Protrka N., Katunarić M., Filipović I., Verzak Z. Caries prevalence in heroin addicts. *Acta Clin Croat*. **2013**, 52(4), 436-43.
16. Du M., Bedi R., Guo L., Champion J., Fan M., Holt R. Oral health status of heroin users in a rehabilitation centre in Hubei province, China. *Community Dent Health*, **2001**, 18(2), 94-8.
17. Dukić W., Dobrijević T. T., Katunarić M., Lesić S. Caries prevalence in chronic alcoholics and the relationship to salivary flow rate and pH. *Cent Eur J Public Health*, **2013**, 21(1):43-7.
18. Vehkalahti M., Nikula-Sarakorpi E., Paunio I. Evaluation of salivary tests and dental status in the prediction of caries increment in caries-susceptible teenagers. *Caries Res*, **1996**, 30(1), 22-8.
19. Girardin F., Hearmon N., Negro F., Eddowes L., Bruggmann P., Castro E. Increasing hepatitis C virus screening in people who inject drugs in Switzerland using rapid antibody saliva and dried blood spot testing: A cost-effectiveness analysis. *J Viral Hepat*. **2019,** 26(2), 236-245.
20. Di Fazio V., Wille S. M. R., Toennes S. W., van Wel J. H. P., Ramaekers J. G., Samyn N. Driving under the influence of cocaine: Quantitative determination of basic drugs in oral fluid obtained during roadside controls and a controlled study with cocaine users. *Drug Test Anal*, **2018,** 10.
21. Fiorentin T. R., Scherer J. N., Marcelo M. C. A., Sousa T. R. V., Pechansky F., Ferrão M. F., Limberger R. P. Comparison of Cocaine/Crack Biomarkers Concentrations in Oral Fluid, Urine, and Plasma Simultaneously Collected From Drug Users. *J Anal Toxicol*, **2018**, 42(2), 69-76.
22. Cone E. J. Oral fluid results compared to self reports of recent cocaine and heroin use by methadone maintenance patients. *Forensic Sci Int.* **2012**, 10(215), 88-91.
23. Kunkel F., Fey E., Borg D., Stripp R., Getto C. Assessment of the use of oral fluid as a matrix for drug monitoring in patients undergoing treatment for opioid addiction. *J Opioid Manag*. **2015**, 11(5), 435-42.
24. Grabenauer M., Moore K. N., Bynum N. D, White R. M., Mitchell J. M., Hayes E. D., Flegel R. Development of a Quantitative LC-MS-MS Assay for Codeine, Morphine, 6-Acetylmorphine, Hydrocodone, Hydromorphone, Oxycodone and Oxymorphone in Neat Oral Fluid. *J Anal Toxicol*. **2018,** 42(6), 392-399
25. Pesce A., West C., Gonzales E., Rosenthal M., West R., Mikel C., Almazan P., Latyshev S., Horn P. Illicit drug use correlates with negative urine drug test results for prescribed hydrocodone, oxycodone, and morphine. *Pain Physician*, **2012**, 15(5), E687-92.
26. Rook E. J., Hillebrand M. J., Rosing H., van Ree J. M., Beijnen J. H. The quantitative analysis of heroin, methadone, and their metabolites and the simultaneous detection of cocaine, acetylcodeine, and their metabolites in

Downloaded from www.periodico.tchequimica.com

human plasma by high-performance liquid chromatography coupled with tandem mass spectrometry. *J Chromatogr B Analyt Technol Biomed Life Sci*. **2005**, 824(1-2), 213-21.
27. Wasels R., Belleville F. Gas chromatographic-mass spectrometric procedures used for the identification and determination of morphine, codeine, and 6-monoacetylmorphine. *J Chromatogr A*. **1994**, 674(1-2), 225-34.
28. Presley L., Lehrer M., Seiter W., Hahn D., Rowland B., Smith M., Kardos KW, Fritch D., Salamone S., Niedbala R. S., Cone E. J. High prevalence of 6-acetylmorphine in morphine-positive oral fluid specimens. *Forensic Sci Int*, **2003**, 133(1-2), 22-5.
29. Sordi M. B., Massochin R. C., Camargo A. R., Lemos T., Munhoz E. A. Oral health assessment for users of marijuana and cocaine/crack substances. *Braz Oral Res*, **2017**, 31, 102.

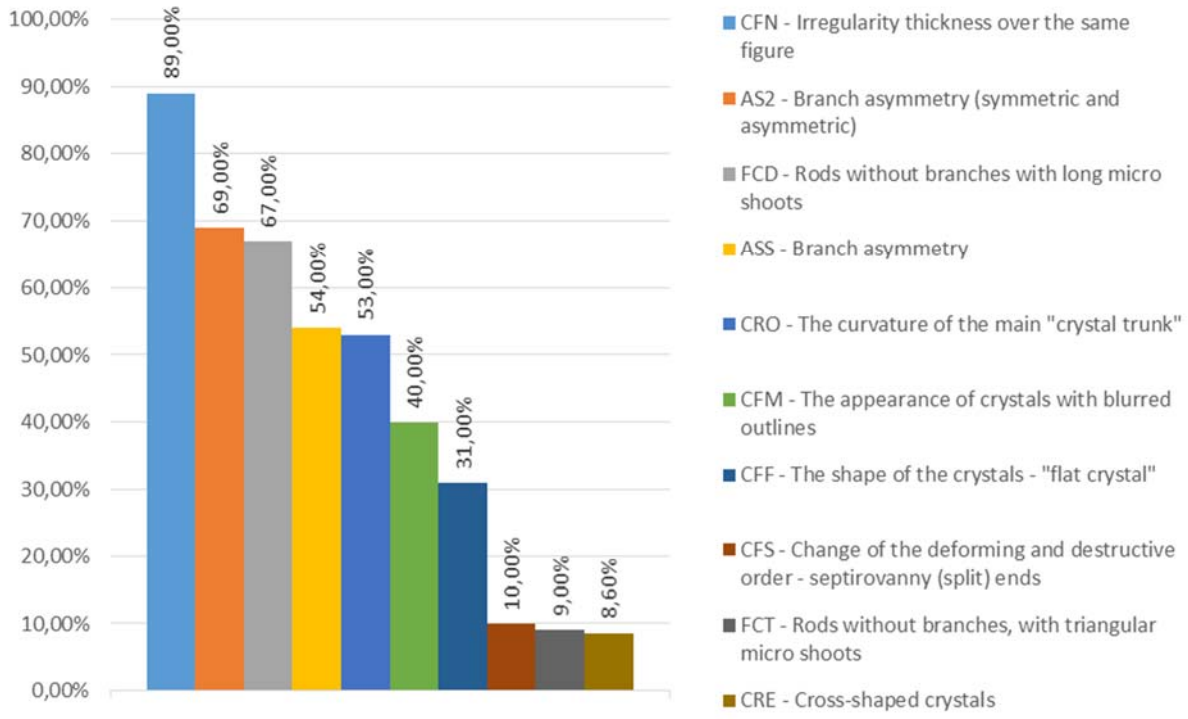

Figure 1. *The frequency of occurrence of qualitative signs of crystallograms of oral fluid in patients of the control group as a percentage*

Downloaded from www.periodico.tchequimica.com

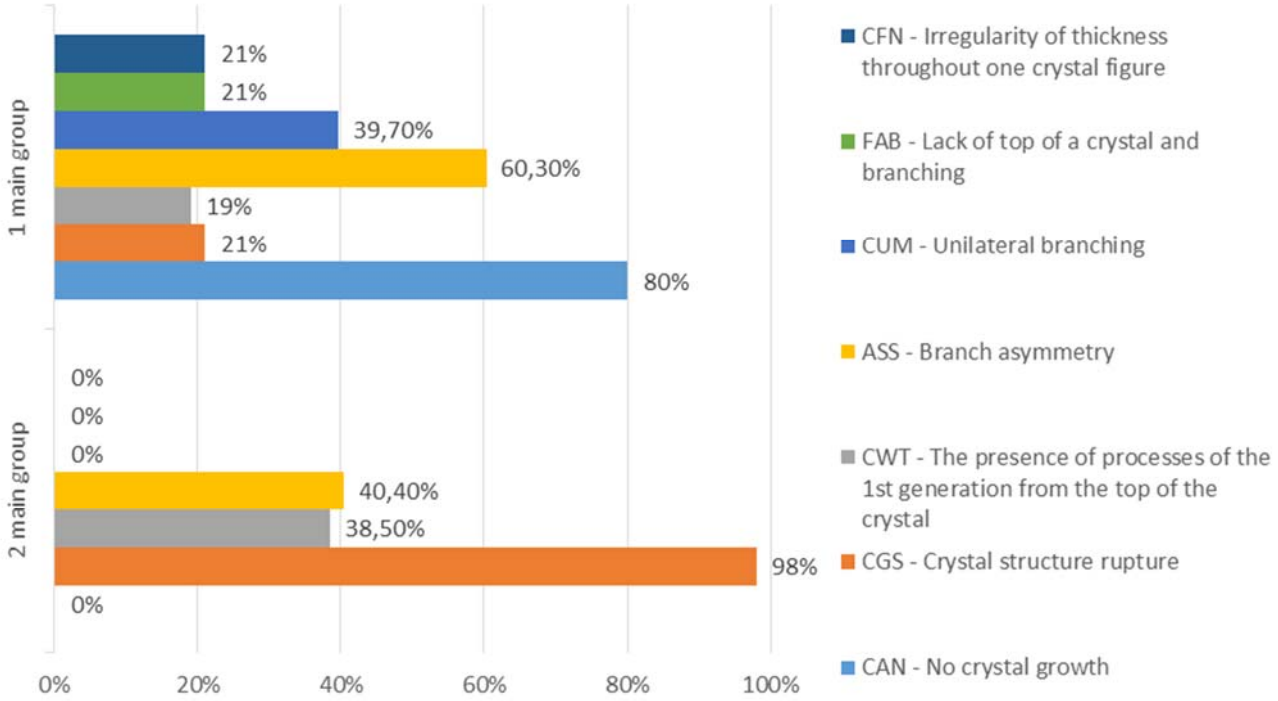

Figure 2. The frequency of detection of qualitative morphological signs in patients of the first and second main groups (as a percentage)

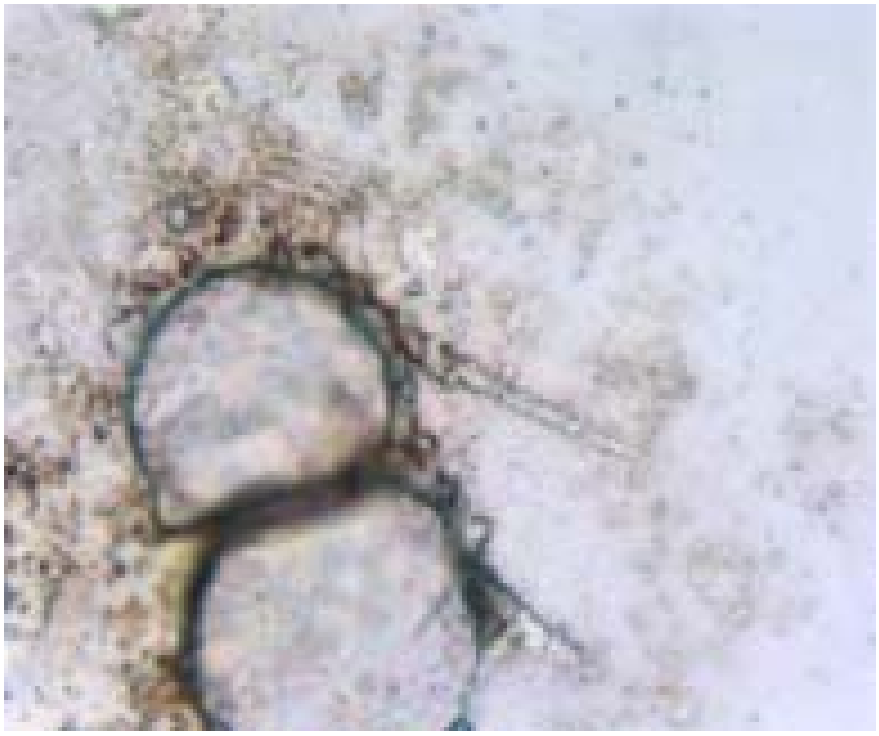

Figure 3. *Needle-like short spines, the lack of crystal growth – CAN*

Downloaded from www.periodico.tchequimica.com

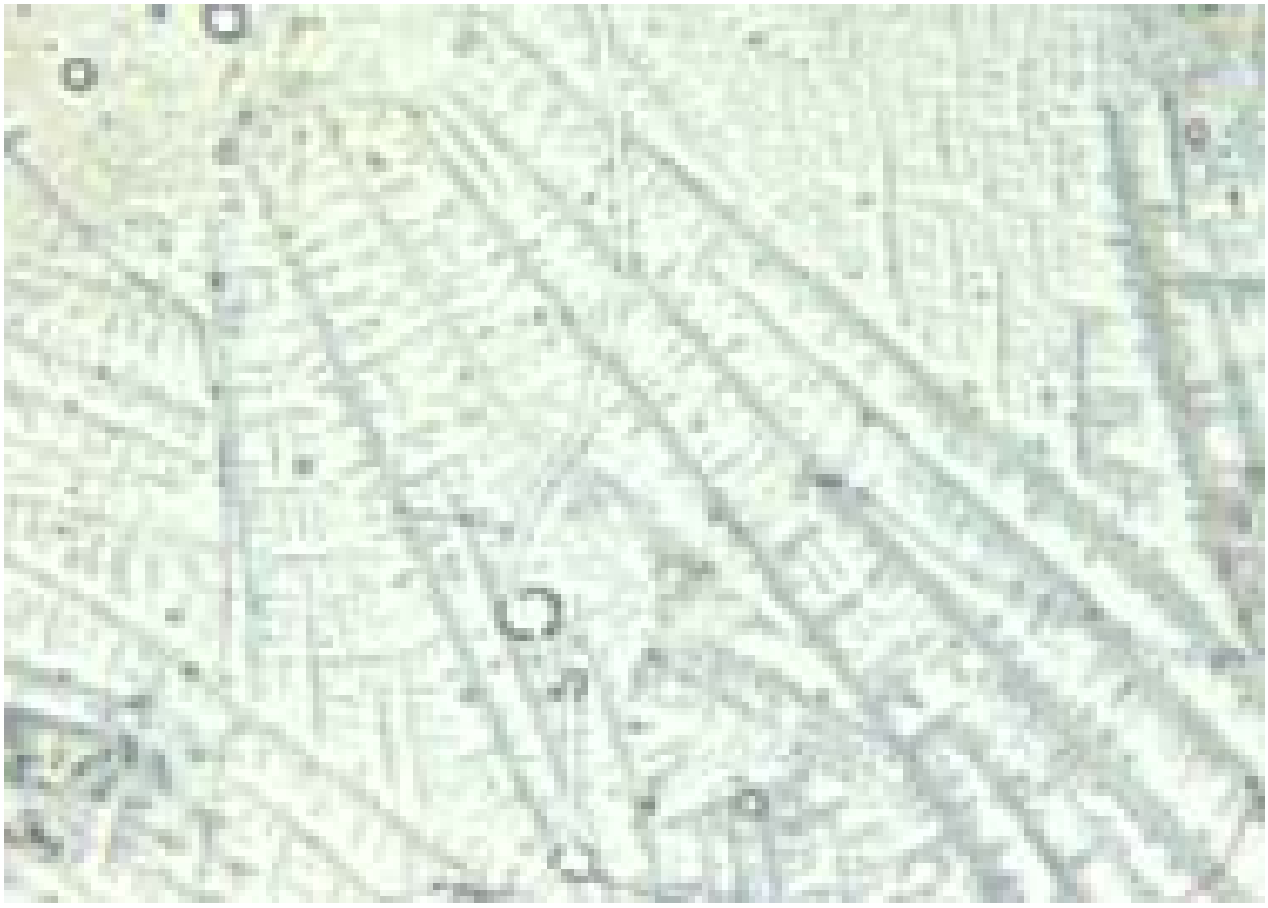

Figure 4. *Gap crystal structure – CGS, Appendix 1-generation departs from the top of the crystal – CWT*

Downloaded from www.periodico.tchequimica.com

PERIÓDICO TCHÊ QUÍMICA
ARTIGO ORIGINAL

DESENVOLVIMENTO DE UM SISTEMA DE MULTIPLICAÇÃO *IN VITRO* PARA *RUBUS LOGANOBACCUS* L.

DEVELOPMENT OF AN *IN VITRO* MULTIPLICATION SYSTEM FOR *RUBUS LOGANOBACCUS* L.

ایجاد سیستم ازدیاد درون شیشه ای برای *Rubus loganobaccus* L.

SAEIDEH, Ekbatan Hamadani[1], HOSSEIN, Lari Yazdi* [2], MOHAMMAD, Hassan Asareh [3], SARA, Saadatmand [4]

[1,4]Islamic Azad University, Science and Research Branch, Faculty of Science, Biology Department

[2]Islamic Azad University, Boroojerd Branch, Faculty of Science, Biology Department

[3]Seed and Plant Certification and Registration Institute

** Correspondence author*
e-mail: Lariyzdi_hossein.iau@yahoo.com

Received 12 June 2019; received in revised form 30 November 2019; accepted 04 October 2019

RESUMO

A variedade *Rubus loganobaccus* L. é um híbrido produzido a partir de um cruzamento *entre Rubus idaeus* e *Rubus ursinus*, conhecido por seus frutos exóticos e distintos. No entanto, ainda não foi introduzido um método comercial de multiplicação econômico, cuja micropropagação como uma técnica confiável poderia ser um procedimento econômico eficiente para gerar materiais vegetais uniformes. Nesse caso, um experimento realizado com gomos de plantas explanta os tratamentos de desinfecção mais adequados, encontrados entre 1 e 5 min em cloreto de mercúrio a 0,1%, no qual gomos saudáveis cresceram sem contaminação por fungos / bactérias. A maior porcentagem de enraizamento (96,66%) e a menor porcentagem de enraizamento (60%) foram observadas nas concentrações de fitohormônios em MS + BA (1 mg·L^{-1}) IBA + (0,1 mg·L^{-1}) e MS + 2ip (1 mg·L^{-1}) + IBA (0,1 mg·L^{-1}), respectivamente. O comprimento médio máximo e mínimo da raiz foram de 3 cm e 1 cm, respectivamente. No estágio de aclimatação da raiz da planta, a porcentagem máxima de vasos sobrevividos e frescos 96,43%, o número médio máximo de ramificações 8,73, o número médio mínimo de ramificações 3,13 nos tratamentos MS + BA (1 mg·L^{-1}) + IBA (0,1 mg·L^{-1}) e meio MS livre de hormônios, respectivamente, o comprimento máximo de ramo 5,22 cm e o comprimento mínimo de ramo 1,71 cm em MS + 2ip (2 mg·L^{-1}) + IBA (0,1 mg·L^{-1}) e AN + BA (1 mg·L^{-1}) + IBA (0,1 mg·L^{-1}), respectivamente, foram observados. No geral, esse protocolo aborda de forma abrangente todo o processo de micropropagação e pode ser ainda mais utilizado na propagação comercial de *Rubus loganobaccus* e produzir materiais vegetais com vantagens superiores aos métodos convencionais.

Palavras-chave: *Hormônios, desinfecção, ácido indol -3-butírico (AIB), meios de crescimento.*

ABSTRACT

The *Rubus loganobaccus* L. variety is a hybrid produced from a cross between *Rubus idaeus* and *Rubus ursinus,* which is well-known for its exatic distinguished fruits. However, a commercial cost-effective multiplication method has not been introduced yet, which micropropagation as a reliable technique could be an efficient economic procedure to generate uniform plant materials. In this case, an experiment carried out using plant buds explants the most appropriate disinfection treatments found out to be 1 to 5 min in 0.1% mercuric chloride in which healthy buds grew with no fungal/bacterial contamination. The highest rooting percentage (96.66%) and the lowest rooting percentage (60%) were observed in concentrations of phytohormones in MS +BA(1 mg·L^{-1}) IBA + (0.1 mg·L^{-1}) and MS + 2ip (1 mg·L^{-1}) + IBA (0.1 mg·L^{-1}), respectively. The maximum and the minimum average root length were 3 cm and 1 cm, respectively. In the acclimatization stage of the plant root, the maximum percentage of survived and fresh pots 96.43%, the maximum average number of branching 8.73, the minimum average number of branching 3.13 in treatments MS + BA(1 mg·L^{-1}) + IBA(0.1 mg·L^{-1}) and hormone-free MS medium, respectively, the maximum branch length 5.22 cm, and the minimum branch length 1.71 cm in MS + 2ip (2 mg·L^{-1}) + IBA (0.1 mg·L^{-1}) and AN + BA (1 mg·L^{-1}) + IBA (0.1 mg·L^{-1}), respectively, were observed. Overall, this protocol comperhensively addresses the whole process of micropropagation and can be further be

Downloaded from www.periodico.tchequimica.com

used in commercial propagation of *Rubus loganobaccus* and produce plant materials with superior advantages over conventional methods.

Keywords: *Hormones, Disinfection, indole -3- butyric acid (IBA), growth media.*

چکیده

واریته *Rubus loganobaccus* L. هیبرید حاصل شده از تلاقی بین *Rubus idaeus* و *Rubus ursinus* می‌باشد که از جهت تولید میوه‌های بسیار جالب توجه شناخته شده است. اگرچه تا کنون روشی مناسب تجاری و از لحاظ اقتصادی به صرفه ارائه نگردیده که از این جهت ریز ازدیادی به‌عنوان روشی مطمئن می‌تواند به منظور تولید مواد گیاهی به شکلی کارآمد و اقتصادی مورد استفاده قرار گیرد. در همین ضمینه آزمایشی صورت گرفت که با استفاده از جوانه‌های گیاه مناسبترین تیمار گندزدایی قرار گیری نمونه‌ها به مدت 1 الی 5 دقیقه در 1% کلرید جیوه مشاهده گردید که در آن جوانه‌های سالم می‌توانند عاری از آلودگی‌های قارچی/باکتریایی رشد نمایند. بالاترین درصد ریشه‌زایی (96.66%) و کمترین درصد ریشه‌زایی (60%) به ترتیب در غلظت‌های MS+ BA(1 mg·L^{-1}) +IBA (0.1 mg·L^{-1}) و MS+ 2ip (1 mg·L^{-1}) + IBA (0.1 mg·L^{-1}) مشاهده گردید. بالاترین و کمترین میانگی طول ریشه نیز به ترتیب 3 و 1 سانتی‌متر مشاهده گردید. در مرحله عادت‌دهی ریشه‌های به شرایط بیرون نیز بالاترین درصد گیاهچه نجات یافته حداکثر 96/43 % حداکثر تعداد میانگین تعداد شاخه جانبی 8/73، حداقل پمیانگین تعداد شاخته جانبی 3/13 به ترتیب در تیمارهای MS+BA(1 mg·L^{-1}) + IBA(0.1 mg·L^{-1}) و محیط کشت MS عاری از هورمون به دست آمد، حداکثر طول شاخه جانبی 5/22 سانتی‌متر و حداقل طول شاخه جانبی 1/71سانتی‌متر به ترتیب در تیمارهای 2ip (2 mg·L^{-1}) + IBA (0.1 mg·L^{-1}) و MS+ AN + BA (1 mg·L^{-1}) + IBA (0.1 mg·L^{-1}) مشاهده گردید. بطورکلی، پروتوکل به دست آمده به صورتی جامع کل فرآیند ریزازدیادی این گیاه را مد نظر قرار داده و می‌تواند بیشتر برای ازدیاد تجاری *Rubus loganobaccus* و تولید مواد گیاهی یا مزایای برتر در مقابل روشهای سنتی مورد استفاده قرارگیرد.

کلمات کلیدی: هورمون، گندزدای، ایندول-3-بوتریک اسید (IBA)، محیط رشد

1. INTRODUCTION:

The *Rubus loganobaccus* variety is a hybrid produced by *Rubus idaeus* and *Rubus ursinus*. The generic name is loganberry and belongs to the family of Rosaceae. Its fruit is red, called the raspberry bear, and it is used as a nutraceutical containing vitamins, fibers, and antioxidants and antimicrobial compounds. The fruits of this plant in European regions are known as healthy snacks (Arencibia, 2013).

This genus is one of the most diverse species in plants, with approximately 740 species (Jennings, 1988). Berries exist not only as fresh fruits but are also generally consumed as frozen fruits, or they are converted into juice, wine, jams, soups, soft foods, and tisanes. In addition, they are used in ice cream and cream of cakes. They are also served beside main courses to make food healthier. The fruit of this plant is rich in vitamin C. One cup of this fruit fulfills 88% of our daily need of vitamin C. Because of its vitamin C, it has antioxidant properties and has the ability to neutralize free radicals (Lee, 2016). Consumption of *Rubus* sp. has grown substantially over the last twenty years. In 1990, the area under cultivation in North America was 4385 hectares, and nearly 90 percent of the product was consumed in the processing industry. (Finn, 2012). Near the valley in Oregon, America food remnants of raspberry have been found that date back to 8000 BCE. The oral tradition of The American Indians (Indigenous peoples of the Americas) has long enjoyed the use of red and black raspberries, and similar fruits in order to take advantage of their medicinal and nutritional properties. (Hummer, 2007). The Rosaceae genus in Iran has 8 herbaceous and shrub often acanaceous species commonly known as raspberries, and often, it is growing in the forest and non-forest shaded areas. Species of Raspberry in Iran are *R. raddeanus, R. ochthodes, R. hyrcanus, and R. persicus,* which in addition to Iran also grow in Russia, Talesh, and the Caucasus (Mozaffarian, 2007). In Rubus loganobaccus species, the plant climbs up to 5 m high (through supporting

Downloaded from www.periodico.tchequimica.com

vegetation). Primocane stems are rounded, or rarely angled, glabrous or with sparse fluff, or non-glandular pilose hairs, prickles -36 mm long, not confined to stem angles. Flowering takes place at the angle of the younger stems. (Evans *et al*., 2007).

Primocane leaves in plants pinnately compound with 3, 5 or 7 leaflets. The leaflets are 5.5 to 8 cm long and 3.5 to 6.5 cm wide. The underpart of leaves is fluffed and generally broadly-ovate to elliptic. The petioles are 3 to 8.5 cm in length. (Evans, 2007) Floricane leaves at the base of the petals contain 3 to 5 leaflets. The length of the leaflets is often 4 to 10.5 cm and 2.5 to 10.5 cm wide. The petiole is 3 to 6.5 cm in length. The inflorescence is subcorymbose with 6 to 12 flowers. The fruits are ovoid to oblong and initially, are green, and when they ripen, they turn dark red to dull black color. Flowering mainly happens late in the spring and summer. (Evans, 2007) Tissue culture is the best way to reduce propagation costs some of the plants (due to mass production) and increases the production of secondary metabolites in medicinal plants. In-plant propagation by tissue culture techniques, which is known as micropropagation, cultivation of apical or axillary buds is used in a suitable and nutrient culture medium. Laboratory plants that have been propagation with this method have been healthy in most species and are more similar and nearer to the actual species.

Micropropagation methods can produce many plants in a short time and can be profitable for off-season production with better market opportunities. Tissue culture provides a quick method for the propagation of fructiferous products and can produce a large number of virus-free, genetically similar plants in a relatively short time and little space without being affected by seasonal variation. The use of *in vitro* micropropagation is more rational and more economical. Methods of biotechnology in the cultivation and production of new raspberry cultivars that are better adapted to local soil and climatic conditions are valuable. The first experiments were carried out for the *in vitro* cultivation of raspberries in 1970. There is also information on how to use this method in Bulgaria. The application of *in vitro* propagation has been documented in a large number of *rubus* cultivars. However, micropropagation requires a lot of experimental research to optimize the conditions in all its stages (Stelkunova, 1970).

2. MATERIALS AND METHODS:

To carry out micropropagation, the plant was obtained from the "CFD" Co. located in Tehran. Several branches that had a leaf (There was an axillary bud in the axil of a leaf) were separated by scissors from the pots. Brushing on branches was done to remove soil and dirt on the branches and leaves. Then the branches were cut with scissors so that each part contains an axillary bud. The parts were placed on a filter and placed on a plastic beaker under running water for 5 hours (Figure 1).

The parts containing the buds were removed with the aid of a forceps and surgical blade. They were then placed in 2 ml vials after being infected. Approximately 2 to 3 weeks later, the buds evolved on isolated parts as a rosette of leaflets. The growth room temperature in which the vials were stored was 24 °C for the day and 18 °C for the night. 16 hours of light and 8 hours of darkness, the intensity of light was 4 to 5 thousand luxuries. (Figure 2). The buds were divided into two groups and were placed into two autoclaved glass containers. There were 2 treatments at this stage:

1) 1 to 5 minutes in 0.1% mercuric chloride
2) 2 to 7 minutes in 0.1% mercuric chloride. In the rooting stage, for each rooting treatment, there were 6 containers (except for treatment 5) in which 5 explants were planted in each glass. The 6 treatments prepared for rooting are shown in Table 1.

In this article, the treatments using the acronym LB are contracted form of the tested loganberry. After the rooting stage, in the respective six treatments and after spending the required time (2 to 3 weeks) for sufficient growth of the plant and its roots (in the growth room), the plants were transferred to the pots filled with soil and kept under the greenhouse condition. In this stage, the plants were removed from the intended treatments (jelly) with the aid of forceps, and after washing the roots with water and removing the jellies, sticking to them (to prevent contamination in the pots), they were transferred to the pots. The plants were planted in a pot and placed in a shaded house where the temperature of the day was 27 °C and the night time temperature was 18 °C and relative humidity was 40 to 50%. To avoid dehydration, plants were covered with transparent plastic covers, which were gradually removed. After 3 weeks of acclimatization, plants continued to grow without

Downloaded from www.periodico.tchequimica.com

cover and in a normal mode. 12 treatments were prepared in accordance with Table 2 in order to obtain the best suitable breeding environment (Proliferation = the number of branches per plant) and the best environment for producing the highest possible branches for this plant. In each container, five explants were planted that, after adequate growth, the plants of each treatment were removed from the sterile containers by forceps and measured with the ruler. The longest branch of each plant was measured. Statistical analysis was performed using SPSS software using Duncan's test.

3. RESULTS AND DISCUSSION:

1.3 Results in primary sterility:

Of the 27 buds in treatment 1, all were healthy and free from fungal and bacterial contamination, and all germinated. Of the 28 buds in treatment 2, there was one fungal contamination, and 22 germinated. (Table 3; Figure 1).

2.3 Rooting results:

The highest percentage of rooting was observed in LB2, and LB6 treatments, and the lowest percentage of rooting was observed in LB4 treatment. The highest mean root length in LB1 and LB2 was by 2-3 cm. The lowest mean root length in LB4 and LB6 was by 1 cm. LB2 and LB3 treatments were produced medium-thick branches and were produced in terms of the thickness of thin branches in LB1, LB4, LB5, and LB6 treatments. In terms of root density, only roots of LB4 treatment had moderate density. In the remnant treatments (LB1, LB2, LB3, LB5, and LB6) in LB2, LB3, and LB5 treatments, secondary roots were produced, and in LB1, LB4 and LB6 treatments, the secondary roots were not produced (Table 4). As shown in Graphic 2, the highest percentage of rooting (96.66 %) is in treatments 2 and 6. The lowest percentage of rooting (60) is in treatment 4 (Table 4; Figure 2). A container containing rooting treatment (2 b) Container containing rooting treatment (1) c) Container containing rooting treatment (3) d) Container containing rooting treatment (4) e) Container containing rooting treatment (5) f) Container containing rooting treatment (6).

3.3 The result of soil root acclimatization

In the stage of acclimatization of the roots of the plants, the highest percentage of survived and fresh pots in treatment 6 was seen (96.43). The lowest percentages of survived and fresh were seen in treatment 2 (45/45). The highest percentage of droopy pots in treatment 2 was seen (54/55). The lowest percentage of droopy pots was seen in treatment 6 (3.57%). The quality of plants grown in the pots was good, and the most extended plant stem length (in pots) was for treatment 6. The lowest plant stem length (in pots) belonged to treatment 2 (Table 5; Figures 3, 4, 10).

4.3 Branching

In all treatments, plants in the containers, in addition to the micropropagation coefficient (branching) and the measurement of the length of the branches, were examined in terms of being survived and fresh, being green, branching thickness, and rooting potential (Figure 5 and 6). In the branching stage, 12 treatments were used, with the highest average branching (8.73), which belongs to LB2 treatment.

The lowest branching average (3.13) is for LB10 treatment. In LB1, LB3, LB4, LB5, LB6, LB7, LB8, LB9, and LB12 treatment roots were not produced, and in LB2 treatment, 87.33% of the plants did not produce root, and 12.97% of the plants produced root. In all treatments, different thicknesses of the branches were seen from very thin, thin, medium to thick. In LB1, LB2, LB3, LB7, LB8, and LB9, LB10, LB11, and LB12 treatments, 100% of plants' leaves were green. In LB4, LB5, and LB6 treatments, all leaves were not green, and a small percentage was yellow. In all treatments, 100% of the plants were fresh, and drooping was not seen (Tables 6 and 7; Figure 11).

At first, *in vitro* propagation was conducted by Broome and Zimmerman (1978) on Blackberry Bramble and Harper (1978) on Black raspberry. Since then, several reports have been published in the *in vitro* propagation of Rubus species. Zimmerman *et al*., (1986) concluded in their study that the best medium for cultivating tissue of different cultivars of raspberry was MS medium (Klokonos, 1986). In a 1985 study, Welander reported that a very poor proliferation rate was obtained from only shoot tips, but better results were achieved with nodal segments. (Welander, 1985).

In a study by Stoevska *et al*. on *Rubus Idaeus* in 1995, apical and axillary buds on active-growing, one-year shoots of Alena Shopska and Samodiva (two cultivars of *Rubus Idaeus*) plants have been used. This study was conducted to determine the possibility of micropropagation. The initial development of the explants and propagation was done in 2 media.

The medium of V2 (Anderson) with 1,

Downloaded from www.periodico.tchequimica.com

2.5, and 5 mg·L^{-1} concentrations of BAP and MS medium with concentrations of 0.1, 0.5, and 2 of IBA was used. Medium V1 was found to be more appropriate. The best propagation coefficient for the Alena Shopska variety was 6.86 ±0.13, and for the samodiva variety, it was 5.53 ± 0.24. They also concluded that the length of the branches decreased as BAP concentration increased. The percentage of rooted shoots extremely was affected by the composition of the nutrient medium and the concentration of IBA. The use of higher Auxin doses of IBA 2 mg·L-1 resulted in the formation of undesirable calluses in the root of the micro-cutting, and the developed roots remained short and backward (Stoevskaya et al., 1995).

In a study conducted by Valentina Isac and *et al*. in 2012 on the micropropagation of several cultivars of Rubus Idaeus, it includes: (Ruvi, Citria, Gradina, Heritage, Cayuga, The Latham, Malling Promise, Malling Exploit, Willamette, Gustar, Vely, Autumn Bliss and Opal). Transfer explants were grown on the original medium to a nutrient medium with 3.0 mg·L^{-1} BA and 0.1 mg·L^{-1} IBA to stimulate differentiation of axillary buds. The raspberry micropropagation takes place over 25-30 days with the MR of 15 to 41.9 (plantlets / explant), depending on the variety. It is relevant that in *in-vitro* routine micropropagation work, more than 2/3 of raspberry varieties have had MR higher than 6 reaching a maximum of 41.9 shoots per initial explant in 'Ruvi' (Valentina Isac, 2012).

In a study, conducted by Jafari Najaf-Abadi and her colleague in 2009 in Iran, to provide the best conditions for *in vitro* propagation of the thornless trailing blackberry, axillary buds were used as explants. Explants were cultured on MS medium containing 2 mg·L^{-1} BA. In a two-weeks period afterward, to proliferate shoots, 12 various treatment with culture medias MS and AN and hormonal concentrations 3 of BA (0, 2 and 3 mg·L^{-1}), single or with GA3 (0, 0.2, 0.5 and 1 mg·L^{-1}) were used. The most significant number of branches with an average of 3.33 and the maximum branch length with an average of 5.87 cm was produced in medium containing 2 mg·L^{-1} BA and 0.5 mg·L^{-1} GA3 and in the experiment involving the application of various levels of IBA (0, 0.5, 1 and 2 mg·L^{-1}) added to MS medium used to evaluated rooting formation in plantlets. A concentration of 2 mg·L^{-1} IBA creates a more significant number of roots and maximum root length. In this medium, four roots with a root length average of 7.83 cm were produced. Of the hardened *in vitro* produced plants approx. ofter 30 days, 85% of rooted micro-cutting tolerated the open-field condition and completely adopted. In order to increase the growth of axillary buds and reduce the apical dominance in shoot cultures, one or more cytokinins are commonly incorporated into the medium at the propagation stage (Jafari Najaf-Abadi and *et al*., 2009). Bobrowski *et al*. (1996) reported that the best medium to propagate branch in blackberry was obtained in MS medium with BA (1.0 and 2.0 mg·L^{-1}). But GA3 didn't improve the propagation rate.

In research on *Rubus* species reported that if BA concentration decreased by 2 mg·L^{-1}, the propagation of axillary buds would not increase, and when the concentration of BA increases to 4 mg·L^{-1}, the propagation of axillary buds decreases. They found that GA3 was essential for propagation in three of the four species used and had significant effects on the complex hormone system. It was known that GA3 could synergistically act with auxins (Wei, 1992).

In 2005, Villa and others selected blackberry axillary buds as explants, and after sterilization, they transferred MS culture medium to 2 mg·L^{-1} BA. The greatest number of branches with an average of 3.33 and the maximum branch length with an average of 5.87 cm was produced in medium containing 2 mg·L^{-1} BA and 0.5 mg·L^{-1} GA3 (Villa and *et al.*, 2005).
Gonzales *et al*. (2000) conducted a study on three species of blueberries (*Vaccinium* cultivar), blackberry (Smoothstem cultivar), and raspberry (Gradina cultivar). Blueberry germination was achieved in WPM with MS vitamins for 15 days and then 30 days in the same culture medium with Zeitin mM 18. The best result was obtained in the same culture medium as mM 25 2ip. (Gonzales *et al*., 2000).

Jin-Hu Wu *et al.* (2009) investigated the factors affecting the efficiency of micropropagation of 32 selections of Rubus. They studied the pre-treatment and early culture phases. Using a Chilling temperature at 4°C in a 6-week period as a pre-treatment led to the enhancement of establishing stage under *in vitro* condition; it was witnessed that 65% of cultures post chilling had normal healthy growth. Hormonal factors such as BA found to be the most appropriate among the three media considered to improve branch development, 3 to 7 branches, or developed plantlets in average recorded per nodal explant. Modification of the level of BA from 0.5 mg·L^{-1} to 3 mg.L^{-1} in a sub-culture to another positively improved the

Downloaded from www.periodico.tchequimica.com

difficulties involved in Rubus micropropagation with long-term exposure to the high levels of BA. The decrease in chlorosis accompanied by enhancement of the quality of plant materials through lowering the concentration of MS macro- and micro-elements to one-third, with combination with0.49 µM IBA and 0.05% activated charcoal, ultimately subjected to the low light intensity (17 µmol m^{-2} s^{-1}). Since response to *in vitro* condition varied considerably, therefore various micropropagation protocols were applied depending on the genotype (Jin-Hu *et al*., 2009).

In a study conducted by Djurdjina Ruzic and his colleague in 2006, the blackberry cultivar Čačanska bestrna was successfully micropropagated. Buds from the branches cut during dormancy (end of January) were used as the initial explants. MS media with BA and IBA or NAA and GA3 were used for the propagation stage. The most significant values of the propagation index were obtained on medium within BA 1.0, IBA 0.1, and GA3 0.1 mg·L^{-1}. The branches had small nodular callus and a high number of bud rudiments in the basal section of branches (Ruzic, 2006).

In a study, Alexandru (2016) presented a protocol for the regeneration of *Rubus loganobaccus* by *in vitro* micropropagation. The Apical buds were used as the explants in the MS culture medium. Branch regeneration was done on MS 100% media gelled with plant agar with different concentration of BAP (0.3; 0.4; 0.5; 0.6 mg·L^{-1}). Results were obtained on 0.3 and 0.4 mg.L^{-1} concentration of BAP, at higher concentrations (0.5, 0.6 mg·L^{-1}) the buds inhibited. The highest branch regeneration results were obtained on MS medium containing BAP (0.4 mg·L^{-1}), generating a number of 8 branches per test tube. When BAP concentration increased above 0.5 mg·L^{-1}, the propagation rate of branches decreased (Mîrza Alexandru, 2016). Georgieva *et al.* (2016) in a protocol for the propagation of berries by Bioreactor, reported that propagation (in MS medium supplement 0.05 BAP mg.1 / 05 mg.L^{-1}, 1 IBA and 0.03 GA3), mg.L^{-1}, 130 mg·L^{-1}, sucrose) and rooting (MS without hormones supplement 30 gr l sucrose) in a solid medium strawberry plants propagation coefficient for 4 weeks was 1.9 (Georgieva, 2016).

In 2006, Zawadzka and Orlikowska conducted a study on the factors affecting the micropropagation of the five cultivars of Raspberry Red (Beskid, Canby, Malling Seedling, Norna, Veten) using MS culture medium. There was no significant difference in the number of leaves obtained from branches cultured on media containing TDZ or BAP. The regeneration medium contained 0.1 mg·L^{-1} TDZ. At higher concentrations, TDZ caused leaf blackening or induced hyperhydration, usually followed with necrosis of the adventitious branches. From the three auxins tested, IBA (IBA, IAA, and NAA) effectively induced micropropagation in all of the cultivars, and NAA gave poor results with all of the cultivars tested (Zawadzka, 2006).

In a study conducted by Jafari Najaf Abadi and her colleagues in 2011 in Iran to study the micropropagation of thornless raspberries by using axillary bud explants, axillary buds were chosen as explants. After sterilization, they transferred the MS culture medium to 2 mg·L^{-1} BA. After 2 weeks, the explants were transferred to a proliferation culture medium containing 12 growth regulators of BA (0, 2 and 3 mg·L^{-1}) and GA3 (0, 0.2, 0.5, and 1 mg·L^{-1}). The greatest number of branches with an average of 3.33 and the maximum branch length with an average of 5.87 cm was produced in medium containing 2 mg·L^{-1} BA and 0.5 mg·L^{-1} GA3. In rooting treatment, basic MS culture medium with 4 IBA concentrations was used. The concentration of 2 mg·L^{-1} IBA produced the highest (4 roots) and the longest root (7.83 mm long) (Jafari Najafabadi, 2009).

Mozaffarzadeh *et al.* (2014) in Iran, the effect of culture medium on the micropropagation of the idaeus *Rubus* raspberry plant using axillary buds in two different culture medium was studied. The axillary buds were cultured on MS medium, and after one-month elongated branches were cut and transferred to the different culture mediums (MS and ½ MS supplement BA hormone 1 mg·L^{-1} and GA3 0.5 mg·L^{-1}) in four replications for proliferation experiments. After one month, the proliferation traits such as a number of nodes and stem length were measured in different treatments, and the average of the traits was compared using variance analysis. The best medium for micropropagation of this plant was MS medium (Mozaffarzadeh, 2009). Jin-Hu *et al*., in a 2009 study, concluded that thornless genotypes were easier to start than the bramble genotypes because there was little contamination. Apical buds were more straightforward to cultivate than axillary buds because the cultures that started from the apical buds produced several branches at a faster rate than those produced by axillary buds. However, axillary buds are still reliable

Downloaded from www.periodico.tchequimica.com

explants source, especially if the initiation cultures stage is developed for multi-branch evolution. (Jin-Hu *et al*., 2009).

In order to establish the optimal conditions for micropropagation in two raspberry cultivars Rasberry (Opal, Cayuga), the results showed that generally, stimulation of multiple shoots or bud formation is achieved by culturing explants on medium supplemented with relatively high levels of cytokinins. TDZ has been shown to promote branch regeneration in woody plant species. The TDZ induced organogenesis via a reduced dominance of the apical meristem, resulting in the formation of adventitious and/or axillary buds directly on the cultured branch tips. Cytokinins act early during branching initiation to control meristem activity and GAs act at later stages, regulating cell division and expansion to control shoot elongation.

Various factors can influence the response of explants culture, including the maternal genotypes, its growing conditions, and the time of the choice of the explants, the culture medium, and the culture conditions. In general, the replication of selected explants is not only influenced by different species of plants but also in a particular species, and different genotypes have different replication. Generally, it is better that young tissue of living cells should be used as explants because young tissue-forming cells have small vacuole, and the ratio of the nucleus to the whole cell is high (Omidi, 2015). Applying appropriate methods for selecting and sterilizing healthy explants can significantly affect the success of the plant tissue culture project. Two of the most important physical factors affecting cultivars are heat and light. In general, more cultures are kept at a temperature of 20 to 28 °C. It should be noted that in many species, there is a direct relationship between the proper temperature of the tissue culture and the proper temperature of the maternal plant in normal conditions. (Omidi, 2015).

Light is used as an indispensable factor in the differentiation and morphogenesis cultivars. The most common light used in tissue culture is light from a fluorescent lamp that has some red light in its range. One of the reasons for using a Fluorescent lamp in tissue culture is low heat production. Photoperiod can be effective in controlling sleep and germination of cells, and its effect is similar to the effect of cytokinins. Although tissue culture of genotypes and different plant species has different responses to light, a photoperiod of 16 hours is recommended in most cultures for regeneration (stemming). In some experiments, the adverse effects of light on the root have been reported Seedlings obtained from tissue culture have an incomplete cuticle and often have an inappropriate root system. When these seedlings are transported to the soil, they quickly undergo water shortage, growth retardation, and even death. To resolve this problem, it is essential to create proper roots and to acclimatize to the soil conditions (Omidi, 2015).

5. CONCLUSIONS:

Factors affecting the micropropagation process in *Rubus loganobaccus* vary remarkably, which in this study, the phytohormonal factor found to be a significant factor in branching. Additionally, rooting as another critical step in the production of micropropagated plants showed a significant dependency on hormonal treatments. In general, in this multi-purpose study, a considerably effective disinfection method for *Rubus loganobaccus* bud explants was developed in addition to a multiplication system with high branching and the rooting rate, which can be employed in commercial propagation programs. All the abovementioned outcomes could be advantageous when it comes to production of propagation material of *Rubus loganobaccus* and enable the producer to lessen their costs while increasing their rate as well as financial benefits.

6. ACKNOWLEDGMENTS

We would like to thank Azad Islamic University Science and Research Branch for supplying laboratory equipment to this study.

7. REFERENCES

1. Alexandru, M. *J. Botany*. 2016, 1 (12).
2. Alional, M., Petronenal, CR., Marius, D. U.S.A.M.V. Iasi, Romania. 2003.
3. Ariel, D., Vergara, A. C., Quiroz, K., Carrasco, B., Gonzales, G. R. *Scientia Horti*. 2013, (160):49-53.
4. Bobrowski, V. L., Mello-Farias Paulo, C., Peters, J. A. *Rev Bras De Agrociencia*. 1996, (2): 17-2.
5. Evans, M., Hains, E. R., Arate, K. *Aust. Syst. Botany*. 2007, (20): 187-251.
6. Finn, C. E., Clark, J.R. *Springer Sci.* 2012, 151-190..

Downloaded from www.periodico.tchequimica.com

7. Georgieva, L., William, S. *J. Agri. Sci*. 2016, 22 (5): 745–751.
8. Gonzales, M. V., Lopez, M., Valdes, A. E., Ordas, R. J. *Ann. App. Biol*. 2003; 137: 73–78.
9. Hummer, K.E., Janick, J. *Acta Horti*. 2007, (759): 89-10.
10. Isac, V., Coman, M. *Fruit growing Res. J*., 2012: 28:1-6.
11. Jennings, D. L. Academic, London, 1988;pp. 193.
12. Jin-Hu, H. T. *Plant Cell Tiss Organ Cult*. 2009, (99):17–25.
13. Klokonos, N. P., Solov-eva, I. I. 1986, (9):44-47.
14. Lee, J. *NFS J*. 2016, (2): 15–18.
15. Mozafarzadeh, F. The 13th Iranian Conference on Plant Breeding and the 3rd Iranian Seed Science and Technology Conference, Tehran, Iran. 2013.
16. Mozaffarian, V. A Dictionary of Iranian Plant Names Latin,English, Persian, Farhang Moaser Publication, Tehran, Iran, 2007.
17. Najafabadi, A. J. The 7th Iranian Horticultural Congress , Tehran, Iran, 2011.
18. Najaf-Abadi, A. J., Hamidoghli, Y. *Aust. J. Crop Sci.* 2009, 3(4):191-194.
19. Omidi, M. *Tehran Uni. Press*, 2015, 6-13.
20. Ruzic, D. *Agriculturae Conspectus Scientifcus*. 2006, 71 (4) : 149-153.
21. Sobczykiewicz, D. *Springer, Berlin*. 339–353.
22. Stelkunova S. E., Popov Lu. G. *Physiol. Na rasteniata*. 1970, (17): 618-622.
23. Stoevska, T., Trifonova, A., Karadocheva, D*. Biotechnol. Equip*. 1995 (9): 27-30.
24. Villa, F., Araujo, AG., Salles Pio. LA., Pasqual, M. *Ciênc agrotec, Lavras*. 2005, 29(3): 582-589.
25. Wei, J., Ying, G., Shen-zhi, Z. *Scientia Horti*. 1992, (49): 335-340.
26. Welander, M. J. *Horti. Sci*. 1985, (60):493-499.
27. Zawadzka, M., Kasel, J. F. *Ornam. Plant Res*. 2006 (14): 105-115.
28. Zimmerman, RH. *Kluwer, The Netherlands*, 1991, 231–246.

Table 1. *Specification of rooting treatments*

Treatment No.	Treatment name	Specifications of each treatment
1	LB1	MS – H
2	LB2	MS+ 1/2 NH_4NO_3 +1/2K(NO_3)
3	LB3	MS+1/2 NH_4NO_3 +1/2K(NO_3)+ IBA(0.1) mg
4	LB4	MS+1/2 NH_4NO_3 +1/2K(NO_3)+ IBA(0.1) mg + sucrose
5	LB5	MS+1/2 NH_4NO_3 +1/2K(NO_3) + IBA(0.5) mg
6	LB6	MS+1/2 NH_4NO_3 +1/2K(NO_3) + IBA(1) mg

Introduction of treatments Table 1:
Treatment No. 1 (LB1): MS-H: (Murashige and Skoog medium) - Hormone
Treatment No. 2 (LB2): MS + 1/2 NH_4NO_3 + 1/2$(NO_3)_2$
Treatment No. 3 (LB3): MS + 1/2 NH_4NO_3 + 1/2$(NO_3)_2$ and indole -3- butyric acid (IBA) 0.1mg
Treatment No. 4 (LB4): MS + 1/2 NH_4NO_3 + 1/2$(NO_3)_2$ and indole -3- butyric acid (IBA) 0.1mg + sucrose
Treatment No. 5 (LB5): MS + 1/2 NH_4NO_3 + 1/2$(NO_3)_2$ and indole -3- butyric acid (IBA) 0.5mg
Treatment No. 6 (LB6): MS + 1/2 NH_4NO_3 + 1/2$(NO_3)_2$ and indole -3- butyric acid (IBA) 1mg

Downloaded from www.periodico.tchequimica.com

Table 2. *Information on twelve branching treatments*

Treatment No.	Treatment name	Specifications of each treatment
1	LB1	MS + BA(0.5) mg 2ip(0.5) mg IBA(0.1) mg
2	LB2	MS + BA(1) mg IBA(0.1) mg
3	LB3	MS + BA(2) mg IBA(0.1) mg
4	LB4	MS + 2ip(1) mg IBA(0.1) mg
5	LB5	MS + 2ip(2) mg IBA(0.1) mg
6	LB6	MS + BA(1) mg 2ip(1) mg IBA(0.1) mg
7	LB7	MS + BA(0.5) mg 2ip(0.5) mg IBA(0.5) mg
8	LB8	MS + BA(0.5) mg 2ip(0.5) mg IBA(0.1) mg GA(0.5) mg
9	LB9	IBA(0.1) mg GA(0.5) mg BA(1) mg 2ip(1) mg + MS
10	LB10	MS – H
11	LB11	IBA(0.1) mg BA(1) mg + (AN)
12	LB12	IBA(0.1) mg BA(0.5) mg 2ip(0.5) mg + (AN)

Introduction of treatments Table 2:

Treatment No. 1 (LB1): Murashige and Skoog medium (MS) + Benzyl adenine (BA) 0.5 mg, 2ip (isopentenyidenine) 0.5mg, indole -3- butyric acid (IBA) 0.1 mg
Treatment No. 2 (LB2): Murashige and Skoog medium (MS) + Benzyl adenine (BA) 1 mg, indole -3- butyric acid (IBA) 0.1 mg
Treatment No. 3 (LB3): Murashige and Skoog medium (MS) + Benzyl adenine (BA) 2 mg, indole -3- butyric acid (IBA) 0.1 mg
Treatment No. 4 (LB4): Murashige and Skoog medium (MS) + 2ip (isopentenyidenine) 1mg, indole -3- butyric acid (IBA) 0.1 mg
Treatment No. 5 (LB5): Murashige and Skoog medium (MS) + 2ip (isopentenyidenine) 2mg, indole -3- butyric acid (IBA) 0.1 mg
Treatment No. 6 (LB6): Murashige and Skoog medium (MS) + Benzyl adenine (BA) 1 mg, 2ip (isopentenyidenine) 1 mg, indole -3- butyric acid (IBA) 0.1 mg
Treatment No. 7 (LB7): Murashige and Skoog medium (MS) + Benzyl adenine (BA) 0.5 mg, 2ip (isopentenyidenine) 0.5mg, indole -3- butyric acid (IBA) 0.5 mg
Treatment No. 8 (LB8): Murashige and Skoog medium (MS) +Benzyl adenine (BA) 0.5 mg, 2ip (isopentenyidenine) 0.5mg, indole -3- butyric acid (IBA) 0.1 mg, Gibberellic acid (GA) 0.5 mg
Treatment No. 9 (LB9): Murashige and Skoog medium (MS) + indole -3- butyric acid (IBA) 0.1 mg Gibberellic acid (GA) 0.5 mg, Benzyl adenine (BA) 1 mg, 2ip(isopentenyidenine)1 mg
Treatment No. 10 (LB10): Murashige and Skoog medium (MS) – Hormone
Treatment No. 11 (LB11): Anderson (AN) + indole -3- butyric acid (IBA) 0.1 mg Benzyl adenine (BA) 1 mg
Treatment No. 12 (LB12): Anderson (AN) + indole -3- butyric acid (IBA) 0.1 mg Benzyl adenine (BA) 0.5 mg 2ip (isopentenyidenine) 0.5 mg

Table 3. *Sterile treatment results*

Treatment name	number	Duration of stay in treatment	Contamination (bacterial, fungal)	Final Health (Germinated Number)
1	27	5 minutes	--	27
2	28	7 minutes	1	22 (5 were not germinated)

Downloaded from www.periodico.tchequimica.com

***Table 4**. The results of the effects of rooting treatments*

Treatment name	Average of rooting	Percentage of rooting	The average length of roots	Branch thickness	roots density	secondary roots
LB1	23	76.66	2-3 cm	Thin	High	Not have
LB2	29	96.66	3 cm	medium-thick	High	have
LB3	28	93.33	1-2 cm	medium-thick	High	have
LB4	18	60	1 cm	Thin	Medium	Not have
LB5	32	91.42	1-2 cm	Thin	High	have
LB6	29	96.66	1 cm	Thin	High	Not have

***Table 5**. Root acclimatization results*

Rooting treatment No.	Total number of pots containing this treatment	Number of survived and fresh pots	Percentage of survived and fresh pots	Number of droopy pots	Percentage of droopy pots	Quality	Plant stem length
1	25	15	60	10	40	Good	1-3 cm
2	22	10	45.45	12	54/55	Good	1-2 cm
3	27	25	92,60	2	7/40	Good	3-5 cm
4	19	17	89.47	2	10/53	Good	1-3 cm
5	32	26	81/25	6	18/75	Good	3-5 cm
6	28	27	96/43	1	3/57	Good	2-6 cm

Downloaded from www.periodico.tchequimica.com

***Table 6**. Branching treatments results*

Treatment name	Average branching	Rooting / lack of root	Branch thickness	Green / yellow plant	Fresh/ droopy plant
LB1	7.76	No Root 100	Thin 23.30 Medium 51.93	Green 100	Fresh 100
LB2	8.73	No Root 87.03 Rooting 12.97	Very thin 45.80 Thin 41.22 Medium 12.97	Green 100	Fresh 100
LB3	6.28	No Root 100	Thin 47.77 Medium 52.22	Green 100	Fresh 100
LB4	7.03	No Root 100	Thin 40.75 Medium 37.91 Thin to medium 21.32	Green 93.83 Yellow 6.11	Fresh 100
LB5	6.10	No Root 100	Thin 75.26 Medium 11.57 Thick 13.15	Green 96.31 Yellow 3.68	Fresh 100
LB6	6.25	No Root 100	Thin 51.2 Thick 48.8	Green 75.2 Yellow 24.8	Fresh 100
LB7	6.40	No Root 100	Medium 100	Green 100	Fresh 100
LB8	3.88	No Root 100	16.49 Thin 83.5 Medium	Green 100	Fresh 100
LB9	3.16	No Root 100	36.84 Thin 63.15 Medium	Green 100	Fresh 100
LB10	3.13	Long and multiple roots 100	84.04 Medium 15.95 Thick	Green 100	Fresh 100
LB11	4.56	No Root 100	36.84 Medium 63.15 Thick	Green 100	Fresh 100
LB12	5.28	No Root 100	16.66 Thin 83.33 Medium	Green 100	Fresh 100

Downloaded from www.periodico.tchequimica.com

Table 7 - *Branch length results*

Raw	Treatment name	The average branch length of each treatment
1	LB1	3.11 cm
2	LB2	3 cm
3	LB3	1.86 cm
4	LB4	2.46 cm
5	LB5	1.71 cm
6	LB6	2 cm
7	LB7	2.33 cm
8	LB8	2.2 cm
9	LB9	1.8 cm
10	LB10	4.48 cm
11	LB11	5.22 cm
12	LB12	1.8 cm

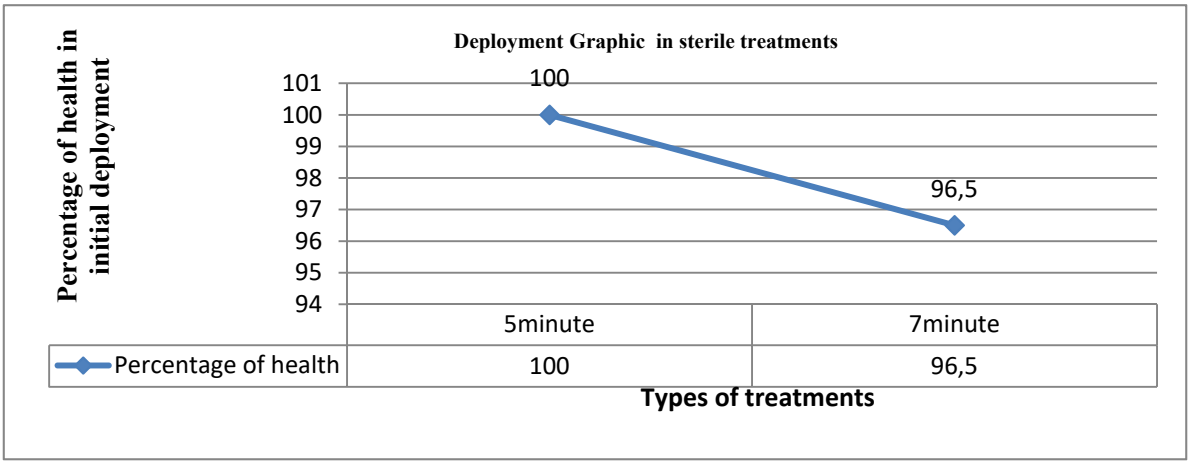

Figure 1. *Deployment graphic in sterile treatments*

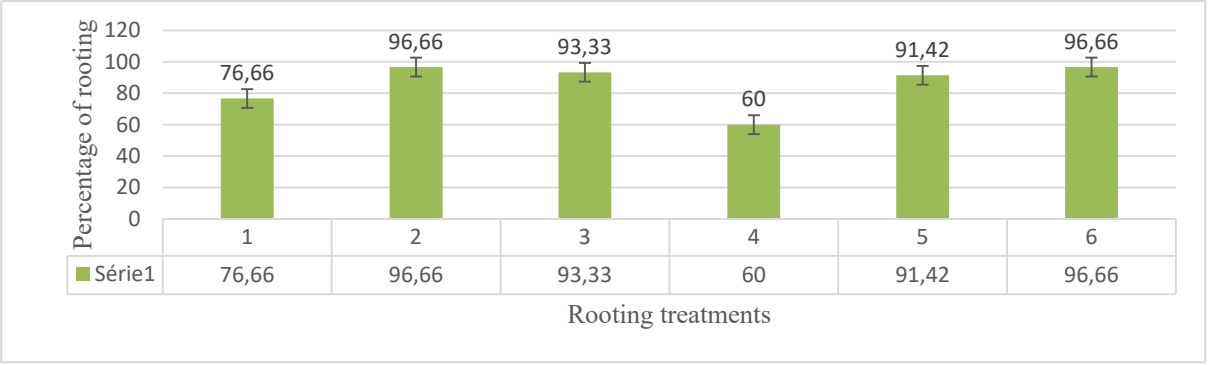

Figure 2. *Comparison of treatment rooting percentage*

Downloaded from www.periodico.tchequimica.com

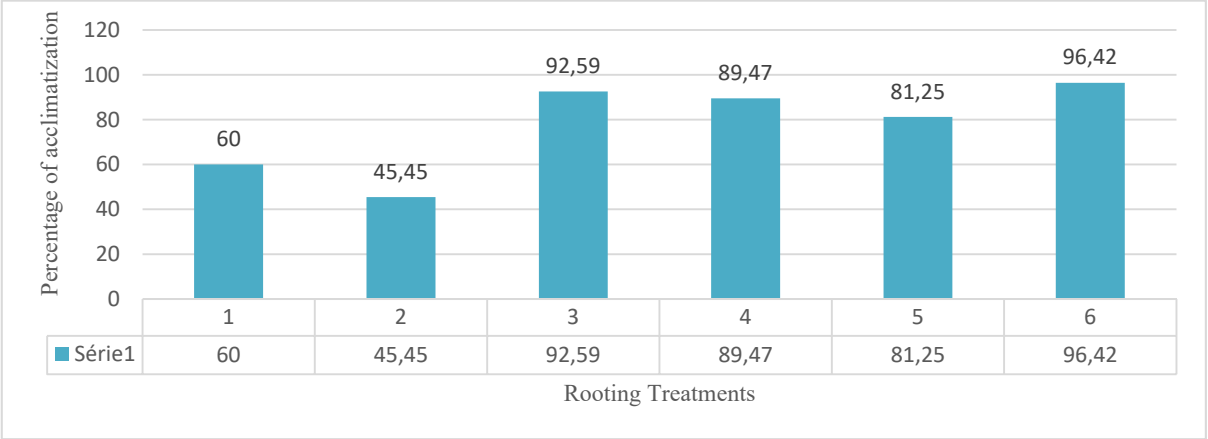

Figure 3. *Comparison of rooting treatments acclimatization in soil*

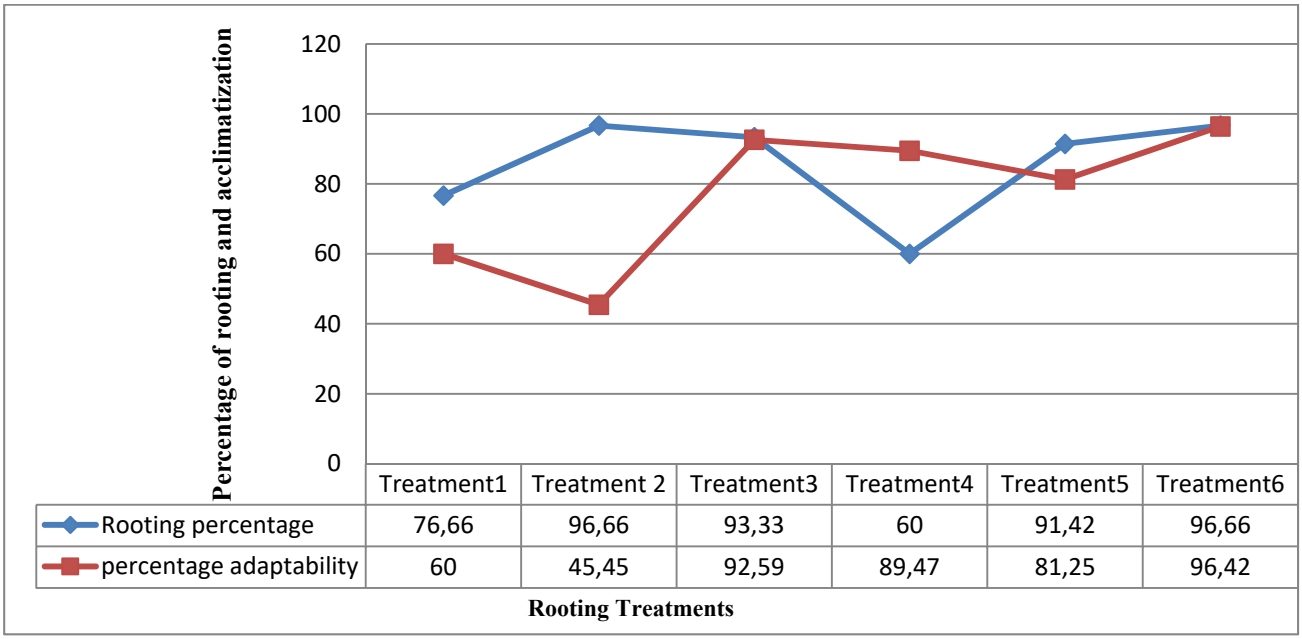

Figure 4. *Comparison of rooting and acclimatization percentage of the root in the soil*

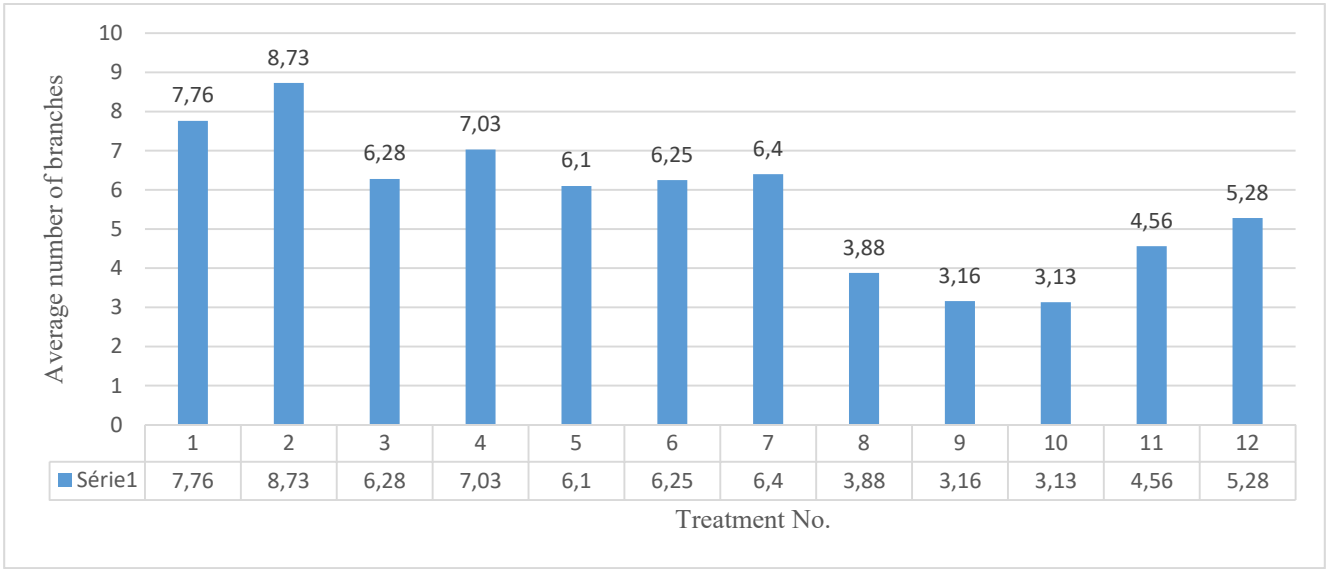

Figure 5 *: Comparison of the percentage of branching of the treatments*

Downloaded from www.periodico.tchequimica.com

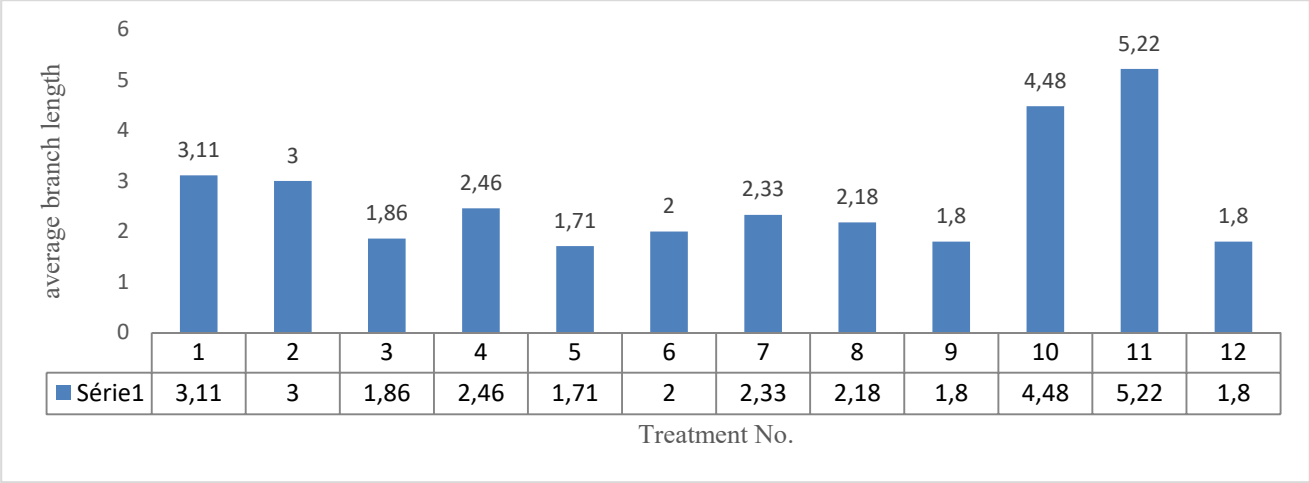

***Figure 6**: Comparing of branch length of branching treatments*

***Figure 7**. Plant specimen in a pot within the greenhouse*

***Figure 8**. Initial parts (containing buds) planted in vials before and after the production of leaflets.*

Downloaded from www.periodico.tchequimica.com

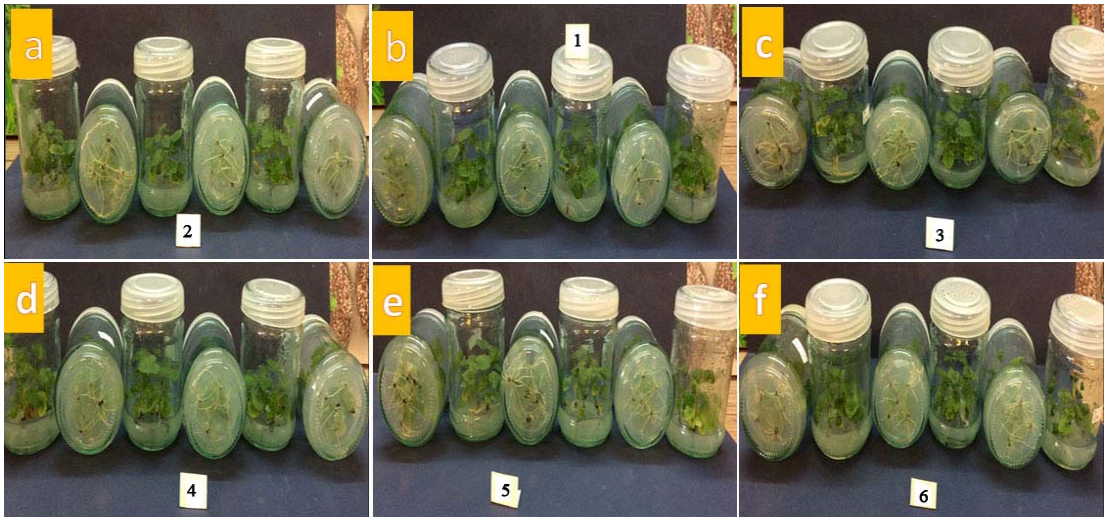

Figure 9. *Rooting images in relevant treatment*

Figure 10. *Rooting treatments at the stage of acclimatization to the soil.*

Downloaded from www.periodico.tchequimica.com

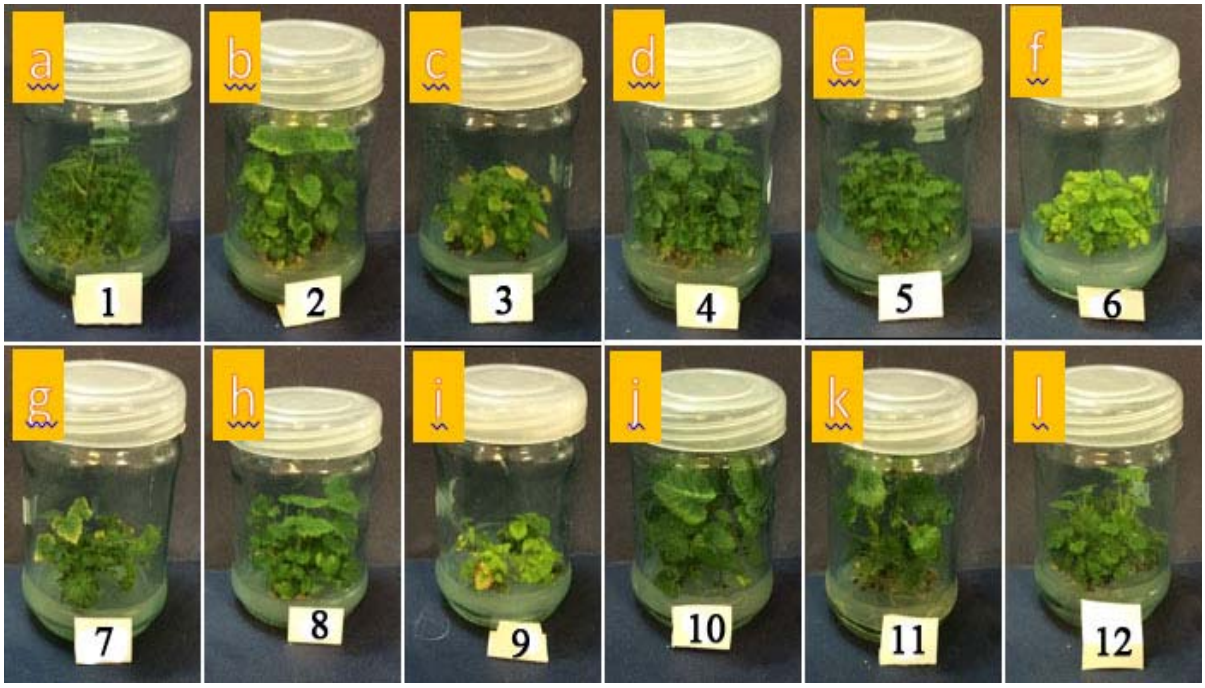

Figure 11. *Containers were containing branching treatment (1 to 12) after branching.*

PERIÓDICO TCHÊ QUÍMICA
ARTIGO ORIGINAL

O ENSINO DE QUÍMICA E O ALUNO DO ENSINO MÉDIO: UM ESTUDO DE CASO NA EDUCAÇÃO BÁSICA ESTADUAL DO MUNICÍPIO DE ESTEIO, BRASIL.

THE CHEMISTRY TEACHING AND THE HIGH SCHOOL STUDENT: A CASE STUDY IN THE STATE BASIC EDUCATION OF ESTEIO CITY, BRAZIL.

FRANCO,Vanessa de Assunção*[1]; BEDIN, Everton[2];

[1,2] Universidade Luterana do Brasil

** Autor correspondente*
e-mail: vanessafrancoo85@gmail.com

Received 24 July 2019; received in revised form 04 October 2019; accepted 12 October 2019

RESUMO

É constante objeto de discussão e reflexão no meio acadêmico as dificuldades dos alunos em compreender os conteúdos e conceitos da disciplina de Química na Educação Básica e a própria prática pedagógica desenvolver-se de forma contextualizada. Considerando essa premissa, este trabalho teve por objetivo investigar e entender os fatores que dificultam o processo de ensinagem de Química nos 2º e 3º anos do Ensino Médio de uma escola pública estadual de Esteio/RS, dando-se ênfase à metodologia adotada pela professora, a participação ativa dos alunos em sala de aula e a relação destes com o ensino de química. Para essa pesquisa exploratória um estudo de campo de cunho quali-quantitativo foi conduzido por meio da observação *in loco* de 15 horas/aula e posterior aplicação de um questionário aos alunos. Os dados, interpretados e refletidos com base na observação e em autores da área, foram expostos por meio de gráficos percentuais, considerando o total dos respondentes (15 alunos do 2º ano e 8 alunos do 3º ano do Ensino Médio). Ao término, os resultados das análises das respostas dadas pelos estudantes revelam aspectos que indicam que há uma grande inconformidade nos processos de ensino e aprendizagem dessa disciplina e uma incoerência em relação ao dizer e fazer pedagógico, corroborando com o atual sistema educacional, o qual não condiz com uma aprendizagem expressiva no ensino de química, merecendo uma profunda reflexão. Portanto, constata-se que as novas metodologias de ensino, assim como as teorias filosóficas e epistemológicas, surgidas nas últimas décadas, ainda não conseguiram provocar mudanças nas velhas práticas pedagógicas.

Palavras-chave*: Aperfeiçoamento Docente, Contextualização, Ensinagem.*

ABSTRACT

It is the constant object of discussion and reflection in the academic environment the students' difficulties in understanding the contents and concepts of the chemistry discipline in basic education and the pedagogical practice itself develop in a contextualized way. Considering this premise, this study aimed to investigate and understand the factors that hinder the teaching process of Chemistry in the 2nd and 3rd years of high school of a state public school in Esteio / RS, emphasize the methodology adopted by the teacher the active participation of students in the classroom and their relation with chemistry teaching. For this exploratory research, a qualitative and quantitative field study was conducted through on-site observation of 15 hours/class and subsequent application of a questionnaire to students. The data, interpreted and reflected based on the observation and authors of the area, were exposed through percentage charts, considering the total of respondents (15 students in the second graders and 8 students in the third graders in high school). At the end, the results of the analysis of the answers given by the students reveal aspects that indicate that there is a great nonconformity in the teaching process of this subject and an inconsistency in the pedagogical saying and doing, corroborating the current educational system, which is not consistent with an expressive learning in chemistry teaching, deserving a deep reflection. Therefore, the new teaching methodologies, as well as philosophical and epistemological theories, emerged in recent decades, still failed to bring about changes in the old pedagogical practices.

Keywords: Teacher Improvement, Contextualization, Teaching.

Downloaded from www.periodico.tchequimica.com

1. INTRODUÇÃO

Acredita-se que hoje o principal desafio em todo o Brasil, e principalmente no Estado do Rio Grande do Sul, é a falta de qualidade na Educação Básica, oferecida às crianças e jovens de forma pública. Com o passar do tempo, muitos alunos foram "inseridos" em escolas públicas, supersaturando-as em relação à própria infraestrutura e, em contrapartida, os recursos públicos destinados a estas não aumentaram na mesma proporção. Em consequência disto, as condições físicas destas escolas pioraram, o salário dos professores manteve-se constante, as taxas de evasão e reprovação aumentaram e à qualidade dos processos de ensino e aprendizagem diminuiu. (Neri; Buchmann, 2007; Bedin, 2015; Moraes; Bedin, 2017).

Em decorrência do supracitado, uma realidade inquestionável nas escolas públicas do Estado gaúcho, acredita-se que melhorar a qualidade no processo de ensinagem seja muito difícil, mas não impossível. Os governantes buscam, de forma legítima, se movimentar, ouvindo para atender, dentro do possível, as diferentes demandas da população, porém, nas pesquisas de opinião pública, em geral, a segurança, a saúde e, às vezes, o emprego aparecem como preocupação maior. Isto deriva da concepção de que a educação de qualidade não é, "ainda", uma demanda de todos ou para todos; logo, apesar de os discursos políticos e eleitorais fomentarem a educação, na prática a mesma não tem sido prioridade dos governos (Abreu, 2009; Ranieri; Alves, 2018).

Segundo a Lei de Diretrizes e Bases da Educação Nacional (LDB – Lei nº 9.394/96), uma das principais finalidades da educação é preparar o indivíduo para o exercício da cidadania, qualificando-o para o mercado de trabalho. Neste aporte, as OCN (Orientações Curriculares Nacionais, 2008) apontam que a importância da área de Ciências da Natureza, Matemática e suas Tecnologias, no desenvolvimento intelectual do estudante de Ensino Médio, encontra-se na qualidade e não na quantidade de conceitos trabalhados, nos quais deve-se abranger, quase que exigindo a interdisciplinaridade, os quatro componentes curriculares: Física, Química, Biologia e Matemática.

Assim, cada componente, independente de ter sua razão de ser, seu objeto de estudo, seu sistema de conceitos e seus procedimentos metodológicos, deve associar-se às atitudes e valores dos outros. No conjunto, "a área corresponde às produções humanas na busca de compreensão da natureza e sua transformação, do próprio ser humano e de suas ações, mediante a produção de instrumentos culturais e nas interações sociais" (Neto; Carvalho, 2008, p. 2).

Em particular, o ensino de Química transformou-se em preocupação premente nos últimos anos, pois, apesar das OCN apontarem um contexto para o trabalho docente, além das dificuldades apresentadas pelos alunos em interpretar e aprender Química, muitos não sabem o motivo pelo qual a estudam, visto que nem sempre esse conhecimento é construído de tal maneira que o mesmo possa entender a sua importância e/ou vincular à sua existência (Saucedo; Bedin, 2018; Finger; Bedin, 2019).

A Química é uma ciência que está constantemente presente em nossa sociedade, em produtos consumidos, em medicamentos e tratamentos médicos, na alimentação, nos combustíveis, na geração de energia, nas propagandas, na tecnologia, no meio ambiente, nas consequências para a economia, dentre outros. Portanto, é necessário que o cidadão tenha o mínimo de conhecimento químico para poder participar ativamente na sociedade tecnológica atual (Martins et al., 2003; Bedin, 2015), a fim de que seja capaz de "tomar decisões fundamentadas em informações e ponderadas as diversas consequências decorrentes de tal posicionamento" (Santos; Schnetzler, 1996, p. 29).

O professor de química, ao desenvolver seu componente curricular em sala de aula, na grande maioria das escolas públicas gaúchas, insiste na perpetuação de uma metodologia tradicional, dotada de um grande volume teórico e voltado para as práticas de memorização de fórmulas, símbolos e leis (Bedin, 2019). Neste desenho, Bedin (2019, p. 102) afirma que "metodologias docentes que se concentram em cálculos matemáticos e memorização de fórmulas e nomenclatura de compostos, sem a validação de fenômenos e conceitos, infelizmente, ainda hoje, são tradicionais no ensino de química". Ainda, segundo o autor, "existe ausência quase total de experimentos e aulas diversificadas, limitando-se ao livro didático ou aula expositiva que concerne ao estudante a passividade, sem instigação de curiosidade ou problemas que o leve a pensar sobre os fenômenos científicos" (Bedin, 2019, p. 102).

Além disso, os conteúdos continuam ser simplesmente "transmitidos" pelos professores

Downloaded from www.periodico.tchequimica.com

de forma completamente desvinculada da realidade dos alunos (Saucedo; Bedin, 2018). Na concepção de Lima e Leite (2012), por exemplo, essa prática escolar, mas não somente ela, tem contribuído de modo exorbitante para a disseminação da ideia de que a Química é uma disciplina cujos conteúdos são difíceis de serem apreendidos, além de seus conhecimentos não fazerem sentido à vida cotidiana dos sujeitos.

Logo, é preciso modificar a visão construída sobre o ensino de química, buscando uma prática pedagógica e uma aprendizagem centrada no aluno que o qualifiquem na medida em que compreende que aprender é um ato necessário e revestido de concepções e ideologias típicas de cada cultura. O aprender implica em cultivar todas as potencialidades de cada pessoa; abrange as dimensões essenciais do sujeito em toda a sua riqueza e na complexidade das suas expressões e dos seus compromissos (Bedin, 2012). Ou seja, refere-se ao desenvolvimento global e interconectado do corpo, da mente, da inteligência, da sensibilidade e do sentido ético.

Assim, cabe ao professor planejar e conduzir esse processo contínuo de ações que possibilitam aos estudantes, inclusive àqueles que apresentam dificuldades, especificidades e singularidades, construir e significar os conceitos aprendidos em suas múltiplas dimensões, individual e coletivamente, dando significado ao processo de ensinagem (Anastasiou, 2006; Bedin; Del Pino, 2019a). Neste sentido, "torna-se necessário uma reflexão sobre a prática docente, favorecendo o uso de novas metodologias de ensino, pois, muitas vezes, tem-se conhecimento de que, dependendo da forma com que o professor administra e desenvolve sua aula, pode-se derivar em exacerbadas fragmentações entre a teoria e a prática, posteriormente, a emersão da dicotomia entre o dizer e o fazer pedagógico. (Bedin; Del Pino, 2016, p. 1413).

Assim, "entende-se que o trabalho do professor de química não deve se limitar a transmitir conteúdos e significados de símbolos e fórmulas, mas favorecer as atividades psico-cognitivas dos estudantes, fazendo com que os mesmos se tornem importantes personagens na assimilação e ressignificação de conceitos" (Bedin, 2019, p. 102). Esta ação é necessária para que não se constitua entre os sujeitos uma sensação de desconforto em função das dificuldades de aprendizagem existentes neste processo. De modo geral, é preciso que o ensino de química seja desenvolvido de forma contextualizada e interdisciplinar, gerando nos alunos interesse e curiosidade pela ciência, bem como potencialidades em aprender e relacionar o conteúdo estudado ao próprio cotidiano (Finger; Bedin, 2019; Bedin, Del Pino, 2019b, 2019c).

Segundo Bedin (2019, p. 103), "esta ação é importante porque se a implantação do conhecimento químico for planejada em relação ao aluno, pode propiciar um conjunto de práticas preestabelecidas que têm o propósito de contribuir para que este se aproprie de conteúdos sociais e culturais de maneira crítica e construtiva, ressignificando-os a partir dos conhecimentos estabelecidos pelo currículo em sala de aula". Ademais, pode-se demonstrar a importância da química para o desenvolvimento científico e tecnológico da humanidade, refletindo sobre as aplicações práticas desta ciência no cotidiano dos alunos, mas, principalmente, pela análise crítica de suas utilidades, do uso de seus recursos naturais e do respeito ao meio ambiente (Zucco, 2011; Pereira, 2014).

Deste modo, o ensinar química se define em função de o aluno aprender expressivamente seus significados científicos nas diferentes dimensões históricas, sociais, culturais, políticas e econômicas, a fim de utilizar esses conhecimentos para significar a própria existência e a de sua comunidade (Bedin, 2019; Bedin, Del Pino, 2019c). Portanto, instigar e problematizar a práxis pedagógica e as práticas e posturas dos estudantes é uma forma de pensar a importância do trabalho coletivo destes para potencializar o processo de ensinagem no contexto educativo brasileiro. Afinal, de acordo com Bedin e Del Pino (2019c, p. 133), para ser um professor de química, hoje, é preciso "apresentar condições significativas de saberes teóricos e metodológicos, competências e habilidades e, principalmente, conseguir estar em constante aperfeiçoamento e atualização em seu desempenho pedagógico".

Diante do exposto, este trabalho teve por objetivo apresentar e refletir criticamente sobre uma atividade investigativa realizada na Educação Básica, a qual buscou entender quais são os fatores que dificultam os processos de ensino e aprendizagem de Química nos 2º e 3º anos do Ensino Médio, dando-se ênfase à metodologia adotada pela professora, a participação ativa dos alunos em sala de aula e a relação destes com o ensino de química.

2. MATERIAIS E MÉTODOS

A presente pesquisa classifica-se como

Downloaded from www.periodico.tchequimica.com

exploratória, pois teve por objetivo averiguar conhecimentos acerca da visão dos alunos do Ensino Médio sobre a Química e a metodologia de ensino do professor dessa disciplina. A forma de coleta de dados se caracterizou pela técnica de estudo de campo numa abordagem quanti-qualitativa, fornecendo subsídios teóricos e empíricos necessários para o desenvolvimento do trabalho (André, 2005). A pesquisa foi realizada no início do ano letivo, durante os meses de março e abril de 2019. O universo dessa pesquisa se consistiu em 15 alunos do 2º ano e 8 alunos do 3º ano do turno da noite, pertencentes a uma escola pública de Ensino Médio da rede estadual da cidade de Esteio/RS.

Na abordagem quantitativa, o instrumento utilizado para a coleta e, posteriormente, análise e interpretação dos dados foi um questionário semiestruturado para os discentes. O questionário foi composto com treze questões: dez questões fechadas, as quais traziam possíveis respostas (hipóteses), e três questões abertas, solicitando a elaboração de respostas construídas a partir da concepção deste. Na abordagem qualitativa, os comentários, as críticas, as reações e as manifestações de sentimentos e emoções dos alunos foram observados e anotados durante 15 horas/aula *in loco*. Esta prática de observação foi de extrema relevância para o processo de reflexão, análise e interpretação dos dados coletados por meio do questionário e analisados de forma quantitativa.

Ao tocante, os dados abaixo, expostos por meio de gráficos percentuais e refletidos com base em teóricos da área, consideram o total de alunos das duas turmas observadas, correspondendo a esta realidade e à interpretação dos autores à luz da observação; logo, qualquer análise destes dados pode gerar interpretação diferenciada.

3. RESULTADOS E DISCUSSÃO

Para a exposição dos dados, preservou-se a identidade de todos os envolvidos. Responderam o questionário um total de 23 alunos; sendo 15 alunos do 2º ano e 8 alunos do 3º ano do Ensino Médio. A maior parte destes tinha entre 16 e 22 anos, onde 61% eram do sexo feminino e 39% do sexo masculino. Os respondentes foram os alunos presentes em sala de aula no último dia da observação *in loco*.

Durante a análise das respostas do questionário, algumas pontuações não passaram despercebidas. A falta de atenção demonstrada pela grande maioria dos discentes foi notória, pois, além de assinalarem respostas divergentes e contraditórias em questões complementares, os sujeitos deixaram algumas questões objetivas sem resposta.

O questionário disposto aos alunos apresentava as seguintes questões: “Por que você está cursando o Ensino Médio?”, “Você pretende realizar outro curso após o término do Ensino Médio?”, “O que você entende por Química?”, “Como você considera o ensino de química?”, “Qual seu grau de interesse no estudo da disciplina Química?”, “Seu professor estimula você a estudar Química?”, “Qual seu grau de dificuldade na disciplina Química?”, “Como você considera a metodologia de ensino empregada pelo professor?”, “Quais os recursos didáticos utilizados pelo seu professor de Química?”, “O professo relaciona o conteúdo de Química com assuntos do seu dia a dia?”, “Que sugestão você daria para melhorar as aulas de química?” e “De exemplos da aplicação da química em seu cotidiano”.

A seguir, para melhor discussão dos resultados, apresenta-se as análises e reflexões dos dados por meio de agrupamento de questões, intensificando-os com uma discussão.

Questões 1 e 2: Por que você está cursando o Ensino Médio? Você pretende realizar outro curso após o término do Ensino Médio?

As duas primeiras questões objetivaram entender o motivo que leva os alunos a cursar e a concluir o Ensino Médio, dando ênfase ao interesse destes após a conclusão do mesmo. Ou seja, por meio de opções de resposta disponibilizadas aos alunos, estes deveriam pontuar com ênfase o grau de objetivo futuro. As opções de resposta, assim como o grau de concordância dos alunos em relação a cada uma, podem ser vistos nas Figuras 1 e 2.

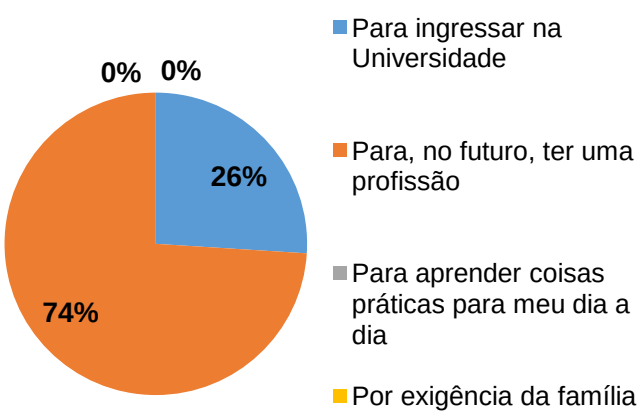

Figura 1: *Motivos para cursar o ensino médio*

Downloaded from www.periodico.tchequimica.com

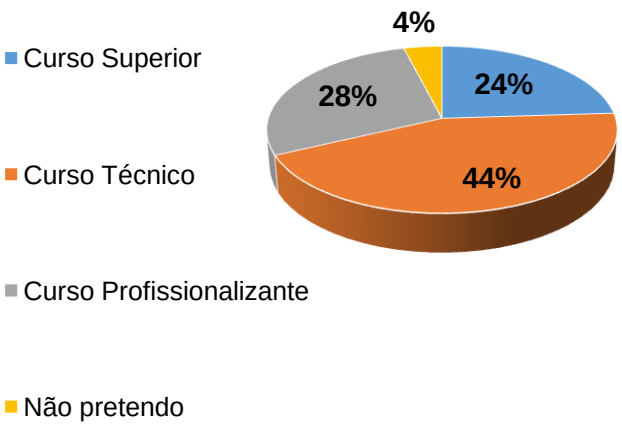

Figura 2: *Interesse dos alunos em realizar cursos após o ensino médio.*

Na Figura 1, percebe-se que a maioria dos alunos 74% (17 alunos) respondeu que o principal motivo para cursar o Ensino Médio seria para, no futuro, ter uma profissão ou reconhecimento melhor. Do mesmo modo, 26% dos sujeitos apontaram a possibilidade de prestar vestibular para ingressar em uma universidade.

Assim, pode-se avaliar que a intenção primeira, da maioria dos alunos matriculados na Educação Básica, referente a este grupo de sujeitos, é a busca de uma profissão; a ideia de conseguir um emprego melhor, não necessariamente está vinculada a necessidade de um diploma superior. Portanto, é cogente mencionar a necessidade de o professor desenvolver os conceitos e conteúdos da ciência química de forma contextualizada as vivências do sujeito, instigando-o aprender conceitos práticos relacionados ao seu cotidiano (Finger; Bedin, 2019). Afinal, é imprescindível que o ensino de química de ênfase a realidade do sujeito, instigando-o a pensar quimicamente os fenômenos naturais que ocorrem em seu entorno, uma vez que, para muitos destes alunos, o término do Ensino Médio significa o término da relação com a química teórica.

Referente ao interesse daqueles com o intuito em realizar uma atividade profissional após o término do Ensino Médio, averígua-se na Figura 2 que as respostas dos sujeitos apontam para à intenção do aperfeiçoamento por meio de um curso técnico ou profissionalizante e não, usualmente, via graduação, objetivando o mercado de trabalho de forma mais rápida.

Neste sentido, percebe-se que o ensino de química deve ter vistas para a aprendizagem social do sujeito à luz da interpretação desta ciência em suas diferentes dimensões. Chassot (2006) lembra que a transmissão dos conhecimentos químicos deve ser encharcada de realidade, e isso não significa o reducionismo que virou modismo, mas sim o ensino de química dentro de uma concepção que destaque o papel social dessa ciência. Todavia, de acordo com Bedin e Del Pino (2018a, p. 66), "associar o contexto, o interesse e o desejo sobre o que aprender dos diferentes alunos às ideias e aos conceitos científicos do componente curricular de química, em um viés democrático e qualitativo da vivência do aluno, é uma tarefa complexa e, ao mesmo tempo, não singular". O que implica pensar na necessidade de o professor aperfeiçoar-se intradisciplinarmente, buscando mobilizar competências, habilidades e atitudes para instigar no aluno uma formação sólida e consciente sobre esta ciência.

Apesar das dificuldades que o professor de química encontra, esta disciplina tem seguido uma forte tendência à contextualização dos conteúdos, sendo importante que o professor apresente ao aluno fatos concreto, observável e mensurável, incorporando ao currículo aspectos sociocientíficos, tais como questões ambientais, políticas, econômicas, éticas, sociais e culturais relativas à ciência e a tecnologia (Bedin; Del Pino, 2015). Estes aspectos auxiliarão o aluno quando prestar processos seletivos para ingressar em outros cursos, pois esta intenção fica evidente quando os discentes são questionados sobre o que pretendem cursar após o Ensino Médio. Os cursos técnicos e cursos profissionalizantes foram os mais apontados, somando juntos 72%. Realizar um curso superior foi também um item bastante assentado pelos sujeitos, sendo 22%, o que confirma, indiferente das porcentagens, que a maior parte destes pretende continuar os estudos após o término do Ensino Médio.

Questões 3, 4 e 5: O que você entende por Química? Como você considera o ensino de química? Qual seu grau de interesse pelo estudo da disciplina de Química?

Quando perguntado aos alunos o que entendiam por química, 30% não responderam a questão; dos outros 70%, obteve-se as seguintes respostas: *"É o estudo da matéria e suas propriedades", "É um estudo científico e importante", "É a ciência que estuda a matéria sua composição e as transformações de cada substância química", "É o estudo científico da matéria e suas propriedades", "Algo muito importante e explicativo sobre como funciona as coisas no nosso cotidiano", "É um estudo*

Downloaded from www.periodico.tchequimica.com

científico", "Estudo da matéria", "É muito preciso e é usado em praticamente tudo que usamos ou comemos", "Química é a mistura é composição dos elementos", "Estudo sobre animais, corpo humano, estudo da ciência, estudo da matéria", e "Estudo da natureza".

A partir de uma interpretação minuciosa das respostas desta questão é possível verificar que a maioria dos alunos tem uma noção básica do que é química e o que esta ciência estuda. Neste sentido, acredita-se que o professor, como o principal agente articulador do processo de ensinagem, deve criar condições necessárias para ativar a inteligência dos alunos, instigando-os a pensar e refletir a química para a cidadania. É importante que, de modo particular, o professor investigue quais são os motivos e as reais expectativas dos alunos em relação à disciplina de Química, pois isto lhe possibilitaria buscar soluções para superar as dificuldades na própria ação, ampliando os conhecimentos e a percepção dos sujeitos acerca desta ciência.

Ademais, um bom mestre deve ter, como principal preocupação, o objetivo de "gerar laços favoráveis entre seu discípulo e o conteúdo que ensina, para que ambos, professor e aluno, descubram o prazer de aprender" (Becker, 2010 p. 44). É hora de "o sujeito começar a aprender a partir da própria ação, para que o professor assuma o papel de mediador/facilitador do processo de aprendizagem, e não mais de um mero transmissor de informações, de modo que o ambiente de ensino passe a ser percebido de forma dinâmica e dialógica" (Bedin; Del Pino, 2018a, p. 68). Neste sentido, as figuras 3 e 4 demonstram a importância e o interesse que os alunos relacionam à disciplina.

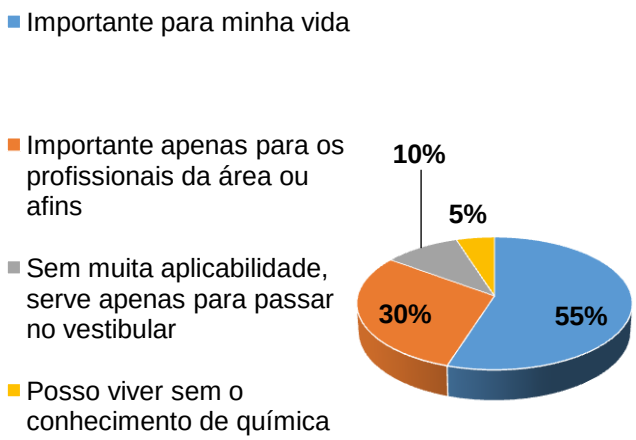

Figura 3: *Importância relacionada à Química*

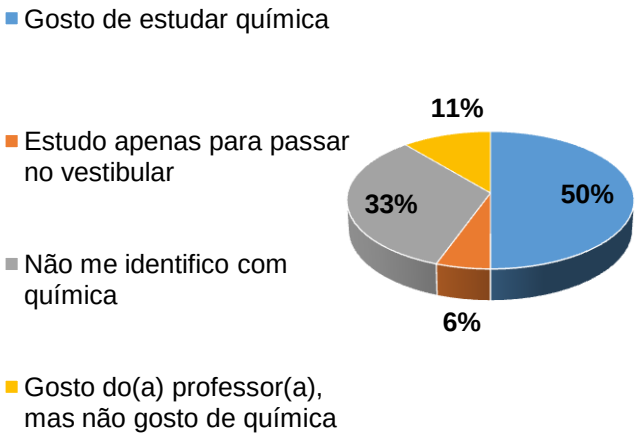

Figura 4: *Interesse dos alunos pela disciplina*

Conforme a Figura 3, 55% dos alunos avaliaram o ensino de Química como sendo importante para a vida, 30% consideraram-no importante apenas para os profissionais da área ou afins, 10% dos alunos o perceberam sem muita aplicabilidade, mas necessário, pois é um assunto do vestibular. Contudo, ainda, um dos discentes acredita ser possível viver sem nenhum conhecimento sobre química. É inquietante que, ainda, há alunos que não conseguem entender a importância da ciência química, pois não compreendem e não percebem suas aplicações. Ademais, é questionável que um aluno que se encontra no término da Educação Básica não consiga vincular esta ciência com algo do seu cotidiano, afirmando poder viver sem a mesma. A respiração humana, por exemplo, é um processo inteiramente químico.

Neste aporte, é sagaz afirma que, por meio da observação durante as aulas, não se percebeu, em nenhuma turma, ações e práticas contextualizadas ou investigativas referentes à ciência, por vezes atividades monótonas e corriqueiras (como leitura de livro e resolução de exercícios) eram desenvolvidas pelo professor. Não somente, mas acredita-se que a ação docente pode contribuir efetivamente para a disseminação de uma visão distorcida dessa ciência, reforçando a predominância de aversão dos educandos em relação aos seus conceitos. Doutras vezes, foi possível perceber que os estudantes não conseguiam compreender o assunto explorado em sala de aula; logo, ao não questionarem sobre, os sujeitos acabavam perdendo o interesse e a curiosidade sobre a química, deixando-o passar vagarosamente.

Entretanto, no que se refere ao interesse dos educandos pela disciplina de Química, 50%

dos alunos assinalaram gostar de Química, 33% disseram não se identificar com os conteúdos de química, 11% relataram gostar do professor, mas não da matéria e, ainda, 6% apenas estudam para passar no vestibular. No gráfico 4, revela-se que metade dos alunos não se sente estimulada a gostar dos conteúdos químicos, não demonstra interesse e curiosidade pela disciplina. Segundo Santos *et al*. (2012, p. 424), o não gostar dos conteúdos de disciplinas como Química, Física e Matemática está associado ao fato de a metodologia de ensino dessas ciências estar, ainda, "supervalorizar a memorização de fórmulas, regras e cálculos, em detrimento do desenvolvimento de habilidades e competências essenciais para que o aluno exerça a cidadania".

No entanto, para Alarcão (2010), estimular o estudo e fazer os alunos gostarem de uma disciplina consiste em o professor estabelecer uma afinidade entre o estudante e o conteúdo estudado, ter como princípio norteador de sua prática pedagógica a preocupação em dar liberdade e responsabilidade ao aluno, para que ele possa, por meio das atividades pedagógicas, adquirir sua autonomia e superar as dificuldades enfrentadas no processo de ensinagem. Assim, acredita-se que o conhecimento será construído e ressignificado pelo sujeito a partir das interações entre os pares e destes com sua realidade, afinal "o conhecimento é um produto da atividade intelectual individual e social de cada estudante; logo, os professores devem criar contextos sociais para sustentar essa produção" (Bedin; Del Pino, 2018b, p. 67). Ainda, segundo os autores, o aluno, "ao não participar do próprio processo de formação, não consegue lograr satisfação de aprender a aprender, intervir de forma crítica e reflexiva na realidade, construir argumentos e ideias próprios e fundamentados cientificamente, desenvolver a capacidade problematizadora, o pensamento autônomo e o espírito científico-investigativo" (Bedin; Del Pino, 2018a, p. 66).

Ainda, refletindo a partir das respostas dos estudantes, é possível perceber que para o desenvolvimento de uma boa prática em sala de aula há a necessidade de o professor desenvolver competências para aliar os conhecimentos teóricos com a prática. Abordar os conteúdos de forma contextualizada faz parte do processo de aprendizagem, além de facilitá-lo e potencializá-lo. Além disso, não se deve deixar de considerar que para um conhecimento amplo e de qualidade, se faz necessário que sejam estudados também modelos explicativos microscópicos. Assim, acredita-se que estas ações, vinculadas a competências e habilidades docentes, sejam significativas o suficiente para despertar nos sujeitos o gosto pela ciência química, instigando-os a pensar e vivenciar esta ciência, potencializando, ainda, a constituição de inteligências e atitudes que configuram a formação de um sujeito crítico e ativo.

Questões 6, 7, 8 e 9: Seu professor estimula você a estudar Química? Qual seu grau de dificuldade na disciplina Química? Como você considera a metodologia de ensino empregada pelo professor? Quais os recursos didáticos utilizados pelo professor de Química?

Dentre os 23 alunos, 21 destes (91%) afirmaram que se sentem estimulados pelo professor a estudar química, o restante, dois alunos (8%), não partilharam da mesma opinião. O sentir-se estimulado é importante porque a relação professor-aluno deve ser desprovida de imposições e ser baseada no respeito, na cooperação e no crescimento, de maneira que o aluno seja levado a interagir ativamente no processo de desenvolvimento cognitivo (Vygotsky, 2010). Apesar de a grande maioria sentir-se estimulada pelo professor, quando perguntados sobre seu grau de dificuldade na disciplina de química, apenas um aluno relatou não ter dificuldade, 52% disseram ter baixo grau de dificuldade e 45% afirmaram ter grau intermediário de dificuldade. Assim, percebe-se que para a grande parte dos alunos a Química é uma ciência bastante complicada e que, indiferente de o professor estimular e instigar o aluno à aprendizagem, a mesma só ocorrerá se o sujeito sentir emoção em compreendê-la. Logo, é preciso despertar no aluno o interesse pela química e, quiçá, este seja despertado a partir de um ensino contextualizado, propiciando-lhe um entendimento expressivo sobre a ciência.

Afinal, a compreensão e o entendimento dos conteúdos e dos conceitos Químicos estão associados à maneira pela qual o professor os explora, de tal modo que ele pode dificultar ou facilitar o entendimento do aluno. A metodologia que o professor utiliza para abordar os conteúdos em sala de aula é essencial para a produção do conhecimento pelo aluno. Nessa concepção, o professor em exercício precisa preparar sua aula e conhecer os conceitos químicos necessários para conduzir metodologicamente o desenvolvimento cognitivo dos seus alunos (Castro, 2008).

No que concerne ao aspecto metodológico do docente, 74% dos alunos

Downloaded from www.periodico.tchequimica.com

afirmaram que a metodologia adota é ativa, com discussão e diálogo sobre os assuntos estudados; 13% dos sujeitos consideram as aulas dinâmicas e citam a utilização de recursos além do quadro, pincel ou livro didático; os outros 13% dos alunos veem as aulas como sendo monótonas e com o professor apenas escrevendo no quadro. Em corroboração a estes últimos, no tempo de observação, constatou-se que o professor não demonstrou aprofundamento nas informações transmitidas. Possivelmente, isto seja decorrência de sua formação inicial, pois o mesmo é formado em Ciências Biológicas e não em Química. Apesar deste fato, é essencial que o professor domine profundamente os conhecimentos teóricos necessários para um bom desenvolvimento de sua prática, apresentando objetivos reais e significados expressivos a presença do aluno. Dessa maneira, os alunos depositarão credibilidade na prática docente, e instigarão o docente a explorar os conteúdos com maior confiança e domínio.

Além disto, é importante que o professor saiba que o tipo de metodologia usada para abordar o conteúdo da disciplina trabalhada influencia na motivação do aluno para o estudo (SAVIANI, 2011). Mas que "[...]somente a utilização de processos, o emprego de técnicas e mudanças nas ações didáticas não são suportes o suficiente para fazer o estudante compreender e aplicar conceitos e métodos em seu dia a dia (Bedin, 2015 apud Bedin; Del Pino, 2018a, p. 66). Ou seja, é preciso desenvolver um ensino em que o aluno consiga relacionar o contexto com a ciência, para construir saberes significativos e expressivos a própria formação.

A figura 5 apresenta as respostas dadas pelos alunos ao apontarem os recursos didáticos utilizados, em sala de aula, pelo professor.

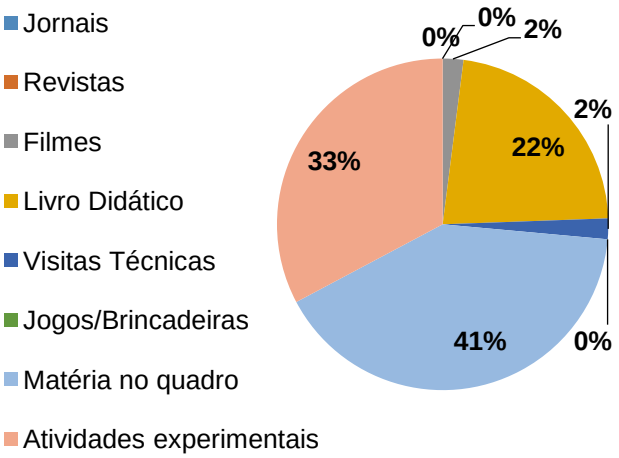

Figura 5: *Recursos didáticos utilizados pelo professor*

A partir dos dados presentes no gráfico 5, fica explicito que a matéria passada no quadro é a ação mais comum do professor, seguida pelas atividades experimentais e pelo uso do livro didático. Na visão de Pérez Gómez (1998, p. 83), "o professor deve levar em consideração e aplicar todos os recursos didáticos disponíveis e adequados, mesmo os mais comuns como o quadro-de-giz, o giz, o livro didático, os jogos, as brincadeiras". Afinal, esses instrumentos, quando bem utilizados pelo professor em suas aulas, podem se tornar aliados poderosos na exploração dos conteúdos e promover o entendimento e a compreensão dos alunos. Se essa dimensão metodológica, em conjunto com as demais, for corretamente trabalhada, possibilitará garantias ao professor de estar desenvolvendo aulas de qualidade (Sant'Anna; Sant'Anna, 2004).

Neste sentido, vale ressaltar a importância de desenvolver aulas práticas na própria sala de aula, por meio de experiências simples produzidas a partir de materiais alternativos, envolvendo a participação dos alunos. Aqui, cabe a criatividade e a disponibilidade do professor em proporcionar a execução de experimentos criativos, simples e participativos, que deem bons resultados para melhoria do processo de ensinagem (Neves *et al.,* 2006). Em colaboração, Hoernig e Pereira (2004) afirmam que quando o aluno observa e/ou manipula o objeto que está a estudar, ele consegue compreender melhor o conteúdo associado, pois a experimentação do concreto estimula o desenvolvimento do raciocínio, faz com que os conceitos relacionados adquiram significado e a compreensão dos conteúdos assuma sentido.

Questões 10, 11 e 12: O professor relaciona o conteúdo de Química com assuntos do seu dia a dia? De exemplos da aplicação da química em seu cotidiano. Que sugestão você daria para melhorar as aulas de química?

Para a maior parte dos alunos (82%) o professor relaciona o conteúdo ministrado em aula com assuntos do dia a dia, tornando, assim, a matéria de Química mais interessante e potencializada. Todavia, ajuíza-se que durante a observação não se percebeu ações de contextualização pelo professor, mas de processos em que o mesmo exemplifica as substâncias presentes na sociedade. Indiferente da ação do professor é sagaz pontuar que a abordagem do conteúdo programático deve levar

Downloaded from www.periodico.tchequimica.com

em conta a vivência do sujeito e a sua participação, mesmo por meio de exemplos extraídos do cotidiano. Essa prática reforça o conteúdo passado no quadro e àquele presente no livro didático, propiciando aos sujeitos aulas mais dinâmicas e capazes de incentiva-los ao estudo da Química (Pozo; Crespo, 2009).

Corroborando as ideias acerca da Química no cotidiano, as orientações apresentadas nos PCN+ destacam que "não se procura uma ligação artificial entre o conhecimento químico e o cotidiano, restringindo-se a exemplos apresentados apenas como ilustração ao final de algum conteúdo; ao contrário, o que se propõe é partir de situações problemáticas reais e buscar o conhecimento necessário para entendê-las e procurar solucioná-las" (Brasil, 2002, p. 93). Assim, entende-se que "o ensino de química deve estar entrelaçado e contextualizado ao conhecimento da realidade do educando, favorecendo momentos em que este possa atuar como autor na construção dos próprios saberes" (Bedin, 2019, p. 103).

Neste aporte, saber o que chama a atenção dos alunos para uma aula de Química é essencial, haja vista que esta ciência faz parte do cotidiano do ser humano. Independe da visão de ensino aplicada, a valorização do cotidiano do aluno apresenta grande influência no processo de ensinagem, pois um conhecimento químico associado à realidade do mesmo lhe possibilita uma compreensão mais significativa dos conteúdos, o que pode traduzir-se num processo de ensino mais eficaz (Brasil, 2008).

Os alunos identificaram como exemplos, em seu cotidiano, que teriam relação com a Química: *alimentos, produtos de limpeza, cosméticos e de higiene pessoal, medicamentos, estados físicos da água, ar, combustíveis e bebidas*. Os exemplos citados pelos discentes não são muito diferentes daqueles apresentados nas pesquisas de Cardoso e Colinvaux (2000). Segundo os autores, os exemplos apresentados levam a acreditar na hipótese de que o professor destes alunos teria estabelecido uma efetiva relação entre o que é ensinado nas aulas de Química e situações do cotidiano. Todavia, destaca-se que os estados físicos da água, por exemplo, não apresentam uma especificidade em química, já que se trata de um processo físico. Assim, é cabível questionar se estas relações que os alunos apontam do contexto com a química, realmente, foram construídos em sala de aula, pois podem, simplesmente, derivarem de uma discussão em um ensino não formal.

Referente a última questão, àquela que solicitava ao aluno para sugerir ações para melhorar as aulas de química, estão: - a promoção de mais aulas práticas, pois um dos alunos afirmou que *"fica mais fácil de compreender a matéria com a realização de experimentos"*; - o aumento do número de aulas de Química por semana, pois, atualmente, nas escolas estaduais do Rio Grande do Sul são ministradas, com pequenas exceções, duas aulas semanais, o que implica na ausência de abordagens de diferentes temas ou de novas metodologias de ensino, limitando-se a uma abordagem mais conteúdista; - um grupo de alunos, afirmou estar satisfeito com as aulas e que não seriam necessárias alterações, pois as *"aulas de Química já são excelentes"*, como afirma um dos estudantes. Outro aluno confirma: *"o ensino está ótimo, o que deveria melhorar são os comportamentos dos colegas nas aulas. Eles atrapalham quem quer prestar atenção em todas as disciplinas"*, indicando que o problema não é específico das aulas de Química, mas da turma em si. Outros aspectos citados foram: "clareza nas explicações" o que exige do professor um domínio maior do conteúdo e de suas múltiplas dimensões, "incentivo aos trabalhos em grupo", fomentando a necessidade de o aluno relacionar-se cognitivamente com o outro e "usar o Datashow nas aulas", apontando a necessidade de o aluno "observar" a química por meio de outros óculos.

4. CONCLUSÕES

Este trabalho possibilitou identificar alguns aspectos importantes que estão relacionados ao desenvolvimento do processo de ensinagem da disciplina de Química no Ensino Médio gaúcho. A partir da análise das respostas dadas pelos alunos ao questionário, aplicado na etapa de trabalho de campo desta pesquisa, foi possível realizar algumas discussões e reflexões sobre as concepções adquiridas por estudantes da rede de ensino pública, sendo esta uma forma de preparar os futuros professores para a elaboração de metodologias que possam ser desenvolvidas nas aulas, deixando-as mais interessantes para prender a atenção do aluno e ensinar Química com qualidade.

Em relação às questões, cujas respostas apresentaram um caráter positivo quantitativamente acentuado, constatou-se que alguns elementos, relacionados à prática pedagógica do professor de Química dessa

Downloaded from www.periodico.tchequimica.com

escola, estão contribuindo de forma positiva para um aprendizado satisfatório da disciplina. Dentre esses elementos merecem destaque: qualidade da relação professor-aluno e os recursos didáticos utilizados pelo professor. O profissional docente de Química, precisa estar bem preparado para buscar mecanismos apropriados e capazes de tornar o processo de ensinagem livre de obstáculos que atrapalhem o seu bom rendimento. Além disso, o uso de experimentos durante as aulas de Química estimula os alunos, a um maior interesse pelo conteúdo abordado, tornando-as mais agradáveis e dinâmicas. Embora não tenha sido citado observado experimentos durante a pesquisa *in loco,* sabe-se que estes não precisam necessariamente de vidrarias e reagentes caros e sofisticados, mas devem ser relacionados ao cotidiano e desenvolvidos em uma perspectiva investigativa.

Por outro lado, outros elementos cujas respostas apresentaram um caráter negativo quantitativamente acentuado merecem destaque. Dentre esses elementos, a dificuldade de compreensão do conteúdo por grande parte dos alunos e a supervalorização de conteúdo passado no quadro estão, de maneira intrínseca, mas não somente estes, relacionados à qualidade da formação do professor. Com um processo formativo inadequado, a maioria dos profissionais desta ciência insiste em práticas pedagógicas adquiridas a partir de heranças culturais, da época em que estavam na escola, ou que lhes foram repassadas por colegas com mais experiência.

Afinal, de acordo com Bedin e Del Pino (2019, p. 72), o professor, "a partir de suas vivências e especificidades, assumindo como espelho de profissão os próprios professores, acaba por reproduzir estilos de ser professor a partir de seus mestres; logo, durante o curso de graduação, é necessária uma formação docente pautada na reflexão sobre a identidade docente e, principalmente, na ação pedagógica, pois neste arcabouço de ações aprende-se o que reproduzir e o que não reproduzir em razão dos efeitos negativos e positivos da sua experiência acadêmica". Desse modo, cabe aqui uma reflexão a respeito do processo da formação continuada de professores, se é que a esse profissional é dada a possibilidade de se atualizar-se e aperfeiçoar-se. Nesta perspectiva, Libâneo (2006, p. 20) denuncia que "os conteúdos dos cursos de licenciatura [...] quase nunca têm correspondência com as situações concretas de sala de aula, não ajudando os professores a formar um quadro de referência para orientar sua prática".

Ademais, tem-se que a partir desta pesquisa, pôde-se constatar que as novas metodologias de ensino, assim como as teorias filosóficas e epistemológicas, surgidas nas últimas décadas, ainda não conseguiram provocar mudanças nas velhas práticas pedagógicas; logo, ressalta-se que é essencial e urgente a implantação de ações que visam um processo de formação mais adequada desses professores para atuarem no ensino de química do Ensino Médio, ficando a cargo da escola e dos cursos de formação de professores a obrigação de instigar e possibilitar a estes sujeitos ações e processos que configurem esta prática. Afinal, acredita-se que quando o professor mudar a sua forma de trabalhar em sala de aula, instigando nos alunos competências, habilidades e atitudes, talvez, estes possam despertar interesse e curiosidade pela ciência química, percebendo-a como parte integrante de seu contexto.

6. REFERÊNCIAS:

1. Abreu, M. Lições do Rio Grande: Referencial Curricular para as escolas estaduais In: *Rio Grande do Sul. Secretaria de Estado da Educação*. Porto Alegre: Secretaria de Estado da Educação do Rio Grande do Sul, **2009**.
2. Alarcão, I. *Professores reflexivos em uma escola reflexiva*. São Paulo: Cortez, **2010**.
3. Anastasiou, L. G. C. Ensinar, aprender, apreender e processos de ensinagem. In. Anastasiou, L. G., Alves, L. *Processos de ensinagem na universidade: pressupostos para as estratégias de trabalho em aula*. 6. ed.- Joinville, SC : UNIVILLE, **2006**.
4. André, M. A. *Estudo de caso em pesquisa e avaliação educacional*. Brasília: Liberlivros, **2005**.
5. Becker, F. *O caminho da aprendizagem em Jean Piaget e Paulo Freire*: da ação à operação. Petrópolis, RJ: Vozes, **2010**.
6. Bedin, E. Filme, experiência e tecnologia no ensino de ciências química: uma sequência didática. *Revista de Educação, Ciências e Matemática*, v. 9, n. 1, **2019**.
7. Bedin, E. *A emersão da interdisciplinaridade no ensino médio politécnico*: relações que se estabelecem de forma colaborativa na qualificação dos

Downloaded from www.periodico.tchequimica.com

processos de ensino e aprendizagem à luz das tecnologias de informação e comunicação. 2015. 512 f. Tese (Tese de Doutorado) – Programa de Pós Graduação em Ciências: Química da Vida e Saúde, Universidade Federal do Rio Grande do Sul, Porto Alegre, RS, **2015**.

8. Bedin, E. *Formação de professores de química: um olhar sobre o Pibid da Universidade Federal de Uberlândia*. **2012**.
9. Bedin, E., Del Pino, J. C. A formação inicial de professores de química a partir da integração e da cooperação nas rodas de conversa: um caso específico. *Revista Debates em Ensino de Química*, v. 4, n. 2 (esp), p. 68-85, **2019a**.
10. Bedin, E., Del Pino, J. C. DICUMBA: uma proposta metodológica de ensino a partir da pesquisa em sala de aula. *Ensaio Pesquisa em Educação em Ciências (Belo Horizonte),* v. 21, **2019b**.
11. Bedin, E., Del Pino, J. C. Análise de Atitudes: proposições docentes sobre a utilização de Rodas de Conversa na formação inicial de professores. *Revista de Estudos e Pesquisas sobre Ensino Tecnológico (EDUCITEC)*, v. 5, n. 11, **2019c**.
12. Bedin, E., Del Pino, J. C. A metodologia Dicumba como uma tempestade de possibilidades para o desenvolvimento do ensino de Química. *Revista Brasileira De Ensino De Ciências E Matemática*, v. 1, n. 1, **2018a**.
13. Bedin, E., Del Pino, J. C. Aprendizagem Colaborativa nas Redes Sociais e a qualificação dos Processos de Ensino e Aprendizagem. *Interacções,* nº. 48, pp. 65-84, **2018b.**
14. Bedin, E., Del Pino, J. Rodas de Conversas na Universidade-Formação Docente Tecnológica em Ciências: metodologias de cunho interdisciplinar. *Tecné Episteme y Didaxis TED*, **2016**.
15. Bedin, E., Del Pino, J. C. Seminário Integrado e Projetos de Aprendizagem: uma proposta metodológica para a construção de saberes. *Ciência e Natura*, v. 37, n. 3, p. 796-807, **2015**.
16. Brasil, Ministério da Educação, Secretaria de Educação Básica (org.) Estratégia para o ensino de Ciências, **s/a.**
17. Brasil. Lei de Diretrizes e Bases. *Lei nº 9.394/96*, de 20 de dezembro de 1996. BRASIL, **1996**.
18. Brasil. Ministério da Educação. *PCN+ ensino médio*: Orientações Educacionais complementares aos Parâmetros Curriculares Nacionais: Ciências da Natureza, Matemática e suas tecnologias. Brasília, DF: MEC/SEMTEC, p. 93, **2002**.
19. Brasil, Ministério da Educação, Secretaria de Educação Básica (org.) *Orientações Curriculares para o Ensino Médio: Ciências da Natureza, Matemática e suas Tecnologias.* Brasília, **2008**.
20. Cardoso, S. P., Colinvaux, D. Explorando a motivação para estudar Química. *Química Nova*, 23 (3), **2000**, p. 401-404.
21. Castro, P. A., Tucunduva, C. C., Arns, E. M. A importância do planejamento das aulas para organização do trabalho do professor em sua prática docente. *Athena, Revista Científica de Educação*, v. 10, n. 10, jan./jun. **2008**.
22. Chassot, A. *Alfabetização científica*: questões e desafios para a educação. 4ª. Edição. Ijuí, Editora: Unijuí, **2006**.
23. De Moraes, C. S., Bedin, E. Indisciplina e falta de autonomia em sala de aula: fatores que influenciam nos processos de ensino-aprendizagem. *Pedagogia em Foco*, v. 12, n. 8, p. 114-133, **2017**.
24. Finger, I., Bedin, E. A contextualização e seus impactos nos processos de ensino e aprendizagem da ciência química. *Revista Brasileira de Ensino de Ciências e Matemática*, v. 2, n. 1, p. 8-24, **2019**.
25. Hoernig, A. M., Pereira, A. B. As aulas de ciências iniciando pela prática: o que pensam os alunos. *Revista Brasileira de Pesquisa em Educação em Ciências*, v. 4, n. 3, P. 19-28, **2004**.
26. Libâneo, J. C. *Democratização da Escola pública*: a pedagogia crítico-social dos conteúdos, Loyola, São Paulo, **2006**.
27. Pozo, J. I., Crespo, M. Á. G. *A aprendizagem e o ensino de ciências*: do conhecimento cotidiano ao conhecimento científico. Porto Alegre: Artmed, v. 5, **2009**.
28. Lima, J. O. G., Leite, L. R. O processo de ensino e aprendizagem da disciplina de Química: o caso das escolas do ensino

Downloaded from www.periodico.tchequimica.com

médio de Crateús/Ceará/Brasil. *Revista Electrónica de Investigación en Educación en Ciencias*, Buenos Aires, v. 7, n. 2, **2012**.

29. Martins, A. B., Santa Maria, L. C., Aguiar, M. R. M. P. As drogas no ensino de Química. *Química nova na escola*, v. 18, n. 2, p. 18, **2003**.
30. Neri, M., Buchmann, G. *Monitoramento das metas educacionais de Dakar*. Estudo de casa do Brasil (2000–2005) para o global monitoring da UNESCO, **2007**.
31. Neto, C. O. C., Carvalho, R. C. P. S. Dificuldades no ensino-aprendizagem de química no ensino médio em algumas escolas públicas da região sudeste de Teresina. *Anais PIBIC*, UESPI, **2008**.
32. Neves, M. S., Moreira, M. A., Caballero, S. M. C. Repensando o papel do trabalho experimental, na aprendizagem da física, em sala de aula: um estudo exploratório. *Investigações em ensino de ciências*. Porto Alegre. Vol. 11, n. 3 dez. **2006.**
33. Pereira, L. B. *A influência do Enem na prática pedagógica da disciplina de química*: o ponto de vista dos professores. 118 p (Dissertação de Mestrado) – Universidade Católica de Petrópolis, Programa de Pós- Graduação Stricto Sensu em Educação, Petrópolis, **2014**.
34. Pérez Gomes, A. I. Ensino para a compreensão. Sacristán, J. G., Pérez Gómez, G. *Compreender e transformar o ensino,* p. 67-98, Artmed, Porto Alegre, **1998**.
35. Ranieri, N. B. S., Alves, A. L. A. (org.). *Direito à educação e direitos na educação em perspectiva interdisciplinar*. São Paulo: Cátedra UNESCO de Direto à Educação/Universidade de São Paulo (USP), **2018**.
36. Sant'Anna, I. M., Sant'Anna, V. M. *Recursos educacionais para o ensino: quando e por quê?*, Vozes, Petrópolis – Rio de Janeiro, **2004**.
37. Santos, D. G., Borges, A. P. A., Borges, C. O., Marciano, E. P., Brito, L. C. C., Carneiro, G. M. B., Epoglou, A., Nunes, S. M. T. A química do lixo: utilizando a contextualização no ensino de conceitos químicos. *Revista Brasileira de Pós-Graduação*, Brasília, DF, v. 8, n. 2, p. 421-443, **2012**.
38. Santos, W. L. P., Schnetzler, R. P. Função social: o que significa ensino de química para formar o cidadão? *Química Nova na Escola pesquisa*. n.4, p. 28-34, nov **1996**.
39. Saucedo, C. dos S., Bedin, E. Estágio em Química: o Meio Ambiente em um Ensino Contextualizado. *Revista de Ensino, Educação e Ciências Humanas* 19.3, p. 344-352, **2018.**
40. Saviani, D. *Pedagogia histórico-crítica: primeiras proximações*. 11. ed. revisada. Campinas, SP: Autores Associados, **2011**, p. 89-111.
41. Vygotsky, L. S. Aprendizagem e desenvolvimento na Idade Escolar. In: Vigostky, L., Luria, A., Leontiev, A. N. *Linguagem, desenvolvimento e aprendizagem*. São Paulo: Ícone, **2010**.
42. Zucco, C. Química para um mundo melhor. *Química Nova*, v. 34, n. 5, p. 733-733, **2011**.

Downloaded from www.periodico.tchequimica.com

PERIÓDICO TCHÊ QUÍMICA
ARTIGO ORIGINAL

ESTUDO DO EFEITO EM PÓ DE SEMENTES DE ESPINHEIRO-MARÍTIMO NA PRODUÇÃO DE PRODUTOS À BASE DE CARNE DEFUMADA A PARTIR DE CARNE DE CAMELO E DE BOVINO

STUDY OF SEA BUCKTHORN SEED POWDER EFFECT ON THE PRODUCTION OF COOKED-SMOKED MEAT PRODUCTS FROM CAMEL MEAT AND BEEF

MAKANGALI, Kadyrzhan[1*]; KONYSBAEVA, Damilya[2]; ZHAKUPOVA, Gulmira[1]; GORBULYA, Viktoriya[2]; SUYUNDIKOVA, Zhanar[3];

[1]S. Seifullin Kazakh agrotechnical University, Department of Food Technology and Processing Products

[2]S. Seifullin Kazakh agrotechnical University, Department of Plant Protection and Quarantine

[3]Kostanay State Pedagogical University, Department of Natural Sciences

** Correspondence author*
e-mail: kadr_90.taz@mail.ru

Received 01 October 2019; received in revised form 13 October 2019; accepted 14 October 2019

RESUMO

As propriedades de consumo da carne dependem em grande parte da composição física e química. O valor da carne de camelo é determinado pelo seu alto teor de nutrientes, em uma forma facilmente digerível, necessária para o funcionamento normal do corpo. No entanto, o principal obstáculo ao uso de carne de camelo na produção de embutidos é a dureza da carne e a fraca capacidade de ligação da mistura da carne de camelo. Assim, pesquisas nessa área são relevantes. Este artigo representa o estudo do efeito de sementes de espinheiro-marítimo em pó nos indicadores de qualidade de produtos à base de carne defumada cozida a partir de carne de camelo e carne bovina. Nesse sentido, estudou-se a composição química do pó de sementes de espinheiro-marítimo que apresentou alto teor de proteínas e polissacarídeos. Verificou-se que o pó das sementes de espinheiro-marítimo é uma fonte de substâncias biologicamente ativas como tocoferol 62,15 ± 2,13 mg / 100 g, carotenóides 4,21 ± 0,22 mg / 100 g e flavonóides 1,54 ± 0,06% .06% justificando, assim, a escolha do pó das sementes de espinheiro-marítimo como parte do produto de carne defumada cozida a partir de carne de camelo e carne bovina. Foi cientificamente comprovado que o pó das sementes de espinheiro-marítimo aumenta os parâmetros funcionais e tecnológicos, melhora as características estruturais, mecânicas e de cor do produto acabado. Em particular, aumenta o rendimento do produto em 6,8%, o teor de umidade em 9,35%, a capacidade de ligação à umidade em 2%, a capacidade de retenção de gordura em 3,5%; a força de cisalhamento foi de 5,8 N / m. Como resultado do estudo, foi proposto o uso de sementes de espinheiro-marítimo em pó na produção de produtos à base de carne de camelo e bovina.

Palavras-chave: Carne de camelo, processamento de carne, composição química, propriedades funcionais e tecnológicas, flavonóides.

ABSTRACT

Consumer properties of meat largely depend on the physical and chemical composition. The value of camel meat is determined by its high content of nutrients in an easily digestible form necessary for the normal functioning of the body. However, the main obstacle to the use of camel meat in the production of sausage products is meat hardness and weak moisture-binding capacity of camel meat. Thus, research in this area is relevant. This article represents the study of sea buckthorn seed powder effect on the quality indicators of cooked-smoked meat products from camel meat and beef. In this regard, the chemical composition of the sea buckthorn seed powder was studied, which showed a high content of proteins and polysaccharides. It was found that the powder from the sea buckthorn seeds is a source of such biologically active substances as tocopherol 62.15 ± 2.13 mg/100 g, carotenoids 4.21 ± 0.22 mg/100 g, and flavonoids 1.54 ± 0.06%.06%. The choice of powder from the sea buckthorn seeds as part of cooked-smoked meat product from camel meat and beef is justified. It has been scientifically proven that the powder from the sea buckthorn seeds boosts the functional and technological parameters, improves the structural, mechanical and color characteristics of the finished product. In particular, it increases the product yield by 6.8%, the moisture content by 9.35%, the moisture-binding capacity by 2%, the fat-holding capacity by 3.5%; the shearing force was 5.8 N/m. As a result

Downloaded from www.periodico.tchequimica.com

of the study, the use of sea buckthorn seed powder in the production of meat products from camel meat and beef has been proposed.

Keywords: Camel meat, meat processing, chemical composition, functional and technological properties, flavonoids.

1. INTRODUCTION

The development of mass food under market relations is directly related to the solution of such tasks as improving the quality of the products made, switching to a labile range of meat products considering the consumers' demand. Development of formulations and technologies of new types of products with original or unique organoleptic indicators with maximum use of all resource sources including non-traditional raw materials is promising and cost-effective (Lisitsyn *et al,*2007).

The camel meat is an unconventional type of raw meat; its properties resemble horsemeat. It is of red color without marbling, tough, dense texture, peculiar smell. Due to its easy digestibility by the human body, camel meat (and fat) is used as diet meat. However, these qualities of camel meat have not been sufficiently studied (Kadim, I. T. *et al*, 2013, Abdelhadi *et al*, 2012, Abril *et al*, 2001, and etc.).

In the Republic of Kazakhstan and in neighboring countries (Russian Federation, Uzbekistan, Turkmenistan) people mainly are occupied with dairy camel breeding as well as breeding to produce wool and further processing products. Meat camel breeding is very far behind in development due to the high content of connective tissue in camel meat, its coarse-fibred structure, which causes meat hardness that is a major obstacle to its widespread use. For this reason, camel meat is mainly used for food only at home (Lisitsyn *et al*, 2018).

In order to improve the quality of sausage made from camel meat, Kalalou and other scientists (Kalalou *et al*,2004) used Selected Lactic Acid Bacteria. The proposed method has shown good results in organoleptic characteristics and structural and mechanical properties of the product. However, the process of production of camel sausage using lactic acid bacteria requires very strict control of microbiological indicators in the maturation process.

Abdel Moneim and E. Suliman (Abdel Moneim *et al*, 2014) studied the sensory characteristics, juiciness, consistency of camel meat sausage as well as the effect of the season, the age of the meat-producing animal and the time of raw meat storage for the sausage production on these indicators. As a result of the study, scientists propose using fresh or frozen raw meat.

Engy (Engy, F. Zaki, 2017) studied the possibility of adding protein emulsion in the production of camel meat sausages. The study suggested the addition of protein emulsion in an amount of 4%, which improves the organoleptic characteristics, moisture-binding capacity, fat-holding capacity, juiciness, consistency of the finished product.

Minimal costs for the breeding and management of camels, the high yield of meat products, fat and other products shows the need to process camel meat and thereby obtain additional resources of raw meat.

In this regard, the development of high-quality meat products from camel meat requires scientifically based methods and modes of its processing, the use of intensive processing methods and effective salting methods.

This study was aimed at developing a new cooked-smoked meat product from camel meat using powder from sea buckthorn seeds in order to activate the maturation processes and impart the improved structural and mechanical parameters, organoleptic indicators, and physical and chemical parameters to the finished product.

2. MATERIALS AND METHODS

2.1 Samples

Laboratory studies of test samples were held in the research laboratory of the V.M. Gorbatov All-Russian Research Institute of the Meat Industry (Moscow, Russian Federation). The test sample of cooked-smoked meat product from camel meat was made from the meat of the Kazakh double-humped camel (Bactrian) at the age of two; camel meat and beef were purchased at Daulet-Beket LLP camel farm (Akshi village, Almaty region, Kazakhstan). Powder from the sea buckthorn seeds was purchased from The Semins' Private Apiary (Moscow, Russian Federation).

Downloaded from www.periodico.tchequimica.com

The test samples were produced at the meat processing research center of Almaty Technological University (Almaty, Republic of Kazakhstan).

2.2 Chemical composition

The chemical composition of meat and meat products was determined by commonly known methods.

Two-hundred grams of product sample were placed in plastic containers, frozen and then dried in a thermal freeze dryer (Modulyol-230, Milford-UK) for 5 days under 100-mbar pressure at −50 °C. The frozen dry samples were ground to a homogeneous mass in a grinder (Panasonic-Mixergrinder-Model MX119N-Japan) for chemical analyses. The moisture was determined by weighing 200 g meat sample before and after drying in a thermal freeze dryer for 5 days. The proximate chemical composition of the product was determined according to the standard methods of the AOAC (2000).

Protein was determined using a Foss Kjeltec 2300 nitrogen/protein analyzer (State standard P 50258). Fat was determined by Soxhlet extraction method using petroleum ether (State standard 23042-86). Ash content was determined by ashing samples in a muffle furnace at 500 °C for 24 h (State standard 31727-2012)

2.3 Determination of the pH

Determination of the pH of meat and meat products. The pH of meat products was monitored using a portable pH meter (Hanna waterproof pH meter, Model Hi 9025) fitted with a plastic body open junction, conic (Hanna FC200B) and a temperature adjusting probe. The pH probe and the thermometer were inserted into the product to a similar depth (2 cm).

2.4 Mineral composition

A mixed standard solution was prepared from a 1000 µg/ml multi-element solution (Darmstadt, Germany) and inhouse standard reference materials used for validation of the method. Evaluation of mineral levels in the samples was carried out after complete digestion using a Milestone 1200 MDR microwave system at a temperature of 200 °C in closed (PTFE) vessel. In brief 5 ml of conc. HNO_3 and 1 ml of 30% H_2O_2 were added to each digestion vessel. They were then heated to 200 °C over a 5-min period and then held at 200 °C for another 20 min. The digest obtained was collected in 50-ml volumetric flasks and made up to volume. Measurements were carried out on the ICP-OES system (Perkin Elmer Model 3300) equipped with a low-flow Gem Cone nebulizer in addition to an ultrasonic nebulizer for low concentrations.

2.5 Sensory indicators of meat products

Sensory evaluation was carried out using score assessment. Ten points scores of intensity and desirability scales were used in the experiment. There was from 1 point (very slight) to 10 point scores of intensity (very strong) and similar for desirability: from 1 point (undesirable) to 10 point (very much desirable). All processed meat products were sensory investigated by six-panel. Products were prepared as half of chubs and 2.5 mm slices and presented to panelists on disposable dishes in white glow light (250 1x). The next sensory parameters were investigated: 1-taste, 2 – smell and aroma, 3 – appearance, 4 – consistency, 5 – view at the cut, 6 – juiciness. (State standard 9793-74, 23041-78).

3. RESULTS AND DISCUSSION:

Sea buckthorn seeds are one of the by-products of the sea buckthorn berries processing. Being a natural concentrate of biologically active substances, sea buckthorn seeds are not widely used. Like any recycled material, sea buckthorn seeds can be considered as a cheap, economically feasible plant component (Lamo *et al*, 2014).

The seeds of sea buckthorn are a natural concentrate of proteins, fats, and carbohydrates (Table 1). Analysis of the chemical composition of seeds showed that seeds contained a significant amount of dietary fiber.

Unlike sea buckthorn pulp, seeds contain slightly fewer carotenoids and ascorbic acid. However, this raw material is rich in such natural antioxidants as tocopherols. Sea buckthorn seeds are far superior to other berries and nuts in this essential protective combination of cell membranes.

Recently, flavonoid compounds were of considerable interest not only as vitamin-like substances but also as strong antioxidants. The presence of flavonoids in the seeds increases the value of the latter. The data obtained show that buckthorn seeds are a promising source of functional ingredients.

Downloaded from www.periodico.tchequimica.com

Table 1. *Chemical composition of sea buckthorn seeds*

Indicator	Content
Proteins, %	20.06±1.15
Lipids, %	12.07±0.65
Carbohydrates, %, including:	
Cellulose	14.21±0.68
Pectin	2.46±0.05
Starch	0.51±0.55
Mono- and disaccharide	1.25±0.52
Minerals %	3.3
Carotenoids, mg	4.21±0.22
Flavonoids, %	1.54±0.06
Tocopherol, mg	62.15±2.13
Ascorbic acid, mg	6.54±0.32
Thiamine, mg	1.02±0.07
Riboflavin, mg	0.25±0.01
Pantothenic acid B3, mg	0.35±0.02
Nicotinic acid B5, mg	0.38±0.02
Pyrodoxine hydrochloride B6, mg	0.26±0.02
Folic acid Bc, mg	0.056±0.06

Analysis of the amino acid composition of seeds (Table 2) showed a high content of arginine and histidine, which are essential for children, in the non-essential amino acids. Seed proteins also contain a lot of glycines and glutamic acid, which are used separately as flavoring agents.

Table 2. *The amino acid composition of proteins of sea buckthorn seeds (mg/100 g of product)*

Amino Acid Name	Sea Buckthorn Seeds
Essential Amino Acids	
Valin	888
Leucine	1998
Phenylalanine	847
Lysine	1085
Methionine	24
Threonine	655
Tryptophan	297
Isoleucine	745
6538	8583
Non-essential Amino Acids	
Cystine	208
Arginine	5608
Alanine	637
Aspartic	1239
Glycine	2810
Serine	1515
Proline	857
Histidine	577
Tyrosine	519
Glutamic	6317

Further, the amino acid score of proteins in the sea buckthorn seed powder (Table 3) was studied in comparison with other seeds.

The method of chemical scores allows establishing the likely efficiency of utilization of the studied protein in the first approximation. It has been established that all essential amino acids are present in the protein of the powder from sea buckthorn seeds; the content of lysine, the basic amino acid that limits the nutritional value of vegetable proteins in the sea buckthorn seeds, is approximately at the same level as oilseeds.

Vitamins are biologically active substances that are necessary for the implementation of the mechanisms of enzymatic catalysis, the normal course of metabolism, maintaining homeostasis, and biochemical provision of body functions. The vitamin composition of the seeds of sea buckthorn is presented in table 4.

Table 4. *Vitamin composition of sea buckthorn seeds*

Indicators	Content
Carotenoids, mg %	6.01 ± 0.22
Flavonoids, mg %	2.2 ± 0.06
Tocopherol, mg %	88.7 ± 2.13
Ascorbic acid, mg %	9.34 ± 0.32
Thiamine, mg %	1.45 ± 0.07
Riboflavin, mg %	0.35 ± 0.01
Pantothenic acid B3, mg %	0.5 ±0.02
Nicotinic acid B5, mg %	0.54 ±0.02
Pyridoxine hydrochloride B6, mg %	0.37 ±0.02
Folic acid Bc, mg %	1.14 ±0.06

Thus, the sea buckthorn seeds have a huge energy potential, because they contain a significant number of proteins, fats, and carbohydrates. Experimental studies have shown the high nutritional value of sea buckthorn seeds, which is characterized by the presence of water- and fat-soluble vitamins, including the ones of antioxidant action.

3.1 Study of the effect of sea buckthorn seed powder on the functional and technological properties of the finished product.

When forming the structural-mechanical and functional-technological properties of meat products, the content of structure-forming agents — polysaccharides in the system and their qualitative composition — are of particular importance. The carbohydrate-water and carbohydrate-lipid interactions are associated

Downloaded from www.periodico.tchequimica.com

with the properties of polysaccharides; therefore, water and fat-holding capacity are some of the mandatory indicators for evaluating the functional ingredient for sausage production.

Traditionally, starch, wheat flour is used in the production of sausages as a moisture-holding component, the chemical composition of which contains not less than 70% of carbohydrates, about 65% of which is starch with the feature of high moisture-binding capacity.

Figure 1 presents the results of the study of the functional and technological properties of the powder of sea buckthorn seeds.

The analysis of the data in Figure 1 shows that sea buckthorn seeds have high functional and technological properties. The moisture-holding capacity of the seeds of sea buckthorn compared to the traditionally used wheat flour is 8% higher, and the fat-holding capacity of the seeds of sea buckthorn compared to the widely used wheat and rice flour is higher by 10% on average.

The experimentally determined values of moisture- and fat-holding capacity of sea buckthorn seed powder do not fully reflect the nature of moisture-binding and holding under conditions closest to the actual sausage production technology, therefore, for more accurate formulation of the recipe, test samples were made and studied, which included the minced meat with the addition of 5%, 10%, and 15% of sea buckthorn seed powder.

Functional and technological properties were defined as a set of indicators that characterize the levels of moisture-binding capacity, pH, moisture, and sensory characteristics.

One of the main physical and chemical indicators that normalize the technological process is the pH. This indicator determines the features of structure formation in the finished product as well as the shelf life (Figure 2).

An increase in the pH value by 0.4-0.8 was observed in the test samples with an increase in the amount of the powder from sea buckthorn seeds introduced, which is caused by a higher pH value of sea buckthorn seeds.

It was established that the sample with the addition of 10% of the plant component when reaching the pH value of 6.5-6.7, the minced meat has a pronounced taste, flavor, delicate texture, it binds water well, i.e. acquires the properties required to produce high-quality sausages.

In the production of sausages, quality indicators related to the moisture content and moisture-binding capacity, which affects the yield of finished products, are of particular importance.

Technological properties and some physical and chemical indicators of the test samples are presented in Table 5.

With the addition of the sea buckthorn seed powder, the moisture-binding capacity of minced meat increases due to the increase in pH.

Analysis of the study results showed that the highest moisture-binding capacity value is observed with the addition of 15% of the sea buckthorn seed powder into the minced meat. The increase in moisture-binding capacity allows increasing the yield of finished products by 9.35%, which will help to increase the economic efficiency of minced meat production.

At the stage of development of the composition of the test samples, the effect of the dose of the sea buckthorn seed powder added in the amount of 5%, 10% and 15% on the rate of elastic-plastic deformation of minced meat was studied. The results of experimental studies are presented in Figure 3.

The data presented in Figure 3 showed that with the addition of 15% of sea buckthorn seed powder, the deformation force increased by 54%, which leads to undesirable compaction of the minced meat system.

When adding 10% of sea buckthorn seed powder, the structure is compacted by 43% compared to the control, which according to literary data, is within the recommended limits.

To clarify the optimal amount of powder from sea buckthorn seeds, test samples of cooked smoked sausages were made with a different dose of added powder from sea buckthorn seeds and their organoleptic characteristics were studied (Figure 4).

The data presented in Figure 4 showed that cooked smoked sausage with the addition of 10% of hydrated sea buckthorn seed powder has the best organoleptic properties. Increasing the amount of powder from the sea buckthorn seeds to 15% leads to a deterioration in the taste and aroma of sausages.

In order to achieve an intensive and stable coloring of meat products, sodium nitrite is added in the amount prescribed by the formulation, as part of the curing mixture.

Under the action of curing ingredients, a significant amount of metmyoglobin is formed,

Downloaded from www.periodico.tchequimica.com

which prevents the formation of nitroso myoglobin. Therefore, the process of metmyoglobin recovery to myoglobin during curing is essential.

Optimum reducing conditions are created at pH 5.7, i.e. close to the isoelectric point of the proteins of the meat, however, the moisture-binding capacity of the meat is minimal. In our case, the pH values of meat systems are in the range of 6.4-6.7, which creates optimal conditions for good moisture-binding. To obtain a good color under these conditions, the presence of reducing substances in a sufficiently large amount is required, which is achieved by adding the powder from the sea buckthorn seeds.

Reducing sugars (for example, glucose) are used to create reducing conditions. When glucose is used with sucrose, the color is significantly improved. Sucrose itself does not create reducing conditions, however, the intermediate products of its anaerobic decomposition (phosphoglyceraldehyde, fructose-6-phosphate, etc.), which are formed under the action of bacterial enzymes, have a significant reducing (recovering) effect.

Such biologically active substances with reducing properties as tocopherol, carotenoids, flavonoids, ascorbic acid present in the sea buckthorn seeds allow refusing the addition of glucose.

Ascorbic acid not only restores the oxidative forms of heme pigments, but also protects nitroso pigments from oxidation, and enhances the antibacterial properties of nitrite relative to *Cl. Botulinum,* inhibits the reaction of peroxide oxidation and prevents the formation of alkylating mutagens like nitrosamines from nitrites (by 32-35%).

Due to the presence of biologically active substances with regenerating properties in sea buckthorn seeds, the process of colouring formation in finished meat products was studied with a study of the residual degree of stability of nitroso pigments, sodium nitrite content and nitroso pigments content. Table 6 presents the colour stability of the finished product with a different dose of sea buckthorn seeds added.

Following the data presented in table 6, the colour stability of the finished meat products increased with the introduction of the powder from sea buckthorn seeds; thus, with the introduction of 5%, it increased by 4.5%, with the introduction of 10% it increased by 5%, which may be due to the high reducing activity of tocopherols, flavonoids, reducing sugars and ascorbic acid present in the sea buckthorn seed composition.

4. CONCLUSIONS:

The results of the study have shown that the addition of powder from sea buckthorn seeds in an amount of not more than 10% helps to improve the functional and technological properties of minced meat. Sea buckthorn seeds bind water due to the protein system and polysaccharides, as a result of which the stability of the finished product is maintained, the losses during heat treatment are reduced, the juiciness and the yield of the product increases. In addition, the introduction of 10% of the sea buckthorn seed powder contributes to the colour stability of the finished product. In connection with the above, the amount of added hydrated powder from sea buckthorn seeds in the recipe of cooked smoked camel meat and beef sausage is approved at 10%.

5. ACKNOWLEDGMENTS:

The study was performed as part of the research work No.0457/GF4 Study of the Functional and Biocorrective Characteristics of Plant-Animal Complexes and the Development of the Technology of National New-Generation Meat Products on their Basis Using Local Raw Materials funded by the Ministry of Science and Education of the Republic of Kazakhstan.

6. REFERENCES:

1. Abdelhadi, O. M. A., Babiker, S. A., Picard, B., Jurie, C., Jailler, R., Hocquette, J. F., & Faye, B. *Meat Science*, **2012,** *90*, 139–144.

2. Abril, M., Campo, M. M., Onenc, A., Sanudo, C., Alberti, P., & Negueruela, A. I. *Meat Science*, **2001,** 58, 69–78.

3. Abdel Moneim, Suliman Selma, Fadlalmola, Babiker, Omer, Arabi, Safa M. Ibrahim (2014). *Food and Public Health*, **2014,** 4(6): 293-300.

4. Al-Bachir, M., & Zeinou, R. *Meat Science*, **2009,** 82, 119–124.

5. Al-Sheddy, I., Al-Dagal, M., & Bazaraa, W. A. *Journal of Food Science,* **1999,** 64, 336–339.

6. AOAC. *Official methods of analysis of the Association of Analytical Chemists (17th ed.).* Gaithersburg, *Maryland*, 2000.

Downloaded from www.periodico.tchequimica.com

7. Belew, J. B., Brooks, J. C., McKenna, D. R., & Savell, J. W. *Meat Science,* **2003,** 64, 507–512.

8. Bouton, P. E., Harris, P. V., & Shorthose, W. R. *Journal of Food Science*, **1972,** 37, 351–355.

9. Engy, F. Zaki. *International Journal of Environment. Agriculture and Biotechnology* , **2017,** 2(5): 2481-2486.

10. Fatima Theyab Al meqbaali, Hosam Habib, Aws Othman, Saeda Al-Marzooqi, Alia Al-Bawardi, Javed Yasin Pathan, Serene Hilary, Usama Souka, Suleiman Al-Hammadi, Wissam Ibrahim, Carine Platat. *Emirates Journal of Food and Agriculture*. **2017;**29(11):822-832.

11. Heneiksen-larsen, K. B., Lexell, J., & Sjostrom, M. *Histochemistry Journal*, **1983,** 15, 167–178

12. Kadim, I. T., Mahgoub, O., Al-Marzooqi, W., Al-Zadgali, S., Annamali, K., & Mansour, M. H. *Meat Science,* **2006,** 73, 619–625.

13. Kadim, I. T., Mahgoub, O., & Purchas, R. W. *Meat Science,* **2008,** 80, 555–569.

14. Kadim, I. T., Al-Karousi, A., Mahgoub, O., Al-Marzooqi, W., Khalaf, S. K., Al-Maqbali, R. S., Raiymbek, G. *Meat Science,* **2013,** 93(3), 564–571.

15. Kalalou I, Faid M and Ahami AT. *Electronic Journal of Biotechnology*, **2004,** 7(3): 243–248.

16. Larmo, Yang B, Hyssälä J, Kallio HP, Erkkola R. *Maturitas,* **2014,** 79(3):316-21.

17. Lisitsyn A. *Meat and healthy food*. Lisitsyn A., Sisenko E.I, Chernukha I.M, Aleksakhina V.A, Semenova A.A, Durnev A.D. V.M. Gorbatov All-Russian Research Institute of the Meat Industry, Moscow, 2007.

18. Lisitsyn A., Makangali K., Uzakov Y., Taeva A., Konysbaeva D., Gorbulya, V. *Current Research in Nutrition and Food Science journal*, **2018,** 6(2): 536-551.

19. Mancini, R. A., & Hunt, M. C. *Meat Science,* **2005,** 71, 100–121.

20. Mulvihill, B. *British Nutrition Foundation. Nutrition Bulletin,* **2001**, 26, 295–299.

21. Rees, M. P., Trout, G. R., & Warner, R. D. *Meat Science,* **2003,** 65, 791–804.

22. Shariatmadari, R., & Kadivar, M. *52nd International Congress of Meat Science and Technology*, Dublin, Ireland, 2006.

23. State standard P 50258.

24. State standard 9793-74 Meat products. Methods for determining moisture.

25. State standard 23042-86 Meat and meat products. Methods for determining fat.

26. State standard 25011-81 Meat and meat products. Methods for the determination of protein.

27. State standard 31727-2012 (ISO 936:1998) Meat and meat products. Method for determining the mass fraction of total ash.

28. State standard 23041-78 Meat and meat products.

29. Wood, J. D., Enser, M., Fisher, A. V., Nute, G. R., Sheard, P. R., Richardson, R. I., Hughes, S. I., & Whittington, F. M. *Meat Science*, **2008,** 78, 343–358.

Downloaded from www.periodico.tchequimica.com

Table 3. Amino acid score of the sea buckthorn seed powder

Amino Acids	FAO protein	Sea buckthorn Seeds	Sunflower Seeds
Lysine	5.5	56.27	62.0
Threonine	4.0	59.326	107.5
Leucine	7.0	81.4	92.8
Isoleucine	4.0	53.12	90.0
Tryptophan	1.0	84.71	160.0
Valin	5.0	64.18	104.0
Methionine + Cystine	3.5	10.17	108.0
Tyrosine + Phenylalanine	6.0	59.66	128.0
Utilisation Ratio		0.15	0.62

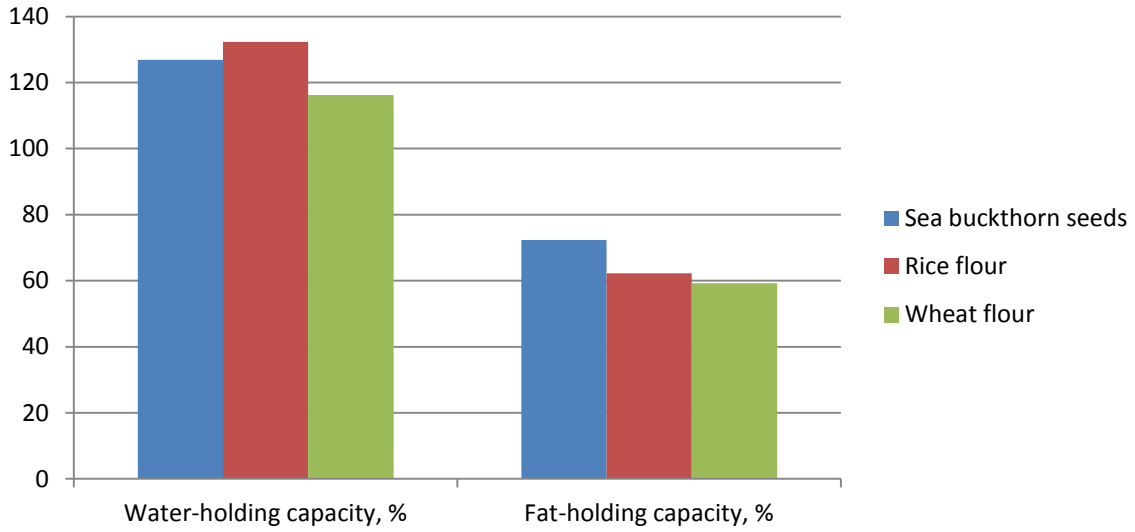

Figure 1. *Water- and fat-holding capacity of the sea buckthorn seeds powder*

Table 5. *Technological, physical, and chemical indicators of test samples with the added sea buckthorn seed powder*

Indicators	Control	Test		
		Amount of sea buckthorn seeds, %		
		5	10	15
pH	6.0	6.4	6.7	6.8
Moisture content,%	52.6	56.61	61.95	66.51
Moisture-binding capacity, %	72.15	73.23	74.15	78.26
Yield, %	85	88.2	91.8	94.35

Downloaded from www.periodico.tchequimica.com

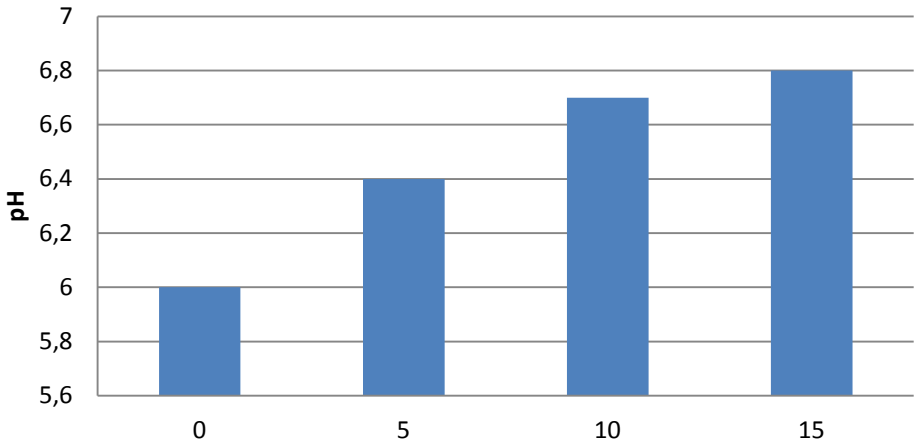

Figure 2. *The pH value of the minced meat with the addition of sea buckthorn seed powder*

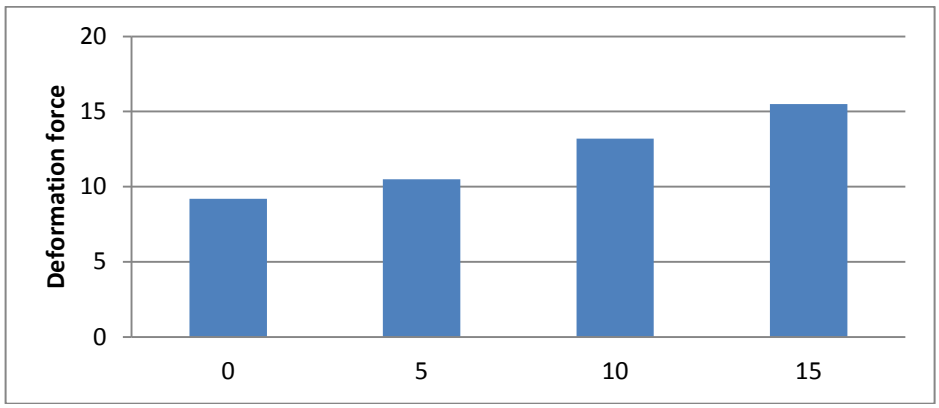

Figure 3. *The change in the minced meat deformation force with the addition of different amounts of sea buckthorn seeds*

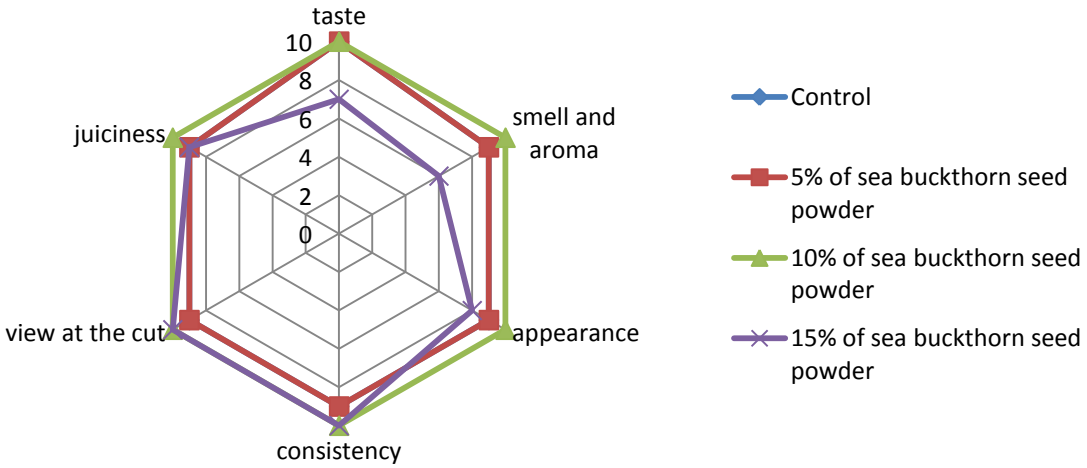

Figure 4. *Organoleptic properties of cooked-smoked sausages with different amounts of added sea buckthorn seed powder*

Table 6. *The colour stability of the finished product*

Indicators	Control	Sea buckthorn seed powder, %	
		5	10
Stability, %	89.3±2.1	94.3±2.3	95.8±1.9
Residual amount of sodium nitrite, %	0.0040±0.0001	0.0030±0.0001	0.0020±0.0001

Downloaded from www.periodico.tchequimica.com

PERIÓDICO TCHÊ QUÍMICA
ARTIGO ORIGINAL

O POTENCIAL DA GERAÇÃO DE ENERGIA A PARTIR DE LODO DE FRIGORÍFICO E SERRAGEM DE MADEIRA

THE POTENTIALITY OF THE ENERGY GENERATION FROM SLAUGHTERHOUSE SLUDGE AND WOOD SAWDUST

MENEZES, Kadja Maisa da Silva[1*]; PRADOS, Carolina Porto[2]; FIGUEREDO, Kytéria Sabina Lopes de[3];

[1,2] Universidade Federal do Tocantins, Campus Universitário de Gurupi, Colegiado de Ciências Exatas e Biotecnológicas, Gurupi, Tocantins, Brasil

[3] Universidade Federal Rural do Semi-Árido - UFERSA, Curso de Engenharia Ambiental**,** Mossoró, Rio Grande do Norte, Brasil

** Autor correspondente*
e-mail: carolinaprados@mail.uft.edu.br

Received 05 August 2019; received in revised form 18 October 2019; accepted 18 October 2019

RESUMO

A utilização de resíduos para produção de energia através de processos como pirólise, combustão e extração de óleos é uma solução sustentável para problemas ambientais sérios como a centralização da matriz energética em materiais não renováveis e poluentes e o volume de resíduos sólidos urbanos. Nesse contexto, este trabalho objetivou analisar o potencial energético de duas biomassas de resíduos sólidos: lodo de abatedouro municipal e serragem de madeira gerados na cidade de Gurupi –TO. Foram avaliados os teores de umidade, voláteis, cinzas e carbono fixo através da análise imediata e poder calorífico superior (PCS) e inferior (PCI) para todas as amostras coletadas. Na análise imediata verificou-se que a amostra de lodo apresentou teor de cinzas superior ao da serragem e ambas apresentaram elevados teores de voláteis. A serragem apresentou maior poder calorífico (4882 cal kg^{-1}) que o lodo (3952,5 cal kg^{-1}), mas o processo de obtenção de energia a partir do lodo requer menor quantidade de calor. Pode-se concluir ainda que ambos os materiais apresentam alternativas viáveis para obtenção de energia.

Palavras-chave: Poder Calorífico; biomassa; Fontes renováveis de energia.

ABSTRACT

The use of waste for energy production through processes like pyrolysis, combustion and oil extraction is a sustainable solution to serious environmental problems like centralization of the energy matrix in non-renewable materials and pollutants and the volume of urban solid waste. In this context, this work aimed to analyze the energy potential of two solid waste biomasses: municipal slaughter sludge and wood sawdust generated in the city of Gurupi –TO. Were evaluated the contents of humidity, volatile content, ash, fixed carbon through the immediate analysis and upper (PCS) and lower (PCI) calorific value were evaluated for all samples collected. In the immediate analysis it was found that the sludge sample had higher ash content than the sawdust and both had high volatile contents. The sawdust presented higher calorific power (4882 cal kg-1) than the sludge (3952.5 cal kg-1), but the process of obtaining energy from the sludge requires less heat. It can also be concluded that both materials present viable alternatives for obtaining energy.

Keywords: Calorific Value, biomass, Renewable sources of energy.

Downloaded from www.periodico.tchequimica.com

1. INTRODUÇÃO

A geração de energia a partir de resíduos sólidos que acarretam em graves impactos ambientais representa uma solução sustentável para gestão desses resíduos que tem sido problemática para a maioria dos países nos últimos anos (Chen, 2018; Song; Li; Zeng, 2015). Em especial os provenientes de processos industriais e sanitários devido ao potencial poluidor e os resíduos de maior volume pelas complicações logísticas. Para essa finalidade é essencial compreender a disponibilidade e o rendimento energético nos materiais, o que pode ser feito através de uma análise imediata e medida ou estimativa do poder calorífico (Chen, 2018; Milbrandt *et al*., 2018).

Ao estabelecer um caminho sustentável econômica e ambientalmente para o aproveitamento energético ocorre a reinserção na cadeia produtiva, transformando os resíduos em matéria prima e aumentando o seu ciclo de vida. Sendo que a aplicabilidade está condicionada à composição química, propriedade físicas e potencial poluidor do material residual. Pode-se dizer que trata-se de uma forma de reciclagem já que envolve submeter os resíduos a um processo de transformação química que levará à geração de algum produto de valor mercadológico como no caso da produção de energia (Borowski *et al*., 2002; Nozela *et al*., 2018).

Os países industrializados geram volumes significativos de resíduos e efluentes com composição química significativamente variada dependendo do processo industrial de que é proveniente. Esse tipo de resíduo geralmente tem um potencial danoso pela presença de metais pesados, poluentes orgânicos persistentes além de caráter extremo de acidez ou basicidade, ou seja, são quimicamente agressivos (Song; Li; Zeng, 2015). O lodo sanitário, por outro lado, é um problema difuso. Independentemente do tipo de atividade econômica, no mínimo o lodo sanitário residencial e proveniente de estações de tratamento de água e esgoto existirão (Guerra; Angelis, 2005).

Por outro lado, em localidades cuja economia é pautada na produção de produtos alimentícios, principalmente carnes, o volume de lodo sanitário é potencializado. Esse tipo de resíduo, apresenta alto teor de materiais voláteis, de óleos, e umidade, além de contaminantes biológicos. A periculosidade, nesses casos, está associada à presença de poluentes orgânicos persistentes, resíduos de fármacos e, a depender da alimentação dos animais, metais pesados. Pode-se adicionar ainda ao rol de resíduos que geram preocupação, os resíduos sólidos urbanos compostos de plástico, madeira, papel, metais e resíduos de alimentos, que por si só, não são tão potencialmente danosos, mas representam uma preocupação devido ao volume que ocupam (Ahmad *et al*., 2014).

Para a produção energética a serragem, que apesar de apresentar baixo potencial poluidor ocupa volume significativo, armazena quantidade significativa de energia nas macromoléculas orgânicas que a constitui. Outro resíduo que se destaca, principalmente pela oferta e ausência de destinação sustentável é o lodo sanitário, que também é constituído de compostos orgânicos que pode ter a energia das ligações químicas aproveitada.

Para Torquato (2016) as propriedades mais importantes que possibilitam a avaliação do potencial de uma biomassa para se transformar em combustível envolvem: o poder calorífico, a temperatura de ignição, análise elementar e imediata. Para o poder calorífico, a bomba calorimétrica possibilita sua análise empírica, onde “emprega-se uma determinada massa do material combustível a ser analisado, submetendo-o posteriormente à combustão completa dentro da cela reacional do calorímetro, que se encontra saturada de oxigênio” (Torquato, 2016, p. 37). Já, para a análise imediata, que determina teor de umidade, voláteis, cinzas e carbono fixo possibilitando a estimativa do poder calorífico, pode-se empregar mufla ou análise termogravimétrica. As mesmas envolvem o aquecimento seguido de pesagem para determinar cada um desses teores (Torquato, 2012).

O presente trabalho objetivou empregar algumas tecnologias para reciclar resíduos comumente gerados no município de Gurupi como, por exemplo, amostras de lodo provenientes de abatedouro municipal e a serragem da madeireiras, convertendo-os em energia. Soluções como esta apresentam uma série de vantagens, passando pela diversificação da matriz energética do país e pela diminuição dos impactos causados pela decomposição dos resíduos.

2. MATERIAIS E MÉTODOS

As amostras de biomassas usadas neste estudo são provenientes do Munícipio de Gurupi - TO sendo:

Downloaded from www.periodico.tchequimica.com

a - *lodo de abatedouro*: fornecido pelo Matadouro Municipal Gurupi: Grupo Paulon Maia (GAM) (Figura 1);

Figura 1. *Amostras de lodo antes da secagem*

b - *serragem*: fornecida pela Madeireira São Sebastião (Figura 2).

Figura 2. *Amostras de serragem antes da secagem*

Previamente aos ensaios, com exceção da análise de umidade, as amostras de lodo e de serragem foram submetidas ao processo de secagem em estufa de esterilização secagem digital 150 L Edutec. Nas seguintes condições:

a - Lodo: 24 horas à (100 ± 5) °C (Torquato, 2012) e
b – Serragem: 24 horas à (105 ± 2) °C (Quirino *et al.*, 2005).

2.1. Análise Imediata

As biomassas em estudo foram submetidas às análises de teor de umidade, cinzas, voláteis, carbono fixo e poder calorífico (real e estimado). As medições e análises foram realizadas no Laboratório de Química Analítica, do Complexo Laboratorial II, da Universidade Federal do Tocantins (UFT) - Campus Gurupi. As análises de cinzas e voláteis foram realizadas utilizando o forno mufla (GP Científica com um programador de temperatura DIGImec tipo FHMP). O poder calorífico foi estimado com base nos dados da análise imediata empregando-se as equações disponíveis na literatura.

2.1.1 Determinação da Umidade

O teor de umidade foi determinado de acordo com o método da Norma ASTM D 3173-85, em que pesou-se uma amostra de aproximadamente 1,000 g (m_1) a temperatura ambiente (quintuplicata) em cadinho de porcelana com peso constante já pré-determinado. Em seguida as amostras foram aquecidas na estufa com temperatura adequada ao tipo da amostra:

a - Lodo: 1 hora à temperatura 100 °C (Colen, 2011);

b - Serragem: 1 hora à temperatura 105±2 °C (NBR 8112).

Prosseguiu-se colocando os cadinhos contendo as amostras em um dessecador por 30 minutos para o resfriamento e em seguida os mesmos foram pesados. Esta operação foi repetida até peso constante já com amostra e a massa computada como m_2 para o cálculo da umidade, conforme descrito na Equação 1 onde m_1 é a massa da biomassa antes da secagem e m_2 é a massa da biomassa após a secagem.

$$Umidade(\%) = \frac{m_1 - m_2}{m_1} \times 100 \qquad \text{(Eq. 1)}$$

2.1.2 Determinação de matéria volátil

As amostras resultantes da determinação do teor de umidade foram aquecidas em uma mufla nas condições específicas para cada amostra:

a - Lodo: 60 minutos à temperatura 550 °C (ASTM D 2415-66);

b - Serragem: 7 minutos à temperatura 850 °C (NBR 8112).

Em seguida os cadinhos foram dispostos em dessecador para resfriamento durante 30 minutos. Os cadinhos contendo as amostras foram pesados até massa constante, anotaram-se as massas finais para cálculo do teor de matéria volátil (m_3).

O teor de material volátil foi calculado segundo a Equação 2 onde m_2 é a massa da biomassa antes da calcinação e m_3 é a massa da biomassa após a calcinação.

$$Teor\ de\ voláteis(\%) = \frac{m_2 - m_3}{m_2} \times 100 \qquad \text{(Eq. 2)}$$

2.1.3 Determinação do teor de cinzas

As amostras resultantes do procedimento anterior foram colocadas novamente em forno mufla nas temperaturas adequadas aos tipos de amostras:

a - Lodo: 1 hora à temperatura 900 °C (ASTM D 2415-66);

Downloaded from www.periodico.tchequimica.com

b - Serragem: 7 horas à temperatura 700 °C (NBR 8112).

Os cadinhos contendo as amostras foram pesados até massa constante, anotou-se as massas finais para cálculo do teor de cinzas (m_4).

O teor de cinzas foi calculado segundo a Equação 3 onde m_3 é massa da biomassa antes da pirólise e m_4 é a massa da biomassa após da pirólise.

$$Teor\ de\ cinzas(\%) = \frac{m_3 - m_4}{m_3} \times 100 \qquad \text{(Eq. 3)}$$

2.1.4 Carbono fixo

O valor do carbono fixo foi calculado de modo simultâneo ao andamento das análises imediatas com base na fórmula indireta sendo obtido pela diferença entre a amostra total e os teores de cinzas e voláteis segundo Ribeiro (2018) expresso pela Equação 4 onde Cf é o carbono fixo, V (%) é o percentual de voláteis e Cz (%) refere-se ao percentual de cinzas.

$$Cf = 100 - (V\% + Cz\%) \qquad \text{(Eq. 4)}$$

2.2. Determinação do poder calorífico

O poder calorífico superior (PCS) também foi estimado para as biomassas cujas análises foram realizadas em forno mufla. Para estimar o cálculo do poder calorífico das amostras utilizou-se modelos matemáticos com correlação com análise imediata destas. Esta análise fundamenta-se na soma dos calores desprendidos na combustão dos elementos que compõe o material chamado de poder calorífico superior da amostra (PCS) com erro absoluto de 3,74% (Ferreira *et al*., 2014; Channiwala e Parikh, 2002).

O PCS estimado foi determinado com base na análise imediata através da Equação 5 para determinação de ambas as biomassas. Já os poderes caloríficos inferior (PCI) e poder calorífico líquido (PCL) foram estimados de acordo com as equações 6 e 7 (Brand, 2010) onde U é o percentual de umidade.

$$PCS = 84{,}5104 \times (Cf) + 37{,}2601 \times (V\%) - 1{,}8642 \times (Cz\%) \qquad \text{(Eq. 5)}$$

$$PCI = PCS - 324 \qquad \text{(Eq. 6)}$$

$$PCL = \left[PCI \times \frac{100 - U}{100}\right] - (6 \times U) \qquad \text{(Eq. 7)}$$

Os valores do poder calorífico (real) foram medidos no Departamento de Engenharia Florestal da Universidade de Brasília (UnB).

O Poder calorífico superior (PCS) das biomassas também foram determinados em bomba calorimétrica, modelo C 2000 basic da IKA em conformidade com a Norma ASTM 3286-66. As amostras foram secas previamente em estufa durante 24 horas, as amostras foram colocadas em cadinho metálico e este posicionado dentro da bomba calorimétrica.

3. RESULTADOS E DISCUSSÃO:

3.1. Análise Imediata

A Tabela 1 apresenta os resultados da análise imediata da umidade, voláteis cinzas e carbono fixo para as duas biomassas analisadas.

Tabela 1. *Resultados dos valores médios da análise imediata: umidade, teor de voláteis, cinzas, carbono fixo.*

Propriedade (% m/m)	***Biomassa***	
	Lodo	***Serragem***
Umidade	(6,39±0,67)	(10,26±1,57)
Voláteis	(70,88±1,28)	(74,47±4,49)
Cinzas	(19,91±1,17)	(1,29±0,09)
Carbono Fixo	(2,81±0,30)	(24,25±4,48)

Fonte: Autores, 2019

3.1.1 Umidade

Os resultados para umidade estão demonstrados na Tabela 1. É possível observar que a umidade do lodo foi inferior à da serragem e a precisão da medida para o lodo foi superior.Os valores de umidade obtidos estão próximos aos encontrados em outros estudos. Souza (2010) por exemplo, encontrou um valor médio de 11,6% para serragem. Em estudo da avaliação energética desse tipo de material, Moulin (2010) encontrou valor médio de 10%. Em análise do lodo de uma estação de tratamento na cidade de Palmas -TO durante estação de chuva. Teixeira (2014) encontrou 6,85% de umidade.

O teor de umidade do lodo e da serragem é uma medida de extrema relevância para o aproveitamento energético pois está ligado ao consumo de energia durante a queima dessas biomassas. Um material com alta umidade demanda maior gasto energético na etapa de secagem do preparo do material. Segundo Vieira (2012) para escolher um combustível a umidade se torna um fator crucial, sendo valores acima de 50 % inexequíveis, pois a partir desse ponto a

Downloaded from www.periodico.tchequimica.com

energia liberada torna-se insuficiente para a combustão. Assim, o lodo e a serragem analisadas estão dentro da faixa de umidade ideal para produção de energia de acordo com esse parâmetro.

3.1.2 Voláteis

A proporção de voláteis presentes no resíduo é determinante no aproveitamento energético, principalmente para embasar o método a ser aplicado. Os voláteis são inversamente proporcionais ao carbono fixo. Além disso, o material volátil auxilia na ignição, porém quem mantém a chama é o carbono fixo.

O teor de material volátil variou entre 68,18 % a 72,15% com desvio médio de 1,28 para as amostras de lodo. Vale destacar que para conversão energética do lodo via pirólise Yang *et al*., (2005) recomenda teor de volátil entre 65 e 85 %, demonstrando a aplicabilidade dos resíduos estudados para geração de energia empregando a pirólise.

Por outo lado, Telmo *et al*., (2010) estipulou para biomassa lenhosa teor de voláteis variando entre 76% para 86%, assim como Białowiec *et al*., (2017) que obteve um valor médio para voláteis para serragem muito próximo: 77,6 ± 0,25% m/m. O resultado para serragem na presente pesquisa permaneceu entre 67,53% e 77,52% aproximando-se então dos materiais estudados por esses autores.

3.1.3 Cinzas

O valor médio de cinza da serragem foi de 1,29%, dentro da normalidade, conforme resolução SAA 11 (2015) que considera valor inferior a 1,5% como aceitável e desejável para serragem. Nogueira e Lora (2003), verificaram o baixo teor de cinzas presentes em diversos tipos de biomassas, principalmente na serragem, considerando satisfatório um teor de cinza de 0,09%. Por outro lado em amostras de lodo espera-se percentuais mais elevados de cinzas, no presente estudo o resultado foi em torno de 20% próximo ao encontrado por Yang *et al*., (2005) que obteve valores entre 5% a 20%.

O teor de cinzas também é um parâmetro importante para o aproveitamento energético é desejável que se tenha o menor teor de cinzas possível. Assim como a umidade, o percentual de cinzas também interfere no poder calorífico causando perda de energia prejudicando a transferência de calor (Vieira, 2012). Para Vieira (2012) altas concentrações de cinzas podem diminuir o poder calorífico, afetar a transferência de calor e podem ainda causar perda de energia havendo necessidade de sua remoção. Para Chaves *et al*., (2013) as cinzas correspondem às substâncias que não entraram em combustão cuja forma sólida não serve para uso energético.

É importante destacar ainda que teores de cinzas elevado no lodo, no processo de pirólise, favorece o contato entre os metais das cinzas e a matéria orgânica, fazendo com que reações de desprendimento dos voláteis ocorram em temperaturas mais baixas, levando ao aumento no rendimento da fração gasosa (Colen, 2011). Assim esse tipo de material é melhor aproveitado na pirólise para produção de biogás.

3.1.4 Carbono Fixo

Os valores de carbono fixo ficaram próximos de 3%, para o lodo isso pode ter acontecido pelo alto teor de voláteis e cinzas presentes na amostra, e devido à natureza do lodo digerido.. Nota-se que os valores encontrados são inferiores ao esperado por Arazo (2017) de 14,1% e por Yang *et al*., (2005) na faixa de 7% a 20%. Para serragem o valor médio encontrado foi de 24,25% sendo abaixo do pesquisado por Tumuluru, *et al*., (2011) cujo carbono fixo variou de 28 a 35%. Vieira (2012) argumenta que quanto maior o percentual de carbono fixo presente na amostra mais lentamente o combustível irá queimar. É provável, portanto, que a serragem apresente maior poder calorífico devido ao maior tempo de queima.

3.2. Poder calorífico

A estimativa do poder calorífico da serragem e do lodo de acordo com as equações 5 a 7 estão apresentados na tabela 2.

Tabela 2. *Resultados dos valores médios do poder calorífico estimado*

Poder Calorífico (Kcal kg^{-1})	***Biomassa***	
	Lodo	***Serragem***
PCS	2829,64	4.821,51
PCI	2.505,64	4.497,51
PCL	2.504,70	4.496,58

Fonte: Autores, 2019

O PCS da serragem é maior que o do lodo porque a serragem tem o teor de carbono fixo superior (24,25% m/m) ao do lodo, determinados na análise imediata. Essa relação direta do carbono fixo com o poder calorífico

Downloaded from www.periodico.tchequimica.com

proporciona ganho de poder energético. Além disso, a serragem possui alto teor de voláteis que juntamente com o carbono fixo são características determinantes para o poder calorífico. Uma biomassa ideal para produção de energia precisa apresentar baixa umidade, baixo teor de cinzas e teores elevados de voláteis, carbono fixo e PCS (Vieira, 2012).

As amostras de serragem apresentaram baixa umidade e poder calorífico alto o que demonstra que a relação entre essas propriedades é inversamente proporcional. Segundo Ribeiro (2018) isso ocorre devido à diminuição das hidroxilas da biomassa que faz com que aumente o teor de carbono fixo e, consequentemente, eleva o poder calorifico das amostras. Além disso nota-se maior facilidade de decomposição da biomassa quando existe baixa umidade e voláteis com menor pressão de vapor.

O valor médio calculado para o poder calorífico superior do lodo de abatedouro foi 11,85 MJ kg^{-1} inferior ao valor observado por Silva (2011) de 16,2 MJ kg^{-1} e 21,80 MJ kg^{-1} encontrado por Teixeira, (2014). Para a serragem analisada encontrou-se PCS 24,32 MJ kg^{-1} superior ao estimado por Telmo, *et al*., (2010) que variou de 20,2 e 20,5 MJ kg^{-1} respectivamente, para amostras de madeira (macia ou dura). Assim, a serragem foi a que apresentou o melhor rendimento energético.

O poder calorífico superior obtido pela bomba calorimétrica para a serragem foi de 4.882,5 kcal kg^{-1} e para o lodo foi de 3952,5 kcal kg^{-1}. Fixando esses valores como valores reais observa-se que há um desvio de 1,27 % e de 39,7% nos valores obtidos para a serragem e para o lodo respectivamente. A maior discrepância para a medida do poder calorífico do lodo pode estar relacionada ao elevado teor de umidade e voláteis que agrega possibilidade de erro ao processo de pesagem durante a análise imediata e à presença de outros elementos químicos como nitrogênio e hidrogênio que também influenciam na quantidade de energia liberada.

Já o poder calorífico inferior estimado a partir do obtido em bomba calorimétrica foi de 3.268,50 kcal kg^{-1} para o lodo e de 4.558,50 kcal kg^{-1} para a serragem. O poder calorífico inferior reflete o valor mais preciso de energia que pode ser gerado, uma vez que calcula a energia após a perda da umidade.

Assim, observa-se que ambas as amostras apresentam poder calorífico adequado à geração de energia. O carvão, normalmente empregado em termoelétricas, segundo o Ministério de Minas e Energia (MME, 2007) apresentam poder calorífico de 2.400 kcal kg^{-1}, valor inferior às biomassas estudadas.

Segundo Brand (2000) os valores de PCS para madeira em geral situa-se na ordem de 4300 kcal kg^{-1} e do PCI, obteve-se um valor médio de 4000 kcal kg^{-1}. Assim, os valore encontrados para o PCI da serragem foram bastante satisfatórios, já que os valores médios pelos dois métodos analisados variam entre 3.982 a 4.558 kcal kg^{-1} para serragem.

4. CONCLUSÕES:

Foi possível verificar que a serragem apresentou características mais atrativas à reciclagem energética. O maior teor de cinzas do lodo, por exemplo, diminui seu poder calorífico consideravelmente. Além do teor de carbono fixo mais elevado da serragem também proporcionar maior potencial de geração de energia para essa biomassa. Apesar disso, deve-se considerar a elevada oferta do lodo e o seu potencial poluidor caso não haja uma destinação adequada.

A análise imediata proporcionou ainda a aquisição de dados determinantes à seleção do processo gerador de energia. Devido aos teores de voláteis para o lodo e para serragem serem altos revela-se um rendimento interessante para a produção de biogás.

Pode-se dizer que os resultados de poder calorífico apresentados pelas biomassas estudadas superiores ao do carvão utilizado nas termoelétricas são um indicativo da sua aplicabilidade como combustível na geração de energia.

Portanto, as propriedades físico-químicas e a capacidade de combustão das biomassas analisadas indicam que o uso do lodo do Matadouro Municipal de Gurupi e da serragem da Madeireira São Sebastião é uma alternativa eficaz para a eliminação dos grandes volumes destes resíduos e uma alternativa de diversificação da matriz energética.

5. AGRADECIMENTOS:

Ao Programa de Pós-graduação em Química da Universidade Federal do Tocantins e à CAPES pela concessão da bolsa.

6. REFERÊNCIAS:

Downloaded from www.periodico.tchequimica.com

1. Ahmad, M. I. *et al*. Anaerobic digestion of waste from a slaughterhouse. Journal of Environmental Chemical Engineering, **2014**, 2, 3, 1320.
2. ABNT. Associação Brasileira de Normas Técnicas. NBR - 8112 (MB1857): Carvão Vegetal -Análise Imediata. **1986.**
3. Arazo, R. O. *et al*. Bio-oil production from dry sewage sludge by fast pyrolysis in an electrically-heated fluidized bed reactor. Sustainable Environment Research, **2017**, 27, 1, 14.
4. ASTM D 2415-66. Standard Test Method for ash Determination, **1986**.
5. ASTM D 3173-85. Standard Test of Humity, **1985**.
6. ASTM D 3286-66. Standard Test Method for The Gross Calorific Power Value by Bomb Calorimeter.**1986**.
7. Białowiec, A. *et al*. The RDF/SRF torrefaction: An effect of temperature on characterization of the product – Carbonized Refuse Derived Fuel. Waste Management, **2017**, 70, 100.
8. Borowski, H. C. *et al*. Análise de um modelo de cogeração a partir de resíduos sólidos urbanos. Revista Tecnologia, **2002**.
9. Brand, M. A. Energia de biomassa florestal. Rio de Janeiro: Inter ciência, 131, **2010**.
10. Brand, M. A. Rendimento do processo produtivo e energético da matéria-prima de uma indústria de base florestal. Dissertação (Mestrado em Ciências Florestais), Setor de Ciências Agrárias, Universidade Federal do Paraná, Curitiba, **2000**, 163.
11. Channiwala, S.A; Parikh, P.P. A Unified Correlation for Estimating HHV of Solid, Liquid and Gaseous Fuels. Fuel, **2002,** 81, 1063**.**
12. Chaves, Antônio M. Brito *et al*. Características energéticas da madeira e do carvão vegetal de clones de Eucalyptus spp. Enciclopédia Biosfera, Centro Científico Conhecer, Goiânia, **2013.** 9, 17, 542.
13. Chen, Y. C. Evaluating greenhouse gas emissions and energy recovery from municipal and industrial solid waste using waste-to-energy technology. Journal of Cleaner Production, **2018**, 192, 269.
14. Colen, A. G. N. Caracterização físico-química e química do lodo de esgoto para aplicação como fonte de energia em processo de pirólise. Dissertação (Mestrado em Agroenergia). Universidade Federal do Tocantins. Palmas, **2011**, 159.
15. Ferreira, I. T. M. *et al*. Estimativa do potencial energético de resíduos celulósicos de fabricação de papel através de análise imediata. Revista Brasileira de Energias Renováveis, **2014,** 3, 297.
16. Guerra, R. C.; Angelis, D. F. D. Classificação e biodegradação de lodo de estações de tratamento de água para descarte em aterro sanitário. Arquivos do Instituto Biológico, **2005**, 72, 1, 91.
17. MME, Ministério de Minas e Energia. Plano Nacional de Energia 2030. Brasília (DF), 2007.
18. Milbrandt, A. *et al*. Wet waste-to-energy resources in the United States. Resources, Conservation and Recycling, **2018,** 137, 47.
19. Moulin, J. C. Avaliação energética da maravalha gerada em uma serraria no município de jerônimo Monteiro - ES. Monografia - Centro de ciências Agrárias. Universidade Federal do Espirito Santo, Espirito Santo, **2010**, 20.
20. Nogueira, L. A. H.; Lora, E. E. S. Dendroenergia: fundamentos e aplicações. 2° ed. Rio de Janeiro: Interciência, **2003**, 200.
21. Nozela, W. C. *et al*. Mixture of biomass to energy reuse. Journal of Thermal Analysis and Calorimetry, **2018**, 131, 1, 769.
22. Quirino, W.F. *et al*. Poder calorífico da madeira e de resíduos lignocelulósicos. Biomassa & Energia, **2005**, 1, 2, 182.
23. Ribeiro, K. P. Caracterização fisico-química do lodo de estação de tratamento de esgoto para aproveitamento como biomassa energética. Dissertação (Mestrado - Programa de Pós-Graduação em Biocombustíveis), Universidade Federal dos Vales do Jequitinhonha e Mucuri. Diamantina, **2018,** 53**.**
24. Silva, J. O. Caracterização do potencial

Downloaded from www.periodico.tchequimica.com

energético e estudo físico-químico do lodo da estação de tratamento de esgoto do DMAE - Uberlândia - MG. Dissertação (Mestrado em Química), Universidade Federal de Uberlândia. Uberlândia, MG, **2011,** 66.

25. Song, Q.; LI, J.; Zeng, X. Minimizing the increasing solid waste through zero waste strategy. Journal of Cleaner Production, 104, 210, **2015**.
26. Souza, F; R. Compósito de lodo de estação de tratamento de água e serragem de madeira para uso como agregado graúdo em concreto. TESE (Doutorado em ciências e engenharia dos materiais) - Instituto de Química, Universidade de São Paulo, São Paulo, **2010.**
27. Teixeira, L. F. Estudo do processo de pirólise termocatalítica como alternativa ao aproveitamento do lodo de esgoto doméstico. Dissertação (Mestrado em Agroenergia) – Universidade Federal do Tocantins. Palmas, **2014**. 108
28. Telmo, C.; Lousada, J.; Moreira, N. Proximate analysis, backwards stepwise regression between gross calorific value, ultimate and chemical analysis of wood. Bioresource Technology, **2010**, 101, 11, 3815.
29. Thipkhunthod, P.; *et al*. Predicting the heating value of sewage sludges in Thailand from proximate and ultimate analyses. Fuel, **2005**, 84, 857.
30. Torquato, L. D. M. Estudo de degradação térmica e caracterização de lodos provenientes de diferentes sistemas de tratamento de esgotos. Dissertação (mestrado) - Universidade Estadual Paulista Júlio de Mesquita Filho, Instituto de Química, Araraquara, **2012**, 109.
31. Torquato, L. D. M. Estudo de viabilidade do emprego de lodo de esgoto e resíduos agrícolas para a geração de bioenergia. Tese (doutorado) - Universidade Estadual Paulista Júlio de Mesquita Filho, Instituto de Química, Araraquara, **2016**, 227.
32. Tumuluru, J. S. A. Effect of pellet die diameter on density and durability of pellets made from high moisture woody and herbaceous biomass. Carbon Resources Conversion, **2018**, 1, 54.
33. Vieira, A. C. Caracterização da biomassa proveniente de resíduos agrícolas. Dissertação (Mestrado) - Curso de Energia na Agricultura, Universidade Estadual do Oeste do Paraná, Cascavel, **2012**, 72.
34. YANG, Y. BIN *et al*. Effect of fuel properties on biomass combustion. Part II. Modelling approach - Identification of the controlling factors. Fuel, **2005**, 84, 16, 2130.

Downloaded from www.periodico.tchequimica.com

PERIÓDICO TCHÊ QUÍMICA
ARTIGO ORIGINAL

NOVO MÉTODO PARA A ESTIMATIVA DAS CONSTANTES DE ESTABILIDADE DE COMPLEXOS COM O EDTA

A NEW METHOD FOR CONSTANT ESTIMATE STABILITY OF COMPLEX WITH EDTA

PEREIRA, Francisco Claudece(*); LIMA, Francisco José Santos

Universidade Federal do Rio Grande do Norte, Instituto de Química, Centro de Ciências Exatas e da Terra, CP 1524, CEP 59072-970, Natal-RN, Brasil, (84) 3342-23-23.

** Autor correspondente*
e-mail: claudece@ufrnet.br

Received 17 May 2019; received in revised form 13 October 2019; accepted 19 October 2019

RESUMO

O presente trabalho descreve uma nova metodologia na área de química analítica, que possibilita o cálculo da constante de estabilidade (de equílibrio ou de formação), dos compostos de coordenação gerados entre todos os cátions metálicos da tabela periódica, excetuando os metais alcalinos (grupo 1), juntamente com o ligante ácido etilenodiamintetraacético. A sistemática é de simples utilização, apresentando baixo custo e permitindo obter, em brevissimo tempo, o conhecimento da dimensão das constantes de formação condicional, para todos os metais coordenados com o agente complexante, para qualquer valor de pH investigado. Em adição, o método também é extensivo para outros ligantes que apresentem a mesma propriedade química de reação, que o ácido etilenodiamintetraacético realiza com os íons metálicos na mesma proporção estequiométrica de ligação. Para a execução deste estudo foram empregadas soluções do cátion cobre (II), em uma concentração de $1{,}0x10^{-2}$ mol L^{-1} e do agente complexante, também apresentando a mesma concentração do metal. O ensaio foi conduzido em um sistema tamponante, constituido de hidróxido de amônia e o sal cloreto de amônio, em um valor de pH constante igual a 10,0. O método permite o seu emprego nos procedimentos experimentais desenvolvidos tanto, em um laboratório químico, quanto em uma sala de aula, utilizada durante a realização das atividades teóricas. O agente quelante apresenta um amplo espectro de aplicação nas indústrias de produtos alimentícios, também na geração de materiais de limpeza em geral, bem como na indústria da fotografia, na produção têxtil, na manufatura do papel e similares, borrachas e afins, polímeros e derivados, dentre outras linhas de produção que destinam seus manufaturados para o consumo humano.

Palavras-chave: *Ácido Etilenodiamintetraacético (EDTA); Complexação; Planilhas; Titulação.*

ABSTRACT

The present work describes a new methodology in analytical chemistry, which makes it possible to calculate the stability constant (equilibrium or formation) of the coordination compounds generated between all metallic cations in the periodic table, except for alkali metals (group 1) together with the ethylene diamine tetraacetic acid binder. The system is simple to use, inexpensive, and allows the knowledge of the size of the conditional formation constants for all metals coordinated with the complexing agent to be investigated at any pH value investigated. In addition, the method is also extensive for other binders having the same chemical reaction property as ethylenediamine tetraacetic acid performs with metal ions in the same stoichiometric bonding ratio. For the execution of this study, solutions of copper (II) cation was employed, at a concentration of $1.0x10^{-2}$ mol L^{-1} and the complexing agent, also presenting the same concentration of metal. The assay was conducted in a buffering system consisting of ammonium hydroxide and ammonium chloride salt at a constant pH of 10.0. The method allows its use in experimental procedures developed both in a chemical laboratory and in a classroom, used during the theoretical activities. The chelating agent has a wide spectrum of application in the food product industries, also in the generation of cleaning materials in general, as well as in the photography industry, textile production, paper manufacture and the like, rubbers and the like, polymers and derivatives, among other production lines intended for its manufacture for human consumption.

Keywords: *Ethylenediaminetetraacetic Acid (EDTA); Complexation; Spreadsheets; Titration.*

Downloaded from www.periodico.tchequimica.com

1. INTRODUÇÃO

O ácido etilenodiamintetracético (EDTA) é uma molécula orgânica que apresenta a capacidade de complexar metais na forma iônica e covalente. É um ácido poliprótico que possui quatro grupamentos de ácido carboxílico, dois centros amina, com um par de elétrons livre em cada átomo de nitrogênio. Sua fórmula molecular é mostrada na Figura 1. É um composto sintetizado em escala industrial, utilizando os reagentes etilenodiamina, formaldeído, e uma fonte segura de cianeto (NaCN). Sua produção mundial supera cifras na ordem de 200.000 toneladas por ano (Sinex, 2018).

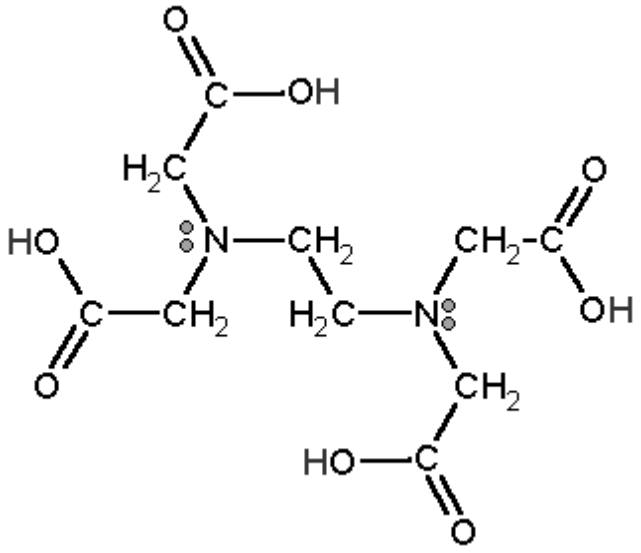

Figura 1: *Fórmula molecular do EDTA.*

Além dos quatro hidrogênios ionizáveis, o EDTA pode adicionar mais dois protóns nas suas respectivas funções amina. A estrutura, completamente protonada é a forma típica encontrada nos livros texto. A propriedade mais inerente do EDTA é a sua capacidade reacional com os metais para formar complexos na proporção de 1:1. Seus grupamentos carboxilatos, previamente desprotonados, ligam-se ao íon metálico em análise. Geralmente, as constantes de equilíbrio de formação dos seus complexos, principalmente para os metais de transição, são elevadíssimas; por conseguinte, todas as suas reações de coordenação são termodinamicamente favoráveis. Quase a totalidade de suas reações são dependentes dos valores de pH do meio reacional. As dimensões das constantes de formação de seus complexos aumentam com a carga do cátion, e com a diminuição de seu respectivo raio iônico. Considerando a sua particular propriedade, de complexar quase todos os metais da tabela periódica, é usualmente empregado na indústria alimentícia, como agente sequestrante. A prévia reação de complexação de um íon metálico, pode evitar reações secundárias deste íon com outras espécies presentes em uma matriz de interesse. Neste sentido, alguns trabalhos mostram o emprego de complexos de ferro-EDTA, em cereais, a fim de suprir deficiências de ferro. Nesta mesma linha de investigação, há relatos do emprego clínico de EDTA, a fim de remediar os efeitos indesejáveis do saturnismo (contaminação por chumbo). Nestes casos, os pacientes são tratados com doses intravenosas diária do complexo [Ca-EDTA]. No organismo humano contaminado com Pb^{+2}, há uma permuta entre o Ca^{+2} (no complexo) e o íon Pb^{+2}, para formar outro complexo [Pb-EDTA], o qual apresenta uma constante de estabilidade muito maior que o complexo anterior. Assim, o novo complexo com o chumbo é descartado pelo trato urinário (Sinex, 2018).

O EDTA é um ligante quelante, largamente utilizado como agente seqüestrante em vários processos químicos, com a finalidade de reagir com uma gama de íons metálicos. Os principais usos do EDTA são destacados nas indústrias de limpeza, detergentes domésticos, indústria fotográfica, têxtil, fabricação de papel, herbicidas, na manufatura de couro, borrachas, polímeros, etc. Estima-se que a europa, somente no ano de 1987, consumiu cerca de 30.000 toneladas desta formulação química. Dados mais recentes, estima que a indústria de produtos domésticos, consome cerca de 200.000 tonelada ao ano. Seu emprego na indústria de celulose consiste em inativar íons metálicos, responsáveis por processos catalíticos, que podem provocar a decomposição do branqueador utilizado na manufatura do papel. Considerando que este setor de produção tem buscado formas distintas de tratamento, a fim de eliminar processos envolvendo a aplicação de cloro, é esperado que o consumo de EDTA e similares, apresente elevado aumento no futuro (Sillanpaa e Sihvonen, 1997; Karl e Giger, 1996; Quintana e Reemtsma, 2007; Nowack *et al*. 1996).

Na agricultura, EDTA é usado como ingrediente na fertilização do solo, uma vez que apresenta a capacidade de melhorar a biodisponibilidade de micronutrientes para as plantas (Viipsi *et al*. 2012). Também destaca-se como importante agente empregado na manufatura de materias de limpeza. Sua

Downloaded from www.periodico.tchequimica.com

utilização como sequestrante de metais permite a substituição de fosfatos nestes produtos industrializados. Contudo, o EDTA apresenta alta recalcitrância de sua biodegrabilidade ambiental. Em vários países europeus, há legislação vedando o seu uso como princípio ativo de formulações industriais de uso higiênico (Sinex, 2018). É largamente utilizado na indústria farmacêutica, na condição de agente antioxidante e como preservativo de medicamentos, além de apresentar propriedades bactericidas, quando utilizado em preparações oftalmológicas (Belal *et al*. 1998).

O agente orgânico encontra larga aplicação no tratamento de águas de descartes, impregnadas com metais pesados, e na remediação de solos contaminados com estes íons, bem como com espécies radioativas. Todavia, o uso indiscriminado de EDTA, para o tratamento de águas e de solos contaminados com metais pesados, tem apresentado alguns efeitos colaterais, uma vez que os complexos formados apresentam uma fraca biodegradabilidade e, por conseguinte, tem alterado o equilíbrio de sistemas aquáticos. Assim sendo, a contaminação dos corpos d'água por complexos com EDTA, tem apresentado notória preocupação (Wu *et al*. 2011; Yang e Lee, 2005; Yang e Davis, 1999). Em efluentes de tratamento de águas residuais, concentrações de até 18 μM têm sido relatados devido a sua lenta biodegradabilidade. Pós-descarga, sua presença persiste como um dos principais poluentes nos rios, lagos e nos lençóis freáticos (Nowack *et al*. 1996).

Uma vez que o agente quelante apresenta uma alta afinidade para complexar íons divalente, conhecidamente tóxicos, tais como, Pb^{+2}, Cd^{+2}, Hg^{+2}, o emprego de EDTA no tratamento de solos contaminandos por estes agentes nocivos, pode aumentar a biodisponibilidade destes metais, devido a formação de compostos de coordenação com alta solubilidade e, portanto, suas remoções de sedimentos adsorvidos (Peraferrer *et al*. 2012).

Uma forma de determinar o nível de complexação, de um uma entidade química em uma amostra, é medir a quantidade total do metal e a quantidade de sua forma livre, após a reação de coordenação. A diferença entre estes dois valores é o teor de sua forma complexada. A quantidade de metais livre em um ambiente denota o teor desta espécie, disponível para os micro-organismos e, esta medida, não é tão simples de ser efetuada, uma vez que outras espécies também estão presentes na matriz submetida à análise (Vega e Weng, 2013).

Os dados sobre a toxicidade de EDTA disponíveis na literatura, são escassos e insuficientes. Devido a sua baixa capacidade de absorção, a toxicidade humana do composto livre é baixissima. A molécula não apresenta efeitos genotóxicos diretos, nem é uma substância cancerígena. Os seus complexos apresentam uma alta estabilidade e, por isso, são pouco biodegradáveis em um tratamento biológico de águas residuais (Sorvari e Sillanptaa, 1996). Embora o EDTA não seja tóxico aos humanos e a biota, a sua persistência no meio ambiente gera grandes preocupações, uma vez que o ligante apresenta a capacidade de gerar complexos solúveis com quase todos os metais da tabela periódica. Sua presença, em locais destinados ao descarte deliberado de metais tóxicos e radioativos, pode provocar a migração destas espécies para outras áreas, promovendo uma disseminação de espécies altamente nocivas aos seres vivos (Willett e Rittmann, 2003). Além do mais, EDTA livre também apresenta forte resistência à sua degradação por ação de bactérias e, por isso, pode acumular-se no solo e em corpos d`água.

Considerando que o EDTA também é utilizado para estudar a mobilidade de metais das séries dos lantanídios e dos actinídios (terras raras), este ligante passa a ser considerado como resíduo radioativo (Furukawa *et al*. 2007). Uma concentração de 31,4 mM ja foi registrada, onde o EDTA foi usado para descontaminar equipamentos radioativos da indústria nuclear. Há registros na literatura, dando conta de que resíduos contendo, tanto agentes como metais radioativos e seus complexos, quando despostos no solo, persistem durante um tempo considerável (Nowack *et al*. 1996).

O EDTA é comercializado nos Estados Unidos desde 1948 e, até os dias atuais, é considerado o agente quelante mais empregado para sequestrar metais. Adicionalmente, o EDTA tem encontrado largo emprego, nos últimos 50 anos, em ações governamentais dos americanos para o controle de quantidades de radionuclídeos e metais pesados, provenientes da fabricação de armas nucleares e nos processos com material radioativo. Com este emprego, uma considerável quantidade de dejetos de EDTA e Me-EDTA, têm sido descartadas no meio ambiente sem qualquer tratamento adequado. Estudos têm apontado que a presença de EDTA livre é um dos maiores constituintes do rio Reno na Europa. Todavia, a maior concentração de EDTA é encontrada em regiões onde armas nucleares

Downloaded from www.periodico.tchequimica.com

são produzidas (Willett e Rittmann, 2003).

O EDTA apresenta um largo espectro de aplicações baseado na sua habilidade de complexar íons metálicos. Na indústria nuclear encontra emprego como importante agente de descontaminação. Utilizado como ator, na limpeza de águas contendo cátions radioativos, a sua melhor função é a lixiviabilidade de cátions imobilizados, ou que apresentam baixa mobilidade em uma matriz qualquer, possibilitando desta forma, sua fácil biodegradabilidade (Chitra *et al*. 2004).

Alguns estudos de complexação, empregando radionuclídeo, também têm encontrado destaque na literatura. As terras raras (plutônio e tório) foram avaliadas através de seus complexos com EDTA. O Pu^{+4} forma um complexo neutro com o EDTA, em meio ácido, e apresenta logaritmo da constante de formação de 26,44. Em valores de pH mais elevados, complexos hidroxilados podem ser formados, do tipo $[Pu(OH)Y]^{-}$ e $[Pu(OH)_2Y]^{-2}$, cujos logaritmos das constantes de formação assumem valores de 21,95 e 15,29; respectivamente. Sob condições de pH neutro, e na presença de excesso do ligante, os autores postulam a existências do $[Pu(Y)_2]^{-4}$, cujo logaritmo da constante de formação apresentaria o valor de 35,39. De forma análoga, Th^{+4} foi empregado a fim de formar complexos com o EDTA. Os resultados apontam uma ligeira distorção com relação aos dados obtidos com o plutônio. Somente o complexo hidroxilado $[Th(OH)_2Y]^{-2}$ apresentou um logaritmo da constante de formação de 39,5. Os demais resultados não apontaram concordância, quando comparado com os resultados obtidos para o outro nuclídeo (Roach, 2008).

Em adição, as constantes de estabilidades dos complexos de EDTA, com os metais Am^{+3}, Cm^{+3} e Eu^{+3} foram determinados a temperatura ambiente, em um intervalo de concentração variando 0,1 a 6,60 mol L^{-1} de $NaClO_4$ utilizando a técnica de titulação potenciométrica. A formação de somente complexos na proporção de 1:1 [M-EDTA], onde (M = Am^{+3}, Cm^{+3} e Eu^{+3}), foi observada sob as condições experimentais empregadas. Constatou-se uma forte dependência, das constantes de dissociação e das constantes de estabilidade, em toda uma ampla faixa de força iônica investigada (Thakur *et al*. 2014; Choppin *et al*. 2007).

Um trabalho de revisão, apresentando as várias técnicas e procedimentos operacionais para a quantificação de EDTA, nas mais diversificadas matrizes é apresentado por (Sillanpaa e Sihvonen, 1997). O manuscrito é amplo e apresenta uma gama de técnicas e metodologias para o monitoramento direto e indireto do agente quelante. Esta revisão poderá ser de grande valia para investigações de natureza quantitativa desta espécie química.

O presente trabalho tem como finalidade, apresentar uma nova metodologia analítica para estimar as dimensões das constantes de formação condicional dos complexos de EDTA com qualquer íon metálico que apresente a propriedade de formar compostos de coordenação com este agente quelante.

2. DESENVOLVIMENTO

Os recursos utilizados no presente trabalho foram os programas computacionais, EXCEL (pacote de recursos da Microsoft OFFICE 2007) e o programa ORIGIN (versão 6,0; da Microcal software, Inc.). O programa EXCEL permitiu a construção das planilhas eletrônicas, enquanto o ORIGIN foi empregado para gerar os gráficos correspondentes aos dados obtidos nas planilhas do EXCEL.

As planilhas eletrônicas podem ser construídas, através de uma simulação de uma titulação potenciométrica, no qual são estimulados os dados referentes ao consumo de uma solução titulante (solução em uma bureta), contra os valores do co-logaritmo da concentração molar do metal. Com a obtenção destes dois parâmetros (simulados) é possível gerar um gráfico, conhecido como “curva volumétrica”, onde são graficados os valores de pMe^{+n} (eixo das ordenadas) contra os valores de consumo de uma solução titulante (no eixo das abscissas). A correta manipulação dos dados gerados nesta titulação permite a obtenção de vários gráficos e, a sua devida interpretação, possibilita a conclusão de diversas observações. A geração e o emprego de planilhas eletrônicas do EXCEL, como ferramenta analítica de obtenção e interpretação de dados, é bastante documentada na literatura (Harris, 2001; Pereira *et al*. 2016).

Os dados apresentados neste trabalho foram obtidos através de comandos efetuados no programa EXCEL. Estes comandos permitem que sejam calculados os valores de pMe^{+n} e o número de mols ou quantidade de matéria (n), das espécies no meio reacional, através da

Downloaded from www.periodico.tchequimica.com

simulação de consumo de uma solução do titulante de concentração conhecida. Para a realização desta operação, emprega-se a equação (modificada) da constante de formação condicional (Kfc), conforme descrição na literatura (Perin e Dempsey, 1974; Harris, 2001). Com os valores arbitrados do consumo do titulante, contra um volume conhecido de uma solução do titulado, cuja concentração também é conhecida, é possivel gerar os parâmetros que permitirão obter os gráficos correpondentes ao experimento planejado. No momento da construção da planilha é necessário arbitrar valores de consumo do titulante. A partir destes valores, e os devidos comandos necessários no programa computacional, o EXCEL efetua os cálculos esperados.

3. RESULTADOS E DISCUSSÃO

Conforme discussão já apresentada, o EDTA é um agente quelante que apresenta a propriedade de formar complexos com praticamente todos os metais da tabela periódica. Em adição, independentemente do estado de oxidação do metal submetido à reação de complexação, a estequiometria do EDTA com este metal, sempre será na proporção de 1:1. Em adição, todos os complexos do EDTA são solúveis e incolores em soluções diluídas em meio aquoso.

O íon metálico escolhido para a realização deste trabalho foi o cobre (Cu^{+2}). Uma aliquota de 50,0 mL da solução de Cu^{+2}, em uma concentração molar de $1{,}0x10^{-2}$ mol L^{-1} foi empregada. Para a realização da reação de complexação, uma solução de EDTA na mesma concentração do Cu^{+2} foi escolhida para a condução das simulações. O procedimento foi realizado em sistema tamponante (NH_4OH/NH_4Cl) em valor de pH 10,0.

Considerando que a molécula do EDTA (Figura 1), apresenta quatro sítios carboxilatos; estes terminais, após etapa prévia de desprotonação, funcionarão como centros de complexação do metal. Devido a reação de coordenação do metal, ocorrer com mais de um sítio da molécula do ligante, este processo também é chamado de quelação.

O processo de desprotonação do EDTA pode ser representado através da seguinte sequência:

$H_4Y \Leftrightarrow H^+ + H_3Y^-$; $pKa_1 = 2{,}00$ (Eq. 1);

$H_3Y^- \Leftrightarrow H^+ + H_2Y^{-2}$; $pKa_2 = 2{,}66$ (Eq. 2);

$H_2Y^{-2} \Leftrightarrow H^+ + HY^{-3}$; $pKa_3 = 6{,}16$ (Eq. 3);

$HY^{-3} \Leftrightarrow H^+ + Y^{-4}$; $pKa_4 = 10{,}24$ (Eq. 4).

Assim, a fração (α) do EDTA na forma Y^{-4} (αY^{-4}), será:

$(\alpha Y^{-4}) = [Y^{-4}] / \{[H_4Y] + [H_3Y^-] + [H_2Y^{-2}] + [HY^{-3}] + [Y^{-4}]\}$ (Eq. 5).

Esta relação pode ser melhor representada pela expressão:

$(\alpha Y^{-4}) = [Y^{-4}] / [EDTA]$ e, por conseguinte: $[Y^{-4}] = (\alpha Y^{-4})\,[EDTA]$ (Eq. 6).

onde [EDTA] é a concentração total de todas as formas de EDTA livre na solução. O termo “livre” indica a parcela do EDTA não complexado no meio reacional.

Os valores da fração do EDTA na forma (Y^{-4}) é função direta dos valores do pH do meio reacional. Estes valores de (αY^{-4}), com a sua correspondente relação com o pH, pode ser facilmemente encontrado nos livros texto (Harris, 2001; Skoog *et al*. 1997).

3.1. Complexos de EDTA

A constante de formação (Kf) de qualquer metal com o EDTA é a própria contante de equilíbrio (Keq.) para a reação de complexação. Seja a expresão genérica:

$M^{+n} + Y^{-4} \Leftrightarrow MY^{(n-4)}$ (Eq. 7).

$Kf = [MY^{(n-4)}] / [M^{+n}]\,[Y^{-4}]$ (Eq. 8).

Os valores da constante de formação (Kf) dos complexos com EDTA são elevadíssimas. Os mesmos podem facilmente ser consultados

Downloaded from www.periodico.tchequimica.com

nos livros textos (Harris, 2001; Skoog *et al*. 1997).

3.1.1. Constante de Formação Condicional (KFC)

A equação 8 descreve a reação de qualquer íon metálico com a espécie (Y^{-4}). Contudo, em valores de pH abaixo de 10,0 outras espécies do EDTA encontram-se no meio reacional, como (H_3Y^-), (HY^{-3}), etc. Desta forma, a constante de formação assume a expressão:

$$Kf = [MY^{(n-4)}] / [M^{+n}] [Y^{-4}] \quad \text{(Eq. 8)}$$

e

$$[Y^{-4}] = (\alpha Y^{-4}) [EDTA] \quad \text{(Eq. 6).}$$

$Kf = [MY^{(n-4)}] / [M^{+n}] (\alpha Y^{-4}) [EDTA]$. Sendo que: $Kf(\alpha Y^{-4})$= Kfc= constante de formação condicional ou constante de formação efetiva.

$$Kfc = [MY^{(n-4)}] / [M^{+n}] [EDTA] \quad \text{(Eq. 9).}$$

Desta forma, todos os cálculos que envolvem o uso da Kfc será precedido de uma consulta nos livros textos sobre os valores da constante de formação (Kf) do complexo, bem como o valor da fração do EDTA na forma Y^{-4} (αY^{-4}) em relação ao valor de pH do sistema tamponante no qual será conduzida a reação (Perin e Dempsey, 1974; Harris, 2001; Skoog *et al*. 1997).

Da expressão anterior é possível a dedução da relação:

$$pM^{+n} = \log Kfc + \log\{[ligante]/[complexo]\} \quad \text{(Eq. 10).}$$

onde os termos entre cochetes denotam concentração molar (mol L^{-1}) do ligante (EDTA) e do complexo (metal-EDTA) (Perin e Dempsey, 1974).

Considerando que as reações de formação de complexos entre EDTA e íons metálicos sempre ocorre na proporção de 1:1 e, considerando também que a co-existência simultânea entre o excesso de EDTA e seu complexo formado, ambos encontrando-se no mesmo ambiente reacional; no caso de uma titulação, este ambiente é o matraz; pode-se resumir a Equação 10, a expressão:

$$pM^{+n} = \log Kfc + \log\{n(ligante)/n(complexo)\} \quad \text{(Eq. 11).}$$

onde n= número de mols das espécies. Desta forma, quando o número de mols do EDTA e sua forma complexada forem iguais, o co-logaritmo da concentração do metal (pM^{+n}) será o valor do logarítmo da constante de formação condicional (Kfc) do complexo e, como Kfc= Kf (αY^{-4}), para um dado valor de pH de um sistema tampão. Assim, é possível estimar o valor da constante de equilíbrio (Keq.) ou constante de formação do complexo (Kf).

O presente trabalho foi simulado a partir da escolha da tomada de uma alíquota de 50,0 mL de uma solução de íons Cu^{+2} na concentração de $1{,}0 \times 10^{-2}$ mol L^{-1} em um sistema tamponante constituido de NH_4OH/NH_4Cl, pH 10,0. O titulante escolhido foi uma solução de EDTA na concentração de $1{,}0 \times 10^{-2}$ mol L^{-1}. Os dados desta titulação potenciométrica são apresentados na Tabela 1. A equação química representativa deste processo é mostrada na Equação 12.

$$Cu^{+2} + EDTA \leftrightarrow [Cu\text{-}EDTA] \quad \text{(Eq. 12).}$$

Considerando que o processo reacional do metal com o EDTA ocorre na proporção de 1:1 e, uma vez que as concentrações do íon metálico e do agente complexante são as mesmas, o volume de equivalência ou volume estequiométrico (VE) será de 50,0 mL (coluna A16) da Tabela 1. Neste volume todo o metal deixará de existir na forma livre e passará a sua forma complexada {[Cu-EDTA]}.

Na presente tabela a coluna “A” representa os volumes escolhidos de EDTA que foram permitidos escoar da bureta. Na coluna “B” são apresentados os números de mols (n) do EDTA. Estes valores podem ser calculados através da multiplicação dos volumes de EDTA que fluiram da bureta (em L) pela sua concentração ($1{,}00 \times 10^{-2}$ mol L^{-1}). Estes valores crescem linearmente até o volume estequiométrico (volume reacional entre o íon metálico e o complexante). Todas as quantidades de matéria (n) de EDTA, após o

Downloaded from www.periodico.tchequimica.com

volume de equivalência (coluna B17 a B49), denotam o excesso do EDTA no meio reacional. A coluna “C” expressa o número de mols do Cu^{+2} livre. A medida que o EDTA flui da bureta a concentração do Cu^{+2} livre diminui e vai a zero no volume de equivalência (C16). A coluna “D” apresenta os dados do número de mols (n) do complexo [Cu-EDTA]. O mesmo começa a ser formado a partir da primeira adição do complexante (D2) e segue aumentando até o limite de sua formação (D16). A partir deste ponto se mantém constante ao longo do experimento. A coluna “E” mostra os dados sobre as concentrações molares do Cu^{+2}. Os valores apresentam o mesmo comportamento da coluna “C” até o valor do volume de equivalência. A partir deste ponto os valores calculados denotam as concentrações molares do íon metálico que se desprende do complexo e retorna a sua condição inicial (coluna E16 a E49). Na coluna “F” é possível observar os valores da concentração molar do complexo [Cu-EDTA]. Os valores compreendidos entre (F1 a F16) apresentam uma relação linear de crescimento, representando a formação do complexo até o volume de equivalência. Após este volume, os valores tendem a diminuir, a medida que aumenta o volume do meio reacional, devido a efeitos de diluição da concentração molar do complexo (coluna F16 a F49). Na coluna “G” são encontrados os valores da função co-logarítmica da concentração molar dos íons cobre (pCu^{+2}) extraídos da coluna “E”. Na coluna “H” são reportados os excessos do EDTA a partir do fim da reação quimica (H17 a H49).

3.1.1.1. Construção da Curva Volumétrica Representativa para o Ensaio

Uma vez apresentado os valores e a metodologia de obtenção dos dados mostrados na Tabela 1, é possível a criação de gráficos que permitem uma avaliação mais criteriosa sobre o sistema escolhido para ser investigado. Por exemplo, o uso dos dados da coluna “A”, volume do EDTA (mL) empregados na composição do eixo “x”, juntamente com os valores da coluna “G” (função co-logaritmo da molaridade do Cu^{+2} = pCu^{+2}) na construção do eixo “y” obtén-se o gráfico chamado de curva volumétrica para a titulação de 50,0 mL de Cu^{+2}, na concentração de $1{,}00x10^{-2}$ mol L^{-1}, em meio tampão pH 10,0, com o titulante EDTA na concentração equimolar. O gráfico resultante é mostrado na Figura 2.

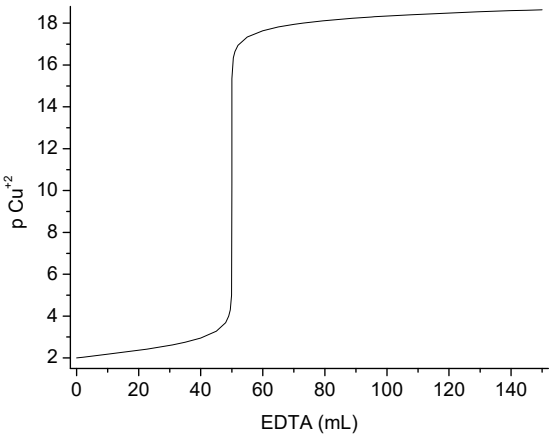

Figura 2: *Curva volumétrica teórica da titulação de 50,0 mL de Cu^{+2} $1{,}00x10^{-2}$ mol L^{-1}, em meio NH_4OH/NH_4Cl, pH 10,0 com EDTA equimolar.*

Em conformidade com a equação 12, o volume de equivalência é de 50,0 mL de EDTA. A escolha de se trabalhar com o excesso do titulante, no dobro do volume de equivalência, foi para monitorar os valores representativos do resíduo do Cu^{+2} que si dissocia da forma complexada {[Cu-EDTA]} e retorna a sua condição livre, de acordo com a equação que representa o equilíbrio na equação 12. Estes valores são mostrados na coluna “E” na Tabela 1 para as quantidades compreendidas entre (E17 a E49). De forma extensiva, os valores da função co-logarítmo desta concentração molar ($p[Cu^{+2}] = -\log[Cu^{+2}]$) são apresentados na coluna “G”, no intervalo entre G17 a G49.

O gráfico apresenta apenas um evento químico, conforme discussão prévia. É notório que o agente complexante (EDTA) realize somente uma reação de coordenação na proporção de 1:1 com qualquer íon metálico passível de complexação com o agente quelante. Desta forma, a curva volumétrica mostrada na Figura 2, apresenta apenas uma elevação. Na curva também é possível constatar que o ponto de equivalência corresponde a 50,00 mL. O grande excesso, na adição do EDTA após este ponto (adição do dobro do volume de equivalência), é somente para gerar os dados que são destacados no presente texto, como àqueles mostrados na coluna “B” da Tabela 1, para os valores estabelecidos entre (B17 a B49). Esta faixa de valores denota as quantidades de matéria (número de mols) excedente do agente complexante que passa a sobrar no meio reacional. Na mesma línea de raciocínio, as quantidades de matéria (número de mols) do complexo Cu-EDTA são mostradas na coluna

Downloaded from www.periodico.tchequimica.com

"D". Para a mesma região em estudo (região de excesso do ligante), estes valores estão compreendidos no intervalo entre D17 a D49. Estes valores são indiferentes frente às posteriores adições do ligante.

Assim, tomando os valores do pCu^{+2}, no intervalo entre G17 a G49 (coluna "G" da Tabela 1) como componentes do eixo "x" no sistema cartesiano, contra os valores no número de mols do complexo (D17 a D49) da referida tabela, como integrantes do eixo "y" do mesmo gráfico, juntamente com os valores compreendidos entre B17 a B49 (coluna "B" da mesma tabela), no mesmo eixo "y", é possivel a geração do gráfico mostrado na Figura 3.

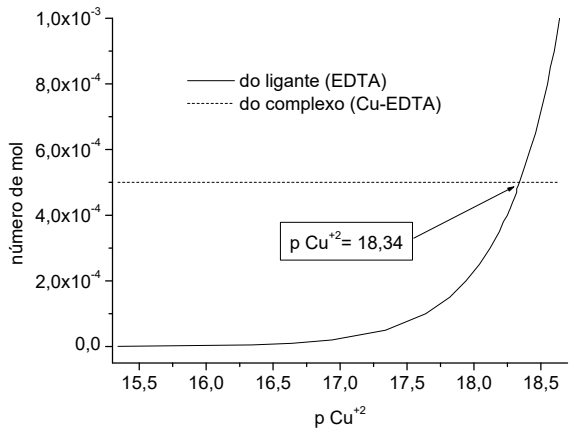

Figura 3: *Gráfico do número de mol do EDTA e do complexo Cu-EDTA contra a função pCu^{+2}, para a região de excesso de EDTA 1,0x10^{-2} mol L^{-1}, na titulação de 50,0 mL de Cu^{+2} 1,0x10^{-2} mol L^{-1} em meio tamponado pH 10,0.*

A referida figura foi construída através do emprego dos dados gerados na simulação de uma titulação de complexação do cátion cobre II e o ligante EDTA, ambas soluções em uma concentração de 1,0x10^{-2} mol L^{-1}. Porém os pares ordenados utilizados nesta figura são aqueles que reportam a consumação total da referida reação entre as duas espécies, onde o número de mols (n) do complexo [Cu-EDTA] não sofre nenhuma alteração, ou seja, estes valores são constantes (curva pontilhada na figura). Por outro lado, após a completa reação entre os dois reagentes, adições posteriores do titulante (EDTA), promovem um aumento em sua concentração (e no seu número de mols), no meio racional, uma vez que não há mais íons do metal capaz de participar do processo reacional. Neste caso, a concentração do EDTA livre tende a aumentar e, o gráfico dos pares ordenados deste comportamento, gera uma curva ascendente (curva cheia na figura 3). A ascenção desta curva intercepta a curva da função constante (curva pontilhada na figura 3) em um único ponto. Este ponto é o par ordenado (18,34; 5,0x10^{-4}). O valor referente ao eixo "y" denota a igualdade existencial no valor do número de mols (n) das duas espécies, ou seja, o complexo [Cu-EDTA] e o excesso do ligante (EDTA). O valor atribuido ao eixo "x" representa a função co-logaritmo da concentração do Cu^{+2} livre, ou seja, a pequena quantidade do metal que consegue si dissociar do complexo e retornar a sua condição iônica (metal livre). Este mesmo valor corresponde ao logaritmo da constante de formação condicional (log Kfc), de acordo com a equação 11. Aplicando a relação exponencial neste valor, chega-se a própria constante de formação condicional (Kfc). Sabendo-se que Kfc é a multiplicação entre a constante de equilíbrio do complexo (Keq.), pela fração do EDTA no valor de pH do sistema tampão empregado na titulação, é possível calcular o valor puro da constante de equilíbrio para o complexo metal-EDTA. No presente caso, a constante de equilibrio ou de formação para o complexo [Cu-EDTA] é 6,30x10^{18} (Harris, 2001; Skoog *et al*. 1997).

4. CONCLUSÕES

A metodologia proposta apresenta um novo sistema de tratamento de dados que pode se empregado para estimar as constantes de estabilidade (de equilíbrio ou de formação) de qualquer complexo formado entre o EDTA e os metais que são capazes de reagir com o ligante a fim de formar compostos de coordenação. O método é de simples utilização e fácil manuseio dos parâmetros gerados em uma titulação. Em adição, o mesmo pode ser aplicado para qualquer outro processo de complexação onde, o ligante empregado apresenta a mesma propriedade que o EDTA oferece aos metais, ou seja, a interação de 1:1 entre o agente complexante e o metal em uso.

5. REFERÊNCIAS:

1. Belal, F.; Aly, F. A.; Walash, M. I.; Kenawy, I. M.; Osman, A. M.; Il Farmaco, **1998**, 53, 365.

Downloaded from www.periodico.tchequimica.com

2. Chitra, S.; Paramasivan, K.; Sinha, P. K.; Lal, K. B.; Journal of Cleaner Production, **2004**, 12, 429.
3. Choppin, G. R.; Thakur, P.; Mathur, J. N.; Inorganica Chimica Acta, **2007**, 360, 1859.
4. Furukawa, K.; Takahashi, Y.; Sato, H.; Geochimica et Cosmochimica Acta, **2007**, 71, 4416.
5. Harris, D. C.; *Análise Química Quantitativa,* 5ª edição, LTC editora, Rio de Janeiro, **2001**, cap. 13.
6. Karl, F. G.; Giger, W.; War. Res., **1996**, 30, 1, 122.
7. Nowack, B.; Luzenkirchen, J.; Behra, P.; Sigg, L.; Environ. Sci. Technol., **1996**, 30, 2397.
8. Peraferrer, C.; Martínez, M.; Poch, J.; Villaescusa, I.; Arch. Environ. Contam. Toxicol., **2012**, 63, 484.
9. Pereira, F. C.; Lima, F. J. S.; Silva, A. O; Revista Virtual de Química, **2016**, 8, 6, 1889.
10. Perin, D. D., Dempsey, B., *Buffers for pH and Metal Ion Control.* Chapman and Hall, New York, **1974,** cap. 7.
11. Quintana, J. B.; Reemtsma, T.; Journal of Chromatography A, **2007**, 1145, 110.
12. Roach, M. J. K.; Science of the Total Environment, **2008**, 396, 1.
13. Sillanpaa, M.; Sihvonen, M. L.; Talanta, **1997,** n. 44, p. 1487.
14. Sinex, S. A.; *EDTA – A Molecule With a Complex Story,* disponivel em: http://www.chm.bris.ac.uk/motm/edta/edtah.htm, acessado em abril de **2019**.
15. Skoog, D. A.; West, D. M.; Holler, F. J.: *Fundamentals of Analytical Chemistry,* 7ª ed., Harcourt College Publishers, USA, **1997**.
16. Sorvari, J.; Sillanptaa, M.; Chemosphere, **1996**, 33, 6, 1119.
17. Thakur, P.; Xiong, Y.; Borkowski, M.; Choppin, G. R.; Geochimica et Cosmochimica Acta, **2014**, 133, 299.
18. Vega, F. A.; Weng, L.; Water Research, **2013**, 47, 363.
19. Viipsi, K.; Sjöberg, S.; Shchukarev, A.; Tõnsuaadu, K.; Applied Geochemistry, **2012**, 27, 15.
20. Willett, A. I.; Rittmann, B. E.; Biodegradation, **2003**, 14, 105.
21. Wu, P.; Zhou, J.; Wang, X.; Dai, Y.; Dang, Z.; Zhu, N.; Li, P.; Wu, J.; Desalination, **2011**, 277, 288.
22. Yang, J. K.; Davis, A. P.; Journal of Colloid and Interface Science, **1999**, 216, 77.
23. Yang, J. K.; Lee, S. M.; Journal of Colloid and Interface Science, **2005**, 282, 5.

Downloaded from www.periodico.tchequimica.com

Tabela 1: *Dados obtidos de uma titulação simulada de 50,0 mL de Cu^{+2} 1,0x10^{-2} mol L^{-1} com EDTA 1,0x10^{-2} mol L^{-1} em meio tampão pH 10,0.*

	A	B	C	D	E	F	G	H
	EDTA (mL)	**n (EDTA) (mol)**	**n (Cu^{+2}) (mol)**	**n ([Cu-EDTA]) (mol)**	**[Cu^{+2}] (mol L^{-1})**	**[Cu-EDTA] (mol L^{-1})**	**pCu^{+2}**	**[EDTA] (mol L^{-1})**
1	0,00	0,00	5,0x10^{-4}	0,00	1,00x10^{-2}	0,00	2,00	
2	2,00	2,00x10^{-5}	4,8x10^{-4}	2,00x10^{-5}	9,23x10^{-3}	3,85x10^{-4}	2,03	
3	5,00	5,00x10^{-5}	4,5x10^{-4}	5,00x10^{-5}	8,18x10^{-3}	9,09x10^{-4}	2,09	
4	10,00	1,00x10^{-4}	4,0x10^{-4}	1,00x10^{-4}	6,67x10^{-3}	1,67x10^{-3}	2,18	
5	15,00	1,50x10^{-4}	3,5x10^{-4}	1,50x10^{-4}	5,38x10^{-3}	2,31x10^{-3}	2,27	
6	20,00	2,00x10^{-4}	3,0x10^{-4}	2,00x10^{-4}	4,29x10^{-3}	2,86x10^{-3}	2,37	
7	25,00	2,50x10^{-4}	2,5x10^{-4}	2,50x10^{-4}	3,33x10^{-3}	3,33x10^{-3}	2,48	
8	30,00	3,00x10^{-4}	2,0x10^{-4}	3,00x10^{-4}	2,50x10^{-3}	3,75x10^{-3}	2,60	
9	35,00	3,50x10^{-4}	1,5x10^{-4}	3,50x10^{-4}	1,76x10^{-3}	4,12x10^{-3}	2,75	
10	40,00	4,00x10^{-4}	1,0x10^{-4}	4,00x10^{-4}	1,11x10^{-3}	4,44x10^{-3}	2,95	
11	45,00	4,50x10^{-4}	5,0x10^{-5}	4,50x10^{-4}	5,26x10^{-4}	4,74x10^{-3}	3,28	
12	48,00	4,80x10^{-4}	2,0x10^{-5}	4,80x10^{-4}	2,04x10^{-4}	4,89x10^{-3}	3,69	
13	49,00	4,90x10^{-4}	1,0x10^{-5}	4,90x10^{-4}	1,01x10^{-4}	4,95x10^{-3}	4,00	
14	49,50	4,95x10^{-4}	5,0x10^{-6}	4,95x10^{-4}	5,03x10^{-5}	4,97x10^{-3}	4,30	
15	49,90	4,99x10^{-4}	1,0x10^{-6}	4,99x10^{-4}	1,00x10^{-5}	4,99x10^{-3}	5,00	
16	50,00	5,00x10^{-4}	0,0	5,00x10^{-4}	4,76x10^{-11}	5,00x10^{-3}	10,32	0,00
17	50,05	5,00x10^{-7}	0,0	5,00x10^{-4}	4,54x10^{-16}	4,99x10^{-3}	15,34	5,00x10^{-6}
18	50,50	5,00x10^{-6}	0,0	5,00x10^{-4}	4,54x10^{-17}	4,97x10^{-3}	16,34	4,98x10^{-5}
19	51,00	1,00x10^{-5}	0,0	5,00x10^{-4}	2,27x10^{-17}	4,95x10^{-3}	16,64	9,90x10^{-5}
20	52,00	2,00x10^{-5}	0,0	5,00x10^{-4}	1,13x10^{-17}	4,90x10^{-3}	16,95	1,96x10^{-4}
21	55,00	5,00x10^{-5}	0,0	5,00x10^{-4}	4,54x10^{-18}	4,76x10^{-3}	17,34	4,76x10^{-4}
22	60,00	1,00x10^{-4}	0,0	5,00x10^{-4}	2,27x10^{-18}	4,54x10^{-3}	17,64	9,09x10^{-4}
23	65,00	1,50x10^{-4}	0,0	5,00x10^{-4}	1,51x10^{-18}	4,35x10^{-3}	17,82	1,30x10^{-3}
24	70,00	2,00x10^{-4}	0,0	5,00x10^{-4}	1,13x10^{-18}	4,17x10^{-3}	17,95	1,67x10^{-3}
25	75,00	2,50x10^{-4}	0,0	5,00x10^{-4}	9,07x10^{-19}	4,00x10^{-3}	18,04	2,00x10^{-3}
26	80,00	3,00x10^{-4}	0,0	5,00x10^{-4}	7,56x10^{-19}	3,85x10^{-3}	18,12	2,31x10^{-3}
27	85,00	3,50x10^{-4}	0,0	5,00x10^{-4}	6,48x10^{-19}	3,70x10^{-3}	18,19	2,59x10^{-3}
28	88,00	3,80x10^{-4}	0,0	5,00x10^{-4}	5,97x10^{-19}	3,62x10^{-3}	18,22	2,75x10^{-3}
29	90,00	4,00x10^{-4}	0,0	5,00x10^{-4}	5,67x10^{-19}	3,57x10^{-3}	18,25	2,86x10^{-3}
30	91,00	4,10x10^{-4}	0,0	5,00x10^{-4}	5,53x10^{-19}	3,55x10^{-3}	18,26	2,91x10^{-3}

Downloaded from www.periodico.tchequimica.com

31	92,00	$4,20x10^{-4}$	0,0	$5,00x10^{-4}$	$5,40x10^{-19}$	$3,52x10^{-3}$	18,27	$2,96x10^{-3}$
32	93,00	$4,30x10^{-4}$	0,0	$5,00x10^{-4}$	$5,27x10^{-19}$	$3,49x10^{-3}$	18,28	$3,01x10^{-3}$
33	94,00	$4,40x10^{-4}$	0,0	$5,00x10^{-4}$	$5,15x10^{-19}$	$3,47x10^{-3}$	18,29	$3,06x10^{-3}$
34	95,00	$4,50x10^{-4}$	0,0	$5,00x10^{-4}$	$5,04x10^{-19}$	$3,45x10^{-3}$	18,30	$3,10x10^{-3}$
35	96,00	$4,60x10^{-4}$	0,0	$5,00x10^{-4}$	$4,93x10^{-19}$	$3,42x10^{-3}$	18,31	$3,15x10^{-3}$
36	97,00	$4,70x10^{-4}$	0,0	$5,00x10^{-4}$	$4,82x10^{-19}$	$3,40x10^{-3}$	18,32	$3,20x10^{-3}$
37	98,00	$4,80x10^{-4}$	0,0	$5,00x10^{-4}$	$4,72x10^{-19}$	$3,38x10^{-3}$	18,33	$3,24x10^{-3}$
38	99,00	$4,90x10^{-4}$	0,0	$5,00x10^{-4}$	$4,63x10^{-19}$	$3,36x10^{-3}$	18,33	$3,29x10^{-3}$
39	100,00	$5,00x10^{-4}$	0,0	$5,00x10^{-4}$	$4,54x10^{-19}$	$3,33x10^{-3}$	18,34	$3,33x10^{-3}$
40	105,00	$5,50x10^{-4}$	0,0	$5,00x10^{-4}$	$4,12x10^{-19}$	$3,23x10^{-3}$	18,38	$3,55x10^{-3}$
41	110,00	$6,00x10^{-4}$	0,0	$5,00x10^{-4}$	$3,78x10^{-19}$	$3,12x10^{-3}$	18,42	$3,75x10^{-3}$
42	115,00	$6,50x10^{-4}$	0,0	$5,00x10^{-4}$	$3,49x10^{-19}$	$3,03x10^{-3}$	18,46	$3,94x10^{-3}$
43	120,00	$7,00x10^{-4}$	0,0	$5,00x10^{-4}$	$3,24x10^{-19}$	$2,94x10^{-3}$	18,49	$4,12x10^{-3}$
44	125,00	$7,50x10^{-4}$	0,0	$5,00x10^{-4}$	$3,02x10^{-19}$	$2,86x10^{-3}$	18,52	$4,29x10^{-3}$
45	130,00	$8,00x10^{-4}$	0,0	$5,00x10^{-4}$	$2,83x10^{-19}$	$2,78x10^{-3}$	18,55	$4,44x10^{-3}$
46	135,00	$8,50x10^{-4}$	0,0	$5,00x10^{-4}$	$2,67x10^{-19}$	$2,70x10^{-3}$	18,57	$4,59x10^{-3}$
47	140,00	$9,00x10^{-4}$	0,0	$5,00x10^{-4}$	$2,52x10^{-19}$	$2,63x10^{-3}$	18,60	$4,74x10^{-3}$
48	145,00	$9,50x10^{-4}$	0,0	$5,00x10^{-4}$	$2,39x10^{-19}$	$2,56x10^{-3}$	18,62	$4,87x10^{-3}$
49	150,00	$1,00x10^{-3}$	0,0	$5,00x10^{-4}$	$2,27x10^{-19}$	$2,50x10^{-3}$	18,64	$5,00x10^{-3}$

OBSERVAÇÕES:

1) Constante de formação do complexo Cu-EDTA: K [Cu-EDTA] = $6,30x10^{18}$.
2) Constante de formação condicional do complexo Cu-EDTA: Kfc [Cu-EDTA] = $2,21x10^{18}$.
3) Alíquota de Cu^{+2} de concentração molar de $1,0x10^{-2}$ mol L^{-1} = 50,00 mL.
4) Concentração molar do EDTA = $1,00x10^{-2}$ mol L^{-1}.
5) Número de mols (n) do Cu^{+2} = $5,00x10^{-4}$ mol.
6) Logaritmo da constante de formação condicional do complexo {(log Kfc) [Cu-EDTA]} = 18,34.
7) Fração do EDTA na forma Y^{-4} em valor de pH 10,0 (αY^{-4}) = 0,35.

Downloaded from www.periodico.tchequimica.com

PERIÓDICO TCHÊ QUÍMICA
ARTIGO ORIGINAL

ESTUDO DE ESPECTROSCÓPIA-IV DA IMOBILIZAÇÃO DE COMPOSTOS DE SELÊNIO EM COLÁGENO BIOMODIFICADO

IR-SPECTROSCOPIC STUDY OF IMMOBILIZATION OF SELENIUM COMPOUNDS ON BIOMODIFIED COLLAGEN

ИК–СПЕКТРОСКОПИЧЕСКОЕ ИССЛЕДОВАНИЕ ИММОБИЛИЗАЦИИ СОЕДИНЕНИЙ СЕЛЕНА НА БИОМОДИФИЦИРОВАНОМ КОЛЛАГЕНЕ

GLOTOVA, Irina Anatolievna[1]; GALOCHKINA, Nadezhda Alekseevna[2*]; SELEMENEV, Vladimir Fedorovich[4] ; PEREGONCHAYA, Olga Vladimirovna[3] ; SOKOLOVA , Svetlana Anatol'evna[3].

[1] Voronezh State Agrarian University named after Emperor Peter the Great, The Faculty of Technology and Merchandizing, Department of Merchandizing Technique and Commodity Expertise.

[2] Voronezh State Agrarian University named after Emperor Peter the Great, The Faculty of Technology and Merchandizing, Department of technology of storage and processing of agricultural products.

[3] Voronezh State Agrarian University named after Emperor Peter the Great, The Faculty of Technology and Merchandizing, Department of chemistry.

[4] Voronezh State University, The Faculty of Technology and Merchandizing, Department of Analytic Chemistry, Chemical faculty

** Autor correspondente*
e-mail: galochkina.na@mail.ru

Received 12 June 2019; received in revised form 30 September 2019; accepted 19 October 2019

RESUMO

O objetivo do trabalho foi pesquisar as características espectrais de substâncias de colágeno produzidas por bioengenharia, utilizando preparações complexas de proteases colagenolíticas obtidas antes e após a imobilização de compostos de selênio em meios ácidos e alcalinos, e comparar o grau de interação das preparações de selênio com a matriz de colágeno após sua imobilização, e sua influência na conformação de moléculas de proteína. Os resultados da imobilização de preparações de selênio em colágeno biomodificado pelo método de espectroscopia no infravermelho foram apresentados, analisados e discutidos. O colágeno biomodificado foi obtido a partir de resíduos de corte de carne (veias e tendões) por hidrólise seqüencial de peróxido alcalino e enzimático com a preparação de colagenase alimentar. As seguintes fontes de selênio foram usadas como compostos com propriedades bioprotetoras para posterior imobilização em proteínas de colágeno biomodificadas: 4,4-di [3 (5-metildiprazolil)] selenida (DMDPS) com o conteúdo de 0,657g de DMDMS em 100 cm^3 e selenito de sódio . Os espectrogramas foram feitos para produtos de biomodificação de colágeno antes da sorção de compostos de selênio (à taxa de 1,2 g^{-6} de selênio em 1 g de colágeno) em ambientes ácido (pH = 5) e alcalino (pH = 10) em uma pesquisa de influência de compostos de selênio em espectros IR de produtos de biomodificação de colágeno. Foi estabelecido que a imobilização ocorreu por reação uma química de preparações de selênio com grupos funcionais das cadeias laterais de moléculas de proteína, e seu grau varia na faixa de Na_2SeO_3 (pH = 5) > 4,4-di [3 (5-metildiprazolil)] selenida (DMDPS) > Na_2SeO_3 (pH = 10). Demonstrou-se que, sob a interação de produtos de selênio com colágeno, não há alteração nas conformações de suas moléculas.

Palavras-chave: *Selênio, colágeno biomodificado, selenito de sódio, 4,4-di [3 (5-metildiprazolil)] selenida (DMDPS), imobilização*.

ABSTRACT

The aim of the work was to research the spectral characteristics of collagen substances bioengineered by using complex collagenolytic proteases preparation obtained before and after the immobilization of selenium compounds in acidic and alkaline media and to comparate the degree of interaction of selenium preparations

Downloaded from www.periodico.tchequimica.com

with collagen matrix upon immobilization and its influence on the conformation of protein molecules. The results of the immobilization of selenium preparations on biomodified collagen by the IR spectroscopy method are presented, analyzed, and discussed. Biomodified collagen was obtained from beef trimming waste (veins and tendons) by sequential peroxide-alkaline and enzymatic hydrolysis with the food collagenase preparation. The following sources of selenium were used as compounds with bioprotective properties for subsequent immobilization on biomodified collagen proteins: 4,4-di[3(5-methyldiprazolil)]selenide (DMDPS) with the content of 0,657g DMDMS in 100 cm^3 and sodium selenite. Spectrograms are carried out for products of biomodification of collagen before sorption of compounds of selenium, (at the rate of 1.2 g^{-6} of selenium on 1 g of collagen) in acid (pH =5) and alkaline (pH =10) environments at a research of influence of compounds of selenium on IR spectrums of products of biomodification of collagen. It was established, that the immobilization takes place by a chemical reaction of selenium preparations with functional groups of the side chains of protein molecules, and its degree varies in the range Na_2SeO_3 (pH=5) > 4,4-di[3(5-methyldiprazolil)]selenide (DMDPS) > Na_2SeO_3 (pH=10). It is shown that under the interaction of selenium products with collagen, there is no change in the conformations of its molecules occurred.

Keywords: *Selenium, biomodified collagen, sodium selenite, 4,4-di[3(5-methyldiprazolil)]selenide (DMDPS), immobilization.*

АННОТАЦИЯ

Цель работы – исследовать спектральные характеристики коллагеновых субстанций, биомодифицированных с применением комплексного препарата коллагенолитической протеиназы, полученные до и после иммобилизации соединений селена в кислой и щелочной средах, на основе чего дать сравнительную оценку степени взаимодействия селеновых препаратов с коллагеновой матрицей при иммобилизации и их влияния на конформацию белковых молекул. Представлены, проанализированы и обсуждены результаты иммобилизации препаратов селена на биомодифицированном коллагене методом ИК-спектроскопии. Биомодифицированный коллаген был получен из отходов жиловки говядины (жилки и сухожилия) путем последовательного перекисно-щелочного и ферментативного гидролиза с использованием ферментного препарата “Коллагеназа пищевая”. В качестве источника селена были использованы искусственно синтезированная органическая форма селена для последующей иммобилизации на биомодифицированных коллагеновых белках: 4,4-ди [3 (5-метилдипиразолил)]селенид (ДМДПС) с содержанием 0,657 г ДМДПС в 100 $см^3$ и селенит натрия , Спектрограммы проведены для продуктов биомодификации коллагена после сорбцией соединений селена (из расчета 1,2 мкг селена на 1 г коллагена) в кислой (pH = 5) и щелочной (pH = 10) средах при исследовании влияния соединений селена на ИК-спектры продуктов биомодификации коллагена. Установлено, что иммобилизация проходит путём химического взаимодействия препаратов с функциональными группами боковых цепей молекул белка, а его степень изменяется в ряду Na_2SeO_3 (pH=5) > ДМДПС > Na_2SeO_3 (pH=10). Показано, что при взаимодействии селеновых препаратов с коллагеном не происходит изменения конформаций его молекул.

Keywords: *селен, биомодифицированный коллаген, селенит натрия, 4,4-ди[3(5-метилдипиразолил)]селенид (ДМДПС), иммобилизаци*

1. INTRODUCTION

The development and application of sorption biomaterials as carriers of biologically active substances is a promising direction in biotechnology (Dyankova and Solak, 2014; Benavides *et al.*, 2012; Holyavka *et al.*, 2014; Kovaleva, *et al.* 2011; Olshannikova *et al.*, 2018; Holyavka *et al.*, 2017). Proteins have Wide possibilities of using as polysorbates, in connection with the presence of a large number of potential binding, which is located in the side radicals of amino acids (Kuznetsova and Glushko, 2007; Chi H Lee, 2001; Yamada *et al.*, 2014; Dharmendra, 2013).

In some works, the collagen is used as a carrier of biologically active substances. The authors of these works apply enzymology engineering methods using general proteolytic activity enzyme preparations (Protosubtilin, Savinase, Neutrase 1.5 MG) and collagenolytic activity enzyme preparation (Collagenase from hepatopancreas of the Kamchatka crab) to improve the sorption capacity of collagen (Kovaleva *et al.*, 2011; Kovaleva *et al.*, 2011; Galochkina *et al.*, Glotova *et al.*, 2015)

Selenium is one of the essential microelements. It is involved in the immune, antioxidant and detoxification systems of the body. The protective property of selenium from ionizing radiation, toxic effects of nitrates and

Downloaded from www.periodico.tchequimica.com

nitrites and heavy metals is well known. Selenium has a positive effect on the quality of life of organisms, including increases resistance to stress, reduces the rate of development of various age-related diseases.The development of more improving technologies for food fortification with essential micronutrients, including selenium, is a promising method of correcting diet (Glotova, *et al.*, 2014; Galochkina *et al.*, 2012).

The aim of the work is to research the spectral characteristics of collagen substances bioengineered by using complex collagenolytic proteases preparation obtained before and after the immobilization of selenium compounds in acidic and alkaline media. On the base of these data, we can give a comparative evaluation of the degree of interaction of selenium preparations with collagen matrix upon immobilization and its influence on the conformation of protein molecules.

2. MATERIAL AND METHODS

To obtain a functional collagen substance were used: veins and tendons, which were allocated in the trimming of cattle in the sausage department of the meat processing plant (JSC "Donskoy", Voronezh, PE "Four penguins", Voronezh) in cutting of beef according to GOST 779; the enzyme preparation "Food Collagenase" (Technical Conditions 2639-001-4554109-98, manufacturer CJSC "Bioprogress", Shchelkovo, Moscow region).

The hepatopancreas of the Kamchatka crab is the source of the enzyme preparation "Food Collagenase". It is the organ, which combines the functions of the liver and pancreas in the crab's digestive tract. The hepatopancreas is a complex of collagenolytic proteases, the molecular weight of which is in the range 23-36 κDa, this complex is adapted to the biodegradation of native collagen according to the physiological characteristics of crab nutrition (Glotova et al., 2014).

Taking into account the need to minimize the number and duration of technological operations, the consumption of chemical reagents and biocatalysts to obtain collagen hydrolyzate with a large number of ionogenic groups for immobilizing selenium in DMDPA, it is advisable to carry out operations for the isolation, purification and biomodification of collagen from the veins and tendons of cattle in accordance with supports sequence presented in Figure 1.

The raw material - vein, tendon, fascia, were allocated at the stage of trimming, after that they were washed with running water and were placed in a peroxide-alkaline solution. This solution contained sodium hydroxide with a concentration of 10 % and hydrogen peroxide – 3 %. The processing for 6-10 h in hydromodule 1:2-2,5 provides a uniform interaction of the peroxide-alkaline solution with the feedstock. After that, the liquid fraction was separated by decantation or centrifugation, and the solid residue of collagen was washed with water and neutralized to pH 8,0-8,5. This interval is in the border region of pH, favorable for the collagenolytic activity's manifestation of the preparation "Food Collagenase". Collagen hydrolyzate was obtained by exposure for 2.5-3.0 hours at 36-38°C with the preparation of "Food Collagenase" in the amount of 0.02 % by the weight of collagen (Glotova and Galochkina, Patent, 2015; Glotova *et al.*, 2015; Majorov A. F. *et al.*,1992) .

The following sources of selenium were used as compounds with bioprotective properties for subsequent immobilization on biomodified collagen proteins: 4,4-di[3(5-methyldiprazolil)]selenide (DMDPS) Technical Conditions 9291-007-59582032 with the content of 0,657g DMDMS in 100 cm^3 (artificially synthesized organic form of selenium, the manufacturer – Limited Liability Company "Safron", Moscow, sanitary-epidemiological conclusion №77.99.13.003.T.000518.03.06). The aggregate state is white powder, in 2002, allowed as a dietary supplement. According to state scientific institution All-Russian veterinary research institute of pathology, pharmacology and therapy of the Russian Academy of agricultural sciences DMDPS currently is the most low-toxic compound of selenium with low cumulative (Glotova et al., 2013); sodium selenite (FSP 42-0250-1024-01) the manufacturer is the firm "MCD chemicals" ("MCD", Moscow);

We studied the impact of selenium compounds on the IR spectra of the products of biomodification collagen. We conducted a survey of these products' spectrograms before and after sorption of selenium compounds, (at the rate of 1.2 mcg of selenium per 1 g of collagen (Glotova and Galochkina, 2015) in the acidic (pH = 5) and alkaline (pH = 10) environments.

The samples of the researched substances with collagen immobilized selenium products were pre-dried at a temperature of 36 °C for 24 hours to obtain IR spectra. After that the

Downloaded from www.periodico.tchequimica.com

samples were carefully ground in an agate mortar to obtain a homogeneous fine powder, and then tablets were made with pre-dried and ground powder of optically pure single-crystal KBr in the ratio of 0.1 mg of sample in 100 mg potassium bromide (Ramasamy Sripriya *et al.*, 2015; Gudkov *et al.*, 2018).

IR spectra of the collagen substances were obtained on a spectrometer with Fourier transform (with ATR) "Vertex-70" (Germany), for subsequent processing, the program GRAMS 4/32 was used.

3. RESULTS AND DISCUSSION

IR spectra of collagen before and after immobilization of DMDPS are presented in fig. 2. The spectra contain two distinct spectral ranges with the wavenumber of 900-1800 cm^{-1} (long-wave) and 2800-3700 cm^{-1} (short-wave). The first region characterizes the fluctuations of collagen molecules' fragments and bonds between the atoms in these molecules. The second area characterizes the valence vibrations of C-H-bonds, OH-bonds in the hydration shells of functional groups, specifies the presence of free water with the normal network of hydrogen bonds and additionally includes the wide absorption spectral band of the vibrations in N-H bonds.

These maximums of the original sample spectra of collagen (fig. 2a, curve 1) adequately explain the structure and functional composition of the protein (Ramasamy Sripriya *et al.*, 2015; Shkutina *et al.*, 2004). Spectral bands 2923 and 2852 cm^{-1} characterize valence vibrations of C-H bonds in the main chain and side radicals of protein molecules stretching. The peak 1453cm^{-1} characterizes their deformational vibrations. The frequencies 1549 and 1636 cm^{-1} correlate to vibrations of the peptide bonds (respectively, the "amide II and amide I»). The maximum 1746 cm-1 correlate to valence vibrations C=O bonds. The salt form of carboxyl groups can be identified by the presence of 1549 and 1333 cm^{-1} absorption bands, which characterize asymmetric and symmetric vibrations of the carboxylate anions of aspartic and glutamic acids. Frequency 1638 cm^{-1} simultaneously corresponds to the salt form of carboxyl groups valence vibrations and the deformation vibrations of amino groups, which are included in the amino acid diaminocarbenes residues. The 3080 cm^{-1} band indicates vibrations of C-H in the aromatic nuclei of phenylalanine and tyrosine residues.

The number of peaks (1243, 1133, 1080, 1021 cm^{-1}) is evident on the left part of the long-wave region of the spectrum. They are due to oscillations of the carbon skeleton of protein, deformed OH, valence CO, and other vibrations. The dependence of the absorption value on the wavenumber for collagen adsorbed selenium preparation (Figure 2A, curve 2) is not qualitatively different from the curve for the original sample. Some differences are in the deviation of the maxima by a few cm^{-1}, which corresponds to the accuracy of the IR spectroscopy method. The form of the spectra remains practically unchanged by varying the pH. Spectrograms were almost identical for the samples with different pH values. Presumably, the interaction of collagen and selenium preparation DMDPS is absent. This can not be confirmed unequivocally since the intensity of the absorption bands on spectrograms is different. To obtain comparable data, we applied the method of processing spectra using the baseline method (Ewing and Kazarian, 2017) . As standard, the maxima (1453 cm^{-1} in the long-wavelength region and 2923 cm^{-1} in the short-wavelength) were chosen. The most appropriate data baseline method is given if the bands that are close in frequency to the analyzed bands are taken as standard. In Fig. 3 shows the relative heights of the maxima in different regions of the spectra.

Immobilization of sodium selenite on collagen in an acidic medium causes a sharp decrease in the intensity of the 1743 cm^{-1} band of C = O vibrations in undissociated carboxyl groups. Immobilization of sodium selenite on collagen also leads to a significant increase in the absorption intensity of asymmetric (1551 cm^{-1}) and less pronounced increase in symmetrical (1397 cm^{-1}) vibrations of carboxylate ions (Fig. 2b, curves 1, 3). This is due to the course of reactions between the functional groups of collagen and sodium selenite (figure 4). In a weakly acidic medium (pH = 5) the process proceeds:

The hydroselenite of sodium formed as a result of the reaction (Figure 4) reacts with the amino groups of the protein to form a mixed sodium-ammonium salt:

$$R\text{-}NH_2 + NaHSeO_3 \rightarrow R\text{-}NH_3 + SeO_3\text{-}Na^+$$

As a result, selenium is fixed on the protein matrix. A certain contribution to the maximum value of 1551 cm^{-1} is made by the vibrations of the $–NH_3^+$ groups (Cherkasov and Pasechnik, 1991).

In an alkaline medium (pH = 10), reaction (fig. 4) can not proceed, since the carboxyl groups of the protein are completely

Downloaded from www.periodico.tchequimica.com

deprotonated, and strong immobilization of selenite on the protein is difficult. Apparently, the selenium ion weakly interacts with the collagen matrix. This fact is indicated by a slight increase in the relative heights of the peaks (h / h_{st}) in comparison with the original sample under these conditions (Figures 3b No. 3 and No. 1, maxima of 1635 and 1397 cm^{-1}).

The immobilization of DMDS on collagen (Fig. 3b, No. 4), as well as the immobilization of sodium selenite, causes a sharp decrease in the content of free carboxyl groups (1746 cm^{-1}) with the simultaneous increase in carboxylate ions (1638, 1549 cm^{-1}). This indicates a possible chemical interaction of the selenium preparation with the protein. The process follows the scheme (figure 5):

In this case, a carboxylate ion of the protein and charged quaternary ammonium are formed. The presence of the quaternary ammonium ion is confirmed by the presence of maxima of 3308 cm^{-1} (corresponding to the hydrated water of the amino group) and 1638 cm^{-1}. The relative height of the peaks h / h_{st} in Fig. 3b, which corresponds to asymmetric and symmetric vibrations of carboxylate ions, in the case of DMDS is less than in the sample that adsorbed sodium selenite at pH = 5 but greater than the one sorbed at pH = 10. This is due to the fact that reaction (3) is less intense than in reaction (1) because of the spatial difficulties in the sorption of a large-size DMDPS molecule compared to sodium selenite.

It is necessary to take into account the following results that we obtained. First, the calculation of h / h_{st} at a maximum of 3308 cm^{-1} relatives to the standard band of 2983 cm^{-1} showed that these values in the series:

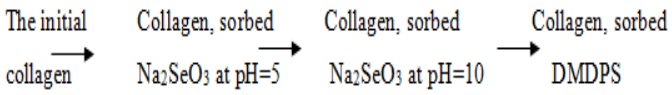

change as 0.25-2.36-0.62-0.76. This fact points to the highest water content in collagen samples with immobilized sodium selenite at pH = 5. The reason for this is an increase in the water content in the hydrated shells of carboxylate ions and of quaternary nitrogen of collagen.

Secondly, the almost complete coincidence of the values of h/h_{st} in the region of «fingerprints» for all the samples under study makes it possible to assume that the immobilization of selenium preparations has an insignificant effect on the conformation of collagen molecules.

4. CONCLUSIONS

The immobilization of selenium preparations on the collagen occurs by their chemical interaction with the carboxyl and amino groups of the protein molecules side chains, with the formation of oppositely charged ions.
The degree of interaction between selenium preparations with collagen varies among: Na_2SeO_3 (pH=5) > DMDPS > Na_2SeO_3 (pH=10).
The immobilization of selenium preparations on the collagen causes an increase in the content of the water of hydration and does not affect the conformation of protein molecules.

5. ACKNOWLEDGMENT

The studies were carried out using the equipment of Common Use Center at Voronezh State University.

6. REFERENCES

1. DYANKOVA S., SOLAK A., Biopolymer matrix systems for incorporation of biologically active substances. Agricultural science and technology; v. 6, p.104-110, 2014. (in Russian)
2. BENAVIDES S., VILLALOBOS-CARVAJAL R., REYES J.E. Physical mechanical and antibacterial properties of alginatefilm: Effect of the cross linking degree and oregano essential oil concentration. Journal of Food Engineering; v.110(2), p.232-239, 2012.
3. HOLYAVKA M.G., KOVALEVA T.A., KARPOV S.I., SEREDIN P.V., ARTYUKHOV V.G Investigation of mechanisms of interaction between inulinase from kluyveromyces marxianus and the matrices of ion exchange resins and fiber. Biophysics; v.59(2), p. 223-229, 2014. (in Russian)
4. KOVALEVA T.A., BELENOVA A.S., SHATALOV G.V. Immobilization of lipase on poly(N-Vinyl pyrrolidone). Bulletin of Experimental Biology and Medicine; v.151(4) , p. 415-417, 2011. (in Russian)
5. OLSHANNIKOVA S.S., KOROLEVA V.A., KHOLYAVKA M.G., PANKOVA S.N., BELENOVA A.S., KONDRATEV M.S., SAMCHENKO A.A., KABANOV A.V., ARTYUKHOV V. G. The adsorption immobilization of bromelain on chitosan matrices. Journal of Biotechnology; v. 280(5) , p. 68, 2018. (in Russian)
6. HOLYAVKA M. G., ARTYUKHOV V. G.,

Downloaded from www.periodico.tchequimica.com

KONDRATYEV M. S., SAMCHENKO A. A., KABANOV A. V., KOMAROV V. M., TERENTYEV V. V. The molecular mechanism of adsorption immobilization of inulinase on polymer matrices. Biophysics; v.62(1) , p. 5-11, 2017. (in Russian)
7. KUZNETSOVA L. S., GLUSHKO A. A., Technological research noninvasive of wound coverings with the juice of plantain and analysis of the adsorption of biologically active substances juice on collagen. Modern problems of science and education; v.6, URL: https://science-education.ru/en/article/view?id=11775 , 2013. (in Russian)
8. CHI H LEE, ANUJ SINGLA, YUGYUNG LEE Biomedical applications of collagen. International Journal of Pharmaceutics; v.221, p. 1–22, 2001.
9. YAMADA S., YAMAMOTO K., IKEDA T., Yanagiguchi K., Hayashi Y. Potency of Fish Collagen as a Scaffold for Regenerative Medicine. BioMed Research International; URL: http://dx.doi.org/10.1155/2014/302932 , 2014
10. DHARMENDRA KUMAR A review on collagen based drug delivery systems. International Journal of Pharmacy Teaching & Practices; v. 4(4), p. 811-820, 2013.
11. KOVALEVA T. A., MAKAROVA T. A., SLIVKIN A. I., KOROTKOVA E. V. Adsorbcionnaya immobilizaciya , iz Aspergillus awamori na kollagene. Voprosy biologicheskoj, medicinskoj i farmacevticheskoj himii; v.11, p.19-22, 2011. (in Russian)
12. KOVALEVA T. A., MAKAROVA E. L., KOROTKOVA E.V. Sorbciya glyukoamilazy iz Aspergillus awamori na kollagene. Vestnik Voronezhskogo gosudarstvennogo universiteta. Seriya: Himiya. Biologiya. Farmaciya; v.1, p. 32-36, 2011. (in Russian)
13. GALOCHKINA N. A., LITOVKIN A. N., GLOTOVA I. A., SVESHNIKOVA I. A. Issledovanie molekulyarno-massovogo raspredeleniya belkovyh frakcij pri modifikacii pishchevyh biopolimernyh system. Sovremennye naukoemkie tekhnologii; v.5(1), p.187-187, 2014. (in Russian)
14. GLOTOVA I. A., GALOCHKINA N. A., SHAKHOV S. V., MATEEV E. Z., KADIRBAEV M. K. Biocatalytic Properties and Substrate Specificity of Proteinase Preparations From Different Sources. Research Journal of Pharmaceutical, Biological and Chemical Sciences; v.6(1), p.1640-1645; URL: http://www.rjpbcs.com/2015_6.1.html, 2015. (in Russian)
15. GLOTOVA I. A., GALOCHKINA N. A. Effect of selenium sources on biochemical processes during swelling and germination of wheat grain. Himija rastitel'nogo syr'ja; 4 DOI: 10.14258/jcprm.2017041849, 2017. (in Russian)
16. GALOCHKINA N. A., GLOTOVA I. A., PARSHIN P. A., PRYANISHNIKOV V. V. Improving the technology of enrichment of food of animal origin. Myasnaya industriya; v.10, p.35-38, 2012. (in Russian)
17. GLOTOVA I. A., GALOCHKINA N. A. Justification of the conditions for obtaining functional biomodified collagen substances. Bulletin of biotechnology and physico-industrial biology. Yu.A. Ovchinnikov; v.10(1), p.10-19, 2014. (in Russian)
18. Patent 2542123 Rossijskaya Federaciya, MPK51 A23L 8/0.3 Sposob polucheniya polifunkcional'noj dobavki dlya obogashcheniya selenom pishchevyh produktov / Glotova I.A., Galochkina N.A.; Voronezh State Agrarian University named after Emperor Peter the Great. - № 2013134911/13; zayavl. 24.07.13; opubl. 20.02.2015, Byul. № 5. (in Russian)
19. GLOTOVA, I. A., GALOCHKINA N. A., KURCHAEVA E. E. Selenium-deficient population conditions and ways of their nutritional correction. Food Industry; v. 12, p.74-77, 2013. (in Russian)
20. RAMASAMY SRIPRIYA, RAMADHAR KUMAR A Novel Enzymatic Method for Preparation and Characterization of Collagen Film from Swim Bladder of Fish Rohu. Food and Nutrition Sciences; v. 6, p.1468-1478, 2015. (in Russian)
21. GUDKOV M., GLOTOVA I., SHAKHOV S., PUGACHEVA I., GALOCHKINA N., BOKADAROV S., LOBACHEVA N Investigation of polymer interaction with nanoscale modifier and development of its identification algorithm. Actual Issues of Mechanical Engineering; p.187-192, 2018. (in Russian)
22. SHKUTINA I.V. STOYANOVA O.F.,

Downloaded from www.periodico.tchequimica.com

SELEMENEV V.F. IK spektroskopiya dlya issledovaniya kompleksa inulaza-nositel'.Vestnik VGU. Seriya: Himiya. Biologiya. Formaciya; v.1: p.110 – 113, 2004. (in Russian)
23. EWING A. V., KAZARIAN S. G. Infrared spectroscopy and spectroscopic imaging in forensic. Analyst; v.142(2), p.257-272, 2017.
24. CHERKASOV A. N. PASECHNIK V. A. Membrany i sorbenty v biotekhnologii. Himiya. – 239 p. 1991. (in Russian)
25. Patent 2112036 Rossijskaya Federaciya, MPK C12N 9/64 Method for producing collagenase/ Sposob poluchenija kollagenazy / MAJOROV A.F., ALBULOV A.I., SAMUJLENKO A. Ja.; 5067815/13, zayavl.09.10.1992 opubl. 27.05.1998 (in Russian)

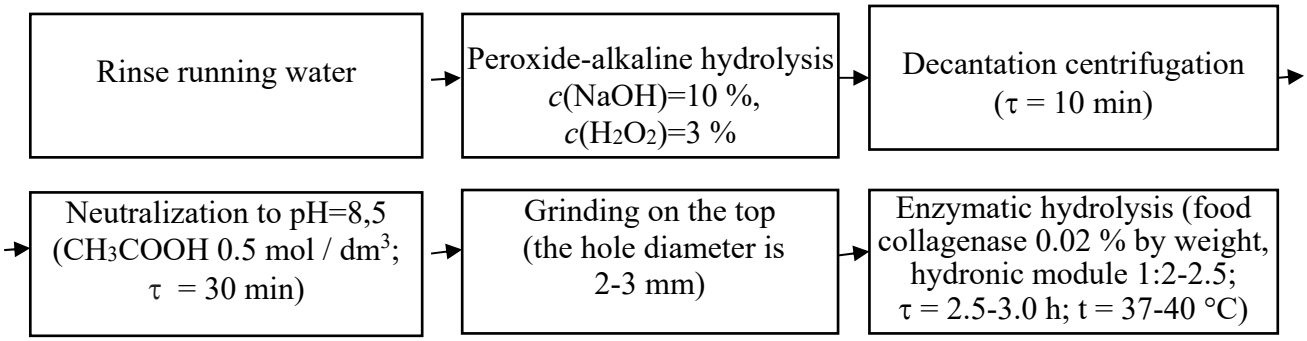

Figure 1 *Sequence of operations in the preparation of collagen biomodination product for the subsequent modification of DMDPS*

Downloaded from www.periodico.tchequimica.com

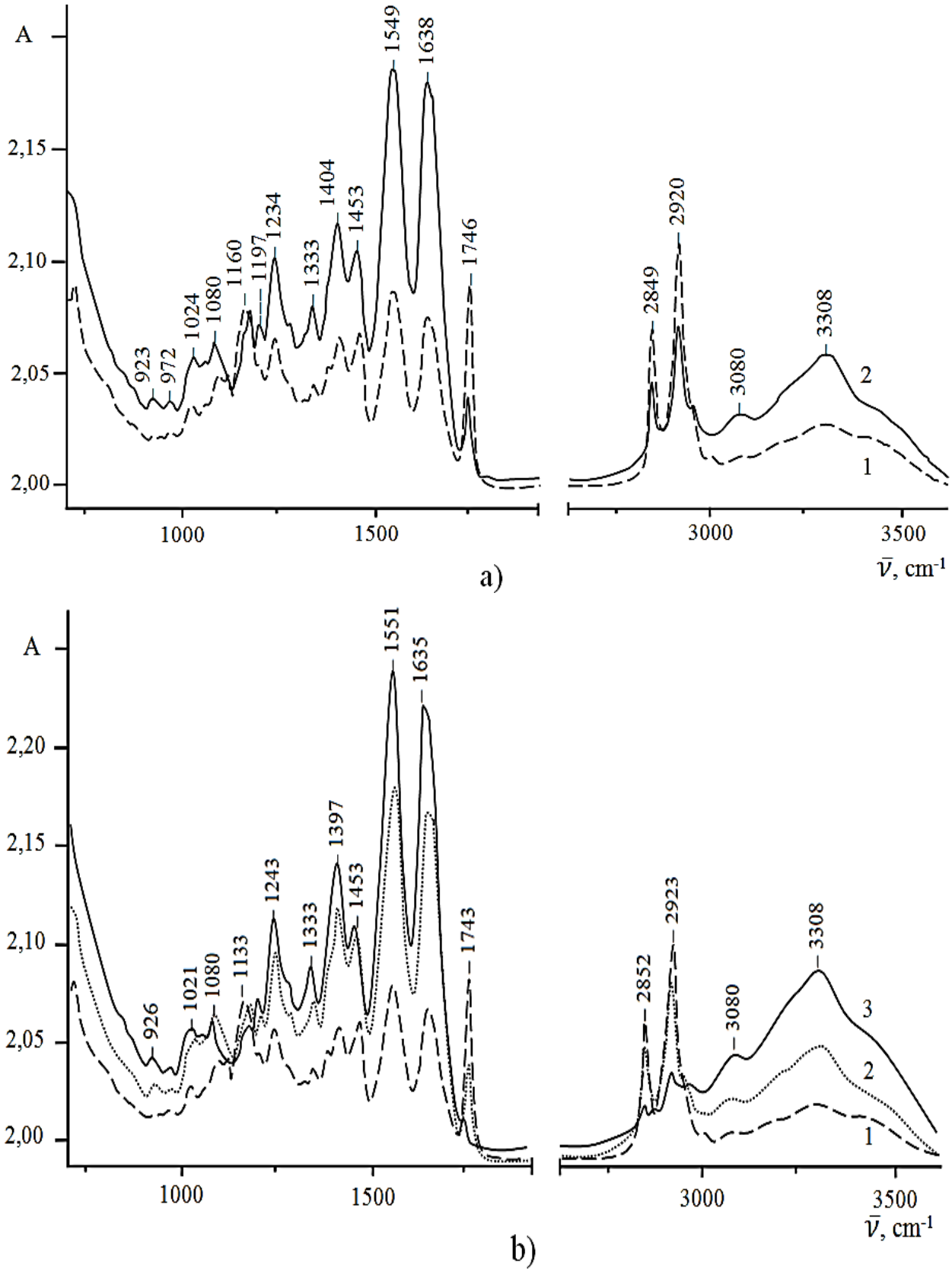

Figure 2 *IR spectra of collagen substances before and after adsorption of DMDPS (a): 1 – initial sample, 2 – sample after adsorption of DMDPS; and during immobilization of sodium Selenite (b): 1 – initial sample, 2 – sample after sorption of sodium selenite (pH=10), 3 – sample after sorption of sodium selenite (pH=5)*

Downloaded from www.periodico.tchequimica.com

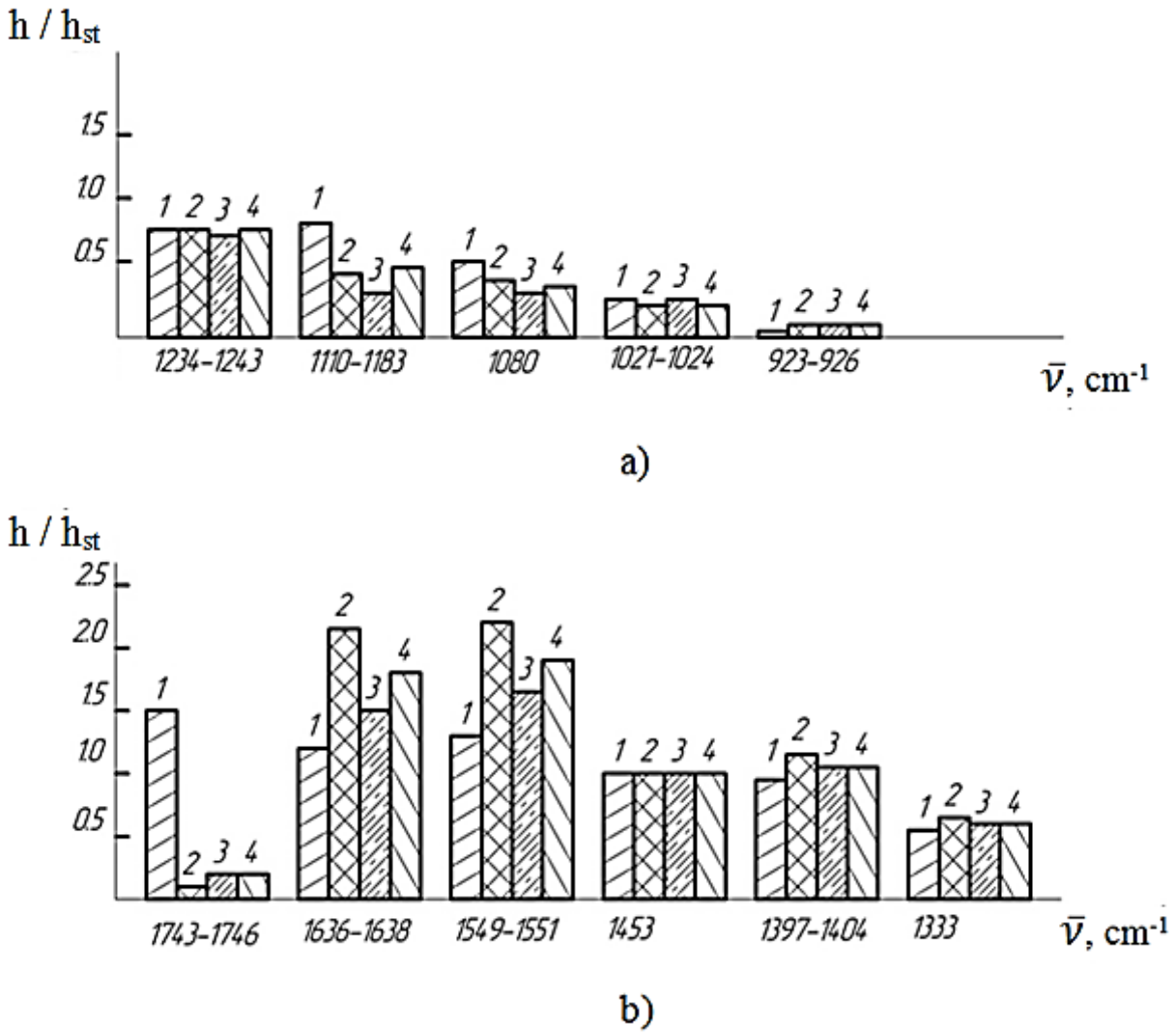

Figure 3 *The ratio h / h_{st} of the peaks of the IR spectra of the initial collagen (1); collagen with immobilized Na_2SeO_3 at pH = 5 (2); and at pH = 10 (3); and DMDPS (4): a - in the wavelength range 923-1243 cm^{-1}; b - in the wavelength interval 1333-1746 cm^{-1}*

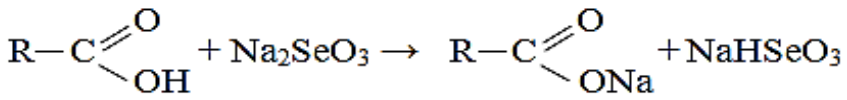

Figure 4 *The scheme of interaction of sodium selenite with functional groups in the collagen matrix, R is the matrix of collagen*

Downloaded from www.periodico.tchequimica.com

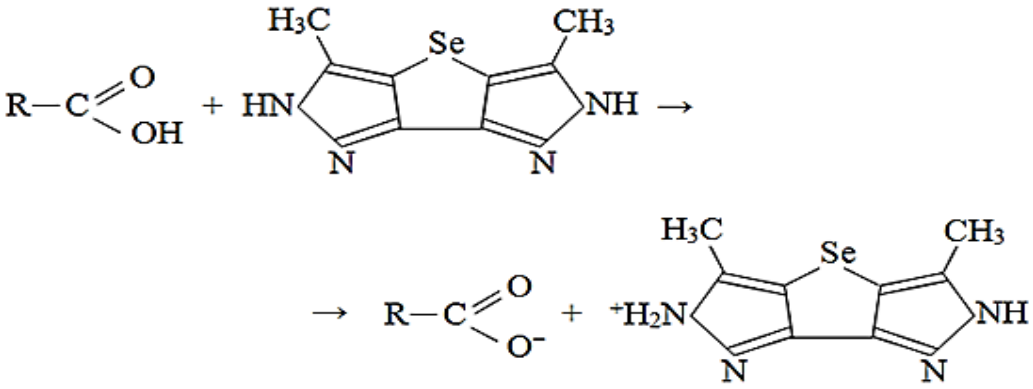

Figure 5 *Possible interaction of DMDPS with functional groups in the collagen matrix*

Downloaded from www.periodico.tchequimica.com

PERIÓDICO TCHÊ QUÍMICA
ARTIGO ORIGINAL

NOVO MÉTODO VOLTAMÉTRICO PARA DETERMINAÇÃO DE FENANTRENO EM ÁGUA SUBTERRÂNEA

NEW VOLTAMMETRIC METHOD FOR DETERMINATION OF PHENANTHRENE IN GROUNDWATER

FERREIRA, Ana Paula Mota[1*]; TEIXEIRA, Erico June Neves[2]; OLIVEIRA, Iolanda Miranda de[3]; PINHEIRO, Helilma de Andréa[4], MARQUES, Aldaléa Lopes Brandes[5*]

[3] Universidade Federal do Maranhão, São Luís - MA, Brasil. Av. dos Portugueses, 1966 - São Luís – MA.

[1,4,5]Programa de PG em Biodiversidade e Biotecnologia da Amazônia Legal-Rede BIONORTE, Universidade Federal do Maranhão, São Luís - MA, Brasil. Av. dos Portugueses, 1966 - São Luís - MA - CEP: 65080-805

[2] Programa de PG em Química, Universidade Federal do Maranhão, São Luís- MA, Brasil. Av. dos Portugueses, 1966 - São Luís - MA - CEP: 65080-805

* *paula_ufma@hotmail.com; aldalea.ufma@hotmail.com*

Received 12 August 2019; received in revised form 21 September 2019; accepted 21 October 2019

RESUMO

Este trabalho propõe um novo método para a determinação de Fenantreno (FEN) em meio aquoso com um eletrodo de carbono vítreo modificado com ftalocianina de cobalto (ECV / CoPc), utilizando voltametria de pulso diferencial (VPD), cuja oxidação de FEN ocorre entre 1,3 e 1,4 V. O eletrodo foi modificado com uma solução metanólica de CoPc 1x10^{-3} mol·L^{-1} contendo Nafion 10%. Para medições voltamétricas no modo Pulso Diferencial foram utilizadas uma amplitude de 0,7V e uma velocidade de varredura (ν) de 0,04V s^{-1}. Os parâmetros experimentais foram otimizados para fins de determinação de FEN em água subterrânea, cuja amostra foi coletada em um poço de água de um posto de combustível de São Luis-MA. Sob essas condições otimizadas, uma curva analítica foi obtida na faixa de concentração de 0,49; a 2,4 µM, com um limite de detecção de 1,2 x 10^{-10} mol·L^{-1}. O método foi aplicado em uma amostra real de água subterrânea de um poço de água localizado em um posto de combustível e foi encontrada uma concentração média de 0,037 µM FEN (n = 5), apresentando um coeficiente de variação de 0,88, o que indica uma boa precisão. A exatidão foi avaliada pelo teste de recuperação, cujo valor médio foi de 99,9%. Esses resultados indicam que o procedimento proposto é uma boa alternativa para a análise de FEN em água natural.

Palavras-chave: *Fenantreno; águas subterrâneas; posto de combustível; Voltametria*

ABSTRACT

This work proposes a new method for the determination of phenanthrene (FEN) in aqueous medium with a cobalt phthalocyanine modified glassy carbon electrode (ECV / CoPc), using Differential Pulse Voltammetry (VPD), whose oxidation of FEN occurs between 1,3 and 1,4 V. The electrode was modified with a 1x10^{-3} mol·L^{-1} CoPc methanolic solution containing 10% Nafion. For voltammetric measurements in Differential Pulse mode, an amplitude of 0.7V and a scan rate of 0.04V s^{-1} were used. Experimental parameters were optimized for the purpose of determination of FEN in groundwater collected in a water well of a São Luis-MA fuel station. Under these optimized conditions, an analytical curve was obtained in the 0.49 to 2,4 µM concentration range, with a detection limit of 1,2 x 10^{-10} mol·L^{-1}. The method was applied to a real groundwater sample from a water well located at a fuel station, and an average concentration of 0.037 µM FEN was found (n = 5), presenting a variation coefficient of 0.88, indicating good precision. Accuracy was assessed by the recovery test, whose average value was 99.9%. These results indicate that the proposed procedure is a good alternative for the analysis of FEN in natural water.

Keywords: *Phenanthrene; groundwater; Fuel station; Voltammetry*

Downloaded from www.periodico.tchequimica.com

1. INTRODUÇÃO

A contaminação de águas subterrâneas por derivados de petróleo tem merecido cada vez mais atenção. Os postos distribuidores de combustíveis se constituem como alvo de maior preocupação, pois se encontram dispersos por todo o território nacional. A quantidade de combustível estocada nos postos de combustíveis, se derramada no solo, pode ser suficiente para inviabilizar o consumo de milhões de metros cúbicos de água subterrânea (GEBARA *et al*, 2013; REGO *et al*, 2007; OLIVEIRA, 2013).

O lançamento acidental de quantidades significativas de combustível no solo, em um posto distribuidor, pode ocorrer de diversas maneiras, tais como: corrosão dos tanques ou das tubulações fabricados em aço, transbordamentos ou derramamentos que acontecem durante as operações de descarga de combustível, dentre outras (OLIVEIRA e OLIVEIRA, 1998).

Os vazamentos em postos de combustíveis provocam vários problemas ao meio ambiente, causados por diversos compostos, como é o caso dos Hidrocarbonetos Policíclicos Aromáticos (HPAs).

Os HPAs são de especial relevância ambiental porque exibem características mutagênicas e carcinogênicas mesmo em concentrações muito baixas. A introdução de HPAs no ambiente é originada de atividades antrópicas, que ocorre através de uma grande variedade de rotas. As principais rotas são as indústrias químicas e as refinarias, a produção de petróleo e gás natural, processos de combustão estacionária, transporte e postos de gasolina (MONTEIRO, DE OLIVA & TAVARES, 2016). A sua presença na água representa um risco iminente à saúde humana. Apesar da hidrofobicidade destes compostos, diversos estudos evidenciaram a presença de HPAs na água tais como antraceno, fluoreno, pireno, naftaleno, fluoranteno, fenantreno e etc. (VIDAL E BECKER, 2006; TROVÃO, 2006; MONTEIRO, DE OLIVA e TAVARES, 2016)

Para esta pesquisa foi selecionado o Fenantreno (C_4H_{10}), um HPA representativo, pois é um composto orgânico neutro que contém 3 anéis aromáticos e apresenta propriedades ambientais como solubilidade em água, coeficiente de partição octanol-água (K_{ow}) e pressão de vapor similares as dos outros HPAs. A estrutura do Fenantreno é similar à de HPAs de pesos moleculares maiores e mais carcinogênicos, como benzo (a) pireno, e por isso ele é considerado um composto representativo, que pode dar uma indicação geral do comportamento dos HPAs (KHODADOUST *et al*. 2004).

No Brasil a Portaria de Consolidação nº 05 do MS de 28 de outubro de 2017, no anexo 7, que define o padrão de potabilidade de água para consumo humano, preconiza somente o benzo (a) pireno, com valor máximo permitido de 0,7 mg L^{-1} como uma substância de análise semestral obrigatória.

Não há um mapeamento de todas as áreas contaminadas do Brasil, bem como o conhecimento de outros contaminantes.

O presente trabalho tem como objetivo desenvolver um método alternativo para a determinação do Fenantreno (FEN) em água subterrânea, usando técnica eletroanalítica. Amostras reais de águas subterrâneas de postos de combustíveis foram coletadas em postos de revenda de combustíveis em São Luís - MA, nas quais o HPA (FEN) foi analisado, empregando o método eletroanalítico proposto neste trabalho.

2. PARTE EXPERIMENTAL

2.1. Instrumentação

Os experimentos eletroquímicos foram realizados no potenciostato modelo autolab-2 da Metrohm acoplado a um computador dotado de um software GPES (General Purpose Electrochemical System) (FERREIRA, 2014) e utilizando a técnica de voltametria de pulso diferencial.

As medidas voltamétricas foram realizadass em uma célula eletroquímica confeccionada em vidro com capacidade de 20 mL, contendo os seguintes eletrodos: eletrodo de referência Ag/AgCl (eletrodo de prata com cloreto de prata) contendo KCl 3,0 mol·L^{-1}, eletrodo auxiliar de platina (Pt) e o eletrodo de trabalho de Carbono Vítreo (ECV). Um sistema de banho ultrassom foi utilizado para possíveis partículas de alumina proveniente do processo de polimento (realizado com lixamento em Feltro) que ficam impregnadas na superfície do eletrodo.

A resposta eletroquímica do Fenantreno foi realizada utilizando um ECV não modificado e modificado com CoPc em solução tampão BR 0,2 mol·L^{-1} como eletrólito suporte, usando as técnicas CV e VPD.

2.4. Procedimento de Análise Voltamétrica

A análise Voltamétrica de Fenantreno em água foi realizada em uma célula eletroquímica

Downloaded from www.periodico.tchequimica.com

contendo 10 mL de tampão BR 0,1 mol·L^{-1} (pH 2,0) utilizando-se eletrodo de carbono vítreo previamente modificado com CoPc.

Os voltamogramas foram registrados de acordo com os parâmetros da Tabela 1, na técnica de voltametria de pulso diferencial.

2.5. Coleta e preparo da amostra real

A amostra de água subterrânea foi coletada em um posto de combustível na região central de São Luís – MA, em um poço localizado no posto, utilizando o procedimento de coleta do Ministério da saúde (SABBAG, 2013.). Após a coleta, as amostras foram armazenadas no refrigerador na temperatura de aproximadamente 10 °C, por um prazo máximo de 20 dias, foram filtradas em filtrilo (0,45 μm) para posterior realização dos experimentos.

3. RESULTADOS E DISCUSSÃO:

A Figura 1 descreve o estudo realizado por VPD com o objetivo de caracterizar o comportamento eletroquímico (processos de redução e oxidação) do eletrodo quimicamente modificado por CoPc. O voltamograma em cor verde mostra a resposta do ECV na ausência do analito FEN. Enquanto o voltamograma vermelho e preto, mostram a resposta na presença do analito.

Quando o eletrodo modificado com CoPc é colocado na presença de FEN, observa-se uma redução significativa no potencial de oxidação do FEN, de 0,16V, bem como um aumento significativo na corrente de oxidação deste analito. Sendo assim, esse resultado sugere que a CoPc produz a catálise da reação de oxidação do FEN.

3.2. Estudos da Oxidação Eletroquímica do FEN sobre ECV/CoPc

O estudo de dependência do potencial de pico (E_p) velocidade de varredura do eletrodo ECV/CoPc, na presença e ausência de FEN (5.0×10^{-3}M), foi realizado por Voltametria Cíclica (VC) e é apresentado na Figura 2. O voltamograma cíclico de FEN (figura não mostrada) mostra um processo redox irreversível na região anódica, em um potencial próximo de 1,35V, o que está de acordo com a Teoria de Laviron (LAVIRON, 1979). Este tipo de comportamento é característico desse tipo de composto.

Para sistemas irreversíveis, E_p varia linearmente com ν e com o Log (ν), como foi observado para o presente sistema e é apresentado na Figura 2, (A) e (B), respectivamente (ALEXIOU & LEVER, 2001; BRAININA, 1987).

Com o propósito de se obter maiores informações sobre reação de oxidação eletroquímica do FEN sobre ECV/CoPc, foi também realizado um estudo do efeito da velocidade de varredura sobre a corrente de pico (I_p), referente a oxidação do FEN sobre o eletrodo modificado, conforme mostra a Figura 3.

Para um pico de adsorção irreversível, de acordo com a teoria de Laviron (LAVIRON, 1979), uma relação linear entre Ip e a velocidade de varredura (ν) é descrito conforme a Equação 1:

$$Ip = \frac{nFQ}{4RT}$$

(Eq. 1)

- I_p é expressa em amperes e Q (área do pico no voltamograma, em coulomb. A Equação 1 indica que n (número de elétrons) pode ser calculado, enquanto Q é obtida sob uma determinada velocidade de varredura. Com base nisto o número de elétrons calculado pela Equação 1, como sendo n = 1. O mecanismo da reação é descrito na Figura 4.

O mecanismo de oxidação do fenantreno consiste na formação de um cátion radical. Esse cátion radical formado inicialmente pode ser oxidado por reação com o Co^{3+} como mediador da reação.

Como o número de elétrons envolvidos na oxidação de fenantreno é de aproximadamente a 1, sugere-se, que um grupo hidroxílico é introduzido ao anel aromático. A medida que o cátion radical é inicialmente formado, estes serão solvatados por moléculas de água, ou seja, o componente polar do solvente usado. A hidratação pode promover a perca de um protón, o que significa que eventualmente, um grupo hidroxílico é introduzido ao anel aromático, formando como produto final a 9,10-fenantraquinona (LOPES & ANDRADE, 1996)

3.3. Otimização das Condições Experimentais visando aplicação analítica do sensor eletroquímico

Para obter melhor resposta analítica, os estudos de otimização das condições experimentais foram realizados na presença de $1x10^{-4}$ mol·L-1 de FEN.

Inicialmente, foi realizado um estudo dos parâmetros operacionais do equipamento visando

Downloaded from www.periodico.tchequimica.com

a possível aplicação do sensor ECV/CoPc na determinação de FEN, cujas melhores respostas obtidas foram incluidas na Tabela 2.

Posteriormente, foi realizado um estudo de otimização dos parâmetros experimentais da solução, onde variou-se um parâmetro de cada vez, enquanto os demais foram mantidos constantes. Diferentes eletrólitos foram avaliados: tampão Britton Robinson (BR), (mistura de 50 mL de uma solução H_3BO_3 0,2 mol·L^{-1} com 50mL de CH_3COOH 0,2 mol·L^{-1} e 50mL de H_3PO_4 0,2 mol·L^{-1}), ácido sulfúrico 0,2 mol^{-1}, ácido clorídrico 0,2 mol^{-1} e tampão McIlvaine (mistura 50 mL de Na_2HPO_4 0,2 mol·L^{-1} com 50mL de ácido cítrico 0,2 mol·L^{-1}). O pH de cada solução de eletrólito foi ajustado, quando necessário, pela adição, gota a gota, de NaOH 2 mol·L^{-1}.

Após a escolha do eletrólito, realizou-se um estudo com diferentes concentrações do eletrólito escolhido (Tampão BR). A concentração de CoPc foi variada na faixa de 10^{-5} a 10^{-3} mol·L^{-1}. Os resultados coletados estão inseridos na Tabela 3, cujos valores escolhidos foram utilizados para os estudos posteriores, quais sejam, o estudo de interferentes, a curva analítica, estudo estudo estatístico e aplicação em amostras reais.

3.4. Curva analítica para FEN

Depois de determinadas as melhores condições analíticas, para quantificação de FEN, uma curva analítica foi obtida a partir de alíquotas de uma solução padrão de FEN, adicionadas à solução do eletrólito suporte (Tampão BR) na célula eletroquímica, sendo as correntes medidas para cada nova concentração. Os voltamogramas e a curva analítica são apresentados na Figura 5.

A Figura 5 (B) mostra uma dependência linear (coeficiente de correlação igual a 0,99) entre a concentração de FEN e a corrente de pico, cuja relação linear apresentou um coeficiente angular de 14,43 μA.L.μmol^{-1} e um coeficiente linear próximo de zero (-1,3), o qual poderia ser usado na correção do cálculo da concentração, caso este método fosse usado na determinação do analito. Entretanto, optou-se pelo método de adição padrão na aplicação do procedimento em amostra real.

A partir do cálculo do desvio padrão médio das medidas de corrente do branco, calculou-se o limite de detecção, como sendo 2,9x10^{-10} mol·L^{-1}. O baixo valor do limite de detecção é atribuído à boa sensibilidade analítica do método nas condições otimizadas.

3.6. Aplicação do Método na amostra real

O método proposto foi aplicado na determinação do FEN, em amostra real de água subterrânea de um poço localizado em um posto de combustível, coletada em um posto de revenda de combustível em São Luis-MA, como visto na Figura 6.

A concentração de FEN na amostra particular da Figura A foi calculada a partir da equação da reta: I (μA) = 1,45 + 17,90 [FEN], sendo encontrado o valor de 0,040 μM de FEN.

Uma concentração média de 0,037 μM de FEN foi obtida da análise feita em replicata, obtendo-se um coeficiente de variação através do estudo da reprodutibilidade (n=5) de 0,88, indicando precisão adequeda. A exatidão foi avaliada pelo teste de recuperação, cujo valor médio obtido foi de 99,9 %.

3.7. Comparação com outros métodos da literatura

Uma comparação da performance analítica do sensor estudado na determinação de HPAs, com outros da literatura é apresentada na Tabela 4.

Pode-se verificar que o sensor proposto, apresentou, nas condições aplicadas, uma sensibilidade, em termos de limite de detecção, melhor do que a maioria dos analitos apresentados nesta tabela. Por outro lado, apesar do analito ser o fenantreno, o único trabalho que apresentou maior sensibilidade (LD: 0,123 10^{-12} mol·L^{-1}), o eletrodo é diferente e a técnica usada foi a voltametria cíclica, que é pouco aplicada, analiticamente.

4. CONCLUSÂO

Um sensor eletroquímico (ECV/CoPc) simples, de resposta rápida e sensível, foi desenvolvido para a determinação eletroanalítica de FEN em água. Os melhores resultados analíticos foram obtidos em tampão BR 0,2 mol·L-1, pH = 2,0, com a técnica VPD. Com amplitude de 0,07 V e velocidade de varredura de 0,04 V, faixa linear adequada (4,9x10^{-7} a 2,4x10^{-6} mol·L^{-1}) foi obtida para FEN. Os resultados demonstraram que o analito apresentou somente um pico de oxidação, à 1,35 V. Boa performance analítica foi obtida em termos de limite de detecção, precisão e exatidão. Devido a simplicidade do método e os bons resultados analíticos obtidos na aplicação em amostra real de água subterrânea, o sensor ECV/CoPc apresenta-se como uma boa e confiável alternativa para a determinação do HPA FEN em amostras de água.

Downloaded from www.periodico.tchequimica.com

5. AGRADECIMENTOS:

Os autores agradecem a CNPq (PQ 2017, Process 310664/2017-9), FINEP (Research Project RECOL 05/Subproject NANOPET), ANP (Research Project PMQC/BIOPETRO, No. 1.029/2016-ANP-007.639), e CAPES (PROCAD-AM) pelo apoio financeiro e bolsas recebidas.

6. REFERÊNCIAS

1. ALEXIOU, C.; LEVER, A. P. L. Coordination Chemistry Reviews, 2001, v. 216-217, p. 45-54.
2. ALLINGER, N. L. (1983). *Química orgânica*. Reverté.
3. BRAININA, K. Z. Talanta, 1987, v 34, p. 41-50
4. CARUSO, F. S. M; ALABURDA, J. Revista do Instituto Adolfo Lutz, 67(1):1-27, 2008.
5. CORSEUIL, X. H. Revista Engenharia Sanitária e Ambiental, 1997, v.2, n.2, p.50-54.
6. FERREIRA, A. P. M. ; PEREIRA, L. N. DOS S. ; DA SILVA, I. S. ; TANAKA, S. M. C. N. ; TANAKA, A. A. ; ANGNES, L. Electroanalysis, v. 26, n. 10, p. 2138-2144, 2014.
7. FOAN, L.; SIMON, V. Journal of Chromatography A, 2012, v. 1256, p. 22–31.
8. GEBARA, S. S.; RÉ-POPPI, N.; DO NASCIMENTO, A. L. C. S.; & JUNIOR, J. L. R. Química Nova, 2013, v.36, p.1030-1037.
9. GERMAN, Natalija; ARMALIS, Saulius. chemija, 2012, v. 23, n. 2.
10. KHODADOUST, Amid P.; REDDY, Krishna R.; MATURI, Kranti. Environmental Engineering Science, 2004, v. 21, n. 6, p. 691-704.
11. JUNIOR, G. G. Dissertação (mestrado em quimica) - Universidade Federal do Triângulo Mineiro, Uberaba – MG, 2017.
12. LAVIRON, E. Journal of Electroanalytical Chemistry and Interfacial Electrochemistry, 1979, v. 101, n. 1, p. 19-28.
13. LOPES, Wilson A.; ANDRADE, JB de. Química Nova, 1996, v. 19, n. 5, p. 497-516.
14. MONTEIRO, D. D. S., DE OLIVA, S. T., & TAVARES, T. M. (2016). *Revista Eletrônica de Gestão e Tecnologias Ambientais*, *4*(2), 129-140.
15. MEIRE, R. O.; AZEREDO, A.; TORRES, J. P. M., 2007, v. 11, p. 188–201.
16. NETTO, A. MOREIRA, J. C., DIAS, A. E. X., ARBILLA, G., FERREIRA, L. F. V., OLIVEIRA, A. S., & BAREK, J. Química Nova, 2000, p.765-773.
17. NI, Y.; WANG, P.; SONG.; LIN, X.; KOKOT, S. Analytica Chimica Acta, 821 (2014) 34
18. OLIVEIRA, R. Dissertação de Mestrado – Universidade Federal da Bahia, Salvador, BA, 2003.
19. OLIVEIRA, L. I.; LOUREIRO, C. O. São Paulo: Associação Brasileira de Águas Subterrâneas, 1998.
20. QIAO, M., QI, W., LIU, H., & QU, J. Journal of Chromatography A, 2013, v. 1291, p. 129-136.
21. R.E. Sioda, B. Frankowska. Journal of Electroanalytical Chemistry. 2008, V.612 , p.147–150.
22. SABBAG, S. K. Orientações técnicas para coleta, acondicionamento e transporte de amostras de solo. 2013
23. SEHATNIA, B.; SABZI, R.E.; KHEIRI, F.; NIKOO, A. Journal of Applied Electrochemistry. 44 (2014) 727–733.
24. SUZY, D. DE L.; ANDREA, F. DE O.; ROSSEAN, G.; DANILA, S. C.; ZORAIDY, M. DE L.; EDUARDO, B. DE M. Mato Grosso, Brasil. Rev. Ambient. Água, 2017, vol. 12, n. 2.
25. TOVIDE, O., JAHEED, N., MOHAMED, N., NXUSANI, E., SUNDAY, C. E., TSEGAYE, A., BAKER, P. G. (2014). *Electrochimica Acta*, *128*, 138-148.
26. TROVÃO, Renata Silva. 2006. Tese de Doutorado. Universidade de São Paulo.
27. VIDAL, Ruth Maria Bonfim; BECKER, Helena. Arquivos de Ciências do Mar, 2006, v. 39, n. 1-2, p. 34-43.
28. VYSKOCIL, Vlastimil; BAREK, Jiri. Current Organic Chemistry, 2011, v. 15, n. 17, p. 3059-3076.
29. YARDIM, Y.; KESKIN, E.; LEVENT, A.; ÖZSÖZ, M.; ŞENTÜRK. Z. Talanta, 80 (2010) 1347.
30. ZACHARA, A.; GAŁKOWSKA, D.; JUSZCZAK, L. Food Control, 2017, v. 80, p. 45–51, 1.

Downloaded from www.periodico.tchequimica.com

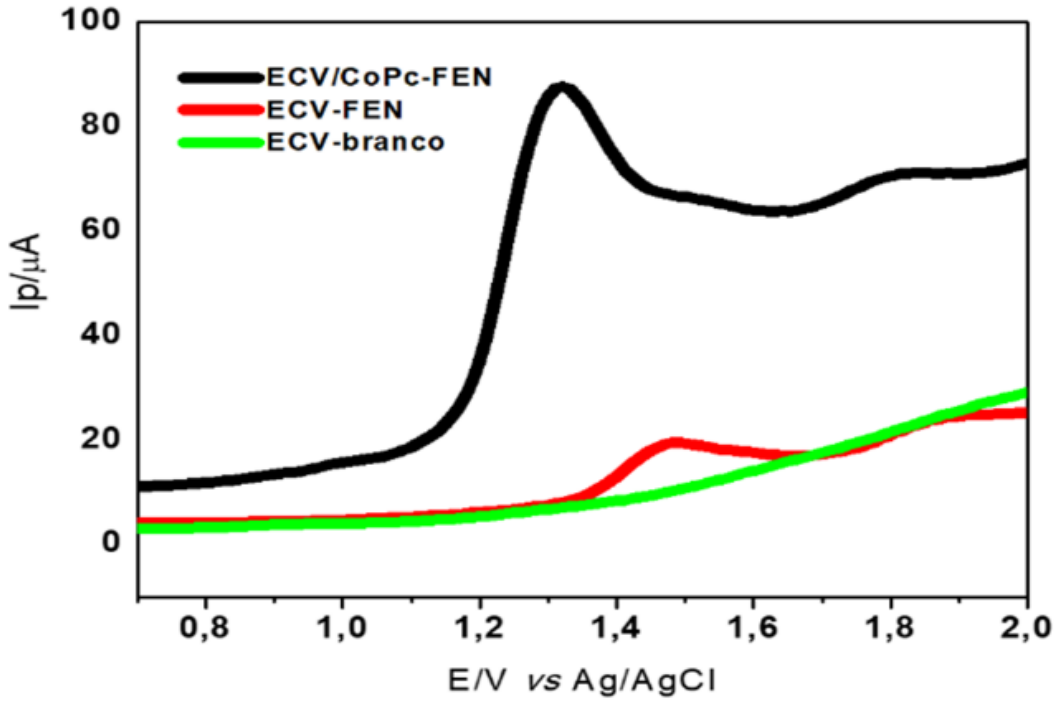

Figura 1. *Voltamogramas de PD (A) branco (B) ECV usando 1x10^{-3} mol·L^{-1} de FEN (C) ECV/CoPc usando 1x10^{-3} mol·L^{-1} de FEN. Tampão Britton Robinson (0,2 mol·L^{-1}, pH 2); Amplitude: 0,07 V; velocidade: 0,05 V s^{-1}*

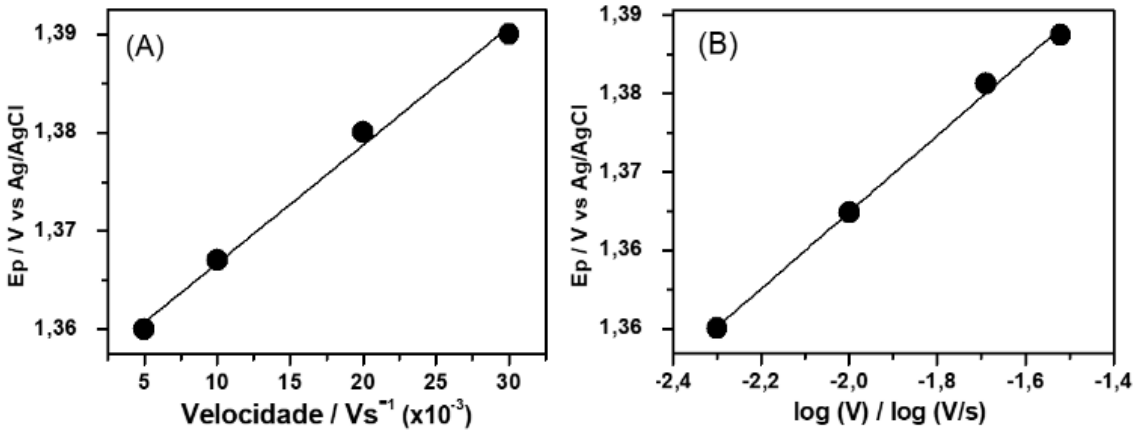

Figura 2. *Gráfico da dependência de (A) Potencial de pico com o a velocidade de varredura e (B) potencial de pico com o logaritmo da velocidade de varredura.*

Downloaded from www.periodico.tchequimica.com

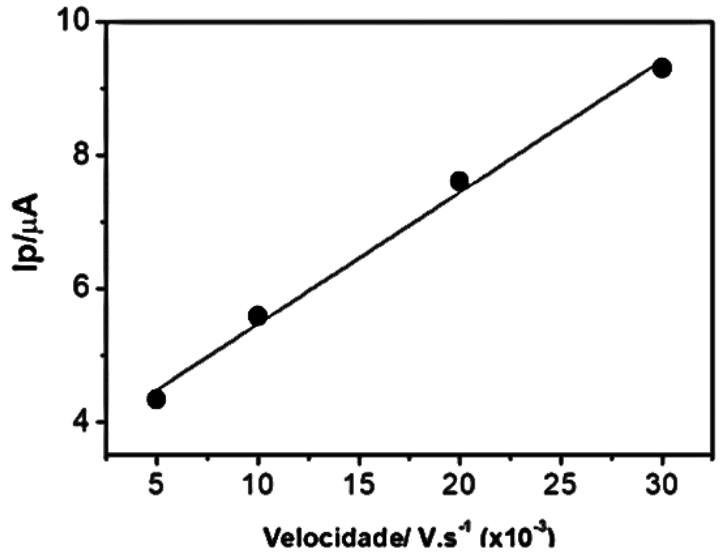

Figura 3. *Gráfico da dependência da velocidade de varredura com a corrente.*

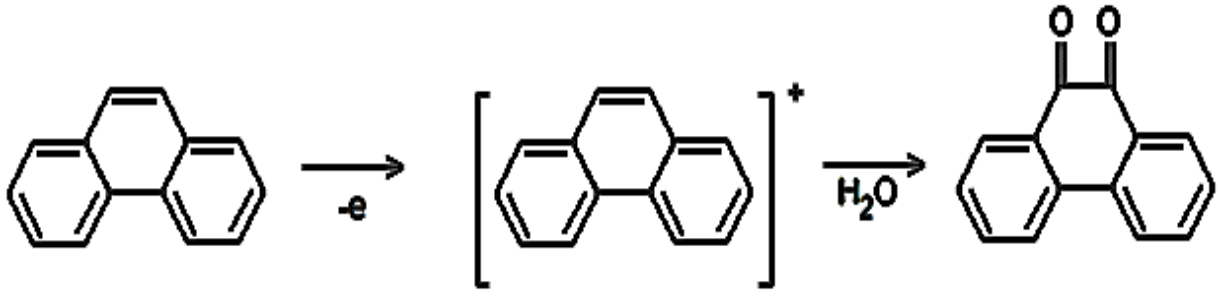

Figura 4. *Mecanismo de oxidação do FEN*

Downloaded from www.periodico.tchequimica.com

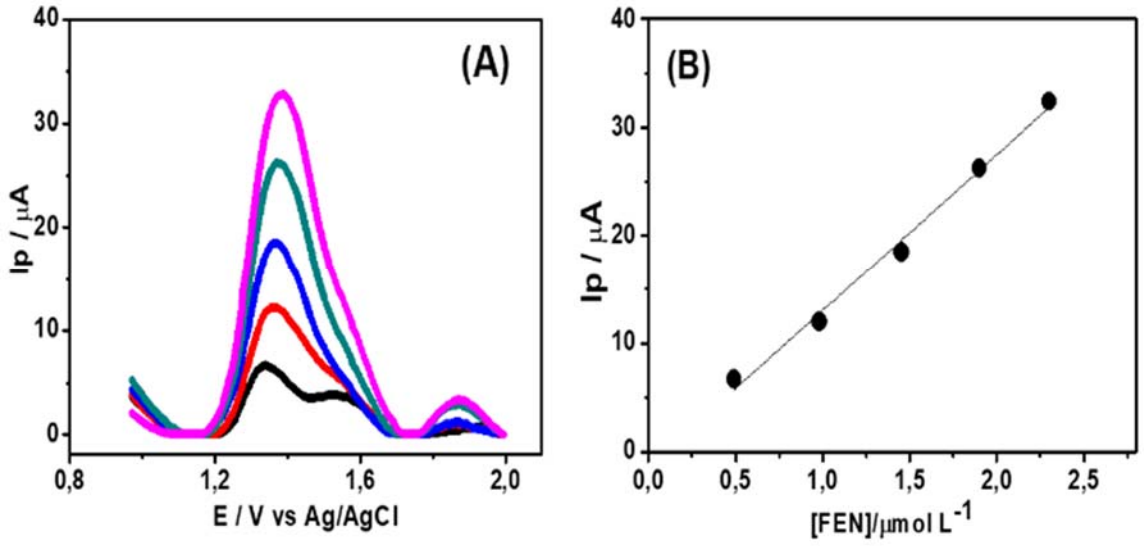

Figura 5. ***(A)*** *Voltamogramas de Pulso Diferencial empregando-se o ECV/CoPc em diferentes concentrações de FEN (0,49; 0,99; 1,5; 1,9 e 2,4 µmol·L^{-1}) em Tampão BR 0,2 mol·L^{-1}, pH 2, ν = 0,04 V s^{-1}, amplitude de pulso de 0,07 V.* ***(B)*** *- Curva analítica de FEN.*

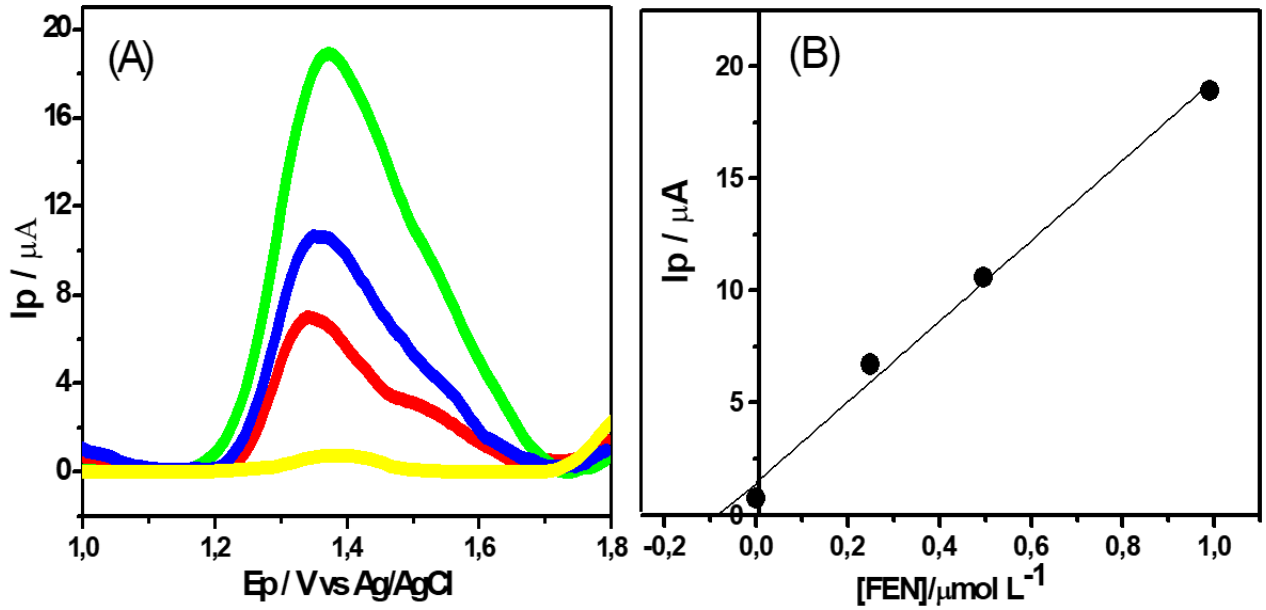

Figura 6. (A) *Voltamogramas de Pulso Diferencial do ECV/CoPc, aplicado em amostra real de água subterrânea na determinação de FEN, pelo método de adição padrão. [FEN]: 0,25 a 1,0 µM; [Tampão BR] = 0,2 mol·L^{-1}, pH= 2, ν = 0,04 V s^{-1}, amplitude de pulso: 0,07 V.* ***(B)*** *Curva de adição padrão referente a* ***(A)***.

Downloaded from www.periodico.tchequimica.com

Tabela 1 - *Parâmetros utilizados para a obtenção das medidas voltamétrica da VPD*

PARÂMETROS	VALORES
Amplitude (V)	0,02 a 0,1
ν (V s^{-1})	0,01 a 0,05
Tempo de pulso (s)	0,2 a 0,6

Tabela 2. *Resumo das condições otimizadas para VPD.*

PARÂMETROS OTIMIZADOS	VALORES OBTIDOS
Amplitude	0,7 V
Velocidade de varredura	0,04 V s^{-1}

Tabela 3. *Resumo dos parâmetros experimentais da solução*

PARÂMETROS	VALORES OTIMIZADOS
Concentração da CoPc	10^{-3} mol·L^{-1}
% Nafion	10 %
Eletrólito suporte	Tampão Britton Robinson
Concentração do eletrólito	0,2 mol·L^{-1}
pH	2,0

Tabela 4: *Determinações analíticas envolvendo HPAs por métodos voltamétricos.*

Eletrodo	Analito	Técnica	LOD (mol·L^{-1})	Ref.
ECV / CoPc	Fenantreno	DPV	2,9 x 10^{-10}	[Este trabalho]
PANI/WO_3/GR/GCE	Fenantreno	CV	0,12 x10^{-12}	[TOVIDE *et al*, 2014]
Eletrodo de pasta de carbono	Naftaleno	SWV	12 x10^{-6}	[GERMAN & ARMALIS, 2012]
Eletrodo de pasta de carbono	Fluoreno	SWV	6,4 x10^{-6}	[GERMAN & ARMALIS, 2012]
Eletrodo de pasta de carbono	Antraceno	SWV	1,2 x10^{-6}	[GERMAN & ARMALIS, 2012]

Downloaded from www.periodico.tchequimica.com

PERIÓDICO TCHÊ QUÍMICA
ARTIGO ORIGINAL

TECNOLOGIAS PARA PREVISÃO DA CONDIÇÃO FUNCIONAL DA MÃO APÓS O TRATAMENTO CIRÚRGICO DA DOENÇA (CONTRATURA) DE DUPUYTREN

TECHNOLOGY FOR PROGNOSIS OF THE FUNCTIONAL STATUS OF HAND AFTER SURGICAL TREATMENT OF DUPUYTREN'S DISEASE (CONTRACTURE)

ТЕХНОЛОГИИ ПО ПРОГНОЗИРОВАНИЮ ФУНКЦИОНАЛЬНОГО СОСТОЯНИЯ КИСТИ ПОСЛЕ ХИРУРГИЧЕСКОГО ЛЕЧЕНИЯ БОЛЕЗНИ (КОНТРАКТУРЫ) ДЮПЮИТРЕНА

MIKUSEV, Gleb I. [1*]; BAIKEEV, Rustem F. [2]; MAGOMEDOV, Ruslan O. [3]; MIKUSEV, Ivan E. [4]; MISHAKIN, Timur S. [5]

[1] City Clinical Hospital No. 7 of Kazan, Department of Traumatology, Kazan – Russian Federation

[2] Kazan State Medical University, Department of Biochemistry, Kazan – Russian Federation

[3] Republican Clinical Hospital of Tatarstan Republic Health Ministry, Diagnostic Department, Kazan – Russian Federation

[4] City Clinical Hospital No. 7 of Kazan, Department of Traumatology, Kazan – Russian Federation

[5] Kazan Federal University, Department of Management in the Social Sphere., Kazan – Russian Federation

** Correspondence author*
e-mail: g.mikusew@mail.ru

Received 05 September 2019; received in revised form 20 October 2019; accepted 21 October 2019

RESUMO

A doença de Dupuytren é um problema agudo e multifacetado que afeta não apenas a medicina, mas também a psicologia e a vida social, uma vez que a pessoa que perdeu a capacidade de desempenhar suas funções socialmente significativas experimenta sofrimento moral e físico. Desde a primeira descrição da doença de Dupuytren até o presente, questões de etiologia, patogênese, classificação, métodos de tratamento e características das medidas preventivas desta doença permanecem discutíveis. Portanto, o principal objetivo do trabalho foi analisar a tecnologia para prever o estado funcional da mão após o tratamento cirúrgico da doença (contratura) de Dupuytren. O estudo foi realizado no Departamento de Microcirurgia da Mão do Hospital Clínico Republicano do Ministério da Saúde da República do Tartaristão. O número total de pacientes sob observação foi de 258, com idades entre 21 e 80 anos. Os resultados da pesquisa foram agrupados em 6 combinações. Foi determinado que três grupos de fatores afetam o grau de cura: A (sexo, idade, objetivo da doença, período de exame, nível de gravidade); B (local de residência, trabalho físico e mental, maus hábitos); C (experiência do cirurgião, tipos de operações, anestesia, seção, plasticidade da pele, tratamento reconstrutivo, cicatrização, etc.). Verificou-se que é possível obter a restauração completa da função da mão direita em 67,5% e da mão esquerda em 59,9% em períodos superiores a um ano.

Palavras-chave: *contratura de Dupuytren, tecnologia de prognóstico, estado funcional da mão, prognóstico, cirurgia.*

ABSTRACT

Dupuytren's disease is an acute and multifaceted problem that affects not only medicine but also psychology, social life, since a person who has lost the ability to perform his/her socially significant functions experiences moral and physical suffering. From the first description of Dupuytren's disease to the present, questions of etiology, pathogenesis, classification, treatment methods, and features of the preventive measures of this disease remain debatable. Therefore, the main goal of the paper was to analyze the technology for predicting the functional state of the hand after surgical treatment of Dupuytren's disease (contracture). The study was conducted at the Department of Hand Microsurgery of the Republican Clinical Hospital of the Ministry of Health of the Republic of Tatarstan. The total number of patients under observation was 258, age 21-80

Downloaded from www.periodico.tchequimica.com

years. The research results were grouped into 6 combinations. It has been determined that three groups of factors affect the recovery degree: A (gender, age, examination period, severity); B (place of residence, physical and mental work, bad habits); C (surgeon's experience, types of operations, anaesthesia, section, skin plastic, reconstructive treatment, healing, etc.). It has been found that it is possible to achieve full restoration of the function of the wrist on the right hand in 67.5% of patients and on the left hand in 59.9% of patients in periods of more than one year.

Keywords: *Dupuytren's contracture, prognosis technology, functional status of hand, prognosis, surgery.*

АННОТАЦИЯ

Болезнь Дюпюитрена является острой и многогранной проблемой, затрагивающую не только медицину, а также психологию, социальную жизнь, поскольку человек, потерявший возможность выполнять свои социально значимые функции, испытывает моральные и физические страдания. С первого описания болезни Дюпюитрена и до сегодняшнего времени дискуссионными остаются вопросы этиологии, патогенеза, классификации, методов лечения, особенностей проведения профилактических мероприятий данного заболевания. Поэтому основная цель работы заключается в анализе технологии по прогнозированию функционального состояния кисти после хирургического лечения болезни (контрактуры) Дюпюитрена. Исследование было проведено в отделении микрохирургии руки Республиканской клинической больнице Министерства здравоохранения Республики Татарстан. Общее количество пациентов, над которыми происходило наблюдение, составило 258, возраст 21-80 лет. Результаты исследований были сгруппированы в 6 комбинаций. Определено, что на степень излечения влияют три группы факторов: А (пол, возраст, назначение болезни, период обследования, степень тяжести); В (место жительства, физическая и умственная работа, вредные привычки); С (опыт хирурга, виды операций, анестезия, сечение, кожная пластика, восстановительное лечение, заживление и др.). Установлено, что возможно достичь полного восстановления функции кисти на правой руке у 67,5%, на левой руке – у 59,9% в периоды более одного года.

Ключевые слова: *контрактура Дюпюитрена, технология прогноза, функциональное состояние кисти, прогноз, хирургия.*

1. INTRODUCTION

Dupuytren's disease (Dupuytren's contracture – DC) is chronic, progressing cicatricial degeneration of palmar aponeurosis, accompanied by flexion contracture of fingers of hand. Dupuytren's contracture is a progressive fibrous proliferation of the palmar fascia of the hand. It is a tumor (growth) but not a cancer. There is no known cause or etiology for Dupuytren's. It is considered an inherited condition (Gonzalez and Gonzalez, 1990; Becker *et al.*, 2015; Ten Dam *et al.*, 2016) and not related to the type of job or hand use. The disease is metabolic and genetic in nature. Surgical treatment for today is the most radical and effective though radiotherapy with soft X-rays (Zirbs *et al.*, 2014) and collagenase injections (Muppavarapu *et al.*, 2015; Verheyden, 2015) are applied.

However the question on indications to operative treatment is not solved definitively; search of the optimal surgical access considering anatomic-physiological singularities of skin of palmar surface of hand providing good vision and freedom of manipulations proceeds; the question on volume of excision of palmar aponeurosis in relation with possibility of recurring and the further advance of pathological process is not solved. Methods of operations and guiding of the postoperative period at patients need classification and specification (Crean *et al.*, 2011). The extent of excision of palmar aponeurosis increases among need fasciotomy (Badois *et al.*, 1993; Lermusiaux *et al.*, 1997), subcutaneous fasciotomy (Kelly and Clifford, 1959; Luck, 1959), segmental fasciectomy (Moermans, 1991; Moermans, 1996), limited fasciectomy (Lubahn *et al.*, 1984; Chick and Lister, 1991; McCash, 1964; Maravic and Landais, 2005), dermo-fasciectomy (Hueston, 1963), total (radical) fasciectomy (McIndoe and Beare, 1958).

The resulting effect of DC treatment is influenced not only by the operation's choice but by series of factors: grade of expression of contracture, prescription of disease, heredity, social premises, age, type of job of the patient. The complications of surgical treatment of DC originating in the long-term postoperative period (LPP) are classified as 1. Disease relapse; 2. Disease extension 3. Disease advance(origin or augmentation of pathological process on not operated hand) (Mikusev *et al.*, 2007) which does

Downloaded from www.periodico.tchequimica.com

not refer to the group of postoperative complications as can originate without the fact of operation, however, if it happens after operation, it is reasonable to consider it for two reasons: 1. Recovery is important for the patient, that is the total absence of signs of disease, 2. The adequate understanding of the correct approach on a method, a range and tactics of operative treatment at palmar fibromatosis should be based on that fact that the palmar fibromatosis is benign fibroproliferative tumor, with genetic background (Ten Dam, E.P. *et al.*, 2016; Becker *et al.*, 2015) according to ICD – 10 – a fascial fibromatosis of unknown etiology (M-720) (International Statistical Classification…, 2010), and relapse, extension and advance are clinical implication of dynamics of tumor growth.

All three types of long-term outcomes lead to disturbance of hand's function, affect results of treatment and are the indication for repeated operation. In turn, the outcome prognosis of the functional status of hand (FSH) after operation is the important element of postoperative follow-up of the patient and preventive maintenance of deterioration in its status. Evidently that the long experience of DC treatment gained by specialists needs the quantitative analysis which has already allowed to tap some trends in recovery of FSH at operative DC treatment, in particular, short – and long-term efficiency of surgical treatment (Crean *et al.*, 2011). Thus each group of researchers analyses types of operations traditional for their clinics. The extension of the detailed analysis of operative DC treatment by the techniques used in our clinic will allow to perform the further optimization of volume and technique of operations at DC. The research goal is to develop a technology of prognosis of the functional status of hand after surgical DC treatment, depending on 1. Factors of biology of the patient, 2. Lifestyle of the patient, 3. Technical–surgical components of operation and rehabilitation treatment.

Research was approved by committee on ethics of State Budget Educational Institution of High Professional Education "Kazan State Medical University" of Health Ministry of Russia; the protocol of meeting No.8 from October, 28th, 2014. Necessary HIPAA consent was obtained from each patient.

2. MATERIALS AND METHODS

Research was led on the basis of the Tatarstan Republic medical institution (Russian Federation), in Kazan – in hand microsurgery unit of Scientific Practical Traumatology Centre of the State Autonomic Healthcare Institution «Republican Clinical Hospital of Health Ministry of Tatarstan Republic». The total quantity of operated patients with DC has constituted 258 patients at the age of 21-80 years. The total quantity of the operated hands was 343: 191 operations (55.7 %)on the right hands, 152 (44.3 %) operations on the left hands. Exclusion criteria for both groups were: age <18 years, pregnant women, and arthroplasty or arthrodesis of the treated joint and stretching, and fat grafting (McInerney and Clover, 2015).

Dupuytren's disease (contracture) was parted on three grades and classified according to the grade of contracture of fingers of hand (Bejul, 1926) (Mikusev, 2001): I grade– induration of palmar aponeurosis without flexion contracture in joints of fingers; II grade – induration of palmar aponeurosis with flexion contracture in MTP joint to an angle 100°; III grade – induration of palmar aponeurosis with flexion contracture in MTP joint to an angle <100° and flexion contracture in proximal inter phalanx joint. In chapter "results" are presented both a grade of classification according to A.P. Bejul, and contracture angle in grades (Table 8) for the purpose of comparison to other classifications (Luck, 1959; Henry and Meyerding, 1936; Iselin and Iselin, 1967; Tubiana and Michon, 1961). DC localization (DC grade is the affected finger of hand/quantity of patients with lesion of the given finger/proportion in%): the right hand, I grade – 1/17/6, 6; 2/15/5, 8; 3/47/18, 2; 4/20/7, 8; 5/32/12, 4 (p<0, 001). II grade – 1/6/2, 3; 2/5/1, 9; 3/40/15, 5; 4/81/31, 4; 5/21/8, 1 (p >0, 98). III grade – 1/2/0, 8; 2/2/0, 8; 3/8/3, 1; 4/40/15, 5; 5/23/8, 9 (p >0, 98). The left hand, I grade – 1/45/17, 5; 2/17/6, 6; 3/48/18, 6; 4/45/17, 5; 5/30/11, 6 (p<0, 001). II grade – 1/5/1, 9; 2/8/3, 1; 3/33/12, 8; 4/60/23, 3; 5/35/13, 6 (p >0, 98). III grade – 1/2/0, 8; 2/3/1, 2; 3/11/4, 3; 4/39/15, 1; 5/60/23, 3 (p >0, 98).

Exsected part of PA. A – the partial excision of changed bands, stretched to one finger – 1; to two fingers – 1+2; to three fingers – 1+2+3; to four fingers – 1+2+3+4; B – excision of proximal part – 1; C – excision of proximal and middle parts – 1+2; D – total excision – 1+2+3. E – sphenoidal excision of middle part of PA and longitudinal bands of distal department of PA with conservation of cross fibers at level of distal third of the metacarpal bones, stretched to four fingers – 1+2+3+4 (Ea); to three fingers – 1+2+3 (Eb); to two fingers – 1+2 (Ec); to one finger – 1 (Ed); α = 20° – 30°. The following types of operations on palmar aponeurosis have been made to the patients (Figure 1, Table 1): A – limited (partial)

Downloaded from www.periodico.tchequimica.com

fasciectomy (Brenner, 1997; Hueston, 1961) (Figure 1 – A), B – limited (partial) excision of proximal part of PA (Figure 1 – B), (Dabrowski, 1967), C – limited (partial) excision of proximal and middle parts of PA (Figure 1 – C) (Mikusev, 2001), D – total (radical) fasciectomy (McIndoe and Beare, 1958) (Figure1 – D), E – limited (partial) sphenoidal excision of middle part of PA and longitudinal bands of distal department of PA with conservation of cross fibres at level of a distal third of metacarpal bones (Figure 1 – E) (Mikusev, 2001). Sphenoidal excision of middle part of PAis made in a cross direction with deviation from a perpendicular on an angle α = 20°– 30°; excision of PA is stretched to four (Ea), to three (Eb), to two (Ec) or to one (Ed) finger independence from scale of operation.

Status localis after surgical treatment was estimated on periods 1 year and more after operation. The following points were considered as LPC: 1. Relapse 2. Extension 3. Advance. The functional status of hand(FSH) after operation was estimated according to the original scale (table 2) (Magomedov *et al.*, 2013) where FSH and the patient's cure were estimated. The cure was appreciated as complete recovery of hand function (i.e. the patient considers itself healthy; postoperative cicatrix is hardly noticeable, elastic, soft; sensitivity on hand and fingers is normal; flexion contractures are not present; hand function is recovered) and absence of LPC (relapse, extension, advance) on both hands (Table 2).

The authors did not use famous questionnaires on estimation of extremities' state after operation as Canadian Occupational Performance Measure (COPM) in relation to the Disabilities of Arm, Shoulder, and Hand (DASH) questionnaire and the Michigan Handout comes Questionnaire (MHQ), as they are not absolutely adequate at lesions of hand (van de Ven-Stevens *et al.*, 2015). We have analyzed 222 factors and their combinations registered at follow-up of patients with DC at developing of system of the functional hand status prognosis. We have divided them into three groups (Appendix, Supplement 1): A (118 factors) **–** the factors determining the biological status of the patient (gender, age, prescription of disease, examination period, grade of DC lesion, heredity, the associated diseases, surgical history and traumas, the disease beginning, laboratory analyses, etc.); B (20 factors) **–** the factors presenting lifestyle of the patient (residence, physical and mental job, bad habits, etc.); C (84factors) – the factors presenting technical-surgical components of operations and rehabilitation treatment (the experience of the surgeon, types of operations, anesthesia, section, dermal plasty, rehabilitation treatment, healing, etc.). Statistical analysis was has been made with the application of software package SPSS (v.13.0). Discriminate function analysis has been used for developing of prognosis system of surgical treatment efficiency. Criterion χ^2andaccuracy of classification was applied for the analysis of qualitative indices.

3. RESULTS AND DISCUSSION:

The detailed analysis of cure from DC was conducted according to following factors of clinical-statistical characteristics of patients with DC and its combination: type of operation, the technique of surgical manipulations, in dice's coefficient (number of patients/cure, %) – it should be appreciated that the combination of type and technique of operations leads up the number of clinical alternatives to 35. The results in our researches have been grouped in 6 combinations. Groups have been generated by the following principle (Table 3): 1 right (No. 2, 5) or left (No. 3, 6) operated hands; 2. Both (No. 1, 4) operated hands; 3. one (No. 1, 2, 3) or various types (No. 4, 5, 6) of operations.

85 patients were operated on both hands, 173 patients were operated only on one, right or left hand. Groups (at the analysis of section type) have been generated by following principle (Table 4): 1. right (No. 2, 5) or left (No. 3, 6) operated hands; 2. Both (No. 1, 4) operated hands; 3 operated by one (No. 1, 2, 3) or various sections' types (No. 4, 5, 6).

Recovery of hand function was determined as: excellent, good, fair, bad (Table 5).

Result (at developing of FSH prognosis technology) was estimated as excellent even with LPC as recovery of movements' function of fingers of hand was the most important fact for the patient was. We used 2 approaches:

I. We prognosticated an outcome, according to scale of FSH estimation: excellent/good/fair/bad (Table 6), considered the effect of combination of factors of groups A + B + C: 1. right, left or both hands are operated 2. right hand is operated3.left hand is operated. (Table 6, No. 1-3); factors of groups A + B: 4. right, left or both hands are operated; 5. right hand is operated; 6. left hand is operated. (Table 6, No. 4-6); factors of group C: 7. operation type; 8.

Downloaded from www.periodico.tchequimica.com

Operated right, left or both hands are operated; 9. right hand is operated; 10. Left hand is operated (Table 6, No. 7-10);

II. Prognosticated outcome: complete functions recovery (Table 7), result estimation: excellent (yes/ no). Impact of factors' combination of groups: A + B + C (Table 7, No. 1-3); factors of groups A + B (Table 7, No. 4-6); factors of group C (Table 7, No. 7-10).

The clinical example on prognosis of long-term postoperative complications after interventions concerning Dupuytren's disease (contracture) based on the analysis of factors A + B + C (right, left or both hands are operated) is presented according to the equation No.1 Table 7. (Appendix, Supplement 2).

Absence of LPC at the patient in the postoperative period reflects the fact that the biological substance of tum our has been eliminated in maximum. The minimum injury of the anatomy of the biomechanics and apparatus which is tightly related to palmar aponeurosis (Figure 2 (Netter, 2003), Figure 3 (Moermans, 1997)) is essential at choice and making operation from the point of view of conservation or recovery of FSH.

The basic question at estimation of DC treatment touches periods of observation after operation. Traditionally, the observation periods at the effectiveness' analysis of treatment are parted: < 6 months – short-term, > 6 months – long-term observations (Crean *et al.*, 2011). Periods of treatment and follow-up after operation concerning DC before working capacity recovery constitute 45-82 days. However, we think that period of the beginning of the analysis from 6 months is not reasonable, as process of healing and recovery of hand function after operation can constitute more than 6 months, especially at intra-operative complications: neuropraxia, nerve injury, arterial injury, flexor ten-don injury, or early postoperative complications: hematoma, infection, skin; therefore observation period ≥ 1 year is justified.

The criterion of efficiency is not today the general notion. The state estimation is used:

1. Finger (Smith and Breed, 1994; Foucher *et al.*, 1995; Tripoli and Merle, 2008),

2. Hands (Smith and Breed, 1994; Foucher *et al.*, 1995),

3. Joint (Macnicol, 1984; Foucher *et al.*, 1992a; Kjeldal and Nygaard, 1998; Coert *et al.*, 2006),

4. Arm (Makela *et al.*, 1991; Moermans, 1996; Constantinou and Deutinger, 1996; Foucher *et al.*, 2003). Additional complication to the classification of treatment's results is the application of several classifications according to DC grades that complicates classification of results' estimation. Separation of DC into three grades (Luck, 1959), four grades (Iselin and Iselin, 1967) is used. DC classification in five grades (Henry and Meyerding, 1936; Tubiana and Michon, 1961) is applied in the majority of clinics. In the postoperative period, in period ≥ 1 year, DC is characterized by disturbance of hand function (the long-term results) in several cases.

Cure, depending on operation type, > 50 % was attained in cases No. 2, 5, 6 (Table 3). Minimum cure was in groups No. 1, 4 in operation «E» (group No.1) or in combination with other operations (group No.4) on both hands. Low cure from DC at operations in both hands reflects not so much negative impact of operation of type «E» as scale of Dupuytren's injury of the patient's organism. Cure, depending on section type on palm > 50 % was attained in cases No.2, 6 (Table 4). Minimum cure was in groups No. 1, 4 (Table 4). A low cure from DC at operations on both hands also reflects the scale of Dupuytren's injury of the patient's organism. The obtained data shows that cumulative surgical DC treatment by various types of operations (the partial excision of changed bands, excision of proximal part, excision of proximal and middle part, total excision, sphenoidal excision of PA) allows to provide free status of the patient – absence of disturbances of hand function in periods ≥ 1 year on the right hand in 67, 5 % of cases, on the left hand – in 59, 9 % of cases. The proportion of the bad results did not exceed 4, 6 % (Table 5).

The estimation of outcomes of DC treatment of the patients by various groups of specialists, by means of descriptive statistics of finger (Foucher *et al.*, 1995; Smith and Breed, 1994; Tripoli and Merle, 2008), hand (Smith and Breed, 1994; Foucher *et al.*, 1995), joint (Macnicol, 1984; Foucher *et al.*, 1992a; Foucher *et al.*, 1992b; Kjeldal *et al.*, 1998; Coert *et al.*, 2006), arm (Makela *et al.*, 1991; Moermans, 1996; Constantinou and Deutinger, 1996; Foucher *et al.*, 2003) and the one-parameter analysis (Nieminen and Lehto, 1986; Norotte *et al.*, 1988; Bulstrode *et al.*, 2005;) does not allow to gain the analysis of results, i.e. prognosis of outcome for the individual patient. Adequate mathematical analysis has allowed to develop a system on result prognosis– the functional hand status in the postoperative period at the patient

Downloaded from www.periodico.tchequimica.com

with Dupuytren's disease (contracture). It is presented in the form of a combination of the equations (Table 6, Table 7). From 3 (the equation No. 8) to 9 (the equation No. 3) parameters became essential for FSH prognosis (excellent/good/fair/bad) (Table 6) from 222 parameters of the anamnesis and follow-up of the patient, depending on operation type. The equations on FSH prognosis (excellent / good/ fair / bad) are characterized by accuracy of classification of 53, 3-66, 0 % (Table 6). The impact of factors of group "C" at operations is not approximated in the form of the equation: the right hand (the equation No. 9) is operated; the left hand (the equation No.10) (Table 6) is operated. Their number includes equation No.7 (Table 6) where accuracy of classification has constituted only 30, 6 % as the mathematical model should present not less than 50 % of patients according to the common rule.

In the paper to explore factors that were most related to functional recovery as measured by DASH in patients with Dupuytren's disease, the three variables "need to take special precautions", "avoid using the hand in social context", and health-related quality of life (EQ-5D index) explained 62,1 % of the variance in DASH, where the first variable had the greatest relative effect (Engstrand *et al.*, 2015), i.e. the IR number is restricted and has no analytical representation in the form of the equation. From 1 (the equation No. 7; No.10) to 13 (the equation No. 2) parameters have appeared essential from 222parameters of the anamnesis and follow-up of the patient, depending on operation type in our research for FSH prognosis (excellent: yes/ no) (Table 7). The equations for FSH prognosis (excellent: yes/no) are characterized by accuracy of classification of 57, 4-77, 0 % (Table 7). Accuracy of factor of group "C" as «the right hand is operated» is not approximated in the form of the equation (the equation No. 9) (Table 7).

The gained results have solved a series of tasks:

1. The factors hindering (21 factors: A factors – 11; B factors – 1; C factors – 9) and favoring (9 factors: A factors– 5; B factors – 3; C factors – 1) to FSH recovery (Table 8).

2. Possibility to prognosticate result of operative DC treatment of hand in terms of its functional status (excellent/good/fair/bad), depending on DC localization, type of operation, technique of section, etc.

3. The resource of the surgeon in FSH improving is restricted by choice of technique of operative measure and by algorithm of postoperative follow-up at the stage of surgical DC treatment. The research has framed the possibility to adjust the result of treatment on preoperative stage is operatively – technical and rehabilitation parts of the patient's follow-up (Table 8):

A. Negative factors: at operative DC treatment on the right hand: by surgeon with the general surgical experience more than 30 years (C_{13}); application of curly section on fingers (C_{28}), sphenoidal excision of middle part of PA with longitudinal bands of distal department of PA (C_6), application in the postoperative period of rehabilitation treatment (dia dynamic currents, variable electric field of ultrahigh frequency, ultra-violet irradiation) (C_{35}); at operative DC treatment on the left hand: by surgeon with general surgical experience 16 – 20 years (C_{51}); application of curly section on palm (C_{66}), the partial excision of palmar aponeurosis (C_{42}), healing by second intention (C_{80}); combination of the partial excision of palmar aponeurosis on one hand and sphenoidal excision of middle part of PA with longitudinal bands of distal department of PA on other hand, made in various periods (C_{83}). B. Positive factors: at operation on the left hand: the free dermal plasty on 4 finger (C_{73}).

4. CONCLUSIONS:

The detailed analysis of cure from DC was conducted according to following factors of clinical-statistical characteristics of patients with DC and its combination: type of operation, the technique of surgical manipulations, in dice's coefficient (number of patients/cure, %) – it should be appreciated that the combination of type and technique of operations leads up the number of clinical alternatives to 35.

1. The effectiveness analysis of alternatives of surgical treatment allows to state that it is possible to achieve complete recovery of hand function on the right hand in 67,5 %, on the left hand – in 59,9 %in periods more than one year.

2. Factors of groups A, B, C influencing recovery of the functional status of hand are determined.

3. Informative ness of prognosis technology of the functional status of hand (excellent / good/ fair / bad) on the basis of factors A, B, C of patients constitutes: A+B+C: 61,6 – 65,4 % (p=0,0001); A+B: 59,9 – 66,0 % (p=0, 0001); C: 53,3 % (p=0, 0001).

Downloaded from www.periodico.tchequimica.com

4. Informative ness of prognosis technology of the functional status of hand (excellent: yes/ no) on the basis of factors A, B, C of patients constitutes: A+B+C: 65, 8 – 77, 0 % (p=0, 0001); A+B: 58,1– 69,0 % (p=0, 0001); C: 57,4 – 61,8% (p = 0,028 – 0,033).

6. REFERENCES:

1. Badois, F.J., Lermusiaux, J.L., Masse, A.C., Kuntz, D. *Revue du Rhumatisme,* **1993***, 60*, 692-697.
2. Becker, K., Tinschert, S., Lienert, A., Bleuler, P.E., Staub, F., Meinel, A., Rößler, J., Wach, W., Hoffmann, R., Kühnel, F., Damert, H.-G., Nick, H.-E., Spicher, R., Lenze, W., Langer, M., Nürnberg, P., Hennies, H.C. *Clin Genet*, **2015**, *87*(5), 483-754.
3. Brenner, P. *Plastische Chirurgie – Handchirurgie. Breitnersche Operationslehre*, **1997**, *14*, 215-222.
4. Bulstrode, N.W., Jemec, B., Smith, P.J. *Journal of Hand Surgery-American Volume,* **2005**, *30*, 1021-1025.
5. Chick, L.R., Lister, G.D. *Hand Clinics*, **1991**, *7*(4), 715-719.
6. Coert, J.H., Nerin, J.P., Meek, M.F. *Annals of Plastic Surgery*, **2006**, *57*, 13-17.
7. Constantinou, E., Deutinger, M. *Acta Chirurgica Austriaca*, **1996**, *28*, 163-165.
8. Crean, S.M., Gerber, R.A., Hellio, Le Graverand, M.P., Boyd, D.M., Cappelleri, J.C. *Journal of Hand Surgery (European Volume)*, **2011**, *36*, 396-407.
9. Dabrowski, T. *ACTA Medica Polona*, **1967**, *8*(4), 499-504.
10. Engstrand, A.C., Krevers, B., Kvist, J. *Journal of Hand Therapy*, **2015**, *28*(3), 255-259.
11. Foucher, G., Cornil, A.C., Lenoble, E. *Annales de Chirurgie de la Main et du Membre Superieur*, **1992a**, *11*, 362-366.
12. Foucher, G., Cornil, A.C., Lenoble, E. *Chirurgie*, **1992b**, *118*, 189-194.
13. Foucher, G., Cornil, A.C., Lenoble, E., Citron, N. *International Journal of Orthopaedics*, **1995**, *19*, 285-258.
14. Foucher, G., Medina, J., Navarro, R. *Journal of Hand Surgery: British & European Volume*, **2003**, *28*, 427-431.
15. Gonzalez, S.M., Gonzalez, R.I. *Western Journal of Medicine*, **1990**, *152*(4), 430-433.
16. Henry, W., Meyerding, M.D. *Archives of Surgery*, **1936**, 32(2), 320-333.
17. Hueston, J.T. *Plastic and Reconstructive Surgery*, **1961**, *27*, 569-585.
18. Hueston, J.T. *Plastic and Reconstructive Surgery,* **1963**, *31*, 66-69.
19. International Statistical Classification of Diseases and Related Health Problems 10th Revision. – World Health Organization, **2010**, https://www.who.int/classifications/icd/ICD10Volume2_en_2010.pdf, accessed September 2019.
20. Iselin, M., Iselin, F. *Maladie de Duputren,* Brussels: Flammarion, **1967**.
21. Kelly, A.P.Jr., Clifford, R.H. *Bulletin American Society of Plastic and Reconstructive Surgeons*, **1959**, *24*, 505-510.
22. Kjeldal, I., Nygaard, H.P. *Journal of Hand Surgery: British & European Volume*, **1998**, *13*, 257-258.
23. Lermusiaux, J.L., Lellouche, H., Badois, J.F., Kuntz, D. *Revue du Rhumatisme,* **1997**, *64*(12), 775-776.
24. Lubahn, J.D., Lister, G.D., Wolfe, T. *Journal of Hand Surgery-American Volume*, **1984**, *9A*(1), 53-58.
25. Luck, V. *Journal of Bone and Joint Surgery,* **1959***, 41*, 635–664.
26. Macnicol, M.F. *International Journal of Orthopaedics*, **1984**, *8,* 55-89.
27. Magomedov, R.O., Mikusev, G.I., Baykeev, R.F. *Bulletin of Traumatology and Orthopedy named after N.N. Priorov*, **2013**, *1*, 10-17.
28. Makela, E.A., Jaroma, H., Harju, A., Anttila, S., Vainio, J. *Journal of Hand Surgery: British & European Volume*, **1991**, *16*, 272-274.
29. Maravic, M., Landais, P. *Journal of Hand Surgery: British & European Volume*, **2005**, *30*(5), 484-487.
30. McCash, C.R. *British Journal of Plastic Surgery*, **1964**, *17*, 271-280.
31. McIndoe, A.H., Beare, R.L. (1958). *American Journal of Surgery*, **1958**, *95*(2), 197-203.
32. McInerney, N.M., Clover, A.J. *Plastic and Reconstructive Surgery,* **2015**, *135*(6), 1066e-1067e.

Downloaded from www.periodico.tchequimica.com

33. Mikusev, G.I., Baykeev, R.F., Mikusev, I.E., Magomedov, R.O. Bulletin of Traumatology and Orthopedy named after N.N. Priorov, 2007, 4, 65-69.

34. Mikusev, I.E. Dupuytren's contracture (questions of aetiology, pathogenesis and operative treatment), Kazan: Tatpoligraf, 2001.

35. Moermans, J.P. *Journal of Hand Surgery: British & European Volume*, **1991**, *16*(3), 243-254.

36. Moermans, J.P. *Journal of Hand Surgery: British & European Volume*, **1996**, *21*, 797-800

37. Moermans, J.P. *Journal of Plastic Surgery*, **1997**, *20*, 240-245.

38. Muppavarapu, R.C., Waters, M.J., Leibman, M.I., Belsky, M.R., Ruchelsman, D.E. *The New York Hand & Wrist Center,* **2015**, *10*(2), 260-265.

39. Netter, F.H. *Atlas of Human Anatomy*, London: Icon Learning Systemsp, **2003**.

40. Nieminen, S., Lehto, M. *Ann Chir Gynaecol,* **1986**, *75*, 164-167.

41. Norotte, G., Apoil, A., Travers, V. *Ann Chir Main*, **1988**, *7*, 277-281.

42. Smith, P., Breed, A.C. *Journal of Hand Surgery-American Volume*, **1994**, *19*, 840-843.

43. Ten Dam, E.P., van Beuge, M.M., Bank, R.A., Werker, P.M. *Journal of Cell Communication and Signaling,* **2016**, *10*(1), 33-40.

44. Tripoli, M., Merle, M. *Journal of Hand Surgery (European Volume)*, **2008**, *33*, 779-782.

45. Tubiana, R., Michon, J. *Mémoires. Académie de Chirurgie,* **1961**, *87*, 887-888.

46. van de Ven-Stevens, L.A., Graff, M.J., Peters, M.A., van der Linde, H., Geurts, A.C. *Journal of the American Physical Therapy Association*, **2015**, *95*(5), 750-757.

47. Verheyden, J.R. *Journal of Hand Surgery (European Volume)*, **2015**, *40*(2), 133-140.

48. Zirbs, M., Anzeneder, T., Bruckbauer, H., Hofmann, H., Brockow, K., Ring, J., Eberlein, B. *Journal of the European Academy of Dermatology and Venereology*, **2014**, *29*(5), 904-911.

Downloaded from www.periodico.tchequimica.com

Table 1. *Allocation of patients by types of the operations*

	Hand (proportion of operations)	
Operation type	The right hand (%)	The left hand (%)
A	The partial excision of the changed bands of PA – 3 (1, 6)	The partial excision of the changed bands of PA – 3 (2, 0)
B	Excision of proximal part of PA – 2 (1, 0)	Excision of proximal part of PA – 5 (3, 3)
C	Excision of proximal and middle parts of PA – 21 (11, 0)	Excision of proximal and middle parts of PA – 17 (11, 2)
D	Total excision of PA – 3 (1, 6)	Total excision of PA – 7 (4, 6)
E	Sphenoidal excision of middle part of PA with longitudinal bands of distal department of PA – 162 (84, 8)	Sphenoidal excision of middle part of PA with longitudinal bands of distal department of PA – 120 (78, 9)
	Σ = 191 (55.7)	Σ = 152 (44.3)

Table 2. *Grade scale of cure from DC and the functional status of hand after operation at patients with DC on periods ≥ 1 year (Magomedov et al., 2013)*

Estimation Parameter, No	Sign	Scale			
		4	3	2	1
1. Cure of the patient	1. Opinion of the patient on treatment outcome	No complain regarding the hand's function	Satisfied	Not completely satisfied	Not satisfied
2. The functional status of hand	2. Postoperative cicatrix	Negligible-elastic, soft	Just noticeable, Slightly astringent, slightly indurated	Noticeable, astringent, indurated	Explicitly noticeable – strongly astrigent, rough
	3. Sensitivity	Normal	Sensitivity is lowered	Sensitivity – is sharp lowered	Sensitivity – is completely lacking on two-three fingers
	4. A flexion contracture-*	not present	In proximal – an interphalanx joint > 160°	In proximal interphalanx joint ≤ 160°	Does not differ from preoperative situation or is expressed in a greater extent
	5.Hand's function	recovered	good	improved	restricted
	6. LPC	not present	present	present	present

The note: Estimation of recovery of function of hand after operation (1 – 5 points): 20 points – excellent, 15 points – good, 10 points –fair, 5 points – bad, Cure from DC (1 – 6 points): 24 cure; <24 –cure is absent. * – 1800, the fingers can be completely unbent in all joints. Position of the bent phalanx at an angle 1600 is admissible

Downloaded from www.periodico.tchequimica.com

Table 3. *Cure of patients from DC at operation on one or both hands: recovery of function of hand without LPC, depending on type of the operation*

Combination of localization and operation type	Number of patients (258)	Localization and type of operations		Cure from DC on periods ≥ 1 year (number of patients/%)
		The right hand	The left hand	
1	63	E	E	22/34, 9
2	94	E	-*	48/51, 1
3	55	-	E	22/40, 0
4	22	A, B, C, D, E	A, B, C, D, E	5/22, 7
5	12	A, C, D	-	7/58, 3
6	12	-	A, B, C, D	8/66, 7

The note. Type of operations: A – the partial excision of changed bands of PA; B – excision of proximal part of PA; C – excision of proximal and middle parts of PA; D – total excision of PA, E-wedge excision of middle part of PA with longitudinal bands of distal part of PA.

-* – operation only on one hand

Table 4. *Cure of patients from DC at operation on one or both hands: recovery of function of hand without LPC depending on section type on palm*

No	Number of patients (258)	Section type on palm		Cure from DC on periods ≥ 1 year (number of patients / %)
		The right hand	The left hand	
1	44	I*	I	12/27, 3
2	74	I	-**	40/54, 0
3	49	-	I	20/40, 8
4	41	I, II, III, IV, V	I, II, III, IV, V	9/21, 9
5	32	II, III, IV, V	-	15/46, 9
6	18	-	II, III, IV, V	10/55, 5

The note: -*I – arched (semi-oval), II – “Z”-shaped, III – linear, IV – curly (wavy), V – after Devis.

-** – operation only on one hand.

Table 5. *Recovery of function of hand (number of hands / %) of operated DC patients on observation period ≥ 1 year*

Recovery of hand’s function estimation	Total, number of hands / %	Operation localization	
		The right hand, number of hands/%	The left hand, number of hands/%
	343/100	191/100	152/100
Excellent	220/64,1	129/67,5	91/59,9
Good	88/25,7	47/24,6	41/27,0
Fair	26/7,6	13/6,8	13/8,5
Bad	9/2,6	2/1,1	7/4,6

Downloaded from www.periodico.tchequimica.com

Table 6. *Prognosis of the functional status of hand after DC operation*

Medical indice	Factors	No	Combination of operations	Canonical discriminant equation(CDE) (A – the factors determining the biological status of the patient; B – life style of the patient; C– technical-surgical components of operations – treatment)	P	CDE meaning as criterion of prognosis of the functional status of hand in the postoperative period	Accuracy of classification
The functional status of hand in the postoperative period, (excellent, good, fair, bad)	Impact of combination of factors A+B+C	1	operated right, left or both hands	CDE = – 0.554 + 3.102 • A_{65} +1.279 • A_{10} + 0.498 • A_{52} – 0.466 • A_{12} + 3.631 • C_2 +3.415 • C_{62} +3.366 • C_{13} +2.555 • C_{44}	0.0001	excellent<–0. 160 ≤ good <0.349 ≤ bad <1.378 ≤ fair	62. 4
		2	operated right hand	CDE = – 0.241+5. 431 • A_{54}+3.081 • A_{72} +2.605 • A_{83}– 1.098 • A_{112}– 2.167 • A_{76} +2.848 • C_{13}	0.0001	bad <–1.316 ≤ excellent <–0, 137 ≤ good <1.756 ≤ fair	65. 4
		3	operated left hand	CDE = – 0. 685+6.533 • A_{12} +2. 131 • A_{15}+1.979 • A_{64} +0. 589 • A_{52}+0.015 • A_{65}– 3. 553 • A_{55}– 3.692 • A_{42}+6.320 • B_{11} +6.042 • C_{42}	0.0001	excellent <– 0.265 ≤ good <0.310 ≤ fair<2.375 ≤ bad	61. 6
		4	operated right, left or both hands	CDE = – 0.547+10.387 • A12+2.126 • A10+1.443 • A52 +0.495 • A65	0.0001	excellent <– 0.031 ≤ good <0.264 ≤ fair<1.213 ≤ bad	61. 2
		5	operated right hand	CDE = – 0.130 +6.388 • A76+2.346 • A112–1.848 • A83–4.793 • A54	0.0001	bad <–0. 898 ≤ excellent <0.047 ≤ good<2.755 ≤ fair	66. 0
		6	operated left hand	CDE = – 0.732 +7.517 • A12+1.824 • A15 +1.537 • A64 +0.805 • A52+0.077 • A65 +4.897 • B11	0.0001	excellent <– 0.153 ≤ good <0.219 ≤ fair<1.657 ≤ bad	59. 9

Downloaded from www.periodico.tchequimica.com

		7	operation type	CDE = – 0.201 +8.413 • C82 + 7.526 • C83 + 3.904 • C81 + 2.575 • C84	0, 0001	good<–0.168 ≤ excellent <0.394 ≤ bad <1.143 ≤ fair	30. 6
		8	operated right, left or both hands	CDE = – 0.077+9. 145 • C42 +6.296 • C2-0.145 • C68	0, 0001	good<–0.129 ≤ excellent <0.366 ≤ bad <0.893 ≤ fair	53. 3
		9	operated right hand	is not approximated	–	–	–
		10	operated left hand	is not approximated	–	–	–

Table 7. *Impact of factors of groups A, B, C on the functional status of hand after DC operation*

Medical indice	Factors	No	Combination of operations	Canonical Discriminant Equation (CDE) (A – the factors determining the biological status of the patient; B – life style of the patient; C – technical-surgical components of operations – treatment)	P	CDE meaning as criterion of prognosis of functional status of hand after DC operation (excellent: yes/ no)	Accuracy of classification %
The functional status of hand in the postoperative period, ≥ 1 year (excellent, others)	Impact of combination of factors A+B+C	1	operated right, left or both hands	CDE = – 0. 776 + 3. 122 · A_{67} + 3. 035 · C_{13}+1. 535 · A_{10} +1. 325 · A_{52} + 1. 135 · C_{80} + 1. 075 · C_{51} + 0. 499 · A_{95} – 0. 812 · A_{71}–1. 565 · C_{73}–1. 814 · B_{10}	0. 0001	Yes <0. 127 <No	72. 9
		2	operated right hand	CDE = – 2. 944 + 2. 028 · B_{10} + 1. 267 · B_{14} + 1. 216 · A_{57} +1. 060 · B_5 + 1. 037 · A_{71} +0. 708 · A_{32} + 0. 029 · A_{107} – 0. 994 · C_{35}– 1. 018 · C_6–1. 065 · A_{25}–1. 541 · A_{85}–3. 070 · B_9–3. 671 · C_{13}	0. 0001	No < – 0. 281 <Yes	77. 0
		3	operated left hand	CDE = – 1.446+1.864 · A65 +1.258 · A52+1.016 · A64 + 0.078 · A109– 2.348 · A20	0.0001	Yes <0.101 <No	65.8

Downloaded from www.periodico.tchequimica.com

		4	operated right, left or both hands	CDE = –0.683+2.975 · A67 +1.971 · A10+1.685 · A52 + 0.744 · A95–1.102 · A71 –2.278 · B10	0.0001	Yes <0.095 <No	69.0
		5	operated right hand	CDE = 0.181+4.215 · B9 + 2.249 · A85 +1.985 · A1 –0.823 · A32–1.333 · A71	0.0001	Yes <0.167 <No	58.1
		6	operated left hand	CDE= – 1.415 +2.492 · A39 + 1.854 · A65+1.067 · A52 +0.940 · A64 +0.076 · A109 –2.209 · A20	0.0001	Yes <0.105 <No	68.4
		7	operation type	CDE = –0.109+9.375 · C83	0.028	Yes <0.028 <No	61.2
		8	operated right, left or both hands	CDE = –1.975+2.037 · C66 +1.339 · C28	0.001	Yes <0.050 <No	57.4
		9	operated right hand	is not approximated			
		10	operated left hand	CDE = –0.143+7.252 · C42	0.033	Yes <0.036 <No	61.8

Table 8. Impact of factors of groups A, B, C on the functional status of hand after operation

No	The factors hindering to the recovery of function status of hand	No	The factors advancing the recovery of function status of hand
1	A_1 – period of examination of the right hand: 1 – 2 years	1	A_{20} – age: 71 – 80 years
2	A_{10} – period of examination of the left hand: 11 – 15 years	2	A_{32}–diagnosis: the right hand: 4 finger of
3	A_{25} – diagnosis: the right hand: 2 finger of I grade (there is no contracture)		II grade (an angle of contracture from 179^0 to 100^0)
4	A_{39} – diagnosis: the left hand: 1 finger of II grade (an angle of contracture from 179^0 to 100^0)	3	A_{57}– heredity, the brother
5	A_{52} – diagnosis: the left hand: 5 finger of III grade (a contracture angle < 100^0)	4	A_{71} –osteochondrosis (associated
6	A_{64} – Ledderhose disease		diseases)
7	A_{65} – epiarticular finger pulps, the right hand	5	A_{107} –haemoglobin increase
8	A_{67} – Peyronie disease		
9	A_{85} – fracture of spinal column (surgical history and traumas)	6	B_5–physical job: 11 – 20 years
10	A_{95} – prescription of disease, the left hand: 1 – 5 years	7	B_{10}– mental job: 1 – 5 years
11	A_{109} – ESR increase	8	B_{14} – mental job: 31 – 40 years
12	B9 –physical job more than 50 years	9	C73 – on the left hand: the free dermal plasty on 4 finger

Downloaded from www.periodico.tchequimica.com

13	C6 – on the right hand: sphenoidal excision of middle part of PA with longitudinal bands of distal department of PA
14	C13 – on the right hand: the common experience of the surgeon: more than 30 years
15	C28 – on the right hand: curly section on fingers
16	C35 – on the right hand: rehabilitation (ultrahigh frequency treatment, ultraviolet irradiation)
17	C42 – on the left hand: the partial excision of PA (character of operation)
18	C51 – on the left hand: the common experience of the surgeon: 16-20 years
19	C66 – on the left hand: curly section on palm
20	C80 – on the left hand: healing by secondary intention
21	C83 – combination of the partial excision of palmar aponeurosis on one hand and sphenoidal excision of middle part of PA with longitudinal band of distal department of PA on other hand in different periods

Downloaded from www.periodico.tchequimica.com

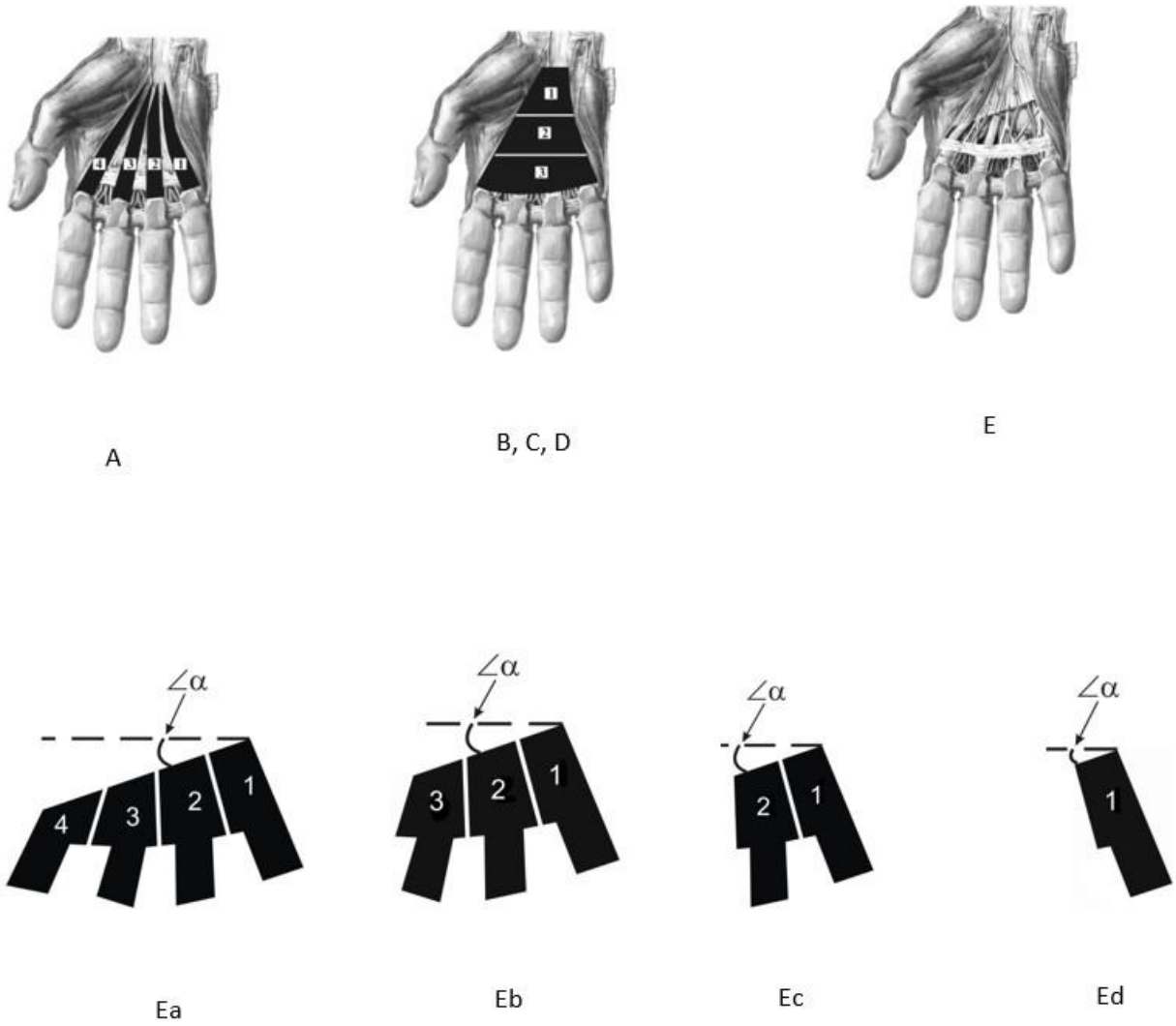

Figure 1. *Topographic surgery of palmar aponeurosis (PA) at DC*

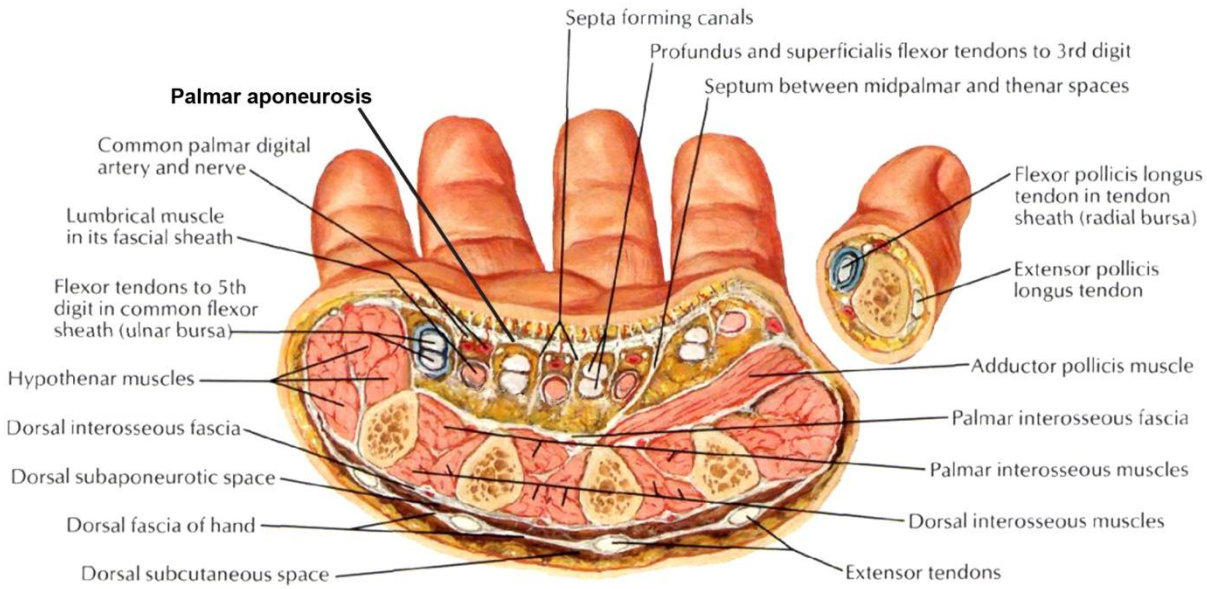

Figure 2. *Normal anatomy of cross section of the lower third of right hand (Netter et al., 2003)*

Downloaded from www.periodico.tchequimica.com

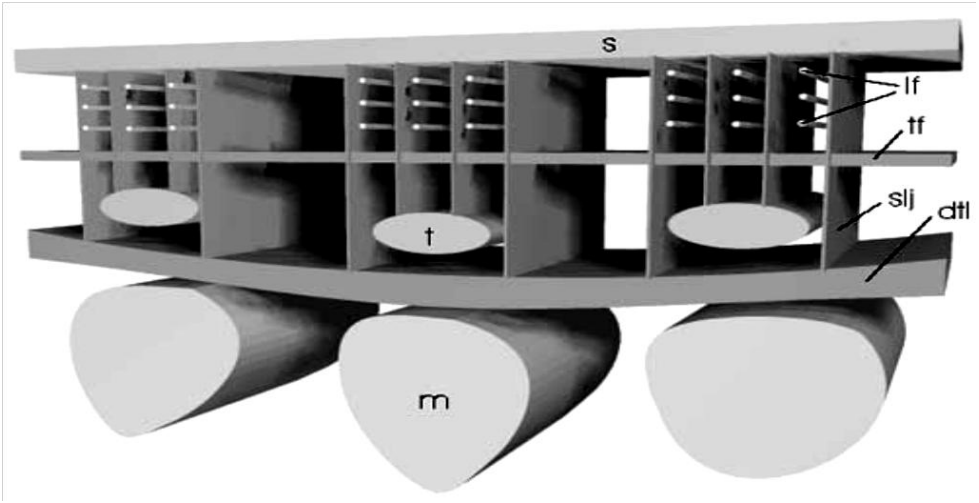

Figure 3. *Biomechanic structure of AP (Moermans, 1997). S – skin, lf – longitudinal fibers, tf – cross fibres, slj – Legueu and Juvara septum, t – tendons, dtl – deep transverse ligament, m – metacarpal bone*

Downloaded from www.periodico.tchequimica.com

APPENDIX, SUPPLEMENT 1

Factors of the anamnesis and follow-up of the patient, surveyed at development of efficiency prognosis technology of surgical measures of Dupuytren's disease (contracture):

A -Factors determining the biological status of the patient (gender, age, disease prescription, examination period, grade of DC lesion, heredity, the associated diseases, surgical history and traumas, the disease beginning, laboratory analyses, etc.): Period of examination of the right hand: A1 – 1-2 years, A2 – 3-5 years, A3 – 6-10 years, A4 – 11-15 years, A5 – 16-20 years, A6 – more than 20 years; Period of examination of the left hand: A7 – 1-2 year, A8 – 3-5 years, A9 – 6-10 years, A10 – 11-15 years, A11 – 16-20 years, A12 – more than 20 years; the gender of the patient: A13 – male, A14 – female; Age of the patient: A15 – 20-30 years, A16 –31-40 years, A17 – 41-50 years, A18 – 51-60 years, A19 – 61-70 years, A20 – 71-80 years, A21 – more 80 years; DC diagnosis on the right hand (affected finger/ DC grade): A22 – 1/I grade, A23 – 1/II grade, A24 – 1/III grade, A25 – 2/I grade, A26 – 2/II grade, A27 – 2/III grade, A28 – 3/I grade, A29 – 3/II grade, A30 – 3/III grade, A31 – 4/I grade, A32 – 4/II grade, A33 – 4/III grade, A34 – 5/I grade, A35 – 5/II grade, A36 – 5/III grade, A37 – atypical form of DC on the right hand; DC diagnosis on the left hand (affected finger/DC grade): A38 – 1/I grade, A39 – 1/II grade, A40 – 1/III grade, A41 – 2/I grade, A42 – 2/II grade, A43 – 2/III grade, A44 – 3/I grade, A45 – 3/II grade, A46 – 3/III grade, A47 – 4/I grade, A48 – 4/II grade, A49 – 4/III grade, A50 – 5/I grade, A51 – 5/II grade, A52 – 5/III grade, A53 – atypical form of DC on the left hand; DC presence in the inheritance at: A54 – mothers, A55 – sister, A56 – father, A57 – brother, A58 – grandmothers, A59 – aunts, A60 – cousin, A61 – grandfathers, A62 – uncles, A63 – cousin; A64 – Leclderhose disease, presence of epiarticular fingers' pulps: A65 – the right hand, A66 – the left hand; A67 – Peyronie disease, Associated diseases: A68 – cardio-vascular system, A69 – respiratory organs, A70 – gastro-intestinal tract, A71 – osteochondrosis, A72 – diabetes, A73 –central nervous system, A74 – pneumatic hammer disease, A75 – oncology, A76 – general diseases, A77 – blade-humerus per arthritis, A78– other; Surgical history and traumas on: A79 –gastro-intestinal tract, A80 – respiratory organs, A81 – the right upper extremities, A82–the left upper extremities, A83 – fracture of ribs, A84 – pelvic fracture, A85 – fracture of spinal column; DC origin in the anamnesis: A86 – acute trauma, A87 – chronic trauma, A88 – spontaneous DC origin; Prescription of origin of disease on the right hand: A89 – 1-5 years, A90 – 6-10 years, A91 – 11-15 years, A92 – 16-20 years, A93 – 21-30 years, A94 – more than 30 years; Prescription of origin of disease on the left hand: A95 – 1-5 years, A96 – 6-10 years, A97 – 11-15 years, A98 – 16-20 years, A99 – 21-30 years, A100 – more than 30 years; Rhesus factor of blood of the patient: A101 – positive, A102 – negative; Blood group of the patient: A103 – O (I), A104 – A (II), A105 – B (III), A106 – AB (IV); Common analysis of blood, meaning: A107 –haemoglobin, A108 – leucocytes, A109 – ESR; Common analysis of urine, meaning: A110 –specific gravity, A111 – response, A112 – transparency, A113 – colour, A114 – fiber, A115 – glucose, A116 – epithelium, A117 – leucocytes, A118 – crystals.

B – the factors presenting life style of the patient (residence, physical and mental job, bad habits, etc.): Place of residence of the patient: B1– city, B2 – village ; physical job during the life: B3 – 1-5 years, B4 – 6-10 years, B5 – 11-20 years, B6 – 21-30 years, B7 – 31-40 years, B8 – 41-50 years, B9 – more than 50 years; mental job during the life: B10 – 1-5 years, B11 – 6-10 years, B12 – 11-20 years, B13 – 21-30 years, B14 – 31-40 years, B15 – 41-50 years, B16 – more than 50 years; B17 – smoking; B18 – alcohol intake; B19 – physical job during the life; B20 – playing sports.

C – the factors presenting technical-surgical components of operations, treatment (the experience of the surgeon, types of operations, anesthesia, section, dermal plasty, rehabilitation treatment, healing, etc.) : C1 – operated right hand; operative measure on the right hand: C2 – the partial excision of PA, C3 – total excision of PA, C4 – excision of apex of PA, C5 – excision of proximal and middle parts of PA, C6 – sphenoidal excision of middle part of PA with longitudinal bands of distal department of PA; Common experience of the surgeon making operation on the right hand: C7 – 1-2 years, C8 – 3-5 years, C9 – 6-10years, C10 – 11-15 years, C11 – 16-20 years, C12 – 21-30 years, C13 – more than 30 years; Specialized experience of the surgeon making operation on the right hand: C14 – 1-2 year, C15 – 3-5 years, C16 – 6-10 years, C17 – 11-15 years, C18 – 16-20 years, C19 – 21-30 years, C20 – more than 30 years; Type of the anesthesia at operation on the right hand: C21 – intravenous regional, C22 – conduction, C23 – intubation narcosis, C24 – intravenous narcosis; Section type on palm of the right hand: C25 –linear, C26 – curly; section type on fingers of the right hand: C27 – linear, C28 – curly; Free dermal plasty on the right hand on: C29 – palms, C30 –

Downloaded from www.periodico.tchequimica.com

the first finger, C31 – the second finger, C32 – the third finger, C33 – the fourth finger, C34 – the fifth finger; Postoperative after treatment on the right hand: C35 – diadynamic currents, variable electric field of ultrahigh frequency, ultra-violet irradiation, C36 – electrophoresis (phonophoresis) Lydasums, C37 – physiotherapy exercises, massage, C38 – paraffin therapy, fango therapy; Healing on the right hand: C39 – primary, C40 – secondary; C41 – operated left hand; Operative measure on the left hand: C42 – partial excision of PA, C43 – total excision of PA, C44 – excision of apex of PA, C45 – excision of proximal and middle parts of PA, C46 – sphenoidal excision of middle part of PA with longitudinal bands of distal department of PA; Common experience of the surgeon making operation on the left hand: C47 – 1-2 years, C48 – 3-5 years, C49 – 6-10years, C50 – 11-15 years, C51 – 16-20 years, C52 – 21-30 years, C53 – more than 30 years; Specialized experience of the surgeon making operation on the left hand: C54 – 1-2 year, C55 – 3-5 years, C56 – 6-10 years, C57 – 11-15 years, C58 – 16-20 years, C59 – 21-30 years, C60 – more than 30 years; Type of anesthesia at operation on the left hand: C61 – intravenous regional, C62 – conduction, C63 – intubation narcosis, C64 – intravenous narcosis; Section type on palm of the left hand: C65 – linear, C66 – curly; Section type on fingers of the left hand: C67 – linear, C68 – curly; Free dermal plasty on the left hand on: C69 – palms, C70 – the first finger, C71 – the second finger, C72 – the third finger, C73 – the fourth finger, C74 – the fifth finger; Postoperative after treatment on the left hand: C75 – dia dynamical currents, variable electric field of ultrahigh frequency, ultra-violet irradiation, C76 – electrophoresis (phonophoresis) Lydasums, C77 – physiotherapy exercises, massage, C78 – paraffin therapy, fango therapy; Healing on the left hand: C79 – primary, C80 – secondary; C81 – excision of apex of PA (on the right or left hand); C82 – the partial excision of PA on one hand and total excision of PA on other hand; C83 – the partial excision of PA on one hand and sphenoidal excision of middle part of PA with longitudinal bands of distal department of PA on other hand; C84 – section on fingers: linear + curly.

Downloaded from www.periodico.tchequimica.com

APPENDIX, SUPPLEMENT 2

Patient X.: 56 years old, case history No. 3546/101516, citizen. Complaints of the patient at entering: callosity of palmar surface of both hands, more in projections of the fourth fingers, periodic pain in these fingers after an exercise stress, a flexion contracture of the fourth fingers of both hands that frames difficulties during work and self-care. Anamnesismorbi. There were indurations on a palmar surface of left (A95) and the right hands about three years ago, then bands were formed with slow development of their flexion contracture on the fourth fingers of both hands. Indurations on foot appeared about a year ago (Leclderhose disease). X. was not treated anywhere.

Anamnesisvitae:

Past diseases: acuterespiratory diseases, brain contusion twice.

The right-handed person, smokes a little, took alcoholic drinks much. DC and Leclderhose disease were at the big brother and at the uncle (paternal father). Worked at office: mental job during one and a half year (B10); then work edas mechanic during 25 years.

The epidemiological anamnesis: X. wasn't in contact to infections. Tuberculosis, syphilis, virus hepatitis: denies. Surgical history: injury of soft tissues of the left hip. The allergologic anamnesis is not confounded. Hemotransfusions were not made earlier.

Data of physical examination:

Common status is satisfactory. Consciousness is clear. Integuments have physiological color. Tongue is pure, wet. Breath is vesicular, respiratory frequency is 16 movements in a minute, conducted from both sides. Both halves of thorax participate in breath symmetrically. Arterialpressure is 124/70 mm of mercury. Pulse is 72 beats per minute, rhythmic, filling up is satisfactory. Abdomenhas regular form, participates in the breath act, at palpation is soft, painless. Lien is not palpated. Pasternatsky symptom is negative from both sides. Liver is not palpated. Defecation and diuresis are not broken.

Status localis:

The right hand:

Visually there is a local hyperkeratosis of the oval form on palmar surface of hand in the field of distal palmar cord at level of 4 MTR joint of 0.4x 0.8 x 10-2m, band is spread from area of hyperkeratosis of palm on the proximal phalanx of 4 finger. There is flexion contracture of 4 finger in MTR joint at the angle 1550.

Palpatory: there is dense band, going in direction to 4 finger and passing to the proximal phalanx of 4 finger, skin over band is thickened. On palmar surface of hand in distal palmar cord under a skin there are small local indurations: at level of 2, 3, 5 MTR joints in the form of nodes of 0,4 x 0,6 x 10-2m, on ulnar border of 1 finger at level of MTR joint in the form of node from 0,3 x 0,4 x 10-2m. Function of 1, 2, 3, 5 fingers is complete, 4 finger is flex in total volume, the extension to the angle presented above.

The left hand:

Visually: there is a local hyperkeratosis of the oval form on palmar surface of hand in distal palmar cord at level of 4 MTR joint of 0.7 x 1.0 x 10-2m, band is spread from area of hyperkeratosis of palm on the proximal phalanx of 4 finger. There is flexion contracture of 4 finger in MTR joint at the angle 1350.

Palpatory: there is dense band, going in direction to 4 finger and passing to the proximal phalanx of 4 finger, skin over band is thickened. On palmar surface of hand in the field of distal palmar cord under skin there are small local indurations: at level of 3, 5 of MTR joints in the form of nodes from 0.5 x 0.7 x 10-2m, on ulnar border of 1 finger at level of MTR joint in the form of node from 0,4 x 0.5 x 10-2m. Function of 1, 3, 5 fingers is complete, 4 finger is flex in a total volume, an extension to the angle presented above.

Palpatory: there are local indurations in the form of nodes on medial border of the middle of plantar surface of both feet. On the right foot: 0.3x 0.5 x 10-2m, on the left foot: 0.5x 0.6 x 10-2m.

Downloaded from www.periodico.tchequimica.com

Diagnosis: Dupuytren's contracture of 1, 2, 3, 5 fingers of I grade, 4 finger of II grade of the right hand; 1, 3, 5 fingers of I grade, 4 finger of II grades of the left hand. Leclderhose disease of both feet.

It is planned: to make operation on the left hand: excision of proximal and middle parts of palmar aponeurosis, band on 4 finger, dermal "Z" plasty. Surgical experience of the operating doctor is 18 years (C51).

Operation: excision of proximal and middle parts of palmar aponeurosis, band on 4 finger, dermal "Z" plasty.

Physiotherapeutic treatment is given in the postoperative period. Healing was by secondary intention (C80).

Mathematical calculation of prognosis of functional status of hand is made:

Canonical Discminant Equation (DCE) = – 0.776 + 0.499 · (1) – 1.814 · (1) + 1.135 · (1) + 1.075 · (1) = 0.12

According to DCE meaning = 0.127 for the given equation (Table 6, the equation No.1) we conclude that patient X. will have an excellent result of FSH recovery.

Control examination was eight years ago.

Hand function is recovered completely, the patient is happy with result, result is excellent.

Correctness of the calculation is demonstrated.

Downloaded from www.periodico.tchequimica.com

PERIÓDICO TCHÊ QUÍMICA
ARTIGO ORIGINAL

EFEITO DA IRRADIAÇÃO DE VIGA ELETRÔNICA DE ALTA CORRENTE NA RESISTÊNCIA À CORROSÃO DE ÓXIDO DE SULFETO DE REVESTIMENTOS DE NI-CR-AL-Y-PLASMA

EFFECT OF HIGH-CURRENT ELECTRON BEAM IRRADIATION ON RESISTANCE OF SULFIDE-OXIDE CORROSION OF NI-CR-AL-Y ION-PLASMA COATINGS

ВЛИЯНИЕ ОБЛУЧЕНИЯ СИЛЬНОТОЧНЫМИ ЭЛЕКТРОННЫМИ ПУЧКАМИ НА СОПРОТИВЛЕНИЕ СУЛЬФИДНО-ОКСИДНОЙ КОРРОЗИИ ИОННО-ПЛАЗМЕННЫХ ПОКРЫТИЙ NI-CR-AL-Y

BYTSENKO, Oksana A. [1,2*]; SHATILOV, Aleksey V. [3]; DANEKO, Aleksandr I. [4]; FILONOVA, Elena V. [5]; MARKOV, Alexey B. [6]

[1,3] Chernyshev Moscow Machine-Building Enterprise, Moscow – Russian Federation

[2,4] Moscow Aviation Institute (National Research University), Moscow – Russian Federation

[5] All-Russian Scientific Research Institute of Aviation Materials, Moscow – Russian Federation

[6] Tomsk Scientific Center of the Siberian Branch of the Russian Academy of Sciences, Tomsk – Russian Federation

** Correspondence author*
e-mail: oksiwear@yandex.ru

Received 02 October 2019; received in revised form 20 October 2019; accepted 21 October 2019

RESUMO

Recentemente, o aparecimento de aceleradores de feixes de elétrons de alta corrente e poderosos lançamentos de íons contribuiu para a criação de efeitos únicos de fluxos de energia concentrados nos materiais. A melhoria dos processos de produção e o desenvolvimento de novos processos tecnológicos, tanto para fabricação de motores de aeronaves domésticos quanto para armas de aviação, continua sendo uma questão urgente. A confiabilidade dos motores depende da confiabilidade das pás da turbina, que são as peças mais carregadas, pois são expostas a cargas estáticas, dinâmicas e cíclicas e também sofrem tensões térmicas cíclicas. Portanto, o principal objetivo do trabalho foi analisar o efeito da irradiação com feixes de elétrons de alta corrente na resistência à corrosão por óxido-sulfeto de revestimentos do íon-plasma Ni-Cr-Al-Y. Para atingir esse objetivo, a irradiação por feixes foi realizada na instalação automatizada dos feixes de elétrons do complexo RITM-SP. A modificação da camada superficial do revestimento do íon-plasma SDP 2 + VSDP 16 usando feixes de elétrons de alta corrente com duração de microssegundos de acordo com o modo selecionado permitiu aumentar significativamente a resistência à corrosão por óxido-sulfeto. A análise da superfície e microestrutura das amostras após o teste de corrosão por óxido-sulfeto (SOC) permitiu determinar os diferentes efeitos do meio no revestimento das amostras, dependendo do estado da superfície das amostras. No processo de estudo da microestrutura das amostras, também foi constatado que as rachaduras individuais que estavam na superfície das amostras após a modificação não receberam seu desenvolvimento durante o teste. Verificou-se que certos tipos de crateras nem sempre são o foco do aparecimento de danos por corrosão, ou seja, a existência desses tipos de crateras e seus efeitos sobre a resistência à corrosão por óxido-sulfeto não são simples.

Palavras-chave: *corrosão por óxido-sulfeto, modificação por feixes de elétrons de alta corrente, revestimentos de íon-plasma condensados, estado de fase estrutural, estudo de microestrutura.*

ABSTRACT

Recently, the emergence of accelerators of high-current electron beams and powerful electron ion beams has contributed to the creation of unique effects of concentrated energy flows on materials. Upgrading of production processes and development of new technological processes of both domestic aircraft propulsion engineering and aviation arms remain topical and needed. Engine operational reliability depends on that of

Downloaded from www.periodico.tchequimica.com

turbine blades. They are the most loaded details because they are experienced to action of static, dynamic and cyclic loadings as well as are subjected to cyclic thermal stresses. Therefore the main objective of our paper is to analyze the effect of high-current electron beam irradiation on-resistance of sulfide-oxide corrosion (SOC)of Ni-Cr-Al-Yion-plasma coatings. To achieve this purpose, beam irradiation was performed using the RITM-SP complex automated electron-beam setup. Modification of surface layer of SDP 2+VSDP16 ion-plasma coating by microsecond high-current electron beams of selected mode made it possible to increase considerably the SOC resistance. An analysis of the surface and microstructure of samples after SOC testing enabled to determine different effects of medium on sample coating depending on the state of the sample surface. When investigated samples microstructure, we found that after modification certain cracks on sample surface did not develop in the course of testing. It was found that some craters were not necessarily centers of corrosion damage origin, i.e., the existence of given types of craters and their impact on SOC resistance stability are ambiguous.

Keywords: *sulfide-oxide corrosion, modification by high-current electron beams, condensed ion-plasma coatings, structural-phase state, investigation of microstructure.*

АННОТАЦИЯ

В последнее время появление ускорителей сильноточных электронных пучков и мощных электронных пусков ионов поспособствовало созданию уникальных воздействий концентрированных потоков энергии на материалы. Совершенствование процессов производства и разработка новых технологических процессов как отечественного авиационного двигателестроения, так и авиационного вооружения остается актуальным вопросом. Надежность работы двигателей зависит от надежности работы лопаток турбины, которые являются наиболее нагруженными деталями, так как подвергаются действию статических, динамических, циклических нагрузок, а также испытывают циклические термические напряжения. Поэтому основная цель работы заключается в анализе влияния облучения сильноточными электронными пучками на сопротивление сульфидно-оксидной коррозии ионно-плазменных покрытий Ni-Cr-Al-Y. Для достижения поставленной цели проводилось облучение пучком на комплексной автоматизированной электронно-пучковой установке «РИТМ-СП». Модифицирование поверхностного слоя покрытия ионно-плазменного покрытия СДП 2+ВСДП 16 с помощью сильноточных электронных пучков микросекудной длительности по выбранному режиму позволило значительно повысить сопротивление сульфидно-оксидной коррозии. Анализ поверхности и микроструктуры образцов после испытания на сульфидно-оксидную коррозию (СОК) позволил определить разное влияние среды на покрытие образцов в зависимости от состояния поверхности образцов. В процессе исследования микроструктуры образцов также было обнаружено, что отдельные трещины, которые были на поверхности образцов после модифицирования, не получили своего развития в процессе проведения испытания. Было установлено, что отдельные виды кратеров не всегда являются очагом зарождения коррозионных повреждений, т.е. существование данных типов кратеров и их влияние на стойкость к сопротивлению сульфидно-оксидной коррозии не однозначна.

Ключевые слова: *сульфидно-оксидная коррозия, модифицирование сильноточными электронными пучками, конденсированные ионно-плазменные покрытия, структурно-фазовое состояние, исследование микроструктуры.*

1. INTRODUCTION

Upgrading of production processes and development of new technological processes of both domestic aircraft propulsion engineering and aviation arms remain topical and needed. The efforts of designers and technologists who developed and made aeronautical engineering were always directed, first of all, at growth of reliability and controllability (and recently at ecological problems) of production and products as well (Baranov *et al.*, 2007; Tishkov and Firsanov, 2011; Terentyev *et al.*, 2012; Plankovsky *et al.*, 2013; Nesterov *et al.*, 2018; Kachanov *et al.*, 2017).

One of the most important areas in growth of reliability of modern gas turbine engines (GTE) and aviation arms as well as in development of the newest construction solutions is provision of required service parameters for materials used to product especially loaded details (including GTE and primarily high pressure turbine rotor blades (Muboyajyan *et al.*, 2012; Kononov *et al.*, 2013; Budinovsky, and Smirnov, 2015; Ivashko *et al.*, 2019). However, even at stability of strength properties of materials used for production of the

Downloaded from www.periodico.tchequimica.com

above details, the turbine blades may break in the course of operation (Cai *et al.*, 2016; Zhou *et al.*, 2017; Blesman *et al.*, 2018). One of the main reasons for that is intense material damage at high-temperature corrosion under the action of static and vibration loads.

An analysis of the performed investigations shows (Kablov, 2001; Shulov *et al.*, 2010; Shulov *et al.*, 2013; Shulov *et al.*, 2015; Kosmin and Budinovsky, 2016) that both character and intensity of turbine blade damages at high temperature corrosion are determined by the following factors: (i) anti-corrosion properties of protective coatings, (ii) level of active static and vibration loads, (iii) operating temperature of turbine blades, as well as (iv) concentration of corrosion-active substances in fuel combustion products. In some cases, high-temperature corrosion acts as an independent disturbing factor (Budinovskii and Muboyadzhan, 2003; Shejko *et al.*, 2017; Ivanov *et al.*, 2018; Braceras *et al.*, 2018). In this connection investigation of mechanisms of corrosion damage and its kinetics is one of the problems for developing new materials and coatings as well as making a system for monitoring technical condition of blades.

One of the solutions for the problem of increasing SOC resistance is the deposition of protective coatings. Application of high energy vacuum-plasma technology seems to be most reasonable for this technology (Bhat *et al.*, 2018; Chanda *et al.*, 2018; Pillis *et al.*, 2018). The MAP-type vacuum-plasma plants developed at the All-Russian Institute of Aviation Materials to deposit heat resistant coatings on turbine blades are used widely and successfully in aircraft propulsion engineering (Muboyajyan *et al.*, 2012; Kachanov *et al.*, 2017). Such plants ensured increasing service life of turbine blades to 600 hoursby deposing double-layer SDP 2+VSDP16 coatings to 100 μm thick (Kononov *et al.*, 2013).

The process of changing physical-chemical properties of surface layers of GTE rotor blades may be presented as the following conditional scheme: 1) destruction of protective coatings owing to erosion/corrosion damage or cracking at considerable amplitudes of thermotension; 2) formation and condensation (at blade surfaces)of sulfur-containing and other corrosion-active compounds at their penetration into engine flow part; 3) formation of Ni sulfide and Cr sulfide at the "alloy–dross" interface.

In the course of exploitation, the defects inherent in condensed multicomponent ion-plasma coatings (presence of a micro drop fraction in plasma that leads to low local adhesion even after high-temperature diffusion annealing; no uniformity of phase components distribution over surface and depth; high roughness of coating) may lead to reduction of heat resistance of coating and its resistance to SOC. Some measures are needed for their leveling (Kahraman *et al.*, 2016; Sentry *et al.*, 2018). Therefore,it is expedient to modify surface layers of condensed ion-plasma coatings using a high-current pulsed electron beam (HPEB) (Shulov *et al.*, 2010; Shulov *et al.*, 2013; Shulov *et al.*, 2015; Bytsenko *et al.*, 2015; Kosmin and Budinovsky, 2016; Bytsenko *et al.*, 2017a).

The objective of the present work is an investigation of the effect of modifying coating surface layers on resistance to SOC by using HPEB condensed ion-plasma NiCrAlY coatings.

2. MATERIALS AND METHODS

The objects of investigation were the samples made of high-temperature JS32 nickel alloy with condensed multicomponent SDP 2+VSDP16 ion-plasma coating deposited according to the series technology (without modifying and with subsequent modifying by HPEB) (Bytsenko *et al.*, 2015; Bytsenko *et al.*, 2017b). HPE Birradiation was made with a complex automated electron-beam plant "RITM-SP" using the following mode: electron energy E = 20 keV and pulse number N = 10, with further thermal treatment for two hours in a vacuum at 1050ºC.

The SOC testings were performed in accordance with PI 1.2A-503-98. The testing mode was cyclic: (i) deposition of salt crust samples by sputtering solution of Na_2SO_4+ NaCl salts on a hot surface; (ii) exposure at a specified temperature of 800°C for one hour; (iii) air cooling. The total testing period was ten cycles. Testing of samples (put into alundum crucibles) was performed in a chamber electric resistance furnace with air. Coating resistance to SOC was estimated before and after irradiation using the gravimetric method with analytical balance (accurate to ±0.0002 g). To determine the kinetics of the SOC process, the samples were weighed in one, five and ten cycle intervals of testing.

The surface condition was investigated using a LEXT OLS 3100 laser confocal microscope, with further computer processing of images obtained (Bytsenko *et al.*, 2016; Bytsenko *et al*., 2017). The investigation of the coating

Downloaded from www.periodico.tchequimica.com

microstructure was performed using a Leica DM IRM optical microscope and a VERIOS 460 scanning electron microscope with an X-MAX 80energy dispersive X-ray microanalyzer.

3. RESULTS AND DISCUSSION:

In the initial state, the coated samples have a uniform surface with single particles of drop phase (Figure 1a). For the most part, the samples with modified coating have a homogeneous shiny surface with a small amount of craters (Figure 1b). Such defects as multi-ring, adjacent and nick-like craters as well as cracks are observed at some sample surfaces after modification. They indicate the instability of irradiation conditions (Figure 1c).

For SOC testing the samples with initial coating (sampleNo1), defectless modified coating (sample No 17) and modified coating with defects (samples No 3 and No 15) were elected. After SOC testing the masses of samples with initial coating practically remained the same after one, five and ten SOC cycles. The mass of the sample with defect less modified coating did not change too. The masses of samples with modified coating with defects decreased by 0.0036 g for the sample No 15 after one cycle and by 0.0467 g for the sample No 3 after five cycles.

After one cycle of testing, the unmodified coating practically does not differ from the initial one (homogeneous, with single particles of drop phase). After five cycles, single areas with corrosion are observed on the sample surfaces. The corrosion-struck coating areas are of greenish tint (Figure 2a). After one cycle of SOC testing, the defect less modified coating became mat. And no corrosion nidi were observed at the sample surface after ten cycles of testing (Figures 2b, 2c). The surfaces of samples with modified coatings with defects have corrosion damages even after one cycle of SOC testing. The corrosion nidi are predominantly near defects and along the sample edge (Figures 3d, 3e). Our investigations of sample surfaces after corrosion testing performed with a LEXT laser confocal microscope (Figure 3) showed that after five cycles of testing the surface of a sample with initial coating becomes rougher than before testing. There are corrosion nidi at the sample surface (shown with arrows in Figure 3c). After ten cycles of testing, the surface roughness decreases, and corrosion is observed over the whole sample surface (Figure 3e).

After five cycles, a sample surface with defect less modified coating is less affected with corrosion than unmodified one and partially preserves the initial condition (see highlights in Figure 3d). After ten cycles, corrosion occurs uniformly over the whole sample surface; no corrosion nidi (pits) are observed (Figure 3f).

After HPEB irradiation and five cycles, a coated sample No3 with defects (as well as that with defect less modified coating) partially preserves the initial (prior to testing) surface condition (Figures 3g, 3h). When comparing with the defect less modified coating, the given sample demonstrates strong corrosion near defects and along its edges. After SOC testing, the microstructure of sample surfaces was studied by the methods of optical and scanning electron microscopy (Figures 4 and 5). It was found that corrosion damage of unmodified coating is uniform (Figure 4a). The corrosion-struck depth increases with the number of cycles (five and ten) from ~6.0 μm to ~25.0 μm (Figure 5a). After ten cycles, single deeper corrosion damages of coating are observed. A uniform corrosion damaging of surface is also observed for a sample with defect less modified coating (Figure 4b). The depth of corrosion damaging is ~1.0 μm at five cycles and ~10 μm at ten cycles (Figure 5b). For the sampleNo3 with defects of modified coating. corrosion damaging after five cycles is ~5.0 μm deep; the sample coating is partially damaged near the sample edge and defects.

An analysis of sample surfaces and microstructure after SOC testing showed different effect of medium on sample coatings depending on the condition of sample surfaces. The reason for such different conditions of surface layer after SOC testing at samples No 3 and No 15 with modified coating is the presence of defects after coating deposition and further irradiation. The appearance of damage centers due to SOC is related to coating peeling after irradiation owing to poor adhesion of coating to substrate. Another cause is the instability of irradiation modes. This is indicated by the presence of the following crater types: multi-ring, adjacent and nick-like. It is known (Shulov *et al.*, 2015) that craters of such types are the most dangerous with respect to corrosion resistance (Figure 6).

4. CONCLUSIONS:

It should be noted that multi-ring and adjacent craters not necessarily served as centers of origin of corrosion damages, i.e., presence of craters of such types and their effect on SOC resistance tolerance are not too

Downloaded from www.periodico.tchequimica.com

unambiguous. When investigating the microstructure of samplesNo3 andNo15, it was found that after modifying some cracks on the sample surfaces did not grow in the course of SOC testing.

When analyzing the data obtained, one can conclude that HPEB modification of the surface layer of the SDP 2+VSDP16 coating by the chosen mode made it possible to considerably increase SOC resistance. The corrosion damage of unmodified coating was from ~6.0 μm to ~25.0 μm (at five and ten cycles) while that of modified defectless coating was ~1.0 μm at five cycles and~10 μm at ten cycles(i.e., 2.5 times smaller).

5. ACKNOWLEDGMENTS:

This work was made with financial support from the Russian Fund of Fundamental Investigations (Grant No14-08-97046 –Volga region_a).

6. REFERENCES:

1. Baranov, N.A., Nesterov, V.A., Polyansky, V.V. *Bulletin of the Moscow Aviation Institute*, **2007**, *14*(1), 13-19.
2. Bhat, R., Bekal, S., Chitharanjan Hegde, A. *Analytical and Bioanalytical Electrochemistry,* **2018**, *10*(12), 1562-1573.
3. Blesman, A.I., Postnikov, D.V., Polonyankin, D.A. *Journal of Physics: Conference Series,* **2018***, 1115*(3), Article number 032022. doi:10.1088/1742-6596/1115/3/032022
4. Braceras, I., Ibáñez, I., Domínguez-Meister, S., Urgebain, A., Sánchez-García, J. A., Larrañaga, A., Garmendia, I. *Surface and Coatings Technology,* **2018**, *355*, 174-180.
5. Budinovskii, S.A., Muboyadzhan, S.A. *Metal Science and Heat Treatment,* **2003**, *45*(5-6), 183-188.
6. Budinovsky, S.A., Smirnov, A.A. *Proceedings of VIAM. Electronic Journal,* **2015**, *4*, http://viam-works.ru, accessed April 2019.
7. Bytsenko, O.A., Filonova, E.V., Markov, A.B. *News of Materials Science. Science and Technology,* **2017a**, *2*(26), 9.
8. Bytsenko, O.A., Filonova, E.V., Markov, A.B. *The effect of intense beams on the surface layers of modern heat-resistant alloys with ion-plasma coatings of various compositions,* London: Interaction of Radiation with Solid, **2015**.
9. Bytsenko, O.A., Filonova, E.V., Markov, A.B., Belova, N.A. *Proceedings of VIAM. Electronic Journal,* **2016**, *6*(42), http://viam-works.ru, accessed July 2019.
10. Bytsenko, O.A., Grigorenko, V.B., Lukina, E.A. Aviation Materials and Technologies*,* **2017b**, *S*, 498-515
11. Cai, J., Lv, P., Guan, Q., Xu, X., Lu, J., Wang, Z., Han, Z. *ACS Applied Materials and Interfaces,* **2016**, *8*(47), 32541-32556.
12. Chanda, U.K., Behera, A., Roy, S., Pati, S. *International Journal of Hydrogen Energy,* **2018**, *43*(52), 23430-23440.
13. Ivanov, Y., Koval, N., Krysina, O., Moskvin, P., Petrikova, E., Tolkachev, O. *Key Engineering Materials*, **2018**, *781*,131-136
14. Ivashko, S.K., Orekhova, V.V., Petukhov, I.G. *Electrometallurgy,* **2019**, *1*, 11-17.
15. Kablov, E.N. *Cast blades of gas turbine engines (alloys, technology, coatings)*, Moscow: MISiS, **2001**.
16. Kachanov, E.B., Schegolev, D.V., Cherkasov, V.V. *Light Alloy Technology,* **2017**, *2*, 66-74.
17. Kahraman, H., Cevik, I., Dündar, F., Ficici, F. *Arabian Journal for Science and Engineering,* **2016**, *41*(5), 1961-1968.
18. Kononov, V.V., Gnatenko, O.V., Gaiduk, S.V., Naumik, V.V. *Engine Engineering Bulletin,* **2013**, *1*, 133-138.
19. Kosmin, A.A., Budinovsky, S.A. *Collection of Reports of the Scientific and Technical Conference*, Moscow, Russian Federation, **2016**, 7.
20. Muboyajyan, S.A., Alexandrov, D.A., Gorlov, D.S. *Aviation Materials and Technologies,* **2012**, *S*, 71-81.
21. Nesterov, V.A., Kukushkin, D.Yu., Kozlov, .P. *Collection of Abstracts of Reports of the XLIV International Youth Scientific Conference*, Moscow, Moscow Aviation Institute, **2018**, 281-282.
22. Pillis, M.F., de Oliveira, M.C.L., Antunes, R.A. *Applied Surface Science,* **2018**, *462*, 344-352.
23. Plankovsky, S.I., Golovin, I.I., Sirenko, F.F. *Aerospace Engineering,* **2013**, *6*(103), 8-14.

Downloaded from www.periodico.tchequimica.com

24. Sentry, M., Bouazza, A., Al-Mahaidi, R., Mahawish, A. *Environmental Geotechnics,* **2018**, *5*(6), 356-370.

25. Shejko, S., Shalomeev, V., Mishchenko, V. *Materials Science and Technology Conference and Exhibition*, **2017**, *1* (2017), 238-244.

26. Shulov, V.A., Engelko, V.I., Gromov, A.N. *Hardening Technologies and Coatings*, **2013**, *11* (107), 15-19.

27. Shulov, V.A., Paykin, A.G., Bytsenko, O.A. *Hardening Technologies and Coatings,* **2010**, *3*, 34-38.

28. Shulov, V.A., Teryaev, D.A., Shirvanyants, G.G. *Russian Journal of Non-Ferrous Metals,* **2015**, *56*(3), 333-338. DOI: 10.3103/S1067821215030190.

29. Terentyev, V.V., Ionov, A.V., Bolkhovitin, M.S. *Russian Engineer*, **2012**, *S5*, 44-47

30. Tishkov, V.V., Firsanov, V.V. *Bulletin of Tula State University. Technical Science Series,* **2011**, *5-1,* 261-266.

31. Zhou, C., Guan, Q. -., Cai, J., Wu, J., Li, C. *Zhongguo Youse Jinshu Xuebao/Chinese Journal of Nonferrous Metals,* **2017**, *27*(9), 1879-1888.

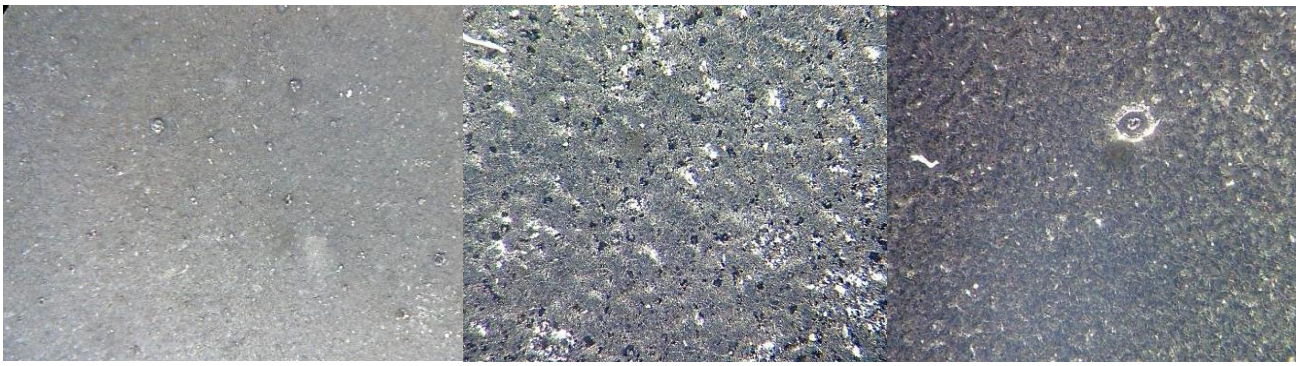

a) *b)* *c)*

Figure 1. *Condition of sample surfaces before SOC testing (x7): a) initial coating; b) modified coating; c) multi-ring crater at the modified coating surface*

Downloaded from www.periodico.tchequimica.com

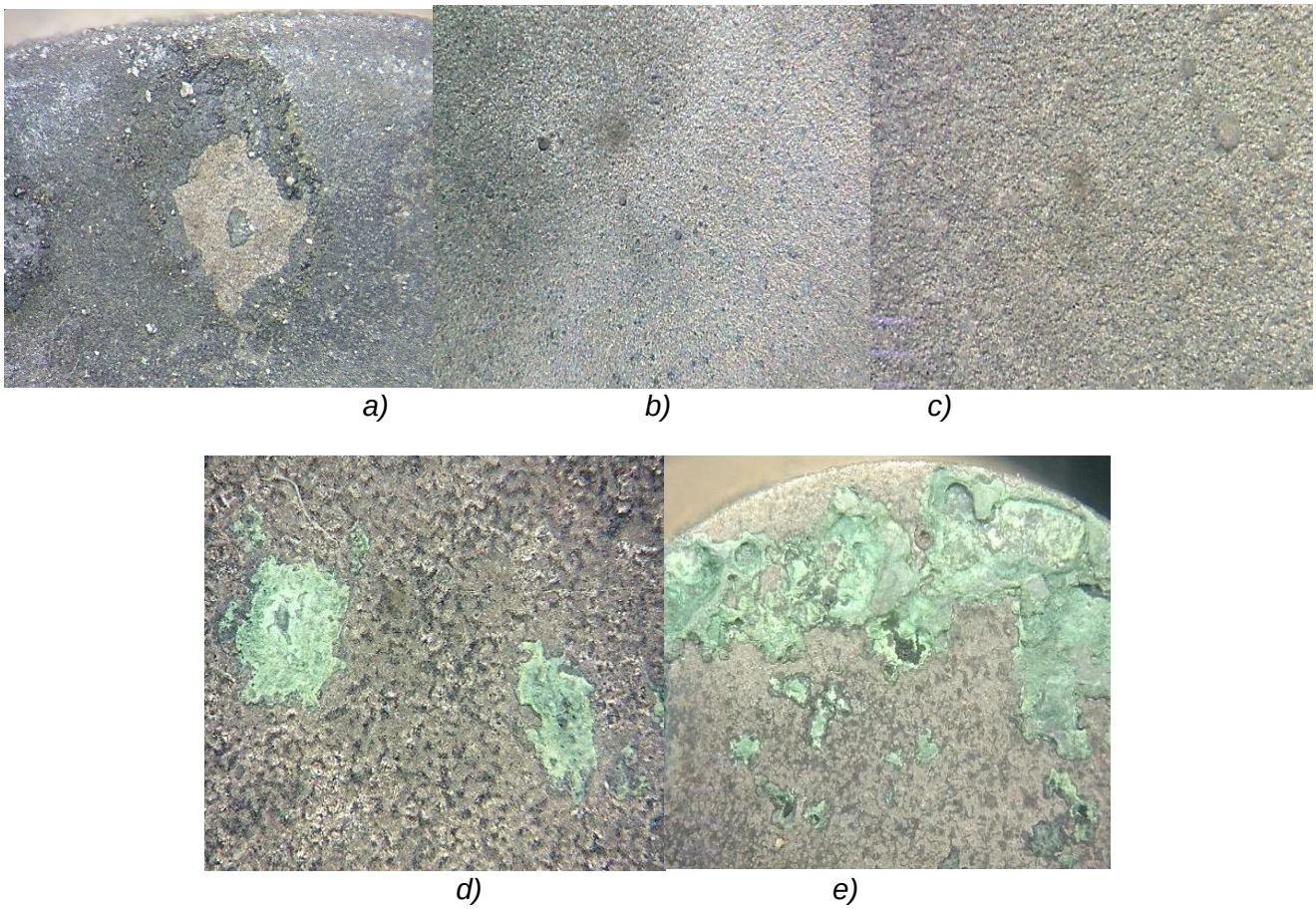

Figure 2. *Condition of sample surfaces after SOC testing (x7): a) initial coating after five cycles of testing; b) defectless modified coating after five cycles of testing; c) defectless modified coating after ten cycles of testing; d) modified coating with defects (sample No15) after one cycle of testing; e) modified coating with defects (sample No 3) after five cycles of testing*

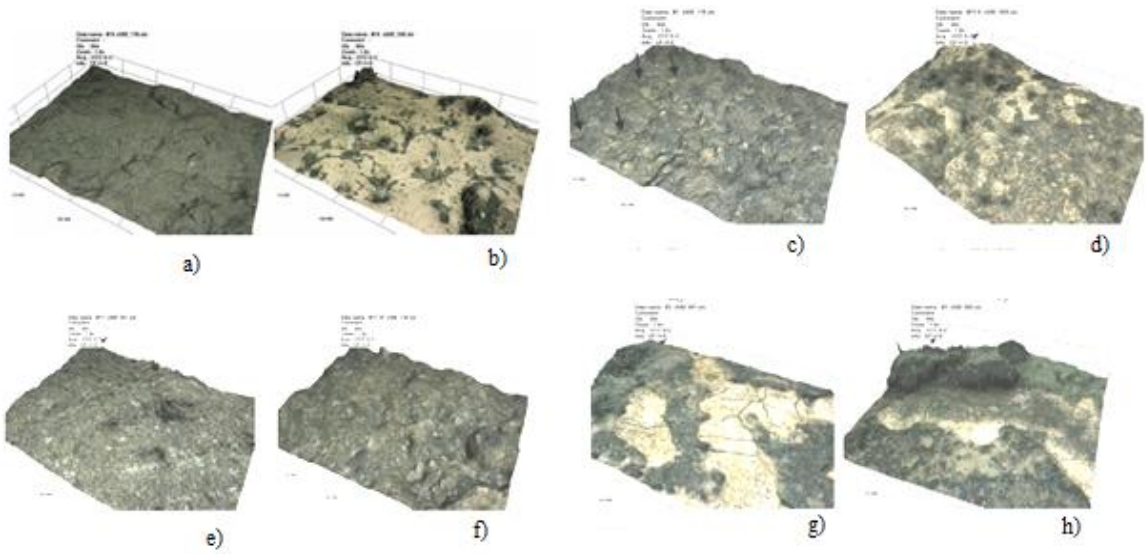

Figure 3. *3D images of sample surfaces (x500): a) unmodified coating in the initial condition; b) defectless modified coating in the initial condition; c) unmodified coating after five cycles of testing; d) defectless modified coating after five cycles of testing; e) unmodified coating after ten cycles of testing; f) defectless modified coating after ten cycles of testing; g) modified coating with defects (sample No3) after five cycles of testing; h) modified coating with defects (sample No15) after five cycles of testing*

Downloaded from www.periodico.tchequimica.com

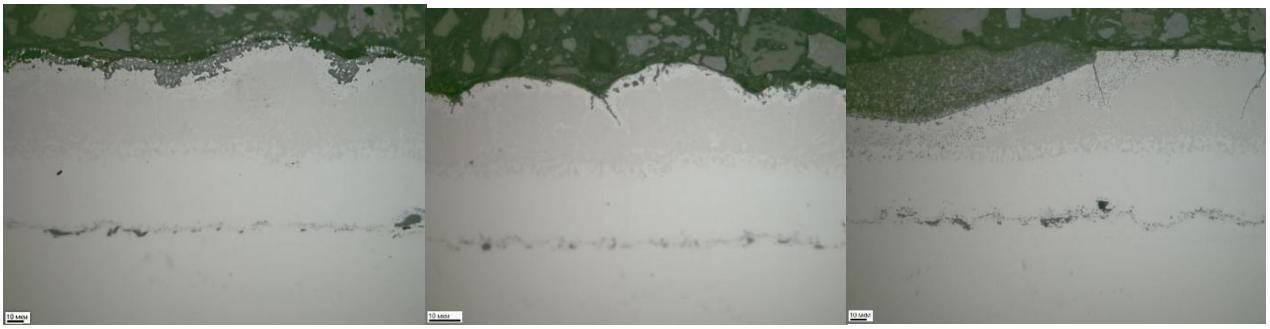

a) b) c)

Figure 4. *Microstructure of surface layer after SOC testing (x200): a) unmodified coating after five cycles of testing; b) defectless modified coating after ten cycles of testing; c) modified coating with defects after five cycles of testing*

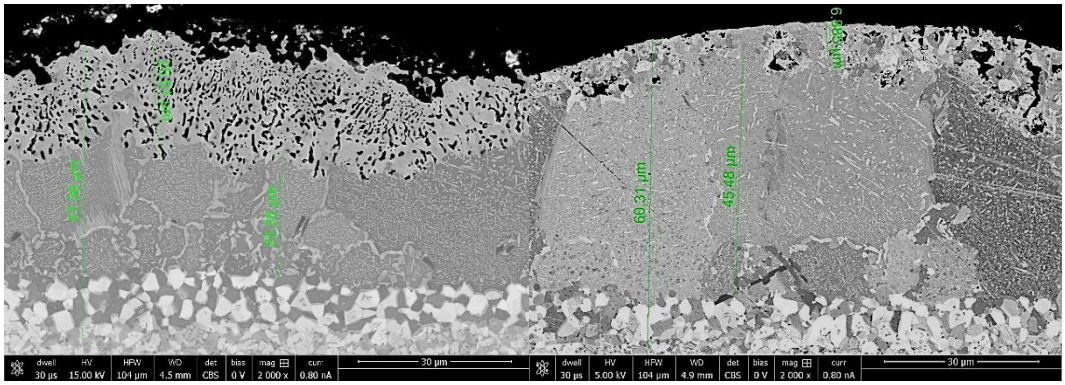

a) b)

Figure 5. *Coating microstructure after SOC testing (x2000): a) unmodified coating after ten cycles of testing; b) defectless modified coating after ten cycles of testing*

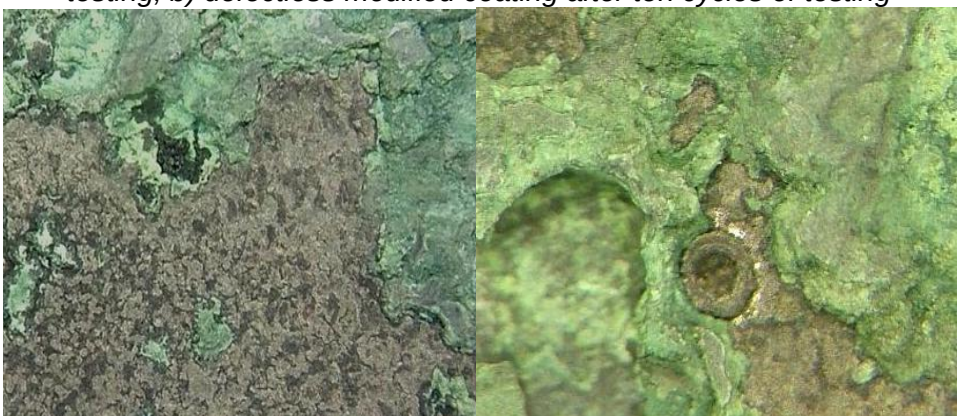

a) b)

Figure 6. *Effect of SOC on the surface of sample with crater-like defects (x20): a) condition of a nick-like crater after five cycles of testing; b) condition of a multi-ring crater after five cycles of testing*

Downloaded from www.periodico.tchequimica.com

PERIÓDICO TCHÊ QUÍMICA
ARTIGO ORIGINAL

DESENVOLVIMENTO E APLICAÇÃO DE UM MÉTODO DE TRIAGEM RÁPIDA PARA DETERMINAÇÃO DE NOVAS SUBSTÂNCIAS PSICOCATIVAS E SEUS METABOLITOS EM URINA

DEVELOPMENT AND APPLICATION OF A RAPID SCREENING METHOD FOR DETERMINATION OF NEW PSYCHOACTIVE SUBSTANCES AND THEIR METABOLITES IN URINE

РАЗРАБОТКА И ПРИМЕНЕНИЕ БЫСТРОГО СКРИНИНГОВОГО МЕТОДА ДЛЯ ОПРЕДЕЛЕНИЯ НОВЫХ ПСИХОАКТИВНЫХ СОЕДИНЕНИЙ И ИХ МЕТАБОЛИТОВ В МОЧЕ

SHESTAKOVA, Kseniia Mikhailovna[1]*; SAVCHUK, Sergey Alexandrovich[2]; MESONZHNIK, Natalia Vladimirovna[3]; KUHARENKO, Alexey Vladimirovich[4]; APPOLONOVA, Svetlana Alexandrovna[5]

[1,2,3,4,5] Institute of Translational Medicine and Biotechnology, I. M. Sechenov First Moscow State Medical

[2] Russian Center of Forensic Medical Expertise.

** Correspondence author*
e-mail: ksenia.shestakova@labworks.ru

Received 06 June 2019; received in revised form 20 September 2019; accepted 21 October 2019

RESUMO

O surgimento contínuo de novas substâncias psicoativas no mercado negro de drogas ilegais, bem como a falta de informações sobre sua influência no corpo humano, enfrenta vários desafios em sua determinação por técnicas analíticas padrão. Além disso, o rápido metabolismo de novas substâncias psicoativas se revela na ausência de possibilidade na identificação de suas estruturas nativas em fluidos biológicos. Este estudo apresenta um novo método de triagem para determinação de 137 substâncias psicoativas, incluindo seus metabólitos. O método 'diluir e disparar' foi escolhido como a técnica preferida de preparação de amostras. e consistiu na diluição 1:5 das amostras de urina com a solução de acetonitrila e água (30:70), seguida de ionização por *eletrospray* - cromatografia líquida - análise em espectrometria de massa em tandem. O método qualitativo desenvolvido foi validado de acordo com os requisitos do Escritório das Nações Unidas sobre Drogas e Crime, que incluíam avaliação de seletividade, limites de detecção, precisão e estabilidade. Além disso, o método apresentado foi testado em 50 amostras de urina positivas certificadas contendo diferentes drogas de abuso. A análise confirmatória foi realizada usando uma abordagem de espectrometria de massa de alta resolução. O método de triagem apresentado oferece a possibilidade de determinação simultânea de canabinóides sintéticos (96), analgésicos opióides (16), estimuladores (13), alucinógenos (5), benzodiazepínicos (5) e medicamentos não classificados (10) durante uma corrida. As avaliações de validação do novo método mostraram altas taxas de especificidade, seletividade, precisão e estabilidade intra e inter-dias, com o limite de detecção variando de 1 a 5 $ng \cdot mL^{-1}$. Ao mesmo tempo, testes de 50 amostras positivas mostraram excelente aplicabilidade do método de triagem desenvolvido para análises preliminares de rotina em laboratórios toxicológicos.

Palavras-chave*: Espectrometria de massa por cromatografia, métodos de triagem, novas substâncias psicoativas.*

ABSTRACT

The ongoing appearance of new psychoactive substances on the black market of illegal drugs, as well as the lack of information on their influence on the human body, faces several challenges in their determination by standard analytical techniques. Moreover, the rapid metabolism of new psychoactive substances reveals in the absence of possibility in the identification of their native structures in biological fluids. This study presents a new screening method for determination 137 psychoactive substances including their metabolites. 'Dilute-and-shoot' method was chosen as the preferable sample preparation technique, and consisted of 1:5 dilution of urine specimens with the solution of acetonitrile and water (30:70) followed by electrospray ionization – liquid

Downloaded from www.periodico.tchequimica.com

chromatography-tandem mass spectrometry analysis. The developed qualitative method was validated according to United Nations Office on Drugs and Crime requirements that included assessment of selectivity, limits of detection, precision, and stability. In addition, the presented method was tested on 50 certified positive urine specimens containing different drugs of abuse. The confirmatory analysis was performed using a high-resolution mass-spectrometry approach. The presented screening method provides the possibility of simultaneous determination of synthetic cannabinoids (96), opioid analgesics (16), stimulators (13), hallucinogens (5), benzodiazepines (5) and non-classified drugs (10) during one run. The validation assessments of the novel method have shown high rates of its specificity, selectivity, intra- and inter-day precision and stability with the limit of detection ranged from 1 to 5 $ng \cdot mL^{-1}$. At the same time, tests of 50 positive samples showed excellent applicability of the developed screening method for routine preliminary screening analysis in toxicological laboratories.

Keywords: *Chromatography-mass spectrometry, screening methods, new psychoactive substances*.

АННОТАЦИЯ

Активное появление новых психоактивных препаратов на черном рынке наркотических средств, а также отсутствие достаточной информации об их влиянии на организм формирует ряд трудностей в их обнаружении рутинно используемыми аналитическими методами. Более того, за счет активного метаболизма психоактивных препраатов определениеих нативных структур в биологических жидкостях становится практически невозможным. Таким образом, в данной работе представлен новый скрининговый метод, направленный на определение 137психоактивных препаратов и их метаболитов.Метод "'Dilute-and-shoot' был выбран как наиболее предпочтительный метод проподготовки. Он заключался в разведении образца в отношении 1:5 смесью ацетонитрил: вода (30:70) с последующим анализомметодом жидкостной хроматографии - тандемной масс-спектрометрии. Разработанный метод был валидирован в соответствии с требованиями Управления ООН по наркотикам и преступности, включающим оценку селективности, предела обнаружения, точности и стабильности Подтверждающий анализ проводился с использованием масс-спектрометрии высокго разрешения. Представленный метод дает возможность одновременного определения синтетических каннабиноидов (96), опиоидных анальгетиков (16), стимуляторов (13), галлюциногенов (5), бензодиазепинов (5) и неклассифицированные соединения (10) во время одного инструментального анализа. Валидация нового метода продемонстрировала высокие уровни специфичности, селективности, точности и стабильности, с диапазоном предела обнаружения 1-5 нг/мл. Помимо этого, апробация на 50 положительных образцах показала отличную практическую значимость разработанного скринингового метода для рутинного предварительного скринингового анализа в токсикологических лабораториях.

Ключевые слова: *Хромато-масс-спектрометрия, скрининговая методика, новые психоактивные вещества.*

1. INTRODUCTION

In recent years drug abuse has become an ongoing global problem mainly because of the yearly emergence of new psychoactive substances (NPS) on the black market of illegal drugs (Simolka *et al.*, 2012). NPS also referred to as "designer drugs" has become a worldwide phenomenon that attracts special attention to scientific and toxicological societies (Grabenauer *et al.,* 2016). Following the United Nations Office on Drugs and Crime (UNODC, 2013), the amount of seized NPS and its recreational use are remarkably growing since 2010th.Currently, more than 800 NPS are under control by the European Monitoring Centre for Drugs and Drug Addiction (EMCDDA), and thus, it has become a common obstacle (UNODC, 2018; Savchuk *et al.*, 2017).

NPS imitate the mechanisms of action of "traditional" illegal drugs showing hallucinogenic (e.g., 1p-LSD, 2C-I), stimulant (e.g., methylon, PVP), sedative (e.g., etizolam, clonazolam) or euphoric (e.g., carfentanyl, 3-methylfentanyl) effects and are usually synthesized by altering chemical structures of the already controlled compounds with minor modifications (Gómez-Ruiz *et al.*, 2007; Savchuk *et al.*, 2017). For this reason, until these substances are not included in the list of prohibited and controlled illegal drugs, they can unpunishably be dispersed all over the world. Usually, they are sold with the trade names "research chemicals", "bath salts" or" exotic

Downloaded from www.periodico.tchequimica.com

incenses".

Generally, the use of blood or saliva as a biological matrix for screening methods of illegal drugs may provide indications of recent exposure and link intoxication to the causative agents (Dresen *et al.*, 2011; Castaneto *et al.*, 2015). Nevertheless, urine is still the most common and applicable matrix in toxicological laboratories due to its non-invasive collection, longer detection time windows, and higher metabolite concentrations (Abdulaziz *et al.*, 2016).

Due to the lack of the appropriate information concerning interactions of NPS with other drugs, as well as their possible impurities and unknown consumed amount of the drug, it is usually challenging to choose the adequate dosage during its illegal consumption (Gurney *et al.*, 2014). Moreover, the higher binding affinity of NPS to receptors (mainly cannabinoid and opioid receptors) compared with one the of traditional drugs, results in a higher severity of the side effects(Keller *et al.*, 2009; Yeakel *et al.*, 2013). As a result, the number of severe intoxications increases that is mostly associated with the need for emergency medical service and occasionally– deaths (Buser *et al.*, 2014; Mir *et al.*, 2011, Centers for Disease Control and Prevention, 2013). At the same time, in several cases, the utilization of NPSs for medical purposes is legal, while its non-medical usage is under specific control almost all over the world.

The still increasing appearance of NPS on the black market and number of overdose cases urges scientists to the creation of fast, accurate, and sensible methodologies for the precise determination of the NPS along with traditional drugs of abuse. Moreover, rapid appearance and variety of physic-chemical properties of each NPS cause several difficulties in their determination in biological matrixes during forensic and toxicological investigations. Therefore, it is needed to develop fast, selective, and sensitive approaches.

Analytical methods routinely used in toxicological laboratories are mainly focused on the determination of parent compounds. At the same time, the main issue in the identification of synthetic NPS, especially synthetic cannabinoids, is their fast metabolism resulting in the fact that most of the native compounds could not be detected in commonly used matrixes, even after first minutes of its consumption (Tyrkko *et al.*, 2013).

For this reason, it is needed to develop a screening method that will cover the preliminary determination of the most spread illegal drugs, including NPS, together with their primary active metabolites.

Chromatographic separation methods, coupled with mass-spectrometric determination techniques, are commonly applied in different toxicological studies providing high rates of sensitivity, selectivity, and specificity (Ibáñez *et al.*, 2013). Until recently, the most preferred mass-spectrometric approaches in terms of routine toxicological analysis were GC-MS methods (Tsujikawa *et al.*, 2014). However, GC-MS is usually time consuming and in most cases, requires steps of extraction and derivatization. For this reason, fast dilute-and-shoot LC-MS/MS screening methods have become the most prevalent techniques usually used for preliminary screening analysis (Xu *et al.*, 2007; Aszyk *et al.*, 2016; Wu *et al.*, 2012). During the last several years, many methods for illegal drug screening have been published. Table 1 represents comparison between last released screening methods with various sample preparation and instrumental approaches.

Thus, this study aimed to develop a fast LC-MS/MS qualitative screening method for the determination of 137 psychoactive substances and their metabolites, including the most popular NPS, in the urine. The method was approved on 50 confirmed positive samples providing high levels of sensitivity and detectability, along with short and simple sample preparation.

2. MATERIALS AND METHODS

2.1. Chemicals

Chemicals were purchased from LGC standards, Cayman Chemical and Sigma-Aldrich. All utilized solvents were of HPLC grade. Acetonitrile, formic acid, and methanol were purchased from Merk (USA).

2.2. Biological material

Urine samples from 50 positive drug users were obtained from cases investigated in the certified toxicological laboratories and were verified by gas chromatography with electron impact mass spectrometry (GC-MS-EI) and UPLC-Q-TOF (information not presented). Drug-free blank urine samples for the development and validation of the method were collected from region specimen banks and were confirmed not to

Downloaded from www.periodico.tchequimica.com

have any drugs of abuse. The certified urine with the quantified amount of the screened drugs was purchased from the WHO UNODC professional blind tests.

2.3. Specimen procedure

The dilute-and-shoot method for the developed screening procedure was as follows:100 µl of urine was transferred to a plastic 1.5 ml Eppendorf vial with the following addition of 150 µl of a mixture containing acetontrile:water (70:30). The resulted solution was after vortexed for 15 seconds and centrifuged 5 min at 15000 rpm. After 40 µl of supernatant was transferred to a new vial with the addition of 60 µl of *Milli-Q® ultrapure water*, vortexed, and transferred to a vial for LC-MS analysis.

2.4. Chromatographic and mass-spectrometric conditions

The LC-MS analysis was conducted using the UPLC ACQUITY system connected to a Xevo TQ-S micro IVD System (Waters Corporation, USA) with an electrospray source operated in positive and negative ion ionization mode. The separation was achieved using chromatographic column Acclaim RSLC 120 AC18, 2.2 µm, 100×2.1mm equipped with guarding column: Acquity UPLC® BEH C18, 5.0×2.1 mm (Waters Inc. USA) maintained at 40°C. Mobile phases consisted of 0.1% formic acid in water with the addition of 2 mM ammonia formate and 1% of acetonitrile (mobile phase A) and 0.1% formic acid in acetonitrile with the addition of 2 mM ammonia formate and 1% of water (mobile phase B). The flow rate was 0.5 ml/min with elution gradient program as follows: 0 min - 1% B, 1 min - 1% B, 8 min - 99% B, 9 min - 99% B, 9 min -99%B, 9.1 min - 1% B, 10.99 min - 1% B, 11 min - 1% B. The total run time was 11 minutes. Ions were registered in both positive and negative ionization in the Selected Reaction Monitoring (SRM) mode by monitoring precursor ions and its two fragment-ions. The mass detector parameters were as follows: cone voltage – 25V,desolvation gas flow rate - 1000 L/h, source temperature – 148°C, desolation gas temperature – 600°C, capillary voltage - 2000V. The equipment maintenance and data analysis were performed using Mass Lynx V4.2.

2.5. Validation

Validation of the presented qualitative screening method was performed according to the UNODC requirements for validation of analytical methods for testing of illegal drugs (UNODC, 2009).

The full qualitative validation procedure was undertaken for 12 drugs of abuse related to different classes of controlled drugs (synthetic cannabinoids, opioids, phenylamines, benzodiazepines). The validation assessment consisted of estimation of selectivity, limits of detection (LOD), precision, and stability of the developed screening method. For the selectivity study, the drug-free blank urine samples collected from health individuals were analyzed in three replicates and were compared to the analyzed three replicates of QC samples, which contained compounds being under validation. Further, there were calculated relative standard deviations of analyzed compounds that did not exceed 15% and 20% in the extreme points, respectively. The precision of the developed method was conducted by analyzing the reproducibility of the received results based on 5 repeated analyses of spiked samples at three concentration levels: lowest (5 ng/ml), medium (50 ng/ml) and highest (150 ng/ml). The stability study was undertaken to assess the stability of the analytes during short andlong-term storage. For this purpose, there were conducted comparison analyses of samples right after its sample preparation, in 72 hours of its storage at +4°C.

2.6. Testing on real positive samples

The method was tested on 50 confirmed positive urine samples. For this purpose, urine samples were provided by toxicological laboratories from different regions of the Russian Federation for round multicentral comparative studies. All provided samples were confirmed and reported before to be positive by means of employing traditional gas-chromatography mass-spectrometry methods.

2.7. Confirmatory high resolution LC-MS method

The confirmatory analysis was performed using UHPLC-QTOF-MS, contained Bruker Elute liquid chromatography coupled to high-resolution quadruple time-of-flight mass-spectrometer. Chromatographic separation was performed using ACQUITY UPLC BEH C18 (100 x 2.1 mm) (BRU-18C182-100 mm). Temperatures of the column and autosampler were maintained at 40 °C and 4 °C, respectively. Mobile phase A contained 1% of Methanol in water with the addition of 5 mM ammonia formate in 0.1% formic acid, while Mobile phase B consisted of methanol with five mM ammonia formate in 0.1% formic acid. The flow rate was 0.2 ml/min. The gradient elution was

Downloaded from www.periodico.tchequimica.com

as follows: 0 min - 1% B, 1 min - 1% B, 8 min - 99% B, 9 min - 99% B, 9 min -99%B, 9.1 min - 1% B, 10.99 min - 1% B, 11 min - 1% B. Ionization was performed in a positive electrospray mode with m/z range 30-1000 m/z. ESI source parameters were: capillary voltage - 4500V; N_2 temperature 220 °C with flow rate 8 l/min and collision energy - 7eV.

3. RESULTS AND DISCUSSION

The presented screening LC-MS/MS method was developed for the determination of 137 illegal drugs, including "traditional illegal drugs" (such as amphetamines or 'marihuana'), NPSs, and their main active metabolites. In many cases, NPS is abused together with traditional drugs of abuse. Therefore, the goal of this study was to establish a method that covers different classes of the most spread drugs of abuse. As a result, the developed screening method allows the opportunity for simultaneous determination of synthetic cannabinoids (88), opioid analgesics (16), stimulators (13), hallucinogens (5), benzodiazepines (5) and non-classified drugs (10) during one LC-MS run (Table 2).

3.1. Optimization of the instrumental methods

Optimization of the separation conditions is one of the critical steps in the development of screening methods. It serves for the identification of all analyzed analytes by separation of their isomers, elimination interfering signals, and certifying elution of all compounds of interest within the selected gradient. Moreover, chromatographic optimization may serve for the establishment of the retention time for all screened compounds that result in in narrow and symmetrical peaks of each analyte. Due to the big difference in the chemical nature of the screened compounds, in the presented study, it was considered to use the C18 phase column, which, to our knowledge, is one of the most optimal stationary phases commonly used for the routine toxicological analysis. To provide appropriate conditions for protonation of basic groups in several NPS it is more common to use buffers with acidic pH. Optimization of the mobile phase composition for HPLC systems plays a key role in the quality of chromatographic separation. Thus, in this study there were tested several components of mobile phase B, such as: pure acetonitrile; acetonitrile + 0.1% formic acid; acetonitrile + 2mM ammonium formate + 0.1% formic acid; acetonitrile + 2mM ammonium formate + 1% water + 0.1% formic acid; pure methanol. The utilization of pure acetonitrile or methanol by itself, as well as with the addition of 1% water, gave good and intensive peaks for only neutral or weakly acidic analytes. At the same time, the addition of organic modifiers (such as 2mM ammonia formate) increased the sensitivity for mostly all of the screened compounds.

Therefore, according to the received results it was found out that the best separation of all analytes presented in the method (at the low signal-to-noise ratio and high rates of sensitivity and resolution) could be achieved using following mobile phases: phase A – deionized water + 0.1% formic acid + 2mM ammonia formate + 1% acetonitrile; phase B – acetonitrile + 0.1% formic acid + 2mM ammonia formate + 1% distillated water.

Besides that, to increase sensitivity in the determination of NPS, the maintenance of mass-spectrometry optic and fragmentation conditions of parent ions was conducted. For this reason, there were analyzed certified urine samples containing morphine in the concentration of 0.1 µg/ml. Cone voltages and collision energies were optimized.

For the following optimization step of the study, there were determined main MRM transitions of each compound. Using Masslynx software, at least two MRM transitions were selected for each of the analytes. Ionization was performed using ESI, maintained in both positive and negative mode. Negative ESI provided better detectability for the acid derivatives. Optimized MRM transitions and collision energies for positive and negative ESI are presented in Tables3 and 4, respectively.

3.2. Optimization of the sample preparation step

The assessment of linearity and sensitivity of the optimized LC-MS conditions demonstrated good results that allowed performing the following optimization of the sample preparation method. 'Dilute-and-shoot' was chosen to be the method of choice for our preliminary screening method as it is the most rapid technique, as well as provides fewer chances of loosing target compounds (as could be present while using solid-phase or liquid-liquid extractions). To find out the appropriate conditions for the 'Dilute-and-shoot' method, to 100 µl of the certified urine, containing Morphine (in concentration 100 ng/ml), there were added different solvent solutions: Pure acetonitrile, Acetonitrile (AcN):water (H_2O) (7:1); 150 µl of the mixture AcN : H_2O with consequent addition of 60 µl of H_2O to the 40 µl of the initial mixture.

Downloaded from www.periodico.tchequimica.com

It was found out that the third approach was the most optimal for the NPS screening, since the addition of water obstructs the elution of the substance in the form of two peaks, while the presence of the organic phase contributes to the sensitivity of the target analytes signals.

3.3. Validation

Validation was performed for 12 selected compounds related to the most spread classes of prohibited substances and was aimed to confirm that the method was satisfied for the determination of leading groups of illegal drugs. The method proved to be selective and specific for the tested compounds by the analysis of blank urine samples that showed the absence of any interfering signals. At the same time, analysis of the quality control solutions at the concentration equal to 5 ng/ml provided purity of all received signals, regarded to analyzed compounds. The precision assessment was performed by analyzing the reproducibility of signals received from analysis at three concentration levels: 5 ng/ml, 50 ng/ml, and 150 ng/ml.

After three repeats of the analysis at each concentration level, the relative standard deviation of the received signals was not more than 15% at high concentrations and 20% – at low concentrations. The received LODs of all analyzed compounds were between the limit of 0.5-10 ng/ml. Furthermore, the already prepared samples were stable during long-term storage for 72 hours at +4°C, by calculating relative standard deviations (RSDs) of the signals immediately after preparation of the samples, in 72 hours. The signals at each time-point remained approximately unchanged (RSD < 15%) that proved the stability of the analyzed substances (Table 5).

The selected gradient program was established in the way that it could separate the main components of the method. The presented method includes 350 MRM transitions with the respected cycle of 0.015 seconds for each compound.

3.4. Application of the method on real positive samples

Real urine samples that contained markers of drug abuse were obtained from different authorized toxicological laboratories. All samples were before examined to be positive using complex routine methods, usually utilized in forensic laboratories. Thus, the method was tested on 50 proved positive cases, associated with the presence of NPS and traditional drugs of abuse (Table 6).

It should be noted that most of the synthetic cannabinoids, were not identified in their native structures, but were presented in the form of its leading derivatives, mostly carboxylic moieties, produced by the expense of losing methoxy-, amide- or adamantyl- groups. Alternately, most of the synthetic cathinones were detected predominately in their native forms. Notably, not all compounds, determined by GC-MS, were identified by the developed approach. This fact could be associated with the absence of preliminary extraction and extremely low concentration of the analyzed compounds.

An example of one of the positive samples is presented in Figure 1. It includes chromatograms received using the developed preliminary screening method as well as the results of a confirmatory analysis performed using high resolution mass-spectrometry (as described in 2.8).

The results of the application of the method showed that the developed approach might find practical applications for clinical purposes. The constant rise of new "designer drugs" poses a critical issue due to the difficulties in their determination using preexisting analytical methods. As a result, the full extent of the effects of these new drugs on body is unknown. Moreover, such limitations are critical in the identification of appropriate detoxification methods and consequent therapy during overdoses. Most NPS quickly metabolize, and so, it is usually impossible to determine the parent structures of these drugs. Therefore, investigations of NPS metabolism should be conducted to evaluate the main biomarkers of illegal drug consumptions. Compared to “traditional narcotics”, NPSs have a higher potency, and extremely low concentrations are consumed. Consequently, highly sensitive analytical methods should be developed to determine the NPS metabolites. Here, a proposed 'dilute-and-shoot' shoot method is rapid, showing high sensitivity with a total sample preparation time of one specimen about 5 minutes. The developed approach makes it possible to determine the main drugs of abuse including NPS and their metabolites within 15 minutes, being a perfect approach for preliminary drug analysis.

.

4. CONCLUSIONS:

A novel methodology was developed, a sensitive and fast LC-MS/MS method for the determination of 137 illegal drugs, including NPS

Downloaded from www.periodico.tchequimica.com

and their metabolites in urine. The presented method gives the possibility for the determination of parent substances, as phase I and phase II metabolites. The developed approach provided excellent performance in terms of turnaround, selectivity, and sensitivity. The utilization of a diluting-shoot sample preparation technique resulted in the establishment of a rapid approach with a total run-time of about 15 minutes. Moreover, the developed method could potentially be utilized for preliminary screening purposes in chemical toxicological laboratories being easily transformed between different LC-MS/MS instruments.

5. ACKNOWLEDGMENTS:

The study was supported by the Russian Academic Excellence Project 5-100.

6. REFERENCES

1. Simolka, K., Lindigkeit, R., Schiebel, H.M., Papke, U., Ernst, L., Beuerle, T. *Anal. and Bioanal. Chem.*, **2012**, *404(1)*, 157-171.
2. Grabenauer, M., Moore, K. N., Brian, F. Final Summary Overview. **2016**
3. UNODC.*https://www.unodc.org/documents/scientific/Global_Smart_Update_2018,* **2018,** *19.*
4. Savchuk, S., Appolonova, S., Pechnikov, A., Rizvanova, L., Shestakova, K. *Forensic Toxicol.*, **2017**, *3,* 359-368.
5. Gomez-Ruiz, M., Hernandez, M., de Miguel, R., Ramos, *J. Mol. neurobiol.*, **2007**, *36(1),* 3-14.
6. Dresen, S., Kneisel, S., Weinmann, W., Zimmermann, R., Auwarter, V. *J Mass Spectrom.*, **2011**, *46(2),* 163-71.
7. Castaneto, M. S., Wohlfarth, A., Desrosiers, N. A., Hartman, R. L., Gorelick, D. A., Huestis, M. A. *Drug Metab. Rev.*, **2015,** *47(2),* 124-174.
8. Aldlgan, A.A., Torrance, H.J. *TrAC Trends in Analytical Chemistry*, **2016**, *80*, 444-457.
9. Gurney, S.M., Scott, K., Kacinko, S., Presley, B., Logan, B. *Forensic Sci. Rev.,* **2014***, 26,* 53–78.
10. Keller, T., Keller, A., Tutsch-Bauer, E., Monticelli, F. *Leg. Med. (Tokyo)*, **2009**, *11,* 98-9.
11. Yeakel, J.K., B.K. Logan. *J. Anal. Toxicol.*, **2013**, *37(8),* 547-51.
12. Buser, G. L., Gerona, R. R., Horowitz, B. Z., Vian, K. P., Troxell, M. L., Hendrickson, R. G. *Clin. Toxicol. (Phila)*, **2014**, *52(7),* 664-73.
13. Mir, A., Obafemi, A., Young, A., Kane, C. *Pediatrics*, **2011**, *128(6),*1622-7.
14. Murphy, T.D., Weidenbach, K.N., Van Houten, C., Gerona, R.R., Moran, J.H., Kirschner, R.I., Marraffa, J.M., Stork, C.M., Birkhead, G.S., Newman, A., Hendrickson, R. *MMWR.*, **2013,** *62(6)*, 93.
15. Tyrkko, E., Pelander, A., Ketola, R., Ojanpera, I. *Anal. Bioanal. Chem.*, **2013**, *405,* 6697–6709.
16. Ibáñez, M., Bijlsma, L., Nuijs, ALN, Sancho, J.V., Haro, G., Covaci, A., Hernández, F. *J. Mass Spectrom.*, **2013**, *48,* 685–694.
17. Tsujikawa, K., Yamamuro, T., Kuwayama, K., Kanamori, T., Iwata, Y.T., Inoue, H. *Forensic Toxicology*, **2014**, *32*(2), 201-207.
18. Xu, R.N., Fan, L., Rieser, M.J. and El-Shourbagy, T.A. *J. of Pharm. and Biomed. Anal.*, **2007,** *44*(2), 342-355.
19. Aszyk, J., Kot-Wasik, A. *Monatsh. Chem*, **2016**, *147,* 1407–1414.
20. Wu, A. Hb., Gerona, R., Armenian, P., French, D., Petrie, M., Lynch, K. L. *Clinical Toxicology*, **2012**, *50(8),* 733-742.
21. Ambach, L., Hernández Redondo, A., König, S., Weinmann, W. *Drug Test Anal.,* **2014**, *6(4),* 367-75.
22. Ambach, L., Redondo, A.H., König, S., Angerer, V., Schürch, S., Weinmann, W. *Bioanalysis,* **2015**, *7(9),* 1119-36.
23. Beck, O., Rausberg, L., Al-Saffar, Y., Villen, T., Karlsson, L., Hansson, T., Helander, A.. *Drug Test Anal.,* **2014***, 6(5),* 492-9.
24. Tang, M.H., Ching, C.K., Lee, C.Y., Lam, Y.H., Mak, T.W. *J Chromatogr B Analyt Technol Biomed Life Sci.,* **2014**, *969,* 272-84.
25. Shin, M., Ji, D., Kang, S., Yang, W., Choi, H., Lee, S. *Arch. Pharm.,* **2014**, *37(6),* 760-72.
26. Verplaetse, R., Decabooter, S. Cuypers, E. *J. of Forensic Toxicol. and Pharmacol.,* **2013** (Doctoral dissertation, Cleveland State University).
27. Kozak, M., Rezai, T., *Thermo fisher application note.* **2018**, *449.*
28. Fagiola, M., Hahn, T., Avella, J. *J. Anal. Toxicol.,* **2018**, *1; 42(8),* 562-569.
29. Al-Saffar, Y., Stephanson, N.N ., Beck, O. *J Chromatogr. B Analyt. Technol. Biomed. Life Sci.*, **2013**, *930,* 112-20.
30. UNODC. **2009**. Available at <https://www.unodc.org/documents/about-unodc/AR09_LORES.pdf>. Access 20 october, 2019.

Downloaded from www.periodico.tchequimica.com

Table 1. *Description of screening methods with various sample preparation and instrumental approach*

Analyzed compounds	Sample preparation	Instrumental analysis	Ref.
Screening of 64 NPS in Dry Blood spots (DPS) phenethylamines cathinones piperazines tryptamines	1.10 µl of blood pipetted onto the DBS, diffused and dried for 3 hours; 2. DBS were punched and collected in the Eppendorf tube; 3. Extraction: +500 µl MeOH + 10 µl IS; vortex (15 min); 4. Supernatant + 10 µl 0.25% HCl MeOH and reconstitution in 100 µl of H_2O	RP-LC-MS/MS Run time – 10 min Scheduled multiple reaction monitoring (sMRM)	(Ambach *et al.*, 2013)
Quantitative analysis of 56 NPS in whole blood and urine Stimulant and hallucinogenic NPS (piperazines, tryptamines, amphetamines, cathinones)	Blood samples: SPE at PH 6, elution by Rapid and simple LC-MS/MS screening of 64 novel psychoactive substances using dried blood spots. Urine samples: LLE in 0.1M NaOH with ethyl acetate	LC-MS/MS ESI(+) sMRM	(Ambach *et al.*, 2015)
Determination of 40 NPS and 4 their metabolites Piperazines (8) Amphetamines (4) Synthetic cathinones (28) and related metabolites (4)	Urine SPE on cation exchange extraction (SOLA SCX); Elution with 2% NH4OH in dichloromethane/2-propanol (95:5, v/v).	LC-HRMS Screening and confirmation - in full scan and data dependent MS^2.	(Beck *et al.,* 2014)
93 drugs of abuse and their metabolites 47 convential metabolites (28 parents and 19 metabolites) 46 NPS (44 parent drugs and 2 metabolites)	Urine SPE pH 6. SPE cartridges (Waters Oasis MCX, 3 cc, 60 mg)	UHPLC-MS/MS ESI (+/-) MRM	(Tang *et al.,* 2014)
35 drugs of abuse and metabolites: Amphetamines (7); THC-COOH; Opiates (6); Cocainics (3); Benzodiazepines (16); others (2)	SPE (pH 5) using the Bond ElutPlexa PCX column Elution with chloroform–isopropyl alcohol (80:20) and 3 ml chloroform–isopropyl alcohol–ammonium hydroxide (80:20:3)	LC/MS/MS ESI (+/-)	(Shin *et al.,* 2014)
414 compounds of illegal drugs	Protein precipitation with acetonitrile and 5-fold dilution	LC-MS/MS sMRM-IDA-EPI	(Verplaetse*et al.,* 2013)
	Urine and plasma SPE 9 Thermo Scientific Hypersep Verify CX 200 mg mixed mode cartridges	LC-MS/MS	(Kozak *et al.,* 2018)
50 NPS in postmortem samples (region, blood, and urine)	whole blood or urine LLE at Ph>9 with 70:30 *n*-butyl chloride:ethyl acetate	LC-MS/MS	(Fagiola*et al.*,2018)
26 “legal highs”	Urine five-fold dilution	LC-MS/MS ESI (+)	(Al-Saffar *et al.*, 2013)

Table 2. *List of the compounds included in the developed screening method with their chemical names, brutto-formulas collision energies (positive ESI mode)*

Synthetic cannabinoids				
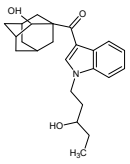	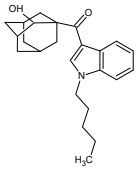	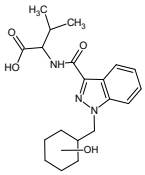	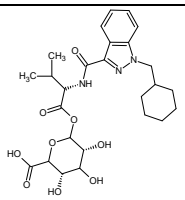	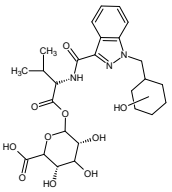
AB–001 M1 (diHydroxylation)	AB–001 M2 (Hydroxylation)	AB–CHMINACA M1 (Carboxylation, hydroxylation of deaminated moity)	AB–CHMINACA M2 (Carboxylation, Glucuronidation)	AB–CHMINACA M3 (Carboxylation, Hydroxylation, Glucuronidation)
$C_{24}H_{31}NO_3$ 381.5078	$C_{24}H_{31}NO_2$ 365.5084	$C_{20}H_{27}N_3O_4$ 373.4461	$C_{26}H_{35}N_3O_9$ 533.5708	$C_{26}H_{35}N_3O_{10}$ 549.5702
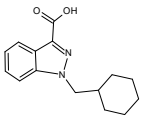	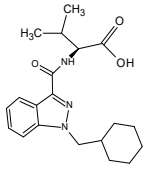	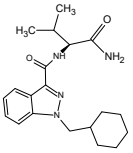	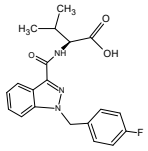	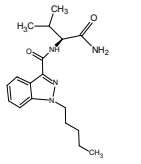
AB–CHMINACA M4 (Carboxylation, Hydrolysis of amide)	AB–CHMINACA M5 (Carboxylation)	AB–CHMINACA	AB–FUBINACA M1 (Carboxylation)	AB–PINACA
$C_{15}H_{18}N_2O_2$ 258.1368	$C_{20}H_{27}N_3O_3$ 357.4467	$C_{20}H_{28}N_4O_2$ 356.4692	$C_{20}H_{20}FN_3O_3$ 369.3895	$C_{18}H_{26}N_4O_2$ 330.4246
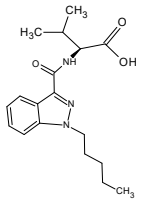	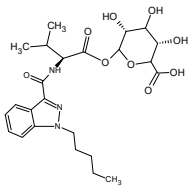	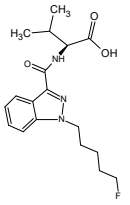	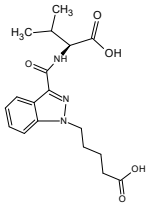	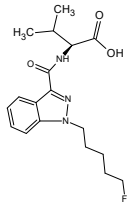
AB–PINACA M1 (Carboxylation)	AB–PINACA M2 (Amide hydrolysis, Glucuronidation)	AB–PINACA–F M1 (Carboxylation)	AB–PINACA–F M2(Oxidative defluorination, amide hydrolysis)	AB–PINACA–F M3 (dicarboxylation, Glucuronidation)
$C_{18}H_{26}N_3O_3$ 331.4094	$C_{24}H_{34}N_3O_9$ 507.5335	$C_{18}H_{24}FN_3O_3$ 349.3998	$C_{18}H_{23}N_3O_5$ 361.3923	$C_{24}H_{31}N_3O_{11}$ 537.5164
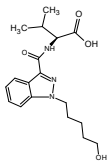	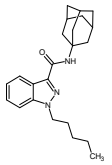	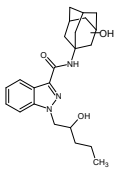	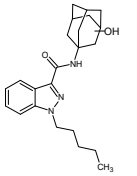	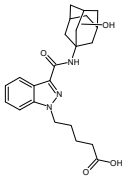
AB–PINACA–F M4 (Defluorination, amide hydrolysis)	AKB–48	AKB–48 M1 (Dihydroxylation)	AKB–48 M2 (Hydroxylation)	AKB–48 M3 (Hydroxylation, Carboxylation)
$C_{18}H_{25}N_3O_4$ 347,4088	$C_{23}H_{31}N_3O$ 365.5117	$C_{23}H_{31}N_3O_3$ 397.5105	$C_{23}H_{31}N_3O_2$ 381.5111	$C_{23}H_{29}N_3O_4$ 411.4941
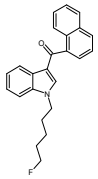	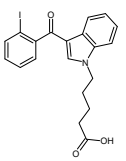	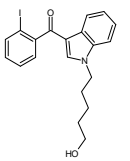	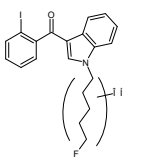	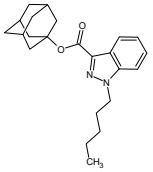
AM–2201	AM–694 M1 (Defluorinization Carboxylation)	AM–694 M2 (Defluorinization Hydroxylation)	AM–694 M3 (Hydroxylation)	APINAC

Downloaded from www.periodico.tchequimica.com

$C_{24}H_{22}FNO$
359.4360

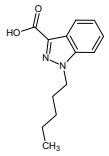

APINAC M1 (Carboxylation)

$C_{13}H_{16}N_2O_2$
232.2783

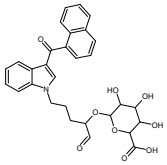

JWH –018 M1 (Carboxylation, Glu)

$C_{30}H_{29}NO_9$
547.5526

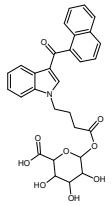

JWH–073 M2 (Carboxylation, Glu)

$C_{29}H_{27}NO_9$
533.5260

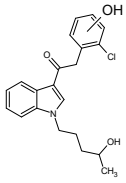

JWH–203 M3 Dihydroxylation

$C_{21}H_{22}ClNO_2$
371.8673

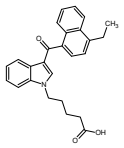

JWH–210 M3 (Carboxylation)

$C_{26}H_{25}NO_3$
399.4816

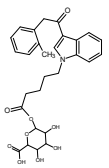

JWH–251 M2 (Carboxylation, Glu)

$C_{20}H_{18}INO_3$
447.2663

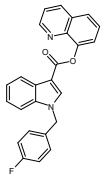

FUB–PB22

$C_{25}H_{17}FN_2O_2$
396.4131

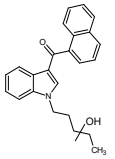

JWH –018 M2 (Hydroxylation)

$C_{24}H_{23}NO_2$
357.4450

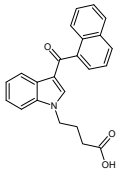

JWH–073 M3 (Carboxylation)

$C_{23}H_{19}NO_3$
357.4019

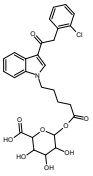

JWH–203 M4 (Carboxlation, glu)

$C_{27}H_{28}ClNO_9$
545.9655

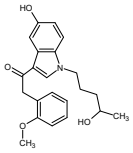

JWH–250 M1 Dihydroxylation

$C_{22}H_{25}NO_4$
367.4382

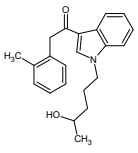

JWH–251 M3 (Hydroxylation)

$C_{20}H_{20}INO_2$
433.2828

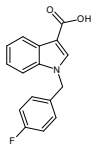

FUB–PB22 M1 (Carboxylation)

$C_{16}H_{12}NO_2F$
269.2704

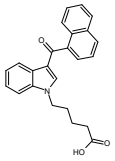

JWH –018 M3 (Carboxylation)

$C_{24}H_{21}NO_3$
371.4284

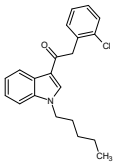

JWH–203

$C_{21}H_{22}ClNO$
339.8585

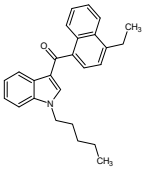

JWH–210

$C_{26}H_{27}NO$
369.4987

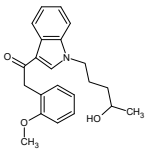

JWH–250 M2 (Hydroxylation)

$C_{22}H_{25}NO_3$
351.4388

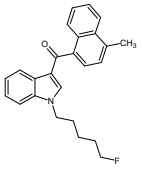

MAM–2201

$C_{20}H_{19}IFNO_2$
451.2732

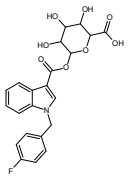

FUB–PB22 (Carboxylation, Glu)

$C_{22}H_{20}FNO_8$
445.3945

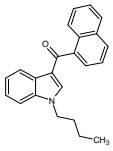

JWH–073

$C_{23}H_{21}NO$
327.4189

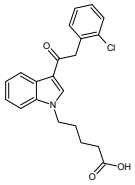

JWH–203 M1 (Carboxylation)

$C_{21}H_{20}ClNO_3$
369.8414

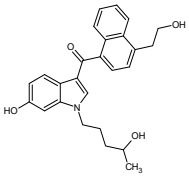

JWH–210 M1 (Trihydroxylation)

$C_{26}H_{27}NO_4$
417.4969

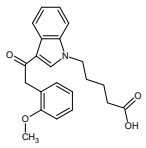

JWH-250 M3 (Carboxylation)

$C_{22}H_{23}NO_4$
365.4223

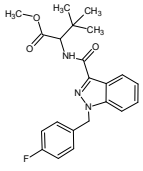

MDMB(N)–Bz–F

$C_{23}H_{30}N_2O_2$
366.4965

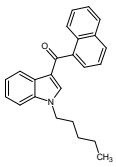

JWH–018

$C_{24}H_{23}NO$
341.4455

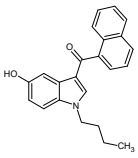

JWH–073 M1 (Hydroxylation at indazole)

$C_{23}H_{21}NO_2$
343.4183

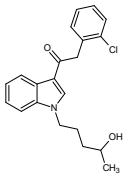

JWH–203 M2(4-pentyl hydroxylation)

$C_{21}H_{22}ClNO_2$
355.8579

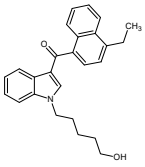

JWH–210 M2 (Hydroxylation)

$C_{26}H_{27}NO_2$
385.4981

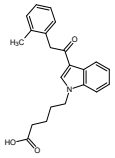

JWH–251 M1 (Carboxylation)

$C_{22}H_{23}NO_3$
349.4223

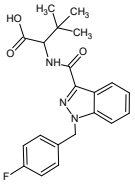

MDMB (N)–Bz–F M1 (Carboxylation)

Downloaded from www.periodico.tchequimica.com

$C_{28}H_{31}NO_9$ 525.5470 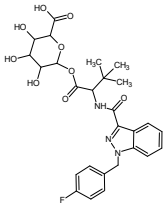 MDMB (N)–Bz–F M2 (Carboxylation, Glu)	$C_{22}H_{25}NO_2$ 335.4394 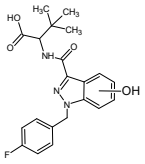 MDMB (N)–Bz–F M3 (indazole Hydroxylation)	$C_{25}H_{24}FNO$ 373.4626 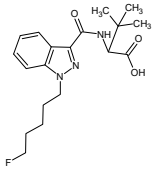 MDMB(N)–2201 M1 (Carboxylation)	$C_{22}H_{24}FN_3O_3$ 397.4427 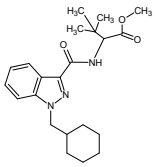 MDMB–CHMINACA	$C_{21}H_{23}FN_3O_3$ 383.4161 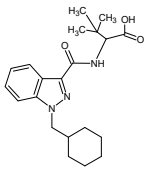 MDMB–CHMINACA M1 (Carboxylation)
$C_{27}H_{31}FN_3O_9$ 559.5402 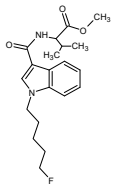 MMB–2201	$C_{21}H_{23}FN_3O_4$ 399.4155 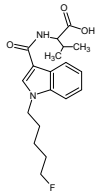 MMB–2201 M1 (Carboxylation)	$C_{19}H_{26}FN_3O_3$ 363.4264 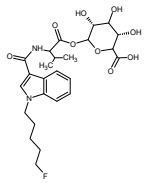 MMB–2201 M2 (Carboxylation, glu)	$C_{22}H_{31}N_3O_3$ 385.4998 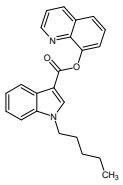 PB–22	$C_{21}H_{29}N_3O_3$ 371,4732 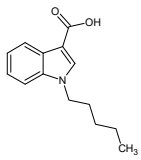 PB–22 M1 (Carboxylation, Ester hydrolysis)
$C_{20}H_{27}FN_2O_3$ 362.4384 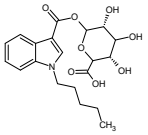 PB–22 M2 (Carboxylation, Glu)	$C_{19}H_{25}FN_2O_3$ 348.4118 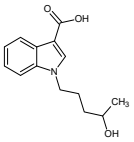 PB–22 M3 (Carboxylation, hydroxylation)	$C_{25}H_{33}FN_2O_9$ 524.5359 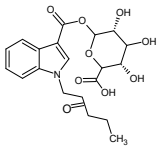 PB–22 M4 (Carboxylation, ketone formation, glu)	$C_{23}H_{22}N_2O_2$ 358.4330 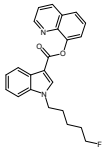 PB–22F	$C_{14}H_{17}NO_2$ 231.2903 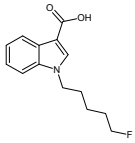 PB–22F M2 (Carboxylation, Ester hydrolysis)
$C_{20}H_{25}NO_8$ 407.4144 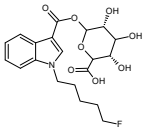 PB–22F M3 (Carboxylation, Glu)	$C_{14}H_{17}NO_3$ 247.2897 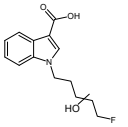 PB–22F M4 (Carboxylation, Hydroxylation)	$C_{20}H_{23}NO_9$ 421.3979 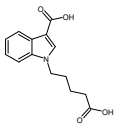 PB–22F M5 (Carboxylation, defluorination)	$C_{23}H_{21}N_2O_2F$ 376.4334 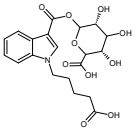 PB–22F M6 (Carboxylation, defluorination, glu)	$C_{14}H_{16}NO_2F$ 249.2807 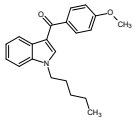 RCS–4
$C_{20}H_{24}NO_8F$ 425.4049 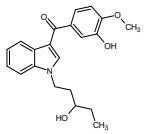 RCS–4M1(Dihydroxylation)	$C_{14}H_{16}NO_3F$ 265.2801 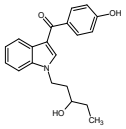 RCS–4 M2 (O-demethyl-OH)	$C_{14}H_{15}NO_4$ 261.2732 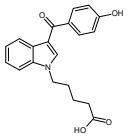 RCS–4 M3 (Hydroxylation)	$C_{20}H_{23}NO_{10}$ 437.3973 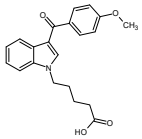 RCS–4 M4 (HO-phenyl-oxo-)	$C_{21}H_{23}NO_2$ 321.4128 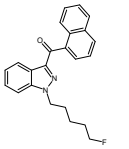 THJ–2201
$C_{21}H_{23}NO_4$ 353.4116 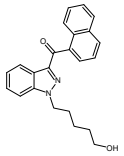 THJ–2201 M1 (defluorination)	$C_{20}H_{21}NO_3$ 323.3856 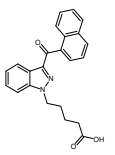 THJ–2201 M2 (Carboxylation,	$C_{21}H_{23}NO_3$ 337.3692 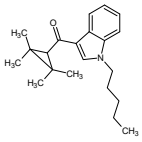 UR–144	$C_{22}H_{25}NO_3$ 351.3957 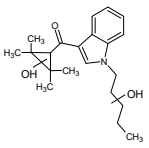 UR–144 M1 (Dihydroxylation)	$C_{23}H_{21}FN_2O$ 360.4240 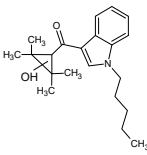 UR–144 M (Hydroxylation)

Downloaded from www.periodico.tchequimica.com

$C_{23}H_{22}N_2O_2$ 358.4330	defluorination) $C_{23}H_{20}N_2O_3$ 372.4165	$C_{21}H_{29}NO$ 311.4611	$C_{21}H_{29}NO_3$ 343.5599	$C_{21}H_{29}NO_2$ 327.4605
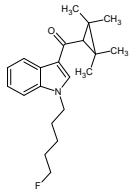 XLR–11 $C_{21}H_{28}FNO$ 329.4515	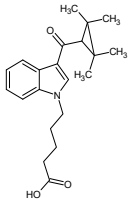 XLR-11 M1 (Carboxylation, defluorination) $C_{21}H_{27}NO_3$ 341.4440	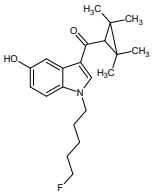 XLR11 M2 (Hydroxylation at indazole) $C_{21}H_{28}FNO_2$ 345.4509		
Synthetic opioids				
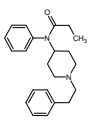 Fentanyl $C_{22}H_{28}N_2O$ 336.4705	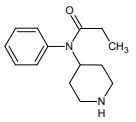 Norfentanyl $C_{14}H_{20}N_2O$ 232.3214	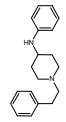 Fentanyl M $C_{19}H_{24}N_2$ 280.4072	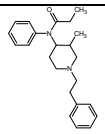 3-methylfentanyl $C_{23}H_{30}N_2O$ 350.4971	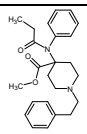 Carfentanyl $C_{24}H_{30}N_2O_3$ 394.5066
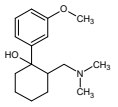 Tramadol $C_{16}H_{25}NO_2$ 263.3752	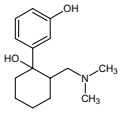 O-desmethyl-tramadol $C_{15}H_{23}NO_2$ 249.3486	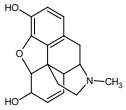 Morphine $C_{17}H_{19}NO_3$ 285.3377	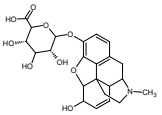 Morphine-glucuronide $C_{23}H_{27}NO_9$ 461.4618	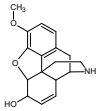 Norcodeine $C_{17}H_{19}NO_3$ 285.3377
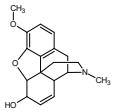 Codeine $C_{18}H_{21}NO_3$ 299.3643	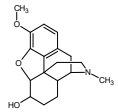 Dihydrocodeine $C_{18}H_{23}NO_3$ 301.3801	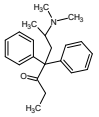 Methadone $C_{21}H_{27}NO$ 309.4452	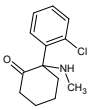 Ketamine $C_{13}H_{16}ClNO$ 237.7252	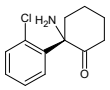 Norketamine C12H14ClNO 223.6987
Halucinogens				
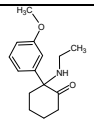 Methoxetamine $C_{15}H_{21}NO_2$ 247.3327	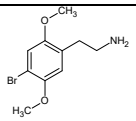 2-CB $C_{10}H_{14}BrNO_2$ 260.1277	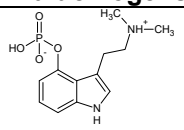 Psilocybin $C_{12}H_{17}N_2O_4P$ 284.2481	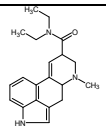 LSD $C_{20}H_{25}N_3O$ 323.432	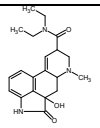 LSD (2-oxo-3-OH) $C_{20}H_{25}N_3O_3$ 355.4308
Stimulators				
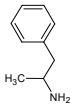 Amphetamine $C_9H_{13}N$ 135.2062	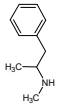 Methamphetamine $C_{10}H_{15}N$ 149.2328	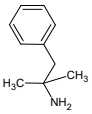 Fentermine $C_{10}H_{15}N$ 149.2328	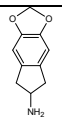 MDAI $C_{10}H_{11}NO_2$ 177.1998	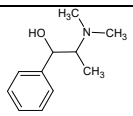 Methylephedrine $C_{11}H_{17}NO$ 179.263
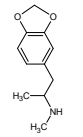 MDMA $C_{11}H_{15}NO_2$ 193.2423	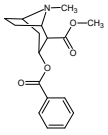 Cocaine $C_{17}H_{21}NO_4$ 303.3529	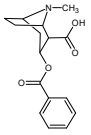 Benzoylecgonine $C_{17}H_{21}NO_4$ 289.3264	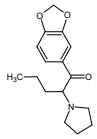 MDPV $C_{16}H_{21}NO_3$ 275.3428	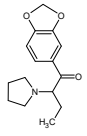 MDPBP $C_{15}H_{19}NO_3$ 261.3163

Downloaded from www.periodico.tchequimica.com

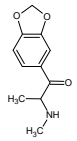 Methylone $C_{11}H_{13}NO_3$	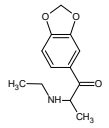 Ethylone $C_{12}H_{15}NO_3$	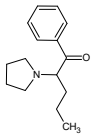 PVP $C_{15}H_{21}NO$		
207.2258	221.2524	231.3333		
Benzodiazepines				
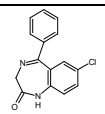 Nordiazepam $C_{15}H_{11}ClN_2O$ 270.7136	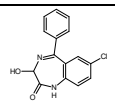 Oxazepam $C_{15}H_{11}ClN_2O_2$ 286.7130	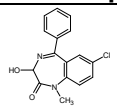 Temazepam $C_{16}H_{13}ClN_2O_2$ 300.7396	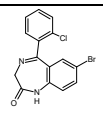 Fenazepam $C_{15}H_{10}BrClN_2O$ 349.6097	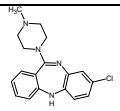 Clozapine $C_{18}H_{19}ClN_4$ 326.8233
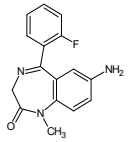 7-Amino flunitrazepam $C_{16}H_{14}FN_3O$ 283.3002				
Other substances				
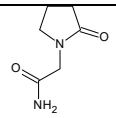 Pyracetam $C_6H_{10}N_2O_2$ 142.1558	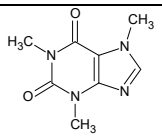 Caffeine $C_8H_{10}N_4O_2$ 194.1906	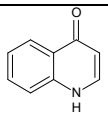 Hydroxyquinoline C_9H_7NO 145.1579	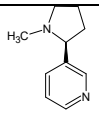 Nicotine $C_{10}H_{14}N_2$ 162.2316	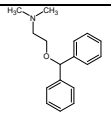 Dimedrol $C_{17}H_{21}NO$ 255.3547
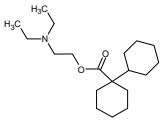 Dicycloverine $C_{19}H_{35}NO_2$ 309.4867	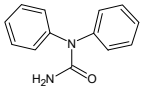 Carbamazepine $C_{15}H_{12}N_2O$ 236.2686	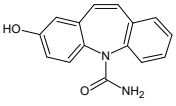 hydroxycarbamazepin $C_{15}H_{12}N_2O_2$ 252.2679	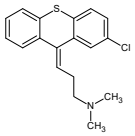 Chlorprotixen $C_{18}H_{18}ClNS$ 315.8602	

***Table 3**. List of the compounds included in the developed screening method with their chemical names, brutto-formulas collision energies(negative ESI mode)*

#	Name	Brutto-formula	$[M+H]^+$	Fragment ions	CE (eV)
Synthetic cannabinoids					
1	AB–001 M1 (dihydroxylation)	$C_{24}H_{31}NO_3$	382	151, 167	15
2	AB–001 M2 (Hydroxylation)	$C_{24}H_{31}NO_2$	366	151,188	18
3	AB–CHMINACA M1 (Carboxylation, hydroxylation of deaminated moity)	$C_{20}H_{27}N_3O_4$	374	257,356	13
4	AB–CHMINACA M2 (Carboxylation, Glucuronidation)	$C_{26}H_{35}N_3O_9$	534	241,312	13
5	AB–CHMINACA M3 (Carboxylation, Hydroxylation, Glucuronidation)	$C_{26}H_{35}N_3O_{10}$	550	257, 238	13
6	AB–CHMINACA M4 (Carboxylation, Hydrolysis of amide group)	$C_{15}H_{18}N_2O_2$	259	145, 241	13
7	AB–CHMINACA M5 (Carboxylation)	$C_{20}H_{28}N_4O_3$	358	145,241	13
8	AB–CHMINACA	$C_{20}H_{28}N_4O_2$	357	257, 328	13
9	AB–FUBINACA M1 (Carboxylation)	$C_{20}H_{20}FN_3O_3$	370	253,324	15
10	AB–PINACA	$C_{18}H_{26}N_4O_2$	331	286, 313	15

Downloaded from www.periodico.tchequimica.com

11	AB–PINACA M1 (Carboxylation)	$C_{18}H_{25}N_3O_3$	332	145, 215	15
12	AB–PINACA M2 (Amide hydrolysis, Glucuronidation)	$C_{24}H_{34}N_3O_9$	508	145, 215, 286	15
13	Ab–Pinaca–F M1 (Carboxylation)	$C_{18}H_{24}FN_3O_3$	350	177, 145, 213, 233, 304, 332	25
14	AB–PINACA–F M2 (Oxidative defluorination, amide hydrolysis)	$C_{18}H_{23}N_3O_5$	362	217, 245	15
15	AB–PINACA–F M3 (dicarboxylation, Glucuronidation)	$C_{24}H_{31}N_3O_{11}$	538	245, 298	15
16	AB–PINACA–F M4 (Oxidative defluorination, amide hydrolysis)	$C_{18}H_{25}N_3O_4$	348	213, 302	10
17	AKB–48	$C_{23}H_{31}N_3O$	412	133, 151, 215	15
18	AKB–48 M1 (Dihydroxylation)	$C_{23}H_{31}N_3O_3$	398	131, 133, 151	15
19	AKB–48 M2(Hydroxylation)	$C_{23}H_{31}N_3O_2$	382	133, 151	15
20	AKB–48 M3 (Hydroxylation, Carboxylation)	$C_{23}H_{29}N_3O_4$	412	133, 151	15
21	AM–2201	$C_{24}H_{22}FNO$	360	155, 232	15
22	AM–694 M1 (Defluorinization, Carboxylation)	$C_{20}H_{18}INO_3$	448	231, 203	15
23	AM–694 M2 (Defluorinization, Hydroxylation)	$C_{20}H_{20}INO_2$	434	203, 231	15
24	AM–694 M3 (Hydroxylation)	$C_{20}H_{19}IFNO_2$	452	231, 221	15
25	APINAC	$C_{23}H_{30}N_2O_2$	367	135, 215	15
26	APINAC M1 (Carboxylation)	$C_{13}H_{16}N_2O_2$	232	216, 145	14
27	FUB–PB22	$C_{25}H_{17}FN_2O_2$	397	109, 224	15
28	FUB–PB22 M1 (Carboxylation)	$C_{16}H_{12}NO_2F$	270	109, 226	15
29	FUB–PB22 (Carboxylation, Glucuronidation)	$C_{22}H_{20}FNO_8$	446	109, 270	15
30	JWH–018	$C_{24}H_{23}NO$	342	155, 214	15
31	JWH –018 M3 (Carboxylation)	$C_{24}H_{21}NO_3$	372	155, 244	15
32	JWH –018 M1 (Carboxylation, Glucuronidation)	$C_{30}H_{29}NO_9$	548	155, 244	15
33	JWH –018 M2 (Hydroxylation)	$C_{24}H_{23}NO_2$	358	155, 230	15
34	JWH–073	$C_{23}H_{21}NO$	328	155, 200	18
35	JWH–073 M1 (Hydroxylation at indazole)	$C_{23}H_{21}NO_2$	344	155, 171	18
36	JWH–073 M2 (Carboxylation, Glucuronidation)	$C_{29}H_{27}NO_9$	534	155, 230	18
37	JWH–073 M3 (Carboxylation)	$C_{23}H_{19}NO_3$	358	155, 230	18
38	JWH–203	$C_{21}H_{22}ClNO$	340	125, 214	15
39	JWH–203 M1 (Carboxylation)	$C_{21}H_{20}ClNO_3$	370	125, 200	15
40	JWH–203 M2 (4-pentyl hydroxylation)	$C_{21}H_{22}ClNO_2$	356	186, 204	15
41	JWH–203 M3 (Dihydroxylation)	$C_{21}H_{22}ClNO_2$	372	125	15
42	JWH–203 M4 (Carboxlation, Glucuronidation)	$C_{27}H_{28}ClNO_9$	546	218, 200	15
43	JWH–210	$C_{26}H_{27}NO$	370	183, 214	15
44	JWH–210 M1 (Trihydroxylation)	$C_{26}H_{27}NO_4$	418	199, 215	15
45	JWH–210 M2 (Hydroxylation)	$C_{26}H_{27}NO_2$	386	183, 214	12
46	JWH–210 M3 (Carboxylation)	$C_{26}H_{25}NO_3$	400	137, 197	12
47	JWH–250 M1 (Dihydroxylation)	$C_{22}H_{25}NO_4$	368	121, 137	15
48	JWH–250 M2 (Hydroxylation)	$C_{22}H_{25}NO_3$	352	121, 137	15
49	JWH-250 M3 (Carboxylation)	$C_{22}H_{23}NO_4$	366	121, 137	15
50	JWH–251 M1 (Carboxylation)	$C_{22}H_{23}NO_3$	350	105, 200	15
51	JWH–251 M2 (Carboxylation, Glucuronidation)	$C_{28}H_{31}NO_9$	526	105, 200	15
52	JWH–251 M3 (Hydroxylation)	$C_{22}H_{25}NO_2$	336	105, 130	15
53	MAM–2201	$C_{25}H_{24}FNO$	374	141, 169	18
54	MDMB(N)–Bz–F	$C_{22}H_{24}FN_3O_3$	398	253, 253	12

Downloaded from www.periodico.tchequimica.com

55	MDMB (N)–Bz–F M1 (Carboxylation)	$C_{21}H_{23}FN_3O_3$	384	253, 338	12
56	MDMB (N)–Bz–F M2 (Carboxylation, Glucuronidation)	$C_{27}H_{31}FN_3O_9$	560	338, 384	12
57	MDMB (N)–Bz–F M3 (Hydroxylation at indazole)	$C_{21}H_{23}FN_3O_4$	400	253, 324	12
58	MDMB(N)–2201 M1 (Carboxylation)	$C_{19}H_{26}FN_3O_3$	364	318, 233	15
59	MDMB–CHMINACA	$C_{22}H_{31}N_3O_3$	386	241, 326	12
60	MDMB–CHMINACAM1 (Carboxylation)	$C_{21}H_{29}N_3O_3$	372,5	145, 241	12
61	MMB–2201	$C_{20}H_{27}FN_2O_3$	364	144, 232	12
62	MMB–2201 M1 (Carboxylation)	$C_{19}H_{25}FN_2O_3$	349.5	144, 232	12
63	MMB–2201 M2 (Carboxylation, glucuronidation)	$C_{25}H_{33}FN_2O_9$	525.5	349.4, 232	12
64	PB–22	$C_{23}H_{22}N_2O_2$	359	144, 214	10
65	PB–22 M1 (Carboxylation, Ester hydrolysis)	$C_{14}H_{17}NO_2$	232	118, 132	12
66	PB–22 M2 (Carboxylation, glucuronidation)	$C_{20}H_{25}NO_8$	408	214, 232	12
67	PB–22 M3 (Carboxylation, hydroxylation)	$C_{14}H_{17}NO_3$	248	186, 174	12
68	PB–22 M4 (Carboxylation, ketone formation, glucuronidation)	$C_{20}H_{23}NO_9$	246	144, 184	12
69	PB–22F	$C_{23}H_{21}N_2O_2F$	377	232, 144	10
70	PB–22F M2 (Carboxylation, Ester hydrolysis)	$C_{14}H_{16}NO_2F$	250	118, 132, 206	10
71	PB–22F M3 (Carboxylation, Glucuronidation)	$C_{20}H_{24}NO_8F$	426	232, 250	10
72	PB–22F M4 (Carboxylation, Hydroxylation)	$C_{14}H_{16}NO_3F$	266	118, 144	10
73	PB–22F M5 (Carboxylation, oxidative defluorination)	$C_{14}H_{15}NO_4$	262	118 ,144, 172, 244	10
74	PB–22F M6 (Carboxylation, oxidative defluorination, glucuronidation)	$C_{20}H_{23}NO_{10}$	438	244, 260	10
75	RCS–4	$C_{21}H_{23}NO_2$	322	107, 135	15
76	RCS–4 M1 (Dihydroxylation)	$C_{21}H_{23}NO_4$	354	151, 230	15
77	RCS–4 M2 (O-demethyl-HO-chain-)	$C_{20}H_{21}NO_3$	324	121, 153	15
78	RCS–4 M3 (Hydroxylation)	$C_{21}H_{23}NO_3$	338	121, 144	15
79	RCS–4 M4 (HO-phenyl-oxo-)	$C_{22}H_{25}NO_3$	352	107, 135	15
80	THJ–2201	$C_{23}H_{21}FN_2O$	361	145, 177	18
81	THJ–2201 M1 (Oxidative defluorination)	$C_{23}H_{22}N_2O_2$	359	155, 231	15
82	THJ–2201 M2 (Carboxylation, Oxidative defluorination)	$C_{23}H_{20}N_2O_3$	373	155, 355	15
83	UR–144	$C_{21}H_{29}NO$	312	125, 214	20
84	UR–144 M1 (Dihydroxylation)	$C_{21}H_{29}NO_3$	344	186, 214	12
85	UR–144 M2 (Hydroxylation)	$C_{21}H_{29}NO_2$	328	214, 230	12
86	XLR –11	$C_{21}H_{28}FNO$	330	125, 232	15
87	XLR-11 M1 (Carboxylation, Oxidative defluorination)	$C_{21}H_{27}NO_3$	342	101, 125, 171, 244	15
88	XLR11 M2 (Hydroxylation at indazole)	$C_{21}H_{28}FNO_2$	346	125, 248	15
	Opioid analgetics				
1	Fentanyl	$C_{22}H_{28}N_2O$	337	105,132	15
2	Norfentanyl	$C_{14}H_{20}N_2O$	233	55,84	10
3	Fentanylmet	$C_{19}H_{24}N_2$	281	105,188	20
4	3-methylfentanyl	$C_{23}H_{30}N_2O$	351	105,202	25
5	Carfentanyl	$C_{24}H_{30}N_2O_3$	395	134,246	20
6	Tramadol	$C_{16}H_{25}NO_2$	264	136,187	15
7	O-desmethyl-tramadol	$C_{15}H_{23}NO_2$	250	121,131	15
8	Morphine	$C_{17}H_{19}NO_3$	286	153,165	30
9	Morphine-3-glucuronide	$C_{23}H_{27}NO_9$	462	201,229	22
10	Morphine-6-glucuronide	$C_{23}H_{27}NO_9$	462	201,229	21
11	Norcodeine	$C_{17}H_{19}NO_3$	286	193,215	15
12	Codeine	$C_{18}H_{21}NO_3$	300	183,199	15
13	Dihydrocodeine	$C_{18}H_{23}NO_3$	302	201,227	15
14	Methadone	$C_{21}H_{27}NO$	310	247,265	15

Downloaded from www.periodico.tchequimica.com

15	Ketamine	$C_{13}H_{16}ClNO$	238	220,125	15
16	Norketamine	$C_{12}H_{14}ClNO$	224	179,125	15
	Halucinogens				
1	Methoxetamine	$C_{15}H_{21}NO_2$	248	121,175	37
2	2-CB	$C_{10}H_{14}BrNO_2$	260	228,243	25
3	Psilocybin	$C_{12}H_{17}N_2O_4P$	285	160,205	15
4	LSD	$C_{20}H_{25}N_3O$	324	180, 223, 281	20
5	LSD M1 (2-oxo-3-OH)	$C_{20}H_{25}N_3O_3$	356.5	237, 265	20
	Stimulators				
1	Amphetamine	$C_9H_{13}N$	136	119,91	15
2	Methamphetamine	$C_{10}H_{15}N$	150	91,119	15
3	Fentermine	$C_{10}H_{15}N$	150	133,105	15
4	MDAI	$C_{10}H_{11}NO_2$	178	131,161	10
5	Methylephedrine	$C_{11}H_{17}NO$	180	131,147	15
6	MDMA	$C_{11}H_{15}NO_2$	194	135,163	15
7	Cocaine	$C_{17}H_{21}NO_4$	304	150,182	15
8	Benzoylecgonine	$C_{17}H_{21}NO_4$	290	119,168	15
9	MDPV	$C_{16}H_{21}NO_3$	276	175, 135	15
10	MDPBP	$C_{15}H_{19}NO_3$	262	191,161	15
11	Methylone	$C_{11}H_{13}NO_3$	208	132,160	15
12	Ethylone	$C_{12}H_{15}NO_3$	222	174,204	20
13	PVP	$C_{15}H_{21}NO$	232	91,161	18
	Benzodiazepines				
1	Nordiazepam	$C_{15}H_{11}ClN_2O$	271	140, 210	15
2	Oxazepam	$C_{15}H_{11}ClN_2O_2$	287	241,269	15
3	Temazepam	$C_{16}H_{13}ClN_2O_2$	301	255, 283	15
4	Fenazepam	$C_{15}H_{10}BrClN_2O$	349	105, 169	15
5	Clozapine	$C_{18}H_{19}ClN_4$	327	84,296	12
6	7-aminoflunitrazepam	$C_{16}H_{14}FN_3O$	284	264, 236	10
	Others				
1	Pyracetam	$C_6H_{10}N_2O_2$	143	126, 98	10
2	Caffeine	$C_8H_{10}N_4O_2$	195	110, 138	15
3	Hydroxyquinoline	C_9H_7NO	146	118, 128	5
4	Nicotine	$C_{10}H_{14}N_2$	163	106, 131	5
5	Dimedrol	$C_{17}H_{21}NO$	256	152, 167	15
6	Dicycloverine	$C_{19}H_{35}NO_2$	310	155, 165	10
7	Carbamazepine	$C_{15}H_{12}N_2O$	237	194, 175	15
8	2-hydroxycarbamazepine	$C_{15}H_{12}N_2O_2$	253	210, 180	15
9	Chlorprotixen	$C_{18}H_{18}ClNS$	316	231, 271	15

Downloaded from www.periodico.tchequimica.com

Table 4. *List of the compounds included in the developed screening method with their chemical names, brutto-formulas collision energies(negative ESI mode)*

#	Name	Brutto-formula	$[M+H]^+$	Fragment ions	CE
1	Phenobarbital	$C_{12}H_{12}N_2O_3$	231	144,188	15
2	THC-COOH	$C_{21}H_{28}O_4$	343	191,245	15
3	Nordiazepam	$C_{15}H_{11}ClN_2O$	269	241,223	15
4	Oxazepam	$C_{15}H_{11}ClN_2O_2$	285	257,205	15
5	Morphine	$C_{17}H_{19}NO_3$	284	248,108	15
6	AB–FUBINACA M1(Carboxylation)	$C_{20}H_{20}FN_3O_3$	368	322,215	15
7	MDMB(N)–2201 M1(Carboxylation)	$C_{19}H_{26}FN_3O_3$	362	318,185	15
8	MMB–2201 M1(Carboxylation)	$C_{19}H_{25}FN_2O_3$	347.5	303,184	15
9	MDMB–CHMINACAM1(Carboxylation)	$C_{21}H_{29}N_3O_3$	370.5	343,214	15
10	AB–CHMINACA M5 (Carboxylation)	$C_{20}H_{27}N_3O_3$	356	213,312	15
11	AB–CHMINACA M5 (Hydroxylation)	$C_{20}H_{27}N_3O_4$	371	229,238	15
12	AB–PINACA–F M1 (Carboxylation)	$C_{18}H_{24}FN_3O_3$	348	185,205	15
13	AB–PINACA–F M2(Oxidative defluorination to COOH, amide hydrolysis)	$C_{18}H_{23}N_3O_5$	360	260,216	15
14	AB–PINACA–F M4 (Oxidative defluorination, amide hydrolysis)	$C_{18}H_{25}N_3O_4$	346	113,169	15
15	PVP	$C_{15}H_{21}NO$	230	114,184	15
16	Benzoylecgonine	$C_{17}H_{21}NO_4$	288	208,125	15
17	MDMB–CHMINACAM1(Carboxylation)	$C_{21}H_{29}N_3O_3$	370	326,243	15
18	MDMB (N)–Bz–F M1 (Carboxylation)	$C_{21}H_{23}FN_3O_3$	382	336,294	15
19	PB–22 M1 (Carboxylation, Ester hydrolysis)	$C_{14}H_{17}NO_2$	230	127,155	15
21	PB–22F M2(Carboxylation, Ester hydrolysis)	$C_{14}H_{16}NO_2F$	248	204,136	15
22	XLR-11 M1 (Carboxylation, Oxidative defluorination)	$C_{21}H_{27}NO_3$	340	171,240	15

Table 5. *Validation parameters of the method*

Name of compounds	LOD ng/ml	Reproducibility RSD,%			RT RSD,%	Stability 72 hr RSD,%
		5 ng/ml	50 ng/ml	150 ng/ml		
Amphetamine	1	3.3	3.3	0.77	3.05	2.93
Buprenorphine	0.5	1.17	1.17	2.51	2.01	2.24
7-amino flunitrazepam	1	8.79	8.79	2.89	0.52	2.42
Nordiazepam	5	0.71	0.71	0.71	2.00	0.18
Morphine	0.5	6.32	6.32	2.61	2.84	3.29
Oxazepam	5	1.4	1.4	1.33	0.55	1.54
Temazepam	5	2.41	2.41	2.59	0.96	2.19
APINAC	5	4.98	4.98	12.65	0.24	10.7
Cocaine	5	4.98	4.98	10.30	1.17	7.75
THC-acid	5	8.88	8.88	1.77	0.59	1.11
Methylecgonine	5	8.61	8.61	19.08	1.84	2.88
Benzoylecgonine	5	7.69	5.12	4.38	1.45	3.18

Downloaded from www.periodico.tchequimica.com

Table 6. *List of the tested samples*

№	Detected compounds		
1	Tramadol	26	PVP
2	Cocaine, amphetamine, methamphetamine	27	AB-Chminaca
3	AB-chminaca, THC	28	AB-Chminaca, AB-fubinacaMDMB(N)-2201 AB-Fubinaca
4	a-PVP, AB-chminaca	29	AB-chminaca
5	Morphine	30	Ab-fubinaca
6	a-PVP, dimedrol, codeine, Morphine	31	AB-fubinaca
7	AB-chminaca	32	pvp
8	PB-22, AB-chminaca, MDMB(N)-2201	33	AB-PINACA-F MDMB-Bz-F MDMB-2201
9	AB-fubinaca, 5F-ab-pinaca, MDMB(N)-2201	34	AB-fubinaca
10	5F-AB-PINACA, AB-fubinaca, PVP	35	PVP, AB-Chminaca
11	MDMB(N)-2201	36	AB-Chminaca
12	MDMB(N)-2201, 5F-ab-pinaca	37	MDMB(N)-2201
13	AB-chminaca, 5F-AB-PINACA, MDMB(N)-Bz-F	38	Morphine
14	AB-chminaca, 5F-AB-PINACA, MDMB(N)-2201, PVP	39	Morphine, ketamine
15	aPVP, ethylon, methoxetamine	40	MDPV, phenobarbital
16	AB-chminaca, 5F-AB-PINACA, MDMB(N)-2201	41	PVP, AB-Chminaca
17	AB-chminaca, 5F-AB-PINACA, XLR-11, AB-PINACA	42	Methadone, MMB-2201 MDMB-2201
18	PB-22F	43	PVP, MDPV
19	PB-22	44	AB-Chminaca, AB-fubinaca, MDMB-chminaca
20	MDPBP	45	PB-22F, AB-PINACA-F
21	MDPBP, PVP, AB-Chminaca	46	Mephedrone, PVP
22	MDPBP	47	PVP
23	PVP, MDMB(N)-2201 , carbamazepine	48	Amphetamine, methamphetamine, carfentanyl, 3-methylfentanyl, methadone
24	PVP	49	MDMB-Chminaca, AB-fubinaca
25	MDMB(N)-2201	50	THJ-2201

Downloaded from www.periodico.tchequimica.com

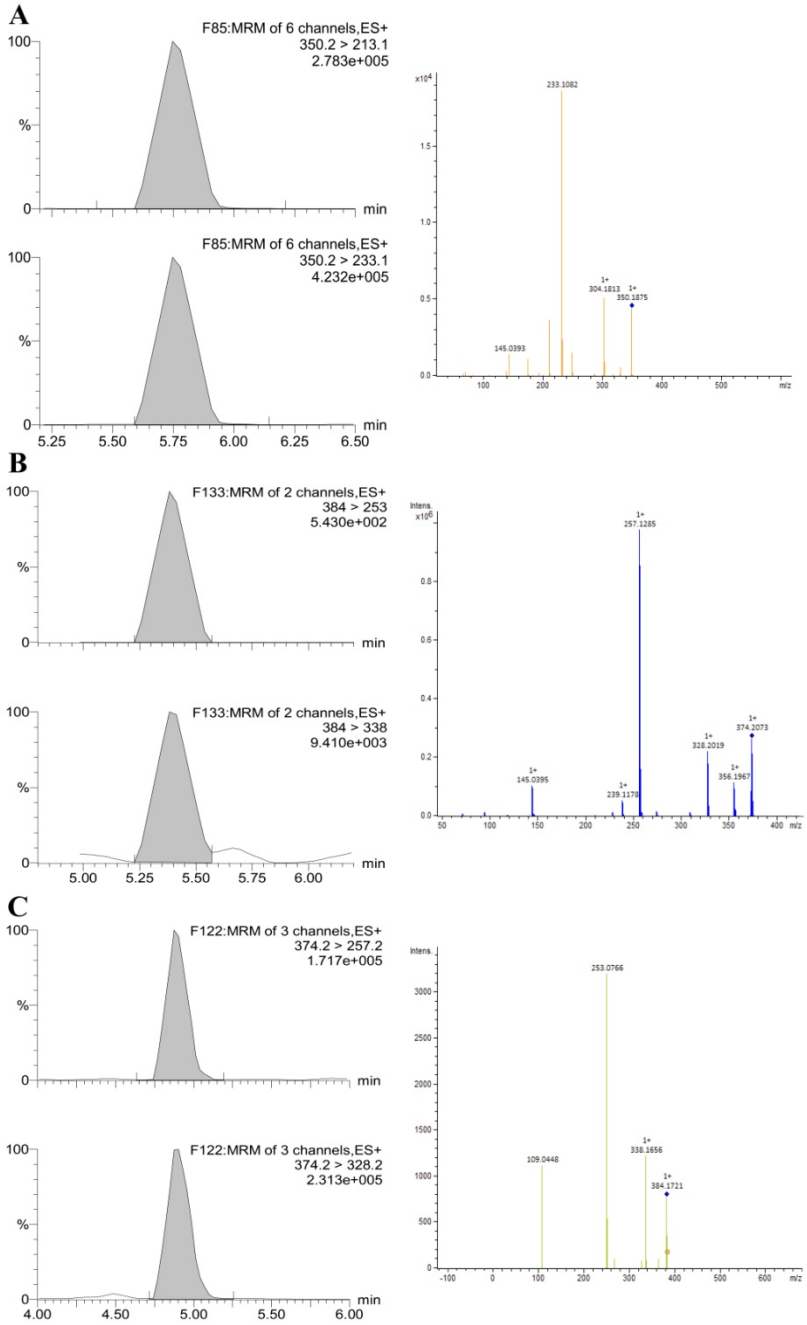

Figure 1. *Results for the tested sample №13 showing chromatograms and confirmatory Q-TOF spectra of **A**–5F-AB-PINACA M1; **B** - MDMB(N)-Bz-F M1 and **C** -AB-CHMINACA M4.*

PERIÓDICO TCHÊ QUÍMICA
ARTIGO ORIGINAL

INFLUÊNCIA DO TIPO DE SOLO E DA CULTURA ANTERIOR NA SUPRESSÃO DO FUSÁRIO POR BACTÉRIAS FORMADORAS DE ESPOROS LOCAIS

THE INFLUENCE OF SOIL TYPE AND PRECEDING CROP ON THE SUPPRESSION OF FUSARIUM BY INDIGENOUS SPORE-FORMING BACTERIA

ВЛИЯНИЕ ТИПА ПОЧВЫ И ПРЕДШЕСТВУЮЩЕЙ КУЛЬТУРЫ НА ПОДАВЛЕНИЕ *FUSARIUM*МЕСТНЫМИ СПОРООБРАЗУЮЩИМИ БАКТЕРИЯМИ

PRAZDNOVA, Evgeniya V. [1*];GOROVTSOV, Andrey V. [2,3]; CHISTYAKOV, Vladimir A. [4]; VASILCHENKO, Nikita G. [5]; KUKHARENKO, Lidiya E. [6];

[1]Southern Federal University, Academy of Biology and Biotechnology, Department of Genetics, 194/1 Stachki Ave., zip code 344090, Rostov-on-Don – Russian Federation

[2]Federal Rostov Agricultural Research Center, 1 Institutskaya Str., zip code 346735, Rassvet – Russian Federation

[3] Southern Federal University, Academy of Biology and Biotechnology, Department of Biochemistry and Microbiology, 194/1 Stachki Ave., zip code 344090, Rostov-on-Don – Russian Federation

[4] Southern Federal University, Academy of Biology and Biotechnology, Laboratory of Experimental Mutagenesis,194/1 Stachki Ave., zip code 344090, Rostov-on-Don – Russian Federation

[5] Southern Federal University, Academy of Biology and Biotechnology, Department of Genetics,194/1 Stachki Ave., zip code 344090, Rostov-on-Don – Russian Federation

[6] LLC Rostov Management Company, 152151, 18 Perovsky Lane, Rostov – Russian Federation

** Correspondence author*
e-mail: ldsz@rambler.ru

Received 29 May 2019; received in revised form 30 August 2019; accepted 14 September 2019

RESUMO

Restaurar e melhorar a fertilidade do solo, aumentar a produtividade das plantas cultivadas é uma das tarefas da produção agrícola. As bactérias do solo formadoras de esporos estão atraindo crescente interesse como agentes de biocontrole, mas a questão da influência das condições locais do solo no desenvolvimento de antagonismo em estirpes bacterianas locais não é bem conhecida. Portanto, o principal objetivo do trabalho é estudar a influência do tipo de solo e de culturas anteriores na intensidade das interações antagônicas entre as bactérias do solo da ordem *Bacillales* e os fungos fitopatogênicos. Para identificar as espécies e estirpes especificadas, os autores utilizaram o método de Sanger, a detecção de produtos de sequenciamento foi realizada automaticamente por eletroforese capilar. O critério para classificar um microrganismo como uma espécie específica foi considerado homologia de pelo menos 97%. Este estudo apresenta novas evidências sobre o efeito do tipo de solo e cultura anterior no nível de antagonismo em relação a *Fusarium* e *Plectosphaerella*. Como resultado, determinou-se que o tipo de solo e a cultura anterior influenciam as interações antagonistas fúngico-bacterianas. A atividade antagonista mais forte entre todos os isolados bacterianos foi encontrada em bactérias isoladas de *Albic Phaeozem*. A maior atividade antagônica contra *F. Graminearum* é representada por estirpes isoladas de solos nos quais o trigo de inverno era a cultura anterior.

Palavras-chave: *Bacillus, Paenibacillus, Fusarium*, *biocontrole, antagonismo, tipo de solo, rotação de culturas.*

ABSTRACT

Restoring and improving soil fertility, increasing the productivity of cultivated plants is one of the objectives of agricultural production. The aim of the present work was to study the antagonistic interactions between the soil bacteria of the order *Bacillales* and phytopathogenic fungi. The spore-forming soil bacteria attract increasing interest as biocontrol agents, but little is known about the influence of local soil conditions on

Downloaded from www.periodico.tchequimica.com

the development of antagonism in indigenous bacterial strains. This can lead to unsuccessful attempts of bacterial antagonists isolation. To determine the sequences of primary nucleotide DNA, the authors used the Sanger sequencing method, the detection of sequencing products was performed automatically, using the method of capillary electrophoresis. Homology of at least 97% was considered as the criterion for classifying a microorganism as a certain species. This study presents new data on the influence of soil type and preceding crop on the level of antagonism against *Fusarium* and *Plectosphaerella*. The results show that both the soil type and preceding crop influence the fungal-bacterial antagonistic interactions. The strongest antagonistic activity among all bacterial isolates was found in bacteria isolated from *AlbicPhaeozem*. The highest antagonistic activity against *F. graminearum* was shown by strains that were isolated from soils on which winter wheat was the preceding crop.

Keywords: *Bacillus, Paenibacillus, Fusarium, biocontrol, antagonism, soil type, crop rotation.*

АННОТАЦИЯ

Восстановление и повышение плодородия почвы, рост продуктивности культурных растений – одна из задач сельскохозяйственного производства. Спорообразующие почвенные бактерии привлекают все больший интерес в качестве агентов биоконтроля, но вопрос о влиянии местных почвенных условий на развитие антагонизма у местных штаммов бактерий недостаточно изучен. Поэтому основная цель работы заключается в изучении влияния типа почв и предшествующих культур на интенсивность антагонистических взаимодействий между почвенными бактериями отряда *Bacillales* и фитопатогенными грибами. Для идентификации выделенных видов и штаммов авторами был использован метод Сэнгера, детекцию продуктов секвенирования осуществляли автоматически методом капиллярного электрофореза. Критерием для отнесения микроорганизма к определенному виду считалась гомология не менее 97%. В данном исследовании представлены новые данные о влиянии типа почвы и предшествующей культуры на уровень антагонизма в отношении *Fusarium* и *Plectosphaerella*. В результате было определено, что тип почвы и предшествующая культура влияют на грибково-бактериальные антагонистические взаимодействия. Наиболее сильная антагонистическая активность среди всех бактериальных изолятов была обнаружена у бактерий, выделенных из *Albic Phaeozem*. Наибольшая антагонистическая активность против *F. Graminearum* представлена штаммами, которые выделялись из почв, на которых озимая пшеница являлась предшествующей культурой.

Ключевые слова: *Bacillus, Paenibacillus, Fusarium, биоконтроль, антагонизм, тип почвы, севооборот.*

1. INTRODUCTION

Due to the growing demand of the population for high-quality and safe agricultural products, there is a need to develop competent approaches and strategies for the cultivation of agricultural crops. The most important branch of agriculture is crop production.

The specialization of farming associated with repeated or permanent cultivation of agricultural plants leads to a number of problems. One of these problems is soil fatigue, which is caused by the depletion of the reserves of organic and mineral substances necessary for plant growth and development (Triberti *et al*., 2016). In addition to the depletion of soil resources, this approach leads to the increased damage caused by various diseases. In grain crops, these include root rot, fusarium head blight, brown rust, scab and late blight in potatoes, cercosporiosis in sugar beet, and many other diseases of agricultural crops.

These diseases are caused by soil phytopathogenic microorganisms, remaining on crop residues and multiplying in the presence of suitable climatic conditions under permanent sowing (Bankina *et al*., 2017; Benitez *et al*., 2017).

Winter wheat is one of the main crops cultivated in Russia. That is why fusarium head blight has become widespread. The disease is observed in most regions where wheat is grown and causes serious losses up to 25-30% of the yield (Gagkayeva *et al*., 2012; Gagkaeva, Gavrilova, 2014).The causative agents of this group of diseases are the fungi of the genus *Fusarium*. These fungi pose a serious threat to humans and farm animals due to the production of mycotoxins, namelyfumonisine (Tamura *et al*., 2015), zearalenone(Brodehl *et al*., 2014), and the trichothecin series toxins: deoxynivalenol (DON), T-2-toxin and HT2-toxin.The toxins accumulate in the seeds of plants (Jimenez-Garcia *et al*., 2018; Szabó *et al*., 2016).

Downloaded from www.periodico.tchequimica.com

There are various ways to protect the crops from phytopathogenic fungi, with chemical fungicides being the most commonly used tool. However, in a number of works, it was shown that the effectiveness of the fungicides decreases steadily due to the gradual development of resistance to active substances (Becker R. *et al*., 2010; Gasich *et al*., 2015).At present, the vector of research has shifted from the search for chemicals to the search for bacteria and their metabolites, which show antagonistic properties to various fungal pathogens of agricultural crops (Parnell *et al*., 2016). This is due to the demand for food free of agrochemical residues and the use of organic farming (Moreno-Velandia *et al*., 2019).

One of the promising groups of microorganisms that differ both in their ability to effectively resist phytopathogens and to show phytostimulating properties is the aerobic spore-forming soil bacteria of the order Bacillales.

International experience indicates a high efficiency of using biological preparations based on bacteria of this order to control Fusarium. In particular, their effectiveness has been demonstrated in such crops as corn, cucumber, and potatoes (Cavaglieri *et al*., 2005; Chen *et al*., 2010; Sadfi *et al*., 2001).The mechanism of action is the colonization of plant root during seed germination and the suppression of pathogenic fungi by excretion of chitinolytic enzymes, siderophores and specific antimicrobial peptidesbelonging to the fengycin, iturin and surfactin families. Aerobic spore-forming bacteria are frequently used in biopharmacology and biotechnology (Cochrane and Vederas, 2016). Their ability toform endospores allow them to be formulated with longer shelf-life due to higher resistance to stress conditions (Lazarovits *et al*., 2014). Both biotic and abiotic factors affect the expression of genes related to antagonistic activity in *Bacillus* species (Díaz *et al*. 2013; Zapata and Díaz, 2012). This can lead to unsuccessful attempts of bacterial antagonists isolation from a number of environments.

It is known that soil bacteria are highly sensitive to local soil and climatic conditions – the type of soil, temperature, humidity, the composition of local microbial communities. Therefore, it is important to study the influence of these conditions on the incidence of antagonistic stains of soil bacteria. This approach allows increasing the chances to isolate a potent bacterial strain. At the same time, the strains of bacteria isolated from a specific region should be a perfect choice as a biocontrol agent for the same region.

This paper is aimed to evaluate the influence of soil conditions and cultivated crops on the incidence and strength of antagonism in soil bacteria against *Fusarium*s pecies.

2. MATERIALS AND METHODS

2.1.Soil sampling sites and methods

Soil samples were collected from agricultural fields located in the Labinsky and Kanevskoy districts of the Krasnodar region (southern Russia) (Figure 1). The sampling sites were located in steppe zone (1 and 2) or foothill zone (3-8). Soils were classified as Haplic Phaeozem, Albic Phaeozem, Luvic Chernozem, and Haplic Chernozem.Each marker represents approximate location of the sampling sites, as from two to seven separate fields were sampled at each location. The total number of fields that have been sampled was 28.

All but two fields were used for growing winter wheat, and the rest were used for growing winter barley. The preceding crops were soybean, corn, sugar beet. sunflower, winter wheat, and peas. The sampling sites location and corresponding soil types and crops are presented in Table 1.

Each field was sampled according to generally accepted methods (Gregorich and Carter, 2007). Ten subsamples of soil were collected from the 0-10 cm layer in the corners and the middle of each field. Then the subsamples were thoroughly mixed.

2.2. Isolation of fungal strains

The fungal strains were isolated from plant residues of wheat and corn, collected from fields 1, 5, 6 and 7. 10 g of plant residues were thouroughly grinded, then stirred with sterile water on a rotary shaker for 30 min. The resulting suspension was plate on wort agar supplemented with streptomycin and grown for 5 days at 25 ºC. The colonies with morphology characteristic of *Fusarium sp.* were isolated, and grown on sucrose-water agar to enhance the production of macroconidia (Mansour *et al*., 2012). Five strains of *Fusarium sp.* were isolated and used for further studies and species-level identification.

Strain Fus 1 was isolated from corn stem residues from site 1 (soil type – Haplic Chernozem), Poc 6.1 from site 6 (soil type – Luvic Chernozem), Poc 6.2.1 and Poc 6.2.2 from site 7(soil type – Haplic Phaeozem), Ple1 from

Downloaded from www.periodico.tchequimica.com

site 5 (soil type – Albic Phaeozem).

2.3 Isolation of bacterial strains with antagonistic properties

The bacterial strains were isolated from the mixed soil samples. The soil was mixed with sterile water at a ratio 1:10 and ground with a rubber pestle to separate the bacterial cells from the soil particles. The resulting soil suspension was shaken in conical flasks at a rotary shaker for 30 min. To isolate spore-forming bacteria, the soil suspension was heated to 80 ºC for 20 min. After cooling to room temperature, the dilutions were prepared and plated on the agar medium, that was composed of 50% wort agar and 50% nutrient agar.

At the same time, the pure culture of *Fusarium graminearum*(Fus 1) that had been grown on wort agar for 7 days prior to the experiment was washed with sterile 0,85% saline solution to obtain the suspension of conidia. The conidia in the resulting suspension were counted under the microscope using a hemocytometer, and the suspension was diluted to 10^4 cells/ml. 50 µl of this suspension was plated on the same plates that were inoculated with soil suspension.

The colonies of bacterial strains were observed after 5 days of incubation at 30ºC. The colonies with antagonistic properties were suppressing the growth of the fungus (Figure 2).These strains were isolated and transferred to the same medium for further study.

2.4The measurement of antagonistic activity of the bacterial isolates

A total of 1040 strains of aerobic spore-forming bacteria have been isolated from the 28 mixed soil samples. The antagonistic activity of the isolates was measured by the method of inhibition zone diameter. The pure culture of each strain was subcultured on a fresh nutrient agar slant and incubated for 18 h to obtain a culture in the logarithmic growth phase. Then one loop of biomass was inoculated to the perimeter of an agar plate. Five strains of bacteria were tested on the same plate, and the test was performed in triplicate. The center of the plate was inoculated with the mycelium of *Fusarium graminearum*, and allowed to grow for 7 days.

The inhibition zone was measured as a perpendicular between the edge of the bacterial colony and the edge of the visible growth of the mycelium of the fungus.

The 202 strains exhibiting the highest antagonistic activity (inhibition zone diameter >12 mm) was then tested against 4 additional fungal isolates to compare with their activity against *F. graminearum*.

2.5. The identification bacterial and fungal isolates

The genotypic characterization of the strains was based on sequence analysis of ribosomal genes. Conservative primers of genes encoding 18S RNA were used for the primary identification of fungi (Innis *et al*., 2012). To establish the phylogenetic relationship of related species, the method of comparing nucleotide sequences encoding the 5.8 S rRNA gene and the internal transcribed spacers ITS1 and ITS2 (Naumova *et al*., 2007), as well as sequences encoding the D1 / D2 gene of the 26S p RNA, was also used.

Variable regions of genes encoding 16S rRNA were used to identify bacteria.

The criterion for classifying a microorganism to a particular species was considered to be homology of at least 97%.

DNA isolation. The isolation of DNA was performed with AmpliTube RV M-SorbTube kit (Syntol, Russia). The bacterial cells were grown on solid nutrient agar for 20 hours. The biomass was washed from the plates with a sterile saline solution and then centrifuged at 3000 g for 15 min. The pellet was frozen in liquid nitrogen and heated to 60 ºC thrice. The quantity of DNA was estimated using Qubit 3.0 fluorimeter.

DNA purification was performed using the Genomic DNA Purification Kit (Syntol, Russia).

PCR reaction was performed with PCR Screen Mix Kit (Evrogen, Russia). The total volume of the PCR mixture was 25 µL. The concentration of primers was 0.5 mkM for all primer pairs (Table 1). Amplification was performed in thermal cycler T100 Thermal Cycler (Bio-Rad, USA). The protocol of amplification:

1. Preliminary denaturation at 95 °C – 3 min
2. 35 cycles of amplification as described above
3. Denaturation at 95 °C - 30 sec
3. Annealing of primers at the optimal temperature (Table 2) – 30 sec
4. Elongation at 72 °C – 30 sec
6. The last elongation at 72 °C – 5 min

Conditions for ***electrophoresis*** of PCR samples were: 1.0% agarose gel, 5 V/cm in TAE buffer for 30 minutes. If it was not possible to establish the species belonging only using

Downloaded from www.periodico.tchequimica.com

16SRNA, species-specific primers (Table 2) were used for accurate identification of some bacterial strains.Sequencing was performed on an AE3000 automatic sequencer. For the analysis of sequences, a specialized computer programs BLAST (Basic Local Alignment Search Tool), and RDB II (Ribosomal Database Project II) were used.

Sequencing. Determination of primary nucleotide DNA sequences was performed by Sanger method with gene-specific primers and Big dye terminator v3.1 Cycle Sequencing Kit with modification (Applied Biosystems, USA) in a volume of 10 µl.

The reading was carried out with both primers (forward and reverse). The reaction was carried out using the Veriti amplifier (Applied Biosystems, USA). Detection of sequencing products was carried out automatically by capillary electrophoresis on the device ABI PRISM 3730 (Applied Biosystems, USA). The results were manually checked for mis-called nucleotides in Sequencing Analysis v. 5.4 software (Applied Biosystems, USA).

3. RESULTS AND DISCUSSION:

3.1 Identification of strains

Strains of fungi. The primary screening of the GenBank database showed that the strains studied belong to the following systematic group: *Eukaryota; Fungi; Dikarya; Ascomycota; Pezizomycotina; Sordariomycetes; Hypocreomycetidae; Hypocreales; Nectriaceae; Fusarium*.

Strain Fus1. Phylogenetic kinship analysis conducted using strains of closely related microorganisms showed that the closest to the studied strain are *Fusariumculmorum, Fusariumgraminearum (Gibberellazeae), Fusariumasiaticum.* Due to the ambiguity of the molecular identification of the Fus 1 strain, its macro- and micromorphological studies were carried out when grown on potato-glucose agar (PDA) and diagnostic medium, water clove agar (CLA), ensuring efficient formation and uniformity of macroconidia (Leslie and Summerell, 2006). The characteristic morphology of macroconidia (Figure 4) with a conical apical cell and a sole basal indicates the strain belongs to the species *Fusariumgraminearum.* According to the results of the analysis of the nucleotide sequence that encodes part of the rRNA genes, as well as on the basis of morphological analysis, it was established that the strain under study is closest to the species *Fusariumgraminearum* (99% homology).

Strains 6.2.1, Poc 6.2.2, Poc.6.1.Based on the 18S analysis, nucleotide sequences encoding the 5.8 S rRNA gene and internal transcribed ITS1 and ITS2 spacers, and analysis of the D1 / D2 domain, it was found that the strains studied are closest to *Fusariumoxysporum* (98% homology).

Strain Ple1. Based on a similar analysis of 18S, 5.8 S rRNA gene and internal transcribed ITS1 and ITS2 spacers, this strain was identified as *Plectosphaerellacucumerina (*formerly *Fusariumtabacinum)(98%* homology*).*

Bacterial strains. A phylogenetic comparative study carried out using typical strains of closely related bacteria and results of analysis of sequences of variable regions of genes encoding 16S rRNA showed that *Paenibacilluspeoriae* was the closest to the studied strains R 3.13(99%), R 4.5 (99%), O 1.27(99%).The strain R 4.24 was identified as *Paenibacillus jamilae* (99%), and the strain R 5.31 as *Paenibacillus polymyxa* (99%). Sequencing of strains R 4.6 and V 3.14 and primary screening of the GenBank and RDP-II database showed that the strains belong to the following systematic Bacteria groups; *Firmicutes; Bacillales; Bacillaceae; Bacillus*, and the homology with several species of the genus *Bacillus* was 99% for both strains.When carrying out PCR analysis of the studied strain using the species-specific primers Bamy-f and Bamy-r, a PCR fragments of 747 bp was obtained (Figure 5). That indicates that the strain can be attributed to the species *Bacillus amyloliquefaciens*, the homology with which was, according to database analysis, 98% for R 4.6 and 99% V 3.14.

1. PCR fragment obtained using primers Bval-f and Bval-r

2. PCR fragment obtained using primers secYsubF and secYsubR

3. PCR fragment obtained using primers secYlichF and secYlichR

4. PCR fragment obtained using primers Bamy-f and Bamy-r

5. PCR fragment obtained using primers Bmoj-f and Bmoj-r

6. PCR fragment obtained using primers Batr-f and Batr-r

7. PCR fragment obtained using primers Bson-f and Bson-r

Downloaded from www.periodico.tchequimica.com

8. DNA Marker 1kb DNA GeneRuler (10000, 8000, 6000, 5000, 4000, 3500, 3000, 2500, 2000, 1500, 1000, 750, 500, 250 bp, from bottom to top)

Amplification of a fragment of 747 bp using primers Bamy-f and Bamy-r indicates that the strain can be attributed to the species *Bacillus amyloliquefaciens* (Table 3).

3.2Statistical analysis of the results on growth inhibition

The analysis of the fungal growth inhibition, caused by the most active strains of bacteria has shown, that thesensitivity to the antagonistic substances, produced by bacteria varied significantly in different fungal species. *F. oxysporum* was more resistant than *F. graminearum*. The growth inhibition zone for that species was 1.72 – 1.50 times smaller, depending on the strain. *P. cucumerina*demonstrated intermediate resistance level (Table 4).

To find out how the sensitivity of different fungal strains depends on the properties of individual bacterial strains, a correlation analysis was performed. If the potent bacterial strains, producing larger quantities of antifungal substances suppress all the fungi to a greater extent, that will result in a strong positive correlation between the data sets fordifferent fungal species. The correlation matrix is presented in Table 5.

The results show that for the most of fungal species, the correlation is positive and statistically significant, but its strength is weak, assuming that there are additional factors determining the extent of inhibition of each fungus by a certain bacterial strain.

To determine whether the resistance to bacterial strains is species- or strain-specific, we performed cluster analysis of the available data. The results are presented in Figure 6.

As shown in Figure 6, three species of phytopathogenic fungi form separate clusters, based on their inhibition by 202 bacterial strains. At the same time, all three strains of *F. oxysporum*formed a single cluster, suggesting that the resistance to inhibition by bacterial strains is more species-specific than strain-specific.

Interestingly, within the *F. oxysporum* cluster, two strains were separated from the third one. Both of these strains (*F. oxysporum* 2 and 3) were isolated from Haplic Phaeozem while *F. oxysporum 1* was isolated from Luvic Chernozem. This led to the assumption that soil type could play a significant role in the formation of fungal-bacterial antagonistic interactions.

3.3 The influence of soil type on the antagonistic properties of bacterial strains

The largest number of bacterial strains was isolated from chernozems of various types (of all 1040 strains, 912 were isolated from soils belonging to chernozems). The strongest antagonistic activity was characteristic of bacteria isolated from Albic Phaeozem(on average the diameter of the suppression zone was 15.95 mm, which is 1.63 higher than that of Luvic Chernozemstrains, and 2.79 times higher than strains of Haplic Chernozem) (Figure 7,8).

However, the influence of soil type had a different pattern for the selection of 202 most active bacterial strains. The dependence of the inhibition zone from the soil type was largely similar for *F. graminearum*, but it was completely different in other fungal strains (Figures 2,3). All three strains of *F. oxysporum* had average suppression zone below 15 mm, irrespective of the soil type. *P. cucumerina* was more sensitive to the bacterial antagonism, but the influence of the soil type was also insignificant.

3.4 The influence of preceding crop on the antagonistic properties of bacterial strains

The influence of the preceding crop on the antagonistic activity of bacteria was assessed since it is known that the preceding crop affects the development of root rot in cultivated crops (Peralta *et al*., 2018). This determines the frequency of phytopathogenic fungi and antagonist bacteria interaction, and as a result, the further resistance of agrocenosis to plant pathogens.

It can be clearly noted that the greatest antagonistic activity against *F. graminearum*was shown by those strains that were isolated from soils on which winter wheat was the preceding crop (the diameter of the growth inhibition zone was significantlyhigher than that of strains isolated from soils with any different preceding crop). (Figure 9).

The strains, isolated from fields with different preceding crops demonstrated less pronounced antagonistic properties against *F. oxysporum* compared to *F. Graminearum* (Figure 10). The preceding crops that were associated with the highest level of antagonism against

Downloaded from www.periodico.tchequimica.com

fungal species, other than *F. graminearum* were corn and soybean. However, this difference was statistically significant only in *F. oxysporum 3*.

4. Discussion

The growth suppression of phytopathogenic fungi that have been studied in this paper depends on the antifungal activity of bacterial strains. The mechanisms, underlying this activity involve the secretion of various metabolites that interact with fungal hyphae and lead to their lysis.

The strains of bacteria with the highest antifungal activity tested in this research belong to the genera *Bacillus* and *Paenibacillus*. A number of metabolites with antifungal activity are described in the literature for these genera:

1) Enzymes of the chitinolytic complex, glucanases and other lytic enzymes that can destroy the cell wall of fungi.
2) Polyketides – bacillaene, difficidin, macrolactin.
3) Oligopeptides.
4) Lipopeptides.

Chitinases. Some species of the *Bacillus* genus are capable of secreting chitinases, so they can use chitin as a carbon source (Wang and Chang, 1997). The following enzymes of the chitinolytic complex of bacteria are known to degrade chitin: exochitinase (capable of cleaving dimeric units of the polymer chain from the non-reducing end), endochitinase (cleaving chitobiose to N-acetylglucosamine) and N-acetylglucosaminidase (Howard *et al.*, 2003).

However, many strains with fungicidal activity do not possess chitinolytic enzymes.

Polyketides. Polyketides are one of the largest groups of bacterial secondary metabolites. They are represented by ensembles of fatty acids synthesized by polyketide synthases (PKS), nonribosomal enzymes with a modular structure (Hertweck, 2009). Polyketides have a wide range of biological effects, including antifungal activity. Polyenes have the highest antifungal activity among them (Bookshelf, 2010). They bind to ergosterol in the membrane of fungal cells and, thus, weaken the membrane, causing the leakage of K^+ and Na^+ ions, which leads to cell death (Harunari *et al.*, 2017).

Non-ribosomally synthesized peptides, and lipopeptides are also secondary metabolites of fungi and bacteria (Mongkolthanaruk, 2012). The genera *Bacillus* and *Paenibacillus* are capable of producing such metabolites as surfactins, fengicins, fusaricidins, polymyxins, lichenisine, iturins, locillomucin. The enzymes of the family of nonribosomal peptide synthases (NRPS) synthesizing them have a domain structure and different functional sites (domains) of the protein molecule participate in the synthesis of one peptide antimycotic (Walsh, 2016).

The resulting peptides are short oligomers 2-48 amino acids long. They often include atypical elements such as D-amino acids, methylated versions of standard amino acids, non-proteinogenic, hydroxylated and glycosylated residues. They can exist in the cell as a heterogeneous mixture of isoforms that differ in the length of the alpha chain. It was shown that these compounds are resistant to heating to 100 °C and the action of proteinase K (Zalila-Kolsi *et al.*, 2016), which is probably due to the presence of atypical amino acids and their stereoisomers in their structure.The ratio of NRP is often specific for different strains of the same species, and activity against different strains of fungi also varies.

The mechanism of action of these oligopeptides and lipopeptides is associated with a violation of the integrity of the membranes. In this study, we found, that the bacterial strains from the same soils had a significantly lower impact on *F. oxysporum*in comparison to *F. graminearum*. The sensitivity of different species and strains of fungi to the action of these lipopeptides often depends on the phospholipid composition, the presence of sphingomyelin and the sterol content in the membranes. However, the observed effect could have been influenced by the initial selection of bacterial strains using *F. graminearum*as a target. This selection could lead to variation in genetic response in presence of different fungal species.

The genes that provide the processes of non-ribosomal synthesis, although they are expressed quite independently, may be influenced by the same regulators. In particular, it is known that the strain *B. subtilis* 168 does not produce NRP due to mutations in the sfp and DegQ genes, with NRPS genes present in its genome (Tsuge *et al.*, 2005). There may also be epigenetic regulatory mechanisms that facilitate the adaptation of bacteria to a particular phytopathogen antagonist. Thus, it has been shown that the synthesis of fungicidal lipopeptides, at least iturins, and fengicins, is modulated by chemical signaling substances

Downloaded from www.periodico.tchequimica.com

secreted by the pathogenic fungus into the rhizosphere (Cawoy *et al.*, 2015).

The fact that the bacteria that were isolated from the fields where wheat had been growing in the previous cycle of crop rotation showed the greatest activity against *F. graminearum* leads to an assumption that genetic and epigenetic adaptation of the mechanisms of antifungal activity to these conditions took place. *F. graminearum*is mainly affecting small-grain cereal crops, though it can be found in several weed species (Supronienе *et al*., 2019).At the same time, *F. oxysporum* is known to have a much broader host range (Dean *et al*., 2012). Our results show that the level of antagonism against *F. oxysporum* did not significantly depend on the preceding crop, contrarily to what was found for*F. graminearum.* It is known, that within the *F. oxysporum* species there are so-called *formae speciales*– groups of lineages that are specialized to cause the disease in particular plant species (Kistler, 2001). The results suggest that the bacteria do not adapt to express antagonism against a particular *formae speciales*, but rather against the *F. oxysporum* species as a whole. This leads to similar patterns of antagonistic activity for different strains of *F. oxysporum.*

The cases of soils being suppressive to some soil-borne diseases are well-documented in the literature (Steinberg*et al*., 2019). At the same time, the influence of soil type on the level of bacterial antagonism against the phytopathogenic fungi has not been widely reported. The mechanisms that may contribute to the extent of pathogens suppression may include direct parasitism of soil bacteria on pathogenic fungal species or indirect mechanisms like competition for iron or causing the systemic resistance in host plants (Adesina*et al*., 2007; Han *et al*., 2000).

There is some evidence that soils that are suppressive to *Fusarium* wilts are most frequently neutral or alkaline (Alabouvette *et al*., 1996). However, our results have shown, that the most potent antagonistic bacteria were found in Albic Phaeozem, with pH levels varying from 5,5 to 6,0. This finding can be explained by the fact that in acidic soils the crops are more frequently affected by *Fusarium*wilt (Fang *et al*., 2012). The lowest level of *F. graminearum* growth inhibition was found in Haplic Chernozem and can be attributed to the high pH (at average, 7,5) and high content of $CaCO_3$characteristic to this soil type. These conditions intensify the competition for iron and are highly unfavorable for the phytopathogenic soil fungi (Steinberg*et al*., 2019). To conclude, the results suggest, that soil types that are suppressing *Fusarium* due to their physico-chemical properties are less likely to develop biological suppression from increased incidence of potent antagonistic bacterial strains. This is probably due to more frequent competition between the bacteria and fungi in disease-conductive soil types. The lack of crop rotation further increase the chances of bacteria and fungi to meet in the rhizosphere of the host plant.

4. CONCLUSIONS:

Thus, it was established that soil type could influence fungal-bacterial antagonistic interactions. The strongest antagonistic activity among all bacterial isolates was found in bacteria isolated from Albic Phaeozem. However, this effect does not not manifest for all selected strains of phytopathogens. The strongest dependence was found in antifungal activity against *F. graminearum.* The influence of the preceding crop on the antagonistic activity of bacteria was also determined. The greatest antagonistic activity against *F. graminearum* was shown by strains that were isolated from soils on which winter wheat was the preceding crop.

The most effective antagonists that were identified belonged to the genera *Bacillus* and *Paenibacillus*. These bacterial genera are known for a wide variety of nonribosomally synthesized metabolites, the production of which can be regulated by external factors. We couldhypothesize that, during the crop rotation, the microbial part of the biocenosis adapts to specific phytopathogens and adjusts its metabolism to the most effective fight against them. All of these factors should be considered when selecting agents for the biocontrol of fungal diseases of crops.

5. ACKNOWLEDGMENTS:

This publication was financially supported by the Southern Federal University.

6. REFERENCES:

[1] Adesina, M.F., Lembke, A., Costa, R., Speksnijder, A., Smalla, K. *Soil Biology and Biochemistry*, **2007**, *39*(11), 2818-2828.

[2] Alabouvette, C., Hoeper, H., Lemanceau, P., Steinberg, C. *Soil Biochemistry*, **1996**, *9*(1), 371-413.

Downloaded from www.periodico.tchequimica.com

[3] Basic Local Alignment Search Tool, http://www.ncbi.nlm.nih.gov/blast, accessed September 2019.

[4] Bookshelf, N. *Polyene Antifungal Drugs,* Galveston: University of Texas Medical Branch at Galveston, **2010**.

[5] Brodehl, A., Möller, A., Kunte H.J., Koch, M., Maul, R. *FEMS Microbiology Letters*, **2014**, *359*, 124–130.

[6] Cawoy, H., Cawoy, H., Debois, D., Franzil, L., De Pauw, E., Thonart, P., Ongena, M. *Microbial Biotechnology*, **2015**, *8*(2), 281-295.

[7] Cochrane, S.A., Vederas, J.C.*Medicinal Research Reviews*, **2016**, *36*, 4–31. https://doi.org/10.1002/med.21321

[8] Dean, R., Van Kan, J.A., Pretorius, Z.A., Hammond-Kosack, K.E., Di Pietro, A., Spanu, P.D., Rudd, J.J., Dickman, M., Kahmann, R., Ellis, J., Foster, G.D. *Molecular Plant Pathology*, **2012**, *13*(4), 414-430.

[9] Díaz, A, Smith, A, Mesa, P, Zapata, J., Caviedes, D., Cotes, A.M. *IOBC-WPRS Bulletin*, **2013**, *86*, 89–94

[10] Fang, X., You, M.P., Barbetti, M.J. *European Journal of Plant Pathology*, **2012**, *134*(3), 619-629.

[11] Gregorich, E.G., Carter, M.R. *Soil sampling and methods of analysis*, Boca Raton: CRC Press, **2007**.

[12] Han, D.Y., Coplin, D.L., Bauer, W.D., Hoitink, H.A. *Journal of Phytopathology,* **2000**, *90*(4), 327-332.

[13] Harunari, E., Komaki, H., Igarashi, Y. *Beilstein Journal of Organic Chemistry*, **2017**, *13*, 441.

[14] Hertweck, C. *Angewandte Chemie International Edition*, **2009**, *48*(26), 4688-4716.

[15] Howard, M.B., Ekborg, N.A., Weiner, R.M., Hutcheson, S.W. *Journal of Industrial Microbiology and Biotechnology*, **2003**, *30*(11), 627-635.

[16] Innis, M.A., Gelfand, D.H., Sninsky, J.J., White, T.J. *PCR protocols: a guide to methods and applications*, Cambridge: Academic Press, **2012**.

[17] Kistler, H.C. Evolution in host specificity in Fusarium oxysporum. In B.A. Summerell, J.F. Leslie, D. Backhouse, W.L. Bryden, L.W. Burgess (Eds.), *Fusarium: Paul E. Nelson Memorial Symposium, Pennsylvania State University–1997. American Phytopathological Society, St. Paul, MN*, **2001**, p.112-115

[18] Lazarovits, G., Turnbull, A., Johnston-Monje, D. *Encyclopedia of Agriculture and Food Systems*, **2014**,*4*, 388–399.

[19] Leslie, J.F., Summerell, B.A. *The Fusarium Laboratory Manual*, Ames: Blackwell Publishing, **2006**.

[20] Mansour, M.B., Goh, Y.K., Vujanovic, V. *Annals of Microbiology*, **2012**, *62*(3), 965-971.

[21] Mongkolthanaruk, W. *Journal of Microbiology and Biotechnology*, **2012**, *22*(12), 1597-1604.

[22] Moreno-Velandia, C.A., Izquierdo-García, L.F., Ongena, M., Kloepper, J.W., Cotes, A.M. *Plant and Soil*, **2019**, *435*(1-2), 39-55.

[23] Naumova, E.S., Serpova, E.V., Naumov, G.I. *Biochemistry*, **2007**, *72* (12), 1659-1667.

[24] Ribosomal Database Project II, http://www.cme.msu.edu, accessed September 2019.

[25] Steinberg, C., Edel-Hermann, V., Alabouvette, C., Lemanceau, P. *Modern Soil Microbiology*, **2019**, *5*, 343.

[26] Suproniene, S., Kadziene, G., Irzykowski, W., Šneideris, D., Ivanauskas, A., Sakalauskas, S., Serbiak, P., Švėgžda, P., Auskalniene, O., Jedryczka, M. *Fungal Ecology*, **2019**, *37*, 30-37.

[27] Tamura, M., Mochizuki, N., Nagatomi, Y., Harayama, K., Toriba, A., Hayakawa, K. *Toxins*, **2015**, *7*, 582–592.

[28] Tsuge, K., Inoue, S., Ano, T., Itaya, M.,Shoda, M. *Antimicrobial Agents and Chemotherapy*, **2005**, *49*(11), 4641-4648.

[29] Walsh, C.T. *Natural Product Reports*, **2016**, *33*(2), 127-135.

[30] Wang, S.L., Chang, W.T. *Applied and Environmental Microbiology*, **1997**, *63*(2), 380-386.

[31] Zalila-Kolsi, I., Afif, B.M., Hacina, A., Sameh, S., Zina, N., Slim, T., Kaïs, J.

Downloaded from www.periodico.tchequimica.com

Microbiological Research, **2016**, *192*, 148-158.

[32] Zapata, J, Díaz, A. Evaluaciones en invernadero y selección de prototipos a base de rizobacterias. In: Díaz A (ed) *Estrategias de control biológico de* Fusarium oxysporum *en el cultivo de uchuva (*Physalis peruviana*),* Bogotá: Produmedios, **2012**, 62–70

Table 1. *Primers used for sequencing*

Gene	Primer sequence
Fungi	
18S rRNA	NS1 -GTAGTCATATGCTTGTCTC NS4 – CTTCCGTCAATTCCTTTAAG
ITS1 and ITS2 spacers	ITS1 – TCCGTAGGTGAACCTGCG ITS4 – TCCTCCGCTTATTGATATGC
D1/D2 gene of 26S rRNA	NL-1 GCATATCAATAAGCGGAGGAAAG NL-4 GGTCCGTGTTTCAAGACGG
Bacteria	
16S RNA	**8F** – AGA GTTTGA TCC TGG CTC AG **926R –** CCG TCA ATT CCT TTR AGT TT **1492R –** GGT TAC CCT TGT TAC GAC TT

Table 2. *Primers used for PCR identification*

Species	Primers	Tm. °C	Amplicon size, bp
Bacillus subtilis	secYsubF TTATATCACGGCTTCGAT secYsubR CGGTAGTTTCGTTTCACCA	57	1050
Bacillus amyloliquefaciens	Bamy-f AAATCTGCCCGTATCGTCGGT Bamy-r GTGAGCATTGGCGTCACGGCG	60	747
Bacillus licheniformis	secYlichF TTACATCACAGCTTCTAT secYlichR CGATAGTTTCGTTTTACCA	57	1050
Bacillus atrophaeus	Batr-f CACCCTCACGGAGATTCCGCA Batr-rAATTCTTTCTTTCCCTGATGG	54	541
Bacillus mojavensis	Bmoj-f CGTTATCGTATCCCGGGCA Bmoj-r AAAATTCTTTCTTTCCCTGAC	60	685
Bacillus vallismortis	Bval-f CGGATGTTCGTGACGGTTTAC Bval-rCCGCAGTCGGGAAGTCAGGA	60	538
Bacillus sonorensis	Bson-f CTTGTTCAAGGCCATGGG Bson-r CCAAATGATGTTTGAAGT	57	684

Downloaded from www.periodico.tchequimica.com

Table 3. *The results of identification of fungi and bacteria*

Strain	Genbank accession number(s)	Species, according to rRNA gene analysis	% of gomology
Fus 1	MN083273 (28 S) MN089640 (5,8 S /ITS1, ITS2)	*Fusarium graminearum*	99
Poc 6.2.1	MN219593 (18 S) MN219583 (5.8 S) MN219634 (D1/D2 26 S)	*Fusarium oxysporum*	98
Poc 6.2.2	MN219651 (18 S) MN219656 (5.8 S) MN219658 (D1/D2 26 S)	*Fusarium oxysporum*	98
Poc 6.1	MN103524.1 (18 S) MN219565 (D1/D2 26 S)	*Fusarium oxysporum*	98
Ple1	MN396230 (18 S) MN396231 (5.8 S)	*Plectosphaerella cucumerina*	98
R 3.13	MN220147 (16 S)	*Paenibacillus peoriae*	99
R 4.5	MN220138 (16 S)	*Paenibacillus peoriae*	99
R 4.6	MN220139 (16 S)	*Bacillus amyloliquefaciens*	*97*
R 4.24	MN220140 (16 S)	*Paenibacillus jamilae*	99
R 5.31	MN220144 (16 S)	*Paenibacillus polymyxa*	99
R 6.14	MN220145 (16 S)	*Paenibacillus peoriae*	99
V 3.14	MN220146 (16 S)	*Bacillus amyloliquefaciens.*	99
O 1.27	MN219728 (16 S)	*Paenibacillus peoriae*	98
K 1.14	MN219707 (16 S)	*Paenibacillus jamilae*	99.
O 2.11	MN220137 (16 S)	*Paenibacillus peoriae*	99

Table 4.*The average growth inhibition zone diameters*

Species	Inhibition zone diameter
F. graminearum	22,441±0,810
F. oxysporum 1	12,995±0,632
F. oxysporum 2	14,946±0,570
F. oxysporum 3	14,559±0,536
P. cucumerina	19,941±0,878

Data presented as mean±0,95 confidence intervals

Table 5. *The correlations between the diameters of the growth inhibition zones for different fungal strains*

	Fungal species	1	2	3	4	5
1	*F. graminearum*	1.000				
2	*F. oxysporum 1*	0.237*	1.000			
3	*F. oxysporum 2*	0.218*	0.350*	1.000		
4	*F. oxysporum 3*	0.381*	0.281*	0.368*	1.000	
5	*P. cucumerina*	0.106	0.217*	0.296*	0.321*	1.000

** – correlation is significant at p<0,05*

Downloaded from www.periodico.tchequimica.com

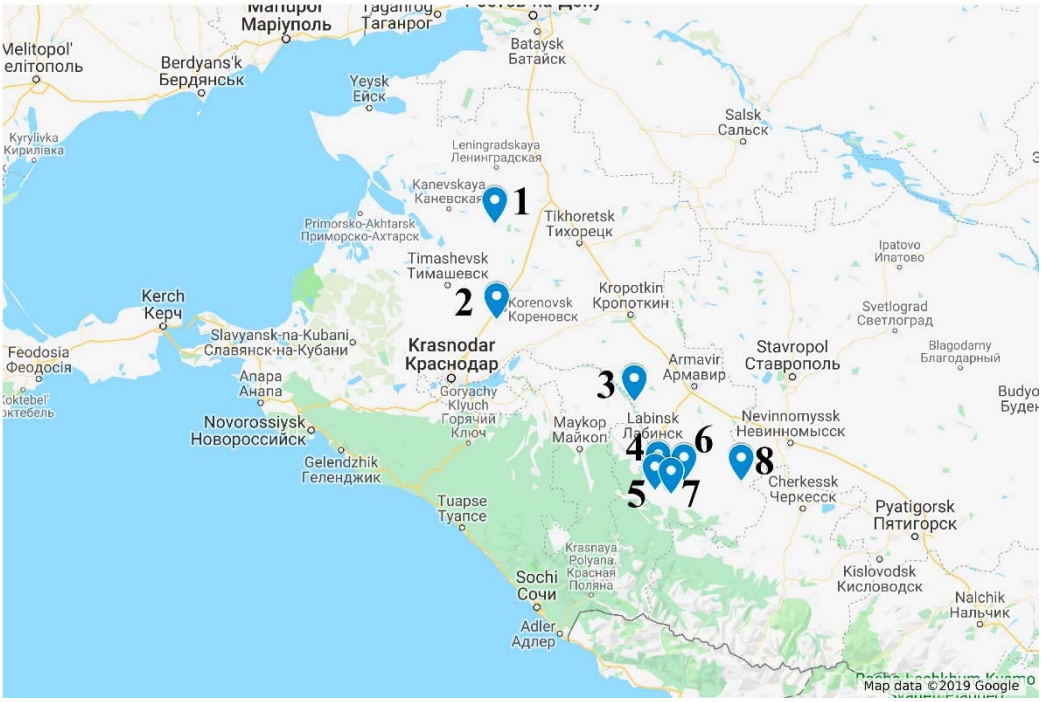

Figure 1. *The locations of the soil sampling sites*

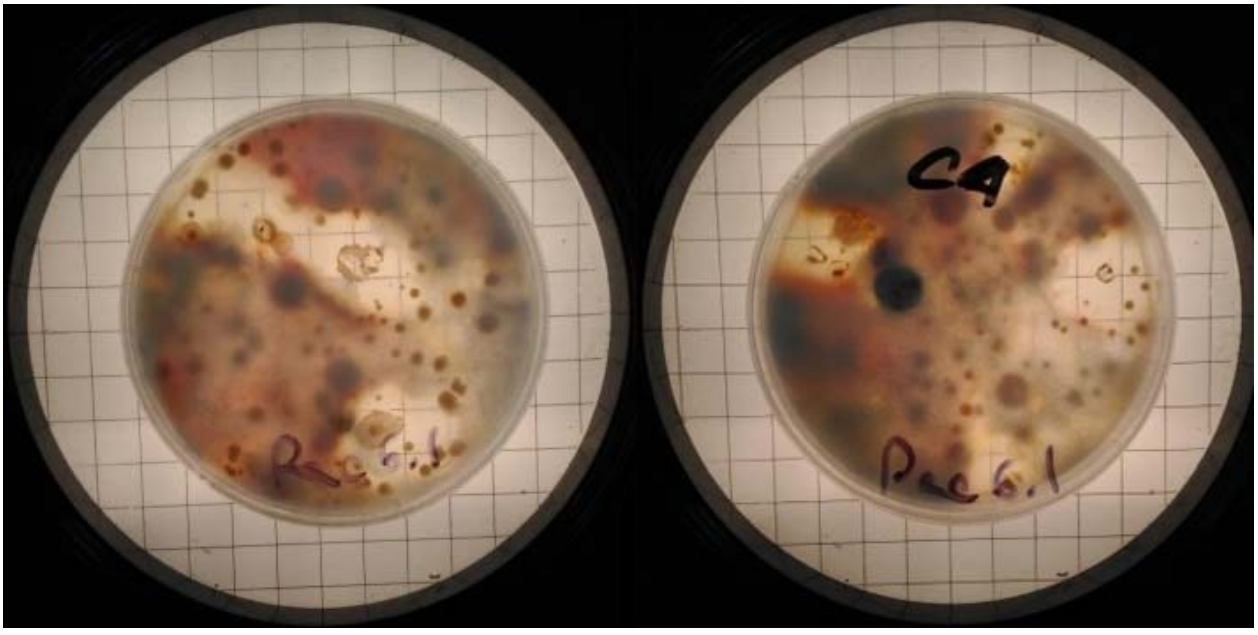

Figure 2. *The primary isolation of strains with antagonistic properties*

Downloaded from www.periodico.tchequimica.com

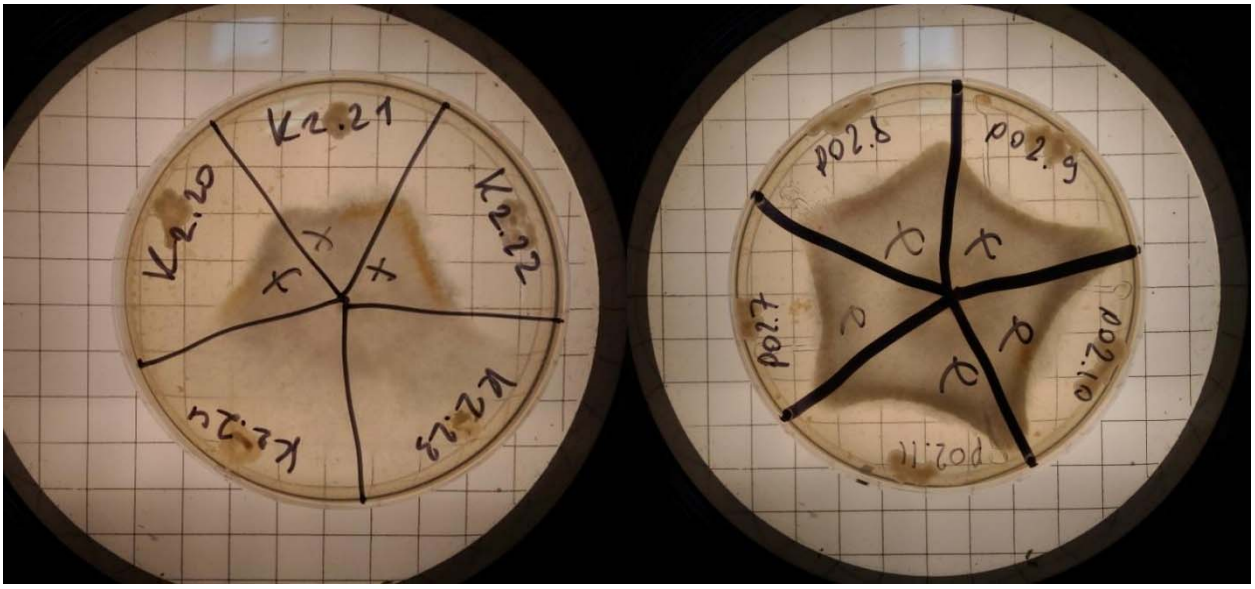

Figure 3. *The measurment of the inhibition zone diameters*

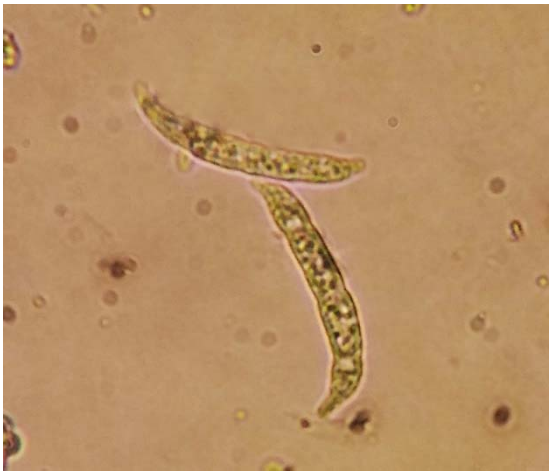

Figure 4. *The characteristic morphology of macroconidia of Fus1 strain on diagnostic medium.*

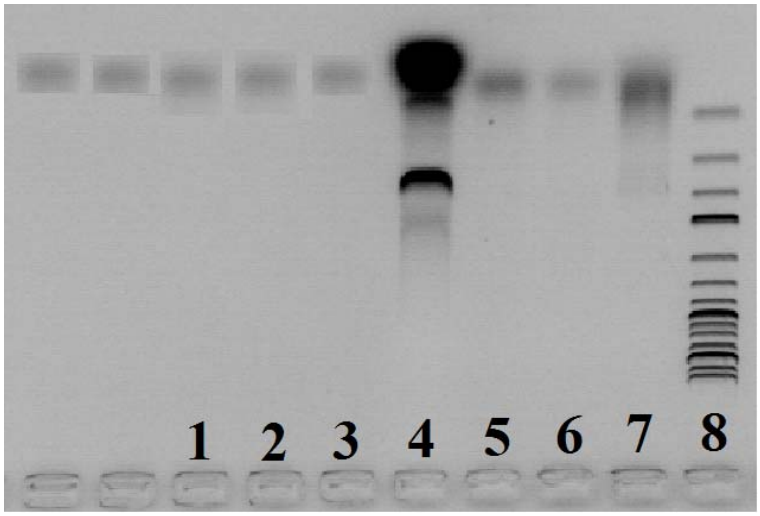

Figure 5. *PCR analysis of strain R 4.6 using species-specific primers*

Downloaded from www.periodico.tchequimica.com

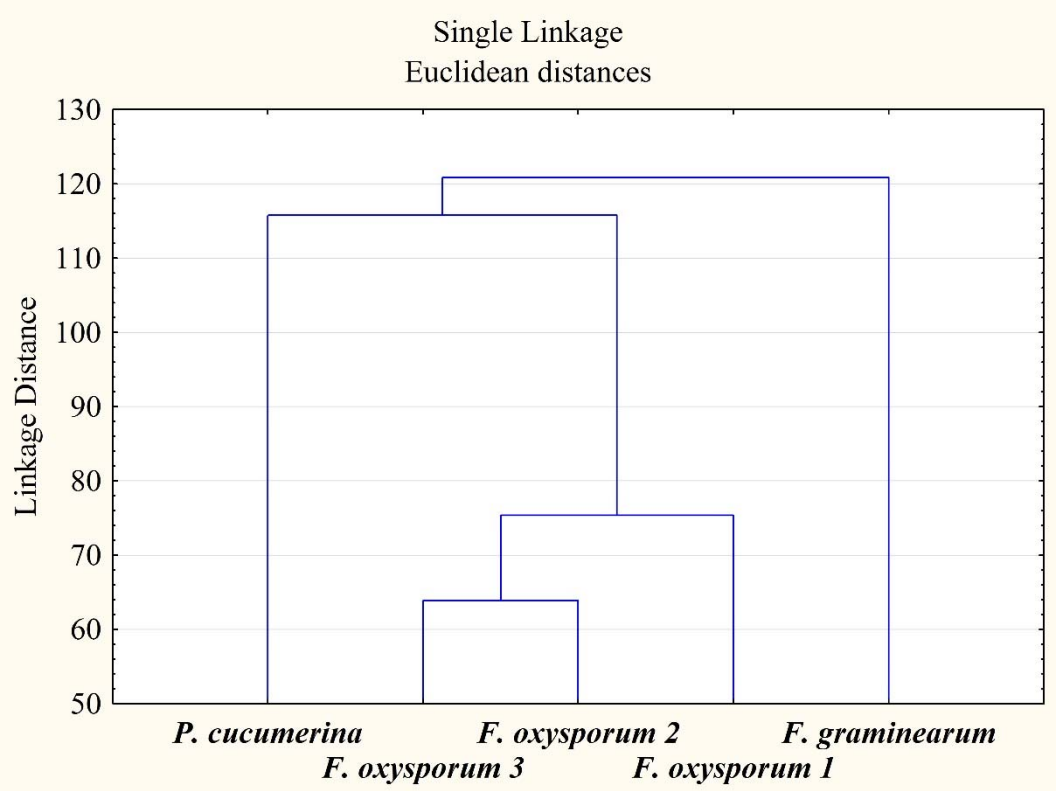

Figure 6. *The results of cluster analysis based on growth inhibition zone diameters*

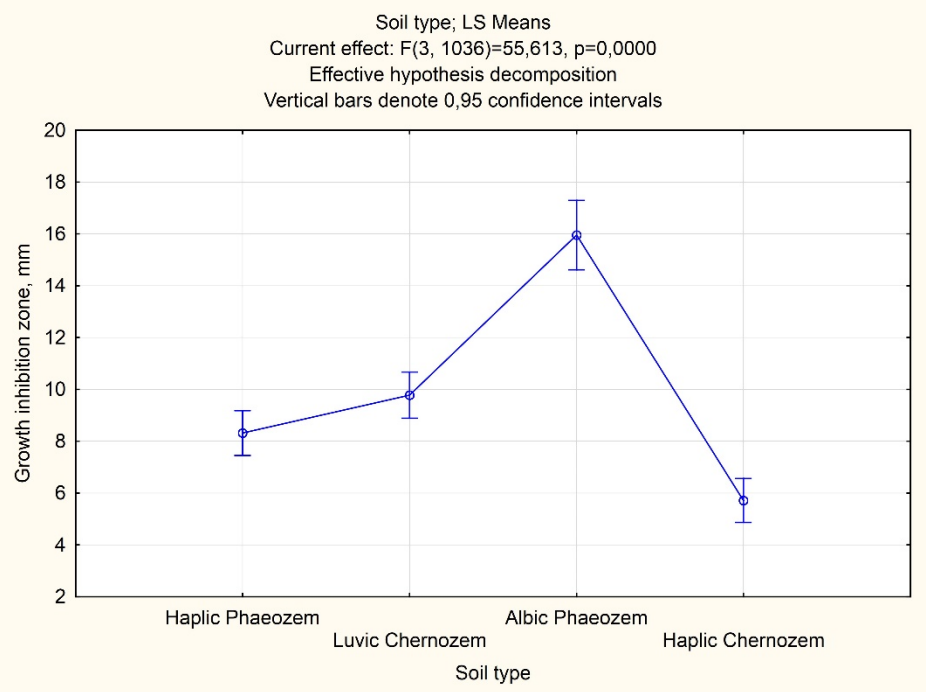

Figure 7. *The growth inhibition of F. graminearum caused by the bacterial isolates from different soil types*

Downloaded from www.periodico.tchequimica.com

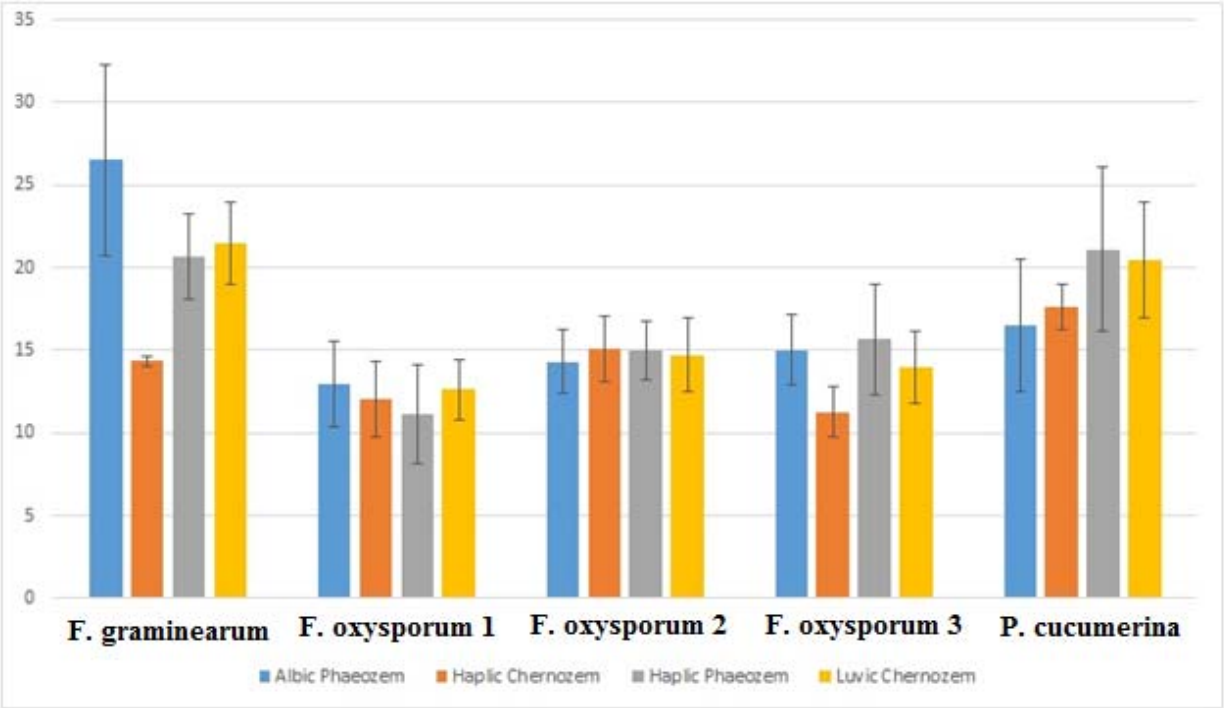

Figure 8. *The growth inhibition of fungal strainscaused by the bacterial isolates from different soil types*

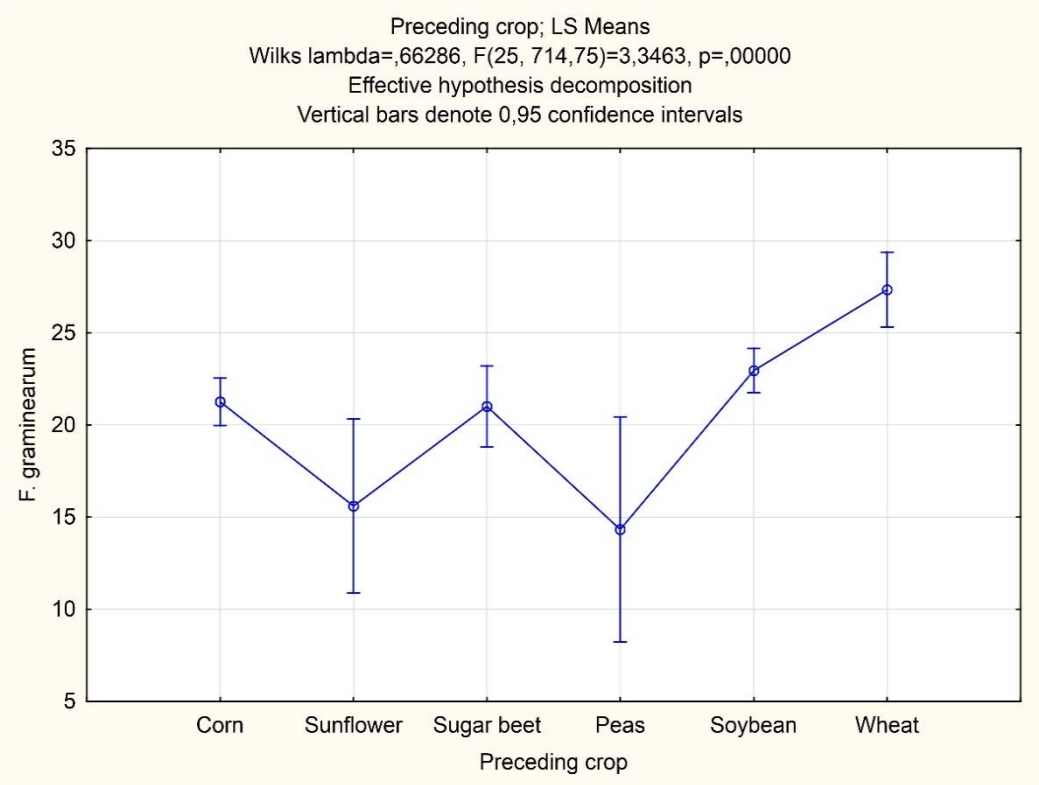

Figure 9. *The growth inhibition of F. graminearum caused by the bacterial isolates from fields with different preceding crops*

Downloaded from www.periodico.tchequimica.com

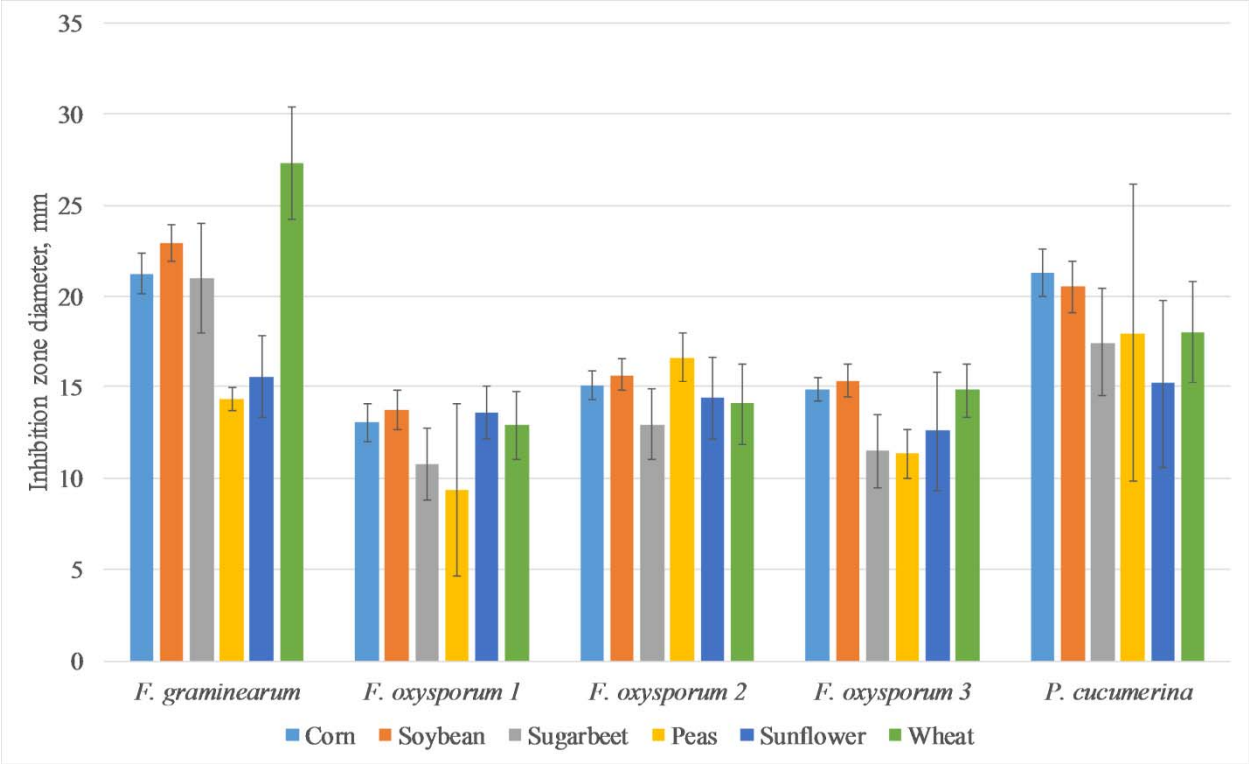

Figure 10. *The growth inhibition of fungal strains caused by the bacterial isolates from fields with different preceding crops*

Downloaded from www.periodico.tchequimica.com

PERIÓDICO TCHÊ QUÍMICA
ARTIGO ORIGINAL

PRODUÇÃO DE LATICÍNIOS À BASE DE LEITE DE CAMELO PARA FINS ESPECIAIS

PRODUCTION OF A DAIRY PRODUCT BASED ON CAMEL MILK FOR SPECIAL PURPOSES

DIKHANBAYEVA Fatima[1]; ZHAKSYLYKOVA Gulshat[1]; SYZDYKOVA Laila[1]; SMAILOVA Zhuldyz[2]; TASTURGANOVA Elmira[1*]

[1]Almaty technological university, Department of «Technology of food products», Almaty, Kazakhstan

[2]Korkyt ata Kyzylorda state University, Department of «Professional education», Kyzylorda, Kazakhstan

**Correspondence author*
@-mail: 66bel@bk.ru

Received 05 August 2019; received in revised form 22 October 2019; accepted 22 October 2019

RESUMO

O manuscrito discute a possibilidade de produzir um produto lácteo à base de leite de camelo para fins especiais. A nutrição especializada destina-se a todos os grupos populacionais e grupos de risco devido ao conteúdo de ingredientes funcionais específicos e à composição equilibrada ou enriquecida de substâncias alimentares. O grupo de risco, além de crianças e pessoas com problemas de saúde, são os idosos, para os quais é fornecida uma nutrição especial. Fermentos probióticos são utilizados na produção de laticínios fermentados, bem como na fabricação de manteiga e queijo. O fermento é introduzido no produto e vêsenvolve-se sob condições controladas. No processo de fermentação que ocorre dessa maneira, as bactérias formam substâncias que conferem ao leite fermentado suas propriedades características, como acidez (pH), sabor, aroma e consistência. A diminuição do pH que ocorre durante a fermentação pelas bactérias lactose em ácido lático tem um efeito conservador no produto, melhorando o valor nutricional e a digestibilidade. Ao contrário do leite de vaca, o leite de camelo é mais saturado com vitaminas e ácidos graxos poliinsaturados. É um medicamento natural biológico curativo, bem como um modulador imunológico para o corpo humano. O leite de camelo é o alimento comum para a sociedade pastoral e uma rica fonte de nutrientes com valor terapêutico. O processamento do leite pode melhorar as propriedades nutricionais, aumentar a digestibilidade das macromoléculas e torná-lo seguro contra micróbios nocivos. A proporção ideal (1:1) de fermentos probióticos para bebidas fermentadas de leite - novas Bio Drinks à base de leite de camelo - foi estabelecida.

Palavras-chave: Leite, leite de camelo, produtos lácteos, produtos para fins especiais, fermento, fermentação.

ABSTRACT

The manuscript discusses the possibility of producing a dairy product based on special-purpose camel milk. Specialized nutrition is intended for all population groups and risk groups due to the content of targeted functional ingredients and balanced or enriched composition of food substances. The risk group, in addition to children and persons with impaired health, are elderly people, for whom a special nutrition is provided. Probiotic ferments are used in the production of fermented dairy products, as well as in butter and cheese making. The leaven is introduced into the product and allowed to develop in it under controlled conditions. In the process of fermentation taking place in this way, bacteria form substances that give the fermented milk product its characteristic properties, such as acidity (pH), taste, aroma, and consistency. The decrease in pH occurring during fermentation by lactose bacteria to lactic acid has a preservative effect on the product while improving nutritional value and digestibility. Unlike cow's milk, camel's milk is more saturated with vitamins and polyunsaturated fatty acids. It is a healing biological natural medicine, as well as an immune modulator for the human body. Camel milk is the common food for pastoral society and a rich source of nutrients with therapeutic value. Milk processing can improve the nutritional properties, increase the digestibility of macromolecules and make it safe from harmful microbes. The optimal ratio (1:1) of probiotic ferments for fermented milk drinks – new Bio Drinks based on camel milk - was established.

Keywords: Milk, camel milk, dairy product, special-purpose products, ferment, fermentation

Downloaded from www.periodico.tchequimica.com

1. INTRODUCTION

When developing foods for special uses, it is necessary to take into account the principles laid down in the concepts of rational, well-balanced, therapeutic, and functional nutrition. The formulation of the product should be developed in accordance with the priority task set for each product, namely: managing essential and other nutrients in the diet. One of the areas of development of dairy foods for particular uses is the enrichment of milk and dairy products (Pasko O. V., 2005).

Currently, some studies are being conducted aimed at producing specialized fermented dairy products that are significantly superior to whole milk, since the number of low-molecular-weight immunoregulatory peptides increases dramatically during the fermentation process. Fermented dairy products containing probiotics and prebiotics can be used to prevent and treat certain diseases (e.g., intestinal and immune diseases) (Siavash Iravani *et al,* 2015). As a result of the use of such products, the state of the microflora of the digestive tract is normalized and the body's immunity improves.

One of the challenges faced by public health professionals is to demonstrate the effectiveness of nutrition education to improve the attitude to the nutrient-dense foods (Deborah J. Nolan-Clark *et al, 2011*). Dairy products are a key source of many nutrients that are not sufficiently consumed since children and adults do not consume the recommended amounts from this food group [4]. It is also recommended using dairy products as the preferred source of calcium and vitamin D in the elderly people (Olivier Ethgen *et al, 2015*). Milk can reduce damage to the intestinal tissue and protects children from enterocolitis (Layla Panahipour *et al,* 2018).

In order to provide the population with the foods, including dairy products that meet modern requirements of nutrition science, the new raw materials are intensively being searched for. In this connection, creating a scientific and practical rationale for the possibility of using camel milk in order to expand raw materials and produce foods that meet the requirements of a balanced diet (Tasturganova E. *et al,* 2018) seems very relevant.

In their article, some scientists stated that camel milk in Kazakhstan is mainly consumed after being fermented. Fermented camel milk, which is called shubat, is usually produced in the traditional way. Changes in the mineral composition of camel milk during fermentation have been studied rarely, especially for heavy metals. This study was aimed at assessing changes in the content of heavy metals and trace elements in the fermentation process (Meldebekova A. *et al,* 2008).

The scientists also claim that dairy products and shubat are used in folk medicine and in several clinics in Kazakhstan to treat tuberculosis, chronic gastritis, colitis and other diseases (Saitmuratova, O.K. *et al,* 2015).

A camel is a multipurpose animal with a huge production potential. Camel milk is a key food in arid and semi-arid regions of African and Asian countries. The quality of milk is influenced by various bacteria contained in milk, as described in the article by some scientists (Abera, T. *et al,* 2016).

Changes in the composition of dromedary milk have been studied by including common parameters, such as protein, total fat, lactose, basic minerals (calcium, phosphorus, and iron) and vitamin C (Konuspayeva, G. *et al,* 2010).

Foreign scientists have been developing production technologies for dairy food based on camel milk. With the addition of a stabilizer, camel milk yogurt was made. Stabilizers were added to improve the texture of the product (Al-Zoreky, N.S. *et al,* 2015). A fermented food produced from spontaneously fermented camel milk that contains several types of bacteria can be used in the production of dairy functional foods (Soleymanzadeh, N *et al,* 2016).

This study of scientists was intended to characterize the dominant microflora in shubat, a special fermented food made of camel milk. Seven shubat samples examined contained lactic acid bacteria and yeast as the dominant microorganisms (Rahman, N. *et al,* 2009).

Due to the growing demand for avoiding the use of chemical additives in foods, bacteriocins can have a significant potential in food preservation. Of the eleven strains of *Lactobacillus acidophilus* derived from camel milk, three strains demonstrated inhibitory activity against foodborne pathogens. *L. acidophilus AA105* showed antimicrobial

Downloaded from www.periodico.tchequimica.com

activity of a wide range (Abo-Amer, A.E. *et al,* 2013).

The key features of camel milk compared to other types of milk are fats with low content of fatty acid and unsaturated fatty acid. Proteins are rich in lactoferrin and lysozyme but have a lack of β-lactoglobulin. It has a higher percentage of total salts, free calcium, protective proteins, and vitamin C, as well as some micro minerals, namely iron, copper, and zinc. Physical and chemical properties. It has been proven that high stability of camel milk is the highest at pH 6.8, and it ferments relatively slowly compared to bovine milk. Camel milk is successfully processed to produce a variety of foods, such as fermented milk, soft cheese, etc. Camel milk has been traditionally used in different regions of the world as a natural adjuvant for the treatment of various human diseases (Singh, R. *et al,* 2017).

In this regard, in order to provide the population with food products that meet the modern requirements of nutrition science, the development of technology of dairy products based on camel milk is an urgent task.

2. MATERIALS AND METHODS

2.1. Samples

Laboratory studies of prototypes were carried out in the research laboratory of Kemerovo State University (Kemerovo, Russian Federation). Prototypes of fermented milk drinks from camel milk were made from the milk of the Kazakh double-humped camel (Bactrian) at the age of 4 years; camel milk was bought at the camel farm LLP "Daulet-Beket" (Akshi village, Almaty region, Kazakhstan).

Prototypes were manufactured in the research center of milk processing of Almaty technological University (Almaty, Republic of Kazakhstan).

2.2 Chemical composition

Dairy product (bio drink) based on camel milk for special uses. On the appliance, "Laktan" was defined as proteins, fats, and carbohydrates dairy product. As a result, the calorie content of the finished product is calculated. According to the following characteristics, the tasting Commission assessed the quality of the dairy product: color, taste, odor, and texture.

2.3 Sensory indicators of meat products

Sensory evaluation was carried out using score assessment. Five points scores of intensity and desirability scales were used in the experiment. There was from 1 point (very slight) to 5 point scores of intensity (very strong) and similar for desirability: from 1 point (undesirable) to 5 points (very much desirable). Prototypes of dairy products were examined using five panels. The products were prepared in the form of fermented milk drinks (yogurt). The following sensory parameters were studied: 1-taste, 2-smell, and aroma, 3-appearance, 4-consistency, 5-color.

3. RESULTS AND DISCUSSION:

The first stage of the process flow begins with the sanitization of equipment. With the deterioration of the sanitary parameters of the finished product, a thorough analysis and additional control of the process flow is conducted to identify the causes of the secondary contamination of the product; they check the quality of the starter, as well as the sanitary and hygienic state of the workshop.

Milk is pasteurized at a temperature of 63°C with a holding for 30 minutes or at 72°C with a holding for 20 minutes. Heat treatment of milk is usually combined with homogenization. Homogenization at a temperature not lower than 55°C and a pressure of 17.5 MPa improves the texture of the bio drink and prevents the isolation of whey.

Pasteurized and homogenized milk is immediately cooled in the regenerative section of the pasteurization unit down to the temperature of fermentation with pure cultures of lactic acid bacteria: using thermophilic cultures – to 37°C. A starter should be immediately added to the milk cooled down to the fermentation temperature.

Before adding to milk, the starter is thoroughly mixed with water, then poured into the milk with constant stirring. The mixture is stirred for 15 minutes. Then yeast is added to ferment lactose. The mixture is stirred for 20 minutes.

Milk ripening takes 8 hours. During this

Downloaded from www.periodico.tchequimica.com

time, milk proteins swell, the lactic acid process slows down or stops completely, lactic acid microorganisms stop developing. The end of the fermentation is determined by the acidity, which should be slightly lower than the acidity of the finished product. When the required acidity is reached, the bio drinks are immediately cooled down to a temperature not higher than 4°C, and then poured into sterile containers. The finished bio drink is stored until sold at a temperature of 0-2°C. The finished products are monitored for the presence of coliform bacteria and a microscopic slide from one or two batches at least every 5 days. Special attention should be paid to equipment in direct contact with the product in the production process.

Formulation of dairy product (bio drink) based on camel milk for special Purposes

Table 1. *Formulation of the Dairy Food (Bio Drink) Production Based on Camel Milk for Special Purposes*

Raw materials and components	**Consumption, L per 100 L of product**
Camel milk Fat content – 3.92 % Non-fat milk solids – 10.61 %	100
Probiotic starter, kg	0.4
Yeast to ferment lactose, wipe samples from culture medium, CFU/g	

Table 2. *Nutrition Value of the Dairy Food (Bio Drink) Production Based on Camel Milk for Special Purposes*

Parameters, UoM	**Dairy product (bio drink)**
Energy value, kcal	67.24
Proteins, g	3.24
Fats, g	3.92
Carbohydrates, g	4.75

As can be seen from this table, the energy value of the dairy product (bio drink) is 64.41 kcal.

In order to determine the quality of the dairy product based on camel milk, it was tasted.

The quality assessment criterion for the dairy product based on camel milk was organoleptic indicators, such as color, odor/aroma, appearance, taste, texture.

Table 3. *Organoleptic Indicators of the Dairy Food (Bio Drink) Production Based on Camel Milk for Special Purposes*

Indicator	**Description**
1. Dairy product (bio drink)	
Color	Milk white, with a pale a yellowish tinge
Taste and odor	Odor: fermented milk, refreshing, rather sharp
Texture	Liquid, homogeneous, foaming, free from impurities

4. CONCLUSIONS:

Camel milk has a specific taste, rich in vitamins and polyunsaturated fatty acids. As a result of microbiological control, compliance of camel milk with microbiological safety and quality requirements and detection of microbiological contamination of raw materials was determined. The content of lactic acid microorganisms with probiotic properties in Bio Drink No. 1, their contents 5*106 CFU/g in the Bio Drink number 2, the content of 3.7*106 CFU/g in the Bio Drink, No. 3, content of 4*106 CFU/g in the Bio Drink No. 4, the content of 3.6*106 CFU/g was determined. The qualitative and quantitative composition was also determined, which established: 1:1 starter for fermentation of Bio Drinks.

5. REFERENCES:

1. Pasko O. V.: *Scientific bases of technology of products for special food. Monograph. – Omsk: Publishing house of Omsk Institute of business and law,* **2005**.

2. Siavash Iravani, Hassan Korbekandi, Seyed Vahid Mirmohammadi. *Journal of Food Science and Technology*, **2015**, 52, Issue 8, 4679–4696.

3. Deborah J. Nolan-Clark, Elizabeth P. Neale, Yasmine C. Probst, Karen E. Charlton, Linda C. Tapsell. *Consumers' salient beliefs regarding dairy products in the functional food era: a qualitative study using concepts from the theory of planned behaviour. BMC Public Health*, **2011**, 11:843.

4. Erin E Quann, Victor L Fulgoni III, Nancy Auestad. *Nutrition Journal*, **2015**, 14:90.

Downloaded from www.periodico.tchequimica.com

5. Olivier Ethgen, Mickaël Hiligsmann, Nansa Burlet, Jean-Yves Reginster. *Archives of Public Health,* **2015**, 73:48.

6. Layla Panahipour, Shayesteh Nasserzare, Zeinab Amer, Friedrich Brücke, Alexandra Stähli, Alexandra Kreissl, Nadja Haiden, Reinhard Gruber. *Clinical Oral Investigations*, **2019**, 23, Issue 4, 1959–1966.

7. Tasturganova E, Dikhanbaeva F, Prosekov A, Zhunusova G, Dzhetpisbaeva B, Matibaeva A. *Current Research in Nutrition and Food Science Journal* **2018**, 6(2), 491-499.

8. Meldebekova A., Konuspayeva G., Diacono E., Faye B. *Impact of Pollution on Animal Products,* **2008***,* 117-123.

9. Saitmuratova, O.K., Yakubova, F.T. & Sagdiev, N.Z. *Chemistry of Natural Compounds,* **2015**, 51, 810–812.

10. Abera, T., Legesse, Y., Mummed, B. et al. *Ethiopian Somali regional state. BMC Research Notes*, **2016.**

11. Konuspayeva, G., Faye, B., Loiseau, G. et al. *Tropical Animal Health and Production*. **2010**, 42(3), 495–499.

12. Al-Zoreky, N.S. & Al-Otaibi, M.M. *Food Science and Biotechnology*, **2015**, 24(2), 601–606.

13. Soleymanzadeh, N., Mirdamadi, S. & Kianirad, M. *Dairy Science & Technology*. **2016**, 96(4), 443–457.

14. Rahman, N., Xiaohong, C., Meiqin, F. et al. *World Journal of Microbiology and Biotechnology*.**2009**, 25(11) 1941–1946.

15. Abo-Amer, A.E. *Applied Biochemistry and Microbiology.* **2013**, 49(3), 270–279.

16. Singh, R., Mal, G., Kumar, D. et al. *Agricultural Research*, **2017**, 6(4) 327–340.

17. Lisitsyn A., Makangali K., Uzakov Y., Taeva A., Konysbaeva D., Gorbulya, V. *Current Research in Nutrition and Food Science journal*, **2018,** 6(2): 536-551.

18. Akinloye, A.M. and O.O. Adewumi. *Int. J. Develop. Sustain*, **2014**, 3 (1): 150-161.

19. Al haj, O.A. and H.A. Al Kanhal. *Int. Dairy J.* **2010**, 20(12): 811-821.

20. Amira, A.B., S. Besbes, H. Attia and C. Blecker. *Int. J. Food Prop*, **2017**, 20 (sup1): S76-S93.

21. AOAC. Official method of analysis. Association of Official Analytical Chemists.17th Ed. Association of Official Analytical Chemists, Washington, DC, USA, **2000.**

22. Berhe, T., E. Seifu, R. Ipsen, M.Y. Kurtu and E.B. Hansen. *Int. J. Food Sci*. **2017,** 2017: 8.

23. Bintsis, T. and P. Papademas. *Global Cheese making Technology*, **2017,** 120-156.

24. Dagostin, J.L.A., D. Carpine and M.L. Masson. *Food Bioprocess Technol*., **2013** 6(11): 3017 –3028.

25. Dubey, U.S., M. Lal, A. Mittal and S. Kapur. *Emir. J. Food Agric.,* **2016,** 28(3): 164-176.

26. García, V., S. Rovira, K. Boutoial, D. Álvarez and M. B. López. A. *J. Dairy Sci. Technol.,* **2014,** 95(2):197-208.

27. Ghada, Z.A. *The Egyptian J. Hospital Med*., **2005,** 21: 116 – 130.

28. Hailu, Y, E. Seifu and Z. Yilma. A*fr. J. Food Sci. Technol.,* **2014,** 5(3): 90-95.

29. Hailu, Y., E.B. Hansen, E. Seifu, M. Eshetu and R. Ipsen. *Int. Dairy J*., **2014** 60: 62-69.

30. Hailu, Y., E.B. Hansen, E. Seifu, M. Eshetu, M.A. Petersen, R. Lametsch, F. Rattray and R. Ipsen*. Int. Dairy J*., **2018**, 81: 122-130.

31. Keceli, T., N. Sahan and K. Yasar. *Aust. J. Dairy Technol*.,**2017,** 61: 32-36.

32. Khalesi, M., M. Salami, M. Moslehishad, J. Winterburn and A.A. Moosavi-Movahedi. *Trend. Food Sci.* Technol., **2017,** 62: 49-58.

33. Mukhametov, A., Dautkanova D., Zhakupova G. *J.Eng.Applied Sci*., **2018,** 13 (Special Issue 8): 6462-6466, 2018.

34. Konuspayeva, G., B. Camier, N. Aleilawi, M. Al-Shumeimyri, K. Al-Hammad, K. Algruin, F. Alshammari, E. Beaucher and B. Faye. *Int. J. Dairy Technol.,* **2017,** 70: 92-101.

35. Konuspayeva, G., B. Faye and G. Loiseau. *J. Food Comp. Anal.,* **2009,** 22(2): 95-101.

Downloaded from www.periodico.tchequimica.com

36. Lamichhane, P., A.L. Kelly and J.J. Sheehan. *J. Dairy Sci.,* **2018,** 101(3): 2692-2709.

37. Marshal, R.T. Standard methods for determination of dairy products.16th Ed. American Public Health Association, **1992,** Washington, D.C..

38. Metzger, L.E, D.M. Barbano, M.A. Rudan and P.S. Kindsted. *J. Diary Sci.,* **2000,** 84:648-658.

39. Ortiz Araque, L.C., M. Darré, C.M. Ortiz, J.F. Massolo and A.R. Vicente. *Int. J. Dairy Technol*., **2018,** 71(2): 340-346.

40. Rashmi, A., N. Bhojak and J. Rajani. *Int. J. Eng. Sci. Invent.* **2013,** 2(1): 7-10.

41. Abzhanova, Matibaeva A., Bulambayeva A., Dzhetpisbaeva, B.S., Serikkyzy, M.S., Rskeldiyev, B.A. *Asian Journal of Microbiology, Biotechnology & Environmental Sciences Paper*, **2018,** 20:26-35

42. Sánchez-Muñoz, M., M. Valdez-Solana, C. Avitia-Domínguez, P. Ramírez-Baca, M. Candelas- Cadillo, M. Aguilera-Ortíz, J. Meza-Velázquez, A. Téllez-Valencia and E. Sierra-Campos. *Foods,* **2017,** 6(8): 62.

43. Seth, K. and U. Bajwa. *J. Food Sci. Technol.,* **2015,** 52(3):1561–1569.

44. Stahl, T., H.I. Sallman, R. Duehlmeier and U. Wernery. *J. Camel Pract. Res*., **2006,** 13(1): 53-57.

45. Wernery, U. *J. Camel Pract. Res*., **2006,** 13(1): 15-26.

Downloaded from www.periodico.tchequimica.com

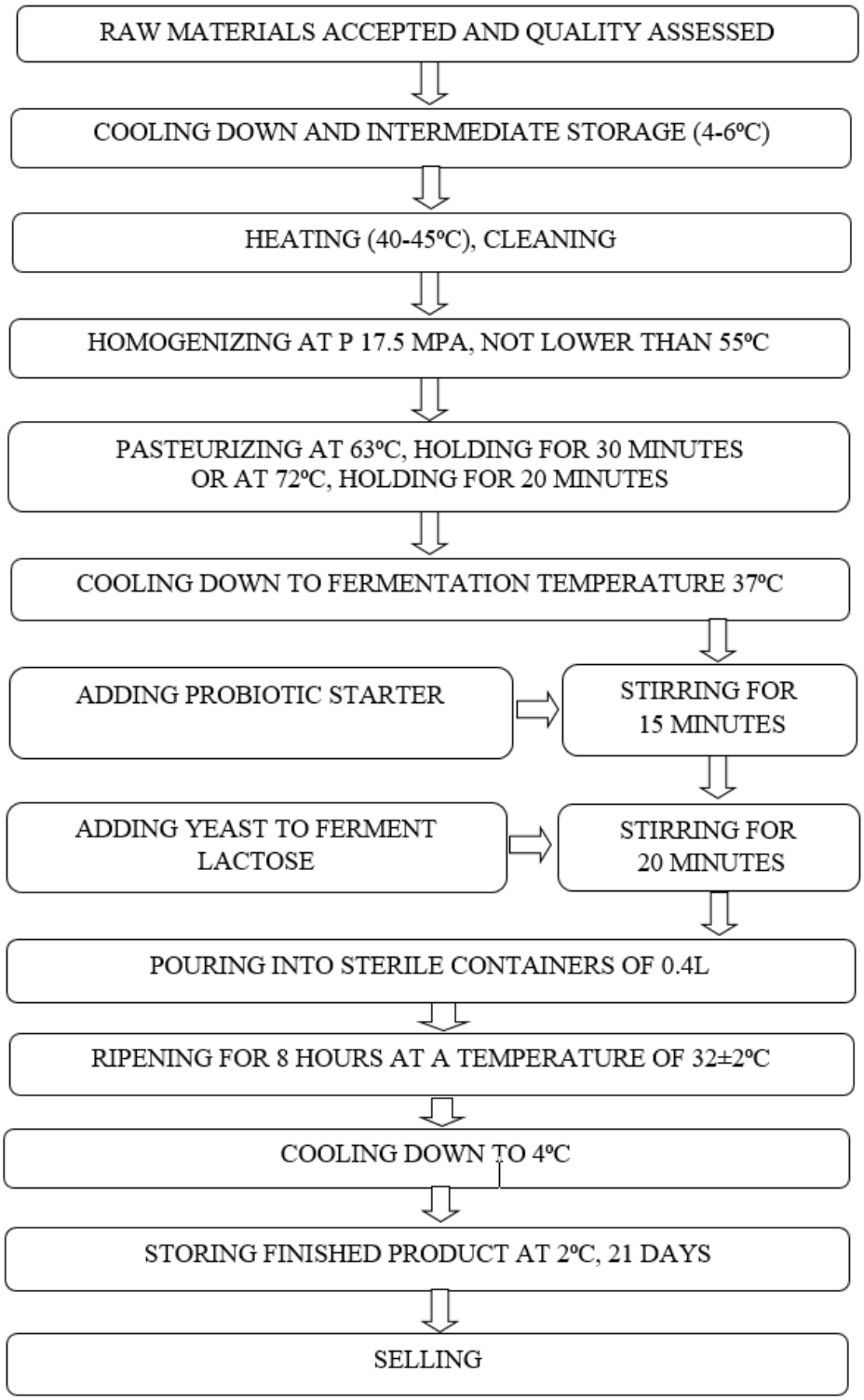

Figure 1. *Process Flow of the Dairy Food (Bio Drink) Production Based on Camel Milk for Special Purposes*

Downloaded from www.periodico.tchequimica.com

PERIÓDICO TCHÊ QUÍMICA
ARTIGO ORIGINAL

MUDANÇA DE FASE EM SISTEMAS HIDROGEOQUÍMICOS DE EQUILÍBRIO LOCAL COMO MECANISMO DE OCORRÊNCIA DE PRECURSORES FLUÍDICOS DE TERREMOTOS

PHASE REARRANGEMENT IN LOCAL BALANCED HYDROGEOCHEMICAL SYSTEMS AS A OF FLUID EARTHQUAKE PRECURSORS MECHANISM OCCURRENCE

ФАЗОВАЯ ПЕРЕСТРОЙКА В ЛОКАЛЬНО-РАВНОВЕСНЫХ ГИДРОГЕОХИМИЧЕСКИХ СИСТЕМАХ КАК МЕХАНИЗМ ВОЗНИКНОВЕНИЯ ФЛЮИДНЫХ ПРЕДВЕСТНИКОВ ЗЕМЛЕТРЯСЕНИЙ

ABDULLAEV, Abdulazyz U.[1*];

[1] Institute of Seismology, Laboratory of Hydrogeodynamics, 75A Al-Farabi Str., zip code 050060, Almaty – Republic of Kazakhstan

** Correspondence author*
e-mail: u.abdullaev@mail.ru

Received 30 June 2019; received in revised form 02 September 2019; accepted 22 October 2019

RESUMO

Cientistas de todo o mundo estão fazendo grandes esforços para resolver o problema da previsão de terremotos. Várias dezenas de diversos fenômenos e sinais foram descobertos que poderiam servir como precursores de terremotos. Mas esses efeitos descobertos se mostraram muito instáveis e tinham um caráter de mosaico no tempo e na área de seu desenvolvimento. Eles nem sempre apareceram e nem antes de cada forte terremoto. Existem muitos casos em que terremotos ocorreram sem o aparecimento de precursores. Tais "fenômenos" instáveis não nos permitem formular modelos adequados para a preparação de fortes terremotos e métodos para prevê-los. Entre os precursores bem estudados e encorajadores de terremotos, os mais promissores são as anomalias hidrogeodinâmicas e hidrogeoquímicas, que têm antecedentes científicos razoavelmente sólidos. Nesta classe de precursores, o mecanismo de sua formação durante a preparação de terremotos permanece discutível. Há perguntas sobre a fonte de concentrações anormais e seu transporte durante um curto período de tempo nos pontos de observação. No presente estudo se afirma que o principal mecanismo para a ocorrência de anomalias exóticas de fluidos transientes é a reestruturação interfásica no sistema hidrogeoquímico mais equilibrado localmente nos objetos de observação como reação aos efeitos da preparação de fortes terremotos. A reestruturação da fase interna no próprio sistema hidrogeoquímico é realizada através do relaxamento estrutural como resultado da ocorrência de reações físico-químicas de troca rápida.

Palavras-chave: *geodinâmica moderna, transições de fase, estado físico das águas subterrâneas, estresse tectônico, previsão de terremotos.*

ABSTRACT

Scientists all over the world are making tremendous efforts to solve the problem of earthquake prediction. Dozens of different phenomena and signs that could serve as precursors of earthquakes are found. But these effects were very unstable and had a mosaic character in the propagation of development and time. They appeared not always and not before every major earthquake. There are many cases where earthquakes occurred without the manifestation of any precursors. Such non-stationary phenomena do not allow formulating adequate strong earthquakes preparing models and their methods of predicting. Among well-studied and encouraging earthquake precursors, hydrogeodynamic and hydrogeochemical anomalies are considered to be the most promising, which has a sufficiently substantiated scientific background. In this class of precursors, the mechanism of their formation during the preparation of earthquakes remains debatable. There are several problems due to abnormal concentration sources and their transport during a little time period in the observation points. In the proposed work, it is proved that the main mechanism of the occurrence of exotic transient fluid anomalies is the interphase rearrangement in the local balanced hydrogeochemical system as a reaction to strong earthquakes factors preparing influence. The internal phase reorganization in the hydrogeochemical system is realized through structural relaxation as a result of the occurrence of rapid physicochemical reactions exchange.

Downloaded from www.periodico.tchequimica.com

Keywords: *modern geodynamics, phase transitions, the physical state of groundwater, tectonic stress, earthquake prediction.*

АННОТАЦИЯ

Ученые во всем мире прилагают громадные усилия для решения проблемы прогнозирования землетрясений. Обнаружены несколько десятков различных явлений и признаков, которые могли бы служить предвестниками землетрясений. Но эти обнаруженные эффекты оказались весьма неустойчивыми и имели мозаичный характер как во времени, так и на площади их развития. Они проявлялись не всегда и не перед каждыми сильными землетрясениями. Имеются немало случаев, когда землетрясения происходили без проявления каких-либо предвестников. Такие нестационарные «феномены» не позволяют сформулировать адекватные модели подготовки сильных землетрясений и методы их прогноза. Среди хорошо изученных и обнадеживающих предвестников землетрясений наиболее перспективными считаются гидрогеодинамические и гидрогеохимические аномалии, которые имеют достаточно обоснованные научные предпосылки. В этом классе предвестников дискуссионным остается механизм их формирования в процессе подготовки землетрясений. Существуют вопросы источника аномальных концентраций и их транспорт за небольшой отрезок времени в пунктах наблюдений. В предлагаемой работе доказывается, что основным механизмом возникновения экзотических быстротечных флюидных аномалий является внутрифазовая перестройка в самой локально-равновесной гидрогеохимической системе в объектах наблюдения как реакция её на воздействие факторов подготовки сильных землетрясений. Внутренняя фазовая перестройка в самой гидрогеохимической системе реализуется путем структурной релаксации в результате протекания быстрых обменных физико-химических реакций.

Ключевые слова: *современная геодинамика, фазовые переходы, физическое состояние подземных вод, тектонический стресс, прогноз землетрясения.*

---

1. INTRODUCTION

Underground water-gas systems as the most mobile component of the earth's crust in various geostructures are sensitive locally-equilibrium hydrogeochemical systems with a very thin structural-phase ratio in the rock-water-gas triad. Such systems are sensitive to external influences and adequately respond to them (Abdullaev, 2002). The formation of the physicochemical composition of underground fluids is directly dependent on the composition of the host rocks and the hydrogeological conditions for their localization (Posokhov, 1975; Driver, 1985; Kraynov and Shvets, 1992). An important area of research to identify the main mechanisms of the occurrence of hydrogeochemical precursors of earthquakes is the dynamics of rapid changes in the ion-salt composition in the hydrogeochemical systems themselves (Talabi, 2018; Warsaw, 1985). It is necessary to proceed from the postulate that in calm seismic situations in conditions of "rest" of the geological environment, the functioning of water-gas systems in time is characterized by local equilibrium in individual hydrogeological structures (Hörbrand *et al.,* 2018).

Studies of the relationship and interdependence of the chemical composition of groundwater and external factors (changes in atmospheric pressure, temperature, tidal forces of the Moon and the Sun) and endogenous factors (the occurrence of earthquakes) were carried out on the analysis of long-term continuous observations at the Almaty Seismic Active Prognostic Testing Ground (APF) in Southeast Kazakhstan (Figure 1), where since 1980. continuous monitoring of variations in a wide range of parameters of the gas chemical composition of groundwater is carried out in order to search for earthquake precursors. To understand the causes and mechanisms of the occurrence of exotic spatiotemporal hydrogeochemical anomalies that occur on the eve and in the periods and implementation of strong earthquakes, we consider the main key properties of these phenomena. According to (Abdullaev, 2002; Nikolaev, 1984), such anomalies are intermittent alternating changes of the so-called “indicative” parameters, which have 4 main morphogenetic groups: “bays”, “humps”, “jump-pulsation” and spontaneous “bursts” that are in amplitude altered surpass background levels by 20-50% to 100%, and sometimes times (Movchan and Yakovleva, 2017). They in the square have the property of “flickering” in time (Aitaliev *et al.,* 2005; O'Neill *et al.,* 2018).

In genetic terms, they are "returnable" i.e.,

Downloaded from www.periodico.tchequimica.com

after the event, and the “marker” parameter returns to its original level. The last property of the anomalies is long-range action, which is found in tens and hundredths of a km. from the source of earthquakes, i.e., they arise not only in the focal zone, but also far beyond its borders. A long search for adequate mechanisms reflecting all these phenomenal properties leads us to the conclusion that they must be “in themselves” and appear due to tectonic factors of earthquake preparation. In this aspect, we proposed a phenomenological model of the formation of exotic seismohydrogeochemical anomalies in the field of tectonic forces and the interaction of reversible chemical processes occurring between substances (Figure 2, right block) and a locally equilibrium open hydrogeochemical system (central block). In this model, all processes are reversible and can develop everywhere and not only in the focal zone covered by the influence of abnormal stresses but also beyond. The most important properties of exotic hydrochemical anomalies are explained quite convincingly here. in this interconnection, all processes universally occur at the vapor-water contact: (hydrolysis, dissolution, precipitation, ion exchange, complex formation, fluid migration, sorption-absorption, wringing of pore solutions, and many others, which are shown in the left block of Figure 2.

In this model, all processes are reversible and can develop everywhere and not only in the focal zone covered by the influence of abnormal stresses but also beyond. The most important properties of exotic hydrochemical anomalies are explained quite convincingly here. in this interconnection, all processes universally occur at the vapor-water contact: (hydrolysis, dissolution, precipitation, ion exchange, complex formation, fluid migration, sorption-absorption, wringing of pore solutions, and many others, which are shown in the left block of Figure 2 (Sobolev, 1993).

2. MATERIALS AND METHODS

To elucidate the mechanism of the ongoing restructuring in hydrogeochemical (GHC) systems on the effect of seismic processes, the salt composition of groundwater was calculated at the GHG stations Tau-Turgen, Gorelnik, and Chushkaly for 1990. and 1995 (Figure 1) due to the occurrence of two strong earthquakes in this area (Baysorunskoye, K = 15.3 and Kegenskoye, K = 13.7). Recalculation of chemical analyzes of groundwater from the ionic form to salt was carried out in accordance with the solubility of salts. In the first place, sparingly soluble, and then increasingly soluble compounds are combined. Thus, according to daily observations at the stations, by converting the results of chemical analyzes from the ionic form to the salt form, a possible hypothetical salt composition was calculated. Using the equivalent form for expressing the chemical composition of groundwater, it is easy to calculate combined ions in salts from the ion-equivalent form. (Posokhov, 1975; Driver, 1985; Kraynov and Shvets 1992; Laptev, 1995).

The ionic form of the chemical composition of groundwater is fully characteristic only of low salinity waters (Rouhi and Kalantari, 2019). With an increase in the concentration of dissolved salts between the ions, the interaction intensifies, and the process of association develops. Associated neutral pairs of $CaSO_4^0$, $MgSO_4^0$, $CaCO_3^0$ or charge-carrying molecules $Mg(HCO_3)^{2+}$, $Ca(HCO_3)^{2+}$ are formed in the solution. The ability of atoms and ions to attach or hold electrons is determined by their electronegativity, which in turn is a characteristic of the generalized acid-base properties of elements, i.e. a measure of how typical for a given element the role of a donor (cationic acid) or an acceptor (base anion) of an electron in compounds (Mattos *et al.,* 2018).

3. RESULTS AND DISCUSSION:

The general scheme of the binding of ions to salts according to the degree of solubility is as follows: Ca^{2+} ions first bind sequentially with HCO_3-, SO_4^{2-}, Cl^- depending on its content, and then Mg^{2+} and Na^+ bind in the same sequence. On the example of several strong earthquakes that occurred at the Almaty landfill in 1990-1995, we see that at the stations of Chushkaly, Turgen and Gorelnik the possible calculated salts of sodium, calcium, and potassium are Na_2SO_4, $NaHCO_3$, NaC1, $Ca(HCO_3)_2$, $CaCO_3$, K_2CO_3 the ratio of the concentration of these salts in the hydrogeochemical system itself on the eve of strong earthquakes in time has changed: some increase and others decrease, and the change in salt concentration is in antiphase due to a decrease in some and an increase in other salts. This process is clearly visible on the example of the temporary course of salts at the GKH station of Chushkaly during the period of the strong May and Baysorun earthquakes in 1990. in the center of the Almaty seismic-prognostic test site (Figures 3, 4), where a strong event (K = 15) was preceded by three impulse disturbances.

Figure 4 shows the course of the $CaHCO_2$ salt change at Tau-Turgen station in connection with the indicated earthquakes, which experiences an abrupt change in concentration before the May

Downloaded from www.periodico.tchequimica.com

earthquake, increasing before the Baysorun event. Figure 5 clearly shows the course of the change in Mg salts over time using another strong Kegen earthquake in 1995 as an example. (K = 13.7). Theoretically calculated mineralization of thermal waters on the eve of strong earthquakes shows that a change in the course of mineralization itself can also indicate a change in the geodynamic state around a given well (Figure. 6). Similar calculations at the Tau-Turgen station show that salt formation or decomposition of salts in the rock-water system occurs in the same way as in the first case: the concentrations of some salts increase, while others decrease in antiphase. As a result, a certain stable variation corridor is preserved, which can be seen in salt calculations $Mg(HCO_3)_2$ and $MgSO_4$ (Figure 3). At the same time, salt concentrations change sharply in the antiphase before and during events.

This process is universal and can occur at various depths. The aforesaid can be imported by the example of GHC anomalies, manifested on the eve of the Baysorun earthquake on 11/11/1990. K = 15.3 at stations in the Issyk-Kul depression, where we see at different depths (well 6-163 m. Well 20-520 m) the same process is out of phase changes in carbonate equilibrium at station Jets-Oguz at a distance of 65 km from the epicenter. At Dolinka station, at a depth of 1183 m, the antiphase ion change is clearly visible $SO4^{2-}$ and Cl (Figure 7) during the course in time before the strong Baysorun earthquake at a distance of 45 km from the epicenter. Observations show that a few days before the seismic events, the concentrations of some salts in both cases ($NaHCO_3$, NaC1, $Mg(HCO_3)_2$) harply increased, and some decreased (Na_2SO_4, $CaCO_3$, K_2CO) in the form of a deep bay, and then returned to original values. Clear instabilities are observed in the balance of salts, i.e., a sharp increase in mineralization before the push and a sharp decrease during the event due to an increase in the proportion of reduced salts (Figure 6). Interestingly, after the seismic event, the level of mineralization recovered.

All these facts indicate that during the preparation and implementation of strong seismic events, the additional substance does not enter the equilibrium GHC system from afar, and anomalies appear as a result of structural relaxation. at the local site of the “steam-water-gas” system. At the same time, theoretical calculations showed that, on the eve of the earthquake, a rather intense association process might be taking place. In connection with the action of abnormal stresses in the locally-equilibrium system, an internal phase rearrangement occurs in full accordance with the action of the well-known law in the physical chemistry of Le Chatelier (Abdullaev, 1991).

An analysis of the ionic-structural relationships of thermal waters and dynamic parameters (flow rate, level, annular pressure) on the eve of earthquakes shows an extremely unstable geodynamic situation that develops spasmodically in time until the stress release (Baimakhan *et al.*, 2009a, Baimakhan et al., 2009b). To describe the dynamic instability in underground water-gas systems in physical chemistry, the concept of “entropy” (s) is usually used as a thermodynamic function of the state of the system, showing the level of chaos or ordering of the system (Abdullaev, 2002; Abdullaev and Tinibaeva, 2007; Abdullaev, 1991; Kraynov and Shvets, 1992; Nicholas and Prigogine, 1979). In statistical thermodynamics, entropy is the concept of the degree of disorder in the location and movement of a large number of homogeneous structural elements (molecules, ions, atoms, complexons) in some isolated systems. It can be defined by the well-known Boltzmann-Planck Equation (Equation 1).

Where P – the number of different (equally probable) microstates of some isolated system, k=1,3810-16 erg / deg (Boltzmann constant). It seems to us that the time course of the development of internal structural relaxation of a local equilibrium GHC system during the formation of concentration anomalies is better characterized in physical and chemical terms through a thermodynamic state – entropy (s).

The vibrational nature of the entropy factor of the basic chemical reactions of carbonate equilibrium in hydrogeochemical systems indicates the formation or decay in time of hydrogeochemical dissipative structures of local partial equilibria. In the thermodynamic aspect, this means an extremely rapid change in the energy state of the system through fluctuations and energy release. This transition is reflected in the course of entropy (S) as the cumulative state of the controlled system, in the form of an alternating jump from “+” to “-”, which is illustrated in the fundamental deterministic model in the coordinates: time (x) and intensity of fluctuations (y) in on the eve of the tectonic earthquake (Figure 8). The aforementioned fleeting changes in the basic phase rearrangements in the local equilibrium system in the rock-water-gas triad are fully explained in the framework of the theory of self-organization of geodynamic systems (Nicholas and Prigozhin, 1979) and self-organized

Downloaded from www.periodico.tchequimica.com

criticality, quite convincingly recently disclosed by P. Buck (2014).

The leading elementary partial equilibrium, of which the local physicochemical equilibrium of the hydrogeochemical system as a whole is taken, is taken as homogeneous basic state elements (its main cells). A theoretical analysis of the information content of such systems shows that main partial equilibria Equations can be distinguished in them, namely (Derr *et al.,* 1974):

– carbonate (Equation 2);

– chlorine sulfate (Equation 3);

– silicate (Equation 4);

– equivalent cation exchange (Equation 5);

– gas exchange (N_2, O_2, CO_2, CH_4).

In real hydrogeochemical systems, all elementary equilibria are closely interconnected and develop in conjunction, as indicated in our phenomenological model (Figure 6). К As our experience and direct observations show, the most sensitive equilibrium, extremely fast and the first to respond to changes in the stress-strain state (VAT), is carbonate equilibrium (Abdullaev, 1997; Kraynov and Shvets, 1992; Driver, 1985). It is possible to isolate and calculate the thermodynamic parameters of the following three basic (model Equations) chemical reactions of carbonate equilibrium (Equations 6-8). Where K_p – equilibrium constant

Calculations show that Gibbs free energy (ΔGe), for example, GGH station Gorelnik on these reactions has the following meaning: a=-6622 cal/mol, b=-2656 cal/mol, c=-1063 cal/mol. Obviously, when a GC system is exposed to the deformation of different signs, a chemical reaction primarily occurs with a smaller energy reserve. It starts earlier and is subject to a much larger oscillatory process than a chemical reaction with a large supply of energy. Based on the foregoing and comparing these reactions with each other in the energy aspect, we can distinguish as a basic chemical reaction of the form: b) as the most sensitive to external energy influences (Equation 9). All these reactions are, of course, the result of the development in groundwater of physico-chemical processes of dissolution, precipitation, complexing, hydrolysis, drainage of gas components from tectonic cracks. From a physical and chemical point of view, a locally-equilibrium hydrogeochemical system in seismically active regions can be represented as a conditional ball consisting of interconnected conjugate partial equilibria that can be deformed into an ellipse under the influence of anomalous stresses (σ_{an}) during the preparation of a tectonic earthquake (Figure 9).

As a result of this, a total disturbance (ξ) is generated in the system as a result of the transformation of the “ball” into an “ellipsoid”. Such a model is a further development and confirmation of our ideas that the GCH system in seismically active areas is a very thin physicochemical system with an easily excitable and mobile medium that is sensitive to geodynamic changes. Therefore, it adequately reflects transient geodynamic processes, including the preparation of earthquakes.

4. CONCLUSIONS:

In the search for real mechanisms for the emergence of hydrogeochemical precursors of earthquakes, numerous researches, and experimental studies have been conducted. They mainly concentrated within the framework of the concept of transporting new portions of solutions of different composition or individual components to the epicentre zone. Even with the assumption of super-diffusion or convection, or rapid mixing of various fluids in a sound field, it is difficult to imagine the possibility of the occurrence of observed concentration increases of certain components in groundwater by 20-100% or more during the day or several days on the eve of major earthquakes and at distances of tens and hundreds of kilometres from their epicentre. Of course, there should be a completely different mechanism for the emergence of short-term exotic hydrogeochemical precursors, which arise at the observation sites, and it should be able to explain the diversity and phenomenal properties of these anomalies.

In this regard, proposed and justified by us in this work the phenomenological model of interconnections between fast-flowing (sometimes spontaneous) tectonic stresses and the preparation of strong earthquakes most convincingly explains that phase restructuring in open HGC systems is not only the main mechanism for generating anomalies but also the main reason for their occurrence in significant area in seismically active areas during periods of earthquake preparation. These achievements certainly advance the theory of seismic catastrophe prediction.

To elucidate the mechanism of the ongoing restructuring in hydrogeochemical (GHC) systems on the effect of seismic processes, the salt composition of groundwater was calculated at the GHG stations Tau-Turgen, Gorelnik, and

Downloaded from www.periodico.tchequimica.com

Chushkaly for 1990. and 1995 due to the occurrence of two strong earthquakes in this area (Baysorunskoye, K = 15.3 and Kegenskoye, K = 13.7).

It is proved that the main mechanism of the occurrence of exotic transient fluid anomalies is the interphase rearrangement in the local balanced hydrogeochemical system as a reaction to strong earthquakes factors preparing influence. The internal phase reorganization in the hydrogeochemical system is realized through structural relaxation as a result of the occurrence of rapid physicochemical reactions exchange.

6. REFERENCES:

1. Abdullaev, A.U. Hydrogeochemical and hydrogeodynamic studies in the earthquake prediction system in Kazakhstan in: *Earthquake prediction and deep geodynamics. Papers of the international symposium* (pp. 196-220), Almaty: Evero, **1997**.
2. Abdullaev, A.U. Le Chatelier Brown's principle as a likely mechanism for the occurrence of geochemical anomalies in geodynamic processes in: *Comprehensive study of earthquake forecast in Kyrgyzstan* (pp. 95-99), Bishkek: İlim, **1991**.
3. Abdullaev, A.U., *Fluid Mode of the Earth's Crust as a Reflection of Modern Geodynamic Processes,* Almaty: Evero, **2002**.
4. Abdullaev, A.U., Tinibaeva, G.M. *Geodynamics and Geoecology of the High Regions in the 21st Century,* **2007**, *2*, 12-15.
5. Aitaliev, Sh.M., Baimakhan, R.B., Sydykov, A.A., Muzdakbaev, M.M. *Moving factors of regional geodynamics of the Caspian Sea: Proceedings of the 16th International Conference on Soil Mechanics and Geotechnical Engineering: Geotechnology in Harmony with the Global Environment*, *Vol. 2*, Amsterdam: IOS Press, **2005**.
6. Baimakhan, R.B., Danaev, N.T., Baimakhan, A.R., Salgaraeva, G.I., Rysbaeva, G.P., Kulmaganbetova, Zh.K., Avdarsolkyzy, S., Makhanova, A.A., Dashdorj, S. *Geotechnical Aspects of Underground Construction in Soft Ground – Proceedings of the 6th International Symposium, IS-SHANGHAI 2008*, **2009**, pp. 751-755.
7. Baimakhan, R.B., Takishov, A.A., Avdarsolkyzy, S.A., Rysbayeva, G.P., Altynbekov, Sh., Kulmaganbetova, Zh.K., Aliyeva, A.M., Salgarayeva, G.I., Zhakashbayev, B.Zh. *Proceedings of the 17th International Conference on Soil Mechanics and Geotechnical Engineering: The Academia and Practice of Geotechnical Engineering*, **2009**, Vol. 2, pp. 1826-1828.
8. Buck, P. *How Nature Works: A Theory of Self-Organized Criticism*, Moscow: Libroskom, **2014**.
9. Derr, V.E., Post, M.J., Schwiesow, R.L., Calfee, R.F., McNice, G.T. *A theoretical analysis of the information content of lidar atmospheric returns*, Boulder, Colo: Environmental Research Laboratories, **1974**.
10. Driver, J. *Geochemistry of Natural Waters*, Moscow: Mir, **1985**.
11. Hörbrand, T., Baumann, T., Moog, H.C. *Geothermal Energy*, **2018**, *6*(1), 20.
12. Kraynov, S.R., Shvets, V.M. *Hydrogeochyme*, Moscow: Nedra, **1992**.
13. Laptev, F.F. *Water analysis*, Moscow: Gosgeoltekhizdat, **1955**.
14. Mattos, J.B., Cruz, M.J.M., De Paula, F.C. F., Sales, E.F. *Journal of South American Earth Sciences*, **2018**, *88*, 275-286.
15. Movchan, I.B., Yakovleva, A.A. International *Journal of Mechanical Engineering and Technology*, **2017**, *8*(12): 926-932.
16. Nicholas, G., Prigogine, I. *Self-organization in Nonequilibrium Systems (From Dissipative Structures to Ordering through Fluctuations)*, Moscow: Mir, **1979**.
17. Nikolaev, A.V. (ed.). *Hydrogeodynamic earthquake precursors*, Moscow: Institute of Physics of the Academy of Sciences of the USSR, **1984**.
18. O'Neill, C., Turner, S., Rushmer, T. *Philosophical Transactions of the Royal Society A: Mathematical, Physical and Engineering Sciences,* **2018**, *376*(2132), 20170414.
19. Posokhov, E.V. *General hydrogeochemistry*, Leningrad: Nedra, **1975**.

Downloaded from www.periodico.tchequimica.com

20. Rouhi, H., Kalantari, N.. *Water Science and Technology: Water Supply,* **2019**, *18*(2), 357-370.
21. Sobolev, G.A. *Earthquake Forecast Basics*, Moscow: Nauka, **1993**.
22. Talabi, A.O. *ARPN Journal of Engineering and Applied Sciences*, **2018**, *13*(9), 3063-3075.
23. Warsaw, G.M. (ed.). *Hydrogeochemical earthquake precursors*, Moscow: Nauka, **1985**.

$$S = k * 1nP/ \quad \text{(Eq. 1)}$$

$$CO_2 + H_2CO_3 \leftrightarrow 2H + HCO_3 \leftrightarrow 2H + CO_0 \quad \text{(Eq. 2)}$$

$$2NaC1 \leftrightarrow Ca(Mg)SO_4 \quad \text{(Eq. 3)}$$

$$2H_2O + SiO_2 \leftrightarrow H_4SiO_4 \quad \text{(Eq. 4)}$$

$$2Na^{+}\ (K^{+}) \leftrightarrow Ca^{2+}(Mg)^{2+1} \quad \text{(Eq. 5)}$$

$$H_2O + [CO_2]^{K}{}_{p} \rightarrow H_2CO_3 \quad \text{(Eq. 6)}$$

$$Ca^{2+} + [CO_3]^{K2-}{}_{p} \rightarrow CaCO_3 \quad \text{(Eq. 7)}$$

$$C0_3^{2-} + [H^{+}]^{K}{}_{p} \rightarrow HCO_3 \quad \text{(Eq. 8)}$$

$$CO_3^{2-} + H^{+K}{}_{p} \rightarrow HCO_3^{-} \quad \text{(Eq. 9)}$$

Figure 1. *Almaty seismic hydrogeochemical prognostic test site in South-East Kazakhstan*

Downloaded from www.periodico.tchequimica.com

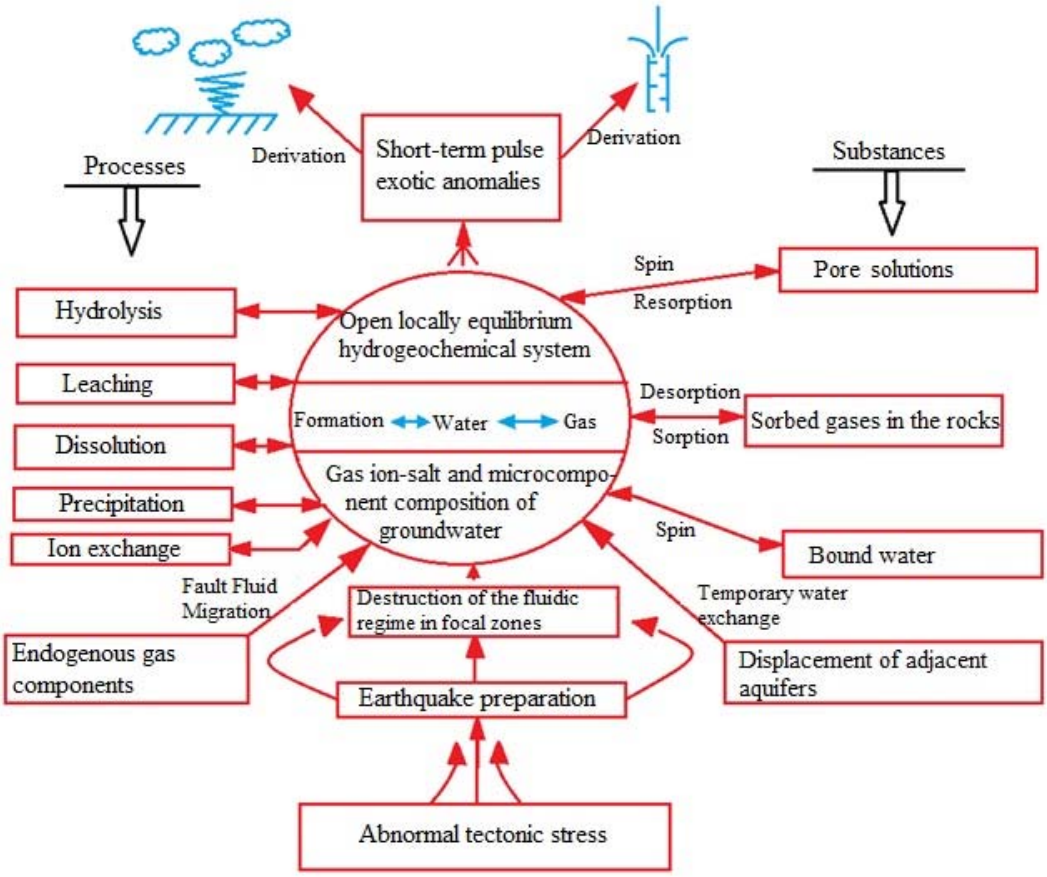

Figure 2. *Phenomenological model of the formation of exotic temporary hydrogeochemical anomalies in the underground waters of seismically active regions during the periods of preparation of strong earthquakes*

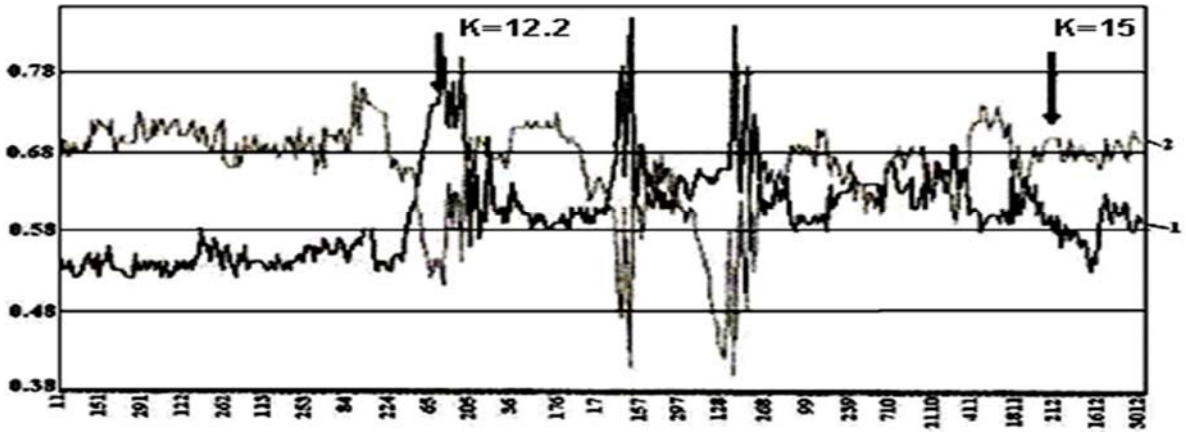

Figure 3. *Time course of antiphase changes of calcium salts at Chushkaly station on the eve of the May (03.05.1990, K = 12.2) and Baysorun earthquakes (11/12/1990, K = 15): 1 – $CaCO_3$; 2 – $Ca(HCO_3)_2$*

Downloaded from www.periodico.tchequimica.com

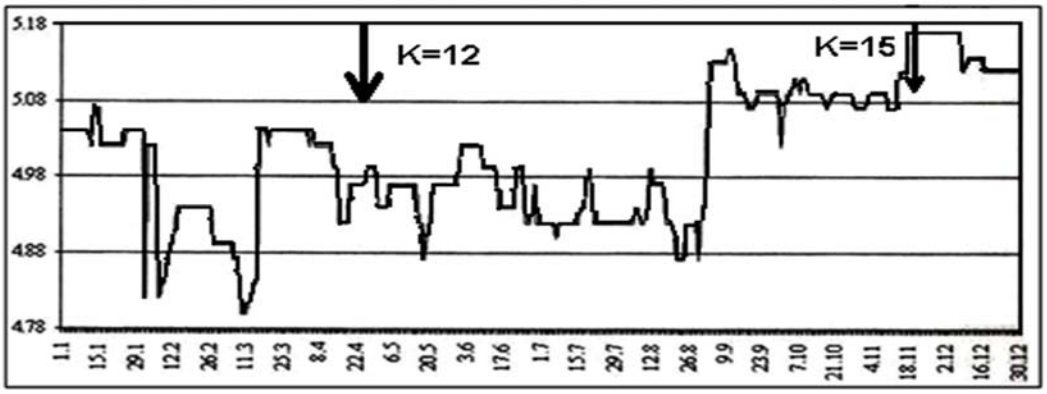

Figure 4. *The time course of changes in Ca $(HCO_3)_2$ in time in 1990 at station Tau-Turgen before strong earthquakes*

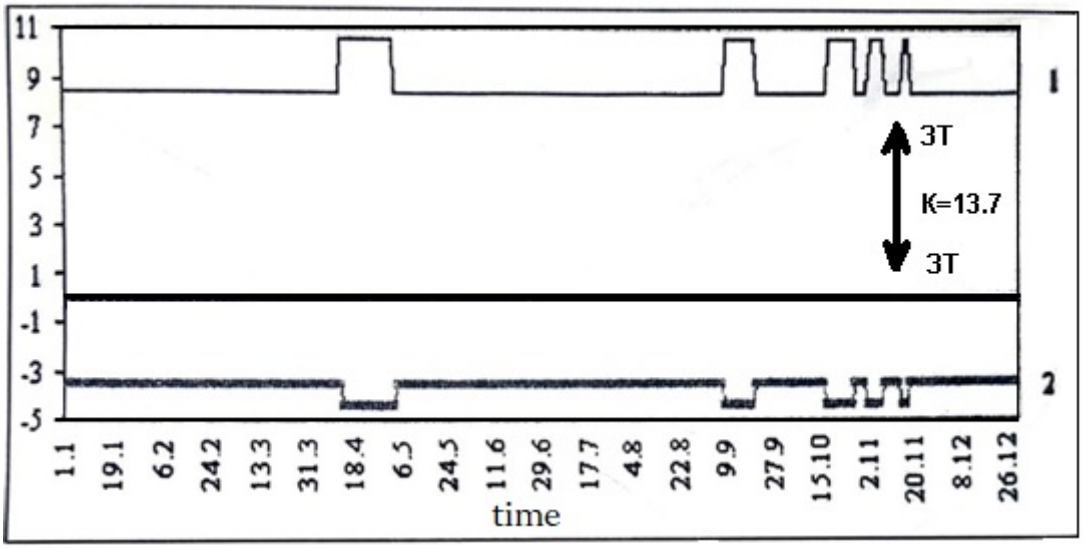

Figure 5. *Distribution of Mg salts in antiphase due to the Kegen earthquake (30/10/1995, K=13.7) at the Tau-Turgen station: 1 – $Mg(HCO_3)_2$, 2 – $Mg\ SO_4$*

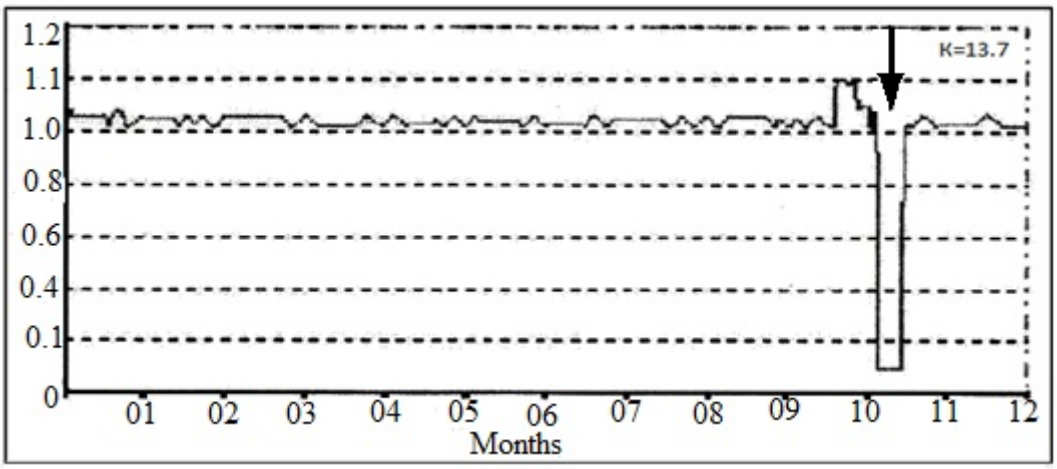

Figure 6. *The course of the estimated mineralization of thermal mineral waters at the Tau-Turgen station on the eve of the Kegen earthquake (31/10/1995, K=13.7)*

Downloaded from www.periodico.tchequimica.com

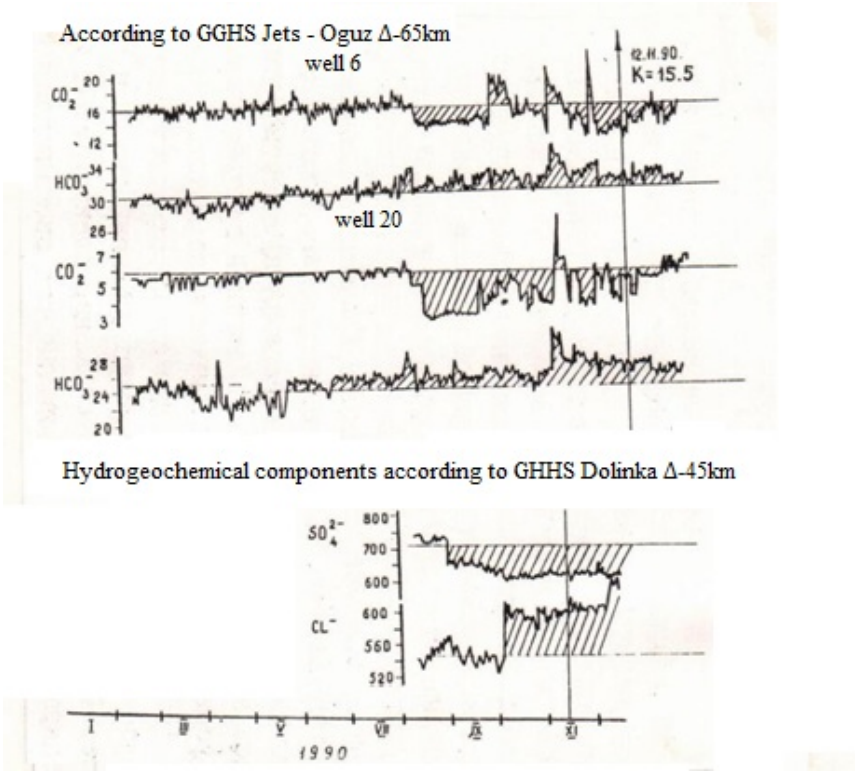

Figure 7. *GHC manifestations of anomalies before the Baysarun earthquake (11/12/90) in the Issyk-Kul depression at various depths*

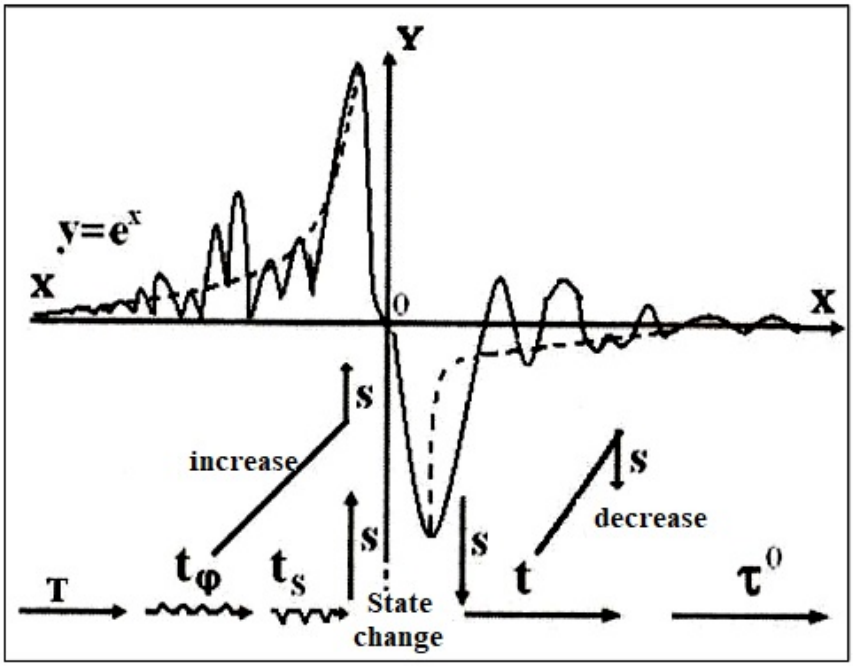

Figure 8. *A fundamental model for the development of the time course of entropy (S) of a local equilibrium GHC system (LHHHC) under the influence of tectonic stress*

Downloaded from www.periodico.tchequimica.com

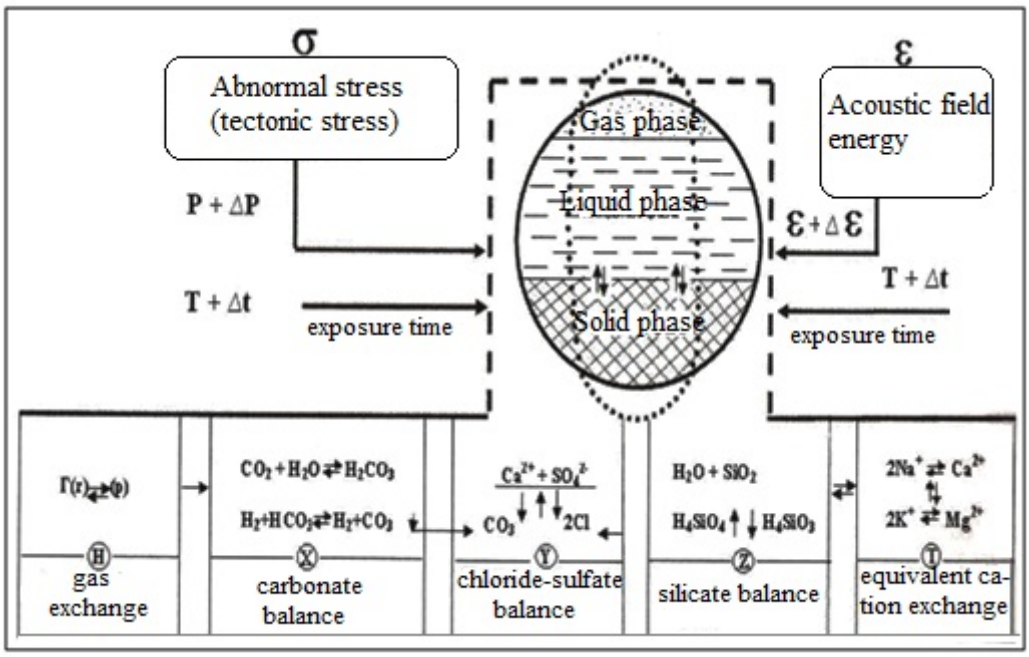

Figure 9. *Phenomenological model of phase adjustment in locally equilibrium physicochemical systems with a generation of dissipative concentration anomalies (Abdullaev, 2002)*

Downloaded from www.periodico.tchequimica.com

PERIÓDICO TCHÊ QUÍMICA
ARTIGO ORIGINAL

ESTUDO DO EFEITO DE CONSERVANTES MULTICOMPONENTES NA QUALIDADE DE PRODUTOS DE CARNE DE CAVALO COZIDA E DEFUMADA

STUDYING THE EFFECT OF MULTICOMPONENT PICKLE ON THE QUALITY OF COOKED AND SMOKED HORSE MEAT PRODUCT

KALDARBEKOVA, Madina[1*]; UZAKOV, Yasin[1]; CHERNUKHA, Irina[2]; KURMANBEKOVA, Akmaral[1], JETPISBAYEVA, Bagila[1]

[1] Almaty Technological University, Department of «Technology of food products»

[2] M. Gorbatov Federal Research Center for Food Systems of Russian Academy of Sciences

** Correspondence author*
e-mail: kadr_90.taz@mail.ru

Received 17 October 2019; received in revised form 22 October 2019; accepted 23 October 2019

RESUMO

A injeção de conservantes multicomponentes contendo proteínas e carboidratos no tecido muscular da carne de cavalo, seguido de massagens, tende a amaciar a carne e melhorar as características organolépticas do produto acabado. A análise dos dados obtidos mostrou que a introdução de aditivos no conservante multicomponente contribuiu para o processo de retenção de umidade na carne de cavalo. Um importante indicador físico e químico dos produtos à base de carne é a capacidade de retenção de umidade, que afeta a consistência dos produtos acabados e o processo de deterioração microbiológica, uma vez que a quantidade de umidade não ligada depende do crescimento do número de microrganismos. É difícil superestimar a importância do pH na tecnologia da carne, pois o valor do pH determina a adequação da carne crua ao processamento. O aumento máximo da capacidade de ligação de umidade da amostra de controle de carne de cavalo em até 70% é alcançado após 90 minutos de massagem e, em seguida, ocorre uma diminuição na hidrofilicidade do sistema devido à destruição física das fibras musculares. O valor de pH se correlaciona com a capacidade de ligação da umidade das matérias-primas e afeta a segurança do produto e sua capacidade de armazenamento. A relação do pH e da capacidade de retenção de umidade com a consistência da carne não está em dúvida. Nesse sentido, no decorrer de estudos experimentais, foram determinados o pH, a capacidade de retenção de umidade e a tensão de punção. Na amostra 1, que continha um extrato de *Goji berries*, a capacidade de retenção de água aumentou 3,4%. Nas amostras 2 (continha farinha de trigo-sarraceno) e 3 (continha um extrato de *Goji berries* e farinha de trigo- sarraceno), com o uso combinado de farinha de trigo-sarraceno e *Goji berries*, que demonstraram altas propriedades de intumescimento, a capacidade de retenção de água aumenta em 6,1% e 7,2 %, respectivamente, 2,7% e 3,8% a mais, respectivamente. Os dados obtidos mostraram que a introdução de aditivos vegetais tem um efeito positivo na consistência do produto de carne defumada cozida, nos protótipos de propriedades estruturais e mecânicas assim como a força de cisalhamento nos protótipos, que foi reduzida em 7, 13 e quase 20%, respectivamente.

Palavras-chave: carne de cavalo, salmoura multicomponentes, propriedades organolépticas, funcionais e tecnológicas, desenvolvimento tecnológico.

ABSTRACT

The multicomponent pumping pickle containing protein and carbohydrate components injected into the muscle tissue of horse meat, followed by massaging, tends to tenderize meat and improve the organoleptic characteristics of the finished product. Analysis of the data obtained showed that the introduction of additives to the multicomponent pickle contributed to the moisture-holding process in horse meat. An important physical and chemical indicator of meat products is the moisture-holding ability, which affects the consistency of finished products and the process of their microbiological spoilage since the amount of unbound moisture depends on the growth of the number of microorganisms. It is difficult to overestimate the importance of pH in meat technology, as the pH value determines the suitability of raw meat for processing. The maximum increase in the moisture-binding capacity of the control sample of horse meat up to 70% is achieved through 90 minutes of massaging, and then there is a decrease in the hydrophilicity of the system due to the physical destruction of muscle fibers. The pH value correlates with the moisture-binding capacity of raw materials and affects the safety of the product and its storage capacity. The relationship of pH and moisture- holding ability with the consistency

Downloaded from www.periodico.tchequimica.com

of meat is not in doubt. In this regard, in the course of experimental studies, pH, moisture-holding ability and puncture voltage were determined. In Sample 1, which contained an extract from Goji berries, the water-holding capacity is increased by 3.4%. In Samples 2 (contained buckwheat flour) and 3 (contained an extract from Goji berries and buckwheat flour), with the combined use of buckwheat flour and goji berries, which demonstrated high swelling properties, the water-holding capacity increases by 6.1% and 7.2%, respectively additional 2.7% and 3.8%. The obtained data showed that the introduction of vegetable additives has a positive effect on the consistency of cooked-smoked meat product, in the prototypes on structural and mechanical properties, as well as shear force in the prototypes which has been reduced by 7, 13 and almost 20%, respectively.

Keywords: horse meat, multi-component brine, organoleptic, functional and technological properties, technology development.

1. INTRODUCTION

Horse meat has been known as a food raw material for more than a thousand years. Horse meat is widely used for the preparation of meat products in the countries of Central Asia, Russia, some countries in Western Europe, e.g. France, Sweden, Belgium, and Japan. Horse meat has a high nutritional value. Compared to other widely used types of raw meat, horse meat is characterized by the highest protein content with optimal amino acid composition, vitamins A and B, hypoallergenic properties, a series of lipids with low atherogenicity, with a minimum level of carbohydrates (Uzakov, 2006).

According to Arihara, the development of functional meat products requires using natural antioxidants. This direction has been worked out and new functional meat products have been developed. Some studies were conducted before concerning the effect of pumpkin seeds on whole-piece horse meat products. No literature available provides information or applications of goji berries in restructured horse meat products (Silvius S., 2014 and etc.).

A method of producing meat products is known, which provides for the preparation of raw materials, the preparation of brine with the introduction of an enzyme preparation, syringing, aging in brine, molding, cooking, Smoking and cooling (Russia, Patent No. 2030884, A23L 1/31, publ. 1995). The disadvantage of the method is the use of an expensive enzyme preparation pepsin.

Russian scientists have developed a method of producing meat product from the rib part of beef by salting, massaging, introducing spices, aging in milk, molding, Smoking, cooking (Russia, Patent No. 1785642, A23L 1/31, publ. 1993). The disadvantage of the method is a long process of massaging and aging up to 48 hours.

Scientists have developed a method for the production of dried meat delicacies from horse meat (Kazakhstan, Patent No. 29358, A23L 1/31, publ. 2006.01). The disadvantage of the method is the use of an expensive bacterial preparation TEXELDCM-1.

Regular use of goji berries improves gastrointestinal function, increases energy levels, improves sleep, reduces fatigue and stress significantly. Goji berries have antioxidant and anti-inflammatory properties (Makangali, 2018; Arihara, 2006 and etc.)

The purpose of the work was to study the effect of multicomponent pumping pickle on the quality indicators of cooked and smoked horsemeat product.

2. MATERIALS AND METHODS

2.1 Samples

Laboratory studies of test samples were held in the research laboratory of the V.M. Gorbatov All-Russian Research Institute of the Meat Industry (Moscow, Russian Federation). In this study, cooled horse meat (pH 5.56) and horse fat were used. Horse meat was purchased from Kainar LLP (Almaty, Kazakhstan).

The test samples were produced at the meat processing research center of Almaty Technological University (Almaty, Republic of Kazakhstan).

The reference pickle contained table salt, sodium nitrite, sugar, and water. The pickle samples additionally contained the following: Sample 1 contained an extract from goji berries, Sample 2 contained buckwheat flour, and Sample 3 contained an extract from goji berries and buckwheat flour.

The meat product was shaped of semi-circular pieces not heavier than 0.4 kg with a thickness of about 10 cm. The meat pieces were injected with brine containing 2.5 kg salt and 150 g sugar per 100 kg of raw material with a density of 1.0923–1.1065 g/c and then were flooded with

Downloaded from www.periodico.tchequimica.com

the rest brine and were refrigerated. The salted meat was massaged in tenderizer for 40 min. The meat product was boiled in cooking-smoking chambers to a temperature in the center of 74-75^{0}C for 2–2.5 h until the temperature at the center of the product had reached 72^{0}C. The boiled product was chilled and smoked for 30 min at a smoke temperature of 40^{0}C.

2.2 Chemical composition

The chemical composition of meat and meat products was determined by commonly known methods.

Two-hundred grams of product sample were placed in plastic containers, frozen and then dried in a thermal freeze dryer (Modulyol-230, Milford-UK) for 5 days under 100-mbar pressure at −50 °C. The frozen dry samples were ground to a homogeneous mass in a grinder (Panasonic-Mixergrinder-Model MX119N-Japan) for chemical analyses. The moisture was determined by weighing 200 g meat sample before and after drying in a thermal freeze dryer for 5 days. The proximate chemical composition of the product was determined according to the standard methods of the AOAC (2000).

Protein was determined using a Foss Kjeltec 2300 nitrogen/protein analyzer (State standard P 50258). Fat was determined by Soxhlet extraction method using petroleum ether (State standard 23042-86). Ash content was determined by ashing samples in a muffle furnace at 500 °C for 24 h (State standard 31727-2012)

2.3 Determination of the rheological properties

The following indicators were determined in the finished products: the total water content by drying to a constant weight; water-binding capacity (WBC) by pressing method; water-holding capacity (WHC) by Vartanyan method; heat treatment losses by the difference of sample mass before and after heat treatment; cutting force with a Warner-Bratzler device.

Determination of the pH of meat and meat products. The pH of meat products was monitored using a portable pH meter (Hanna waterproof pH meter, Model Hi 9025) fitted with a plastic body open junction, conic (Hanna FC200B) and a temperature adjusting probe. The pH probe and the thermometer were inserted into the product to a similar depth (2 cm).

2.4 Mineral composition

A mixed standard solution was prepared from a 1000 µg/ml multi-element solution (Darmstadt, Germany) and inhouse standard reference materials used for validation of the method. Evaluation of mineral levels in the samples was carried out after complete digestion using a Milestone 1200 MDR microwave system at a temperature of 200 °C in closed (PTFE) vessel. In brief 5 ml of conc. HNO_3 and 1 ml of 30% H_2O_2 were added to each digestion vessel. They were then heated to 200 °C over a 5-min period and then held at 200 °C for another 20 min. The digest obtained was collected in 50-ml volumetric flasks and made up to volume. Measurements were carried out on the ICP-OES system (Perkin Elmer Model 3300) equipped with a low-flow Gem Cone nebulizer in addition to an ultrasonic nebulizer for low concentrations.

2.5 Sensory indicators of meat products

Sensory evaluation was carried out using score assessment. Five points scores of intensity and desirability scales were used in the experiment. There was from 1 point (very slight) to 5 point scores of intensity (very strong) and similar for desirability: from 1 point (undesirable) to 5 points (very much desirable). All processed meat products were sensory investigated by six-panel. Products were prepared as half of chubs and 2.5 mm slices and presented to panelists on disposable dishes in white glow light (250 1x). The next sensory parameters were investigated: 1-taste, 2 – smell and aroma, 3 – appearance, 4 – consistency, 5 – view at the cut, 6 – juiciness. (State standard 9793-74, 23041-78).

3. RESULTS AND DISCUSSION:

The pickle ingredients were selected due to their functional properties and the required organoleptic characteristics of the finished horsemeat product. The concentration of each ingredient in the pickle was defined taking into account the established rates of their use and the allowable content of each ingredient in the finished product, as well as the amount of pickle to the mass of pumping material (Table 1).

After the different variants of multicomponent pumping pickle were injected into horse meat, the water-binding capacity of the reference and test samples was studied. Changes in the hydrophilic characteristic of horse meat in the process of massaging were studied;

Downloaded from www.periodico.tchequimica.com

the results of the research are presented in Figure 1.

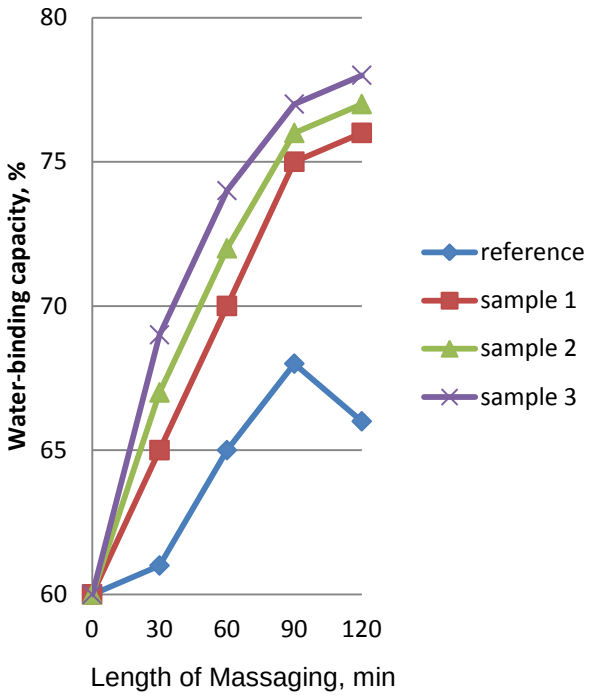

Figure 1. *Water-binding capacity of horse meat in the course of massaging*

The maximum increase in the water-binding capacity of the reference sample of horse meat to 70% is achieved after 90 minutes of massaging, and then the hydrophilic property of the system reduces due to the physical destruction of muscle fibers.

With the introduction of the protein component to the pickle, WBC of horse meat (Sample 1) stabilizes and increases to 76% after 90 minutes of massaging. Goji berries added to the pickle contribute to the additional stabilization of the meat system due to their ability to increase the stickiness both inside the meat pieces and on the surface.

The pickle with buckwheat flour injected into the horse muscle tissue contributes to the formation of a single matrix due to the interaction of the negatively charged surface of the polysaccharide with salt-soluble muscle proteins and cations. In addition, buckwheat flour has a high drying capacity, which also leads to increased WBC of the sample.

An extract of goji berries and buckwheat flour was added to Sample 3. After 90 minutes of massaging Sample 3 reached the maximum WBC value of 79% and stabilized it at this level.

The process of color formation is important for the cooked and smoked product; the process was studied by determining the content of nitric oxide pigments in the samples when the raw material was left curing for 4 hours after massaging (Figure 2).

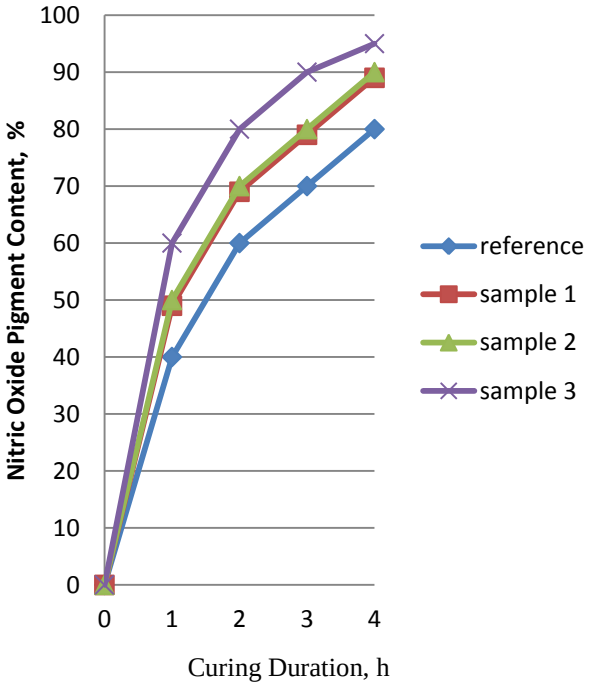

Figure 2. *Accumulation of nitric oxide pigments in the horse meat muscle tissue when curing*

As a result of biochemical transformations of the meat pigment – myoglobin –during curing, the product color is formed and stabilized. Among the factors affecting the process of color formation, an important role is played by reducing agents, e.g. reducing sugars and ascorbates.

Figure 2 shows that the introduction of an extract from goji berries into the pickle accelerates the formation of nitric oxide pigments.

The introduction of buckwheat flour, which plays an important process role, has virtually no effect on the color formation of the products.

The greatest acceleration of the color formation process in horse meat product is observed in the pickle with the combined use of an extract from goji berries and buckwheat flour (Sample 3). Goji berries contain ascorbic acid, which contributes to the conversion of sodium nitrite to nitric oxide, recovers metmyoglobin already contained in raw materials, binds oxygen well, and thereby protects meat pigments from oxidation.

After massaging and curing, the process parameters of the cured horse meat were determined (Table 2).

Downloaded from www.periodico.tchequimica.com

Analysis of the data obtained showed that the introduction of additives to the multicomponent pickle contributed to the water-holding process in horse meat. In Sample 1, WHC is increased by 3.4%. In Samples 2 and 3, with the combined use of buckwheat flour and goji berries, which have high swelling properties, WHC increases by 6.1 and 7.2%, i.e. by an additional 2.7 and 3.8%.

Polysaccharide-containing additives contribute most to the water-holding process in the meat system due to their high hydrophilic capacity. This has been proven by the results of the study of mass losses after heat treatment of cured horse meat (Table 2). The data shows a significant reduction in losses with the introduction of carbohydrate additives. The use of a series of process additives in the pumping pickle is aimed at improving the cohesive adhesion processes in the meat system. Goji berries and buckwheat flour are involved in both intra- and interphase changes.

The introduction of goji berries and buckwheat flour to the pickle contributes to the formation of a solid spatial grid after the heating-cooling cycle. Thus, the complex combination of proteins and carbohydrates makes it possible to benefit from the synergistic effect of the pickle components for the formation of high-quality indicators of cooked and smoked horse meat.

After massaging and curing, some samples of cooked and smoked horse meat products were developed. Consistency of meat products is an important qualitative parameter, which can be examined with the help of the shear stress value (Figure 3).

The data obtained showed that the introduction of additives had a positive effect on the consistency of the product; in the samples, the shear force decreases, respectively, by 7, 13 and almost 20%. The greatest effect is manifested in Sample 3 with the entire complex of additives.

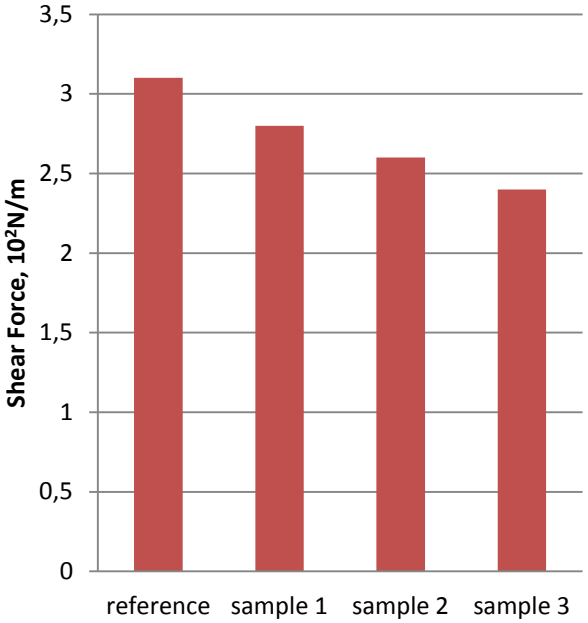

Figure 3. *Shear stress of the cooked and smoked horse meat*

The data presented in Figure 4 showed that Sample 3 had the best organoleptic characteristics with the introduction of goji berries and buckwheat flour. The data obtained showed that under the influence of multicomponent pumping pickles, finished products acquire a stable color and delicate texture. Due to the high water-holding capacity of the meat system, the juiciness of the products is formed, which improves the taste.

4. CONCLUSIONS:

Thus, the introduction of an extract of goji berries and buckwheat flour, which contains a number of functional components, to the pickle, contributes to the formation and stabilization of the quality indicators of the cooked and smoked horsemeat product. The multicomponent pickle consisting of an extract of goji berries and buckwheat flour helps to bind water through the protein system and polysaccharides, which maintains the stability of the finished product, reduces heat treatment losses, increases the juiciness and the yield of the product. The introduction of goji berries also contributes to the stability of the color of the finished product.

5. ACKNOWLEDGMENTS:

The study was performed as part of the research work No.0457/GF4 Study of the Functional and Biocorrective Characteristics of Plant-Animal Complexes and the Development of

Downloaded from www.periodico.tchequimica.com

the Technology of National New-Generation Meat Products on their Basis Using Local Raw Materials funded by the Ministry of Science and Education of the Republic of Kazakhstan.

6. REFERENCES:

1. Silvius S., Horse Meat Consumption - Between Scandal and Reality. 2nd Global Conference on business, economics, management and tourism, 30-31 October 2014, Prague, Czech Republic.

2. Arihara, K. *Meat Sci.,* **2006**, 74: 219-229.

3. Makangali K., Lisicyn A., Uzakov Y., Taeva A., Konysbaeva D., Gorbulya, V. *Current Research in Nutrition and Food Science Journal*, **2018,** 6(2): 536-551.

4. Kolesnikova N., Bazhenova B. A. *Meat series,* **2012**, 3, 70-72.

5. Seeram, N.P., *J. Agric. Food Chem*., **2008,** 56: 627-629.

6. Amagase, H. and D.M. Nance. *J. Altern. Complement. Med.,* **2008,** 14: 403-412.

7. Rohlik, B.O., P. Pipek and J. Panek. *Czech J. Food Sci.,* **2013,** 31: 307-312.

8. Amagase, H. and N.R. Farnsworth. *Food Res. Int.*, **2011,** 44: 1702-1717.

9. State standard 9793-74 Meat products. Methods for determining moisture.

10. State standard 23042-86 Meat and meat products. Methods for determining fat.

11. State standard 25011-81 Meat and meat products. Methods for the determination of protein.

12. State standard 31727-2012 (ISO 936:1998) Meat and meat products. Method for determining the mass fraction of total ash.

13. State standard 23041-78 Meat and meat products.

14. Abril, M., Campo, M. M., Onenc, A., Sanudo, C., Alberti, P., & Negueruela, A. I. *Meat Science*, **2001,** 58, 69–78.

15. Abdel Moneim, Suliman Selma, Fadlalmola, Babiker, Omer, Arabi, Safa M. Ibrahim (2014). *Food and Public Health*, **2014,** 4(6): 293-300.

16. Al-Bachir, M., & Zeinou, R. *Meat Science*, **2009,** 82, 119–124.

17. Al-Sheddy, I., Al-Dagal, M., & Bazaraa, W. A. *Journal of Food Science,* **1999,** 64, 336–339.

18. AOAC. *Official methods of analysis of the Association of Analytical Chemists (17th ed.).* Gaithersburg, *Maryland*, 2000.

19. Belew, J. B., Brooks, J. C., McKenna, D. R., & Savell, J. W. *Meat Science,* **2003,** 64, 507–512.

20. Bouton, P. E., Harris, P. V., & Shorthose, W. R. *Journal of Food Science*, **1972,** 37, 351–355.

21. Engy, F. Zaki. *International Journal of Environment. Agriculture and Biotechnology* , **2017,** 2(5): 2481-2486.

22. Fatima Theyab Al meqbaali, Hosam Habib, Aws Othman, Saeda Al-Marzooqi, Alia Al-Bawardi, Javed Yasin Pathan, Serene Hilary, Usama Souka, Suleiman Al-Hammadi, Wissam Ibrahim, Carine Platat. *Emirates Journal of Food and Agriculture*. **2017;**29(11):822-832.

23. Heneiksen-larsen, K. B., Lexell, J., & Sjostrom, M. *Histochemistry Journal*, **1983,** 15, 167–178

24. Kadim, I. T., Mahgoub, O., Al-Marzooqi, W., Al-Zadgali, S., Annamali, K., & Mansour, M. H. *Meat Science,* **2006,** 73, 619–625.

25. Kadim, I. T., Mahgoub, O., & Purchas, R. W. *Meat Science,* **2008,** 80, 555–569.

26. Kadim, I. T., Al-Karousi, A., Mahgoub, O., Al-Marzooqi, W., Khalaf, S. K., Al-Maqbali, R. S., Raiymbek, G. *Meat Science,* **2013,** 93(3), 564–571.

27. Kalalou I, Faid M and Ahami AT. *Electronic Journal of Biotechnology*, **2004,** 7(3): 243–248.

Downloaded from www.periodico.tchequimica.com

Table 1. *Composition of pumping pickle*

Component	Content of pickle components, kg per 100 kg			
	Reference	**Sample 1**	**Sample 2**	**Sample 3**
Goji berries	-	+	+	+
Buckwheat flour	-	-	+	+
Goji berries + buckwheat flour	-	-	-	+
phosphates	+	+	+	+
Table salt	+	+	+	+
Sodium nitrite	+	+	+	+
Granulated sugar	+	+	+	+
Water	+	+	+	+
Total	100	100	100	100

Table 2. *Process parameters of horse meat*

Parameter	Reference	Sample 1	Sample 2	Sample 3
Water-holding capacity,%	82.5±2.0	85.3±1.7	89.0±1.8	89.9±1.6
Medium pH	5.71±0.1	5.7±0.1	5.7±0.1	6.2±0.2
Heat treatment losses, %	38.9±0.5	35.8±0.8	23.9±0.6	20.8±0.6

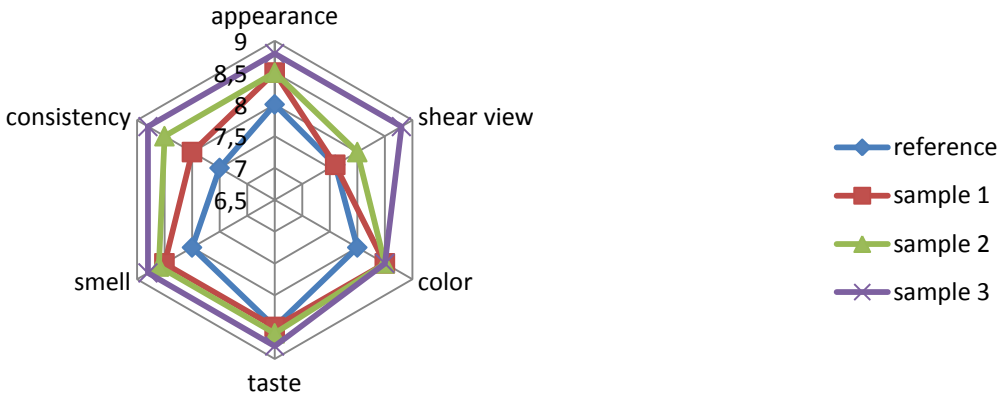

Figure 4. *Organoleptic evaluation of cooked and smoked horse meat products*

Downloaded from www.periodico.tchequimica.com

PERIÓDICO TCHÊ QUÍMICA
ARTIGO ORIGINAL
Note: This study is the continuation and expansion of a previously published study.

JUSTIFICATIVA PARA O USO DO COMPLEXO TERAPÊUTICO E PROFILÁTICO PARA EVITAR INTOLERÂNCIA A ACRILATOS EM PACIENTES COM HIPERFUNÇÃO DAS GLÂNDULAS TIREOIDES

RATIONALE FOR THE USE OF THERAPEUTIC AND PROPHYLACTIC COMPLEX TO PREVENT INTOLERANCE TO ACRYLATES IN PATIENTS WITH HYPERFUNCTION OF THE THYROID GLANDS

ОБОСНОВАНИЕ ПРИМЕНЕНИЯ ЛЕЧЕБНО-ПРОФИЛАКТИЧЕСКОГО КОМПЛЕКСА ДЛЯ ПРЕДУПРЕЖДЕНИЯ НЕПЕРЕНОСИМОСТИ К АКРИЛАТАМ У БОЛЬНЫХ С ГИПЕРФУНКЦИЕЙ ЩИТОВИДНОЙ ЖЕЛЕЗЫ

[1]SEVBITOV, Andrei[*]; [2]ZHAD'KO, Sergei; [1]ERSHOV, Kirill; [1]BORISOV, Vitaliy; [1]MIRONOV, Sergey

[1]Department of Propaedeutic of Dental Diseases
of I. M. Sechenov First Moscow State Medical University (Sechenov University)

[2] Department of prosthetic dentistry
of V. I. Vernadsky Crimean Federal University, Medical Academy named after S. I. Georgievsky

** Correspondence author*
e-mail: avsevbitov@mail.ru

Received 12 June 2019; received in revised form 29 October 2019; accepted 11 November 2019

RESUMO

Este estudo é dedicado à análise do efeito da prótese removível de acrílico sobre os tecidos mucosos e duros da cavidade oral de pacientes com hipertireoidismo e, também, para justificar a aplicação de uma gama de medidas curativas e profiláticas baseadas na preparação "*Endonorm*" para prevenção de eventos de intolerância em pacientes com patologia mencionada. As alterações morfológicas e funcionais da glândula tireoide afetam o estado geral do corpo humano, incluindo os tecidos da cavidade oral, e essas deficiências geralmente se manifestam pela perda precoce de dentes devido a cárie e doenças periodontais. As manifestações orais da tireotoxicose incluem aumento da suscetibilidade à cárie, doença periodontal, aumento do tecido extraglandular da tireóide, osteoporose maxilar ou mandibular, dentição acelerada e síndrome da boca ardente. Este problema nesses pacientes, em particular aqueles que sofrem de hiperfunção da glândula tireóide, deve ser resolvido por meio de terapia medicamentosa complexa para aumentar a resistência e reduzir o nível de sensibilização do corpo. "*Endonorm*" é uma mistura de extratos vegetais secos de *Potentilla alba Linnaeus*, preparado de acordo com tecnologia especial, o principal componente ativo do produto é a Albinina. Objetivo de estudar os indicadores de atividade semelhante à tripsina da saliva mista em pacientes com hiperfunção da glândula tireóide, cujas próteses foram fabricadas pelo método padrão de compressão e usando medidas terapêuticas e profiláticas propostas. Após a definição da aplicação de próteses removíveis, o aumento da atividade enzimática da saliva em 17%, em comparação com os índices, anteriores ao início da prótese. Estabeleceu que a faixa de medidas curativa e profilática proposta permite evitar o risco de desenvolvimento de eventos de intolerância ao acrilato e normalizar os índices estudados 1 mês após a prótese.

Palavras-chave: *hipertireoidismo (hiperfunção da glândula tireóide), alergia, prótese removível.*

ABSTRACT

This investigation is devoted to the analysis of acrylic removable denture's effect on the mucous and hard tissues of the oral cavity of patients with hyperthyroidism and, also, to rationale for application the curative and prophylactic range of measures based on the preparation "Endonorm" for precaution of events of intolerance of patients with mentioned pathology. Morphological and functional changes in the thyroid gland

Downloaded from www.periodico.tchequimica.com

affect the general state of the human body, including tissues of the oral cavity, and these impairments usually manifest by the early loss of teeth due to caries and periodontal diseases. Oral manifestations of thyrotoxicosis include increased susceptibility to caries, periodontal disease, enlargement of extraglandular thyroid tissue, maxillary or mandibular osteoporosis, accelerated teething, and burning mouth syndrome. This problem in such patients, in particular, those suffering from hyperfunction of the thyroid gland, should be resolved by means of complex medicinal therapy to increase resistance and reduce the level of body sensitization. “Endonorm” is a mixture of dry vegetable extracts of white cinquefoil, prepared according to special technology, the main active component of the product is Albinin. Purpose of studying the indicators of trypsin-like activity of mixed saliva in patients with hyperfunction of the thyroid gland, whose dentures were manufactured by standard compression method, and by using proposed therapeutic and prophylactic measures. After the applying of removable dentures was defined, the increase of saliva’s enzyme activity on 17% as compared with indices, which was before the beginning of the prosthesis. It established that the proposed curative and prophylactic range of measures permits to prevent the risk of development of events of acrylate intolerance and to normalize the studied indices on 1 month after the prosthesis.

Keywords: *hyperthyroidism (hyperfunction of the thyroid gland), allergy, removable denture.*

АННОТАЦИЯ

Данное исследование посвящено изучению влияния акриловых съемных протезов на слизистую и твердые ткани полости рта у больных с гиперфункцией щитовидной железы и обоснованию применения лечебно-профилактического комплекса на основе препарата «Эндонорм» для профилактики явлений непереносимости у больных с указанной патологией. Морфофункциональные изменения щитовидной железы оказывают влияние как на организм человека в целом, так и на ткани полости рта в частности, что проявляется ранней утратой зубов вследствие кариеса и заболеваний пародонта. К проявлениям тиреотоксикоза в полости рта относятся: повышенная восприимчивость к кариесу, пародонтит, увеличение экстрагландулярной ткани щитовидной железы, верхнечелюстной или нижнечелюстной остеопороз, ускоренное прорезывание зубов и синдром жжения в полости рта. Данная проблема у таких больных, в частности страдающих гиперфункцией щитовидной железы, должна быть решена путем комплексной терапии с применением медикаментозных препаратов для повышения резистентности и снижения уровня сенсибилизации организма. Препарат «Эндонорм» представляет собой смесь произведенных по особой технологии сухих растительных экстрактов лапчатки белой (лат. *Potentilla alba Linnaeus*), основным действующим началом которой является субстанция Альбинин. Цель исследования: изучить показатели трипсиноподобной активности смешанной слюны у больных с гиперфункцией щитовидной железы, съемные протезы которым были изготовлены традиционным компрессионным методом и с применением предлагаемого лечебно-профилактического комплекса. Было выявлено увеличение ферментативной активности слюны после наложения съемных протезов на 17 % по сравнению с показателями до начала протезирования. Установлено, что предлагаемый лечебно-профилактический комплекс позволяет предупредить риск развития явлений непереносимости к акрилатам и нормализовать изучаемые показатели через 1 месяц после протезирования.

Ключевые слова: *гиперфункция щитовидной железы, аллергия, съемные протезы*.

1. INTRODUCTION

On the features of the structure and function of the thyroid gland.

The thyroid gland (glandula thyroidea) is a gland of internal secretion, and it is part of the endocrine system, synthesizes a number of hormones necessary to maintain homeostasis of the body.

The thyroid gland is a symmetrical organ, consisting of two lobes and an isthmus. The right and left lobes are adjacent directly to the trachea, the isthmus is located on the anterior surface of the trachea. Some authors separately allocate in a thyroid gland a pyramidal share. In the normal (euthyroid) state, the mass of the thyroid gland is from 20 to 65 g, and the size of the lobes depends on the sex and age characteristics and can vary widely enough. During puberty, there is an increase in the size and weight of the thyroid gland, and in old age, respectively, it decreases. In women during pregnancy, there is also a temporary increase in the size of the thyroid gland, which independently, without

Downloaded from www.periodico.tchequimica.com

treatment, takes place within 6-12 months after birth.

The thyroid gland synthesizes two iodine-containing hormones-thyroxine (T4) and triiodothyronine (T3), and one peptide hormone — calcitonin. In the tissue of the thyroid gland, the accumulation of the amino acid tyrosine occurs, which is deposited and stored in the form of a protein-thyroglobulin (a building material for the synthesis of thyroid hormones). In the presence of molecular iodine and the inclusion of the enzyme thyroid peroxidase (TPO), the synthesis of hormones T3 and T4 occurs.Thyroxine (T4) and triiodothyronine (T3) are synthesized in the apical part of the thyroid epithelium. Calcitonin (thyrocalcitonin) is produced by the parathyroid glands as well as the C-cells of the thyroid.

Thyroid hormones are the main regulators of homeostasis of the human body. With their direct participation, the main metabolic processes occur in tissues and organs, the formation of new cells and their structural differentiation, as well as genetically programmed death of old cells (apoptosis). Another equally important function of thyroid hormones in the body is to maintain constant body temperature and energy production (the so-called calorific effect). Thyroid hormones regulate the body's oxygen consumption by tissues, oxidation processes, and energy production, as well as control the formation and neutralization of free radicals. Throughout life, thyroid-stimulating hormones affect the mental, mental and physical development of the body. Deficiency of hormones at an early age leads to growth retardation, can cause bone diseases, and their deficiency during pregnancy-significantly increases the risk of cretinism of the unborn child due to underdevelopment of the brain in the prenatal period. Thyroid hormones are also responsible for the normal functioning of the immune system — they stimulate the cells of the immune system, the so-called T-cells, with which the body fights infection.

According to the world Health Organization (who) among endocrine disorders, thyroid diseases occupy the second place after diabetes. More than 665 million people in the world have an endemic goiter or suffer from other thyroid pathologies; 1.5 billion people face the risk of iodine deficiency diseases. At the same time, according to statistics, the increase in the number of thyroid diseases in the world is 5% per year.

According to various data, from 15 to 40% of the population of Russia suffer from thyroid pathologies, while in some regions, the percentage of patients in need of thyroid treatment is close to 95%. Statistics show that every second person living in Moscow and the Moscow region has a violation of the function or structure of the thyroid gland.

Among the possible causes of thyroid pathologies can be primarily identified poor environmental conditions, lack of iodine and other nutrients in the diet, as well as increasingly common genetic disorders.

Features of the influence of the thyroid gland on the oral cavity

Morphological and functional changes in the thyroid gland affect the general state of the human body, including tissues of the oral cavity, and these impairments usually manifest by early loss of teeth due to caries and periodontal diseases (Evstratenko *et al.*, 2018; Mazzeo *et al.*, 2013; Voloshina *et al.*, 2018). Oral manifestations of thyrotoxicosis include increased susceptibility to caries, periodontal disease, enlargement of extraglandular thyroid tissue, maxillary or mandibular osteoporosis, accelerated teething, and burning mouth syndrome.

Burning mouth syndrome, a condition that causes burning pain in the mouth, and Sjogren's syndrome, a condition that causes dry mouth, are more common in people with thyroid disease.

Patients who have thyroid disease present a problem for dental treatment. Awareness of the status and current stage of treatment is important to understand the possible changes required for dental treatment. The duration of therapy and the current status are important for understanding the metabolic control of patients. The main complications in patients with hyperthyroidism and hypothyroidism are associated with concomitant heart disease (Silva *et al.*, 2019; Dukić *et al.*, 2013; Vehkalahti *et al.*, 1996).

Dentists are required to be aware of the various aspects of the treatment of the disease that can affect the patient.

In turn, the problem of the relationship between oral tissues and materials used for manufacturing of removable orthopedic structures is one of the main in clinical orthopedic dentistry (Girardin *et al.*, 2019; Timoshin *et al.*, 2018, 2019; Sevbitov *et al.*, 2018). Acrylic dental materials are widely used for the manufacture of removable complete or partial dentures. (Timoshin, Sevbitov, *et al.* 2018).

Downloaded from www.periodico.tchequimica.com

Acrylic plastics in dentistry - as a method of treatment of dental diseases that have arisen on the background of thyroid diseases

A new page in the history of dentistry began in 1935 when the acrylic polymers are beginning to be introduced into dental practice.

Today, acrylic polymers are the main material for the manufacture of medical prostheses around the world.

Currently, dental polymers are 80% of all medical polymers and are represented primarily by polymers and copolymers of alkyl methacrylates.

Commodity form of basic materials is a set of powder-liquid (Kolodkina *et al.*, 2018; Vereshchagina *et al.*, 2004; Gerasimov *et al.*, 1993; Gozha *et al.*, 2010).

The powder may contain the following components a suspension polymer or a methacrylic acid-based copolymer with a General formula.

CH2=C(CH3)-COOR, where R-hydrocarbon radical; initiator; dye; stabilizer; turbid. The liquid is a solution in a monomer (methyl methacrylate - MMA) of target additives. When mixing separately stored powder with liquid, a molding mass is formed, which, depending on the composition of the powder and liquid, is cured (polymerized) by heating or spontaneously. After curing, the monomer forms a matrix of the curing product (polymerizate), in which the polymer – powder balls are distributed. The cured polymer-monomer mixture has a heterogeneous structure, which is due to the presence of "old" and "new" polymer in the polymer.

Dental prostheses in the oral cavity are affected by a complex of factors: physical, chemical, biological in an aggressive chemical environment, which is saliva. They are subjected to strong mechanical pressure when processing food. In turn, the material from which the prosthesis is made, directly affects the environment of the oral cavity, its mucous membrane, the body as a whole. Interaction of high-molecular compounds with the human body is a complex multifactorial process (Saxena *et all*, 2019)

In this regard, the materials used in prosthetic dentistry must meet the following medical and technical requirements:

- sufficient strength to ensure the integrity of the prosthesis;

- the necessary elasticity, eliminating deformation under the influence of chewing forces;

- high impact resistance;

- low density;

- sufficient thermal conductivity;

- high wear resistance;

- indifference to the action of saliva and various food additives;

- lack of adsorption capacity to nutrients and

the microflora of the oral cavity;

- a good imitation of natural color and color fastness;

- harmless to the tissues of the oral cavity and the body as a whole.

However, not yet found such materials that are fully would meet all the requirements. Synthetic acrylic plastics have many necessary qualities, including those that put polyacrylates out of competition with other plastics as construction materials for medicine: low water absorptiveness mechanical strength chemical inertness high manufacturability and low cost (Rech-Ortega *et al.*, 2019)

But the use of acrylic polymers has significant drawbacks.

It should be noted that studies relating to pathology the mucous membrane of the oral cavity in using removable plate prostheses are given considerable attention in both domestic and foreign literature.

Researchers dealing with this rather complex problem, different opinions are expressed about the etiology of these phenomena and the required methods of treatment. According to some authors, pathological reactions of the oral mucosa occur due to irritation of nerve elements at different levels of the reflex chain of the autonomic Central nervous system.

In the occurrence of prosthetic stomatitis, certain value it is attached to microorganisms, and the amount of microflora is greatly influenced by the microrelief of the surface of the plate prosthesis the presence of micro-steps, porosity.

The accumulated data to date allow us to conclude that most likely any removable prosthesis is a complex stimulus of mechanical, chemical, chemical-toxic, thermally insulating and sensitizing nature. Although in each case, a single pathogenic factor may be decisive. And

Downloaded from www.periodico.tchequimica.com

depending on the influence of which of the pathogenic factors is considered by researchers, certain methods of influence on the polymer dentures are used.

Etiology of allergic stomatitis in such conditions has not yet been clearly established, but most likely, it is related to immune response to irritating substance (Zholudev *et al.*, 2004, 2005). Some authors suggest that stomatitis is a sign of intolerance to acrylic plastics occurring in cases where, for unexplained reasons, the human immune system reacts to the appearance of molecules that it cannot recognize (Kasatkina *et al.*, 2010; Kalyvradzhiyan *et al.*, 2010; Lepilin *et al.*, 2003; Nartikova *et al.*, 1977). It is known that in patients with symptoms of endocrinopathy, phenomena of intolerance occur 20% more often than in people who do not have such pathologies. This fact is caused by general metabolism disorder, increased sensitivity and weak immune response (Paschina *et al.*, 1968; Kuznetsova *et al.*, 2018; Platonova *et al.*, 2018;).

According to some authors, the problem of intolerance to acrylates in patients, in particular, suffering from hyperfunction of the thyroid gland, should be solved with the help of complex drug therapy to increase resistance and reduce the level of sensitization of the body (Sevbitov *et al.*, 1999, 2004; Mamedov *et al.*, 2019; Yumashev *et al.*, Semenycheva *et al.*, 2019, Yumashev *et al.*, 2019).

Drug "Endonorm". History of creation.

"Endonorm", is a mixture of dry vegetable extracts of white cinquefoil, prepared according to special technology, the main active component of the product is Albinin.

Extract of the root of white Lapchatki, standardized substance Albinin, is the main active component of the drug, and other components are enhancing and modulating the effect of the first.

Each capsule contains Lapchatka white root extract 200 mg, grass extract succession 80 mg, kelp powder 70 mg, licorice root extract 50 mg.

Due to the biochemical characteristics of each of the components, the effect of their mutual strengthening in the treatment of diseases of the thyroid gland is created.

Studies have shown that the presence of a sum of phenolic compounds in the white Retina (Potentilla alba L.) affects the production of the anterior pituitary thyroid-stimulating hormone, contributes to the normalization of the morphological structure of thyroid tissue and the return of the thyroid gland to the euterioid state.

Licorice naked (Glycyrrhiza glabra L.) due to glycyrrhizic acids normalize the adrenal glands, immune, and reproductive systems restore hormonal imbalance of the body.

Polyphenolic compounds contained in a Series of three-part (Bidens tripartita L.) have immunomodulatory activity, allow to achieve a maximum therapeutic effect in diffuse toxic goiter and autoimmune thyroiditis.

Laminaria saccharina (Laminaria saccharina L.) due to the presence of a wide range of macro - and microelements normalizes biochemical processes in the tissues of the thyroid gland.

Cinquefoil white is quite well known in the folk medicine of Russia and European countries. Its dosage forms are recommended in the complex treatment of various diseases, including the elimination of such disorders of the thyroid gland as: hypothyroidism (hypofunction), hyperthyroidism (hyperfunction, thyrotoxicosis, Graves 'disease-graves'), autoimmune thyroiditis (Hashimoto's thyroiditis), euthyroid goiter (diffuse, nodular/multi-nodular), hyperplasia of the thyroid gland.

Albinin, contained in the white Lapchatke (Potentilla alba L.), affects the production of the anterior pituitary thyroid-stimulating hormone, normalizes the morphological structure of thyroid tissue, returns the thyroid gland to the euthyroid state.

"Endonorm" is recommended as a dietary Supplement-a source of glycyrrhizic acid and tannins, an additional source of iodine.

Downloaded from www.periodico.tchequimica.com

Figure 1. Lapchatka white.

Lat. Name - Potentilla alba Linnaeus; Department-Magnoliophyta; Class-Magnoliopsida; Order-Rosales; Family-Rosaceae; Genus-Potentilla; Species-alba L.

Lapchatka white is a modest, perennial, and low herbaceous medicinal plant, with a branched rhizome and a height of no more than 30 centimeters, which ends with a rosette of palmately dissected leaves into 5 leaflets. The white color of the petals indicates cross-pollination by nocturnal insects. Blooms in April-June, fruits in June-July. Fruits are dry ovoid, hairy at the base, achenes. Seeds are spread by insects and birds.

On the territory of the Russian Federation grows mainly in the southern regions of the European part to the Urals. Prefers light, especially oak and pine forests, copses, edges and meadows, grassy slopes, and shrubs. Thickets almost do not form. On 1 m2 there are no more than 2-3 plants. It is listed in the regional Red books, in particular, in the Red book of Moscow, Smolensk, Ryazan, Lipetsk, and other regions. It is also listed in the Red book of the Republic of Belarus (resolution of the Ministry of natural resources of Belarus No. 14 of 09.06.2004).

Raw material base Lapchatki white insignificant, because insufficiently studied methods of introduction of plants in culture. That is why it is extremely difficult to find a real and properly harvested root of lapchatki white. For the same reason, officially buy in pharmacies rhizomes and roots Lapchatki white can not. There are experimental plots of several hundred square meters (vegetative method of reproduction is used — by dividing the root), the largest of which is located in the Bryansk region (Bryansk region, Unechsky district, D. Sands, SHPP "Ginseng").

Lapchatka white grows in nature very slowly - from seed to adult plants with a rhizome length of 20-30 centimeters takes 10-15 years. Seeds have low germination, and germination time is stretched, seedlings develop slowly. On the rhizome of adult Lapchatki white there are many dormant buds, thanks to which,with the help of vegetative reproduction from cuttings 1-1.5 cm long, you can grow a whole plant. From one rhizome, you can get a few dozen cuttings. Cuttings are planted in spring or autumn. After 4-5 years after painstaking care of cuttings grow plants suitable for subsequent planting. By this time, the underground part (rhizome and storing roots) also reaches the optimal weight. In the future, the rate of development of the plant is significantly reduced.

For the treatment of diseases of the thyroid gland in folk medicine, raw Lapchatki white began to be used since the XVIII century. At the same time, the underground part is used as raw material — rhizomes and roots, which are harvested in the autumn, after the death of the above-ground mass. It should be noted that the grass Lapchatki white does not have thyroid-stimulating activity. The plant becomes suitable for preparation of medicinal raw materials for the 3-4 year of vegetation. In folk medicine, a decoction of the herb Lapchatki white is used to treat uterine prolapse. Lapchatka white also shows antibacterial activity, so it is used for colitis, enterocolitis, dysentery and other gastrointestinal diseases. Five are used for the prevention and treatment of diseases of the liver, the gastrointestinal tract, in particular, pus. It is used as a local wound healing agent, for this powder from dry grass is sprinkled with boils, boils, carbuncles, abscesses.

A study of the Lapchatka white.

Stage 1. Beginning. The 1970s.

The first clinical trials of Lapchatka white Were conducted by Ukrainian researchers G. K. Smyk and V. V. Krivenko in the early 1970s on the basis of the Clinical hospital under the Council of Ministers of the USSR, and the results of their studies were published in the" Pharmaceutical journal " [1975]. At this same time, about Lapchatke, a white published several articles (Smyk G. K., Krivenko W. W. 1975; Prikhodko E. I. 1976; Smyk G. K. 1982). Candidate of medical Sciences Prikhodko Elena Ivanovna, who observed patients with thyroid disorders, who were treated with white Lapchatka, stated a good therapeutic effect-up to full recovery.

But, unfortunately, research and experiments with Lapchatka white were suspended due to the lack of raw materials and funding.

Stage 2. From 1983 to 1999.

Russia's first Bloodroot white began to grow Kunitsyn, Vladislav Viktorovich. Since 1983, Kunitsyn began to actively promote and distribute

Downloaded from www.periodico.tchequimica.com

white Lapchatka. Writing from Kiev Botanical gardens is a plant, he started to practice agricultural techniques of cultivation and breeding adults. He has accumulated a large number of letters and grateful responses from people completely rid of various diseases of the thyroid gland. His numerous appeals to all authorities-from the Minister of health of the USSR and various research institutes, to the editors of magazines and Newspapers-year after year contributed to the popularization of the medicinal properties of the plant among herbalists, phytotherapists and other people associated with folk medicine. During this period, he published many articles about Lapchatka Belaya in various popular publications. Based on his personal experience, Vladislav Viktorovich notes that white Lapchatka is effective in treating the thyroid gland both with its increased and decreased function. In 1999, he met a doctor-phytotherapist, candidate of medical Sciences Kayukova Valentina Anatolyevna.

In LLC SHPP, "Ginseng" were planted the first few roots of Lapchatki white and started its industrial cultivation.

Stage 3.

In 2000, the doctor-phytotherapist Kayukova Valentina Anatolyevna set an extensive experiment to study the medicinal properties of the plant with the open publication of medical histories in the newspaper "Green Doctor". Over the course of several years of painstaking work, she managed to observe more than 500 patients in total. Valentina Anatolyevna initiated a new wave of clinical studies of Lapchatka Belaya (after more than 20 years) and did a great job of analyzing the accumulated material. Until now, this work has no analogues and is of interest to readers not only in terms of the results obtained but also the conclusions and recommendations for the use of Lapchatki white for medicinal purposes.

As a result of the research conducted at the research Institute of inorganic chemistry SB RAS (Novosibirsk), the chemical composition of this plant was established. The underground part contains carbohydrates (starch), iridoids, saponins, phenol carboxylic acids, flavonoids (quercetin), tannins (gallotanin) up to 17% (maximum in the flowering phase). The above-ground part contains iridoids, saponins, phenol-carboxylic acids, flavonoids (rutin), tannins (up to 6%). Phenol-carboxylic acids and their derivatives (n-coumaric, ellagic acids), flavonoids (quercetin, kaempferol, cyanidin) were found in the leaves. Lapchatka is a concentrator Mn, Zn, Cu, Ce, Co, Fe, Si, Al and for Si, Al, Zn, Mn their content exceeds the criterion of the degree of concentration of mineral elements for non-traditional plants in 1.7, 2.5, 3.0, 4.0 times, respectively. It should be noted that white Cinquefoil also contains elemental iodine and anion of iodic acid.

In 2001, Semenova E. F. and Presnyakova E. V. at the I Russian scientific-practical conference "Actual problems of innovation with non-traditional plant resources and the creation of functional products" announced a report on the chemical composition of white Lapchatka and its use for medicinal purposes.

And finally, only in 2005, 40 years later, from the extract of roots and rhizomes of Lapchatki white was isolated active substance-Albinin (Albinin), which has thyroid-stimulating and gonadotropic activity. In particular, this substance is one of the main components of the drug “Endonorm.”

Purpose: to study the indicators of trypsin-like activity of mixed saliva in patients with hyperfunction of the thyroid gland, whose dentures were manufactured by standard compression method, and by using proposed therapeutic and prophylactic measures.

2. MATERIALS AND METHODS

For this purpose, examined 34 patients (18 females and 16 males) aged 40 – 60 years with hyperfunction of the thyroid gland. Patients were divided into two groups. The first group (17 subjects) included orthopedic patients, treated with removable prostheses made by traditional compressive method from Ftorax. Orthopedic patients of the second group (17 subjects) received laminar removable dental prostheses with a double-layer basis made using the proposed technique of saturation lamina with “Endonorm”.

Individual gaskets in a double-layer basis of a removable denture were made by a direct method using GC “Coe-Soft” dental plastic.

All patients were examined at the baseline

Downloaded from www.periodico.tchequimica.com

and 2 weeks, 1 and 3 months after orthopedic treatment. Trypsin-like activity (TLA) of mixed saliva was measured by a spectrophotometric method based on a determination of the rate of N-Benzoyl-L-arginine removal from the synthetic N-Benzoyl-L-arginine of ethyl ester substrate (Reanal).

To implement this method, we diluted 0.5 ml of saliva to 2 ml with 0.05 M Tris-HCL buffer (pH 8.0) and, after its pre-incubation, added 1 ml of BAEE solution for 5 minutes. The reaction was carried out in a spectrophotometer thermostated cuvette (at 25 ^{0}C). The rate of spontaneous hydrolysis of BAEE was monitored by optical density increase at 253 nm every 5 minutes within 30 minutes interval and compared with a reference sample. The activity was calculated according to Equation 1:

$$TLA = \Delta D250^{30} \times 3 / (1/1 \times 0.5 \times 30) - \Delta D250^{30} \text{ µmol/ml.} \quad \text{(Eq. 1)}$$

where $\Delta D250^{30}$ is the increase of optical density in 1 ml of the sample at 253 nm within 30 minutes;

3 – sample volume (ml);

0.5 – the amount of saliva taken for analysis (ml);

1.1 – the increase in optical density at 253 nm, corresponding to the formation of 1 µmol BAEE in 1 ml of the sample;

30 – reaction time (min).

The results were expressed in micromoles of hydrolyzed substrate per minute per milliliter.

Analysis of obtained results was made by the method of variation statistics using Student's t-test, A p-value <0.05 was considered significant.

3. RESULTS AND DISCUSSION:

Trypsin-like activity (TLA) of mixed saliva in hyperthyroid patients before prosthetics was 47.95 ± 1.56 µmol/ml in the first group and 47.90 ± 1.55 µmol/ml in the second group, where the proposed therapeutic and prophylactic complex is applied (Fig. 2, Table 1).

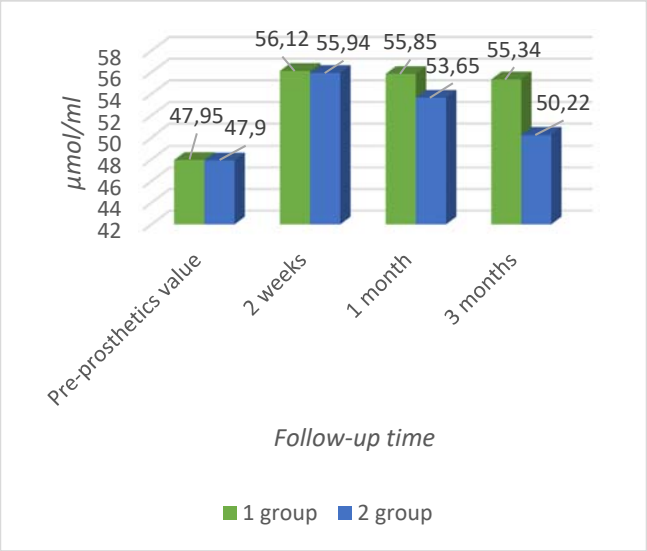

Figure 2. *The trypsin-like activity of mixed saliva after the imposition of laminar removable dentures in orthopedic patients with thyroid hyperfunction (µmol/ml)*

Table 1. The trypsin-like activity of mixed saliva after the imposition of laminar removable prostheses in orthopedic patients with hyperfunction of the thyroid gland (µmol/ml)

Study group	Pre-prosthetics value	Follow-up time		
		2 weeks	1 month	3 months
1 group, n=17	47.95 ±1.56	56.12 ±1.72, p<0.05	55.85 ±1.68, p<0.05	55.34 ±1.49, p<0.05
2 group, n=17	47.90 ±1.55	55.94 ±1.48, p<0.05	53.65 ±1.50, p>0.05	50.12 ±1.63, p>0.05

By the second week of follow-up increase of values in both groups was observed: for example, the value of trypsin-like activity in the first group was 56.12 µmol/ml, in the second group - 55.94 µmol/ml, that corresponded to a 17% increase comparing to baseline (pre-prosthetics) data. We assume that this reaction was caused by an adaptive response to the presence of a foreign body (removable prosthesis) and did not require any correction of therapeutic measures.

Further monitoring of TLA in mixed saliva showed sufficiently high TLA values in the first group of patients (55.85 ± 1.68 µM/ml), while in the second group we noted stabilization of TLA (53.65 ± 1.50 µmol/ml), p> 0.05.

By the 3rd month in the first group, TLA still remained at a sufficiently high level (55.34 ± 1.49 µmol/ml, p <0.05), but in the second group

Downloaded from www.periodico.tchequimica.com

evaluated parameter approached baseline value (p> 0.05).

By the second week of follow-up increase of values in both groups was observed: for example, the value of trypsin-like activity in the first group was 56.12 μmol/ml, in the second group - 55.94 μmol/ml, that corresponded to a 17% increase comparing to baseline (pre-prosthetics) data. We assume that this reaction was caused by an adaptive response to the presence of a foreign body (removable prosthesis) and did not require any correction of therapeutic measures.

Further monitoring of TLA in mixed saliva showed sufficiently high TLA values in the first group of patients (55.85 ± 1.68 μM/ml), while in the second group we noted stabilization of TLA (53.65 ± 1.50 μmol/ml), p> 0.05.

By the 3rd month in the first group, TLA still remained at a sufficiently high level (55.34 ± 1.49 μmol/ml, p <0.05), but in the second group evaluated parameter approached baseline value (p> 0.05).

Two weeks after the application of removable dentures, we observed an increase of saliva enzymatic activity in both groups. This phenomenon was considered to be an adaptive response of the patient's body to the presence of removable acrylic prostheses. Further observation (1 month after orthopedic treatment) showed a sufficiently high level of TLA in the first group of patients and normalization of the studied parameters in the second group (received proposed therapeutic and prophylactic complex). TLA value was an indicator of the correctness of the chosen orthopedic and medical tactics; especially it suggested that developed integrated approach based on the use of gasket, saturated with the "Endonorm" was etiopathogenetic. Three months after orthopedic treatment with removable prostheses, the level of TPA in the first group of patients remained sufficiently high, but in the second group it was close to pre-prosthetics values. Obtained results indicate early adaptation and elimination of negative effects of the acrylic basis in hyperthyroid patients of the second group and suggest the need for correction of therapeutic measures in the first group of patients by means of application of the proposed complex.

4. CONCLUSIONS:

It was revealed that after applying removable laminar prostheses in hyperthyroid orthopedic patients, violation of the enzymatic activity of mixed saliva is observed. In two weeks, trypsin-like activity was 17% higher compared to the baseline value. This fact was considered as the cumulative effect of thyroid dysfunctions and the effects of acrylic plastics.

It has been established that the use of the proposed curative and prophylactic complex based on "Endonorm" and the use of "Coe-Soft" gaskets in patients with thyroid hyperfunction can prevent the development of intolerance to acrylic removable prostheses.

5. ETHICS COMMITTEE:

All research methods under this article have been conducted in accordance with the relevant guidelines and regulations. All experimental protocols were approved by the Local ethics Committee of I. M. Sechenov First Moscow State Medical University (Sechenov University) protocol number № 10-16 от 09.11.2016. Prior to the study, informed consent was obtained from all patients for the upcoming study.

6. ACKNOWLEDGMENTS:

This work was done at Sechenov University with supported by the "Russian Academic Excellence Project 5-100".

7. REFERENCES:

1. Evstratenko, V. V., Sevbitov, A. V., Platonova, V. V., Selifanova, E. I., Dorofeev, A. E. The characteristics of crystallization of mixed saliva in patients using heroin and methadone. *Klinichescheskaya Laboratornaya Diagnostika*, **2018**, 63(4), 223-227.

2. Mazzeo, M. A., Linares, J. A., López, M. M., Bachmeier, E., Wietz, F. M., Galván, V., Valentinuzzi, M. C., Riveros, J. A., Finkelberg, A. Analysis of saliva samples from oncological patients treated with 5-fluorouracil and leucovorin calcium by scanning electron microscopy with energy dispersive system. *Journal of Oral Pathology and Medicine*, **2013**, 42(10), 788-792.

3. Voloshina, I. M., Borisov, V. V.,

Downloaded from www.periodico.tchequimica.com

Sevbitov, A. V., Davidyants, A. A., Mironov, S. N., Kuznetsova, M. Yu., Ergesheva, E. V. Distinctive features of microcrystallization of mixed saliva in children with different levels of activity of the carious process. *Asian Journal of Pharmaceutics*, **2018**, 12(S3), 1017-1020.

4. Silva, P. D. C., Santos, B. L. C. D., Soares, G. L., Oliveira, W. A. D. Anti-Candida albicans activity of the association of citronelal with anfotericin B or with cetoconazole. *Periodico Tche Quimica*, **2019**, 16(31), 223-234

5. Dukić, W, Dobrijević, T. T., Katunarić, M., Lesić S. Caries prevalence in chronic alcoholics and the relationship to salivary flow rate and pH. *Cent Eur J Public Health*, **2013**, 21(1):43-7.

6. Vehkalahti, M, Nikula-Sarakorpi, E, Paunio, I. Evaluation of salivary tests and dental status in the prediction of caries increment in caries-susceptible teenagers. *Caries Res*, **1996**, 30(1), 22-8.

7. Girardin, F, Hearmon, N, Negro, F, Eddowes, L, Bruggmann, P, Castro, E. Increasing hepatitis C virus screening in people who inject drugs in Switzerland using rapid antibody saliva and dried blood spot testing: A cost-effectiveness analysis. *J Viral Hepat*. **2019,** 26(2), 236-245.

8. Timoshin, A. V., Sevbitov, A. V., Ergesheva, E. V., Mironov, S. N., Kozhemov, S. I., Pustokhina, I. G., Danshina S. D. Experience in the use of collagen phytoplates in the treatment of gingivitis. *Opcion*. **2019**, 35(S21), 582-598.

9. Timoshin, A. V., Sevbitov, A. V., Drobot, G. V., Yumashev, A. V., Timoshina, M. D. Use of bioresorbable plates on the basis of collagen and digestase for treatment of diseases of oral mucosa (review of clinical cases). *International Journal of Green Pharmacy*. **2018**, 12(S1), 290-296.

10. Sevbitov, A. V., Dorofeev, A. E., Davidyants, A. A., Ershov, K. A., Timoshin, A. V. Assessment of pain perception of elderly patients with different levels of dentophobia during surgical dental appointment. *Asian Journal of Pharmaceutics*. **2018**, 12(S3), 1012-1016.

11. Timoshin, A. V., Sevbitov, A. V., Ergesheva, E. V., Boichuk, A. V., Sevbitova, M. A. Experience of treatment of aphthous lesions of oral mucosa by preparations on the basis of collagen and digestase. *Asian Journal of Pharmaceutics.* **2018**, 12(1), 284-287.

12. Kolodkina, V. I., Arutyunov, A. V., Sirak, S. V., Ivashchenko, V. A., Skorikova, L. A., Andriutsa, N. S., Tsymbalov, O. V., Risovanniy, S. I. Cytological characteristics of oral cavity tissues of experimental animals when using photo polymeric material. *Medical News of North Caucasus.* **2018**, 13(4), 637-641.

13. Vereshchagina, G. V., Trapkova, A. A. Some mechanisms of action of thyroid hormones. *Advances in modern biology*. **2004**, 97 (3), 447-457.

14. Gerasimov, G. A., Petunina, N. A. Iodine and autoimmune diseases of the thyroid gland. *Problems of endocrinology*. **1993**, 39 (3), 52 - 54.

15. Gozha, L. D., Talalai, T. Yu., Arunov, T. I. Functional disorders of saliva in toxic-chemical stomatitis caused by metal prostheses. *Dentistry for all*. **2010**, 3, 53-56.

16. Zholudev, S. E., Zhmakin, I. Treatment and prevention of prosthetic stomatitis in persons older than 55 years, that use removable plate prostheses. *Dentist*. **2004**, 9, 21-24.

17. Zholudev, S. E. Ways to improve the adaptation in people with problems of tolerability of removable denture materials. *Maestro dentistry*. **2005**, 19, 5-11.

18. Kasatkina, E. P. Iodine deficiency diseases in children and adolescents. *Eligible doctor.* **2010**, 10, 14-18.

19. Kalyvradzhiyan, E. S., Podoprigora, A. V., Komarova, Yu. N., Bobeshko, M. N. Clinical and experimental substantiation of

Downloaded from www.periodico.tchequimica.com

the use of modified adhesive composition based on polysaccharides to improve the period of adaptation to removable denture plate prosthesis. *Modern orthopedic dentistry*. **2010**, 13, 31-36.

20. Lepilin, A. V., Rubin, V. I., Proshin, N. G. The effect of removable plate prostheses made of acrylic plastics on the structural and functional properties of the cellular membranes of the oral mucosa. *Stomatology*. **2003**, 1, 51-54.

21. Nartikova, V. F., Oglobina, O. G. Modern methods in biochemistry, M, **1977**.

22. Paschina, T. S., Egorova, G. P. Modern methods in biochemistry, M, 1968.

23. Kuznetsova, M. Yu., Nevdakh, A. S., Platonova, V. V., Sevbitov, A. V., Dorofeev, A. E. Evaluation of effectiveness of a preparation on the basis of phytoecdysteroids for treatment of traumatic injuries of oral mucosa in orthodontic patients. *International Journal of Green Pharmacy.* **2018**, 12(S1), 297-300.

24. Platonova, V. V., Sevbitov, A. V., Shakaryants, A. A., Dorofeev, A. E. The experimental clinical substantiation of treatment of patients with odontogenic phlegmon of maxillofacial area using delargin in complex therapy. *Klinicheschеskaya Laboratornaya Diagnostika*. **2018**, 63(5), 293-296.

25. Sevbitov, A. V., Persin, L. S., Slabkobskaia, A. B., Pankratova, N. V. The morphological status of the maxillodental system in children living in an area contaminated by radionuclides as a result of the accident at the Chernobyl Atomic Electric Power Station. *Stomatologiya*. **1999**, 78(6), 41-42.

26. Sevbitov, A. V. Remote effects of the Chernobyl accident: evaluation of the maxillodental status of the children. *Stomatologiia*. **2004**, 83(1), 44-47.

27. Mamedov, A. A., Morozova, N. S., Yumashev, A. V., Dybov, A. M., Nikolenko, D. A. Criteria for provisional restorations used in preparation for comprehensive orthodontic and orthopedic rehabilitation. *Periodico Tche Quimica*. **2019**, 16(32), 647-655.

28. Yumashev, A. V., Semenycheva, I., Rakhadilov, B., Tsymbal, A. Development of biocompatible coatings for dental implants based on transition metal nitrides. *Journal of Global Pharma Technology*. **2019**, 11(5), 22-28.

30. Yumashev, A. V., Koneva, E. S., Borodina, M. A., Lipson, D. U., Nedosugova, A.B. Electronic apps in assessing risk and monitoring of patients with arterial hypertension. *Prensa Medica Argentina*. **2019**, 105(4), 235-245.

31. Saxena, N., Habelitz, S., Marshall, G. W., Gower, L. B. Remineralization of demineralized dentin using a dual analog system. *Orthodontics and Craniofacial Research.* **2019**, 22(S1), 76-81.

32. Rech-Ortega, C., Fernández-Estevan, L., Solá-Ruíz, M. F., Agustín-Panadero, R., Labaig-Rueda, C. Comparative in vitro study of the accuracy of impression techniques for dental implants: Direct technique with an elastomeric impression material versus intraoral scanner. *Medicina Oral Patologia Oral y Cirugia Bucal.* **2019**, 24(1), 89-95.

Downloaded from www.periodico.tchequimica.com

PERIÓDICO TCHÊ QUÍMICA
ARTIGO ORIGINAL

ANÁLISE PROSPECTIVA DE PARÂMETROS DE ESPECTRO LÍPIDICO E MARCADORES INFLAMATÓRIOS VASCULARES COMO VARIANTE DE UMA ABORDAGEM PERSONALIZADA AO PROGNÓSTICO DE EVENTOS CORONÁRIOS INDESEJÁVEIS EM PACIENTES COM DOENÇA CARDÍACA CORONÁRIA APÓS ANGIOPLASTIA

PROSPECTIVE ANALYSIS OF LIPID SPECTRUM PARAMETERS AND VASCULAR INFLAMMATORY MARKERS AS A VARIANT OF A PERSONIFIED APPROACH TO PROGNOSIS OF UNDESIRABLE CORONARY EVENTS IN PATIENTS WITH CORONARY HEART DISEASE AFTER ANGIOPLASTY

ПРОСПЕКТИВНЫЙ АНАЛИЗ ПАРАМЕТРОВ ЛИПИДНОГО СПЕКТРА И МАРКЕРОВ СОСУДИСТОГО ВОСПАЛЕНИЯ КАК ВАРИАНТ ПЕРСОНИФИЦИРОВАННОГО ПОДХОДА К ПРОГНОЗУ НЕЖЕЛАТЕЛЬНЫХ КОРОНАРНЫХ СОБЫТИЙ У ПАЦИЕНТОВ С ИШЕМИЧЕСКОЙ БОЛЕЗНЬЮ СЕРДЦА ПОСЛЕ АНГИОПЛАСТИКИ

PETELINA, Tatiana I.[1*]; MUSIKHINA, Natalia A.[2]; GAPON, Liudmila I.[3]; DYACHKOV, Sergey M.[4]; SHAROYAN, Yuliya A.[5];

[1,2,3,4,5] Tomsk National Research Medical Center of the Russian Academy of Sciences, Tyumen Cardiology Research Center, 111 Melnikaite Str., zip code 625026, Tomsk – Russian Federation

** Correspondence author*
e-mail: petelina@cardio.tmn.ru

Received 05 September 2019; received in revised form 20 October 2019; accepted 23 October 2019

RESUMO

A relevância do estudo se deve ao fato de que o papel ambíguo dos mediadores bioquímicos no desenvolvimento de complicações da angioplastia com colocação de stent e a falta de consenso quanto ao tempo dos parâmetros laboratoriais são determinados para esclarecer abordagens ao estudo de parâmetros bioquímicos que indicam a natureza do curso da doença arterial coronariana e o desenvolvimento de possíveis complicações indesejáveis após intervenção coronária percutânea. O objetivo deste artigo foi analisar os parâmetros do espectro lipídico e marcadores da resposta inflamatória vascular em pacientes com doença arterial coronariana em grupos com angina de peito estável e angina de peito instável após angioplastia com colocação de stent para monitorar a dinâmica de parâmetros bioquímicos e identificar preditores de vasos coronários indesejados. Pacientes com doença arterial coronariana com estenose arterial coronariana significativa (n=95) revelados após angiografia coronária no ponto de aumento máximo no nível de marcadores de reação inflamatória (três meses após angioplastia) foram divididos em 2 grupos – pacientes com angina de peito estável e persistente (n=77) até o final do estudo, e pacientes com um episódio pós-revascularização desenvolvido de angina instável (n=18) após angioplastia com colocação de stent. Foi estabelecido que pacientes com angina instável no estágio inicial apresentaram um risco significativamente maior de desenvolver instabilidade do fluxo sanguíneo coronariano no período pós-revascularização devido aos níveis inicialmente elevados de homocisteína e proteína C reativa altamente sensível. Os resultados obtidos são muito importantes para a implementação de um programa ideal para o monitoramento de pacientes com doença arterial coronariana, melhorando medidas para aumentar a adesão à terapia no estágio ambulatorial do tratamento.

Palavras-chave: *angina de peito, angioplastia, colocação de stent, espectro lipídico, marcadores de inflamação.*

ABSTRACT

The relevance of the study is due to the fact that the ambiguous role of biochemical mediators in the development of angioplasty complications with stenting and the lack of consensus on the timing of laboratory indicators determine to specify the approaches to the study of biochemical parameters that indicate the nature of the course of coronary heart disease (CHD) and the development of possible undesirable complications after

Downloaded from www.periodico.tchequimica.com

percutaneous coronary intervention. This article aims to analyze the parameters of lipid spectrum and markers of vascular inflammatory reaction in patients with CHD, in groups with stable angina and unstable angina episode after angioplasty with stenting, to trace the dynamics of biochemical parameters and to reveal the predictors of undesirable coronary events. Patients with CHD with significant coronary artery stenosis (CKS, n=95) revealed after coronary angiography (CAG) at the point of maximum increase in the markers of the inflammatory response (3 months after angioplasty) are divided into 2 groups – patients with stable angina pectoris (AP, n=77) until the end of the study and patients with a developed post-revascularization episode of unstable angina (UA, n=18) after angioplasty with stenting. It was established that patients with UA at the initial stage have a significantly higher risk of developing coronary blood flow instability in the post-revascularization period due to initially elevated levels of homocysteine and rf-CRP. The results obtained are very important for the implementation of an optimal program for monitoring patients with coronary artery disease, improving measures to increase adherence to therapy at the outpatient stage of treatment.

Keywords: *angina pectoris, angioplasty, stenting, lipid spectrum, markers of inflammation*.

АННОТАЦИЯ

Актуальность исследования обусловлена тем, что существует неоднозначное отношение к роли биохимических медиаторов в развитии осложнений после ангиопластики со стентированием и отсутствует консенсус по срокам проведения лабораторных исследований, которые отражают характер течения ИБС и временные точки для развития возможных нежелательных осложнений. Целью данной статьи является анализ параметров липидного спектра и маркеров сосудистой воспалительной реакции у пациентов с ИБС в группах со стабильной стенокардией и нестабильным приступом стенокардии после ангиопластики со стентированием, для отслеживания динамики биохимических показателей и выявления предикторов нежелательных коронарных сосудов. Пациенты с ишемической болезнью сердца (ИБС) с выявленным значимым коронарным стенозом артерий (ЗКС, n=95) после проведенной коронароангиографии (КАГ) в точке максимального повышения уровня маркеров воспалительной реакции (3 месяца после ангиопластики) разделены на 2 группы – пациенты с сохраняющейся стабильной стенокардией (СС, n=77) до конца исследования и пациенты с развившимся постреваскуляризационным эпизодом нестабильной стенокардии (НС, n=18) после ангиопластики со стентированием. Установлено, что пациенты с НС на исходном этапе имеют достоверно более высокий риск развития нестабильности коронарного кровотока в постреваскуляризационом периоде за счет исходно повышенных уровней гомоцистеина и вч-СРБ. Полученные результаты очень важны для осуществления оптимальной программы по наблюдению за пациентами с ИБС, улучшению мер по повышению приверженности к терапии на амбулаторном этапе лечения.

Keywords: *стенокардия, ангиопластика, стентирование, липидный спектр, маркеры воспаления.*

1. INTRODUCTION

Cardiovascular diseases (CVD) remain the main cause of disability and mortality in developed countries, of which more than half of cases are atherothrombotic diseases, in particular, coronary artery disease (CAD) (Karpov *et al.,* 2010). A characteristic feature of CAD are unpredictable acute coronary events (ACE), the main pathogenetic factor of which is a breach in the integrity of the unstable atherosclerotic plaque, causing the formation of a blood clot in the coronary artery lumen. Currently, there is an active search for biochemical markers that can predict the development of acute atherothrombotic events. These include serum lipid spectrum parameters and markers of systemic and local activity of vascular inflammation, the most studied of which are C-reactive protein (CRP), interleukins-6,8 (IL), matrex metalloproteinases (MMP-2 and 9), CD40 receptor–CD40 ligand signaling system and others (Zykov *et al.,* 2011; Gusev *et al.,* 2012; Afanasieva *et al.,* 2016; Ezhov *et al.,* 2017; Mironova and Mironov, 2018).

Coronary stenting is one of the most common methods for treating patients with various forms of CAD, characterized by an effective restoration of coronary circulation and stabilization of a patient's condition. The prognosis in patients after percutaneous coronary intervention (PCI) depends on many factors (Schiele *et al.,* 2018; Solow *et al.,* 2018; Tanaskovic *et al.,* 2018). Clinical prognostic parameters, such as gender, age and presence of diabetes mellitus (DM) were studied as predictors of poor prognosis (Golukhova and Kuznetsova, 2016; Golukhova *et al.,* 2016; Tomilova *et al.,* 2017; Muhsin and Ibrahim, 2018; Sergienko and Ansheles, 2018). However, while

Downloaded from www.periodico.tchequimica.com

the clinical and angiographic parameters of coronary complications of angioplasty are well known, changes in laboratory data that contribute to their development are presented insufficiently. According to published data, CRP, levels of plasminogen activator inhibitor-1, von Willebrant factor activity, erythrocyte sedimentation rate, levels of eosinophils and myeloperoxidase are predictors of poor prognosis after PCI with stenting and implantation of drug-eluting stents, but the results are often inconsistent (Ndrepepa *et al.,* 2014; Getz and Reardon, 2014; Bibek *et al.,* 2015; Moon *et al.,* 2016; Petelina *et al.,* 2017; Mukherjee *et al.*, 2018). An ambiguous role of biochemical mediators in the development of complications after angioplasty with stenting and a lack of consensus regarding timing of determination require specification of their importance for the course of post-revascularization CAD and the development of possible coronary adverse events (Velibey *et al.,* 2016; Parsa *et al.,* 2018; Czubaszewski *et al.,* 2018; Fracassi *et al.,* 2018; Kosaki *et al.,* 2018; Manati *et al.,* 2018; Sihag *et al.,* 2018; Trasca *et al.,* 2018; Le Gall *et al.,* 2018).

Patients with CAD and significant coronary stenosis of the arteries (SCS, n = 95) (SCS, n=95) after coronary angiography, at the point of maximum increase in the level of markers of the inflammatory reaction (3 months after angioplasty) are divided into 2 groups – patients with persistent stable angina pectoris (SA, n=77) until the end of the study and patients with post-revascularization episodes of unstable angina (UA, n=18).

Changes in biochemical parameters showed a prolonged nature of the vascular inflammatory response with a tendency to decrease in the parameters after 6 months in the SA group and after 12 months of follow-up in the group with post-revascularization UA episodes. In the group of patients with SCS, an increase in low density lipoproteins by 1 mmol/L increased the probability of post-revascularization unstable angina 7.387 times. It was found that patients with UA at baseline had a significantly higher risk of coronary circulation instability in post-revascularization period due to initially elevated levels of homocysteine and hsCRP.

The initial increase in the levels of atherogenic lipid fractions and systemic prolonged nature of the vascular inflammatory reaction after angioplasty with stenting are prognostic factors for the development of coronary adverse events (Tenekecioglu *et al.,* 2016; Sirtori *et al.,* 2017).

This article aims to analyze the parameters of lipid spectrum and markers of vascular inflammatory reaction in patients with CHD, in groups with stable angina and unstable angina episode after angioplasty with stenting, to trace the dynamics of biochemical parameters and to reveal the predictors of undesirable coronary events.

2. MATERIALS AND METHODS

The study was conducted at the emergency cardiology department of the Tyumen Cardiology Research Center and Tomsk National Research Medical Center of the Russian Academy of Sciences. The study involved 143 patients with coronary artery disease. The distribution of the patients was based on the following parameter - severity of coronary stenosis defined as ≥75% narrowing of the artery lumen diameter. After selective CAG, the groups of patients with significant coronary stenosis, SCS (n = 95), initially stable angina (SA, n = 53) and unstable angina (UA, n = 42) were identified.

The study parameters were evaluated at baseline, when the patient was admitted to the hospital, before CAG and 3, 6 and 12 months after angioplasty with drug-eluting stent implantation during standard therapy (ACE inhibitors, β-adrenergic blockers, disaggregants – clopidogrel and/or acetylsalicylic acid, statins). The mean follow-up was 12±1.4 months.

The study protocol is approved by the Institutional Ethics Committee. Before inclusion in the study, each study participant gave a written informed consent to the use of study results for scientific purposes.

The diagnosis of CAD, criteria for stable and unstable angina pectoris, dyslipidemia, severity of hypertension, CHF and obesity were verified according to the modern national and international clinical guidelines for diagnosis and treatment developed by the expert committee of the Russian Society of Cardiology, World Health Organization, American Heart Association and European Society of Cardiology, respectively.

Venous blood was collected in disposable tubes of the Vacuette system (Japan) on an empty stomach and the blood was centrifuged for 15 minutes at 2500 rpm in a Sigma centrifuge (Germany). Patients' blood serum was aliquoted for further freezing (at -70 °C).

The parameters of lipid metabolism were studied using the Cobas Integra 400 plus biochemical automatic analyser (Switzerland).

Downloaded from www.periodico.tchequimica.com

Total cholesterol (TC), triglycerides (TG), HDL and LDL were determined using a direct enzymatic colorimetric method; concentrations of apolipoproteins A-I (Apo A-I), apolipoproteins B (Apo-B) and lipoproteins a (Lp (a)) were determined using immunoturbidimetry using analytical kits and control materials by Roche Diagnostics Gmb (Germany).

The following biochemical markers of inflammation were determined: highly sensitive C-reactive protein (hsCRP, reference values 0-3.0 mg/L) – using an immunoturbidimetric method with the C-reactive protein hs analytical kit (BioSystem, Spain) on a Clima MC-15 open type analyser (Spain); interleukin-1β (IL-1β, reference values 0-5.0 pg/mL), interleukin-6 (IL-6), interleukin-8 (IL-8), tumour necrosis factor-α (TNF-α, reference values 0-8.11 pg/mL) – "sandwich" and homocysteine (HYC, reference values 5.0–15.0 μmol/L) – by competitive methods (solid-phase chemiluminescent enzyme immunoassay) on the IMMULITE 1000 analyser (Siemens Diagnostics, USA); soluble CD40 – ligand (sCD40 L) by the method of "sandwich immunoassay" using the Human sCD40L Elisa kits on the Bender MedSystems analyser, Austria; CD40 receptor and matrix metalloproteinase-9 (MMP-9, reference values 20.3-77.2 ng/mL) – Bender MedSystems and eBioscience company, Austria; tissue inhibitor of metalloproteinase-1 (TIMP-1, reference values 92-116 ng/mL)) – Human TIMP-1 Elisa K.t Invitrogen, USA on the Personal Lab analyser, Italy.

Parameters of endothelial functional activity in blood serum: levels of nitrites (reference value 3.77±0.87 nmol/L) were determined on the Humalyzer 2000 Human biochemical analyser (Germany, 1995) and endothelin-1-21 (reference values 0.2-0.7 fmol/L) – on the Dynatech enzyme immunoassay analyser (Germany, 1989).

A comprehensive assessment of the vasculature condition was carried out using a high-tech method – selective CAG using the Diagnost ARC A, Poly diagnost C, Integris Allura (Phillips, Holland) angiographic units according to the standard Judkins method of femoral access. Percutaneous coronary intervention was performed using transluminal balloon coronary angioplasty (TBCA) with stenting.

Statistical methods. Statistical data processing was performed using the Statistica application software package (SPSS Inc, version 11.5). To assess the normality of distribution, the Kolmogorov – Smirnov criterion was used. The Student's t-test was used to detect differences between the groups in quantitative variables of normal distribution; the non-parametric Mann-Whitney test was used to compare qualitative and quantitative values that were not normal. The groups were compared using the Wilcoxon test for paired measurements. Data is presented as mean values with standard deviations (M±SD). Significance of differences was detected at $p<0.05$. The relationship between signs was evaluated using the Pearson and Spearman rank correlation coefficients for quantitative and qualitative values, respectively. To identify predictors among the total number of parameters studied, the binary logistic regression was used.

3. RESULTS AND DISCUSSION:

According to the previously obtained results of a prospective observation in general groups of patients who underwent angioplasty with stenting, the signs of correction of initially elevated levels of atherogenic lipid fractions, parameters of vascular inflammatory response and endothelial dysfunction were observed within 12 months. A significant decrease in atherogenic fractions of TC, LDL, HDL and TG was observed after 6 months with baseline SA and after 12 months with baseline UA. A prolonged response of systemic highly sensitive C-reactive protein (hs-CRP) and local inflammatory reactions (TNF-α, homocysteine, IL-1β, MMP-9) were observed with a maximum after 3 months and a decrease with a tendency to target levels after 6 months in SA and after 12 months in UA after angioplasty with stenting.

Parallel unidirectional growth of the parameters of vascular inflammatory response at "3 months" point after angioplasty, together with persisting hypercholesterolemia, identifies patients with SCS, regardless of the clinical manifestation of CAD, as patients at very high risk of early restenosis and the process of prolonged indolent inflammatory reaction up to the end point of follow-up does not exclude late atherothrombotic complications.

Over the last years, as the frequency of percutaneous coronary interventions with stenting has increased, more and more attention has been focused on solving problems associated with atherothrombosis and restenosis inside stents, which are detected in approximately 10–40% and 0.87–2.2% of cases during the first year after stent placement, respectively (Cassese *et al.,* 2014; Chen *et al.,* 2014; Darvishpour *et al.,* 2016; Palur Ramakrishnan *et al.,* 2017; Persic *et*

Downloaded from www.periodico.tchequimica.com

al., 2018).

As a starting point for the development of restenosis, a combined involvement is considered – mechanical damage to the intima and media of the arteries with aggravated local inflammatory reaction, as well as hypersensitivity to stent materials, involving eosinophilic granulocytes in the reaction process (Gabbasov *et al.,* 2010; DeSart *et al.,* 2016; Lee *et al.,* 2016).

Taking into account the peak of inflammatory response activation after 3 months of follow-up, we analysed changes in the markers of the lipid profile and vascular inflammatory response in patients with persistent SA and patients with episodes of UA in post-revascularization period. It was established that in the patients with SCS after angioplasty with stenting (n=95), stable condition in the patients from the initial groups was maintained over the period of further analysed follow-up in 81.1% of cases (n=77); development of post-revascularization UA episodes was observed in 18.9% of cases (n=18). It was found that post-revascularization episodes of UA in 72.2% of cases (n=13) were significantly (p=0.02) more often in the patients with initial instability of the coronary circulation at the initial stage of the study, and only in 27.8% of cases (n=5) – in patients with SA at baseline. In the patients with post-revascularization episodes of UA after diagnostic CAG, restenosis of the operated coronary vessel was detected in 4 cases (1.3%).

Comparative characteristics of clinical and historical parameters in patients after angioplasty with stenting according to the clinical course of CAD, reported during the observation, are presented in Tables 1-2.

According to Table 1, patients with SA and post-revascularization episodes of UA were comparable for incidence and history of tobacco smoking, family history of CAD, history of MI, and presence and history of CAD, type 2 diabetes.

In accordance with the data presented in Table 2, patients in both groups did not significantly differ in a number of parameters considered as possible risk factors for adverse coronary events. The majority of patients were men with single vessel SCS, CAD mainly associated with exertional angina (EA) II FC in combination with grade 3 hypertension, CHF II FC (NYHA) and grade I obesity.

Comparative characteristics of lipid spectrum parameters in patients with SA and with post-revascularization episode of UA are presented in Table 3. The point of maximum increase of the studied parameters and the end point of the study are presented.

As can be seen from Table 3, no significant differences were revealed in the comparative description of the level of atherogenic fractions between groups of patients with SA and post-vascularization episode of UA at the point of 3 and 12 months of angioplasty with stenting.

A significant decrease in TC and LDL ($p<0.05$) was found while the level of parameters above the reference values was maintained during a prospective analysis of the lipid spectrum parameters in patients with SA. The constancy of high values of TG and LP (a) levels was revealed. A significant decrease in VLDL and Apo B/Apo A-I parameters was registered, their target level after 12 months was observed. The statistically significant increase in Apo A-I can be traced in the reference values. A prospective analysis of lipid spectrum parameters in patients with a post-revascularization UA episode did not reveal a significant decrease in elevated levels of total cholesterol, LDL, TG and LP (a). A significant decrease in the level of VLDL reaches the limits of the reference interval after 12 months. No significant change in the content of the antiatherogenic fraction represented by HDL and Apo A-I was detected in the initial and prospective stages.

According to the data presented in Table 4, patients with SA and post-revascularization UA episode did not significantly differ in the degree of activation of systemic and local inflammatory responses represented by hyperproduction of hsCRP and TNF-α, MMP-9, homocysteine, respectively, and endothelial dysfunction in the form of elevated plasma endothelin-1 concentrations and reduced nitrite levels.

A prospective analysis of inflammatory markers in patients with SA revealed a significant decrease in elevated levels of hsCRP, TNF-α, and homocysteine with the achievement of a standard interval of values 12 months after angioplasty with stenting. Despite a significant decrease in the concentration of MMP-9 following 12 months after angioplasty, the target marker level was not observed. A statistically significant decrease in the values of the cytokine cascade (IL-1β, IL-6, IL-8), CD 40, sCD 40L and an increase in TIMP-1 were detected within the reference range. Endothelial dysfunction showed hyperproduction of plasma endothelin-1 and a significant increase in the level of nitrites 12 months after angioplasty. A prospective analysis

Downloaded from www.periodico.tchequimica.com

of inflammatory markers in the group of patients with a post-vascularization UA episode revealed an increased content of hsCRP, TNF-α and homocysteine after 3 months and a significant decrease in the above values up to the reference range following 12 months after angioplasty with stenting. Despite a significant decrease in the level of MMP-9, an increased concentration of the marker was observed after 12 months. Constant endothelin-1 hyperproduction and a tendency to increased nitrite following 12 months after angioplasty with stenting are observed.

Direct correlations of prolonged activation of vascular inflammatory response and endothelial dysfunction markers with clinical and historical parameters were characteristic during the analysed observation period. Thus, in the group of SA patients, VLDL and LP (a) were positively correlated with homocysteine (p=0.02, r=0.3; p=0.01, r=0.4, respectively), homocysteine with the fact of smoking and HF functional class (p=0.01, r=0.4; p=0.01, r=0.4, respectively), hsCRP with HF functional class and compliance with therapy (p=0.02, r=0.4; p=0.001, r=0.8, respectively), TNF-α with HF functional class (p=0.03, r=0.4), and endothelin-1 with hypertension grade (p=0.02, r=0.4).

In the group of patients with a post-revascularization UA episode, TNF-α is positively correlated with body mass index, CHF FC (NYHA), family history of CAD (p=0.02, r=0.4; p=0.02, r=0.4; p=0.01, r=0.8; respectively), hsCRP with CHF FC (NYHA), the multi-vascular nature of the significant damage in the coronary bed, the number of angina episodes (p=0.01, r=0.3, p=0.03, r=0.4; p=0.03, r=0.4, respectively), homocysteine level with the presence of type 2 diabetes (p=0.03, r=0.4), endothelin-1 level with a history of myocardial infarction (MI) (p=0.01, r=0.6).

The identified correlation coincides with studies that indicate a close relationship between clinical and laboratory parameters (Moon *et al.,* 2016; Getz and Reardon, 2014; Cassese *et al.,* 2014; Chen *et al.,* 2014). According to the goal of our work, a multivariate analysis (binary logistic regression) was used to identify the main predictors that determine the maximum development of UA in the post-revascularization period in patients with SCS after stenting. The initial set of variables included: lipid profile parameters and markers of vascular inflammation. The final model included: low density lipoproteins, triglycerides, total cholesterol and endothelin-1. As a result of the analysis of variables, the most essential parameters were selected and a model with three variables was created. The encoding of the values of essential parameters is presented in Table 5. The technical result was expressed using the formula of the obtained linear function (Equation 1).

In order to classify the entire set into subgroups using the obtained linear function, a logit-transformation with the calculation of the separation point is applied (Equation 2). Where P is the probability that an event of interest will occur – unstable angina: e is a mathematical constant equal to 2.718; F is the value of the regression equation.

Exp (B) for logistic regression coefficients specifies the degree of change in the relative risk of an event of interest for a particular variable B. For example, increase in low-density lipoproteins increases the probability of an event of interest 7.387 times compared to the baseline risk (relative risk of outcome).

The specificity of this model was 70.1%; sensitivity was 75.0%; on average, 71.1% of the initial grouped observations are correctly classified. An indicator of the prediction accuracy for an episode of post-revascularization unstable angina is the area under the ROC curve – for our model it was 0.715 (P<0.001), which corresponds to the good quality of the model, Figure 1.

Therefore, in the general group of patients with SCS, an increase in low-density lipoproteins by 1 mmol/L increased the risk of post-revascularization unstable angina 7.387 times compared to baseline risk (OR=1.76; 95% CI 1.95 – 27.8353; p=0.027). Our data is indirectly consistent with the data of Mihaylova B. et al., who showed that the reduction of LDL cholesterol by 1 mmol/L reduced the risk of cardiovascular complications by 20% (Mihaylova *et al.,* 2012).

It should be mentioned that, based on clinical and historical data, the binary logistic regression method showed that the risk of SCS increased 2.8 times in men (OR=2.761; 95% CI: 1.41 – 5.39; p=0.003); when LDL levels in men increased by 1 mmol/L, the risk of SCS further increased 1.8 times (OR=1.76; 95% CI 1.23 – 2.53; p=0.002).

In addition, the same method showed that in the patients with UA episodes at the initial stage of the study, the risk of unstable coronary circulation in post-vascularization period increased 4.1 times (OR=4.07; 95% CI 1.32-12.59; p=0.02).

All cases of recurrent UA episodes (n = 13) in the group with baseline UA were recorded with

Downloaded from www.periodico.tchequimica.com

hyperhomocysteinemia (>15 μmol/L) detected at the initial stage of the study with mean homocysteine level of 16.52 μmol/L, or 10.1% higher than the upper limit of normal.

Hyperhomocysteinemia correlated both with a repeated episode of UA (p=0.04 and r=0.4) and hyperproduction of hs-CRP (p=0.02 and r=0.5), indicating a vicious circle of interaction between local inflammation in atherosclerotic plaque, repeated coronary adverse event and activation of systemic inflammatory response, which is consistent with literature data (Bibek *et al.,* 2015; Ndrepepa *et al.,* 2014; Moon *et al.,* 2016).

Therefore, a summary of available data of laboratory blood tests allows determination of biochemical markers that can reliably predict significant coronary stenosis and adverse events in post-revascularization period for different clinical variants of the course of CAD at the initial stage of examination, when patients are admitted to the hospital, prior to angioplasty with stenting – these are male gender, elevated levels of LDL, and hyperhomocysteinemia. The established set of parameters can be considered as a variant of a personified approach to prognosis of coronary adverse events in patients with CAD after angioplasty with stenting and can determine the choice of rational tactics of drug therapy.

4. CONCLUSIONS:

From a practical point of view, it is important for a physician who works with patients to know what time points after a transcutaneous intervention are most dangerous for the development of coronary complications. Our data suggests that almost the entire postoperative year can be dangerous in terms of the development of complications. Elevated levels of atherogenic lipid parameters and markers of vascular inflammation, i.e. hs-CRP, TNF-α, homocysteine, endothelin-1 and MMP-9, from the beginning of follow-up to the maximum rise at the point of "3 months" after angioplasty, may indicate a risk of the development of early coronary complications, such as early restenosis and atherothrombosis, and the failure to achieve the target levels of the studied parameters at the final stage of follow-up (endothelin-1, nitrite, MMP-9) may indicate of a systemic slow vascular inflammatory response in patients with CAD with a probability of late atherothrombotic complications.

The implementation of an optimal program to increase patients' adherence to therapy, in particular, with statins and antiplatelet agents, which maintain the target levels of LDL cholesterol and reduce the risk of thrombosis, together with dynamic monitoring of laboratory markers, are two main directions that can protect a patient from coronary events in postoperative period.

5. REFERENCES:

1. Afanasieva, O.I., Utkina, E.A., Artemieva, N.V., Ezhov, M.V., Adamova, I.Yu., Pokrovsky, S.N. *Kardiologiya*, **2016**, *56*(6), 5-11.
2. Bibek, S., Xie, Y., Gao, J., Wang, Z., Wang, J., Geng, D. *Inflammation*, **2015**, *38*(1), 159-169.
3. Cassese, S., Byrne, S., Tada, T., Pinieck, S., Joner, M., Ibrahim, T., King, L.A., Fusaro, M., Laugwitz, K.L., Kastrati, A. *Heart*, **2014**, *100*, 153-159.
4. Chen, J., Chen, Y., Tian, F., Han, Y., Jing, J., Liu, J., Wang, J., Zhou, S. *Zhonghua Xin Xue Guan Bing Za Zhi*, **2014**, *42*, 14-18.
5. Czubaszewski, Ł., Straburzyńska-Lupa, A., Migaj, J., Straburzyńska-Migaj, E. *Cardiology Journal*, **2018**, *25*(6), 701-708.
6. Darvishpour, A., Pashaki, N.J., Salari, A., Nejad, M.T., Barari, F. *Journal of Mazandaran University of Medical Sciences*, **2016**, *26*(137), 206-210.
7. DeSart, K., O'Malley, K., Schmit, B., Lopez, M.-C., Moldawer, L., Baker, H., Berceli, S., Nelson, P. *Journal of Vascular Surgery*, **2016**, *64*(3), 766-778.
8. Fracassi, F., Vetrugno, V., Mandurino-Mirizzi, A., Cosentino, N., Panicale, S., Caprari, P., Niccoli, G., Crea, F. *Coronary Artery Disease*, **2018**, *29*(8), 638-646.
9. Gabbasov, Z.A., Kozlov, S.G., Saburova, O.S., Titov, V.N., Lyakishev, A.A. *Cardiology*, **2010**, *1*, 7-12.
10. Getz, G.S., Reardon, C.A. *Thromb Vasc Biol*, **2014**, *34*(4), 695-696.
11. Golukhova, E.Z, Kuznetsova, E.V. *Diabetes Mellitus*, **2016**, *19*(5), 406-413.
12. Golukhova, E.Z., Grigoryan, M.V.,

Downloaded from www.periodico.tchequimica.com

Ryabinina, M.N. *Rational Pharmacotherapy in Cardiology*, **2016**, *5*, 528-535.

13. Gusev, D.E., Potievsky, B.G., Raychevin, N., Sirkin, A.L. *Cardiology*, **2012**, *4*, 4-8.
14. Ezhov, M.V., Sergienko, I.V., Kukharchuk, V.V. *VIreview*, **2017**, *44*, 175-183.
15. Karpov, Yu.A., Samko, A.N., Buza, V.V. *Coronary angioplasty and stenting*, Moscow: Medical News Agency, **2010**.
16. Kosaki, R., Minoura, Y., Ogura, K., Oishi, Y., Tanaka, L., Arai, K., Nomura, K., Sakai, K., Sekimoto, T., Nisikura, T., Tsujita, H., Kondo, S., Tsukamoto, S., Hamazaki, Y., Kobayashi, Y. *Journal of Cardiology*, **2018**, *72*(6), 494-500.
17. Le Gall, G., Kirchgesner, J., Bejaoui, M., Landman, C., Nion-Larmurier, I., Bourrier, A., Sokol, H., Seksik, P., Beaugerie, L. *PLoS ONE*, **2018**, *13*(8), e0201991.
18. Lee, M.-J., Park, S.-D., Kwon, S.W., Woo, S.-I.Email Author, Lee, M.-D., Shin, S.-H., Kim, D.-H., Kwan, J., Park, K.-S. *American Journal of Cardiology*, **2016**, *118*(9), 1323-1328.
19. Manati, W., Pineau, J., Puertas, R.D., Morel, E., Quadiri, T., Bui-Xuan, B., Chevalier, P. *Cardiology Journal*, **2018**, *25*(6), 708-713.
20. Mihaylova, B., Emberson, J., Blackwell, L., Keech, A., Simes, J., Barnes, E., Voysey, M., Gray, A., Collins, R., Baigent, C. (Eds.). *Cholesterol Treatment Trialists' (CTT) Collaborators, The effects of lowering LDL cholesterol with statin therapy in people at low risk of vascular disease: meta-analysis of individual data from 27 randomised trials*, Lancet, **2012**.
21. Mironova, T.F., Mironov, V.A. *Materials of the 12th International Conference on Mechanics, Resource and Diagnostics of Materials and Structures*. Ekaterinburg, Russian Federation, **2018**, 030043.
22. Moon, A., Choi, D., Jahng, S. *Fibrinolysis*, **2016**, *27*, 70-76.
23. Muhsin, A., Ibrahim, S.S. *International Journal of Research in Pharmaceutical Sciences*, **2018**, *9*(S2), 78-82.
24. Mukherjee, K., Sequira, L., Vaz, C.J. *Journal of Clinical and Diagnostic Research*, **2018**, *12*(12), LC01-LC05.
25. Ndrepepa, G., Braun, S., Tada, T., Guerra, E., Schunkert, H., Laugwitz, K.L., Kastrati, A. *Cardiovasc. Revasc. Med*, **2014**, *15*, 131-13.
26. Palur Ramakrishnan, A.V.K., Varghese, T.P., Vanapalli, S., Nair, N.K., Mingate, M.D. *Cardiovascular Therapeutics*, **2017**, *35*(1), 64-70.
27. Parsa, A., Sadeghi, M., Roghani, F., Golshani, J., Khani, A., Yazdekhasti, S. *Iranian Heart Journal*, **2018**, *19*(1), 52-60.
28. Persic, V., Bastiancic, A.L., Rosovic, I., Raljevic, D., Samsa, D.T., Bastiancic, L., Miskulin, R., Boban, M., Laskarin, G. *Medical Hypotheses*, **2018**, *115*, 72-76.
29. Petelina, N., Musikhina, L., Gapon, V., Kuznetsov, E., Gorbatenko, I., Emeneva I. *Integrative Obesity and Diabetes*, **2017**, *3*(2), 1-8.
30. Schiele, F., Ecarnot, F., Chopard, R. *European Journal of Preventive Cardiology*, **2017**, *24*(3), 88-100.
31. Sergienko, I.V., Ansheles, A.A. Rational *Pharmacotherapy in Cardiology*, **2018**, *14*(1), 77-87.
32. Sihag, B.K., Jain, D., Subramanian, G. *Journal of Clinical and Diagnostic Research*, **2018**, *12*(12), OC17-OC21.
33. Sirtori, C.R., Labombarda, F., Castelnuovo, S., Perry, R. *Annals of Medicine*, **2017**, *49*(2), 134-141.
34. Solow, E.B., Vongpatanasin, W., Skaug, B., Karp, D.R., Ayers, C., de Lemos, J.A. *Clinical and Experimental Rheumatology*, **2018**, *36*(6), 1031-1037.
35. Tanaskovic, S., Radak, D., Aleksic, N., Calija, B., Maravic-Stojkovic, V., Nenezic, D., Ilijevski, N., Popov, P., Vucurevic, G., Babic, S., Matic, P., Gajin, P., Vasic, D., Rancic, Z. *Journal of Vascular Surgery*, **2018**, *68*(1), 118-127.

Downloaded from www.periodico.tchequimica.com

36. Tenekecioglu, E., Bourantas, C.V., Abdelghani, M., Sotomi, Y., Suwannasom, P., Tateishi, H., Onuma, Y., Yılmaz, M., Serruys, P.W. *Expert Review of Cardiovascular Therapy*, **2016**, *14*(9), 1053-1070.

37. Tomilova, D.I., Karpov, Y.A., Lopukhova, V.V. *Russian Journal of Cardiology*, **2017**, *8*, 7-12.

38. Trasca, S.P., Florescu, C., Dinescu, V.C., Puiu, I., Dinescu, S.N., Tudorascu, D.R., Bica, E.C., Vasile, R.C., Romanescu, F.M., Bunescu, M.G., Cioatera, N., Goanta, E.V. *Revista de Chimie*, **2018**, *69*(12), 3600-3604.

39. Velibey, Y., Guvenc, T.S., Alper, A.T. *Journal of Thoracic Disease*, **2016**, *8*(9), 2353-2356.

40. Zykov, K.A., Nuraly, E.Y., Kaznacheeva, E.I., Kuznetsova, T.V., Spring, E.B., Masenko, V.P. *Cardiology Messenger*, **2011**, *1*, 23-33.

$$F = 0.927 + 2.000 \times LDL + 1.355 \times TG - 2.288 \times TC \quad \text{(Eq. 1)}$$

$$P = 1/(1+e^{(-F)}) \quad \text{(Eq. 2)}$$

Table 1. *Characterization of risk factors in patients with stable angina and with a post-vascularization episode of unstable angina (M±SD)*

Parameter	Patients with SA (n=77)	Patients with UA episode (n=18)
Fact of smoking	29.9% (n=23)	22.2% (n=4)
Family history of CAD	24.4% (n=19)	11.1% (n=2)
CAD without hypertension	10.4% (n=8)	27.8% (n=5)
History of MI	44.2% (n=34)	44.4% (n=8)
Dyslipidemia	94.8% (n=73)	94.4% (n=17)
Type 2 diabetes	33.8% (n=26)	27.8% (n=5)
CAD duration, years	6.95±5.87	9.26±7.43
Smoking history, years	10.43±1.19	9.75±2.3
DM 2 type duration, years	4.67±2.46	5.44±2.61

Note: n – number of patients, % – percentage of the total subjects in the group

Downloaded from www.periodico.tchequimica.com

Table 2. *Characteristics of clinical and historical parameters of patients with stable angina and with a post-revascularization episode of unstable angina (M±SD)*

Parameter	Patients with SA (n=77)	Patients with UA episode (n=18)
Men	68.8% (n=53)	83.3% (n=15)
Single vessel SCS	57.1% (n=44)	61.1% (n=11)
Multi-vessel SCS (≥2 CA)	42.9% (n=33)	38.9% (n=7)
Exertional angina, FC		
I	6.5% (n=5)	5.6% (n=1)
II	62.3% (n=48)	72.2% (n=13)
III	31.2% (n=24)	22.2% (n=4)
Hypertension, grade		
1	6.5% (n=5)	11.1% (n=2)
2	14.3% (n=11)	16.7% (n=3)
3	68.8% (n=53)	44.4% (n=8)
CHF (NYHA) FC		
I	5.2% (n=4)	5.6% (n=1)
II	79.2% (n=61)	66.7% (n=12)
III	15.6% (n=12)	27.8% (n=5)
Dyslipidaemia	94.8% (n=73)	94.4% (n=17)
Obesity		
0	32.5% (n=25)	16.7% (n=3)
I	46.8% (n=36)	50.0% (n=9)
II	15.6% (n=12)	22.2% (n=4)
III	5.2% (n=4)	11.1% (n=2)
Age, years	60.47±9.54	57.17±10.11

Note: n – number of patients, % – percentage of the total subjects in the group

Table 3. *Comparative characteristics of lipid spectrum parameters in patients with stable angina and with post-vascularization episode of unstable angina (M±SD)*

Parameter	Patients with SA (n=77)		Patients with UA episode (n=18)	
	after 3 months	after 12 months	after 3 months	after 12 months
TC (mmol/L)	4.9±0.88	4.64±0.85*	4.71±1.22	4.7±1.15
HDL (mmol/L)	1.13±0.26	1.18±0.28	1.03±0.2	1.08±0.21
LDL (mmol/L)	2.82±0.78	2.46±0.81*	2.77±1.02	2.6±0.96
VLDL (mmol/L)	0.69±0.23	0.63±0.25*	0.77±0.19	0.55±0.23*
TG (mmol/L)	1.87±0.65	1.74±0.45	1.95±0.54	1.76±0.5
Apo B (mg/dl)	102.94±27.72	94.23±24.6*	95.52±18.8	97.73±22.9
Apo A-I (mg/dl)	142.15±30.32	151.47±26.5*	135.67±31.92	147.08±16.9
Apo B/Apo A-I	0.74±0.3	0.66±0.32*	0.7±0.2	0.65±0.19
LP (a) (mg/dl)	35.33±22.01	27.01±10.61	25.58±20.6	24.46±17.55

Note: n – number of patients; significance of differences in groups of patients with SA and with an UA episode 3 and 12 months after angioplasty with stenting: * $p<0.05$

Downloaded from www.periodico.tchequimica.com

Table 4. *Comparative characteristics of inflammatory markers and endothelial dysfunction parameters in patients with stable angina and with a post-revascularization episode of unstable angina (M±SD)*

Parameter	Patients with SA (n=77)		Patients with UA episode (n=18)	
	after 3 months	after 12 months	after 3 months	after 12 months
CD 40 (ng/mL)	104.42±38.2	90.81±28.42*	86.53±21.9	77.98±21.65
sCD40L (ng/mL)	3.64±0.83	3.24±0.72	3.35±0.72	2.99±0.91
CD 40/sCD 40L	29.25±8.76	29.15±8.73	24.85±7.06	26.53±9.11
TIMP-1(ng/mL)	96.59±19.98	106.44±28.0*	97.88±23.3	105.48±23.5
MMP-9 (ng/mL)	115.68±29.0	88.19±31.12*	129.8±16.6	85.72±28*
IL-1β (pg/mL)	5.07±1.77	4.47±1.85*	4.43±1.74	4.1±1.2
IL-6 (pg/mL)	3.89±2.32	3.18±1.5*	4.27±2.95	3.4±1.89
IL-8 (pg/mL)	23.52±20.48	17.92±14.64*	19.65±13.0	15.32±9.45
TNF-α (pg/mL)	11.26±4.81	6.99±3.19*	11.41±4.69	7.02±2.67*
hsCRP (mg/L)	3.47±0.81	2.78±0.94*	3.4±0.94	2.52±0.93*
homocysteine (μmol/L)	17.94±5.99	10.77±5.44*	16.72±4.95	10.42±3.6*
nitrites (nmol/ml)	2.59±1.06	3.29±0.98*	2.67±1.12	3.07±0.91
endothelin-1 (fmol/l)	1.07±0.5	1.05±0.55	0.95±0.51	1.05±0.41

Note: n – number of patients; significance of differences in the groups of patients with SA and UA episode 3 and 12 months after pangioplasty with stenting: * $p<0.05$

Table 5. *Encoding values of essential features*

Parameter	Variable	Type	Unit of measurement
Low density lipoprotein	LDL	Quantitative	mmol/L
Triglycerides	TG	Quantitative	mmol/L
Total cholesterol	TC	Quantitative	mmol/L

Downloaded from www.periodico.tchequimica.com

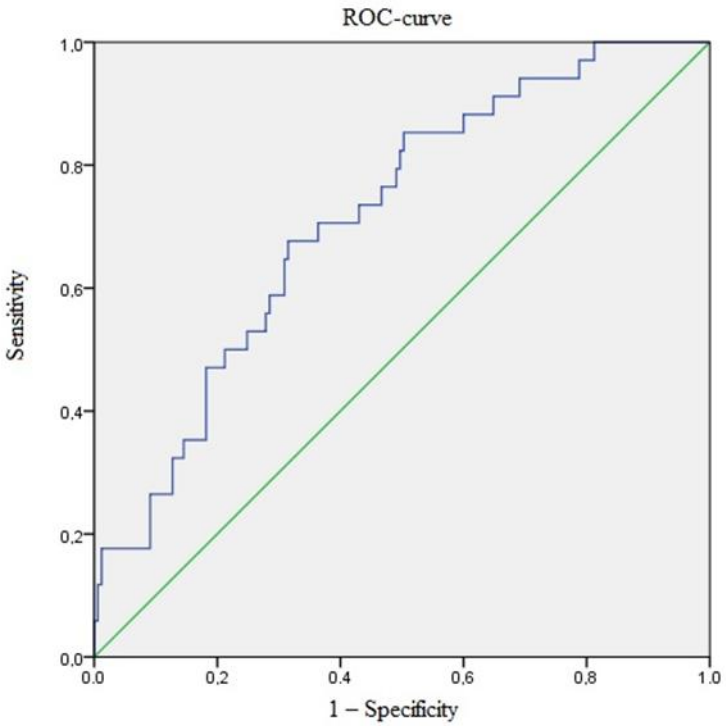

Figure 1. *ROC-curve: area under the ROC-curve is 0.715 (P<0.001)*

Downloaded from www.periodico.tchequimica.com

PERIÓDICO TCHÊ QUÍMICA
ARTIGO DE REVISÂO

CÁLCULO DO NÃO-EQUILÍBRIO DE SISTEMAS QUE CONSISTEM NO CONJUNTO DE SUBSISTEMAS DE EQUILÍBRIO LOCAL

CALCULATION OF THE NONEQUILIBRIUM SYSTEMS CONSISTING OF AN AGGREGATE OF LOCALLY-EQUILIBRIUM SUBSYSTEMS

РАСЧЁТ НЕРАВНОВЕСНОСТИ СИСТЕМ, СОСТОЯЩИХ ИЗ СОВОКУПНОСТИ ЛОКАЛЬНО-РАВНОВЕСНЫХ ПОДСИСТЕМ

RYNDIN, Vladimir V.[1*];

[1,] S. Toraigyrov Pavlodar State University, Department of Mechanics and Oil and Gas Engineering, 64 Lomov Str., zip code 140008, Pavlodar – Republic of Kazakhstan

** Correspondence author*
e-mail: rvladvit@yandex.kz

Received 20 June 2019; received in revised form 30 September 2019; accepted 22 October 2019

RESUMO

A segunda lei da termodinâmica (SLT) baseia-se no postulado do não-equilíbrio, segundo o qual existe uma propriedade objetiva da matéria – o "não-equilíbrio", que caracteriza a distribuição desigual da matéria e do movimento no espaço. Uma nova formulação da SLT é dada em relação ao conjunto de subsistemas de equilíbrio local que compõem o sistema de não-equilíbrio: quando ocorrem processos reais (irreversíveis), o não-equilíbrio do sistema isolado (SI) diminui e, nos processos reversíveis, o não-equilíbrio no sistema de subsistemas de equilíbrio local não muda completamente (o incremento de não-equilíbrio de um tipo totalmente compensado por diminuição do não-equilíbrio de qualquer outro tipo). Como característica quantitativa do sistema de não-equilíbrio, consideramos o trabalho máximo que pode ser feito quando o sistema de não-equilíbrio entra em equilíbrio. O artigo fornece uma confirmação calculada das disposições teóricas do conceito de não-equilíbrio e seu aparato matemático por exemplos de determinação da perda de não-equilíbrio de SI durante a operação do motor térmico que executa um ciclo irreversível e o estado de não-equilíbrio do sistema adiabático (SA). Foram dados os esquemas do SI consistindo de um corpo quente, o ambiente e um fluido de trabalho que executa um ciclo de Carnot imperfeito em temperatura, bem como um SA consistindo do ambiente e um fluido de trabalho, cuja expansão dá o trabalho a um receptor externo. Se demonstra que o trabalho externo do sistema adiabático deve ser determinado não pela diminuição do potencial termodinâmico do fluido de trabalho, como geralmente é aceito, mas pela diminuição do potencial de todos os corpos do SA (fluido de trabalho e ambiente). Como resultado, expressões analíticas são obtidas para o cálculo prático do não-equilíbrio e sua redução durante processos reais em sistemas que consistem no conjunto de subsistemas de equilíbrio local, o que é novo em termodinâmica.

Palavras-chave: *segunda lei da termodinâmica, postulado de não-equilíbrio, amount of nonequilibrium, calculation of nonequilibrium.*

ABSTRACT

The basis of SLT is the postulate of nonequilibrium, according to which there is an objective property of matter – “nonequilibrium”, which characterizes the uneven distribution of matter and motion in space. A new formulation of the SLT is given in relation to the set of locally equilibrium subsystems that make up the nonequilibrium system: when real (irreversible) processes occur, the nonequilibrium of the isolated system (IS) decreases, and in reversible processes the nonequilibrium in the system of locally equilibrium subsystems does not change (the increment of one kind of nonequilibrium completely compensated by a decrease in the disequilibrium of some other kind). The maximum work that can be done when the nonequilibrium system goes into equilibrium is considered as a quantitative characteristic of the nonequilibrium system. The article provides a calculated confirmation of the theoretical provisions of the concept of nonequilibrium and its mathematical apparatus by examples of determining the loss of IS disequilibrium during operation of a heat engine performing an irreversible cycle and the nonequilibrium state of an adiabatic system (AS). Schemes of an IS consisting of a hot body, the environment, and a working fluid performing a temperature-imperfect Carnot cycle are given, as well as an AS consisting of the environment and a working fluid, upon expansion of which work is given to an

Downloaded from www.periodico.tchequimica.com

external work receiver. It is shown that the external work of the adiabatic system should be determined not by the decrease in the thermodynamic potential of the working fluid, as is generally accepted, but by the decrease in the potential of all AS bodies (the working fluid and the environment). As a result, analytical expressions are obtained for the practical calculation of nonequilibrium and its reduction during real processes in systems consisting of an aggregate of locally-equilibrium subsystems, which is new in thermodynamics.

Keywords: *second law of thermodynamics, postulate of nonequilibrium, amount of nonequilibrium, calculation of nonequilibrium.*

АННОТАЦИЯ

В основу ВЗТ положен постулат неравновесности, согласно которому существует объективное свойство материи – «неравновесность», характеризующее неодинаковость распределения вещества и движения в пространстве. Даётся новая формулировка ВЗТ применительно к совокупности локально-равновесных подсистем, составляющих неравновесную систему: при протекании реальных (необратимых) процессов неравновесность изолированной системы (ИС) уменьшается, а в обратимых процессах неравновесность в системе локально-равновесных подсистем не изменяется (приращение неравновесности одного вида полностью компенсируется уменьшением неравновесности какого-либо другого вида). В качестве количественной характеристики неравновесности системы рассматривается максимальная работа, которая может быть совершена при переходе неравновесной системы, в равновесное состояние. В статье даётся расчётное подтверждение теоретических положений концепции неравновесности и её математического аппарата на примерах определения потери неравновесности ИС при работе тепловой машины, осуществляющей необратимый цикл, и неравновесности адиабатной системы (АС). Приведены схемы ИС, состоящей из горячего тела, окружающей среды и рабочего тела, совершающего неидеальный по температуре цикл Карно, а также АС, состоящей из окружающей среды и рабочего тела, при расширении которого отдаётся работа внешнему приёмнику работы. Показано, что внешняя работа адиабатной системы должна определяться не по убыли термодинамического потенциала рабочего тела, как общепринято, а по убыли потенциала всех тел АС (рабочего тела и окружающей среды). В результате получены аналитические выражения для расчёта на практике неравновесности и её уменьшения при протекании реальных процессов в системах, состоящих из совокупности локально-равновесных подсистем, что является новым в термодинамике.

Keywords: *второй закон термодинамики, постулат неравновесности, количество неравновесности, расчет неравновесности.*

1. INTRODUCTION

The second law of thermodynamics (SLT) attracts the attention of scientists of many specialties, including philosophers. The analytical expression of the second law of thermodynamics is the inequality of Rudolf Clausius in 1850 (Equation 1).

According to this record, the entropy of a nonequilibrium isolated system $S_{\text{noneq.IS}}$ in irreversible processes increases, while in reversible processes, it remains. The question arises, which property of matter (motion, the form of motion, or other property) is quantitatively preserved in the IS during the course of reversible (ideal) processes. The modern thermodynamics does not have the answer to this question. Ignorance (misunderstanding) of the essence of SLT led to the appearance of various formulations (about twenty formulations of LST (Putilov were proposed) (Putilov, 1971; Freitas *et al.*, 2016) and an abundance of material devoted to clarifying the meaning of these formulations (Reyf, 1972; Wald, 2001; Martyushev and Seleznev, 2006; Rakopoulos and Giakoumis, 2006; Liu and Liu, 2008; Ben-Naim, 2010; Seifert, 2012; Bejan, 2016; D'Alessio *et al.,* 2016; Chen *et al.*, 2017; Altaner, 2017; Martyushev and Celezneff, 2017; de Oliveira, 2019; Marbœuf *et al.,* 2019; Ptaszyński and Esposito, 2019; Sellitto and Di Domenico, 2019; de Blasio, 2019; Borin and Sukhorukov, 2019).

As Moran notes, no wording fully reflects all aspects of the SLT given by other formulations. Many authors (Moran *et al.,* 2014) see the reason for the lack of a uniform formulation of the SLT as the diversity of thematic areas covered by the second law (Guo *et al.,* 2019).

When clarifying the formulations of SLT, contradictions arise both within individual textbooks and between textbooks of different authors: A.I. Andryushchenko (Andryushchenko,

Downloaded from www.periodico.tchequimica.com

1975), H.D. Baehr (Baehr, 1973), P. Calabrese (Calabrese, 2018), L. Chen and A. Tsutsumi (Chen and Tsutsumi, 2018), E. Fermi (Fermi, 1937), R. Hołyst and A. Poniewierski (Hołyst and Poniewierski, 2012), V.I. Krutov (Krutov *et al.,* 1991); Vukalovich and Novikov (Vukalovich and Novikov, 1968), Novikov (Novikov, 1984), C. Borgnakke, R.E, Sonnag, (Borgnakke and Sonnag, 2009), B. Callen (Callen, 1985), V.A. Kirillin (Kirillin *et al.,* 1983), Ch. Kittel (Kittel, 1993), D. Kondepudi and Prigogine (Kondepudi and Prigogine, 2015), I.R. Krichevsky (Krichevsky, 1970), B.H. Lavenda (Lavenda, 2010), R. Morales-Rodriguez (Morales-Rodriguez, 2016), M.J. Moran (Moran *et al.,* 2014). R.C. Srivastava (Srivastava *et al.,* 2007). These formulations indirectly describe the consequences arising from the SLT or are redundant (for example, the statement about heat removal in the cycle). One single formulation is needed (as is customary in other laws), from which various existing formulations should flow (or be considered redundant) as consequences. If there is a unified formulation of SLT, the need to introduce many formulations will become redundant.

This SLT formulation, based on the postulate “on the existence and change of nonequilibrium”, is given by Ryndin V. V.: “The total (complete) nonequilibrium of an isolated system cannot increase – in reversible (ideal) processes it does not change, but in real (irreversible) processes it is reduced.” In this paper, instead of the existing concept of equilibrium, which underlies the SLT, the concept of nonequilibrium is introduced. According to this concept, the cause of all processes is nonequilibrium – a property of matter, due to the uneven distribution of the concentration of motion in space.

The following types of nonequilibrium are distinguished: thermal and baric, due respectively to the difference in temperature and pressure in space; mechanical (kinetic and potential), electrical, chemical. To assess the nonequilibrium of the entire system, consisting of a set of locally-equilibrium subsystems, the concept of complete nonequilibrium is introduced as the sum of all types of nonequilibrium of an isolated system (Khantuleva and Shalymov, 2017; Yuan and Yung, 2018; Cao *et al.,* 2019; Patitsas, 2019).

The processes in which the total nonequilibrium of the IS does not change (the growth of the nonequilibrium of one type is completely compensated by the decrease in the nonequilibrium of the other type) will be those reversible processes that are considered in thermodynamics; in irreversible processes, the nonequilibrium of the IS decreases (Saikhanov, 2017). The analytical expression of this formulation is the inequality (Equation 2). Where Λ is nonequilibrium (the amount of nonequilibrium), which is understood as the maximum work obtained in an adiabatic system (AS), or could be obtained in an isolated system during the course of reversible processes that bring the nonequilibrium system to an equilibrium state. Equation 2 is the opposite Clausius Equation 1 – the total entropy of IS cannot decrease. As a result of this generalization, the change in the entropy of the IS dS_{IS} used to record the SLT acquired the meaning of one of the characteristics of the change in the nonequilibrium state of the IS (Chakraborty *et al.,* 2017; Dutt, 2018; Kudinov *et al.,* 2018; Park, 2018; Sobolev, 2018).

2. MATERIALS AND METHODS

2.1. The nonequilibrium of isolated system

In the concept of nonequilibrium, an isolated system is understood to mean a nonequilibrium system consisting of a set of locally-equilibrium (quasi-equilibrium) subsystems (sources and receivers of heat, receivers and sources of work, working fluid, environment, small and finite elements of the flow) that interact with each other, but do not interact with other systems that are not part of the isolated system in question.

Since when real processes take place, IS tends to an equilibrium state, when the system loses its ability to do work (transfer motion in an ordered form), then the maximum work performed by the system upon its transition to an equilibrium state is accepted as a quantitative measure of the system’s nonequilibrium Λ (Equation 3).

To calculate the maximum (possible) work in thermodynamics, such values as thermodynamic potentials, heat exergy, and flow exergy are used.

In isolated systems, in the course of real processes, the ordered motion (OM) is transformed into the chaotic motion (CHM), i.e., the dissipation (scattering) of the OM occurs. The equilibrium state in the system occurs when all the OM (work) completely goes into chaotic motion (heat) (Equation 4).

This work is called possible work, lost working capacity, or energy loss. It is estimated through an increase in entropy $\Delta S_{\text{noneq.IS}\rightarrow\text{eq.st}}$ during the transition of IS from a given nonequilibrium state to an equilibrium state,

Downloaded from www.periodico.tchequimica.com

according to the Gouy – Stodola equation Kirillin (1983) (Equation 5). Where T_{AM} is the temperature of the equilibrium ambient medium (AM) (atmosphere or large body of water), which does not change upon the transition of a nonequilibrium system to an equilibrium state (T_{AM} = const).

In the general case, when there is no liquid AM, it takes T_{CBmin} – the variable body temperature with the lowest temperature (cold body temperature) during heat transfer or the temperature of the thermodynamic system when it interacts with work sources (cargo, spring, flywheel, capacitor, battery), which themselves are not characterized by temperature, and Equation 3 taking into account Equation 5 takes the form (Equation 6).

The change in the IS nonequilibrium (recall: increment (plus sign) (Equation 7), decrease (minus sign) (Equation 8)). Equation 9, during its transition to the equilibrium state, can be represented as the difference between the nonequilibrium values in the final (equilibrium state Λ2, when the nonequilibrium state is zero $\Lambda_{eq.st} \equiv 0$) and in the initial Λ2 – nonequilibrium state defined by Equation 6 (Equation 10).

Equation 10 for changing IS nonequilibrium in an elementary process, taking into account inequality (1) for changing IS entropy $\mathrm{d}S_{\mathrm{noneq.IS}} \geq 0$, and $T_{\mathrm{CB\,min}} \geq 0$ can be written as (Equation 11). Equation 11 is confirmed by the postulate of nonequilibrium (Equation 2) put forward by the author – the nonequilibrium of an isolated system cannot increase. If to proceed from the primacy of Equation 2, then Clausius Equation 1 follows from Equation 11 $\mathrm{d}S_{\mathrm{IS}} \geq 0$. Equation 10 in differential form for the decrease of the nonequilibrium ($-\mathrm{d}\Lambda$) of the system can be written (Equation 12) and in the integral form (Equation 13).

2.2. The nonequilibrium of the adiabatic system

If the thermodynamic potential in the general case is denoted by the symbol Π (“pi” Greek), then the amount of system nonequilibrium will be determined by the potential difference of the system in the nonequilibrium state $\Pi_{\mathrm{noneq.st}}$ and the equilibrium state $\Pi_{\mathrm{eq.st}}$ (let's call it “potential difference” $\Delta\Pi^{*}$), which is equal to the maximum work of the system when it goes to the equilibrium state (Equation 14). For a final decrease in nonequilibrium, Equation 14 can be written as (Equation 15). In differential form, this equation will take the form (Equation 16). Where $\mathrm{d}\Pi_{\mathrm{eq.st}} \equiv 0$, since during the transition of the system to the equilibrium state, all processes cease and, therefore, changes in all values are equal to zero.

The potential difference of the adiabatic system performing the work decreases in any processes (reversible and irreversible). However, only in reversible (index “o”) processes the potential difference decrease, equal to the decrease in the thermodynamic potential, will be equal to the maximum external work of the nonequilibrium system (Equation 17).

In the case of irreversible processes, the external (superscript “e”) work of system results in less loss of the potential difference (decrease of the thermodynamic potential) (Equation 18).

Consequently, the general condition for the transition of a system from a more nonequilibrium state to a less nonequilibrium state (more equilibrium) has the form (Equation 19).

According to this expression, external work is equal to a decrease in the potential difference, or a decrease in the thermodynamic potential in reversible processes and less than this decrease in irreversible processes.

2.3. Heat exergy and flow exergy as a measure of nonequilibrium change

When heat Q_1 is transferred from a hot body with temperature T_1 to an ambient medium with a constant temperature T_0, thermal nonequilibrium equal to the ideal cycle of Carnot (ICC) is lost (Equation 20).

The value E_Q, equal to the maximum work that can be obtained in an ideal cycle of Carnot due to the supplied heat Q_1, if the cold body is an ambient medium of constant parameters, it is customary to call heat exergy. Thus, heat exergy, in accordance with Equation 20, is a quantitative characteristic of the change in the thermal nonequilibrium of the hot body – ambient medium system.

When a unit mass substance flows from a large-capacity tank with pressure p1 and temperature T_1 into the ambient medium with constant parameters p_0 and T_0, nonequilibrium is lost, a measure of which is the work performed by the flow in an ideal turbine. The maximum specific work obtained from a unit mass flow element when it expands in the turbine to the AM parameters is called specific flow exergy (Equation 21) (Krutov *et al.,* 1991).

Downloaded from www.periodico.tchequimica.com

The exergy of the flow (flow of the substance) will be a measure of the change in the nonequilibrium of the reservoir-AM system during the transfer of a single portion of the substance into the ambient medium of the constant parameters the author (Equation 22).

The following are examples of calculating nonequilibrium and its changes in an isolated and adiabatic system.

3. RESULTS AND DISCUSSION:

3.1. Calculation of the loss of nonequilibrium of an isolated system during operation of a heat engine performing an irreversible cycle

Let a non-equilibrium isolated system consist of a hot body (HB) with a constant temperature T_{HB}, an ambient medium with a constant temperature T_0, a working body that performs an irreversible cycle (for example, Carnot's cycle, nonideal on temperature (CCNT) in which heat is supplied at $T_1 < T_{\text{HB}}$, and heat is removed at $T_2 = T_0$) and the work receiver (WR) (Figure 3). When heat is removed from the HB in the amount of Q_1, the thermal nonequilibrium of the HB-AM system will change (decrease) into the exergy of this heat Equation 20 (Equation 23). As a result of the implementation in the temperature range from T_1 to T_0 irreversible by the temperature of Carnot-cycle, work is performed that is allocated to the work receiver, as a result of which the mechanical nonequilibrium between WR and other IS bodies increases (arises) by the value of W_{CCNT} (Equation 24).

The complete change in the nonequilibrium state of the IS during the operation of the irreversible (real) cycle is determined by the sum of the changes in the thermal (23) and mechanical (24) nonequilibrium systems $(\Delta\Lambda_{\text{WB}} = 0)$ (Equation 25). Decrease (loss) of IS nonequilibrium (Equation 26). From expression (25), it can be concluded that the decrease in the nonequilibrium state of the adiabatic system HB-WR-AM (the maximum work that can be done by the nonequilibrium AS due to the heat Q) is equal to the exergy of heat, which in turn consists of external useful work W_{CCNT} and lost work W_{loss} (see Figure 1) (Equation 27).

Therefore, the external work W^e performed by the nonequilibrium adiabatic system during an irreversible cycle in it is less than the maximum possible work (heat exergy) for the work of losses, which in the general case can be caused by both the finite temperature difference between the working fluid and heat sources, and friction of piston.

Consider the second method for determining the loss of IS nonequilibrium, according to Equation 22, after determining the change in the IS entropy. When heat is removed from the HB in the amount (Equation 28), its entropy will decrease by (Equation 29).

This heat is supplied to the heat engine, where it is divided into two parts: one part is converted into work supplied to the WR in the amount (Equation 30), and the other part in the amount (Equation 31) is allocated to the cold body, in which the ambient medium is taken.

As a result of the supply of heat Q_2 to the ambient medium (CB), its entropy will increase by a value (Equation 32). Adding this change in entropy with a change in the entropy of the HB (Equation 29), a complete change in the entropy of a nonequilibrium isolated system during an irreversible cycle is obtained (changes in the entropy of WB and PD during the cycle are zero) (Equation 33).

Replacing Q_2 with Equation 31, the increment (since $T_1 < T_{\Gamma\text{T}}$) of the entropy (Equation 34) is obtained. Loss of IS nonequilibrium (Equation 22), taking into account that (Equations 35-36) (in Figure 1, the lost work is depicted as the area of the rectangle a78ba).

Comparing Equation 36 and Equation 26, it can be concluded that both methods of calculating the decrease in the IS nonequilibrium give the same results. At the same time, the calculation of the total change in the IS nonequilibrium (loss, dissipation of the possible work) as the sum of the change in the thermal and mechanical nonequilibrium according to Equation 25 is more visual than through the change in the entropy of the IS.

3.2. Calculation of the nonequilibrium of the adiabatic system

Let the nonequilibrium adiabatic system (nonequilibrium AS) consist of a working body (WB) located in a cylinder with a movable piston, and a liquid ambient medium (ambient medium, along with the liquid ambient medium (for example, the atmosphere), includes receivers (sources) of work that perceive the work of the adiabatic system; the nonequilibrium adiabatic system (Noneq.AS) together with the sources (receivers) of work form a nonequilibrium isolated system (Noneq.IS)) (AM), with constant parameters p_0 and T_0 (Figure 2).

Downloaded from www.periodico.tchequimica.com

To ensure the lifting of the load without acceleration (which means that the calculation does not need to take into account the change in the kinetic energy of the load and the piston) with variable gas pressure on the piston and constant mass of the load, a special device is used. The device consists of a gear rack 1, gear 2, and cam 3 and ensures equality of moments relative to the axis of the cam of constant gravity and variable resulting gas pressure and AM forces on the piston by changing the arm length of gravity (Figure 2).

This nonequilibrium AS is capable of performing work, for example, in lifting the load, only until the moment of equilibrium establishment in it. The maximum external work W^e_{max} obtained from this system at the moment of establishing the barometric ($p = p_0$) and thermal ($T = T_0$) equilibrium in it will be the initial amount of nonequilibrium of such a system.

The equation of the first law of thermodynamics (FLT) for the nonequilibrium adiabatic ($\delta Q^e = 0$) system can be written as Equation 37, where Equation 38.

Further, the transformations are reduced to expressing the change in internal energy (IE) of ambient medium (AM) through the WB parameters, which is possible with reversible processes. Unlike nonequilibrium AS, the ambient medium can exchange both heat and work with the working body; therefore, for AM, the FLT equation has the form Equation 39, where Equation 40.

In order to maximize external work, the processes must proceed reversibly inside nonequilibrium AS, i.e., without dissipation (conversion of ordered motion into chaotic motion) of ordered motion both when moving the piston (in the absence of friction between the piston and the cylinder liner), and when heat transfer. The latter is ensured by the use of an ideal heat engine (IHE) in the event of a finite temperature difference between the WB and the AM, or heat exchange during an infinitely small temperature difference between the WB and the AM, when the IHE work can be neglected in comparison with the transferred heat.

Note that here authors consider the reversibility of processes in a purely nonequilibrium system ($p \neq p_0$, $T \neq T_0$), while the existing concept of reversibility assumes the reversibility of processes in systems close to the equilibrium state (in quasi-equilibrium systems). According to the concept of nonequilibrium in reversible processes, the complete nonequilibrium of an isolated system does not change. In this example, the decrease in the nonequilibrium AS is compensated by the increase in the mechanical nonequilibrium of the receiver of work (load) with respect to the nonequilibrium AS.

Evidence of the reversibility of the processes (lack of dissipation), according to the SLT, is the invariance of entropy (the absence of ordered motion dispersion between the AM molecules) of an isolated or adiabatic system (Equation 41), where (Equation 42). Assuming that the volume of nonequilibrium AS is unchanged Equation 43, Equation 44 follows. Substituting Equation 42 and Equation 44 into Equation 40, authors express the change in the internal energy of the AM through changes in the entropy and volume of the WB (Equation 45).

Substituting Equation 45 into Equation 38, the following expressions for maximum external work are obtained:

a) at a small decrease in the nonequilibrium of the adiabatic system ($-d\Lambda$) (Equation 46);

b) upon complete transition of the system to the equilibrium state ($\Lambda_{eq.st} = 0$) (Equation 47), where the value (Equation 48) is uniquely determined by the state parameters of both the WB and the AM, i.e., it is a function of the state of the parameters of this nonequilibrium system.

Since, in accordance with Equation 47, the decrease of the function Z is equal to the external work of nonequilibrium AS, this function can be considered as the potential of a nonequilibrium system consisting of a working body and the ambient medium, whose parameters (AM) do not change as the entire nonequilibrium system transitions to the equilibrium state. The potential function Z is sometimes considered as a generalizing potential for thermodynamic potentials. For example, in the work of A. I. Andryushchenko (1975), it is noted that "in the reactions of systems that maintain a constant volume V and temperature T, the maximum work (Equation 49), where (Equation 50). At $T_0 = T$ there are (Equation 51) and (Equation 52).

These transformations cannot be considered correct for two reasons. First, the transition from the potential function Z (Equation 48) to Z_V (Equation 50) is possible not at V = const, but at V = 0; at the same time, with a constant volume (Equation 53). Secondly, the expression for the potential function Z (Equation 50) includes the internal energy and entropy of only the working body (without AM), and the expression for the Helmholtz energy contains the total values of the

Downloaded from www.periodico.tchequimica.com

IE and entropy of the entire nonequilibrium system (WB and AM). Hence (Equation 54).

Consider some specific examples of determining the amount of nonequilibrium of a system consisting of WB and AM. Let the system be in a thermally ($T_1 > T_0$) and barically ($p_1 > p_0$) nonequilibrium state. As reversible processes of the transition of the system to the equilibrium state, first authors take the isentropic process 1–2s (without external heat transfer and friction) of the expansion of the working body to a final temperature $T_{2s} = T_0$, and then the isothermal process 2s–0 to a final pressure $p_{2T} = p_0$ (Figure 3).

The amount of nonequilibrium of such a system in accordance with Equation 47 will be equal to the decrease in the potential function Z (Equation 55).

To simplify, suppose that the working body is an ideal gas, whose internal energy does not change at a constant temperature. Consequently, a change in IE could only occur in the adiabatic process of 1-2s. In accordance with the FLT, the decrease in the internal energy of the adiabatic system is equal to the external work performed by the system (WB) on the external ambient medium (for the working body, the external ambient medium is a liquid ambient medium and a work receiver) (Equation 56). This work is depicted as the area 12s451 of Figure 3.

Since the change in the entropy of the WB occurs only in the isothermal process, the product $T_0\Delta S_{\mathrm{WB}}$ gives the heat of the isothermal process, which in the case of an ideal gas is equal to the external work in the isothermal process 2s–2T (depicted as the area 2s2T342s of the Figure 3 (Equation 57). Given that (Equation 58), then the last term in the right-hand side of Equation 55 can be represented as the external work of a liquid AM (for it, the external medium is the working body and the work receiver) (Equation 59).

This work is negative and is depicted as the area 3562_T3 of Figure 3. The total work performed by the nonequilibrium AS upon its transfer to the equilibrium state will be equal to the sum of the works (Equations 56, 57, 59) (Equation 60).

Comparing this expression for works with (Equation 55), it can be concluded that, indeed, a decrease in the potential function Z gives the maximum work of the nonequilibrium adiabatic system, consisting of WB and a liquid AM with constant parameters, upon its transition to the equilibrium state (Equation 61). This work characterizes the nonequilibrium of this system $\Lambda_{\mathrm{noneq.AS}}$ and is depicted as a hatched area of the figure in Figure 3.

The external work of the nonequilibrium AS can also be calculated as the technical work of the piston $W_{\mathrm{tech.piston}}$ (this work is transferred from the piston to the receiver of work through the rod or connecting rod) in the absence of friction in adiabatic and isothermal processes, if to neglect the change in the mechanical energy of the piston (Equation 62).

Consider the case when the system is in a barically nonequilibrium state ($p_1 > p_0$), but in a thermal equilibrium state ($T_1 = T_0$). The amount of baric nonequilibrium of such a system can be determined from (55) and (60), taking into account the fact that the transition of the nonequilibrium AS to the equilibrium state occurs in an isothermal process and, therefore, for an ideal gas $\Delta U_{\mathrm{WB}} = 0$ (Equation 63).

Since the volume and temperature of the entire nonequilibrium AS are constant ($V_{\mathrm{noneq.AS}} = \mathrm{const}$; $T = T_0 = \mathrm{const}$), external work not related to changing the total volume of such a system $W^{*\mathrm{o}}_{V,T}$, until the nonequilibrium is completely lost, will be equal to the decrease in the Helmholtz potential (isochoric-isothermal potential) for throughout nonequilibrium AS (Equation 64). Strictly speaking, the temperature of the AM as a result of heat removal decreases. However, due to its large size, the decrease in the temperature of the ambient medium (atmosphere) is insignificant. Where for an ideal gas in an isothermal process $\Delta U_{\mathrm{WB}} = 0$, and since the process is reversible, the change in the entropy of the nonequilibrium AS is zero ($\Delta S_{\mathrm{noneq.AS}} = 0$).

In accordance with the equation of FLT for the decrease in the IE of the ambient medium can be written (Equation 65), since the heat given off by AM is equal and opposite in sign to the heat received by the working body (Equation 66), in the isothermal process of an ideal gas, all external heat goes to the working heat to perform external work (Equation 67), since the volume of the entire nonequilibrium AS is constant, then (Equation 68).

Substituting Equation 65 for the decrease in the IE of the ambient medium into Equation 64, the expression for external work $W^{*\mathrm{o}}_{V,T}$ is obtainted, that is not related to a change in the total volume of the system, i.e., the maximum work performed by the barically nonequilibrium system WB-AM of constant volume upon its transition to equilibrium state, or – for the amount of baric nonequilibrium of such a system (Equation 69).

Downloaded from www.periodico.tchequimica.com

As you can see, the maximum external work that can be transferred from the baricaly nonequilibrium adiabatic system to the consumer of the work is less than the work of changing the volume of the WB in the isothermal process to the work of displacing the ambient medium (performed against the constant pressure of the AM p_0).

If, for the calculation of the work, use Equation 51 for the potential function Z_V or for the Helmholtz potential F_T is used, written for the working body, then (Equation 70) can be obtained.

Consequently, the potential function Z_V and the Helmholtz potential F_T, calculated for a working body in an equilibrium state, are potentials for the work of the volume change performed by the working body in an isothermal process. However, the losses of these potentials are not equal to the external work performed by the nonequilibrium AS in the isothermal process (Equation 69) (Equation 71), which means that they do not characterize the change in the nonequilibrium of any system.

A measure of the nonequilibrium state of the WB-AM system during the course of the isochoric-isothermal process in it in accordance with (Equation 64) is the decrease in the isochoric-isothermal potential $-\Delta F_{\mathrm{V,T}}^{\mathrm{noneq.AS}}$, calculated for the entire nonequilibrium system, and not for one working body.

From here there is a general conclusion, that the potentials of locally-equilibrium systems (for example, the working body in a cylinder) and their decrease that are determined in thermodynamics courses do not characterize the change in any nonequilibrium state and do not give the value of the external work performed by the nonequilibrium system, which includes this locally-equilibrium system. Only a decrease in the thermodynamic potential calculated for the entire set of bodies of a nonequilibrium system is equal to a decrease in the nonequilibrium system, and hence the external work of this system as it transitions to an equilibrium state.

4. CONCLUSIONS:

This article is a continuation of the concept of nonequilibrium, based on the postulate "about nonequilibrium and its change" and the basis of the SLT. It provides calculations of nonequilibrium and its changes for two systems: an isolated system during operation of a heat engine and an adiabatic system. Based on the results of this work, the following conclusions can be drawn:

1) the diagrams of nonequilibrium systems consisting of quasi-equilibrium subsystems are given – adiabatic, consisting of a working body in a cylinder and a liquid AM and an isolated system consisting of an adiabatic system and a receiver of work;

2) the second law of thermodynamics should be used to consider the behavior of just such quasi-equilibrium systems, and not a separate body (working body), as is often practiced;

3) calculations of the nonequilibrium state of the adiabatic system are given by the decrease of the thermodynamic potential recorded for the entire set of bodies of the nonequilibrium system, and by the technical work of the piston in a reversible process;

4) the potentials of locally-equilibrium systems (for example, the working body in the cylinder) determined in thermodynamics courses and their decrease do not characterize the change in any nonequilibrium and do not give the value of the external work performed by the nonequilibrium adiabatic system;

5) a methodology for calculating thermal and baric nonequilibrium is given, and the corresponding expressions for calculating this nonequilibrium were obtained;

6) the above calculations are a practical confirmation of the validity of the postulate of nonequilibrium, introduced by the author on the basis of the second law of thermodynamics.

5. REFERENCES:

1. Altaner, B. *Journal of Physics A: Mathematical and Theoretical*, **2017**, *50*(45), 454001.
2. Andryushchenko, A. I. *Fundamentals of technical thermodynamics of real processes*, Moscow: Vysshaya shkola, **1975**.
3. Baehr, H. D. *Thermodynamics: An Introduction to the Basics and Their Technical Applications*, Berlin-Heidelberg-New York: Springer-Verlag, **1973**.
4. Bejan, A. *Advanced Engineering Thermodynamics*, Durham: Duke University, **2016**.
5. Ben-Naim, A. *Discover Entropy and the Second Law of Thermodynamics: A Playful Way of Discovering a Law of Nature*, Singapore: World Scientific Pub Co Inc,

Downloaded from www.periodico.tchequimica.com

2010.

6. Borgnakke, C., Sonnag, R. E. *Fundamentals of Thermodynamics*, Ann Arbor: University of Michigan, **2009**.
7. Borin, A., Sukhorukov, E. *Physical Review B*, **2019**, *99*(8), 085430.
8. Calabrese, P. *Physica A: Statistical Mechanics and its Applications*, **2018**, *504*, 31-44.
9. Callen, B. *Thermodynamics and Introduction to Thermostatics*, New York: John Wiley and Sons, **1985**.
10. Cao, F., Wu, J., Li, Y., Ngai, T. *Langmuir*, **2019**, *35*(27), 8910-8920.
11. Chakraborty, S., Chatterjee, S., Barma, M. *Physical Review E*, **2017**, *96*(2), 022128.
12. Chen, L., Tsutsumi, A. *Chemical Engineering Transactions*, **2018**, *70*, 949-954.
13. Chen, Z.-S., Li, C., Wang, G. *Journal of Engineering Thermophysics*, **2017**, *38*(8), 1589-1596.
14. D'Alessio, L., Kafri, Y., Polkovnikov, A., Rigol, M. *Advances in Physics*, **2016**, *65*(3), 239-362.
15. de Blasio, C. Introduction to entropy and second law. *In: Green Energy and Technology*, Basingstoke: Springer Nature, **2019**.
16. de Oliveira, M. J. *Revista Brasileira de Ensino de Fisica*, **2019**, *41*(1), e20180174.
17. Dutt, A.K. *Journal of Physical Chemistry B*, **2018**, *122*(50), 12049-12059.
18. Fermi, E. *Thermodynamics*, New York: Prentice-Hall, Inc, **1937**.
19. Freitas, R., Asta, M., De Koning, M. *Computational Materials Science,* **2016**, *112*, 333-341.
20. Guo, Y., Jou, D., Wang, M. *Physical Review B*, **2019**, *98*(10), 104304.
21. Hołyst, R., Poniewierski, A. *Thermodynamics for Chemists, Physicists and Engineers*, Dordrecht: Science+Business Media, **2012**.
22. Khantuleva, T. A., Shalymov, D. S. *Philosophical Transactions of the Royal Society A: Mathematical, Physical and Engineering Sciences*, **2017**, *375*(2088), 20160220.
23. Kirillin, V. A., Sychev, V. V., Sheyndlin, A. E. *Technical Thermodynamics*, Moscow: Energoatomizdat, **1983**.
24. Kittel, Ch. *Thermal physics*, New York: John Willey and Sons, **1993**.
25. Kondepudi, D., Prigogine, I. *Modern Thermodynamics: From Heat Engines to Dissipative Structurers,* New Delhi: John Wiley and Sons, **2015**.
26. Krichevsky, I. R. *Concepts and foundations of thermodynamics*, Moscow: Chemistry, **1970**.
27. Krutov, V. I., Isayev, S. I., Kozhinov, A. I. *Technical Thermodynamics*, Moscow: Vysshaya shkola, **1991**.
28. Kudinov, V. A., Eremin, A. V., Kudinov, I. V., Zhukov, V. V. *Combustion, Explosion and Shock Waves*, **2018**, *54*(6), 649-653.
29. Lavenda, B.H. *A New Perspective on Thermodynamics*, Berlin: Springer Science+Business Media, **2010**.
30. Liu, Y., Liu, Y.-J. *Separation and Purification Technology*, **2008**, *61*(3), 229-242.
31. Marbœuf, A., Claisse, A., Le Tallec, P. *Journal of Computational Physics*, **2019**, *390*, 66-92.
32. Martyushev, L. M., Celezneff, V. *Entropy*, **2017**, *19*(3), 126.
33. Martyushev, L. M., Seleznev, V. D. *Physics Reports*, **2006**, *426*(1), 1-45.
34. Morales-Rodriguez, R. *Thermodynamics: Fundamentals and Its Application in Science*, Kongens Lyngby: Technical University of Denmark, **2016**.
35. Moran, M. J., Shapiro, H. N., Boettner, D. D., Balley, M. B. *Fundamentals of Engineering 28 Thermodynamics*, New York: John Wiley and Sons, **2014**.
36. Novikov, I. I. *Thermodynamics*, Moscow: Mashinostroenie, **1984**.
37. Park, H. *Journal of the Korean Physical Society*, **2018**, *72*(12), 1413-1420.
38. Patitsas, S. N. *Physical Review E*, **2019**, *100*(2), 022116.
39. Ptaszyński, K., Esposito, M. *Physical Review Letters*, **2019**, *122*(15), 150603.
40. Putilov, K.A. *Thermodynamics*, Moscow: Nauka, **1971**.

Downloaded from www.periodico.tchequimica.com

41. Rakopoulos, C.D., Giakoumis, E. G. *Progress in Energy and Combustion Science*, **2006**, *32*(1), 2-47.
42. Reyf, F. *Statistical physics: Berkeley physics course*, Berkeley: The University in Berkeley, McGraw; Hill Book Company, **1972**.
43. Saikhanov, M.B. *Theoretical and Mathematical Physics*, **2017**, *191*(1), 572-579.
44. Seifert, U. *Reports on Progress in Physics*, **2012**, *75*(12), 126001.
45. Sellitto, A., Di Domenico, M. *Continuum Mechanics and Thermodynamics*, **2019**, *31*(3), 807-821.
46. Sobolev, S.L. *Physical Review E*, **2018**, *97*(2), 022122.
47. Srivastava, R. C., Subit, K.S., Abhay, K.J. *Thermodynamics: A core course*, New Delhi: Prentice-Hall of India Private Limited, **2007**.
48. Vukalovich, M .P., Novikov, I.I. *Technical Thermodynamics*, Moscow: Energiya, **1968**.
49. Wald, R. M. *Living Reviews in Relativity*, **2001**, *4*, 6.
50. Yuan, H. Y., Yung, M.-H. *Physical Review A*, **2018**, *98*(2), 022125.

$$\mathrm{d}S_{\mathrm{noneq.IS}} \geq 0 \qquad \text{(Eq. 1)}$$

$$\mathrm{d}\Lambda_{\mathrm{noneq.IS}} \leq 0 \quad \mathrm{d}\Lambda_{\mathrm{noneqIS}} \leq 0 \qquad \text{(Eq. 2)}$$

$$\Lambda \equiv \Lambda_{\mathrm{noneq.IS}} \equiv W^{\max}_{\mathrm{noneq.st}\rightarrow\mathrm{eq.st}}. \qquad \text{(Eq. 3)}$$

$$W^{\max}_{\mathrm{noneq.st}\rightarrow\mathrm{eq.st}} = W^{\max}_{\mathrm{loss}} = Q_{\mathrm{diss}}. \qquad \text{(Eq. 4)}$$

$$W^{\max}_{\mathrm{diss}} = W^{\max}_{\mathrm{noneq.st}\rightarrow\mathrm{eq.st}} = T_{\mathrm{AM}}\Delta S_{\mathrm{noneq.st}\rightarrow\mathrm{eq.st}} \qquad \text{(Eq. 5)}$$

$$\Delta\Lambda_{\mathrm{noneq.IS}} = W^{\max}_{\mathrm{diss}} = W^{\max}_{\mathrm{noneq.st}\rightarrow\mathrm{eq.st}} = T_{\mathrm{CB\,min}}\Delta S_{\mathrm{noneq.IS}\rightarrow\mathrm{eq.st}} \qquad \text{(Eq. 6)}$$

$$\Delta x = x_2 - x_1 \qquad \text{(Eq. 7)}$$

$$-\Delta x = x_1 - x_2 \qquad \text{(Eq. 8)}$$

$$\Delta\Lambda = \Lambda_2 - \Lambda_1 \qquad \text{(Eq. 9)}$$

$$\Delta\Lambda_{\mathrm{noneq.IS}} = \Lambda_{\mathrm{eq.st}} - \Lambda_{\mathrm{noneq.IS}} = -\Lambda_{\mathrm{noneq.IS}} = -W^{\max}_{\mathrm{noneq.st}\rightarrow\mathrm{eq.st}} = -T_{\mathrm{CB\,min}}\,\Delta S_{\mathrm{noneq.IS}\rightarrow\mathrm{eq.st}}. \qquad \text{(Eq. 10)}$$

$$\mathrm{d}\Lambda_{\mathrm{IS}} = -T_{\mathrm{CB\,min}}\mathrm{d}S_{\mathrm{IS}} \leq 0 \qquad \text{(Eq. 11)}$$

$$-\mathrm{d}\Lambda = \delta W_{\mathrm{loss}} = \delta W_{\mathrm{diss}} = T_{\mathrm{CB\,min}}\mathrm{d}S_{\mathrm{diss}} \qquad \text{(Eq. 12)}$$

$$-\Delta\Lambda = W_{\mathrm{loss}} = W_{\mathrm{diss}} = T_{\mathrm{CB\,min}}\Delta S_{\mathrm{diss}} \qquad \text{(Eq. 13)}$$

$$\Lambda_{\mathrm{AS}} = \Delta\Pi^{*} = \Pi_{\mathrm{noneq.st}} - \Pi_{\mathrm{eq.st}} = W^{\max}_{\mathrm{noneq.st}\rightarrow\mathrm{eq.st}} = W^{\mathrm{e}}_{\max} \qquad \text{(Eq. 14)}$$

Downloaded from www.periodico.tchequimica.com

$$-\Delta\Lambda_{AS}^{max} = -\Delta(\Delta\Pi^*)_{max} = \Lambda_1 - \Lambda_2 = \Lambda_{noneq.st} - \Lambda_{eq.st} = \Lambda_{noneq.st} = \\ = \Pi_{noneq.st} - \Pi_{eq.st} = \Pi_1 - \Pi_2 = -\Delta\Pi_{max} = W_{noneq.st\rightarrow eq.st}^{max} = W_{max}^{e}.$$ (Eq. 15)

$$-d\Lambda_{AS} = -d(\Delta\Pi^*) = -d\Pi_{noneq.st} + d\Pi_{eq.st} = -d\Pi_{noneq.st} \equiv -d\Pi = \delta W_{max}^{e} = \delta W^{eo}$$ (Eq. 16)

$$\delta W^{eo} = \delta W_{max}^{e} = -d(\Delta\Pi^*)$$ (Eq. 17)

$$\delta W^{e} < -d(\Delta\Pi^*) = -d\Pi$$ (Eq. 18)

$$\delta W^{e} \leq -d(\Delta\Pi^*) = -d\Pi$$ (Eq. 19)

$$-\Delta\Lambda_{therm} = W_{ICC} - Q_1(1 - T_0/T_{noneq}) - E_{Q^5}$$ (Eq. 20)

$$e_x = w_{typ}^{max} = h - h_0 + T_0(s_0 - s)$$ (Eq. 21)

$$e_{x1} = h_1 - h_0 + T_0(s_0 - s_1) = w_{tur}^{max} = -\Delta\lambda_{reserv\text{-}AM}$$ (Eq. 22)

$$\Delta\Lambda_{therm} = \Delta\Lambda_{HB\text{-}AM} = -E_{Q_1} = -Q_1(1 - T_0 / T_{HB}) < 0$$ (Eq. 23)

$$\Delta\Lambda_{mech} = \Delta\Lambda_{WR} = W_{CCNT} = Q_1(1 - T_0 / T_1) > 0$$ (Eq. 24)

$$\Delta\Lambda_{noneq.IS} = \Delta\Lambda_{therm} + \Delta\Lambda_{WB} + \Delta\Lambda_{mech} = \Delta\Lambda_{noneq.AS} + \Delta\Lambda_{WR} = -E_{Q_1} + W_{CCNT} = \\ = -Q_1(1 - T_0 / T_{HB}) + Q_1(1 - T_0 / T_1) = -Q_1 T_0(1/T_1 - 1/T_{HB}) = -W_{loss}.$$ (Eq. 25)

$$-\Delta\Lambda_{noneq.IS} = W_{loss} = Q_1 T_0(1/T_1 - 1/T_{HB}).$$ (Eq. 26)

$$-\Delta\Lambda_{noneq.AS} = E_{Q_1} = W_{CCNT} + W_{loss} \equiv W^{e} + W_{loss}$$ (Eq. 27)

$$Q_{HB} = -Q_1 < 0$$ (Eq. 28)

$$\Delta S_{HB} = Q_{HB}/T_{HB} = -Q_1/T_{HB} < 0$$ (Eq. 29)

$$W^{e} = W_{CCNT} = Q_1(1 - T_0/T_1)$$ (Eq. 30)

$$Q_2 = Q_1 - W_{CCNT} = Q_1 T_0/T_1$$ (Eq. 31)

$$\Delta S_{CB} = Q_2/T_0$$ (Eq. 32)

$$\Delta S_{noneq.IS} = \Delta S_{HB} + \Delta S_{CB} = -Q_1/T_{HB} + Q_2/T_0$$ (Eq. 33)

$$\Delta S_{noneq.IS} = \Delta S_{diss} = -Q_1/T_{HB} + Q_1/T_1 = Q_1(1/T_1 - 1/T_{HB}) > 0$$ (Eq. 34)

Downloaded from www.periodico.tchequimica.com

$$T_{\mathrm{CB\,min}} = T_0 \quad \text{(Eq. 35)}$$

$$-\Delta\Lambda_{\mathrm{noneq.IS}} = W_{\mathrm{loss}} = T_0\Delta S_{\mathrm{noneq.IS}} = Q_1 T_0(1/T_1 - 1/T_{\mathrm{HB}}) \quad \text{(Eq. 36)}$$

$$\mathrm{d}U_{\mathrm{noneq.AS}} + \delta W^{\mathrm{e}}_{\mathrm{max}} = \mathrm{d}U_{\mathrm{WB}} + \mathrm{d}U_{\mathrm{AM}} + \delta W^{\mathrm{e}}_{\mathrm{max}} = 0 \quad \text{(Eq. 37)}$$

$$\delta W^{\mathrm{e}}_{\mathrm{max}} = -\mathrm{d}U_{\mathrm{noneq.AS}} = -\mathrm{d}U_{\mathrm{WB}} - \mathrm{d}U_{\mathrm{AM}} \quad \text{(Eq. 38)}$$

$$\delta Q^{\mathrm{e}}_{\mathrm{AM}} = \mathrm{d}U_{\mathrm{AM}} + \delta W^{\mathrm{e}}_{\mathrm{AM}} = \mathrm{d}U_{\mathrm{AM}} + p_0\mathrm{d}V_{\mathrm{AM}} \quad \text{(Eq. 39)}$$

$$\mathrm{d}U_{\mathrm{AM}} = \delta Q^{\mathrm{e}}_{\mathrm{AM}} - p_0\mathrm{d}V_{\mathrm{AM}} = T_0\mathrm{d}S_{\mathrm{AM}} - p_0\mathrm{d}V_{\mathrm{AM}} \quad \text{(Eq. 40)}$$

$$\mathrm{d}S_{\mathrm{noneq.AS}} = \mathrm{d}S_{\mathrm{WB}} + \mathrm{d}S_{\mathrm{AM}} = 0 \quad \text{(Eq. 41)}$$

$$\mathrm{d}S_{\mathrm{AM}} = -\mathrm{d}S_{\mathrm{WB}} \quad \text{(Eq. 42)}$$

$$\mathrm{d}V_{\mathrm{noneq.AS}} = \mathrm{d}V_{\mathrm{WB}} + \mathrm{d}V_{\mathrm{AM}} = 0 \quad \text{(Eq. 43)}$$

$$\mathrm{d}V_{\mathrm{AM}} = -\mathrm{d}V_{\mathrm{WB}} \quad \text{(Eq. 44)}$$

$$\mathrm{d}U_{\mathrm{AM}} = -T_0\mathrm{d}S_{\mathrm{WB}} + p_0\mathrm{d}V_{\mathrm{WB}} \quad \text{(Eq. 45)}$$

$$\delta W^{\mathrm{e}}_{\mathrm{max}} = -\mathrm{d}U_{\mathrm{WB}} + T_0\mathrm{d}S_{\mathrm{WB}} - p_0\mathrm{d}V_{\mathrm{WB}} = \\ = -\mathrm{d}(U_{\mathrm{WB}} - T_{\mathrm{AM}}S_{\mathrm{WB}} + p_{\mathrm{AM}}V_{\mathrm{WB}}) = -\mathrm{d}Z = -\mathrm{d}\Lambda; \quad \text{(Eq. 46)}$$

$$W^{\mathrm{e}}_{\mathrm{max}} = -\Delta Z = Z_1 - Z_2 = -\Delta\Lambda_{\mathrm{max}} = -(\Lambda_{\mathrm{eq.st}} - \Lambda_{\mathrm{noneq.st}}) = \Lambda_{\mathrm{noneq.st}} = \Lambda \quad \text{(Eq. 47)}$$

$$Z = U_{\mathrm{WB}} - T_{\mathrm{AM}}S_{\mathrm{WB}} + p_{\mathrm{AM}}V_{\mathrm{WB}} = U - T_0S + p_0V \quad \text{(Eq. 48)}$$

$$L_{\mathrm{max}} = Z_{\mathrm{V1}} - Z_{\mathrm{V2}} \quad \text{(Eq. 49)}$$

$$Z_{\mathrm{V}} = U - T_0S \quad \text{(Eq. 50)}$$

$$Z_{\mathrm{V}} = U - TS = F \quad \text{(Eq. 51)}$$

$$L_{\mathrm{max}} = F_1 - F_2 \quad \text{(Eq. 52)}$$

$\Delta Z = \Delta Z_V$. (Eq. 53)

$$Z_{\mathrm{V}} = U_{\mathrm{WB}} - TS_{\mathrm{WB}} \neq F = U_{\mathrm{WB\text{-}AM}} - TS_{\mathrm{WB\text{-}AM}} = U_{\mathrm{WB}} + U_{\mathrm{AM}} - T(S_{\mathrm{WB}} + S_{\mathrm{AM}}) \quad \text{(Eq. 54)}$$

$$\Lambda_{\mathrm{noneq.AS}} = Z_1 - Z_{2\mathrm{T}} = Z_1 - Z_0 = U_1 - T_0S_1 + p_0V_1 - \\ -U_0 + T_0S_0 - p_0V_0 = -\Delta U_{\mathrm{WB}} + T_0\Delta S_{\mathrm{WB}} - p_0\Delta V_{\mathrm{WB}}. \quad \text{(Eq. 55)}$$

$$W^{\mathrm{e}}_{1-2s} = -\Delta U_{\mathrm{WB}} \quad \text{(Eq. 56)}$$

Downloaded from www.periodico.tchequimica.com

$$W_{\mathrm{T}}^{\mathrm{e}} = Q_{\mathrm{T}} = T_0 \Delta S_{\mathrm{WB}} \quad \text{(Eq. 57)}$$

$$\Delta V_{\mathrm{WB}} = -\Delta V_{\mathrm{AM}} \quad \text{(Eq. 58)}$$

$$W_{\mathrm{AM}}^{\mathrm{e}} = p_0 \Delta V_{\mathrm{AM}} = -p_0 \Delta V_{\mathrm{WB}} < 0 \quad \text{(Eq. 59)}$$

$$W_{\mathrm{noneq.AS\,max}}^{\mathrm{e}} = W_{1-2s}^{\mathrm{e}} + W_{\mathrm{T}}^{\mathrm{e}} + W_{\mathrm{AM}}^{\mathrm{e}} = -\Delta U_{\mathrm{WB}} + T_0 \Delta S_{\mathrm{WB}} - p_0 \Delta V_{\mathrm{WB}} \quad \text{(Eq. 60)}$$

$$-\Delta Z = W_{\mathrm{noneq.AS\,max}}^{\mathrm{e}} = \Lambda_{\mathrm{noneq.AS}} \quad \text{(Eq. 61)}$$

$$\Lambda_{\mathrm{noneq.AS}} = W_{\mathrm{tech.piston}} = \int_1^{2\mathrm{T}} (p - p_{\mathrm{AM}})\,\mathrm{d}V = \int_1^{2\mathrm{s}} p\mathrm{d}V + \\ + \int_{2\mathrm{s}}^{2\mathrm{T}} p\mathrm{d}V - p_{\mathrm{AM}} \Delta V = W_{1-2s}^{\mathrm{e}} + W_{\mathrm{T}}^{\mathrm{e}} + W_{\mathrm{AM}}^{\mathrm{e}} = W_{\mathrm{noneq.AS\,max}}^{\mathrm{e}}. \quad \text{(Eq. 62)}$$

$$\Lambda_{\mathrm{noneq.AS}} = T_0 \Delta S_{\mathrm{WB}} - p_0 \Delta V_{\mathrm{WB}} = W_{\mathrm{T}}^{\mathrm{e}} + W_{\mathrm{AM}}^{\mathrm{e}} = W_{\mathrm{noneq.AS\,max}}^{\mathrm{e}} \quad \text{(Eq. 63)}$$

$$W_{\mathrm{noneq.AS}}^{\mathrm{e}} = W_{V,T}^{*\mathrm{o}} = -\Delta \Pi_{V,T}^{\mathrm{noneq.AS}} = -\Delta F_{V,T}^{\mathrm{noneq.AS}} = (F_1 - F_2)_{V,T}^{\mathrm{noneq.AS}} = \\ = U_1 - TS_1 - U_2 + TS_2 = -\Delta U_{\mathrm{noneq.AS}} + T\Delta S_{\mathrm{noneq.AS}} = -(\Delta U_{\mathrm{WB}} + \Delta U_{\mathrm{AM}}) + \\ + T(\Delta S_{\mathrm{WB}} + \Delta S_{\mathrm{AM}}) = -\Delta U_{\mathrm{WB}} - \Delta U_{\mathrm{AM}} = -\Delta U_{\mathrm{AM}} = \Lambda_{\mathrm{baric}}, \quad \text{(Eq. 64)}$$

$$-\Delta U_{\mathrm{AM}} = -Q_{\mathrm{AM}}^{\mathrm{e}} + W_{\mathrm{AM}}^{\mathrm{e}} = Q_{\mathrm{T}} + p_{\mathrm{AM}} \Delta V_{\mathrm{AM}} = W_{\mathrm{T}}^{\mathrm{e}} - p_0 \Delta V_{\mathrm{WB}} \quad \text{(Eq. 65)}$$

$$Q_{\mathrm{T}} = -Q_{\mathrm{AM}}^{\mathrm{e}} \quad \text{(Eq. 66)}$$

$$Q_{\mathrm{T}} = W_{\mathrm{T}}^{\mathrm{e}} \quad \text{(Eq. 67)}$$

$$\Delta V_{\mathrm{AM}} = -\Delta V_{\mathrm{WB}} \quad \text{(Eq. 68)}$$

$$W_{V,T}^{*\mathrm{o}} = W_{\mathrm{noneq.AS}}^{\mathrm{e}} = W_{\mathrm{T}}^{\mathrm{e}} - p_0 \Delta V_{\mathrm{WB}} = (\int p\mathrm{d}V)_{\mathrm{T}} - \\ - \int p_0 \mathrm{d}V = \int (p - p_{\mathrm{AM}})\mathrm{d}V = W_{\mathrm{tech.piston}} = \Lambda_{\mathrm{baric}}. \quad \text{(Eq. 69)}$$

$$W^{\mathrm{e}} = -\Delta Z_{\mathrm{V}} = -\Delta F_{\mathrm{T}} = F_{\mathrm{WB_1}} - F_{\mathrm{WB_2}} = U_{\mathrm{WB_1}} - TS_{\mathrm{WB_1}} - U_{\mathrm{WB_2}} + TS_{\mathrm{WB_2}} = \\ = -\Delta U_{\mathrm{WB}} + T_0 \Delta S_{\mathrm{WB}} = T_0 \Delta S_{\mathrm{WB}} = Q_{\mathrm{T}} = W_{\mathrm{T}}^{\mathrm{e}} = W_{\mathrm{WB_T}}^{\mathrm{e}} \neq \Lambda_{\mathrm{baric}} = W_{\mathrm{T}}^{\mathrm{e}} - p_0 \Delta V_{\mathrm{WB}}. \quad \text{(Eq. 70)}$$

$$-\Delta Z_{\mathrm{V}} = -\Delta F_{\mathrm{T}} \neq \Lambda_{\mathrm{baric}} = W_{\mathrm{T}}^{\mathrm{e}} - p_0 \Delta V_{\mathrm{WB}} \quad \text{(Eq. 71)}$$

Downloaded from www.periodico.tchequimica.com

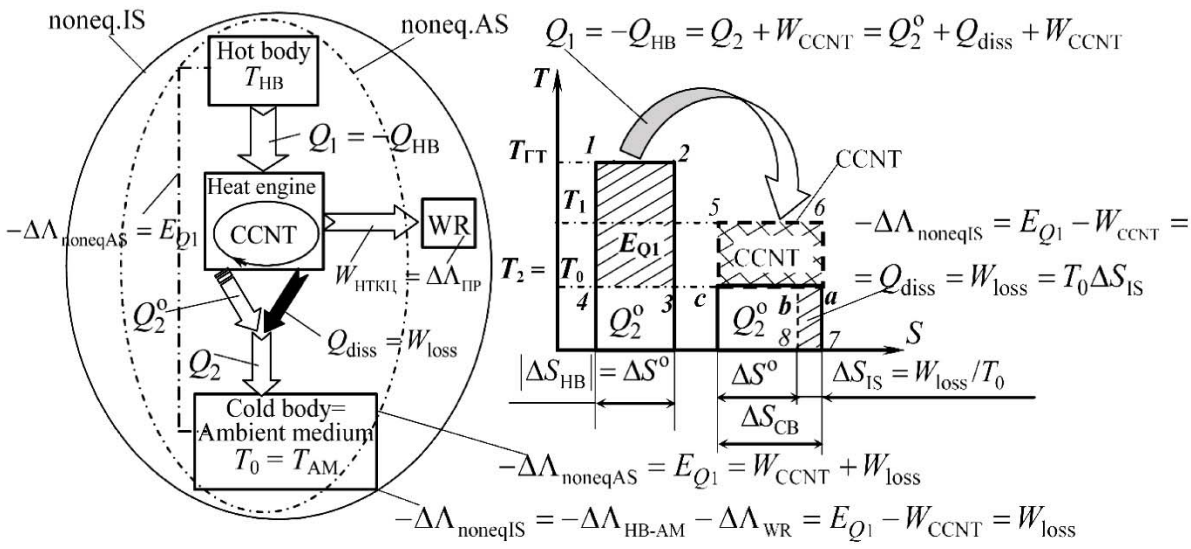

Figure1. *To the calculation of the loss of nonequilibrium of IS during the operation of the heat engine*

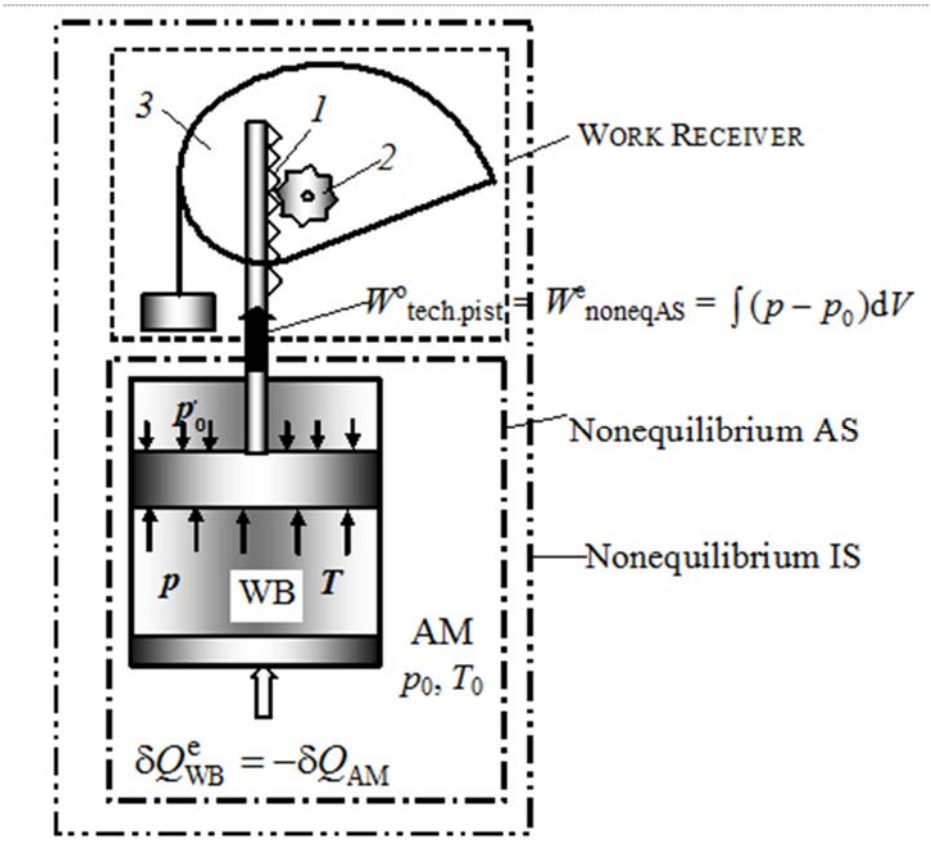

Figure 2. *Scheme and boundary of a nonequilibrium adiabatic system*

Downloaded from www.periodico.tchequimica.com

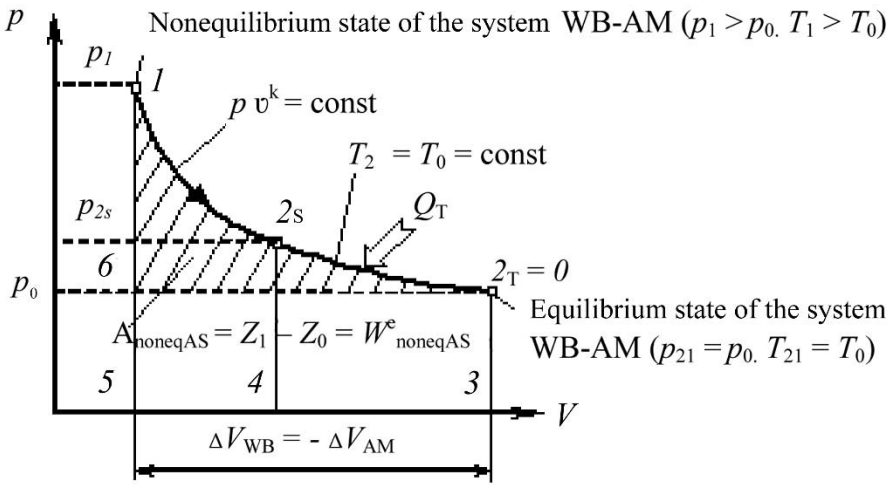

Figure 3. *To the calculation of the nonequilibrium of the adiabatic system*

Downloaded from www.periodico.tchequimica.com

PERIÓDICO TCHÊ QUÍMICA
ARTIGO ORIGINAL

AVALIAÇÃO ECONÔMICA DO PROJETO DE AGRICULTURA DE PRECISÃO NO CAZAQUISTÃO

ECONOMIC ASSESSMENT OF PRECISION AGRICULTURE PROJECT IN KAZAKHSTAN

ЭКОНОМИЧЕСКАЯ ОЦЕНКА ПРОЕКТА ТОЧНОГО ЗЕМЛЕДЕЛИЯ В КАЗАХСТАНЕ

AITKHOZHIN, Serik K.[1*]; BALKIBAYEVA, Aida M.[2]; RAMAZANOVA, Raushan H.[3]; YERMEKOV, Farabi K.[4]; KARSYBAYEVA, Karlygash A.[5];

[1,2,5] Saken Seifullin Kazakh Agrotechnical University; Management Department, 62 Pobedy Ave., zip code 010011, Nur-Sultan – Republic of Kazakhstan

[3] Saken Seifullin Kazakh Agrotechnical University; Soil Science and Agrochemistry Department, 62 Pobedy Ave., zip code 010011, Nur-Sultan – Republic of Kazakhstan

[4] Saken Seifullin Kazakh Agrotechnical University; Land Management, Architecture and Design Department, 62 Pobedy Ave., zip code 010011, Nur-Sultan – Republic of Kazakhstan

** Correspondence author*
e-mail: dep_agr@mail.ru

Received 12 June 2019; received in revised form 06 October 2019; accepted 23 October 2019

RESUMO

Os documentos que discutem a eficácia das tecnologias inteligentes na agricultura no Cazaquistão ainda não foram publicados. O tópico não possui diferenças regionais e atrai grande atenção da comunidade acadêmica. Portanto, para tomar decisões sobre o uso de tecnologias digitais, os agricultores devem ser informados sobre sua eficácia e o que devem fazer quando aplicadas. A avaliação econômica e a análise custo-benefício foram usadas para comparar as tecnologias agrícolas tradicionais e digitais na produção de grãos. Os agricultores ricos de países desenvolvidos usam a tecnologia digital de maneira extremamente ampla, reduzindo os custos operacionais para trabalho assalariado e recursos produtivos. Neste estudo, os autores tentaram avaliar a hipótese de significativa eficiência econômica e ambiental na aplicação de ferramentas de tecnologia de precisão. O objetivo deste trabalho é avaliar, do ponto de vista econômico, os resultados da aplicação de elementos de agricultura de precisão que podem contribuir para o estudo da eficácia das tecnologias digitais nos níveis global e local. Este estudo mostra que, com o uso de modernas tecnologias digitais na produção, uma fazenda em determinadas circunstâncias pode aumentar a produção de trigo em pelo menos 25 a 30%. O lucro bruto das tecnologias agrícolas tradicionais foi de US $ 31 por hectare, enquanto o da tecnologia digital foi de US $ 54.

Palavras-chave: *tecnologia agrícola digital, sistema de informações de gerenciamento agrícola, agricultura digital, agronomia de precisão, agricultura de precisão.*

ABSTRACT

The matter of the effectiveness of applying smart technologies in agriculture of the Republic of Kazakhstan will be of interest to the academic community, regardless of territorial affiliation. The relevance of the research is in the need to inform farmers on the efficiency of such technologies and how to use them. Economic valuation, cost-benefit analysis were used to compare traditional and digital agricultural technologies in grain production. Wealthy farmers from developed countries widely use digital technology, reducing operating costs for wage labour and productive resources. In this research, the authors attempted to prove the hypothesis of significant economic and environmental efficiency in the application of precision technologies. The purpose of this paper is to evaluate the results of the application of precision farming tools from an economic standpoint, these results can contribute to the study of the efficiency of digital technologies at the global and local levels. This research displays that with application of modern digital technologies in production, under certain circumstances, a farm can increase wheat yield by at least 25-30%. Gross profit with traditional technologies in agriculture amounted to 31 US dollars per hectare, while application of digital technologies brought 54 US dollars per hectare.

Downloaded from www.periodico.tchequimica.com

Keywords: *digital agriculture technologies, farm management information system, digital farming, precision agriculture, precision farming*.

АННОТАЦИЯ

Тема эффективности применения умных технологий в сельском хозяйстве Республики Казахстан будет интересна для академического сообщества вне зависимости от территориальной принадлежности. Актуальность исследования обусловлена необходимостью информирования фермеров о том, насколько такие технологии эффективны, и как их использовать. Экономические оценки, анализ затрат и прибыли был использован для сравнения традиционных и цифровых технологий сельского хозяйства в производстве зерна. Богатые фермеры из развитых стран широко применяют цифровые технологии, сокращая операционные расходы на наемный труд и производственные ресурсы. В этом исследовании авторы сделали попытку доказать гипотезу о значительной экономической и экологической эффективности применения точных технологий. Целью данной работы является оценка с экономической точки зрения результатов применения инструментов точного земледелия, данные результаты могут внести вклад в исследования эффективности цифровых технологий на глобальном и местном уровнях. Это исследование показывает, что с применением современных цифровых технологий в производстве, при определенных обстоятельствах, ферма может увеличить урожай пшеницы как минимум на 25-30%. Валовая прибыль с традиционными технологиями в сельском хозяйстве составила 31 доллар США за гектар, в то время как с применением цифровых технологий – 54 доллара США за гектар.

Ключевые слова: *цифровые сельскохозяйственные технологии, информационная система управления фермой, цифровое сельское хозяйство, точное земледелие, точное сельское хозяйство*.

1. INTRODUCTION

Modern agriculture technologies are changing to address farmers' needs for effective production. World practice in applying digital technologies is not so long, accounts only a few decades. Therefore, studies on this subject are relatively new. In Kazakhstan, precision technologies are used only by big companies, and it is not nation spread. State incentives to introduce precision agriculture in combination with digital technologies launched in 2018 for nine model agricultural entities and calculations on its efficiency were made. For this article, we choose three farms with more relevant and complete data.

Informational technologies have been entering into almost every sector of the economy rapidly over the last decades. They came into agriculture as well. Smart farming, farm management information system, digital farming, precision agriculture, and precision farming are the new definitions related to the digital world. Developed and developing countries face these innovations and adopt them carefully (Takhumova *et al.*, 2016). Developed countries apply start-of-art tools in agriculture particularly for cultivation of their main specialized crops. The US largest corn farms have double the precision agriculture adoption rates of all farms: 70-80 % vast of large farms use mapping, about 80 percent use guidance systems, and 30-40 percent use variable rate application (Schimmelpfennig, 2016). Yet this type of technologies even in top countries used selectively. Australian grain growers have readily adopted machine guidance and auto steer, and a majority have access to yield monitoring, but the rate of use of many crops and soil sensors remains comparatively low (Bramley and Ouzman, 2019). Although precision agriculture technology has been available in Australia late period, it has been estimated that only around 3% of Australian grain growers use some form of technology (Price, 2004; Bellon-Maurel and Huyghe, 2017).

When a farm conducts spraying on external landmarks, that is, without navigation systems, up to 4% of the crops remain unprocessed, and another 11% are processed twice. In addition, if on 11% of the area the company receives only a loss from the waste of materials, then the loss from the raw 4% can be much greater. Results of the evaluation of the gross economic effect of precision agriculture tools are still arguable and situational. Overall, precision agriculture technologies can reduce operating costs by preventing farmers from over applying inputs (Schimmelpfennig, 2016; Esenam, 2017; Higgins *et al.,* 2017; Popović *et al.,* 2017, Matyushenko *et al.*, 2018).

Downloaded from www.periodico.tchequimica.com

The simple analysis of adoption versus non-adoption shows precision agriculture technology adoption positively and significantly associated with higher profitability (Castle *et al.,* 2017; Castle, 2016). Reports for 2016 show those cost savings ranging from USD 13 to more than USD 25 per acre when growers use global positioning systems yield or soil maps in conjunction with auto-steer and variable-rate technology when applying inputs (Crumment, 2017; Ivanova and Merkulova, 2018).

Another economic benefit of using digital technologies was found, like between USD 5-44 per ha, which related to "higher grain and fertilizer prices and depended on levels of soil nutrients in the different zones" (Robertson *et al.,* 2018). In addition, the benefits outweigh the associated costs for cereal farms in excess of 80 ha for the lowest price system to 200 – 300 ha for the more sophisticated systems (Godwin *et al.,* 2003).

In Russia case, investments in 2012 with the minimal cost, including AgGPS EZGuide 250 on parallel driving with AG15 antenna with Omnistar XP correction by calculation were USD 2.919 for each combine and 200 USD additionally for the next months. Therefore, these investments will be paid back in the first year of implementation without including yield growth up to 5-10% (Igoshin, 2012). Additionally, with positive correlation between applying precision agriculture and economic benefits some studies presented controversial results. The small influence was found for US corn producers (Schimmelpfennig, 2016; Deichmann *et al.,* 2016; Schuster, 2017).

Precision agriculture tools such as variable rate of fertilizer application were not profitable in wheat and barley, sometimes profitable in corn, and profitable in sugar beet. Profitability correlated closely with the per acre gross revenue earning potential of the crops grown (Swinton and Lowenberg-DeBoer, 2001). Farm size, the shape of the field, and other factors are indicated to be valuable for the economic impact of operations adopted digital technologies (Paraforos *et al.,* 2016; Paraforos *et al.,* 2017; Skvortsov *et al.,* 2018; Shamshiri *et al.,* 2018).

Hired labour costs are 60 to 70 percent lower with any of the three precision agriculture technologies on small corn farms (140-400 cropland acres), while hired labour costs are higher on large farms that have adopted precision mapping and guidance (Schimmelpfennig, 2016). Research projects in Colorado, Kansas, and Nebraska showed the greatest return occurs in the most irregularly shaped fields. The payback is less than one year all the way up to around 120 acres in size. In the case of small, square fields, the payback is 2.38 years (Smith *et al.,* 2013). The application of precision technology in agriculture depends on experience of farmers, size of their business the most (Castle *et al.,* 2016).The use of Internet of things spreads not only on open space soil based crops but also in greenhouses. A not very expensive device, which needed three-tier open source software platform at local, edge, and cloud planes, was proposed for greenhouse cultivation (Řezník *et al.,* 2016; Zamora-Izquierdo *et al.,* 2019).

Information strategy with site-specific information to determine the economically optimal uniform rate of lime provides an average increase in the annual return of $14.38 ha in Indiana. (Bongiovanni and Lowenberg-DeBoer, 2000).

Consideration of the factors, which contribute to the stabilisation and growth of efficiency in grain production, will make it possible to develop a well-specified set of actions, which are aimed at solving the problems of the branch development. A serious limitation to precision nutrient management in Kazakhstan is the availability of fertilizers to farmers. Fertilizer supplies to farmers in Kazakhstan are inadequate even for P, which is mined in Kazakhstan with more exports of P fertilizer exceeding 3 billion US$ annually (Carrer *et al.,* 2017; Lindblom *et al.,* 2017; Waltz, 2017; Daum *et al.,* 2018; Pierce, 2018).

In order to ensure efficient agricultural production (in response to the changing natural conditions, to expectations and demands of consumers, as well as to the requirements of the state concerning ecological agricultural production), farmers must run their farms and do their business not only in accordance with agrotechnical requirements. They must also apply state-of-the-art digital technologies. In the course of utilisation of state-of-the-art digital technologies, it is always necessary to comply with a certain logistics chain. That is, it is necessary to know how to start and how to complete planting and harvesting of the agricultural crops. In accordance with the numerous studies, crop yields are the most important factor, which determines the profitability of grain production. As a rule, the greater crop yields, the lower costs of production/prime costs and labour costs per 1 metric tonne of the products and, respectively, the higher profitability of these products.

Precision farming in grain production consisted of several stages:

– selection of fields with relatively uniform soil fertility and compilation the electronic fields

Downloaded from www.periodico.tchequimica.com

map;

– accurate pre-sowing tillage, sowing, differential fertilizer, and plant protection products;

– identification of the state of crops, yield forecast, and grain quality based on remote monitoring systems.

The aim of this paper is to evaluate from an economic perspective the results of implementation precision farming elements, which can contribute to the studies on digital technologies efficiency globally, and locally. Papers discussing the efficiency of smart technologies in agriculture with Kazakhstani cases were not published yet. Therefore, in respect of making decisions concerning the application of digital technologies, farmers need to be informed how it is effective and what they should do while applying them.

Wealthy farmers over the world have been applying digital technologies more and more, cutting operation expanses on hired labour and production recourses. In this study, we tried to evaluate the hypothesis of significant economic and environmental efficiency of application the precision technologies tools (Friedrich *et al.,* 2016; Kudari and Patil, 2017).

2. MATERIALS AND METHODS

In Kazakhstan state project called Digital Kazakhstan was formed for the period 2018-2022, which considered agriculture as one of the five directions for implementation. According to this project in 2019, the information on the food chain, livestock, planting from the farm to retail will be collected for transparency monitoring. In 2020, the entire electronic platform e-Agro trade for food will be designed. Finally, for 2022 National Project on spatial data infrastructure is planned (Digitalization of economy branches, 2018). In 2018, precision agriculture was applied for nine pilot farms. We selected three farms with more representative data for the purpose of this study in order to evaluate how effective digital technologies in agriculture of Kazakhstan.

In this study, we collected soil analysis, field history, and space maps, cost analysis and made calculations on how much expenses and profit were made for one ha of land with smart agriculture technologies. In the course of implementation of this project, investigations were based on the principles of the systematic and integrated approach, of the economic analysis, and of the comparative analysis. We have begun our study of farms from the study of history of their fields during 10-year period in order to find answers to the following questions: which agricultural crops have been planted by the relevant farm during this period of time and what are volumes of the mineral fertilisers, which were introduced to these fields. All these data have been collected in order to determine the efficiency of the application of the mineral fertilisers by relevant farms, as well as in order to determine degree of influence of these fertilisers upon the crop yields of the cultivated crop. In addition to the study of history of the relevant fields in the course of development of agricultural production, we have calculated all expenses, which are connected with production of the agricultural crop. Particularly, such calculations for the wheat and rape were made in accordance with the technological flow chart.

Before submission of our recommendations to farms we have conducted analysis of agrochemical properties of soils from 1(one) ha in order to determine level of content of those forms of nitrogen, phosphorus, and potassium, which are accessible for nutrition of crops, as well as in order to ensure further calculation of the relevant rates of application of fertilisers. Following the analysis, which we have performed, we have calculated, how much monetary funds any farm must spend (investments in acquisition of agricultural equipment, mineral fertilisers, herbicides and fungicides, seed treatment, equipping of the specialised machines and vehicles) in order to ensure that this farm will generate profits from each cultivated hectare in accordance with the technology of the bitmap precision agriculture.

We have been performed our study with the help of field methods; that is, we have obtained all the data on the basis of primary data collection.

This pilot project was duly developed and performed by the interdisciplinary research group (27 scientists of Saken Seifullin Kazakh Agrotechnical University) in cooperation with the Competences Centre of the National Chamber of Entrepreneurs of the Republic of Kazakhstan in accordance with the instructions of the Ministry of Agriculture of the Republic of Kazakhstan. The main goal of this project was formulated as follows: approbation and introduction of digital technologies on the basis of 9 pilot farms in Akmola, Karaganda, Kostanay, and North Kazakhstan regions with subsequent dissemination of successful experiences among farmers of the Republic of Kazakhstan.

Since the beginning of the implementation of this pilot project, a group of scientists has carried

Downloaded from www.periodico.tchequimica.com

out a broad range of activities, which are required for the introduction of precision farming technologies. Electronic maps of fields were developed for each pilot area. A training stage for farm specialists concerning the application of these technologies was organised and carried out. Audit of technical fleets of the pilot farm was carried out along with the provision of pieces of advice concerning the acquisition of special equipment for precision farming. Electronic agrochemical cartograms of the pilot fields were developed. Calculations in respect of application of the required rate of fertilisers were made. We have also developed electronic maps with respect to the following factors: weed infestation of crops; degree of their infection with plant diseases, pest colonisation of plants. These electronic maps were submitted to the relevant farms. Therefore, these farms have succeeded in performance of local treatments, as well as in suppression of diseases at the early stages of their development.

In order to determine degree of efficiency of the precision farming technologies from the economic point of view, in 2018 we performed economic calculations on the basis of the data, which were collected from three farms in Akmola, Karaganda, and Kostanay regions: "Akmola Phoenix" JSC, "Naydorovskoye" LLP and “Troyana" LLP. In the course of our calculations, we have used the method of timing, observation, and data analysis with the help of Excel software.

In order to optimise expenses of farms in the course of cultivation of various agricultural crops along with the relevant decrease in the costs of production in the branch of crop cultivation, we have calculated expenses in respect of each of these farms and have conducted an analysis of their possibilities. As a rule, various systems of criteria are used in the course of calculation of the economic efficiency in grain production. As concerns food cereals, it is usual to calculate the following parameters: crop yields (1); costs of production per one centner of the product (2); labour costs per one centner (3); profits per one hectare (4); the level of profitability (5).

The data concerning the application of mineral fertilisers, concerning seed application rate, as well as data on the profitability of production with the help of traditional agro-technology, as well as in accordance with new agro-technology have been entered to Excel forms. These forms were used in the course of development the following matrixes: "Matrixes of application of mineral fertilisers with the help of traditional technology, as well as with the help of precision farming technology", "Matrixes for calculation of the seed application rate", and "Forecast matrix of profitability".

The "Forecast matrix of profitability" with the help of its main parameters presents economic calculations of expenses ("Indirect expenses for wheat production" and "Direct expenses in accordance with the flow process chart for wheat production"). In addition, this Matrix presents "Calculations of sums for the purchase of seeds, fertilisers, and herbicides (in the case of planning the crop yields at the level of 10 centner/hectare)". Results of all calculations have been compiled in the relevant table "Calculation of the income section of the company budget". This Table includes the following items of income: parameters "Crop yields", "Gross production", "Refraction", "Gross collection, taking into consideration refraction", "Costs of production", and "Gross profits". Calculations of the "income item" were made in accordance with the actual planted acreage in hectares, as well as in tenge per one hectare. Table 1 presents crop yields of wheat in three (3) pilot farms in 2018.

As we can see, average crop yields of wheat on 3 pilot areas have increased following the introduction of certain components of precision farming. The average crop yields were approximately equal to 30 centner/hectare. Therefore, it is possible to draw a logical conclusion that introduction of components of digital technologies into the production of wheat is equal to not less than 5 centner/hectare. In addition, introduction of the technology of precision farming has demonstrated that it is possible to save 9% of fuel and lubricant materials at the expense of utilisation of the system of parallel driving, as well as it is possible to save 27% of mineral fertilisers and 31% of pesticides at the expense of their differentiated application (Akhmetshin *et al.*, 2018).

3. RESULTS AND DISCUSSION:

We assumed that precision agriculture affects positively on operational results of production. In accordance with our calculations, gross profits on the relevant areas (in the conditions of three pilot farms) have achieved the level of 54 US Dollars per one hectare in the course of production of wheat with the help of digital technologies. Similar investigations were carried out by other scientists. The application of digital technologies can be an efficient method of farming under certain circumstances. Certain agricultural crops, for example, fruits and vegetables cannot be fully subject to digitalisation,

Downloaded from www.periodico.tchequimica.com

robotization, and automation, not least because of the complexity of these technologies and lack of qualified human resources in rural areas (Vasconez *et al.,* 2018; Vogt, 2017). The efficiency of digital technologies is also connected with the minimisation of the resources, which are used in the course of production. For instance, reducing the quantity of agrochemicals required. It could also reduce costs, risk of crop damage and excess herbicide residue, as well as potentially reduce environmental impact (Partel *et al.,* 2019).

In our research, we have studied wheat. It turned out that digital technologies are applicable to the production of this crop, and these technologies can result in an increase in the economic efficiency of production. Within the framework of this project, we have developed electronic maps of fields of the relevant farms. These electronic maps were used as the cartographic base for performance of the agricultural chemical survey (Figures 1-3). Taking into account orientation of this project to precision farming, this agricultural chemical survey has been carried out with the help of GPS receivers in order to ensure soil sampling in accordance with the grid sheet survey (coordinate referencing). For the first time, grid of sampling of soils from the elementary plots was approbated provided that area of each elementary plot is equal to one hectare instead of the previously accepted areas in the Republic of Kazakhstan, which were equal to 75 hectares on the rainfed lands and 10 hectares on the irrigated lands (Kingwell and Pannell, 2005; Swinton and Lowenberg-DeBoer, 1998). On the basis of the agrochemical survey, which we have performed, as well as on the basis of integration of the data of the agrochemical analysis of soils, we have developed agrochemical cartograms of availability of soils with humus and movable forms of nutrients (Figures 4-5). In accordance with the results obtained, it was established that there were substantial losses of humus within the entire surveyed area of arable soils as compared with the similar virgin lands virgin lands. There is no doubt that this fact exerts influence upon the crop yields of cultivated crops. There is a lack of a considerable extent of those forms of nitrogen and phosphorus, which are accessible for nutrition in the soils of the surveyed fields. Therefore, the set of actions, which are aimed at increase of the humus content, must include the following actions: application of organic fertilizers; introduction of perennial grasses into the succession of crops; green manuring, etc. At the same time, increase of level of the efficient of soil fertility is possible in the case of application of mineral fertilisers. On the basis in the methodology of calculation of rates of fertilisers, which was developed by Professor V.G. Chernenok (Saken Seifullin Kazakh Agrotechnical University), we have calculated rates of fertilisers, which contribute to increasing rate the content of the movable phosphorus and content of the nitrate-nitrogen up to optimal levels.

In accordance with the electronic maps, which were developed in the course of this project, the following facts were established: there is strong degradation of soils within the fields of the pilot farms, while content of micronutrients in these soils is not sufficient in order to ensure growth of crops within the fields of the pilot commercial farms (Figures 1-5). In accordance with the analysis of soils, it was established that the introduction of both phosphorus and nitrogen is insufficient practically in all commercial farm units (except for "Troyana" LLP). This fact exerts essential influence upon the level of crop yields of these commercial farm units. In the course of investigations of the main agrochemical characteristics of soils on the fields of these commercial farms, we have determined optimal rates of application of fertilisers and calculated relevant effects from the proposed recommendations.

Soils in Kazakhstan should respond to precision agriculture because many soils are degraded, and soil fertility is often low as fertilizer application in Kazakhstan has declined over the last 30 years. Micronutrients may be important in Kazakhstan soils as nutrient deficiencies may be occurring given soil degradation, low fertilizer use, and low humus content (Franzen, 2008; Pierce, 2018).

In Table 2, performance expectations of wheat production have been modelled with consideration of the conducted research and economic evaluation. According to our calculations, the optimal area, from which the introduction of precision farming technology should be started, is not less than 2 thousand ha. The comparison of two technologies and their economic efficiency is represented below. The average yield in three areas with the use of tradition technology is 1.2 tons per hectare, while if to take the minimum increment of 0.5 tons per hectare when introducing digital technologies, yield can reach 1.7 tons per hectare. With the price of USD 131.5 per 1 ha profit from an area of 2 thousand hectares is USD 54 per hectare. Therefore, it is noticeable that the use of precision farming technology not only improves crop yield but also increases gross profit from its trading even taking into account refraction.

Downloaded from www.periodico.tchequimica.com

In the case of the introduction of digital technologies, the farm will need additional investments in the amounts of USD 37 per one hectare. In addition to these investments, they will need outsourcing services with respect to consultations and technical support. In order to ensure wide dissemination of technologies of the precision farming among farmers, it is very important to organise relevant training, introductory courses in respect of digital technologies and technologies of the precision farming on the basis of the specific pilot commercial farm units, which would be capable to of demonstrating their successful experiences.

In addition to this training, the first stage of the introduction of digital technologies will be possible in the case of governmental support and partial indemnification of farmers' expenses in connection with these technologies. For those farmers, who plan introduction of the precision farming, it is necessary to envisage the following actions, which will require additional expenses: agrochemical analysis (revealing of the easy-hydrolysable nitrogen and movable phosphorus); acquisition of mineral fertilisers, installation of the system, which will ensure differentiated application of fertilisers and parallel driving, device for application of the main rate of fertilisers, expense for crop protection products, consultancy servicing.

4. CONCLUSIONS:

Therefore, in the course of organisation the productive activities, it is necessary to comply with certain requirements. The most important requirement is very simple: timely performance of all works and activities, which are envisaged by the relevant technologies, including compliance with the agro technical requirement beginning from the preparation of soil for the future sowing of cereal crops and up to their harvesting. In order to comply with this requirement, it is necessary to have certain production resources, material, and technical resources and labour resources, which must be in rational proportions depending on the crop yields of various crops, as well as depending on the accepted technologies of their production. Therefore, it is necessary to study the procedure of implementation of the plan in respect of all agro technical actions (1); determine the efficiency of all such actions (additional yield per one centner) (2). Then it would be necessary to calculate the influence of each such action upon the level of crop yields (3) and upon the gross production (4) of the relevant crop.

It is possible to separate three big groups among the factors of cultivation efficiency of cereal crops: agro technical, technical, as well as organisational and economic factors. As concerns, the first group, utilisation of the prospective varieties and hybrids and application of the scientifically substantiated systems of farming, are the most important factors as of today. Application of the progressive systems and machine is the most important factor in the second group, while a combination of marketing and governmental regulation is the most important factor in the third group.

In accordance with our calculations, “Akmola Phoenix" JSC, "Naydorovskoye" LLP, and “Troyana" LLP can increase their gross profits with the help of digital technologies from USD 31 up to USD 54 per one hectare of wheat.

If these farms are guided by all recommendations, which were submitted for them by the experts in the sphere of digitalisation, then they can increase the crop yields of wheat by 25-35 % in perspective. At the same time, they can increase such parameters as income and profits.

5. ACKNOWLEDGMENTS:

We are grateful to Nurlan M. Kaskatayev for help in writing this article. We offer the whole family sincere condolences in connection with the irreparable loss.

6. REFERENCES:

1. Akhmetshin, E.M., Kopylov, S.I., Lobova, S.V., Panchenko, N.B., Kostyleva, G. *International Journal of Energy Economics and Policy*, **2018**, *8*(4): 169-177.
2. Bellon-Maurel, V., Huyghe, C. *OCL – Oilseeds and fats, Crops and Lipids*, **2017**, *24*(3), D307.
3. Bongiovanni, R., Lowenberg-DeBoer, J. *Precision Agriculture*, **2000**, *2*, 55-70.
4. Bramley, R.G.V., Ouzman, J. *Precision agriculture*, **2019**, *20*(1), 157-175.
5. Carrer, M.J., de Souza Filho, H.M., Batalha, M.O. *Computers and Electronics in Agriculture*, **2017**, *138*(1), 11-19.
6. Castle, M.H. *Masters thesis*, University of Nebraska-Lincoln, United States, **2016**.
7. Castle, M.H., Lubben, B.D., Luck, J.D. Mieno, T. *Agricultural Economics*, **2017**, *June*.

Downloaded from www.periodico.tchequimica.com

8. Castle, M.H., Lubben, B.D., Luck, J.D. *Agricultural Economics*, **2016**, *1*, 49.
9. Crumment, D. https://www.farm-equipment.com/blogs/6-opinions-columns/post/13649-ahead-of-the-curve-economic-benefits-of-using-precision-farming, accessed February **2017**.
10. Daum, T., Buchwald, H., Gerlicher, A., Birner, R. *Computers and Electronics in Agriculture*, **2018**, *153*, 144-150.
11. Deichmann, U., Goyal, A., Mishra, D. *Agricultural Economics (United Kingdom)*, **2016**, *47*, 21-33.
12. Digitalization of economy branches, https://digitalkz.kz/ru/cifrovizaciya-otraslei-economiki/, accessed January **2018**.
13. Esenam, A. *International Sugar Journal*, **2017**, *119*(1422), 108-117.
14. Franzen, D. https://www.ndsu.edu/fileadmin/soils/pdfs/1176.1.pdf, accessed January **2008**.
15. Friedrich, J., Klingner, S., Becker, M., Schneider, M. *Landtechnik*, **2016**, *71*(2), 35-42.
16. Godwin, R.J., Richards, T.E., Wood, G.A., Welsh, J.P., Knight, S.M. *Biosystems Engineering*, **2003**, *84*(4), 533-545.
17. Higgins, V., Bryant, M., Howell, A., Battersby, J. *Journal of Rural Studies*, **2017**, *55*, 193-202.
18. Igoshin, A.A., *Bulletin of NGIEI*, **2012**, *5*(12), 2-8.
19. Ivanova, E.V., Merkulova, E.Y. *Quality – Access to Success*, **2018**, *19*(S2), 130-134.
20. Kingwell, R., Pannell, D. *Australian Journal of Agricultural Research*, **2005**, *56*, 553-561.
21. Kudari, M.B., Patil, S.L. International Journal of *Agricultural and Statistical Sciences*, **2017**, *13*(1), 297-301.
22. Lindblom, J., Lundström, C., Ljung, M., Jonsson, A. *Precision Agriculture*, **2017**, *18*(3), 309-331.
23. Matyushenko, I.Y., Shtal, T.V., Piddubna, L.I., Piddubnyi, I.O., Kvitka, Y.M. *Journal of Advanced Research in Law and Economics*, **2018**, *9*(4), 1343-1361.
24. Paraforos, D.S., Vassiliadis, V., Kortenbruck, D., Stamkopoulos, K., Ziogas, V., Sapounas, A.A., Griepentrog, H.W. *Computers and Electronics in Agriculture*, **2017**, *142*, 504-514.
25. Paraforos, D.S., Vassiliadis, V., Kortenbruck, D., Stamkopoulos, K., Ziogas, V., Sapounas, A.A., Griepentrog, H.W. *IFAC-PapersOnLine*, **2016**, *49*(16), 324-329.
26. Partel, V., Kakarla, Ch. Ampatzidis, Y. *Computers and Electronics in Agriculture*, **2019**, *157*, 339-350.
27. Pierce, F.J. *Final Report on the Digital Technologies in Agriculture Project*, New York: Oxford University Press Inc., **2018**.
28. Price, P. *Spreading the PA message*, Canberra: Grains Research and Development Corporation, **2004**.
29. Popović, T., Latinović, N., Pešić, A., Zečević, Ž., Krstajić, B., Djukanović, S. *Computers and Electronics in Agriculture*, **2017**, *140*, 255-265.
30. Řezník, T., Kepka, M., Charvát, K., Charvát, K., Horáková, S., Lukas, V. *IOP Conference Series: Earth and Environmental Science*, **2016**, *34*(1), 012031.
31. Robertson, M., Lyle, G. Bowden, J.W. *Field Crops Research*, **2018**, *105*, 211-220.
32. Schimmelpfennig, D. https://www.ers.usda.gov/webdocs/publications/80326/err-217.pdf?v=0, accessed October **2016**.
33. Schuster, J. Resource: *Engineering and Technology for Sustainable World*, **2017**, *24*(1), 20-21.
34. Shamshiri, R.R., Weltzien, C., Hameed, I.A., Yule, I.J., Grift, T.E., Balasundram, S.K., Pitonakova, L., Ahmad, D., Chowdhary, G. *International Journal of Agricultural and Biological Engineering*, **2018**, *11*(4), 1-14.
35. Skvortsov, E.A., Skvortsova, E.G., Sandu, I.S., Iovlev, G.A. *Economy of Region*, **2018**, *14*(3), 1014-1028.
36. Smith, C.M., Dhuyvetter, K.C., Kastens, T.L., Kastens, D.L., Smith, L.M. *Journal of the ASFMRA*, **2013**, 185-206.
37. Swinton, S.M., Lowenberg-DeBoer, J. *Proceedings of the 3rd European Conference on Precision Agriculture,* Montpellier, France, **2001**.
38. Swinton, S.M., Lowenberg-DeBoer, J.

Downloaded from www.periodico.tchequimica.com

Journal of Production Agriculture, **1998**, *11*, 439-446.

39. Takhumova, O.V., Lovyannikova, V.V., Konovalova, I.A. *Actual Problems of Economics*, **2016**, *184*(10): 228-234.
40. Vasconez, J.P., Kantor, G.A. Cheein, F.A. A. *Biosystems Engineering*, **2018**, *179*, 35-48.
41. Vogt, S. https://grdc.com.au/resources-and-publications/grdc-update-papers/tab-content/grdc-update-papers/2017/02/the-economics-of-precision-agriculture, accessed February **2017**.
42. Waltz, E. *Nature Biotechnology*, **2017**, *35*(5), 397-398.
43. Zamora-Izquierdo, M.A., Santa, J., Martinez, J.A., Martinez, V., Skarmeta, A.F. *Biosystems engineering*, **2019**, *177*, 4-17.

***Table 1**. Crop yields of the spring wheat in 2018, centner/hectare*

Farms	Cultivated area, hectare	Average crop yields in the region, centner/hectare	Crop yields on the pilot field, centner/hectare	Growth rate, centner/hectare
Akmola region				
"Akmola-Phoenix" JSC	500	12.9	18.0	+5.1
Karaganda region				
"Naydorovskoye" LLP	250	11.6	50.2	+38.6
Kostanay region				
"Troyana" LLP	400	13.7	22.0	+8.3

***Table 2**. The calculated rate of wheat production in traditional and precision farming technologies*

Parameters	Per one ha in physical terms		Per one ha in monetary terms	
	Traditional technology	Application of digital technologies	Traditional technology	Application of digital technologies
Crop yields, 12 c/ha	12	17	-	-
Gross collection/croppage, ton	1.2	1.7	158	210
Refraction, 10%, ton	0.12	0.17	-	-
Gross collection, taking into consideration tret/refaction, ton	1.08	1.53	142	201
Costs of production, USD			111	148
Additional costs for precision farming, USD			-	37
Gross profits, USD			31	54

Downloaded from www.periodico.tchequimica.com

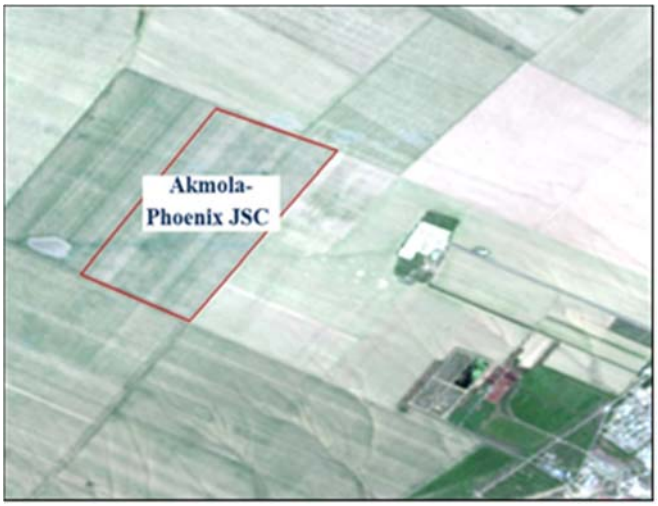

Figure 1. *The electronic map of field within the pilot area of "Akmola Phoenix" JSC, 500 hectares*

Figure 2. *The electronic map of field within the pilot area "Naydorovskoye"LLP, 250 hectares*

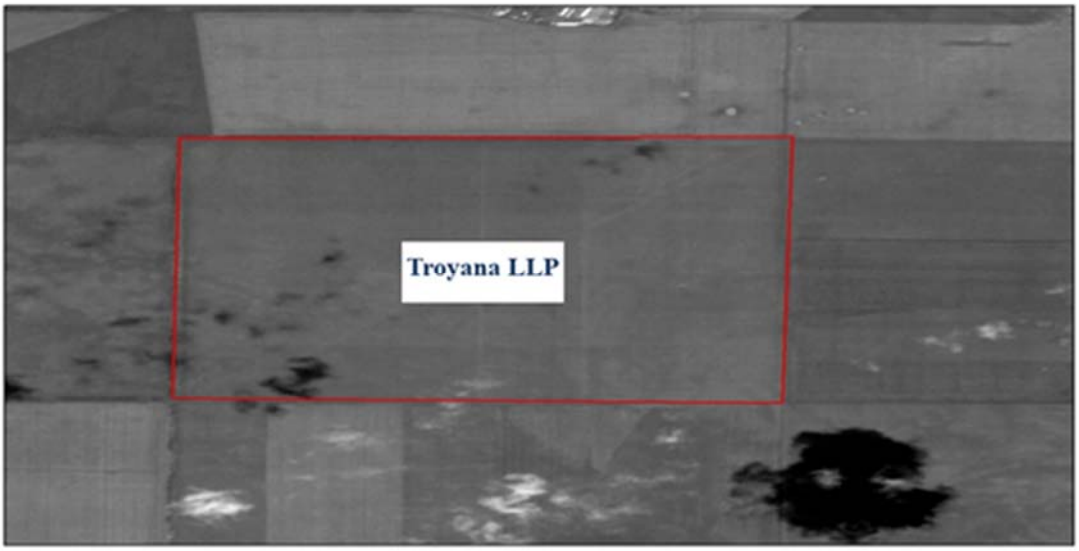

Figure 3. *The electronic map of field within the pilot area of «Troyana» LLP, 400 hectares*

Downloaded from www.periodico.tchequimica.com

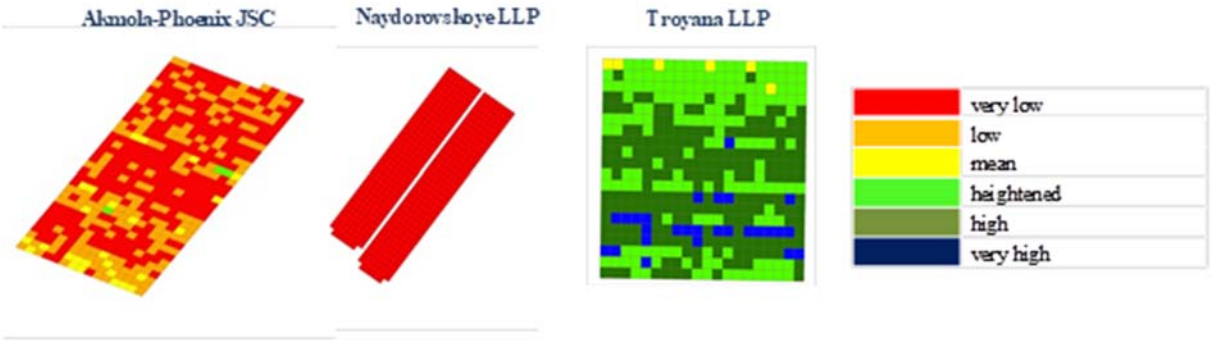

Figure 4. *Agrochemical cartogram of the easy-hydrolysable nitrogen'scontent, mg/kg*

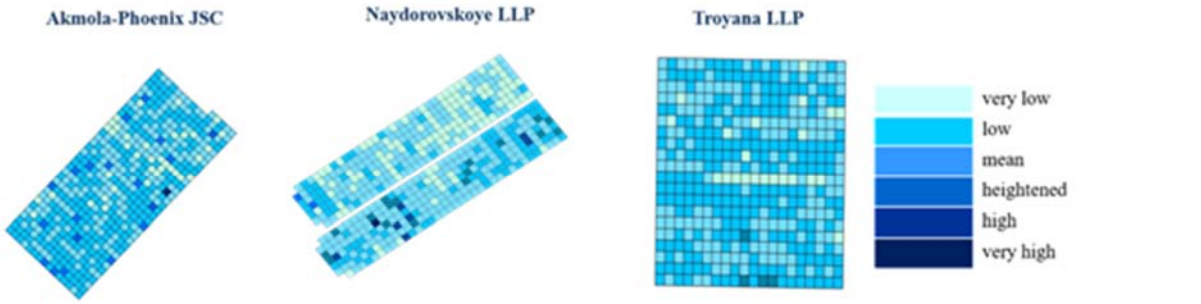

Figure 5. *Agrochemical plan/cartogram of the content of the movable phosphorus, mg/kg*

Downloaded from www.periodico.tchequimica.com

PERIÓDICO TCHÊ QUÍMICA
ARTIGO ORIGINAL

ÍON SULFATO EM ÁGUAS SUBTERRÂNEAS DA BACIA DO RIO MAYMA (ALTÁI DO NORTE, RÚSSIA)

SULFATE ION IN THE GROUNDWATER IN THE BASIN OF MAYMA RIVER (NORTHERN ALTAI, RUSSIA)

СУЛЬФАТ-ИОН В ПОДЗЕМНЫХ ВОДАХ БАССЕЙНА Р. МАЙМА (СЕВЕРНЫЙ АЛТАЙ, РОССИЯ)

KOCHEEVA, Nina A.[1*]; ROLDUGIN, Vladimir V.[2]; KATZ, Valentina E.[3]; MANANKOVA, Tatyana I.[4];

[1, 4] Gorno-Altai State University, Department of Geography and Environmental Management, 1 Lenkina Str., zip code 649000, Gorno-Altaisk – Russian Federation

[2, 3] JSC "GEOLOGICAL ENTERPRISE" ALTAI-GEO", 52 Zavodskaya Str., zip code 649100, Maima – Russian Federation

** Correspondence author*
e-mail: nina_kocheewa@mail.ru

Received 29 May 2019; received in revised form 06 September 2019; accepted 23 October 2019

RESUMO

A relevância do problema investigado é que a maioria da população mundial sofre com a falta de água potável. Uma parte significativa da água na superfície da Terra é caracterizada por baixa qualidade e não é adequada para uso doméstico. É por isso que é importante investigar as causas das mudanças na composição qualitativa da água e encontrar maneiras de influenciá-la. O objetivo do artigo é estudar o conteúdo de íons sulfato nas águas do norte de Altái pelo exemplo da bacia do rio Mayma. Os dados foram analisados de duas fontes diferentes em dois laboratórios para obter resultados mais precisos. O estudo mostrou que o conteúdo de íons sulfato na água é influenciado por fatores como precipitação, características geológicas, características da paisagem. Diferentes condições de temperatura e umidade em diferentes épocas do ano também afetam esse indicador. Gelo e neve congelados podem acumular íons sulfato criados por fatores antropogênicos e, consequentemente, durante o derretimento, os íons sulfato caem nas águas subterrâneas e nas águas dos rios. O indicador estudado também é afetado pela temperatura do ar e da água subterrânea, cujo aumento pode ser causado por terremotos. Devido ao grande número de fatores que afetam o conteúdo do íon sulfato na água, é bastante difícil determinar a causa exata de flutuações significativas. Portanto, o trabalho comprova a importância de uma análise abrangente dos materiais factuais e do estudo de todos os fatores acima. Os materiais de artigos podem ser úteis no estudo adicional da composição qualitativa das águas de Altái do Norte, bem como em sua aplicação prática para melhorar a composição da água potável.

Palavras-chave: *composição qualitativa da água, precipitação atmosférica, água potável, terremotos nas montanhas, fator antropogênico.*

ABSTRACT

The relevance of the investigated problem is that the majority of the world's population suffers from a lack of drinking water. A significant part of the water on the surface of the Earth is characterized by low quality and is not suitable for home use. That is why it is important to investigate the causes of changes in the qualitative composition of water and find ways to influence it. The aim of the article is to study the content of sulfate ion in the waters of Northern Altai by the example of the Maima river basin. The data was analyzed from two different sources in two laboratories for more accurate results. The study showed that the content of sulfate ions in water is influenced by such factors as precipitation, geological features, landscape features. Different temperature and humidity conditions at different times of the year also affect this indicator. Ice and snow can accumulate sulfate ions created by anthropogenic factors, and, accordingly, during melting, sulfate ions get into groundwater and river waters. The studied indicator is also affected by air temperature and groundwater temperature, the increase of which can be caused by earthquakes. Due to the large number of factors affecting the content of sulfate ion in water, it is rather difficult to determine the exact cause of significant fluctuations. Therefore, the work proves the importance of a comprehensive analysis of factual materials and the study of all

Downloaded from www.periodico.tchequimica.com

of the above factors. Article materials can be useful in further studying the qualitative composition of the waters of the Northern Altai, as well as for their practical application to improve the composition of drinking water.

***Keywords**: qualitative composition of water, precipitation, drinking water, mountain earthquakes, anthropogenic factor.*

АНОТАЦИЯ

Актуальность исследованной проблемы состоит в том, что большинство населения планеты страдает от недостатка питьевой воды. Значительная часть воды на поверхности Земли характеризуется низким качеством и не подходит для домашнего употребления. Именно поэтому важно исследовать причины изменения качественного состава воды и найти способы влияния на него. Цель статьи заключается в исследовании содержимости сульфат иона в водах Северного Алтая на примере бассейна реки Майма. Был произведен анализ данных из двух разных источников в двух лабораториях для большей точности результатов. Исследование показало, что на содержание сульфат ионов в воде влияют такие факторы, как атмосферные осадки, геологические особенности, особенности ландшафта. Разный режим температуры и влажности в разные времена года также влияют на данный показатель. Замерзший лед и снег могут аккумулировать сульфат ионы, создавшиеся антропогенными факторами, и, соответственно, во время таяния, сульфат ионы попадают в подземные воды и воды рек. На изучаемый показатель влияет также температура воздуха и температура подземных вод, повышение которой может быть связано с активизацией сейсмической деятельности. В связи с большим количеством факторов, влияющих на содержание сульфат иона в воде, определить точную причину значительных колебаний достаточно сложно. Поэтому работа доказывает важность комплексного анализа фактических материалов и исследования всех вышеперечисленных факторов. Материалы статьи могут быть полезными при дальнейшем изучении качественного состава вод Северного Алтая, а также для практического их применения для улучшения состава питьевой воды.

***Ключевые слова**: качественный состав воды, атмосферные осадки, питьевая вода, горные землетрясения, антропогенный фактор.*

---

1. INTRODUCTION

As noted by V. I. Vernadsky: "Throughout the geological history, we observe a very close connection between water and life, both in the aquatic environment and on land" (Vernadsky, 2003). Natural waters (underground and surface) are needed in various sectors of the national economy and the industrial sector. Up to 68% of surface and 32% of GW are used for household purposes (Danilov-Danilyan *et al*., 2005). According to some American scientists, in 2015, almost half of the world's population (3 billion people) will live in countries experiencing water shortages (Danilov-Danilyan *et al*., 2005; Trofimov *et al*., 2000; Yazvin, 2003). Therefore, today much attention is paid to the study of the quality of water suitable for household purposes.

Noteworthy is the statement of some researchers (Jaramillo and Destouni, 2014) that "the individual and cumulative effects of various factors of changing water resources are still difficult to distinguish and are largely unknown, especially on a global scale." In this paper (Jaramillo and Destouni, 2014), data of 859 hydrological basins for the period 1901-2008 were analyzed. The world spectrum of various sizes and directions of changes in the Budyko space (Budyko, 1980) was studied, from which climatic and landscape drivers are pointed out, for example, changes in land use and water use, which are necessary to explain at least in 74% of the basins studied (Kiryukhin *et al.*, 1998). The impact of such landscape factors on the change in water resources is basically the opposite of the effects of atmospheric climate change, according to the authors of the work (Jaramillo and Destouni, 2014). An important component of the study of natural waters is their chemical composition.

Mountains are an important component of the nature of the Earth. Most often, they are a gravity drain area for adjacent aligned spaces, which leads to the study and monitoring of the dynamics and composition of the natural waters of mountainous countries. The work (Tague and Grant, 2009) considers the dynamics of GW in the Alps due to climate change. Landscape and climatic features in the Alps determine the patterns of snow cover formation, which affects the hydrological and hydrogeological regime of natural waters.

Downloaded from www.periodico.tchequimica.com

The relationship of land use, topography, composition of rocks and composition of PS was considered in the work (Schot and Van der Wal, 1992), where it was pointed out that intensive anthropogenic impact provokes oxygen depletion and subsequent low oxidation-reduction potentials that lead to denitrification, dissolution of manganese and iron oxides and changes in the content of sulfates. Thus, the study of the dynamics and composition of the GW is today conducted in different regions and at different levels (Robertus, 2010). The Republic of Altai is no exception.

In the Republic of Altai, almost one third of the exploited natural water provides drinking needs (Roldugin *et al*., 2018; Report on the stat, 2016). The largest consumer of this type of water is the city of Gorno-Altaisk and two large villages (Mayma and Kyzyl-Ozek). These settlements are located in the valley of Mayma river which is the right tributary of Katun river (Figure 1). The purpose of this work is to study the content of sulfate ion in the natural waters of Northern Altai (using the example of the Mayma river basin).

2. MATERIALS AND METHODS

The paper presents the results of the analysis of data on the content of sulfate ion in natural waters, groundwater temperature and air temperature, as well as a seismic activity over the period 1999-2016. The use of a data complex from different sources and the results of the analysis of two laboratories makes it possible to compare and monitor the results obtained, which increases the reliability of the study.

The distance in a straight line between the outermost OP is about 20 km (Figure 1). The height of the study area varies from 260 to 450 m above sea level, which determines 190 m difference in elevation on the territory of 20 km. Modern research tools and graphics allow to visualize the main geomorphological features of the study area and get a general idea of the relief and the hydrological and transport network.

A long study of the geological structure of Gorny Altai revealed its main laws and features, which include a sharp transition from the mountains to the plains of Western Siberia – the “face” of Altai (Ryabchikov and Gvozdetsky, 1978). Maps (geological, minerals, etc.) of the new generation reflect minerogenic subdivisions identified on the basis of various types of geological analysis. The published materials indicate that the “ore cluster” assumed in the study area is “confined to terrigenous-carbonate and siliceous-terrigenous-carbonate formations of the Eskong Formation and the Barotal series. As a rule, ore minerals are associated with a fine impregnation of pyrite and cord-like excretions of organic material, indicating hydrogen sulphide contamination of sedimentation pools” (Fedak *et al*., 2011).

In the northern part of the study area (OP in Novaya St.), alluvial sediments of the r. Katun are water-bearing minerals (Figure 2, Table 1), which overlap the bedrock. The thickness of water-bearing deposits varies widely – from 10 meters on the slopes of the terraces to 42 meters in the coastal zone (Katz *et al.,* 1996). In the southern part, alluvial deposits of the Mayma river are the water-bearing minerals, whose power varies widely. The basin of the Mayma river, like the whole Northern Altai, is located in a zone of sharply continental climate. The average long-term air temperature in January is minus 13.8 ºC, in July it is 18.7 ºC according to the Gorno-Altai CHEM (Gorno-Altai Center for Hydrometeorology and Environmental Monitoring) (average for the period 1971-2000). During the same period, the average rainfall over the winter is 153 mm, during the spring it is 137 mm, the contribution of summer is 310 mm, and that of autumn is 140 mm.

The landscape diversity of the Maima District is relatively small. In total, 4 geoms are distinguished: bald peaks and subbald peaks; mountain taiga South Siberian; subtaiga South Siberian; forest-steppe south-siberian. On the territory of the region, groups of facies of the mountain-taiga South-Siberian group of geoms sharply predominate, among which the class of middle-mountain slope cedar and birch-larch middle-mountain and low-mountain facies is distinguished (Zhuravleva *et al.,* 2016), which are characteristic of the slopes of the ridges bounding Mayma river Landscape structure of the basin of Mayma river is reflected on the map, published in work by Zolotov (2012). The length of the river is 60 km (Ryabchikov and Gvozdetsky, 1978), almost half of which runs through residential areas.

3. RESULTS AND DISCUSSION:

3.1. The condition of ion sulfate in water nowadays

Sulfate ions are present in almost all surface and GW, belonging to the most important anions that determine the quality and class of water in all regions of the World (Peristaya *et al*., 2011; Kiryukin *et al*., 1988; Shvartsev and

Downloaded from www.periodico.tchequimica.com

Savichev, 2006). The content of this component in natural waters is not constant and varies under the influence of various factors (Report on the state…, 2016): from geographic location to the activation of seismic processes. Today, one of the most comprehensive lists of published results of hydrogeological and hydrochemical works performed in the Republic of Altai is given in (Katz *et al.,* 1996). The number of works devoted to various aspects of the chemical composition of natural waters increased after the strong earthquake of 2003.

The data on OP in Novaya street show that the difference between the minimum and maximum content of sulfate ion is 38%, which is not surprising as the number of samples is small (Figure 2). However, this number is still significant and should have a justification. The following factors were considered as environmental factors that may affect the content of sulfate ion: precipitation (Tague and Grant, 2009); geological features (Tague and Grant, 2004); landscape features (Jaramillo and Destouni, 2013; Jaramillo and Destouni, 2014). The correlation of precipitation in the year of testing with the content of sulfate ion was-0.4 (Spearman's correlation coefficient). The indicator of non-parametric statistics was used because of the small amount of data, which makes it impossible to use parametric analysis methods. According to these data, it is possible to talk about the tendency to reduce the sulfate ion content.

3.2. The influence of temperature

Features of the temperature and humidity regime of the study area consist of uneven precipitation at different periods of the year (Sukhova, 2009). This preconditions the analysis of precipitation during the winter (Figure 2) and the summer period of the year.

The relationship between the content of sulfate ion and the external environment consists of reducing the sulfate ion content in the years of high snow cover, which causes a smaller depth of soil freezing and a greater amount of melt water that penetrates to different depths in different parts of the basin. At this point of observation, no correlation was recorded between the amount of precipitation in the summer period and the content of sulfate ion in the groundwater. In the course of the work, there was a tendency of a closer connection of the sulfate-ion content with the amount of winter precipitation compared to the air temperature. This does not contradict the basic laws of the behavior of meltwater and GW in the conditions of Siberian mountains, as well as the results of the analysis of data of another OP – a well in Severnaya street. It is located at the foot of Tugaya mountain in the city of Gorno-Altaisk. The well section is illustrated in Table 1.

The monitoring of chemical elements content, water temperature and radon activity were adjusted here. This OP is characterized by the largest amount of data compared to the rest of the network. Regime observations were started in January 2004. Using the entire array of accumulated data, the correlation coefficients were calculated (Table 2).

3.3. Seismic and radon activity

Correlation coefficients were obtained between: the content of sulfate ion and the amount of precipitation – minus 0.18; sulfate ion content and radon activity of 0.14; sulfate ion content and seismic activity of 0.39. The latter provided a basis for studying the relationship between the content of sulfate ion and seismic activity in the time interval immediately following the strong earthquake of 2003 with the epicenter in the South-East Altai – for the period 2004-2006. The correlation coefficient for this period of time showed a higher value – 0.42. The result obtained is consistent with the data from a study of the hydrochemical effects of the earthquake on December 23, 2003 in the south-eastern part of Iran (Malakootian and Nouri, 2010). Standard statistical methods established the most significant reaction of chemical compounds in the first year after the earthquake (Malakootian and Nouri, 2010).

The authors could not ignore the study of the relationship between seismic and radon activity according to the data from Severnaya street OP for the entire observation period. The authors of this work confirmed the trends identified in the course of the earlier study (Peristaya *et al.,* 2011; Katz *et al.,* 2015) and obtained a statistically significant correlation coefficient between these characteristics equal to 0.93.

The obtained data of the correlation analysis determined the interest in the water temperature dynamics in the well in Severnaya street (Figures 3, 4). The average water temperature in the well in 2004 was 35.7 ° C, in 2017 – 13.4 ° C. Dispersion analysis allows you to demonstrate the identified differences and prove their significance. Two peaks in the graph (Figure 4) indicate an abnormal temperature increase. The analysis showed the statistical

Downloaded from www.periodico.tchequimica.com

significance of the first of them, which was conducted in 2004-2006.

To verify the significance of the peak temperature in the period 2011-2012 the temperature dispersion analysis was performed for the period 2007–2018. It is established that 2007 is also included in the period of an abnormal increase in water temperature. Its anomalous decrease in 2010 also draws attention. Perhaps this decrease in water temperature is due to the weather conditions. To test this hypothesis, the data of HMS (hydrometeorological station) Kyzyl-Ozek on the air temperature for ten years 2006-2015 were analyzed. It was in 2010 that the lowest average temperature of the year in the period under study was recorded. Perhaps here is one of the reasons for lowering the temperature of groundwater. This idea is consistent with another result, which consists in the fact that throughout the study period, the temperature of the GW in Severnaya street fell to the minimum at the end of winter – in early spring. The same trend is scheduled for OP in Novaya street.

In 2007, the highest air temperature was noted, which perhaps affected the temperature of the groundwater. It should be noted that the seismic activity in 2007 and 2010 was at the minimum level, which suggests a significant role for geographical conditions in the supply of sulfates in GW and during its temperature. However, it does not contradict the idea that seismic activation leads to an increase in the temperature of the groundwater. An indirect confirmation of this idea are the features of the geological structure of the OP in Novaya street (Table 1) and Severnaya street.

OP data in Severnaya street provide the opportunity for a multilateral study of the status and dynamics of the quality of GW in this area. The results obtained by the authors of this work are consistent with the results for other mountain areas (Guseva *et al*., 2013).

3.4. A connection between various factors

A significant fluctuation of the sulfate-ion content in the water of wells was revealed, the causes of which are difficult to establish for some sites. These difficulties are determined by the nature of the object of the study and a small amount of data. Unfortunately, these conditions today are the norm and are characteristic of most OPs (Yazikov and Shatilov, 2004), which leads to incomplete hydrogeological and hydrochemical information. With this type of testing, it is possible to talk only about trends (Novaya Street, Monday), and in some cases only about introducing new data into use. To convincingly explain the dynamics of sulfate ion and other components, it is necessary to continue monitoring with the study of the landscape features of the territory.

A large data array (for example, the OP Severnaya street) makes it possible to establish patterns and confirm them by quantitative methods. A tendency has been revealed towards the connection of the studied component, sulfate ion, with environmental factors: water and air temperature, as well as with the amount of precipitation. Mathematical indicators of this connection are different and often do not reach high values. The authors suggest that the mechanism of this relationship is more complex than the direct dependence of one indicator on another. The combination of factors is the most possible variant. The conditions of the mountainous area create some balance, which is easily broken when activating, for example, the technogenic factor. An example is the OP in Novaya street. At the same time, high-speed, energy-intensive natural processes, such as earthquakes, are capable of interfering with the “traditional” fluctuations of the state of its components for the given territory. An example is the OP in Severnaya street.

Analysis of our data shows that the minimum content of sulfate ion is typical for precipitation. This suggests that snow and rain are not a source of sulfate ion in the GW. At the same time, in the snow that had lain all winter, more sulfates are accumulated than in the snow that just fell. The reason may be the anthropogenic effect on snow cover, for example, aerosols from motor vehicle emissions. In the rivers and streams of the Maima river basin sulfate ion content is lower than in well water and also does not reach the TLV value.

The processes of atmospheric portage of anthropogenic and natural anthropogenic substances from economically developed regions can be an important factor in the formation of the chemical composition of natural waters. Nevertheless, according to hydrochemical indicators, surface and groundwater in the basin of Maima river is generally characterized as “clean”, and the ecological and geochemical state of the basin of the study area can be assessed as satisfactory.

The temperature of groundwater rises during the earthquake. This increase can be

Downloaded from www.periodico.tchequimica.com

considered instantaneous compared with the time it takes to return to its average values. The greatest increase in the temperature of the groundwater and the longest period of its return to the mean value is observed for the aquifer confined to the deposits of the Vendian-Cambrian age. This is important to note due to the fact that the depth of observation wells drilled in ancient and Quaternary sediments is comparable (Table 1).

4. CONCLUSIONS:

In this paper, only the sulfate ion content was considered, but the chemical composition of natural water was analyzed over a large spectrum of components. It needs to be emphasized that all the components in the natural waters of the study area do not exceed the TLV for fishery and cultural and community water use. There can be different reasons for this phenomenon. The fact that the snow that had lain all winter contained more sulfates than the snow that just fell proves a possibility of anthropogenic influence. Also there is no correlation in the amount of precipitation in the summer period and the content of sulfate ion in the groundwater. The causes of significant fluctuation of the sulfate-ion content in the water of wells are difficult to establish. Because the investigation fully depends on the nature of the object of the study, on external conditions and as result of this dependence there is small amount of data.

The work done has shown that at all observation points of the monitoring network of the TLV sulfate ion are not exceeded and the condition of the groundwater is satisfactory for this component. The study revealed a very close relationship between the seismic activity and radon activity (correlation coefficient 0.93), which determines the relationship between the sulfate ion content and the radon activity.

The authors consider the complex of factual material and the results obtained as a unique phenomenological array, which can serve as a basis for assessing the ecological status of the Mayma river and identify factors affecting the formation of the composition of the natural waters of the territory. Practical investigation and learning of data showed that earthquakes, processes of atmospheric portage of anthropogenic and natural anthropogenic substances, time of year can be among these factors. In addition, our study demonstrates the importance of spatial analysis of the current state of natural waters for understanding the context of hydrological changes, within which any sustainable water management plan should be located.

5. ACKNOWLEDGMENTS:

The research work was carried out in the framework of the project of the Ministry of Education and Science of the Russian Federation state project “Economic and social adaptation of the man to the natural and climatic conditions of the Altai Mountains in the second half of the Holocene” (No. 33.1971.2017 /ПЧ).

6. REFERENCES:

1. Ryabchikov, A.M., Gvozdetsky, N. A. (Eds.) *Altai Territory: Atlas,* Moscow-Barnaul. Publishing House of the Research Institute of Mountain Nature Management, **1978**.
2. Budyko, M.I. *Climate in the past and the future,* Leningrad. Hydrometeoizdat (Hydrometeorological Publishing House), **1980.**
3. Danilov-Danilyan, V. I., Losev, K.S., Rafe, I. E. *Before the Main Challenge of Civilization: A Look from Russia,* Moscow. INFRA-M, **2005**.
4. Destouni, G., Jaramillo, F., Prieto, C. *Nature Climate Change*, **2013**, *3(3). https://www.nature.com/articles/nclimate1719, accessed 15 August 2018.*
5. Fedak, S. I., Turkin, Yu. A., Gusev, A. I., Shokalsky, S. P. Rusanov, G. G., Borisov, B. A., Belyaev, G. M., Leontyeva, E. M. *State Geological Map of the Russian Federation. Scale 1: 1,000,000 (third generation). Altai-Sayan Series,* St. Petersburg. Russian Geological Research Institute, **2011**.
6. Guseva, N. V., Kopylova, Yu. G., Leushina, S. K. *Bulletin of the Tomsk Polytechnic University,* **2013***, 322 (1),* 141–146.
7. Jaramillo, F., Destouni, G. *Geophysical Research Letters,* **2014**, *41 (23)*, 8377–8386.
8. Katz, V. E., Kudryavtseva, T. N., Chentsova, N. P. *Results of Geological and Environmental Studies and Mapping of 1: 1,000,000 Scale of the Altai Territory and the Altai Republic.* GE "Altai-Geo", **1996.** *https://rfgf.ru/catalog/docview.php?did=2e0b8e3c8bd17b3cd9d68ca6503e367a, accessed 20 August.2018*
9. Katz, V. E., Shitov, A. V., Roldugin, V. V.

Downloaded from www.periodico.tchequimica.com

Modern Problems of Hydrogeology, Engineering Geology and Hydro-geo-ecology of Eurasia, **2015**, 424–428.

10. Kiryukhin, V. A., Korotkov, A. I., Pavlov, A. N. *General Hydrogeology.* Leningrad. Nedra. **1988**.
11. Malakootian, M., Nouri, J. *International Journal of Environmental Research,* **2010**, *4(3),* 443–454.
12. Peristaya, L. F. Indina, I. V., Peristy, Yu. A., Kozyreva, A. N. *Belgorod State University Scientific Bulletin. Series: Natural Sciences,* **2011**, *17 (21 (116))*, 75–84.
13. Robertus, U. V. (ed.) *Report on the State and Protection of the Environment of Altai Republic in 2010*. Gorno-Altaisk. Altai Regional Institute of Ecology, **2016**.
14. Roldugin, V.V., Kats, V.E., Kocheeva, N.A. Astrakhan *Bulletin of Environmental Education,* **2018**, *1*, 60–69.
15. Schot, P. P., Van der Wal, J. *Journal of Hydrology*, **1992**, *134 (1-4),* 297–313.
16. Shvartsev, S. L., Savichev, O. G. *Computational Technologies,* **2006***, 11 (S6),* 67–78.
17. Sukhova, M.G. *Bioclimatic Conditions of Human Activity in the Altai-Sayan Mountain Country.* Tomsk. Tomsk University Publishing house, **2009**.
18. Tague, C., Grant, G. E. *Water Resources Research*, **2004**, *40 (4). https://agupubs.onlinelibrary.wiley.com/doi/10.1029/2003WR002629, accessed 15 August 2018.*
19. Tague, C., Grant, G. E. *Water Resources Research*, **2009**, *45 (7). https://agupubs.onlinelibrary.wiley.com/doi/10.1029/2008WR007179, accessed 15 August 2018.*
20. Trofimov, V.T., Ziling, D.G., Baraboshkina, T.A., Bogoslovskiy, V. A., Zhigalov, A. D., Harkina, M. A., Hachinskaya, N. D., Tsukanova, L. A., Kasyanova, N. A., Krasilova, N. S*. Ecological Functions of the Lithosphere.* Moscow. Publishing House of Moscow State University, **2000**.
21. Vernadsky, V.I. *History of Natural Waters,* Moscow. Nauka, **2003**.
22. Yazikov, E. G., Shatilov, A. Yu. *Geo-ecological Monitoring: Tutorial.* Tomsk. TPU publishing house, **2004**.
23. Yazvin, L.S. *Exploration and Protection of Subsoil Riches*, **2003**, *10*, 13–19.
24. Zhuravleva, O. V., Karanin, A. V., Kocheeva, N. A., Babin, V. G., Malkov, P. Y., Minaev, A. I., Suhova, M. G., Fedotkin,a N. V., Ebel, A. V. *Creating a Protected Area as a Factor in Stabilizing the State of the Environment in the Urbanized Territories of Northern Altai. Gorno-Altaysk*. GAGU Publishing House, **2016**. http://elib.gasu.ru/index.php?option=com_abook&view=book&id=180:sozdanie-prirodookhrannoj-territorii-kak-faktor-stabilizatsii-sostoyaniya-okruzhayushchej-sredy-urbanizirovannykh-territorij-severnogo-altaya&catid=8:ecology&Itemid=166, accessed 20 August 2018.
25. Zolotov, D. V., Lubenets, L. F., Chernykh, D. V. *World of Science, Culture, Education*, **2012**, *2 (33),* 360–369.

Downloaded from www.periodico.tchequimica.com

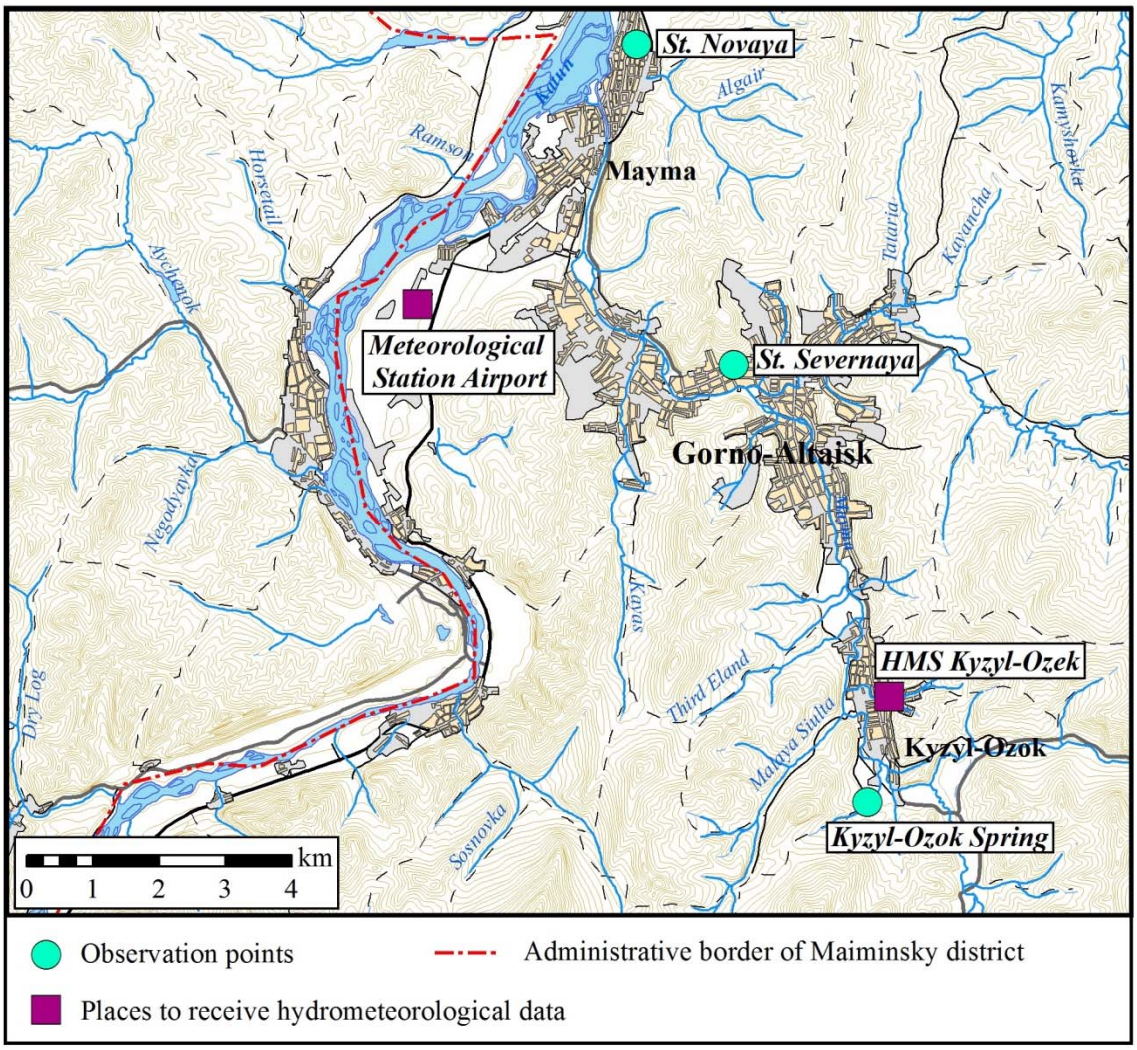

Figure 1. *Scheme of observation points (compiled by V. V. Roldugin) (Roldugin, 2018)*

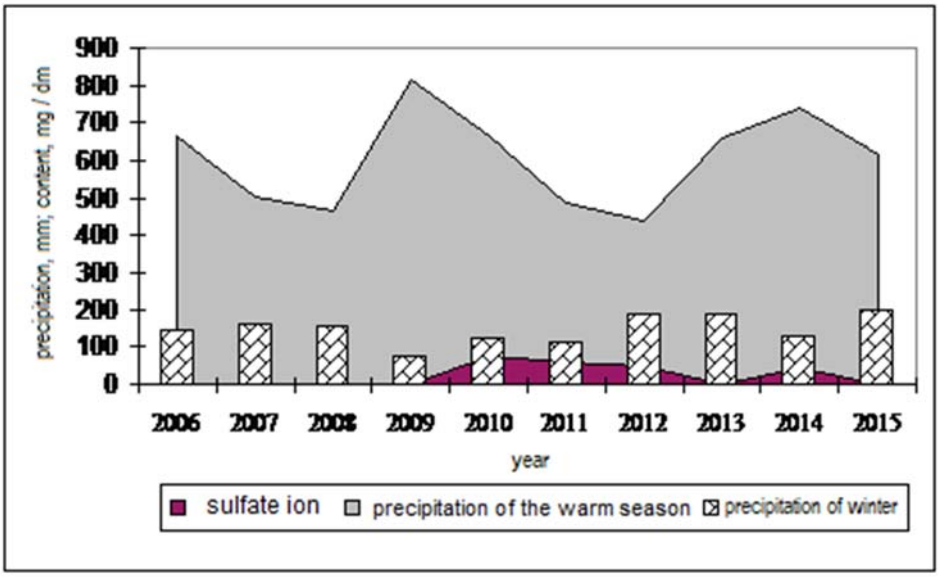

Figure 2. *The amount of precipitation and the content of sulfate ion in the water well in Novaya Street*

Downloaded from www.periodico.tchequimica.com

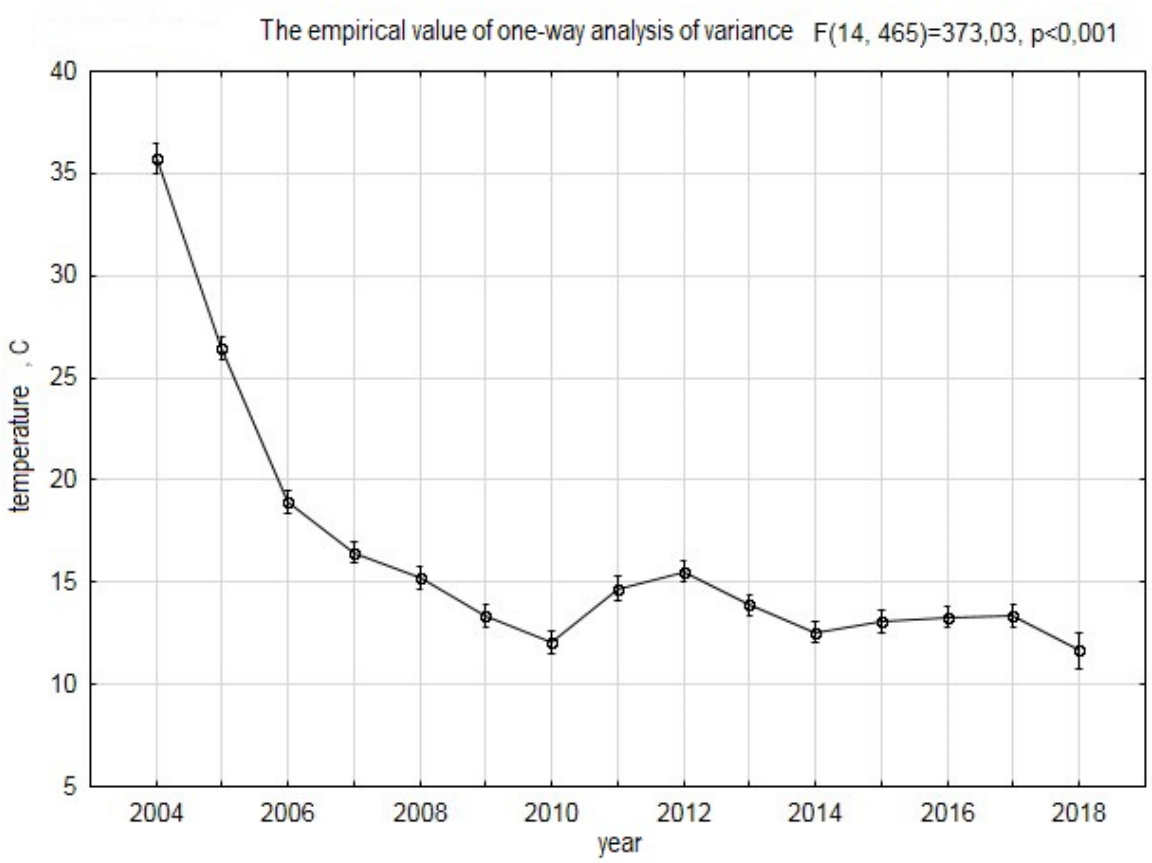

Figure 3. *Dispersion analysis of the well water temperature in Severnaya Street for the period 2004-2018*

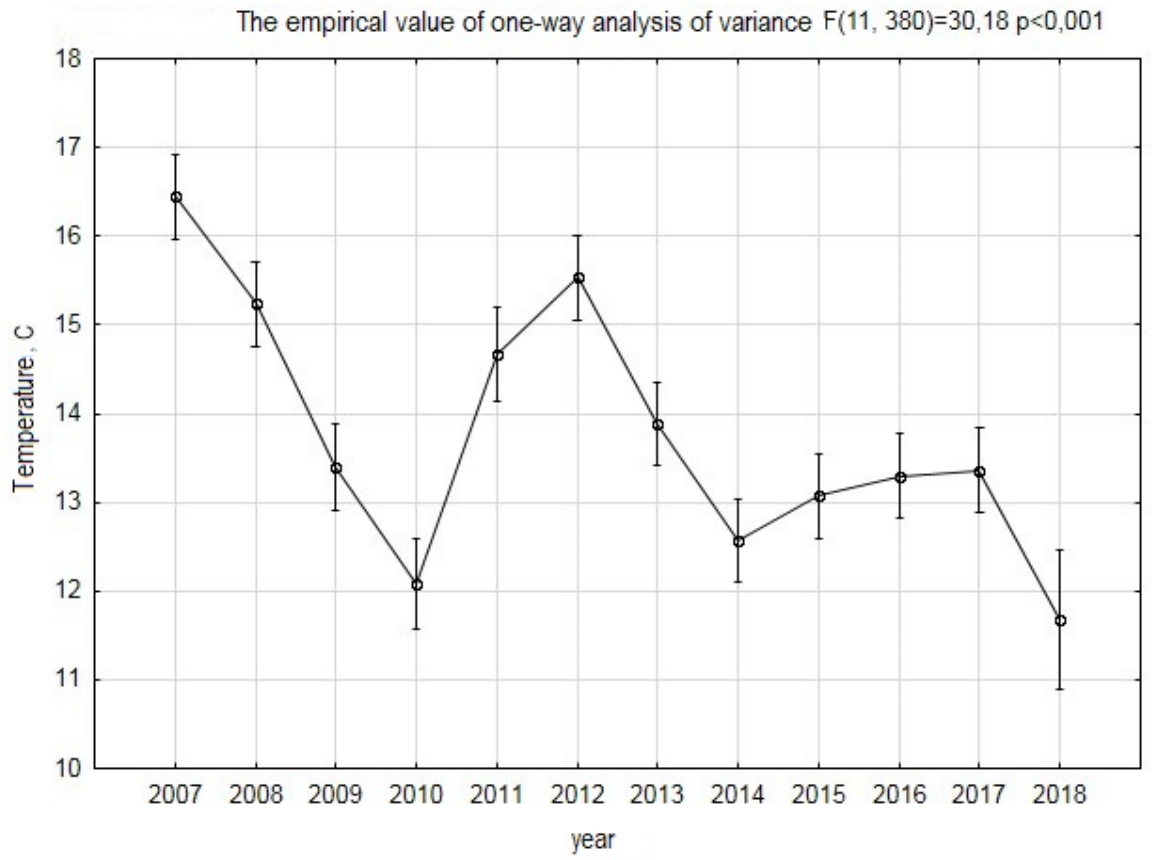

Figure 4. *Dispersion analysis of the well water temperature in Severnaya Street for the period 2007-2018*

Downloaded from www.periodico.tchequimica.com

Table 1. *Well cut in Severnaya Street.*

Geological index	Lithological composition of reservoirs	Depth, м	Layer thickness, м	Go-technical cut	Well casing	
					diametr, мм	depth, м
Q_{III-IV}	Rubble deposits	9	9	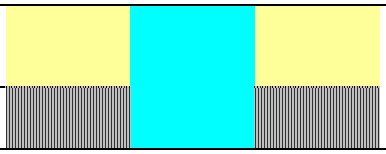	100	10
V-Є	Shale rock	10	1			

Table 2. *Correlation of hydrochemical indicators and characteristics of the environment according to OP in Severnaya Street (Gorno-Altaisk)*

	Content of fluorine	Water temperature,ºC
Content of radon	-0.6	0.0
Seismic activities	-0.2	- 0.27
SO_4/Cl	0.3	-0.3

Downloaded from www.periodico.tchequimica.com

PERIÓDICO TCHÊ QUÍMICA
ARTIGO ORIGINAL

DETERMINAÇÃO EXPERIMENTAL DE CARACTERÍSTICAS DA RESISTÊNCIA À FENDILHAÇÃO E MODELAGEM TEÓRICA DE PROCESSOS DE DESENVOLVIMENTO DE FENDAS EM AMOSTRAS DE PLÁSTICO DE CARBONO SOB CONDIÇÕES DE PRODUÇÃO ADITIVA

EXPERIMENTAL FINDING OF FRACTURE TOUGHNESS CHARACTERISTICS AND THEORETICAL MODELING OF CRACK PROPAGATION PROCESSES IN CARBON FIBER SAMPLES UNDER CONDITIONS OF ADDITIVE PRODUCTION

ЭКСПЕРИМЕНТАЛЬНОЕ ОПРЕДЕЛЕНИЕ ХАРАКТЕРИСТИК ТРЕЩИНОСТОЙКОСТИ И ТЕОРЕТИЧЕСКОЕ МОДЕЛИРОВАНИЕ ПРОЦЕССОВ РАЗВИТИЯ ТРЕЩИН В ОБРАЗЦАХ УГЛЕПЛАСТИКА В УСЛОВИЯХ АДДИТИВНОГО ПРОИЗВОДСТВА

DOBRYANSKIY, Vasiliy N.[1*]; RABINSKIY, Lev N.[2]; TUSHAVINA, Olga V.[3];

[1,2] Moscow Aviation Institute (National Research University), Institute of General Engineering Training, 4 Volokolamskoe shosse, zip code125993, Moscow – Russian Federation

[3] Moscow Aviation Institute (National Research University), Institute of Aerospace, 4 Volokolamskoe shosse, zip code 125993, Mosco – Russian Federation

** Correspondence author*
e-mail: dobryanskijvn@mail.ru

Received 25 May 2019; received in revised form 01 October 2019; accepted 24 October 2019

RESUMO

A urgência do problema mencionado neste artigo é que, com o desenvolvimento da tecnologia aeroespacial, a demanda por materiais de boa qualidade aumentou. Uma questão importante é garantir durabilidade em condições de cargas de longo prazo e em condições de desenvolvimento de danos. Um dos critérios que garante a resistência do material é a resistência à fendilhação. O objetivo do artigo é estudar a resistência à fendilhação entre camadas (tenacidade à fratura) sob carga em condições de separação e cisalhamento transversal, dureza entre camadas, bem como o efeito da temperatura na dureza entre camadas, propriedades mecânicas de tração. É feita uma comparação dos valores de resistência à fendilhação entre camadas GIC (separação) e GIIC (cisalhamento), bem como propriedades mecânicas de tração e dureza entre camadas de amostras de fibra de carbono. Os principais métodos para estudar esse problema foram o método de feixe curto, o método DCB, o método ENF. Os resultados dos dados experimentais foram comparados com a modelagem dos processos de aparência e desenvolvimento de fendas nos complexos de elementos finitos ABAQUS e Ansys, com base nos modelos VVCT, elementos coesivos. Foram encontrados desvios do experimento e foram tiradas conclusões de que o ponto de aplicação da carga deve ser deslocado da borda da amostra, o que reduzirá a separação inicial e aumentará a rigidez da amostra. Devido ao fato de que o modelo da zona de coesão ser muito sensível aos parâmetros de entrada, é necessário conhecer muitos parâmetros e levar em consideração um grande número de fatores. Estudos têm mostrado como usar o modelo VCCT para obter a carga crítica da germinação da primeira fenda. A técnica de pesquisa pode ser usada para novas experiências, inclusive para simular estratificação adicional com menos erros.

Palavras-chave: *material compósito polimérico, fibra de carbono, parâmetro de resistência à fendilhação entre camadas, modelagem, parâmetro de escala da teoria dos gradientes.*

ABSTRACT

The relevance of the problem stated in this article is that the development of aerospace technology increased the demand for good quality materials. An important issue is ensuring durability in conditions of long-term loads and in conditions of damage development. One of the criteria that ensure the toughness of the material is crack resistance. The aim of the work is to study the interlayer crack resistance (fracture toughness) under loading under conditions of separation and transverse shear, interlayer strength, as well as the effect of temperature on interlayer strength, mechanical tensile properties. A comparison of the values of interlayer crack resistance G_{IC} (separation) and G_{IIC} (shear) and of mechanical tensile properties and interlayer strength of

Downloaded from www.periodico.tchequimica.com

carbon fiber samples is made. The main methods for studying this problem were the short-beam method, the DCB method, the ENF method. The results of the experimental data were compared with modeling the processes of the appearance and development of cracks in the finite element complexes ABAQUS and Ansys based on the VVCT models, cohesive elements. Deviations from the experiment were found and conclusions were drawn that the point of application of the load had to be shifted from the edge of the sample, which will reduce the initial separation and increase the stiffness of the sample. Due to the fact that the cohesion zone model is very sensitive to input parameters, it is necessary to know many parameters and take into account a large number of factors. The practical importance of this work is to show how to use the VCCT model to obtain the critical load of the germination of the first crack. The research technique can be used for further experiments, including simulation further stratification with low inaccuracy.

Keywords: *polymer composite material, carbon fiber, interlayer crack resistance parameter, modeling, scale parameter of gradient theory.*

АНОТАЦИЯ

Актуальность заявленной в данной статье проблемы состоит в том, что с развитием авиакосмичной техники вырос спрос на материалы хорошого качества. Важным вопросом есть обеспечение прочности в условиях длительных нагрузок и в условиях развития повреждений. Один из критериев, который обеспечивает прочность материала, является трещиностойкость. Цель статьи заключается в исследовании межслоевой трещиностойкости (вязкости разрушения) при нагружении в условиях отрыва и поперечного сдвига, межслоевой прочности, а также влияния температуры на межслоевую прочность, механических свойств при растяжении. Приводится сравнение значений межслоевых трещиностойкостей G_{IC} (отрыв) и G_{IIC} (сдвиг), а также механических свойств при растяжении и межслоевой прочности образцов углепластиков. Основными методами к исследованию данной проблемы были метод короткой балки, метод DCB, метод ENF. Результаты экспериментальных данных были сопоставлены с моделированием процессов появления и развития трещин в конечно-элементных комплексов ABAQUS и Ansys на основе моделей VVCT, когезионных элементов. Были обнаружены отклонения от эксперимента и сделаны выводы, что точку приложения нагрузки необходимо сместить от края образца, что сократит величину изначального расслоения и увеличит жесткость образца. По причине того, что модель когезионной зоны является очень чувствительной к входным параметрам, необходимо знать множество параметров и учитывать большое количество факторов. Исследования показали, как с помощью модели VCCT получить критическую нагрузку прорастания первой трещины. Методика проведения исследования может быть использована для дальнейших опытов, в том числе для того, чтобы смоделировать дальнейшее расслоение с меньшей погрешностью.

Ключевые слова: *полимерный композиционный материал, углеродное волокно, параметр межслоевой трещиностойкости, моделирование, масштабный параметр градиентной теории.*

---

1. INTRODUCTION

To create modern aerospace technology, we need materials with high strength, hardness, heat resistance, corrosion resistance, other characteristics, and the combination of these properties. Fiber composites based on polymer matrices are promising structural materials, as they have high specific characteristics of strength and rigidity. Currently, these materials are increasingly being used as part of aviation, space, transport and other structures (Kablov, 2012; Borschev and Gusev, 2014). For example, in promising aircraft products, the weight of polymer composite material in project exceeds 50%: Boeing 787 (USA) – 50%, Airbus A380 (Europe) – 30%, Airbus A 350 (Europe) – 50% (Krylov *et al.*, 2016; Savin, 2012). In a promising Russian-made aircraft of MS-21 family, a composite design of wing and tail structures was introduced (Savin, 2014). This is caused by the requirements for the weight efficiency of products, to satisfy which it is necessary to use materials with a high level of specific properties (Shejko *et al.*, 2017). The use of composite materials in the aviation industry significantly reduces material consumption of structures, increases material use rate up to 90%, reduces the number of equipment and dramatically reduces the complexity of manufacturing structures by several times reducing the number of parts included in them (Savin, 2014).

Nonetheless, there are many problems specific to layered composite materials that limit their scope of application. One of the main issues that are uncounted in the design of structures made of polymer composite materials is ensuring durability under conditions of long-term loads and

Downloaded from www.periodico.tchequimica.com

conditions of damage development. In particular, such parameters as interlayer strength and crack resistance (Yakovlev *et al.*, 2014) are important and determining for strength. The importance of these characteristics is caused by the fact that cracks begin to develop in the weakest point of polymer composite material – the matrix and the interfacial zone (Figure 1).

Studies have shown that the behavior of composite materials under static and cyclic loading cannot be reliably described by classical theories. For a more accurate assessment of the durability and resource characteristics of the material, comprehensive tests are required, including tests aimed at determining the parameters of crack resistance. To assess the stress-strain state of multilayer structures, we can use the final parameter of fracture mechanics – the intensity of energy release (Finogenov and Erasov, 2003). Then, the Virtual Crack Closure Technique (VCCT) is used (Liu and Islam, 2013; Krueger, 2013; Senthil *et al.*, 2013). Now, one of the main tools for numerical solution of problems of modeling bundle growth is the finite element method (Landry and La Plante, 2012; Muñoz *et al.*, 2006).

The use of interface elements based on the CZM (Cohezive Zone Model) model (Kuznetsova *et al.*, 2015) allows us to study the initiation and development of the bundle without specifying the initial defect and rearrangement of the finite element mesh during its propagation. Theoretical and experimental study of crack resistance parameters is a relevant problem of modern mechanics of composite materials. Thus, the relevant task is to study the mechanical properties, and, in particular, the crack resistance parameters of carbon fiber based on experimental and theoretical methods (Lurie *et al.*, 2015; Lomakin *et al.*, 2017; Formalev and Kolesnik, 2017; Kolesnik *et al.*, 2015; Lomakin *et al.*, 2018; Lurie *et al.*, 2017; Bulychev *et al.*, 2018; Formalev *et al.*, 2016; Rabinsky and Turchavina, 2019; Kakhramanov *et al., 2017;* Rabinsky and Turchavina, 2018). To determine the mechanical characteristics of PCM, a number of experimental studies were carried out using standard methods: the study of shear strength by the short beam method, the study of tensile strength, the finding the specific work of delamination under tear conditions G_{IC} according to the DCB method and under transverse shear G_{IIC} according to the ENF method.

2. MATERIALS AND METHODS

Mechanical tests were performed at Instron 5969 test equipment. This machine and the set with which it is equipped to meet all that is required by the ASTM (ASTM: Active Russian Standards, 2019) standards that describe the test procedure.

2.1. Interlayer shear durability of short plates

To study the durability of short plates, the samples were tested for three-point bending. 3 batches were tested, 7 samples for each. The testing base for the first batch was 10 mm, for the second – 8.55 mm, for the third – 8.6 mm. The loading roller of the testing machine has a radius of 5 mm, and radius of supports is 2 mm. The samples were rectangular plates, the parameters of which are 15×2.44×4.95; 12×2.15×4.37; 12×2.16×4.28 respectively for the first, second and third parties (Figure 2). All the samples were measured and numbered. The geometry of the samples and the value of the base were recorded in protocol, as well as in program. Each sample was checked for defects prior to installation into the test machine. During testing, the nature of the destruction of the sample was determined using a camera with big magnification (Figure 3).

2.2. The tension tests

The tension tests were conducted according to ASTM D3039 Standard Test Method (ASTM: Active Russian Standards, 2019) for Tensile Properties of Polymer Matrix Composite Materials. The nature of the method is as follows: a tensile load is applied to the sample, the vector of which coincides with its main axis, at a constant speed until a fracture occurs, or until the stress (load) or deformation (tension) reaches the specified value (Figure 4). During the test, the load and elongation of the sample are being measured (Figure 5).

2.3. Finding the magnitude of specific work of separation in terms of separation G_{IC} according to the DCB method

Finding the magnitude of the specific work of the separation under separation conditions was performed according to ASTM D5528 (ASTM: Active Russian Standards, 2019). The specific work of separation is the limit of the ratio of change in elastic energy accumulated in the sample when it is loaded to the infinitely small increment of the area of the interlayer crack.

Downloaded from www.periodico.tchequimica.com

The method consists in testing under conditions of loading by separation of a sample with preliminary separation at its end located at the center of thickness. Tearing forces are applied to the sample through loops (Figure 6) that adhere to opposite surfaces at one end of the sample. In the time of the test, the applied force and crack length are recorded.

2.4. Finding the magnitude of the specific work of stratification under transverse shear conditions G_{IIC} according to the ENF method

The procedure of the test is described in the standard ASTM D7905 (ASTM: Active Russian Standards, 2019) (Figure 7). The nature of the method is to make the test with a constant speed of loading a three-point bend of the sample in the form of beam, at the end of which stratification is performed, located in the center of the thickness. During testing, the applied force, the displacement of the central support and the length of the crack were recorded.

3. RESULTS AND DISCUSSION:

Based on the data obtained, graphs of the dependence of the load on displacements during the interlayer shear were constructed (Figure 8). Figure 9 shows the results of tensile testing of samples. The calculation of the value of specific work of separation in terms of separation G_{IC} and under shear conditions G_{IIC} was carried out in full accordance with ASTM D5528 and D7905 (ASTM: Active Russian Standards, 2019). Based on the experimental data, the graphs were made (Figure 10, 11). The experimental data were compared with the model of the processes of appearance and development of cracks in the finite element complexes ABAQUS and Ansys based on the VVCT models and cohesive elements (Figure 12).

As a result of the numerical calculation at the first stage, the following dependences were received (Figure 13). The obtained dependencies cannot be considered reliable. The critical load deviation from the experimental is about 15%. There is also a significant discrepancy between the elasticity properties. It can be caused by many factors:

- mistakes made during experimental studies, which led to the assignment of incorrect material constants;
- inaccurate specification of the boundary conditions: during the experiment, some samples deviated from horizontal arrangement, which was caused by the asymmetric arrangement of the loops;
- inaccurate setting of the properties of CZM material: for example, Artificial Damping Coefficient can significantly affect the critical load (Figure 14) (this ratio of artificial damping is needed to stabilize the numerical solution, the smaller it is, the smaller the integration step over time), as well as critical delamination energy (Figure 15); in addition, the value of critical energy of separation in processing the results had a significant scatter, to the extent of difference in two or more times.

Another factor that affects the results is the application of loading to the sample. It can be that the loop that was used in the experiment contacted by the entire surface with the sample. Moreover, the force was applied through the loop mechanism. All this could cause redistribution of stresses in contact zone of the loop and the sample. In the process of modeling, it was supposed that this way, the point of application of the load could be shifted from the edge of the sample, which, in turn, will reduce the value of initial delamination and increase the stiffness of the sample (Figure 1-6).

4. CONCLUSIONS:

We have performed an experimental and theoretical study of the mechanical properties of composite materials reinforced with carbon filler. As a result, the testing procedure for PCM aimed at research was developed. interlayer strength, as well as the effect of temperature on interlayer strength; mechanical properties of composites materials; determining the magnitude of the specific work of delamination under separation conditions G_{IC} according to the DCB method and under transverse shear conditions G_{IIC} according to the ENF method. An experimental base was developed, practical recommendations for further studies of layered PCMs were offered. Carbon fiber samples with different densities of reinforcing filler were tested. A comparison was made of the values of parameters for interlayer crack resistance G_{IC} and G_{IIC}, and interlayer strength, mechanical tensile properties for different batches of samples.

A significant effect of temperature on the interlayer strength of layered PCMs was demonstrated. The results of the experimental data were compared with modeling of processes of appearance and development of cracks in the finite element complexes ABAQUS and Ansys based on the VVCT models, cohesive elements,

Downloaded from www.periodico.tchequimica.com

and gradient theory of elasticity; the scale parameter of gradient theory of elasticity was identified. By using the VCCT model, it was possible to obtain only the critical load of the growth of the first crack, further stratification using this model could not be modeled, the results obtained did not correlate with experimental data at all.

The cohesion zone model is very sensitive to input parameters. To find solutions within the framework of this model, it is necessary to know the parameters of crack resistance, which can only be learned by experiment on special samples using certain methods. This model also requires a fine mesh and exact adjustment of the solver. Within the framework of this model, it was possible to track the appearance of the first crack, and also to trace the further development of the crack within the first three growth stages with an acceptable error.

5. ACKNOWLEDGMENTS:

The work was carried out with the financial support of the state project of the Ministry of Education and Science project code 2.9219.2017 / 8.9.

6. REFERENCES:

1. ASTM: *Active Russian Standards*, **2019**, https://www.astm.org/DATABASE.CART/russian.html, accessed 4 October 2019.
2. Borschev, A. V., Gusev, Yu. A. *The Aviation Materials and Technologies,* **2014**, *S2*, 34-38.
3. Bulychev, N. A., Kuznetsova, E. L., Bodryshev, V. V., Rabinskiy, L. N. *Nanoscience and Technology. An International Journal,* **2018**, *9 (2)*, 91-97.
4. Finogenov, G. N., Erasov, V. S. *The Aviation Materials and Technologies,* **2003**, *3*, 62-67.
5. Formalev, V. F., Kolesnik, S.A. *Journal of Engineering Physics and Thermophysics*, **2017**, *90 (6)*, 1302-1309.
6. Formalev, V. F., Kolesnik, S. A., Kuznetsova, E. L., Rabinskii, L. N. *High Temperature*, **2016**, *54 (3)*, 390-396.
7. Formalev, V. F., Kolesnik, S. A., Kuznetsova, E. L., Rabinskiy, L. N. *International Journal of Pure and Applied Mathematics*, **2016**, *111 (2)*, 303-318.
8. Kablov, E.N. *Bulletin of Russian Academy of Sciences*, **2012**, *82 (6)* .520-530.
9. Kakhramanov, R. M., Knyazeva, A. G., Rabinskiy, L. N., Solyaev, Y. O. *High Temperature,* **2017**, *55 (5*), 731-736.
10. Kolesnik, S. A., Formalev, V. F., Kuznetsova, E. L. *High Temperature,* **2015**, *53 (1)*, 68-72.
11. Krueger, R. *Applied Mechanics Reviews,* **2013**, *57 (1-2)*, 109-143.
12. Krylov, V. D., Yakovlev, N. O., Kurganova, Yu. A., Lashov, O. A. *The Aviation Materials and Technologies*, **2016**, *40 (1)*, 79-85.
13. Kuznetsova, E. L., Leonenko, D. V., Starovoitov, E. I. *Mechanics of Solids*, **2015**, *50 (3)*, 359-366.
14. Landry, B., La Plante, G. *Composites Part,* **2012**, *43 (2)*, 533-541.
15. Liu, P. F., Islam, M. M. *Composite Structure,* **2013**, *106*, 47-56.
16. Lomakin, E. V., Lurie, S. A., Belov, P. A., Rabinskii, L. N. *Reports of Physics*, **2017**, *62 (1)*, 46-49.
17. Lomakin, E. V., Lurie, S. A., Rabinskiy, L. N., Solyaev, Y. O. *Reports of Physics,* **2018**, *63 (4)*, 161-164.
18. Lurie, S. A., Kuznetsova, E. L., Rabinskii, L. N., Popova, E. I. *Mechanics of Solids*, **2015**, *50 (2)*, 135-146.
19. Lurie, S. A., Solyaev, Y. O., Lizunova, D. V., Rabinskiy, L. N., Bouznik, V. M., Menshykov, O. *International Journal of Heat and Mass Transfer,* **2017**, *109*, 511-519.
20. Muñoz, J. J., Galvanetto, U., Robinson, P. *International Journal of Fatigue*, **2006**, *28 (10)*, 1136-1146.
21. Rabinskiy, L. N., Tushavina, O. V. *Periodico Tche Quimica*, **2018**, *15 (1)*, 321-329.
22. Rabinsky, L. N., Tushavina, O. V. *STIN*, **2019,** *4*, 22-26.
23. Rabinskiy, L. N., Tushavina, O. V. *INCAS Bulletin,* **2019**, *11 (Special Issue)*, 203-211.
24. Savin, S. P. *News of Samara Scientific Center of the Russian Academy of Sciences,* **2012**, *4 (2)*, 686-693.
25. Senthil, K., Arockiarajan, A., Palaninathan, R., Santhosh, B., Usha, K. M. *Composite Structure,* **2013**, *106,* 139-149.
26. Shejko, S., Shalomeev, V., Mishchenko, V. *Materials Science and Technology Conference and Exhibition*, **2017**, *1 (2017)*, 238-244.
27. Yakovlev, N. O., Akolzin, S. V., Shvets, S. M. *Materials Science News. Science and Technology,* **2014**, *4*, 1-10.

Downloaded from www.periodico.tchequimica.com

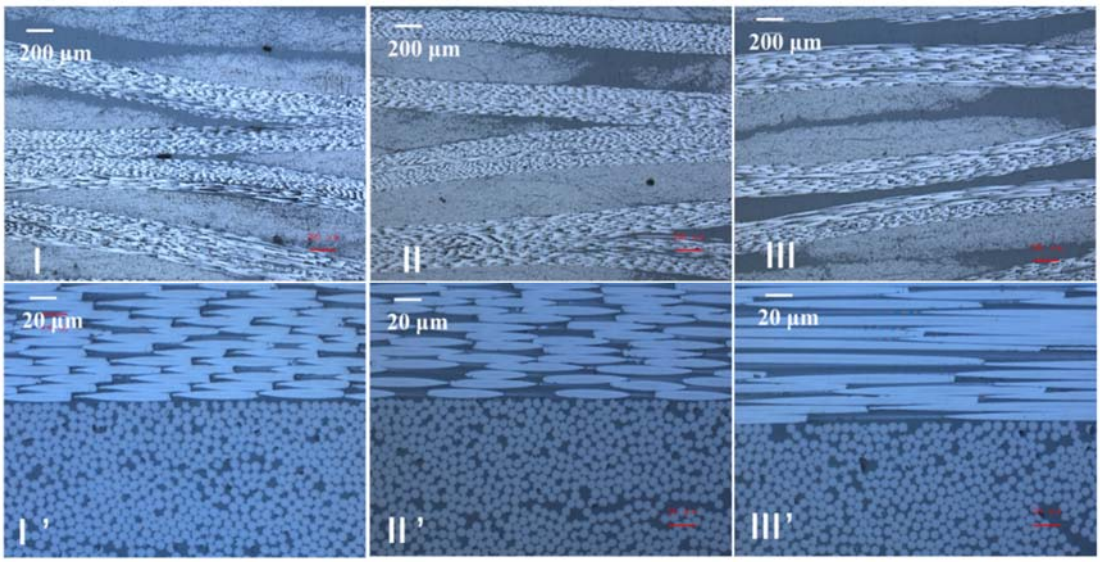

Figure 1. *The structure of polymer composite material*

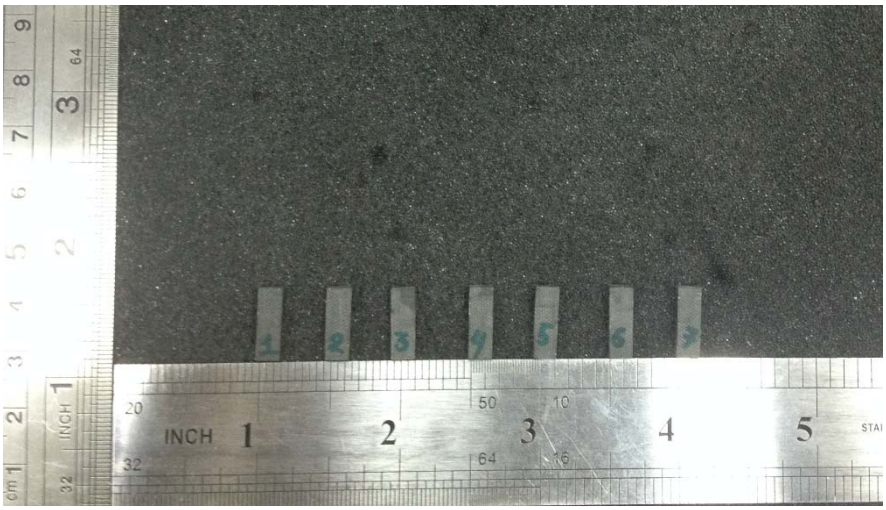

Figure 2. *Samples for studying the durability at the interlayer shear*

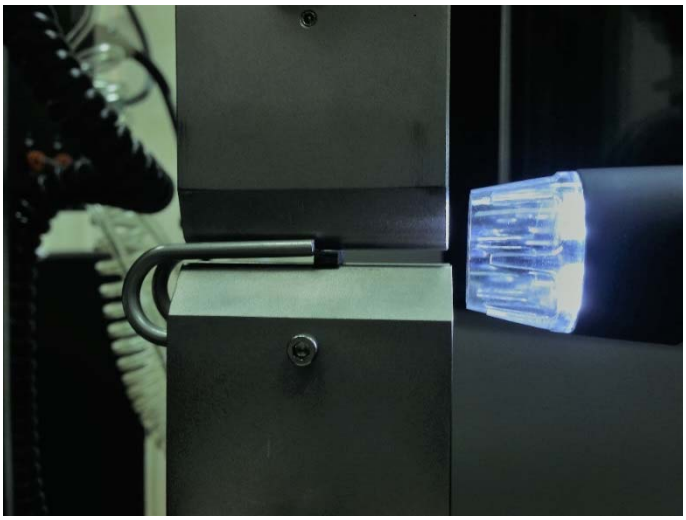

Figure 3. *View of a sample placed in the testing machine. On the right is the magnification camera*

Downloaded from www.periodico.tchequimica.com

Figure 4. *Labeled tensile test sample mounted in mechanical grips before and after the test*

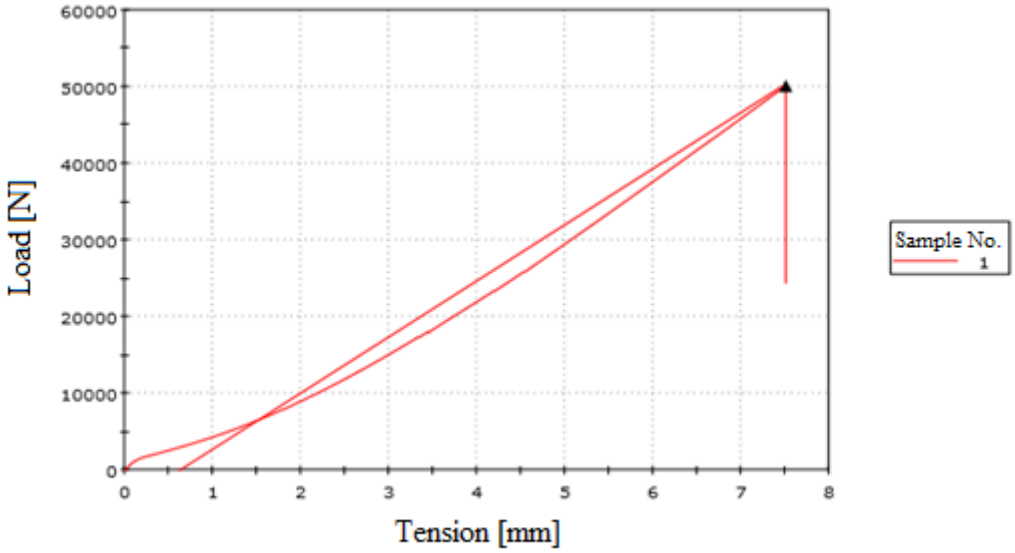

Figure 5. *Load-displacement diagram for tensile testing sample*

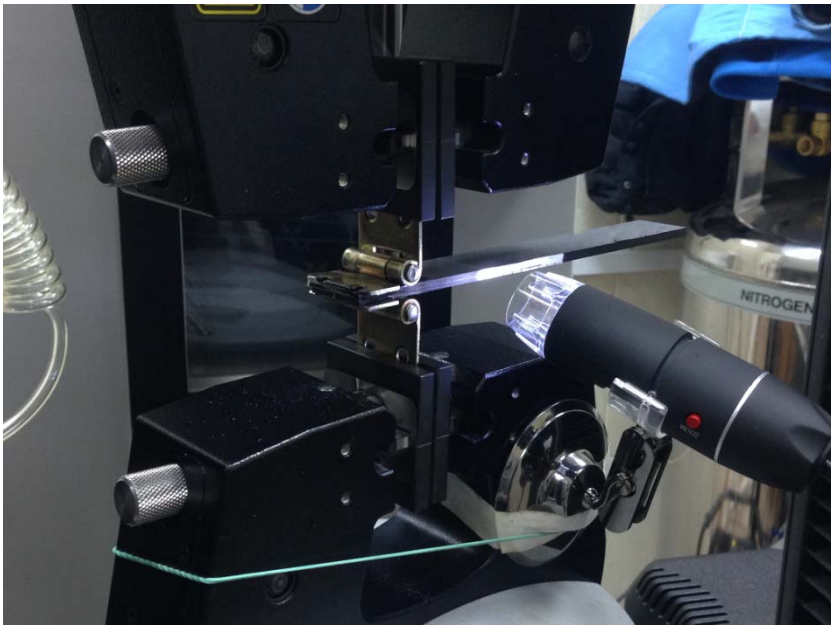

Figure 6. *Testing according to ASTM D5528 (ASTM: Active Russian Standards, 2019)*

Downloaded from www.periodico.tchequimica.com

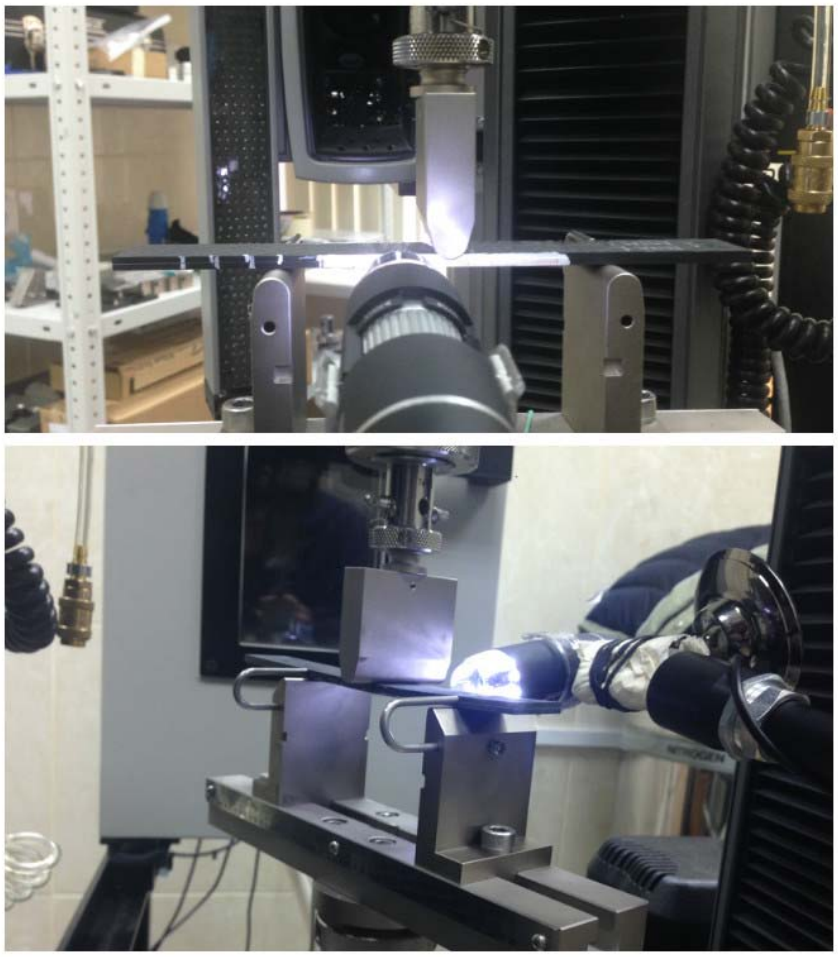

Figure 7. *Tests according to ASTM D7905*

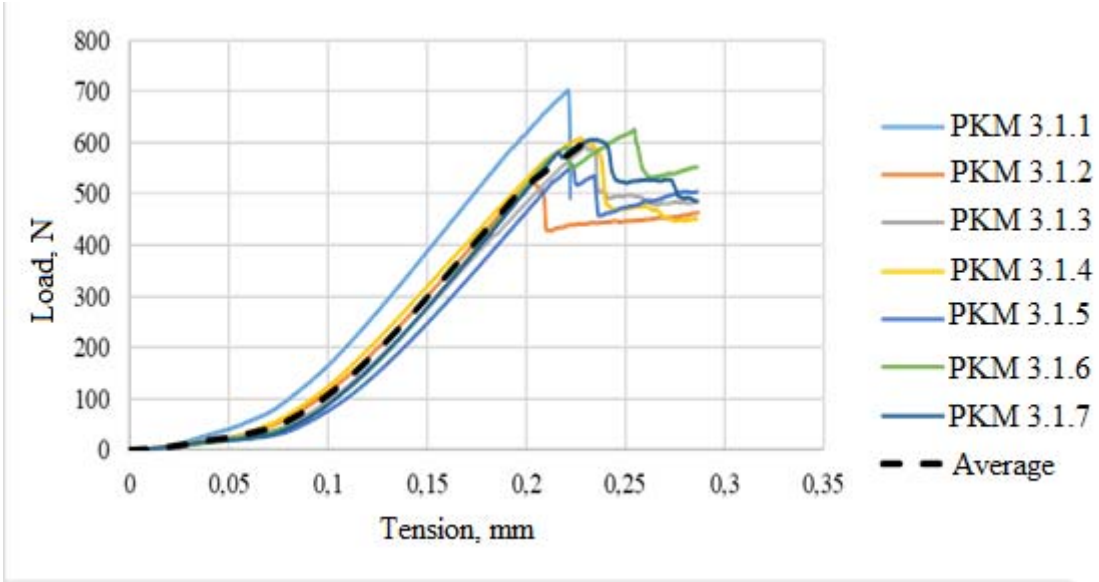

Figure 8*. The Load-displacement diagram*

Downloaded from www.periodico.tchequimica.com

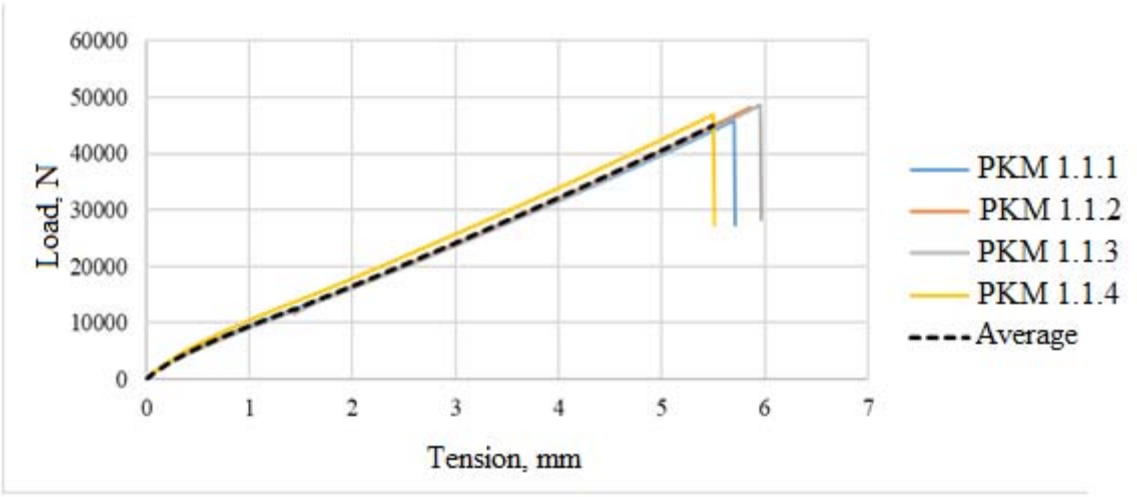

Figure 9. *Diagram of load-displacement for RMB 1.1*

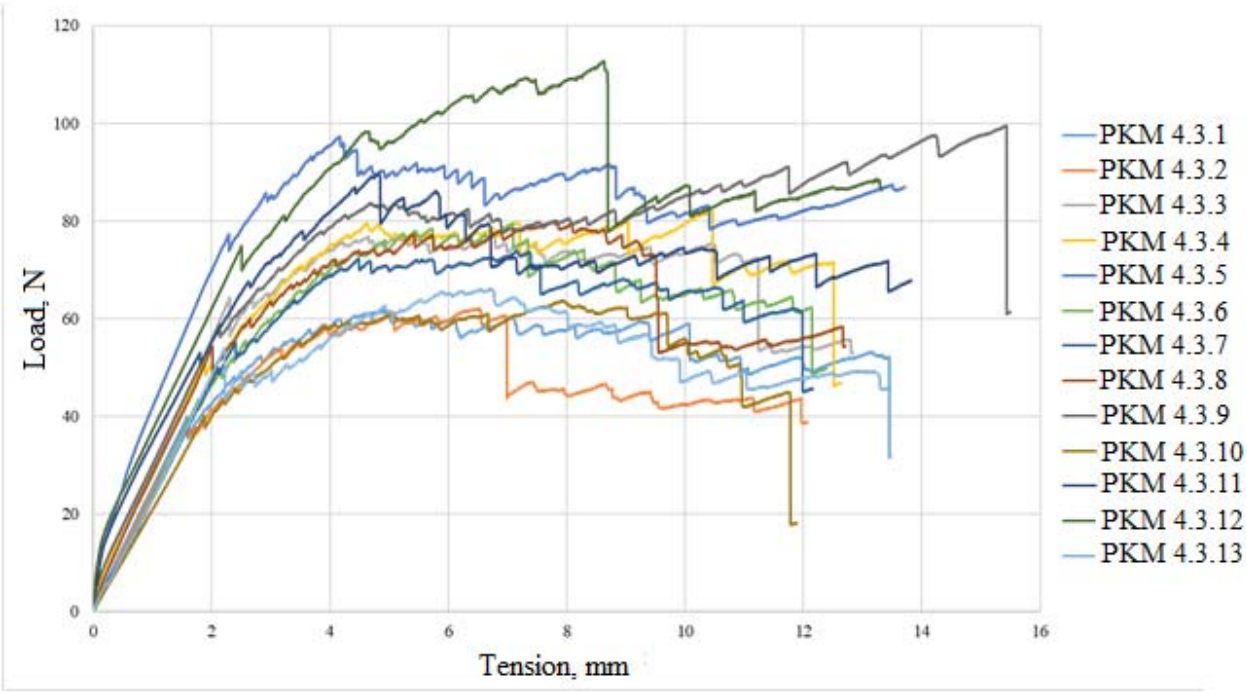

Figure 10. *The Load-displacement diagram in tests on fracture toughness by DCB method*

Downloaded from www.periodico.tchequimica.com

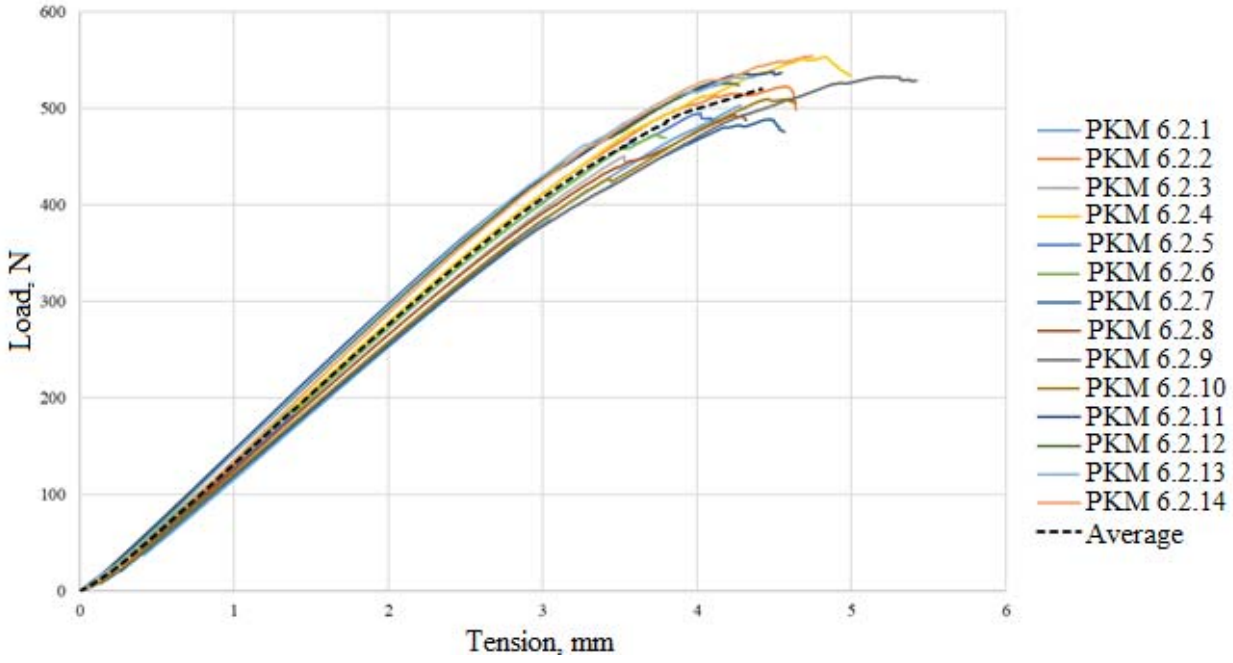

Figure 11. *The Load-displacement diagram on fracture toughness tests according to ENF*

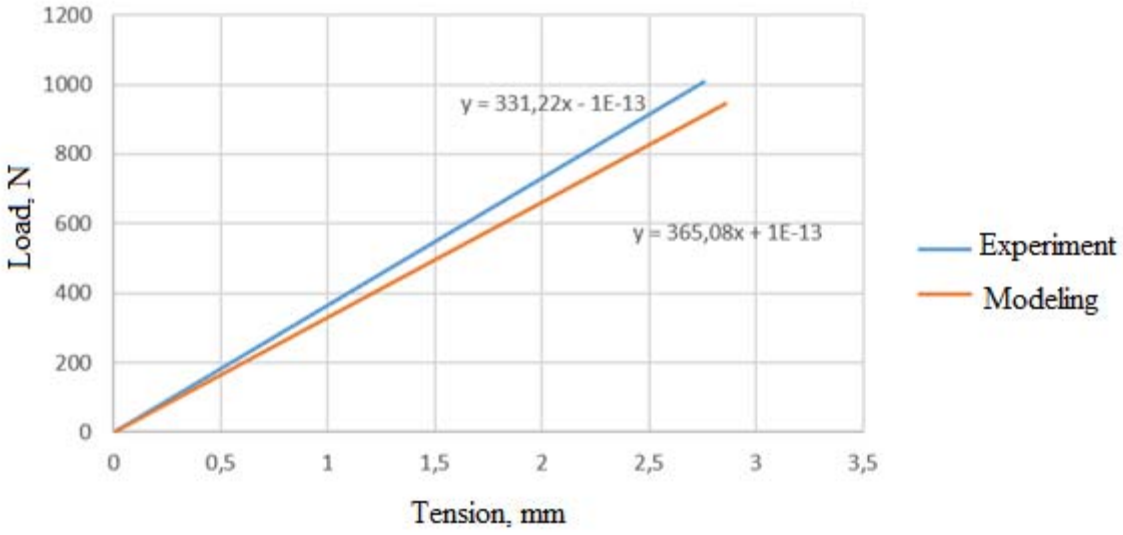

Figure 12. *Comparison of experimental and simulation results with the use of the VCCT model*

Downloaded from www.periodico.tchequimica.com

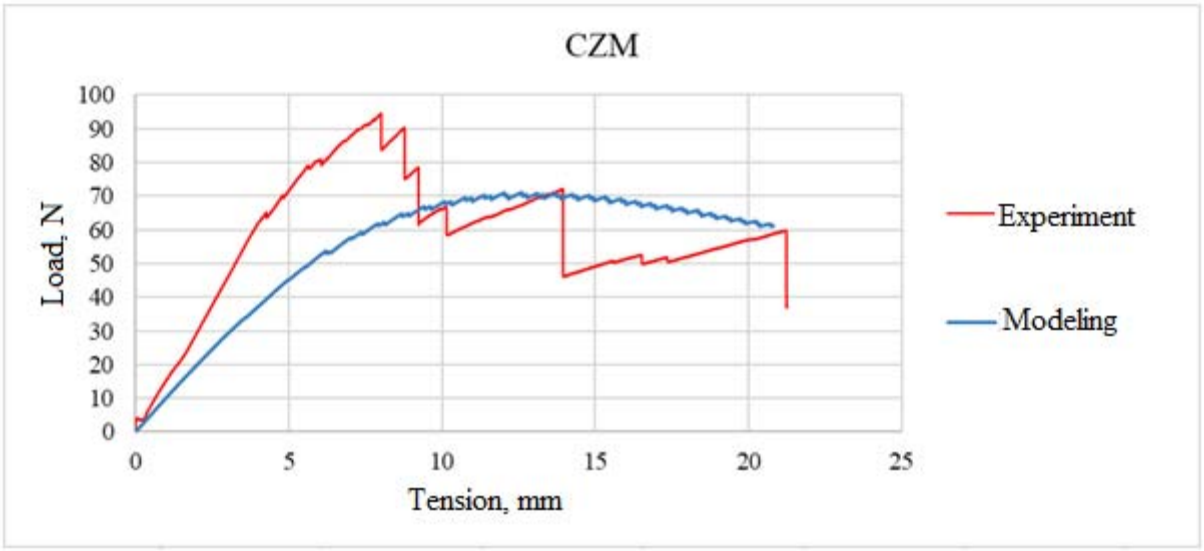

Figure 13. *Comparison of simulation and experiment data*

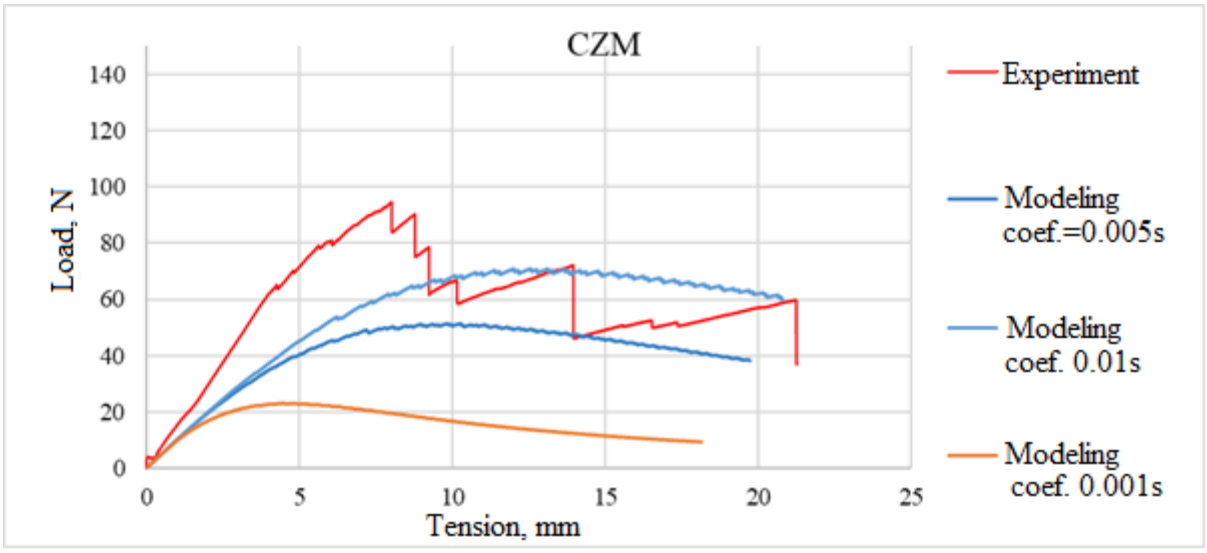

Figure 14. *Influence of damping coefficient*

Downloaded from www.periodico.tchequimica.com

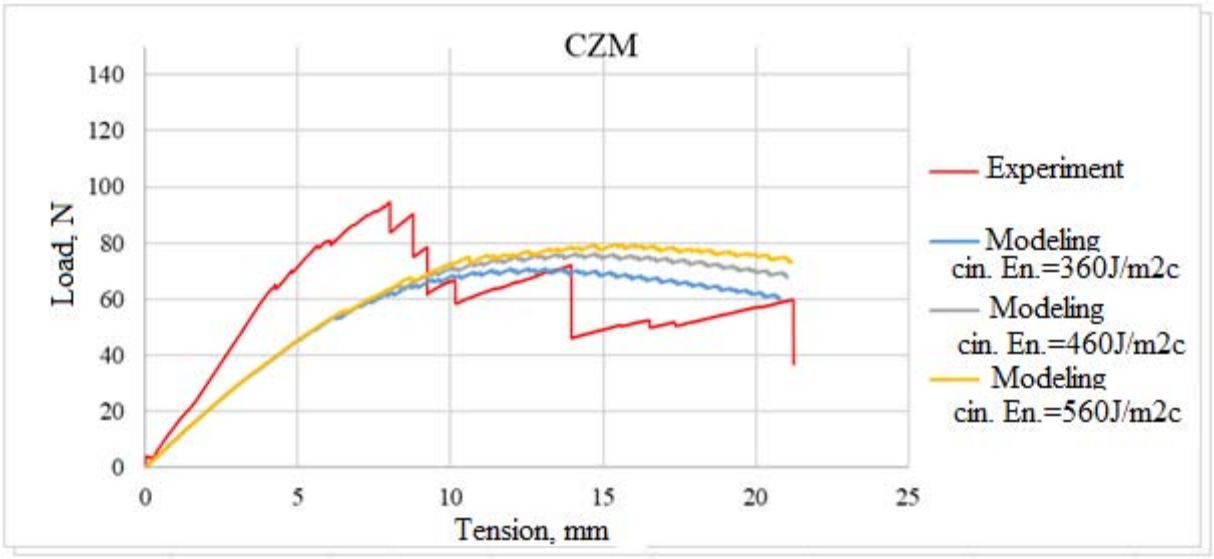

Figure 15. *The influence of critical energy of stratification*

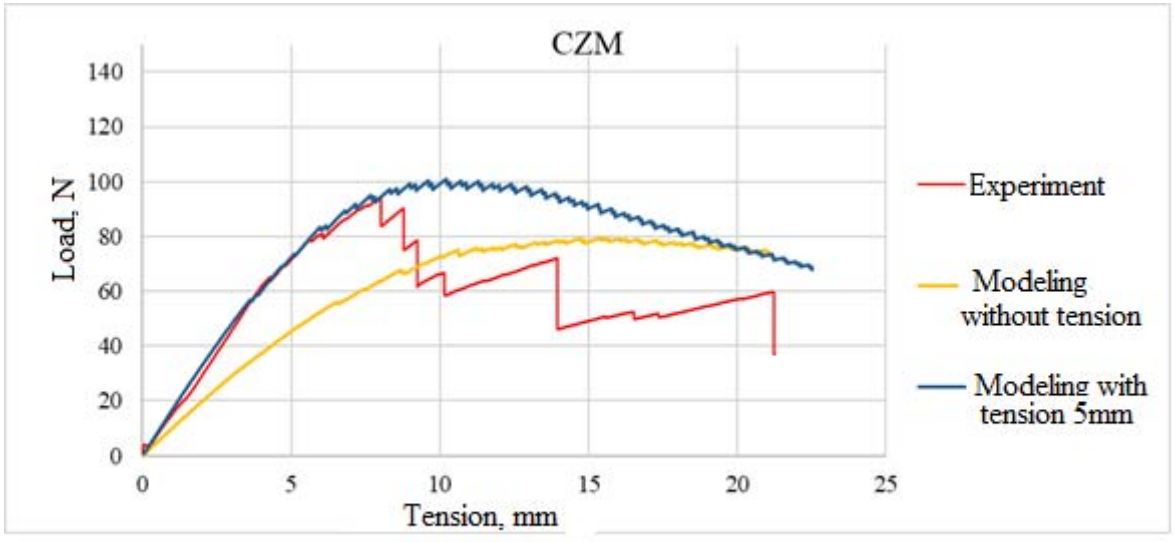

Figure 16. *Influence of point of load application*

Downloaded from www.periodico.tchequimica.com

PERIÓDICO TCHÊ QUÍMICA
ARTIGO ORIGINAL

PURIFICAÇÃO DE ELETRÓLITO ALCALINO DE PRODUTOS DE REAÇÃO DISSOLVADOS DURANTE A OPERAÇÃO DA FONTE DE CORRENTE QUÍMICA DE AR E ALUMÍNIO

PURIFICATION OF ALKALINE ELECTROLYTE FROM DISSOLVED REACTION PRODUCTS DURING WORK OF THE AIR-ALUMINUM CHEMICAL CURRENT SOURCE

ОЧИСТКА ЩЕЛОЧНОГО ЭЛЕКТРОЛИТА ОТ РАСТВОРЕННЫХ ПРОДУКТОВ РЕАКЦИИ В ПРОЦЕССЕ РАБОТЫ ВОЗДУШНО-АЛЮМИНИЕВОГО ХИМИЧЕСКОГО ИСТОЧНИКА ТОКА

OKOROKOVA, Nadezhda S.[1*]; PERCHENOK, Aleksandr V.[2]; SUVOROVA, Elena V.[3]; FARMAKOVSKAYA, Ariadna A.[4]

[1,3,4] Moscow Aviation Institute (National Research University), Department of Physical Chemistry, 4 Volokolamskoe shosse, zip code 125993, Moscow – Russian Federation

[2] LLC “Energoclub”, 26/21 Zoi and Aleksandra Kosmodemyanskikh Str., zip code 125130, Moscow – Russian Federation

** Correspondence author*
e-mail: ok.nadezhda@mail.ru

Received 22 May 2019; received in revised form 01 October 2019; accepted 23 October 2019

RESUMO

A relevância do artigo se baseia no fato de que a criação de usinas de energia elétrica com fontes de corrente química de ar e alumínio está na fase de desenvolvimento e teste de amostras e protótipos. O objetivo do artigo é calcular as dimensões do circuito eletrolítico e do cristalizador. Foram realizados estudos experimentais da cinética do processo de decomposição de soluções de aluminato de potássio na faixa de temperatura e composição correspondentes às condições operacionais de usinas de energia elétrica com fontes de corrente química de ar e alumínio para diversos fins. O artigo apresenta os resultados da aplicação de vários métodos de purificação do eletrólito alcalino a partir de produtos de reação dissolvidos formados durante a operação de uma fonte de corrente química de ar e alumínio. Os parâmetros cinéticos da decomposição de soluções de aluminato são determinados experimentalmente, dependendo da temperatura, da concentração de alumínio dissolvido, da concentração de hidróxido de alumínio da semente e do tamanho da superfície da semente. As dimensões dos sistemas de purificação de eletrólitos de produtos de reação dissolvidos - o circuito de eletrólitos e o cristalizador – foram calculadas, o que aumentou significativamente o tempo de operação contínua de usinas com base na fonte de corrente química de ar e alumínio. Foi mostrado que, para uma usina de 100 W, o volume do cristalizador é de 1,3 L com uma concentração de sementes de 20% em peso. A massa de água consumida durante a operação da usina por 6 horas é de 1,4 kg.

Palavras-chave: *Instalação eletroquímica, purificação de eletrólitos, soluções supersaturadas de aluminato, cristalização, processo de decomposição da solução*.

ABSTRACT

The relevance of the article is based on the fact that the state of work on the creation of power sources (PS) with AA chemical current sources (CCS) is at the stage of development and testing of prototypes. The purpose of this article is to calculate dimensions of the electrolyte circuit and the crystallizer. There were experimental studies of the decomposition kinetics of the process solutions of potassium aluminate in the range of temperatures and compositions corresponding to operating conditions with PS AA CCS for various purposes. This study presents the results of applying various methods of cleaning an alkaline electrolyte from dissolved reaction products formed during the operation of an air-aluminum (AA) chemical current source (CCS). The kinetic parameters of decomposition of aluminate solutions were experimentally determined, depending on temperature, the concentration of dissolved aluminum, concentration of initial aluminum hydroxide and the size of the first surface. The dimensions of the electrolyte purification systems from dissolved reaction products — electrolyte circuit and crystallizer — were calculated, which significantly increased the time continuous operation of power

Downloaded from www.periodico.tchequimica.com

sources (PS) based on AA CCS. It was demonstrated that for a 100 W power supply, the crystallizer volume should be 1.3 l with initial concentration of 20 % of mass. The mass of water consumed during the operation of the PS for 6 hours is 1.4 kg.

Keywords: *Electrochemical installation, electrolyte purification, supersaturated aluminate solutions, crystallization, solution decomposition process.*

АННОТАЦИЯ

Актуальность статьи заключается в том, что состояние работ по созданию энергоустановок (ЭУ) с ВА химическими источниками тока (ХИТ) находятся на стадии разработки и испытания макетных и опытных образцов. Цель статьи – провести расчет габаритов электролитного контура и кристаллизатора. Были проведены экспериментальные исследования кинетики процесса декомпозиции растворов алюминатов калия в интервале температур и составов, соответствующим условиям работы ЭУ с ВА ХИТ различного назначения. В работе приведены результаты применения различных методов очистки щелочного электролита от растворённых продуктов реакции, образующихся при работе воздушно-алюминиевого (ВА) химического источника тока (ХИТ). Экспериментально определены кинетические параметры процесса декомпозиции алюминатных растворов, в зависимости от температуры, концентрации растворенного алюминия, концентрации затравочного гидроксида алюминия и величины затравочной поверхности. Проведены расчеты габаритов систем очистки электролита от растворенных продуктов реакции – электролитного контура и кристаллизатора, позволяющих существенно увеличить время непрерывной работы энергоустановок (ЭУ) на основе ВА ХИТ. Показано, что для ЭУ мощностью 100 Вт объем кристаллизатора составляет 1,3 л при концентрации затравки 20 мас.%. Масса воды, расходуемой при работе ЭУ в течение 6 часов, равна 1,4 кг.

Ключевые слова: *Электрохимическая установка, очищение электролита, пересыщенные алюминатные растворы, кристализация, процесс декомпозиции растворов*.

---

1. INTRODUCTION

One of the most effective and promising electrochemical systems is oxygen- (air-) aluminum pair (O 2 / Al or AA) with aqueous electrolytes. Currently, the state of work on the creation of power sources (PS) with AA chemical current sources (CCS) is at the stage of development and testing of prototypes. They have high specific energy consumption (up to 700 W · h / kg) and a unique set of working properties: long-term storage before work and during pauses, complete explosion and fire safety, the absence of toxic components and work products, which determines the possibility of widespread use in various equipment (Skvortsov *et al.,* 2016; Skvortsov *et al.,* 2018).

An additional positive quality of the considered CCS is the possibility of using and processing the resulting reaction products. The resulting aluminum hydroxide can be a feedstock for aluminum production. In this case, the system can be considered as mechanically rechargeable with charge and discharge processes separated in space and time. Therefore, in terms of the energy, cost, technological, and operational characteristics, the oxygen-aluminum electrochemical pair is one of the most effective and promising combinations. The schematic diagram of AA CCS with alkaline electrolyte is shown in Figure 1. The main reactions and the place of their occurrence are shown there.

As we can see from the scheme, the main products of the AA CCS reaction are soluble aluminates and solid aluminum hydroxide $Al(OH)_3$. Currently, the causes of the functional failure of the AA CCS and the parameters affecting the resource of PS based on them are determined. It was demonstrated that the time of one operation cycle is limited by the process of passivation of the working surface of the anode with a film consisting of reaction products. We have developed several methods that can significantly increase the time of continuous operation of power units with AA CCS. The main ones are the use of corrosion inhibitors and anode depassivators in an electrochemical reaction (Pushkin *et al.,* 2018; Farmakovskaya *et al.,* 2018a; Farmakovskaya *et al.,* 2018b; Okorokova *et al.,* 2015a; Egan *et al.,* 2013; Li and Bjerrum, 2002; Doche *et al.,* 1997; Okorokova *et al.,* 2015b; Okorokova *et al.,* 2010; Okorokova *et al.,* 2011; Pushkin, 2014; Karonik *et al.,* 1988; Shao *et al.,* 2002; Soler *et al.,* 2007).

In addition, an analysis of the operability of AA CCS and PS based on them also showed that

Downloaded from www.periodico.tchequimica.com

in regimes with high current densities, the time of continuous operation and the life of the PS are limited both by passivation of the aluminum anode and destruction of the gas diffusion cathode by the formed dissolved and solid reaction products. It is possible to achieve an improvement in characteristics of the cell and increase in the operating life of electric actuator if conditions are created that reduce the concentration of reaction products in the electrolyte (Skvortsov *et al.,* 2000; Akbarov *et al.,* 2018; Burkov *et al.,* 2018; Gavryushin *et al.,* 2018).

The easiest way to clean the electrolyte from dissolved aluminates is the decomposition of supersaturated aluminate solutions by crystallization on seed aluminum hydroxide, followed by removal of solid $Al(OH)_3$.

Nonetheless, the available information on the kinetic parameters of the crystallization process and currently developed devices and methods for calculating such crystallizers relate to the processes of industrial production of aluminum and solutions of sodium aluminates. Thus, the development of a methodology for calculating a system for purifying an electrolyte from dissolved aluminates and crystals of aluminum hydroxide as applied to AA CCS is a very urgent task. In this study, we present the results of studies on the application of various methods of purification of alkaline electrolyte from dissolved reaction products formed during the operation of AA CCS. The kinetic parameters of the decomposition of aluminate solutions are experimentally determined, depending on temperature, the concentration of dissolved aluminum, the concentration of initial aluminum hydroxide and the size of the surface. The dimensions of electrolyte purification systems from dissolved reaction products — the electrolyte circuit and the crystallizer — were calculated, which made it possible to significantly increase the continuous operation time of the PS based on AA CCS.

2. MATERIALS AND METHODS

As was mentioned, to ensure long-term operation of a power source with high and stable characteristics, it is necessary to conduct continuous or periodic cleaning of the electrolyte from dissolved reaction products.

A decrease in the concentration of aluminum in the electrolyte supersaturated with aluminates can also occur during natural crystallization. Nonetheless, due to the tendency of alkaline aluminate solutions to high supersaturations, this process either does not develop at all or proceeds at an insufficient rate.

The composition of aluminate solutions can be characterized by the concentration of alkali, aluminum, and aluminum hydroxide expressed in mass %, g/l or mol/l. While, the widely used characteristic of the studied solutions is the supersaturation value for aluminum, determined by three main values: absolute supersaturation C, relative supersaturation d and degree of supersaturation p, which are respectively equal to (Equations 1-3). Where C – is the concentration of aluminum in the solution, C_p – is the equilibrium concentration of aluminum.

In some cases, to characterize aluminate solutions, the values of alkaline and acid N modules representing molar ratios were used (Equations 4-5).

The features and behavior of aluminate solutions, in particular, the possibility of high supersaturation, stability, and delay of the decomposition process, reflect the patterns inherent in both true and colloidal systems. Thus, there are several different theories of the nature of aluminate solutions – colloidal, saline and mixed.

The salt theory, which treats aluminate solutions as ionic systems consisting of complex aluminate ions, is the most widely used. Aluminate solutions with a degree of supersaturation not exceeding p = 0.8 are characterized by six-fold coordination, leading to the formation of anions $Al(OH)_6^{3-}$. An increase in the degree of supersaturation promotes the polymerization of ions according to the scheme (Equation 6).

With ion dehydration $Al(OH)_4^-$ asymmetric oxyanions formed $AlO(OH)_2^-$ polymerize due to hydrogen bonds. It is also possible to have dehydration of concentrated solutions according to the scheme (Equation 7).

Usually, in solutions with alkali concentration of more than 10 mass% and a degree of supersaturation of more than one, the process of ion polymerization also occurs. $Al(OH)_4^-$. While, the most stable polymer groups are those that, with varying degrees of polymerization, do not change the sign and number of charges. This condition is satisfied in the case of combining ions $Al(OH)_4^-$ into dimers, trimers, and ultimately into polymers. Thus, the formation of polymer compounds of aluminum ions can be as follows (Equation 8) or in general form (Equation 9).

This polymerization scheme takes into account the possible association of aluminum ions by forming bridges $-Al-O-Al-$. Additional confirmation of the course of polymerization of

Downloaded from www.periodico.tchequimica.com

anions $Al(OH)_4^- \rightleftarrows AlO_2^- + 2H_2O$ is provided by the fact that when a certain concentration of aluminum is reached, all hydroxyl ions will be bound into these polymers. Nonetheless, a much larger amount of aluminum can be dissolved in such solutions, for which it is necessary to have free OH – ions , the formation of which is possible as a result of the polymerization of aluminum anions according to Equation (9).

In the absence of strong decomposition initiators (solid phases, impurities, additives), aluminate solutions are quite stable and can stay in a metastable state for a long time. The polymerization process in this case, in this case, is balanced by the depolymerization process. For decomposition of an aluminate solution, it is necessary that the polymerization process ends with polycondensation – the release of a solid phase $Al(OH)_3$. Therefore, the course of the decomposition process in supersaturated aluminate solutions is determined by many factors, one of which is in which concentration range it occurs

A stable state of solution corresponds to concentrations less than or equal to equilibrium, and its crystallization without changing the state is impossible. The metastable range can be divided into two zones. The first one is between the equilibrium concentration and the concentration below which spontaneous crystallization is practically impossible, but possible using seed crystals. The second zone corresponds to concentrations at which spontaneous formation of crystals is possible, but, as a rule, crystallization does not occur immediately, but after a certain period of time, called the induction time (period).

The zone of the labile state of supersaturated aluminate solution is characterized by the fact that crystallization in it occurs instantly. For a complete understanding of the behavior of aluminate solutions formed during the operation of AA CCS and the course of the formation of solid reaction products in them, it was necessary to determine the boundaries of the metastable and labile zones of the state of solutions depending on alkali concentration and temperature.

We have chosen a method based on measuring the time of induction of spontaneous crystallization of solution with varying degrees of supersaturation. It was believed that the concentration of solutions that have an induction time tending to infinity corresponds to the first zone of the metastable region. The concentration of solutions with finite induction time corresponds to the second zone of metastability.

The induction time of the self-decomposition process, tending to zero, have solutions located in the labile region of the state. Nonetheless, the determination of true limiting supersaturations by this method is fraught with serious difficulties, consisting of the difficulty of accurate experimental measurement of extremely small values of induction periods. Thus, it is practically considered that if the time before the start of the crystallization process does not exceed one minute, the solution is in a labile state. Experiments were done for three alkali concentrations of 12, 16 and 20 mass% in the temperature range from 303 to 353 K. The experimental data are presented in Figures 2-4.

Based on the obtained data, the influence of temperature on the position of the boundaries of metastable and labile regions of the state of studied solutions was established (Figures 5-6).

Figure 5 demonstrates the absolute amount of aluminum that can be dissolved in an alkali solution corresponding to the working concentration of the electrolyte (20 mass%), and Figure 6 shows the real degrees of supersaturation that can be attained in one or another area of the state of the studied supersaturated aluminate solutions. The obtained results indicate that an increase in the concentration of alkali and, accordingly, the amount of hydroxide ions, leads to an increase in concentration of dissolved aluminum.

Nonetheless, the width of the metastable region has not changed. The relative size of the metastable region (Figure 6), in this case, decreases significantly. The obtained temperature dependences (Figure 5) demonstrate that with increasing temperature the metastable region narrows and, accordingly, the stability of aluminate solutions decreases, which, apparently, is a consequence of an increase in the rate of ion diffusion $Al(OH)_4^-$ accelerating the processes of polymerization and polycondensation.

Considering the abovementioned, we came to the conclusion that in the PS based on AA CCS it is necessary to carry out the forced decomposition of the electrolyte, in which supersaturated aluminate solutions crystallize on specially introduced seed crystals either in the electrolyte circuit or in a special device — the crystallizer according to the reaction (Equation 10).

For calculation of the dimensions of electrolyte circuit and crystallizer, we made experimental studies of the kinetics of decomposition of potassium aluminate solutions in

Downloaded from www.periodico.tchequimica.com

the temperature and composition range corresponding to the operating conditions of PS with AA CCS for various purposes and obtained data on the rates of this process depending on various factors. We studied solutions with a potassium alkali concentration of 12-22 mass% in the temperature range 293-333 K.

As initiating crystals, specially prepared or industrial aluminum hydroxide was used. The specific surface of the seed crystals was calculated based on the measurement of the particle size distribution of initiating aluminum hydroxide. Then, we proceeded from the following considerations that if particles are assumed to be spherical and identical in size, then their specific surface is equal to (Equation 11). Where r is the density of seed; d 1 is particle diameter of the seed.

3. RESULTS AND DISCUSSION:

As it was shown by the differential particle size distribution curves (Figure 7), the aluminum hydroxide used for the seed was a polydisperse powder, the specific surface of which was determined as the sum of the specific surfaces of the particles in the entire size range (Equation 12). Where N_1 – is a fraction of particles of diameter d i in the measured sample.

The total seed surface in solution was (Equation 13). Where C_s – is the concentration of seed.

Since the decomposition rate constant is directly proportional to the seed surface, the linear growth constant of crystals, k_{log}, was calculated from the slope of the straight line $k_{dec} = f(S)$, and then k_{dec} (Equation 14). Where $K_v = 3a/b$ – is coefficient of matching the volume of powder particles with their surface; a, b – volumetric and surface form factor; for particles with a diameter of 2 to 20 μm, the coefficient $K_{v\,is}$ estimated at 2.9.

The rate constants of the crystallization process of aluminum hydroxide at various temperatures were used to calculate the activation energy of this process according to the Arrhenius equation (15). Where Ea – is the activation energy of the decomposition process.

The crystallization process of aluminum hydroxide is characterized by the energy of activation equal to 54 ± 2 kJ/mol and does not depend on the composition of aluminate solution and the type of seed aluminum hydroxide.

Kinetic curves of the decomposition process of studied solutions, showing the dependence of the processing speed on various factors are shown in Figures 8 and 9 .The effect of alkali concentration on the decomposition of supersaturated aluminate solutions is shown in Figure 8, and the effect of temperature is shown in Figure 9. As we can see from the above data, an increase in alkali concentration and temperature leads to a decrease in the stability of aluminate solutions and an increase in the rate of their decomposition.

A typical kinetic dependence is illustrating the effect of the concentration of dissolved aluminum on the decomposition rate shown in Figure 10. It is non-linear and, regardless of other parameters, is described by a second-order kinetic equation (16):

where k_{dec} – is the deposition rate constant; C and C_{eq} are the current and equilibrium aluminum concentrations, respectively.

Processing the obtained experimental data using a derived equation shows that the crystallization rate constant depends on the amount of seed (Figure 11) and, accordingly, the seed surface (Figure 12).

The studies of decomposition processes allowed us to determine the main parameters of the PS cleaning units – the electrolyte circuit and the crystallizer – and to maintain the optimal electrolyte composition at the input of the AA battery. The optimal parameters of the electrolyte circuit were estimated based on obtained values of decomposition rates. The time interval necessary for the crystallization process to take place was calculated by the formula (Equation 17). Where – dC / dt – is the crystallization rate. ΔC Al is the increase in the concentration of dissolved aluminum in electrolyte, which is equal to (Equation 18). Where C_{Al}^{1} , C_{Al}^{2} – are respectively, the concentration of aluminum at the input and output of the battery; M_{Al} – second consumption of aluminum; Q_{el} – electrolyte consumption through the battery.

The time required for decomposition should be provided by corresponding lengths of the electrolyte path in the circulation circuit and its speed (Equation 19). Where n – is the number of contour sections in which crystallization occurs; l i, W i – are respectively, the length and velocity of the electrolyte flow in these areas. Estimates performed according to formulas 17-19 and experiments carried out on PS prototypes showed that at medium work capacities and high decomposition rates corresponding to high concentrations of dissolved aluminum, the crystallization process could occur in the

Downloaded from www.periodico.tchequimica.com

electrolyte circulation circuit.

To reduce the concentration of dissolved aluminum, it is possible to increase the amount of seed in the electrolyte, which will inevitably lead to a significant increase in energy costs for pumping the electrolyte and decrease the resource and reliability of the operation of PS units, therefore, in some cases it is necessary to intensify the process of electrolyte purification. As we mentioned above, it is possible to use a crystallizer, in which it is possible to create the required concentrations of the seed. Then, the required dimensions of the simplest crystallizer can be calculated using Equations (20) and (21). Where t_{cr} – is the time of the electrolyte stays in a crystallizer, L_{cr} – is the length of the crystallizer; W_{el} is the electrolyte flow rate in the crystallizer.

The volume of the crystallizer can be determined by the formula (Equation 22).

A schematic diagram of a continuous submersible crystallizer is demonstrated in Figure 13.

4. CONCLUSIONS:

The boundaries of metastable and labile regions of the state of supersaturated aluminate solutions were determined on model solutions corresponding to working concentrations of the primary electrolytes of AA CCS.

The experiments conducted for three KOH alkali concentrations of 12, 16, and 20 mass % in the temperature range from 303 to 353 K allowed us to determine the absolute amount of aluminum that can be dissolved in alkali solution corresponding to the working electrolyte concentration (20 wt%), as well as real degrees of supersaturation that can be achieved in a particular area of existence of studied supersaturated aluminate solutions. The obtained results indicate that an increase in the concentration of alkali and, accordingly, the amount of hydroxide ions, leads to an increase in the concentration of dissolved aluminum.

Nonetheless, the width of the metastable region is practically unchanged, and the relative size of the metastable region is significantly reduced. The obtained temperature dependences show that with increasing temperature the metastable region narrows and, accordingly, the stability of aluminate solutions decreases, which, apparently, is a consequence of an increase in the rate of ion diffusion $Al(OH)_4^-$ accelerating processes of polymerization and polycondensation.

On model solutions, the kinetic parameters of decomposition of aluminate solutions were experimentally established, in relation to the composition of the solutions obtained during the operation of AA CCS in various modes, depending on temperature, the concentration of dissolved aluminum, concentration of seed aluminum hydroxide and the seed surface. As seed crystals, we used specially prepared or industrial aluminum hydroxide with known particle size distribution. Based on differential particle size distribution curves, the total seed surface in solution was calculated.

For solutions with an alkali concentration of 12-22 mass% in the temperature range of 293-333 K, it was demonstrated that an increase in alkalinity and temperature of solutions with the same degree of supersaturation increases the decomposition rate. The dependence of decomposition rate on aluminum concentration is nonlinear and is described by a second- order kinetic equation. The crystallization rate constant depends on the amount of seed and, accordingly, the seed surface. Based on the values of the rate constants of the crystallization of $Al(OH)_3$ at various temperatures, the activation energy of this process was calculated, which is 54 ± 2 kJ / mol and it does not depend on the composition of the aluminate solution and the type of seed aluminum hydroxide.

We made calculations on the dimensions of electrolyte purification systems from dissolved reaction products – electrolyte circuit and crystallizer. Experiments were done on PS prototypes, and they demonstrated that at medium operating powers and high decomposition rates corresponding to high concentrations of dissolved aluminum (p = 1.5), the crystallization process takes place in the electrolyte circulation circuit.

In order to reduce concentration of dissolved aluminum, it is possible to increase the amount of seed in electrolyte, which inevitably leads to a significant increase in energy costs for pumping the electrolyte and a decrease in the resource and reliability of operation of PS units, therefore, in some cases, to intensify the process of cleaning electrolyte, it is necessary to use a special device – a crystallizer, in which It is possible to create the required seed concentration.

Since the decomposition rate depends on temperature, the concentration of alkali and aluminum, and the amount of seed, the choice of the optimal design and operation of the mold is also largely determined by characteristics and operating conditions of the PS. Thus, to determine

Downloaded from www.periodico.tchequimica.com

the minimum mass and size of the mold, multi-parameter optimization should be done taking into account the given characteristics.

Evaluation calculations have demonstrated that for a 100 W power supply, the crystallizer volume should be 1.3 l at a seed concentration of 20 mass% The mass of water consumed during the operation of the PS for 6 hours is 1.4 kg.

5. REFERENCES:

1. Akbarov, R.D., Zhilisbaeva, R.O., Tashpulatov, S.S.H., Cherunova, I.V., Bolysbekova, R.T. *Izvestiya Vysshikh Uchebnykh Zavedenii, Seriya Teknologiya Tekstil'noi Promyshlennosti*, **2018**, *2018*(5), 188-192.
2. Burkov, S.I., Zolotova, O.P., Sorokin, B.P., Turchin, P.P., Talismanov, V.S. *Journal of the Acoustical Society of America*, **2018**, *143*(1), 16-22
3. Doche, M. L., Novel-Cattin, F., Durand, R., Rameau, J. J. *Journal of Power Sources*, **1997**, *65*, 197-207.
4. Egan, D.R., Ponce de León, C., Wood, R. J.K., Jones, R.L., Stokes, K.R., Walsh, F.C. *Journal of Power Sources*, **2013**, *236*, 293-310.
5. Farmakovskaya, A., Okorokova, N., Pushkin, K., Sevruk, S., and Suvorova, E. *2018 International Theoretical and Practical Conference on Alternative and Smart Energy,* Voronezh, Russian Federation, **2018a**.
6. Farmakovskaya, A., Okorokova, N., Pushkin, K., Sevruk, S., Suvorova, E. 2019. *2018 International theoretical and practical conference on alternative and smart energy*, Voronezh, Russian Federation, **2018b**.
7. Gavryushin, S.S., Skvortsov, P.A., Skvortsov, A.A. *Periodico Tche Quimica*, **2018**,*15*(30), 678-686.
8. Karonik, V.V., Klochkova, L.L., Kulakov, E.B., Sevruk, S.D., Farmakovskaya, A.A. *Collection of Scientific Works of the Moscow Power Institute (MEI),* **1988**, *169*, 28-33.
9. Li, Q., Bjerrum, N.J. *Journal of Power Sources*, **2002**, *110*, 1-10.
10. Okorokova, N.S., Prokofev, M.V., Pushkin, K.V., Sevruk, S.D., Suvorova, E.V., Farmakovskaya, A.A. *Trudy MAI*, **2015b**, *83*.
11. Okorokova, N.S., Pushkin, K.V., Sevruk, S.D., Farmakovskaya, A. A. *Russian utility patent No. 105528*, **2010**.
12. Okorokova, N.S., Pushkin, K.V., Sevruk, S.D., Farmakovskaya, A.A. *Russian utility patent No. 116257*, **2011**.
13. Okorokova, N.S., Sevruk, S.D., Suvorova, E.V., Farmakovskaya, A.A. *Russian Metallurgy (Metally)*, **2015a**, *2015*(13), 1174-1178.
14. Pushkin, K.V. *29th Congress of the International Council of the Aeronautical Sciences,* Central Aerohydrodynamic Institute named after professor N. E. Zhukovsky, St. Petersburg, Russian Federation, **2014**.
15. Pushkin, K.V., Sevruk, S.D., Okorokova, N.S., Farmakovskaya. A.A. *Periódico Tchê Química*, **2018**, *15*(S1), 414-425.
16. Shao, H.B., Wang, J.M., Zhang, Z., Zhang, J.Q., Cao, C.N. *Materials Chemistry, and Physics*, **2002**, *77*, 305-309.
17. Skvortsov, A., Zuev, S., Koryachko, M., Glinskiy, V. *Microelectronics International*, **2016**, *33*(2), 102-106.
18. Skvortsov, A.A., Orlov, A.M., Frolov, V.A., Gonchar, L.I., Litvinenko, O.V. *Physics of the Solid State*, **2000**, *42*(10), 1861-1864.
19. Skvortsov, A.A., Pshonkin, D.E., Luk'yanov, M.N., Rybakova, M.R. *Periodico Tche Quimica*, **2018**, *15*(30), 421-427.
20. Soler, L., Macanas, J., Munoz, M., Casado, J., *Journal of Power Sources*, **2007**, *169*, 144-149.

Downloaded from www.periodico.tchequimica.com

$$\Delta C = C - C_p \quad \text{(Eq. 1)}$$

$$d = \Delta C / C_p \quad \text{(Eq. 2)}$$

$$d = \Delta C / C_p \quad \text{(Eq. 3)}$$

$$\alpha = n(K_2O)/n(Al_2O_3) \quad \text{(Eq. 4)}$$

$$N = n(Al_2O_3)/n(K_2O) \quad \text{(Eq. 5)}$$

$$2Al(OH)_6^{3-} \rightleftarrows Al_2(OH)_{11}^{5-} + OH^- \rightleftarrows Al_2(OH)_{10}^{4-} + 2OH^- \quad \text{(Eq. 6)}$$

$$Al(OH)_4^- \rightleftarrows AlO_2^- + 2H_2O \quad \text{(Eq. 7)}$$

$$Al(OH)_4^- + Al(OH)_4^- \rightleftarrows Al_2(OH)_7^- + OH^- \quad \text{(Eq. 8)}$$

$$nAl(OH)_4^- \rightleftarrows Al_n(OH)_{3n+1}^- + (n-1)OH^- \quad \text{(Eq. 9)}$$

$$[Al(OH)_4]^- \rightarrow OH^- + Al(OH)_3 \downarrow \quad \text{(Eq. 10)}$$

$$S_{sp} = {}^{6}/_{r \cdot d_1} \quad \text{(Eq. 11)}$$

$$S_{sp} = {}^{6}/_{r \cdot S(N_i/d_i)} \quad \text{(Eq. 12)}$$

$$S = S_{sp} \cdot C_s \quad \text{(Eq. 13)}$$

$$k_{dec} = k_{lg} \cdot S \cdot r \cdot K_v \quad \text{(Eq. 14)}$$

$$\frac{d \ln K}{dT} = \frac{E_a}{(R \cdot T^2)} \quad \text{(Eq. 15)}$$

$$-\frac{dC}{dt} = k_{dec}\left(C - C_{eq}\right)^2 \quad \text{(Eq. 16)}$$

$$\Delta t_{dec} \geq \frac{\Delta C_{Al}}{-dC/dt} \quad \text{(Eq. 17)}$$

$$\Delta C_{Al} = \Delta C_{Al^1} - \Delta C_{Al^2} = \frac{M_{Al}}{Q_{el}} \quad \text{(Eq. 18)}$$

$$\Delta t_{dec} = \sum n \Delta t_i = \sum \frac{l_i}{W_i} \quad \text{(Eq. 19)}$$

$$dt_{cr} = L_{cr}/W_{el} \quad \text{(Eq. 20)}$$

$$V_{cr} = \frac{dC_{Al} \cdot Q_{el}}{dC/dt} \quad \text{(Eq. 21)}$$

Downloaded from www.periodico.tchequimica.com

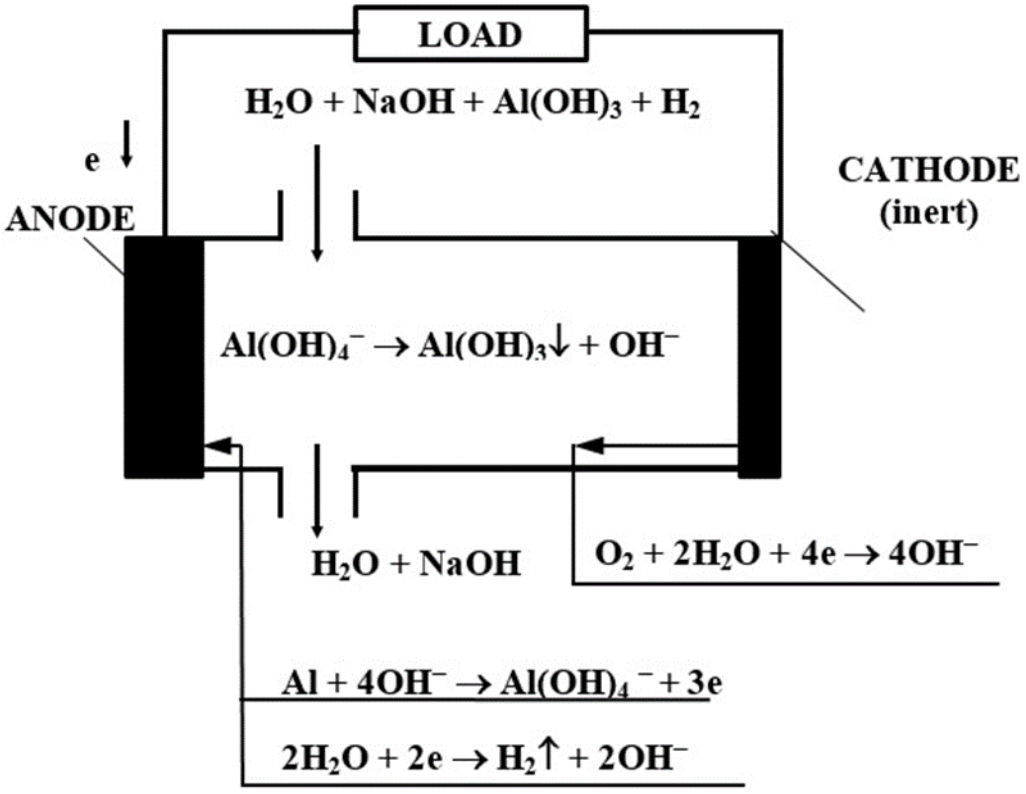

Figure 1. *Schematic diagram of AA CCS*

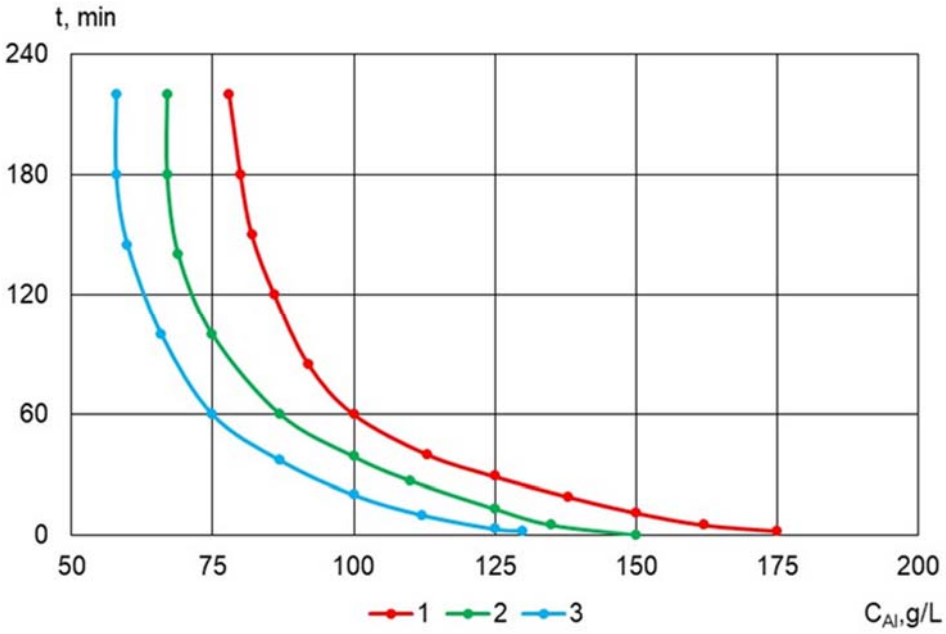

Figure 2. *The dependence of induction time of the decomposition of aluminate solution on the concentration of aluminum; alkali concentration – 20 mass%. 1 – temperature 303K, 2 – temperature 333K, 3 – temperature 353K*

Downloaded from www.periodico.tchequimica.com

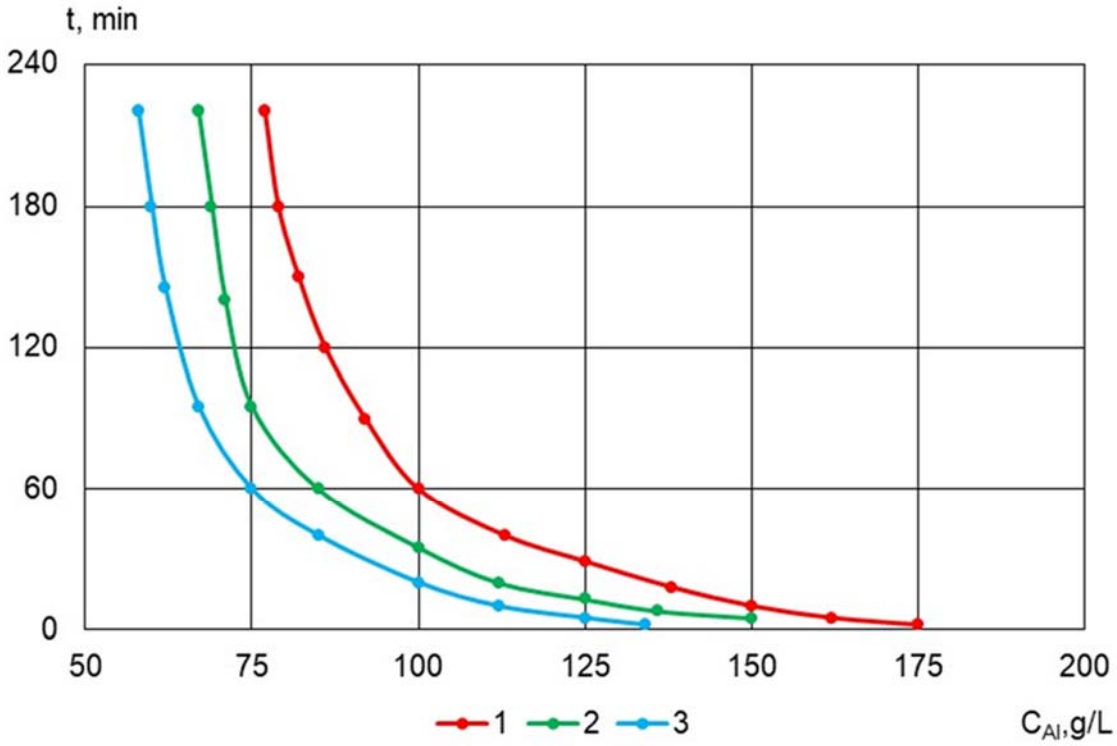

Figure 3. *The dependence of the induction time of the decomposition of the aluminate solution on the concentration of aluminum; alkali concentration – 16 mass%. 1 – temperature 303K, 2 – temperature 333K, 3 – temperature 353K*

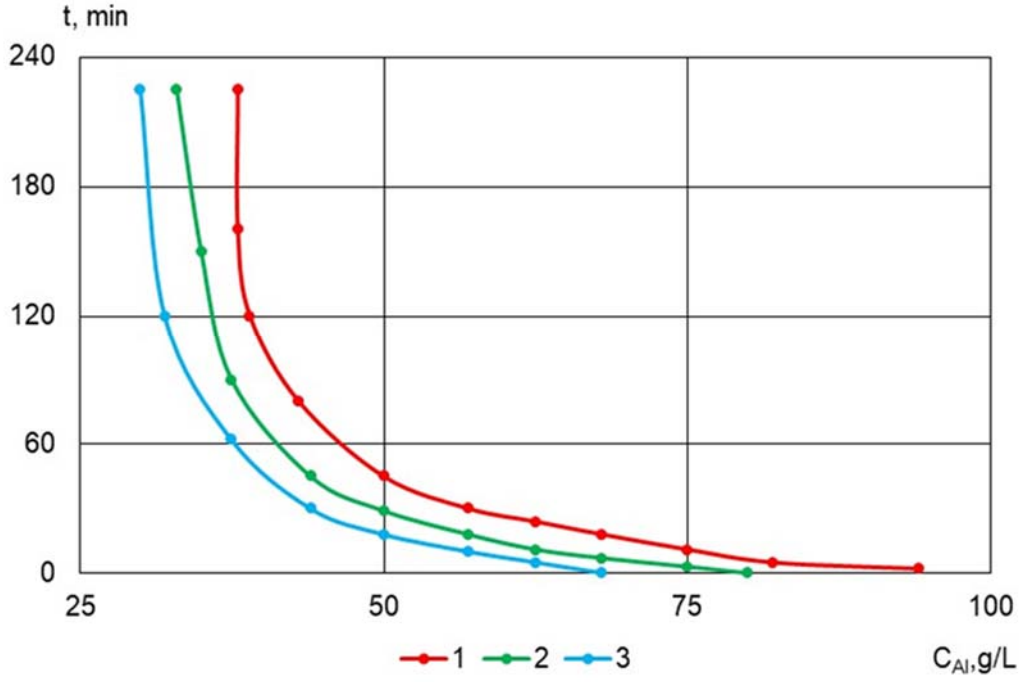

Figure 4. *The dependence of induction time of decomposition of the aluminate solution on the concentration of aluminum; alkali concentration – 12 mass%. 1 – temperature 303K, 2 – temperature 333K, 3 – temperature 353K*

Downloaded from www.periodico.tchequimica.com

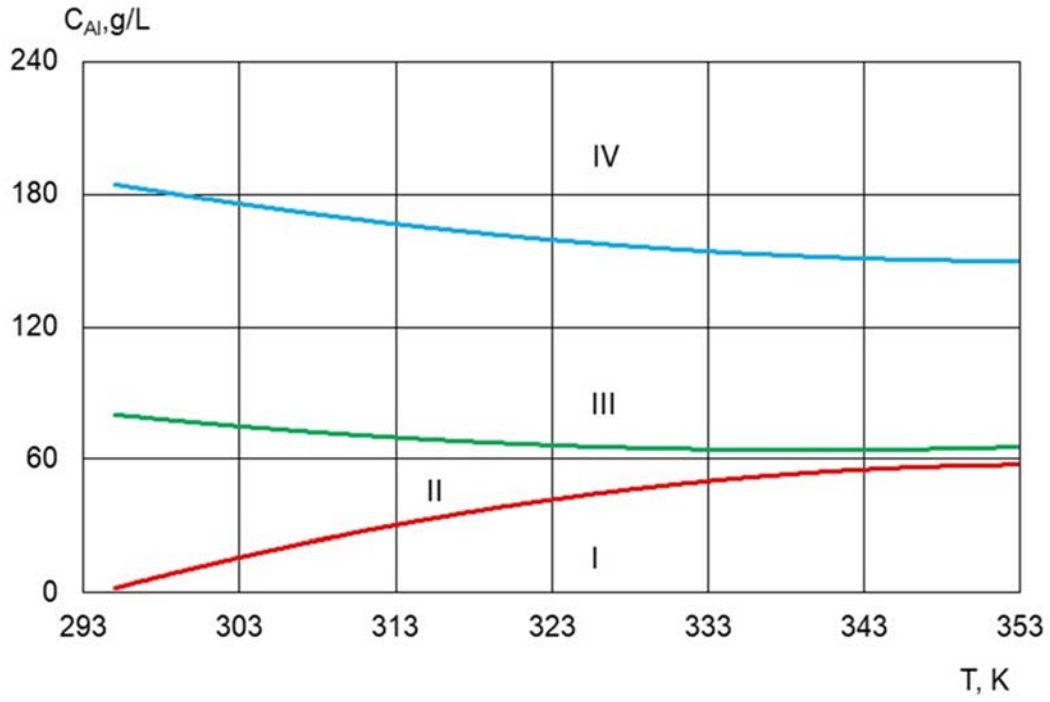

Figure 5. *The boundaries of state regions of aluminate solution depending on temperature; alkali concentration – 20mass%. I is a stable region, II is the first metastable region, III is the second metastable region, IV is a labile region*

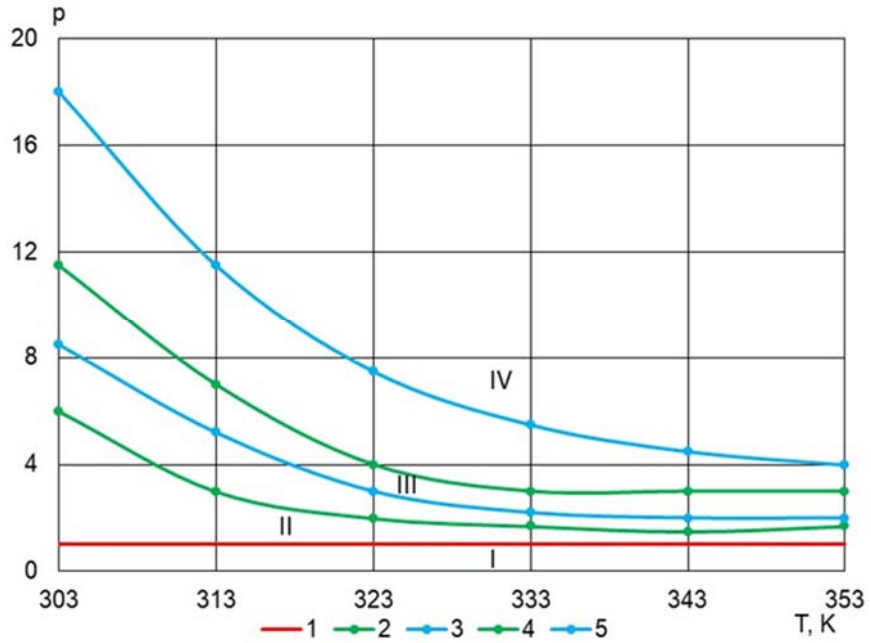

Figure 6. *The boundaries of state regions of aluminate solutions depending on temperature. 2, 4 – a solution of 20 mass% KOH; 3, 5 – solution of 12 mass% KOH; I is a stable region, II is the first metastable region, III is the second metastable region, IV is a labile region*

Downloaded from www.periodico.tchequimica.com

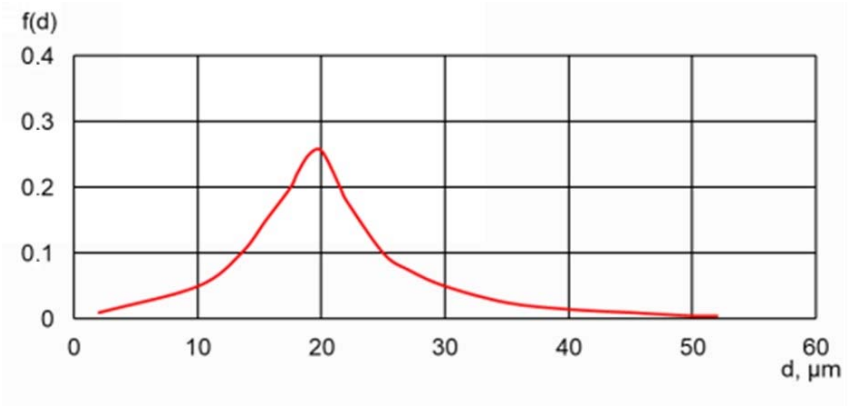

Figure 7. *Differential size distribution curve for the seed crystals*

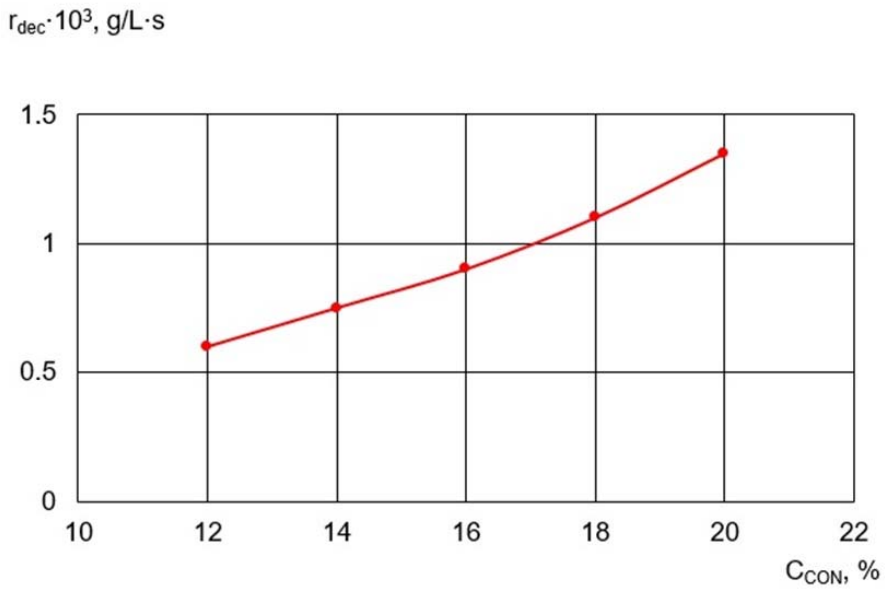

Figure 8*. Dependence of the decomposition rate in aluminate solution on alkali concentration. Temperature – 333 K; degree of supersaturation – 1.5; concentration A1 (OH)* $_3$ *– 2 mass%*

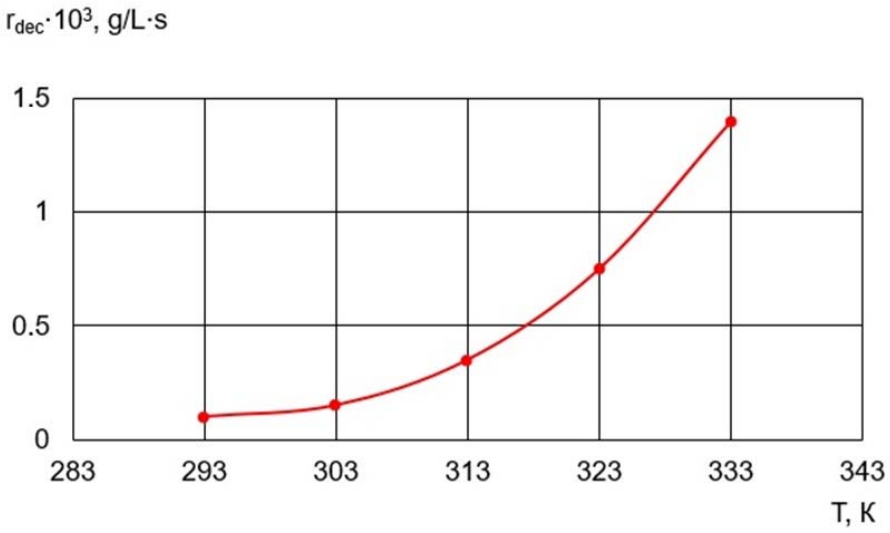

Figure 9*. Dependence of decomposition rate of aluminate solution on temperature. Alkali concentration – 20 mass%; degree of supersaturation – 1.5; concentration A1 (OH)* $_3$ *– 2 mass%*

Downloaded from www.periodico.tchequimica.com

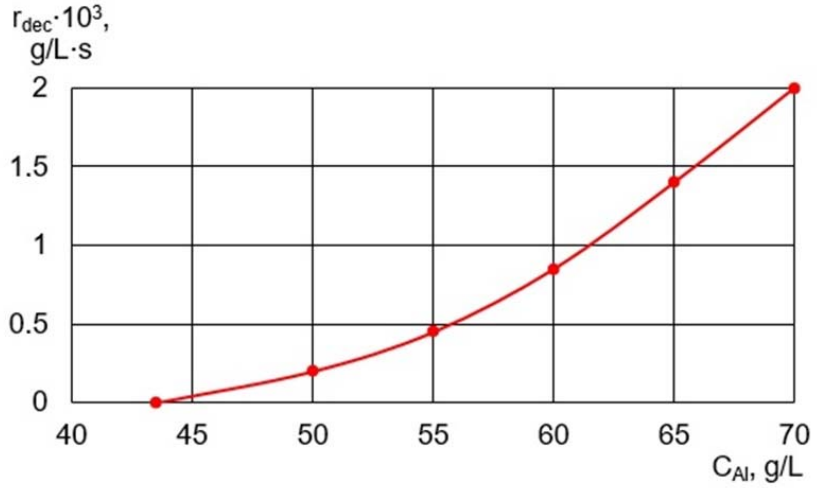

Figure 10. *Dependence of the rate of decomposition of aluminate solution on the concentration of aluminum. Temperature— 333 K; KOH concentration – 20 mass%, A1 (OH) concentration* $_3$ *– 2 mass%*

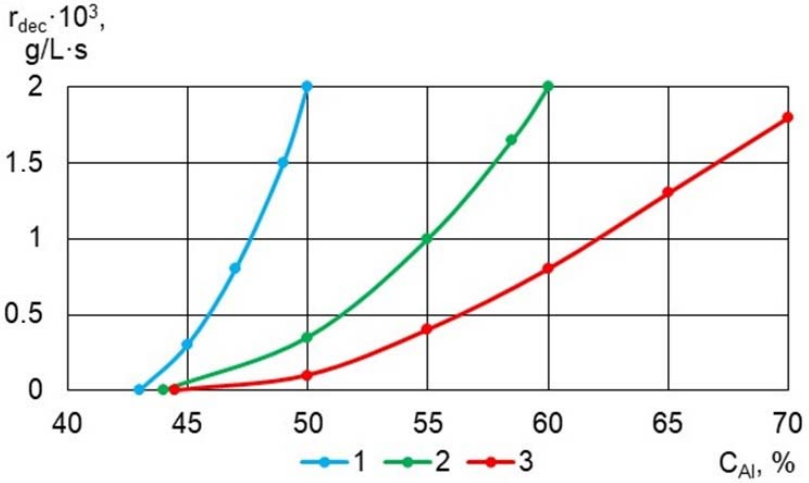

Figure 11*. Dependence of the rate of decomposition of aluminate solution on the concentration of aluminum hydroxide. Temperature – 333K; KOH concentration – 20 mass%; 1 – concentration A1 (OH)* $_3$ *– 6 wt.%; 2 – concentration A1 (OH)* $_3$ *– 4 wt.%, 3 – concentration A1 (OH)* $_3$ *– 2 mass%*

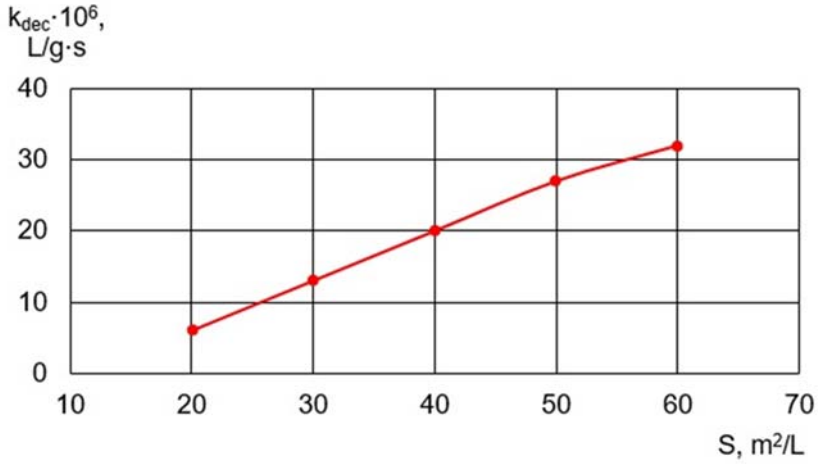

Figure 12*. Dependence of decomposition rate constant on the seed surface. Temperature – 333 K; KOH concentration – 20 mass%*

Downloaded from www.periodico.tchequimica.com

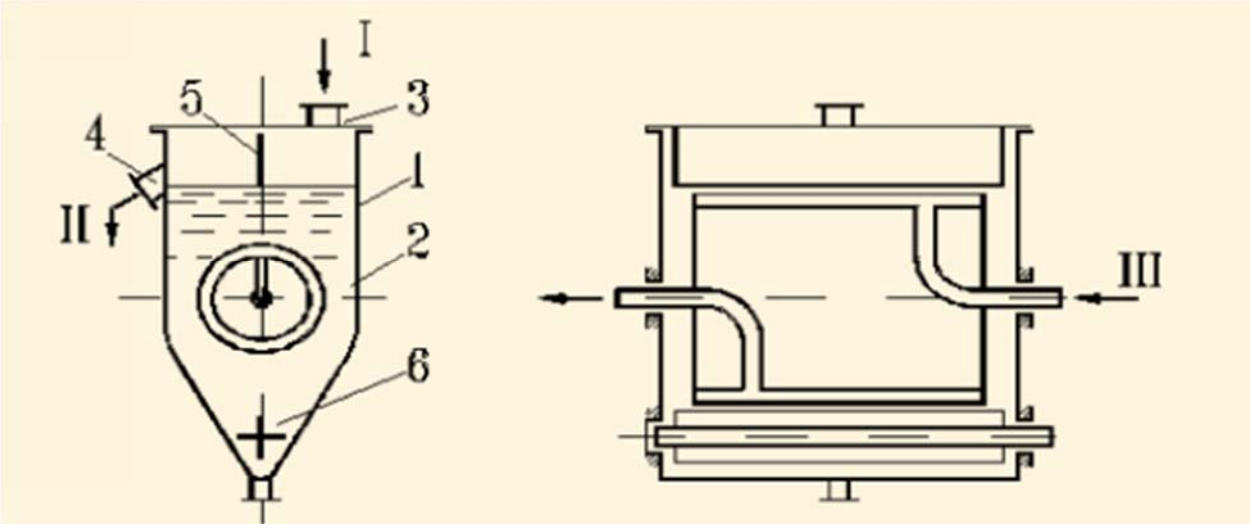

Figure 13. *Scheme of the crystallizer: 1 – housing; 2 – drum; 3 – fitting for introducing the solution; 4 – fitting for withdrawing a suspension of crystals; 5 – a partition; 6 – paddle mixer; I – solution; II – suspension; III – cooling water*

Downloaded from www.periodico.tchequimica.com

PERIÓDICO TCHÊ QUÍMICA
ARTIGO ORIGINAL

BASE DO DESENVOLVIMENTO DA PERSONALIDADE PSICOLÓGICA E PROFISSIONAL DE FUTUROS PSICÓLOGOS EDUCACIONAIS

BASIS OF PSYCHOLOGICAL AND PROFESSIONAL PERSONALITY DEVELOPMENT OF FUTURE EDUCATIONAL PSYCHOLOGISTS

ОСНОВЫ ПСИХОЛОГИЧЕСКОГО И ПРОФЕССИОНАЛЬНОГО РАЗВИТИЯ ЛИЧНОСТИ БУДУЩИХ ПЕДАГОГОВ-ПСИХОЛОГОВ

NAGIMZHANOVA, Karakat M. [1*]; BAIMANOVA, Lyazzat [2]; MAGAVIN, Sabit Sh.[3]; ADZHIBAEVA, Botagoz Zh.[4]; BETKENOVA, Meruert S.[5];

[1] Turan-Astana University, Department of Pedagogy and Psychology, Astana – Republic of Kazakhstan

[2] Sh. Ualikhanov Kokshetau State University, Department of Foreign Language, Kokshetau – Republic of Kazakhstan

[3] S.Seifullin Kazakh AgroTechnical University, Department of Technological Machines and Equipment, Astana – Republic of Kazakhstan

[4] Astana Medical University, Department of Dentistry, Astana – Republic of Kazakhstan

[5] Kazakh National University of the Arts, Department of Social and Humanitarian Disciplines, Astana – Republic of Kazakhstan

** Correspondence author*
e-mail: karakat_4@mail.ru

Received 04 September 2019; received in revised form 20 October 2019; accepted 24 October 2019

RESUMO

As mudanças no sistema de ensino superior atualmente em curso estão associadas à busca e criação de condições psicológicas e pedagógicas para a formação de competências gerais e profissionais que permitam que futuros especialistas realizem seu potencial pessoal e criativo. Portanto, o principal objetivo do trabalho foi analisar os fundamentos do desenvolvimento psicológico e profissional da personalidade dos futuros professores-psicólogos. Para atingir esse objetivo, os autores utilizaram o método de análise e as abordagens metodológicas de atividade autorreguladora do sujeito orientada à personalidade. Foi estabelecido que o desenvolvimento fisiológico e profissional dos psicólogos educacionais, especialmente nos estágios iniciais, desempenha um papel decisivo na criação das bases para o bem-estar da comunidade. Foi determinado que, para resolver problemas psicológicos (dos adultos e crianças), os profissionais precisam do conhecimento profundo da disciplina e do uso de habilidades criativas. A formação de um professor-psicólogo prossegue ao longo de sua carreira profissional. A universidade estabelece as bases para qualidades profissionais e significativas profissionalmente de um especialista, que posteriormente garantem a formação profissional da personalidade no processo de atividade psicológica e pedagógica. Com base em dados gráficos, os autores estabeleceram as características do desenvolvimento dos principais componentes e sua relação na estrutura da prontidão da pessoa. O estudo apresentado contribuirá para a formação de prontidão da pessoa para as atividades profissionais de futuros professores-psicólogos.

Palavras-chave: *distinção profissional, psicólogos educacionais, desenvolvimento pessoal, sistema educacional moderno.*

ABSTRACT

Changes in the system of higher professional education that are currently taking place are associated with the search and creation of psychological and pedagogical conditions for the formation of general and professional competencies that allow future specialists to realize their personal and creative potential. Therefore, the main objective of the paper was to analyze the basics of the psychological and professional personality development of future teachers-psychologists. To achieve this objective, the authors employed the

Downloaded from www.periodico.tchequimica.com

analysis method, subject-activity, and personality-oriented methodological approaches. It was established that the physiological and professional development of educational psychologists, especially in the early stages, plays a decisive role in laying the foundations for the welfare of the community. It was determined that to solve psychological problems (of adults and children), practitioners require in-depth knowledge of the discipline, the application of creative skills. The becoming of a teacher-psychologist continues throughout their entire professional career. The university lays the foundation for professionally significant and personal qualities of a specialist, which subsequently ensure the professional becoming of the personality in the process of psychological and pedagogical activity. Based on the graphic data, the authors established the features of the development of the main components and their relationship in the structure of personal readiness. The presented research will contribute to the maturation of personal readiness for the professional activities of future teachers-psychologists.

Keywords: *professional distinctiveness, educational psychologists, personal development, modern educational system.*

АННОТАЦИЯ

Изменения в системе высшего профессионального образования, происходящие в настоящее время, связаны с поиском и созданием психолого-педагогических условий для формирования общих и профессиональных компетенций, позволяющих будущим специалистам реализовать свой личностный и творческий потенциал. Поэтому основная цель работы заключается в анализе основ психологического и профессионального развития личности будущих педагогов-психологов. Для достижения поставленной цели авторами использован метод анализа, субъектно-деятельностные и личностно-ориентированные методологические подходы. Установлено, что физиологическое и профессиональное развитие педагогических психологов, особенно на ранних этапах, играет решающую роль в создании основ для благополучия сообщества. Определено, что для решения психологических проблем (взрослых и детей) практикам необходимы глубокие знания дисциплины, применение творческих навыков. Становление педагога-психолога протекает на протяжении всей профессиональной деятельности. В вузе закладываются основы профессионально значимых и личностных качеств специалиста, которые в последующем обеспечивают профессиональное становление личности в процессе психолого-педагогической деятельности. На основе графических данных авторами установлены особенности развития основных компонентов и их взаимосвязи в структуре личностной готовности. Представленное исследование поспособствует формированию личностной готовности к профессиональной деятельности будущих педагогов-психологов.

Ключевые слова: *профессиональная индивидуальность, педагогические психологи, личное развитие, современная образовательная система.*

1. INTRODUCTION

Today, the practice of educational psychology is taking place in a complex, challenging and ever-changing context where professional confidence is difficult to maintain and where it is easy for EP practitioners to lose sight of the beliefs, hopes, and aspirations with which they entered the profession. Educational Psychologists in several case study interviews expressed concerns about the extent to which they have the requisite knowledge and skills to enable them to work in this wider context. Many feel that, whilst their initial training has prepared them for this wider role … [they] need additional training to ensure that they are able to fulfill the new role expected of them.

Several reasons have been put forward to explain why many EP practitioners appear to be experiencing something of an identity crisis (Cameron and Monsen, 2005). Such professional anxiety has surfaced in the form of rifts within the profession about the nature of professional training for the EP practitioners of the future; uncertainty about their professional role in a new children's workforce, and a lack of corporate confidence in their ability to influence future developments in services for children and young people (Lunt and Majors, 2000; Norwich, 2005; or the extended summer 2005 debate on EPNET on what constitutes the 'basic' work of an educational psychologist). Of course, educational psychology is not the only profession to be living in 'interesting' times. However, educational psychologists appear to be suffering from a double whammy: pressure from central and local government to squeeze into a new service model for children and young people and self-doubts about the relevance of their skills and knowledge in this new millennium environment. Lunt and Majors (2000) have argued that somewhere along the way EP seems to have lost their

Downloaded from www.periodico.tchequimica.com

psychology, a point supported by Norwich (2005) who claims: theoretical concepts are applied to produce practical principles and techniques, with their origins often not known or ignored by practitioners.

A recent DfES document on the Educational Psychology Service views the work of educational psychologists in broad terms as providing "assessment, consultation, advice and training to early year's settings, schools, families and the Local Education Authority". Curran, Gersch and Wolfendale (Curran *et al.*, 2003) have offered a more pragmatic, if traditional, service delivery model and outlined three potential levels at which EPs can operate:

- The **individual** (for example, assessment and intervention with an individual child).
- The **organization** (for example, in a school providing in-service training of teachers).
- The **system** (for example, in a Local Education Authority which is developing innovatory, special or additional education provision).

Within the profession itself, the aforementioned EPNET debate eventually resulted in a one-sentence description of 'basic work' which read more like a worthy political statement than a precise role description: "Educational Psychologists are applied psychologists who primarily address issues within children's development and learning, whilst supporting equal opportunities relating to removal of barriers in culture, race, gender, disability, and social disadvantage, ultimately promoting inclusion at all these levels." A list of the key features of educational psychological practice has been provided by Gersch (2004) and this includes: helping children; employing effective interpersonal skills; listening to children and adults; being objective and dispassionate; creative problem solving; offering practical help; assisting and facilitating when things get stuck; applying research to real-life problems; being empirically grounded; evaluating interventions and actions (using evidence-based criteria); working directly and through others, and adding value to people's lives. While all of these are worthy tasks, none of them could be viewed as being exclusive to the EP practitioner.

How to achieve a measure of professional distinctiveness has been the subject of considerable debate within the profession. Some journal contributors have recommended an improved strategy for EP service delivery (Evans, 2005) or a more cohesive practitioner approach to major problem areas such as social, emotional and behavioral difficulties (Rees *et al.*, 2003). Others have called for a critical evaluation of the theoretical foundations of expert practice in general (Moore, 2005) and the practice of educational psychology in particular (Leadbetter, 2005). At the 'big picture' level, Baxter and Frederickson (Baxter and Frederickson, 2005) have argued that educational psychologists should be widening their practice beyond the traditional special needs client groups and promoting positive development outcomes for all children (Lysytsia *et al.*, 2019).

Interesting though these recommendations are, they still do not address the particular and distinctive contribution of the EP or provide a convincing answer to the question posed by the Special Educational Needs and Disability Division/Children'sWorkforce Unit, (Smith, 2005) viz. "What is it that EPs bring to a situation that is different from what others bring?" In short, how can we respond to the blunt challenge from Wood (1998): "Okay, then: what do EPs develop?"

1.1. Blurring the distinctiveness factor

In highlighting the distinctive component of applied psychology, there are several natural and imposed barriers to be overcome. In the first place, all professional problem solvers (from plumbers to psychologists) employ some kind of systematic problem– solving procedure. Such a procedure often includes components like a systematic investigation of the problem situation, clarification of the problem itself, a clear perspective of what needs to be done to overcome the problem, a strategy for achieving this and monitoring or follow-up to see that the outcome has been achieved and has overcome or reduced the original problem. Clearly, then, systematic problem solving, like the solution-focused approach advocated by Stobie, Boyle, and Woolfson (Stobie *et al.*, 2005) is by no means the sole prerogative of the practicing EP.

Secondly, in all human life psychology is ubiquitous: the simplest and the most complex features of people's behavior have a psychological explanation lurking somewhere! Sometimes, this psychological component is obvious and, therefore, clients are likely to view a psychological explanation as unspectacular, everyday and ordinary ("Our psychologist often tells us what we know already!") On other

Downloaded from www.periodico.tchequimica.com

occasions, when the explanation is not at all obvious, parents, teachers and others who are being asked to implement an EP-recommended strategy for change may express more than a degree of skepticism.

Thirdly, for all applied psychologists, there remain the twin challenges of linking highly specific, frequently-piecemeal research with the urgent and often-messy demands of the real world. The task of making this link between the problem under discussion and the recommended approaches to understanding and managing this problem intelligible to people who may not have a background in psychological research and theory requires considerable creativity and high-level communication skills.

In a sentence, then, applied psychologists are required to use psychology in a creative and innovative way, so as to provide an integrated and coherent perspective of complex environments (e.g., school, homes, children's homes, etc), the complex problems and situations which occur in such environments (e.g., critical incidents, parental uncertainty, teacher stress, children's learning and behavior difficulties, etc) and the complex needs of people which results from such problems (e.g., reassurance, insight, skill deficits, challenges to current belief systems, etc).

Achieving a transparent connection between psychology and the problems of adults and children will require applied practitioners to utilize sophisticated consultation processes and an in-depth knowledge of the discipline, so that they can provide people with a deeper understanding of problematic situations, offer research-based, creative and effective ways of managing these problems, and also promote proactive approaches to minimize the occurrence and impact of such problems in the first place.

What then are the distinguishing features of applied psychology practice? To answer this question, it is necessary to move beyond the conventional, but narrow, focus on practice improvement to uncover some of the higher-order conceptual processes which are likely to make the EP's perspective different from those of other professional groups. In this paper, I would like to discuss five distinctive factors and readers are invited to consider their own additions to this list:

(a) Adopting a psychological perspective of the nature of human problems.

(b) Drawing on the knowledge base of psychology to uncover mediating variables which may provide an explanation of why certain events may be related.

(c) Unraveling problem dimensions using sophisticated models which can be used to navigate through a sea of complex human data and to provide a simple but useful map of the interaction between people factors and aspects of their living/ learning environments.

(d) Using information from the research and theoretical database in psychology to recommend evidence-based strategies for change.

(e) Promoting innovative concepts or big ideas which are underpinned by psychological research evidence and theory and which can enable clients to spot potential opportunities for positive change.

These arguably distinctive aspects of applied psychology practice will now be discussed in turn. The psychologist adds a distinct perspective, asks particular types of questions and uses validated interventions and tools. This perspective is grounded in scientific psychology on the one hand and a commitment to evidence-based practice and scientific methods on the other. Applied psychologists approach human problems with specific and well-established psychological perspectives in mind. In psychology, it is generally accepted that human behavior is most usefully viewed from an eco-systemic perspective which emphasizes the complex, interdependent and recurring nature of the links between a variety of contextual, personal, and interpersonal variables. Such a stance involves:

- Adopting an interactive rather than single-factor view of problems or problem situations (Morton, 2004; Cameron and Monsen, 2005).

- Recognizing that human problems have different levels or layers, ranging from within-person to within-home, school, community and beyond (Curran *et al*., 2003).

- Attempting to understand and reconcile the different perspectives which people may bring to a particular problem situation (as an illustration, accounts of the widely differing attributions of disruptive behavior held by pupils, parents, and teachers can be found in Miller, 2003).

- Unpicking the human factors which can hasten or hinder the process of desired change, especially: gaining commitment to change,

Downloaded from www.periodico.tchequimica.com

understanding group processes, recognizing the power of people's belief systems, and employing sophisticated procedures to encourage joint planning of monitoring, evaluation, reflection, and personal/professional development. In particular, psychologists often find themselves introducing the possibility of change to children, teachers and parents who, themselves, may see no need for such change and, while this presents a tough professional challenge, strategies have been developed to help a 'reluctant' client to move from a pre-contemplation to a contemplation of change stance (McNamara, 1998).

The distinctive advantage of all these psychological perspectives is that a rich and multi-layered picture of the problem situation is constructed, while stereotyping, especially of persons from diverse backgrounds, is reduced and common biases, snap judgments and unwarranted explanations are minimized.

1.2. Uncovering mediating variables

In the education sector, many new approaches to problems (e.g., the introduction of the literacy or numeracy hours) could be said to exist at the a-theoretical level: an exclusive focus on previous success or failure contexts is not uncommon. It is the a-theoretical model which is in operation when a previously successful headteacher is invited to take control of a failing school, presumably in the hope that the success formula will travel with him/ her. A-theoretical research is mainly concerned with knowing that certain (often-unspecified) factors seem to be regularly associated with particular outcomes. Theoretical research, on the other hand, attempts to discover why particular variables (e.g., the 'weak' headteacher) seem to generate specific outcomes (e.g., the 'failing' school). In other words, it is the nature of the relationship between input and outcome which is the focus of the interest for the psychologist and it is this quest for explanatory factors which is the reason of psychological research and theory.

Therefore, the emphasis of most research and theory in psychology is upon the mediating or explanatory variables, i.e., those factors which not only offer reasons for the occurrence of particular human phenomena at a certain point in time but also provide explanations which can be generalized to other similar situations. While applied psychology can often provide insight into those aspects of human behavior which are unusual, complex, exotic and bizarre, it can also illuminate the common-place by challenging what may appear to many as the obvious links between human problems (and successes) and their antecedents, contexts, and outcomes. A global example of mediating variables in action concerns the apparently obvious and super-glued relationship between a lack of resources, on one hand, and the poverty, unhappiness, and ill-health which results from such a deficit, on the other (Rymashevskaya *et al.*, 2017).

Yet, well-meaning, early attempts to tackle poverty by throwing resources at the problem produced minimal benefits or occasionally negative outcomes for the people concerned. Clearly, there were other powerful mediators at work and a careful investigation led Devitt (1977) to identify another key factor (as well as disease) that mediated the impact of limited resources and the outcomes, especially for people in rural areas. This turned out to be the poverty-generated, self-defeating beliefs of people which led them to narrow their horizons for change. In short, a lack of basic resources not only sapped the energy for physical work (the lay person's explanation) but also closed people's minds to the possibilities, opportunities and the need for change (the mediating psychological variable).

Another example of the importance of the mediating variable (this time from educational psychology) is the all-too-frequently reported link between reading disability and disruptive behavior. In their research which attempted to tease out some of the mediating variables which connects these two problem areas, Willcutt and Pennington (2000) confirmed a gender component (boys with poor reading ability exhibited externalized behaviors like attention disorder, oppositional disorder, and conduct disorder, whilst girls with similar difficulties tended to exhibit internalized behavior, especially depression). While the uncovering of such a gender variable may not immediately seem to be remarkable, this knowledge can alert the teacher to the often hidden effects of reading disability on the emotional well-being of girls (a deeper understanding of the problem), but also indicates that a gender factor should be taken into consideration when approaches to teaching and management are being considered (a more appropriate teaching strategy).

A 'grounded' classroom example might be the child or young person who annoys and disturbs others at work has difficulty staying on-task for more than a few minutes and who seems to have a worryingly-low level of intrinsic motivation. Frequently invoked teacher explanations for such problems may include low

ability, poor home background, or even the suspicion of attention deficit hyperactivity disorder. A more insightful psychological hypothesis might be that this child may believe that he or she can only learn when an adult is giving one-to-one attention and indicating exactly which tasks needed to be done because his or her belief about learning was that it should be an effortless activity (Dweck and Leggett, 1988).

A psychological perspective provides a teacher with a way to 'get hold of' a complex situation and to think about the problem and possibilities in the light of views of human meaning. This advantage is not only afforded by mere knowledge about concepts, principles, and theories; it is only manifested when those ideas are tied together as coherent frames that suggest when and how the ideas can be used (Anderson *et al.*, 1995).

So, one necessary task of the EP practitioner might be to use psychology to challenge what appears to be 'commonsense' or 'common practice' explanations by creating a cognitive dissonance which encourages the consideration of alternative explanations for problems. In the case of the latter, Wagner (1995) has argued that the task for the psychologist is to create this disturbance in a client's current thinking to allow a change of perception to occur and cautions that this new perspective might be resisted or rejected, unless there was an at least some level of congruence with existing perceptions, beliefs or constructs. However, she also points out that changes in perspective do frequently occur and are well recognized across the fields of both theoretical and applied psychology as a cognitive shift, a re-framing/reconstruction of a problem, or the employment of a new hypothesis.

Many of the problems on which applied psychologists are asked for advice present as messy and complex situations which are difficult to unpick, contain information black holes, lack well-established procedures for management and have unclear processes and outcomes. To uncover some of the subtle features that may be underpinning such problems, practitioners require an approach that can bring a systematic and logical analysis to bear on the problem without over-simplifying the real-life complexity of the problem situation (e.g., classrooms are complex, crowded and exceptionally busy places, within which groups of students who differ considerably in interests, abilities, and needs have to be managed), or underestimating the impact (both positive and negative) of human perceptions or recognizing the vested interests which can lead to clients bringing about or resisting change.

Problem analysis is a process by which information is structured and analyzed in a way that aids a deeper understanding by both client(s) and by the consultant (Monsen *et al.*, 1998). Of central importance in problem, analysis is the generation of hypotheses that are based on a combination of psychological research and theory and also on the nature of the problem situation. However, rather than a search for the 'right' single conceptualization of a problem, psychologists using a problem analysis protocol will seek those psychological factors which provide the most plausible and logical representation of the problem and which have higher probability than other 'explanations'. The objective is to provide a 'best fit' which encapsulates the main features of the situation and leads to a clear intervention plan based on evidence-based practice (Cameron and Monsen, 2005; Vinichenko *et al.*, 2019).

For the EP practitioner, the use of a problem analysis protocol ensures that close touch with the knowledge base in psychology is maintained and the often-covert, yet complex and sophisticated theoretical basis which often underpins psychological advice becomes transparent. Much of the time, such high-level reasoning in EP practice remains private and therefore inaccessible to clients, colleagues, and employers, so protocols, like problem analysis, can enable EPs to articulate the often-sophisticated background thinking which underpins their distinctive contribution to the assessment and management of problems. The art of being wise is the art of knowing what to leave out.

1.3. Analysis of evidence-based recommendations

Effective professional advice should go beyond the warm glow of sympathetic support, which seems to meet the practitioner's needs more than the service user's (Gameson *et al.*, 2003). Within the last decade, the central government has made it clear that support professionals in education, in common with other professional groups, must base their practice on the best possible evidence of what works. While evidence-based practice has been an important aspect of psychology for many decades, such an approach has been less obvious in the field of education in general, especially when compared with developments in health services where its influence has been strongly felt.

Downloaded from www.periodico.tchequimica.com

One outcome of this relatively recent requirement to identify and apply best practice has been the publication of a number of reviews and meta-analyses of psychological interventions (Harrington, 2001; Carr, 2002; Fonagy *et al.*, 2002; Wilson *et al.*, 2003). The international 'Cochrane collaboration' has been providing an updated database of clinical trials and systematic reviews which indicates that interventions have proven effectiveness, while the UK Cochrane Centre in Oxford and the NHS Centre for Reviews and Assimilation in York have specific briefs to review and promote effective practice, particularly for Health Service decision-making. For schools, an Educational Review Group has been set up in the University of London Institute of Education (the EPPI-Centre) where one recent review topic has been behavior management. Some effectiveness reviews from this Group have already begun to appear (Evans *et al.*, 2003). In the case of social, emotional and behavioral difficulties, a service-led summary of general findings and themes emerging from reviews of psychological interventions has been provided by Cameron and Faulkner (Cameron and Faulkner, 2005). Of course, many questions about the effectiveness of different types of psychological intervention with children who have emotional, social and behavioral difficulties remain unanswered; however, a clearer picture of the more effective strategies for change which can be used at a variety of different levels, including the individual child, the classroom, the family, the school and the community, is now beginning to emerge.

While not all researchers and practitioners are professionally comfortable with such an emphasis on outcomes over processes (Lewis, 1998; Connor-Smith and Weisz, 2003), nevertheless there is now general agreement among applied psycholo1gists that the 'best possible evidence' should guide professional practice and advice in health, child-care and education (Frederickson and Cline, 2002). Distinctively, educational psychologists are one of the very few professional groups (and possibly the only one in LEAs) who have specific knowledge and skills in research design, are competent in statistical analysis and who are trained to take a constructively critical stance to research findings in general. In an era when it often appears that the education and social care systems are over-concerned with bureaucratic detail, depressive reality, quick fixes and professional scapegoating, it can often seem that there are severe limitations placed on informed innovation and creativity. Such are the demands for psychological advice and the increasing administrative pressures to meet statutory deadlines, that it can be only too easy for EP practitioners to miss opportunities for change or lose sight of potential connections between the 'big picture' of children's needs and the research/theoretical knowledge base in psychology which can indicate promising approaches to such problems.

Psychology has long been a powerful force for positive change in our society: its historical contributions to the development of people, in general, have been huge (Zimbardo, 2004). Educational psychology, in particular, has encouraged the growth of significant improvements in early years education, learning and behavior difficulties (especially with regard to specific learning difficulties, autistic spectrum disorder, attention deficit hyperactive disorder), severe learning difficulties and challenging behavior, bullying in schools, friendlessness, critical incident management in schools … the list is a gratifyingly long one! Harrington (2001) has envisioned 'real applied psychology' as opening people's minds to what they can do, rather than creating the illusion of helping by offering complex explanations for why they cannot do it. A few particular contenders which meet the 'Harrington criterion' (and which the reader might like to supplement) could include the concept of empowerment; resilience and vulnerable children; positive psychology and emotional well-being.

"I cannot keep crying forever. I will try hard, so, someday I hope my child will appreciate she is born …" (Devitt, 1997). Far better than any scientific review paper could do, this comment from an unknown Japanese mother highlights the importance of giving parents, teachers, care staff and other direct contact personnel, not only the skills but also conferring on them the status/beliefs to be able to intervene positively on behalf of their children. Studies in the area of outcome have shown that there are specific experiences which are central to the outcomes of empowerment, especially the experience of achievement, a sense of being in control of events, hopefulness and optimism, and the experience of both instrumental and emotional support (Epps and Jackson, 2002; Nunkoosing, 2000; Rappaport, 1984).

As well as applying to significant adults in the lives of children, the principle of empowerment can also be extended to the latter group, where self-management approaches can enable the children and young people themselves to take control of their own lives (Doran and

Downloaded from www.periodico.tchequimica.com

Cameron, 1994; Cameron, 1998). Self-management strategies can also include anger management and self-control. Improving self-management can, therefore, include the teaching of coping skills which children and young people can use at school and beyond, and also helping them to minimize the use of common but self-defeating adolescent strategies such as self-blame, worry and opting-out (Sukhodolsky *et al.*, 2002; Connor, 2002; Faupel, 2004; Lewis and Frydenberg, 2002; Frydenberg *et al*., 2004).

The concept of resilience, especially in the case of vulnerable children, can be viewed as a combination of those factors which can cushion the child from the effect of negative life experiences, including parental rejection, abuse and neglect and which can enable a child or young person to successfully cope with their life. A resilient child has been succinctly described as one who works well, loves well and expects well, notwithstanding profound life adversity (Werner and Smith, 1982). Fonagy, Steele, Steele, Higgett, & Target (Fonagy *et al.*, 1994) have provided a summary of the research and theory which underpin the concept of resilience, while other writers have suggested how the concept of resilience can be employed with vulnerable children in school (Jackson and Martin, 1998) and in EP practice (Dent and Cameron, 2003).

1.3. Positive psychology

Positive psychology addresses the study of positive aspects of experience with a view to improving the quality of individual and community life. It encompasses such diverse topics as well-being, joy, the psychology of happiness, flow and optimal experience, personal stress, wisdom, creativity, imagination, well-being in old age and characteristics of positive groups, institutions and communities (for further details see the seminal article by Seligman and Csickzentmihalyi (2000)). The main themes of positive psychology are the positive experience (what can make one experience better than another); the positive personality (what can make one individual happier than another); and the positive context (what can make one environment more enabling than another) (Seligman, 2002). Of particular interest to EPs is the concept of 'flow' or 'optimal experience' which is an emotional state characterized by complete and timeless involvement in a task, accompanied by intrinsic motivation and self-satisfaction (Csikszentmihalyi, 1997). Creating the conditions whereby disaffected pupils can obtain flow experience in the classroom presents a creative challenge to psychologists and teachers alike, but could provide a reluctant learner with the opportunity to sample the joys, rather than the frustrations, of learning.

Although this particular development in psychology is still in its early stages, there are exciting possibilities here to support the initiative on promoting children's mental health within early years and school settings, by focusing proactively on the enhancement of the emotional and personal well-being of children and young people, rather than relentlessly pursuing a reactive response to problems when these have been well established. Big ideas like empowerment, resilience and the creation of emotional well-being are intrinsically, excitingly seductive, can provide deeper insight into familiar situations and are likely to revive positive feelings about the tasks in hand. Above all, they can rekindle the sometimes submerged enthusiasm and high aspirations of direct contact staff.

The distinctive dimension of these and other big ideas lurking around in the contemporary psychology knowledge base is that they have got strong foundations in applied research, rather than being merely based on the more traditional antecedents (e.g., anecdotal evidence, feel-good speculation or a belief that surely it must do some good) which appear to underpin so many new initiatives in education today.

2. MATERIALS AND METHODS

2.1. Analysis of the study to identify the professional qualities of students

Summarize the data discussed in the Experiment assessed professional and psychological development of the student's personality. Object of the research: 90 students of the "Turan-Astana" university at the age of 17-22 participated in the study. Methods of psychological research:

– 16-factor test of Cattell (type);

– Modified methodology of John Holland's profession selection survey;

– As a basic method of research, a non-standardized interview was conducted on the theme "The level of professional development of a person".

Multiple-factor research of individuals. Cattell's survey.

Purpose: This survey is designed to explore sixteen individual factors and it gives a lot

Downloaded from www.periodico.tchequimica.com

of information about the individual's personality as constitutional factors.

This survey consists of 187 questions. It is recommended to write one of the answer options "no", "yes", "do not know" on the registration form. Note: You are asked to answer several questions. The aim is to find out about your behavior, your interests, and the skill. There are no questions with “correct” and “wrong” answers. Various researched people are asked to answer questions depending on their distinctive features. If you want to find out suggestions and information about the distinctive features that describe your character in various situations, try to give precise and realistic answers. When answering questions, you choose one of the three options. The number of answers on the blank must match the number of queries. By choosing the option "a", you mark the left square, if you select the option "b", then you mark the middle one and if you choose the option "c", you select the right square.

Remember by answering:

- Questions are very short. Therefore, imagine yourself in the light of the content of the question and do not stop on each small things.
- Do not spend a lot of time thinking. Answer what comes first to your mind.
- Try to answer several questions in 1 minute. Then you will finish answering the test in 35 minutes.
- Try to avoid unclear responses that come to your mind suddenly.
- Do not skip any question. You should answer all questions.
- If you have some questions that cannot be linked to your own behavior, try to give more concise answers. Do not try to look good with your own answers. Show your thoughts in a freeway.

The second method in our study is a modified methodology of John Holland’s profession selection survey. The methodology is a typological study of the person, the test is developed by John Holland (Holland *et al.*, 2005). The stimulating material of the test is unique to similar questionnaires and consists of 40 dichotomic alternatives, each of which is presented in a specific profession. The researched person needs to choose one of these. In other words, he/she has to answer the hypothetical question. On the psychological basis of the specialty used in the test, the author assigned 6 scales to 6 person types: realistic; research; artistic; social; business; conventional.

Each type corresponds to 14 professions. It equates scales to quantities and allows to compare clarity of any type in all researchers.

The key.

1. Realistic: 1,2,3,4,5,16,17,18,19,21,31,32,33,34 – all A.
2. Research: 1B, 6A, 7A, 8A, 9A, 16B, 20A, 22A, 23A, 24A, 31B, 35A, 36A, 37A.
3. Artistic: 5B, 9B, 12B, 14B, 15B, 19B, 21B, 24B, 27B, 29B, 30B, 34B,41A,42B.
4. Social: 2B, 6B, 10A, 11A, 12A, 17B, 20B, 25A, 26A, 27A, 36B, 38A, 39A, 41B.
5. Business: 4B, 8B, 11B, 13B, 15A, 23B, 26B, 28B, 30A, 33B, 35B, 37B, 39B,40B.
6. Conventional: 3B, 7B, 10B, 13A, 14A, 18B, 22B, 25B, 28A, 29A, 32B, 40A, 42A, 38B.

Characteristics of types:

1. Realistic – non-social, emotionally stable, and chivalrous people who are focused on the current. This type deals with specific objects and ways how to use these objects. It wants to engage in activities that need motor skills, flexibility, and accuracy. People of this type choose a profession that needs precise action: electrician, mechanic, etc. This type of people is characterized by non-verbal mathematical abilities.

2. Research – workaholic, non-social, precise, independent, ingenious, they like to solve tasks that require abstract thinking and prefer scientific professions such as botany, astronomer, physicist, etc. This type is intelligent, whose both verbal and non-verbal abilities are highly developed.

3. Artistic – complex approach to the world and life, flexibility, originality, independence in decision-making, a distinctive feature than surrounding people. In relationships, it relies on their own sensations, emotions, imagination, and intuition. People of this type like to engage in activities with creative nature. Their verbal abilities are superior, but not always. Motor and perception abilities are high. They dream high even when they are young and are characterized by an accent given on their "I".

4. Social type sets goals and opportunities that allow them to communicate with the surrounding environment. It has a social skill and needs social connections. The main characteristics are intercourse, aspiration to education and upbringing, humanism, tenderness, psychological orientation to man. Activities that this type likes are teaching and treatment. Specialties that fit this type are doctors

Downloaded from www.periodico.tchequimica.com

and psychologist. It tries to keep away from intellectual issues. It solves problems by focusing on emotions, feelings and communication skills. It is depended on the group and surrounding views, it is active. Verbal abilities are developed better than non-verbal abilities.

5. Business type chooses goals, values, and goals that can demonstrate their power, enthusiasm, intensity, precedence, and love for adventure. It wants a leader role and only then, meets its need to gain recognition of others. It is a manager, director, journalist, reporter, artist, diplomat, and sales managers. He does not like handicapped activities, activities that require concentration and intellectual effort. Desirous of verbally-guided tasks with leadership and authority. Aggressive, like to maintain the line of management.

6. Conventional type is characterized by a wish for clearly defined activities and they like to be managed. It adheres to traditions and traditional views and its attitude towards problems has stereotypical-practical and clear properties. Characteristic features: rigid, conservative, dependent. It likes jobs related to office and accounting. Engagement skills are well developed. Non-verbal mathematical talents are good. The weak organizer and leader, their decisions depend on the opinions of others and surrounding people.

Our research was conducted between 2016 and 2018, and its results were compared. The study included 90 students at the age of 17-22 from Turan-Astana University, who are studying at the 1st and 4th courses. It is classified by the following specialties: Pedagogy and Psychology, Psychology. The main criteria for dividing research objects into groups was their specialization.

3. RESULTS AND DISCUSSION

As a result of the research, the following became known:

1. Factors influencing the choice of a profession were found: level of professional plan formation; interest and information levels of the chosen specialty; motives of professional self-definition of students.

2. The main motives of professional development and learning;

3. Determining the degree of readiness for professional activity: the main motives of professional activity; realistic level of expectations of postgraduate education; level of professional mobility; the degree of professional attractiveness of the researchers.

4. The impact and relationships between the professional and personal development of the objects of the research;

5. During studying research groups, some difficulties were identified and its dynamics was examined.

Difference between the groups of students who were included in the study on these indicators was determined. In our study, the relative performance parameters of the 1st and 4th-year students are as follows.

1. In the majority of 4th-year students (78.6%), we can notice that an intermediate type of professional plan is formed. The exact type is typical for specialty groups only. According to the groups participated in general study 21.2% show a specific type. These results are shown by the results of the study. Most students in the 1st year demonstrate the intermediate type of life plan; 24.5% and 21.0% of students have real-life plans. Detected data indicate that the self-determining process of young people takes a long term (Figure 1).

So the difference between the two groups can be calculated by using the t criterion of the Student (Equation 1):

$$t = \frac{X^1 ap - X^2 ap}{\sqrt{m_1^{2} + m_2^{2}{}_2}} \qquad \text{(Eq. 1)}$$

where X^{1}_{ap} is an arithmetic meaning of the first statistical group; X^{2}_{ap} is an arithmetic meaning of the second statistical group; m_1 is an error of the arithmetic average meaning of the first statistical group; m_2 is an error of the arithmetic average meaning of the second statistical group. In determining the difference between the arithmetic average meanings of two groups, parameter $t_{эм}$ is 3.2, i.e. $t\ (3,2) > t_{0,01}$ (2,639), so the difference between the arithmetic average meanings of two statistical groups is statistically significant.

2. Also among the 1st year students, 64.3% students show a medium degree of interest in the selected profession, only 28.2% (on profession TOURISM) show a high degree of interest (7.3%), and among the 4th year students, a medium degree has 75.2%, and a high degree is 24.8% (Figure 2). In determining the difference between the arithmetic average meanings of two

Downloaded from www.periodico.tchequimica.com

groups, parameter $t_{эм}$2.9, i.e. t (2.9)> $t_{0,01}$ (2.639), so the difference between the arithmetic average meanings of two statistical groups is statistically significant.

3. The degree of information awareness on the selected profession is noticed among the students of the profession TOURISM and Psychology, but students of Psychology are aware less. These parameters show that 16% of the results of the study in real terms for students of the 1st year have a high degree of awareness, 33.6% – a medium level and 50.4% – higher than low parameters. Thus, the reason for the high level of awareness among high school pupils is related to the increase in the quality of professional campaign work (Figure 3).

4. External factors influence mostly the choice of profession of respondents. 35.7% of respondents (biologists and pedagogues-psychologists) are motivated by their parents and close relatives, and 35.7% (other psychologists) are motivated with the need to address their own and relatives' problems, and 28.6% (TURISM) are interested in the profession that they have chosen. These results show that the impact of parental influence on children's future profession is reduced (Figure 4).

5. For our first-year students (71.4%), there is a tendency of indirect motives of study and professional development; only 28.6% (biologists) are the direct motives. Direct motives include "creative work or research" (a cognitive motive group), and among indirect motives, there are the motive for being a professional in their profession prevails (achievement motives group). In contrast, the 4th year students have mostly a direct motivation that is 56% while indirect motives are 44% (Figure 5).

In determining the difference between the arithmetic average meanings of two groups, the parameter $t_{эм}$ is -3.6, i.e. t (3.6)>$t_{0,01}$ (2.639), so the difference between the arithmetic average meanings of two statistical groups is statistically significant.

6. For 71.4% of our 1st-year students, the indirect motive of education and professional development prevails; only 28.6% of the direct motives are the priority. Direct motives include "creative work or research" (a cognitive motive group), and among indirect motives, there are the motive for being a professional in their profession prevails (achievement motives group). In contrast, the 4th year students have mostly a direct motivation that is 56% while indirect motives are 44% (Figure 6). In determining the difference between the arithmetic average meanings of two groups, the parameter $t_{эм}$ is -3.6, i.e. t (3.6)> $t_{0,01}$ (2.639), so the difference between the arithmetic average meaning of two statistical groups is statistically significant.

7. For 71.4% of the 1st year students in the studied group, the prevailing influence is an external positive motivation in professional activities. Motivations for personal development of students in the profession of pedagogy-psychologist: "expanding own views", "possibility of intellectual and spiritual growth and social motives: "to help others", "to be useful for the society, etc. The motives of achievement of biologists: "to become a professional in own profession", "to have a well-paid job", "to achieve a certain status", and 28.6% (TOURISM) have prevailing inner motives. In addition, the 4th year students with a high level of internal motivation are 68%, and those whose external motives are 32% (Figure 7). In determining the difference between the arithmetic average meaning of two groups, the parameter $t_{эм}$2.8, i.e. t (2.8)>$t_{0,01}$(2.639), so the difference between the arithmetic average meaning of two statistical groups is statistically significant.

8. True expectations after graduation of the higher education. 35.7% of the 4th year students are characterized by high realistic expectations, 21.5% have lower, and 42.8% have medium expectations. For the 1st year students, medium is 81.1%, and 10.3% is higher, and 8.6% is lower. In determining the difference between the arithmetic average meaning of two groups, the parameter $t_{эм\ -}$ is 3,1, i.e. t (3,1)> $t_{0,01}$ (2,639), so the difference between the arithmetic average meaning of two statistical groups is statistically significant (Figure 8).

9. A profession mobilization capacity. All 42.8% of the 4th year students have a high profession mobilization capacity, 35.7 % show medium, and 21.5 % show levels of this capacity. 1st-year students: Most students have 62.1% of medium, 22.4% – low, 14.5% – high level of the capacity (Figure 9). In determining the difference between the arithmetic average meanings of two groups, the parameter $t_{эм}$ is 2.9, i.e. t (2.9)>$t_{0,01}$ (2.639), so the difference between the arithmetic average meanings of two statistical groups is statistically significant.

10. In the 4th year course 35.7% are characterized by a high professional level, 42.8% – medium and 21.5% – low. This result is based on the average of 70% for the 1st year students, 29.4% – low and 1.3% is for the highest level

Downloaded from www.periodico.tchequimica.com

(Figure 10). In determining the difference between the arithmetic average meaning of two groups, the parameter $t_{эм}$ is 4.3, i.e. t (4.3)>$t_{0,01}$ (2,639), so the difference between the arithmetic average meanings of two statistical groups is statistically significant.

11. Each student of the considered group is distinguished by the peculiarities of interconnection and interactions in the processes of personal and professional development. For example, biologists and psychologists are interconnected closely with these processes. However, for the students of the psychology profession are the key factor is self-fulfillment and personality development, and it is accompanied by personal development. Professional development is one of the few attempts to pursue psychological development on the one hand and, on the other hand, there are only several directions of realization of a psychologist. However, students in the profession biology, on the contrary, have a clear differentiation of professional and personal development. Professional development and prospects of acquiring a certain status, increasing the material wellbeing and so on is only a tool. Thus, professional activities and possible career achievements are the priority for the biological respondents.

Each student passes the following stages in the formation of his/her personal and college student status: adaptation; socialization; creation of a different age society.

4. CONCLUSIONS:

As educational psychologists become clearer about their distinctive contribution in the changing world of early childhood, school-age and post-16 developments, their respective work with children and young people is, paradoxically, likely to become both richer and broader, rather than narrow and introverted. Indeed, when EPs begin to draw more heavily on their own knowledge base in contemporary psychology, previously obscured connections with other disciplines begin to emerge, as the following possibilities illustrate:

• Closer links between educational psychology and clinical neuropsychology.

• Improved collaborative practice involves helping teachers and careers to support children who are experiencing bereavement, be it through the death of a loved-one or parental break-up.

• A reduction in the number of young people involved in crime or who become victims of crime through psychological input into youth offending projects.

• Multidisciplinary collaboration for children with autism.

• Improved childcare practice which promotes the concept of ‘authentic warmth’ in residential and foster homes for looked-after children.

• Improving services for young people in the light of the rediscovered link between insecure attachment and later violence.

Applied psychology can, therefore, help people to understand themselves and others, enable them to maximize developmental opportunities and encourage them to recognize/celebrate diversity among people. Psychology is concerned with understanding how individuals and groups learn and develop and how this informs the development of society: most certainly, it is not about putting people into pigeonholes or labeling people, even though it has often been employed for this purpose. Part of the power of psychology stems from the fact that it draws upon a research and theoretical knowledge base which seeks to understand the complexity of human experience and eschews simple answers to complex questions

Similarly, applied psychologists who identify with the claim of Gale, that psychology is possibly the most powerful force for positive change in human development, are also likely to believe that the benefits of the discipline cannot be restricted to a few people only. In the case of educational psychology, the delivery of high impact, educational and child psychology services in the future will encourage EPs to move away from an over-involvement with both schools and special educational needs and also to develop the confidence in their discipline to challenge mundane and often marginal administration duties, currently demanded by LEAs. Instead, EPs of the future will be required to develop a distinctive professional role and a secure identity which will allow them not only to benefit many more children and young people and the significant adults in their lives but also to ensure that psychological research, theory, and practice is at the forefront of local and national decision making.

Downloaded from www.periodico.tchequimica.com

5. REFERENCES:

1. Anderson, L. M., Blumenfeld, P. R., Pintrick, P. R., Clark, C. M., Marx, R.W., Peterson, P. *Educational Psychology,* **1995**, *30*, 143-157.
2. Baxter, J., Frederickson, W. *Educational Psychology in Practice,* **2005**, *21*(2), 87-102.
3. Cameron, R.J. *Psychology in education portfolio,* Windsor: NFER-Nelson, **1998**.
4. Cameron, R.J., Falkner, J. *Managing the emotional, social and behavioural difficulties of children and young people: A psychological perspective,* Kingston-upon-Thames: Surrey Children's Service, **2005**.
5. Cameron, R.J., Monsen, J. *Educational Psychology in Practice,* **2005**, *21*(3), 283-fcv306.
6. Carr, A. *What works for children and adolescents? A critical review of psychological interventions with children, adolescents and their families,* London: Routledge, **2002**.
7. Connor, M.J. *Anger management training: A review of research findings concerning effectiveness,* Kingston-upon-Thames: Surrey Children's Service, **2002**.
8. Connor-Smith, J.K., Weisz, J.R. *Child and Adolescent Mental Health,* **2003**, *8*(1), 3-10.
9. Csikszentmihalyi, M. *Finding flow: The psychology of engagement with everyday life,* New York: Harper Collins, **1997**.
10. Curran, A., Gersch, I.S., Wolfendale, S. *Applied psychology: Current issues and new directions,* London: Sage, **2003**.
11. Dent, R.J., Cameron, R.J. *Educational and Child Psychology,* **2003**, *19*(1), 3-19.
12. Devitt, P. *Notes on poverty-orientated community development*, London: Overseas Development Institute, **1997**.
13. Doran, C., Cameron, R. J. *Educational Psychology in Practice,* **1994**, *11*(2), 15-23.
14. Dweck, C., Leggett, E. L. *Psychology Review,* **1998**, *95*(2), 256-273.
15. Epps, S., Jackson, B.J. *Empowered families, successful children: Early intervention programmes that work,* Washington, DC: American Psychology Ass, **2002**.
16. Evans, J., Harden, A., Thomas, J., Benefield, P. *Support for pupils with emotional and behavioural difficulties (EBD) in mainstream primary classrooms: A systematic review of the effective-ness of interventions.* London: EPPI-Centre, Institute of Education, **2003**.
17. Evans, S. *Educational Psychology in Practice,* **2005**, 21(2), 131-146.
18. Faupel, A.W. *Emotional literacy: Assessment and intervention,* Windsor: NFER-Nelson, **2004**.
19. Fonagy, P., Steele, M., Steele, H., Higgett, A., Target, M. *Journal of Child Psychology and Psychiatry,* **1994**, *35*(2), 231-257.
20. Fonagy, P., Target, M., Cottrell, D., Phillips, J., Kurtz, Z. *What works for Whom? Acritical review of treatments for children and adolescents,* London: Guildford, **2002**.
21. Frederickson, N., Cline, T. *Special educational needs, inclusion and diversity,* Buckinghamshire: Open University, **2002**.
22. Frydenberg, E., Lewis, R., Bugalshi, K., Cotta, A., McCarthy, C., Luscombe-Smith, N., Poole, C. *Educational Psychology in Practice,* **2004**, *20*(2), 118-134.
23. Gameson, J., Rydderch, G., Ellis, D., Carroll, T. *Educational Psychology in Practice,* **2003**, 20(4), 96-115.
24. Gersch, I. *The Psychologist,* **2004**, 17(3), 142-145.
25. Harrington, R. *Child Psychology and Psychiatry,* **2001**, *6*, 65.
26. Holland, J., Dance, R., McManus, N., Stitt, C. *Lost for words: Loss and bereavement awareness training,* London: Jessica Kingsley, **2005**.
27. Jackson, S., Martin, P.Y. Surviving the care system: Education and resilience. *Journal of Adolescence,* **1998***, 21*, 569-583.
28. Leadbetter, J. *Educational and Child Psychology,* **2005***, 22*(1), 18-28.
29. Lewis, J. *Children & Society,* **1998**, *12*(2), 136-140.

Downloaded from www.periodico.tchequimica.com

30. Lewis, R., Frydenberg, E. *British Journal of Educational Psychology,* **2002**, *72*, 419-431.
31. Lysytsia, N., Martynenko, M., Bielikova, N., Gron, O., Us, M. *Entrepreneurship and Sustainability Issues*, **2019**, *7*(1), 336-352. http://doi.org/10.9770/jesi.2019.7.1(25).
32. Lunt, I., Majors, K.E. *Educational Psychology in Practice,* **2000**, *15*(4), 237-245.
33. McNamara, E. *Motivational interviewing: A form teacher's manual,* Merseyside: Positive Behaviour Management, **1998**.
34. Miller, A. *Teachers, parents and classroom behaviour: A psychosocial approach,* Maidenhead: Open University Press, **2003**.
35. Monsen, J. Graham, B., Frederickson, N., Cameron, R. J. *Educational Psychology in Practice,* **1998**, *13*(4), 234-244.
36. Moore, J. *Educational Psychology in Practice,* **2005**, *21*(2), 103-116.
37. Morton, J. *Understanding development disorders: A causal modelling approach,* Oxford: Blackwell, **2004**.
38. Norwich, B. *School Psychology International,* **2005**, *26*(4), 387-397.
39. Nunkoosing, K. *Empowerment,* Portsmouth: University of Portsmouth, **2000**.
40. Rappaport, J. *Prevention in Human Services,* **1984**, *3*, 1-7.
41. Rees, C., Farrell, P., Rees, P. *Educational Psychology in Practice*, **2003**, *19*(1), 35-47.
42. Rymashevskaya, N., Malysheva, M., Pisklakova-Parker, M. *Entrepreneurship and Sustainability Issues*, **2017**, *5*(1), 138-149.
42. Seligman, M. *Authentic happiness: Using your new positive psychology to realize your potential for lasting fulfilment,* London: Brealey, **2002**.
43. Seligman, M., Csikszentmihalyi, M. *American Psychologist,* **2000**, *55*(1), 5-14.
44. Smith, P. *Review of the functions and contribution of educational psychologists in England and Wales in light of Every Child Matters: Change for children,* London: DfES, **2005**.
45. Stobie, I., Boyle, J., Woolfson, L. *School Psychology International,* **2005**, *26*(1), 5-28.
46. Sukhodolsky, D. Solomon, R., Perine, J. *Journal of Child and Adolescent Group Therapy,* **2002**, *10*(3), 159-170.
47. Vinichenko, M.V., Klementyev, D.S., Rybakova, M.V., Malyshev, M.A., Bondaletova, N.F., Chizhankova, I.V. *Entrepreneurship and Sustainability Issues*, **2019**, 7(1), 92-104.
48. Wagner, P. *School consultation: A handbook for practising educational psychologists.* London: Educational Psychology Consultation Service, **1995**.
49. Werner, E.E., Smith, R.S. *Vulnerable but invincible: A longitudinal study of resilient children and youth,* New York: McGraw Hill, **1982**.
50. Willcutt, E., Pennington, B. *Journal of Child Psychiatry,* **2000**, *41*(8), 1039-1048.
51. Wilson, S.J., Lipsey, L.W., Derzon, J.H. *Journal of Consulting and Clinical Psychology,* **2003**, *71*(1), 136-149.
52. Wood, A. *Special Children,* **1998**, *2*, 12-13.
53. Zimbardo, P.G. *American Psychologist,* **2004**, *59*(5), 339-355.

Downloaded from www.periodico.tchequimica.com

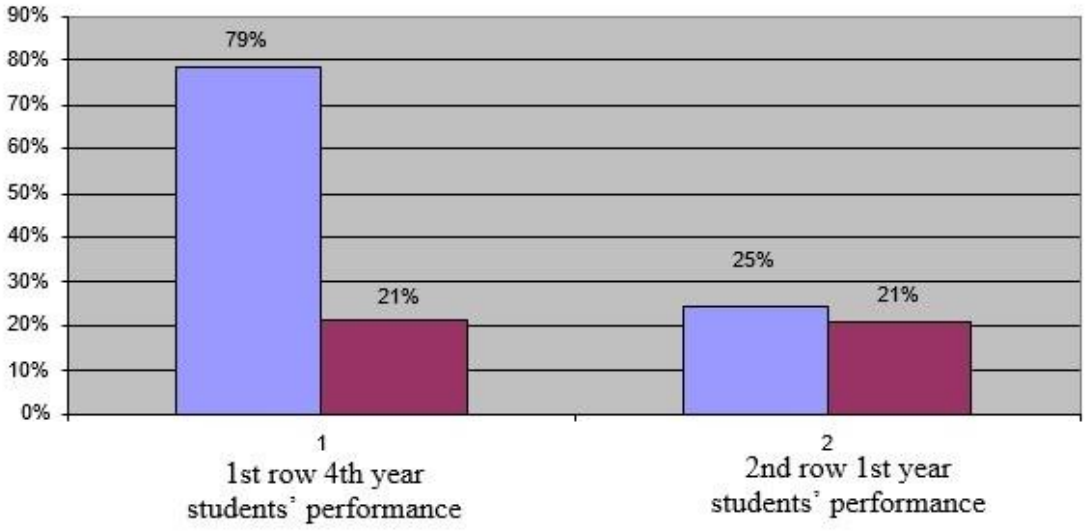

Figure 1. *1st and 4th year students. Relative percentage ratio of students` professional plans*

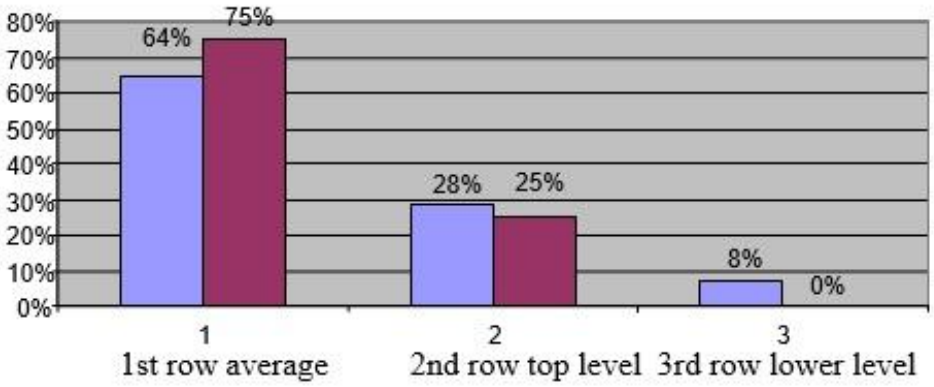

Figure 2*. Percentage of students of 1st and 4th year students' interest in their chosen specialty*

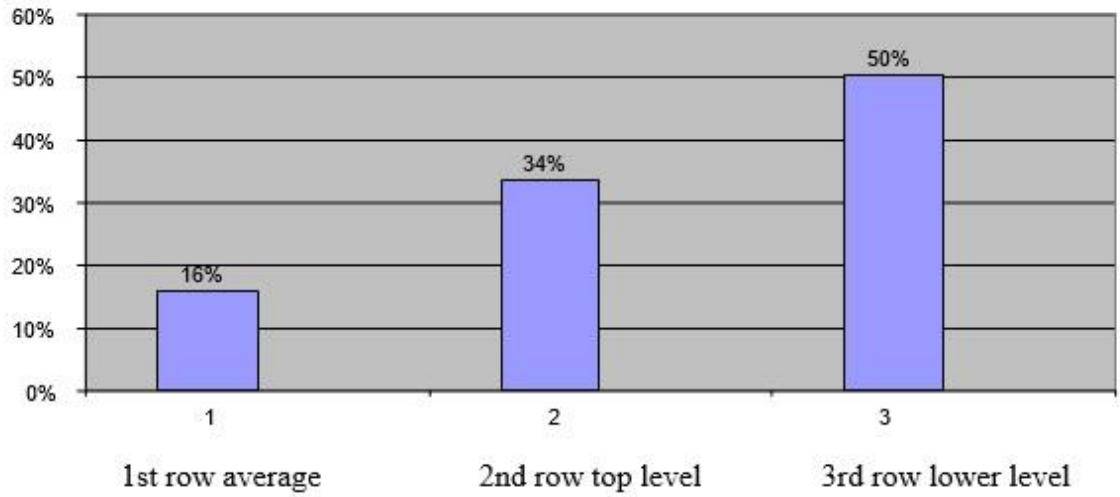

Figure 3*. Indicators of 1st year students on selected specialties*

Downloaded from www.periodico.tchequimica.com

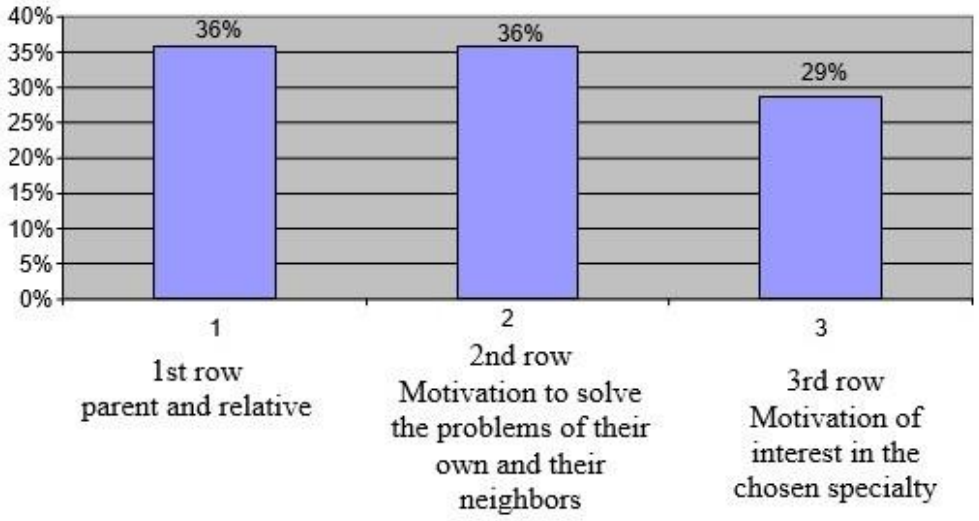

***Figure 4**. Indicators of the basic motivational factors of the students in the chosen specialty*

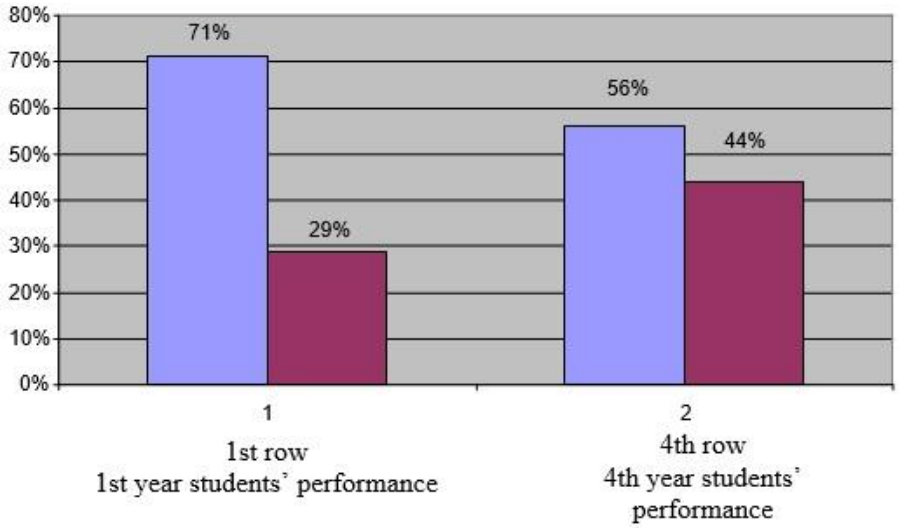

***Figure 5**. Study and professional development of the 1st and 4th year students' relative indices of motives*

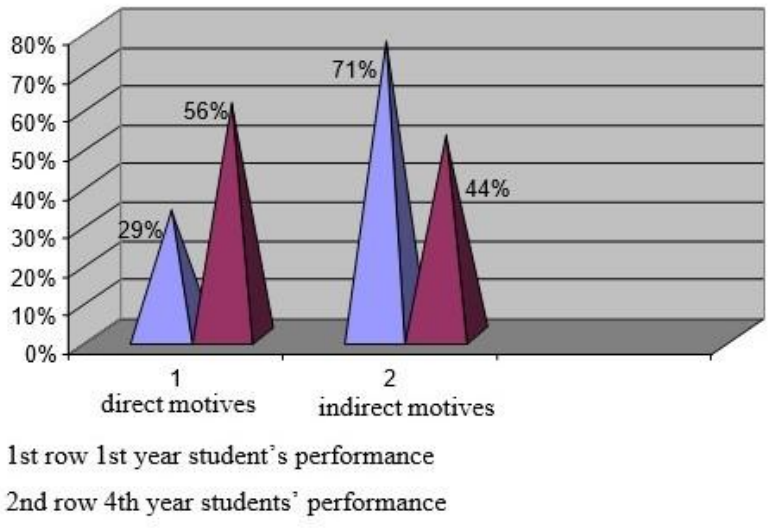

***Figure 6**. Comparison of the level of formation of direct and indirect motives of the 1st and 4th year students in the specialty*

Downloaded from www.periodico.tchequimica.com

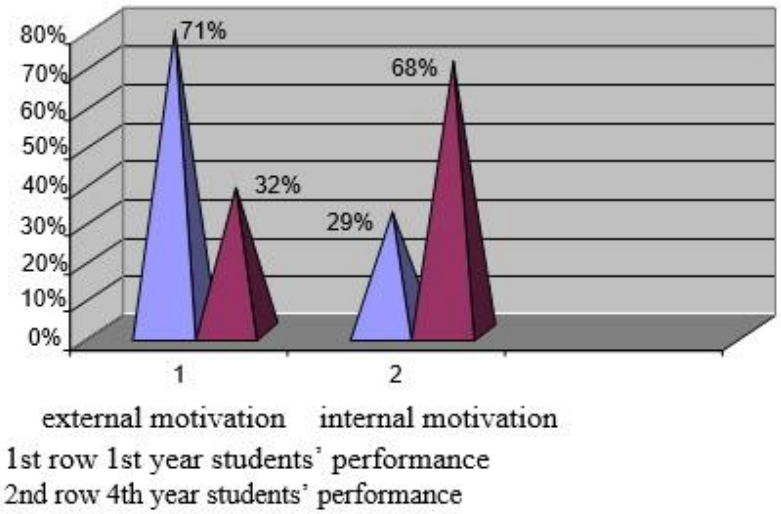

***Figure 7**. Comparison of the level of formation of the internal and external motivation of students of the 1st and 4th year students in the specialty*

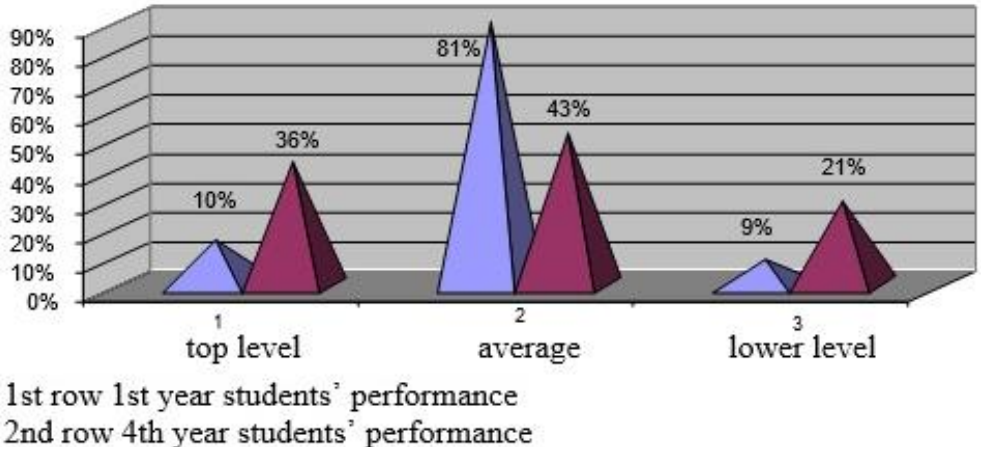

***Figure 8**. Comparison of the level of students' expectations after graduation from the 1st year and 4th year students*

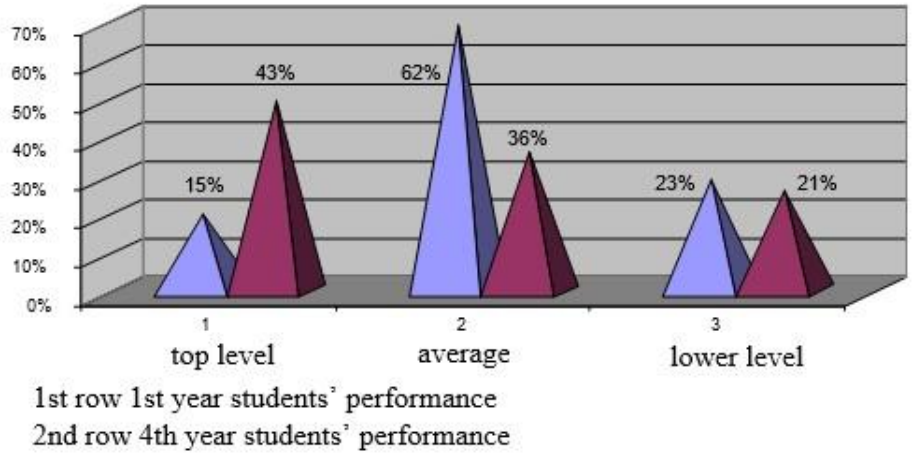

***Figure 9**. Comparative performance indicators of the 1st and 4th year students' professional concentration levels*

Downloaded from www.periodico.tchequimica.com

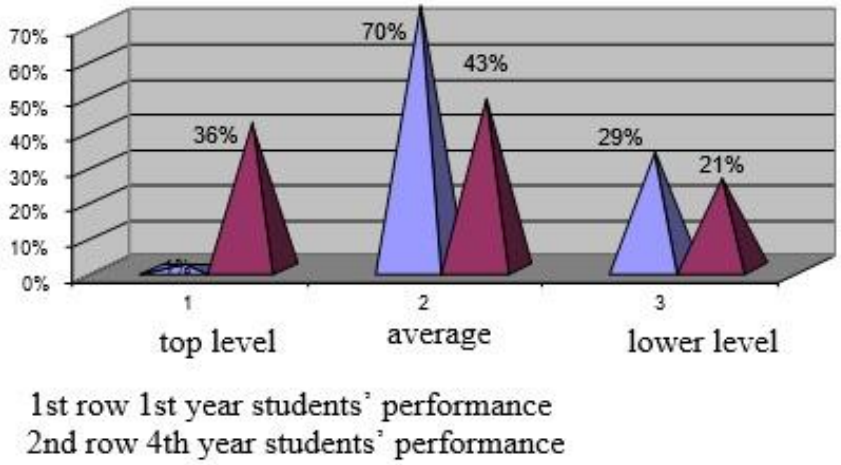

***Figure 10**. Comparative indicators of the level of professional success of the 1st year and 4th year students*

PERIÓDICO TCHÊ QUÍMICA
ARTIGO ORIGINAL

FORMAÇÃO AMBIENTALMENTE ORIENTADA NO PROCESSO DO PROGRAMA PROFISSIONAL PARA ESTUDANTES

ENVIRONMENTALLY-ORIENTED TRAINING IN THE PROCESS OF THE PROFESSIONAL PROGRAMME FOR STUDENTS

ЭКОЛОГИЧЕСКИ ОРИЕНТИРОВАННОЕ ОБУЧЕНИЕ В ПРОЦЕССЕ ПРОФЕССИОНАЛЬНОЙ ПРОГРАММЫ ДЛЯ СТУДЕНТОВ

DLIMBETOVA, Gaini K.[1*]; ABENOVA, Saulet U.[2]; MANDYKAYEVA, Almagul R.[3]; STUKALENKO, Nina M.[4]; BAKIROVA, Kulzhakhan S.[5];

[1,2,3] L.N. Gumilyov Eurasian National University, Department of Social Pedagogics and Self-Knowledge, Nur-Sultan – Republic of Kazakhstan

[4] Branch of JSC "National Center for Professional Development “Orleu”", Institute of Professional Development in Akmola region, Kokshetau – Republic of Kazakhstan

[5] Abai Kazakh National Pedagogical University, Department of Geography, Ecology, and Tourism, Nur-Sultan – Republic of Kazakhstan

** Correspondence author*
e-mail: gainid@mail.ru

Received 04 September 2019; received in revised form 20 October 2019; accepted 24 October 2019

RESUMO

Os processos químicos formam a base para a existência de toda matéria viva e inanimada. Além disso, a base para o desenvolvimento do mundo material e a determinação das características dos objetos e materiais pertence à área de assunto do processamento químico. Nesse sentido, o uso de recursos naturais torna-se um problema urgente, a fim de determinar a possibilidade de sua máxima conservação com um uso mais intensivo. Para os estudantes da Faculdade de Química, isso é especialmente importante, pois são eles que implementam os processos de produção química que causam os danos mais significativos ao meio ambiente. Além disso, a principal tarefa da ecologização é minimizar os danos recebidos. Manter o equilíbrio a esse respeito é a relevância da pesquisa. A inovação da pesquisa é determinada pelo fato de que, pela primeira vez, a competência ambiental é considerada um processo de futuro apoio profissional ao trabalho na indústria química. No processo de pesquisa, foi utilizado o método longitudinal que incluiu um experimento paralelo do qual participaram os grupos controle e experimental. Os autores assumem que a competência ambiental deve ser determinada no início do trabalho de cada profissional e influenciá-los aplicando conhecimentos especializados. O artigo revela as características metodológicas e essenciais da aplicação da competência ambiental na formação profissional de estudantes veteranos. O uso da abordagem proposta permitirá às autoridades regionais exercer controle operacional e modelar os cenários para o desenvolvimento dos processos de ecologização do território devido à ecologização da educação, levando em consideração as mudanças ambientais externas.

Palavras-chave: *competência ecológica, tomada de medidas, treinamento, estudantes, especialidade química.*

ABSTRACT

Chemical processes form the basis for the existence of all living and inanimate matter. Moreover, the basis for the development of the material world and the determination of the objects’ and materials’ features belongs to the subject area of chemical processing. In this regard, the use of natural resources becomes an urgent problem in order to determine the possibility of its maximum conservation with more intensive use of it. For students of the Faculty of Chemistry, this is especially important since it is they who implement the processes of chemical production that cause the most significant harm to the ecological environment. In addition, the main task of ecologization is to minimize the damage received. Maintaining balance in this regard is the relevance of the research. The novelty of the research is determined by the fact that for the first time environmental competence is considered as a process of future professional support of work in the chemical industry. In the process of research, it was used the longitudinal method, which included a parallel experiment,

Downloaded from www.periodico.tchequimica.com

in which participated the control and the experimental groups. The authors assume that environmental competence should be determined at the beginning of the work of each professional and influence them by applying specialized knowledge. The article reveals the methodological and essential characteristics of applying environmental competence in the professional training of senior students. The use of the proposed approach will allow the regional authorities to exercise operative control and model the scenarios for the development of the processes of ecologization of the territory due to the ecologization of education, taking into account the external environment changes.

Keywords: *ecological competence, taking measures, training, students, chemical specialty*.

АННОТАЦИЯ

Химические процессы составляют основу существования всего живого и неживой материи. Вместе с тем, основа развития материального мира и определение свойств объектов и материалов принадлежит предметной области химического процессинга. В связи с этим, использование природных ресурсов становится насущной проблемой для того, чтобы определить возможность максимального его сохранения при более интенсивном его использовании. Для студентов химического факультета это особенно актуально, так как именно они реализуют процессы химического производства, которые наносят экологической среде наибольший вред. Вместе с тем, основная задача экологизации состоит в том, чтобы минимизировать полученный вред. Сохранение равновесия в данном ключе и составляет актуальность проводимого исследования. Новизна исследования определяется тем, что впервые экологическая компетенция рассматривается как процесс будущего профессионального обеспечения работы в химической промышленности. В процессе исследования использовался продольный метод, который включал параллельный эксперимент, в котором участвовали две группы: контрольная и экспериментальная. Авторы определяют, что экологическая компетенция должна быть определена в начале работы каждого профессионала и влиять на применение им специальных знаний. В статье раскрывается методологическая и сущностная характеристика применения экологической компетенции в профессиональной подготовке студентов старших курсов. Использование предложенного подхода позволит региональным властям осуществлять оперативный контроль и моделировать сценарии развития процессов экологизации территории вследствие экологизации образования с учетом изменений внешней среды.

Ключевые слова: *экологическая компетентность, принятие мер, обучение, студенты, химическая специальность.*

1. INTRODUCTION

A characteristic feature of the last century was the impetuous unrestrained striving for economic and technological development. Ignorance, and in most cases – ignoring the laws of nature leads to terrible consequences, the proof of this is the environmental crisis of our time, which is caused by the depletion of vital natural resources (Lee *et al.,* 2016). Planetary cataclysms, such as increased volcanic activity or icing, soil degradation or desertification of fertile lands, snowballed a significant change in the biosphere and from time to time put the human community before the choice of dying or changing lifestyles: migrating, resorting to tillage and switching to settled or introduce some new forms of management (Lowan-Trudeau, 2017). But until XX century, on Earth, people did not face such changes, as a result of which nature would find itself in a state of unstable equilibrium, and people – before the choice between death and a fundamentally different way of being (Richardson *et al.,* 2016; Maslennikov *et al.,* 2017; Akhmetshin *et al.,* 2019a; Akhmetshin *et al.,* 2019b).

Over the past 50 years, the deterioration of most ecosystems in the biosphere can be observed, catastrophic depletion of soil, mineral resources, a significant decrease in bioproductivity and biodiversity, unprecedented pollution of the Earth's surface; hydrosphere and atmosphere are associated with the intensive growth of the planet's population and the development of scientific and technological progress (Lopes *et al.,* 2014). It is the need to meet the increasing needs of human society led to a massive expansion of the volume of economic activity, changes in the proportions of the world economy, technique and technology, production capacity, product range, production, and personal consumption. The world has developed production and consumption patterns that do not meet the conditions for the healthy coexistence of man and nature (Kim *et al.,* 2017; Rusko and Lumnitzer, 2017; Isakova, 2018).

One of the most potent levers out of the

Downloaded from www.periodico.tchequimica.com

crisis, which has been developed in the relationship of man with nature, is environmental education. Noting the social orientation of environmental problems, N. Reimers pointed out that one of the ways out of the environmental crisis is regulated co-evolution in the “society-environment” system. At the present stage, mankind should understand its inalienability from nature, revise its principles and beliefs, assess the truth formulated 400 years ago by the English philosopher F. Bacon "We cannot control nature except by submitting to it" (Flagg and Bates, 2016; Genc *et al.,* 2018; Grishaeva *et al.,* 2018).

Due to the expansion of human activity, social ecology is actively developing – a science that studies the patterns of society’s impact on the biosphere and changes in it, affects every single person and society as a whole. The goal of social ecology is the formation of knowledge about the harmonious relationship between society and nature, the principles of rational environmental management, worldview beliefs that nature that surrounds us is our home, and its preservation is a condition for the survival of humanity. Environmental consciousness and culture are formed by using the principles and methods of environmental education and training (Grodzinska-Jurczak, 2000; Adler *et al.,* 2016; Manzheley, 2016; Kaigorodova *et al.,* 2017).

An essential role in the awareness of a person of their place in nature belongs to environmental ethics. Ecological ethics is the study of the fundamentals of relations with nature, based on the recognition of the moral status of nature, high appreciation of its values, respect for the right to the harmonious existence of all components of natural ecosystems (Pryor *et al.,* 2005). The subject of ecological ethics is the studies of the foundations of the moral attitude of a person to nature, the analysis of stereotypes of human behavior that lead to environmental problems, the search for ethical ideals of the relationship of man to nature that will help overcome the ecological crisis (Lee, 2007). Ecological ethics is designed to identify new principles and new approaches to relationships in the “man-nature” system, new behaviors that will contribute to solving environmental problems. Ethics in an ecological sense is a restriction of freedom of action in the struggle for existence. Ecological ethics is based on the principle of the 20th-century German philosopher Albert Schweitzer - the principle of reverence for life, the central idea of which is the postulate “all living beings are worth living.” The great humanist wrote: “The more we look into nature, the more we realize that we are connected with everything living in nature. A person cannot live only for themselves - we must realize that any life is a value”, because ethics, in their opinion, is “a person’s unlimited responsibility for everything living on the Earth” (Mueller, 2009; Marekha and Omelyanenko, 2017).

Man is the only creature that can control and manipulate the environment, destroy or preserve it. Knowledge of the consequences of environmental impact is an essential element of human culture. The present and the future are more determined by a person. In turn, the actions that a person will do are determined by their education. In order to understand the essence of the concept of ecological culture and its components, it is worth considering the concept of culture and its relationship with nature in a general sense (Fateev and Fateeva, 2016; Zeleeva and Asafova, 2016; Sitarov and Urekeshova, 2017; Cherdymova *et al.,* 2018).

The goal of the experiment’s formative stage, which lasted during 2015-2018, was the practical verification of the effectiveness of the technology to form an environmental culture of students of the chemistry faculty in the process of professional training (Sasongko *et al.*, 2019).

2. LITERATURE REVIEW

The realization of the goal and main tasks of the formation of ecological culture is based on the principles of the interrelation of theoretical knowledge with the practical activity of students; the inclusion of ecological aspects in the structure of subject, special generalizing topics; the combination of classroom activities in nature (excursions, field camps, tourist trips); the use of problematic teaching methods (role-playing games, environmental clubs, research activities, experiments, observations); a combination of classroom and extracurricular environmental work (Kimmerer, 2012; Aleksandrova *et al.,* 2019; Sagiyeva *et al.*, 2018).

The future chemist should be able to assess historical and modern processes and problems in the life of the country, trends in educational development, have high mortality, possess organizational and professional skills, professionally solve problems according to their social consequences, be fluent in a foreign language, use one of the additional foreign languages professionally (Schleicher, 1989).

The main production functions that the future chemist should possess include: a

Downloaded from www.periodico.tchequimica.com

predictive one, which implies awareness of environmental situations, the ability to solve them, the preparation of laboratory instruments, utensils, reagents for chemical analysis; technical - the ability to assess the pollution of the hydrosphere, atmosphere, biosphere; technological - the ability to take samples and conduct analyses of agricultural products, to make practical decisions to reduce environmental pollution (Gough, 2017). The content of production functions, which consist of the tasks and skills of future chemists, are presented in the formula of production functions, typical tasks of activity and skills that a chemist should have (Brown, 1992; Aliyeva *et al.,* 2016).

From the point of view of the issue that is solved in our research, it is significant that the characteristics of the age period of student chemists are the search for harmony in the natural world and the comprehension of one's own position in relations with him (Sofluau and David, 2018). At this age, the predominantly aesthetic, contemplative perception of nature is especially pronounced, the relation to which is objective in nature (Schleicher, 1975; Schleicher, 1989). Interaction with the natural world is carried out on the basis of mastering the technologies of aesthetic development of natural objects, namely: manifestations of sensual aesthetic susceptibility to them; individual semantic assessment of their life conditions; emotional responsiveness in situations of communication with them; and, finally, in the ability to find a cultural form of preserving and expressing one's impression of these objects (in drawings, poems, photographs, music) (Liu and Chai, 2012). Consequently, it is appropriate to note the role of excursions into nature, during which students through emotions can feel the beauty of nature, its uniqueness; there is an enrichment of the motives of a responsible attitude to nature and the development of environmentally literate behavior (Generalov, 1998). It is worth focusing on the fact that adolescence itself is associated with the formation of such personal qualities as responsibility, perseverance, frugalism, benevolence, self-criticism, readiness to perform various tasks, which determine the result of harmonious interaction with nature and the formation of ecological culture (Anderson, 2008).

We share the opinion that the goal of modern vocational education is the appropriate preparation of chemists to implement rational activities aimed at protecting and improving the state of the environment, preventing civilizational threats and solving global environmental problems associated with human activities (Harding *et al.,* 2018). Thus, the formation of the ecological culture of future chemists provides for the mastery of in-depth environmental knowledge, relevant environmental skills and abilities, due to the presence of motivation and value orientations regarding environmental activities aimed at preserving the environment, which are formed during the study of academic disciplines, expand and refined over many occupations and turning into beliefs (Gevorgyan and Adanalyan, 2009).

3. MATERIALS AND METHODS

In the course of professional training of future students of the Faculty of Chemistry, the level of formation of indicators of motivational, axiological, cognitive, reflective and practical criteria of ecological culture was diagnosed. In the process of research, it was used the longitudinal method, which included a parallel experiment, in which two groups participated: the control and the experimental. Their composition was identical in all control and neutral characteristics that could affect the consequences of the experiment.

Experimental and control groups were identified (the number of students, respectively, 152 and 163). Diagnostics covered students of the III and IV years of study. In the control groups (CG), the educational process took place according to the traditional program of studying environmental disciplines, and in the experimental groups (EG), the technology of forming an ecological culture was developed in the learning process. Comparison of both research objects was carried out both before the experiment and after it. This made it possible to compare the initial and final characteristics of the process of forming an ecological culture, namely, ecological knowledge, and motivation, value orientations regarding the nature, environmental awareness, and nature conservation activities of students of the chemical faculty, thus proving the effectiveness to introduce the proposed technology into the educational process.

According to the results of the input diagnostics, four levels of forming the criteria of ecological culture in the CG and the EG students (primary, medium, sufficient, high) were inserted. According to a specific structure of ecological culture, a questionnaire for students was developed, which was used to study the criteria for the formation of ecological culture among future students of the Faculty of Chemistry. The

Downloaded from www.periodico.tchequimica.com

questionnaire contained blocks of characteristics that should be evaluated by students at various stages of experimental work.

The first block of the questionnaire contained questions (positions 1-3), aimed at studying the prerequisites for selection by future chemists of professional activity. The second block (positions 4-5) is aimed at determining the importance of students' formed knowledge related to the performance of their professional duties. The third block of the questionnaire (position 6-7) was meant to research the level of awareness development of one's own involvement in environmental protection activities and the value orientations of the chemist, which have a positive effect on the process of ecological culture formation. The fourth block (position 8) was designed to determine the level of development of the relevant skills. The formative experiment was carried out in several stages. A significant place in the experimental work was occupied by the diagnosis of the level of motivation, the formation of relevant knowledge, skills, and personal qualities of students, which were carried out in two stages – at the beginning and at the end of the experiment. The level of formation of each of chemical faculty students' environmental criteria was evaluated on the basis of the developed indicators.

4. RESULTS AND DISCUSSION:

Let dwell on the evaluation of specific criteria. Thus, the motivational criterion envisaged the formation of a sustainable motivation for conscious environmental activity among future students of the chemistry department.

As can be seen from the data presented in Figure 1, students' motivation increases in the process of experimental work, which indicates a conscious choice of their future profession. To assess the level of motor development of the professional activities of students of the chemical faculty, we chose K. Zamfir's method in A. Rean's modification, based on the concept of external and internal motivation. Having an internal type of motor activity in itself is essential for the individual. With the external type of motivation, there is the desire to meet other needs, external to the content of the activity itself in the basis of professional activity. Most of the students indicated that they were seeking to preserve nature (0.84), where they will be able to participate in environmental protection measures (0.76), while they will be implemented precisely in the field of ecology (0.72). Other motives are not so important (Table 1).

Severity indicators of each type of motivation (internal motivation IM, external positive motivation IPM, and external negative ENM) are calculated by the formulas (Equations 1-3). The results of the calculations are shown in Table 2.

The general motivational complex can be represented in the form of inequality: IM (4,02) >IPM (2,73) >ENM (2,08). This inequality indicates that the motivational complex for the choice of the profession of students of experimental groups belongs to the optimal motivational complex. Thus, most of the students of the chemical faculty who took part in the experiment deliberately expressed a desire to preserve nature following internal motives.

Axiological criterion envisaged the development of awareness of the need for a responsible attitude to nature in the process of the professional activity. To check the level of formation of a specific list of value orientations, we have prepared scales containing indicators by the degree of importance and level of formation in the respondents' self-assessment (sections were taken twice – before and after the experiment. The results of valuable orientations formation are shown in Table 3.

In the course of the experiment, such value orientations as the realization that not only man but also every kind of animal and plant has the right to exist as a result of a long evolution (0.69-0.89), the ability to observe nature (0, 72-0.89), the improvement of their personal inner world on the feeling of human unindifference, dignity, care, mutual aid (0.71-0.88), the desire to preserve the flora and fauna (0.73-0.9), the desire to multiply the wealth of nature (0.7-0.88).

According to the cognitive criteria for the formation of ecological culture, it assumed the level of assimilation of ecological knowledge and its implementation in the process of professional activity, when the knowledge gained is transformed into ecosystem understanding. To check the level of formation of professional environmental knowledge among students, we have prepared scales that contain indicators of the level of formation of the relevant knowledge in the self-assessment of respondents from the experimental and control groups (sections were made twice – before and after the experiment). The results are shown in Table 4.

The level of formation of professional

Downloaded from www.periodico.tchequimica.com

environmental knowledge among students of experimental groups (Figure 2) for the experiment was the lowest with regard to knowledge concerning objects, phenomena, and environmental processes (0.64). After the experiment, the level of knowledge formation has changed significantly. Knowledge of the conservation of plant and animal world has reached a high level (0.92).

The level of knowledge on economic approaches to environmental protection remains insufficient, although, comparing with the initial, there is a tendency to growth (0.75 at the beginning of the experiment and 0.86 at the end) and knowledge on the protection of atmospheric air, water resources, soil (0, 76 at the beginning of the experiment and 0.86 at the end).

It is worth noting that among students there is a tendency to receive modern environmental education, which will contribute to the development of their professionalism.

The practical criterion covered the skills and abilities that contribute to the formation of ecological culture. The results of the dynamics of the level of professional (gnostic, design, constructive, organizational, communicative) skills formation necessary to form the environmental culture among students of the chemical faculty are shown in Figure 3.

Among the Gnostic skills after the experiment, then the ability to analyze and evaluate the state of the environment (0.9), analyze, select and apply optimally suitable research methods in professional activities (0.89) gained the highest development. The lowest level was gained by the ability to analyze the general ecological state of the region by indicator organisms (0.83), analyze the possibilities of ecological imbalance during professional activities (0.84), analyze economic losses from the air, water, and land pollution (0.84).

Design skills have gained positive dynamics throughout the experiment. The ability to develop proposals for the creation of natural protected areas (0.91), to develop recommendations for rationing and limiting the anthropogenic impact on the environment (0.89), to determine the types of economic losses from environmental pollution by enterprises (0.88) has gained unique development. However, in our opinion, students lack practical experience acquired in the course of their professional activities, as evidenced by the insufficiently formed skills to design trends and ways to accelerate progress and methods to neutralize negative phenomena (0.84) and predict the dynamics and design a model of the state of the biosphere time and space (0.82).

Among constructive skills there is a positive trend in the development of such skills as choosing the most appropriate methods and ways to overcome the environmental crisis (0.71 at the beginning of the experiment and 0.9 after its completion), to realize the goals and objectives of developing an environmentally stable society by selecting information methods of environmental education (0.69 at the beginning of the experiment and 0.87 after its completion), determine the types, methods and stages of work for the organization of the system of environmental monitoring (0.68 at the beginning of 0.84 to experiments and after its completion). However, attention should be paid to the types and methods of environmental monitoring and the use of computer technology in assessing the state of the environment. In the block of organizational skills, the highest level of formation has been acquired by the ability to promote the formation of an environmental outlook (0.89), to carry out environmental protection measures (0.89), to encourage everyone to systematical, purposeful, continuous communication with the environment in the process of various activities (0.88).

Communicative skills have turned out to be the most developed, namely: to develop communication skills in a team (0.89), to participate in discussions and the choice of optimal solutions (0.9), to organize the work of a group of subordinates (0.87), to manage their emotions, behavior in time of communication with the leadership (0.9), to stimulate the interest of the younger generation in solving environmental problems of our time (0.88). This indicates that students are already ready to work in a team; that's why it is advisable to attract students to participate in public environmental associations, research work, environmental festivals, competitions, tourism. After the experiment, communication skills (0.89) and organizational skills (0.88) reach a high level of development.

The reflexive criterion (Figure 4) provided for the development of self-awareness, self-realization, which will help in future professional activity. Data analysis suggests that a significant part of students are aware of their own involvement in the implementation of environmental activities, without which it is impossible to guarantee the environmental safety of the environment and society. Among the self-realization types of own involvement in environmental protection activities, the largest

Downloaded from www.periodico.tchequimica.com

tendency for growth compared with the initial level during the experiment was: development of environmental responsibility (0.89), assessment of the environmental situation and implementation of environmental protection measures in accordance with environmental legislation (0.88), encouraging the younger generation to actively protect the environment through the formation of relevant value orientations, knowledge, intelligence skills (0.89). The summarized data on the levels of indicators' formation of the ecological culture of the chemical faculty students are presented in Table 5.

Thus, according to the motivational criterion high level was reached by 36.2% of the students of the experimental groups, whereas in the control groups – only 14.3%, sufficient – 44.6% and 40.1%, respectively, there has been a decrease in the medium – 16.0% and 36, 9% respectively and the initial level – 3.2% and 8.7%. The identified positive changes among the students of experimental groups indicate significant changes in the motivational sphere, the dominance of professionally oriented motives relating to nature, interest in solving modern environmental problems, the presence of environmentally valuable orientations and incentives to carry out professional activities.

According to the axiological criteria a high level was reached by 35.6% of the students of the experimental groups, 15.6% – by the students of the control groups, 46.5% and 38.8%, respectively, reached sufficient level, 14.5% and 37.3% – medium, and the initial level was reached respectively by 3.4% and 8.3%. These data indicate the formation of ideological environmental positions, which become vital principles, determine the nature of its activities as a future specialist in the field of ecology.

According to the cognitive criterion a high level was reached by 38.2% of the students in the experimental groups, 14.5% – students of the control groups, 43.6% and 40.2%, respectively – the sufficient level, 14.1% and 37.1%, respectively – the medium level, respectively – 4.1% and 8.2% – beginner. The data obtained indicate an increase in the volume of professional knowledge acquired by future specialists on ecology, environmental protection and rational environmental management, an understanding of the positive and negative anthropogenic impact on the environment, and understanding the causes of the current environmental crisis in the country (Pechancová *et al.*, 2019).

Thus, according to the reflexive criterion a high level was reached by 37.4% of the students of the experimental groups, whereas in the controls – only 15.4%, sufficient – 42.4% and 40.4%, respectively, a decrease in the medium level – 16.9% and 36, respectively, and the initial level, respectively, – 3.3% and 8.2%. These indicators show that students are aware of their own involvement in solving environmental problems and the ability to make environmental-friendly decisions.

According to the practical criterion, a high level was reached by 36.4% of students of experimental groups, 15.2% – in the control groups, 42.3% and 39.8%, respectively, – sufficient, 17.8% and 36.4%, respectively, – beginner, and 3.5% and 8.6% reached the beginner level. The revealed positive changes testify to the mastery of general professional and specialized skills of interaction with the environment.

Evaluation of experimental data allowed us to detect not only the high efficiency of the proposed technology for the formation of an environmental culture of the chemical faculty students but also to trace the positive dynamics of the quality indicators growth.

According to the data obtained, the increase in indicators of a high level of ecological culture formation among students of experimental groups according to the motivational criterion was 23% and only 0.9% among the control groups; a sufficient level – respectively 7.3% and 3.1%; by axiological criterion, this increase was at a high level of 21.8% (2.0%), sufficient – 10.1% (2.2%); according to the cognitive criterion, respectively, at a high level – 24.8% (1.2%); according to the reflexive criterion, this increase was at a high level of 23.3% (1.5%); according to practical criteria, respectively, at a high level – 22.1% (0.7%).

Results analysis of a series of sections of the formative experiment stage have shown a decrease in the number of students who had an initial level of ecological culture according to the above-given criteria, respectively, an increase in students of experimental groups was – 6.9%, – 5.9%, – 5.2%, – 6 , 2%, – 6.4%; in the control groups – 1.2%, – 0.9%, – 1.0%, – 1.1%, – 1.1%.

In both compared categories, there was a decrease in the number of students with a medium level of ecological culture, but this tendency is more pronounced in experimental groups. Consequently, a decrease in the proportion of students who had initial and medium levels of ecological culture led to an

Downloaded from www.periodico.tchequimica.com

increase in the number of students with sufficient and high levels. These indicators are more clearly expressed in the experimental groups. The dynamics of the formation levels of the ecological culture of chemical faculty students in control (CG) and experimental (EG) groups are reflected in Figures 5 and 6.

After finishing the pedagogical experiment, the methods of mathematical processing of numerical data using the Kolmogorov-Smirnov λ-criterion have been used, and a point has been found where the sum of the discrepancies between the empirical distributions in the EG and CG is the greatest, and the significance of differences is evaluated (Tables 6-10).

Let us formulate the null hypothesis (H0) about the normal distribution: the empirical distributions of the levels of formation of motivational, axiological, cognitive, reflexive and practical criteria of the ecological culture of the CG and the EG do not differ. H1: the empirical distributions of the levels of formation of the motivational, axiological, cognitive, reflective and practical criteria of the ecological culture of the CG and the EG are different.

The critical value is taken as follows: $\lambda_{0.05} = 1.36$. According to the λ-criterion, since 2.34> 1.36, the discrepancies between the empirical distributions in the EG and CG are certain (Equation 4). Therefore, the hypothesis H1 is accepted.

The critical value is taken as follows: $\lambda_{0,05} = 1,36$. According to the λ-criterion, since 2,46>1,36, the discrepancies between the empirical distributions in the EG and CG are certain (Equation 5). Therefore, the hypothesis H1 is accepted.

The critical value is taken as follows: $\lambda_{0,05}=1,36$. According to the λ-criterion, since 2,40>1,36, the discrepancies between the empirical distributions in the EG and CG are certain (Equation 6). Therefore, the hypothesis H1 is accepted.

The critical value is taken as follows: $\lambda_{0,05}=1,36$. According to the λ-criterion, since 2,13>1,36, the discrepancies between the empirical distributions in the EG and CG are certain (Equation 7). Therefore, the hypothesis H1 is accepted.

The critical value is taken as follows: $\lambda_{0,05}=1,36$. According to the λ-criterion, since 2,10>1,36, the discrepancies between the empirical distributions in the EG and CG are certain (Equation 8). Therefore, the hypothesis H1 is accepted. The calculations made show that the critical values of $\lambda_{0.10}\approx1.23$ and $\lambda_{0.05}\approx1.36$ are significantly less than the actual (empirical) values. Therefore, the null hypothesis is rejected, which means that the CG and the EG are not homogeneous.

Currently, there is no single method for assessing sustainable development and the impact of education on the social environment and its development is an urgent problem in the scientific environment. For this purpose, an indicative system for assessing the level of the ecologization of territory due to the ecologization of education is proposed. The method of aggregation based on four groups of indicators (ecological, economic, social, international and innovative) was applied when constructing. The set of indicators includes sub-indicators, integral indicators and an aggregative indicator of the highest order to assess the level of ecologization of the territory due to the ecologization of education. A distinctive feature of the proposed system is the inclusion of the indicators characterising not only the three traditional spheres of impact on the environment - economic, ecological and social but also the indicators characterising the sphere of international and innovative activity. A comprehensive assessment allows to identify shortcomings in the ecologization of the territory due to the ecologization of education and take them into account in the operative order when adjusting the programmes of its development.

The initial set of subindicators is formed from indicators used in different international assessment methodologies of sustainable development (United Nations Commission on Sustainable Development, OECD and World Bank) and integral indicators (EDP, HDI, ESI, LPI, EF GPI, ISEW) grouped by the main directions of assessment of the ecologization level of the territory due to ecologization of education and types of economic activity (Table 11).

For expert assessment, it was proposed an ordinal scale from "0" to "5" points which allows to order the considered sub indicators and reveal hidden ordering with the help of experts. The result of the assessment is the formation of a basic set of sub indicators to assess the level of ecologization of the territory due to the ecologization of education in five main directions. According to the author, the formation of an additional set of sub indicators is advisable to carry out by the method of expert selection, taking into account the dependence between the

Downloaded from www.periodico.tchequimica.com

sub indicators (Table 12) based on constructing matrix dependence.

The most significant will be the sub indicators which gained the highest point in ranking by the independence degree and compliance with the objectives of the territorial programme of ecologization (Table 13).

For the effective application of the proposed system of indicators to assess the level of ecologization of the territory due to the ecologization of education, it is necessary to determine the threshold values that indicate the output of controlled sub indicators beyond the permissible range (Table 14). It should be taken into account that the changes of the values of sub indicators have different gradation depending on the direction of change – positive or negative. The transition of the sub indicator from one range to another reflects the effectiveness of decisions taken at the territorial level in the field of ecologization.

Direction of sub indicator value changes:

A – permissible range of sub indicator values;

B – range of values which characterise a small deviation of sub indicator within the variable norm;

C – range of values which characterise a deviation of sub indicator within the threat to ecologization;

D – range of values which characterise a deviation of sub indicator in the direction of deecologisation.

The use of the indicative system of indicators for assessing the level of ecologization of territory due to the ecologization of education with clearly identified ranges of permissible and critical values will allow the regional authorities to exercise control in the operative order and model the scenarios of development of the processes of ecologization of the territory due to ecologization of education including a movable external environment.

For the effective implementation of the indicative system for assessing the level of ecologization of the territory due to the ecologization of education proposed by the author, a sequence of actions for its implementation is proposed. The calculation of the aggregated indicator to assess the level of ecologization of the territory due to the ecologization of education is carried out by the formula (Equation 9). Where Lge – aggregative indicator of the level of ecologization of the territory due to the ecologization of education; Lec – integral economic indicator; Lecg – integral ecological indicator; Lim – integral indicator of international and innovative activities; Ls – integral social indicator.

For practical use of the aggregated indicator of the highest order, it was developed a criterion assessment systematising the values of the levels of ecologization of areas due to the ecologization of education (Table 15).

5. CONCLUSION:

The dynamics of the values of the highest aggregative indicator, that is, ecologization level allows to determine the trajectory of sustainable development of the territory, identify the need to create interrelated programmes of territorial development in the field of ecologization. Besides, the aggregative indicator provides an opportunity to measure and monitor the level of ecologization of the territory due to the ecologization of education. The use of the proposed approach will allow the regional authorities to exercise operative control and model the scenarios for the development of the processes of ecologization of the territory due to the ecologization of education, taking into account the external environment changes.

Consequently, the effectiveness of the technology of forming ecological culture among the chemical faculty students in the process of vocational training has been proved with the methods of mathematical statistics. The results of the control sections of the experiment's developmental phase have confirmed the effectiveness of the proposed learning technology. In the course of the study, we have also determined the levels of formation of ecological culture indicators according to motivational, axiological, cognitive, reflexive and practical criteria. Positive changes have been revealed among the students of experimental groups, which confirms the effectiveness of the experimental technology influence and testifies to the effectiveness of the chosen pedagogical conditions, which ensured the viability of the model, in particular, the targeted design of an information-ecological educational environment; ensuring positive motivation of students of the chemical faculty to the formation of ecological culture; education of the need for continuous professional self-improvement among students of the chemical faculty; attracting students of the Chemistry Faculty to environmental activities, which has led to an increase in the levels of

Downloaded from www.periodico.tchequimica.com

ecological culture.

6. REFERENCES:

1. Adler, I., Zion, M., Mevarech, Z.R. *Journal of Research in Science Teaching*, **2016**, *53*(4), 620-663.
2. Akhmetshin, E.M., Mueller, J.E., Yumashev, A.V., Kozachek, A.V., Prikhodko, A.N., Safonova, E.E. *Journal of Entrepreneurship Education*, **2019a**, *22*(1), 1-12.
3. Akhmetshin, E.M., Pavlyuk, A.V., Ling, V. V., Mikhailova, M.V., Shichiyakh, R.A., Kozachek, A.V. *Journal of Entrepreneurship Education*, **2019b**, *22*, 1-12.
4. Aleksandrova, O., Hroznyi, I., Vinnikova, N., Chuvasova, N. *Naukovyi Visnyk Natsionalnoho Hirnychoho Universytetu*, **2019**, *2019*(2), 153-162.
5. Aliyeva, A., Dlimbetova, G., Bakirova, K., Shaimerdenova, G. *Springer Proceedings in Complexity*, **2016**, 347-352.
6. Anderson, D. *Vocations and Learning*, **2008**, *1*(2), 105–29.
7. Brown, M. *Research in Science Education*, **1992**, *22*(1), 63–71.
8. Cherdymova, E.I., Afanasjeva, S.A., Parkhomenko, A.G., Ponyavina, M.B., Yulova, E.S., Nesmeianova, I.A., Skutelnik, O.A. *EurAsian Journal of BioSciences*, **2018**, *12*(2), 167-174.
9. Fateev, V.N., Fateeva, I. *Anthropologist*, **2016**, *23*(1-2), 148-151.
10. Flagg, J.A., Bates, D.C. *International Journal of Sustainability in Higher Education*, **2016**, *17*(4), 489-505.
11. Genc, M., Genc, T., Rasgele, P.G. *International Research in Geographical and Environmental Education*, **2018**, *27*(4), 326-340.
12. Generalov, M. B. *Chemical and Petroleum Engineering*, **1998**, *34*(9), 611–19.
13. Gevorgyan, S., Adanalyan, A. A Comparison Of Ecological Education And Sustainable Development Education in Allen-Gil, S., Stelljes, L., Borysova, O. (Eds.): *Addressing Global Environmental Security Through Innovative Educational Curricula* (57-61), Dordrecht: Springer Netherlands, **2009**.
14. Gough, A. *Cultural Studies of Science Education*, **2017**, *12*(4), 889–905.
15. Grishaeva, Y.M., Tkacheva, Z.N., Medvedkov, A.A., Volgin, A.V., Krylov, P.M., Litvinenko, V.V. *Man in India*, **2017**, *97*(14), 1-9.
16. Grodzinska-Jurczak, M. *Environmental Science and Pollution Research*, **2000**, *7*(4), 235–38.
17. Harding, K.L., Aguayo, V.M., Masters, W.A., Webb, P. *BMC Public Health*, **2018**, *18*(1), 470.
18. Isakova, A. *Materials of the 18th International Multidisciplinary Scientific Geoconference: "International Multidisciplinary Scientific GeoConference Surveying Geology and Mining Ecology Management"*. Albena, Bulgaria, **2018**, 115-122.
19. Kaigorodova, G.N., Kosarenko, N.N., Shapovalov, D.A., Sayfutdinova, G.B., Sharonov, I.A., Ignatov, S.B., Kartushina, I.G. *Eurasian Journal of Analytical Chemistry*, **2017**, *12*(7), 1079-1088.
20. Kim, E.-J.A., Asghar, A., Jordan, S. *Canadian Journal of Science, Mathematics and Technology Education*, **2017**, *17*(4), 258–70.
21. Kimmerer, R.W. *Journal of Environmental Studies and Sciences*, **2012**, *2*(4), 317–23.
22. Lee, S.-O. *Asia Pacific Education Review*, **2007**, *8*(2), 194–204.
23. Lee, S.-S., Hung, D., Teh, L. W. *Educational Research for Policy and Practice*, **2016**, *15*(1), 55–70.
24. Liu, Z., Chai, Y.J. A Multimedia Based Natural Forest Park for Ecological Education in Xie, A., Huang, X. (Eds.): *Advances in Computer Science and Education* (397–402), Heidelberg: Springer Berlin Heidelberg, **2012**.
25. Lopes, A., Boyd, P., Andrew, N., Pereira, F. *Higher Education*, **2014**, *68*(2), 167–83.
26. Lowan-Trudeau, G. *Cultural Studies of Science Education*, **2017**, *12*(1), 119–28.
27. Marekha, I., Omelyanenko, V. *Economic Annals-XXI*, **2017**, *162*(11-12), 9-12.
28. Maslennikov, V., Grishina, O., Lyandau,

Downloaded from www.periodico.tchequimica.com

Y., Kalinina, I. *Proceedings of the 30th International Business Information Management Association Conference, IBIMA 2017 – Vision 2020: "Sustainable Economic development, Innovation Management, and Global Growth"*. Madrid, Spain, **2017**.

29. Manzheley, I.V. *Teoriya i Praktika Fizicheskoy Kultury*, **2016**, *2016-January*(12), 38-40.
30. Mueller, M.P. *Science & Education*, **2009**, *18*(8), 1031–56.
31. Pechancová, V., Hrbáčková, L., Dvorský, J., Chromjaková, F., Stojanovic, A. *Entrepreneurship and Sustainability Issues*, **2019**, *7*(2), 825–41. http:// doi.org/10.9770/jesi.2019.7.2(3).
32. Pryor, A., Carpenter, C., Townsend, M. *Journal of Outdoor and Environmental Education*, **2005**, *9*(1), 3–13.
33. Richardson, G.B., Castellano, M.E., Stone, J.R., Sanning, B.K. *Evolutionary Psychological Science*, **2016**, *2*(1), 58–69.
34. Rusko, M., Lumnitzer, E. *Proceedings of the 15th IEEE International Conference on Emerging eLearning Technologies and Applications*. Stary Smokovec, Slovakia, **2017**.
35. Sagiyeva, R., Zhuparova, A., Ruzanov, R., Doszhan, R., Askerov, A. Entrepreneurship and Sustainability Issues, *6*(2): 711–28. http:// doi.org/10.9770/jesi.2018.6.2(17).
36. Sasongko, G., Huruta, A.D., Pirzada, K. *Entrepreneurship and Sustainability Issues*, **2019**, *7*(1), 166–76. http:// doi.org/10.9770/jesi.2019.7.1(13). Sitarov,
37. V.A., Urekeshova, L. *Regional Science Inquiry*, **2017**, *9*(2), 187–96.
38. Schleicher, K. *International Review of Education*, **1975**, *21*(2), 231–60.
39. Schleicher, K. *International Review of Education*, **1989**, *35*(3), 257–81.
39. Sofluau, R., David, D.O. *Journal of Rational-Emotive & Cognitive-Behavior Therapy*, **2018**, *36*(1), 89–97.
40. Zeleeva, V.P., Asafova, E.V. *Mathematics Education*, **2016**, *11*, 4, 549-558.

Downloaded from www.periodico.tchequimica.com

$$IM = \frac{Value6+Value7}{2} \quad \text{(Eq.1)}$$

$$IPM = \frac{Value1+Value2+Value5}{3} \quad \text{(Eq. 2)}$$

$$ENM = \frac{Value3+Value4}{2} \quad \text{(Eq. 3)}$$

$$\lambda = d_{\max}\sqrt{\frac{n_e n_k}{n_e + n_k}} = 0,264\sqrt{\frac{152*163}{152+163}} = 2,34 \quad \text{(Eq. 4)}$$

$$\lambda = d_{\max}\sqrt{\frac{n_e n_k}{n_e + n_k}} = 0,277\sqrt{\frac{152*163}{152+163}} = 2,46 \quad \text{(Eq. 5)}$$

$$\lambda = d_{\max}\sqrt{\frac{n_e n_k}{n_e + n_k}} = 0,271\sqrt{\frac{152*163}{152+163}} = 2,40 \quad \text{(Eq. 6)}$$

$$\lambda = d_{\max}\sqrt{\frac{n_e n_k}{n_e + n_k}} = 0,24\sqrt{\frac{152*163}{152+163}} = 2,13 \quad \text{(Eq. 7)}$$

$$\lambda = d_{\max}\sqrt{\frac{n_e n_k}{n_e + n_k}} = 0,237\sqrt{\frac{152*163}{152+163}} = 2,1 \quad \text{(Eq. 8)}$$

$$Lge = \frac{Lec + Lecg + Lim + Ls}{4} \quad \text{(Eq. 9)}$$

Downloaded from www.periodico.tchequimica.com

Table 1. *The distribution of motives to make a choice of the profession for the students of the chemical faculty of experimental groups*

Value	Motives	EG
1	Pursuance of the nature conservation	0.82
2	Desire to participate in environmental activities	0.76
3	The desire for self-realization, namely in the sphere of ecology	0.72
4	The desire to be competitive in the labor market	0.51
5	The desire to be spiritually rich as well as cultural and beneficial to society	0.44
6	Desire to reach social prestige	0.41
7	It is unmodern to be uneducated	0.3

Table 2. *Motivational complex for the choice of profession by the students of experimental groups*

IM	IPM	ENM
4.02	2.73	2.08

Table 3. *Indicators' dynamics of the formation of value orientations among students of experimental and control groups+*

Value Orientations	EG before the experiment	EG after the experiment	CG before the experiment	CG after the experiment
Realizing that not only a person but also every kind of animal and plant has the right to exist as a result of a long evolution	0.69	0.89	0.68	0.82
Realizing that every intrusion into nature can lead to positive as well as negative circumstances for people's health	0.74	0.88	0.7	0.84
Realizing oneself being a part of nature	0.73	0.87	0.67	0.83
Development of the congtive interest to solving the ecological issues	0.74	0.89	0.69	0.85
Ability to observe nature	0.72	0.89	0.71	0.8
Improving one's own inner world through realizing the sense of personal unindifference, dignity, carefulness and mutual help	0.71	0.88	0.7	0.78
Realizing one's uniqueness and singularity of nature	0.79	0.9	0.72	0.82
Development of the aesthetic feeling of nature, desire to see, create and learn the beautiful	0.71	0.86	0.7	0.83
Desire to preserve the flora and fauna	0.73	0.9	0.73	0.84
Desire to increase the wealth of nature	0.7	0.88	0.68	0.85
Realizing the fact that ecological situation threatens the needs and interests of a person	0.76	0.9	0.73	0.83
Studying the reasons of ecological crisis, ways of its avoiding for the benefit of a person as well as nature	0.72	0.88	0.67	0.77

Downloaded from www.periodico.tchequimica.com

Using scientific-technological achievements of the STR in the professional activities	0.69	0.84	0.69	0.76
Desire to preserve nature as an element of cultural environment	0.75	0.9	0.73	0.83

Table 4. *The level of formation of professional knowledge among students of experimental and control groups*

Knowledge	EG before the experiment	EG after the experiment	CG before the experiment	CG after the experiment
Levels of biological life organisation	0.71	0.89	0.66	0.81
Theories of the origin and evolution of life on Earth	0.73	0.91	0.64	0.79
Biological diversity of the organisms at species, cenotic and ecosystem level	0.76	0.9	0.69	0.78
Main terms and laws of ecology	0.77	0.91	0.68	0.8
Dependence of the organism on the area of inhabitance on different stages of the life circle	0.75	0.89	0.61	0.75
Structure, components, biosphere dynamics	0.78	0.88	0.7	0.82
Populations, ecosystems, biocenoses	0.76	0.9	0.73	0.83
Composition and structure of the Earth and the earth's crust	0.74	0.88	0.72	0.84
Geomorphological landscapes	0.71	0.89	0.7	0.8
Biochemical cycles of substances in the biosphere	0.71	0.9	0.69	0.78
Patterns of formation of natural resources, their distribution	0.7	0.9	0.72	0.81
Sources of pollution and development of measures to improve the state of the environment	0.74	0.91	0.73	0.77
Person’s influence on nature, ecological crisis	0.76	0.89	0.75	0.82
Global ecological problems, disasters, ways to overcome them	0.72	0.9	0.69	0.76
Definiton and prediction of environmental risk	0.71	0.88	0.72	0.8
Relationship of pollution of regions with the state of vegetation and human health	0.72	0.9	0.7	0.79
Protection of flaura and fauna	0.74	0.92	0.73	0.81
Methods of measuring environmental parameters, devices and their principles of work	0.75	0.88	0.74	0.79
Nature Reserve Fund	0.72	0.89	0.69	0.81
Objects and subjects of environmental monitoring	0.64	0.88	0.66	0.78
Types of environmental monitoring	0.67	0.9	0.69	0.76
Monitoring of the atmosphere, hydrosphere, lithosphere, biological	0.67	0.9	0.68	0.78

Downloaded from www.periodico.tchequimica.com

resources				
Methods of physical and chemical analysis	0.66	0.9	0.7	0.79
Landscapes	0.69	0.9	0.68	0.8
Environmental safety standards for air, water usage, soil, radiation safety of environmental components (MPC, MPD)	0.68	0.9	0.66	0.79
Air, soil, water protection	0.76	0.86	0.7	0.78
Types, ways, scales of natural resources usage; depletion, restoration and replacement of natural resources	0.73	0.89	0.71	0.82
Concept of environmental protection activity	0.76	0.89	0.72	0.83
Economic approaches to the protection of the environment	0.75	0.86	0.73	0.79
Regulatory framework, government regulation and management in the field of environmental examination	0.74	0.89	0.75	0.8
Types of ecological examination	0.73	0.9	0.71	0.77

Table 5. *Formation of the ecological culture of the chemical faculty students (the formative stage of the experiment)*

Criteria	**Motivational**		**Axiological**		**Cognitive**		**Reflexive**		**Practical**	
	EG	**CG**	**EG**	**CG**	**EG**	**CG**	**EG**	**CG**	**EG**	**CG**
Levels	**%**	**%**	**%**	**%**	**%**	**%**	**%**	**%**	**%**	**%**
High	36.2	14.3	35.6	15.6	38.2	14.5	37.4	15.4	36.4	15.2
Sufficient	44.6	40.1	46.5	38.8	43.6	40.2	42.4	40.4	42.3	39.8
Medium	16	36.9	14.5	37.3	14.1	37.1	16.9	36	17.8	36.4
Beginner	3.2	8.7	3.4	8.3	4.1	8.2	3.3	8.2	3.5	8.6

Table 6. *Calculation of the λ-criterion for comparing empirical distributions in the EG and CG of the indicators of the motivational criterion formation (the formative stage of the experiment)*

Levels	**Empirical frequency**		**Empirical relative frequency**		**Cumulative empirical relative frequency**		**Discrepancies d=Σ f*e-Σ f*k**
	fe	**fk**	**f*e**	**f*k**	**Σ f*e**	**Σ f*k**	
High	55	23	0.362	0.143	0.362	0.143	0.219
Sufficient	68	65	0.446	0.401	0.808	0.544	0.264
Medium	24	60	0.16	0.369	0.968	0.913	0.055
Beginner	5	14	0.032	0.087	1	1	
Total	152	163	1	1			

Table 7. *Calculation of the λ-criterion for comparing the empirical distributions in the EG and CG of the formation of axiological criterion indicators (the formative stage of the experiment)*

Levels	**Empirical frequency**		**Empirical relative frequency**		**Cumulative empirical relative frequency**		**Discrepancies d=Σ f*e-Σ f*k**
	fe	**fk**	**f*e**	**f*k**	**Σ f*e**	**Σ f*k**	
High	54	25	0.356	0.156	0.356	0.156	0.2
Sufficient	71	63	0.465	0.388	0.821	0.544	0.277
Medium	22	61	0.145	0.373	0.966	0.917	0.049
Beginner	5	14	0.034	0.083	1	1	
Total	152	163	1	1			

Downloaded from www.periodico.tchequimica.com

Table 8. *Calculation of the λ-criterion for comparing the empirical distributions in the EG and CG of the formation of cognitive criterion indicators (the formative stage of the experiment)*

Levels	Empirical frequency		Empirical relative frequency		Cumulative empirical relative frequency		Discrepancies d=Σ f*e-Σ f*k
	fe	fk	f*e	f*k	Σ f*e	Σ f*k	
High	58	24	0.382	0.145	0.382	0.145	0.237
Sufficient	66	66	0.436	0.402	0.818	0.547	0.271
Medium	21	60	0.141	0.371	0.959	0.918	0.041
Beginner	6	13	0.041	0.082	1	1	
Total	152	163	1	1			

Table 9. *Calculation of the λ-criterion for comparing the empirical distributions in the EG and CG of the formation of reflexive criterion indicators (the formative stage of the experiment)*

Levels	Empirical frequency		Empirical relative frequency		Cumulative empirical relative frequency		Discrepancies d=Σ f*e-Σ f*k
	fe	fk	f*e	f*k	Σ f*e	Σ f*k	
High	57	25	0.374	0.154	0.374	0.154	0.22
Sufficient	64	66	0.424	0.404	0.798	0.558	0.24
Medium	26	59	0.169	0.36	0.967	0.918	0.049
Beginner	5	13	0.033	0.082	1	1	
Total	152	163	1	1			

Table 10. *Calculation of the λ-criterion for comparing the empirical distributions in the EG and CG of the formation of practical criterion indicators (the formative stage of the experiment)*

Levels	Empirical frequency		Empirical relative frequency		Cumulative empirical relative frequency		Discrepancies d=Σ f*e-Σ f*k
	fe	fk	f*e	f*k	Σ f*e	Σ f*k	
High	55	25	0.364	0.152	0.364	0.152	0.212
Sufficient	64	65	0.423	0.398	0.787	0.55	0.237
Medium	27	59	0.178	0.364	0.965	0.914	0.051
Beginner	5	14	0.035	0.086	1	1	
Total	152	163	1	1			

Table 11. *Group of indicators in the directions of ecologisation and economic activities to assess the ecologisation level of the territory due to the ecologisation of education*

Considered calculation method	Main identified advantages	Main identified disadvantages	Adjusted set of indicators based on the results of expert assessment	Indicators proposed by the author
United Nations Commission on Sustainable Development	Indicators used in the methodology are divided into 4 groups: social, economic, ecological (with subgroups: water resources, land resources, other natural resources, atmosphere and waste) and	Indicators used do not have a strongly pronounced specificity and can be simultaneously attributed to the other directions of ecologisation	GRP per capita; Percentage of GRP allocated on environmental protection; Environmental taxes and subsidies; Amount of additional financing for sustainable development after	Share of environmental entrepreneurship in the territory Share of the population of the territory engaged in the ecological sector Ecological costs index Ecology economisation index

Downloaded from www.periodico.tchequimica.com

	organisational. Three types of indicators indicate "Driving force indicators", "Current state Indicators" and "Response Indicators". The set of indicators in the group corresponds to the following sections: "Agenda for the 21st century": economic development, change of consumption pattern, financial resources and mechanisms. Among the indicators used there are 5 indicators that directly characterise the process of ecologisation (No. 45, 63 – 66) in the economic direction	1992; Adjusted net national income per capita; National product per capita adjusted for ecological damage

Table 12. *Dependences of subindicators of assessing the ecologisation level of territory due to the ecologisation of education*

Name of subindicator group	**Conventional name**	**Dependency characteristics**	**Dependency description**	**Expert importance, points**
Indicators-substitutes	IS	Change of one subindicator in a pair directly affects the value of the second indicator	Directly proportional	1
Complementary subindicators	CS	Increase of one of the su-indicators in a pair leads to the decrease of the second one	Inversely proportional	2
Independent subindicators	InS	Both subindicators are independent	No dependency	3

Downloaded from www.periodico.tchequimica.com

Table 13. *Dependency matrix of sub-indicators to assess the ecologisation level*

Name of arbitrary subindicator	Ordinal number of indicator	1	2	3	4	5	Final assessment of the dependence of subindicators, points
Coefficient of environmental friendliness of production	1		CS = 2	InS = 3			5
Coefficient of environmentally friendly production	2	CS = 2		IS = 1			3
Development index of ecological branding	3	InS = 3	IS = 1	-			4

Table 14. *Range of values of subindicators (fragment)*

Name of subindicator	Name of the integral indicator on the selected topic Ecological indicator – I_{ecg} Range of values of the integral indicator, %						
	D	C	B	A	B	C	D
Coefficient of environmental friendliness of production	< 0	0–10	10–20	20–33	34–45	46–50	> 51
Coefficient of environmentally friendly production	< 0	0–10	10–20	20–33	34–45	46–50	> 51
Development index of ecological branding	< 0	0–10	10–20	20–33	34–45	46–50	> 51

Downloaded from www.periodico.tchequimica.com

Table 15. *Value gradation of the aggregative indicator of ecologisation of territory due to the ecologisation of education*

Level's name	**0 level "Zero"**	**1 level "Elementary"**	**2 level "Basic"**	**3 level "Medium"**	**4 level "High"**	**5 level "Advanced"**
Degree characteristics	absence of ecologisation process in all spheres of activity	developments in the direction of the implementation of the process of ecologisation of the territory due to the ecologisation of education	presence of the most common and necessary spheres of ecologisation of the territory due to the ecologisation of education for development	development of ecologisation of the territory	active process of integration of economy and ecology	assessment of the real development of ecologisation of the territory due to the ecologisation of education as a process
Value of integral indicators						
Economic indicator	[0–0.05]	[0.051–0.08]	[0.081–0.1]	[0.11–0.2]	[0.21–0.3]	[0.31–0.4]
Ecological indicator	[0–0.05]	[0.051–0.08]	[0.081–0.1]	[0.11–0.2]	[0.21–0.3]	[0.31–0.4]
Indicator of international and innovative activities	[0–0.05]	[0.051–0.08]	[0.081–0.1]	[0.11–0.2]	[0.21–0.3]	[0.31–0.4]
Social indicator	[0–0.05]	[0.051–0.08]	[0.081–0.1]	[0.11–0.2]	[0.21–0.3]	[0.31–0.4]
Aggregative indicator of the ecologisation level of the territory due to the ecologisation of education	[0–0.05]	[0.051–0.08]	[0.081–0.1]	[0.11–0.2]	[0.21–0.3]	[0.31–0.4]

Downloaded from www.periodico.tchequimica.com

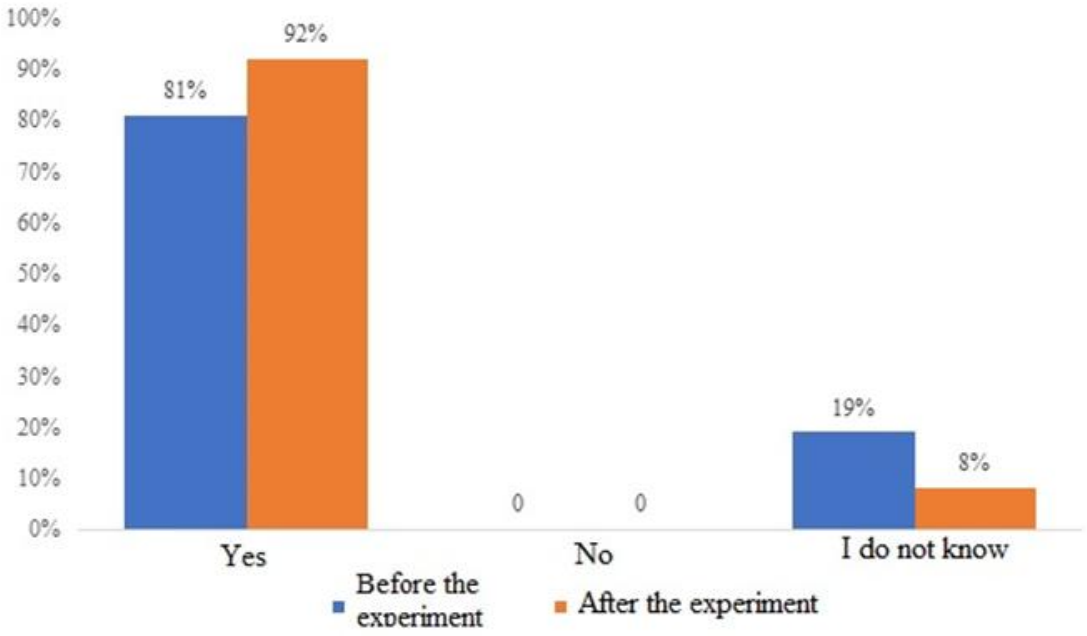

Figure 1. *Motivation dynamics*

Downloaded from www.periodico.tchequimica.com

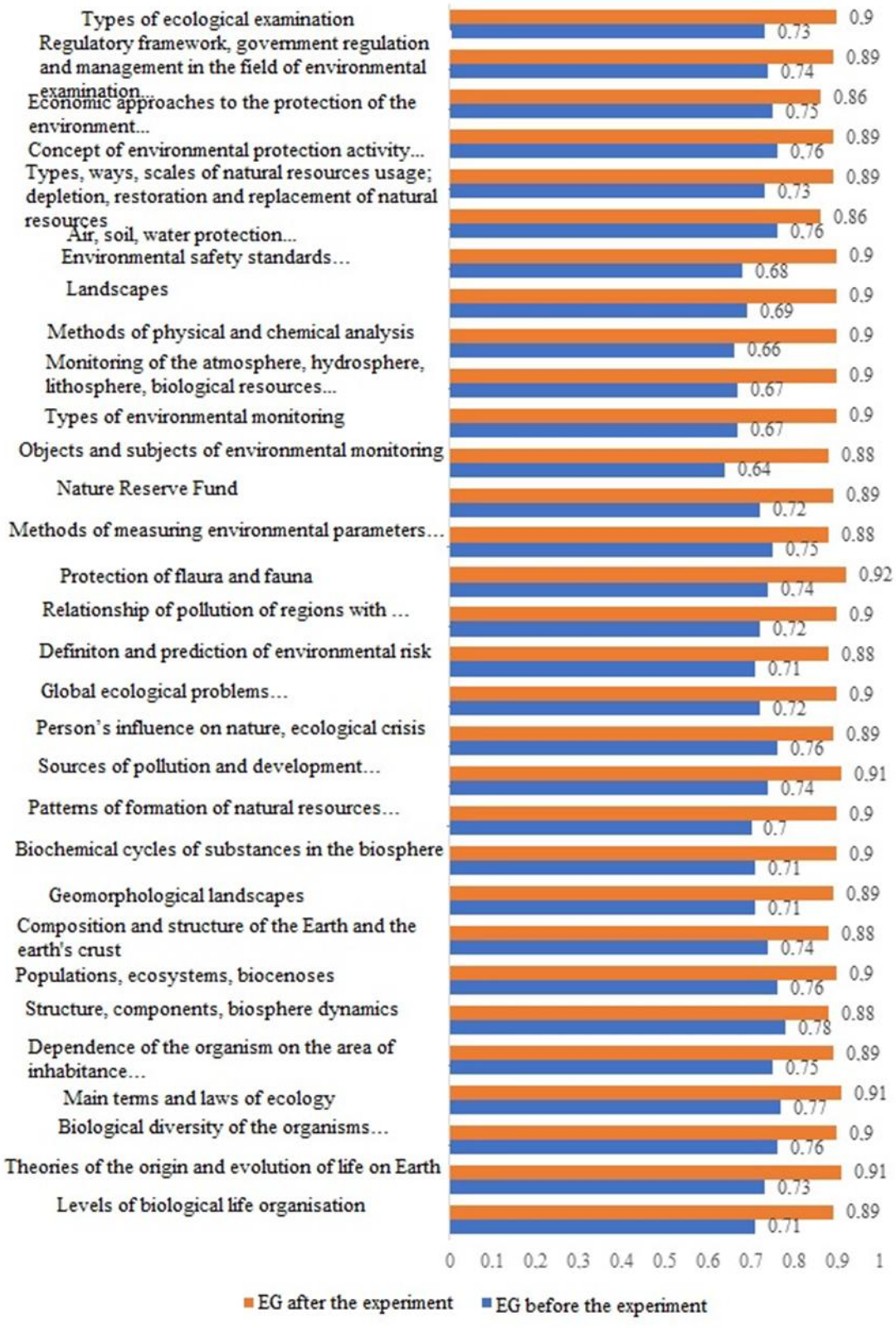

Figure 2. *The level of development of professional environmental knowledge (experimental groups)*

Downloaded from www.periodico.tchequimica.com

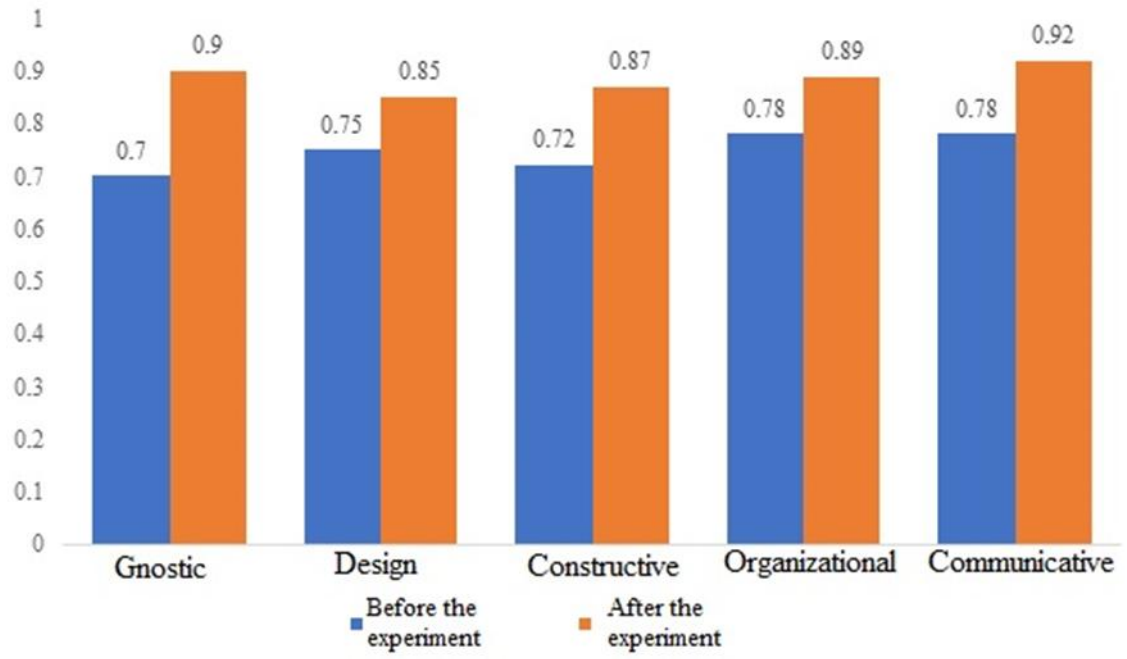

Figure 3. *Dynamics of the level of professional skills development necessary for the formation of an ecological culture (experimental groups)*

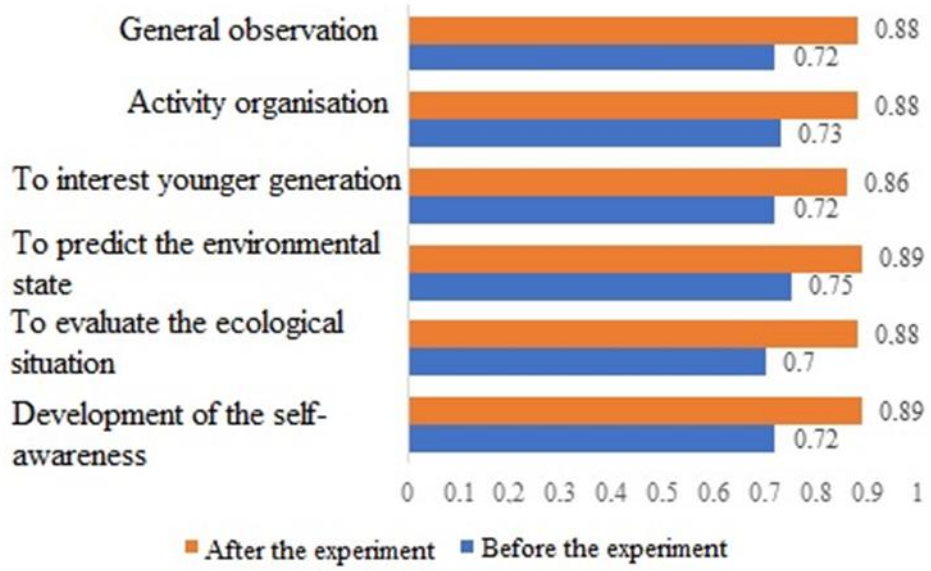

Figure 4. *Types of self-awareness of environmental activities (experimental groups)*

Downloaded from www.periodico.tchequimica.com

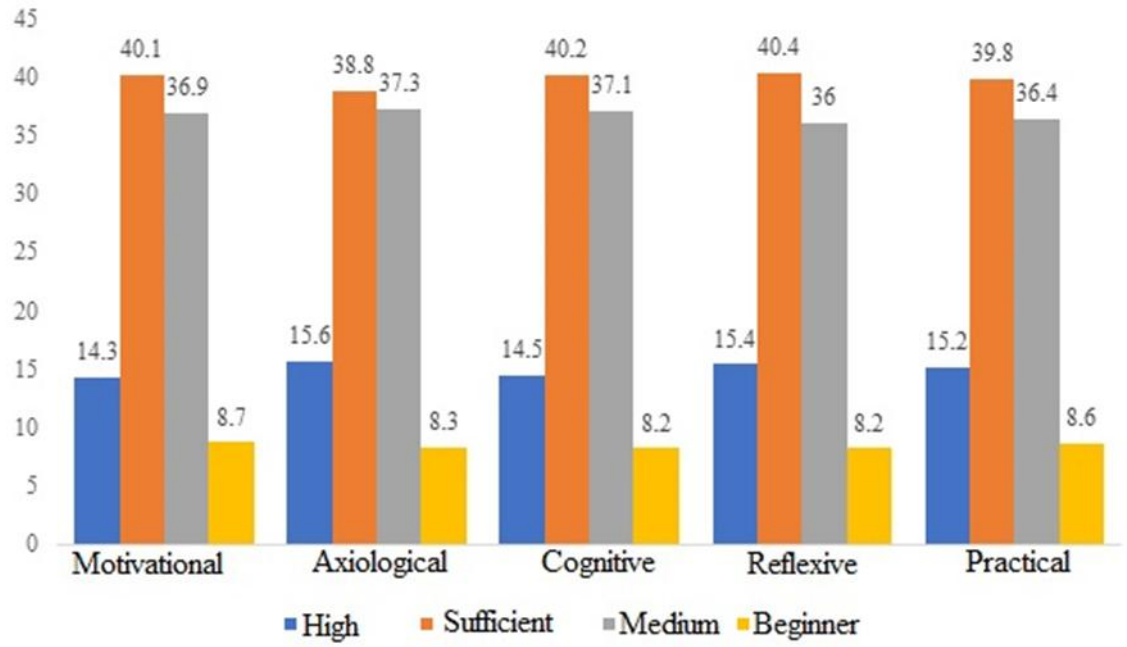

Figure 5. *Level dynamics of the ecological culture formation among the future students of the chemical faculty (control groups)*

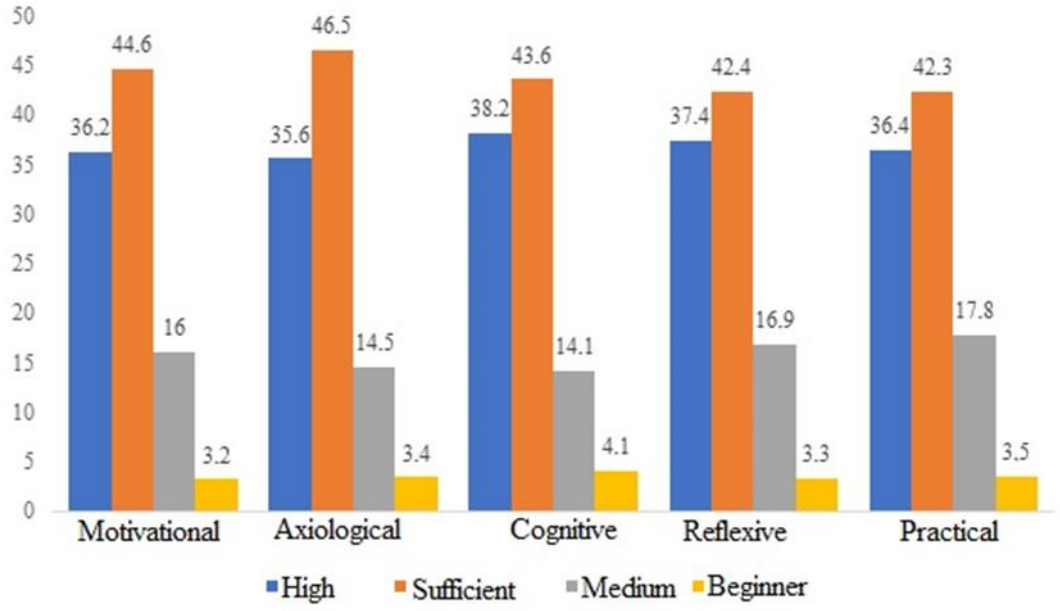

Figure 6. *Level dynamics of the ecological culture formation among the future students of the chemical faculty (experimental groups)*

Downloaded from www.periodico.tchequimica.com

PERIÓDICO TCHÊ QUÍMICA
ARTIGO DE REVISÃO

OS CAMINHOS DE MELHORIA DOS MÉTODOS DE TRATAMENTO DA HIPOSPÁDIAS EM CRIANÇAS: REVISÃO DE LITERATURA

THE WAYS OF IMPROVEMENT OF THE METHODS OF HYPOSPADIAS TREATMENT IN CHILDREN: LITERATURE REVIEW

СОВЕРШЕНСТВОВАНИЕ СПОСОБОВ ЛЕЧЕНИЯ ГИПОСПАДИИ У ДЕТЕЙ: ОБЗОР ЛИТЕРАТУРЫ

ZHARKIMBAYEVA, Almira D.[1*]; DYUSEMBAYEV, Azat A.[2]; AUBAKIROV, Maratbek T.[3]; GAMZAYEVA, Yesmira M.[4];

[1,2,3,4,5] Semey State Medical University, Department of Pediatric Surgery and Orthopedics, 103 Abay Str., zip code 071400, Semey – Republic of Kazakhstan

** Correspondence author*
e-mail: zhar_77@mail.ru

Received 02 October 2019; received in revised form 20 October 2019; accepted 24 October 2019

RESUMO

A relevância do estudo se deve ao fato que a hipospádia é uma malformação congênita do sistema urogenital em meninos. A taxa de incidência de hipospádia varia em diferentes países. O principal fator etiológico no desenvolvimento desse defeito é o desequilíbrio hormonal da mãe que é causado por várias razões. A correção da hipospádia é realizada apenas cirurgicamente. Atualmente, muitos métodos cirurgicos são utilizados, mas, apesar disso, o número de complicações no pós-operatório permanece alto. O objetivo do artigo foi estudar os resultados do tratamento cirúrgico da hipospádia em crianças após vários métodos de uretroplastia utilizando diferentes enxertos. Foram pesquisados os artigos no único banco de dados eletrônico Pub Med, Elsivier, Scopus, Web of Science de 2007 a 2018. Foram examinados 265 artigos de tratamento da hipospádia usando os seguintes métodos: método TIP (placa incisada tubularizada), Mathieu, GTIP (placa incisada tubularizada de enxerto) e uretroplastia em dois estágios de Bracka. As complicações mais comuns em vários estudos foram seguintes: fístula, estenose da luz neurouretral e deformidade peniana secundária. Assim, os métodos existentes de tratamento cirúrgico desse defeito em crianças não levam à completa eliminação da ocorrência de complicações pós-operatórias. Nesse sentido, o tratamento das hipospádias permanece relevante e requer o desenvolvimento de novos métodos de uretroplastia.

Palavras-chave: *crianças, métodos TIP, GTIP e Bracka, complicações.*

ABSTRACT

The relevance of the study is due to the fact that hypospadias is a congenital defect of the urogenital system in boys. The incidence rate of hypospadias differs in different countries. The main etiological factor of this defect development is a hormonal imbalance of different origin in mothers. Hypospadias can be corrected only surgically. Currently, there are a number of surgical approaches used, but still, the number of complications in the postoperative period remains high. The purpose of the article was to evaluate the outcomes of surgical correction of hypospadias in children observed after different approaches to urethroplasty involving transplanting. The authors performed a search for articles in electronic databases Pub Med, Elsevier, Scopus, Web of Science for the period from 2007 to 2018. The authors reviewed 265 articles dedicated to the correction of hypospadias by the following methods: TIP (tabularized incised plate), Mathieu, GTIP (graft tabularized incised plate) and two-stage Bracka urethroplasty. The most widespread complications mentioned in different studies were fistulas, stenosis of the urethral neo-meatus, and secondary deformation of the penis. Current approaches to surgical correction of hypospadias in children do not provide complete recovery from post-operative complications. Due to this fact, the issues of treatment of hypospadias remain relevant, requiring the development of new approaches to urethroplasty.

Keywords: *children, TIP, GTIP and Bracka methods, complications.*

Downloaded from www.periodico.tchequimica.com

АННОТАЦИЯ

Актуальность исследования обусловлена тем, что гипоспадия является врожденным пороком развития мочеполовой системы у мальчиков. Показатель частоты встречаемости гипоспадии различается в разных странах. Основным этиологическим фактором развития данного порока является гормональный дисбаланс матери, вызванный различными причинами. Коррекция гипоспадии осуществляется только хирургическим путем. В настоящее время применяются множество оперативных методик, но несмотря на это, количество осложнений в послеоперационном периоде остается высоким. Цель статьи – изучить исходы хирургического лечения гипоспадии у детей после различных методов уретропластик с использованием разных трансплантатов. Проведен поиск статей в единых электронных базах данных Pub Med, Elsivier, Scopus, Web of Science с 2007 года по 2018 год. Рассмотрены 265 статей лечения гипоспадии с применением следующих способов: TIP (tubularized incised plate) метода, Mathieu, GTIP (graft tubularized incised plate) и двухэтапной уретропластики Bracka. Наиболее распространенными осложнениями в различных исследованиях были свищ, стеноз просвета неоуретры и вторичная деформация полового члена. Таким образом, существующие методики оперативного лечения данного порока у детей не приводят к полному устранению возникновения послеоперационных осложнений. В связи с этим лечение гипоспадии остается актуальным и требует разработок новых способов уретропластики.

Ключевые слова: *дети, TIP, GTIP и Bracka методы, осложнения.*

1. INTRODUCTION

Hypospadias is the second widespread congenital anomaly of external male genital organs, giving the leading position to cryptorchism. It is diagnosed in 1 in 200–300 newborn babies. The degree of hypospadias can vary from insignificant to severe, depending on the localization of the urethral meatus (Bouty *et al.,* 2015; Canning*,* 2016; Aydogmus *et al.,* 2017; Bhat *et al.,* 2017; Dokter *et al.,* 2018).

According to the performed systematic review of 169 original articles, the incidence rate of hypospadias varies significantly in different countries from 4 to 43 cases per 10,000 newborns. Some research data indicates the increase in the incidence rate of hypospadias in China, Australia, USA, and Europe (van der Zanden *et al.,* 2012). Monitoring of congenital anomalies, conducted by the European register by 19 forms, showed that in Moscow, during the past 4 years, hypospadias occupied the 4th place and its incidence rate was 8.86% of the total diagnosed congenital anomalies of the development (Rudin *et al.,* 2013). A major European research that included more than 5.8 million newborns in 23 UEROCAT registers for the period from 2001 to 2010 showed that the general incidence rate of hypospadias was 18.61 per 10,000 of births (Bergman *et al.,* 2015). European Surveillance of Congenital Anomalies (EUROCAT) is a network of registers of congenital anomalies in Europe that is financed by the EU and exists for more than 30 years. It operates according to the standard methodology for registering the data on the cases of congenital anomalies at birth, death of a fetus older than 20 weeks of gestation age and miscarriage, and anomalies of fetus development. EUROCAT surveils three spheres: incidence rate, primary preventive measures, and prenatal screening. In general, in Europe, the performed analysis on the relative risks based on mothers' age showed that teenage mothers have a higher risk of NCA development (non-chromosomal congenital anomalies) as compared to elder mothers aged 35–44, who did not have that risk, and that the age of mothers itself does not contribute to the risk of NCA development (Loane *et al.,* 2009). General incidence rate of hypospadias in Rotterdam is 38 cases per 10,000 of the living population. In Mainz, from 2001 to 2010, the incidence rate was 36.83 per 10,000 births (Pierik *et al.,* 2002; Ayob and Arnold, 2016).

One of the studies, conducted for the analysis of mothers' age, showed that the highest incidence rate of the total hypospadias in six age groups of mothers was in the group of teenage mothers as compared to the mothers aged from 25 to 29 years old (Bergman *et al.,* 2015).

Retrospective analysis of the database ECLAMC the Latin American Collaborative Study of Congenital Malformations (ECLAMC) contained the data on the newborns that were diagnosed with hypospadias from January 1989 to December 2012. The study excluded the countries that lacked or provided incomplete information. The final analysis included 159 hospitals from six counties of South America. The researchers examined 4,020,384 of newborns and diagnosed 4,537 cases of hypospadias, which gave the incidence rate of 11.3 per 10,000 of newborns. The analysis of the tendencies revealed a global increase in the hypospadias

Downloaded from www.periodico.tchequimica.com

incidence rate by 0.2 cases per 10,000 newborns annually (h<0.0001). This made the increase by 3.3% for the studied period. Totally, 82.2% of cases were diagnosed as isolated hypospadias, the rest 17.8% of hypospadias cases were associated with other anomalies. The most widespread associated anomaly was cryptorchism, which was observed in 15.3% of cases. The present study provides epidemiologic based proof that during the past twenty years, an incidence rate of hypospadias increased in different countries of South America. Reports from other countries show the increase in hypospadias incidence rate from 1 to 4% (Fernández *et al.,* 2017). The study of temporary tendencies and geographical variations of the incidence rate of isolated anomalies, multiple anomalies and general cases in China from 1996 to 2008 showed that the rate were 7.64, 1.39 and 9.03 per 10,000 births, respectively. The highest incidence rate (12.10 per 10,000 births) was registered in the eastern region. Increasing tendencies and differences in the incidence rate of hypospadias by the classification of urban (5.28%) and rural (9.79%) regions and geographical location were the following: in eastern region – 9.08%, in central region – 9.08%, and in western region – 6.57%. These rates indicate the fact that the impact on the environment and mothers' age can play a crucial role in the development of hypospadias (Li *et al.,* 2012). The incidence rate of hypospadias in Poland is 17.9 per 10,000 births (Kowal *et al.,* 2015). According to some researchers, the total incidence rate in the Danish county Funen was 16.9 per 10,000 births. For the period of 1986-1999, as compared to 2000-2009, the incidence rate of hypospadias nearly doubled from 12.2 in the first period to 23.7 in the second one, but in 2008, the incidence rate decreased, especially the rate of simple cases as compared to the severe ones (Nissen *et al.,* 2015).

In the case of extracorporal fertilization, the incidence rate of hypospadias increases by 5 times (Makazhanov, 2012; Badawy *et al.,* 2018). Many studies were conducted for the children who were conceived due to assisted reproductive technology (ART). In the general population, 3% of the survived newborns have one serious congenital anomaly at birth. According to the authors, the main causes of congenital anomalies are genetic factors that also provoke spontaneous preterm abortions in the first trimester (Kermani *et al.,* 2012; Gong and Cheng, 2017). Distal form (glans penis, coronal, or subcoronal) of hypospadias in newborns are registered in 60–65% of cases, mid penile form – in 20–30% of cases, and proximal (posterior penile, penoscrotal, scrotal, or perineal) form – in 10–15% of cases (Singal *et al.,* 2016; Alsaywid *et al.,* 2017; Ollivier *et al.,* 2018).

2. MATERIALS AND METHODS

The most widespread complication after the urethroplasty is urethrocutaneous fistula. After the primary Duckett urethroplasty with a preputial island flap, successful closure of the fistula was registered in 6.55%, and in 33.5% of cases, recurrent unfavorable outcome was registered. The potential factors for the development of fistulas are patients' age, fistula size, localization and quantity of fistulas after the primary urethroplasty, the duration of the operation time, the length of the neo-urethra, time of the fistula closure and post-operative infections. It was established that the recurrent fistula was observed in patients with ucf diameter of 2 mm and more. The authors also believe that the application of caudal regional anesthesia does not prevent the development of urethrocutaneous fistula (Menon *et al.,* 2017; Kreysing and Höhne, 2016; Seleim *et al.,* 2017; Han *et al.,* 2018; Kagantsov and Surov, 2018).

W. Snodgrass and N. Bush in their study made a review of widely used surgical methods of restoration for distal and proximal hypospadias, their complications, functions of urinary tracts and esthetic results. The obtained data indicate that the tip is more preferable than Mathieu. In all the cases of primary hypospadias, only two methods were used: tip and two-step prepitual grafts (Snodgrass and Bush, 2016; Snodgrass and Bush, 2017). To compare the complications after the urethroplasty for the distal hypospadias, the authors performed a systematic review of the information in the databases Medline, Embase, and Cochrane from 1990 to 2009. According to the data obtained in 23 publications, 15 series of reports and 1,892 cases of tip method operations and 10 series of reports on 1,496 cases of Mathieu method operations, the following complication rates were revealed: meatus stenosis, neo-urethra strictures, and fistulas were observed in 6.9% of cases after tip urethroplasty (tabularized incised plate) and 6.7% after Mathieu urethroplasty (Snodgrass and Bush, 2016; Chandrasekharam, 2016).

One of the studies was focused on the comparison of the treatment outcomes of hypospadias by the methods of tip and urethroplasty without urethral plate incision. The general rate of urethrocutaneous fistula after tip

Downloaded from www.periodico.tchequimica.com

was 36%, and after urethroplasty without urethral plate incision – 32%. The second complication in the rating was meatus stenosis – 27.4%. Penis edema was registered in 7.55% of cases, hematoma – in 1.9% of cases, infection of urinary tracts – in 1.9% of cases in both groups (Wilkinson *et. al.,* 2012).

The authors show the results of two-step urethroplasty with buccal mucous graft. In 1/3 of patients, graft fibrosis developed after the first step. Complications after the second step of the surgery were registered in 34% of patients: urethral stenosis, glandular split, fistula, balatinis xerotica obliterans (Leslie *et al.,* 2011; Faure *et al.*, 2016). Thus, general complications registered after the correction of hypospadias included urethrocutaneous fistula, meatus stenosis, neo-urethra stenosis, urethra diverticula or urethrocele, which can lead to the development of infection, esthetic defects, hair growth in the urethra, splattering or abnormal urine flow, erectile dysfunction, balatinis xerotica obliterans leading to the strictures. In the majority of cases, postoperative complications are usually revealed at the early stage within the first months after the surgery, but some complications such as fistula, neo-urethral stenosis, and recurrent deformation of the penis can be registered at later stages (Kendigelen *et al.,* 2016; Keays and Dave, 2017; Faasse and Liu, 2017). The average time of the diagnostics of complications such as glans penis deformation was 2 months, of urethral fistula, meatostenosis, stricture and diverticula of the urethra – 6 months. Control examination of the patients in the post-operative period was performed in 1.2 weeks and 1.3 and 6 months, and further one time a year until the completion of penis growth (Tiryaki *et al.,* 2016).

In the majority of cases, hypospadias has isolated character, but it can also be associated with other anomalies, especially those that are located in the urogenital tract (Bouty *et al.,* 2015). Hypospadias is one of the most widespread congenital anomalies. However, its etiology remains understudied. The study on the role of genetic and ecologic factors in the development of familial aggregation of hypospadias was conducted. Monogenic mode of inheritance of hypospadias in families and association with genetic defects in the biosynthesis of androgens indicates on the genetic background (Schnack *et al.,* 2007). Heritability of hypospadias is high, around 65–75%, and the risk of its development is estimated as elevated (12–20-fold in the first degree of family relatives) (Schnack *et al.,* 2007). The results of the conducted cohort study of the familial aggregation of hypospadias within the couples of male twins and first, second and third-degree relatives showed that the genetic inheritance is observed equally often patrilineally and matrilineally, and the risks of hypospadias recurrence for brothers and sons are similar. The main role in familial hypospadias can be played by genetic factors and not by general environmental ones (Schnack *et al.,* 2007; Li *et al.*, 2016; Kim *et al.,* 2016; Kozyrev *et al.,* 2017).

Other causes of hypospadias in children include genetic polymorphisms, identified in FGF8 and FGFR2 genes, that were observed in a minor share of cases. Since the development of male reproductive organs is an AR-dependent process, it can be suggested that polymorphisms, identified in FGF8 and FGFR2 genes in boys with hypospadias, can prevent AR-responses during the development of the urethra (Beleza-Meireles *et al.,* 2007; Sadeghi *et al.,* 2017).

A longitudinal study that included vegetarian women showed that the influence of phytoestrogens on the development of a male reproductive system and confirmed that the incidence rate of hypospadias in newborn boys was higher (North and Golding, 2000). Urogenital anomalies, including hypospadias, are met in 22% of cases in newborns with Ellis-van Creveld syndrome (EVC) (Kowal *et al.,* 2015). Hypospadias was described in more than 200 other syndromes, like WAGR, (Wilms tumor, Aniridia, Genitourinary defect, mental Retardation complex), Denys-Drash syndrome (genitourinary defects and susceptibility to WT) and Smith-Lemli-Opitz syndrome (congenital anomaly of heart, lungs, kidneys, gastrointestinal tract and genitals). The genetic basis of these syndromes is the mutation in the genes, like C31 in children with Denys-Drash syndrome or DHCR7 in children with Smith-Lemli-Opitz syndrome (Bouty *et al.,* 2015; Nakamura *et al.,* 2018).

The group of chemical substances that were studied in terms of influence on hypospadias development is pesticides. Some of them can be destructive for the endocrine system. A major study in Australia, based on professional data of newborns registration, reported on the elevated risk associated with heavy metals but not with other chemical groups of substances. Prospective cohort study conducted in Denmark gave some limited proof that professional impact of such endocrine destructive substances, such as phthalate ester ethers, alkyl-phenols, and bis-phenols, on future mothers, in general, elevated the risk of hypospadias development (Morales-Suárez-

Downloaded from www.periodico.tchequimica.com

Varela *et al.,* 2011). Urethral closure depends on the transformation of testosterone into dihydrotestosterone (DHT) (anabolic steroid of 5α-reductase type II), binding of DHT ligand with nuclear apparatus of androgen and the following respective androgen receptors activities (AR). The last two studies highlighted the influence of progesterone on the increase in the risk of hypospadias development (Carmichael *et al.,* 2012; de Andrade *et al.,* 2017; Wilkinson *et al.,* 2017; Wong *et al.,* 2018; Wu *et al.,* 2018).

Hypospadias develops as a result of the anomalous or incomplete formation of the urethra during the first weeks of embryonal development. There are two stages in the development of exterior reproductive organs in humans: early hormone-independent stage (5–8 weeks of the gestation) and hormone-dependent stage (8–12 weeks) (Blaschko *et al.,* 2012). Embryogenesis: Primary gonads are formed between the 4th and 5th weeks of the fetus development. The presence of Y-chromosome provides the development of the testicles. The formation of the posterior urethra by splitting of the primary cloaca into the primitive rectum and urogenital sinus occurs between the 30th and 40th day of the embryo life. Urogenital sinus or vesicourethral channel develops into the bladder and posterior urethra. By the 43–45th day (the length from the coccyx to the crown of head is 15 mm), the posterior urethra is completely formed and opens as ostium urogenitale. The development of the anterior urethra starts at the beginning of the 3rd month. On the 5th week of gestation, genital eminence develops in a form of tissue cranially to cloaca; on the 6th week, urethral folds and scrotal rolls appear. It is suggested that Y-chromosome encodes the synthesis of protein Y-antigen that contributes to the conversion of indifferent gonad into testicular tissue. Embryogenic phenotypic differences develop in two directions: differentiation of inner ducts and outer genitals. At the early stages of development, an embryo contains both female (paramesonephric) and male (mesonephric) ducts.

Internal genital organs develop from Wolffian and Mullerian ducts that are located nearby each other in an embryo at the early stages of development. During the development of a male embryo, Mullerian ducts begin to degenerate at the 6th week, which indicates on even earlier differentiation of germinal epithelium and activation of hormonal activity of the formed gonad. In male embryos, Wolffian ducts develop into epididymis, seminal ducts, and seminal vesicles, while Mullerian ducts disappear. Female embryos have Mullerian ducts develop into fallopian tubes, uterus and upper part of the vagina and Wolffian ducts regress. Outer genitals and urethra in embryos of any sex develop from urogenital sinus and genital eminence, genital folds, and hills. Development of the urethra from the urethral plate is described in the works of different authors. According to Herzog and Howard, quick growth of urethral duct from urethral plate coincides with the intensive development of Wolffian bodies on the 6th – 10th week of gestation. The closure of urethral ducts begins around the meatus of the urogenital sinus, gradually spreading upwards to the glans penis strictly by the median line. This process begins from the 10th – 11th week of the embryo life and completes by the end of the 14th week. By this time, when the length of an embryo from the coccyx to the crown of head reaches 80mm, the outer urethral meatus opens on the volar surface of the penis under its glans. Glandular section is formed independently from the isolated urethral plate. The migration of the outer urethral meatus to the top of the glans penis is observed from the 15th to the 20th week of gestation. Herzog used to identify outer urethral meatus in a fetus located on the lower surface of the glans penis at the 4th month of the gestation.

Fetal testicles can synthesize a protein called anti-Mullerian factor that reduces paramesonephric ducts in male embryos. On the 8th week of gestation, when the gonads differentiated into testicles on males (XY), a hormone-dependent phase of differentiation begins. Besides, starting on the 10th week of gestation, first, under the influence of chorion gonadotrophic hormone (CGH), and then, under the influence of luteinizing hormone (LH), fetal testicles begin to synthesize a lot of testosterone that affects undifferentiated outer genitals leading to their masculinization. During the 5th week of pregnancy, mesodermal cells spread on the cloaca membrane and form a couple of cloaca folds. These folds are located along the line anterior to the cloaca membrane to form genital tubercle. At the end of the 2nd month, the tubercle is 1.5 mm high. However, at this stage, it is still impossible to identify visually a male embryo from a female one. The differences in the exterior structure of the genitals appear by the end of the 3rd month (50–55 mm) when in female embryos this tubercle begins to bend down and in male embryos, it remains straight. By this time, male embryos have closure of the urethral duct started from the bottom to the top. The formation of genital tubercle completes by the 6th week. A week later, scrotum folds and urethral plate

Downloaded from www.periodico.tchequimica.com

appear in the bottom of the tubercle. Genital tubercle is growing, transforming into a penis, urogenital sinus develops into a prostate and prostatic part of the urethra, and genital folds merge forming a male urethra. The meatus is formed by the retraction of epithelial tissue inside the glans penis and merges with the distal end of the forming urethra in the area of fossa navicularis. The fusion of urethral folds is the key stage in the formation of a penis. Penile skin, including the foreskin, develops from ectodermal tissue that covers the whole penis. According to other authors, the formation of the urethra coincides with the formation of the foreskin and frenulum that are the two formations that are also deformed in males with hypospadias. The development of the foreskin coincides with the completion of urethral duct closure under the glans penis. On the 3rd month of gestation, there is a focus of epithelization on the top of the glans penis is observed. It is a plastic material for the formation of inner and outer layers of the foreskin. It is believed that epithelial layers, that cover the glans, fuse with the epithelial cover of the closed urethral duct and form the frenulum. By the end of the 1st trimester, the genitals get formed completely. It should be noted that inner male genitals (genital ducts) are formed under a direct action of testosterone, while the external genitals develop under the influence of the active metabolite T-DHT (dihydrotestosterone), which is produced in cells in the presence of a specific enzyme – 5 alfa-reductase (Bouty *et al.,* 2015; Shirazi *et al.,* 2016).

3. RESULTS ANS DISCUSSION:

As a rule, hypospadias is an isolated anomaly, but it can represent one of the peculiarities of more than 200 different syndromes. The diagnostics includes the collection of anamnesis, clinical examination, evaluation of local status, laboratory analyses and diagnostic instrumental methods. The associated anomalies in the development of urogenital ducts are widespread in newborns with proximal hypospadias. The most common anomalies are groin hernia, cryptorchism, and renal agenesia. For this reason, proximal hypospadias requires thorough evaluation. The presence of one or both testicles can indicate such a condition as an androgenetic syndrome or combined gonad dysgenesis. In this case, it is necessary to investigate the karyotype and perform ultrasound scanning of urinary tracts and inner genitals. Besides, endoscopic examination of the urethra and bladder during the surgery to exclude the urogenital sinus. If hypospadias is associated with kidney and renal tract anomalies, it is necessary to perform advanced clinical examination using urodynamic tests, X-ray imaging (excretory urography, urethrocystography), radioisotope and endoscopic methods of diagnostics (Manzoni *et al.*, 2004).

Based on the results of the life and diseases anamnesis, local status, and laboratory and instrumental data, the form of hypospadias is identified. But precise diagnostics of the hypospadias form, degree of cavernous bodies deformity, and quality of the urethra are possible to perform only under general anesthesia, which often results in the change of initially indicated surgical treatment plan.

The study of outcomes of surgical treatment of different forms of hypospadias in children, based on the data obtained by foreign and Russian researchers, showed that the problem of this anomaly correction remains acute because different complications are observed in both early and late postoperative period. Surgical treatment for hypospadias targets the restoration of penis function and anatomy. The main task of the treatment is to reconstruct a direct, esthetically normal penis with the urethral meatus located in the proper place (Ziada *et al.,* 2011).

One of the main aspects of hypospadias treatment is the age of a patient. It is still disputable when the correction of the anomaly should be more feasible. Earlier, foreign authors had a different opinion on the age when the treatment should start. Some authors recommended starting the radical correction at the age of six months, others recommended to wait until one year of age. Presently, the American Academy of Pediatrics and European experts recommend that the correction of hypospadias has to be performed at the age of 6 – 12 months. When it is not possible to perform it earlier for any reason, the treatment can be started at the age of 3-4 years old (Manzoni *et al.*, 2004).

Surgical treatment of different forms of hypospadias has its peculiarities. Currently, for the formation of the glanular part of the urethra and urethral duct, different methods are used, like the methods of Duplay, Snodgrass, Mathieu, Duckett and two-phase methods. According to the research data, normally formed spongy tissue in the glans never involves urethra and the ends of the corona do not touch each other. Urethral duct is “suspended” in the ventral surface of the

Downloaded from www.periodico.tchequimica.com

glans penis. Often, glanuloplasty is performed as follows: the formed urethral duct is encircled by the ends of the glans, creating a continuous sleeve around the distal part of the artificial urethra, which may cause complications. Due to this, an important role plays the formation of glanular part of the urethra that influences the effectiveness of the urinal flow. Insignificant resistance to the urinal flow in glanular part of the urethra leads to the increase in micturation pressure in the proximal part of the neo-urethra and, as a result, the risk of urinary fistula (Staroverov and Kazanskaya, 2016). The main drawback of the Mathieu technique is a round shape of the meatus instead of a slot-like one (Yesildag *et al.,* 2004) which, probably, leads to the development of stenosis and fistula. This fact also proves that the conducted randomized study on the primary hypospadias with distal forms (glanular, subglanular, midshaft) that was corrected with two methods of urethroplasty: conventional TIP Snodgrass and combined Mathieu-IP (urethra incised-plate). As a result, meatus stenosis and urethral fistula developed as a complication in 21.8% of cases after TIP Snodgrass and in 2.9% of cases after Mathieu-IP. Thus, the combined method with urethral plate incision reduces the rate of complications and improves the esthetic effect (Khalil *et al.,* 2017). To correct moderate and severe torsion of a penis with a distal form of hypospadias, some authors propose to perform a decutanization with the excision of fibrous remnants. If the torsion remains completely or partially, it is recommended to fix a flap of fibrous tunic of the penis to the periosteum of the pubic bone, which is considered a more reliable and efficient method of the torsion correction. Torsion of a penis is a rotation of cavernous bodies around the radial axis. It is identified by the displacement of the “median raphe” from the central line going along the ventral surface of a penis from the corona to the scrotum and perineum. These authors believe that vast mobilization of the urethra to the perineum does not lead to the correction of torsion and only minimally improves the angle of penis rotation. Further studies are needed for the deep and detailed understanding of the pathogenesis of a congenital torsion of a penis (Elbakry *et al.,* 2013).

Urethroplasty, which is a method of surgical correction for hypospadias, is performed by the method of tabularized incised plate (TIP), application of cutaneous flaps and transplants. From the mid 90’s, the TIP method became widespread in the correction of distal, proximal and re-operational hypospadias. According to the author, TIP potentially simplifies surgical solutions and techniques, has a low rate of complications and better esthetic effect. However, to achieve optimal results, it is necessary to pay special attention to the surgical details and understand the counter-indications to the procedure (Snodgrass, 2005).

Formation of the neo-urethra using buccal mucosa was first proposed by Humby in 1941 (Humby, 1941; Elsheikh and Fayad, 2011) and Mirabet in 1964 (Mirabet-Ippolito, 1964; Stein *et al.,* 2006). In 1993, el-Kasaby et al. (el-Kasaby *et al.,* 1993) were the first to report about the application of a buccal mucosa transplant in the restoration of penile and bulbar structures in 20 adult men without hypospadias. In 2001, Asopa et al. (Asopa *et al.,* 2001) described the technique of dorsal implantation of a buccal flap for the restoration of front urethral strictures. In 1995, severe forms of hypospadias were corrected with two-stage Bracka urethroplasty (Bracka, 1995).

Application of buccal mucosa as a transplant for urethra replacement was a revolutionary method in the management of serious cases of hypospadias (Manzoni *et al.*, 2004). According to the authors, the skin defect on the ventral surface of a penis is replaced by the buccal mucosa flap with further formation of artificial urethra or buccal mucosa can be used as a graft into a narrow urethral path (Snodgraft), which allows for the formation of the urethra with a diameter that is suitable for the patient’s age. Such operations became widespread from the beginning of the 2000’s in adult and pediatric patients. Thus, the patients, who were operated using this technique, were mainly children, and some authors believe that it is difficult to evaluate the final results. This provokes some concerns about the application of this method. In this case, the urethra is formed from a tissue that is not homologous to the tissue of a penis, and the experience of hypospadias treatment shows that all the cases of the registered penis cancer development were caused by the application of non-homologous tissues. The buccal mucosa flap is tightly sutured to the cavernous bodies, which is an obligatory condition for its engraftment. Thus, the formed urethral duct in a child remains fixed to the cavernous bodies and the urethra loses mobility, which is necessary for its elongation during the erection. In adult patients with the formed penis, this does not lead to serious complications, but in children, it is not known yet, how this surgery will influence on their sexual life. During the plastics with unattached

Downloaded from www.periodico.tchequimica.com

flaps, there is a risk of trophic failure in the graft, which leads to its necrosis (Staroverov and Kazanskaya, 2016). Some authors believe that the method of grafting with the inner layer of the foreskin for the straightening of a penis remains underestimated. This approach was offered in the 1960's by A.M. Cloutier but did not become widespread (Cloutier, 1962).

One of the most widespread problems in hypospadias is the development of fistulas. To reduce the risk of fistula development, it is necessary to follow some rules: optimal choice of glanuloplasty based on anatomic peculiarities, use of the optic tools, quickly degrading suture material, protection of sutures with the dartos fascia, slight penis compression to avoid hematomas and allow for the revascularization, immobilization of the penis and proper urine diversion in postoperative period. Although the TIP is a simple and popular method of urethroplasty, the rate of post-operational complications varies from 11.1 to 33.3%, on average, 21.8% (Van Putte and De Win, 2016). The drawbacks of TIP urethroplasty are high rate of urethral-cutaneous fistula (0–33%) and meatus stenosis that requires regular dilation. These complications are more serious as compared to other complications because of narrow urethral duct and flat, shallow glans (Elbakry *et al.,* 2016).

According to Grosos et al. (Grosos *et al.,* 2014), urethral fistula developed after Duplay urethroplasty in 9.1% of cases. According to Sharma data, it developed in 20% of cases after TIP urethroplasty (Sharma *et al.,* 2013). The authors of the study compared the outcome of urethroplasty for the correction of distal hypospadias by the conventional TIP method and modified TIP method with the use of intact and laterally enlarged plate. General rate of the complications was 16.8% and 5.6%, respectively. These conclusions confirm that the most widespread post-operational complication is urethral-cutaneous fistula (Van Putte and De Win, 2016).

Other authors use the PAWGs method of urethroplasty that involves post-auricular Wolfe grafts. Such grafts are thicker than the inner layer of the foreskin, but of the same thickness or thinner than the buccal flap taken from the oral cavity. Significant drawbacks of PAWGs method are keloid scars that sometimes develop on the donor part. Sometimes, synechias developed in the reconstructed urethral duct, which required the replacement of post-auricular skin with the mucous. If the donor's skin was taken closer to the mastoid bone, the treated child may have hair growing in the meatus of neo-urethra (Bracka, 2008).

For objective functional and esthetic evaluation of the urethroplasty outcome for the correction of hypospadias by different methods, Holland et al. in 2001 proposed the system of HOSE scoring (Hypospadias Objective Scoring Evaluation System). For the evaluation of the functional outcome of the treatment, five objective elements are used: position and forms of the meatus, evaluation of the urine flow, straightness of the penis, absence of fistula and any other complications (van der Toorn *et al.,* 2013; Holland *et al.,* 2001). The proposed system of the evaluation is simple and can be measured clinically when the written consent from parents is obtained and in the presence of a qualified clinician that will perform the evaluation procedure. The total score for the evaluation equal to 14 was recommended as an acceptable result (Al-Adl *et al.,* 2014).

Prospective study was conducted for the evaluation of the esthetic and functional outcome of the correction of primary hypospadias with two methods of urethroplasty: MIUP (midline incision of the urethral plate) and TIP (tabularized incised plate) with the grafting of unattached flap of the foreskin, performed from 2012 to 2015. The method of G-TIP included standard steps of Snodgrass urethroplasty. The result was estimated by the HOSE system (Hypospadias Objective Scoring Evaluation System). Despite the fact that esthetic results were acceptable (>14 points in 96% of patients), the most often complications after the urethroplasty were urethrocutaneous fistula, suture scars and transplant on the edge of slot-like meatus, neo-urethra stricture in the place of incision after MIUP and in the graft area after G-TIP, as well as penis angulation by 10–30 degrees (Gupta *et al.,* 2016). Traditionally, the methods of choice for the correction of proximal forms of hypospadias are two-step Bracka operations with the use of buccal mucous graft, post-auricular graft and double isle flap urethroplasty (Sakr *et al.,* 2017).

The prospective study conducted in 2013–2015 focused on the evaluation of esthetic and functional treatment results after the two-step urethroplasty with buccal and tongue mucous grafts. After the first step, the following complications were revealed: infection, penis edema, skin ecchymosis, residual chord, graft rejection or contracture. In the area of donor skin flap, wet dressing was observed and patients complained about the pain that required pain management in 69% of cases. After the second

Downloaded from www.periodico.tchequimica.com

step of urethroplasty, the complications were skin ecchymoses, penis edema, bleeding, fistulas, and meatus stenosis. Thus, general complications rate was 23% (Gupta *et al.,* 2016).

In one of conducted studies on urethroplasty with buccal and tongue mucous for the correction of front strictures of the urethra, Kumar A., Das S.K. et al. highlight earlier post-operational complications in the lingual donor area as compared to buccal area, and in later post-operational period such complications as tightness, discomfort and numbness were observed only in the group, where a buccal flap was used (Kumar *et al.,* 2010). Similar results were presented in the report by Pal D.K., Gupta D.K. et al. in the group, where lingual flap was used. In early post-operational period, the patients had scrambled speech, in the group with BMG (buccal mucosal graft), salivary changes were observed, tightness, pain in the donor area and numbness, difficulties with mouth opening, recurrent urethral stenosis (Pal *et al.,* 2016). According to Sharma A.K et al., the preparation of lingual graft took less time than buccal graft (Sharma *et al.,* 2013).

Despite the application of different methods of urethroplasty and unattached grafts and pedicle flaps, the rate of postoperative complications remains high. The right choice of the method of operation provides good functional and esthetic result and reduces the risk of post-operational complications. The analysis of the published information on the treatment outcomes in patients with hypospadias and the search results in the databases of the scientific journals proved the necessity in the development of optimal methods of correction for the urethroplasty in children with hypospadias.

4. CONCLUSIONS:

The review of numerous studies allowed the authors to suggest that the incidence rate of hypospadias, in general, in different countries tends to increase annually. The authors established that the main cause of hypospadias was a failure of endogen stimulation of the penis development, which results in the malformation of the urethra and the adjoining structures. There are a number of different methods of urethroplasty and unattached grafts or pedicle flaps used, but still, the number of complications in post-operative period remains high. The right choice of the surgery provides good functional and esthetic results and reduces the risk of the development of post-operative complications.

The analysis of the data on the outcomes of the treatment for hypospadias, based on the data obtained from the databases of the published journals, proved the need in the development of optimal variants of urethroplasty in children with hypospadias. The maximum risk factors for the development of complications after urethroplasty grafting include the wrong choice of glanduloplasty (the urethra is placed unacceptably deep), suture material, insufficient inversion of the epithelial edges of a wound, insufficient coverage of the urethroplasty area with the second layer of the tissue, unattached grafts, insufficient hemostasis, ischemic necrosis of tissues, method and duration of the urine deprivation in the post-operative period. For this reason, long-term observation of patients is required.

5. REFERENCES:

1. Al-Adl, A.M., El-Karamany, T.M., Bassiouny, A.S. *Arab Journal of Urology,* **2014**, *12*(2), 116–126.
2. Alsaywid, B.S., Mohammedkhalil, A.K., Mesawa, A.A., Alzahrani, S.Y., Askar, A.H., Abuznadah, W.T., Jafarzadehpour, E., Nouri, S. *Urology Annals,* **2017**, *9*(2), 141–144.
3. Asopa, H.S., Garg, M., Singhal, G.G., Singh, L., Asopa, J., Nischal, A. *Urology,* **2001**, *58*, 657–9.
4. Aydogmus, Y., Bagbanci, S., Demirbas, A., Hascicek, A.M. *Archivos Espanoles de Urologia*, **2017**, *70*(8), 740-745.
5. Ayob, F., Arnold, R. *Anaesthesia*, **2016**, *71*(7), 759-763.
6. Badawy, H., Orabi, S., Hanno, A., Abdelhamid, H. *Journal of Pediatric Urology*, **2018**, *14*(1), 28.e1-28.e8.
7. Beleza-Meireles, A., Lundberg F., Lagerstedt, K., Zhou, X., Omrani, D., Frise´n, L., Nordenskjo¨ld, A. *European Journal of Human Genetics,* **2007**, *15*, 405–410.
8. Bergman, J.E.H., Loane, M., Vrijheid, M., Pierini, A., Nijman, R.J.M., Addor, M.-C. Barisic, I., Beres, J., Braz, P., Budd, J., Delany, V., Gatt, M., Khoshnood, B., Klungsoyr, K., Martos, C., Mullaney, C., Nelen, V., Neville, A., O'Mahony, M., Queisser-Luft, A., Randrianaivo-Ranjatoelina, H., Rissmann, A., Rounding, C., Tucker, D., Wellesley, D., Zymak-

Downloaded from www.periodico.tchequimica.com

Zakutnya, N., Bakker, M., de Walle, H. *World Journal of Urology,* **2015**, *33*(12), 2159–2167.

9. Bhat, A., Bhat, M., Sabharwal, K., Bhat, A., Kumar, R. *African Journal of Urology*, **2017**, *23*(2), 94-99.
10. Blaschko, S.D., Cunha, G.R., Baskin, L.S. *Differentiation,* **2012**, *84*(3), 261–268.
11. Bouty, A., Ayers, K.L., Pask, A., Heloury, Y., Sinclair, A.H. *Sexual Development,* **2015**, *9*(5), 239– 259.
12. Bracka, A. *British Journal of Urology,* **1995**, *76* (Suppl. 3), 31–41.
13. Bracka, A. *Indian Journal of Urology,* **2008**, *24*(2), 210–218.
14. Canning, D.A. *The Journal of Urology*, **2016**, *196*(3), 881-882.
15. Carmichael, S.L., Shaw, G.M., Lammer, E.J. *Birth Defects Research Part A: Clinical and Molecular Teratology,* **2012**, *94*(7), 499–510.
16. Chandrasekharam, V.V.S. *Journal of Pediatric Urology*, **2016**, *12*(2), 129-130.
17. Cloutier, A.M. *Plast Reconstr Surg Transplant Bull,* **1962**, *30*, 368–73.
18. de Andrade, E.C., de Castro Paiva, K.C., da Silva Guedes, S., Souza, M.L.C., Pereira, M.N., Miana, L.P., de Figueiredo, A.A., de Bessa, J., Jr., Netto, J.M.B. *Journal of Pediatric Urology*, **2017**, *13*(4), 352.e1-352.e7.
19. Dokter, E.M., Mouës, C.M., Rooij, I.A.L.M.V., Biezen, J.J.V.D. *European Journal of Pediatric Surgery*, **2018**, *28*(2), 200-206.
20. Elbakry, A., Hegazy, M., Matar, A., Zakaria, A. *Arab Journal of Urology,* **2016**, *14*(2), 163–170.
21. Elbakry, A., Zakaria, A., Matar, A., El Nashar, A. *Arab Journal of Urology,* **2013**, *11*(1), 1–7.
22. el-Kasaby, A.W., Fath-Alla, M., Noweir, A.M., el-Halaby, M.R., Zakaria, W., el-Beialy, M.H. *The Journal of Urology,* **1993**,*149*, 276–8.
23. Elsheikh, M.G., Fayad, A.A. *Open Journal of Urology,* **2011**, *1*(1), 4–7.
24. Faasse, M.A, Liu, D.B. *Journal of Pediatric Urology*, **2017**, *13*(4), 354.e1-354.e5.
25. Faure, A., Bouty, A., Nyo, Y.L., O'Brien, M., Heloury, Y. *Journal of Pediatric Urology*, **2016**, *12*(5), 286.e1-286.e7.
26. Fernández, N., Pérez, J., Monterrey, P., Poletta, F.A., Bägli, D.J., Lorenzo, A.J., Zarante, I. *International Brazilian Journal of Urology*, **2017**, *43*(2), 325–-334.
27. Gong, E.M., Cheng, E.Y. *Journal of Pediatric Urology*, **2017**, *13*(5), 457-467.
28. Grosos, C., Bensaid, R., Gorduza, D.-B., Mouriquand, P. *Journal of Pediatric Urology,* **2014**, *10*(6), 1232–1237.
29. Gupta, V., Yadav, S.K., Alanzi, T., Amer, I., Salah, M., Ahmed, M. *Arab Journal of Urology,* **2016**, *14*(4), 299–304.
30. Han, W., Zhang, W., Sun, N. *International Urology and Nephrology,* **2018**, *50*(2), 191–195.
31. Holland, A.J., Smith, G.H., Ross, F.I., Cass, D.T. *British Journal of Urology*, **2001**, *88*(3), 255–258.
32. Humby, G. *British Journal of Surgery,* **1941**, *29*, 84–92.
33. Kagantsov, I.M., Surov, R.V. *Urologiia*, **2018**, *5*, 81-87.
34. Keays, M.A., Dave, S. *Canadian Urological Association Journal,* **2017**, *11*(1–2Suppl1), 48–53.
35. Kendigelen, P., Tutuncu, A.C., Emre, S., Altindas, F., Kaya, G. *Regional Anesthesia and Pain Medicine*, **2016**, *41*(5), 610-615.
36. Kermani, R.M., Nedaeifard, L., Nateghi, M.R., Fazeli, A.S., Ahmadi, E., Osia, M.A., Jafarzadehpour, E., Nouri, S. *Archives of Iranian Medicine,* **2012**, *15*(4), 228–231.
37. Khalil, M., Gharib, T., El-shaer, W., Sebaey, A., Elmohamady, B., Elgamal, K. *Arab Journal of Urology,* **2017**, *15*(3), 242–-247.
38. Kim, M.H., Im, Y.J., Kil, H.K., Han, S.W., Joe, Y.E., Lee, J.H. *Anaesthesia*, **2016**, *71*(7), 773-778.
39. Kowal, A., Mostowska, A., Mydlak, D., Eberdt-Gołąbek, B., Misztal, M., Jagodziński, P.P., Hozyasz, K.K. *Central European Journal of Urology,* **2015**, *68*(2), 257–262.
40. Kozyrev, G.V., Protasov, A.A., Nikolaev, V.V., Abdullaev, F.K., Abdulkarimov, G.A.,

Downloaded from www.periodico.tchequimica.com

Karmanov, M.E. *Urologiia*, **2017**, *5*, 63-68.

41. Kreysing, L., Höhne, C. *Paediatric Anaesthesia*, **2016**, *26*(3), 329-330.
42. Kumar, A., Das, S.K., Trivedi, S., Dwivedi, U.S., Singh, P.B. *Urologia Internationalis,* **2010**, *84*(1), 78–83.
43. Leslie, B., Lorenzo, A. J., Figueroa, V., Moore, K., Farhat, W.A., Bägli, D.J., Pippi Salle, J.L. *The Journal of Urology,* **2011**, *185*(3), 1077–1082.
44. Li, H.-B., Xu, Y.-M., Fu, Q., Sa, Y.-L., Zhang, J., Xie, H. *Asian Journal of Andrology*, **2016**, *18*(3), 467-470.
45. Li, Y., Mao, M., Dai, L., Li, K., Li, X., Zhou, G., Wang, Y., Li, Q., He, C., Liang, J., Zhu, J. *Birth Defects Research Part A: Clinical and Molecular Teratology*, **2012**, *94*(1), 36–41.
46. Loane, M., Dolk, H., Morris, J.K. *BJOG An International Journal of Gynecology & Obstetrics,* **2009**, *116*(8), 1111–1119.
47. Makazhanov, M.A. *Scientific-Practical Journal of Medicine, "Vestnik KazNMU"* **2012**. Available from: https://kaznmu.kz/press/2012/01/27/гипоспадия-определение-распростран/, accessed April 2019.
48. Manzoni, G., Bracka, A., Palminteri, E., Marrocco, G. *British Journal of Urology,* **2004**, *94*(8), 1188–1195.
49. Menon, P., Rao, K.L.N., Handu, A., Balan, L., Kakkar, N. *Journal of Pediatric Urology*, **2017**, *13*(3), 292.e1-292.e7.
50. Mirabet-Ippolito, V. *Modification de la Técnia de Mcindoe Para El Tratamiento de Los Hipospadias,* Valencia: DT, **1964**.
51. Morales-Suárez-Varela, M.M., Toft, G.V., Jensen, M.S., Ramlau-Hansen, C., Kaerlev, L., Thulstrup, A.-M., Llopis-González, A., Olsen, J., Bonde, J.P. *Environ Health*, **2011**, *10*, 3.
52. Nakamura, M., Moriya, K., Nishimura, Y., Nishida, M., Kudo, Y., Kanno, Y., Kitta, T., Kon, M., Shinohara, N. *BMC Pediatrics*, **2018**, *18*(1), 179.
53. Nissen, K.B., Udesen, A., Garne, E. *Congenital Anomalies (Kyoto)*, **2015**, *55*(1), 37–41.
54. North, K., Golding, J. *British Journal of Urology,* **2000**, *85*(1), 107–113.
55. Ollivier, M., Paris, F., Philibert, P., Garnier, S., Coffy, A., Fauconnet-Servant, N., Haddad, M., Guys, J.M., Reynaud, R., Faure, A., Merrot, T., Wagner, K., Bréaud, J., Valla, J.S., Dobremez, E., Gaspari, L., Daures, J.-P., Sultan, C., Kalfa, N. *Journal of Urology*, **2018**, *200*(4), 890-894.
56. Pal, D.K., Gupta, D.K., Ghosh, B., Bera, M.K. *Urology Annals,* **2016**, *8*(2), 157–162.
57. Pierik, F.H., Burdorf, A., Nijman, J.M.R., de Muink Keizer-Schrama, S.M.P.F., Juttmann, R.E., Weber, R.F.A. *Human Reproduction,* **2002**, *17*(4), 1112–1115.
58. Rudin, Yu.E., Marukhnenko, D.V., Garmanova, T.N. *Experimental and Clinical Urology*, **2013**, *4*, 110–114.
59. Sadeghi, A., Mirshemirani, A., Tabari, A.K., Sadeghian, N., Rozroukh, M., Ghoroubi, J., Mohajerzadeh, L., Sarafi, M. *Iranian Journal of Pediatrics*, **2017**, *27*(6), e7752.
60. Sakr, A., Elkady, E., Abdalla, M., Fawzi, A., Kamel, M., Desoky, E., Seleem, M., Omran, M., Elsayed, E., Khalil, S. *Arab Journal of Urology,* **2017**, *15*(3), 236–241.
61. Schnack, T.H., Zdravkovic, S., Myrup, C., Westergaard, T., Christensen, K., Wohlfahrt, J., Melbye, M. *American Journal of Epidemiology,* **2007**, *167*(3), 251–256.
62. Seleim, H.M., Morsi, H., Elbarbary, M.M. *Journal of Pediatric Urology*, **2017**, *13*(3), 290.e1-290.e7.
63. Sharma, A.K., Chandrashekar, R., Keshavamurthy, R., Nelvigi, G.G., Kamath, A.J., Sharma, S., Venkatesh, G.K. *International Journal of Urology,* **2013**, *20*(12), 1199–1203.
64. Shirazi, M., Mahmoudi, H., Nasihatkon, B., Ghaffaripour, S., Eslahi, A. Pakistan *Journal of Medical Sciences*, **2016**, *32*(1), 125-129.
65. Singal, A.K., Dubey, M., Jain, V. *World Journal of Urology*, **2016**, *34*(7), 1019-1024.
66. Snodgrass, W., Bush, N. *Urology Annals,* **2016**, *8*(4), 403–408.
67. Snodgrass, W., Bush, N.C. *Journal of Pediatric Urology*, **2017**, *13*(3), 289.e1-289.e6.

Downloaded from www.periodico.tchequimica.com

68. Snodgrass, W.T. *British Journal of Urology,* **2005**, *95*(4), 683–693.
69. Staroverov, O.V., Kazanskaya, I.V. *Andrology and Genital Surgery,* **2016**, *17*, 77–84.
70. Stein, R., Schröder, A., Thüroff, J. W. *British Journal of Urology,* **2006**, *97*(4), 871–889.
71. Tiryaki, S., Ələkbərova, V., Dokumcu, Z., Ergun, R., Tekin, A., Yagmur, I., Ulman, I., Avanoglu, A. *Journal of Pediatric Urology*, **2016**, *12*(6), 395.e1-395.e6.
72. van der Toorn, F., de Jong, T.P.V.M., de Gier, R.P.E., Callewaert, P.R.H., van der Horst, E.H.J.R., Steffens, M.G., Hoebeke, P., Nijman, R.J.M., Bush, N.C., Wolffenbuttel, K.P., van den Heijkant, M.M.C., van Capelle, J-W., Wildhagen, M., Timman, R., van Busschbach, J.J. *Journal of Pediatric Urology,* **2013**, *9*(6 Pt B), 1006–1016.
73. van der Zanden, L.F.M., van Rooij, I.A.L.M., Feitz, W.F.J., Franke, B., Knoers, N.V.A.M., Roeleveld, N. *Human Reproduction Update,* **2012**, *18*(3), 260–283.
74. Van Putte, L., De Win, G. *Arab Journal of Urology,* **2016**, *14*(4), 312–316.
75. Wilkinson, D.J., Farrelly, P., Kenny, S.E. *Journal of Pediatric Urology,* **2012**, *8*(3), 307–312.
76. Wilkinson, D.J., Green, P.A., Beglinger, S., Myers, J., Hudson, R., Edgar, D., Kenny, S.E. *Journal of Pediatric Urology*, **2017**, *13*(5), 481.e1-481.e6.
77. Wong, Y.S., Pang, K.K.Y., Tam, Y.H. *Hong Kong Medical Journal*, **2018**, *24*(3), 238-244.
78. Wu, M. Chen, F., Xie, H., Lv, Y., Huang, Y., Liu, Y., Ye, W. *International Urology and Nephrology*, **2018**, *50*(10), 1795-1800.
79. Yesildag, E., Tekant, G., Sarimurat, N., Buyukunal, S.N.C. *The Journal of Urology,* **2004**, *171*(6), 2623–2625.
80. Ziada, A., Hamza, A., Abdel-Rassoul, M., Habib, E., Mohamed, A., Daw, M. *The Journal of Urology,* **2011**, *185*(6), 2483–2486.

ANEX 1 - LIST OF ABBREVIATIONS

TIP – tubularized incised plate

GTIP – graft tubularized incised plate

NCA – non-chromosomal congenital anomalies

ECLAMC – the Latin American Collaborative Study of Congenital Malformations

DHT – dihydrotestosterone

AR – androgen receptor

LH – luteinizing hormone

HOSE – Hypospadias Objective Scoring Evaluationg system

UCF – urethrocutaneous fistula

MIUP – the midline incision of the urethral plate

PAWGs – post-auricular Wolfe grafts

Downloaded from www.periodico.tchequimica.com

PERIÓDICO TCHÊ QUÍMICA
ARTIGO ORIGINAL

DESENVOLVIMENTO SUSTENTÁVEL DE INSTITUIÇÕES EDUCACIONAIS NO CONTEXTO DA INTRODUÇÃO DE ELEMENTOS DA EDUCAÇÃO À DISTÂNCIA NO PROCESSO DE APRENDIZAGEM

SUSTAINABLE DEVELOPMENT OF EDUCATIONAL INSTITUTIONS IN THE CONTEXT OF THE INTRODUCTION OF ELEMENTS OF DISTANCE EDUCATION IN THE LEARNING PROCESS

УСТОЙЧИВОЕ РАЗВИТИЕ ОБРАЗОВАТЕЛЬНОГО УЧРЕЖДЕНИЯ В УСЛОВИЯХ ВНЕДРЕНИЯ ЭЛЕМЕНТОВ ДИСТАНЦИОННОГО ОБРАЗОВАНИЯ В ПРОЦЕСС ОБУЧЕНИЯ

AITBAYEVA, Bakyt M.[1*]; MAULENOVA, Asemgul M.[2]; AKHMETZHANOVA, Zhanar B.[3]; KENZHEBEKOVA, Zhibek A.[4]; RAKHIMBAYEVA, Bagira O.[5];

[1,2,3,4,5] Academician E.A. Buketov Karaganda State University, Department of Practical Course of the Kazakh Language, Karaganda – Republic of Kazakhstan

** Correspondence author*
e-mail: izmalkov@mail.ru

Received 30 August 2019; received in revised form 20 October 2019; accepted 24 October 2019

RESUMO

A educação a distância é essencialmente a base para o desenvolvimento de instituições educacionais que fornecem serviços inovadores que não podem ser obtidos em outros lugares. Acredita-se que a educação a distância substitua a educação tradicional como parte da simplificação e barateamento do processo educativo. Ao mesmo tempo, as principais tendências mundiais indicam a necessidade do desenvolvimento de elementos de autoeducação e a expansão da natureza geográfica das propostas educacionais. A relevância do estudo reside no fato de ser necessário distinguir entre o uso de métodos de educação a distância na esfera tradicional e no campo da formação de profissionais. O artigo apresenta o conceito de necessidade de integrar os elementos da educação a distância no processo de formação de professores universitários. Os autores acreditam que os professores usam as mesmas técnicas na elaboração de cursos e na aplicação de tecnologias de treinamento que no ensino a distância. Portanto, o uso de tecnologias de educação a distância pode ser mostrado como base para o desenvolvimento de programas de educação continuada e educação profissional adicional. Os autores propuseram um estudo sobre a necessidade e suficiência do uso de tecnologias de educação a distância e as possibilidades de sua integração no processo de pós-graduação. A importância prática do estudo é determinada pelo fato de que são reveladas as possibilidades de desenvolvimento independente de professores não apenas como sujeitos do processo educacional, mas também como sujeitos de treinamento.

Palavras-chave: Educação a distância, professor, estrutura, desenvolvimento, treinamento.

ABSTRACT

Distance education is essentially the basis for the development of educational institutions that provide innovative services, which cannot be obtained elsewhere. It is believed that distance education is a substitute for the traditional as part of simplifying and cheapening the learning process. At the same time, the leading global trends suggest the need for the development of elements of self-education and the expansion of the geographical nature of educational offers. The relevance of the study is that it is necessary to distinguish between the use of distance education methods in the traditional sphere and the sphere of training professionals. The paper presents the concept of the need to integrate elements of distance education in the process of preparing university teachers. The authors believe that teachers in drawing up courses and applying learning technologies use the same techniques as in distance learning. Therefore, the use of distance learning technologies can be shown as the basis for the development of advanced training programs and additional professional education. The authors proposed a study on the need and sufficiency of the use of distance education technologies and the possibilities for their integration into the process of postgraduate education. The practical significance of the work is determined by the fact that the possibilities of self-development of teachers

Downloaded from www.periodico.tchequimica.com

are fully disclosed, not only as subjects of the educational process but also as subjects of training.

Keywords: Distance education, teacher, structure, development, training.

АННОТАЦИЯ

Дистанционное образование по своей сути является основой для развития учебных заведений, которые оказывают инновационные услуги, которые не могут быть получены в других местах. Считается, что дистанционное образование является заменой традиционному как части упрощения и удешевления процесса обучения. При этом ведущие мировые тенденции говорят о необходимости развития элементов самообразования и расширении географического характера образовательных предложений. Актуальность исследования заключается в том, что требуется разграничить использование методики дистанционного образования в традиционной сфере и сфере подготовки профессионалов. В работе представлена концепция о необходимости интеграции элементов дистанционного образования в процесс подготовки преподавателей вузов. Авторы полагают, что преподаватели при составлении курсов и применении технологий обучения используют такие же приемы, как и при обучении в дистанционной сфере. Поэтому применение дистанционных образовательных технологий может быть показано как основа для развития программ повышения квалификации и дополнительного профессионального образования. Авторами предложено исследование о необходимости и достаточности применения технологий дистанционного образования и возможностей по их интеграции в процесс последипломного образования. Практическая значимость работы определяется тем, что полностью раскрыты возможности самостоятельного развития преподавателей не только как субъектов учебного процесса, но также и как субъектов обучения.

Ключевые слова: Дистанционное образование, преподаватель, структура, развитие, обучение.

1. INTRODUCTION

Among the trends in the development of distance education in pedagogical theory and practice, the leading ones are the following: deepening the connection with the modernisation of pedagogical education on a modern scientific basis; design and implementation for lifelong learning and education of population; usage as a means of ensuring a quick response to the results of globalisation and other global processes; improving the quality of teaching and methodological support of the organisation of distance education (Holmberg, 1989; Akhmetshin *et al.,* 2019; Aleksandrova *et al.,* 2018; Aleksandrova *et al.,* 2019).

The system requirements for the teacher in the conditions of distance education are: an innovative orientation of his/her personality and readiness for innovations in the professional and pedagogical being; readiness for interpersonal dialogue with an organiser and subjects of the educational distance process; comprehensive competence in matters of psychology and pedagogy of professional self-education and self-education, personality psychology and the theory and technology of distance education; the ability to expand and deepen the experience of creative self-developing activities. (Huett *et al.,* 2008)

The set of these requirements is directly related to the teacher's readiness category for distance education in the system of continuing education, the structure of which is defined as an integral personality property reflecting the holistic interaction of motivational and value (increasing awareness of the need to master the theory and technology of distance education by means of self-education at the self-value level), cognitive (formation of personally assigned knowledge of modern information technology training, the basics of its organisation in higher education, ways of professional activity based on information and communication technologies for the purposes of professional development and self-development) and operational (a set of actions and operations related to the use of distance education technologies in professional activities) components (Booker, 1998).

Often they reveal the main features of the organization of distance education in the system of continuing education of teachers, with an emphasis from teaching to the independent cognitive activity of teachers; increased demand for the formation of teachers' readiness for distance education (ensuring their compulsory computer literacy as subjects of the educational process); changes in the ways of interaction between the subjects of the educational process, due to the advent of appropriate means of distance education technologies; flexibility of organizational forms and methods in accordance with the levels of actual readiness of teachers for distance education, time and place of conducting

Downloaded from www.periodico.tchequimica.com

classes (Guri-Rozenblit, 1993). The fact of the absence of the systemic nature of the distance education of a teacher as a result of the unreasonableness of the corresponding system in the scientific and pedagogical theory (Fraser, 2017) is updated.

2. LITERATURE REVIEW

Defining the conceptual positions of the distance education model in the system of continuing education of teachers, we took into account the following methodological principles (Branon and Essex, 2001):

– a systematic approach that focuses on disclosing the integrity of pedagogical objects, identifying various types of communication in them and bringing them into a single theoretical picture (Wen *et al.,* 2019). In accordance with this approach, teachers in distance education in the system of continuous education explore as an integral system, ordered by a plurality of interrelated components, which is a holistic formation (Rabinovich *et al.,* 2017);

– the concept of enhancing the cognitive activity, aimed at obtaining new knowledge, new information, which is implemented in order to obtain new knowledge and consciously use them in practice (Guri-Rosenblit, 2005). Cognitive activity is manifested in the teacher's attitude to the content and process of activity, in the mobilization of volitional efforts to achieve learning objectives (Hermansson, 1988). That is, cognitive activity is associated with an interest in the learning process, a need for expanding one's own horizons, the intensification of cognitive activity is characterized not only by the features of the activity itself but also by the attitude of students to the activity process (Montoya and Soledad, 2013);

– personality-oriented approach, which is based on the leading ideas of the humanization of education, provides a broad view of the content of education of humanities students, ways of learning activities, the expected result; allows a teacher to perceive a student as a communicative person, to identify and reveal their own capabilities, their ego (Berge and Muilenburg, 2001). Its essential features are the subject-subject humane cooperation of all participants in the educational process; diagnostic and stimulation method of knowledge; activity-communicative activity of students, their development and self-development; designing by a teacher (and later by students) individual achievements in all types of activities, their sensitive developments; consideration of the range of personal needs and capabilities of a person in obtaining quality education in the content and methods (Walker and Fraser, 2005);

– modular approach: modular technology is based on maximum programmability, structural clarity in the organization of the pedagogical process (Hoppers, 2000). Learning objectives take into account the capabilities of students (teachers), and at each stage of education, they determine the basic level of knowledge and skills (Tabata and Johnsrud, 2008). Based on autonomous portions of adapted educational content to the intellectual characteristics of each, this approach allows to more independently or fully independently work with the proposed individual program (McVey, 2018). The learning process based on the modular approach allows to: differentiate and integrate the learning content by grouping educational modules that provide the development of the discipline's content is reduced, full or in-depth versions and corresponding structured content aimed at mastering knowledge and skills, solving specific learning tasks (Stella and Gnanam, 2004). There is a reorientation of focuses in the educational process, that is, the process of directed learning, and not the teaching process, becomes the main thing.

3. MATERIALS AND METHODS

A pedagogical experiment involved studying the state of distance learning in the continuing education system (Rovai and Lucking, 2003). Based on its results, theoretical principles, which naturally complement the theory and methodology of vocational education, have been formulated (Kerimbayev *et al.,* 2017). In the process of conducting a stating experiment, a number of tasks have been implemented:

– subjects of diagnosis have been highlighted;

– criteria, tools, methods, and levels of diagnosis have been substantiated;

– the current state of readiness of teachers for the organization of distance education in the system of continuing education has been determined;

– the state of development of professional and pedagogical competence has been determined;

– a cross-section, analysis, and interpretation of its data have been conducted;

Downloaded from www.periodico.tchequimica.com

– a training system in the continuing education system has been developed.

The pedagogical experiment provided for the introduction of the distance education system in continuing education in the educational process of educational institutions.

The statistical results of the surveys have been summed up taking into account the number of questions, the maximum possible number of points received for answering the question, and the sum of points in accordance with the level of formedness of the readiness criterion. The result summarised in the table helped to determine indicators of the levels of formedness of the relevant criteria for the readiness of teachers to organize distance education in the system of continuing education. The points for each readiness criterion were added and the achieved level was calculated by the formula (Equation 1). Wherein P – the level of readiness to distance education, $\sum n$ – total sum of points of a respondent, $\sum m$ – maximum sum of points.

Having qualimetric indicators on the methods of diagnostics of the identified levels of readiness (motivational and value, cognitive and operational) of teachers to organisation of distance education in the system of continuing education, we correlated the amounts of points received into the relevant component of competence with the total number of points earned and converted to percentages. Then we compared the results to identify the components which will require more attention. Statistical analysis of the results was carried out using Microsoft Excel spreadsheets.

The general level of teachers' readiness for the organization of distance education in the system of continuing education of teachers was calculated as the arithmetic mean of all the criteria according to the formula (Equation 2). Wherein Σ – initial level of preparedness; a – number of participants at the appropriate level of readiness criteria, n – the number of readiness criteria (motivational and value, cognitive and operational).

In order to assess the effectiveness of approbation of the methodological system, the experiment toolkit was conducted to determine levels of teachers for organizing distance education in the system of continuing education of teachers after the experiment was determined (Lee, 2003). Having obtained as a result of the final cross-section of the data on shifts in the levels of formedness of the main criteria of readiness among teachers, we estimated the significance of these changes and made conclusions regarding the effectiveness of the introduction of the corresponding system.

4. RESULTS AND DISCUSSION:

At the beginning of the experiment, testing was carried out according to the adapted method. This method allowed to show changes in the motivational and value criteria of readiness for distance education. As a result of this survey, we obtained such data (Figure 1), namely: 90% of respondents chose No. 1 – to be a highly qualified specialist, No. 3 – to successfully continue their educational activities, No. 4 – to successfully carry out scientific activities and No.10 – to ensure success of professional activity; 75% chose No. 6 – to master new professional knowledge; 33% chose No. 7 – to be constantly ready for innovation, No. 2 – to receive a certificate, No. 8 – not to skip classes of the training cycle, and No. 12 – to achieve respect among colleagues.

The following motives were not chosen: No. 5 – to receive a cash bonus; № 9 – to keep up with colleagues; No. 11 – to # meet pedagogical requirements; No. 13 – to be an example for colleagues; No. 15 – to avoid conviction and administrative penalties; No. 16 – to get intellectual satisfaction.

Comparison of the data showed that the majority of teachers increased the number of cognitive motives – to be a highly qualified specialist and get a certificate (by 5%), to successfully continue their educational activities (by 55%), to successfully carry out research activities (by 17%), to ensure the success of their professional activities (by 55%). This indicates the effectiveness of the introduction of a system of continuing education for teachers.

After statistical processing of the results of the experiment according to the levels of formation of the criteria of teachers' readiness to organize distance education in the system of continuing education of teachers, we were convinced of significant achievements. This is evidenced by the combined experimental data of Table 1. The results of the formative stage of the experiment on the motivational and value criterion showed that 4.2% of teachers lack a steady cognitive interest in organizing distance education in the system of continuing education of teachers, these teachers do not understand the advantages that distance learning technologies provide them in comparison with

Downloaded from www.periodico.tchequimica.com

traditional teaching methods.

In the process of observation, the interest of teachers in the development of their own distance courses, the use of cloud services was detected, but when designing an e-learning course, some teachers needed help and did not strive for self-improvement. Also, they were not trying to master modern distance education opportunities in the organization of their professional activities. However, the number of teachers with a sufficient level of readiness (by 60.5% compared with the ascertaining stage) and high (by 16.6%) increased significantly. The dynamics of the development of motivational and value criterion of teachers' readiness at the formative stage has significantly increased in comparison with the ascertaining one. The graphic interpretation of the results before and after the experiment is shown in Figure 2.

The study of the level of teachers' readiness for tutoring activities according to the level of formedness of operational criteria showed an increase in the number of respondents with sufficient and high levels. This is evidenced by the data in Table 1. Observations demonstrated that teachers, after the introduction of the developed methodological system, not only have improved their skills to use various forms and methods of organizing distance education in universities, but also have learned how to work in the information-educational environment and the system of continuing education of teachers. Thus, the best teachers have coped with the development of e-learning courses for teachers, which, in our opinion, is due to the activation of their intrinsic motivation, and therefore there are no low and average points, there are a small number of points above the average, the overwhelming number is high.

Data analysis showed that the number of teachers with a sufficient level of readiness (by 56.2% compared with the ascertaining stage) and high (20.8%) increased significantly. The histogram presented in fig. 4 reflects the dynamics of teachers' readiness to organize distance education in the system of continuing education of teachers according to the levels of formation of the operational criterion before and after the experiment.

So, the results of the pedagogical experiment showed that in terms of the motivational and value indicator of readiness almost all teachers changed their attitude towards the problem of distance education in the system of continuing education of teachers in a positive way. In accordance with the cognitive indicator of readiness, teachers have developed a steady knowledge of the theory of distance education, the use and development of distance education technologies in working with teachers. According to the operational indicator of readiness, the necessary skills for developing and implementing distance education technologies have been formed for the respective functional competence.

The data in Table 1 and Figures 2, 3 show the advantage of a high and sufficient level of teachers' readiness to organize distance education in the system of continuing education of teachers according to all defined criteria, which confirms the effectiveness of the developed methodological system. The general level of teachers' readiness for the organization of distance education in the system of continuing education of teachers was calculated as the arithmetic mean of all the criteria according to the formula (Equation 2). Wherein Σ – the initial level of preparedness; a – number of participants at the appropriate level of readiness criteria, n – the number of readiness criteria (motivational and value, cognitive and operational).

The final state of formedness of teachers' readiness for tutoring activities was determined. The generalized results of the experiment are summarised in Table 2, and the graphical interpretation is shown in Figure 4.

The effectiveness of teacher training for tutoring activity is indicated by the efficiency coefficient, which was calculated using the formula (Equation 3). Wherein Rafter – medium, sufficient and high indicator of preparedness of teachers to tutoring activity after the experiment (in %); Before – medium, sufficient and high indicator of preparedness of teachers to tutoring activity before the experiment (in %).

The effectiveness of the developed methodological system can be discussed in the case when K > 1.

In our study, K = 95.8 / 37.5≈58.38 (motivation and value criterion of readiness);

K = 97.9 / 37.5≈60.4 (cognitive);

K = 97.9 / 41.7≈56.2 (operational);

K = 97.9 / 39.6≈58.3 (total level of readiness).

The final stage of the experiment showed that the majority of teachers have risen to the highest level of readiness for tutoring activities. According to the results of the statistical processing of the questionnaires of participants in

Downloaded from www.periodico.tchequimica.com

the experiment, a significant increase in the parameters of all indicators of the levels that were measured was stated. The data testifies to the effectiveness of the developed methodical system of training teachers for the organization of distance education in the system of continuous education.

For the final statistical confirmation of the effectiveness of the experiment, it is necessary to compare the experimental data before and after the experiment, therefore, to calculate the Pearson criterion. The empirical value of the motivational and value criterion is 58.62, of the cognitive one is 61.05, of the operational one, is 59.37, and the general level of readiness is 59.68, which exceeds the critical value $\chi crit^2$ = 7.81 for the degree of freedom v = 3 and α = 0,05. Disagreements between ascertaining and forming stages of the experiment can be considered reliable. So, the effectiveness of the developed teaching and methodical subsystem, with the help of which it is possible to form motivational and value, cognitive and operational components of teachers' readiness for organizing distance education in the system of continuous education, is statistically confirmed.

The experimental subsystem of the professional and pedagogical improvement of organizers of distance education has confirmed its effectiveness and suggests the continuation of work on improving the professional competence of modern teachers of pedagogical universities and disseminating the experience we have gained. In order to assess the effectiveness of the above-mentioned system, a toolkit of the ascertaining stage of the experiment was used to verify the efficient changes in the levels of formation of motivational and value, cognitive and operational criteria of readiness for the implementation of distance education in the system of continuing education.

As a result of this survey, we received the following data (Figure 5): 87% of respondents chose No. 1 – to be a highly qualified specialist, No. 3 – to successfully continue their educational activities and No. 4 – to successfully carry out scientific activities; 78% chose No. 6 – to acquire new professional knowledge, and No. 10 – to ensure the success of their professional activities; 45% chose No. 7 – to be constantly ready for innovation, and number 8 – not to skip classes of the training cycle; 38% chose No. 2 – to get a certificate, No. 13 – to be an example for colleagues, and No. 16 – to get intellectual satisfaction.

The following motives were not chosen: No. 5 – to receive a cash bonus; № 9 – to keep up with colleagues; No. 11 – to meet pedagogical requirements; No. 12 – to achieve respect among colleagues; No. 15 – to avoid conviction and administrative penalties. Comparison of data with the ascertaining stage of the experiment showed that the majority of teachers increased the number of cognitive motives – to be highly qualified specialist (by 17%), to successfully continue their educational activities (by 24%), to successfully carry out scientific activities (by 100%), to master new professional knowledge (by 35%), to ensure the success of professional activity (by 23%). This indicates the effectiveness of the implementation of a distance education system in continuing education.

After statistical processing of the results of the formative stage of the experiment according to the levels of formation of the criteria of teachers' readiness for the introduction of distance education in the system of continuous education, we were convinced of significant achievements. The results of this work are reflected in Table 3.

Data analysis (Figure 6) on the motivational and value criterion of readiness shows (average value) that 27.1% of the respondents of the experimental groups lack a steady cognitive interest in distance education in the system of continuing education. These teachers do not understand the advantages provided by technology distance education compared to traditional teaching methods.

Also, they are not trying to master modern distance education opportunities in the organization of their professional activities. In the process of observation, we recorded the interest of teachers in the use of distance learning courses, cloud technologies, but in designing an individual plan they need the help of a teacher and do not strive for self-improvement. We recorded no need to use elements of distance education in the educational process of the university. However, the number of teachers with an average level of readiness (by 23.9%) and sufficient (6.6%) increased significantly. In our opinion, this is the influence of irreversible processes in the computerization of society and education as well. Experts understand the advantages of distance education, but in solving professional problems, they partially apply traditional methods.

In our opinion, the next indicator of the effectiveness of experimental work is positive

Downloaded from www.periodico.tchequimica.com

changes regarding the levels of teachers' readiness for distance education in the system of continuing education by levels of the formedness of cognitive criteria. As in the study of the motivational and value criterion of teachers' readiness for distance education in the system of continuous education, significant dynamics in the cognitive criterion of experimental groups in comparison with the ascertaining stage is observed.

Analysis of the data from Table 3 shows that after the introduction of the appropriate methodology, 32.5% (average value) of the respondents in the experimental groups experienced a low level of cognitive criterion formedness. These teachers have almost no knowledge of the use of existing distance learning software, webinar software, cloud technology capabilities, and the capabilities of remote education hardware. Teachers do not know the features of online services in the organization of distance education in the system of continuing education. However, the number of respondents with a high level of readiness (by 2.4%), sufficient (by 4.7%) and medium (by 24.0%) increased significantly. This indicates that teachers have in-depth knowledge of hardware, software, and methodological support in organizing distance education, their integration to develop their own information resources, personal cloud environment, as well as knowledge of the theoretical foundations of the use of distance education and its organization.

The statistical data of the input and output controls on the cognitive criterion convincingly proved that the subsystem introduced by us is rather efficient. The quantitative results of the study in the experimental and control groups are presented in Figure 7.

The study of the level of teachers' readiness for distance education in the system of continuing education by the levels of formedness of the operational criterion showed an increase in the number of respondents with medium, sufficient and high levels. This is evidenced by the data in Table 3. Thus, the respondents of the experimental groups, after the introduction of the relevant system, not only improved their skills and abilities to use various distance education technologies but also learned how to work in the information-educational environment and in the system of continuing education of teachers.

Data analysis showed that the number of respondents with a high level of readiness (by 4.0%), sufficient (by 10.1%) and medium (by 14.2%) increased significantly. However, on average low is 20.5%. Observations showed that the teachers coped with the individual plan best of all as regards the creation of a personal blog and an electronic portfolio, which, in our opinion, is due to the activation of their intrinsic motivation; the overwhelming amount is high. This indicates the presence of experience of teachers with the site of the system of continuous education.

The histogram presented in Figure 8, reflects the dynamics of teachers' readiness for distance education in the system of continuous education by the levels of formedness of the operational criterion.

So, the results of the pedagogical experiment showed that in terms of the motivational and value indicator of readiness almost all teachers changed their attitude towards the problem of distance education at the university and in the system of continuing education.

Accordingly, according to the cognitive readiness indicator, teachers have developed a steady knowledge of the theory of distance education, the use of distance education technologies in high school and in the system of continuous education. According to the operational readiness indicator, the necessary skills and skills of distance education technologies in the university and in the system of continuing education are formed for the respective functional competence.

The data in Table 3 and Figures 8-10 show the advantage of a sufficient and average level of teachers' readiness for distance education in the system of continuing education on all defined criteria that confirm the effectiveness of the implementation of the proposed educational and methodical system. The general level of teachers' readiness for distance education in the system of continuous education was calculated as the arithmetic mean of all criteria using (Equation 1). The final state of the preparedness of teachers for distance education in the system of continuous education was determined. The generalized results of the experiment are summarized in Table 4, and the graphical interpretation is shown in Figure 9.

The effectiveness of the methodological system of training teachers for distance education in the system of continuous education determines the efficiency ratio, which was calculated by the formula (Equation 4). Wherein R_{EG} is the medium, sufficient and high readiness of the

Downloaded from www.periodico.tchequimica.com

respondents of the experimental groups (in%, it was calculated as the arithmetic average);

R_{KG} is an average, sufficient, and high readiness indicator of respondents of control groups (in %, it was calculated as an arithmetic average).

It is possible to speak about the effectiveness of a methodical system in the case when K> 1.

In our study, K = 70.9/38.3≈32.6 (motivational and value criterion of readiness);

K = 67.4 / 36.3≈31.1 (cognitive);

K = 79.4 / 50.1≈29.3 (operational);

K = 73.2 / 41.6≈31.6 (total readiness level).

The data testifies to the effectiveness of the methodological system developed by us for preparing teachers for distance education in the system of continuous education.

Similar diagnostic methods were used to identify the readiness status of respondents in control groups. Analysis of the state of readiness of teachers for distance education in the system of continuous education by the levels of formation of the criteria is given in Table 5.

In the control groups during the experiment, there were positive changes in the aspects of enhancing the readiness of teachers for distance education and increasing their psychological-pedagogical competence. These changes should be explained by the activity of a small number of members of control groups in self-education and non-formal education. Moreover, in some higher educational institutions and institutes of advanced education, it already corresponds to the course for computerization and advanced training of teachers, although the corresponding process has not yet gained an appropriate character, and it significantly activates specific teachers and practitioners who have increased their readiness for distance education.

For the final statistical confirmation of the effectiveness of the experiment, it is necessary to compare the data of the ascertaining stage with the formative stages of the experiment by calculating the Pearson criterion for motivational and value, cognitive, operational criteria and the general level of readiness. The empirical value of the EG1 criterion is 69.30, respectively; 61.63; 54.53; 60.14; EG 2 – 84.91; 58.21; 72.80; 68.75; EG 3 – 80.64; 68.57; 84.54; 73.96. Discrepancies between experimental and control groups can be considered significant. This exceeds the critical value $\chi 2kr = 7.81$ for the degree of freedom $v = 3$ and $\alpha = 0.05$.

So, the pedagogical experiment showed the effectiveness of the developed system of distance education for teachers. The final stage of the experiment showed that the majority of teachers have risen to the highest level of readiness for distance education in the system of continuous education. According to the results of the statistical processing of questionnaires of participants in the experiment, a significant increase in the parameters of all indicators of measurable levels was found. The effectiveness of the introduction of the developed system of distance education in the continuing education of teachers in the development of professional and pedagogical competence was checked taking into account the comparative method of scientific research, the essence of which is to compare the results of the ascertaining stage with what is forming during experimental work. The total number of respondents remained unchanged.

At the formative stage of the experiment, similar methods were used to diagnose the development of the professional and pedagogical competence of teachers, which were used at the ascertaining stage. The same diagnostic evaluation parameters and levels are used. Having qualimetric indicators on the methods of diagnostics of the identified levels of development of professional and pedagogical competence of teachers with diagnostic units, we correlated the amounts of points received into the appropriate component of competence with the total number of points earned and converted to percentages that were calculated using formula (Equation 4). Then we compared the results to identify the components which will require more attention. Statistical analysis of the results was carried out using Microsoft Excel spreadsheets.

The data in Table 6 indicate an increase in the level of development of the professional and pedagogical competence of teachers in the formative stage of the pedagogical experiment. The most effective was the level of development of the professional and pedagogical competence of teachers of experimental groups, where the system of distance education was fully implemented in the continuing education of teachers.

To build a histogram, the indicators of professional and pedagogical competence of teachers at each stage of the study from table 1-6 were chosen. According to the results, histograms 11-13 could be constructed. So, the dynamics of the development of levels of

Downloaded from www.periodico.tchequimica.com

professional and pedagogical competence of teachers in accordance with the blocks is clearly seen.

Analysis of the data (Figure 10) demonstrates that after the introduction of the corresponding model of a teacher, the experimental groups almost do not have a low level of theoretical and methodological training (on average, 5.6%). However, the number of teachers with a sufficient level (by 5.0%) and high (by 3.9%) increased.

Such results indicate that the respondents of the experimental groups better mastered the theoretical and methodological knowledge, which are stable and complex. In addition, sufficient and medium levels of theoretical and methodological training demonstrate that teachers are capable of consciously transforming professional and theoretical knowledge in accordance with their specialty; systematically exhibit targeted independent cognitive activity, which, in turn, expands the pedagogical potential of specialists, predetermines an active search for ways to learn new things, comprehension of new information, its theoretical interpretation.

The statistical data of input and output testing on theoretical and methodological blocks have convincingly proved that the introduced system of distance education in the continuing education of teachers is quite effective. We consider positive changes in the levels of development of professional and pedagogical competence of teachers in psychological and pedagogical blocks as another indicator of the effectiveness of experimental work. As in the study of the theoretical and methodological block of professional and pedagogical competence of teachers, significant dynamics in the psychological and pedagogical training of respondents in experimental groups is observed: a high level increased by 5.0% on average; sufficient by 3.0%. However, the low level is almost absent – 5.4% (Figure 11).

The data in table 6 and figures 10, 11 show the advantage of a sufficient and medium level of development of professional and pedagogical competence of teachers in all defined blocks, which confirms the effectiveness of the introduction of the developed distance education system in the continuing education of teachers. Such results make it possible to state that EG respondents are much better able to practically direct and effectively adapt their knowledge and skills in solving specific psychological and pedagogical problems based on comparison, analysis, synthesis, generalization, systematization, and forecasting. The increase in the manifestations of psychological and pedagogical training in the EG indicates positive changes in the development of professional and pedagogical competence of teachers, their ability to transform professional and life experience at a level higher than reproductive.

The general level of development of professional and pedagogical competence of teachers was calculated as the arithmetic average of all diagnostic blocks according to Equation 3. The final state of professional and pedagogical competence in the experimental groups was determined. The generalized experimental results are summarised in Table 7, and a graphical interpretation of the results of the forming experiment is presented in Figure 12.

The effectiveness of the distance education system in the continuing education of teachers is evidenced by the efficiency coefficient, which was calculated by Equation 4. Wherein R_{EG} is a sufficient and high level of development of professional and pedagogical competence of teachers after the experiment (in %); R_{KG} – a sufficient and high level of development of professional and pedagogical competence of teachers before the experiment (in %).

It is possible to speak about the effectiveness of the developed system in the case when $K > 1$.

In our study, K = 94.3 / 83.7≈10.6 (theoretical and methodological preparation);

K = 94.6 / 85.6≈9.0 (psychological and pedagogical);

K = 94.7 / 84.9≈9.8 (general level of professional and pedagogical competence).

The data indicate the effectiveness of the distance education system that we developed in the continuing education of teachers in experimental groups.

For final statistical confirmation of the effectiveness of the experiment, it is necessary to compare the experimental data of the ascertaining stage with the formative by calculating the Pearson criterion from the data for the theoretical, methodological, psychological and pedagogical blocks and the general level of development of the professional and pedagogical competence of teachers. The empirical value of the EG 1 criterion is 19.25, respectively; 12.07; 16.11; EG 2 – 17.58; 18.78; 18.93; EG 3 – 18.84; 18.39; 19.47.

Downloaded from www.periodico.tchequimica.com

Discrepancies between experimental and control groups can be considered significant. This exceeds the critical value $\chi^2 kr = 7.81$ for the degree of freedom $v = 3$ and $\alpha = 0.05$.

5. CONCLUSIONS:

So, the pedagogical experiment showed the effectiveness of the developed distance education system in the continuing education of teachers. The experiment demonstrated that most teachers increased the level of professional and pedagogical competence.

The essential characteristics of the basic definitions of scientific research determined by the analysis of philosophical, psychological, pedagogical and methodological literature, indicate that the appeal to distance learning is a reaction of scientists to the needs of society in the training of specialists capable of learning throughout their lives, ready to work in conditions of fierce competition in an informationally colored educational space.

Distance learning in the system of lifelong education is an interdisciplinary pedagogical category that characterizes the degree of individualization, intensity and controllability subordinated to the goals of professional development of teachers' independent cognitive activity by means of information and communication technologies via indirect interaction (synchronous and asynchronous) with participants of the educational process remote from each other under the guidance of a tutor. The leading essential characteristics of distance learning are: its basic competence in the use of information and communication technologies for their own professional development and overall development; individualized independent nature of the process of increasing the level of readiness for the organization of personality-oriented distance learning; indirect interaction (diverse communication links) of distance learning organisers with participants in the educational process using electronic means.

The research concept corresponds to the specifics of the problem of the effectiveness of the theoretical and methodological support of distance learning, which requires an optimal combination of systemic, competent, personal and active, and technological methodological approaches to its solution, the choice of a modelling method as the leading tactical means of searching for patterns, principles, content and operating conditions of a particular system. Its technological component has provided the basis of scientific research on the search for distance learning technology, professional components that contributed to the creative nature of this process and increasing of the level of professional and pedagogical competence of teachers to the planned level, and in general – the functioning of the developed system at the required level of quality.

The distance education model in the system of continuing education is such an ideal object that makes it possible to identify the relations within a subject of modeling, display them graphically, focus on solving basic problems, and logically predict distance learning as a systemic formation. The designed corresponding model is an integrated set of interconnected blocks of components: methodological (main approaches: competency-based, personal and active, technological); theoretical (principles of the functioning of the distance education system, the content of distance learning, the matrix of communicative relations of its organizers, organizational and pedagogical conditions for the effectiveness of distance learning as a system); educational and methodological support (educational and methodological support of the process of formation of readiness for distance learning, educational and methodological subsystem of professional and pedagogical improvement of distance learning organizers); effective (increasing the level of professional and pedagogical competence as a consequence of the quality functioning of the distance learning system).

The distance learning system meets the needs of an individual in continuing education as a means of professional development throughout life and has such holistic characteristics: the ability to stimulate the process of acquiring a professional-pedagogical and information and communication culture; the presence of two orientation vectors (promoting creative processes in society and the development of a personality of a teacher in educational and professional environments); readiness for self-organization of movement in the general system of higher education as relatively autonomous and multicomponent.

6. REFERENCES:

1. Akhmetshin, E. M. Mueller, Ju. E., Yumashev, A. V., Kozachek, A. V., Prikhodko, A. N., Safonova, E. E. *Journal of Entrepreneurship Education*, **2019**,

Downloaded from www.periodico.tchequimica.com

22(1), 1528-2651.

2. Aleksandrova, O., Batchenko, L., Dielini, M., Lavryk, U. *Naukovyi Visnyk Natsionalnoho Hirnychoho Universytetu*, **2018**, *4*, 157-165.
3. Aleksandrova, O., Hroznyi, I., Vinnikova, N., Chuvasova, N. Naukovyi *Visnyk Natsionalnoho Hirnychoho Universytetu*, **2019**, *2019*(2), 153-162.
4. Berge, Z. L., Muilenburg, L. *TechTrends*, **2001**, *45*(4), 40.
5. Booker, H. M. *International Advances in Economic Research,* **1998**, *4*(2), 202.
6. Branon, R. F., Essex, Ch. *TechTrends,* **2001**, *45*(1), 36.
7. Fraser, W. J. *Turkish Online Journal of Distance Education,* **2017**, *18*(4), 35-51.
8. Guri-Rosenblit, S. *Higher Education*, **2005**, *49*(4), 467–93.
9. Guri-Rozenblit, S. *International Review of Education*, **1993**, *39*(4), 287–306.
10. Hermansson, G. L. *International Journal for the Advancement of Counselling*, **1988**, 11(4), 255–63.
11. Holmberg, B. *Higher Education Policy,* **1989**, *2*(2), 63–64.
12. Hoppers, W. *International Review of Education*, **2000**, *46*(1), 5–30.
13. Huett, J., Moller, L., Foshay, W. R., Coleman, C. *TechTrends,* **2008**, *52*(4), 66–70.
14. Kerimbayev, N., Kultan, J., Abdykarimova, S, Akramova, A. *Education and Information Technologies*, **2017**, *22*(5). 2125–39.
15. Lee, J.-Y. *Asia Pacific Education Review*, **2003**, *4*(2), 181–88.
16. McVey, M. *International Review of Education*, **2018**, *64*(2), 269–72.
17. Montoya, R., Soledad, M. *International Journal of Educational Technology in Higher Education*, **2013**, *10*(2), 414–30.
18. Rabinovich, T., Pierre, B., Fedorenko, I. *Journal of Financial Services Marketing*, **2017**, *22*(3), 126–31.
19. Rovai, A. P., Lucking, R. *Educational Technology Research and Development*, **2003**, *51*(2), 5.
20. Stella, A., Gnanam, A. *Higher Education*, **2004**, *47*(2), 143–60.
21. Tabata, L. N, Johnsrud, L. K. *Research in Higher Education*, **2008**, *49*(7), 625.
22. Walker, S. L., Fraser, B. J. *Learning Environments Research*, **2005**, *8*(3), 289–308.
23. Wen, J., Zhang, W., Shu, W. *The Journal of Supercomputing*, **2019**, *75*(2), 719–31.

$$P = \frac{\sum n 100\%}{\sum m} \quad \text{(Eq. 1)}$$

$$\sum = \frac{(a_1 + a_2 + a_3)}{n} \quad \text{(Eq. 2)}$$

$$K = \frac{R_{after}}{R_{before}} \quad \text{(Eq. 3)}$$

$$K = \frac{R_{EG}}{R_{KG}} \quad \text{(Eq. 4)}$$

Downloaded from www.periodico.tchequimica.com

Table 1. *The state of readiness of teachers for the organization of distance education in the system of continuing education of teachers (final cross-section, in %)*

Criterion of readiness	Levels	Ascertaining stage	Formative stage
Motivational and value	High	4.2	20.8
	Sufficient	6.2	66.7
	Medium	27.1	8.3
	Low	62.5	4.2
Cognitive	High	4.2	22.9
	Sufficient	4.1	62.5
	Medium	29.2	12.5
	Low	62.5	2.1
Operational	High	4.2	25.0
	Sufficient	6.3	62.5
	Medium	31.2	10.4
	Low	58.3	2.1

Table 2. *General characteristics of the levels of teachers' readiness for the organization of distance education in the system of continuing education of teachers (final cross-section, in %)*

Level of readiness	Ascertaining stage	Formative stage
High	4.2	22.9
Sufficient	6.2	64.6
Medium	29.2	10.4
Low	60.4	2.1

Table 3. *General characteristics of the levels of teachers' readiness for the organization of distance education in the system of continuous education (final cross-section, in %)*

Criterion of readiness	Levels of readiness	EG 1		EG 2		EG 3	
		Ascertaining stage	Formative stage	Ascertaining stage	Formative stage	Ascertaining stage	Formative stage
Motivational and value	High	2.4	6.4	3.3	7.6	2.4	6.4
	Sufficient	7.1	13.3	8.3	15.1	7.6	14.4
	Medium	28.4	50.3	26.8	51.9	28.5	53.2
	Low	62.1	30.0	61.6	25.4	61.5	26.0
Cognitive	High	1.2	3.6	2.3	4.1	1.6	4.5
	Sufficient	7.1	11.0	7.0	12.0	6.3	11.5
	Medium	27.0	51.2	29.1	52.2	27.5	52.3
	Low	64.7	34.2	61.6	31.7	64.6	31.7
Operational	High	1.2	6.1	2.3	7.6	1.6	6.5
	Sufficient	7.1	15.2	7.0	18.6	6.9	17.6
	Medium	39.8	52.6	43.9	55.9	40.5	58.3
	Low	51.9	26.1	46.8	17.9	51.0	17.6

Downloaded from www.periodico.tchequimica.com

Table 4. *The general level of teachers' readiness for distance education in the system of continuous education (final slice, in%)*

Levels of readiness	ER 1		ER 2		ER 3	
	Ascertaining stage	Formative stage	Ascertaining stage	Formative stage	Ascertaining stage	Formative stage
High	1.5	5.4	2.6	6.4	1.9	5.8
Sufficient	7.1	13.1	7.6	15.2	6.9	14.5
Medium	32.0	51.4	32.8	53.4	32.4	54.6
Low	59.4	30.1	57.0	25.0	58.8	25.1

Table 5. *The state of readiness of the participants of control groups for distance education in the system of continuous education (final cross-section, in %)*

Criterion of readiness	Level of readiness	CG 1	CG 2	CG 3
Motivational and value	High	2.8	2.6	2.6
	Sufficient	8.5	8.9	8.7
	Medium	27.7	29.0	28.2
	Low	61.0	59.5	60.5
Coginitive	High	2.4	2.5	1.9
	Sufficient	7.3	7.4	6.7
	Medium	26.2	29.1	27.3
	Low	64.1	61.0	64.1
Operational	High	1.4	2.1	1.8
	Sufficient	7.2	7.6	6.9
	Medium	40.2	43.5	40.1
	Low	51.2	46.8	51.2

Table 6. *The results of pedagogical diagnostics of the assessment of the levels of development of professional and pedagogical competence of teachers in diagnostic units (final cross-section, in%)*

The focus of vocational teacher training	Levels	EG 1		EG 2			EG 3
		Ascertaining stage	Formative stage	Ascertaining stage	Formative stage	Ascertaining stage	Formative stage
Theoretical and methodological training	High	14.6	18.8	13.4	17.0	12.9	16.7
	Sufficient	42.7	47.9	44.3	49.1	44.5	49.4
	Medium	25.9	27.3	26.4	28.3	26.5	28.5
	Low	16.8	6.0	15.9	5.6	16.1	5.4
Psychological and pedagogical training	High	14.3	20.6	12.4	16.0	11.3	16.0
	Sufficient	47.0	48.2	45.5	48.7	43.9	48.1
	Medium	27.1	26.1	26.5	29.9	29.0	30.1
	Low	11.6	5.1	15.6	5.4	15.8	5.8

Downloaded from www.periodico.tchequimica.com

Table 7. *The general level of development of professional and pedagogical competence of teachers (total cross-section, %)*

Levels	EG 1		EG 2		EG 3	
	Ascertaining stage	**Formative stage**	**Ascertaining stage**	**Formative stage**	**Ascertaining stage**	**Formative stage**
High	14.7	20.3	12.8	16.7	12.2	16.7
Sufficient	45.6	48.5	44.9	48.7	44.4	48.7
Medium	26.0	26.1	26.7	29.3	27.6	29.2
Low	13.7	5.1	15.6	5.3	15.8	5.4

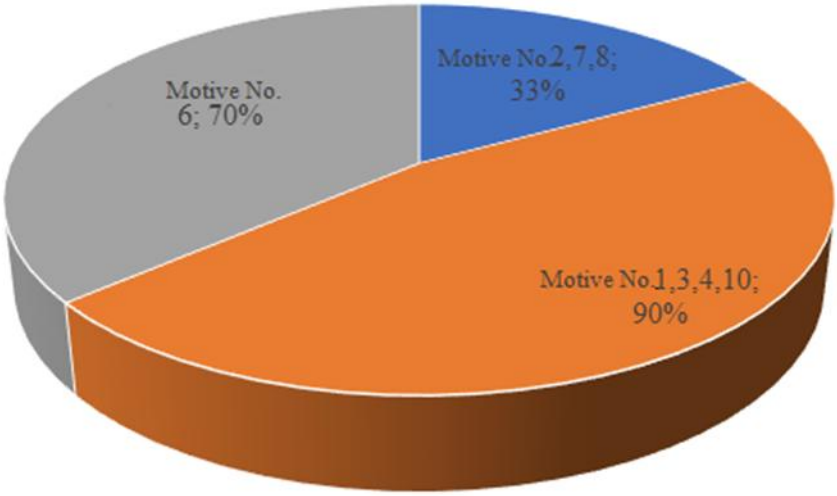

Figure 1. *The result of the final diagnosis of motivational and value criterion of teachers' readiness for distance education in the system of continuing education of teachers*

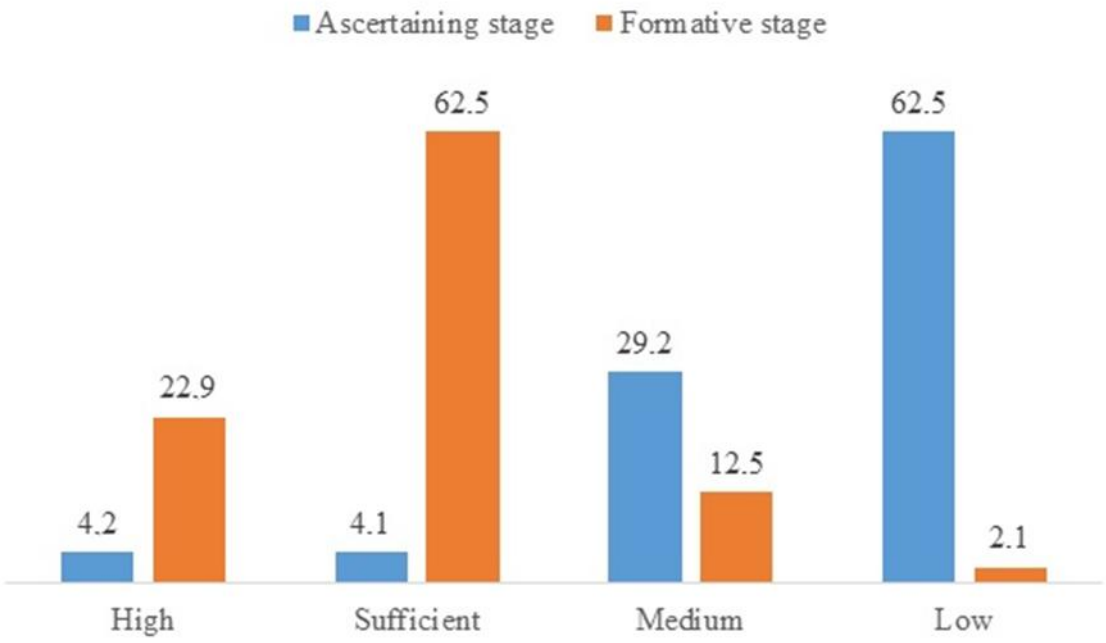

Figure 2. *The state of readiness of teachers for the organization of distance education in the system of continuing education of teachers by levels of formedness of cognitive criteria (final cross-section, in%)*

Downloaded from www.periodico.tchequimica.com

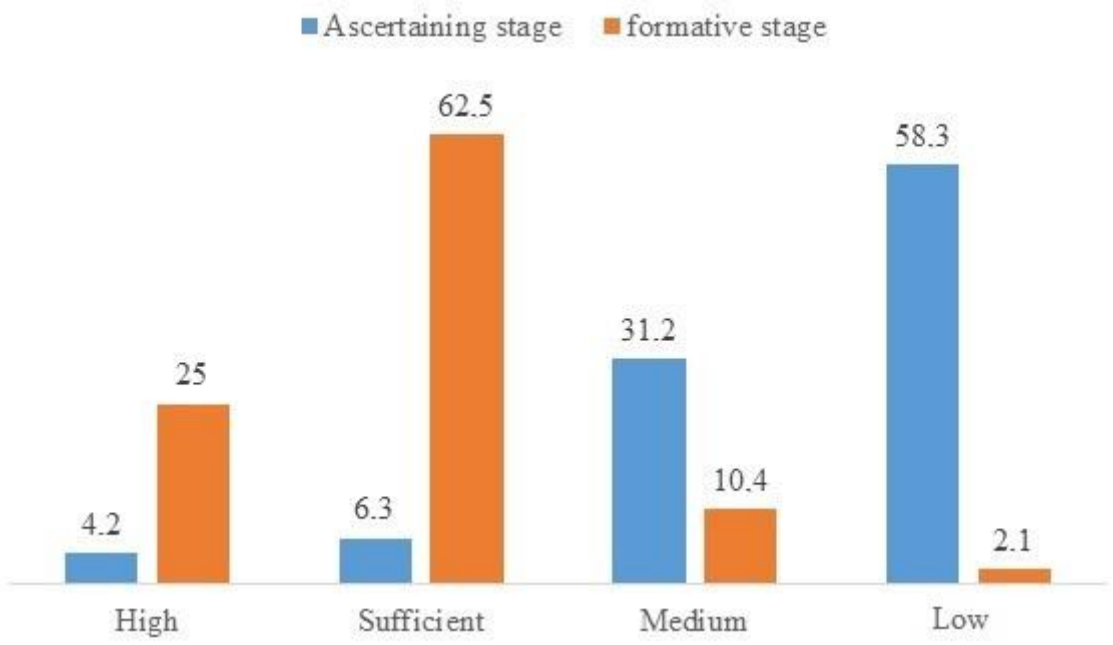

Figure 3. *The state of readiness of teachers for the organization of distance education in the system of continuing education of teachers by the levels of formation of operational criteria (final cross-section, in %)*

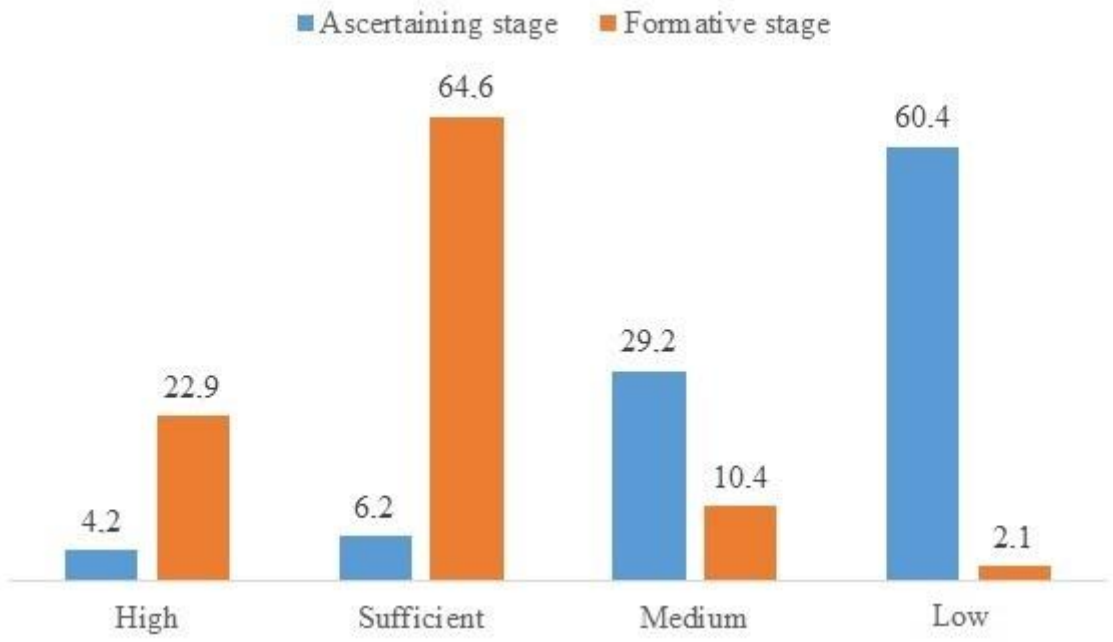

Figure 4. *General characteristics of the levels of teachers' readiness for the organization of distance education in the system of continuous education (total cross-section, %)*

Downloaded from www.periodico.tchequimica.com

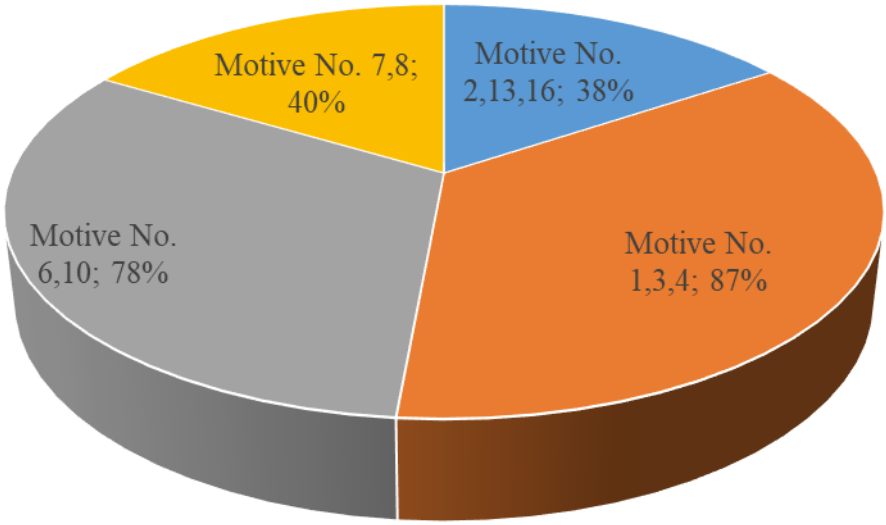

Figure 5. *The result of the final diagnosis of motivational and value criterion of readiness for distance education in the system of continuing education*

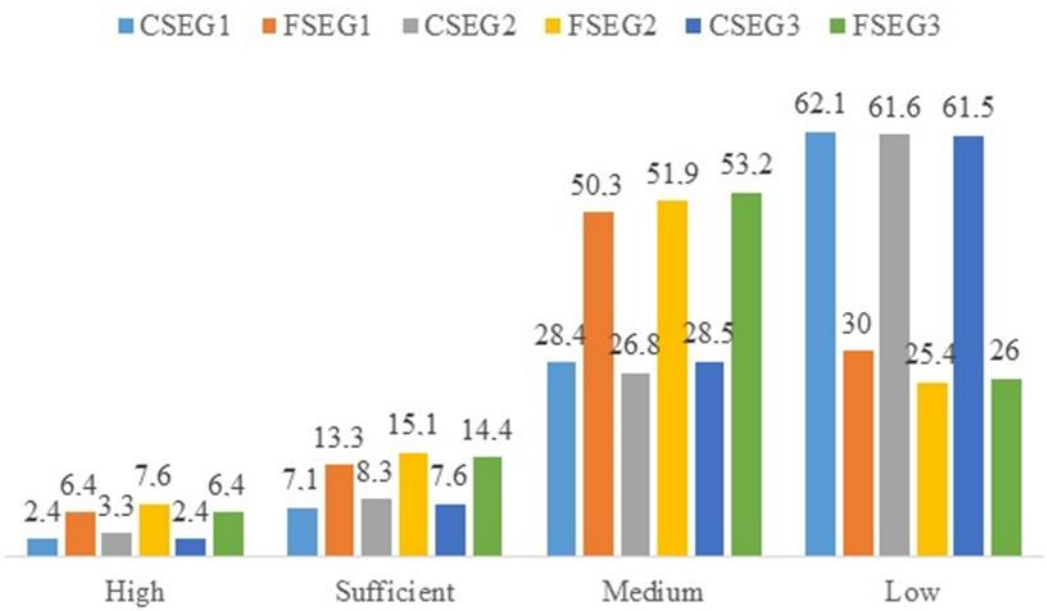

Figure 6. *The state of readiness of teachers for distance education in the system of continuous education by levels of formedness of motivational and value criteria (final cross-section, in %)*

Downloaded from www.periodico.tchequimica.com

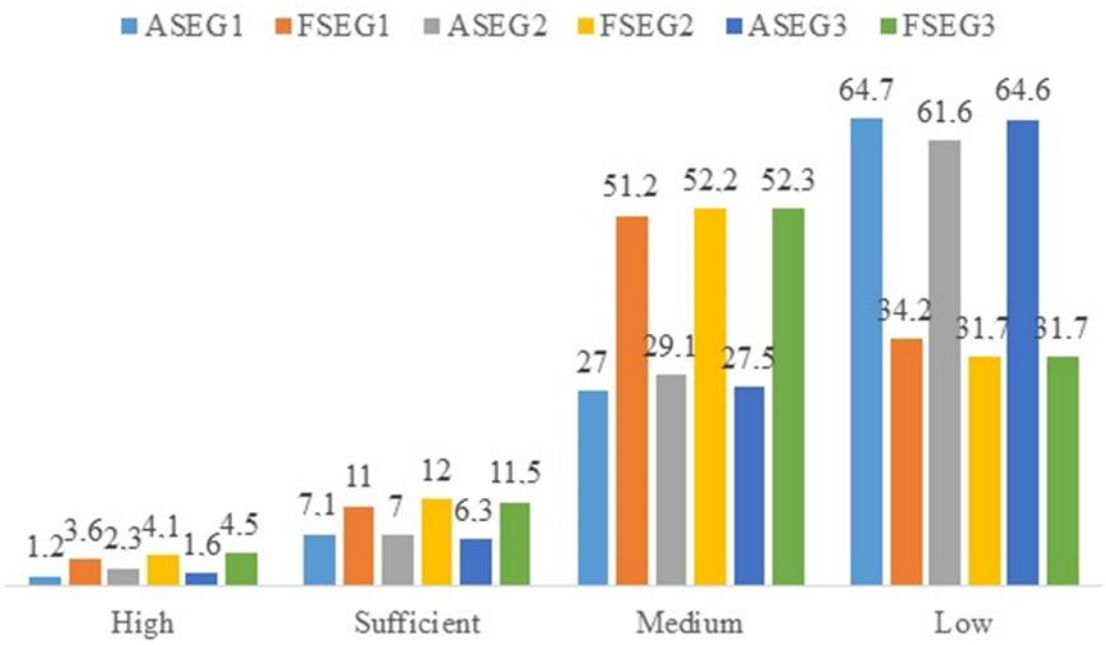

Figure 7. *The state of readiness of teachers for distance education in the system of continuous education by levels of formedness of cognitive criteria (final cross-section, in %)*

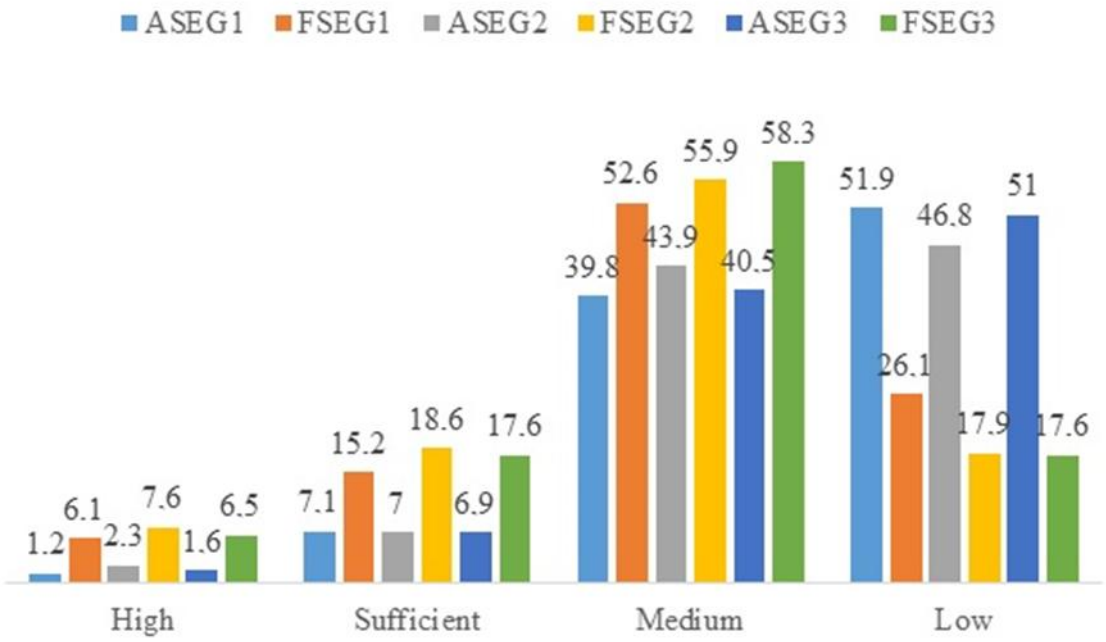

Figure 8. *The state of readiness of teachers for distance education in the system of continuous education by levels of formedness of operational criteria (final cross-section, in %)*

Downloaded from www.periodico.tchequimica.com

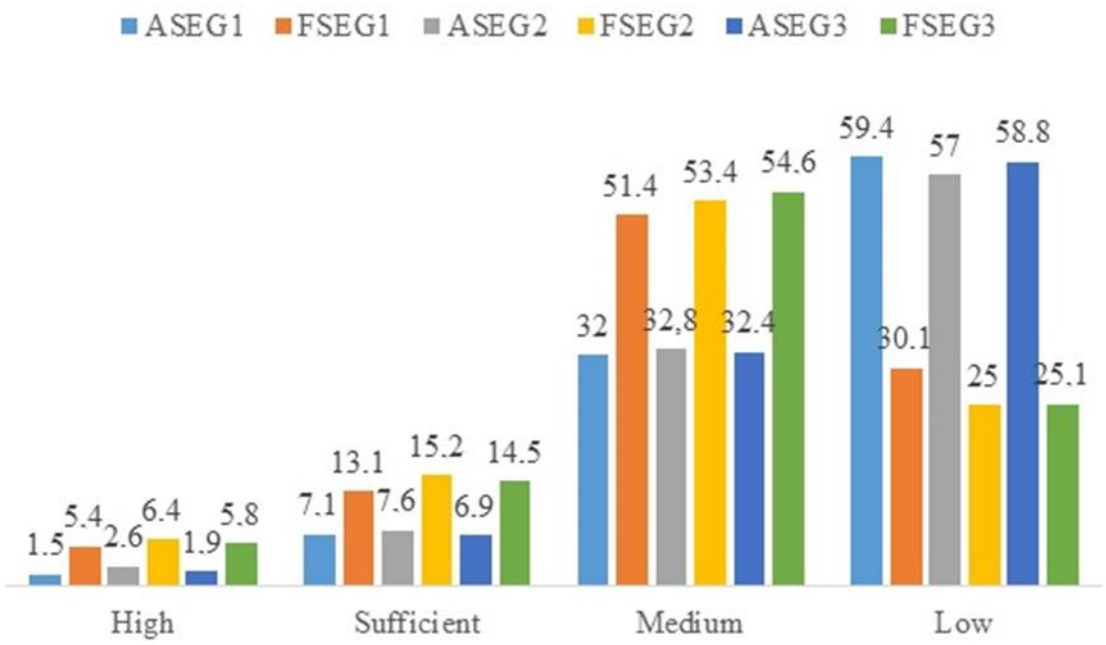

Figure 9. *General results of teachers' readiness levels for distance education in the system of continuing education (final cross-section,%)*

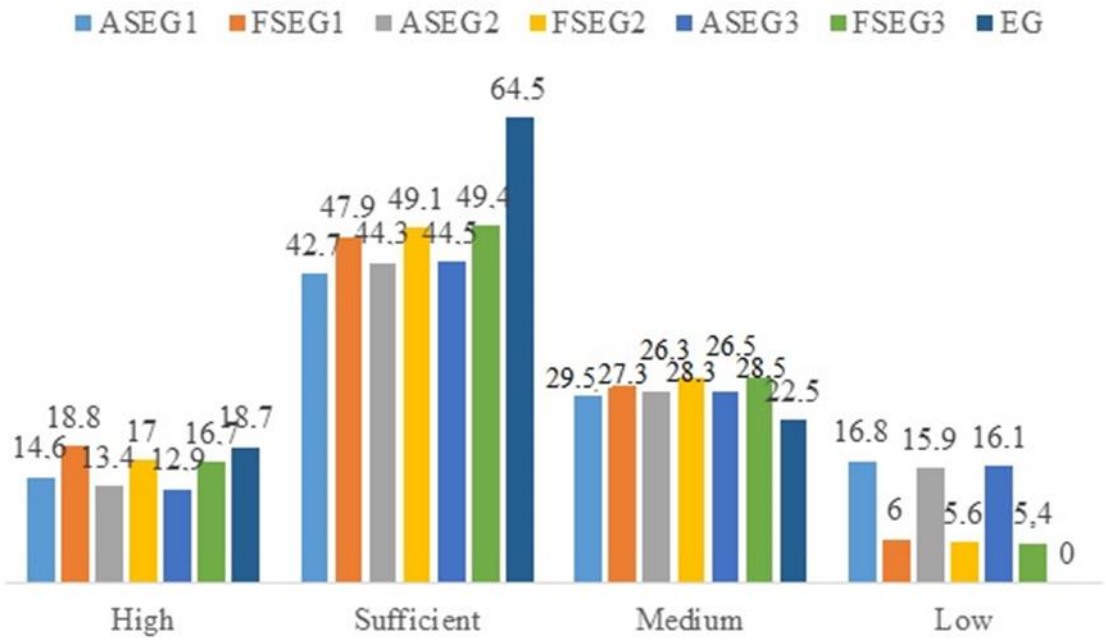

Figure 10. *A diagram on the comparison of the development levels of the theoretical and methodological training of teachers (final cross-section,%)*

Downloaded from www.periodico.tchequimica.com

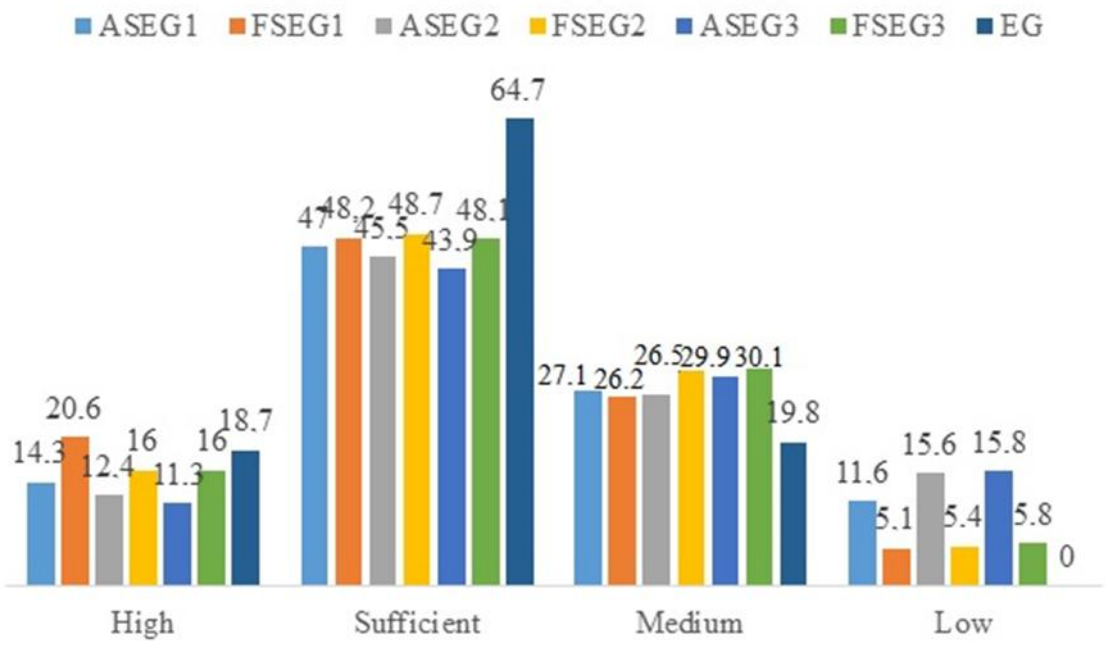

Figure 11. *A diagram on the comparison of the levels of development of psychological and pedagogical training of teachers (final cross-section, %)*

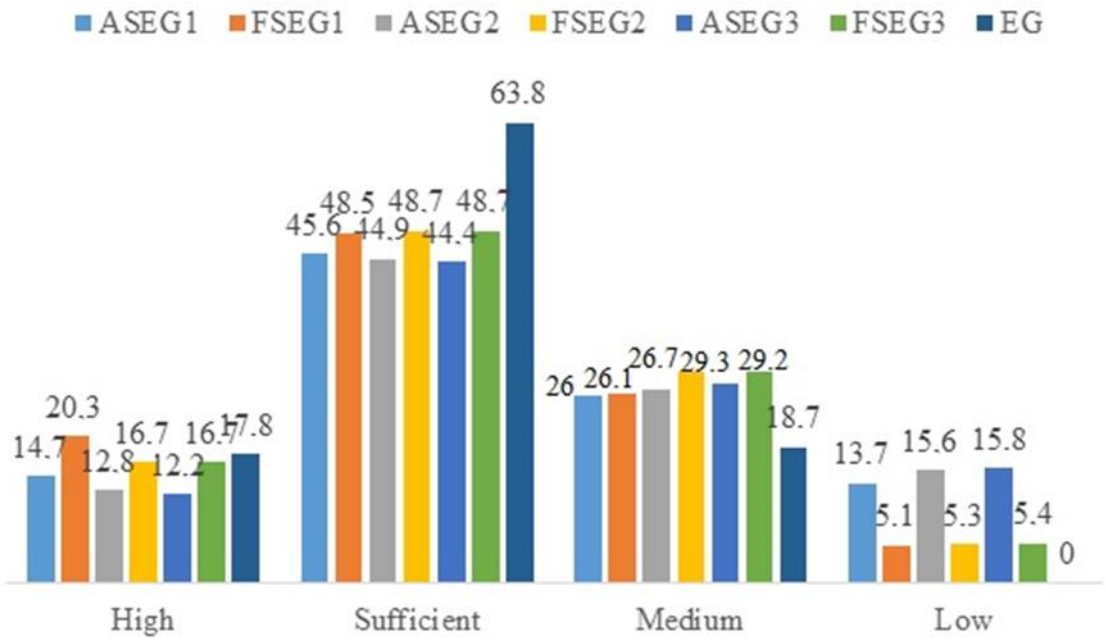

Figure 12. *A diagram on the comparison of the levels of development of professional and pedagogical competence of teachers (final section, %)*

Downloaded from www.periodico.tchequimica.com

PERIÓDICO TCHÊ QUÍMICA
ARTIGO ORIGINAL

DINÂMICA DA FORMAÇÃO DA COMPETÊNCIA INTERCULTURAL PROFISSIONAL DE PROFESSORES ENTRE ESTUDANTES ESTRANGEIROS

DYNAMICS OF FORMATION OF FUTURE TEACHERS' PROFESSIONAL INTERCULTURAL COMPETENCE AMONG FOREIGN STUDENTS

ДИНАМИКА ФОРМИРОВАНИЯ ПРОФЕССИОНАЛЬНОЙ МЕЖКУЛЬТУРНОЙ КОМПЕТЕНТНОСТИ ИНОСТРАННЫХ СТУДЕНТОВ-БУДУЩИХ УЧИТЕЛЕЙ

AKHTARIEVA, Raziya F.[1*]; IBRAGIMOVA, Elmira R.[2]; PUCHININA, Olga P.[3];

[1] Elabuga Institute of Kazan Federal University, Department of Pedagogy, Kazan – Russian Federation

[2] Elabuga Institute of Kazan Federal University, Department of Russian Language and Literature, Kazan – Russian Federation

[3] Elabuga Institute of Kazan Federal University, Department of English Philology and Cross Cultural Communications, Kazan – Russian Federation

** Correspondence author*
e-mail: raziya-a@yandex.ru

Received 29 August 2019; received in revised form 20 October 2019; accepted 25 October 2019

RESUMO

Na ciência russa, o interesse permanece na formação da competência intercultural dos estudantes. Os processos intensivos de migração que ocorrem no mundo levam à interação social de representantes de diferentes comunidades e nações. A relevância deste estudo esta baseada no fato de que a competência profissional intercultural é considerada uma condição necessária para os processos de aculturação dos estudantes estrangeiros no ambiente educacional multiétnico da universidade. A necessidade de aumentar a competitividade das universidades russas no campo dos serviços educacionais internacionais determina a necessidade de criar condições adequadas nas instituições de ensino russas para o pleno desenvolvimento da personalidade dos estudantes estrangeiros como profissionais num determinado campo de atividade de acordo com a ordem social entre os estados. O artigo apresenta os resultados do estudo da dinâmica da formação da competência intercultural profissional de futuros professores entre estudantes estrangeiros que vivem na Rússia de 0 a 5 anos. Foram realizados diagnósticos do nível geral de tolerância dos estudantes pesquisados, tipos de identidade étnica, identidade étnica positiva. As atitudes em relação às estratégias de aculturação também foram investigadas. O estudo realizado com base nos resultados de uma pesquisa escrita revelou o grau de formação dessa competência entre os entrevistados.

Palavras-chave: *tolerância, competência intercultural, identidade étnica, aculturação, adaptação sociocultural.*

ABSTRACT

Russian science remains interested in the formation of the intercultural competence of students. Intensive migration processes taking place in the world lead to the social interaction of representatives of different communities and nations. The relevance of this study lies in the fact that it considers the professional intercultural competence as a necessary condition of acculturation processes among foreign students in polyethnic educational environment of the university. The need to increase competitiveness of Russian higher education institutions in the area of international educational services necessitates creation of appropriate conditions in Russian educational institutions for the full development of a personality of a foreign student as a professional in a particular field of activity in accordance with the social order between the states. The article presents the results of studying the dynamics of formation of future teachers' professional intercultural competence among foreign students living in Russia from 0 to 5 years. The authors carried out diagnostics of the general level of tolerance among the interviewed students, types of ethnic identity, and positive ethnic identity. The attitudes towards acculturation strategies were also investigated. The study based on the results of a written survey revealed the degree of formation of this competence among the respondents.

Downloaded from www.periodico.tchequimica.com

Keywords: *tolerance, intercultural competence, ethnic identity, acculturation, sociocultural adaptation.*

АННОТАЦИЯ

В российской науке сохраняется интерес к вопросам формирования межкультурной компетентности учащейся молодежи. Интенсивные миграционные процессы, происходящие в мире, приводят к социальному взаимодействию представителей разных общин и наций. Актуальность данного исследования состоит в том, что рассмотрена профессиональная межкультурная компетентность как необходимое условие аккультурационных процессов у студентов-инофонов в полиэтнической образовательной среде вуза. Необходимость повышения конкурентоспособности российских вузов в сфере международных образовательных услуг диктует потребность в создании соответствующих условий в российских образовательных учреждениях для полноценного развития личности иностранного студента как профессионала, в той или иной сфере деятельности в соответствие с социальным заказом между государствами. В статье представлены результаты изучения динамики формирования профессиональной межкультурной компетентности иностранных студентов-будущих учителей со стажем проживания в России от 0 до 5 лет. Авторами проводится: диагностика общего уровня толерантности опрошенных студентов, типов этнической идентичности, позитивной этнической идентичности; а также исследуются установки на стратегии аккультурации. Проведенное авторами исследование по результатам письменного опроса позволяет выявить степень формирования у респондентов данной компетенции.

Ключевые слова: *толерантность, межкультурная компетентность, этническая идентичность, аккультурация, социокультурная адаптация.*

1. INTRODUCTION

The socio-cultural conditions in which modern society lives, allow us to say that in any team: in the classroom, in a student group, in an enterprise or the office – there cannot be people who think alike, look at life the same way, belong to the same nation and profess the same faith, etc. Intensive migration processes taking place in the world, lead to the social interaction of representatives of different communities and nations. The problem of intercultural communication is also relevant to modern Tatarstan due to its multi-ethnic composition and multi-confessionalism. The transformation of Russian society forms the need to analyze the social and cultural background of intercultural communication, as well as trends in its dynamics (Lukiyanova *et al.*, 2018a).

Education of foreign students is a matter of prestige of the country, so it is dealt with by the experts. The governments of all countries strive to create good conditions for the education of young people from abroad, considering the prestige of education in the world ranking. It is noteworthy that in Russia, the same as in the US, the educational system does not divide students into ‘we’ and ‘they’. Russia strives to ensure that its universities in the rankings are on a par with the best educational institutions in the UK, USA, France, Germany, etc. And it succeeds (Training of foreign students in Russia, 2019).

In a ranking of countries with the best system of higher education 2016, British company QS has indicated the US and the UK among the leaders, as it is easy to guess. The top 5 also included Germany, Australia, and Canada, slightly inferior to them were France and the Netherlands. Foreign experts placed Russia on the 26th place out of 50 (the rating is closed by the UAE, Estonia, and Pakistan). In general, this result can be called quite good for our country, because this issue is not engaged in the country for a long time. These results became possible due to the high quality of education in Russian universities, which determines the growth of the number of foreign students from year to year. The government pays special attention to this issue, because the more there are students from other countries, the higher the University is evaluated according to the criteria of international rankings — QS or Times Higher Education (Lukiyanova *et al.*, 2018b).

As for the universities themselves, for them, the admission of foreigners is not only a matter of prestige but also an opportunity to receive additional income. By the way, the cost of education for citizens of other countries in the Russian universities, as a rule, does not differ from the fee for education for the Russians (most programs are taught in Russian, and English-speaking ones are more expensive). The number of foreign students in Russia is expected to triple by 2025. The number of visitors is growing not only from Africa and the Arab countries but also from the European Union. A large proportion of

Downloaded from www.periodico.tchequimica.com

students come from the CIS and countries of the former socialist camp. If until recently Moscow was the most popular city among foreigners, many foreign students tried to study at its universities, now the educational institutions of other Russian cities are in demand. A worthy place in the list is occupied by Kazan: nowadays, quite a number of different scientific and educational organizations is concentrated in the capital of Tatarstan. There are more than 30 universities, including one Federal University and two national research universities. Besides, the Kazan scientific center includes 4 research institutes. Finally, the republic has its own Academy of Sciences with 6 research institutes. A special place in the list of universities of the Republic of Tatarstan is taken by the Kazan Federal University, a university that has the status of federal since 2010 but as a university, it has a 215-year history. Today, after the merger of several universities under the auspices of the Federal University, over 600 educational programs are implemented in the KFU, more than 44.000 students, including more than 6.000 foreign students, which is about 14% of the total number of students studying at the Kazan Federal University (Akhmetshin *et al.*, 2019).

According to the 'Russian education' portal, most often foreign students choose natural sciences, medicine, philology, as well as programs related to culture and art. The most popular sector universities, which train specialists in economics and management, finance and management, civil service (foreigners studying in 179 of them), automotive, energy, technology, and industrial universities (99), humanitarian-social (112) and classical universities (95) and educational institutions, which have the specialization of 'Culture and Art" (72). Most often, the citizens of other countries choose undergraduate (59.5 thousand people), the next is specialist (43.2 thousand people), and the last one is the master's degree (10.99 thousand people). In our study, we examined the dynamics of the formation of future teachers' professional intercultural competence among foreign students, that is, the students who are trained in the field of 'Pedagogical Education', which specializes the Elabuga Institute of Kazan Federal University (Bocheliuk *et al.*, 2019).

The relevance of this study lies in the fact that the authors have considered professional intercultural competence as a necessary condition of acculturation processes among foreign students in the polyethnic educational environment of the university. It is desirable to lay the foundation for the formation of the future specialists' competence of professional intercultural interaction as early as at school – both in the educational and extracurricular activities – to develop at the university in the process of classroom and extracurricular activities (Volchik and Maslyukova, 2019).

Since 2014, the number of foreign students in the Elabuga Institute of the KFU has been growing every year. So, if the number of foreign students in 2014 reached only 40 people, at present, there are more than 900 foreigners. The increase in their number requires certain knowledge, skills to successfully regulate the functioning of a multinational team.

2. LITERATURE REVIEW

Currently, the problem of formation of intercultural competence is particularly relevant for the graduates specializing in the language profiles of the pedagogical studies. This is because although the students have a fairly high level of foreign language communicative competence very often, they do not possess the necessary amount of knowledge of the intercultural character and intercultural communication skills. All this leads to a misunderstanding at the level of cultural meanings and images, as well as cultural shock.

The problem has become the subject of numerous studies for more than 30 years, among both foreign and Russian scientists such as S. Ter-Minasova, G. Andreeva, N. Gromova, N. Garskova, I. Khaleeva, V. Safonov, V. Furmanova, G. Elizarova, T. Dmitrenko, A. Leont'ev, I. Bim, R. Milrud and R. Maximov, P. Sysoev, V. Oshchepkova, Samovar L. A., Porter R. E., McDaniel E. R., Roy, C. S., Byram M., Neuner G., D. Buttjes, etc. (Andreeva, 2009; Gromova, 2010; Khaleeva, 2000; Safonova, 2014; Furman, 2009; Elizarova, 2005; Dmitrenko, 2009; Leontyev, 2008; Bim, 2007; Galskova, 2004; Milrud and Maksimova, 2017; Sysoev, 2004; Oshchepkova, 2004; Samovar *et al.*, 2013; Neuner, 2012; Buttjes, 2000; Byram, 2004).

Foreign researchers define this concept in different ways. Thus, according to Brian Spitzberg (2000), it reflects the relevance and effectiveness of behavior in a particular situation of communication. According to Larry Samovar and Richard Porter, intercultural competence is the degree of efficiency and productivity of contact with the representatives of other cultures. By this term K. Knapp means "the ability to

Downloaded from www.periodico.tchequimica.com

achieve an equally successful understanding of other cultures and communication communities, as well as the representatives of their culture" (Soldatova, 2006), i.e., intercultural competence, in his opinion, is the ability to reach an understanding of one's own and someone else's culture. This scientist focuses on the behavioral aspect of dealing with the representatives of another culture. J. Lehtonen (Lehtonen, 2003) believes that for successful communication in another culture, a foreigner needs to know not only the language but also the country's history, society, art, economy, or he/she must possess comprehensive knowledge about the culture of the country. H. Spencer-Oatey, P. Franklin (Spencer-Oatey and Franklin, 2009) believe that this is "the ability to recognize, respect, appreciate and productively use both in relation to themselves and to others – cultural conditions, determinants of perception, decision-making, feelings and actions in order to create conditions for mutual adaptation and development of synergetic forms of cooperation, living together, tolerance to existing differences, effective orientation concerning the peculiarities of interpretation and formation of the world" (Solodukhin, 2009). At the same time, this competence assumes that a person should possess the ability to "form shared meanings and experiences on the basis of mastering knowledge about the uniqueness of the language, values and norms, experiences and behavioral algorithms of each other" (Solodukhin, 2009). Professor Michael Biram of the English University of Durham (Byram, 2004) is also actively engaged in the problems of intercultural communication. Its model is the basis for many foreign studies. According to the scientist, intercultural communication consists of the following five components: relations, knowledge, skills of interpretation and correlation, skills of discovery and interaction, critical awareness of culture or political education. Representatives of different cultures, who have formed intercultural competence, should be open to each other, curious, ready to abandon prejudices about native and foreign culture; know about social groups, their activities in their own and foreign countries, about the general processes of personal and social interaction; they must be able to interpret a document or an event of a foreign culture, explain it and compare it with the phenomena of their culture; be able to acquire new knowledge about culture, the ability to operate with knowledge, skills in the conditions of communication and interaction in real time. S. Markova notes that in the process of acculturation, each person simultaneously solves two major problems: he/she seeks to preserve his/her cultural identity and is included in another culture. First, there is acculturation shock, which is replaced by one of the solutions to this problem and gives four main strategies of acculturation: assimilation, integration, separation, and marginalization (Markova, 2015).

Most of the Russian scientists such as N. Guez, G. Elizarova, T. Larina, I. Solovyev, V. Furmanova, N. Vasiliev (Ghez *et al.*, 1982; Elizarova, 2005; Larina, 2005; Solovieva, 2013; Furmanova, 2009) agree that intercultural competence is an ability that allows an individual to realize him/herself within the framework of intercultural communication. Thus, N. Vasilyeva believes that an intercultural competence includes "the knowledge of life habits, mores, customs, attitudes of this society, forming individual and group attitudes; individual motivations, forms of behavior, non-verbal components (gestures, facial expressions), national and cultural traditions, and value systems" (Vasilyeva, 2017). According to N. Galskova, intercultural communication is an indicator of completeness of a person's ability to participate effectively in intercultural communication. E. Kuznetsova expresses the idea of "ethno-pedagogical readiness, defining it as the result of a process of ethno-pedagogical training, and an integrative quality of personality". This quality of personality is represented as a set of motivational-value, cognitive, emotional-volitional, and activity-creative components aimed at the implementation of educational activities in the multi-ethnic region (Kuznetsova, 2001). The prevalence of ethnopedagogy in the educational process, according to T. Pochtareva should be considered "as one of the tools for constructing ethnic and broad-based education leading to the mastery of the learning values of the national and world culture" (Pochtareva, 2007).

3. MATERIALS AND METHODS

The article presents the results of a study on the formation of intercultural competence, which was attended by foreign 1-5-year students of the Elabuga Institute of the Kazan Federal University. The total sample size was 169 people. The ethnic composition of the sample as a whole – Turkmen respondents, more precisely, students from Turkmenistan. According to the objectives of our study, they were divided into two groups. Group A included students studying at non-linguistic faculties (Mathematics and Natural

Downloaded from www.periodico.tchequimica.com

Sciences, Psychology and Pedagogy, Engineering and Technology, Economics and Management, Law), and Group B included the students of the Faculty of Philology and History and the Faculty of Foreign Languages.

It should be noted that in the process of learning, the respondents from Group A study such subjects as 'Ethnology', 'Sociology', while the students of the Engineering-Technological Faculty, studying at the profiles of the Decorative Art and Design and Technology and Supplementary Education, have the opportunity to attend classes on such subjects as 'Decoration Items and Interior Design', 'Cooking', 'Design-School Education', 'Culture of the Houses, Arts and crafts', 'Fundamentals of Applied and Decorative Arts', 'Modern Decorative Art', 'Creation of Art Objects', 'Technology of Creation of Authors' Dolls' where they get closer acquainted with national culture of the people living in the territory of the Republic of Tatarstan. The main tasks of the technology of folk arts and decorative-applied art are as follows: the introduction of not only Russian but also foreign students to the multinational culture, aesthetic education of the individual, the development of artistic taste and acquaintance with the deep sense of popular commercial art and decorative-applied arts, which is the wise ideas and moral precepts of the people (Wati *et al.*, 2019).

The students who form the basis of Group B learn the language and culture of other countries. Foreign students of the Faculty of Philology and History study in-depth Russian and English languages, while the students of the Faculty of Foreign Languages learn English, German and Chinese languages. In the process of learning, they also become acquainted with the culture and traditions of the country of the studied language and the multinational Republic of Tatarstan, and also establish cross-cultural contacts in the process through various practices and training, while participating in international conferences (Todorov *et al.*, 2018).

In the study, the indicators of intercultural competence were the expression of ethnic identity (person's awareness of his/her belonging to a certain ethnic group); the level of ethnic tolerance (the ability of a person to show tolerance for unfamiliar lifestyle of representatives of other ethnic communities, their behavior, national traditions, customs, feelings, opinions, ideas, beliefs, etc.); as well as the establishing of intercultural interaction.

We studied foreign students-respondents' behavioral attitudes to different socio-ethnic groups by using the scales of acculturation strategy authored by John Berry. Besides, we applied the express-survey 'Tolerance Index' (Soldatova and Shaigerova, 2003), the methodical development of G. Soldatova and S. Ryzhova, 'Types of Ethnic Identity', which allows diagnosing ethnic identity and its transformation in the context of ethnic tensions.

K. Knapp proposed a model of intercultural competence, which he defined as "the ability to achieve an equally successful understanding of both representatives of other cultures and communication communities, as well as the representatives of their culture", and identified the following features of this ability:

- understanding based on communicative activities and behaviors from culturally determined cognitive schemes;
- knowledge models and communication actions, interpreting them in their own and studied culture and language;
- willingness to accept the intercultural context of communication;
- understanding based on communicative activities and behaviors from culturally determined cognitive schemes;
- knowledge of a variety of communication behaviors in intercultural interaction;
- general knowledge of the relationship between culture and communication, including the dependence of the way of thinking and behavior on the culture-specific characteristics of thinking, as well as the differences between cultures determined by these characteristics;
- a set of strategies to stabilize the interaction, i.e., to solve the frictions and problems arising in the process of communication (Knapp and Knapp-Pot-thoff, 1990).

In 'Cross-Cultural Psychology. Research and Application', Berry D. V., Portinga A. H., Sigall M. H. suggest that "cultural contacts in the socio-political context of the group influence the culture and behavior of the individual. They are carried out along with the contacts between populations, which are the result of historical and contemporary events such as colonial expansion, international trade, invasions, and migration. These contacts lead to another acculturation procedural variable involving the mutual influence of the contacting groups" (Berry *et al.*, 2007, Matsumoto, 2003). The acculturation strategies identified by J. Berry are as follows: assimilation

Downloaded from www.periodico.tchequimica.com

(a variant of acculturation in which a person fully accepts the values and norms of a particular culture, abandoning its rules and values); integration (identification with the old culture and the new one); separation (the denial of a foreign culture while maintaining the identification with their culture. In this case, the representatives of the non-dominant group prefer a greater or lesser degree of isolation from the dominant culture); marginalization (option of acculturation, manifested in the loss of identity with their own culture and the lack of identification with the culture of the majority. This situation arises from the inability to maintain one's own identity (usually due to some external reasons) and the lack of interest in obtaining a new identity (perhaps due to discrimination or segregation on the part of this culture) – allowed to investigate acculturation expectations (Berry *et al.*, 2016). In the analysis of the scales, we calculated the percentage of positive answers ('agree') to the relevant group of questions.

4. RESULTS AND DISCUSSION:

After the implementation of the methods, quantitative results of the qualitative indicators were obtained. The high level of tolerance of the foreign students surveyed is shown by the results of the 'Tolerance Index' express questionnaire – more than 80 points (Figure1).

The methodical development of G. U. Soldatova and S. V. Ryzhova 'Types of Ethnic Identity' (Soldatova and Ryzhova, 2011) allowed diagnosing the ethnic identity and its transformation in the conditions of interethnic tension. The diagnostic results are presented in Table 1.

The results of the survey presented in Figure 1 clearly show that the dynamics of tolerance in Groups A and B are not the same. The overall level of the students' tolerance in the 1st and 2nd years from both groups is approximately the same (85 and 86 points, respectively). But from the 2nd year, in Group A there is a decrease in this level to 82 points. The overall level of tolerance in Group A to the end of university education is reduced. In Group B, the maximum level of tolerance reaches the beginning of the 4th year, and in the 5th year, these indicators remain at the same level. The questionnaire by G. Soldatova and S. Ryzhova (2011) 'Types of Ethnic Identity', consisting of two scales that are relevant to hypo-identity (ethnic nihilism and ethnic indifference), the scale of norm, that is, increased positive ethnic identity, and three scales corresponding to the transformation of identity by type of hyper-identity (ethnic egoism, ethnic isolationism, and ethnic fanaticism), allowed the study to conclude that most of the foreign students showed 'normal' results; among 64.3% of Group A students the scale 'Norm' prevails, among the students of Group B this number was higher – 71%. The results on the other scales are also almost the same. Thus, among the surveyed students of both groups, the second most frequent, after the 'Norm', was the scale of 'Ethnic Difference' (18% and 19%, respectively), the third in Group A – 'Ethnic Egoism' (12%), in Group B – 'Ethnic Nihilism' (5.8%). According to the 'Ethnic Nihilism' scale, Group A respondents scored fewer points (5% and 5.8%, respectively) compared to the second group. At the same time, the students of Group B have a scale of 'Ethnic Egoism' in the frequency of choice inferior to the first group (12% and 4%, respectively). On the scale of 'Ethnic Isolationism' and 'Ethnic Fanaticism', we found a very low degree of intensity of these types of identity (ethnic isolationism – 0.5% and 0.2%, respectively; ethnic fanaticism 0.2% and 0%, respectively). This result suggests that this part of foreign students retains the right of self-determination on the ethnic grounds, which remains important in the process of self-assessment (Mathis, 2003).

Thus, the students of the language faculties: the Faculty of Philology and History and the Faculty of Foreign Languages have a high level of ethnic identity indicators. They combine a positive attitude to their ethnic group and to other ethnic groups, to establishing intercultural contacts, and are committed to such transformation as hypo-identity, the erosion of ethnic identity. The indifference to the ethnic criterion in the context of globalization is natural in the modern world for most spheres of interaction. It can lead to the devaluation of the values of their culture and the loss of its uniqueness (Sugandini *et al.*, 2019).

The students of non-linguistic faculties showed a slightly different level of ethnic identity. The transformation of the ethnic consciousness of most respondents in this group has the type of hyper-identity. It is expressed in the forms of ethnic egoism and ethnic fanaticisma that can manifest itself in the contempt of members of other nationalities and cultures, the exaggeration of the importance of their own culture against others, and the sense of the people' superiority. As for the foreign students studying at the EI of the CFU, ethnic fanaticism is not the predominant

Downloaded from www.periodico.tchequimica.com

type of ethnic identity in any foreign student groups. These types are mainly expressed in a harmless form at the verbal level. This is manifested in the division of people based on the formula ‘my people – not my people’.

The most pronounced type is positive ethnic identity (norm) (Table 2) predominates in 100% of the subjects. In its structure, the positive image of own ethnic group is correlated with the positive value attitude to other ethnic groups. Ethnic identity, according to the ‘norm’ type is characterized by high tolerance and readiness for interethnic contacts. It is a condition of peaceful intercultural interaction in the multi-ethnic educational environment of the university. As can be seen from the results of the survey presented in Table 2, the maximum values on this scale are observed among the foreign students studying at the faculties of Philology and History and Foreign Languages (Group B). If in the first year the indicator has minimal values, then from the second year the dynamics is increasing. It reaches the maximum values to the fourth-rate (17.20). At this level, it lasts until graduation (17.52). In Group A, the range of values on this scale also varies slightly (from 15.43 to 12.16): first in the downward direction (at the 1st and 2nd years), and then, at senior courses, this indicator begins to rise.

As can be seen from the results presented in Table 3, in the conditions of intercultural interaction for the surveyed students of Group B the first place was taken by the integration strategy. Yet the indicators on the scale of ‘integration’ are declining every year. If students in the first year of study gave preference to this strategy (77.27%), by the fifth year of study, this figure decreased by 54.05%. The second most frequent strategy for Group B respondents is assimilation and separation (24.14% and 22.74%, respectively, for the sample as a whole). It should be noted that the indicators on a scale of ‘assimilation’ in different courses changed (14.18% to 24.14%), indicators on a scale of ‘separation’ are uneven: if in the first year 4% the respondents gave preference to this strategy, then in the second year the indices increased to 13.80%, while in the third, on the contrary, decreased by almost half (8.96%). Interestingly, in the fourth year, there is a sharp jump in the direction of increasing this figure to 22.74%. Positive responses on the scale of ‘marginalization’ were recorded in 6.81% of the students in this group. It should be noted that the strategy of marginalization is preferable for the first-year students compared to the separation strategy (4.55%). Most Group A respondents, as well as Group B respondents, chose the integration strategy (75.01%). The next most frequent acculturation strategies are separation (22.01%), and assimilation (19.76%).

Thus, the study allows us to draw the following conclusions. During the entire period of study, the subjects recorded a high level of general tolerance, the ethnic identity of the type ‘norm’ (positive ethnic identity), the predominance of establishing ‘integration’ as a strategy of acculturation. The dynamics of the foreign students’ intercultural competence indicators from the language and non-language faculties (Group B and Group A) are different, and at different stages of training, it is abrupt. Comparative analysis showed that in quantitative terms, the positivity of the dynamics of the structural components of intercultural competence is demonstrated in Group B. In our opinion, the content of the education that students learn based on the specifics of the faculty plays an important role here. The curriculum at the language faculties includes disciplines, the development of which allows the student to master the cultural wealth of the country of the studied language. The cultural environment of the city where the higher educational institution is located is of great importance in the formation of professional intercultural competence of future teachers among the foreign students.

In our case, it is the city of Elabuga, which has a thousand-year history, rich cultural heritage of which is vividly represented in the Elabuga State Historical, Architectural, and Art Museum and Reserve. Foreign students have an opportunity to participate in a variety of cultural events held by this institution in conjunction with the Elabuga Institute. After all, learning a foreign language involves familiarizing with the language consciousness of the people whose language is being studied. The main components of this content are spheres, topics, situations of communication, philological and regional knowledge, language skills, speech, educational and compensatory skills.

Country knowledge is considered by modern science as a component of cultural studies and, accordingly, socio-cultural competence. Regarding the training of future teachers, the introduction to professional background knowledge, i.e., the knowledge of social groups, is a must to study profile for successful professional communication in the target language. Various extracurricular activities are held in the Elabuga Institute for formation of

Downloaded from www.periodico.tchequimica.com

professional intercultural competence, thus contributing to integration process: national holidays (‘Christmas’, ‘National Christmas Tree’, ‘Navruz’, ‘Sabantuy’, ‘Day of Slavic Written Language’, and ‘Mother Language Day’), projects devoted to the memorable dates of historical significance (‘Victory in the War’, ‘Immortal Regiment’, the conference days of the institute), the anniversaries of outstanding figures of culture, literature, science and folk heroes (Stakheev Readings, Makhmutov Readings, Khlebnikov Readings, and Creative Works by Rasil Valeev), open lectures (Open lecture for the students on ‘The Moral lessons of creative works by L. Tolstoy’ in the framework of the year devoted to L. Tolstoy in 2018), festivals (Festival of Peoples’ Friendship), competitions (competition of readers dedicated to the Mother Language Day, creative competition ‘Каурый каләм’, the contest of photos ‘A Day in the EI CFU’), meetings of the literary club ‘Planet Writer’ (in the framework of the year devoted to L. Tolstoy), the cinema club meetings (‘Poetry Meeting’ in the framework of the annual international poetry festival ‘Ladomir’, literary drawing room ‘The Link of Times’ (meeting with a member of the Russian Union of Writers Tatiana Rolich)), ‘Dedication to Profession’ for the students of the 1st year, ‘Start’ students teaching school, participation in the ‘Total Dictation’ test etc. The University successfully uses the adaptive potential of social and cultural activities of students, which is concluded in the following:

- creation and translation of cultural samples that contribute to the formation of personality and its social adaptation in the university environment;
- maintaining the traditions and continuity of generations, ensuring the evolutionary transition of the individual from one stage of socialization to another;
- optimization of the process of the individual’s norms and values correlation with the norm and values of the society, and the development of personal worldview;
- filling the free time of the students with developmental, personality shaping content;
- ensuring social and cultural integration, communication, freedom in the choice of leisure activities, and development of the motivational and emotional sphere of personality;
- formation, development, and satisfaction of personal needs in self-realization, self-education, creativity, group support, reference, and identity;
- development of adaptive abilities of the person at its entry into various microenvironments.
- ensuring the social mobility of the individual (Osipenkova, 2007).

All the above listed performs the following educational tasks: the education of the students' universal, civil-patriotic and national feelings of consciousness and behavior in high school. They are aimed at the formation among the foreign students of not only the ideas about the culture and traditions of different nationalities, but also at the formation of their ability to comply with universal norms of morality and behavior, the willingness to correctly perceive national values, and their desire to enrich themselves with the knowledge of these values.

5. CONCLUSIONS:

Based on the study, it can be assumed that the dynamics of intercultural competence of future teachers among foreign students is manifested in the following. First-year students of all faculties get acquainted with the specifics of the learning process in the Russian university, immersed in the process of obtaining new knowledge, thus manifesting the cognitive component of intercultural competence. This stage (otherwise called the ‘honeymoon’, the entry-stage) is characterized by high rates of intercultural competence.

The second-year students begin and continue the stage of ‘cultural shock’. During this period, foreign students begin to comprehend the knowledge received in the educational and extracurricular time, not only their attitude to the specificity of the studied material is formed, but also the contradictions are revealed, that is, the emotional component of intercultural competence is manifested. At this stage, there is a slight decrease in the intercultural competence; foreign students of the third year of study move to the stage of immersion. In this period, the motivational-value component of intercultural competence is manifested, because namely starting from the third year a student has the opportunity to put the previously obtained ethnocultural knowledge on practice, that is, they can work on projects, do an internship, to practice, for example, in a summer camp, or participate in conferences, etc. If the student has successfully passed the first two stages, then there is strengthening and growth of positive dynamics of the professional intercultural competence indicators. Otherwise, the reduction

Downloaded from www.periodico.tchequimica.com

of these indicators is possible.

The stage of stabilization or adaptation is typical for senior students (fourth and fifth year of study). During this period, the acquired knowledge, skills, and ethnocultural character continue to be implemented in practice (industrial (pedagogical), pre-diploma practice, projects, and final qualifying works). This is how the behavioral component of intercultural competence is manifested. The result of this stage is the consolidation of the dynamics of the intercultural competence indicators of the previous stage, and the stage of immersion. The results allow us to justify the need to develop a system of measures aimed at the formation of positive ethnic identity of future teachers among foreign students.

6. REFERENCES:

1. Akhmetshin, E.M., Pavlyuk, A.V., Ling, V.V., Mikhailova, M.V., Shichiyakh, R.A., Kozachek, A.V. *Journal of Entrepreneurship Education*, **2019**, *22*, 1-12.
2. Andreeva, G.M. *Social psychology today: searches and reflections (collection),* Moscow: MPSI, **2009**.
3. Berry, D.V., Purtinga, A.Kh., Seagall, M.H. *Cross-cultural psychology. Research and application.* Kharkov: Gumanitarnyy tsentr, **2007**.
4. Berry, D.V., Purtinga, A.Kh., Sigall, M.Kh., Dassin, P.R. *Foreign students in Russia: who comes to the country and why*, **2016**, https://www.ucheba.ru/article/2895 accessed January 2019.
5. Bim, I.L. *Competences in education: design experience,* Moscow: Nauchno-vnedrencheskoye predpriyatiye “INEK”, **2007**.
6. Bocheliuk, V., Panov, M., Nechyporenko, V., Pozdniakova-Kyrbiatieva, E. *Astra Salvensis*, **2019**, *7*(13), 275-288
7. Buttjes, D. *Landeskundliches Lernen im Fremdsprachenunterricht*, Paderborn: Schoningh, **2000**.
8. Byram, M. *Sprogforum*, **2004**, *6*(18), 8-13.
9. Dmitrenko, T.A. *Methods of teaching English at a university,* Moscow: MELI, **2009**.
10. Elizarova, G.V. *Culture and foreign language teaching,* St. Petersburg: KARO, **2005**.
11. Furmanova, V.P. *Intercultural communication in the theory and practice of teaching foreign languages at a university,* Saransk: Mordovian State University named after N.P. Ogarev, **2009**.
12. Galskova, N.D. *Foreign Languages at School,* **2004**, 1, 3-8.
13. Ghez, N.I., Lyakhovitsky, M.V., Mirolyubov, A.A., Folomkina, S.K., Shatilov, S.F. *Methods of teaching foreign languages in high school*, Moscow: Vysshaya shkola, **1982**.
14. Gromova, N.M. *Business communication in a foreign language: teaching methodology*, Moscow: Magistr, **2010**.
15. Khaleeva, I.I. *Proceedings of the Russian Academy of Education*, **2000**, *1*, 20–29.
16. Knapp, K., Knapp-Pot-thoff, A. *Zeitschrift fur Fremdsprachenforschung*, **1990**, *1*, 62–93.
17. Kuznetsova, E.V. *Ethnopedagogical preparation of pedagogical students for work in a multi-ethnic region,* Astrakhan: Astrakhan State Pedagogical University, **2001**.
18. Larina, T.V. *Foreign Languages in High School,* **2005**, *3*, 47-51
19. Lehtonen, J. Globalization, National Cultures, and the Paradox of Intercultural Competence, **2003**. http://viesti.jyu.fi/laitos/lehtonen/globalization.html, accessed September 2019.
20. Leontyev, A.A. *Psychology of communication,* Moscow: Smysl; Izdatelskiy tsentr “Akademiya”, **2008**.
21. Lukiyanova, M.N., Zayarnaya, I.A., Kadyrov, M.A. Public Policy and Administration, **2018a**, *17*(4), 586-599
22. Lukiyanova, M.N., Akulich, O.V., Shvarova, E.V., Kadyrov, M.A., Titova, E.V., Hasanov, S.L. *Journal of Applied Economic Sciences*, **2018b**, *13*(4), 906-922.
23. Markova, S.D. *Modern Research and Innovation,* **2015**, *12*. http://web.snauka.ru/issues/2015/12/60006, accessed September 2019.
24. Mathis, V.I. *Pedagogy of interethnic communication,* Barnaul: Altai State

Downloaded from www.periodico.tchequimica.com

Pedagogical University, **2003**.

25. Matsumoto, D. *Psychology and culture.* St. Petersburg: Piter, **2003**.
26. Milrud, R.P., Maksimova, I.R. *Foreign Languages at School,* **2017**, *7*, 2-11.
27. Neuner, G. *The Role of Sociocultural Competence in Foreign Language Teaching and Learning.* Strasbourg: Council of Europe/Council for Cultural Co-operation, **2012**.
28. Oshchepkova, V.V. *Language and culture of Great Britain, USA, Canada, Australia, New Zealand,* Moscow: Glossa Press Publishing House, **2004**.
29. Osipenkova, N.A. *Socio-cultural activity as a factor in the social adaptation of students.* St. Petersburg: St. Petersburg Humanitarian University of Trade Unions, **2007**.
30. Pochtareva, T.V. *Formation of ethnocultural competence of students in a multi-ethnic educational environment,* Stavropol: Stavropol State University, **2007**.
31. Safonova, V.V. *Co-study of languages and cultures in the mirror of world trends in the development of modern language education,* **2014**. https://cyberleninka.ru/article/n/soizuchenie-yazykov-i-kultur-v-zerkale-mirovyh-tendentsiy-razvitiya-sovremennogo-yazykovogo-obrazovaniya, accessed September 2019.
32. Samovar, L.A., Porter, R.E., McDaniel, E.R., Roy, C.S. *Communication Between Cultures*, Wadsworth: Cengage Learning, **2013**.
33. Soldatova, G.U. *Over the barriers: man, text, communication,* Moscow: Smysl, **2006**.
34. Soldatova, G.U., Ryzhova, S.V. Types of ethnic identity, **2011**. https://bitly.su/C6iL, accessed September 2019.
35. Soldatova, G.U., Shaigerova, L.A. *Workshop on psychodiagnostics and the study of personality tolerance,* Moscow: Moscow State University, **2003**.
36. Solodukhin, V.I. *Integration of the activities of socio-cultural institutions in the formation of specialists of ethnocultural associations: a system-structural approach,* Moscow: FGOUVPO "Moscow State University of Culture and Arts", **2009**.
37. Solovieva, E.N. The role of intercultural communication in modern education, **2013**. https://cyberleninka.ru/article/n/rol-mezhkulturnoy-kommunikatsii-v-sovremennom-obrazovanii, accessed September 2019.
38. Spencer-Oatey, H., Franklin, P. *Intercultural interaction: a multidisciplinary approach to intercultural communication,* New York: Palgrave Macmillan, **2009**.
39. Spitzberg, B. *A model of intercultural communication competence,* Belmont: Wadsworth, **2000**.
40. Sugandini, D., Susilowati, Ch., Pambudi, A., Aw, S., Muafi, Siswoyo, M. *Entrepreneurship and Sustainability Issues*, **2019**, *7*(1), 413-424. http://doi.org/10.9770/jesi.2019.7.1(29).
41. Sysoev, P.V. *The concept of multicultural language education,* Moscow: Moscow State University named after M.V. Lomonosov, **2004**.
42. Todorov, G.N., Kalinina, A.V., Rybakova, A.I. *Entrepreneurship and Sustainability Issues*, **2018**, *5*(4), 992-1007. http://doi.org/10.9770/jesi.2018.5.4(20).
43. Vasilyeva, N.N. Intercultural competence. Strategies and techniques for achieving it, **2017**. https://www.researchgate.net/publication/318252107_Mezkulturnaa_kompetentnost_kak_neobhodimaa_sostavlausaa_professionalnoj_podgotovki_uristov, accessed September 2019.
44. Volchik, V., Maslyukova, E. *Entrepreneurship and Sustainability Issues*, **2019**, *6*(4), 2095-2109. http://doi.org/10.9770/jesi.2019.6.4(38).
45. Wati, L.N., Primiana, H.I., Pirzada, K., Sudarsono, R. *Entrepreneurship andSustainability Issues*, **2019**, *7*(1): 52-68. http://doi.org/10.9770/jesi.2019.7.1(5).

Downloaded from www.periodico.tchequimica.com

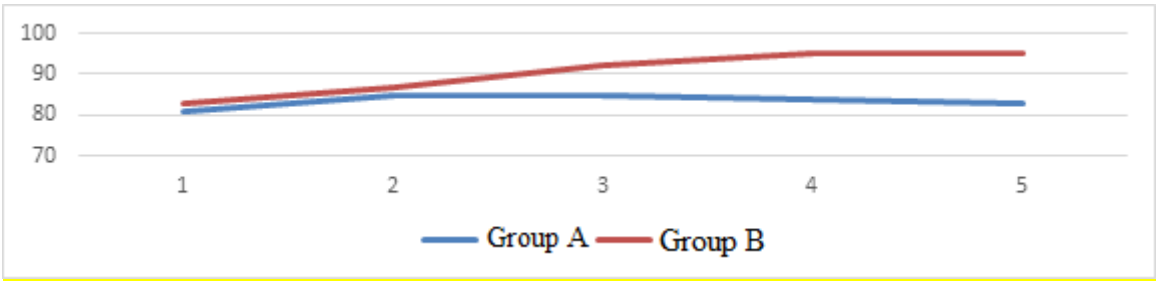

Figure 1. *Express Diagnostics 'Tolerance Index' (Diagnostics of the General Level of Tolerance of the Surveyed Students)*

Table 1. Types of Ethnic Identity Diagnostics' Results (%) ('Types of Ethnic Identity' (G.U. Soldatova, S.V. Ryzhova))

	Ethnic Nihilism	Ethnic Indifference	Norm	Ethnic Egoism	Ethnic Isolationism	Ethnic Fanaticism
Group A	5	18	64.3	12	0.5	0.2
Group B	5.8	19	71	4	0,2	0

Table 2. The Results of the Diagnosis of Ethnic Identity by Type 'Norm' (Positive Ethnic Identity) ('Types of Ethnic Identity' (G. Soldatova, S. V. Ryzhova))

	1 year	2 year	3 year	4 year	5 year
Group A	15.10	12.16	12.44	13.74	15.43
Group B	13.22	17.44	18.68	17.20	17.52

Table 3. Attitudes to Acculturation Strategies

	Separation					Marginalization					Integration					Assimilation				
Groups	1	2	3	4	5	1	2	3	4	5	1	2	3	4	5	1	2	3	4	5
Group A	7.35	10.87	13.37	13.5	22.01	5.32	8.87	9.5	13.63	6.13	75.01	66.55	61.78	55.28	52.10	12.32	13.71	15.22	17.59	19.76
Group B	4	13.80	8.96	22.74	12.05	4.55	3.5	10.75	2.7	9.76	77.27	67.31	64.21	54.55	54.05	14.18	15.39	16.08	20.01	24.14

PERIÓDICO TCHÊ QUÍMICA
ARTIGO ORIGINAL

CARACTERÍSTICAS DA COMPETITIVIDADE DOS PRODUTOS DO EMPREENDEDORISMO INDUSTRIAL

COMPETITIVE PECULIARITIES OF INDUSTRIAL ENTERPRISES' PRODUCTS

ОСОБЕННОСТИ КОНКУРЕНТОСПОСОБНОСТИ ПРОДУКЦИИ ПРОМЫШЛЕННЫХ ПРЕДПРИЯТИЙ

UKUBASSOVA, Galiya S.[1*]; AMIRBEKOVA, Ainur B.[2]; PRIMZHAROVA, Kalyash K.[3]; DARIBAYEVA, Adaskhan K.[4]; ISMAILOVA, Diana T.[5]

[1,2] Kazakh University of Economics, Finance and International Trade, Department of Economics, Nur-Sultan – Republic of Kazakhstan

[3] Narxoz University, Department of Public Administration, Almaty – Republic of Kazakhstan

[4] Kazakh University of Economics, Finance and International Trade, Department of International Trade and Law, Nur-Sultan – Republic of Kazakhstan

[5] Kazak University of Technology and Business, Department of Management and Tourism, Nur-Sultan – Republic of Kazakhstan

** Correspondence author*
e-mail: ukubasova_g@mail.ru

Received 29 August 2019; received in revised form 20 October 2019; accepted 25 October 2019

RESUMO

As empresas aumentam seus indicadores financeiros para atingir suas metas de desenvolvimento. A fonte de desenvolvimento pode servir como uma estratégia desenvolvida e como uma versão especializada do programa, que se baseia na consecução de certos indicadores financeiros. Particularmente, pode ser a questão da constante garantia de lucro e do aumento e otimização de processos internos que são considerados como base do funcionamento constante da empresa. A consideração do que pode ser visto como a competitividade da produção determina a relevância do estudo. A inovação do estudo está no fato de que não apenas uma certa estratégia para atingir as metas é considerada a base da competitividade, mas também uma estratégia para a formação do ambiente interno sustentável da empresa, que pode ser implementado considerando as necessidades de produção e seu potencial desenvolvimento. Como base para aumentar a competitividade da indústria química e a operação sustentável da empresa, os autores consideram o ambiente interno. Prevê-se que a implementação do aumento da resistência interna seja realizada com base na avaliação do sistema de cooperação externa. O significado prático do trabalho é determinado pela necessidade de formar uma certa relação entre estabilidade interna e as possibilidades de mudança externa.

Palavras-chave: *indústria química, produtos, competitividade, empresa, desenvolvimento econômico.*

ABSTRACT

Industrial enterprises are improving their financial performance to achieve their development goals. The source of development can serve as a developed strategy and a specialized version of the program, which is based on the achievement of certain financial indicators. Particularly, it can be the issue of constant ensuring of profit, and of the increase and optimization of internal processes which are considered as a basis of steady functioning of the enterprise. Consideration of what can be viewed as the competitiveness of production, namely determines the relevance of the study. The novelty of the study is in the fact that not only a certain strategy in achieving the targets is considered as the basis of competitiveness, but also a strategy for the formation of internal sustainable environment of the enterprise, which can be implemented considering the needs of production and its potential development. As a basis for increasing the competitiveness of the chemical industry and sustainable operation of the enterprise, the authors consider the internal environment. The implementation of the increase in internal resistance is expected to be conducted based on the evaluation of the system of external cooperation. The practical significance of the work is determined by the need to form a certain relationship between internal stability and the possibilities of external change.

Downloaded from www.periodico.tchequimica.com

Keywords: *chemical industry, products, competitiveness, enterprise, economic development.*

АННОТАЦИЯ

Промышленные предприятия повышают свои финансовые показатели для достижения поставленных целей развития. Источником развития может служить как разработанная стратегия, так и специализированная версия программы, которая основывается на достижении определенных финансовых показателей. В частности, речь может идти как о постоянном обеспечении прибыли, так и о повышении и оптимизации внутренних процессов, которые считаются основой устойчивого функционирования предприятия. Рассмотрение того, что можно считать конкурентоспособностью производства и определяет актуальность проводимого исследования. Новизна исследования определяется тем, что в качестве основы конкурентоспособности рассматривается не только определенная стратегия в достижении плановых показателей, но также и стратегии формирования внутренней устойчивой среды предприятия, которая может быть реализована с учетом потребностей производства и его потенциального развития. В качестве основы для повышения конкурентоспособности предприятия химической промышленности авторы рассматривают внутреннюю среду как основу для обеспечения устойчивого функционирования предприятия. Реализацию повышения внутренней устойчивости предполагается проводить на основе оценки системы внешнего сотрудничества. Практическая значимость работы определяется необходимостью формирования определенного соотношения между внутренней устойчивостью и возможностями внешнего изменения.

Ключевые слова: *химическая промышленность, продукция, конкурентоспособность, предприятие, экономическое развитие.*

1. INTRODUCTION

For the enterprises operating in imperfect competition markets, the ability to foresee the situation and to create and consolidate their competitive advantages is of particular importance. Many studies on competitiveness are conditioned by different positions of scientists, and the lack of a unified approach to the definition of the object of study. There is no systematic approach to the definition of competitiveness: its various elements are considered separately from each other, the relationship between them is not fully considered (Mingaleva *et al.*, 2020). A gross methodological error is the use of a methodology based on an endogenous view of the market system, according to which the main problem of existing market participants is the preservation of the enterprise as a market entity, and the means of its solution is the rationalization of market behavior on the basis of an effective competition strategy (Ivashchuk, 2013; Negrych, 2013; Pylypenko and Murtazina, 2013). When using the system-praxeological approach, such an understanding of competitiveness as an integrated property of the economic system is realized, which determines the implementation of the goals and the results of functioning necessary and sufficient for the active positioning of the system in the market space (Atanelishvili and Silagadze, 2018; Sharafutdinov *et al.,* 2018; Akhmetshin *et al.,* 2018a; Akhmetshin *et al.,* 2018b).

The current state of the chemical industry market is characterized by constant changes in the external environment and environmental requirements (Gribust, 2018), the variability of consumer demand, the presence of many enterprises of different forms of ownership, providing almost every economic entity with the right to enter the external market, increasing uncertainty, and risk (Zhang and Niu, 2013). In the context of the formation of market relations, the main factor in the success of modern enterprises is to ensure their competitiveness both now and in the future.

In the conditions of increasing dynamism and uncertainty of the external environment, strategic management is effective for solving these problems (Rusinova, 2014). Strategic management is a multifaceted, formal and behavioral management process, through which effective strategies are formulated and implemented, which help to balance the potential of the enterprise with the capabilities of the external environment to achieve the goal. The stages of strategic management, which is a kind of decision-making process, include as follows (Chursin and Makarov, 2015a): awareness of the need to make a decision; diagnosis and restructuring of the problem; formulation of options for further action; adoption of one or more options for implementation; implementation of decisions; monitoring and evaluation of results.

Downloaded from www.periodico.tchequimica.com

The approach to strategic management is based on strategic analysis, which performs the following tasks (Xin, 2013):

–collection and processing of information for management decision-making on strategic issues;

–analysis of existing strategies and assessment of their dynamism and ability to adapt to changes in the external environment;

–assessment of prospects and competitive opportunities of the enterprise;

–analysis of strategic alternatives for decision-making on investment and financing of production development, marketing, and sales organization and other issues;

–operational analysis of the implementation of strategies and their adjustment; providing top management with reliable, relevant strategic information.

Such an approach is formed by their requirements, which are fully implemented within one or more enterprises based on several positions that are fully justified economically for a particular enterprise (Silagadze, 2019).

2. LITERATURE REVIEW

The need to determine the key factors affecting the competitiveness of the enterprise, in particular, its components, determines the relevance of this issue and is discussed in this section. By the factors, we understand the conditions, causes, parameters, indicators that affect the economic process, and the result of this process. The factors are dynamic in time and space and interact closely (Čoćkalo *et al.,* 2019).

The study of the influence of the external and internal environment is reflected in the works of many scientists: mostly of Western school. Factor analysis of competitiveness and the study of the mechanism of its geno- and phenotypic characteristics formation allow us to assert the general equilibrium of the effects of the internal and external environment on the level of economic systems' competitiveness (Kruzhilin *et al.,* 2018). However, this equilibrium theoretically exists only in the long term as a general trend. In the short term, non-equilibrium models with internal or external competitiveness phenotype are real.

Economic-logical, economic-mathematical, and heuristic methods of analysis are used in the analysis of individual components of the external and internal environment. One of the most popular methods of analysis and assessment of the environment is SWOT-analysis, which involves the search for opportunities and threats contained in the external environment of the enterprise; study of the strengths and weaknesses of the enterprise; and the determination of chain links between these two groups of factors (Tao and Li, 2018).

The study on the identification and evaluation of certain factors affecting the company is the subject of many works. The purpose of analyzing these works was to identify and distribute the factors of competitiveness of the enterprise (Beausang, 2003). There are more than 40 factors of the internal environment, which were determined as a result of the study of their impact on the competitiveness and competitive sustainability of the enterprise. The factors to be considered when choosing each competitive strategy (low-cost strategy, differentiation strategy, and focus) include as follows: production, financial, marketing, technological, innovative, labor, information, management, time, and spatial (Shtal *et al.,* 2018a).

One of the important factors affecting the preservation of competitiveness in the future, that is, the competitiveness of the enterprise, is its innovative activity. Modern competition has some features – enterprises compete not so much for the possession of capital resources and material values, but for the ability to develop and implement innovations. Scientific and technological progress requires enterprises to use advanced technologies and equipment. The progressive scientific knowledge embodied in them allows enterprises not only to adapt to the existing external conditions but also to actively influence them. Also, innovative development of the enterprise leads to new qualitative changes not only in the production sphere, but also in scientific and technical, organizational, and managerial one.

However, it should be noted that the key aspect of innovation is the issue of financing. Innovation requires significant financial resources, and therefore for effective innovation it is advisable to create conditions for the gradual accumulation of domestic and foreign resources.

In the framework of the approach, which investigated the static and dynamic financial characteristics of the enterprise, it is noted that the current, short-term financial characteristics reflect the financial condition of the enterprise, and the financial stability of the entity – a dynamic

Downloaded from www.periodico.tchequimica.com

characteristic that reflects the stability of the financial condition of the enterprise in the long term (Li *et al*., 2018). To assess the static availability of financial resources, the liquidity indicators and capital structure are used, for which a normative value is set. The main source for the calculation of indicators is the balance sheet of the enterprise, compiled on a certain date (Liu and Zhu, 2017). To assess the dynamic availability of financial resources, profitability and turnover indicators are calculated, the source of information on which is the balance sheet of the enterprise and the profit and loss statement, which can be published in the public press (Chursin and Makarov, 2015b). The indicators for assessing financial stability do not have regulatory (threshold) values, so for comparison, as a rule, the industry average value or data of leading competitors are used (Nesterenko *et al.,* 2019). In the set of indicators describing financial stability, it is necessary to additionally include the indicators characterizing the cash flow, its structure and dynamics. The source for the calculation of the data is the statement of the cash flows of the enterprise, which is included in the annual reporting of the economic entity (Conti and Giaccaria, 2001).

An important factor affecting the competitiveness of the enterprise is its personnel (Lawton and Hodges, 1999). Human resources – the most active factor that enables the company to adapt and develop, so it is important not only the available number and qualification of personnel, but also to analyze future needs in personnel; the presence and successful implementation of personnel-strategy – recruitment, selection, appointment, promotion, release, consolidation, retraining, personnel evaluation, training and development of personnel, as well as an effective system of motivation and remuneration system. The corporate culture of the enterprise plays an important role (An *et al.,* 2019).

According to the system approach, the stability of the system primarily depends on the stability of its individual elements, representing the structure of the system, and the quality of the system management. The quality of management depends on the management structure, management processes, management methodology (Gilroy, 1998). By the management structure, we mean the functional and organizational structure, the system of organizational relations, the interaction between the supreme governing bodies, norms, standards, etc. By the processes of management, we mean the system planning, communication, development processes, and execution management solutions, and process management. That is, organizational and technological, socio-organizational and information processes. By the methodology of management, we mean the vision, objectives, strategies, policies, methods, functions, that is, the organizational and methodological processes, theoretical and methodological processes (Shtal *et al.,* 2018b).

The effectiveness of management depends on the application of scientific methods in the systematic approach to it (Chursin and Makarov, 2015c). Such methods include as follows: golden proportion, soft resonance control, cognitive analysis and control, reflexive control, and system approach to management. Assessment of the impact of the environment on the company can be carried out considering the factors proposed above. The approach to defining the factors of influence of environment on the company can be used to develop the indicators of the external environment's impact.

3. MATERIALS AND METHODS

In order to function and compete effectively, it is necessary to constantly monitor and respond appropriately, both in terms of commercialization and expansion of services, and in terms of organizational and technical improvement of production. One of the factors that provide high-quality services and maintenance is the use of modern technologies and equipment in the production process.

Technical and technological resource support is the basis for the functioning of the chemical industry. It is the technique and technology that ensure the process of providing the service. The current level of development of the chemical industry makes it possible to offer a particular service in a variety of areas – both in the user segment and in the industrial sector. The level of technology (generation) mainly determines the level of evaluation of the enterprise by consumers. Accordingly, this affects the percentage of the market volume occupied by the chemical industry. And this in its turn – the volume of revenues from activities, and development opportunities.

Based on this, the indicators showing the competitiveness of the chemical industry on the component that determines the stability of the production system are as follows: level of application of advanced technologies to the

Downloaded from www.periodico.tchequimica.com

technological processes and equipment; area of presence of the chemical industry; share of innovative equipment.

Accordingly, the evaluation of the variable X2 – sustainability of the production system (Equation 1). Where X_{21} – the level of application of advanced technological technologies, processes, and equipment; X_{22} – area of presence of the chemical industry; X_{23} – share of innovative equipment.

The personnel management system consists of such elements as the planning of the number of personnel, recruitment, and selection of personnel, training and professional development, analysis of work efficiency, and personnel rotation. The planning is carried out to optimize the number and professional level of personnel. For this purpose, we conduct a systematic analysis of the workforce of the enterprise and the forecast of changes in personnel for a certain period, considering the development strategy of the enterprise and personnel policy.

X_3 variable estimation – the stability of the personnel (Equation 2). Where X_{31} – skill level of personnel; X_{32} – the level of personnel management efficiency; X_{33} – level of the corporate culture.

Estimation of X_{33} – the level of corporate culture is carried out according to the following indicators: X_{331} – the type of organization; X_{332} – the degree of aggressiveness of the head; X_{333} – the homogeneity of the culture.

X_4 variable estimation – financial and investment performance (Equation 3). Where X_{41} – return on sales; X_{42} – return on equity.

For the financial condition, the maximum and minimum levels can be the best and worst recorded in the industry or in the region, or the values of the indicators of the enterprise itself, or the values obtained based on expert assessments. Indicators need to be normalized, and then the value will be from 0 to 1 (Equation 4). Where a_{jmin} – minimum value of the j indicator; a_{jmax} – maximum value of j indicator; a – actual value of j indicator.

The factors influencing the competitiveness of the enterprises also includes the application of modern management techniques. It is also facilitated by a flexible organizational structure and the presence of the mission. An effective system of management of the chemical industry contributes to the continuous satisfaction of the growing needs of consumers, improving performance by streamlining and optimizing processes, the implementation of such goals as improving the level of customer service, improving competitiveness and efficiency in the future, ensuring profitability, strengthening partnerships and the positive image of the enterprise.

An important factor hindering the further progress of the chemical industry is the imperfection of the organizational and economic management mechanism. The influence of this factor on the competitiveness of the chemical industry is enhanced due to the increased sensitivity of the industry to it. This is due to the specifics of the industry, namely the peculiarities of the organization of the production process, which is not localized within a single enterprise, that is, in creating a service and providing it to the user, several organizationally and financially separate enterprises participate that perform technological operations. Hence the urgent need for a well-organized system of interaction of all participants in the production of chemical products (Yerseitova *et al.*, 2018).

Variable estimation X_5 – management quality (Equation 5). Where X_{51} – the level of the management structure; X_{52} – level of application of modern management methods.

Formation and improvement of the management structure is an ongoing process, the purpose of which is to improve the efficiency of the enterprise. A fast-growing chemical industry with a relatively short service life cycle is characterized by a change in the management structure. To analyze the effectiveness of the management structure as one of the factors of competitiveness, it is necessary to investigate the following things: the effectiveness of achieving the goals, objectives, and strategies of the enterprise; the efficient allocation of resources of the enterprise; speed of response to changes; efficiency of interaction between employees and customers; adaptability to internal and external factors and speed of response.

4. RESULTS AND DISCUSSION:

We will assess the competitiveness of Talas Investment Company (Zhambyl Region, Republic of Kazakhstan). The company's activity is the chemical industry. The company is focused on the implementation of the latest achievements in the chemical industry, using fiber-optic communication lines and digital processing in the management of chemical equipment, providing the highest quality products.

Downloaded from www.periodico.tchequimica.com

Based on the data provided by Talas Investment Company, the level of tactical competitiveness of the enterprise was determined. The calculation considered two factors of competitiveness of services – the quality of services and maintenance, as well as the cost of services. The calculated level of tactical competitiveness of the enterprise is 0.55, which falls within 0.5-0.75 and corresponds to grade C – as average. The composition of indicators for assessing the internal competitiveness of the chemical industry, their gradation (levels) are shown in Table 1.

X_1 variable estimation – Sustainability of the marketing system', which was carried out on elements using the scale of the point estimate, is given in Table 2.

The value of the indicator is at two levels – medium and low. We calculate the μ value for these levels:

—— 18;

—— 19.

Thus, variable X_1 – Sustainability of the marketing system corresponds to level H – as low.

Variable estimation X_2 – Sustainability of the production system consists of the evaluation of variables: X_{21} – Level of application of advanced technologies to technological processes and equipment (Table 3), X_{22} – area of presence, X_{23} – share of innovative equipment.

Variable estimation of the level of the advanced technologies applied to the technological processes and equipment, which was carried out on the elements using the scale of the score, is given in Table 3.

We calculate the value μ for the levels – medium and high, respectively, the parameters of the membership function:

—— 23;

—— 24.

The share of the territory of Zhambyl Region, where Talas Investment Company is present, is 75%. We calculate the value μ for the levels – as medium and high, respectively, the parameters of the membership function:

—— 75;

—— 80.

Variable X_{22} – Area of presence corresponds to level B – as high.

The share of equipment used by Talas Investment Company is 95%. We calculate the value μ for the level – as high according to the parameters of the membership function:

100.

Variable X_{23} – share of innovative equipment corresponds to level B – as high. Variable X_2 – Sustainability of the production system corresponds to level B – as high.

Variable estimation X_3 – sustainability of the personnel consists of the evaluation of variables: X_{31} – Skill level of personnel (Table 4), X_{32} – Level of personnel management efficiency (Table 5), X_{33} – Level of corporate culture (Table 6).

Variable X_{31} – Skill level of personnel corresponds to level C – as average.

We calculate the value of μ for the levels of medium and high, respectively, the parameters of the membership function:

—— 34;

—— 35.

Variable X_{32} – Level of personnel management efficiency corresponds to level B – as high.

Degree of aggressiveness of the head coincides with the type of organization. The culture is preliminary homogenous.

We calculate the value of μ for the levels – intermediate and aggressive according to the parameters of the membership function:

—— 29;

—— 30.

Variables X_{331} – type of organization, X_{332} – degree of aggressiveness of the head corresponds to level P – as intermediate. Variable X_{333} – the homogeneity of the culture corresponds to level O – as homogenous. Variable X_{33} – Level of corporate culture corresponds to level B – as high. Variable X_3 – sustainability of the personnel corresponds to level B – as high.

X_4 variable estimation – financial and investment performance (Table 7) consists of evaluation of variables: X_{41} – net return on sales, X_{42} – return on equity (Table 6).

Variable X_{41} – net return on sales

Downloaded from www.periodico.tchequimica.com

corresponds to level C – as average; X_{42} – return on equity corresponds to level H – as low, X_4 – financial and investment performance corresponds to level C – as average.

Variable estimation X_5 – management quality consists of the evaluation of variables: X_{51} – the level of the management structure (Table 8), X_{52} – level of application of modern management methods (Table 9).

We calculate the value μ for the level C – as average according to the parameters of the membership function:

16.

Variable X_{51} – the level of the management structure corresponds to level C – as average.

We calculate the value μ for the levels – medium and low, respectively, the parameters of the membership function:

Variable X_{52} – level of application of modern management methods according to level C – as average. Variable X_5 – management quality corresponds to level C – as average. X_6 variable estimation – level of social responsibility of the enterprise (Table 10).

We calculate the value μ for the level C – as average according to the parameters of the membership function:

18.

Variable X_6 – Level of social responsibility corresponds to level C – 'what is required'. Estimate of other variables and the resulting estimate is summed up in Table 11.

According to Table 11, strategic competitiveness of Talas Investment Company corresponds to the level of C-C, for which the attack leader – flank attack, the frontal attack is a recommended strategy. The results of the proposed method do not contradict to the results obtained with the use of classical techniques, such as SWOT analysis, GE/McKinsey multifactor model, and others, but unlike the existing ones, the following advantages can be noted: complexity, consistency, considering the dynamics of indicators in space and time, and specifics of the chemical industry. The results of the competitiveness assessment of Talas Investment Company, which are obtained at this stage, are the basis for further configuration of the competitiveness assessment model.

The problem points of the proposed methodology include the lack of an exhaustive list of evaluation elements, which, on the one hand, indicates its incompleteness, and, on the other, ensures its flexibility and adaptability to the changing conditions of functioning.

5. CONCLUSIONS:

The analysis of the competitive environment of the chemical industry 'Talas Investment Company' shows that the chemical industry is developing dynamically and increasing its competitive advantage. Competition occurs not only among the most promising sub-sector of consumer goods but also among the enterprises providing services for the industrial production of certain chemicals. This is due to the development of technologies for processing products by chemical conversion and expansion of their application. Based on the survey it was found that for most of the chemical industry, the lack of a comprehensive system of adequate assessment of competitiveness, the lack of interconnection of management decisions and evaluation results are the reasons for low competitiveness.

In such conditions, for the modern enterprise of the chemical industry, the issue of assessment and ensuring the competitiveness not only now, but also for the prospect, is extremely important. According to the proposed method of assessing the competitiveness of the enterprise, we developed a technique for the chemical industry, considering the specifics of its activities. The following factors influencing competitiveness of the enterprise of chemical industry are defined: use of modern technologies and equipment; strong production, research, and experimental base; qualified personnel; stable financial position; pricing and assortment policy; application of modern management methods; social responsibility of the enterprise.

In the course of the work, recommendations on the choice of competitive strategy of the chemical industry are formed, which are based on the results of assessing its competitiveness: tactical competitiveness, competitiveness, and strategic competitiveness.

6. REFERENCES:

1. Akhmetshin, E., Morozov, I., Pavlyuk, A., Yumashev, A., Yumasheva, N., Gubarkov, S. *European Research Studies Journal*, **2018a**, *21*(1), 352-361.

Downloaded from www.periodico.tchequimica.com

2. Akhmetshin, E.M., Pavlyuk, A.V., Kokorev, A.S., Lazareva, T.G., Artemova, E.I. *Journal of Applied Economic Sciences*, **2018b**, *13*(8), 2309-2322.
3. An, M.-H., Ri, G.-Y., Rim, G.-N. *Journal of the Knowledge Economy*, **2019**, 1-27.
4. Atanelishvili, T., Silagadze, A. *Bulletin of the Georgian National Academy of Sciences*, **2018**, *12*(4), 163-166.
5. Beausang, F. *Third World Multinationals: Engine of Competitiveness or New Form of Dependency?* London: Palgrave Macmillan, UK, **2003**.
6. Chursin, A., Makarov, Y. (Eds.). Formation of the Firm Competitiveness MIS Systems. In *Management of Competitiveness: Theory and Practice* (pp. 289–343), Cham: Springer International Publishing, **2015a.**
7. Chursin, A., Makarov, Y. (Eds.). Quantitative Evaluation of the Firm Competitiveness. In *Management of Competitiveness: Theory and Practice* (pp. 193–260), Cham: Springer International Publishing, **2015b**.
8. Chursin, A., Makarov, Y. (Eds.). Theoretical Bases of Competitiveness Management. In *Management of Competitiveness: Theory and Practice* (pp. 83–131), Cham: Springer International Publishing, **2015c**.
9. Čoćkalo, D., Jordjević, D., Bogetić, S., Bakator, M., Bešić, C. Competitiveness of Domestic Enterprises in Changing Markets and Industry 4.0. In Monostori, L., Majstorovic, V. D., Hu, S. J., Djurdjanovic, D. (Eds.): *Proceedings of the 4th International Conference on the Industry 4.0 Model for Advanced Manufacturing* (pp. 113–127), Cham: Springer International Publishing, **2019**.
10. Conti, S., Giaccaria, P. (Eds.). Competitiveness and development: from enterprise to place. In *Local Development and Competitiveness* (pp. 133–155), Dordrecht: Springer, Netherlands, **2001**.
11. Gilroy, B. M. International Competitiveness, Multinational Enterprise Technology Clubs, and the Government Interface. In Koch, K.-J., Jaeger, K. (Eds.): *Trade, Growth, and Economic Policy in Open Economies: Essays in Honour of Hans-Jürgen Vosgerau* (pp. 13–30), Berlin, Heidelberg: Springer Berlin Heidelberg, **1998**.
12. Gribust, I. *World Ecology Journal*, **2018**, *8*(2), 11-21.
13. Ivashchuk, I. *Skhid*, **2013**, *1*(121), 19-23
14. Kruzhilin, S., Baranova, T., Mishenina, M., Zaitseva, M. Regional specificity creation of protective afforestations along highways. *World Ecology Journal*, **2018**, *8*(2), 22-32.
15. Lawton, T. C., Hodges, M. R. Promoting Competitiveness: inward investment incentives and enterprise policy. In Lawton, T. C. (Ed.): *European Industrial Policy and Competitiveness: Concepts and Instruments* (pp. 204–225), London: Macmillan Education UK, **1999**.
16. Li, J., Li, M., Gao, Y., Li, J., Su, H., Huang, M. (Eds.). Corporate Level: New Driving Forces and Models for Enhancing the Competitiveness of Chinese Enterprises. In *China's Provincial Economic Competitiveness and Policy Outlook for the 13th Five-year Plan Period (2016-2020)* (pp. 203–235), Singapore: Springer Singapore, **2018**.
17. Liu, J., & Zhu, X. Human Capital Investment: The Fundamental Means to Promote Enterprise Competitiveness. In Liu, Y. (Ed.): *New Interpretations on the Development of China's Non-Governmental Enterprises* (pp. 209–229), Singapore: Springer Singapore, **2017**.
18. Mingaleva, Z., Deputatova, L., Starkov, Y. Management of Organizational Knowledge as a Basis for the Competitiveness of Enterprises in the Digital Economy. In Antipova, T. (Ed.): *Integrated Science in Digital Age* (pp. 203–212), Cham: Springer International Publishing, **2020**.
19. Negrych, O. *Skhid*, **2013**, *3*(123), 45-49
20. Nesterenko, S., Rozumenko, S., Kravets, O., Redko, L. Managing Competitiveness of the Enterprise: Theoretical-Methodological Aspect. In Nadykto, V. (Ed.): *Modern Development Paths of Agricultural Production* (pp. 483–492). Cham: Springer International Publishing, **2019.**
21. Pylypenko, O., Murtazina, N. *Skhid*, **2013**, *4*(124), 61-65

Downloaded from www.periodico.tchequimica.com

22. Rusinova, O. *Skhid*, **2014**, *4*(130), 58-62.

23. Sharafutdinov, R.I., Gerasimov, V.O., Akhmetshin, E.M., Yumashev, A.V., Pavlyuk, A.V., Luzina, T.V. Inclusive growth index assessment in the regions of the Volga Federal District of the Russian Federation. *Proceedings of the 31st International Business Information Management Association Conference – Innovation Management and Education Excellence through Vision 2020* (pp. 3890-3902). Milan, Italy, **2018**.

24. Shtal, T. V., Bondarenko, L. M., Ukubassova, G. S., Amirbekuly, Y., Toiboldinova, Z. G. *Espacios*, **2018a**, *39*(12), 23.

25. Shtal, T. V., Polyakova, Y. O., Hasanov, E. L., Ukubassova, G. S., Kozhabaeva, S. A. *Utopia y Praxis Latinoamericana*, **2018b**, *23*(82), 64-82.

26. Silagadze, A. *Bulletin of the Georgian National Academy of Sciences*, **2019**, *13*(2), 142-145.

27. Tao, M., Li, Z. Research on the Construction of Enterprise Brand Competitiveness Evaluation System Based on the Integration of SWOT and AHP Model. In Tavana, M., Patnaik, S. (Eds.): *Recent Developments in Data Science and Business Analytics* (pp. 55–62), Cham: Springer International Publishing, **2018**.

28. Xin, Z. Research on the Relationship Between Enterprise Innovation and the Formation of Core Competitiveness. In Qi, E., Shen, J., Dou, R. (Eds.): *The 19th International Conference on Industrial Engineering and Engineering Management* (pp. 1625–1632), Berlin, Heidelberg: Springer Berlin Heidelberg, **2013**.

29. Yerseitova, A., Issakova, S., Jakisheva, L., Nauryzbekova, A, Moldasheva, A. *Entrepreneurship and Sustainability Issues*, **2018**, *6*(2): 558–576. http:// doi.org/10.9770/jesi.2018.6.2(7).

30. Zhang, H., Niu, Z. Influence Mechanism of Lean Production to Manufacturing Enterprises' Competitiveness. In Qi, E., Shen, J., Dou, R. (Eds.): *The 19th International Conference on Industrial Engineering and Engineering Management* (pp. 805–813), Berlin, Heidelberg: Springer Berlin Heidelberg, **2013**.

$$X_2 = f(X_{21}, X_{22}, X_{23}) \quad \text{(Eq. 1)}$$

$$X_3 = f(X_{31}, X_{32}, X_{33}) \quad \text{(Eq. 2)}$$

$$X_4 = f(X_{41}, X_{42}) \quad \text{(Eq. 3)}$$

$$X_j = \frac{a_{jf} - a_{i\min}}{a_{j\max} - a_{j\min}} \quad \text{(Eq. 4)}$$

$$X_5 = f(X_{51}, X_{52}) \quad \text{(Eq. 5)}$$

Downloaded from www.periodico.tchequimica.com

Table 1. *Indicators of Complex Components of Internal Competitiveness for the Chemical Industry*

Complex components of internal competitiveness	Indicators/Gradations (Levels)		
	1st	2nd	3rd
Sustainability of the marketing system	The effectiveness of the marketing service: the level of efficiency of sales promotion and after-sales service, modern advertising system, and marketing research Gradations (levels) and evaluation of the indicator are determined by experts		
Sustainability of the production system	B, C, H Level of application of advanced technologies, technological processes, and equipment	B, C, H Area of the presence of the enterprise	B, C, H Share of equipment, or share of own sales channels
	Gradations (levels) and evaluation of the indicator are determined by experts		
Sustainability of the personnel	B, C, H Skill level of personnel	B, C, H Level of personnel management efficiency	B, C, H Level of the corporate culture
	Gradations (levels) and evaluation of the indicator are determined by experts		
Financial and investment performance	B, C, H Return on sales P/Q_{sales}	B, C, H	B, C, H Return on equity P/K_{part}
Management quality	B, C, H Level of application of modern management methods		B, C, H The level of the management structure
	Gradations (levels) and evaluation of the indicator are determined by experts		
Level of social responsibility	B, C, H		B, C, H
	Gradations (levels) and evaluation of the indicator are determined by experts No – failure to comply with the requirements of mandatory social responsibility = H What is required – compliance with the requirements of mandatory social responsibility = C Voluntary – voluntary social responsibility, social mission = B		

Table 2. *Point Variable Estimation of X_1 – Sustainability of the Marketing System*

Elements	Points		
	1	2	3
Implementation of market segmentation	1		
Study of consumer needs and preferences	1		
Study of the competitors		2	
The level of control over the quality of services		2	
Trademark use		2	
Consideration of the elasticity of demand in setting the price	1		
Application of discount system from the price		2	
The use of progressive methods of sales	1		
Level of service		2	
Estimate of the services' efficiency	1		
Estimate of the promotional activities' effectiveness	1		
Total		16	

Downloaded from www.periodico.tchequimica.com

Table 3. *Estimate of the Level of the Advanced Technologies Applied to the Technological Processes and Equipment*

Elements	Estimate
Competitiveness of the technologies used	3
Ensuring the necessary level of quality and competitiveness of products (services)	3
Degree of compliance of equipment and technologies with market features and volumes	2
Capacity building (expansion of existing capacities)	3
Efficiency	2
Flexibility	3
Complexity	3
Universality	2
Ease of adaptation	1
Total	22

Table 4. *Estimate of the Level of Personnel Qualification in Talas Investment Company*

Indicator	Values
Number of employees in the unit on average, persons	120
Number / share of employees working in the specialty, with higher education, persons/ %	110/92
Number of marketers, persons	5
Number / share of marketers with the 'master' qualification level, or the degree of Candidate (Doctor) of Economic Sciences, persons/ %	1/20
Number/share of employees raising their qualification level, persons/ %	7/8.4

Table 5. *Estimate of the Level of the Personnel Management Efficiency (Motivation Of Personnel)*

Elements	Points		
	1	2	3
Application of methods for direct material remuneration (wages, bonuses, participation in profits)			3
Application of methods for indirect material remuneration (tuition fees, insurance, and pension provision)			3
Application of non-material motivation methods (flexible working hours)			3
Creating conditions for internal motivation (interesting work, opportunities for success, and self-realization)			3
Creating conditions for external motivation: recognition, promotion			3
Training of management personnel in motivation methods		2	
Use of the evaluation system for the working contribution to the results			3
System of staff participation in the profits		2	
Personnel participation in enterprise management		2	
Relations with trade unions	1		
Adaptation of personnel to the system of state regulation of labor relations		2	
Personnel recruitment, estimate and placement			3
Selection, estimate, and placement of management personnel (training, retraining and advanced training, formation of the managers' reserve, current assessment and certification, work with consultants and young specialists)			3
Total	33		

Downloaded from www.periodico.tchequimica.com

Table 6. *Determining the Type of Organization and the Degree of Aggressiveness of the Head*

Elements	Points		
	1	**2**	**3**
Active attitude to life and business			3
Encouraging reasonable risk		2	
Admittance of errors, non-standard situations		2	
Level of competition			3
Encouraging personnel training			3
Value of time			3
Level of regulation of the organization members' actions		2	
Value of the vertical and horizontal control			3
Value of standards and norms	1		
Support of beliefs and attitudes (myths, religion, rites, and rituals), tolerance		2	
Degree of discrimination (gender, age, etc.)			3
Total		26	

Table 7. *Results of X_{41}, X_{42} Estimates*

	a_{jmax}	a_{jmin}	a_{jf}	X_{ij}^{h}	**Estimate**
X_{41}	0.5	-0.15	0.18	0.5	C
X_{42}	0.3	-0.01	0.03	0.1	H

Table 8. *Estimate of the Management Structure Level*

Elements	Points
Commitment of the enterprise	3
Flexibility of the organizational structure	3
Transparency of the organizational structure	3
Efficiency of the enterprise	2
Proportionality of the number and complexity of the manager's tasks to the available time for their solution	1
Spirit of cooperation	2
Awareness of managers	1
Total	15

Downloaded from www.periodico.tchequimica.com

Table 9. *Estimate of the Level of the Modern Management Methods Application (Processes and Management Methodology)*

Elements	Points		
	1	2	3
Research and diagnostics of the current management system (the use of analytical materials for the study of the management system, organizational diagnosis, technical and economic calculations in various areas and opportunities for the development of the organizational system)		2	
Monitoring of changes in the external and internal environment	1		
Research, experiments, modeling, calculations in various areas to improve the efficiency and effectiveness of the control system	1		
The study of literary sources, the generalization of the world experience of successful enterprises (the results of research, domestic and foreign best practices in the construction of management systems of enterprises working effectively)	1		
Generalization and balancing of the organizational cutoff of other domestic and foreign prosperous enterprises	1		
Monitoring of legislative documents, norms, and standards for building of a management system		2	
Development of plans and programs for organizational development of the enterprise	1		
Application of strategic processes for monitoring and coordination of activities		2	
Use of modern information technologies			3
Creation of data and knowledge banks for the management decision support system	1		
Increase of the organizational and technical level of activity of separate management units and executors			3
Implementation of the system of improving the organization and working conditions	1		
Total		19	

Table 10. *Estimate of Level of the Enterprise's Social Responsibility*

Elements	Points		
	1	2	3
Production of quality products and services for consumers			3
Creation of attractive jobs		2	
Payment of legal salaries and investment in human development		2	
Strict compliance with legal requirements: tax, labor, environmental, etc.			3
Building good-faith relationships with all stakeholders		2	
Efficient business focused on creating added economic value and increasing the welfare of its shareholders		2	
Consideration of public expectations and generally accepted ethical standards in business practices	1		
Contribution to the formation of civil society through the partnership programs and projects of local community development	1		
Total		16	

Downloaded from www.periodico.tchequimica.com

Table 11. *Summary Estimate of Competitiveness of the 'Talas Investment Company' Chemical Industry Enterprise and its Components*

Complex Components	Indicators	Estimate of the Indicator	Estimate of Complex Indicator	Estimate
Internal Competitiveness				
Sustainability of the marketing system			H	
Sustainability of the production system	Level of application of advanced technologies to technological processes and equipment	C	B	
	Area of presence	B		
	Share of innovative equipment	B		
Sustainability of the personnel	Skill level of personnel	C	B	C
	Level of personnel management efficiency	B		
	Level of the corporate culture	B		
Financial and investment performance	Return on sales	C	C	
	Return on equity	H		
Management quality	The level of the management structure	C	C	
	Level of application of modern management methods	C		
Level of social responsibility			C	
External actions				
Supplier pressure			C	
Consumer pressure			B	
Level of competition			C	C
Level of state pressure			B	
Level of STP effect			B	

Downloaded from www.periodico.tchequimica.com

PERIÓDICO TCHÊ QUÍMICA
ARTIGO ORIGINAL

O EFEITO DE CAMADAS DIELÉTRICAS FINAIS DO SILÍCIO NA DINÂMICA DE AQUECIMENTO DE INTERCONEXÃO EM CHOQUE TÉRMICO

THE EFFECT OF THIN DIELECTRIC LAYERS AT SILICON ON INTERCONNECTION HEATING DYNAMICS AT THERMAL SHOCKS

ВЛИЯНИЕ ТОНКИХ ДИЭЛЕКТРИЧЕСКИХ СЛОЕВ НА КРЕМНИИ НА ДИНАМИКУ НАГРЕВА МЕЖСОЕДИНЕНИЙ В УСЛОВИИ ТЕПЛОВЫХ УДАРОВ

SKVORTSOV, Arkadiy A.[1*]; ZUEV, Sergey M.[2]; KORYACHKO, Marina V.[3]; SKVORTSOVA, Anna A.[4]

[1,4] Moscow Polytechnic University, Department of Dynamics, Durability of Machines and Resistance of Materials, Moscow – Russian Federation

[2] Moscow Polytechnic University, Department of Electrical Equipment and Industrial Electronics, Moscow – Russian Federation

[3] Moscow Polytechnic University, Department of Physics, Moscow, – Russian Federation

** Correspondence author*
e-mail: skvortsovaa2009@yandex.ru

Received 30 August 2019; received in revised form 20 October 2019; accepted 25 October 2019

RESUMO

A relevância do estudo se deve ao fato de que, nas condições de desenvolvimento da micro e nanoeletrônica, é necessário prestar atenção aos sistemas de comutação resistiva, que são a base nas estruturas dessas áreas da eletrônica. O trabalho trata da investigação do papel de finas camadas dielétricas de óxido e nitreto de silício na dinâmica de aquecimento de interconexão em placas monocristalinas de silício. O método principal para o estudo desse problema é o método do experimento, que permite identificar as características da influência da subcamada dielétrica nos regimes térmicos de sistemas multicamadas. É mostrado que a passagem de pulsos de corrente (amplitude de até $6 \cdot 10^{10}$ A/m^2 e uma duração de até 600 μs) leva a danos térmicos das interconexões até a interrupção do circuito elétrico. A natureza da destruição depende fortemente da qualidade da deposição de filmes dielétricos e metálicos, bem como do estado da interface metal-dielétrica. Verificou-se que os oscilogramas da inclusão, obtidos durante a passagem de um pulso de corrente, refletem claramente a mudança nos parâmetros dimensionais (h_2) e térmicos (λ_2) das subcamadas dielétricas; foram considerados os mecanismos de degradação térmica dos sistemas de metalização de alumínio com subcamadas dielétricas finas relacionadas à sua fusão; verificou-se que a formação de zonas fundidas está relacionada à redução local da seção transversal do filme e, consequentemente, ao aparecimento de uma zona fundida que se coagula em quedas no curso da corrente de pulso e promove a interrupção do circuito elétrico. O método proposto pode ser aplicado para avaliar as propriedades térmicas de filmes finos de dielétricos.

Palavras-chave: *comutação resistiva, interface metal-dielétrico, estrutura para altas temperaturas.*

ABSTRACT

The relevance of the study is due to the fact that in the conditions of development of micro-and nanoelectronics, it is necessary to pay attention to resistive switching systems, which are the basis in the structures of these areas of electronics. The work deals with the investigation of the role of thin dielectric layers of silicon oxide and nitride on interconnection heating dynamics at monocrystalline silicon plates. The leading method to the study of this problem is the method of experiment, which allows identifying the features of the influence of the dielectric sublayer on the thermal regimes of multilayer systems. It is shown that passage of current pulses (amplitude up to $6 \cdot 10^{10}$ A/m^2 and duration up to 600 μs) leads to thermal damage of interconnections right up to breaking the electric circuit. The character of destruction strongly depends on the quality of deposition of dielectric and metal films as well as on the state of the dielectric-metal interface. It was found that the oscillograms of the inclusion, taken during the passage of a current pulse, clearly reflect the change in the dimensional (h_2) and thermal (λ_2) parameters of the dielectric sublayers; considered the thermal degradation mechanisms of the aluminum metallization systems with thin dielectric sublayers related to its melting; it was found that formation of

Downloaded from www.periodico.tchequimica.com

melted zones is related to local reduction of film cross-section and consequently to the appearance of a melted zone that coagulates into drops in the course of current pulse passing and promotes breaking the electric circuit. The proposed method can be applied to assess the thermal properties of thin films of dielectrics.

Keywords: *resistive switching, metal-insulator interfaces, structure for high temperature.*

АННОТАЦИЯ

Актуальность исследования обусловлена тем, что в условиях развития микро- и наноэлектроники необходимо уделять внимание резистивным коммутационным системам, которые являются основой в структурах этих областей электроники Работа посвящена изучению роли тонких диэлектрических слоев оксида и нитрида кремния на динамику нагрева межсоединений на пластинах монокристаллического кремния. Ведущим методом к исследованию данной проблемы является метод эксперимента, позволяющий выявить особенности влияния диэлектрического подслоя на тепловые режимы многослойных систем. Показано, что прохождение токовых импульсов амплитудой до $6 \cdot 10^{10}$ A/m^2 и длительностью до 600 μs приводит к тепловому разрушению межсоединений вплоть до обрывов электрической цепи. Характер разрушений сильно зависит от качества нанесения диэлектрической пленки и пленки металла, а также состояния межфазной границы диэлектрик-металл. Обнаружено, что осциллограммы включения, снимаемые в процессе прохождения импульса тока, четко отражают изменение размерных (h_2) и тепловых (λ_2) параметров диэлектрических подслоев; рассмотрены механизмы тепловой деградации систем алюминиевой металлизации с тонкими диэлектрическими подслоями, связанные с её оплавлением; выявлено, что образование участков расплава связано с локальным уменьшением поперечного сечения пленки и, как следствие, появлению расплавленного участка, который в процессе прохождения импульса сворачивается в капли и способствует обрыву токопроводящей линии. Предложенная методика может быть применена для оценки тепловых свойств тонких пленок диэлектриков.

Ключевые слова: *резистивное переключение, интерфейс металл-диэлектрик, структура для высоких температур.*

1. INTRODUCTION

It is well known that the resistive commutation systems (along with p-n junctions) are the key elements in the micro- and nanoelectronic structures (Shejko *et al.*, 2016, Ambrogio *et al.,* 2017; Shejko *et al.*, 2017; Iskovych-Lototsky *et al.*, 2019). This fact is related to a large extent to the constant tendency to structure miniaturization (Bermejo *et al.,* 2016; Long *et al.*, 2016) (which correspondingly results in increasing "thermal" loads on them), as well as requires structure operation speed (Hofmann *et al.,* 2004)

In this connection much attention is being given to metal-insulator-semiconductor structures and physical-mechanical processes that are basic to their operation: solid-state reactions at interfaces (Popok *et al.,* 2016; Dornic *et al*., 2018; Pichkur *et al.*, 2015), diffusion and aggregation of complexes, generation-recombination processes of charge carriers (Woirgard *et al.,* 2015; Brincker *et al*., 2018), problems of heat conduction in multilayer media (Skvortsov *et.al.*, 2016a; Hu *et, al*., 2012) and other transport phenomena (van Soestbergen *et al.,* 2010; Nguyen *et al.,* 2011; Hadała *et al.,* 2011).

It is also known that a semiconductor crystal is subjected to high thermoelastic stresses in the power of electronic devices, especially under the pulsed operating conditions (Gavryushin *et al.,* 2018a; Gavryushin *et al.,* 2018b). In this case, the metallization systems, contacts, and near-contact areas of a semiconductor structure are the most "vulnerable", because they have many interfaces and geometrical heterogeneities (Orlov *et al.*, 2003b; Skvortsov and Karizin, 2012; Skvortsov *et al.,* 2016a; Ruffilli *et al.,* 2017;). Therefore, the purpose of the present work is an investigation of the effect of thin dielectric layers on the heating dynamics of interconnections on silicon under a surface thermal shock.

2. MATERIALS AND METHODS

In this work, the metal-semiconductor and metal-dielectric-semiconductor structures were studied. The monocrystalline silicon plates oriented in the (111) and (100) directions served as substrates. They were doped with phosphorus (it is the intentional introduction of impurities into an intrinsic semiconductor for the purpose of modulating its electrical, optical and structural properties); their resistivity varied in the

Downloaded from www.periodico.tchequimica.com

ρ = 1…0.01 Ω·cm range. When studying the Al-Si binary systems, a 30…50 μm *n*-epitaxial layer was deposited on some plates to prevent current flow through the semiconductor. Thin silicon oxide SiO_2 or silicon nitride Si_3N_4 films were deposited on some plates to compare temperature dependencies of λ_2 values. Aluminum (as the most popular metallization material in semiconductor structures) served as the conductive metal film (Beshajova and Martin, 2018). Registration of temperature changes in a thin-film structure was made using a test structure as a metallization track. Square current pulses were passed through it, with registering voltage drop U(t) from a part of the test structure. From the U(t) oscillograms, one can judge the dynamics of system heating in the course of current pulse passing. Moreover, the processes of irreversible degradation related to the appearance of melted regions in the structure are clearly reflected in the U(t) oscillograms. It was established that a potential-jump in the U(t) curve is definitely related to the appearance of melted Al fragments on the region analyzed.

Silicon nitride films were prepared using pyrolytic deposition of dichlorosilane with ammonia onto silicon plates at reduced pressure (~50 Pa) in the temperature range of 700-900°C. Deposition of silicon nitride films was realized at a specialized plant (Figure 1). It involved a quartz reactor (a quartz tube 100 mm in diameter (1, Figure 1) with a temperature-controlled zone), afore vacuum evacuation system (operating in the continuous mode with pump speed to 30 l/s) and a working gas (monosilane SiH4 and ammonia NH_3) feed system. A diffusion furnace provided a uniform temperature of operating zone at a length of 700 mm with an accuracy of ± 2 ºC.

The thermal oxide was grown in diffusion furnaces using the standard technology (Birouk and Madi, 2011) in the temperature range of 1150-1250°C in dry oxygen. A number of specimens a to isothermal annealing at 550°C in the inert atmosphere to stabilize contact properties and improve adhesion. The process of silicon thermal oxidation in oxygen or water vapor is usually described with resulting chemical reactions (Equations 1 and 2).

The films of thermal silicon oxide were grown in a flow reactor with vertical plates (Figure 2) in "dry" oxygen (O_2) and in "wet" oxygen – with the presence of water vapor (O_2 + H_2O).

A choice of oxidation method was determined by the required thickness and properties of the formed oxide. The required thin (< 0.5 μm) oxide films were grown in dry oxygen. To this end, the boats with plates (2, Figure 2) were gradually moved into the furnace heated to 800÷900 °C. To prevent substrates warping, the temperature was gradually raised to the required value (900 - 1200 °C) and was supported in the course of oxidation with an accuracy of ± 1 °C. After completing the oxidation process, the temperature in the furnace was gradually reduced, and the substrates were taken out.

The formation of test structures was performed with optical photolithography (Figure 3, a-d). The investigation of test structures was made using the voltmeter-ammeter method from the electrical response taken from different structure areas in the passage of single current pulses of different forms (Skvortsov *et al.,* 2018; Skvortsov *et al.,* 2016b). The experimental investigation of degradation processes was performed for the test structures (Figure 3, e) from the switching oscillograms $U(t)$. They were taken by the appropriate probes in the course of current pulse passage and were recorded with a digital oscillograph.

The temperature dynamics of metallization track $T_1(t)$ was calculated from the variation of voltage drop $U(t)$ (Equation 3).

Here R_0 = 0.88 Ω is the metallization track resistance at T_0 = 290 K measured with the voltmeter-ammeter method; α = 0.0043 K^{-1} is the aluminum temperature coefficient of resistance.
The metallographic studies of the results of degradation processes were performed using a digital optical 3D microscope Keyence VHX6000.

3. RESULTS AND DISCUSSION:

It was noted that the temperature variations of the structures under investigation were judged from the switching oscillograms. Figure 4 presents the typical results of these investigations for systems with a dielectric SiO_2 sublayer. The obtained curves are described by known Equation 4 (Orlov *et al.*, 1996).

Here and further the indices "1", "2" and "3" apply, correspondingly, to the aluminum metallization, dielectric sublayer, and semiconductor substrate; h is thickness; λ is thermal conductivity: c, d and a are, correspondingly, thermal capacity, density, and thermal conductivity.

Because all the parameters depend on temperature, so as before (Orlov *et al.,* 2003a), we used their temperature-averaged values to calculate T_1. To this end, the studied temporal

Downloaded from www.periodico.tchequimica.com

interval was divided into small time intervals Δt. The averaged value of each parameter was calculated as the average integral value taken by it in all elementary intervals. (E.g., the average integral value of b is Equation 5). One can see from Equation 4 that the structure heating dynamics depends on the current strength and parameters of the semiconductor matrix, as well as on thermal conductivity and thickness of the intermediate dielectric film.

The thickness of dielectric sublayer strongly influences the thermal conditions of multilayer systems (see Figure 4). To illustrate, changing the intermediate film thickness h_2 of silicon oxide from 0.1 μm to 0.16 μm increases temperature T_1 of Al film from 390 K to 440 K at t = 400 μs from the moment of pulse switching (Figure 4, dashed line). This leads to an earlier structure overheating: at the same current density $j = 5.5 \cdot 10^{10}$ A/m^2, the thicker is the intermediate semiconductor layer, the quicker is metallization tracks warm-up (Figure 4).

The presence of dielectric sublayers with different λ_2 values is also clearly represented on oscillograms at the passage of current pulses. There is a big difference between the heat-conducting properties of silicon oxide films and silicon nitride films at different temperature modes of metal layers operation when passing current pulses of the same electric power. This is clearly shown in Figure 5.

Thus the switching oscillograms clearly represent a variation of the dimensional (h_2) and thermal (λ_2) parameters of sublayers. Using the experimental switching oscillograms and the data on thicknesses of dielectric films, we calculated the temperature dependences of λ_2 values for the studied SiO_2 and Si_3N_4 films from the following Equation 5.

The results of the calculations from Equation 6 are presented in Figure 6.

It can be observed that the obtained results agree well with the known literature data for films of silicon oxide (Zhu *et al.*, 2018; Gu and Wang, 2018) and silicon nitride (Fong *et al.,* 2016). Thus the proposed procedure can be applied to estimate thermal properties of thin dielectric films.

Earlier (Skvortsov *et al.,* 2018; Skvortsov *et al.,* 2016a) we revealed that, at high-power electric pulses (pulse duration $\tau \sim 500$ μs and pulse power P_i = 5…17 W), the degradation processes in the binary metallization systems are related to formation of a melted zone (when the metal melting temperature is achieved) and contact melting processes that occur at the metal-semiconductor interface.

Contrary to the Al-Si systems, the presence of thin dielectric films on semiconductor surface prevents the processes of contact melting in the metal-semiconductor system. Therefore, the beginning of the degradation processes is related solely to Al melting. It is accompanied by an abrupt potential-jump $U(t)$ at the oscillograms followed with its oscillation and a jump related to conducting channel breakdown. Growth of current density to the $j \sim 8 \cdot 10^{10}$ A/m^2 values appreciably promotes complete melting of the test structure (Figure 7).

Formation of melted zones has been discussed earlier (Brincker *et al.,* 2018). We ascribed this to the processes of electric transfer and thermal diffusion in the defective areas of metal track. Local reduction of film cross-section leads to an increase of current density and consequently to the appearance of a melted zone. In this case, melted metal coagulates into drops, and the conducting line breaks.esults should be presented concisely. Also, point out the significance of the results and place the results in the context of other work and theoretical background.

4. CONCLUSIONS:

It was considered the effect of thin dielectric layers of silicon oxides and silicon nitrides on heating dynamics of interconnections at monocrystalline silicon plates using the oscillographic method. It was found that the switching oscillograms taken in the course of current pulse passing clearly reflect the variation of the dimensional (h_2) and thermal (λ_2) parameters of dielectric sublayers. Using the experimental switching oscillograms and the data on the thicknesses of dielectric films, we calculated the temperature dependences of the SiO_2 films and Si_3N_4 films studied. This proved that the proposed method could be applied to assess the thermal properties of thin films of dielectrics.

It was also shown that passage of current pulses with amplitude up to $6 \cdot 10^{10}$ A/m^2 and duration up to 600 μs results in thermal damage of interconnections right up to breaking the electric circuit. We considered the thermal degradation mechanisms of the aluminum metallization systems with thin dielectric sublayers related to its melting. It was found that

Downloaded from www.periodico.tchequimica.com

formation of melted zones is related to local reduction of film cross-section and consequently to the appearance of a melted zone that coagulates into drops in the course of current pulse passing and promotes breaking the electric circuit.

5. ACKNOWLEDGMENTS:

The reported study was funded by RFBR according to the research project No. 18-29-27005.

6. REFERENCES:

1. Ambrogio, S., Magyari-Köpe, B., Onofrio, N., Mahbubul, I.M., Duncan, D., Nishi, Y., Strachan, A. *Journal of Electroceramics,* **2017**, *7*, 1-4.
2. Bermejo, R., Krautgasser, C., Deluca, M., Pletz, M., Supancic, P., Aldrian, F., Danzer, R. *Journal of Microelectronics and Electronic Packaging*, **2016**, *13*(1), 17-22.
3. Beshajova, I.P., Martin, M. *Proceedings of the International Spring Seminar on Electronics Technology*, **2018**, *2018*, Article number 8443684.
4. Birouk, B., Madi, D. *Applied Physics A: Materials Science and Processing*, **2011**, *104*(2), 739-748.
5. Brincker, M., Walter, T., Kristensen, P.K., Popok, V.N. *Journal of Materials Science: Materials in Electronics*, **2018**, *29*(5), 3898-3904.
6. Dornic, N., Ibrahim, A., Khatir, Z., Tran, S.H., Ousten, J.-P., Ewanchuk, J., Mollov, S. *Microelectronics Reliability*, **2018**, *88-90*, 462-469.
7. Fong, S.W., Sood, A., Chen, L., Kumari, N., Asheghi, M., Goodson, K.E., Gibson, G.A., Wong, H.-S.P. *Journal of Applied Physics*, **2016**, *120*(1), 015103.
8. Gavryushin, S.S., Skvortsov, P.A., Skvortsov, A.A. *Periodico Tche Quimica*, **2018a**, *15*(Special Issue 1), 174-181.
9. Gavryushin, S.S., Skvortsov, P.A., Skvortsov, A.A. *Periodico Tche Quimica*, **2018b**, *15*(30), 678-686.
10. Gu, H., Wang, H. *Computational Materials Science*, **2018**, *144*, 133-138.
11. Hadała, B., Cebo-Rudnicka, A., Malinowski, Z., Gołdasz, A. *Archives of Metallurgy and Materials*, **2011**, *56*(2), 367-377.
12. Hofmann, M., Gemming, T., Wetzig, K. *Analytical and Bioanalytical Chemistry*, **2004**, *379* (4), 547-553.
13. Hu, C.-K., Ohm, J., Gignac, L.M., Breslin, C.M., Mittal, S. *Journal of Applied Physics*, **2012**, *111*, 093722.
14. Iskovych-Lototsky, R.D., Bulyha, Y.V., Kobylyanska, I.M., Kotyra, A., Kalizhanova, A., Amirgaliyev, Y.d, *Przeglad Elektrotechniczny*, **2019**, *95*(4), 36-40.
15. Long, S.B., Liu, Q., Lv, H.B., Liu, M. *Scientia Sinica: Physica, Mechanica et Astronomica,* **2016**, 46(10), 107-111
16. Nguyen, T.A., Joubert, P.-Y., Lefebvre, S., Chaplier, G., Rousseau, L. *Microelectronics Reliability*, **2011**, *51*, 1127-1135.
17. Orlov, A.M., Kostishko, B.M., Skvortsov, A.A. *Structures. Inorganic Materials*, **1996**, *32*(3), 246-249.
18. Orlov, A.M., Skvortsov, A.A., Litvinenko, O.V. *Technical Physics*, **2003a**, *48*(6), 736-741.
19. Orlov, A.M., Skvortsov, A.A., Solov'ev, A.A. *Zhurnal Eksperimental'noj i Teoreticheskoj Fiziki*, **2003b**, *123*(3), 590-599.
20. Pichkur, V., Lazarenko, M., Alekseev, O., Kovbasa, V., Lazarenko, M. *Eastern-European Journal of Enterprise Technologies*, **2015**, *1*(6), 52-56
21. Popok, V.N., Pedersen, K.B., Kristensen, P.K., Pedersen, K. *Microelectronics Reliability*, **2016**, *58*, 58-64.
22. Ruffilli, R., Berkani, M., Dupuy, P., Lefebvre, S., Weber, Y., Legros, M. *Microelectronics Reliability*, **2017**, *76-77*, 507-511.
23. Shejko, S., Shalomeev, V., Mishchenko, V. *Materials Science and Technology Conference and Exhibition 2017, MS and T 2017*, **2017**, *1*, 238-244.
24. Shejko, S., Yechyn, S., Demchenko, N. *Materials Science and Technology Conference and Exhibition 2016, MS and T 2016*, **2016**, *1*, 353-358.

Downloaded from www.periodico.tchequimica.com

25. Skvortsov, A., Zuev, S., Koryachko, M., Glinskiy, V. *Microelectronics International*, **2016a**, *33*(2), 102-106.
26. Skvortsov, A.A., Karizin, A.V. *Journal of Experimental and Theoretical Physics*, **2012**, *114*(1), 85-88.
27. Skvortsov, A.A., Zuev, S.M., Koryachko, M.V. *Key Engineering Materials*, **2018**, *771*, 118-123.
28. Skvortsov, A.A., Zuev, S.M., Koryachko, M.V., Glinskiy, V.V. *Microelectronics International*, **2016b**, *33*(2), 102-106.
29. van Soestbergen, M., Mavinkurve, A., Rongen, R.T.H., Jansen, K.M.B., Ernstb, L.J., Zhang, G.Q. *Electrochimica Acta*, **2010**, *55*, 5459-5469.
30. Woirgard, E., Arabi, F., Sabbah, W., Martineau, D., Theolier, L., Azzopardi, S. *Microelectronics Reliability*, **2015**, *55*(9-10), 1961-1965.
31. Zhu, W., Zheng, G., Cao, S., He, H. *Scientific Reports*, **2018**, *8*(1), 10537.

$Si + O_2 = SiO_2$ (Eq. 1)

$Si + 2H_2O = SiO_2 + 2H_2$ (Eq. 2)

$$U(t) = I(t)R_0\left[1+\alpha(T_1(t)-T_0)\right]. \quad \text{(Eq. 3)}$$

$$T_1 = T_0 + \frac{I^2 \bar{R}_1}{S}\left(\frac{h_2}{\bar{\lambda}_2} + \frac{1}{\bar{c}_3 \bar{d}_3}\sqrt{\frac{t}{\bar{a}_3}}\right) \quad \text{(Eq. 4)}$$

$$\bar{b} = \frac{1}{\Delta T}\int_{T_0}^{T_1} b(T)\,dT \quad \text{(Eq. 5)}$$

$$\bar{\lambda}_2 = \frac{h_2}{\left(\frac{\Delta T_1 \cdot S}{I^2 \bar{R}_1} - \frac{1}{\bar{c}_3 \bar{d}_3}\sqrt{\frac{t}{\bar{a}_3}}\right)} \quad \text{(Eq. 6)}$$

Downloaded from www.periodico.tchequimica.com

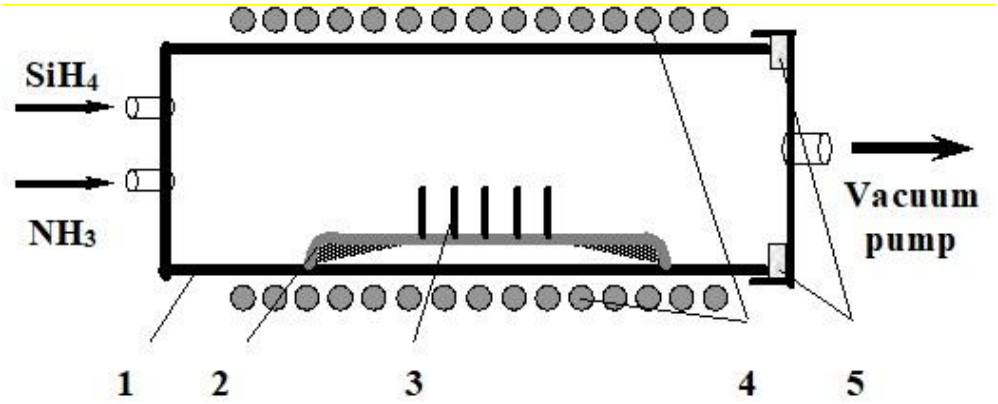

Figure 1. *Diagram of installation for deposition of pyrolytic silicon-based films: 1 – quartz reactor, 2 – boat for silicon plates 76 mm in diameter, 3 – vertical silicon plates, 4 – resistance heater, 5 – compactors*

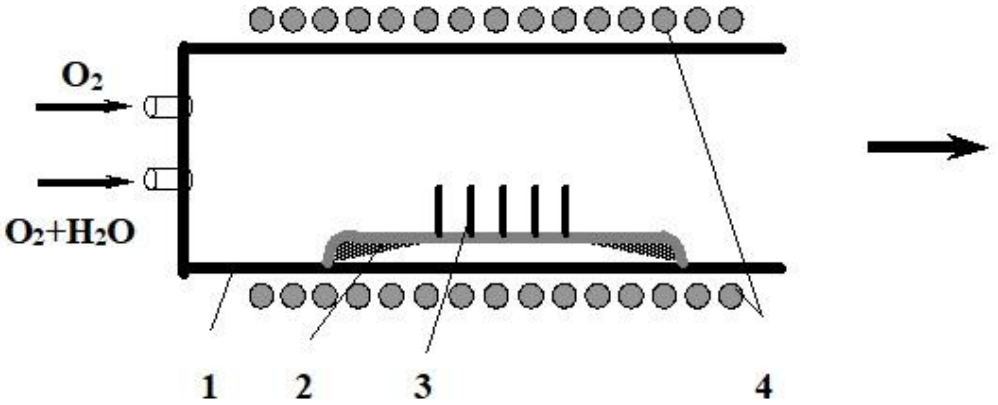

Figure 2. *Diagram of installation for growth of thin silicon oxide films:* ***1 –*** *quartz reactor,* ***2 –**** *boat for silicon plates 76 mm in diameter,* ***3 –*** *vertical silicon plates,* ***4 –*** *resistance heater providing temperature in the isothermal zone to 1200 °C*

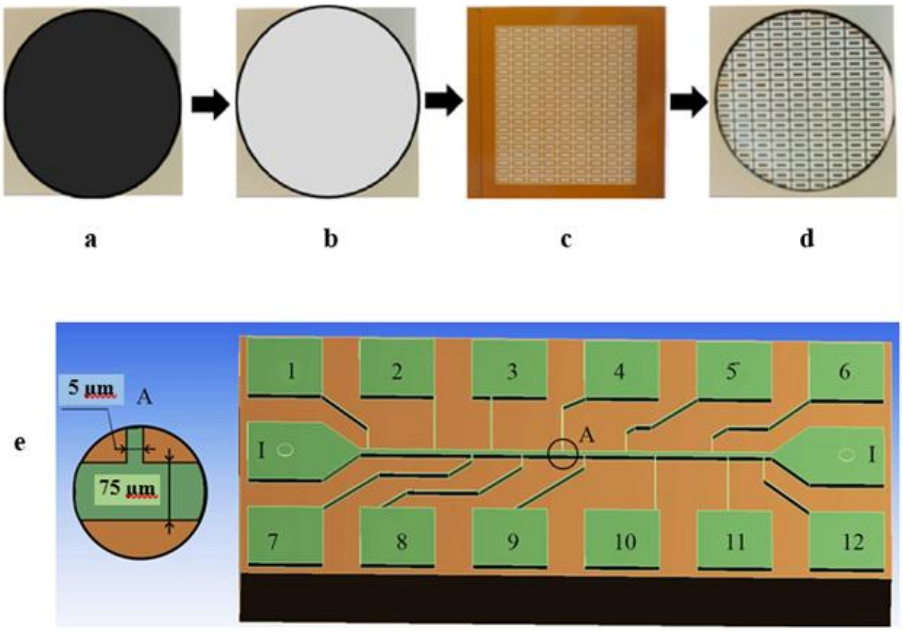

Figure 3. *Photographs of a 76 mm silicon plate (a) with a sprayed aluminum film (b), a working photomask (c) and a silicon plate after structures formation (d). A 3D model of a metal film-semiconductor plate test structure (e) to study temperature modes of metallization tracks: I – current area, 1-12 – contact areas to record oscillograms*

Downloaded from www.periodico.tchequimica.com

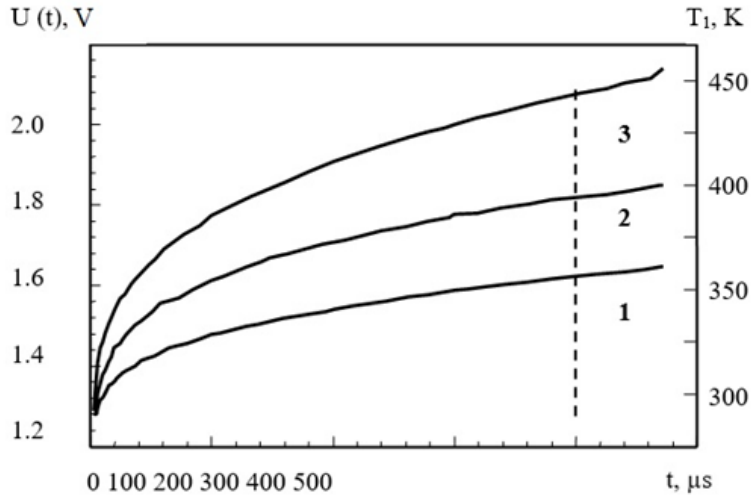

***Figure 4**. Switching oscillograms taken from an area of the Si-SiO_2-Al system test structure at passage of a single current pulse (amplitude of $5.5 \cdot 10^{10}$ A/m^2) at different thicknesses of dielectric sublayer: 1 – $h_2 = 0$; 2 – $h_2 = 0.1$ μm; 3 – $h_2 = 0.16$ μm; $h_1 = 2.5$ μm. The pulse duration of 450 μs*

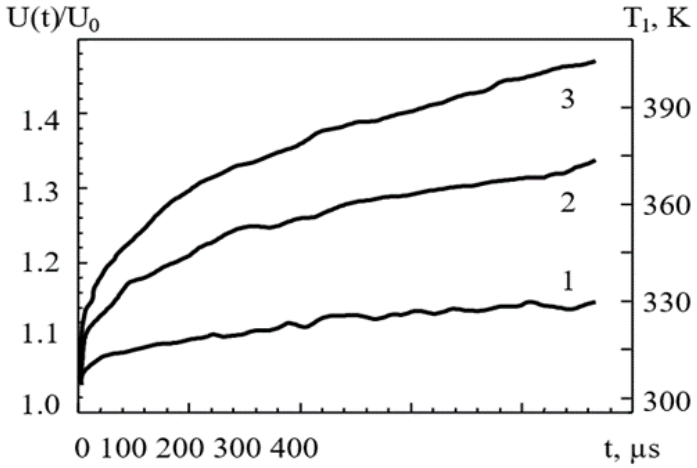

***Figure 5**. Switching oscillograms of a Si-dielectric-Al system at the passage of a single current pulse (amplitude $j = 3 \cdot 10^{10}$ A/m^2, duration 450 μs); $h_1 = 5$ μm, $h_2 = 0.1$ μm: **1** – $h_2 = 0$; **2** – Si_3N_4; **3** – SiO_2*

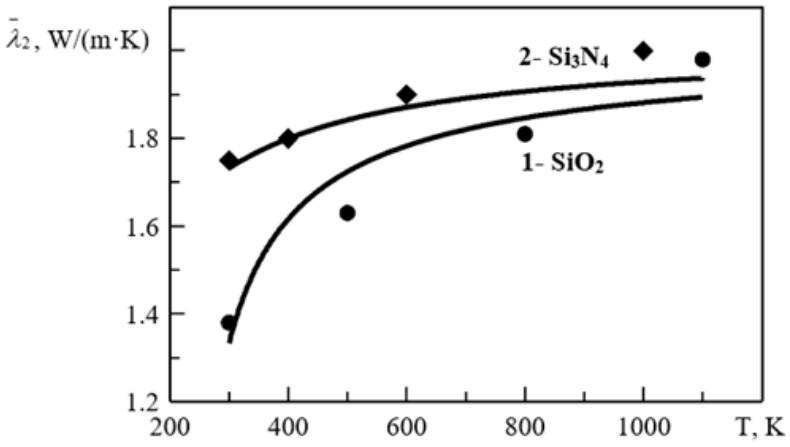

***Figure 6**. Results of calculation of temperature dependences of $\bar{\lambda}_2$ for SiO_2 films (**1**) and Si_3N_4 films (**2**): ● – the experimental data for SiO_2 films from (Zhu et al., 2018; Gu and Wang, 2018), ♦ – those for Si_3N_4 films from (Fong et al., 2016)*

Downloaded from www.periodico.tchequimica.com

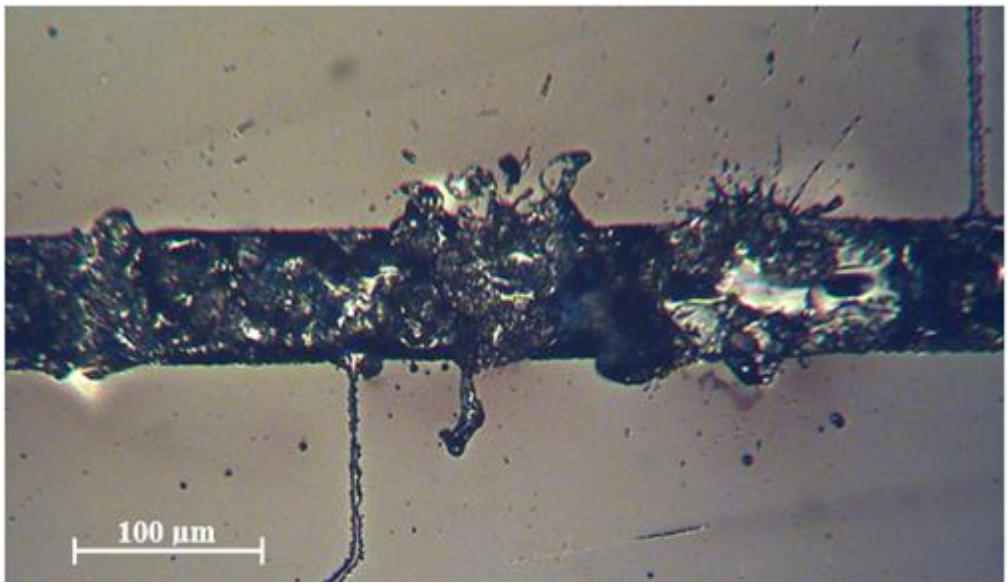

***Figure 7**. Photograph of melting fragment of an Al-SiO_2-Si test structure after the passage of a square current pulse (amplitude $j = 8 \cdot 10^{10}$ A/m^2 and duration τ = 500 µs)*

Downloaded from www.periodico.tchequimica.com

PERIÓDICO TCHÊ QUÍMICA
ARTIGO ORIGINAL

SISTEMA DE AVALIAÇÃO DA QUALIDADE ORIENTADA PELA WEB PARA ÁGUAS SUPERFICIAIS DA BACIA DO RIO

WEB-ORIENTED QUALITY ASSESSMENT SYSTEM FOR SURFACE WATERS OF RIVER BASIN

ВЕБ-ОРИЕНТИРОВАННАЯ СИСТЕМА ОЦЕНКИ КАЧЕСТВА ПОВЕРХНОСТНЫХ ВОД РЕЧНОГО БАССЕЙНА

JAMALOV, Jalal K.[1*]; NURSEITOV, Daniyar B.[2]; GOTOVTSEV, Alexey V.[3];

[1,2] Satbayev University, Institute of Information and Telecommunication Technologies, Almaty – Republic of Kazakhstan

[3]Russian Academy of Sciences, Institute of Water Problems, Moscow – Russian Federation

** Correspondence author*
e-mail: j.jamalov@norlist.kz

Received 30 August 2019; received in revised form 20 October 2019; accepted 25 October 2019

RESUMO

Este artigo apresenta o SaaS (software como serviço) que permite criar modelagem de cenário de transferência de poluição para fontes difusas de poluição usando o exemplo da bacia do rio Ili (República do Cazaquistão). Foi analisado o desenvolvimento de tecnologias que determinam o estado hidrológico do lago e da água. A praticabilidade de modelar as descargas e a distribuição de poluentes foi comprovada. O software FORTRAN (Programa de Simulação Hidrológica), um modelo de computador que nos permite modelar a concentração de compostos de nitrato (NO_3), amônia total e consumo de oxigênio bioquímico com resolução de um dia para o período de 1980 a 2016, foi descrito. O modelo foi calibrado usando os dados de observações de campo de seis postos hidrológicos, o que possibilitou a obtenção de valores satisfatórios de vazão de água. Para trabalhar com o sistema, foi desenvolvida uma interface gráfica que permite ao usuário que não está familiarizado com o software FORTRAN fazer cálculos. Foi implementado um algoritmo para o início automatizado de cálculos de cenário com pós-processamento e apresentação de resultados. A abordagem baseada na Web facilita o acesso multiusuário, único e rápido ao sistema de qualquer lugar do mundo. A eficiência dos resultados da programação foi investigada e a dinâmica das mudanças após o uso do software FORTRAN foi estabelecida.

Palavras-chave: *rio Ili, modelagem, poluentes, sistema de informação geográfica, software.*

ABSTRACT

This article presents the Software as a service system that allows creating scenario modeling of pollution transfer for diffuse sources of pollution using the example of the Ili river basin (Republic of Kazakhstan). The development of technologies that determine hydrological state of the lake and water in it are analyzed. The practicability of modeling the discharges and distribution of pollutants is substantiated. The FORTRAN Hydrological Simulation Program software, a computer model that allows us to model the concentration of nitrate compounds (NO_3), total ammonium, and biochemical oxygen consumption with one day time resolution for the period from 1980 to 2016 was described. The model was calibrated using the field observations data from 6 hydrological posts, which made it possible to obtain satisfactory water discharge values. To work with the system, a graphical interface was developed which allows the user who is not familiar with the FORTRAN Hydrological Simulation Program software to make calculations. Implemented was an algorithm for automated starting of scenario calculations with post-processing and presentation of results. The web-based approach facilitates multi-user, one-time and fast access to the system from anywhere in the world. The efficiency of results of programming was investigated and the dynamics of changes after using the FORTRAN Hydrological Simulation Program software was established.

Keywords*: Ili River, modeling, pollutant, geoinformation system, software.*

Downloaded from www.periodico.tchequimica.com

АНОТАЦИЯ

В данной статье представлена SaaS (программное обеспечение как услуга) система, позволяющая производить сценарное моделирование переноса загрязнения для рассеянных источников загрязнения на примере бассейна реки Или (Республика Казахстан). Проанализировано развитие технологий, которые определяют гидрологическое состояние озера и воды в нем. Изучены текущие данные об исследуемом регионе, а именно о русле реки, озерах, суб-бассейнах и точках сбора метеорологической информации. Были определены входные данные, в том числе цифровая модель рельефа Или-Балхашского региона, карты речных сетей, карты землепользования, карты почв, метеорологические данные. Обоснована целесообразность моделирования сбросов и распространения загрязняющих веществ. Описана, полученная в программном обеспечении Hydrological Simulation Program FORTRAN, компьютерная модель, которая позволяет моделировать концентрацию нитратных соединений (NO_3), общего аммония (TAM), и биохимическое потребление кислорода с ежедневным временным разрешением на период с 1980 по 2016 года. Произведена калибровка модели с использованием данных натурных наблюдений 6 гидрологических постов, что позволило получить удовлетворительные значения расходов воды. Для работы с системой разработан графический интерфейс, позволяющий пользователю, не знакомому с программным обеспечением Hydrological Simulation Program FORTRAN, производить расчеты. Реализован алгоритм автоматизированного запуска сценарных расчетов с пост-обработкой и представлением результатов. Веб-ориентированный подход обеспечивает многопользовательский, единовременный и быстрый доступ к системе из любой точки мира. Изучена эффективность результатов программирования и выяснена динамика перемен после использования программного обеспечения Hydrological Simulation Program FORTRAN.

Ключевые слова: *река Или, моделирование, загрязняющие вещества, геоинформационная система, программное обеспечение.*

1. INTRODUCTION

A web-based system was developed using ASP.NET MVC technology, which provides the possibility to model the concentration of pollution and water flow for any part of the river network for a given time period. The river basin was selected as the region for study, or since the river is one of the largest transboundary rivers connecting the Republic of Kazakhstan and China, and is also one of the most important sources of fresh water for the Republic of Kazakhstan. It provides about 80% of the total water inflow to Lake Balkhash, of which 70% is formed in China (Kovalov *et al, 2017*; Akbayeva *at al.*, 2019). This is described in detail in these publications (Dostay *et al*., 2013; Pueppke *et al*., 2018a). Since the beginning of intensive economic activity, the volume of pollution increased (Pueppke *et al*., 2018b). A decrease in water flow has provoked a violation of the natural state of the ecosystem, including the hydrological state of the lake (Zonn *et al*., 2018). With regard of these problems, it is necessary to analyze water consumption, to assess water quality and to apply effective water management (Talismanov *et al.*, 2017; Talismanov *et al.*, 2018a; Talismanov *et al.*, 2018b). The use of GIS technologies significantly simplifies the presentation of spatial information, and also provides a convenient and user-friendly interface for working with geo-data. Figure 1 demonstrates the starting page of the system, which presents the current data on the studied region, namely:

1) the main bed of the Ili River, taking into account external tributaries;

2) bathymetry of Lake Balkhash and Kapchagai reservoir, obtained during the field studies described in paragraph 2.5;

3) the isolines of Lake Balkhash and Kapchagai reservoir, calculated based on bathymetry data and Landsat 8 image processing;

4) Divided into sectors the Ili River sub-basin, obtained as a result of processing digital elevation model and map of the river network described in clause 2.2;

5) points of collection of meteorological information obtained for the processing of the European Center for Medium-Range Weather Forecasts (ECMWF Reanalysis datasets ERA-Interim), described in clause 2.2.

Storage and visualization of layers is implemented by Geoserver tools and the OpenLayers open library. To simulate the assessment of changes in concentration of fertilizers, as well as scenarios for reducing the flow of water to the territory of the Republic of Kazakhstan, a hydrological model has been developed. Simulation modeling is considered as an essential methodical supplement for obtaining

Downloaded from www.periodico.tchequimica.com

information about dynamics of distributed parameters of water bodies. Similar studies assessing water quality using the HSPF model were presented (Alarcon and Sassenrath, 2017). Software integration of the model, as well as recommendations for model calibration are presented (Lampert and Wu, 2015; Lampert and Wu, 2018; Alarcon and Sassenrath, 2016; Alarcon *et al*., 2017; Terleev *et al*., 2019). The methodology of research is described in detail in paragraph 2.

2. MATERIALS AND METHODS

In order to create a hydrological model, the following input data were defined in the HSPF software: 1) Digital elevation model of the Ili-Balkhash area; 2) River Networks Maps; 3) Land use map; 4) Soil map; 5) Meteorological data. The algorithm for automated data processing was developed and presented in Figure 2.As can be seen from Figure 2, the following tools were involved in algorithm:

1) The Watershed Delineation Tool (WDT) is a tool implemented in Better Assessment Science Integrating point & Non-point Sources software (BASINS 4.1) (EPA: Better Assessment…, 2019), which provides for the separation of collecting basin into sub-basins, described in section 2.2.

2) Hydrological Simulation Program - Fortran - a program that builds a hydrological model (Donigian *et al*., 1983).

3) WDMUtil (Watershed Data Management Utility) is an utility for processing time series of meteorological information (Brignoli *et al*., 2017).

4) Publish module - module of automatic publishing of vector layers at the server

5) Geoserver - a server for storing and presenting spatial information

The mechanism of changing the configuration file User Control Input (UCI) has been implemented via web interface, which allows generating various modeling scenarios.

2.1. Computational tools

By using HSPF, a computer model was obtained for modeling the basin hydrology, diffuse sources of pollution and water quality, Figure 3. Figure 3 shows a model in the HSPF software. But physically, the model is a generated UCI file, which can be changed using any programming language with the observance of the syntax of the HSPF. The developed writing mechanism, written in the Python programming language, provides the correct file changing, and allows to make changes without opening the software. Figure 4 shows a recording functions.

The write_to_uci function writes to configuration file. An entry includes a set of parameters, based on which the function defines the following: 1) the section of river for which the calculation is performed; 2) pollutant, function of pollutant can be used for both point and not point sources of pollution; 3) number of time series in which the result of calculation will be written. The write_to_wdmout function creates a time series in the file. A time series must be created for each new parameter written in UCI file, otherwise the calculations will be performed with an error.

In order to obtain most accurate results, the model is calibrated using data from 6 hydrological posts of Table 1 and cross-section data obtained during field observations described in clause 2.4. Table 1 presents the data of hydro stations that constantly monitor the Ili River. They provide the data on hydrological and hydrochemical regimes of the river.

2.2. Processing of data

Data sets (DEM, River net, Land Use) with a spatial resolution of 30 m were used to divide catchment basin into sub-basins. DEM and River net data were obtained from the ASTER Global Digital Elevation Model V2 open database (ASTGTM) and USGS HydroSHEDS. Land use data are taken from the Global Land Cover 2000 Project (GLC 2000) of the Science and Knowledge Service of the European Commission. The results of the processing of land use data are in Table 2, which shows land cover for the studied region. For a visual representation of the land use data, sub-basins were shown in Google Earth software in Figure 5.

As it can be seen from Figure 5, the cover of shrubs, evergreen areas comprise up to 30% of the current cover of the Ili river basin. Grass cover, closed-open areas cover approximately 12% of the catchment area, and tree cover, areas of mixed type of leaves reach up to 8%. Eroded soils and badlands take 32% of the catchment area. Hydrological processes, in its turn, vary over time and depend on changes in the state of environment, and to assess pollution of dispersed sources, a sequence of hourly precipitation, evaporation, temperature, and other meteorological data is required. Table 3 shows all

Downloaded from www.periodico.tchequimica.com

the meteorological parameters that were used in calculations.

Meteorological data from ECMWF ERA-Interim reanalysis data set for the period 1979–2016 was used. Data from 6 points, which are displayed in Figure 1, were extrapolated to the catchment area. Temperature data were used to estimate potential total evaporation (PEVT) for the catchment of Ili river. The Penman-Monteith equation was used to generate the PEVT dataset to develop the model.

2.3. Hydrological modeling and water quality modeling

A field survey was done to measure the baseline flux as well as to collect water samples and measure the total concentration of pollutants during May-June 2017. During the research work, field data were obtained from 20 cross-sections. Figure 6. Starting from the hydrological border post - the quay of Dubun approximately every 20 km downstream in the straight sections of the river with one canal, transverse profiles were constructed. The cross-sectional area of the river was instrumentally measured to determine the flow of water, which, in turn, is necessary to determine the transferred mass of the solute. Along the entire length of the river, without taking into account the Kapshagai reservoir, in the upper flow of the Ili River, 10 transverse profiles were built (Figure 6: red line with points) before merging with the Kapshagai reservoir, and 9 transverse profiles (Figure 6: green line with points) downstream the Ili River from the Kapshagay HPP to Kunaevsky Automobile Bridge. Samples of water and bottom sediments were sampled for chemical analysis in the stationary laboratory of the Institute of Geography for ionic composition of water (NO_3, NH_4, BOD, Ca_2^+, Mg_2^+, Na^+, K^+, SO_4^{2-}, Cl^-, HCO_3^-) and so on.

These field and laboratory measurements were utilized to partially validate the simulated results. Table 4 shows the data of measurements. As it can be seen from table 3, the concentration of suspended sediments increases with decreasing water consumption, regardless of the direction of movement.

2.4. Development of the web system

The web application was developed on the ASP.NET MVC platform. An ASP.NET MVC application works on the Model View Controller model. This model makes it possible to separate the presentation (interface), model (data) and application logic into 3 separate components, so that each component can be changed independently, which greatly increases the efficiency and flexibility of the system. The system interface is comprised of two functional parts. The first panel was developed to render the map. All manipulations with geospatial data were visualized for this area (markers, scaling, geolocation, contours, etc.). Another panel was used to display information on both the initial (space-time coordinates) and calculated concentrations of pollutants.

The information panel also allows to see the coordinates of the mouse pointer as it moves around the map. A function that facilitates map display is functionality based on two APIs: ESRI ArcGIS for JavaScript and OpenLayers. Depending on the request, the scripts in the application may work with one or both of them. This makes the system an easy object-oriented technology for embedding maps into web applications.

The scheme of user interaction with system is shown in Figure 7. CreateOrder and ShowResult views were developed for working with the system (Bespalov *et al.*, 2019). The CreateOrder view is for dispersed sources of pollution; it should be selected from the options offered, and for point sources it is possible to create with the designation of the name and the indication of the daily load, Figure 8

The ShowResult view is intended to show the calculation results. The main part of the screen is dedicated to a map with layers of the river basin. The layers are interactive and by clicking on one of them, the information about it can be revealed. The ShowResult view is presented in Figure 9.In the upper right corner there is a panel for managing layers, with which you can enable or disable the corresponding layers. In addition, the results can be displayed as a table by clicking the "View data" button. Initialization of the map and displaing of layers is implemented using the OpenLayers open library:

```
var basemap = new ol.layer.Tile({
      source: new ol.source.XYZ({
         attributions: new ol.Attribution({
            html: 'Tiles &copy; <a
href="http://services.arcgisonline.com/ArcGIS/' +

'rest/services/World_Imagery/MapServer">ArcGIS</a>'
         }),
         url:
'http://server.arcgisonline.com/ArcGIS/rest/services/' +
            'World_Imagery/MapServer/tile/{z}/{y}/{x}'
      })
   })
```


Downloaded from www.periodico.tchequimica.com

The source of geo-data is the open source software Geoserver, integrated with PostgreSQL DBMS, Figure 10. The layers that have been manipulated in Geoserver can be obtained via Web Map Service WMS protocol:

```
var wmsUrl = '@geoserverUrl/geoserver/localhost/wms';
var meteoLayer = new ol.layer.Tile({
    visible: true,
    source: new ol.source.TileWMS({
        ratio: 1,
        url: wmsUrl,
        params: {
            'LAYERS': 'localhost:balkash_meteo',
            'FORMAT': 'image/png',
            'VERSION': '1.1.1',
            'STYLES': '',
            'SERVICE': 'WMS',
            tiled: true,
        },
        serverType: 'geoserver'
    }),
        zIndex: 3    });
```

In addition to the basic map, there are three more layers: a layer of catchment basins, a layer of river sections and a layer of meteorological data points. These layers are requested from the web application controller, which, in turn, receives them from Geoserver and sends them to display, where they are shown as vector images.

2.5. Scenario calculations

The performed scenario calculations are aimed at predicting changes in ecology of the Ili-Balkh region in order (hypothetically) to reduce the likelihood of depletion of Lake Balkhash. Four technical reports (Pueppke *et al*., 2018a; Zonn *et al*., 2018; Severskiy *et al*., 2016; Propastin, 2012) were employed to approximate “natural” conditions (that is, not disturbed by human activity). Besides increasing anthropogenic load, there are natural factors that reduce inflow, such as climate change and changes in the glaciers of the basin, described in detail in the report (Severskiy *et al*., 2016). Based on the report data, glacial systems in large basins, such as Balkhash (Central Asia), change simultaneously, linearly and with identical speeds. The average reduction rates of the Zailiysky – Kungei glaciers (the mountain system of Tien Shan, Central Asia) and the upper reaches of Ili for the period 1955/56–2008. amounted to 0.76%, 0.75% and 0.73% per year, respectively. The decrease in water inflow will cause a decrease in the level of Lake Balkhash, which will bring the following problems: increasing water salinity; increasing the concentration of pollutants; desertification of the area.

The research described in the report (Propastin, 2012) show that the maximum value of the absolute height of a water mirror was observed in July 2005 with a value of 342.52 m. This level of water in the lake was accompanied by an increased amount of sediment and temperature. This research will be taken into account for the further development of the hypothesis. Therefore, the following experiments will be conducted: 1. scenario with decreasing inflow by 13%, increase in precipitation; 2. scenario with decreasing inflow by 22%, reduced evaporation value; 3. scenario with decreasing inflow by 28%.

3. RESULTS AND DISCUSSION:

3.1 Results of simulation with reduced inflows

The monthly average water inflow for July 2005 was - 29,420 cubic feet per second or ~ 900 cubic meters per second (m^3 / s). The Figure 7 represents that at the maximum level, the average annual inflow into the lake is ~ 500 cubic meters per second. Although, the shallowing dynamics of the lake were observed until 2004 (Guillaume and Rizzolio, 2004). Losses were estimated at approximately 150 square kilometers of water surface. Accordingly, the hypothesis that when the inflow value is 500 m^3 / s, the maximum value of the lake level is reached. Figure 11 shows the results of inflow modeling at the river mouth.

Water inflow determines the amount of water flowing through the cross-sectional area of flow per unit of time. There is a pronounced low value of water inflow in 1991, due to low precipitation and high evaporation. The reverse situation was monitored in 2002, when high precipitation and low evaporation were recorded. In general, the average value of the water inflow is around ~ 450 m^3 / s.

3.2. Results of modeling changes in concentration of nitrogenous compounds

Figure 12 presents modeling of BOD (biochemical oxygen demand) for 3 scenarios. The mass concentration of oxygen dissolved in water, which is necessary under certain conditions of biological oxidation, is turning into water by organic and / or inorganic substances. Figures 13 and 14 sum up the annual volumes of nitrogenous compounds calculated using water consumption. In conditions of the considered

Downloaded from www.periodico.tchequimica.com

scenarios, where this influence (exact discharges) is not taken into account, the initial sources were expressed in increasing concentration with decreasing amount of water in all three scenarios, Figures 12, 13, 14. In the presence of external discharges this ratio will be even greater.

The dynamics of increasing BOD concentration is observed in conditions of decreasing water inflow, so an increase in concentration will entail a disruption of the biological self-purification process of the reservoir. The processes of biological self-purification are associated with consumption of oxygen dissolved in the water of the reservoir. To prevent disruption in the oxygen regime in a water body, the amount of organic matter entering the water bodies with sewage should not exceed a certain value corresponding to the amount of oxygen coming from the atmosphere. With the increase in household load the use of nitrate fertilizers increases, which in turn leads to an increase in the concentration of nitrogenous compounds in the water. Therefore, the dynamics of a sharp increase in the concentration of NO_3 and NH_4 in 1991 under conditions of low consumption were monitored. The specifics of increasing concentration prevail in each of the scenarios.

4. CONCLUSIONS:

This study shows that a web-based approach makes it easier for users to work with models targeted for specialized users. The implementation of this system allows users who have no experience with BASINS or HSPF to make scenario calculations. In the current implementation, only one geographic region has been considered, but thanks to MVC technology, it will be sufficient to add a new hydrological model for another region and it will not take much effort. The hydrological model and sediment transport model presented in this study can provide good estimates of sediment concentrations and inflow values on a daily, monthly, and annual time scale. The model calculates the total concentrations of pollutants that follow a seasonal pattern corresponding to what actually happens in the Ili river basin. The peak precipitation concentration values coincide with peak fluxes. This demonstrates that higher loads and deposits are formed during events with low flow rates. Scenarios 1, 2 and 3 decrease the power of peak flow events. While decreasing flow peaks, these scenarios also lead to an increase in pollutant concentrations. Scenario 3 provides the highest concentration for each year. The maximum increase for indicators is following: 1) BOD (biochemical oxygen demand) - in 2002, with an increase in water consumption - by 37%; 2) NO_3 (nitrates) - in 1991, at the lowest water consumption - by 39%; 3) TAM (Ammonium ion (NH_4^+)) - in 1992, with a reduced water flow rate - by 22%

In conclusion, the results of scenario modeling demonstrate that the hypothesis is correct in terms of reducing the volume of peak flows in total flow, i.e. If the drainage basin of the Ili river is restored to the approximate initial (natural) discharge of water, sediment transport and water will be more appropriate in current land use / land cover conditions.

5. ACKNOWLEDGMENTS:

We would like to thank reviewers for useful commentaries. The work is supported by the grant No 1049 \ GF4 of the Ministry of Education and Science of the Republic of Kazakhstan.

6. REFERENCES:

1. Akbayeva, L., Tulegenov, E., Omarbayeva, A., Kobetaeva, N., Nurgalieva, Z., Nurkeyev, Y., Martišová, P., Vietoris, V., Zhanabayev, A. *Journal of Food Sciences,* **2019**, *13(1)*, 25-31
2. Alarcon, V. J., Hernandez, A. J. P., Alcayaga, H. *17th International Conference on Computational Science and Its Applications*, Trieste, Italy, **2017**, 613-625.
3. Alarcon, V. J., Sassenrath, G. F. *16th International Conference on Computational Science and Its Applications*, Beijing, China, **2016**, 33-43.
4. Alarcon, V. J., Sassenrath, G. F. *International Journal of Agricultural and Environmental Information Systems,* **2017**, *8(2)*, 20-31.
5. Bespalov, Y.G., Vysotska, O., Porvan, A., Linnyk, E., Stasenko, V. A., Doroshenko, G. D., Omiotek, Z., Amirgaliyev, Y. Proceedings of *the International Scientific Internet Conference on Computer Graphics and Image Processing and 48th International Scientific and Practical Conference on Application of Lasers in Medicine and Biology,* CRC Press/Balkema, Leiden, **2019**, 101-110.

Downloaded from www.periodico.tchequimica.com

6. Brignoli, M. L., Espa, P., Batalla, R. J. *Journal of Soils and Sediments,* **2017**, I, 2187-2201.

7. Donigian, Jr. A. S. B., Haith, D. A., Walter, M. F. *HSPF Parameter Adjustments to Evaluate the Effects of Agricultural Best Management Practices.* Athens: U.S. EPA Environmental Research Laboratory, **1983**, 107 p.

8. Dostay, Z., Alimkulov, S., Tursunova, A., Myrzakhmetov, A. *Arabian Journal of Geosciences,* **2013**, *6(8)*, 3041-3047.

9. EPA: *Better Assessment Science Integrating Point and Nonpoint Sources (BASINS)*, **2019**. https://www.epa.gov/exposure-assessment-models/basins, accessed 20 April 2019.

10. Guillaume, Le S., Rizzolio, D. *UNEP Global Resource Information Database 'United Nations Environment Programme – Lake Balkhash"*, **2004**. https://na.unep.net/siouxfalls/datasets/datalist.php, accessed: 15 March 2019.

11. Kovalov, K. M, Alekseev, O. M., Lazarenko, M. M., Zabashta, Y. F., Grabovskii, Y. E., Tkachov, S. Y. *Nanoscale Research Letters*, **2017,** *12*, Article number 468.

12. Lampert, D. J., Wu, M. *Journal of Computing in Civil Engineering,* **2018**, *32(4)*, 166-174.

13. Lampert, D. J., Wu, M. *Environmental Modelling and Software* **2015**, *68*, 166-174.

14. Propastin, P. *Lakes and Reservoirs: Research and Management,* **2012**, *17(3)*, 161-169.

15. Pueppke, S. G., Iklasov, M.K., Beckmann, V., Nurtazin, S. T., Thevs, N., Sharakhmetov, S., Hoshino, B. *Sustainability,* **2018a**, *10(4)*, 1234.

16. Pueppke, S. G., Nurtazin, S. T., Graham, N. A. *Water,* **2018b**, *10(5),* 541.

17. Severskiy I., Vilesov E., Armstrong R., Kokarev A., Kogutenko L., Usmanova Z., Morozova V., Raup B. *Annals of Glaciology,* **2016**, *57(71)*, 382-394.

18. Talismanov, V. S., Popkov, S. V., Karmanova, O. G., Zykova, S. S., Chernobrovkina, A. P. *Journal of Pharmaceutical Sciences and Research,* **2017**, *9(12)*, 2372-2375.

19. Talismanov, V. S., Popkov, S. V., Zykova, S. S., Karmanova, O. G. *Journal of Pharmaceutical Sciences and Research,* **2018a**, *10(2)*, 328-332.

20. Talismanov, V. S., Popkov, S. V., Zykova, S.S., Karmanova, O.G. *Journal of Pharmaceutical Sciences and Research,* **2018b**, *10(4)*, 950-955.

21. Terleev, V., Mirschel, W., Nikonorov, A., Ginevsky, R., Lazarev, V., Pavlova, V., Topaj, A., Pashtetsky, V., Dunaieva, I., Popovych, V., Melnichuk, A., Layshev, K. *Advances in Intelligent Systems and Computing,* **2019**, *983*, 449-461.

22. Zonn, I. S., Zhiltsov, S. S., Parkhomchik, L. A., Markova, E. A. *Handbook of Environmental Chemistry,* **2018**, *85,* 153-167.

Downloaded from www.periodico.tchequimica.com

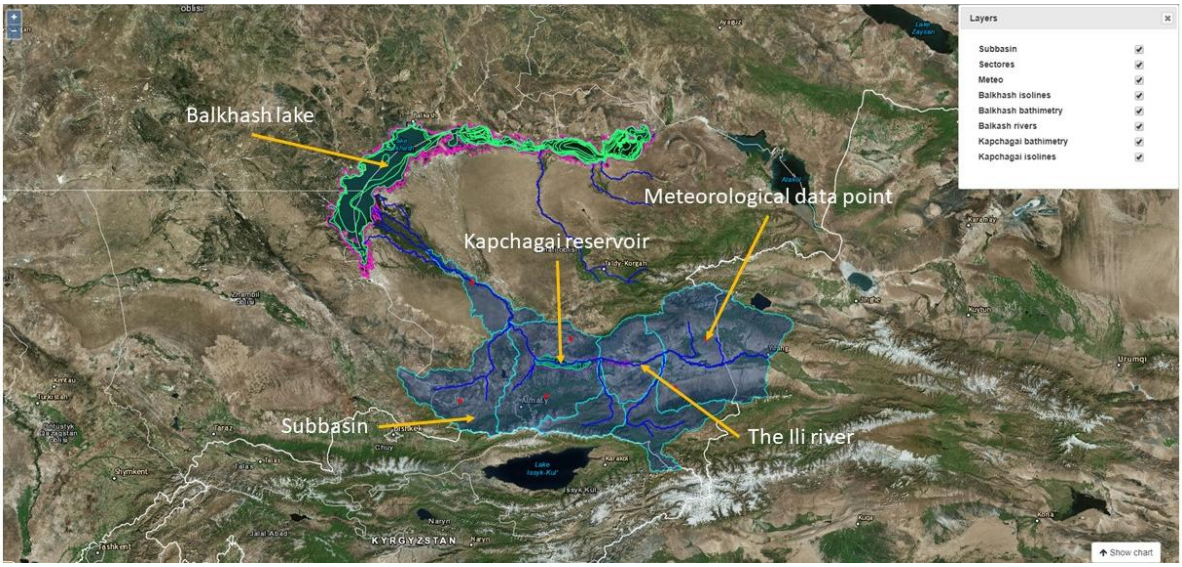

***Figure 1**. Start window of the system with current data on the region*

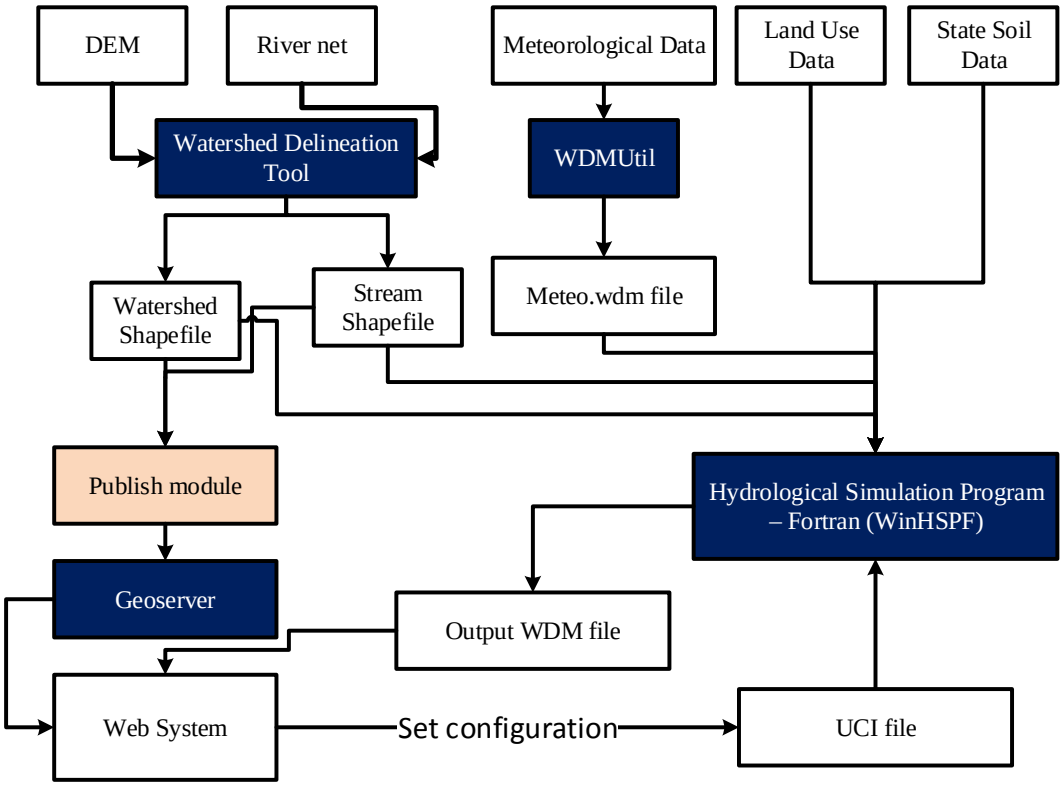

***Figure 2**. Schematic representation of calculation algorithm*

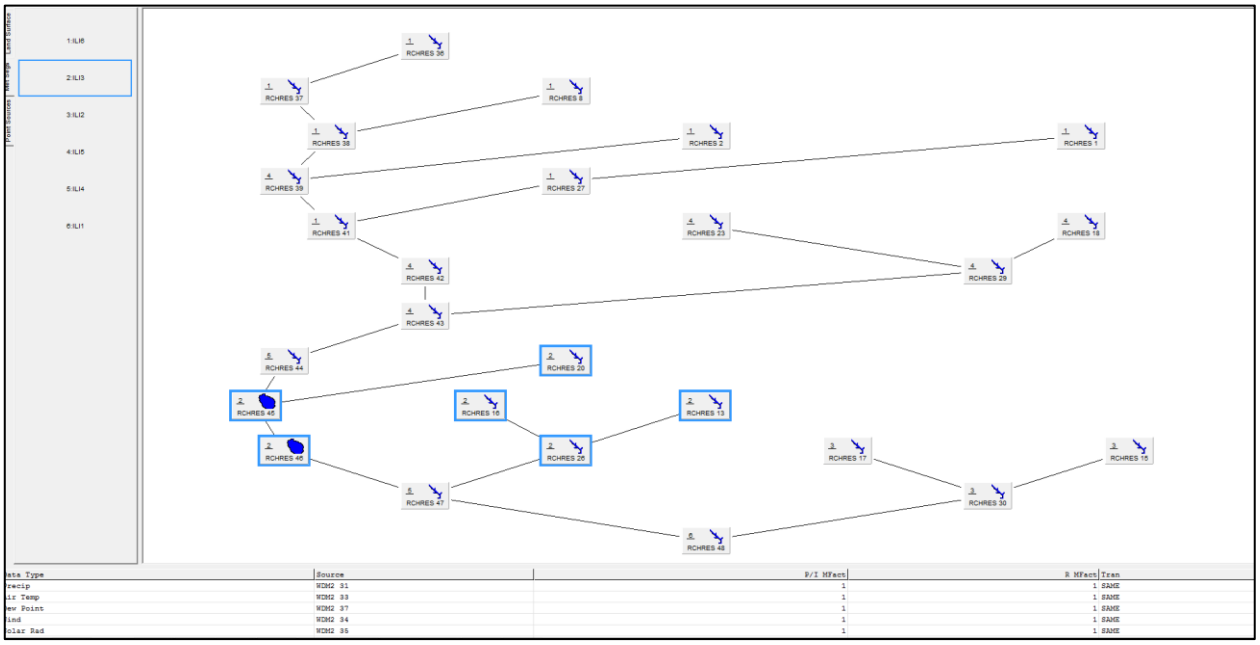

Figure 3. *Computer model of the Ili river basin*

```
File  Edit  Format  Run  Options  Window  Help
import os, sys, re, datetime
def write_to_uci(ucifile_path, operation_type, operation_number,
                 operation_section,section_variable_name, dataset_number, constituent_name):
#     -operation type (e.g., PERLND, IMPLND, RCHRES)
#     -operation number (e.g., 101, 102)
#     -operation section (e.g., PWATER, SEDMNT, HYDR)
#     -section variable name (e.g., PERO, SURO, SURS)
    if os.path.isfile(ucifile_path):
        try:
                file=open(ucifile_path,"r")
                indata=file.read().split('\n')
                outdata=''
                for line in indata:
                        ext_target_line = re.search("END EXT TARGETS", line)
                        if ext_target_line is None:
                                outdata+=line+"\n"
                        else:
                                outdata += operation_type +"  "+operation_number+" "+operation_section+"    "+section_variable_name+"
                                1 1          AVER WDM1  "+dataset_number+" "+constituent_name+"    1 ENGL AGGR REPL\n"
                                outdata += "END EXT TARGETS \n"
                file.close()
                file=open(ucifile_path,"w")
                file.write(outdata)
                file.close()
        except:
            exit(1)

def write_to_wdmout(wdmfile_path, scenario, location, dataset_number, constituent_name):
    from pyhspf import WDMUtil
    wdm = WDMUtil()
    if os.path.isfile(wdmfile_path):
        try:
            wdm.open(wdmfile_path,'rw')
            #dsns = wdm.get_datasets(wdmfile)
            #print(dsns)
            #tstypes = [wdm.get_attribute(wdmfile, n, 'TSTYPE') for n in dsns]
            #print(tstypes)
            attributes = {
                    'TSTYPE': constituent_name,
                    'TCODE ': 4,
                    'TSSTEP': 1,
                    'TSFORM': 1,
                    'IDSCEN': scenario,
                    'IDLOCN': location
                      }
            wdm.create_dataset(wdmfile_path, dataset_number, attributes)
            wdm.close(wdmfile_path)
        except:
            exit(1)
```

Figure 4. Screenshot of UCI file write code

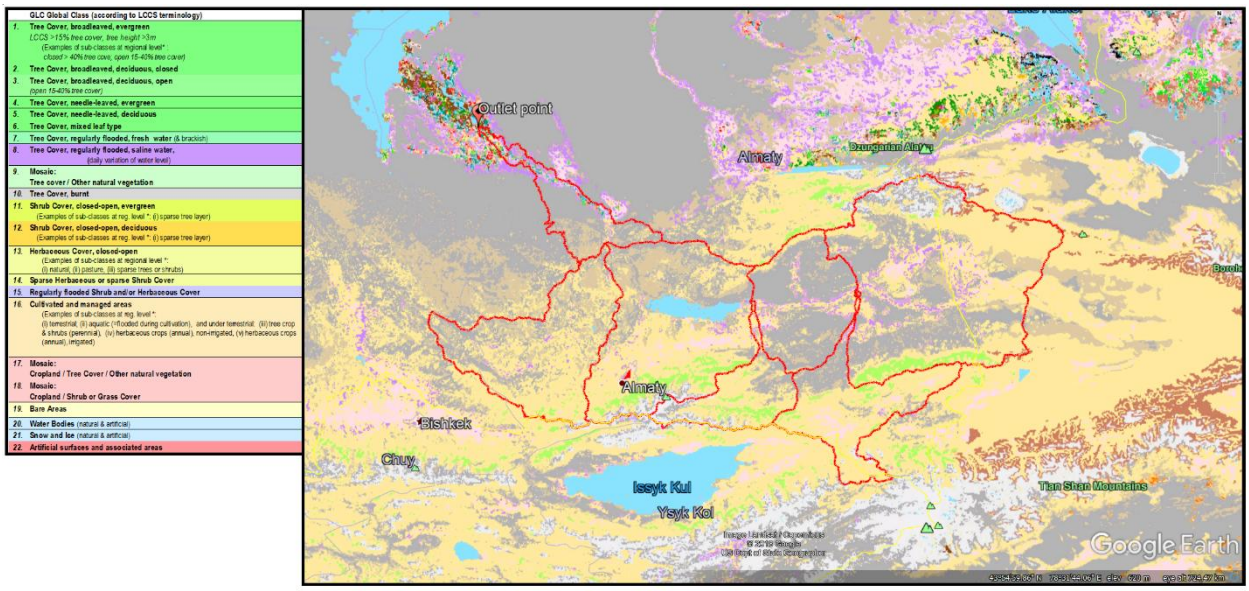

Figure 5. *Land use and land cover map for the Ili river catchment area. The research area is covered mainly by shrubs, patches of stony and eroded soil. For the purpose of hydrological modeling, the catchment area was divided into 7 sub-basins (red lines)*

Figure 6. *Geolocation of data collection points*

Downloaded from www.periodico.tchequimica.com

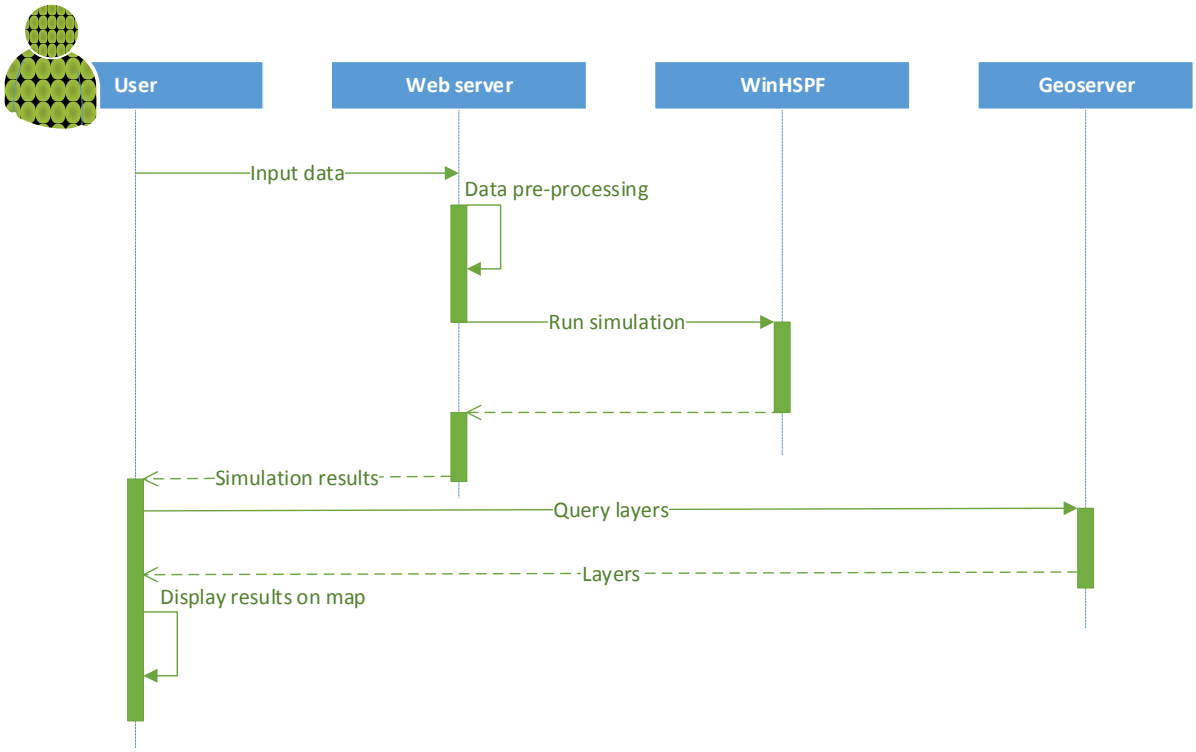

Figure 7. *The diagram of sequence*

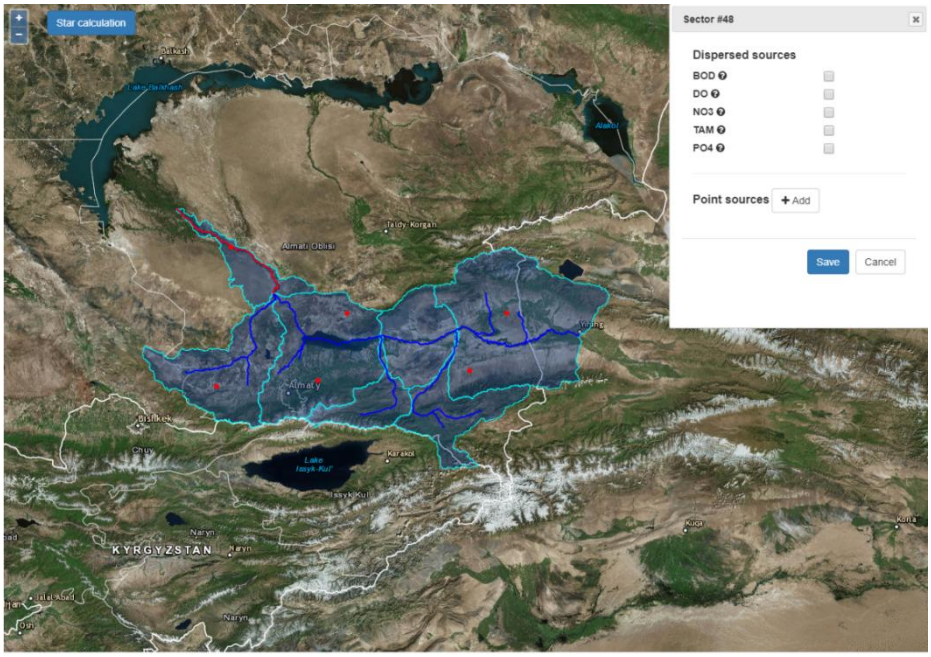

Figure 8*. CreateOrder view*

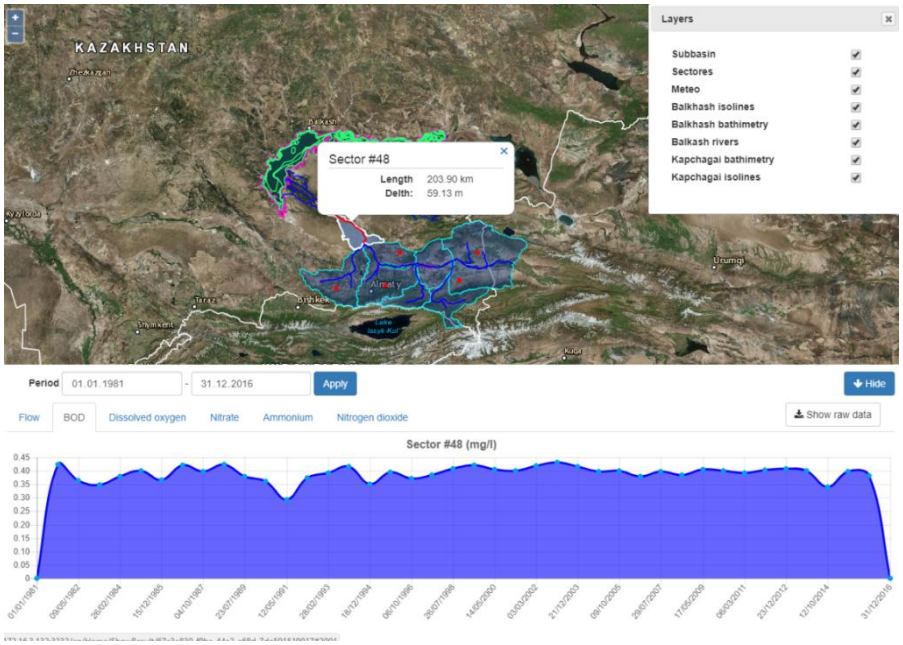

Figure 9. *ShowResult view*

Type of	Headline	Title	Storage	Included	Native SRS
	balkash_isolines	localhost:balkash_isolines	postgis_database	✔	EPSG:32643
	balkash_meteo	localhost:balkash_meteo	postgis_database	✔	EPSG:32643
	balkash_rivers	localhost:balkash_rivers	postgis_database	✔	EPSG:32644
	balkhash	localhost:balkhash	postgis_database	✔	EPSG:32643
	balkhash_bathimetry	localhost:balkhash_bathimetry	postgis_database	✔	EPSG:32643
	kapshagai_bathimetry	localhost:kapshagai_bathimetry	postgis_database	✔	EPSG:32643
	kapshagai_topo_isolines	localhost:kapshagai_topo_isolines	postgis_database	✔	EPSG:32643
	river_net	localhost:river_net	postgis_database	✔	EPSG:32643
	sub_basin	localhost:sub_basin	postgis_database	✔	EPSG:32643
	sub_basin_3857	localhost:sub_basin_3857	postgis_database	✔	EPSG:3857

Figure 10. *Layers published in Geoserver*

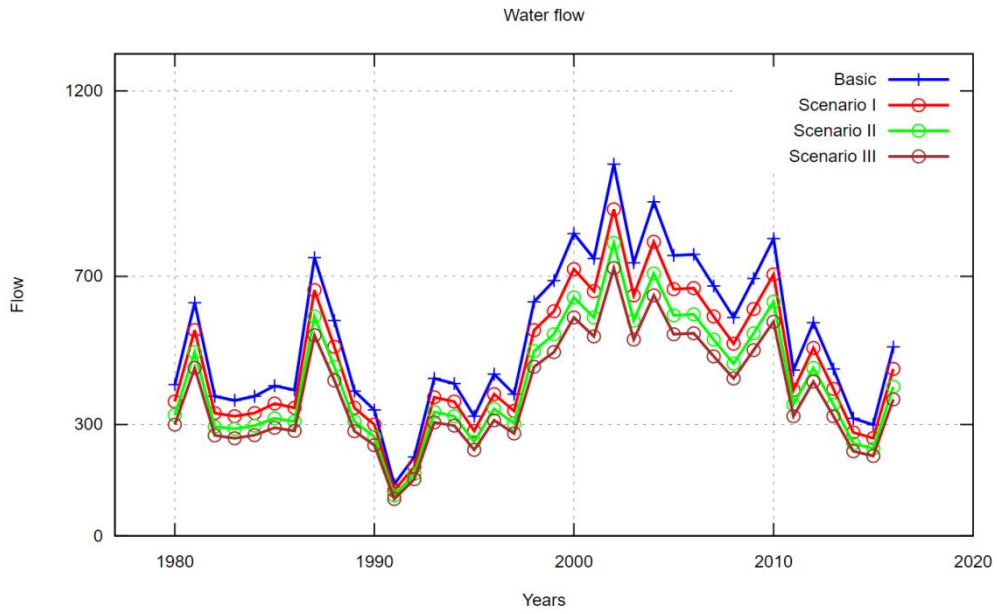

Figure 11. *Results of water inflow modeling (m3 / s)*

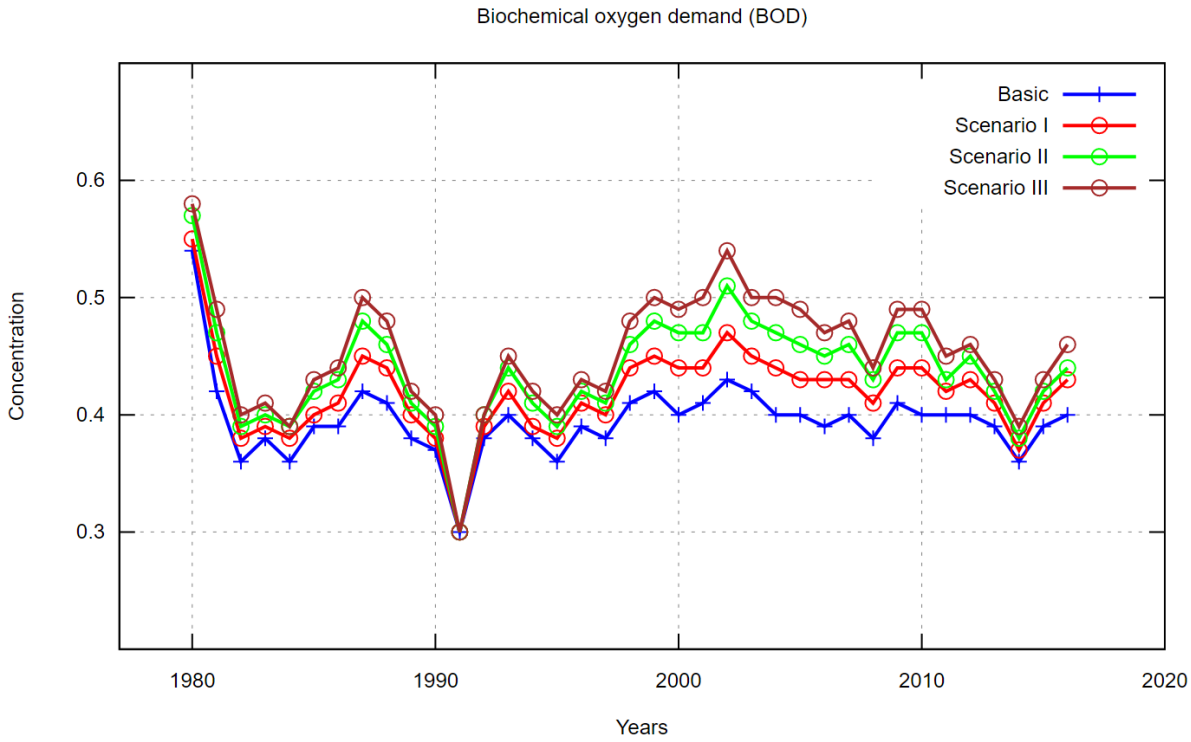

Figure 12. *Results of BOD concentration modeling (mg / L)*

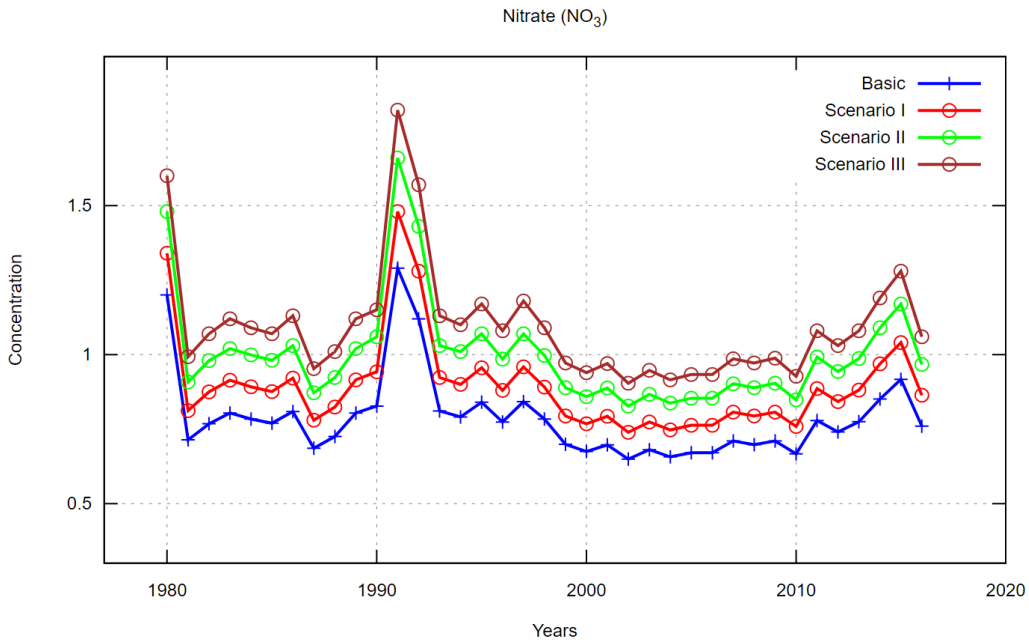

Figure 13. *Nitrate modeling results*

Downloaded from www.periodico.tchequimica.com

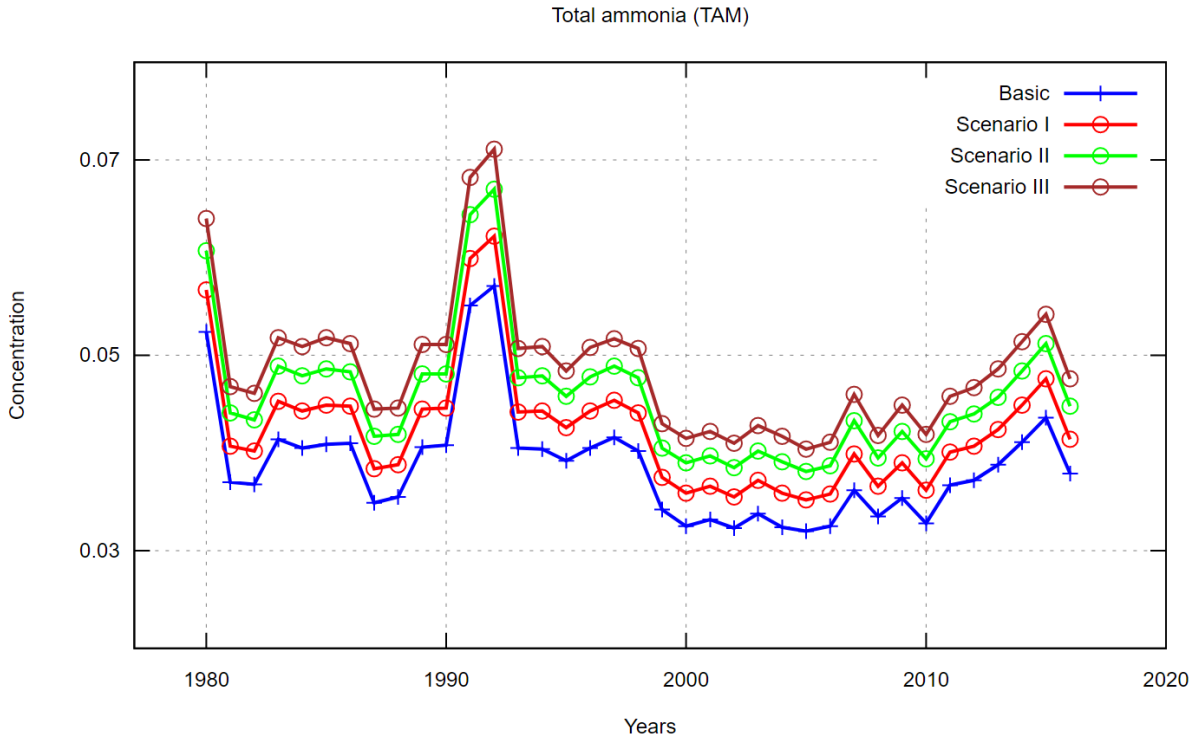

Figure 14. *Total Ammonia modeling results*

Downloaded from www.periodico.tchequimica.com

***Table 1**. The main points of quality control of surface waters in the Ili river basin*

Waterbody code	Location	Post code	Distance from the outfall, km	Catchment area, square km
113200001	pier dobyn	14003	723	64388
113200002	Tekes village	14022	331	1770
113200001	164 km above the Kapchagai hydroelectric station	14004	607	85400
113200483	Malybay village	14160	40	4300
113200001	Kapchagai hydroelectric station	14011	434	111000
113200001	Ushzharma village	14014	264	129000

***Table 2.** Land use and land cover in Ili river catchment*

Land use or land cover	Percent cover
Shrub Cover, closed-open, evergreen	30%
Bare areas	32%
Herbaceous cover, closed-open	12%
Tree Cover, regularly flooded, saline water	2%
Tree Cover, mixed leaf type	8%
Shrub Cover, closed-open, deciduous	9%
Others	7%

***Table 3.** Meteorological data*

Data set	Description of parameter
PREC	Amount of precipitation (mm / hour)
CLOU	Overcast (0-10)
ATEM	Air temperature (°F)
WIND	Wind speed (mph)
SOLR	Solar radiation (MJ / m^2)
PEVT	Evaporation (inches)
Dewp	Temperature of dew point

***Table 4.** Measured stream flow and total suspended sediment concentration at or near the Ili river delta*

Location	Stream flow (m^3/s)	Total suspended sediment (mg/L)
Downstream	400	860
Upstream	500	780
Upstream 1	480	820
Average	460	820

PERIÓDICO TCHÊ QUÍMICA
ARTIGO ORIGINAL

MODELAGEM NUMÉRICA E *SOFTWARE* PARA DETERMINAR OS PARÂMETROS ESTÁTICOS E DE LIGAÇÃO DOS ORGANISMOS EM CRESCIMENTO NO PROCESSO DE TRANSFERÊNCIA ADITIVA NÃO ESTACIONÁRIA DE CALOR E MASSA

NUMERICAL MODELING AND SOFTWARE FOR DETERMINING THE STATIC AND LINKAGE PARAMETERS OF GROWING BODIES IN THE PROCESS OF NON-STATIONARY ADDITIVE HEAT AND MASS TRANSFER

ЧИСЛЕННОЕ МОДЕЛИРОВАНИЕ И ПРОГРАММНОЕ ОБЕСПЕЧЕНИЕ ДЛЯ ОПРЕДЕЛЕНИЯ СТАТИЧЕСКИХ И КИНЕМАТИЧЕСКИХ ПАРАМЕТРОВ РАСТУЩИХ ТЕЛ В ПРОЦЕССЕ НЕСТАЦИОНАРНОГО АДДИТИВНОГО ТЕПЛОМАССОПЕРЕНОСА

KUZNETSOVA, Ekaterina L.[1*]; RABINSKIY, Lev N.[2];

[1] Moscow Aviation Institute (National Research University), Faculty of Applied Mechanics, Moscow – Russian Federation

[2] Moscow Aviation Institute (National Research University), Department of Engineering Graphics, Moscow – Russian Federation

** Correspondence author*
e-mail: lareyna@mail.ru

Received 03 September 2019; received in revised form 20 October 2019; accepted 26 October 2019

RESUMO

Atualmente, os métodos de impressão tridimensional de produtos a partir de polímeros, metais e materiais cerâmicos são amplamente utilizados. As tecnologias de síntese camada a camada possibilitam a obtenção de produtos de alta qualidade com características mecânicas suficientemente altas, próximas às realizadas com os processos tecnológicos tradicionais. Um problema relacionado foi resolvido, incluindo o cálculo da temperatura no produto e da área de operação em torno dele em uma configuração plana com base em duas abordagens diferentes. Um corpo extensível camada por camada apresenta o problema instável de condução de calor. A cada passo, a altura da região computacional aumenta devido ao preenchimento de uma nova camada de pó. Uma etapa do cálculo é determinada pelo intervalo entre duas passagens consecutivas do laser. A distribuição de temperatura encontrada em cada etapa é usada como condições iniciais para os cálculos na próxima etapa. O campo de temperatura obtido como resultado da solução do problema implementado no produto em questão com uma etapa de 1000 (após a aplicação e a fusão de 1000 camadas) é ainda mais comparado com a solução do problema quase-estacionário para o produto de dimensões finitas. Usando o exemplo da geometria simples, é mostrado que uma solução quase estacionária pode fornecer uma estimativa satisfatória do estado térmico macroscópico do produto em crescimento.

Palavras-chave: *crescimento de produtos em camadas, aquecimento a laser, modelagem, condutividade térmica não estacionária, corpo em crescimento, tecnologias aditivas.*

ABSTRACT

Currently, methods of three-dimensional printing of products from polymer, metal and ceramic materials are widely used. Layer-by-layer synthesis technologies make it possible to obtain high-quality products with sufficiently high mechanical characteristics close to those realized using traditional technological processes. A related problem is solved, including calculating the temperature in the product and the operation area surrounding it in a flat setting based on two different approaches. For a layer-by-layer extensible body, the unsteady heat conduction problem is stated. At each step, the height of the computational region increases due to the filling of a new layer of powder. One time step of the calculation is determined by the interval between two consecutive passes of the laser. The temperature distribution found at each step is used as the initial conditions for the calculations at the next step. The temperature field obtained as a result of solving the problem that is implemented in the product in question with a step of 1000 (after applying and melting 1000 layers) is further compared with the solution of the quasi-stationary problem for the finite dimensions product. Using the example of the simple geometry taken, it is shown that a quasi-stationary solution can provide a satisfactory estimate of the macroscopic thermal state of the growing product.

Downloaded from www.periodico.tchequimica.com

Keywords: *layer-by-layer product growth, laser heating, modeling, non-stationary thermal conductivity, growing body, additive technologies.*

АННОТАЦИЯ

В настоящее время широко распространены методы трехмерной печати изделий из полимерных, металлических и керамических материалов. Технологии послойного синтеза позволяют получать изделия высокого качества, обладающие достаточно высокими механическими характеристиками, близкими к тем, которые реализуются при использовании традиционных технологических процессов. Решается сопряженная задача, включающая расчет температуры в изделии и окружающей его рабочей области в плоской постановке на основе двух различных подходов. Для послойно наращиваемого тела ставится нестационарная задача теплопроводности. На каждом шаге увеличивается высота расчетной области вследствие засыпки нового слоя порошка. Один временной шаг расчета определяется интервалом между двумя последовательными проходами лазера. Найденное на каждом шаге распределение температуры используется в качестве начальных условий для проведения расчетов на последующем шаге. Поле температур, полученное в результате решения задачи которое реализуется в рассматриваемом изделии с шагом 1000 (после нанесения и проплавления 1000 слоев) и в дальнейшем сравнивается с решением квазистационарной задачи для изделия конечных размеров. На примере рассмотренной простой геометрии показано, что квазистационарное решение может дает удовлетворительную оценку макроскопического теплового состояния выращиваемого изделия.

Ключевые слова: *послойное выращивание изделий, нагрев лазером, моделирование, нестационарная теплопроводность, растущее тело, аддитивные технологии.*

1. INTRODUCTION

Currently, methods of three-dimensional printing of products from polymer, metal and ceramic materials are widely used (Guo and Leu, 2013; Uriondo *et al.,* 2015). Layer-by-layer synthesis technologies make it possible to obtain high-quality products with sufficiently high mechanical characteristics close to those realized using traditional technological processes (Skvortsov *et al.,* 2000; Murr *et al.,* 2012; Skvortsov *et al.,* 2012; Kablov, 2015; Smurov *et al.,* 2015; Bikas *et al.,* 2016; Shejko *et al.,* 2016; Skvortsov and Karizin, 2017).

A significant part of the work is devoted to modeling of physical phenomena at the micro level or only in the vicinity of a local high-energy source, leading to the melting of the powder (King *et al.,* 2015; Khairallah *et al.,* 2016) and heating is carried out using a laser or an electronic beam. Other works are related to the simultaneous or sequential modeling of macroscopic temperature fields in the process of layer-by-layer synthesis and the residual stress strain behavior of the products obtained. The main result of such calculations is an estimation of the effectiveness of the applied technological modes for obtaining high-quality products in which minimal negative effects of permanent deformations and residual stresses are implemented (Riedlbauer *et al.,* 2012). The process is accompanied by multiple laser passes on the surface of the parts. Modeling of such processes is carried out in the framework of the unrelated problem of thermoelastic behavior: the non-stationary problem of thermal conductivity is solved, and the product stress strain behavior is determined on the basis of the solution of the quasi-static problem of thermoelastic behavior. To speed up numerical calculations, methods of creating adaptive finite element meshes are used (Keller *et al.,* 2013). When using finite element packets to accelerate numerical calculations, the finite element mesh can be enlarged so that each finite element contains several sintered layers (Orlov *et al.,* 2003; Gorchakov *et al.,* 2004; Dmitriev *et al.,* 2011).

In the study of residual stress strain behavior, it can be used an assumption about the insignificant influence of trajectory of the heating source (laser or electronic beam) on the surface of the product (Knyazev *et al.,* 2007: Formalev and Kolesnik, 2017; Kakhramanov *et al.,* 2017; Formalev et al., 2018a; Rabinskiy *et al.,* 2018; Rabinsky and Tushavina, 2019b).

2. MATERIALS AND METHODS

The problem is considered in a flat setting. It is assumed that the wall is quite extended and the heat transfer at its remote faces can be neglected, then the same thermal mode is realized in each section perpendicular to the direction of motion. The process of layer-by-layer synthesis of a thin vertical wall is shown in Figure 1. As a result of the calculation, it is necessary to

Downloaded from www.periodico.tchequimica.com

determine the thermal state of the synthesis operation area, which includes the product itself, non-sintered powder surrounding it and the working platform, schematically shown in Figure 1a. For this purpose, at each step corresponding to a new poured layer, we solve the unsteady heat conduction problem. Then, for a layer-by-layer growing body, we come to periodic local heating of its surface, associated with the action of a laser. Shrinkage loss of powder is neglected at a first approximation.

The region in which the calculation is carried out is denoted by Ω_i. This region consists of a working platform (Equation 1) and from a growing region (Equation 2), which includes the growing product and non-sintered powder surrounding it. Accordingly, piecewise constant properties corresponding to the materials of the platform, the synthesized product, and the powder are set in the region Ω_i. In this example, the wall is located in the center of the computational region and has a thickness d. We will carry out the calculation for half of the region, taking into account the symmetry of the problem shown in Figure 1b, which also shows the coordinate system used in the calculations.

The generalized mathematical model should take into account unsteady heat conduction, unsteady and non-uniform mass loss, arbitrary orientation of the principal axes of the heat conductivity tensor, complex heat transfer at free boundaries, the presence of heat fluxes, the direction of which deviates significantly from the direction of the normal to the boundaries, the non-convexity of the boundaries during mass growth, as well as curvilinear coordinate systems.

The problem is solved in an unsteady setting, taking into account the method for determining the moment of beginning and end of mass growth under substantially unsteady conditions.

3. RESULTS AND DISCUSSION:

Based on the refined software system that implements the above methods, the influence of the computational region curvature, the degree of anisotropy, the orientation of the principal axes of the thermal conductivity tensor on the two-dimensional non-stationary temperature field is explored, and it is presented the nature of the isotherms at the outer boundary during heating with mass growth (Mykhalevskiy, 2018; Mykhalevskiy, 2019).

To solve this problem, we use the one-dimensional equation of unsteady heat conduction, taking into account the terminal velocity of propagation of the heat wave and scale effects (Lomakin *et al.,* 2018) (Equation 3).

The balance of thermal energy at the inner boundary of the layer (Equation 4).

Continuity of heat fluxes and temperatures at the boundary $w1$ between the liquid film and the body (Equation 5)

In the mathematical model (3-5), the following designations are used: τ, T, λ, c, ρ – respectively, temperature, thermal conductivity, heat capacity, density; δ_T – body thickness; q – heat flux density; Indices: $w1$, $w2$ – respectively, the outer and inner borders of the body; eff – effective;

At each *i*-th step of the calculation, the region height Ω_i is increased by the thickness of one layer *h.* In the resulting region in the time interval $t \in [(i-1)\Delta t,\ i\Delta t]$ the problem of non-stationary thermal conductivity is solved.

Where T_i (*x, y, t*) – the temperature field, which is realized in the computational region Ω_i at the *i*-th calculation step, Equation 6 – the heat flux vector, $k(x, y, T_i)$, C_p (x, y, T_i), p (x , y) – the coefficients of thermal conductivity, heat capacity and density, the values of which are given piecewise constant functions of coordinates and continuous temperature functions. The solution of unsteady heat conduction problems was considered in (Babaytsev *et al.,* 2015; Lurie *et al.,* 2015; Koshoridze *et al.,* 2017; Lomakin *et al.,* 2018a; Lomakin *et al.,* 2018b; Formalev *et al.,* 2018b; Formalev *et al.,* 2018c; Formalev and Kolesnik, 2019; Rabinskiy and Tushavina, 2019a; Nikitin *et al.,* 2019; Rabinskiy *et al.,* 2019; Babaytsev *et al.,* 2019)

As the initial conditions for problem (1), we use the solution obtained in the previous calculation step, which is extrapolated to the new layer added as follows:

Here (i – 1) h is the maximum height of the computational region at the previous calculation step, that is, the sum of the thicknesses of the layers already applied.

In the recorded initial conditions (Equation 7), the found temperature distribution on the surface of the product at the previous calculation step is, in fact, extended by one new layer upwards for performing calculations at a new step. This assumption is based on the small thickness of the applied layers, which almost

Downloaded from www.periodico.tchequimica.com

instantly warm up to the substrate temperature after their application and, at the same time, slightly affect the macroscopic thermal state of the product.

At the first calculation step $i=i_{0,}$ it is assumed that the region under consideration Ω_{i_0} uniformly warmed up to ambient temperature T_0. This medium is air or an inert gas in which synthesis is carried out and which is supplied to blow and chill down the product and to prevent oxidation of its surface.

As the boundary conditions at the lower and lateral boundaries of the computational region $\Omega_{i,}$ the heat transfer condition is set according to Newton's law (Equation 8). Where the heat transfer coefficient α is a parameter of the model and it is determined by the arrangement of the processing chamber used for the synthesis of equipment, n is the vector of a unit external of the normal to the boundary of the region.

At the upper boundary of the region, heat transfer by radiation according to the Stefan-Boltzmann law and heat supply are additionally taken into account due to the action of the heating source (Equation 9).

Here, σ – the Stefan-Boltzmann constant, ε – the degree of blackness of the surface, $q(x,t)$ – the heat flux supplied to the surface of the product under the action of a laser. It is assumed that the temperature of the walls of the chamber, where the heat is exchanged by radiation, is equal to the ambient temperature T_0 .

In the calculations, we assume that the modeling wall is rather thin, and the velocity of the heating source v is quite large (usually from several tens of millimeters to several meters per second). Therefore, at the upper boundary of the wall in the laser operating zone, we will set a constant value with respect to the *x*-coordinate for the heat flux supplied simultaneously to the entire melted surface of the product. In the selected coordinate system, this is a section of the boundary with the coordinate $y=ih$ in the range $-d/2 \le x \le d/2$. For approximate calculations, we assume that this function $q(x,t)$ is piecewise constant in time and has the following form (Equation 10). Where $t_0=d/v$ is the operating time of heating, which is determined by the width of the wall and the velocity of the source.

Let us consider the growing process, starting with step $i_0=1000$, to avoid creating too small finite element mesh. We are talking about layer-by-layer growing of a thin vertical wall made of stainless steel. We set the parameters of the problem in the form: - the thickness of one layer h = 20 μm, the width of the considered part of the operation area L = 3 cm, the wall thickness d = 1 mm, the maximum height H = 3 cm, the thermal conductivity of the powder is 0.01, and the density is 0.5 from the corresponding characteristics of the sintered material, the melting temperature T_{melt} = 1400 C. The calculations are carried out under the assumption that the characteristics of the materials vary linearly depending on the temperature and that the working platform and the wall are made of the same material.

At above temperatures the material characteristics we consider constant. The calculation time at each step (the time between the actions of the heating source) Δt = 25 seconds. The heat transfer coefficient α on the surface will be set equal to the case of natural and forced (intense blowing) convection. The ambient temperature T_0 = 25C, the degree of blackness of the surface ε = 0.5. The velocity of the heating source v = 2 m/s, the power P = 100W, the efficiency coefficient η = 0.4, the radius of the heating spot r = 120 μm. The calculations are carried out for the maximum number of steps N = 1500.

As a result of the calculations, the following results were obtained: Figure 2 shows a diagram of temperature changes along the *y* coordinate, throughout the height of the wall. Here, on one graph, temperature profiles are applied at different points in time in the growing product. All graphs are constructed, 10 seconds later, after exposure to the laser, that is, at the moment when the surface of the product manages to cool down after the next intense heating. With an increase in the heat transfer coefficient at the boundaries of the computational region , shown in Figure 2b, the wall warms up less, but the temperature difference throughout its height increases. For the case of low heat transfer coefficient shown in Figure 2a, the product actually overheats. Thus, according to the modeling results, we can see that the specified synthesis mode is unacceptable and requires correction.

4. CONCLUSIONS:

The problems of heat and mass transfer are one of the most important problems of mathematical physics. This is due to both their widespread distribution and the determining influence on the efficiency of thermal, diffusion

Downloaded from www.periodico.tchequimica.com

and chemical apparatuses.

The problems of thermal conductivity and diffusion have wide practical application. The ability to solve such problems allows you to get the most important information about the process. For example, for a thermal process, it is possible not only to calculate the stationary temperature field, heat fluxes and average temperatures of individual structural elements and the apparatus as a whole, but also to determine the nature of the change (profiles, differences, gradients) of temperatures at individual points of the structural elements of the apparatus, to predict possible thermal diffusion effects, find the optimal parameters and offer a control circuit for this unit or installation.

The scientific paper gives the results of a numerical solution of the plane problem of incremental growth of a thin vertical wall in the process of its layer-by-layer laser growing. In the proposed modeling method, a finite element mesh is built at each new calculation step, and solutions at different calculation steps are joined by redefining and extrapolating the initial conditions.

The approach used makes it possible to obtain, with a sufficient degree of accuracy, synthesis parameters for a specific geometry region of the growing product. The region for which the solution is framed should be large enough so that during the growing process the necessary mode can be realized in it.

5. ACKNOWLEDGMENTS:

The work was carried out with the financial support of the state project of the Ministry of Education and Science project code 2.9219.2017/8.9.

6. REFERENCES:

1. Babaytsev, A.V., Dobryanskiy, V., Solyaev, Y.O. *Lobachevskii Journal of Mathematics*, **2019**, *40*(7), 887-895.
2. Babaytsev, A.V., Kornev, Y.V., Semenov, N.A. *International Journal of Nanomechanics Science and Technology*, **2015**, *6*(4), 261-280.
3. Bikas, H., Stavropoulos, P., Chryssolouris, G. *International Journal of Advanced Manufacturing Technology*, **2016**, *83*, 389–405.
4. Dmitriev, A.I., Skvortsov, A.A., Koplak, O.V., Morgunov, R.B., Proskuryakov, I.I. *Physics of the Solid State*, **2011**, *53*(8), 1547-1553.
5. Formalev, V.F., Kolesnik, S.A. *High Temperature*, **2017**, *55*(4), 564-569.
6. Formalev, V.F., Kolesnik, S.A. *Journal of Engineering Physics and Thermophysics*, **2019**, *92*(1), 52-59.
7. Formalev, V.F., Kolesnik, S.A., Kuznetsova, E.L. *High Temperature*, **2018a**, *56*(5), 727-731.
8. Formalev, V.F., Kolesnik, S.A., Kuznetsova, E.L. *Periodico Tche Quimica*, **2018b**, *15*(S1), 426-432.
9. Formalev, V.F., Kuznetsova, E.L., Kuznetsova, E.L. *Periodico Tche Quimica*, **2018c**, *15*(S1), 377-389.
10. Gorchakov, A.I., Semenova, A.V., Syrovatskaya, Yu.V., Shcherbakov, Yu.V., Yasnitskij, L.N. *Fizika i Khimiya Obrabotki Materialov*, **2004**, *1*, 43-47.
11. Guo, N., Leu, M.C. *Frontiers of Mechanical Engineering*, **2013**, *8*(3), 215–243.
12. Kablov, E.N. *Intelligence & Technology*, **2015**, *2*(11), 52-55.
13. Kakhramanov, R.M., Knyazeva, A.G., Rabinskiy, L.N., Solyaev, Y.O. *High Temperature*, **2017**, *55*(5), 731-736.
14. Keller, N., Neugebauer, F., Xu, H., Ploshikhin, V. *LightMAT*, **2013**, *3*(5).
15. Khairallah, S.A., Anderson, A.T., Rubenchik, A., King, W.E. Laser powder- *Acta Materialia*, **2016**, *108*, 36-45.
16. King, W.E., Anderson, A.T., Ferencz, R.M., Hodge, N.E., Kamath, C., Khairallah, S.A., Rubenchik, A.M. *Applied Physics Reviews*, **2015**, *2*(4), 41304.
17. Knyazev, A.G., Pobol, I.L., Gordienko, A.I., Demidov, V.N., Kryukova, O.N., Oleshchuk, I.G. *Physical Mesomechanics*, **2007**, *10*(5), 105-119.
18. Koshoridze, S.I., Levin, Y.K., Rabinskiy, L.N. *Russian Metallurgy (Metally),* **2017**, *13*(1), 1194-1201.
19. Lomakin, E., Rabinskiy, L.N., Radchenko, V. *Meccanica*, **2018a**, *53*(15), 3831-3838.
20. Lomakin, E.V., Lurie, S.A., Belov, P.A., Rabinskiy, L.N. *Doklady Physics*, **2018a**, *63*(12), 503–507.

Downloaded from www.periodico.tchequimica.com

21. Lurie, S.A., Kuznetsova, E.L., Rabinskii, L.N., Popova, E.I. *Mechanics of Solids*, **2015**, *50*(2), 135-146.

22. Murr, L.E., Gaytan, S.M., Ramirez, D.A., Martinez, E., Hernandez, J., Amato, K.N., Shindo, P.W., Medina, F.R., Wicker, R.B. *Journal of Materials Science & Technology*, **2012**, *28*(1), 1–14.

23. Mykhalevskiy, D. *Eastern-European Journal of Enterprise Technologies*, **2018**, *6*(9-96), 16-21.

24. Mykhalevskiy, D.V. *Latvian Journal of Physics and Technical Sciences*, **2019**, *56*(1), 41-52.

25. Nikitin, P.V., Tushavina, O.V., Shkuratenko, A.A. *Incas Bulletin*, **2019**, *11*(Special Issue), 191-201.

26. Orlov, A.M., Skvortsov, A.A., Solov'ev, A.A. *Journal of Experimental and Theoretical Physics*, **2003**, *96*(3), 523-530.

27. Rabinskiy, L.N., Tushavina, O.V. *Incas Bulletin*, **2019a**, *11*(Special Issue), 203-211.

28. Rabinskiy, L.N., Tushavina, O.V. *Periodico Tche Quimica*, **2018**, *15*(S1), 321-329.

29. Rabinskiy, L.N., Tushavina, O.V. *STİN*, **2019b**, *4*, 22-26.

30. Rabinskiy, L.N., Tushavina, O.V., Fedotenkov, G.V. *Asia Life Sciences, Supplement*, **2019**, *19*(1), 149-162.

31. Riedlbauer, D., Mergheim, J., McBride, A., Steinmann, P. *Proceedings in Applied Mathematics and Mechanics*, **2012**, *12*, 381–382.

32. Shejko, S., Yechyn, S., Demchenko, N. “The method for determination of the influence of the stress-strain state of metal on the structural transformations in the low-alloy steel”. *Materials of the Science and Technology Conference and Exhibition 2016 (T 353-358*), Salt Lake City, USA, **2016**.

33. Skvortsov, A.A., Karizin, A.V. *Solid State Phenomena*, **2017**, *269*, 78-90.

34. Skvortsov, A.A., Orlov, A.M., Frolov, V.A., Gonchar, L.I., Litvinenko, O.V. *Physics of the Solid State*, **2000**, *42*(10), 1861-1864.

35. Skvortsov, A.A., Orlov, A.M., Zuev, S.M. *Russian Microelectronics*, **2012**, *41*(1), 31-40.

36. Smurov, I.Y., Konov, S.G., Kotoban, D.V. *Science and Technology*, **2015**, *2*(14), 11–22.

37. Uriondo, A., Esperon-Miguez, M., Perinpanayagam, S. *Journal of Aerospace Engineering*, **2015**, *229*(11): 2132–2147.

Ω_P = {0≤ $x \le L$, - $H \le y \le 0$} (Eq. 1)

Ω_L = {0≤ $x \le L$, 0≤ $y \le ih$ } (Eq. 2)

$$\left(\lambda_{yy}\right)_{eff}\frac{d^2T}{dy^2}-\Pi\left(c\rho\right)_f\cdot v_f\frac{dT}{dy}=\rho C_p\frac{\partial T}{\partial t}+\tau\frac{\partial^2 T}{\partial t^2}+\frac{k_V}{l_T^2}T,\quad 0<y<\delta_T\,. \tag{Eq. 3}$$

$$\left(\lambda_{yy}\right)_{eff}\left.\frac{dT}{dy}\right|_{w2}=q_{w2},\ y=0\,. \tag{Eq. 4}$$

$$\lambda_f\left.\frac{dT}{dy}\right|_{w1}=\left(\lambda_{yy}\right)_{eff}\left.\frac{dT}{dy}\right|_{w1},\ T_f\big|_{w1}=T\big|_{w1},\ y=\delta_T\,. \tag{Eq. 5}$$

Downloaded from www.periodico.tchequimica.com

$$\mathbf{q} = -k\nabla T_i \qquad \text{(Eq. 6)}$$

$$T_i\left(x,y,0\right) = \begin{cases} T_{i-1}(x,y,\, i\Delta t), & y \le \left(i-1\right)h \\ T_{i-1}(x,(i-1)h,i\Delta t), & \left(i-1\right)h \le y \ge i\,h \end{cases} \qquad \text{(Eq. 7)}$$

$$x = 0, x = L, y = -H:\ \mathbf{q}\cdot\mathbf{n} = \alpha\left(T_i - T_0\right) \qquad \text{(Eq. 8)}$$

$$y = i\,h:\ \mathbf{q}\cdot\mathbf{n} = \alpha\left(T_i - T_0\right) + \sigma\varepsilon\left(T_i^4 - T_0^{\,4}\right) + q\left(x,t\right) \qquad \text{(Eq. 9)}$$

$$q\left(x,t\right) = \begin{cases} q_0, & t \le t_0 \ \cup\ |x| \le d/2 \\ 0, & t > t_0 \end{cases} \qquad \text{(Eq. 10)}$$

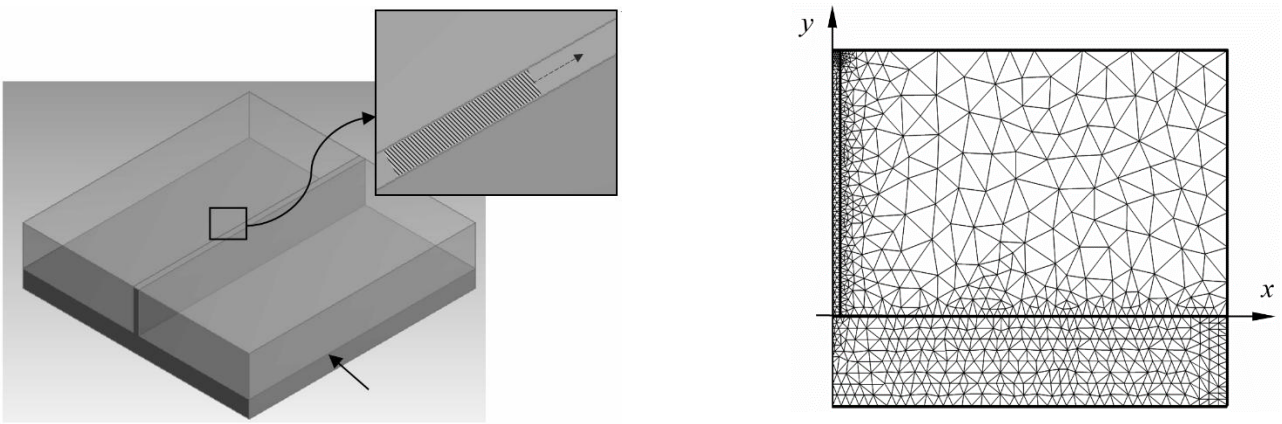

a) *b)*

Figure 1. *The problem setting of layer-by-layer sintering of a thin vertical wall: a) a schematic demonstration of the nature of movement of the laser beam on the surface of the sintered product; b) a finite element model for solving a problem in a flat setting. The cross section of the sintered wall is shown*

Downloaded from www.periodico.tchequimica.com

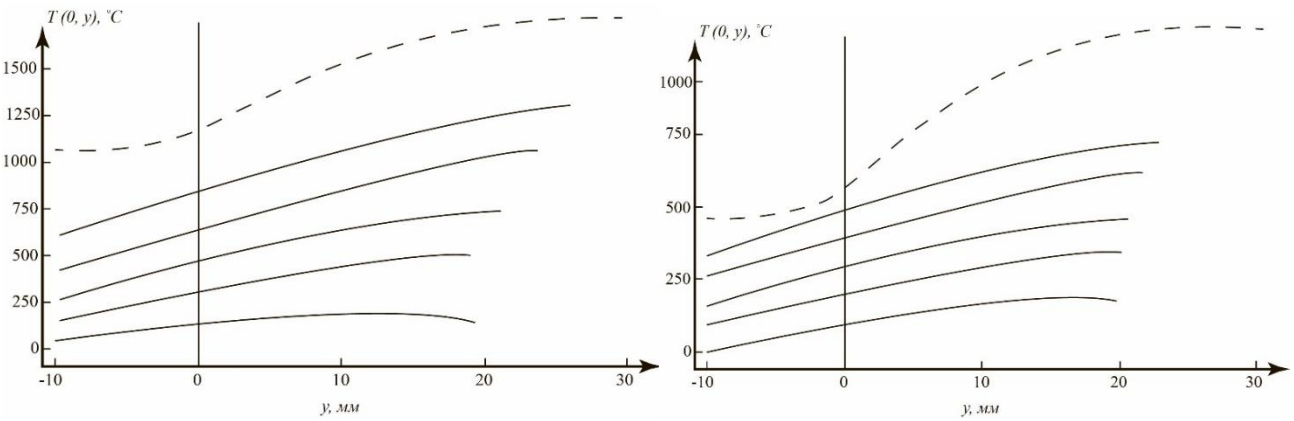

a) *b)*

Figure 2. *Change in the temperature profile T(0, y) throughout the height of the growing wall and in the platform below it. Temperature profiles that occur every 10 calculation steps are shown. The profiles are constructed for time moments preceding the next laser exposure, that is, when the surface of the product manages to cool down after the action of the previous laser pulse. The dashed line shows the solution, without taking into account the growth of the product and without taking into account the pulsed action of the laser*

Downloaded from www.periodico.tchequimica.com

PERIÓDICO TCHÊ QUÍMICA
ARTIGO ORIGINAL

METODOLOGIA PARA O CÁLCULO DE PROJETO DE ESTRUTURAS COMPOSITAS DE PAREDES ESPESSAS QUE OPERAM NAS CONDIÇÕES DE CARREGAMENTO EM ALTA VELOCIDADE

DESIGN CALCULATION TECHNIQUE FOR THICK-WALLED COMPOSITE CONSTRUCTIONS OPERATING UNDER HIGH-SPEED LOADING

МЕТОДИКА ПРОЕКТИРОВОЧНОГО РАСЧЕТА ТОЛСТОСТЕННЫХ КОМПОЗИТНЫХ КОНСТРУКЦИЙ, РАБОТАЮЩИХ В УСЛОВИЯХ ВЫСОКОСКОРОСТНОГО НАГРУЖЕНИЯ

BABAYTSEV, Arseniy V.[1*]; RABINSKIY, Lev N.[2];

[1,2] Moscow Aviation Institute (National Research University), Institute of General Engineering Training, Moscow – Russian Federation

** Correspondence author*
e-mail: Ar77eny@gmail.com

Received 03 September 2019; received in revised form 20 October 2019; accepted 26 October 2019

RESUMO

O artigo apresenta uma metodologia para o cálculo da estrutura axissimétrica de paredes espessas, composta por uma barra de aço (componente de reforço) e uma camisa externa de paredes espessas feita de fibra de carbono. A estrutura é carregada com calor linear distribuído ao longo de seu comprimento, associado à pressão externa ativa e forças inerciais. A metodologia baseia-se num modelo unidimensional da barra composta de seção variável levando em consideração as deformações transversais que são necessárias na análise da estrutura de paredes espessas operando sob pressão. Na abordagem proposta, a geometria do produto é dividida em seções e aproximada por fragmentos na forma de cones truncados e, no caso particular, de cilindros. Como resultado dos cálculos, é determinada a distribuição das tensões normais de tração/compressão na carcaça e na haste de reforço, bem como as tensões tangenciais no limite do contato. Como resultado dos cálculos de teste, é mostrada uma consistência bastante boa do modelo unidimensional considerado com modelagem refinada de elementos finitos. Foi estabelecido que a concentração de tensões de cisalhamento é realizada devido à presença de deformações substancialmente não homogêneas nas áreas de mudanças bruscas na geometria, uma redução no raio da casca (aparência de efeitos de arestas) e na área de um aumento acentuado no raio do chanfro da carcaça, onde a pressão externa está no lugar.

Palavras-chave: *estruturas compostas, barra de seção variável, carregamento em alta velocidade, cálculo de projeto, compósito de paredes espessas.*

ABSTRACT

The scientific paper presents a technique for calculating a thick-walled axially symmetrical construction consisting of a steel rod (reinforcing component) and an external thick-walled shell made of carbon fiber. The construction is loaded with linear load distributed along its length, associated with the operating external pressure, and inertial forces. The technique is based on a one-dimensional model of a composite rod of variable cross-section, roughly taking into account transverse deformations, which is necessary when analyzing a thick-walled construction operating under pressure. In the proposed approach, the geometry of the product is divided into sections and approximated by fragments in the form of truncated cones and, in the particular case, in the form of cylinders. As a result of calculations, the distribution of normal tensile/compression stresses in the shell and in the reinforcing rod, as well as tangential stresses at the boundary of their contact, are determined. As a result of test calculations, a fairly good consistency of the considered one-dimensional model with refined finite-element modeling is shown. It has been established that the concentration of shear stresses is realised due to the presence of substantially inhomogeneous deformations in the areas of sharp changes in geometry, a reduction in the radius of the shell (the appearance of edge effects), and in the area of a sharp increase in the radius of the bevel of the shell where external pressure is in place.

Keywords: *composite constructions, variable cross section rod, high-speed loading, design calculation, thick-walled composite.*

Downloaded from www.periodico.tchequimica.com

АННОТАЦИЯ

В работе представлена методика расчета толстостенной осесимметричной конструкции, состоящей из стального стержня (армирующего компонента) и внешней толстостенной оболочки, выполняемой из углепластика. Конструкция нагружается распределенной вдоль ее длины погонной нагрузкой, связанной с действующим внешним давлением, и инерционными силами. Методика основана на одномерной модели составного стержня переменного сечения, приближенно учитывающей поперечные деформации, что необходимо при анализе толстостенной конструкции, работающей под давлением. В предложенном подходе геометрия изделия разбивается на участки и аппроксимируется фрагментами в форме усеченных конусов и, в частном случае, цилиндров. В результате расчетов определяется распределение нормальных напряжений растяжения/сжатия в оболочке и в армирующем стержне, а также касательные напряжения на границе их контакте. В результате тестовых расчетов показана достаточно хорошая согласованность рассмотренной одномерной модели с уточненным конечно-элементным моделированием. Установлено, что концентрация напряжений на сдвиг реализуется из-за наличия существенно неоднородных деформаций в областях резкого изменения геометрии, уменьшение радиуса оболочки (появление краевых эффектов) и в области резкого увеличения радиуса скоса оболочки, где действует внешнее давление.

Keywords: *композитные конструкции, стержень переменного сечения, высокоскоростное нагружение, проектировочный расчет, толстостенный композит.*

1. INTRODUCTION

Design calculations based on one-dimensional approximate models of rods and beams of variable cross section can be effectively used in the development of axially symmetrical constructions of high-fineness ratio. Similar one-dimensional models are used, for example, in the design of columns and supports, including composite ones (Mossakovsky, 1990; Volchkov, 2007; Berezovskii *et al.*, 2015; Dudchenko, 2016; Lomakin *et al.*, 2018a), and (Lurie et al., 2015; Babaytsev *et al.*, 2017; Kakhramanov *et al.*, 2017; Rabinskiy and Tushavina, 2018; Formalev *et al.*, 2018a; Formalev *et al.*, 2018b; Lomakin *et al.*, 2018b; Rabinskiy and Tushavina, 2019a; Formalev and Kolesnik, 2019; Rabinskiy *et al.*, 2019; Nikitin *et al.*, 2019; Rabinskiy and Tushavina, 2019b; Babaytsev *et al.*, 2019). Such models make it possible, at a first approximation, to evaluate the construction strength and determine the loading conditions of its elements (compartments, sections) for further refined numerical calculations. In addition, simplified calculations can be useful for choosing the basic geometric parameters, layout, and structural arrangement of the designed products. Naturally, one-dimensional calculations are not sufficient, even during preliminary design study, but they can be considered basic, reducing the problem to the problem solved by the most simple methods from the structural resistance course (Rabinskiy and Tushavina, 2019c; Babaytsev *et al.*, 2019).

In this scientific paper, we consider the task of designing a composite axially symmetrical product consisting of a steel cylindrical rod (reinforcing component) located in the central part and a thick-walled shell surrounding it, made of carbon fiber and having an external diameter that varies along the axis of the product (see Figure 1). Intensive pressure having an effect on the outer surface of the shell in the rear part of the construction leads to large accelerations in the axial direction and, accordingly, to large values of inertial loads (Mykhalevskiy, 2018; Akbarov *et al.*, 2018; Mykhalevskiy and Horodetska, 2019). As a result, the construction operates under difficult stress conditions (all-round compression in the rear part, longitudinal compression in the front part, shear at the contact boundary of the shell and the rod, and in the region of change in the cross-section of the shell, etc.), which, however, at a first approximation, can be reduced to a simple one-dimensional case of loading a variable cross section composite rod (Dmitriev *et al.*, 2011; Skvortsov *et al.*, 2000). The task of the calculation in such a simplified model is to determine the tensile/compression stresses in the shell and in the rod, as well as to determine the tangential stresses in the zone of their contact (Yasnitskii, 1989; Gorchakov *et al.*, 2004; Skvortsov *et al.*, 2012). To assess the strength and integrity of the construction, the found stresses are compared, respectively, with the tensile strength of the shell material, the yield strength of the metal rod and the shear strength (resistance of collapse) of their contact joint.

A distinctive feature of the calculations is the relatively small aspect ratio of the products under consideration and the presence of

Downloaded from www.periodico.tchequimica.com

significant external pressure. In this case, neglecting the transverse deformations of the composite shell in the radial and circumferential directions leads to significant calculation errors. To take these deformations into account, at a first approximation, we use the technique proposed in (Kornev *et al.*, 2018), in which, practically, one can use the solution of the Lamé problem on deformations of a thick-walled hollow cylinder under pressure (Sedov, 1970). Initially, in (Kornev *et al.*, 2018), calculations were carried out only for the endings of the construction under consideration. In this work, the technique (Kornev *et al.*, 2018) is generalized to the case of an arbitrary number of sequentially arranged compartments of a given conical or cylindrical shape, for which a solution is framed taking into account the matching conditions at the boundaries of their contact. Since the geometry of the compartments is known in the case under consideration, the solution can be framed using the integral form of the equilibrium equations for each compartment of the product, in contrast to (Kornev *et al.*, 2018), where the equilibrium equations in differential form were used. The reliability of the proposed technique for design calculations is verified by the example of the typical geometry of the product under consideration, for which precise numerical calculations by the finite element method are carried out.

Note that in the model used, only the longitudinal characteristics of the product materials are available, therefore, in the general case, the technique turns out to be fair for both isotropic and anisotropic composite materials of the shell. The manufacturing technology of the shell is also insignificant, and it can be performed, for example, in the form of a thick-walled layered composite or by winding, etc.

2. MATERIALS AND METHODS

We consider an axially symmetrical composite construction in the form of a cylindrical steel rod and an external composite shell of variable cross section (see Figure 1). The structure is loaded with an external pressure p having an effect on the surface of the rear conical part of the shell (see Figure 3a). The pressure leads to an all-round compression of the rear part of the product, and its projection onto the central axis leads to the acceleration of the construction in the longitudinal direction a and to the corresponding inertial loads. Provided that the rod can be slightly longer than the shell, this can be taken into account by attaching the masses m0 and m1 at the front and rear ends of the rod.

2.1. Acceleration of the product and average shear stresses on the thread

First of all, we determine the acceleration of the product at a given pressure. If we know the whole mass of the product *m* (the shell, the rod and, if there are attached masses) and the maximum cross-sectional area of the rear part of the product *S*, which is under pressure, will be found Equation 1. Further, at a "zero-order" approximation, we estimate the shear linear force having an effect in the direction of the axis of the rod in the region of the threaded contact with the shell. We replace the impact of the shell on the rod by a distributed linear force $\overline{T}$ constant in magnitude (this is the main simplification at this stage of calculating the "zero-order" approximation) and having an effect in the longitudinal direction. By writing down the equation of equilibrium for the rod as a solid body, we find (Equation 2). Where m_c – the mass of the rod, Equation 3 – the cross-sectional area of the rod, ρ_c _ the density of the rod material, L – the length of the rod and Equation 4 – the diameter of the rod.

Then crosscutting linear effort is determined from the following Equation 5. The average tangential stresses on the thread are determined from the ratio (Equation 6).

2.2. Model of the integral composite rod

To frame a solution at a first approximation, we shall frame a solution in a one-dimensional setting, considering the equilibrium of the product only in the direction of its axis of symmetry. To do this, we integrate all the acting loads by the cross section and by the outer surface of the product, and remove them to the central axis. At a first approximation, we assume that all stresses are constant by the cross section of the shell and the rod. This approach allows us to evaluate the normal tensile/compression stresses in the outer shell $\sigma_0(z)$ and in the rod $\sigma_c(z)$, as well as tangential stresses at the boundary of their contact $\tau(z)$. The outer duct of the real product is approximated by piecewise linear sections, that is, the axially symmetrical geometry of the shell is approximated by sections in the form of truncated cones and cylinders. The

Downloaded from www.periodico.tchequimica.com

rod is modeled as a cylinder. It is assumed ideal contact between the rod and the shell.

In order to frame a solution, let us consider the truncated part of the product fragment presented in Figure 2. This figure shows the external loads and internal stresses having an effect on the truncated fragment of the shell and the rod (shown by hatching). We write down the equations of equilibrium and strain compatibility conditions for *i*-th product fragment within which the axial coordinate varies in the range $z_{i-1} \le z \le z_i$. We obtain the following ratios:

1) The equilibrium condition of the outer shell element (Equation 7). Where Equation 8 – the cross-sectional area of the considered *i*-th element of the shell at the point *z,* Equation 9 – the radius of the cross section of the fragment at a given point, $R_i(0)$ – the radius of the initial section of the fragment, α_i – taper angle of the fragment (for cylindrical fragments α_i = 0, $\sigma_0(z)$ – stresses in the current section of the shell fragment, $\sigma_0(z_{i-1})$ – stresses having an effect on the left boundary of the shell fragment under consideration (at the initial point *z* = 0, these stresses are equal to the operating pressure *p*, and then they are determined based on the solution in the previous section of the product), Equation 10 – the volume of the shell fragment, Equation 11 – the volume of the rod fragment, Equation 12 – the resultant of shear stresses having an effect on the contact of the shell fragment and the rod.

2) The equilibrium condition of the rod element is determined using Equation 13. Where Equation 14 – the cross-sectional area of the rod; and at the starting point, the stresses are calculated taking into account the operating pressure and the mass attached (Equation 14).

3) strain compatibility conditions with approximate allowance for the operating pressure are written as follows (Equation 15) (Kornev *et al.*, 2018). Where E_s, E_o, ν_s, ν_o – elastic moduli and Poisson's ratios of the materials of the rod and the shell, respectively.

For the shell fragments on which pressure does not have an effect Equation 7 reduces to a simpler ratio (Equation 16), which determines the equality of longitudinal deformations in the rods and in the shell. A detailed derivation of the ratio (Equation 7) was presented in (Kornev *et al.*, 2018) based on the solution of the Lamé problem for a thick-walled cylinder loaded with pressure.

From the written down three Equations 7 – 17, three unknown functions are determined: $\sigma_0(z)$, $\sigma_c(z)$, $T(z)$. The tangential stresses at the contact of the rod and the shell are determined from the Equation 18.

These stresses, in contrast to the solution of the "zero" approximation (Equation 6), turn out to be variable by the length of the rod. The found stress values are compared with the corresponding maximum permissible stresses for the materials of the shell, the rod and their threaded connection.

3. RESULTS AND DISCUSSION:

3.1. Initial data

We consider an example of product geometry presented in Figure 3. The total length of the product is 500 mm. The maximum cross-sectional diameter d_{max} = 160 mm, and its area, respectively (Equation 19). The diameter of the reinforcing rod is 20 mm. Operating pressure *p* = 300 MPa. The rod material is steel with properties ρ_s = 7850 kg/m^3, E_s = 200 GPa, ν_s = 0.3. Yield strength of steel under tension and compression σ_s =±355 MPa. The material of the composite shell is carbon laminate with a density ρ_o = 1500 kg/m^3 and with characteristics in the direction of the product axis E_o = 60 GPa, ν_o = 0.35, σ_o = +1100/-700 MPa. The shear strength (resistance of collapse) of the joint is 120 MPa. Attached masses at the ends of the rod are absent. The total mass of the construction *m* = 4.47 kg.

On the basis of (Equation 1) we find the acceleration of the product for the given conditions of the problem *a* = 1.341 m/s. This acceleration is quite large, however, it is less than the speed of sound in the materials under consideration, therefore, at a first approximation, all calculations, including numerical ones, can be carried out in a quasi-static setting. The average tangential shearing stress is determined from (Equation 6) and is $\overline{\tau} = 114$ MPa. Thus, from a simple design calculation of the "zero" approximation, it follows that the strength margin of the joint under given loading conditions can be quite large (more than 114.3 MPa), if, due to the optimal choice of the product geometry, an approximately constant shear force along the length of the rod can be realized. Structural failure can occur only due to the uneven distribution of shear forces, that is, the presence of a concentration of shear stresses on the mount, which can be associated, for example,

Downloaded from www.periodico.tchequimica.com

with a sharp change in the size of the cross section of the outer shell.

3.2. Numerical modeling

To verify the results of design calculations, we will carry out numerical modeling applying the finite element method with the use of Ansys Workbench software, taking into account the axial symmetry of the problem. An example of a finite element model of the product is shown in Figure 3. The average size of the elements is ~ 1.5 mm; the total number of elements in the model is ~ 16274. The pressure is set in the region of the rear part of the product (at the border highlighted in color in Figure 3) and is balanced by the inertial forces associated with acceleration in the longitudinal direction of the product. The threaded connection is not drawn – an ideal contact is set between the rod and the shell along a smooth boundary, remote from the central axis by a distance equal to the radius of the rod. The calculation is carried out in a linearly elastic setting under the assumption of small strains, at the quasi-static approximation. The results of numerical modeling are presented in Figure 4. It shows the distribution of normal stresses in the longitudinal direction and tangential stresses in the plane of the model section (*zr).*

3.3. Comparison of analytical and numerical calculations

Figure 5 shows a comparison of the results of design calculations by the analytical method described in section 2.2., with the results of numerical modeling presented in section 3.2. It shows the distribution of normal stresses in the longitudinal direction in the rod (on the central axis) and in the shell. The distribution of tangential stresses at the contact boundary of the shell and the rod is shown in Figure 5c.

From the calculation results it follows that the concentration of shear stresses is realized due to the presence of substantially inhomogeneous strains in the areas of sharp changes in geometry, a decrease in the radius of the shell (the emergence of edge effects), and in the region of a sharp increase in the radius of the bevel of the shell, where external pressure has an effect. In these places, a fastener cut may begin. This can be eliminated by strengthening these areas, in particular, by increasing the radius. The estimation by the model of the integral composite rod (see section 2.2), gives significant errors, although the found value of 390 MPa approximately corresponds to the level of effective stresses. Normal stresses turns out to be negative along the entire length of the rod and in the shell in front part of the product. Positive tensile stresses are realized in the shell material in the rear part of the product, where external pressure has an effect. These stresses *exceed* the specified tensile strengths of materials.

The obtained analytical solution is quite close to the results of numerical modeling. It can be seen that the tangential force in the analytical solution is overestimated in the concentration region, and thus designing on the basis of this solution provides an additional margin of safety for the joint. This approximate solution can be used for preliminary product design and for choosing the geometry of the outer shell, which provides shear strength of the fastener and tensile-compressive strength of the rod and the shell without taking into account the concentration associated with the uneven distribution of stresses over the shell cross section (see Figure 5).

In general, further consideration requires an improved three-dimensional calculation with layered analysis. And speaking of composites – it is necessary to take into account the complex criteria of a combined stress, layer-by-layer analysis.

4. CONCLUSIONS:

1. The technique for calculating a thick-walled axially symmetrical construction has been considered.

2. A one-dimensional model of a composite rod of variable cross section, approximately taking into account transverse strains, was regarded. As a result of calculations, the distribution of normal tensile/compression stresses in the shell and in the reinforcing rod, as well as tangential stresses at the boundary of their contact, are determined.

3. As a result of test calculations, a fairly good consistency of the considered one-dimensional model with improved finite-element modeling is shown. Normal stresses in the longitudinal direction and tangential stresses in the plane of the model section under consideration were obtained using the described technique and the finite element method. A comparative analysis of the results obtained was carried out. Recommendations are given for further consideration of such constructions.

Downloaded from www.periodico.tchequimica.com

5. ACKNOWLEDGMENTS:

The work was carried out with the financial support of the state project of the Ministry of Education and Science project code 2.9219.2017/8.9.

6. REFERENCES:

1. Akbarov, R.D., Zhilisbaeva, R.O., Tashpulatov, S.S.H., Cherunova, I.V., Bolysbekova, R.T. I*zvestiya Vysshikh Uchebnykh Zavedenii, Seriya Teknologiya Tekstil'noi Promyshlennosti*, 2018, 2018-January(5), 188-192
2. Babaytsev, A., Dobryanskiy, V., Solyaev, Y. *Lobachevskii Journal of Mathematics*, **2019**, *40*(7), 887-895. DOI: 10.1134/S1995080219070059.
3. Babaytsev, A.V., Prokofiev, M.V., Rabinskiy, L.N. *International Journal of Nanomechanics Science and Technology,* **2017**, *8*(4), 359-366. DOI: 10.1615/NanoSciTechnolIntJ.v8.i4.60.
4. Berezovskii, V.V., Shavnev, A.A., Solyaev, Y.O., Lur'e, S.A. *Russian Metallurgy (Metally)*, **2015**, *10*, 790-794.
5. Dmitriev, A.I., Skvortsov, A.A., Koplak, O.V., Morgunov, R.B., Proskuryakov, I.I. Physics of the Solid State, **2011**, *53*(8), 1547-1553.
6. Dudchenko, A.A. Calculation, design and manufacturing technology of thermostable composite rod. *Composite Materials Constructions*, **2016**, *1*, 3-11.
7. Formalev, V.F., Kolesnik, S.A. *Journal of Engineering Physics and Thermophysics*, **2019**, *92*(1): 52-59.
8. Formalev, V.F., Kolesnik, S.A., Kuznetsova, E.L. *Periodico Tche Quimica*, **2018a**, *15*(Special Issue 1), 426-432.
9. Formalev, V.F., Kuznetsova, E.L., Kuznetsova, E.L. *Periodico Tche Quimica*, **2018b**, *15*(Special Issue 1): 377-389.
10. Gorchakov, A.I., Semenova, A.V., Syrovatskaya, Yu.V., Shcherbakov, Yu.V., Yasnitskij, L.N. *Fizika i Khimiya Obrabotki Materialov*, **2004**, *1*, 43-47.
11. Kakhramanov, R.M., Knyazeva, A.G., Rabinskiy, L.N., Solyaev, Y.O. *High Temperature*, **2017**, *55*(5), 731-736.
12. Kornev, Yu.V., Emelyanov, S.V., Lukyanova, A.Yu., Semenov, N.A., Semenov, P.E., Babaytsev, A.V. *Composites: Mechanics, Computations, Applications*, **2018**, *9*(4), 283-295. DOI: 10.1615/CompMechComputApplIntJ.2018025142.
13. Lomakin, E., Rabinskiy, L., Radchenko, V. *Meccanica*, **2018a**, *53*(15), 3831-3838. DOI: 10.1007/s11012-018-0919-y.
14. Lomakin, E.V., Lurie, S.A., Belov, P.A., Rabinskiy, L.N. *Doklady Physics*, **2018b**, *63*(12), 503–507.
15. Lurie, S.A., Kuznetsova, E.L., Rabinskiy, L.N., Popova, E.I. *Mechanics of Solids*, **2015**, *50*(2), 135-146.
16. Mossakovsky, V.I. *The strength of rocket structures,* Moscow: Vysshaya shkola, **1990**.
17. Mykhalevskiy, D. *Eastern-European Journal of Enterprise Technologies,* **2018**, *6*(9-96), 16-21
18. Mykhalevskiy, D.V., Horodetska, O.S. *Journal of Mechanical Engineering Research and Developments*, **2019**, *42*(2), 2019, 50-57
19. Nikitin, P.V., Tushavina, O.V., Shkuratenko, A.A. *Incas Bulletin*, **2019**, *11*(Special Issue), 191-201. DOI: 10.13111/2066-8201.2019.11.S.19.
20. Rabinskiy, L.N., Tushavina, O.V. *Incas Bulletin*, **2019a**, *11*(Special Issue), 203-211. DOI: 10.13111/2066-8201.2019.11.S.20;
21. Rabinskiy, L.N., Tushavina, O.V. *Periodico Tche Quimica*, **2018**, *15*(Special Issue 1), 321-329.
22. Rabinskiy, L.N., Tushavina, O.V., Fedotenkov, G.V. *Asia Life Sciences*, **2019b**, Supplement 19(1), 49-162.
23. Rabinsky, L.N., Tushavina, O.V. *STİN*, **2019c**, *4*, 22-26.
24. Sedov, L.I. *Continuum Mechanics*, Moscow: Nauka, **1970**.
25. Skvortsov, A.A., Orlov, A.M., Frolov, V.A., Gonchar, L.I., Litvinenko, O.V. *Physics of the Solid State*, **2000**, *42*(10), 1861-1864.
26. Skvortsov, A.A., Orlov, A.M., Zuev, S.M. *Russian Microelectronics*, **2012**, *41*(1), 31-40.
27. Volchkov, O. D. *The strength of launch*

Downloaded from www.periodico.tchequimica.com

vehicles. Moscow: MAI Publishing House, **2007**.
28. Yasnitskii, L.N. *Mechanics of Solids*, **1989**, *24*(2), 90-96.

$$a = pS/m \quad \text{(Eq. 1)}$$

$$m_c a = pS_c + \bar{T}L \quad \text{(Eq. 2)}$$

$$S_c = \pi d_c^2 / 4 \quad \text{(Eq. 3)}$$

$$d_c = 2R_c \quad \text{(Eq. 4)}$$

$$\bar{T} = \left(m_c a - pS_c\right)/L \quad \text{(Eq. 5)}$$

$$\bar{\tau} = \frac{\bar{T}}{2\pi R_c} \quad \text{(Eq.6)}$$

$$\sigma_0(z)S_i(z) = \sigma_0(z_{i-1})S_i(z_{i-1}) + \rho_0 a V_i(z) + T(z) - p\left(S_i(z) - S_i(z_{i-1})\right) \quad \text{(Eq. 7)}$$

$$S_i(z) = \pi\left(R_i^2(z) - R_p^2\right) \quad \text{(Eq. 8)}$$

$$R_i(z) = R_i(0) + \left(z - z_{i-1}\right)\tan\alpha_i \quad \text{(Eq. 9)}$$

$$V_i(z) = \frac{1}{3}\pi\left(z - z_{i-1}\right)\left(R_i^2(0) + R_i(0)R_i(z) + R_i^2(z)\right) - V_c(z) \quad \text{(Eq. 10)}$$

$$V_c(z) = \pi R_p^2\left(z - z_{i-1}\right) \quad \text{(Eq. 11)}$$

$$T(z) = 2\pi R_c \int_{z_{i-1}}^{z} \tau(x)dx \quad \text{(Eq. 12)}$$

$$\sigma_c(z)S_c = \sigma_c(z_{i-1})S_c + \rho_c a V_c(z) - T(z) \quad \text{(Eq. 13)}$$

$$S_c = \pi R_c^2 / \quad \text{(Eq. 14)}$$

$$\sigma_c(0) = \frac{m_0 a}{S_c} - p \quad \text{(Eq. 15)}$$

$$E_c\sigma_0 = E_0\sigma_c \quad \text{(Eq. 16)}$$

$$\sigma_0(z) = \frac{E_0}{E_c}\left(\sigma_c(z) + 2\nu_c p\right) - 2\nu_0 p \quad \text{(Eq. 17)}$$

Downloaded from www.periodico.tchequimica.com

$$\tau(z) = \frac{d}{dz}\left(\int_{z_{i-1}}^{z} \tau(x)dx \right) = \frac{1}{2\pi R_c} \frac{dT(z)}{dz} \qquad \text{(Eq. 18)}$$

$$S = \frac{\pi \cdot d_{\max}{}^2}{4}. \qquad \text{(Eq. 19)}$$

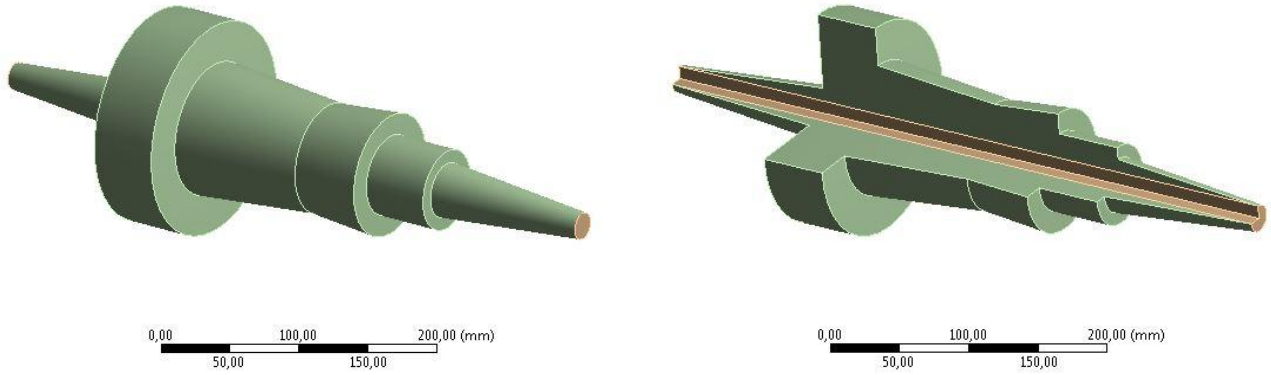

Figure 1. *Integral composite rod: 1 – steel reinforcing component, 2 – external composite shell of variable cross section*

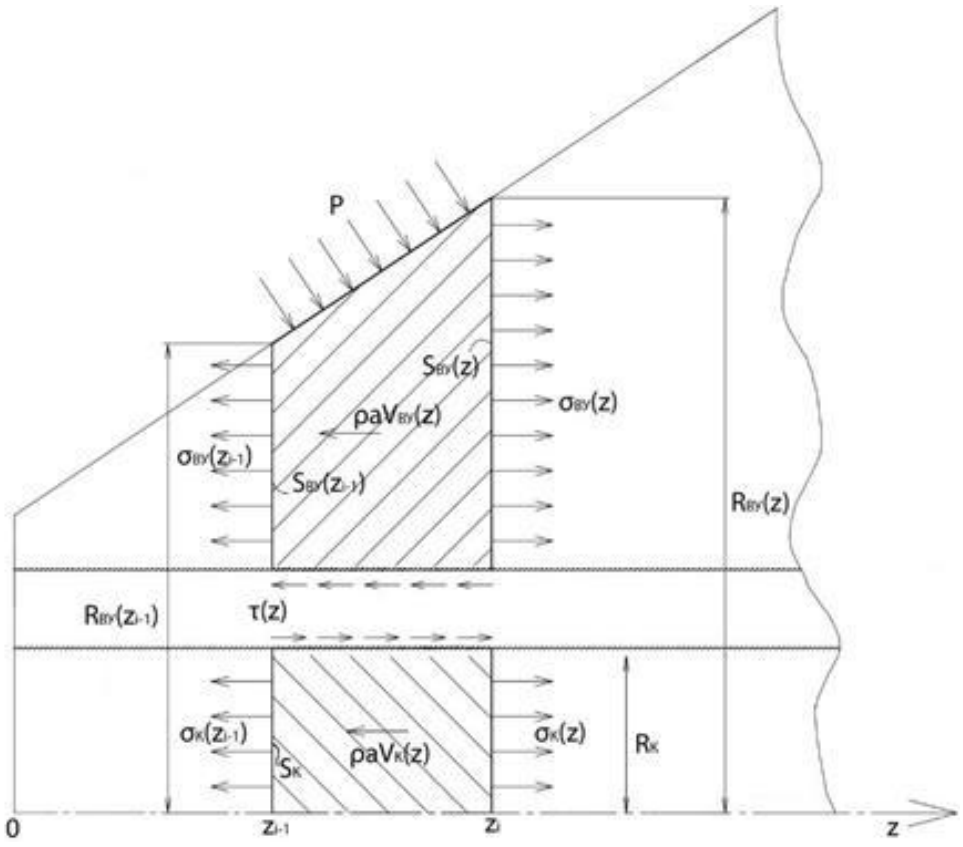

Figure 2. *Fragment of the rod and the outer shell, and the loads having an effect on them*

Downloaded from www.periodico.tchequimica.com

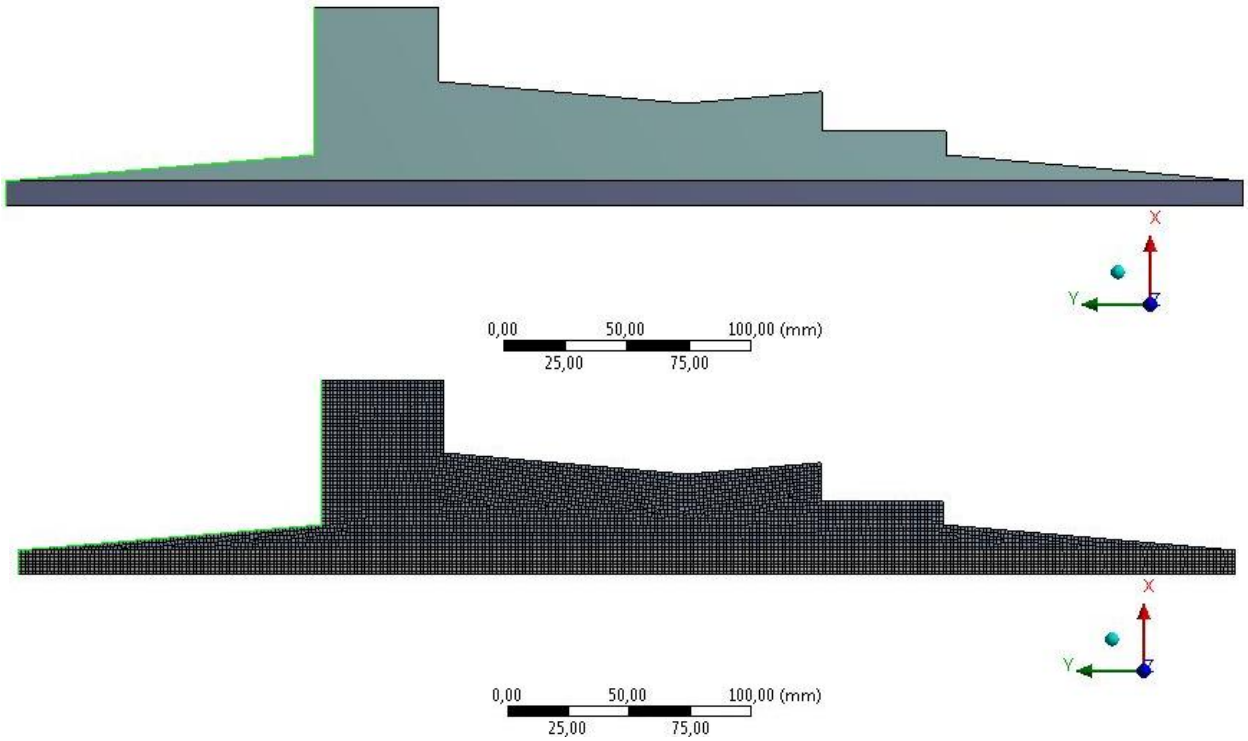

Figure 3. *An example of the considered geometry of the product and its finite element model. The zone of external pressure effect is shown in color*

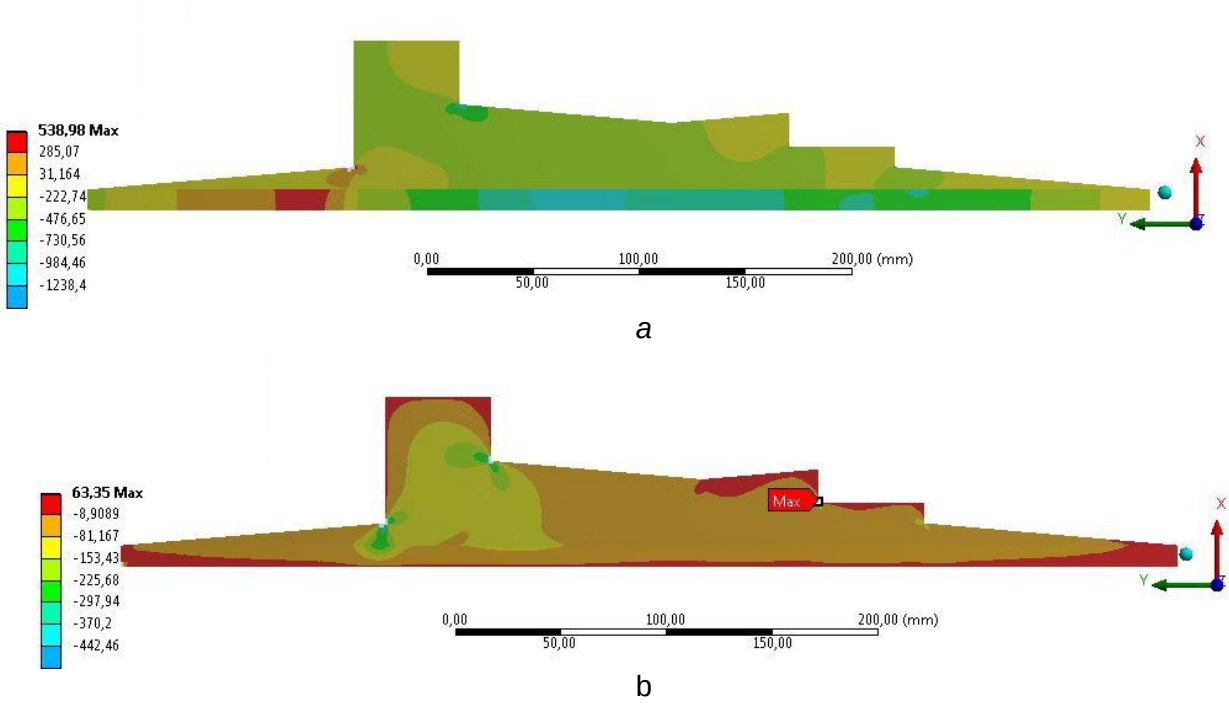

Figure 4. *The results of finite element modeling, a: normal stresses in the longitudinal direction, b: tangential stresses in the plane of the considered model section*

Downloaded from www.periodico.tchequimica.com

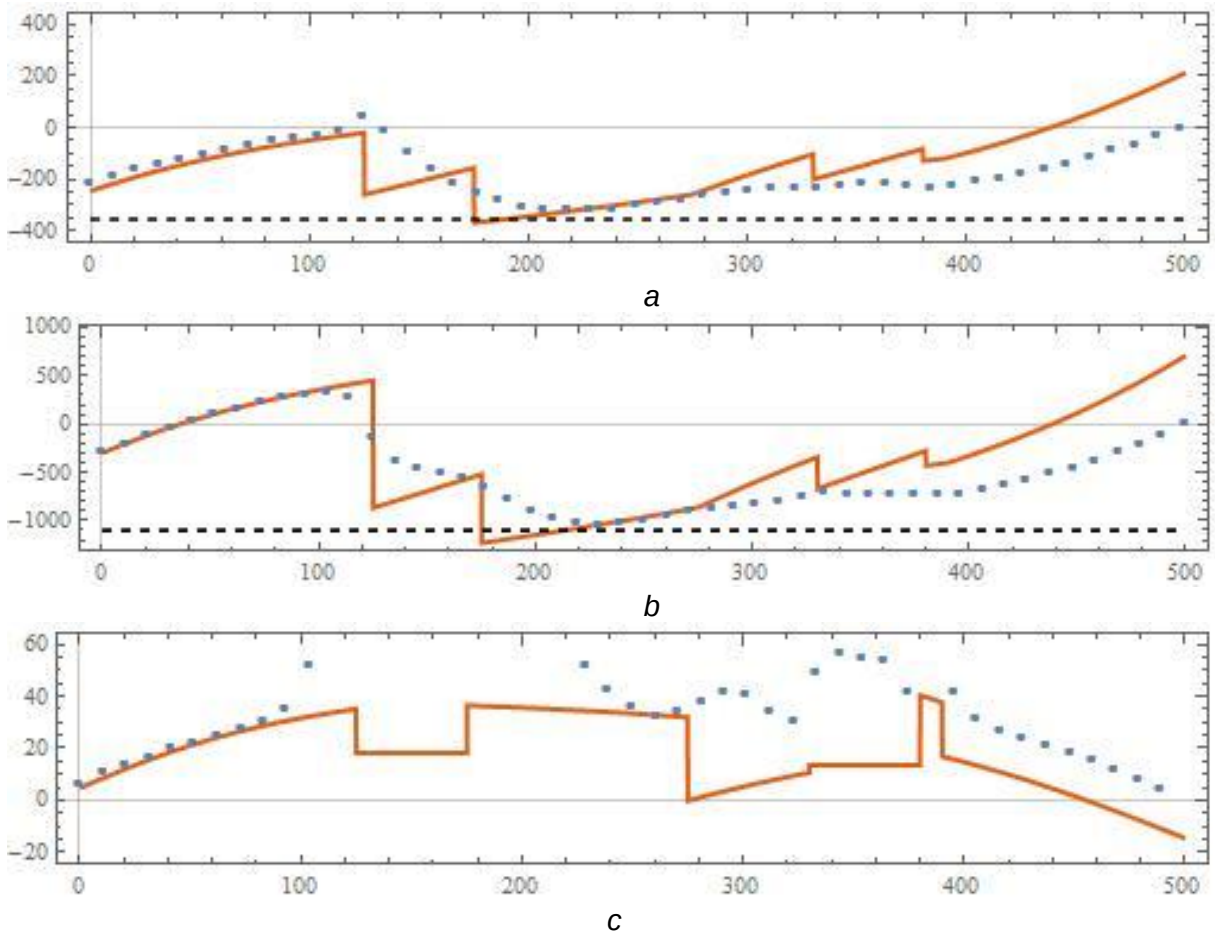

Figure 5. *Comparison of the results of analytical (solid lines) and numerical (points) modeling, a: longitudinal stresses in the rod Sc(z) [MPa], b: longitudinal stresses in the shell So(z) [MPa], in: tangential stresses at the contact τ(z) [MPa]. Dotted lines show the corresponding stress limits*

Downloaded from www.periodico.tchequimica.com

PERIÓDICO TCHÊ QUÍMICA
ARTIGO ORIGINAL

AVALIAÇÃO DA DURABILIDADE DOS REVESTIMENTOS EM DIFÍCEIS CONDIÇÕES DE ESTRESSE

ASSESSMENT OF DURABILITY OF COATINGS IN DIFFICULT STRESS CONDITIONS

ОЦЕНКА ПРОЧНОСТИ ПОКРЫТИЙ В УСЛОВИЯХ СЛОЖНОГО НАПРЯЖЕННОГО СОСТОЯНИЯ

GETMANOV, Alexandr G.[1*]; RABINSKIY, Lev N.[2];

[1] Moscow Aviation Institute (National Research University), Department of Spacecraft Engineering, Moscow – Russian Federation

[2] Moscow Aviation Institute (National Research University), Department of Engineering Graphics, Moscow – Russian Federation

** Correspondence author*
e-mail: getmanov@mai.ru

Received 12 September 2019; received in revised form 20 October 2019; accepted 26 October 2019

RESUMO

Foram estudadas as propriedades mecânicas de revestimentos protetores à base de epóxi-poliéster aplicados a substratos de aço. Foram determinadas as características mecânicas dos revestimentos, bem como sua influência no comportamento das amostras sob carga mecânica. Testes de amostras com revestimentos, criados por métodos de nanoindentação, com posterior processamento de dados experimentais usando modelos analíticos simplificados padrão e usando modelagem numérica de elementos finitos, foram realizados. Em ensaios de tração, foi demonstrado que a presença de revestimentos leva a alterações na natureza da fratura das amostras. Nos testes de estabilidade, os resultados dos dados experimentais foram comparados com os resultados dos cálculos analíticos e numéricos, que demonstraram o efeito dos revestimentos na estabilidade de amostras de paredes finas. As propriedades mecânicas das amostras com revestimentos em um ou nos dois lados da amostra foram estudadas, o que também confirmou o módulo elástico dos revestimentos estudados em um nível de até 10 GPa (com o valor médio para materiais a granel até 3,5 GPa). No processo de teste em temperatura elevada, foi estabelecida a importância de garantir um aperto constrito das amostras na ausência dos quais ocorre um aumento significativo no erro de medição. Devido a deformações de temperatura, a rigidez das amostras é reduzida e, consequentemente, diverge das condições do selo rígido adotado nos cálculos. Os resultados obtidos visam desenvolver ideias sobre propriedades mecânicas bem como métodos para alterar e calcular propriedades mecânicas, revestimentos de proteção finos usados em várias indústrias e, em particular, uma ampla classe de revestimentos usados para proteger elementos estruturais das estruturas de aeronaves contra a corrosão.

Palavras-chave: *resistência do revestimento, tensões residuais, revestimentos protetores, modelagem de elementos finitos, módulo de elasticidade.*

ABSTRACT

The mechanical properties of protective powder coatings based on epoxy-polyester applied to steel substrates were studied. The mechanical characteristics of coatings, as well as their influence on the behavior of samples under mechanical loading, were determined. Tests of samples with coatings, created by Nano indentation methods, with subsequent processing of experimental data using standard analytical simplified models and using numerical finite element modeling were performed. In tensile tests it was demonstrated that presence of coatings leads to changes in the nature of fracture of the samples. In stability tests, the results of experimental data were compared with the results of analytical and numerical calculations, which demonstrated the effect of coatings on the stability of thin-walled samples. The mechanical properties of samples with coatings on one or both sides of the sample were studied, which also confirmed the elastic modulus of the studied coatings at a level of up to 10 GPa (with the average value for bulk materials up to 3.5 GPa). In the process of testing at elevated temperature, the importance of ensuring tight clamping of the samples was established, in the absence of which significant increase in the measurement error takes place. Due to temperature deformations, stiffness of the samples is reduced and, accordingly, deviate from conditions of hard seal

Downloaded from www.periodico.tchequimica.com

assumed in calculations. The results obtained are aimed at developing an understanding about mechanical properties, as well as about methods for changing and calculating mechanical properties, thin protective coatings used in various industries and, in particular, a wide class of coatings used to protect aircraft structural components from corrosion.

Keywords: *coating rigidity, residual stresses, protective coatings, finite element modeling, elastic modulus.*

АННОТАЦИЯ

Исследуются механические свойства защитных порошковых покрытий на эпоксидно-полиэфирной основе, нанесенных на стальные подложки. Определены механические характеристики самих покрытий, а так же их влияние на поведение образцов при механическом нагружении. Проведены испытания образцов с покритями методами наноиндентирования с последующей обработкой экспериментальных данных с использованием стандартных аналитических упрощенных моделей, так и с использованием численного конечно-элементного моделированяи. В испытаниях на растяжение показано, что наличие покрытий приводит к изменению характера разрушения образцов. В испытаниях на устойчивость проведено сопоставление результатов экспериментальных данных и результатов аналитических и численных расчетов, которые показали влияние наличия покрытий на устойчивость тонкостенных образцов. Исследованы механические свойства образцов с покрытиям, нанесенными с одной или с двух сторон образца, которые также подтверждают значения модуля упругости исследуемых покрытий на уровне до 10 ГПа (при обычном значении для объемных материалов до 3.5 ГПа). В процессе проведения испытаний при повышенной температуре установлена важность обеспечения плотного зажима образцов, в отсутствие которого, происходит значительное увеличение погрешности проводимых измерений – вследствие температурных деформаций жесткость закрепления образцов снижается и, соответственно, отклоняются от условий жесткой заделки, принимаемой в расчетах. Полученные результаты направлены на развитие представлений о механических свойствах, а также о способах измерения и расчета механических свойств, тонких защитных покрытий, применяемых в различных отраслях промышленности и, в частности, широкого класса покрытий, применяемых для защиты от коррозии элементов конструкций авиационной техники.

Keywords: *прочность покрытий, остаточные напряжения, защитные покрытия, конечно-элементное моделирование, модуль упругости.*

1. INTRODUCTION

Polymer coatings are widely used in various fields of technology to protect structural elements from corrosion, and to provide electrical insulation, to control the frictional characteristics of surfaces, for decorative purposes, etc. (Gavrilova *et al.,* 2009) Getting reliable identification of mechanical properties of coatings is an important task from the point of view of ensuring their durability and wear resistance during operation (Gavrilova *et al.,* 2009; Gavrilov *et al.,* 2009). In the present dissertation, we provide the determination of the mechanical properties of coatings based on epoxy-polyester that are used to protect the structural elements of aircraft from corrosion. Based on the sequence of experimental studies and theoretical calculations, the elastic modulus of coating material is determined, the residual stresses acting in it, resulting from use of heat treatment during coating process (Zezin *et al.,* 2012a; Zezin *et al.,* 2012b; Gavrilov *et al.,* 2012).

The results can be used to assess the strength and durability of coating materials, and to assess their impact on the mechanical behavior of protected thin-walled structures. When doing strength calculations of large-sized structures, the influence of coatings can be neglected if the wall thickness of the products significantly exceeds the thickness of the coatings and stiffness of coatings is much lower than stiffness of material of the structure. Nonetheless, if the thickness of the coating is comparable with the thickness of the structural element and if the coatings have sufficient rigidity, then their influence cannot be neglected in certain loading cases. From the point of view of strength calculations, thin-walled metal structural elements with polymer coatings can be represented in the form of two- or three-layer plates (depending on whether the coating is applied on one or both sides) with stiffer middle layer of metal and much more pliable outer layers -coatings. Now, not many experimental and theoretical works are known in which macroscopic mechanical behavior of such structural elements of this kind is analyzed taking into account the effects of the influence of residual stresses. We can note a wide variety of works in the field of study of functional gradient

Downloaded from www.periodico.tchequimica.com

thin-walled structures with coatings. However, in these structures it is usually assumed that the stiffness of the surface layers is higher compared to the inner area. Such structures are, for example, metal products with ceramic coatings or with hardened surface areas. The study of thin-walled structures with rigid middle layer and pliable thin outer layers has not received much attention. In linear problems of statics, experiments show that the influence of thin coatings can be neglected. Nonetheless, in more specific problems, for example, under conditions of finite strains, nonlinear elasticity, stability and vibration loading problems of thin-walled structures with coatings, neglect of influence of coatings can lead to calculation errors. Therefore, in this work, we study the intrinsic properties of mechanical coatings, evaluate residual stresses acting in them and their strength, and analyze the effect of coatings on the mechanical behavior of thin steel plates under static loading.

2. MATERIALS AND METHODS

Let us evaluate the strength of the coating in conditions of separation tests of cantilever-fixed sample. In order to do this, we consider the option of testing samples in the form of thin metal plates (strips) with coatings fixed at one end to a rigid substrate (Figure 1). Fixing to the substrate is realized by high-strength adhesive joints, the cohesive and adhesive strength of which exceeds the adhesive strength of the coating to the substrate and, accordingly, provides the possibility of changing the latter in this experiment. The plate is loaded by force at free end directed vertically upwards, while the rigid substrate is fixed on lower surface. So, the separation of the plate from the substrate is ensured. By high-strength adhesive, as it was said, the fracture is localized at the boundary of the coating with the substrate and, thus, in tests, it is possible to determine the maximum load at which this destruction begins. The destruction mechanism is complex in this case since both normal and shear stresses act in the presented test scheme in the coating and in the substrate. The maximum of these stresses is located at the point where the rigid substrate ends (x = L – a). We are performing calculations to estimate these stresses. In the calculations, we assume that the thickness of coating hc and the adhesive joint ha can be neglected and the problem of deformations of beam of thickness h fixed at one end on a steel substrate of thickness H can be considered. The shear force and bending moment arising in the beam determine the level of stress at the boundary of its contact with a substrate and, accordingly, the desired stress level in coating.

The length of the cantilever beam extending beyond the rigid skid is a. Thus, the moment and shear force acting at the separation point are (Equation 1).

In the fixation area x <La the beam deflections and its curvature remains zero, and, therefore, in the framework of classical beam theory, in this area in the beam, both moment and shear forces are equal to zero. Therefore, from the point of view of classical theory, the beam stays in unstressed state in fastening zone, and only at the boundary of the fastening zone concentrates bending moment and cutting force applied to it. Therefore, the classical theory does not allow us to estimate the level of stresses acting in the area of contact between the beam and rigid substrate (Geodesic…, 2005).

More acceptable estimates for the problem under consideration can be obtained by considering the Timoshenko beam model. This model is an approximation of the real deformed state of the beam, which, generally speaking, must be described, taking into account the effects of compression (Feodosiev, 2013; Grigolyuk and Tolkachev, 1980). By resolving shear deformations in the beam, it is possible to evaluate how its stress-strain state changes in fastening area, where there is no deflection and the curvature remains zero (the shifts are acceptable: the lower surface of beam remains in full contact with rigid substrate, and the upper moves relative to the lower due to externally applied load transmitted from loose end of the beam).

In the case of small deflections, the beam curvature in the framework of Tymoshenko model is determined by the following relation (Equation 2) (Grigolyuk and Tolkachev, 1980). Where y (x) – is the deflection of the beam, – is bending moment – is shearing force, E – is Young's modulus of beam material (metal sample, in this case), G – is shear modulus of the beam, I = bh $^{3/12}$ – is iteration moment in beam section, F = bh cross-sectional area, 5/6 – correction ratio introduced in the theory of Tymoshenko (Timoshenko and Gere, 2002), the hatch denotes the derivative in the x direction (Beam Deflection…, 2019).

Given that in the fastening area, the beam curvature equals zero, and the cutting force is related to the moment (Equation 3), the differential equation for bending moment has the

Downloaded from www.periodico.tchequimica.com

form (Equation 4).

The boundary conditions for this equation are determined from (1) on the right end and on condition of absence of load on the left, that is, it is possible to use conditions of the form (Equation 5) or (Equation 6).

It is impossible to satisfy both conditions in terms of moment and shear force (4) since in the recorded model there are not enough constants for this. Fulfillment of this condition at the remote end of the fixed beam is mandatory since it implies the absence of angles of rotation of the beam sections, which is performed either in case of symmetry of problem under consideration or in case of sufficient length of the beam fixing area.

The general solution to problem (2) has this form (Equation 7).

Given the boundary conditions (4) and simplifications, we get the distribution of internal force factors and transverse load in the fastening area (Equation 8).

Let us note that shearing force in (6) determines the shear stresses that are realized in the beam and at the boundary of its contact with the substrate. The nature of the distribution of tangential stresses over the thickness of the beam outside the area is described by a parabolic dependence, however, in the contact area this dependence deviates from the classical law, primarily because the tangential stresses on the lower surface of the beam cease to be zero due to its conjugation with the substrate. By analogy with the classical approach, it is suggested to introduce the following estimate to determine desired tangential stresses at the contact of the beam with the substrate using the correction factor (Equation 9).

These stresses (9) lead to the cut of the coating from the substrate. Normal stresses that lead to separation of coating are estimated based on distributed nominal load (8). Value is linear load, respectively, normal stresses are determined by the following relationship, in which we also introduce a correction factor (Equation 10).

The ratio k_σ, k_τ are proposed to calculate by comparison of the obtained solutions with numerical modeling for the problem under consideration (see below).The maximum tangential and normal stresses that can be used in the processing of experimental data are realized at the boundary of the pinning area and have the form (taking into account the definition for α in 3)) (Equation 11-12). Where ν – is the Poisson coefficient of the beam material.

From the obtained solutions (9) – (12), it can be seen that the stresses decay exponentially with distance from the boundary of the fastening area (in accordance with the Saint-Venant principle). The maximum values of these stresses depend on the parameters of the model. They are proportional to the applied load and length of loose end of the sample protruding beyond the substrate, and proportional to the width of the sample and the square of its thickness. With a sufficiently large extent of the fastening area (L >> a), the tangential stresses practically cease to depend on its length, since the free end of the beam ceases to influence at the point x = 0 (Equation 13).

In this case, constant relationship between tangential and normal stresses is realized, which is determined by the Poisson's ratio of beam material (Equation 14).

In case of a small length of the fastening area, the effect of the end of the beam, at which the zero load is set (x = 0), is still insignificant. Figure 2 shows that with an increase in the relative length of the substrate (in fractions of the sample thickness), the level of maximum tangential stresses rapidly decreases and reaches an asymptotic value. Changing this level is realized within 5% of the asymptotic value for any value of the Poisson's ratio characteristic of structural materials.

As a result, for processing the experimental data, we can use the simplest relations (13), (14), in which it remains only to determine the correction coefficients. This was accomplished by comparing the results of calculations with numerical modeling. A two-dimensional model was considered within the framework of planar stress state hypothesis, presented in Figure 3. The model consists of a steel beam and a steel substrate, between which the conditions of ideal contact with respect to displacements and stresses are indicated. At the loose end of the beam, a load is applied, acting in the vertical direction and distributed at the end of the beam. The bottom surface of the base is fixed, or symmetry conditions are set on the left border of the beam (this condition corresponds to loading sample according to the three-point bending scheme, which is easy to implement in experiments using standard equipment).

In calculations, square elements of the second order (with quadratic approximation) are used. The material of the entire model is steel.

Downloaded from www.periodico.tchequimica.com

The coating on the beam and the adhesive bond layer are not shown under the assumption that their thickness is small.

We are considering models with different lengths and thicknesses of beams. The thickness of the beam always stays 3 elements. A small “skew” of 0.5 mm in size was made at the boundary of the beam fixing area, which ensures the independence of the solution from the mesh size (otherwise, a right angle and stress concentration arise). In the calculations, the load value was set as 5 N. The length of the entire model was 100 mm, the width was set equal to 10 mm.

3. RESULTS AND DISCUSSION:

To process the test results for samples with coatings, numerical, and analytical calculations were performed. The influence of residual stresses on identification results for Young's modulus of coatings was estimated. In the calculations, estimates for the values of residual stresses were used, both according to the classical relations (Stony, Boll), and according to the refined formulas that take into account deformations in the plane of sample and its deformation, for plates of small thickness.

A study was made of the effect of coatings on the mechanical behavior of samples under conditions of testing on tension and stability at normal and elevated temperatures. In tensile tests it was demonstrated that presence of coatings leads to changes in the nature of fracture of the samples. In stability tests, the results of experimental data were compared with the results of analytical and numerical calculations, which demonstrated the effect of coatings on the stability of thin-walled samples. In the process of testing at elevated temperature, the importance of ensuring tight clamping of the samples was established, in the absence of which significant increase in the measurement error takes place – due to temperature deformations, stiffness of the samples is reduced and, accordingly, deviate from conditions of hard seal assumed in calculations.

4. CONCLUSIONS:

A technique is proposed for assessing the strength of contact of coatings with the substrate under the action of normal and shear stresses in bending tests. As a result of experiments and simulations, strength estimates of coatings under consideration were obtained.

The obtained results can be used to assess the durability of protective coatings, to assess the optimality of some technological modes of their manufacture, and to predict the occurrence of technological defects and defects that arise during operation.

As a result of the conducted research, it is possible to perform tests for thermal conditions and thermal cycling in the future. The main theoretical provisions for doing these works are considered in (Formalev et al., 2015; Formalev et al., 2017; Babaytsev et al., 2017; Lomakin et al., 2017; Kakhramanov et al., 2017; Bulychev et al., 2018; Formalev et al., 2018; Kuznetsova et al., 2018; Lomakin et al., 2018; Nikitin et al., 2019; Rabinskiy et al., 2019; Rabinskiy and Tushavina, 2019a; Rabinskiy and Tushavina, 2019b; Formalev and Kolesnik, 2019).

5. ACKNOWLEDGMENTS:

This work was carried out with the financial support from the Ministry of Science and Higher Education of the Russian Federation within the State Assignment No 9.1077.2017/PCh.

6. REFERENCES:

1. Babaytsev, A.V., Prokofiev, M.V., Rabinskiy, L.N. *International Journal of Nanomechanics Science and Technology*, **2017**, *8*(4), 359-366.
2. Beam Deflection – Math24. https://www.math24.net/beam-deflection/, accessed January **2019**.
3. Bulychev, N.A., Kuznetsova, E.L., Bodryshev, V.V., Rabinskiy, L.N. *Nanoscience and Technology: An International Journal*, **2018**, *9*(2), 91-97.
4. Feodosiev, V.I. *Selected tasks and questions on the resistance of materials*, Moscow: Ripol Klassic, **2013**.
5. Formalev, V.F., Kolesnik, S.A. *Journal of Engineering Physics and Thermophysics*, **2019**, *92*(1), 52-59.
6. Formalev, V.F., Kolesnik, S.A., Kuznetsova, E.L. *High Temperature*, **2018**, *56*(5), 727-731.
7. Formalev, V.F., Kolesnik, S.A., Kuznetsova, E.L. *High Temperature*, **2015**, *53*(5), 697-702.
8. Formalev, V.F., Kolesnik, S.A., Kuznetsova, E.L. *High Temperature*,

Downloaded from www.periodico.tchequimica.com

2017, *55*(5), 761-766.

9. Gavrilov, D.G., Mamonov, S.V., Martirosov, M.I., Rabinsky, L.N. Nanoindentation of powder coatings on a polyester and epoxy-polyester basis. *Materials of the All-Russian Scientific and Technical Conference "New Materials and Technologies" (*112-113*).* Moscow Aviation Institute, Moscow, Russian Federation, **2012**.
10. Gavrilov, D.G., Martirosov, M.I., Rabinsky, L.N. 2009. Powder paints: properties, technology features, advantages and prospects. *Materials of the II All-Russian scientific-practical school-seminar "Computer engineering in industry and universities" (58-60).* Moscow Aviation Institute, Moscow, Russian Federation, **2009**.
11. Gavrilova, D.G., Mamonova, S.V. Martirosov, M.I., Rabinskiy, L.N. Nanostructured coatings: experimental studies. *Materials of the First All-Russian Scientific and Technical School – Seminar "Computer Engineering in Industry and Universities" (pp. 24-25).* Moscow Aviation Institute, Moscow, Russian Federation, **2009**.
12. Geodesic – Wikipedia. https://en.wikipedia.org/wiki/Geodesic, accessed June **2005.**
13. Grigolyuk, E.I., Tolkachev, V.M. *Contact problems of the theory of plates and shells*, Moscow: Mashinostroyeniye, **1980**.
14. Kakhramanov, R.M., Knyazeva, A.G., Rabinskiy, L.N., Solyaev, Y.O. *High Temperature*, **2017**, *55*(5), 731-736.
15. Kuznetsova, E.L., Kuznetsova, E.L., Rabinskiy, L.N., Zhavoronok, S.I. *Journal of Vibroengineering*, **2018**, *20*(2), 1108-1117.
16. Lomakin, E.V., Lurie, S.A., Belov, P.A., Rabinskii, L.N. *Doklady Physics*, **2017**, *62*(1), 46-49.
17. Lomakin, E.V., Lurie, S.A., Rabinskiy, L.N., Solyaev, Y.O. *Doklady Physics*, **2018**, *63*(4), 161-164.
18. Nikitin, P.V., Tushavina, O.V., Shkuratenko, A.A. *Incas Bulletin*, **2019**, *11*(S2019), 191-201.
19. Rabinskiy, L.N., Tushavina, O.V. Fedotenkov, G V. *Asia Life Sciences, Supplement,* **2019**, *19*(1), 149-162.
20. Rabinskiy, L.N., Tushavina, O.V. *Incas Bulletin*, **2019a**, *11*(S2019), 203-211.
21. Rabinsky, L.N., Tushavina, O.V. *STİN*, **2019b**, *4*, 22-26.
22. Timoshenko, S.P. Gere, Dzh. *The mechanics of material,* Moscow: Villiams, **2002**.
23. Zezin, Yu.P., Lomakin, E.V., Mamonov, S.V., Martirosov, M.I., Rabinsky, L.N., Chistyakov, P.V. *Factory laboratory. Material Diagnostics*, **2012a**, *78*(8), 61-63.
24. Zezin, Yu.P., Lomakin, E.V., Mamonov, S.V., Martirosov, M.I., Rabinsky, L.N., Chistyakov, P.V. *News of the Saratov University. New series. Series "Mathematics. Mechanics. Computer science",* **2012b**, *12*(3), 74-80.

$$M(L-a)=Pa, \quad Q(L-a)=P \qquad \text{(Eq. 1)}$$

$$\frac{d^2y(x)}{dx^2}=\frac{M(x)}{EI}-\frac{5}{6GF}\frac{dQ(x)}{dx} \qquad \text{(Eq. 2)}$$

$$Q(x)=\frac{dM(x)}{dx} \qquad \text{(Eq. 3)}$$

$$\underline{x<L-a}:\frac{d^2M(x)}{dx^2}-\alpha^2M(x)=0 \quad \alpha^2=\frac{5GF}{6EI} \qquad \text{(Eq. 4)}$$

$$\underline{x=L-a}:M(x)=Pa \quad \underline{x=0}:M(x)=0 \qquad \text{(Eq 5)}$$

Downloaded from www.periodico.tchequimica.com

$$\underline{x = L - a}: \frac{dM(x)}{dx} = Q(x) = P \quad \underline{x = 0}: M(x) = 0 \qquad \text{(Eq. 6)}$$

$$M(x) = C_1 e^{\alpha x} + C_2 e^{-\alpha x} \qquad \text{(Eq. 7)}$$

$$M(x) = Pa\frac{sh(\alpha x)}{sh(\alpha(L-a))} \quad , Q(x) = \alpha Pa\frac{ch(\alpha x)}{sh(\alpha(L-a))}, \qquad \text{(Eq. 8)}$$

$$q(x) = \alpha^2 Pa\frac{sh(\alpha x)}{sh(\alpha(L-a))}$$

$$\tau_{xz} = k_\tau \frac{Q(x)}{bh} = k_\tau \frac{aP\alpha}{bh}\frac{ch(\alpha x)}{sh(\alpha(L-a))} \qquad \text{(Eq. 9)}$$

$$\sigma_z = k_\sigma \frac{q}{b} = k_\sigma \frac{aP\alpha^2}{bh}\frac{sh(\alpha x)}{sh(\alpha(L-a))} \qquad \text{(Eq. 10)}$$

$$\tau_{\max} = \tau_{xz}(L-a) = k_\tau \frac{aP}{bh}\sqrt{\frac{5GF}{6EI}}cth\left((L-a)\sqrt{\frac{5GF}{6EI}}\right) = \qquad \text{(Eq. 11)}$$

$$= k_\tau \frac{aP}{bh^2}\sqrt{\frac{5}{1+\nu}}cth\left(\frac{L-a}{h}\sqrt{\frac{5}{1+\nu}}\right)$$

$$\sigma_{\max} = \sigma_z(L-a) = k_\sigma \frac{aP}{b}\frac{5GF}{6EI} = k_\sigma \frac{Pa}{bh^2}\frac{5}{1+\nu} \qquad \text{(Eq. 12)}$$

$$t_{\max}\Big|_{L^\circ\ ¥} = k_t \frac{aP}{bh^2}\sqrt{\frac{5}{1+n}} \qquad \text{(Eq. 13)}$$

$$\frac{t_{\max}}{s_{\max}}\Big|_{L^\circ\ ¥} = \frac{k_t}{k_s}\sqrt{\frac{1+n}{5}} \qquad \text{(Eq. 14)}$$

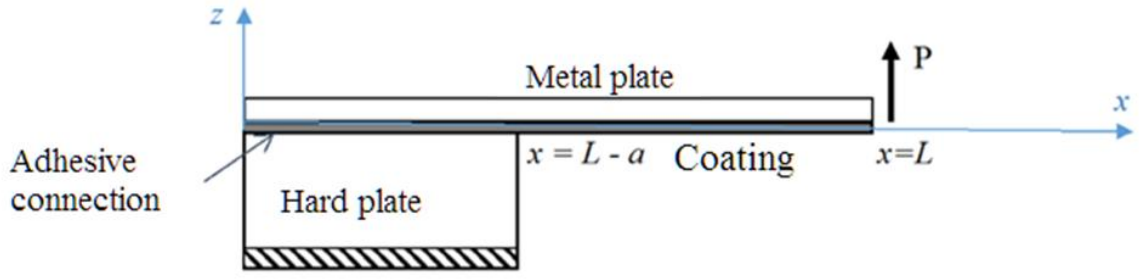

Figure 1. *Testing setup for coated samples cantilevered on a rigid substrate*

Downloaded from www.periodico.tchequimica.com

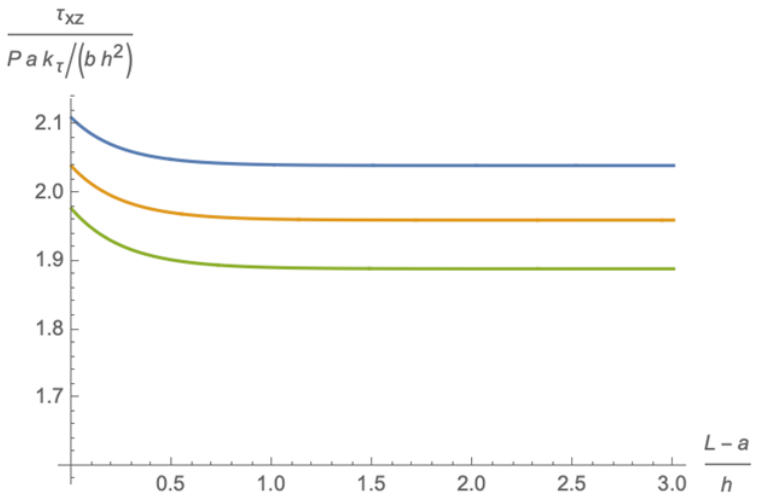

Figure 2. *Dependence of maximum tangential stresses at the separation point on dimensions of the sample fixing area. Colors: blue – $\nu = 0.2$, yellow – $\nu = 0.3$, green – $\nu = 0.4$*

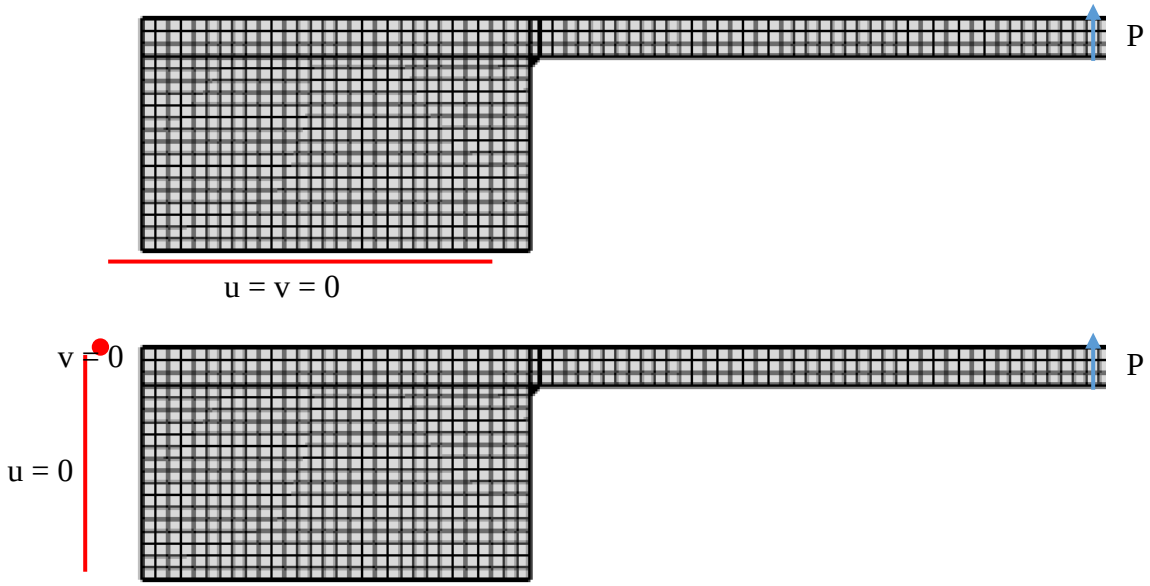

Figure 3. *The finite element model of the beam fixed to the substrate, loaded according to the cantilever (top) and three-point (bottom) bending scheme*

Downloaded from www.periodico.tchequimica.com

PERIÓDICO TCHÊ QUÍMICA
ARTIGO ORIGINAL

AVALIAÇÃO DA EFICIÊNCIA DE ENDURECIMENTO COM O MECANISMO DE TRANSFERÊNCIA DE CALOR MASSA CONVECTIVO DURANTE A LIGA SUPERFICIAL A LASER NO MODO DE REFUXO

EVALUATION OF HARDENING EFFICIENCY WITH CONVECTIVE HEAT AND MASS TRANSFER MECHANISM DURING LASER SURFACE ALLOYING IN REFLOW MODE

ОЦЕНКА ЭФФЕКТИВНОСТИ УПРОЧНЕНИЯ ПРИ КОНВЕКТИВНОМ МЕХАНИЗМЕ ТЕПЛОМАССОПЕРЕНОСА ВО ВРЕМЯ ЛАЗЕРНОГО ПОВЕРХНОСТНОГО ЛЕГИРОВАНИЯ В РЕЖИМЕ ОПЛАВЛЕНИЯ

BELASHOVA, Irina S.[1*]; Rabinskiy, Lev N.[2]; TURSHAVINA, Olga V.[3]

[1,2] Moscow Aviation Institute (National Research University), Department of Advanced Technologies, Moscow – Russian Federation

[3] Moscow Aviation Institute (National Research University), Department of Managing Exploitation of Space-Rocket Systems, Institute of Aerospace, Moscow – Russian Federation

** Correspondence author*
e-mail: Irina455@inbox.ru

Received 03 September 2019; received in revised form 20 October 2019; accepted 26 October 2019

RESUMO

O estágio atual de desenvolvimento de tecnologia exige muito das características operacionais das peças. Vários componentes e peças de máquinas, ferramentas de corte de metal, elementos estruturais metálicos trabalham sob condições de maior atrito, altas cargas específicas, altas temperaturas, uma ampla gama de velocidades e exposição a ambientes agressivos, por exemplo. Portanto, a melhoria da qualidade, confiabilidade, eficiência e produtividade de máquinas, ferramentas, equipamentos e outros produtos de engenharia mecânica, reduzindo seu consumo específico de material e consumo de energia, é alcançada principalmente pelo uso de materiais e tecnologias de endurecimento progressivo para aumentar a força, a resistência ao desgaste, à resistência, à corrosão e outras propriedades físicas e mecânicas das peças de máquinas e ferramentas. Portanto, o principal objetivo do trabalho foi avaliar a transferência de massa durante a adição superficial a laser no modo fusão. Para avaliar a eficácia das tecnologias de endurecimento de superfície, propõe-se o uso de dois novos parâmetros – desgaste reduzido e microdureza integrada reduzida da camada superficial modificada. Com base na análise dos dados experimentais sobre o desgaste de uma fresa de aço de cromo-tungstênio-zircônio e U10, processada pelo laser com manchas no modo de fusão, se mostra a existência de uma correlação entre os parâmetros inseridos e a equação de regressão foi obtida. A abordagem proposta para avaliar a eficácia do endurecimento da superfície pode ser usada não apenas no caso particular de modificação a laser, mas também para qualquer outra tecnologia para criar revestimentos funcionais com gradiente.

Palavras-chave: *endurecimento superficial, resistência ao desgaste, desgaste reduzido, microdureza integral reduzida, liga a laser.*

ABSTRACT

The modern stage of equipment development imposes increased requirements for the performance characteristics of parts. Different components and parts of machines, metal-cutting tools and metal structural elements work in the conditions of high friction, high specific loads, high temperatures, a wide range of speeds and impact of aggressive media, for instance. Therefore, improvement the quality, reliability, economical efficiency and productivity of machines, tools, equipment and other engineering products as well as reduction of their specific material consumption and energy consumption is achieved primarily by the use of materials and progressive strengthening technology that improve the hardening, wear resistance, corrosion resistance and other physical and mechanical properties of machine parts and tool. Therefore, the main objective of the paper was to evaluate the mass-transfer during laser surface alloying in the reflow mode. To evaluate the effectiveness of surface hardening technology, it was proposed to use two new parameters – reduced wear and reduced integrated micro hardness of the modified surface layer. Based on an analysis of the experimental data

Downloaded from www.periodico.tchequimica.com

on the wear of a cutter made of HVG and U10 steel, processed by a laser with smears in the reflow mode, the existence of a correlation between the entered parameters is demonstrate and the regression equation is obtained. The proposed approach to evaluating the effectiveness of surface hardening can be used not only in the special case of laser modification but also for any other technology for creating gradient and functional coatings.

Keywords: *surface hardening, wear resistance, reduced wear, reduced integral micro hardness, laser alloying.*

АННОТАЦИЯ

Современный этап развития техники предъявляет повышенные требования к эксплуатационным характеристикам деталей Различные узлы и детали машин, металлорежущие инструменты, металлические элементы конструкций работают в условиях повышенного трения, больших удельных нагрузок, высоких температур, широкого диапазона скоростей, воздействия агрессивных сред и т д. Поэтому повышение качества, надежности, экономичности и производительности машин, инструмента, оборудования и других изделий машиностроения, снижение их удельной материалоемкости и энергопотребления достигается прежде всего применением материалов и прогрессивных упрочняющих технологий, позволяющих повысить прочность, износостойкость, коррозионную стойкость и другие физико-механические свойства деталей машин и инструмента. Поэтому основная цель работы заключается в оценке массопереноса во время лазерного поверхностного легирования в режиме оплавления. Для оценки эффективности технологий поверхностного упрочнения предложено использовать два новых параметра – приведенный износ и приведенную интегральную микротвердость модифицированного поверхностного слоя. На основе анализа экспериментальных данных износа резца из стали ХВГ и У10, обработанного лазером с обмазками в режиме оплавления, показано существование корреляционной связи между введенными параметрами и получено уравнение регрессии. Предложенный подход к оценке эффективности поверхностного упрочнения может быть использован не только в частном случае лазерного модифицирования, но и для любой другой технологии создания градиентно-функциональных покрытий.

Ключевые слова: *поверхностное упрочнение, износостойкость, приведенный износ, приведенная интегральная микротвердость, лазерное легирование*.

1. INTRODUCTION

Obvious advantages of laser technologies of surface hardening are high heating and cooling rates, lack of contact during processing, locality and the ability to process hard-to-reach areas, absence of deformation of the work pieces and the relative simplicity of technology, as well as possibility to modify the surface of materials to obtain new physical, mechanical and operational characteristics (Moldagozhieva *et al.*, 2017; Burkov *et al.*, 2018). The modification method is especially effective for parts that operate under sliding friction, abrasive and erosive wear and for tool hardening, namely, for cutting tools of simple shape and small dimensions of the cutting edge. Thus, it makes, inexpensive low-alloy tool steels, modified layers of high hardness, strength, wear resistance, heat resistance, similar in properties to high-alloy high-speed steels (Orlov *et al.*, 2003; Skvortsov *et al.*, 2009; Skvortsov and Karizin, 2012; Skvortsov *et al.*, 2016; Skvortsov and Karizin, 2017). Therefore, alloying the surface of such steels is done according to the regimes providing possibility of modification, i.e. with surface melting. When the surface is melted as a result of laser exposure, the alloying elements of coating are mixed with the base material and they interact.

The mechanism of mass transfer during laser alloying is quite complex and does not have common interpretation. In number of works (Borovsky *et al.*, 1982; Arutyunyan *et al.*, 1988) it was shown that the circulation process and movement of the melt due to *thermocapillary effect are the* basis of transfer process. On the surface of melt, the temperature decreases from the center of irradiation to the edge of liquid bath. As the melt temperature changes, the surface tension force also changes, increasing toward the edges of liquid bath. Due to a change in the surface tension force, melt moves from the center of liquid bath to its edge; this movement of the melt on surface is transmitted inward due to the forces of viscous friction. An approximate calculation of the motion of melt and the shape of its surface suggests evaluating velocities of the motion of molten metal and the role of surface tension forces.

The calculations shown by the authors of (Borovsky *et al.*, 1982) for iron, with width and depth of melting zone of 2.0 and 0.2 mm,

Downloaded from www.periodico.tchequimica.com

respectively, and temperature difference in the central and regional parts of 500^0 C, showed that the mass of the melt in the surface layer can move at a speed of the order of 1-3 m / c, and its internal areas – with a speed of 3-4 times less. The mass transfer model based on thermocapillary effect accounts for the observed high rates of mass transfer and melt mixing. In the work (Arutyunyan *et al.*, 1988), the authors, exploring the possibility of alloying 10X18H9T tantalum steel under the action of monochromatic radiation, explain the characteristic depths of tantalum penetration (to a depth of about 100 nm) by *diffusion in liquid phase.* The nature of concentration profiles of tantalum and calculation of diffusion coefficient, which is estimated to be of the order of 10^{-8} m^2 / s, which is characteristic of diffusion in liquid phase, are presented.

In the works (Belashova, 2004; Belashova andTarasova, 2008; Belashova et al., 2009), the fact of the ***parallel action of*** *convective and thermal diffusion mass transfer* during laser irradiation is established *,* which is some obstacle to obtaining a stably uniform doped layer: the action of the first mechanism leads to significant inhomogeneity of melting bath, and due to the second, the convective flows of alloying are continuously dissolving elements. Despite the fact that action of the second mechanism leads to a more uniform distribution of alloying elements over melting bath, the microstructure of the layer remains extremely uneven, areas with different etchability are observed, which are located in different parts of melting bath (Figure 1).It was also established : that both various etchability and abrupt changes in micro hardness are associated with changes in the concentration of alloying elements in the volume of melting both. These micro hardness jumps are characteristic of the mixing mechanism during laser alloying and they do not depend on the type of alloying element.

Laser technologies of surface hardening differ both in the depth of the modified layer and in the nature of change of its properties along depth. Thus, the problem arises of choosing the optimal technology parameters, in particular, the compositions of alloying ingredients that provide the greatest wear resistance of the modified surface layer. To get a theoretical solution to this problem by methods of mathematical modeling is currently quite difficult, based on the above alloying mechanism, and the fact that experimental studies of wear processes are very time-consuming and lengthy. So, it seems appropriate to use other criteria for quantifying the effectiveness of laser technologies of surface hardening, which have correlation with wear resistance and allow experimental determination at smaller cost.

In this work, for the criterion, it is proposed to use a new characteristic – ***reduced integral micro hardness.*** The definition of the introduced parameter is given below and, based on the processing of experimental data, it was demonstrated that there is a significant correlation between it and the wear resistance of the modified surface layer.

2. MATERIALS AND METHODS

As the studied materials, low alloyed and carbon tool steels HVG and U8-U10 were selected. Samples were pre-heated by the standard treatment for each type of steel in a tempering temperature from 780-800 $^{\circ}$C and low temperature tempering, 180-220 ^{o} C. The powders were deposited in form of coating with an organic binder. Hardening was performed on a "Quantum-16" laser machine of pulsed action with a telescopic nozzle that improves collimation of radiation. The samples were processed after laser had reached stable operation. The radiation power density was varied both by changing the pulse energy and focal length, i.e. position of the surface of sample relative to the focal plane of output lens of the laser optical system (ΔF). Depending on power density and thickness of saturating coating (δ), various structures of hardened zones were obtained that have specific for this mechanism and difficult to predict micro hardness distribution over cross section of melt pool. Micro hardness was measured on PMT-3 instrument with load of 0.98 N.

The geometric dimensions of the spot were calculated from the diameter and thickness of laser irradiation area. The diameter of laser exposure area is the distance between boundaries of structural transformations on the metal surface; the thickness of laser exposure area is the maximum distance in the center of phase transformations to the initial structure.

The wear resistance was determined during wear of the sample after laser alloying by friction paired with a counter body on SMT-1 friction machine. The counter body was made of 30 HGSA steel after heat treatment with hardness of 50 ... 56 HRC. The disk rotation frequency was 300 rpm, the force of pressure of the test sample to the disk was 240 N. The specific pressure was 1.2 MPa. As coolant (cutting fluid) AKVOL-3 was used, which filled the

Downloaded from www.periodico.tchequimica.com

test chamber. Then, the samples were ground until reaching the contact surface of 95% using diamond paste AFM 40/28. Prior to the test, the samples were washed, dried and weighed on analytical balance with an accuracy of 0.05 mg. Given the number of revolutions of disk and the load on the sample, after 30 minutes, weighing of frayed samples was repeated.

During the tests, the moment of friction was registered and the coefficient of friction was determined; The temperature of samples was measured using a thermocouple and a potentiometer.

In order to study kinetics of laser alloying and the phenomenon of mass transfer, distribution of elements in the alloying areas was studied by X-ray spectral and radiographic analyzes.

When alloying, heating was done to temperatures exceeding the melting temperature. Thus, the laser exposure area consists of a melting area and a thermal influence area. These characteristics were measured using a metallographic microscope with an accuracy of 0.01 mm.

3. RESULTS AND DISCUSSION:

To quantify the effectiveness of surface hardening technologies, authors proposed to use a new parameter – reduced wear Y equal to the ratio of wear of modified surface layer to tool wear in the absence of hardening in the same operating conditions (tests).Reduced wear Y is a dimensionless quantity that characterizes the decrease in wear (increase wear resistance) of modified surface layer. In absence of hardening, specified wear Y the base metal is assumed to be 1. Nonetheless, the experimental determination of reduced wear Y is very laborious and time consuming. Thus, it seems appropriate to try using other criteria for quantifying the effectiveness of surface hardening technologies, which have correlation with the wear Y and allowing experimental determination with less cost.

As it was noted above, one of the parameters of modified surface layer, which is not difficult to determine experimentally, is its micro hardness. Figure 2 displays the distribution of micro hardness of depth of hardened layer by doping with various coating saturating. It is easy to see that the nature of change in micro hardness in depth for different compositions of alloying composition is significantly different. For example, when doping from coating, where titanium is the saturating medium, a layer with depth of up to 50 μm with high micro hardness (up to 18000 MPa) is obtained on the surface of sample, then it drops to 10300 MPa, and evens out at depth of 100 to 150 μm at hardness values of 11700-13000 MPa. For the coatings in which niobium is the main alloying component, the graphs have a completely different look: on the surface of sample, the hardness values do not exceed 13000 MPa, then at depth of about 50 μm the micro hardness of layer sharply increases to 16000-18000 MPa and then decreases to 13000 MPa by depth of 100-150 μm.

It brings a question: is it possible to use any characteristic of the micro hardness distribution non-uniform in depth as a criterion for quantifying the effectiveness of laser technologies of surface hardening, i.e., is there a correlation between such a characteristic and reduced wear. To make it easy, peak (maximum) micro hardness values could be used for this purpose. Nonetheless, this approach was not successful: it was not experimentally possible to establish a correlation between this parameter and wear resistance (Belashova, 1998). This is because of the fact that under conditions of operation of products from tool steels, the work of the entire layer as a whole is important, i.e. its integral characteristic. Thus, as a desired criterion, it is proposed to use a new characteristic – the reduced integral micro hardness of modified surface layer Y', which is calculated by the Equation 1.

Where h - is depth of the modified layer; H_{μ}^{0} - is micro hardness of the base metal; $H_{\mu}(x)$ - is micro hardness of the modified layer at a point at a depth x, $0 \le x \le h$.

From the formula (1) it follows that the reduced integrated micro hardness of the modified surface layer Y' is dimensionless quantity and characterizes the change in micro hardness of the entire modified layer with respect to the micro hardness of homogeneous layer of base metal of the same thickness. In the absence of hardened layer, the parameter Y' should be assumed equal to 1.Let us note that, in contrast to the peak values of micro hardness, the reduced integral micro hardness of modified surface layer Y' *characterizes properties of the entire modified layer.*

The advantage of introduced parameter is

Downloaded from www.periodico.tchequimica.com

the simplicity of its calculation directly from experimental data: the value of reduced integral micro hardness is proportional to the area of curved trapezoid, limited from above by the graph of micro hardness of modified layer in depth. When tabulating the dependence of micro hardness over depth of modified layer, the area of curved trapezoid can be calculated using simple quadrature formulas, for example, the trapezoid formula.

To confirm the existence of correlation between reduced wear Y and reduced integral micro hardness Y' of modified surface layer, results of experimental studies of the wear of a cutter made of HVG and U10 steel, treated with laser with smears in flash mode, were used (Belashova, 1998) .Titanium, niobium and carbon (graphite) were chosen as alloying elements for the surface modification and hardening of the studied instrumental steels.

During experiments, chemical composition of saturating coating was varied. The elements that participate in compounds form a triple system, therefore, to select the content of components in compounds, the simplex lattice method proposed by Scheffe (Scheffe, 1963) for constructing “composition-property” diagrams were used.

As we know, a measure of tightness of functional relationship between two random variables is the pair correlation coefficient. The value can vary from 0 to ± 1.If it comes close to zero, then the connection is either completely absent or is substantially nonlinear. If it comes close to ± 1, then the connection is linear. At the range of intermediate values, the relationship is stronger, the closer the correlation coefficient to unity. For processing experimental results provided in (Belashova, 1998), the method for calculating the correlation coefficients proposed in (Novik and Arsov, 1980) was used. As a result of calculations, the pair correlation coefficient for reduced wear Y and reduced integral micro hardness Y' modified surface layer was equal to $-0{,}73$, which allows us to conclude that there is a significant linear relationship between these two parameters. The corresponding linear regression model has the following look Equation 2.

Therefore, when conducting experiments on selecting the optimal parameters of hardening technologies that provide the greatest wear resistance of modified surface layer, it is possible to exclude laborious tests of wear resistance and use reduced integral micro hardness as an optimization criterion Y' of modified surface layer, the finding of which requires less time (Rabinsky and Tushavina, 2019; Formalev *et al.*, 2018a; Kakhramanov *et al.*, 2017; Lomakin *et al.*, 2018; Lomakin *et al.*, 2017; Formalev *et al.*, 2018b; Formalev and Kolesnik, 2019; Babaytsev *et al.*, 2017; Formalev *et al.*, 2017; Bulychev *et al., 2018;* Rabinskiy and Tushavina, 2019a; Nikitin et al., 2019; Rabinskiy and Tushavina, 2019b*).*

4. CONCLUSIONS:

To assess the effectiveness of laser technologies of surface hardening, it was proposed to use two new parameters – reduced wear and reduced *integrated micro hardness of* modified surface layer. Based on analysis of experimental data on the wear of cutter made of HVG and U10 steel, processed by laser with smears in reflow mode, the existence of correlation relationship between the introduced parameters was demonstrated. Considering that the experimental studies of wear processes are very laborious and lengthy, the presence of correlation between the entered parameters can significantly reduce the complexity of research when assessing the effect of a particular type of alloying coating on cutting properties of instrumental materials.

The proposed approach to assessing the effectiveness of surface hardening can be used not only for the particular case of laser modification, but also for any other technology of creating gradient-functional coatings.

The possibility of evaluating hardening efficiency under various thermal conditions is outlined in.

5. ACKNOWLEDGMENTS:

The work was carried out with the financial support of the state project of the Ministry of Education and Science, project code: 9.9074.2017/БЧ.

6. REFERENCES:

1. Arutyunyan, R.V., Baranov, V.YU., Bolshov, L.A. *Surface: Physics, Chemistry, Mechanics*, **1988**, *5*, 129-137.
2. Babaytsev, A.V., Prokofiev, M.V., Rabinskiy, L.N. *International Journal of Nanomechanics Science and Technology*, **2017**, *8*(4), 359-366.
3. Belashova, I.S. *High Technology,* **2004***, 10*, 36-40.

Downloaded from www.periodico.tchequimica.com

4. Belashova, I.S. *MyTOM,* **1998**, *1*, 2-4.
5. Belashova, I.S., Tarasova, T.V. *High Technology*, **2008**, *1*, 74-85.
6. Belashova, IS, Svetushkov, N.N., Tarasova, T.V. *Collection of scientific papers "Modern methods of obtaining and research of nanostructured materials and coatings", Moscow, Russian Federation,* **2009**, 148-160.
7. Borovsky, I.P., Gorodsky, D.D., Sharaseev, I.M. *DAN USSR,* **1982**, *263*(3), 616-618.
8. Bulychev, N.A., Kuznetsova, E.L., Bodryshev, V.V., Rabinskiy, L.N. *Nanoscience and Technology: An International Journal*, **2018**, *9*(2), 91-97.
9. Burkov, S.I., Zolotova, O.P., Sorokin, B.P., Turchin, P.P., Talismanov, V.S. Journal of the Acoustical Society of America, **2018**, *143*(1), 16-22
10. Formalev, V.F., Kolesnik, S.A. *Journal of Engineering Physics and Thermophysics*, **2019**, *92*(1), 52-59.
11. Formalev, V.F., Kolesnik, S.A., Kuznetsova, E.L. *High Temperature*, **2018a**, *56*(5), 727-731.
12. Formalev, V.F., Kolesnik, S.A., Kuznetsova, E.L. *High Temperature*, **2017**, *55*(5), 761-766.
13. Formalev, V.F., Kolesnik, S.A., Kuznetsova, E.L. *Periodico Tche Quimica*, **2018b**, *15*(Special Issue 1), 426-432.
14. Kakhramanov, R.M., Knyazeva, A.G., Rabinskiy, L.N., Solyaev, Y.O. *High Temperature*, **2017**, *55*(5), 731-736.
15. Lomakin, E.V., Lurie, S.A., Belov, P.A., Rabinskii, L.N. *Doklady Physics*, **2017**, 62(1), 46-49.
16. Lomakin, E.V., Lurie, S.A., Rabinskiy, L.N., Solyaev, Y.O. *Doklady Physics*, **2018**, *63*(4), 161-164.
17. Moldagozhieva, Z.D., Zhilisbayeva, R.O., Kucharbaeva, K.Zh., Toktarbayeva, A.T., Tashpulatov, S.Sh. *Izvestiya Vysshikh Uchebnykh Zavedenii, Seriya Teknologiya Tekstil'noi Promyshlennosti,* **2017**, *371*(5), 65-659
18. Nikitin, P.V., Tushavina, O.V., Shkuratenko, A.A., *Calculation of heat transfer on the catalytically active surface of high-speed aircraft*, INCAS Bulletin, **2019**, *11*(Special Issue), 191 – 201. DOI: 10.13111/2066-8201.2019.11.S.19.
19. Novik, F.S., Arsov, Ya.B. *Experiment planning.* Moscow: Mashinostroyeniye, **1980**.
20. Orlov, A.M., Skvortsov, A.A., Solov'ev, A.A. *Zhurnal Eksperimental'noj i Teoreticheskoj Fiziki*, **2003**, *123*(3), 590-599.
21. Rabinskiy, L.N., Tushavina, O.V. *INCAS Bulletin*, **2019a**, *11*(Special Issue), 203-211, DOI: 10.13111/2066-8201.2019.11.S.20;
22. Rabinskiy, L.N., Tushavina, O.V., Fedotenkov, G.V. *Asia Life Sciences,* **2019b**, *19*(1), 149-162, 2019
23. Rabinsky, L.N., Tushavina, O.V. *STİN*, **2019**, *4*, 22-26.
24. Scheffe, G. *Analysis of variance,* Moscow: Fizmatgiz, **1963**.
25. Skvortsov, A., Zuev, S., Koryachko, M., Glinskiy, V. *Microelectronics International*, **2016**, *33*(2), 102-106.
26. Skvortsov, A.A., Karizin, A.V. *Journal of Experimental and Theoretical Physics*, **2012**, *114*(1), 85-88.
27. Skvortsov, A.A., Karizin, A.V. *Solid State Phenomena*, **2017**, *269*, 78-90.
28. Skvortsov, A.A., Orlov, A.M., Muradov, V.E. *Technical Physics Letters*, **2009**, *35*(7), 606-609.

Downloaded from www.periodico.tchequimica.com

$$Y' = \frac{1}{hH_{\mu}^{0}} \int_{0}^{h} H_{\mu}(x)dx \qquad \text{(Eq. 1)}$$

$$Y = 1{,}29 - 4{,}55 \times Y\text{¢} \qquad \text{(Eq. 2)}$$

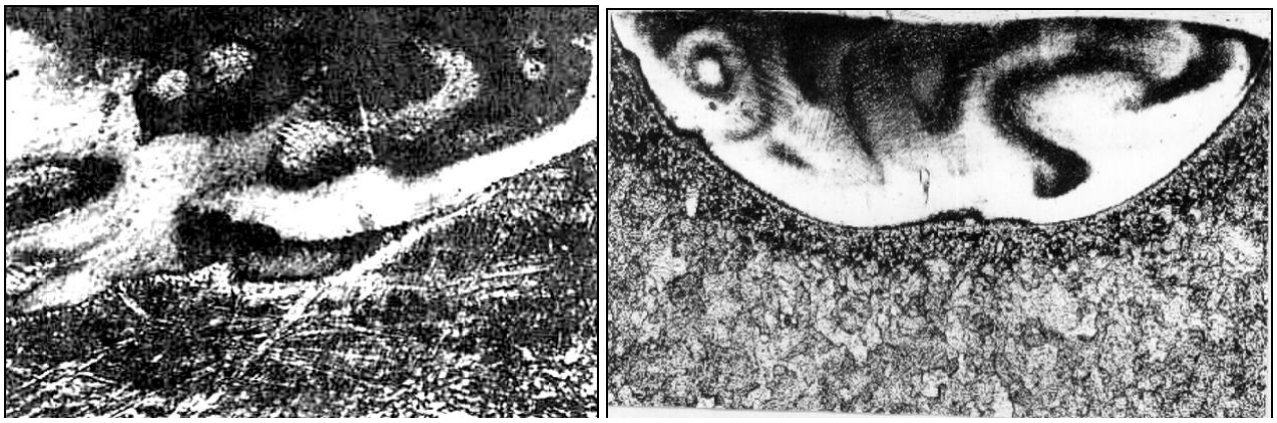

a b

Figure 1. *Microstructures of laser exposure zones: a) – is steel U10, pulse energy E_{imp} = 20 J, coating density δ = 5 mg / cm ^{2}, coating composition: titanium-niobium-carbon; b) – is steel 12X13, E_{imp} = 15 J, δ = 4 mg / cm ^{2}, laser cementation, (x250)*

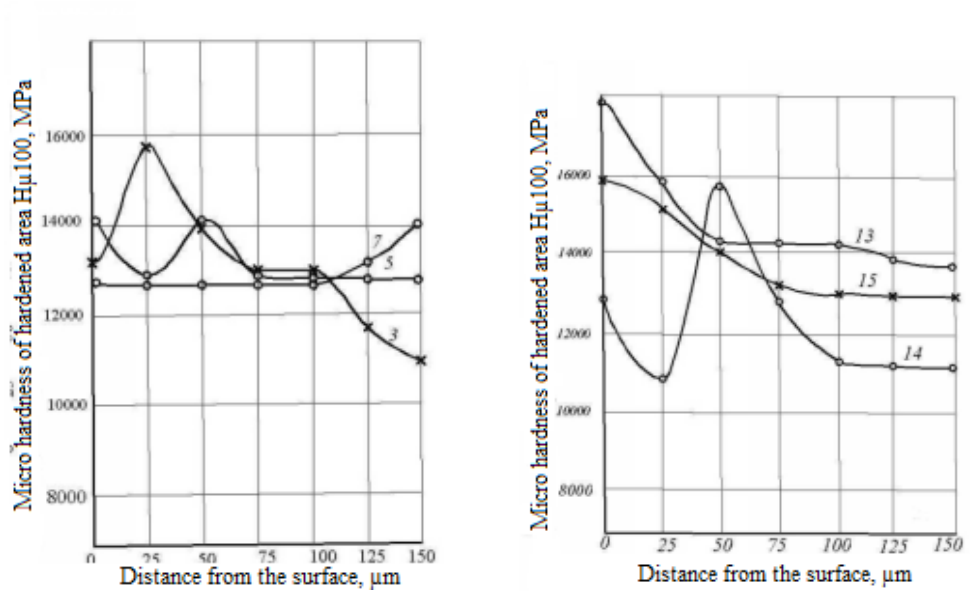

Figure 2. *Micro hardness distribution over the depth of hardened layer upon alloying with various saturating coatings (the choice of compositions according to Scheffe method [5]):*
1 – Ti: Nb: C = 1: 1: 1; 2 – Nb: C = 2: 1; 3 – Ti: C = 2: 1; 4 – Nb: C = 1: 1;
5 – Ti: Nb = 1: 1; 6 – Nb: C = 5: 1; 7 – Ti: C = 5: 1; 8 – Ti: Nb: C = 1: 1: 2;
9 – Ti: Nb: C = 2: 4: 1; 10 – Ti: Nb: C = 4: 2: 1; 11 – Nb (100%); 12 – Ti (100%);
13 – Ti: Nb = 1: 1; 14 – Ti: Nb = 1: 3; 15 – Ti: Nb = 3: 1

Downloaded from www.periodico.tchequimica.com

PERIÓDICO TCHÊ QUÍMICA
ARTIGO ORIGINAL

ORIGEM E PROPAGAÇÃO DE SÓLITONS DE TEMPERATURA COM TRANSFERÊNCIA DE CALOR DE ONDA NA ÁREA LIMITADA DURANTE PROCESSOS TECNOLÓGICOS ADICIONAIS

ORIGINATION AND PROPAGATION OF TEMPERATURE SOLITONS WITH WAVE HEAT TRANSFER IN THE BOUNDED AREA DURING ADDITIVE TECHNOLOGICAL PROCESSES

ВОЗНИКНОВЕНИЕ И РАСПРОСТРАНЕНИЕ ТЕМПЕРАТУРНЫХ СОЛИТОНОВ С ВОЛНОВЫМ ТЕПЛООБМЕНОМ В ОГРАНИЧЕННОЙ ОБЛАСТИ В ХОДЕ АДДИТИВНЫХ ТЕХНОЛОГИЧЕСКИХ ПРОЦЕССОВ

FORMALEV, Vladimir F. [1*]; KOLESNIK, Sergey A. [2]; KUZNETSOVA, Ekaterina L. [3]; RABINSKIY, Lev N.[4];

[1,2,3] Moscow Aviation Institute (National Research University), Institute No. 9 "General Engineering", Moscow – Russian Federation

[4] Moscow Aviation Institute (National Research University), Department of Material Sciences, Moscow – Russian Federation

** Correspondence author*
e-mail: formalev38@yandex.ru

Received 30 August 2019; received in revised form 24 October 2019; accepted 27 October 2019

RESUMO

Neste trabalho, com base em análises de problemas na transferência de calor por ondas em corpos delimitados, a teoria de ondas isoladas termicamente (solitons) foi desenvolvida para investigar os processos de transferência de calor na vizinhança inicial e nas proximidades do corpo delimitado. As escalas de tempo são proporcionais ao tempo de relaxamento (nanossegundos) e as escalas da variável espacial são medidas em nanômetros. Uma nova solução analítica para a transferência de calor por ondas foi obtida com base na equação do calor do tipo hiperbólico sob a ação de vários sólitons, com base nos quais foram analisadas a interação dos sólitons entre si, a absorção e a reflexão dos sólitons a partir dos limites do corpo. Tendo analisado um grande volume de resultados, verificou-se que os sólitons térmicos são refletidos diferentemente dos sólitons mecânicos, uma vez que a energia térmica do sóliton é primeiro absorvida pelo limite de isolamento térmico nas paredes com isolamento térmico e, em seguida, a energia é rejeitada pela condutividade térmica na direção oposta. Verificou-se que a diferença de temperatura no interior do sóliton é negativa na direção de condução e positiva na direção refletida. Os resultados podem ser utilizados na interação térmica de radiação de alta potência com superfícies sólidas, bem como em problemas da mecânica quântica.

Palavras-chave: *sóliton térmico, velocidade da onda térmica, corpo limitado, condutividade térmica, equação de calor do tipo hiperbólico.*

ABSTRACT

Within this work, based on analyses of problems on wave heat transfer in bounded bodies, the theory of thermally isolated waves (solitons) is developed to investigate the heat transfer processes in the initial time vicinity and in the vicinity of the bounded body, that is the time scales are commensurate with the relaxation time (nanoseconds), and the scales of the spatial variable are measured in nanometers. A new analytical solution of the wave heat transfer based on the heat conduction equation of hyperbolic type under the action of a series of solitons was received, based on which the interaction of individual solitons with each other, absorption and reflection of the solitons from the body boundaries was analyzed. Analysis of a large number of results made clear that thermal solitons reflect not as mechanical ones, since first there is absorption of the soliton thermal energy by the heat-insulated boundary on the heat-insulated walls, and then the energy is rejected by the thermal conductivity in the opposite direction. It was found that the temperature gradient inside the soliton is negative in the forward direction and positive in the reflected direction. The results of the paper can

Downloaded from www.periodico.tchequimica.com

be used in thermal interaction of high-power radiation with solid surfaces, as well as in the problems of quantum mechanics.

Keywords: *thermal soliton, heatwave velocity, bounded body, thermal conductivity, hyperbolic type heat equation.*

АННОТАЦИЯ

В рамках данной работы, на основе анализа проблемы волнового теплообмена с ограничением тепла, была разработана теория термоизолированных волн (солитонов) для изучения процессов теплообмена около начального момента времени и вблизи ограниченного тела, т.е. процесс, когда временные масштабы соизмеримы со временем релаксации (наносекундами), и масштабы пространственной переменной измеряются в нанометрах. Новое аналитическое решение волнового теплообмена было получено на основе уравнения теплопроводности гиперболического типа под действием ряда солитонов, на базе которых было проанализировано взаимодействие солитонов друг с другом, поглощение и отражение солитонов от границ тела. Проанализировав большой объем результатов было установлено, что тепловые солитоны отражаются не так, как механические, ввиду того, что сначала происходит поглощение тепловой энергии солитона теплоизолирующей границей на теплоизолированных стенках, а затем энергия отбрасывается теплопроводностью в обратном направлении. Было обнаружено, что перепад температуры внутри солитона отрицательный в проводящем направлении и положительный в отраженном направлении. Результаты работы могут использоваться при тепловом взаимодействии мощного излучения с твердыми поверхностями, а также в задачах квантовой механики.

Ключевые слова: *тепловой солитон, скорость тепловой волны, ограниченное тело, теплопроводность, уравнение теплопроводности гиперболического типа.*

1. INTRODUCTION

It is well known that heat transfer with convection, thermal conductivity, and radiation at the micro-level occurs by individual quanta, the time intervals between which depend significantly on the free path length between the molecules, as well as on the degree of excitation of the degrees of freedom, mainly vibrational for the solids. Hence it immediately follows that there is a time lag of the heat flow from the temperature gradient. The lag time between the heat flux and the temperature gradient is called the relaxation time. It is very small for solids (Equation 1) (Lykov, 1967).

There are conditions for the occurrence of a heatwave in a solid body since the relaxation time accounted for in the heat transfer, leads to a finite velocity of the heat flow propagation, in contrast to the infinite velocity of heat propagation, determined by the classical Fourier's law. Such wave heat transfer is characterized by the presence of moving the first kind discontinuity of the temperature field with decreasing discontinuity amplitudes due to thermal energy dissipation. If you are considering not a continuous (over time) heat input into the solid, but a pulse one, which takes place in real heat exchange, then a series of isolated pulses (solitons) having front and rear discontinuity, at wave motion inside the body, should hypothetically retain the basic geometric and thermal physical properties, taking into account the significant dissipation of heat (Belov *et al.*, 2014, Sokolov and Ryabinov, 2015).

Theoretically, the wave heat transfer is described by the heat equation of hyperbolic type with the wave term (the second temperature derivative in time) and the dissipative term (the first temperature derivative in time). Based on this equation the wave heat transfer was studied in papers (Zarubin and Kuvyrkin, 2000; Kartashov, 2001; Shashkov *et al.*, 2004; Zarubin *et al.*, 2018). In a paper (Kartashov, 2016) the analysis of wave heat transfer based on two relaxation times (by heat transfer and elasticity) was carried out.

It should be noted that wave heat transfer occurs not only because of the presence of the relaxation time but also because of the nonlinearity of the thermal physical properties of the medium, depending on temperature (Samarskiy *et al.*, 1987; Kolesnik, 2014; Kolesnik *et al.*, 2015; Gidaspov and Severina, 2015; Gidaspov *et al.*, 2016; Lurie *et al.*, 2017; Bulychev *et al.*, 2017; Bulychev *et al.*, 2018a; Lomakin *et al.*, 2018; Gidaspov *et al.*, 2018; Bulychev *et al.*, 2018b). Paper (Formalev, 2012) contains the first theoretically obtained thermal shock waves in nonlinear medium and the conditions of their occurrence.

Downloaded from www.periodico.tchequimica.com

The purpose of this paper is a theoretical study of the propagation and interaction of isolated thermal pulses (solitons) inbounded bodies, determining of the properties of thermal solitons at reflection from the body boundaries, collision of solitons reflected from the right boundary and moving in a straight direction, their dissipation and the final formation of the temperature distribution under the action of a group of solitons.

2. MATERIALS AND METHODS

The problem is set to analyze the dynamics of motion and reflection of a series of isolated heat waves (solitons) of rectangular shape with the temperature amplitude T_0, acting on the left boundary of a bounded rod, based on the wave equation of thermal conductivity. Such problems arise in quantum mechanics when the body is irradiated with powerful pulses of thermal energy of various origins.

Mathematically, the problem is formulated as follows (Equations 2 – 6), where τ_r – relaxation time – the time of the heat flux rate lag $q(x,t)$ from the temperature gradient in compliance with the law of heat conduction Vernotte-Cattaneo-Lykov, which is the Equation 7) in one-dimensional case. Based on Equation 7 the wave heat transfer Equation 2 was derived; $\eta(z)$ – Heaviside function ($\eta(z)=1$ at $z>0$, $\eta(z)=0$ at $z<0$); T_0 – absolute temperature value in a single heat pulse, acting during the time t_1 (this value is called the *pulse support); d* – time lag between the pulses; x,t – spatial and time variables; a – thermal conductivity m^2/s; K – number of solitons.

Replacing Equation 8 the problem (Equations 2–6) can be reformulated in relation to function $T_1(x,t)$, but with zero initial condition $T_1(x,0)=0$. Further replacing $T_1(x,t)$ by $T(x,t)$, the problem (Equations 2–6) can be cast without loss of generality with homogenous initial values (Equation 9). Herewith the final solution of Equation 1 and Equations 3–11 should be added with the value of T_e. As the relaxation time τ_r in solid bodies has order of $10^{-12} \div 10^{-14} s$, it is expedient (Equation 2, Equations 4–6 and Equation 8) to change to the non-dimensional variables, wherefore the Equation 1 is multiplied by τ_r, and then divided by τ_r^2. After that, authors derive the below non-dimensional variables (Equations 10–13). Embedding the non-dimensional variables Equation 9 in correlations (Equations 2, 4–6, 9) authors get the problem of wave heat transfer in a dimensionless form (replacing the non-dimensional variables $\overline{T}$, $\overline{t}$, $\overline{x}$, $\overline{l}$, $\overline{t_1}$, $\overline{d}$ with T, t, x, l, t_1, d) (Equations 14 – 18).

As the velocity v of the heatwave is determined by Equations 19 (Lykov, 1967), from the equation, Equation 20 Equation 21 is obtained that is Equation 22 following that $\overline{t}=\overline{x}$. Thus, in the problem Equation 14–17 of the heat transfer the dimensionless special variable x coincides with the non-dimensional time variable t.

To solve the problem Equation 14–17 the source function method (Green) is applied. To get the Green function, $G(\overline{x},\xi,\overline{t})$ it is needed to place the unit capacity source at a point of $\overline{x}=\xi$, and in compliance with the general theory formulate the problem to define this function, using the zero conditions for this function in the space-time boundary (Equations 23–27), where $\delta(\overline{x}-\xi)$ – the Dirac function. If the solution to the problem (Equations 23–27) for the function $G(x,\xi,t)$ is obtained, the solution to the problem (Equations 14–17) will be in time integral form $\tau<t$ (Equation 28) (Rabinskiy and Tushavina, 2019). By substitution Equation 29 Equation 23 is reduced to the parabolic type. Substituting Equation 29 in Equation 23 and putting to zero the ratio at $\partial V/\partial\overline{t}$, authors get $\mu=1/2$, where the problem (Equations 23–27) turns into the problem (Equations 30-34). Problem (Equations 30–34) can be solved by the method of separation of variables with the presentation of Equation 35. Eigenvalues λ_n and their related proper functions $X_n(\overline{x})$ of the Sturm-Liouville problem is given by (Equation 36) and functions $\theta_n(\overline{t})$ equal to (Equations 37–38). Meeting Equation 38 the initial conditions Equation 33 and Equation 34, the ratios A_n, are obtained (Equation 39). Thus the function Equation (38) is given by Equation 40. Herewith the problem solution Equations 30–34 is the function (Equation 41), where Equation 42. Considering Equation 29 and Equation 41 the solution of Equations 23–25 for the source function

Downloaded from www.periodico.tchequimica.com

$G(\bar{x},\xi,\bar{t})$ in Equation 43. Substituting Equation 43 into Equation 28, authors get the solution of Equations 23–25 for the function $\bar{T}(x,t)$ given by Equation 44, where Equation 46. Equation 44 – is the solution of the original problem Equations 14–25 of the wave heat transfer for the group of K isolated heat waves (solitons).

3. RESULTS AND DISCUSSION:

Calculation of wave heat transfer in bounded bodies was done for a single thermal soliton with the pulse support in time $\bar{t}_1 = 0.5$, for two solitons with pulse supports $\bar{t}_1 = 0.5$ and period between them equal to Equation 47 and three solitons with pulse supports $\bar{t}_1 = 0.5$ and period between them equal to Equation 48. Results are presented in Figures 1-5 respectively, demonstrating the dynamics of isolated heat waves in bounded rod under conditions when the right boundary is heat isolated (Equation 49):

As the dimensionless time (Equation 50) and dimensionless spatial variable (Equation 51) equal each other, supports of the heat waves in time (time periods, in which the wave amplitude is above zero, and equals to zero outside these periods) are equal to supports with a spatial variable.

Input data for all results had the below values: time supports (as well as space supports) were taken equal to 0.5, dimensionless rod length (Equation 52) was taken equal to 3, maximum relative temperature (Equation 53) of solitons, entering the body on the left boundary, equals to 1 and the absolute temperature T_0 can be general.

Figures 1-2 presents dynamic motion of one soliton, having the front and the rear first kind discontinuity, herewith the temperature profile inside the support is decreasing $\left(\frac{\partial \bar{T}}{\partial \bar{x}} < 0\right)$ according to the heat power dissipation. Herewith the temperature before the front edge of the soliton equals the initial value (zero in this case), and behind the left edge, the temperature profile is different to the initial for some value (Figure 1).

Having reached the right end of the rod, the soliton energy is used to increase the temperature of the right thermally insulated boundary, and since the temperature to the left of the right boundary is approximately equal to the initial one, an isolated heatwave is formed in the opposite direction (reverse wave). The edges in the reverse wave change their places – the rear edge becomes the front one, and the front edge is rear one.

Now the temperature on the new front edge is lower than that on the rear one, and between them, the temperature distribution is determined by Equation 34 with $\frac{\partial \bar{T}}{\partial \bar{x}} > 0$ (Figure 2). Having reached the left boundary of the rod, the temperature of the left boundary of the soliton takes a boundary value equal to zero (Figure l, $\bar{t} = 6.5$).

Figure 3 shows the dynamics of motion, reflection, and interaction of two solitons with supports $\bar{t}_1 = 0.5$ and the period of time (and space) equal to 2.5. Temperature distribution, motion dynamics, and reflections are maintained in the same quality as for the variant in Figures 1-2 except for the interaction of the soliton reflected from the right boundary and moving in a straight direction from the left boundary to the right one (Figure 3, $\bar{t} = \{4; 4.5; 5\}$). In Figure 3 ($\bar{t} = 4.5$), the left and the right solitons converged into one, and its amplitude is the sum of the decreasing amplitudes of the "left" and the "right" solitons (Figure 3 ($\bar{t} = 4$)). The solitons diverge (Figure 3 ($\bar{t} = 5$)) preserving all qualitative and geometric characteristics except for the amplitudes, which go on to decrease (Figure 3 ($\bar{t} = 5$)) due to the dissipation of thermal energy.

Figures 4-5 shows the motion dynamics of three solitons with supports $t_1 = 0.5$ and periods of time (and the spatial variable) equal to $\bar{d} + \bar{t}_1 = 1$. It evidences all properties of single and double solitons. In addition, the interaction of a large number of solitons with the right body boundary shows that after reflection the number of "bursts" with the largest amplitudes is preserved (in this case there are three of them). Due to the smaller gap between the solitons compared to the options in Figures 1-3, the temperature at these intervals is much higher than the initial value, that is, a continuous temperature field is formed.

4. CONCLUSIONS:

On the basis of a new analytical solution of the problem of wave heat transfer in bounded bodies, a formation mechanism of an unsteady temperature field was defined using a series of

Downloaded from www.periodico.tchequimica.com

isolated thermal waves (solitons) at times proportional to several times of thermal relaxation, that is, at times of nanosecond durations with a heat depth of several nanometers. The mechanism of thermal solitons reflection from the opposite body boundary is set, according to which all soliton energy is absorbed by the heat -isolated wall, and then the inverse wave of the thermal soliton is formed, having the same geometric and kinematic properties as the direct wave taking into account the dissipation. In addition, the interaction mechanism between direct and reflected solitons is defined, according to which the total energy of the merged soliton (the temperature profile amplitude) is below the sum of soliton powers before their meeting. Herewith the temperature gradient inside the soliton is negative in the forward direction and positive in the reflected direction.

The merged solitons then diverge, continuing to move in the same directions as before the merger, preserving their geometric and kinematic characteristics, and taking into account the absorption (dissipation) of thermal energy.

5. ACKNOWLEDGMENTS:

The work was carried out with the financial support of the state project of the Ministry of Education and Science project code 2.9219.2017 / 8.9.

6. REFERENCES:

1. Belov, P.A., Kobets, L.P., Borodulin, A.S. *Inorganic Materials: Applied Research*, **2014**, *5*(4): 403-406.
2. Bulychev, N.A., Kazaryan, M.A., Chaikov, L.L., Averyushkin, A.S., Krasovskii, V.I., Feofanov, I.N., Rasmagin, S.I., Zadorin, D.A., Zakharyan, R.A. *XIII International Conference on Pulsed Lasers and Laser Applications AMPL-2017*, **2017**, *12*, 183-189.
3. Bulychev, N.A., Kazaryan, M.A., Kirichenko, M.N., Garibyan, B.A., Morozova, E.A., Chernov, A.A. *Proceedings – SPIE*, **2018a**, *10614*(10614OZ), 2-6.
4. Bulychev, N.A., Kuznetsova, E.L., Bodryshev, V.V., Rabinskiy, L.N. *Nanoscience and Technology: an International Journal*, **2018b**, *9*(2), 91-97. DOI: 10.1615/NanoSciTechnolIntJ.2018025703
5. Formalev, V.F. *High Temperature*, **2012**, *50*(6), 744-748.
6. Gidaspov, V.Yu., Golubev, V.K., Severina, N.S. *Bulletin of the South Ural State University, Series: Mathematical Modelling, Programming and Computer Software*, **2016**, *9*(3), 94-104.
7. Gidaspov, V.Yu., Moskalenko, O.A., Severina, N.S. *High Temperature*, **2018**, *56*(5), 751-757.
8. Gidaspov, V.Yu., Severina, N.S. *High Temperature*, **2015**, *53*(4), 526-530.
9. Kartashov, E.M. *Analytical Methods in Theory of Heat Conduction of Solid Bodies*, Moscow: Visshaya Shkola, **2001**.
10. Kartashov, E.M. *Journal of Engineering Physics and Thermophysics*, **2016**, *89*(2), 346-356.
11. Kolesnik, S.A. *Mathematical Models and Computer Simulations*, **2014**, *6*(5), 480-489.
12. Kolesnik, S.A., Formalev, V.F., Kuznetsova, E.L. *High Temperature*, **2015**, *53*(1), 68-72.
13. Lomakin, E.V., Lurie, S.A., Rabinskiy, L.N., Solyaev, Y.O. *Reports of Physics*, **2018**, *63*(4), 161-164.
14. Lurie, S.A., Solyaev, Y.O., Lizunova, D.V., Rabinskiy, L.N., Bouznik, V.M., Menshykov, O. *International Journal of Heat and Mass Transfer*, **2017**, *109*, 511-519.
15. Lykov, A.V. *Theory of Heat Conduction*, Moscow: Vischaya Shkola, **1967**.
16. Rabinskiy, L.N., Tushavina, O.V. INCAS Bulletin, **2019**, *11*(Special Issue), 203-211. DOI: 10.13111/2066-8201.2019.11.S.20.
17. Samarskiy, A.A., Galaktionov, V.A., Kurdyumov, S.P., Mihajlov, A.P. *Modes with aggravation in problems for quasilinear parabolic equations*, Moscow: Nauka, **1987**.
18. Sokolov, N.S., Ryabinov, V.M. Soil Mechanics and Foundation Engineering, **2015**, *52*(1): 18-22.

Downloaded from www.periodico.tchequimica.com

19. Shashkov, A.G., Bubnov, A.V., Yanovskij, S.Yu. *Heat conduction wave phenomena*, Moscow: URSS, **2004**.
20. Zarubin, V.S., Kuvyrkin, G.N. *Mathematical modeling of thermomechanics*, Moscow: Fizmatlit, **2000**.
21. Zarubin, V.S., Kuvyrkin, G.N., Savelyeva, I.Yu. *International Journal of Heat and Mass Transfer*, **2018**, *116*, 833-839.

$\left(\sim 10^{-12} - 10^{-14} \mathrm{s} \right)$, (Eq. 1)

$$\tau_r \frac{\partial^2 T}{\partial t^2} + \frac{\partial T}{\partial t} = a \frac{\partial^2 T}{\partial x^2}, \ 0 < x < l, \ t > 0; \quad \text{(Eq. 2)}$$

$$T(x,0) = T_e = const, \quad 0 \le x \le l; \quad \text{(Eq. 3)}$$

$$\frac{\partial T(x,0)}{\partial t} = 0, \ 0 \le x \le l; \quad \text{(Eq. 4)}$$

$$T(0,t) = T_0 \sum_{k=1}^{K} \left[\eta\left(t - \left(k \cdot d + (k-1)t_1\right) + d\right) - \eta\left(t - k\left(d + t_1\right) + d\right) \right] = \varphi(t), \ t > 0; \quad \text{(Eq. 5)}$$

$$\frac{\partial T(l,t)}{\partial x} = 0, \ t > 0, \quad \text{(Eq. 6)}$$

$$q(x,t) = -\frac{\partial T(x,t)}{\partial x} - \tau_r \frac{\partial q(x,t)}{\partial t}, \quad \text{(Eq. 7)}$$

$$T(x,t) = T_1(x,y) + T_e \quad \text{(Eq. 8)}$$

$$T(x,0) = 0, \ 0 \le x \le l. \quad \text{(Eq. 9)}$$

$$\overline{T}(x,t) = T(x,t) / T_0; \quad \text{(Eq. 10)}$$

$$\overline{t} = t / \tau_r; \ \overline{x} = \frac{x}{\sqrt{a\tau_r}}; \quad \text{(Eq. 11)}$$

$$\overline{l} = l / \sqrt{a\tau_r}, \ \overline{t_1} = t_1 / \tau_r; \quad \text{(Eq. 12)}$$

$$\overline{d} = d / \sqrt{a\tau_r}. \quad \text{(Eq. 13)}$$

$$\frac{\partial^2 \overline{T}}{\partial t^2} + \frac{\partial \overline{T}}{\partial t} = \frac{\partial^2 \overline{T}}{\partial x^2}, \ 0 < \overline{x} < \overline{l}, \ \overline{t} > 0; \quad \text{(Eq. 14)}$$

$$\overline{T}(\overline{x},0) = 0, \ 0 \le \overline{x} \le \overline{l}; \quad \text{(Eq. 15)}$$

Downloaded from www.periodico.tchequimica.com

$$\frac{\partial \overline{T}\left(\overline{x},0\right)}{\partial \overline{t}}=0,\ \ 0\le \overline{x}\le \overline{l};$$ (Eq. 16)

$$\overline{T}\left(0,\overline{t}\right)=1\cdot\sum_{k=1}^{K}\left[\eta\left(\overline{t}-\left(k\cdot\overline{d}+\left(k-1\right)\overline{t_1}\right)+\overline{d}\right)-\eta\left(\overline{t}-k\left(\overline{d}+\overline{t_1}\right)+\overline{d}\right)\right]=\varphi\left(\overline{t}\right),\ \overline{t}>0;$$ (Eq. 17)

$$\frac{\partial \overline{T}\left(\overline{l},\overline{t}\right)}{\partial \overline{x}}=0,\ \ \overline{t}>0./$$ (Eq. 18)

$$v=\sqrt{a/\tau_r}$$ (Eq. 19)

$$v=x/t$$ (Eq. 20)

$$v=\sqrt{a\tau_r}\cdot\overline{x}/\tau_r\cdot\overline{t}=\sqrt{a/\tau_p}\overline{x}/\overline{t}=\sqrt{a/\tau_r},$$ (Eq. 21)

$$\sqrt{a/\tau_r}=\sqrt{a/\tau_r}\overline{x}/\overline{t}$$ (Eq. 22)

$$\frac{\partial^2 G}{\partial \overline{t}^{\,2}}+\frac{\partial G}{\partial \overline{t}}=\frac{\partial^2 G}{\partial \overline{x}^{\,2}},\ \ 0<\overline{x}<\overline{l},\ \ 0<\xi<\overline{l}\ ,\overline{t}>0;$$ (Eq. 23)

$$G\left(\overline{x},\xi,0\right)=0,\ \ 0\le\overline{x}\le\overline{l},\ \ 0<\xi<\overline{l}\ ;$$ (Eq. 24)

$$\frac{\partial G\left(\overline{x},\xi,0\right)}{\partial \overline{t}}=1\cdot\delta\left(\overline{x}-\xi\right),\ \ 0\le\overline{x}\le\overline{l},\ \ 0<\xi<\overline{l}\ ;$$ (Eq. 25)

$$G\left(0,\xi,\overline{t}\right)=0,\ \ \overline{t}>0,\ \ 0<\xi<\overline{l}\ ;$$ (Eq. 26)

$$\frac{\partial G\left(\overline{l},\xi,\overline{t}\right)}{\partial \overline{x}}=0,\ \ t>0,\ \ 0<\xi<\overline{l}\ ;$$ (Eq. 27)

$$\overline{T}\left(\overline{x},\overline{t}\right)=\int_0^{\overline{t}}\varphi\left(\tau\right)\left[\frac{\partial}{\partial\xi}G\left(\overline{x},\xi,\overline{t}-\tau\right)\right]_{\xi=0}d\tau.$$ (Eq. 28)

$$G\left(\overline{x},\xi,\overline{t}\right)=V\left(\overline{x},\xi,\overline{t}\right)\cdot\exp\left(\mu\overline{t}\right)$$ (Eq. 29)

$$\frac{\partial^2 V}{\partial \overline{t}^{\,2}}-\frac{1}{4}V=\frac{\partial^2 V}{\partial \overline{x}^{\,2}},\ \ 0<\overline{x}<\overline{l},\ \ 0<\xi<\overline{l}\ ,\overline{t}>0;$$ (Eq. 30)

$$V\left(\overline{x},\xi,0\right)=0,\ \ 0\le\overline{x}\le\overline{l},\ \ 0<\xi<\overline{l}\ ;$$ (Eq. 31)

$$\frac{\partial V\left(\overline{x},\xi,0\right)}{\partial \overline{t}}=1\cdot\delta\left(\overline{x}-\xi\right),\ \ 0\le\overline{x}\le\overline{l},\ \ 0<\xi<\overline{l}\ ;$$ (Eq. 32)

$$V\left(0,\xi,\overline{t}\right)=0,\ \ \overline{t}>0,\ \ 0<\xi<\overline{l}\ ;$$ (Eq. 33)

Downloaded from www.periodico.tchequimica.com

$$\frac{\partial V\left(\overline{l},\xi,\overline{t}\right)}{\partial\overline{x}}=0,\ \ t>0,\ \ 0<\xi<\overline{l}\ .$$ (Eq. 34)

$$V=X\left(\overline{x}\right)\cdot\theta\left(\overline{t}\right).$$ (Eq. 35)

$$\lambda_n=\frac{\pi\left(1/2+n\right)}{l},\ \ X_n\left(\overline{x}\right)=\sin\left(\lambda_n\overline{x}\right),\ \ n=0,1,2,...,l$$ (Eq. 36)

$$\theta_n\left(\overline{t}\right)=A_n\cdot\sin\left(\overline{t}\sqrt{\lambda_n^2-1/4}\right)+B_n\cdot\cos\left(\overline{t}\sqrt{\lambda_n^2-1/4}\right)$$ (Eq. 37)

$$V\left(\overline{x},\overline{t}\right)=\sum_{n=0}^{\infty}\theta_n\left(\overline{t}\right)\cdot X_n\left(\overline{x}\right)=\sum_{n=0}^{\infty}\Bigg[A_n\sin\left(\overline{t}\sqrt{\lambda_n^2-1/4}\right)+$$
$$+B_n\cdot\cos\left(\overline{t}\sqrt{\lambda_n^2-1/4}\right)\Bigg]\sin\left(\lambda_n\overline{x}\right).$$ (Eq. 38)

$$B_n=0,\ \ A_n\left(\xi\right)=\frac{2}{\overline{l}}\ \frac{\sin\left(\lambda_n\xi\right)}{\sqrt{\lambda_n^2-1/4}}.$$ (Eq. 39)

$$V\left(\overline{x},\xi,\overline{t}\right)=\sum_{n=0}^{\infty}\frac{2}{\overline{l}}\frac{\sin\left(\lambda_n\xi\right)}{\sqrt{\lambda_n^2-1/4}}\sin\left(\overline{t}\sqrt{\lambda_n^2-1/4}\right)\cdot\sin\left(\lambda_n\overline{x}\right).$$ (Eq. 40)

$$V\left(\overline{x},\xi,\overline{t}\right)=\sum_{n=0}^{N}\frac{2}{\overline{l}}\frac{\sin\left(\lambda_n\xi\right)}{\sqrt{\left|\lambda_n^2-1/4\right|}}\mathrm{sh}\left(\overline{t}\sqrt{\left|\lambda_n^2-1/4\right|}\right)\sin\left(\lambda_n\overline{x}\right)+$$
$$+\sum_{n=N+1}^{\infty}\frac{2}{\overline{l}}\frac{\sin\left(\lambda_n\xi\right)}{\sqrt{\lambda_n^2-1/4}}\sin\left(\overline{t}\sqrt{\lambda_n^2-1/4}\right)\sin\left(\lambda_n\overline{x}\right),$$ (Eq. 41)

$$N<\frac{\overline{l}}{2\pi}-\frac{1}{2}\ \ 42$$ (Eq. 42)

$$G\left(\overline{x},\xi,\overline{t}\right)=\sum_{n=0}^{N}\left(\frac{2}{\overline{l}}\frac{e^{-\overline{t}/2}}{\sqrt{\left|\lambda_n^2-1/4\right|}}\mathrm{sh}\left(\overline{t}\sqrt{\left|\lambda_n^2-1/4\right|}\right)\right)\sin\left(\lambda_n\overline{x}\right)\sin\left(\lambda_n\xi\right)+$$
$$+\sum_{n=N+1}^{\infty}\left(\frac{2}{\overline{l}}\frac{e^{-\overline{t}/2}}{\sqrt{\lambda_n^2-1/4}}\sin\left(\overline{t}\sqrt{\lambda_n^2-1/4}\right)\right)\sin\left(\lambda_n\overline{x}\right)\sin\left(\lambda_n\xi\right).$$ (Eq. 43)

$$\overline{T}\left(\overline{x},\overline{t}\right)=\int_0^{\overline{t}}\varphi\left(\tau\right)\left(\frac{\partial}{\partial\xi}G\left(\overline{x},\xi,\overline{t}-\tau\right)\right)_{\xi=0}d\tau=$$
$$=\int_0^{\overline{t}}\varphi\left(\tau\right)\sum_{n=0}^{N}\left[\frac{2}{\overline{l}}\frac{e^{-\left(\overline{t}-\tau\right)/2}}{\sqrt{\left|\lambda_n^2-1/4\right|}}\mathrm{sh}\left(\overline{t}-\tau\right)\sqrt{\left|\lambda_n^2-1/4\right|}\right]\times\times\lambda_n\cdot\sin\left(\lambda_n\overline{x}\right)d\tau+\int_0^{\overline{t}}\varphi\left(\tau\right)\sum_{n=N+1}^{\infty}\left[\frac{2}{\overline{l}}\frac{e^{-\left(\overline{t}-\tau\right)/2}}{\sqrt{\lambda_n^2-1/4}}\right.$$
$$\left.\sin\left(\left(\overline{t}-\tau\right)\sqrt{\lambda_n^2-1/4}\right)\right]\lambda_n\cdot\sin\left(\lambda_n\overline{x}\right)d\tau,$$ (Eq. 44)

Downloaded from www.periodico.tchequimica.com

$$\lambda_n = \frac{\pi(1/2+n)}{l},\ n = 0,1,2,...;\ . \quad \text{(Eq. 45)}$$

$$\varphi(\tau) = \sum_{k=1}^{K}\left[\eta\left(\tau - \left(k\cdot\bar{d} + (k-1)\bar{t}_1\right) + \bar{d}\right) - \eta\left(\tau - k\left(\bar{d}+\bar{t}_1\right) + \bar{d}\right)\right]. \quad \text{(Eq. 46)}$$

$$\bar{d} + \bar{t}_1 = 2.5\left(\bar{d} = 2\right) \quad \text{(Eq. 47)}$$

$$\bar{d} + \bar{t}_1 = 1\ \left(\bar{d} = 0.5\right). \quad \text{(Eq. 48)}$$

$$\left(\frac{\partial\bar{T}\left(\bar{l},\bar{t}\right)}{\partial\bar{x}} = 0\right). \quad \text{(Eq. 49)}$$

$$\bar{t} = t/\tau_r \quad \text{(Eq. 50)}$$

$$\bar{x} = x/\sqrt{a\tau_r} \quad \text{(Eq. 51)}$$

$$\bar{l} = l/\sqrt{a\tau_r} \quad \text{(Eq. 52)}$$

$$\bar{T} = T/T_0 \quad \text{(Eq. 53)}$$

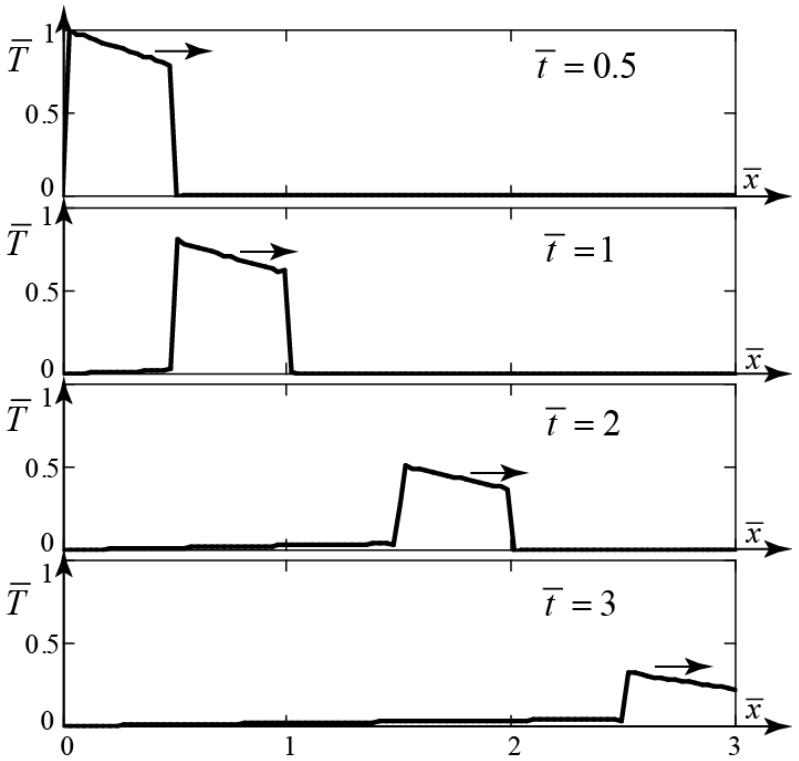

Figure 1. *Motion dynamics and reflection from the right boundary of one temperature soliton with the support* $\bar{t}_1 = 0.5$ *in bounded space* $\bar{t} = \{0.5; 1.0; 2.0; 3.0\}$

Downloaded from www.periodico.tchequimica.com

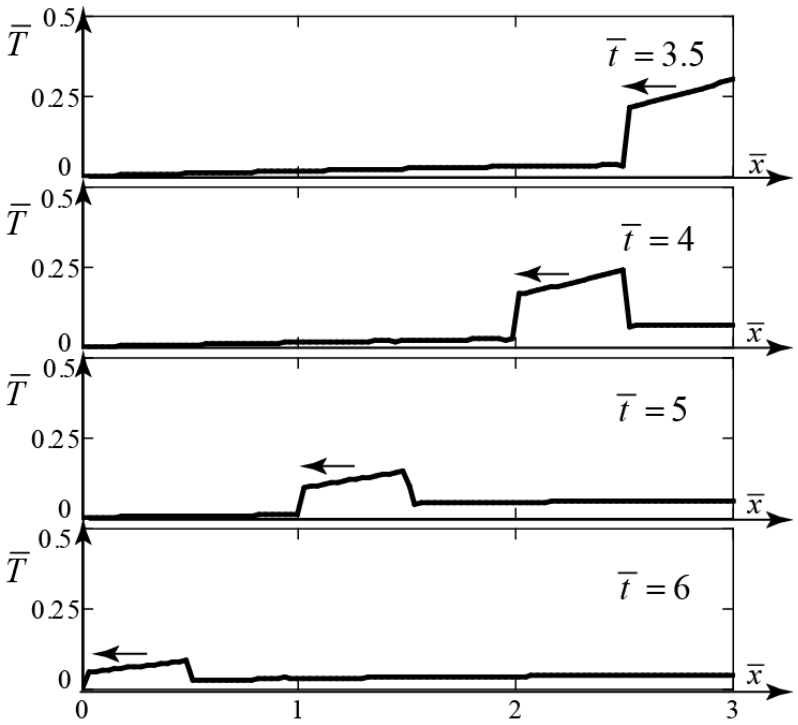

Figure 2. *Motion dynamics and reflection from the right boundary of one temperature soliton with the support* $\overline{t}_1 = 0.5$ *in bounded space* $\overline{t} = \{3.5; 4.0; 5.0; 6.0\}$

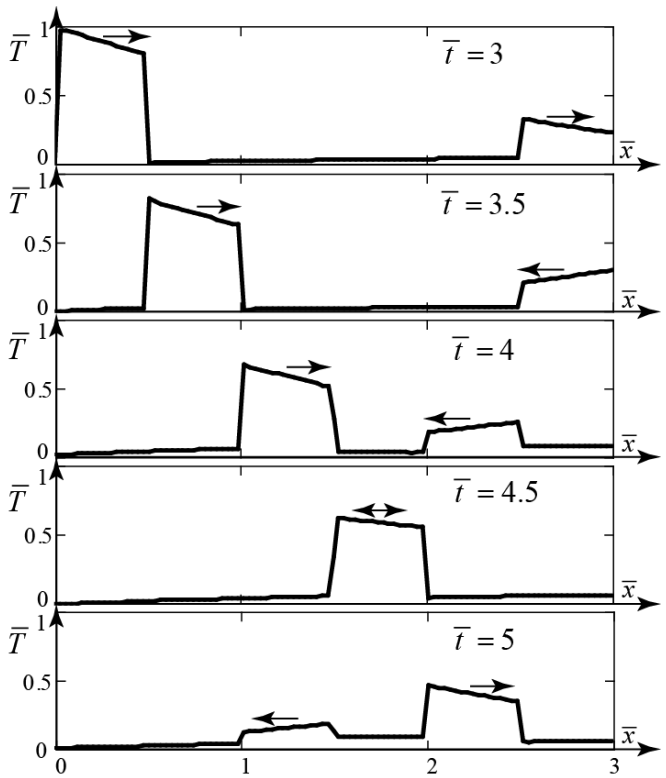

Figure 3. *Motion, correlation dynamics, and reflection from the right boundary of two temperature solitons with the supports* $\overline{t}_1 = 0.5$ *and the period* $\overline{d} + \overline{t}_1 = 2.5$ *in bounded space:*

$\overline{t} = \{3; 3.5; 4.0; 4.5; 5.0\}$

Downloaded from www.periodico.tchequimica.com

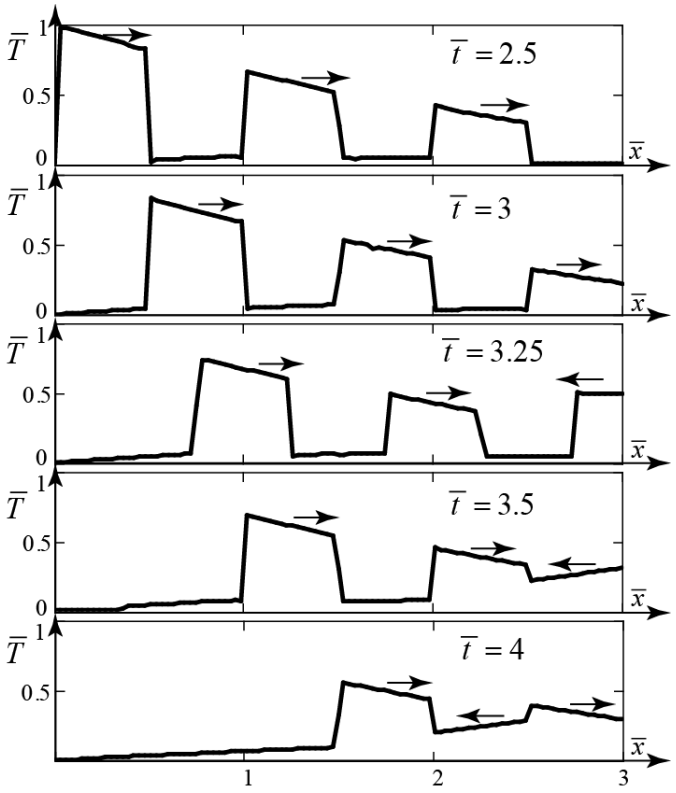

Figure 4. *Motion, correlation dynamics, and reflection from the right boundary of three temperature solitons with the supports* $\overline{t}_1 = 0.5$ *and the period* $\overline{d} + \overline{t}_1 = 1$ *in bounded space:* $\overline{t} = \{2.5; 3.0; 3.25; 3.5; 4.0\}$

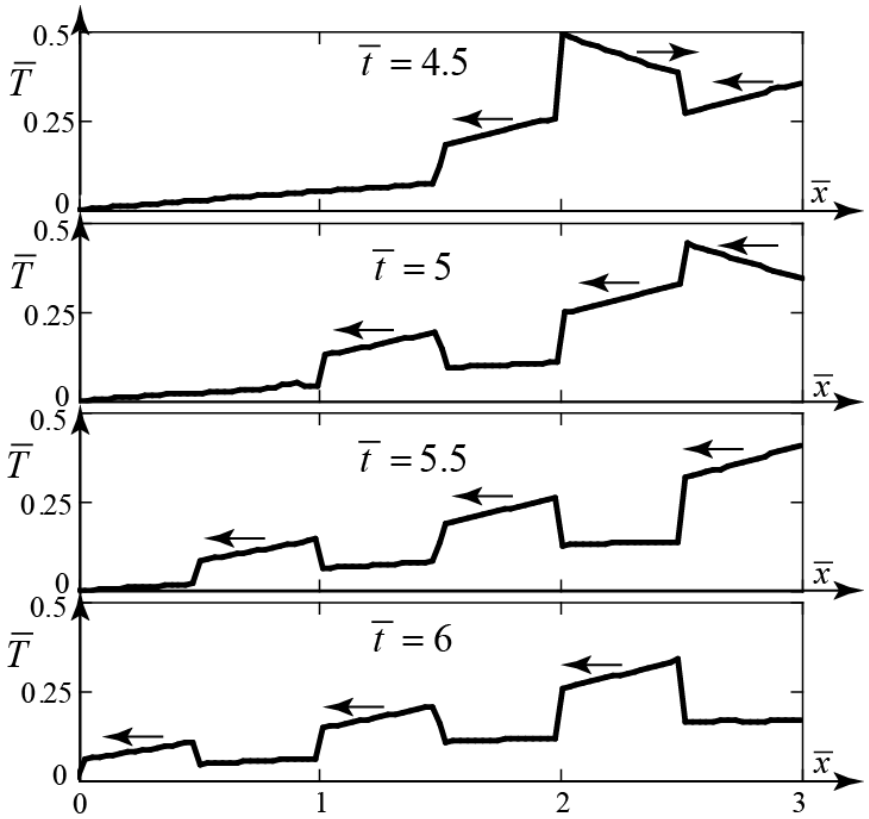

Figure 5. *Motion, correlation dynamics, and reflection from the right boundary of three temperature solitons with the supports* $\overline{t}_1 = 0.5$ *and the period* $\overline{d} + \overline{t}_1 = 1$ *in bounded space:* $\overline{t} = \{4.5; 5.0; 5.5; 6.0\}$

Downloaded from www.periodico.tchequimica.com

PERIÓDICO TCHÊ QUÍMICA
ARTIGO ORIGINAL

CARACTERIZAÇÃO ESTRUTURAL DO ÁCIDO 2-AMINO-2-OXOACÉTICO POR DIFRAÇÃO EM PÓ DE RAIO-X E QUÍMICA QUÂNTICA

STRUCTURAL CHARACTERIZATION OF 2-AMINO-2-OXOACETIC ACID BY X-RAY POWDER DIFFRACTION AND QUANTUM CHEMISTRY

DELGADO, Gerzon E.[1*]; BELANDRIA, Lusbely M.[1], GUILLEN, Marilia[1], MORA, Asiloé J.[1], SEIJAS, Luis E.[2]

[1] Laboratorio de Cristalografía, Departamento de Química, Facultad de Ciencias, Universidad de Los Andes, Mérida 5101, Venezuela

[2] Laboratorio de Procesos Dinámicos em Química, Departamento de Química, Facultad de Ciencias, Universidad de Los Andes, Mérida 5101, Venezuela

** Correspondence author*
e-mail: gerzon@ula.ve

Received 04 July 2019; received in revised form 27 October 2019; accepted 27 October 2019

RESUMO

O ácido 2-amino-2-oxoacético ou ácido carbamoil fórmico ou ácido oxâmico é um ingrediente farmacêutico ativo (API) de grande importância principalmente por ser um inibidor da desidrogenase láctica (LDH). Atua como um inibidor das vias metabólicas de células tumorais e exibiu atividade anticâncer significativa contra células de carcinoma nasofaríngeo (NPC) in vitro e pode ser considerado como uma droga potencial para o tratamento do diabetes tipo 2. Além disso, esse composto poderia ser usado como um componente no projeto de arquiteturas supramoleculares baseadas em ligações de hidrogênio através das funcionalidades complementares de ligação de hidrogênio dos grupos funcionais carbonila e amida presentes. A difração de raios X de cristal único é a técnica mais poderosa para determinar a estrutura cristalina de pequenas moléculas. No entanto, para vários materiais, incluindo o ácido oxâmico, pode ser complicado cultivar cristais únicos de tamanho e qualidade adequados que os tornem apropriados para a análise da estrutura. Por esse motivo, o estudo estrutural foi realizado com difração de raios X em pó, um processo significativamente mais desafiador do que a determinação de estruturas a partir de dados de cristal único. O ácido oxâmico foi caracterizado por técnicas espectroscópicas de FT-IR e RMN, análise térmica de TGA-DSC, cálculos semi-empíricos de PM7 e difração de raios X por pó. O composto do título cristaliza no sistema monoclínico com grupo espacial Cc, Z = 4 e parâmetros celulares unitários *a*= 9.4994(4) Å, *b*= 5.4380(2) Å, *c*= 6.8636(3) Å, β= 107.149(2)°, V= 338.79(2) Å^3. A molécula tem uma conformação trans. A estrutura molecular e o empacotamento de cristais são estabilizados principalmente pelas ligações intra e intermoleculares de hidrogênio O - H ••• O e N - H ••• O. A caracterização estrutural deste tipo de composto API é importante para entender seus mecanismos de ação devido a seus consideráveis efeitos biológicos. Em particular, este estudo estrutural permitiria o exame subsequente de suas propriedades medicinais como um agente antitumoral e antidiabético.

Palavras-chave: ácido oxâmico, difração de raios-X, cálculo PM7, ligação de hidrogênio

ABSTRACT

2-amino-2-oxoacetic acid, carbamoyl formic acid, or oxamic acid is an active pharmaceutical ingredient (API) of great importance mainly because is an inhibitor of lactic dehydrogenase (LDH). It acts as an inhibitor to the metabolic pathways of the tumor cells and exhibited significant anticancer activity against nasopharyngeal carcinoma (NPC) cells *in vitro* and can be considered as a potential drug for the treatment of type 2 diabetes. Also, this compound could be used as a building block in the design of supramolecular architectures based on hydrogen bonds through the complimentary hydrogen-bond functionalities of the carbonyl and amide functional groups present. Single-crystal X-ray diffraction is the most powerful technique for crystal structure determination of small molecules. However, for several materials, including oxamic acid, it could be complicated to grow single crystals of suitable size and quality that make them appropriated to structure analysis. For this reason, the structural study was conducted with powder X-ray diffraction which is a process significantly more challenging than structure determination from single-crystal data. Oxamic acid has been characterized by FT-IR and NMR spectroscopic techniques, thermal TGA-DSC analysis, semi-empirical PM7 calculations, and X-ray powder

Downloaded from www.periodico.tchequimica.com

diffraction. The title compound crystallizes in the monoclinic system with space group *Cc*, Z=4, and unit cell parameters *a*= 9.4994(4) Å, *b*= 5.4380(2) Å, *c*= 6.8636(3) Å, β= 107.149(2)°, V= 338.79(2) Å^3. The molecule has a *trans* conformation. The molecular structure and crystal packing are stabilized mainly by intra- and inter-molecular O--H···O and N--H···O hydrogen bonds. The structural characterization of this type of API compound is important to understand its mechanisms of action due to its considerable biological effects. In particular, for oxamic acid, this structural study would allow subsequent examination of its medicinal properties as an antitumor and antidiabetic agent.

Keywords: oxamic acid, powder X-ray diffraction, PM7 calculation, hydrogen bonding.

1. INTRODUCTION

2-amino-2-oxoacetic acid, carbamoyl formic acid, or oxamic acid is an active pharmaceutical ingredient (API) of great importance mainly because is an inhibitor of lactic dehydrogenase (LDH), acts as an inhibitor to the metabolic pathways of the tumor cells (Papaconstantinou and Colowick, 1961; Zhao *et al*., 2011; Li *et al*., 2013) and exhibited significant anticancer activity against nasopharyngeal carcinoma (NPC) cells *in vitro* (Li *et al*., 2013). Recently, it was demonstrated that oxamic acid improved glycemic control and insulin sensitivity in db/db mice, and therefore it can be considered as a potential drug for the treatment of type 2 diabetes (Ye *et al*., 2016). On the other hand, oxamic acid is normally generated from the oxidation of organic compounds containing nitrogen functional groups, as aniline, sulfanilic acid and azo dyes (Leitner *et al*., 2002), and is highly refractory to chemical oxidation and conventional processes as ozonation and photolysis (Kerna *et al*., 2007).

From the molecular point of view (Figure 1), oxamic acid (H_2NCO-$COOH$), the monoamide of the oxalic acid (HOOC-COOH), is the isoelectronic and isosteric analog of pyruvic acid (H_3CCO-$COOH$), one of the most important chemical compound in biochemistry. However, the NH_2 group of oxamic acid makes it chemically more active, since having hydrogen donor groups (NH) and, in turn, hydrogen acceptor groups (C=O), is capable of forming interesting supramolecular arrangements in the solid-state (Aakeröy *et al*., 1996). That is why this compound begins to be used as a building block in the design of supramolecular architectures based on hydrogen bonds through the complimentary hydrogen-bond functionalities of the carbonyl and amide functional groups (Da Cunha *et al*., 2018). Molecules containing the oxamate group ($C_2O_3N_2$−) have been synthesized during the past three decades due to their role as chelate ligands in coordination chemistry (Orge *et al*., 2015).

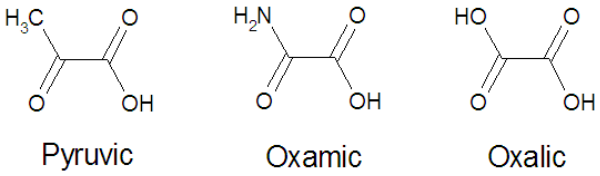

Figure1. *Pyruvic, Oxamic and Oxalic acid chemical structures.*

A search of the Cambridge Structural Database (CSD version 5.40, Nov 2018) (Groom and Allen, 2014) revealed that there are only 12 entries containing the oxamate fragment, transition-metal complexes were not included, all salts. The crystal structure of 2-amino-2-oxoacetic acid has not been reported.

Single-crystal X-ray diffraction is the most powerful technique for crystal structure determination of small molecules. However, for several materials, it could be complicated to grow single crystals of suitable size and quality that make them appropriated to structure analysis. It is difficult to recrystallize the oxamic acid reason why its structure has not been determined. Therefore, the structural study was carried out using powder X-ray diffraction, which is a process significantly more challenging than structure determination from single-crystal data (Harris and Williams, 2014).

In this work, and as part of ongoing structural studies on amino acid derivatives with active biologically molecules (Ávila *et al*., 2004; Mora *et al*., 2005; 2013; 2017; Seijas *et al*., 2010; Delgado *et al*., 2012; 2015; 2016a; 2016b; 2019; Fernández *et al*., 2018), including the derivative nicotinamidium oxamate (Delgado *et al*., 2015), it has been reported the spectroscopic, theoretical and powder X-ray diffraction study of 2-amino-2-oxoacetic, oxamic acid (**I**).

2. MATERIALS AND METHODS

Oxamic acid (2-amino-2-oxoacetic acid) 98% was a commercial material, purchased from Aldrich Co. (O3750), and was used as received.

Attempts to recrystallize the acid in various solvents was unsuccessful.

2.1 FT-IR and NMR spectroscopic studies

The FT-IR spectrum for the title compound was recorded on a Perkin Elmer 1600 spectrometer employing a KBr disc, in the region from 400 to 4000 cm-1 (Figure 2). The bands at 3352 and 3244 cm-1 are typical of the asymmetric tension of N-H group. The bands at 1732 and 1682 cm-1 may be assigned to the carbonyl groups (C=O). Furthermore, the symmetric 1238 cm-1 tension band of CO group, indicates that the oxamic acid is in neutral form.

^{1}H-NMR and ^{13}C-NMR spectra were recorded on a Bruker Avance 400 model spectrometer in DMSO-d_6 solution: ^{1}H NMR (400 MHz, DMSO-d6) δ=11.01 (s, OH), δ=7.68 (s, NH_2). ^{13}C NMR (100.6 MHz, DMSO-d6) δ=162.0 (C=O amide), δ=159.8 (C=O carboxy).

2.2 Thermal analysis

Melting point was determined on an Electrothermal Model 9100 apparatus. Thermal analysis of oxamic acid was performed in a Perkin-Elmer TGA7 coupled with a DSC console. The sample was heated from 25 to 600 °C at a rate of 10 °C min-1, under a nitrogen flux of 100 ml min-1 (Figure 3). A sharp endothermic peak observed at 206 °C corresponds to the compound melts, which was further confirmed by melting point analysis (205-206 °C). The sample decomposed completely at 290 °C.

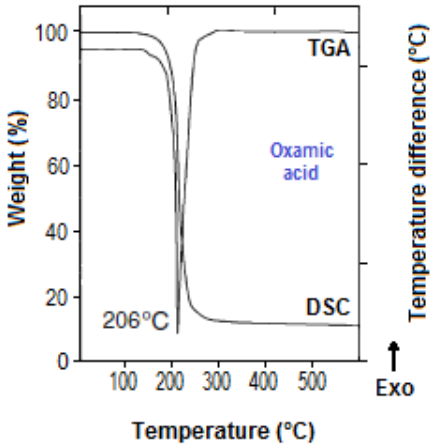

Figure 3. *Thermal analysis plot, TGA and DSC, for* ***(I)****.*

2.3 Theoretical calculations

In order to complete and improve the initial model for further Rietveld refinement (Rietveld, 1969), it was decided to perform a geometry optimization of the solid, employing the semi-empirical quantum mechanics method PM7 (Stewart, 2013). In addition, the reported average unsigned errors for bond length in organic compounds containing C, H, N, O are around 0.01 Å. The initial lattice parameters for the crystal was obtained from the X-ray diffraction pattern indexing and the non-hydrogen atomic positions were obtained from the crystal structural solution found by direct methods using the program Expo2009 (Altomare *et al*., 2009) in the *Cc* monoclinic space group. From the Direct Methods solution, we are not able to assign the N and O atoms of the molecules, and it was decided to perform an optimization geometry considering four conformers (Figure 4), and hydrogen atoms were placed depending on the atom assignments. All the calculations were performed using Gaussian09 (Frisch *et al*., 2009); the lattice parameters were fixed to the experimental values and the atomic positions were optimized.

For all the calculations the basis set 6-31++G(d,p) was employed. The initial structure was built up using bond distances and angles of crystal structure reported in this work. To visualize non-covalent interactions Non-Covalent-Index (NCI) based on the analysis of the electron density was used (Jhonson *et al*., 2010). This approach has the ability to highlight interactions on the low density, low gradient regime. NCI analysis allows us to identify different types of chemical interactions in terms of the electron density and its gradient.

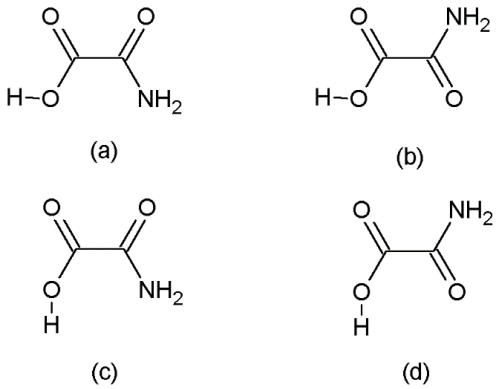

Figure 4*. Conformers, cis and trans, considered for the geometrical optimization of* ***(I)****.*

The NCI analysis is based on a 2D plot of the reduced gradient density (RGD) *vs* the electron density (ρ) where: RGD= $1/2(3\pi^2)^{1/3}.|\nabla\rho|/\rho^{4/3}$. When inter or intramolecular interaction is present, the RGD goes to cero as a result of the presence of critical points in the

Downloaded from www.periodico.tchequimica.com

electron density between the interacting fragments.

2.4. X-ray powder diffraction

The X-ray powder diffraction pattern for 2-amino-2-oxoacetic acid was collected at room temperature in a Siemens D5005 diffractometer using monocromatized CuKα radiation. A small quantity of the sample was ground mechanically in an agate mortar and pestle and mounted on a flat holder covered with a thin layer of grease. The samples were scanned from 15-65° 2θ, with a step size of 0.02° and counting time of 10s. Silicon was used as an external standard.

From the powder pattern, the 20 first measured reflections were completely indexed using the program Dicvol04 (Boultif and Löuer, 2004), which gave a unique solution in a monoclinic cell with parameters *a* = 9.50 Å, *b* = 5.44 Å, *c* = 6.86 Å, β = 107.1° in a *C*-type cell. The Rietveld refinement (Rietveld, 1969) was carried out using the Fullprof program (Rodriguez-Carvajal, 2018) with the unit cell parameters indexed and the atomic positions theoretically optimized. The angular dependence of the peak full width at half maximum (FWHM) was described by the Cagliotti's formula (Cagliotti *et al*., 1958). Peak shapes were described by the parameterized Thompson-Cox-Hastings pseudo-Voigt profile function (Thompson *et al*., 1987). The background variation was described by a polynomial with six coefficients. Restraints were applied to bond distances (deviations ±0.01 Å) and bond angles (deviations ±1°) using average values derived from the CSD [10]. The isotropic atomic displacement parameters were refined as one overall Uiso for the non-hydrogen atoms starting from a value of 0.03 $Å^2$. The isotropic displacement coefficients of each of the hydrogen atoms were calculated as 1.3 times the value of the temperature factor of their riding non-hydrogen atom. The refinement was stable and convergence was readily achieved. All geometrical calculations were done using the program Platon (Spek, 2003). Table 1 summarizes the crystal data, intensity data collection and Rietveld refinement details for the title compound. Figure 5 shows the observed calculated and different profile for the final cycle of the refinement. Table 2 shows the atomic coordinates and selected geometrical parameters for 2-amino-2-oxoacetic acid.

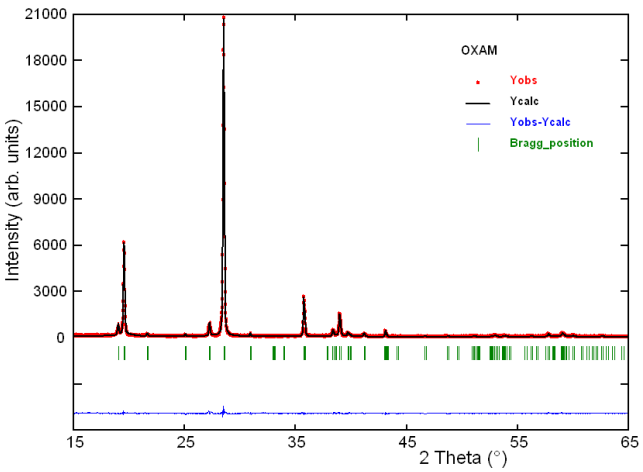

Figure 5. *Rietveld refinement plot for(**I**).*

CCDC-1500810 contains the supplementary crystallographic data for this paper. These data can be obtained free of charge from the Cambridge Crystallographic Data Centre via www.ccdc.cam.ac.uk/data_request/cif.

3. RESULTS AND DISCUSSION:

The 2-amino-2-oxoacetic acid crystallizes in the non-centrosymmetric space group *Cc* with one molecule in the asymmetric unit. Figure 6 shows the molecular structure and the atom-labeling scheme of the title compound. Bond distances, bond angles, and torsion angles are presented in Table 2, and are in agreement with experimental average values found in the 12 entries with oxamate fragments, searched in the Cambridge Structural Database (CSD, version 5.40, Nov 2018) (Groom and Allen, 2014).

This compound crystallizes in a neutral form, unlike the oxamate fragments found in the crystal structural database. The neutral character of the amino acid is confirmed by a clear difference in the values for C1-O1 and C1-O2 bond distances (Table 2). The molecule is essentially plane with maximal deviations of 0.001(1) Å in C1, and adopts a *trans* conformation with the acid and amide groups on opposite sides of the molecule [torsion O1-C1-C2-N2 = 178.6(2) Å].

Downloaded from www.periodico.tchequimica.com

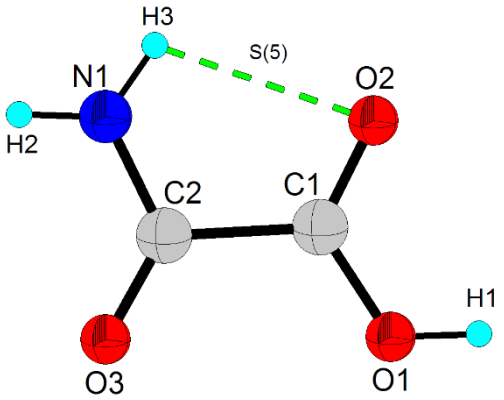

Figure 6. *The molecular structure of (**I**) showing the atomic numbering scheme.*

The molecular structure and crystal packing are stabilized by one intermolecular O–H···O and three N–H···O hydrogen bonds, reinforced by one N–H···O intramolecular interaction (Table 3). The intramolecular N1–H3···O2 gives rigidity to the oxamate molecule with graph-set motif S(5) (Etter, 1990).

The intramolecular interactions O1–H1···O3 and N3–H3···O2 produces a hydrogen bond that connect two molecules by a typical heterosinton amide-acid with graph-set $R^2_2(8)$. The N1–H3···O3 hydrogen bonds form infinite chains which run along the *c* axis with graph-set notation C(4) and produce another heterosinton $R^2_2(8)$ with the N1–H2···O2 interaction. Together, these hydrogen-bond patterns produce a 14-atom cycle described by $R^3_4(14)$, which are connected by amide-acid $R^2_2(8)$ dimers (Figure 7). These chains which extend along the *c* and *b* axis resulting in a lamellar packing type with layers of chains stack along the diagonal of *ca* plane with an average interplanar separation of 5.18 Å (Figure 8).

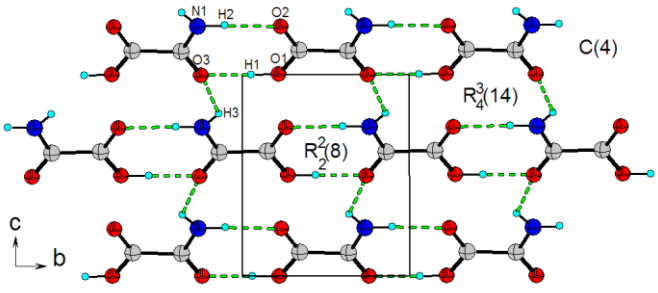

Figure 7. *A portion of the crystal packing shows all intermolecular N--H···O and O--H···O intramolecular hydrogen bonds formed in (**I**).*

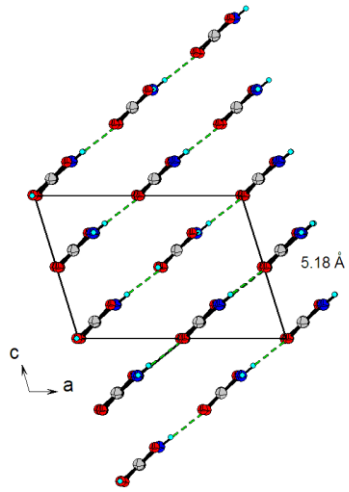

Figure 8. *Packing view of (**I**) showing the extended chains in the ca plane and separated 5.18 Å along the diagonal.*

Figure 9 shows a graph of RGD vs sing(λ_2)ρ, where each of the points has been colored with the corresponding value of sing (λ_2)ρ. As mentioned above, the peaks in the graph are coupled with non-covalent interactions and the value of the density where RGD tends to zero is associated with the strength of the interaction, the negative sign indicates whether the interaction is attractive, while the positive sign indicates repulsive interactions. The hydrogen bonds interactions are in agree the experimental results and the NCI analysis of the non-covalent interactions indicates that the force of the hydrogen bonds decreases in the following order: O1–H1···O3 (i) > N1–H2···O2 (ii) > N1–H3···O3 (iii) > N1–H3···O2.

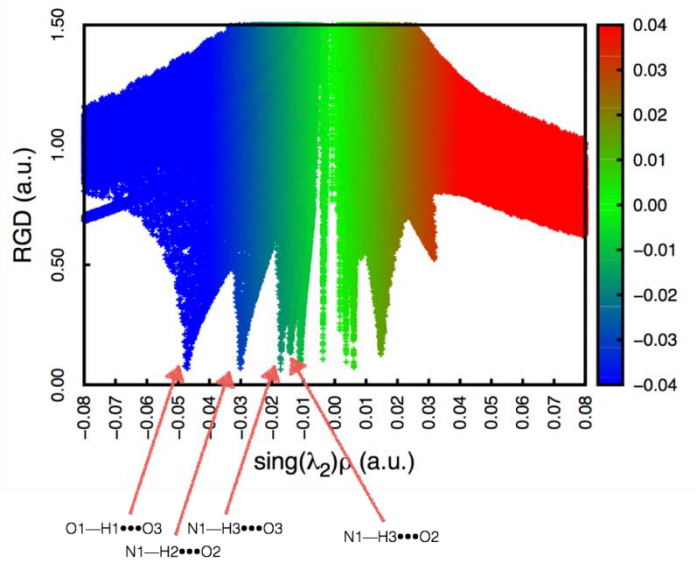

Figure 9*. RGD diagram shows the hydrogen bond interactions in agree with the experimental results in (**I**).*

Downloaded from www.periodico.tchequimica.com

4. CONCLUSIONS:

2-amino-2-oxoactic acid, oxamic acid, an active pharmaceutical ingredient (API) of great importance mainly as possible anti-tumor and anti-diabetes agent, has been structurally characterized by theoretical and experimental techniques. The impossibility of obtaining adequate crystal for single-crystal diffraction study made it necessary to use powder X-ray diffraction complemented by PM7 calculations to establish its crystal structure.

Oxamic acid crystallizes in the monoclinic system with space group *Cc*, Z=4, and unit cell parameters *a*= 9.4994(4) Å, *b*= 5.4380(2) Å, *c*= 6.8636(3) Å, β= 107.149(2)°, V= 338.79(2) Å^3. The bond lengths and bond angles are very close to the corresponding ones found in Cambridge structural database. The molecule has a *trans* conformation. The molecular structure and crystal packing are stabilized mainly by intra- and inter-molecular O--H···O and N--H···O hydrogen bonds.

The structural characterization of oxamic acid can contribute to the chemical and pharmaceutical industries because of its potential use as antitumor and antidiabetic agent.

5. ACKNOWLEDGMENTS:

This work was supported by CDCHT-ULA (Grant C-1990-17-08-B) and FONACIT (Grants LAB-97000821).

6. REFERENCES:

1. Papaconstantinou, J., Colowick, S.P. *J. Biol. Chem*. **1961**, 236, 278.
2. Zhao, Y., Liu, H., Liu, Z., Din, Y., LeDoux, S.P., Wilson, G.L., Voellmy, R., Lin, Y., Lin, W., Nahta, R., Liu, B., Fodstad, O., Chen, J., Wu, Y., Price , J.E., Tan, M. *Cancer Res*. **2011**, 71, 4585.
3. Li, X., Lu, W., Hu, Y., We, S., Qian, C., Wu, W., Huang, P. *Int. J. Oncol*., **2013**, 43, 1710.
4. Ye, W., Zheng, Y., Zhang, S. Yan, L., Cheng, H., Wu, M. *Plos One*, **2016**, 11, e,0150303
5. Leitner, N.K.V., Berger, P., Legube, B. *Environ. Sci. Technol*. **2002**, 36, 3083.
6. Kerna, A., TilleybIain, E., Hunter, S. *J. Biotechnol.*, **2007**, 29, 6.
7. Aakeröy, C., Hughes, D., Nieuwenhuyzen, M. *J. Am. Chem. Soc*., **1996**, 118, 10134.
8. Da Cunha, T.T., Oliveira, W.X.C., Marzano, I.M., Pinheiro, C.B., Pereira-Maia, E.C., Pereira, C.L.M. *J. Mol. Struc*. **2018**, 1149, 803.
9. Orge, C.A., Pereira, M.F., Faria, J.L. *Appl. Catal. B*, **2015**, 174-175, 113.
10. Groom, C.R., Allen, F.H. *Angew. Chem. Int. Ed*., **2014**, 53, 662.
11. Harris, K.D.M., Williams, P.A. in *Structure from Diffraction Methods*, ed. by D.W. Bruce, D. O'Hare, R.I. Walton, Wiley, Chichester, **2014**.
12. Ávila, E.E., Mora, A.J., Delgado, G.E., Ramírez, B., Bashas, A., Koteich, S. *Acta Cryst. C*, **2004**, 60, o759.
13. Mora, A.J., Ávila, E.E., Delgado, G.E., Fitch, A.N., Brunelli, M. *Acta Cryst. B*, **2005**, 61, 96.
14. Seijas, L.E., Delgado, G.E., Mora, A.J., Brunelli, M., Fitch, A.N. *Powder Diffr*. **2010**, 25, 235.
15. Delgado, G.E., Seijas, L.E., Mora, A.J., Gonzalez, T., Briceño, A. *J. Chem. Cryst*. **2012**, 42, 968.
16. Mora, A.J., Belandria, L.M., Ávila, E.E., Seijas, L.E., Delgado, G.E., Miró, A., Almeida, R., Brunelli, M., Fitch, A.N. *Cryst. Growth Design*, **2013**, 13, 1849.
17. Delgado, G.E., Varela, K.N., Mora, A.J., Bruno, J., Atencio, R. *Mol. Cryst. Liq. Cryst*. **2015**, 609, 218.
18. Delgado, G.E., Mora, A.J., González, T., Uzcátegui, J., Lobaton, R., Marroquín, G. *Mol. Cryst. Liq. Cryst*. **2016**a, 625, 225.
19. Delgado, G.E., Guillén, M., Ramírez, J.W., Mora, A.,J., Contreras, J.E., Chacón, C. *Powder Diffr*. **2016**b, 31, 242.
20. Mora, A.J., Belandria, L.M., Delgado, G.E., Seijas, L.E., Lunar, A., Almeida, R. *Acta Cryst. B*, **2017**, 73, 968.
21. Fernández, L.E., Delgado, G.E., Maturano, Tótaro, R.M., Varetti, E.L. *J. Mol. Struct*. **2018**, 1168, 84.
22. Delgado, G.E., Mora, A.J., González, T., Santos, I., Rivas, P., Seijas, L.E. *J. Tchê Quím*. **2019**, 16, 875.
23. Rietveld, H.M. *J. App. Cryst*. **1969**, 2, 65.

Downloaded from www.periodico.tchequimica.com

24. Stewart, J.J. *J. Mol. Model*., **2013**, 19, 1.

25. Altomare, A., Camalli, M., Cuocci, C., Moliterni, A., Rizzi, R., Corriero, N., Falcicchio, A. *J. Appl. Cryst*. **2009**, 42, 1197.

26. Frisch, M.J. *et al*. Gaussian 09, Gaussian, Inc., **2009**.

27. Jhonson E. R., Keinan S., Mori-Sánchez P., Contreras-García, J., Cohen' A.J., Yang, W. *J. Am. Chem. Soc*. **2010**, 132, 6498.

28. Boultif, A., Löuer, D. *J. Appl. Cryst*. **2004**, 37, 724.

29. Rodriguez-Carvajal J. Fullprof, version 6.2, **2018**, LLB, CEA-CNRS, France.

30. Cagliotti, G., Paoletti, A., Ricci, F.P. *Nucl. Instrum*. **1958**, 3, 223.

31. Thompson, P., Cox, D.E., Hastings, J.B. *J. App. Cryst*. **1987**, 20, 79.

32. Spek, A.L. *J. Appl. Cryst*. **2003**, 36, 7.

33. Etter, M.C. *Acc. Chem. Res*. **1990**, 23, 120.

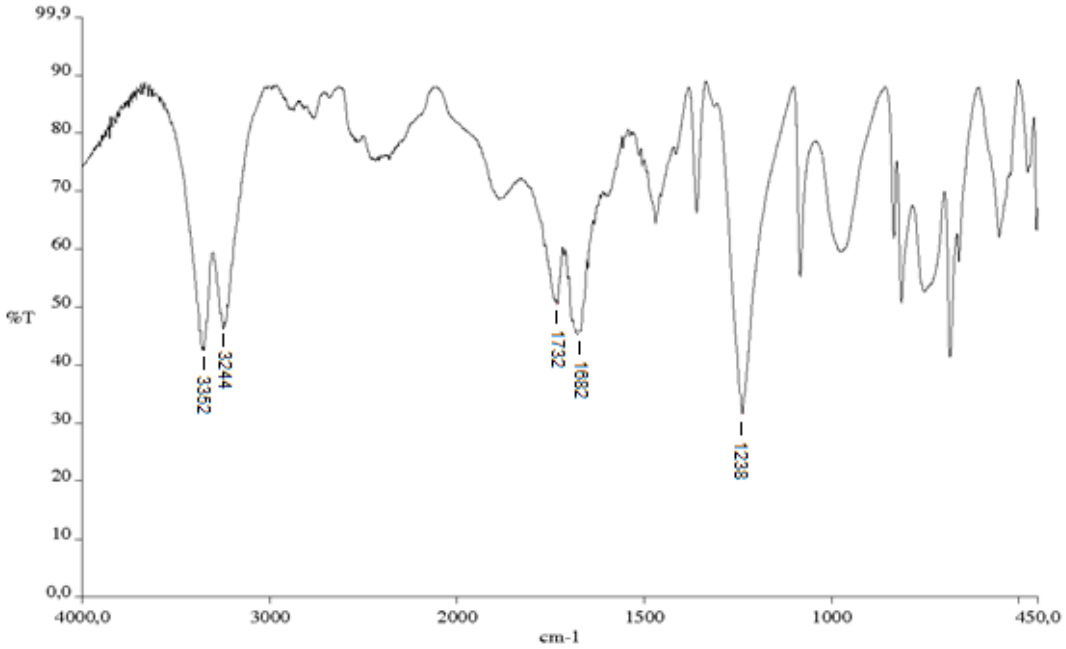

***Figure 2**. FT-IR spectrum for (**I**).*

***Table 1**. Results of the Rietveld refinement for oxamic acid (**I**).*

Molecular formula	$C_2H_3NO_3$	CCDC	1500810
Molecular weight	89.05 (g/mol)		
Crystal system	Monoclinic	D_{calc}	1.752 (g/cm^3)
Space group	*Cc* (N° 9)	N° step intensities	2501
Z	4	N° independent reflections	153
a	9.4994(4)Å	Peak-shape profile	Pseudo-Voigt
b	5.4380(2) Å	R_{exp}	5.2 %
c	6.8636(3) Å	R_p	7.7 %
β	107.149(2)º	R_{wp}	7.2 %
V	338.79(2) Å^3	S	1.4

$R_{exp} = 100\ [(N\text{-}P+C) / \sum_w(y_{obs}^2)]^{1/2}$ $R_{wp} = 100\ [\sum_w|y_{obs} - y_{calc}|^2 / \sum_w|y_{obs}|^2]^{1/2}$

$R_p = 100\ \sum|y_{obs} - y_{calc}| / \sum|y_{obs}|$ $S = [R_{wp} / R_{exp}]$ N-P+C: number of degrees of freedom

Downloaded from www.periodico.tchequimica.com

Table 2. *Atomic coordinates and geometrical parameters (Å, deg) for oxamic acid (**I**).*

Atom	*x*	*y*	*z*	foc	B (Å^2)
C1	0.1069(2)	1.1538(2)	-0.3812(2)	1	0.15(3)
C2	0.1067(2)	0.8628(2)	-0.3851(2)	1	0.15(3)
O1	-0.0056(2)	1.2762(2)	-0.4988(2)	1	0.15(3)
O2	0.2078(2)	1.2632(2)	-0.2635(2)	1	0.15(3)
O3	0.0108(2)	0.7437(2)	-0.5023(2)	1	0.15(3)
N1	0.2299(2)	0.7632(2)	-0.2609(2)	1	0.15(3)
H1	-0.0059(2)	1.4402(2)	-0.5006(2)	1	0.45(4)
H2	0.2372(2)	0.6025(2)	-0.2572(2)	1	0.45(3)
H3	0.3008(2)	0.8578(2)	-0.1929(2)	1	0.45(3)

C1-O1	1.313(2)	C2-O3	1.209(2)
C1-O2	1.210(2)	C2-N1	1.341(2)
C1-C2	1.582(2)	N1-C2-C1	113.4(1)
O1-C1-C2	120.0(1)	O2-C1-C2	119.9(2)
O3-C2-C1	122.9(1)	O1-C1-O2	120.0(1)
O1-C1-C2-N1	178.6(2)	O1-C1-C2-O3	4.9(3)
O2-C1-C2-O3	-178.3(2)	O2-C1-C2-N1	-4.6(2)

Table 3. *Hydrogen bonds geometry (Å, deg) (D-donor; A-acceptor; H-hydrogen) for (**I**).*

D--H···A	D--H	H···A	D···A	D--H···A
N1--H3···O2 (intra)	1.030	2.310	2.697(7)	101.00
O1--H1···O3$^{(i)}$	1.030	1.670	2.694(7)	176.00
N1--H2···O2$^{(ii)}$	1.030	1.720	2.744(7)	169.00
N1--H3···O3$^{(iii)}$	1.030	2.040	3.049(4)	168.00
N1--H2···O1$^{(iii)}$	1.030	2.600	2.993(4)	102.00

Symmetry codes: $^{(i)}$ x, 1+y, z, $^{(ii)}$ x, -1+y, z, $^{(ii)}$ ½+x, -½-y, ½+z

Downloaded from www.periodico.tchequimica.com

PERIÓDICO TCHÊ QUÍMICA
ARTIGO ORIGINAL

DADOS DE DIFRACÇÃO DE RAIOS-X PARA UM NOVO COMPOSTO DE PIRAZOLINE

X-RAY POWDER DIFFRACTION DATA FOR A NEW PIRAZOLINE COMPOUND

DELGADO, Gerzon E.[1*], DELGADO-NIÑO, Pilar[2], LOBATON, Robert[3], LIEW, Suk-Ming[4], JAMALIS, Joazaizulfazli[4]

[1] Laboratorio de Cristalografía, Departamento de Química, Facultad de Ciencias, Universidad de Los Andes, Mérida, Venezuela

[2] Facultad de Ingeniería, Universidad Libre, Bogotá, Colombia

[3] Laboratorio de Análisis Farmacéutico, Departamento de Análisis y Control, Facultad de Farmacia y Bioanálisis, Universidad de Los Andes, Mérida, Venezuela

[4] Department of Chemistry, Faculty of Science, Universiti Teknologi Malaysia, Skudai Johor, Malaysia

** Correspondence author*
e-mail: gerzon@ula.ve

Received 03 October 2019; received in revised form 27 October 2019; accepted 27 October 2019

RESUMO

As pirazolinas são agentes importantes na química medicinal como um suporte promissor para estudos de modificação estrutural e desenvolvimento de medicamentos devido à sua ampla gama de atividades biológicas como, por exemplo, atividade anticâncer, antifúngica, antibacteriana, antidepressiva, anticonvulsivante, antitubercular, antioxidante, antileishmanial e anti-inflamatória. Estes compostos heterocíclicos podem ser preparados ao refluxo da chalcona com hidrato de hidrazina e acetato de sódio anidro na presença de ácido acético glacial. A caracterização estrutural, estrutura molecular e cristalina desses compostos orgânicos permite estudar suas propriedades biológicas para conhecer suas aplicações potenciais. Portanto, o uso do XRPD é muito importante, pois permite obter um registro para ser usado como método de identificação. O objetivo desta investigação foi obter e reportar dados de difração de pó de raios-X de boa qualidade do composto pirazolina 1- (3- (4-iodofenil) -5- (3-metil tiofen-2-il) -4,5 -di-hidro-1H-pirazol-1-il) etan-1-ona, que pode ser usado como potencial agente antimicrobiano e anticâncer. O padrão de pó foi indexado no grupo espacial monoclinico I2 / a com os parâmetros celulares unitários *a* = 25.440(5) Å, *b* = 5.124(2) Å, *c* = 26.261(6) Å, β = 105.75(2)° and figures of merit M_{20}= 38.2 and F_{20}= 66.6 (0.00573, 53). Todas as linhas medidas foram indexadas e são consistentes com o grupo espaço monoclínico. O padrão de pó será incluído no banco de dados do arquivo de difração de pó para ser usado como referência.

Palavras-chave: Difração de raios X, pirazolina, agente antimicrobiano e anticancerígeno.

ABSTRACT

Pyrazolines are important agents in medicinal chemistry as a promising scaffold for structural modification and drug development studies due to their wide range of biological activities such as anticancer, antifungal, antibacterial, antidepressant, anticonvulsant, antitubercular, antioxidant, antileishmanial and anti-inflammatory activity. These heterocyclic compounds can be prepared by refluxing chalcone with hydrazine hydrate and anhydrous sodium acetate in the presence of glacial acetic acid. The structural characterization, molecular and crystalline structure, of these organic compounds, allows studying their biological properties to know their potential applications. Hence the use of XRPD is very important because it allows obtaining a record to be used as a method of identification. The aim of this investigation was to obtain and reported good quality X-ray powder diffraction data the pyrazoline compound 1-(3-(4-iodophenyl)-5-(3-methyl thiophen-2-yl)-4,5-dihydro-1H-pyrazol-1-yl)ethan-1-one, which could be used as potential anti-microbial and anti-cancer agent. The powder pattern was indexed in the monoclinic space group *I*2/*a* with unit cell parameters *a* = 25.440(5) Å, *b* = 5.124(2) Å, *c* = 26.261(6) Å, β = 105.75(2)° and figures of merit M_{20}= 38.2 and F_{20}= 66.6 (0.00573, 53). All measured lines were indexed and are consistent with the monoclinic space group. The powder pattern will be included in the Powder Diffraction File database to be used as a reference.

Keywords: Powder X-ray diffraction, pyrazoline, anti-microbial agent, anti-cancer agent.

Downloaded from www.periodico.tchequimica.com

1. INTRODUCTION

The 5-membered heterocyclic compounds type pyrazolines are important agents in medicinal chemistry as a promising scaffold for structural modification and drug development studies due to their wide range of biological activities such as anticancer, antifungal, antibacterial, antidepressant, anticonvulsant, antitubercular, antioxidant, antileishmanial and anti-inflammatory activity (Kumar *et al*., 2013; Deng *et al*., 2012; Özdemir *et al*., 2007; Rani *et al*., 2011; Insuasty *et al*., 2012; 2013; 2015; Montoya *et al*., 2014; Moreno *et al*., 2018). Acetylated pyrazolines have been found to be more active than the non-acetylated pyrazolines (Khalil *et al*., 2012; Monga *et al*., (2014); Al-Maqtari *et al*., 2015). It has been reported that the introduction of the acetyl group at first position enhances the molluscicidal activity as well as increases the stability of pyrazolines (Mishriky et al., 1996). Moreover, pyrazolines are extensively useful synthons in organic chemistry and also, they have played a crucial role in the development of theory in heterocyclic chemistry (Ahmad *et al*., 2016; Shivalingegowda *et al*., 2017; Naveen *et al*., 2018; Sathish *et al*., 2018).

The method most used, by its simplicity, in the synthesis of pyrazolines is by refluxing chalcone with hydrazine hydrate and anhydrous sodium acetate in the presence of glacial acetic acid for 24 hours (Shaaban *et al*., 2012; Levai, 1997; 2002). An alternative route involves 1,3-dipolar cycloaddition of nitrile imines to carbon-carbon double bond of arylmethylene compounds (Farag *et al*., 1994; 1997).

An excellent method of crystalline solids characterization, of different chemical nature, is the Powder X-ray diffraction (PXPD). This method together with single-crystal X-ray diffraction are the more powerful techniques for crystal structure determination. X-ray diffraction patterns are very useful for the identification of new materials and hence the importance of reporting in the appropriate database: Powder Diffraction File of the International Centre for Diffraction Data (ICDD, 2017).

In this work, and as part of ongoing structural studies on active biologically molecules (Delgado *et al*., 2015; Delgado *et al*., 2016a; 2016b; Delgado *et al*., 2017; Delgado *et al*., 2018a; 2018b; Delgado *et al*., 2019a; 2019b; 2019c), a new *N*-acetylated pyrazoline was studied using PXRD technique. The X-ray powder diffraction data for 1-(3-(4-iodophenyl)-5-(3-methyl thio phen-2-yl)-4,5-dihydro-1H-pyrazol-1-yl)ethan-1-one is reported. This compound was prepared among a series of chalcone and pyrazoline derivatives as potential anti-cancer and anti-microbial agents (Al-Maqtari *et al*., 2015).

The crystal structure of this compound was studied from single-crystal X-ray diffraction and crystallizes with monoclinic symmetry in the space group *I*2/*a* (Delgado *et al.*, 2019c). The objective of this investigation is to obtain a good quality X-ray powder pattern, reliable values of d-spacing and relative intensity of observed *hkl* reflections, of the mentioned pyrazoline.

2. MATERIALS AND METHODS

2.1. Synthesis and specimen preparation

A mixture of the iodinated chalcone (**1**) (0.8 mmol), hydrazine hydrate (2 mL) and sodium acetate (2.0 mmol) in glacial acetic acid (15 mL) was refluxed for 24 hours (Figure 1). Crushed ice was then added and the reaction mixture was stirred again for 30 minutes. The resulting solid (**2**) was filtered using a pump vacuum, washed with cold distilled water, dried and recrystallized from methanol.

2.2. Fourier-transform infrared (FTIR) and nuclear magnetic resonance (NMR)

The chemical structure of pyrazoline (**2**) was elucidated using FTIR, ^{1}H NMR and ^{13}C NMR. Spectroscopic data were recorded using the FTIR Spectrometer Frontier (ATR-FTIR), Bruker Advancer 400 MHz and 300 MHz NMR spectrometer (^{1}H and ^{13}C NMR) in $CDCl_3$ or DMSO-d_6 using TMS as the internal standard. Brown solid (30.26% yield), m.p. 120-124ºC.

ATR-FTIR ν (cm^{-1}): 3109 (C-H sp^2), 2921 (C-H sp^3), 1656 (C=O), 1583 and 1406 (C=C aromatic), 1320 (C-N), 1006 (N-N), 717 (C-S), 659 (C-I)

^{1}H NMR 400 MHz, ($CDCl_3$) δ (ppm): 7.78 (dd, J = 8.4 Hz, 2H, H-3' and H-5'), 7.48 (d, J = 8.4 Hz, 2H, H-2' & H-6'), 7.06 (d, J = 4.8 Hz, 1H, H-5), 6.76 (d, J = 4.8 Hz, 1H, H-4), 5.86 (d, J_{xa} = 4.4 Hz, J_{xb} = 11.6 Hz, 1H, H_x), 3.68 (d, J_{bx} = 11.6 Hz, J_{ba} = 17.6 Hz, 1H, H_b), 3.20 (d, J_{ax} = 4.4 Hz, J_{ab} = 17.6 Hz, 1H, H_a), 2.41 (s, 3H, acetyl-CH_3), 2.34 (s, 3H, thiophene-CH_3)

^{13}C NMR 300 MHz, (DMSO-d_6) δ (ppm): 168.26 (C=O), 154.31 (C=N), 139.36 (C-2), 138.50 (C-3' and C-5'), 134.14 (C-3), 131.29 (C-1'), 130.90 (C-5), 129.28 (C-2' and C-6'), 123.50 (C-5), 54.71 (pyrazoline-CH), 42.45 (pyrazoline-

Downloaded from www.periodico.tchequimica.com

CH_2), 22.55 (acetyl-CH_3), 14.35 (thiophene-CH_3).

2.3. X-ray powder diffraction data

Powder diffraction data was collected at room temperature 298(1) K. A small quantity of the sample was ground mechanically in an agate mortar and pestle. The resulting fine powder, sieved to 106 μm, was mounted in a zero background holder covered with a thin layer of petroleum jelly (Buhrke *et al*., 1998). XRPD pattern was recorded with a Siemens D5005 diffractometer operating in Brag-Brentano geometry equipped with a Cu target X-ray tube (40 kV, 30 mA) and a diffracted beam graphite monochromator. The specimen was scanned from 5-65° 2θ, with a step size of 0.02° and counting time of 10 s. Quartz was used as an external standard. The software package Highscore Plus v3.0 was used to eliminate the $K\alpha_2$ component, establish the positions of the peaks and determine the peak intensities of the diffraction peaks.

3. RESULTS AND DISCUSSION:

The X-ray powder pattern of the pyrazoline (**2**) is shown in Figure 2. The 20 first peak positions were indexed using the program DICVOL04 (Boultif and Louër, 2004), which gave a unique solution in a monoclinic cell. This result confirms the crystal structure reported (Delgado *et al*., 2019a).

The complete powder diffraction dataset was reviewed in the monoclinic space group *I*2/a, using the software Highscore Plus v3.0. All measured lines were indexed and were consistent with the mentioned space group. From this analysis, the refined unit-cell parameters obtained were: *a* = 25.440(5) Å, *b* = 5.124(2) Å, *c* = 26.261(6) Å, β = 105.75(2)°, V = 3294.7(3) $Å^3$, Z = 8, with figures of merit M_{20}= 38.2 (de Wolff, 1968) and F_{20}= 66.6 (0.00573, 53) (Smith and Snyder, 1979). The calculated and observed values of XRD data are listed in Table 1. The unit cell parameters and space group assignment were validated by a Le-Bail fit (Le Bail, 2005) of PXRD data using a pseudo-Voigt peak profile function (Thompson *et al.,* 1987) with program Fullprof (Rodríguez-Carvajal, 2018) available in the software package WinPlotr (Roisnel and Rodríguez-Carvajal, 2001).

Figure 2 shows the very good fit between the observed and calculated patterns.

4. CONCLUSIONS:

The new pyrazoline, 1-(3-(4-iodophenyl)-5-(3-methyl thiophen-2-yl)-4,5-dihydro-1H-pyrazol-1-yl)ethan-1-one, was prepared by refluxing an iodinated chalcone with hydrazine hydrate and anhydrous sodium acetate. Spectroscopic studies confirmed the molecular structure of the heterocyclic compound. This is a new pyrazoline derivative with potential anti-microbial and anti-cancer properties. The powder pattern was indexed in the monoclinic space group *I*2/*a* with unit cell parameters *a* = 25.440(5) Å, *b* = 5.124(2) Å, *c* = 26.261(6) Å, β = 105.75(2)° and figures of merit M_{20}= 38.2 and F_{20}= 66.6 (0.00573, 53). All lines of powder pattern data were indexed and are consistent with the *I*2/*a* monoclinic space group. The X-ray powder diffraction data for the title compound is reported and will be included in the PDF database to be used as a reference.

5. ACKNOWLEDGMENTS:

This work was supported by FONACIT (Grant LAB-97000821).

6. REFERENCES:

1. Kumar, H., Saini, D., Jain, S., Jain, N. Eur. *J. Med. Chem*. **2013**, 70, 248.
2. Deng, H., Yu, Z-Y., Chen, M-J., Tao, K., Hou, T-P. *Chem. Biol. Drug. Des*. **2012**, 79, 279.
3. Özdemir, Z., Kandilci, H.B., Gümüşel, B., Calis, Ü., Bilgin, A. *Eur. J. Med. Chem*. **2007**, 42, 373.
4. Rani, M., Yusuf, M., Khan, S.A., Sahota, P.P., Pandove, G. *Arab. J. Chem*. **2011**, 8, 174.
5. Insuasty, B., Chamizo, L., Muñoz, J., Tigreros, A., Quiroga, J., Abonía, R., Nogueras, M., Cobo, J. *Archiv. Pharm*. **2012**, 345, 275.
6. Insuasty, B., Montoya, A., Becerra, D., Quiroga, J., Abonia, R., Robledo, S., Vélez, I.D., Upegui, Y., Nogueras, M., , J. *Eur. J. Med. Chem*. **2013**, 67, 252.
7. Montoya, A., Quiroga, J., Abonia, R., Nogueras, M., Cobo, J., Insuasty, B. *Molecules*, **2014**, 19, 18656.
8. Insuasty, B., Ramírez, J., Becerra, D., Echeverry, C., Quiroga, J., Abonia, R.,

Downloaded from www.periodico.tchequimica.com

Robledo, S.M., Vélez, I.D., Upegui, Y., Muñoz, Ospina, V., Nogueras, M., Cobo, J. *Eur. J. Med. Chem*. **2015**, 93, 401.

9. Moreno, L.M., Quiroga, J., Abonia, R., Ramírez-Prada, J., Insuasty, B. *Molecules*, **2018**, 23, 1956.
10. Khalil, N.A., Ahmend, E.M., El-Nassan, H.B., Ahmed, O.K., Al-Abd, A.M. *Arch. Pharm. Res*. 2012, 35, 995.
11. Monga, V., Goyal, K., Steindel, M., Malhotra, M., Rajani, D.P., Rajani, S.D. *Med. Chem. Res*. 2014, 23, 2019.
12. Al-Maqtari, H.M., Jamalis, J., Sirat, H.M. *Jurnal Teknologi*, 2015, 77, 55.
13. Mishriky, N., Asaad, F.M., Ibrahim, Y.A, Girgis, A.S. *Indian J. Chem*. **1996**, 35B, 935.
14. Ahmad, N.A., Naveen, S., Kumara, K.K., Jamalis, J., Lokanath, N.K. *Der Phar. Chem*. **2016**, 8, 49.
15. Shivalingegowda, N., Ming, L.S., Jamalis, J., Kumar, C.S.A., Lokanath, N.K. *Chem. Data Coll*. **2017**, 7-8, 58.
16. Naveen, S., Ahmad, N.S., Deepa Urs, M.V., Lingegowda, N.S., Jamalis, J., Reddy, K.R., Lokanath, N.K. *Chem. Data Coll*. **2018**, 17-18, 132.
17. Sathish, M., Meenakshi, G., Xavier, S., Sebastian, S., Periandy, S., Ahmad, N.A., Jamalis, J., Rosli, M., Fun, H.K. J. Mol. Struct. **2018**, 1164, 420.
18. Shaaban, M.R., Mayhoub, A.S, Farag, A.M. *Expert Opin. Ther. Patents*, **2012**, 22, 253.
19. Levai, A. *Chem. Heterocycl. Compd*. **1997**, 33, 647.
20. Levai, A. *J. Heterocyclic. Chem*. **2002**, 39, 1.
21. Farag, A.M., Abbas, I.M., Abdallah, M.A. *J. Chem. Res. S*, **1994**, 286, 7.
22. Farag, A.M., Kheder, N.A., Budesinsky, M. *Tetrahedron*, **1997**, 53, 9293.
23. ICDD-PDF-2 (Database), International Centre for Diffraction Data, Newtown Square, PA, USA, **2017**.
24. Delgado, G.E., Mora, A.J., Contreras, J.E., Chacón, C. *Powder Diffr*. **2015**, 30, 178.
25. Delgado, G.E., Mora, A.J., González, T., Uzcátegui, J., Lobaton, R., Marroquín, G. *Mol. Cryst. Liq. Cryst*. **2016**a, 625, 225.
26. Delgado, G.E., Rodríguez, J.A., Mora, A.J., Bruno-Colmenárez, J., Uzcátegui, J., Chacón, C. *Mol. Cryst. Liq. Cryst*. **2016**b, 629, 96.
27. Delgado, G.E., Belandria, L.M., Mora, A.J., Bruno, J., Marroquín, G. *J. Tchê Quím*. **2017**, 14, 66.
28. Delgado, G.E., Osal, E., Mora, A.J., González, T., Palma, A., Bahsas, A. *J. Struct. Chem*. **2018**a, 59, 1248.
29. Delgado, G.E., Henao, J.A., Quintana, J.A., Al-Maqtari, H.M., Jamalis, J., Sirat, H.M. *J. Struc. Chem*. **2018**b, 59, 1493.
30. Delgado, G.E. Mora, A.J. González, T., Santos, I., Rivas, P., Seijas, L.E. *J. Tchê Quím*. **2019**a, 16, 347.
31. Delgado, G.E., Delgado-Niño, P., Jamalis, J. *J. Tchê Quím*. **2019**b, 16, 878.
32. Delgado, G.E., Liew, S.M., Jamalis, J., Cisterna, J., Cárdenas, A., Brito, I. *J. Chi. Chem. Soc*. **2019**c, In press.
33. Boultif, A., Louër, D. *J. Appl. Cryst.* **2004**, 37, 724.
34. Buhrke, V., Jenkins, R., Smith, D. *Preparation of specimens for X-ray fluorescence and X-ray diffraction analysis* (Wiley, New York), pp. 141-142. **1998**.
35. de Wolff, P.M. *J. Appl. Crystallogr*. **1968**, 1, 108
36. Smith, G.S., Snyder, R.L. *J. Appl. Crystallogr*. **1979**, 12, 60.
37. Le Bail, A. *Powder Diffr*. **2005**, 20, 316.
38. Thompson, P., Cox, D.E., Hastings, J.B. *J. Appl. Cryst*. **1987**, 20, 79.
39. Rodriguez-Carvajal J Fullprof, version 6.0, LLB, CEA-CNRS, France, **2018**.
40. Roisnel, T., Rodríquez-Carvajal, J. *Mater. Sci. Forum*, **2001**, 378-381, 118.

Downloaded from www.periodico.tchequimica.com

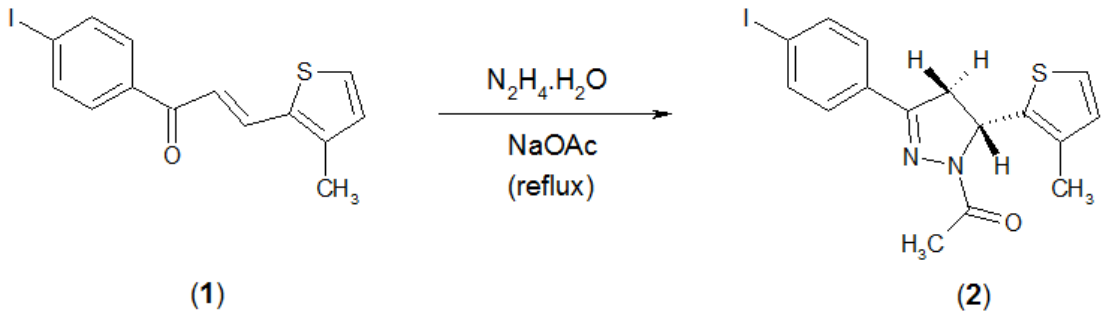

(**1**) (**2**)

Figure 1. *Chemical synthesis of the title pirazoline (**2**) from an iodinated chalcone.*

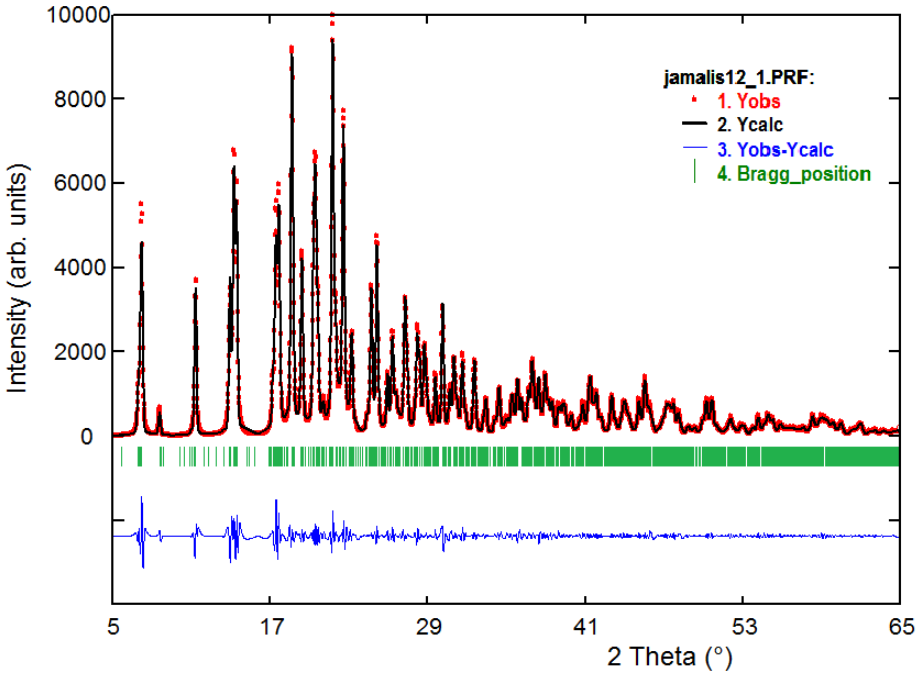

Figure 2. *Observed (red) and calculated (black) XRD patterns of the pirazoline (**2**) from the Le Bail refinement. Vertical bars (green) indicate the positions of the Bragg peaks. The lower trace depicts the difference between the experimental and calculated intensity values.*

Table 1. *X-ray powder diffraction data of 1-(3-(4-iodophenyl)-5-(3-methylthiophen-2-yl)-4,5-dihydro-1H-pyrazol-1-yl)ethan-1-one.*

$2\theta_{obs}$ (°)	d_{obs} (Å)	$(I/I_o)_{obs}$	*h*	*k*	*l*	$2\theta_{cal}$ (°)	d_{cal} (Å)	$\Delta 2\theta$ (°)
6.995	12.62597	9.7	1	0	-1	6.988	12.63999	0.008
7.218	12.23747	46.1	2	0	0	7.218	12.23746	0.000
8.578	10.30047	5.6	1	0	1	8.577	10.30063	0.000
11.341	7.79618	31.3	3	0	-1	11.340	7.79700	0.001
13.997	6.32213	23.9	2	0	-2	14.002	6.31982	-0.005
14.255	6.20840	53.9	3	0	1	14.255	6.20810	-0.001
14.464	6.11893	50.5	4	0	-1	14.422	6.13683	0.042
17.211	5.14798	9.6	2	0	2	17.205	5.14981	0.006
17.444	5.07965	46.9	4	0	-2	17.439	5.08137	0.006
17.670	5.01543	107	1	1	0	17.679	5.01287	-0.009
18.675	4.74765	75.8	0	1	1	18.661	4.75123	0.014
19.427	4.56558	39.1	2	1	-1	19.393	4.57354	0.034
20.310	4.36897	39.5	1	0	-3	20.327	4.36544	-0.017
20.457	4.33788	56.9	3	1	0	20.458	4.33761	-0.001
20.634	4.30100	26.3	2	1	1	20.651	4.29759	-0.017
21.071	4.21294	6.4	3	0	-3	21.067	4.21360	0.003
21.770	4.07906	100.0	6	0	0	21.770	4.07918	0.001
21.988	4.03925	22.8	1	1	-2	21.993	4.03837	-0.005
22.592	3.93262	73.0	4	1	-1	22.594	3.93228	-0.002
23.234	3.82530	22.3	3	1	-2	23.234	3.82539	0.001
24.716	3.59925	32.1	4	1	1	24.740	3.59573	-0.025
25.146	3.53856	51.0	5	1	0	25.146	3.53866	0.001
25.930	3.43344	14.3	3	0	3	25.931	3.43325	-0.001
26.317	3.38381	25.6	3	1	2	26.318	3.38361	-0.002
26.851	3.31765	4.1	1	1	-3	26.813	3.32232	0.038
27.278	3.26675	32.2	0	1	3	27.274	3.26720	0.004
27.426	3.24941	18.1	3	0	-4	27.437	3.24818	-0.011
28.224	3.15931	25.2	1	1	3	28.212	3.16067	0.012
28.395	3.14068	18.7	4	0	3	28.380	3.14231	0.015
28.761	3.10149	19.9	6	0	2	28.739	3.10389	0.023
29.583	3.01719	15.3	2	1	3	29.585	3.01700	-0.002
30.135	2.96316	4.9	6	1	1	30.136	2.96307	-0.001
30.703	2.90967	11.1	2	0	4	30.703	2.90968	0.000
31.010	2.88153	16.4	5	1	2	31.004	2.88207	0.006
31.275	2.85773	8.2	7	1	-2	31.273	2.85790	0.002
31.648	2.82486	20.7	6	1	-3	31.641	2.82547	0.007
31.881	2.80479	5.9	9	0	-1	31.883	2.80461	-0.002
32.554	2.74831	17.2	1	1	-4	32.532	2.75009	0.022
33.263	2.69136	4.2	4	1	-4	33.287	2.68945	-0.024
33.440	2.67746	10.2	4	1	3	33.429	2.67837	0.012
34.104	2.62688	3.8	1	1	4	34.101	2.62708	0.003
34.481	2.59897	8.3	1	0	-5	34.484	2.59877	-0.003
35.013	2.56070	5.2	0	2	0	35.012	2.56077	0.001
35.422	2.53206	6.2	2	1	4	35.453	2.52991	-0.031
35.885	2.50044	11.3	10	0	-2	35.885	2.50045	0.000
36.170	2.48141	8.0	2	2	-1	36.144	2.48316	0.026
36.681	2.44802	12.1	6	0	-5	36.684	2.44783	-0.003

Downloaded from www.periodico.tchequimica.com

PERIÓDICO TCHÊ QUÍMICA
ARTIGO ORIGINAL

USO DE REDES NEURAIS ARTIFICIAIS PARA A DIFERENÇA DE TEMPO NA LOCALIZAÇÃO DO ALVO DE CHEGADA COM BASE NA TRANSFORMADA DE COSSENO DISCRETA REDUZIDA

USING ARTIFICIAL NEURAL NETWORKS FOR TIME DIFFERENCE OF ARRIVAL TARGET LOCALIZATION BASED ON REDUCED DISCRETE COSINE TRANSFORM

ИСПОЛЬЗОВАНИЕ ИСКУССТВЕННЫХ НЕЙРОННЫХ СЕТЕЙ ДЛЯ РАЗНИЦЫ ВО ВРЕМЕНИ ЛОКАЛИЗАЦИИ ЦЕЛИ ПРИХОДА НА ОСНОВЕ УМЕНЬШЕННОГО ДИСКРЕТНОГО КОСИНУСНОГО ПРЕОБРАЗОВАНИЯ

SHEVGUNOV, Timofey [1];

[1] Moscow Aviation Institute (National Research University), Department of Theoretical Radio Engineering, Moscow – Russian Federation

** Correspondence author*
e-mail: shevgunov@gmail.com

Received 30 August 2019; received in revised form 27 October 2019; accepted 28 October 2019

RESUMO

As coordenadas angulares da fonte de pulso são determinadas pela comparação dos sinais recebidos simultaneamente por vários canais. Para resolver esse problema, o uso de redes neurais é importante. Este artigo discute a aplicação da abordagem de rede neural artificial (RNA) na tarefa de localização de destino. O estudo foi realizado com base em uma técnica de extração de características realizada por uma transformada discreta de cosseno que permitiu obter uma representação compacta da energia do sinal submetido ao processamento digital. O autor define um esquema para estimar o ângulo de chegada do sinal com base na diferença de tempo entre as estimativas de chegada e os problemas estreitos de estimativa de atrasos constantes como parâmetros informativos incorporados nos sinais recebidos que são cópias ruidosas e fracas do sinal de referência. A estrutura do dispositivo adaptativo foi usada para sintetizar a conexão direta da RNA, que é equipada com um conjunto abreviado dos coeficientes de transformada discreta de cosseno (TDC) mais sensíveis e que fornecem uma representação exaustiva do processo aleatório cíclico estacionário de primeira ordem. Um estudo da precisão da estimativa do atraso foi realizado para avaliar o desempenho de RNAs com diferentes tamanhos de sua camada oculta e diferentes números de coeficientes de TDC em suas entradas. Foi provado que cinco coeficientes de TDC são suficientes para distinguir a mudança de fase em toda a faixa. Por sua vez, isso leva a uma estimativa confiável do atraso produzido pela RNA treinada, que contém oito neurônios em sua camada oculta.

Palavras-chave: *estimativa de atraso, ciclo-estacionariedade, perceptron multicamada, sinal de referência, estrutura de elementos adaptativos.*

ABSTRACT

The angular coordinates of the pulse source are determined by comparing the signals received simultaneously on several channels. To solve this issue, the application of neural networks is highly important. In this article, the application of the artificial neural network (ANN) approach to the task of target localization is discussed. The research was performed on the basis of a feature extraction technique executed by a discrete cosine transform, which allowed to obtain a compact representation of the signal energy subjected to digital processing. The author defines the angle-of-arrival estimation scheme based on time difference of arrival estimators and the particular problem of estimating constant delays as informative parameters embedded into received signals that are noisy and damped copies of the reference signal. The adaptive element framework is used for synthesis of the feedforward ANN which is fed with the reduced set of the most sensitive discrete cosine transform (DCT) coefficients, which provide a concise representation of the first-order cyclostationary random process. The investigation on the delay estimation accuracy has been carried out to evaluate the performance of the ANNs with different size of their hidden layer and various numbers of the DCT coefficients at their input. It has been proved that five DCT coefficients are enough for the discrimination of the phase shift in the whole range. In turn, it results in the reliable delay estimation produced by the trained ANN that contains

Downloaded from www.periodico.tchequimica.com

eight neurons in its hidden layer.

Keywords: *delay estimation, cyclostationarity, multilayer perceptron, reference signal, adaptive element framework.*

АННОТАЦИЯ

Угловые координаты импульсного источника определяются путем сравнения сигналов, принятых одновременно несколькими каналам. Для решения данной проблемы важное значение имеет применение нейронных сетей. В данной статье обсуждается применение подхода искусственной нейронной сети (ИНС) к задаче целевой локализации. Исследование проводилось на основе методики выделения признаков, выполняемой дискретным косинусным преобразованием, что позволило получить компактное представление энергии сигнала, подвергнутого цифровой обработке. Автор определяет схему оценки угла прихода сигнала, исходя из разницы во времени оценок прихода и узкую проблематику оценки постоянных задержек в качестве информативных параметров, внедренных в принимаемые сигналы, которые являются шумными и затухающими копиями опорного сигнала. Структура адаптивного устройства используется для синтеза прямой связи ИНС, которая снабжается сокращенным набором наиболее чувствительных коэффициентов дискретного косинусного преобразования (ДКП), что обеспечивает исчерпывающее представление циклостационарного случайного процесса первого порядка. Исследование точности оценки задержки было проведено для оценки производительности ИНС с различным размером их скрытого слоя и различным числом коэффициентов ДКП на их входе. Доказано, что пяти коэффициентов ДКП достаточно для различения фазового сдвига во всем диапазоне. В свою очередь, это приводит к достоверной оценке задержки, производимой обученной ИНС, которая содержит восемь нейронов в своем скрытом слое.

Ключевые слова: *оценка задержки, циклостационарность, многоуровневый перцептрон, опорный сигнал, структура адаптивных элементов.*

1. INTRODUCTION

The problem of angle of arrival estimation consists in determining the bearing, which is the angle between the signal source, where the signal originates, and the direction choses to be the reference of the passive radar system, i.e., the direction to the North. It is known that the optimal solution to this problem can be obtained via the maximum likelihood estimator (MLE) that maximizes the likelihood function over all bearings with a given measurement obtained by the set of sensors. Although the great advantage of this method is thought to be the highest potential accuracy, it suffers from the disadvantage that is that the direct implementation has no close-form expression and, therefore, will require high computational efforts for obtaining the numerical solution of the underlying optimization problem with required accuracy. This paper introduces an alternative approach based on multi-layer perceptron type ANNs which is based on the alternative representation of the received signal via discrete cosine transformation Discrete Cosine Transform (DCT) rather than the canonical Fourie series basis.

It was shown in (Efimov *et al.*, 2014) that a low-cost, high-speed, compact solutions for a number of avionics-related tasks are available via the approach based on artificial neural networks (ANN) (Hassoun, 1995). Being aligned to that approach, this paper presents the results of research focused on the tasks of the target detection problem (Rihaczek and Hershkowitz, 2000). One of the issues raised in the target detection is known as the position location that determines one's ability to estimate the coordinates of the particular target using its radio emission. There are several techniques to solve the positioning but angle of arrival (AOA) and time difference of arrival (TDOA) are the only which are vital enough to be implemented for the avionics. Since one can easily realize that there is nothing but time delay estimation (Dubrovin *et al.*, 2014; Shevgunov *et al.*, 2014) is in the key point of both techniques. This makes important the developing of a robust algorithm of time delay estimation based on feature extraction. The direct time delay evaluation originated on those features nonlinear combining can be successfully performed in the ANN-basis. Although the optimal solution based on maximum likelihood approach can be naturally extended for ANN (Shevgunov and Efimov, 2019a), it will require too much computational resources.

The offered approach uses DCT to obtain a set of the DCT coefficients from the received signal. Then, selection is used to reduce number of coefficients in the selection, hence getting

Downloaded from www.periodico.tchequimica.com

Reduced Cosine Transform Coefficients (RDCTC) set. The phase shift embedded in the original signal will also be encoded into RDCTC set. Since the form of the reference signal is known a series of RDCTC sets can be synthesized in advance and used as training data to the Neural Network. Reduced size of the DCT coefficient set guarantees relatively small size of the network itself.

Using these synthesized RDCTC sets to train network one can obtain the neural network designed specifically for the known reference signal; since the neural network is featured with the ability to handle noisy and incomplete data this solution becomes both accurate and efficient in terms of calculation cost. The ANN trained once can be easily replicated to perform within other systems which resemble the same architecture. It opens the road to fast processing of the signal and further developing algorithms which can be implemented in small-size computers carried onboard as well as low-cost mass produced systems working autonomously or being asked with low rate.

2. MATERIALS AND METHODS

The single-station model being considered in this paper contains a passive radar system and the signal source. The passive radar system is equipped with antenna system of at least two sensors. The local coordinates of the sensors within the radar system are known with high accuracy. The signal source which bearing is to be estimated emits the unknown signal which can be considered as a realization of first-order stationary process with a known power spectrum spectral density (PSD). This model fits well the real signals belonging to the class of man-made amplitude modulated signals used in modern radar and communication systems.

One of the important problems within position location task is calculating delay between two signals received at the specially separated points. The prime concept of angle-of-arrival (AOA) estimation technique is shown in Figure 1.

The signal $s(t)$ radiated by a radio source (RS) is received at two spatially separated points where signals can be expressed in the following forms (Equations 1, 2), where K_1 and K_2 are dimensionless attenuation ratios, T_1 and T_2 are time delays and n_1 and n_2 are noises for the first and second points correspondingly.

Considering the instance of the first-order cyclostationary signal (Shevgunov *et al.*, 2018a) $s(t)$ with the circular frequency ω, the points separated by the distance d being not farther than the half of its wavelength and noises uncorrelated with each other as well as with the signal, one can obtain the following expressions for the received signals (Equations 3, 4), where amplitude A is assumed to be random (Shevgunov, 2019) while the phases φ_1 and φ_2 can be used for evaluation of angle of arrival (Equation 5), where c is a phase speed e.g. the speed of light.

There are few approaches to determine phase shift between two harmonics. The most widely used technic is cross-correlation. One of its efficient applications is shown in (Chan *et al.*, 1999). But not all approaches involve the cross-correlation, the algorithm of direct phase estimation is based on neural networks and was originally introduced in (Shaltaf and Mohammad, 2009).

In order to implement successfully this group of algorithms, one needs at first to determine such features of the signal which will most effectively embed the information about the delay or phase shift. Those features are obviously expected to be very sensitive to the changes in the delay. It was shown in (Efimov and Shevgunov, 2014), that a subset of Direct Cosine Transform coefficients can be used for that purpose. This subset can be used to decode the value of phase shift which allows one to calculate time delay.

The Discrete Cosine Transform is a transform with even harmonic functions basis. Although there are 8 types of DCT due to the symmetry property; in this paper, the author uses the most thoroughly researched type described in (Oppenheim *et al.*, 1999) as the normalized DCT-II and defined by the following Equations 6, 7, 8.

That transform was chosen among the others sue to its property known as “energy compression”: the coefficients of the sequence are concentrated at some range of indices with higher density rather than in Discrete Fourier Transform (DFT) or any other types of DCT. This property is illustrated by 3D-plot shown in Figure 2 where the actual values of DCT coefficients are plotted against coefficient number and values of the time delay measured in the part of harmonic period.

The results depicred in Figure 2 indicate that some of coefficients are less sensitive to the phase shift; hence, the usage of the whole set of DCT coefficients is redundant. The criteria of how to choose the most sensitive of the phase shift

Downloaded from www.periodico.tchequimica.com

coefficients must be defined. In paper (Shaltaf and Mohammad, 2009), the criteria of class L_1 based on the sum of absolute difference (SAD) is proposed (Equation 9), where R_m is the m-th DCT coefficient under analysis, φ_n are possible phase values of the received signal defined with some predefined steps. Alternatively to the SAD, L_2 criteria can be used, in which the sequential selection of the coefficients containing the major part of the energy (Equation 10).

Generally speaking, both criteria led to the same results in selecting the most sensitive DCT coefficients (R) in order to form RDCTC sets. These RDCTC sets are to be used later as training data for the artificial neural network.

3. RESULTS AND DISCUSSION:

3.1. ANN synthesis

The solution investigated in this paper is based on the application of ANN that is considered to be a versatile mathematical model inspired by biological neural networks formed by the neural cells of animals. For the problem under consideration, an ANN could be mainly considered as a computational system that performs some transformation upon the input data vector (Equation 11), where **p** is the input data vector, α is the output value of the bearing to be estimated, H stands for the functional transform performed over **p** by the neural network, **Q** is the network topology descriptor, **Θ** is the arranged set neural network inner parameters.

Even if the mapping between input and output data cannot be expressed analytically in closed form, in case of neural network it is possible (according to the universal approximation theorem (Haykin, 1994)) to increase the number of the training samples causing network transform function to converge to the desired function. Moreover, trained neural network is believed to be able to perform the desired functional transform with a given accuracy. That can be achieved via its training which goal is to determine the vector of inner network parameters **Θ** defined for a given topology **Q** using a series of S training patterns that are input-output data sample pairs $[(p_1, \alpha_1), (p_2, \alpha_2), \ldots, (p_S, \alpha_S)]$.

The series of training patterns is calculated deterministically based on a single station mathematical model for the whole value range of the bearing parameter a. The direct transform from bearing ai to input data matrix Xi is thought to be known (Equation 12). The structural graph of feed-forward neural network known as multi-layer perceptron (MPL) is shown in Figure 3.

The network can solve the task of estimation of the constant delay be easily built using adaptive elements (Efimov and Shevgunov, 2012a). This network is built from neurons united into two layers traditionally called hidden and output ones. Each neuron embeds the summing element and the functional transform; for the hidden layer hyperbolic tangent function is used. The output layer is chosen to be relevant to its functional transform element and contains only summation element.

Using adaptive elements as a starting point makes synthesizing the most classes of neurons way easier (Efimov and Shevgunov, 2012b). Such approach provides network structure to be plain and simple yet allows creating complex transfer functions. This implements the paradigm known as network's point of view which means all elements are quite identical in terms of signal propagation that also allows introducing new types of elements easily while any new elements would be able to represent various systems considering their parts as masked sub-networks (Hagan *et al.*, 2002).

A regular or linear separating neuron can be synthesized by means of a set of amplifying elements, a summing element and a functionally transforming element performing the required transformation function. Each amplifier is connected to a certain summing element input thus implementing synoptic weight.

The structural scheme of a regular neuron with 3 inputs is shown in Figure 4. Its synaptic weights are represented by the amplifiers in the left-hand part of the scheme, where the weighted signals are summed together and then transmitted to the functionally transforming element that embeds the necessary activation function.

The overall transform functions of regular neuron define as follow (Equation 13). According to the back-propagation characteristics of the underlying elements the back-propagation function and the structural scheme in case of back-propagation for regular neuron define as shown in the Figure 5.

The transform function in that case has the formula defined in the expression below

Downloaded from www.periodico.tchequimica.com

(Equation 14), where *g* is the first derivative of the activation function (Equation 15).

One can easily see that the transformation of the graph shown in Figure 4 into the graph shown in Figure 5 is straightforward. Thus, each amplifier has been transformed into the amplifier of the same weight, the combiner has turned into the hub. However, the non-linear element implementing the activation function is replaced by the linear amplifier which weight is equal to the its derivative evaluated at the same argument.

3.2. Numerical simulation

As input signal $s(t)$ for the numerical modeling the estimated cyclostationary signal (Shevgunov *et al.*, 2018b) of the frequency Ω_0. The sampling period was chosen to be T in accordance with the sampling theorem. We assumed that, for the sake of the simulation, the signal was delayed with constant delay D However, it is important to note that this delay will vary from one experiment to another in order to estimate how this change in its value will affect the coefficient of DCT coefficients.

A series of DCT transforms were performed on each input signal related to various delay values. The statistics has been collected and those results are depicted in the single plot which is shown in Figure 6. There one can see the difference in the behavior of DCT coefficients of different number. Thus, those which belong to small values vary significantly while other, with grater index value, take small values.

Figure 6 clarifies an important point which consists in the issue that, despite the fact that all DCT coefficients are sensitive to the value of the delay (Knapp and Carter, 1976) in the signal, the most sensitive to that change are only a few coefficients marked there as R_1, R_2 and R_3. These results also indicate that no matter how sensitive any coefficient to the value of the delay is, it is sensitive only for the delay changes in some range, for example R_1 coefficients is only sensitive to the change in ranges [0.18 – 0.4] and [0.6 – 0.86]. That means R_1 will improve quality of the estimation only for the values within these ranges; outside of them the coefficient will be almost useless. In order to cover all possible values of the time delay changes, one needs to pick a few DCT coefficients so their ranges of sensitivity will overlap. In this particular case, we need at least 3 coefficients to obtain appropriate estimation procedure. As a matter of fact, the problem of how to combine the information of three coefficients and use it in an optimal way rises.

The whole outlook of the SAD ability could be presented by the dependency of SAD, written in Equation 8, from the number of DCT coefficient as it shown in Figure 7 where the SAD is depicted against the number of the coefficient in DCT representation. One can easily see that coefficient R_2 is the most sensitive to the information about the angle, which is stored in the signal. The coefficient R_1 has the close value of the SAD measure, though it is smaller. The SAD value for R_3 is half as much as for R_2. The other coefficient, which R_5 is the greatest one among, do not exceed a third of what it takes for R_3.

After the indices of the most sensitive DCT coefficients have been determined, the next step is selecting optimal neural network topology (Efimov and Shevgunov, 2013) in order to make it efficient in the estimation of phase-shift value. The numerical modeling was performed to choose the topology leading to lower value of Mean Square Error (MSE). The parameter of the topology to be optimized is the size of the hidden layer. A series of 40 experiments was performed for each size of hidden layer in order to rule out the effect of the random initial synaptic weights. In each experiment the value of MSE for neural network with the hidden layer of given size was estimated, taken values were averaged afterwards. The obtained dependency between MSE and the hidden layer size is shown in Figure 8.

The curve shown in Figure 8 means that the more neurons is in the hidden layer, the more accurate estimation will be achieved. However, the excessive accuracy has no sense in practice since there are other source of errors which have to be taken into account. That is why it is so important to strike a balance between the size of the network and computational cost. The other factor considered above is the size of RDCTC, and it can be reasonable to assess these factors simultaneously.

In fact, the set of experiments were carried out to estimate the influence of both the size of the hidden layer and the number of the most sensitive DCT coefficients. The results are compiled into the diagram shown in Figure 9; the value of MSE are depicted with intensity of grayscale. The plot is divided into square cells which is for pair value (*Number of neurons*, *Number of DCT coefficients*). The lighter the cell is, the greater the value of the error is.

Downloaded from www.periodico.tchequimica.com

The analysis above shows that it is enough to take 5 most sensitive DCT coefficients while the ANN contains 8 neurons in the hidden layer. The results of the numerical simulation indicate that MSE generally decreases as the number of DCT coefficients in the RDCTC sets or the number of the neurons in the hidden layer increases (Haykin, 1994; Shevgunov and Efimov, 2019b). It is important to note that the drawback of the increase of either size of hidden layer or the size of RDCTC sets is the increase of the calculation cost.

4. CONCLUSIONS:

The present paper reflects the current advances in the ANN-based signal processing related to implementation in modern onboard systems. The concept of adaptive elements has been used as a clear yet effective tool forming the framework for the synthesis of the artificial neural networks which are able to solve the estimation of the angle of arrival which is the crucial part of the target localization problem. The adaptive element approach consists in building up a graph for the backpropagation where the graph that is used at the feed forward stage is given.

It was shown that the neural networks provide a researcher the strong framework for effective time delay estimating algorithm. The estimation procedure relies on the feature extraction technique carried out by discrete cosine transform which appropriate type allows obtaining the compact energy representation of signal undergone to the digital processing. It has been shown that there is a small subset of discrete cosine transform coefficients which are extremely sensitive to the changes in the delay. Since each of those coefficients in the subset is sensitive only in a range of the delay variation, the effective non-linear combination must be employed instead of the individual coefficients processed separately. It was also shown that DCT coefficient with smaller indices are more valuable since they vary greater than those of higher indices.

The feed-forward neural network, which was chosen in the class of multilayer perceptron, appears to be the most computationally effective architecture which allows one to build up the best combination via the training process. The DCT coefficients chosen to be included into the RDCTC set are used as the input of the ANN while the value of the delay is the output parameter, which the ANN is trained to fit. The optimization problem for the number of features enough for signal representation and for the number of elements in the hidden layer was also solved as the illustrative example in the current research. It was shown that the set containing 5 DCT coefficients could achieve the error rate less than 10-9 if the ANN containing 8 neurons in its hidden layer is applied. Since time delay estimation is the core of commonly used position location techniques, i.e. angle of arrival and time difference of arrival, ANN provides the reliable foundation for the robust integrated procedure.

5. ACKNOWLEDGMENTS:

This work was supported by state assignment of the Ministry of Education and Science of the Russian Federation (project 8.8502.2017/BP).

6. REFERENCES:

1. Chan, Yu., So, H., Ching, P. *IEEE Transactions on Signal Processing*, **1999**, *47*(4), 1193-1198.
2. Dubrovin, A., Nikishov, V., Shevgunov, T. *Tyrrhenian International Workshop on Digital Communication: Enhanced Surveillance of Aircraft and Vehicles* (*ESAV-2014*), Rome, Italy, **2014**, 87-92. doi: 10.1109/TIWDC-ESAV.2014.6945451.
3. Efimov, E., Shevgunov, T. *Journal of Radio Electronics*, **2012**, *8*, 2-7.
4. Efimov, E., Shevgunov, T. *The Works of MAI*, **2012**, *51,* http://trudymai.ru/upload/iblock/6c6/razrabotka-i-issledovanie-metodiki-postroeniya-neyronnykh-setey-na-osnove-adaptivnykh-elementov.pdf?lang=en&issue=51, accessed September 2019.
5. Efimov, E., Shevgunov, T. *The Works of MAI*, **2013**, *68*, http://trudymai.ru/upload/iblock/831/831084817b0416a99a825dd9868f02d5.pdf?lang=en&issue=68, accessed September 2019.
6. Efimov, E., Shevgunov, T. *XXXI General Assembly of the International Union of Radio Science* (*URSI GASS 2014*), Beijing, China, **2014**. doi: 10.1109/URSIGASS.2014.6929360.
7. Efimov, E., Shevgunov, T., Valaytite, A., Sadovskaya, E. *29th Congress of International Council of the Aeronautical Sciences* (*ICAS-2014*), St. Petersburg, Russian Federation, **2014**, *10.5.2*, 1-15.

Downloaded from www.periodico.tchequimica.com

8. Hagan, M., Demuth, H., Beale, M. *Neural Network Design*. Oklahoma: Martin Hagan, **2002**.

9. Hassoun, M. *Fundamentals of Artificial Neural Networks*. Cambridge: MIT Press, **1995**.

10. Haykin, S. *Neural Networks: A Comprehensive Foundation*. New York: Macmillan Coll Div, **1994**.

11. Knapp, C., Carter, G. *IEEE Transactions on Acoustic, Speech and Signal Processing*, **1976**, *24*(4), 320-327.

12. Oppenheim, A.V., Schafer, R.W., Buck, J.R. *Discrete-Time Signal Processing*. Upper Saddle River: Prentice Hall, **1999**.

13. Rihaczek, A., Hershkowitz, S. *Theory and Practice of Radar Target Identification*. Norwood: Artech House, **2000**.

14. Shaltaf, S., Mohammad, A. *American Journal of Applied Sciences*, **2009**, *6*(4), 703-708.

15. Shevgunov, T. *Journal of Physics: Conference Series*, **2019**, *1163*(1), 1-6. doi: 10.1088/1742-6596/1163/1/012037.

16. Shevgunov, T., Dubrovin, A., Nikishov, V. *XXXI General Assembly of the International Union of Radio Science* (*URSI GASS 2014*), Beijing, China, **2014**. doi: 10.1109/URSIGASS.2014.6929038.

17. Shevgunov, T., Efimov, E. *Artificial Intelligence and Algorithms in Intelligent Systems*. Berlin: Springer, **2019a**. doi: 10.1007/978-3-319-91189-2_15.

18. Shevgunov, T., Efimov, E. *Cybernetics and Automation Control Theory Methods in Intelligent Algorithms, Proceedings of 8th Computer Science On-line Conference*, **2019b**, *3*, 164-173. DOI: 10.1007/978-3-030-19813-8_18.

19. Shevgunov, T., Efimov, E., Kuznetsov, Yu. *2018 Baltic URSI Symposium*, Poznan, Poland, **2018a**, 901-904. doi: 10.23919/URSI.2018.8406726.

20. Shevgunov, T., Efimov, E., Zhukov, D. *Proceedings of National Research University Higher School of Economics, Moscow, Russian Federation*, **2018b**, 1-4. DOI: 10.1109/MWENT.2018.8337271.

$$s_1(t) = K_1 \cdot s(t - T_1) + n_1(t), \quad \text{(Eq. 1)}$$

$$s_2(t) = K_2 \cdot s(t - T_2) + n_2(t), \quad \text{(Eq. 2)}$$

$$x_1(t) = A \cdot \cos\left(\omega \cdot t + \varphi_1\right), \quad \text{(Eq. 3)}$$

$$x_2(t) = A \cdot \cos\left(\omega \cdot t + \varphi_2\right), \quad \text{(Eq. 4)}$$

$$\cos\alpha = \frac{c\left(\varphi_2 - \varphi_1\right)}{\omega\, d} \quad \text{(Eq. 5)}$$

$$X[k] = \sqrt{\frac{2}{N}} \cdot \beta[k] \cdot \sum_{n=0}^{N-1} \Psi_{n,k}, 0 \le k \le N-1 \quad \text{(Eq. 6)}$$

$$\Psi_{n,k} = x[n] \cdot \cos\left(\frac{\pi \cdot k \cdot (2n+1)}{2N}\right), \quad \text{(Eq. 7)}$$

Downloaded from www.periodico.tchequimica.com

$$\beta[k]=\begin{cases}\frac{1}{\sqrt{2}}, k=0;\\ 1, \quad 1\le k\le N-1.\end{cases}$$ (Eq. 8)

$$SAD(m)=\sum_{n=0}^{N-1}\left|R_m(\varphi_{n+1})-R_m(\varphi_n)\right|$$ (Eq. 9)

$$ME(m)=\sum_{n=0}^{N-1}\left|R_m(\varphi_n)\right|^2 ./$$ (Eq. 10)

$\alpha = H(\mathbf{Q}, \mathbf{\Theta})(\mathbf{p})$. (Eq. 11)

$X_i = F(\alpha_i)$. (Eq. 12)

$$\mathbf{y}_f = f\left(\sum_{i=1}^{N}(x_{f,i}w_i)\right)$$ (Eq. 13)

$$\mathbf{y}_{b,i} = x_b g\left(\sum_{i=1}^{N}(x_{f,i}w_i)\right)$$ (Eq. 14)

g(v) = df(v)/dv. (Eq. 15)

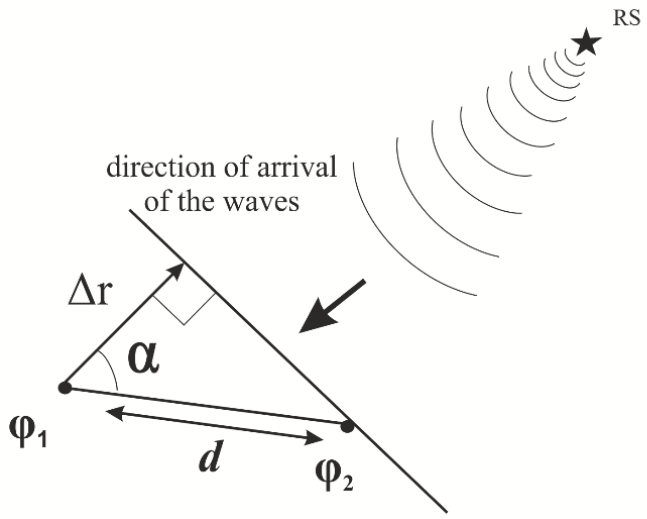

***Figure 1**. Received signals at two spatially separated points*

Downloaded from www.periodico.tchequimica.com

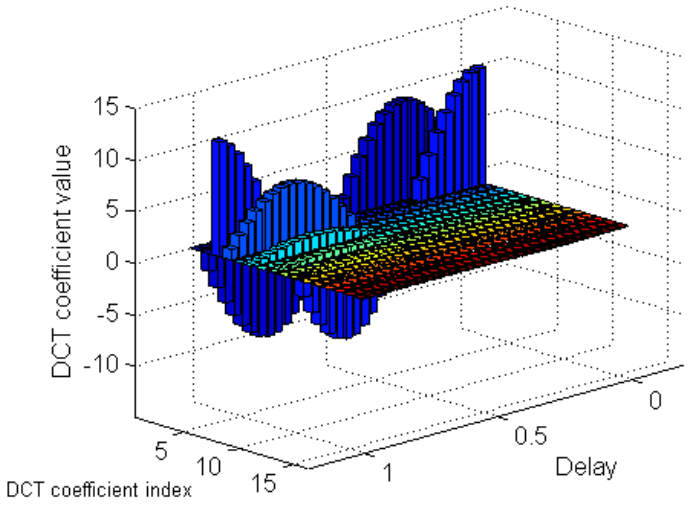

***Figure 2**. DCT energy compression*

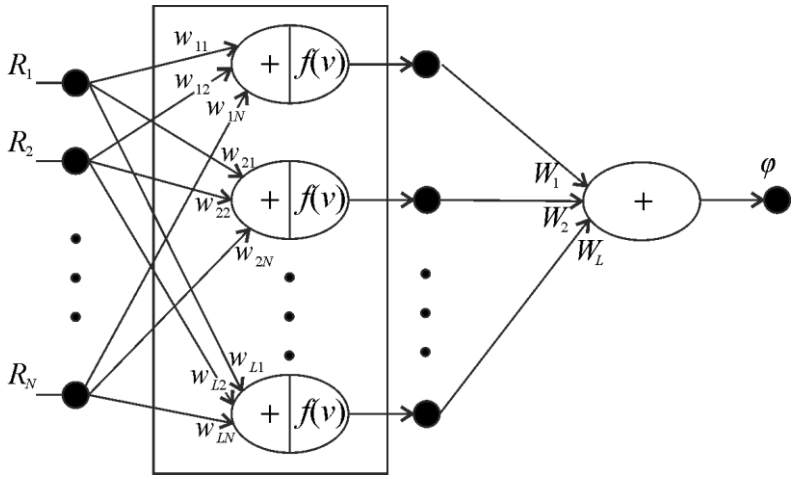

***Figure 3**. Multilayer perceptron as ANN angle evaluator*

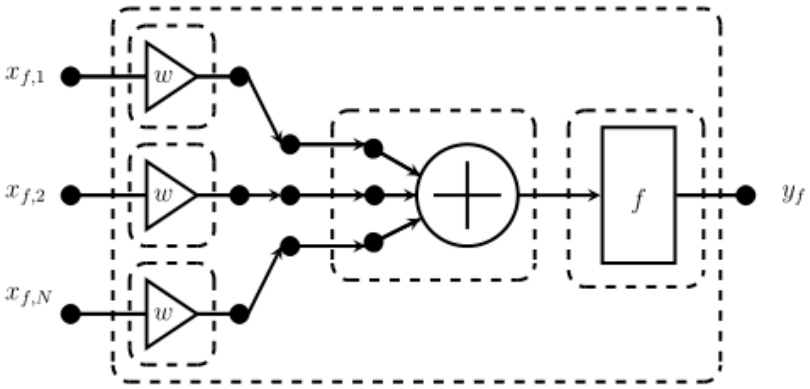

***Figure 4**. Regular neuron with three inputs during feed-forwarding*

Downloaded from www.periodico.tchequimica.com

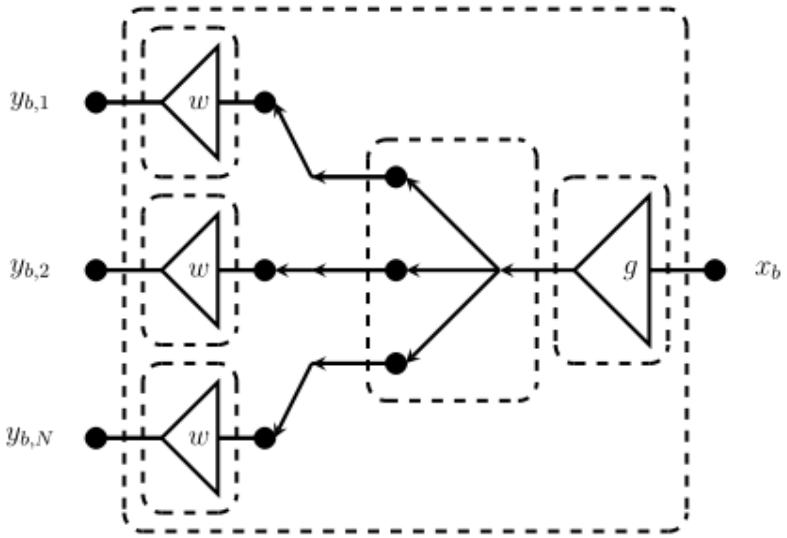

***Figure 5**. Three-input neuron during back-propagation*

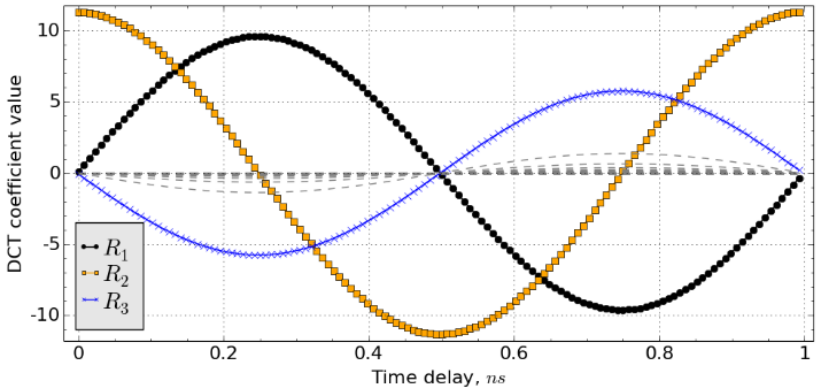

***Figure 6**. DCT values dependency on the phase shift*

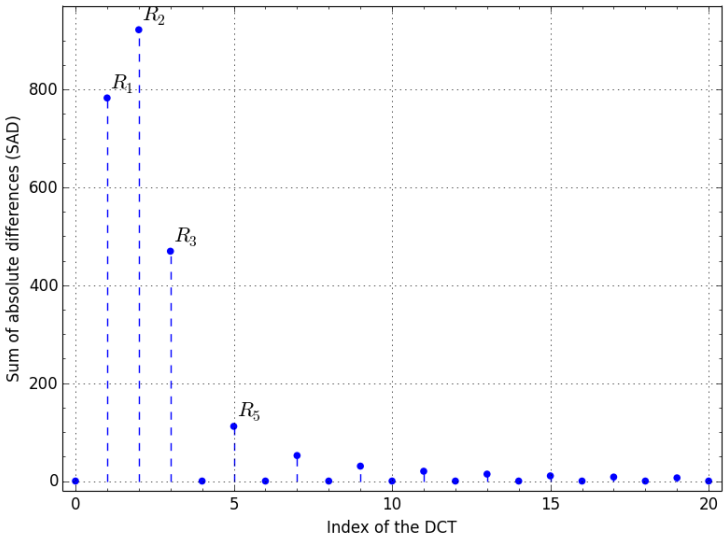

***Figure 7**. SAD evaluated for various DCT coefficients*

Downloaded from www.periodico.tchequimica.com

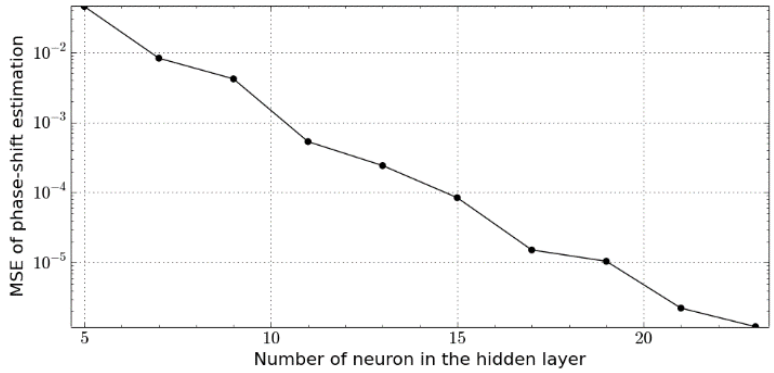

***Figure 8**. MSE against the number of neurons in the hidden layer*

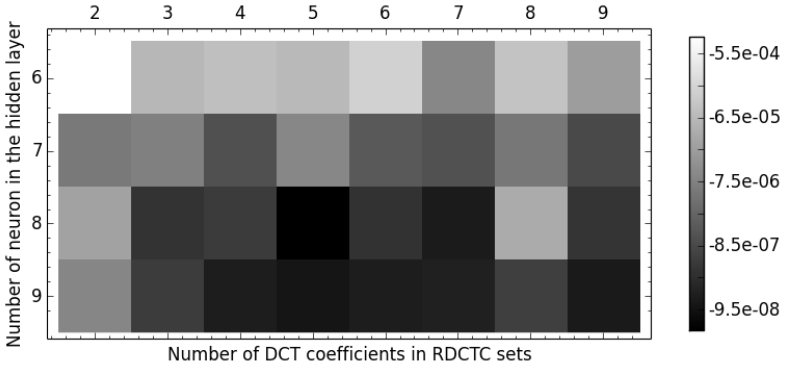

***Figure 9**. MSE against the number of neuron in the hidden layer and size of the RDCTS sets*

Downloaded from www.periodico.tchequimica.com

PERIÓDICO TCHÊ QUÍMICA
ARTIGO ORIGINAL

ANÁLISE GEOMÉTRICA DO FLUXO SUPERSÔNICO EM DOIS CORPOS AXIALMENTE SIMÉTRICOS USANDO O MÉTODO DE PROCESSAMENTO DE IMAGEM DIGITAL

GEOMETRY ANALYSIS OF SUPERSONIC FLOW AROUND TWO AXIALLY SYMMETRICAL BODIES USING THE DIGITAL IMAGE PROCESSING METHOD

ГЕОМЕТРИЧЕСКИЙ АНАЛИЗ СВЕРХЗВУКОВОГО ОБТЕКАНИЯ ДВУХ ТЕЛ ВРАЩЕНИЯ С ПРИВЛЕЧЕНИЕМ МЕТОДА ЦИФРОВОЙ ОБРАБОТКИ ИЗОБРАЖЕНИЯ

BODRYSHEV, Valeriy V.[1*]; KORZHOV, Nikolay P.[2]; NARTOVA, Lidiya G.[3]; RABINSKIY, Lev N.[4];

[1,2,3,4] Moscow Aviation Institute (National Research University), Department of Engineering Graphics, Moscow – Russian Federation

** Correspondence author*
e-mail: NioBVV@mail.ru

Received 03 September 2019; received in revised form 27 October 2019; accepted 28 October 2019

RESUMO

O artigo é dedicado ao estudo das leis geométricas de interseção de duas ondas de choque oblíquas formadas durante o fluxo supersônico em torno de dois corpos localizados no ângulo de ataque zero. Foram determinadas as coordenadas dos pontos de contato das ondas de choque com as superfícies dos modelos dos corpos axissimétricos. Os sistemas de análise de decisão e suporte à decisão são baseados na atração dos resultados do processamento de fotos (quadros de vídeo) pelo parâmetro da intensidade da imagem. Esse método permite determinar os ângulos de inclinação das ondas de choque com um alto grau de probabilidade e, portanto, identificar com mais precisão os pontos de contato da onda de choque com a superfície investigada. Foi feita uma análise dos quadros de vídeo da interação das ondas de choque usando o método de processamento de imagem digital de acordo com o parâmetro de intensidade da imagem. Foram apresentadas fórmulas que determinam o ponto de interseção das ondas de choque decorrentes do movimento supersônico de dois corpos axissimétricos próximos um do outro. As coordenadas do ponto de contato da onda de choque de saída com a superfície do segundo objeto foram determinadas levando em consideração a diferença nos ângulos de inclinação das ondas de choque de entrada e de saída. A disponibilidade de estatísticas suficientes permitiu identificar relações teóricas entre a vazão do gás, os parâmetros geométricos dos objetos, as distâncias entre eles, densidade, pressão e intensidade da imagem nas fotografias. O método de processamento de imagem digital pode ser aplicado à análise de ondas de choque durante o fluxo supersônico em torno de corpos com uma extremidade "embotada". A frente da onda de choque, neste caso, é descrita por uma curva de segunda ordem, na análise da qual é necessário selecionar uma parte dessa curva, substituindo-a com certa precisão por um segmento de linha reta (linha Mach).

Palavras-chave: *densidade de fluxo de gás, intensidade de imagem, processamento digital de imagens de sombra, onda de choque, interferência aerodinâmica.*

ABSTRACT

The scientific paper covers the research of the geometric laws of the intersection of two angle shock waves formed upon supersonic flow with zero incidence of two bodies. The positions of shock waves engaging with the surfaces of the models of axially symmetrical bodies are determined. Systems of analysis and decision support are based on the involvement of photographs (video frames) processing results by the image intensity parameter. This method facilitates the identification of the shock wave angle with a higher rate of probability, and, therefore, the more precise definition of the engagement points of the shock wave with the researched surface. This paper analyses the video frames of the interaction of shock waves using the digital image processing method by the image intensity parameter, the formulas determining the intersection point of shock waves, that occur upon the supersonic motion of two axially symmetric bodies near each other, are determined. The positions of the point of contact of the outgoing shock wave with the surface of the second object were determined, factoring in the difference in the the incoming and outgoing shock wave angles. The availability of sufficient statistics allowed to identify theoretical relationships between the gas flow rate, the geometric

Downloaded from www.periodico.tchequimica.com

parameters of objects, the distances between them, density, pressure and image intensity in photographs. The method of digital image processing can be applied to the analysis of shock waves during the flow around a supersonic stream of bodies with a "blunt" end. The shock wave front in this case is described by a second-order curve, upon the analysis of which it is necessary to select a portion of this curve, replacing it with some accuracy by a straight line segment (Mach line).

Keywords: *gas flow density, image intensity, digital processing of shadow images, compressive shock wave, aerodynamic interference.*

АННОТАЦИЯ

Статья посвящена исследованию геометрических законов пересечения двух косых скачков уплотнения, образующихся при сверхзвуковом обтекания расположенных при нулевом угле атаки двух тел. Определены координаты точек контакта ударных волн с поверхностями моделей осесимметричных тел. Системы анализа и поддержки принятия решений основываются на привлечении результатов обработки фотографий (видеокадров) по параметру интенсивность изображения. Данный метод позволяет определить углы наклона ударных волн с большой долей вероятности, и, следовательно, более точно выявить точки контакта ударной волны с исследуемой поверхностью. В работе был проведен анализ видеокадров взаимодействия ударных волн с применением метода цифровой обработки изображения по параметру интенсивность изображения, представлены формулы, определяющие точку пересечения ударных волн, возникающих при сверхзвуковом движении двух осесимметричных тел вблизи друг друга. Были определены координаты точки касания исходящего скачка уплотнения с поверхностью второго объекта с учетом отличия углов наклона приходящей и исходящей ударной волны. Наличие достаточной статистики позволило выявить теоретические зависимости между скоростью газового потока, геометрическими параметрами объектов, расстояниями между ними, плотностью, давлением и интенсивностью изображения на фотографиях. Метод цифровой обработки изображений может быть применен для анализа скачков уплотнения при обтекании сверхзвуковым потоком тел с «затупленным» концом. Фронт ударной волны в этом случае описывается кривой второго порядка, при анализе которой необходимо выделить участок этой кривой, заменив с некоторой точностью ее отрезком прямой линии (линией Маха).

Ключевые слова: *плотность газового потока, интенсивность изображения, цифровая обработка теневых снимков, скачок уплотнения, аэродинамическая интерференция.*

1. INTRODUCTION

The studies of supersonic flows implemented in conditions of a group flight of airborne vehicles under various conditions of their relative position refer to the problems of aerogas dynamics. A detailed analysis of the gas-dynamic structure of their interaction is important for explaining the effects of aerodynamic interference and predicting the forces and torques that arise (Dmitriev *et al.*, 2011; Babaytsev *et al.*, 2015). An in-depth study of the features of the development of such complex flows requires the involvement of both experimental and computational methods (Sokolov and Ryabinov, 2015).

In (Derunov *et al.,* 2009), the results of numerical calculations of supersonic flow around two axially symmetrical bodies located at angles of attack were compared with experimental data. The calculations were based on solving the Euler equations. In (Zabrodin *et al.,* 1995; Volkov and Derunov, 2005; Volkov and Derunov, 2006), the flow around two similar bodies at zero angle of attack was studied; in (Eremin *et al.,* 2002), the possibilities of numerical calculation of aerodynamics during the separation of rocket stages were shown. In (Volkov, 1998; Brodetsky *et al.,* 1998), the effects of aerodynamic interference with the surface of an axially symmetrical body with a conical head were studied, and in (Brodetsky *et al.,* 1999), two similar bodies. In (Chaplin *et al.,* 2016; Chaplin *et al.,* 2011; Chaplin, 2009; Bulat and Uskov, 2015), the results of a study of the models of axially symmetrical bodies with various configurations of the nose part streamlined by an air supersonic flow are presented.

The work includes both experimental results of blowing in a wind tunnel at M = 2.43, and calculations for various conditions of interaction between bodies. The forces and torques forcing on the model were measured for different variants of the arrangement of bodies, and dimensionless aerodynamic coefficients were calculated.

In this scientific paper, in order to study the processes of interaction of gas-dynamic

Downloaded from www.periodico.tchequimica.com

shock waves of supersonic flow, using the method of digital processing of video frames is proposed (Tarasenko *et al.,* 2015; Bodryshev *et al.,* 2016; Tarasenko *et al.,* 2017; Bodryshev *et al.,* 2018). This method makes it possible to more accurately determine the angle of the shock wave on the Mach line (Bodryshev *et al.,* 2016; Bodryshev *et al.,* 2018; Rabinskiy and Tushavina, 2019b; Rabinskiy and Tushavina, 2019a; Nikitin *et al.,* 2019; Rabinskiy *et al.,* 2019), evaluate the "strength" of the crossing waves, their dependence on the geometry of the objects, and determine changes in the angles of shock waves after the point of impact. This allows us to more accurately calculate the coordinates of the engagement point of the shock wave peak with the surface of the "neighboring" object.

2. MATERIALS AND METHODS

2.1. Method for Determining the Geometric Parameters of the Compressive Shock Wave Zone

During the movement of supersonic axially symmetrical vehicles in conditions of a group flight, compressive shock waves arise in front of them, the shape of which depends on the fore part of a particular vehicle, the angle of the interaction of objects (Chaplin *et al.,* 2016). In front of the vehicle, which has an ogive shape, intermediate between a cone and an ellipsoid, which further turns into a cylindrical one, an attached conical compressive shock wave with a peak at the apex of the ogive-shaped body arises.

When flowing around bodies with a "blunt" end, the front of the shock wave is described by a quadric curve, in the analysis of which a section of this curve is usually distinguished, replacing with a certain accuracy by a straight line segment (the Mach line). When two or more similar vehicles move close to each other, interaction (interference) of compressive shock waves occurs, as a result of which shock waves have an effect on the bodies of moving vehicles. This leads to a change in the pressure field structure on the vehicle bodies, a change in the aerodynamic torque curves and, in the final version, it can lead to a change in their subsequent trajectories of motion, and increase the likelihood of a collision.

Figure 1 shows a diagram of a shock wave structure (*SWS*) formed in the space between models. The incoming shocks until they intersect preserve the shape of a classical cone. The generators of the cones until they intersect with each other constitute straight lines. The intersection line of the cones (shock waves) is a quartic curve. Beyond the intersection line, the shocks become quartic surfaces, shear surfaces, or the so-called extruded surfaces, i.e., surfaces formed by the displacement of an arbitrary generator along an arbitrary guide track. In this case, the generators of the shear surface are generators of a variable type (Figure 1, *b*).

2.2. Digital Image Processing Method for Assessing the Position of Crossing Shock Waves

Figure 2 shows the results of an experimental study on supersonic flow around two bodies (Chaplin *et al.,* 2016). Both bodies have the same shape in the fore part; the distance between the axes of the models is 2.94*D* (*D* is the diameter of the cylindrical part of the model). The displacement of the fore parts of the models relative to each other is $\Delta x = 0$. The angle between the axes of the models is $\psi = 0$.

For this option, the attached conical compressive shock waves with a peak at the apex of the ogive-shaped body should be identical to each other. The initial analysis of this photograph by the image intensity parameter showed the need to make adjustments to the initial experimental data given by the authors. Thus, the distance between the axes of the models in the area of the head parts is equal to 2.78*D*, the distance in the area of the tail parts is equal to 2.93*D*. That is, there is some deviation of the object axes from parallel alignment. It is also confirmed by the results of measuring the angles between incoming compressive shock waves.

3. RESULTS AND DISCUSSION:

3.1. The Geometric Parameters of the Compressive Shock Wave Zone

Let us consider the pattern of the intersection of oblique conical compressive shock waves formed by the movement of two identical objects with conical heads in the plane of symmetry (Figure 3). The rate of the first object M_1, the second object M_2. The distance between the model axes is equal to H. The displacement of the fore parts of the models relative to each other is Δx. The angle between the model axes is $\psi = 0$.

The angles between the generators of the attached conical compressive shock waves and their axes are called Mach angles. They are related to the Mach number according to the

Downloaded from www.periodico.tchequimica.com

following ratios (Equations 1, 2). The coordinates of the point of intersection of two shock waves $A_0(x_0, y_0)$ are determined by solving two equations (Equation 3). When equating the right parts, Equation 4 is gotten.

The coefficients *c* and *d* are determined based on the values of the point coordinates $A_1(x_1, y_1)$ and $A_2(x_2, y_2)$ (Equations 5, 6). When solving Equations 1-5 consistently, the generalized equations for determining the coordinates x_0, y_0 (Equations 7, 8) are obtained. In this case, the distances H_1 and H_2 from the point of intersection of the shock waves $A_0(x_0, y_0)$ are determined by the dependencies (Equation 9).

When the values of the point coordinate $A_0(x_0, y_0)$ and the values of the angles θ and φ are known, the coordinates of the intersection points $A_3(x_3, y_3)$ and $A_4(x_4, y_4)$ of the outgoing shock waves with objects shall be defined according to dependencies (Equations 10, 11). The geometric calculations presented above proceed from the variant of the head parts of objects made in the form of a classical cone for which ratios (Equation 1) are valid. At the same time, in real constructions, the shape of the head part can differ significantly from the conical one and have, for example, the shape of an ogive-shaped body.

Therefore, when determining the values of the angles of the conical compressive shock waves outgoing from the nose parts of the objects, their correction is necessary. It is also necessary to know the exact values of the oblique angles θ and φ. A quantitative assessment of the angles of the compressive shock waves depending on the rate of the incoming flow can be performed using the method of digital processing of shadow images by the image intensity parameter. Such a method is given in (Tarasenko *et al.,* 2015). Further development and capability enhancement of its application for various problems of supersonic gas dynamics are presented in (Bodryshev *et al.,* 2016; Tarasenko *et al.,* 2017; Bodryshev *et al.,* 2018; Abashev *et al.,* 2018).

3.2. Assessing the Position of Crossing Shock Waves

Figure 2, *b* shows a photograph display of Figure 2, *a* in functional form $L = f(x, y)$. Here L is the image intensity. Further processing is performed as follows. The image area is divided into discrete cells. Each cell can contain from *1* to *n* pixels along the *x* axis and *1* to *m* pixels along the *y* axis. The cell size (*m* and *n*) depends on the necessary accuracy in estimating the value of the flow rate, and it is determined by practical rationality. Cell parameters *x*, *y* are fixed by the coordinates of its center or any angle of the cell (for example, the bottom-left angle). Thus, the image is stored in the form of a two-dimensional array (i.e., a matrix in size $m \times n$), in which each element with coordinates (*x*, *y*) corresponds to the accepted cell coordinate.

Since *L* for a shadow image characterizes the rate of change in the gas flow density (Tarasenko *et al.,* 2015; Bodryshev *et al.,* 2016), then the change in *L* determines the dynamics of the flow rate. Figure 4, *a*, as an example, shows graphs of the changes in *L* in longitudinal sections *1* and *2*. Section *2* passes through the point of intersection of the shock waves. In both sections, the graphs of the changes in the image intensity look identical when the flow passes through the compressive shock waves. The minimal intensities L_{1min}, L_{2min} are observed on the shock line (the flow rate is minimal, the pressure is maximal), immediately after the shock occurs the image intensities L_{1max} and L_{2max} are maximal (the flow rate increased, and the pressure decreased). But the length of the burst area of the image intensity is greater in section 2 ($\Delta 2$ is larger than $\Delta 1$ by about 2.5 times).

The amplitudes of increase and attenuation of the image intensity on the line of the compressive shock waves are larger when the flow passes the interference point of shock waves. Thus, the intensity of the *shock wave process*, which is characterized by the ratio of static pressures before and after the *shock wave process*, is higher when the flow passes the interference point. Most likely, this is the reason for the change in the values of the oblique angles of compressive shock waves after their interaction. Figure 4, *b* shows that after the shock wave interaction at point A, each of them continues to grow in the same direction as previously. The hypothesis that after shock waves encounter, each can be represented as one reflected from an imaginary plane passing through the intersection point of these shocks is not correct.

In order to determine the true oblique angle of the shock wave of the Mach cone, outgoing from the head of the object, it is necessary to obtain the exact direction of the straight line, which forms the Mach cone. For this purpose, the method of least squares by discrete points is used. It is expedient to apply two options for using this method based on the condition

Downloaded from www.periodico.tchequimica.com

(Figure 5) (Bodryshev *et al.,* 2016). Here L_i - the intensity in the *i*-th cell, L_{LV} - the limiting value of the intensity.

1. By the coordinates of the extreme cells in the initial stage of the shock wave.

2. By the coordinates of the cells that determine the beginning of the shock wave using the Freeman chain code.

Here, the cells are defined as a sequence according to an eight-linked lattice. The equations of the line when using the method of least squares are as follows in Equations 12, 13. Hence the oblique angle of the compressive shock wave φ is in Equation 14 where N is the number of cells with measurement L_i. Thus, processing the "lines" 1-1, 1-2, 2-1, 2-2 (Figure 2) the angles $\alpha, \beta, \varphi, \theta$ are determined.

Using this method, all the angles of the lines of compressive shock waves before they intersect at point A_0 and after it were calculated. The obtained values of the angles of incoming and outgoing compressive shock waves are shown in Figure 2, *a*. The values of incoming compressive shock waves from identical test models are not equal to each other, and they differ from the value of the Mach cone angle, determined by the ratio (Equation 2).

At the claimed flow rate in the experiment under study, M = 2.43, the angles for both shocks should be 24.3°. The difference between the theoretical angle φ and the experimentally measured angle may be due to the fact that the shape of the head of the models under test has an ogive shape, rather than a conical shape, for which the angle of the Mach cone is determined. In addition, as shown above, the axes of the models during the test are not completely parallel. The digital image processing method can also be used to analyze compressive shock waves during a supersonic flow around bodies with a "blunt" end. The shock wave front, in this case, is described by a quadric curve, in the analysis of which it is necessary to separate a section of this curve, replacing it with a certain accuracy by a straight line segment (the Mach line).

4. CONCLUSIONS:

The analysis of video frames of the shock waves interaction was made using the method of digital image processing by the parameter image intensity. There are formulas that determine the point of intersection of shock waves arising from the supersonic motion of two axially symmetrical bodies close to each other. The angles of shock waves were determined both by the traditional method depending on the gas flow rate and by using the digital image processing method, which allows more accurate determination of the wave oblique angle before and after the point of intersection of the shock waves.

The coordinates of the point of contact of the outgoing compressive shock wave with the surface of the second object are determined, taking into account the difference in the oblique angles of the incoming and outgoing shock wave. This makes it possible to more accurately predict the distribution of pressure on the vehicle bodies and to calculate the aerodynamic torque characteristics.

The availability of sufficient statistics makes it possible to identify theoretical ratios between the gas flow rate, the geometric parameters of objects, the distances between them, density, pressure, and image intensity in photographs.

5. ACKNOWLEDGMENTS:

This work has been partially supported by RFBR, project No. 17-01-00837.

6. REFERENCES:

1. Babaytsev, A.V., Kornev, Y.V., Semenov, N.A. *International Journal of Nanomechanics Science and Technology,* **2015**, *6*(4), 261-280.
2. Bodryshev, V.V., Abashev, V.M., Korzhov, N.P., Tarasenko, O.S*. Bulletin of Tula State University. Section Engineering,* **2018**, *6*, 458–467.
3. Bodryshev, V.V., Abashev, V.M., Tarasenko, O.S., Mirolyubova, T.I. *Electronic Journal "Transactions of Moscow Aviation Institute",* **2016**, *88*, http://trudymai.ru/published.php?ID=70428, accessed 20 April 2019.
4. Brodetsky, M.D., Derunov, E.K., Kharitonov, A.M., Zabrodin, A.V., Lutsky, A.E. *Thermophysics and Aeromechanics*, **1998**, *5(3),* 301–306.
5. Brodetsky, M.D., Derunov, E.K., Kharitonov, A.M., Zabrodin, A.V., Lutsky, A.E. *Thermophysics and Aeromechanics*, **1999**, *6(2),* 165–172.
6. Bulat, P.V., Uskov, V.N. *Collection of scientific articles of the International*

Downloaded from www.periodico.tchequimica.com

Scientific Division of the ITMO University "Mechanics and Energy Systems", **2015**, 24–39.

7. Chaplin, R., *Aerodynamic Interference Between High-Speed SlenderBodies*, Ph.D. Thesis, Cranfield University, Cranfield, England, **2009**.
8. Chaplin, R., MacManus, D., Leopold, F., Martinez, B., Gauthier, T., Birch, T*. Computers and Fluids,* **2011**, *50(1)*, 155–174.
9. Chaplin, R., MacManus, D.G., Leopold, F., Martinez, B., Gauthier, T., Birch, T. *AIAA Journal*, **2016**, *54(7),* 2017–2033.
10. Derunov, E.K., Volkov, V.F., Zheltovodov, A.A., Maximov, A.I.. *Thermophysics and Aeromechanics,* **2009**, *16(1),* 13–20
11. Dmitriev, A.I., Skvortsov, AA., Koplak, O.V., Morgunov, R.B., Proskuryakov, I.I. *Physics of the Solid State*, **2011**, *53*(8), 1547-1553.
12. Eremin, V.V., Mikhalin, V.A., Rodionov, A.V. *Aeromechanics and Gas Dynamics*, **2002**, *1*, 24–35.
13. Nikitin, P.V., Tushavina, O.V., Shkuratenko, A.A*. INCAS Bulletin*, **2019**, *11,* 191–201, DOI: 10.13111/2066-8201.2019.11.S.19.
14. Rabinskiy, L. N., Tushavina, O. V. *INCAS Bulletin,* **2019a**, 11, 203–211, DOI: 10.13111/2066-8201.2019.11.S.20;
15. Rabinskiy, L.N., Tushavina, O.V., Fedotenkov, G.V. *Asia Life Sciences*, **2019**, *19(1),* 149–162.
16. Rabinskiy, L.N., Tushavina, O.V. *STİN*, **2019b**, *4*, 22–26.
17. Sokolov, N.S., Ryabinov, V.M. Soil Mechanics and Foundation Engineering, **2015**, *52(1)*: 18–22.
18. Tarasenko, O.S., Bodryshev, V.V., Abashev, V.M. *Bulletin of Tula State University. Technical Science*, **2017**, *2*, 290–302.
19. Tarasenko, O.S., Bodryshev, V.V., Abashev, V.M. *Electronic Journal "Transactions of Moscow Aviation Institute",* **2015**, *83,* http://trudymai.ru/published.php?ID=62032, accessed 20 April 2019.
20. Volkov, V.F. *International Conference on the Methods of Aerophysics Research.* Novosibirsk, Russia, **1998**, 228–233.
21. Volkov, V.F., Derunov, E.K. *Physics Engineering Journal*, **2006**, *79(4),* 81–90.
22. Volkov. V.F., Derunov. E.K. *Computational Methods and Programming*, **2005**, *6(1),* 75–85.
23. Zabrodin, A.V., Lutsky, A.E., Brodetsky, M.D., Derunov, E.K. *Thermophysics and Aeromechanics,* **1995***, 2(2),* 97–102.

$$sin\alpha=\frac{1}{M_1};\ sin\beta=\frac{1}{M_2} \quad \text{(Eq. 1)}$$

$$\alpha=arcsin(\frac{1}{M_1});\ \beta=arcsin(\frac{1}{M_2}) \quad \text{(Eq. 2)}$$

$$y_0=tg(\alpha)x_0+c;\ y_0=tg(\beta)x_0+d \quad \text{(Eq. 3)}$$

$$x_0=\frac{c-d}{tg(\alpha)-tg(\beta)} \quad \text{(Eq. 4)}$$

$$c=y_1-tg(\alpha)x_1 \quad \text{(Eq. 5)}$$

$$d=y_2-tg(\beta)x_2 \quad \text{(Eq. 6)}$$

$$y_0=(x_0-x_1)tg(arcsin(\frac{1}{M_1}))+y_1 \quad \text{(Eq. 7)}$$

Downloaded from www.periodico.tchequimica.com

$$x_0=\frac{y_1-y_2-tg(\arcsin(\frac{1}{M_1})x_1+tg(\arcsin(\frac{1}{M_2})x_2}{tg(\arcsin(\frac{1}{M_1})-tg(\arcsin(\frac{1}{M_2})} \quad \text{(Eq. 8)}$$

$$H_1=y_1\text{-}0{,}5D_1\text{-}y_0;\ H_2=y_0+0{,}5D_1\text{-}y_2 \quad \text{(Eq. 9)}$$

$$y_3 = y_0+H_1;\ y_4 = y_0 - H_2 \quad \text{(Eq.10)}$$

$$x_3= x_0 - \frac{H_1}{tg(\varphi)};\ x_4=x_0 - \frac{H_1}{tg(\theta)} \quad \text{(Eq. 11)}$$

$$x\cos(\varphi) + y\sin(\varphi) = d \quad \text{(Eq. 12)}$$

$$d = \frac{1}{N}\sum_{i=1}^{N}(x_i\cos(\varphi) + y_i\sin(\varphi) \quad \text{(Eq. 13)}$$

$$\varphi = 2\text{arctg}\left(\frac{1}{2}\frac{N\sum_{i=1}^{N}x_iy_i-\sum_{i=1}^{N}x_i\sum_{i=1}^{N}y_1}{\left\{N\sum_{i=1}^{N}x_i^2-\left(\sum_{i=1}^{N}x_i\right)^2\right\}-\left\{N\sum_{i=1}^{N}y_i^2-\left(\sum_{i=1}^{N}y_i\right)^2\right\}}\right) \quad \text{(Eq. 14)}$$

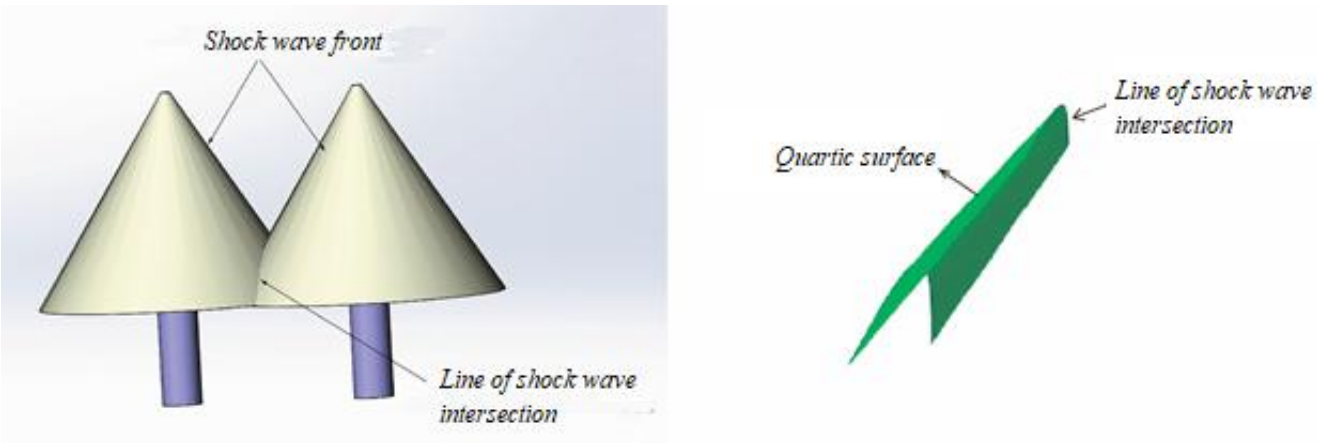

Figure 1. *The geometric pattern of the intersection of shock waves (a) and the surface shape of the compressive shock wave after the intersection of shock waves (b)*

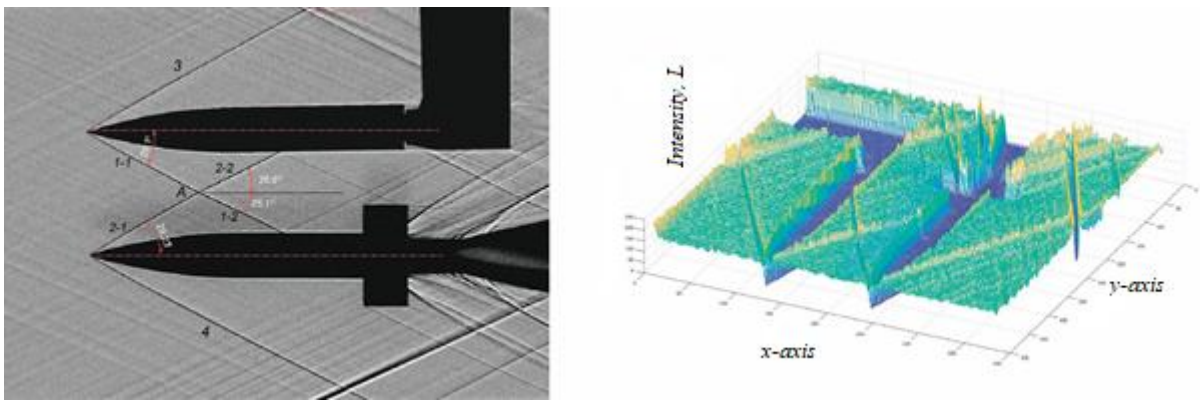

Figure 2. *The video frame of the shock wave intersection zone (a) and the corresponding mapping of the function L=f(x, y) (b)*

Downloaded from www.periodico.tchequimica.com

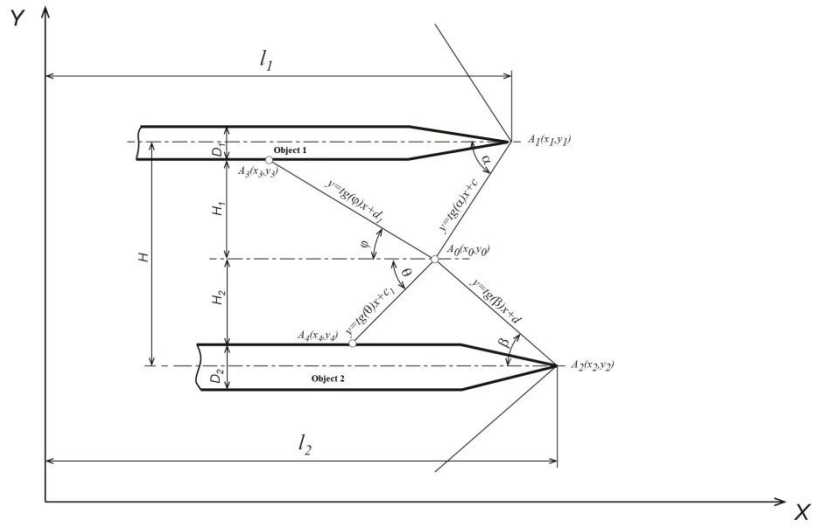

Figure 3. *The pattern of the intersection of oblique conical compressive shock waves*

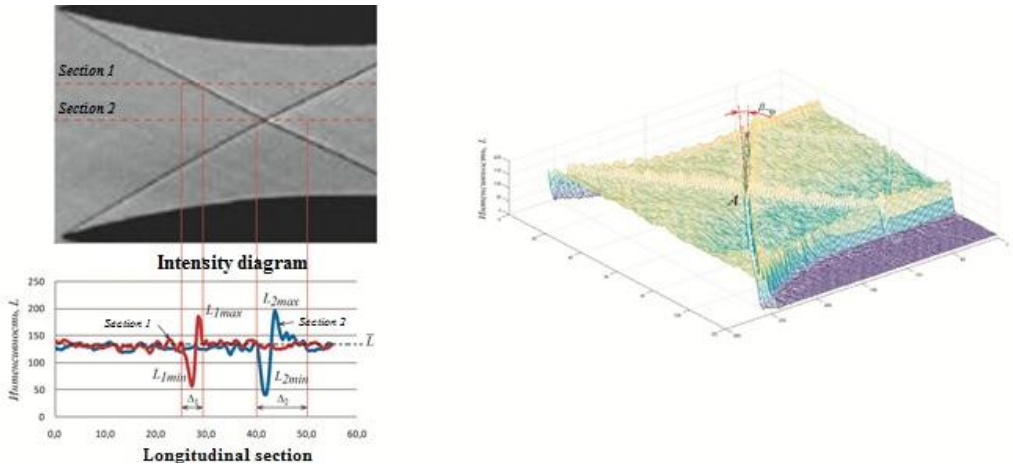

Figure 4. *Dynamics of changes in image intensity in longitudinal sections (a), display of changes in the angle of the shock wave flow after the intersection point (b)*

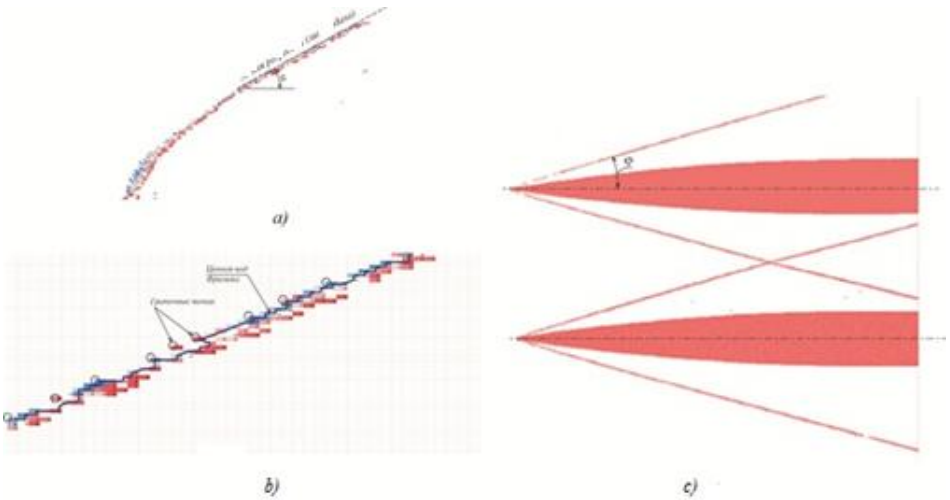

Figure 5. *Example of displaying an array of cells located in the compressive shock wave: a - with the given condition $L_i \geq L_{LV}$, b - on the Mach shock line, c - the pattern of shock waves intersection*

Downloaded from www.periodico.tchequimica.com

PERIÓDICO TCHÊ QUÍMICA
ARTIGO ORIGINAL

ABORDAGEM ESPECTRAL DA AVALIAÇÃO DE UMA SÉRIE TEMPORÁRIA DE MUDANÇA DE POTÊNCIA NAS UNIDADES DE MEDIÇÃO DE SUBESTAÇÃO E SUA APLICAÇÃO NOS MODOS DE CONTROLE DOS SISTEMAS DE MEDIÇÃO DE ELETRICIDADE DE SUBESTAÇÃO

SPECTRAL APPROACH TO THE ESTIMATION OF THE TIME SERIES OF THE POWER CHANGE IN THE SUBSTATION METERING UNITS AND ITS APPLICATION IN THE CONTROL MODES OF SUBSTATION ELECTRICITY METERING SYSTEMS

СПЕКТРАЛЬНЫЙ ПОДХОД К ОЦЕНКЕ ВРЕМЕННОЙ СЕРИИ ИЗМЕНЕНИЯ МОЩНОСТИ В ПОДСТАНЦИОННЫХ УЧЕТНЫХ УСТРОЙСТВАХ И ЕГО ПРИМЕНЕНИЕ В РЕЖИМАХ УПРАВЛЕНИЯ ПОДСТАНЦИОННЫМИ СИСТЕМАМИ УЧЕТА ЭЛЕКТРОЭНЕРГИИ

PICHUGIN, Vladimir N.[1*]; YAGIN, Evgene V.[2]; LUKISHIN, Alexander V.[3]; PAKHOMOVA, Olga A.[4]; HAZOV, Andrey Yu.[5];

[1,2,4] Chuvash State University named after I.N. Ulyanov, Department of Higher Mathematics and Information Technologies, Chuvashia – Russian Federation

[3,5] Chuvash State University named after I.N. Ulyanov, Department of Humanities and Economic Disciplines, Chuvashia – Russian Federation

** Correspondence author*
e-mail: vladimir_iii@mail.ru

Received 13 September 2019; received in revised form 28 October 2019; accepted 28 October 2019

RESUMO

Para criar os modelos de superfícies estendidas nas partes de ondas longas e ondas curtas do espectro de ondas, é necessário conhecer as características de dispersão dos obstáculos da fita, idealmente localizados tanto no espaço livre quanto em uma superfície estendida. Os métodos para o estudo remoto de superfícies estendidas, com base na análise de sinais gerados pela reflexão ou radiação de ondas eletromagnéticas que passam por neoplasias, permitem visualizar a topografia, características e tipo de vários locais, tamanhos de vários objetos. Um dos métodos de pesquisa eficazes é resolver o problema da difração de ondas eletromagnéticas por um objeto infinitamente estendido no espaço livre. O objetivo deste estudo é caracterizar ondas eletromagnéticas durante a difração de ondas eletromagnéticas em objetos que podem ser usados como sistemas de radar. Foram utilizados o método de processamento estatístico de dados experimentais de testes de campo e a descrição matemática da situação do radar eletromagnético, bem como sua simulação computacional. O resultado deste estudo pode ser formulado como o desenvolvimento de métodos analíticos e de software para analisar o padrão de difração de ondas eletromagnéticas no modo de recepção de ondas múltiplas em um objeto infinitamente estendido no espaço livre, bem como um método de software para calcular características de difração em frequências que excedem a frequência base, levando em consideração a falta de homogeneidade dos campos eletromagnéticos nessas condições. Os resultados da pesquisa utilizados no desenvolvimento da metodologia universal para o projeto e desenvolvimento de sistemas de radar capazes de funcionar adequadamente em um ambiente eletromagnético são de importância prática. Os resultados deste estudo vão permitir uma completa descrição do quadro eletrodinâmico da propagação de ondas e sua difração, ou seja, a consideração às propriedades de difração dos sistemas de radar nos permitirá desenvolver uma direção para sua produção e propagação mais amplas.

Palavras-chave: *sistemas de radar do tipo slot, ondas eletromagnéticas, funções espectrais, integral de Fourier, equações de onda.*

ABSTRACT

In order to create models of extended surfaces in the long and short wavelength parts of the wave spectrum, it is necessary to know the dispersion characteristics of tape-like obstacles perfectly located both in free space and on an extended surface. Methods of remote studying of extended surfaces, based on an

Downloaded from www.periodico.tchequimica.com

analysis of signals that are generated by reflection or radiation of electromagnetic waves passing neoplasms allows us to view the topography, characteristics, and type of the different locations, sizes of various objects. One of the effective methods of study is to solve the problem of diffraction of electromagnetic waves on an infinitely extended object in free space. The purpose of this study is characteristics of electromagnetic waves during diffraction of electromagnetic waves at objects that can be used as radar systems. The method of statistical processing of experimental data from field tests and mathematical description of electromagnetic radar situation, as well as its computer simulation were used. The result of this study can be formulated as the development of analytical and software methods for analyzing diffraction pattern of electromagnetic waves in multi-wave mode of reception on infinitely extended object in free space, as well as a software method for calculating diffraction characteristics at frequencies exceeding the basic frequency, taking into account the inhomogeneity of electromagnetic fields in these conditions. The practical significance is the research results used in the development of a universal technique for design and development of radar systems capable of working adequately in conditions of electromagnetic environment in question. The results of this research will allow a complete description of the electrodynamic picture of wave propagation and its diffraction, namely, taking into account the diffraction properties of radar systems will allow us to develop a direction for their wider production and distribution.

Keywords: *slot type radar systems, electromagnetic waves, spectral functions, Fourier integral, wave equations.*

АННОТАЦИЯ

Для создания моделей протяженных поверхностей в длинноволновой и коротковолновой частях спектра волны необходимо знать дисперсионные характеристики ленточных препятствий, идеально расположенных как в свободном пространстве, так и на протяженной поверхности. Методы дистанционного изучения протяженных поверхностей, основанные на анализе сигналов, генерируемых отражением или излучением электромагнитных волн, проходящих новообразования, позволяют нам просматривать топографию, характеристики и тип различных мест расположения, размеров различных объектов. Одним из эффективных методов исследования является решение проблемы дифракции электромагнитных волн на бесконечно протяженном объекте в свободном пространстве. Целью данного исследования является характеристика электромагнитных волн при дифракции электромагнитных волн на объектах, которые могут быть использованы в качестве радиолокационных систем. Использован метод статистической обработки экспериментальных данных полевых испытаний и математического описания электромагнитной радиолокационной обстановки, а также его компьютерное моделирование. Результат этого исследования может быть сформулирован как разработка аналитических и программных методов анализа дифракционной картины электромагнитных волн в многоволновом режиме приема на бесконечно вытянутом объекте в свободном пространстве, а также программный метод расчета дифракционных характеристик на частотах. превышение базовой частоты с учетом неоднородности электромагнитных полей в этих условиях. Практическое значение имеют результаты исследований, использованные при разработке универсальной методики проектирования и разработки радиолокационных систем, способных адекватно работать в условиях электромагнитной обстановки. Результаты этого исследования позволят полностью описать электродинамическую картину распространения волны и ее дифракции, а именно учет дифракционных свойств радиолокационных систем позволит нам разработать направление для их более широкого производства и распространения.

Ключевые слова: *радиолокационные системы щелевого типа, электромагнитные волны, спектральные функции, интеграл Фурье, волновые уравнения.*

1. INTRODUCTION

In a multi-location study of the earth's surface, a quantitative description of the phenomena caused by repeated structure and taking into account the influence of the underlying surface properties on the characteristics of the received signals are of great importance (Immoreev, 2009) .An analysis of characteristics of scattering electromagnetic waves by an ideally conducted ribbon screen located on flat boundary of the conducting dielectric half-space allows us to study problems associated with sharp change in electro physical properties of the earth's surface and the presence of well-reflecting objects located on it (Likhachev and Usov, 2010; Orlov *et al.,* 2003; Golovin, 2004).

There are some solutions for ideally conducting discs and bands that make it possible to obtain multi-location estimates of characteristics of wave scattering (Kurkchan *et al.,* 2016; He *et al.,* 2008; Özdenvar and McMechan, 1997). Nonetheless, these solutions are inapplicable in radiometric research, because

Downloaded from www.periodico.tchequimica.com

The parameters of thermal radiation of the medium are determined by active losses of electromagnetic waves in the medium, i.e., the possibility of radiometric observation of objects is conditioned by the difference in their absorption capacity. In these studies, the problem of diffraction by an infinitely extended tape in free space is considered. In Loshilov *et al.* (2010, Daus and Kharchenko, 2018), the problems were reduced to a system of pair integral equations with respect to spectral functions for surface current densities solved by the moment method. Similar problems for impedan ribbon (Figure 1) and for slit in the impedan shield can also be solved by the eigenfunction method (Semyonov and Loschilov, 2011; Loshilov *et al.,* 2012; Skianis, 2014; Gatignol *et al.,* 2010; Orofino and Pedersen, 1993).

2. MATERIALS AND METHODS

The infinite impedan ribbon and the infinite slit in impedan screen are represented as coordinate surfaces ξ = 0 in the elliptical coordinate system of Figure 2.

The diffraction field of an arbitrarily oriented slit in the screen in a Cartesian coordinate system independent of its orientation is determined by substituting the relations for field components in the elliptical system into formulas that relate vector functions to the indicated coordinate systems (Bashly *et al.,* 2017; Yao *et al.,* 2001; Inverarity, 2003). To do this, it is necessary to express the gap field in an elliptical coordinate system associated with gap for the case when the electric field vector $\dot{\bar{E}}$ or magnetic field strength $\bar{H}$ of incident wave is oriented along the slit. The indicated expressions are obtained as a result of expressing a boundary problem by the method of dividing variable based on expansion of plane wave in series according to Mathieu function (Kultin, 2015; Pichugin *et al.,* 2013; Badylevich *et al.,* 2003).

Let us apply the Cartesian coordinate system XYZ so that the plane of the screen coincides with the plane XY, and the plane of incidence of electromagnetic wave coincided with the plane ZY. The direction of the normal to the front of incident plane wave forms an angle γ with axis OZ.Linear slit of infinite length and finite width $2h$ is angled τ relative to the axis OZ (Figure 2) (Pichugin and Bugrova, 2013; Li *et al.,* 2015; Morgunov, 2004). In general, the field of an incident plane electromagnetic wave in free space has the form Equations 1 and 2. The total field is the sum of the incident and diffracted by ribbon fields (Equations 3, 4 and 5). Equation 6 is the solution for complex amplitudes satisfying the radiation conditions at infinity (Equation 7), where $(\pm)$ – are spectral densities for the amplitudes in the upper and lower half-spaces (Equations 8-16). Looking for solution of the wave inhomogeneous equation in the form of the Fourier expansion we get Equations 17, 18 and 19.

3. RESULTS AND DISCUSSION:

The spectral density depends on the distribution of external current in space. At that, the integral is taken only at those points in space where there are existing points. Then we need to solve the wave equation (Equations 20, 21). Let us see the expansion of the Fourier function (Equations 22, 23 and 24) where $g(x_1)$- is spectral density, this expression can be interpreted as an infinite set of plane homogeneous waves located in the positive and negative direction of the axis x with phase speeds (Equation 25) where x_1- plays the role of wave number, amplitude of these waves $g(x_1)$ does not depend on coordinate x. Therefore, the solution of the wave equation is in Equations 26, 27 and 28.

Solution for complex amplitudes satisfying the wave equation and depending on transverse coordinates x and z, and radiation conditions at infinity, can be recorded in the form of the Fourier integral. We shell use the variable separation method, the Fourier method to solve the wave equation (Equation 29). Then divide it by XYZ (Equations 30-33) minding the equality of the left and right sides of the equation and their independence, we assume that they are equal to some separation constant, let minding the equality of the left and right sides of the equation and their independence, we assume that they are equal to some separation constant, let (Equations 34-37), thus we reduce the first equation by Y and get a new system of equations (Equations 38, 39).

Let us consider the homogeneous equation (Equation 40). If we take into account (Equation 41) then (Equations 42, 43), where (Equations 44, 47). Let us separate the variables (Equation 48). Then we shell move on to dimensionless spatial variables (Equations 49, 50) then we get a system of equations in the form (Equation 51, 52).

To solve inhomogeneous wave equations, we use Fourier expansion. The function X (u) is defined on the interval $-\infty \leq u \leq \infty$ therefore,

Downloaded from www.periodico.tchequimica.com

its expansion into the Fourier integral is (Equation 53). Analogically for function Z(v) (Equation 54). Therefore, for the vector potential $\vec{A}(x,z)$we have (Equations 55, 56) where (Equation 57).

Let us consider the internal integral (Equations 58, 59). By putting an expression for $\vec{A}(u,v)$in the wave equation (Equations 38, 39 and 40) we get Equation 60 by comparing Equations 53, 54 and Equations 55-59. We can see that the spectral plane of the desired function $\vec{A}(u,v)$ differs from the spectral plane of external current decomposition $-\vec{j}^{st}$ only a factor $-\frac{1}{a^2}-(k^2-p_0^2-\varepsilon^2-w^2)$. We can determine the spectral plane of the desired function $\vec{g}(\varepsilon)$.For this, we multiply Equations 55-59 by complex conjugate functions $\frac{1}{2\pi a^2}e^{-i\varepsilon' u-iw'v}$ where ε', w' are fixed values ε, w, then integrate over the entire infinite space (Equations 61, 62). Then we transfer the stroke from wave numbers $\varepsilon' and\ w'$spatial coordinates $u\ and\ v$ (Equation 63).

This expression determines spectral density g(u,v) in the expansion (Equations 53, 54). It depends on distribution of the external current in the space, and integral (Equation 63) is calculated only at those points in the space where currents exist (Equation 64). S denotes a cross section of volume of sources x by the plane y = const. Let us calculate integral w (Equations 65, 66 and 67). Transition to the plane of complex variable w and putting $k^2<\varepsilon^2+p_0^2$, which does not limit the generality of the results obtained, we note that in the integrand there are two singular points (bands): one in the upper half-plane w = iw′; another in the lower half-plane: w = iw'. For $(v-v')<0$ integral L can be supplemented by vanishing integral in circle of infinitely large radius in the upper half-plane, where at $w\to i\infty$ the integrand tends to zero. Then the integral will be (Equations 68, 69). There is no special singular point in infinity (Equation 70). Thus, Green's function is equal to (Equation 71)

Let us substitute Equations 29-33 into Equations 42, 43 taking into account Equations 45-47, finite functions of surface electric densities and magnetic currents (Equation 72). Then we consider the Fourier transform to find the spectral density $\vec{a}_{\pm}(\varepsilon)$ (Equation 73).

We will take the inverse Fourier to transform from this system, for this we multiply the left side of the equation by complex conjugate functions $e^{-i\varepsilon' u}$ and integrate the resulting expression over the space where currents exist, i.e. via variable and ranging from -1 to 1 (across the width of the cavity) (Equation 74). We'll use (Equatian 75) and get (Equation 76). Let us consider the vector potential through the spectral density (Equation 77). We shell to solve the internal integral (Equation 78).

Each function $t(z)$ regular in circle $|z-a|<\rho$ decomposes into a power series converging in the circle (Equation 79) where the coefficient is determined by the formulas (Equation 80) or (Equation 81) where $\rho_1<\rho$ this Taylor power series in vicinity of point z = a (Equation 82). Let us multiply the first equation by vector $\vec{v}_0$and replace $\vec{\varepsilon}\to\varepsilon$ (Equation 83). Then, combining the spectral densities for magnetic and electric currents, we obtain (Equation 84). We shell apply the mean value theorem (Equation 85). The average value $\frac{1}{b-a}\int_a^b f(x)dx$ on the interval [-a; b] (Equation 86).

The spectral density depends on the distribution of external current. In its turn, the distribution of external current on the tape is associated with fulfillment of the boundary conditions of impedance type on the surface of tape above and below, i.e. on the coordinate plane v =0, for tangential components of the fields $\vec{E}_t$ and $\vec{H}_t$ the relation is satisfied (Equation 88) where H – are waves with capacitive nature, E – are waves with inductive nature.

The presence of the surface impedance can be considered as a condition for the existence of a surface wave in second medium. A plane impedance (dielectric structure) tape is virtually modeled as waveguide, waveguide-type waves can naturally exist in it. Outside of tape (layer) there is a surface wave above and below. Critical frequencies for a planar dielectric waveguide are (Equation 87). The condition $w=w_{kr}^{(n)}$ meets condition φ = φ* the Brewster angle, where φ – is angle of incidence of the wave. At φ = φ* outside the layer, an ordinary uniform wave propagates along the tape, and consequently, a longitudinal component at the boundary H_y or $E_y$is lost, which means that there is no dependence on the type of polarization, i.e. at $f\le f_{kr}(\varphi\le\varphi^*)$ waveguide type wave inside the tape (layer) is destroyed. Outside the tape on plane v=0, the following expressions are valid (Equation 89). For current systems outside tape |u|>1, integral equations (Equation 89) are equal 0 (Equation 90).

The system of Equations 89, 90 is the initial point for solving asymptotic or numerical

Downloaded from www.periodico.tchequimica.com

methods. Then, it is solved by the method of moments; for this case, unknown functions of the current density are expanded in a series according to the complete system of functions orthogonal to width of the tape.

For numerical analysis of spectral functions by (Equations 89, 90, a software simulator was created in RAD Studio development environment (Pichugin *et al,* 2015; Skvortsov *et al.,* 2012; Skvortsov and Karizin, 2017). The software simulator was designed to simulate spectral characteristics in long and short wavelengths of the spectrum (Figures 3-4). Performing a numerical analysis, we can notice that a jump occurs on the surface of the magnetic field and electric field: the jump in magnetic field is equal to the surface density of external electric current (Equation 91). The jump in electric field is equal to surface density of external magnetic current.

4. CONCLUSIONS:

During the research, corresponding algorithm was developed for asymptotic or numerical simulation of diffraction pattern of electromagnetic waves in multi-wave mode of reception on an infinitely extended object in free space, as well as a software method for calculating diffraction characteristics at frequencies exceeding the fundamental frequency, taking into account inhomogeneity of electromagnetic fields in these conditions. The developed methodology for researching characteristics of electromagnetic waves during diffraction of electromagnetic waves at objects can be used in design and development of radar systems capable of working adequately in the conditions of electromagnetic environment under consideration. Based on the provisions and conclusions, a software tool was developed. The results of the study can become the basis for development of means of electromagnetic compatibility of radar objects. Based on the recommendations developed in this study, new methods can be developed to improve the efficiency of radar systems.

5. REFERENCES:

1. Badylevich, M.V., Iunin, Yu.L., Kveder, V.V., Orlov, V.I., Osip'yan, Yu.A. *Journal of Experimental and Theoretical Physics*, **2003**, *97(3),* 601–605.
2. Bashly, P.N., Manuilov, B.D., Derkachev, K.V. *Journal of Communications Technology and Electronics*, **2017**, *1(62),* 41–47.
3. Daus, Yu.V., Kharchenko, V.V. *Applied Solar Energy*, **2018**, *54(1)*, 71–76.
4. Gatignol, P., Potel, C., Bedrici, N. Applied *Physics Letters*, **2010**, *96(4),* 044103.
5. Golovin, Yu.I. *Physics of the Solid State*, **2004**, *46(5),* 789–824.
6. He, B.-S., Zhang, H.-X., Han, L.-H., Zhang, J. *Oil Geophysical Prospecting*, **2008**, *43(6),* 656-661+684.
7. Immoreev, I.Y. *Radio engineering and electronics*, **2009**, *54*, 5–31.
8. Inverarity, G.W. *SIAM Journal on Scientific Computing,* **2003**, *24(2),* 645–651.
9. Kultin, N.B. *Bases of programming in Delphi Embarcadero*. Saint-Peterburg. Bkhv-Peterburg, **2015**.
10. Kurkchan, A.G., Manenkov, S.A., Negorozhina, E.S. *Journal of Communications Technology and Electronics*, **2016**, *3(61),* 224–233.
11. Li, G.-R., Wang, H.-M., Li, P.-S., Gao, L.-Z., Peng, C.-X., Zheng, R. *Acta Physica Sinica,* **2015**, 64(14), 148102.
12. Likhachev, V.P., Usov, N. Non-linear radar method. Patent RU2382380C1, **2010**. https://patents.google.com/patent/RU2382380C1/ru. Accessed 20 February 2019.
13. Loshilov, A.G., Bibikov, T.H., Semyonov, E.V., Malyutin, N.D. 22-th International Crimea Conference "Microwave and telecommunication technology", Sevastopol, Ukraine, **2012**.
14. Loshilov, A.G., Semenov, V.E., Malyutin, N.D., Misyunas, A.O., Iljin, A.A. *Papers of the Volume State University of control systems and radio electronics*, **2010**, *2(22), 1*, 166–170.
15. Morgunov, R.B. *Physics-Uspekhi,* **2004**, *47(2),* 125–147.
16. Orlov, A.M., Skvortsov, A.A., Solov'ev, A.A. *Journal of Experimental and Theoretical Physics*, **2003**, *96(3),* 523–530.
17. Orofino, D.P., Pedersen, P.C. *IEEE Transactions on Ultrasonics, Ferroelectrics, and Frequency Control,*

Downloaded from www.periodico.tchequimica.com

1993, *40(3),* 238–249.

18. Özdenvar, T., McMechan, G.A. *Geophysical Prospecting*, **1997**, *45(3),* 403-420.
19. Pichugin, V.N., Bugrova, I.G. *The study of diffraction of electromagnetic waves on the nonlinear scatterers.* Moscow. Scientific and information journal of the research Institute of education and science "Education. Science. Scientific personnel", **2013**.
20. Pichugin, V.N., Fedorov, R.V., Nemkova, M.P., Veryaskina, M.A. *Ecology, Environment and Conservation*, **2015**, *21*, AS1–AS5.
21. Pichugin, V.N., Pryanikov, V.S., Sedelnikov, Y.E. *Antenna array of slotted radiators in multiwave reception mode.* Cheboksary. Publishing house of the Chuvash University, **2013**.
22. Semyonov, E., Loschilov, A.G. Measurements of the nonlinearity is of the Ultra Wideband Signals Transformation. Rijeka. InTech, **2011**. https://www.intechopen.com/books/ultra-wideband-communications-novel-trends-system-architecture-and-implementation/measurements-of-the-nonlinearity-of-the-ultra-wideband-signals-transformation. Accessed 20 February 2019.
23. Skianis, G.A. *SpringerPlus*, **2014**, *3(1),* 729.
24. Skvortsov, A.A., Karizin, A.V. *Solid State Phenomena*, **2017**, *269*, 78–90.
25. Skvortsov, A.A., Orlov, A.M., Zuev, S.M. *Russian Microelectronics*, **2012**, *41(1)*, 31–40.
26. Yao, D.-Z., Ding, D.-H., Wang, R.-H., Hu, C.-Z. *Wuhan University Journal of Natural Sciences,* **2001**, *6(4),* 787–790.

$$\dot{\vec{E}} = \dot{\vec{E}}_0\left(\vec{x}_0\cos(\alpha_1) + \vec{y}_0\cos(\alpha_2) + \vec{z}_0\cos(\alpha_3)\right)e^{-i\kappa\left(x\cos(\gamma_1) + y\cos(\gamma_2) + z\cos(\gamma_3)\right)} \quad \text{(Eq. 1)}$$

$$\dot{\vec{H}} = \dot{H}_0\left(\sqrt{\frac{\dot{\mu}\mu_0}{\dot{\varepsilon}\varepsilon_0}}\right)^{-1}\left(\vec{x}_0\cos(\beta_1) + \vec{y}_0\cos(\beta_2) + \vec{z}_0\cos(\beta_3)\right)e^{-i\kappa\left(x\cos(\gamma_1) + y\cos(\gamma_2) + z\cos(\gamma_3)\right)} \quad \text{(Eq. 2)}$$

$$\left.\begin{matrix}\vec{H}=\vec{H}_{pad}+\vec{H}_{dif}\\ \vec{E}=\vec{E}_{pad}+\vec{E}_{dif}\end{matrix}\right\}\begin{cases}\vec{E} = -i\omega\mu_a\vec{A}^{\text{Э}} + \frac{1}{i\omega\varepsilon_a}grad\ div\ \vec{A}^{\text{Э}} - rot\ \vec{A}^{\text{М}}\\ \vec{H} = -i\omega\varepsilon_a\vec{A}^{\text{Э}} + \frac{1}{i\omega\mu_a}grad\ div\ \vec{A}^{\text{М}} - rot\ \vec{A}^{\text{Э}}\end{cases} \quad \text{(Eq. 3)}$$

$$\vec{A}(x,y,z) = \vec{A}(x,z)e^{-ip_0 y\frac{1}{a}} = \vec{A}(x,z)e^{-ip_0\frac{y}{a}} = \vec{A}(x,z)e^{-ik_0 a\sin\theta\cos\varphi_0 y\frac{1}{a}} = \vec{A}(x,z)e^{-ik_0\sin\theta\cos\varphi_0 y} \quad \text{(Eq. 4)}$$

$$p_0 = k\sin\theta\cos\varphi_0 = k_0 a\sin\theta\cos\varphi_0 \quad \text{(Eq. 5)}$$

$$\vec{A}\left(\frac{x}{a};\frac{z}{a}\right) = \frac{1}{2\pi}\int_{-\infty}^{\infty}\vec{a}_{\pm}(\varepsilon)e^{i(\varepsilon\frac{x}{a}\pm w\frac{z}{a})}d\varepsilon \quad \text{(Eq. 6)}$$

$$\vec{a}_{\pm}(\varepsilon) = \frac{1}{2}\frac{z_0}{iw}(\vec{J}^{m}(\varepsilon) \mp \overrightarrow{M}^{-1}[\vec{v}_0\vec{J}^{e}(\varepsilon)]) \quad \text{(Eq. 7)}$$

$$w = \sqrt{k^2 - \varepsilon^2 - {p_0}^2} \quad \text{(Eq. 8)}$$

$$w = \sqrt{k^2 - \varepsilon^2 - (k\sin\theta\cos\varphi_0)^2} \quad \text{(Eq. 9)}$$

$$\vec{A}(x,y,z) = \int_v \dot{\overrightarrow{J^{\text{ст}}}}(x',y',z')G(x,y,z,x',y',z')dx'dy'dz' \quad \text{(Eq. 10)}$$

$$G(x,y,z,x',y',z') = \frac{1}{(2\pi)^3}\iiint_{-00}^{00}\frac{e^{-i\gamma_1(x-x')-i\gamma_2(y-y')-i\gamma_3(z-z')}}{x_1^2+x_2^2+x_3^2-k^2}dx_1dx_2dx_3 \quad \text{(Eq. 11)}$$

Downloaded from www.periodico.tchequimica.com

$$\gamma = \sqrt{x_1^2 + x_2^2 - k^2} \quad \text{(Eq. 12)}$$

$$w = \sqrt{k^2 - \varepsilon^2 - p_0^2} \quad \text{(Eq. 13)}$$

$$-x_2 = \sqrt{x_1^2 + x_3^2 - k^2} = \gamma \quad \text{(Eq. 14)}$$

$$\frac{\partial^2 A}{\partial x^2} + \frac{\partial^2 A}{\partial y^2} + \frac{\partial^2 A}{\partial z^2} + k^2 A = \dot{\overrightarrow{J^{st}}} \quad \text{(Eq. 15)}$$

$$A(x,y,z) = X(x)Y(y)Z(z) \quad \text{(Eq. 16)}$$

$$\vec{A}(x,y,z) = \frac{1}{(2\pi)^3} \iiint_{-00}^{00} g(x_1,x_2,x_3)\, e^{-ix_1x - ix_2y - ix_3z} dx_1 dx_2 dx_3 \quad \text{(Eq. 17)}$$

$$Y(y), Z(z) = X(x) = \frac{1}{\sqrt{2\pi}} \int_{x_1=-00}^{00} g(x_1) e^{-ix_1x} dx_1 \quad \text{(Eq. 18)}$$

$$g(x_1,x_2,x_3) = -\frac{1}{(2\pi)^3} \iiint_{-00}^{00} \frac{j_{(x,y,z)}^{\text{CT}} e^{-ix_1x - ix_2y - ix_3z}}{k^2 - x_1'^2 - x_2'^2 - x_3'^2} dxdydz \quad \text{(Eq. 19)}$$

$$\frac{\partial^2 \vec{A}}{\partial x^2} + \frac{\partial^2 \vec{A}}{\partial y^2} + \frac{\partial^2 \vec{A}}{\partial z^2} + k^2 \vec{A} = -\dot{\vec{j}}^{st} \quad \text{(Eq. 20)}$$

$$A(x,y,z) = X(x)Y(y)Z(z) \quad \text{(Eq. 21)}$$

$$X(x) = \frac{1}{\sqrt{2\pi}} \int_{x_1=-00}^{00} g(x_1) e^{-ix_1x} dx_1 \quad \text{(Eq. 22)}$$

$$Y(y) = \frac{1}{\sqrt{2\pi}} \int_{x_2=-00}^{00} g(x_2) e^{-ix_2y} dx_2 \quad \text{(Eq. 23)}$$

$$Z(z) = \frac{1}{\sqrt{2\pi}} \int_{x_3=-00}^{00} g(x_3) e^{-ix_3z} dx_3 \quad \text{(Eq. 24)}$$

$$v_{av} = \frac{\omega}{x_1} \quad \text{(Eq. 25)}$$

$$\frac{\partial^2 \vec{A}}{\partial x^2} + \frac{\partial^2 \vec{A}}{\partial z^2} - \vec{A}(x,z) e^{-i\frac{p_0 y}{a}} \left(\frac{-ip_0}{a}\right)^2 + k_0^2 \vec{A}(x,z) - \dot{\vec{j}}^{\text{CT}} \quad \text{(Eq. 26)}$$

$$\frac{\partial^2 \vec{A}(x,y,z)}{\partial x^2} + \frac{\partial^2 \vec{A}(x,y,z)}{\partial z^2} - \vec{A}(x,z) e^{-i\frac{p_0 y}{a}} \left(k_0^2 - \left(\frac{p_0}{a}\right)^2\right) - \dot{\vec{j}}^{\text{CT}} \quad \text{(Eq. 27)}$$

$$\frac{\partial^2 \vec{A}(x,y,z)}{\partial x^2} + \frac{\partial^2 \vec{A}(x,y,z)}{\partial z^2} + \vec{A}(x,z) \frac{1}{a} \left(k_0^2 - {p_0}^2\right) = -\dot{\vec{j}}^{st} \quad \text{(Eq. 28)}$$

$$Z\left(\frac{\partial^2}{\partial x^2} + \frac{\partial^2}{\partial y^2} + k_0^2\right) XY + XY \frac{\partial^2}{\partial z^2} Z = 0 \quad \text{(Eq. 29)}$$

$$\frac{1}{XY}\left(Y \frac{\partial^2 X}{\partial x^2} + X \frac{\partial^2 Y}{\partial y^2} + k_0^2 XY\right) + \frac{1}{Z} \frac{\partial^2 Z}{\partial z^2} = 0 \quad \text{(Eq. 30)}$$

$$Y = A(x,z) e^{-i\frac{P_0 Y}{a}} \quad \text{(Eq. 31)}$$

$$\frac{1}{XY}\left(Y \frac{\partial^2 X}{\partial x^2} + XY\left(k_0^2 - \left(\frac{P_0}{a}\right)^2\right)\right) + \frac{1}{Z} \frac{\partial^2 Z}{\partial z^2} = 0 \quad \text{(Eq. 32)}$$

Downloaded from www.periodico.tchequimica.com

$$\frac{1}{XY}\left(Y\frac{\partial^2 X}{\partial x^2}+XY\left(k_0^2-\left(\frac{P_0}{a}\right)^2\right)\right)=-\frac{1}{Z}\frac{\partial^2 Z}{\partial z^2} \quad \text{(Eq. 33)}$$

$$\varepsilon^2=\Gamma^2 \quad \text{(Eq. 34)}$$

$$\begin{cases}\frac{1}{XY}\left(Y\frac{\partial^2 X}{\partial x^2}+XY\left(k_0^2-\left(\frac{P_0}{a}\right)^2\right)\right)=\varepsilon^2\\ -\frac{1}{Z}\frac{\partial^2 Z}{\partial z^2}=\varepsilon^2\end{cases} \quad \text{(Eq. 35)}$$

$$\begin{cases}Y\frac{\partial^2 X}{\partial x^2}+XY\left(k_0^2-\left(\frac{P_0}{a}\right)^2\right)=XY{\varepsilon_0}^2\\ \frac{\partial^2 Z}{\partial z^2}=-Z{\varepsilon_0}^2\end{cases} \quad \text{(Eq. 36)}$$

$$\begin{matrix}Y\frac{\partial^2 X}{\partial x^2}+XY\left(k_0^2-{\varepsilon_0}^2-\left(\frac{P_0}{a}\right)^2\right)=0\\ \frac{\partial^2 Z}{\partial z^2}+Z\varepsilon^2=0\end{matrix}; \quad \text{(Eq. 37)}$$

$$\begin{cases}\frac{\partial^2 X}{\partial x^2}+X\left(k_0^2-{\varepsilon_0}^2-\left(\frac{P_0}{a}\right)^2\right)=0\\ \frac{\partial^2 Z}{\partial z^2}+Z{\varepsilon_0}^2=0\end{cases} \quad \text{(Eq. 38)}$$

$$\begin{cases}w_0^2=k_0^2-\varepsilon_0^2-\left(\frac{P_0}{a}\right)^2\\ w=(k_0a)^2-(\varepsilon_0a)^2-(P_0)^2\\ w=k^2-\varepsilon^2-P_0^2\end{cases} \quad \text{(Eq. 39)}$$

$$\frac{\partial^2\vec{A}(x,y,z)}{\partial x^2}+\frac{\partial^2\vec{A}(x,y,z)}{\partial y^2}+\frac{\partial^2\vec{A}(x,y,z)}{\partial z^2}+k_0^2\vec{A}(x,y,z)=0 \quad \text{(Eq. 40)}$$

$$\vec{A}(x,y,z)=\vec{A}(x,z)e^{-\frac{ip_0y}{a}} \quad \text{(Eq. 41)}$$

$$\left(\frac{\partial^2}{\partial x^2}+\frac{\partial^2}{\partial z^2}\right)\vec{A}(x,z)e^{-\frac{ip_0y}{a}}-\vec{A}(x,z)e^{-\frac{ip_0y}{a}}\left(\frac{p_0}{a}\right)^2+k_0^2\vec{A}(x,z)e^{-\frac{ip_0y}{a}}=0 \quad \text{(Eq. 42)}$$

$$\left(\frac{\partial}{\partial x^2}+\frac{\partial^2}{\partial z^2}\right)\vec{A}(x,z)+\vec{A}(x,z)\frac{1}{a^2}(k^2-p_0^2)=-\vec{j}^{\text{CT}} \quad \text{(Eq. 43)}$$

$$k=k_0a \quad \text{(Eq. 44)}$$

$$\vec{A}(x,z)=\vec{X}(x)\vec{Z}(z) \quad \text{(Eq. 45)}$$

$$\vec{Z}(z)\frac{\partial^2\vec{X}(x)}{\partial x^2}+\vec{X}(x)\frac{\partial^2\vec{Z}(z)}{\partial z^2}+\vec{X}(x)\vec{Z}(z)\ \frac{1}{a^2}(k^2-p_0^2)=-\vec{j}^{st} \quad \text{(Eq. 46)}$$

$$Z\frac{\partial^2 X}{\partial x^2}+X\frac{\partial^2 Z}{\partial z^2}+XZ\ \frac{1}{a^2}(k^2-p_0^2)=0 \quad \text{(Eq. 47)}$$

$$\begin{cases}\frac{\partial^2 Z}{\partial z^2}+Z\frac{1}{a^2}(k^2-\varepsilon^2-p_0^2)=0\\ \frac{\partial^2 X}{\partial x^2}+X\frac{1}{a^2}\varepsilon^2=0\end{cases} \quad \text{(Eq. 48)}$$

$$u=\frac{x}{a} \quad \text{(Eq. 49)}$$

Downloaded from www.periodico.tchequimica.com

$$v = \frac{z}{a} \quad \text{(Eq. 50)}$$

$$\begin{cases} \frac{\partial^2 Z}{\partial v^2} + Zw^2 = -\vec{J}^{st} \\ \frac{\partial^2 X}{\partial u^2} + X\varepsilon^2 = -\vec{J}^{st} \end{cases} \text{k} \quad \text{(Eq. 51)}$$

$$w = \sqrt{k^2 - \varepsilon^2 - p_0^2}, \quad \text{(Eq. 52)}$$

$$\vec{X}(u) = \frac{1}{\sqrt{2\pi}} \int_{\varepsilon=-\infty}^{\infty} \vec{g}(\varepsilon) e^{-i\varepsilon u} d\varepsilon \quad \text{(Eq. 53)}$$

$$\vec{Z}(v) = \frac{1}{\sqrt{2\pi}} \int_{w=-\infty}^{\infty} \vec{g}(w) e^{-iwu} dw \quad \text{(Eq. 54)}$$

$$\vec{A}(u,v) = \frac{1}{2\pi} \int_{w=-\infty}^{\infty} \int_{\varepsilon=-\infty}^{\infty} \vec{g}(\varepsilon, w) e^{-i\varepsilon u - iwv}\, dw d\varepsilon \;\; (iu) \quad \text{(Eq. 55)}$$

$$k^2 = \varepsilon^2 + p_0^2 + \gamma^2 \quad \text{(Eq. 56)}$$

$$\gamma = \gamma_0, -\gamma^2 = w^2, \;\; w_1 = -i\gamma, \;\; w_2 = i\gamma \quad \text{(Eq. 57)}$$

$$L = \int_{w=-\infty}^{\infty} e^{-iwv} \vec{g}(w)\, dw \quad \text{(Eq. 58)}$$

$$\vec{A}(x,z) = \int_s \vec{J}^{\text{CT}}(x', z') G(x, z; x', z') dx' dz' \quad \text{(Eq. 59)}$$

$$\vec{A}(x,z) = \int_s \vec{J}^{\text{CT}}(x', z') G(x, z; x', z') dx' dz' \quad \text{(Eq. 60)}$$

$$-\frac{1}{2\pi} \iint_{-\infty}^{\infty} \dot{\overrightarrow{J^{st}}}(u, v)\, e^{i\varepsilon' u + iw' v} du dv = \iint_{-\infty}^{\infty} (k^2 - p_0^2 - \varepsilon^2 - w^2) g(\varepsilon, w) \delta(\varepsilon' - \varepsilon) \delta(w' - w) d\varepsilon dw \quad \text{(Eq. 61)}$$

$$-\frac{1}{2\pi} \iint_{-\infty}^{\infty} \dot{\overrightarrow{J^{st}}}(u, v)\, e^{i\varepsilon' u + iw' v} du dv = (k^2 - p_0^2 - \varepsilon^2 - w^2) g(\varepsilon', w') \quad \text{(Eq. 62)}$$

$$(k^2 - \varepsilon^2 - p_0^2 - w^2) g(\varepsilon, w) = -\frac{1}{2\pi} \iint_{-\infty}^{\infty} \vec{J}^{st}(u', v') e^{i\varepsilon u' + iwv'} du' dv' \quad \text{(Eq. 63)}$$

$$\vec{A}(u,v) = \int_s \vec{J}^{st}(u', v') G(u, v, u', v') du' dv' =$$
$$\int_s \vec{J}^{st}(u', v') \left(\frac{1}{(2\pi)^2} \iint_{-\infty}^{\infty} \frac{e^{i(u-u')\varepsilon - i(v-v')w}}{k^2 - \varepsilon^2 - p_0^2 - w^2} d\varepsilon dw \right) du' dv' \quad \text{(Eq. 64)}$$

$$L = -\int_{-\infty}^{\infty} \frac{e^{-i(v-v')w}}{(w - iw')(w + iw')}\, dw \quad \text{(Eq. 65)}$$

$$w' = \sqrt{k^2 - \varepsilon^2 - p_0^2} \quad \text{(Eq. 66)}$$

$$w' = \sqrt{\varepsilon^2 + p_0^2 - k^2} \quad \text{(Eq. 67)}$$

$$L_{(z-z')<0} = \int_\Gamma t(w) dw = \sum_{j=1}^{n} \int_{\gamma_j} f(w) dw + \int_{\gamma_R} f(w) dw \quad \text{(Eq. 68)}$$

$$\int_F f(w) dw = 2\pi i \left(\sum_{j=1}^{n} \underset{w=w_j}{res}\, t(w) + \underset{w=\infty}{res}\, t(w) \right) \quad \text{(Eq. 69)}$$

$$L_{(v-v')<0} = 2\pi i \underset{w=-iw'}{res} f(w) = \frac{\pi e^{-w'(v-v')}}{w'} \quad \text{(Eq. 70)}$$

Downloaded from www.periodico.tchequimica.com

$$G(u,v;u',v') = \frac{1}{4\pi}\int_{\infty} \frac{e^{-i(u-u')\varepsilon \pm w'(v-v')}}{w'} d\varepsilon \quad \text{(Eq. 71)}$$

$$\begin{cases} \vec{j}^{e}(u) = \frac{iw}{2\pi z_0}\widetilde{M}\left[\int_{-\infty}^{\infty}[\vec{v}_0\vec{a}_{+}(\varepsilon)]e^{i\varepsilon u}d\varepsilon - \int_{-\infty}^{\infty}[\vec{v}_0\vec{a}_{-}(\varepsilon)]e^{i\varepsilon u}d\varepsilon\right] \\ \vec{j}^{m}(u) = (-)\frac{iw}{2\pi z_0}\int_{-\infty}^{\infty}\left[\vec{v}_0[\vec{v}_0\vec{a}_{+}(\varepsilon)]\right]e^{i\varepsilon u}d\varepsilon - \frac{iw}{2\pi z_0}\int_{-\infty}^{\infty}\left[\vec{v}_0[\vec{v}_0\vec{a}_{-}(\varepsilon)]\right]e^{i\varepsilon u}d\varepsilon \end{cases} \quad \text{(Eq. 72)}$$

$$\begin{cases} (\pm)\frac{z_0}{iw}\widetilde{M}^{-1}\vec{j}^{e}(u)_{\pm} = \frac{1}{2\pi}\int_{-\infty}^{\infty}[\vec{v}_0\vec{a}_{\pm}(\varepsilon)]e^{i\varepsilon u}d\varepsilon \\ (-)\frac{z_0}{iw}\vec{j}^{m}(u)_{\pm} = \frac{1}{2\pi}\int_{-\infty}^{\infty}\left[\vec{v}_0[\vec{v}_0\vec{a}_{\pm}(\varepsilon)]\right]e^{i\varepsilon u}d\varepsilon \end{cases} \quad \text{(Eq. 73)}$$

$$\begin{cases} (\pm)\frac{z_0}{iw}\widetilde{M}^{-1}\int_{-1}^{1}\vec{j}^{e}(u)e^{-i\varepsilon' u}du = \int_{-1}^{1}\frac{1}{2\pi}\int_{-\infty}^{\infty}[\vec{v}_0\vec{a}_{\pm}(\varepsilon)]e^{i(\varepsilon-\varepsilon')u}dud\varepsilon \\ (-)\frac{z_0}{iw}\int_{-1}^{1}\vec{j}^{m}(u)e^{-i\varepsilon' u}du = \int_{-1}^{1}\frac{1}{2\pi}\int_{-\infty}^{\infty}\left[\vec{v}_0[\vec{v}_0\vec{a}_{\pm}(\varepsilon)]\right]e^{i(\varepsilon-\varepsilon')u}dud\varepsilon \end{cases} \quad \text{(Eq. 74)}$$

$$\frac{1}{2\pi}\int_{-\infty}^{\infty} e^{i(\varepsilon-\varepsilon')u}dud\varepsilon = \delta(\varepsilon-\varepsilon') = \begin{cases}\infty; at\ \varepsilon' = \varepsilon \\ 0; at\ \varepsilon' \neq \varepsilon\end{cases} \quad \text{(Eq. 75)}$$

$$\begin{cases} (\pm)\frac{z_0}{iw}\widetilde{M}^{-1}\int_{-1}^{1}\vec{j}^{e}(u)e^{-i\varepsilon' u}du = \int_{-1}^{1}[\vec{v}_0\vec{a}_{\pm}(\varepsilon)]\delta(\varepsilon-\varepsilon')d\varepsilon \\ (-)\frac{z_0}{iw}\int_{-1}^{1}\vec{j}^{m}(u)e^{-i\varepsilon' u}du = \int_{-1}^{1}\left[\vec{v}_0[\vec{v}_0\vec{a}_{\pm}(\varepsilon)]\right]\delta(\varepsilon-\varepsilon')d\varepsilon \end{cases} \quad \text{(Eq. 76)}$$

$$\vec{A}(u,v) = \frac{1}{2\pi}\int_{-\infty}^{\infty}\int_{-\infty}^{\infty} g(\varepsilon,w)e^{-iu\varepsilon - iwv}dwd\varepsilon \quad \text{(Eq. 77)}$$

$$L = \int_{-\infty}^{\infty}\frac{e^{-iwv}dw}{k^2-\varepsilon^2-p_0^2-w^2} = \int_{-\infty}^{\infty}\frac{e^{-iwv}dw}{(-)(w-iw')(w+iw')} \quad \text{(Eq. 78)}$$

$$t(z) = \sum_{n=0}^{\infty} C_n(z-a)^n \quad \text{(Eq. 79)}$$

$$C_n = \frac{1}{n!}t^n(a) \quad \text{(Eq. 80)}$$

$$C_n = \frac{1}{2\pi i}\int_{|\varepsilon-a|=\rho_1}\frac{t(\varepsilon)d\varepsilon}{(\varepsilon-a)^{n+1}} \quad \text{(Eq. 81)}$$

$$\left.\begin{matrix}\sum_{n=0}^{\infty} C_n(z-a)^n \\ \sum_{n=-1}^{-\infty} C_n(z-a)^n = \sum_{n=1}^{\infty}\frac{C_{-n}}{(z-a)^n}\end{matrix}\right\} \quad \text{(Eq. 82)}$$

$$\begin{cases} (\mp)\frac{z_0}{2iw}\widetilde{M}^{-1}\left[\vec{v}_0\left(\int_{-1}^{1}\vec{j}^{e}(u)e^{-i\varepsilon u}du\right)\right] = a_{\pm}(\varepsilon) \\ \frac{z_0}{2iw}\int_{-1}^{1}\vec{j}^{\text{M}}(u)e^{-i\varepsilon u}du = a_{\pm}(\varepsilon) \end{cases} \quad \text{(Eq. 83)}$$

$$a_{\pm}(\varepsilon) = \frac{z_0}{2iw}\left[\vec{j}^{\text{M}}(\varepsilon) \mp \widetilde{M}^{-1}[\vec{v}_0\vec{j}^{e}(\varepsilon)]\right] \quad \text{(Eq. 84)}$$

$$a_{\pm}(\varepsilon) = \left(\vec{a}^{\text{M}}{}_{\pm}(\varepsilon) + \vec{a}^{e}{}_{\pm}(\varepsilon)\right)\frac{1}{2} \quad \text{(Eq. 85)}$$

$$\vec{A}(u,v) = \frac{1}{2\pi}\int_{-\infty}^{\infty}\vec{a}_{\pm}(\varepsilon)\, e^{i\varepsilon u \pm iwv}d\varepsilon \quad \text{(Eq. 86)}$$

$$w_{\text{кр}}^{(n)} = \frac{n\pi}{d}\frac{c}{\sqrt{\varepsilon_1\mu_1 - G_2\mu_2}} = 2\pi f \quad \text{(Eq. 87)}$$

Downloaded from www.periodico.tchequimica.com

$$\left.\begin{array}{l}\vec{E}_t(x,y,{}^{+}0)=zz_0[\vec{v}_0,\vec{H}_t(x,y,{}^{+}0)]\\ \vec{E}_t(x,y,{}^{-}0)=zz_0[\vec{v}_0,\vec{H}_t(x,y,{}^{-}0)]\end{array}\right\} as\ |x|<a\ or\ |a|<1 \qquad \text{(Eq. 88)}$$

$$\begin{cases}\dfrac{1}{4\pi}\displaystyle\int_{-\infty}^{\infty}\left\{(Z\widetilde{M}+\widetilde{I})\vec{j}^{\,m}(\varepsilon)\right\}l^{i\varepsilon u}d\varepsilon=(-)2z\vec{H}_t^{\,u}\\ \dfrac{1}{4\pi}\displaystyle\int_{-\infty}^{\infty}\left\{(\widetilde{M}+Z\widetilde{I})\vec{j}^{\,l}(\varepsilon)\right\}l^{i\varepsilon u}d\varepsilon=-2[\vec{n}\vec{H}_t^{\,n}]\end{cases} \qquad \text{(Eq. 89)}$$

$$\begin{cases}\dfrac{1}{4\pi}\displaystyle\int_{-\infty}^{\infty}\vec{j}^{\,m}(\varepsilon)l^{\,i\varepsilon u}du=0\\ \dfrac{1}{4\pi}\displaystyle\int_{-\infty}^{\infty}\vec{j}^{\,l}(\varepsilon)l^{\,i\varepsilon u}du=0\end{cases} \qquad \text{(Eq. 90)}$$

$$\left[V_0\left(H_t^{pad}(u_2+0)-H_t^{pad}(u_2-0)\right)\right]=j_i(u) \qquad \text{(Eq. 91)}$$

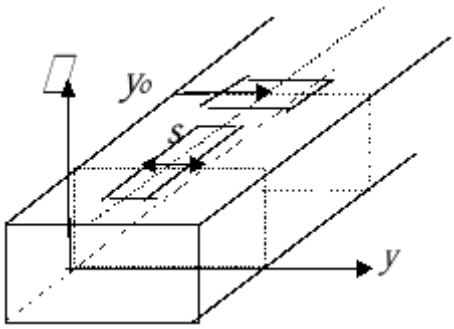

Figure 1. *Waveguide-slot type of radar system*

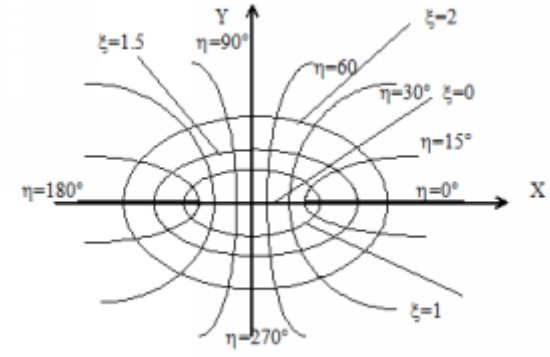

Figure 2. *The model of the antenna system (diffuser)*

Downloaded from www.periodico.tchequimica.com

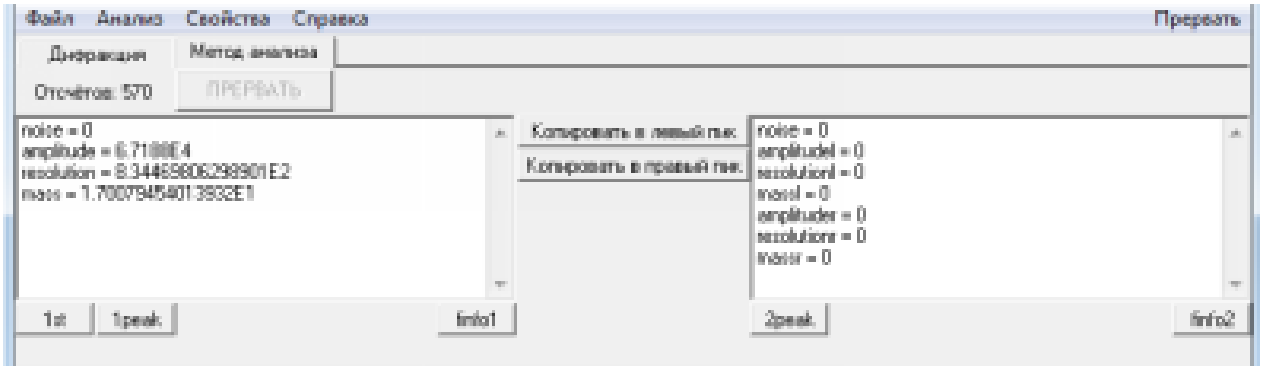

Figure 3. *Spectral Characterization Analysis Results*

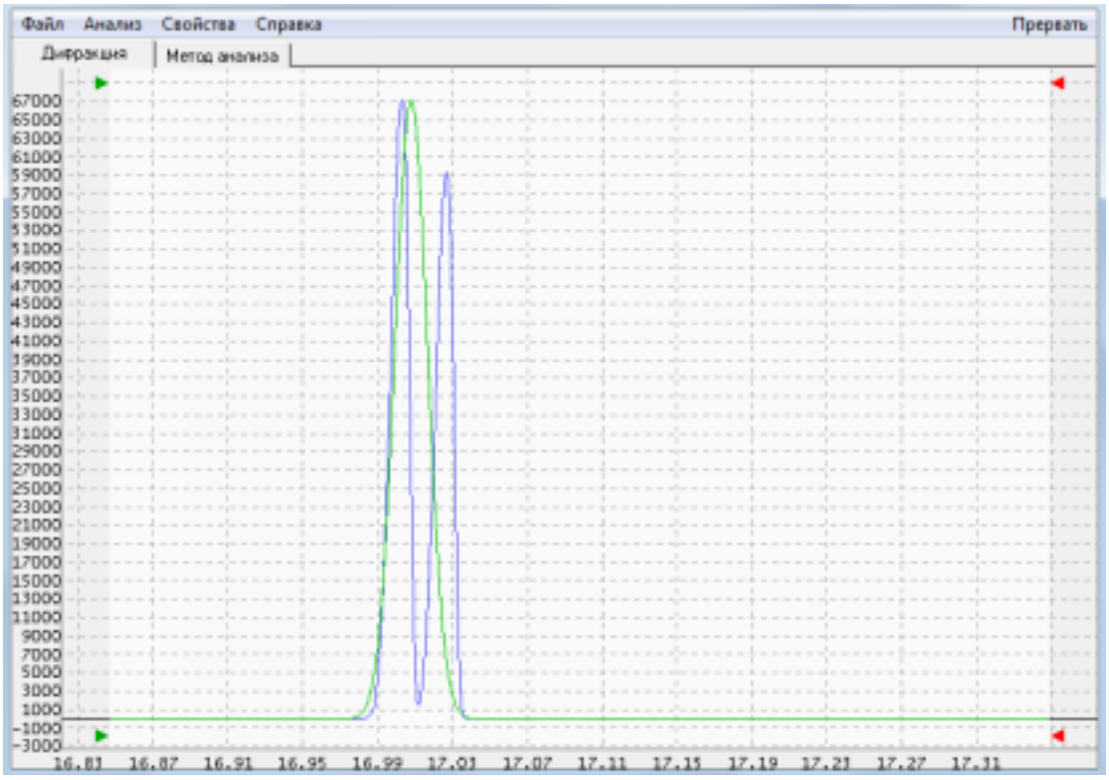

Figure 4. *The study of spectral characteristics in a software simulator*

PERIÓDICO TCHÊ QUÍMICA
ARTIGO ORIGINAL

ESTADO NO DOMÍNIO DOS REVESTIMENTOS RESISTENTES AO CALOR PARA LIGAS E AÇOS DE NÍQUEL À PROVA DE CALOR

STATE IN THE FIELD OF HEAT-RESISTANT COATINGS FOR HEAT-PROOF NICKEL ALLOYS AND STEELS

СОСТОЯНИЕ ВОПРОСА В ОБЛАСТИ ЖАРОСТОЙКИХ ПОКРЫТИЙ ДЛЯ ЖАРОПРОЧНЫХ НИКЕЛЕВЫХ СПЛАВОВ И СТАЛЕЙ

TERENTIEVA, Valentina S.[1]*; ASTAPOV, Alexey N.[2]; RABINSKIY, Lev N.[3];

[1,2,3] Moscow Aviation Institute (National Research University), Department of Advanced Materials and Technologies for Aerospace Application, Moscow – Russian Federation

** Correspondence author*
e-mail: k903ter@mai.ru

Received 30 August 2019; received in revised form 28 October 2019; accepted 28 October 2019

RESUMO

Atualmente, em muitos setores como, por exemplo, aviação, espacial (foguetes) e engenharia é dada atenção especial ao aumento das características táticas e técnicas dos produtos que estão sendo criados, aumentando sua confiabilidade e economia. A solução de problemas requer o uso de materiais que possam trabalhar em ambientes agressivos sob cargas pesadas, altas temperaturas, pressões e vibrações, o que determina a relevância do problema descrito no artigo. O objetivo do artigo foi realizar uma análise crítica de revestimentos desenvolvidos na Rússia com diversas características de composição, propriedades tecnológicas e operacionais, do ponto de vista da possibilidade de usá-los para fornecer um sistema confiável de proteção de material sob condições que causam corrosão por gás de alta temperatura e erosão da camada superficial. No trabalho foram considerados os principais métodos de proteção de materiais como pulverização térmica, pulverização a plasma, feixe de elétrons, pulverização por catodo de arco elétrico a plasma, deposição a vácuo, tratamento químico-térmico, revestimento por difusão à base de alumínio. Entre os métodos mais eficazes, destacaram-se o método de síntese autopropagável a alta temperatura, o método da química do plasma de alta energia e os métodos de deposição física no vácuo. Também foram destacados os tipos de revestimentos (de óxido, metálicos, intermetálicos, de esmalte de vidro, de vidro cristalino e vitrocerâmico) e suas características. Foi dada especial atenção aos revestimentos resistentes ao calor à base de esmaltes refratários uma vez que suas vantagens incluem baixo custo e a possibilidade de aplicá-los diretamente em peças sem *primers*, subpêlos, protetores. Foi identificada uma série de soluções técnicas que protegem as ligas da corrosão e erosão por gases de alta temperatura durante operações de longo prazo em produtos de aeronaves a altas temperaturas. Os resultados do artigo podem ser úteis para pesquisas posteriores, pois os desenvolvimentos individuais não são informativos do ponto de vista da solução de problemas específicos e exigem testes de bancada caros do resultado técnico declarado.

Palavras-chave: *resistência ao calor, revestimento, ligas de níquel, revestimentos vitrocerâmicos, tecnologias de aplicação.*

ABSTRACT

Currently, in many industries, special attention is paid to increasing the reliability and economy of the products. Solving problems requires the use of materials that can work in difficult conditions, which determines the relevance of the problem stated in the article. The purpose of the article was to conduct a critical analysis of coatings developed in Russia that are diverse in composition, technological and operational properties, from the standpoint of the possibility of using them to provide a reliable material protection system under conditions that cause high-temperature gas corrosion and surface layer erosion. The main methods of materials protection were considered in the work: thermal spraying, plasma spraying, electron beam, plasma electric arc cathode spraying, vacuum deposition, chemical-thermal treatment, diffusion coating based on aluminum. Among the more effective methods, the method of self-propagating high-temperature synthesis, the method of high-energy plasma chemistry, the methods of physical deposition in vacuum are noted. The types of coatings were also highlighted and their short characteristics were given. Particular attention was paid to heat-resistant coatings based on refractory enamels since their advantages include low cost and the possibility of applying them directly

Downloaded from www.periodico.tchequimica.com

to parts. A number of technical solutions have been identified that protect the alloys from high-temperature gas corrosion and erosion under long-term operation in aircraft products at high temperatures. The results of the article may be useful for further research since individual developments are uninformative from the standpoint of solving specific problems and require expensive bench testing of the claimed technical result.

Keywords: *heat resistance, coating, nickel alloys, glass-ceramic coatings, application technologies.*

АННОТАЦИЯ

В настоящее время во многих отраслях особое внимание уделяется повышению надежности и экономичности продукции. Решение проблем требует использования материалов, способных работать в сложных условиях, что и определяет актуальность проблемы, изложенной в статье. Целью статьи является проведение критического анализа разработанных в России покрытий, отличающихся по составу, технологическим и эксплуатационным свойствам, с точки зрения возможности их использования для обеспечения надежной системы защиты материалов в условиях, вызывающих высокую температуру. газовая коррозия и эрозия поверхностного слоя. В работе рассмотрены основные методы защиты материалов: термическое напыление, плазменное напыление, электронный луч, плазменное электродуговое катодное напыление, вакуумное напыление, химико-термическая обработка, диффузионное покрытие на основе алюминия. Среди наиболее эффективных методов отмечены метод самораспространяющегося высокотемпературного синтеза, метод химии плазмы высоких энергий, методы физического осаждения в вакууме. Также были выделены типы покрытий и даны их краткие характеристики. Особое внимание было уделено термостойким покрытиям на основе тугоплавких эмалей, поскольку к их преимуществам относятся низкая стоимость и возможность нанесения их непосредственно на детали. Был определен ряд технических решений, которые защищают сплавы от высокотемпературной газовой коррозии и эрозии при длительной эксплуатации авиационных изделий при высоких температурах. Результаты статьи могут быть полезны для дальнейших исследований, поскольку отдельные разработки являются неинформативными с точки зрения решения конкретных задач и требуют дорогостоящего стендового тестирования заявленного технического результата.

Ключевые слова: *жаростойкость, покрытие, никелевые сплавы, стеклокерамические покрытия, технологии нанесения.*

1. INTRODUCTION

Presently, in many industries (aviation, space, rocket, engineering), special attention is paid to increasing the tactical and technical characteristics of the products being created, increasing their reliability, resource, and economy. Solution of problems requires the use of materials capable of operating in various aggressive environments, under cyclic and alternating loads, high temperatures, pressures, vibrations, including when interacting with high-speed high-enthalpy flows of gases (air, fuel combustion products) (Tomarov and Shipkov, 2018).

High-temperature gas corrosion of nickel alloys and alloy steels is accompanied by the formation of scale on their surface, which is represented by phases of variable composition, as well as zones of inner oxidation under hardened layers (Burkov *et al.*, 2018). As a result, the de-alloying of alloys, especially those containing Nb, Mo, and W, takes place, and for steels, there is also decarburization. Changes in chemical composition, in turn, lead to deterioration in the mechanical properties of materials and their operational characteristics (Thomas *et al.*, 2018).

The problems are significantly aggravated by the using of alloys under the influence of high-speed flows of oxygen-containing gases (Astapov and Terentieva, 2014; Astapov and Terentieva, 2016; Terentieva and Astapov, 2018). As a result, their oxidation processes are significantly accelerated, which are accompanied by the destruction and delamination of formed oxide films and local plastic deformation of the surface layers. In supersonic and hypersonic flows, local gas corrosion and selective oxidation of individual alloy components are intensified, surface microrelief in the form of roughness, corrosion-erosion pits and caverns are more intensively developing, which, in turn, increases gas turbulence in boundary regions and erosive destruction of materials.

Protection of alloys from high-temperature gas corrosion and erosion using thin-layer heat-resistant coatings in many cases is the only possible way to realize their heat-proof characteristics and functional properties (Tomarov and Shipkov, 2018).

Downloaded from www.periodico.tchequimica.com

The requirements for protective coatings can be very diverse depending on the service time, which can range from a few seconds to thousands of hours, and on working conditions. Heat-resistant coatings, in addition to actually effective protection against oxidation and erosion, high physical and chemical compatibility with the base material, should have increased heat resistance and mechanical strength, and in addition, they should have low catalyticity and certain optical properties (radiation, reflection). The minimal catalytic activity on the surface at exothermic reactions of heterogeneous recombination of atoms and ions of high-speed flows reduces the chemical component of aerodynamic heating to the smallest value.

A high degree of blackness of the coating makes it possible to intensify the process of re-emission of the received heat into the surrounding space, which is important when organizing thermal protection systems for bodies of high-speed aircraft. While ensuring the thermal conditions of the flow paths of propulsion systems, the coating should have a high heat-reflecting ability in order to maximize heat dispersion through the material (Tomarov *et al.,* 2018).

Extensive literature, including inventions, articles, monographs (Astapov and Terentieva, 2014; Abraimov and Eliseev, 2001; Terentieva, 2008; Kablov *et al., 1999*; Gayamov *et al.,* 2014), is devoted to various types of heat-resistant coatings and methods for applying them to heat-proof structural materials, in particular, high-alloy chromium-nickel alloys and steels. It seems appropriate to make a critical analysis of coatings developed in Russia that are diverse in composition, technological and operational properties, from the standpoint of the possibility of using the accumulated theoretical knowledge and applied experience in relation to the tasks of providing a reliable protection system for the abovementioned structural materials under conditions that cause high-temperature gas corrosion and surface erosion layers (Astapov and Terentieva, 2016).

2. MATERIALS AND METHODS

2.1. Single-layer heat resistant coatings

Among the many single-layer heat-resistant coatings, oxide, metal, intermetallic and enamel coatings are widely used (mainly for protecting the blades of gas turbine engines (GTE) and for technological use) (Shao *et al*., 2019). Purely *oxide coatings* based on refractory oxides (Al_2O_3, Cr_2O_3, Y_2O_3, La_2O_3, MgO, BeO, ZrO_2, HfO_2, ThO_2 or a combination thereof), applied, as a rule, by various methods of thermal spraying, are not very promising due to the high brittleness of oxides, a significant difference in the thermos-physical characteristics of the base materials and coatings, which lead to cracking of the protective layer during quick changes in temperature, thermal cycling and thermal shock, and also due to absence of reserve component, providing restoration of the coating at in case of random defects (Astapov and Terentieva, 2016). At the same time, refractory oxides are widely used as an integral part of complex – multilayer, composite heat-resistant coatings, especially if needed, in addition to protection against high-temperature gas corrosion, to provide thermal insulation properties of the surface layers of the protected parts.

The use of single-layer *intermetallic* and/or *ceramic* oxygen-free compounds (aluminides, silicides, borides, carbides, nitrides) and their compositions as protective coatings is also unpromising for practically the same reasons. Due to the significant difference in temperature coefficients of the linear expansion of refractory oxides, high-temperature intermetallic compounds, ceramics, and protected structural materials, the coatings are in tension state after application. During the cooling process, a partial relaxation of tensile stresses occurs, which is accompanied by cracking. Mono-coatings, with the exception of enamel, are used mainly as functional layers in complex – multilayer, composite systems for protecting heat-proof alloys (Shao *et al.,* 2019).

Single-layer *metal* coatings (mainly in Me-Cr-Al-Y system, where Me is Ni, Ni-Co) are still used to protect GTE blades up to 1050-1100 °C. Since the 80s of the XX century, they have replaced traditional diffusion aluminide coatings, in which, at high temperatures, the “resorption” of diffusion layers occurs and the aluminum content is unacceptably reduced. Most of multicomponent coatings of this system (Abraimov, 1993; Abraimov and Eliseev, 2001; Abraimov and Geykin, 2018; Kolomytsev, 1979; Terentieva, 2008) are formed by methods based on the processes of vacuum physical evaporation of materials with their subsequent condensation (vacuum-arc, electron-beam, magnetron), as well as using plasma spraying methods.

2.2. Multilayer, composite heat-resistant coatings

The works (Muboyadzhyan, 2011; Kablov

Downloaded from www.periodico.tchequimica.com

et al., 1999; Kablov *et al.,* 2007), demonstrate the original technological processes developed at FSUE “VIAM” for producing ion-plasma diffusion, condensed and condensation-diffusion coatings for protecting nickel blade alloys from high-temperature gas corrosion in the temperature range of 1000-1100 °C and 1100-1200 °C. For complex alloying of ion-plasma diffusion coatings, the deposition of condensed nickel-based sublayers is proposed. Alloying elements included in the nickel sublayer should modify the coating, and the sublayer becomes an obstacle to the dissolution of refractory alloy elements in the diffusion coating layer. In some cases, thin (~ 3–5 μm) anti-diffusion barrier layers of metal carbides are used, made, for example, by high-energy plasma chemistry (Muboyadzhyan *et al.,* 2010; Muboyadzhyan, 2010; Muboyadzhyan, 2011; Kablov *et al.,* 2007). It was mentioned that condensation-diffusion coatings have significantly higher protective properties compared to conventional condensed coatings. Nonetheless, they provide no information about their properties, except for the extreme temperature range of their protective ability (1000-1200 °C).

The authors of work (Poklad *et al.,* 2010) mention that the combined use of two or more technologies makes it possible to more successfully solve the problems of increasing the operability of heat-resistant coatings of Ni(Co)-Cr-Al systems up to 1200 °C. This is connected to the expansion of the usability of complex alloying with refractory elements (Ta, Re, W), effectively inhibiting the diffusion "resorption" of coatings, and micro additives (Y, La, Ce, Hf, Si), thus increasing their functional properties. The concentration limits of the content of the elements in high-temperature coatings of this system are provided.

Of interest is the information (Samoilenko, 2006) on the effect of various elements involved in mutual diffusion in the systems “nickel alloy – aluminide coatings (complex, conditioned, combined)” on the destabilization of chemical and phase compositions of coatings, their structure and, as a consequence, on the decrease of protective resource. The conclusions that were made confirm the need to suppress diffusion processes between a heat-resistant coating and a protected heat-proof alloy. For these purposes, coatings are alloyed with elements that, being in β- or γ ′ -phase, impede diffusion processes, or participate in formation of inner coating zone containing carbides and intermetallic compounds that impede mutual diffusion of the elements. A similar effect is made by diffusion barrier layers created in the surface layers of the protected alloys with a purpose to inhibit diffusion into the coating of refractory elements (Mo, Nb, V, Ta). The latter, entering the coating, reduce protective properties of the oxide film, lead to the loss of Al and, thereby, significantly reduce stability of the β phase and durability of the protective systems. This circumstance lets us conclude that stability of β-phase can be rather effectively controlled by targeted alloying and the creation of barrier layers, thereby solving the problem of increasing the mechanical properties of coatings while maintaining high resistance to gas corrosion and surface erosion.

2.3. Heat-resistant coatings

Attention to heat-resistant silicate enamels in aeronautical engineering is primarily conditioned by fact that, characterized by a simple formation technology and low cost, many of them can provide antioxidant protection and special surface properties (erosion resistance, anticatalyticity, emissivity) of elements of heat-loaded structures from heat-proof materials in a fairly wide temperature range. Another advantage of enamel coatings is the possibility of applying them directly to parts without any primers, undercoats, protectors.

Almost all enamels are applied by slip technology from pre-melted frits – oxide alloys synthesized at high temperatures (from 800-1000 °C for low-melting compositions, 1200-1400 °C – for medium-melting compositions and up to 1600-1650 °C – for refractory). The technological process of enameling is established (Vargin *et al.,* 1958; Solntsev and Tumanov, 1976; Solntsev, 1984; Appen, 1974; Appen, 1976) and includes:

- preparation of slip suspension (slip);
- surface preparation of protected material (degreasing, hydro-sandblasting, etching in a soda bath);
- applying of slip (with a spray gun, dipping, dousing or brush);
- drying of layer (air or oven at 50-100 °C);
- heat treatment (firing) with a purpose to reflow the enamel and firmly fix it on the surface of the product. In case of defects, the burnt enamel is removed (by sandblasting, etching in an alkaline bath), and after that, the enameling process is repeated.

Frit compositions for enamel coatings used to protect steel and nickel alloys from high-temperature gas corrosion which are produced in

Downloaded from www.periodico.tchequimica.com

Russia, the USA, Japan, France, Germany, and other developed countries, as a rule, range within the following limits in terms of the content of the main components, mass. %: SiO_2 – 25÷85, BaO – 20÷50, B_2O_3 – 0÷20, Al_2O_3 – 0÷5, MgO – 0÷3, CaO – 0÷5 (Solntsev, 1984). To improve the adhesive properties of formed coatings, the so-called adhesion oxides — CoO, NiO, MoO_3 — are introduced into the frits in small amounts. With the purpose to increase the functional characteristics of coatings (chemical resistance, resistance to erosion, degree of blackness, heat-reflecting ability), fillers are included (Cr_2O_3, Al_2O_3, TiO_2, ZrO_2, CeO_2, $ZrSiO_4$, SiB_4, SiC) through the mixture for welding upon receipt of the frit or in the form of mill additives in the preparation of the slip. Depending on the chemical and physical-mineralogical composition, glass-enamel (glassy), glass-crystalline (glass-metal) and glass-ceramic coatings can be distinguished.

3. RESULTS AND DISCUSSION

3.1. Research on single-layer heat resistant coatings

The advantages and disadvantages of vacuum spreading methods are quite fully presented in studies (Kablov *et al.,* 1999; Muboyadzhyan, 2010), the authors of which, on the basis of comparative multi-parameter analysis, demonstrated that the most preferred method (in terms of the combined parameters of density, adhesion, structural perfection of coatings combined with simplicity and reliability of equipment, performance, and process accuracy) is the vacuum-arc evaporation of alloys. Another step forward was the original high-energy ion-plasma technology developed at FSUE “VIAM” and the creation of ion-plasma systems MAP-1M, MAP-2, MAP-3. A significant amount of developed thin-layer ion-plasma diffusion, condensed, and condensation-diffusion coatings for protecting turbine blades from high-temperature gas corrosion using this method is presented in literature (Muboyadzhyan *et al.,* 2010; Muboyadzhyan, 2011; Kablov *et al.,* 1999; Kablov *et al.,* 2007). The main chemical systems with these coatings, their abbreviations and applications are given in works (Muboyadzhyan, 2011; Kablov *et al.,* 1999; Kablov *et al.,* 2007).

The monographs (Abraimov, 1993; Abraimov and Eliseev, 2001; Abraimov and Geykin, 2018; Kolomytsev, 1979; Terentieva, 2008) describe the most significant theoretical and experimental data obtained by Russian and international researchers in the process of developing protective coatings mainly for nickel-blade alloys. Attention is directed to the technology for producing diffusion coatings, which, according to the authors, will remain the most common for a long time. These coatings include, primarily, the technologies of powder and slip alitization, chromoalitization, aluminosilication, characterized by simplicity and economy. While they are used as basic ones, a large number of new coating compositions have been created in which Al and Cr remain the main alloying elements. They are present in almost all high-temperature coatings since they provide the formation of oxide film with high protective properties. The compositions of many coatings include one or more microalloying elements (Hf, Zr, Y, La, Ce, Yb), designed to improve the adhesive ability of protective films. In order to increase the thermochemical stability, metal coatings are alloyed with refractory elements (Ta, Re, Ru, Nb, W), which inhibit the diffusion "resorption" of protective layers.

A brief review of Russian materials for making single-layer condensed coatings and developed abroad (grades, chemical composition) is given in (Terentieva, 2008). Condensed coatings of the same chemical systems as diffusion ones have better properties in general since the method opens up the possibility of producing coatings of a given composition with a constant or specified distribution of alloying elements in thickness.

The use of nickel, cobalt, iron, or combinations thereof, as well as a set of alloying elements, as a basis for coatings of the Me-Cr-Al-Y system, depends on the purpose of the coatings, the material of the parts to be protected, and their operational conditions. An analysis of literature in the field of development of heat-resistant coatings for the protection of parts made of heat-proof nickel alloys and steels shows that a positive solution to the problem is usually associated with an individual approach to both the choice of coating composition and method of its formation, even within the same method. Thus, it makes no sense to consider the countless number of developed compositions of heat-resistant coatings and methods for their application from the standpoint of applicability or improvement. But attention should be paid to practicability of choosing a basic system and concentration ratio of the components of protective coatings. Therefore, from analysis of general characteristic of the properties of electron-beam coatings of Me-Cr-Al-Y systems

Downloaded from www.periodico.tchequimica.com

(Me – Ni, Co, Fe and their combination) (Terentieva, 2008) it follows that coatings have the highest protective ability on blade nickel alloys (type ZhS_6U) Ni-Cr-Al-Y, and the maximum heat resistance and high ductility are found in Ni-Co-Cr-Al-Y coatings. Coatings of Fe-Cr-Al-Y system are, usually, unstable on nickel alloys and are not recommended for use. 37% Cr in coatings of the Co-Cr-Al system is seen as a threshold concentration at which reliable protection of nickel alloys from gas corrosion is ensured for a wide temperature range. Small additives Y, Hf, Si significantly improve protective ability of coatings (Ni, Co)-Cr-Al, but their number also has its limits, for example, in Co-Cr-Al-Y – no more than 0.2-0.3% for reasons of maintaining sufficient ductility (Terentieva, 2008).

Followers of the school of Kolomytseva P.T. still continue to develop and improve heat-resistant protective coatings obtained by chemical-thermal treatment by powder mixtures and diffusion saturation in circulating gas medium (Abraimov, 1993; Abraimov and Eliseev, 2001; Abraimov and Geykin, 2018). The patents (Arzamasov *et al*., 2006; Eliseev *et al.,* 2007) offer methods for the formation of thin-layer (30–40 μm) of chromoaluminide coatings on the ZhS_6U alloy in a circulating halide medium using different sources of diffusing elements and different technological methods for chromoalification.

Various techniques are included in technological cycle of producing aluminide coatings (Eliseev *et al.,* 2003a; Eliseev *et al.*, 2003b; Eliseev *et al.,* 2003c; Eliseev *et al.,* 2007): changing the chemical composition of successively applied layers, using pre-melted ingots of special alloys, from which transition coating layers are formed by various spraying methods. At the same time, it is mentioned that, due to the shortcomings of the methods of electron beam, plasma and electric arc cathode sputtering from ingots (high porosity of the resulting coatings and the unevenness of their thickness, especially on complex parts), diffusion coatings based on aluminum are preferable, in particular: gas, or slip, or powder alitization, chromoalation, aluminosilicon.

In (Levashov *et al.,* 2009), an effective method was proposed for increasing the life of blades made of ZhS_6U alloy by applying electro spark alloying coatings using a KhTN-61 alloy made by self-propagating high-temperature synthesis to form a coating from consumable electrode. The phase composition of the coatings after one minute of treatment according to the given optimal regime is: cobalt-based solid solution and double carbides (Nb, Ti) C and (Mo, Ti) C. The presented test results show that this method of coating formation allows the creation of high-quality multifunctional antifriction alloys on the ZhS_6U alloy (decrease in the friction coefficient by 5 times), wear-resistant (increase in wear resistance by more than 10 times), including layers with increased hardness (at thickness of 40 μm H_μ = 5.2 GPa). Despite the effectiveness of the considered method, a significant increase in the wear resistance, hardness, and antifriction of the resulting coatings, it remains doubtful that with this phase composition it is possible to provide protection against high-temperature gas corrosion even at moderately high temperatures.

The significant disadvantages of most diffusion saturation methods include prolonged exposure to high temperatures (1050–1230 °C) (Abraimov and Eliseev, 2001) during the formation of coatings of optimal thicknesses (80–100 μm), which cannot but adversely affect the structure stability of the protected nickel alloys, and, therefore, its properties. Moreover, it is very problematic to use these methods on "delicate" thin-walled structural elements of the flow paths of propulsion systems, which, as a rule, have complex geometry of surfaces to be protected and sufficiently large overall dimensions.

Enamel coatings are discussed in another section of this article. The developers of almost all single-layer coatings, including the above-mentioned coating, in their subsequent publications, state that two-, three-stage, mainly multilayer, complex, combined composite heat-resistant coatings have the best protective properties. They are obtained in various ways, within the same method – condensation (using electron beam, cathode, plasma, laser, and other technologies), diffusion (powder, slip, gas technologies), and by a combination of different methods and specific technics.

3.2. Specifics of multilayer, composite heat-resistant coatings

The work (Kablov *et al.,* 2007) shows the advantages and possibilities of using high-energy ion-plasma technology for applying protective and hardening multicomponent coatings based on industrial application experience for this technology. The features of ion-plasma multicomponent condensed coatings of Ni(Co, Ni-Co)-Cr-Al-Y systems developed at the VIAM Federal State Unitary Enterprise are highly dispersed structure in the initial state (~ 0.1 μm), high adhesion (> 100 MPa), high deposition

Downloaded from www.periodico.tchequimica.com

accuracy and relatively low cost. Depending on the composition, they can provide at a minimum thickness of about 50 μm long protection blade alloys from hot gas corrosion up to temperatures of 800-1100 °C. Coatings are successfully used both as independent protection since they have a minimal effect on the mechanical characteristics of the base material, and as a part of sublayers for air-diffusion and heat-protective coatings. For example, a recent report (Smirnov and Budinovsky, 2017) about a significant increase in service characteristics of the currently used heat-resistant condensation-diffusion coatings of composition Ni-Cr-Al-Ta-Re-Y-Hf + Al-Ni-Y to protect the widely used heat-proof blade alloy ZhS_{32} by creating an internal nitride barrier layer by ion-plasma technology at MAP-2 installation. A similar positive effect was obtained by the authors of works (Gayamov *et al.,* 2014) when creating heat-resistant ion-plasma coatings for Al-Ni-Cr-Y system with a sublayer formed from the heat-resistant alloy of the Ni-Cr-Al-Ta-Hf-Re-Y system due to the formation of a thin barrier layer containing tantalum carbide particles.

Worthy of attention are the works (Kuznetsov *et al.,* 2007; Kuznetsov *et al.,* 2011; Lesnikov *et al.,* 2012) devoted to the creation of a coating system for protection against high-temperature gas corrosion of internal cavity and external path surface of single-crystal high pressure turbine blades (HPT) of modern gas turbine engines made of carbon-free heat-proof alloys with a high content of refractory elements (Re, Ru, Ta). A particularity of these blades is the “openwork” design with a complex system of internal cavities and perforations with a size of ~ 0.5–1.0 mm. The temperature of the outer and inner surfaces of the HPT blades varies around 250-300 °C, and the temperature of the outer path surface 1150-1250 °C. The authors believe that the solution of such complex problems is possible only by combining various methods and technologies of coating formation (gas circulation, thermal diffusion saturation, high-energy ion-plasma technology, reactive deposition during magnetron evaporation). They introduce the developed diffusion-condensation coating, formed by sequential alitization, then applying the chromium-aluminum layer by the gas circulation method, then the main layer, consisting of β-phase (Ni, Co) Al with a high Al content and alloyed 1 at.% Cr ion-plasma technology. It is stated that at present, gas circulation coatings are the most effective and, in fact, the only ones for protecting the internal cavity and perforations of cooled HPT blades. To protect the external tract surface, an ion-plasma coating of the Al-Ni-Cr-Y system has been developed. The temperature-time resource of the HPT blades protected by this complex coating is estimated as – 1150 °C, 1000 h.

The research results presented in work (Kachalin and Mednikov, 2013) show the possibility of creating heat-resistant nanostructured coatings on the details of the gas paths of aviation and space technology using physical methods of deposition in vacuum, in particular, the magnetron method in forming such coatings. It is stated that recently heat-resistant and erosion-resistant nanostructured coatings have been developed that not only protect chrome-nickel alloys from high-temperature gas corrosion at temperatures above 1000 °C but also have resistance to shock dynamic effects. It is stated that to ensure the long-term performance of the blades at t > 1000 °C, combined diffusion-conditioned multilayer coatings (based on the Ni-Cr-Al-Si-O system) containing a barrier sublayer of Ni-Cr-Al-Si nano-layer structure have been developed, inhibiting the diffusion of atoms at the boundary with the protected alloy and, thus, stabilizing the main phase of NiAl for a sufficiently long period. The addition of oxygen during the magnetron sputtering of Ni-Cr-Al-Si (or Cr-Al-Si) material helps to obtain heat-resistant protective coatings based on oxides of the mentioned systems. The structure of the coatings is a combination of microlayers with sizes from 0.5 to 3–4 μm; each of them consists of nano-layers with sizes from 20 to 40 nm. The static heat resistance of structural alloys (for example, EI652, EP693) with these coatings in the air of a chamber laboratory furnace at t = 1050 ° C, 50 hours increases by no less than 4-5 times. The test results of samples of EP693 alloy with the same coating for drop-impact erosion (droplet diameter of 800 μm, collision velocity of 250 m/s) demonstrated that no ablation occurs in the first 500-600 min, i.e. the duration of the incubation period of the ablation of the mass of the alloy protected by the coating increases by 4-6 times.

Thus, the results of numerous studies have shown that the main trends in improving heat-resistant coatings are: 1. transition from single-layer to two- and multilayer coatings, which, along with the heat resistance, make it easier to provide the required set of properties (anti-erosion, wear-resistance, tribological, special); 2. creation of diffusion barriers, since the main mechanism for the exhaustion of protective properties of coatings at high temperatures is diffusion process in the systems with “substrate-

Downloaded from www.periodico.tchequimica.com

coating" and "coating-environment".

At the same time, a large reserve remains in the use of layers of heat-resistant ceramic compounds in the coating structure. There are also promising, but still weak, attempts to use nanotechnology in the development of coatings, the development of which currently goes in two ways: the creation of nanostructured coatings (with the size of individual grains in the range of 1–100 nm in three directions) and nano-layer structures with thickness of each layer within nanometer range.

3.3. Heat-resistant coatings based on refractory enamels

A wide range of enamel resource coatings has been developed to ensure the performance of materials in question at temperatures of 900-1100 °C for a long time and 1200 °C for a short time, including operation in high-speed aggressive gas flows. Among these developments, the majority belongs to heat-resistant coatings for effective protection of parts and assemblies of gas turbine engines and turbo-pump units (Solntsev *et al.,* 2001; Solntsev *et al.,* 2002; Solntsev *et al.,* 2004b; Solntsev *et al.,* 2006; Solntsev *et al.,* 2008; Solovieva *et al.,* 2009; Kablov *et al.,* 2016); some technical solutions aimed at increasing the reliability of the structural elements of liquid rocket engines (for manned and cargo spacecraft, strategic ballistic missiles, space stations) (Solntsev, 2009; Prilepsky *et al.,* 1993); there are practically no developments in the field of protection of heat-loaded parts of gliders of hypersonic aircraft and their propulsion systems (Astapov *et al.,* 2019a). The latter, first of all, is caused by temperature-time factors, significantly limiting the possibility of applying traditional structural materials in so-called hot structures. They are usually made of more heat-proof materials – alloys based on refractory metals (Nb, Mo, W), graphites, carbon composites (Astapov and Rabinskiy, 2017; Yurishcheva *et al.,* 2018; Astapov *et al.,* 2019e; Astapov and Terentieva, 2014; Astapov and Terentieva, 2016; Terentieva and Astapov, 2018) and high-temperature ceramics (Astapov *et al.,* 2019b; Astapov *et al.,* 2019c; Astapov *et al.,* 2019d). Though, the problem of ensuring the short-term performance of steels and nickel alloys at temperatures of 1250-1350 °C under the influence of high-speed flows (air, fuel combustion products) remains extremely important.

Known enamel coating (Solntsev *et al.,* 2001), designed to protect high-temperature nickel alloys from destruction from high-temperature gas corrosion in a high-speed gas stream during operation. The coating contains SiO_2, B_2O_3, Al_2O_3, BaO, CaO, MgO, TiO_2, Cr_2O_3 as well as mineral complex compound based on SiO_2. The coating is formed using slip-firing technology, heat treatment is done at a temperature of 1100-1200 °C for 2-5 minutes. The authors declare a significant increase in properties for heat-proof nickel alloys protected by this kind of coating at working temperatures of 1100 °C and higher, namely: heat resistance more than 10 times at 1100 °C, heat resistance 4 times at $1100 \leftrightarrow 20$ °C and 9 times at $1200 \leftrightarrow 20$ °C, the expansion of effective softening range of more than 150 °C. Unfortunately, it is not indicated under what conditions all the above characteristics of the properties are obtained. Apparently, it was tested in thermal furnaces under conditions of natural air convection, since there is no information about the influence of high-speed flows of hot gases on the structure and properties of coatings.

Later, the same authors patented a different composition (Solntsev *et al*., 2002) of an effective glass-enamel coating for protection of heat-proof alloys from destruction under conditions that cause gas corrosion. The advantages include a decrease in temperature of coating formation to room temperature, an increase in continuity (by 6-10%), heat resistance (by ~ 1.5-2 times) and heat resistance at temperatures exceeding 1000 °C (more than 10 times), which is confirmed by experimental data. Since the coating is formed at room temperature, it can be used not only as a resource but also as a repair tool with the possibility of application in field (airfield, polygon) conditions.

Glass-crystal coatings, in comparison with glass-enamel ones, have higher protection properties (Solntsev, 2009). Coatings of this group are characterized by a high degree of cohesion of silicon-oxygen framework, and, as a consequence, have enhanced characteristics of heat resistance, temperature resistance, and thermodynamic stability in aggressive environments containing abrasive particles.

In work (Solntsev, 2010), it is reported that for a wide range of parts made of heat-proof alloys (combustion chambers, afterburners, heat pipes, stabilizers), a series of glass-crystal coatings (EVK-103, EVK-103M, EVK-112, EVK-75, EVK-127), stable in high-speed gas flows at temperatures of 900-1000 °C for a long time and 1200 °C for a short time. These coatings are characterized by strong adhesion to the surface

Downloaded from www.periodico.tchequimica.com

of alloys, bulk micro-crystallization, gas density, strong chemical bonding, high heat and heat resistance characteristics. Publication (Solntsev *et al.,* 2014), presents a glass-crystal coating of EVK-104M with system SiO_2-BaO-B_2O_3-Al_2O_3. The coating is operational for a long time ineffective protection of parts from high-temperature gas corrosion at higher extreme temperatures (1050 °C for a long time) and, like the previous ones, up to 1200 °C for a short time (when temperature peaks). The use of coating can significantly reduce the rate of oxidation of alloys (on VZh159 alloy – by 5-8 times).

In work (Denisova, 2018), new high-temperature glass-ceramic coatings based on the refractory frits of the BaO-Al_2O_3-SiO_2 system and silicon tetraboride SiB_4 are presented. It was declared that in terms of a combination of operational properties and advantages in application technology, they surpass domestic and foreign counterparts. Additive SiB_4 brings the temperature of formation of coatings closer to the temperatures of operation. The results of experimental verification indicate that they can provide effective protection of nickel alloys and heat resistant steels against high-temperature gas corrosion and ignition up to 1250 °C for more than 100 high performance of glass-ceramic coatings in strong oxidizing environments is associated with amorphous structure of their matrices, optimization of the ratio of refractory ceramic particles and glass-forming components, and the presence of bulk micro crystallization.

In works (Solntsev, 2009; Solntsev, 2014), the possibilities of using theoretical experience obtained at the "VIAM" Federal State Unitary Enterprise on example of development of reaction-curable thermoregulating erosion-resistant coatings for reusable thermal protection of materials (quartz tiles) of the Buran reusable spacecraft were demonstrated. Using silicon tetraboride (SiB_4) and silicon hexaboride (SiB_6) in the development of temperature-controlled firing “black” coatings formed as a result of chemical reactions between atmospheric oxygen, borides and high-silica matrix glass, provided the necessary complex of functional properties at operational temperatures up to 1250 °C: high degree of blackness ($\varepsilon \geq 0.9$), low catalyticity of the surface (constant of velocity of heterogeneous recombination of atoms $K_w \sim 1$ m/s), very high characteristics of heat resistance, thermostability and thermoelasticity.

Promising are some concepts based on the use of refractory oxides and more complex synthetic compositions of oxygen-free ceramics, and oxides having a common structure-forming component. As such components, Si, B, and other elements can be used. When protecting thin-walled parts of complex configuration, arises a problem of lowering the temperature of coating formation while maintaining the basic operational properties. In work (Solntsev *et al.,* 2004a), to solve the problem it was proposed to use the reaction curing effect when chemically active components (borides and fusible borosilicate glasses) are introduced into silicate systems. The latter can actively interact with components of the silicate system with the formation of liquid borosilicate phase, which bonds the particles of the refractory phase and promotes the relaxation of thermoelastic stresses. Such coatings are formed over a wide temperature range of 1120-1160 °C. The effectiveness of their protective action is not worse than that of glass-crystal coatings. In (Solntsev *et al.,* 2004a), a comparative analysis of the averaged properties of glass enamel, glass crystalline, refractory, and reaction-cured coatings was carried out. The presented data indicate that, according to the combined criteria of formation temperature, heat resistance (1000-1100 °C ↔ 20 °C mode) and time to failure in a gas stream at 1000, 1100, 1200 °C, refractory coatings are in the lead, and the properties of glass-crystalline and reaction-cured coatings are almost the same.

The authors of the patent (Prilepsky *et al.,* 1993) developed a glass-ceramic coating with a favorable set of properties for protection of alloy steel products working in high-temperature gas flow conditions, with high surface blackness values (ε = 0.78-0.84), and heat resistance (600-950 h at 1000 °C) and temperature resistance (920 ↔ 20 °C 500-1000 heat exchange). The protective capacity of the coating is provided by its composition, which, in addition to oxides SiO_2, TiO_2, Al_2O_3, Cr_2O_3, CaO, BaO, MnO, CoO, MoO_3, contains oxygen-free compounds SiC and SiB_4. The latter are introduced in order to increase the service life and emissivity. The thin-layer coating (40–60 μm) is applied in the form of an aqueous slip layer, which is then briefly burned at temperatures of 1130-1200 °C. Also, the coating has a favorable set of technological properties – opacity, wetting ability, continuity, strong adhesion to the base. In conditions of interaction with high-speed gas flows, the coating loses its working capacity at temperatures above 1200 °C. This is because of the transition of coating to a viscous-fluid state, in which the resistance to mechanical entrainment (erosion) is significantly weakened, which leads either to formation of a wavy (different thickness) surface with local

Downloaded from www.periodico.tchequimica.com

defects, or to partial or complete runoff of the coating, or to its blowing off, i.e. to expose the substrate.

The authors of this invention were able to solve these problems (Astapov *et al.,* 2019a) by applying a coating layer 60–70 μm thick over the specified coating, containing, in addition to the previously considered components, an additional mill additives Al_2O_3 and Cr_2O_3. In the process of formation, takes place the surface crystallization of the coating and the formation of highly dispersed crystals of barium aluminosilicate with the composition $BaAl_2Si_2O_8$ ranging in size from 0.5 to 1.5–2 μm (less often up to 3–4 μm), concentrated exclusively in the surface layer with a thickness of 3–5 μm. Their refractoriness (melting point 1760 °C), high thermodynamic stability and location contribute to an additional increase in surface resistance to erosion entrainment, which positively affects the allowable working temperature of the coating. During high-temperature operation of coated products, coagulation of $BaAl_2Si_2O_8$ crystals and gradual spreading of crystallization deep into the coating layer are registered. The partial dissolution of Al_2O_3 in the barium silicate glass phase increases the viscosity of the matrix by creating a unified glass-forming framework. As a result, there is an increase in temperature resistance and resistance to erosion of the coating, expanding the limits of its short-term performance on the protected alloys – up to 1350 °C.

In summary: analyzing the presented data, it should be noted that glass enamels, refractory, glass crystalline, and reaction-cured coatings belong to the class of high-resource coatings, characterized by a combination of high physicochemical, technological, and corrosion-resistant properties. Coatings can protect structural elements from heat-proof nickel alloys and steels from high-temperature exposure to aggressive media at temperatures up to 1200-1250 °C (for a short time up to 1350 °C). Nonetheless, there is no information on the effectiveness of the protective action and mechanisms of operability of these coatings in high-speed gas flows (with rare exceptions (Astapov *et al.,* 2019a), or they are very scarce and uninformative (Solntsev *et al.,* 2004a).

4. CONCLUSIONS

A critical analysis of many years of research by conducted by Russian scientists in the field of creating single-layer and multi-layer heat-resistant coatings for heat-proof nickel alloys and steel for protection against high-temperature gas corrosion, including operation under conditions of interaction with high-velocity high-enthalpy flows of oxygen-containing gases, was carried out. Depending on the chemical and structural-phase composition, the following types of coatings were distinguished – oxide, metallic, intermetallic, glass-enamel, glass-crystal and glass-ceramic. Single-layer coatings cannot provide some of the numerous requirements for the surface of structural materials. Thus, in recent years, the main attention has been paid to the development of the architecture of multilayer, composite protective coatings. So, single-layer coatings are mainly used as intermediate layers in the "substrate – heat-resistant coating" system, where they perform barrier-compensation functions.

A significant place in this review is given to coatings based on refractory enamels. Now, a wide range of enamel resource coatings has been developed to ensure the performance of materials in question for temperatures of 900-1100 °C for a long time and 1200 °C for a short time, including operation in high-speed aggressive gas flows. Among these developments, the vast majority belongs to heat-resistant coatings for the effective protection of parts and assemblies of gas turbine engines and turbopump units; some technical solutions are aimed at increasing the reliability of the structural elements of liquid rocket engines; there are practically no developments in the field of protecting heat-loaded parts of gliders of hypersonic aircraft and their propulsion systems. The latter, primarily, is caused by temperature-time factors, significantly limiting the possibility of using traditional structural materials in high-temperature structures.

A number of technical solutions have been found; they protect the alloys from high-temperature gas corrosion and erosion during long-term operation in aircraft products at temperatures up to 1200-1250 °C with the possibility of short-term temperature peaks up to 1300-1350 °C. Some developments seem to be effective, however, they are uninformative from the standpoint of solving specific problems and require expensive testing of the claimed technical result in conditions that mimic operational conditions as applied to a particular alloy and specific features of structural elements made of the material.

5. ACKNOWLEDGMENTS

Downloaded from www.periodico.tchequimica.com

The work was supported by the Russian Foundation for Basic Research (project code 17-08-01527-a).

6. REFERENCES:

1. Abraimov, N.V. *High temperature materials and coatings for gas turbines*, Moscow: Mashinostroyeniye, **1993**.
2. Abraimov, N.V., Eliseev, Yu.S. *Chemical-thermal treatment of heat-proof steels and alloys*, Moscow: Intermet Inzhiniring, **2001**.
3. Abraimov, N.V., Geykin, V.A. *Temperature resistant coatings and welding in gas turbine engines,* Moscow: Nauka i tekhnologii, **2018**.
4. Appen, A.A. *Temperature resistant inorganic coatings,* Leningrad: Khimiya, **1976**.
5. Appen, A.A. *The chemistry of glass*, Leningrad: Khimiya, **1974**.
6. Arzamasov, B.N., Eliseev Yu.S., Abraimov N.V., Simonov V.N. RF. Patent 2270880, MPK C23C10 / 14 (2006.01), **2006**.
7. Astapov, A.N., Barabanov, B.N., Eremina, A.I., Lifanov, I.P. Patent 2679774 RF, MPK C03C 8/14 (2006.01), **2019a**.
8. Astapov, A.N., Lifanov, I.P., Prokofiev, M.V. *Russian Metallurgy (Metally),* **2019b**, *6*, 640–646. DOI: 10.1134/S0036029519060065.
9. Astapov, A.N., Pogozhev, Yu.S., Prokofiev, M.V., Lifanov, I.P., Potanin, A.Yu., Levashov, E.A., Vershinnikov, V.I. *Ceramics International,* **2019c**, 45(5), 6392–6404. DOI: 10.1016/j.ceramint.2018.12.126.
10. Astapov, A.N., Pogozhev, Yu.S., Prokofiev, M.V., Potanin, A.Yu., Levashov, E.A., Vershinnikov, V.I., Rabinskiy, L.N. *International Journal of Heat and Mass Transfer*, **2019d**, *140,* 12–20. DOI: 10.1016/j.ijheatmasstransfer.2019.05.100.
11. Astapov, A.N., Rabinskiy, L.N. *Solid State Phenomena,* **2017**, *269*, 14–30. DOI: 10.4028/www.scientific.net/SSP.269.14.
12. Astapov, A.N., Terentieva, V.S. *Russian Journal of Non-Ferrous Metals,* **2016**, *57(2),* 157–173. DOI: 10.3103/S1067821216020048.
13. Astapov, A.N., Terentieva, V.S. *Thermal Processes in Engineering*, **2014**, 6(1), 2–11.
14. Astapov, A.N., Zhestkov, B.E., Lifanov, I.P., Rabinskiy, L.N., Terentieva, V.S. *Arabian Journal for Science and Engineering,* **2019e**, *44(6),* 5323–5334. DOI: 10.1007/s13369-018-3585-4.
15. Burkov, S.I., Zolotova, O.P., Sorokin, B.P., Turchin, P.P., Talismanov, V.S. *Journal of the Acoustical Society of America*, **2018**, *143*(1), 16-22.
16. Denisova, V.S. *Space Engineering and Technology*, **2018**, *2*(21), 24–32.
17. Eliseev, Yu.S., Abraimov, N.V., Simonov, V.N., Shkretov, Yu.P. Patent 2308541 RF, MPK C23C26/00 (2006.01), C23C10/6 (2006.01), **2007**.
18. Eliseev, Yu.S., Dushkin, A.M., Shkretov, Yu.P., Abraimov, N.V. Patent 2213801 RF, MPK C23C4/16 (2000.01), C23C4/08 (2000.01), **2003a**.
19. Eliseev, Yu.S., Dushkin, A.M., Shkretov, Yu.P., Abraimov, N.V. Patent 2213802 RF, MPK C23C14/16 (2000.01), C23C4/08 (2000.01), **2003b**.
20. Eliseev, Yu.S., Dushkin, A.M., Shkretov, Yu.P., Abraimov, N.V. Patent 2212473 RF, MPK C23C28/00 (2000.01), **2003c**.
21. Gayamov, A.M., Budinovsky, S.A., Muboyadzhyan, S.A., Kosmin, A.A. *Electronic Scientific and Technical Journal*, **2014**, *1,* 1–11. DOI: 10.18577/2307-6046-2014-0-1-1-1.
22. Kablov, E.N., Muboyadzhyan, S.A., Budinovsky, S.A., Lutsenko, A.N. *Metals*, **2007**, *5,* 23–34.
23. Kablov, E.N., Muboyadzhyan, S.A., Budinovsky, S.A., Pomelov, Y.A. *Conversion in Engineering,* **1999**, *2,* 42–47.
24. Kablov, E.N., Solntsev, S.S., Rosenenkova, V.A., Denisova, V.S. Patent 2598657 RF, MPK C03C 8/14 (2006.01), **2016**.
25. Kachalin, G.V., Mednikov, A.F. *Natural and Technical Sciences,* **2013**, *4,* 187–194.
26. Kolomytsev, P.T. *Heat resistant diffusion coatings,* Moscow: Metallurgiya, **1979**.
27. Kuznetsov, V.P., Lesnikov, V.P., Konakova, I.P., Popov, N.A., Moroz, E.V. *Promising Materials*, **2011**, *13,* 469–480.
28. Kuznetsov, V.P., Lesnikov, V.P., Muboyadzhyan, S.A., Repina, O.V. *Metallurgy and Heat Treatment of Metals*, **2007**, *5,* 41–48.
29. Lesnikov, V.P., Kuznetsov, V.P., Konakova,

Downloaded from www.periodico.tchequimica.com

I.P., Moroz, E.V. *Bulletin of the Samara State Aerospace University named after Academician S.P. Korolev,* **2012**, *3-1(34),* 211–216.

30. Levashov, E.A., Kudryashov, A.E., Zamulaeva, E.I., Pogozhev, Yu.S., Sanin, V.N., Andreev, D.E., Yukhvid, V.I. *News of higher educational institutions. Powder metallurgy and functional coatings,* **2009**, *2,* 33–38.
31. Muboyadzhyan, S.A. *All materials. Encyclopedic Reference*, **2011**, *3*, 26–30.
32. Muboyadzhyan, S.A. *Russian Chemical Journal,* **2010**, *1,* 103–109.
33. Muboyadzhyan, S.A., Aleksandrov, D.A., Gorlov, D.S. *Metals*, **2010**, *5,* 39–51.
34. Poklad, V.A., Shkretov, Yu.P., Abraymov, N.V. *Engine*, **2010**, *4,* 4–8.
35. Prilepsky, V.N., Dudova, S.V., Drum, B.N. Timoshenko, V.P. Patent 2000278 RF, MPK C03C8/02 (1990.01), **1993**.
36. Samoilenko, V.M. *Scientific Bulletin of Moscow State Technical University of Civil Aviation,* **2006**, *108,* 112–114.
37. Shao, G., Lu, Y., Hanaor, D.A.H., Cui, S., Jiao, J., Shen, X. *Corrosion Science,* **2019**, *146,* 233–246.
38. Smirnov, A.A., Budinovsky, S.A. *Electronic Scientific and Technical Journal,* **2017,** *1(49),* 11–24. DOI: 10.18577/2307-6046-2017-0-1-2-2.
39. Solntsev, S.S. *All materials. Encyclopedic Reference*, **2009**, *1,* 26–40.
40. Solntsev, S.S. *Electronic Scientific and Technical Journal,* **2014**, *2,* 1–21. DOI: 10.18577/2307-6046-2014-0-2-1-1.
41. Solntsev, S.S. *Protective technological coatings and refractory enamels*, Moscow: Mashinostroyeniye, **1984**.
42. Solntsev, S.S. *Russian Chemical Journal*, **2010**, *LIV(1)*, 25–33.
43. Solntsev, S.S., Isaeva, N.V., Shvagireva, V.V., Maksimov, V.I. *Conversion in Engineering*, **2004a**, *4*, 77–80.
44. Solntsev, S.S., Isaeva, N.V., Shvagireva, V.V., Solovieva, G.A. Patent 2163897 RF, MPK C03C 8/14 (2000.01), **2001**.
45. Solntsev, S.S., Isaeva, N.V., Shvagireva, V.V., Solovieva, G.A. Patent 2273609 RF, MPK C03C 8/22 (2006.01), **2006**.
46. Solntsev, S.S., Isaeva, N.V., Shvagireva, V.V., Solovieva, G.A. Patent 2328472 RF, MPK C03C 8/22 (2006.01), **2008**.
47. Solntsev, S.S., Isaeva, N.V., Shvagireva, V.V., Solovieva G.A. Patent 2191165 RF, MPK C 03C8/22 (2000.01), C04B41/86 (2000.01), **2002**.
48. Solntsev, S.S., Isaeva, N.V., Shvagireva, V.V., Solovieva, G.A. Patent 2239616 RF, MPK C04B41/86 (2000.01), C03C8/22 (2000.01), **2004b**.
49. Solntsev, S.S., Shvagireva, V.V., Isaeva, N.V., Solovieva, G.A. *Electronic Scientific and Technical Journal,* **2014**, *6,* 1–9. DOI: 10.18577/2307-6046-2014-0-6-4-4.
50. Solntsev, S.S., Tumanov, A.T. *Protective coatings of metals when heated,* Moscow: Mashinostroyeniye, **1976**.
51. Solovieva, G.A., Grashchenkov, D.V., Isaeva, N.V., Shvagireva, V.V. Patent 2358925 RF, MPK C03C 8/14 (2006.01), **2009**.
52. Terentieva, V.S. *Heat resistant coatings for gas turbines*, Moscow: MAI-PRINT Publishing House, **2008**.
53. Terentieva, V.S., Astapov, A.N. *Russian Journal of Non-Ferrous Metals*, **2018**, *59(6),* 709–718. DOI: 10.3103/S1067821218060172.
54. Thomas, K., Vincent, S., Barbadikar, D., Kumar, S., Anwar, R., Fernandes, N. IOP *Conference Series: Materials Science and Engineering,* **2018**, *346(1),* 012010.
55. Tomarov, G.V., Shipkov, A.A. *Thermal Engineering*, **2018**, *65(8)*, 493–503.
56. Tomarov, G.V., Shipkov, A.A., Komissarova, T.N. *Thermal Engineering*, **2018**, *65(8),* 504–514.
57. Vargin, V.V., Antonova, E.A., Gutorova, L.L., Litvinova, E.I. *Technology of enamel and metal enameling,* Moscow: Gosstroyizdat, **1958**.
58. Yurishcheva, A.A., Astapov, A.N., Lifanov, I.P., Rabinskiy, L.N. Key *Engineering Materials*, **2018**, *771,* 103–117. DOI: 10.4028/www.scientific.net/KEM.771.103.

Downloaded from www.periodico.tchequimica.com

PERIÓDICO TCHÊ QUÍMICA
ARTIGO ORIGINAL

IDENTIFICAÇÃO DO ALVO DE DISPERSÃO COM BASE NA FUNÇÃO RADIAL DE REDES NEURAIS ARTIFICIAIS NA PRESENÇA DE RUÍDO NÃO ESTACIONÁRIO

SCATTERING TARGET IDENTIFICATION BASED ON RADIAL BASIS FUNCTION ARTIFICIAL NEURAL NETWORKS IN THE PRESENCE OF NON-STATIONARY NOISE

РАСПРЕДЕЛЕНИЕ ЦЕЛЕВОЙ ИДЕНТИФИКАЦИИ НА ОСНОВЕ РАДИАЛЬНОЙ ФУНКЦИИ ИСКУССТВЕННЫХ НЕЙРОННЫХ СЕТЕЙ В ПРИСУТСТВИИ НЕСТАЦИОНАРНОГО ШУМА

SHEVGUNOV, Timofey[1]*; EFIMOV, Evgeniy[2]; KIRDYASHKIN, Vladimir[3];

[1,2] Moscow Aviation Institute (National Research University), Department of Theoretical Radio Engineering, Moscow – Russian Federation

[3] Moscow Aviation Institute (National Research University), Department of Radar, Navigation, and Avionics, Moscow – Russian Federation

** Correspondence author*
e-mail: shevgunov@gmail.com

Received 30 August 2019; received in revised form 28 October 2019; accepted 28 October 2019

RESUMO

O artigo discute o problema do reconhecimento de alvos de radar realizado em imagens de radar complexas. Uma abordagem de rede neural artificial (ANN) com uma função de base radial (RBF) é proposta para identificar dispersadores de pontos localizados em uma imagem de radar. O conceito atualizado de blocos adaptativos simples como base para a montagem da rede permite o desenvolvimento de um esquema de extração de recursos baseado em ANN para processamento bidimensional de sinais. Foi demonstrado que ANN que implementa unidades de processamento neural de RBF pode ser usada para identificar alvos de radar descritos por um conjunto de dispersores individuais mesmo quando a distância relativa entre os dispersores é comparável ou menor que a largura efetiva de cada dispersor. A abordagem apresentada neste artigo foi a utilização da rede neural com a função de base radial especialmente sintetizada (RBF), usada para aproximar imagens de radar selecionadas transmitidas à sua entrada. Os resultados obtidos indicaram uma alta precisão na estimativa de centros individuais de dispersores na presença de ruído, o que não se limita ao caso estacionário, mas é considerado ciclostacionário. Também foi mostrado que os parâmetros que descrevem as coordenadas dos centros de dispersão podem ser extraídos com sucesso da ANN treinada após cerca de cem épocas passadas no processo de treinamento da ANN, que é realizado usando o método de descida com gradiente modificado. O principal resultado foi uma demonstração da possibilidade de usar redes neurais para análise automática de imagens de radar, que é parte integrante do conjunto de tarefas que formam o problema do reconhecimento de alvos. O algoritmo proposto implementa uma abordagem para identificar sistemas feitos usando procedimentos de treinamento em redes neurais.

Palavras-chave: *classificação do difusor, não estacionário, ciclo-estacionário, imagem de radar integrada, alvos de radar.*

ABSTRACT

The paper deals with the radar target discrimination problem performed on complex radar images. The approach based on radial basis function (RBF) artificial neural network (ANN) is proposed for the identification of point scatterers placed within a radar image. The renewed concept of simple adaptive units as the foundation for network assembling allows one to design an ANN-based feature extraction scheme for the two-dimensional signal processing. It was shown that ANN implementing RBF neural processing units could be applied for the identification of radar targets described by the set of separated scatterers, even in cases where the relative distance between the scatterers is comparable to or less than the effective width of each scatterer. The obtained results indicate a high accuracy estimation of separate scatterer centers in the presence of noise which is not limited to the stationary case but supposed to be cyclostationary. It was also shown that the parameters describing the coordinates of scattering centers could be successfully extracted from the trained ANN after about one hundred epochs spent on ANN training process, which is carried out by means of modified gradient

Downloaded from www.periodico.tchequimica.com

descent method. The main result is to demonstrate the possibility of using neural networks to automatically analyze radar images, which is an integral part of a set of tasks that form the target recognition problem. The proposed algorithm implements an approach of identification systems made using a neural network training procedures.

Keywords*: scatterer estimation, non-stationarity, cyclostationarity, complex radar image, radar targets.*

АННОТАЦИЯ

В статье рассматривается проблема распознавания радиолокационных целей, выполняемая на сложных радиолокационных изображениях. Подход, основанный на искусственной нейронной сети (ANN) с радиальной базисной функцией (RBF), предлагается для идентификации точечных рассеивателей, размещенных в радиолокационном изображении. Обновленная концепция простых адаптивных блоков как основы для сборки сети позволяет разработать схему извлечения признаков на основе ANN для двумерной обработки сигналов. Было показано, что ANN, реализующий нейронные блоки обработки RBF, может применяться для идентификации радиолокационных целей, описываемых набором отдельных рассеивателей, даже в тех случаях, когда относительное расстояние между рассеивателями сопоставимо или меньше эффективной ширины каждого рассеивателя. Подход, представленный в этой статье, состоит в использовании нейронной сети с особо синтезированной радиальной базисной функцией (RBF), которая используется для аппроксимации отобранных радиолокационных изображений, передаваемых на ее вход. Полученные результаты указывают на высокую точность оценки отдельных центров рассеивателей при наличии шума, который не ограничивается стационарным случаем, а предполагается, что он является циклостационарным. Также было показано, что параметры, описывающие координаты центров рассеяния, могут быть успешно извлечены из обученного ANN после примерно ста эпох, потраченных на процесс обучения ANN, который осуществляется с помощью модифицированного метода градиентного спуска. Основным результатом является демонстрация возможности использования нейронных сетей для автоматического анализа радиолокационных изображений, что является неотъемлемой частью набора задач, формирующих проблему распознавания целей. Предложенный алгоритм реализует подход идентификации систем, выполненных с использованием процедур обучения нейронной сети.

Ключевые слова: *оценка рассеивателя, нестационарность, циклостационарность, комплексное радиолокационное изображение, радиолокационные цели.*

1. INTRODUCTION

One of the important problems solved by modern smart radar systems is target identification. The possible approach to its solution is the machine-based analysis of radar images which can be performed by means of automated scattering analysis of the radar targets. The conceptual idea here is a decomposing the whole image under processing into point scatterers (Rihaczek and Hershkowitz, 2000) which are rather simple elements whose appearance can have a clear physical explanation. It allows each scatterer to be reproduced as a part of mutually interconnected structure supported by the appropriate artificial neural network (ANN) (Efimov *et al.,* 2014; Sandu *et al.*, 2018).

The authors of the current paper found out (Efimov and Shevgunov, 2012b) that the existing methods of ANN design require some modifications in order to allow considering the neural networks as identification techniques rather than approximation models only. The essential benefit (Efimov and Shevgunov, 2012a) is that neural networks organized as identification models provide one with the powerful tool to perform effective parameter estimation procedure. The complex model can be decomposed into simpler blocks, which are mirrored in the appropriate units in the network graph (Dubrovin *et al.,* 2014; Koltunov *et al.*, 2018). It means that not only can a successfully trained network be used for representing the revealed dependency, but it can also extract the values of internal parameters featuring its elements. Having been extracted, these values can be reversely mapped into the values related the original model parameters. In many widespread cases (Shevgunov *et al.,* 2014), there would be a simple one-to-one reference between model parameters and some of network parameters.

A typical radar image to be processed is assumed to be obtained by a radar system performing azimuthal scanning with a high resolution in both distance and angle dimensions. The system operating in centimeter wavelength

Downloaded from www.periodico.tchequimica.com

range (Shevgunov and Efimov, 2019a) emits coherent pulses using the same antenna, working with time division, both for the transmission and the echo measuring receive. The scanning cycle is inevitably carried out in the presence of noise that can be modeled as stationary or non-stationary, e.g. cyclostationary (Shevgunov, 2019; Shevgunov *et al.,* 2018a), process. The general concept of the scatterer identification approach is the estimation of parameters describing the set of scatterers involved in target's representation such as the coordinate of their centers within the target as the most important information to characterize its geometrical form in any further processing. This information being acquired could be passed to the customized classification systems, which can be a data-driven system organized on machine-learning principles that will form internal features working as anchors for the process of the automatic target identification.

The approach presented in this paper consists of using particularly synthesized radial basis function (RBF) neural network which is used for approximating sampled radar images given to its input. As soon as the approximation has finished successfully, the Cartesian coordinates of the scatterers are taken from the parameters of the neurons directly, which is proved by the intense numerical calculations whose results are presented in order to estimate the practical viability. It was shown in (Efimov and Shevgunov, 2014) that the ability of neural networks to operate on distorted, noisy and incomplete data sets alongside with the properties of RBF-neurons allows them to be applied in the scatter based target identification. The rest of this paper is organized as follows. Materials and Methods introduce the short outlook of the radar image model. The ANN-based solution for the problem identification of multiple scatterers and the numerical simulation are described in Results and Discussion. The paper ends with conclusion depicting the further development of the processing based on ANN.

2. MATERIALS AND METHODS

The basic model of a complex radar target (Henderson and Lewis, 1998) considers the radar target to be represented as a set of individual scatterers mounted on a stiff backbone. This model supposes that echo-response signals received during observation are to be determined as a superposition of the responses from each individual scatterer. Each of these individual responses possesses in the first consideration the form of the probe pulse emitted by the radar system. The physical model lying behind point scatterers is based on the assumption of the electromagnetic wave reflecting from the sharp edges of the man-made objects such as aircraft. Moreover, complex objects can be expressed as a unique superposition of scatterers as if they all were hold of a stiff frame. The model proposed has a few deliberately introduced simplifications. At first, non-linear distortions caused by signal reflection from a scatterer are thought to be compensated. At second, the changes in the positions of the scatterers are considered insignificant whatever they have been caused, i.e., due to antenna moving or micro vibration. Finally, the total inaccuracy of the reflection process could be represented in the model by means of the additive noise component.

The proposed model of space-time radar echo response signal of a complex radar target is used to generate test input radar image. Since a high resolution in both distance (denoted by ρ) and angle (denoted by φ) for the observed radar target is assumed, the signal could be described with Equation 1 where $\dot{x}_p(t,\theta)$ stands for complex-valued space-time radar signal echoed from p-th individual scatterer, $\dot{s}(t-\tau_p)$ is the slice of the radar image across the distance (in fact, the form of this slice will correspond to the form of probe pulse), $f_A^2(\theta-\varphi_p)$ is a term for squared antenna pattern, φ_p determines the main beam direction of the antenna. The term *n(t)* describes the additive noise which exhibits stationary or cyclostationary properties (Shevgunov *et al.,* 2018b; Shevgunov and Efimov, 2019b) in the frequency band width enough for efficient functioning of the radar system. The schematic structure of the reflected signal is shown in Figure 1, where one can see red thin solid line as the three-dimensional plot of the wave in the time domain. The amplitude response depends on the scanning angle due to the particular radiation pattern of the antenna as well as on the back-scattering radiation pattern of the scatterer under investigation. Since the latter is assumed to be a great deal wider than the former, one can conclude that the response envelope will resemble the squared radiation pattern of the antenna, which is depicted via thin blue solid line.

The example of a complex radar image possessing three individual scatterers generated according to the introduced model for the complex radar target is shown in Figure 2 where the intensity varies – the lighter pixels are, the greater values of the function they represent.

Downloaded from www.periodico.tchequimica.com

Nevertheless, one can bear in mind that the image is visualized only by the absolute value of the original complex-valued 2D function (1) and any information about the phase is omitted there. As one can note in Figure 2, two of three pulses are close to each other. Therefore their responses overlapping was chosen intentionally to investigate whether the proposed ANN algorithm is able to distinct them successfully and to what extent. The third pulse has the greatest intensity and located far separately from the others. The probe pulse range waveform and antenna cross-range pattern are both assumed to have shape of the Gaussian curves. The typical value of the width of the antenna cross-range pattern is 1–5 degree while the effective pulse width is from 1–10 ns which determines the temporal and spatial resolution for further processing.

3. RESULTS AND DISCUSSION:

3.1. Neural Network Design

Scattering center coordinates are usually considered (Chen and Andrews, 1980) to be the most relevant parameter for the target identification. Thus in (Konovaluk *et al*., 2010; Chen and Ling, 2002 the prolific way to the identification using parametric methods for pole estimation in the frequency domain authors has been proposed. The coordinates of the poles on the virtual complex plane can be used then to evaluate geometrical centers of the scatters. Although this approach demonstrates high accuracy and has proven suboptimal nature, it suffers from high calculation cost and the requirement to perform accurate deconvolution of the radar image that is a naturally ill-conditional problem. Authors of the current work have proposed in (Efimov and Shevgunov, 2013) alternative solution based on ANN-framework since taking into consideration the fact that Radial Basis Function (RBF) neural networks perfectly correspond to the model (1). The proposed approach contains the following steps:

Step 1. Radar image sampling.

Step 2. The preparation of the training set is made of the radar image samples.

Step 3. RBF neural network synthesis.

Step 4. Training of the ANN using the set as the input data.

Step 5. Extraction RBF neurons parameters are performed to directly calculate coordinates of individual scatterers.

The structural scheme of RBF artificial neural network is shown in Figure 3. It consists of input signals x and y representing coordinates of a point belonging to the image to be processed and the output z representing the intensity at this point; the block marked with “+1” introduces bias input. The training set consists of samples whose x and y coordinates in the image are used as input data, and the signal intensity in that point is used as target output data. Hence, the problem can be now overlooked as the task of approximation of the target radar image with neural network.

The output signal generated by ANN is defined by the Equation 2 where x_a is output network signal as the approximated radar image, ρ and φ stand for distance and antenna azimuthal angle correspondingly, P denotes the number of RBF neurons within the network, g_p is the partial output signal taken as weighted output of p-th RBF neuron. The key point to highlight is that single RBF neuron is targeting a particular part of the image which best corresponds to the neurons output signal. Therefore, by selecting activation function of the neuron in accordance to the probe pulse form and antenna pattern, one can expect that each single RBF neuron will target one individual scatterer provided the training process is successful. The parameters of the neurons are available after the training and can be directly used for calculating the estimated parameters of the scatterers, which are the coordinates of their centers and the effective widths.

The structure RBF-neuron is of particular interest as it is a special type of neuron that not only uses a radial basis function as its activation function but also has another input combiner. Structural scheme of RBF neuron during feed-forwarding is shown in Figure 4. In case of two-dimensional input data, the neuron will have 3 inputs: two are for coordinates x and y, and the extra one is for bias. The latter is marked with “+1”. The transformation function can be easily written from the scheme of the neuron in Figure 4. Thus, the output signal is defined by the Equation 3 where x_0 and y_0 are the coordinates of the centers, k_x and k_y are scale multipliers. The argument inside the parenthesis of the term f in the transfer function above can be expressed in the form of the canonical equation of an ellipse or an ellipsoid if the dimension would be greater than two (Equation 4) where the following substitutions are applied (Equation 5).

In the case of Gaussian function taken for the activation function f, the output signal of one RBF-neuron will be equal to unity at the central

Downloaded from www.periodico.tchequimica.com

point and rapidly decreasing bell around. The individual knowledge of the adaptive elements behavior during their back-propagations opens the option for constructing a structural scheme of RBF neuron for back-propagation as it is seen in Figure 5.

3.2. Numerical Simulation

Since any strict theoretical investigation on the estimation ability of ANN is always challenging, the numerical simulation is a helpful tool that is used in order to estimate practical accuracy of the proposed procedure. In this section, the numerical simulation is being conducted according to the five-step plan developed in the previous section. In the first step, the described above allocation of three individual scatterers was used to synthesize the radar image of a complex target. Basically, the radar image previously shown in Figure 2 undergoes the sampling procedure, which is performed with the equal sampling steps in both dimensions. The discrete points, or samples, of the image are shown in Figure 6 by means of circles, which area is proportional to the intensity of the wave received at each point in the two-dimensional plot. Since the value is superposition of all the scatteres involved in imaging their values are not decaying smoothly from the center down to the side of the bell curved shown in Figure 2.

The second step consists in getting all the samples together in order to form the training set as the set of ordered pairs *{(x, y), z},* where *x* and *y* are spatially coordinated of each sample and *z* is the absolute value of the intensity of the reflected field at the point with the given position. In the third step, there is synthesized the ANN based on RBF architecture described in the previous section. Since the number of RBF-neuron corresponds to the number of scatterers, this quantity is assumed to be known and equal to three. The activation function is chosen Gaussian in accordance with the form of probe pulse and antenna pattern possessed by model (1). The assumption of the Gaussian bell is not critical for the overall performance as it will be seen it further.

In the fourth step, the training set containing all the samples was used to train the RBF ANN network in the batch mode with the gradient descent method. The choice of the gradient descent method was made due to its relative simplicity even at the cost of slower convergence in comparison with the second-order method. However, the latter are required computationally expensive procedures such as the matrix inversion, which is the gradient descent method is free of. For the purpose of controlled training process, the objective function was defined as the mean-squared error (MSE) function, which evaluates the difference between the source radar image and the solution evaluated at particular point by the synthesized RBF ANN. In addition, it evaluates the overall network performance while the training goes on and gets the clue about the epoch number when the training process can be stopped. The learning curve during the training is shown in Figure 7 as the value of the MSE curve plotted against the number of iteration or epoch.

The curve in Figure 7 can be split into two parts. In the first part, the error is large but decreases rapidly while, in the second part, the error is rather small but goes down slowly. One can see that the low level of MSE is achieved just after 100 training iterations; hence, the approximated radar image fits the source radar image accurately to process further. Besides, Figure 7 shows that the value of MSE is still decreasing at the end of the training process but notably slower than it took place at the beginning.

In the last step, the parameters of the scatterers are immediately extracted from the adaptive elements which the neurons consist of. Since the training process has finished successfully, the neurons contain the values related to the positions of the scatterers. The reconstructed scatterers are shown in Figure 8 alongside with the true ones. The black solid lines depict the two-sigma level of each scatterer in the model whereas the dashed blue line illustrates the same for the scatterers estimated by the RBF ANN. It is clear that the centers of all scatterers are accurately estimated despite the fact that two of them were chosen in the model to be partially overlapping. However, the effective widths of the scatterers are not estimated so accurately. The width of two of the scatterers was estimated smaller as one can see in Figure 8 that the blue ellipses are inside the black ones. This phenomenon could be explained by their lesser influence on the overall MSE value and will be discussed in the next section in more details.

4. CONCLUSIONS:

The series of Monte-Carlo simulation clearly indicates that RBF neural network can be successfully used for accurate estimating the centers of the individual scatterers with signal-to-noise ratios down to 5 dB. However, the accuracy

Downloaded from www.periodico.tchequimica.com

of the parameter describing the effective width of each scatterer is rougher. The explanation of this phenomenon consists in the difference in the influence caused by parameters of both types on the overall target function to be minimized during ANN training prosses. Thus, that function is significantly more sensitive to the change of the position of the scatter due to the fact that the greater values of the reconstructed image are primarily concentrated in the neighborhood of their center. Since the target function is quadratic, the greater values serve as additional weights. In contrast, the estimated values of scatterer width may vary in the wider range without any significant change in the target function that can be enough to adjust them even in the later training epochs. Nevertheless, the positions of the scatterers are considered to be more robust features as they are strongly related to the physical geometry of the target while the intensity of the reflection, which determines the width, will vary depending on many factors, the most important of which is the angle of the incident electromagnetic wave.

The paper reflects the current advances in the ANN based signal processing in regards to tasks related to the modern signal processing systems. The main result of the paper is demonstrating a possible way how neural networks can be used for automated radar image analysis which is the essential part of a set of tasks forming target recognition problem. The proposed algorithm carries out the system identification approach reached via neural network learning procedure. Thus. the radar image is firstly approximated by RBF networks where each RBF-neuron preserves the information about the point scatterer of the possible targets. The adaptive element concept chosen for ANN synthesis is extremely suitable for the second stage when the values of parameters are being extracted and further transformed into parameters of the multiscatterer model. The research, whose some results are presented in the paper, is bound to be continued as it is expected to be naturally developed into a universal scatter estimator that can be used for the automated scatterer identification and further reconstruction of the target shape carried out by means of another ANN belonging to the class of multilayer perceptrons.

5. ACKNOWLEDGMENTS:

This work was supported by the state assignment of the Ministry of Education and Science of the Russian Federation (project 8.8502.2017/BP).

6. REFERENCES:

1. Chen, C., Andrews, H. IEEE *Transactions on Aerospace and Electronic Systems*, **1980**, *16(1),* 2–14.
2. Chen, V., Ling, H. *Time-Frequency Transforms for Radar Imaging and Signal Analysis,* Norwood: Artech House, **2002**.
3. Dubrovin, A., Nikishov, V., Shevgunov, T. *Tyrrhenian International Workshop on Digital Communication: Enhanced Surveillance of Aircraft and Vehicles*, Rome: IEEE, **2014**, 87–92. DOI: 10.1109/TIWDC-ESAV.2014.6945451.
4. Efimov, E., Shevgunov, T. *XXXI General Assembly of the International Union of Radio Science*, Beijing: IEEE, **2014**. DOI: 10.1109/URSIGASS.2014.6929360.
5. Efimov, E., Shevgunov, T. *The Works of MAI,* **2012a**, *51.* http://trudymai.ru/upload/iblock/6c6/razrabotka-i-issledovanie-metodiki-postroeniya-neyronnykh-setey-na-osnove-adaptivnykh-elementov.pdf?lang=en&issue=51, accessed 15 April 2019.
6. Efimov, E., Shevgunov, T. *Journal of Radio Electronics,* **2012b**, *8*, 2-7. 3.
7. Efimov, E., Shevgunov, T. *The Works of MAI,* **2013**, *68*. http://trudymai.ru/upload/iblock/831/831084817b0416a99a825dd9868f02d5.pdf?lang=en&issue=68, accessed 15 April 2019.
8. Efimov, E., Shevgunov, T., Valaytite, A., Sadovskaya, E. *29th Congress of International Council of the Aeronautical Sciences*, St. Petersburg, **2014**, 1–15.
9. Henderson, F., Lewis, A. *Principles and applications of imaging radar. Manual of remote sensing.* 3rd ed., Somerset: John Wiley and Sons, **1998**.
10. Koltunov, I.I., Panfilov, A.V., Poselsky, I.A., Chubukov, N.N., Krechetov, I.V., Skvortsov, A.A. *Journal of Mechanical Engineering Research and Development*, **2018**, *41*(4), 37-39.
11. Konovaluk, M., Gorbunova, A., Kuznetsov, Yu., Baev, A. *4-th All-Russian Conference Radiolocation and radio communication*, Moscow, Russian

Downloaded from www.periodico.tchequimica.com

Federation, **2010**.

12. Rihaczek, A., Hershkowitz, S. *Theory and Practice of Radar Target Identification*, Norwood: Artech House, **2000**.
13. Shevgunov, T. *Journal of Physics: Conference Series*, **2019**, *1163(1)*, 1–6. DOI: 10.1088/1742-6596/1163/1/012037.
14. Sandu, C., Deaconu, M., Silivestru, V., Olariu, C.-T., Sandu, C.-R. *INCAS Bulletin*, **2018**, *10(4)*, 141-151.
15. Shevgunov, T., Dubrovin, A., Nikishov, V. *XXXI General Assembly of the International Union of Radio Science*, Beijing, China, **2014**. DOI: 10.1109/URSIGASS.2014.6929038.
16. Shevgunov, T., Efimov, E. Artificial Neural Networks Implementing Maximum Likelihood Estimator for Passive Radars. In: R. Silhavy (Ed.), *Artificial Intelligence and Algorithms in Intelligent Systems*, Berlin: Springer, **2019a**, 144–153. DOI: 10.1007/978-3-319-91189-2_15.
17. Shevgunov, T., Efimov, E. *Proceedings of 8th Computer Science On-line Conference*, **2019b**, *3*, 164–173. DOI: 10.1007/978-3-030-19813-8_18.
18. Shevgunov, T., Efimov, E., Kuznetsov, Yu. *2018 Baltic URSI Symposium*, Poznan, **2018a**, 901–904. DOI: 10.23919/URSI.2018.8406726.
19. Shevgunov, T., Efimov, E., Zhukov, D. *Proceedings of National Research University Higher School of Economics*, Moscow, Russia, **2018b**, 1–4. DOI: 10.1109/MWENT.2018.8337271.

$$\dot{x}(t,\theta) = \sum_{p=1}^{P} \dot{x}_p(t,\theta) + n(t) = \sum_{p=1}^{P} \dot{a}_p \cdot \dot{s}\left(t-\tau_p\right) \cdot f_A^2\left(\theta-\varphi_p\right) + n(t) \quad \text{(Eq. 1)}$$

$$x_a(\rho,\varphi) = \sum_{p=1}^{P} g_p\,(\rho,\varphi) \quad \text{(Eq. 2)}$$

$$z = f\left(k_x(x_0+x)^2 + k_y(y_0+y)^2\right) \quad \text{(Eq. 3)}$$

$$z = f\left(w(x,y)\right),\ \frac{(x-x_1)^2}{c^2} + \frac{(y-y_1)^2}{d^2} = 1. \quad \text{(Eq. 4)}$$

$$x_1 = -x_0, y_1 = -y_0,\ c = \sqrt{w/k_x}, d = \sqrt{w/k_y} \quad \text{(Eq. 5)}$$

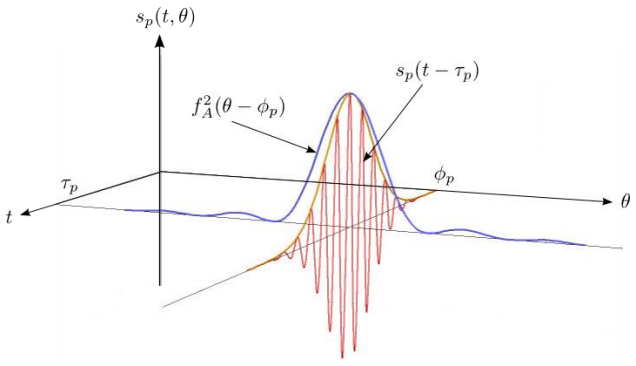

Figure 1. *The structure of space-time radar echo response signal of complex radar target*

Downloaded from www.periodico.tchequimica.com

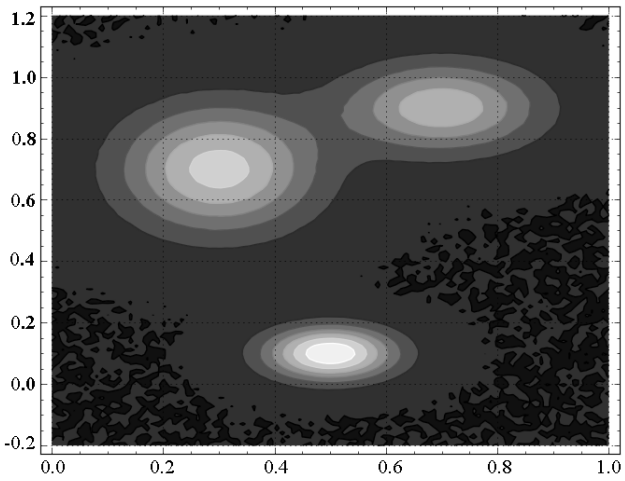

Figure 2. *The example of a radar image with three scatterers*

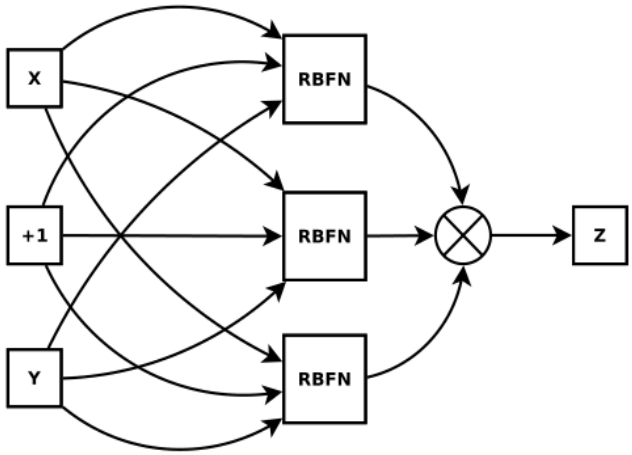

Figure 3. *RBF neural network*

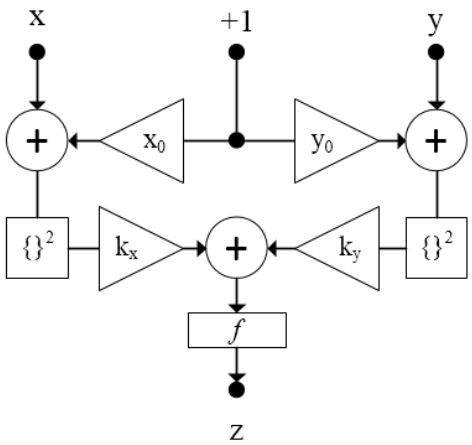

Figure 4. *The scheme of RBF neuron for feed-forwarding*

Downloaded from www.periodico.tchequimica.com

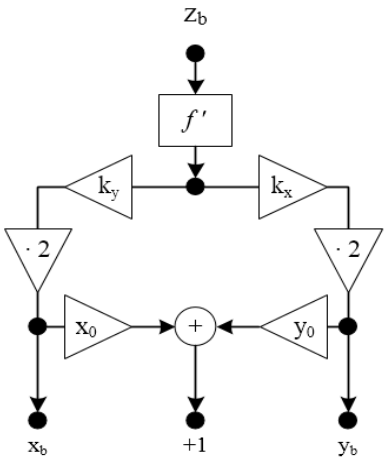

Figure 5. *Structural scheme of RBF neuron for backpropagation*

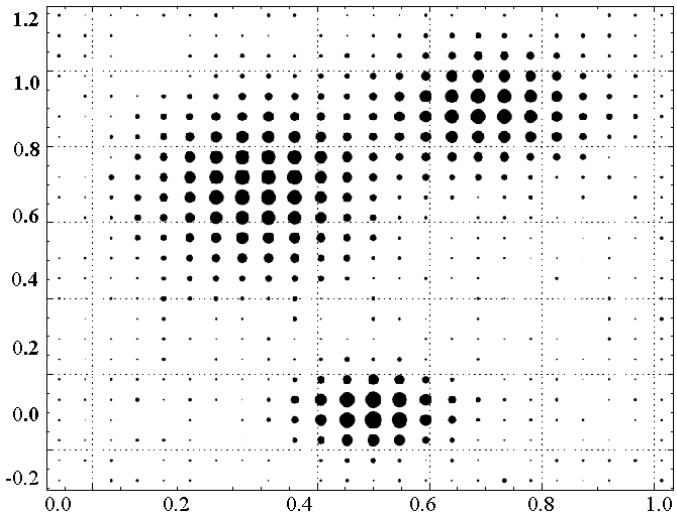

Figure 6. *Sampled radar image*

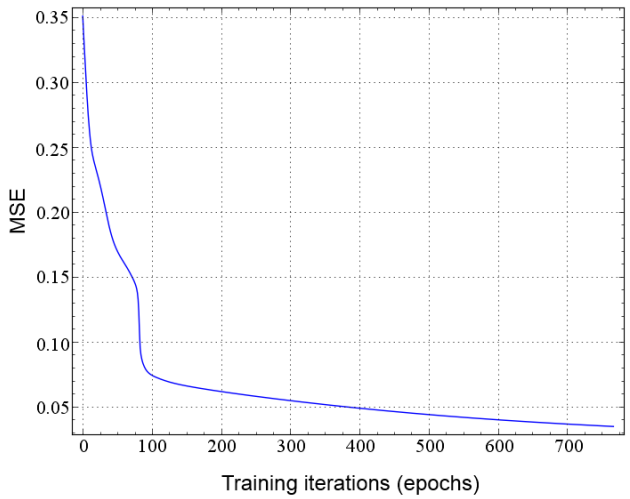

Figure 7. *Training process*

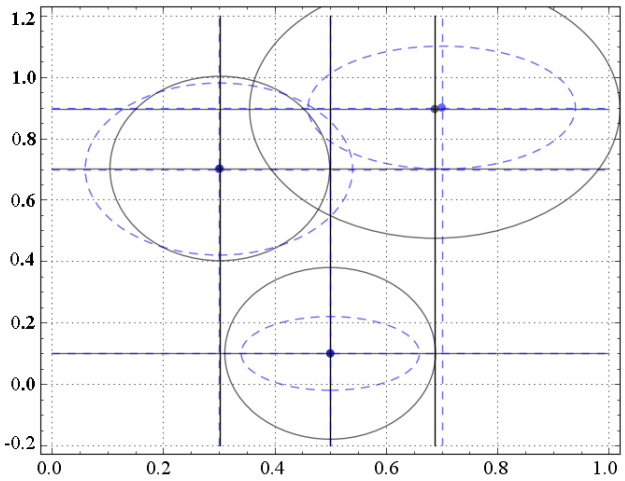

Figure 8. *Original and reconstructed scatterers*

Downloaded from www.periodico.tchequimica.com

PERIÓDICO TCHÊ QUÍMICA
ARTIGO ORIGINAL

DEFORMAÇÃO DE ESTRUTURAS DE ARAME DO TIPO HELICOIDAL

DEFORMATION OF THE HELICAL TYPE WIRE STRUCTURES

ДЕФОРМАЦИЯ ПРОВОЛОЧНЫХ КОНСТРУКЦИЙ СПИРАЛЬНОГО ТИПА

DANILIN, Alexander N.[1*]; RABINSKIY, Lev N.[2]; ZHAVORONOK, Sergey I.[3];

[1] Institute of Applied Mechanics of the Russian Academy of Sciences, Moscow – Russian Federation

[2] Moscow Aviation Institute (National Research University), Department of Material Sciences, Moscow – Russian Federation

[3] Institute of Applied Mechanics of the Russian Academy of Sciences, Department of Mechanics of Smart and Composite Materials and Systems, Moscow – Russian Federation

** Correspondence author*
e-mail: andanilin@yandex.ru

Received 30 August 2019; received in revised form 28 October 2019; accepted 28 October 2019

RESUMO

A análise de linhas aéreas de transmissão de energia envolve a modelagem da estática e das vibrações dos condutores. A solução de tais problemas exige estritamente a devida consideração da estrutura interna do condutor, em particular para sistemas de segurança energética, e a confiabilidade do suporte de informações e telecomunicações para aeródromos e sistemas de aviação, bem como para linhas aéreas de transmissão de energia sujeitas a ventos fortes, especialmente em condições de gelo. Devido à complexidade das estruturas de arame, surgem problemas conhecidos ao avaliar suas deformações, rigidez, capacidade de carga. Por exemplo, a rigidez à flexão de um condutor pode variar significativamente dependendo de sua deformação. Portanto, a rigidez pode variar ao longo do eixo do condutor e no tempo. Este artigo propõe um novo modelo para a deformação de estruturas de arame semelhante aos condutores típicos das linhas aéreas de transmissão de energia. Tais projetos incluem não apenas condutores e cabos, mas também braçadeiras em espiral projetadas para tensionar, pendurar, conectar, proteger e reparar os condutores. Com base na média de energia, cada camada de arame é considerada como um invólucro cilíndrico anisotrópico elástico equivalente. Portanto, o condutor ou braçadeira em espiral pode ser modelado como um sistema de invólucros embutidos um no outro e interagindo por meio de pressão e atrito. No processo do estudo, foram feitos cálculos que permitiram formular equações para as matrizes de flexibilidade e rigidez das estruturas em espiral. O problema da interação da braçadeira de tensão com a camada do condutor externo é formulado e resolvido. Finalmente, o mecanismo de transferência de força da braçadeira para o condutor foi investigado.

Palavras-chave: *condutor, braçadeira espiral, média de energia, invólucro cilíndrico de membrana, carga admissível.*

ABSTRACT

Analysis of overhead power transmission lines (OPL) involves the simulation of statics and oscillation. Solving such problems strictly requires the proper accounting of the internal conductor structure, in particular for power safety and reliability systems of information-telecommunication supply of aerodromes and aircraft systems, as well as for overhead transmission lines subjected to intense wind, especially in icing conditions. Due to the complexity of wire structures, known issues arise in the estimates of their deformations, stiffness, bearing capacity, etc. For instance, the bending stiffness of the conductor can vary considerably. Consequently, the stiffness can vary along the conductor axis as well as in time. This paper proposes a new deformation model of wire structures similar to typical OPL conductors. Such structures include not only conductors and cables, but spiral clamps intended for tension, suspension, joining, protection, and repair of conductors. Based on energy averaging each wire layer is considered as an equivalent elastic anisotropic cylindrical shell. Therefore a conductor or a spiral clamp can be modeled as a system of shells nested into each other and interacting by means of pressure and friction forces. In the process of the study, calculations were made that made it possible to formulate equations for the matrices of flexibility and cruelty of spiral structures. The interaction problem for a tension clamp with an external wire layer of a conductor has been formulated and solved. Finally, the mechanism of the force transfer from the clamp on the conductor has been investigated.

Downloaded from www.periodico.tchequimica.com

Keywords: *Conductor, spiral clamp, energy averaging, membrane cylindrical shell, bearing capacity.*

АННОТАЦИЯ

Анализ воздушных линий электропередачи (ОПЛ) включает моделирование статики и колебаний проводников. Решение таких задач строго требует надлежащего учета внутренней проводниковой структуры, в частности, для систем энергетической безопасности и надежности информационно-телекоммуникационного обеспечения аэродромов и авиационных систем, а также для воздушных линий электропередачи, подверженных сильному ветру, особенно в условиях обледенения. Из-за сложности проволочных конструкций возникают известные проблемы при оценке их деформаций, жесткости, несущей способности и т.д. Например, изгибная жесткость проводника может значительно варьироваться в зависимости от его деформации. Следовательно, жесткость может изменяться как вдоль оси проводника, так и во времени. В этой статье предлагается новая модель деформации проволочных конструкций, аналогичная типичным проводникам ОПЛ. Такие конструкции включают не только проводники и кабели, но и спиральные зажимы, предназначенные для натяжения, подвешивания, соединения, защиты и ремонта проводников. На основе усреднения энергии каждый слой проволоки рассматривается как эквивалентная упругая анизотропная цилиндрическая оболочка. Поэтому проводник или спиральный зажим могут быть смоделированы как система оболочек, вложенных друг в друга и взаимодействующих посредством сил давления и трения. В процессе исследования были произведены вычисления, которые позволили сформулировать уравнения для матриц гибкости и жестокости спиральных структур. Сформулирована и решена задача взаимодействия натяжного зажима с внешним проводным слоем проводника. Наконец, механизм передачи силы от зажима на проводник был исследован.

Ключевые слова: *Проводник, спиральный зажим, усреднение энергии, мембранная цилиндрическая оболочка, допустимая нагрузка.*

---

1. INTRODUCTION

In engineering, wire structures similar to OPL conductors are considered usually as flexible uniform rods or cables with average stiffness parameters. At the same time, their internal structures are neglected. This approach is used, for instance, in computing conductors' sag between supports, or in simulating conductor vibrations under wind flows (Glazunov, 1956; Boshnyakovich, 1971). However, such models do not allow describing the known effects during the conductor deformation (Dubois *et al.*, 1991; Costello, 1997; Cardou and Jolicoeur, 1997; Papailiou, 1997; Pilkey, 2002; Hong *et al.,* 2005; Feyrer, 2007; Goudreau *et al.*, 2010; Foti and Martinelli, 2011), and their use in calculations can lead to unacceptable errors (Papailiou, 1997; Orlov *et al.*, 2003a; Orlov *et al.*, 2003b, Sokolov and Ryabinov, 2015).

Two assumptions about the joint deformation of wire spirals are used to calculate the bending or torsional conductor stiffness. They can be interpreted as "opposite" in meaning and define the lower and upper bounds of the theoretical estimate. Indeed, the first one assumes the independent wire deforming while the second one assumes their coupled deforming, i.e. wire spirals are rigidly connected into one, forming a kind of monolithic rod. However, comparative calculations show (Vinogradov, 2005) that the upper and lower stiffness values calculated by both methods for the selected conductor or cable can differ by more than 70 times. Uncertainty in the knowledge of stiffness or damping conductor parameters leads to errors and inefficiency of the existing calculation algorithms. Wrong physical and mechanical ideas about the deformation of wires and similar systems destroy the integrity of the mathematical model is accurate in many other aspects. It is, of course, possible to use the "detailed" finite element simulation of wire structures (Fekr *et al.,* 1999, Lévesque *et al.*, 2011); however, this way is extremely time-consuming. On the other hand, the results strongly depend on the geometry of contact surfaces formed by the solving algorithm. Thus, the "direct" finite element simulation approach is practically unacceptable when investigating the dynamic behavior of wire structures or optimizing their structures.

An "intermediate" simulation strategy is based on the averaging of the mechanical properties of wire spirals in each wire layer of a conductor. For instance, one can consider the deformation of an arbitrary spiral wire and then use the assumption of coupling all wires of a layer or the whole conductor (Costello, 1997; Cardou and Jolicoeur, 1997; Hong *et al.*, 2005;

Downloaded from www.periodico.tchequimica.com

Rawlins, 2005a; Rawlins, 2005b; Feyrer, 2007; Rawlins, 2009; Goudreau *et al.*, 2010; Foti and Martinelli, 2011; Shejko *et al.*, 2016). However, it is difficult to introduce a correct model of layer interaction, taking into account the forces of pressure and friction between adjacent layers.

A method of energy averaging treating each wire layer as an equivalent anisotropic cylindrical shell has been proposed in (Shalashilin *et al.*, 2005; Danilin *et al.*, 2011a; Danilin *et al.*, 2011b). As a result, conductors are considered as systems of cylindrical shells embedded in each other and interacting by means of pressure and friction forces. The further development of this approach is presented below.

In the engineering practice, a new class of problems related to the design and manufacture of spiral-type clamps for conductors suspending, tensioning, connecting, protecting, and repairing appeared recently (Vinogradov *et al.*, 1994; Ryzhov, 1998; Vinogradov *et al.*, 1998; Ryzhov and Tsvetkov, 2005; Preformed Line Products…, 2007; Anosov *et al.*, 2015; Catalog APRESA…, 2019). One or more wire layers of limited length form the typical spiral clamp that could be well combined with conductors due to its flexibility. Moreover, a spiral clamp is integrated after installation with the conductor into almost monolithic structure, and the layers of a spiral clamp mounted on a conductor could be considered as additional external layers of limited length.

The clamp design requires the load-bearing capacity as well as the optimal design parameters, i.e., the length of the clamping, direction, and pitch (angle of rising) of the spirals, to be determined accurately, otherwise the clamping could be inefficient and even lead to damaging of the core of the structure. The appropriate estimate becomes possible only considering spiral structures as systems of wire layers interacting by means of pressure and friction forces, as shown below.

2. MATERIALS AND METHODS

Let us consider the equilibrium of a helical rod in the osculating plane (Figure 1), and let (Equation 1) be the radius of curvature, where α is the angle of ascent and (Equation 2). The equilibrium equations of forces referenced to the axis and normal to the rod can be then formulated as follows (Equation 3). while the equilibrium of momenta gives the known relation (Equation 4). Let S be the helix length along its axis, and L be the length of a turning pitch along the conductor axis (Equation 5). Let us consider hence the deformation of the helix rod under the loads inducing internal forces being constant along the rod length.

First, let us apply the force *P* along the conductor axis, as shown in Figure 2a. The resulting momentum in the rod cross-section may be decomposed into the bending momentum $M_b(P)$ and torque $M_t(P)$ (Equation 6). Also, the longitudinal force arises in the wire cross-section (Equation 7). The effect of shearing forces on the rod deformation is neglected. Let us consider hence the loading of the helical rod in the plane normal to the *x*-axis by the external torque *M*. The bending momentum M_b and torque M_t arise in the cross-sections of the rod (Figure 2b) (Equation 8).

Let the transversal load q directed along the curvature radius of the rod, and let the points of the rod axis translate strictly along the curvature radii; this displacement referred hereinafter as w is constant along the rod under the given load q. Then, only the longitudinal force arises in the rod cross-sections (Equation 9). Where (Equation 1) is the curvature radius of the rod in the osculating plane. In general, the overall bending, torsional, and longitudinal reactions appear in the rod cross-section under the simultaneous action of three external loads (Equation 10).

As a result, the potential energy of the helix strain can be represented as follows (Equation 11). Where EJ_z, GJ_t, EF are bending, torsional and longitudinal stiffness of the helical rod corresponding to the momenta M_b, M_t, and the force N. Substituting (Equation 10) into (Equation 11) and accounting for (Equation 5), we obtain finally (Equation 12).

Let us define the elongation Δ of the helical rod along the axis x, the angle φ of rod twisting around the axis x, and the area Sw as generalized displacements, and let introduce the conjugated generalized forces (Equation 13). The generalized displacement *Sw* corresponds to the force intensity *q*. Indeed, the work of the force on the displacement *w* is determined as follows (Equation 14). Assuming that *w* remains constant within a coil of length *S*, we have hence (Equation 15) which determines the required conjugated “force-displacement” pair. Substituting the forces P and M expressed through P^*, M^*

Downloaded from www.periodico.tchequimica.com

, and q accordingly to (Equation 13) into (Equation 12) we obtain the following strain energy formulation (Equation 16). As provided by the Castigliano theorem, the generalized displacements are defined as (Equation 17). The corresponding matrix formulation is represented as (Equation 18). Where the elements of the matrix (Equation 19) are introduced below (Equation 20). Where (Equation 21) is the dimensionless factor.

Let us consider hence the cylindrical shell of radius r and length L elastically equivalent to the system of helical rods (wires). Let the shell be loaded at its ends by the longitudinal force T, the torque H, and the internal pressure p (Figure 3). The loads P_1, M_1, q_1 acting on the separate rod of the system, and the loads acting on the shell are interrelated as follows (Equation 22). Where n is the number of rods. Introduction of the relative elongation and the relative twist angle for the cylindrical shell and accounting for (Equation 22) leads to the matrix relation (Equation 23). The elements of the matrix (Equation 24) are determined as follows (Equation 25).

As we treat the conductor as a rod with specific mechanical properties, we could establish the relationships between the forces acting on the rod, and its strains within Hookean law (Equation 26). Where ε, θ, and κ are the relative elongation, the relative twist angle, and the curvature of the rod axis, respectively; N, H, M are longitudinal forces, twisting and bending moments in the rod; B and R are the flexibility and rigidity matrices, i.e. $R = B^{-1}$. The traditional definition of tensile, torsional, and bending stiffness follows directly from (Equation 26) if the matrices B and R are diagonal (i.e., for the isotropic rod considered in the principal central axes).

The conductor is a system consisting of a core (central wire) and wire layers modeled as anisotropic cylindrical membranes accordingly to (Equation 23), (Equation 25). Let us assume the conductor layers laid without gap and interference fit. The layers are numbered from 1 to *n,* and the index “0” is assigned to the core. Thus, for the *i*-th layer, Equation 23 takes the form (Equation 27). Here $T^{(i)}$ denotes the longitudinal force in the shell mid surface, which is related to the force $N^{(i)}$ acting on the shell as usually (Equation 28). And $r^{(i)}$ is the radius of the mid surface of the *i*-th layer.

Eliminating $p^{(i)}$ from the Equation (27), we reduce them to the following form (Equations 29-30). So that (Equation 31). For the whole wire, the longitudinal force N and the torque H are computed by summation of the forces and momenta acting on the core and the layers (Equation 32). Let us assume the contact between wires being ideal with no relative sliding; as a result, their deformations are equal (Equation 33). The following matrix formulation of the equations (Equation 32) can be obtained (Equation 34).

Substituting hence (Equation 31) into (Equation 34), accounting for (Equation 31), we obtain (Equation 35). Where $E^{(0)}$ and $G^{(0)}$ are moduli for tension and shear of the core, (Equation 36) is the area (Equation 37) is the polar moment of inertia and $d^{(0)}$ is the diameter of the core wire.

The resulting stiffness matrix R is defined for the stretched and twisted wire. It is expected that the elements $R_{12} = R_{21}$ are small as compared to the diagonal R_{11} and R_{22} due to the counter winding of the conductor layers. In any case, the angles of winding layers can be selected so that its elements out of the diagonal vanish, then R_{11} and R_{22} can be interpreted as classic stiffness of the conductor on stretching and torsion. The Equations 29-30 allow determining the bending and torsional stiffness of the wire structure. First, let us consider the torsion. At $T = 0$ it follows from (Equation 29) (Equation 38). When the wire is twisted by an angle θ, all layers are twisted equally (Equation 39).

At the same time, the torque H is defined by the summation of the torques of layers (Equation 40). Therefore, taking into account (Equation 38)-(Equation 40), we have (Equation 41). Let denote the torsional conductor stiffness as GJ_t, where G is some shear modulus. Thus, (Equation 42), and on the basis of the (Equation 41), we obtain (Equation 43). For the core and the *i*-th layer we have (Equation 44). Where $E^{(i)}$, $\mu^{(i)}$ are the moduli of elasticity and the Poisson's ratio of the layer material. Thus (Equation 45).

Let us consider hence the conductor bending stiffness. The curvature κ, the curvature radius, ρ and the bending moment are interrelated by the following formula (Equation

Downloaded from www.periodico.tchequimica.com

46). The bending moment M_b is defined as follows (Equation 47). When the flat cross-sections hypothesis is fulfilled, the fiber elongation is introduced as (Equation 48). If the *i*-th bend is treated as a shell consisting of longitudinal fibers in which the stresses (Equation 49) act, then Hooke's law for a longitudinal fiber in the form (Equation 50) follows from (Equation 29), (Equation 30). Accounting for (Equation 46)-(Equation 48), we obtain (Equation 51).

In particular, for the circular cross-section of radius $r^{(i)}$ and thickness $d^{(i)}$ we have (Equation 52). Thus, the bending stiffness of the *i*-th layer can be defined as follows (Equation 53). As the axes curvature of all the layers and the conductor is assumed to equal, we have (Equation 54). Therefore, considering (Equation 53), we define the bending stiffness of a conductor as (Equation 55).

3. RESULTS AND DISCUSSION:

The torsional and bending stiffness of aluminum-steel conductors (AS series, Russia) were calculated (Boshnyakovich, 1971; Glazunov, 1956). The typical cross-section of an AS conductor is shown in Figure 4. The aluminum conductive layers are referred hereinafter as 1 and 2, and the steel core is formed by the layer 3 and the central wire 4. The used data are presented below in Tables 1 and 2. The first columns of the Tables contain the conductors' marks in the form of the ratio of nominal cross-section areas of aluminum and steel parts (mm^2). In the second column, the sums of the number of wires in layers are given; the value of each term of the sum gives the number of wires in the layer while the number of terms corresponds to the number of layers. The nominal wire diameters and the lay ratios defined by the formula (Equation 56) are presented in the third and fourth columns, respectively. Here *L* is the twist step, r is the radius of the layer (i.e. radius of the circle on which the centers of cross-sections of wires lie), and *d* is the diameter of wires. Thus, (Equation 56), and finally (Equation 57) accordingly to the second formula (Equation 5).

The calculation results are presented below in Table 3. The first column contains the wire mark; the second is the outer wire's diameter (i.e. the diameter of the corresponding circumcircle). The third and fourth columns contain bending and torsional stiffness obtained using (Equation 55) and (Equation 45), respectively. The fifth column contains the values of the torsional stiffness obtained as (Equation 58). Where d is the outer diameter of the wire (in millimeters), and the numerical coefficient dimension is $\mathrm{N}\times\mathrm{m}^2/\mathrm{mm}^4$ (Koch, 2001). This formula was obtained at the Montefiore Institute (Belgium, University of Liège) (Dubois *et al.*, 1991) as a result of extensive analysis of the experimental data. Comparison of the 4th and 5th columns of Table 3 indicates a good correlation of the theoretical prediction given by the proposed model and the known experimental data.

A typical spiral type fittings is a spiral tension clamp (Figure 5) consisting of one or more layers formed by wire strands using special friction coatings (Catalog APRESA…, 2019; Preformed Line Products…, 2007). Spiral clamps are used for suspending and tensioning OPL conductors and cables. Its installation can be carried out manually by sequential coiling of the layers. The main problem of the clamp design is to find optimal values for its parameters (the clamp length, direction, and pitch (winding angle) of the spirals, and the coefficients of friction). Otherwise, the clamp may not function effectively and even cause damage to the core.

The spiral clamp can be reduced to an equivalent cylindrical shell as well as to a conductor layer. To solve the problem of interaction of the clamp with the conductor, we could consider the equilibrium of the elementary ring of the shell with the length dx equivalent to the clamp. The shell element is loaded by the longitudinal force T, the circumferential force (Equation 59), and the friction force f with longitudinal and circumferential components referred hereinafter as f_x and f_y. The ring element of length dy in the circumferential direction is shown in Figure 6, while the equilibrium equations are written as follows (Equation 60).

Let us assume the frictional force be distributed over the contact surface between the clamp and the cable as (Equation 61), where p is the contact pressure and k_T is the friction factor. Let also the force f be directed along the resultant shearing force vector formed by the forces T and h (Equation 62). The contact pressure p for given forces T, h, and the radial displacement w_0 corresponding to the interference fit of the clamp is determined from

Downloaded from www.periodico.tchequimica.com

the third equation (Equation 23) as (Equation 63).

The displacement w_0 is given by the difference between the initial radii of the conductor and the clamp if the reduction in the diameter of the cable due to its interaction with the clamp is neglected. The displacement w_0 is assumed positive if the initial radius of the clamp is less than the radius of the conductor. If the initial values T_0 and H_0 are given by the fastening conditions of the clamp on the support at $x=0$, then the equations (Equation 60), (Equation 62) allow one to formulate the Cauchy problem (Equation 64). Where the pressure p is given by (Equation 63). The problem statement (Equation 64) assumes that the clamp is so lengthy that the mutual interference of its ends could be neglected, i.e. the semi-infinite shell is considered.

Let us consider the condition of the fastening of the clamp on the support with unconstrained rotation, i.e. $H_0=0$, as a first approximation. Then the second equation (Equation 64) has the solution $H(x)\equiv 0$, and the corresponding Cauchy problem for the first equation (Equation 64) takes the form (Equation 65). The solution of the Cauchy problem (Equation 65) can be written as follows (Equation 66). Let us note that the solution (Equation 66) has the asymptotic component (Equation 67) (see Figure 7). The minimum length $l_{\min}$ of the clamp corresponding to the force T_0 can be obtained from the solution (Equation 66) as (Equation 68).

Let us consider hence the problem of interaction for the system shown in Figure 8, consisting of a clamp, the outer layer of a conductor and the inner part of it, which we will call the core. The equilibrium equations of the clamp and the outer layer of the conductor have the form (Equation 69). And the force $N^{(3)}$ in the conductor core is determined by the equilibrium condition as follows (Equation 70). If we assume that the frictional forces $f^{(1)}$ and $f^{(2)}$ arising between the layers are proportional to the pressure forces $p^{(1)}$ and $p^{(2)}$ between the layers, then (Equation 71).

As before, we assume that the friction forces are directed along with the resultant shearing force between the layers. Then (Equation 72). The pressure $p^{(1)}$ between the clamp and the conductor is determined by the ratio (37) (Equation 73). The pressure $p^{(2)}$ between the external layer of the conductor and its core is determined by the same ratio, but written for the external layer, taking its deflection equal to zero (Equation 74).

As before, we assume that the clamp on the support can freely rotate. Then for Equation 40, taking into account the notation (Equation 71)–(Equation 74), we obtain the following Cauchy problem (Equations 75-78). In the case of rigid fixing of the clamp on the support, when $\theta^{(1)}=0$, from the second equation, taking into account the expression for $p^{(1)}$ (Equation 73), it follows that (Equation 79).

Then the initial conditions for equations (Equation 75) are written in the form (Equation 80). Where $H_0^{(1)}$ is given by formula (Equation 79). As an example, let's consider the problem of the interaction of the tension clamp NS-17.1-01 (according to the ESSP catalog, XI.2004) and the conductor AS 150/24. Clamp parameters: radius of the middle surface $r^{(1)}=10.45\,\text{mm}$; diameter of wires $d^{(1)}=3.8\,\text{mm}$; tensile modulus $E^{(1)}=200\,\text{kN}/\text{mm}^2$; Poisson's ratio $\mu^{(1)}=0.29$; angle of inclination of the wires relative to the conductor cross-section $\alpha^{(1)}=67^\circ$; the number of wires $n^{(1)}=14$; interference fit $w_0^{(1)}=0,9\,\text{mm}$. The friction coefficient between the shells simulating the layers of the clamp and the conductor was assumed to be equal to $k_T^{(1)}=0.6$.

The parameters of the conductor outer layer: radius of the middle surface $r^{(2)}=7.2\,\text{mm}$; diameter of wires $d^{(2)}=2.7\,\text{mm}$; tensile modulus $E^{(2)}=63\,\text{kN}/\text{mm}^2$; Poisson's ratio $\mu^{(2)}=0.34$; the angle of inclination of the wires relative to the conductor cross-section $\alpha^{(2)}=103.6^\circ$; the number of wires $n^{(2)}=16$; technological interference $w_0^{(2)}=0.2\,\text{mm}$. The coefficient of friction between the shell modeling the outer conductor layer and the cylindrical surface of the conductor core (the inner part of the conductor) was taken to be equal to $k_T^{(2)}=0.15$.

Figure 9 shows, respectively, the dependence of the forces $T^{(i)}$ and the torques $H^{(i)}$, acting in the clamp $(i=1)$ and the outer conductor layer $(i=2)$ from the longitudinal coordinate x. Changing the tensile force in the inner conductor part (core) along the *x*-coordinate

Downloaded from www.periodico.tchequimica.com

is shown in Figure 10a. Figure 10b shows the distribution of pressure $p^{(i)}$ between the clamp and the outer conductor layer, as well as between the outer layer of the conductor and its internal part. Figure 11 shows the distributions of rotation angles of the clamp cross-sections $(i=1)$ and the outer conductor layer $(i=2)$ relative to the axis x .

In Figures 9-11, solid lines represent the solution of the initial value problem (Equation 75), (Equation 80), when the turn of the clamp is forbidden (the case of rigid fastening). The dashed lines correspond to the initial value problem (Equation 75), (Equation 78) when the clamp on the support can turn freely. The initial force in the clamp was calculated as (Equation 81), where the force $N_0^{(1)}$ was taken equal 23kN

4. CONCLUSIONS:

1. An approach to the modeling of multilayer wire structures of a regular structure has been developed, taking into account the interaction of wire layers by the forces of pressure and friction. Each layer is represented from the position of energy averaging as an anisotropic cylindrical shell, and the wire structure itself is considered as a system of cylindrical shells enclosed into each other, between which slip is permitted, taking into account the forces of pressure and friction.

2. On the basis of the developed approach, formulas for calculating the stiffness and compliance matrices are obtained, which allow evaluating the torsion and bending stiffness of the conductor taking into account its internal structure and the interaction of the layers between each other.

3. On the example of the problem of the interaction of the OPL conductor with the tension spiral clamp, a method of analysis of the bearing capacity and the structural efficiency of the spiral clamps is shown.

5. ACKNOWLEDGMENTS:

This work has been partially supported by RFBR, project No. 17-01-00837.

6. REFERENCES:

1. Anosov, Yu.V., Danilin, A.N., Kurdyumov, N.N. *Trudy MAI*, **2015**, *80*. Available at: http://trudymai.ru/upload/iblock/52d/52d17b8352c66b0785561cb93d236c66.pdf?lang=ru&issue=80.
2. Boshnyakovich, A.D. *Mechanical modeling of conductors and cables of power lines*, Leningrad: Energy, **1971**.
3. Cardou, A., Jolicoeur, C. *Applied Mechanics Reviews*, **1997**, *50*(1), 1-14.
4. Catalog APRESA. Accesorios preformados. Parcela 155 SEVILLA-7 (Spane), **2019**. http://www.plp-spain.com/index.php/es/, accessed October 2019.
5. Costello, G.A. *Theory of wire rope*, New-York: Springer-Verlag, **1997**.
6. Danilin, A.N., Kuznetsova, E.L., Rabinsky, L.N., Tarasov, S.S. *Nonlinear World*, **2011a**, *9*(10), 635-645.
7. Danilin, A.N., Zakharov, A.P., Kuznetsova, E.L. Kurdyumov, N.N., Tarasov, S.S. *Nonlinear World*, **2011b**, *11*(4), 234-242.
8. Dubois, H., Lilien, J.L., Dal Maso, F. *Scientifique de l'Association des Ingénieurs Électriciens sortis de l'Institut Électrotechnique Montefiore*, **1991**, *1*, 46-62.
9. Fekr, M.R., McClure, G., Farzaneh, M. *Computers & Structures*, **1999**, *72*, 301-316.
10. Feyrer, K. *Wire ropes: tension, endurance, reliability*, Berlin, New York: Springer-Verlag, **2007**.
11. Foti, F., Martinelli, L. A model for the cyclic biaxial bending of stranded ropes. *Proceedings of the 20th Congress of the AIMETA (p. 240)*, Bologna, Italy, September 12-15, **2011**.
12. Glazunov, A.A. *Basics of the mechanical part of overhead power lines*, Moscow-Leningrad: Gosenergoizdat. **1956**.
13. Goudreau, S., Lévesque, F., Cardou, A., Cloutier, L. *IEEE Transactions on Power Delivery*, **2010**, *25*(4), 2997-3006.
14. Hong, K-J., Der Kiuregian, A., Sackman, J.L. *Journal of Engineering Mechanics*, **2005**, *131*(5), 500-511.
15. Koch, G.H. *Advanced Materials & Processes*, **2001**, 36-38. Available at: https://www.asminternational.org/documents/10192/1755223/amp15908p036.pdf/0

Downloaded from www.periodico.tchequimica.com

26e7c61-4606-424e-9ade-3455865aba71.

16. Lévesque, F., Goudreau, S., Cloutier, L., Cardou, A. *Tribology International*, **2011**, *44*(9), 1014-1023.
17. Papailiou, K.O. *IEEE Transactions on Power Delivery*, **1997**, *12*(4), 1576-1588.
18. Pilkey, W.D. *Analysis and design of elastic beams. Computational Methods*, New York: Wiley & Sons, **2002**.
19. Preformed Line Products (PLP). Energy Product Catalog. **2007**. Available at: http://preformed.com.
20. Rawlins, C.B. *Analytical elements of overhead conductor fabrication*. Palo Alto: Fultus Corporation, **2005a**.
21. Rawlins, C.B. Flexure of a single-layer tensioned cable at rigid support. *Proceedings of the 6th International Symposium on Cable Dynamics (pp. 363-370)*, Charleston, USA, September 19-22, **2005b**.
22. Rawlins, C.B. *Journal of Sound and Vibration*, **2009**, *323*(1-2), 232-256.
23. Ryzhov, S.V. *Electrical Stations*, **1998**, *1*, 8-11.
24. Ryzhov, SV, Tsvetkov, Yu.L. *Elektro*, **2005**, *2*, 32-36.
25. Shalashilin, V.I., Danilin, A.N., Volkov-Bogorodskiy, D.B. Model of overhead line conductor with the interaction of layers. *Proceedings of the 6th International Symposium on Cable Dynamics,* Charleston *(pp. 371-377)*, USA, September 19-22, **2005**.
26. Shejko, S., Yechyn, S., Demchenko, N. Materials Science and Technology Conference and Exhibition 2016, MS and T 2016, **2016**, *1*, 353-358.
27. Sokolov, N.S., Ryabinov, V.M. *Soil Mechanics and Foundation Engineering*, **2015**, *52(1)*, 18-22.
28. Vinogradov, A.A. *Vibrations of conductors of overhead power lines under wind*, Moscow: Publishing house CJSC, "Elektrosetstroyproekt", **2005**.
29. Vinogradov, A.A., Ryzhov, S.V., Shtelmakh, A.A. *Energy Construction*, **1994**, *3*, 60-61.
30. Vinogradov, A.A., Ryzhov, S.V., Tishchenko, A.V. *Electrical Stations*, **1998**, *1*, 3-11.
31. Orlov, A.M., Skvortsov, A.A., Solov'ev, A.A. Zhurnal Eksperimental'noj i Teoreticheskoj Fiziki, **2003a**, *123*(3), 590-599.
32. Orlov, A.M., Skvortsov, A.A., Solov'ev, A.A. Journal of Experimental and Theoretical Physics, **2003b**, *96*(3), 523-530.

$$\rho = r/\cos^2\alpha \qquad \text{(Eq. 1)}$$

$$d\theta = ds/\rho \qquad \text{(Eq. 2)}$$

$$\frac{dN}{ds} - \frac{Q}{\rho} + t = 0; \quad \frac{dQ}{ds} + \frac{N}{\rho} - q = 0, \qquad \text{(Eq. 3)}$$

$$dM/ds = Q \qquad \text{(Eq. 4)}$$

$$S = \frac{2\pi r}{\cos\alpha}; \quad L = S\left|\sin\alpha\right| = 2\pi r\frac{\left|\sin\alpha\right|}{\cos\alpha}. \qquad \text{(Eq. 5)}$$

$$M_b(P) = Pr\sin\alpha, \quad M_t(P) = P\,r\cos\alpha. \qquad \text{(Eq. 6)}$$

$$N(P) = P\sin\alpha. \qquad \text{(Eq. 7)}$$

Downloaded from www.periodico.tchequimica.com

$$M_b(M) = -M\cos\alpha,\ M_t(M) = M\sin\alpha. \quad \text{(Eq. 8)}$$

$$N(q) = q\rho = \frac{qr}{\cos^2\alpha} \quad \text{(Eq. 9)}$$

$$\begin{aligned} M_b &= M_b(P) + M_b(M) = P\,r\sin\alpha - M\cos\alpha, \\ M_t &= M_t(P) + M_t(M) = P\,r\cos\alpha + M\sin\alpha, \\ N &= N(P) + N(q) = P\sin\alpha + q\,r/\cos^2\alpha. \end{aligned} \quad \text{(Eq. 10)}$$

$$U = \frac{1}{2}\int_0^S \left(\frac{M_b^2}{EJ_z} + \frac{M_t^2}{GJ_t} + \frac{N^2}{EF}\right) ds \quad \text{(Eq. 11)}$$

$$U = \frac{1}{2} S\left[\frac{(P\,r\sin\alpha - M\cos\alpha)^2}{EJ_z} + \frac{(P\,r\cos\alpha + M\sin\alpha)^2}{GJ_t} + \frac{(P\sin\alpha + qr/\cos^2\alpha)^2}{EF}\right]. \quad \text{(Eq. 12)}$$

$$\begin{aligned} P^* &= P + N(q)\sin\alpha = P + qr\sin\alpha/\cos^2\alpha, \\ M^* &= M + N(q)\,r\cos\alpha = M + qr^2/\cos\alpha. \end{aligned} \quad \text{(Eq. 13)}$$

$$A_q = \int_0^S w\,q\,ds \quad \text{(Eq. 14)}$$

$$A_q = q\,Sw \quad \text{(Eq. 15)}$$

$$\begin{aligned} U = \frac{1}{2} S\Bigg\{ &\frac{1}{EJ_z}\left[P^* r\sin\alpha - M^*\cos\alpha - qr^2(\mathrm{tg}^2\alpha - 1)\right]^2 + \\ &+ \frac{1}{GJ_t}\left(P^* r\cos\alpha + M^*\sin\alpha - 2qr^2\,\mathrm{tg}\,\alpha\right)^2 + \frac{1}{EF}\left(P^*\sin\alpha + qr\right)^2\Bigg\}. \end{aligned} \quad \text{(Eq. 16)}$$

$$\Delta = \frac{dU}{dP^*};\quad \varphi = \frac{dU}{dM^*};\quad Sw = \frac{dU}{dq}. \quad \text{(Eq. 17)}$$

$$\left[\Delta\ \ \varphi\ \ Sw\right]^T = A\left[P^*\ \ M^*\ \ q\right]^T \quad \text{(Eq. 18)}$$

$$A = \left\| a_{ij} \right\|\ \ (i, j = 1, 2, 3) \quad \text{(Eq. 19)}$$

$$\begin{aligned} &a_{11} = Sr^2\left(\frac{1+\psi}{EJ_z}\sin^2\alpha + \frac{\cos^2\alpha}{GJ_t}\right);\quad a_{12} = a_{21} = Sr\left(\frac{1}{GJ_t} - \frac{1}{EJ_z}\right)\sin\alpha\cos\alpha; \\ &a_{22} = S\left(\frac{\sin^2\alpha}{GJ_t} + \frac{\cos^2\alpha}{EJ_z}\right);\quad a_{13} = a_{31} = -Sr^3\left(\frac{\mathrm{tg}^2\alpha - (1+\psi)}{EJ_z} + \frac{2}{GJ_t}\right)\sin\alpha; \\ &a_{23} = a_{32} = -Sr^2\left(\frac{2\mathrm{tg}^2\alpha}{GJ_t} + \frac{1-\mathrm{tg}^2\alpha}{EJ_z}\right)\cos\alpha;\quad a_{33} = Sr^4\left[\frac{(1-\mathrm{tg}^2\alpha)^2 + \psi}{EJ_z} + \frac{4\mathrm{tg}^2\alpha}{GJ_t}\right]. \end{aligned} \quad \text{(Eq. 20)}$$

$$\psi = J_z/Fr^2 \quad \text{(Eq. 21)}$$

Downloaded from www.periodico.tchequimica.com

$$P_1 = T\,2\pi r/n,\ M_1 = H/n\ ,\ q_1 = p2\pi r\,L/(nS), \qquad \text{(Eq. 22)}$$

$$\left[\varepsilon\ \ \theta\ \ w\right]^T = B\left[T\ \ H\ \ p\right]^T, \qquad \text{(Eq. 23)}$$

$$B = \left\|b_{ij}\right\|\ \ (i, j = 1,2,3) \qquad \text{(Eq. 24)}$$

$$b_{11} = \frac{2\pi r^3}{n\left|\sin\alpha\right|}\left(\frac{1+\psi}{EJ_z}\sin^2\alpha^{(i)} + \frac{\cos^2\alpha}{GJ_t}\right),\quad b_{12} = \frac{r}{n}\,\mathrm{sign}\,\alpha\cos\alpha\left(\frac{1}{GJ_t} - \frac{1}{EJ_z}\right),$$
$$b_{13} = -\frac{2\pi r^4}{n}\sin\alpha\left(\frac{\mathrm{tg}^2\alpha - 1 - \psi}{EJ_z} + \frac{2}{GJ_t}\right),\quad b_{22} = \frac{1}{n\left|\sin\alpha\right|}\left(\frac{\sin^2\alpha}{GJ_t} + \frac{\cos^2\alpha}{EJ_z}\right),$$
$$b_{21} = 2\pi r\,b_{12},\quad b_{23} = -\frac{2\pi r^3}{n}\cos\alpha\left(\frac{2\mathrm{tg}^2\alpha}{GJ_t} + \frac{1-\mathrm{tg}^2\alpha}{EJ_z}\right), \qquad \text{(Eq. 25)}$$
$$b_{31} = b_{13},\ b_{32} = \frac{b_{23}}{2\pi r},\ b_{33} = \frac{2\pi r^5}{n}\left|\sin\alpha\right|\left[\frac{(1-\mathrm{tg}^2\alpha)^2 + \psi}{EJ_z} + \frac{4\mathrm{tg}^2\alpha}{GJ_t}\right].$$

$$\left(\varepsilon\ \ \theta\ \ \kappa\right)^T = B\left(N\ \ H\ \ M\right)^T \quad \text{or} \quad \left(N\ \ H\ \ M\right)^T = R\left(\varepsilon\ \ \theta\ \ \kappa\right)^T. \qquad \text{(Eq. 26)}$$

$$\left(\varepsilon^{(i)}\ \ \theta^{(i)}\ \ 0\right)^T = B^{(i)}\left(T^{(i)}\ \ H^{(i)}\ \ p^{(i)}\right)^T \qquad \text{(Eq. 27)}$$

$$N^{(i)} = 2\pi r^{(i)}\,T^{(i)} \qquad \text{(Eq. 28)}$$

$$\left(\varepsilon^{(i)}\ \ \theta^{(i)}\right)^T = \bar{B}^{(i)}\left(T^{(i)}\ \ H^{(i)}\ \right)^T; \qquad \text{(Eq. 29)}$$

$$\bar{B}^{(i)} = \left\|\bar{b}_{kl}\right\| = \begin{pmatrix} b_{11}^{(i)} - \dfrac{b_{13}^{(i)}b_{31}^{(i)}}{b_{33}^{(i)}} & b_{12}^{(i)} - \dfrac{b_{13}^{(i)}b_{32}^{(i)}}{b_{33}^{(i)}} \\ b_{21}^{(i)} - \dfrac{b_{23}^{(i)}b_{31}^{(i)}}{b_{33}^{(i)}} & b_{22}^{(i)} - \dfrac{b_{23}^{(i)}b_{32}^{(i)}}{b_{33}^{(i)}} \end{pmatrix};\quad k,\ l = 1,2, \qquad \text{(Eq. 30)}$$

$$\left(T^{(i)}\ \ H^{(i)}\ \right)^T = C^{(i)}\left(\varepsilon^{(i)}\ \ \theta^{(i)}\ \right)^T;\quad C^{(i)} = \left\|c_{pq}^{(i)}\right\| = \left(\bar{B}^{(i)}\right)^{-1};\quad p,\ q = 1,2. \qquad \text{(Eq. 31)}$$

$$N = N^{(0)} + \sum_{i=1}^{n} N^{(i)} = N^{(0)} + 2\pi\sum_{i=1}^{n} r^{(i)}T^{(i)};\quad H = H^{(0)} + \sum_{i=1}^{n} H^{(i)}. \qquad \text{(Eq. 32)}$$

$$\varepsilon^{(i)} = \varepsilon,\ \ \theta^{(i)} = \theta;\quad i = 0,\ 1,\ ...,\ n. \qquad \text{(Eq. 33)}$$

$$\begin{pmatrix} N \\ H \end{pmatrix} = \begin{pmatrix} N^{(0)} \\ H^{(0)} \end{pmatrix} + \sum_{i=1}^{n}\begin{pmatrix} 2\pi r^{(i)} & 0 \\ 0 & 1 \end{pmatrix}\begin{pmatrix} T^{(i)} \\ H^{(i)} \end{pmatrix}. \qquad \text{(Eq. 34)}$$

$$\begin{pmatrix} N \\ H \end{pmatrix}^T = R\begin{pmatrix} \varepsilon \\ \theta \end{pmatrix}^T,\ R = \begin{pmatrix} E^{(0)}F^{(0)} & 0 \\ 0 & G^{(0)}J_t^{(0)} \end{pmatrix} + \sum_{i=1}^{n}\begin{pmatrix} 2\pi r^{(i)} & 0 \\ 0 & 1 \end{pmatrix}C^{(i)} \qquad \text{(Eq. 35)}$$

Downloaded from www.periodico.tchequimica.com

$$F^{(0)} = \pi d^{(0)2}/4 \quad \text{(Eq. 36)}$$

$$J_t^{(0)} = \pi d^{(0)4}/32 \quad \text{(Eq. 37)}$$

$$\theta^{(i)} = \bar{b}_{22}^{(i)} H^{(i)}. \quad \text{(Eq. 38)}$$

$$\theta^{(i)} = \theta; \quad i = 0,1,...,n. \quad \text{(Eq. 39)}$$

$$H = \sum_{i=0}^{n} H^{(i)}. \quad \text{(Eq. 40)}$$

$$H = \sum_{i=0}^{n} \theta^{(i)} c_{22}^{(i)} = \theta \sum_{i=0}^{n} c_{22}^{(i)}. \quad \text{(Eq. 41)}$$

$$\theta = H / (GJ_t) \quad \text{(Eq. 42)}$$

$$GJ_t = \sum_{i=0}^{n} c_{22}^{(i)}. \quad \text{(Eq. 43)}$$

$$b_{22}^{(0)} = \frac{1}{G^{(0)} J_t^{(0)}} \approx \frac{10}{G^{(0)} d^{(0)4}}; \quad J_t^{(i)} = 0.1 d^{(i)4}; \quad J_b^{(i)} = 0.05 d^{(i)4}; \quad G^{(i)} = \frac{E^{(i)}}{2(1+\mu^{(i)})}; \quad \text{(Eq. 44)}$$

$$GJ_t = 0.1 G^{(0)} J_t^{(0)} + \sum_{i=1}^{n} c_{22}^{(i)}. \quad \text{(Eq. 45)}$$

$$\kappa = \rho^{-1} = M_b / EJ_b \quad \text{(Eq. 46)}$$

$$M_b = \int_F y \sigma \, dF \quad \text{(Eq. 47)}$$

$$\varepsilon = y \rho^{-1} \quad \text{(Eq. 48)}$$

$$\sigma^{(i)} = T^{(i)}/d^{(i)} \quad \text{(Eq. 49)}$$

$$\varepsilon^{(i)} = \bar{b}_{11}^{(i)} T^{(i)} = \bar{b}_{11}^{(i)} d^{(i)} \sigma^{(i)} \quad \text{(Eq. 50)}$$

$$E^{(i)} J_b^{(i)} = M_b^{(i)} \rho^{(i)} = \rho \int_F y \frac{\varepsilon^{(i)}}{\bar{b}_{11}^{(i)} d^{(i)}} dF = \frac{1}{\bar{b}_{11}^{(i)} d^{(i)}} \int_{F^{(i)}} y^2 dF^{(i)}. \quad \text{(Eq. 51)}$$

$$\int_{F^{(i)}} y^2 dF^{(i)} = \pi r^{(i)3} d^{(i)}. \quad \text{(Eq. 52)}$$

$$E^{(i)} J_b^{(i)} = \frac{\pi r^{(i)3}}{\bar{b}_{11}^{(i)}}. \quad \text{(Eq. 53)}$$

$$M_b = \sum_{i=0}^{n} M_b^{(i)}. \quad \text{(Eq. 54)}$$

Downloaded from www.periodico.tchequimica.com

$$EJ_b = M_b\rho = \rho\sum_{i=0}^{n} M_b^{(i)} = \rho\sum_{i=0}^{n}\frac{E^{(i)}J_b^{(i)}}{\rho} = 0.05d^{(0)4}E^{(0)} + \pi\sum_{i=1}^{n} r^{(i)3}c_{11}^{(i)}. \quad \text{(Eq. 55)}$$

$$m = L/(2r+d) \quad \text{(Eq. 56)}$$

$$\alpha = \mathrm{Arctg}\left(L/2\pi r\right) \quad \text{(Eq. 57)}$$

$$GJ_t = 0.00027\,d^4, \quad \text{(Eq. 58)}$$

$$h = H/(2\pi r^2) \quad \text{(Eq. 59)}$$

$$\frac{dT}{dx} = -f_x, \quad \frac{dH}{dx} = -2\pi r^2 f_y. \quad \text{(Eq. 60)}$$

$$f = k_T p \quad \text{(Eq. 61)}$$

$$f_x = f\sin\beta, \quad f_y = f\cos\beta;$$
$$\sin\beta = \frac{|T|}{\sqrt{T^2+h^2}}, \quad \cos\beta = \frac{|h|}{\sqrt{T^2+h^2}}; \quad h = \frac{H}{2\pi r^2}. \quad \text{(Eq. 62)}$$

$$p = \frac{w_0 - b_{31}T - b_{32}H}{b_{33}}. \quad \text{(Eq. 63)}$$

$$\frac{dT}{dx} = -k_T p\,\sin\beta, \quad \frac{dH}{dx} = -2\pi r^2 k_T p\cos\beta\,;$$
$$T(0) = T_0\,,\ H(0) = H_0\,, \quad \text{(Eq. 64)}$$

$$\frac{dT}{dx} = -k_T\frac{w_0 - b_{31}T}{b_{33}} = -k_T\left(a_0 + a_1T\right); \quad T(0) = T_0 \quad \left(a_0 = \frac{w_0}{b_{33}}, \quad a_1 = -\frac{b_{31}}{b_{33}}\right). \quad \text{(Eq. 65)}$$

$$T(x) = T_\infty + \left(T_0 - T_\infty\right)e^{-k_T a_1 x}, \quad T_\infty = -\frac{a_0}{a_1}. \quad \text{(Eq. 66)}$$

$$T_\infty = \lim_{x\to\infty} T = -\frac{w_0}{|b_{31}|}. \quad \text{(Eq. 67)}$$

$$l_{\min} = \frac{1}{k_T a_1}\ln\left(1 - \frac{T_0}{T_\infty}\right). \quad \text{(Eq. 68)}$$

Downloaded from www.periodico.tchequimica.com

$$2\pi r^{(1)}\frac{dT^{(1)}}{dx}=-f_x^{(1)}\,2\pi\left(r^{(1)}-\frac{d^{(1)}}{2}\right),\quad \frac{dH^{(1)}}{dx}=-f_y^{(1)}\,2\pi\left(r^{(1)}-\frac{d^{(1)}}{2}\right)^2,$$

$$2\pi r^{(2)}\frac{dT^{(2)}}{dx}=f_x^{(1)}2\pi\left(r^{(2)}+\frac{d^{(2)}}{2}\right)-f_x^{(2)}\,2\pi\left(r^{(2)}-\frac{d^{(2)}}{2}\right),\qquad \text{(Eq. 69)}$$

$$\frac{dH^{(2)}}{dx}=f_y^{(1)}\,2\pi\left(r^{(2)}+\frac{d^{(2)}}{2}\right)^2-f_y^{(2)}\,2\pi\left(r^{(2)}-\frac{d^{(2)}}{2}\right)^2,$$

$$N^{(3)}+T^{(1)}\,2\pi r^{(1)}+T^{(2)}\,2\pi r^{(2)}=T_0^{(1)}\,2\pi r^{(1)}\qquad \text{(Eq. 70)}$$

$$f^{(1)}=k_T^{(1)}p^{(1)},\ \ f^{(2)}=k_T^{(2)}p^{(2)}\qquad \text{(Eq. 71)}$$

$$f_x^{(1)}=f^{(1)}\sin\beta^{(1)},\ \ f_y^{(1)}=f^{(1)}\cos\beta^{(1)},$$

$$\cos\beta^{(1)}=\left|h^{(1)}\right|\Big/\sqrt{T^{(1)^2}+h^{(1)^2}},\ \ \sin\beta^{(1)}=\left|T^{(1)}\right|\Big/\sqrt{T^{(1)^2}+h^{(1)^2}},$$

$$h^{(1)}=H^{(1)}\Big/\left(2\pi r^{(1)^2}\right),$$

$$f_x^{(2)}=f^{(2)}\sin\beta^{(2)},\ \ f_y^{(2)}=f^{(2)}\cos\beta^{(2)},\qquad \text{(Eq. 72)}$$

$$\cos\beta^{(2)}=\left|h_{12}\right|\Big/\sqrt{T_{12}^2+h_{12}^2},\ \ \sin\beta^{(2)}=\left|T_{12}\right|\Big/\sqrt{T_{12}^2+h_{12}^2},$$

$$h^{(2)}=H^{(2)}\Big/\left(2\pi r^{(2)^2}\right),$$

$$T_{12}=T^{(1)}\left(r^{(1)}/r^{(2)}\right)+T^{(2)},\ \ h_{12}=h^{(1)}\left(r^{(1)}/r^{(2)}\right)+h^{(2)}.$$

$$p^{(1)}=\left(w_0^{(1)}-b_{31}^{(1)}T^{(1)}-b_{32}^{(1)}H^{(1)}\right)\Big/b_{33}^{(1)}\qquad \text{(Eq. 73)}$$

$$p^{(2)}=p^{(1)}\left(r^{(1)}/r^{(2)}\right)-\left(b_{31}^{(2)}T^{(2)}+b_{32}^{(2)}H^{(2)}\right)\Big/b_{33}^{(2)}\qquad \text{(Eq. 74)}$$

$$\frac{dT^{(1)}}{dx}=-f_x^{(1)}\left(1-\frac{d^{(1)}}{2r^{(1)}}\right),\quad \frac{dH^{(1)}}{dx}=-f_y^{(1)}\,2\pi r^{(1)^2}\left(1-\frac{d^{(1)}}{2r^{(1)}}\right)^2,$$

$$\frac{dT^{(2)}}{dx}=f_x^{(1)}\left(1+\frac{d^{(2)}}{2r^{(2)}}\right)-f_x^{(2)}\left(1-\frac{d^{(2)}}{2r^{(2)}}\right),\qquad \text{(Eq. 75)}$$

$$\frac{dH^{(2)}}{dx}=f_y^{(1)}\,2\pi r^{(2)^2}\left(1+\frac{d^{(2)}}{2r^{(2)}}\right)^2-f_y^{(2)}\,2\pi r^{(2)^2}\left(1-\frac{d^{(2)}}{2r^{(2)}}\right)^2;$$

$$f^{(1)}=k_T^{(1)}p^{(1)},\ \ f^{(2)}=k_T^{(2)}p^{(2)};$$

$$p^{(1)}=\left(w_0^{(1)}-b_{31}^{(1)}T^{(1)}-b_{32}^{(1)}H^{(1)}\right)\Big/b_{33}^{(1)},\ \ p^{(2)}=p^{(1)}\left(r^{(1)}/r^{(2)}\right)-\left(b_{31}^{(2)}T^{(2)}+b_{32}^{(2)}H^{(2)}\right)\Big/b_{33}^{(2)};\qquad \text{(Eq. 76)}$$

$$f_x^{(1)}=f^{(1)}\sin\beta^{(1)},\ \ f_y^{(1)}=f^{(1)}\cos\beta^{(1)},\ \ f_x^{(2)}=f^{(2)}\sin\beta^{(2)},\ \ f_y^{(2)}=f^{(2)}\cos\beta^{(2)};\qquad \text{(Eq. 77)}$$

$$T^{(1)}(0)=T_0^{(1)},\ T^{(2)}(0)=0,\ H^{(1)}(0)=H^{(2)}(0)=0\qquad \text{(Eq. 78)}$$

Downloaded from www.periodico.tchequimica.com

$$H_0^{(1)} = -\left(b_{22}^{(1)} - b_{23}^{(1)} \frac{b_{32}^{(1)}}{b_{33}^{(1)}} \right)^{-1} \left[\frac{b_{23}^{(1)}}{b_{33}^{(1)}} w_0^{(1)} + \left(b_{21}^{(1)} - b_{23}^{(1)} \frac{b_{31}^{(1)}}{b_{33}^{(1)}} \right) T_0^{(1)} \right] \quad \text{(Eq. 79)}$$

$$T^{(1)}(0) = T_0^{(1)},\ T^{(2)}(0) = 0,\ H^{(1)}(0) = H_0^{(1)},\ H^{(2)}(0) = 0 \quad \text{(Eq. 80)}$$

$$T_0^{(1)} = N_0^{(1)} / (2\pi r^{(1)}) \quad \text{(Eq. 81)}$$

Table 1. *Parameters of conductive (aluminum) part of AS conductors*

AS conductors	Number of wires in the layers	Wire diameter, mm	Lay ratio
1	2	3	4
120/19	10+16	2.40	15, 12
120/27	12+18	2.20	15, 12
150/19	9+15	2.80	15, 12
150/34	12+18	2.50	15, 12
185/24	9+15	3.15	15, 12
240/39	10+16	3.40	15, 12
185/128	24+30	2.10	15, 12
300/39	9+15	4.00	15, 12
300/66	12+18	3.50	15, 12
330/30	10+16+22	2.98	15, 12, 10
330/43	12+18+24	2.80	15, 12, 10
400/22	10+16+22+28	2.57	18, 15, 13, 11
400/64	10+16	4.37	15, 12
400/93	12+18	4.15	15, 12
300/204	24+30	2.65	15, 12
500/26	8+14+20	3.90	15, 12, 10
500/64	12+18+24	3.40	15, 12, 10
550/71	12+18+24	3.60	15, 12, 10
600/72	12+18+24	3.70	15, 12, 10
650/79	15+21+27+33	2.90	18, 15, 12, 10

Downloaded from www.periodico.tchequimica.com

Table 2. *Parameters of cores – steel part of AS conductors*

AS conductor	Number of wires in the layers	Wire diameter, mm	Lay ratio
1	2	3	4
120/19	1+6	1.85	20
120/27	1+6	2.20	20
150/19	1+6	1.85	20
150/34	1+6	2.50	20
185/24	1+6	2.10	20
240/39	1+6	2.65	20
185/128	1+6+12+18	2.10	25, 20, 15
300/39	1+6	2.65	20
300/66	1+6+12	2.10	25, 20
330/30	1+6	2.30	20
330/43	1+6	2.80	20
400/22	1+6	2.00	20
400/64	1+6	3.40	20
400/93	1+6+12	2.50	25, 20
300/204	1+6+12+18	2.65	25, 20, 18
500/26	1+6	2.20	20
500/64	1+6	3.40	20
550/71	1+6	3.60	20
600/72	1+6+12	2.20	25, 20
650/79	1+6+12	2.30	25, 20

Table 3. *Stiffnesses of AS conductors*

AS conductors	d, mm	EJ_b, N·m^2	GJ_t, N·m^2	GJ_t^{exp}, N·m^2
1	2	3	4	5
120/19	15.15	113.6	15.37	14.22
120/27	15.40	125.3	16.50	15.19
150/19	16.75	166.8	23.03	21.25
150/34	17.50	208.9	27.50	25.32
185/24	18.90	269.5	37.18	34.45
240/39	21.55	463.1	62.60	58.23
185/128	23.10	835.9	82.66	76.88
300/39	23.95	695.4	96.14	88.84
300/66	24.50	812.2	101.48	97.28
330/30	24.78	807.5	103.77	101.81
330/43	25.20	867.2	120.92	108.88
400/22	26.56	1041.6	163.73	134.36
400/64	27.68	1261.3	170.52	158.50
400/93	29.10	1615.0	200.79	193.61
300/204	29.15	2119.1	209.61	194.95
500/26	30.00	1684.2	244.93	218.70
500/64	30.60	1885.4	262.89	236.73
550/71	32.40	2369.7	330.42	297.54
600/72	33.20	2632.8	360.17	328.03
650/79	34.70	3134.4	468.10	391.45

Downloaded from www.periodico.tchequimica.com

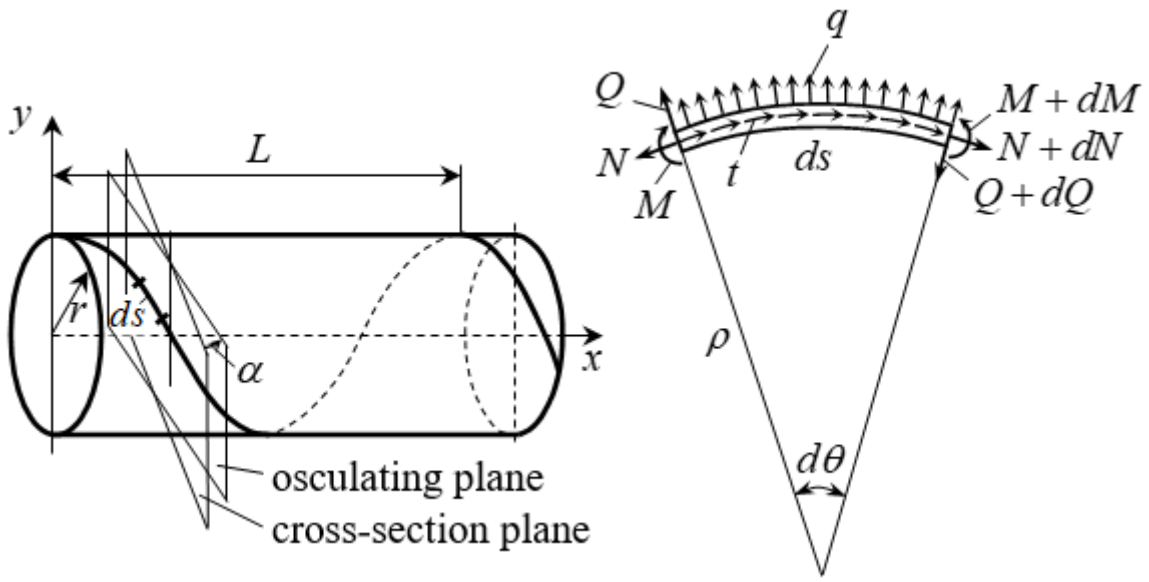

Figure 1. *The equilibrium of the differential element of the helical rod in the osculating plane*

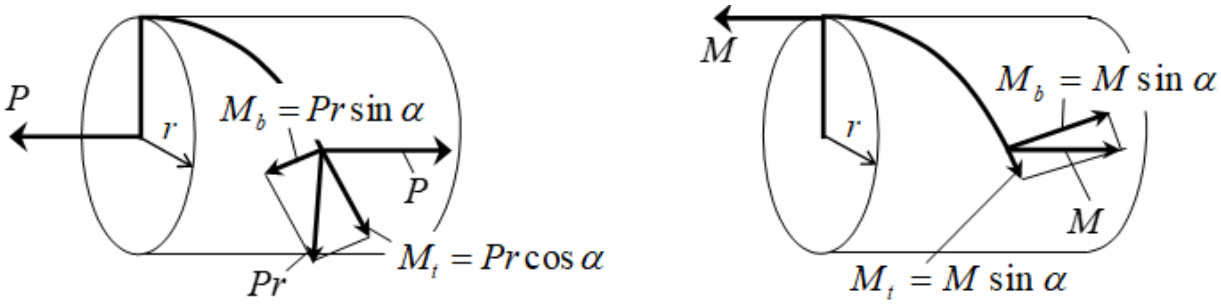

Figure 2. *Momenta in the cross section of the helical rod from the action of external force factors: a) Momenta from the action of longitudinal force; b) Momenta from the action of torque)*

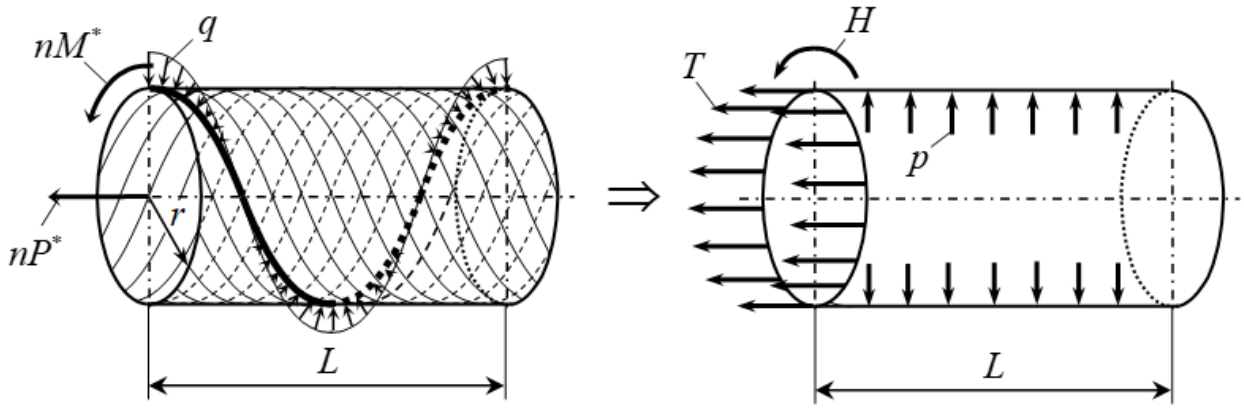

Figure 3. *The reduction of the conductor layer to an equivalent shell*

Downloaded from www.periodico.tchequimica.com

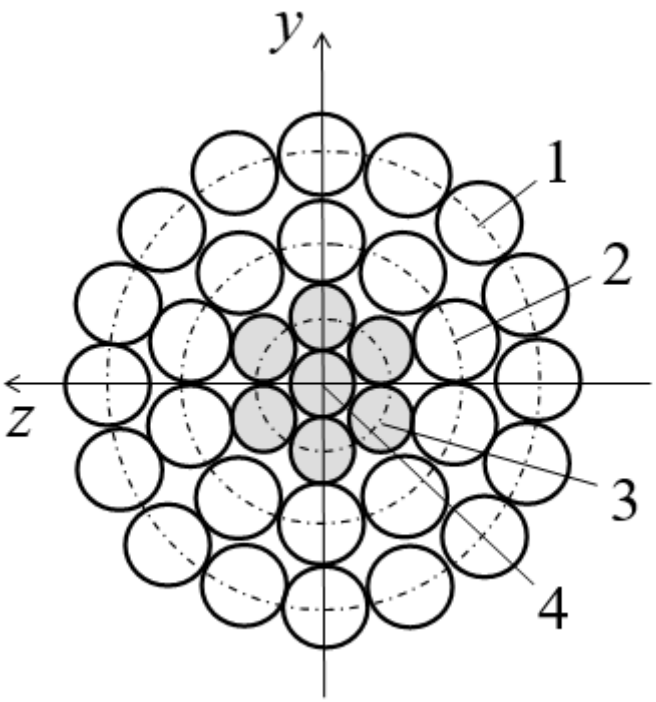

Figure 4. *AS conductor construction*

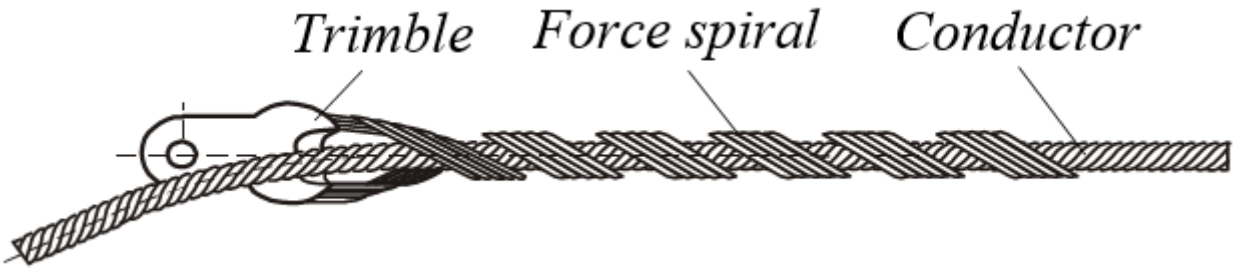

Figure 5. *Spiral tension clamp on the conductor*

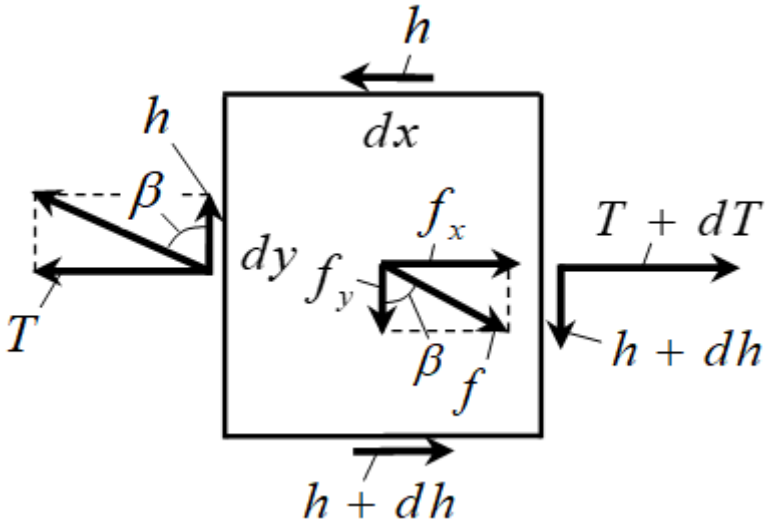

Figure 6. *Equilibrium of an element of an equivalent shell ring*

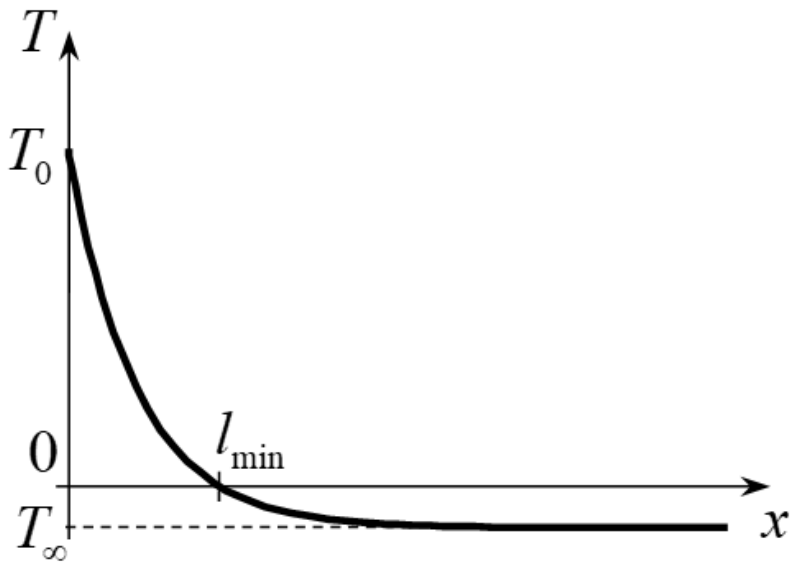

Figure 7. *Type of function (Equation 51)*

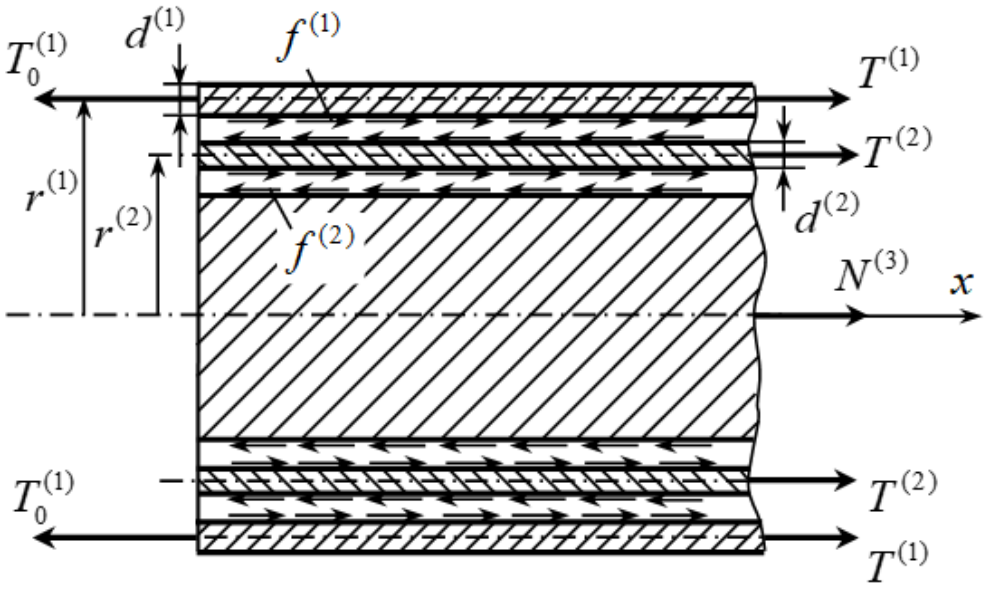

Figure 8. *The interaction of the clamp, the outer layer of the conductor and its internal part*

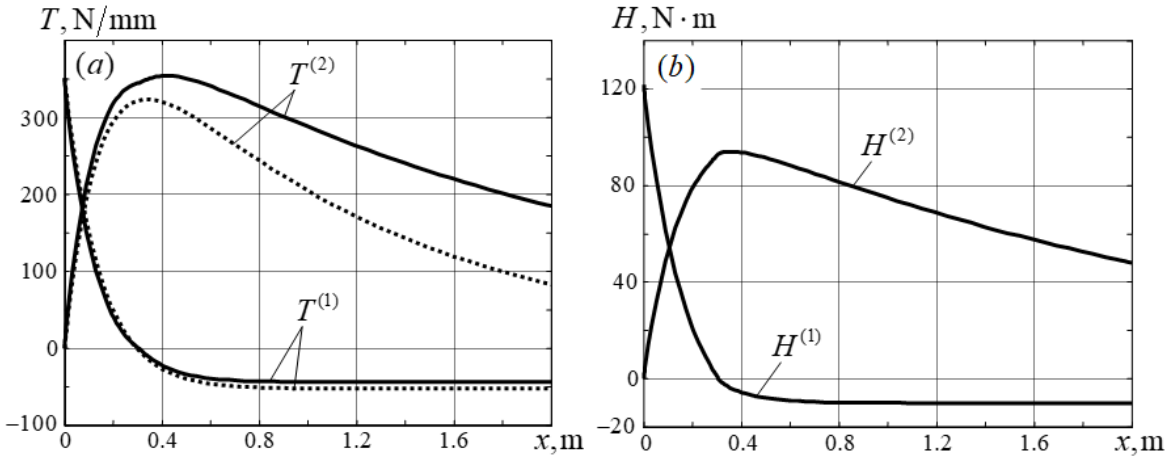

Figure 9. *The variation of the longitudinal force (a) and torque (b) in the clamp and outer conductor layer along with the coordinates*

Downloaded from www.periodico.tchequimica.com

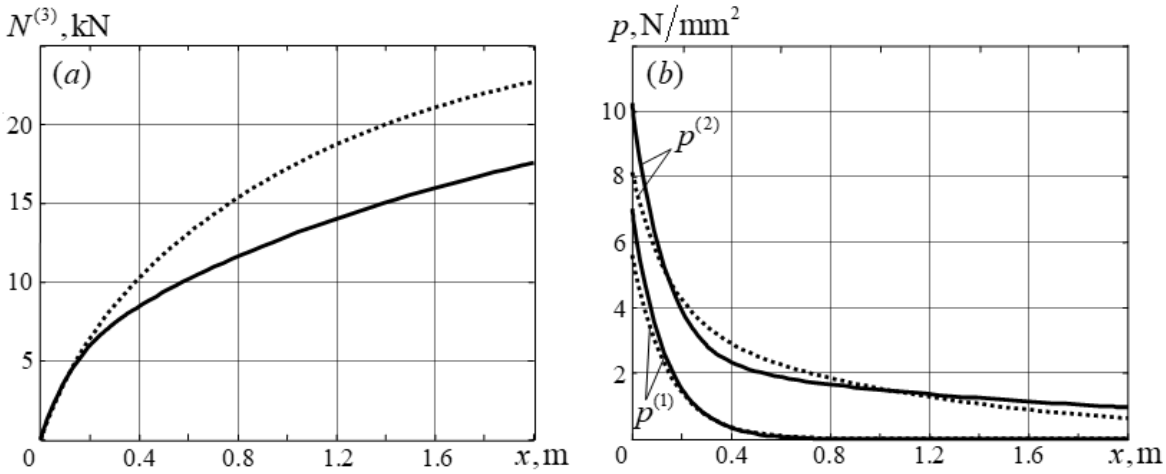

Figure 10. *The variation of the tensile force* $N^{(3)}$ *(a) in the inner conductor part and the internal pressure* $p^{(i)}$ *(b) between the clamp and the outer conductor layer* $(i=1)$*, and between the outer layer of the conductor and its inner part* $(i=2)$ *along the coordinate* x

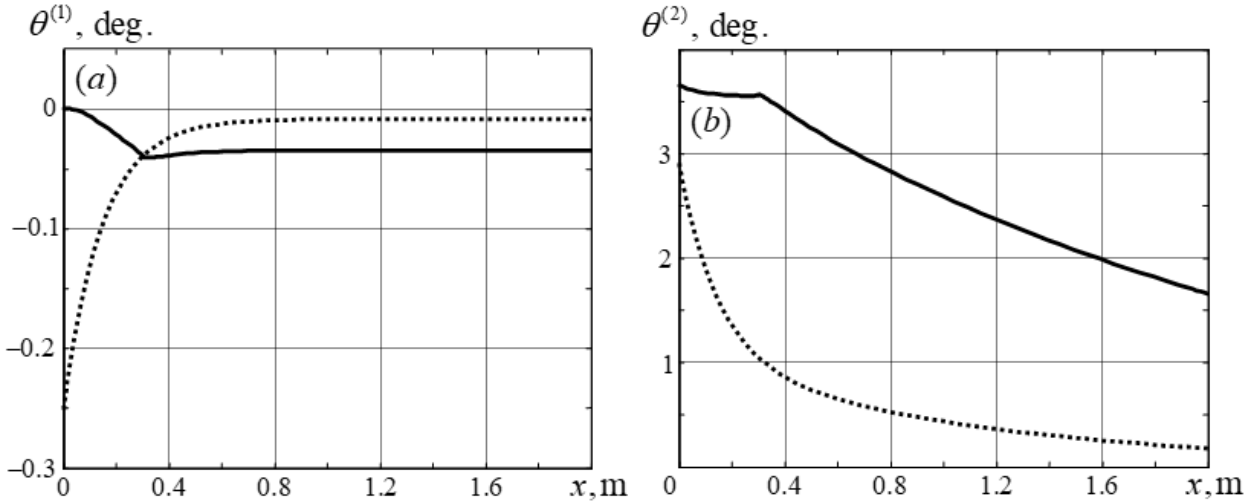

Figure 11. *The variation of rotation angles of clamp cross sections* $\theta^{(1)}$ *(a) and cross-sections of outer conductor layer* $\theta^{(2)}$ *(b) along the coordinate* x

Downloaded from www.periodico.tchequimica.com

PERIÓDICO TCHÊ QUÍMICA
ARTIGO ORIGINAL

TEOR TOTAL DE FENÓLICOS E ANTOCIANINA DE DOIS CULTIVOS DE UVA VERMELHA (*VITIS VINIFERA* L.) CVS SAHEBI E HALAGHO CONFORME AFETADOS PELA SEVERIDADE DA PODA E COMPRIMENTO DA CANA

TOTAL PHENOLICS AND ANTHOCYANIN CONTENT OF TWO RED GRAPE (*VITIS VINIFERA* L.) CVS SAHEBI AND HALAGHO CULTIVARS AS AFFECTED BY PRUNING SEVERITY AND CANE LENGTH

فنل کل و محتوای آنتوسیانین دو کلتیوار انگور قرمز صاحبی و حلقو و تاثیر پذیری آنها از شدت هرس و طول شاخه

MAHTAB, Zonouri[1]; DAVOOD, Bakhshi[2]*; ESMAEIL, Fallahi [3]; ISA, Arji[4]

[1]University of Guilan, Faculty of Agricultural Sciences, University Campus 2, Department of Horticultural Science

[2]University of Guilan, Faculty of Agricultural Sciences, Department of Horticultural Science

[3]University of Idaho, Parma Research and Extension Center, Parma

[4] Agricultural and Natural Resources Research and Education Center, Department of Crop and Horticultural Science Research

** Corresponding Author*
e-mail: bakhshi-d@guilan.ac.ir

Received 06 August 2019; received in revised form 20 September 2019; accepted 28 October 2019

RESUMO

Uma uva popular e importante a 'Sahebi' e uma uva local menos conhecida a 'Halagho' do Irã foram estudadas para desmascarar a influência da severidade da poda e do comprimento da cana nos potenciais bioativos da fruta; teor total de fenólicos e antocianinas nas quais eles afetaram significativamente. Nesta investigação, foram estudados os efeitos de 4, 6 e 8 gemas por cana com intensidade de poda leve, moderada e severamente podada e sua interação no curso de dois anos consecutivos, 2017 e 2018 nas variedades 'Sahebi' e 'Halagho'. Os resultados revelaram diferenças marcantes que, em qualquer cultivar, o conteúdo fenólico da polpa foi 2 a 5 vezes maior em 2017 em comparação com 2018 com a 'Halagho' severamente podada no mais alto (5,14 mg/g DW). Considerando que 'Halagho' podada levemente com 6 gomos por cana teve o maior conteúdo de antocianina da casca (1,09 mg/g DW), na mesma condição, mas com a poda severa 'Halagho' apresentou o maior conteúdo de antocianina na polpa (0,86 mg/g DW) enquanto no segundo ano, em 2018, podada severa ou levemente esse tipo com 6 gemas por cana teve um aumento significativo no acúmulo de compostos fenólicos (10 mg/g DW). A partir dos resultados deste experimento, pode-se concluir que a poda das videiras é um estressor e gera fitoquímicos aprimorados que podem possivelmente mitigar as consequências negativas. No entanto, a variação nas propriedades bioquímicas manifestou uma dependência notável da cultivar de uva, além do fator tempo, que foi mais pronunciado na variedade 'Halagho' do que na 'Sahebi'. Até certo ponto, o efeito das cultivares foi predominante nas diferenças de duas cultivares.

Palavras-chave: *polpa de bagas; qualidade da baga; casca das bagas; fecundidade de brotos; fitoquímicos.*

ABSTRACT

A popular and important grape ‘Sahebi’ and a less known local grape ‘Halagho’ in Iran, were studied to unmask the influence of pruning severity and cane length on fruit bioactive potentials; total phenolic and anthocyanin content in which they affected significantly. In this investigation, effects of 4, 6 and 8 buds per cane with pruning intensity as light, moderate and severely pruned and their interaction in the course two consecutive years, 2017 and 2018 in ‘Sahebi’ and ‘Halagho’ were studied. Results revealed striking differences which in either cultivar, pulp phenolic content was 2 to 5 fold higher in 2017 compared to 2018 with the severely pruned ‘Halagho’ at the highest (5.14 mg/g DW). Whereas, lightly pruned ‘Halagho’ with 6 buds per canes had the highest peel anthocyanin content (1.09 mg/g DW), in the same condition but with severely pruning ‘Halagho’ showed the highest anthocyanin content in pulp (0.86 mg/g DW) while in the second year, 2018, severely or lightly pruned this type with 6 buds per cane had a significant increase in phenolic compound accumulation (10 mg/g DW).

Downloaded from www.periodico.tchequimica.com

From the results of this experiment, it could be concluded that the pruning of the vines is a stressor and generates enhanced phytochemical constitutes to possibly mitigate the negative consequences. However, variation in the biochemical properties manifested a notable grape cultivar dependency in addition to the time factor, which was more pronounced in 'Halagho' than 'Sahebi'. To some extent the effect of cultivars on the differences of two cultivars was predominant.

Keywords: *berry pulp; berry quality; berry peel; bud fruitfulness; phytochemicals*

چکیده

یک رقم انگور محبوب و مهم 'صاحبی' و انگور محلی کمتر شناخته شده 'حلقو' در ایران ، برای آشکار کردن تأثیر شدت هرس و طول شاخه بر پتانسیل‌های بیوشیمیایی میوه مورد مطالعه قرار گرفتند. میزان فنل کل و آنتوسیانین کل در آنها به طور قابل توجهی تحت تأثیر قرار گرفت. در این تحقیق ، اثرات 4 ، 6 و 8 جوانه در هر شاخه با شدت هرس به عنوان سبک، متوسط و شدید و برهم کنش آنها در طی دو سال متوالی ، 2017 و 2018 در 'صاحبی' و 'حلقو' بررسی شد. نتایج نشان داد که در هر دو رقم اختلاف قابل توجهی وجود دارد، میزان فنل پالپ در سال 2017 در مقایسه با سال 2018 با هرس شدید 'حلقو' 2 تا 5 برابر بیشتر بوده و در بالاترین سطح (5/14 میلی گرم در گرم وزن خشک) قرار داشت. در حالی که ، هرس متوسط صورت گرفته در 'صاحبی' با 6 جوانه در هر شاخه دارای بالاترین میزان آنتوسیانین پوست (1.09 میلی گرم در گرم وزن خشک) را داشت، در همان شرایط اما با هرس شدید 'حلقو' دارای بالاترین میزان آنتوسیانین در پالپ بود (0.86 میلی گرم در گرم وزن خشک. در حالی که در سال دوم 2018، 'حلقو' هرس شدید یا سبک با 6 جوانه در هر شاخه افزایش قابل توجهی در تجمع ترکیب فنلی (10 میلی گرم در گرم خشک) را داشت. از نتایج این آزمایش می توان نتیجه گرفت که هرس انگور یک عامل تنش زا است و باعث افزایش ترکیبات فیتوشیمیایی می‌گردد تا با پیامدهای منفی تنش مقابله نماید. با این حال ، تغییر در خواص بیوشیمیایی علاوه بر عامل زمان، وابستگی قابل توجهی به رقم انگور را نشان می‌دهد، که این میزان در 'حلقو' از 'صاحبی' برجسته تر بود. تا حدودی اثر ارقام بر اختلاف دو رقم غالب بود.

کلمات کلیدی: پالپ حبه، کیفیت حبه، پوست حبه، باروری جوانه، فیتوشمیایی

1. INTRODUCTION

Grapevine (*Vitis vinifera* L.) is one of the most valuable agricultural crops worldwide. Archeological and historical discoveries suggest the Near-East region between the Black and Caspian seas where its early domestication could have been taken place (Myles *et al*., 2011).

The very first traces of grape cultivation detected in the north of Zagros mountains-Iran (McGovern, 2017). Considering the criticality of grape fruit, knowledge on almost every aspect in particular secondary metabolites in grapevine is expanding which helps vine growers to develop new cultivation techniques to modify and improve grape quality (Azuma, 2018). From which plant management can significantly contribute to improving viticultural practices in order to control plant physiological response, reflecting on enhancement table grape yield and quality. As a key task, pruning remains a manual operation that can largely influence a spectrum of quality and quantity properties (Billikopf and Norton, 1992; Keller, 2015).

As mentioned earlier, pruning is a cultural task with multidimensional effects which improving bud fruitfulness by selecting buds in appropriate positions as well as control of shoot numbers and their placement of vine and enhancement of fruit quality in general and lessening the fluctuation in average annual yield in long-term (Groumpos *et al*., 2015). Moreover, grapes enriched of an array of phenolic constitutes in the peel, seeds, and pulp which possess notable biological properties specifically antioxidant activity (Casazza *et al*., 2010). Being known for high nutritional and health values, fresh grape consumption is experiencing a significant and constant increase. In fresh fruits, texture and color attributes for the assessment of freshness and enjoyment of eating (Peneau *et al*., 2006).

Also, the peel of the red grape compose of a large number of phytochemicals, because polyphenolics specifically anthocyanins in berry distributed unevenly with main concentration in peels (Adams, 2006; Godevac *et al*., 2010) which confers numerous health benefits (Zhang *et al*., 2011), and since all phenolics contain at least one aromatic ring, they can consequently absorb UV light effectively (Cote *et al*., 2010). The grape polyphenol compounds are chiefly classified as

Downloaded from www.periodico.tchequimica.com

flavonoids (C6C3C6 skeleton) with a high level of anthocyanins (Garrido and Borges, 2013). Owing to their capability in quenching oxidants, anthocyanins are found to be accumulated in response to myriad number of environmental stresses (Braidot *et al*., 2008; Song *et al*., 2015). Additionally, they are potent bioactive constitutes with anti-inflammatory and anticancer activities (Xia *et al*., 2010).

The quantification of the quality traits of the grapevine can indeed provide viticulturists with invaluable practical knowledge, enable them to operate field tasks in a more efficient manner which ultimately leads to higher yield and filling the gap between supplies vs. demand (Barbagallo *et al*., 2011). The concentration and composition of phenolic compounds in red grapes differ with grape cultivars (Costa *et al*., 2014). In mountain vineyards, vines are trained by the head training systems, which due to its cost-effectiveness as well as low maintenance requirement is economically feasible. The lack of incident radiation in the clusters and excessive crop loads decrease quality.

Iran is one of the renown producers of table grapes and processed products such as juice and raisin in the world (FAO, 2014). Having an enormous variability of grapes in Iran, now various local grape cultivars being bred, albeit so far no significant attention on behalf of scholars has been paid to them. As a case in point, there is no published report concerning the berry phenolic content of 'Halagho' and 'Sahebi' grapes, native red grape cultivars which the former cultivar mostly coltivated in the west of Iran while the later cultivar is popular and coltivated widly. Hence, the purpose of current research was to evaluate the phenolic content and total anthocyanins of berries of those two abovementioned cultivars in the full ripening stage (e.g., in various parts: peel, pulp, and whole berry) to explore the effects of combined pruning severity and different bud numbers per cane in common vineyard conditions.

2. MATERIALS AND METHODS

2.1. Site description

The experiment was carried out in two consecutive growing seasons, 2017 and 2018, in a commercial vineyard located in Sarbarzeh region of Kermanshah province, in the west of Iran (34°45′46″N; 47°11′34″ E, 1923 m asl). Two seeded red table grape varieties,'Sahebi' and 'Halagho' from 20 year-old vines with head training at a spacing of 1.5 by 2.5 m in an east-west row orientation in a relatively equal status were used. Both cultivars were hardwood cutting-originated, irrigated with drip irrigation. During each phenological period the irrigation applied in addition to possible precipitation.

2.2. Pruning programs

The 20 years old vines that annually moderately pruned by the owner in this study defined as 'control'. Our concentration in this experiment was on exploring the possible impacts of the length of canes and the severity of pruning. Pruning plan was applied in late - Apr in 2017 and late- Mar in 2018 (Because of local weather conditions. Pruning severity treatments have consisted of two types of pruning; lightly pruned with the formula 40 + 20 and severely pruned with 20 + 20 formula (Ahmedullah and Himelrick, 1989). Afterward, in the number of buds per cane, substitute cane (two-node spur) were pruned with 2 bud lengths and by randomly with respective treatments: pruning, 4, 6 and 8 buds on the cane and different pruning intensity of light and intensity). To repeat this experiment in 2018, the substitute canes (two-node spur) pruned and each on cane, two buds remained exchanged.

2.3. Sampling

Specimens were collected at the berry fully ripe stage, based on the red color appearance. Picking grape bunches was carefully randomized throughout the vines for each cultivar. Vines were well managed, uniform in size, and had no nutrient deficiency or pest damage. At least 10 cluster samples were taken from each vine.

2.4. Biochemical analyzes

2.4.1. Fruit material and extract preparation

Briefly, grape samples were manually separated into peel and seeds. Berries were cut longitudinally with a razor blade, and seeds were carefully removed from each berry. The pulp on the inner face of berry peel was removed using an end-flattened spatula. Peel of freshly harvested grapes was directly separated, weighed and then pulverized with liquid nitrogen to ensure full phenolic extraction. Of each specimen 500 mg was mixed with 1.5 ml solvent containing 85% methanol and 15% acetic acid. Mixtures then incubated at 4 °C in the dark for 24 h. The extracts were centrifuged at 10000 rpm for 10 min, using Whatman filter papers the solvents removed from the extracts. The mixtures stored at 4 °C before use.

Downloaded from www.periodico.tchequimica.com

2.4.2. Total phenolic content

Total phenolic content (thereafter; TPC) in the grape extracts were evaluated colorimetrically according to the Folin-Ciocalteu colorimetric method (Singleton and Rossi, 1965) with slight modification. Briefly, 70 µl the grape extracts were mixed with 1 ml Folin-Ciocalteu reagent 10%, then added to 130 µl double distilled water. After 6 min, 7.5% sodium carbonate solution was added. The mixture was allowed to react at room temperature in the dark for 90 min, and then, the absorbance was measured at 760 nm. The results were expressed as milligrams of gallic acid equivalents (GAE) per gram dry weight. Gallic acid was employed as a calibration standard. The measurements were compared to a standard curve of prepared gallic acid solutions and expressed as mg gallic acid equivalents per gram dry weight (GAE/g DW) ($y=3.0912x+0.0502$, $y^2= 9962$) of peel and pulps. The standard curve was generated with 0.10, 0.20, 0.30 and 0.40 mg gallic acid/L by a UV-vis double-beam spectrophotometer (T80+UV/VIS PG Instrument Ltd) at the wavelength of 750 nm.

2.4.3. Total anthocyanin content

Using Wrolstad (1976) method with some change the total anthocyanin content (thereafter; TAC) was measured. The absorbance of the anthocyanin containing extract, described above, was then measured at 520 and 700 nm in two reference pH 1.0 and 4.5 buffers against a blank of reagents according to Longo and Vasapollo (2006). The calculation of cyanidin 3-glucoside (C3G) was done using Equations 1 and 2.

$$A= (A_{510} - A_{700})_{pH\ 1.0} - (A_{510} - A_{700})_{pH\ 4.5} \quad \text{(Eq. 1)}$$

$$\text{TMA content} = (\Delta A \times MW \times DF \times Ve \times 1000) / (\varepsilon \times 1 \times C) \quad \text{(Eq. 2)}$$

Where A is absorbance, MW is the molecular weight of cyanidin-3-glucoside (449.2), DF is the dilution factor (1), Ve is the extract volume, ε is the molar absorptivity coefficient of cyanidin-3-glucoside (29,600), and M is the mass of the berries extracted and C is the concentration of the grape extract in milligrams per milliliter. The final results expressed as mg/g DW of anthocyanin.

2.5. Statistical analysis

The experimental design used was a split-split plot with three replicates. The main factors consisted of time (year) with two levels (2017 and 2018) and grape cultivars with two levels (‘Sahebi’ and ‘Halghoo’). The severity of pruning (light, moderate and severe) was considered as sub-plot factor and number of buds per cane (4, 6, 8 buds per cane) as sub-sub (or split-split) factors. Analysis of variance was performed using the SAS statistical package (version 9.4; SAS Institute, Cary, NC, USA). Differences among treatments were assessed by Duncan’s range test at the level of 1% and 5%.s

3. RESULTS AND DISCUSSION

A notably valuable insight into the impacts of pruning practice on phytochemical contents of two important Iranian red grapes was acquired, in which in terms of time factor the TPC of the grape peel, as well as pulps in either cultivar, was significantly higher in 2017 than 2018, by comparison (Table 1 and 2). Interestingly enough, TPC of the whole berry in 2018 was significantly higher when compared with 2017 (Table 3). Whereas to some extent, similar to the TPC behavior pattern, in 2017, TAC of peel, pulp, and whole berry was higher in 2017 than in 2018 (Tables 4, 5 and 6). In 2017, as negative consequences of pruning, imposing stress, and significant decrement in yield and fruit size by comparison to control were witnessed.

By 2018, vines reached stable physiological conditions, which as a result, enhancement in fruit growth was observed. Increasing the amount of phenolic compounds in peel and pulp in 2017 compared to 2018 can also be justified by the fact that due to increased light penetration into the crown of vines, in all forms of pruning severity light, moderate and severe.

Archer and Strauss (1989) reported that the fruit composition is affected by the microclimate inside the crown, in shade conditions, the quality of fruit in grapes is greatly reduced. In fact, with the increase of light penetration into the vines, phenolic compounds increased in 2017, but in 2018, by creating a coating on grape fruit clusters, reduced light intensity and phenolic compounds decreased. The phenolic content was significantly lower in the grape pulp when compared with peel (Table 2). The content of phenolics seems to be a tissue specific trait. Phenolics were lower in pulp compared to peel which is in accordance with other scholars (Pantelic, 2016), unlike pulp, the grape peel contains a large array of phenolic compounds (Nile *et al*., 2013).The accumulation of secondary metabolites is a strategy of plant

Downloaded from www.periodico.tchequimica.com

defense against stress.

Vine response to stress at the berry level resulted in the accumulation of secondary metabolites in pulp and peel as a defense against cell degradation (Ferrandino and Lovisolo, 2013).

On the other hand, considering the fact that parameters such as yield, TSS, TA and number of berries per bunch showed a statistically significant increase in 2018 (data not shown), hence, it could be pointed that increase in volume of yield may lead to lessen the concentration of phytochemicals of interests in this experiment. In 2017, peel phenols of 'Sahebi' were significantly lower than 'Halagho' in all pruning levels and number of buds per cane (Table 1).

Differences in the phenolic compounds of various grape cultivars have also been proven in others' studies (Rodriguez-Montealegre, 2006; Orak, 2007; Pantelic, 2016). The grape cultivar exerts a significant influence on the phenolic composition (Dani *et al*., 2007; De Pascali *et al*., 2014).The concentration and composition of phenolic compounds in red grapes differ with grape cultivars (Costa *et al*., 2014).

In which in this study regardless of the factor of year, the two grapes type almost followed a consistant pattern since the compounds targeted in 'Sahebi' where lower in general when capered to 'Halagho'. The difference in phenolic contents in the peel of cultivated grapes couldbe partly attributed to the genotypes (Montealegre *et al*., 2006).Peel morphological and structural characteristics, as dictated by the cultivar, seem to exert a direct effect on the extractability of phenolic compounds (Rolle *et al*., 2009). Biochemically, flavonoids and anthocyanins are important determinants of antioxidant capacity and quality of fruit.

Acylated derivatives of anthocyanin greatly affect its stability and color intensity.In this study, there was a significant difference between the anthocyanin and phenol compounds in 'Halagho' and 'Sahebi', indicating the genetic difference and the enzymes involved in the bio production of the compounds in different cultivars reported by other researchers (Yonekura-Sakakibara, 2009).

Severe and moderate pruning of 'Halagho' during 2018 lead to a significant increase in TPC in the whole berry. In 2017, severely and lightly pruned of 'Sahebi' compared with control treatment, and maintenance of 4, 6 or 8 buds per cane showed a significant decrease in total phenol content in the whole berry which showed no significant difference at all (Table 3).

In the case of the interaction between years, grape cultivars, pruning severity and the number of buds per cane showed that 'Halagho', when pruned in 2017 with 6 or 4 buds per cane, showed peel anthocyanin content which was not significantly affected by treatments. In 2018, peel anthocyanin content in both cultivars decreased without any significant difference (Table 4). In severely pruned 'Halagho' in 2017 and the maintenance of 6 buds per cane increased pulp anthocyanin significantly compared to other treatments.

The pulp anthocyanin in both cultivars decreased significantly in 2018 (Table 5). Severe pruning of 'Sahebi' in 2017 with 4 buds per cane increased TAC in the whole berry which was not significantly different from the other treatments. In 2018, TAC was significantly decreased in both cultivars compared with 2017. However this difference was not significantly different (Table 6). The results of this experiment indicated that the pruning of two cultivars, 'Halagho' and 'Sahebi' (in particular the 'Halagho'), in 2017, increased anthocyanin content in the peel, pulp, and whole berry as compared in 2018. In all pruning levels, a self-regulating branch growth was found leading to an increase in compounds such as anthocyanin and total phenols. In red grapes, such as 'Halagho' and 'Sahebi', anthocyanins are an important group of phenolic compounds (Yang *et al*., 2009) because of their valuable nutritional and medicinal benefits and visual quality of their color. The peel color plays an important role in determining fruit quality of table grapes, mainly due to the composition and the content of anthocyanins (Paredes-Lopez *et al*., 2010). It is shown that the quantity and quality of anthocyanins in grape berries greatly influence the quality of red grapes (Boss *et al*., 1996). Phenolics in the plant kingdom are important because of their function in the defense system. Pruning has a significant effect on the accumulation of these compounds. In order to synthesize anthocyanin in grapevine berries and to balance juice compounds, clusters should receive direct sunlight (Spayd *et al*., 2002). Due to the high temperature for producing high quality fruits and berries with maximum color, it should be prevented from exposing clusters to long-term exposure to sunlight (Bergqvist *et al*., 2001). In confirmation of this point, the results of this research showed that the pruning of the

Downloaded from www.periodico.tchequimica.com

'Halagho' in light form in 2017 and keeping 6 buds per cane or the severe pruning of this cultivar in 2017 and keeping 4 buds per cane increased anthocyanin content in the peel. These results are consistent with reports from Shinomiya *et al*. (2015). Vine or cluster exposure to low temperature and high light intensity enhances anthocyanin accumulation which was not seen in the current work. This might be due to the training system used in this study. High temperature and/or shading treatments reduce berry peel coloration. Reports of increasing anthocyanin accumulation due to sunlight exposure have helped growers to avoid poor peel coloration by incorporating light quality control methods, such as shoot positioning and light reflectors around the fruiting zone. In a vineyard, the training system determines the light interception for a certain amount of leaf area and consequent bud and fruit exposure to sunlight (Reynolds and Heuvel, 2009). Bunch sunlight and UV exposure significantly increase anthocyanins content in the grape (Song *et al*., 2015). In particular, temperature and irradiance are critical because of their direct effect on the synthesis and accumulation of polyphenols in the berries (Keller, 2010). The effects of light on grapevine physiology have been exploited to address grape berry quality: different training systems, influencing the vine light use efficiency exert pivotal consequences on berry quality (Petrie *et al*., 2009).

The reduction of the anthocyanin level in 2018 can also be due to branch growth. The anthocyanin levels in the whole berry, pulp and peel are significantly lower than in 2017. It has been proved that phenolic biosynthesis may be induced in response to different abiotic elicitors (Song *et al*., 2015). In 2017, the number of canes was reduced due to differences in pruning intensity compared to 2018. The number of cane per plant in the year 2016 was significantly higher than in 2017 and 2018, and there was a significant difference at the probability level of 1%. But in 2018, due to the stability of the number of canes, the intensity of pruning was reduced and became stable. Vine vigor and viticulturaL practice of the grapes may also impact on grape anthocyanin concentration. The vigor parameters including main shoot length and total shoot length were positively correlated to yield; were negatively correlated with berry anthocyanin production (Baluja *et al*., 2012). The low number of shoots per canopy volume can lead to a reduction in the intensity and even to a complete cessation of various metabolic processes (Jones, 1992) which was concluded in the current work (data was not shown).

4. CONCLUSIONS

Phenolic constitutes possess a large quantity of biochemical properties from which grapes are their renowned source with undisputable importance in the daily diet of people worldwide. Whereas, pruning as a critical practice if adopted un appropriately like pruning all mature canes by local grape growers, heavy exploitation of stored nutritional material of the tree and therefore, reduction in vines vigourity, as well as quality, would be the aftermath. The results obtained are reliable proof that the pruning program can negative or positively influence phenolic compound concentration in grape. More, the grape cultivars show different sensitivity to the type of viticultural practice which was observed in 'Sahebi' and 'Halagho'. These findings are valuable to improve viticultural practices in grape production, allowing the improvement of grape quality to forecast the potential crop before pruning. Nonetheless, applying this pruning program on the same cultivars with other training systems further needs to be investigated. Additionally, the locality is another crucial factor that understands its effectiveness on these two cultivars is essential. Ultimately, the present work expands the knowledge of appropriate pruning and management on two Iranian red grape cultivars for grape growers.

ACKNOWLEDGMENTS

We thank the Department of Horticultural Sciences of the University of Guilan for supplying equipment to this study.

REFERENCES

1. Adams, D. O. *Am. J. Enol. Vitic*, 2006, 57(3): 249-256.
2. Ahmedullah, M., Himelric, D. C. *Grape management*, 1989, 383-471.
3. Archer, E., Strauss, H. C. S. *Afri. J. Enol. Vitic*, 1989, 10(2): 74-76.
4. Azuma, A. *J. Hortic*, 2018, 59-63.
5. Baluja, J., Diago, M. P., Goovaerts, P.,Tardaguila, J. *Precision Agric*, 2012, 13:457-472.
6. Barbagallo, M. G., Guidoni, S., Hunter, *J. J. S. Afr. J. Enol. Vitic*, 2011, 32: 129-136.
7. Battista, F., Tomasi, D., Porro, D., Caicci, F., Giacosa, S., Rolle, L. Italian J. *Food*

Downloaded from www.periodico.tchequimica.com

Sci, 2015, 27: 136-141.

8. Bergqvist, J., Dokoozlian, N., Ebisuda, N. *Amer. J. Enol. Viti*, 2001, 52(1): 1-7.
9. Billikopf, G., Norton, M. *California Agric*, 1992, 46 (5): 12-13.
10. Boss, P. K., Davies, C., Robinson, S. P. *Plant Physiol*, 1996, 111(4):1059-1066.
11. Braidot, E., Zancani, M., Petrussa, E., Peresson, C., Bertolini, A., Patui, S., Macri, F., Vianello, A. *Plant Signaling and Behav*, 2008, 3: 626-632.
12. Casazza, A. A., Aliakbarian, B., Mantegna, S., Cravotto, G., Perego, P. J. *Food Engi*, 2010, 100: 50-55.
13. Costa, E., Cosme, F., Jordao AM, Mendes-Faia, A. Int. J vine and wine sci, 2014, 48:51-62.
14. Cote, J., Caillet, S., Doyon, G., Sylvain, J. F., Lacroix, M. *Critical Rev. Food Sci*. *Nutri*, 2010, 50: 872-888.
15. Dani, C., Oliboni, L. S., Vanderlinde, R., Bonatto, D., Salvador, M., Henriques, J. A. P. *Food Chem. Toxic*, 2007, 45: 2574-2580.
16. De Pascali, S. A., Coletta, A., Del Coco, L., Basile, T., Gambacorta G, Fanizzi, F.P. *Food Chem*, 2014, 161, 112-119.
17. Ferrandino, A., Lovisolo, C. *Environ Experi Bot*, 2013, 114-124.
18. Garrido, J., Borges, F. *Food Res. Inter*, 2013, 54:1844-1858.
19. Godevac, D., Tesevic, V., Velickovic, M., Vujisic, L. J., Vajs, V, Milosavljevic, S. *J. Serb*. *Chem. Soc*, 2010, 75: 1641-1652.
20. Gomez Gallego, M. A., Sanchez-Palomo E, Hermosın-Gutierrez I, Gonzales Vinas MA. J Europ. *Food Res. Technol*, 2013, 236:647-658.
21. Groumpos, P. P., Antigoni, A. P., Groumpos, P., Vasileios, P. *IFAC-PapersOnLine*, 2015, 48-24: 015-020.
22. Hogan, S., Zhang, L., Li, J., Zoecklein, B., Zhou, K. LWT - *Food Sci. and Tech*, 2009, 42: 1269-1274.
23. Intrigliolo, D. S., Castel, J. R. (2011). *Irriga. Sci*, 29:443-454.
24. Jones, H. G. *Cam. Uni. Press*, *Cambridge*, 1992
25. Katalinic, V., Smole Mozina, S., Skroza, D., Generalic, I., Abramovic, H., Milos, M., Ljubenkov, I., Piskernik S, Pezo I, Terpinc P, Boban, M. *Food Chem*, 2010, 119: 715-723.
26. Keller, M. The Science of Grapevines: Anatomy and Physiology. *Acad. Press*. 2015.
27. Keller, M. J. *Grape and Wine Res*, 2010, 16: 56-69.
28. Longo, L., Vasapollo, G. *Food Chem*, 2006, 94(2), 226-231.
29. Mannini, F., Mollo, A., Lale Demoz, P. *Agric Vitis*, 2010, 127: 142-147.
30. McGovern, P., Jalabadze, M., Batiuk, S., Callahan, M. P., Smith, K. E., Hall, G. R., Kvavadze, E, Maghradze D, Rusishvili N, Bouby L, Failla O, Cola G, Mariani L, Boaretto E, Bacilieri R, This P, Wales, N, Lordkipanidze, D. *Proce. Nation. Acad. of Sci*, 2017, 114, 10309-E10318.
31. Montealegre, R. R., Peces, R. R., Vozmediano, J. L. C., Gascuena, J. M., Romero, E. G. *J. Food Comp. Anal*, 2006, 19(6-7): 687-693.
32. Myles, S., Boyko, A. R., Owens, C. L., Rown, P. J., Grassi, F., Aradhya, M. K., Prins, B., Reynolds, A., Chia, JM., Ware, D., Bustamante, C. D., Buckler, E. S. *Proce. Nation. Acad. of Sci*, 2011, 108 (9): 3530-3535.
33. Nile, S. H., Kim, S. H., Ko, E. Y, Park, S. W. *BioMed Res Int*, 2013, 71: 65-80.
34. Orak, H. H. *Sci. Hort*, 2007, 111: 235-241.
35. Pantelic, M. M., Zagorac, D. C. D., Davidovic, S. M., Todic, S. R., Beslic, Z. S., Gasic, U. M., Tesic, Z. L., Natic, M. M. *Food Chem*, 2016, 211: 243-252.
36. Paredes-Lopez, O., Cervantes-Ceja, M. L., Vigna-Perez, M., Hernandez-Perez, T. *Plant Foods for Human Nutri*, 2010, 65: 299-308.
37. Peneau, S., Hoehn, E., Roth, H. R., Escher, F., Nuessli, *J. Food Qual. Pref*. 17: 9-19.
38. Petrie, P. R., Trought, M. C. T., Howell, G. S., Buchan, G. D., Palmer, J. W. *Amer. J. Enol. Vitic*, 2009, 60 (2): 173-182.
39. Reynolds, A. G., Heuvel J. *Am. J. Enol. Vitic*, 2009, 60: 251-268.

Downloaded from www.periodico.tchequimica.com

40. Rodriguez-Montealegre, R., Romero-Peces, R., Chacon-Vozmediano, J. L., Martinez Gascuena, J., Garcia-Romero, E. *J. Food Comp. Anal*, 2006, 19: 687-693.

41. Rolle, L., Torchio, F., Zeppa, G., Gerbi, V. *Amer. J. Enol. Vitic*, 2009, 60:93-97.

42. Satisha, J., Ramteke, S. D., Shikhamany, S. D*. Ind. J Horti*, 2000, 57(1): 9-12.

43. Shinomiya, R., Fujishima, H., Muramoto, K., Shiraishi, M. *Scientia Horti*, 2015, 193: 77-83.

44. Singleton, V. L., Rossi, J. R. *Amer. J. Enol. Vitic*, 1965, 16: 144-158.

45. Song, J., Smart, R., Wang, H., Dambergs, B., Sparrow, A., Qian, M. C. *Food Chem*, 2015, 173: 424-431.

46. Spayd, S. E., Tarara, J. M., Mee, D. L., Ferguson, J. *Amer. J. Enol. Vitic*, 2002, 53(3): 171-182.

47. Wrolstad, R. E. *Corvallis*, *Ore: Oregon Agric Expt Station Bull*, 1976, 624.

48. Xia, E. Q., Deng, G. F., Guo, Y. J., Li, H. B. *Int. J Mol*. *Sci*, 2010, 11: 622-646.

49. Yang, J., Martinson, T. E., Liu, R. H. *Food Chem*, 2009, 116: 332-339.

50. Yonekura-Sakakibara, K., Nakayama, T., Yamazaki, M., Saito, K. *Springer*. New York: 2009, 169-190.

51. Zhang, A., Fang, Y., Li, X., Meng, J., Wang, H., Li, H. *Mol*, 2011, 16: 2846-2861

Table 1: *Peel phenolic content of 'Sahebi' and 'Halagho' grapes pruned during the years 2017 and 2018*

Peel phenolic content (mg/g DW)					
		2017		2018	
Treatment	Number of buds per cane	Halagho	Sahebi	Halagho	Sahebi
control	Moderately pruned	43.81 a	28.80 d	19.10 e	12.00 e
Severely pruned	4	42.51 a	27.71 d	20.5 e	14.40 e
	6	31.44 c	26.85 d	23.90 e	12.10 e
	8	38.15 ab	29.10 d	21.30 e	12.20 e
Lightly pruned	4	39.76 ab	27.45 d	20.90 e	14.50 e
	6	34.00 bc	26.59 d	25.50 e	14.00 e
	8	43.27 a	28.51 d	21.20 e	14.20 e

Meanes with the same letters in each column and row show no significant difference in Duncan's multiple range test at $p \leq 5\%$.

Downloaded from www.periodico.tchequimica.com

***Table 2**: Pulp phenolic content in 'Sahebi' and 'Halagho' grapes pruned during the years 2017 and 2018*

Pulp phenolic content (mg/g DW)					
		2017		2018	
Treatment	Number of buds per cane	Halagho	Sahebi	Halagho	Sahebi
Control	Moderately pruned	4.05bc	2.65de	1.38fg	0.61g
Severely pruned	4	3.68bcd	3.29cd	0.94fg	0.79fg
	6	3.27cd	2.71de	1.42fg	0.72fg
	8	5.14a	2.70de	1.10fg	0.81fg
Lightly pruned	4	3.29cd	2.89cde	0.84fg	0.84fg
	6	3.05cde	2.65de	1.86ef	0.80fg
	8	4.56ab	2.63de	0.80fg	1.17fg

Meanes with the same letters in each column and row show no significant difference in the Duncan's multiple range test at $p \leq 5\%$.

***Table 3**: Total phenolic content of the whole berry in 'Sahebi' and 'Halagho' grapes pruned during the years 2017 and 2018*

Total phenol content in the whole berry (mg/g DW)					
		2017		2018	
Treatment	Number of buds per cane	Halagho	Sahebi	Halagho	Sahebi
Control	Moderately pruned	6.23efgh	4.60i	7.74bcde	7.25cdef
Severely pruned	4	5.50hi	4.70i	8.37bc	8.12bc
	6	5.63ghi	4.48i	10.00a	7.28cdef
	8	5.30hi	4.62i	7.02cdefg	7.50bcde
Lightly pruned	4	6.38efgh	4.65i	7.62bcde	7.41bcdef
	6	5.57ghi	5.94fghi	8.86ab	7.92bcd
	8	6.42defgh	4.75i	7.60bcde	8.36bc

Meanes with the same letters in each column and row show no significant difference in Duncan's multiple range test at $p \leq 5\%$.

Downloaded from www.periodico.tchequimica.com

Table 4**:** *Peel anthocyanin content in 'Sahebi' and 'Halagho' grapes pruned during the years 2017 and 2018*

Peel anthocyanin content (mg/g DW)					
		2017		2018	
Treatment	Number of buds per cane	Halagho	Sahebi	Halagho	Sahebi
Control	Moderately pruned	0.93 a-c	0.95 a-c	0.03 f	0.03 f
Severely pruned	4	1.07 a	0.78 b-e	0.04 f	0.04 f
	6	0.88 a-d	0.62 de	0.03 f	0.11 f
	8	1.00 ab	0.63 de	0.03 f	0.04 f
Lightly pruned	4	0.69 c-e	0.97 ab	0.03 f	0.04 f
	6	1.09 a	0.55 e	0.04 f	0.03 f
	8	0.94 a-c	0.74 b-e	0.03 f	0.04 f

Meanes with the same letters in each column and row show no significant difference in Duncan's multiple range test at $p \leq 5\%$.

Table 5: *Pulp anthocyanin content in 'Sahebi' and 'Halagho' grapes pruned during the years 2017 and 2018*

Pulp anthocyanin content (mg/g DW)					
		2017		2018	
Treatment	Number of buds per cane	Halagho	Sahebi	Halagho	Sahebi
Control	Moderately pruned	0.48 c	0.51 c	0.007 d	0.001 d
Severely pruned	4	0.62 bc	0.55 c	0.003 d	0.011 d
	6	0.86 a	0.52 c	0.006 d	0.002 d
	8	0.49 c	0.70 b	0.004 d	0.043 d
Lightly pruned	4	0.48 c	0.55 c	0.001 d	0.005 d
	6	0.49 c	0.51 c	0.001 d	0.006 d
	8	0.51 c	0.51 c	0.003 d	0.003 d

Meanes with the same letters in each column and row show no significant difference in Duncan's multiple range test at $p \leq 5\%$.

Downloaded from www.periodico.tchequimica.com

***Table 6**: Total anthocyanin content in 'Sahebi' and 'Halagho' grapes pruned during the years 2017 and 2018*

Total anthocyanin content (mg/g DW)					
		2017		2018	
Treatment	number of buds per cane	Halagho	Sahebi	Halagho	Sahebi
control	moderately pruned	0.51 a	0.33 c	0.031 d	0.024 d
Severely pruned	4	0.38 a-c	0.40 a-c	0.030 d	0.031 d
	6	0.48 ab	0.34 bc	0.030 d	0.092 d
	8	0.43 a-c	0.37 bc	0.023 d	0.026 d
Lightly pruned	4	0.48 ab	0.35 bc	0.027 d	0.026 d
	6	0.34 bc	0.36 bc	0.028 d	0.026 d
	8	0.38 a-c	0.28 c	0.025 d	0.028 d

Meanes with the same letters in each column and row show no significant difference in Duncan's multiple range test at $p \leq 5\%$.

Downloaded from www.periodico.tchequimica.com

PERIÓDICO TCHÊ QUÍMICA
ARTIGO ORIGINAL

A COMPREENSÃO SUBJETIVA DO ESTUDANTE AO USAR RECURSOS EDUCACIONAIS ABERTOS

SUBJECTIVE UNDERSTANDING OF THE STUDENT WHEN USING OPEN EDUCATIONAL RESOURCES

СУБЪЕКТНОЕ ПОНИМАНИЕ СТУДЕНТА ПРИ ИСПОЛЬЗОВАНИИ ОТКРЫТЫХ ОБРАЗОВАТЕЛЬНЫХ РЕСУРСОВ

BAZYLOVA, Baglan[1*]; ZHUSUPOVA, Zhanna[2]; KAZHIGALIEVA, Gulzhan[3]; ONALBAYEVA, Aigul[4]; KALININA, Valentina[5];

[1,3,4,5] Kazakh State Women's Teacher Training University, Department of Russian Language and Literature, Almaty – Republic of Kazakhstan

[2] K. Zhubanov Aktobe Regional State University, Department of Pedagogy, Psychology and Primary Education, Aktobe – Republic of Kazakhstan

** Correspondence author*
e-mail: baglan_5_3@mail.ru

Received 11 September 2019; received in revised form 20 October 2019; accepted 29 October 2019

RESUMO

A relevância do estudo se deve ao fato de que os recursos educacionais abertos têm a capacidade de se livrar do desenho metodológico básico que complica o processo de aprendizagem entre os estudantes, ou seja, de usar a experiência internacional no ensino e na aquisição de conhecimento. Este estudo mostra aspectos do funcionamento dos recursos educacionais abertos e sua base tecnológica. A novidade do trabalho reside na formação de um modelo de uso de recursos educacionais abertos na preparação de cursos especializados do Departamento de Química Aplicada. Os autores mostram que a eficácia do uso de recursos educacionais abertos depende diretamente da proporção de aprendizagem on-line e do isolamento tecnológico das disciplinas. Em particular, não apenas os processos educacionais são levados em consideração na implementação do programa de química aplicada, mas também outras disciplinas que exigem a troca de experiências entre países e o uso de uma ampla gama de equipamentos tecnológicos e uma estrutura on-line. Em particular, se considera o treinamento no exemplo de bancos de dados, redes de informação e outras estruturas espacialmente distribuídas. A importância prática do estudo é determinada pelo fato de que o uso de recursos educacionais abertos não só intensificará o processo educacional na universidade, mas também determinará a possibilidade de integração no espaço educacional global.

Palavras-chave: *Recurso educacional, eficácia educacional, departamento de química aplicada, ensino superior.*

ABSTRACT

The relevance of the study is determined by the fact that open educational resources carry the ability to overcome the basic methodological construct complicating the learning process among students and namely the use of international experience while learning and obtaining knowledge. This study shows the aspects of functioning open educational resources and their technological basis. The novelty of the work was the formation of a model for the use of open educational resources in training of specialized courses of the Department of applied chemistry. The authors showed that the effectiveness of open educational resources use depends directly on the share of online learning and technological isolation of subjects. In particular, not only learning processes in the implementation of the program in applied chemistry, but also other disciplines that require the exchange of experience between countries and the use of a wide range of technological equipment and online structure are considered. In particular, training on the example of databases, information networks, and other spatially distributed structures are considered too. The practical significance of the study is defined by the fact that the use of open educational resources will not only intensify the learning process at the university, but also to determine the possibility of integration into the world educational space.

Keywords: *Educational resource, educational efficiency, Department of applied chemistry, higher education.*

Downloaded from www.periodico.tchequimica.com

АНОТАЦИЯ

Актуальность исследования обусловлена тем фактом, что открытые образовательные ресурсы имеют способность изживать основную методологическую конструкцию, усложняющую процесс обучения среди студентов, а именно использовать международный опыт при обучении и получении знаний. В данном исследовании показаны аспекты функционирования открытых образовательных ресурсов и их технологическая база. Новизна работы заключается в формировании модели использования открытых образовательных ресурсов при подготовке специализированных курсов кафедры прикладной химии. Авторы показывают, что эффективность использования открытых образовательных ресурсов напрямую зависит от доли онлайн-обучения и технологической изоляции предметов. В частности, учитываются не только учебные процессы при реализации программы по прикладной химии, но и другие дисциплины, которые требуют обмена опытом между странами и использования широкого спектра технологического оборудования и онлайн-структуры. В частности, рассматривается обучение на примере баз данных, информационных сетей и других пространственно распределенных структур. Практическая значимость исследования определяется тем, что использование открытых образовательных ресурсов позволит не только интенсифицировать учебный процесс в университете, но и определить возможность интеграции в мировое образовательное пространство.

Ключевые слова: *Образовательный ресурс, образовательная эффективность, кафедра прикладной химии, высшая школа.*

1. INTRODUCTION

In situations where information technologies are becoming more affordable, pedagogues have found that digital educational resources are an important part of the learning process. In 1994, the term "training object" was introduced into the circulation to refer to digital materials that are being developed for multiple-use (Cheung, 2019).

In 1998, based on a study of the essence of the concept, "open content" showed that the principles of the movement of "open software" can also be applied to the content of the resource (or its content) (Sampson *et al*., 2012; Li, 2016; Delimont *et al.*, 2016; Crozier, 2018). According to the classical definition, the term "open" means granting additional copyright permissions to information in excess of those granted by standard copyright law (Kourbetis and Boukouras, 2014; Rahayu and Sapriati, 2018; Kinskey *et al.,* 2018; Adygezalova *et al.* 2018).

These additional permissions are expressed as follows: Reuse – the right to reuse the material in its unaltered form (Pande, 2018); Revise – the right to adapt, correct, modify or alter the content of the material itself (Peters, 2017); Remix – the right to combine the original or revised content of the material with other objects to create something new (Sherimon *et al.,* 2018a); Redistribute – right to share copies of the original material (Sherimon *et al.,* 2018b; Tappeiner *et al*., 2019; Lin, 2019).

In 2002, Massachusetts Institute of Technology (MIT) made a significant contribution to the development of the concept of open educational resources when it launched the "Open Course Ware" project while opening free access to the materials of its training courses. Since 2018, the world organization of UNESCO has been actively supporting initiatives to create open educational resources on the Internet (hereinafter-OER). According to the experts of this organization, OER is of particular importance in developing countries since their use can significantly increase access to quality higher education and lifelong learning, as well as ensure the full participation of universities in the creation of the world system of higher education (Annand and Jensen, 2017; Mishra, 2017; Xiao *et al.*, 2018; Navarrete and Luján-Mora, 2018; Horn *et al.*, 2018; Tappeiner *et al.,* 2019; Vogus, 2019; Aleksandrova *et al.*, 2019).

According to UNESCO's definition, open educational resources are training, educational or scientific resources placed in the public domain or distributed under a license that permits their free use or processing. Open educational resources include complete courses, teaching materials, modules, textbooks, videos, texts, software and any other means, materials or technologies used to provide access to knowledge (Volchik and Maslyukova, 2019).

The purpose of the pedagogical experiment was to identify the differences

Downloaded from www.periodico.tchequimica.com

between the two empirical distributions.

2. LITERATURE REVIEW

The world pedagogical community has developed many practical recommendations regarding general principles for creating and using open educational resources. Here are some of them (Duval *et al*., 2011). It would be advisable for higher education institutions:

– develop different strategies for using OER in their own scientific and educational activities (Banerjee, 2018);

– encourage the creation of new and adaptation of existing educational resources to achieve the objectives of the institution in various fields of activity (educational process, scientific and economic activities). This primarily will be an effective step towards the establishment of an educational repository of a higher education institution (Hou *et al*., 2013);

– encourage the scientific and pedagogical staff of the educational institution to create OER by using moral and material measures (Rennie and Mason, 2010);

– provide access to the OER of all interested persons, primarily students, and teachers, subject to the copyright of the developers;

– encourage the open publication of scientific works of the educational institution, which will contribute to the improvement of its world and national ranking (Minguillón, 2010).

It would be advisable for scientific and pedagogical staff of higher educational institutions:

– grant their own research the status of "open" in order to increase their scientific authority (Schaffert, 2010);

– create teams together with students to develop OER, which will enhance their learning activities (Kopp *et al.*, 2017);

– use the principle of openness to promote their own discipline. Experts note that it can be not only parts of educational information but also booklets, promo videos, presentations of training courses, photos, works of the best students (Becker, 2012; Jaggars *et al.*, 2018);

– use OER for creating communities of practitioners from relevant fields of scientific activity, which will stimulate the expansion of professional contacts between teachers of different educational institutions (Li, 2013; Li and Wong, 2015; Feldman-Maggor *et al.*, 2016).

In Russia, some steps have been taken to promote open educational resources. Thus, Magna Charta Universitatum, signed in 1999, includes in academic freedom the open access to information, with exceptions provided by law, including scientific information through the development of open electronic archives (University institutional repositories), open electronic journals of universities and the ability to freely maintain relationships with their colleagues in any part of the world (Cheung, 2018).

Educational resources give the benefits that students need them to get additional information on these issues to share their views and discuss the learning process with other students and the teacher (Nasongkhla and Donaldson, 2018). Teachers have the opportunity to create courses more effectively using multimedia resources that require special technical and media skills, learn new teaching methods, create resources and discuss them with colleagues, join professional communities. Educational institutions can demonstrate educational and scientific programs to a wide audience, attract more applicants, reduce the cost of developing training courses. It is clear that any educational institution or scientist while creating an open educational resource strives to ensure that its copyrights are respected. The international community has developed a specific mechanism sponsored by Creative Commons (Li and Wong, 2015; Hilton, 2016; Islim and Cagiltay, 2016; Cobb, 2018; Hajri *et al.*, 2019).

3. MATERIALS AND METHODS

A pedagogical experiment can cover a group of students, a faculty, a University or several universities. The determining role in the experiment belongs to the scientific hypothesis. Based on the observations, the hypothesis has been formulated that the introduction of OER will contribute to the expansion of the information educational environment of the University and its structuring and forensic methodology of use of OER will contribute to the formation of ICT competences of future bachelors of the Department of applied chemistry increasing the level of their training. By means of pedagogical experimentation reliability of the hypothesis on increasing level of professional training of applied chemistry bachelors has to be checked.

Experiments always involve some kind of comparison, usually between a control group of

Downloaded from www.periodico.tchequimica.com

students trained using the traditional method (without using OER), and an experimental group, in our study it is a group of students who studied using OER. Scientific and pedagogical work was carried out during 2013-2018 and covered five stages of scientific and pedagogical search:

1) Diagnostic stage (2013-2014), – during period in which the state of training bachelors of Department of applied chemistry in higher education in Russia and abroad has been analyzed; identified and formulated were contradictions that can be solved through the introduction of distance learning technologies in universities, based on a systematic approach, by deploying a system of support for distance learning at all levels of training: from pre-University training, training bachelors, specialists and masters, to postgraduate education and training of scientific and pedagogical workers;

2) Prognostic stage (2014), at that stage, were defined the main goals and objectives of the study, implemented the prediction results and developed the program of pedagogical experiment and formulated the main principles and provisions of OER use; OER has been rolled out within the University;

3) Organizational stage (2014), which identified the list of disciplines of chemical cycle, disciplines of cycle of professional and practical training of the future bachelors of the Department of applied chemistry; determined were the control and experimental groups for carrying out the pedagogical experiment; prepared were educational and working programs of the disciplines that were included in the pedagogical experiment;

4) Practical phase (2014-2017), in which was developed and implemented e-learning courses of the following disciplines: "Basics of distance learning", “Chemistry of higher organic compounds", "Organic chemistry", "Analytical chemistry", "Chemistry of higher inorganic compounds" for students of 1-4 courses held sections of knowledge to track changes in learning outcomes of students in the experimental groups.

5) Synthesis stage (2017-2018), which reviewed experimental work: performing tasks, achieving goals and documenting results of the experiment; prepared the relevant conclusions on the results of the experiment.

Tasks of pedagogical experiment: identify the requirements for the preparation of bachelors of the Department of applied chemistry in universities in Russia and abroad; identify the requirements for the material and technical support of the experimental site; analyze existing teaching methods using ICT and OER; prepare guidelines for the use of distance learning technologies on the preparation of bachelors of the Department of applied chemistry; conduct a survey among teachers and students to determine the status, problems and prospects of training bachelors of the Department of applied chemistry; by results of pedagogical experiment to formulate conclusions and to define prospects of further research of a problem; identify the differences in the preparation of bachelors of the Department of applied chemistry on traditional methods and training from training with the use of OER.

Goals of pedagogical experiment: teach students to understand the essence of processes and phenomena arising in the professional activities of chemical technology specialists; form students' ability to think, to give estimates, to analyze the received educational data; develop skills of working with OER universities; develop students' skills and abilities to use OER in independent work.

The following research methods were used to achieve the goals, objectives, tasks and hypothesis testing: theoretical analysis of psychological-pedagogical, scientific-technical and educational-methodical literature on the subject of research; study and generalization of pedagogical experience; didactic modeling; method of information analysis for the formulation of basic definitions and concepts used in the study; learning experience and collecting information about the learning process and the use of OER in the preparation of bachelors of the Department of applied chemistry; modeling of pedagogical processes for the deployment of OER universities; monitoring and testing method to determine the readiness of students and teachers to use OER; survey methods; inquiries and interviews with teachers and students on the use of OER; pedagogical experiment to confirm the effectiveness of the proposed method of using OER in the preparation of bachelors of the Department of applied chemistry; statistical processing of experimental data and their interpretation; generalization and prognostic methods for formulating conclusions, recommendations and determining directions for further research.

Fisher’s criterion is designed to compare two samples by frequency of occurrence of the effect (indicator) of interest to the researcher. The

Downloaded from www.periodico.tchequimica.com

larger it is, the more significant are the differences. The criterion evaluates the reliability of differences between the percentages of the two samples in which the effect of interest (indicator) is registered. Figuratively speaking, the 2 best pieces cut from 2 pies are compered and it is decided which one is really bigger. The essence of Fisher's angular transformation is to convert percentages into values of the central angle, which is measured in radians. A larger angle φ will correspond to a larger percentage, and a smaller fraction will correspond to a smaller angle, but the ratio is not linear: By increasing divergence between the angles φ1 and φ2 and increasing the number of samples the value of the criterion increases. With higher value φ* more likely it is that the differences are significant.

Hypotheses. H0: The proportion of individuals who exhibit the studied effect in sample 1 is not more than in sample 2. H1: The proportion of individuals who exhibit the studied effect in sample 1 is more than in sample 2. Graphical representation of the criterion φ*. The angular transformation method is somewhat more abstract than the other criteria. The formula followed by E.V. Gubler in calculating the values φ assumes that 100% will be formed by the angle φ = 3,142, i.e. the rounded value π = 3,14159 ... This allows us to represent the comparable samples in the form of two semicircles, each of which symbolizes 100% of the size of your sample. Percentages of subjects with the effect will be presented as sectors formed by central angles φ. The criterion φ* makes it possible to determine whether one of the angles is statistically significantly superior to the other for given sample sizes.

Limitations of criterion φ*. 1. None of the matched fractions should be equal to zero. Formally, there are no obstacles to the application of the φ method in cases where the proportion of observations in one of the samples is 0. However, in these cases, the result may be unduly inflated. 2. There is no upper limit in the criterion φ. Samples can be arbitrarily large.

The lower limit is 2 observations in one of the samples. However, the following ratios in the number of the two samples should be observed: if there are only 2 observations in one sample, there should be at least 30 in the second sample; if one of the samples has only 3 observations, the second should have at least 7; if one of the samples has only 4 observations, the second should have at least 5; by $n_1, n_2 \geq 5$ any comparisons are possible. In principle, it is possible to compare samples that do not meet this condition, for example, with the ratio $n_1=2$, $n_2=15$, but in these cases, it will not be possible to identify significant differences. The criterion φ* has no other restrictions.

4. RESULTS AND DISCUSSION:

Within the first phase of the study (2013-2014) was carried out a stating stage of pedagogical experiment, which goal was the allocation of competences of bachelors of the Department of applied chemistry and the study of the level of competences of future specialists in accordance with the curriculum. The training content of bachelors of Department of applied chemistry has been analyzed as well as training methods and means were selected and the leading role of ICT in the preparation of bachelors of Department of applied chemistry defined. The available software and hardware used in the learning process have been analyzed: hardware, multimedia equipment, local and global networks, software and the like.

The investigations carried out allowed to conclude that the level of formation of professional competences of bachelors of the Department of applied chemistry is insufficient, and the introduction of OER in the educational process of the University in the information society and the requirements of the labor market requires a systematic approach. Literary sources analyzed provided an opportunity to conclude that the formation of professional and cultural information of the bachelors Department of applied chemistry should be widely introduced in the educational process ICT and OER through the OER resources and services, as a part of integrated University IOS, providing support for the educational process on a daily, part-time (distance) forms of education.

In order to determine the readiness of students to use ICT in the educational process was conducted entrance survey. As a result of the survey among 132 first-year students of the training direction "Chemical technologies" it was determined that: 99% of students have e-mail and use it; 99% of students can register on websites and download files from the Internet; 87.5% of students are familiar with chat and forum; 99% of students passed computer testing; 40% of students are familiar with OER; Internet usage level: 17.5% – beginner, 77.5% – advanced user, 5% – specialist; most students have an average level of chemical disciplines 7-9 points on a 12-point scale (60%), the remaining 40% have sufficient and high levels.

Downloaded from www.periodico.tchequimica.com

The conclusions obtained as a result of statistical processing of students' answers to the questionnaire provided an opportunity to determine the need to improve the level of formation of professional competencies through the systematic use of OER in the educational process on the basis of OER.

During the second stage of the study (2014-2015), the state of development of the research problem was determined, the program of experimental research was created. The existing methods of training using OER have been analyzed. The educational and working program of the experimental discipline "Chemistry of higher organic compounds" was developed. Classes in the discipline of the CHOHOC with the use of OER have been started. The analysis of the training level on 1st-year students, their knowledge, skills, and abilities in the disciplines of chemical and technological orientation has been developed.

The search stage of the pedagogical experiment was conducted at the Russian technological University at the faculty of chemical technologies. To increase the level of formation of professional competences of bachelors of the Department of applied chemistry in RTU-MIREA, since 2014-2015, it was proposed to conduct classes using OER and OER tools that implement them: providing remote consultations, organization of forums and chats of the most complex issues of educational programs of disciplines, automated entrance control, computer-oriented lectures and laboratory work, computer testing and surveys.

As approbation in the educational process of the developed method of using OER was chosen discipline of free choice of higher education institution "Chemistry of higher organic compounds", which is studied in the first year in the second semester. The educational and methodical complex of discipline "Chemistry of higher organic compounds" was created with the following content: general information about the course, entrance control from course, theoretical training material of course module, materials for the practical training for the course module, students' independent work, attendance control, ongoing monitoring from course, reports on the implementation of tasks for classes and independent work of the module, topical control on module, module control, semester control on the course (examination), monitoring the safety of knowledge (delayed control, the rector's control, AAC (Fateev and Fateeva, 2016).

According to the results obtained after the entrance survey, the adjustment of the structure of CHOHOC course, its methodical system of training and relevant didactic materials was carried out, and namely: all lectures on the course are relaunched as format*.ppt (presentations); most of the lectures of the course are presented in flash format (videos); task of all laboratory work is set out in the OER; mobile access to UIS of discipline in OER is set up; module for sending reports of activities and assessments was configured.

The results of statistical processing of semester control on CHOHOC discipline showed the effectiveness of developed methods of OER using, which contributed to improving the quality of student performance in the discipline "Chemistry of higher organic compounds". To study the effectiveness of the developed methodology of OER using by means of OER the students passed the output test.

Figure 1 shows the statistics of answers of students' experimental group (132 people) on the issues of the output survey, in which they noted that the system of support distance learning helps them in the preparation of such learning activities as: lectures (33.3%), laboratory work (70.8%), practical exercises (33.3 per cent), independent work (33.3 per cent), and modular control (54.2%), and final test (50%). As a result, the level of cognitive activity of students increased.

Thus, during the second phase of the study: analysis of the training level by bachelors of the Department of applied chemistry was carried out; OER was set up; OER for disciplines "Organic chemistry", "Analytical chemistry", “Methods of physical and chemical analysis” was prepared; manual for working with OER of universities was developed; method of OER using in the electronic training course through means of OER was developed.

On the third forming stage of the pedagogical experiment (2015-2017) has been identified and verified the efficiency and effectiveness of the proposed method of using OER in teaching these subjects: “Organic chemistry” of 2 courses, "Analytical chemistry" of 3 courses, "Physical and Chemical Methods of analysis" in the 4th year.

The experiment covered up to 303 students of specialty "Chemical technology" (undergraduate). Statistical processing of results of scientific-pedagogical experiment and evaluation of the effectiveness of the developed technique use of distance learning technologies

Downloaded from www.periodico.tchequimica.com

in training of bachelors in Department of applied chemistry in the RTU-MIREA was carried out by using methods of mathematical statistics. The aim of the pedagogical experiment was to identify the differences between the two empirical distributions. Comparison of indicators of success of training of students of experimental and control groups of the specified disciplines by means of Fisher's criterion has been carried out. At the forming stage of the pedagogical experiment, the following results were obtained.

While checking the effectiveness of the proposed methodology for the OER using by teaching the discipline "Organic chemistry" (OC) in the 2nd year it has been found that the formulated hypothesis H1 proportion of students in the experimental group, which according to the results of the semester exam on the discipline OC have got a score of "excellent" or "good" more than in the control group. This means that the quality of student performance of the experimental group according to the results of semester control at the rate is higher than the quality of education of students in the control group, indicating that the efficiency of the proposed method of using OER in teaching discipline OC. Figure 2 shows a diagram of success when comparing the CG and the EG on the subject "Organic chemistry".

When testing the effectiveness of the proposed method of OER using in teaching on discipline "Analytical chemistry" (ANCM) for a 3 course it has been found that according the formulated hypothesis H1 the proportion of students in the experimental group, who according to the results of the semester examination in the discipline ANCM have "excellent" or "good" more than in the control group. This means that the quality of student performance of the experimental group according to the results of semester control at the rate of ANCM is higher quality of academic performance of students in the control group, indicating that the efficiency of the proposed method of using OER in teaching discipline ANCM. Figure 3 shows a diagram of success when comparing the CG and the EG in the discipline "Analytical chemistry".

When testing the effectiveness of the proposed method of OER using in teaching the discipline "Physical and chemical methods of analysis" (PCHMA) in the 4th year it was revealed that according to the formulated hypothesis H1 the proportion of students who, according to results of the semester examination for the discipline PCHMA have a positive assessment in the experimental group more than in control group. This means that the level of training success of students of the experimental group is higher than the level of performance of students of the control group, which indicates the effectiveness of the proposed method of using OER in teaching the discipline of PCHMA. Figure 4 shows the diagram of success at comparison of KG and EG on discipline "Methods of physical and chemical analysis". The results of the statistical processing of pedagogical studies data from four of these curriculum areas of training chemical technology confirm the effectiveness of the proposed methods of using distance learning technologies in training of bachelors in Department of applied chemistry, resulting in improving outcomes and/or quality of performance.

The application of the proposed method of OER using contributed to improving the quality of student performance, which makes it possible to confirm the hypothesis of the study in terms of improving the level of professional training of future specialists in chemical technologies. In Table 1 the distribution of semester exam scores on the discipline "Chemistry of higher organic compounds" at the ascertaining stage of pedagogical experiment is given. Control and experimental groups at the forming stage of the pedagogical experiment were formed in this way (Table 2):

– control group (CG) included the 1st year students of RTU-MIREA, who studied at the specialty "Chemical technology": in the second semester of the 2012-2013 academic year (group KT 801, PR 802) and in 2013-2014 (group KT 901, PR 902). Students of the control group were trained according to the traditional method (without the use of OER);

– experimental group (EG) included the 1st year students of RTU-MIREA, who studied at the specialty "Chemical technology": in the second semester of the 2014-2015 academic year (group KT 101, PR 102) and in 2015-2016 (group KT 111, PR 112). Students of the experimental group were trained according to the traditional method (with the use of OER).

The scheme of formation of KG and EG at the forming stage of the experiment on the discipline "Chemistry of higher organic compounds" by years of training are presented in table 4.2. Analysis of the semester exam results in 2012-2013 and 2013-2014 in the CHOHOC discipline allows us to conclude that the primary grade is "satisfactory" (D-E), which indicates an

Downloaded from www.periodico.tchequimica.com

insufficient level of knowledge on this discipline (Table 3).

To test the hypothesis that there were no differences between the knowledge levels of students in the control and experimental groups, the results of a semester exam in general chemistry were selected, which were processed through the multifunction criterion φ* by Fisher (F is a criterion Fisher's angular transformation). By using the criterion is evaluated the significance of differences between the proportions (in percent) of two empirical samples in which the effect of interest by a researcher is recorded.

Fisher's criterion has insignificant limitations: 1) none of the particles to be compared should not be equal to zero; 2) lower boundary for the number of observations in the sample for the criterion will be equal to 2, but it is necessary to adhere to certain ratios in the number of both samples: if n_1=2, so n_2≥30; if n_1=3, so n_2≥7; if n_1=4, so n_2≥5; by n_1=5 and n_2≥5 any comparisons are possible;

3) the upper limit for the number of observations in the sample for the criterion is practically absent, that is, the samples can be arbitrarily large.

There are no other restrictions for the Fisher's criterion. The distribution of final grades in control and experimental groups according to the results of the semester exam in the discipline "General Chemistry" of 1st-year students is shown in Tables 4 and 5. Table 6 summarized data on the results of the semester exam in the discipline "General chemistry" in the control and experimental groups. Note that the final grade in the discipline "General chemistry" for the experimental groups of 100 points system was transformed into the traditional four-point scale.

Based on the data given in table 6, firstly the reliability of the absence hypothesis, from a statistical point of view, of differences between the quality indicators of the teaching "General chemistry" of students in experimental and control groups has to be checked. Hypotheses will be formulated: H0: The percentage of students passed the semester exam in "General chemistry" with grade "excellent" or "good" in the experimental group is no more than in the control group; H1: The proportion of students passed the semester exam in "General chemistry" with grade "excellent" or "good" in the experimental group is greater than in the control group.

A table that actually represents a table of empirical frequencies according to two values of the attribute: students who got grades "5" or "4", and students who received grades "3" or "2" (Table 7) is constructed. At the same time, only proportions corresponding to observation are used in the calculations, for which the effect takes place. Based on the data given in Table 8 and despite the fact that the quality indicator for the semester exam in "General Chemistry" is 33.3% and 38.9%, respectively in favor of the experimental group, while using Fisher's criterion, the hypothesis that there are no differences between the knowledge levels of students in the control (n = 66) and experimental (n = 54) groups, thus "quality of performance" is selected as an indicator for comparison.

As can be seen from Table 7 the level of achievement of students in the control group in comparison with the student achievement level of the experimental group in the discipline "General chemistry" is 0.6% lower. The performance indicator in the discipline "General chemistry" for the experimental group is higher in comparison with the control groups by 5.6%. For the average score, there are the following results: 3.4 and 3.4 of semester exam in "General chemistry" for control and experimental groups. According to the corresponding Table 9, the value of IP correspond to the shares of 33.3% and 38.9% in the corresponding groups:

$$\varphi_1(38.9\%) = 1.347$$

$$\varphi_2(33.3\%) = 1.230$$

Then the empirical definition φ* using the formulae is calculated (Equation 1). Where angle φ_1 corresponds to a larger proportion; angle φ_2 corresponds to a smaller fraction; n_1 is the number of observations in the first sample (experimental groups); n_2 is the number of observations in the second sample (control groups).

In the case (Equation 2) crucial importance φ^*_{kr} that corresponds to the levels of statistical significance accepted in psychological and pedagogical research is equal (Equation 3). Thus, there is inequality $\varphi^*_{emp} = 0.64 < \varphi^*_{kr} = 1.64$. That is, the empirical value is in the zone of insignificance and the hypothesis H0 is accepted. This means that reliably, with a significance level of α = 0.05, the student performance indicator of the experimental group according to the results of the semester exam in the discipline "General chemistry" does not differ from the student learning quality indicator of the control group.

Downloaded from www.periodico.tchequimica.com

As the results of statistical data processing confirm, the differences between the control and experimental groups are insignificant, which allows us to verify the effectiveness of the OER methodology using the example of CHOHOC discipline. Let us now check the reliability of the hypothesis that there is no, from a statistical point of view, differences between the student achievement levels of the experimental and control groups from the CHOHOC course (Table 10). Hypotheses will be formulated: H0: The percentage of students passed the semester exam in "Chemistry of higher organic compounds" with grade “excellent” or “good” in the experimental group is no more than in the control group; H1: The proportion of students who passed the semester exam in "Chemistry of higher organic compounds" with grade “excellent” or “good” in the experimental group is greater than in the control group.

A table of empirical frequencies according to two values of the attribute: students who got grades "5" or "4", and students who received grades "3" or "2" (Table 11) is constructed. According to the corresponding table, the value of the cell size corresponding to the shares of 89.4% and 96.3% in the corresponding groups is determined:

$$\varphi_1(96.3\%) = 2.754$$
$$\varphi_2(89.4\%) = 2.478$$

Then the empirical definition φ* is calculated (Equation 4). Thus, there is inequality $\varphi^*_{emp} = 1.51 < \varphi^*_{kr} = 1.64$. It means that the empirical definition value $\varphi^*_{emp} = 1.51$ is in the zone of insignificance and the hypothesis H0 is accepted. This means that the success level of students from the experimental group is higher than the success level of students from the control group.

Let us verify the reliability of the hypothesis of the absence, from a statistical point of view, of differences between the quality levels of student performance in control and experimental groups in the discipline "Chemistry of higher organic compounds" (Figure 5). Hypotheses are formulated: H0: The percentage of students passed the semester exam in "Chemistry of higher organic compounds" with grade “excellent” or “good” in the experimental group is no more than in the control group; H1: The proportion of students who passed the semester exam in "Chemistry of higher organic compounds" with grade “excellent” or “good” in the experimental group is greater than in the control group.

A table of empirical frequencies according to two values of the attribute: students who got grades "5" or "4" and students who received grades "3" or "2" (Table 12) is constructed. According to the corresponding table, the values of the cell size correspond to the shares of 42.4% and 66.7% in the corresponding groups:

$$\varphi_1(66.7\%) = 1.911$$
$$\varphi_2(33.3\%) = 1.418$$

Then the empirical definition φ* is calculated (Equation 5). Thus, there is inequality $\varphi^*_{emp} = 2.68 > \varphi^*_{kr} = 2.31$. That is, empirical significance $\varphi^*_{emp} = 2.68$ is in the zone of significance and the hypothesis H1 is accepted, but hypothesis H0 is not accepted. This means that reliably the student success quality indicator of the experimental group according to the results of semester control in the discipline “Chemistry of higher organic compounds” with a significance level ∝=0.01, from a statistical point of view, differs significantly from the student quality indicator of the control group. The results of statistical processing of semester control data on the “Chemistry of higher organic compounds” discipline showed the effectiveness of the developed methodology for using OER, which contributed to improving the quality of student performance in the discipline “Chemistry of higher organic compounds”.

5. CONCLUSIONS:

Summing up the study, it is to be noted that the open educational resources can give free access to education for everyone, but mainly for non-traditional groups of students, expanding opportunities for higher education. Open educational resources are by no means an alternative to classical education. This is only a means to obtain versatile, deep, professional information.

Open educational resources were examined and it was determined that it is impossible to use these open sources only as additional forms of education. Modern forms of using network resources for educational purposes are largely limited only by their consideration as a consequence of an auxiliary resource for traditional classroom education. Our analysis showed that any educational resources inherently can exist only if combined with the

Downloaded from www.periodico.tchequimica.com

information environment that every educational institution should have. In this regard, open educational resources can be used as an element of traditional learning.

The hypothesis of the study on the example of three subjects was examined, it determined the possibility of monitoring the quality of teaching. Subjects – "Organic Chemistry" (OCH) in the 2nd year, "Analytical Chemistry" (ACH) in the 3rd year, "Physicochemical Analysis Methods" (PCHAM) in the 3rd year. For each discipline, the shares of students were identified who, according to the results of the semester exam in the discipline, have positive marks and compared the indicators in experimental and in control groups. An analysis of all distributions and statistical processing showed that the assumption of which group of students got better after using the developed methodology showed that the hypotheses were set correctly and, on the whole, the results of the experimental group were 20-30% higher than that of the control group. Therefore, it can be said that the analysis of the indicators of introducing open educational resources has shown that the introduction of the chemical-technological cycle into the process of teaching disciplines is generally 20-30% more successful than using only its own or traditional methods and methods of circumcision. Such an advantage is expressed not only in an increase in quantitative indicators of grades but also subject to the development of competencies of the students themselves.

An additional condition that was not fully shown in the work was the formation of an understanding that, in addition to quantitative assessment, it is worth talking about the qualitative execution of the proposed project. In a qualitative way, the use of OER will contribute to the formation of a higher level of performance and professional fitness in general. The application of the proposed methodology for the use of OER contributed for improving the quality of academic performance of students in the Department of chemical technology, which makes it possible to conclude that the hypothesis of the study is confirmed in terms of increasing the level of professional training of future specialists in the Department of chemical technology.

6. REFERENCES:

1. Adygezalova, G.E., Allalyev, R.M., Kiseleva, A.V., Grigorieva, N.A. *Journal of Advanced Research in Law and Economics*, **2018**, *9*(1), 6–14.
2. Aleksandrova, O., Hroznyi, I., Vinnikova, N., Chuvasova, N. *Naukovyi Visnyk Natsionalnoho Hirnychoho Universytetu*, **2019**, *2*, 153-162.
3. Annand, D., Jensen, T. *International Review of Research in Open and Distance Learning*, **2017**, *18*(4), 1-15.
4. Banerjee, K. How to Incorporate Open Educational Resources (OER) into the Infrastructure and Pedagogy for Promoting Ubiquitous Learning. In: K.C. Li, K.S. Yuen, B.T.M. Wong (Eds.), *Innovations in Open and Flexible Education*, Singapore: Springer Singapore, **2018**, 177–184.
5. Becker, P.A. Dutch Repository for Open Educational Resources in Software Engineering: Does Downes' Description Fit? In: S. Kurbanouglu, U. Al, P.L. Erdougan, Y. Tonta, N. Uçak (Eds.), *E-Science and Information Management,* Berlin, Heidelberg: Springer Berlin Heidelberg, **2012**, 71–78.
6. Cheung, S.K.S. A Study on the University Students' Use of Open Educational Resources for Learning Purposes. In: Cheung, S.K.S., Jiao, J., L.-K. Lee, X. Zhang, K.C. Li, Z. Zhan (Eds.), *Technology in Education: Pedagogical Innovations*, Singapore: Springer Singapore, **2019**, 146–155.
7. Cheung, S.K.S. Perceived Usefulness of Open Educational Resources Between Full-Time and Distance-Learning Students. In: S.K.S. Cheung, L. Kwok, K. Kubota, L.-K. Lee, J. Tokito (Eds.), *Blended Learning. Enhancing Learning Success,* Cham: Springer International Publishing, **2018**, 357–367.
8. Cobb, D. *International Education Journal*, **2018**, *17*(3), 15-29.
9. Crozier, H. *Serials Librarian*, **2018**, *74*(1-4), 145-150.
10. Delimont, N., Turtle, E.C., Bennett, A., Adhikari, K., Lindshield, B.L.L. *Research in Learning Technology*, **2016**, *24*, article number 29920.
11. Duval, E., Verbert, K., Klerkx, J. Towards an Open Learning Infrastructure for Open Educational Resources: Abundance as a Platform for Innovation. In: C.S. Calude, G. Rozenberg, A. Salomaa (Eds.), *Rainbow of Computer Science: Dedicated to Hermann Maurer on the Occasion of His 70th Birthday*, Berlin, Heidelberg: Springer Berlin

Downloaded from www.periodico.tchequimica.com

Heidelberg, **2011**, 144–156. https://doi.org/10.1007/978-3-642-19391-0_11.

12. Fateev, V.N., Fateeva, I. *Anthropologist*, **2016**, *23*(1-2), 148-151.
13. Feldman-Maggor, Y., Rom, A., Tuvi-Arad, I. *Chemistry Education Research and Practice*, **2016**, *17*(2), 283-295.
14. Hajri, H., Bourda, Y., Popineau, F. *Communications in Computer and Information Science*, **2019**, *1022*, 166-190.
15. Hilton, J.L., *Educational Technology Research and Development*, **2016**, *64*(4), 573-590.
16. Horn, E.A., Anderson, R., Pierick, K. *Information Discovery and Delivery*, **2018**, *46*(4), 197-203.
17. Hou, J., Lu, H., Qi, Y. Promoting Development and Use of OER: The Case of Open Educational Resources Consortium of Chinese Universities. In: S.K.S. Cheung, J. Fong, W. Fong, F.L. Wang, L.F. Kwok (Eds.), *Hybrid Learning and Continuing Education*, Berlin, Heidelberg: Springer Berlin Heidelberg, **2013**, 313–321.
18. Islim, O.F., Cagiltay, K. *Eurasia Journal of Mathematics, Science and Technology Education*, **2016**, *12*(3), 559-567.
19. Jaggars, S.S., Folk, A.L., Mullins, D. *Performance Measurement and Metrics*, **2018**, *19*(1), 66-74.
20. Kinskey, C., King, H., Lewis Miller, C. *Open Learning*, **2018**, *33*(3), 190-202.
21. Kopp, M., Gröblinger, O., Zimmermann, C. Increasing Educational Value: The Transformation of MOOCs into Open Educational Resources. In: C. Delgado Kloos, P. Jermann, M. Pérez-Sanagustín, D.T. Seaton, S. White (Eds.), *Digital Education: Out to the World and Back to the Campus*, Cham: Springer International Publishing, **2017**, 223–232.
22. Kourbetis, V., Boukouras, K. Accessible Open Educational Resources for Students with Disabilities in Greece: They are Open to the Deaf. In: C. Stephanidis, M. Antona (Eds.), *Universal Access in Human-Computer Interaction. Universal Access to Information and Knowledge*, Cham: Springer International Publishing, **2014**, 349–357.
23. Li, C.-Y. *International Journal of Technology and Human Interaction*, **2016**, *12*(3), 106-125.
24. Li, K.C., Wong, B.T.-M. Computer Literacy and Use of Open Educational Resources: A Study of University Students in Hong Kong. In: K.C. Li, T.-L. Wong, S.K.S. Cheung, J. Lam, K.K. Ng (Eds.), *Technology in Education. Transforming Educational Practices with Technology,* Berlin, Heidelberg: Springer Berlin Heidelberg, **2015**, 206–214.
25. Li, Y. Constructing and Sharing Open Educational Resources: Policy and Capacity. In: J. Lam, K.C. Li, S.K.S. Cheung, F.L. Wang (Eds.), *Knowledge Sharing through Technology*, Berlin, Heidelberg: Springer Berlin Heidelberg, **2013**.
26. Lin, H. *International Review of Research in Open and Distance Learning*, **2019**, *20*(3), 1-18.
27. Minguillón, J. Analyzing Hidden Semantics in Social Bookmarking of Open Educational Resources. In: S. Sánchez-Alonso, I.N. Athanasiadis (Eds.), *Metadata and Semantic Research,* Berlin, Heidelberg: Springer Berlin Heidelberg, **2010**, 8–17.
28. Mishra, S. *Distance Education*, **2017**, *38*(3), 369-380.
29. Nasongkhla, J., Donaldson, A.J. Using Trust Telling and Amicable Inquiry for Open Educational Resources to Strengthen a University Network in Thailand. In: B. Hokanson, G. Clinton, K. Kaminski (Eds.), *Educational Technology and Narrative: Story and Instructional Design*, Cham: Springer International Publishing, **2018**, 39–50. https://doi.org/10.1007/978-3-319-69914-1_4.
30. Navarrete, R., Luján-Mora, S. *Universal Access in the Information Society*, **2018**, *17*(4), 755-774.
31. Pande, J. *International Journal of Information Technology,* **2018**, *10*(3), 339–347. https://doi.org/10.1007/s41870-018-0126-z.
32. Peters, M.A. (Ed.). Open Educational Resources (OER). *In: Encyclopedia of Educational Philosophy and Theory,* Singapore: Springer Singapore, **2017**, 1712. https://doi.org/10.1007/978-981-287-588-4_100716
33. Rahayu, U., Sapriati, A. *Turkish Online Journal of Distance Education*, **2018**, *19*(4), 163-175.

34. Ragulina, Y.V., Semenova, E.I., Zueva, I.A., Kletskova, E.V., Belkina E.N. *Entrepreneurship and Sustainability Issues*, **2018**, *5*(4), 890–898. http://doi.org/10.9770/jesi.2018.5.4(13).

35. Sampson, D.G., Zervas, P., Chloros, G. Towards Community-Based Open Educational Resources: Tools for Developing and Managing IEEE LOM Application Profiles. In: A. Jimoyiannis (Ed.), *Research on e-Learning and ICT in Education*, New York: Springer New York, **2012**, 283–294. https:// doi.org/10.1007/978-1-4614-1083-6_21.

36. Schaffert, S. Strategic Integration of Open Educational Resources in Higher Education. In: U.-D. Ehlers, D. Schneckenberg (Eds.), *Changing Cultures in Higher Education: Moving Ahead to Future Learning,* Berlin, Heidelberg: Springer Berlin Heidelberg, **2010,** 119–131. https://doi.org/10.1007/978-3-642-03582-1_11

37. Sherimon, V., Al Shuaily, H.S., Thirupathi, R. *Advances in Intelligent Systems and Computing*, **2018a**, *725*, 891-902.

38. Sherimon, V., Al Shuaily, H.S., Thirupathi, R. Effectiveness of Integrating Open Educational Resources and Massive Open Online Courses in Student Centred Learning. In: M.E. Auer, T. Tsiatsos (Eds.), *Interactive Mobile Communication Technologies and Learning*, Cham: Springer International Publishing, **2018b**, 891–902.

39. Tappeiner, L., DiSanto, J.M., Lyons, K. Expanding Access to Education through Open Educational Resources (OERs). In: K.S. Wolfe, K. Lyons, C. Guevara (Eds.), *Developing Educational Technology at an Urban Community College*, Cham: Springer International Publishing, **2019**, 135–146.

40. Volchik, V., Maslyukova, E. Trust and development of education and science. *Entrepreneurship and Sustainability Issues*, **2019**, 6(3), 1244–1255. http:// doi.org/10.9770/jesi.2019.6.3(27).

41. Vogus, B. *Public Services Quarterly*, **2019**, *15*(3), 242-247.

42. Xiao, J., Wang, M., Jiang, B., Li, J. *Journal of Ambient Intelligence and Humanized Computing*, **2018**, *9*(3), 667–677.

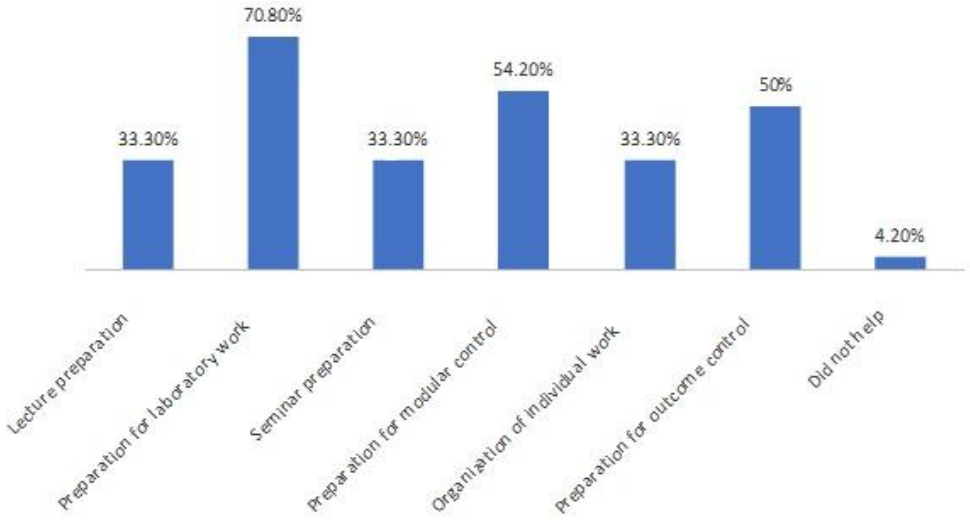

Figure 1. *Diagram of distribution of students' responses on survey results in OER*

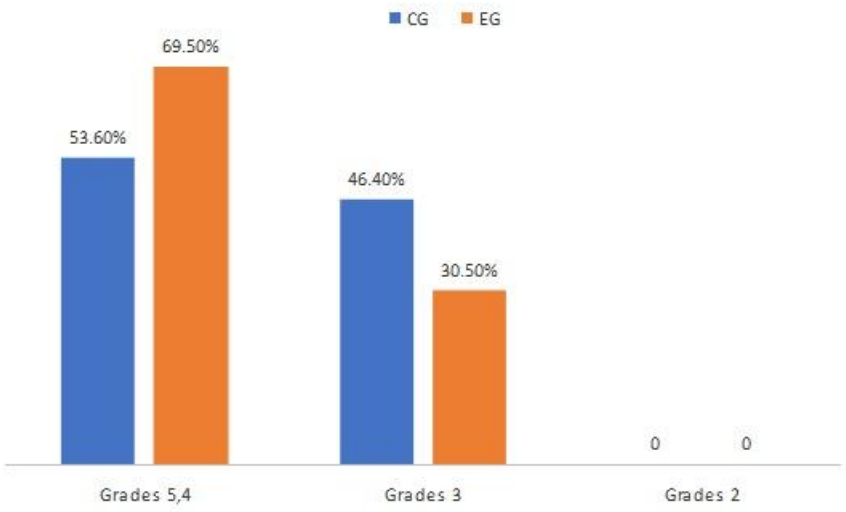

Figure 2. *Diagram of student's academic standing in KG and EG on discipline "Organic chemistry"*

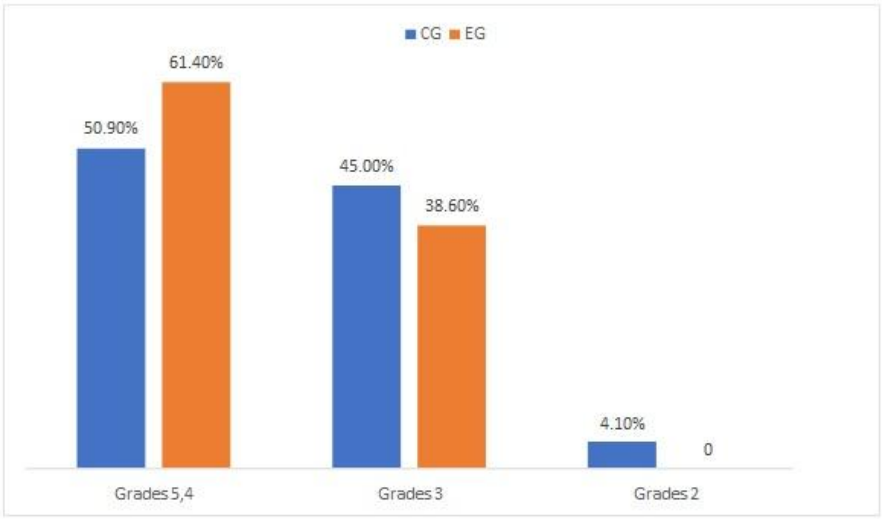

Figure 3. *Diagram of students' academic standing in KG and EG on discipline "Analytical chemistry"*

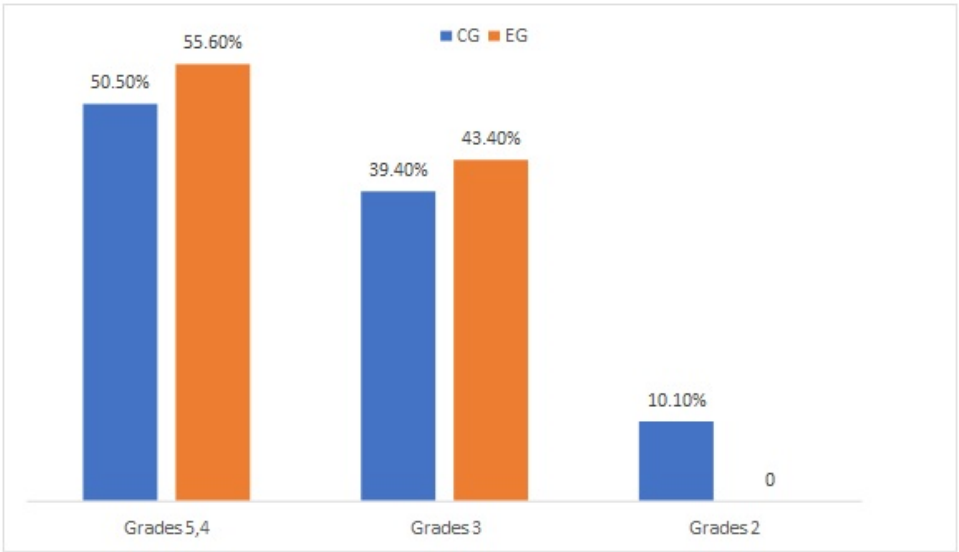

Figure 4. *Diagram of student's academic standing in KG and EG on discipline "Physical and chemical methods of analysis"*

Downloaded from www.periodico.tchequimica.com

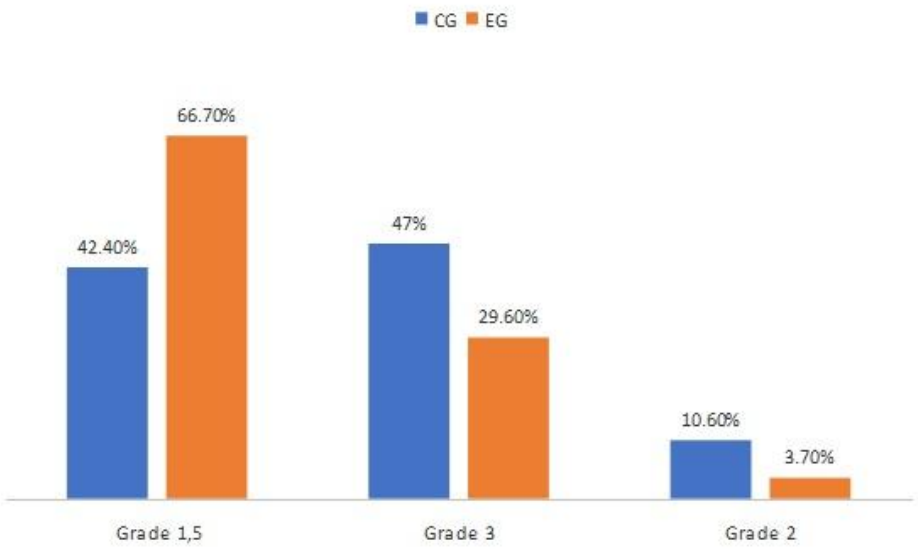

Figure 5. *Diagram of success level of students from CG and EG in the discipline "Chemistry of higher organic compounds"*

Table 1. *Distribution of semester exam scores on the discipline "Chemistry of higher organic compounds" in 2012-2014*

Years of study	Group	Headcount	Number of students assessed				Percentage of students assessed			
			2	3	4	5	2	3	4	5
2012-2013	KT-801	17	1	9	5	2	5.9%	52.9%	29.4%	11.8%
	PR-802	18	5	9	3	1	27.8%	50%	16.7%	5.5%
	Total	35	6	18	8	3				
2013-2014	KT-901	18	0	10	6	2	0.0%	55.6%	33.3%	11.1%
	PR-902	13	1	3	7	2	7.7%	23.1%	53.8%	15.4%
	Total	31	1	13	13	4				

Table 2. *Summary table of student assessment and quality of student assessment in control groups*

Group	Academic performance	Of successful students
KT-801	94.1%	41.2%
PR-802	71.5%	22.2%
KT-901	100%	44.4%
PR-902	92.3%	69.2%

Table 3. *Scheme of the formation of control and experimental groups at the forming stage of the pedagogical experiment in the CHOHOC discipline*

Groups	Number of students (by the academic years)				Total
	2012-2013	2013-2014	2014-2015	2015-2016	
Control	35	31			66
Experimental			36	18	54
Total:	35	31	36	18	120

Downloaded from www.periodico.tchequimica.com

Table 4. *Distribution of semester exam grades on "General chemistry" of 2012-2014 in control group*

Group	Number of students	Grade	Distribution of grades			
			2012-2013		2013-2014	
			Number of students were assessed	Share of students were assessed, %	Number of students were assessed	Share of students were assessed, %
KT	35	“2”	0	0	0	0
		“3”	8	47	12	66.7
		“4”	7	41.2	4	22.2
		“5”	2	11.8	2	11.1
PR	31	“2”	3	16.7	1	7.7
		“3”	12	66.7	8	61.5
		“4”	1	5.5	2	15.4
		“5”	2	11.1	2	15.4

Table 5. *Distribution of semester exam grades on "General chemistry" of 2014-2015 in experimental group*

Group	Number of students	Grade	Distribution of grades			
			2012-2013		2013-2014	
			Number of students were assessed	Share of students were assessed, %	Number of students were assessed	Share of students were assessed, %
KT	35	“2”	0	0	0	0
		“3”	13	72.2	1	11.1
		“4”	2	11.1	8	88.9
		“5”	3	16.7	0	0
PR	31	“2”	2	11.1	1	11.1
		“3”	10	55.6	6	66.7
		“4”	4	22.2	1	11.1
		“5”	2	11.1	1	11.1

Table 6. *Distribution of semester exam grades on "General chemistry" of 2014-2015 in control and experimental groups*

Group	Number of students	Grade	Distribution of grades	
			Number of students were assessed	Share of students were assessed, %
CG	66	“2”	4	6.1
		“3”	40	60.6
		“4”	14	21.2
		“5”	8	12.1
EG	54	“2”	3	5.5
		“3”	30	55.6
		“4”	15	27.8
		“5”	6	11.1

Downloaded from www.periodico.tchequimica.com

Table 7. *Table for calculations by Fisher's criterion when comparing two groups by the proportion of students with rating "5" or "4" and "3" or "2"*

Group	Grades 4 or 5		Grades 3 or 2		Total
	Number of students	%	Number of students	%	
CG	22	33.3	44	66.7	66
EG	21	38.9	33	61.1	54
Total	43		77		120

Table 8. *Level of achievement of students in discipline "General chemistry"*

Group	Success	Number of students assessed	Average grade
CG	93.9	33.3	3.4
EG	94.5	38.9	3.4

Table 9. *Distribution of semester exam grades on "Chemistry of higher organic compounds" discipline of 2014-2015 in experimental groups*

Group	Staff strength	Number of students assessed				Share of students assessed, %			
		2	3	4	5	2	3	4	5
KT-101	18	0	5	10	3	0.0%	27.8%	55.6%	16.6%
PR-102	18	1	3	11	3	5.5%	16.7%	61.1%	16.7%

Table 10. *Distribution of semester exam grades on "Chemistry of higher organic compounds" discipline of 2014-2015 in experimental groups*

Group	Staff strength	Number of students assessed				Share of students assessed, %			
		2	3	4	5	2	3	4	5
KT-111	9	0	4	5	0	0.0%	44.4%	55.6%	0.0%
PR-112	9	1	4	3	1	11.1%	44.4%	33.3%	11.1%

Table 11. *Table for calculations by Fisher's criterion when comparing two groups by the proportion of students with positive ratings on the final control at discipline "Chemistry of higher organic compounds"*

Group	Grades 3-5		Grade 2		Total
	Number of students	%	Number of students	%	
CG	59	89.4	7	10.6	66
EG	52	96.3	2	3.7	54
Total	111		9		120

Table 12. Table for calculations by Fisher's criterion when comparing two groups by the proportion of students with ratings "5" or "4" and "3" or "2" on the final control at discipline «Chemistry of higher organic compounds"

Group	Grades 3-5		Grade 2		Total
	Number of students	%	Number of students	%	
CG	28	42.4	38	57.6	66
EG	36	66.7	18	33.3	54
Total	64		56		120

Downloaded from www.periodico.tchequimica.com

$$\varphi^* = (\varphi_1 - \varphi_2)\sqrt{\frac{n_1 n_2}{n_1 + n_2}} \quad \text{(Eq. 1)}$$

$$\varphi^*_{emp} = (1.347 - 1.230)\sqrt{\frac{54 * 66}{54 + 66}} \approx 0.64 \quad \text{(Eq. 2)}$$

$$\varphi^*_{kr} = \begin{cases} 1.64 (p \leq 0.05) \\ 2.31 (p \leq 0.01) \end{cases} \quad \text{(Eq. 3)}$$

$$\varphi^*_{emp} = (2.754 - 2.478)\sqrt{\frac{52 * 59}{52 + 59}} \approx 1.51 \quad \text{(Eq. 4)}$$

$$\varphi^*_{emp} = (1.911 - 1.418)\sqrt{\frac{54 * 66}{54 + 66}} \approx 2.68 \quad \text{(Eq. 5)}$$

Downloaded from www.periodico.tchequimica.com

PERIÓDICO TCHÊ QUÍMICA
ARTIGO ORIGINAL

LINEARIZAÇÃO DA UMIDADE RELATIVA SOBRE O OCEANO PACÍFICO NA LINHA EQUATORIAL

LINEARIZATION OF RELATIVE HUMIDITY OVER THE PACIFIC OCEAN ON THE EQUATORIAL LINE

DÍEZ, César Manuel[1*]; SOLANO, Carlos Javier

[1] Universidad Nacional de ingeniería. Facultad de Ciencias, Unidad de Postgrado, Lima – Peru

** Correspondence author*
e-mail: cdiezch@uni.pe

Received 19 August 2019; received in revised form 28 October 2019; accepted 30 October 2019

RESUMO

O sistema atmosférico é regido pela interação de muitos parâmetros meteorológicos causando dependência entre eles, ou seja, umidade e temperatura, ambos adequados diante de qualquer anomalia, como tempestades, furacões, eventos El Niño Oscilação Sul (ENSO). Portanto, entender perturbações da variação de umidade ao longo do tempo pode fornecer um indicador de qualquer fenômeno oceanográfico. Os dados anuais de umidade relativa ao redor da linha Equatorial do Oceano Pacífico foram processados e analisados para compreender a evolução temporal de cada conjunto de dados, apreciar anomalias, tendências, histogramas e propor uma maneira de prever episódios anômalos como eventos ENSO, observando anormalidade dos coeficientes de correlação de lag entre cada par de boias. Os conjuntos de dados foram retirados do projeto Rede Transoceânica de Oceano / Triângulo de Atmosfera Tropical (TAO / TRITON), matriz dirigida pelo *Pacific Environmental Laboratory* (PMEL) da Administração Nacional Oceânica e Atmosférica (NOAA) e pela Agência Japonesa de Ciências da Terra-Marinha e Tecnologia (JAMSTEC). Todos os conjuntos de dados foram processados e o código foi elaborado pelo autor ou adaptado da Mathworks Inc. Mesmo ocorrências de umidade relativa no lado leste do Oceano Pacífico parecem oscilar harmonicamente, enquanto ocorrências no lado oeste não, devido ao tamanho de suas amplitudes de oscilações. Esse fato pode ser observado nos histogramas que mostraram formas de pico no lado leste do oceano e gaussianos no oeste; As funções de correlação de defasagem mostraram que nenhum par de boias sincroniza flutuações, mas as boias ocidentais são afetadas diante dos eventos do ENSO, especialmente entre 1997-98. Definitivamente, as correlações de atraso nas boias ocidentais são determinantes para detectar eventos ENSO.

Palavras-chave*: Correlação Lag, eventos ENSO, Função de Distribuição Discreta, Umidade Relativa, Processo de Dados.*

ABSTRACT

The atmosphere system is ruled by the interaction of many meteorological parameters, causing a dependency between them, i.e., moisture and temperature, both suitable in front of any anomaly, such as storms, hurricanes, El Niño-Southern Oscillation (ENSO) events. So, understanding perturbations of the variation of moistness along the time may provide an indicator of any oceanographic phenomenon. Annual relative humidity data around the Equatorial line of the Pacific Ocean were processed and analyzed to comprehend the time evolution of each dataset, appreciate anomalies, trends, histograms, and propose a way to predict anomalous episodes such ENSO events, observing abnormality of lag correlation coefficients between every pair of buoys. Datasets were taken from the Tropical Atmosphere Ocean / Triangle Trans-Ocean Network (TAO/TRITON) project, array directed by Pacific Environmental Laboratory (PMEL) of the National Oceanic and Atmospheric Administration (NOAA), and the Japan Agency for Marine-Earth Science and Technology (JAMSTEC). All the datasets were processed, and the code was elaborated by the author or adapted from Mathworks Inc. Even occurrences of relative humidity in the east side of the Pacific Ocean seem to oscillate harmonically, while occurrences in the west side, do not, because of the size of their amplitudes of oscillations. This fact can be seen in the histograms that show Peak shapes in the east side of the ocean, and Gaussians in the west; lag correlation functions show that no one pair of buoys synchronize fluctuations, but western buoys are affected in front of ENSO events, especially between 1997-98. Definitely, lag correlations in western buoys are determined to detect ENSO events.

Keywords*: Lag correlation,* ENSO events*, Discrete Distribution Function, Relative Humidity, Data process.*

Downloaded from www.periodico.tchequimica.com

1. INTRODUCTION

The atmosphere is thermodynamic permeable container plenty of gases (air), with a shape of a sphere that envelops the Earth. Continuously, these gases are going from one place to another inside this container in any direction, forming hurricanes (Uccellini and Ten Hoeve, 2019), storms (Gomez, Carter, Trustrum, Page, and Orpin, 2013), or just moving as winds (Xu et al., 2019), absorbing or detaching vapor water from their environment (Behar, Sbarbaro, Marzo, and Moran, 2019), reason why this gas, might be structured into two kinds, wet and dry, which percentage depends on many meteorological parameters (Xu, Huang, Zhang, and Li, 2018). Vapor water (Lawrence, 2016) may be formed upon sea surface because of the refracted radiations (Maksin et al., 2018), evaporations of surface waters (Kolehmainen et al., 2017), turbulence (Cuxart, and Jiménez, 2006), or because of rain (Chakraborty, Talukdar, Saha, Jana, and Maitra, 2017), among others.

Nevertheless, vapor water is affected by solar radiation (Riavo et al., 2016), dust concentration (Csavina, Field, Félix, Corral-Avitia, Sáez, and Betterton, 2014), biological processes (Quagliarini, Gianangeli, D'Orazio, Gregorini, Osimani, Aquilanti, and Clementi, 2019), temperature (Njau, 1994).

All these happenings criticize the amount of moisture presented in the air, affecting not only the natural environment, such as ships or embarkations travelling around, that may contain subtle merchandise such foods, electronic equipment, or the equipment of the embarkations themselves (Ju, Zhao, Mujumdar, Fang, Gao, Zheng, and Xiao, 2018, and Testaa, Maranob, Ambrogib, Boracchib, Casulac, Biganzolib, and Moroni, 2017); their crew (Buonocore, De Vecchi, Scalco, and Lamberts, 2018); or the skin (Klaassen, Schipper, and Masen, 2016).

But winds may displace these vapors to adjoining areas affecting contiguous populations (Lima, Ha Ahna, and Hwan Jeongb, 2018), animals (Xiong, Meng, Gao, Tang, Zhang, 2017), climates (Sahin & Cigizoglu, 2012), systems (Gehan, Sallam, and Elsayed, 2015), or things (Zhan, Wang, Cao, L. Li, and C. Li, 2010), provoking phenomena (A.K. Singha, H. Singha, Singhb, and Sawhneyb, 2002), change concentration of gases in the atmosphere (Gubb, Blanusa, Griffiths, and Pfrang, 2018).

As have been seen, quantification of relative humidity, which is derived from environmental temperatures (Lin and Hubberd, 2003), is very important, due to its atmosphere-ocean interaction side effect, and also may be a useful parameter for forecasting (Ruano, Ferreira, and Mendes, 2010), hydro-climate studies (Lee, Zhan, and Pei, 2015), determine the consumption of energy in buildings (Mba, Meukam, Kemajou, 2016).

This project processed the relative humidity data from PMEL-NOAA (PMEL-NOAA) network to analyze particularities in time, a proposal that will be sustainable observing anomalies in the time series of each dataset, analyzing their trends, kind of oscillations (Yang, 2019), amplitudes. Discrete distribution functions to understand frequencies of occurrences and basic statistics. Finally, lag correlation functions, (Zebende, Brito, Silva, and Castro, 2018), between every pair of buoys of the grid to see trends between each couple. A small change in the lags of relative humidity (Rhee, Im, Kim, and Song, 2019) may be an important change in the atmosphere of the datasets (Ross et al, 2018), because of the repercussions in the adjacent areas (Sloane and Wolff, 1985), or any adjacent areas may influence in the ocean (Seidov et al., 2015). Relative humidity in this grid tends to be null in each dataset, discarding the options of covariance of any two datasets, and open another option, such parabolic relationship (El Massoud, 2005), or any chaotic system (McNeal, Petcovic, Bals-Elsholz, and Ellis, 2019).

2. MATERIALS AND METHODS

2.1. Data

This investigation pretended to examine the evolution in time of Relative Humidity in the Pacific Ocean, (Liua, Hana, Lia, Tianc, and Liud, 2018), trends (Bettio, 2008), normalized discrete distribution functions, and interprets interactions of Relative Humidity along the Equatorial Line in the Pacific Ocean. Reason why, annual data of relative humidity at 3 meters of altitude, between 137º E and 95º W meridians, and between 9º N and 8º S latitudes of sixty-nine buoys since 1980 (see figure 1), were handled from the Tropical Atmosphere Ocean / Triangle TransOcean Network (TAO/TRITO) project of the Pacific Marine Environment Laboratory (PMEL), directed by the National Oceanic and Atmospheric Administration (NOAA) around the equatorial line of the Pacific Ocean.

Downloaded from www.periodico.tchequimica.com

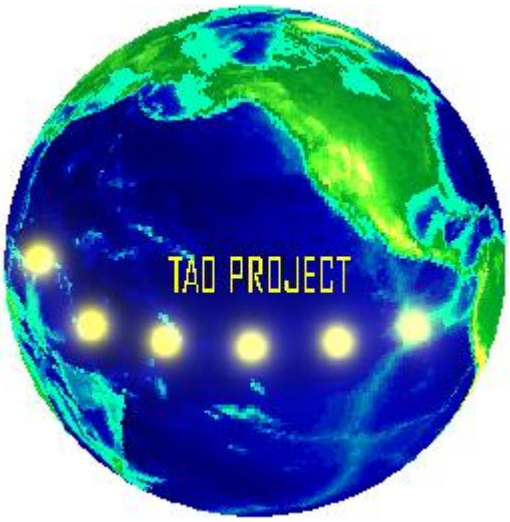

Figure 1. *Location of the grid of Relative humidity located at the TAO/TRITON Project, in the Equatorial line of the Pacific Ocean of PMEL-NOAA. Adapted from MatLab (Mathworks Inc.).*

2.2. Anomalies in Relative Humidity

The first arrangement was the analysis of sequential data, applied to time data collected from the whole moored instruments for the TAO//TRITON project, through their time series and their anomalies (Emery & Thomson, 2007), organized by latitudes and longitudes (Dare and Ebert, 2017). The trends and amplitudes vary along the time and may be an indicator in front of ENSO events, (Ambrosino, Thinová, Briestensky, and Sabbarese, 2019).

2.3. Statistical model

The second process applied to these data was the normalization of discrete relative distribution functions, (Cook, 2015) of the frequencies of occurrences of Relative Humidity, (Zhu L., Li, Y. & Jiang, Z., 2017). Considering a bin of one unit of size, for each dataset of the grid, "it will be represented a set of measured values, n_j, with j=1, …, m, in the finite widths elements (bins) of a partition of the range of allowed values of the dataset", (Pruneau, 2017) as indicated in Eq. 1, appreciating location, spread and symmetry of the pile of data, and the shapes of the probability density functions (Grace, 2015), and the number of humps (Wilks, 2006).

$$frequency\ density = \frac{frequency}{class\ width} \quad \text{Eq. 1}$$

Finally, the last arrangement was the analysis of trends of the temporal evolution of each buoy respect each other, dataset by dataset, it could be feasible to linearize them respect each other by lag correlation functions, (Chung and Power, 2017, and Gerhards, Schramm, and Schmid, 2019), that avows figure out how well relative humidity of each dataset correlates in time respect to other datasets, defined in Eq. 2,

$$\tau(x,y) = \frac{\frac{1}{N-1}\sum_{i=1}^{N}(x_i-\bar{x})(y_i-\bar{y})}{\sqrt{\frac{1}{N-1}\sum_{i=1}^{N}(x_i-\bar{x})^2}=\sqrt{\frac{1}{N-1}\sum_{i=1}^{N}(y_i-\bar{y})^2}} \quad \text{Eq 2}$$

where:
$\bar{x}$: mean value of the x dataset (x buoy).
$\bar{y}$: mean value of the y dataset (y buoy).
N: length of the data set.
x_i: any value of x dataset.
y_i: any value of y dataset.

If τ values trends to zero, means that relative humidity between the pair of buoys parameterized is scattered randomly without any relationship. The ranges could increase until τ = 1, which means that datasets are dependent respect each other (Pickard and Emery, 2007).

All these processes were implemented using Matlab 2009a student version, and the codes were performed or adapted to this project from the functions of the software themselves.

3. RESULTS AND DISCUSSION:

3.1 Time evolution of relative humidity in the Pacific Ocean around the Equatorial line.

There should a relationship between temperature and moisture in the atmosphere of the tropical waters of the Pacific Ocean. It is known by the oceanographers that temperatures in this atmosphere have very small defined ranges as Relative Humidity does. In the Northeast of the Pacific Ocean, Relative Humidity fluctuates quasi harmonically inside the 64 % and 92 % interval of range around the continuous average line along the time. There would be appreciated an increment of Relative Humidity in some buoys in front of hot ENSO events (Wang and McPhaden, 2001), such in the 8º N 156º E and 8º N 165º E in 1997-98, as can be seen in figure 2, (a) and (b); and other lower peaks such 2000, as can be seen in figure 3, (a) and (b), in the 2º N 156º E buoy in the year 1998, and in the 2º N 165º E buoy in 1997, respectively.

Observing buoys located in the Southeast of the Pacific Ocean, the harmonic oscillations

Downloaded from www.periodico.tchequimica.com

have a major period of oscillations, achieving periods of 5 years around the continuous average value in the 0º N of latitude, see figure 4 (a), (0º N 156º E). But Southern latitudes have not standard behavior, presenting some of them, occurrences up the mean average value for more than 10 years, as can be seen in figure 4 (b). (5º S 156º E), and ranges of Relative Humidity are slightly bigger than northern buoys.

The time evolution of Relative Humidity in the Northwest of the Pacific Ocean almost oscillates harmonically with constant amplitudes around the average line, near the eastern surface. Abnormal oscillations are observed and, only in the 8º N 155º W, it is observed one wavelength up the time average line, 1997-98, and one oscillation below this line between 2013-14 in the 5º N 140º W buoys, see figure 5 (a) and (b), respectively.

In the Southwest of the Pacific Ocean, sinusoidal oscillations up and down the continuous average line are observed, but in the 8º S latitudes, as it is appreciated in the 5º S 170º W and 8º S 125º W positions, respectively, see figure 6 (a) and (b). Nevertheless, exceptions occur; some buoys do not oscillate during few years since 1997 as 5º S 155º W and 5º S 110º W buoys do. Past this period, there is another long period, almost 10 years, where occurrences happen above the time average line, it means, oscillations happen up this line, as indicates figure 6 (c) and (d).

There should an inverse or direct dependence of Relative Humidity with temperatures, depending on the location of the buoy, the reason why it will be recommended to correlate both variables. And also, it is seen that moisture is perturbed when an ENSO event is taking place.

3.2 Discrete Distribution Function of Relative humidity over the Pacific Ocean in the Equatorial line.

It has been found a dependence on the occurrences of Relative Humidity respect colder or hotter periods in the Pacific Ocean around the Equatorial line. Besides, ranges are very similar in the east and the west sides of the grid. Observing annual histograms, it is seen that expected values for every buoy address to 80%, and extreme values do not exceed 60% in the lower limit and 94 % in the upper one. The shorter scale parameters of a probability density function of the observations are founded in the Northeast of the Pacific Ocean, see figure 7, (a) and (b); and the bigger ones in the Southwest side, see figure 8, (a) and (b).

This contrast is reflected by the increase of means values of Relative Humidity in the west of the Pacific Ocean. The histograms at the 5º N latitude, just in the 155º W, 140º W, and 125º W meridians, have Gaussians shapes, but no one histogram has Gaussians shapes, see figure 9, (a), (b), and (c); major peaks are located in the eastern part of the Ocean, and lower peaks are located in the western part, achieving values of Relative Humidity of 100%, as could be seen in figure 10 (2º S 125º W).

By the seen in these histograms, it is possible to say that air temperature and relative humidity have a corresponding relationship in the area of the Pacific Ocean around the Equatorial line, and mean value increase in the west side of the network.

3.3 Linearization of Relative Humidity over the Pacific Ocean in the Equatorial line.

Linearization of annual Relative Humidity in the Pacific Ocean over the Equatorial line between each pair of buoys shows that there are not a couple of buoys that correlate with each other. Observing plots of lag correlations of buoys located in the East of this area of the ocean, i.e. 0º N 156º E and 2º N 147º E, and 0º N 156º E and 2º N 165º E, see figure 11 (a), and (b), respectively; or buoys located in the west side, i.e. 0º N 125º W and 0º N 140º W, and 8º S 180º W and 9º N 140º W, see figure 12, (a) and (b), respectively; or buoys of the east and west of the Pacific Ocean, i.e. 0º N 156º E and 8º S 180º W, and 2º N 147º E and 8º S 180ºW, see figure 13, (a) and (b), respectively, have around zero values along the time. It means that, every buoy has occurrences independently of each other; see figure 12, (a) and (b).

All the occurrences of lag correlation functions of relative humidity near the Equatorial line are very close to the expected values. In spite of that, it is appreciated that some buoys are perturbed several times, modifying slightly their directions. This fact is observed in the lag correlation between 0º N 156º E and 2º N 147º E, in the years 1997, 2004, 2001, as it could be seen figure 11 (a); in the lag correlation between 0º N 156º E and 2º N 165º E in 1997, 2002, 2006, and 2011, see figure 12 (b).

4. FUTURE PREDICTIONS:

Analysis of relative humidity in front of temperatures, as SST, Air T, upper temperatures

Downloaded from www.periodico.tchequimica.com

(Wang and McPhaden, 2001) would be able to achieve an interaction forward ENSO events.

Taking short periods of time and subgrids (Weber and Mass, 2019) to linearize Relative Humidity, will allow focussing on variations of this parameter respect to ENSO events.

5. CONCLUSIONS:

It has been seen that some amplitudes of oscillations of time series of Relative Humidity are constants, and trend to oscillate periodically. Other buoys oscillate with variable amplitudes but with values near the extreme values of the ranges of Relative Humidity. Values of Relative Humidity for all the buoys oscillate harmonically; so, there should be a dependence of their expected value.

Occurrences of Relative Humidity oscillate in front of the time, but no one buoy synchronizes respect the others. These oscillations have small periods, especially in the Northern side of the Pacific Ocean, or large periods, especially in the Southern side of the ocean. Shapes of histograms are very similar, extreme values are characteristic of the side of the ocean, eastern or western, being bigger ranges near the American Continent. Even Relative Humidity of each buoy oscillates around 80%, no one buoy correlates with another buoy.

It is recommendable to compare short periods of time series of Relative Humidity in front of ENSO events since Relative Humidity is suitable for these events. And, also, a method to predict ENSO events means lag correlation functions, there would be working with shorter periods (Subramanian, Juricke, Dueben, and Palmer, 2019).

6. ACKNOWLEDGMENTS:

I would like to express my gratitude to Facultad de Ciencias and Facultad de Ingeniería Ambiental of Universidad Nacional de Ingeniería, Centro de Tecnoligías de la Información y Comunicaciones (CTIC-UNI), and Clever for their cooperation on this Project. I would like to thank my Mother Teresa Chirinos, my Sister Teresa Díez, My wife Miriam Loayza and my two little children, Abbie and Paul, for enabling me to continue on this Project supporting and encouraging me in spite of all the time it took me away from them. I would like to greatly thanks Manuel and Raul Chirinos Coya for the orientation to develop the programs to process the data for PMEL-NOAA.

7. REFERENCES:

1. Ambrosino, F., Thinová, Lenka., Briestensky, M., and Sabbarese, C. Anomalies identification of Earth's rotation rate time series (2012-2017) for possible correlation with strong earthquakes occurrences. Geodesy and Geodynamics, **2019**, 5.
2. Behar, O., Sbarbaro, D., Marzo, A., and Moran, L. A simplified methodology to estimate solar irradiance and atmospheric turbidity from ambient temperature and relative humidity. Renewable and Sustainable Energy Reviews, **2019**, 6.
3. Bettio, L. Seasonal climate summary southern hemisphere (winter 2007): a developing La Niña and a positive Indian Ocean Dipole. Australian Meteorological Magazine, **2008**, 11.
4. Buonocore, C., De Vecchi, R., Scalco, V., Lamberts, R. Influence of relative air humidity and movement on human thermal perception in classrooms in a hot and humid climate. Building and Environment, **2018**, 17.
5. Chakraborty, R., Talukdar, S., Saha, U., Jana, S., Maitra, A. Anomalies in relative humidity profile in the boundary layer during convective rain. Atmospheric Research, **2017**, 10.
6. Chung, Ch. T. Y. and Power, S. B. The nonlinear impact of El Niño, La Niña and the Southern oscillation on seasonal and regional Australian precipitation, **2017**, 21.
7. Cook, N. A statistical model of the seasonal-diurnal wind climate at Adelaide. Australian Meteorological and Oceanography Journal, **2015**, 23.
8. Cuxart, J and Jiménez, M. A. Mixing Processes in a Nocturnal Low-Level Jet: An LES Study. Journal of the Atmospheric Science, **2006**, 14.
9. Csavina, J., Field, J., Félix O., Corral-Avitia, A. Y., Sáez, A. E., Betterton, E. A. Effect of wind speed and relative humidity on atmospheric dust concentrations in semi-arid climates. Science of the Total Environment, **2014**, 8.

Downloaded from www.periodico.tchequimica.com

10. Dare, R. A., and Ebert, E. E. Latitudinal variations in the accuracy of model-generated forecasts of precipitation over Australia and South-east Asia. Journal of Southern Hemisphere Earth System Science, **2017**, 25.

11. El Massoud, M. On solvability of a parabolic system arising in physical oceanography. Journal of Mathematical Analysis and Applications, **2005**, 13.

12. Enrico Quagliarini, E., Gianangeli, A., D'Orazio, M., Gregorini, B., Osimani, A., Aquilanti, L., and Clementi, F. Effect of temperature and relative humidity on algae biofouling on different fired brick surfaces. Construction and Building Materials, **2019**, 9.

13. Emery, W. J., & Thomson, R. E. *Data Analysis Methods in Physical Oceanography.* Colorado, USA: Elsevier. **2006**.

14. Gehan, A.H., Sallam A, Elsayed, E.A. Estimating relations between temperature, relative humidity as independent variables and selected water quality parameters in Lake Manzala, Egypt. Ain Shams Engineering Journal, **2015**, 14.

15. Gerhards, C., Schramm, M., and Schmid, A. Use of the Weibull distribution function for describing cleaning kinetics of high-pressure water in the food industry. Journal of Food Engineering, **2019**, 26.

16. Gomez, B., Carter, L., Trustrum, N. A., Page, M. J., and Orpin, A. R. Coherent rainfall response to middle- and late-Holocene climate variability across the mid-latitude South Pacific. The Holocene, **2013**, 6.

17. Grace, W. Using the stretched Exponential Distribution to Model Runs of Extremes in a Daily Meteorological Variable. Australian Meteorological and Oceanography Journal, **2015**, 12.

18. Gubb, C., Blanusa, T., Griffiths, A., Pfrang, C. Can houseplants improve indoor air quality by removing CO2 and increasing relative humidity? Springer Nature, **2018**, 11.

19. Ju, H. Y., Zhao, S. H., Mujumdar, A.S., Fang, X. M., Gao, Z. J., Zheng, Z. A., Xiao, H. W. Energy-efficient improvements in hot air drying by controlling relative humidity based on Weibull and Bi-Di. Food and Biproducts Processing, **2018**, 44.

20. Klaassen, M., Schipper, D. J., Masen, M.A. Influence of the relative humidity and the temperature on the In-vivo friction behavior of human skin. Biotribology, **2016**, 31.

21. Kolehmainen, J., Sippola, P., Raitanen, O., Ozel, A., Boyce, Ch. M., Saarenrinne, P., and Sundaresan, S. Effect of humidity on triboelectric charging in a vertical vibrated granular bed: Experiments and modeling. Chemical Engineering Science, **2017**, 11.

22. Lawrence, M. G. The relationship between Relative Humidity and the Dewpoint Temperature in Moist Air. Bulletin of the American Meteorological Society, **2004**, 10.

23. Lee, H. F., Zhang, D. D., and Pei, Q. Reconstruction of the geographic extent of drought anomalies in northwestern China over the last 539 years and its teleconnection with the Pacific Ocean. The Holocene, **2015**, 14.

24. Liua, W., Hana, Y., Lia, J., Tianc, X., Liud, Y. Factors affecting relative humidity and its relationship with the long-term variation of fog-haze events in the Yangtze River Delta. Atmospheric Environment, **2018**, 8.

25. Lima, D. K., Ha Ahna, B., Jeongb, J. H. Method to control an air conditioner by directly measuring the relative humidity of indoor air to improve the comfort and energy efficiency. Applied Energy, **2018**, 9.

26. Lin, X. And Hubbard, K. G. Uncertainties of Derived Dewpoint Temperature and Relative Humidity. American Meteorological Society, **2003**, 4.

27. Maksic, J., Shimizu, M. H., Sampaio de Oliveira, G., Venancio, I. M., Cardoso, M., and Ferreira, F. A. Simulation of the Holocene climate over South America and Impacts on the vegetation. The holocen, **2018**, 13.

28. Mba, L., Meukam, P., Kemajou, A. Application of artificial neural network for predicting hourly indoor air temperature and relative humidity in modern building humid region. Energy and Buildings,

Downloaded from www.periodico.tchequimica.com

2016, 11.

29. McNeal, P., Petcovic, H., Bals-Elsholz, T., and Ellis, T. Seeing weather through chaos. Bulletin of the American Meteorological Society, **2019**, 14.
30. Njau, E. C. Expressions for Wind Speed, Relative Humidity, Rainfall, Absolute Humidity, Vapor Pressure and Dew Point As Functions Of Temperature*. Renewable Energy, **1994**, 6.
31. Pickard, G. L., & Emery, W. J. *Descriptive Physical Oceanography. An Introduction.* Burlington, USA: Butterworth Heinemann, **2007**.
32. PMEL-NOAA, N. O. *Global Marine Moored Buoy Array*. Retrieved from https://www.pmel.noaa.gov/tao/drupal/disdel/. **2015**.
33. Pruneau, C. A. *Data Analysis Techniques for Physical Scientists.* New York: Cambridge University Press, **2017**.
34. Rhee, J., Im, J., Kim, J., and Song, S. J. Humidity effects on the aerodynamic performance of a transonic compressor cascade. International Journal of Heat and Mass transfer, **2019**, 9.
35. Riavo, N., Voarintsoa, G., Brook, G. A., Liang, F., Marais, E., Hardt, B., Cheng, H., Edwards R. L., and Railsback, L. B. Stalagmite multi-proxy evidence of wet and dry intervals in northeastern Namibia: Linkage to latitudinal shifts of the Inter-Tropical Convergence Zone and changing solar activity from AD 1400 to 1950. The Holoce, **2016**, 13.
36. Ross, M. E., Vicedo-Cabrera, A. M., Kopp, R. E., Song, L., Goldfarb, D. S., Pulido, J., Warner, S., Furth, S. L., and Tasian, G. E. Assessment of the combination of temperature and relative humidity on kidney stone presentations. Environment Research, **2018**, 9.
37. Ruano, A. E., Ferreira, P. M., and Mendes, H. MOGA Design of Temperature and Relative Humidity Models for Predictive Thermal Comfort. IFAC Proceedings Volumes, **2010**, 6.
38. Sahin, S. & Cigizoglu, H. K. The effect of the relative humidity and the specific humidity on the determination of the climate regions in Turkey. Springer / Verlag, **2012**, 12.
39. Seidov, D., Antonov, J. J., Arzayus, K. M., Baranova, O. K., Biddle, M., Boyer, T. P., Johnson, D. R., Mishonov, A. V., Paver, C., and Zweng, M. M. Oceanography north of 60º from World Ocean Database. Progress in Oceanography, **2015**, 21.
40. Singha, A. K., Singha, H, Singhb, S.P., Sawhneyb, R.L. Numerical calculation of psychrometric properties on a calculator. Building and Environment, **2002**, 4.
41. Sloane, Ch. S., and Wolff, G. T. Prediction of Ambient light scattering using a physical model responsive to relative humidity: Validation with measurements from Detroit. Atmospheric Environment, **1985**, 12.
42. Subramanian, A., Juricke, S., Dueben, P., and Palmer, T. A stochastic representation of subgrid uncertainty for dynamical core development. Bulletin of the American Meteorological Society, **2019**, 11.
43. Testaa, F., Maranob, G., Ambrogib, F., Boracchib, P., Casulac, A., Biganzolib, E., Moroni, P. Study of the association of atmospheric temperature and relative humidity with bulk tank milk somatic cell count in dairy herds using Generalized additive mixed models. Research in Veterinary Science, **2017**, 7.
44. Uccellini, L. W., and Ten Hoeve, J. E. Evolving the National weather service to build a weather-ready nation. Bulletin of the American Meteorological Society, **2019**, 20.
45. Weber, N. J. and Mass, C. F. Subseasonal weather prediction in a global convection-permitting model. Bulletin of the American Meteorological Society, **2019**, 11.
46. Wang, W. and McPhaden, M. Surface Layer Temperature Balance in the Equatorial Pacific during the 1997-98 El Niño and 1998-99 La Niña. Journal of Climate, **2001**, 15.
47. Wilks, D. S. *Statistical Methods in the Atmospheric Sciences.* USA. **2006**.
48. Xiong Y., Meng Qing-Shi, Gao J., Tang Xiang-Fang, Zhang Hong-fu. Effects of relative humidity on animal health and welfare. ScienceDirect, **2017**, 6.
49. Xu, J., Zhu, F., Wang, S., Zhao, X.,

Downloaded from www.periodico.tchequimica.com

Zhang, M., Ge, X., Wang, J., Tian, W., Wang, L., Yang, L., Ding, L., Lu, X., Chen, X., Zheng, Y., Guo, Z. Impact of relative humidity on fine aerosol properties via environmental wind tunnel experiments. Atmospheric Environment, **2019**, 9.

50. Xu, X., Huang, Z., Zhang, X., and Li, Z. A novel humidity measuring method based on dry-bulb temperatures using artificial neural network. Building and Environment, **2018**, 8.
51. Yang, Z-Ch. Hourly ambient air humidity fluctuation evaluation and forecasting based on the least-squares Fourier-model. Measurement, **2019**, 12.
52. Zebende, A.A. Brito, A.M. Silva Filho, A.P. Castro. ρDCCA applied between air temperature and relative humidity: An hour/hour view. G.F. Physica A, **2018**, 10.
53. Zhan, X., Wang, Y., Cao, L., Li, L., Li, Ch. Determining critical relative humidity by measuring air humidity in equilibrium directly. European Journal of Pharmaceutical Sciences, **2010**, 4.
54. Zhu L., Li, Y. & Jiang, Z. Statistical Modeling of CMIP5 Projected Changes in Extreme West Spells over China in the Late 21st Century. Jurnal of Meteorological research, **2017**, 18.

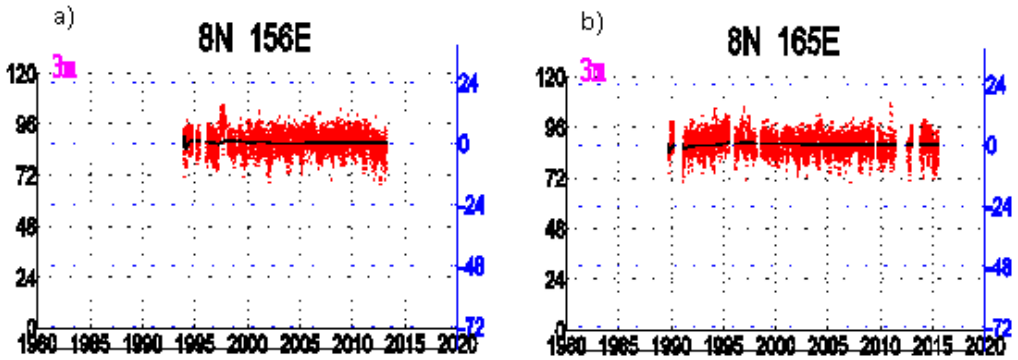

Figure 2. *Increment of Relative Humidity occurrences above time average line at a) 8º N 156º E, b) and pronounced at 8º N 165º E.*

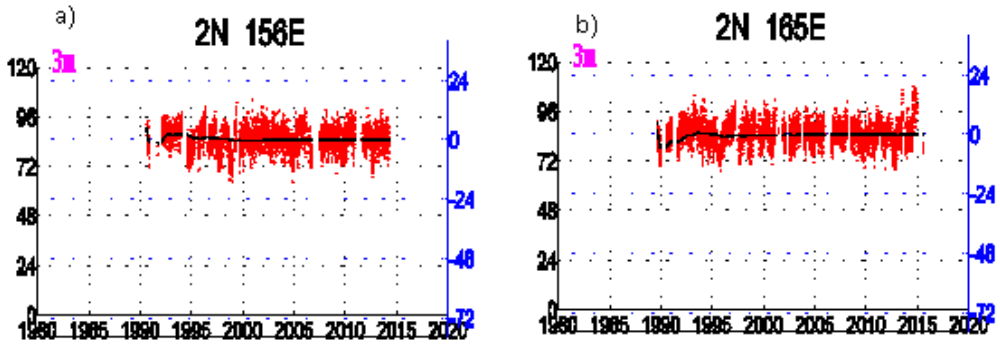

Figure 3. *Reduction of Relative Humidity occurrences below time average line at a) 2º N 156º E, b) and pronounced at 2º N 165º E.*

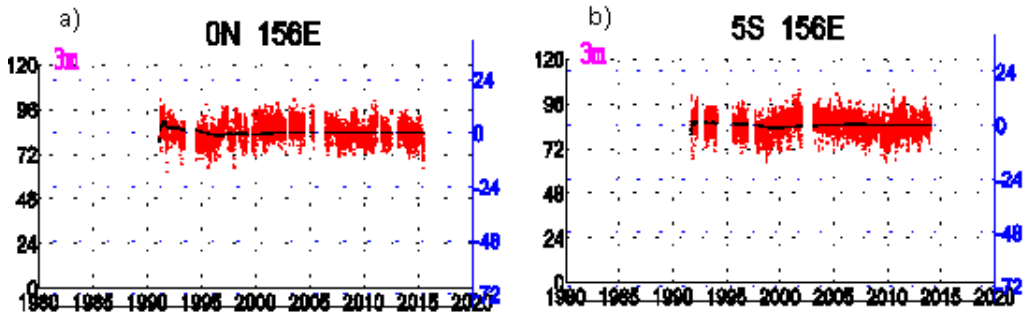

Figure 4. *Normal oscillation of Relative Humidity above and below time average line during long period from 1997 at a) 0º N 156º E, and at b) 5º S 156º E.*

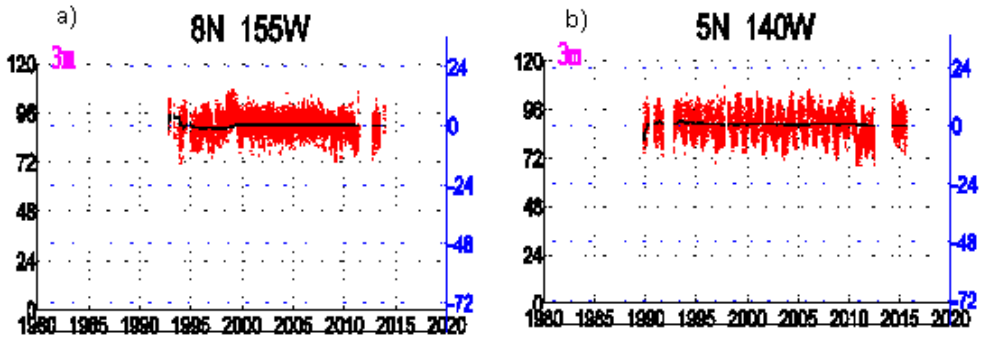

Figure 5. *Abnormal oscillation of Relative Humidity in the northwest of the Pacific Ocean around the Equatorial line, oscillating a) above, at 8º N 155º W, and b) below, at 5º N 140º W, the time average line.*

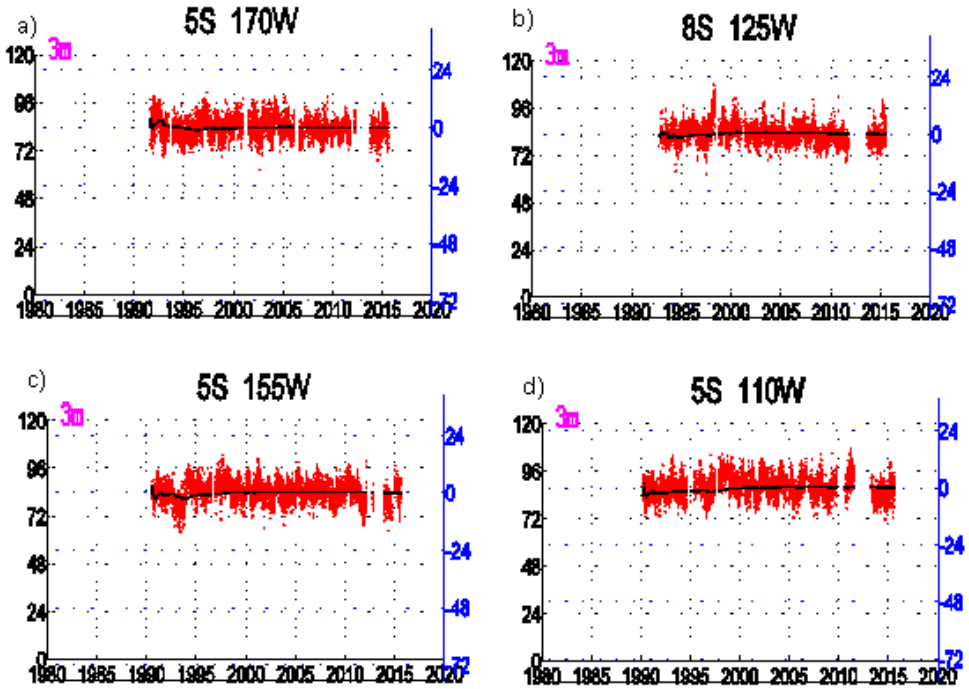

Figure 6. *Sinusoidal oscillations of Relative Humidity in the southwest of the Pacific Ocean around the Equatorial line in normal conditions at a) 5º S 170º W, b) 8º S 125º W, and abnormal conditions at c) 5º S 155º W, and d) 5º S 110º W locations.*

Downloaded from www.periodico.tchequimica.com

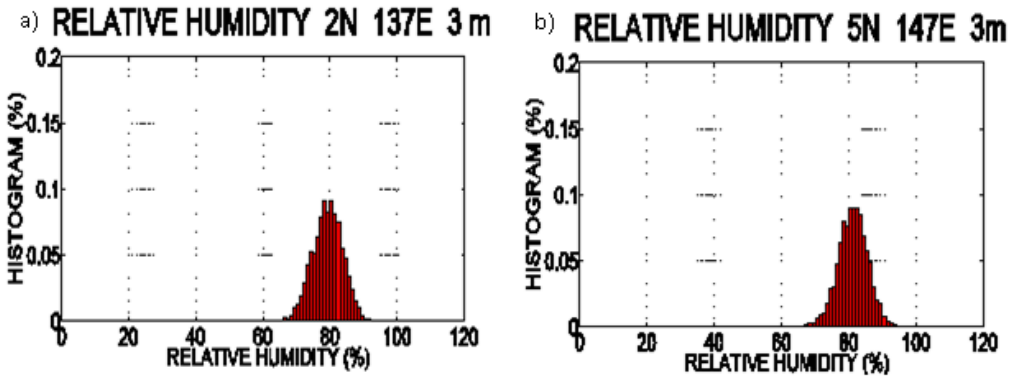

Figure 7. *Discrete PDF of Relative Humidity in the northeast of the Pacific Ocean in the Equatorial line at a) 2º N 137º E, and b) 5º N 147º E.*

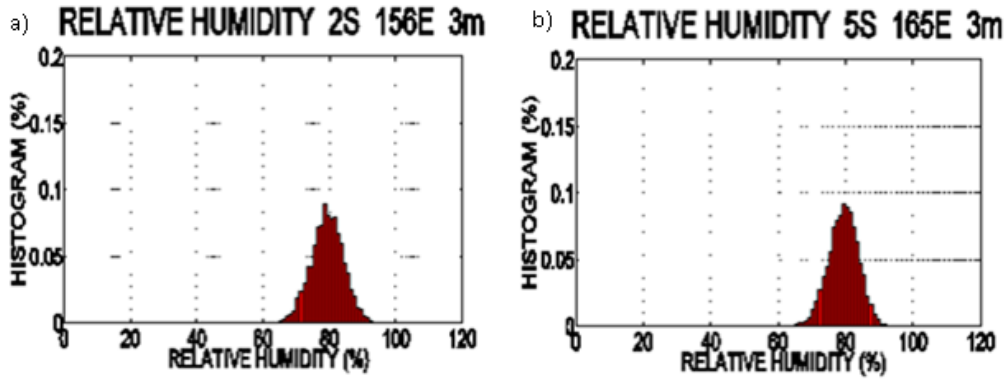

Figure 8. *Discrete PDF of Relative Humidity in the southeast of the Pacific Ocean in the Equatorial line at a) 2º S 156º E, and b) 5º S 165º E.*

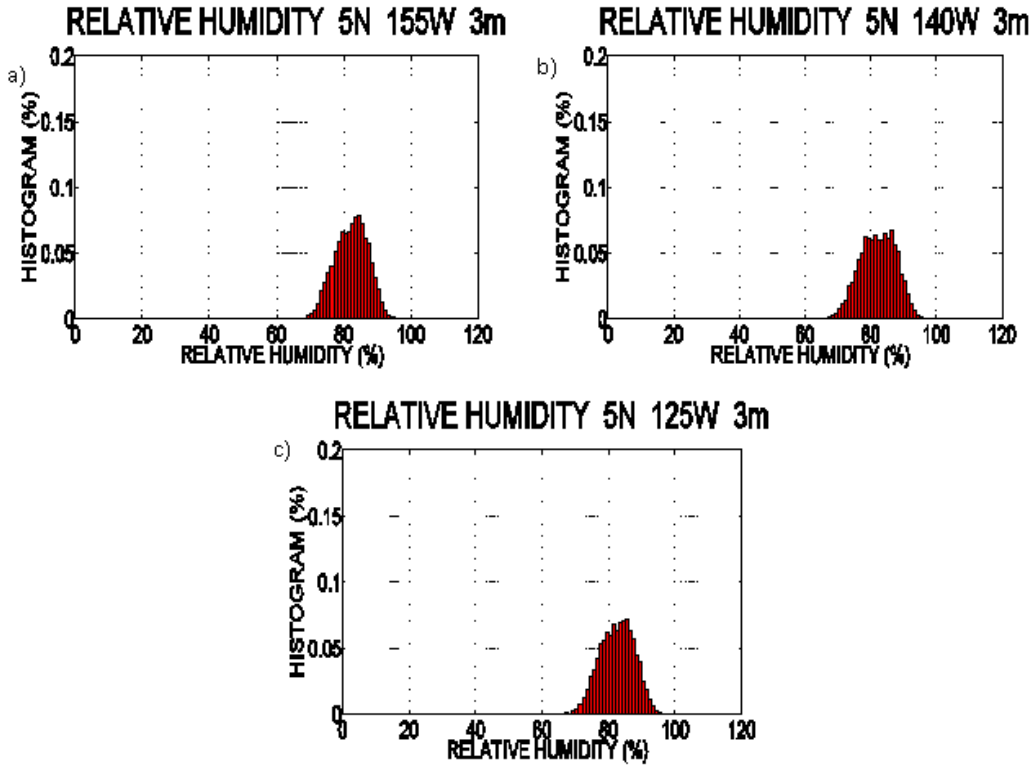

Figure 9*. Gaussian shapes of Discrete PDF of Relative Humidity in the Pacific Ocean at the Equatorial line at a) 5º N 155º W, b) 5º N 125º W, and c) 5º N 140º W.*

Downloaded from www.periodico.tchequimica.com

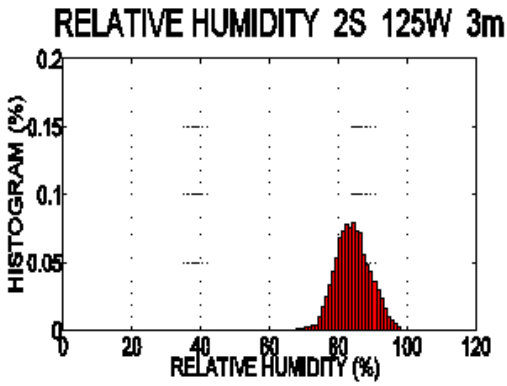

Figure 10. *Lower peaks of Discrete PDF of Relative Humidity in the Pacific Ocean at the Equatorial line at 2º S 125º W.*

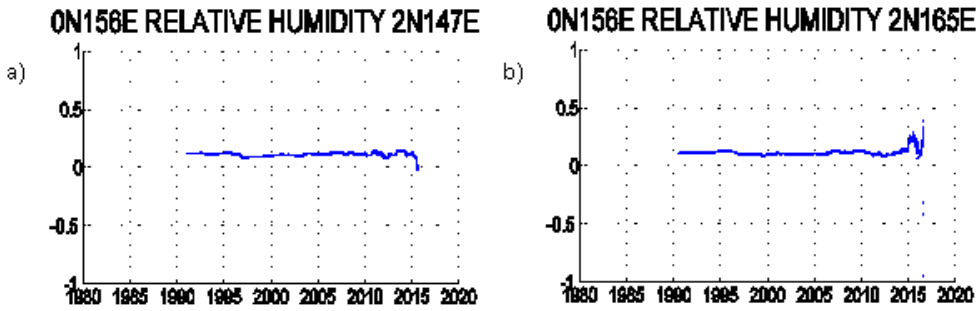

Figure 11. *Lag correlation functions of PDF of Relative Humidity in the east side of the Pacific Ocean at the Equatorial line between a) 0º N 156º E and 2º N 147º E, and b) 0º N 156º E and 2º N 165º E.*

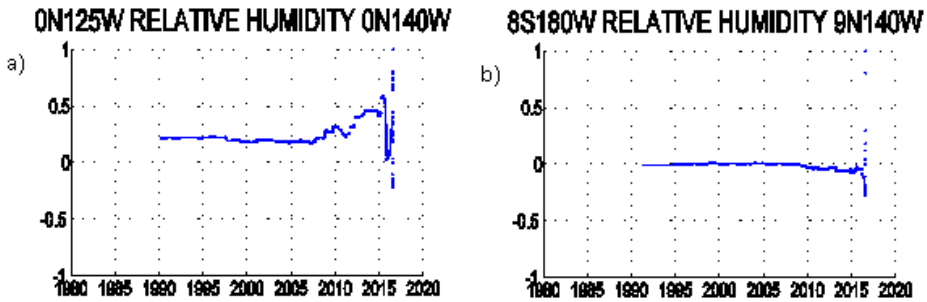

Figure 12. *Lag correlation functions of PDF of Relative Humidity in the west side of the Pacific Ocean at the Equatorial line between a) 0º N 125º W and 0º N 140º W, and b) 8º S 180º W and 9º N 140º W.*

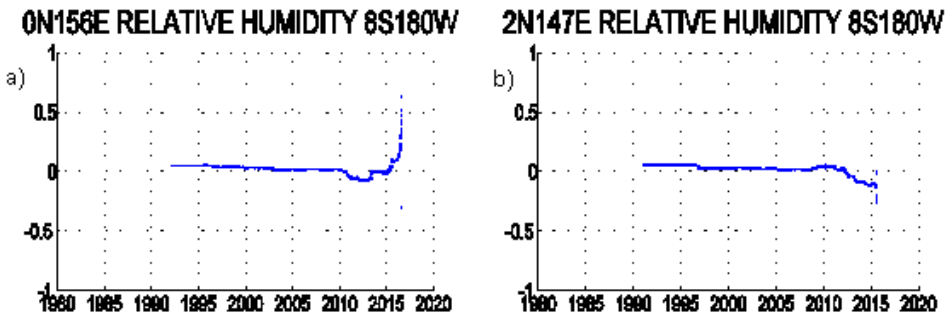

Figure 13. *Lag correlation functions of PDF of Relative Humidity between the east and west sides of the Pacific Ocean at the Equatorial line between a) 0º N 156º E and 8º S 180º W, and b) 2º N 147º E and 8º S 180º W.*

Downloaded from www.periodico.tchequimica.com

PERIÓDICO TCHÊ QUÍMICA
ARTIGO ORIGINAL

DIAGNÓSTICOS BIOECOLÓGICOS DO SOLO CONTAMINADO POR ÓLEO REMEDIADO COM SORVENTES POLIMÉRICOS

BIOECOLOGICAL DIAGNOSTICS OF OIL-CONTAMINATED SOIL REMEDIATED WITH POLYMERIC SORBENTS

БИОЭКОЛОГИЧЕСКАЯ ДИАГНОСТИКА НЕФТЕЗАГРЯЗНЕННОГО ПОЧВОГРУНТА, ВОССТАНАВЛИВАЕМОГО ПОЛИМЕРНЫМИ СОРБЕНТАМИ

VASILIEV, Sergey I.[1] *; FOMINA, Natalya V.[2]; LAPUSHOVA, Lyubov A.[3], FEDOTOVA, Arina S.[4]; ZHURAVLEV, Dmitry N.[5];

[1] Siberian Federal University

[2,4] Krasnoyarsk State Agrarian University

[3] Krasnoyarsk Branch of Irkutsk State Transport University

[5] NPF Ekosorb LLC

** Correspondence author*
e-mail: s-vasilev1@yandex.ru

Received 22 June 2019; received in revised form 24 October 2019; accepted 30 October 2019

RESUMO

O impacto antropogênico nos ecossistemas ao redor dos campos de petróleo desenvolvidos causou problemas ambientais que afetaram todos os habitats dos organismos vivos. O método de sorção é considerado o mais eficiente e ambientalmente aceitável para a remoção de substâncias petrolíferas do solo. As vantagens dos sorventes poliméricos são a capacidade de remover vários contaminantes para praticamente qualquer concentração residual, ausência de contaminantes secundários e controlabilidade do processo de sorção. A atividade enzimática do solo é um indicador de seu estado ecológico e pode ser usada para avaliar o grau de contaminação, a intensidade da exposição e a eficiência da remediação. A análise enzimática é realizada através do estudo dos níveis de atividade das enzimas envolvidas em diferentes processos bioquímicos no solo. Isso pode fornecer informações mais confiáveis sobre mudanças no estado do solo. Nesta pesquisa, o diagnóstico bioecológico do solo contaminado com óleo foi realizado através do estudo das enzimas oxidativas (catalase) e hidrolíticas (urease, protease e invertase) antes e após a aplicação dos sorventes. Com base na comparação dos dados obtidos no estudo da atividade enzimática e celulolítica do solo com uma alteração na contagem microbiana total, nas propriedades morfológicas e biológicas dos microrganismos do solo e nas alterações hematológicas e bioquímicas nos modelos biológicos em relação às taxas de aplicação do sorvente, revelou uma correlação entre os índices de atividade biológica do solo, composição quantitativa e específica dos microrganismos. As reações químicas que ocorrem no solo, associadas ao metabolismo, decomposição e síntese de substâncias orgânicas, migração de compostos químicos, mobilização de nutrientes, são realizadas com a ajuda de enzimas. A alta sensibilidade, precisão, simplicidade relativa e fácil operação de métodos para determinar a atividade das enzimas do solo permitiram que fossem utilizados em estudos para avaliar a intensidade e a direção dos processos bioquímicos essenciais para a vida e fertilidade do solo. A atividade do solo serviu como um indicador integral do impacto ambiental.

Palavras-chave: *solo, poluição, petróleo, sorventes poliméricos, enzima*.

ABSTRACT

The anthropogenic impact on ecosystems around developed oil fields has caused environmental issues that affect all habitats of living organisms. The sorption method is considered the most efficient and environmentally acceptable for the removal of petroleum substances from the soil. The advantages of polymeric sorbents are the ability to remove various contaminants to almost any residual concentration, absence of secondary contaminants, and sorption process controllability. The enzymatic activity of soil is an indicator of its ecological state and it can be used to assess the degree of contamination, the intensity of exposure, and efficiency of remediation. The enzymic analysis is performed by studying the activity levels of enzymes involved

Downloaded from www.periodico.tchequimica.com

in different biochemical processes in soil. This can give more reliable information on changes in the state of the soil. In this research, the bioecological diagnostics of oil-contaminated soil was carried out by studying oxidative enzyme (catalase) and hydrolytic enzymes (urease, protease, and invertase) before and after application of sorbents. Based on a comparison of data obtained in study of enzyme and cellulolytic activity of the soil with a change in the total microbial count, morphological and biological properties of soil microorganisms and hematological, biochemical changes in biological models with regard to application rates of sorbent, it was revealed a correlation between the indices of biological activity of the soil, quantitative and specific composition of microorganisms. Chemical reactions occurring in the soil, associated with metabolism, decomposition, and synthesis of organic substances, migration of chemical compounds, mobilization of nutrients, are carried out with the help of enzymes. High sensitivity, accuracy, relative simplicity and easy operation of methods for determining the activity of soil enzymes allowed them to be used in studies in assessing the intensity and direction of biochemical processes that are essential for soil life and fertility. The activity of soil served an integral indicator of the environmental impact.

Keywords: *soil, pollution, petroleum, polymeric sorbents, enzyme.*

АННОТАЦИЯ

Увеличение техногенного воздействия на экосистемы в районах освоения нефтяных месторождений вызвало ряд экологических проблем, охватывающих все среды обитания живых организмов и растений. Сорбционный метод очистки почвы и грунта от нефтепродуктов является наиболее эффективным и экологически приемлемым способом. Преимуществом данного метода является возможность удаления загрязнений чрезвычайно широкой природы практически до любой остаточной концентрации, а также отсутствие вторичных загрязнений и управляемость процессом. Ферментативная активность почвы является показателем ее экологического состояния, поэтому может применяться для оценки как степени ее загрязнения, интенсивности воздействия и эффективности ремедиации. Ферментативный анализ необходимо проводить изучая уровни активности ферментов, участвующих в разных биохимических процессах в почве, что позволит получить более достоверную информацию об изменении ее состояния. Биоэкологическая диагностика нефтезагрязненной почвы и грунта в данной работе проводилась при изучении окислительного фермента (каталаза) и гидролитических (уреаза, протеаза и инвертаза) до и после применения сорбентов. На основе сопоставления данных, полученных при изучении ферментативной и целлюлозолитической активности почвы с изменением общего микробного числа, морфо-биологических свойств микроорганизмов почвы и гематологических, биохимических изменений биологических моделей с учетом дозы внесения сорбента, выявлены корреляции между показателями биологической активности почвы, количественным и видовым составом микроорганизмов. Химические реакции, протекающие в почве, связанные с обменом веществ, разложением и синтезом органических веществ, миграцией химических соединений, мобилизацией питательных элементов и т.д., осуществляются с помощью ферментов. Высокая чувствительность, точность, относительная простота и нетрудоемкость методов определения активности почвенных ферментов позволили использовать их в исследованиях при оценке интенсивности и направленности важнейших для жизни и плодородия почвы биохимических процессов. В данной работе активность почвенных ферментов принята как интегральный показатель воздействия факторов среды.

Ключевые слова: *почвогрунт, загрязнение, нефть, полимерные сорбенты, ферменты.*

1. INTRODUCTION

When studying the mechanism of oil-contaminated soil remediation with sorbents, a researcher should pay equal attention to the initial indicators, the analysis of processes occurring in petroleum substances in the soil, and the principles of sorption of the introduced pollutants by the sorbents. There are dozens of sorbent brands, both organic and polymer-based, that are used in oil spill response operations (Vasiliev and Melkozerov, 2011; Aznauryan, 2009).

The soil cover diagnostics with biochemical methods, in particular, with the help of enzyme indicators, has now been proven highly efficient. The enzymatic activity of soil was studied for different objects and, regardless of the aim of the research, this indicator is always considered as an integral expression of the action of environmental factors and interdependent processes occurring in the soil (Aznauryan, 2009; Dolgova, 1975; Kolesnikov *et al*., 2007; Kireeva *et al.*, 2001; Fomina, 2013; Novoselova, 2004; Khaziyev and Fatkhiyev, 1981; Khaziyev *et al*., 1988; Schemelinina *et al.,* 2007; Kireeva *et al.,*

Downloaded from www.periodico.tchequimica.com

1998). The influence of petroleum substances on soil enzymes includes direct impact, such as inhibiting, destroying or activating enzymes, and indirect impacts, such as changing the soil enzyme pool as a result of inhibiting the growth of soil mesofauna and plants. Enzymatic activity in oil-contaminated soils during remediation can help validate the effect of remediation on the properties of disturbed soils. Therefore, enzymatic activity, associated with the transformation of compounds of the main biogenic elements, is a complex representative indicator (Fomina, 2013). At the same time, the sorption mechanism in fertile soil remediation after oil spills needs to be studied further (Vasilyev *et al.,* 2015).

2. MATERIALS AND METHODS

The subject of the study was an oil-contaminated mixture of soil and peat, with pH = 7.2, C_{org} = 18.9%, and N = 1.07%. To simulate the contamination, oil from the Surgut deposit was introduced in concentrations of 6 g per 1 kg of soil (low) and 60 g per 1 kg of soil (high). Polymeric sorbents Unisorb-M, Unisorb-bio, and Unisorb-Ferro (Melkozerov *et al.,* 2019; Zhuravlev *et al.,* 2006) were used to remediate the soil. These sorbents are produced by the scientific and production organization LLP “Ekosorb”, Krasnoyarsk Russia, there is a positive experience of their usage in the elimination of industrial accidents both in oil fields and in the liquidation of the accident at the Sayano-Shushenskaya hydroelectric station.

Ten soil samples were collected, including a control sample with no oil or sorbent introduced, a sample with oil, a sample with oil and Unisorb-M, a sample with oil and Unisorb-bio, and a sample with oil and Unisorb-Ferro (Melkozerov *et al.,* 2014, 2017). The soil was sampled according to GOST 17.4.3.01-83 Nature protection. Soils. General requirements for sampling. The laboratory and analytical studies were performed using generally accepted methods in soil science and biology (Kazeev *et al.,* 2003; Khaziyev, 2005). Catalase determination was carried out according to the Johnson and Temple (1964) method by titration with 0.1 n $KMnO_4$ solution, the activity was expressed in ml of 0.1 n $KMnO_4$ / g dry soil for 20 minutes. The protease activity was determined by the method of Hoffmann and Teicher (1957) at a wavelength of 650 nm and expressed in mg of amine nitrogen/10 g of soil over 20 hours. Urease activity was established by the method of Scherbakova (1983) by colorimetrication at a wavelength of 400 nm and expressed in mg of ammonium nitrogen/10 g of dry soil for 4 hours. The invertase activity was studied by the method of colorimetric according to Hoffmann and Pallauf (1965) at a wavelength of 578 nm and expressed in mg of glucose/g of dry soil for 24 hours. All indicators of soil enzymatic activity were recalculated, taking into account soil moisture content per 1 g of soil.

In this research, the indicators of enzymatic activity are used as diagnostic criteria for validating the environmental safety and performance of sorbents, introduced to localize the oil contamination of soil (Vinogradova *et al.,* 2015; Prudnikova *et al.,* 2017). Redox enzymes have always received much attention because of their significant role in soil-forming processes (Pakharkova *et al.,* 2015; Volova *et al.,* 2017). The activity of this group of enzymes indicates the intensity of oxidation and the humification of organic substances.

3. RESULTS AND DISCUSSION

Earlier, it was established that the activity of soil enzymes is a sensitive indicator of the biological state of the soil (Aznauryan, 2009; Dolgova, 1975).

The catalase activity of contaminated soil varied depending on the concentration of oil. The high concentration reduced the activity to 0.35 0.1 n $KMnO_4$ ml per 1 g of soil in 20 minutes, while the low concentration increased it to 0.43 0.1 n $KMnO_4$ ml per 1 g of soil in 20 minutes. The catalase activity of the uncontaminated control sample was 0.37–0.39 0.1 n $KMnO_4$ ml per 1 g of soil in 20 minutes on average (Figure 1). The sorbents increased the catalase activity in the first and second cases, and in case of high contamination, the catalytic activity indicators were similar to those of the control sample (Figure 1).

In case of low contamination, the catalase activity increased to 0.42, 0.44, and 0.45 0.1 n $KMnO_4$ ml per 1 g of soil in 20 minutes with applied sorbents Unisorb-Ferro, Unisorb-M, and Unisorb-bio, respectively. There was a clear stimulation of catalase activity, especially with Unisorb-bio that contains a complex of hydrocarbon-oxidizing microorganisms.

The proteolytic activity of the uncontaminated control sample was 0.70–0.71 mg of amine nitrogen per 1 g of soil in 20 hours, while the high contamination gave a 1.5-time decrease in the activity and applied sorbent Unisorb-M reduced it by half to 0.35 mg of amino nitrogen per 1 g of soil in 20 hours (Figure 2). On the contrary, sorbent Unisorb-bio-enhanced the

Downloaded from www.periodico.tchequimica.com

proteolytic activity to 1.05 mg, which can be explained by its composition (microorganisms).

Having considered the indicators of proteolytic activity in contaminated soil in low concentration (6 mg/kg), it was found that in this concentration, oil has a stimulating effect on proteolysis (0.79 mg). With Unisorb-M and Unisorb-bio, it was 0.90 and 0.96 mg, respectively. It should be noted that the highest indicators of this enzyme were also observed in the case of high contamination in the experiment with Unisorb-bio (Figure 2).

Sorbent Unisorb-Ferro reduced the proteolytic activity in both cases, yielding 0.31 and 0.53 mg of amine nitrogen per 1 g of soil in 20 hours, thus approaching the activity values of the uncontaminated soil sample in case of high contamination.

Since urease participates in nitrogen metabolism, the study of its activity is absolutely necessary for diagnostics of contaminated soil. The initial urease activity of uncontaminated soil was 0.63 mg of ammonium nitrogen per 1 g of soil in 4 hours. The introduction of oil at low concentration resulted in an increase in the urease activity to 0.93 mg of ammonium nitrogen per 1 g of soil in 4 hours. In the samples with sorbents, the urease activity also increased and did not vary significantly; it was 0.96–1.05 mg of ammonium nitrogen per 1 g of soil in 4 hours (Figure 3).

In the samples with high contamination, the urease activity decreased from 0.63 mg (in the control sample) to 0.46 mg of ammonium nitrogen per 1 g of soil in 4 hours, and in the samples with Unisorb-M and Unisorb-Ferro, to 0.39 and 0.43 mg of ammonium nitrogen per 1 g of soils in 4 hours, respectively. A notable stimulation of urease activity was observed when using Unisorb-bio, containing germ cultures that affect the nitrogen metabolism in oil-contaminated soil.

Having analyzed the data on the invertase activity, it was found that in case of low contamination, its activity doubles on average. The sorbents also increased the invertase activity from medium 14.3 mg of glucose per 1 g of soil in 24 hours to enriched 32.9–36.9 mg of glucose per 1 g of soil in 24 hours (Figure 4) on Zvyagintsev's scale (1978).

A high level of soil contamination reliably reduced the invertase activity from 14.4 mg to 13.5 mg of glucose per g of soil in 24 hours, and with sorbents Unisorb-M and Unisorb-bio, to 12.9 and 13.6 mg of glucose per g of soil in 24 hours, respectively. It should be noted that at this level of contamination, only Unisorb-Ferro enhanced the invertase activity, showing the remediation performance of 18.9 mg of glucose per 1 g of soil in 24 hours.

The comparative study of enzyme activity was carried out to validate the 'unmarred' effect of sorbents on uncontaminated soil (Table 1). It was determined that the catalase activity does not differ from that of the control sample, while the urease activity, on the contrary, decreases by half, except for the samples with sorbent Unisorb-bio.

The protease activity decreases insignificantly; at that, and the smallest decrease was observed in the samples with Unisorb-bio, most likely due to sorption (Table 1). The invertase activity after the application of the studied sorbents decreased insignificantly in the samples with Unisorb-M and Unisorb-bio, while Unisorb-Ferro did not significantly change its activity as compared to the control sample.

The enzymatic activity of oil-contaminated soil validated the performance of the studied sorbents. It can be observed in the increase in the enzyme activity in case of low contamination and the return of indicators to the control values in case of high contamination. The only exceptions are enzymes involved in nitrogen metabolism: significant contamination increased the activity only in samples with Unisorb-bio due to the presence of carbohydrate-oxidizing microorganisms.

4. CONCLUSION

When introduced into uncontaminated soil, sorbents Unisorb-M and Unisorb-bio yield an insignificant decrease in the invertase activity, while Unisorb-Ferro does not reduce the invertase activity as compared to the control sample.

The increase in the activity of soil enzymes after the introduction of Unipolymer polymeric sorbents at minimal contamination and the return to the control values at maximum contamination confirm the effective performance of the studied sorbents for remediation of oil-contaminated soil.

The application of the Unisorb series sorbents to the oil-contaminated soil with a low level of contamination (6 g of oil per 1 kg of soil) doubles the invertase activity.

At a higher level of contamination (60 g of oil per 1 kg of soil), the urease activity decreases from 0.63 mg as in the control sample to 0.46 mg of ammonium nitrogen per 1 g of soil in 4 hours.

The application of sorbents Unisorb-M and Unisorb-Ferro at high contamination reduces

Downloaded from www.periodico.tchequimica.com

the urease activity to 0.39 and 0.43 mg per 1 g of soil, respectively, while sorbent Unisorb-bio, containing germ cultures, reliably stimulates the urease activity and increases the nitrogen metabolism in oil-contaminated soil.

At the high level of contamination, sorbent Unisorb-Ferro reduces the proteolytic activity to 0.31 and 0.53 mg of amine nitrogen per 1 g of soil in 20 hours, thus approaching the proteolytic activity of uncontaminated soil.

The performance of the studied sorbents can be validated only in comparison to the performance in an uncontaminated soil sample. It was determined that all the studied sorbents did not significantly change the activity of catalase and invertase as compared to the control sample. However, they can reduce the activity of urease and protease, probably by reducing the activity of microorganisms in the soil.

The materials of this article can be useful for EHS professionals and students who study the environment of the northern petroleum provinces of Russia.

5. REFERENCES

1. Aznauryan, D. K. Izmeneniye ekologo-biologicheskikh svoystv pochv Yuga Rossii pri zagryaznenii neftyu [Changes in ecological and biological properties of soils in the South of Russia due to oil contamination]. PhD Dissertation, Southern Federal University, Rostov-on-Don, **2009.** (in Russian).
2. Dolgova, L. G. Biokhimicheskaya aktivnost pochvy pri zagryaznenii [Biochemical activity of soil at contamination]. *Pochvovedeniye [Soil Science],* **1975,** 4, 113–118 (in Russian).
3. Fomina, N. V. Izmeneniye biogennykh svoystv pochvy pod vliyaniyem tekhnogennogo zagryazneniya [Changes in soil biogenic properties under the influence of technogenic pollution]. Saarbrucken: Lap Lambert Academic Publishing, **2013.**
4. GOST 17.4.3.01–83. Nature protection. Soils. General requirements for sampling, **2008.** Available at: http://docs.cntd.ru/document/1200012800 (in Russian).
5. Kazeev, K. Sh., Kolesnikov, S. I., Valkov, V. F. (2003) Biologicheskaya diagnostika i indikatsiya pochv: metodologiya i metody issledovaniy [Biological diagnostics and indication of soil: Methodology and methods of research]. Rostov-on-Don: Rostov State University, **2003**. (in Russian).
6. Khaziyev, F. Kh. Metody pochvennoy enzimologii [Methods of soil enzymology]. Moscow: Nauka, **2005.** (in Russian).
7. Khaziyev, F. Kh., Fatkhiyev, F. F. Izmeneniye biokhimicheskikh protsessov v pochvakh pri neftyanom zagryaznenii i aktivatsiya razlozheniya nefti [Changes in biochemical processes in soils under oil contamination and activation of oil decomposition]. *Agrokhimiya [Agrochemistry],* **1981,** 10, 102–111. (in Russian).
8. Khaziyev, F. Kh., Tishkina, E. I., Kireeva, N. A. Vliyaniye nefteproduktov na biologicheskuyu aktivnost pochv [Effect of petroleum products on soil biological activity]. *Biologicheskiye nauki [Biological Sciences],* **1988,** 10, 93–99. (in Russian).
9. Kireeva, N. A., Novoselova, E. I., Khaziyev F. Kh. Carbohydrase activity in oil-contaminated soils. *Eurasian Soil Science*, **1998,** 31(12), 1314–1318.
10. Kireeva, N. A., Vodopyanov, V. V., Novoselova, E. I., Onegova, T. S., Zhdanova, N. V. Mikrobiologicheskaya rekultivatsiya neftezagryaznennykh pochv [Microbiological remediation of oil-contaminated soils]. Moscow: VNIIOENG, **2001.** (in Russian).
11. Kolesnikov, S. I., Tatosyan, M. L., Aznauryan, D. K. Izmeneniye fermentativnoy aktivnosti chernozema obyknovennogo pri zagryaznenii neftyu i nefteproduktami v modelnykh eksperimentakh [Changes in enzymatic activity of black earth contaminated with petroleum and oil products in simulation experiments]. Doklady Rosselkhozakademii [Reports of the Russian Academy of Agricultural Sciences], **2007**, 5, 32–34 (in Russian).
12. Melkozerov, V. M., Baryshev, I. E., Vasilyev, S. I., Matveykina, Ya. V., Fedotova, A. S. Features of the development of native microflora of oil-contaminated soils under sorption effects. Geology and petroleum potential of the West Siberian megabasin (experience, innovation). *Bulletin of Tyumen Industrial University*, **2014**, 2, 191–196.
13. Melkozerov, V. M., Vasiliev, S. I., Velp A. Ya., Krylyshkin, R. N. Effektivnaya likvidatsiya avariynykh razlivov nefti i nefteproduktov s primeneniyem sovremennykh tekhnologiy i polimernykh

Downloaded from www.periodico.tchequimica.com

sorbentov [Efficient elimination of oil and oil product spills using modern technologies and polymeric sorbents]. *Sistemy. Metody. Tekhnologii [Systems. Methods Technology],* **2010**, 3, 115–123. (in Russian).
14. Melkozerov, V. M., Vasilyev, S. I., Zhuravlev, D. N., Lapushova, L. A., Fedotova, A. S. Investigation of the characteristics of the modified sorbents of the Unipolymer and Unisorb series. *Environmental protection in the oil and gas complex, Moscow, VNIONG*, **2017**, 3, 13–17.
15. Melkozerov, V. M., Zhuravlev, D. N., Sharipov, I. A., Vildanov, A. A., Vasilyev, S. I. The study of the properties of polymeric sorbents of various modifications used to eliminate oil spills in the water areas of the Arctic zone. *Environmental protection in the oil and gas complex, Moscow, VNIONG*, **2019,** 1, 49–55.
16. Novoselova, E. I. Strukturno-funktsionalnaya transformatsiya biogeotsenoza pri neftyanom zagryaznenii i puti yego vosstanovleniya [Structural and functional transformation of biogeocenosis under oil contamination and ways to remediate it]. Ufa: Bashkir State University Pub, **2004**. (in Russian).
17. Pakharkova, N. V., Prudnikova, S. V., Gekk, A. S., Larkova, A. N., Korosteleva, N. S. Optimization of plant selection for the bioremediation of soils polluted by oil and oil products in the conditions of Southern Siberia. *Bulletin of Krasnoyarsk State Agrarian University*, **2015**, 8, 28–33.
18. Rudnikova, S. V., Vinogradova, O. N., Trusova, M. Y. Specific character of bacterial biodegradation of polyhydroxyalkanoates. *Doklady Biochemistry and Biophysics*, **2017**, 473(1), 94–97.
19. Schemelinina, T. N., Novoselova, E. I., Kireeva, N. A., Markarova, M. Yu. Diagnostirovaniye stepeni zagryaznennosti pochv neftyu po pokazatelyam fermentativnoy aktivnosti [Diagnosing the degree of soil contamination with oil by enzymatic activity]. *Vestnik of Orenburg State University*, **2007,** 75, 432–434. (in Russian).
20. Vasiliev, S. I., Melkozerov, V. M. Okhrana okruzhayushchey sredy i ratsionalnoye nedropolzovaniye pri razrabotke, ekspluatatsii neftyanykh mestorozhdeniy, transportirovke nefti i nefteproduktov [Environmental protection and rational subsoil use in the development and operation of oil fields and the transportation of petroleum and oil products]. Saarbrucken, Lap Lambert Academic Publishing, **2011.**
21. Vasilyev, S. I., Miloserdov, E. E., Bulchayev, N. D. Environmental problems in the development and exploitation of oil and gas fields in Eastern Siberia. *Mining industry*, **2015,** 3, 88.
22. Vinogradova O. N., Prudnikova S. V., Zobova N. V., Kolesnikova V. L. Microbiological degradation of poly-3-hydroxybutyrate in samples of agrogen-transformed soils. *Journal of the Siberian Federal University. Biology*, **2015**, 8(2), 199–209.
23. Volova, T. G., Prudnikova, S. V., Vinogradova, O. N., Syrvacheva, D. A., Shishatskaya, E. I. Microbial Degradation of Polyhydroxyalkanoates with Different Chemical Compositions and Their Biodegradability. *Microbial Ecology*, **2017,** 73(2), 353–367
24. Wang, H., Fischer, T., Wieprecht, W., Möller, D. A predictive method for crude oil volatile organic compounds emission from soil: Evaporation and diffusion behavior investigation of binary gas mixtures. *Environmental Science and Pollution Research*, **2015**, 22(10), 7735–7743.
25. Zhuravlev, D. N., Vasiliev, S. I., Voskresensky, A. G., Lubinets, G. G., Parshenok, A. G. Composition for polymeric sorbent. Patent 2663743 MCP B 01J 20/26 B 01J 20/24 (2006/01), Moscow, RF, Russian Federation, **2006.**
26. Johnson, J. L.; Temple, K. L. Some variables affecting the measurement of 'catalase activity' in soil. *Soil Science Society of America Proceedings*, **1964,** 28:, 207–209.
27. Hoffmann G., Teicher K. Enzyme systems of our arable soils. VII. Proteases. *Z. PflErnähr Düng. Bodenk.*, **1957**, 77, 243–251.
28. Scherbakova T. A. Enzymatic activity of the soil and the transformation of organic matter. Minsk: Science and Technology, **1983.**
29. Hoffmann, G., Pallauf, J. Advances in Enzymology and Related Areas of Molecular Biology, **1965.**

Downloaded from www.periodico.tchequimica.com

Table 1. *Average activity of soil enzymes with the application of sorbents*

Experiment option	Catalase, 0.1 n $KMnO_4$ ml per 1 g of soil in 20 min	Urease, mg of ammonium nitrogen per 1 g of soil in 4 h	Protease, mg of amine nitrogen per 1 g of soil in 20 h	Invertase, mg of glucose per 1 g of soil in 24 h
Control sample (clean soil)	0.38±0.02	0.63±0.17	0.70±0.27	14.4±2.4
Soil + Unisorb-M	0.38±0.01	0.30±0.10	0.58±0.12	13.5±2.1
Soil + Unisorb-bio	0.37±0.02	0.48±0.12	0.61±0.25	13.2±2.0
Soil + Unisorb-Ferro	0.38±0.02	0.37±0.02	0.55±0.12	14.0±2.2

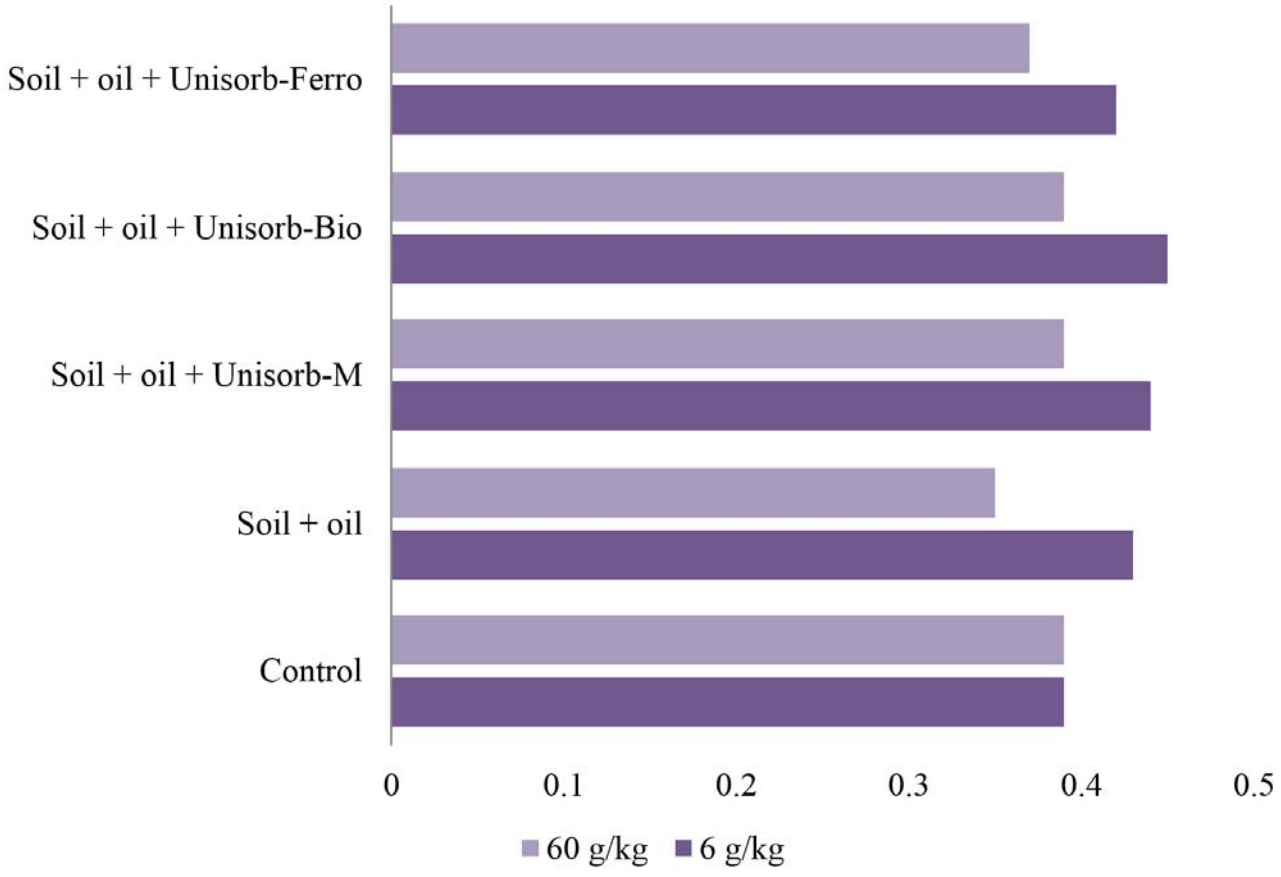

Figure 1. *Catalase activity in oil-contaminated soil*

Downloaded from www.periodico.tchequimica.com

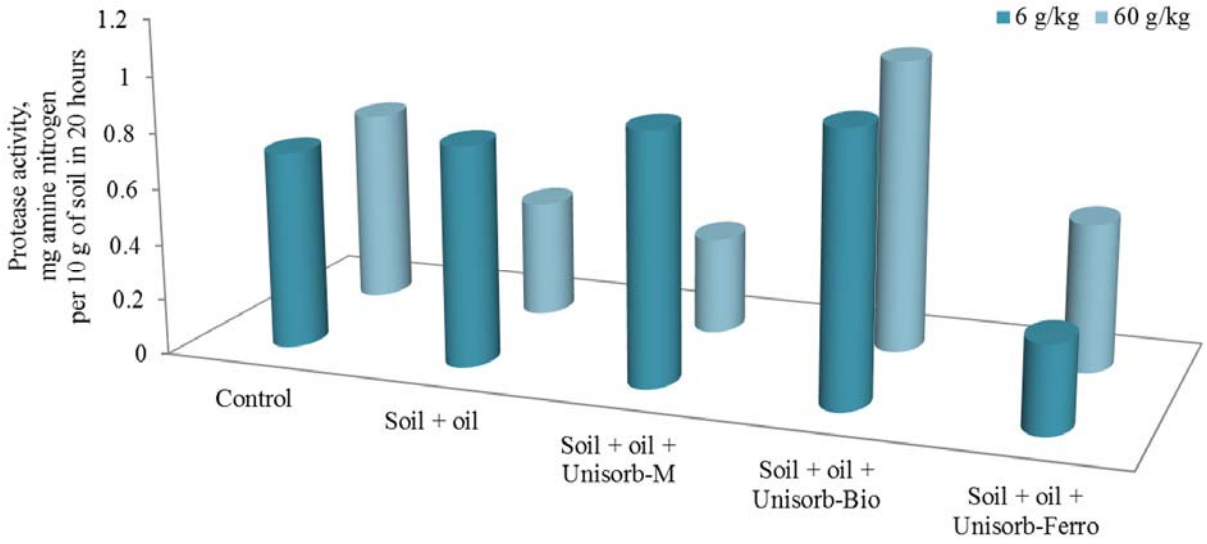

Figure 2. *Protease activity in oil-contaminated soil*

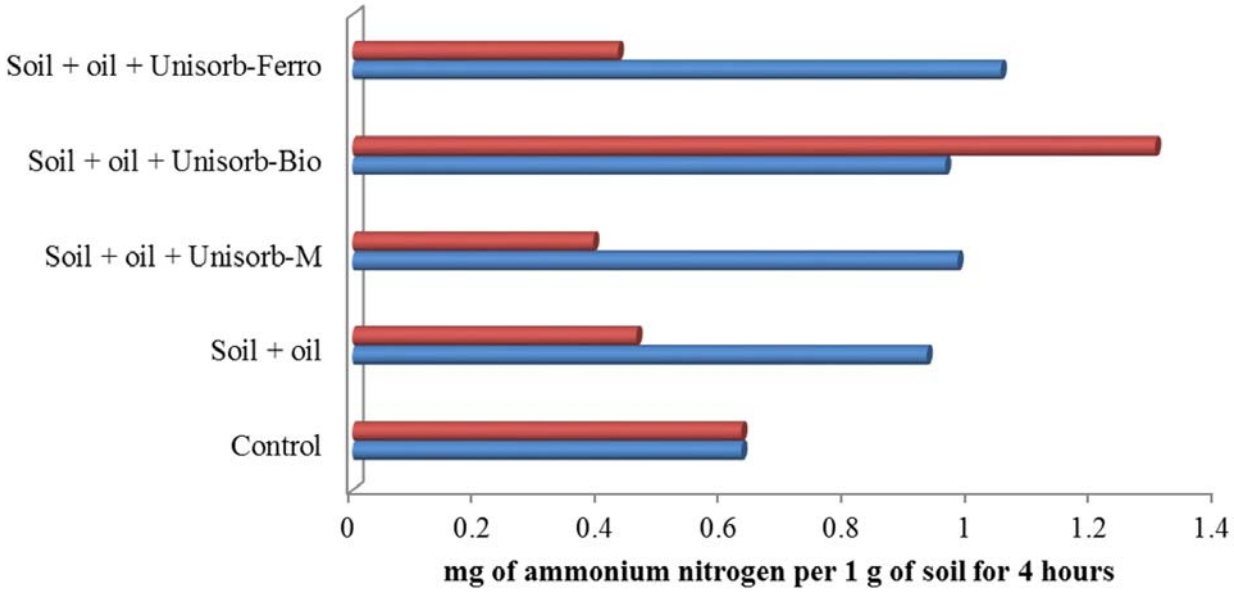

Figure 3. *Urease activity in oil-contaminated soil*

Downloaded from www.periodico.tchequimica.com

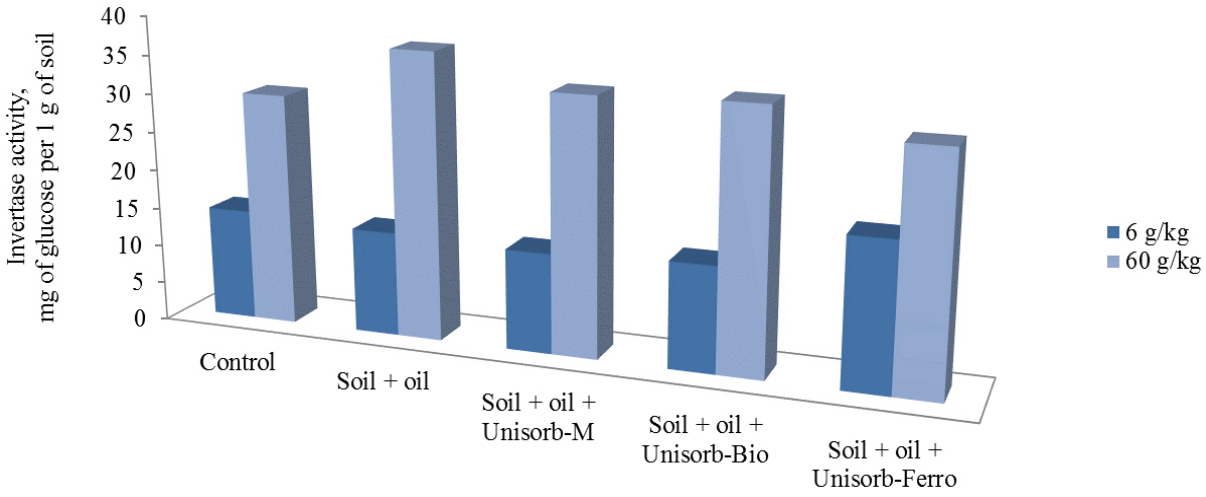

Figure 4. *Invertase activity in oil-contaminated soil*

Downloaded from www.periodico.tchequimica.com

PERIÓDICO TCHÊ QUÍMICA
ARTIGO ORIGINAL

VALIDAÇÃO DE METODOLOGIA PARA MODELAR EFEITOS DE PERDA DE ESTABILIDADE EM PEÇAS DE PAREDES FINAIS FABRICADAS USANDO A TECNOLOGIA SLM

VALIDATION OF METHODOLOGY FOR MODELING EFFECTS OF LOSS OF STABILITY IN THIN-WALLED PARTS MANUFACTURED USING SLM TECHNOLOGY

ВАЛИДАЦИЯ МЕТОДИКИ МОДЕЛИРОВАНИЯ ЭФФЕКТОВ ПОТЕРИ УСТОЙЧИВОСТИ ТОНКОСТЕННЫХ ДЕТАЛЕЙ, ИЗГОТАВЛИВАЕМЫХ С ИСПОЛЬЗОВАНИЕМ ТЕХНОЛОГИИ SLM

DOBRYANSKIY, Vasiliy N.[1*]; RABINSKIY, Lev N.[2]; TUSHAVINA, Olga V.[3];

[1,2] Moscow Aviation Institute (National Research University), Institute of General Engineering Training, Moscow – Russian Federation

[3] Moscow Aviation Institute (National Research University), Institute of Aerospace, Moscow – Russian Federation

** Correspondence author*
e-mail: dobryanskijvn@mail.ru

Received 30 August 2019; received in revised form 20 October 2019; accepted 30 October 2019

RESUMO

As tecnologias de manufatura aditiva possibilitam fabricar qualquer produto em camadas com base no modelo de computador 3D, mas esse problema não é bem conhecido. Portanto, o artigo considera o problema de descrever os efeitos da perda de estabilidade decorrente da impressão tridimensional de produtos que contenham elementos cujo comprimento exceda significativamente a espessura ou o tamanho característico da seção transversal. O comportamento de tais elementos, do ponto de vista da mecânica dos materiais, pode ser descrito usando modelos de placas ou vigas. Foram comparados os resultados dos cálculos obtidos usando o modelo de condutividade térmica e termoelasticidade não estacionária com dados experimentais para o elemento específico do produto impresso no qual ocorre perda de estabilidade. Foi constatado que, nos momentos iniciais, é realizado o menor coeficiente de impacto crítico, o que, por sua vez, o torna o fenômeno mais perigoso. A possibilidade de alterar os parâmetros de impressão e a geometria do produto para excluir esses efeitos foi investigada. O elemento estrutural considerado pode perder estabilidade durante o processo de construção. Os resultados da solução do problema espectral mostraram que, com o tempo, o valor do efeito crítico diminui e tende assintoticamente a um valor mínimo fixo.

Palavras-chave: *fusão seletiva a laser, estado termomecânico, estruturas de paredes finas, tensão residual, validação.*

ABSTRACT

Additive manufacturing technologies make it possible to manufacture any product in layers based on a 3D computer model, but this issue is understudied. Therefore, this paper considers the problem of describing the effects of buckling arising in the three-dimensional printing of products containing elements whose length significantly exceeds their thickness or the characteristic size of the cross section. The behavior of these elements, from the point of view of material mechanics, can be described using models of plates or beams. In this study, we compare the results of calculations obtained using the model of non-stationary thermal conductivity and thermos-elasticity with experimental data for a specific element of printed product in which stability loss occurs. It was concluded that, at the initial moments of time, the lowest critical impact coefficient is realized, which in turn makes it the most dangerous phenomenon. The possibility of changing print parameters and product geometry to exclude the mentioned effects has been investigated. The considered structural element may lose stability during the building process. The results of solving the spectral problem indicated that over time the value of the critical effect decreases and asymptotically tends to a fixed minimum value.

Keywords: *selective laser melting, thermomechanical state, thin-walled structures, residual stress, validation.*

Downloaded from www.periodico.tchequimica.com

АННОТАЦИЯ

Аддитивные технологии производства позволяют изготавливать любое изделие послойно на основе компьютерной 3D-модели, но данный вопрос не является хорошо изученным. Поэтому в работе рассматривается проблема описания эффектов потери устойчивости, возникающих при трехмерной печати изделий, содержащих элементы, длина которых значительно превышает их толщину или характерный размер поперечного сечения. Поведение таких элементов, с точки зрения механики материалов, может быть описано с использованием моделей пластин или балок. В настоящей работе проводится сопоставление результатов расчетов, полученных с использованием модели нестационарной теплопроводности и термоупругости, с экспериментальными данными для конкретного элемента напечатанного изделия, в котором произошла потеря устойчивости. Одним из выводов, которые авторы представляют в статье, является то, что в начальных моментах времени реализуется наименьший коэффициент критического воздействия, что в свою очередь делает его наиболее опасными явлением. Исследована возможность изменения параметров печати и геометрии изделия для исключения данных эффектов. Рассмотренный элемент конструкции может терять устойчивость в процессе наращивания. Результаты решения спектральной задачи показали, что с течением времени значение критического воздействия уменьшается и асимптотически стремится к фиксированному минимальному значению.

Ключевые слова: *селективное лазерное сплавление, термомеханическое состояние, тонкостенные конструкции, остаточное напряжение, валидация.*

1. INTRODUCTION

The problem of predicting the residual stress-strain state of products obtained by methods of additive technologies is not completely resolved yet (Luo and Zhao, 2018; Yan *et al.*, 2018). This problem is in many respects similar to the known effects arising in the process of welding metal products (Dong and Brust, 2000), which were thoroughly researched and largely solved in the 1970-1990s. In three-dimensional product printing, the volume of added material is much more significant than in welding, and description of these processes requires development of new algorithms that take into account the increase of the part, the multiscale nature of the processes that are being implemented, and the thermal and thermomechanical state of various parts of the product under local intense heating from moving source (Kim *et al.*, 2004; Kakhramanov *et al.*, 2017; Ngo *et al.*, 2018; Bandyopadhyay and Traxel, 2018).

In this study, we consider the problem of describing unusual defects that may occur during three-dimensional printing of thin-walled parts, and which are associated with the phenomenon of loss of stability through the action of macroscopic fields of compressive stresses that arise in some versions of the product geometry when they are unevenly heated (Santos *et al.*, 2018). A specific example of a core element was considered, during printing of which these effects appeared and led to its curvature, which is unacceptable from the point of view of using the construction (Fig. 1). The product was created from 316 l steel and manufactured using standard printing settings on a Renishaw laser fusion system.

2. MATERIALS AND METHODS

The problem of modeling the thermomechanical state of synthesized product in three-dimensional quasi-static formulation of the problem of thermo-elasticity was considered. External influence follows from solutions of problem of unsteady heat conduction. Equations of the static equilibrium have the form (Equation 1). Kinematic relations correspond to geometrically linear theory of elasticity for plane elements (Equation 2). The defining equations of linear thermos-elastic medium have the form (Equation 3), where temperature field follows from solution of the heat conduction problem described below. Boundary conditions correspond to rigid termination of one of the side surfaces, the remaining side surfaces were free from bonds. Front surfaces were also free (Equation 4). The heat conduction problem was considered in unsteady setting for plane elements (Equation 5). At boundary conditions corresponding to absence of heat exchange with the external environment (Equation 6) and in homogeneous initial conditions (Equation 7). On one of the lateral surfaces, the field of heat flux vector with finite carrier was set, directed normally to the given surface and decreasing exponentially. The position of non-zero flux is defined by the point modeling center of the spot

Downloaded from www.periodico.tchequimica.com

of the laser beam (Equation 8).

The accepted law of distribution of amplitude of heat flux over time is presented in Figure 2. The solution to heat conduction problem has general form $T = T(x, y, z, t)$.

The problem was being solved using the finite element method. Since the geometric areas of calculation were parameterized, then for each set of parameters its own finite element mesh was used for each types of analysis. The grid was formed by volumetric tetrahedral four-node elements. Thermomechanical state of parts at various stages of the synthesis was simulated (Fig. 3). The model was fixed by the end surfaces. In the heat conduction problem, initial and boundary conditions (Equations 6–7) are applied to all surfaces. A laser source impacts the model in the center of the upper plane (Equation 8). The problem can be solved in an unsteady setting. The solution of the problem of thermal conductivity will be the temperature field specified in the table at the points corresponding to nodes of the finite element grid $T = T_{i,k}$ (*i* – is the node number, *k* – is the moment of time).The linear thermos-elasticity problem can be solved numerically in three-dimensional formulation. Lower side surface is rigidly pinched (Equation 4). The temperature field is used as a load at a fixed moment of time in accordance with the solution of previous problem. In this calculation, the allowable exposure time in one zone and the critical impact value at which the “deformation” of the structural element occurs were analyzed.

3. RESULTS AND DISCUSSION:

The obtained solution of thermos-elasticity problem corresponds to the subcritical state of simulated system. The problem of stability of the equilibrium state for discrete analogue of original problem is considered in the bifurcation formulation, that is, it can be reduced to the eigenvalue problem for the operator of homogeneous initial-boundary value problem of bending deformation under strains corresponding to the thermos-elasticity problem. Then, the temperature field generated by source and causing subcritical stress state acts as one-parameter loading of the system. The load parameter will be the coefficient at the amplitude of heat flux, i.e. (Equation 9).

The result of solving the spectral problem can be a set of eigenvalues and eigenvectors of a discrete analogue of the original problem, while the smallest positive value is taken as critical. Similar problems with the study of temperature effects were considered in works (Knyazeva et al., 2007; Riedlbauer et al., 2012; Keller et al., 2013; Lurie *et al*., 2015; Formalev and Kolesnik, 2018; Rabinsky and Tushavina, 2019a; Rabinskiy and Tushavina, 2019b; Formalev and Kolesnik, 2019).

The result of integrating the equations of unsteady heat conduction was a solution in form of isothermal contours similar to concentric circles, while the density decreased with increasing time (temperature gradients decreased). When calculating the linear thermos-elasticity problem, the obtained stress fields had high gradients at the initial time instants, which quickly decreased over time. Figure 4 shows kinds of the first form of buckling for various degrees of body growth.

The results of solving the spectral problem have demonstrated that over time the value of critical effect decreases and asymptotically tends to a fixed minimum value. Figure 5 shows graphs of the dependence of logarithm of coefficient of critical impact on time.

4. CONCLUSIONS:

Based on the results obtained, the following conclusions can be made. The considered structural element may lose stability during the growing process. The most dangerous are initial moments of time, since the smallest critical impact coefficient is realized in them. To ensure a stable growth process, we should implement the following measures:

– to provide maximum number of supporting elements, since an increase in the number of bonds will raise the value of critical impact coefficient;

– to realize a high speed of the laser beam, in order to prevent overheating of a local zone, which will lead to "deformation";

– to reduce the thermal effect, if possible, minimize the power of the laser beam at the initial stages of element formation, if this is permissible in terms of working process.

5. ACKNOWLEDGMENTS:

The work was carried out with the financial support of the state project of the Ministry of Education and Science project code 2.9219.2017 / 8.9.

Downloaded from www.periodico.tchequimica.com

6. REFERENCES:

1. Bandyopadhyay, A., Traxel, K.D. *Additive Manufacturing*, **2018**, *22*, 758-774. DOI: 10.1016/j.addma.2018.06.024
2. Dong, P., Brust, F.W. *Journal of Pressure Vessel Technology*, **2000**, *122*(3), 329-338.
3. Formalev, V.F., Kolesnik, S.A. *High Temperature,* **2017**, *55*(4), 564-569.
4. Formalev, V.F., Kolesnik, S.A. *Journal of Engineering Physics and Thermophysics,* **2019**, *92*(1), 52-59.
5. Formalev, V.F., Kolesnik, S.A., Kuznetsova, E.L. *High Temperature*, **2018**, *56*(5), 727-731.
6. Kakhramanov, R.M., Knyazeva, A.G., Rabinskiy, L.N., Solyaev, YuO. *High Temperature*, **2017**, *55*(5), 731-736.
7. Keller, N., Neugebauer, F., Xu, H., Ploshikhin, V. *Light MAT Conference,* **2013**, *3*(5), 34-43.
8. Kim, H., Lin, Y., Tseng, T.-L. B. *Rapid Prototyping Journal*, **2004**, *24*(3), 645-669. DOI: 10.1108/RPJ-03-2017-0048
9. Knyazeva, A.G., Pobol, I.L., Gordienko, A.I., Demidov, V.N., Kryukova, O.N., Oleshchuk, I.G. *Physical Mesomechanics,* **2007**, *10*(5), 105-119.
10. Luo, Z., Zhao, Y. *Additive Manufacturing*, **2018**, *21*, 318-332. DOI: 10.1016/j.addma.2018.03.022
11. Lurie, S.A., Kuznetsova, E.L., Rabinskii, L.N., Popova, E.I. *Mechanics of Solids,* **2015**, *50*(2), 135-146.
12. Ngo, T.D., Kashani, A., Imbalzano, G., Nguyen, K.T.Q., Hui, D. *Composites Part B: Engineering*, **2018**, *14*, 172-196. DOI: 10.1016/j.compositesb.2018.02.012
13. Rabinskiy, L. N., Tushavina, O.V. *INCAS Bulletin*, **2019b**, *11*(Special Issue), 203-211. DOI: 10.13111/2066-8201.2019.11.S.20.
14. Rabinsky, L.N., Tushavina, O.V. *STİN*, **2019a**, 4, 22-26.
15. Riedlbauer, D., Mergheim, J., McBride, A., Steinmann, P. *Proceedings in Applied Mathematics and Mechanics,* **2012**, *12*, 381-382. DOI: 10.1002/pamm.201210179
16. Santos, L.S., Gupta, S.K., Bruck, H.A. *Additive Manufacturing*, **2018**, *23*, 235-245. DOI: 10.1016/J.ADDMA.2018.08.002
17. Yan, Z., Liu, W., Tang, Z., Liu, X., Zhang, N., Li, M., Zhang, H. *Optics and Laser Technology*, **2018**, *106*, 427-441. DOI: 10.1016/j.optlastec.2018.04.034

$$\frac{\partial \sigma_{xx}}{\partial x}+\frac{\partial \tau_{xy}}{\partial y}+\frac{\partial \tau_{xz}}{\partial z}=0,$$
$$\frac{\partial \tau_{yx}}{\partial x}+\frac{\partial \sigma_{yy}}{\partial y}+\frac{\partial \tau_{yz}}{\partial z}=0, \qquad \text{(Eq. 1)}$$
$$\frac{\partial \tau_{zx}}{\partial x}+\frac{\partial \tau_{zy}}{\partial y}+\frac{\partial \sigma_{zz}}{\partial z}=0.$$

$$\varepsilon_{xx}=\frac{\partial u_x}{\partial x},\ \varepsilon_{yy}=\frac{\partial u_y}{\partial y},\ \varepsilon_{zz}=\frac{\partial u_z}{\partial z},$$
$$\varepsilon_{xy}=\frac{1}{2}\left(\frac{\partial u_x}{\partial y}+\frac{\partial u_y}{\partial x}\right),$$
$$\varepsilon_{yz}=\frac{1}{2}\left(\frac{\partial u_y}{\partial z}+\frac{\partial u_z}{\partial y}\right), \qquad \text{(Eq. 2)}$$
$$\varepsilon_{xz}=\frac{1}{2}\left(\frac{\partial u_x}{\partial z}+\frac{\partial u_z}{\partial x}\right),$$

Downloaded from www.periodico.tchequimica.com

$$\sigma_{xx} = \lambda(\varepsilon_{xx} + \varepsilon_{yy} + \varepsilon_{zz}) + 2\mu\varepsilon_{xx} - (3\lambda + 2\mu)\alpha T,$$
$$\sigma_{yy} = \lambda(\varepsilon_{xx} + \varepsilon_{yy} + \varepsilon_{zz}) + 2\mu\varepsilon_{yy} - (3\lambda + 2\mu)\alpha T,$$
$$\sigma_{zz} = \lambda(\varepsilon_{xx} + \varepsilon_{yy} + \varepsilon_{zz}) + 2\mu\varepsilon_{zz} - (3\lambda + 2\mu)\alpha T,$$
$$\sigma_{xy} = 2\mu\varepsilon_{xy}, \sigma_{yz} = 2\mu\varepsilon_{yz}, \sigma_{xz} = 2\mu\varepsilon_{xz}. \quad \text{(Eq. 3)}$$

$$u_x = u_y = u_z = 0,\ z = 0, \quad \text{(Eq. 4)}$$

$$\frac{\partial T}{\partial t} = a\left(\frac{\partial^2 T}{\partial x^2} + \frac{\partial^2 T}{\partial y^2} + \frac{\partial^2 T}{\partial z^2}\right) + \frac{Q}{\rho c}, \quad \text{(Eq. 5)}$$

$$-nq = 0, \quad \text{(Eq. 6)}$$

$$T = 0,\ t = 0. \quad \text{(Eq. 7)}$$

$$q0 = \frac{2\eta P}{\pi r_0^2} e^{\frac{-2r2}{r_0^2}} \quad \text{(Eq. 8)}$$

$$q0 = \lambda \frac{2\eta P}{\pi r_0^2} e^{\frac{-2r2}{r_0^2}} \quad \text{(Eq. 9)}$$

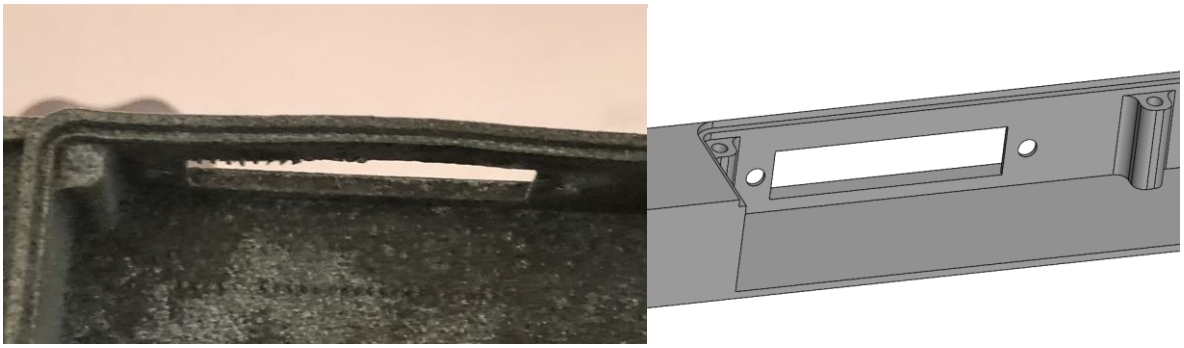

a *b*

Figure 1. *Fragment of product in which the loss of stability occurred, a: initial geometry of model, b: manufactured product containing defect*

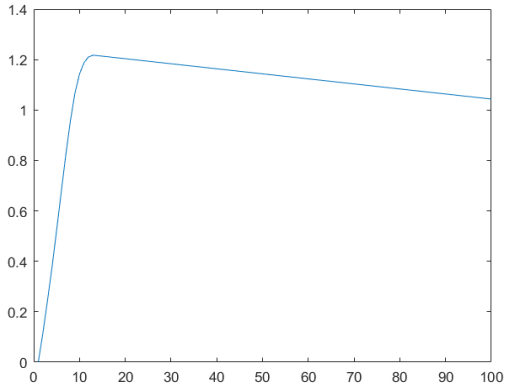

Figure 2.*The accepted law of distribution of amplitude of the heat flux in time*

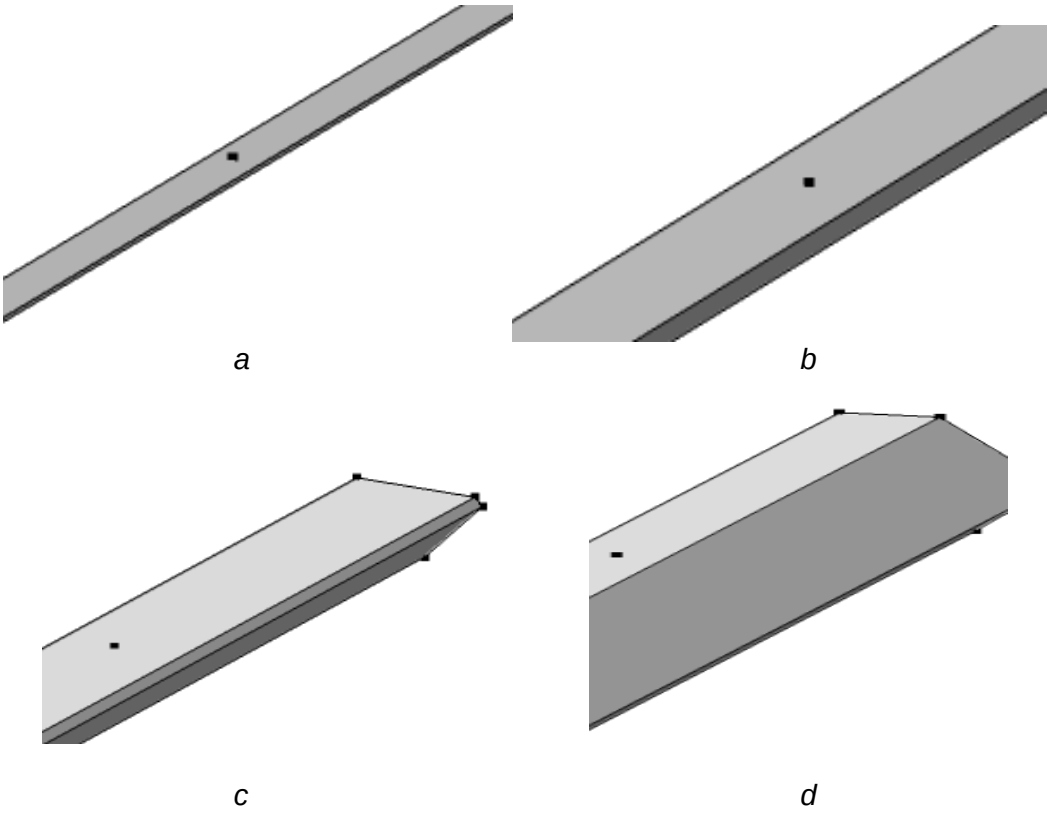

Figure 3. *Element geometry for 10%, 25%, 50% and 100% of growth*

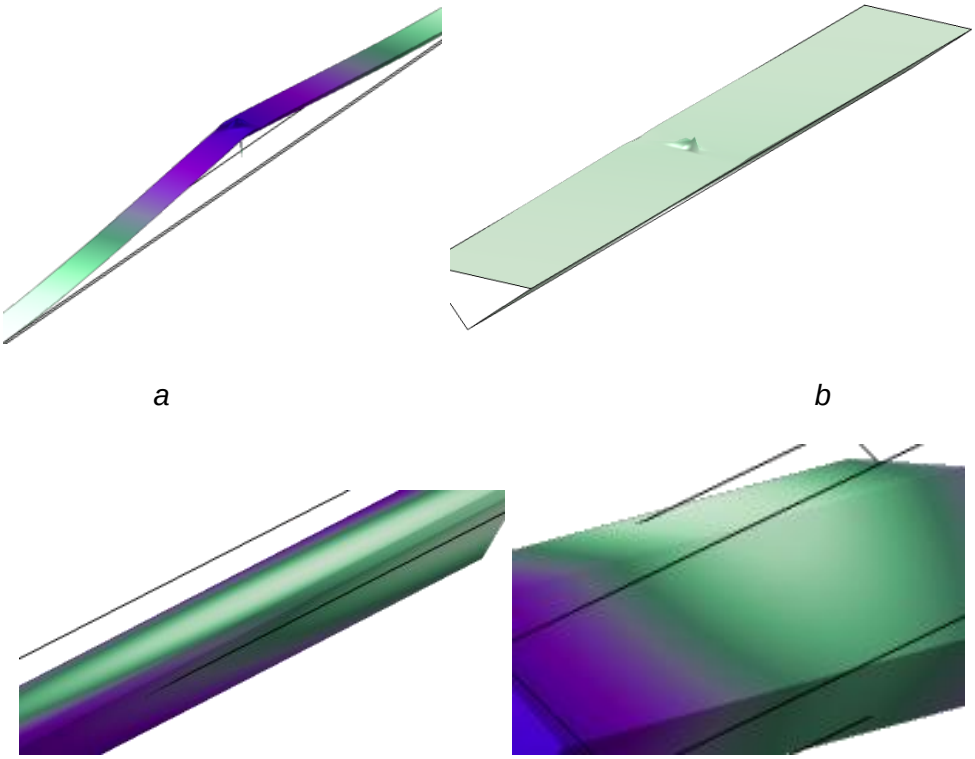

a *b*

c *d*

Figure 4. *The first form of stability loss (a -10%, b – 25%, c – 50 %, and d – 100% of part growth)*

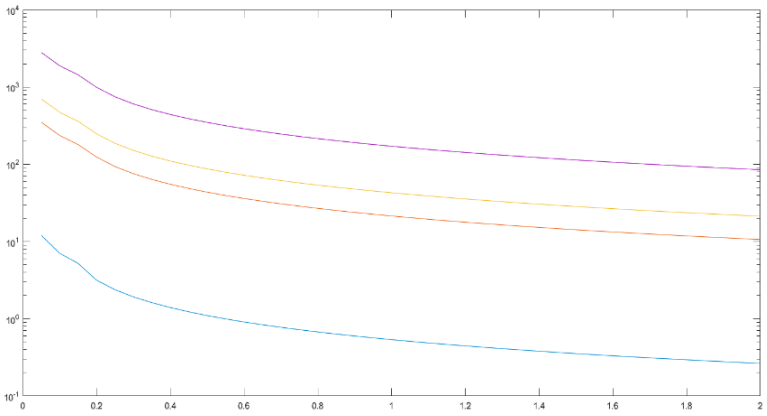

Figure 5. *The dependence of logarithm of coefficient of critical impact on time for different degrees of body growth (10%, 25%, 50%, 100%)*

Downloaded from www.periodico.tchequimica.com

PERIÓDICO TCHÊ QUÍMICA
ARTIGO ORIGINAL

ESTUDO DA INFLUÊNCIA DE EFEITOS TÉRMICOS E CLIMÁTICOS NO DESEMPENHO DA PROTEÇÃO TÉRMICA DE TELHAS DE VEÍCULOS ESPACIAIS

INVESTIGATION OF THE INFLUENCE OF THERMAL AND CLIMATE EFFECTS ON THE PERFORMANCE OF TILED THERMAL PROTECTION OF SPACECRAFT

ИССЛЕДОВАНИЕ ВЛИЯНИЯ ТЕПЛОВЫХ И КЛИМАТИЧЕСКИХ ВОЗДЕЙСТВИЙ НА РАБОТОСПОСОБНОСТЬ ПЛИТОЧНОЙ ТЕПЛОВОЙ ЗАЩИТЫ КОСМИЧЕСКИХ ЛЕТАТЕЛЬНЫХ АППАРАТОВ

RABINSKIY, Lev N.[1]*; TUSHAVINA, Olga V.[2];

[1] Moscow Aviation Institute (National Research University), Institute of General Engineering Training, Moscow – Russian Federation

[2] Moscow Aviation Institute (National Research University), Institute of Aerospace, Moscow – Russian Federation

** Correspondence author*
e-mail: rabinskiy@mail.ru

Received 30 August 2019; received in revised form 31 October 2019; accepted 31 October 2019

RESUMO

O artigo discute as questões de proteção térmica de veículos espaciais sob vários tipos de efeitos térmicos e climáticos. Durante a preparação para o lançamento, vários tipos de formação de gelo são possíveis na superfície da estrutura telhada, consistindo em telhas de quartzo com proteção contra o calor. É muito importante durante a operação determinar as tensões normais e tangenciais durante a formação de gelo e o efeito do gelo formado nas lacunas entre as telhas. É necessário calcular a durabilidade e os indicadores da proteção térmica de telhas nos estágios ativos do voo da nave espacial. Foi criado um modelo matemático que permite, com um grau de precisão suficiente, estudar a estrutura telhada quanto à resistência, cisalhamento e rasgo das telhas quando exposto ao gelo. A resistência, cisalhamento e rasgo das telhas sob a influência do gelo foram calculados. Estudos teóricos e experimentais foram comparados. Os cálculos realizados permitiram mostrar que as telhas não entrariam em colapso sob a carga considerada. A resistência do substrato suporta as forças de cisalhamento emergentes. Foram obtidos os valores da resistência de aderência do gelo que aparece na superfície do revestimento protetor térmico de fibra de quartzo. Foi demonstrado que a proporção de tangentes no estado estressado das telhas não excede 10%. O modelo matemático proposto para o estudo das características da proteção térmica de telhas de uma veículo espacial descreve adequadamente os processos em estudo. Estudos experimentais mostraram concordância satisfatória com os resultados teóricos. Os cálculos realizados para determinar as tensões de cisalhamento finais no substrato mostraram que a resistência do substrato suporta as forças de cisalhamento emergentes. A consideração das condições climáticas pode reduzir significativamente os riscos no projeto de proteção térmica de aeronaves modernas. Os resultados deste artigo podem ser usados em pesquisas adicionais e também podem ser levados em consideração ao projetar aeronaves.

Palavras-chave: *veículo espacial, processo de formação de gelo, telhas de quartzo com proteção térmica, período de preparação antes do lançamento, lacunas entre as telhas.*

ABSTRACT

The article discusses the thermal protection of spacecraft under various types of thermal and climatic influences. During the pre-launch preparation, several types of icing are possible on the surface of the tiled structure, consisting of quartz heat-shielding tiles. It is very important in the process of operation, to determine normal and shear stresses during icing and the impact of ice formed in the tile gaps. It is necessary to calculate the strength and performance of the tiled thermal protection in active stages of flight of spacecraft. A mathematical model was constructed that allows, with a sufficient degree of accuracy, to research the tiled structure for strength, shear and tearing of the tile when exposed to ice. Calculations for strength, shear, and tearing of tiles under the influence of ice were performed. Theoretical and experimental studies were compared. The performed calculations made it possible to show that the tile will not collapse under the considered load.

Downloaded from www.periodico.tchequimica.com

The strength of the substrate withstands the emerging shear forces. The values of the adhesion strength of ice appearing on the surface of quartz fiber heat-protective coating were obtained. It was demonstrated that the proportion of tangents in the stressed state of the tile does not exceed 10%. The proposed mathematical model for studying the characteristics of the tiled thermal protection of a spacecraft adequately describes the processes under study. Experimental studies have shown satisfactory agreement with theoretical results. The calculations performed to determine the ultimate shear stresses in the substrate showed that the strength of the substrate withstands the emerging shear forces. Consideration of climatic conditions can significantly reduce risks in the design of thermal protection of modern aircraft. The results of this study can be used in further studies, and they can also be taken into account in the construction of aircraft.

Keywords: *spacecraft, icing process, quartz heat-shielding tiles, prelaunch period, tile gaps.*

АННОТАЦИЯ

В статье рассматриваются вопросы теплозащиты космических аппаратов при различных видах тепловых и климатических воздействий. Во время подготовки к запуску возможны несколько видов обледенения на поверхности черепичной конструкции, состоящей из кварцевых теплозащитных плиток. Очень важно в процессе эксплуатации определять нормальные и касательные напряжения при обледенении и воздействие льда, образующегося в зазорах плитки. Необходимо рассчитать прочность и показатели плиточной теплозащиты на активных этапах полета космического корабля. Была построена математическая модель, которая позволяет с достаточной степенью точности исследовать плиточную структуру на прочность, сдвиг и разрыв плитки при воздействии льда. Были выполнены расчеты на прочность, сдвиг и разрыв плитки под воздействием льда. Теоретические и экспериментальные исследования были сопоставлены. Выполненные расчеты позволили показать, что плитка не будет разрушаться при рассматриваемой нагрузке. Прочность подложки выдерживает возникающие сдвиговые усилия. Получены значения адгезионной прочности льда, появляющегося на поверхности термозащитного покрытия из кварцевого волокна. Было продемонстрировано, что доля касательных в напряженном состоянии плитки не превышает 10%. Предложенная математическая модель для изучения характеристик плиточной тепловой защиты космического аппарата адекватно описывает изучаемые процессы. Экспериментальные исследования показали удовлетворительное согласие с теоретическими результатами. Расчеты, выполненные для определения предельных напряжений сдвига в подложке, показали, что прочность подложки выдерживает возникающие сдвиговые силы. Учет климатических условий позволяет значительно снизить риски при проектировании тепловой защиты современных самолетов. Результаты этой статьи могут быть использованы в дальнейших исследованиях, а также могут быть приняты во внимание при конструировании самолетов.

Ключевые слова: *космический летательный аппарат, процесс обледенения, кварцевые теплозащитные плитки, период предстартовой подготовки, межплиточные зазоры*.

1. INTRODUCTION

In the process of operation, the surface of the spacecraft is exposed to various physical and mechanical fields that adversely affect flight performance. This increases the risk of deterioration of aerodynamic characteristics, increase in passive mass, likelihood of individual tiles failing or tearing off the structure under the action of forces when ice is formed in the tile gaps of systems and aggregates, as well as the possibility of destruction of the thermal barrier coating. The causes of ground icing of bodies and structures in natural climatic conditions are fairly well understood (Bogorodsky and Gavrilov, 1980; Trude, 1983; Trunov, 1983; Afanasyev and Tushavina, 2016), and the main mechanisms of ice formation during prelaunch preparation are identified (Sandu *et al.*, 2018).

The study of the influence of climatic effects such as radiation, icing, rain, fog during the operation of spacecraft on performance of structural elements with porous heat-shielding material is of paramount importance (Orlov *et al.*, 2003; Shejko *et al.*, 2016, Daus and Kharchenko, 2018). Taking into account the above-mentioned negative features in operation, the adhesive strength and stiffness of casing of modern spacecraft were studied.

To solve this problem, a mathematical model has been developed that correctly describes the stress-strain state, which allows us to examine tiled structure for strength, shear, and tear. The development of mathematical model that takes into account unsteady thermal processes under the influence of physical and mechanical fields of various physical nature was considered in works (Kolesnik *et al.,* 2015; Kuznetsova *et al.,* 2015; Lurie *et al.,* 2015; Afanasyev and Tushavina, 2016; Danilin *et al.,*

Downloaded from www.periodico.tchequimica.com

2016; Prokofiev *et al*., 2016; Babaytsev *et al.,* 2017; Lomakin *et al.,* 2017; Kakhramanov *et al.,* 2017; Formalev and Kolesnik, 2017a; Formalev and Kolesnik, 2017b; Lurie *et al.,* 2017a; Lurie *et al.,* 2017b; Bulychev *et al.,* 2018; Formalev *et al.,* 2018a; Formalev *et al.,* 2018b; Kuznetsova *et al.,* 2018; Lomakin *et al*., 2018; Rabinskiy and Tushavina, 2019; Rabinskiy *et al.,* 2019).

2. MATERIALS AND METHODS

The installation diagram of heat-shielding tiles on the glider surface is shown in Figure 1 which schematically displays the method of tiled thermal protection of spacecraft from various types of thermal fields of various physical nature. In this case, the thermal protection of the airframe consists of quartz tile 1 with coating 2 lying on damping substrate 3. Thermal protection insulation tile consists of quartz ceramics with significant porosity of up to 90%. There is a gap 4 between the tiles, which can be filled with liquid that turns into ice. Between the quartz tile 1 and substrate 3 is an adhesive layer 5. The entire heat-protection structure rests on the casing 6.

The need to study the stress-strain state and strength of heat-protection tiles during icing is one of the most important during storage and transportation of the product in open atmospheric conditions, since the moisture contained in the pores of thermal insulation during freezing forms significant forces that can not only cause damage but also destroy the thermal protection system, then, during aerodynamic heating in flight, such damage can cause an emergency or complete destruction of the spacecraft.

Thus, the need to study the stress-strain state and strength of heat-protective tiles during icing is one of the most important issues during the storage and transportation of the product in open atmospheric conditions (Trude, 1983). The finding of the stress-strain state and strength of heat-shielding tiles is divided into two stages — the determination of spacer stresses in a heat-protection coating and also normal, and shear stresses in the substrate-tile system. Installation of heat-shielding tiles on the glider casing using Figure 1. presented in the form (Figure 2).

In accordance with the design scheme, a tile with a layer of ice in load conditions can be represented in the form of a beam, shown in Figure 3. Then, due to the freezing of the gap, the beam will be extended by an amount $\varepsilon_0\delta$ and total length $l_{pl}+\delta(1+\varepsilon_0)$ will be decreased by this amount due to compression forces N_s (Equation 1). In the equation E_{pl}, E_l, F_{pl}, F_l are modules of elasticity and cross-sectional area of tiles and ice, respectively, ε_0 – linear relative expansion of water during freezing. Let's transform Equation 1 to the form of Equation 2. Using well-known inequality in Equation 2 $\frac{E_l F_l l_{pl}}{E_{pl} F_{pl} \delta} \square\ 1+\varepsilon_0$ we'll get Equation 3. Then the expression for spacer stresses will be expressed like Equation 4.

3. RESULTS AND DISCUSSION:

3.1. Determination of normal and tangential stresses in the substrate-tile system

A scheme of the shear stresses arising in the damping substrate made of felt material and located between the heat-shielding tiles and the structure of the spacecraft is shown in Figure 4. To determine the stress-strain state in the substrate-tile system, a beam element has to be cut at a distance x from the axis of symmetry y. Equilibrium Equation 5 for a tile with respect to the longitudinal axis x will have the look of Equations 5, 6. In these expressions $\sigma(x), \tau(x)$ are normal and tangential stresses in section, σ_0 is stress at the origin. Then the longitudinal movement in the tile will have a look of Equation 7 and the angular displacement will be Equation 8. As a result, the tangential stress in felt substrate will take the form of Equation 9.

Equation 9 will be differentiated twice with respect to the variable x, the differential equation is obtained for distribution of tangential stresses along the substrate Equations 10, 11. G_f, ν are the shear modulus of the felt and Poisson's ratio respectively. The solution of the Equation 10 will have the form of Equation 12. Constants of integration C_1 ,C_2 and unknown voltage σ_0 at the origin are taken from boundary conditions (Equations 13-15).

By substituting Equations 6-9 into Equations 13-15, taking into account Equation 12, a system of equations is gotten for determining the constants C_1 ,C_2 and σ_0 (Equations 16-18). Using the solution of Equations 16-18, the expressions for the constants are gotten (Equations 19-21). Then, using Equations 19-21, the analytical expressions are determined for normal and tangential stresses for quartz tile and damping substrate

Downloaded from www.periodico.tchequimica.com

(Equations 22, 23). Using Equation 11 finally Equations 24, 25 are gotten. The fraction of shear stresses in the stress state of the tile can be written in the form of relations (Equation 26). Longitudinal displacements $u(x)$ of heat-protective tiles will be determined via known relations (Equation 27). Figures 6-7 show the relationship between the ratio of shear stresses to normal and the distribution of displacements depending on the length of the heat-shielding tile. The following values of the parameters included in Equations 26-27 are accepted.

3.2. Experimental research of tiled thermal protection of spacecraft

The schematic diagram of the installation for studying the adhesion strength of ice is presented in Figure 8. Cooling and temperature control of model 7 was done in a climatic chamber 6 by nitrogen vapor at atmospheric pressure. The dimensions of the climate chamber were $560 \times 240 \times 230$ мм. Nitrogen was directed to the thermostat from Dewar 1 vessel. The temperature at thermostat was controlled using the thermostat 5 before they entered climate chamber 6. Sample 7 was installed in grips 8, mounted on power frame. Loading of the sample is performed using the movement of beam 10 moving along the power columns 9. Dimensions of test samples are $195 \times 10 \times 3$ мм.

During the experiment, the gas temperature in the thermostat was measured with a thermometer with measuring scale from -50 ° C to 0 ° C and a division value of 0.1 degrees. The temperature in chamber was controlled by thermostat 5. The sample was cooled by the gas temperature in the thermostat of 279 K. Thermostating was done for at least 30 min (Figures 9-11).

4. CONCLUSIONS:

Hereby:

- The performed calculations on the strength of tile under the conditions of ice formation in inter-tile gaps made it possible to show that the tile will not collapse under the considered load.
- The calculations performed to establish the ultimate shear stresses in the substrate showed that the strength of the substrate withstands the emerging shear forces.
- The calculations of stresses arising due to freezing of moisture in the heat-insulating layer of damping substrate made it possible to confirm the tensile strength of the substrate.
- Based on the results of experimental research on a test bench, the values of the adhesion strength of ice appearing on the surface of quartz fiber heat-protective coating were obtained.
- It was demonstrated that the proportion of tangents in the stressed state of the tile does not exceed 10%.
- The suggested mathematical model for the study of performance of tiled thermal protection of spacecraft adequately describes the processes under study.
- The performed calculations have demonstrated the ability to predict the performance of promising aerospace products.
- The experimental studies have demonstrated a satisfactory agreement with theoretical results.
- The calculations performed to determine the ultimate shear stresses in the substrate showed that the strength of substrate withstands the arising shear forces
- Consideration of climatic conditions allows to significantly reduce risks in the design of thermal protection of modern aircraft

5. ACKNOWLEDGMENTS:

The work has been conducted with the financial support of the grant of the Russian Foundation for Basic Research (grant No. 17-01-00837-a).

6. REFERENCES:

1. Afanasyev, V.A., Tushavina, O.V. *Bulletin of the Moscow Aviation Institute,* **2016**, *23(4),* 95–101.
2. Babaytsev, A.V., Prokofiev, M.V., Rabinskiy, L.N. *International Journal of Nanomechanics Science and Technology*, **2017**, *8(4),* 359–366. DOI: 10.1615/NanoSciTechnolIntJ.v8.i4.60.
3. Bogorodsky, V.V., Gavrilov, V.P. *Ice. Physical properties. Modern methods of glanciology,* Leningrad: Gidromethioizdat, **1980**.
4. Bulychev, N.A., Kuznetsova, E.L., Bodryshev, V.V., Rabinskiy, L.N. *Nanoscience and Technology. An International Journal*, **2018**, *9(2),* 91–97. DOI:

Downloaded from www.periodico.tchequimica.com

10.1615/NanoSciTechnolIntJ.2018025703.

5. Daus, Yu.V., Kharchenko, V.V. *Applied Solar Energy*, **2018**, *54(1)*: 71–76.
6. Danilin, A.N., Kuznetsova, E.L., Kurdyumov, N.N., Rabinskiy, L.N., Tarasov, S.S. *PNRPU Mechanics Bulletin*, **2016**, *4*, 187–199.
7. Formalev, V.F., Kolesnik, S.A. *High Temperature*, **2017a**, *55(4),* 564–569.
8. Formalev, V.F., Kolesnik, S.A. *Journal of Engineering Physics and Thermophysics*, **2017b**, *90(6),* 1302–1309.
9. Formalev, V.F., Kolesnik, S.A., Kuznetsova, E.L. *High Temperature*, **2018a**, *56(3),* 393–397.
10. Formalev, V.F., Kolesnik, S.A., Kuznetsova, E.L. *High Temperature*, **2018b**, 56(5), 727–731.
11. Kakhramanov, R.M., Knyazeva, A.G., Rabinskiy, L.N., Solyaev, Y.O. *High Temperature*, **2017**, *55(5),* 731–736.
12. Kolesnik, S.A., Formalev, V.F., Kuznetsova, E.L. *High Temperature*, **2015**, *53(1),* 68–72.
13. Kuznetsova, E.L., Kuznetsova, E.L., Rabinskiy, L.N., Zhavoronok, S.I. *Journal of Vibroengineering*, **2018**, *20(2),* 1108–1117.
14. Kuznetsova, E.L., Leonenko, D.V., Starovoitov, E.I. *Mechanics of Solids*, **2015**, *50(3),* 359–366.
15. Lomakin, E.V., Lurie, S.A., Belov, P.A., Rabinskii, L.N. *Doklady Physics*, **2017**, *62(1),* 46–49.
16. Lomakin, E.V., Lurie, S.A., Rabinskiy, L.N., Solyaev, Y.O. *Doklady Physics,* **2018**, *63(4),* 161–164.
17. Lurie, S.A., Kuznetsova, E.L., Rabinskii, L.N., Popova, E.I. *Mechanics of Solids*, **2015**, *50(2),* 135–146.
18. Lurie, S.A., Rabinskiy, L.N., Polyakov, P.O., Sitnikov, S.A., Solyaev, Y.O. *International Journal of Nanomechanics Science and Technology*, **2017a**, *8(4)*, 347–358. DOI: 10.1615/NanoSciTechnolIntJ.v8.i4.50.
19. Lurie, S.A., Solyaev, Y.O., Lizunova, D.V., Rabinskiy, L.N., Bouznik, V.M., Menshykov, O. *International Journal of Heat and Mass Transfer*, **2017b**, *109*, 511–519.
20. Orlov, A.M., Skvortsov, A.A., Solov'ev, A.A. Zhurnal Eksperimental'noj i Teoreticheskoj Fiziki, **2003**, *123(3)*, 590-599.
21. Prokofiev, M.V., Vishnevskii, G.E., Zhuravlev, S.Y., Rabinskiy, L.N. *International Journal of Nanomechanics Science and Technology,* **2016**, *7(2),* 97–105. DOI: 10.1615/NanomechanicsSciTechnolIntJ.v7.i1.40.
22. Rabinskiy, L.N., Tushavina, O.V. *INCAS Bulletin,* **2019**, *11,* 203–211. DOI: 10.13111/2066-8201.2019.11.S.20.
23. Rabinskiy, L.N., Tushavina, O.V., Fedotenkov, G.V. *The Asian International Journal of Life Sciences*, **2019**, *19(1),* 149–162.
24. Sandu, C., Deaconu, M., Silivestru, V., Olariu, C.-T., Sandu, C.-R. *INCAS Bulletin*, **2018**, *10*(4), 141–151.
25. Shejko, S., Yechyn, S., Demchenko, N. Materials Science and Technology Conference and Exhibition 2016, MS and T 2016, **2016**, *1*, 353-358.
26. Trude, P. (ed.). *Physics and mechanics of ice*, Moscow: Mir, **1983**.
27. Trunov, O.K. *Protecting aircraft from ground icing,* Moscow: GOSNNIGA, **1983**.

Downloaded from www.periodico.tchequimica.com

$$\frac{N_s l_{pl}}{E_{pl}F_{pl}} + \frac{N_s(1+e_0)d}{E_l F_l} = e_0 d \quad \text{(Eq. 1)}$$

$$N_s = \frac{\varepsilon_0 E_l F_l}{1+\varepsilon_0 + \frac{E_l F_l l_{pl}}{E_{pl}F_{pl}\delta}} \approx \varepsilon_0 E_{pl} F_{pl} \frac{\delta}{l_{pl}} \quad \text{(Eq. 2)}$$

$$N_s \approx \varepsilon_0 E_{pl} F_{pl} \frac{\delta}{l_{pl}} \quad \text{(Eq. 3)}$$

$$\sigma_R = \frac{N_S}{F_{pl}} = \varepsilon_0 \frac{N_S}{F_{pl}} = \varepsilon_0 E_{pl} \frac{\delta}{l_{pl}} \quad \text{(Eq. 4)}$$

$$\Sigma x = 0 \qquad \sigma(x) H_{pl} b - \int_0^x \tau(x) b dx - \sigma_0 H_{pl} b = 0 \quad \text{(Eq. 5)}$$

$$\sigma(x) = \frac{1}{H_{pl}} \int_0^x \tau(x) dx + \sigma_0 \quad \text{(Eq. 6)}$$

$$\delta(x) = \int_0^x \frac{\sigma(x)}{E_{pl}} dx = \frac{1}{E_{pl}} \int_0^x \left[\frac{1}{H_n} \int_0^x \tau(x) b dx + \sigma_0 \right] dx \quad \text{(Eq. 7)}$$

$$\gamma(x) = \frac{\delta(x)}{H_f} \quad \text{(Eq. 8)}$$

$$\tau(x) = G_f \gamma(x) = \frac{G_f}{E_{pl} H_{pl} H_f} \int_0^x \left[\int_0^x \tau(x) dx + \sigma_0 H_n \right] dx \quad \text{(Eq. 9)}$$

$$\frac{d^2 t(x)}{dx^2} = k^2 t(x) \quad \text{(Eq. 10)}$$

$$k^2 = \frac{G_f}{E_{pl} H_{pl} H_f} \quad \text{(Eq. 11)}$$

$$t(x) = C_1 e^{kx} + C_2 e^{-kx} \quad \text{(Eq. 12)}$$

$$\tau(x)\big|_{x=0} = 0 \quad \text{(Eq. 13)}$$

$$\sigma(x)\big|_{x=\frac{l_{pl}}{2}} = \sigma_R \quad \text{(Eq. 14)}$$

$$\delta(x)\big|_{x=\frac{l_{pl}}{2}} = H_f \gamma(x)\big|_{x=\frac{l_{pl}}{2}} \quad \text{(Eq. 15)}$$

$$C_1 + C_2 = 0 \quad \text{(Eq. 16)}$$

Downloaded from www.periodico.tchequimica.com

$$\frac{1}{H_n k}\left(C_1 e^{k\frac{l_{pl}}{2}} - C_2 e^{-k\frac{l_{pl}}{2}} - C_1 + C_2\right) + \sigma_0 = \sigma_R \quad \text{(Eq. 17)}$$

$$\frac{1}{E}\int_0^x \left[\frac{1}{H_{pl}}\int_0^x \tau(x) b dx + \sigma_0\right] dx \Bigg|_{x=\frac{l_{pl}}{2}} = \frac{C_1 e^{kx} + C_2 e^{-kx}}{G}\Bigg|_{x=\frac{l_{pl}}{2}} \quad \text{(Eq. 18)}$$

$$C_1 = \sigma_R \frac{l_{pl} H_{pl} k^2 G_f}{2\left(H_{pl} H_f k^2 E_{pl} - G_f\right)\left(e^{k\frac{l_{pl}}{2}} - e^{-k\frac{l_{pl}}{2}}\right) + k l_{pl} G_f\left(e^{k\frac{l_{pl}}{2}} - e^{-k\frac{l_{pl}}{2}}\right)} \quad \text{(Eq. 19)}$$

$$C_2 = -\sigma_R \frac{l_{pl} H_{pl} k^2 G_f}{2\left(H_{pl} H_f k^2 E_{pl} - G_f\right)\left(e^{k\frac{l_{pl}}{2}} - e^{-k\frac{l_{pl}}{2}}\right) + k l_{pl} G_f\left(e^{k\frac{l_{pl}}{2}} - e^{-k\frac{l_{pl}}{2}}\right)} \quad \text{(Eq. 20)}$$

$$\sigma_0 = 2\sigma_R \frac{\left(e^{kl_{pl}} - e^{-kl_{pl}}\right)\left(H_f H_n k^2 E_{pl} - G_f\right) + k l_{pl} G_f}{\left(e^{kl_{pl}} - e^{-kl_{pl}}\right)\left(2H_f H_n k^2 E_{pl} - 2G_f\right) + k l_{pl} G_f\left(e^{kl_{pl}} + e^{-kl_{pl}}\right)} \quad \text{(Eq.21)}$$

$$\tau(x) = \sigma_R \frac{l_{pl} H_n k^2\left[e^{k\left(\frac{l_{pl}}{2}+x\right)} - e^{k\left(\frac{l_{pl}}{2}-x\right)}\right]}{2\left(e^{kl_{pl}-1}\right)\left(H_f H_n k^2 \frac{E_{pl}}{G_f} - 1\right) + k l_{pl}\left(e^{kl_{pl}} + 1\right)} \quad \text{(Eq. 22)}$$

$$\sigma(x) = \sigma_R \frac{2\left(e^{kl_{pl}} - 1\right)\left(H_f H_n k^2 \frac{E_{pl}}{G_f} - 1\right) + k l_{pl}\left[e^{k\left(\frac{l_{pl}}{2}+x\right)} + e^{k\left(\frac{l_{pl}}{2}-x\right)}\right]}{2\left(e^{kl_{pl}} - 1\right)\left(H_f H_n k^2 \frac{E_{pl}}{G_f} - 1\right) + k l_{pl}\left(e^{kl_{pl}} + 1\right)} \quad \text{(Eq. 23)}$$

$$\tau\left(x\right) = \sigma_R \frac{H_{pl} k\left[e^{k\left(\frac{l_{pl}}{2}+x\right)} - e^{k\left(\frac{l_{pl}}{2}-x\right)}\right]}{e^{kl_{pl}} + 1} \quad \text{(Eq. 24)}$$

$$\sigma\left(x\right) = \sigma_R \frac{e^{k\left(\frac{l_{pl}}{2}+x\right)} + e^{k\left(\frac{l_{pl}}{2}-x\right)}}{e^{kl_{pl}} + 1} \quad \text{(Eq. 25)}$$

$$\frac{\tau(x)}{\sigma(x)} = H_{pl} k \frac{1 - e^{-2kx}}{1 + e^{-2kx}} \quad \text{(Eq. 26)}$$

Downloaded from www.periodico.tchequimica.com

$$u(x)=\int_0^x \frac{\sigma(x)}{E_{pl}}dx=\frac{\sigma_R}{E_{pl}\left(e^{kl_{pl}}+1\right)}\int_0^x\left[e^{k\left(\frac{l_{pl}}{2}+x\right)}+e^{k\left(\frac{l_{pl}}{2}-x\right)}\right]dx=\frac{2\sigma_R sh(kx)}{E_{pl}k\left(1+e^{-kl_{pl}}\right)} \quad \text{(Eq. 27)}$$

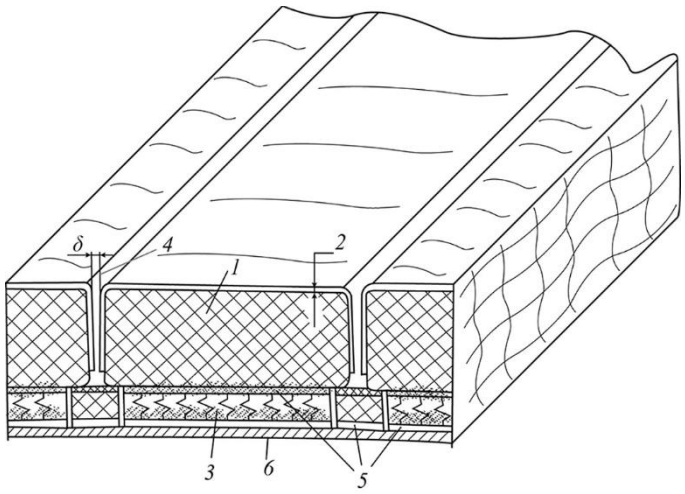

Figure 1. *Location of heat-shielding tiles on the airframe*

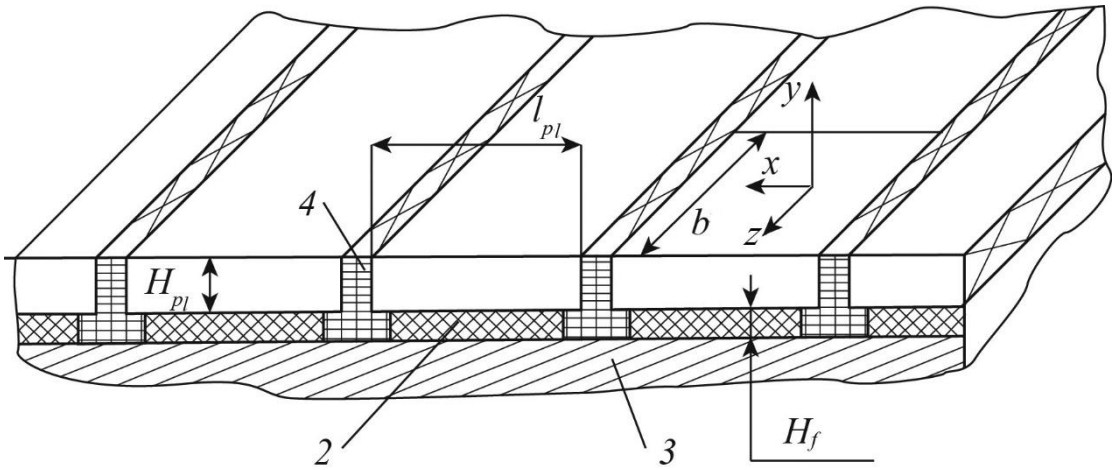

Figure 2. *Layout of heat-protective tiles on the airframe*

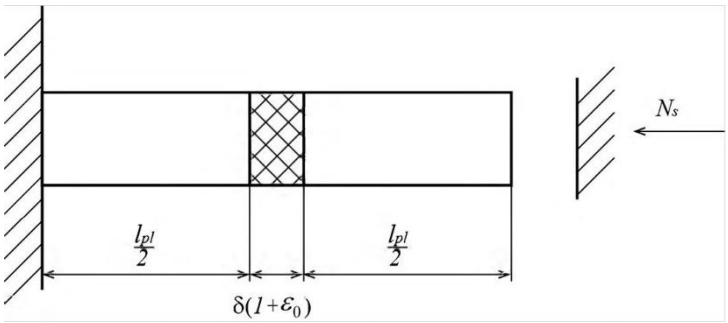

Figure 3. *Design scheme for determining spacer stresses*

Downloaded from www.periodico.tchequimica.com

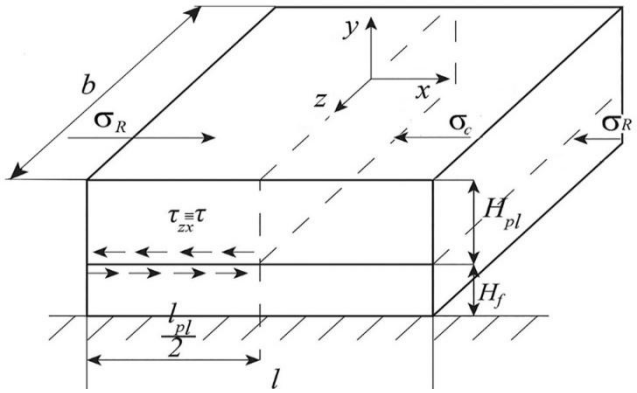

Figure 4. *Stress state in substrate-tile system*

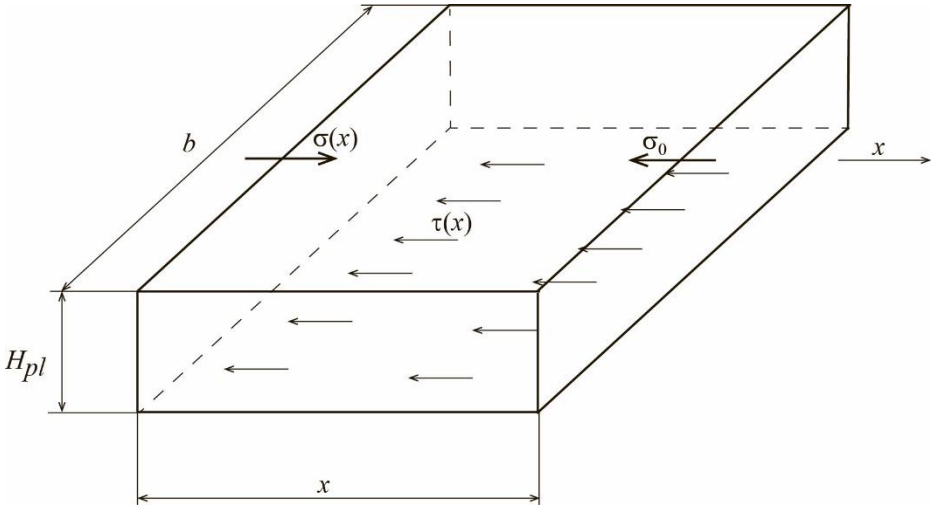

Figure 5. *Beam element for the equilibrium equation*

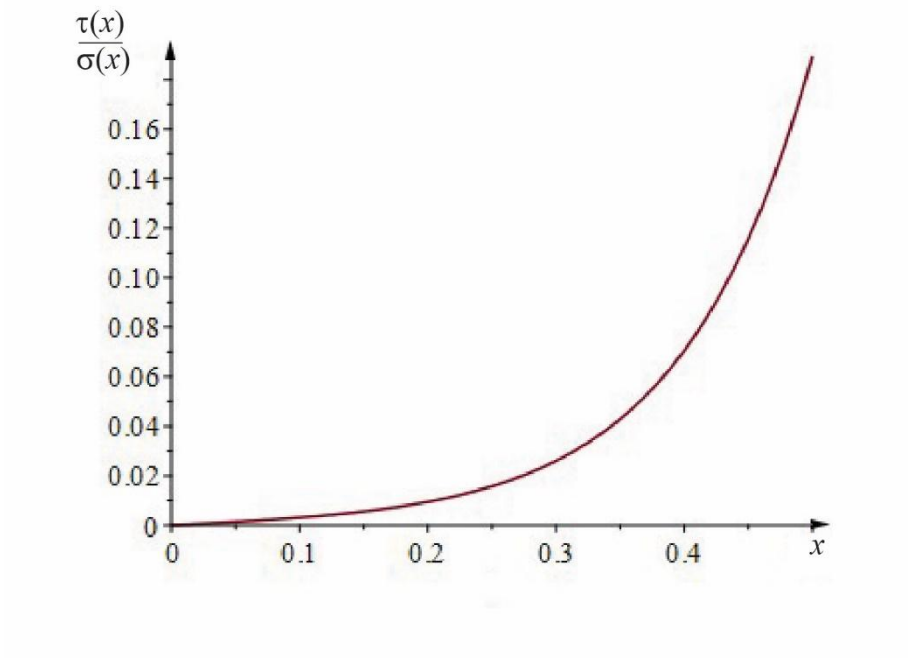

Figure 6. *Tile shear ratio in stresses state*

Downloaded from www.periodico.tchequimica.com

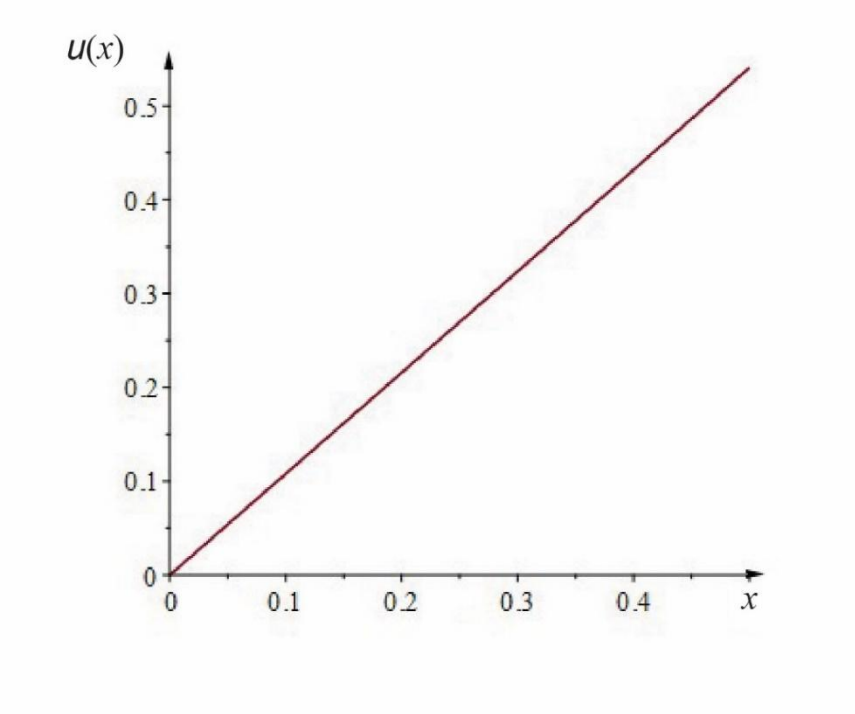

Figure 7. *The longitudinal movement of the tile*

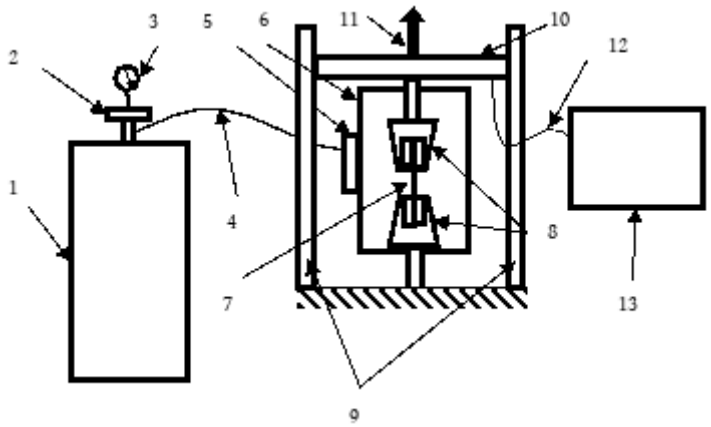

Figure 8. *Schematic diagram of installation for studying adhesion strength of ice: 1 – dewar vessel with nitrogen; 2 – gear; 3 – pressure gauge; 4 – hose for supplying nitrogen to chamber; 5 – thermostat; 6 – climate chamber; 7 – test sample; 8 – captures; 9 – power columns; 10– load traverse; 11 – direction of movement of traverse; 12 – data transmission cable, 13 – information output and processing monitor*

Downloaded from www.periodico.tchequimica.com

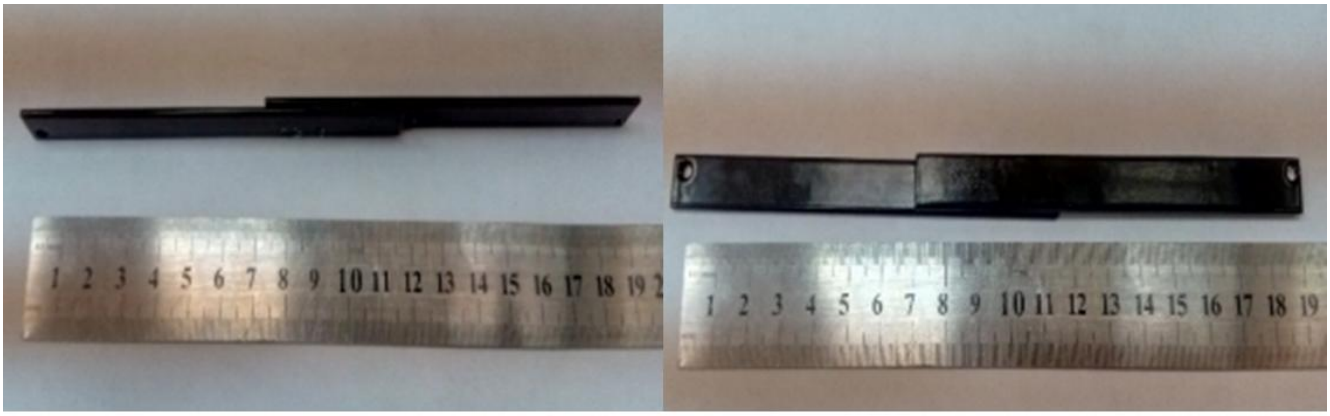

Figure 9. *Picture of the test sample*

Figure 10. *Picture of the sample in installation*

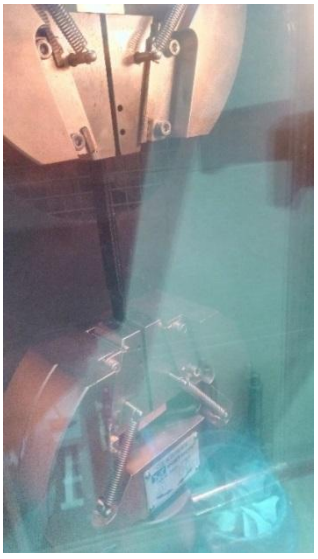

Figure 11. *Picture of the sample during testing*

Downloaded from www.periodico.tchequimica.com

PERIÓDICO TCHÊ QUÍMICA
ARTIGO ORIGINAL

INVESTIGAÇÃO DA DINÂMICA DE SISTEMAS MECÂNICOS NÃO LINEARES COM LONGAS LINHAS DE ALIMENTAÇÃO ATRAVÉS DA MODELAGEM DIGITAL

INVESTIGATION OF THE DYNAMICS OF NONLINEAR MECHANICAL SYSTEMS WITH LONG POWER LINES THROUGH DIGITAL MODELING

ИССЛЕДОВАНИЕ ДИНАМИКИ НЕЛИНЕЙНЫХ МЕХАНИЧЕСКИХ СИСТЕМ С ДЛИННЫМИ ЛИНИЯМИ ПИТАНИЯ ЧЕРЕЗ ЦИФРОВОЕ МОДЕЛИРОВАНИЕ

KONDRATENKO, Leonid A.[1]*; MIRONOVA, Lyubov I.[2]; DMITRIEV, Vladimir G.[3]; EGOROVA, Olga V.[4]; SHEMIAKOV, Aleksandr O.[5];

[1] National Research Nuclear University MEPhI (Moscow Engineering Physics Institute), Department of Power Engineering, Moscow – Russian Federation

[2,3] Moscow Aviation Institute (National Research University), Department of Machine Science and Machine Components, Moscow – Russian Federation

[4] Moscow Aviation Institute (National Research University), Faculty of Applied Mechanics, Moscow – Russian Federation

[5] Moscow Aviation Institute (National Research University), Moscow – Russian Federation

** Correspondence author*
e-mail: kondrat.leonid@yandex.ru

Received 30 August 2019; received in revised form 31 October 2019; accepted 31 October 2019

RESUMO

Muitos dos mecanismos usados na indústria contêm links de entrada e saída conectados por longas linhas de força. Aumentar a eficiência e a vida útil dos sistemas mecânicos com longas filas é de grande importância para a economia do país. Para um uso mais racional desses dispositivos, é importante manter esses modos de operação com a máxima precisão, geralmente incluindo a velocidade necessária do atuador e a tensão nas linhas. Tais parâmetros podem mudar espontaneamente, dependendo das condições de operação do sistema. Na presença de várias influências, tarefas semelhantes para determinar os regimes e parâmetros marcados, indicando a necessidade de sua mudança, só podem ser resolvidas com a ajuda da teoria e dos métodos de pesquisa correspondentes. O artigo apresenta os problemas e o método de estudar sistemas mecânicos de duas camadas com um número infinito de graus de liberdade com base nas equações de momento e momento de momento em forma diferencial. São propostas transformações com o uso de equações de ondas conhecidas, que possibilitam levar explicitamente em consideração as oscilações das velocidades de movimento e tensões nas linhas de força dos sistemas mecânicos ao descrever processos dinâmicos. A solução de sistemas de equações diferenciais parciais é dada usando a transformada de Laplace, que possibilitou obter equações gerais de movimento e, após algumas simplificações, proceder a equações diferenciais ordinárias que levam em consideração as características dinâmicas de sistemas com parâmetros distribuídos. O método Runge-Kutta modernizado obteve soluções e realizou simulação numérica de processos transitórios no acionamento hidráulico, cujos resultados têm boa convergência com experimentos em larga escala.

Palavras-chave: *equações diferenciais, parâmetros distribuídos, sistema mecânico, atuador hidráulico, características de frequência.*

ABSTRACT

Many of the mechanisms used in industry contain input and output links connected by long lines of force. Increasing the efficiency and service life of mechanical systems with long lines is of great importance for the country's economy. For a more rational use of these devices, it is important to maintain these operating modes with maximum accuracy, usually including the required speed of the actuator and the voltage in the lines. Such parameters can spontaneously change depending on the operating conditions of the system. In the presence of various influences, similar tasks to determine the marked regimes and parameters indicating the

Downloaded from www.periodico.tchequimica.com

need for their change can be solved only with the help of the corresponding theory and research methods. The article presents the problems and the method of studying two-tier mechanical systems with an infinite number of degrees of freedom on the basis of the equations of momentum and moment of momentum in differential form. Transformations with the use of well-known wave equations are proposed, which made it possible to explicitly take into account the oscillations of the speeds of motion and stresses in the force lines of mechanical systems when describing dynamic processes. The solution of systems of partial differential equations is given using the Laplace transform, which made it possible to obtain general equations of motion and, after some simplifications, proceed to ordinary differential equations that take into account the dynamic features of systems with distributed parameters. The modernized Runge-Kutta method obtained solutions and carried out numerical simulation of transient processes in the hydraulic drive, the results of which have good convergence with full-scale experiments.

***Keywords**: differential equations, distributed parameters, mechanical system, hydraulic drive, frequency characteristics.*

АННОТАЦИЯ

Многие из используемых в промышленности механизмов содержат входные и выходные звенья, соединенные длинными силовыми линиями. Такие механизмы широко используются в технологии глубокого сверления в коллекторах теплообменников, гребных валов, турбо-сверлильных валов с длиной отверстий до семи метров и других критических конструкций, а также в процессах бурения нефтяных и газовых скважин длиной вращающихся линий электропередач, достигающих нескольких километров. Повышение эффективности и срока службы механических систем с длинными линиями имеет большое значение для экономики страны. Для более рационального использования этих устройств важно поддерживать эти режимы работы с максимальной точностью, обычно включая требуемую скорость привода и напряжение в линиях. Такие параметры могут самопроизвольно меняться в зависимости от условий работы системы. При наличии различных воздействий аналогичные задачи по определению отмеченных режимов и параметров, указывающих на необходимость их изменения, могут быть решены только с помощью соответствующей теории и методов исследования. В статье представлены проблемы и методика изучения двухуровневых механических систем с бесконечным числом степеней свободы на основе уравнений импульса и момента импульса в дифференциальной форме. Предложены преобразования с использованием известных волновых уравнений, которые позволили при учете динамических процессов явным образом учитывать колебания скоростей движения и напряжений в силовых линиях механических систем. Решение систем дифференциальных уравнений в частных производных дается с помощью преобразования Лапласа, что позволило получить общие уравнения движения и после некоторых упрощений перейти к обыкновенным дифференциальным уравнениям, учитывающим динамические особенности систем с распределенными параметрами. Модернизированный метод Рунге-Кутты позволил получить решения и провести численное моделирование переходных процессов в гидроприводе, результаты которого хорошо сходятся с полномасштабными экспериментами.

***Ключевые слова**: дифференциальные уравнения, распределенные параметры, механическая система, гидравлический привод, частотные характеристики.*

1. INTRODUCTION

Used in industry, many mechanisms are mechanical systems containing input and output links interconnected by long force lines. Such mechanisms are widely used in the technology of deep drilling of holes in the headers of heat exchangers, propeller shafts, turbodrill shafts with hole lengths up to seven meters and other responsible structures, as well as in oil and gas well drilling processes when the length of rotating force lines reaches several kilometers. The given examples show that the increase in efficiency and service life of mechanical systems with long lines is of great importance for the country's economy.

For more rational use of these devices, it is important to maintain the specified (target) modes of operation with maximum accuracy, usually including the required speed of movement of the executive body and the voltage (pressure) in the lines. Such parameters may spontaneously change depending on the system operating conditions. In the presence of various impacts, similar tasks by definition of the noted modes and parameters, indicating the need for their changes, can be solved only with the appropriate theory and research methods (Yasnitskii, 1989). While designing such structures, the dynamic properties of the system can be assessed using traditional methods, for example, frequency analysis. However, for the implementation of technological

Downloaded from www.periodico.tchequimica.com

operations, it is important to know the regularity of the movement of the executive body (cutter, cutting part of the drill, etc.), as well as stresses arising in structural elements (Kondratenko and Mironova, 2018a). In addition, for their more effective application, it is necessary to maintain rational modes of operation with maximum accuracy, for example, maintain the required speed the executive body at given loads.

The design of two-link mechanisms often constitute the input link, which is the engine, and the output link is the executive body (the cutting part of the drill, chisel, mill, etc.), rigidly interconnected by force lines. Such simple mechanisms Babakov I.M. refers to systems with an infinite number of degrees of freedom (Babakov, 1958). The study of processes in the long force lines of mechanical systems usually described using differential equations in partial derivatives, has been the subject of a number of papers, for example, (Sirazijeva *et al.*, 2004, Kondratenko and Mironova, 2018a; Kondratenko and Mironova, 2018b; Kondratenko and Mironova, 2018c; Babakov, 1958; Popov, 1977; Sedov, 1970; Voronov, 1981; Frolov, 2000; Markin, 2010; Kondratenko, 2005, Vlasova et al., 2016). However, only in (Kondratenko and Mironova, 2018a); Popov, 1977; Kondratenko and Mironova, 2018c), the authors take into account the presence of a load on the output. Traditionally, the description is constructed using partial differential equations.

Due to the fact that significant oscillatory phenomena occur in systems with long lines, it is very important to find a way to calm the oscillations. This path is associated with overcoming serious difficulties. To solve problems of this kind, it was proposed in (Berezyanskij and Kondratev, 1988) to use the expansion theory in the form of an infinite family of commuting self-adjoint operators with the corresponding projection spectral theorem. With this approach, theorems of representation of positive definite functions of an infinite number of variables in a layer are established and the infinite-dimensional problem of moments is studied. The role of operators is played by a countable family of differentiations with respect to various variables, infinite families of shifts, etc. However, the application of this theorem very often gives negative answers. The main question was investigated only in certain particular cases when in this way the values of optimal control actions were obtained, both for the problems of program control and for certain problems of the synthesis of systems with feedback. In addition to the above-mentioned studies related to the use of results relating to the problem of moments, problems are known about controlling linear parabolic and hyperbolic systems (Godunov and Ryabenkij, 1977). However, such decisions are justified so far only for individual special cases.

In some cases, similar problems are solved by an approximate method with the replacement of the corresponding functional equations by suitable finite-dimensional difference schemes. As a result, the problem of optimal control of an approximating system described by equations in finite differences or by a system of ordinary differential equations is obtained. Wherein, for a finite-dimensional system, it becomes necessary to consider the maximum principle and estimate the convergence of approximating controls. However, the questions of substantiating such a finite difference approximation have not been studied enough. In mechanical engineering, it is quite rare to find situations when the calculation of oscillations (vibrations) of a particular structural element can be carried out accurately. As a rule, technical calculations are approximate. The main assumptions are made when choosing a calculation scheme. At the same time, the insignificant features of the system are ignored and only its main parameters that determine the nature of the phenomenon are highlighted, although in some cases minor features can have a great influence on the operation of the mechanism. n many cases, systems with distributed masses are replaced by systems with concentrated masses, parts of complex geometric shapes (springs, crankshafts, etc.) are usually reduced to an equivalent straight beam, nonlinear elastic elements are often replaced by equivalent linear ones, etc. Simulation of such systems is also possible with the help of analog machines. However, the complexity of creating a model, low accuracy of results, and low mobility of machines significantly limit the spread of this method.

In most cases, mechanical systems operate under the action of variable external influences in the presence of various nonlinearities, including significant ones (backlash, pressure and displacement restrictions, dead band). Periodic effects can be approximated by harmonic functions, the response of the system to which is conveniently described by frequency characteristics. Often the impacts are sporadic. For example, during deep drilling, getting a carbide particle under the cutting blade will cause a sharp change in the

Downloaded from www.periodico.tchequimica.com

moment of resistance, which in turn may distort the hole trajectory or disturb the surface layer. It is very difficult to describe the behavior of the system in such cases using frequency methods. It requires calculations that take into account fluctuations in the time domain. Therefore, the study of issues of dynamics and the determination of the actual values of speeds and voltages, characterizing the features of power transmission, is very important for developing solutions to improve the efficiency of these devices. An attempt to solve the noted problems was undertaken in the proposed article.

2. MATERIALS AND METHODS

In this question, the performance of the devices in question is determined by the transmitted power, i.e., the speed of movement of the executive body and the stress in the force line. When these parameters deviate from rational values, there is a need to study the Equations 1, 2 (Kondratenko *et al.,* 2018; Babakov, 1958). Here Ω is the speed of movement of the technological object; t is the time; ζ_i is the coordinates of the system; f_i is the speed of change of coordinates. In this case, the study is reduced to solving Equation 3. Usually, in the study of dynamic processes in mechanical systems, the tasks of determining changes in coordinates, vibration shapes (Kolovskij, 1989; Ualiev and Ualiev, 2006; Vulfson, 1990) are solved. For this purpose, the methods of the theory of elasticity are used, for example, they use the Equation 4 (Kondratenko *et al.,* 2018; Frolov, 1995; Yavorskij and Detlaf, 1974) the solution of which is sought in Equation 5.

Here ν, E is the mass and elastic characteristics of the mechanical line; f_k is the section area; $Q_н$ is the intensity of the external load; H_k, θ_k, p_k, α_k is constants determined from the initial conditions. In the case of using the Lagrange equation of the 2nd kind (Equation 6) considered are the kinetic (T) and potential energy (U) oscillations, taking into account Equation 7 where q is the generalized coordinate.

The parameters of the movement of the mechanism from this equation are determined after some transformations. The indicated equations that underlie many papers on the dynamics of machines, for example (Babakov, 1958; Kolovskij, 1989; Ualiev and Ualiev, 2006; Vulfson, 1990), allow, for given boundary conditions, to estimate the change in the displacements of the elementary volume of a bar, column, and other parameters in time and space. However, such information, if it is necessary to take into account the interrelationship of a large number of factors, is, on the one hand, redundant, since it is often enough to know under what conditions self-oscillations occur of the rotation frequency of a technological object (executive body), i.e. stability is lost, and under what conditions the system is stable. On the other hand, without explicitly taking into account the second variable (stress), complete information about the dynamics of the stress state in the course of work cannot be received, which makes it difficult to estimate the likelihood of a part breaking or disrupting the mechanism. In the case of using systems with long force lines, there is also the problem of describing the behavior of the mechanism under standard disturbance (impacts), for example, step disturbance.

Studies show, for example (Postnikov, 1974; Reiner, 1958), that an intermediate variable (stress) is not always linearly related to displacement. However, the described methods do not take this feature into account. In addition, depending on the stresses, the position of the executive body may change, which will result in changes in indicators boring of aperture, drilling of wells for oil and gas. In this regard, there is a need to develop a method where the oscillations of both speeds and stresses, as well as the influence of various nonlinearities, are explicitly taken into account.

3. RESULTS AND DISCUSSION:

3.1. The Conclusion of the Original Equations

To solve this problem, when considering longitudinal oscillations in a straight solid rod in the absence of mass forces, the equation of momentum in differential form was used (Equation 8) (Sedov, 1970) and the equation of longitudinal vibrations (Equation 9) where Equation 10; u is moving along the x axis; σ is longitudinal (normal) voltage; ρ is the density of the material; E is the modulus of elasticity. From Equations 8, 9 the Equation 11 is obtained. Integrating Equation 3 over x, assuming that for $x = 0$, $\sigma = \text{const}$, and then differentiating over t the result obtained, the expression is arrived at Equation 12 (Kondratenko, 2005).

Denote the current value of the stress σ_x by σ. Given that the surface forces acting on each point of the cross section of an elementary volume are directed in the opposite direction from the direction of the speed of movement,

Downloaded from www.periodico.tchequimica.com

Equations 8, 12 are rewritten in the form Equations 13, 14. When considering torsional vibrations, the deplanation of sections is assumed to be absent. Then the elastic oscillations are described by the Equation 15 (Kondratenko, 2005; Kondratenko *et al.,* 2017b) where φ, *x* is the angle of rotation of the section line and the coordinate with zero in the center of the driving link; G is material shear modulus. From the equation of angular momentum for a finite volume of a continuous medium in the absence of viscous friction in the material (Sedov, 1970), after the known transformations (Kondratenko, 2005; Kondratenko *et al.,* 2017b), it is possible to obtain for the elementary volume of the rod with an outer radius r with ρ = const the equation of angular momentum in the differential form Equation 16 where Ω is rotation speed, Equation 17; τ is the maximum tangential stresses in torsion. From Equations 14, 16 the Equation 18 is arrived at. After integrating Equation 18 along the x coordinate and subsequent differentiation by t, the Equation 19 is gotten. The system of Equations 16, 19 makes it possible to describe the changes in the tangential stresses on the outer cylindrical surface in an elementary volume and the speed of movement of the elementary sections of the trunk.

Assuming that G = const, ρ = const and performing the one-dimensional Laplace transform of these equations with zero initial conditions (Ivanov *et al.,* 1971), Equation 20 is obtained (Equation 21) where *s* is a complex variable, Equation 22, ω is the frequency of circular oscillation. Suppose that the process of transferring motion during a shift is similar to the process of transferring motion during longitudinal vibrations. In this case, following the phenomelogical Zener model (Reiner, 1958) for the elementary volume, the equation of motion can be written in the form Equation 23 where θ, η is deformation and viscosity; G_1, G_2 is isothermal and adiabatic shear modulus. If Equation 23 is rewritten in operator form and then using the Laplace transform with zero initial conditions, then Equation 24 can be obtained where a_ε is the relaxation constant (Equations 25, 26). From here for the generalized modulus of elasticity can be written (Equation 27). Here G_u, G_υ are, respectively, the ordinates of the complex function G_ω ($j\omega$) along the real and imaginary axes.

It is further assumed that the features of the interaction of transverse waves with the interface are similar to the interactions of longitudinal waves and are largely determined by the wave resistance (Equations 28, 29) (Yavorskij and Detlaf, 1974) where a_2 is the speed of movement of the transverse waves. If to consider the harmonic oscillations propagating along the line, it can be introduced into consideration the wave resistance in operator form – impedance $Z_b(j\omega)$ (Equation 30) (Kondratenko and Mironova, 2018c; Kondratenko *et al.,* 2017a). Assuming the material density is constant with regard to Equations 27–29, the transformed Equation 30 is written in the form Equation 31. Here are the following ratios (Equation 32) where ψ (ω) is the generalized function of internal friction. Internal friction ψ in solids can play a significant role. It is known, for example, that magnesium alloys and a number of other materials have very good vibration-insulating properties, largely due to internal friction. At the same time, for steels, because of the smallness, this value is often neglected. Then Equation 33, ψ (ω) = 0. Dynamic features of force line with parameters distributed along the length are characterized by the operator coefficient of wave propagation, which, based on Equation 20 in Laplace images with these assumptions, can be written in the form Equation 34.

Differentiating Equation 16 with respect to the x coordinate, then eliminating the derivative $d\Omega(s)/dx$ using Equation 19 and applying Equation 34, Equation 35 is obtained (Kondratenko, 2005; Kondratenko *et al.,* 2017b). This equation is a 2nd order differential equation with constant coefficients. Its solution after the introduction of hyperbolic functions (Kondratenko, 2005; Kondratenko *et al.,* 2017b) under boundary conditions for x = 0 (Equations 36, 37), has the form Equation 38. Having solved the system of Equations 16, 19 in the manner described above with respect to Ω(s, x), Equation 39 is obtained and for the boundary conditions for: x = 0 (Equations 40, 41) finally, there will be Equation 42. If in the process of oscillation, the output link does not miss the angular momentum that is supplied to this link, then disturbance waves are reflected from the end of line. The case of a matched load will be considered when there are no reflected waves in the system. In this case, the boundary conditions are the following relations (Equations 43-45) (Kondratenko, 2005; Kondratenko and Mironova, 2018c). Here, W_{p2} is the geometric polar moment of the resistance of the section of the line of the executive body with the moment of inertia *J;* h_k, M_c is the coefficients of friction loss and moment of resistance acting on the executive body; *l* is the length of the line. The coefficient h_k takes into account only friction

Downloaded from www.periodico.tchequimica.com

losses proportional to the speed of the load.

Jointly solving Equations 38, 42 taking into account the specified boundary conditions, the equation of motion of the executive body of the system is obtained (Equations 46, 47). Having performed similar transformations as applied to longitudinal vibrations in solid lines, Equations 11, 12, the equation of motion is obtained (Kondratenko, 2005; Ivanov *et al.,* 1971), which has almost the same form as Equation 46.

If to carry out transformations similar to those described for a volumetric hydraulic actuator (Popov, 1977; Kondratenko, 2005), then, assuming that the leakage through the hydraulic motor is significantly higher than the leakage through the pump, the equation of motion can be obtained (Equation 48) (Kondratenko *et al*., 2017a; Rabinskiy and Tushavina, 2019a; Rabinskiy and Tushavina, 2019b; Kamke, 1959; Nikitin *et al.,* 2019). Here are the following ratios (Equations 49, 50) where τ is tightness criterion of volumetric hydraulic actuator; ϑ_{0s} is the coefficient of elasticity; $E_g(s)$, $\Psi(s)$ are polynomials obtained during transformations; w is the volumetric constant of the hydraulic motor; Q is pump flow rate; $\theta_{01}(s)$ is the operator coefficient of wave propagation in the pressure line; J is the moment of inertia of rotating parts; c is the coefficient of friction loss proportional to the pressure differential; h is the coefficient of friction loss proportional to the speed of movement; ρ_0, κ is the density and bulk modulus of elasticity of the liquid; Ω is the frequency of rotation of the output shaft; M_r - the moment of resistance; L is the length of the hydraulic line; K_u is coefficient leakages in the volumetric engine. In this case, the boundary conditions were determined by the balance of the flows rate fluid entering the pipelines and resulting from them.

3.2. Solving Systems of Equations

Since the mechanisms usually have nonlinearities, including substantial ones, the solution of such problems is possible only by a numerical method. Considering the similarity of equations describing the dynamics of mechanical and hydraulic systems (Kondratenko, 2005), as well as a simpler fixation of oscillations in the hydraulic drive, the development of a method for numerical simulation of dynamic processes in mechanical systems was based on comparing simulation results with field tests of hydraulic drive. To solve this problem, the Equation 48 has to be algebraically decomposed into Equations 51, 52. Here p is the differential pressure on the hydraulic motor. The correctness of the decomposition is checked by the reverse decision. From the Equation 31 the transfer function of the influence of oscillations of the pump flow rate is obtained on the pressure drop at $M_r = 0$ (Equation 53). The complex functions $\Psi(s)$ and $\vartheta(s)$ in Equation 32 will be replaced by their real parts $\Psi(\omega)$ and $\vartheta(\alpha)$ (Equation 54).

Figure 1 shows the calculated ratios of the modules of real and imaginary parts of the functions $\vartheta(i\omega)$, $\Psi(i\omega)$. The calculations were carried out for hydraulic IID. It can be seen from the graphs that the real parts of the functions significantly exceed their imaginary parts in modulus in almost the entire frequency range. Turning to the originals of Equations 51, 52, Equations 55, 56 are obtained. Simulation was carried out for electrohydraulic drive with parameters: J = 34 N*cm*s^2; w = 11.3 cm^3 / rad; h = 17N*cm*s; æ =1.4*10^{3}MPa; ρ_0 = 870 kg / m^3; f_1=f_2=3.13 cm^2; τ=0.05(N*cm*s)$^{-1}$; a_{1m}=5,36*10^{-2} s; a_{2m}= 5,76*10^{-4}c^2; K_{mu} = 0.02 1 / (B). Safety valves in both lines are set to a pressure of p = 15 MPa. The length of each of the two hydraulic lines was l = 22 m. For example, taking into account Equations 55, 56 for the hydraulic drive, a system of Equations 57-60.

Here $U(t)$, a_{1m}, a_{2m} is respectively, the control voltage, the coefficients of the control mechanism; γ is angle of rotation of the control mechanism roller; p_1, p_2 is respectively, the pressure in the pressure and make-up lines; Δp is pressure differential on the hydraulic motor, Equation 61; Q_T is theoretical maximum flow rate of the pump; Q_{k1}, Q_{k2} is leakage through valves; V_1 is volume of fluid in the line. The Equation 35 was solved using the 4th order Runge-Kutta method (Kondratenko *et al.,* 2018; Kamke, 1959).

3.3. Simulation Results

Modeling was carried out using a PC with counting steps H = 10^{-4}; 2*10^{-4} sec. The error did not exceed 10%. The control signal was changed according to the law (Equation 62). For each settable frequency ω with U_0 = 10 V, U_a = 5 V for 10 sec. the counts calculated the values of the input coordinate U, as well as the liquid flow Q supplied to the system and the values of the other variables. After analyzing the obtained numerical values, the amplitude of the oscillations of the pressure differential A_p and the phase shift φ of forced oscillations the differential pressure relative to the oscillations of the flow were determined. Then calculated the value of

Downloaded from www.periodico.tchequimica.com

Equation 63. In addition, the frequency response was calculated from the transfer function (Equation 53) using complex functions. Also for the marked hydraulic drive, experimental frequency characteristics were obtained. The results of all calculations and natured experiments are shown in Figure 2. It can be seen from them that the numerical simulation performed by the method described above very accurately reflects the processes in the system with distributed parameters of elastic lines (Kondratenko and Mironova, 2018c).

4. CONCLUSIONS:

The proposed method for solving systems of nonlinear differential equations that take into account the distributed parameters of the power lines of the mechanisms allows us to conduct various numerical experiments to study the parameters of motion and the stressed state in various mechanical systems and obtain adequate results. Here, with a constant counting step each of the four stages of the calculation cycle, nonlinear factors were taken into account (friction, unidirectional rotation, pressure limitation). For each input frequency of forced oscillations ω was recalculated the values of α and the functions $\Psi(\omega)$, $\vartheta_s(\alpha)$. If to consider that during the operation of virtually any mechanism oscillations are generated, the frequency of which depends on the speed of movement of the executive body, then the proposed method can be used to obtain not only frequency characteristics but also oscillograms of transients in the considered systems.

5. ACKNOWLEDGMENTS:

The investigation was made in Moscow Aviation Institute and supported financially by the Russian Foundation for Basic Researches under Grant No. 19-01-00675 and by the Grant of the President of the Russian Federation No. MK-3869-2019.8.

6. REFERENCES:

1. Babakov, I.M., *Oscillation theory*, Moscow: GTTL, **1958**.
2. Berezyanskij, Yu.M., Kondratev, Yu.G. *Spectral methods in infinite-dimensional analysis,* Kiev: ANUSSR, Naukova Dumka, **1988**.
3. Frolov, K.V. *Engineering. Encyclopedia. Volume 1-3: Dynamics and strength of machines. Theory of Mechanisms and Machines,* Moscow: Mashinostroenie, **1995**.
4. Frolov, K.V*., Engineering. Encyclopedia. Volume I-4: Automatic control. Theory*, Moscow: Mashinostroenie, **2000**.
5. Godunov, S.K., Ryabenkij, V.S. *Difference schemes*, Moscow: Nauka, **1977**.
6. Ivanov, V.A., Chemodanov, B.K., Medvedev, V.S. *Mathematical foundations of the theory of automatic control*, Moscow: Vysshaya shkola, **1971**.
7. Kamke, E. *Handbook of ordinary differential equations,* Leipzig: B.G. Teubner, **1959**.
8. Kolovskij, M.Z. *Car dynamics*, Leningrad: Mashinostroenie, **1989**.
9. Kondratenko, L., Dmitriev, V., Mironova, L. *Vibroengineering Procedia*, **2017a**, *12*, 231–236. DOI: 10.21595/vp.2017.18743.
10. Kondratenko, L., Mironova, L. *International Journal of Mathematical, Engineering and Management Sciences*, **2018a**, *3(4),* 315–334.
11. Kondratenko, L.A., Mironova, L.I. 2018. *International Conference on Modern Trends in Manufacturing Technologies and Equipment*. Sevastopol, Russia, **2018b**.
12. Kondratenko, L.A., Mironova, L.I. *Engineering and Automation Problems,* **2018c**, 1, 92–97.
13. Kondratenko, L.A., Mironova, L.I., Dmitriev, V.G., Kuznetsova, E.L. *Periódico Tchê Química*, **2018**, *15(1),* 126–137.
14. Kondratenko, L.A., Terekhov, V.M., Mironova, L.I. *Engineering & Automation Problems*, **2017b**, *1*, 133–137.
15. Kondratenko, L.A., *Vibrations and speed regulation methods of movement of technological objects*, Moscow: MRSU, **2005**.
16. Markin, D.N., *Theoretical foundations of electroacoustics*, Saint-Petersburg: SPbGUKiT, **2010**.
17. Nikitin, P.V., Tushavina O.V., Shkuratenko, A.A. *Incas Bulletin,* **2019**, *11,* 183–190. DOI: 10.13111/2066-8201.2019.11.S.19.
18. Popov, D.N., *Dynamics and regulation of hydro-pneumatic systems*, Moscow: Mashinostroenie, **1977**.
19. Postnikov, V.S. *Internal friction*, Moscow:

Downloaded from www.periodico.tchequimica.com

Metallurgiya, **1974**.

20. Rabinskiy, L.N., Tushavina, O.V. *Incas Bulletin*, **2019a**, *11,* 203–211. DOI: 10.13111/2066-8201.2019.11.S.20.
21. Rabinskiy, L.N., Tushavina, O.V. *STİN*, **2019b**, *4*, 22–26.
22. Reiner, M. *Rheology*, Berlin-Guttingen-Heideiberg: Springer-Veriag, **1958**.
23. Sedov, L.I. *Continuum Mechanics,* Moscow: Nauka, **1970**.
24. Sirazijeva, L.F., Stepin, S.N., Makhotkina, L.Yu. *Lakokrasochnye Materialy i Ikh Primenenie*, **2004**, *10*, 25-28.
25. Ualiev, G., Ualiev, Z.G. *Mathematical modeling of the mechanical systems dynamics with variable characteristics*, Almaty: Kazakh National Pedagogical University, **2006**.
26. Vlasova, O., Kovalenko, V., Kotok, V., Vlasov, S. *Eastern-European Journal of Enterprise Technologies*, **2016**, *5(5-83)*, 33-39.
27. Voronov, A.A., *Fundamentals of the theory of automatic control. Special linear and nonlinear system,* Moscow: Ehnergoizdat, **1981**.
28. Vulfson, M.I. *Fluctuations of machines with cyclic mechanisms*, Leningrad: Mashinostroenie, **1990**.
29. Yasnitskii, L.N. *Mechanics of Solids*, **1989**, *24(2)*, 90-96.
30. Yavorskij, B.M., Detlaf, A.A. *Handbook of physics,* Moscow: Nauka, **1974**.

$$\frac{\partial \Omega}{\partial t} = \sum_{i=1}^{n} \frac{\partial \Omega}{\partial \zeta_i} f_i \qquad \text{(Eq. 1)}$$

$$f_i = \frac{d\zeta_i}{dt} \qquad \text{(Eq. 2)}$$

$$\frac{d\zeta_i}{dt} = f_i\left(t,\ \zeta_1,\ \zeta_{2,}\ ...,\ \zeta_n\right)\text{b} \qquad \text{(Eq. 3)}$$

$$\nu \frac{\partial^2 u}{\partial t^2} - \frac{\partial\left[Ef_k\left(\partial x / \partial t\right)\right]}{\partial x} = Q_n\left(x,t\right) \qquad \text{(Eq. 4)}$$

$$u\left(x,t\right) = \sum_{k=1}^{\infty} H_k \theta_k\left(x\right) \sin\left(p_k t + \alpha_k\right) \qquad \text{(Eq. 5)}$$

$$\frac{d}{dt}\left(\frac{\partial T}{\partial \dot{q}}\right) - \frac{\partial T}{\partial q} = Q \qquad \text{(Eq. 6)}$$

$$Q = -\frac{dU}{dq} \qquad \text{(Eq. 7)}$$

$$\rho \frac{\partial \upsilon}{\partial t} = \frac{\partial \sigma}{\partial x} \qquad \text{(Eq. 8)}$$

$$\frac{\partial^2 u}{\partial t^2} = \frac{E}{\rho} \frac{\partial^2 u}{\partial x^2} \qquad \text{(Eq. 9)}$$

$$\upsilon = \frac{\partial u}{\partial t} \qquad \text{(Eq. 10)}$$

Downloaded from www.periodico.tchequimica.com

$$\frac{1}{\rho}\frac{\partial \sigma}{\partial x} = \frac{E}{\rho}\frac{\partial^2 u}{\partial x^2} \quad \text{(Eq. 11)}$$

$$\frac{1}{E}\frac{\partial \sigma_x}{\partial t} = \frac{\partial \upsilon}{\partial x} \quad \text{(Eq. 12)}$$

$$\rho\frac{\partial \upsilon}{\partial t} = -\frac{\partial \sigma}{\partial x} \quad \text{(Eq. 13)}$$

$$\frac{1}{E}\frac{\partial \sigma}{\partial t} = -\frac{\partial \upsilon}{\partial x} \quad \text{(Eq. 14)}$$

$$\frac{\partial^2 \varphi}{\partial t^2} = \frac{G}{\rho}\frac{\partial^2 \varphi}{\partial x^2} \quad \text{(Eq. 15)}$$

$$\rho r\frac{\partial \Omega}{\partial t} = -\frac{\partial \tau}{\partial x} \quad \text{(Eq. 16)}$$

$$\Omega = \frac{\partial \varphi}{\partial t}\,\mathrm{d} \quad \text{(Eq. 17)}$$

$$G\frac{\partial^2 \varphi}{\partial x^2} = -\frac{1}{r}\frac{\partial \tau}{\partial x} \quad \text{(Eq. 18)}$$

$$rG\frac{\partial \Omega}{\partial x} = -\frac{\partial \tau}{\partial t} \quad \text{(Eq. 19)}$$

$$\rho r\, s\, \Omega(s) = -\frac{d\tau(s)}{dx} \quad \text{(Eq. 20)}$$

$$rG\frac{d\Omega(s)}{dx} = -s\tau(s) \quad \text{(Eq. 21)}$$

$$s = j\omega\,\mathrm{g} \quad \text{(Eq. 22)}$$

$$\tau + \frac{\eta}{G_2}\frac{d\tau}{dt} = G_1\theta + \eta\frac{d\theta}{dt} \quad \text{(Eq. 23)}$$

$$\tau(s)\left(s + \frac{1}{a_\varepsilon}\right) = \theta(s)G_2\left(s + \frac{1}{k_b\alpha_\varepsilon}\right) \quad \text{(Eq. 24)}$$

$$a_\varepsilon = \frac{\eta}{G_2} \quad \text{(Eq. 25)}$$

$$k_b = \frac{G_2}{G_1} \quad \text{(Eq. 26)}$$

Downloaded from www.periodico.tchequimica.com

$$G_{\omega}(s)=\frac{\tau(s)}{\theta(s)}=G_u(\omega)+jG_{\upsilon}(\omega) \quad \text{(Eq. 27)}$$

$$-\frac{\tau}{\Omega}=\rho a_2 \quad \text{(Eq. 28)}$$

$$a_2=\sqrt{\frac{G}{\rho}} \quad \text{(Eq. 29)}$$

$$Z_b(j\omega)=\frac{\tau(j\omega)}{\Omega(j\omega)} \quad \text{(Eq. 30)}$$

$$Z_b(j\omega)=\frac{j\omega G_u(\omega)\sqrt{\rho/G_u(\omega)}\sqrt{1+j\dfrac{G_{\upsilon}(\omega)}{G_u(\omega)}}}{j\omega}=\frac{G_u(\omega)\theta(j\omega)}{j\omega}j \quad \text{(Eq. 31)}$$

$$\theta(j\omega)=\pm\sqrt{\frac{j\omega}{G_u(\omega)}[\rho j\omega+\psi(\omega)]} \quad \text{(Eq. 32)}$$

$$G_u=(\omega)=G=const \quad \text{(Eq. 33)}$$

$$\theta(s)=\pm s\sqrt{\frac{\rho}{G}} \quad \text{(Eq. 34)}$$

$$\frac{\partial^2\tau(s)}{\partial x^2}-\theta^2(s)\tau(s)=0 \quad \text{(Eq. 35)}$$

$$\tau(s,x)=\tau_1(s,0) \quad \text{(Eq. 36)}$$

$$\frac{\partial\tau(s,x)}{\partial x}=-\frac{rG}{s}\theta^2(s)\Omega_1(s,0) \quad \text{(Eq. 37)}$$

$$\tau(s,x)=\tau_1(s,0)ch\left[\theta(s)x\right]-\frac{rG}{s}\theta(s)\ \Omega_1(s,0)sh\left[\theta(s)x\right] \quad \text{(Eq. 38)}$$

$$\frac{\partial^2\Omega(s)}{\partial x^2}-\theta^2(s)\ \Omega(s)=0 \quad \text{(Eq. 39)}$$

$$\Omega(s,x)=\Omega_1(s,0) \quad \text{(Eq. 40)}$$

$$\frac{\partial\Omega(s,x)}{\partial x}=-\frac{s\tau_1(s,0)}{rG} \quad \text{(Eq. 41)}$$

Downloaded from www.periodico.tchequimica.com

$$\Omega(s,x)=\Omega_1(s,0)ch\ [\theta(s),x)]-\frac{s\tau_1(s,0)sh\ [\theta(s)x]}{\theta(s)rG} \quad \text{(Eq. 42)}$$

$$\Omega(s,0)=\Omega_1(s);\ \Omega(s,l)=\Omega_2(s) \quad \text{(Eq. 43)}$$

$$\tau(s,0)=\tau_1(s);\ \tau(s,l)=\tau_2(s) \quad \text{(Eq. 44)}$$

$$\tau_2(s)=\frac{M_c(s)+h_k\Omega_2(s)+Js\ \Omega_2(s)}{W_{p2}} \quad \text{(Eq. 45)}$$

$$\Omega_2(s)\left[1+h_k\vartheta_k(s)s+J\vartheta_k(s)s^2\right]=\frac{\Omega_1(s)}{chA}-M_c(s)\vartheta_k(s)s \quad \text{(Eq. 46)}$$

$$\vartheta_k(s)=\vartheta_{k0}Z_n(s);\ \vartheta_{k0}=\frac{l}{GrW_{p2}};\ Z_k(s)=\frac{thA}{A};\ A=\theta(s)l \quad \text{(Eq. 47)}$$

$$\Omega(s)\left\{s^2J\vartheta_s(s)+s[J\tau_k+\vartheta_s(s)h]+1-c+\tau_k h\right\}=$$
$$=Q(s)(1-c)\Psi(s)-M_r(s)\left[\vartheta_s(s)s+\tau_k\right] \quad \text{(Eq. 48)}$$

$$\vartheta_s(s)=\frac{1}{E_g(s)}\vartheta_{0s}(s)Z(s);\ \tau_k=\frac{K_u}{w^2};\ \vartheta_{0s}=\frac{Lf_1}{\kappa w^2} \quad \text{(Eq. 49)}$$

$$Z(s)=\frac{thA_1}{A_1};\ \theta_{01}(s)=\sqrt{\frac{\rho_0}{\kappa}};\ A_1=\theta_{01}(s)L \quad \text{(Eq. 50)}$$

$$Q(s)\Psi(s)=w\,\Omega(s)+\tau_k w^2 p(s)+\vartheta_s(s)w^2 sp(s) \quad \text{(Eq. 51)}$$

$$p(s)w\ (1-c)=M_r(s)+h\,\Omega(s)+Js\ \Omega(s) \quad \text{(Eq. 52)}$$

$$W_{pq}(s)=\frac{P(s)}{Q(s)}=\frac{(Js+h)\Psi(s)}{s^2J\vartheta_s(s)+s\left[J\tau_k+\vartheta_s(s)h\right]+1-c+\tau_k h} \quad \text{(Eq. 53)}$$

$$\alpha=l\omega\sqrt{\frac{\rho}{\kappa}} \quad \text{(Eq. 54)}$$

$$Q(t)\Psi(\omega)=w\,\Omega(t)+\tau w^2 p(t)+\vartheta(\alpha)w^2\frac{dp}{dt} \quad \text{(Eq. 55)}$$

$$p(t)w\ (1-c)=M_c(t)+h\,\Omega(t)+J\frac{d\Omega}{dt} \quad \text{(Eq. 56)}$$

$$\frac{V_1}{\kappa}Z_1(\omega)\frac{dp_1}{dt}=\gamma(t)Q_T\Psi(\omega)-w\,\Omega(t)+Q_{k2}-Q_{k1}-\tau_k w^2\Delta p(t)-0{,}1\tau_k w^2 p_2(t) \quad \text{(Eq. 57)}$$

Downloaded from www.periodico.tchequimica.com

$$\frac{V_1}{\kappa} Z_1(\omega) \frac{dp_1}{dt} = -\gamma(t) Q_T \Psi(\omega) + w\,\Omega(t) - Q_{k2} + Q_{k1} - \tau_k w^2 p_1(t) \quad \text{(Eq. 58)}$$

$$\Delta pw = M_c(t) + h\,\Omega(t) + J\frac{d\Omega}{dt} \quad \text{(Eq. 59)}$$

$$K_u U(t) = \gamma(t) + a_{1m}\frac{d\gamma}{dt} + a_{2m}\frac{d^2\gamma}{dt^2} \quad \text{(Eq. 60)}$$

$$\Delta p = p_1 - p_2 \mathrm{f} \quad \text{(Eq. 61)}$$

$$U = U_0 + U_a \sin(\omega t)\mathrm{f} \quad \text{(Eq. 62)}$$

$$L = 20\lg\left(\frac{A_p}{Q_a}\right)\mathrm{f} \quad \text{(Eq. 63)}$$

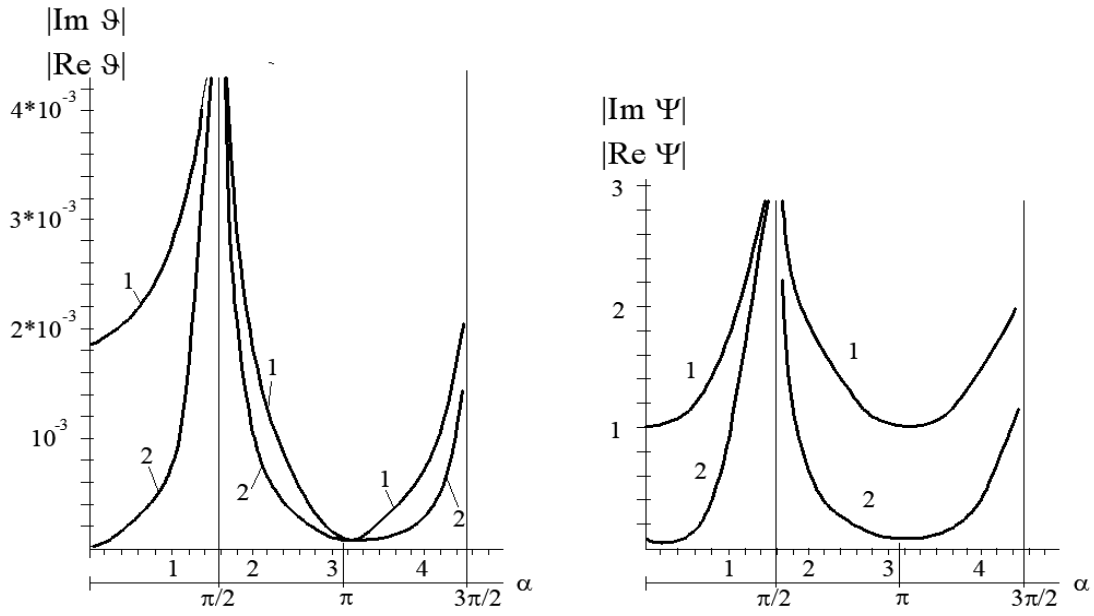

Figure 1. *The ratio of the modules of the real (1) and imaginary (2) parts of the functions $\vartheta(i\omega)$, $\Psi(i\omega)$ for the IID hydraulic drive*

Downloaded from www.periodico.tchequimica.com

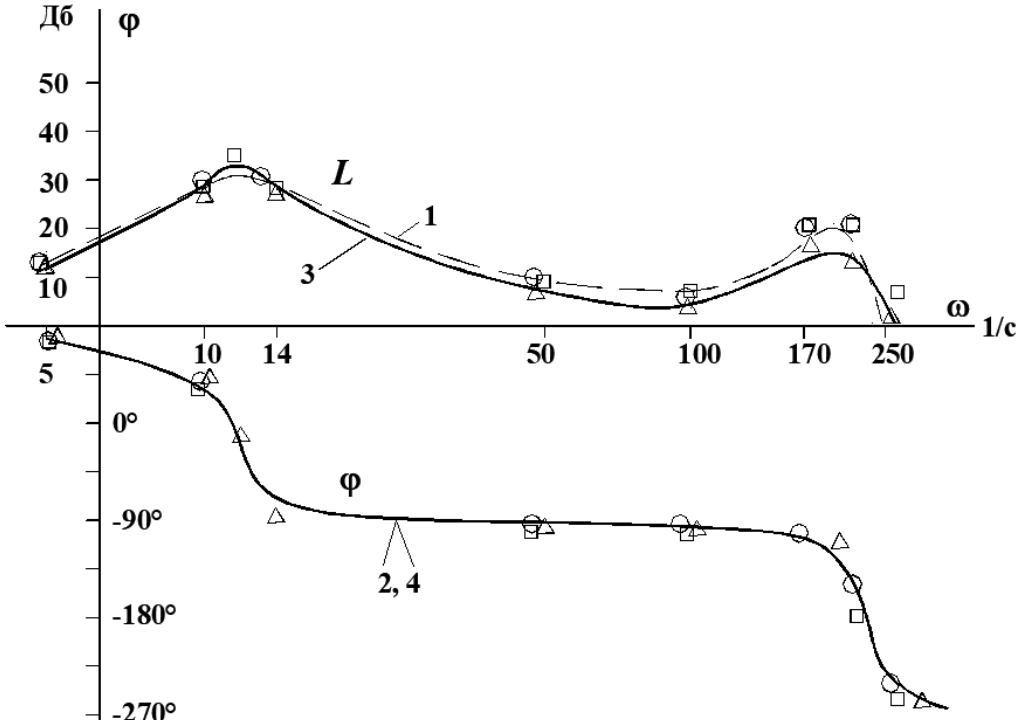

Figure 2. *Logarithmic amplitude (L) and phase (φ) frequency characteristics of the ghydraulic drive: curves 1, 2 is calculated curves of the simulation model; curves 3, 4 is curves obtained by experiment*

Downloaded from www.periodico.tchequimica.com

PERIÓDICO TCHÊ QUÍMICA
ARTIGO ORIGINAL

MOVIMENTO CONTROLADO POR CAMPO ELÉTRICO DE GOTÍCULAS DE LIGA LÍQUIDA SOBRE A SUPERFÍCIE DE SEMICONDUTORES

MELT DROPS MOVEMENT OVER SEMICONDUCTOR SURFACES CONTROLLED BY ELECTRIC FIELD

УПРАВЛЯЕМОЕ ЭЛЕКТРИЧЕСКИМ ПОЛЕМ ПЕРЕМЕЩЕНИЕ КАПЕЛЬ РАСПЛАВА ПО ПОВЕРХНОСТИ ПОЛУПРОВОДНИКОВ

SKVORTSOV, Arkadiy A.[1]*; KORYACHKO, Marina V.[2]; ZUEV, Sergei M.[3]; DEMCHENKOVA, Anastasiya A.[4];

[1,4] Moscow Polytechnic University, Department of Mechanics of Materials, Moscow – Russian Federation

[2] Moscow Polytechnic University, Department of Physics, Moscow – Russian Federation

[3] Moscow Polytechnic University, Department of Industrial Electronics, Moscow – Russian Federation

** Correspondence author*
e-mail: skvortsovaa2009@yandex.ru

Received 28 October 2019; received in revised form 31 October 2019; accepted 31 October 2019

RESUMO

Os problemas de formação de zonas fundidas e sua subsequente migração sobre a superfície do material são interessantes do ponto de vista do desenvolvimento de novos métodos tecnológicos para formar estruturas microeletrônicas. Tais gotas podem ser usadas como elementos primários de trabalho de microlentes e refletores, displays e pesadores. O objetivo deste trabalho foi estudar estudos de processos de eletromigração de inclusões à base de prata e alumínio fundidas sobre superfícies de cristais semicondutores de germânio e alumínio. As questões de formação e movimento de gotas fundidas sobre as superfícies de cristais de semicondutores de silício e germânio são consideradas dentro da estrutura da abordagem eletrocapilar. É mostrado por um exemplo de sistemas Ge-Ag e Si-Al que a migração acelerada está relacionada à contribuição de um componente eletrocapilar que relaciona a força de tensão superficial de quedas de derretimento à diferença de potencial elétrico na interface. O experimento consistiu em aplicar grãos de metal na superfície das amostras e aspirar a câmara onde foram criadas pressão excessiva e temperatura da superfície. Iniciou-se a migração de inclusões por poderosos pulsos de corrente. Foi feita uma análise do efeito da corrente direta em uma gota de fundido depositada na superfície de uma matriz cristalina. Uma análise da composição das gotículas foi realizada usando o método AES, cujos resultados mostraram a relação entre as concentrações de prata e germânio. Avaliações quantitativas são dadas para taxas de migração em sistemas sob fluxo de corrente direta, bem como sob cargas de corrente pulsada. Durante o experimento, verificou-se que a energia necessária para separar a gota da matriz rígida não foi consumida. O valor da densidade de transferência de carga superficial foi estimado. Os resultados do trabalho podem ser utilizados para desenvolver novos métodos tecnológicos para a formação de estruturas microeletrônicas e seu uso para fins práticos.

Palavras-chave: *estruturas microeletrônicas, efeito eletrocapilar, campo elétrico.*

ABSTRACT

The problems of molten zones formation and their subsequent migration over material surface are of interest from the viewpoint of developing novel technological methods of forming microelectronic structures. Such drops can be used as primary working elements of microlenses and reflectors, displays, weighers. The aim of this work was experimental studying processes of electromigration of molten silver- and aluminum-based inclusions over surfaces of germanium and aluminum semiconductor crystals. The issues of formation and motion of molten drops over the surfaces of silicon and germanium semiconductor crystals are considered within the framework of the electrocapillary approach. It is shown by an example of Ge-Ag and Si-Al systems that accelerated migration is related to the contribution of an electrocapillary component that relates surface tension force of melt drops to electric potential difference at the interface. The experiment consisted in applying metal grain to the surface of the samples and vacuuming the chamber where excessive pressure and the

Downloaded from www.periodico.tchequimica.com

surface temperature were created. Migration of inclusions by powerful current pulses was initiated. An analysis of the effect of direct current on a drop of melt deposited on the surface of a crystalline matrix was made. An analysis of the droplet composition was carried out using the AES method, the results of which showed the relationship between silver and germanium concentrations. Quantitative evaluations are given for migration rates in systems under direct current flow as well as under pulsed current loads. During the experiment, it was found that the energy required to detach the droplet from the rigid matrix was not consumed. The value of the surface charge transfer density was estimated. The results of the work can be used to develop new technological methods for the formation of microelectronic structures and their use for practical purposes.

Keywords: *microelectronic structures, electrocapillary effect, electric field.*

АННОТАЦИЯ

Проблемы формирования расплавленных зон и их последующей миграции по поверхности материала представляют интерес с точки зрения разработки новых технологических методов для формирования микроэлектронных структур, которые можно использовать в качестве основных рабочих элементов микролинз и отражателей, дисплеев, весов. Целью данной работы является экспериментальное изучение процессов электромиграции расплавленных включений на основе серебра и алюминия над поверхностями кристаллов полупроводника германия и алюминия. В рамках электрокапиллярного подхода рассматриваются вопросы образования и движения расплавленных капель над поверхностями полупроводниковых кристаллов кремния и германия. На примере систем Ge-Ag и Si-Al показано, что ускоренная миграция связана со вкладом электрокапиллярного компонента, который связывает силу поверхностного натяжения капель расплава с разностью электрических потенциалов на границе раздела. Эксперимент заключался в нанесении металлического зерна на поверхность образцов и вакуумировании камеры, в которой создавалось избыточное давление и температура поверхности. Была инициирована миграция включений мощными импульсами тока. Миграция расплавленных зон контролировалась с помощью оптической микроскопии. Был проведен анализ влияния постоянного тока на каплю расплава, осажденного на поверхности кристаллической матрицы. Анализ состава капель был выполнен с использованием метода AES, результаты которого показали взаимосвязь между концентрациями серебра и германия. Были даны количественные оценки для скоростей миграции в системах при постоянном токе, а также при импульсных токовых нагрузках. В ходе эксперимента было установлено, что энергия, необходимая для отделения капли от жесткой матрицы, не расходуется. Было оценено значение плотности поверхностного переноса заряда. Результаты работы могут быть использованы для разработки новых технологических приемов формирования микроэлектронных структур и их использования в практических целях.

Ключевые слова: *микроэлектронные структуры, электрокапиллярный эффект, электрическое поле.*

1. INTRODUCTION

The problems of molten zones formation and their subsequent migration over material surface are of interest from the viewpoint of both developing novel technological methods of forming microelectronic structures (Anson *et al*., 1999; Mills and Su, 2006; Siewiorek *et al.,* 2016; Lischner *et al.,* 2016; Liu *et al.,* 2017; Eisaabadi and Nouri, 2018) and application of such drops as primary working elements of microlenses and reflectors (Shi, 2008; Wang *et al.,* 2011; Zohrabi *et al.,* 2016; He *et al.,* 2019), displays, weighers (Zhongping *et al*., 1995; Kang and Shin, 2001; Evtukh *et al.,* 2003; Ahmadi *et al.,* 2011; Heikenfeld and Steckl, 2005; Chen *et al*., 2014). Strong heating and melting of metal tracks deposited on semiconductor or dielectric are under operation of microelectronic devices (Cisse Haba *et al.,* 2005; Orlov *et al*., 2004; Lischner *et al.,* 2016; Skvortsov *et al*., 2017). Such processes start to appear at the local rise of temperature produced by high current densities $j = 10^9$-10^{10} A/m^2. The developed electric transport processes lead to damage of the metallization layer structure and directed transport of the liquid substance formed both in the volume of semiconductor plate and over its surface. The melted zones formed on the surface coagulate into drops and are expelled by the current along the lines of force of the electric field.

That is why electric field is often considered as a controlling factor of inclusions geometry at directed motion of zones under electrocapillary effect (Ahmadi *et al.,* 2011; Ahmadi *et al.,* 2012; Ahmadi *et al*., 2013; Mishra *et al.,* 2016; Orlov and Makhmud-Akhunov, 2018; Xu *et al*., 2019). Indeed, when applying potential difference Δφ, the value of drop surface charge changes according to the Lippmann equation (Liu

Downloaded from www.periodico.tchequimica.com

et al., 2015; Ahmadi *et al.,* 2011; Mishra *et al.*, 2016; Feng *et al*., 2016; Orlov *et al.*, 2018) (Equation 1) where σ is surface tension of a molten drop, φ is electric potential and e_0^* is electric charge surface density. The aim of this work was experimental investigation of electromigration of molten silver- and aluminum-based inclusions over surfaces of germanium and silicon semiconductor crystals.

2. MATERIALS AND METHODS

Experimental investigation of surface migration processes was performed for the Ag-Ge system. The specimens were single crystalline *p*-Ge 4×4×15 mm^3 bars with resistivity of 30 Ω·cm. A metal grain with diameter *d* to 200 μm was put on the crystal surface, and the chamber was vacuumized to residual pressure of ~50 Pa. Then argon was filled into the chamber producing a small excess pressure. The Ge surface temperature was created by an external resistance heater and passing a direct electric current through the crystal. The experimental technique is stated in detail in (Skvortsov *et al*., 2018; Li *et al.,* 2019).

On reaching the eutectic temperature T_e, contact melting began accompanied by the appearance of a rainbow halo as a ring around the formed drop. The halo front extended for a distance (Equation 2) (where τ_p is time of front propagation). Appearance of a halo (observed in practically all experiments on surface migration) is related to fast surface diffusion of Ag and formation of the thinnest melt film at the single crystal surface. In all experiments, the melt drops moved toward the negative electrode and changed practically instantly the direction of their motion when changing the polarity of the external voltage source. In this case, only the direction of motion changed while the speed became constant. This ruled out considerable effect of temperature gradient along the specimen. Besides, no evident immersion of a drop into the matrix was observed at a surface mass transfer. This indicated an insignificant temperature difference in the radial direction that apparently was determined by the application of an external resistance heater.

An analysis of drop composition (mass transfer at T = 1123 K) was made by the AES method. The specimen was put into a high-vacuum (10^{-7} Pa) chamber of the Auger electron spectrometer 09 IOS 10-005. Surface cleaning was made for 5 min. with Ar ions (ion energy of 4 keV). The AES results showed that the ratio C_{Ag}/C_{Ge} between concentrations of silver (C_{Ag}) and germanium (C_{Ge}) in the area of crystallized inclusion was 0.47. The obtained ratio is somewhat low as compared with the data of the equilibrium phase diagram (C_{Ag}/C_{Ge} = 0.55). The observed difference is due to the process of inclusion crystallization that leads to changing the concentration ratio in favor of germanium.

3. RESULTS AND DISCUSSION:

The results of investigations showed that in all experiments melt drops of the Ag-Ge system moved toward the negative electrode and reversed the direction of their motion practically instantly at the reversal of polarity of the external voltage source. In this case, only the direction of motion changed while drops velocity remained constant. This excluded appreciable influence of temperature gradient along the specimen. In this case, much attention was paid to the creation of experimental conditions preventing drops dipping into a matrix. This was achieved by minimization of temperature difference in the radial direction due to the selection of modes of an external heater and current flow through the specimen (Figure 1).

In case of drop immersion into a matrix, the motion mechanisms will be limited by the melting-crystallization processes. This will lead to an essential reduction of drop migration velocity (Schiaffino and Sonin, 1997; Yan and Fan, 2001; Gamboa *et al*., 2002; Gamboa *et al*., 2011). Besides, at such surface mass transfer, a recrystallized track will remain behind a molten inclusion. This also indicates dissolution-crystallization processes at the front and back walls of the drop (Geguzin and Krivoglaz, 1971; Orlov and Skvortsov, 2007; Skvortsov *et al*., 2016a; Skvortsov *et al.,* 2016b; Kumar *et al*., 2017). The specific character of surface transfer with speed *w* is related to the occurrence of the electrocapillary effect. The essence of the supposed effect is laminar movement of liquid (in drop volume) under action of gradient of the electrostatic field according to Equation 1. In this case, *w* has to increase as inclusion size grows; which was observed in the experiment (Figure 2).

For the Al-Si system, migration of inclusions was initiated by high-power current pulses passing through thin metal films deposited on the silicon surface. A thermal shock promoted the formation of molten zones and their migration (Sobolev and Usherenko, 2006). This was controlled with methods of optical microscopy (as

in the Ag-Ge system). The technique of test structures formation and experimentation is given in detail in (van Soestbergen *et al*., 2010; Skvortsov *et al*., 2016c). The main experimental results are presented in Figure 2. The results of (Orlov *et al.,* 1989a; Orlov *et al.,* 1989b) were used for quantitative estimation of surface charge density in the systems considered. For them, an analysis was made of direct current impact on a melt drop put on the surface of a crystalline matrix. It was shown that one of the mechanisms of surface movement of a drop may be related to a version of electrocapillary motion (Equation 3) where η is melted dynamic viscosity; *E* is electric field strength in the inclusion.

Equation 4 is mechanical force; S_k is the area of drop contact with matrix; *d* is drop height; *a* is drop size in the contact region. The electric field strength *E* in the drop was estimated taking into account the effect of electric field perturbation by an inclusion (Equation 5). Equation 6 is the electric field strength in a matrix far from an inclusion; ρ_1 and ρ_2 are the resistivities of an inclusion and matrix, respectively. In these experiments $\theta = 0$, so Equation 7 has to be considered in Equation 3. Assuming that the drops are hemispherical (Equations 8, 9, 10), Equation 3 becomes Equation 11

It follows from the experimental data that the energy required to tear the drop back off the rigid matrix is not spent: $\Delta\sigma \rightarrow 0$. Thereby Equation 5 with regard to Equation 12 may be written as Equation 13. This gives linear dependence on ℓ. The obtained relation makes it possible to quantitatively estimate the value of surface density of charge transfer from the experimental data (Figure 3). The results of the calculation are presented in Table 1.

4. CONCLUSIONS:

Thereby the present work contains investigation of formation and migration of Ag- and Al-based molten zones. Carried out experiments consisted in passing a constant electric current through a crystal. Upon reaching the eutectic temperature, contact melting began, a rainbow halo in the form of a ring around the formed drop appeared, which was observed in almost all experiments on surface migration. Drops of the melt moved toward the negative electrode and changed their direction of motion when the polarity of the external voltage source changed, and when the direction changed, the speed remained constant. This phenomenon excluded a significant effect of the temperature gradient along the sample. It was also pointed out that the temperature difference in the radial direction is insignificant due to the absence of an obvious immersion of a drop in the matrix.

Migration of inclusions by powerful current pulses was initiated. An analysis of the effect of direct current on a melt drop deposited on the surface of a crystalline matrix established that one of the mechanisms of the surface motion of a drop can be associated with a variant of electrocapillary motion. During the experiment, it was found that the energy required to detach the droplet from the rigid matrix is not consumed. The value of the surface charge transfer density was also estimated. The numerical values of charge surface density for the Ag-Ge system (e_0*= 80…120 Q/m2) and Al-Si system (e_0*=776 Q/m2) in the considered temperature range were obtained from an analysis of experimental data. The quantitative evaluations of migration rates in the systems at direct current flow (to 20 m/s) and at impulse current loads (to 30-40 m/s) are given.

5. ACKNOWLEDGMENTS:

This work was carried out as part of the RFBR project No. 18-07-00564.

6. REFERENCES:

1. Ahmadi, A., Buat, M.D., Hoorfar, M. *Journal of Micromechanics and Microengineering*, **2013**, *23(4),* 045001.
2. Ahmadi, A., Devlin, K.D., Hoorfar, M. *Microfluidics and Nanofluidics*, **2012**, *12(1-4),* 295–305.
3. Ahmadi, A., Holzman, J.F., Najjaran, H., Hoorfar, M. *Microfluid Nanofluid*, **2011**, *10*, 1019–1032.
4. Anson, J.P., Drew, R.A.L., Gruzleski, J.E. *Metallurgical and Materials Transactions*, **1999**, *30B*, 1027–1032.
5. Chen, L.-C., Shiu, J.-W., Cheng, W.-Y., Lo, K.-L., Chang, R.-L. *21st International Display Workshops,* **2014**, *2*, 1162–1165.
6. Cisse Haba, T., Ablart, G., Camps, T., Olivie, F. *Chaos, Solitons and Fractals*, **2005**, *24(2)*, 479–490.
7. Eisaabadi, G., Nouri, A. *International Journal of Metalcasting,* **2018**, *12(2),* 292–297.
8. Evtukh, A., Hartnagel, H., Litovchenko, V.,

Yilmazoglu, O. *Materials Science and Engineering A,* **2003**, *353(1-2),* 27–35.

9. Feng, J., Liu, B., Tian, Y., Zhang, B. *17th International Conference on Electronic Packaging Technology*, China, **2016**, 348–351.
10. Gamboa, R.M., Brito, M.C., Serra, J.M., Alves, J.M., Vallera, A.M. *Solar Energy Materials & Solar Cells,* **2002**, *72*, 173–181.
11. Gamboa, R.M., Brito, M.C., Serra, J.M., Maia Alves, J., Vallêra, A.M. *Journal of Crystal Growth,* **2011**, *324(1),* 26–30.
12. Geguzin, Ya.E., Krivoglaz, M.A. *Motion of macroscopic inclusions in solid,.* Moscow: Metallurgiya, **1971**.
13. He, Z., Gou, F., Chen, R., Yin, K., Zhan, T., Wu, S.-T. *Crystals*, **2019**, *9(6),* 292.
14. Heikenfeld, J. Steckl, A.J. *Applied Physics Letters*, **2005**, *86(1),* 011105.
15. Kang, S.H., Shin, E. *Solid-State Electronics*, **2001**, *45(2),* 341–346.
16. Kumar, S., Kumar, P., Pratap, R. *Journal of Physics D: Applied Physics*, **2017**, *50(39)*, 39LT02.
17. Li, Y., Sun, S., Gao, Y., Yao, Y., Galstyan, E., Rudra, P., Rathi, M., Dutta, P., Pouladi, S., Ryoua, J.H., Selvamanickam, V. *Journal of Applied Crystallography,* **2019**, *52(4),* 898–902.
18. Lischner, D.J., Basseches, H., D'Altroy, F.A. *ECS Journal of Solid State Science and Technology*, **2016**, *132(12),* 2997–3001.
19. Liu, Q., Zou, R., Wu, J., Xu, K., Lu, A., Bando, Y., Golberg, D., Hu, J. *Nano Letters*, **2015**, *15(5),* 2809–2816.
20. Liu, X., Li, Y., He, Y. *Physical Metallurgy and Materials Science,* **2017***, 48(3),* 1264–1272.
21. Mills, K.C., Su, Y.C. *International Materials Reviews,* **2006**, *51(6),* 329–351.
22. Mishra, K., van den Ende, D., Mugele, F. *Micromachines*, **2016**, *7(6),* 102. doi: 10.3390/mi7060102.
23. Orlov, A.M., Belashchenko, D.K., Oborin, L.A. *Inorganic materials*, **1989a**, *25(2),* 851–854.
24. Orlov, A.M., Belashchenko, D.K., Shimansky, A.F., Oborin, L.A. *Inorganic materials*, **1989b**, *25(3),* 437–439.
25. Orlov, A.M., Makhmud-Akhunov, M.Y., Kuznetsova, K.V. *Technical Physics*, **2018**, *63(11),* 1576–1581.
26. Orlov, A.M., Skvortsov, A.A. *Inorganic Materials*, **2007**, *43(5),* 471–474.
27. Orlov, A.M., Skvortsov, A.A., Salanov, A.A. Semiconductors, 2004, 38(4), 376–379.
28. Schiaffino, S., Sonin, A.A. *Journal of Fluid Mechanics*, **1997**, *343*, 95–110.
29. Shi, F. *Journal of Shenyang Jianzhu University (Natural Science),* **2008**, *24(6),* 1014–1019.
30. Siewiorek, A., Sobczak, N., Sobczak, J., Kudyba, A., Kozera, R., Boczkowska, A. *Journal of Materials Engineering and Performance*, **2016**, *25(8),* 3348–3357.
31. Skvortsov, A.A., Khripach, N.A., Papkin, B.A., Pshonkin, D.E. *Microelectronics International*, **2018**, *35(4),* 197–202.
32. Skvortsov, A.A., Khripach, N.A., Zaletov, D.V., Pshonkin, D.E. *Research Journal of Pharmaceutical, Biological and Chemical Sciences,* **2016b**, *7(6),* 998–1003.
33. Skvortsov, A.A., Koryachko, M.V., Skvortsov, P.A. *International Conference on Actual Problems of Electron Devices Engineering*, Saratov, Russian Federation, **2016c**.
34. Skvortsov, A.A., Pshonkin, D.E., Luk'yanov, M.N., Rybakova, M.R. *Solid State Phenomena*, **2017**, *269*, 31–36.
35. Skvortsov, A.A., Zuev, S.M., Koryachko, M.V., Glinskiy, V.V. *Microelectronics International*, **2016a**, *33(2),* 102–106.
36. Sobolev, V.V., Usherenko, S.M. *Journal De Physique. IV:JP*, **2006**, *134*, 977–982.
37. van Soestbergen, M., Mavinkurve, A., Rongen, R.T.H., Jansen, K.M.B., Ernst, L.J., Zhang, G.Q. *Electrochimica Acta*, **2010**, *55(19)*, 5459–5469.
38. Wang, G.-W., Zheng, H.-X., Yao, S.-Y., Zhang, F.-S. *Materials Science Forum*, **2011**, *663-665*, 654–657.
39. Xu, X., Zhang, Y., Sun, L. *Indian Journal of Physics*, **2019**, *93(4),* 427–438.
40. Yan, M., Fan, Z. *Journal of Materials Science*, **2001**, *36*, 285–295.
41. Zhongping, H., Panao, Ch., Shudan, Zh., Yong, C., Baoping, W. *Proceedings of the IEEE International Vacuum Microelectronics Conference*, Portland, OR, USA, **1995**, 18–22.

Downloaded from www.periodico.tchequimica.com

42. Zohrabi, M., Cormack, R.H., Gopinath, J.T. *Optics Express*, **2016**, *24(21),* 23798–23809.

$$\frac{\partial\sigma}{\partial\varphi} = e_0^* \quad \text{(Eq. 1)}$$

$$x \approx \sqrt{\tau_p} \quad \text{(Eq. 2)}$$

$$w = \frac{d}{\eta}\left(e_0^* E + \frac{F_m}{S_k} - \frac{a\Delta\sigma}{S_k}\right) \quad \text{(Eq. 3)}$$

$$F_m = 2mg\sin\theta \quad \text{(Eq. 4)}$$

$$E = \frac{3\rho_1}{2\rho_1 + \rho_2} E_0 \quad \text{(Eq. 5)}$$

$$E_0 = jp_2 \quad \text{(Eq. 6)}$$

$$F_m / S_k = 0 \quad \text{(Eq. 7)}$$

$$d = r = \ell / 2 \quad \text{(Eq. 8)}$$

$$a = 2r \quad \text{(Eq. 9)}$$

$$S_k = \pi r^2 \quad \text{(Eq.10)}$$

$$w = \frac{1}{\eta}\left(e_0^* Er - \frac{2\Delta\sigma}{\pi}\right) \quad \text{(Eq. 11)}$$

$$\ell = 2r \quad \text{(Eq. 12)}$$

$$w = \frac{1}{\eta} e_0^* E \frac{\ell}{2} \quad \text{(Eq. 13)}$$

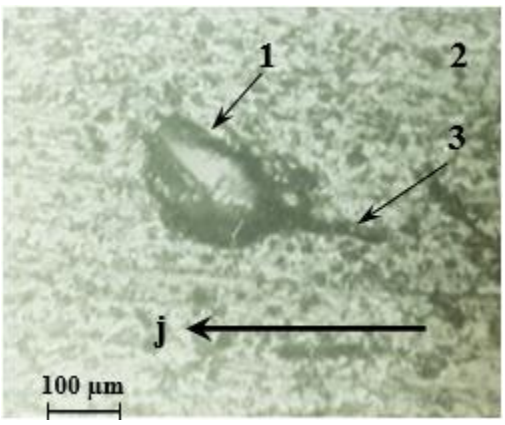

Figure 1. *A photograph of moving Ag-Ge melt drop over surface of Ge single crystal: 1 – moving drop; 2 –Ge surface; 3 – track (the arrow shows direction j of current density vector coinciding with the drop migration direction)*

Downloaded from www.periodico.tchequimica.com

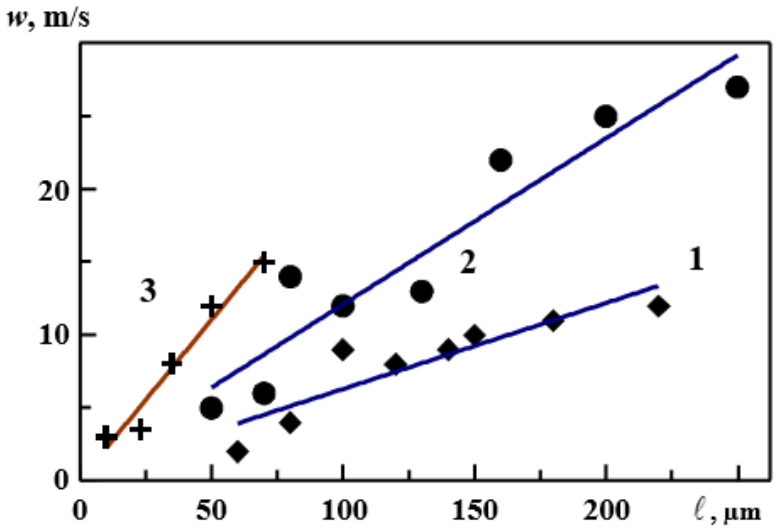

***Figure 2**. Dimensional dependence of surface migration velocities of melt drops: 1, 2 – silver-based over Ge surface at temperatures T = 973 K and 1043 K, respectively; 3 – aluminum-based over Si surface at T = 893 K*

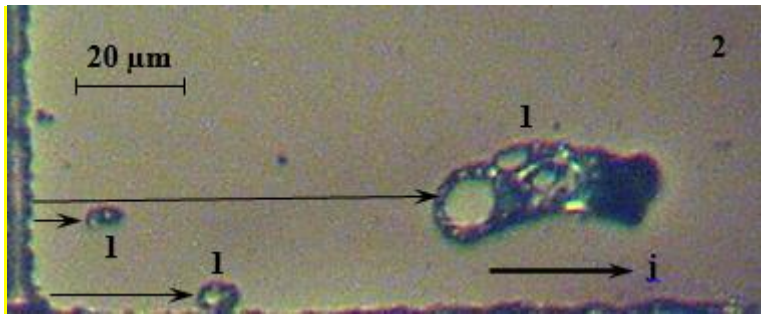

***Figure 3.** A photograph of electromigration processes at a silicon single crystal surface after current pulse (energy to 250 mJ, duration of 500 μs) passing through a sprayed aluminum film: 1 – migrating melt drops; 2 – silicon surface (the arrow shows direction j of current density vector coinciding with the direction of molten zones migration)*

***Table 1.** The values of calculated and experimental data on Ag- and Al-based inclusions migration over silicon and germanium surfaces*

№	Parameter	Dimensionality	Temperature, K		
			1043	**973**	**893**
1	System	-	Ag-Ge	Ag-Ge	Al-Si
2	$\Delta w l \Delta \ell$, 10^6	1/s	0.11	0.06	0.22
3	η, 10^{-3}	Pa·s	1.5	1.9	3.0
4	E	V/m	3.0	2.7	1.7
5	e_0^*	Q/m^2	110	84.4	776

Downloaded from www.periodico.tchequimica.com

PERIÓDICO TCHÊ QUÍMICA
ARTIGO DE REVISÃO

POTENCIAL DE USO DA GOMA DA MANGA (*MANGIFERA INDICA*) EM SISTEMAS FARMACOLÓGICOS

POTENTIAL USE OF MANGO GUM (*MANGIFERA INDICA*) IN PHARMACOLOGICAL SYSTEMS

SILVEIRA, M. C. A.[1*]; GLÓRIA, R. S. L.[2]; BARBOSA, K. M.[3]; SANTOS, L. S. S.[1]

[1] Universidade Federal do Tocantins, Programa de Pós Graduação em Biotecnologia

[2] Universidade Federal do Tocantins, Curso de Engenharia de Bioprocessos e Biotecnologia

[3] Universidade Federal do Tocantins, Programa de Pós Graduação em Química

**Mauren Cristine Agustini da Silveira*
e-mail: maurencriz@uft.edu.br

Received 10 July 2019; received in revised form 30 September 2019; accepted 31 October 2019

RESUMO

A possibilidade do uso de polímeros naturais ou modificados para formulação de nanocápsulas contendo fármacos é uma opção farmacêutica para casos em que é necessário o aumento de meia vida de medicações no organismo e diminuição dos efeitos colaterais, podendo serem usados também para melhor direcionamento farmacológico ao sítio alvo, relacionados a baixo custo de produção com estas características e disponibilidade renovável. Gomas e mucilagens têm sido estudadas para uso em sistemas anternativos naturais de administração de medicamentos. A goma proveniente do tronco da *Mangifera indica* tem poucos estudos direcionados a este propósito, apesar de ter apresentado resultados promissores em trabalhos anteriores. Caracterização das vias de formação da goma são explanadas, assim como sua extração e purificação. Foi confirmada a semelhança das propriedades da goma Acácia amplamente utilizada em blendas de comprimidos. A goma de M. indica também foi utilizada para liberação acelerada de fármacos. A versatilidade desta goma associa-se com a presença de mucilagem. Modificações químicas da goma M. indica e misturas entre outras gomas podem ser realizadas para adaptar suas propriedades às diversas formas de liberação controlada de fármacos. Vários compostos isolados com propriedades farmacêuticas são demonstrados. Características físico químicas de vários artigos sobre esta goma foram compilados. As técnicas já utilizadas para a formação de nanocápsulas através da goma de M. indica estão apresentadas. São relatadas várias pesquisas utilizando especificamente a goma de M. indica provinda do tronco da mangueira utilizada como liberação de fármacos . Estes estudos justificam um resumo das propriedades farmacêuticas para entrega de fármacos já realizados com esta goma. Estudos complementares para aproveitamento e valorização do cultivo da mangueira são sugeridos.

Palavras-chave: *Mangifera indica*, goma, polissacarídeos, nanocarreador, liberação controlada

ABSTRACT

The possibility of using natural or modified polymers to formulate drug-containing nanocapsules is a pharmaceutical option for cases in which an increase in the half-life of medications in the body and a decrease in side effects is required, and may also be used for better pharmacological targeting of the site. Related to low production costs with these characteristics and renewable availability. Gums and mucilages have been studied for use in natural alternative drug delivery systems. The gum from the trunk of *Mangifera indica* has few studies aimed at this purpose, although it has shown promising results in previous studies. Characterization of the gum formation pathways are explained, as well as their extraction and purification. The similarity of properties of Acacia gum widely used in tablet blends has been confirmed. *Mangifera indica* gum was also used for accelerated drug release. The versatility of this gum is associated with the presence of mucilage. Chemical modifications of the *Mangifera indica* gum and mixtures among other gums may be made to adapt their properties to the various forms of controlled drug release. Several isolated compounds with pharmaceutical properties are demonstrated. Physical chemical characteristics of several articles on this gum have been compiled. The techniques already used for the formation of nanocapsules through *Mangifera indica* gum are presented. Several studies have been reported specifically using *Mangifera indica* gum from the Mango trunk used as drug release. These studies justify a summary of the pharmaceutical properties for drug delivery

Downloaded from www.periodico.tchequimica.com

already performed with this gum. Complementary studies for utilization and valorization of Mango cultivation are suggested.

Key-words: *Mangifera indica, gum, polysaccharide, nanocarrier, controlled release*

1. INTRODUCTION

Plant gum and mucilage have been studied as an alternative to obtain natural polymers to reduce side effects and improve drug distribution to the target site, in addition to the therapeutic properties of polysaccharides present in species that can be absorbed by the body (KULKARNI *et al*., 2011). When a polymer is great studied, and a lot of data is produced, it becomes easier for it to be approved by regulatory authorities (NGWULUKA; OCHEKPE; ARUOMA, 2014). Polymers can be found in microorganism, algal, and plant metabolism products in the form of parts of cotyledons, mucilage or gum (ROCHA, G. M.; CÉSAR, P.; SOUZA, A., 2017; RAJESWARI; GOKA, 2017; RODRIGUES; PAULA; COSTA, 1993; SHARMA *et al*., 2016).

Vegetable gums are composed of heteropolysaccharides, generally (PINHEIRO A.C. *et al*., 2010). A still little explored gum comes from the stem of *M. indica*, a plant typical of tropical countries whose fruit is Mango (BIRDWOOD, 1862). Gums dissolve in water through the formation of hydrogen bridges. In solution, polymer molecules can be organized into an orderly structure called the micelle, which is stabilized by hydrogen bonds. The micelle immobilizes the water, and as the intermolecular association extends, the viscosity is increased, or there is conversion to a gel that has liquid-solid-like characteristics or viscoelasticity (HAMDANI; WANI; BHAT, 2019; TORCHILIN, 2006). Most gums reduce the surface tension of water (FACCIO, 2015).

Mucilage is usually produced in seed-coat cells, in leaves, in the bark, in the middle lamella, and some roots. They are part of a physiological process of the plant (KHAN; PARVEZ; SHARMA, 2015; U. RAGHU *et al*., 2019). Mucilage is a hydrocolloid that does not dissolve in water because it is partially hydrophilic, little branches (SARKAR *et al*., 2018). As a result, in contact with water forms gels and viscous substances. They are formed by more linear polymers and gums by branched polymers (HIRST; JONES, 1958; KHAN; PARVEZ; SHARMA, 2015). Both gum and mucilage are involved in the composition of hemicelluloses. These consist of sugars such as glucoses, mannose, and xylose, while those produced by gum and mucilage are galactose and arabinose (PRAJAPATI *et al*., 2013).

Mucilage is formed by neutral sugars of L-arabinose, D-galactose, L-rhamnose, and D-xylose and may even contain galacturonic acid. Pectin is an acidic polysaccharide and the main component of mucilage (PILETTI, 2011).

The gums are the result of the pathological reaction of the plant in response to microorganism attacks, water stress, or pre-healing of cuts (ASPINALL, 1970; JOEL; FAHN, 1980). *M. indica* produces both as resinous gum and mucilage. Up to now, the studies carried out have characteristics compatible as much drug delivery formulations as high solubility and delayed distribution time (CHOUDHARY; PAWAR, 2014).

Studies have reported that mango gum has antiviral (SILVA; DUARTE; VIEIRA FILHO, 2014), anthelmintic (MARIMUTHU, 2001; MUTHUKUMARAN, 2017), and antibacterial properties (BAYONA, 2016; SHARMA *et al*., 2016). This property is due to the presence of alkyl groups of the aromatic compound. The more halogenated, the greater the antimicrobial power and position substituents enhance the effect (GONZAGA, 2008). It has also been suggested that lipophilia affects this property (SILVA *et al*., 2010). They can be used in binders with Arabica-like gum effectiveness (MOGOŞANU; GRUMEZESCU, 2015), diluents (NAYAK *et al*., 2011), tablet disintegrants (HEMALATHA; SRIKANTH; SAI, 2017), suspended colloidal protectors, gel gelling agents, oral liquid thickeners, suppository, and nanoparticles (DUFRESNE; LIN, 2015; GHAYEMPOUR *et al*., 2015; HAMDANI; WANI; BHAT, 2019; OGAJI *et al*., 2012; THAKUR; THAKUR, 2015).

2. CHEMICAL COMPOSITION OF GUM AND MUCILAGE

To identify the polymer, one must determine its structure. Its properties depend on its chemical composition and chain conformation (NGWULUKA; OCHEKPE; ARUOMA, 2014). A comprehension of the morphology, size, and surface chemistry of natural polymers is essential

Downloaded from www.periodico.tchequimica.com

to define their properties and possible uses for pharmaceutical purposes (KUMAR DHAKA *et al*., 2017; KUMAR *et al*., 2010).

In the case of gums, this determination is complex, as there are several chains of different intertwined properties, on the other hand, there is a range of techniques to feature and to identify these chains (BHATIA, 2016; SELLÉS *et al*., 2002; VINOD *et al*., 2008; YANG; ZHANG, 2009). Natural polymers are generally amorphous or semicrystalline (GONZÁLEZ-MARTÍNEZ *et al*., 2017; OLAYEMI; SALIHU; ALLAGH, 2013). They have a higher solubility than highly crystalline polymers (PATHAK *et al*., 2014).

Gum and mucilage have an undefined number of monosaccharides in hydrolysis. These may be pentoses if derived from xylan, or hexoses if derived from starch and cellulose. Gum-forming polysaccharides have pyranosidic (hexagonal) rings and furanosidic (pentagonal) rings, with different types of glycosidic bonds and several forms of D and L enantiomers. Sucrose, for example, is a non-reducing sugar composed of a pyranosidic ring with a furasidic ring attached by carbons 1 and 2 (HIRST; JONES, 1958). Gum has its composition significant amounts of calcium, potassium and magnesium salts present in uronic acids (HIRST; JONES, 1958). The mucilage is made up of ester groups of sulfuric acid (ASPINALL, 1970). Both gum and mucilage have galactose and arabinose. The resins have terpenes (GIGANTE, 2005) and do not dissolve in water, becoming glassy in contact with air after their viscous formation in the stem. These data may direct the isolation and characterization of the main gum compounds (CHOUDHARY; PAWAR, 2014; KULKARNI *et al*., 2011; RAVINDRAKULLAI REDDY; MANJUNATH, 2013; SHARMA *et al*., 2016). Most gums dissolve in water and are, therefore, hydrophilic. This feature allows the binding with active principles of also hydrophilic drugs (LACCHIA; GUERREIRO, 2009; LÓPEZ-COBO *et al*., 2017). So, for the introduction and release of these drugs in the body, depending on the target site, there must be an affinity for lipophilic substances. Because such adaptations are necessary, the structure of certain polymers is modified. Modification of a polymer may alter its degree of crystallinity (SANTOS *et al*., 2016). Figure 1 shows the metabolism pathways of mucilage, gum, and resin formation.

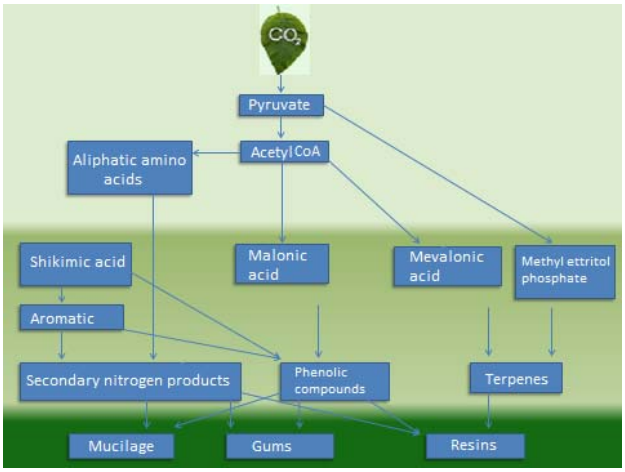

Figure 1: *Pathways of exudates plant metabolism*

All in all, gum and mucilage differ to branches their chains, ability to gel and form solution-insoluble masses, and presence of terpenes. Table 1 brief the differences between gum, mucilage, and resin.

Table 1: *Main characteristics of gum, mucilage, resins, and latex. (Adapted from LANGENHEIN, 2003)*

	Primary components	**Solubility**	**Secretor tissue**
Gums	Polysaccharides	Water soluble	Cavities
Mucilage	Polysaccharides	Water soluble	Epidermal cells, trichomes, ducts cavities
Resin	Terpenoids, phenolic compounds	Liposoluble	Canals, Blisters, Cavities, Trichomes, Epidermal cells
Latex	Terpenoids, phenolic compounds, carbohydrates	Liposoluble	Laticifers

3. MIXTURES AND CHEMICAL MODIFICATION

Modification methods include grafting, crosslinking, derivative formation, and polymer mixing, changing their physicochemical properties. However, this modification should not alter biological properties (NGWULUKA; OCHEKPE; ARUOMA, 2014).

The polymer-polymer mix is easier and more convenient, as chemical reactions are not necessary for the synthesis of new polymers (NOKHODCHI *et al*., 2015; RIBEIRO *et al*., 2017). Bonding occurs by Van der Waals forces,

Downloaded from www.periodico.tchequimica.com

hydrogen bonds, dispersion forces, covalent bonding (crosslinking), or ionic bonding. Grafting involves covalent adhesion of monomers in the polymer chain. SAH (2016) defines polymerization as “Curing” in which there is the polymerization of oligomers to form structures that adhere to the substrate by physical forces.

There is polymer mixture to increase retention and retard drug release, for example, alginate and carob gum in the manufacture of microspheres and mixtures of natural and synthetic gums such as carboxymethylcellulose with carob gum and methacrylate for hydrogel production (KHAN; PARVEZ; SHARMA, 2015). Another example is the addition of Guar gum and Xanthan gum on *M. indica* seed polymer to improve both gums, or alone to grow the viscosity of the *M. indica* seed gum (NAWAB *et al*., 2016).

Methods of modification by chemical reactions may increase solubility through carboxymethylation, carbamoylation, or cyanoethylation. Otherwise, they can increase solvent affinity through acetylation or deacetylation (LIMA *et al*., 2018), incorporate drugs through phosphorylation (SANTOS *et al*., 2016), produce analogs, depolymerize, add properties antivirals, anticoagulants through sulfation (MARQUES *et al*., 2017), and add sensitivity to radiation through esterification for diagnostic detection (SANTOS *et al*., 2016; NGWULUKA; OCHEKPE; ARUOMA, 2014; PATHAK *et al*., 2014). These are methods that modify viscosity and alter absorption (ROCHA, G.; CÉSAR, P.; SOUZA A., 2017; SIERAKOWSKI, 1988). Natural polymers such as cashew gum, locust bean gum, starch, hemicellulose, xylan, guar gum was carboxymethylated (FEDELI *et al*., 2015; MONTEIRO *et al*., 2015), Guar gum and *Cassia tora* gum were carbamoylated (SARKAR *et al*., 2018), Tamarind seed gum and *C. tora* were cyanoethylated (NGWULUKA; OCHEKPE; ARUOMA, 2014).

It is possible to modify a gum to alter adhesive and mucilaginous properties while maintaining the hydrophilic capacity with a viscosity at low concentrations. Separating the mucilaginous part would lead to the loss of the possibility of alteration (PRAJAPATI *et al*., 2013). Hydrocolloids are used for rheological and sensory modifications in foods in order to change their texture and physical stability (ROCHA, 2017). Plasticizers added to the galactomannan/starch blend alter the hydration of the formed films (SOARES, 2009). Okra mucilage was modified by acrylamide graft for the development of polymeric materials in wastewater treatment (MISHRA; CLARK; PAL, 2008). Modification of Hibiscus mucilage for a suspending agent (EDWIN J, EDWIN S, DOSI S, RAJ A, 2007). Increased adhesive capacity of *Manilkara zapota* seed (SUDARSHAN; SUNIL B, 2015).

4. CHARACTERIZATION METHODS

As gum can come mixed with mucilages and resins, there are techniques for characterizing these mixtures (LEAL, 2014). Chemically most gum is recognized to contain hydroxyl (OH-), ether (COC), acetyl (CH3CO-), carboxyl (-COO-), aliphatic groups, and carbonyl (-C = O) groups (PADIL *et al*., 2018).

Some simple tests can be performed to assess the presence of other substances in the gum. Nadi reagent indicates the presence of blue-colored terpenes. Lipophilic substances become colorless in a mix of chloroform and ethanol. The test with tannic acid and iron (III) chloride detects the presence of mucilage, as long as it is rich in proteins. Schiff's reagent (PAS) for neutral polysaccharides (RODRIGUES, 2007). Molish's test confirms the presence of carbohydrate with a violet color present using 100 mg of dry gum or mucilage powder added to Molisch's reagent and sulfuric acid solution (SANT '*et al*., 2006). The Ruthenium test detects pectin, and plant mucilage with the presence of pink in a simple mixture of the reagent with the mucilaginous gum observed under the microscope. Most mucilages are derived from uronic acids (galacturonic and glucuronic). The 0.2 N iodine test with 10 mg gum becomes colorless if there are polysaccharides in the gum and the enzyme assay with 0.5 ml benzidine in alcohol with a gum solution in 20 ml water detects enzyme in the presence of a blue color (RAVINDRAKULLAI REDDY; MANJUNATH, 2013).

The term resin is used to define gums using the indication that resins have terpenes (FIGUEIREDO *et al*., 2007).

Techniques may be used to determine the structure, chain conformation, sugar identification, molecular weight, degree of polydispersity and crystallinity. These characteristics influence properties such as solubility, stability, and drug release (ALBUQUERQUE, 2017; ROCHA, G.; CÉSAR P.; SOUZA A., 2017; MARQUES *et al*., 2017; SANTOS *et al*., 2016). X-ray diffraction is the

Downloaded from www.periodico.tchequimica.com

main technique used to determine the degree of crystallinity of a polymer. The presence and position of the characteristic peaks in the diffractogram indicate the degree of crystallinity and the type of crystalline structure obtained. The adsence characteristic peaks in the spectrum are indicative of the complete amorphous nature of the polymer (GHALANDARI *et al*., 2014; LIU *et al*., 2007).

Structural characterizations are performed with Fourier transform infrared spectroscopy (FTIR), liquid nuclear magnetic resonance (NMR) (one and two dimensions), solid-state NMR, Raman spectroscopy, gas chromatography (GC), mass spectroscopy GC (MS), and high-performance liquid chromatography (NDINGA; JM, 2015). Techniques such as gel electrophoresis, differential scanning calorimetry, wide-angle X-ray diffraction, and X-ray diffraction are used for polymorphism determination (WANG *et al*., 2015).

Molecular weights and polydispersity of gum and mucilage can be determined by size exclusion by chromatography (SEC), gas chromatography (GC), and viscometry/rheometry (YANG; ZHANG, 2009). Viscosity can be used to estimate molecular weight as it is a direct reflection of molecular weight. Waters® is promoting a chromatographic technique called Advanced Polymer Chromatography System (APC™) that offers a better resolution for molecular weight determination, but only for low molecular weight samples (NGWULUKA; OCHEKPE; ARUOMA, 2014). Polysaccharides of different molecular weights and sizes may be separated using precipitants such as ethanol, methanol, and acetone, or by performing gel chromatography. Sephadex, Sephacryl, and Sepherose are mostly used gels. Polysaccharides may be acidic or basic and can be separated with cetyltrimethylammonium bromide (CTAB) or cetylpyridinium chloride (CPC), which may form a complex precipitate with the acid polysaccharide. They can also be separated by ion-exchange cellulose chromatography, for example, DEAE-Cellulose column, DEAE-Sepharose column (WANG *et al*., 2015). The combination of techniques provides more accurate data such as chemical and morphological structures on a molecular scale (NGWULUKA; OCHEKPE; ARUOMA, 2014). Any modification on the polymer surface influences the degree of encapsulation and drug release, as well as the interaction with cells (YANG; ZHANG, 2009).

Thermal analyses such as differential exploratory calorimetry (DSC) elucidate physical and chemical changes during thermal processes (EMEJE *et al*., 2009; HOMBREIRO PEREZ *et al*., 2000; SANTOS *et al*., 2016). By exposing a polymer to a temperature range, it is possible to identify glass transition temperatures, crystallization, melting and decomposition (EMEJE *et al*., 2009; MOHAN, 2017; PATHAK *et al*., 2014). Materials behave differently below and above their glass transition temperatures (LIN; DUFRESNE, 2015). The mechanical properties of a polymer depend on the glass transition temperature, and it depends on the molecular weight (FATHI; MOHEBBI; KOOCHEKI, 2016; SANTOS *et al*., 2016; YANG; ZHANG, 2009). Other less commonly used thermal techniques are dynamic mechanical thermal analysis (DMTA), thermally simulated current spectroscopy (TSC), and dilatometry (DIL) (NGWULUKA; OCHEKPE; ARUOMA, 2014).

Rheological behavioral analyses such as the viscoelastic behavior of a polymer also depend on molecular weight, directly influencing the later ability of the polymer formed either in tablets, scaffolds, micro, or nanocapsules to release the drug (MOHAN, 2017; THAKUR; THAKUR, 2015; TORCHILIN, 2006). The influence is around hardness, compression, suspendability, zeta potential capacity, flow shear effects, frequency and temperature effects on polymers, ability to behave like gel, paste, viscous liquid, depending on the chosen polymer use and measured through a rheometer (NGWULUKA; OCHEKPE; ARUOMA, 2014). Intrinsic viscosity decreases with increasing ionic strengths of the solution (VASQUEZ *et al*., 2015).

The ability of the polymer to gel depends on the ionic strength, pH, and temperature (RIBEIRO *et al*., 2016; WU *et al*., 2009). Polysaccharide gums may exhibit neutral charge, negative charge, or positive charge according to the presence of various chemical groups attached to individual monosaccharide units (FISZMAN; VARELA, 2013).

The forming of the polymers is up to on the polysaccharides. They may exhibit some conformations in solutions, such as coils, semi-flexible currents, stiff currents, and helical currents, including single, double, and triple-helical chains and describe the flexibility of polymeric chains in solutions (YANG; ZHANG, 2009). An example is the conformational change of Gellan gum in the face of temperature changes. Its polysaccharide has a repeat unit helix shapes, 1,3-b-D-glucose, 1,4-b-D-glucuronic acid, 1,4-b-D-glucose and 1,4-a-L-rhamnose. The

Downloaded from www.periodico.tchequimica.com

ellipticity at 202 ηm decreases with cooling and increases with heating (YANG; ZHANG, 2009).

In vivo testing of toxicological and histopathological reactions is required for safe drug use (PATHAK *et al*., 2014). It is a primary part of drug research. The classification of the tests depends to on the purpose of the drug administration route. The need for sterility of the drug produced, for example, intravenously, is not the same for oral use (JAKKI *et al*., 2016; KROKIDA, 2017; MORA-HUERTAS; FESSI; ELAISSARI, 2010; MUSYANOVYCH; LANDFESTER, 2014; Ribeiro *et al*., 2017). Characteristics for the polymer-drug conjugate to be practical is that the polymeric carrier is non-toxic and non-immunogenic, MW high enough to ensure long circulation times, but <40 kDa for non-biodegradable polymers to ensure renal elimination upon release of the drug adequate loading capacity, potency of the conjugate throughout transport, but easily cleaved upon arrival at the target and the ability to reach intended tissue by active as well as passive means (LIECHTY *et al*., 2010).

5. PHARMACEUTICAL USE OF GUM OF *M. INDICA*

The *M. indica* gum, Anacardeaceae family, has amorphous and semicrystalline parts and has shown both hydrophilicity and hydrophobicity when diluted in both water and alcohol and precipitates the polymers (AHMED; ABBAS, 2018; GARG *et al*., 2018; NAYAK *et al*., 2011, 2012; SHINGALA *et al*., 2010). Only the work by Singh *et al*., 2010, reported the initial alcohol extraction to form diclofenac sodium delayed-release tablets.

Mango gum has been sold by Indians to heal cracked feet (ANJANEYULU; RADHIKA, 2000). It was used by Filipinos to cure parasitic skin disease, Syphilis, and Herpes (NUSSINOVITCH, 2009).

M. indica gum polymer has rare data obtained though promising for drug delivery because of its lower toxicity, higher biodegradability, responsiveness, and adaptability to nanotechnology (ALAM; PARVEZ; SHARMA, 2014; CHANDRAJITH; MARAPANA, 2018; MARIMUTHU JAYAKUMAR, 2001; RAI *et al*., 2007). *M. indica* gum has already been used for metformin immediate release tablets (HEMALATHA; SRIKANTH; SAI, 2017).

In 1965 it was isolated from the gum, a cyclotriterpenoid that is a viral cycle blocker (SILVA; DUARTE; VIEIRA FILHO, 2014), which became known as mangiferolic acid (CORSANO; MINCIONE, 1965).

In turn, the work of Vinod *et al*. (2013) reported the gum to be slightly soluble in water, forming a thick gel, practically insoluble in alcohol, chloroform, and acetone.

6. PHYTOLOGY IN GUM PRODUCTION OF *M. INDICA*

Gum is produced in response to infection or healing by tissue injury. (MENESTRINA *et al*., 1998). They are formed in ducts within which there are pseudo vacuoles that produce and store proteins. (BHOSALE; OSMANI; MOIN, 2014; SHARMA *et al*., 2016) Polysaccharides are transported to the vacuoles by Golgi vesicles. Proteins form spherical or crystalline structures. Polypeptides tend to form hexamers because the vacuolar pH value is low (SCHNIZL, 2001).

Gum formation was studied by MARIMUTHU *et al*. In his conclusion he showed that there is a large increase in ATP molecules, the concentration of mitochondria near the exudate ducts, higher carbohydrate concentration in the months March to May, when gum and resin exudates are produced (MARIMUTHU, 2001).

Carbohydrates are lysed into monomers by the large concentrated enzymatic activity at the site. The secreted lipids are oxidized and form aromatic resins. There is increased lipase activity at the sites near the ducts. With the action of ATP on mevalonic acid, there is the incorporation of acetate to isoprenes, terpenes, and fatty acids. The amount of resin was verified about increased cytoplasm peroxidase activity, cell nucleus position, and lipid location (JOEL, 1980; JOEL; FAHN, 1980).

7. EXTRACTION AND PURIFICATION

The extraction of *M. indica* gum is done by slashing the trunk of the tree during the rainless months. Gum production can be enhanced by the use of Etefon, a plant stimulator (LIMA *et al*., 2001). Gum can be produced near mucilage, which makes separation difficult and can be detected by chemical tests using red Ruthenium that detects mucilage if it is red (CHOUDHARY; PAWAR, 2014; HEMALATHA; SRIKANTH; SAI, 2017 ; NAYAK *et al*., 2012; PATHAK *et al*., 2014; PRADO; DEMARCO, 2018; WET; ROBBERTSE; COETZEE, 2016). This mucilage is pinkish-yellow, unlike the white matter that comes out of

Downloaded from www.periodico.tchequimica.com

the fruit stalk. This white substance is called latex and has 5- [2 (Z) -heptadecenyl] resorcinol, skin irritant (BANDYOPADHYAY; GHOLAP; MAMDAPUR, 1985).

Some authors found the gum to be whitish (NAYAK *et al*., 2012), other browns (AHMED; ABBAS, 2018), and others are yellowish. The consistency also varies, being viscous or more hardened (ALAM; PARVEZ; SHARMA,2014;CHANDRAJITH;MARAPANA,2018; HEMALATHA; SRIKANTH; SAI, 2017; NAYAK *et al*., 2011; NDINGA; JM, 2015; SARKAR *et al*., 2018).

The form of gum purification also has slight variations. Most dry the gum first, then grind it and use continuous extraction with water. Others pass through sieve no. 80 before diluting with water (AHMED; ABBAS, 2018; RODRIGUES; PAULA; COSTA, 1993). But alcohol extraction has also been done (SHINGALA *et al*., 2010). Right after dilution, partial or not, most add twice the amount of acetone to the solution formed (GHAYEMPOUR; MONTAZER; MAHMOUDI RAD, 2015; HEMALATHA; SRIKANTH; SAI, 2017; LIMA *et al*., 2018; MARIMUTHU; JAYAKUMAR, 2001; RIBEIRO *et al*., 2016; VASANTRAO PATIL *et al*., 2014). After precipitation, the precipitate is centrifuged to recover the precipitate and dried at 50 ° C (JAKKI *et al*., 2016; VINOD R, [s.d]). Some prefer to dry the solution without centrifugation and still others dry before acetone is added (KUMAR AYAK; SWAMY, 2011).

Figure 2 was obtained from the work of Kahanzada *et al*. (2004), and collaborators from Pakistan. Shows gummy mango in response to the attack of *Botryodiplodia theobromae* fungi purposely inoculated for study.

8. *MANGIFERA INDICA* GUM ISOLATED COMPOUNDS

Volatile terpene compounds, mostly unoxygenated sesquiterpenes such as beta-elemene (6.7%), beta-caryophyllene (9.8%) (Figure 2-A), alpha-humolene (3.4%), beta-chamigrene (4.5%), and alpha (31.9%) and beta-selinene (31.3%) (Figure 2-B) were found in samples of M. Indica resin gums by Kovats retention index and by solid-phase microextraction (NDINGA; JM, 2015). Also found were amylose, α-arabinofuranosyl, β-galactopyranosyl (Figure 2-C) (PATHAK *et al*., 2014). Viradabine (Figure 2-D) is an anti-viral, anti-herpetic drug whose active ingredient is arabinofuranosil.

As much in leaf as fruit and gum were found: β-pinene, α-felandrene, 3-carene, β-elemene, α-gurjunene, β-caryophyllene, α-humulene, α-selinene, β-selinene, and caryophyllene oxide. Elemene has apoptosis antiproliferative activity, and beta caryophyllene has antibacterial activity (ANJANEYULU; RADHIKA, 2000; CHANDRAJITH; MARAPANA, 2018). Elemene and selinene contribute to the floral and hibernal aroma, respectively (NDINGA; J-M, 2015). As their compositions are low in exudates, they do not have odorous characteristics but are in greater proportion in leaves and fruits (NDINGA; J-M, 2015).

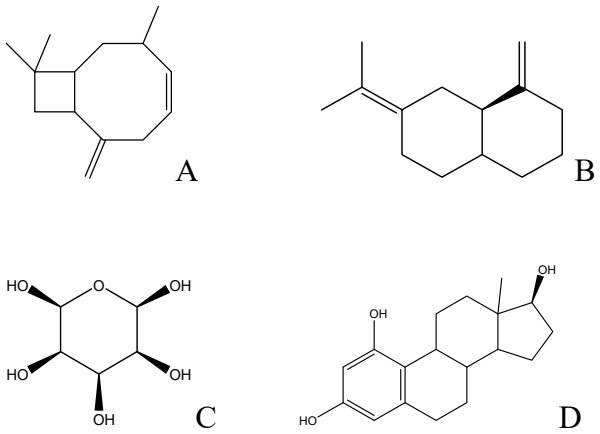

Figure 2: *Some compounds isolated from Mangifera indica gum.*

CORSANO and MINCIONE (1965), isolated from the acidic part of *Mangifera* gum, indicates a compound they named manguiferolic acid (Figure 3), which was the first example of triterpenic acid with a cyclopropane ring.

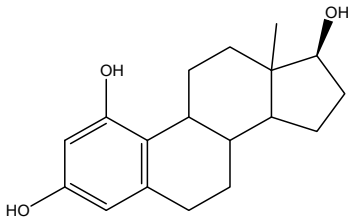

Figure 3: *Manguiferolic acid chemical structure*

In 1968 the same authors isolated ambonic acid from the same acidic part of the resin (Figure 4) (CORSANO; MINCIONE, 1968).

Downloaded from www.periodico.tchequimica.com

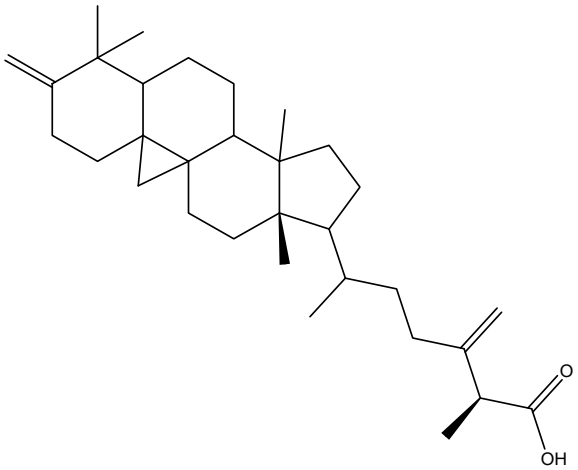

Figure 4: *Ambonic acid chemical structure*

In 1980 Joel and Fahn isolated tannic acid (Figure 5) from Mango gum (LIN; DUFRESNE, 2015). The property of acid is to be a binder used as a collagen cross-linkage agent in orthodontic restorations (OLIVEIRA *et al*., 2017).

In the work of Elouma *et al*. (2015), there is a difference between the gum samples obtained from the several plants about the percentage of the main elements. The samples were obtained from trees from the same region and at the same time. The analyzes were repeated two years after the first one, and the variance did not change. Therefore, the difference of the proportion of the elements between the samples is not due to the volatility of the compounds. According to the author, it may be due to a chemical transformation of some components of gum exudates under thermodynamically specific conditions. And β-elemene presents up to 64% has an anti-proliferative effect on cancer cells (PURI; SHARMA; NAGPAL, 2016). There are also reports of nonvolatile compounds ethers, aldehydes, ketone acids, lactones and phenols (NDINGA; J-M, 2015).

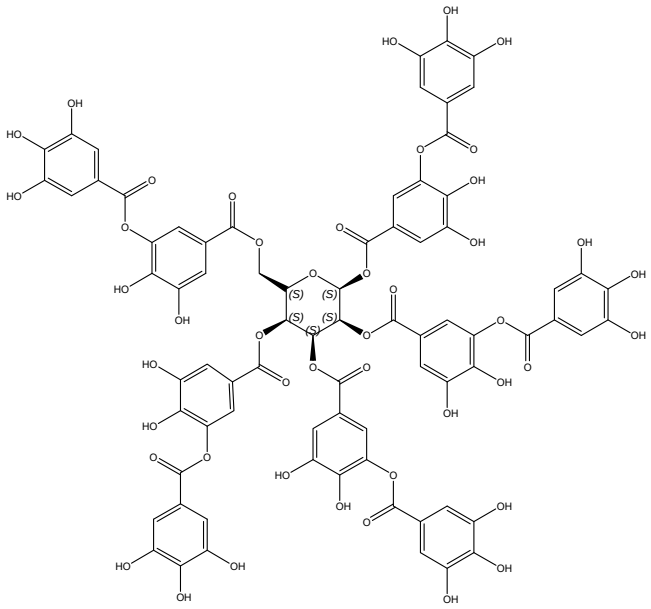

Figure 5: *Tannic acid chemical structure*

Manguiferin (Figure 6) was isolated from the bark of the *M. indica* tree. Being the active ingredient of VIMANG®, it promises to avoid oncogenesis (TREVISAN *et al*., 2008). A study conducted with Cuban and Brazilian cultivars revealed data confirming the presence of high proportion of manguiferin in the bark of the trees (71.40 g / kg of dry material), with no benzoic acid in Brazilian cultivars, which encourages the research of xanthan derivatives to from Manga by-products (SELLÉS *et al*., 2002).

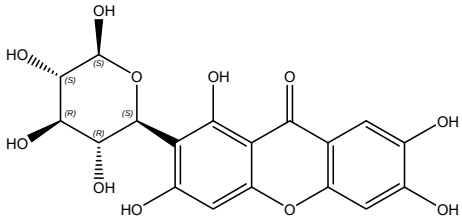

Figure 6: *Manguiferin*

9. PHYSICAL-CHEMICAL CHARACTERISTICS OF *MANGIFERA INDICA* GUM

Alkali metal salts of linear polysaccharides are highly ionized in water, and the distribution of the ionic charge throughout the molecule tends to keep it in an extended form because of Coulomb repulsion. This repulsion between carboxylate anions repels polysaccharide molecules and promotes a high degree of solution stability (ASPINALL, 1970; BASKAR, 2013; BHOSALE; OSMANI; MOIN, 2014). Extended independent polysaccharide chains produce highly viscous solutions, so hydration of the particular carboxylate anion leads to solution stability and solution viscosity (AMORIM *et al*., 2007).

In the presence of multivalent cations (such as

calcium), intra and intermolecular saline bridges are established. The interconnection between polysaccharide molecules leads to gel formation and, if extensive, precipitation. As salts formed from monovalent cations are stable over the range of the pH scale, molecular instability occurs at very high pH values due to the normal alkalosis degradation process. As the pH is reduced to about 3, carboxylic acid groups are formed, and as the hydrogen ion concentration of the solution increases, this ionization is passed on. Under repressed ionization conditions, uncharged carboxylic acid groups lose large amounts of associated water, polysaccharide molecules do not repel and, being linear, readily associate from a gel or precipitate (WANG; ELLIS; ROSS-MURPHY, 2000).

The properties of Mango gum presented a real density of 0.74 g / ml (CARR, 1965) considered low about other natural gums. The lower the density, the greater the porosity of the substance (HABIBI; LUCIA, 2012; SIERAKOWSKI, 1988).

The link between the compressibility index and flowability is inversely proportional (CARR *et al*., 1965). Being low compressibility between 11 to 15%, high between 16 to 20%, and very high above 31% (CARR, 1965). Bulk mass and bulk density give insight into particle packing and disposition and the compaction profile of a material (SARKAR *et al*., 2018). Solubility may be explained by the nature of the gum's molecular structure and mixtures as certain proteins or monosaccharide structures. The less linear the polymer, the more soluble (ABDULLAH, 2010; GARG *et al*., 2017; SIRISHA; DSOUZA, 2016). Linear polysaccharides take up more space and are more viscous than highly branched compounds of the same molecular weight. The gels are easier formed as of branched compounds and uniform because extensive interaction along chains is not possible (BHOSALE; OSMANI; MOIN, 2014).

Water holding capacity (WHC) and oil holding capacity (OHC) depend on the protein fraction present in the structure. It was found among 14 natural gums that WHC ranged from 34.66 to 1024.66 (g water / 100 g gum) (SARKAR *et al*., 2018). WHC varies depending on factors such as the hydrophilic - hydrophobic balance of amino acids in the protein molecule, as well as protein-associated carbohydrate and lipid fractions. There is no direct correlation between solubilization and water retention capacity, as each parameter is dependent on a different structural aspect of the biopolymer chain (MOGHIMI *et al*., 2015; MONTEIRO *et al*., 2015; RAJESWARI; GOKA, 2017). A 6% concentration of Mango gum has the same binding power as 10% starch and 5% is comparable to the binding power of Arabian gum (RAI *et al*., 2007; SINGH *et al*., 2010). Most gum does not dissolve if they are in a concentration greater than 5% (CHOUDHARY; PAWAR, 2014).

Rest angle is a measure of the resistance of dust to flow under gravity due to frictional forces resulting from the surface properties of the granules (ABDULLAH, 2010; OLAYEMI; SALIHU; ALLAGH, 2013). Different gum showed different angles of rest, ranging from 38.13 to 39.80°. As the angle of repose decreases, the binding level of the granules increases. This may be due to the reduction in the cohesive forces of larger granules formed at the highest bonding level (SARKAR *et al*., 2018; ABDULLAH, 2010). VINOD, 2013, found that Mangifera gum has good compressibility with moderate flow.

Chemical stimuli (pH, redox potential, ionic strength, and chemical agents) induce a response by altering the molecular interactions between polymer and solvent (by adjusting the hydrophobic/hydrophilic balance) or between the polymer chains (influencing crosslinking or the integrity of the polymer main chain, by propensity for hydrophobic association or electrostatic repulsion). Changes may occur in transitions in solubility, hydrophilic-hydrophobic balance, and conformation (ACHILLEOS; HATTON; VAMVAKAKI, 2012; GU *et al*., 2018; SALIM *et al*., 2014). These changes manifest themselves in a number of ways, such as the transition from polymer chains (collapse of a macromolecule from an expanded coil state to an ideal coil state to a collapsed globule state, or vice versa It is also analogous to behavior swelling of a cross-linked polymer gel), swelling / depletion of covalently cross-linked hydrogels, sol-gel transition of physically cross-linked hydrogels and self-assembly of amphiphilic polymers (FISZMAN; VARELA, 2013; MEMIOLU *et al*., 2002; PURI; SHARMA; NAGPAL, 2016; TIWARI *et al*., 2012; YANG; ZHANG, 2009).

The variation in pH in the body allows a selectivity of polymer / target site interaction. The stomach has pH 2.5, in the intestine, the pH is 6.2-7.5. Within cells, in endosomes, the pH is between 5.0 to 6.8, in lysosomes between 4.5 and 5.5. In the vicinity of cancer cells, tissue pH becomes more acidic (6.5) (CHANG *et al*., 2017; GU *et al*., 2018; LIECHTY *et al*., 2010). Delivery of nanoparticles or microparticles through the gastrointestinal tract occurs through passive absorption at a concentration gradient on the

Downloaded from www.periodico.tchequimica.com

intestinal surfaces, as determined by three primary factors: ionization extent, molecular weight, and oil/water partition coefficient of the drug (LIECHTY *et al*. al., 2010).

Scientists have devoted an effort to develop or find polymers that can exploit these pH variations to selectively provide drugs for specific intracellular or extracellular sites of action (BANIK; BROWN, 2014). Jakki *et al*. (2016) obtained anionic polymer nanoparticles from Manga gum for drug delivery in the treatment of Alzheimer's. NAYAK *et al*. (2012), found that *Mangifera indica* gum is a pH sensitive polymer, therefore, an intelligent polymer that can be used in controlled drug release. Kuppusamy *et al*. (2013) confirmed that *M. indica* gum is a non-toxic anionic polymer suitable for ocular drug delivery system

10. GUM NANOCAPSULES

Polymeric nanoparticles can be made of various polymers and can be modified in hydrophilicity and lipophilia, size and functionalized with different molecules to meet therapeutic needs (BHATIA, 2016), (LIN; DUFRESNE, 2015; RANA *et al*., 2011; SAH *et al*., 2016; TOWLE; WHISTLER, 2012).

The aim of using nanocapsules as drug carriers is to make the therapeutic dose as constant as possible (BASTO *et al*., 2016; BIZERRA; SILVA, 2016; KOTHAMASU *et al*., 2012; LIECHTY *et al*., 2010; MORA- HUERTAS; FESSI; ELAISSARI, 2010; PRABHAKAR; TAPAN; RATAN, 2013), enabling fewer drug doses and reducing side effects, either by substituting excipients or by directing the drug to the target site (YI *et al*., 2018). As shown in figure 7, there are several types of technologies for modifying drug release kinetics at the plasma level.

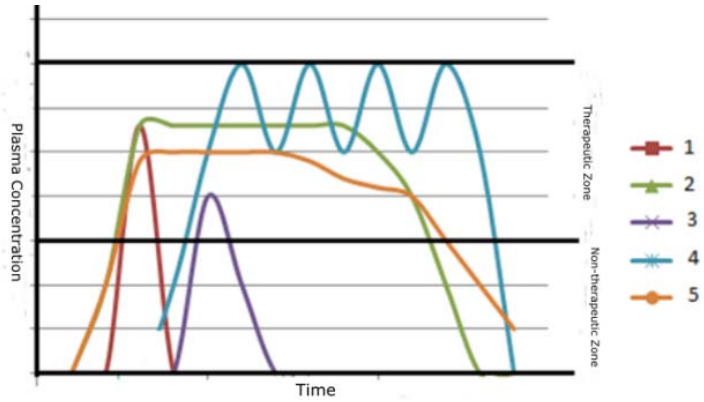

Figure 7: *Plasma Profile at 1: Conventional Release 2: Sustained Release 3: Delayed Release 4: Repeated Release 5: Extended Release. (Adapted from VEIGA, 1988).*

A means of targeted drug delivery by the body, reducing the interference of the individual's chemical and physiological barriers on the drug and reducing side effects was found through nanotechnology (FEDELI *et al*., 2015; MARQUES *et al*., 2017; MOSQUEIRA; SANTOS MAGALHAES, 2007; MUSYANOVYCH; LANDFESTER, 2014). With nanocarriers it is possible to distribute aliquots smaller than 100 nanometers of drug without being degraded or modified by the body's natural defense systems and fluids, being able to reach the target site (ACHILLEOS; HATTON; VAMVAKAKI, 2012; ANTON *et al*., 2007; GU *et al*., 2018; SALIM *et al*., 2014; WANG; WANG, 2013).

The objective of the technique is to obtain capsules of uniform size, good biodispersibility (BRUM JUNIOR, 2011; KOTHAMASU *et al*., 2012) resistant when far from the target site and with easy release directed to the action site or with gradual release of content, in both cases, with no release peaks within the therapeutic range, maintaining constant release over a longer period of time (BASTO *et al*., 2016; IVERSEN; SKOTLAND; SANDVIG, 2011; MOGOŞANU; GRUMEZESCU, 2015). To achieve this goal, microscopic drug encapsulation techniques were formulated with a pH-resistant sheath that could easily pass between or encompassed cell membranes and release the pharmaceutical content either near or within the target cell, prevent recognition of the body's defenses and allow surface changes to conjugate proteins that function as a molecular targeting site (CARDOSO; LIMA; QUEIROZ, C, 2013; COUVREUR *et al*., 2002; LEAL, 2014; NAWAZ ; ROHAN; GOWDA, 2011; OGAJI; NEP; AUDU-PETER, 2012; SILVA *et al*., 2003; YALAVARTHI; CHOWDARY VADLAMUDI, 2012).

The first patent registered with the nanocapsule technique was filed in 1963 and accepted in 1969 developed by Henn Ruus in the United States. The author cites some substances chosen to formulate nanocapsules from 0.1 to 450 microns: "Cellulose and synthetic polymers, including polyethylene, polypropylene, polymethyl methacrylate, polymethacrylate" (HENN RUUS, 1969). The objects of the invention include a simple method for encapsulating water or hydrophobic substances with an insoluble and infusible high molecular weight polymer shield with high uniformity of thickness, dry, and free

flow. For substances for pharmacological purposes, the author comments on the need for the chosen materials to be non-toxic. In prior U.S. Patent No. 2,712,507 of 1955, filed in 1953, Green (1955) obtained microcapsules with Arabica coacervation shell but worked only for hydrophobic and acid-resistant substances.

The active drug release system can also be used at the nanoscale through monolithic erosion systems such as nanospheres (EMEJE *et al*., 2009; GHALANDARI *et al*., 2014).

In this case, there are no reservoirs, and the drug becomes involved in the polymer constituent web, adsorbed on the surface or inside, being distributed by erosion (HOLKEM *et al*., 2015; VRIGNAUD; BENOIT; SAULNIER, 2011). In nanocapsules, the drug may be in the nucleus or polymeric membrane (CAMARGO *et al*., 2013; COUVREUR *et al*., 2002; KOTHAMASU *et al*., 2012).

11. NANOCAPSULE FORMATION TECHNIQUES USING PRE-FORMED POLYMERS

Emulsification-solvent, evaporation, salting-out, emulsification-solvent diffusion, solvent displacement (nanoprecipitation) are the main techniques for obtaining nanoparticles used for their ease of operation, speed, and lower cost. However, the solvent displacement technique allows nanocapsules and nanospheres to be obtained. Nanoparticle characterization analyzes include pH, toxicity, mean size distribution, surface charge (Zeta potential), absorbed drug content, and infrared spectroscopy (FTIR), chemical stability, physical stability, and toxic capacity (FRANCO, 2013; JOSÉ, J.; CORRÊA, 2015; RIBAS, 2013).

12. SUMMARY OF PHARMACOLOGICAL RESEARCH CARRIED OUT ABOUT MANGO GUM

12.1. AHMED & ABBAS (2018)

Extraction and evaluation of *Mangifera indica* gum as a sustained release polymer in Glinbenclamide matrix tablets

It has been found that M. indica gum collected at low cost has the good swelling capacity, good flow and suitability for Glinbenclamide controlled release tablet matrix formulations, the more concentrated the gum purity, the higher the delay in drug release time, between 9,55% and 10,89% in 24 hours. The formulations were evaluated for various parameters such as weight uniformity, friability, percent content, hardness, and in vitro dissolution studies.

12.2. HEMALATHA *et al*. (2017)

Formulation and evaluation of bilayered tablets containing an immediate release layer of Glimepiride complexed with Mangifera indica gum and sustained release layer containing Metformin HCl by using HPMC as release retardant.

Development of a two-layer Glimepiride and Metformin tablet using *M. gum* as immediate release polymers and HPMC as a sustained release layer. Glimepiride and metformin are oral hypoglycemic drugs. Bilayer tablets were evaluated by parameters such as thickness, diameter, weight variation, hardness, friability, disintegration, and in vitro release studies. The drug content uniformity study showed uniform drug dispersion throughout the formulation.

12.3. NAWAB *et al*. (2016)

Effect of Guar and Xanthan gums on functional properties of mango (*Mangifera indica*) kernel starch.

This research was done on gum extracted from *M. indica* seed. The effects of different concentrations of Guar gum and Xanthan gum on the functional properties of Mango seed gum were studied. Both gums increased the water absorption of the seed gum. The addition of Xanthan gum appeared to reduce swelling power and solubility at higher temperatures, while Guar gum increased solubility and swelling. The addition of both gums produced an increase in the viscosity peak of the seed gum. The binding temperature of the seed gum was higher than that of the gum-modified seed gum, indicating the ease of gelatinization. Guar gum accelerated retreat, but Xanthan gum delayed the phenomenon during seed gum cooling.

12.4. JAKKI *et al*. (2016)

A novel anionic polymer as a carrier for CNS delivery of an anti-Alzheimer drug.

Herbal polymers can be used for controlled drug release and also help direct the drug to the site of action. Mango gum polymeric nanoparticles (NPs) were a vehicle for the central nervous system (CNS) administration using the drug Donepezil (DZP). NPs were prepared by modified ion gelation and emulsion cross-linking method. The diameter of the NPs was 90-130

Downloaded from www.periodico.tchequimica.com

nm. DZP-loaded NPs were almost spherical in shape, without hemolysis at therapeutic doses. In vivo studies have shown that the brain target has been reached. Thus, based on the above results, the water-soluble fraction extracted from mango gum is a suitable nanoparticle candidate for brain-targeted drug delivery.

12.5. BAYONA (2016)

Evaluación de la actividad antibacteriana in vitro de la resina de *Mangifera indica* sobre cepas de *Escherichia coli, Staphylococcus aureus*, y *Pseudomonas aeruginosa.*

The antibacterial activities were satisfactory, suggesting the natural safety of this resin as a drug formulation.

12.6. MAHAMMED & GOWDA (2014)

Formulation and evaluation of mango gum microspheres as targeted drug delivery to colon.

Mango phosphate reticular microspheres were emulsified using sodium phosphate as a cross-linking agent for the treatment of colon cancer by encapsulating the drug Methotrexate. Particle size was increased as polymer concentration increased and with increasing agitation rate decreased particle size.

12.7. VINOD (2013)

Formulation and evaluation of Nicorandil sustained release matrix tablets using natural gum *Mangifera indica* as a release modifier.

Tablets are having as a gum *M. indica* was used for the controlled release of Nicorandil. The physicochemical and phytochemical properties were evaluated. The granules were evaluated for resting angle, bulk density, density, compressibility index, weight uniformity, active ingredient content, thickness, friability, hardness and dissolution *in vitro*. The prepared tablets showed 86.5% to 97.8% erosion release at stable 12h for 3 months.

12.8. NAYAK *et al*. (2012)

A novel binding agent for pharmaceutical formulation from *Mangifera indica* tree.

The gum extracted from *M. indica* was subjected to toxicity and pre-formulation studies as to its suitability as a tablet binding agent compared to starch using Lornoxicam as a drug. The prepared granules were evaluated for percentage average particle size, total porosity, compressibility index and dispersion properties, content uniformity, hardness, friability, disintegration time, and dissolution in vitro. The pills had good physicochemical properties, and drug release was over 90% in 90 minutes.

12.9. NAYAK *et al*. (2011)

An in vitro evaluation of *Mangifera indica* gum as a potential excipient for oral controlled-release matrix tablet.

The propose was to develop Lornoxicam tablets with *M. indica* gum for sustained release once a day, in different proportions of the drug. *M. indica* gum was used as matrix-forming material, and microcrystalline cellulose was used as diluent. As the proportion of gum in the matrix was increased, there was a corresponding decrease in drug release, reaching 98%. A swelling study was also performed to study the dispersibility of gums at different concentrations. Formulation stability was observed for 3 months.

12.10. NAYAK *et al*. (2011)

The exploitation of *Mangifera indica* gum as a novel natural gelling agent in the designing of gel formulation.

To study the gelling properties of *M. indica* gum, gels were prepared using Ceclofenac as a model drug. The gels were evaluated for drug content, viscosity determination, in vitro permeability (across the dialysis membrane), irritation tests, and skin stability. They did not produce dermatological reactions and were well tolerated by the guinea pig. Stability study revealed that the gel formulations were physically stable and without syneresis. Briefly, *M. indica* gum can be used as a pharmaceutical excipient in gel formulations by replacing some synthetic gelling polymers after modifications.

12.11. SIVAKUMAR *et al*. (2010)

Design and characterization of Diclofenac sodium tablets containing *Mangifera indica* resin as release retardant.

M. indica gum was used as a retardant in the development of sustained-release drug formulation employing diclofenac sodium as a drug model. The manufactured tablets were made physicochemical analysis and in vitro release studies. *M. indica* resin exhibited an excellent retarding effect on drug release even at its low concentrations (4% w / w). They showed drug release for more than 12 houres.

12.12. SINGH *et al*. (2010)

Evaluation of *Mangifera indica* gum as a tablet binder.

Tablets using *M. indica* gum as a binder with the drug Paracetamol were prepared and

Downloaded from www.periodico.tchequimica.com

evaluated for physicochemical characteristics. The friability of the tablets ranged from 1.12 to 0.26%, and the disintegration time was from 3 to 8 minutes. Arabica gum was compared at a concentration of 5% (w/w).

12.13. DIXIT *et al*. (2014)

Characterization of tabletting properties of mango gum.

Data on physical, thermal, and sorption properties of *M. indica* gum were performed. These data were identical to those obtained in Singh's work (2010). The aim of the research by Dixit *et al.* was to analyze in vitro release capacity using 2.5% Mango gum for ketoprofen tablet manufacture, which obtained a release rate of 95.07% within 30 minutes, indicating that a fast release and binder property in the conventional matrix.

Research on the anticancer potential with *M. indica* seed extract was conducted by Wu *et al*. (2015), indicating the effectiveness of rectal colon cancer treatment and prevention.

13. CONCLUSIONS

The properties of Mango stem gum have been little explored, but with the results already analyzed, it is possible to direct some possibilities of use.

A great number of researchs were conducted in Asian countries. Much of the research has been limited to physicochemical research and tableting, not delving into the potential for nanocapsule formation.

It is verified that *M. indica* gum has polymers with properties for the controlled release of drugs, both fast and delayed. Indeed, physicochemical characteristics indicate that nanocapsules can be formulated for controlled oral drug release. Besides the regional differences that characterize the *M. indica* gum polymers, the period of collection, the temperature to which the gum is subjected can interfere in the composition of the obtained polymers.

The common characteristics between Mango gum and Arabian gum (Acacia gum) can be explored by testing the same associations between gums for modification of the required characteristics.

Modification of the gum by association with other gums can be tested among other regional gums, such as Cashew gum, Tamarind seed gum or even with *M. indica* mucilage itself at various concentrations.

The physicochemical characteristics of regional gums present differences found in the literature that can be used, such as the difference in the percentage of polysaccharides and mucilage in the gum, whose characteristic may allow, for example, the development of nanocapsules for the release of hydrophilic and hydrophobic drugs same time, using modified *M. indica* gum. In addition to the pH-responsive gum, it is possible to isolate both its hydrophilic and hydrophobic parts for the different mechanisms of controlled drug release.

14. REFERENCES

1. ABDULLAH. Cohesiveness and Flowability Properties of Silica Gel Powder. Physics International, v. 1, n. 1, p. 16–21, 2010.
2. ACHILLEOS, D. S.; HATTON, T. A.; VAMVAKAKI, M. Light-regulated supramolecular engineering of polymeric nanocapsules. Journal of the American Chemical Society, v. 134, n. 13, p. 5726–5729, 4 abr. 2012.
3. AHMED, E. S. Y.; ABBAS, E. S. E. Extraction and Evaluation of *Mangifera indica* Gum as a Sustained Release Polymer in Glibenclamide Matrix Tablets. UK Journal of Pharmaceutical Biosciences, v. 6, n. 4, p. 01, 1 ago. 2018.
4. ALAM, M. T.; PARVEZ, N.; SHARMA, P. K. FDA-Approved Natural Polymers for Fast Dissolving Tablets. Journal of Pharmaceutics, v. 2014, p. 1–6, 27 abr. 2014.
5. ALAMGIR, A. N. M. Phytoconstituents—Active and inert constituents, metabolic pathways, chemistry and application of phytoconstituents, primary metabolic products, and bioactive compounds of primary metabolic origin. In: Progress in Drug Research. [s.l.] Birkhauser Verlag AG, 2018. v. 74p. 25–164.
6. ALBUQUERQUE, P. Avaliação de atividades biológicas de membrana e gel da galactomanana extraída das sementes de Cassia grandis com biomoléculas imobilizadas. [s.l.] Universidade Federal de Pernambuco, 2017.
7. AMORIM, L. V. *et al*. Influence of ionic strength on the viscosities and water loss of bentonite suspensions containing polymers. Materials Research, v. 10, n. 1, p. 53–56, 29 set. 2007.
8. ANJANEYULU, V.; RADHIKA, P. Triterpenoids and Steroids from *Mangifera indica Linn.* Indian Journal of Chemistry, v. 39B, p. 883–893, 2000.
9. ANTON, N. *et al*. Nano-emulsions and nanocapsules by the PIT method: An investigation on the role of the temperature cycling on the emulsion phase inversion. International Journal of Pharmaceutics, v. 344, n. 1–2, p. 44–52, 1 nov. 2007.
10. ASPINALL, G. O. Gums and Mucilages. Advances in Carbohydrate Chemistry and Biochemistry, v. 24, n. C, p. 333–379, 1970.

Downloaded from www.periodico.tchequimica.com

11. BANDYOPADHYAY, C.; GHOLAP, A. S.; MAMDAPUR, V. R. Characterization of Alkenylresorcinol in Mango (*Mangifera indica L*.) Latex. J. Agric. Food Chem, v. 33, n. 3, p. 377–379, 1985.
12. BANIK, B. L.; BROWN, J. L. Polymeric Biomaterials in Nanomedicine. In: Natural and Synthetic Biomedical Polymers. [s.l.] Elsevier Inc., 2014. p. 387–395.
13. BASKAR, D. Plant, exudates and mucilages. J. Adv. Pharm. Edu. & Res., v. 03, n. 04, p. 387–402, 2013.
14. BASTO, S. *et al*. Emulsão e microemulsão: novos sistemas de liberação controlada de fármacos no tratamento veterinário. UFRPE, v. 10, n. 1–4, p. 25–33, 2016.
15. BAYONA, Q. F, J. Evaluación de la actividad antibacteriana in vitro de la resina de *Mangifera indica* sobre cepas de *Escherichia coli*, *Staphylococcus aureus*, y *Pseudomonas aeruginosa*. Universidad de Santander, Cucuta, 2016.
16. BHATIA, S.; Plant Derived Polymers, Properties, Modification & Applications. In: Natural Polymer Drug Delivery Systems. [s.l.] Springer International Publishing, 2016. p. 119–184.
17. BHOSALE, R. R.; OSMANI, R. A. M.; MOIN, A. Natural gums and mucilages: A review on multifaceted excipients in pharmaceutical science and research. International Journal of Pharmacognosy and Phytochemical Research, v. 6, n. 4, p. 901–912, 2014.
18. BIRDWOOD, G. Catalogue of the economic products of the presidency of Bombay. A catalogue of the government central museum.pp:386, 1862.
19. BIZERRA, A.; SILVA, V. Sistemas de liberação controlada: Mecanismos e aplicações. Revista Saúde e Meio Ambiente-RESMA, v. 3, n. 2, p. 1–12, 2016.
20. BRITO, G. F. *et al*. Biopolímeros, Polímeros Biodegradáveis e Polímeros Verdes. n. 2, p. 127–139, 2011.
21. BRUM JUNIOR, L. Desenvolvimento e avaliação da atividade e farmacocinética de nanopartículas lipídicas sólidas contendo a associação de Quinina e Doxiciclina. PortoAlegre, 2011.
22. CAMARGO, Z. *et al*. Nanocápsulas poliméricas deformáveis no encapsulamento de bioativos.Brasil, 2013.
23. CARDOSO, M.; LIMA, P.; QUEIROZ, R. P. Nanomedicina: Aplicação da nanotecnologia na medicina. 2013.
24. CARR, R. L. Evaluating flow properties of solids. Chem Eng J , v. 72, p. 163–168, 1965.
25. CHANDRAJITH, V. G.; MARAPANA, R. Physicochemical and Phytochemical Characters of Bark Exudates of *Mangifera indica*. Chemistry Research Journal, v. 3, n. 3, p. 88–91, 2018.
26. CHANG, R. *et al*. Amphiphilic peptide nanoparticles for use as hydrophobic drug carriers and antibacterial agentsUS, 2017.
27. CHOUDHARY, P. D.; PAWAR, H. A. Recently Investigated Natural Gums and Mucilages as Pharmaceutical Excipients: An Overview. Journal of Pharmaceutics, v. 2014, p. 1–9, 7 abr. 2014.
28. CORSANO, S.; MINCIONE, E. Triterpenoids from *Mangifera indica*: I. The structure of mangiferolic acid. Tetrahedren Letters, v. 28, p. 2377–2381, 1965.
29. CORSANO, S.; MINCIONE, E. The absolute configuration of ambonic acid at C-25. Chemical Communications (London), n. 13, p. 738–739, 1968.
30. COUVREUR, P. *et al*. Nanocapsule technology: a review. Crit. Rev. Therapeutic Drug Carrier Systems, v. 19, n. 2, p. 99–134, 2002.
31. DIXIT, M. *et al*. Characterization of Tabletting Properties of Mango Gum. Research & Reviews: A Journal of Drug Formulation, Development and Production, v. 1, n. 1, 2014.
32. DUFRESNE, A.; LIN, N. 7 Characterization of Polysaccharide Nanocrystal-Based Materials.Polysaccharide-Based Nanocrystals: Chemistry and Applications, First Edition. Edited by Jin Huang, Peter R. Chang, Ning Lin and Alain Dufresne. by Chemical Industry Press. Published by Wiley-VCH Verlag GmbH & Co. KGaA, 2015.
33. EDWIN J, EDWIN S, DOSI S, RAJ A, G. S. Application of hibiscus leaves mucilage as suspending agent. Indian. J Pharm Educ Res, v. 41, p. 373–375, 2007.
34. EMEJE, M. *et al*. Isolation, characterization and formulation properties of a new plant gum obtained from Cissus refescence . International Journal of Green Pharmacy, v. 3, n. 1, p. 16, 15 abr. 2009.
35. FACCIO, C. Caracterização e uso da mucilagem do jaracatiá [Carica quercifolia (a. st.-hil.)Hhieron] na adsorção de papaína. Santa Catarina, 2015.
36. FATHI, M.; MOHEBBI, M.; KOOCHEKI, A. Introducing Prunus cerasus gum exudates: Chemical structure, molecular weight, and rheological properties. Food Hydrocolloids, v. 61, 2016.
37. FEDELI, E. *et al*. Nanoobjects formed by ionic PAMAM dendrimers: hydrophilic/lipophilic modulation and encapsulation properties. Soft Matter, v. 11, n. 30, p. 6009–6017, 14 ago. 2015.
38. FIGUEIREDO, A. *et al*. Histoquímica e citoquímica em plantas: princípios e protocolos. Lisboa, 2007.
39. FISZMAN, S.; VARELA, P. The role of gums in satiety/satiation. A review. Food Hydrocolloids, v. 32, n. 1, p. 147–154, 2013.
40. FRANCO, N. Nanopartículas e suas Aplicações em Ciências Farmacêuticas O Estado da Arte. Porto, 2013.
41. ROCHA, G. M.; CÉSAR, P.; SOUZA, A. Inovação tecnológica em fármacos e

Downloaded from www.periodico.tchequimica.com

medicamentos. 1. ed. Olinda: Livro Rápido, 2017.
42. GARCES, J.; MUÑOZ, A.; ANTON, J. Pharmaceutical preparation for improving the bioavalability of drugs which are difficult to absorband a procedure for obtaining it United States Patent, n. 5,736,161. 1998.
43. GARG, A. *et al*. Nanomedicine: Emerging Trends in Treatment of Malaria. In: Antimicrobial Nanoarchitectonics: From Synthesis to Applications. [s.l.] Elsevier Inc., 2017. p. 475–509.
44. GARG, A. *et al*. Applications of natural polymers in mucoadhesive drug delivery: An overview. Advance Pharmaceutical Journal, v. 3, n. 2, p. 38–42, 26 jun. 2018.
45. GHALANDARI, B. *et al*. The new insight into oral drug delivery system based on metal drugs in colon cancer therapy through β-lactoglobulin/oxali-palladium nanocapsules. Journal of Photochemistry and Photobiology B: Biology, v. 140, p. 255–265, 2014.
46. GHAYEMPOUR, S.; MONTAZER, M.; MAHMOUDI RAD, M. Tragacanth gum as a natural polymeric wall for producing antimicrobial nanocapsules loaded with plant extract. International Journal of Biological Macromolecules, v. 81, p. 514–520, 1 nov. 2015.
47. GIGANTE, B. Natural Resins. Conservar Patrimônio, v. 1, p. 33–46, 2005.
48. GONZAGA, W. A. Preparação e Avaliação Farmacológica de Derivados dos Lipídios Fenólicos do Líquido da Casca da Castanha de Caju. Brasília, 2008.
49. GONZÁLEZ-MARTÍNEZ, D. A. *et al*. Characterization of a novel complex coacervate based on whey protein isolate-tamarind seed mucilage. Food Hydrocolloids, v. 72, 2017.
50. GOSWAMI, S.; NAIK, S. Natural gums and its pharmaceutical application. Journal of Scientific and Innovative Research, v. 3, n. 1, p. 112–121, 2014.
51. GU, M. *et al*. Applications of stimuli-responsive nanoscale drug delivery systems in translational researchDrug Discovery TodayElsevier Ltd, , 1 maio 2018.
52. HABIBI, Y.; LUCIA, L. A. Polysaccharide building blocks : a sustainable approach to the development of renewable materials. [s.l.] John Wiley & Sons, 2012.
53. HAMDANI, A. M.; WANI, I. A.; BHAT, N. A. Sources, structure, properties and health benefits of plant gums: A review. International Journal of Biological Macromolecules, v. 135, p. 46–61, ago. 2019.
54. HEMALATHA, S.; SRIKANTH, P.; SAI, M. Formulation and Evaluation of Bilayered Tablets Containing Immediate Release Layer of Glimepiride Complexed with *Mangifera indica* Gum and Sustained Release Layer Containing Metformin HCL by Using HPMC as Release Retardant. International Journal of Pharmaceutical and Clinical Research, v. 9, n. 6, 17 ago. 2017.
55. HENN RUUS. Method of encapsulation. Niagara Falls, , 1969.
56. HIRST, E. L.; JONES, J. K. N. The gums and mucilages of plants. In: Aufbau · Speicherung · Mobilisierung und Umbildung der Kohlenhydrate / Formation · Storage · Mobilization and Transformation of Carbohydrates. [s.l.] Springer Berlin Heidelberg, 1958. p. 500–517.
57. HOLKEM, A. T. *et al*. Preparation techniques of nanotechnology systems applied to food. Ciência e Natura, v. 37, n. Ed. Esp., p. 87–96, 2015.
58. HOMBREIRO PEREZ, M. *et al*. The preparation and evaluation of poly(e-caprolactone) microparticles containing both a lipophilic and a hydrophilic drug. Journal of Controlled Release. v. 65, p. 429-438, 2000.
59. IVERSEN, T. G.; SKOTLAND, T.; SANDVIG, K. Endocytosis and intracellular transport of nanoparticles: Present knowledge and need for future studies. Nano Today, v.6, n. 2. p.176-185.abr. 2011.
60. JAKKI, S. L. *et al*. Novel anionic polymer as a carrier for CNS delivery of anti-Alzheimer drug. Drug Delivery, v. 23, n. 9, p. 3471–3479, 21 nov. 2016.
61. JOEL, D. M.; FAHN, A. Ultrastructure of the Resin Ducts of *Mangifera indica L*. (Anacardiaceae). 2. Resin. Secretion in the Primary Stem Ducts. Annals of Botany, v. 46, n. 6, p. 779–783, 1980a.
62. JOEL, D. M.; FAHN, A. Ultrastructure of the Resin Ducts of *Mangifera indica L*. (Anacardiaceae). 3. Secretion of the Protein-polysaccharide Mucilage in the Fruit. Annals of Botany, v. 46, n. 6, p. 785–790, 3 fev. 1980b.
63. JOSÉ, J.; CORRÊA, L. Copal do Brasil: Ocorrência e caracterização físico-química da resina Jutaicica de Santarém. Santarém, 2015.
64. KASGARD, T.; DRUMMOND, C. J. Ordered 2-D and 3-D nanostructured amphiphile self-assembly materials stable in excess solventPhysical Chemistry Chemical Physics, 2006.
65. KHAN, S.; PARVEZ, N.; SHARMA, K. Novel natural mucoadhesive polymers. World Journal of Pharmacy and Pharmaceutical Sciences, v. 4, n. 12, p. 374–388, 2015.
66. KOTHAMASU, P. *et al*. Nanocapsules: The weapons for novel drug delivery systems. BioImpacts, v. 2, n. 2, p. 71–81, 2012.
67. KROKIDA, M. K. Thermal and nonthermal encapsulation methods. [s.l.] CRC Press, 2017.
68. KULKARNI, P. *et al*. Brief introduction of natural gums, mucilages and their applications in novel drug delivery systems-a review. International Journal of Drug Formulation and Research , v. 2, n. 6, p. 54–71, 2011.
69. KUMAR AYAK, R. *et al*. An in vitro evaluation of *Mangifera indica* gum as a potential excipient for oral controled-release matrix tablet.

Downloaded from www.periodico.tchequimica.com

Pharmacologyonline, v. 2, p. 360–391, 2011.
70. KUMAR AYAK, R.; SWAMY, A. V. Explotation of *Mangifera indica* gum as novel natural geling agent in the desing of formulations. Pharmacologyonline, v. 2, p. 522–541, 2011.
71. KUMAR DHAKA, R. *et al*. Conservation and Scientific Techniques for Improvement of Gum and Resin Yielding Tropical Tree Species.Trends in Biosciences. v. 10, n. 1, p. 64-67, 2017
72. KUMAR, V. *et al*. Dissertação de Mestrado. Feasibility of plant based natural polysaccharide as release modifier for the sustained release preparation of diclofenac sodium tablet. Rajiv Gandhi University of Health Sciences, Bangalo re, Karnataka, 2010.
73. LACCHIA, A. P. S.; GUERREIRO, S. M. C. Aspectos ultra-estruturais dos canais secretores em órgãos vegetativos e reprodutivos de Anacardiaceae. Acta Botanica Brasilica, v. 23, n. 2, p. 376–388, 17 set. 2009.
74. LANGENHEIM, J. H. Plant Resins: Chemistry, Evolution, Ecology, and Ethnobotany. 1. ed. Portland: Timber Press, 2003.
75. LEAL, M. G. Tese de Doutorado. Parámetros fisicoquímicos y rasgos estructurales vinculados con el potencial industrial de dos gomas de Anacardiaceae. Facultad Experimental de Ciencias, Maracaibo, 2014.
76. LETCHFORD, K.; BURT, H. A review of the formation and classification of amphiphilic block copolymer nanoparticulate structures: micelles, nanospheres, nanocapsules and polymersomes. Eu. J. Pharm. Biopharm., 65(3):259-69, mar. 2007.
77. LIECHTY, W. B. *et al*. Polymers for Drug Delivery Systems. Annual Review of Chemical and Biomolecular Engineering, v. 1, n. 1, p. 149–173, 11 jun. 2010.
78. LIMA, A. *et al*. Estimulantes químicos na extração da goma de cajueiro (Anacardium occidentale, l.) Chemical stimulants in the extraction of the gum of cashew tree. Ciência Rural, v. 31, n. 3, p. 409–415, 2001.
79. LIMA, M. R. *et al*. Hydrophobization of cashew gum by acetylation mechanism and amphotericin B encapsulation. International Journal of Biological Macromolecules, v. 108, p. 523–530, 1 mar. 2018.
80. LIN, N.; DUFRESNE, A. Surface Modification of Polysaccharide Nanocrystals. In: Polysaccharide-Based Nanocrystals: Chemistry and Applications, Publisher: Wiley Blackwell (ISBN:9783527336197) p. 63–108. Doi: 10.1002/9783527689378.ch3, 2015.
81. LIU, M. *et al*. Synthesis, characterization, and evaluation of phosphated cross-linked konjac glucomannan hydrogels for colon-targeted drug delivery. Drug Delivery, v. 14, n. 6, p. 397–402, ago. 2007.
82. LÓPEZ-COBO, A. *et al*. Use of HPLC- and GC-QTOF to determine hydrophilic and lipophilic phenols in mango fruit (*Mangifera indica L*.) and its by-products. Food Research International, v. 100, p. 423–434, 1 out. 2017.
83. MAHAMMED, N.; GOWDA, D. V. Formulation and evaluation of mango gum microspheres as a targeted drug delivery to colon. Int J Pharm Bio Sci, v. 5, n. 4, p. 126–137, 2014.
84. MARIMUTHU, J.; JAYAKUMAR, M. Gum-Resinosis in *Mangifera indica*. Korean J. Ecol., v. 24, n. 2, p. 121–123, 2001.
85. MARQUES, J. *et al*. Adaptation of targeted nanocarriers to changing requirements in antimalarial drug delivery. Nanomedicine: Nanotechnology, Biology, and Medicine, v. 13, n. 2, p. 515–525, 1 fev. 2017.
86. MEMIOLU, E. *et al*. Amphiphilic β-cyclodextrins modified on the primary face: Synthesis, characterization, and evaluation of their potential as novel excipients in the preparation of nanocapsules. Journal of Pharmaceutical Sciences, v. 91, n. 5, p. 1214–1224, 2002.
87. MENESTRINA, J. M. *et al*. Similarity of monosaccharide, oligosaccharide and polysaccharide structures in gum exudate of Anacardium occidentale. Phytochemistry, v. 47, n. 5, p. 715–721, mar. 1998.
88. MISHRA, A.; CLARK, J. H.; PAL, S. Modification of Okra mucilage with acrylamide: Synthesis, characterization and swelling behavior. Carbohydrate Polymers, v. 72, n. 4, p. 608–615, 10 jun. 2008.
89. MOGHIMI, S. M. *et al*. Polymeric Nanoparticles as Drug Carriers and Controlled Release Implant Devices. In: Nanoparticulates as Drug Carriers. Deakin University: Imperial College Press, 2015. p. 29–42.
90. MOGOŞANU, G. D.; GRUMEZESCU, A. M. Pharmaceutical Natural Polymers: Structure and Chemistry. In: Handbook of Polymers for Pharmaceutical Technologies. [s.l.] Wiley, 2015. v. 1p. 477–519.
91. MOHAN, S. Physicochemical characterisation and binding property of polysaccharide of Solanum betaceum cav in tablet formulation. Chennai, 2017.
92. MONTEIRO, A. A. DE S. *et al*. Efeito da modificação química na solubilidade e intumescimento de microesferas à base de goma do cajueiro carboximetilada e quitosana. Polímeros, v. 25, n. spe, p. 31–39, dez. 2015.
93. MORA-HUERTAS, C. E.; FESSI, H.; ELAISSARI, A. Polymer-based nanocapsules for drug delivery International Journal of PharmaceuticsElsevier B.V., 29 jan. 2010.
94. MOSQUEIRA, V. C. F.; SANTOS-MAGALHAES, N. Application of pharmaceutical nanotechnology to the treatment of malaria. Revista Brasileira de Ciências Farmacêuticas.Vol. 43, n. 4, out./dez., 2007
95. MUSYANOVYCH, A.; LANDFESTER, K. Polymer micro- and nanocapsules as biological carriers with multifunctional properties. Macromolecular Bioscience. Vol. 14, n. 4, p. 458-477, 2014.

Downloaded from www.periodico.tchequimica.com

96. MUTHUKUMARAN, M. Natural gums, mucilage's and their applications in novel drug delivery systems – A comprehensive review. World Journal of Pharmacy and Pharmaceutical Sciences, v. 6, n. 4, p. 921–937, 24 abr. 2017.
97. NAWAB, A. *et al*. Effect of guar and xanthan gums on functional properties of mango (*Mangifera indica*) kernel starch. International Journal of Biological Macromolecules, 2016.
98. NAWAZ, M.; ROHAN, D. D.; GOWDA, D. V. Modified polysaccharide as drug delivery: review. JSS College of pharmacy, v. 11, n. 1, 2011.
99. NAYAK, R. K. *et al*. Aninverto evaluation of *Mangifera indica* gum as a potential excipient for oral controlled - release matrix tablet. Pharmacologyonline, 2011.
100. NAYAK, R. K. *et al*. A Novel Binding Agent For Pharmaceutical Formulation From *Mangifera Indica* Tree. Asian Journal of Biochemical and Pharmaceutical Research Issue, v. 2, n. 1, p. 2012, 2012.
101. NDINGA, E. A.; J-M, O. Characterization of volatile compounds from the gum-resin of *Mangifera indica L*. trunk bark using HS-SPME-GC/MS. Série Pharm. Méd. Trad. Afr, v. 17, n. 2, p. 1–7, 2015.
102. NGWULUKA, N. C.; OCHEKPE, N. A.; ARUOMA, O. I. Naturapolyceutics: The science of utilizing natural polymers for drug deliveryPolymersMolecular Diversity Preservation International, , 2014.
103. NOKHODCHI, A. *et al*. Application of Polymer Combinations in Extended Release Hydrophilic Matrices. In: Handbook of Polymers for Pharmaceutical Technologies. [s.l.] Wiley, 2015. v. 1p. 23–49.
104. NUSSINOVITCH, A. Plant Gum Exudates of the World. Plant Gum Exudates of the World, 2009.
105. OGAJI, I. J.; NEP, E. I.; AUDU-PETER, J. D. Advances in Natural Polymers as Pharmaceutical Excipients. Pharmaceutica Analytica Acta, v. 03, n. 01, 29 fev. 2012.
106. OLAYEMI, O.; SALIHU, B.; ALLAGH, S. Evaluation of the binding properties of Spondias purpurea gum in metronidazole tablet formualtions. International Journal of Pharmacy and Pharmaceutical Sciences, v. 5, n. SUPPL. 2, p. 584–589, 2013.
107. OLIVEIRA, M. D. B. *et al*. Ácido Tânico nos Procedimentos Restauradores. J. Health, v. 19, p. 4–290, 2017.
108. PADIL, V. V. T. *et al*. Tree gum-based renewable materials: Sustainable applications in nanotechnology, biomedical and environmental fieldsBiotechnology AdvancesElsevier Inc., , 15 nov. 2018.
109. PAIPHANSIRI, U.; TANGBORIBOONRAT, P.; LANDFESTER, K. Polymeric nanocapsules containing an antiseptic agent obtained by controlled nanoprecipitation onto water-in-oil miniemulsion droplets. Macromolecular Bioscience, v. 6, n. 1, p. 33–40, 5 jan. 2006.
110. PATHAK, D. *et al*. Physicochemical characterization and toxicological evaluation of plant-based anionic polymers and their nanoparticulated system for ocular delivery. Nanotoxicology, v. 8, n. 8, p. 843–855, 2014.
111. PILETTI, R. Dissertação de Mestrado. Extração da mucilagem da tuna (Cereus hildmaniannus k. Schum) para aproveitamento industrial. Universidade Federal de Santa Catarina. Florianópolis, 2011.
112. PINHEIRO A. C. *et al*.Utilização de revestimentos/filmes edíveis para aplicações alimentares. http://hdl.handle.net/1822/16725.(ISSN: 1645-5878). Braga, 2010.
113. PRABHAKAR, V.; TAPAN, A.; RATAN, R. Magic Bullets - Nanocapsules in Future Medicine. http://ijps.aizeonpublishers.net/content/2013/4/ijps303-308.pdf International Journal of Pharma Sciences , v. 3, n. 4, p. 303–308, 2013.
114. PRADO, E.; DEMARCO, D. Laticifers and Secretory Ducts: Similarities and Differences. Ecosystem Services and Global Ecology, 2018.
115. PRAJAPATI, V. D. *et al*. Pharmaceutical applications of various natural gums, mucilages and their modified forms Carbohydrate Polymers, 15 fev. 2013.
116. PURI, V.; SHARMA, P.; NAGPAL, M. An Update on Some Recent Solubility Enhancers as Pharmaceutical Excipients. Journal of Pharmaceutical Technology, Research and Management, v. 4, n. 1, p. 45–62, 5 maio 2016.
117. RAI, S. *et al*. Oriental medicine *Mangifera indica*. Oriental pharmacy and experimental medicine, v. 7, n. 1, p. 1–10, 2007.
118. RAJESWARI, S.; GOKA, V. Natural polymers: A recent review. World Journal of Pharmacy and Pharmaceutical Sciences, v. 6, n. 8, p. 472–494, 9 ago. 2017.
119. RANA, V. *et al*. Modified gums: Approaches and applications in drug deliveryCarbohydrate Polymers, 30 jan. 2011.
120. RAVINDRAKULLAI REDDY, M.; MANJUNATH, K. Pharmaceutical Applications of Natural Gums, Mucilages and Pectins-A Review. International Journal of Pharmaceutical and Chemical Sciences, v. 2, n. 3, p. 1233–1239, 2013.
121. RIBAS, D. A.Tese de Doutorado. Desenvolvimento de nanocápsulas contendo Cetoprofeno e avaliação in vitro da citotoxicidade. Universidade Federal de Santa Maria, Santa Maria, 2013.
122. RIBEIRO, A. J. *et al*. Gums' based delivery systems: Review on cashew gum and its derivatives Carbohydrate Polymers, 2016. vol. 147, p.188-200. Doi: 10.1016/j.carbpol.2016.02.042.
123. RIBEIRO, L. N. M. *et al*. Advances in Hybrid Polymer-Based Materials for Sustained Drug Release. International Journal of Polymer

Downloaded from www.periodico.tchequimica.com

Science, v. 2017, p. 1–16, 1 nov. 2017.
124. ROCHA, M. C. Dissertação de Mestrado. Extração, propriedades físico -químicas e utilização de mucilagem de chia (*Salvia hispanica l*.) como substituto de gordura em biscoitos. Universidade Federal de Lavras, Lavras, 2017.
125. RODRIGUES, J.; PAULA, R.; COSTA, S. Métodos de Isolamento de Gomas Naturais: Comparação Através da Goma do Cajueiro (Anacardiumoccidentale L). Polímeros: Ciência e Tecnologia -, p. 31–36, 1993.
126. RODRIGUES, R. G. Tese de Doutorado. Análise morfológica e fitoquímica da Fava d'Anta (Dimorphandra mollis Benth). UFV, 2007.
127. SAH, S. K. *et al*. Natural Gums Emphasized Grafting Technique: Applications and Perspectives in Floating Drug Delivery SystemAsian Journal of Pharmaceutics. V. 10 n.2 p. 72-83, 2016.
128. SALIM, M. *et al*. Amphiphilic designer nano-carriers for controlled release: From drug delivery to Diagnostics Med Chem Comm Royal Society of Chemistry,vol. 5, n.11, p. 1602-1618,1 nov. 2014.
129. SANT', B. F. *et al*. Anatomia e histoquímica das estruturas secretoras do caule de Spondias dulcis forst. f. (Anacardiaceae). Sociedade de investigações florestais, v. 30, n. 3, p. 481–489, 2006.
130. SANTOS, P. P. *et al*. Biodegradable polymers as wall materials to the synthesis of bioactive compound nanocapsules. Trends in Food Science and Technology Elsevier Ltd, , 1 jul. 2016.
131. SANTOS, V. M. R. *et al*. Síntese e caracterização de novos copolímeros fosforilados. Polímeros, v. 25, n. spe, p. 19–24, 17 jan. 2016.
132. SARKAR, P. C. *et al*. Studies on physico-chemical and functional properties of some natural Indian gums. Asian Journal of Dairy and Food Research, v. 37, n. 02, 6 jun. 2018.
133. SCHNIZL, Z. The infrastructure of Mucilage Secreting Trichomes of. v. 41, n. 2, p. 227–245, 2001.
134. SELLÉS, A. *et al*. Isolation and quantitative analysis of phenolic antioxidants, free sugars, and polyols from mango (*Mangifera indica L*.) stem bark aqueous decoction used in Cuba as a nutritional supplement. Journal of agricultural and food chemistry, v. 50, n. 4, p. 762–766, 2002.
135. SHARMA, D. R. *et al*. Herbal gums and mucilage as excipients for Pharmaceutical Products. Research Journal of Pharmacognosy and Phytochemistry, v. 8, n. 3, p. 145, 18 out. 2016.
136. SHINGALA, V. K. *et al*. Design and characterization of diclofenac sodium tablets containing *Mangifera indica* resin as release retardant. International Journal of PharmTech Research, v. 2, n. 3, p. 2107–2111, jul. 2010.
137. SIERAKOWSKI, M. R. Tese de Doutorado. Aspectos Estruturais da mucilagem de Pereskia aculeata, Mill (ora-pro-nobis). Curitiba: Universidade Federal do Paraná, 1988.
138. SILVA, F. C.; DUARTE, L. P.; VIEIRA FILHO, S. A. Celastráceas: Fontes de triterpenos pentacíclicos com potencial atividade biológica. Revista Virtual de Quimica, v. 6, n. 5, p. 1205–1220, 2014.
139. SILVA, L. L. *et al*. Composição química, atividade antibacteriana in vitro e toxicidade em Artemia salina do óleo essencial das inflorescências de Ocimum gratissimum L., Lamiaceae. Brazilian Journal of Pharmacognosy, v. 20, n. 5, p. 700–705, out. 2010.
140. SINGH, A. K. *et al*. Evaluation of *Mangifera indica* gum as tablet binder. International Journal of PharmTech Research, v. 2, n. 3, p. 2098–2100, jul. 2010.
141. SINGH, A. K.; PANNER, S.; SIVAKUMAR, T. Isolation, characterization and formulation properties of a new plant gum obtained from *Mangifera indica*. International Journal of Pharmaceutical and Biomedical Research (IJPBR), v. 1, n. 2, p. 35, 2010.
142. SIRISHA, V. L.; DSOUZA, J. S. Polysaccharide-based nanoparticles as drug delivery systems. In: Marine OMICS: Principles and Applications. CRC Press, 2016. p. 643–682.
143. SOARES, C. E. A. Tese de Doutorado. Caracterização estrutural e potencial da galactomana de Adenanthera pavonina L. como produção de filmes comestíveis bioativos. Universidade Federal do Ceará, Fortaleza, 2009.
144. SOUTO, E. B.; SEVERINO, P.; SANTANA, M. H. A. Preparação de nanopartículas poliméricas a partir de polímeros pré-formados: parte II. Polímeros, v. 22, n. 1, p. 101–106, 27 jan. 2012.
145. SUDARSHAN, S.; SUNIL B, B. In vivo mucoadhesive strength appraisal of gum Manilkara Zapota. Brazilian Journal of Pharmaceutical Sciences, v. 51, n. 3, p. 689–698, 1 jul. 2015.
146. THAKUR, V. K.; THAKUR, M. K. Handbook of Polymers for Pharmaceutical Technologies. [s.l.] Wiley, 2015. v. 2
147. TIWARI, G. *et al*. Drug delivery systems: An updated review. International journal of pharmaceutical investigation, v. 2, n. 1, p. 2–11, jan. 2012.
148. TORCHILIN, V. Nanoparticules as Drug Carriers. 1. ed. Londres: Imperial College Press, 2006.
149. TOWLE, G. A.; WHISTLER, R. L. Chemical Modification of Gums. In: Industrial Gums: Polysaccharides and Their Derivatives: Third Edition. [s.l.] Elsevier Inc., 2012. p. 53–67.
150. TREVISAN, M. T. S. *et al*. Characterization and Quantitation of Polyphenolic Compounds in Bark, Kernel, Leaves, and Peel of Mango (

Downloaded from www.periodico.tchequimica.com

Mangifera indica L.) . Journal of Agricultural and Food Chemistry, v. 56, n. 14, p. 5599–5610, 2008.
151. U. RAGHU, A. A. HINDUSTAN, K. HARITHA, J. ANJI, G. SUDHAKAR, G. V. Review Article Quick Reference to the Matrix Forming Gums and Mucilage. Journal, International Science, Modern Sciences, Pharmaceutical Pharmacy, Industrial Education, Pharmaceutical, v. 4, n. 3, p. 61–66, 2019.
152. VASANTRAO PATIL, S. *et al*. Natural binders in tablet formulation. International Journal of PharmTech Research, v. 6, n. 3, p. 1070–1073, 2014.
153. VASQUEZ, E. *et al*. Influence of the Ionic Strength in the Intrinsic Viscosity of Xanthan Gum. An Experimental Review. Journal of Polymer and Biopolymer Physics Chemistry, v. 3, n. 1, p. 12–18, 2015.
154. VEIGA, F. J. G. Medicamentos orais de liberação controlada: comprimidos matriciais hidrófilos. Boi. Fac. Farm. Coimbra, v. 12, n. 2, p. 17–87, 1988.
155. VINOD R. Formulation and Evaluation of Nicorandil Sustained Release Matrix Tablets Using Natural Gum *Mangifera Indica* as Release Modifier. Asian Journal of Biomedical and Pharmaceutical Sciences; vol. 3, n.18, p. 54-60, 2013.
156. VINOD, V. T. P. *et al*. Compositional analysis and rheological properties of gum kondagogu (*Cochlospermum gossypium*): A tree gum from India. Journal of Agricultural and Food Chemistry, v. 56, n. 6, 2008.
157. VRIGNAUD, S. *et al*. Aqueous core nanocapsules: A new solution for encapsulating doxorubicin hydrochloride. Drug Development and Industrial Pharmacy, v. 39, n. 11, p. 1706–1711, nov. 2013.
158. VRIGNAUD, S.; BENOIT, J. P.; SAULNIER, P. Strategies for the nanoencapsulation of hydrophilic molecules in polymer-based nanoparticles Biomaterials, nov. 2011. Doi:10.1016/j.biomaterials.2011.07.057.
159. WANG, A.; WANG, W. Gum-g-copolymers: Synthesis, properties, and applications. In: Polysaccharide Based Graft Copolymers. Springer-Verlag Berlin Heidelberg. ISBN: 9783642365669 p. 149–203, 2013.
160. WANG, C. Z. *et al*. Chemical constituents and structural characterization of polysaccharides from four typical bamboo species leaves. Molecules, v. 20, n. 3, p. 4162–4179, 1 mar. 2015.
161. WANG, H.; HALAS, N. J. Mesoscopic au “meatball” particles. Advanced Materials, v. 20, n. 4, p. 820–825, 18 fev. 2008.
162. WANG, Q.; ELLIS, P. R.; ROSS-MURPHY, S. B. The stability of guar gum in an aqueous system under acidic conditions. Food Hydrocolloids, v. 14, n. 2, p. 129–134, 2000.
163. WET, E.; ROBBERTSE, P. J.; COETZEE, J. Ultrastructure of the stigma and style of *Mangifera indica L*. South African Journal of Botany, v. 56, n. 2, p. 206–213, 2016.
164. WU, C.-Y. *et al*. Different Mechanisms of Seed Kernel Extract from *Mangifera indica* on the Growth of Two Colon Cancer Cell Lines. Food and Nutrition Sciences, v. 06, n. 04, p. 421–428, 23 mar. 2015.
165. WU, Y. *et al*. An investigation of four commercial galactomannans on their emulsion and rheological properties. Food Research International, v. 42, n. 8, 2009.
166. YALAVARTHI,P.R.;CHOWDARY VADLAMUDI, H. Design and Assessment of Colon Specific Drug Delivery of Mefenamic Acid using Modified Pulsincap Technique and Hupu Gum. Indo American Journal of Pharmaceutical Research. (ISSN: 2231-6876) v. 2, n. 9, 2012.
167. YANG, L.; ZHANG, L. M. Chemical structural and chain conformational characterization of some bioactive polysaccharides isolated from natural sources. Carbohydrate Polymers, v. 76, n. 3, p. 349-361, 9 abr. 2009.
168. YI, Q. *et al*. Bioreducible nanocapsules for folic acid-assisted targeting and effective tumor-specific chemotherapy. International Journal of Nanomedicine, v. 13, p. 653–667, 31 jan. 2018.

Downloaded from www.periodico.tchequimica.com

PERIÓDICO TCHÊ QUÍMICA
ARTIGO ORIGINAL

ESTADO DEFLETIDO DO SEMICONDUTOR DA ÁREA DE CONTATO PRÓXIMO NA ELETRODEGREGAÇÃO DA FAIXA DE METALIZAÇÃO NA SUPERFÍCIE

DEFLECTED STATE OF SEMICONDUCTOR NEAR-CONTACT REGION AT ELECTRO-DEGRADATION OF METALLIZATION TRACK ON ITS SURFACE

НАПРЯЖЕННО-ДЕФОРМИРОВАННОЕ СОСТОЯНИЕ ПРИКОНТАКТНОЙ ОБЛАСТИ ПОЛУПРОВОДНИКА ПРИ ЭЛЕКТРОДЕГРАДАЦИИ ДОРОЖКИ МЕТАЛЛИЗАЦИИ НА ЕГО ПОВЕРХНОСТИ

SKVORTSOV, Arkadiy A.[1*]; ZUEV, Sergey M.[2]; KORYACHKO, Marina V.[3]; VOLOSHINOV, Evgeniy B.[4];

[1] Moscow Polytechnic University; Department of Dynamics, Strength of Machines and Resistance of Materials, Moscow – Russian Federation

[2] Moscow Polytechnic University; Department of Industrial Electronics, Moscow – Russian Federation

[3,4] Moscow Polytechnic University; Department of Physics, Moscow – Russian Federation

** Correspondence author*
e-mail: SkvortsovAA2009@yandex.ru

Received 30 August 2019; received in revised form 31 October 2019; accepted 01 November 2019

RESUMO

É sabido que um estado não homogêneo de estresse ocorre em compostos de materiais diferentes após aquecimento. Na avaliação da resistência das juntas, é necessário levar em consideração as especificações físicas dos elementos soldados, as dimensões geométricas e as condições de temperatura de sua operação. O objetivo da pesquisa foi realizar a análise do estado de tensão-deformação da zona de contato de um semicondutor mediante eletrodegradação de uma trilha de metalização em sua superfície. Estruturas de metal semicondutor de película fina foram pesquisadas. Como substratos, foram usadas bolachas monocristalinas de silício dopadas com fósforo, orientadas nas direções (111) e (100), com resistividade no intervalo ρ = 1 ... 0,01 Ω.cm e 30 ... 50 μm. A camada n-epitaxial foi depositada em uma parte das bolachas. Como um filme metálico condutor, foi utilizado alumínio com espessura de 1 ... 2 μm. A estrutura do teste foi formada por fotolitografia óptica. Os oscilogramas da inclusão de U (t) no processo de passagem do pulso de corrente foram obtidos pelas sondas correspondentes de locais potenciais e registrados por um osciloscópio de armazenamento digital. Um procedimento de estimativa para a região sob tensão de semicondutores no aquecimento superficial local de uma área de superfície metalizada com pulso elétrico foi fornecido. O tamanho calculado da região do substrato de silício deformado foi comparado com o experimental sob passagem de pulsos elétricos quadrados. Foi estimada a região desviada, que depende da duração e amplitude do pulso elétrico. Uma não uniformidade considerável da pista de metalização após a passagem do pulso elétrico foi fixada experimentalmente.

Palavras-chave: *aquecimento de semicondutores, estado de tensão, fusão por contato, área de tensão-deformação.*

ABSTRACT

It is well known that a nonhomogeneous state of stress occurs in compounds of dissimilar materials upon heating. Uon the assessment of the strength of the joints, it is necessary to factor in the physical specifications of the soldered elements, the geometric dimensions and temperature conditions of their operation. The purpose of the research was to perform the stress-strain state analysis of the contact zone of a semiconductor upon electrodegradation of a metallization track on its surface. Thin-film metal-semiconductor structures were researched. As substrates, it was used phosphorus-doped silicon single-crystal wafers oriented in the (111) and (100) directions, with a resistivity in the range ρ = 1 ... 0.01 Ω.cm, and a 30 ... 50 μm n-epitaxial layer was deposited on a part of the wafers. As a conductive metal film, aluminum 1 ... 2 μm thick was used. The test structure was formed by optical photolithography. The oscillograms of the U(t) inclusion in the process

Downloaded from www.periodico.tchequimica.com

of passage of the current pulse were taken by the corresponding probes from potential sites and recorded by a digital storage oscilloscope. An estimation procedure for the semiconductor stressed region at local surface heating of a metallized surface area with electric pulse was given. The calculated size of deformed silicon substrate region was compared with the experimental one under passage of square electric pulses. It was estimated the deflected region that depends on duration and amplitude of electric pulse. A considerable nonuniformity of the metallization track after electric pulse passage was fixed experimentally.

Keywords: *semiconductor heating, stressed state, contact melting, deflected region.*

АННОТАЦИЯ

Хорошо известно, что в соединениях разнородных материалов при нагреве возникает неоднородное напряженное состояние. При оценке прочности соединений необходимо учитывать физические характеристики спаянных элементов, геометрические размеры и температурные режимы их работы. Цель исследования – провести анализ напряженно-деформированного состояния приконтактной области полупроводника при электродеградации дорожки металлизации на его поверхности. В работе исследовались тонкопленочные структуры металл-полупроводник. В качестве подложек использовались легированные фосфором кремниевые монокристаллические пластины, ориентированные в направлении (111) и (100), с удельным сопротивлением в диапазоне ρ=1…0.01 Ω.cm, а на части пластин был нанесен 30…50- μm n-эпитаксиальный слой. В качестве проводящей металлической пленки был использован алюминий толщиной 1…2 μm. Формирование тестовой структуры осуществлялось методом оптической фотолитографии. Осциллограммы включения U(t) в процессе прохождения импульса тока снимались соответствующими зондами с потенциальных площадок и фиксировалось цифровым запоминающим осциллографом. Приведена методика оценки области напряженного состояния полупроводника при локальном поверхностном нагреве металлизированного участка поверхности импульсом тока. Проведено сопоставление результатов расчета размера деформированной области кремниевой подложки с экспериментом в условиях прохождения прямоугольных токовых импульсов. Проведена оценка напряженно-деформированной области, которая зависит от длительности и амплитуды электрического импульса. Экспериментально зафиксирована существенная неоднородность дорожки металлизации после прохождения импульса.

Ключевые слова: *нагрев полупроводника, напряженное состояние, контактное плавление, напряженно-деформированная область.*

1. INTRODUCTION

It is well known that heating compounds of dissimilar materials leads to appearance of a non-uniform stressed state (Kapitonov *et al.*, 2017; Kashniyal and Pandey, 2018; Lim and Meguid, 2019; Dong and Wang, 2019). In the course of heating such compound, stresses in the layers of elements increase at the expense of thermal expansion. This may result in the destruction of the layer (Dang *et al.*, 2017; Shejko *et al.*, 2017; Chen *et al.*, 2018; Xu *et al.*, 2018; Ishitani *et al.*, 2018; Bojita *et al.*, 2018). When estimating joint efficiency, one has to take into account the physical characteristics of soldered elements as well as their geometric sizes and temperature modes of their operation (Sirazijeva *et al.*, 2004, Li *et al.*, 2016; Skvortsov *et al.*, 2016; Mailman *et al.*, 2017; Romashevskiy et al., 2018; Voss *et al.*, 2018; Çiçek *et al.*, 2019).

Earlier it has been shown that electric current $I(t)$ flowing along the X-axis leads to appearance of (i) a heat flow with density (Equation 1) (here l, b, and R are respectively length, width, and resistance of the metallization track) and (ii) a temperature field $T(x,y,z)$ (Equation 2) (Skvortsov *et al.*, 2016).

Here the X, Y and Z coordinate axes are directed along length, width and into a plate, respectively; λ is plate heat conduction; T_0 is temperature of environment; (Equation 3) is silicon thermal diffusivity; (Equation 4) is integral exponent.

Equation 2 describes temperature distribution over the surface of plate with a square heating source. Decreasing a minimum topological size of joint elements leads to the problem of "thermal overloads" in the layers (Hu *et al.*, 2012; Zhao *et al.*, 2018; Joi et al., 2019). This may result in destruction of contacts and near-contact regions (Zheng *et al.*, 2017; Amrastanov *et al.*, 2018; Tsai, 2018; Kreiml *et al.*, 2019). On a number of occasions technologists try to apply the methods of correcting mechanical stresses by additional oxidizing the reverse side of silicon plates (Lee *et al.*, 2017; Nguyen *et al.*, 2018; Yao *et al.*, 2019). Nevertheless, in some cases partial destruction of joint integrity (Makara

Downloaded from www.periodico.tchequimica.com

et al., 2015; Bondariev *et al.*, 2018) as well as mechanical damage of the sample under investigation (up to crack formation) (Tsay and Wu, 2017; Hu *et al.*, 2018; Brincker *et al.*, 2018; Ishii *et al.*, 2018; Wang *et al.*, 2019; Mikhelashvili *et al.*, 2019) are observed. In this connection the problem of mechanism of the observed phenomena seems to be urgent.

It is known (Skvortsov *et al.*, 2006; Skvortsov *et al.*, 2016; Moser *et al.*, 2019) that passage of an electric pulse through metallization track may result in processes of (i) contact melting (as the eutectic melting temperature T_{eu} achieves 850 K at the Al-Si interface) and (ii) aluminum film melting (as the aluminum melting temperature T_{Al} achieves 934 K). It was established by the authors in their earlier works (Skvortsov *et al.*, 2006; Skvortsov *et al.*, 2016) that development of processes of contact melting and electro-degradation for the Al-Si systems can appear when heating thin-film systems by an electric pulse of energy up to 250 μJ and interval duration of 50…1000 μs.

The purpose of the research was to perform the stress-strain state analysis of the contact zone of a semiconductor upon electrodegradation of a metallization track on its surface.

2. MATERIALS AND METHODS

Thin-film metal-semiconductor structures were studied in this work. As substrates, we used phosphorus-doped silicon single-crystal wafers oriented in the (111) and (100) directions with a resistivity in the range ρ=1…0.01 Ω.cm, and on parts of the plates was applied 30…50- μm n-epitaxial layer. High-resistance layers prevented shunting of metallization systems, facilitating thermal field analysis. As a conductive metal film, aluminum 1 ... 2 μm thick was used. The test structure was formed by optical photolithography and is shown in Figure 1. The developed measuring complex consisted of a master oscillator, a current pulse shaper of various shapes (rectangular, sawtooth, sinusoidal, etc.) and a digital storage oscilloscope. The current pulse shaper of various shapes, which is part of the installation, provided the following parameters: current adjustment range up to 60 A; the duration of the leading and trailing edges from 10 μm, respectively; maximum pulse duration from 1 ms; maximum pulse repetition rate of at least 0.2 Hz. The measuring complex was used to record temperature operating conditions and defect formation in semiconductor structures under pulsed influences.

The registration of temperature changes in the surface layers of silicon was carried out using the test structure described earlier. Through it pulses of various shapes were passed with the recording of the waveforms U (t). The oscillograms of the inclusion of U (t) during the passage of the current pulse were taken by the corresponding probes from potential sites and recorded by a digital storage oscilloscope.

3. RESULTS AND DISCUSSION:

A typical $U(t)$ dependence when passing square electric pulses of different amplitudes (pulse duration τ_i = 500 μs) is presented in Figure 1. The feature of switching oscillograms and construction of safe area of the metallization system are presented in Figure 2. The points on the oscillograms 1-7 show the moments of oscillogram deviation related to the beginning of contact melting processes at the Al-Si interface and Al film melting. Current pulse power was no more than 170 mJ. It should also be stressed that, at considered parameters of single electric pulses (Kreiml *et al.*, 2019; Li *et al.*, 2016; Kim *et al.*, 2018; Yao *et al.*, 2019; Lu and Yeh, 2019) passing through the metallization-substrate track, the melting-crystallization processes may be wave-like (Figure 3).

3.1. Explosive loading factors in the metallization systems

The main acting factors of explosive-loading in the metallization systems are relaxation of tangential stresses (Msolli *et al.*, 2018; Wang *et al.*, 2019) and concomitant formation of macro-deformations. They lead to formation in the silicon substrate of a deflected wake whose stressed state is close to biaxial or triaxial compression. Detonation in the moment of explosive current pulse passing through metallization is realized in the sliding mode. In this case, 3D configurations of metal flow are realized. A substantially nonhydrostatic stressed state of metal is typical for them. Under these conditions, the role of deviator component of stress tensor increases (Skvortsov *et al.*, 2006). Because of this, relaxation of tangential stresses becomes considerably easier. The final result of this is formation of a deflected wake with σx0 ≈ σz0 ≈ σд. Configuration of a wake appearing in the relaxed material at explosive detonation in the moment of current pulse (with critical current density) passing through metallization (width b_0

Downloaded from www.periodico.tchequimica.com

and thickness δ_0) is sketched in Figure 4.

Cross sizes (v and w) of the region within which relaxation of tangential stresses occurred depend on the thermal shock mode, energy and geometric parameters of Al metallization, physical-mechanical properties of material and substrate geometry, etc. To estimate approximately v and w, let us suppose that (Equation 5) and (Equation 6) (here q_0 is the linear mass of conditional charge) and ascribe the basic part of energy of real wave field to a conditional wave of profile compression. This wave is symmetric about the x-axis; its duration is ~δ0D-1 (Skvortsov *et al.*, 2006). Because of assumption of equality between the kinetic and potential energies in such wave, the total specific energy in it is determined from the following formula (Equation 7). Here σR is stress that is normal to the curvilinear front of a shock wave, cc is propagation velocity of a weak plastic wave, D is propagation velocity of a shock wave, E is Young modulus and R is distance from the x-axis.

Let us liken action of a thin film on semiconductor to successive elastic collisions of mass q0 elements (zone I_0 Solid, Figure 2) moving along a normal to the Z-axis at speeds proportional to $\sqrt{2Q_0}$. Here Q_0 is specific heat of explosion with very big mass of metal whose density is ρ_1 (i.e., one can write down $\rho_1\delta_0^2 c_c^2 D^{-2}$). Hence the energy delivered to the substrate in the moment of explosion pulse passing is expressed by (Equation 6). It follows from Equations 7-8 that (Equation 9).

Thus, the sizes of deflected region will be determined by the stress values in a wave sufficient to achieve deflected state in the substrate. Equation 9 allows to apply the theory of explosive loading for analysis of thermoelastic state of the metal-semiconductor systems. Moreover, variation of "explosive pulse" can affect the size of deflected substrate region. This may result later in formation of point and linear defects, appearance of friction near the thermal shock source and even to system damage.

3.2. Consequences of increasing impulsive action power

Increasing of pulse power action (zone II Liquid, Figure 1) leads to degradation processes in the aluminum metallization system, taking into account electric transport and development of the contact melting processes. The state of the Al-Si interface after crystallization is presented in Figure 5. The contact interaction at pulse advancing to the metal-semiconductor system may be described by the following model. Geometry of the problem is such. There are two solid-state objects: a plate (Si) and a bar (Al). At the instant of an electric pulse (with critical current density) transmission, the aluminum film (Figure 5) is melting and, under action of electric transport (zone II Liquid, Figure 2) and thermal expansion, realizes microscopic travel over the silicon substrate surface. The bar is sliding over the plate with a given speed. In this case, the resulting friction produces heat, thus performing heating both things.

In the general case, the given problem is nonlinear. To simplify calculation, we allow an ideal contact between the contacting surfaces. A natural convective heat exchange with environment is organized on the object surfaces. Calculations were performed using the ANSYS program complex where the mechanical-thermal properties of materials were specified, a finite-element model was developed, boundary conditions and loadings were applied (Figure 6).

At first let a bar is forced down into a plate under the action of surface tension (at the instant of applying a pulse with critical current density) and let this lasts for 0.5 μs. Then the bar will move along the plate due to electric transport. The absolute thermal contact is applied by default. This means that temperature does not drop as heat is transferred from one surface to another. However, numerous “real” conditions lead to the conclusion that thermal conductivity of a real thermal contact differs from absolute one.

Course of computation was controlled by the use of construction of a force convergence graph. The contact stresses calculated in the course of work in the ANSYS program complex are presented in Figure 7. Their numerical values for the structure studied with given geometric parameters lie in the range from 16 to 18 MPa.

4. CONCLUSIONS:

Thereby an analysis of a deflected state of semiconductor near-contact region at electro-degradation of metallization track on its surface revealed some important aspects related to construction of a chart of regions of safe and critical activity of aluminum-silicon contact. This made it possible to perform rapid analysis of safe operation modes for the structures under investigation. We estimated a deflected region depending on electric pulse duration and amplitude. An analysis performed in the ANSYS system from solution of contact problem for the

Downloaded from www.periodico.tchequimica.com

aluminum-silicon system showed that considerable stresses appear in the contact region. They may result in formation of defects in the near-contact region as well as have an influence upon geometry and formation of wavy geometry of a crystallized aluminum film after its melting.

5. ACKNOWLEDGMENTS:

The reported study was funded by RFBR according to the research project No. 18-07-00564.

6. REFERENCES:

1. Amrastanov, A.N., Seregina, E.V., Stepovich, M.A., Filippov, M.N. *Journal of Surface Investigation*, **2018**, *12*(4), 778-782.
2. Bojita, A., Boianceanu, C., Purcar, M., Florea, C., Simon, D., Plesa, C.-S. *Microelectronics Reliability*, **2018**, *87*, 142-150.
3. Bondariev, V., Gorushko, V., Pilipenko, V., Solodukha, V. *High Temperature Material Processes*, **2018**, *22*(1), 1-6.
4. Brincker, M., Walter, T., Kristensen, P.K., Popok, V.N. *Journal of Materials Science: Materials in Electronics*, **2018**, *29*(5), 3898-3904.
5. Chen, Y.-L., Wu, J., Lee, C.C. *Journal of Materials Science: Materials in Electronics*, **2018**, *29*(12), 10037-10043.
6. Çiçek, O., Kurnaz, S., Bekar, A., Öztürk, Ö. *Composites Part B: Engineering*, **2019**, *174*, article number 106987.
7. Dang, G.T., Kawaharamura, T., Furuta, M., Allen, M.W. *Applied Physics Letters*, **2017**, *110*(7), article number 073502.
8. Dong, A., Wang, H. *Annalen der Physik*, **2019**, *531*(7), 1800440.
9. Hu, C.-K., Ohm, J., Gignac, L.M., Breslin, C.M., Mittal, S., Bonilla, G., Edelstein, D., Rosenberg, R., Choi, S., An, J.J., Simon, A.H., Angyal, M.S., Clevenger, L., Maniscalco, J., Nogami, T., Penny, C., Kim, B.Y. *Journal of Applied Physics*, **2012**, *111*(9), Article number 093722.
10. Hu, X., Liu, H., Wang, X., Zhang, X., Shan, Z., Zheng, W., Li, H., Wang, X., Zhu, X., Jiang, Y., Zhang, Q., Zhuang, X., Pan, A. *Advanced Optical Materials*, **2018**, *6*(12), 1800293.
11. Ishii, T., Yamakawa, H., Kanaki, T., Miyamoto, T., Kida, N., Okamoto, H., Tanaka, M., Ohya, S. *Scientific Reports*, **2018**, *8*(1), article number 6901.
12. Ishitani, Y., Aoki, T., Funabashi, H., Morita, K. *Applied Physics Letters*, **2018**, *113*(19), article number 192105.
13. Joi, A., Venkatraman, K., Tso, K.-C., Dictus, D., Dordi, Y., Wu, P.-W., Pao, C.-W., Akolkar, R. *ECS Journal of Solid State Science and Technology*, **2019**, *8*(9), 516-521.
14. Kapitonov, S.S., Bespalov, N.N., Il'in, M.V., Gulyaev, I.V. *Russian Electrical Engineering*, **2017**, *88*(6), 351-354.
15. Kashniyal, U., Pandey, K.P. *Vacuum*, **2018**, *152*, 109-113.
16. Kim, W.K., Melnick, C., Shim, J.H., Kaviany, M. *Journal of Nuclear Materials*, **2018**, *511*, 148-163.
17. Kreiml, P., Rausch, M., Terziyska, V.L., Winkler, J., Mitterer, Ch., Cordill, M.J. *Scripta Materialia*, **2019**, *162*, 367-371.
18. Lee, J.-G., Kim, D.-H., Eom, S.-K., Roh, S.-H., Seo, K.-S., Kim, H.-S., Kim, H., Cha, H.-Y., Byun, Y.-C. *Journal of the Korean Physical Society*, **2018**, *72*(1), 166-170.
19. Li, Y., Lee, H.-T., Saka, M. *Microelectronics Reliability*, **2016**, *65*, 178-183.
20. Lim, L.Y., Meguid, S.A. *Materials and Design*, **2019**, *164*, Article number 107543.
21. Lu, C.-L., Yeh, M.-K. *Microelectronic Engineering*, **2019**, *213*, 47-54.
22. Mailman, A., Leitch, A.A., Yong, W., Steven, E., Winter, S.M., Claridge, R.C.M., Assoud, A., Tse, J.S., Desgreniers, S., Secco, R.A., Oakley, R.T. *Journal of the American Chemical Society*, **2017**, *139*(6), 2180-2183.
23. Makara, V.A., Steblenko, L.P., Vesna, G.V., Naumenko, S.N., Kurilyuk, A.N. *Physics of the Solid State*, **2015**, *57*(2), 349-352.
24. Mikhelashvili, V., Yofis, S., Shacham, A., Khanonkin, I., Eyal, O., Eisenstein, G. *Journal of Applied Physics*, **2019**, *126*(5), article number 054501.
25. Moser, S., Zernatto, G., Kleinbichler, M., Nelhiebel, M., Zechner, J., Cordill, M.J., Pippan, R. *JOM*, **2019**, *71*(10), 3399-3406.
26. Msolli, S., Alexis, J., Kim, H. *Advanced Engineering Materials*, **2017**, *19*(8), article

Downloaded from www.periodico.tchequimica.com

number 1700109.

27. Nguyen, M.-C., On, N., Ji, H., Nguyen, A.H.-T., Choi, S., Cheon, J., Yu, K.-M., Cho, S.-Y., Kim, J., Kim, S., Jeong, J., Choi, R. *IEEE Transactions on Electron Devices*, **2018**, *65*(6), 2492-2497.
28. Romashevskiy, S.A., Tsygankov, P.A., Ashitkov, S.I., Agranat, M.B. *Applied Physics A: Materials Science and Processing*, **2018**, *124*(5), article number 376.
29. Shejko, S., Shalomeev, V., Mishchenko, V. *Materials Science and Technology Conference and Exhibition 2017, MS and T 2017*, **2017**, *1*, 238-244.
30. Sirazijeva, L.F., Stepin, S.N., Makhotkina, L.Yu. *Lakokrasochnye Materialy i Ikh Primenenie*, **2004**, *10*, 25-28.
31. Skvortsov, A.A., Orlov, A.M., Rybin, V.V. *Technical Physics Letters*, **2006**, *32*(3), 240-242.
32. Skvortsov, A.A., Zuev, S.M., Koryachko, M.V., Glinskiy, V.V. *Microelectronics International*, **2016**, *33*(2), 102-106.
33. Tsai, C.-Y. *Microelectronics Reliability*, **2018**, *91*, 335-343.
34. Tsay, C.-Y., Wu, P.-H. *Japanese Journal of Applied Physics*, **2017**, *56*(3), article number 03BA02.
35. Voss, L.F., Murphy, J.W., Shao, Q., Henderson, R.A., Frye, C.D., Stoyer, M.A., Nikolic, R.J. *Applied Physics Letters*, **2018**, *113*(24), article number 24103.
36. Wang, M., Zhao, L., Fourmeau, M., Nelias, D. *Journal of the Mechanics and Physics of Solids*, **2019**, *122*, 472-488.
37. Xu, T., Ji, G.P., Cao, Z.X., Ji, A.L. *Journal of Physics D: Applied Physics*, **2018**, *51*(5), article number 055303.
38. Yao, Y., Chalifoux, B.D., Heilmann, R.K., Schattenburg M.L. *Optics Express*, **2019**, *27*(2), 1010-1024.
39. Zhao, J., Zhai, J., Lu, Y., Liu, N. *International Journal of Heat and Mass Transfer*, **2018**, *120*, 241-249.
40. Zheng, D., Yu, C., Zhang, Q., Wang, H. *Nanotechnology*, **2017**, *28*(50), article number 505201.

$q = I^2R/lb$ (Eq. 1)

$$T(y,\tau)-T_0=\frac{I^2R}{2\pi\lambda lb}\left[(\frac{b}{2}-y)E_1(\frac{(b/2-y)^2}{4a\tau})+(\frac{b}{2}+y)E_1(\frac{(b/2+y)^2}{4a\tau})\right]$$
$$+\frac{I^2R\sqrt{a\tau}}{\sqrt{\pi\lambda lb}}\left[\Phi(\frac{b/2-y}{\sqrt{4a\tau}})+\Phi(\frac{b/2+y}{\sqrt{4a\tau}})\right] \quad \text{(Eq. 2)}$$

$a = \lambda/(cd)$ (Eq. 3)

$$E_1(z)=\int_z^\infty \exp(-\xi)\frac{d\xi}{\xi} \quad \text{(Eq. 4)}$$

$b_0 = \delta_0$ (Eq. 5)

$$\rho_0 = q_0\delta_0^{-2} \quad \text{(Eq. 6)}$$

$$U = \pi R\delta_0 c_c \sigma_R^2 (DE)^{-1} \quad \text{(Eq. 7)}$$

$$U \approx \frac{q_0^2 Q_0 D^2}{\rho_1 \delta_0 c_c^{\ 2}} \quad \text{(Eq. 8)}$$

Downloaded from www.periodico.tchequimica.com

$$\sigma_R(R) \approx \frac{\delta_0 \rho_0^{\,2}}{\pi R \rho_1} \left(\frac{D}{c_c}\right)^3 Q_0 E$$

(Eq. 9)

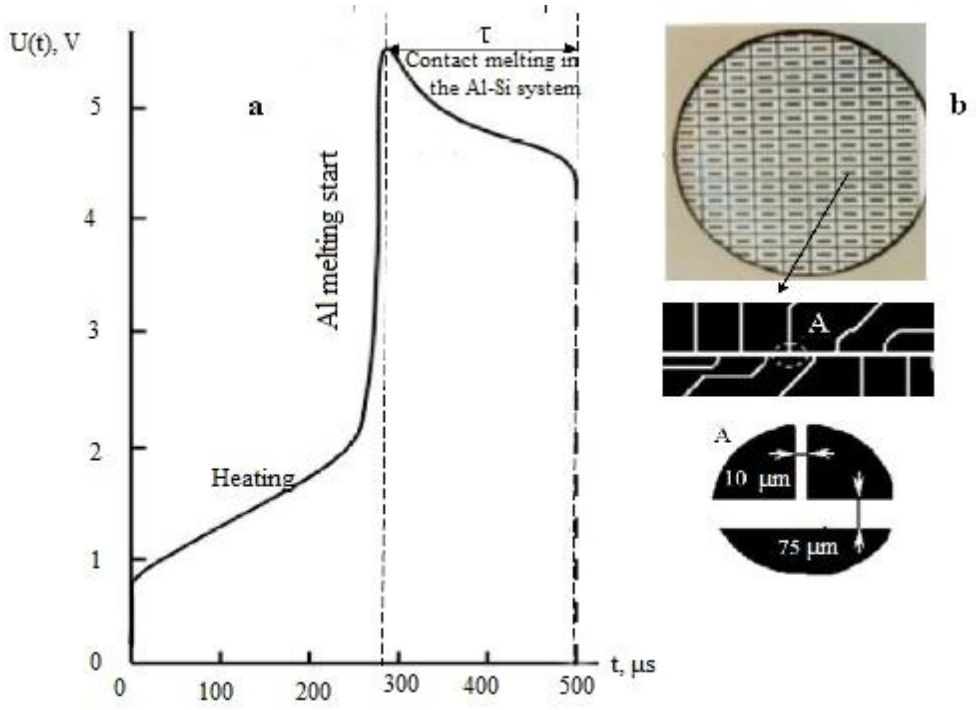

Figure 1. *a – Appearance of switching oscillograms U(t) at a single current pulse passing through an Al metallization track on Si. Al film thickness of 3 μm; length and width of 5 mm and 50 μm, respectively; Si substrate thickness of 1 mm; pulse duration τ = 500 μs, amplitude j =5.8·10^{10} A/m^2. τ zone is contact melting duration; b – Appearance of test structures used when performing experiment*

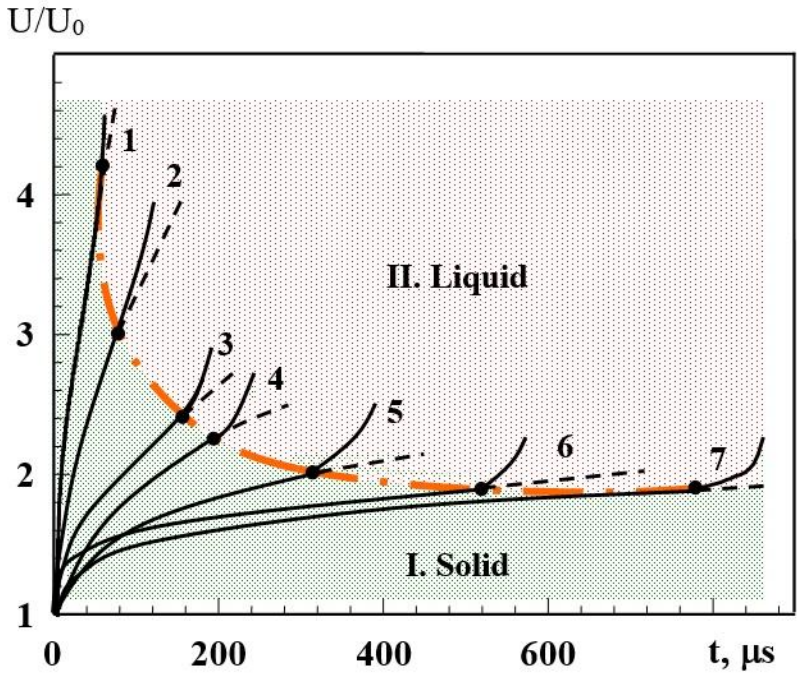

Figure 2. *Chart of safe operation region of an Al-Si contact (I. Solid is bounded above by a dash-dotted line) constructed on the basis of switching oscillograms taken at passing through the structure of a single square current pulse with amplitude (in A/m^2): 1 – j = 8.8·10^{10}; 2 – 8.6·10^{10}; 3 – 8.2·10^{10}; 4 – 6.7·10^{10}; 5 – 6.6·10^{10}; 6 – 6.1·10^{10}; 7 – 5.8·10^{10}*

Downloaded from www.periodico.tchequimica.com

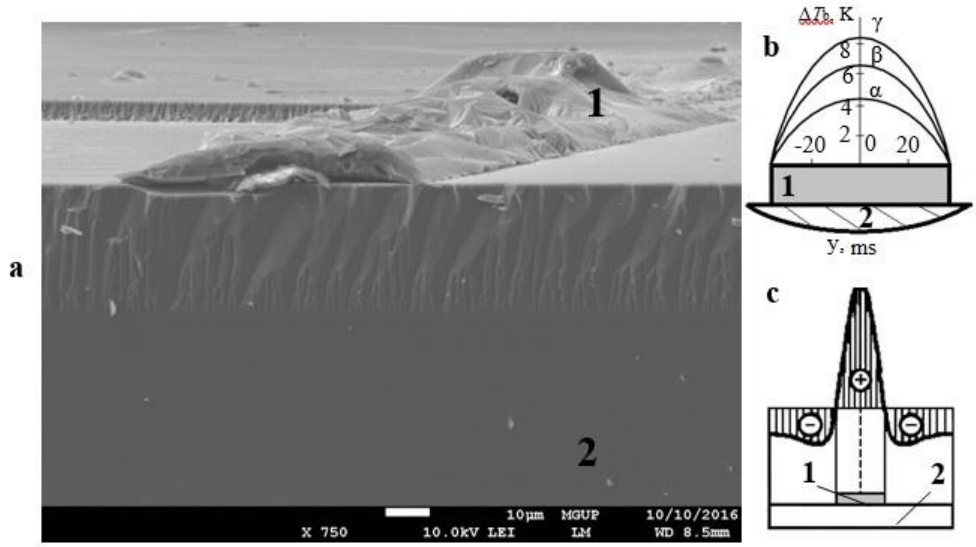

Figure 3. *a – wave-like form of Al metallization (1) on Si substrate (2) after a current pulse passing through it (melting); b – ΔT_b temperature profile of metallization track at passing a current pulse with duration τ_0 = 1000 μs and amplitude (in A/m^2): α – 2.0×10^{10}; β – 2.8×10^{10}; γ –3.5×10^{10}; c – stress diagram in the metal-substrate system at a moment of current pulse passing*

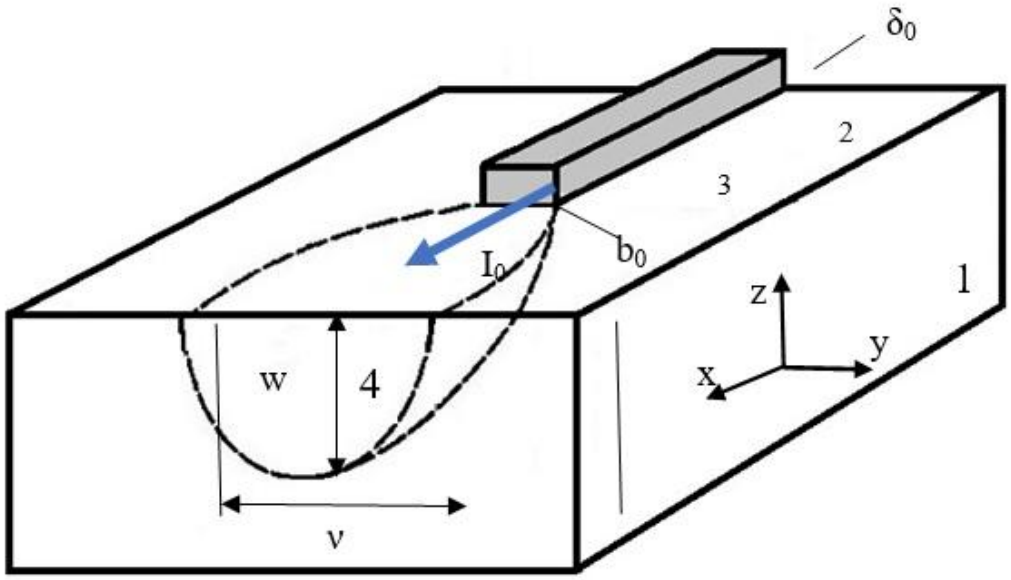

Figure 4. *Configuration of "momentary" deflected region produced in the Si substrate by an explosive current pulse passing through Al metallization in the sliding supersonic detonation mode: 1 – Si substrate, 2 – Al metallization, 3 – detonation front, 4 – track contour; the I0 arrow shows direction of current motion*

Downloaded from www.periodico.tchequimica.com

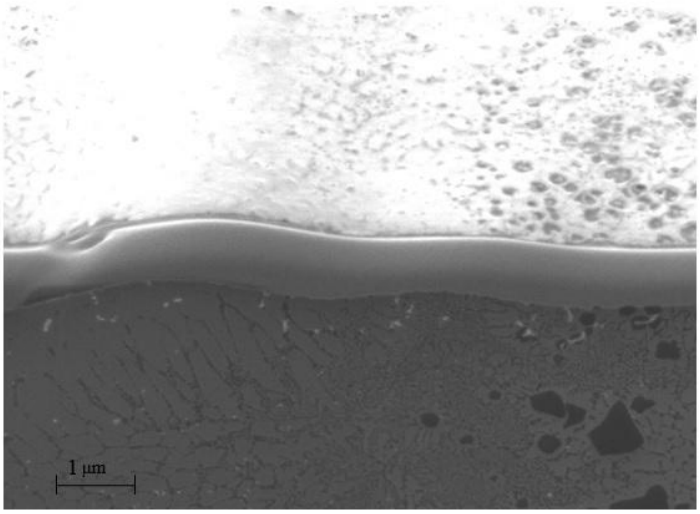

Figure 5. *Scanning electron microscope picture of wave-like parts of the Al-Si metallization system after passing a critic current pulse*

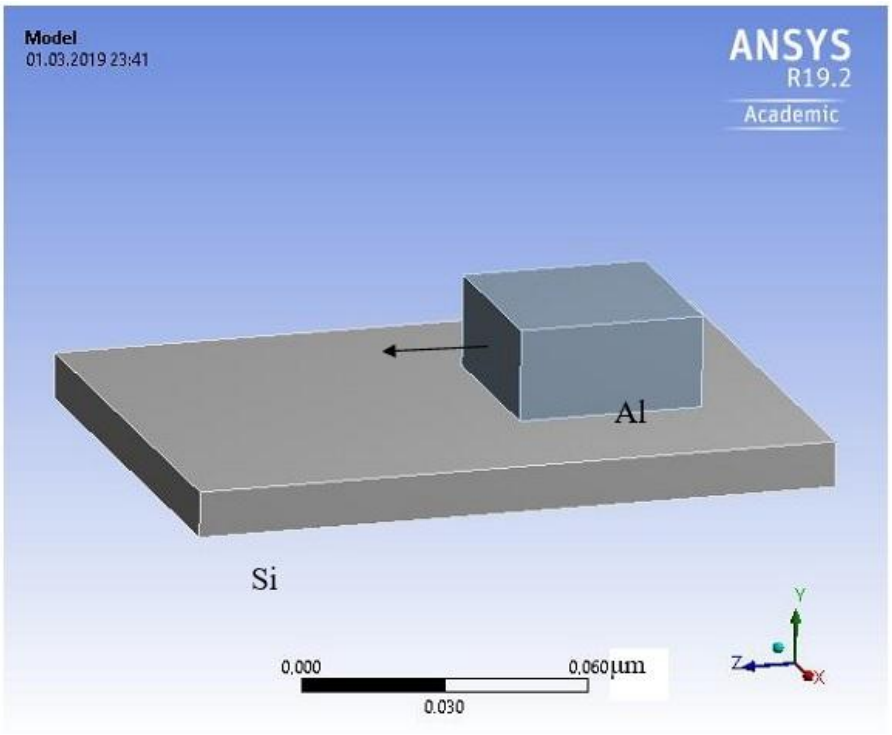

Figure 6. *3D model used for calculations, arrow shows direction of electric current flow*

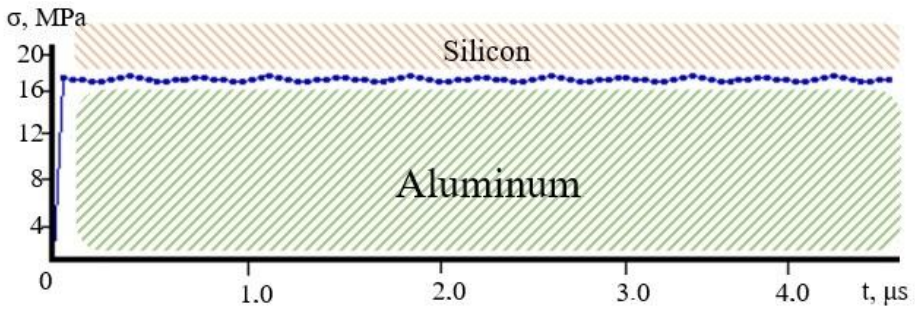

Figure 7. *Contact stresses at the Al-Si interface*

Downloaded from www.periodico.tchequimica.com

PERIÓDICO TCHÊ QUÍMICA
ARTIGO ORIGINAL

SÃO OS PACIENTES COM NEFROPATIA DIABÉTICA DIFERENTES EM RELAÇÃO A PARÂMETROS DE ULTRASSOM RENAL E ACHADOS DE SONOGRAFIA DOPPLER COMPARADOS COM HISTOPATOLOGIA RENAL?

ARE PATIENTS WITH DIABETIC NEPHROPATHY DIFFERENT REGARDING RENAL ULTRASOUND PARAMETERS AND DOPPLER SONOGRAPHY FINDINGS COMPARED WITH RENAL HISTOPATHOLOGY?

GHADI, Armin[1]; BAGHERI, Seyed Morteza[1*]; HORI, Honey[1]; ROOSTAEE, Ayda[1]; GHADAMZADEH, Mustafa[1];

[1] Department of Radiology, Hasheminejad Kidney Center (HKC), Iran University of Medical Sciences, Tehran, Iran

** Autor correspondente*
e-mail: bagherii.m@iums.ac.ir

Received 26 August 2019; received in revised form 08 October 2019; accepted 02 November 2019

RESUMO

Os achados de ultrassonografia (US) e sonografia Doppler dos vasos renais podem fornecer informações úteis sobre o suprimento estrutural e vascular de pacientes que sofrem de doença renal crônica (DRC). O objetivo deste estudo foi comparar os achados da US de pacientes com nefropatia diabética com os achados patológicos de sua biópsia renal. Neste estudo descritivo, os parâmetros ultrassonográficos, incluindo índice de resistividade (IR), tamanho e volume renal, ecogenicidade cortical e medular e achados histopatológicos da biópsia renal (fibrose, inflamação e cronicidade) de 60 pacientes (27 mulheres e 33 homens) com nefropatia diabética internados no centro renal Hasheminejad (HKC) de Teerã foram extraídos e analisados. Dos 60 pacientes, fibrose intersticial (FI) em 47 pacientes, inflamação intersticial (II) em 50 pacientes e sinais de cronicidade em 43 pacientes no relatório de patologia foram observados. Pacientes com FI apresentaram maior comprimento renal, maior volume sinusal, ecogenicidade grosseira e ecogenicidade medular anormal, significativamente. A presença de II foi associada a maior comprimento renal, maior volume renal e sinusal, maior ecogenicidade cortical e mais pacientes com ecogenicidade grosseira e ecogenicidade medular anormal. A observação da cronicidade foi significativamente correlacionada com maior volume sinusal e mais pacientes com borda renal irregular. De acordo com os achados deste estudo, comprimento e volume renal, volume do seio renal e presença de ecogenicidade grosseira e ecogenicidade medular anormal estão fortemente correlacionados com os achados histopatológicos renais em pacientes com nefropatia diabética. O IR não é um marcador adequado para identificar alterações tubulo-intersticiais nesses pacientes.

Palavras-chave: *Ultrassonografia, Doppler, Índice Resistivo, Doença Renal Crônica, Biópsia renal.*

ABSTRACT

Ultrasonography (US) findings and Doppler sonography of renal vessels can provide useful information on the structural and vascular supply of patients suffering from chronic kidney disease (CKD). The purpose of this study was to compare the US findings of patients with diabetic nephropathy with the pathologic findings of their renal biopsy. In this descriptive study, US parameters including resistivity index (RI), renal size and volume and cortical and medullary echogenicity, and histopathological findings of renal biopsy (fibrosis, inflammation and chronicity) of 60 patients (27 women and 33 men) with diabetic nephropathy admitted in Hasheminejad kidney center (HKC) of Tehran were extracted and analyzed. Of 60 patients, interstitial fibrosis (IF) in 47 patients, interstitial inflammation (II) in 50 patients and signs of chronicity in 43 patients in pathology report were observed. Patients with IF had larger renal length, higher sinus volume, coarse echogenicity, and abnormal medullary echogenicity, significantly. The presence of II was associated with larger renal length, higher renal and sinus volume, higher cortical echogenicity, and more patients with coarse echogenicity and abnormal medullary echogenicity. The observation of chronicity was significantly correlated with higher sinus volume and more patients with irregular renal rim. According to the findings of this study, renal length and volume, renal sinus volume, and the presence of coarse echogenicity and abnormal medullar echogenicity strongly correlate with renal histopathologic findings in patients with diabetic nephropathy. RI is not a suitable marker for identifying tubulointerstitial changes in these patients.

Downloaded from www.periodico.tchequimica.com

Keywords: *Ultrasonography, Doppler Ultrasound, Resistive Index, Chronic Kidney Disease, Renal biopsy.*

1. INTRODUCTION

Chronic kidney disease (CKD) is one of the major growing issues in the public health system, worldwide (Nahas and Bello, 2005). Only a small population of patients with renal dysfunction experience a rapid decline in renal function and often they are presented with a chronic impairment of renal function (Eriksen and Ingebretsen, 2006). Diabetes mellitus (DM) is one of the main causes of CKD, other health problems and diabetic nephropathy is the most common cause of end-stage renal disease (ESRD) (Ritz and Orth, 1999, Ghajari et al., 2017). The diagnosis of CKD in patients with DM and the prognosis of it, especially their long-term prognosis is of great importance. The major predictors of renal function decline in these patients are arterial hypertension (HTN), proteinuria, and baseline renal function (Bigé et al., 2012). Histological findings of renal biopsy, including the presence of interstitial fibrosis (IF) are also associated with renal function and long-term prognosis of CKD (Nath, 1992).

Ultrasonography (US) findings and Doppler sonography of renal vessels can provide useful information on the structural and vascular morphology of patients suffering from CKD. Unlike histopathologic studies, US is a non-invasive method to evaluate patients who are at risk of renal impairment (Ghadirpour et al., 2014). Several studies in recent years have shown the relationship between US parameters (especially renal resistive index (RI)) and tubulointerstitial and vascular damage of the kidneys (Sugiura and Wada, 2009).

Despite the promising results in various studies, US parameters are less used in CKD management (Buturović-Ponikvar and Višnar-Perovič, 2003). The aim of the study was to compare the sonographic findings of patients with diabetic nephropathy with the pathologic findings of the renal biopsy in these patients so that this low-risk and safe method can be used as an alternative to more risky diagnostic methods such as biopsy and imaging with contrast media.

2. MATERIALS AND METHODS

2.1 Study design and setting

This descriptive cross-sectional study was performed from October to May in 2017-2018. The study was done at Hasheminejad Kidney Center (HKC), a referral academic hospital affiliated to Iran University of Medical Sciences, Tehran and was approved by the ethics committee (code#: IR.IUMS.FMD.REC.1396.9411282017) of Iran University of Medical Sciences. The research was carried out according to the Helsinki Declaration and informed written consent was obtained from all participants.

2.2. Participants

This study included 60 patients with DM referred to the Hasheminejad kidney center (HKC) for renal biopsy. History and demographic information were taken from all participants.

The inclusion criteria were:

1. Patients with diabetic nephropathy (proteinuria > 0.5 g/24h) (Gross et al., 2005)
2. Age > 20 years

The exclusion criteria were:

1. Polycystic kidney disease
2. Post-renal CKD
3. Acute kidney injury
4. Patients with one kidney
5. Renal tumors
6. Asymmetry of the kidneys (> 2 cm difference in renal length)

2.3 Ultrasonographic and histopathologic evaluation

US examination was performed 24 hours before the renal biopsy. U.S and Doppler US examinations were performed by a single radiologist with 10 years biopsy experience unaware of patient information, by a 3.5 MHz abdominal convex transducer with a PHILIPS Acuson 500. For each patient, renal length, volume, renal sinus volume, and cortical and medullary thickness was measured for both kidneys. Renal cortical echogenicity was assessed and recorded as Grade 1, 2 and 3, as

Downloaded from www.periodico.tchequimica.com

being light, moderate, and advanced, respectively (Gross et al., 2016). Corticomedullary differentiation and medullary echogenicity were evaluated as normal, increased and decreased. The presence of coarse echogenicity was also evaluated (normal, slightly or considerable). Renal rim was recorded as either regular or irregular. The presence of inflammatory changes, surrounding fat, fatty infiltration of the renal parenchyma, and renal displacement during inhalation was also recorded. RI was calculated by the following formula using built-in software: (systolic flow velocity - diastolic flow velocity) / systolic flow velocity. The RI was measured five times on each kidney and the average value was recorded (Kim et al., 1992).

Renal biopsies were performed by using ultrasonographic localization of the lower pole of the left kidney. All renal biopsy specimens were reviewed on light microscopy, immunofluorescence, and electron microscopy (Ikee et al., 2005; Spyridopoulos et al., 2010). The presence of renal interstitial fibrosis (IF), interstitial inflammation (II) and chronicity were evaluated.

2.4 Statistical analysis

Statistical analysis was performed by SPSS software V22, SPSS Inc., Chicago, IL, USA. The Kolmogorov-Smirnov test was used to assess the normality of the data distribution. Chi-square test and repeated measures ANOVA were used for statistical comparison of results between. The significant threshold was considered to be less than 0.05.

3. RESULTS AND DISCUSSION:

Of 60 patients enrolled in this study, 27 (45%) were female and 33 (55%) were male (Table 1). Of these patients, we observed interstitial fibrosis (IF) in 47, interstitial inflammation (II) in 50 and signs of chronicity in 43 patients. As it is demonstrated in table 2-4, there were no significant differences in the sex distribution, mean age and the number of patients with HTN between cases with the presence of either histopathologic finding and patients without them (all with p-value > 0.05). The mean age of patients with IF in their renal specimen and without it, was 49.91 ± 15.13 43.00 ± 13.00 years, respectively. The mean age of patients with II was 49.14 ± 14.99 years and in cases without II was 44.80 ± 14.48 years. In patients with positive findings regarding chronicity, the mean age was 49.26 ± 15.67 years and in patients with negative findings, it was 46.29 ± 12.82 years. The glomerular filtration rate (GFR) values were significantly lower in patients with positive findings in their renal biopsy all with p-value < 0.001 (35.72 ± 12.32, 37.18 ± 26.00 and 35.02 ± 27.06 in patients with IF, II and chronicity compared to 79.00 ± 12.32, 84.70 ± 6.46 and 70.59 ± 19.62 in patients without them, respectively).

In table 2, US findings are demonstrated based on the presence of interstitial fibrosis in the renal biopsy. As it is shown, there was no significant difference in renal volume, RI, renal cortex, medulla and cortex on medulla thickness, medulla/cortex and parenchyma/renal diameter ratio, cortex echogenicity, Corticomedullary differentiation, renal rim contour and the presence of inflammatory changes, surrounding fat, fatty infiltration of the renal parenchyma, and renal displacement during inhalation, whether IF was present or not. The RI was higher in patients with fibrosis (0.68 ± .11 and 0.67 ± .10 compared to 0.65 ± .02 and 0.65 ± .03 in right and left kidney, respectively) with no significant difference (both with p-value = 0.401). Patients with fibrosis had a larger right kidney (111.02 ± 9.40 mm compared to 104.15 ± 4.34 mm) with p-value = 0.020. The sinus volume was 33.84 ± 12.10 cc in right kidney and 35.30 ± 11.28 cc in the left kidney in patients with IF and 23.77 ± 8.56 cc in right kidney and 22.54 ± 9.23 cc in left kidney in patients without IF. This difference was significant (p-value = 0.007 and 0.004, respectively). The fibrosis was associated with more patients with renal coarse echogenicity (17 cases of slight and 6 cases of considerable coarse echogenicity compared to none in patients without IF) and abnormal medullar echogenicity (15 patients with decreased and 7 with increased echogenicity, whereas all of the patients without fibrosis were normal regarding this US parameter) with p-value = 0.006 and 0.008, respectively.

In table 3, US findings are shown based on the presence of interstitial inflammation in the renal biopsy. We observed no significant difference comparing patients with II and patients without it, regarding RI, renal cortical, medullar and cortex on medulla thickness, medulla to cortex and parenchyma to diameter ratio, Corticomedullary differentiation, renal rim contour and the presence of inflammatory changes, renal surrounding fat, fatty infiltration of the renal parenchyma, and renal displacement during inhalation. The RI was 0.68 ± .10 and 0.65 ± .03 in the right kidney and 0.66 ± .10 and 0.65 ± .03 in the left kidney, in patients with and without

Downloaded from www.periodico.tchequimica.com

inflammation, respectively, with no significant difference (both with p-value = 0.611). The presence of inflammation was associated with larger kidney and larger renal volume, significantly (111.02 ± 9.11 mm and 196.88 ± 50.02 cc compared to 102.10 ± 2.18 mm and 134.30 ± 17.48 cc in right and 110.76 ± 11.32 mm and 192.92 ± 75.71 cc compared to 103.00 ± 4.83 mm and 139.50 ± 10.29 cc in left kidney) all with p-value < 0.05. The sinus volume was 33.79 ± 11.71 cc in right kidney and 35.21 ± 10.91 cc in left kidney in patients with II and 21.00 ± 7.79 cc in right kidney and 19.10 ± 7.53 cc in left kidney in patients without inflammation. This difference was significant (p-value = > 0.001 and 0.001, respectively). The coarse echogenicity was recorded only in patients with inflammation (17 cases of slight and 6 cases of considerable coarse echogenicity) which was significant with p-value =0.024. Patients with increased cortical echogenicity (17 grade 2 and 7 grade 3) and abnormal medulla echogenicity (15 patients with decreased and 7 with increased echogenicity) were also observed only in the case of II, with p-value = 0.018 and 0.031, respectively.

In table 4, US findings are demonstrated based on the presence of chronicity in the renal biopsy. There was no significant difference comparing patients with and without chronicity regarding RI, renal medullar thickness, medulla to cortex and parenchyma to diameter ratio, cortical and medullar echogenicity, Corticomedullary differentiation, and the presence of inflammatory changes, renal surrounding fat, fatty infiltration of the renal parenchyma, and renal displacement during inhalation. The RI was higher in the presence of chronicity with no significant difference (0.68 ± .11 and 0.65 ± .04 in the right kidney and 0.67 ± .11 and 0.64 ± .03 in the left kidney, with p-value = 0.219 and 0.84, in patients with and without chronicity, respectively (Table 5). The presence of chronicity was also associated with larger kidney and larger renal volume, significantly (112.05 ± 9.18 mm and 198.00 ± 40.74 cc compared to 103.18 ± 4.17 mm and 157.24 ± 65.20 cc in right and 112.28 ± 11.11 mm and 196.33 ± 71.72 cc compared to 102.35 ± 6.15 mm and 152.88 ± 64.49 cc in left kidney) all with p-value < 0.05. The sinus volume was 34.92 ± 12.18 cc in right and 36.22 ± 11.42 cc in the left kidney in patients with chronicity and 23.59 ± 7.42 cc in right and 23.35 ± 8.14 cc in left kidney in patients without chronicity. This difference was significant both with p-value < 0.001. Higher cortical thickness was observed in patients with positive chronicity in renal biopsy in both kidneys (8.69 ± 2.67 mm and compared to 7.46 ± 1.18 mm in right and 9.48 ± 5.93 mm compared to 7.13 ± .42 mm in left) with p-value = 0.046 and 0.004, respectively. The thickness of the portion of cortex lying on medulla was also higher in patients with chronicity sign which was significant in the left kidney (8.21 ± 1.99 mm and compared to 7.11 ± .45 mm with p-value = 0.004) (Table 6). The coarse echogenicity and irregular renal rim contour were observed only in patients with chronicity (17 cases of slight and 6 cases of considerable coarse echogenicity and 10 patients with irregular rim) with p-value =0.001 and 0.025, respectively (Table 7).

U.S is a useful diagnostic tool in nephrology conditions. In many of the renal disorders, US is used as the first line of diagnosis, due to its non-invasive nature and its low cost and the ability to evaluate different parts of the kidney and its parenchyma (Lucisano et al., 2015). However, it is still less used in evaluating the structural changes and management of CKD (Pellerito and Polak, 2012). The aim of this study was to investigate the relationship between US findings and renal histopathology in patients with diabetic nephropathy.

Based on the findings of this study, the interstitial fibrosis was associated with larger kidney, higher renal sinus volume, and more patients with coarse echogenicity and abnormal medullar echogenicity (i.e. decreased or increased). The presence of interstitial inflammation in the renal biopsy had a significant relationship with larger kidney, larger renal and sinus volume, higher cortical echogenicity, and more patients with coarse echogenicity and abnormal medullar echogenicity (i.e. decreased or increased). The observation of chronicity was significantly correlated with larger kidney, higher cortical thickness, higher renal sinus volume, and more patients with irregular renal rim contour and coarse echogenicity. There was no significant difference between the pathologic findings of the renal biopsy specimen of patients with diabetic nephropathy and their mean RI.

Moghazi et al. conducted a study regarding the relationship of US findings with renal histopathological findings in 207 patients with CKD (Moghazi et al., 2005). They concluded that among US parameters, cortical echogenicity associated best with the renal histopathology. There was a significant correlation between renal size and glomerular sclerosis and tubular atrophy and between parenchyma thickness and tubular atrophy. Furthermore, the most important determinants of cortical echogenicity were tubular atrophy and interstitial inflammation and not the

Downloaded from www.periodico.tchequimica.com

fibrosis. In 86% of patients in higher grades of CKD, renal length of < 20 cm and cortical echogenicity > 1 were recorded. They reported that even though size or echogenicity alone are not adequate factors in diagnosing the irreversible chronic renal disease, but the probability of a curable disease in patients with smaller kidney and higher cortical echogenicity is very low. In comparison, in the present study, higher renal size and sinus volume and the presence of coarse echogenicity were associated with all of the renal histopathologic findings (i.e. fibrosis, inflammation, and chronicity). Also, there was no comparison between the severity of renal function and size. Similar to the Moghazi et al. study, there was an association between cortical echogenicity and interstitial inflammation and not the interstitial fibrosis. The lack of correlation between interstitial fibrosis and cortical echogenicity seems surprising, Given that it is widely assumed that collagen fibrils play an important role in acoustic backscatter of tissue (Rosenfield et al., 1978; Insana et al., 1991; Price et al., 1980). In another study conducted by Hricak et al. on the qualitative assessment of echogenicity (Hricak et al., 1982), no relation was found with IF.

In a Lucisano et al. study on 72 patients with stages 1-4 of CKD (Lucisano et al., 2015), it was found that parenchymal thickness and renal length were highly correlated with GFR and could be appropriate tools for evaluating renal function in these patients. Based on the findings of this study, correction of US parameters with the height of patients would strengthen the association of these parameters with the GFR. In the Hricak et al. study, a relationship was also observed between renal length and histopathologic findings including sclerosis (Hricak et al., 1982). On the other hand, Beland et al. concluded that cortical thickness compared with renal length is a better indicator of renal function and it has a stronger relationship with GFR (Beland et al., 2010). In the present study, renal length was associated with interstitial fibrosis, inflammation, and chronicity in renal biopsy of patients with diabetic nephropathy.

Van et al. also showed that both renal length and volume are associated with renal function measured by GFR in the elderly, but the renal length has low specificity in the prediction of renal impairment (Van et al., 2013). The main problem with measuring renal volume using ultrasound is the difficulty in measuring the true renal volume due to using of the ellipsoid formula to measure the renal volume, while the kidney is not a true ellipsoid.

In our study, cortical thickness was only associated with chronicity and not the presence of inflammation or interstitial fibrosis. Furthermore, medulla thickness was not significantly correlated with any of the renal histopathologic findings. In the Moghazi et al. study, there was no correlation between renal parenchymal and cortical thickness and pathologic findings (Moghazi et al., 2005). The poor correlation of histopathological findings with these measurements may be due to the poor accuracy and reproducibility of these parameters. Also, in the presence of poor Corticomedullary differentiation, such as patients with moderate to advanced CKD, the cortex and medulla interface is hard to evaluate and it is more appropriate to measure the parenchymal thickness (sum of cortex and medulla), instead (Beland et al., 2010).

In Yaprak et al. study, a different method was used to evaluate renal function. In this study, renal length and parenchymal thickness and echogenicity were calculated and summed up as a CKD ultrasound score (Yaprak et al., 2017). It was concluded that there is a correlation between CKD ultrasound score and eGFR and this score can be used to differentiate between grades 3-5 and 1-2 of CKD. Relationships between RI and several pathological renal conditions such as glomerulosclerosis and tubulointerstitial and vascular injuries, as well as diabetes have been reported in some studies (Bakker et al., 1999; Moradi et al., 2011; Hedayatifar et al., 2017, Shirin et al., 2016, Sugiura et al., 2016; Mostbeck et al., and Platt et al., 1990).

Despite the strength of the present study, it is subject to a number of limitations and should be interpreted in view of its limitations. The main limitation was the small sample size. Also, US parameters were not compared with renal function markers including creatinine and GFR. Furthermore, RI was not analyzed in different stages of nephropathy.

4. CONCLUSIONS:

According to the findings of this study, renal length and volume, renal sinus volume, and the presence of coarse echogenicity and abnormal medullar echogenicity strongly correlate with renal histopathologic findings (presence of fibrosis, inflammation, and chronicity) in patients with diabetic nephropathy. Also, RI is not a suitable marker for identifying

Downloaded from www.periodico.tchequimica.com

tubulointerstitial changes in these patients. Increased cortical echogenicity and thickness are associated with interstitial inflammation and chronicity, respectively.

5. ACKNOWLEDGEMENTS:

The present study was supported by a grant from the Vice-chancellor for Research, Iran University of Medical Science, Iran.

6. CONFLICTS OF INTEREST:

No conflicts are declared

7. REFERENCES:

1. Bakker J., Olree M., Kaatee R., de Lange E.E., Moons K.G., Beutler J.J., Beek F.J. *Radiology*. **1999**, 211, 623-8.
2. Beland M.D., Walle N.L., Machan J.T., Cronan J.J. *American J Roentgenol*. **2010**, 195,146-9.
3. Bigé N, Lévy P.P., Callard P., Faintuch J.M., Chigot V., Jousselin V., Ronco P., Boffa J.J. *BMC Nephrol*. **2012**, 13,139.
4. Buturović-Ponikvar J, Višnar-Perovič. *Eur J Radiol*. **2003**, 46, 115-22.
5. El Nahas A.M., Bello A.K. *The Lancet*., **2005**, 365, 331-40.
6. Eriksen B.O., Ingebretsen O.C. *Kidney Int*. **2006**, 69, 375-82.
7. Ghadirpour A., Tarzamni M.K., Naghavi-Behzad M., Abedi-Azar S., Koushavar H., Nezami N. *Med Ultrason*. **2014**,16,95-9.
8. Ghajari H., Nouhjah S., Shahbazian H., Valizadeh R., Tahery N. *Diabetes Metab Syndr*. **2017**, 11, 455-8.
9. Gross J.L., De Azevedo M.J., Silveiro S.P., Canani L.H., Caramori M.L., Zelmanovitz T. *Diabetes care*. **2005**, 28, 164-76.
10. Gulek B., Soker G., Erken E., Adam F.U., Varan H.I., Ada S., Alparslan N.Z., Kaya O., Erken E., Durgun B. *Open J Radiol*. **2016**, 6, 18.
11. Hedayatifar S., Bagheri S.M., Khajehasani F. *Biomed Res*. **2017**, 28, 5378-82.
12. Hricak H., Cruz C., Romanski R., Uniewski M.H., Levin N.W., Madrazo B.L., Sandler M.A., Eyler W.R. *Radiology*. **1982**, 144, 141-7.
13. Ikee R., Kobayashi S., Hemmi N., Imakiire T., Kikuchi Y., Moriya H., Suzuki S., Miura S. *Am J Kidney Dis*. **2005** Oct 1; 46(4):603-9.
14. Insana M.F., Hall T.J., Fishback J.L. *Ultrasound Med Biol*. **1991**, 17, 613-26.
15. Kim S.H., Kim W.H/, Choi B.I., Kim C.W. *Clin Radiol*. **1992** Feb 1; 45(2):85-7.
16. Lucisano G., Comi N., Pelagi E., Cianfrone P., Fuiano L., Fuiano G. *J Ultrasound Med*. **2015**, 34, 299-306.
17. Moghazi S., Jones E., Schroepple J., Arya K., Mcclellan W., Hennigar R.A., O'Neill W.C. *Kidney Int*. **2005**, 67, 1515-20.
18. Moradi M., Sirous M., Esmaeili H., Hosseini S.M. *J Isfahan Med Sch*. **2011**, 28, 1168-72.
19. Mostbeck G.H., Kain R., Mallek R., Derfler K., Walter R., Havelec L., Tscholakoff D. Duplex. *J Ultrasound Med*. **1991**, 10, 189-94.
20. Nath K.A. *Am J Kidney Dis*. **1992**, 20, 1-7.
21. Pellerito J., Polak J.F. Introduction to Vascular Ultrasonography E-Book. Elsevier Health Sciences, **2012**.
22. Platt J.F., Ellis J.H., Rubin J.M., DiPietro. M.A., Sedman A.B. *Am J Roentgenol*. **1990**, 154, 1223-7.
23. Price R.R., Jones T.B., Goddard J., James J.R. A.E. *Radiol Clin North Am*. **1980**, 18, 21.
24. Ritz E., Orth S.R. *New Engl J Med*. **1999**, 34, 1127-33.
25. Rosenfield A.T., Taylor K.J., Crade M., DeGraaf C.S. *Radiology*. **1978**, 128, 737-44.
26. Shirin M., Sharif M., Gurung A., Datta A. *Bangladesh Med Res Counc Bull*. **2016**, 41,125-30.
27. Spyridopoulos T.N., Kaziani K., Balanika A.P., Kalokairinou-Motogna M., Bizimi V., *Med Ultrason*. **2010**, 12,228-32.
28. Sugiura T., Nakamori A., Wada A., Fukuhara Y. *Clin Nephrol*. **2004**,61,119-26.
29. Sugiura T., Wada. *Nephrol Dial Transplant*. **2009**, 24, 2780-5.
30. Van N.D., Velghe A., Petrovic M., Vandewiele C., Lameire N., Voet D., Afschrift M. *J Nephrol*. **2003**,16, 658-62.
31. Yaprak M., Çakır Ö., Turan M.N., Dayanan R., Akın S., Değirmen E., Yıldırım M., Turgut F. *Int Urol and Nephrol*. **2017**, 49, 123-31.

Downloaded from www.periodico.tchequimica.com

Table 1. *Patients' sex distribution*

Gender	Frequency	Percent	Valid Percent	Cumulative Percent
Female	27	45.0	45.0	45.0
Male	33	55.0	55.0	100.0
Total	60	100.0	100.0	-

Table 2. *Ultrasonography findings based on the presence of interstitial fibrosis in the renal biopsy*

Characteristic	Without fibrosis	With fibrosis	P-value
No.	13	47	
Age (y)	43.00 (13.00)	49.91 (15.13)	.116
GFR (ml/min)	79.00 (12.32)	35.72 (12.32)	< .001
Sex			
Female	7 (53.8)	20 (42.6)	.469
Male	6 (46.2)	27 (57.4)	
Hypertension			
No	6 (46.2)	21 (44.7)	.925
Yes	7 (53.8)	26 (55.3)	
Renal volume (RK) (cc)	170.23 (69.94)	190.94 (45.42)	.083
Renal volume (LK) (cc)	171.92 (62.25)	187.36 (74.70)	.253
Renal sinus volume (RK) (cc)	23.77 (8.56)	33.84 (12.10)	.007
Renal sinus volume (LK) (cc)	22.54 (9.23)	35.30 (11.28)	.004
Renal length (RK) (mm)	104.15 (4.34)	111.02 (9.40)	.020
Renal length (LK) (mm)	104.62 (5.19)	110.81 (11.69)	.070
RI (RK)	.65 (.02)	.68 (.11)	.401
RI (LK)	.65 (.03)	.67 (.10)	.464
Cortex thickness (RK) (mm)	8.00 (.71)	8.43 (2.69)	.891
Cortex thickness (LK) (mm)	7.23 (.44)	9.25 (5.72)	.098
Medulla thickness (RK) (mm)	8.54 (1.42)	8.00 (2.35)	.687
Medulla thickness (LK) (mm)	8.46 (2.13)	8.54 (3.30)	.588
Cortex on medulla thickness (RK) (mm)	8.00 (.71)	8.35 (2.09)	.805
Cortex on medulla thickness (LK) (mm)	7.23 (.44)	8.08 (1.94)	.098
Medulla/cortex (RK)	1.15 (.39)	.97 (.32)	.163
Medulla/cortex (LK)	1.17 (.32)	.98 (.25)	.107
Parenchyma/diameter (RK)	.69 (.38)	.63 (.64)	.408
Parenchyma/diameter (LK)	.68 (.37)	.61 (.61)	.596

*GFR: Glomerular filtration rate, RK: Right kidney, LK: left kidney, RI: Resistive index

Downloaded from www.periodico.tchequimica.com

Table 3. *Ultrasonography findings based on the presence of interstitial fibrosis in the renal biopsy*

Characteristic	**Without fibrosis**	**With fibrosis**	**P-value**
Cortex echogenicity, No (%)			
Grade 1	10 (76.9)	26 (55.3)	
Grade 2	3 (23.1)	14 (29.8)	.236
Grade 3	0 (0)	7 (14.9)	
Coarse echogenicity, No (%)			
Normal	13 (100)	24 (51.1)	
Slightly	0 (0)	17 (36.2.3)	.006
Considerable	0 (0)	6 (12.8)	
Inflammatory changes, No (%)			
No	0 (0)	7 (14.9)	.139
Yes	13 (100)	40 (85.1)	
Medulla echogenicity, No (%)			
Normal	13 (100)	25 (53.2)	
Decreased	0 (0)	15 (31.9)	.008
Increased	0 (0)	7 (14.9)	
Corticomedullary differentiation, No (%)			
Normal	3 (23.1)	10 (21.3)	
Decreased	0 (0)	11 (23.4)	.146
Increased	10 (76.9)	26 (55.3)	
Renal rim, No (%)*			
Regular	13 (100)	37 (78.7)	.068
Irregular	0 (0)	10 (21.3)	
Fat surrounding the kidney, No (%)			
No	10 (100)	41 (87.2)	.232
Yes	0 (0)	6 (12.8)	
Fatty infiltration of the renal parenchyma, No (%)			
No	10 (100)	40 (85.1)	.193
Yes	0 (0)	7 (14.9)	
Renal displacement during inhalation, No (%)			
No	10 (100)	44 (93.6)	.412
Yes	0 (0)	3 (6.4)	

Downloaded from www.periodico.tchequimica.com

Table 4. *Ultrasonography findings based on the presence of interstitial inflammation in the renal biopsy*

Characteristic	Without inflammation	With inflammation	P-value
No.	10	50	
Age (y)	44.80 (14.48)	49.14 (14.99)	.564
GFR (ml/min)	84.70 (6.46)	37.18 (26.00)	< .001
Sex, No (%)			
Female	7 (70)	20 (40)	.082
Male	3 (30)	30 (60)	
Hypertension, No (%)			
No	6 (60)	21 (42)	.296
Yes	4 (40)	29 (58)	
Renal volume (RK) (cc)	134.30 (17.48)	196.88 (50.02)	< .001
Renal volume (LK) (cc)	139.50 (10.29)	192.92 (75.71)	.011
Renal sinus volume (RK) (cc)	21.00 (7.79)	33.79 (11.71)	.001
Renal sinus volume (LK) (cc)	19.10 (7.53)	35.21 (10.91)	< .001
Renal length (RK) (mm)	102.10 (2.18)	111.02 (9.11)	< .001
Renal length (LK) (mm)	103.00 (4.83)	110.76 (11.32)	.018
RI (RK)	.65 (.03)	.68 (.10)	.611
RI (LK)	.65 (.03)	.66 (.10)	.611
Cortex thickness (RK) (mm)	8.30 (.48)	8.35 (2.63)	.586
Cortex thickness (LK) (mm)	7.30 (.48)	9.11 (5.56)	.245
Medulla thickness (RK) (mm)	7.80 (.26)	8.18 (2.39)	.311
Medulla thickness (LK) (mm)	7.40 (.77)	8.75 (3.30)	.402
Cortex on medulla thickness (RK)	8.30 (.48)	8.27 (2.05)	.585
Cortex on medulla thickness (LK) (mm)	7.30 (.48)	8.01 (1.90)	.245
Medulla/cortex (RK)	.94 (.04)	1.02 (.37)	.874
Medulla/cortex (LK)	1.01 (.09)	1.03 (.30)	.937
Parenchyma/diameter (RK)	.80 (.37)	.61 (.62)	.080
Parenchyma/diameter (LK)	.79 (.35)	.59 (.60)	.131

*GFR: Glomerular filtration rate, RK: Right kidney, LK: left kidney, RI: Resistive index

Downloaded from www.periodico.tchequimica.com

Table 5. *Ultrasonography findings based on the presence of interstitial inflammation in the renal biopsy*

Characteristic	Without inflammation	With inflammation	P-value
Cortex echogenicity, No (%)			
Grade 1	10 (100)	26 (52)	
Grade 2	0 (0)	17 (34)	.018
Grade 3	0 (0)	7 (14)	
Coarse echogenicity, No (%)			
Normal	10 (100)	27 (54)	
Slightly	0 (0)	17 (34)	.024
Considerable	0 (0)	6 (12)	
Inflammatory changes, No (%)*			
No	0 (0)	7 (14)	.208
Yes	10 (100)	43 (86)	
Medulla echogenicity, No (%), No (%)*			
Normal	10 (100)	28 (56)	
Decreased	0 (0)	15 (30)	.031
Increased	0 (0)	7 (14)	
Corticomedullary differentiation, No (%)			
Normal	3 (30)	10 (20)	
Decreased	0 (0)	11 (22)	.249
Increased	7 (70)	29 (58)	
Renal rim, No (%)*			
Regular	10 (100)	40 (80)	.121
Irregular	0 (0)	10 (20)	
Fat surrounding the kidney, No (%)*			
No	7 (100)	44 (88)	.333
Yes	0 (0)	6 (12)	
Fatty infiltration of the renal parenchyma, No (%)*			
No	7 (100)	43 (86)	.291
Yes	0 (0)	7 (14)	
Renal displacement during inhalation, No (%)*			
No	7 (100)	47 (94)	.506
Yes	0 (0)	3 (6)	

Downloaded from www.periodico.tchequimica.com

Table 6. *Ultrasonography findings based on the presence of chronicity in the renal biopsy*

Characteristic	Without chronicity	With chronicity	P-value
No.	17	43	
Age (y)	46.29 (12.82)	49.26 (15.67)	.297
GFR (ml/min)	70.59 (19.62)	35.02 (27.06)	< .001
Sex, No (%)			
Female	11 (64.7)	16 (37.2)	.054
Male	6 (35.3)	27 (62.8)	
Hypertension, No (%)			
No	6 (35.3)	21 (48.8)	.342
Yes	11 (64.7)	22 (51.2)	
Renal volume (RK) (cc)	157.24 (65.20)	198.00 (40.74)	.001
Renal volume (LK) (cc)	152.88 (64.49)	196.33 (71.72)	.004
Renal sinus volume (RK) (cc)	23.59 (7.42)	34.92 (12.18)	< .001
Renal sinus volume (LK) (cc)	23.35 (8.14)	36.22 (11.42)	< .001
Renal length (RK) (mm)	103.18 (4.17)	112.05 (9.18)	< .001
Renal length (LK) (mm)	102.35 (6.15)	112.28 (11.11)	.001
RI (RK)	.65 (.02)	.68 (.11)	.219
RI (LK)	.64 (.03)	.67 (.11)	.084
Cortex thickness (RK) (mm)	7.46 (1.18)	8.69 (2.67)	.046
Cortex thickness (LK) (mm)	7.13 (.42)	9.48 (5.93)	.004
Medulla thickness (RK) (mm)	7.82 (1.81)	8.23 (2.32)	.299
Medulla thickness (LK) (mm)	8.05 (2.00)	8.72 (3.40)	.817
Cortex on medulla thickness (RK) (mm)	7.76 (.75)	8.48 (2.15)	.259
Cortex on medulla thickness (LK) (mm),	7.11 (.45)	8.21 (1.99)	.004
Medulla/cortex (RK)	1.10 (.35)	.97 (.33)	.160
Medulla/cortex (LK)	1.13 (.28)	.98 (.26)	.227
Parenchyma/diameter (RK)	.59 (.39)	.67 (.65)	.375
Parenchyma/diameter (LK)	.59 (.37)	.64 (.63)	.445

*GFR: Glomerular filtration rate, RK: Right kidney, LK: left kidney, RI: Resistive index

Downloaded from www.periodico.tchequimica.com

Table 7. *Ultrasonography findings based on the presence of chronicity in the renal biopsy*

Characteristic	Without chronicity	With chronicity	P-value
Cortex echogenicity, No (%)			
Grade 1	10 (58.8)	26 (60.5)	
Grade 2	7 (41.2)	10 (23.3)	.125
Grade 3	0 (0)	7 (16.3)	
Coarse echogenicity, No (%)			
Normal	17 (100)	20 (46.5)	
Slightly	0 (0)	17 (39.5)	.001
Considerable	0 (0)	6 (14)	
Inflammatory changes, No (%)*			
No	0 (0)	7 (16.3)	.077
Yes	17 (100)	36 (83.7)	
Medulla echogenicity, No (%), No (%)*			
Normal	13 (76.5)	25 (58.1)	
Decreased	4 (23.5)	11 (25.6)	.180
Increased	0 (0)	7 (16.3)	
Corticomedullary differentiation, No (%)			
Normal	3 (17.6)	10 (23.3)	
Decreased	4 (23.5)	7 (16.3)	.767
Increased	10 (58.8)	26 (60.5)	
Renal rim, No (%)*			
Regular	17 (100)	33 (76.7)	.025
Irregular	0 (0)	10 (23.3)	
Fat surrounding the kidney, No (%)*			
No	14 (100)	37 (86)	.140
Yes	0 (0)	6 (14)	
Fatty infiltration of the renal parenchyma, No (%)*			
No	14 (100)	36 (83.7)	.122
Yes	0 (0)	7 (16.3)	
Renal displacement during inhalation, No (%)*			
No	14 (100)	40 (93)	.310
Yes	0 (0)	3 (7)	

Downloaded from www.periodico.tchequimica.com

PERIÓDICO TCHÊ QUÍMICA
ARTIGO ORIGINAL

FORMAÇÃO DE FLUXOS HETEROGÊNEOS SUPERSÔNICOS EM ACELERADORES DINÂMICOS A GÁS COM GRANDE ALONGAMENTO

FORMATION OF THE SUPERSONIC HETEROGENEOUS STREAMS IN THE GAS-DYNAMIC ACCELERATORS WITH GREAT ELONGATION

ФОРМИРОВАНИЕ СВЕРХЗВУКОВЫХ ГЕТЕРОГЕННЫХ ПОТОКОВ В ГАЗОДИНАМИЧЕСКИХ УСКОРИТЕЛЯХ С БОЛЬШИМ УДЛИНЕНИЕМ

NIKITIN, Petr V.[1]*; RABINSKIY, Lev N.[2]; TUSHAVINA, Olga V.[3];

[1] Moscow Aviation Institute (National Research University), Institute of Aerospace, Department of Aerospace Thermal Engineering, Moscow – Russian Federation

[2] Moscow Aviation Institute (National Research University), Institute of General Engineering Education, Department of Perspective Materials and Technologies of Aerospace Designation, Moscow – Russian Federation

[3] Moscow Aviation Institute (National Research University), Institute of Aerospace, Department of Managing Exploitation of Space-Rocket Systems, Moscow – Russian Federation

** Correspondence author*
e-mail: petrunecha@gmail.com

Received 25 October 2019; received in revised form 04 November 2019; accepted 04 November 2019

RESUMO

O presente artigo descreve os resultados da investigação experimental e teórica da dinâmica dos gases e da troca de calor no decurso de um fluxo supersônico da mistura gás-pó dentro dos aceleradores gasodinâmicos axialmente simétricos, que possuem pequenas seções críticas (dcrítico = 1...3 mm) e alongamento substancial (L/dcrítico de 70 a 200). A necessidade de realização de tais investigações foi determinada por dois aspectos. O primeiro é o desenvolvimento de tecnologias de inovação com o objetivo de formar revestimentos resistentes ao calor e outros revestimentos com várias funções e propriedades necessárias (formação desses revestimentos com a ajuda de correntes heterogêneas supersônicas). A segunda é a criação de fluxos heterogêneos supersônicos, necessários para o desenvolvimento de investigações experimentais de processos de desgaste erosivo e corrosivo de componentes estruturais de aeronaves de alta velocidade que voam em anomalias atmosféricas (nuvens de chuva e poeira). Para criar um modelo matemático mais confiável da corrente de fluxos heterogêneos não isentrópicos em aceleradores dinâmicos a gás com grande alongamento, uma série de estudos experimentais foi realizada. Os parâmetros de fluxo de gás viscoso foram calculados usando o modelo clássico da camada limite plana. A significância das características do fluxo de gás portador, a dispersão de partículas e seu material para acelerar partículas no fluxo heterogêneo foram esclarecidas. O estudo mostrou que o projeto de microaceleradores dinâmicos a gás deve ser realizado levando em consideração o aumento da espessura da camada limite ao longo das paredes do acelerador de partículas. Também foi esclarecido o entendimento da dinâmica dos gases do fluxo e da transferência de calor de misturas heterogêneas em aceleradores supersônicos dinâmicos a gás com uma concentração de massa de partículas de pó ("fase K") na corrente de até 15%.

Palavras-chave: *gás portador, "fase K", revestimentos multifuncionais, anomalias atmosféricas, transferência de calor entre fases.*

ABSTRACT

The present article describes results of the experimental and theoretical investigation of gas dynamics and heat exchange in the course of a supersonic flow of the gas-powder mixture within the axially symmetric gas-dynamic accelerators, which have small critical cross-sections (dcritical from 1 to 3 mm) and substantial elongation (L/dcritical from 70 to 200). The necessity of performance of such investigations was determined by two aspects. The first is the development of the innovative technologies with the purpose of formation of the heat-resistant coatings and other coatings with various functions and necessary properties (formation of such coatings with the help of supersonic heterogeneous streams). The second is the creation of the supersonic

Downloaded from www.periodico.tchequimica.com

heterogeneous streams, which are required for the development of experimental investigations of processes of the erosive and corrosive wear of structural components of the high-speed air vehicles, which conduct flights in atmospheric anomalies (rain clouded sky and dust-in-air conditions). This study describes the entire cycle of the experimental investigations, which were performed with the purpose of construction of the more reliable mathematical model of flow of the nonisentropic heterogeneous streams in the gas-dynamic accelerators with great elongation. The viscous gas flow parameters were calculated using the classical model of a flat boundary layer. The value of the characteristics of the carrier gas flow, the dispersion of particles and their material for accelerating particles in a heterogeneous flow were found out. The study showed that the design of gas-dynamic micro accelerators must be carried out taking into account the increase in the thickness of the boundary layer along the walls of the particle accelerator. In addition, this article presents a more detailed description of gas dynamics of flow and heat exchange of the heterogeneous mixtures within supersonic gas-dynamic accelerators with mass concentration of the powder particles ("K-phase") in the stream up to 15%.

Keywords: *gas-carrier, "K-phase", coatings with various functions, atmospheric anomalies, interphase heat exchange.*

АННОТАЦИЯ

В данной статье изложены результаты экспериментального и теоретического исследования газодинамики и теплообмена при сверхзвуковом течении газопорошковой смеси в осесимметричных газодинамических ускорителях с малыми критическими сечениями (dкр = 1...3 мм) и значительным удлинением (L/ dкр = 70... 200). Необходимость в постановке таких исследований обусловлена двумя аспектами. Первый – это разработка инновационных технологий формирования термостойких и других разнофункциональных покрытий с необходимыми свойствами с использованием сверхзвуковых гетерогенных потоков. Второй – создание сверхзвуковых гетерогенных потоков для постановки экспериментальных исследований процессов эрозионно-коррозионного износа элементов конструкции высокоскоростных ЛА, совершающих полёт в атмосферных аномалиях (дождевая и пылевая облачность). В работе с целью создания более достоверной математической модели течения неизоэнтропических гетерогенных потоков в газодинамических ускорителях с большим удлинением проведен цикл экспериментальных исследований. Были проведены расчёты параметров потока вязкого газа на базе использования классической модели плоского пограничного слоя. Было выяснено значение характеристик потока газа-носителя, дисперсности частиц и их материала для ускорения частиц в гетерогенном потоке. Исследование показало, что проектирование газодинамических микроускорителей необходимо осуществлять с учетом нарастания толщины пограничного слоя вдоль стенок ускорителя частиц. Также было уточнено понимание газодинамики течения и теплообмена гетерогенных смесей в сверхзвуковых газодинамических ускорителях с массовой концентрацией частиц порошка («К-фаза») в потоке до 15%.

Ключевые слова: *газ-носитель, «К-фаза», разнофункциональные покрытия, атмосферные аномалии, межфазный теплообмен.*

1. INTRODUCTION

Gasdynamics studies the motion of compressible continuous media and their interaction with solids. Shock application of a load causes the formation of shock waves in the solid, their interference and other processes that form the task, the solution of which will create a technology for the formation of high-quality coatings. The process of formation of a boundary layer increasing in thickness with a viscous gas flow deforms the velocity field across and along the length of the channel, which has a noticeable effect on the kinematics of particles in the case of a heterogeneous mixture flowing in it. Therefore, the development of a design technique for accelerating channels is relevant (Fang *et al.,* 2016; Chernov and Dudin, 2019).

Specific features of flow of the heterogeneous mixture in the gas-dynamic accelerators with great elongation are as follows: 1. formation of process of the adiabatic flow of the heterogeneous mixture within the gas-dynamic duct of accelerators (in this context "adiabatic flow" means the flow without any heat exchange between a stream and the accelerator wall); 2. implementation of process of the interphase heat exchange within the volume of a stream between the nonisothermal high-speed "K-phase" and the nonisothermal gas-carrier. At the present time, these specific features are considered as challenging problems in the sphere of scientific investigations (Suciu *et al.*, 2018).

The first problem of the above-mentioned problems is connected, first of all, with dynamic characteristics of acceleration of the solid phase

Downloaded from www.periodico.tchequimica.com

(of particles) within the high-speed gas-carrier. This solid phase (particles) forms the resulting coating. This process is implemented in the stream of the viscous gas that flows with acceleration in the special channels (gas-dynamic accelerators), which have profiles in accordance with the gas dynamics laws. This problem is increasingly complex owing to the fact that such accelerators must have not only a design-basis profile but relevant elongated shape as well (in order to ensure achievement of the required velocity of particles at the output from the gas-dynamic accelerator).

This problem is connected (in the first instance) with the fact that the length of the channel determines the velocity of particles. Therefore, the channel length determines the most important parameters of the entire technological process, which is implemented in order to ensure application of coatings, such as quality of coating, productivity, coefficient of the powder utilisation, and so on (Nikitin and Stepanenko, 2006; Nikitin, 2010; Mikhatulin *et al.,* 2011).

As it is well known from the gas dynamics, the viscous flow of gases in the channels is accompanied by the formation of the boundary layer, the thickness of which increases. This process deforms the field of velocities both across the channel and along the length of the channel. In the case of the flow of the heterogeneous mixture in the channel, the process of increase of the boundary layer exerts significant influence upon the kinematics of particles, as well as upon distribution of various particles within the stream. Therefore, there is the topical problem of developing relevant methodology, which will ensure designing of the accelerating channels with the purpose of formation of such two-phase streams, which would have optimal parameters (Golosnoy et al., 2009; Hu et al., 2015; *Zhang et al*., 2016; Gusev *et al.,* 2018; Chugunkov *et al.*, 2018; Cui *et al*., 2019).

The second problem of the above-mentioned problems is connected with the interaction of the high-speed particles (which have various degrees of dispersion) with the solid surface. It is known from the mechanics of rigid bodies that impulsive application of a load to the surface of a body causes the formation of shock waves within the body, interference of these waves, as well as other processes. In this situation, the following processes are implemented within the zones of concentration of waves: processes of elastic and plastic deformation, adiabatic transformation of mechanical power into thermal energy, dissipation of energy, dynamic diffusion, possible structural, and phase changes, as well as erosion and corrosion processes (Fedyaev *et al*., 2015; Yin *et al*., 2016).

As the final result, the entire set of these processes forms the multiparameter problem. Development of the mathematical model of this problem, as well as solving and verification of this problem will make it possible to create both innovation technology of formation of the high-quality coatings, which have various goal-seeking functional properties, and the problem of erosive and corrosive wear of structural components of the high-speed air vehicles in the course of flying through the cumulonimbus and dusty clouds (Toma *et al*., 2013; Yin *et al*., 2014; Kornienko *et al*., 2016; Liu *et al.,* 2018).

As it was already noted above, the shaped channel, within which acceleration of the heterogeneous stream is ensured, is the most important component of the test (experimental) stands, which create the supersonic heterogeneous streams with possibilities of parameters changing in a wide range. As concerns actual installations, which are used in the real world, they are based on utilization of the elongated accelerating channels (such as convergent-divergent nozzles; de Laval nozzles), which have a conical shape or a flat (rectangular) shape.

At the same time, these elongated accelerating channels are characterized by small angles of expansion of the supersonic section. Due to the fact that critical cross-sections have small areas (dcritical is changed from 1 mm to 5 mm), relative elongation of such channels can be changed over the wide range (L/dcritical is equal to from 50 to 200). The last fact determines the velocity of the "K-phase" at the perpendicular cut of the channel (Cui *et al.,* 2019; Bogdan *et al*., 2019; Flamant and Clarke, 2019).

As it is known, the key feature of flows of viscous gases within the channels, which are characterised by the elongated shapes, is connected with the fact that the boundary layer, which was created on the surface of walls of these channels, ensures an essential decrease of the actual flow cross-section of the channel as compared with the design/calculated cross-section. This fact decreases both the mass flow rate per second of the stream and the velocity of this stream. If this effect will not be taken into consideration in the process of designing of such

Downloaded from www.periodico.tchequimica.com

channels, then the boundary layer will be closed up inside the nozzle. Therefore, the established turbulent flow occurs within the following sections of such channels (in the downward flow direction). Such flow is similar to the flow, which occurs and then is implemented within the main section of the smooth of the cylindrical tube. As it is known, such flow is accompanied by the intensive dissipation of the stream energy.

As concerns the experimental supersonic gas-dynamic stand, it is understood that this process is the harmful one, because of availability of this process will not make it possible to ensure a rigorous calculation of the stream parameters at the perpendicular cut of the channel (Ovsyannik and Makeeva, 2018; Avezova *et al.,* 2019; Babak *et al.,* 2019). In the course of flow of the heterogeneous mixtures within the accelerators, which are characterized by such shapes due to the small dimensions of particles (within the submicron range), it is possible to consider that motion of the particles along these channels is the motion in the straight line.

2. MATERIALS AND METHODS

Turbulisation of the stream within the channel (due to the fact of the above-mentioned reasons), which occurs, ensures changes both in the nature of motion of particles and in the law of distribution of velocities of particles over the transversal cross-section of the relevant stream. In addition, the relevant energy dissipation effect ensures significant decrease velocity of particles as compared with the design/calculated velocity. For example, many experiments proved that velocities of the particles within the two-phase streams (provided these velocities were measured with the help of the laser Doppler velocimeter system) can be essentially different (up to 50%) as compared with the of the values, which were calculated in accordance with the theory of the adiabatic flows. This is the reason why it is necessary to estimate the influence of the boundary layer upon the dynamics of the flow of the heterogeneous mixture within the channels, which have various elongated shapes.

In the course of performance of this analysis, a certain number of assumptions were accepted. For example, due to the small dimensions of particles, no drops in the temperatures of particles within the volume of these particles were taken into consideration. The last fact is similar to the actual conditions because in accordance with the existing estimates value of the Biot number is changed within the following limits: Bi is equal to from 10^{-3} to 10^{-4}. In addition, it was previously understood that the viscous effects, which (for all intents and purposes) do not depend upon temperature of the surface, due to the fact low levels of the particle temperatures do not exert any essential influence upon the aerodynamic resistance of a particle.

Therefore, in the course of analysis within the framework of the approximated model of the interphase interaction between a particle and the gaseous stream, this fact has made make it possible to analyze the dynamic and thermal problems as two independent problems. In these circumstances, the algorithm of calculation of all other parameters of stream of the viscous gas must be developed in accordance with the classic model of the flat boundary layer (Nikitin *et al.,* 1982).

In this case, the dynamic problem was presented as the system of the integrodifferential equations in Equation 1 where x is the coordinate position along the generatrix of the relevant accelerator, δ^{**} is the thickness of the momentum loss within the boundary layer, while τ_w denotes the shearing surface stresses. The rest parameters are the parameters, which are universally accepted parameters in the mechanics of fluids and gases.

As it is well known, the Mach criterion of the approaching stream M_∞, the temperature factor T_w/T_{gas}, as well as the Reynolds criterion Re_w have no essential influence upon the shape of the velocities profile (distribution) in respect of thickness of the boundary layer. Therefore, Equation 2 has been assumed, where y is the coordinate position along the normal to the accelerator surface, while δ denotes the thickness of the boundary layer in the design/calculated cross-section. In the situation, interconnection between various integral characteristics of the boundary layer was determined in accordance with the following form (Equations 3-5) where δ^* denotes thickness of displacement within the boundary layer. The above-presented system of equations in respect of the boundary layer had made it possible to calculate the supersonic flows, which were registered in the actual supersonic accelerators. in order to perform further calculations The following stagnation parameters of stream were assumed as the initial data: pressure P_0, temperature $T_{0,}$ and geometrical dimensions of actual supersonic accelerators.

Downloaded from www.periodico.tchequimica.com

Table 1 presents certain results of the calculations, which were performed in respect of the axially symmetric gas-dynamic accelerator. It follows from the data, which are presented in the above Table, that values of actual diameters of the output cross-section of accelerator $d_{aver.\ phase}$ and calculated values of this accelerator $d_{aver.\ calculated}$ are different. In addition, actual values of the Mach criterion ($M_{aver.\ phase}$) and values of the Mach criterion, which were calculated in accordance with the adiabatic theory of the ideal flow $M_{aver..p.}$ and the Mach criterion $M_{aver..}$, which was determined in the course of experiments with the same accelerator, do not correspond with each other. By comparison, the above Table presents the data of the article (Alkhimov *et al.,* 2000) in the last two lines of this Table. These results are in satisfactory correlation with each other. It is obvious that there exists a significant influence of the increase of the boundary layer thickness upon the nature of flow of the viscous gas in the elongated gas-dynamic accelerators.

These calculations, which were have been performed with utilization of the above-presented system of Equations 1-5 demonstrate that (for example) the boundary within the conical gas-dynamic accelerator (diameter of critical cross-section $d_{critical}$ of which is equal to 1 mm) layer will be closed up at the distance of *L, which is equal to from 10 to 12 mm* from the critical cross-section. In the case of a further increase of the critical cross-section diameter of the nozzle up to $d_{critical}$ up to 2 mm, the boundary layer will be already closed up at the distance of L, which is equal to from 100 mm up to 120 mm. In accordance with further processes, the turbulent flow will be established in both downward flow directions.

This fact creates essential complications for the application of the gas-dynamic micro accelerators within various experimental stands. It is necessary to perform the designing of such micro accelerators taking into consideration the increase of the boundary layer thickness along the walls of the relevant accelerator of particles. Similar problems have been analyzed in articles (Rabinskiy and Tushavina, 2019a; Rabinskiy and Tushavina, 2019b; Rabinskiy *et al*., 2019).

3. RESULTS AND DISCUSSION:

As it is well known, acceleration of particles within the heterogeneous stream is determined by characteristics of stream of the gas-carrier (velocity of the gas-carrier u_{gas}, density of the same gas-carrier ρ_{gas} and so on), as well as by the degree of dispersion of particles and kind of material of these particles. In addition, the nature of the flow of the gas-carrier within the channel of accelerator plays an important role in this process.

Figure 1 presents the dimensionless set of parameters (Equation 6), where $L_{accelerator}$ denotes length of the relevant accelerator, $d_{час}$ ($d_{particle}$) denotes diameter of a particle, P_i denotes pressure within the design/calculated *i-th* cross-section of this accelerator, $V_{particle,i}$ denotes velocity of a particles within the design/calculated cross-section, $u_{gas,i}$ denotes gas velocity within the design/calculated cross-section (in accordance with the calculations, which were carried out in the article (Alkhimov *et al*., 2000)), Δ denotes relevant experiment (Alkhimov *et al*., 2000), O denotes results of this article, C_f is equal to 0.5, while ● denotes results of this article C_f is equal to 1.0.

Figure 1 presents the results of calculations and measurements of the relative velocity of the aluminum and copper particles as compared with results, which were obtained in (Alkhimov *et al*., 2000). These experiments were performed with the help of the industrial powders, degree of dispersion of which $d_{час}$ is equal to from 2.5 to $25 \cdot 10^{-6}$ meter. Velocity of the gas-carrier within the heterogeneous stream was changed within the limits of V_{gas} *, which* is equal to from 200 to 1200 m/second. Figure 1 presents the results of the computational experiment, which was performed in the Moscow Aviation Institute in accordance with the above-described methodology. Conditions of this experiment are similar to the conditions of the experiment, which was performed in (Alkhimov *et al*., 2000). The single exception is as follows: in this case, calculations were performed for the conical nozzle (Lomakin *et al.,* 2017; Formalev *et al.,* 2018; Formalev and Kolesnik, 2019).

From this point of view, the main complexity of application of this methodology is connected with the fact that shape of particles of the industrial powders, which are utilized in the experimental and technological practice, has essential differences in respect of the spherical shape, for which dependency of the aerodynamic drag coefficient C_f is equal to $f(Re_w)$ and which is already well-known. Therefore, it is possible to explain the fact of difference of results of calculation of the relative velocity for the spherical particles, the value of C_f of which is equal to 0.5, while the value of C_f is equal to 1.0. Figure 1 presents the results of calculations for the particles, which have a nonspherical shape at the

Downloaded from www.periodico.tchequimica.com

value of C_f, *which* is equal to 1.0. As is evident from this Figure, there exists a proper correlation of results of both articles (Figure 2), if C_f *is equal to 1.0*.

4. CONCLUSIONS:

The article presents results of the algorithm of the calculations (in accordance with section 1), which were performed in order to determine the dynamics of the flow of particles as well as dynamics of the interphase heat exchange within the high-speed heterogeneous stream. Kind of the gaseous phase is air; "K-phase" denotes copper particles (Cu) with diameter at the level of 40 micrometers. The shape of the supersonic gas-dynamic accelerator is a conical one.

Figure 2 presents the results of these calculations. It follows from this Figure that the maximum speed of heating of a particle is implemented within the precritical area of the nozzle, that is, in the area of maximum temperature and maximum density of the gas-carrier.

There exists strong influence upon the intensity of heating of a particle within the precritical area of the nozzle, and this influence is connected with the fact that relevant particles stay within this section of the nozzle during relatively prolonged time due to the fact that velocities of the gas-carrier (U_{gas}) and velocities of particles ($V_{particle}$) are small.

5. ACKNOWLEDGMENTS:

This investigation was performed within the framework of the Russian Science Foundation grant in respect of the "Performance of investigations by scientific groups under management of young scientists" event of the Presidential Programme of the Investigation Projects (Agreement No. 19-79-10258 dated August 08, 2019).

6. REFERENCES:

1. Alkhimov, A.P., Klinkov, S.V., Kosyrev, V.F. *Thermophysics and Aeromechanics*, **2000**, *7*, 21–30.
2. Avezova, N.R., Avezov, R.R., Vokhidov, A.U., Rakhimov, E.Y., Gaziev, U.K. *Applied Solar Energy,* **2019**, *55(1),* 30–35.
3. Babak, V., Dekusha, O., Vorobiov, L., Dekusha, L., Kobzar, S., Ivanov, S. *39th IEEE International Conference on Electronics and Nanotechnology.* Kyiv, Ukraine, **2019**, 301–304.
4. Bogdan, M., Błachnio, J., Spychała, J., Zasada, D. *Engineering Failure Analysis*, **2019**, *105*, 337–346.
5. Chernov, V.V., Dudin, V.I. *Russian Metallurgy (Metally),* **2019**, *2019(6),* 629–631.
6. Chugunkov, D.V., Kuzma-Kichta, Yu.A., Seyfelmlyukova, G.A., Lavrikov, A.V., Skurikhina, A.D. *3rd All-Russian Scientific Conference Thermophysics and Physical Hydrodynamics with the School for Young Scientists.* Yalta, Crimea, Ukraine, **2018**.
7. Cui, S., Miao, Q., Domblesky, J.P., Liang, W., Song, Y. *Ceramics International*, **2019**, *45(10),* 12635–12642.
8. Fang, Y., Zuo, S., Liang, X., Cao, Y., Gao, X., Zhang, Z. *Applied Thermal Engineering*, **2016**, *93*, 36–42.
9. Fedyaev, V.L., Galimov, E.R., Gimranov, I.R., Takhaviev, M.S., Morenko, I.V., Fazlyev, L.R. *7th Conference on Low Temperature Plasma in the Processes of Functional Coating Preparation*. Kazan, Russian Federation, **2015**.
10. Flamant, Q., Clarke, D.R. *Scripta Materialia*, **2019**, *173*, 26–31.
11. Formalev, V.F., Kolesnik, S.A. *Journal of Engineering Physics and Thermophysics*, **2019**, *92(1),* 52–59.
12. Formalev, V.F., Kolesnik, S.A., Kuznetsova, E.L.. *High Temperature*, **2018**, *56(3),* 393–397.
13. Golosnoy, I.O., Cipitria, A., Clyne, T.W. *Journal of Thermal Spray Technology*, **2009**, *18(5-6),* 809–821.
14. Gusev, V.M., Buklakov, A.G., Konovalov, P.A., Tyuftyaev, A.S. *Chemical and Petroleum Engineering*, **2018**, *54(5-6),* 298–303.
15. Hu, H., Niu, D., Tang, S., Tang, G. *Journal of Xi'an Jiaotong University*, **2015**, *49(7),* 30–36.
16. Kornienko, E.E., Mul', D.O., Rubtsova, O.A., Vaschenko, S.P., Kuzmin, V.I., Gulyaev, I.P., Sergachev, D.V. *Thermophysics and Aeromechanics,* **2016**, *23(6),* 919–927.
17. Liu, Z., Zhou, J., Wu, H. P*owder Technology*,

Downloaded from www.periodico.tchequimica.com

2018, *338*, 129–139.

18. Lomakin, E.V., Lurie, S.A., Belov, P.A., Rabinskii, L.N. *Doklady Physics*, **2017**, *62(1),* 46–49.
19. Mikhatulin, D.S., Polezhaev, Yu.V., Reviznikov, D.L. *Heat and mass transfer thermochemical and thermoerosive destruction of thermal protection,* Moscow: Publishing house "Yanus-K", **2011**.
20. Nikitin, P.V. *Heterogeneous flows in innovative technologies*, Moscow: Publishing house "Yanus-K", **2010**.
21. Nikitin, P.V., Kocherin, Yu.A., Dikun, Yu.V. *"Study of heat transfer in aircraft": Sat Proceedings of the Moscow Aviation Institute.* MAI, Moscow, **1982**.
22. Nikitin, P.V., Stepanenko, S.A. *"Aviation and Cosmonautics – 2006": materials of the 5th international conference.* Moscow, Russian Federation, **2006**.
23. Ovsyannik, A.V., Makeeva, E.N. *Proceedings of CIS Higher Education Institutions and Power Engineering Associations*, **2018**, *61(1),* 70–79.
24. Rabinskiy, L.N., Tushavina, O.V. *INCAS Bulletin*, **2019a**, *11*, 203–211.
25. Rabinskiy, L.N., Tushavina, O.V. *STIN*, **2019b**, *4*, 22–26.
26. Rabinskiy, L.N., Tushavina, O.V., Fedotenkov, G.V. *Asia Life Sciences*, **2019**, *19(1),* 149–162.
27. Suciu, G., Neamtu, A.S., Neamtu, J., Ditu, M.C., Petrescu, G. *INCAS Bulletin*, **2018**, *10*(4), 181-190.
28. Toma, S.L., Bejinariu, C., Baciu, R., Radu, S. *Surface and Coatings Technology*, **2013**, *220*, 266–270.
29. Yin, S., Meyer, M., Li, W., Liao, H., Lupoi, R. *Journal of Thermal Spray Technology*, **2016**, *25(5),* 874–896.
30. Yin, S., Suo, X., Liao, H., Guo, Z., Wang, X. *Surface Engineering*, **2014**, *30(6),* 443–450.
31. Zhang, C., Chen, Q., Liu, J., Tang, W., Wang, K., Song, J. *Surface and Coatings Technology*, **2016**, *294*, 177–185.

$$\frac{d\delta^{**}}{dx} = \frac{\tau_w}{\rho_\infty \cdot u^2_{\infty,газ}} \qquad \text{(Eq. 1)}$$

$$\frac{u(y)}{u_\infty} = \left(\frac{y}{\delta}\right)^{1/7} \qquad \text{(Eq. 2)}$$

$$\frac{\delta^{**}}{\delta} = 1 - \frac{\delta^{*}}{\delta} - n\int_0^1 \frac{z^{n+1}dz}{\left(1+\frac{k-1}{2}M^2_\infty\right)\left[\left(1-\bar{T}_w\right)z+\bar{T}_w\right]-\frac{k-1}{2}M^2_\infty z^2} \qquad \text{(Eq. 3)}$$

$$\frac{\delta^{*}}{\delta} = 1 - n\int_0^1 \frac{z^{n}dz}{\left(1+\frac{k-1}{2}M^2_\infty\right)\left[\left(1-\bar{T}_w\right)z+\bar{T}_w\right]-\frac{k-1}{2}M^2_\infty \cdot z^2} \qquad \text{(Eq. 4)}$$

$$\frac{\delta}{x} = \frac{0{,}0575}{Re^{0,2}_x}\left(\frac{\delta^{**}}{\delta}\right)^{-0,8} \frac{\left(1+\frac{(k-1)}{2}M^2_\infty\right)^{0,6}}{\left(1+0{,}75\frac{(k-1)}{2}M^2_\infty\right)^{1,05}} \bar{T}_w^{\,0,6}\left(\frac{2}{1+\bar{T}_w}\right)^{1,05} \qquad \text{(Eq. 5)}$$

$$A = \left(d_{час}/L_{уск}\right)^{0,5}\left(\rho_{час}\cdot u^2_{газ}/P_i\right)^{0,5} \qquad \text{(Eq. 6)}$$

Downloaded from www.periodico.tchequimica.com

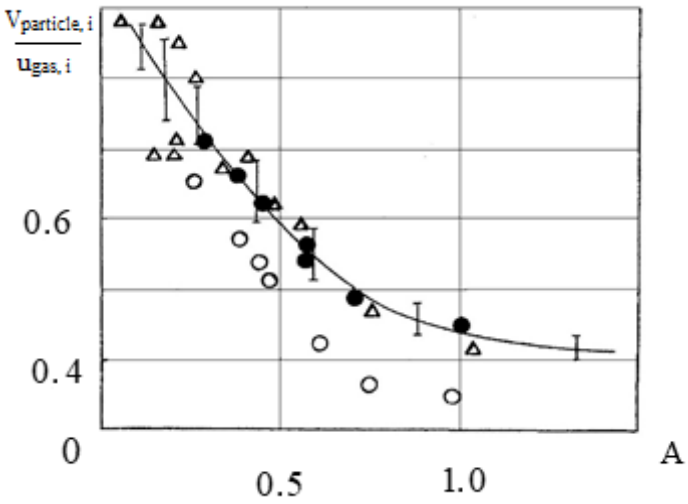

Figure 1. *Change of the relative velocity of a particle depending on the dimensionless set of parameters A*

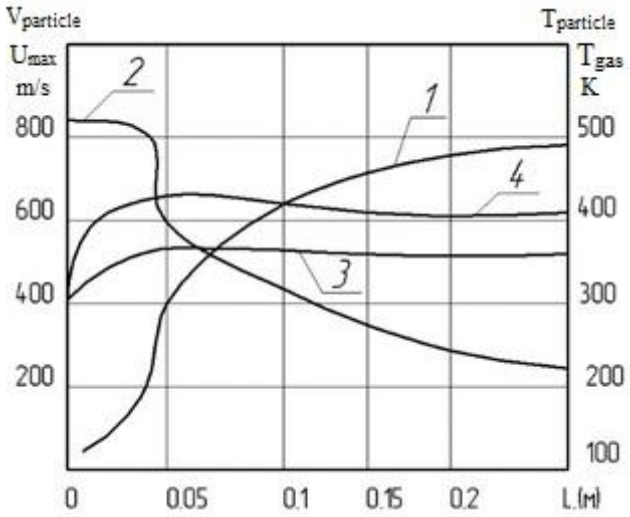

Figure 2. *Distribution of velocities and temperatures of the gas and solid phases along the length of the supersonic of accelerator: 1 is the velocity of the gas phase, 2 is the temperature of the gas phase, 3 is velocity of the cuprum particle, 4 is the temperature of the cuprum particle*

Table 1. *Design/calculated parameters for the axially symmetric gasdynamic accelerator*

$d_{crit.}$	$d_{aver.}$	$M_{aver.\ phase}$	Re_x	$M_{aver..p}$	$d_{aver.\ phase}/d_{aver..p}$	$M_{aver..эк}$
mm	mm	-	-	-	-	-
3.5	12.2	3.45	6.3×105	4.14	0.71	-
4.5	9.5	2.55	4.36×105	3.05	0.84	2.48
4.5	9.5	2.67	5.19×105	3.05	0.845	2.6
2.72	12.65	3.87	1.2×105	4.8	0.67	-
4.72	12.65	2.84	0.27×105	3.58	0.71	-

Downloaded from www.periodico.tchequimica.com

PERIÓDICO TCHÊ QUÍMICA
ARTIGO ORIGINAL

ESPECIAÇÃO GEOQUÍMICA E SIMULAÇÃO DE MODO BATCH NOS AMBIENTES DEPOSICIONAIS DE CARBONATOS

GEOCHEMICAL SPECIATION AND BATCH MODE SIMULATION IN THE CARBONATE DEPOSITIONAL ENVIRONMENTS

KLUNK, Marcos Antônio[1]*; DASGUPTA, Sudipta[2]; DAS, Mohuli[2]; WANDER, Paulo Roberto[1]; DI CAPUA, Andrea[3,4]

[1] University of Vale do Rio dos Sinos, Department of Mechanical Engineering, São Leopoldo, RS, Brazil

[2] Indian Institute of Technology Bombay (IIT Bombay), Department of Earth Sciences, Powai, Mumbai, India.

[3] CNR- Istituto per la Dinamica dei Processi Ambientali-Sezione di Milano, Via Mangiagalli, Milano, Italy

[4] Università Degli Studi di Milano-Bicocca, Piazza della Scienza, Milano, Italy

** Correspondence author*
e-mail: marcosak@edu.unisinos.br

Received 12 August 2019; received in revised form 30 October 2019; accepted 14 November 2019

RESUMO

A modelagem geoquímica tem sido freqüentemente usada para entender e interpretar interações água-rocha em bacias sedimentares. Dados termodinâmicos, parâmetros cinéticos, métodos numéricos, histórico e condições de contorno são fatores que afetam qualquer sistema de modelagem geoquímica. No presente estudo, tentamos estabelecer um modelo de especiação geoquímica comparando a interação da água de formação e da rocha carbonática nos ambientes deposicionais carbonáticos das sucessões cambrianas da área de Bachu e Tarim. Um estudo comparativo da especiação geoquímica foi realizado usando quatro softwares diferentes: PHREEQC™, GWB™, TOUGHREACT™ e GEODELING. GEODELING é um simulador geoquímico onde os detalhes são apresentados mais adiante neste trabalho. Todo o software foi analisado minuciosamente, considerando a distribuição, mobilidade e disponibilidade de espécies químicas em ambientes geológicos. Resultados muito semelhantes na especiação são observados ao trabalhar com sistemas de baixa temperatura. Uma discrepância pode ser observada nos resultados ao trabalhar com altas temperaturas. No entanto, uma formulação completa de Newton-Raphson, o dimensionamento de equações algébricas e a troca de espécies principais ajudam a reduzir a possibilidade de falhas do método numérico usado no PHREEQC™.

Palavras-chave: *Simulação Numérica; Diagênese; GWB™, PHREEQC™, TOUGHREACT™.*

ABSTRACT

Geochemical modeling has been frequently used to understand and interpret water-rock interactions in sedimentary basins. Thermodynamic data, kinetic parameters, numerical methods, boundary history, and boundary conditions are factors affecting any geochemical modeling system. In the present study, we have attempted to establish a geochemical speciation model by comparing the interaction of formation water and carbonate rock in the carbonate depositional settings of Cambrian successions of Bachu and Tarim area. A comparative study of geochemical speciation has been performed using four different software: PHREEQC™, GWB™, TOUGHREACT™, and GEODELING. GEODELING is a geochemical code simulator that we have developed, and the details are presented further in this work. All the software has been analyzed minutely, considering the distribution, mobility, and availability of chemical species in geological environments. Very similar results in speciation are observed while working with low-temperature systems. A discrepancy can be observed in the results while working with high temperatures. However, a thorough Newton-Raphson formulation, scaling of algebraic equations and master-species switching helps to reduce the possibility of failures of the numerical method used in PHREEQC™.

Keywords: Numerical Simulation; Diagenesis; GWB™, PHREEQC™, TOUGHREACT™.

Downloaded from www.periodico.tchequimica.com

1. INTRODUCTION

The scientific community has progressed in geochemical modeling for both natural and hypothetical environments (Manoj *et al.,* 2019; Johnson *et al.,* 2018; Fowler *et al.,* 2018; Somasekhar *et al.,* 2018; Singh *et al.,* 2017). These developments are associated with numerical techniques, which are capable of solving complex mathematical problems, along with incorporating improvements in evaluating capability of computers (Singh *et al.,* 2017). Geochemical modeling studies evolved during the 1960's after the works of Helgeson and James (1968), Helgesson (1967a, 1967b) and Garrels and Mackenzie (1967) made remarkable progress in this field (Apollaro *et al.,* 2019; Eppner *et al.,* 2017). The first simulations were initially studied for understanding the chemical reactions in aquatic environments in order to solve water pollution hazards. These simulations also assessed the diagenetic processes such as natural formation and alteration of rocks (Lai *et al.,* 2018; Limarino *et al.,* 2017; Crémière *et al.,* 2016; Klunk *et al.,* 2015; Udchachon *et al.,* 2011). It is impossible to reproduce the exact behavior of most geochemical systems in the laboratory due to the complexity and diversity in time scale of the reactions in geological environments (Klunk *et al.,* 2018).

It is important to take care of our defined goals and expectations of what the modeling will reveal while producing a geochemical model (Lassin *et al.,* 2018). Our defined goals were to focus on the major issues and to identify the processes which control the geochemical system (Buccianti *et al.,* 2018; Osorno *et al.,* 2015; Mason *et al.,* 2015; Verma, 2012; Bernhard, 1999). These processes might reveal the kind of modeling which is most appropriate for the research of geological environment. Generally, the processes involved in geochemical systems are not simple (Guseva and Kopylova, 2013; Wang *et al.,* 2010; Fritz *et al.,* 2010; Spiteri *et al.,* 2007).

Hence, it can be advantageous to choose simpler models with lesser details as it will provide more results for analysis. In this paper, a comparative study of geochemical speciation using PHREEQC™, TOUGHREACT™, Geochemist's Workbench™ (GWB), and GEODELING has been performed (Alvarez *et al.,* 2018; Klajmon *et al.,* 2017; De Lucia and Kühn 2013; Wolf *et al.,* 2017; Shevalier *et al.,* 2014; Xu *et al.,* 2011; Shabani *et al.,* 2019; Cleverley and Bastrakov 2005; Kong *et al.,* 2013; Sellerino *et al.,* 2019; Bethke 2008, 2002; Parkhurst and Appelo 1999; Xu and Pruess 1998). GEODELING is a software that have developed to fulfill this purpose (Klunk *et al.,* 2017). In this comparative study, the distribution, mobility, and availability of chemical species in geological environments have been verified (Baccar and Fritz, 1993). The efficiency and accuracy of GEODELING software have also been established. The chemical behavior of mineral compounds from the North Sea (Morad *et al.,* 1990) has been modeled in this particular study.

2. MATERIALS AND METHODS

2.1. Geochemical speciation modeling

The concept of speciation is applied to several chemical systems and is most commonly applied in the case of aqueous solutions (Klunk *et al.,* 2017; Batley *et al.,* 2009). These aqueous solutions typically include natural water systems viz., sea, river, lake, and ground waters. The natural water systems are multi-component solutions where a network of interactions is established (Klunk *et al.,* 2017). This leads to the formation of chemical species which have different thermodynamic stability (Ball and Nordstrom, 1991). The diverse chemical behavior of ions that are present in the medium leads to a different quantitative distribution of species, which further depends on the kinetics of the process (Dutta *et al.,* 2010; Peng, 2009; Drever, 1997). Chemical speciation is used to evaluate the distribution of certain chemical species with different chemical forms and oxidation states (Purkait and Mukherjee, 2008; De Stefano *et al.,* 1999; Foti *et al.,* 2000). A geochemical modeling system attempts to map all the reactions and events of the modeled environment (Klunk *et al.* 2018; Chidambaram *et al.,* 2011a). These events include complexation, oxidation, reduction, precipitation, and dissolution. The geochemical model system is also influenced by environmental conditions such as temperature, pH and surface properties (Wu *et al.,* 2015; Foti *et al.* 2004). To fulfill the purpose of our study, a code simulator called GEODELING is being developed. Its functionalities and features have been further explained in this paper.

2.1.1. GEODELING - Speciation Model

GEODELING has been developed from the thermodynamic model based on the numerical method of DISSOL™ (Fritz, 1975, 1981). The mentioned thermodynamic code was expanded through the introduction of kinetic laws governing the geochemical speciation for making numerical

Downloaded from www.periodico.tchequimica.com

simulations possible in time functions (Lasaga, 1984; Helgeson and James, 1968). Therefore, in the kinetic and thermodynamic model of the GEODELING code, the molecular diffusion of the aqueous phase and a porous layer formed by the dissolution or precipitation of minerals control the mineral reaction rates. The speciation code has been applied in the form of the physical, a chemical, aqueous, and geochemical tool with intuitive and interactive interface (Klunk *et al.,* 2017). The language chosen for GEODELING is C++. It is a well-known programming language that has a bias towards programming of the system. It also supports efficient low-level computation, generic programming, object-oriented programming and data abstraction (Dale and Weems, 2014). It also provides impactful and flexible mechanisms for “abstraction” i.e., construction of the language, which allows the programmer to introduce and implement contemporary objects matching the required concepts of an application.

2.1.2. Geochemist's Workbench™ – GWB

Department of Geology in the University of Illinois at Urbana-Champaign developed GWB™ in 1978. GWB™ uses modules SpecE8 in React mode as a speciation model (Bethke, 2008, 2002). An initial geochemical system is set in order to attain thermodynamic equilibrium (Kong *et al.,* 2013). This software automatically installs a specific quantity of water (1 kg) in the system, followed by setting a specific quantity of solutes. During this period, the GWB™ starts calculating and interacting, which further leads to the speciation model. The output data is generated when GWB™ finishes the simulation (Klunk *et al.,* 2018). The information of the output files includes temperature, pressure, ionic strength, pH, solution density, water activity, ionic strength, the mass of solvent, ionic strength, and mass of the rock (Cleverley and Bastrakov, 2005).

An aqueous species index has been generated with the solutes of the simulation. GWB™. solved a particular set of nonlinear algebraic equations (Sellerino *et al.,* 2019). These equations were formulated using the mass action equation and the equilibrium constant. It is also correspondent to aqueous species like minerals or gas from the database simultaneously. GWB™ solves the mass action equation by resolving the system’s mass balance. GWB™ software solves such equations with the aid of Newton-Raphson method (Klunk *et al.,* 2015).

2.1.3. PHREEQC™

PHREEQC™ is a software that has been designed for performing a broad range of geochemical calculations (Klunk *et al.,* 2017; Parkhurst and Appelo, 1999). It is written using programming languages C and C++ (Alvarez *et al.,* 2018; Klajmon *et al.,* 2017). PHREEQC™ is competent for the following functions: (1) calculation of the speciation and saturation index; (2) calculation of the reactions in "batch model" and one-dimensional (1D) transportation; (3) utilization of the Pitzer model for high salinity water outside the application range of the Debye-Huckel theory (Klunk *et al.,* 2015; De Lucia and Kühn, 2013; Pitzer, 1991). The software operates an integral numerical method and allows the solution of standard differential equations to be discerned for reconstructing the three-dimensional (3D) trajectories (Klunk *et al.,* 2018; Parkhurst and Plummer, 1993).

2.1.3. TOUGHREACT™

Xu and Pruess (1998) developed the first version of TOUGHREACT™, which introduces reactive geochemistry heat flow along with multi-phase fluid in TOUGH2™. TOUGHREACT™ requires 64-bit arithmetic for the implementation to be successful (Wolf *et al.,* 2017; Klunk *et al.,* 2015; Zhang, 2013). The code requires understanding of the fundamental equations of fluid flow and non-isothermal multiphase transport occurring within geological environment (Shabani *et al.,* 2019; Klunk *et al.,* 2017; Jin, 2007). It also needs a fundamental knowledge of the numerical solution of the equations which are used to describe similar geological processes (Klunk *et al.,* 2018; Shevalier *et al.,* 2014; Xu *et al.,* 2011; Xu and Pruess, 1998). The simulator has an application in one-dimensional, two-dimensional, or three-dimensional geologic domains, respectively. These domains are comprised of heterogeneous physical and chemical components. Hence, the results can be used for a wide range of geological conditions (Wolf *et al.,* 2017; Pruess *et al.,* 1999). A data base module that employs the thermodynamic equation of state (EOS) monitors the temperature and pressure. The code computes the speciation of the constituent solutes of formation water and marine connate water, which acts as a function of temperature and pressure (Shabani *et al.,* 2019; Pruess, 1991). For discretization, the numerical methods with geometrical parameters are used, which are resolved using the Newton - Raphson method (Xu *et al.,* 2011; Pruess, 1991).

Downloaded from www.periodico.tchequimica.com

2.2. Initial conditions of the water speciation and batch mode simulation

A numerical simulation study was carried out with GWB™, PHREEQC™, and TOUGHREACT™ software, which predicted the geochemical speciation of formation water (from Nordstrom *et al.,* 1994). The deciphered results were compared with our own developed code (GEODELING). The optimum temperatures used for simulations are 25°, 40°, 60°, 80°, 100°, 120°, 140°, 150°, and 160°C, respectively. Baccar and Fritz (1993) studied several interactions between the rock and formation water in different temperatures. The composition of formation water was assembled from Nordstrom *et al.* (1994). The major elements of the chemical composition of formation water are exhibited in Table 1.

Table 1. Composition of the formation water with pH 8.22.

Chemical Species	Composition (mM/L)
K^+	10.45
Na^+	479.32
Ca^{2+}	10.53
Mg^{2+}	54.39
SO_4^{2-}	28.89
Cl^-	559.5

The initial conditions of simulation using the GEODELING have the combination of the chemical species as its starting point. The logarithmic activity of ionic species calculates and represents the contemporary concentrations (Sahu *et al.,* 2016). The effect of interaction between the ions of the solution is eliminated by the activity concentration (Saxena *et al.,* 2012). Modeling of a carbonate rock system was proposed to complement the tests of our own code. In this work, the core samples of Well Batan-5 from the Lower Cambrian Xiaoerbulak Formation in Bachu area (Peng *et al.,* 2018), and that of Well Mabei-1 from the Middle Cambrian Shayilik Formation in North Tarim area have been studied. Dissolution fluids of carbonate rock comprise of meteoric fresh water (mainly consisting of CO_2) and acid fluid (mainly consisting of CO_2 and organic acid) (Chidambaram *et al.,* 2011b). These are related to thermal maturity of organic matter associated with deep hydrothermal fluid (mainly with CO_2) and burial condition (Srivastava 2013; Ponomarev *et al.* 2017b; Moore 1989; Mazzullo and Harris 1992).

Initial conditions have partial pressure amounting to 2.0 MPa of the CO_2 solution (at pH value of about 5.0). The experimental temperatures were set with respect to the burial heat evolution of the Cambrian sedimentary succession in the Bachu Area and the North Tarim Area (Peng *et al.,* 2018). In Bachu Area, the succession is closer to the surface with the highest temperature of 144°C, whereas in the North Tarim Area, the Cambrian succession is buried at greater depth with temperature of about 234°C. The hydrostatic pressure was set at the particular depths, which were correspondent to the temperatures of the strata (slightly adjusted).

The samples are shown to be dolomitic limestone from the section authentication. X-diffraction (Peng *et al.,* 2018) reveals that the dolomitic limestone sample shows calcite concentration of 52.49% and dolomite concentration of 44.18%, respectively.

3. RESULTS AND DISCUSSION

Events that are predicted by numeric simulation between 25° and 160°C with the aid of GWB™, PHREEQC™, and TOUGHREACT™ software as compared to GEODELING, are summarized in Figure 1. Analyzing the trend of simulations, we observed two significant episodes: 1) events developing at low temperatures (25°–100°C) and 2) events developing at high temperatures (120°–160°C). The logarithm of ion activity is dependent on the temperature of the reaction system. We observe similar behavior of the software at low temperatures. The numerical method of software attributes to the unique characteristics at higher temperature, thus causing discrepancy in the results.

We observed the similarity in low-temperature events while correlating the results of GEODELING with the other software. GEODELING reproduces the logarithm of the activity of Mg^{2+}, Ca^{2+}, K^+, and SO_4^{2-} ions for their speciation. Again, the ions like Na+ and Cl- when correlated with GWB™, PHREEQC™, and TOUGHREACT™ software, shows diverse behavior at high temperatures. The saturation index event to carbonate rock shows similar behavior in all the four software. The geochemical modeling predicts the dissolution of calcite and dolomite from the acids fluids found in meteoric fresh water and acid fluid (Fig. 2).

Figure 3a and Figure 3b show the dissolution of calcite and dolomite. It can also be noted that the anhydrite does not get dissolved with its saturation index in the region of precipitation. In the generated models, this mineral did not suffer due to acidic action of the fluid. Such

Downloaded from www.periodico.tchequimica.com

behavior can be seen by the micrograph of Figure 3a.

GEODELING code was built to predict the different species of a geological environment. The simulations of this study permitted a comparative study of GEODELING behavior with speciation of other commercial software (Fig. 1). The results revealed different results for different codes during the modeling of two temperature events. The convergence of outcomes is less evident at high temperatures than at low temperatures. Usually, at low temperatures, the results of the simulation exhibit similar behavior as each software applies identical numerical methods for solving various sets of reactions. At low temperatures (T < 100°C), the similarity of the code results can be observed because of the involvement of low kinetic energy in the reactions. Each simulator possesses its algorithms established on the numerical methods which depend on kinetic and thermodynamic parameters contained in the database.

For higher temperature reactions (120°–160°C), the kinetic energy increases, thereby generating different results irrespective of the model. Accordingly, the GEODELING system produces dissimilar results for sodium and chloride ions. However, when compared to GEODELING, other software such as GWBTM, PHREEQC™, and TOUGHREACT™ have similar approaches while operating with high temperatures. This particular behavior was also observed in calcium and magnesium ions. Generally, GWB™ and TOUGHREACT™ reproduce a similar behavior from 120°C.

These equations depend on kinetic as well as thermodynamic data, thereby directly affecting the medium of the reaction. In the case of temperatures above 120°C, the thermodynamic and kinetic conditions acquire an anomalous behavior assuming constant values of “500” in numeric treatment. The appearance of “500” value is a reference approach to indicate that no value has been calculated. This comparative study revealed two episodes, depending on the temperature. The first and second stage are correspondent to the temperature range of 25°–100°C and 120°–160°C respectively. The first stage verifies the convergence of the results, and the second stage confirms a peculiarity in the numerical method. Users should be cautious while selecting a geochemical speciation software based on the temperature range, as various systems can generate discrepant behaviors.

Batch mode simulations were executed at 25°C, and software packages like GWB™, PHREEQC™, TOUGHREACT™, and GEODELING were employed. These batch mode simulations react in a closed system without flux. Typically, carbonate rock buried at very low depth, and temperature rises slowly. The fluid flow rates are also quite low, limiting the migration of elements en-masse through the rocks. However, over the years, carbonate-rock interactions tend to attain chemical equilibria. The batch mode focuses on achieving that particular steady state. Due to changes in temperature and fluid flow, the water contained in the pores cannot be in chemical equilibrium with its enclosing mineral phases. Therefore, the carbonate reactions are the result of this gradual tendency towards a state of progressive equilibrium, which never accomplishes a finite state. Hence, a condition approximated to a "steady state" is more suitable to describe the chemical state of rocks.

Figure 2 provides the progress of carbonate reactions for different simulations in batch mode. The minerals are initially observed to be far away from equilibrium. Gradually, the minerals achieve the "steady-state" condition. The four geochemical modeling packages manifest similar behavior in the dissolution of dolomite and calcite minerals. We also observed the phenomenon of intense nucleation with the carbonates.

The geochemical results reveal that the dolomitic limestone with calcite concentration of 52.49% has a higher dissolution rate at a particular pressure and temperature than the residual sand. The fine-grained crystalline dolomite with no calcite indicates that dissolution ability of calcite is higher than dolomite under both near-surface and deep burial conditions. Places where calcite and dolomite coexists, also demonstrates that acidic fluid dissolves calcite before dolomite. Therefore, irrespective of rock types, transitional carbonate rocks with higher calcite concentration in burial state are more susceptible to dissolution and henceforth, form high quality reservoirs.

For the residual sand with fine-grained dolomite crystals, observations with the aid of a polarizing microscope and CT scan images demonstrate that the smaller pores expand and integrate, forming bigger pores or caves comprising smooth dissolution edges, after dissolution (thin section images in Figs. 3a – 3b). When observed with the aid of polarizing microscope, the sample consisting of a small proportion of anhydrite showed cracks developing in contact with pores before dissolution, but the trace of dissolution along the cracks cannot be identified after the occurrence of dissolution (thin

Downloaded from www.periodico.tchequimica.com

section images in Fig. 3c). There is a minute variation in the models produced by TOUGHREACT™ as a result of using the numerical method for simulation of the reactions. However, GWB™, PHREEQC™, and GEODELING using almost identical numerical methods at particular range of temperatures reveal similar plots.

4. CONCLUSIONS

The present study of geochemical speciation and batch mode using the application of GWB™, PHREEQC™, and TOUGHREACT™ codes along with GEODELING for the simulating the formation of water and carbonate rocks provides the following conclusions:

1) The reactions at low temperatures (from 25°C to 100°C) consisting of multiple simulators produce similar behaviors. At such temperature range, involving low energy, the thermodynamic parameters, and reaction kinetics behave in accordance with the particularities of each code. GWB™, PHREEQC™, TOUGHREACT™ and GEODELING software used the numerical methods which can attain only limited convergence of results, with high precision in case of reactions involving geological environments at low-temperature.

2) From 120°C to 160°C temperature range with higher kinetic energy and greater intensity of the reactions, the simulations with all the four software generate diverse results. This diversity is due to the utilization of different mass balance equations for calculating chemical speciation by the different software.

3) In this temperature range, the simulators use several mathematical interpolations that are less stable and produce a lower convergence of results. Thereby, each simulator pursues its own ideal set of numerical solutions for achieving the equilibrium.

4) The geochemical speciation was pursued to compare the results of different simulators for predicting the various chemical species of a geological environment. The application of GEODELING allows correlation of results with other software such as GWB™, PHREEQC™, TOUGHREACT™ possessing a high degree of acceptance for low temperatures. Near high temperatures, users need to be cautious while choosing the appropriate geochemical modeling software. The user should undertake a precursory study utilizing the temperature information with the available codes for verifying the convergence.

5) In batch mode simulation at low temperatures (around 25°C), various simulators proliferate altogether divergent behaviors. In this particular range of temperatures with low energy, the thermodynamic parameters and reaction kinetics are treated with respect to the particularities of each code. The numerical methods of GWB™, PHREEQC™ TOUGHREACT™, and GEODELING software have achieved limited convergence of results, with low precision expected for reactions involving carbonate rocks at low-temperature geological environments. Consequently, each simulator perceives its best set of numerical solutions for attaining the equilibrium.

6) Users should be careful while selecting a specific geochemical modeling software because the knowledge of the temperature range is an important factor for choosing a simulator. With the temperature information, the user should commence with a preliminary study of the available codes in order to verify the convergence of the observed results in the formation of water and carbonate rocks.

5. ACKNOWLEDGMENTS

The authors acknowledge the Brazilian agencies CNPq (National Council of Technological and Scientific Development – Brasília, DF, Brazil), CAPES (Coordination for the Improvement of Higher Education Personnel) for the research funding, and the generous assistance of all the people from the company who granted us access to their database and perception information.

6. REFERENCES

1. Manoj, S., Thirumurugan, M., Elango, L. Hydrogeochemical modelling to understand the surface water–groundwater interaction around a proposed uranium mining site. Journal of Earth System Science, **2019**, 128(49), 1-14.
2. Johnson, L. M., Rezaee, R., Kadkhodaie A., Smith, G., Yu, H. Geochemical property modelling of a potential shale reservoir in the Canning Basin (Western Australia), using Artificial Neural Networks and Geostatistical tools; Computers & Geosciences, **2018**, 120, 73-81.
3. Fowler, A. P. G., Ferguson, C., Cantwell, C. A., Zierenberg, R. A., McClain, J., Spycher, N., Dobson, P. A conceptual geochemical model of the geothermal system at Surprise Valley, C. A. Journal of

Downloaded from www.periodico.tchequimica.com

Volcanology and Geothermal Research, **2018**, 353, 132-148.
4. Somasekhar, V., Ramanaiah, S., Sarma, D. S. Geochemical characterization of the siliciclastic rocks of Chitravati Group, Cuddapah Supergroup: Implications for provenance and depositional environment. Journal of Earth System Science, **2018**, 127-154.
5. Singh, C. K., Kumar, A., Shashtri, S., Kumar, A., Kumar, P., Mallick, J. Multivariate statistical analysis and geochemical modeling for geochemical assessment of groundwater of Delhi, India. Journal of Geochemical Exploration, **2017**, 175 59-71.
6. Helgeson, H. C., James, W. R. Activity coefficients in concentrated electrolyte solutions of elevated temperatures. Journal of the American Chemical Society, **1968**, S 130.
7. Helgeson, H. C. Thermodynamics of complex dissociation in aqueous solutions at. elevated temperatures. Journal of Physical Chemistry, **1967a**, 71, 3121-3136.
8. Helgeson, H. C. Solution chemistry and metamorphism. In: Abelson P.H. (ed.) Researches in Geochemistry, v. II, New York, Wiley, **1967b**, 362-404.
9. Garrels, R. M., Mackenzie, F. T. Origin of the chemical compositions of some springs and lakes. Equilibrium concepts in natural water systems. American Chemical Society, **1967**, 67, 222-242.
10. Apollaro, C., Perri, F., Le Pera, E., Fuoco, I., Critelli, T. Chemical and minero-petrographical changes on granulite rocks affected by weathering processes. Frontiers in Earth Science, **2019**, 13(2), 247-261.
11. Eppner, F., Pasquier, P., Baudron, P. A coupled thermo-hydro-geochemical model for standing column well subject to CO_2 degassing and installed in fractured calcareous aquifers. Geomechanics for Energy and the Environment, **2017**, 11, 14-27.
12. Lai, J., Wang, G., Wang, S., Cao, J., Li, M., Pang, X., Qin, Z. Review of diagenetic facies in tight sandstones: Diagenesis, diagenetic minerals, and prediction via well logs. Earth-Science Reviews, **2018**, 185, 234-258.
13. Limarino, C. O., Giordano, S. R., Rodriguez Albertani, R. J. Diagenetic model of the Bajo Barreal formation (Cretaceous) in the southwestern flank of the Golfo de San Jorge Basin (Patagonia, Argentina), Marine and Petroleum Geology, **2017**, 88, 907-931.
14. Crémière, A., Lepland, A., Chand, S., Sahy, D., Kirsimäe, K., Bau, M., Brunstad, H. Fluid source and methane-related diagenetic processes recorded in cold seep carbonates from the Alvheim channel, central North Sea. Chemical Geology, **2016**, 432, 16-33.
15. Klunk, M. A., Damiani, L. H., Feller, G., Rey, M. F., Conceiçao, R. V., Abel, M., De Ros, L. F. Geochemical modeling of diagenetic reactions in Snorre Field reservoir sandstones: a comparative study of computer codes. Brazilian Journal of Geology, **2015**, 45, 29-40.
16. Udchachon, M., Thassanapak, H., Feng, Q., Chonglakmani, C. Geochemical constraints on the depositional environment of Upper Devonian radiolarian cherts from Loei, north-eastern Thailand. Frontiers in Earth Science, **2011**, 5(2), 178-190.
17. Klunk, M. A., Dasgupta, S., Conceiçao, R. V. Computerized geochemical modeling of burial diagenesis of the Eocene turbidite reservoir elements: Urucutuca Formation, Espírito Santo Basin, southeastern Brazil passive margin. Journal of Palaeogeography, **2018**, 7, 12-26.
18. Lassin, A., André, L., Devau, N., Lach, A., Beuvier, T., Gibaud, A., Azaroual, M. Dynamics of calcium carbonate formation: geochemical modeling of a two-step mechanism. Geochimica et Cosmochimica Acta, **2018**, 240, 236-254.
19. Buccianti, A., Lima, A., Albanese, S., De Vivo, B. Measuring the change under compositional data analysis (CoDA): Insight on the dynamics of geochemical systems. Journal of Geochemical Exploration, **2018**, 189, 100-108.
20. Osorno, J., Rangel, A. Geochemical assessment and petroleum systems in the Sinú-San Jacinto Basin, northwestern Colombia. Marine and Petroleum Geology, **2015**, 65, 217-231.
21. Mason, S. E., Corum, K. W., Ramadugu, S. K. Fundamental insights about environmental interface reactivity from DFT calculations of geochemical model systems. Surface Science, **2015**, 631, 48-56.
22. Verma, M. P. GeoSys.Chem: Estimate of reservoir fluid characteristics as first step in

Downloaded from www.periodico.tchequimica.com

geochemical modeling of geothermal systems. Computers & Geosciences, **2012**, 49, 29-37.
23. Bernhard, M. Quality control and reference materials in speciation analysis. Fresenius Journal of Analytical Chemistry, **1999**, 363, 439-445.
24. Guseva, N., Kopylova, Y. Geochemical Mobility of Chemical Elements in Saline Lake Systems in Khakassia (Russia). Procedia Earth and Planetary Science, **2013**, 7, 325-329.
25. Wang, P., Anderko, A., Springer, R. D., Kosinski, J. J., Lencka, M. M. Modeling chemical and phase equilibria in geochemical systems using a speciation-based model. Journal of Geochemical Exploration, **2010**, 106(1-3), 219-225.
26. Fritz, B., Jacquot, E., Jacquemont, B., Baldeyrou-Bailly, A., Rosener, M., Vidal, O. Geochemical modelling of fluid–rock interactions in the context of the Soultz-sous-Forêts geothermal system. Comptes Rendus Geoscience, **2010**, 342(7-8), 653-667.
27. Spiteri, C., Slomp, C. P., Regnier, P., Meile, C., Van Cappellen, P. Modelling the geochemical fate and transport of wastewater-derived phosphorus in contrasting groundwater systems. Journal of Contaminant Hydrology, **2007**, 92(1-2), 87-108.
28. Alvarez, A. C., Blom, T., Lambert, W. J., Bruining, J., Marchesin, D. Analytical and numerical validation of a model for flooding by saline carbonated water. Journal of Petroleum Science and Engineering, **2018**, 167, 900-917.
29. Klajmon, M., Havlová, V., Červinka, R., Mendoza, A., Franců, J., Berenblyum, R., Arild, Ø. REPP-CO_2: Equilibrium Modelling of CO_2-Rock-Brine Systems. Energy Procedia, **2017**, 114, 3364-3373.
30. De Lucia, M., Kühn, M. Coupling R and PHREEQC: Efficient Programming of Geochemical Models. Energy Procedia, **2013**, 40, 464-471.
31. Wolf, J. L., Fischer, S., Rütters, H., Rebscher, D. Reactive Transport Simulations of Impure CO_2 Injection into Saline Aquifers Using Different Modelling Approaches Provided by TOUGHREACT V3.0-OMP. Procedia Earth and Planetary Science, **2017**, 17, 480-483.
32. Shevalier, M., Dalkhaa, C., Humez, P., Mayer, B., Becker, V., Nightingale, M., Zhang, G. Coupling of TOUGHREACT-Geochemist Workbench (GWB) for Modeling Changes in the Isotopic Composition of CO_2 Leaking from a CCS Storage Reservoir. Energy Procedia, **2014**, 63 3751-3760.
33. Xu, T., Spycher, N., Sonnenthal, E., Zhang, G., Zheng, L., Pruess, K. TOUGHREACT Version 2.0: A simulator for subsurface reactive transport under non-isothermal multiphase flow conditions. Computers & Geosciences, **2011**, 37(6), 763-774.
34. Shabani, B., Vilcáez, J. TOUGHREACT-CO_2Bio – a new module to simulate geological carbon storage under biotic conditions (Part 1): the multiphase flow of CO_2-CH_4-H_2-H_2S gas mixtures. Journal of Natural Gas Science and Engineering, **2019**, 63, 85-94.
35. Cleverley, J. S., Bastrakov, E. N. K2GWB: Utility for generating thermodynamic data files for The Geochemist's WorkbenchTM at 0–1000°C and 1–5000 bar from UT2K and the UNITHERM database. Computers & Geosciences, **2005**, 31(6), 756-767.
36. Kong, X-Z., Tutolo, B. M., Saar, M. O. DBCreate: A SUPCRT92-based program for producing EQ3/6, TOUGHREACT, and GWB thermodynamic databases at user-defined T and P. Computers & Geosciences, **2013**, 51, 415-417.
37. Sellerino, M., Forte, G., Ducci, D. Identification of the natural background levels in the Phlaegrean fields groundwater body (Southern Italy). Journal of Geochemical Exploration, **2019**, 200, 181-192.
38. Bethke, C. M. GWB Reaction Modeling Guide-A User's Guide to React and Gtplot. University of Illinois, Urbana, IL, **2008**, 74p.
39. Bethke, C. M. The Geochemists Workbench Version 4.0: A User's Guide. University of Illinois, Urbana, IL, **2002**, 224p.
40. Parkhurst, D. L., Appelo, C. A. J. User's guide to PHREEQC-a computer program for speciation, batchreaction, one-dimensional transport, and inverse geochemical calculations.Water-Resources Investigations Report 99-4259. Reston, Virginia: U.S. Geological Survey, **1999**, 312.
41. Xu, T., Pruess, K. Coupled modeling of non-isothermal multiphase flow, solute transport and reactive chemistry in porous and fractured media: 1. Model development and validation, Lawrence

Downloaded from www.periodico.tchequimica.com

Berkeley National Laboratory Report LBNL-42050, Berkeley, California, **1998**.
42. Klunk, M. A., Ponomarev, A. A., Dasgupta, S., Das, M. Arsenic Speciation in Groundwater using the Softwares PHREEQC, GWB, and GEODELING Southern Brazilian Journal of Chemistry, **2017**, 25 30–35.
43. Baccar, M. B., Fritz, B. Geochemical modelling of sandstone diagenesis and its consequences on the evolution of porosity. Applied Geochemistry, **1993**, 8, 285-295.
44. Morad, S., Bergan, M., Knarud, R., Nystuen, J. P. Albitization of detrital plagioclase in Triassic reservoir sandstones from the snorre field, Norwegian North Sea. Journal of Sedimentary Research, **1990**, 60, 411-425.
45. Batley, G. E., Francesconi, K. A., Maher, W. A. The role of speciation in environmental chemistry and the case for quality criteria. Environmental Chemistry, **2009**, 6(4), 273-274.
46. Ball, J. W., Nordstrom, D. K. User's manual for WATEQ4F, with revised thermodynamic data base and test cases for calculating speciation of major, trace, and redox elements in natural waters. Open-File Report, **1991**, 91-183.
47. Dutta, S., Mallick, M., Mathews, R. P., Mann, U., Greenwood, P. F., Saxena, R. Chemical composition and palaeobotanical origin of Miocene resins from Kerala-Konkan Coast, western India. Journal of Earth System Science, **2010**, 119(5), 711-716.
48. Peng, S. Characterization of solute transport parameters in leach ore: inverse modeling based on column experiments; Frontiers of Earth Science in China, 2009, 3(2), 208-213.
49. Drever, J. I. The Geochemistry of Natural Waters (3rd ed), New Jersey, Prentice-Hall Inc, **1997**, 436p.
50. Purkait, B., Mukherjee, A. Geostatistical analysis of arsenic concentration in the groundwater of Malda district of West Bengal, India. Frontiers of Earth Science in China, **2008**, 2(3), 292-301.
51. De Stefano, C., Gianguzza, A., Piazzese, D., Sammartaus, S. Speciation of low molecular weight carboxylic ligands in natural fluids: protonation constants and association with major components of seawater of oxydiacetic and citric acids. Analytica Chimica Acta, **1999**, 398(1), 103-110.
52. Foti, C., Gianguzza, A., Piazzese, D., Trifiletti, G. Inorganic speciation of organotin (IV) cations in natural waters with particular reference to seawater. Chemical Speciation and Bioavailability, **2000**, 12(2), 41-52.
53. Chidambaram, S., Karmegam, U., Sasidhar, P., Prasanna, M. V., Manivannan, R., Arunachalam, S., Manikandan, S., Anandhan, P. Significance of saturation index of certain clay minerals in shallow coastal groundwater, in and around Kalpakkam, Tamil Nadu, India. Journal of Earth System Science, **2011a**, 120(5), 897-909.
54. Wu, Z., Wu, J., Lu, G. A one-way coupled atmospheric-hydrological modeling system with combination of high-resolution and ensemble precipitation forecasting. Frontiers of Earth Science, **2015**, 10(3), 432-443.
55. Foti, C., Gianguzza, A., Milea, D., Millero, F. J., Sammartano, S. Speciation of trialkyltin(IV) cations in natural fluids. Marine Chemistry, **2004**, 85(3-4), 157-167.
56. Fritz, B. Etude thermodynamique et simulation des réactions entre minéraux et solutions. Application a la géochimie des altérations et des eaux continentals. Sciences Géologiques – Bulletins et Mémoires, **1975**, 41, 152.
57. Fritz, B. Etude therrnodynamique et modélisation des réactions hydrothermales et diagénétiques. Sciences Géologiques – Bulletins et Mémoires, **1981**, 65, 197.
58. Lasaga, A. C. Chemical kinetics of water-rock interactions. Journal of Geophysical Research: Solid Earth, **1984**, 89(B6), 4009-4025.
59. Dale, N. B., Weems, C. Programming and problem solving with C++. Jones Bartlett Publishers, **2014**, 1068p.
60. Pitzer, K. S. Activity coefficients in electrolyte solutions. 2nd edition. C.R,C. Press. Chapter 3. Pitzer, K.S. Ion interaction approach. T D Corr., **1991**, 5-153.
61. Parkhurst, D. L., Plummer, L. N. Geochemical models. In: ALLEY, W. M. Regional ground-water quality. New York: Van Nostrand Reinhold, **1993**, 199-225.
62. Zhang, W. Effect of modeling factors on the dissolution-diffusion-convection process during CO_2 geological storage in deep saline formations. Frontiers in Earth

Downloaded from www.periodico.tchequimica.com

Science, **2013**, 7(2), 238-256.
63. 63 Jin, Y. Theory and application for retrieval and fusion of spatial and temporal quantitative information from complex natural environment. Frontiers in Earth Science, **2007**, 1(3), 284-298.
64. Pruess, K., Oldenburg, C., Moridis, G. TOUGH2 user's guide, Version 2.0, Lawrence Berkeley Laboratory Report LBL-43134, Berkeley, California, **1999**.
65. Pruess, K. TOUGH2: A general numerical simulator for multiphase fluid and heat flow, Lawrence Berkeley Laboratory Report LBL-29400, Berkeley, California, **1991**.
66. Nordstrom, D. K. On the evaluation and application of geochemical models, Appendix 2 in Proceedings of the 5th CEC Natural Analogue Working Group and Alligator Rivers Analogue Project, an international workshop held in Toledo, Spain, EUR 15176 EN, **1994**, 375-385.
67. Sahu, P., Sikdar, P. K., Chakraborty, S. Geochemical evolution of groundwater in southern Bengal Basin: The example of Rajarhat and adjoining areas, West Bengal, India. Journal of Earth System Science, **2016**, 125(1), 129-145.
68. Saxena, A., Sachan, H. K., Mukherjee, P. K., Mukhopadhya, D. K. Fluid–rock interaction across the South Tibetan Detachment, Garhwal Himalaya (India): Mineralogical and geochemical evidences. Journal of Earth System Science, **2012**, 121(1), 29-44.
69. Peng, J., Wang, X., Han, H., Yin, S., Xia, Q., Li, B. Simulation for the dissolution mechanism of Cambrian carbonate rocks in Tarim Basin, NW China. Petroleum Exploration and Development, **2018**, 45(3), 431-441.
70. Chidambaram, S., Prasanna, M. V., Karmegam, U., Singaraja, C., Pethaperumal, S., Manivannan, R., Tirumalesh, K. Significance of pCO_2 values in determining carbonate chemistry in groundwater of Pondicherry region, India. Frontiers in Earth Science, **2011b**, 5(2), 197-206.
71. Srivastava, R. K. Petrological and geochemical characteristics of Paleoproterozoic ultramafic lamprophyres and carbonatites from the Chitrangi region, Mahakoshal supracrustal belt, central India. Journal of Earth System Science, **2013**, 122(3), 759-776.
72. Ponomarev, A. A., Bubnova, A. V., Klunk, M. A. The Use of X-Ray Microtomography to Assess Changes in the Voids Structure of Rocks. Southern Brazilian Journal of Chemistry, **2017b**, 25, 12-16.
73. Moore, C. H. Carbonate diagenesis and porosity. 1st Edition, New York: Elsevier, **1989**, 337p.
74. Mazzullo, S. J., Harris, P. M. Mesogenetic dissolution: Its role in porosity development in carbonate reservoirs; AAPG Bulletin, **1992**, 76(5), 607-620.

Downloaded from www.periodico.tchequimica.com

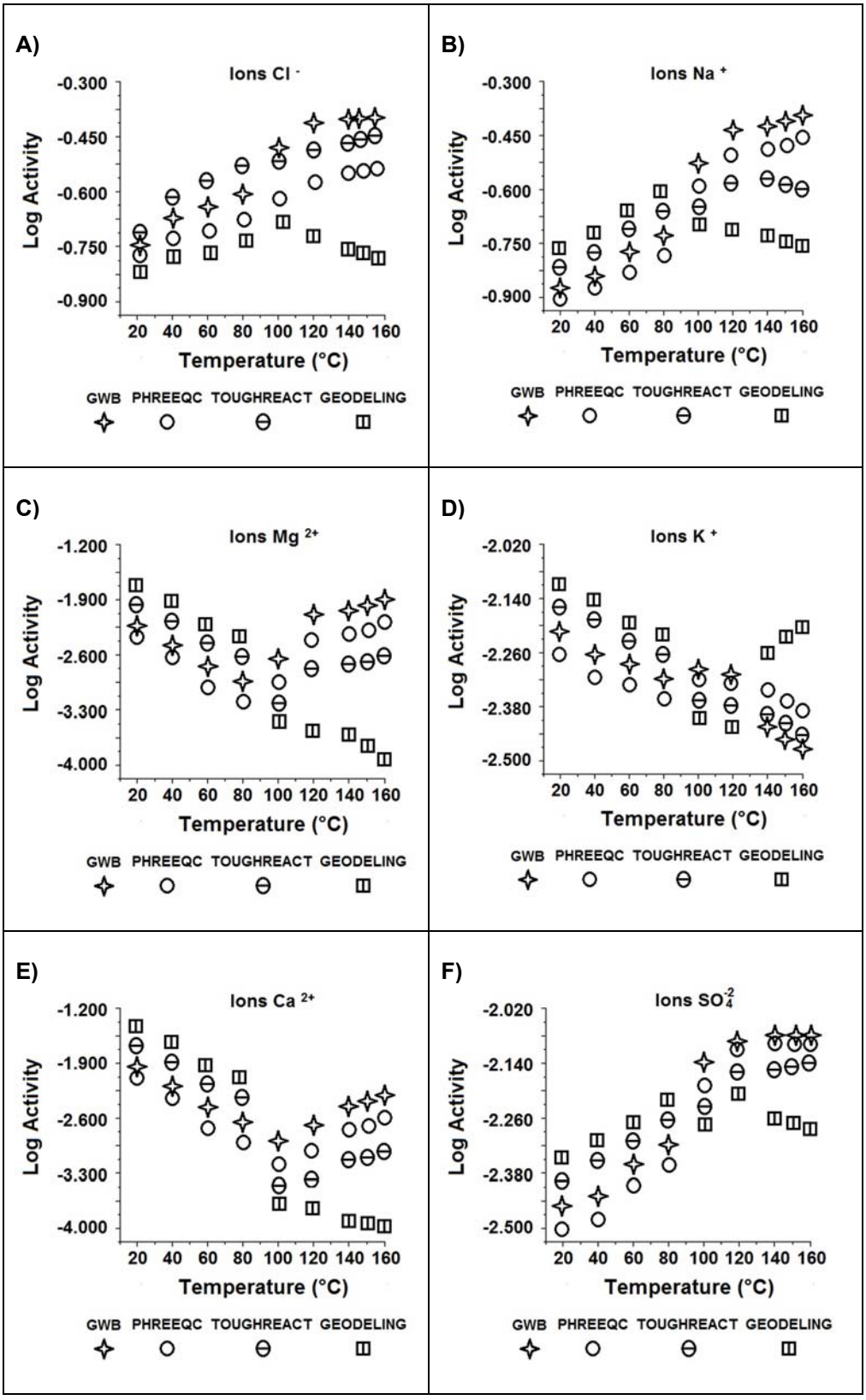

Figure 1. *Speciation model using GWBTM, PHREEQCTM, TOUGHREACTTM and GEODELING.*

Downloaded from www.periodico.tchequimica.com

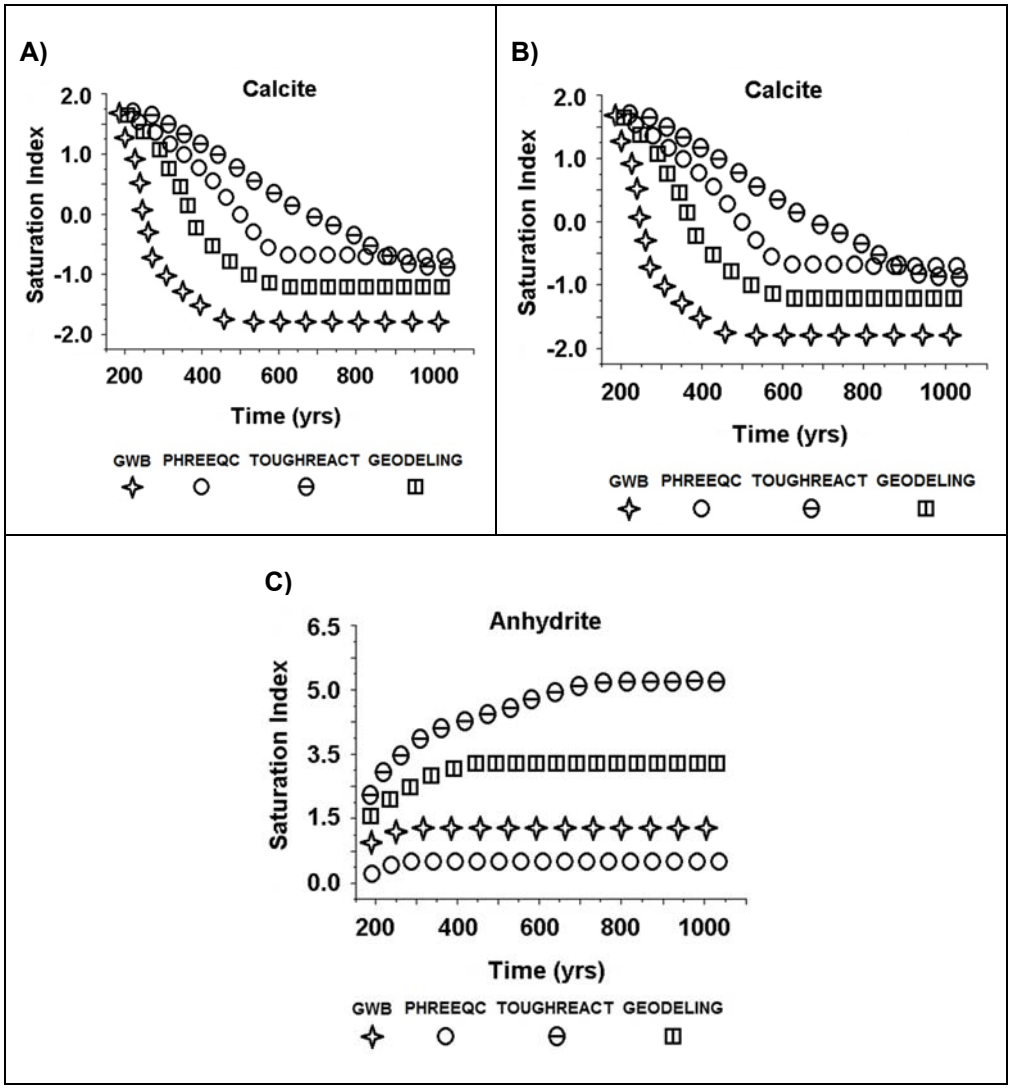

Figure 2. *Case study of a carbonate rock system model. Saturation index acquired with the aid of GWB™, PHREEQC™, TOUGHREACT™ and GEODELING.*

Downloaded from www.periodico.tchequimica.com

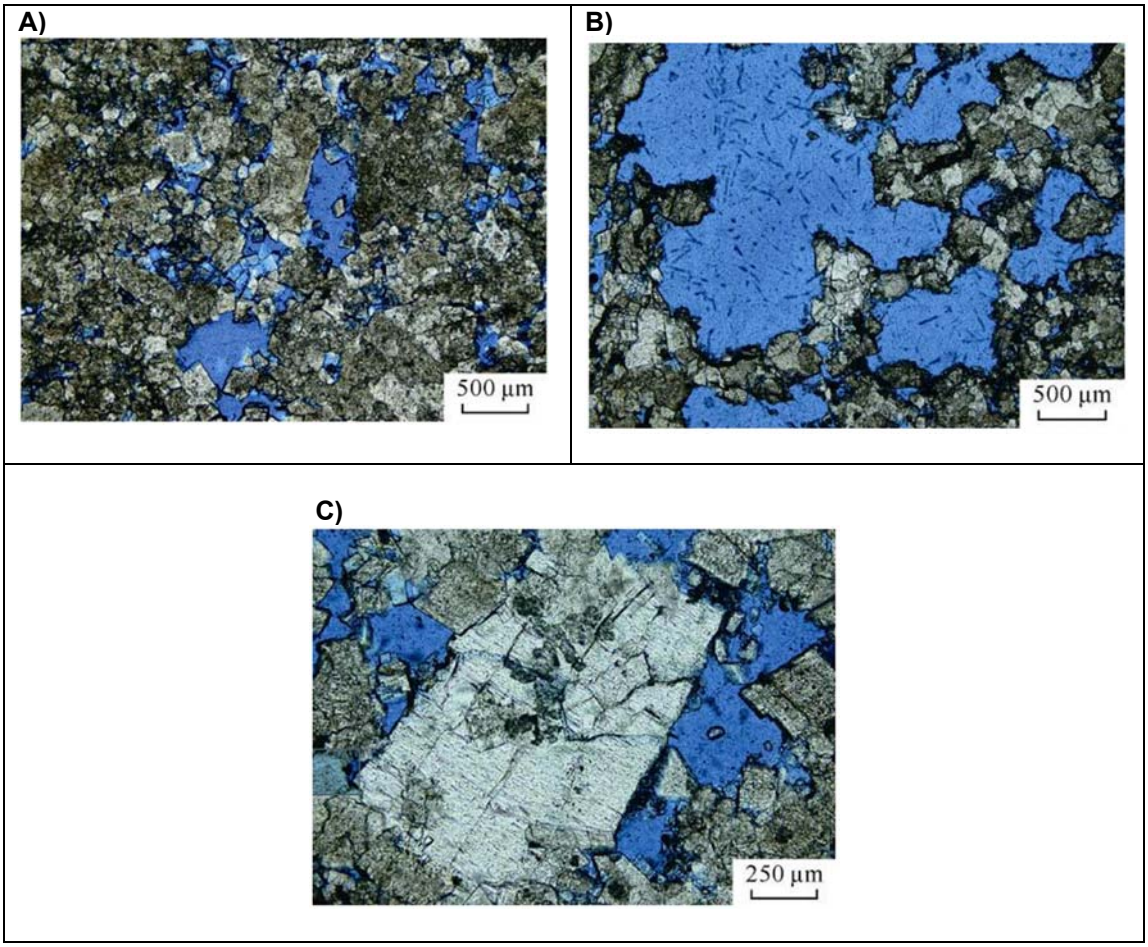

Figure 3. *The characteristics of Cambrian rock samples under microscope. a) Batan Well-5 at the depth of 5785.95m in Xiaoerbulak Formation showing residual sand fine-crystalline dolomite before the dissolution, with developed intercrystalline pores, observed, under single polarization (casting slice); b) Batan Well-5 at the depth of 5785.95m in Xiaoerbulak Formation showing residual sand fine-crystalline dolomite after the dissolution, where the intercrystalline pores are diffused into karst caves with smooth edges, under single polarization (casting slice); c) Batan Well-5 at the depth of 5785.95m in Xiaoerbulak Formation showing residual sand fine-crystalline dolomite after the dissolution where the anhydrite in the intercrystalline cavity remains uneroded, under single polarization (casting slice) (Peng et al., 2018).*

Downloaded from www.periodico.tchequimica.com

PERIÓDICO TCHÊ QUÍMICA
ARTIGO ORIGINAL

SENSIBILIDADE DOS NEURÔNIOS SENSORIMOTORES DO CORTEX DO CÉREBRO DE RATOS A MEDIADORES NO DERRAME HEMORRÁGICO

SENSITIVITY OF RAT BRAIN SENSORIMOTOR CORTEX NEURONS TO MEDIATORS IN HEMORRHAGIC STROKE

ЧУВСТВИТЕЛЬНОСТЬ НЕЙРОНОВ СЕНСОМОТОРНОЙ КОРЫ МОЗГА КРЫС К МЕДИАТОРАМ НА ФОНЕ ГЕМОРРАГИЧЕСКОГО ИНСУЛЬТА

MESHCHERYAKOV Alexandr[1 *]; KOPLIK Elena[2]; VOLKOV Vladimir[3]; IONKINA Helena[4]; BUDNIKOV Mikhail[5]; BORISOVA Elena[6];

[1,3,4,5,6] Sechenov First Moscow State Medical University, Department of Normal Physiology

[2] State Research Institute of Normal Physiology named after P.K. Anokhin RAMS

** Correspondence author*
e-mail: alex_maf@mail.ru

Received 29 May 2019; received in revised form 30 October 2019; accepted 06 November 2019

RESUMO

O problema dos distúrbios da circulação cerebral pós-estresse, o mais grave dos quais é hemorragia cerebral ou derrame hemorrágico, é extremamente urgente. Em relação à taxa de sobrevivência, estudos anteriores mostraram que, no mesmo tipo de situações de conflito, indivíduos resistentes e predispostos a influências estressantes emocionais são claramente distinguidos. No entanto, os mecanismos neurais que fornecem regulação neuromediatória das respostas aos efeitos estressantes ainda são pouco estudados. A análise da sensibilidade neuroquímica à acetilcolina e norepinefrina dos neurônios do córtex sensório-motor de ratos com atividades diferentes de acordo com os parâmetros de comportamento, ou seja, resistência ao estresse emocional influencia antes e após o acidente hemorrágico experimental (AHE). O processo de recuperação após um AHE devido à atividade neural em ratos prognósticos estáveis (VA) e predispostos (NA) a situações estressantes possui características individuais. A influência do estresse agudo antes do desenvolvimento do AHE altera a natureza da atividade dos neurônios do córtex sensório-motor em ratos VA e NA no terceiro e sétimo dia após o AHE. O EHS leva a alterações específicas na sensibilidade dos neurônios à acetilcolina e norepinefrina em ratos VA e NA. A microionoforese da acetilcolina causa a ativação da atividade do impulso neuronal em ratos VA e NA, e essas alterações são as mesmas após o EHS. A influência do estresse agudo antes do desenvolvimento do AHE não altera a natureza das respostas dos neurônios à microionoforese de noradrenalina em animais com AV. Pelo contrário, em ratos NA observou-se perda da sensibilidade dos neurônios à noradrenalina durante o desenvolvimento da AHE contra o estresse. É possível que a influência aguda do estresse antes do desenvolvimento da AHE possa alterar a atividade do sistema noradrenérgico cerebral em ratos NA, que são predispostos prognosticamente às influências do estresse. Os dados obtidos enfatizam a plasticidade da estrutura nervosa central no desenvolvimento da resposta a influências estressantes. (O número do protocolo de aprovação da comissão de ética é 18-15 de 13 de março de 2018.).

Palavras-chave: *Estresse, acidente vascular cerebral hemorrágico, ratos, neurônios, noradrenalina*.

ABSTRACT

The problem of post-stress disorders of cerebral circulation, the most severe of which is cerebral hemorrhage, or hemorrhagic stroke, is extremely urgent. Concerning the survival rate, previous studies have shown that in the same type of conflict situations, individuals resistant and predisposed to emotional stressful influences are clearly distinguished. However, the neural mechanisms providing neuromediatory regulation of responses to stressful effects are still little studied. The analysis of neurochemical sensitivity to acetylcholine and norepinephrine of the sensorimotor cortex neurons of rats having different activity according to behavior parameters, i.e., resistance to emotional stress influences before and after experimental hemorrhagic stroke (EHS) was carried out. The recovery process after an EHS due to neural activity in prognostically stable (VA) and predisposed (NA) to stressful situation rats has individual characteristics. Acute stress influence before EHS

Downloaded from www.periodico.tchequimica.com

development changes the nature of neurons activity of the sensorimotor cortex in VA and NA rats on the third and seventh day after EHS. EHS leads to specific changes in the sensitivity of neurons to acetylcholine and norepinephrine in VA and NA rats. Acetylcholine microionophoresis causes activation of the neuron impulse activity in VA and NA rats, and these changes are the same after EHS. Acute stress influence before EHS development does not change nature of neuron responses to norepinephrine microionophoresis in VA animals. On the contrary, in NA rats loss of neuron sensitivity to norepinephrine during EHS development against stress was noted. It is possible that acute stress influence before EHS development can change brain noradrenergic system activity in NA rats, which are prognostically predisposed to stress influences. The data obtained stress the plasticity of the central nervous structure in development of response to stressful influences. (The ethics commission approval protocol number is 18-15 from 13th of Marth 2018.)

Keywords: *stress, hemorrhagic stroke, rats, neurons, norepinephrine*.

АННОТАЦИЯ

Проблема развития постстрессорных нарушений мозгового кровообращения, самое тяжелое из которых внутри мозговое кровоизлияние, или геморрагический инсульт, является крайне актуальной. Проведенные ранее исследования продемонстрировали, что в однотипных конфликтных ситуациях, по показателю выживаемости, отчетливо выявляются индивиды устойчивые и предрасположенные к эмоциональным стрессорным воздействиям. Однако нейронные механизмы, обеспечивающие нейромедиаторную регуляцию ответов на стрессорные воздействия, мало исследованы. В работе проведен анализ нейрохимической чувствительности к ацетилхолину и норадреналину нейронов сенсомоторной коры головного мозга крыс, имеющих различную активность по параметрам поведения до и после геморрагического инсульта. Процесс восстановления после экспериментального постстрессорного инсульта по показателям нейронной активности у прогностически устойчивых (ВА) и предрасположенных (НА) к стрессорным воздействиям крыс различен. Геморрагический инсульт приводит к специфическим изменениям чувствительности нейронов сенсомоторной коры к норадреналину у ВА и НА крыс. Острое стрессорное воздействие до формирования инсульта не изменяет характера ответов нейронов на микроионофорез медиатора у ВА животных. У НА крыс, напротив, отмечена потеря чувствительности нервных клеток к норадреналину при формировании геморрагического инсульта на фоне стресса. Можно полагать, что острое стрессорное воздействие до формирования геморрагического инсульта может изменять активность норадренергической системы нейронов сенсомоторной коры НА крыс - прогностически предрасположенных к стрессорным воздействиям. Полученные данные еще раз подчеркивают пластичность центральных нервных структур при формировании ответа на стрессорные воздействия. (Протокол этического комитета №18-15 от 13 марта 2018 г.)

Ключевые слова: *стресс, геморрагический инсульт, крысы, нейроны, норадреналин.*

1. INTRODUCTION

The problem of post-stress disorders of cerebral circulation, the most severe of which is cerebral hemorrhage, or hemorrhagic stroke, is extremely urgent (Yumatov, 2001; Lee *et al.,* 2016; Rainforth *et al.,* 2007; Smith and Eskey, 2011). Despite the high amount of works devoted to the study of the mechanisms of the development of post-stroke changes, a number of questions concerning the development of cerebral circulatory disorders in mammals with different prognostic resistance to similar stress loads remain unsolved.

Concerning the survival rate, previous studies have shown that in the same type of conflict situations, individuals resistant and predisposed to emotional stressful influences are clearly distinguished (Sudakov, 1983; Sudakov and Umruhen, 2010). It was shown that previous stress influenced biochemical parameters of the body during stroke development. The stress load before the experimental stroke differently changed the conformational properties of some blood proteins (e.g. albumin) in rats, differing in the parameters of behavior and response to stress (Kalinina *et al*., 2012).

Previous special experiments showed that active rats exhibiting in the “open field” a short latent period of the first movement and exit to the center, and also high locomotor activity on the periphery and, especially, in the center, are animals predictively resistant to stress loads. At the same time, rats that demonstrate a long latent period of the first movement and exit to the center, low activity, both in the center and on the periphery and having high vegetative balance indicators, are animals predictively predisposed to stress loads.

In this regard, rats that demonstrate

Downloaded from www.periodico.tchequimica.com

different locomotor activity in the “open field” test can be divided into two groups: resistant (highly active - VA) and predisposed (low active - NA) to emotional stress influences (Koplik, 2002; Koplik *et al.,* 2005).

Neurochemical and morphological changes in the brain of rats with different behavioral parameters occurring at various stages of the post-stroke period have not been fully studied. The dynamics of neurological symptoms in behaviorally passive (NA) and active (VA) animals with intracerebral hemorrhage (hemorrhagic stroke) are not completely studied (Koplik and Klassina, 2018; Koplik and Pertsov, 2019; Bogolepov *et al.,* 2001; Koplik *et al.,* 2001).

It has been shown that animal resistance to emotional stress closely correlates with genetically determined and individually acquired properties of neurotransmitter processes in various brain structures (Sudakov and Umryukhin, 2010). Thus, in VA and NA due to individual behavior parameters, preliminary emotional stress load changes dynamics of norepinephrine, dopamine, and to a lesser extent, serotonin content in the sensorimotor cortex after modeling hemorrhage in the caudate nucleus of the brain (Ivannikova *et al.,* 2012).

However, the neural mechanisms providing neuromediatory regulation of responses to stressful effects are still little studied (Bogolepov *et al.,* 2004). Considering the above, the purpose of this study was to analyze neurochemical sensitivity of neurons in the sensorimotor cortex of rats having different activity according to behavior parameters, i.e., resistance to emotional stress influences after hemorrhagic stroke.

2. MATERIALS AND METHODS

The experiments were carried out in 24 male rats of the Wistar strain (12 — VA and 12 — NA) with body weight 190–210 g, on the background of experimental hemorrhagic stroke (EHS) before and after stress influence. EHS was modeled by injecting 60 μl of own blood into the caudate nucleus of the left hemisphere (Deinsberger *et al.,* 1996). All control rats underwent a false operation for hemorrhagic stroke 1 day before the experiments.

Two days before the experiments, in which impulse activity was recorded and microionophoretic addition of neuroactive substances into the perineuronal space done, scalping and trepanation of the animal skull were performed under air-ether anesthesia. A micromanipulator was placed on the bones of the skull to introduce 3 channel pencil-type glass microelectrodes into the brain with a tip diameter of 2-4 μm, with the help of which extracellular registration of neurons impulse activity and microionophoretic addition of physiologically active substances to them was done. The recording channel of pencil-type glass three-channel microelectrodes was filled with 3M NaCl solution. For MIP neurotransmitters, 10^{-6} M solutions of Ach and NA in distilled water were used.

On the third (72 hours) and seventh (168 hours) days of influence (Koplik and Klassina, 2018) after EHS development the impulse activity of neurons of the sensorimotor (SM) cortex and microionophoretic (MIP) neurotransmitters behavior (acetylcholine (Ach) and norepinephrine (NA) were recorded: strength current 15-25 nA, with intervals between summing up 2-3 min.) to nerve cells of the SM cortex. The experiments were performed in anesthetized animals - urethane 1g / kg in 3-4 ml of 0.9% NaCl solution, i / p.

The obtained experimental data were statistically treated using nonparametric statistical methods and “Statistica 6” programs.

The character of neuronal activity pattern was analyzed by time-frequency characteristics: the duration of the interpulse intervals was measured. After analog-to-digital conversion, neuronograms were recorded on electronic media. Subsequently, a computer analysis of neurons activity of was carried out according to specially developed programs with the construction of graphs of interval histograms with a piecewise-uneven time scale (Sudakov, 1983; Timoshin, 1992).

A total of 57 neurons were recorded in VA and 48 in NA rats. The number of registered neurons in groups of experimental animals and the experimental scheme are shown in Table 1.
Number of SM neurons in the cortex of rats with different states in groups

3. RESULTS AND DISCUSSION

The performed studies have shown that after EHS SM cortex neurons of the rat are characterized by a single- arrhythmic type of spontaneous impulse activity. In the patterns of the discharge activity of the overwhelming majority (96%) of neurons of both VA and NA rats, the pulse intervals of 600-800 ms duration dominate (Figure 1). Moreover, patterns in the region of 600-700 ms are more characteristic for VA rats, and for NA - 700-800 ms.

Downloaded from www.periodico.tchequimica.com

Our previous experiments showed that the most difficult period in hemorrhagic stroke in NA rats was day 3. During this period, there was a sharp increase in lipid peroxidation indicators and an increase in the antioxidant index, whereas by day 7, opposite мутеы are observed in VA rats compared to NA rats, indicating a higher neurological status in VA rats (Bogolepov *et al*., 2004).

At the same time, the activity patterns of SM cortex neurons had no significant differences on the third and seventh days after EHS, both in VA and in NA animals.

However, the acute stress influence exerted before EHS development changes the character of the impulse activity of the cortical SM cortex neurons in VA and NA rats on the third and seventh days after EHS (Figures 2, 3). Therefore, the analysis of changes in the sensitivity of neurons to neurotransmitters - Ach and NA on the background of EHS was later performed.

Ach MIP was shown to induce activation of the neuron activity in VA and NA rats, and these changes are of the same nature on the third and seventh days after EHS. On the third day, as well as on the seventh day, after stroke, Ach MIP leads to domination of neuron activity patterns in VA rats at intervals of 70-90 ms (Figure 2). At the same time, a discrete dominance of the interpulse intervals within the range of 100-300 ms is characteristic for NA rats. Cancellation of MIP Ach is accompanied by a gradual restoration of the initial activity of neurons within 180 seconds.

Acute stressful influence results in the activation of the discharge activity of neurons in both groups of animals, which is reflected in the dominance in the activity patterns of intervals within the limits of 10-30 ms.

Stressful influence before EHS development does not change the character of the responses of neurons to MIP NA in VA animals. In NA rats, acute stressful influence, before EHS development, is accompanied by a loss of sensitivity of SM cortex neurons to MIP NA on the third and seventh days after stroke (Figure 4).

After EHS, NA unidirectionally changes the impulse activity of SM cortex neurons in VA and NA rats on the third and seventh day. The character of changes in the patterns of neuronal activity has no specific features in animals of both groups, which indicates the absence of differences in the internal noradrenergic mechanisms during EHS development in VA and NA animals (Figures 3, 4).

4. CONCLUSION

Individual characteristics of rets' behavior in the "open field", specifying their resistance to emotional stress, significantly affect the severity of neurological symptoms in case of intracerebral hemorrhage. Predictably stress-resistant rats are characterized by a faster recovery of neurological status, motor, and coordinatory disorders by the seventh day after unilateral hemorrhagic stroke in the caudate nucleus compared with stress-predisposed animals. (Koplik, 2015).

It is the structures of the sensorimotor cortex that participate in the restoration of motor activity after a stroke and are associated with restoring the balance of asymmetric interhemispheric inhibition and corticomotor excitability (McDonnell and Stinear, 2017).

The spontaneous impulse activity of SM cortex neurons in VA and NA rats on the background of EHS is of the same type with weakly expressed specificity.

Acute stressful influence leads to activation of neurons discharge activity in both groups of animals, which is reflected in the dominance in the activity patterns of intervals within 10-30 ms. Moreover, acute stress influence, before EHS development, changes the activity pattern of SM cortex neurons in VA and NA rats on the third and seventh days after EHS.

SM cortex neurons sensitivity to Ach is unidirectional in VA and NA rats on the third and seventh days after EHS on the background of stress. In VA rats, intervals of 70-90 ms duration dominate, and in NA rats – 100-300 ms.

MIP NA unidirectionally changes the spontaneous impulse activity of SM cortex neurons in VA and NA rats on the third and seventh days after EHS. The character of changes in the activity patterns of nerve cells has no specific features in VA and NA animals. This may indicate the identity of noradrenergic mechanisms during EHS development in VA and NA animals. However, prior to EHS development, in NA rats, acute stress influence is accompanied by a loss of sensitivity of SM cortex neurons to MIP NA on the third and seventh day after stroke.

Thus, due to neural activity, the recovery process after post-stress stroke has specific differences in VA and NA animals. EHS leads to changes in neurons sensitivity to NA in VA and NA rats. Acute stress influence before stroke development does not change the character of the neuron responses to MIP mediator in VA animals. On the contrary, in NA rats there was a loss of neurons sensitivity to NA during EHS

Downloaded from www.periodico.tchequimica.com

development on the background of acute stress. Therefore, acute stress influence before EHS development can change the activity of the noradrenergic system of neurons of the SM cortex in rats - prognostically predisposed to stress effects. The data obtained once again emphasize the plasticity of the central nervous structures in development of a response to stressful effects.

5. REFERENCES

1. Bogolepov, N. N., Koplik, E. V., Krivitskaya, G. N. Structural-functional characteristics of neurons in the cerebral cortex of rats with different sensitivities to emotional stress. *Bulletin of Experimental Biology and Medicine*, **2001**, 132(8), 124–128.
2. Bogolepov, N. N., Popova, E. N., Koplik, E. V., Krivitskaya, G. N., Sudakov, K. V. Structural-functional organization of neurons in the cerebral cortex of rats with different levels of resistance to emotional stress in conditions of exposure to delta sleep-inducing peptide. *Neuroscience and Behavioral Physiology*, **2004**, 34(6), 611–616.
3. Deinsberger, W., Vogel, J., Kuschinsky, W., Auer, L. M., Boker, D. K. Experimental intracerebral hemorrhage: description of a double in-jection model in rats. *Neurol. Res.,* **1996,** 5, 475–477.
4. Ivannikova, N. O., Pertsov, S. S., Krylin, V. V. Features of biogenic amines content in the cerebral cortex in experimental hemorrhagic stroke in rats with different behavioral activity. *Bull. expert. biol.and medicine*, **2012**, 153(5), 631–634.
5. Kalinina, V. V., Ivannikova, N. O., Koplik, E. V., Smolina, N. V., Gryzunov, Iu. A., Dobretsov, G. E. Stress effect on the development of hemorrhagic stroke. *Journal Vyssh Nerv Deiat Im I P Pavlova*, **2012,** 62(4), 506–512.
6. Klyueva, L. A. Cellular composition of lymphoid nodules in the trachea wall in rats with different resistance to emotional stress in a model of hemorrhagic stroke]. *Zh Nevrol Psikhiatr Im S S Korsakova*, **2017**, 117(8-2), 63–70. doi: 10.17116/jnevro20171178263-70.
7. Koplik, E. V., Klassina, S. Ya. Features of the dynamics of cardiac activity restoration in rats with different behavior after a post-stress hemorrhagic stroke. *Bulletin of new medical technologies,* **2018,** 25(2), 54–61.
8. Koplik, E. V., Pertsov, S. S. Compensatory capabilities of the cerebral cortex in experimental hemorrhagic stroke in rats with different resistance to emotional stress. In: *Proceedings of conference Modern problems of systemic regulation of physiological functions, Conference proceedings, Halkidiki, Greece, 25-31 may,* pp. 106–109, **2019**,.
9. Koplik, E. V., Salieva, R. M., Gorbunova, A. V. Open field test as a prognostic criterion for resistance to emotional stress in Wistar rats. *Journal of Higher Nervous Activity. I.P. Pavlova*, **2005**, 45(4), 775.
10. Koplik, E. V., Sudakov, K. V., Bogolepov, N. N., Krivitskaya, G. N., Popova, E. N. Structural and functional characteristics of neurons in the sensorimotor cortex of rats with different resistance to emotional stress. *Bulletin of Experimental Biology and Medicine,* **2001**, 132(2), 715–718.
11. Koplik, E. V. Features of lipid peroxidation in the cerebral cortex during experimental hemorrhagic stroke in rats with different behavioral activity. *Academic Journal of Western Siberia,* **2015**, 11(1-56), 69–72.
12. Koplik, E. V. Method for determining the criterion of resistance of rats to emotional stress. *Bulletin of New Medical Technologies,* **2002**, 9(1), 16–18.
13. Lee, Y. C., Lin, C. H., Lin, M. S., Lu, Y., Chang, C. H., Lin, J. W. Comparison of the effects of serotonin-norepinephrine reuptake inhibitors versus selective serotonin reuptake inhibitors on cerebrovascular events. *J Clin Psychiatry*, **2016**, 77(1), e1-7. doi: 10.4088 / JCP.14m09394.
14. McDonnell, M. N., Stinear, C. M. TMS measures of motor cortex function after stroke: A meta-analysis. *Brain Stimul.,* **2017,** 10(4), 721–734. doi: 10.1016/j.brs.2017.03.008
15. Rainforth, M. V., Schneider, R. H., Nidich, S. I. Stress reduction programs in patients with elevated blood pressure: a systematic review and meta – analysis. *Curr. Hypertens Rep.,* **2007**, 6, 520–528.
16. Smith, S. D., Eskey, C. J. Hemorrhagic stroke. *Radiol Clin North Am.,* **2011**, 49(1), 27–45. doi: 10.1016 / j.rcl.2010.07.01.011.
17. Sudakov, K. V., Umryukhin, P. E. Systemic basics of emotional stress. Moscow: Geotar-Media, **2010.**
18. Sudakov, K. V. Systemic mechanisms of brain activity. In *Methodological Aspects of Brain Science [in Russian],* pp. 102–116. Moscow: Meditsina, **1983**.

Downloaded from www.periodico.tchequimica.com

19. Timoshin, D. V. Dynamics of interstimulus intervals in the activity of neurons of the sensorimotor cortex during the development of a food-procuring reflex in the rabbit. *Neuroscience and Behavioral Physiology*, **1992,** 22(5), 370–379.
20. Yumatov, E. A. Cardiovascular reactions in emotional overstrain. *Human Physiology*, **2001,** 6(5), 93–99.

TABLES

Table 1. *The scheme of the experiment*

State of the experimental animals	VA rats after 72 hours	NA rats after 72 hours	VA rats after 168 hours	NA rats after 168 hours
EHS	15	12	18	12
Stress influence - EHS	12	12	12	12

The scheme of the experiments (stages in seconds)						
Background	Ach	After Ach	Break	Background	NA	after NA
180	30	180	300	180	30	180
Total time of one neuron activity registration – 1 080 sec.						

FIGURES

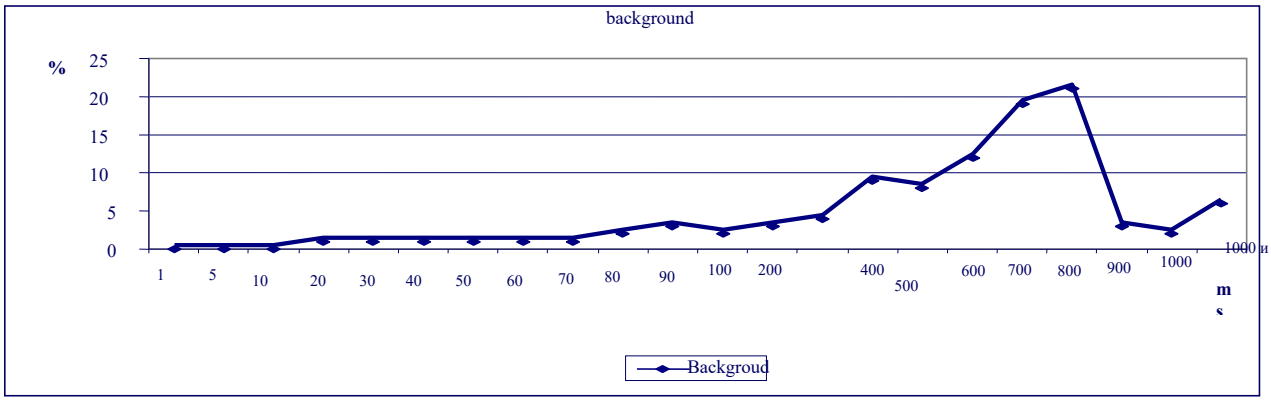

Figure 1. *Histogram of interpulse interval distribution in the patterns of SM cortex neurons activity in the rat after EHS.*

Downloaded from www.periodico.tchequimica.com

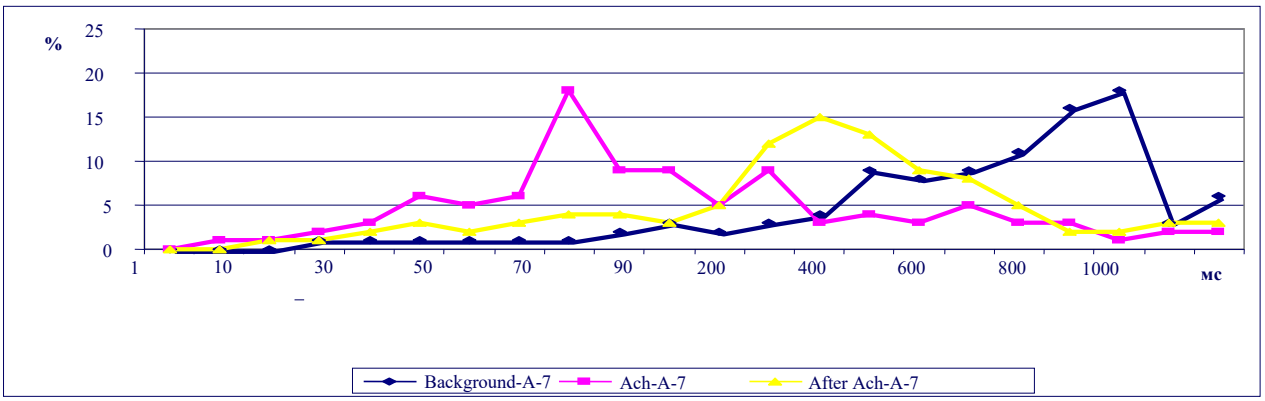

Figure 2. *Histograms of interpulse intervals distribution in the activity patterns of SM cortex neurons in VA rats on the 7th day (168 hours) after EHS with Ach MIP.*

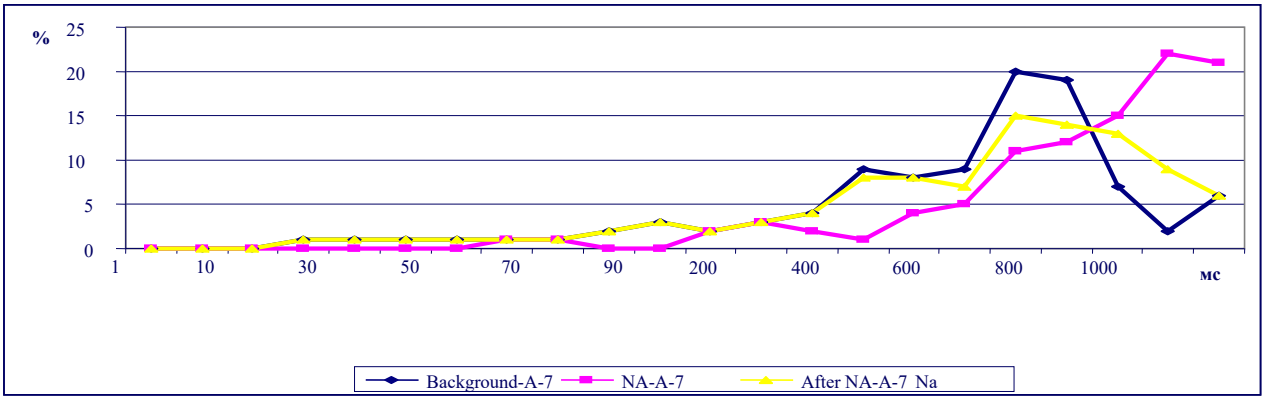

Figure 3. *Histograms of interpulse intervals distribution in the activity patterns of the SM cortex neurons in VA rats on the 7th day (168 hours) after EHS with MIP NA.*

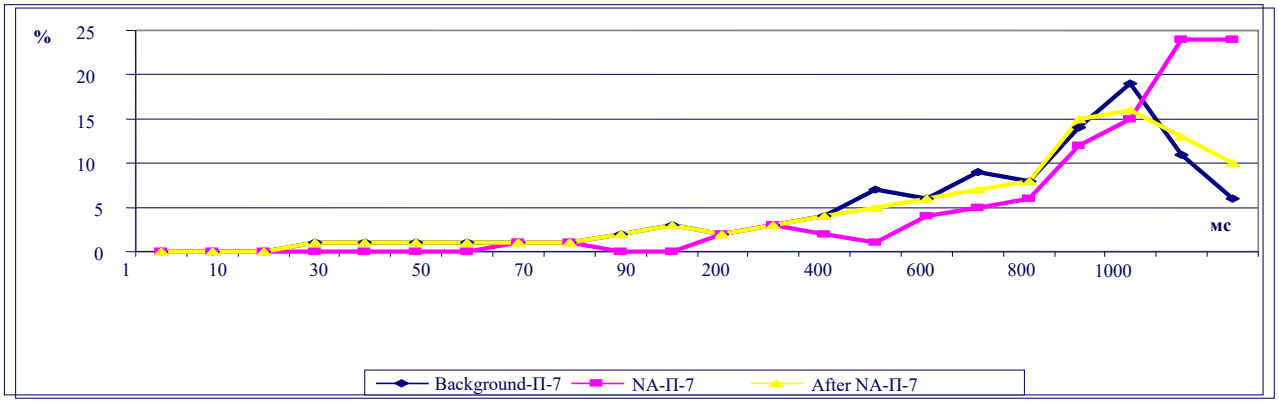

Figure 4. *Histograms of interpulse intervals distribution in the activity patterns of the SM cortex neurons in NA rats on the 7th day (168 hours) after EHS with MIP NA.*

Downloaded from www.periodico.tchequimica.com

PERIÓDICO TCHÊ QUÍMICA
ARTIGO ORIGINAL

MICROFACIAS E ESTUDO GEOQUÍMICO DA FORMAÇÃO DE DALICHAI: UM ESTUDO DE CASO DE ALBORZ CENTRAL NA PROVÍNCIA DE SEMNO, NORTE DO IRÃ

MICROFACIES AND GEOCHEMICAL STUDY OF THE DALICHAI FORMATION: A CASE STUDY OF CENTRAL ALBORZ IN SEMNAN PROVINCE, NORTHERN IRAN

میکروفاسیس و ژئوشیمی سازند دلیچای، منطقه سمنان، البرز مرکزی، ایران

SHAHKARAM, Elmira[1]; ADABI, Mohammad Hossein[2*]; JAHANI, Davoud[3]; VAZIRI, Seyed Hamid[4];

[1,3,4] Department of Geology, North Tehran Branch, Islamic Azad University, Tehran, Iran

[2] Department of Geology, Faculty of Earth Sciences, Shahid Beheshti University, Tehran, Iran

[*] *Corresponding author*
e-mail: m-adabi@sbu.ac.ir

Received 19 June 2019; received in revised form 30 October 2019; accepted 09 November 2019

RESUMO

Os principais depósitos progressivos bajocianos são acúmulo marroquino e calcário cheio de amonites e outros fósseis marinhos que são chamados de 'Formação Dalichai' com 1420m de espessura. Há erosão e limites inconsistentes que distinguem a Formação Dalichai da Formação Shemshak. O limite das formações Dalichai e Lar é isoclino e graduado. A presença de foraminíferos bentônicos, brilhos de esponja e amonites na seção Sharaf alude à existência de marinhos rasos a profundos. Processos diagenéticos como cimentação, micritização, porosidade, acumulação, óxido de ferro e bioturbação são observados na Formação Dalichai. Os carbonatos nessa formação podem ter composição aragonítica primária de acordo com os estudos sobre elementos principais e secundários, isótopos de carbono e oxigênio, e desenhando esses valores uns contra os outros. Em tal condição, a diagênese não marinha influenciou principalmente os carbonatos. Ao comparar Sr/Ca e Mn, pode-se sugerir que um ambiente diagenético semi-fechado para aberto tenha impactos nos carbonatos. A Formação Dalichai e a Formação Lar podem identificar um limite em 1200m de espessura, uma vez que existem mudanças nos Sr/Ca, Sr/Na, Sr e isótopos de carbono e oxigênio a serem estudados. A temperatura do calcário da formação Dalichai foi calculada em 32,9 °C. Em relação à litologia e análise das microfacias da seção Sharaf, são especificadas três microfacias que aparecem como depósitos na rampa externa. Neste estudo, sugere-se que o modelo de rampa homoclinal seja utilizado para essa formação. A seção Sharaf da formação Dalichai envolve composição mineralógica aragonítica na qual a diagênese do enterro influenciou substancialmente.

Palavras-chave: *Microfacias; Formação Dalichai; Diagênese; Ambiente sedimentar; Elementos principais e secundários; Isótopos de oxigênio e carbono*.

ABSTRACT

Top Bajocian progressive deposits are marly accumulation and limestone filled with ammonites and other marine fossils that are called ‘Dalichai formation’ with 1420m in thickness. There are erosion and inconsistent boundary that distinct Dalichai formation from Shemshak formation. The boundary of Dalichai and Lar formations is isocline and graded. The presence of Benthic foraminifera, sponge sparkles, and ammonites in the Sharaf section alludes the existence of shallow to deep open marine. Such diagenetic processes as cementation, micritization, porosity, accumulation, iron oxide and bioturbation are observed in Dalichai formation. The carbonates in this formation could have primary aragonitic composition according to the studies on main and secondary elements, carbon and oxygen isotopes, and drawing these values against each other. In such condition, non-marine diagenesis influenced the carbonates mostly. By comparing Sr/Ca and Mn, a semi-closed to open diagenetic environment can be suggested to have impacts on carbonates. Dalichai formation and Lar formation can identify a boundary in 1200m thickness since there are changes in Sr/Ca, Sr/Na, Sr, and carbon and oxygen isotopes to study. Dalichai formation limestone temperature was calculated 32.9 °C. Regarding lithology and analysis of Sharaf section microfacies, three microfacies are specified that appear as deposits in outer ramp. In this study, the model of Homoclinal ramp is suggested to utilize for such formation. Sharaf section Dalichai Formation entails aragonitic mineralogy composition on which burial diagenesis has substantially influenced.

Downloaded from www.periodico.tchequimica.com

Keywords: *Microfacies; Dalichai Formation; Diagenesis; Sedimentary environment; Main and secondary elements; Oxygen and carbon isotopes.*

چکیده

نهشته‌های پیشرونده باژوسین بالایی از نوع انباشته‌های مارنی و سنگ‌آهک‌های مارنی حاوی آمونیت و دیگر سنگواره‌های دریایی می‌باشد که به آن‌ها سازند دلیچای گفته می‌شود. ضخامت این رسوبات در منطقه شرف 1420 متر می‌باشد. مرز سازند دلیچای با سازند شمشک به صورت ناپیوسته از نوع فرسایشی و با سازند لار به صورت تدریجی و هم شیب است. وجود فرامینیفر بنتیک، سوزن‌های اسفنج و آمونیت در برش شرف بیانگر یک محیط دریای باز کم عمق تا عمیق است. از فرآیندهای دیاژنتیکی در این سازند می‌توان به سیمانی‌شدن، میکرایتی‌شدن، تخلخل، آشفتگی زیستی، تراکم، آهن‌دار شدن اشاره کرد. . مطالعه عناصر اصلی و فرعی، ایزوتوپ‌های اکسیژن و کربن و ترسیم این مقادیر در مقابل یکدیگر، حاکی از این است که کربنات‌های سازند دلیچای دارای ترکیب اولیه آراگونیتی بوده و دیاژنز غیردریایی بیشترین تاثیر را روی آن‌ها گذاشته است. ترسیم نسبت Sr/Ca در مقابل Mn نشان می‌دهد که این کربنات‌ها تحت تاثیر یک محیط نیمه بسته تا باز دیاژنتیکی قرارگرفته‌اند. با استفاده از تغییرات Sr/Na، Sr/Ca و ایزوتوپ اکسیژن و کربن، مرز این سازند با سازند لار در ضخامت 1200 متری مشخص شده است. دمای محاسبه شده برای سنگ آهک‌های دلیچای در برش شرف برابر با 32/9 درجه سانتیگراد می‌باشد. مطالعات سنگشناسی و آنالیز رخساره‌ای در برش شرف منجر به شناسایی سه ریزرخساره شد که در محیط رسوبی رمپ خارجی نهشته شده‌اند. مدل پیشنهادی برای این سازند یک سیستم رمپ هوموکلاین می‌باشد. سازند دلیچای در این برش دارای ترکیب کانی‌شناسی آراگونیتی است و دیاژنز تدفینی بیشترین تاثیر را روی آن گذاشته است.

واژه های کلیدی: *ریزرخساره‌ها، سازند دلیچای، دیاژنز، محیط رسوبی،* عناصر اصلی و فرعی، ایزوتوپ‌های اکسیژن و کربن

1. INTRODUCTION

In northern areas of Alborz mountain, no eupelagic deposits of upper Bajocian, Callovian (Dalichai Formation) and Oxfordian deposits, and Kimmeridgian (Lar Formation) exist and the younger rocks of Jurassic period are directly placed on the older rocks Shemshak deposits. Therefore, the northern and southern areas of Alborz experienced different geographical features from the upper Bajocian era until the last days of the Jurassic period. In their study, Davoudzadeh and Schmidt (1984) stated that the sedimentary basin of the northern Alborz is literary the continued highs of Lesser Caucasus syncline which indicates no sign of Bajocian and Bathonian rocks. However, southern Alborz is abundant with these rocks in many areas. The south parts in Alborz mountain entail sequence of rocks rich with ammonites and some marly and shale limestone in the formation of stratigraphic units. Among these sandstones and herb shales, it can be observed the presence of Shemshak group as well as thick limestone of Lar Formation (Upper Jurassic). The first explanation regarding the breccia of this formation was proposed by Erni (1931), discussing the signs of Bathonian ammonites in them. Later, Erni's suggested breccia was later reviewed by Steiger (1966) that lead the reviewed breccia to investigation by the 12th Iranian Committee of Stratigraphy and announced it as an official stratum unit of middle Jurassic of Alborz mountain. This formation is known to have organized layer of marly limestone and limestone sand along with some layers of marly shale and ammonite fossils including Oppelia and Parkinsonia (Darvishzadeh, 2004) (Figure 6).

2. DEVELOPMENT

2.1. Geographical location

A Sharaf section shows middle Jurassic sedimentary rocks that are considerably spread in the north of Gardaneh-ye Āhūān (A village in Semnan called Jam) and are extremely thick (Figure 3). Alavi-Naini (1972) investigated Jam district as well as a Sharaf section and prepared its geological map with a scale of 1:100000. Semnan-Damghan's main road leads to the Sharaf section. The study area is located between latitudes N 35º 56′ 12.5″ and longitudes E 53º 45′ 51″ (Figure 1).

2.2. Methodology

An appropriate geological section for performing the field studies is selected based on 1:100000 Jam map and analyzing the satellite photos. At first, the section was investigated in terms of geological and tectonic considerations to identify the upper and lower formation edge clearly and allow sampling to takes place. Sharaf section

Downloaded from www.periodico.tchequimica.com

contributed to sampling by providing 149 samples perpendicular to the layers. Meanwhile, such characteristics as apparent thickness, geographical features, layers contact, lithology types, and the direction and dip of the beds were also studied. 137 thin sections were collected from the Sharaf section and examined by an optical microscope. Adopting Dickson methodology (1965), it was attempted to identify calcite and dolomite separately by painting some of the sections with an Alizarian-red-s solution. In the current study, Dunham (1962) and Folk (1962) classification was employed for naming limestone. Identifying the facies and representing the sedimentary environment, Flugel (2010) model and the classification of Burchett and Wright (1992) were adopted by this study. After conducting a detailed study on the carbonate rocks, 50 of them were chosen for the elemental analysis. For specifying main as well as secondary elements, the rocks powders were analyzed by means of atomic absorption spectroscopy of Iranian Geological Organization geochemistry laboratories. The range of primary elements (Ca, Mg) and secondary elements (Na, Sr, Mn) are represented by percentages and ppm, respectively. 18 elemental analyzed powders samples were chosen and transferred to the Central Science Laboratory (CSL) of the University of Tasmania for analyzing oxygen and carbon isotope. The analysis included 15 mg of the sample powder that was exposed to phosphoric acid for 24 hours with a temperature of 25 centigrade. The aim was to evaluate the emission of CO2 of each sample by means of a mass spectrometer (micromass, 602 D). The error value of isotope measurement was ±0.001‰. Samples combined oxygen and carbon isotope is shown with δ (delta) sign, expressed based on parts per thousand (per mile), and evaluated with respect to Pee Dee Blemnite (PDB) standard.

3. RESULTS AND DISCUSSION

3.1. Stratigraphy

Dalichai formation of Alborz mountain range contains limestone, marly and marl limestone, and some layers of shale and siltstone among them. A detrital discontinuity caused by a middle Cimmerian event on siliciclastic deposits of Shemshak Formation companions this sequence. According to Nabavi, Jurrasic sea depth slightly increased in the latest days of the Bathonian stage that gradually constituted more calcareous sediments. In Jam area (35 km Khavar, Semnan), the outcrop of Dalichai formation exists only in north Bactriana of Attari fault (Alborz areas) (Figure 2) (Alavi-Naini, 1972). Sharaf mountain Dalichai formation establishes the alternates of olive-grey marls (Figure 5) and marly and sometimes nodular limestone with 1420m of thickness. This formation is identified by the fine nature of the rocks with a specified erosion in topography and a lower dip comparing to Lar Formation (Figure 3).

3.1.1. Dalichai Formation petrology in Sharaf mountain (Thickness=1420m) (Figure 7)

- Thin to medium limestone in 29m thickness of the layers
- Micro conglomerate in 23m thickness
- Alternate of thin layer limestone with grey to olive shales in 256m thickness.
- Medium layer limestone with shale and marl interlayers in 279m thickness
- Alternate of thin to medium layer limestone with grey shale in 768m thickness
- Thick to massive chert limestone (Lar) in 65 thick

3.2. Microfacies and sedimentary environment

Generally, the shallow open marine is located under the waves power line and in the middle ramp. Besides, the presence of ploids is observable in more shallow parts. These ploids are smaller in size by comparing to those exist in the lagoon environment. Since these species are widely spread across the globe along with an almost uniform condition for them, open marine stratigraphy is of vital importance. Deep open marine location is under the diluvial waves line and in the outer ramp.

Figure 4. Limestone layers of Sharaf section

Figure 5. Dalichai Formation Olive marl of Sharaf

Downloaded from www.periodico.tchequimica.com

section

Figure 6. Dalichai Formation ammonites of Sharaf section

3.2.1. Microfacies of Sharaf section

3.2.1.1. Microfacies of the shallow marine environment (A)

1. A_1 Sandy wackstone:

The microfacies groundmass is entirely constructed with micrites along with quartz grains (Figure 8.A).

2. A_2 Bioclast Sponge Spicules mudstone to wackestone:

Allochem presence is shallow in this microfacies and shaped like sponge spicules with prominent longitudinal and latitudinal sections. Most of the sponge sparkles are formed with silica. There are recognizable stylolite and iron paths in this microfacies, along with a noticeable surface fracture (Figure 8.B).

3.2.1.2 Deep open marine environment microfacies:

3. B Mudstone:

Allochem presence is significantly small (lower than 10%), and the groundmass is fully filled with micrites (Figure 8.C).

3.2.2. Sedimentary environment of the Dalichai Formation in the study section

Quiet environment index with no specific turbulences along with temperate hydrodynamic energy of deep marine and average salinity include a considerable mass of micrites with fine texture, a bivalve thin layer, sponge sparkles, and benthic and pelagic foraminifera, and the absence of sedimentary structures (Casovic *et al*., 2004; Flugel, 2010). Such a condition locates on the outer ramp.

Thus, the microfacies with mud-supported groundmass, benthic and some pelagic foraminifera, bivalve layers, sponge sparkles, and no coarse skeleton particles can be related to shallow to deep open marine. The anaerobic and low oxygen condition has resulted in forming the sponge sparkles. A carbonate ramp system can be regarded for Dalichai Formation microfacies of Sharaf section by studying the microfacies and the areas of formation, their gradually changes and the absence of such indexes as great barrier reefs, slip and failure structures, calsi-turbidite structures, and pisolites and oncoids that are gradually found in carbonate ramps.

Dalichai Formation type of Sharaf section is a low slip carbonate ramp (Homoclinal) that has a continued shoreline to basin glacis, regarding the comparison between the found microfacies and Wilson (1975) and Flugel (2010) standards and the studies on tectonic and stratigraphy conditions of Dalichai Formation.

3.3. Diagenetic processes of Sharaf section Dalichai Formation

3.3.1 Cementation

Diagenetic mainly carries out the cementation effort in which closed cavities become over-saturated by a high amount of flows. Analyzed Dalichai Formation samples by petrography studies indicate that sparrycalcitecement occurs rarely that all samples composition shows homogeneous micrites. In this texture, skeleton particles are appropriately dispersed. Sharaf section cementation process entails mostly the micrites groundmass and shows no cement textures. Only a few of the early samples were constructed with cement (Figure 9). Sharaf section fails to vary in different types of cement and only entails equant, block, and veined cement.

3.3.2 Mechanical Compaction:

The mechanical compaction is easily observed in the Sharaf section due to a low allochem gathering and the presence of mud-supported fabrics. Such compactness is not of vital concern regarding the history of breccia diagenetic.

3.3.3 Chemical Compaction

With an increase in grains and sediment solubility that can result in burden pressure or tectonic stresses, chemical compaction or pressure dissolution occurs (Adabi, 1996). Following this physical compaction, the exposure of chemical compaction provides to the sediments. They can be identified, then, by the pressure solution, stylolite formation, and joint solution that indicates some fractures. Besides, irregular

Downloaded from www.periodico.tchequimica.com

stylolite of different structures is observable in Dalichai formation (Figure 10.B). Calcite vein cement paintings explain the iron calcite presence in Dalichai Formation calcite veins. Since the veins cross the texture and components of the rock, they can have a tectonic origin. In some cases, these veins are cut by a stylolite that may be as the result of burial diagenesis of the diagenetic Dalichai Formation history. Some small scale and multistages fractures are approximately found (Figure 10.A, Figure 10.C).

3.3.4 Porosity

It is defined as a totally empty space ratio over the total volume of rock (Choquette & Pray, 1970). Porosity beginning of a groundmass may take place diagenesis. Sharaf section porosity shows up itself with caivty, intra-grains, inter-grains, channel, and fracture (Figure 11).

3.3.5 Silicification

It is a standard diagenetic process that happens for unsialic sedimanteries with little or sporadic effects (Hesse, 1989., Tucker, 2001). Over-satuarated sialic pore flow is required for carbonate sedimantary silification that can be occurred in any diagenesis stages, including primary, middle, delayed (Tucker, 2001). Each breccia silificaition displays silicious existence on sponge sparkles, as a subsitude for echinoderms fossils, or in the groundmass (Figure 12.C).

3.3.6 Iron Oxide

Carbonate sedimentary iron oxide is a diagenetic process. Mostly stylolite lines, solution veins, porous spaces, and/or in fossil rocks are the hosts for iron components. Iron oxide occues widely and extensively fills empty spaces of inter-grains, intra-grains, stylolite lines, fractures, and sometimes solution veins of micrite groundmass (Figure 11.B).

3.3.7 Dolomitization

Dolomite is a semi-stable mineral that subsitudes its primary crystals with the next stable phases by a sequence process and in the burial and/or metamorphism period (Warren, 1989). Sharaf section dolomitization entails dolo-micrites and limited single crystall replacement (Figure 12.A, Figure 12.B).

3.4 Geochemical analysis

Argonite, high magnasium calcite (Shallow marine and tropical climate), and low magnasium calcite (Deep and cold marine) are the main minerals of marine carbonates. According to some studies (Veizer, 1983, Rao, 1996), the minerals solution Ca and Mg, salinity level, and pressure CO_2 can be changed by exposing to temprature changes. Besides, unstable argonite minerals and high magnasium calcite transfers to a stable diagenetic low magnesium calsite uder the influence of time and diagenetic processes. In this definition, carbonates' primary minerology is a complicated task.

3.4.1. Primary minerology of Dalichai Formation

3.4.1.1 Main and secondary elements

Strontium

Sr changes of bulk carbonate samples in new warm water regions are between 8000 to 10000 ppm per change (Milliman, 1974). Temperate climate Bulk carbonate samples changes indicate 1600 to 5000 ppm (3250 ppm on average) (Rao and Adabi, 1992). The Sr amount in argonite is higher than the amount in calcite since Ca bigger cations (e.g., Sr, and Na) are prefrabley replaced in the argonite orthorhombic system. Almost 1000 ppm (maximum Sr amount) can be replaced in abiotic calcite system (Veizer, 1983).

Dalichain formation lime sample of the Sharaf section is the range of 183 ppm to 420 ppm. This amount is lower than that of recent. It may be as the result of diagenetic processes, particularily meteoric diagenesis (Adabi and Rao, 1991). Figure 13 categorizes Sr and Na amount based on the highest and the lowest rate, including recent argonite warm water with the highest Sr and Na amont, permian tasmanite subarctic limestone, recent temperate carbonate limestone, mozduran aragonite and gordon tasmania areas, Dalichai Maragheh limestone areas (Adabi and Abarghani, 2000), and cretaceous aged fahlian limestone. To specify tropical from non-tropical microfacies, Sr numbers are compared against Na numbers (Winefield *et al*., 1996). As it is evident, Dalichai Formation lime samples are located in aragonite Dalichai Formation of Maraghe breccia due to the mineralogy of an identified composition (Figure 13).

Sodium

The amount of sodium in Dalichai Formation lime samples fluctuates from 742 to 1929 ppm. The level of sanitary, biochemical differentiation, kinetic evidence, mineralogy, and water depth are the factors of sodium centralization in recent carbonate sedimentary deposits (Millman 1974, Winefield *et al*., 1996).

Downloaded from www.periodico.tchequimica.com

Sodium changes in recent aragonite deposits vary between 1500 ppm to 2700 ppm (Milliman, 1974, Adabi and Rao, 1991). Decreases of samples sodium against those of recent aragonite carbonates indicate non-marine diagenetic processes affects (Adabi, 2011).

Manganese

The range of manganese elements of the Dalichai Formation differs between 91 ppm to 749 ppm. Figure 14 illustrates compares Sr and Mn changes and shows that the samples are located in the Mozduran lime aragonite area. Mn diversities indicate diagenetic flow impacts. Mn and Fe amount of recent aragonite deposits display the numbers lower than 50 ppm (Milliman, 1974).

Sr/Ca ration

The diagenesis process in open/closed systems can be established based on the ration of Sr/Ca against Mn. In the study by Brand and Veizer (1981), it is identified the areas for aragonite diagenetic, high magnesium calcite (HMC), and low magnesium calcite (LMC) as illustrated in Figure 15.

In the case of water-rock interaction in open diagenesis systems, the amount of Sr/Ca meets reductions. Water-rock interactions are low in semi-closed, particularly closed, diagenetic systems that result in no obvious diagenesis Sr/Ca phases ratio compared to primary components. Generally, a decrease of magnesium in diagenetic calcite indicates a closed system. The chance of non-marine diagenesis of a semi-closed to open system is high for Dalichai Formation samples due to a low Mn amount and a decrease in Sr/Ca ration.

3.4.1.2 Oxygen and carbon isotopes

Considerable information regarding sedimentation environment temperature, diagenetic temperature, diagenesis processes in a diagenetic environment, salinity, alteration tendency, growth and/or sedimentation rate can be collected by analyzing oxygen 18 and carbon 13 isotopes (Marshall, and Ashton, 1980, Rao, 1996, Adabi *et al*., 2016). Is doing so, carbonates of different areas can be distinguished. Dalichai limestone Oxygen 18 isotopes changes are between -2.49‰ to -4.86‰. This value ranges from +1.42‰ to +3.54‰ for carbon 13 isotopes of Dalichai limestone. Burial diagenesis has influenced the oxygen and carbon isotopes by imposing the changes (Figure 16). These modifications display a major and a minor change in oxygen and carbon isotopes, respectively (Adabi, 2011).

Carbonate isotopes are created from the host lime, which can result in this minor change of carbonate isotope in the isotopically burial model. Besides, there is a lower isotope fractionation between carbon 13 isotope and carbon 12 isotopes by increasing temperature. It can be compared by the fractionation of oxygen 18 isotopes and oxygen 16 isotope that shows a higher value. Thus, there can observe an inclined linear tendency of oxygen and carbon values in burial diagenesis (Lohmann, 1988).

3.4.2. Temperature determination

Typically, the heaviest and the lightest oxygen isotope represents sedimentary environment temperature and diagenetic temperature, respectively (Adabi, 1996). Many equations suggest temperature determination based on oxygen isotope. This study has utilized the equation proposed by Anderson & Arthur (1983) as follows:

$$T^{\circ C} = 16.0 - 4.14(\delta_c - \delta_w) + 0.13(\delta_c - \delta_w)^2$$

In this formula, T represents temperature (centigrade), δ_c represents oxygen isotope content in 25 centigrade (PDB), and δ_w indicates marine oxygen isotope in the case of calcite accumulation (SMOW). The value of δ_w is considered zero for new marine; δ_c value differs in each period, but the period of Jurassic demands the value of -1.2‰ (Anderson & Arthur, 1983).

The temperature of the Dalichai Formation limestone of the Sharaf section has been calculated to be 32.9 centigrade. Regarding the previous explanations, these carbonates are subjected to non-marine diagenesis processes. Their oxygen and carbon isotopes are, thus, extracted, and they show a higher temperature against that of sedimentation processes.

Besides, the are large amounts of Fe (1400-9000 ppm) along with a little presence of Mn (91-749 ppm), and Na (742-1929 ppm) indicates the sedimentary environment unreal temperature which alludes its belongings to the burial very shallow environment.

3.4.3. Sr alterations against oxygen and carbon isotopes

Figures 12 and 13 illustrates Sr changes against oxygen and carbon isotopes, respectively. In both figures, the comparison of recent temperate bulk carbonate samples areas, upper Jurassic areas with aragonite mineralogy, as well as the areas of aragonite Mozduran formation,

Downloaded from www.periodico.tchequimica.com

Ordovician aragonite areas, and Gordon Tasmania aragonite formation areas are displayed (Adabi, 1996). As it is clear, most samples are located in aragonite mineralogy areas of Mozduran.

Carbonate isotopes changes of recent temperate areas show consistency due to the marine origin of the carbonates. Dalichai Formation carbonates expose small alteration and similar mineralogy composition that locates them in the Mozduran aragonites area (Adabi, 1996).

3.4.4. Mn changes against oxygen and carbon isotopes

Mn values of carbonate depend on redox and oxidation circumstances. In the case of the latter, only a few Mn elements can enter carbonate network. However, in redox conditions (half to full reactions), carbonate network accepts higher Mn values in itself (Adabi and Rao, 1991). The centralization of Mn is reduced by decreasing water depth and/or increasing the distance of shoreline. Most of the samples demonstrate the Mn value higher than 200 ppm, which suggests the presence of semi-aerobic or half redox reactions that dominated diagenetic environment. Comparing changes in oxygen isotope 18 and magnesium (Figure 19) of Dalichai Formation limestone implies that all samples are detected in the areas of upper Jurassic aragonite limestone of Mozduran formation and remote of Tasmania recent temperate areas limestone. This figure also reveals that oxygen 18 isotopes become lighter by occurring an increase in Mn value. This alludes alteration processes or non-marine diagenesis impacts.

Carbon 13 isotope can have constant changes in the areas where Mn values of temperate Tasmania limestone are changed. However, due to diagenetic processes, this isotope may vary in aragonite limestone of Mozduran Jurassic and Ordovician aragonite limestone of the Gordon group. Carbon 13 isotope also becomes lighter as the result of an increase in Ma due to non-marine diagenesis impacts (Adabi, 1996).

By drawing the changes in carbon 13 isotope and comparing them to Mn of carbonate samples, it can be mentioned that all samples are discovered in aragonite limestone of Mozduran formation upper Jurassic and are noticeably closed to $\delta^{13}C$ areas of aragonite marine of upper Jurassic due to a lower tendency of alteration (Figure 20).

3.4.5. Sodium changes against oxygen and carbon isotopes

Oxygen 18 isotope values of almost all Dalicahi formation samples are close to the areas of upper Jurassic aragonites with the least alteration tendency. This explains a little influence of non-marine diagenesis on these samples. According to the values of Na against $\delta^{18}O$, it is clear that some samples of Dalichai Formation are spotted in Tasmania Gordon areas of aragonite limestone due to the same composition of mineralogy (Figure 21).

Carbon 13 isotope shows constant changes against carbonate sodium of recent temperate regions due to the marine nature of the carbonates. Regarding non-marine processes, Na values of Mozduran formation aragonitic carbonates meet a reduction by any decrease occurs in $\delta^{13}C$ (Adabi and Rao, 1991). Dalichai Formation carbonates are located in Mozduran aragonites due to their low tendency of alteration and identical mineralogy (Figure 22).

3.4.6. Secondary elements (Sr/Ca, Sr/Na, Sr) changes to distinguish boundaries of formations

An essential element in carbonates analysis is the Sr element. Some researchers, including Winefield *et al*. (1996), suggested the applicability of Sr/Na ratio to distinguish facies and boundaries of formations (Adabi and Asadi Mehmandosti, 2008). Lar and Dalichai Formations can readily be distinguished by considering Sr changes and their ratio to Ca and Na in the stratigraphy column. As Figure 23 illustrates, Sr values and Sr/Ca, Sr/Na changes are evident in Lar and Dalichai Formations boundary. This may prove the chemical composition differentiation of sea water when the formations establishment begins. Thus, both formations boundary can be evidently distinguished.

Obviously, both Lar and Dalichai Formations display different values of secondary elements since there is a dominance of physio-chemical changes in the environment. Besides, specified changes (i.e., shifts) exist in their boundary in 1200m thickness (Figure 23).

3.4.7. Carbon and oxygen isotopes

3.4.7.1. Oxygen 18 isotopes changes of Dalichai and Lar Formations

Drawing oxygen 18 changes against Lar and Dalichai Formations thickness expresses oxygen isotope changes in the boundary of both

Downloaded from www.periodico.tchequimica.com

formations. In Figure 24, it is revealed lower changes of oxygen isotope in Dalichai Formation, particulary Lar Formation boundry. The lowest value of oxygen 18 isotope is observed in Lar – Dalichai Formations boundry. Such changes resulted in a space between them. in the isotope analysis, it was attempted to utilize the samples with the lowest alterations (i.e., those samples that have kept the primary marine characterestics). Oxygen 18 isotopes substantial changes, particulary in two formations boundary, which can be as the result of metaoric waters or burial diagenesis impacts.

3.4.7.2 Carbon 13 isotope changes of Lar and Dalichai Formations

Similar to oxygen 18 isotopes, changes in carbon 13 isotopes in the boundry of two formations are clearly identified. Lar Formation carries a lighter carbon isotope and shows higher fluctuations compared to Dalichai Formation. Figure 25 marks the constant changes in carbon 13 isotope in the stratigraphy column. And the carbon begins to have the lightest value in the Lar Formation boundary.

4. CONCLUSION

- Dalichai Formation considers being the first marine sedimentary of Alborz middle Jurassic with a particular outcrop in south regions. The deposits are formed in a marine environment. Dalichai marly rocks play a guidance role as a slightly green layer that can distinct the dark bottom layers with coals from the Lar Formation top rocks.
- Dalichai Formation thickness of the Sharaf section was estimated at 1420m. Any changes regarding the thickness of the Dalichai Formation in structural zone of central Alborz fail to follow a distinct procedure. It can be as the result of dominance of tectonic conditions over the region, the presence of a tensile phase, inconsistency of sedimentation, and bed rock conditions in the formation time.
- Dalichai Formation displays inconsistent existence on the siliciclastic formation of Shemshak with an erosion nature. Lar limestone formation meets the upper part of the Dalichai Formation, which is consistent and isocline. Dalichai top boundary with Lar Formation is where marly layers disappear, and chert layers emerge.
- Varity of diagenetic processes, including accumulation, stylolitization, cementation, iron oxide, silification, dolomitization, and types of porosity, have imposed effects.
- Regarding microfacies researches, three microfacies have been identified for Sharaf section as follows:
  Outer ramp micro facies:
  C1 Sandy-Wackstone
  C2 Bioclast Sponge Spicules mudstone to wackestone
  D Mudstone
- The proposed model for this formation of the Sharaf section depends on microfacies types, the absence of great barrier reefs, slip and failure structures, calsi-turbidite structures, pisolites, and a Homoclinal ramp.
- Regarding the proposed model, the sedimentary environment of the Sharaf section is an open marine.
- Primary and secondary elements and isotopes analysis of the Dalichai Formation expresses the primary aragonitic mineralogy presence in the formation. by comparing oxygen and carbon isotopes, it can be mentioned a shallow burial diagenesis processes.
- It can be concluded the impacts of non-marine of a semi-closed to open environment on the carbonates according to the changes in secondary elements, particularly Sr/Ca against Mn, and the changes of $\delta^{18}O$ and $\delta^{13}C$ of the formation carbonates.
- In 1200m thickness, the boundary for Lar Formation and Dalichai Formation is evident that is as the result of physio-chemical water changes, diagenetic processes, and Sr/Na, Sr/Ca, and Sr changes. Besides, a shift occurs for oxygen and carbon isotopes in this thickness. This fact can prove the secondary elements changes of this boundary.
- Utilizing Arthur and Anderson's (1983) Equation, Dalichai Formation calculated temperature is 32.9 centigrade. Meteoric and burial types of processes have impacted the carbonates that resulted in carbon and oxygen extraction. Thus, temperature calculation shows a higher a higher number than the real one in time of sediment formation (δ_w = -1.2‰).

5. REFERENCES

1. Adabi, M. H., 2011, Sedimentary Geochemistry, Arian Zamin pub., Second edition, p. 553. (in persian)
2. Adabi, M. H., Abarghani, A., 2003,

Downloaded from www.periodico.tchequimica.com

Investigation of facies of Dalichai Formation (Middle Jurassic) and Lar (Upper Jurassic) and application of isotopic analysis and sub-elements in separation of these two formations in northwest Maragheh in Iran, Journal of science, Tehran university, Vol. 27, No. 1, pp. 39-52. Accessible at: https://journals.ut.ac.ir/article_16684.html (in persian)
3. Darvishzadeh, A., 2005, Geology of Iran, Amirkabir pub., Edition 4, p. 432. (in persian)
4. Adabi, M.H., 1996. Sedimentology and geochemistry of Upper Jurassic (Iran) and Precambrian (Tasmania) carbonate, Unpubl. Ph. D. Thesis, Uni. Tasmania, Australia, 400 p.
5. Adabi, M.H., and Rao, C.P., 1991. Petrographic and geochemical evidence for original aragonitic mineralogy of Upper Jurassic carbonate (Mozduran Formation) Sarakhs area, Iran. Sedimentary Geology, v. 72, p. 253-267.
6. Adabi, M.H., and Asadi Mehmandosti, E., 2008. Microfacies and geochemistery of the Ilam Formation in the Tang-e-Rashid area, Izeh, S.W. Iran: Journal of Asian Earth Sciences, v. 33, p. 267-277.
7. Adabi, M.H., Salehi, M.A, and Ghobeishavi, A., 2010. Depositional environment, sequence stratigraphy, and geochemistry of Lower Cretaceoues carbonates (Fahliyan Formation), South-West Iran. Journal of Asian Earth Sciences, v. 39, p. 148-160.
8. Adabi, M.H., Kakemem, U., and Sadeghi, A., 2016. Sedimentary facies, depositional environment, and sequence stratigraphy of Oligocene-Miocene shallow water carbonate form the Rig Mountain, Zagros basin (SW Iran) Carbonates and Evaporites, p. 1-17.
9. Alavi-Naini, M., Hamedi, A.R., 1972. Map 1:100000 Jam; Geological Survey of Iran.
10. Anderson, T.F., and Arthur, M.A., 1983. Stable Isotopes of oxygen and carbonand theirapplication to sedimentologic and paleoenvironmental problems: in Stable Isotopes in Sedimentary Geology: Soc. Econ. Paleontal. Mineral., Short Course, v. 10, Section 1.1-1.151.
11. Brand, U., and Veizer, J., 1981. Chemical Diagenesis of multicomponent carbonate system, II: stable Isotops: Journal. Sed. Petrology, v. 51, p. 987-997.
12. Burchett, T.P., and Wright, V.P., 1992. Carbonate ramp depositional systems. Sedimentary Geology. v. 79(1-4), p. 3-57.
13. Choqutte, P.W., and Pray, L.C., 1970. Geologic nomenclature and classification of porosity in sedimentary carbonates. American Association of Petroleum Geology bulletin, v. 54(2), p. 207-250.
14. Cosovic, I., Schnell, M., and Springer, A., 2004. Pre-post and combined-equalization single-user bounds for MC-CDMA, in Wireless Technology, 2004. 7th European Conference, p. 321-324.
15. Davoudzadeh, M., Schmidt, K., 1984. A review of the Mesozoic paleogeography and paleotectonic evolution of Iran. Neues Jahrb. Geo. Paleontol. Abh. ISSN 0077-7749, Dtsch, v. 168 (2-3), p. 182-207.
16. Dickson, J.A.D., 1965. A modified staining technique for carbonate in thin section, Natures v. 205, p. 287.
17. Dunham, R.J., 1962. Classification of carbonate rocks according to depositional texture. American Assiciaion of Petroleum Geologist, Memoir v. 1, p. 108-121.
18. Erni, A., 1931. Decouverte du Bathonien fossilifere dans I′ Elbourz. Eclogae geol. Helv., 24: 64-65.
19. Flugel, E., 2010. Microfacies of Carbonate Rocks. Springer- Verlag. Berlin, 1006, p.
20. Folk, R.I., 1962. Spectral subdivision of limestone types. In: Classification of Carbonate Rocks (Ed. By W.E., Ham), p. 62-84. Mem. Am. Ass. Petrol. Geo. 1.
21. Hesse, J., 1989. Silica diagenesis: origin of inorganic and replacement cherts. Earth-Science Reviews, v. 26(1-3). P. 253-284.
22. Lohmann, K.C., 1988. Geochemical patterns of meteoric diagenetic systems and their aplication tostudies of paleokarst: In James, N.P., and Choquette, P.W., (eds), Paleokarst: New York, Springer-Verlag, p. 58-80.
23. Marshall, D.J., and Ashton, M., 1980. Isotopic and trace element evidence for submarine lithification of hardgrounds in the Jurassic of eastern England. Sedimentology, v. 27(3), p. 271-289.
24. Milliman, J.D., 1974. Recent Sedimentary Carbonates, Part 1, Springer-Verlag, Berlin, p. 375.
25. Rao, C.P., 1990. Petrography, trace elements and oxygen and carbon isotops Gordon Group carbonate (Ordovician), Florentone Vally, Tasmania, Australia, Sedimentary Geology, v. 66, p. 83-97.
26. Rao, C.P., 1996. Elemental compositon of marine calcite from modern temperate

Downloaded from www.periodico.tchequimica.com

shelf brachiopods, bryozoans, and bulk carbonates, eastern Tasmania, Australia: Carbonates and Evaporites, v. 11, p. 1-18.
27. Rao, C.P., and Adabi, M.H., 1992. Carbonate minerals, major and minor elements, and oxygen and carbon isotops and their variation with water depth in cool, temperate carbonates, western Tasmania, Australia, Marine Geology, v. 103, p. 249-272.
28. Steiger, R., 1966. Die Geology der West-Firuzkuh-Area (Central Alborz/Iran).
29. Tucker, M.E., 2001. Sedimentary Petrology: An introduction to the origin of sedimentary rocks. Blackwell Scientific Publication, 262 p.
30. Veizer, J., 1983. Trace elements and stable isotops in sedimentary carbonates: In Reeder, R. J., (Eds), Carbonatea, Mineralogy, and Chemistry. Reviews in Mineralogy, Blacksburg, v. 11, p. 265-299.
31. Warren, J.K., 1989. Evaporite Sedimentology: Importance in Hydrocarbon Accumulation: Englewood Cliffs, NJ, Prentice Hall Advanced Reference Series, 285 p.
32. Wilson, J.L., 1975. Carbonate Facies in Geologic History. Springer-Verlog, Newyork, 471 p.
33. Winefield, P.R., Nelson, C.S., and Hodder, A.P.W., 1996. Discriminating temperate carbonates and their diagenetic enviroments using bulk elemental geochemistry: a reconnaissance study based on New Zealand Cenozoic limestones. Carbonates and Evaporites, v.11, p. 19-31.
34. map.iranview.com

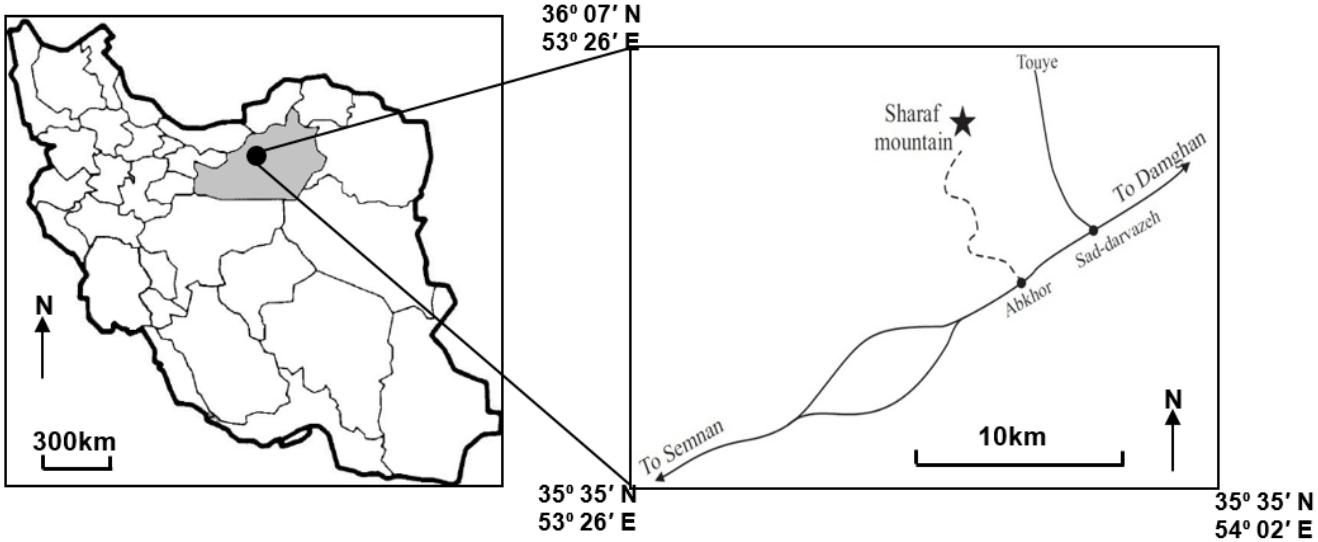

Figure 1*. Location map pf the study area and the section studied.*

Downloaded from www.periodico.tchequimica.com

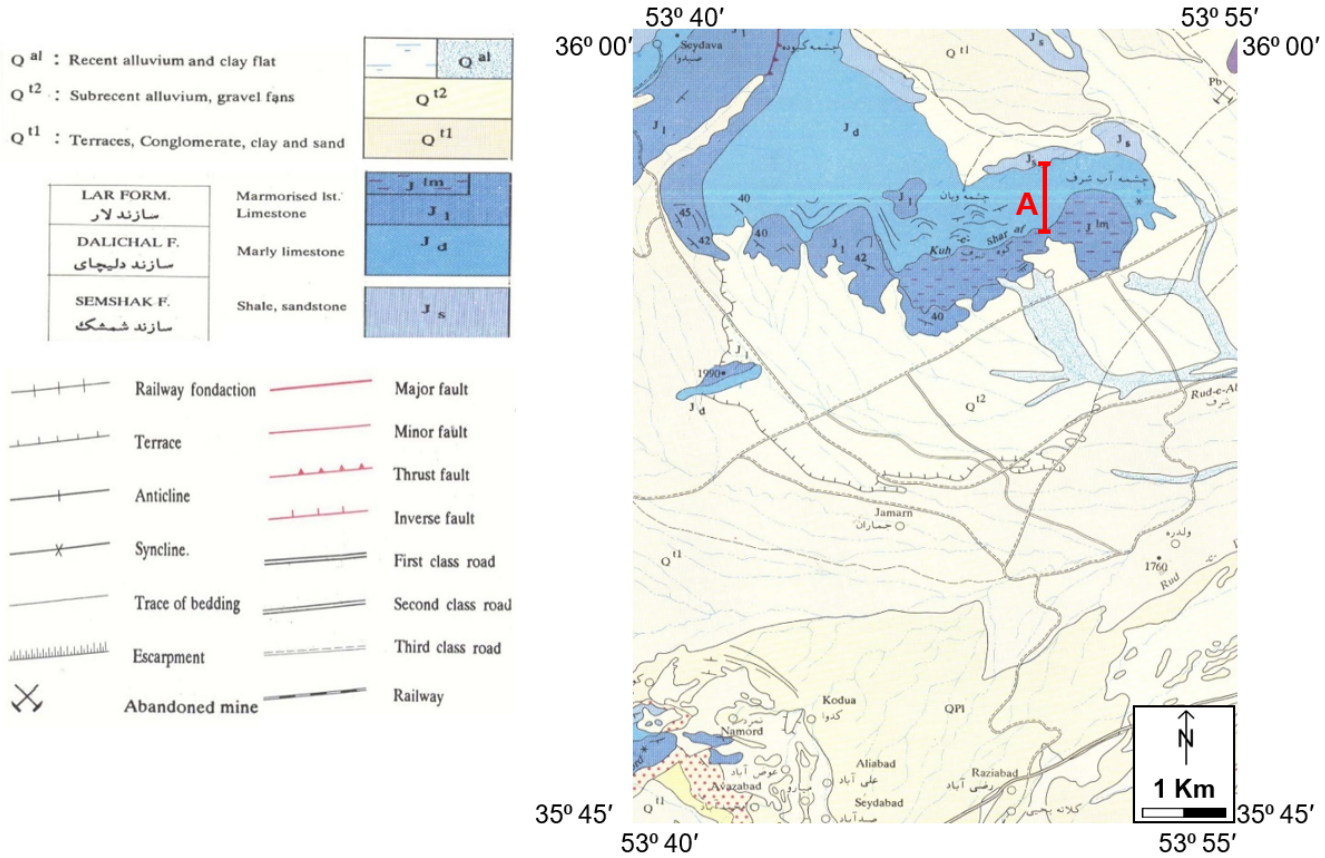

Figure 2. Sharaf section (A) with a geological map of Jam with the scale of 1:100000 (Alavi-Naini and Hamedi, 1972)

Figure 3. Sharaf mountain (southwest view)

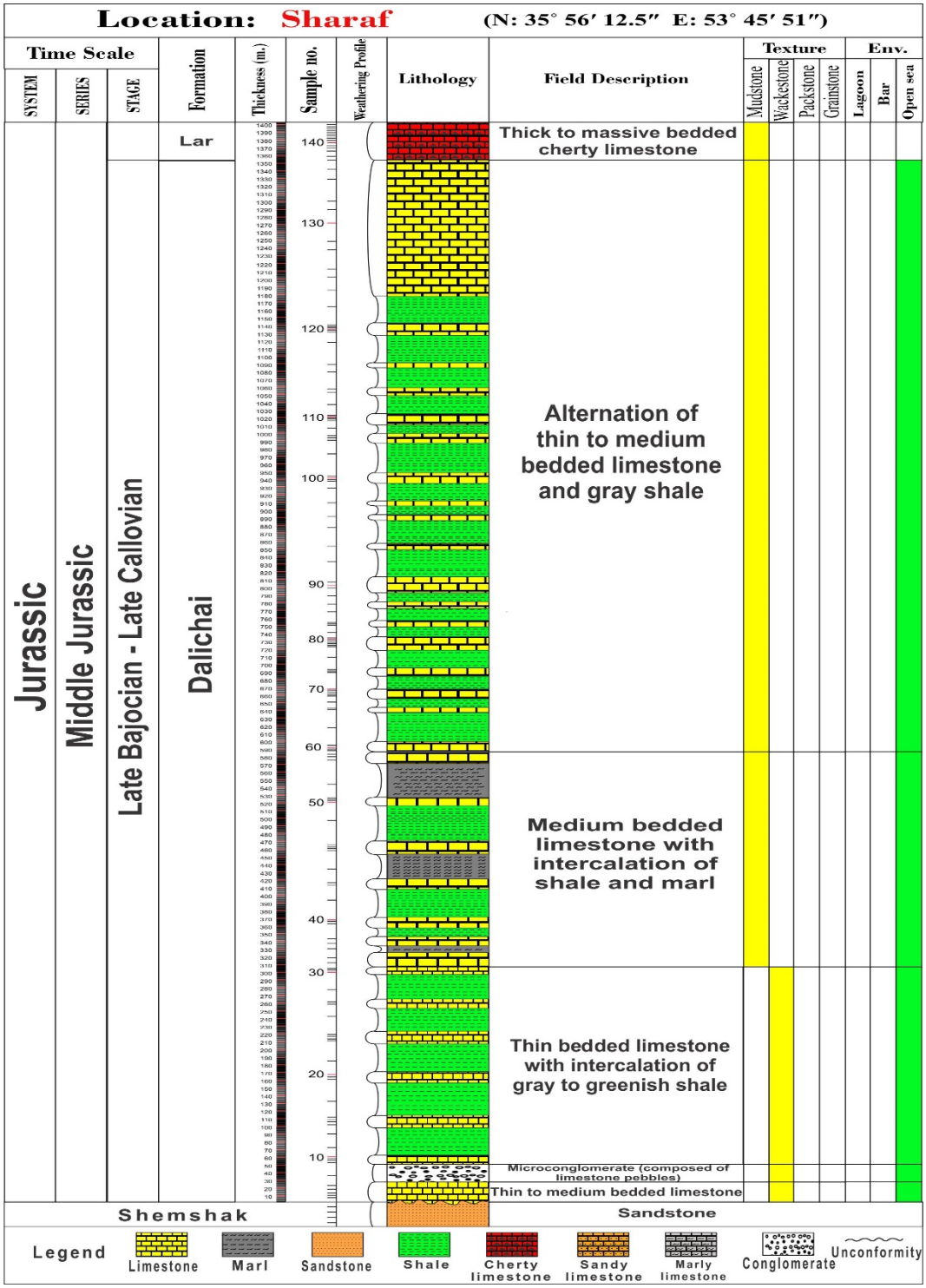

Figure 7. Stratigraphy column of Sharaf section

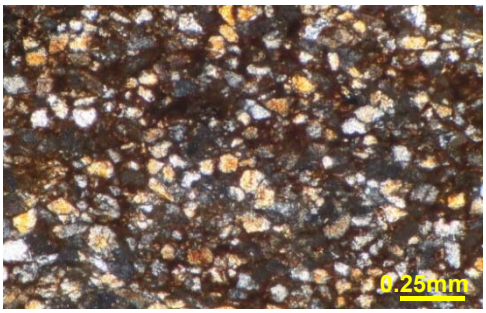

(A). A_1 Sandy-wackstone, section 2

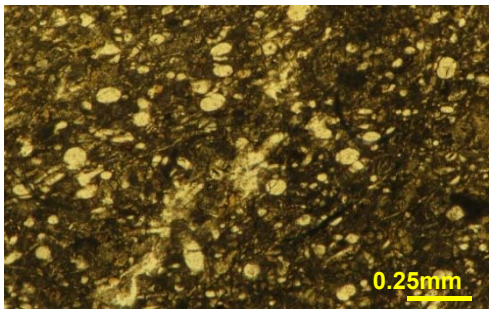

(B). A2 Bioclast Sponge Spicules mudstone to wackestone, section 27

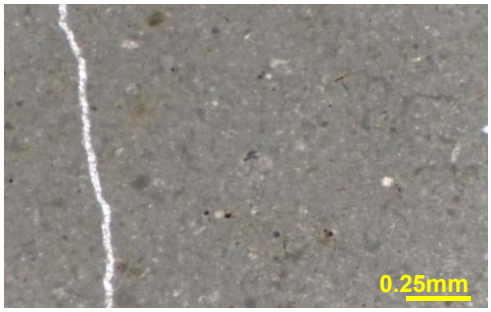

(C). B Mudstone, Section 89

Figure 8. *Microfacies of Dalichai Formation in Sharaf section*

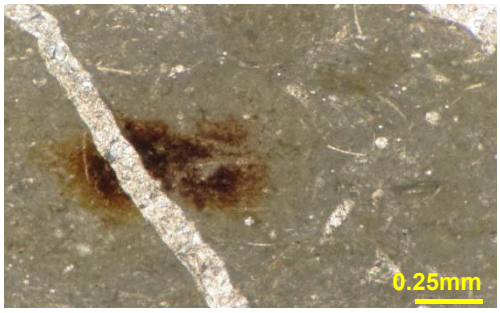

(A). Filler vein cement – Noraml light (PPL) – section 6

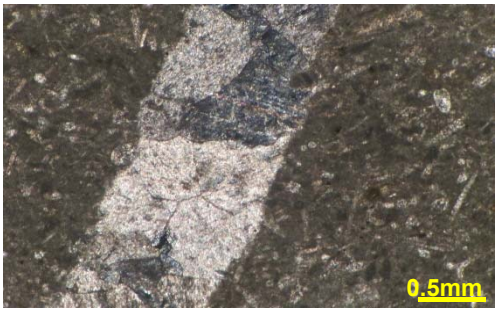

(B). Block cement filling a vein – polarized light (XPL) –section 5

Figure 9. *Dalichai Formation cement types of Sharaf section*

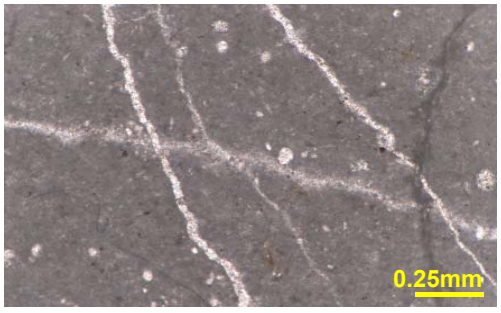

(A). Small scale fractures – normal light (PPL) – section 47

(B). Styolite – Normal light (PPL) – section 108

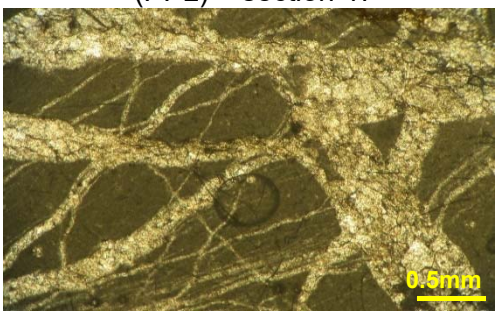

(C). Crossed multistages fractures – Normal light (PPL) – section 47

Figure 10. *Compaction types of Sharaf section*

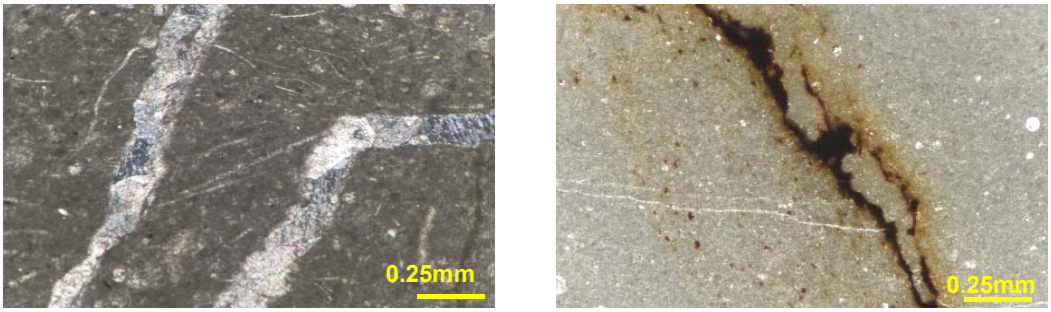

(A). Silicious filled channel porosity - polarized light (XPL), section 16

(B). Iron oxide fracture porosity – normal light (PPL) –section 43

Figure 11. *Porosity type of Sharaf section*

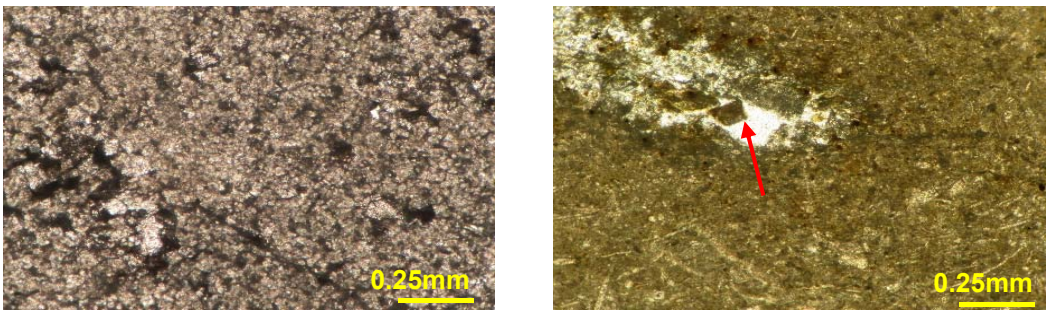

(A). Dolomitization (dolo-micrites) – normal light (PPL) –section 137

(B). Dolomitization – normal light (PPL) – section 7

Figure 12. *Other diagenetic processes of Sharaf section*

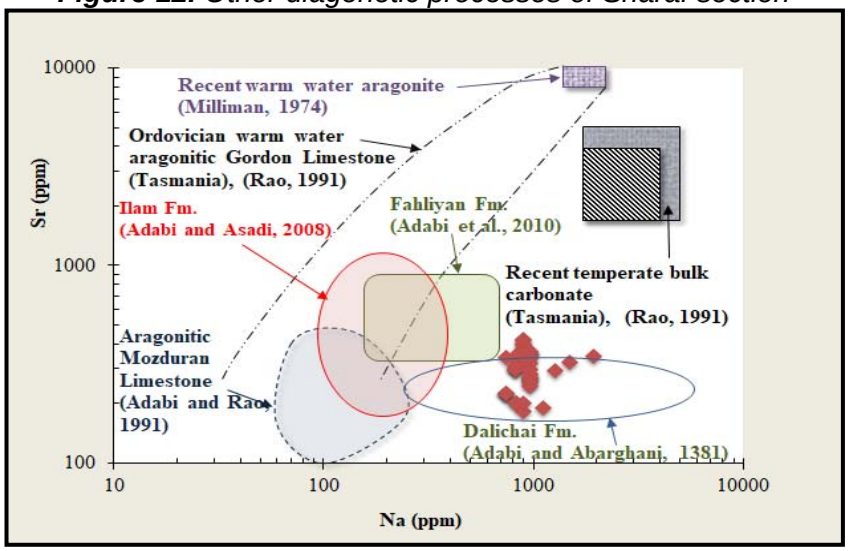

Figure 13. Na *and* Sr changes comparison in Dalichai Formation lime samples of Sharaf section *Regarding some limitations, aragonite mineralogy, and identical diagenetic processes, Dalichai Formation lime samples are located in the area of Maraghe formation (Adabi and Abarghani, 2002)*

Downloaded from www.periodico.tchequimica.com

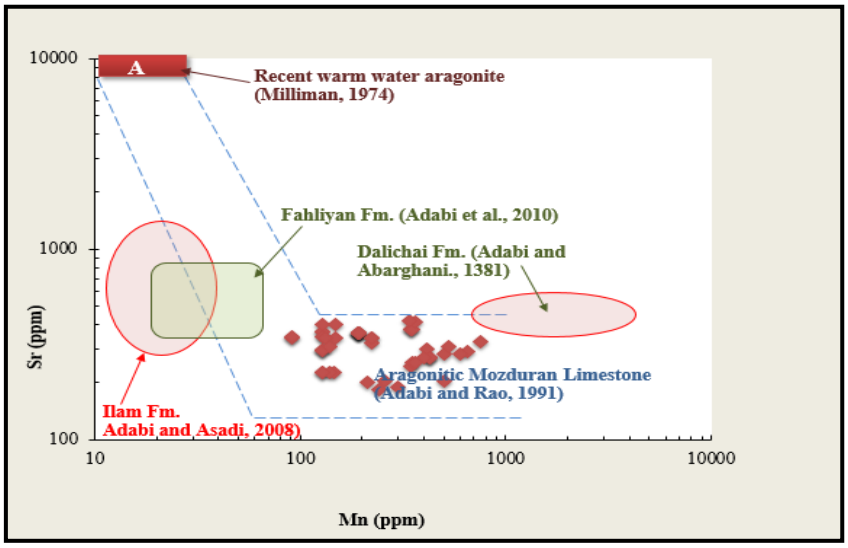

Figure 14. Na and Sr changes comparison in Dalichai Formation lime samples of Sharaf section *Regarding the same aragonite primary mineralogy, samples are located in Mozduran formation. Dalichai Formation limestone of Maraghe shows a high amount of Mn due to the diagenetic flow impacts and the tendency of alteration.*

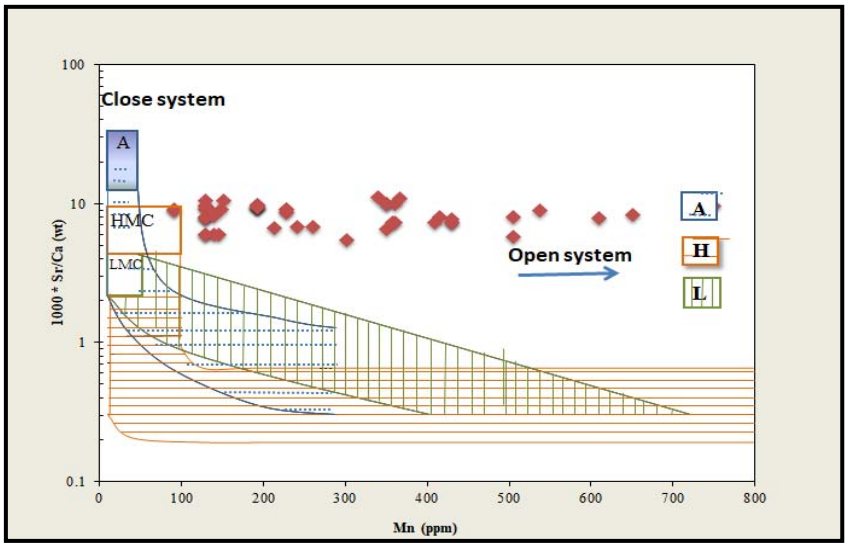

Figure 15. Sharaf section ($\frac{Sr}{Ca}$) changes processes against Mn

Dalichai Formation lime samples are influenced by diagenetic processes of a semi-closed to open system, regarding the established areas by Brand and Veizer (1981)

Downloaded from www.periodico.tchequimica.com

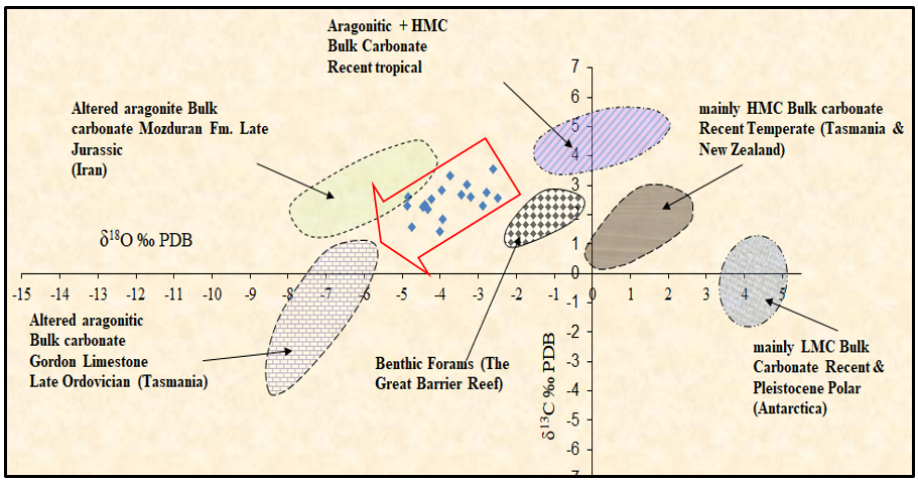

Figure 16. Sharaf section Dalichai Formation diagram of $\delta^{18}O$ against $\delta^{13}C$
The inclined carbon and oxygen tendency indicates shallow burial diagenesis

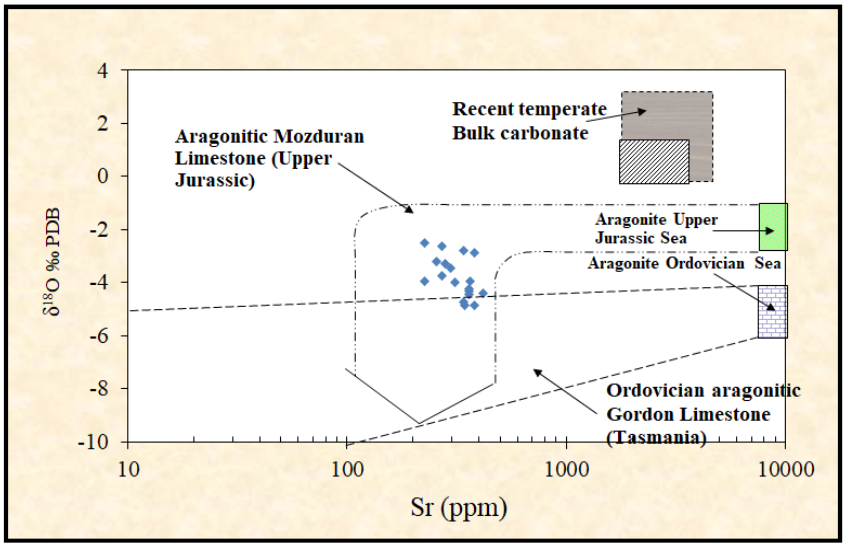

Figure 17. *Changes of $\delta^{18}O$ against Sr values of Dalichai Formation of Sharaf section. Most of the samples are located in the areas of aragonite minerology and many others near upper Jurassic aragonite areas*

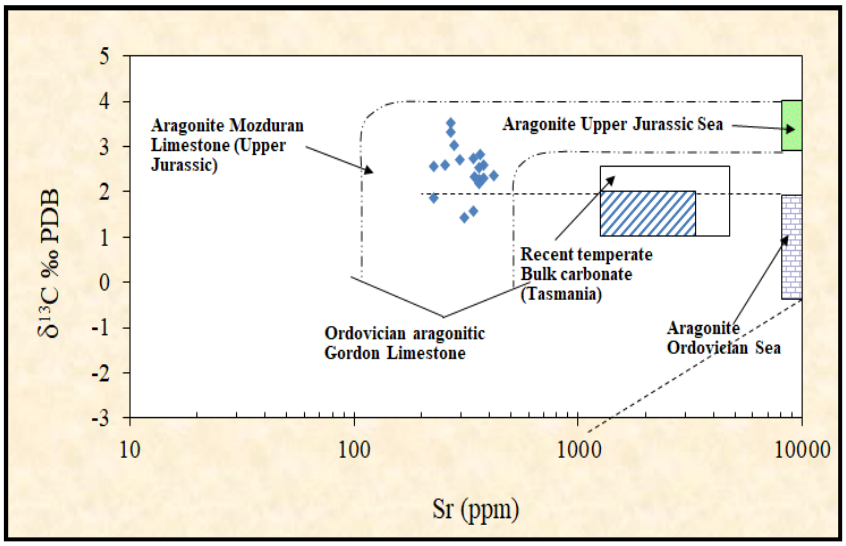

Figure 18. *Changes of Sr values against $\delta^{13}C$ of Dalichai Formation of Sharaf section. The changes are insignificant due to the weak impacts of Diagenesis processes on carbon isotopes*

Downloaded from www.periodico.tchequimica.com

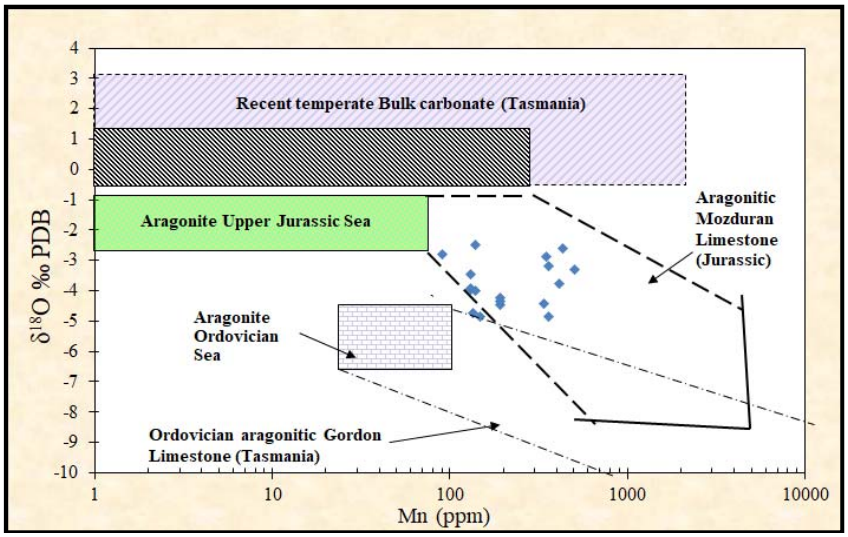

Figure 19. Changes in $\delta^{18}O$ against Mn of Dalichai Formation of Sharaf section

As it is evident, most samples are located in primary aragonite minalorogy composition by comparing to the proposed areas of recent temperate carbonates, Gordon aragonite limestone of Tasmania (Rao, 1990), and aragonite carbonate areas of Mozduran formation upper Jurassic (Adabi, 1996)

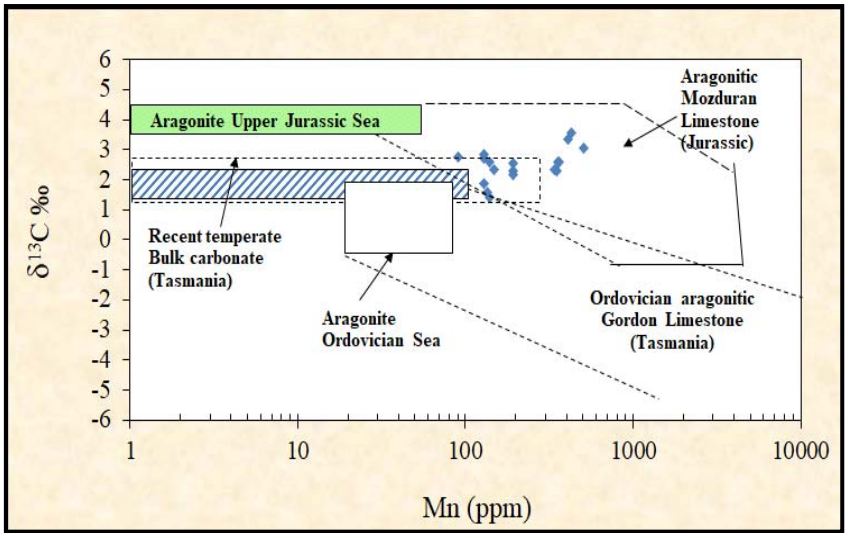

Figure 20. changes in $\delta^{13}C$ against Mn values of Sharaf section Dalichai Formation

Drawings on Mozduran formation limestone areas, carbonate samples areas of recent temperate regions, Tasmania Gordon aragonite areas, upper Jurassic marine aragonites, and Ordovician aragonite marine can allude the similarity of Mn value changes of both aragonite samples of Dalichai Formation and marine aragonites of upper Jurassic that show no relationship to any changes of $\delta^{13}C$

Downloaded from www.periodico.tchequimica.com

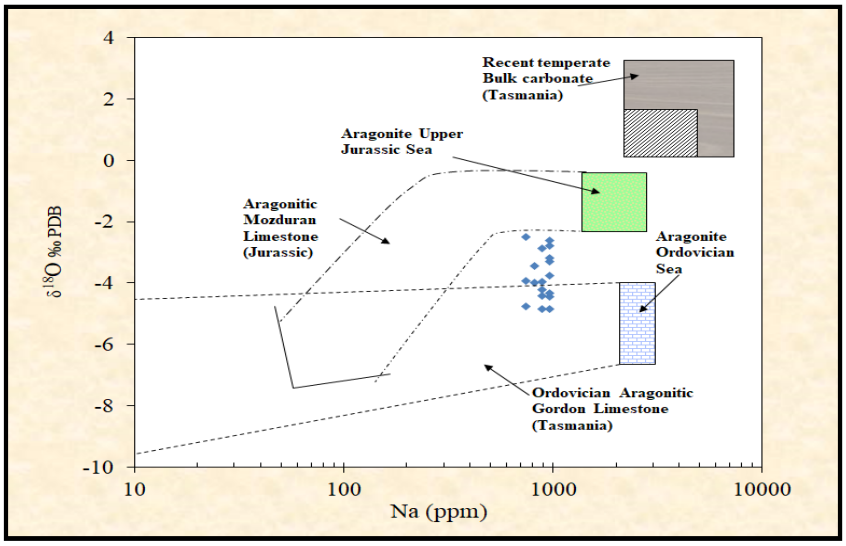

Figure 21. Changes in $\delta^{18}O$ against Na of Dalichai Formation of Sharaf section
It draws Dalichai Formation samples in comparison with proposed carbonates of recent temperate areas, Tasmania Gordon aragonitic limestone (Rao, 1990), and upper Jurassic areas of aragonitic carbonates (Adabi, 1996). As it is evident, most samples are located in aragonites areas of Mozduran upper Jurassic and primary aragonitic mineralogy of Tasmania Gordon.

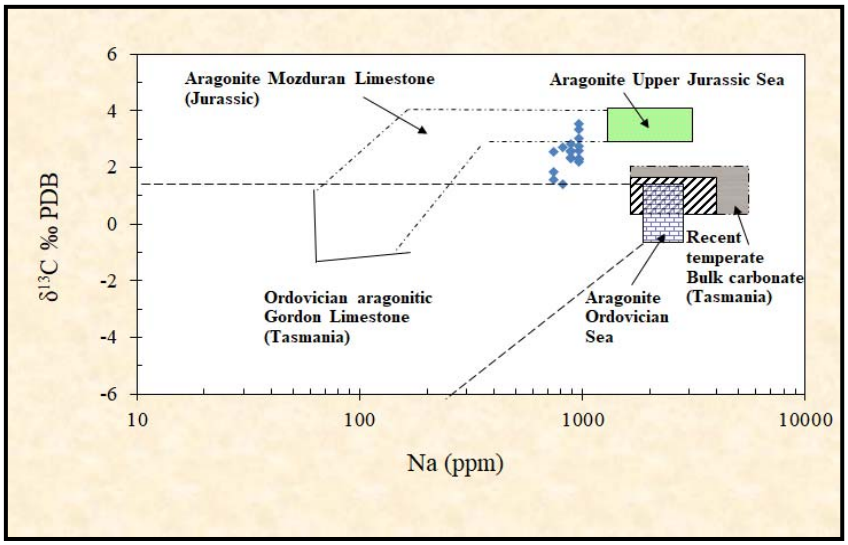

Figure 22. Changes in $\delta^{13}C$ against Na of Dalichai Formation of Sharaf section
It draws Mozduran formation limestone, recent temperate carbonate samples, Gordon Tasmania aragonitic samples, and established areas of marine aragonites of upper Jurassic and Ordovician. Dalichai Formation carbonates are displayed to be in Mozduran aragonites due to a low alteration tendency and identical composition of mineralogy.

Downloaded from www.periodico.tchequimica.com

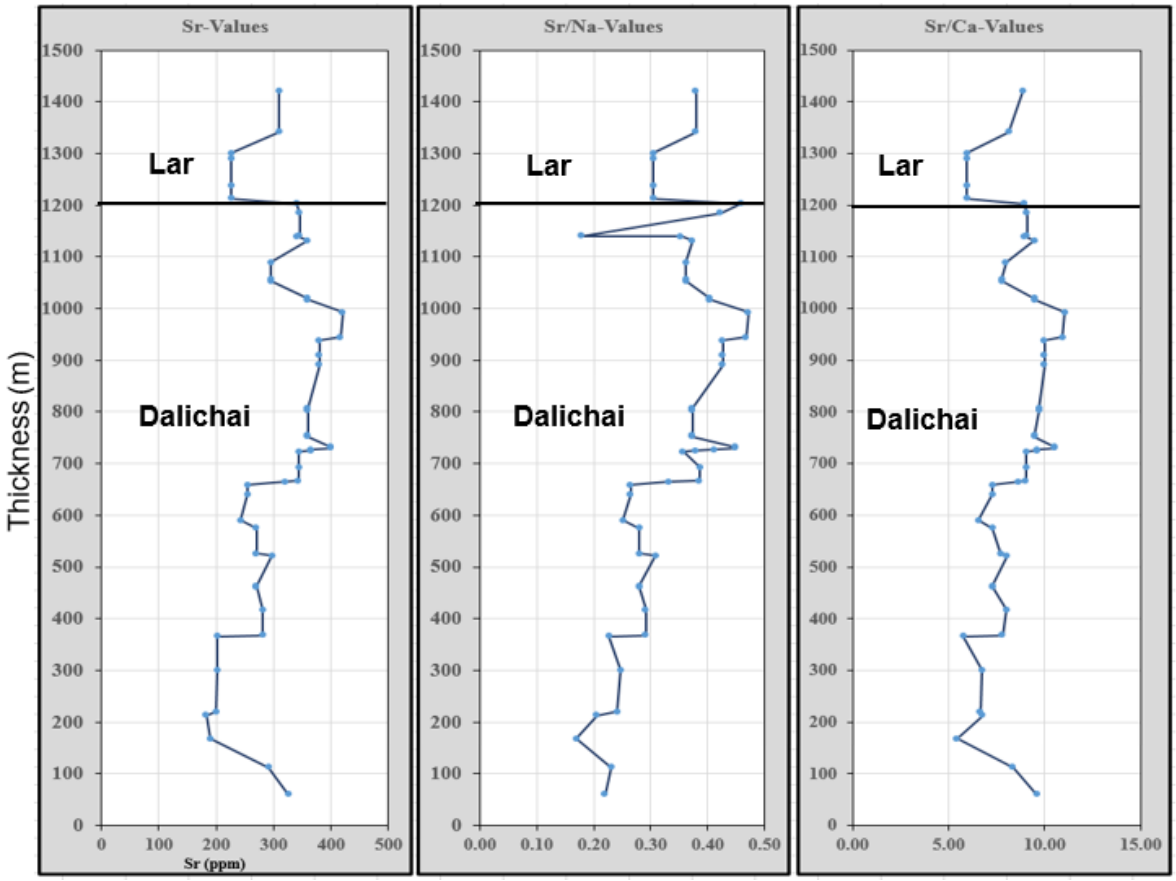

Figure 23. Changes of Sr (A), Sr/Ca (B), and Sr/Na (C). Elements changes in 1200m thickness are sharp.

Downloaded from www.periodico.tchequimica.com

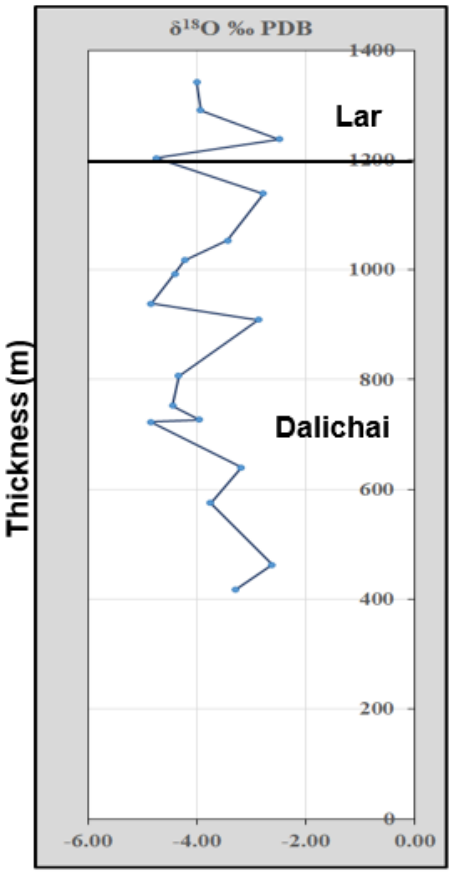

Figure 24. *Oxygen 18 isotope changes in Dalichai and Lar Formations*
Obviously, oxygen isotope suggests different values for both Lar and Dalichai Formations. The boundary for both formations is determine based on the lower value of oxygen isotope of Lar Formation compared with that of Dalichai Formation

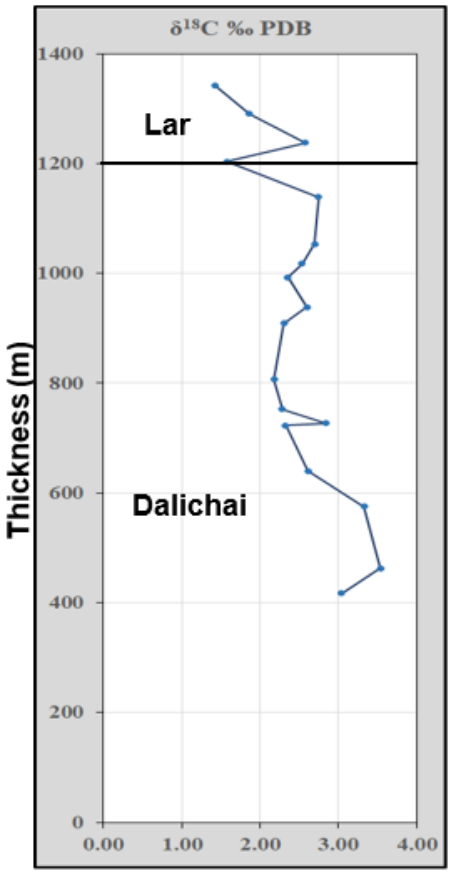

Figure 25. Carbon 13 isotopes for both Lar and Dalichai Formations as regards lighter isotopes of carbon in thickness 1200m, Dalichai *Formation* establishes a boundary that distinct it from Lar Formation. This carbon isotope shift may be the result of non-marine diagenesis processes.

Downloaded from www.periodico.tchequimica.com

PERIÓDICO TCHÊ QUÍMICA
ARTIGO ORIGINAL

ASSOCIAÇÃO DO ALELO DELEÇÃO DA INSERÇÃO / DELEÇÃO POLIMORFISMO DO AIIBB3 INTEGRINA GENE E SÍNDROME METABÓLICA EM NORTISTAS JOVENS

ASSOCIATION OF THE DELETION ALLELE OF THE INSERTION/DELETION POLYMORPHISM OF *αIIbβ3* INTEGRIN GENE AND METABOLIC SYNDROME IN YOUNG NORTHERNERS

АССОЦИАЦИЯ ДЕЛЕЦИОННОГО АЛЛЕЛЯ ПОЛИМОРФИЗМА ВСТАВКИ / ДЕЛЕЦИИ ГЕНА *αIIbβ3* ИНТЕГРИНА И МЕТАБОЛИЧЕСКОГО СИНДРОМА У МОЛОДЫХ ЖИТЕЛЕЙ СЕВЕРА

KORNEEVA Elena V.[1 *]; VOEVODA Mihail I.[2]; SEMAEV Sergey E.[3]; MAKSIMOV Vladimir N.[4];

[1] Surgut State University, Department of Internal Medicine

[2,3,4] Research Institute of Therapy and Preventive Medicine, Department of the Federal State Budgetary Scientific Institution “Federal Research Center Institute of Cytology and Genetics of the Siberian Department of the Russian Academy of Sciences”

** Correspondence author*
e-mail: evkorneeva39@rambler.ru

Received 02 June 2019; received in revised form 30 October 2019; accepted 09 November 2019

RESUMO

A justificativa para o presente estudo é explicada por uma alta disseminação da síndrome metabólica entre a população jovem, que é um dos principais fatores de risco cardiovascular. O estudo visa investigar a associação entre um alelo de deleção do polimorfismo de deleção/inserção no gene da integrina αIIbβ3 e síndrome metabólica em os jovens do norte. Foram examinados 758 jovens de 18 a 44 anos (idade média de 36,62 ± 5,12 anos) com síndrome metabólica e 77 jovens saudáveis e sem distúrbios metabólicos. A transportadora do alelo I associado ao risco cardiovascular foi revelada em 63% dos pacientes examinados que apresentaram risco aumentado de desenvolvimento de distúrbios metabólicos (OR 1,409, IC 95% 0,858-2,311, p = 0,253). Não houve diferença significativa entre as populações nativas e não nativas na taxa de ocorrência do alelo I (62,2% e 64,7%). O genótipo II teve associação significativa com hipertensão arterial (OR 1,377, IC 95% 0,912-2,080, p = 0,073), obesidade (OR 1,335, IC 95% 0,825-2,219, p = 0,071), hipercolesterinemia (OR 1,386, IC 95% 0,977 -1,966, p = 0,115), hipertrigliceridemia (OR 1,232, IC 95% 0,889-1,706, p = 0,097). Foi estabelecido que a população não nativa apresentava maior risco de desenvolvimento de obesidade abdominal, hipertensão arterial e hipercolesterinemia, diferentemente da população nativa que apresentava risco significativamente maior de desenvolvimento de trigliceridemia. Os materiais do artigo podem ser úteis para a avaliação da predisposição genética ao infarto do miocárdio, acidente vascular cerebral e tromboembolismo, o que permitirá a indicação oportuna de medidas preventivas.
.

Palavras-chave: *gene da integrina αIIbβ3, síndrome metabólica, obesidade, hipertensão arterial, hipercolesterolemia, hiperglicemia*.

ABSTRACT

The rationale for the present study is explained by a high spread of metabolic syndrome among the young population, living in an area equivalent to the Far North. The study is aimed at the investigation of the association between a deletion allele of the polymorphism of deletion/insertion in the *αIIbβ3* integrin gene and metabolic syndrome in young residents Khanty-Mansiysk Autonomous Okrug – Ugra (Russia). The 758 young people aged 18-44 (mean age 36.62±5.12 years old) with metabolic syndrome and 77 healthy young people without metabolic disorders were examined. The carriership of the allele I associated with the cardiovascular risk was revealed in 63% of the examined patients that had an increased risk of the development of metabolic disorders (OR 1.409, 95% CI 0.858-2.311, p=0.253). There was no significant difference between the native and non-native populations in the rate of occurrence of allele I (62.2% and 64.7%). Genotype II had significant

Downloaded from www.periodico.tchequimica.com

association with arterial hypertension (OR 1.377, 95 % CI 0.912-2.080, p=0.073), obesity (OR 1.353, 95% CI 0.825-2.219, p=0.071), hypercholesterinemia (OR 1.386, 95% CI 0.977-1.966, p=0.115), hypertriglyceridemia (OR 1.232, 95% CI 0.889-1.706, p=0.097). It was established that the non-native population had a higher risk of the development of abdominal obesity, arterial hypertension, and hypercholesterinemia, unlike the native population that had a significantly higher risk of the development of triglyceridemia. The materials of the article can be useful for the evaluation of genetic predisposition to myocardial infarction, stroke, and thromboembolism, which will allow for timely indication of preventive measures.

Keywords: *αIIbβ3 integrin gene, metabolic syndrome, obesity, arterial hypertension, hypercholesterolemia, hyperglycemia.*

АННОТАЦИЯ

Актуальность исследования обусловлена высоким распространением в настоящее время метаболическим синдромом среди молодого населения, проживающих в местности, приравненной к Крайнему Северу. В связи с этим, данная статья направлена на изучение ассоциации делеционного аллеля полиморфизма вставки / делеции в гене αIIbβ3 интегрина и метаболического синдрома у молодых жителей Ханты-Мансийского автономного округа - Югры. Было обследовано 758 молодых человека в возрасте 18-44 года (средний возраст 36,62±5,12 лет) с проявлениями метаболического синдрома и 77 здоровых молодых людей без метаболических нарушений. Установлено, что носительство аллеля I, связанного с кардиоваскулярным риском, было выявлено у 63% всех обследованных, имевших повышенный риск развития метаболических нарушений (ОШ 1.409, 95% ДИ 0.858-2.311, p=0.253). Среди некоренных и коренных жителей по частоте носительства аллеля I достоверных различий не выявлено – 62,2 % и 64,7 %. Генотип II показал значительную ассоциацию с артериальной гипертензией (ОШ 1.377, 95 % ДИ 0.912-2.080, p=0.073), ожирением (ОШ 1.353, 95% ДИ 0.825-2.219, p=0.071), с гиперхолестринемией (ОШ 1.386, 95% ДИ 0.977-1.966, p=0.115), с гипертриглицеридемией (ОШ 1.232, 95% ДИ 0.889-1.706, p=0.097). Среди некоренного населения установлено увеличение шансов развития абдоминального ожирения, артериальной гипертензии, гиперхолестринемией, в отличие от коренных жителей, у которых определено высоко отношение шансов развития триглицеридемии. Материалы статьи представляют практическую ценность для оценки генетической предрасположенности к инфаркту миокарда, инсульту, тромбоэмболии, что позволит своевременному проведению профилактических мероприятий.

Ключевые слова: *ген αIIbβ3 интегрин, метаболический синдром, ожирение, артериальная гипертензия, гиперхолестеринемия, гипергликемия*.

---

1. INTRODUCTION

It is known that metabolic syndrome, in particular, such components as obesity and insulin resistance, are closely associated with the disorders in the systems of coagulation and fibrinolysis, which leads to the increase in the risk of the development of cardiovascular diseases (Berkovskaya and Butrova, 2009). In patients with obesity, the hyperactivity of thrombocytes, as the main component of metabolic syndrome, is a pathogenetic factor of atherotrombogenesis, which is manifested as an increased adhesion and a capability to aggregate. Such activity of platelets can be associated with the damage of platelet membranes, increased expression of the superficial receptors for the molecules of adhesion, failure of intracellular metabolic processes inside the cells (Boden, 2008; Chromylev, 2015). Platelets aggregate due to the presence of receptors (protein-integrin complexes) located on their surface.

A possible association of different polymorphisms in the integrin gene and thromboembolic complications are described by numerous authors (Kokubo *et al.,* 2007). Integrins are transmembrane glycoproteins that are involved in the intercellular and cellular-matrix interactions and consist of α- and β-subunits. The most widespread is *αIIbβ3* integrin that is located on the long arm on the 17th chromosome in the locus 17q21.32 and expressed on the surface of thrombocytes being a receptor of fibrinogen (Calvete, 1995; Westerbacka *et al.*, 2002; Chernyak and Snezhitskiy, 2018). Trombocytopathyas can develop as a result of a mutation in the genes *αIIbβ3* (Huang *et al.,* 2019).

The study was aimed to investigate the associations between a deletion allele of polymorphism of insertion/deletion in the *αIIbβ3* integrin gene and metabolic syndrome in young northerners.

Downloaded from www.periodico.tchequimica.com

2. MATERIALS AND METHODS

The study was performed in the facilities of Fedorovskaya municipal clinical hospital, the branch of the hospital in vil. Russkinskaya and Surgutskaya municipal clinical hospital №1. 758 young people aged 18-44 (mean age 36.62±5.12 years old) with metabolic syndrome and 77 healthy young people without metabolic disorders were examined. The non-native population was represented by urban and rural populations. The native northern population was represented by Khanty and Mansi. The main criterion for the metabolic syndrome was an increase in the waist measurement to more than 94 cm in men and more than 80 cm in women (Ferreira *et al.,* 2005). Additional criteria were arterial hypertension (AH ≥ 130/85 mmHg), an increase in the level of triglycerides (TG) (≥ 1.7 mmol/L), a decrease in the level of cholesterol HDL (<1.0 mmol/L in men; <1.2 mmol/L in women), an increase in the level of cholesterol LDL > 3.0 mmol/L, hyperglycemia before meal (glucose in plasma before meal ≥ 6.1 mmol/L), glucose intolerance (glucose in plasma 2 hours after the exposure within the range of ≥7.8 and ≤11.1 mmol/L) (Russian Society of Cardiology, 2009). The state of lipid and carbohydrate metabolism was evaluated in blood plasma taken from the fasting ulnar vein from them at least 12 hours after the last meal. The content of blood lipids was determined on a biochemical express analyzer Reflotron Plus (Roche Diagnostics, Switzerland).

The content of LDL cholesterol was evaluated using the Frivald formula at a TG concentration below 4.5 mmol / L: LDL cholesterol = total cholesterol - (HDL cholesterol + TG / 2.2), mmol / L. An oral glucose tolerance test (PTTG) was performed with a load of 75 g glucose. In the morning, after complete fasting for 8-14 hours, blood was taken from the cubital vein from the subjects to determine plasma glucose. 15 minutes before the study, the patients were in a calm state, in a comfortable sitting position. Then they drank 75 g of glucose dissolved in 250-300 ml of water in 5 min. After 2 h, blood was again taken from the peripheral vein, and the plasma glucose level was determined.

The characteristics of the examined patients are presented in Table 1. All the participants underwent anthropometric examination (height, body weight, body mass index (BMI=kg/m^2), waist measurement (WM), blood pressure, total cholesterol, HDL, LDL, triglycerides, carbohydrate metabolism). The molecular-genetic study was performed in the Department of the Federal State Budgetary Scientific Institution “Federal Research Center Institute of Cytology and Genetics of the Siberian Department of the Russian Academy of Sciences. Genome DNA was isolated from venous blood by the method of phenol-chloroform extraction. Polymorphism of *αIIbβ3* integrin was tested with polymerase chain reaction (PCR) with restriction fragment length polymorphism (RFLP).

All the patients signed the form of informed consent for participation in the study. The present study was approved by the Expert Council of the Surgut State University.

The obtained results were processed statistically with a software package SPSS 16.0. The authors estimated the frequency rate of genotypes of the studied single nucleotide polymorphism (SNP) in the ethnic groups with metabolic syndrome and in the control group. The comparison of groups by the frequency rate of genotypes was performed with cross tables using Pearson's chi-square test with the calculation of the error of the mean (m) and mean value (M). In the case of the fourfold table, a two-tailed Fisher-Yates test was applied. The relative risk of the development of the components of metabolic syndrome for a certain allele or genotype was calculated as odds ratio (OR). Confidential interval (CI) was calculated by two-tailed Fisher’s test and Pearson's chi-square test. The data was significant at $p<0.05$.

Table 1. *Characteristics of the examined patients with MS, (M±m)*

Parameters	Values
Bodyweight, kg	83.52 ± 0.03
BMI, kg/m²	32.07±0.49
Waist measurement, cm	91.39±0.85
Glucose level before a meal, mmol/L	5.47±0.55
Glucose level 2 hours after the exposure, mmol/L	6.52±0.012
Total cholesterol, mmol/L	5.47±0.63
Triglycerides, mmol/L	2.54±0.15
HDL mmol/L	1.69±0.16
LDL, mmol/L	3.08±0.011
SBP, mmHg	115.52±0.04
DBP, mmHg	75.29±0.03

3. RESULTS AND DISCUSSION

The spread of genotypes and alleles of the integrin gene *αIIbβ3* among the studied native and non-native populations is presented in Table

Downloaded from www.periodico.tchequimica.com

2. The frequency rate of the carriership of the genotype DD was 14.4%, ID – 45.2%, II – 40.4%. The carriership of the allele I associated with the risk of the development of cardio-vascular diseases was revealed in 63% of the examined patients. There was no significant difference between native and non-native populations by the frequency rate of the carriership of the allele I (62.2% and 64.7%, respectively) (Table 2).

In the group of the native population with metabolic syndrome, the frequency rate of the carriership of genotype II of insertion and deletion polymorphism of *αIIbβ3* integrin gene was 64.9%, and in a certain part of the non-native population with metabolic disorders – 60.5%. In the control group of the native population, the carriership of the genome II was observed by 6.9% more often than in the control group of the non-native population. The frequency rate of the carriership of the genotype II among the non-native population with metabolic syndrome was higher than in the control group (60.5% and 54.2%, respectively). Among the native population, the frequency rate of carriership of the genotype II in patients with metabolic syndrome and the control group was not statistically significant (64.9% and 61.1%, respectively). It was established that the carriers of the allele II of *αIIbβ3* integrin gene had an increased risk of the development of metabolic disorders (OR 1.409, 95% CI 0.858-2.311, p=0.253) (Table 3).

Table 4 shows the results of the study of the association between polymorphisms of *αIIbβ3* gene integrin and the components of metabolic syndrome. Thus, there was a significant association between genotype II and high blood pressure (OR 1.377, 95% CI 0.912-2.080, p=0.073), high BMI (OR 1.353, 95% CI 0.825-2.219, p=0.071), hypercholesterinemia (OR 1.386, 95% CI 0.977-1.966, p=0.115), hypertriglyceridemia (OR 1.232, 95% CI 0.889-1.706, p=0.097) (Table 4).

Figure 1 contains the data on the revealed association of polymorphism of *αIIbβ3* integrin gene with metabolic syndrome among native and non-native young populations. Non-native population had a higher OR of the development of abdominal obesity (OR 1.418, 95% CI 0.797-2.522, p=0.294), arterial hypertension (OR 1.661, 95% CI 1.016-2.714, p=0.251), hypercholesterinemia (OR 1,612, 95% CI 1.043-2.492, p=0.222) unlike native population that had a high OR of the development of triglyceridemia (OR 1.508, 95% CI 0.846-2.688, p=0.295).

The present study was conducted for the investigation of the role of deletion allele of the polymorphism of insertion/deletion in *αIIbβ3* integrin gene in young northerners with metabolic syndrome.

Different authors in their works showed the allele of the deletion II of the αIIbβ3 integrin gene was associated with unfavorable metabolic and vascular effects (Amabile *et al*., 2014). Thus, the Czech authors showed a positive correlation between the expression of αIIbβ3 integrin and hyperglycemia before a meal (r=0.48, p<0.05) (Osmancik *et al.,* 2007). Patients with insulin resistance have a high risk of the development of thrombosis. It was proved experimentally that the removal of the insulin receptor from the surface of a platelet led to an increase in the platelet count, but the influence of insulin on them was blocked. In platelets that did not have insulin receptors, it was established that the aggregation of platelets and the enhancement of the activation of αIIbβ3 integrin were reduced (Moore *et al.,* 2015). It is known that insulin resistance has a genetic background. A high risk of the development of diabetes mellitus type II in 506 patients with disturbances of tolerance to glucose (OR = 5.17, 95% CI 1.76-15.21, p=0.003) was revealed in comparison with patients that changed their lifestyle (Siitonen *et al.,* 2004).

An association between polymorphism of insertion/deletion (I/D) αIIbβ3 and arterial hypertension in patients with diabetes mellitus and without it was established. The rate of frequency of the genotype DD was significantly higher both in patients with arterial hypertension with diabetes (77.14%, p<0.01) and without it (71.43%, p<0.05) in comparison with the control (40%). Besides, allele D was more often observed in patients with hypertonic disease and diabetes (84.29%, p<0.01) and without it (80%, p<0.05) in comparison with control (58.33%). At the same time, it was revealed that genotype DD was associated with a low level of HDL (p=0.001) and a high level of LDL (p=0.017) in comparison with genotypes II and ID in the group of patients with arterial hypertension and without diabetes mellitus type II (Tayel *et al*., 2012). It was established that functions of platelets and activation of αIIbβ3, caused by thrombin, decrease in patients with obesity. A decrease in the activity of sarcoendoplasmic net Ca2 + ATPase (SERCA3) by 48% is also observed. The loss of weight restores the activity of SERCA3 and further transmission of calcium signals, activation of αIIbβ3, aggregation of platelets, and secretion of ADP (Elaïb *et al*., 2019).

On the other hand, some data prove the involvement of insulin in the regulation of the activation of platelets. Thus, in people with

Downloaded from www.periodico.tchequimica.com

normal body weight, insulin can inhibit the aggregation of platelets, unlike in people with obesity that do not have insulin to exert this function, which can contribute to further damage of the vascular wall (Kohler, 2002; Westerbacka *et al.,* 2002). It was established that higher activity of platelets was observed in patients with a more severe degree of ischemic heart disease (Osmancik *et al.,* 2007). In many works, the association between a mutant allele I in *αIIbβ3* integrin gene and the development of myocardial infarction, ischemic heart disease, and thromboembolism was established, especially at a younger age (Chernyak and Snezhitskiy, 2018; Aksyutina *et al*., 2013; Ali Elsidege *et al.*, 2019; Xu *et al*., 2014).

4. CONCLUSION

Thus, in our study, we obtained a significant association of the polymorphism of insertion/deletion in the αIIbβ3 integrin gene with metabolic disorders among young indigenous and non-indigenous patients of the Khanty-Mansiysk Autonomous Okrug-Ugra. Carriage of the allele I, associated with the risk of developing cardiovascular diseases, was observed in 63% of all examined patients with metabolic disorders. In our study, genotype II showed a significant association with arterial hypertension (OR 1.661), obesity (OR 1.418) and hypercholesterolemia (OR 1.612) in young non-indigenous people of the North, in contrast to the indigenous people, who have a high ratio of the chances of triglyceridemia (OR 1.508). The identification of the genotype αIIbβ3 integrin allows for an evaluation of genetic predisposition of young northerners to myocardial infarction, stroke, and thromboembolism, and timely indication of preventive measures.

5. LIST OF ABBREVIATIONS

AO – abdominal obesity,
AH – arterial hypertension,
HCL - hypercholesterolemia,
HCL - hypertriglyceridemia,
HG – hyperglycemia.

6. REFERENCES

1. Aksyutina, N.V., Nikulina, S.Y., Shulman, V.A., Nazarov, B.V., Maximov, V.N., Bezruk, A. P., Balog, A. I., Poplavskaya, E.E., Bespalov, A.B., Kotlovsky, M. Yu., Chernova, A.A. Interconnection between the polymorphism of the gene of glycoprotein integrin alfa and development of acute cerebrovascular event in the family of patients with atrial fibrillation. *Russian Cardiologic Journal*, **2013,** 6(104), 6–10.
2. Ali Elsidege, A. L., Mahdi, H. F., Eldin G. E. S. Association of Fibrinogen Receptor (Integrin αIIbβ3) Polymorphism in Sudanese Ischemic Stroke Patients. *Pak J Biol Sci,* **2019,** 22(2), 59–66.
3. Amabile, N., Cheng, S., Renard, J. M., Larson, M. G., Ghorbani, A., McCabe, E., Griffin, G., Guerin, C., Ho, J. E., Shaw, S. Y., Cohen, K. S., Vasan, R. S., Tedgui, A., Boulanger, C. M., Wang, T. J. Association of circulating endothelial microparticles with cardiometabolic risk factors in the Framingham Heart Study. *Eur Heart J.*, **2014,** 35(42), 2972–2979.
4. Berkovskaya, M.A, Butrova, S.A. Metabolic syndrome as a protrombogenic condition. *Obesity and metabolism*, **2009,** 3.
5. Boden, G. Obesity, and free fatty acids. *Endocrinol Metab Clin North Am*, **2008**, 37, 635–646.
6. Bolton-Maggs, P. H., Chalmers, E. A., Collins, P. W., Harrison, P. , Kitchen, S. , Liesner, R. J., Minford, A. , Mumford, A. D., Parapia, L. A., Perry, D. J., Watson, S. P., Wilde, J. T., Williams, M. D. A review of inherited platelet disorders with guidelines for their management on behalf of the UKHCDO. *British Journal of Haematology*, **2006,** 135, 603–633.
7. Calvete, J.J. On the structure and function of platelet integrin alpha IIb beta 3, the fibrinogen receptor. *Proc Soc Exp Biol Med*, **1995,** 208, 346–60.
8. Chernyak, A. A., Snezhitskiy, V. A. Prospects of the application of biomarkers (adiponectin, P-selectin, integrin β3) as biochemical predictors of restenosis in patients with ischemic heart disease after coronary stenting. *Journal of Grodnenskiy State Medical University*, **2018,** 16(1), 5–11.
9. Chromylev, A.V. Pathogenetic aspects of atherothrombotic risk in patients with obesity and trombophilia. *Obstetrics, gynecology, and reproduction*, **2015,** 3, 45–52.
10. Coller, B.S. αIIbβ3: structure and function. *J Thromb Haemost*, **2015,** 13 Suppl 1(Suppl 1), 17–25.
11. Elaïb, Z.·, Lopez, J.J.·, Coupaye, M,, Zuber, K., Becker, Y,, Kondratieff, A., Repérant, C., Pépin, M., Teillet, F., Msika, S., Denis, C.V., de Prost, D., Rosa, J.P., Bobe, R., Stépanian, A. Platelet Functions are Decreased in Obesity and Restored after

Downloaded from www.periodico.tchequimica.com

Weight Loss: Evidence for a Role of the SERCA3-Dependent ADP Secretion Pathway. *Thromb Haemost*, **2019**, 119(3), 384–396.
12. Ferreira, I., Twisk, J.W.R., van Mechelen, W., Kemper, H.C.G., Stehouwer, C.D.A. Development of Fatness, Fitness, and Lifestyle From Adolescence to the Age of 36 Years: Determinants of the Metabolic Syndrome in Young Adults: The Amsterdam Growth and Health Longitudinal Study. *Arch Intern Med*., **2005**, 165(1), 42–48. doi:10.1001/archinte.165.1.42.
13. Huang, J., Li, X., Shi, X., Zhu, M., Wang, J., Huang, S., Huang, X., Wang, H., Li L., Deng, H., Zhou, Y., Mao, J., Long, Z., Ma, Z., Ye W., Pan, J., Xi, X., Jin, J. Platelet integrin αIIbβ3: signal transduction, regulation, and its therapeutic targeting. *J Hematol Oncol*., **2019**, 12(1), 26.
14. Kohler, H.P. Insulin resistance syndrome: interaction with coagulation and fibrinolysis. *Swiss. Med. Wkly*., **2002,** 132(19–20), 241–52.
15. Kokubo, T., Uchida, H., Choi, E. T. Integrin alpha(v)beta(3) as a target in the prevention of neointimal hyperplasia. *J. Vasc. Surg*., **2007**, (45), 33–38.
16. Moore, S.F., Williams, C.M., Brown, E., Blair, T.A., Harper, M.T., Coward, R.J., Poole, A.W., Hers, I. Loss of the insulin receptor in murine megakaryocytes/platelets causes thrombocytosis and alterations in IGF signalling. *Cardiovasc Res*., **2015,** 107(1), 9–19.
17. Osmancik, P. P., Bednar, F., Móciková, H. Glycemia, triglycerides, and disease severity are best associated with higher platelet activity in patients with stable coronary artery disease. *Journal of Thrombosis and Thrombolysis*, **2007**, 2(24), 105.
18. Siitonen, N, Lindstrom, J, Eriksson, J, Valle, T.T., Hämäläinen, H., Ilanne-Parikka, P., Keinänen-Kiukaanniemi, S., Tuomilehto, J., Laakso, M., Uusitupa, M. Association between a deletion/insertion polymorphism in the alpha2B-adrenergic receptor gene and insulin secretion and type 2 diabetes. The Finnish Diabetes Prevention Study. *Diabetologia,* **2004,** 47, 1416–1424.
19. Tayel, S.I., Khader, H.F., El-Helbawy, N.G., Ibrahim, W.A. Association of deletion allele of insertion/deletion polymorphism in α2B adrenoceptor gene and hypertension with or without type 2 diabetes mellitus. *Appl Clin Genet*., **2012,** 5, 111–118.
20. Westerbacka, J., Yki-Jarvinen, H., Turpeinen, A., Rissanen, A., Vehkavaara, S., Syrjala, M., Lassila, R. Inhibition of platelet-collagen interaction. An in vivo action of insulin abolished by insulin resistance in obesity. Arterioscler. *Thromb. Vasc. Biol*., **2002,** 22, 167–172.
21. Xu, Z., Chen, X., Zhi, H., Gao, J., Bialkowska, K., Byzova, T.V., Pluskota, E., White, G.C. 2nd, Liu, J., Plow, E.F., Ma, Y.Q. Direct interaction of kindlin-3 with integrin αIIbβ3 in platelets is required for supporting arterial thrombosis in mice. *Arterioscler Thromb Vasc Biol.,* **2014**, 34(9), 1961–1967.

Downloaded from www.periodico.tchequimica.com

TABLES

Table 2. *The rate of occurrence of insertion and deletion polymorphism of gene αIIbβ3 in ethnical groups.*

Population	The rate of occurrence of genotypes						The rate of occurrence of alleles			
	DD		ID		II		D		I	
	n	%	n	%	n	%	n	%	n	%
Non-native population (n=569)	93	16.3	255	44.8	221	38.8	441	38.8	697	61.2
Native population (n=266)	33	12.4	122	45.9	111	41.7	188	35.3	344	64.7
Total	126	14.4	377	45.2	355	40.4	649	37	1107	63

Table 3. *The rate of frequency of insertion and deletion polymorphism of αIIbβ3 integrin gene in the studied groups*

Genotype	Control group, n=77		Patients with metabolic syndrome, n=758		OR, 95% CI, p
	n	%	n	%	
Total, n=835					
DD	17	22.1	117	15.4	0.644, 0.363-1.143, p= 0.293
ID	34	44.2	343	45.3	1.045, 0.652-1.676, p=0.241
II	26	33.8	298	39.3	1.409, 0.858-2.311, p=0.253
Allele D	68	44.2	577	38.1	0.777, 0.556-1.086, p=0.171
Allele I	86	55.8	939	61.9	1.287, 0.921-1.798, p=0.171
Non-native population, n=569					
DD	14	23.7	87	17.1	0.631, 0.332-1.200, p=0.328
ID	26	44.1	229	44.9	1.034, 0.601-1.780, p=0.277
II	19	32.2	194	38.0	1.292, 0.728-2.296, p=0.293
Allele D	54	45.8	403	39.5	0.774, 0.528-1.136, p=0.196
Allele I	64	54.2	617	60.5	1.292, 0.880-1.895, p=0.196
The native population, n=266					
DD	3	16.7	30	12.1	0.688, 0.188-2.517, p=0.138
ID	8	44.4	114	46.0	1.063, 0.406-2.785,p=0.491
II	7	38.9	104	41.9	1.135, 0.426-3.026, p=0.500
Allele D	14	38.9	174	35.1	0.849, 0.424-1.701, p=0.355
Allele I	22	61.1	322	64.9	1.178, 0.588-2.360, p=0.355

Downloaded from www.periodico.tchequimica.com

Table 4. *Association between homozygotic II polymorphism of αIIbβ3 integrin and parameters of metabolic syndrome in the studied groups*

Parameter	DD n (%)		ID n (%)		II n (%)		OR, 95% CI, p
Abdominal Obesity (AO)							
Patients with AO	109	14.9	323	44.2	298	40.8	1.353, CI 0.825-2.219, p=0.071
Patients without AO	17	22.1	34	44.2	26	33.8	
Arterial Hypertension (AH)							
Patients with AH	15	14.2	49	46.2	42	39.6	1.377, CI 0.912-2.080, p=0.073
Patients without AH	290	31.9	328	36.2	290	31.9	
Hypercholesterolemia (HCL)							
Patients with HCL	93	12.8	249	53.3	243	33.9	1.386, CI 0.977-1.966, p=0.115
Patients without HCL	23	12.8	96	53.3	61	33.9	
Hypertriglyceridemia (HTG)							
Patients with HTG	26	13.1	87	43.9	85	42.9	1.232, 0.889-1.706, p=0.097
Patients without HTG	98	16.2	277	46.9	229	37.9	
Hyperglycemia (HG)							
Patients with HG	35	13.0	135	50.0	100	37.0	0.812, 0.604-1.092, p=0.050
Patients without HG	92	15.6	249	42.3	247	42.1	

Note: AO – abdominal obesity, AH – arterial hypertension, HCL - hypercholesterolemia, HTG - hypertriglyceridemia, HG – hyperglycemia. p<0.05

FIGURES

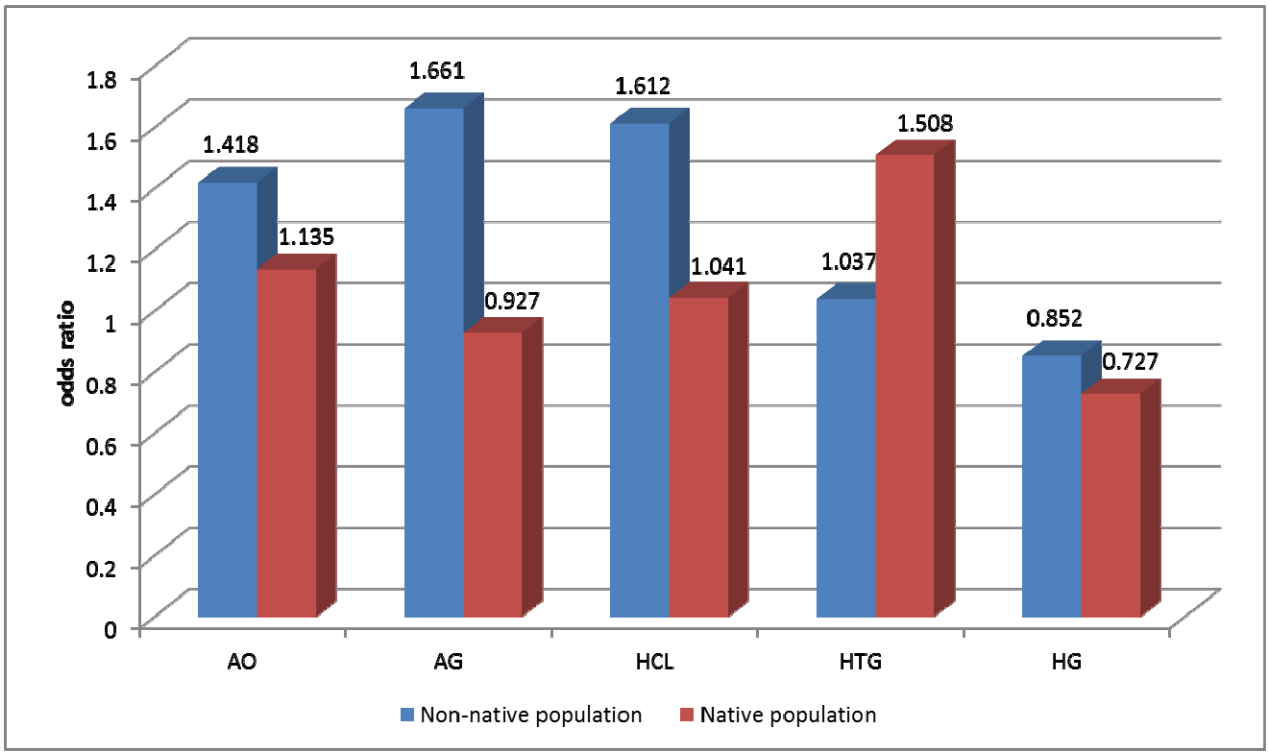

Note: AO – abdominal obesity, AH – arterial hypertension, HCL - hypercholesterolemia, HTG - hypertriglyceridemia, HG – hyperglycemia. p<0.05

Figure 1. *OR of the frequency rate of homozygotic II polymorphism αIIbβ3 with the parameters of metabolic syndrome in the studied ethnic groups.*

Downloaded from www.periodico.tchequimica.com

PERIÓDICO TCHÊ QUÍMICA
ARTIGO ORIGINAL

DESENVOLVIMENTO DE UM MÉTODO PARA AVALIAR OS RESULTADOS DA APRENDIZAGEM ATRAVÉS DO GERENCIAMENTO AUTOMÁTICO DE ENSAIOS

DEVELOPMENT OF A METHOD FOR ASSESSING LEARNING OUTCOMES THROUGH AUTOMATED TESTING MANAGEMENT

РАЗРАБОТКА МЕТОДА ОЦЕНКИ РЕЗУЛЬТАТОВ ОБУЧЕНИЯ ПОСРЕДСТВОМ УПРАВЛЕНИЯ АВТОМАТИЗИРОВАННОГО ТЕСТИРОВАНИЯ

KAZANBAYEVA, Albina S.[1*]; IKLASSOVA, Kainizhamal E.[2]; KULIKOV, Vladimir P. [3];

[1,2,3] M. Kozybayev North Kazakhstan State University, Department of Information and Communication Technologies, 86 Pushkin Str., zip code 150000, Petropavlovsk – Republic of Kazakhstan

** Correspondence author*
e-mail: akazanbaeva83@mail.ru

Received 03 June 2019; received in revised form 20 October 2019; accepted 09 November 2019

RESUMO

A avaliação do conhecimento é uma parte importante do processo pedagógico, pois ajuda a melhorar a qualidade do conhecimento profissional, contribui para a eficácia e eficiência da educação. Este artigo discute a aplicação de várias abordagens para a construção de um sistema especialista difuso de diagnóstico para testar o conhecimento. O objetivo do estudo é otimizar de maneira abrangente o processamento de informações de testes de massa, a fim de obter dados de relatórios, considerar testes claros e difusos, traçar uma analogia entre testes claros e difusos, oferecer e justificar vários esquemas para resumir os resultados dos testes, oferecer nosso próprio protótipo do sistema de teste especialista automatizado que abrange todas as etapas do processo de teste. Em geral, o teste como um problema algorítmico pode ser representado como a tarefa de construir um sistema especialista para avaliar o conhecimento dos sujeitos. Esses sistemas são usados para resolver muitos problemas relacionados ao gerenciamento eficaz, pesquisa científica e afins, onde é necessário obter o resultado com uma quantidade limitada de informações confiáveis. Está estabelecido que a teoria clássica dos testes tem uma série de suposições controversas, e os resultados de sua aplicação têm sérias desvantagens práticas. Portanto, o princípio básico da abordagem no trabalho é a separação da criação de um banco de tarefas de teste e o processo de compilação de testes (banco de material de teste) e o teste.

Palavras-chave: *sistema de treinamento, teste, teste de treinamento, resultados acadêmicos, previsão de desempenho dos estudantes.*

ABSTRACT

Testing knowledge is an important part of the pedagogical process, as it helps to improve the quality of professional knowledge, contributes to the effectiveness and efficiency of training. This article discusses the use of several approaches to building a fuzzy diagnostic expert system for knowledge testing. The aim of the research is a comprehensive optimisation of the process of mass test information processing in order to obtain reporting data, consideration of clear and fuzzy tests, drawing the analogy between clear and fuzzy tests, proposal and justification of different schemes of summing up the testingandproposal of one's own prototype of automated expert testing system which covers all stages of the testing process. Generally speaking, testing, as an algorithmic problem, can be represented as a problem of building an expert system to evaluate knowledge of testees. Such systems are used in solving many problems related to effective management, scientific research, and the like, where it is necessary to get the result with a limited amount of reliable information. It is established that the classical theory of tests has a number of controversial assumptions, and the results of its application have serious practical drawbacks. Therefore, the main principle of the approach in the work is the separation of the creation of a bank of test tasks and the process of compiling tests (bank of test material) and testing.

Keywords: *studying system, testing, training test, educational achievements, student's performance prediction.*

Downloaded from www.periodico.tchequimica.com

АННОТАЦИЯ

Проверка знаний является важной частью педагогического процесса, поскольку она способствует повышению качества профессиональных знаний, способствует результативности и эффективности обучения. В данной статье рассмотрено применение нескольких подходов к построению диагностирующей нечеткой экспертной системы для тестирования знаний. Целью исследования является комплексная оптимизация процесса обработки массовой тестовой информации с целью получения отчетных данных, рассмотрение четких и нечетких тестов, проведение аналогии между четкими и нечеткими тестами, предложение и обоснование различных схем подведения итогов тестирования, предложение своего прототипа автоматизированной экспертной системы тестирования, охватывающей все этапы процесса тестирования. Вообще говоря, тестирование, как алгоритмическая задача может быть представлено как задача конструирования экспертной системы для оценки знаний испытуемых. Подобные системы применяются при решении многих задач, связанных с эффективным управлением, научным поиском и подобных, где требуется получить результат при ограниченном количестве достоверной информации. Установлено, что классическая теория тестов имеет ряд спорных предположений, а результаты ее применения – серьезные практические недостатки. Поэтому в работе основным принципом подхода является разделение создания банка тестовых заданий и процесса составления тестов (банка тестового материала) и тестирования.

Ключевые слова: *система обучения, тестирование, обучающий тест, учебные достижения, прогнозирование успеваемости студентов.*

1. INTRODUCTION

The system of testing the results of studying has been transformed in the direction of quality control of education. One should note that the introduction of innovative educational technology in continuing education is becoming an increasingly effective tool for professional development.

Tests can be used at any stage of studying. Some of them are intended to evaluate the readiness of students to master a new academic course; others are intended to identify specific gaps in knowledge. Also, tests are used to plan the necessary targeted corrective work, predict the further process of studying, and determine the competence of specialists of the organisations (Maslennikov *et al.*, 2017; Aleksandrova *et al.*, 2018). Basic testing includes conducting input, current and interim controls, interim attestation for every discipline, including external evaluation of educational achievements (EEEA), and state final attestation.

The widest possible introduction of information technology in the education system and the solution of the problem of education quality cause the need for research and development of models adequate to the processes of educational activities of higher educational establishment (Naykhanova *et al.*, 2002).

Improving the quality of studying is the main direction of the education system's development. One of the main tasks of the management of education quality in a higher educational establishment is the task of control and evaluation of the quality of studying.In the conditions of the modern information society, automated testing can become the main tool for quality control (Naykhanova and Danilova, 2002; Akhmetshin *et al.*, 2019; Bocheliuk *et al.*, 2019).

In this article, the authors have studied the problems of the development of evaluation of the results of studying by testing. In the course of the research, the analysis of knowledge control systems of students showed that the development of these systems is mainly on an empirical basis. It has neither proper scientific and methodological justification, nor theoretical models of specialist's readiness for professional activity. In connection with the objective needs of university practice, the implementation of the programme to improve the quality of specialists' education, there arises a need to develop a science-based system of control of students' knowledge.

To date, there is a technical problem, namely, to improve the process of automated evaluation of the results of the testing of students. The solution which will allow to improve the efficiency of knowledge control, ensure the objectivity of evaluation of passing a test regarding both the levels of assimilation of test tasks and the test as a whole (Vinogradova and Popov, 2019).

To solve the technical problem, a method of evaluating students' knowledge based on the use of fuzzy logic and the theory of question-answer relations is proposed.

Downloaded from www.periodico.tchequimica.com

2. LITERATURE REVIEW

The research paper (Julliand *et al.*, 2018) presents a test generation method based on the calculation of the achievable and related under-approximation of the abstraction of the event system. Problems of formal description of the processes of studying system and attestation by testing were considered in the research (Bride *et al.*, 2016; Godefroid, 2007; Bué *et al.*, 2011; Godefroid *et al.*, 2005; Tillmann and De Halleux, 2008). In some research papers (Makarov and Sevastyanova, 2020) a method of visualisation and interpretation of the results of stored knowledge monitoring is proposed. The possibility of its use for the analysis of problems of studying at the individual and group levels is justified.

According to the studied material on the use of various methods when developing, as well as conducting the computer testing, there are presented results that will improve the ability to identify not difficult passing the test and perform an individual test points (Makarov and Sevastyanova, 2020; Wise *et al.*, 2019; Wise and Gao, 2017).

There are several approaches to the evaluation of the test task recommended by leading specialists in this field. These developments are based on both international testing experience as well as Russian and Kazakh (special developments were formed, which are distinctive from international recommendations for the preparation of tests, aims, and methodology for evaluating the results).

V.S. Avanesov (Doctor of Education, a leading specialist in the field of the theory of pedagogical measurements) suggests in every task, to give one score for the correct answer and for the incorrect one to give zero. At the same time, he notes the existence of more "advanced" evaluation schemes, for example, in testing centers in Western countries. The task is scaled according to its contribution to the general variation of test points of testees, that is, the evaluation in every case will be different and depend on a certain set of questions. At the end of the test, before putting a mark, the author proposes to conduct the correction of points for guessing (this is relevant for questions with one correct option). For questions with several correct options, he considers it impractical to conduct a correction for guessing.

Some unsolved problems related to the evaluation of the student's level of competence by the method of testing are considered in the research paper (Bershadskaya *et al.*, 2019). In modern research (Muchuchuti *et al.*, 2019), different classification algorithms are compared to predict and improve students' performance.The results obtained help predict the total performance of students in time and develop activities that can improve their final mark.

During the simulation, researchit was proposed as an adaptive, effort-oriented test (Wise and Kingsbury, 2016), which allowed to weaken the wrong orientation on the subject caused by unmotivated passing the test. Some researchers have developed fuzzy rules for changing the level of difficulty in adaptive testing (Lendyuk *et al.*, 2015; Maravić *et al.*, 2016; Mantzaris *et al.*, 2019).To be exact, these are the authors whose research (Özyurt *et al.*, 2012) is dedicated to the process of designing and developing the module of computerised adaptive testing integrated into UZWEBMAT. UZWEBMAT is an expert system that supports an adaptive and intelligent individual e-learning environment. It was dedicated to teaching a probabilistic subject.

The classical theory of tests has a number of controversial assumptions, and the results of its application are serious practical shortcomings. In particular, it was noted that when evaluating the student's knowledge with the help of tests of different levels of complexity, it is possible to get different ideas about the achievements of students. Statistics calculated within the framework of the classical theory of tests allow obtaining the relative position of every testee in the normative sample. However, they cannot be used to objectively evaluate the values of the parameters characterising the level of knowledge of the testees and the complexity of the test tasks. The question "What is the objective evaluation of the level of the student's preparedness on the subject?" the classical theory of tests is still open. There was an attempt to answer this question in the framework of another methodological approach to the creation of pedagogical tests. Also, to the interpretation of test results, within the framework of so-called Item Response Theory (IRT), but as the practice has shown, this theory also has a number of serious shortcomings.

The shortcoming of the existing theories is the fact that one way or another, all these theories suggest the obligatory presence of "aerobatic testing" and a large number of "tests" for every task. In real life, not every higher education establishment can afford it. And this is especially unacceptable for testing students in subjects the content of which varies from year to year (for

Downloaded from www.periodico.tchequimica.com

example, computer science). Given that in the special subject at the intersessional control a clearly insufficient (to determine the quality of the test according to the proposed theories) number of students are tested, and the tests evaluate the knowledge of students not quite objectively.

Of course, the test set "randomly" obtained from the unified to the binary representation of the test poole of tasks will be by far more cumbersome. However, this is partially compensated by dropping "atypical" mistakes and parameterisation of the test task formatting; that is, counting tasks can be generated from formulas based on a random number sensor. Drawings (figures) are also recovered from parameterised random parameters of functioning algorithms. Also, in the same way, it is possible to set variable texts. Obviously, the costs of such a prepared test base will multiply increase, including the time spent by experts and programmers. Apparently, this problem is one of those that prevents such reading of the computer version of testing (Kulikov and Shatilova, 2005).

Reduction of the time spent, especially of the specialists gathered in groups, can be solved by switching to adaptive testing, which, as noted above, is unrealisable on a paper basis, but is actively used by technology leaders (for example, Microsoft).

One of the ways to overcome these difficulties was the development of automated testing on WebTest shell already available at the higher education establishment. All this allows suggesting that it is advisable to conduct the research dedicated to the method of evaluating the results of automated testing.

3. MATERIALS AND METHODS

3.1. Quantitative knowledge criteria

The evaluation system where knowledge is characterised by general terms such as "good", "strong," and "in-depth" is often unsatisfactory. Also, the four-point system, if it is based on subjective ideas about knowledge and intuitive quantitative criteria, slightly changes the situation.

This system satisfactorily performs its functions in the evaluation of knowledge by a person (professor). However, when using technical means of studying and control for the purposes of studying, such a system of marks is fundamentally inapplicable since technical devices do not have intuition. The machine can work only with formalised and quantified information.

Usually, knowledge is determined (with some degree of accuracy) by setting the student elementary control questions and comparing the answers of the student with the answers, which are considered to be deliberately correct (sample).The concept of "elementary control question" in this case is relative. It is elementary only because within the framework of the considered domain, it is not divided into simpler ones. However, its content can be quite complex. The concept of "student's response" is considered in a broad sense. In general sense, it is a response to a request.It can be both deterministic and probabilistic and can be expressed not only in words but also in actions, such as performing certain operations and the like. We introduce the concepts of "elementary knowledge" and "general knowledge".

Elementary knowledge is understood as the knowledge which refers to one elementary question. It is determined by comparing the response information with the sample information. General knowledge we consider as the knowledge that applies to all issues raised within the framework of this topic or course. At the same time, the issue of how many elementary questions need to be asked in order to reliably evaluate the level of general knowledge, as well as the issue of how complex the questions should be, is within the scope of specific methodologies and are not considered here.

We consider that the developed system (model) allows formulating such a (sufficiently large) number of questions that, in all cases will provide sufficiently reliable identification of the level of general knowledge on the topic, course, or their sections. It means that in the framework of model the following condition 'is always met where q is a number of questions which can be posed by means of the model (model capabilities); q' is a number of questions necessary for reliable identification of the level of general knowledge (psychological and pedagogical requirements).

As a quantitative criterion of knowledge, one can use the degree of compliance of Ti information contained in student’s answers to i question and information that in relation to this question is considered to be correct (sample) (Equation 1). Where X_i is the code response information to i question; Xi' is the code of sample information corresponding to i question. Until now, this approach/method had been widely applied. It was proposed a method in which when determining the level of general knowledge, not only the degree of compliance of the information contained in the student's answer with sample

Downloaded from www.periodico.tchequimica.com

information but also the number of mistakes made is taken into account. The degree of noncompliance can be used as a mistake criterion of F_i of the same types of information (Equation 2). We consider T_i value determined by Equation 1 to be the evaluation of knowledge of i question and F_i value determined by Equation 2 to be the mistake that characterises lack of knowledge of i question.

The value of T_i evaluation related to the degree of compliance of directly proportional dependence: the higher the degree of compliance, the higher the evaluation. The value of F_i mistake is inversely proportional to the degree of compliance: the smaller the degree of compliance, the higher the mistake.

This representation of quantitative criteria characterising elementary knowledge is in good agreement with the intuitive representation of the correlation of evaluations and mistakes (the greater the mistake, the lower the evaluation and vice versa). S_i is the general evaluation for i question that can be determined by Equations 3 and 4.

In the first case, it can be obtained on the basis of analysis the evaluation of knowledge of iquestion (traditional "clear" testing) andin the second oneon the basis of analysis proposed by us, that is, taking into account the mistakes made (as the difference of the evaluations of knowledge and mistakes of i question).

3.2. Point and integral evaluation of knowledgelevel

In accordance with the provisions of the mathematical theory of evaluation of the quality of test tasks, the level of knowledge θ can be considered as a general part of correct answers to all conceivable test tasks that display the subject area. By the data of testing, it is possible to find pinpoint $\tilde{\theta}_k$ and/or interval $\left[\tilde{\theta}_k^1;\tilde{\theta}_k^2\right]$ statistical evaluation θ. As it is known from the mathematical statistics course, the point evaluation of the general share is the sampling rate (Wise and Gao, 2017), which is (Equation 5). Where *p* is a part of correct answers oftested/student? Determined, according to (5). This evaluation is unbiased, consistent, and effective, but it is only an approximate value θ. However, the accuracy of the approximation can be considered sufficient for practical conclusions only in case when testee/student was offered a large number of test tasks $(k \to \infty)$. For short tests, the issue of accuracy of the estimate can be solved as follows. By setting δ probability, we determine $\tilde{\theta}_k^1$ and $\tilde{\theta}_k^2$ in the way that the following correlation should perform (Equation 6). In other words, we find θ an interval estimation with δ reliability. Traditionally, the boundaries of $\tilde{\theta}_k^1$ and $\tilde{\theta}_k^2$ confidence intervals for general share are determined like solutions of Equations 7, 8. If k>20, one can use approximate formulas.

3.3. A priori determination of the complexityof the test task (TT)

A priori determination of the complexity of the test task (TT). In classical testology, there are only statistical methods for determining the complexity of the TT. However, in practice, especially for entrance testing, the attempt to establish the level of pre-experimental complexity is particularly relevant because not for every task from the bank of the TT (due to the principle of non-disclosure of the TT before entrance exams) there is a possibility to determine the complexity statistically. However, on the other hand, it is impossible to talk about balanced versions of the entrance TT without taking into account the quality of the TT as a complexity.

Of course, it is difficult to achieve a complete coincidence of the values of a priori and statistical complexity because the quality of the determination of complexity depends not only onhow good and thought-out is the system of determining the complexity of the TT proposed in this research paper, but also on the level of professionalism of the experts who work with it. However, one way or another, the system will self-improve in the process of operating, namely:

1. Correct a priori evaluations of complexity with available statistical evaluations;

2. Evaluate how correct the expert's opinion is and provide relevant information (warn) about it.

For the attempt of a priori determination of the complexity, the first step is to establish the factors (x1, ..xn) affecting the complexity and establish their weight coefficients.A priori complexity of the TT will be considered to be the value determined by Equation 9, where$T(x_i)$ is the quantitative importance of i complexity factor to the TT. Together with experienced professors-experts in the field of entrance test tasks, we have developed a system of factors (reflected in Table

Downloaded from www.periodico.tchequimica.com

1.) that affect the task complexity for a priori determination of the complexity of the test task in any discipline.

According to the system of a priori determination of the TT complexity, the complexity of 20 entrance TT in mathematics was measured and compared with the statistical complexity measured for about 500 university entrants. The results are shown in Figure 1.The measurement error of this experiment was plus or minus 7%, which can be considered acceptable.

3.4. Correction method for guessing

Modern testology, which leaves open the issue of the identification of the testees who simply guessed when answering the test. The approaches to determining the quality of the task in which the proportion of very easy and very complicated questions does not change the status of guessed answers.

Some testologists, in particular, V. S. Avanesov (Doctor of Education, a leading expert in the field of the theory of pedagogical measurements), tried to introduce at the end of the test, before putting marks, the correction of points for guessing. But many testologists fairly disagree. Thus, for example, in the methodical recommendations of the Department of Pedagogy and Psychology of Leningrad Sanitary Hygiene Medical Institute based on the developments of I. M. Sechenov First Moscow State Medical University, the authors note that this formula equally penalises those who "can guess" and those who "can not".

In this research paper, we propose a fundamentally new approach that does not imply mass fining the testees by correcting the points for guessing.

There is a category of questions that testees answered mostly without thinking, namely, by guessing, but the questions did not fall into the category of low-response.Without identifying such questions before determining the level of reliability and validity of the test, we have a high probability that the reliability and validity of the test will be determined incorrectly.

The proposed method allows us to identify a group of testees who with a high probability guessed, and a group of "bad" questions that most students answered at random.

The model of a group of students who answer the test without thinking that is, randomly choose answers was created. If a standard test task consists of a question and 5 answers, a random student gains at random the result of 20% plus or minus 4% of the maximum of one hundred percent. At the same time, the number of people who simultaneously chose correct answers to one question will be at average 20% for each question with a deviation of plus or minus 6%. (If the number of questions ~100, then the number of testees ~300).

Thus, when evaluating the quality of tests, it is logical to exclude from consideration the questions answered by 20 plus or minus 6% of the testees from their total number, and it is logical to assume that students who gained 20 points plus or minus 4% of the total number of points are likely to have guessed.

Further, on the model of "guessing" students the average number of pairs of overlapping questions is calculated, i.e., for each pair of questions the number of identical answers is calculated (for example, if a student answers or does not answer these 2 questions at the same time). With 99% of reliability, this number is 67 % of the total number of students plus or minus 1%.

From real suspicious questions revealed according to the scheme stated in cl.1 (20%+-6%), they distinguish those which the number of pair overlaps is 67% +-1%. The answers to the other questions were not random (for example, cheating or not guessing, but an attempt to think).

The set of remaining real suspicious questions (cl. 3) is checked for the similarity of the distribution according to the Fisher criterion with the set of modelled random questions. In case of a positive result with the reliability adopted when calculating the Fisher statistics, it is possible to decide that the majority of students answered them at random, namely, by guessing. It is logical to exclude these questions from consideration and provide relevant information to the professor.

By excluding the questions which were guessed, it is possible to calculate the test results for one of the proposed methodology. However, in this case, the lowest threshold for students should be the result not lower than 20% +2* 4%=28% from maximum (at the final interval, the spread of the summed up factor formed by a large number of independent causes is evaluated as sigma 2). To the interval from 12% to 28% will fall, the students who guessed, below 12% are those who were consciously mistaken. As can be seen in Table 2 and Figure 2, the results are flat-lining with the help of this methodology.

A more detailed picture can be seen in (Figure. 3) where, in fact, the scale of evaluation

Downloaded from www.periodico.tchequimica.com

"lengthened" by half and became of more "normal" character.

4. RESULTS AND DISCUSSION:

4.1 Bank of Test Tasks

In this research paper, the main principle of the approach is to separate the creation of the bank of test tasks and the process of compiling the tests (bank of test material) and testing. The Bank of Test Tasks should function as an individual complete system, and it can be further used by different testing systems.The main purpose of the Bank of Test Tasks is as entering test results in database storage, pairing this base with the test material base, processing test results, and obtaining the accounting data with the minimum cost of all kinds of resources.

The preparatory stage of organising the testing includes the creation (throughout the academic year) of the Bank of Test Tasks and the Bank of Test Material in the form of an electronic database (DB). Test tasks are classified by topics and complexity levels, which are at the primary level determined by experts (highly qualified professors).

Every test task must comply with a specific rule base for the selection of test tasks, the requirements for which are developed in Chapter 2.

The Expert Data Collection Bank contains the information on expert recommendations (highlyqualified professors) concerning the quality of the test material, division into topics, complexity levels, etc. Test material "verified" by experts is placed to the Bank of Test Tasks, where tasks are classified according to the specified criteria.

The first requirement imposed on any test is the completeness of the coverage of all sections of the subject. To meet this requirement, it is advisable to divide all the questions into several topics and group the questions by topics. In this case, the elements of the division can be both unrelated sections of the subject and a group of issues that satisfy the same properties. For example, if we want to include a question in all tickets of the future test, it is enough to consider this question as an individual topic because every examination paper will include at least one question from every topic. In more detail, the scheme of creating the Bank of Test Tasks reflected in (Figure. 4) and is the following:

The automated test management system block described above can be prepared throughout the academic year.

The object-oriented design technology was used to develop a model of the automated Bank of Test Tasks. The main object of the whole system is a task. Every task is characterised by a category (clear–fuzzy), quality (satisfactory, good and excellent), subject, topic, module it belongs to, complexity, the time required for the answer, the author, and the expert who verified and evaluated it. The elements of studying, module, and subject (for easier qualitative and quantitative evaluation of the Bank of Test Tasks) are also characterised by average time, complexity and number of the TT.

The content of the task and answers can contain text, graphic, and formula information as well as figures. The content of the task can be created directly in the system or imported from an external system.

Every task can correspond to an arbitrary number of answers. At the same time, the task can have one or more correct answers. The number of correct answers is determined by the task category.

4.2 Test generator

The test generation from test tasks can be carried out automatically, and the user can set the required scope and complexity of the test as well as impose other restrictions. Before the beginning of test generation, the system suggests you specify the test structure and the number of required options.

Textstructure:

1. Subject name.
2. Total number of the TT in the test.(N)
3. Number of modules used in the test.(M)

3.1. Module name
3.2. Number of topics used in the test.(L)
3.2.1. Topic name.
3.2.2. Number of TT(K)
3.2.3. Average time for one TT (T)
3.2.4. Average complexity of TT (S)

Rule base for test generation of the topic with the specified K, T.

1. Choose *K* from the BTT and give this massive the name TEST
2. Find Nt (that is Nt is = new test) – average time of TT in TEST
3. D =0
4. If topic No. >1, then T=T+A
5. If Nt >T, then move on to 13 or to 6
6. If Nt =T, then move on to 16 or to 7
7. Delete from TEST massive the task with minimum time (t minimal test), TEST= new TEST

Downloaded from www.periodico.tchequimica.com

8. Copy to new TEST from the BTT the TT which is the nearest by time value (t of the BTT) to t minimal test, to f the BTT>t minimal test, move on to 11

9. Delete from TEST massive the task with maximum time (t maximum test), TEST= new TEST

10. Copy to new TEST from the BTT the TT(the nearest by time value (t of the BTT) to t minimal test, to f the BTT<t minimal test, move on to 11.

11. Find T new in new TEST

12. D new=T-Tnew

13. If D new *D<=0 then move on to 14 otherwise to 5

14. If topic No. =K then if D>0, D= D new, TEST = new TESTotherwise 15

15. If |Dnew |-|D|<=0, то 16 otherwise accurate to within D= D new, TEST= newTEST

16. A=-D

17. Accurate to within DTEST is compiled

To generate a test with a set complexity, a similar rule base is used, with changes in cls. 8 and 10 (the replacement condition of the test task with the same time values is added, if there are none, then the next task in order is checked).

Unit for evaluation of testing results:

Rule base of evaluating the knowledge level of testees. Unit for identifying "guessed" TT:

1. If the complexity of the question is from 0.14 to 0.26, *then* include the question in the category of suspicious and move on to2;

2. If according to the Fisher criterion, the distribution of a "suspicious" question is similar to a set of modelled random questions, so to consider a question to be guessed means to consider it ordinary.

Unit for evaluation of clear testing:

1. *If* it is necessary to evaluate the test in "non-traditional" ways, *then* move on to the Unit for evaluating fuzzy testing *otherwise* evaluate in the traditional way and move on to 2;

2. If it is necessary to evaluate the test, excluding "guessed questions", *then* move on to the unit for identifying "guessed" *TT* and move on to 3 *otherwise* evaluate in the traditional way *and* move on to *4;*

3. If the question is guessed, *then* exclude the question from further consideration and move on to 4;

4. Evaluate the test in the traditional way on a scale of 1 or 0.

5. Question complexity Equation 10 (S_{iq} is the evaluation of answer of q student to i question, w is a number of students in the group).

Unit for evaluation of fuzzy testing:

1. If it is a guessed question, *then* exclude the question from further consideration and move on to;

2. If a priori information on the degree of preparedness of testees is known(an expert can single out the category of "excellent students" *then*move on to the unit for methodology with excellent students, otherwise move on to the unit for universal methodology.

Unit for universal methodology:

1. Correct answer weight t_k (Equation 11) (a_1 ... a_m is the number of correct options of answers).

2. Incorrect answer weight f_j *if* $\forall$ $b_j \neq 0$ *then* (Equation 12), *If* $b_j = 0$ *then* $f_j = 0$. *If* $b_k = 0$, $k \neq j$ *then* (Equation 13) (b_1 ... b_n is the number of incorrect options of answers).

3. Question weight (Equation 14) (S_{iq} is the evaluation of answer of q student to i question, w is a number of students in the group).

Unit for methodology with excellent students

1. Data entry ("excellent students" according to experts);

2. If a student who was entered in the category of "excellent students", scored less than 50% of the maximum, then he should be excluded from the category of "excellent students" and the relevant message to the expert should be provided;

3. Linear programming problem is solved (Equation 15): $x_j \in [-1;0]$, if x_j is an incorrect answer, $x_j \in [0;1]$, if x_j is a correct answer, (a_{i1},...a_{i5}) isvariety of options of answers of i "excellent student" to k question;

4. *f* the sample is the only *then* move on to7otherwisemove on to5;

5. Move on to the unit for universal methodology;

6. Select from the variety of N samples obtained by the methodology with excellent students $X_n = (x_{1n},\ldots x_{5n})$"the closest" to the sample obtained by the universal methodology $X_y=(x_{1y},\ldots x_{5y})$, the one which $\sum_{i-1}^{5}(x_{1i}-x_{yi})^2$ was the

least;

7. Question weight (Equation 16).

4.3. Analyser

The analyseris intended to provide feedback in the system.Internal feedback is the information that comes from a student to the testing program in response to his actions when performing tests.It is intended for self-correction by the testing program of its database and rule base. The information of external feedback in the system under consideration comes to the teacher and is used by him to correct the informative content of the tests or the course of lectures as well as the student's activity. More detailed scheme of the analyser of test tasks is reflected in (Figure 5) and is the following:

Analyser's rule base
If the testing is clear, then perfom unit 1.
If the testing is clear, then perfom unit 2.

Unit 1:

If the guessed questions are identified, then provide the relevant information to the expert.

If there is a priori information on the testees, then provide the information on the validity degree to the expert (the question weight by the methodology with "excellent students") and recommend questions with the validity coefficient of less than 0.3, exclude from the Bank of Test Tasks or make a correction.

If a priori complexity in the Bank of Test Tasks is not equal to a posteriori within the accuracy of 0.01, then adjust the value in the Bank of Test Tasks (and all parametric forms of the TT).

If a posteriori complexity in the Bank of Test Tasks is not equal to a posteriori complexity for the current stage of testing within the accuracy of 0.01, then adjust the value in the Bank of Test Tasks (and all parametric forms of the TT), taking into account the accumulated statistics.

If a priori evaluation of the time required to solve the task in the Bank of Test Task is not equal to a posteriori one within the accuracy of 1 second, then adjust the value in the Bank of Test Task (and all parametric forms of the TT).

If a posteriori evaluation of the time required to solve the task in the Bank of Test Tasks is not equal to a posteriori one for the current stage of testing within the accuracy of 1 second, then adjust the value in the Bank of Test Tasks (and all parametric forms of the TT).

If the reliability coefficient of the test satisfies the expert, *then* memorise the test structure.

Theteststructureincludesnumber of tasks (the best option is parametric) of certain complexity level and time characteristics for every module and subject.

Unit 2:

If the guessed questions are identified, then provide the relevant information to the expert.

If there is a priori information on the testees, then provide the information on the validity degree to the expert (the question weight by the methodology with "excellent students") otherwise provide the information on complexity to the expert (by the universal methodology) and recommend questions with the validity coefficient ofless than 0.3, exclude from the Bank of Test Tasks or make correction.

If a posteriori complexity in the Bank of Test Tasks is not equal to a posteriori complexity for the current stage of testing within the accuracy of 0.01, then adjust the value in the Bank of Test Tasks (and all parametric forms of the TT), taking into account the accumulated statistics.

If a posteriori evaluation of the time required to solve the task in the Bank of Test Tasks is not equal to a posteriori one for the current stage of testing within the accuracy of 1 second, then adjust the value in the Bank of Test Tasks (and all parametric forms of the TT).

If the reliability coefficient of the test satisfies the expert, *then* memorise the test structure.

The test structure includes a number of tasks (the best option is parametric) of certain complexity level and time characteristics for every module and subject. Knowledge control is an integral part of the pedagogical process, especially if we want to consider this process as technological, i.e., one that ensures under certain conditions a guaranteed goal achievement. Although there are individual software tools focused on computerisation of control, however, these tools are not in all cases adequatefor solving the relevant problems of entrance and intersessional testing the solutions of which the ASTM presented in this paper is responsible for.

Downloaded from www.periodico.tchequimica.com

The ASTM can be divided into the following parts: automatic and automated generation of test tasks by the description of the knowledge system, test generation from test tasks, conducting a computerised test survey, and processing of test results.

For effective use of pedagogical testing in practice, it is necessary to have the opportunity to generate a sufficient number of variants of test tasks with minimal time.

Test generation from test tasks can be carried out automatically, and the user can set the required volume and complexity of the test, as well as impose other restrictions.

A computerised survey can be carried out on the basis of tests generated immediately before testing that really allows providing every testee with its own variant (in case of "computer test").

Processing the results of pedagogical testing is an important part of knowledge control and is considered as an element of the iterative process of test development, i.e., the use of test results to modify the test in order to improve its a posteriori evaluations.

The automated test system of management (ATSM) was used to generate tests for entrance in various academic disciplines and intersessional examinations in North Kazakhstan State University and demonstrated its high efficiency.

In more detail, a testing process is as follows. From the Bank of Test Material, the electronic system selects the tasks which satisfy a certain rule base and evaluates the suitability level and the complexity level. The tasks, which do not satisfy the rules base, are not entered into the Bank of Test Tasks. Next, the generator compiles a test with the necessary set of subjects, the number of questions on every topic in the subject, and the set complexity level of questions and time characteristics. After processing the test results, the analyser provides recommendations on how to optimise the test.

The unit for knowledge base and data of model consists of the Bank of Test Materials and Bank of Test Tasks. The Bank of Test Tasks can be replenished with new tasks at any time. The interaction of the units is reflected in Figure 6 with the help of lines.

The expert survey unit consists of the rule base (RB) for selection of test tasks to the bank; rule bases (RB) to evaluate the complexity of tests and answers and unit for data collection from experts (where can be included data about a priori evaluation of the individual qualities of tasks, information on the testes and required test parameters).

Expert survey unit (ESU) is intended to generate and configure the unit for evaluation of test results as well as the decision-making unit (DMU) of the operating part of the ESU.

The test generator is directly engaged in the formation of the test (taking into account the information coming from the EEU about the required set of subjects, the number of questions on each topic in the subject, and general level of test complexity).

Decision-making unit includes the analyser of test results which gives guidelines for optimizing a test (for example, concerning the determination of the TT qualities, adjusts the attributes of tasks in the Bank of Test Tasks, memorises the structure of "successfully formed" tests according to experts) and unit of test results evaluation which depending on the purpose of testing (intersessional or entrance) makes a decision on the TT qualities, assignment of optimal weights to the TT, points distribution or the exclusion of TT from consideration.

The application of the test management system allows to conduct examinations at the higher technological and technical level and increases the evaluation ability of the test.

5. CONCLUSIONS:

Due to the widespread introduction of the test system of knowledge control, the development of control systems based on testing and development of methods for compiling the tests have become particularly relevant.

Optimised test data processing is understood as entering test results in database storage, pairing this base with the test material base, processing test results, and obtaining the accounting data with the minimum cost of all kinds of resources.

The aim of the research was to identify the main evaluation criteria of the test material and test task, the development of generalized formalized approaches to the evaluation of different types of questions of clear and fuzzy tests, statistical analysis of the results.

According to the results of the study, the automated test management system was created, which allows obtaining a priori information on the TT, create tests, conduct testing, and automatically obtain its results. The program includes the schemes of finding the result

Downloaded from www.periodico.tchequimica.com

described in the research paper.

6. REFERENCES:

1. Akhmetshin, E. M., Pavlyuk, A. V., Ling, V. V., Mikhailova, M. V., Shichiyakh, R. A., Kozachek, A. V. *Journal of Entrepreneurship Education*, **2019**, *22*, 1-12.
2. Aleksandrova, O., Batchenko, L., Dielini, M., Lavryk, U. *Naukovyi Visnyk Natsionalnoho Hirnychoho Universytetu*, **2018**, *4*, 157-165.
3. Bershadskaya, M.D., Serova, A.V., Chepurenko, A.Yu., Zima, E.A. *VyssheeObrazovanie v Rossii*, **2019**, *28*(2), 38-50.
4. Bocheliuk, V., Panov, M., Nechyporenko, V., Pozdniakova-Kyrbiatieva, E. *Astra Salvensis*, **2019**, *7*(13), 275-288
5. Bride, H., Julliand, J., Masson, P.-A. *Science of Computer Programming*, **2016**, 132(2), 190-208.
6. Bué, P.-C., Julliand, J., Masson, P.-A. *Lecture Notes in Computer Science (including subseries Lecture Notes in Artificial Intelligence and Lecture Notes in Bioinformatics)*, 6706 LNCS, **2011**, 51-68.
7. Godefroid, P. Compositional dynamic test generation. *The ACM Special Interest Group on Programming Languages*, **2007**, *42* (1), 47-54.
8. Godefroid, P., Klarlund, N. & Sen, K. *Proceedings of the ACM SIGPLAN Conference on Programming Language Design and Implementation (PLDI),* Phoenix, USA, 2005, 213-223.
9. Julliand, J., Kouchnarenko, O., Masson, P.A., Voiron, G. *Programming and Computer Software*, **2018**, *44*, 1-14.
10. Kulikov, V.P., Shatilova, E.M. *Bulletin of EKSTU named after D. Serikbayev*, **2005**, *1*, 2.
11. Lendyuk, T., Sachenko, S., Rippa, S., Sapojnyk, G. *Proceedings of the 2015 IEEE 8th International Conference on Intelligent Data Acquisition and Advanced Computing Systems: Technology and Applications* (IDAACS 2015), **2015**, *2*(7341443), 945-948.
12. Makarov, S.I., Sevastyanova, S.A. *Advances in Intelligent Systems and Computing*, **2020**, *908*, 502-509.
13. Mantzaris, A.V., Walker, T.G., Taylor, C.E., Ehling, D. *Journal of Big Data*, **2009**, *6*(1), Article No.24.
14. Maravić, S., Čisar, P., Pinter, R. *Computers and Education*, **2016**, 92-93, 142-160.
15. Maslennikov, V., Grishina, O., Lyandau, Y., Kalinina, I. *Proceedings of the 30th International Business Information Management Association Conference, IBIMA 2017 – Vision 2020: Sustainable Economic development, Innovation Management, and Global Growth*, Madrid, Spain, **2017**, *2017*, 4376-4384
16. Muchuchuti, S., Narasimhan, L., Sidume, F. *Lecture Notes in Networks and Systems*, **2019**, *69*, 742-755.
17. Naykhanova, L.V., Danilova, S.D. *Theoretical and applied issues of modern information technologies: Materials of the Third All-Russian Scientific and Technical Conference.* Ulan-UdeRussian Federation, **2002**, 170-173.
18. Naykhanova, L.V., Danilova, S.D., Tumashov, S.V., Angaeva, E.Yu. *Collection of Scientific and Methodological Articles*, **2002**, *8*, 114-120.
19. Özyurt, H., Özyurt, O., Baki, A., Güven, B. *Expert Systems with Applications*, **2012**, *39*(10), 9837-9847.
20. Tillmann, N., De Halleux, J. *Lecture Notes in Artificial Intelligence and Lecture Notes in Bioinformatics*, **2008**, 4966 LNCS, 134-153.
21. Vinogradova, N.P., Popov, A.N. *Entrepreneurship and Sustainability Issues*, **2019**, *6*(4), 1798-1806.
22. Wise, S.L., Gao, L. *Applied Measurement in Education*, **2017**, *30*(4), 343-354.
23. Wise, S.L., Kingsbury, G.G. *Journal of Educational Measurement*, **2016,** *53*(1), 86-105.
24. Wise, S.L., Kuhfeld, M.R., Soland, J. *Applied Measurementin Education*, **2019**, *32*(2), 183-192.

Downloaded from www.periodico.tchequimica.com

$T_i = f(X_i, X_i')$, (Eq. 1)

$F_i = f_1(X_i, X_i')$, (Eq. 2)

$S_i = T_i$ (Eq. 3)

$S_i = T_i - F_i$ (Eq. 4)

$$\tilde{\theta}_k = p\,, \quad \text{(Eq. 5)}$$

$$p\left(\tilde{\theta}_k^1 \le \theta \le \tilde{\theta}_k^2\right) = \delta\,, \quad \text{(Eq. 6)}$$

$$\sum_{m=kp}^{k} C_k^m \left(\tilde{\theta}_k^1\right)^m \left(1-\tilde{\theta}_k^1\right)^{k-m} = \frac{1-\delta}{2}, \quad \text{(Eq. 7)}$$

$$\sum_{m=0}^{kp} C_k^m \left(\tilde{\theta}_k^2\right)^m \left(1-\tilde{\theta}_k^2\right)^{k-m} = \frac{1-\delta}{2}. \quad \text{(Eq. 8)}$$

$$AT(x_1,..x_n) = \sum_{i=1}^{n} T(x_i) \quad \text{(Eq. 9)}$$

$$d_i = \frac{w - \sum_{q=1}^{w} s_{iq}}{w} \quad \text{(Eq. 10)}$$

$$t_k = \frac{a_k}{\sum_{k=1}^{m} a_k} \quad \text{(Eq. 11)}$$

$$f_j = -\frac{\prod_{j=1}^{n} b_j}{b_j \sum_{j=1}^{n} \frac{\prod_{j=1}^{n} b_j}{b_j}} \quad \text{(Eq. 12)}$$

$$f_j = -\frac{\prod_{j=1, j\neq k}^{m} b_j}{b_j \sum_{j=1, j\neq k}^{m} \frac{\prod_{j=1, j\neq k}^{m} b_j}{b_j}} \quad \text{(Eq. 13)}$$

$$r_i = 1 + \frac{\sum_{q=1}^{w} s_{iq}}{w} \quad \text{(Eq. 14)}$$

Downloaded from www.periodico.tchequimica.com

$$\sum_{i=1}^{l} r_i = \sum_{i=1}^{l} \sum_{j=1}^{5} a_{ij} \cdot x_j \rightarrow \max \quad \text{(Eq. 15)}$$

$$r_k = \frac{\sum_{i=1}^{l} r_i^k}{l} \quad \text{(Eq. 16)}$$

Table 2. *Test results with the exclusion of suspicious questions*

	Test with all questions		**Test without "suspicious" questions**	
0-19%	9	31%	4	15%
20-39%	17	59%	15	56%
40-59%	2	7%	5	19%
60-79%	1	3%	1	4%
80-100%	0	0	0	0
	29		25	

(Table 2 was presented before Table 1 for editorial reasons, sorry for any inconvenience. Editors)

Downloaded from www.periodico.tchequimica.com

Table 1. *Factors affecting the task complexity for a priori determination of the TT*

Complexity criterion	Criterion qualitative characteristics	Final rank
time required for the perception of task	big	0.0666666666666667
	average	0.065
	small	0.03
time required for solving	big	0.0666666666666667
	average	0.055
	small	0.01
complexity (by avanesov)	level 1	0.111111111111111
	level 2	0.09
	level 3	0.06
	level 4	0.03
	level 5	0.0888888888888889
complexity (by bespalko)	level 0	0.0888888888888889
	level 1	0.0444444444444444
	level 2	0.06
	level 3	0.055
	level 4	0.111111111111111
content	homogeneous (1 topic)	0.07
	homogeneous (several topics)	0.08
meaning	obvious	0.065
	non-obvious, without subtext	0.06
	with subtext	0.085
	a test for intelligence	0.08
by number of elements of actin	1	0.04
	2 or 3	0.08
	>3	0.07
if any additional constructions are required	strictly yes	0.051
	depending on university entrant's level	0.055
	strictly no	0.0666666666666667
time required for solving a task by expert	>60 seconds	0.111111111111111
	40-60	0.1
	20-40	0.03
	5-20	0.06
	<5	0.03
if it can seem obvious at first sight or "confuse"	yes	0.06
	no	0.0222222222222222
topic complexity	high	0.0666666666666667
	medium	0.03
	low	0.04
by links of data structure	worldview minimum	0.0666666666666667
	basic knowledge	0.0222222222222222
	curriculum knowledge beyond basic level	0.08
	extra knowledge besides curriculum	0.0888888888888889
content of tt	calculate	0.0666666666666667
	simplify (use of formulas, laws)	0.04
	text task	0.06
if can be solved orally (without using paper and notes)	strictly yes	0.0666666666666667
	depending on university entrant's level	0.04
	strictly no	0.06

Downloaded from www.periodico.tchequimica.com

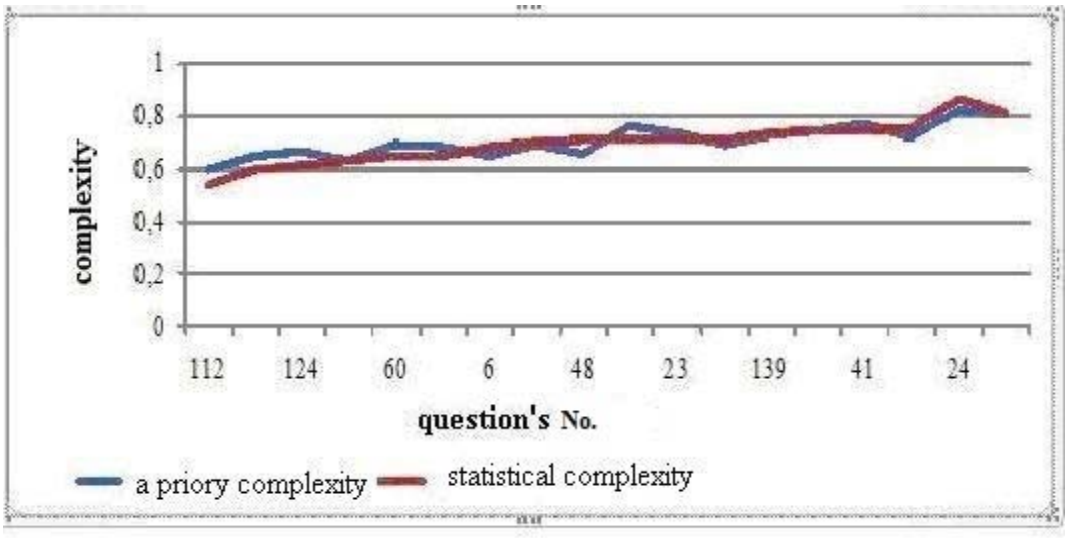

Figure 1. *A priori determination of the difficulty of the test task*

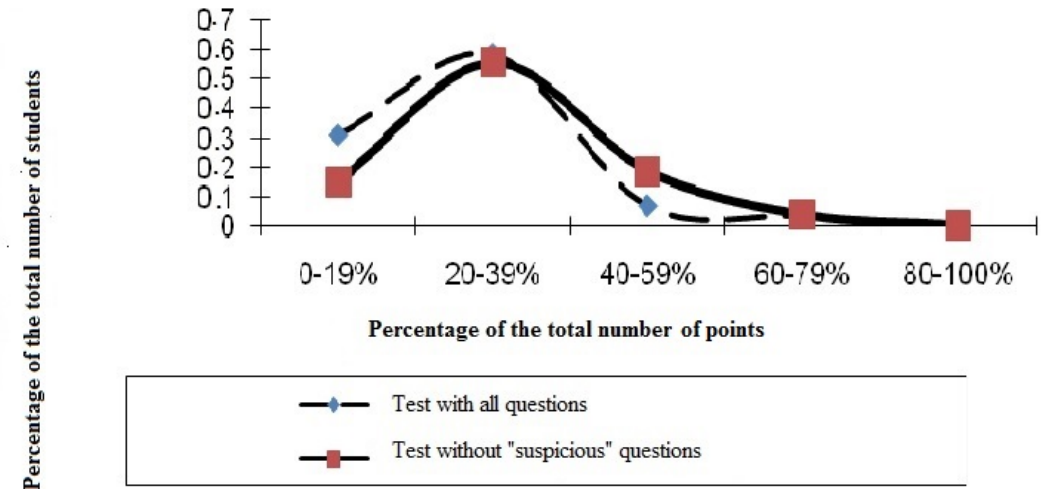

Figure 2. *Testing results diagram*

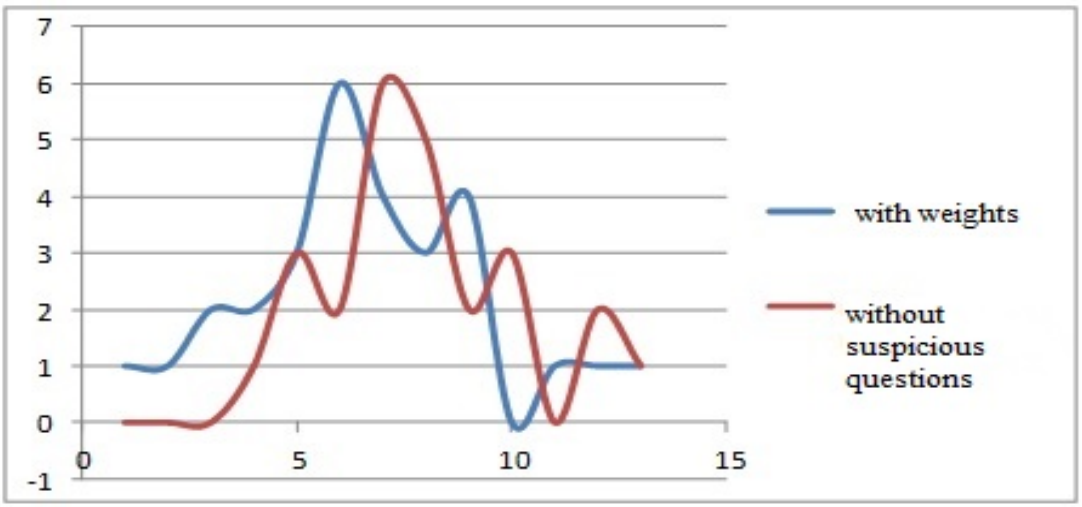

Figure 3. *Evaluation scale of test tasks*

Downloaded from www.periodico.tchequimica.com

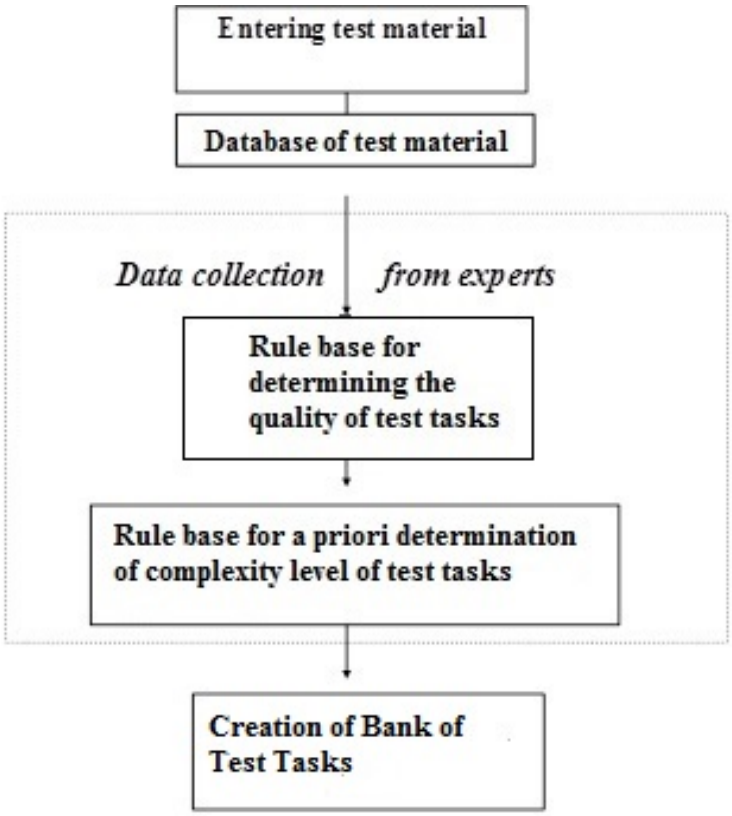

Figure 4. *Scheme of creation of Bank of Test Tasks*

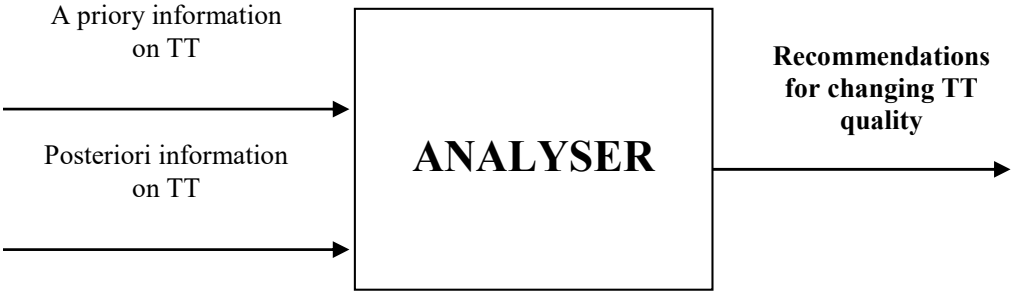

Figure 5. *Scheme of test tasks analyser*

Downloaded from www.periodico.tchequimica.com

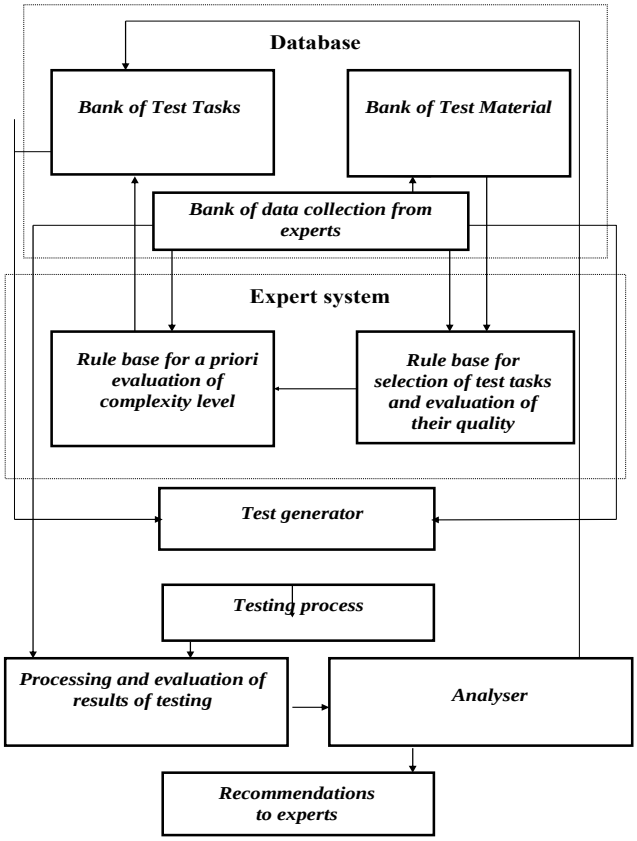

Figure 6. *Structure of an automated system of test management*

Downloaded from www.periodico.tchequimica.com

PERIÓDICO TCHÊ QUÍMICA
ARTIGO ORIGINAL

MATERIAL POLÍMERO E CERÂMICO PARA A FABRICAÇÃO DA CÂMERA DE DESCARGA DE GÁS DO MOTOR DE FOGUETE ELÉTRICO

THE POLYMER-CERAMIC MATERIAL FOR THE MANUFACTURE OF GAS DISCHARGE CHAMBER FOR THE ELECTRIC ROCKET ENGINE

ПОЛИМЕР-КЕРАМИЧЕСКИЙ МАТЕРИАЛ ДЛЯ ИЗГОТОВЛЕНИЯ ГАЗОРАЗРЯДНОЙ КАМЕРЫ ЭЛЕКТРИЧЕСКОГО РАКЕТНОГО ДВИГАТЕЛЯ

NIGMATZYANOV, Vladislav V.[1,2*]; POGODIN, Veniamin A.[3]; RABINSKIY, Lev N.[4]; SITNIKOV, Sergey A.[5];

[1] Research Institute of Applied Mechanics and Electrodynamics, 5 Leningradskoe shosse, zip code 123458, Moscow – Russian Federation

[2] Moscow Aviation Institute (National Research University), Department of Aircraft, Rocket Engines and Power Plants, 4 Volokolamskoe shosse, zip code 125993, Moscow – Russian Federation

[3,4,5] Moscow Aviation Institute (National Research University), Department of Advanced Materials and Technologies of Aerospace Application, 4 Volokolamskoe shosse, zip code 125993, Moscow – Russian Federation

** Correspondence author*
e-mail: vladtamgin@gmail.com

Received 28 June 2019; received in revised form 14 September 2019; accepted 09 November October 2019

RESUMO

O artigo discute a criação do material compósito dielétrico resistente ao calor à base de polímeros de organossilício para a fabricação de uma câmara de descarga de gás do motor de foguete elétrico. Foi proposto o aglutinante que atende aos altos requisitos de resistência à vibração e permeabilidade da câmara de descarga de gás na faixa de megahertz de ondas eletromagnéticas. Com base nesse aglutinante preenchido com pó de nitreto de silício, foi produzido a câmara de descarga de gás; este produto foi totalmente testado como parte do motor de foguete elétrico de laboratório de 200 kW. O estudo das transformações estruturais que ocorrem durante o aquecimento dos materiais foi realizado por análise térmica síncrona. O material obtido como resultado do experimento, cuja base foi SiSiB®PVMQ preenchida com Si_3N_4 a 60% em massa, é caracterizado por várias propriedades que são estruturadas e descritas neste artigo. Como resultado do estudo, foi demonstrado que o material estudado é caracterizado por resistência ao calor de até 400ºC. Com base nessa pesquisa, os autores produziram a câmara de descarga de gás, que foi testada como parte de um modelo de laboratório. Verificou-se que o aumento da perda de massa acima de 400°C é devido ao início do processo de degradação térmica da principal cadeia polimérica.

Palavras-chave: *cerâmica, elastômeros de organossilício, materiais compósitos, motores de foguetes elétricos, câmara de descarga de gás.*

ABSTRACT

This study discusses the creation of heat-resistant dielectric composite material based on organosilicon polymers for the manufacture of gas discharge chamber (GDC) for the electric rocket engine (ERE). A binder has been proposed that meets the high requirements for vibration resistance and electromagnetic permeability of GDC in the megahertz range of electromagnetic waves. Based on this binder filled with silicon nitride powder, GRC was designed; this product was fully tested as part of laboratory 200 kW ERE. The research of structural transformations that occur during heating of materials was carried out by synchronous thermal analysis. The material obtained in the result of the experiment, the basis of which was SiSiB®PVMQ filled with Si3N4 60% by mass, is characterized by a number of properties that are structured and described in this study. As a result of the study, it was demonstrated that the studied material is characterized by heat resistance up to 400 ºC. On the basis of these materials, the authors produced a GDC, which was tested as part of a laboratory model. It was established that the increase in mass loss over 400 °C is due to the initiation of the process of thermal degradation

Downloaded from www.periodico.tchequimica.com

of the main polymer chain.

Keywords: *ceramics, organosilicon elastomers, composite materials, electric rocket engines, gas discharge chamber.*

АННОТАЦИЯ

В работе обсуждаются вопросы по созданию термостойкого диэлектрического композиционного материала на основе кремнийорганических полимеров для изготовления газоразрядной камеры (ГРК) электроракетного двигателя (ЭРД). Было предложено связующее, которое соответствовало высоким требованиям к вибростойкости и электромагнитной проницаемости ГРК в мегагерцовом диапазоне электромагнитных волн. На основе данного связующего, наполненного порошком нитрида кремния изготовили ГРК, данное изделие прошло полное испытания в составе лабораторного ЭРД мощностью 200Вт. Исследование структурных превращений, происходящих при нагреве материалов, проводилось методами синхронного термического анализа. Материал, полученный в результате эксперимента, основой которого стал SiSiB®PVMQ наполненный Si3N4 60% масс., характеризуются рядом свойств, которые структурированы и описаны в данной работе. В результате исследования показано, что исследованный материал характеризуется термостойкостью до 400ºС. Авторами на основе этого материала была изготовлена ГРК, которая прошла испытания в составе лабораторной модели. Установлено, что рост потери массы свыше 400°С обусловлен инициацией процесса термодеструкции основной полимерной цепи полимера.

Ключевые слова: *керамика, кремнийорганические эластомеры, композиционные материалы, электроракетные двигатели, газоразрядная камера.*

1. INTRODUCTION

Space exploration is receiving a lot of attention in such economically leading countries as the USA, China, Japan, India, Russia, and countries of the European Community. Success in the development of near-Earth orbit, the lunar surface, interplanetary space is becoming one of the most important drivers for the development of modern technologies in these countries. One of the areas of intensification of space exploration is widespread use and development of electric rocket engines (ERE), which allow for a significant increase in the mass of payload of the spacecraft (SC) via reducing the mass of the working fluid. It should be mentioned that the longest project in the history of astronautics – the flight of Voyager 1 and Voyager 2 spacecraft to the boundaries of the solar system (NASA, USA, since 1977) became possible to some extent due to the use of electro thermal electric propulsion engines – “hydrazine” engines. In modern space technology, ERE is being developed for use in the correction of orbit of the spacecraft, bringing the spacecraft into the geostationary orbit, and also as a mid-flight engine in interplanetary flights (Antropov *et al.*, 2002; Gorshkov *et al.*, 2008; Loeb, 2015; Sitnikov, 2017; Khartov *et al.*, 2013; Rabinsky *et al.*, 2016a).

Among all types of electric propulsion, the greatest achievements have been reached in the use of ion engines (IE). Thus, XIPS-25 ion engines for orbit reaching and correction has been used for many years on space platforms of Boeing (USA). As sustainer engines, SERT ion engines were used in long interplanetary missions in DEEP SPACE 1 and DAWN missions (ongoing). Japan’s Space Agency’s Hayabusi 1 mission employed the μ-10 ion engine to fly to and from Itokawa asteroid. The mission of Hayabusi 2 to asteroid 1999 JU3 is currently being successfully performed. Currently, ERE is considered to be the main candidate for use as a sustainer engine in planned missions for the exploration of deep space, including when flying to Mars and other objects of the solar system. Unfortunately, due to some objective and subjective reasons in the development of ion engine technology in the Russian Federation, there was a significant retarding behind the world level, attempts to overcome which have been successful in recent years. At the same time, the technological problems of manufacturing the main structural elements of IE are getting significant.

One of the most effective IEs for use as a sustainer engine for long space flights is usually considered a high-frequency ion engine (HFIE) due to its inherent high efficiency and high resource life. The operation of the engine is based on the generation of plasma of the working matter (for example, xenon) and the acceleration of the ionization products by the electromagnetic field of the HF generator (Figure 1)

The ionization of the HFIE working matter

Downloaded from www.periodico.tchequimica.com

is carried out in the volume of a thin-walled bowl of a gas-discharge chamber. An increase in HFIE power to a value of 15 kW and above leads to an inevitable increase in the diameter of the gas distribution system (500 mm and more) while maintaining the chamber thickness at the level of 4 ... 7 mm. Currently, GDC chambers are made of ceramics based on aluminum oxide, silicon nitride (Khartov *et al.*, 2013). The diameter of the existing chambers, with a wall thickness of 4 mm, does not exceed 300 mm, because of low vibration resistance of thin-walled ceramic products and technological difficulties in their obtaining. Therefore, there are prerequisites for the search for alternative materials for GDC HFIE. The main requirements for the GDC material are electromagnetic permeability in the megahertz range, vibration resistance, and heat resistance.

Earlier, the authors of the article made attempts to make GDC from polymer-ceramic composites by the method of molding into a closed form (Rabinsky *et al.*, 2016a; Pogodin *et al.*, 2016a; Poliakov *et al.*, 2016; Ripetsky *et al.*, 2016; Rabinsky *et al.*, 2016b; Pogodin *et al.*, 2016b; Lurie et al., 2011; Pogodin *et al.*, 2019; Formalev et al., 2015). The technology of molding large-sized products from organosilicon rubbers obtained by the polycondensation reaction into a metal form was worked out. As a result, an HFIE chamber with a diameter of 100 mm was manufactured and successfully tested. The material for the chamber was polymethylphenylsiloxane rubber modified with terminal vinyl groups and filled with silicon nitride. The main disadvantage of the material used was the insufficiency of heat resistance, up to 370 °C in a vacuum (Lurie *et al.*, 2011; Pogodin *et al.*, 2019; Formalev *et al.*, 2015).

The material of the chamber – organosilicon polymers, is a high molecular weight compound containing silicon in the main polymer chain bonded to organic substituents in the side frame. Organosilicon polymers are usualy classified depending on the heteroatom in the main polymer chain: polyorganosiloxanes (oxygen), polyorganosilazanes (nitrogen), polycarbosilanes (carbon). Materials based on organosilicon compounds can be used in a temperature range from -120 ° C to 550 ° C, they are good dielectrics transparent to electromagnetic radiation (Andrianov and Sokolov, 1955; Daus and Kharchenko, 2018; Pogodin *et al.*, 2019).

Among organosilicon polymers, polyorganosiloxanes, to the greatest extent, comply with the above requirements for GDC material. Despite the high heat resistance of polyorganosilazanes and polycarbosilanes, materials based on them do not ensure stability of performance for the HFIE chamber material under conditions of contact with ionized gas at temperatures above 300 ° C. Among polyorganosiloxanes, cross-linked polymers have the highest heat resistance; linear polymers, which are characterized by high elongation, have a temperature limit of about 300 ° C (Pogodin *et al.*, 2019; Vinogradov *et al.*, 2016). In theory, cross-linked polymers and composite materials based on them have high heat resistance and can withstand repeated heating in an oxidizing environment up to 550 to 600 ° C. To achieve such heat resistance, it is necessary to modify organosilicon elastomeric composite materials using MQ resins (Vinogradov *et al.*, 2016), also known in the literature under other names: oligotrimethylsiloxysiloxanes, trimethylsiloxysili_ cates, or copolymer MQ-siloxanes.

MQ resins are oligomeric organosilicon compounds the molecules of which contain structural fragments of silicon dioxide [$SiO_{4/2}$] (Q) in the main chain, and trimethylsiloxy [$(CH_3)_3 SiO_{1/2}$] (M) groups (Molchanov and Kim, 1997; Voronkov *et al.*, 1976; Rabinskiy and Tushavina, 2019a; Rabinsky and Tushavina, 2019b).The above mentioned formula corresponds to the spatial highly branched structure .The lower is the Q / M ratio , the less pronounced is the elasticity. At the same time, the glass transition temperature for the polymer rises. At the ratio of M: Q is less than 0.7, the glass transition temperature rises to 200 ° C. So, MQ-siloxanes are characterized by high heat resistance .Co-condensation of MQ Resins with polyorganosiloxanes inhibits the depolymerization of the latter at temperatures above 300 ° C. Thermal degradation of MQ resins begins at temperatures above 400 ° C, with the formation of amorphous silicon oxide .Therefore, by combining the elasticity of linear polyorganosiloxanes and the heat resistance of MQ-siloxanes, it is possible to increase the heat resistance of composite material for the production of FDC HFIE.

2. MATERIALS AND METHODS

The main efforts in the search for material for GDC were directed to the development of GDC, molded from modified polymer-ceramic composites, based on organosilicon rubber, including ones filled with silicon nitride. The obtained material was developed by polymerization by double bonds of vinyl groups at

Downloaded from www.periodico.tchequimica.com

silicon atom and polycondensation by the hydrosilylation reaction (Figure 2).

At the first stage of the work on making GDC molded from modified polymer-ceramic composites, the physicochemical fundamentals of producing composite materials with a polymer matrix and ceramic powder were made as a filler to increase the vibration resistance of large-sized thin-walled products. Technology has been developed for forming large-sized products from organosilicon rubbers into a metal form, made by the polycondensation and polymerization reaction. Laboratory plots were made for these alternative methods of forming billets, including those adapted for further use in additive manufacturing.

At the second stage of works, a set of studies was conducted on the properties of the developed polymer-composite materials modified with MQ resins, which made it possible to formulate recommendations on using and adaptation of the obtained materials in space technology. A product under the SiSiB®PVMQ brand with a viscosity of 50,000 cSt and a refractive index n_D = 1.5490 from Power Chemical Corporation Limited (China) was used as the starting polymer for making the composite material. The catalyst K-21 was used as a hardener. A composite material was prepared by mixing Si_3N_4 powder with SiSiB®PVMQ in the bead mill for 4 hours. The proportion of silicon nitride was 60% of the mass. The structural transformations occurring during heating of materials were studied by synchronous thermal analysis using STA 449 F3 Jupiter instrument from NETZSCH (Germany) (Figure 3) in the differential scanning calorimetry (DSC) mode and with thermogravimetric analysis (TGA) mode.

The samples were heated to 1100 °C in open melting pots of Al_2O_3 with a volume of 0.085 ml at linearly increasing furnace temperature at a rate of 10 °C/min. The melting pots were placed in cylindrical recesses of the upper part of the DSC / TG sensor made of Pt-Rh alloy. The argon flow rate through the measuring cell (a sample and a reference) during the experiment was 50 ml / min. An empty melting pot was used as a reference. The sample and the reference temperatures were measured using built-in S-type thermocouples made of Pt-Rh alloys. The accuracy of temperature measurement was ± 0.3 °C. The change in mass of the samples was recorded with an accuracy of 1 μg. The isothermal drift of weights in the entire temperature range did not exceed 10 μg / h. Data collection and calculations, as well as device operation control, were performed using NETZSCH Proteus Software (Germany) software under MS-Windows OS.

For the best assessment of the properties of materials, the following types of tests were used:

- Isothermal annealing of samples with an exposure of 5 hours in a vacuum electric furnace SCHVE 1.2.5 / 25 at a residual pressure of $P = 6 \cdot 10^{-3}$ *Pa* and measurement of shrinkage after isothermal annealing in a vacuum according to GOST 26433.1-89.

- Measurement of tensile strength at Instron universal testing machine 5960 series for type III samples manufactured in accordance with GOST 269, thickness 2 ± 0.2 mm. The tests were performed at a temperature of 28 ^{0}C and loading speed of 500 mm/min.

- Measurement of the hardness of samples before and after isothermal annealing in vacuum at TSHR instrument in accordance with GOST 253-53.

- Performing vibration testing of the obtained prototypes of GDC HFIE with a diameter of 160 mm in accordance with GOST V 24880-81, GOST RV 20.57.305-98, GOST RV 50674-94, GOST B 22589-86.

- Operational tests of prototypes of GDC HFIE with a diameter of 100 mm on a vacuum stand with a volume of 0.4 m3 (Figure 4).In the pumping system of this testing line, oil-free means of obtaining vacuum were used: a two-stage fore-vacuum pump MU-603 from Kashijama (the first stage is a two-rotor five-stage Roots pump, the second stage is a Roots pump) and four turbo molecular pumps with a magnetic suspension of the Tim-2203LM rotor from Shimats .The pump compartment of the vacuum chamber was equipped with a water-cooled target — an aluminum alloy ion stream receiver with ring conical concentric grooves that reduce reverse flows. The pumping system of the testing line provided a dynamic vacuum of 10^{-3} Pa at xenon flow rates of up to 0.65 mg / s.

3. RESULTS AND DISCUSSION:

Figure 5 shows DTA plots of a SiSiB®PVMQ sample and a SiSiB®PVMQ-based material sample filled with Si_3N_4 60 mass% In argon. In the case of SiSiB®PVMQ, the mass loss of the test samples at 400 °C was about 10% of the mass.

The pyrolysis process is accompanied by thermolysis of organic frame: methyl, vinyl, phenyl

Downloaded from www.periodico.tchequimica.com

substituents at the silicon atom. In the result of pyrolysis, amorphous silicon oxide and silicon carbide are formed. The yield of the pyrolysis residue is about 49%, which is slightly lower than the value obtained based on elemental composition in starting polymer: C – 27.14%; H – 5.55%; Si – 37.00; O – 30.31.The reason for this lies in the occurrence of cyclic depolymerization of linear sections of the polymer chain, loss of silicon and oxygen in the composition of pyrolysis products. The increase in mass loss over 400 °C is due to the initiation of the process of thermal degradation of the polymer chain. Therefore, processes that occur up to 400 °C are mainly associated with the progress of the reaction along unreached functional groups, the telomerization reaction, the intramolecular rearrangement of macromolecules, and removal of low temperature boiling substances. The heat resistance of materials based on SiSiB®PVMQ filled with $Si_3 N_4$ 60 mass%, Slightly higher, according to the schedule of weight loss, 10% corresponds to a temperature of 550 °C. As can be seen from the graph, the proportion of the pyrolysis residue obtained at 1100 °C corresponds to the amount of silicon nitride 60% and 50% of the residue from the polymer part.

The resulting materials based on SiSiB®PVMQ filled with $Si_3 N_4$ 60 mass%, are characterized by the following properties:

- Hardness according to Shore – 50-60 (scale A).
- Density –1.20-1.40 g/cm^3.
- Elasticity – linear elongation – 35-40% of permanent deformation.
- Elongation at break point – 50 to 60%.
- The tensile strength – 6-8 MPa.
- Volume shrinkage after curing: 3-4%.
- Temperature ratio of linear expansion – 1.0 to 1.5 · 10^{-3} K^{-1}
- Dielectric strength – 15 – 20 kV/mm.
- Dielectric loss tangent: – 0.2 to 0.02.

The confirmation of the electrical properties was performed during the test of gas distribution system made from new material as part of a laboratory model of the engine with a diameter of the ion-optical system 160 mm. For this, a ready-made laboratory model of HF IE was used. For this laboratory model, the dependences of ion beam current on the flow rate and the embedded high-frequency power (HF power) when GDC was previously obtained. A vacuum test bench for testing polymer-ceramic GDCs as part of the laboratory model of HF IE provided a dynamic vacuum of 10^{-3} Pa at xenon consumption of up to 0.65 mg/s. The objective of these tests was to compare previously obtained integral characteristics of ceramic and polymer-ceramic GDC engines with new ones when the GDC was replaced by a chamber made of polymer-ceramic materials modified with MQ resins.

4. CONCLUSIONS:

As part of the conducted research, promising materials for creating a gas distribution system were studied – polymer-ceramic materials modified with MQ resins, providing the required electro physical and operational characteristics of the HF IE discharge chambers. During the study, the vacuum thermal stability of polymethylphenylsiloxane rubber modified with MQ-siloxane was investigated to create a polymer-ceramic composite that provides required electrical and operational characteristics of GDC of an electric rocket engine (radio transparency, manufacturability, vibration resistance, and so on). It was demonstrated that the studied material is characterized by high heat resistance. Modification with MQ resins partially blocked depolymerization of the linear part of polymer. In the general composition with silicon nitride, the heat resistance of the binder remains at the same level, due to mineral filling, the mass loss is proportionally reduced. Silicon nitride does not affect the process of thermal degradation with the synergistic effect of increasing heat resistance in the system of silicon nitride – a polymer binder was not found.

Methods of obtaining products from complex ceramic materials based on the use of polymer-ceramic materials modified with MQ resins based on silicone rubber filled with silicon nitride were studied. Experimental elements of technological equipment were created for the production of gas distribution systems from the developed polymer-ceramic materials. It was experimentally confirmed that the operating temperature of the gas distribution system made of silicon nitride-filled rubber modified with MQ resins could reach 400 °C without loss of mechanical and electrophysical properties.

Based on this material, GDC was manufactured, which was tested as part of the laboratory model of HF IE. The obtained dependences of the ion beam current on the flow rate of the working fluid and the enclosed HF power were not inferior to the previously obtained values for an engine with a gas discharge chamber based on alumina ceramics. From the obtained results, it follows that mechanical and

Downloaded from www.periodico.tchequimica.com

electrophysical parameters of the GDC from polymer-ceramic material modified with MQ resins and filled with silicon nitride meet the requirements for gas discharge chambers of HF IE.

5. ACKNOWLEDGMENTS:

The work was conducted in the Moscow Aviation University with the support of the Russian Foundation for Basic Research, project No 18-29-18083/18.

6. REFERENCES:

1. Andrianov, K.A., Sokolov, N.N. *DAN USSR,* **1955**, *101*(1), 81-84.
2. Antropov, N.N., Dyakonov, G.A., Pokryshkin, A.I. *Applied Physics*, **2002**, 1, 37-48.
3. Daus, Yu.V., Kharchenko, V.V. Applied Solar Energy, **2018**, *54*(1), 71-76.
4. Formalev, V.F., Kuznetsova, E.L., Rabinskiy, L.N. *High Temperature*, **2015**, *53*(4), 548-553.
5. Gorshkov, A.S., Muravyov, V.A., Shagayda, A.A. *Hall, and Ion Plasma Engines for Spacecraft,* Moscow: Mashinostroyeniye, **2008**.
6. Khartov, S.A., Balashov, V.V., Sitnikov, S.A. *MAI Proceedings*, **2013**, *63*. http://trudymai.ru/published.php?ID=36114, accessed April 2019.
7. Loeb, H.W., *Acta Astronautica,* **2015**, *116*, 299-306.
8. Lurie, S.A., Belov, P.A., Rabinsky, L.N., Lark, S.I. *Scale Effects in Continuum Mechanics. Materials with Microstructure and Nanostructure,* Moscow: MAI-Print Publishing House, **2011**.
9. Molchanov, B.V., Kim, V.D. *Plastic Masses,* **1997**, *3*, 22-25.
10. Pogodin, V.A., Rabinsky, L.N., Sitnikov, S.A. *STİN,* **2019**, *4*, 20-21.
11. Pogodin, V.A., Sitnikov, S.A., Solyaev, Yu.O. *New Refractories*, **2016a**, *11*, 33-37.
12. Pogodin, V.A., Sitnikov, S.A., Solyaev, Yu.O. *New Refractories*, **2016b**, *11*, 33-37.
13. Poliakov, P.O., Soliayev, Y.O., Sitnikov, S.A. *International Journal of Pure and Applied Mathematics,* **2016**, *111*(2), 319-330.
14. Rabinskiy, L. N., Tushavina, O.V. *INCAS Bulletin*, **2019a**, *11*(Special Issue), 203-211. DOI: 10.13111/2066-8201.2019.11.S.20.
15. Rabinsky, L.N., Sitnikov, S.A., Khartov, S.A. *Abstracts of the V international scientific seminar "Dynamic deformation and contact interaction of thin-walled structures when exposed to fields of various physical nature"* Moscow, Russian Federation, **2016a**, 159-160.
16. Rabinsky, L.N., Sitnikov, S.A., Solyaev, Yu.O. *Materials of the XXII International Symposium "Dynamic and Technological Problems of Mechanics of Structures and Continuous Media" named after A.G. Gorshkova,* Moscow, Russian Federation, **2016b**, *2,* 108-109.
17. Rabinsky, L.N., Tushavina, O.V. *STİN,* **2019b**, *4*, 22-26.
18. Ripetsky, A., Sitnikov, S., Rabinskiy, L. *IOP Conference Series: Materials Science and Engineering*, **2016**, *140*, 1-6.
19. Sitnikov, S.A. *Development of ion erosion-resistant materials based on silicon nitride for discharge chambers of electric rocket engines,* Moscow: Moscow Aviation Institute (National Research University), **2017**.
20. Vinogradov, S.V., Polivanov, A.N., Chuprova, E.A. *Chemical Industry Today*, **2016**, *1*, 13-18.
21. Voronkov, M.G., Mileshkevich, V.P., Yuzhelevsky, Yu.A. *Siloxane bond,* Novosibirsk: Nauka, **1976**.

Downloaded from www.periodico.tchequimica.com

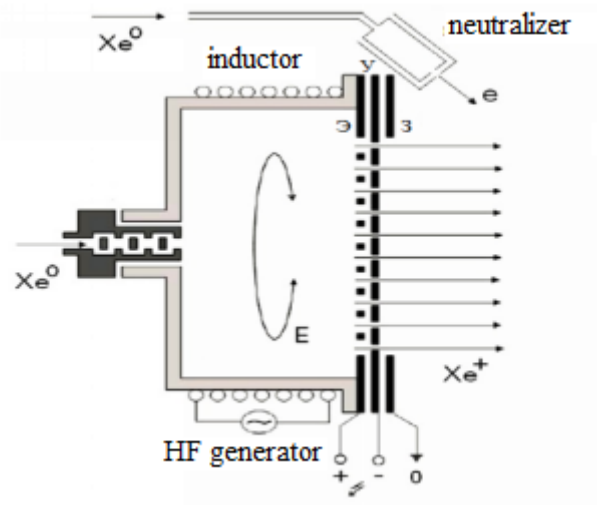

Figure 1. *Schematic diagram of the HFIE operation*

Figure 2. *Forming of test specimens from modified polymer-ceramic composites into a metal mold*

Figure 3. *STA 449 F3 Jupiter device from NETZSCH company (Germany)*

Downloaded from www.periodico.tchequimica.com

Figure 4 *The GDC prototype mounted on the HFIE prototype (left) and the general view of the vacuum testing line for HFIE (right)*

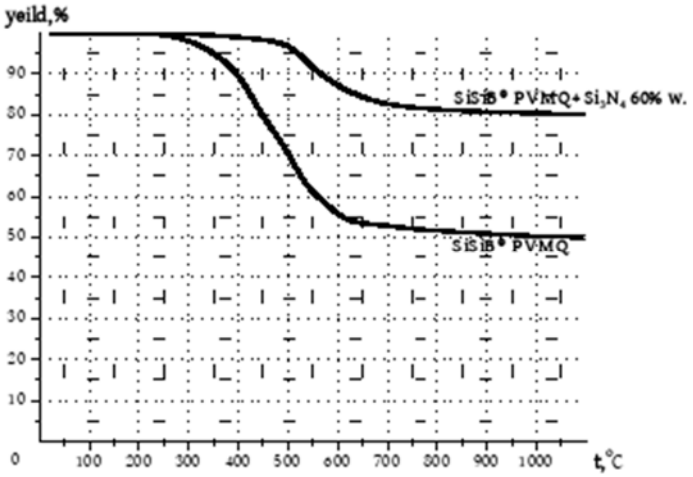

Figure 5. *Dependence of mass loss on temperature during the DTA of a SiSiB®PVMQ sample and a composite material based on SiSiB®PVMQ filled with Si_3N_4 60 mass% in argon medium*

Downloaded from www.periodico.tchequimica.com

PERIÓDICO TCHÊ QUÍMICA
ARTIGO ORIGINAL

ESTUDO DA QUALIDADE DE TRIGO E PÃO DE CLASSE BAIXA OBTIDOS PELO MÉTODO DE ENSAIO ACELERADO

STUDY OF THE QUALITY OF LOW-CLASS WHEAT AND BREAD OBTAINED BY THE ACCELERATED TEST METHOD

ИССЛЕДОВАНИЕ КАЧЕСТВО ПШЕНИЦЫ НИЗКОГО КЛАССА И ХЛЕБА, ПОЛУЧЕННОГО УСКОРЕННЫМ МЕТОДОМ ТЕСТОВЕДЕНИЯ

TURSUNBAYEVA, Sholpan A. [1] *; IZTAYEV, Auyelbek [2] ; MAGOMEDOV, Magomed [3]; YAKIYAYEVA, Madina A. [4] *; MULDABEKOVA, Bayan Zh. [5];

[1,2,4,5] Almaty Technological University, Department "Technology of bread and processing industries", 100Tole Bi st., zip code 050012, Almaty – Kazakhstan

[3] Voronezh State University of Engineering Technologies, Department of Technology of Bakery, Confectionery, Pasta and Grain Processing, 19 Revolutsii str., Voronezh – Russian Federation

** Correspondence authors*
e-mail: yamadina88@mail.ru

Received 18 October 2019; received in revised form 11 November 2019; accepted 11 November 2019

RESUMO

A qualidade do pão é determinada pela qualidade das matérias-primas utilizadas e, principalmente, farinha e água, como principais tipos de matérias-primas. O artigo apresenta os resultados de um estudo das propriedades físico-bioquímicas, indicadores de panificação pelo método acelerado, obtidos a partir de farinha de trigo mole finamente moída 3, 4, 5 e classes externas. Uma massa de cozimento preparada de maneira acelerada por 2-3 minutos pode melhorar suas propriedades reológicas, reduzir o tempo de cozimento para 36 minutos, melhorar a qualidade do pão da farinha de trigo mole de baixa qualidade. De acordo com o objetivo do estudo, foram estudadas as alterações nas propriedades físico-químicas dos grãos de trigo mole 3, 4, 5 e fora das classes, foi obtida farinha de trigo integral moída finamente separadamente do trigo mole de diferentes classes, e foi estudada a qualidade do pão preparado pelo método de teste acelerado da farinha de trigo mole. classes diferentes. Em geral, todas as amostras de trigo podem ser classificadas como recomendadas para consumo, uma vez que aumentaram os parâmetros organolépticos e físico-bioquímicos das propriedades reológicas em comparação com uma amostra de trigo fora da classe. Assim, os resultados de estudos utilizando o método de teste acelerado mostraram que o trigo das classes 3, 4 e 5 estudadas formavam as propriedades necessárias dos produtos semiacabados e contribuíam para melhorar a qualidade dos produtos de panificação e melhorar sua qualidade.

Palavras-chave: *trigo, farinha, qualidade, pão, indicador*.

ABSTRACT

The quality of bread is determined by the quality of the raw materials used, and above all, flour and water as the main types of raw materials. The article presents the results of a study of physico-biochemical properties, indicators of bread baking by the accelerated method, obtained from finely ground soft wheat flour 3, 4, 5, and out-of class. A baking dough prepared in an accelerated way for 2-3 minutes can improve its rheological properties, reduce baking time to 36 minutes, improve the quality of bread from low-quality soft wheat flour. In accordance with the purpose of the study, the changes in the physicochemical properties of soft wheat grains 3, 4, 5 and out-of class were studied, finely ground whole-ground flour separately from different classes of soft wheat grains was obtained, and the quality of bread prepared using the accelerated test method from soft wheat flour was studied, different classes. In general, all wheat samples can be classified as recommended for consumption since they have increased organoleptic and physico-biochemical parameters of rheological properties compared to a wheat sample out-of class. Thus, the results of studies using the accelerated test method showed that wheat of classes 3, 4, and 5 studied formed the necessary properties of semi-finished products and contributed to improving the quality of bakery products and improving their quality

Keywords: *wheat, flour, class, bread, indicator*.

Downloaded from www.periodico.tchequimica.com

АННОТАЦИЯ

Качества хлеба определяются качеством используемого сырья и, прежде всего, муки и воды, как основных видов сырья. В статье приведены результаты исследования физико-биохимических свойств, показателей выпечки хлеба ускоренным методом, полученного из тонкоизмельченной муки зерна мягкой пшеницы 3, 4, 5 и вне классов. Хлебопекарное тесто, приготовленное ускоренным способом в течение 2-3 минут позволяет улучшить его реологические свойства, сократить время выпечки до 36 минут, повысить качество хлеба из муки мягкой пшеницы пониженного качества. В соответствии с целью исследований в работе были исследованы изменения физико-биохимических свойств зерна мягкой пшеницы 3, 4, 5 и вне классов, получена тонкоизмельченная цельносмолотая мука отдельно из зерна мягкой пшеницы разных классов, исследована качества хлеба, приготовленного ускоренным методом тестоведения из муки мягкой пшеницы разных классов. В целом, все образцы пшеницы, можно отнести к рекомендуемым для потребления, поскольку они обладают повышенными органолептическими и физико-биохимическими показателями реологическими свойствами по сравнению с образцом пшеницы вне класса. Таким образом, результаты проведенных исследований с применением ускоренного метода тестоведения показали, что пшеница исследованных 3, 4 и 5 классов формировали необходимые свойства полуфабрикатов и способствовала улучшению качества хлебобулочных изделий и повышению их качества.

Ключевые слова: пшеница, мука, сорт, хлеб, показатель.

1. INTRODUCTION

In recent years, bread has been regarded as a functional food product through which a person receives the biologically active compounds he needs. Based on research by both Kazakhstani and foreign scientists, for the development of a wide range of bakery products, including for dietary nutrition, bread production technologies using innovative methods of making bread are promising and more practical (Pashchenko *et al*., 2008; Auerman, 2002; Moore *et al*., 2009). In the northern regions of Kazakhstan, the specific volumes of low-quality soft wheat harvests are increasing annually. The volumes of 3, 4, and 5 classes of wheat are especially increasing. Restoring the quality of flour, dough, bread in the baking process is of great relevance. For Kazakhstan, which has great potential, the production of wheat grain and the preservation of harvested, improving, and restoring its qualities is of crucial strategic importance.

1.1. Literature analysis and problem statement

The prerequisites for this study is that to achieve a well-loosened structure of the baking dough, and it is necessary to provide for an increased amount of baking yeast, which can cause the manifestation of negative properties of the product. Recently, there has been a lot of talk about yeast, the benefits, and harms of which are being called into question. The thing is that when yeast enters the body during active reproduction, they begin to consume, along with carbohydrates, all those useful vitamins, and minerals that come with food. And this means that a person does not receive them, which in the future leads to their deficiency and depletion of the body (Yakiyayeva *et al*., 2016; Sereev, 2014; Slavin, 2004). Bakery yeast in a duet with flour can upset the acid-base balance. Excessive consumption of buns can lead to the formation of an acidic environment, which is fraught with chronic constipation, gastritis, ulcers, as well as the occurrence of osteoporosis. Stimulate the growth of malignant tumors. This proposition was proved by a scientific experiment conducted by the French scientist Etienne Wolf. Yeast causes diseases of the heart, lungs, and liver (Magomedov *et al*., 2010; Li *et al*., 2013).

To intensify the process of maturation of semi-finished products after kneading, enhanced mechanical processing of dough during kneading is used, the ideas of which were popular already in the 20s. At this time, it began to produce kneading machines intensive principle (Magomedov *et al*., 2007; Mei *et al*., 2016; Sandhu *et al*., 2011).

Professor Elton, together with staff at the British Bakeries Research Institute in Chorleywood in the 1930s, conducted research on the effects of intensive kneading on ripening dough. The results served as the basis for the development of technology for intensive preparation of the dough with a shortened fermentation cycle (Chorleywood method). The

Downloaded from www.periodico.tchequimica.com

main idea of this method was that by increasing by 4-5 times the mechanical processing of the dough against the usual one, it is possible to intensify and accelerate the maturation process of the dough, reducing its fermentation time by 1-1.5 hours (Rolfe, 2000; Weststrat *et al*., 2002; Kim *et al*., 2003; Janssen *et al*., 2017).

The positive effect of mechanical stress during the kneading process on the speed and quality of wheat dough was confirmed by N.F. Prokopenko, V.V. Ionova, V.M. Donchenko. Work in the field of kneading theory, calculation of the operating parameters of kneading machines, and experimental studies of the specifics of processes during intensive kneading were performed at the Ukrainian State University of Food Technologies (I.M. Roiter, A.T. Lisovenko, V.N. Kovbasa, I.N. Litovchenko) Based on these works, a number of fundamentally new dough mixing machines have been created (Roberfroid, 2002; Dziki *et al*., 2014; Han *et al*., 2011).

Scientists have studied the dough kneading in a vacuum, in an atmosphere of air, oxygen, nitrogen, hydrogen and carbon dioxide. The fact of mechanical capture (occlusion) by the test during the mixing process of significant quantities of gas in the atmosphere of which the test is being mixed was established. It was found that if the dough is kneaded in an atmosphere of oxygen enriched air, then these gas bubbles formed in the dough during its kneading are a factor in the oxidative effect of oxygen on the corresponding components of the test, especially on its protein-proteinase complex (Agil *et al*., 2012; Tsyganova *et al*., 2012).

However, none of these methods eliminate the introduction of yeast into the dough. Many of them even require an increase in the amount of yeast added to the dough.

One of the ways of loosening bakery semi-finished products, excluding the introduction of yeast, is the mechanical way of loosening the dough.

A known method of mechanical loosening of dough by knocking down part of it, which consists of the following: part of the dough (in a relatively liquid and cold state) is knocked down for 5 minutes in a special knocking machine of strong and heavy construction. After a break, the whipped mass is fed into a conventional kneading machine, in which the dough is kneaded, which then goes for cutting and baking (Satsaeva *et al*., 2016; Dashen *et al*., 2016; Hemdane *et al*., 2015).

However, these methods were used only for the preparation of dough from wheat flour and did not find application in industry.

An analogue for the creation of innovative equipment and technology for functional bakery products with a shortened production cycle is the development of knock-down functional bread technology from wheat flour by scientists of the Voronezh State Technological University of Engineering Technologies (VSTUET) (Magomedov *et al*., 2010; Rak *et al*., 2018; Ktenioudaki *et al*., 2015).

In recent years, ozone, ions, ozone, ion-ozone, and electronic technology are finding wider applications in the food industry, which has several advantages over special additives and technologies. The use of ion-ozone technology agents with many useful properties (bactericidal, redox, etc.) in food production is the latest trend and represents a promising direction in food production (Fratelli *et al*., 2018; Ukrainets *et al*., 2016; Ye *et al*., 2012). Currently, scientists from the Almaty Technological University are conducting research on the use of ozonized, ionized and ionized water in the production of flour, bakery, pasta, flour confectionery from wheat flour and flour from a mixture of wheat, grain, oilseeds and legumes to improve quality, safety and environmental purity of finished products (Iztaev *et al*., 2018).

In order to solve the above problems, we prepared yeast-free dough and bread from different classes of soft wheat and studied the physico-biochemical, rheological properties, qualities, cooking time, and other indicators.

1.2. Aims and objectives of the study

The purpose of the research work is to use the accelerated test method developed by scientists of Voronezh State University with the aim of improving the physico-biochemical and rheological properties of low-class soft wheat samples.

To fulfill the purpose of the scientific work, we selected samples of soft wheat 3, 4, 5, and out-of classes.

Based on the objectives of the study, the following tasks were set:

- to investigate and determine the physico-biochemical properties of low-class soft wheat flour;

- determine changes in amino acid content and draw comparative conclusions;

- to determine the rheological properties of

Downloaded from www.periodico.tchequimica.com

dough and bread made from soft wheat flour 3, 4, 5, and out-of classes.

2. MATERIALS AND METHODS

The following raw materials were used for the manufacture of the test samples: soft wheat flour 3,4,5 and out of classes, edible salt (GOST R 51574-2000), drinking water (SanPiN 2.1.4.1074-01).

The following research objects were used to conduct experimental studies: grain samples of soft wheat of classes 3, 4, and 5 and wheat out-of class from northern Kazakhstan. These samples were ground at a laboratory mill installation of the Voronezh State University of Engineering Technologies and were intended for baking by the accelerated method of testing bread from whole-ground wheat of the above classes (Figure 1).

Figure 1. *The experimental setup for the preparation of the test accelerated methods*

Studies to determine the physico-biochemical properties of grain, amino acids and proteins were carried out on the basis of the Almaty Technological University, and the production of finely ground and whole flour from different classes of soft wheat and bread baking using the accelerated test method based on the Voronezh State University of Engineering Technologies.

Physico-biochemical and biochemical (moisture, nature, vitreous, quantity, and quality of gluten, grinding size, ash content, mass fractions of fat, protein, fiber, and amino acids) were determined in wheat grain.

In the finished bread, moisture, acidity, porosity, as well as shape stability and specific volume were determined.

The moisture content of the flour was determined by the accelerated method, according to GOST 9404-88. The content of raw gluten was controlled according to GOST 27839-88. The quality of raw gluten was determined by measuring its elastic properties, according to GOST 27839-88. The ash content of flour was determined according to GOST27494-87 using an accelerator - nitric acid and expressed as a percentage. The mass fraction of protein was determined according to GOST 10846-64, the fat content was determined according to GOST 29 033-91, the mass fraction of fiber was carried out according to the Wend method. The mass fraction of amino acids was determined according to M-04-38-2009. The vitreous nature of wheat grains was determined on a diaphragmoscope according to GOST 10987-76, the nature of grain on a liter purk according to GOST 10840-64, the mass fraction of 1000 grains according to GOST 10842-89.

Flour from whole-ground wheat grain was obtained by disintegration-wave grinding on a disintegrator (Figure 2). Wheat grains are fed into the working chamber 2 through the feed funnel 1, which is equipped with a grate for additional removal of weed particles exceeding the size of the grains.

Figure 2. *Appearance of the disintegrator: 1 - loading funnel, 2 - working chamber with grinding disks, 3 - unloading hole, 4 - filter, 5 - electric motor*

The electric motors 6 drive the grinding disks 3 and stand in such a way that the movement of the magnetic disks occurs to meet each other. Due to this design feature, a high

Downloaded from www.periodico.tchequimica.com

number of revolutions (18000-25000 rpm), and a small gap between the pins of the grinding disks, the grains are crushed with a higher degree of dispersion than other types of mills, which allows obtaining a high quality product.

In addition, in a very short period of time, synchronized conditions for the interaction of the field and matter at the atomic-molecular level arise in the chamber. This causes positive changes in the physicochemical state of the surface structure, which is the mechanical activation of the feedstock.

Through the inlet, the gap of which is regulated depending on the selected raw material in accordance with its size, the mass enters the working chamber, where it is ground. Ready flour through the discharge opening 4 is fed into the bag.

3. RESULTS AND DISCUSSION:

Studies were conducted on the physico-biochemical properties of the obtained flour from low classes of common wheat.

Determination of the vitreous nature of wheat samples showed that grains of classes 3 and 4 were vitreous with some content of partially vitreous grains, unlike wheat of class 5 and wheat out-of class, which had more powdery grains.

Table 1 shows the quality indicators of samples of wheat flour.

The quality and quality of bread products depends on the quantity and quality of gluten flour. Gluten in the baking industry has two main functions: it is a plasticizer, that is, it plays the role of a kind of lubricant, which gives the mass of starch grains fluidity, and a binder that combines starch grains into a single test mass. The first property of gluten allows you to mold the dough, the second to keep the form given to the dough. The uniqueness of gluten lies in the fact that the gluten frame formed during the pressing of the dough, which holds the mass of starch grains.

The results obtained indicate that the amount of gluten in a sample of grain, class 3 wheat, is normal, in contrast to samples of class 4 wheat, where the amount of gluten is 2% less and 5% less for wheat.

The quality of gluten shows that the readings of all samples are normal and approximately the same. This is due to the formation of hydrogen bonds between oppositely charged active centers of individual protein molecules due to active microclusters and disulfide bonds due to the oxidation of sulfhydryl groups under the influence of peroxide compounds of treated wheat, which strengthen the protein structure and reduce the activity of proteolytic enzymes.

The results showed a slight improvement in the elastic properties of the gluten prototypes, a decrease in moisture and hydration ability, an increase in the dry gluten content compared to wheat out-of class.

An important indicator of flour is its ash content. Ash content, due to its sharp unevenness in the components of grain, is of great industrial importance as a means of monitoring the grinding process and the quality of the flour. The ash content of the flour and its color are influenced by the ash content of the grain.

As a result of the research, the ash content of only 3 classes of wheat can be considered, although reduced, but the norm. The remaining samples, due to the conducted steel, have a high ash content, i.e., high content of minerals.

Fiber, despite the fact that it is not absorbed by the body, plays an important role in digestion, providing mechanical movement of food along the gastrointestinal tract. The results showed that the control sample and wheat of classes 3 and 4 have good indicators, in contrast to the wheat of class 5, where the fiber content is too high (Magomedov *et al*., 2007).

The protein content in wheat in all samples is below normal, but class 3 wheat is the most acceptable result. The fat content in all samples except class 4 wheat is normal. The wheat of the 3rd class again has the best result.

The change in the physicochemical properties of the grain is probably due to the dissociation of molecules with the formation of reactive compounds and the formation of a larger number of microclusters from wheat associates with an increase in the duration of its processing.

Grinding coarseness (particle size distribution, flour particle size) has a significant effect on the physical, structural, and mechanical properties of the dough and the finished bread. Other things being equal, flour size of its particles in the range of 150 to 400 microns does not significantly affect the quality of bread. But very large grains of particles with a size of 400 to 500 microns do not have time to completely saturate with moisture during the kneading and preserve

Downloaded from www.periodico.tchequimica.com

their individuality. The size of flour from soft wheat varieties was evaluated according to GOST by descent / passage through silk sieves No. 43/35.

The amino acid composition of 3, 4, 5, and non-cool varieties of soft wheat was determined. The results of changes in the content of non-essential and essential amino acids are presented in Figures 3-6 and tables 2-5.

A number of studies have shown that lysine and arginine tend to increase with decreasing wheat protein content (Table 3). The greatest discrepancies are between leucine + isoleucine (table 2). Stable differences in the concentration of amino acids between high- and low-protein wheat have been proved for lysine, which is higher in low-protein wheat, proline, and phenylalanine, which are found in lower amounts in low-protein wheat (table 4).

The results obtained from table 5 indicate that the essential amino acid threonine has the highest concentration among all the essential amino acids in class 3 — 0.16%. Essential amino acids - lysine and phenylalanine are contained in small quantities.

Given the constancy in the content of most amino acids, it seems more likely that such discrepancies reflect differences in different classes of wheat rather than differences in research methods.

Since the quality of bakery products depends not only on the properties of raw materials but also largely on the rheological properties of semi-finished products, it was advisable to study the effect of wheat of classes 3, 4, and 5 on the rheological properties of the dough.

The dough was prepared by mechanical loosening under pressure in an experimental laboratory unit developed at the Department of Technology of Baking, Pasta, and Confectionery at the Voronezh State Technological Academy.

It consists of a whipping chamber, an asynchronous electric motor, a control panel, a compressor, a thermostat, and a discharge opening. The installation works as follows: the recipe components of the dough are fed through the loading hole into the kneading case of the batch mixer, in which the kneading organ is installed in the form of a whisk, driven by an electric motor through a speed variator. At the end of loading, the kneading case of the kneading machine is hermetically closed by a lid and kneading the dough for 3-5 minutes at a kneading organ rotation speed of 5 s-1. Then, atmospheric air under a pressure of 0.3-0.4 MPa is introduced into the chamber through the nozzle under excess pressure into the kneading case.

During the dough kneading, thermostatically controlled water (20-25 °C) is continuously supplied to the shirt of the dough mixer. In this case, the recipe components are knocked down, and the test mass is saturated with air (Magomedov *et al*. 2010).

Baking bread was carried out according to the following conditions: kneading and kneading the dough lasted 3-5 minutes, baking finished bread was carried out 30-35 minutes, without fermentation, and the total time spent on one type of bread was only 33-40 minutes. The results of the study are shown in Fig. 7-8 and in table 6.

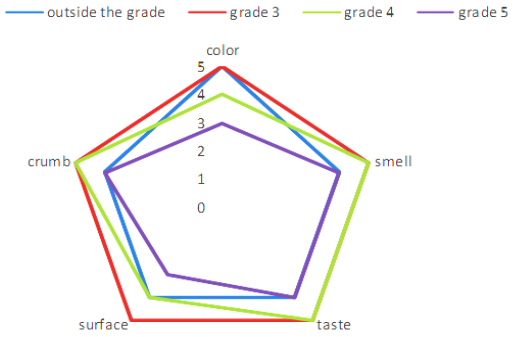

Figure 7. *Profilogram of organoleptic indicators of wheat bread*

From Figures 7 and 8 show that wheat out-of class - the crumb is poorly loosened, the surface is uneven, there are small cracks, the smell is not pronounced, the color is brown.

Class 3 wheat - the bread structure is developed, the crumb is characterized by high porosity. No cracks are observed, the color is yellow-brown, the smell is pleasant. The taste is pleasant and harmonious.

Class 4 wheat - the taste is pleasant. The crumb has a uniform structure. The color is brown, and the surface is flat, the smell is pleasant.

Class 5 wheat - taste with a touch of bitterness, dark brown. The crumb is medium, with highly developed porosity; the shape of the product is not correct.

Based on the results of wheat grains, it was advisable to study its effect on the quality of bread. The quality of bakery products was judged

Downloaded from www.periodico.tchequimica.com

by physico-chemical parameters: humidity, acidity, porosity, as well as shape stability and specific volume. The preparation of the test was carried out in a random manner (table 6).

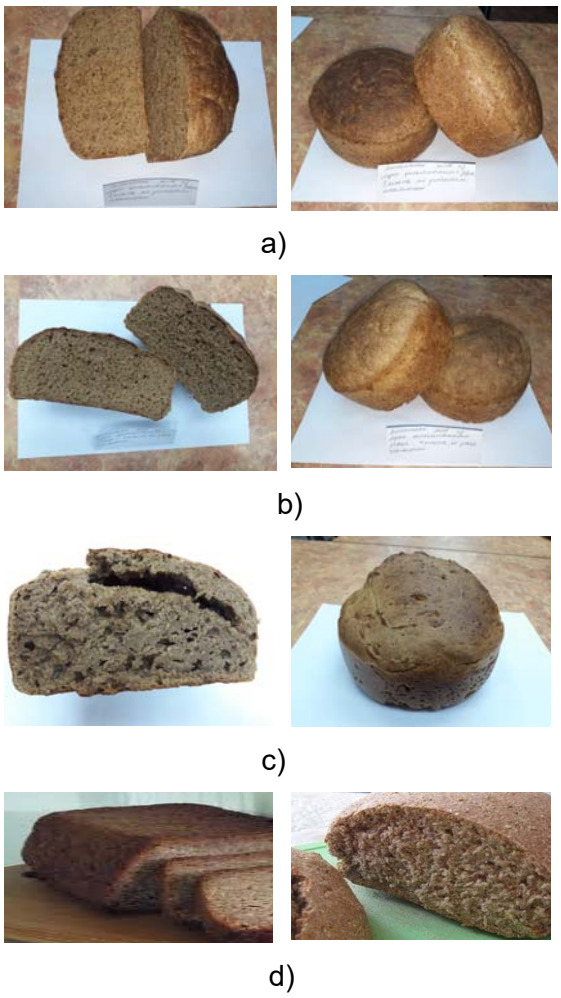

Figure 8. *Type of bread obtained from the accelerated method from whole-ground flour of soft wheat grain of different classes: a) bread learned in an accelerated way from grain of 3 class soft wheat; b) bread, learned in an accelerated way from grain 4 classes of soft wheat; c) bread learned in an accelerated way from grain of class 5 soft wheat; d) bread learned in an expedited way from soft wheat grain out-of class*

For all experimental bread samples, compared with a wheat sample out-of class, an increase in the shape stability index from 0.40 % to 0.50 % (in the third class of wheat), in the specific volume indicator up to 3.6 cm^3/g (in the third class of wheat) was revealed) and porosity from 48 to 52 % (table 6).

The results are due to the strengthening of gluten and a change in the rheological properties of the test.

Table 6. *Change in the quality indicators of bread from different classes of soft wheat*

Samples	Bread quality indicators				
	Formstability, %	**Specific volume of bread, cm^3/g**	**Humidity, %**	**Acidity, degree**	**Porosity, %**
Out-of-class wheat	0,40	3,20	41	4,8	48
wheat 3 class	0,50	3,60	41	4,2	46
wheat 4 class	0,47	3,51	41	4,4	48
wheat 5 class	0,45	3,44	40	4,9	52

An increase in the specific volume indicator for wheat samples of classes 3, 4, and 5 by 125, 117.5, and 112.5% and porosity by 112.6, 111.2, and 108.4%, respectively, was established, which was due to an increase in the plasticity of the dough and an improvement in lifting yeast strength.

4. CONCLUSIONS:

Summing up, we can say with confidence that the use of the accelerated test method allows improving the performance of class 3 wheat dough, as well as ready-made bread made from whole wheat of different classes has the best performance. Thus, it is possible to recommend further study of the rheological properties and quality indicators of wheat bread from different classes.

As a result of the study, it was found that the amount of gluten in class 3 soft wheat flour is normal, and for samples of class 4 soft wheat, the amount of gluten is 2% less and for class 5 wheat less than 5%. Also, the ash content of only 3 classes of wheat was reduced, but it corresponded to the norm, and the remaining samples had elevated ash contents, i.e., high levels of minerals. The protein content in wheat in all samples was below normal, but the most acceptable result was in soft wheat class 3. The fat content in all samples except class 4 wheat was not lower than the established norm. The best result was shown by a sample of wheat class 3.

Downloaded from www.periodico.tchequimica.com

With the intensive mechanical loosening of the dough, starch grains increase in volume, become looser and are easily amenable to the action of amylolytic enzymes. The linear fraction of starch - amylose, which forms the inner part of starch grains, hydrolyzes faster than amylopectin, which constitutes its outer part and has a branched structure.

An important role in the starch hydrolysis by a-amylase is played by proteolytic enzymes. Proteases, by carrying out limited protein cleavage, contribute to the release of amylases from the bound state and also hydrolyze the part of the storage proteins that are firmly bound to the surface of starch granules, while the access of the enzyme to the substrate is facilitated. Under the action of proteolytic enzymes, the complex structure of a protein molecule is simplified, its ability to swell decreases and the solubility of proteins increases.

The main reaction catalyzed by proteolytic enzymes is the hydrolysis of the peptide bond in the molecules of proteins and peptides.

To determine the rheological properties of low-class soft wheat, the dough was prepared and investigated, and the bread was baked. Kneading and kneading the dough was 3-5 minutes, baking the finished bread was carried out for 30-35 minutes, without fermentation, and the total time spent on getting one type of bread was only 33-40 minutes. As a result, it was proved that we used the technology of making dough and bread improves the quality of gluten, increases the rheological properties, and reduces time.

In the study of amino acids, it was determined that the essential amino acid threonine in class 3 is 0.16%, compared with other samples a significantly high amount. It was also found that lysine and arginine tend to increase as the protein content of wheat decreases, and the greatest differences are between leucine + isoleucine.

As a result of the hydrolysis of test proteins under the action of a protease, polypeptides, peptides, amino acids are formed.

Protein molecules contain reactive SH groups that are able to oxidize under the influence of oxygen. When knocking down the components of the dough under pressure, the semifinished product is saturated with atmospheric oxygen.

The addition of the enzyme preparation GC-106 to the dough during intensive churning and saturation with air oxygen increases the solubility of proteins, reduces the ability of the protein molecule to swell, which will provide a significant increase in the foaming of the semi-finished product, a decrease in the specific power per batch, thereby reducing energy consumption, and increasing the elasticity of the foam, its stability.

In addition, the action of enzymes (a-amylase and protease) on starch and protein of flour during churning contributes to the intensive formation of substances that determine the taste and aroma of bread. At this stage, a number of products of enzymatic hydrolysis of proteins and starch (low molecular weight nitrogenous substances, polypeptides, peptides, amino acids, carbonyl compounds) are formed, which participate in the formation of the taste and aroma of the yeast-free product, as well as the melanoid formation that occurs during baking of bread. As a result, melanoidins are formed, which color the peel, and intermediate and by-products of this reaction, which also participate in the formation of the taste and aroma of the finished products.

In Figure 9, a physical model of the degradation of starch and wheat flour protein in a yeast-free dough is presented.

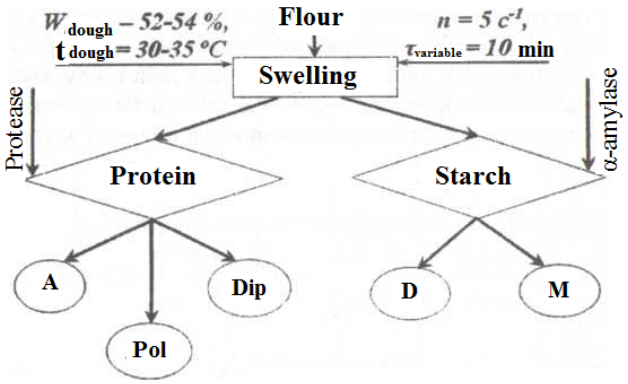

Figure 9. *Physical model of the process of destruction of starch and protein of wheat flour in a yeast-free dough: D – dextrins, M – maltose, A – amino acids, Pol - polypeptides, Dip – dipeptides; W_{dough} – dough humidity,%, t_{dough} – dough temperature, ° C, p - kneading organ rotation frequency, s-1, $\tau_{variable}$ - mixing time, min*

When knocking down the components of the dough under the pressure of compressed air, the semifinished product is intensively saturated with oxygen. At the same time, the structural and mechanical properties of the dough are improved, and its bulk mass is reduced. This is due to a

Downloaded from www.periodico.tchequimica.com

decrease in the number of SH groups and the formation of S-S bonds in the protein structure, which contribute to the strengthening of the protein structure and, accordingly, the foam film. Thus, intensive mixing and knocking down of the test with the saturation of air oxygen in the presence of the enzyme preparation GC-106 accelerates the processes of protein hydrolysis, while their solubility increases, the foaming of the semi-finished product increases, the formation of substances involved in the melanoidin formation reactions intensifies, the specific power for kneading decreases.

Therefore, enzymatic hydrolysis of the main components of flour with a mechanical method of loosening and forcing it will allow you to get the dough and bakery product with optimal structural and mechanical properties and a full-fledged taste and aroma.

We made the following conclusions:

1. The accelerated test method improves physico-biochemical and rheological indicators by almost 2 times;

2. The time to get one type of yeast-free bread is 33-40 minutes, including the preparation and baking process. Compared with traditional methods, this indicator, on average, reduces the time of receipt by 3 times.

3. The resulting bread products are used for functional purposes and provide the population with healthy nutrition.

5. REFERENCES:

1. Agil, R., Hosseinian, F. Dual Functionality of Triticale as a Novel Dietary Source of Prebiotics with Antioxidant Activity in Fermented Dairy Products. J. Plant Foods for Human Nutrition, **2012**, 67 (1), 88–93.
2. Auerman, L. Ya. Technology of baking production: textbook. St. Petersburg: Profession, **2002**, 416.
3. Dashen, M. M, Edia-Asuke, U. A., Amapu, T. Y, et. al. Effect of fermented dough on the organoleptic quality and shelf-life of bread. Journal of Microbiology Research, **2016**, 1 (1), 104–114.
4. Dziki, D., Rozylo, R., Gawlik-Dziki, U., Swieca, M. Current trends in the enhancement of antioxidant activity of wheat bread by the addition of plant materials rich in phenolic compounds. Trends in Food Science & Technology, **2014**, 40, 48-61.
5. Erkmen, O. Uses of Ozone to Improve the Safety and Quality of Foods. J. Gida Teknolojisi, **2001**, 5 (3), 58–64.
6. Fratelli, C., Muniz, D. G., Santos, F. G., Capriles, V. D. Modelling the effects of psyllium and water in gluten-free bread: An approach to improve the bread quality and glycemic response. Journal of Functional Foods, **2018**, 42, 339–345.
7. Han, H. M., Koh, B. K. Antioxidant activity of hard wheat flour, dough and bread prepared using various processes with the addition of different phenolic acids. Journal of Science and Food Agricultural, **2011**, 91, 604-608.
8. Hemdane, S., Leys, S., Jacobs, P. J., Dornez, E., Delcour, J. A., Courtin, C. M. Wheat milling by-products and their impact on bread making. Food Chemistry, **2015**, 187, 280-289.
9. Iztaev, A., Kulazhanov, T., Yakiyayeva, M., Maemerov, M., Iztaev, B., Mamayeva, L. The Efficiency of Ionocavitational Processing and Storage in the Nitrogen Medium of Oilseeds. Journal of Advanced Research in Dynamical and Control Systems, **2018**, 7, 2032–2040.
10. Janssen, F., Pauly, A., Rombouts, I., Jansens, K. J. A., Deleu, L. J., Delcour, J. A. Proteins of Amaranth (Amaranthus spp.), Buckwheat (Fagopyrum spp.), and Quinoa (Chenopodium spp.): A Food Science and Technology Perspective. J. Comprehensive reviews in food science and food safety, **2017**, 16(1), 39-58.
11. Kim, J. G., Yousef, A. E., Khadre, M. A. Ozone and its Current and Future Application in the Food Industry. J. Advances in Food and Nutrition Research, **2003**, 45, 167–218.
12. Ktenioudaki, A., Alvarez-Jubete, L., Smythc, T. J., Kilcawley, K., Rai, D. K., Gallagher, E. Application of bioprocessing techniques (sourdough fermentation and technological aids) for brewer's spent grain breads. Food Research International, **2015**, 73, 107-116.
13. Li, M., Peng, J., Zhu, K. X., Guo, X. N., Zhang, M., Peng, W., & Zhou, H. M. Delineating the microbial and physical–chemical changes during storage of ozone treated wheat flour. J. Innovative Food Science & Emerging Technologies, **2013,** 20, 223–229
14. Magomedov, G. O., Ponomareva, E. I. Scientific and practical fundamentals of

Downloaded from www.periodico.tchequimica.com

the technology of whipped functional bakery products (monograph). Voronezh: VGTA, **2010**, 248.
15. Magomedov, G. O., Ponomareva, E. I., Krutskikh, S. N., Shelest, T. N., Levin, Yu. N. The influence of various factors on the rheological properties of a whipped yeast-free test. J. Storage and processing of agricultural raw materials, **2007**, 5, 42-46.
16. Mei, J., Liu, G., Huang, X., Ding, W. Effects of ozone treatment on medium hard wheat (Triticum aestivum L.) flour quality and performance in steamed bread making. CyTA-Journal of Food, **2016**, 14, 449–456.
17. Moore, J., Luther, M., Cheng, Z., Yu, L. Effects of baking conditions, dough fermentation, and bran particle size on antioxidant properties of whole-wheat pizza crusts. Journal of Agricultural and Food Chemistry, **2009**, 57, 832-839.
18. Pashchenko, L. P., Zharkova, I. M. Technology of bakery products. Moscow: KolosS, **2008**, 389.
19. Rak, V., Yurchak, V., Bilyk, O., Bondar, V. Research into techniques for making wheat bread on hop leaven. Eastern-European Journal of Enterprise Technologies, **2018**, 1 (11 (91)), 4–9.
20. Richardson, D. P. Functional Food and Health Claims. J. The world of Functional ingredients, **2002**, 9, 12–20.
21. Rolfe, R. D. The Role of Probiotic Cultures in the Control of Gastrointestinal Health. The Journal of Nutrition, **2000**, 130 (2), 369S–402S.
22. Roberfroid, M. B. Global view on functional foods: European perspectives. British Journal of Nutrition, **2002**, 88 (S2), S133–S138.
23. Sandhu, H. P., Manthey, F. A., Simsek, S. Quality of bread made from ozonated wheat (Triticum aestivum L.) flour. Journal of the Science of Food and Agriculture, **2011**, 91, 1576–1584.
24. Satsaeva, I. K., Gasieva, V. A., Teboeva, A. K., Farnieva, Ya. S. The way to improve the quality and safety of bakery products from wheat flour by improving the technology of hop yeast. J. Vestnik KrasGAU, **2016**, 2, 118–124.
25. Sereev, I. Effect of spring biomass removal on expression of agronomic traits of winter wheat. World Applied Sciences Journal, **2014**, 30 (3), 322-329.
26. Slavin, J. Whole grains and human health. J. Nutrition Research Reviews, **2004**, 17, 99-110.
27. Tsyganova, T. B., Gakova, O. A. Improving the quality of bakery products based on the regulation of water properties. J. Bakery of Russia, **2012**, 1, 20-21.
28. Ukrainets, A., Kochubei-Lytvynenko, O., Bilyk, O., Zakharevych, V., Vasylchenko, T. A study of the effect of enriched whey powder on the quality of a special-purpose bread. Eastern-European Journal of Enterprise Technologies, **2016**, 2 (11 (80)), 32–41.
29. Wandersleben, T., Morales, E., Burgos-Díaz, C., Barahona, T., Labra, E., Rubilar, M., *et al*. Enhancement of functional and nutritional properties of bread using a mix of natural ingredients from novel varieties of flaxseed and lupine. J. Food Sci-Tech Brazil, **2018,** 91, 48–54.
30. Weststrat, J. A., van Poppel, G., Verschuren, P. M. Functional foods, trends and future. British Journal of Nutrition, **2002**, 88(S2), S233–S235.
31. Yakiyayeva, M., Iztaev, A., Kizatova, M., Maemerov, M., Iztaeva, A., Feydengold, V., Tarabaev, B., Chakanova, Zh. Influence of ionic, ozone ion-ozone cavitational treatment on safety of the leguminous plants and oil-bearing crops at the storage. Journal of Engineering and Applied Sciences, **2016**, 11(6), 1229-1234.
32. Ye, E. Q., Chacko, S. A., Chou, E. L., Kugizaki, M., Liu, S. Greater whole-grain intake is associated with lower risk of type 2 diabetes, cardiovascular disease, and weight gain. The Journal of Nutrition, **2012**, 142, 1304-1313.

Downloaded from www.periodico.tchequimica.com

Table 1. *Quality indicators of wheat flour*

Indicator	Norm on ND	Wheat out-of class	Wheat 3 classes	Wheat 4 classes	Wheat 5 classes
Humidity, %	14,0-15,0	12,6	12,7	12,7	12,8
Nature, g / l	760	787,7	790,5	796,7	813,9
Mass of 1000 grains, g		29,3	37,48	31,88	35,42
Mass fraction of protein, not less than %	14,0	12,4	13,17	11,02	11,26
Mass fraction of fat,%	1,6-3,2	1,74	1,62	1,14	1,16
Mass fraction of fiber,%		8,4	8,7	10,41	9,8
Mass fraction of ash,%	1,97	1,36	1,42	1,37	1,11
Gluten mass fraction, not less than %	28,0	21,57	24,76	22,94	19,77
Gluten quality according to IDK-1, units	20-100	74	76,1	72,5	73,3

Table 2. *Composition of essential and non-essential amino acids of wheat out-of class*

N	Time	Component	Height	Start	End	Area	Conc., mg/l	Mass fraction of amino acids in %
1	7.518		1.262	7.357	7.623	69.78	0.00	0
2	7.677	arginine	0.499	7.623	7.768	16.91	19.0	0,23±0,09
3	10.700	arginine	0.688	10.627	10.808	21.63	10.0	0,12±0,04
4	11.410	tyrosine	0.823	11.323	11.508	28.79	30.0	0,36±0,11
5	12.173	histidine	0.338	12.082	12.250	12.54	12.0	0,14±0,07
6	12.352	leucine + isoleucine	1.224	12.250	12.608	97.07	35.0	0,42±0,11
7	12.692	methionine	0.160	12.608	12.783	7.349	6.10	0,07±0,02
8	12.907	valine	0.775	12.783	13.028	37.02	25.0	0,30±0,12
9	13.182	proline	2.395	13.028	13.332	120.7	74.0	0,89±0,23
10	13.425	threonine	0.512	13.332	13.528	22.42	15.0	0,18±0,07
11	14.052	serine	0.814	13.925	14.162	39.81	21.0	0,25±0,07
12	14.287	alanine	0.802	14.162	14.400	39.05	17.0	0,21±0,05
13	15.377	glycine	1.020	15.232	15.478	55.99	19.0	0,23±0,08

Table 3. *The composition of the interchangeable and essential amino acids of wheat 3 class*

N	Time	Component	Height	Start	End	Area	Conc., mg/l	Mass fraction of amino acids in %
1	7.232		1.202	7.105	7.395	68.17	0.00	0
2	7.458	arginine	0.527	7.395	7.522	14.56	16.0	0,20±0,08
3	10.265	lysine	0.746	10.190	10.437	24.04	12.0	0,15±0,05
4	10.908	tyrosine	1.095	10.820	11.065	38.8	40.0	0,50±0,15
5	11.152	phenylalanine	0.195	11.065	11.223	7.805	7.40	0,09±0,03
6	11.503	histidine	0.071	11.408	11.550	1.477	1.40	0,02±0,01
7	11.753	leucine + isoleucine	1.477	11.633	11.978	109.4	40.0	0,50±0,13
8	12.053	methionine	0.304	11.978	12.128	11.38	9.40	0,12±0,04
9	12.245	valine	0.924	12.128	12.357	39.99	26.0	0,33±0,13
10	12.505	proline	3.052	12.357	12.620	147.3	91.0	1,14±0,30
11	12.703	threonine	0.664	12.620	12.805	24.84	16.0	0,20±0,08
12	13.258	serine	1.022	13.145	13.367	45.76	24.0	0,30±0,08
13	13.468	alanine	0.906	13.367	13.582	39.48	17.0	0,21±0,06
14	14.440	glycine	1.338	14.308	14.588	68.8	23.0	0,29±0,10

Downloaded from www.periodico.tchequimica.com

Table 4. *Composition of interchangeable and irreplaceable amino acids of wheat 4 class*

N	Time	Component	Height	Start	End	Area	Conc., mg/l	Mass fraction of amino acids in %
1	7.437		0.943	7.345	7.548	38.75	0.00	0
2	7.673	arginine	0.478	7.548	7.832	25.43	29.0	0,29±0,12
3	10.735	lysine	0.757	10.657	10.822	23.9	11.0	0,11±0,04
4	11.452	tyrosine	1.070	11.340	11.545	39.04	40.0	0,41±0,12
5	11.642	phenylalanine	0.289	11.545	11.735	12.95	12.0	0,12±0,04
6	12.398	leucine + isoleucine	1.529	12.273	12.630	118.5	43.0	0,44±0,11
7	12.732	methionine	0.181	12.630	12.820	7.985	6.60	0,07±0,02
8	12.950	valine	0.946	12.820	13.068	44.75	30.0	0,30±0,12
9	13.242	proline	2.967	13.068	13.372	156.5	97.0	0,98±0,26
10	13.467	threonine	0.655	13.372	13.585	27.87	18.0	0,18±0,07
11	14.095	serine	0.998	13.968	14.205	47.42	25.0	0,25±0,07
12	14.338	alanine	0.914	14.205	14.452	43.47	18.0	0,18±0,05
13	15.435	glycine	1.288	15.283	15.627	71.55	24.0	0,24±0,08

Table 5. *The composition of the interchangeable and essential amino acids of wheat 5 class*

N	Time	Component	Height	Start	End	Area	Conc., mg/l	Mass fraction of amino acids in %
1	7.370		1.732	7.270	7.532	75.1	0.00	0
2	7.598	arginine	0.486	7.532	7.740	21.23	24.0	0,24±0,10
3	10.588	lysine	0.790	10.520	10.685	23.79	11.0	0,11±0,04
4	11.152	tyrosine	0.214	11.098	11.203	6.899	7.10	0,07±0,02
5	11.290	phenylalanine	1.065	11.203	11.370	34.33	33.0	0,33±0,10
6	12.222	leucine + isoleucine	1.609	12.082	12.473	114.7	42.0	0,43±0,11
7	12.548	methionine	0.207	12.473	12.633	7.876	6.50	0,07±0,02
8	12.765	valine	0.988	12.633	12.892	44.07	29.0	0,29±0,11
9	13.052	proline	2.961	12.892	13.175	142.3	88.0	0,89±0,23
10	13.273	threonine	0.663	13.175	13.360	25.24	16.0	0,16±0,06
11	13.895	serine	1.031	13.773	14.002	45.64	24.0	0,24±0,06
12	14.138	alanine	0.990	14.002	14.240	44.0	19.0	0,19±0,05
13	15.233	glycine	1.356	15.077	15.350	70.59	24.0	0,24±0,08

Downloaded from www.periodico.tchequimica.com

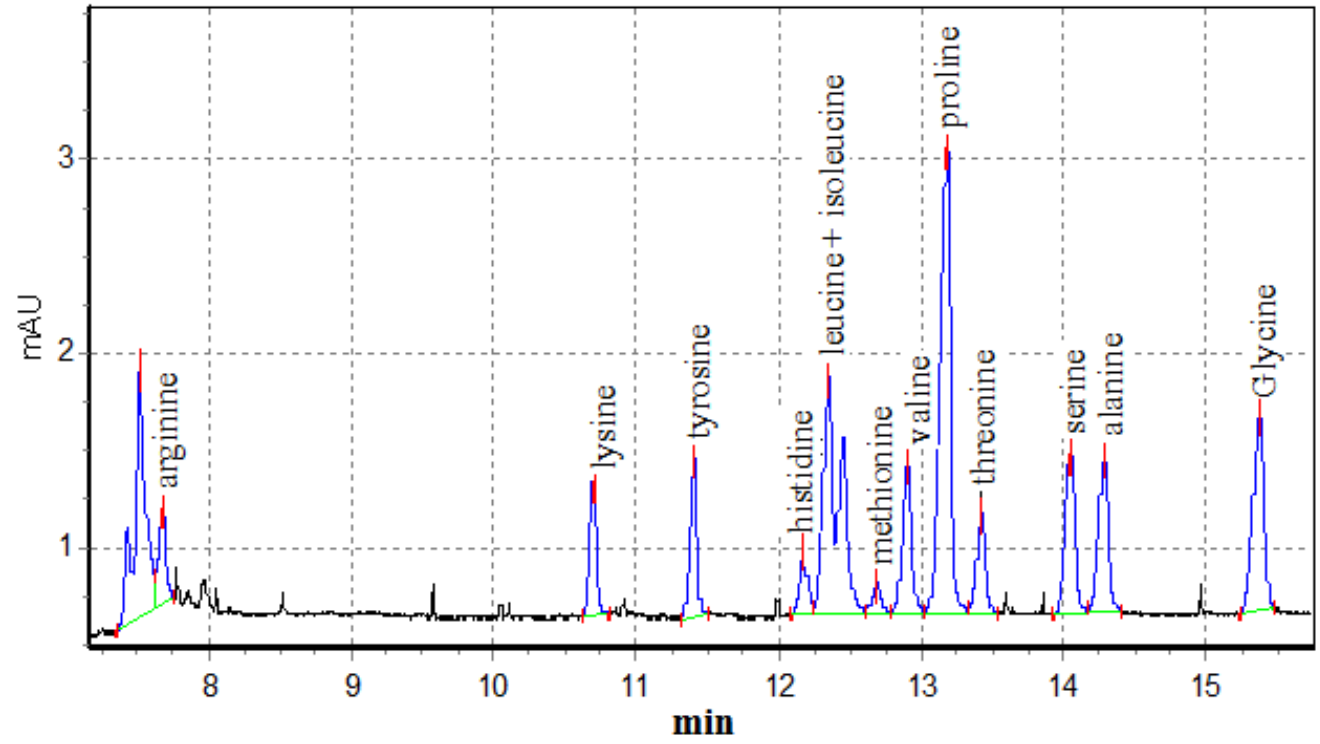

Figure 3. *The composition of the interchangeable and irreplaceable amino acids of wheat out-of class*

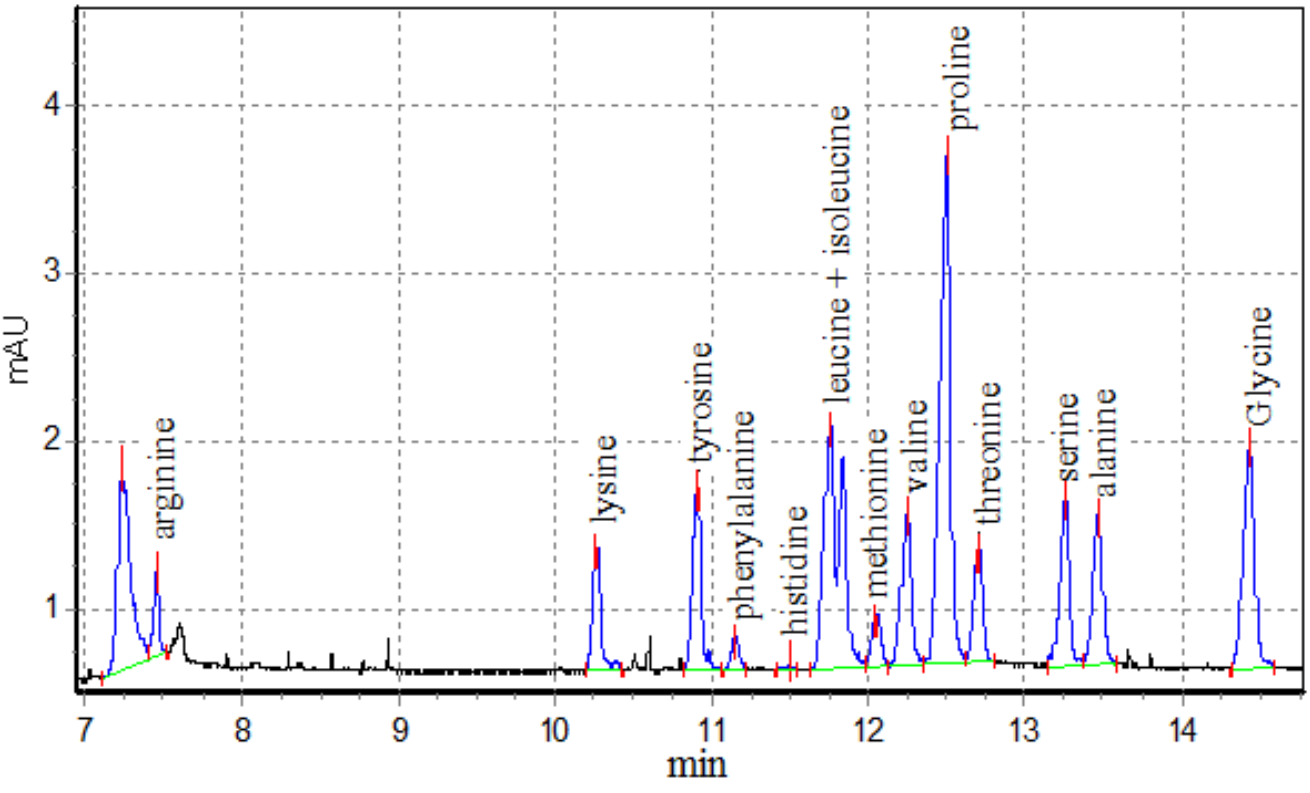

Figure 4. *Composition of interchangeable and irreplaceable amino acids of wheat 3 class*

Downloaded from www.periodico.tchequimica.com

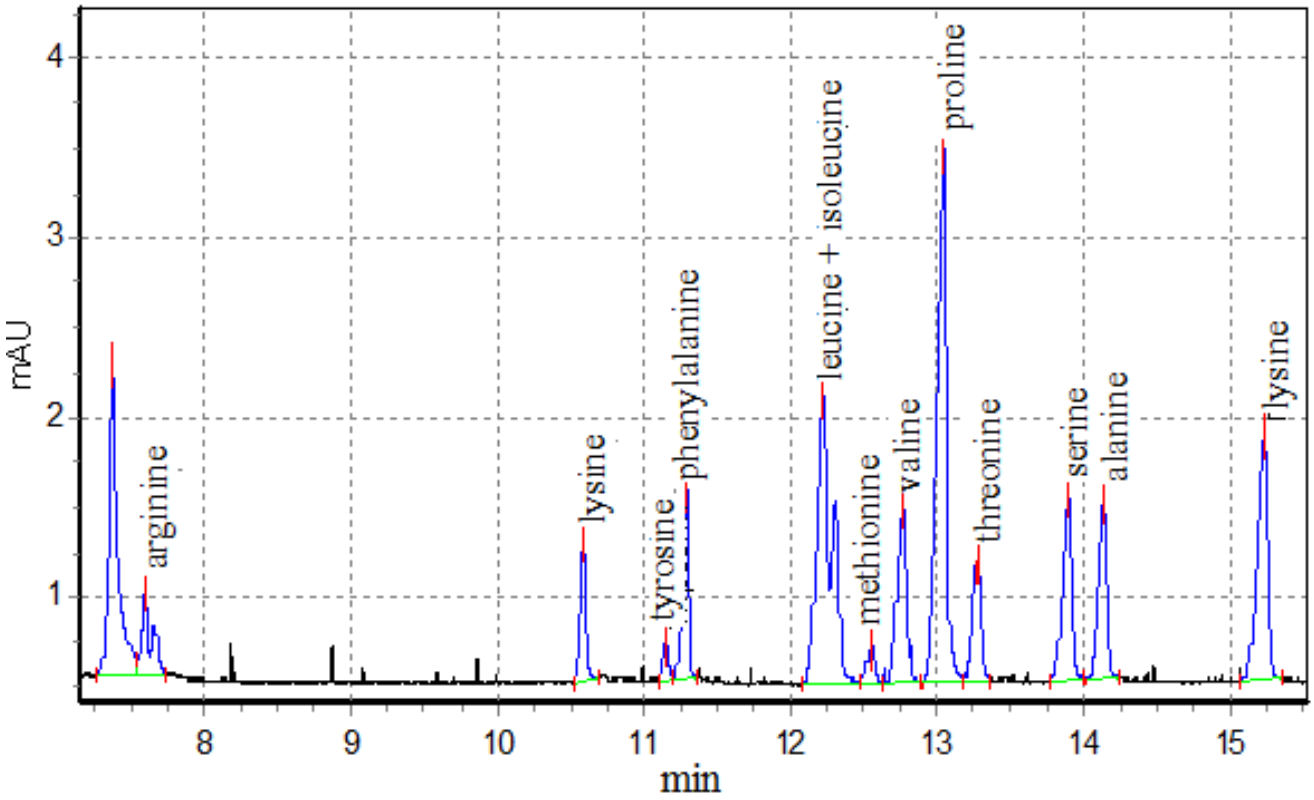

Figure 5. *The composition of the interchangeable and essential amino acids of wheat 4 class*

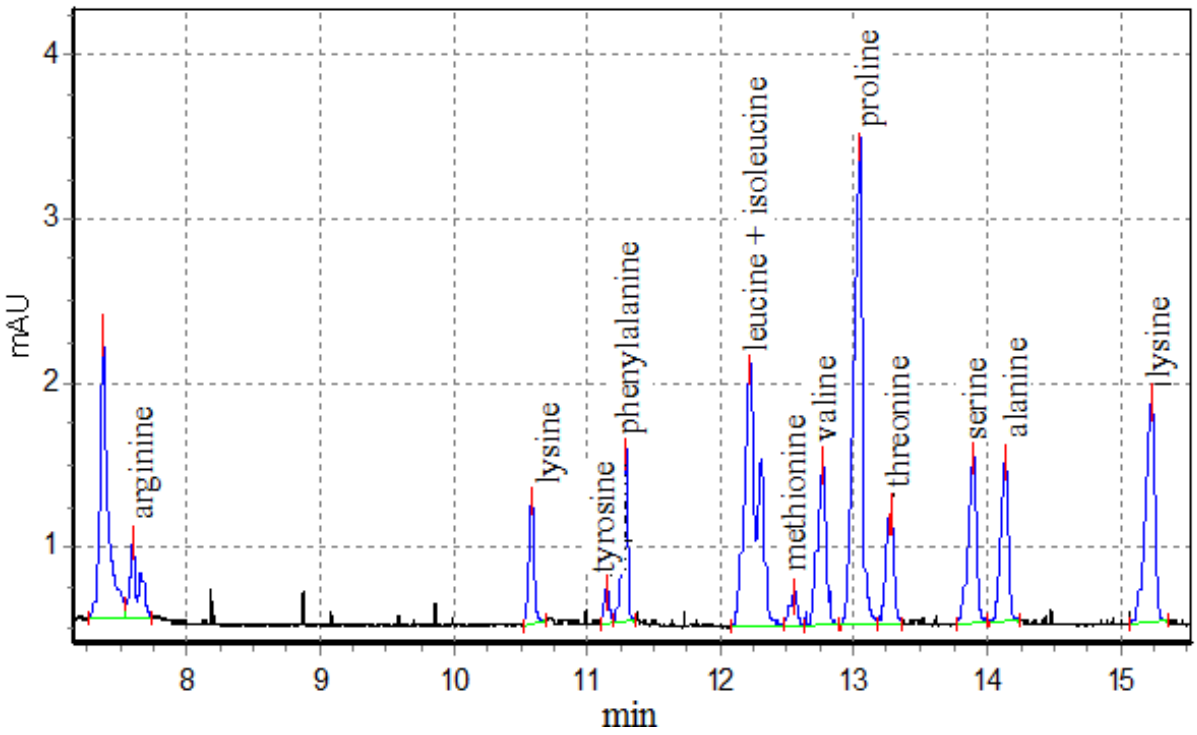

Figure 6. *Composition of interchangeable and essential amino acids of wheat 5 class*

Downloaded from www.periodico.tchequimica.com

PERIÓDICO TCHÊ QUÍMICA
ARTIGO ORIGINAL

APROVEITAMENTO DE LODO ORIUNDO DE ESTAÇÕES DE TRATAMENTO DE ESGOTO SANITÁRIO (ETE) E SUA UTILIZAÇÃO COMO MATÉRIA PRIMA NA FABRICAÇÃO DE TIJOLOS

USE OF SLUDGE FROM SANITARY SEWAGE TREATMENT PLANTS (S.T.P) AND THEIR USE AS RAW MATERIAL IN THE MANUFACTURE OF BRICKS

TARABAI, Monira Kansaon[1*]; AZEVEDO, Sirlei Geraldo de[2]

[1] Graduada em Engenharia Civil através da Faculdade Kennedy-MG

[2] Engenheiro na Companhia de Saneamento Básico de Minas Gerais

**Monira Kansaon Tarabai*
e-mail: monirakansaon@gmail.com

Received 12 January 2019; received in revised form 21 August 2019; accepted 14 November 2019

RESUMO

O presente artigo aborda uma possível solução, quanto à destinação final do lodo oriundo de Estações de Tratamento de Esgotamento Sanitário (E.T.E), visando à preservação ambiental. O resíduo solido gerado, após os processos de tratamento do efluente bruto é altamente contaminante e prejudicial a área na qual é depositado. Diante disso, o aproveitamento do lodo com aplicação de técnicas de reuso, torna-se pertinente, tanto sobre a ótica econômica, quanto sobre a ótica ecológica. Ao substituir o uso de agregados provenientes de jazidas minerais, a argila principal matéria prima na fabricação de produtos cerâmicos (Vieira, 2000), pelo lodo tratado de ETE teremos uma economia das fontes de materiais granulares. Objetivando sua reintegração ao ciclo produtivo através da introdução do lodo como matéria prima incorporada a massa cerâmica na fabricação de tijolos vazados, verificou-se a viabilidade de uso através de análise de desempenho, ao comparado ao tijolo testemunha fabricado em olaria, sem adição de lodo. Foram elaborados corpos de prova com três tipos de amostras: 90% de argila e 10% de lodo; 80% de argila e 20% de lodo; 70% de argila e 30% de lodo. Ensaios de perda de massa, índice de absorção de água e de resistência a compressão foram realizados. Quanto aos testes os corpos de prova com 10% e 20% de lodo foram os que tiveram maior adequação aos requisitos técnicos, mas por se tratar de um maior volume do resíduo para aplicação de técnicas de reuso o tijolo com dosagem de 20% de lodo é o mais indicado. NBR7.7171, de novembro de 1992:Bloco Cerâmico para alvenaria; Especificação NBR 6.461, de junho de 1983: Bloco Cerâmico para Alvenaria - Verificação da resistência à compressão: Método de ensaio; NBR 8.947, de novembro de 1992: Telha Cerâmica- Determinação da massa e da Absorção de Água: Método de Ensaio. Quanto aos testes, o corpo de prova com 20% de lodo foi o que teve maior adequação aos requisitos técnicos e ambientais.
.

Palavras-chave: *Lodo (ETE); Processamento de resíduos; Tijolos cerâmicos.*

ABSTRACT

This paper discusses a possible solution regarding the final disposal of sludge from Sanitary Sewage Treatment Stations (ET), aiming at environmental preservation. The solid waste generated after the wastewater treatment processes is highly contaminating and detrimental to the area in which it is deposited. Given this, the use of sludge with the application of reuse techniques becomes pertinent, both from the economic point of view and from the ecological point of view. By replacing the use of aggregates from mineral deposits, the main clay raw material in the manufacture of ceramic products (Vieira, 2000), by the treated sludge of WWTP we will save on the sources of granular materials. Aiming its reintegration to the production cycle through the introduction of sludge as raw material incorporated in the ceramic mass in the manufacture of hollow bricks, the viability of use was verified through performance analysis, compared to the control brick made of pottery, without the addition of sludge. Specimens were prepared with three types of samples: 90% clay and 10% sludge; 80% clay and 20% sludge; 70% clay and 30% sludge. Mass loss, water absorption index and compressive strength tests were performed. As for the tests, the specimens with 10% and 20% of sludge were the ones that had better adaptation to the technical requirements, but because it is a larger volume of the residue for the application of reuse techniques, the brick with 20% sludge dosage. is the most suitable. NBR7.171, November 1992: Ceramic Block for masonry; Specification NBR 6.461, June 1983: Masonry Ceramic Block - Compressive Strength Check: Test Method; NBR 8.947, November 1992: Ceramic Tile- Determination of Mass and Water Absorption: Test Method.

Downloaded from www.periodico.tchequimica.com

As for the tests, the specimen with 20% of sludge was the one that had the best adaptation to technical and environmental requirements. The present article approaches a possible solution regarding the destination of the sludge coming from Sanitary Sewage Treatment Stations, aiming at environmental preservation. Aiming at its reintegration into the productive cycle through applications of reuse techniques, the sludge became raw material when the ceramic mass was incorporated into the brick fabrication. Three types of samples were elaborated: 90% of clay and 10% of mud; 80% clay and 20% sludge; 70% clay and 30% sludge. As for the tests, the test specimen with 20% of sludge was the one that had more adequacy to the technical and environmental requirements.

Keywords: *Sludge (S.T.P.); Waste processing; Ceramic bricks*.

1. INTRODUÇÃO

O Resíduo sólido, denominado lodo, oriundo das etapas dos tratamentos oferecidos pelas Estações de Tratamento de Esgoto (ETE) é um subproduto dos processos realizados para retirar as cargas poluentes dos esgotos, processos esses, que podem ser físicos, químicos ou biológicos. Em ato contínuo, o efluente é devolvido aos corpos de água receptores como produto final, efluente tratado, em conformidade com os parâmetros, padrões e diretrizes exigidas pelo Conselho Nacional do Meio Ambiente (CONAMA 430/2011). O lodo de esgoto é definido pela CONAMA (375/2006) como sendo uma fonte que potencializa a proliferação de vetores e moléstias, compostos orgânicos persistentes e patógenos em concentrações nocivas à saúde pública e ao meio ambiente, podendo conter poluentes tóxicos, fenóis e os chamados metais pesados em caso de despejos industriais. O resíduo sólido, pastoso, de natureza orgânica, proveniente do pós- tratamento segue para um leito de secagem dentro da própria ETE para o desaguamento, onde diminui de volume e consequentemente o custo com o transporte até um aterro sanitário.

Substituir parte dos agregados provenientes de jazidas minerais finitas pelo lodo, as fontes de materiais granulares estarão sendo poupadas. A exploração deliberada e sem controle pode haurir esse recurso estratégico para o desenvolvimento das atividades econômicas. De acordo com a NBR 9935 (ABNT, 2005) todo esse processo de exploração caracteriza-se por provocar a remoção da cobertura vegetal do local de exploração, causando impactos que podem muitas vezes ser irreversíveis para todo o ecossistema da região.

Visando à preservação ambiental através da aplicação de técnicas de reuso o lodo se tornará matéria prima ao ser incorporado à massa cerâmica, agregando valor a algo que até então gerava custos para ser dispensado.

A indústria cerâmica tem grande aceitação em agregar novos materiais em sua composição, uma alternativa promissora de disposição correta desse resíduo é a incorporação à massa cerâmica (ARAÚJO/2008). O lodo que pode ser adicionado ao processo de preparação da massa cerâmica para auxiliar na correção da umidade (ANDREOLI et al.,2006).

1.1 Referencial Teórico

1.1.1 *Tratamentos de Esgotamento Sanitário*

O efluente é constituído em média de 99,9% de água e 1% de sólidos, desses sólidos 75% é matéria orgânica em decomposição que proliferam microrganismos advindos de fezes humanas e dependendo da saúde da população, pode conter patógeno (NUVOLARI et al., 2011). Apesar da maior concentração do esgoto ser composto por água, ele é altamente contaminante, devido à matéria orgânica presente.

Segundo Azevedo Neto (1973) as águas pluviais com matéria orgânica, devido à lavagem das ruas e campos deveriam passar por um tratamento adequado antes de ser lançadas aos corpos de água, problema recorrente nos dias atuais em conformidade com o artigo de Pacheco Jordão (2015). Ele acrescenta que, apenas 54% da população Brasileira tem acesso às redes coletoras e 46% lançariam seus efluentes diretamente nos corpos de água. Nos períodos de maior índice pluviométrico, onde se esperaria que a qualidade das águas melhorasse ocorre o inverso, a qualidade das águas dos rios piora, pois com a deficiência na coleta e tratamento de esgoto, o carreamento de cargas poluidoras das ruas e campos, aumentam a carga difusa depositadas nas águas.

Von Sperling (2014), elucida sobre os processos de tratamentos de Esgotamento Sanitário, onde o efluente bruto, em ato contínuo passa por vários níveis de tratamento dependendo da qualidade do esgoto e da qualidade que se espera que esse efluente tenha

Downloaded from www.periodico.tchequimica.com

no após tratamento. O primeiro processo é o Tratamento Preliminar considerado físico, onde são retidos os sólidos grosseiros por meio de gradeamento. O segundo processo é o Tratamento Primário também considerado físico, que reduz uma parte significativa da matéria orgânica e sólidos sedimentáveis. Esse método tem eficiência também na remoção dos sólidos flutuantes, principalmente óleos e graxas. O terceiro tratamento é o Tratamento Secundário, onde é removida a matéria orgânica e os sólidos dissolvidos na massa líquida dos esgotos através de reações biológicas, realizadas por micro-organismos: bactérias, protozoários e fungos no processo aeróbio. No anaeróbio, essas reações são realizadas praticamente por apenas bactérias. O quarto tratamento denominado Tratamento Terciário, remove poluentes específicos (micronutrientes), outros poluentes que não foram retidos nos tratamentos primário e secundário, obtendo um tratamento de qualidade superior para os esgotos. Nesse tratamento, compostos como nitrogênio e fósforo são removidos através da desinfecção com adição de radiação ultravioleta, ozônio ou cloro.

De acordo com Maziviero (2011. 106p), com o progressivo aumento populacional, os problemas ambientais resultantes da geração de resíduos das atividades humanas exigirão ações que viabilizem o equilíbrio entre consumo e reuso. No caso do lodo de esgoto não é diferente, pois além do grande volume que exigirá cada vez maiores locais para descarte, existe ainda o problema ambiental, onde a ausência de um tratamento adequado causa sérios danos à área onde é depositado.

1.1.2 *Descarte do Resíduo Sólido gerado*

No Brasil, a CONAMA (resolução 375/2006), seção VIII, preconiza que a estocagem do lodo numa propriedade deve ser feita em local com declividade máxima de até 5%, com distância mínima de segurança de rios, poços, lagos, minas e afins que varia de 15 a 100m e por período máximo de 15 dias. Proíbe. Também que a estocagem seja feita diretamente sobre o solo. O manuseio e carregamento de caminhões na área de estocagem poderão ser feitos com pás carregadeiras de rodas ou retroescavadeiras com caçambas frontais (BRASIL, 2004).

Von Sperling (2001) afirma que, enquanto o lodo permanecer na unidade gerenciadora, ele deverá ser armazenado em local coberto para evitar encharcamento e diminuir o problema de odor. O local deve possuir piso de concreto armado ou asfalto impermeabilizado, de modo a evitar a infiltração do lodo no solo, deve possuir também estruturas de coleta de chorume e de águas pluviais.

Em conformidade com Ferreira et al. (1999), após o tratamento adequado por digestão aeróbia ou anaeróbia o lodo de esgoto pode ser enviado para aterros sanitários (exclusivos ou comuns); para áreas de landfarming, que consiste na degradação biológica do resíduo em uma camada superior, que é periodicamente revolvida para haver aeração; para incineração ou para reciclagem agrícola. A disposição oceânica foi descartada visto que, em países com maior avanço nas tecnologias de disposição de lodo, ela é uma prática totalmente proibida.

Consoante Andrade (1999) a técnica de landfarming, apesar de ser uma alternativa de menor custo, também exige grande disponibilidade de área semelhante à dos aterros.

Estima-se que no Brasil, as alternativas de reuso do lodo gerado nas Estações de Tratamento de Esgoto, seriam pouco utilizadas e teria sua destinação final nos aterros sanitários (WAKI/2016). O processo e a disposição final do lodo representam até 60% do custo operacional de uma ETE (VON SPERLING/2001). O que encarece a reutilização do lodo no que diz respeito à disposição final, são o transporte e o manejo, entretanto através de uma visão sistêmica e planejada é possível identificar os veículos e equipamentos mais adequados em cada etapa do processo, buscando um sistema logístico organizado e eficaz (GODOY/2013).

Nuvolari (2011, 43p) cita em sua obra, que a preocupação com o descarte correto do lodo de esgotos é algo relativamente recente no Brasil. Os processos que englobam a disposição final de 90% do lodo produzido no mundo são: incineração, disposição em aterros e caleação.

1.1.3 *Descontaminação e Reuso do lodo*

O processo de caleação consiste em misturar a cal virgem (CaO) em proporções que variam em função do peso seco do lodo, de modo a promover o aumento do pH numa reação exotérmica que inativa até 90% dos organismos patogênicos e acelera o processo de evaporação, podendo atingir temperaturas de até 80 ºC.

De acordo com os estudos desenvolvidos por Passamani (2001) a higienização do lodo anaeróbio através da caleação por cal virgem hidratada, com dosagens que variaram entre 10 a

Downloaded from www.periodico.tchequimica.com

60%, teores de sólidos totais da ordem de 30% e período de estocagem dos produtos correspondentes a 24 horas, observou-se que essas condições foram suficientes para inviabilizar 100% de ovos de helmintos presentes no lodo.

O tratamento térmico implica no aquecimento do lodo por um determinado período a fim de higienizar e estabilizar o insumo. A temperatura em que o lodo será submetido dispensa o tipo de fonte, sendo eficaz qualquer fonte energética. O método é bastante eficaz na inativação de helmintos, uma vez que as enzimas, que fazem parte da constituição dos microrganismos, diminuam ou percam totalmente sua capacidade funcional, devido à modificação de sua estrutura pelo efeito térmico. Ovos de helmintos e vírus quando inativados termicamente não se tornam viáveis novamente (Hay, 1996).

Em seus estudos Andreolli et al. (2000, 281-312p) obteve um grande êxito em reduzir de forma considerável ovos de helmintos, ao fazer uso de uma estufa, submetendo o lodo a uma temperatura de 80ºC por um período de 5 minutos. Em contrapartida Lima (et al., 2005) concluíram que, se aquecerem lodo por 10 minutos a uma temperatura de 70 ºC, haverá a eliminação quase que total dos ovos.

As ETE's como solução viável podem fazer uso do biogás produzido no sistema para a higienização térmica de todo o lodo produzido, alcançando a completa inviabilização dos ovos de helmintos.

> "No processo de desinfecção para reutilização do resíduo, a queima em fornos ou aplicação da cal são bastante onerosos, mas os benefícios ambientais justificam os custos do tratamento. O desenvolvimento de um trabalho que verifique a possibilidade de utilização do lodo como matéria prima alternativa na indústria cerâmica é uma pesquisa plausível devido aos resultados de pesquisas anteriores com a reutilização do lodo em materiais de construção ter sido satisfatórios [...]. O uso de lodos procedentes de ETE como matéria prima cerâmica pode ser uma alternativa viável, tanto econômica como técnica, reduzindo custos ambientais relacionados à disposição final desses materiais. Além disso, as operações inerentes à indústria cerâmica (fornos com altas temperaturas) fazem com que os riscos sanitários se reduzam ao mínimo (INGUNZA, 2008, p. 2)."

Diante disso, podemos deduzir que ao realizar a queima de tijolos cerâmicos com percentuais de lodo tratado com cal, a uma temperatura de 900º Celsius em altos fornos de uma olaria, pelo período de sete dias, ou com a utilização da Mufla pelo período de quatro horas, todos os contaminantes foram eliminados. Ressaltamos ainda, o processo de secagem em estufa, na qual foram submetidos pelo período de quarenta e oito horas.

1.1.4 *Características do Lodo*

Para implementar uma Estação de Tratamento de Esgotamento Sanitário é necessário fazer um estudo local, levando em consideração vários fatores para adotar o tratamento apropriado. Deve-se avaliar se a área é residencial ou industrial, investigar os hábitos da população, a situação econômica, social, pois todos esses fatores influenciam na composição do efluente bruto e na qualidade do lodo que será produzido no pós-tratamento. A característica do lodo depende da qualidade do esgoto e do processo de tratamento utilizado. O resíduo de esgoto em geral apresenta 40% de matéria orgânica, 4% de nitrogênio e 2% de fosforo; macronutrientes (N, P, K, Ca e Mg) e micronutrientes (Cu, Zn, Mn e Fe) e componentes tóxicos. Com base no peso seco, no Brasil o lodo é composto por sólidos voláteis, nutrientes [...] e a presença de metais pesados em maior quantidade (BETTIOL & CAMARGO/2006).

1.1.5 *Características da Argila*

As argilas em geral são caracterizadas pela alta resistência plástica quando se adiciona água na quantidade certa. São materiais terrosos naturais de granulometria fina. As argilas possuem em sua constituição os chamados argilominerais que são os silicatos hidratados de alumínio, ferro e magnésio. Além dos argilominerais, as argilas contêm outros elementos e minerais, tais como matéria orgânica, sais solúveis e partículas de quartzo, pirita, mica, calcita, dolomita e outros minerais residuais, podendo conter também, minerais não cristalinos ou amorfos. (SOUZA SANTOS, 1989).

De acordo com Vieira (2000) a argila é a principal matéria-prima utilizada na fabricação de

Downloaded from www.periodico.tchequimica.com

produtos cerâmicos, devido a sua alta plasticidade, a resistência mecânica após ser submetida a queima adequada, pela possibilidade da utilização de aplicações e técnicas simples e por ter grandes quantidades à disposição.

Souza Santos (1989) definiu que a argila plástica caulinítica ou em camadas mistas com matéria orgânica, óxidos e hidróxidos de ferro e alumínio, como sendo a mais indicada para a fabricação de blocos e tijolos maciços. As argilas com estas características são geralmente encontradas em margens de rios, lagos ou várzeas (CARVALHO et al., 2000).

1.1.6 *Incorporação do lodo a massa cerâmica*

De acordo com Andreoli (2001, 287p) a adição do lodo de esgoto de forma homogenia, após devida desinfecção seria uma matéria-prima de excelência na fabricação de produtos cerâmicos, como telhas, tubos, tijolos e lajotas. Sua utilização tem-se mostrado uma alternativa viável de destinação adequada. Ainda, segundo Andreoli (2001, 28p) o lodo é adicionado ao processo durante a etapa de preparação da massa cerâmica e auxilia na correção de umidade já que o lodo é um resíduo expansivo na presença de água, isso pode ser feito manualmente, com pás carregadeiras, ou em olarias mais tecnificadas, utilizando-se equipamentos apropriados.

De acordo com Campregher (2006), através de prensagem mecânica, a dosagem de 5% de lodo em base seca e utilizando temperaturas de 950°C, foram obtidos corpos-de-prova que atendem a legislação brasileira nos quesitos absorção, porosidade e resistência à compressão.

2. PARTE EXPERIMENTAL

2.1 Método de abordagem

O projeto de pesquisa tem como finalidade verificar a viabilidade do lodo oriundo do Tratamento de Esgotamento Sanitário através de uma análise de desempenho, ao ser incorporado a massa cerâmica na fabricação de tijolos e comparado ao tijolo testemunha fabricado pela Olaria, sem adição de lodo. Será feito um estudo de viabilidade em relação ao percentual que pode ser acrescido à massa cerâmica na busca por soluções, a fim de dar uma destinação ecologicamente correta para o resíduo. Realizado para fins experimentais o projeto proposto servirá de parâmetro para estudos mais complexos.

O experimento consistiu na fabricação de tijolos cerâmicos vazados, contendo 0%, 10%, 20%, 30% de lodo, com as dimensões de 8,8 x 7,1 x 3,5 mm, foram moldados utilizando-se uma prensa mecanizada em olaria e queimados em forno industrial tipo Hoffman. A fabricação dos corpos de prova seguiu os parâmetros de rotina da indústria cerâmica. Duas unidades de cada corpo de prova forma recolhidos ainda úmidos e encaminhados ao laboratório de materiais de construção da Faculdade Kennedy, para a realização de testes pertinentes e complementadores.

2.1.1 *Produção dos Corpos de Prova:*

a) Destorroamento das matérias-primas, conforme Figuras 03 e 04;
b) Determinação das quantidades de matérias-primas citadas no item 3.2;
c) Peso de cada mistura em balança digital para inferir se todas totalizaram 3.000g, conforme figura. 05;
d) Homogeneização das matérias-primas;
e) Modelagem mecanizada dos corpos de prova;
f) Verificação de peso e dimensões de todos os corpos de prova úmidos;
g) Secagem no tempo e em estufa;
h) Verificação do peso e dimensões de todos os corpos de prova secos;
i) Queima em forno Hoffman e Mufla;
j) Verificação de peso e dimensões de todos os corpos de prova queimados;
k) Ensaios pertinentes.

2.2 Coletas das Matérias-Primas

O lodo utilizado como matéria-prima na modelagem dos corpos de prova foi recolhido do leito de secagem de uma ETE, em forma de torrões secos, proveniente do tratamento anaeróbio UASB. O resíduo foi armazenado em caixa térmica, devidamente lacrada e identificada.

O subproduto utilizado no experimento foi submetido à desinfecção dentro da própria ETE com aplicação da cal. Para um manuseio seguro, foram utilizados equipamentos de proteção individual.

Foram utilizados dois tipos de argila, denominadas argila de várzea, uma rica em dióxido de ferro e outra rica em alumínio, ambas advindas do pátio da própria Olaria, onde foram moldados os corpos de prova.
Para a realização do ensaio de umidade foram

Downloaded from www.periodico.tchequimica.com

recolhidas amostras da argila e do lodo na aquosidade em que foram utilizados. Ambos foram embalados em saco plástico, identificados e encaminhados ao laboratório de materiais de construção da Faculdade Kennedy, para a realização dos devidos ensaios.

2.3 Destorroamento e Quantificação de Matéria-Prima a ser utilizada

Para a modelagem dos corpos de prova o lodo seco foi umedecido e destorroado manualmente e com a utilização de um misturador elétrico. A argila foi destorroada manualmente com a utilização de uma espátula. Todo o procedimento foi realizado em local apropriado, sem risco de ação de intempéries nas dependências da olaria.

2.4 Confecção dos Tijolos

Definido o percentual de lodo a ser acrescido em cada amostragem, às matérias-primas foram dosadas e pesadas para posterior modelagem dos tijolos em três dosagens de lodo, além dos tijolos sem adição de lodo chamado de tijolo-testemunha.

Os tijolos foram moldados com porcentagens diferentes de lodo totalizaram 3.000g de mistura de argila e lodo. As amostras continham: 2700g de argila e 300g de lodo; 2400g de argila e 600g de lodo; 2100g de argila e 900g e 100% de argila de 0% de lodo, a fim de realizar os testes pertinentes em que são submetidos os tijolos convencionais.

Homogeneizados e posteriormente moldados com a utilização de uma prensa mecanizada, denominada marombinha (equipamento com as mesmas funcionalidades da maromba utilizada na produção em larga escala de tijolos padrões) em caráter experimental, pois as dimensões dos corpos de prova não são padronizadas para a utilização na construção civil. Os tijolos úmidos foram pesados e medidos, para serem submetidos a ensaios posteriores.

Uma parte dos corpos de prova foi seca por um período de quatorze dias ao ar livre em pátio coberto na Olaria, e duas amostras com cada porcentagem de lodo incluindo os tijolos testemunhas, foram levadas ao laboratório de materiais de construção da Faculdade Kennedy, para serem secos com a utilização da estufa por um período de 24 horas a uma temperatura de 105º Celsius, a fim de eliminar toda a umidade das peças. Para certificar de que realmente os corpos de prova perderam toda a umidade, após a medição e pesagem, ambos foram novamente submetidos ao processo de secagem por mais 24 horas na estufa a mesma temperatura anterior, totalizando 48 horas. Após o período de secagem os tijolos foram pesados, medidos novamente confirmando a perda de umidade.

Todos os corpos de prova foram timbrados para determinar a dosagem de lodo em sua formulação. Número 01: 10% de lodo, número 02: 20% de lodo, número 03: 30% de lodo e o tijolo sem numeração: 0% de lodo.

A queima dos tijolos se deu de duas formas, a maios parte no forno industrial da indústria e os oito corpos de prova encaminhados ao laboratório foram queimados na Mufla. Os Tijolos que ficaram na Olaria foram queimados em forno industrial Hoffman, a uma temperatura de 900º. Célsius pelo período de sete dias, cujo resfriamento se deu no interior do próprio forno. Os tijolos que foram encaminhados ao Laboratório de química, foram queimados utilizando a Mufla. Em um primeiro momento, o equipamento foi manuseado periodicamente para variar a temperatura, a fim de observar se haveria alguma alteração relevante. Foram colocadas quatro unidades de corpos de prova, um de cada dosagem de lodo incluindo o testemunha. A queima durou quatro horas a temperaturas variáveis e o resfriamento se deu dentro da própria Mufla. No segundo momento os últimos quatro corpos de prova foram inseridos na Mufla e sujeitos a temperatura de 900º. C pelo período de uma hora e meia. O resfriamento também se deu dentro da própria estuda. Após a queima todos foram pesados e medidos.

2.5 Considerações para os Ensaios

Cada tijolo é considerado um corpo de prova. Dentre os tijolos fabricados, de forma aleatória foram escolhidos treze exemplares para a realização dos ensaios, respeitando o que preconiza a norma NBR 15270 (ABNT, 2005). Mesmo se tratando de tijolos fora dos padrões de dimensionamento comercial a norma foi respeitada.

2.6 Ensaio para Determinação do Percentual de Umidade do Lodo e da Argila

As amostras de lodo e argila, enviadas ao laboratório de materiais de construção da Faculdade Kennedy, conforme citado no item 3.1, foram destorroadas manualmente e inseridas em

Downloaded from www.periodico.tchequimica.com

cápsulas que foram pesadas anteriormente. De posse da tara das cápsulas foi registrado o peso de todas as amostras úmidas que foram secas na estufa por vinte e quatro horas. Passado o tempo de secagem todas as amostras foram pesadas novamente. Para certificar de que as amostras perderam toda a umidade, ambas foram submetidas a mais vinte e quatro horas de estufa e confirmado o peso seco.

As Tabelas 1 e 2 foram organizadas para demonstrar a quantidade de umidade contida em cada matéria prima utilizada na confecção dos corpos de prova. Além da umidade, de posse dos resultados da amostragem, podemos determinar com exatidão a quantidade de massa seca da argila e do lodo que foi utilizado na confecção dos corpos de prova. Esse estudo serve de parâmetro para novos experimentos, ao utilizar a massa seca de cada matéria-prima e dosar a umidade ideal para a confecção de corpos de prova.

2.7 Ensaio de Perda de Massa

Para o quesito perda de massa, não há normatização, mas mostra-se pertinente sua análise quanto à homogeneidade das matérias-primas. O percentual de perda de massa (PM) se dá pela Equação 1.

$$\boldsymbol{PM = \frac{Maq - Mdq}{Mdq}\ x\ 100} \qquad \text{(Eq. 1)}$$

Onde Maq é a massa do corpo de prova seco antes da queima e Mdq é a massa depois da queima.

2.8 Ensaio de Índice de Absorção de Água (AA)

A NBR 15270 (ABNT, 2005) item: 5.6 adverte que o índice de absorção não deve ser inferior a 8% nem superior a 22%.

No proposto estudo adotamos a metodologia de submergir os tijolos cerâmicos vazados já queimados em um tanque com água limpa e fria, pelo período de 24 horas. Lembrando que, os tijolos foram pesados antes de serem submergidos para a realização dos cálculos subsequentes referente à absorção de água.

Passado o tempo de imersão os tijolos foram retirados da água e reservados a fim de eliminar o excesso. O percentual de Absorção de Água (AA) é obtido pela Equação 2.

$$\boldsymbol{AA = \frac{Múmido - Mseco}{Mseco} x100} \qquad \text{(Eq. 2)}$$

Onde M úmido é o massa do tijolo saturado e a M seco é a massa do tijolo após a queima.

2.9 Ensaio de Resistência à compressão (RC)

As resistências à compressão dos blocos cerâmicos são normatizadas pela NBR15270 (ABNT, 2005), onde os resultados devem atender aos valores mínimos de ≥ 1,5 Mpa para ensaios na horizontal e ≥ 3,0 MPa para ensaios na vertical.

Os corpos de prova forma capeados com argamassa no traço de 1x1, utilizando areia lavada fina peneirada, cimento CPV ARI e água o suficiente. Uma placa metálica plana foi untada com óleo para evitar que a argamassa grudasse na placa. Em seguida a argamassa foi espalhada sobre a placa e os tijolos assentados na horizontal. Passados vinte e quatro horas os tijolos foram descolados da placa e repetido o capeamento no outro lado das peças. Após o endurecimento da pasta de argamassa os corpos de prova foram imersos em um tanque contendo água fria pelo período de vinte e quatro horas.

Pouco antes do ensaio, os corpos de prova foram retirados do tanque e superficialmente enxugados.

A Resistência à compressão é dada pela Equação 3, onde F é a Forca de ruptura observada no equipamento para o rompimento do corpo de prova, em Kgf, e Āp é a média das áreas das duas faces do corpo de prova cerâmico, em centímetro quadrado. Ao efetuar a equação se obtém a tensão de ruptura. A unidade de medida pode ser expressa em Mpa (Mega Pascal)

$$\boldsymbol{RC = \frac{F}{\bar{A}p}\ x\ 100} \text{ (Eq. 3)}$$

3. Resultados e discussões

3.1 Avaliação dos Tijolos quanto aos Aspectos Físicos

A Tabela 3 expõe uma ementa quanto aos aspectos dos tijolos com adição de lodo em comparação ao tijolo-testemunha.

Em comparação ao tijolo testemunha, os tijolos com percentual de lodo tiveram alteração de odor apenas na fase úmida. Quanto à deformação, apenas algumas peças com porcentagem de 30% apresentaram arestas

Downloaded from www.periodico.tchequimica.com

quebradas e fissuras superficiais, o que leva a deduzir que houve uma homogeneidade irregular. Os tijolos que queimaram no forno industrial por uma semana, a uma temperatura de 900ºC e na Mufla com variação de temperatura pelo período de quatro horas, queimaram de forma regular não apresentando alteração de cor e nem patologias. Os tijolos queimados na Mufla a uma temperatura de 900º Celsius pelo período de uma hora e trinta minutos apresentaram fissuras. Em relação ao peso e dimensões não houve nenhuma variação significativa. Observou-se que a variação aconteceu de acordo com o percentual de lodo adicionado a massa.

3.2 Avaliação dos Tijolos quanto a Dimensão

A Tabela 4 demonstra as médias das dimensões dos tijolos, considerando que a dimensão do tijolo testemunha é de 88x70x35 mm. Em destaque estão os valores que extrapolaram a variação máxima permitida pela NBR 15270/2005 (3 mm para mais ou para menos).

Neste parâmetro os tijolos com 10% de lodo foram reprovados, pois apresentaram variação de comprimento superior ao limite estabelecido pela norma. Esse resultado é um indicativo de que o lodo não tem influência significativa na variação dimensional dos tijolos, o que implica que essa variação se deu devido ao método de fabricação, que não foi padronizado. O método apesar de mecanizado apresentou variações no momento do corte.

3.3 Avaliação dos Tijolos quanto a Perda de Massa

O Gráfico 1, demonstra a massa dos tijolos após a queima em comparação com o tijolo testemunha. A perda de massa é determinada pela variação de dosagens do lodo.

Analisando o gráfico podemos constatar que os tijolos com 10 e 20% de lodo são estatisticamente semelhantes e que a perda de massa está relacionada à adição de lodo que é um resíduo leve, que torna o tijolo mais fácil de ser manuseado o que não implica em variação dimensional. Um menor peso está relacionado com menor densidade resultando em melhor isolamento acústico e maior economia no projeto estrutural.

3.4 Avaliação dos Tijolos quanto a Absorção de Água (AA)

O Gráfico 2 representa a média de Absorção de água dos tijolos fabricados com diferentes dosagens de lodo.

O gráfico mostra uma relação diretamente proporcional entre o aumento da dosagem de lodo e o aumento da Absorção. De acordo com a norma, a absorção de água deve estar entre 8 e 22%. Sendo assim, apenas os tijolos com 30% de lodo não foram reprovados.

Analisando as amostragens em conformidade com a norma os tijolos testemunhas e os com percentuais de lodo com dosagem de 10 e 20%, foram aprovados. A absorção dos tijolos é distinta entre si. Isto implica que há realmente um incremento significativo da absorção quando ao aumento da dosagem de lodo.

4.5 Avaliação dos Tijolos quanto Resistência a Compressão (RC)

Os resultados obtidos na prensa representam a Força de Ruptura em kgf (Quilograma-força). Utilizando a fórmula do item 3.9, encontrou-se a Resistência a Compressão em Mpa (Mega Pascal).

Os valores de Resistência à Compressão dos corpos de prova com percentuais de lodo foram diferentes dos tijolos testemunhas. Os resultados obtidos pelos tijolos com adição de 10%, 20% e 30% de lodo foram diferentes entre si e estatisticamente próximos ou maiores em comparação aos tijolos testemunhas. Isto significa que houve uma redução insignificante da resistência dos tijolos quanto ao aumento da dosagem de lodo, sendo assim os tijolos com 10 e 20% de lodo em sua composição alcançaram os maiores valores de resistência à compressão.

O Gráfico 3 apresenta a variação de resistência dos tijolos em porcentagens. Constatou-se que, apenas os tijolos com 30% de lodo perderam 13% de resistência, os tijolos com dosagem de 10 e 20% de lodo tiveram um percentual de RC acima do tijolo testemunha, respectivamente 45 e 54%.

4. CONCLUSÃO

Em relevância a todos os ensaios realizados e em comparação com o Tijolo testemunha, cujo percentual é de 0% de lodo, constatou-se que: os tijolos não tiveram alteração de odor após a queima; em nenhuma das dosagens constatou-se variações de dimensões consideráveis; os tijolos com 30% de lodo apresentaram fissuras superficiais; os tijolos encaminhados ao laboratório, que passaram pela queima na Mufla a 900º Celsius pelo período de

Downloaded from www.periodico.tchequimica.com

uma hora e trinta minutos apresentaram fissuras em todas as dosagens de lodo e os com queima na Mufla com variações de temperatura entre 700 e 900 ºC pelo período de quatro horas, não apresentaram nenhuma deformação visual; todos os tijolos apresentaram boa resistência mecânica; a adição de lodo não acarretou em perda significativa na massa dos tijolos; a absorção de água está diretamente ligada à dosagem de lodo; os tijolos fabricados com lodo em todas as dosagens absorveram mais água do que o tijolo-testemunha, mas se mantiveram no parâmetro de tolerância; a resistência à compressão foi significativamente aumentada com a adição de lodo nos tijolos de 10 e 20% em comparação ao tijolo testemunha.

Para as condições especificadas neste experimento pode-se concluir que, as dosagens máximas que podem ser incorporadas a massa cerâmica na fabricação de tijolos vazados atendendo aos requisitos técnicos são de 10 e 20% de lodo.

Diante da necessidade de utilizar um volume maior do resíduo, a fim destina-lo de forma ecologicamente correta com aplicação das técnicas de reuso, o tijolo com dosagem de 20% de lodo é o mais indicado.

Em relação às normas ambientais, devido à dificuldade operacional para a realização de análises laboratoriais, visando à determinação de concentrações de metais pesados nas amostras, não classificaremos nos requisitos referentes à classe de periculosidade descrito na NBR10006 (ABNT, 2004c), mas estudos realizados demostraram que os tijolos maciços após a queima, em caso de demolição estão inseridos na classe II A- não perigosos e inertes (DUARTE/2008).

5. REFERÊNCIAS:

1. NBR 7170/83-Tijolo maciço cerâmico para alvenaria–Especificação. Rio de Janeiro: ABNT, 1983b. 4p.
2. NBR 15270-1 2005 – bloco vazado cerâmico para alvenaria – Especificação. Rio de janeiro: ABNT, 1983b. 4p.
3. NBR 6.461, de junho de 1983: Bloco Cerâmico para Alvenaria - Verificação da resistência à compressão: Método de ensaio.
4. NBR 8.947, de novembro de 1992: Telha Cerâmica- Determinação da massa e da Absorção de Água: Método de Ensaio.
5. NBR 7171 – Bloco Cerâmico para Alvenaria – Especificação. Rio de Janeiro: ABNT, 1992. 8 p.
6. ANDRADE NETO, C. O.; ALEM SOBRINHO, P.; MELO, H. N. S.; AISSE, M. M. Decanto-digestores. 117-138 p. In: CAMPOS, J. R. (coord.) Tratamento de esgotos sanitários por processo anaeróbio e disposição controlada no solo. 1. ed. Rio de Janeiro: ABES, 1999. 464 p.
7. ANDREOLI, C.V. et al. Gestão pública do uso Agrícola do lodo de esgoto. In: BERTOL, W. & CAMARGO, O. A. Impactos ambientais de uso agrícola do lodo de esgoto. Jaguariúna, São Paulo: EMBRAPA Meio ambiente, 2000. 281-312p.
8. ANDREOLI, C.V. et al. Alternativas de uso de resíduos do saneamento. Rio de Janeiro: Abes, 2006. 417 p.
9. ANDREOLI, C. V.; PINTO, M. A. T. Introdução. In: ANDREOLI, C. V. Resíduos sólidos do saneamento: processamento, reciclagem e disposição final. Rio de Janeiro: Rima Artes e Textos, 2001. 287 p. (Programa de Pesquisa em Saneamento Básico – PROSAB, 2).
10. ARAÚJO, F. S. D. Influência do lodo de ETE na massa para fabricação de massa vermelha. 2008. 76f. Dissertação (Mestrado em Engenharia de (Materiais)-Centro de Ciências exatas e da Terra, Universidade Federal do Rio Grande do Norte, Natal, 2008).
11. ASSOCIACAO BRASILEIRA DE NORMAS TECNICAS – ABNT. NBR 6460/83 -Tijolo maciço cerâmico– Verificação da resistência à compressão– Método de ensaio. Rio de Janeiro: ABNT, 1983 a. 3p.
12. BETTIOL, W. ; CAMARGO, O. A. A (coord.). Lodo de esgoto: Impactos ambientais na Agricultura. Jaguariúna: Embrapa Meio Ambiente, 2006. Disponível em: www.jaguariuna.cnpm.embrapa.br/ Acesso em: 18 dez.2016.
13. CAMILO GODOY, C. A logística na destinação do lodo de esgoto. São Paulo: Revista Científica Online-Tecnologia-Gestão-Humanismo-ISSN 2238-5819 Disponível em:< https://www.a+logística+na+destinação+do+lodo+de+esgoto> Acesso em 01 jan.2017.
14. CAMPREGHER, N. Estudo da viabilidade da incorporação do lodo da Estação de Tratamento de Efluentes da indústria de papel, celulose e aparas em material

Downloaded from www.periodico.tchequimica.com

cerâmico. Florianópolis, 2006. Dissertação (Mestrado em Engenharia Química). UFSC. Disponível em: http://livros01.livrosgratis.com.br/cp102787.pdf Acesso em: 12 mar. 2017.
15. CARVALHO, O. O.; SOUZA, L. C.; REGO, J. M.; LEITE, J. Y. P. Perfil da Indústria de Cal no Rio Grande do Norte. Relatório: FIERN/SENAI. Natal, 2000. CD-ROM COPASA (companhia de Saneamento de Minas Gerais) – métodos de tratamento do efluente bruto. Disponível em: <http://.copasa.com.br/media2/PesquisaEscolar/COPASA_Esgoto.pdf> Acesso em: 18 ago. 2016.
16. CONSELHO NACIONAL DO MEIO AMBIENTE – CONAMA. Resolução n°375/2006. Define critérios e procedimentos, para o uso agrícola de lodos de esgoto gerados em estações de tratamento de esgoto sanitário e seus produtos derivados, e dá outras providências. Disponível em: < http://www.mma.gov.br/port/conama/res/res06/res37506.pdf>. Acesso em 28 jun. 2016.
17. CONSELHO NACIONAL DO MEIO AMBIENTE – CONAMA. Resolução n°430/11, alterando parcialmente e complementando a Resolução no 357, de 17 de março de 2005. Art. 1□. Dispõe sobre condições do lançamento de efluentes em corpos de água receptores. Disponível em: <http://www.mma.gov.br/port/conama/legiabre.cfm?codlegi=646>. Acesso em: 18 ago. 2016
18. Duarte, A. da C. L. incorporação do lodo de esgoto a massa de cerâmica para fabricação de tijolos maciços: uma alterativa para disposição final do resíduo. Natal/RN, 2008. Dissertação (mestrado). Programa de Pós-Graduação em Engenharia Sanitária. Universidade Federal do Rio Grande do Norte. Disponível em: file:///C:/Users/Sony/Downloads/Dissertacao_Anaxsandra%20Lima%20Duarte%20(1).pdf> Acesso em: 28 ago. 2016.
19. DURANTE-INGUNZA, M. P.; ANDREOLI C. V, NASCIMENTO, R. M.; TINOCO, J.D.; HOPPEN, C.; PEGORINI, E. S. Uso de resíduos do saneamento na fabricação de cerâmica vermelha. 283-359 In: Andreoli C. V (coord.) Alternativas de Uso de Resíduos do Saneamento. Rio de Janeiro: ABES 2006. 471 p.
20. ENVIRONMENTAL PROTECTION AGENCY - EPA. Biosolids technology fact sheet: centrifuge thickening and dewatering. Washington, DC.: Environmental Protection Agency, Sept. 2000. 8 p.
21. FERREIRA, A. C.; ANDREOLI, C. V.; JURGENSEN, D. Produção e características dos biossólidos. 17-25 p. In: ANDREOLI, C. V.; LARA, A. I. (org.) Uso e manejo do lodo de esgoto na agricultura. Rio de Janeiro: PROSAB, 1999. 97 p.
22. INGUNZA, M. P. D. et. al. Uso de lodo de ETE como matéria prima para fabricação de tijolos na região Açu/RN/Brasil. Universidade Federal do Rio Grande do Norte, Natal, [2008]. Disponível em: www.bvsde.paho.org/bvsaidis/uruguay30/BR05431_Durante_Ingunza.pdf Acesso em: 11 jan. 2017.
23. LIMA, E. P. C. et al. Estudo da termo resistência de ovos de helmintos, coliformes Termotolerantes e Encherichia Coli. In 23º. CONGRESSO BRASILEIRO DE ENGENHARIA SANITARIA E AMBIENTAL, 2005 Anais, Campo Grande/MS, 2005. Revista Eletrônica de Gestão e Tecnologia Ambiental. Disponível em:< file:///C:/Users/Sony/Downloads/8792-34688-1-PB.pdf > Acesso em: 28 ago. 2016.
24. MAZIVIERO, G.T. Avaliação do potencial citotóxico, genotóxico e mutagênico de lodo de esgoto por meio dos sistemas – teste allium cepa e tradescantia pallida. 2011. 106f. Dissertação (Mestrado em Ciências Biológicas). UNESP/Rio Claro/SP/2011.
25. MOTTA, J. F. M; ZANARDO, A; CABRAL JR, M. As Matérias-primas Cerâmicas. Parte I: O Perfil das Principais Indústrias Cerâmicas e Seus Produtos. Cerâmica Industrial. 6 (2): 28-39p., 2001
26. NUVOLARI, A. et al. Esgoto sanitário: coleta, transporte, tratamento e reuso agrícola. 2ª ed. Revista, atualizada e ampl.-São Paulo: Blucher, 2011. 43p.
27. PEREIRA, K.L.A. Estabilização de um solo com cimento e cinza de lodo para uso em pavimentos. 2012. 102f. Dissertação (Pós-Graduação em Engenharia Civil). UFRN/Natal/RN/2012.
28. HAY, J. C. Pathogen destruction na biosolid composting. BioCycle, Emmaus, v. 37, n. 6, p.67-76, jun 1996. HAYS, B. D.

Downloaded from www.periodico.tchequimica.com

Potential for parasitic disease transmission with land application of sewage.
29. SOUZA SANTOS, P. Ciência e tecnologia de argilas. 2. ed. São Paulo: Edgard Blucher Ltda., 1989. 499 p.
30. PASSAMANI, F. R. F.; GONÇALVES, R. F. Higienização de lodos de esgotos. In: GONÇALVES, R. F. (coord.). Gerenciamento do lodo de lagoas de estabilização não mecanizadas. Rio de Janeiro: PROSAB/ABES, 1999, cap. 7, p.63-67.
31. PATRICK LWAKI, G. PORTAL DE TRATAMENTO DE ÁGUA. Destinação final de Disponível em: <tratamentodeagua.com. br/artigo/destinacao-final-de-lodos-de-etas-e-etes>. Acesso em 20 ago.2016.
32. VIEIRA, C. M. F.; HOLANDA, J. N. F. de; PINATTI, D. G. Characterization of red ceramic body used in the production of bricks in the region of Campos dos Goytacazes - RJ. Cerâmica 46(297), 2000. Disponivel em:<http://www.scielo.br/scielo.php?script=sci_arttext&pid=&lng=en&nrm=iso>. Acesso em 20 de junho de 2007.
33. VON SPERLING, M. Lodo de esgotos: tratamento e disposição final. Belo Horizonte: Departamentob de Engenharia Sanitária e Ambiental – UFMG; Companhia de Saneamento do Paraná, 2001. 484p.
34. VON SPERLING, M. Introdução à qualidade das águas e ao tratamento de esgotos. Belo Horizonte: Departamento de Engenharia Sanitária e Ambiental – UFMG; 2014. 264-327p.
35. SILVA, M. O. S. A. Manual de operação da ETE Arrudas. Belo Horizonte: Companhia de Saneamento de Minas Gerais – COPASA, 2002. 7 v.

Figura 1. Lodo recolhido do leito de secagem

Figura 2. Argila recolhida do pátio da olaria

Figura 3. Destorroamento do lodo

Figura 4. Destorroamento da argila

Downloaded from www.periodico.tchequimica.com

Figura 5. 90% de Argila-2.700g

Figura 6. Maromba utilizada na produção da Indústria

Figura 7. Marombinha

Figura 8. Modelagem mecanizada dos tijolos

Figura 9. Pesagem dos corpos de prova

Figura 10. Tijolos moldados

Figura 11. Corpo de prova timbrado- 10% de lodo

Figura 12. Tijolos na Estufa para serem secos

Downloaded from www.periodico.tchequimica.com

Figura 13. Tijolos secos dos na Estufa

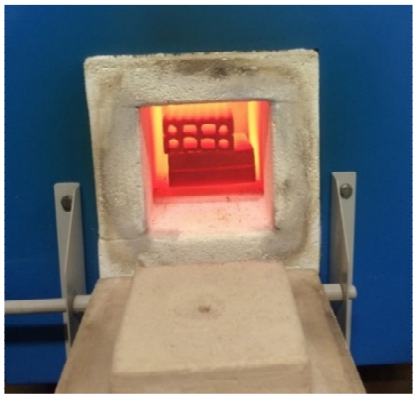

Figura 14. Tijolos queimados na Mufla

Figura 15. Tijolos queimando no forno industrial

Figura 16. Tijolo após a queima sendo medido

Figura 17. Tijolo após a queima sendo pesado teste

Figura 18. Amostra de Argila para realização de

Figura 19. Amostra de lodo para realização de teste

Figura 20. Cápsulas numeradas com amostras

Figura.21-Tijolo pesado antes da queima

Figura 21. Tijolo pesado antes da queima

Figura.22-Tijolo pesado após a queima

Figura 22. Tijolo pesado após a queima

Figura 23. Tijolo imerso em água por 24 horas

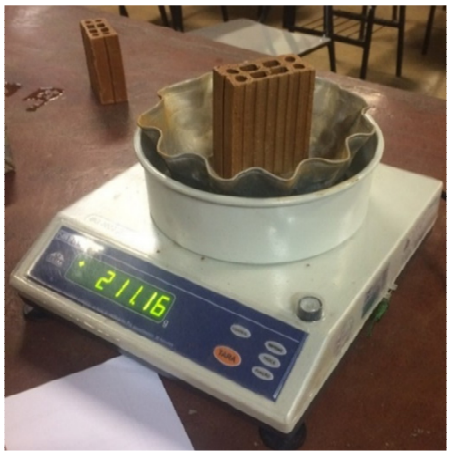

Figura 24. Peso do tijolo após imersão em água por 24 horas

Figura.26-Preparo da argamassa

Figura 25. Preparo da argamassa

Figura.27-Capeamento

Figura 26. Capeamento

Figura 27. Capeamento em ambas as faces

Figura 28. Capeamento dos tijolos em uma face

Figura 29. Pressa utilizada para romper corpos de prova ***Figura 30.***Corpo de prova sendo comprimido

Figura 32. Corpo de prova rompido

Tabela 1. Determinação do Teor de Umidade do Lodo

Teor de Umidade				
Determinação	Nº.	01	02	03
Cápsula	Nº.	85	54	84
Peso bruto úmido	g.	22,04	25,95	24,91
Peso bruto seco	g.	14,90	16,59	16,24
Peso da água	g.	7,14	9,36	8,67
Tara da cápsula	g.	9,58	9,79	9,87
Peso do solo seco	g.	5,32	6,80	6,37
Teor de umidade	%	134,21	137,65	136,11
		Média de umidade: 135,99%		

Fonte: Dados coletados a partir da realização dos ensaios.

Tabela 2. Determinação do Teor de Umidade da Argila

Teor de Umidade				
Determinação	Nº.	01	02	03
Cápsula	Nº.	40	55	41
Peso bruto úmido	g.	29,62	28,94	25,50
Peso bruto seco	g.	24,30	23,86	21,05
Peso da água	g.	5,32	4,63	4,45
Tara da cápsula	g.	7,36	9,49	7,51
Peso do solo seco	g.	16,94	14,37	13,54
Teor de umidade	%	31,40	32,22	32,87
		Média de umidade: 32,16%		

Fonte: Dados coletados a partir da realização dos ensaios.

Tabela 3. Características dos tijolos de acordo com a dosagem de lodo

Características/aspectos	Dosagem de lodo em porcentagem		
	10%	20%	30%
Arestas, fissuras	1	1	2
Coloração	1	1	1
Queima homogenia	1	1	1
Facilidade de corte	1	1	1
Homogeneidade da massa	1	1	1
Odor – tijolo úmido	2	2	2
Odor – tijolo seco	1	1	1
Odor – tijolo queimado	1	1	1
Peso	2	2	2
Regularidade na forma	1	1	1

Legenda: *1 - semelhante ao TT; 2 - pequena alteração; 3 - grande alteração; 4 - deformação completa.*

Fonte: Tabela formulada pela própria autora, mediante análise estética dos corpos de prova 2017.

Downloaded from www.periodico.tchequimica.com

Tabela 4. Variações das dimensões dos tijolos.

Tijolos	Δ comprimento (mm)	Δ largura (mm)	Δ espessura (mm)
Testemunha 1	0	0	0
Testemunha 2	0	0	0
10% de lodo	5	0	2
20% de lodo	1	0	1
30% de lodo	2	1	1

Fonte: Tabela formulada pela própria autora, mediante análise estética dos corpos de prova 2017.

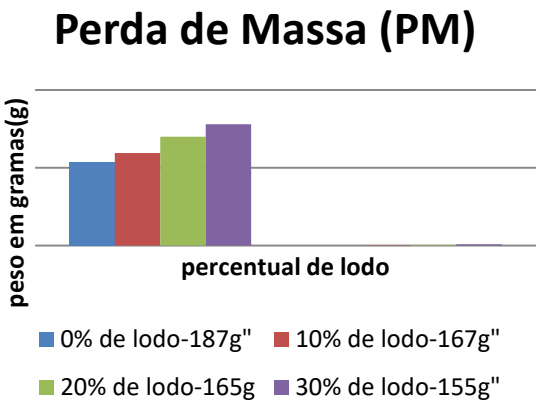

Gráfico 1: Perda de massa dos tijolos após a queima - percentuais de 0% de lodo, 10% de lodo, 20% de lodo e 30% de lodo .

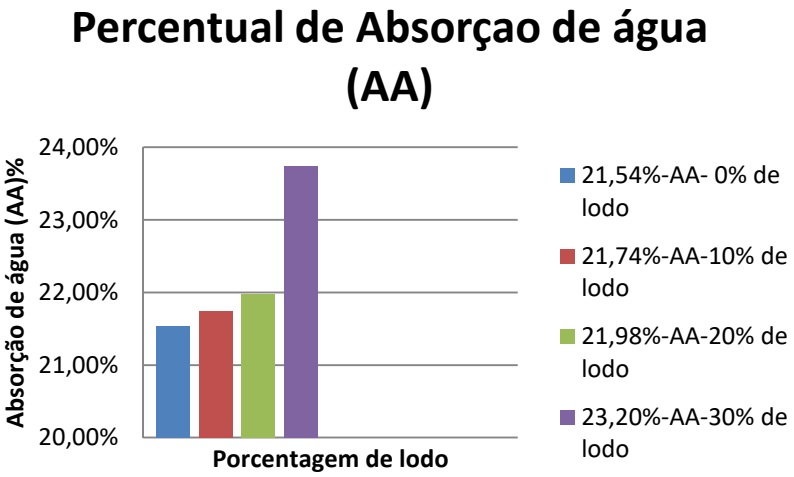

Gráfico 2 Percentual de absorção de água dos tijolos, após imersão em água.

Downloaded from www.periodico.tchequimica.com

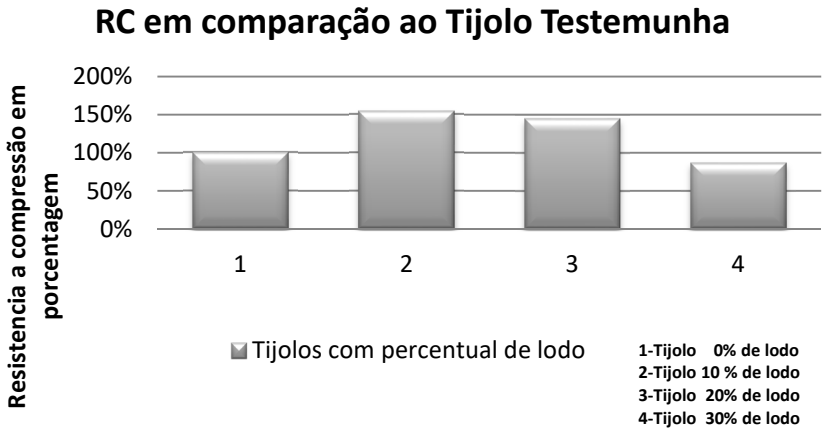

Gráfico 3. Aumento da Resistência a Compressão dos tijolos com 10 e 20% de lodo em relação ao tijolo testemunha.

Downloaded from www.periodico.tchequimica.com

PERIÓDICO TCHÊ QUÍMICA
ARTIGO ORIGINAL

RUMO À REDUÇÃO DO ESFORÇO COMPUTACIONAL NAS PREDIÇÕES DE VIBRAÇÕES INDUZIDAS POR VÓRTICES DE UM RISCADOR CILÍNDRICO

TOWARDS REDUCING COMPUTATIONAL EFFORT IN VORTEX INDUCED VIBRATION PREDICTIONS OF A CYLINDRICAL RISER.

VIDYA, Chandran[1]; SHEEJA, Janardhanan[2]; SEKAR, M[3*];

[1]Department of Mechanical Engineering, Karunya Institute of Technology and Sciences, Tamil Nadu, India

[2]Department of Mechanical Engineering, SCMS School of Engineering and Technology, Kerala, India

[3]Department of Mechanical Engineering, AAA College of Engineering and Technology, Tamil Nadu, India

** Correspondence author*
e-mail: mailtosekar@gmail.com

Received 23 August 2019; received in revised form 30 October 2019; accepted 18 November 2019

RESUMO

As vibrações induzidas pelo fluxo geralmente denominadas vibrações induzidas por vórtices são de grande importância no projeto de *risers* marinhos. Esses *risers* cilíndricos flexíveis sofrem vibrações de amplitude muito alta quando a frequência de derramamento de vórtice corresponde à frequência natural do riser. Tais vibrações são capazes de colocar a segurança da tripulação trabalhando em plataformas *offshore* em questão. Portanto, a previsão de resposta de tais estruturas é considerada muito importante. Embora muito trabalho numérico tenha sido feito neste campo, tratando o problema como uma interação fluido-estrutura bidirecional, o fato de esses trabalhos exigirem esforços computacionais muito altos não o tornou pertinente quando os recursos computacionais de ponta não estão prontamente disponíveis. Uma rápida previsão da resposta estrutural de tais estruturas esbeltas precisa ser útil para os engenheiros em momentos de necessidade. Este artigo aborda uma técnica de solução para esse problema através de um método econômico para previsão rápida e confiável da resposta do riser sob vibração induzida por vórtice, utilizando o esforço computacional mínimo para o número moderado de Reynolds (Re 3 x 10^5). As simulações de fluxo bidimensionais são realizadas usando CFD baseado em RANSE, seguido pelo mapeamento uniforme das forças hidrodinâmicas no *riser* tridimensional. A grade usada para a simulação numérica foi validada com relação aos resultados experimentais do túnel de vento para Re = 5,3 x 10^4. As forças hidrodinâmicas correspondentes aos três primeiros harmônicos da frequência natural do *riser* foram usadas como entrada no solucionador estrutural para analisar o resposta usando o método dos elementos finitos. Obtiveram-se trajetórias do cilindro nos três primeiros modos de vibração, um padrão típico de oito algarismos, característico da vibração de bloqueio. Verificou-se que o método é bastante eficaz no cálculo rápido de problemas de vibração induzidos por fluxo para números de Reynolds baixos e moderados.

Palavras-chave:*CFD; cilindros de fluxo passado; lock-in; resposta estrutural; vibrações induzidas por vórtices*

ABSTRACT

Vibrations induced by flow, generally referred to as vortex induced vibrations, are of great importance in the design of marine risers. These flexible cylindrical risers undergo vibrations of very high amplitude when the vortex shedding frequency matches the natural frequency of the riser. Such vibrations are capable of putting the safety of crew working on offshore platforms in question. Hence the prediction of response of such structures is considered very important. Although a lot of numerical work has been done in this field treating the problem as a two-way fluid structure interaction, the fact that these works demand very high computational efforts has not made it pertinent where high end computing resources are not readily available. A quick prediction of the structural response of such slender structures needs to be handy to the engineers at times of need. This paper addresses a solution technique for such a problem through an economical method for quick and reliable prediction of riser response under vortex induced vibration utilizing minimum computational effort for moderate Reynolds number (Re $\leq$ 3 x 10^5). Two dimensional flow simulations are carried out using RANSE based CFD followed by the uniform mapping of hydrodynamic forces on to the three dimensional riser. The grid used for the numerical simulation has been well validated against wind-tunnel experimental results for Re= 5.3 x 10^4. Hydrodynamic forces corresponding to the first three harmonics of natural frequency of the riser have been used as input in the structural

Downloaded from www.periodico.tchequimica.com

solver to analyse the response using finite element method. Trajectories of the cylinder in the first three modes of vibration have been obtained, a typical eight figure pattern which is characteristic for lock-in vibration. It is found that the method is quite effective in the quick computation of flow induced vibration problems for low and moderate Reynolds numbers.

Keywords: *CFD;flow past cylinders; lock-in;structural response;vortex-induced-vibrations*.

1. INTRODUCTION

Vortex shedding around bluff bodies is natural yet a phenomenon that consumed years of comprehensive studies, for it is well known for the imminent catastrophes it brings with it. Tacoma Narrows Bridge disaster is the worst case one could recall while thinking about vortex shedding. With the ever-rising demand for petroleum products, the development of offshore oilfields has been growing fast over the past century. The drilling facilities are designed in such a way that it enables a prolonged offshore operation for a large period of time starting from a few months to several decades. Numerous studies are being carried out in this field for the proper design of the slender marine risers in ocean. The stability of structures especially those carrying pressurised fluid in them is a topic of research interest. (Ramírez*et al*. 2017, Pezzini, *et al*., 2017) If the bluff structure is not mounted rigidly and the frequency of vortex shedding matches the natural frequency of the structure, the structure begins to resonate, vibrating with harmonic oscillations of large amplitude (Bourguet, 2011). This phenomenon is known as lock-in. During lock-in, vortex shedding frequency shifts to the natural frequency of the structure leading to large amplitude vibrations.

The vortex shedding occurs at a discrete frequency and is a function of the Reynolds number, defined by Equation 1.

$$\mathrm{Re} = \frac{\rho V D}{\mu} \qquad \text{(Eq. 1)}$$

The dimensionless frequency of the vortex shedding, the shedding Strouhal number, $St = f_v D/V$, is approximately equal to 0.2 when the Reynolds number is greater than 1,000. When vortices are shed from the cylinder, uneven pressure distribution develops around the upper and lower surfaces of the cylinder, generating an oscillatory hydrodynamic loading (lift) on the cylinder. This unsteady force given by Equation 2 can induce significant cross flow vibrations on a structure, especially if the "resonance" condition is met.

$$F_L = \frac{1}{2} C_L \rho A V^2 \qquad \text{(Eq. 2)}$$

C_L is the coefficient of lift. The cylinder also experiences a net force along the flow direction and is called the drag force and is given by Equation 3.

$$F_D = \frac{1}{2} C_D \rho A V^2 \qquad \text{(Eq. 3)}$$

where C_D is the drag coefficient.

The phenomenon of lock-in was first observed by Feng during his classical experiment (Feng, 1968). He described the phenomenon observed as matching the frequency of cylinder vibration and fluid force to the natural frequency in a vacuum. Later it was observed that this matching of frequency holds good only for higher values of mass ratio, m*(Blevins, 1990). Further research in the field explains the phenomenon as either large amplitude vibration of the cylinder (Sarpkaya, 1977)or matching of the frequency of cylinder vibration and fluid force (Khalak and Williamson, 1999). Synchronization and lock-in, are often used synonymously, but from the experiments it was shown that, for zero damping and sinusoidal motion, synchronization ($f = f_n$) occurs at only one condition, effective stiffness ratio, $k^*_{eff} = 0$ (Sheils *et al.*, 2001), where k^*_{eff} is defined as in Equation 4.

$$k^*_{eff} = \frac{m^*}{V_R^2} \qquad \text{(Eq. 4)}$$

Matching of vortex shedding frequency with one of the natural frequencies of the structure may not always be the only (sole) reason for lock-in. Contrary to classical lock-in , whereby the

Downloaded from www.periodico.tchequimica.com

oscillation frequency matches the structural natural frequency, in the experiments on stationary cylinder free to oscillate, it was found that the oscillation frequency increases markedly above the natural frequency, through the excitation regime while at the same time it is below the vortex shedding frequency (of the non-oscillating structures) (Khalak and Williamson, 1999). Even though vortex shedding and the vibration induced by it has been a topic of extensive research for several years, due to its intrinsic nature, the researchers are still not able to confidently define the phenomenon and describe the flow physics behind shifting of shedding frequency. Numerous analytical, experimental, and numerical investigations have been carried out in the field of vortex induced vibration (VIV) of long flexible cylinders. Most of these studies focused on the structural response of the cylinders rather than the phenomenon of lock-in (Trim *et al*., 2005; Vandiver *et al*., 2009). Freely oscillating cylinders were modelling as a spring mass system with single or two degrees of freedom (Sekar *et al*., 2009). Experiments in wind tunnels using particle induced velocimetry (PIV) have proved to predict the flow characteristics and structural response with much accuracy (Wang *et al*., 2015). Laboratory experiments and offshore large scale experiments have also been recognized as effective tools for analysis of VIV (Domal and Sharma, 2017; Gao *et al*., 2017). However, for case specific analysis of the problem, experiments are not always possible, and hence most of the researchers rely on computational fluid dynamics (CFD) as a tool for predicting VIV (Daniels *et al*., 2016). Unlike the experiments CFD facilitates detailed study of the flow physics which is otherwise impossible. Three dimensional (3D) numerical simulations are widely accepted in the research community as capable of predicting VIV characteristics accurately. Researchers were under the notion that two dimensional (2D) simulations are acceptable only for lower Reynolds numbers (Re < 250) because of the inherent 3D characteristics of vortices. Later on several researchers have proved that 2D simulations are capable of accurately predicting VIV phenomenon in rigid structure cases (Xie *et al*., 2012). 3D numerical simulation demands high computational resources for flow analysis and also for generation of the 3D computational grid. The objective of the present work is to test the accuracy of 2D numerical simulations in predicting flow characteristics of VIV and to develop an easy and economical tool for comprehensive analysis of vortex shedding and the structural response during VIV. RANSE-based Commercial solver ANSYS Fluent -15, as well as ANSYS Workbench -15, have been used as the tools for the study.

2. MATERIALS AND METHODS

The grid generated for the analysis has been validated using the experimental method. Experiments have been carried out on a subsonic wind tunnel, and the results have been compared with those of numerical studies for the same value of Reynold's number. Details of the material and dimensions of the test cylinder are shown in Table 1.

Table 1. *Geometric specification of the riser and fluid domain*

The diameter of the riser (D)	0.05 m
Distance from inlet to the riser	9 D
Distance from riser to outlet	27 D
Lateral distance from cylinder to both sides	7 D
Cylinder Material (Hollow)	PVC

2.1. CFD Prediction for Vortex Shedding

Geometric modeling and the generation of computational grids around the riser placed in a fluid domain, mimicking ocean environment (still water conditions) have been carried out using ANSYS ICEM CFD.

2.1.1. Creating a computational domain

The geometric specifications of the riser model and the fluid domain with respect to the diameter of the riser are given in Table 1.The length of the riser (L) has been chosen to be 0.4 m, so that the aspect ratio (L/D) is 20. At this value of aspect ratio, the model has been found to account for the three dimensional effects of vortex shedding (Vandiver *et al*., 2009). Figure 1 shows the representation of fluid domain. Domain size has been fixed based on the published domain independency test results (Gutafsson, 2012).

Downloaded from www.periodico.tchequimica.com

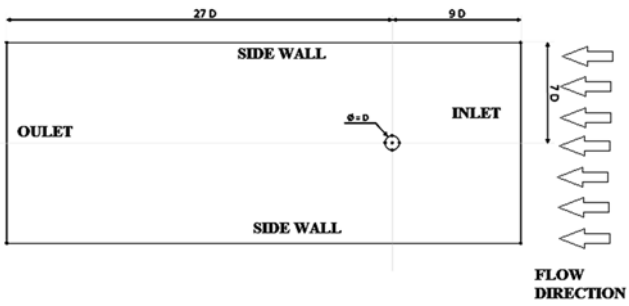

Figure 1. *Dimensions of the fluid domain with the riser*

Meshing or generating the computational grid in the fluid domain around the riser effectively is most important in capturing the vortex shedding phenomenon. The vorticity transport equation represented by Equation 5 gives an insight into the mechanism of generation and transport of vortices.

$$\frac{\partial \omega}{\partial t} + u \cdot \nabla \omega + \omega(\nabla \cdot u) = \omega \cdot \nabla u + \frac{1}{\rho^2} \nabla p + \upsilon \nabla^2 \omega \quad \text{(Eq.5)}$$

The third term on the right hand side of the equation represents the diffusion of vorticity by viscosity. Due to this term, vorticity is generated along solid wall boundaries because of steep velocity gradients. These steep gradients make vortical motion susceptible to numerical dissipation. But in the near wall region, where the mesh is usually very fine, this is not an issue since the fine mesh can capture viscous effects. It is a bigger issue in the far field, where poor resolution can severely weaken and distort the vertical structures (Kamkar, 2011). Hence importance must be given even to the far field wake, where the major concern is the mesh resolution.

2.1.2. Mesh Generation

Mesh element size near the surface of the cylinder is of great importance in case of turbulent flow compared to laminar flow. The interaction between the mean flow and the boundary layer flow is more in turbulent flow, and turbulence plays the most important role in the transport of momentum and hence must be properly resolved, especially at the boundary for better results. To accurately capture the features of flow near the boundary, the spacing of the first grid point should be such that it is well within the laminar sub layer of the boundary layer for turbulent flow and within the boundary layer for laminar flow. In the outset a mesh has been generated, and the drag force computed has been compared with the value obtained through experiments. The experimental set up is described in the previous section. The flow over the cylinder corresponds to a Re =5.3 x 10^4 which is in the laminar flow regime. The boundary layer at Re = 5.3 x 10^4 is laminar before separation, but during vortex shedding the wake of the cylinder turns turbulent in nature at any Re > 300. Hence while meshing the geometry due consideration must given to the possible influence of turbulence on the boundary layer.

From Blasius's solution of the equation for the boundary layer in laminar flow, represented by Equation 6, the boundary layer thickness, considering the boundary layer to be completely laminar, is 1x10^{-3} m.

$$\delta = \frac{4.91 D}{\sqrt{Re_D}} \quad \text{(Eq. 6)}$$

If, for an additional factor of safety, we consider the influence of turbulence on the boundary layer, then the minimum element size near the cylinder wall must be chosen so that it is well with the laminar sub-layer of the boundary layer. The thickness of the laminar sub-layer is obtained from Equation 7.

$$\delta' = \frac{11.6 \upsilon}{V^*} \quad \text{(Eq. 7)}$$

Where V* is the frictional velocity given by Equation 8.

$$V^* = \sqrt{\frac{\tau_0}{\rho}} \quad \text{(Eq. 8)}$$

And τ_0 the wall shear stress is obtained as in Equation 9.

$$\tau_0 = \frac{0.664 \rho V^2}{2\sqrt{Re_D}} \quad \text{(Eq. 9)}$$

For Re = 5.3 x 10^4, the thickness of the laminar sub-layer has been obtained from the Von-Karman momentum integral equation as 2.8 x 10^{-4} m. While generating mesh for computation, 3 x 10^{-4} m has been fixed as the global minimum seed element size with a scale factor of 1. An unstructured mesh has been generated with view that the same mesh may be used for analyzing the

Downloaded from www.periodico.tchequimica.com

variation in flow characteristics with oscillating cylinder. Quad dominant mesh type has been preferred in shell meshing parameters as it suits accurate meshing of curved cylindrical surface. Patch dependent mesh method has been selected since it gives the best quad dominant quality while capturing surface details. Tetra/Mixed mesh type and Robust (Octree) mesh method have been selected for surface meshing. Moreover it is to be observed that the first grid point should exhibit a Y+ (wall normal dimensionless distance) value of less than 1 in case of RANS simulations. Near wall spacing or element size has been calculated as 2 x 10^{-5} from Equation 10.

$$\Delta S = \frac{\mu Y^{+}}{\rho V^{*}} \qquad \text{(Eq.10)}$$

This value of near wall spacing is ensured by fixing maximum element size and height 3 x 10^{-5} m and height ratio 1.05 with 20 numbers of prism layers to cover the entire boundary layer in the part mesh set up of cylinder surface. After a thorough grid independency study, the final mesh for analysis has been chosen with 41,932 elements. Unstructured mesh used for the flow analysis using ANSYS 15 is shown in Figure 2.

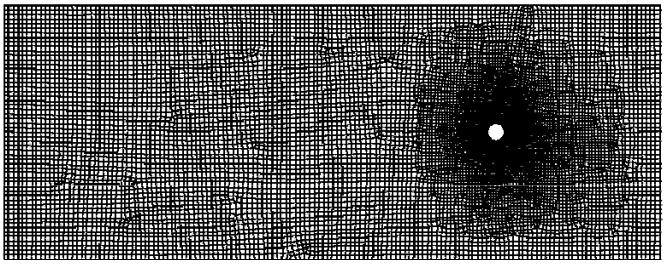

Figure 2. *Unstructured 2D mesh generated in ANSYS ICEM CFD*

2.1.3. Flow Analysis

Flow past the cylinder at Re = 5.3 x 10^4has been simulated using the generated unstructured mesh in ANSYS Fluent -15.Pressure based transient analysis has been carried out. Fluid flowing has been chosen to be water at density 998.2 kg/m^3, and the inlet velocity 1.06m/s in order to match the Re value. k-ω SST turbulence model has been selected, which has been tested against other models and proven to be the most adaptable model to predict the near cylinder and wake flow characteristics (Chandran.*et al*., 2018). Velocity inlet boundary condition has been given at the inlet, pressure outlet at the outlet boundary, and for both sides of the domain, symmetry boundary condition (Chandran *et al.*, 2019). Pressure velocity coupling has been done using PISO scheme. Second order upwind spatial discretization has been selected for momentum and turbulent kinetic energy. Second order implicit transient formulation has been used. The spatial discretization gradient is least squares cell based. Since the simulation has been compared with the results obtained from wind tunnel experiments turbulent intensity has been calculated from the empirical correlation for a duct flow given by Equation 11.

$$I = \frac{V'}{V_{avg}} = 0.16\left(Re_D\right)^{\frac{1}{8}} \qquad \text{(Eq. 11)}$$

Where *V* the root mean square of velocity fluctuations and V_{avg} is the mean flow velocity. For Re = 5.3 x 10^4, the turbulence intensity will be 4 % according to Equation 11 and hence so chosen for analysis. The time step size for the transient simulation has been calculated based on vortex shedding frequency corresponding to Re = 5.3 x 10^4. The time period of vortex shedding has been calculated from the definition of Strouhal number (St) given by Equation 12.

$$St = \frac{fD}{V} \qquad \text{(Eq. 12)}$$

where f is the vortex shedding frequency.

The time period has been obtained as 0.25 seconds from the value of frequency. For accurately capturing the shedding phenomenon one-time period should contain at least 20 time steps. Accommodating 25 time steps per time period, the time step size obtained is 0.01 seconds. Further for ensuring stability of the solution, Courant Friedrichs Lewy (CFL) condition must be satisfied as given by Equation 13.

$$\Delta t = \frac{C_m \Delta x}{V} \qquad \text{(Eq. 13)}$$

where C_m is the maximum allowable CFL number.

For explicit solver C_m =1. Δx is the minimum element size. The time step size obtained from Equation 13 is 3 x 10^{-4} seconds. A time step size of 1 x 10^{-4} seconds has been selected for the transient analysis of the flow with a safety factor. Simulations have been performed for various time step sizes ranging from 1 x 10^{-3} to

Downloaded from www.periodico.tchequimica.com

5 x 10^{-5}. Above a value of 1 x 10^{-4} the results have been found to be independent of time step size. Simulations have been run for 5 seconds, and it took nearly 1.5 hours of physical time to complete the runs on an 8 GB RAM machine. Analysis of flow took 1.36 seconds computational time for reaching convergence. RMS value of coefficient of drag (C_D) obtained from the analysis is 0.63, and that of coefficient of lift (C_L) is 0.61. Shedding frequency has been calculated from the period of oscillation of the lift force. Lift force oscillates about zero mean value at the same frequency as that of vortex shedding. The frequency of oscillation of C_L, and hence that of shedding, has been found to be equal to be 35.7 Hz, which corresponds to a St = 0.28. A relationship between St and Re (Techet, 2005) it is observed that at Re = 5.3 x 10^4 for a smooth cylinder, Strouhal number value is just above 0.3. Hence the obtained shedding frequency value from the numerical simulation has been proved to be in acceptable range.C_D and C_L time histories after convergence for a number of time periods are presented in Figure 3 and Figure 4.

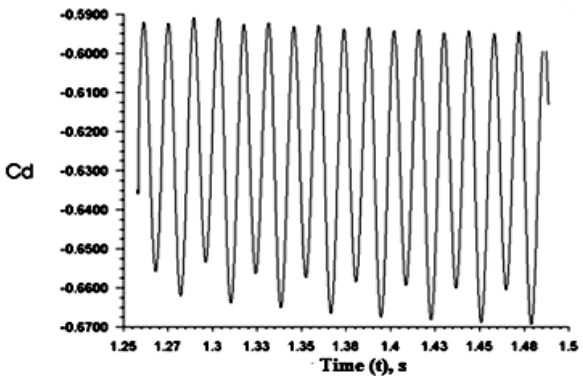

Figure 3. *Time history of the coefficient of drag (C_D) at Re = 5.3 x 10^4*

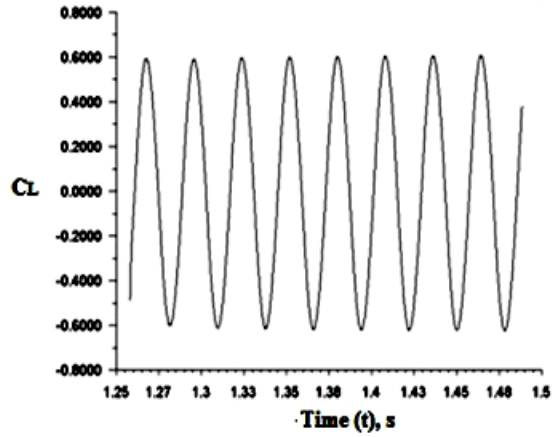

Figure 4. *Time history of the coefficient of lift (C_L) at Re = 5.3 x 10^4*

2.2. Experiment - Flow Past Horizontal Cylinder

Experiments have been conducted with two folded objectives. The first one does a quantitative comparison, and the other one for a qualitative comparison. Quantitative comparisons with the numerical study have been established through a test at moderate Re = 5.3 x 10^4while the qualitative ones employed lower Re tests for flow visualizations, thus proving the efficacy of the mesh at moderate and low Re.

2.2.1. Quantitative Comparisons

A smoke test was carried out in the subsonic wind tunnel of Aerospace Laboratory of Karunya Institute of Technology and Sciences, Coimbatore, India. A horizontal cylinder of diameter 50 mm and length 600 mm fitted with pressure tapings has been used as the model for testing. The compressor of the wind tunnel unit was operated at 600 rpm, which corresponds to 16.4 m/s (Re = 5.3 x 10^4) velocity at the test section. Smoke was inducted into the test section by burning liquid paraffin. Flow patterns and vortex shedding around the cylinder were captured using a high resolution camera.C_D and C_L values have been calculated from the measured pressure distribution. Details of the wind tunnel are as follows.

2.2.1.1. Wind tunnel specification

Test Section Size	:	Cross section = 600 x 600 mm
Length	:	4000 mm
Maximum Speed	:	45 m/s
Contraction Ratio	:	6:1
Contraction Length	:	1.8 m
Entry Section	:	Bell mouthed.
Smoke	:	Provided in the contraction cone
Power	:	22 kW/30 HP AC motor.

An inclined manometer with ethanol as the manometric fluid is fixed on the tunnel. The two limbs of the manometer are connected to the static pressure holes one in the settling chamber just before the contraction and the other to that at the entrance of the test section. The reading on the manometer is very near to the dynamic head of the fluid in the test section, and it serves as a reference for keeping the tunnel speed constant. The tunnel is also provided with a pitot static tube

Downloaded from www.periodico.tchequimica.com

which can be traversed across the tunnel cross section.

Pressure readings have been observed from the pressure ports provided on the circumference of the cylinder. Static and stagnation pressure have also been observed. Plots of pressure distributions around the cylinder and coefficient of pressure are represented in graphs Figure 5(a) and 5(b). C_D has been calculated by integrating $C_p\cos\theta$ over 360° using Simpson's method of integration. The value of C_D obtained from the wind tunnel experiment is 0.62. A comparison of the results obtained from the simulations and experiment are given in Table 2.

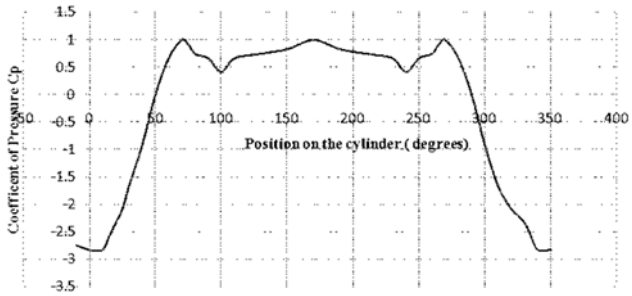

a)

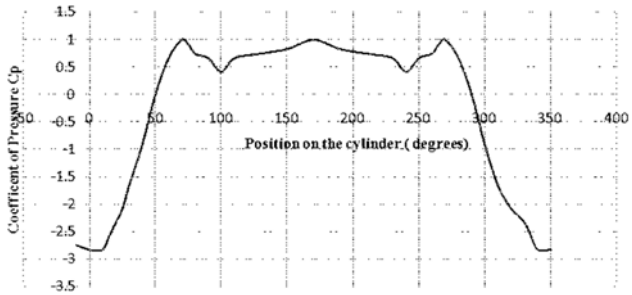

b)

Figure 5. *(a) Pressure distribution around the cylinder at Re = 5.3 x 10^4 (b) Coefficient of pressure around the cylinder at Re = 5.3 x 10^4*

2.2.2. Qualitative Comparisons

An experiment to visualize, study, and analyze the characteristics of wake behind the horizontal cylindrical model has been conducted through smoke injection tests in the wind tunnel. A 50 mm diameter cylinder with 600 mm length has been used for flow visualization. The model is exactly similar to the one used for pressure measurement but without pressure ports. The model which had been used for pressure measurement cannot be used in this scenario because of the risk of the pressure ports getting clogged with smoke particles. The recommended maximum tunnel speed for smoke visualization experiments is 4 m/s. Smoke tests have been performed at 0.6 m/s which corresponds to Re = 2000. Numerical simulations also have been performed using ANSYS Fluent 15 for the same Reynolds number using the previously generated mesh. Results obtained from the experiment and simulations are compared in Table 2. St has been calculated from the frequency of vortex shedding using Equation 12. In numerical simulations the shedding frequency is taken to be equal to the oscillation frequency of lift coefficient. Shedding frequency is obtained as 0.99 Hz and Strouhal number as 0.1995 for Re = 2000. Vortex shedding frequency from the wind tunnel experiment has been calculated by repeatedly noting from the recorded video of shedding phenomenon, the time is taken for shedding 20 vortices from the upper boundary of the cylinder, and then taking the average time observed for the calculation. Results obtained are presented in Table 2 for comparison with those obtained from numerical simulations.

Figures 6(a) and 6(b) represent the flow pattern obtained from the numerical study after convergence at 1.6 seconds of flow and wind tunnel test respectively for flow past cylinder at Re = 2000. Distances to the lower pressure zones (vortices) shed from the cylinder are indicated on a scale of the diameter of the cylinder. The length of the line segment in both figures corresponds to the diameter of the cylinder. The angle of separation of the boundary layer is shown in the wake patterns given in Figures 7(a) and 7(b). The numerical value of the separation angle is given in Table 2. For verification of the results from the present grid, flow analysis has been carried out at Re = 1000, in order to validate the grid using other published numerical works. The RMS value of C_D is found to be 1.24, which is very much comparable with the published results at Re=1000 (C_D= 1.15) (Braza. *et al.,* 1986).

2.3. Force - Frequency Plot and Structural Analysis

Characteristics of flow past cylinder is a topic extensively investigated by researchers. Many have proposed plots from experimental, analytical, and numerical simulation results, which show the relationship between various flow parameters such as. with Re. The present work focuses on a marine riser model of specified dimension. A methodology has been developed to predict the structural response especially the trajectory of any section of the riser under vortex induced vibration. As the first phase, a data sheet has been created using the unstructured 2D mesh

Downloaded from www.periodico.tchequimica.com

given in Figure 2.The sheet gives the numerical results of C_D, C_L, and vortex shedding frequency (f_v) from the 2D simulations performed in ANSYS Fluent-15 for a range of Reynolds number up to the sub critical value and the values have been mapped over the entire length of a 3D cylinder

Simulations have been performed for Re = 100 to 20,000.The velocity of flow has been assumed to be uniform along the span of the cylinder. Using the values of C_D and C_L obtained from the flow analysis lift and drag force acting on a cylindrical riser of 8 m length, and 0.05 m diameter has been estimated. Figures 8(a) and 8(b) show the plot for drag and lift forces on a cylindrical riser model of 0.05 diameter and 8 m length against its vortex shedding frequency.

From the plot, the hydrodynamic forces acting on the cylinder at various frequencies can be obtained. The value of hydrodynamic loads obtained from the plot at a specific frequency has been used as the input for predicting the structural response of the cylinder and the trajectory of any point on the surface of the cylinder.

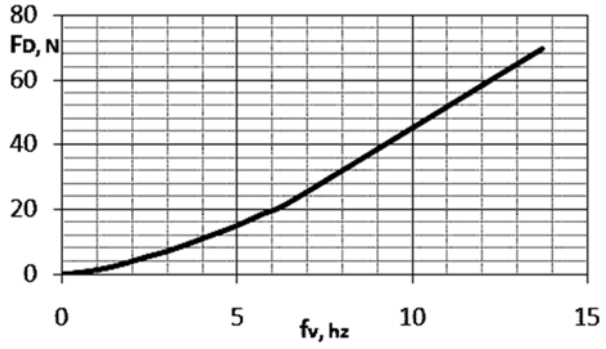

a)

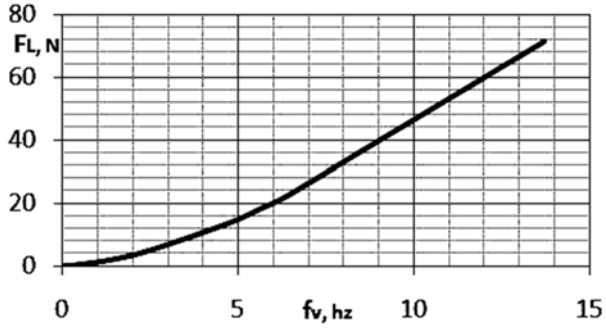

b)

Figure 8. *(a) Drag Force – Frequency plot (b) Lift Force – Frequency plot*

Structural analysis of the cylinder model has been performed in ANSYS Workbench-15. Drag and lift forces acting on the cylinder as a result of vortex shedding have been given as input in the solver. It has been treated as an oscillating force having an amplitude equal to maximum lift in the direction perpendicular to the flow (cross flow) and equal to maximum drag in the direction of flow (in line).The frequency of oscillation of lift and drag forces has also been obtained from flow analysis. It has been observed that the drag coefficient is oscillating about a non-zero value at double the frequency of the lift coefficient. Vortices are shed behind the cylinder at the same frequency as that of the oscillating lift force. When the vortex shedding frequency matches the natural frequency of oscillation of the cylindrical structure, a resonance condition, well known as lock – in vibration occurs, which gives rise to oscillations of very high amplitude. This may bring in extensive damage to the structure and to the working crew. Hence the analysis of the response of structures vibrating at their natural frequencies due to vortex shedding is considered to be most desirable in design of offshore structures.

The cylinder has been modeled in ANSYS Workbench-15 as a hollow vertical, having a thickness of 2.5 x 10^{-3} mm. The material of the riser model has been chosen to be Poly Vinyl Chloride (PVC) of density 1400 kg/m^3. The simulation has been performed as a transient case since it involves time varying forces and deformation. The top end has been modeled fixed in the x and y directions, and the bottom end with motion in x, y, and z direction arrested. Since the riser is a flexible structure, Mechanical ANSYS Parametric Design Language (APDL) has been used as the solver. Stiffness and mass coefficients were provided as input in the damping control of analysis settings of the solver. After performing a grid independency analysis, a mesh having 66,158 elements have been chosen for the response analysis. The meshing of the geometry has been done using tetrahedral elements. The time step size has been chosen to be 5 x 10^{-2} based on the oscillating frequency of hydrodynamic loads. Transient simulation has been performed for 10 seconds. Local displacements at estimated locations of maximum vibration amplitude at the first three modes of vibration were obtained by inserting a displacement probe at the respective locations on the cylinder. Time histories of displacement in the X and Y directions and the trajectory of the cylinder during vibration have been plotted from the probe data.

The first three modes of vibration and the corresponding natural frequencies of the riser in the air have been obtained as 2.99, 9.7, and 20.23

Downloaded from www.periodico.tchequimica.com

Hz, respectively, from the modal analysis. Natural frequencies of the riser in water have been obtained solving Equation 14, considering added mass to be 70% of the total system mass, m_a = 1.12 kg, and stiffness of the riser k = 17.73 N/m. The first three natural frequencies of the riser in water have been obtained as 2.88 Hz, 7.16 Hz, and 9.41 Hz, respectively.

$$\frac{1}{\omega_{n\,water}^2} = \frac{1}{\omega_{n\,air}^2} + \frac{m_a}{k} \qquad \text{(Eq. 14)}$$

Drag and lift forces, corresponding to the identified natural frequencies of the riser, have been obtained from the plotted frequency – force graph. The amplitude of variation of drag force has been observed to be much less compared to the lift force. Lift force has been considered as periodically varying force, which oscillates about zero and acting in the cross flow direction as given in Equation.15 in the structural solver.

$$F(t) = F_0 \cos(\omega_v t) \qquad \text{(Eq. 15)}$$

Drag force oscillates with double the frequency of lift force, and it oscillates about a non-zero value. Drag force has two components, viz. average drag and the fluctuating component of drag force. From the numerical simulation, both RMS value and fluctuation about RMS value of drag forces have been obtained. Drag force is applied to the cylinder in the structural solver, as given by Equation 16.

$$F_D(t) = F_{Davg} + F_D' \cos(2\omega_v t) \qquad \text{(Eq. 16)}$$

Where F_{Davg} is the RMS value of drag force, and F'_D is its fluctuating component. The lift and drag forces obtained from the flow analysis corresponding to the flow regimes at which vortex shedding frequency (ω_v) matches the first three harmonics of the natural frequency of the cylinder (ω_n) have been used for structural analysis. This condition is generally referred to as lock-in condition. The drag force oscillates at double the frequency of lift coefficient. This phenomenon is well established in published literature (Durbin, 2007).

For the identified natural frequencies, structural analysis has been carried out to study various response parameters. A deformation probe has been inserted at z = 4 m for first and third modes of vibrations and at z = 2 m for the second mode to observe the response of the cylinder under oscillating load.

3. RESULTS AND DISCUSSION

It can be observed that the numerical simulation with the grid generated, as shown in Figure 2 in the present work, is capable of replicating the wake pattern behind the cylinder exactly in the way the experiments do. Wake dimensions are comparable in both cases in terms of the span and angle of separation. Quantitative comparisons between the experimental and numerical values presented in Table 2 indicate the reliability in the present numerical predictions. Here the important observation is that at lower Re = 2000, a better prediction of St is achieved (9% deviation from the experimental ones) while at higher Re = 4000, a deviation of 22% is observed from the corresponding experimental value.

From the history of cylinder displacement during the lock-in, it can be observed that, as the frequency of shedding increases, the amplitude of displacement in cross flow direction goes on decreasing and that in the inline direction increases. This is because, at higher Re corresponding to higher shedding frequencies, the value of C_D is also high. A huge number of researchers are focusing on the cross flow response of cylinder. The observation made here emphasizes the need for investigating the inline response during lock-in at higher harmonics of natural frequency.

By plotting the non-dimensional amplitude of the cylinder in IL and CF directions, the trajectory of the probe location has been traced, as shown in Figures 9 (a) – (c) for all three frequency regimes. It can be observed that the cylinder point follows an eight figure trajectory during lock - in. The cylinder is expected to follow an eight figure trajectory due to oscillating lift and drag forces induced by vortex shedding at its wake. In lock-in condition the frequency of the inline vibration is twice that of cross flow vibration, and the trajectory of the cylinder corresponds to “Lissajou figure 8” (Vandiver *et al*., 2009). Trajectory obtained from the numerical study is very much comparable with the response of an 8 m riser model obtained from the experimental study (Liangjie *et al*., 2004). The trajectory from the experiment is given in Figure 10.

The trajectories traced show the increasing importance of accounting for IL response at higher harmonics of natural frequency. The maximum amplitude in the CF direction is obtained to be equal to 2.5D, where D is the diameter of the cylinder when the cylinder locks on to the first

Downloaded from www.periodico.tchequimica.com

natural frequency. During the first natural frequency lock-in vibration, the cylinder traces the same path repeatedly for several cycles of oscillation. But moving to higher harmonics, there is considerable uncertainty in the case of exact path traced. The magnitude of the non-dimensional amplitude of oscillation and the pattern of trajectory matches reasonably well with the published experimental and numerical results.

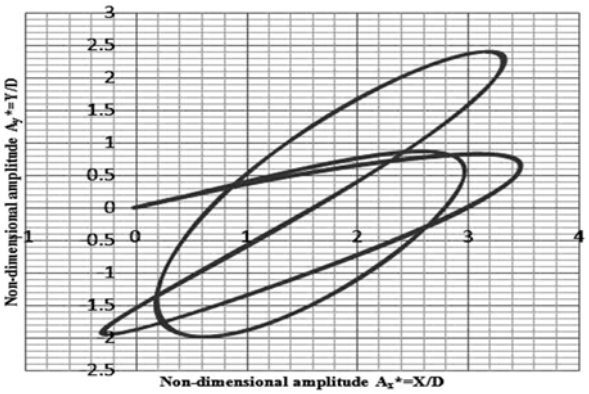

a)

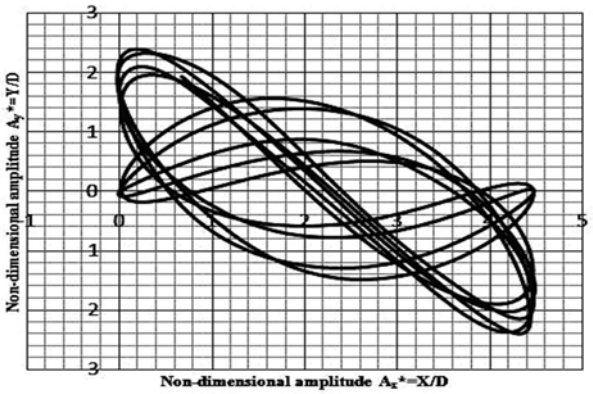

b)

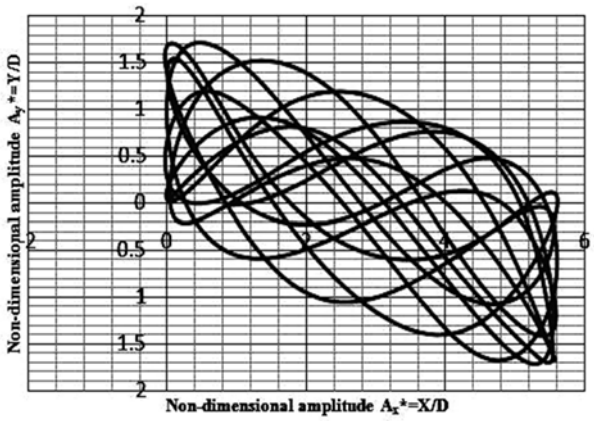

c)

Figure 9. *Trajectory of the cylinder (a) shedding frequency equal to the first harmonic of natural frequency (b) shedding frequency equal to second harmonic of natural frequency* ***(****c) shedding frequency equal to third harmonic of natural frequency*

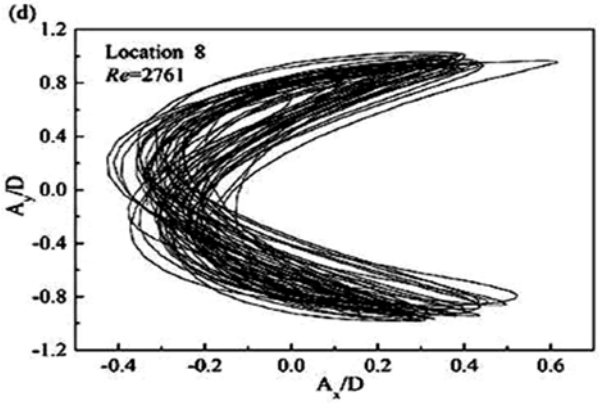

Figure 10. *Trajectory obtained from an experimental study of the response of cylindrical riser*

4. CONCLUSIONS

This paper presents a method that is computationally economic at the same time efficient in predicting VIV of cylindrical risers. Two dimensional flow analysis is capable of predicting the numerical values of hydrodynamics loads, pressure patterns during vortex shedding, the amplitude of oscillation and the trajectory as well for VIV problems. Vortex induced vibration of slender structures especially petroleum risers and mooring cables are one of the important aspects that should never be neglected in their design. Hence a thorough understanding of the loads and responses of such slender structures is essential before its design and deployment. Numerical analysis using two way fluid structure interaction (FSI), which can predict the parameters with considerable accuracy is always not handy for everyone dealing with this type of problem because of the heavy computational requirement needed for such solvers. This method has been proposed in a view to supporting young researchers in the field of the intrinsic flow phenomenon of vortex shedding, who lack high computational facility but may also understand the phenomenon without compromising much accuracy.

The method has been well validated in two stages, initially the grid, which yields the same flow physics as that of conventional experiments and then the structural behaviour which also is in good agreement with similarly published works (Liangjie*et al.*,2004 ,Vandiver*et al.*,2009). On the whole, it is found that the method is quite effective in the quick computation of VIV problems for low and moderate Re. At high Re, 3D studies find their

Downloaded from www.periodico.tchequimica.com

use as 2D predictions do not suffice in providing the minute details of flow physics.

5. AKNOWLEDGEMENT

The authors of this paper wholeheartedly express their gratitude and acknowledgement to Mr. K. Alfred Sunny and Mr. Kumar of Karunya Institute of Science and Technology, Coimbatore, India, for the technical support rendered by them while conducting experiments on the sub-sonic wind tunnel. We also extend our deepest sense of gratefulness to Prof. M. Madhavan, former Principal, SCMS School of Engineering and Technology, Eranakulam, India, for his timely advice and support.

6. REFERENCES

1. Gustafsson, A. Analysis of Vortex-Induced Vibration of Risers, Master's thesis in Applied Mechanics, Chalmers University of Technology, Sweden, **2012**.
2. Blevins, R.D. Flow-Induced Vibration, second ed., Van Nostrand Reinhold, New York, **1990.**
3. Bourguet, R., Karniadakis, G.E., Michael, S., and Triantafyllou, M.S. Lock-in of the vortex-induced vibrations of a long tensioned beam in shear flow, *Journal of Fluids and Structures*, **2011**, 27, 838–847.
4. Braza, M., Chassaing, P., and Minh, H.H. The Numerical Study and Physical Analysis of the Pressure and Velocity Fields in the Near Wake of a Circular Cylinder, *Journal of Fluid Mechanics*, **1986**, 165, 79–130.
5. Chandran, V., Sekar, M., Janardhanan, S., and Menon, V.A. numerical study on the influence of mass and stiffness ratios on the vortex induced motion of an elastically mounted cylinder for harnessing the power. *Energies*, **2018**, 11, 2580.
6. Chandran, V., Sekar, M., Janardhanan, S., Influence of Freqency Ratio on Hydroelastic Response of a Cylinder with Degrees of Freedom under Vortex Induced Vibration., *International Journal of Innovative Technology and Exploring Engineering*, **2019**, 8, 9S3, 307 -312.
7. Daniels, S.J., Castro, I.P., and Xie, Z. Numerical analysis of free stream turbulence effects on the vortex-induced vibrations of a rectangular cylinder, *Journal of Wind Engineering and Industrial Aerodynamics*, **2016**, 153, 13–25.
8. Domala, V., and Sharma, R. An experimental study on vortex-induced vibration response of marine riser with and without semi-submersible, *Journal of Engineering for the Maritime Environment*, **2017.**
9. Durbin, P,A., and Medic, G. Fluid dyanamics with a computational perspective, **2007,** Cambridge University Press, Newyork.
10. Feng, C.C., The measurement of vortex-induced effects in flow past stationary and oscillating circular and D-section cylinders, Master's thesis,**1968**, University of British Columbia.
11. Gao, Y., Fu, S., Xiong, Y., Zhao, Y., and Liu, L. Experimental study on response performance of vortex-induced vibration on a flexible cylinder, *Ships, and Offshore Structures*, **2017**,12, 116–134.
12. Kamkar S.J. Mesh Adaptation Strategies for vortex dominated flows, Ph. D Thesis, **2011**, Stanford University.
13. Keshavarzian, B., and Khosravi, M. Numerical Investigation of the Structural Frequencies Effects on Flow Induced Vibration and Heat Transfer, *Journal of Material and Environmental Science*, **2015**, 6 (7), 1949–1956.
14. Khalak, A., and Williamson, C.H.K. Motions, forces, and mode transitions in vortex-induced vibrations at low mass-damping, *Journal of Fluids and Structures*, **1999**, 13, 813–851.
15. Liangjie, M., Qingyou, L., and Shouwei, Z. Experimental Study of the Vortex-Induced Vibration of Drilling Risers under the Shear Flow with the Same Shear Parameter at the Different Reynolds Numbers, *PLoS ONE*, **2004**, 9, e104806.
16. Pezzini, A., Brião, V,B., and DE BONI, L.A. B. Preliminary study for a cleaning and water reuse system, *PERIÓDICO TCHÊ QUÍMICA* **,2017**, 28, 127–132.
17. Ramírez, Ann-Katrin, P., Wolff, and Carl, F. Building quality infrastructure services for water and sanitation providers in latinamerica – examples from german development cooperation, *PERIÓDICO TCHÊ QUÍMICA*, **2017**, 28, 18–28.
18. Sarpkaya, T., Transverse Oscillations of

Downloaded from www.periodico.tchequimica.com

Circular Cylinder in Uniform Flow, Part I Report No. NPS-69L 77071-R, **1997**, Naval Postgraduate School, Monterey, Calif.

19. Sekar, M., Srinivas, J., Kotaiah, K.R., and Yang, S.H. Stability analysis of turning process with the tailstock-supported workpiece, *Int J Adv. Manuf. Technol*, **2009**, 43, 9–10, 862–871.
20. Shiels, D., Leonard, A.,and Roshko, A. Flow-Induced Vibration of a Circular Cylinder at Limiting Structural Parameters, *Journal Of Fluids And Structures*, **2001**, 15, 3–21.
21. Techet, A.,13.42 Lecture: Vortex induced vibration – MIT open courseware, **2005**, Massachusetts Institute of Technology, USA.
22. Trim, A.D., Braaten, H., Lie, H., and Tognarelli, M.A. Experimental investigation of vortex-Induced vibration of long marine risers. *Journal of Fluids and Structures*, **2005**, 21, 335–361.
23. Vandiver, J.K., Jaiswal, V., and Jhingran, V. Insights on vortex-induced, traveling waves on long risers. *Journal of Fluids and Structures*, **2009**, 25: 641–653
24. Wang, Q., Li, M.,and Xu, S., Experimental study on vortex induced vibration (VIV) of a wide-D-section cylinder in a cross flow,Theoretical and Applied Mechanics Letters, **2015**, 5: 39–44.
25. Xie, F., Deng, J., Xiao, Q., and Zheng, Y.A. Numerical simulation of VIV on a flexible circular cylinder, *Fluid Dynamics Research*, **2012**, 44, 21.

Table 2. *Comparison between wind tunnel experiments and numerical simulations.*

Reynolds Number (Re)	**CoefficientofDrag (C_D)**		**Strouhalnumber (St) (Non-dimensional Frequency)**		**Wake Dimension**	
	Experiment	**Numerical**	**Experiment**	**Numerical**	**Experiment**	**Numerical**
53000	0.62	0.63	NA		NA	
4000	-	-	0.178	0.22	θ = 126°	θ = 120°
2000	-	-	0.183	0.1995	D = 0.05m	D = 0.02m

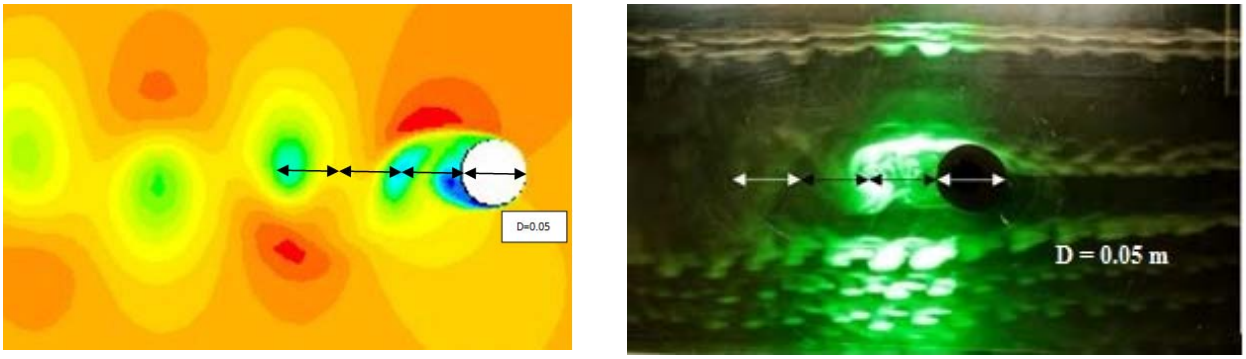

a) *b)*

Figure 6. *Pressure pattern at the wake of the cylinder at Re = 2000 (a) obtained from numerical simulations (b) obtained from the smoke test conducted in the subsonic wind tunnel*

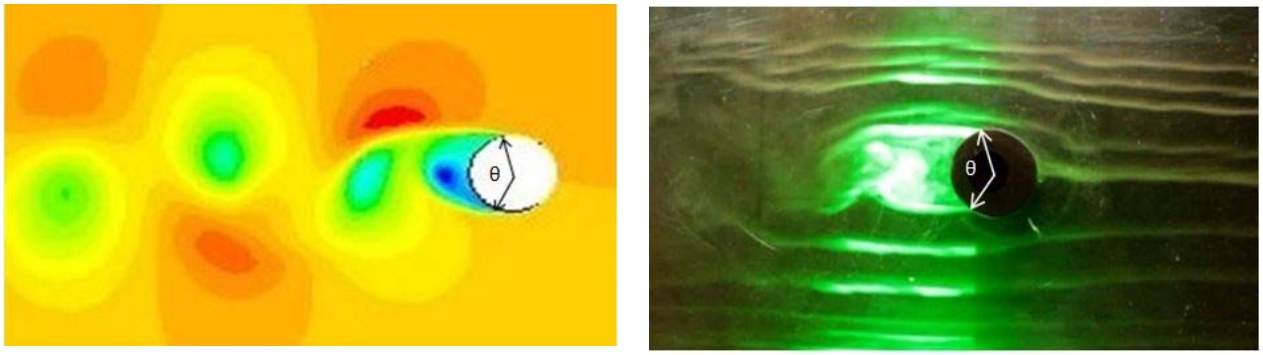

a) *b)*

Figure 7. *Boundary layer separation at the wake of the cylinder at Re = 4000. (a) obtained from numerical simulations (b) obtained from the smoke test conducted in the subsonic wind tunnel*

Downloaded from www.periodico.tchequimica.com

PERIÓDICO TCHÊ QUÍMICA
ARTIGO ORIGINAL

ATITUDE PARA A TECNOLOGIA PARA PROFESSORES DE CIÊNCIA EM TREINAMENTO NA INDONÉSIA: UMA ANÁLISE DE FATOR EXPLORATÓRIO

ATTITUDE TOWARDS TECHNOLOGY FOR PRE-SERVICE SCIENCE TEACHERS IN INDONESIA: AN EXPLORATORY FACTOR ANALYSIS

ROSIDIN, Undang[1]; MASKUR, Ruhban[2]; KADARITNA, Nina[3]; SAPUTRA, Andrian[3,*]

[1,*]Department of Physics Education, Faculty of Teacher Training and Education, University of Lampung, Indonesia

[2]Department of Mathematics Education, Faculty of Tarbiyah and Teacher Training, State Islamic University of Raden Intan Lampung, Indonesia

[3]Department of Chemistry Education, Faculty of Teacher Training and Education, University of Lampung, Indonesia

** Correspondence author*
e-mail: andriansaputra@fkip.unila.ac.id

Received 19 October 2019; received in revised form 09 November 2019; accepted 13 November 2019

RESUMO

O conhecimento e a habilidade tecnológica são cruciais para professores e professores em treinamento, pois afetam diretamente o desempenho, a qualidade da aprendizagem e o acesso mundial mais amplo. Muitos estudos mostraram que a capacidade de um professor em pedagogia integrada à tecnologia é influenciada por sua atitude em relação à tecnologia. O objetivo deste estudo foi utilizar a análise fatorial exploratória para examinar os fatores estruturais, o nível de preferência e a inter-relação entre os componentes da atitude em relação à tecnologia. Os dados foram coletados de 150 professores de ciências em serviço da Universidade Lampung usando o método tradicional de pesquisa. Além disso, foram analisadas variância, comparação de valores médios e coeficientes de Alfa de Cronbach para explicar as contribuições de itens e fatores para a atitude geral em relação à tecnologia. A análise de correlação de Pearson também foi realizada para descobrir a relação entre os componentes. Os resultados confirmaram a validade do instrumento com fatores de carga variando de 0,427 a 0,882. Além disso, o coeficiente total de Cronbach Alpha foi de 0,810, o que informou uma alta consistência interna do instrumento, com cinco componentes de atitude tecnológica, responsáveis por 77,82% da variância. Especificamente, a consequência percebida da tecnologia é identificada como uma preferência atitudinal dominante dos professores de ciências em serviço na Indonésia, seguidos pelas aspirações de carreira e pela diferença de gênero. A análise do momento do produto Pearson revelou uma correlação significativa entre os componentes da atitude em relação à tecnologia.

Palavras-chave: *Atitude em relação à tecnologia; Professor de ciências em treinamento; Análise fatorial exploratória.*

ABSTRACT

Technological knowledge and skill are crucial for teachers and pre-service teachers because they have a direct effect on performance, learning quality, and wider world access. Many studies showed that the ability of a teacher in technology-integrated pedagogy is influenced by their attitude towards technology. The aim of this study was to use exploratory factor analysis in examining the structural factors, the preference level and the interrelationship among components of attitude towards technology. Data was collected from 150 pre-service science teachers in Lampung University by using traditional survey method. Additionally, variance, mean values comparison, and Cronbach Alpha coefficients were analyzed in explaining the contributions of items and factors to the overall attitude towards technology. Pearson correlation analysis was also conducted to find out the relationship among components. The results confirmed the validity of instrument with loading factors ranging from 0.427–0.882. In addition, the total Cronbach Alpha coefficient was 0.810 which informed a high internal consistency of instrument with five components of technological attitude account for 77.82% of variance. Specifically, the perceived consequence of technology is identified as a dominant attitudinal preference of pre-service science teachers in Indonesia, followed by career aspirations and gender difference. Pearson product-moment analysis revealed a significant correlation among components of attitude towards technology.

Downloaded from www.periodico.tchequimica.com

Keywords: *Attitude toward technology; Pre-service science teacher; Exploratory factor analysis.*

1. INTRODUCTION

The rapid development of technology has become a major concern for all elements of society. People in any profession are aware of the great role of Information and Communication Technology (ICT) of the ease of life and national development. In education, ICT mastery is prominent for teachers and pre-service professional teachers in the era of the industrial revolution 4.0. (Warschauer & Matuchniak, 2010). The integration of ICT in learning is an essential strategy in facilitating the shifting from traditional pedagogical paradigms towards constructivist-oriented pedagogies (Chai, Hong & Teo, 2009; Liu, 2011; Keengwe & Georgina, 2013).

By integrating technology, teachers can easily direct students to imagine the complex objects (Tania & Saputra, 2018; Tania et al., 2017; Sang et al., 2010), interpret the abstract concept to concrete things (Sunyono, Tania, & Saputra, 2016; Lee, 2012; Bujak et al., 2013; Wojciechowski & Cellary, 2013), also actively participate in collaborative activities in virtual classes or e-learning schemes (Holcomb & Beal, 2010, Keengwe et al., 2014). The use of various innovations and technology by teachers will lead to higher confidence in integrating technology-pedagogy (Kim et al., 2013; Rienties, Brouwer, & Lygo-Baker 2013), facilitating collaboration between colleagues (Afshari et al., 2009; Ottenbreit-Leftwich et al., 2010; Kim et al., 2013; Tomkins, 2019), and bringing up new innovative ideas (Koehler & Mishra, 2009; Stayer, 2012; Laurillard, 2013). Finally, the application of technology and multimedia in the teaching-learning process can help students enhance their academic achievement (Chiang, Yang, & Hwang, 2014; Alqahtani & Mohammad, 2015) and encouraging students' motivation and confidence in learning (Hazari, North, & Moreland, 2009; Yang & Wu, 2012; Chiang, Yang, & Hwang, 2014).

Recognizing the important role of technology in achieving learning objectives, a professional teacher must take a vital role in teaching, guiding, and motivating in the accomplishment of ICT-integrated learning (Kramarski & Michalsky, 2010; Gilakjani, Lai-Mei, & Ismail, 2013). A research conducted by Hattie (2003) revealed that teacher's effectiveness contributes up to 30% of variance in student achievement, 50% of variance for pre-existing student abilities, and the remaining 20% of variance is influenced by home, school (including administration), and peers. Based on this data, teachers who use student-centered approaches and have good classroom management competencies will increase student achievement to the maximum (Opdenakker & Van Damme, 2006). Furthermore, a competent teacher is characterized by how often she/he uses ICT in multiple ways in the classroom (Whittle Telford, & Benson, 2018).

There are a couple of factors for teachers in integrating ICT into their learning which can be categorized as external and internal factors. External factors include professional teacher development and training, administrative support, positive school environments, adequate technological resources, technology access, technical assistants, adequate planning time, sustained funding for technology, and instructional styles (Eteokleous, 2008). Additionally, the attitude of the principal (Coffland& Strickland, 2004), colleague influences (Oncu, Delialioglu, & Brown, 2008), and parental involvement (Baek, Jong, & Kim, 2008) are also included as external factor. Meanwhile, internal factors include attitudes toward learning, pedagogical beliefs, and personal characteristics (Eteocleous, 2008), individual mindset and teacher's belief (Liu, 2011).

Attitude is undeniably one of the internal factors that greatly determine the success of technology integration in the teaching-learning process. Teo (2008) states that the way teachers use technology for instructional design is very dependent on their attitude toward technology. Despite of the qualified technological tools provided by the school provides, it can only be optimized if the teacher has a positive attitude towards it (Huang & Liaw, 2005). A positive teacher attitude towards technology will be a determining factor for the successful adoption and integration of technology in the teaching and learning process (Van Braak et al., 2004; Huang & Liaw, 2005). Conversely, teachers who have a negative attitude towards the use of ICT will tend to be difficult to accept and adapt technology in their instructional design (Wang & Dostál, 2017).

In particular, Bame et al. (1993) has constructed structural factors of Pupils' Attitude

Downloaded from www.periodico.tchequimica.com

Towards Technology USA (PATT-USA) Survey (de Vries, 1988). Items of PATT-USA are grouped into 5 dimensions i.e. Career Aspirations, Interest in Technology in Schools, Perception of Consequences of Technology, Difficulty of Perception, and Technology as a Subject for Both Genders (Bame et al., 1993). However, Ardies, de Maeyer, & Gijbels (2013) reconstructed the PATT-survey by adding one more dimension in the mediated boredom of technology. By using this PATT-reconstructed survey, this research investigated attitude towards technology of pre-service Indonesian science teachers. Furthermore, information related to the structural factors was used to discuss the preference level of students towards factors and interrelationship among factors.

2. MATERIALS AND METHODS

2.1 Research Design and Participants

This research used a conventional survey design by distributing questionnaires to pre-service science teacher in Lampung Province, Indonesia. Survey research is a procedure in quantitative research in which the researcher conducts a survey of the sample to describe the attitudes, opinions, behavior or characteristics of the population (Creswell, 2012). Furthermore, survey methods have been effectively used to express attitudes towards technology and perceptions of technology implementation in teaching and learning (Norton, McRobbie, & Cooper, 2000; Baek, Jong, & Kim, 2008). The population in this research was pre-service science teachers from the Department of Chemical Education, Physical Education, and Biological Education, Faculty of Teacher Training and Education, University of Lampung. In addition, 150 pre-service science teachers were chosen as research sample by using random sampling technique. Everyone who became a sample filled agreement to participate in this research.

2.2 Instrument and Data Collection

The data collection technique in this research was using attitude towards technology questionnaire (Appendix 1) developed by Ardies, de Maeyer, & Gijbels (2013) which originally consisted of 25 items. The instrument was adapted and transliterated into the Indonesian language (Bahasa), making it easier for research subjects to understand each item in the instrument. Items are then consulted and validated by the judgement of three experts in the field of statistics, psychologists, and education evaluation experts. Furthermore, all items were inserted into google form to facilitate participants in accessing the questionnaire and to simplify the data tabulation.

2.3 Data Analysis

Data analysis in this research was carried out into several stages. In the initial stage, students' answers were coded into 5 levels of Likert scale. The coding results were analyzed whether the data was suitable for EFA based on the Kaiser-Mayer-Olkin (KMO) sampling of adequacy and Bartlett's test of sphericity. Before the EFA process was carried out, the communality coefficient of each item identified would be considered as included in the analysis based on Stevens's (2002) criteria. Items that are maintained in the instrument must have a loading factor of more than 0.40, therefore items with a loading factor of less than 0.40 will automatically be eliminated in the analysis of each item in the instrument. If all of these preliminary procedures have been passed then an EFA can be performed. The estimation of latent factors number proposed in this study was obtained by extracting the main components and of the varimax orthogonal rotation by considering an eigenvalue which is greater than one. In order to obtain the reliability of each factor and total Cronbach Alpha coefficient was used to calculate the validated construction instrument. In addition, the mean and standard deviation were calculated to obtain information related to the dominant preference for the factors forming the technology attitude. In the final stage, correlation analysis of each factor was carried out using the Pearson correlation coefficient.

3. RESULTS AND DISCUSSION

3.1 Structural analysis of attitude towards technology

The results of this study consisted of two parts i.e (a) structure analysis of attitude towards technology and (b) level of preference and interrelationship between attitude dimensions. Structure analysis was carried out by using exploratory factor analysis in which statement items in the questionnaire will be grouped and validated into certain factors based on appropriate statistical criteria. Exploratory factor analysis (EFA) was a statistical method used to reveal the basic structure of variables and identify the fundamental relationships between variables.

Downloaded from www.periodico.tchequimica.com

All measured variables correspond with each latent variable (Schmitt, 2011; Treiblmaier & Filzmoser, 2010). To ensure the EFA results, calculation to Kayser-Mayer-Olkin (KMO) measure of sampling adequacy and Bartlett test of sphericity were used. The KMO test was performed to analyze the suitability of the data for factor analysis by measuring the shared variance in the items (Beavers et al., 2013). The lower the KMO test value, the more suitable the data for factor analysis. Moreover, the Bartlett test of sphericity was used to check whether the correlation matrix was an identity matrix. This method was able to inform variables which were not related and suitable for structural factors (Beavers et al., 2013).

The KMO and Bartlett test values in this study were 0.853 and 2157.349 ($p < 0.05$) respectively, which indicate that a set of research data was suitable for EFA and would produce accurate analysis results. Subsequently, it was necessary to inspect whether all items could be included in the EFA analysis or need to eliminate certain items in the analysis process. This could be done by observing the coefficient of extraction commonalities. Extraction communalities are estimations of variance for each variable that can be explained by factors in a factor solution (UCLA Statistical Consulting Group, 2019). Small values of the commonalities coefficient indicated that variables did not match factor solutions, and may considered to be excluded from the next analysis. Steven (2002) suggested that the threshold value of the communality was 0.40 to determine which items were retained or excluded in EFA. The communality coefficient was greater than 0.40 indicates that the item contributed significantly to latent variables in producing a fit model. Furthermore, item number 10 (I enjoy repairing things at home) has a coefficient of 0.318, it means that the commonality analysis needs to be repeated by removing the item. In the second commonality analysis, it was obtained coefficients ranging from 0.410 – 0.852 which informed that only 23 items could be considered for the EFA analysis.

The verified items were further analyzed by using varimax rotation method and principal component extraction with eigenvalues larger than one for all accepted factors. The results suggested that items were distributed into 5 latent factors with 77.82% of total variance explained (s^2) as shown in Table 1. This construction was different from the result of Ardies et al. (2013) who obtained six factors of technological attitude. The current study found out that the items concerning interest in technology proposed by Ardies's research spread to two factors, namely technological career aspirations and consequence of technology. Full details of the factors are presented as follows:

1. Factor 1 (s^2 = 18.972%) was named technological career aspirations (TCA). It accommodated 6 items exploring job and career ambition in technology, interest concerning work in technology, and interest concerning technology lesson at school.
2. Factor 2 (s^2 = 16.581%) was named as perceived consequence of technology (PCT). It accommodates 6 items exploring the importance of technology and technology lessons, the advantage of technological use at work, interest in technology and technology lessons at school.
3. Factor 3 (s^2 = 13.093%) was named as tediousness towards technology (TTT). It accommodates 4 items exploring technological jobs, hobbies, and machines are boring.
4. Factor 4 (s^2 = 15.554%) was named technology as a subject for both boys and girls (TBG). It accommodates 3 items exploring gender differences in technology.
5. Factor 5 (s^2 = 13.620%) was named as label perceived difficulty of technology (PDT). It accommodates 4 items exploring prerequisites to study technology.

Each item has an absolute value of the loading factor ranging from 0.427–0.882 as shown in table 2. This value meets the criteria of Steven (2002) whereas items retained in factor analysis must have a loading factor greater than 0.4. This result was also supported by reliability analysis using Cronbach's alpha coefficients, while the scores for each factor are 0.753, 0.861, 0.830, 0.796 and 0.755, respectively with 0.810 as the overall coefficient. These indicate that the loading factors have a high internal consistency to evaluate attitudes of teachers' candidates towards technology.

3.2 Preference level and Interrelationships among factors

The preference level analysis was carried out to get specific information related to the dominant attitudinal tendency of pre-service science teachers towards technology in Indonesia. This analysis was performed by comparing the mean values of each factor with a grand mean as suggested by Suprapto (2016). The result of the analysis claimed that the

Downloaded from www.periodico.tchequimica.com

perceived consequence of technology was considered as the most dominant factor from technology attitude with a mean value of 4.013 and a standard deviation of 0.468. The second rank was technological career aspirations with a mean value of 3.885 and a standard deviation value of 0.681, followed by technology as a subject for both boys and girls with mean and standard deviation values of 3.080 and 1.127 respectively. These three factors had a mean value greater than the grand mean (2.960) as shown in Table 2. These findings indicated that pre-service Indonesian science teachers, in the first stage, would direct their feelings toward the positive (or negative) effects of technology on the environment and society when they decided to use or not to use technology in their instructional design. Subsequently, teacher candidates would consider how big their ambition to learn or to master technology-related jobs in the future, by including their gender aspects (Ardies et al., 2014).

The next important information is regarding the relationships among attitudinal factors towards technology. In this study, the interrelationship among factors was analyzed using Pearson product-moment correlation. Pearson correlation test was used to determine the one-on-one correlation between each dependent variable toward the independent variable. The correlation coefficients are ranging from -0.208–0.538 that useful for limited prediction (Creswell, 2012). Furthermore, one factor correlates significantly at the 0.01 and 0.05 levels with other factors as shown in table 3. The results also showed that the items questionnaire affect each other either positively or negatively. This also indicates that the efforts applied to improve an attitude component will directly strengthen or weaken another component.

This study was performed by analyzing structural factors which composed technological attitudes, followed by revealing the preference level and interrelationship among factors. These findings produce an attitude towards technology instrument which has high validity and reliability. The items and latent factors in this instrument were able to explain 77.82% of variance in attitudes towards technology. This percentage of variance meets the standard by Pett, Lackey, & Sullivan (2003) which revealed the cumulative variance extracted by successive factors should be more than 50%. Moreover, variance analysis in each factor was found that technological career aspirations as the greatest variance among others. It means that the attitude towards technology could be described by job and career ambition in technology, interest relating to work in technology, interest relating to technology lessons at school relatively more than others. As in the reliability analysis, Cronbach Alpha coefficients was 0.753; 0.861; 0.830; 0.796; 0.755 for each scale and 0.810 for the instrument overall. According to Nunnally & Bernstein (1994), the alpha values greater than 0.70 could be considered as a minimum measure of internal consistency. In other words, these factors were quite reliable in representing the overall attitudes towards technology. Based on the reliability and validity analysis above, the instrument was believed to be able to produce accurate information about attitude towards technology, especially for teachers and pre-service science teachers.

Preference level analysis based on the comparison between mean and grand mean informed three main factors of the technological attitudes for Indonesian science teacher candidates. There were perceived consequence of technology as the first rank followed by technological career aspirations, and technology as a subject for both boys and girls, respectively. As stated by Suprapto (2016), the comparison between mean and grand mean provide justification related to the degree of attitude (Suprapto, 2016). These results indicate that the pre-service teacher's attitude towards technology is primarily determined by their awareness of the importance of technology and technology education, the benefits of technology use, and interest in technology and technology lessons in schools. This finding is in line with a nationwide survey of fourth to twelfth-grade teachers in the USA by Sheingold& Hadley (1990) and found that the source of their motivation to use technology in teaching and learning were the benefits to their own learning and professional development as teacher. Furthermore, interest in technology would encourage users to intensively interact with technology and explore the use of technology in various situations (Zhao & Frank, 2003). Teachers with more computer experience were more likely to show positive attitudes towards computers (Pope-Davis &Twing, 1991; Moseley and Higgins, 1999; Rozell& Gardner, 1999; Kadijevich&Haapasalo, 2008; Teo, 2008). The next technology attitudes of pre-service science teachers were job and career ambition, interest relating to work, and gender effect in technology. Ardies, Maeyer, &Gijbels (2015), researchers in specific, have studied these factors in their longitudinal studies and concluded that career aspirations and interests in technology depends on gender and become big boosts in addressing

Downloaded from www.periodico.tchequimica.com

technology integration. In addition, students' career aspirations and interests in technology are unsettled, it generally changes in the first cycle of secondary education and continues to decrease over time.

Pre-service teachers trained in Institutions for Teacher Training and Pedagogy would generally obtain courses related to content and professional knowledge integrated technology. For example ICT-based learning, virtual-based learning (e-learning), computer visualization, and various computer applications for specific subjects (for example computational chemistry, computational physics, bioinformatics, etc.). The aims were to introduce, train, and familiarize science teacher candidates in Indonesia to adopt and adapt technology in the teaching-learning process. Positive attitudes and confidence in integrating various technologies in instructional settings were expected by having more interactions and experiences with computer technology. This was also supported by Teo (2008) who surveyed the attitude of Singaporean pre-service teachers' towards computer use and found that years of computer use are positively correlated with positive computer attitudes and the level of computer confidence.

From Pearson correlation analysis, it was found that a factor correlated to each other significantly with confidence levels of 99% and 95%. These results informed that career aspirations affect perceived consequence, tediousness, perceived difficulty toward technology and all these factors could not be separated from gender difference. Several studies supported these findings by stating that attitude towards computer technology constitutes to many variables such as computer experience (Pope-Davis & Twing, 1991; Kadijevich & Haapasalo, 2008; Teo, 2008), perceived usefulness and computer confidence (Rovai & Childress , 2002; Teo, 2008), Age (Pope-Davis &Twing, 1991), gender (Pope-Davis &Twing, 1991; Sadik, 2006; Teo, 2008), training (Tsitouridou & Vryzas, 2003), and subjective norm and facilitating conditions (Teo, 2008). Therefore, all efforts by education stakeholders such as schools, government, education observers, institutions for educational quality assurance, teacher training institutions should start encouraging technology-pedagogy integration and improving technological skills for teachers and pre-service science teachers by encouraging positive attitudes towards technology. Surely, many other factors must be also considered in doing this.

4. CONCLUSIONS:

Exploratory factor analysis applied in this research provided important evidence related to the main factors that characteristically configures the attitudes of pre-service science teachers towards technology. From all factors, perceived consequence of technology, technological career aspirations, and technology as a subject for both boys and girls play an important role in attitude towards technology for Indonesian pre-service science teachers. Based on Cronbach alpha coefficients, there are significant attitudinal correlations among the factors. Finally, statistical judgments confirm that the instruments used in this study have a high validity and reliability. In addition, the evidence presented in this research are expected to be recommendations and catalyst for teachers and teacher candidates to change their mindset and encourage a positive attitude towards technology in education.

5. REFERENCES:

1. Afshari, M., Bakar, K. A., Luan, W. S., Samah, B. A., & Fooi, F. S. Factors Affecting Teachers' Use of Information and Communication Technology. *Int. J. Instr.*, **2009**, *2*(1), 77–104.
2. Alqahtani, M., & Mohammad, H. Mobile Applications' Impact on Student Performance and Satisfaction. *Turk. Online J. Educ. T.*, **2015**, *14*(4), 102-112.
3. Ardies, J., De Maeyer, S., & Gijbels, D. Reconstructing the Pupils Attitude Towards Technology-survey. *Design and Technology Education*, **2013**,*18*(1), 8-19.
4. Ardies, J., De Maeyer, S., Gijbels, D., & van Keulen, H. Students attitudes towards technology. *Int. J. Technol. Des. Ed.*, **2015**, *25*(1), 43-65.
5. Bame, E. A., Dugger, W. E., de Vries, M., & McBee, J. Pupils' attitudes toward technology—PATT-USA. *J. Technol. Stud.*, **1993**, *19*(1), 40-48.
6. Baek, Y.G., Jong, J., & Kim, B. What Makes Teachers Use of Technology in The Classroom? Exploring the Factors Affecting Facilitation of Technology with a Korean Sample. *Comput. Educ.*, **2008**, *50*(8), 224-234.
7. Beavers, A. S., Lounsbury, J. W., Richards, J. K., Huck, S. W., Skolits, G. J., & Esquivel, S. L. Practical Considerations for Using

Downloaded from www.periodico.tchequimica.com

Exploratory Factor Analysis in Educational Research. *Pract. Assess. Res. Eval.*, **2013**, *18*(6), 1-31.

8. Bujak, K. R., Radu, I., Catrambone, R., Macintyre, B., Zheng, R., & Golubski, G. A Psychological Perspective on Augmented Reality in the Mathematics Classroom. *Comput. Educ.*, **2013**, *68*, 536-544.
9. Chai, C. S., Hong, H. Y., & Teo, T. K. G. Singaporean and Taiwanese Pre-Service Teachers' Beliefs and Their Attitude Towards ICT Use: A Comparative Study. *Asia-Pac. Educ. Res.*, **2009**, *18*(1), 117-128.
10. Chiang, T. H. C., Yang, S. J., & Hwang, G. J. An Augmented Reality-Based Mobile Learning System to Improve Students' Learning Achievements and Motivations in Natural Science Inquiry Activities. *Educ. Technol. Soc.*, **2014**, *17*(4), 352-365.
11. Coffland, D., & Strickland, A. Factors Related to Teacher Use of Technology in Secondary Geometry Instruction. *J. Comput. Math. Sci. Teach*., **2004**, *23*(4), 347–365.
12. Creswell, J. W. Educational Research: Planning, Conducting, and Evaluating Quantitative and Qualitative Research (4th ed.). Boston, MA: Pearson, **2012**.
13. Eteokleous, N. Evaluating Computer Technology Integration in a Centralized School System. *Comput. Educ.*, **2008**, *51*(2), 669–686.
14. Gilakjani, A. P., Lai-Mei, L., & Ismail, H. N. Teachers' Use of Technology and Constructivism. *Int*. *J. Mod. Educ. Comput. Sci.*, **2013**, *5*(4), 49.
15. Hazari, S., North, A., & Moreland, D. Investigating Pedagogical Value of Wiki Technology. *J. Inf. Syst. Educ.*, **2009**, *20*(2), 187-198.
16. Holcomb, L. B., & Beal, C. M. Capitalizing on Web 2.0 in the Social Studies Context. *Tech. Trends*., **2010**, *54*(4), 28-33.
17. Huang, H. M., & Liaw, S. S. Exploring Users' Attitudes and Intentions Toward the Web as A Survey Tool. *Comput. Hum. Behav*. **2005**, *21*(5), 729-743.
18. Kadijevich, D., & Haapasalo, L. Factors That Influence Student Teacher's Interest to Achieve Educational Technology Standards. *Comput. Educ.*, **2008**, *50*(1), 262-270.
19. Keengwe, J., & Georgina, D. Supporting Digital Natives to Learn Effectively with Technology Tools. *Int. J. Inform. Comm. Tech. Educ.*, **2013**, *9*(1), 51-59.
20. Keengwe, J., Onchwari, G., & Agamba, J. Promoting Effective E-Learning Practices Through the Constructivist Pedagogy. *Educ. Inform. Tech*., **2014**, *19*(4), 887-898.
21. Kim, C., Kim, M. K., Lee, C., Spector, J. M., & DeMeester, K. Teacher Beliefs and Technology Integration. *Teach. Teach. Educ*., **2013**, *29*, 76-85.
22. Kling, R. Learning about Information Technologies and Social Change: The Contribution of Social Informatics. *Inform. Soc.*, **2000**, *16*(3), 217-232.
23. Koehler, M., & Mishra, P. What is Technological Pedagogical Content Knowledge (TPACK)?. *Contemp. Iss. Tech. Teach. Educ.*, **2009**, *9*(1), 60-70.
24. Kramarski, B., & Michalsky, T. Preparing Preservice Teachers for Self-Regulated Learning in the Context of Technological Pedagogical Content Knowledge. *Learn. Instr.*, **2010**, *20*(5), 434-447.
25. Laurillard, D. Rethinking University Teaching: A Conversational Framework for The Effective Use of Learning Technologies. Routledge, **2013**.
26. Lee, K. Augmented Reality in Education and Training. *Tech. Trends.*, **2012**, *56*(2), 13-21.
27. Liu, S. H. Factors Related to Pedagogical Beliefs of Teachers and Technology Integration. *Comput. Educ.*, **2011**, *56*(4), 1012-1022.
28. Moseley, D. & Higgins, S. Ways Forward With ICT: Effective Pedagogy Using Information and Communications Technology for Literacy and Numeracy in Primary Schools. London: Teacher Training Agency, **1999**.
29. Norton, S., McRobbie, C., & Cooper, T. Exploring secondary mathematics teachers' reasons for not using computers in their teaching: Five case studies. *J. Res. Comput. Educ.*, **2000**, *33*(1), 87–109.
30. Nunnally, J., & Bernstein, I. Psychometric Theory (3rd ed.). New York: McGraw-Hill, **1994**.
31. Opdenakker, M. C., & Van Damme, J. Teacher Characteristics and Teaching Styles as Effectiveness Enhancing Factors of

Downloaded from www.periodico.tchequimica.com

Classroom Practice. *Teach. Teach. Educ*., **2006**, *22*(1), 1-21.

32. Oncu, S., Delialioglu, O., & Brown, C. A. Critical Components for Technology Integration: How Do Instructors Make Decisions? *J. Comput Math. Sci. Teach.*, **2008**, *27*(1), 19–46
33. Ottenbreit-Leftwich, A. T., Glazewski, K. D., Newby, T. J., & Ertmer, P. A. Teacher Value Beliefs Associated with Using Technology: Addressing Professional and Student Needs. *Comput. Educ.*, **2010**, 55(3), 1321-1335.
34. Pett, M. A., Lackey, N. R., & Sullivan, J. J. Making Sense of Factor Analysis: The Use of Factor Analysis for Instrument Development in Health Care Research. Thousand Oaks, CA: Sage, **2003**.
35. Pope-Davis, D. B., & Twing, J. S. The Effects of Age, Gender, and Experience on Measures of Attitude Regarding Computers. *Comput. Hum. Behav*., **1991**, *7*(4), 333-339.
36. Rienties, B., Brouwer, N., & Lygo-Baker, S. (2013). The Effects of Online Professional Development on Higher Education Teachers' Beliefs and Intentions Towards Learning Facilitation and Technology. *Teach. Teach. Educ.*, 29, 122-131.
37. Rovai, A. P., & Childress, M. D. Explaining and Predicting Resistance to Computer Anxiety Reduction among Teacher Education Students. *J. Res. Comput. Educ.,* **2002**, 35(2), 226-235.
38. Rozell, E. J., & Gardner III, W. L. Computer-Related Success and Failure: A Longitudinal Field Study of the Factors Influencing Computer-Related Performance. *Comput. Hum. Behav.*, **1999**, 15(1), 1-10.
39. Sadik, A. Digital Storytelling: A Meaningful Technology-Integrated Approach for Engaged Student Learning. *Educ. Technol. Res. Develop.*, **2008**, 56(4), 487-506.
40. Sang, G., Valcke, M., Van Braak, J., & Tondeur, J. Student Teachers' Thinking Processes and ICT Integration: Predictors of Prospective Teaching Behaviors with Educational Technology. *Comput. Educ.*, **2010**, 54(1), 103-112.
41. Schmitt, T. A. Current Methodological Considerations in Exploratory and Confirmatory Factor Analysis. *J. Psychoeduc. Assess.*, **2011**, 29(4), 304-321.
42. Sheingold, K. & Hadley, M. Accomplished Teachers: Integrating Computers Into Classroom Practice. New York: Centre for Technology in Education, **1990**.
43. Stevens, J. Applied Multivariate Statistics for the Social Sciences. Mahwah, NJ: Erlbaum, **2002**.
44. Suprapto, N. Students' Attitudes Towards STEM Education: Voices from Indonesian Junior High Schools. *J. Turk. Sci. Educ.*, **2016**, 13(3), 75-87.
45. Sunyono, S., Tania, L., & Saputra, A. A Learning Exercise Using Simple and Real-Time Visualization Tool to Counter Misconceptions about Orbitals and Quantum Numbers. *J. Baltic Sci. Educ.*, **2016**, 15(4), 452-463.
46. Tania, L. & Saputra, A. Using Android-Based Equation Plotters as Supporting Tools for Teaching and Learning Atomic Orbitals. *Period. Quim*., **2018**, 15(30), 397-401.
47. Tania, L., Saputra, A., Muntari, I., & Yolanda, N. A Student-Generated Less-Familiar Atomic Orbitals (l = 4–10) Representation Using Simple and Real-Time Visualization Software. *Period. Quim*., **2017**, 18(2), 121-122.
48. Teo, T. Pre-service Teachers' Attitudes Towards Computer Use: A Singapore Survey. *Australas. J. Educ. Tech*, **2008**, 24(4), 413-424.
49. Treiblmaier, H., & Filzmoser, P. Exploratory Factor Analysis Revisited: How Robust Methods Support the Detection of Hidden Multivariate Data Structures in IS Research. *Inform. Manage.*, **2010**, 47(4), 197-207.
50. Tsitouridou, M. & Vryzas, K. Early Childhood Teachers' Attitudes Towards Computer and Information Technology: The Case of Greece. *Inform. Tech. Child. Educ. Ann.*, **2003**, 1, 187-207.
51. UCLA Statistical Consulting Group. Factor analysis: SPSS Annotated Output. Retrieved 06 August, 2019 from https://stats.idre.ucla.edu/spss/output/factor-analysis/
52. Van Braak, J., Tondeur, J., & Valcke, M. Explaining Different Types of Computer Use Among Primary School Teachers. *Eur. J. Psych. Educ*., 2004, 19(4), 407.
53. Warschauer, M., & Matuchniak, T. New Technology and Digital Worlds: Analyzing

Downloaded from www.periodico.tchequimica.com

Evidence of Equity in Access, Use, and Outcomes. *Rev. Res. Educ.*, **2010**, 34(1), 179-225.

54. Whittle, R. J., Telford, A., & Benson, A. C. Teacher's Perceptions of How They Influence Student Academic Performance in VCE Physical Education. *Aust. J. Teach. Educ.*, **2018**, 43(2), 1.
55. Wojciechowski, R., & Cellary, W. Evaluation of Learners' Attitude Toward Learning in ARIES Augmented Reality Environments. *Comput. Educ*., **2013**, 68, 570-585.
56. Yang, Y. T. C., & Wu, W. C. I. Digital Storytelling for Enhancing Student Academic Achievement, Critical Thinking, and Learning Motivation: A Year-Long Experimental Study. *Comput. Educ.*, **2012**, 59(2), 339-352.
57. Zhao, Y., & Frank, K. A. Factors Affecting Technology Uses in Schools: An Ecological Perspective. *Am. Educ. Res. J*., **2003**, 40/4, 807-840.

Table 1. *Items informations, loading factor dan Cronbach α of attitude towards technology questionnaire*

	Factor 1	Factor 2	Factor 3	Factor 4	Factor 5
Factor 1: Technological Career Aspirations (TCA), α = 0.753, s^2 = 18.972%					
TCA1	0.879				
TCA2	0.850				
TCA3	0.801				
TCA4	0.798				
TCA5	0.645				
TCA6	0.492				
Factor 2: Perceived Consequence of Technology (PCT), α = 0.861, s^2 = 16.581%					
PCT1		0.847			
PCT2		0.800			
PCT3		0.789			
PCT4		0.529			
PCT5		-0.427			
PCT6		-0.482			
Factor 3: Tediousness Towards Technology (TTT) α = 0.830, s^2 = 13.093%					
TTT1			0.844		
TTT2			0.840		
TTT3			0.830		
TTT4			0.700		
Factor 4: Technology as a Subject for both Boys and Girls (TBG) α = 0.796, s^2 = 15.554%					
TBG1				0.882	
TBG2				0.881	
TBG3				0.815	
Factor 5: Perceived Difficulty of Technology (PDT), α = 0.755, s^2 = 13.620%					
PDT1					0.758
PDT2					0.724
PDT3					0.656
PDT4					0.606

Downloaded from www.periodico.tchequimica.com

Table 2. *The mean and standard deviation of each factor**

Factor	Mean	Standard Deviation	Ranking
1	3.885	0.681	2*
2	4.013	0.468	1*
3	1.924	0.781	4
4	3.080	1.127	3*
5	1.899	0.682	5

*mean > grand mean

Table 3. *Summary of Pearson correlation for each factors*

	Factor 1	Factor 2	Factor 3	Factor 4	Factor 5
Factor 1	1	0.538**	-0.403**	-0.216**	-0.273*
Factor 2		1	-0.249**	0.210*	-0.208*
Factor 3			1	0.253**	0.323**
Factor 4				1	0.345**
Factor 5					1

***P* > 0.01; **P* > 0.05

APPENDIX 1

Attitude Towards Technology Questionnaire

Directions:
Please tick () in the box one of the five choice (Strongly Disagree (SD), Disagree (D), Neutral (N), Agree (A) and Strongly Agree (SA) for each statement

Items	**Option**				
	SD	**D**	**N**	**A**	**SA**
Technological Career Aspirations					
I would enjoy a job in technology					
I would like a career in technology later on					
Working in technology would be interesting					
I will probably choose a job in technology					
If there was a school club about technology I would certainly join it					
There should be more education about technology					
Perceived Consequence of Technology					
Technology lessons are important					
Technology is very important in life					
Everyone needs technology					
You have to be smart to study technology					
Technology makes everything work better					
I am not interested in technology					

Downloaded from www.periodico.tchequimica.com

Tediousness Towards Technology

Most jobs in technology are boring					
A technological hobby is boring					
I think machines are boring					
I do not understand why anyone would want a job in technology					

Technology as a Subject for both Boys and Girls

Boys are more capable of doing technological jobs than girls Boys know more about technology than girls do this Boys are able to do practical things better than girls					

Perceived Difficulty of Technology

You can study technology only when you are good at both mathematics and science					
To study technology you have to be talented					
Technology is only for smart people					
I would rather not have technology lessons at school					

Downloaded from www.periodico.tchequimica.com

PERIÓDICO TCHÊ QUÍMICA
ARTIGO ORIGINAL

ESTUDO DE PROCESSOS DE DEFORMAÇÃO DE MATERIAIS PLÁSTICOS USANDO PROCESSAMENTO DE IMAGEM DIGITAL

INVESTIGATION OF PROCESSES OF DEFORMATION OF PLASTIC MATERIALS WITH THE HELP OF DIGITAL IMAGE PROCESSING

ИССЛЕДОВАНИЕ ПРОЦЕССОВ ДЕФОРМАЦИИ ПЛАСТИЧНЫХ МАТЕРИАЛОВ С ПРИМЕНЕНИЕМ ЦИФРОВОЙ ОБРАБОТКИ ИЗОБРАЖЕНИЙ

BODRYSHEV, Valeriy V.[1*]; BABAYTSEV, Arseniy V.[2]; RABINSKIY, Lev N.[3];

[1] Moscow Aviation Institute (National Research University), Department of Engineering Graphics, Moscow – Russian Federation

[2] Moscow Aviation Institute (National Research University), Institute of General Engineering Training, Research Department No. 9, Moscow – Russian Federation

[3] Moscow Aviation Institute (National Research University), Institute of General Engineering Training, Moscow – Russian Federation

** Correspondence author*
e-mail: NioBVV@mail.ru

Received 20 October 2019; received in revised form 14 November 2019; accepted 14 November 2019

RESUMO

Atualmente, uma ampla gama de trabalhos está em andamento para criar métodos de correlação usando algoritmos apropriados. Isso é especialmente útil na construção de vetores de deslocamento para avaliar a deformação de materiais com o estabelecimento de correspondência entre as seções de duas imagens, calculando as funções de correlação cruzada e procurando um extremo. O objetivo deste trabalho foi desenvolver um método para avaliar o mecanismo de destruição do material de acordo com a análise da imagem fotográfica pelo parâmetro de intensidade da imagem utilizando a análise multivariada da relação entre a intensidade da imagem. Além disso, este método deve ser usado com a ajuda de análises multivariadas (análise de múltiplos fatores) das relações entre intensidade da imagem e rugosidade da superfície, revelando a geometria da área (volume) de deformação sob várias condições operacionais. O método digital de processamento de fotografias (quadros de vídeo) foi utilizado para estudar a microestrutura e a superfície dos materiais pelo critério de intensidade da imagem durante os testes de deformação mecânica. Os parâmetros quantitativos da intensidade da imagem são comparados com a estrutura do material, a rugosidade da superfície antes e após a destruição das amostras. As imagens utilizadas foram obtidas durante o teste mecânico de amostras de alumínio. Para garantir a confiabilidade dos resultados dos testes, foram testadas seis amostras do mesmo tipo. Um diagrama de tensão-deformação foi criado para cada amostra. Os diagramas de tensão-deformação dos testes mecânicos foram comparados com os diagramas de fotoanálise usando o método descrito acima. Os resultados correlacionaramm-se bem um com o outro, mas, diferentemente do experimento, onde a tensão é medida apenas no local do medidor de tensão, a fotoanálise fornece uma imagem completa da distribuição da tensão em toda a área da amostra. Além disso, foi realizada uma análise multivariada para avaliar as dimensões e formas geométricas dos elementos estruturais.

Palavras-chave: *fotografia (quadro de vídeo), estrutura do material, escala de cinzentos, rugosidade, teste de tração.*

ABSTRACT

As of now, many investigations are performed in order to develop methods of correlation with the help of relevant algorithms. This is especially helpfull for plotting vectors of displacements in order to estimate deformation of various materials, as well as to determine correspondence between sections of two images through calculation of the cross-correlating functions and to ensure seeking of the extremum. The aim of this study was to develop relevant method to estimate mechanism of fracture of materials in accordance with the data of analysis of a photographic image in respect of the parameter of the image intensity. In addition, this method is to be used with the help of the multivariate analysis (multi-factor analysis) of the interrelationship

Downloaded from www.periodico.tchequimica.com

between image intensity, surface roughness, and possibility to determination the geometrical parameters of the deformation area/deformation volume under different conditions of operation. Digital method of processing of photographs/video frames has been used in order to investigate microstructure and surface of materials in respect of criterion of the image intensity in the course of mechanical tests in accordance with deformations. Quantitative parameters of the image intensity were compared to the structure of material, as well as to the surface roughness before and after destruction of samples. The images used were obtained during mechanical testing of aluminium samples. To ensure the validity of the test results, six specimens of the same type were tested. A stress-strain diagram was drawn up for each specimen. Stress-strain diagrams from the mechanical tests were compared with those from the photo analysis using the method described above. The results correlate well with each other, but unlike the experiment, where the strain is measured only at the strain gauge location, the photo analysis provides a complete picture of the strain distribution over the entire specimen area. In addition, a multivariate analysis has been carried out to evaluate the geometric dimensions and shapes of the structure elements.

Keywords: *photograph (video frame), structure of material, grey colour gradation, roughness, tensile strength test.*

АННОТАЦИЯ

В настоящее время проводится большой спектр работ по созданию методов корреляции с применением соответствующих алгоритмов. Это особенно полезно для построения векторов перемещений для оценки деформации материалов, с установлением соответствия между участками двух изображений путем вычисления взаимно-корреляционных функций и поисков экстремума. Целью данной работы является разработка метода оценки механизма разрушения материала по данным анализа фотоизображения по параметру интенсивности изображения с привлечением многофакторного анализа связи между интенсивностью изображения. Кроме того, этот метод должен использоваться с помощью многомерного анализа (многофакторного анализа) взаимосвязей между интенсивностью изображения, шероховатостью поверхности, выявлением геометрии площади (объема) деформации при различных условиях эксплуатации. Цифровой метод обработки фотографий (видеокадров) был использован для исследования микроструктуры и поверхности материалов по критерию интенсивности изображения в процессе механических испытаний по деформациям. Сопоставлены количественные параметры интенсивности изображения со структурой материала, шероховатостью поверхности до и после разрушения образцов. Используемые изображения были получены во время механических испытаний образцов алюминия. Для обеспечения достоверности результатов испытаний были испытаны шесть образцов одного типа. Диаграмма напряжение-деформация была составлена для каждого образца. Диаграммы напряжения-деформации механических испытаний сравнивали с диаграммами фотоанализа с использованием метода, описанного выше. Результаты хорошо коррелируют друг с другом, но в отличие от эксперимента, где деформация измеряется только в месте расположения тензометрического датчика, фотоанализ дает полную картину распределения деформации по всей площади образца. Кроме того, был проведен многомерный анализ для оценки геометрических размеров и форм элементов конструкции.

Ключевые слова: *фотография (видеокадр), структура материала, градация серого цвета, шероховатость, испытание на растяжение.*

1. INTRODUCTION

Due to development of the high-quality recording photographic equipment and video equipment, as well as development of digital methods of the videodata processing in various branches of technology (Znamenskaya *et al.*, 2001; Bessonov *et al.*, 2013, Filippov and Proskokov, 2014; Belov *et al.*, 2014; Berezovskii *et al.*, 2015; Kobets *et al.*, 2016; Bodryshev and Morgunova, 2017a; Babaytsev *et al.*, 2017a; Formalev and Kolesnik, 2017; Formalev and Kolesnik, 2018; Bulychev *et al.*, 2018), there exists the possibility for development of the quick-operating and non-contact methods in order to estimate deformations of materials in various conditions of operation in respect of the parameter of the image intensity of photographs/video frames (Borynyak and Nepochatov, 2007; Volkov, 2010; Sodushkin *et al.*, 2011; Bodryshev and Morgunova, 2017b; Bodryshev, 2017; Bieda *et al.*, 2018; Babaytsev *et al.*, 2019; Ho *et al.*, 2019). This problem is the task of vital importance in the course of investigations of deformation processes and processes of destruction of the structurally nonuniform materials (metals, ceramic materials, composite materials and so on) (Rief *et al.*, 2017; Bodryshev and Morgunova, 2017a; Bulychev *et al.*, 2018; Dzioba and Lipiec, 2018; Rabinskiy *et*

Downloaded from www.periodico.tchequimica.com

al., 2019; Faraji and Torabzadeh, 2019; Hosdez *et al.*, 2019).

At the present time, many investigations are performed in order to develop methods of correlation with the help of relevant algorithms for plotting vectors of displacements in order to estimate deformation of various materials (Sodushkin *et al.*, 2011; Borodulin, 2013; Filippov and Proskokov, 2014; Bodryshev and Morgunova, 2017a; Bodryshev, 2017; Kang and Muhammad, 2017; Wu *et al.*, 2018; Babaytsev *et al.*, 2019), as well as to determine correspondence between sections of two images through calculation of the cross-correlating functions and to ensure seeking of the extremum (Görtan, 2017; Pushkarev et al., 2017; Iwamoto and Kanie, 2017; Yang *et al.*, 2018; Khotinov *et al.*, 2019; Muniandy, 2019; Wang *et al.*, 2019). Calculated values of the deformation parameters will be final results of such method. Investigations of various processes of destruction of plastic materials are described in this article. The article presents investigation of the problem of interrelationship between deformation of surfaces of various materials and the law of variation of the intensity of images of these surfaces.

Goal of the present article was to develop relevant method in order to estimate mechanism of fracture of materials in accordance with the data of analysis of a photographic image in respect of the parameter of the image intensity.

2. MATERIALS AND METHODS

Mechanical tensile strength tests have been performed in order to verify the proposed methodology. These tests were performed with the help of the Instron 5969 (produced of the Great Britain) equipment as well as with the help of the Bluehill 3 software. The sample has been captured and held with the help of special mechanical captures. Speed of performance of these tests has been established at the level of 1 mm/minute. All tests have been performed at room temperature. These tests have been performed with the help of 4 samples up to the moment of destruction of these samples. The samples were made as the platelets with following dimensions: 120 mm in length, 10 mm in width, and 1.4 mm in thickness. All samples were photographed before and after tests. The load – displacement diagram was constructed in accordance with results of these tests.

Photographs or video frames of the material structure of all samples are stored in the files, which have BMP or JPEG extensions. Quality of images is determined in accordance with quantity of pixels within the preassigned section in the range from 72 up to 400 pixels/inch (from 28.35 up to 157.48 pixels/cm).

Before and after tests, the entire area of relevant photograph of the sample under investigation is then splitted into discrete cells, which contain from 1 up to *k* pixels in horisontal direction (axis of abscissas *x*) and from 1 up to *m* pixels in vertical direction (axis of ordinates *y*). Dimension of the cell depends on the required precision of estimation in the course of investigation of the relevant photograph and this dimension must be the same in both variants. Function L=f(x,y) of intensities of images within a cell is quantitative characteristic of these intensities (that is, white colour level within a photograph). This function (in the case of a digital still photograph) is presented as the matrix of integers, which are reduced to the range of gradations from 0 up to 255 (quantisation) (Bodryshev and Morgunova, 2017a; Formalev and Kolesnik, 2017; Shtefan *et al.*, 2019). In the course of investigation of the obtained matrix it is very important to transform this matrix with the help of the coefficient of discreditation (Equation 1). In this case, $\Delta_{measured}$ and Δ_{actual} is share of dimension of components within a digital still photograph and actual value of this dimension, respectively.

Therefore, an image is presented as the two-dimensional function L(xy) along with construction of the relevant diagram, where *x* and *y* are coordinates of the cells within a photograph, while L is intensity of image (brightness) within the preassigned cells (Figure 1). The obtained data are presented in a graphical form as the three-dimensional model xyL (Figure 1b). Further processing of this model makes it possible to determine the following: laws of change of the L=f(x,y) in the longitudinal or transversal cross-sections; any coordinate in any point of the relevant diagram; distance between cells and so on. In the course of investigation of influence of length of the section ($H_{calculated}$), within which measurement of deformation is performed (Figure 2), it is very important to determine exact position of the point of deformation within the sample. Relative deformation ε is determined in accordance with the following expression (Equation 2). Where $H_{calculated\ 0}$ and $H_{calculated}$ is length of the deformation fixation within the initial sample and after destruction of this sample, respectively. It is worthy of note that destruction of material in the second variant (Figure 2b) was observed near the upper jaw for fixation of the

Downloaded from www.periodico.tchequimica.com

sample in the testing machine ($H_{apper\ part}$). In this case, section $H_{calculated}$ is situated in the lower part of the sample and relative deformation is only determined in accordance with the data in respect of tensile of the lower section of the relevant sample.

Figure 3 presents fracture diagram N-ε of the sample 1.1 (Figure 2). In this case, N is load upon the sample. A substantial zone of the material yielding is clearly visible. The following Figure 4 presents digital image of the sample 1.1 after destruction. Zone of the surface deformation near the point of destruction is clearly visible. It is important to determine the structure of this deformation. As concerns transversal direction, this deformation has the wave structure, which is characterised by the amplitude of variation of the image intensity value Equation 3, as well as by parameters of deformation of the relevant material (roughness). In this case $L_{max.Mi}$, $L_{min.Mi}$ are maximum and minimum values of intensity (respectively) within the i-th wave (which is under consideration) of the M-th cross-section.

There are good reasons to analyse the data on the amplitude of variation of the surface deformation of various materials Equation 4 as the criterion of the material deformation. In this case, h_{MaxMi}, h_{MinMi} respectively, are maximum and minimum values of the deformation height within the i-th wave (which is under consideration) of the M-th cross-section.

There are good reasons to perform comparison of these criterions in accordance with the data of the root-mean-square deviation SL and Sh of parameters L and h. For the M-th cross-section, we will have (Equations 5; 6). In this case, L_{Mk} and h_{Mn} is value of L within the k-th cell and value of h in the course of the i-th measurement of the M-th cross-section, respectively, while $\overline{L_M}$ and $\overline{h_M}$ are average values of these parameters. In addition, there are good reasons to analyse standard criterion R_z of the surface roughness as the criterion of deformation (Bodryshev, 2017; Bodryshev and Morgunova, 2017b; Babaytsev *et al.*, 2019).

It is recommended to use method of the contour analysis in order to determine geometrical parameters of sections of deformation near the zone of destruction (Borynyak and Nepochatov, 2007; Bodryshev, 2017). Section is characterised by availability of cells with the range of dispersion of the image intensity Equation 7. In this case, $L_{max.}$ and $L_{min.}$ are minimum and maximum values of the image intensity within the cells of digital display of the sample surface, respectively. The entire area of the section with the preassigned values of ΔL_1 is determined in accordance with the help of the receptor models, which ensure discretisation of space. The receptor method is based on the approximate representation of a geometrical object within the field/space of receptors. From the mathematical point of view, the receptor geometrical model is described by the multitude $A=\{a_{ij}\}$, where (Equation 8). It is assumed that receptor is in the unexcited state, if boundary of the section does not crosses this receptor, as well as if this receptor does not belong to the internal branch.

The obtained matrix, which contains the data "*1*", makes it possible to estimate boundaries of this section, as well as to determine its area. The entire area of the preassigned section S_i is determined with the help of summation of all n cells with parameter "*1*". Then this sum is to be multiplied by the area of one cell. This area is to be determined as the product of the cell width s_{cell} and height h_{cell} (Equation 9). Contour of the section is determined with the help of Freeman chain code (Borynyak and Nepochatov, 2007; Vinogradov, 2015; Bodryshev, 2017; Babaytsev *et al.*, 2017b; Kornev *et al.*, 2018; Rabinskiy and Tushavina, 2019; Rabinsky and Tushavina, 2019). It is reasonable to generalise results of the statistical analysis, which is to be performed with the help of the required quantity of samples on the condition of the preassigned kind of loading, in accordance with the statistical criterions.

3. RESULTS AND DISCUSSION:

On the basis of the data, which are contained in the matrices of digital display of samples and which are presented in Figure 2, Table 1 and Figure 5 present results of calculation of change of the relative deformation ε in the course of variation of the $H_{calculated}$ at different distances from the fixation jaws. It is obvious that relative deformation increases in the course of decrease of the distance $H_{calculated}$. In this case, we observe various kinds of dynamics of change in values of ε depending on position of the point of fracture. Therefore, issue of dependence of the ε value from the position of $H_{calculated}$ is the problem of vital importance.

Let us analyse dynamics of change in S_L and S_h values, as well as dynamics of change in the criterion of roughness R_z of sample 1.1. Figure 6 presents fixed cross-sections in the longitudinal and transversal directions for the

Downloaded from www.periodico.tchequimica.com

upper and lower parts of the sample, which was fractured in the conditions of tensile. Figure 7 presents diagram of change of the image intensity L in the longitudinal cross-section in the centre of the destroyed upper part of the sample (cross-section 6 of the upper part). Roughness of this cross-section was determined with the help of the Mitutoyo Surftest SJ-210 equipment. Chart of change of the roughness is presented in Figure 8 (diagram of the roughness measurement was constructed beginning from the upper end of the deformation section at the distance of 30 mm from the point of destruction). Construction of such charts makes it possible to determine the law of interrelationship between the parameters under investigation.

Comparisons in respect of SL values, as well as in respect of dispersion of roughness Sh have been performed in accordance with the following procedures (Figure 6):

1. Analysis of the data SL and Sh in the longitudinal cross-sections (1.5, 6, 9) of the upper and lower parts of the sample (of the samples).

2. Analysis of the data SL and Sh in the transversal cross-sections of the upper and lower parts of the sample (of the samples).

3. Group analysis of the data SL and Sh in the transversal and longitudinal cross-sections of the upper and lower parts of the sample (of the samples).

4. Performance of analysis of the data SL along with parameters of roughness Rz.

Relevant chart (Figure 9) presents dynamics of change of the data SL, Sh, Rz in the upper part of the fractured sample in the transversal cross-sections 2.5, 5.5, 6.5, 10, 20, and 30 mm (as an example). Clear trend of the interconnected correlation between these parameters is observed. It is possible to determine two sections in the range from 2.5 up to 5.5 mm, where change of SL, Sh, and Rz values is practically inessential, as well as the second section (more than 20 mm), where effect of deformation is an insignificant factor.

Results of performed investigations clearly demonstrate that deformation of surface within the zone of destruction is only determined by the effect of destruction as such, as well as that deformation depends on of the surface roughness of the initial sample to a lesser degree. As concerns the lower part of the sample (Figure 6b), dynamics of change of parameters is different as compared to the dynamics of the upper part (Figure 10) in a certain degree. It is possible that these data can be explained with the help of different "conditions" of deformation of these samples. As concerns the range from 5 up to 18 mm, values of Rz and Sh decrease in the form of waves and have inessential slope, while SL value has a substantial slope. It is reasonable to perform additional investigations in order to analyse this situation.

The following Figure 11 presents dependences of change of the parameters under investigation near the zone of destruction. It is clearly visible that values of SL, Sh, Rz both for the lower section and for the upper section of sample at the distances 3, 6, and 10 mm are practically equal to each other. Therefore, the stressed state within the zone of fracture is practically the same. As concerns estimation of the zone of deformation, there are good reasons to investigate digital matrices of the displayed sections (Figure 12). Due to the fact that expressions (2) and (3) are satisfied and they are valid, it is possible to determine area of the deformed section (S3) with the great degree of accuracy. In this variant, this area is equal to 119 mm^2 and it is determined in accordance with the following expression: S3 = S – S1 – S2. In this case, S, S1, and S2 are the foillowing parameters: total area of part of the image under investigation; area of the sample without any deformations; area of the image beyond the sample, respectively.

The following problems have been solved in the course of this investigation:

1. Estimation of deformation of various samples in the course of destruction on the basis of the length of the fixed section, within which fixation of such deformation occurs.

2. Determination of the law of deformation of the sample cell taking into consideration the dependence of such deformation on dimensions of this cell. These data make it possible to determine the law of deformation within the zone of destruction.

3. Investigation of the interrelationship between surface deformation of sample within the zone of destruction and the law of variation of the image intensity.

4. Determination of the zone of deformation of various materials after destruction.

4. CONCLUSIONS:

1. Mechanical tensile tests were performed. Load-displacement diagrams for all

Downloaded from www.periodico.tchequimica.com

samples under investigation were obtained. Measurements of roughness in different cross-sections before and after tests were made. Charts of changes in roughness were constructed.

2. Deformation processes in the aluminium samples in the condition of the uniaxiual static tensile were investigated in accordance with the method of correlation of digital images before and after destruction.

3. Display of the massive of the image intensity in the upper and lower parts of the fractured sample ensures visual presentation of differences or coincidences of the deformation parameters within these sections.

4. Influence of the length of the section for deformation measurements upon the value of deformation was investigated with the help of the digital method of the sample image processing.

5. The statistically significant interrelationship of the image intensity of surface of the sample under investigation with the root-mean-square deviation of the surface deformation after destruction and parameter of roughness Rz was determined.

6. Geometrical dimensions of the deformation sections near the zone of destruction are determined with the help of the method of contour analysis. In addition, this method is to be used with the help of the multivariate analysis (multi-factor analysis) of the interrelationship between image intensity, surface roughness, and possibility of determination of geometrical parameters of the deformation area/deformation volume under different conditions of operation.

5. ACKNOWLEDGMENTS:

This investigation was performed within the framework of the Russian Science Foundation grant in respect of the “Performance of investigations by scientific groups under management of young scientists” event of the Presidential Programme of the Investigation Projects (Agreement No. 19-79-10258 dated August 08, 2019).

6. REFERENCES:

1. Babaytsev, A.V., Bodryshev, V.V., Morgunova, A.A., Rabinsky, L.N. A combined method for assessing the relationship between the deformation of materials and the roughness of their surface based on digital photographs analysis of digital photographs. *Proceedings of the XXV International Symposium “Dynamic and Technological Problems of Structural Mechanics and Continuous Media” (pp. 27-28)*. Sanatorium Vyatichi, Kremenki, Russian Federation, **2019**.
2. Babaytsev, A.V., Martirosov, M.I., Rabinskiy, L.N. *Russian Metallurgy (Metally)*, **2017a**, *2017*(13), 1170-1175.
3. Babaytsev, A.V., Prokofiev, M.V., Rabonskiy, L.N. *Nanoscience and Technology: an International Journal*, **2017b**, *8*(4), 359-366.
4. Belov, P.A., Kobets, L.P., Borodulin, A.S. *Inorganic Materials: Applied Research*, **2014**, *5*(4), 403-406.
5. Berezovskii, V.V., Shavnev, A.A., Solyaev, Y.O., Lur'e, S.A., Babaytsev, A.V., Kurganova, Y.A. *News of Materials Science. Science and Technology*, **2015**, *3*, 3-10.
6. Bessonov, I.V., Polezhaev, A.V., Kuznetsova, M.N., Nelub, V.A., Buyanov, I.A., Chudnov, I.V., Borodulin, A.S. *Polymer Science – Series D*, **2013**, *6*(4), 308-311.
7. Bieda, M., Jarzębska, A., Koprowski, P., Kawałko, J., Kudłacz, K., Boczkal, S., Faryna, M., Kulczyk, M., Pachla, W., Sztwiertnia, K. *IOP Conference Series: Materials Science and Engineering*, **2018**, *375*(1), 012037.
8. Bodryshev, V.V. *Journal “Technology of materials”*, **2017**, *11*, 8-12.
9. Bodryshev, V.V., Morgunova, A.A. Digital image processing method for identifying the sizes and concentrations of phases of composite materials. *Proceedings of the 16th International Conference “Aviation and Cosmonautics – 2017” (pp. 348)*. MAI, Moscow, Russian Federation, **2017a**.
10. Bodryshev, V.V., Morgunova, A.A. Evaluation of the geometric characteristics of nanosized particles of metal oxides by digital image analysis. *Proceedings of the 16th International Conference “Aviation and Cosmonautics – 2017” (pp. 467–468).* MAI, Moscow, Russian Federation, **2017b**.
11. Borodulin, A.S. *Polymer Science – Series D*, **2013**, *6*(1), 59-62.
12. Borynyak, L.A., Nepochatov, Yu.K. *Technologies in the Electronic Industry*, **2007**, *3*, 82-88.
13. Bulychev, N.A., Kazaryan, M.A., Erokhin, A.I., Averyushkin, A.S., Rabinsky, L.N.,

Downloaded from www.periodico.tchequimica.com

Bodryshev, V.V., Garibyan, B.A. *Metal Technology*, **2018**, *9*, 39–47.

14. Dzioba, I., Lipiec, S. *IOP Conference Series: Materials Science and Engineering*, **2018**, *461*(1), 012018.
15. Faraji, G., Torabzadeh, H. *Materials Transactions*, **2019**, *60*(7), 1316-1330.
16. Filippov, A.V., Proskokov, A.V. *Bulletin of the Moscow State Technical College. N.E. Bauman, a series of "Engineering"*, **2014**, *2*, 100-113.
17. Formalev, V.F., Kolesnik, S.A. *International Journal of Heat and Mass Transfer*, **2018**, *123*, 994–998.
18. Formalev, V.F., Kolesnik, S.A. *Journal of Engineering Physics and Thermophysics*, **2017**, *90*(6), 1302-1309.
19. Görtan, M.O. *IOP Conference Series: Materials Science and Engineering*, **2017**, *194*(1), 012046.
20. Ho, H.C., Chung, K.F., Liu, X., Xiao, M., Nethercot, D.A. *Engineering Structures*, **2019**, *192*, 305-322.
21. Hosdez, J., Langlois, M., Witz, J.-F., Limodin, N., Najjar, D., Charkaluk, E., Osmond, P., Forre, A., Szmytka, F. *International Journal of Solids and Structures*, **2019**, *171*, 92-102.
22. Iwamoto, T., Kanie, S. *Procedia Engineering*, **2017**, *171*, 1272-1278.
23. Kang, J., Muhammad, W. *Journal of Testing and Evaluation*, **2017**, *45*(5), 1587-1600.
24. Khotinov, V.A., Polukhina, O.N., Vichuzhanin, D.I., Schapov, G.V., Farber, V.M. *Letters on Materials*, **2019**, *9*(3), 328-333.
25. Kobets, L.P., Malysheva, G.V., Borodulin, A.S. *Inorganic Materials: Applied Research*, **2016**, *7*(1), 15-19.
26. Kornev, Yu.V., Emelyanov, S.V., Lukyanova, A.Yu., Semenov, N.A. *Composites: Mechanics, Computations, Applications*, **2018**, *9*(4), 283-295.
27. Muniandy, K. *Materials Science and Technology (United Kingdom)*, **2019**, *35*(9), 1016-1027.
28. Pushkarev, O.I., Bochkarev, P.U., Bashkirtseva, I.V. *Procedia Engineering*, **2017**, *206*, 222-227.
29. Rabinskiy, L.N., Tushavina, O.V. *INCAS Bulletin*, **2019**, *11*(Special Issue), 203-211.
30. Rabinskiy, L.N., Tushavina, O.V., Fedotenkov, G.V. *Asia Life Sciences*, **2019**, *19*(1), 149-162.
31. Rabinsky, L.N., Tushavina, O.V. *STIN*, **2019**, *4*, 22-26.
32. Rief, T., Hausmann, J., Motsch, N. *Key Engineering Materials*, **2017**, *742*, 660-665.
33. Shtefan, E., Pashchenko, B., Blagenko, S., Yastreba, S. *Lecture Notes in Mechanical Engineering*, **2019**, 356-363. DOI: 10.1007/978-3-319-93587-4_37
34. Sodushkin, A.I., Kibitkin, V.V., Pleshanov, V.S. *Bulletin of TPU. Management, Computer Engineering and Computer Science*, **2011**, *318*(5), 48-51.
35. Vinogradov, A.A. *Bulletin of PNIPU*, **2015**, *13*, 34-39.
36. Volkov, I.V. *Computer Optics*, **2010**, *34*(1), 82-89.
37. Wang, Y., Meng, W., Xiang, D., Li, S. *Journal of Mechanical Engineering*, **2019**, *55*(1), 81-90.
38. Wu, K., Li, X., Ge, Y., Ruan, S. *International Journal of Advanced Manufacturing Technology*, **2018**, *96*(5-8), 2091-2099.
39. Yang, S.-S., Ling, X., Du, P. *Journal of Central South University*, **2018**, *25*(4), 747-753.
40. Znamenskaya, I.A., Gvozdeva, L.G., Znamensky, N.V. *Visualization methods in gas flow mechanics*, Moscow: Moscow Aviation Institute, **2001**.

Downloaded from www.periodico.tchequimica.com

$k_{discreditation} = \Delta_{measured}/\Delta_{actual.}$ (Eq.1)

$$\varepsilon = \frac{(H_{calculated} - H_{calculated\,0})}{H_{calculated\,0}}$$ (Eq. 2)

$\Delta L_{Mi} = L_{max.Mi} - L_{min.Mi/}$ (Eq.3)

$\Delta h_{ji} = h_{maxMi} - h_{minMi}$ (Eq.*4)*

$$S_{LM} = \frac{\sqrt{\sum_{1}^{k}(L_{Mk} - \overline{L_M})^2}}{k-1};$$ (Eq. 5)

$$S_{hM} = \frac{\sqrt{\sum_{1}^{n}(h_{Mn} - \overline{h_M})^2}}{n-1}.$$ (Eq. 6)

$\Delta L_1 = L_{max.} - L_{min}$ (Eq. 7)

$$a_{ij} = \begin{cases} 1, if\ L_{min} < L_i \leq L_{max} \\ 0,\ if\ L_{min} > L_i > L_{max} \end{cases}$$ (Eq. 8)

$S_i = n \times h_{cell} \times s_{cell}$ (Eq. 9)

Table 1. *Data of the relative deformation depending on the distance from the fixation jaws*

	Relative deformation ε, %		
	sample 1.1	**sample 1.2**	**sample 1.3**
complete sample	10.53	10.38	15.45
0 mm	15.58	10.38	23.61
5 mm	17.91	15.07	27.42
7 mm	19.05	18.84	29.31
9 mm	20.34	23.08	31.48
11 mm	21.82	27.87	34.00

Downloaded from www.periodico.tchequimica.com

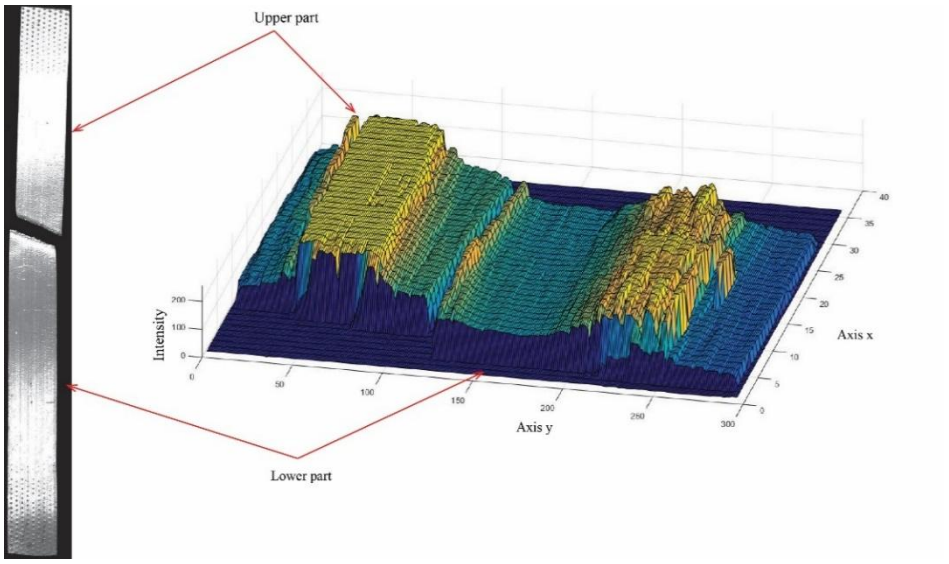

a) b)

Figure 1. *Example of surface of the metal sample, which was destroyed in the course of tensioning (a) and graphical presentation of the function L=f(x,y) of this image (b)*

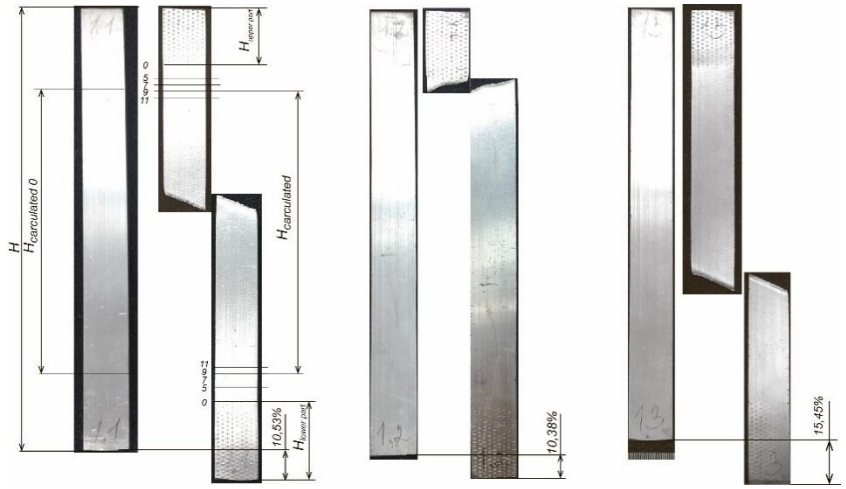

a) b) c)

Figure 2. *Superimposed images of samples before and after tensile strength tests (translations of inscriptions within the above Figure)*

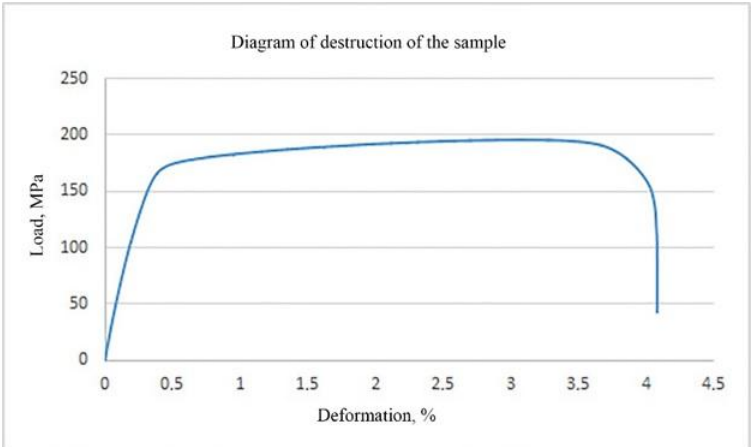

Figure 3. *Diagram of destruction of the plastic material*

Downloaded from www.periodico.tchequimica.com

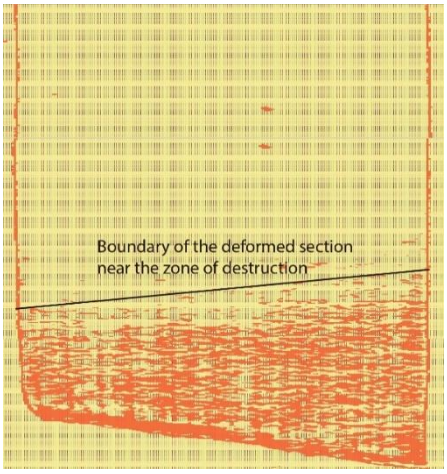

Figure 4. *Digital image of the upper part of the sample after destruction*

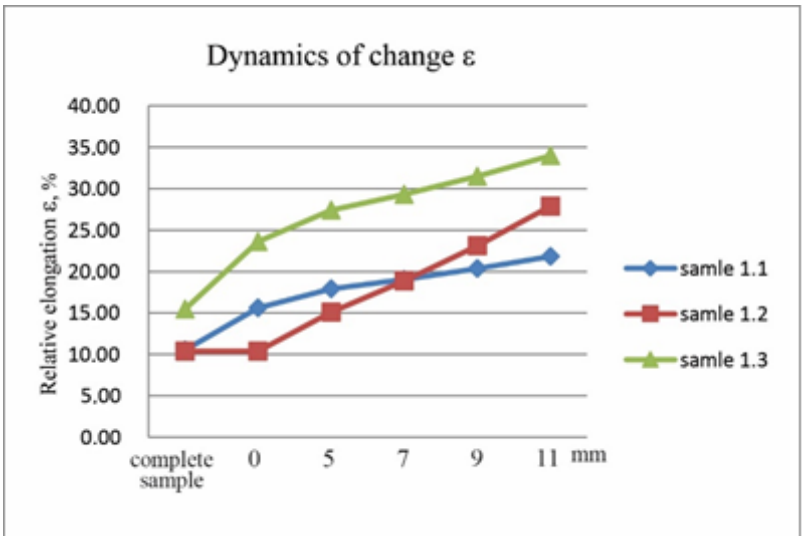

Figure 5. *Chart of change of the relative elongation of samples ε; values of the relative elongation were measured at different distances from the fixation jaws (Figure 4)*

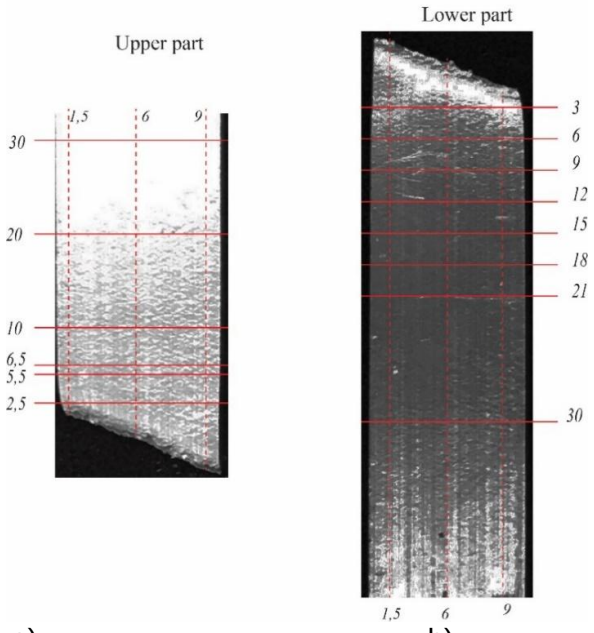

a) b)

Figure 6. *View of the fractured sample along with the preassigned cross-sections, as well as with the points of measurement of L and h values; a – the upper part; b – the lower part*

Downloaded from www.periodico.tchequimica.com

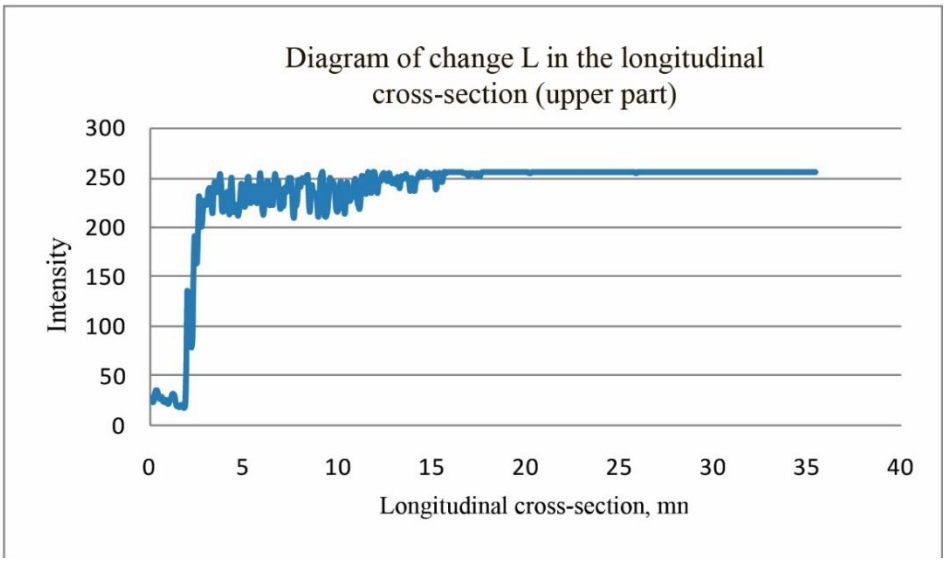

Figure 7. *Diagram of change of the image intensity in the cross-section 6*

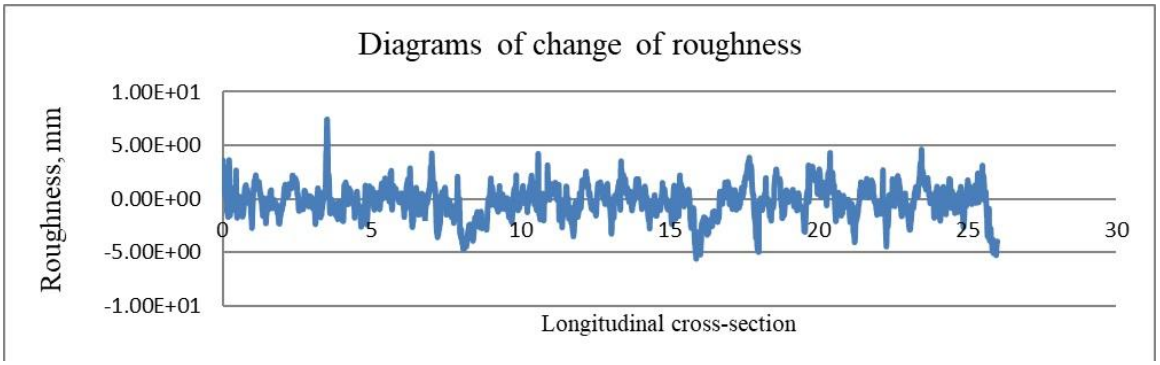

Figure 8. *Diagram of change of roughness in the cross-section 6*

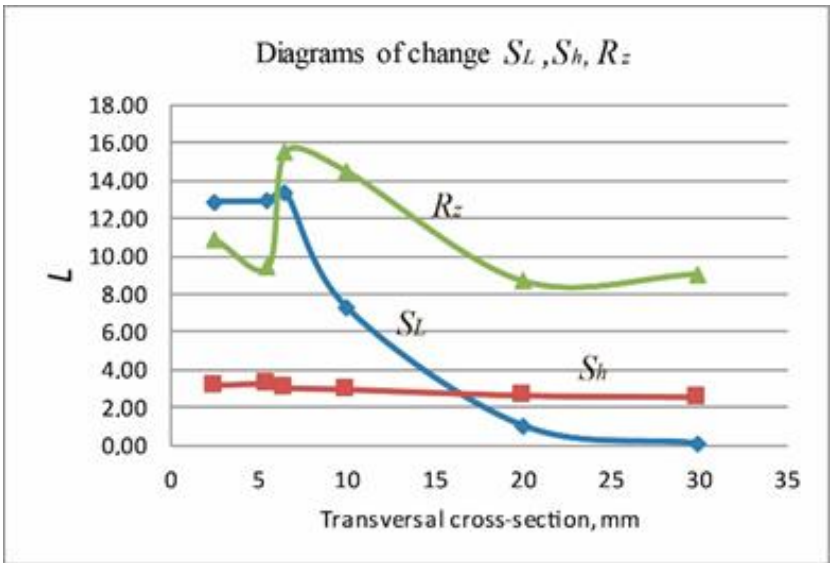

Figure 9. *Comparative diagrams of change of the data SL, Sh, and Rz in the upper part of the fractured sample*

Downloaded from www.periodico.tchequimica.com

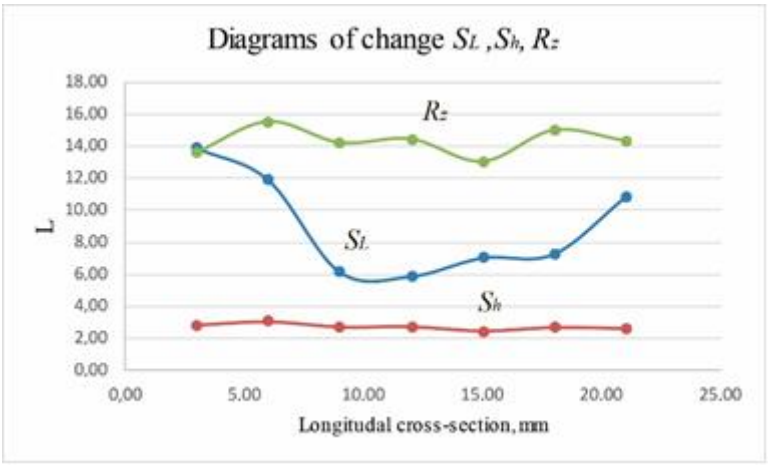

Figure 10. *Comparative diagrams of change SL, Sh, Rz in the lower part of the fractured sample*

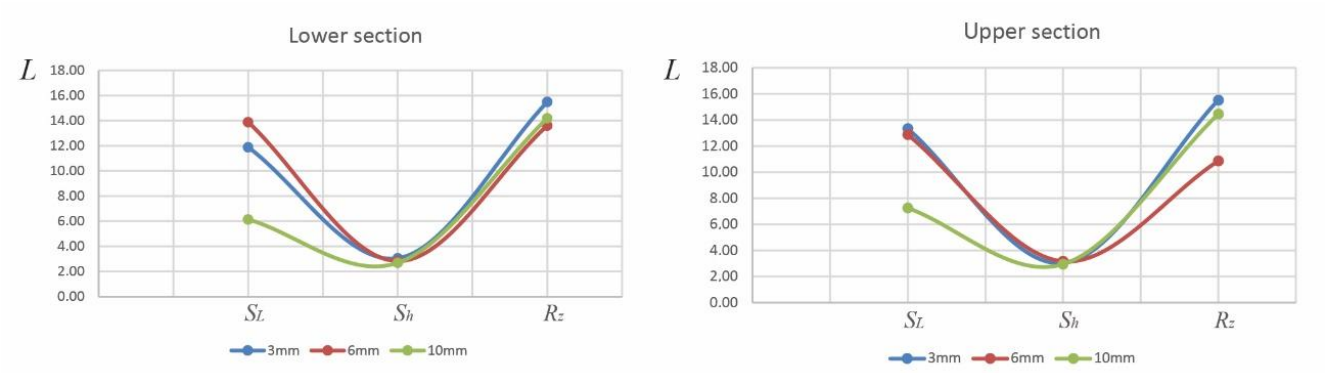

a) *b*)

Figure 11. *Diagrams of change of SL, Sh, and Rz values within the same cross-sections of the upper (a) and lower (b) sections of the destroyed sample*

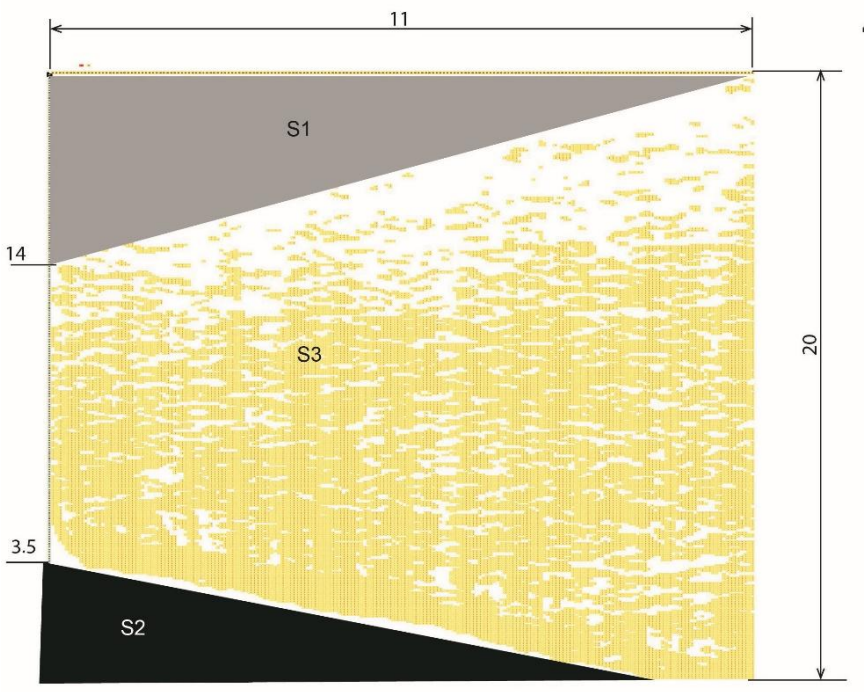

Figure 12. *Digital display of the deformed section of the fractured sample*

Downloaded from www.periodico.tchequimica.com

PERIÓDICO TCHÊ QUÍMICA
ARTIGO ORIGINAL

PROCESSOS DE PARTIDA DO MOTOR DE AUTOMÓVEL USANDO UM DISPOSITIVO DE ARMAZENAMENTO DE ENERGIA CAPACITIVO

THE STARTING PROCESSES OF A CAR ENGINE USING CAPACITIVE ENERGY STORAGES

ПРОЦЕССЫ ПУСКА АВТОМОБИЛЬНОГО ДВИГАТЕЛЯ С ИСПОЛЬЗОВАНИЕМ ЕМКОСТНЫХ НАКОПИТЕЛЕЙ ЭНЕРГИИ

MALEEV, Ruslan A.[1]*; ZUEV, Sergei M.[2]; FIRONOV, Anatoliy M.[3]; VOLCHKOV, Nikolay A.[4]; SKVORTSOV, Arkadiy A.[5];

[1,2,4] Moscow Polytechnic University, Department of Electrical Equipment and Industrial Electronics, Moscow – Russian Federation

[3] Moscow Polytechnic University, Department Ground Means of Transportation, Moscow – Russian Federation

[5] Moscow Polytechnic University, Department of Mechanics of Materials, Moscow – Russian Federation

** Correspondence author*
e-mail: eope@mospolytech.ru

Received 23 October 2019; received in revised form 10 November 2019; accepted 13 November 2019

RESUMO

O artigo apresenta os dados de experimentos relacionados ao processo de partida do motor de automóvel usando um dispositivo de armazenamento de energia capacitivo. É mostrado que os dispositivos de armazenamento de energia capacitivo podem ser usados para iniciar com eficiência o motor de combustão interna. O objetivo do artigo foi estudar os sistemas de partida elétrica de combustão de veículos com o dispositivo de armazenamento de energia capacitivo como fonte de energia elétrica utilizando um aparelho matemático que permitiu analisar o processo de partida do motor de veículo com energia capacitiva. No processo de trabalho, foram obtidas dependências analíticas do tempo e do ângulo de rotação do eixo de manivela do motor de combustão interna (número de cursos de trabalho) dos principais parâmetros do sistema de partida do arrancador elétrico com um momento constante de resistência no eixo do motor de combustão interna. Foram realizados os cálculos matemáticos e modelagem de modos operacionais em produtos de software especializados. Os resultados do experimento mostraram que o processo de rolagem do motor de combustão interna usando o arrancador elétrico quando é alimentado por dispositivos de armazenamento de energia capacitivo é significativamente diferente do processo de rolagem quando alimentado por uma bateria. Em conexão com o amplo uso de baterias em veículos e a busca de soluções tecnológicas alternativas para elas, pode-se dizer que os resultados obtidos neste artigo são de valor prático no quadro da moderna tecnologia de equipamentos elétricos.

Palavras-chave: *carga-descarga, dados experimentais, bateria de armazenamento, solução tecnológica alternativa, equipamentos elétricos modernos.*

ABSTRACT

The article presents data on experiments related to the start-up process of an automobile engine using capacitive energy storage. It is shown that capacitive energy storage devices can be used for efficient start-up of an internal combustion engine. The aim of the article was to study the systems of electric start of vehicles combustion with capacitive energy storage as source of electric energy using a mathematical apparatus that allowed analyzing the process of starting a vehicle engine with capacitive energy. In the course of work, analytical dependences on the time and angle of rotation of the crankshaft of the internal combustion engine (number of working strokes) of the main parameters of the electric starter starting system with a constant moment of resistance on the shaft of the internal combustion engine were obtained. Mathematical calculations and simulation of operating modes in specialized software products were carried out. The results of the experiment showed that the process of scrolling the internal combustion engine with an electric starter when it is powered from capacitive energy storage devices differs significantly from the process of scrolling when powered from a rechargeable battery. Due to the large proliferation of batteries in vehicles and the search for alternative

Downloaded from www.periodico.tchequimica.com

technological solutions to them, it can be said that the results obtained in this article are of practical value in the framework of modern electrical equipment technology.

Keywords: *charge-discharge, experimental data, rechargeable battery, alternative technological solution, modern electrical equipment.*

АННОТАЦИЯ

В статье представлены данные об экспериментах, связанных с процессом запуска автомобильного двигателя с использованием емкостного накопителя энергии. Показано, что емкостные накопители энергии могут использоваться для эффективного запуска двигателя внутреннего сгорания. Целью статьи является изучение систем электрического запуска сгорания транспортных средств с емкостным накопителем энергии в качестве источника электрической энергии с использованием математического аппарата, который позволил проанализировать процесс запуска двигателя транспортного средства с емкостной энергией. В процессе работы были получены аналитические зависимости от времени и угла поворота коленчатого вала двигателя внутреннего сгорания (числа рабочих ходов) основных параметров системы запуска электростартера с постоянным моментом сопротивления на валу двигателя внутреннего сгорания. Проведены математические расчеты и моделирование режимов работы в специализированных программных продуктах. Результаты эксперимента показали, что процесс прокрутки двигателя внутреннего сгорания с помощью электростартера при его питании от емкостных накопителей энергии значительно отличается от процесса прокрутки при питании от аккумуляторной батареи. В связи с большим распространением аккумуляторов в транспортных средствах и поиском альтернативных технологических решений для них можно сказать, что результаты, полученные в этой статье, имеют практическую ценность в рамках современной технологии электрооборудования.

Ключевые слова: заряд-разряд, экспериментальные данные, аккумуляторная батарея, альтернативное технологическое решение, современное электрооборудование.

1. INTRODUCTION

Analysis of the state and development of modern systems of electric starter systems (ESS) shows that their output parameters are affected by electrical and mechanical losses, the design of the drive mechanism, and the operating mode of the starter. The existing constructive and technological measures to improve these factors have reached optimal values, and it is not possible to improve the output parameters of the ESS due to their change (Shi *et al*., 2005; Hata *et al*., 2015; Jung *et al*., 2015; Munakata and Kanamura, 2015; Ogundiran *et al*., 2017).

At present time lead acid rechargeable batteries (AB) are used overwhelmingly as sources of electrical energy in electric starter systems (ESS) of internal combustion engines (ICE) of vehicles. The main disadvantage of it is low utilization of stored energy at negative temperatures, due to the high internal resistance, which complicates the process of starting the internal combustion engine (Keshan *et al*., 2016; Grachev *et al*., 2017; Subramanian, 2017; Kroics, 2018; Kunt, 2018; Ramazanov *et al*., 2018; Dhundhara and Verma, 2018; Sulym *et al*., 2018; Ha, 2019). In this regard, capacitive energy storages (ECs) are very promising. They have significantly lower internal resistances compared with AB and higher specific powers (Cheremisin *et al*., 2015; Karmazin *et al*., 2015;Vatamanu and Bedrov, 2015; Ishmatov *et al*., 2016; Opila, 2017; Dong *et al.,* 2017; Fomin *et al*., 2018; Hulea *et al*., 2018; He *et al*., 2019).

The use of ESS with energy storage devices (CES) makes it possible to maintain the nominal voltage of the vehicle and apply low-voltage CES both on promising and on serial automobile engines with almost no modification of the elements of the ESS (Waters *et al*., 1979; Xie *et al.*, 2016; Crouch, 2017; Luo *et al.,* 2017; Malozyomov *et al.,* 2018; Xu *et al*., 2018; Bae and Park, 2018; Tishkov *et al*., 2019; Kuznetsov and Artemenko, 2019; Shao *et al*., 2019).

The initial dates in the design of ESS are minimum starting speed nmin, average static moment of resistance ICE Ms, corresponding nmin and starting time ts at the limit (minimum) temperature of the reliable starting t0min. Therefore, for a theoretical analysis of the processes occurring in an ESS with an CES in the first approximation, it can be assumed that the shaft of an internal combustion engine is loaded with a constant static moment of resistance Mr. Neglecting also the moment of inertia of the system “electric starter – internal combustion engine”, uneven rotation of the engine shaft and starter inductance, the following

Downloaded from www.periodico.tchequimica.com

main results were obtained (Kroics, 2015; Manla *et al*., 2015; Hiramatsu *et al*., 2015; Saito *et al*., 2015; Geetha and Subramani, 2017; Xu *et al*., 2017).

This article presents the results of a theoretical and experimental study of the ESS ICE with CES. The evaluation of the effectiveness of electric start-up systems using energy storage devices at low temperatures was carried out. The aim of the article was to study the systems of electric start of internal combustion of vehicles with capacitive energy stores as sources of electric energy using a mathematical apparatus, which allowed to analyze the process of starting a car engine using capacitive energy stores. The results obtained as a result of research will be used in the development and justification of the requirements for a start-up system with energy storage devices, which will increase the performance of automotive vehicles at low temperatures.

2. MATERIALS AND METHODS

The study was conducted in the framework of the methodology of the physical foundations of electrical engineering and electronics, including using the method of analogy and forecasting. According to the method proposed by the authors earlier (Maleev *and* Shmatkov, 2013a; Maleev and Shmatkov, 2013b; Korotkov *et al.,* 2015; Maleev *et al*., 2015; Khortov *et al.,* 2016a; Khortov *et al*., 2016b; Skvortsov *et al*., 2016; Akimov *et al.,* 2017; Shmatkov and Lavrikov, 2017; Zuev *et al.,* 2017) and taking into account the assumptions presented above, a mathematical apparatus was used that allowed the authors to analyze the process of starting a car engine using capacitive energy storage devices.

So at a constant moment of resistance M_r, the current intensity of the electric starter (ST) armature will also be constant (Equation 1) (Korotkov *et al*., 2015) where η_{tr} – transmission efficiency from ST to ICE (η_{tr} = 0.85) (Maleev *et al*., 2015); η_{em} – electromagnetic efficiency ST ($\eta_{ем}$ = 0.75-0.95); *i* – is the gear ratio of the drive from the ST to the internal combustion engine; C_m – constant ST; ϕ is the main magnetic flux of ST excitation. If the CES is charged to the initial voltage *Ucoi* and has an internal resistance R_c, then at a constant discharge current $i_c=I_a$ all the main parameters of the ESS will decrease linearly with time *t* (Figure 1).

The voltage at the terminals of the CES (Equation 2) (Maleev and Shmatkov, 2013a) where c – is the capacity of CES. CES voltage under load (Equation 3) (Maleev and Shmatkov, 2013b) where Equation 4 is time constant CES (Akimov *et al*., 2017). EMF at starter anchor (Equation 5) (Khortov *et al*., 2016a) where ΔU_b – voltage drop under brushes ST (with I_a = const, ΔU_a = const); R_w – wire resistance from CES to ST; R_{ST} – the total resistance of the ST, which includes the resistance of the excitation windings and armature (Equation 6) (Skvortsov *et al.,* 2016) is discharge time constant CES. ST armature speed (Equation 7) (Khortov *et al*., 2016b) where c_c – constant ST. Electromagnetic power ST (Equation 8) (Shmatkov and Lavrikov, 2017). Time t_k during which ST rotates (until it stops) (Equation 9) (Zuev *et al*., 2017). CES voltage at which ST stops (Equation 10) (Zuev *et al*., 2017).

According to Equations 1-10, an analysis was made of the starting processes of an automobile engine using capacitive energy storage devices to obtain numerical results.

3. RESULTS AND DISCUSSION:

After stopping ST, it occurs discharge CES on the active resistance in the starter circuit, but this process is not of interest due to the lack of useful work. The dependence of the ESS parameters on the angle of rotation φ of the crankshaft of the ICE and on the number of engine power strokes Npx is much more complicated. The rotation angle φ of the engine crankshaft given by the following relationship (Equation 11): where Equation 12 is the angular frequency of rotation of the engine crankshaft, s^{-1}; n – rotational speed of the engine crankshaft, min^{-1}.

The number of working strokes of the internal combustion engine is determined by the Equation 13. The angular frequency of rotation ω linearly depends on time t (Equation 14) where Equation 15 is maximum angular speed of the crankshaft at the start cranking; tk – cranking time of the engine crankshaft. Substituting Equation 14 into Equation 11 and after transformations, Equation 16 is obtained. From Equation 14, after the conversion, you can get the expression for the current time (Equation 17). Substituting Equation 17 into Equation 16, after transformations, Equation 18 will be gotten where Equation 19 is the full angle of rotation of the engine crankshaft.Equation 20 is obtained from the Equation 18.

The change in φ/ϑ in the function n/nmax

is shown in the Table 1. The dependence of φ/ϑ on n/nmax is shown on the Figure 2. Table 1 shows the values of n and φ obtained in the course of calculations. The adduction of φ⁄θ and n⁄nmax allows us to simplify the calculation and increase the accuracy of the results obtained. The n⁄nmax step was set by the heuristic method in the range from 1.0 to 0.0 with a step of 0.1. The calculation of φ⁄θ in table 1 was carried out according to Equation 20. From the Equation 18 can be obtained the equation that determines the change in the frequency of rotation on the angle of rotation (Equation 21). The dependence of n/n_{max} in the function φ/ϑ is shown in Figure 2. As can be seen, with a frequency of n greater than Equation 22, the crankshaft rotates in the range of the angle of rotation φ from 0 to 75–0.

Figure 3 shows the dependence of φ/ϑ and n/n_{max} on a relative time t/t_k. The obtained results allow to draw the following important conclusions. If the average rotational speed n_{av} is equal to the minimum starting frequency of rotation n_{min}, then within 3/4 of the full angle of rotation of the crankshaft Θ, it will rotate at a frequency greater than n_{min}. This significantly improves the process of mixing, facilitates the ignition of the combustible mixture, increases the efficiency of its combustion, i.e. facilitates the process of starting the engine. In this case, the required start time should be shorter than when powered by the ST from the battery when the engine crankshaft is turned at a frequency of n_{min}.

The Figure 4 shows the dependence of the ESS-parameters on the angle of rotation and the number of working strokes of the ICE – NWS. Experimental studies were carried out in the laboratory of the department "Electrical equipment and industrial electronics" of the Moscow Polytechnic University. The object of the test was the four-cycle, four-cylinder, injection engine of a modern small-volume car with a working volume of 1.7 liters. CES consisted of several dozen individual high-voltage electrolytic capacitors (type K50-17 with a capacity of 200 mkF each (Kwight et al., 1990)) with a total capacity of 0.1277 F. The initial charge voltage for CES was Ucoi = 290 V. As the ST was used own standard industrial DC electromotor (220 V) JB-061-M64 with a front cover, a traction relay and a drive mechanism from a starter 35.3708. The total gear ratio of ST-ICE is 11,7. Figures 5 and 6 show the variation in the instantaneous and average values of the engine crankshaft rotational speed (n and n_{av}), the torque of the starter, adduced to the crankshaft ($M_{st} = M_{sti} \times \eta_{tr}$ and $M_{st.av}$.) and the voltage at the CES-terminals Uc depending on from time t and crank angle φ (number of working strokes N_{ws}) at a temperature of -15C (oil viscosity 1150 mm^2/ s).

As can be seen, the process of scrolling of the internal combustion engine with an electric starter when it is powered from CES is significantly different from the process of scrolling when it powered from an AB (Figure 7). In the initial period of operation, ST develops a large torque (Equation 23), which is necessary to overcome the moment of resistance and dynamic moment. (Figures 5, 6). Then, as the crankshaft is turning, due to a decrease in the viscosity of the oil in the friction pairs of the internal combustion engine and the rotational speed decreases, the torque of the rotational resistance and the torque of the starter M_{st} decreases and most of the time the scrolling occurs with a constant torque.

The rotational frequency n initially increases rapidly during 0.33 s to a value of n_{max} = 520 min^{-1}, and then decreases linearly as it discharges and decreases sharply to zero at the end of the rotation. The average frequency of rotation of its scrolling time t_n = 1.436 s is 327 min^{-1}. The sharp increase in the rotational speed at the initial moment compared with the gradual increase in the frequency when powered from the battery (Figure 7) is due to the high voltage CES. The absence of stages with a constant scrolling frequency is caused by a change in the voltage CES U_c according to its discharge. The voltage at the terminals of the CES – U_c is significantly reduced at the beginning of the scrolling, when the moment of resistance, the torque M_{st} and the required current consumed from the CES to provide this torque are higher. The CES voltage U_c and the rotation frequency n decrease linearly most of the time (from 0.619 s to 1.262 s) while scrolling occurs with practically constant M_{st} (and, therefore, with a constant starter current Ia = 14.9-14.3 A), which corresponds to aforecited theoretical studies.

The sharp decrease in rotational speed at the end of the scrolling process is due to the fact that at a certain voltage CES, the generated power becomes insufficient to overcome the increasing moment of resistance due to compression of the fuel-air mixture in one engine cylinder. Changing of the net power P developed at ST, energy W_{co} and number of strokes N_{px} depending on the time is shown in Figure 8 in addition to the dependencies n, M_{st} and equation 24. At the same time, Figure 8 shows the calculated dependences of the CES-voltage U_{calc} and the crankshaft rotation speed n_{calc}. The

Downloaded from www.periodico.tchequimica.com

maximum of ST-power $P_{2max} = 4471$ W will be developed at the stage of acceleration (t = 0.055 s) at a sufficiently high moment of resistance and voltage of CES.

The CES-energy (Equation 25) during cranking of the engine crankshaft t_s = 1.436 s. is decreasing due to the CES-discharge from 5370 J to 379 J. The engine performs 17 working strokes during the scrolling time t_s. If to think that the cranking of the engine crankshaft occurs with a constant average moment of resistance and an average current of the starter armature 14.6 A , then with the total resistance of the starter circuit (including resistance of the ES, the resistance of the excitation windings and starter armature, the resistance of the collector exact node and resistance of the wires), equal to 9.14 ohms, the estimated time of cranking of the engine crankshaft to the stop $t_к$ is equal to 1.387 s versus 1.436 seconds in the experiment. The calculated values of voltages of CES Ucalc quite closely coincide with the experimental values.

Significant discrepancies between the calculated (n_{calc}) and experimental rotational frequencies of the crankshaft of the ICE are primarily explained by the change in the main magnetic excitation flux of the ST in the scrolling process, which is not taken into account in the calculation. The test results showed that scrolling of the ICE from high-voltage ES comparing to scrolling from AB differs in significantly lower operating currents ($I_{u.av.}$ = 14-20 A versus $I_{u.av.}$ = 200-300 A), more higher rotational frequencies of the engine crankshaft (n_{av} = 327 min^{-l} versus n_{av} = 140 min-I) and significantly less scrolling time (t_s = 1.436 s. versus t_s = 10 s). A decrease in the operating current ST and an increase in the crankshaft speed is explained primarily with an increase in the power supply voltage (CES). The CES as it is discharged. The reduction of operating current ST allows reducing the cross-section of wires from CES to ST, which reduces the mass-dimensional indicators of the ESS. At the same time, heat losses in the ESS are reduced, which increases its efficiency.

Increased engine cranking frequency facilitates the start process and, in accordance with the starting characteristics of the engine, the start time is reduced. Therefore, despite the fact that the scrolling time of the internal combustion engine with NE is reduced, the engine can be started due to an increase in the rotational speed of the engine crankshaft. At the same time, the test results showed that for a reliable start of the ICE of a modern small-sized car with a high-voltage CES at a temperature of -15 °C, the starting characteristics of the injection need to be changed.

4. CONCLUSIONS:

According to the results of the research, the following most important results can be briefly highlighted:

1. Analytical dependences on the time and angle of rotation of the engine crankshaft (the number of working strokes) of the basic parameters of the ESS, with a constant moment of resistance on the engine shaft. The experimental results show the possibilities of practical use of the proposed calculation methods after taking into account the influence of dynamic factors on the characteristics of the ESS in the CES.

2. The influence of dynamic factors on the characteristics of ESS with CES should be taken into account after statistical data processing of ICE with CES of starting tests in different climatic conditions. For reliable start-up of an internal combustion engine with high-voltage CES at a temperature of (-15 ÷ -25) ° C, a change in its starting characteristics is required. Moreover, experimental studies have shown that at temperatures (-20 ÷ -25) ℃ ESS starts were carried out using an electric starter with an additional gearbox.

3. The process of cranking the crankshaft ICE when the electric power from the high voltage CES differs from the power supply from a AB by significantly lower operating currents ST, higher frequencies and smaller scroll time. It is also worth noting that an increase in the value of the capacity of the CES and the value of the initial charging voltage of the CES allows increasing the scroll time, the number of working strokes of the internal combustion engine, the average and maximum rotational speeds of the crankshaft of the engine, and the useful power of the electric starter, however, a detailed analysis of these characteristics is beyond the scope this study.

5. ACKNOWLEDGMENTS:

This work was supported by the Ministry of Education and Science of the Russian Federation, project No. 8.5171.2017/BCh.

6. REFERENCES:

Downloaded from www.periodico.tchequimica.com

1. Akimov, A.V., Varlamov, D.O., Zuev, S.M. *Construction, description of work and diagnostics of the system of electric starter of modern vehicles*, Moscow: Moscow Polytech, **2017**.
2. Bae, S., Park, J.-W. *Journal of Electrical Engineering and Technology*, **2018**, *13(2)*, 631–636.
3. Cheremisin, V.T., Nazevak, V.L., Shatokhin, A.P. *Bulletin of the Tomsk Polytechnic University, Geo Assets Engineering*, **2015**, *326(10),* 54–64.
4. Crouch, D.A. Battery technology for automotive applications. In A. Emadi (Ed.), *Handbook of automotive power electronics and motor drives*, Chicago: Illinois Institute of Technology, **2017**, 677–688.
5. Dhundhara, S., Verma, Y.P. *Energy*, **2018**, *147*, 1108–1128.
6. Dong, L., Xu, Q., Lu, F., Nie, X., He, Y., Wang, Y., Yan, Z. Physica C: *Superconductivity and its Applications*, **2017**, *541*, 16–21.
7. Fomin, O., Sulym, A., Kulbovskiy, I., Khozia, P., Ishchenko, V. *Eastern-European Journal of Enterprise Technologies*, **2018**, *2(1-92),* 63–71.
8. Geetha, A., Subramani, C. *International Journal of Energy Research*, **2017**, *41(13),* 1817–1834.
9. Grachev, P.Yu., Strizhakova, E.V., Tabachinskiy, A.S. *Procedia Engineering*, **2017**, *206*, 386–391.
10. Ha, N. *4th International Conference on Advances in Energy and Environment Research*. Shanghai; China, **2019**.
11. Hata, K., Huang, X., Hori, Y. *54th Annual Conference of the Society of Instrument and Control Engineers of Japan*. Hangzhou, China, **2015**, 1459–1462.
12. He, Y., Wang, X., Zhang, P., Huang, H., Li, X., Shui, Y., Chen, B., Guo, Z. *Energy*, **2019**, *183*, 358–367.
13. Hiramatsu, T., Huang, X., Kato, M., Hori, Y. *IEEJ Transactions on Industry Applications*, **2015**, *135(9),* 898–905.
14. Hulea, D., Cornea, O., Muntean, N. *18th IEEE International Conference on Power Electronics and Motion Control*. Budapest, Hungary, **2018**.
15. Ishmatov, Z., Plotnikov, I., Isaak, B. *9th International Conference on Power Drives Systems*. Perm, Russian Federation, **2016**.
16. Jung, J., Zhang, L., Zhang, J. *Lead-acid battery technologies: Fundamentals, materials, and applications*. Boca Raton, Florida: CRC Press, **2015**.
17. Karmazin, R., Koch, A., Matz, R., Männer, R., Metzger, W., Wolff, A. *11th International Conference and Exhibition on Ceramic Interconnect and Ceramic Microsystems Technologies.* Dresden, Germany, **2015**.
18. Keshan, H., Thornburg, J., Ustun, T.S. *4th IET Clean Energy and Technology Conference*. Kuala Lumpur, Malaysia, **2016**.
19. Khortov, V.P., Skvortsov, A.A., Zuev, S.M. *Automotive Industry*, **2016a**, *10*, 24–27.
20. Khortov, V.P., Skvortsov, A.A., Zuev, S.M., Vorozheikin, V.V. *Automotive Industry*, **2016b**, *12*, 12–16.
21. Korotkov, V.I., Maleev, R.A., Mychka, N.V., Gulin, A.N. *Scientific Peer-Reviewed Journal*, **2015**, *4(26),* 26–31.
22. Kroics, K. *56th International Scientific Conference on Power and Electrical Engineering of Riga Technical University*. Riga, Latvia, **2015**.
23. Kroics, K. *International Exhibition and Conference for Power Electronics, Intelligent Motion, Renewable Energy and Energy Management*. Nuremberg, Germany, **2018**, 1786–1791.
24. Kunt, M.A. *Journal of Automobile Engineering*, **2018**, *232(12),* 1648–1653.
25. Kuznetsov, S.M., Artemenko, I.V. *Materials Science and Engineering*, **2019**, *560(1),* 012173.
26. Kwight, S.M., Mendelevich, Y.A., Chizhkov, Yu.P. *Starting qualities and staring systems of automotive and tractor engines*, Moscow: Mechanical Engineering, **1990**.
27. Luo, Y., Shi, Y., Zheng, Y., Gan, Z., Cai, N. *Energy Procedia*, **2017**, *105*, 4458–4463.
28. Maleev, R.A., Gulin, A.N., Mychka, N.V., Kuznetsova, Yu.A. *Scientific Peer-Reviewed Journal*, **2015**, *4(26),* 51–55.
29. Maleev, R.A., Shmatkov, Yu.M. *Scientific Peer-Reviewed Journal. Series 1. Land Vehicles, Power Plants and Engine*s, **2013a**, *2(16),* 125–129.
30. Maleev, R.A., Shmatkov, Yu.M. *Scientific*

Downloaded from www.periodico.tchequimica.com

Peer-Reviewed Journal. Series 1. Land Vehicles, Power Plants and Engines, **2013b**, *2(16),* 129–133.

31. Malozyomov, B.V., Myatezh, A.V., Smirnov, M.A. *19th International Conference of Young Specialists on Micro/Nanotechnologies and Electron Devices*. Erlagol, Altai, Russian Federation, **2018**, 704–707.
32. Manla, E., Sabbah, M., Nasiri, A. *7th Annual IEEE Energy Conversion Congress and Exposition*. Montreal, Canada, **2015**, 6199–6205.
33. Munakata, H., Kanamura, K. All-solid-state rechargeable batteries. In Q. Xu, T. Kobayashi (Eds.), *Advanced materials for clean energy*, Boca Raton, Florida: CRC Press, **2015**, 271–283.
34. Ogundiran, M.B., Buluku, T.G., Babayemi, J.O., Osibanjo, O. *Journal of Material Cycles and Waste Management*, **2017**, *19(1),* 163–171.
35. Opila, D.F. *American Control Conference*. Seattle, United States, **2017**.
36. Ramazanov, R.F., Fridman, B.E., Kharcheva, K.S., Komarov, O.V., Serebrov, R.A. *Defence Technology*, **2018**, *14(5),* 622–627.
37. Saito, T., Kondo, K., Koseki, T., Mizuma, T. *Electrical Engineering in Japan*, **2015**, *192(2),* 57–67.
38. Shao, H., Narayanasamy, P., Razeeb, K.M., Lynch, R.P., Rhen, F.M.F. *Issues in Environmental Science and Technology*, **2019**, *2019(46),* 150–183.
39. Shi, Y., Wang, Y., Li, P. *Acta Energiae Solaris Sinica,* **2005**, *26(1),* 86–89.
40. Shmatkov, Yu.M., Lavrikov, A.A. *The study of the system of electric starter start vehicles*, Moscow: Moscow Polytech, **2017**.
41. Skvortsov, A.A., Khortov, V.P., Zuev, S.M. *International Journal of Pure and Applied Mathematics*, **2016**, *111(3),* 455–465.
42. Subramanian, K.A. *Biofueled reciprocating internal combustion engines*, Delhi: Indian Institute of Technology, **2017**.
43. Sulym, A.O., Fomin, O.V., Khozia, P.O., Mastepan, A.G. *Naukovyi Visnyk Natsionalnoho Hirnychoho Universytetu*, **2018**, *2018(5),* 79–87.
44. Tishkov, A.I., Konoplev, Y.V., Shevtsov, I.V., Yuev, A.A. *Russian Aeronautics*, **2019**, *62(2),* 321–325.
45. Vatamanu, J., Bedrov, D. *Journal of Physical Chemistry Letters,* **2015**, *6(18),* 3594–3609.
46. Waters, E.D., Saaski, E.W., Martini, W.R. *Proceedings of the Intersociety Energy Conversion Engineering Conference. Boston, Massachusetts*, **1979**, 475–480.
47. Xie, L., Burgers, J., Kawaji, M. *11th IIR Conference on Phase Change Materials and Slurries for Refrigeration and Air Conditioning.* Karlsruhe, Germany, **2016**, 236–245.
48. Xu, Q., Sun, J., Zhao, M., Jiang, X., Mao, Y., Cui, S. *International Conference on Life System Modeling and Simulation, and International Conference on Intelligent Computing for Sustainable Energy and Environment.* Nanjing, China, **2017**, 329–338.
49. Xu, Y., Chen, X., Tian, F., Peng, H., Yan, S. *China International Conference on Electricity Distribution.* Tianjin, China, **2018**, 680–684.
50. Zuev, S.M., Shmatkov, Yu.M., Maleev, R.A., Khortov, V.P., Lavrikov, A.A., Varlamov, D.O. *Electrical equipment and car electronics in basic terms with their explanation in Russian and English*, Moscow: Moscow Polytech, **2017**.

Downloaded from www.periodico.tchequimica.com

$$\mathrm{Ia} = \frac{\mathrm{Mr}}{\eta tr \times \eta \mathrm{em} \times \mathrm{i} \times \mathrm{Cm} \times \phi} \quad \text{(Eq. 1)}$$

$$Uco = Ucoi - \frac{Ia}{c} \times t \quad \text{(Eq. 2)}$$

$$Uc = Uco - Ia \times Rc = Ucoi - \frac{Ia}{C}(t + \tau c) \quad \text{(Eq. 3)}$$

$$\tau_C = R_C \times C \quad \text{(Eq. 4)}$$

$$Ea = Ucoi - \Delta Ua - Ia\,(Rc + Rw + Rs\mathrm{T})\left(1 + \frac{t}{\tau}\right) \quad \text{(Eq. 5)}$$

$$\tau = C \times (R_C + R_W + R_{ST}) \quad \text{(Eq. 6)}$$

$$na = \frac{Ucoi - \Delta Ub - Ia\,(Rc + Rw + R\mathrm{cT})}{Cc \times \emptyset}\left(1 + \frac{t}{\tau}\right) \quad \text{(Eq. 7)}$$

$$p = \left[Ucoi - \Delta Ub - Ia\,(Rc + Rw + Rs\mathrm{T}) \times \left(1 + \frac{t}{\tau}\right)\right] \times Ia \quad \text{(Eq. 8)}$$

$$t\mathrm{K} = ((Ucoi - \Delta Ub) \times c)/Ia - \tau \quad \text{(Eq. 9)}$$

$$Uco\mathrm{K} = Ia \times (Rc + Rw + Rs\mathrm{T}) + \Delta Ub \quad \text{(Eq. 10)}$$

$$\boldsymbol{\varphi} = \int \omega \mathrm{dt} \quad \text{(Eq. 11)}$$

$$\omega = \frac{\boldsymbol{\pi} \times \boldsymbol{n}}{\mathbf{30}} \quad \text{(Eq. 12)}$$

$$N_{WS} = \frac{\boldsymbol{\varphi}}{\boldsymbol{\pi}} \quad \text{(Eq. 13)}$$

$$\boldsymbol{\omega} = \boldsymbol{\omega max} - \frac{\boldsymbol{\omega max}}{\mathbf{t\kappa}} \times \mathbf{t} \quad \text{(Eq. 14)}$$

$$\omega_{max} = \frac{\pi \times n_{max}}{30} \quad \text{(Eq. 15)}$$

$$\boldsymbol{\varphi} = \int \boldsymbol{\omega}\,\mathbf{dt} = \int (\boldsymbol{\omega max} - \boldsymbol{\omega max}/\mathbf{t\kappa} \times \mathbf{t})\mathbf{dt} = \boldsymbol{\omega max} \times \mathbf{t} \times (\mathbf{1} - \mathbf{t}/(\mathbf{2} \times \mathbf{t\kappa})) \quad \text{(Eq. 16)}$$

$$\mathbf{t} = \frac{\boldsymbol{\omega max} - \boldsymbol{\omega}}{\boldsymbol{\omega max}} \times \mathbf{tk} = \left(\mathbf{1} - \frac{\boldsymbol{\omega}}{\boldsymbol{\omega max}}\right) \times \mathbf{tk} \quad \text{(Eq. 17)}$$

$$\varphi = \omega\mathrm{max} \times \left(1 - \frac{\omega}{\omega\mathrm{max}}\right) \times t\kappa \times \left[1 - \frac{\left(1 - \frac{\omega}{\omega\mathrm{max}}\right) \times t\kappa}{2 \times t\kappa}\right] =$$

$$= \frac{t\kappa \times \omega\mathrm{max}}{2} \times [1 - (\frac{\omega}{\omega\mathrm{max}})2] = \Theta \times [1 - (\frac{\omega}{\omega\mathrm{max}})2], \quad \text{(Eq. 18)}$$

$$\vartheta = \frac{\boldsymbol{t\kappa} \times \boldsymbol{\omega max}}{\mathbf{2}} \quad \text{(Eq. 19)}$$

$$\frac{\boldsymbol{\varphi}}{\Theta} = 1 - \left(\frac{\omega}{\omega_{max}}\right)^2 = 1 - \left(\frac{n}{n_{max}}\right)^2 \quad \text{(Eq. 20)}$$

$$n = n_{max} \times \sqrt{\mathbf{1} - \frac{\boldsymbol{\varphi}}{\Theta}} \quad \text{(Eq. 21)}$$

$$n_{av} = \frac{n_{max}}{2} \quad \text{(Eq. 22)}$$

Downloaded from www.periodico.tchequimica.com

$$M_{st} = 280N \times m \quad \text{(Eq. 23)}$$

$$U_c = f(t) \quad \text{(Eq. 24)}$$

$$W_{co} = \frac{C \times U_{c2}}{2} \quad \text{(Eq. 25)}$$

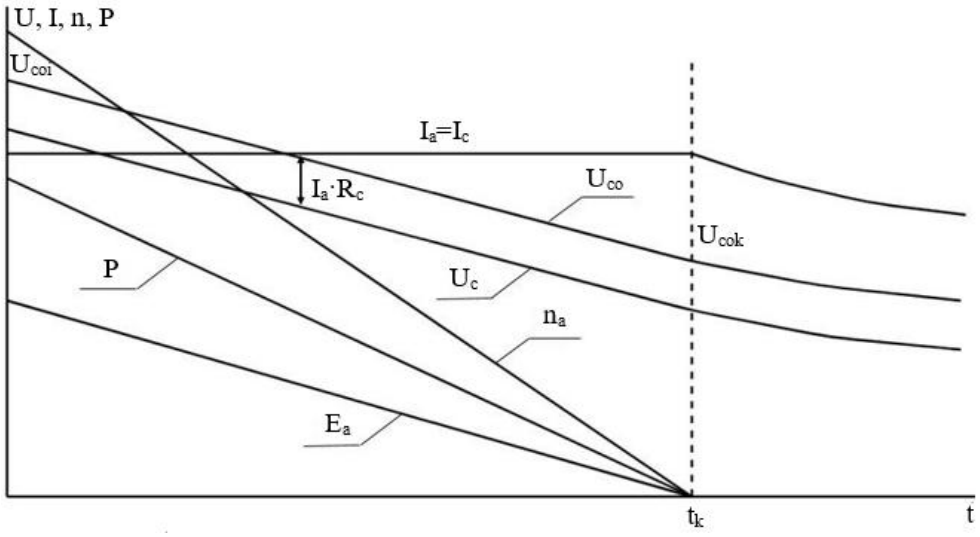

Figure 1. *The dependence of the ESS parameters on time at a constant discharge current*

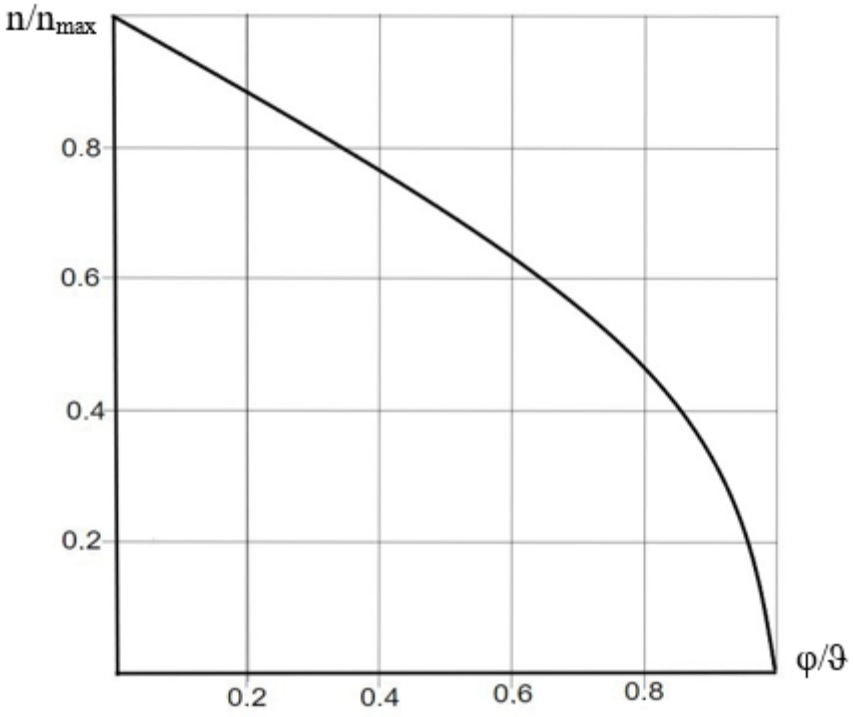

Figure 2. *The dependence of the engine speed on the angle of rotation in relative units*

Downloaded from www.periodico.tchequimica.com

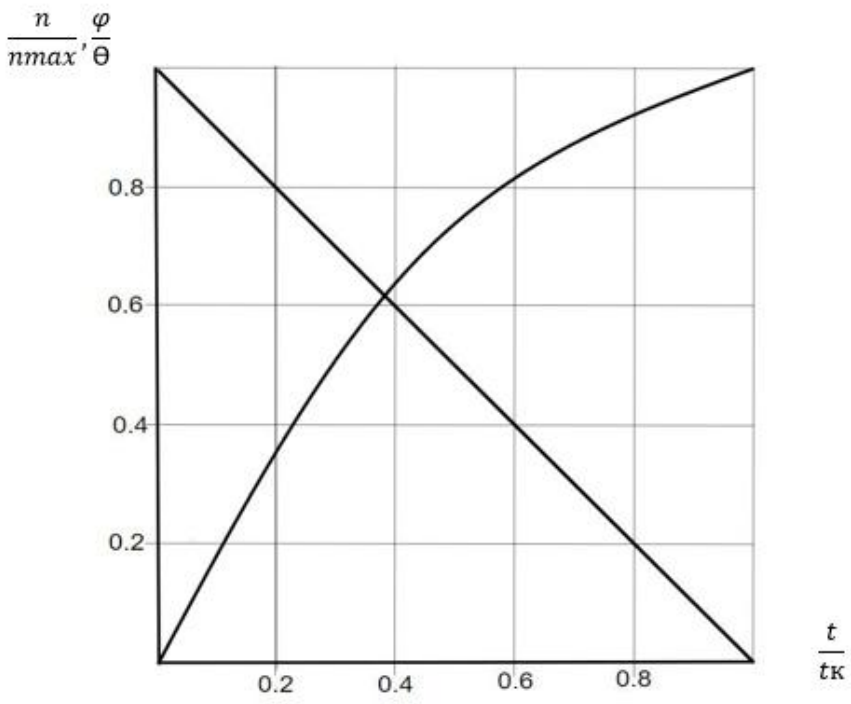

Figure 3. *The dependence of the rotational speed of the crankshaft ICE on the angle of rotation, to the rotation time, in relative units*

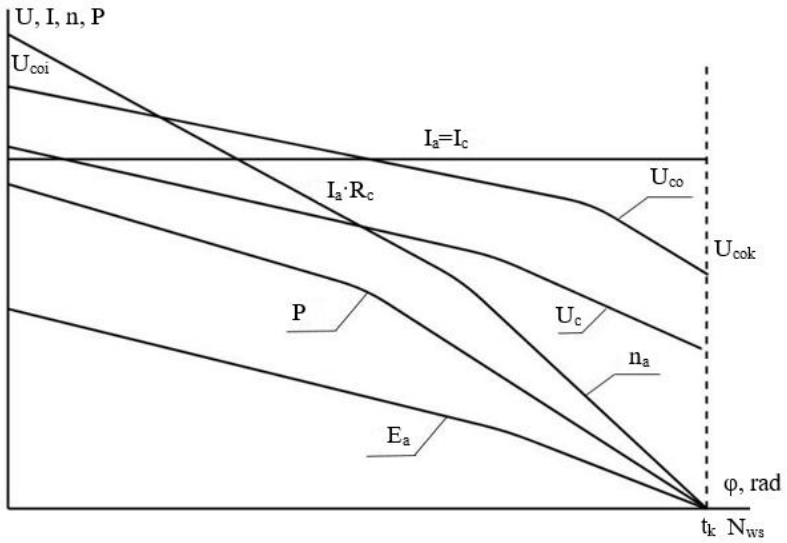

Figure 4. *Estimated change of ESS-parameters on the angle of rotation and the number of working strokes of the engine*

Downloaded from www.periodico.tchequimica.com

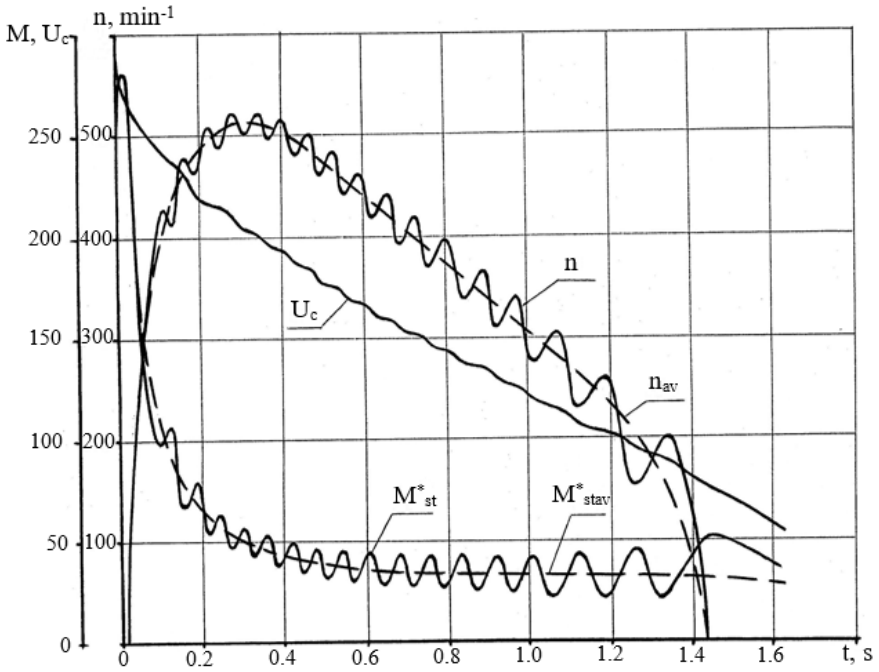

Figure 5. *The dependence of instantaneous and average ESS-parameters to the time cranking of the engine*

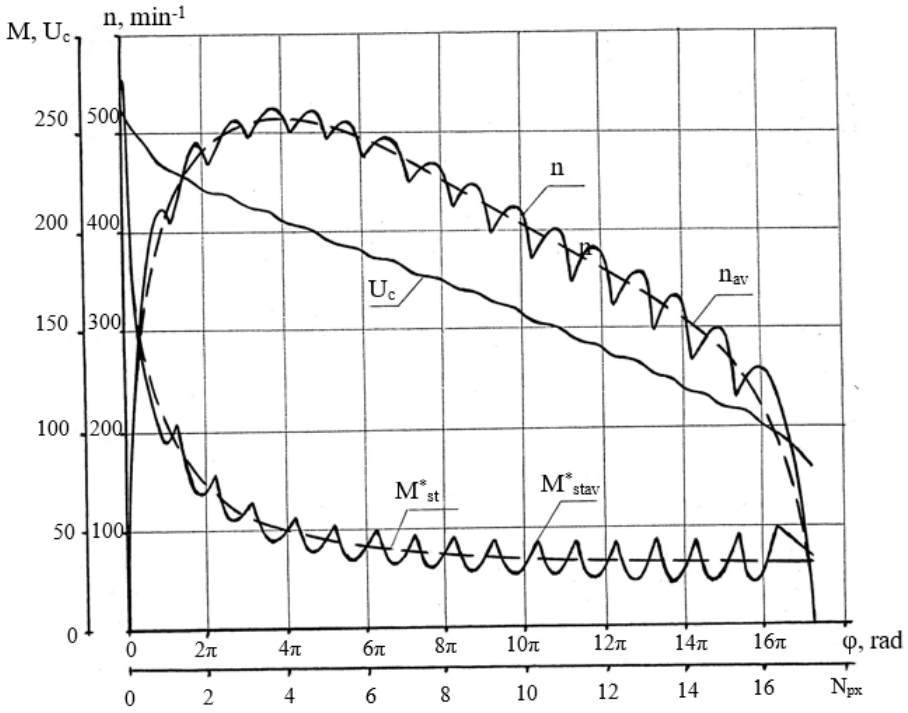

Figure 6. *The dependence of instantaneous and average ESS-parameters on the angle of rotation and the number of working strokes of the engine*

Downloaded from www.periodico.tchequimica.com

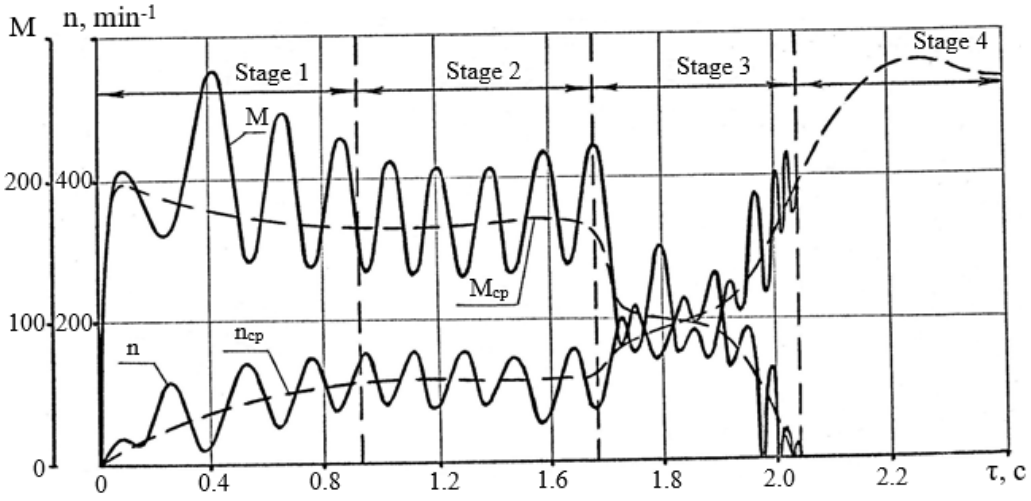

***Figure 7**. The dependence of the frequency and moments of the starter resistance when it powered by a battery*

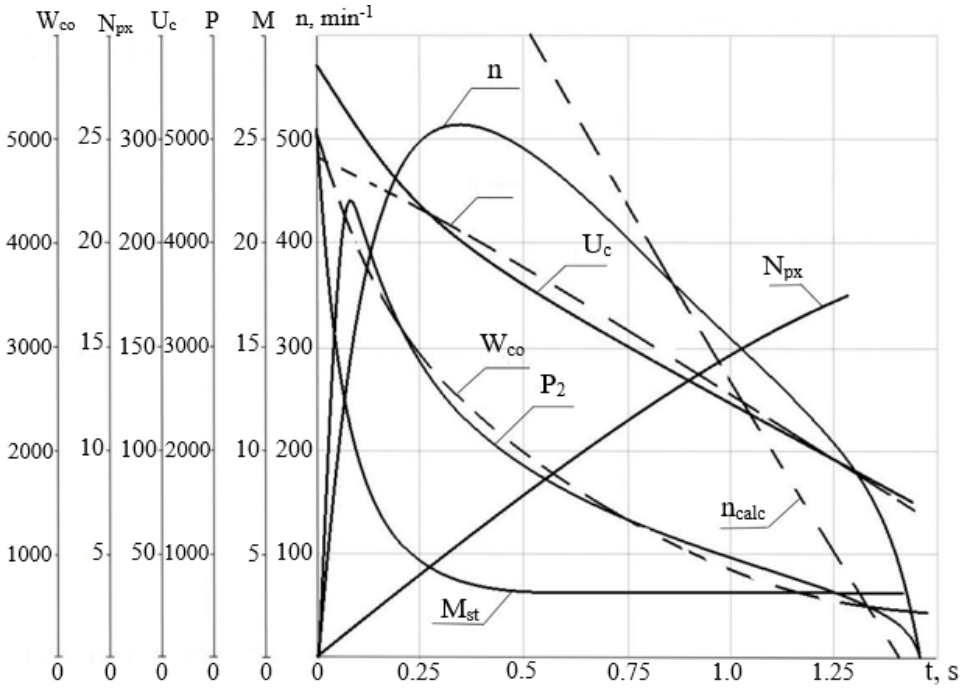

***Figure 8.** Experimental dependencies of the ESS-parameters depending on the engine scrolling time*

***Table 1.** Values of n and φ obtained in the course of calculations*

n/n_{max}	0.9	0.8	0.7	0.6	0.5	0.4	0.3	0.2	0.1	0
φ/ϑ	0.19	0.36	0.51	0.64	0.75	0.84	0.91	0.96	0.99	1.00

Downloaded from www.periodico.tchequimica.com

PERIÓDICO TCHÊ QUÍMICA
ARTIGO ORIGINAL

COMPOSIÇÃO QUÍMICA DOS SOLOS DOS SÍTIOS ARQUEOLÓGICOS AP-MA-05 EM MACAPÁ-AMAPÁ

CHEMICAL COMPOSITION OF AP-MA-05 ARCHAOLOGICAL SITE SOIL IN MACAPÁ-AMAPÁ

XAVIER, Nildineide Soares[1*]; XAVIER, José Renato Magno[2]; COSTA, Jucilene Amorim[3];

[1*] Universidade do Estado do Amapá, Pró-Reitoria de Graduação, Setor de Laboratórios.

[2] Instituto de Desenvolvimento Rural, Coordenação de Assistência Técnica e Extensão Rural

[3] Universidade Federal do Amapá, Pró-Reitoria de Graduação, Faculdade de Geografia.

** Autor correspondente*
e-mail: Nildineide.xavier@ueap.edu.br

Received 19 August 2019; received in revised form 16 October 2019; accepted 13 November 2019

RESUMO

Arqueoantrossolos são solos que registram a ocupação humana e podem ser encontrados em antigos assentamentos habitacionais conhecidos por sítios arqueológicos. Este tipo de solo geralmente apresenta características distintas dos solos circunvizinhos devido a modificações das suas propriedades químicas, causadas pelas atividades humanas passadas e seu estudo auxilia na compreensão à cerca dessas atividades e da organização destas populações pré-históricas. Com isto, o objetivo deste artigo foi caracterizar os solos do sítio arqueológico AP-MA-05 em relação a sua composição química, apontando as alterações sofridas em decorrência da atividade humana pretérita, em comparação a sua área adjacente. A área de estudo está situada no município de Macapá, Estado do Amapá, no *campus* da Universidade Federal do Amapá (UNIFAP). Para o alcance dos objetivos foram coletadas 41 amostras de solo em duas transversais na área do sítio arqueológico e para fins de comparação na área adjacente foi aberta uma trincheira na qual os solos foram coletados para as determinações pertinentes. Os parâmetros químicos foram mensurados através da determinação de pH em água, fósforo disponível, cálcio, magnésio, potássio e alumínio trocáveis e acidez potencial. Os dados químicos demonstraram grande variabilidade nos solos do sítio e fertilidade superior ao solo da área adjacente, inferindo que as alterações observadas são decorrentes das atividades humanas pretéritas, devido aos solos apresentarem mesma origem. As determinações químicas também indicaram o crescimento do sítio no sentido sul, além dos limites estabelecidos em pesquisas anteriores.

Palavras-chave: *Arqueoantrossolo. Fertilidade. Unifap. Amazônia.*

ABSTRACT

Archaeo anthrosols are soils that record human occupation and can be found in ancient housing settlements known by archaeological sites. This type of soil generally presents distinct characteristics of the surrounding soils due to changes in its chemical properties caused by past human activities and its study helps to understand these activities and the organization of these prehistoric populations. Therefore, the objective of this research was to characterize the soils of the archaeological site AP-MA-05 in relation to its chemical composition, pointing to the alterations suffered as a result of past human activity, in comparison to its adjacent area. The study area is in the municipality of Macapá, Amapá State, on the campus of the Federal University of Amapá (UNIFAP). To reach the objectives, 41 soil samples were collected in two transverse lines in the area of the archaeological site and, for the purpose of comparison in the adjacent area, a trench was opened in which the soils were collected for the pertinent determinations. The chemical identification was measured by pH determination in water, available phosphorus, calcium, magnesium, exchangeable potassium and aluminium, potential acidity. The chemical data showed a great variability in the soils of the archaeological site and superior fertility to the soil of the adjacent area, inferring that the alterations observed in the site are due to the previous human activities as the soils present the same origin. The chemical determinations also indicated the growth of the archaeological site in the south direction, outside the limits established in previous researches.

Keywords: *Arqueoantrossolo. Fertility. Unifap. Amazon.*

Downloaded from www.periodico.tchequimica.com

1. INTRODUÇÃO

Os solos predominantes na Região Amazônica pertencem à classe dos Latossolos e Argissolos, sendo estes caracterizados por seu alto grau de intemperismo e por possuir propriedades físicas adequadas ao uso agrícola, entretanto, apresentam fortes limitações químicas. Na Região também ocorrem solos que foram modificadas por processos antrópicos resultantes da ocupação humana pretérita, conhecidos como arqueoantrossolo (KAMPF *et al.,* 2010; PRIMAVESI, 2001).

Estes solos apresentam modificações principalmente nas suas propriedades químicas em decorrência da deposição de resíduos orgânicos e inorgânicos, sendo as maiores contribuições provenientes de produtos de origem animal e vegetal que foram descartados durante as atividades desenvolvidas por populações do passado e que adicionaram certos nutrientes aos solos, conferindo a estes uma maior fertilidade (WOODS, 2009).

Embora agricultores de todo o mundo já houvessem reconhecido que antigas ocupações apresentavam solos férteis, foi somente no início do século 20 que as modificações químicas causadas no solo por estas atividades humanas passaram a ser vistas como evidências para o estudo de assentamentos abandonados (PARNELL; TERRY, 2002).

Os registros mais importantes da ação humana pré-histórica no solo resultam de assentamento e da prática da agricultura. Nos sítios de assentamento, são concentrados grandes volumes de material orgânico resultante da atividade humana como ossos, conchas, sangue, carapaças, fezes, folhas e sementes. Todo esse material é depositado de acordo com o padrão de assentamento da aldeia, que irá definir de que forma a área foi ocupada (KERN, 2009).

As pesquisas pedológicas, arqueológicas e etnográficas têm auxiliado na identificação desses padrões de assentamentos e trouxeram novos conhecimentos sobre a visão da inter-relação dentre homem e meio ambiente. O estudo da composição mineral e química dos solos aplicada a sítios arqueológicos revela que atividades desempenhadas em um mesmo local sob um determinado tempo deixam distintas assinaturas fixas no solo através de anomalias de certos elementos químicos que podem levar a informações conclusivas sobre a forma de assentamento do homem na pré-história (COSTA; KERN, 1999; COSTA; COSTA; KERN, 2013; HASTIK, GEITNER; NEUBURGER, 2013; KERN, 2009; SCHMIDT, 2016).

Tendo em vista o exposto, o objetivo deste artigo foi caracterizar os solos do sítio arqueológico AP-MA-05 em relação a sua composição química, apontando as alterações sofridas em decorrência da atividade humana pretérita, em relação a sua área adjacente (AD).

2. ÁREA DE ESTUDO

A área de estudo compreende ao sítio arqueológico AP-MA-05, que está situado no campus da Universidade Federal do Amapá (UNIFAP), localizada no município de Macapá, Estado do Amapá (Figura 1).

As coordenadas geográficas da área central do sítio são: Latitude 00°00.490'S e Longitude 051°05.142'W, DATUM WGS84. O Igarapé do Zerão é a drenagem mais próxima, a cerca de 600 m, o qual desagua no rio Amazonas, que está a cerca de 2 km da área estudada.

Em relação aos aspectos físicos, a área de estudo se encontra na unidade geológica de cobertura Detrito-laterítica Pleistocênica, caracterizada pela presença de sedimentos argilo-arenosos amarelados. A área de estudo é coberta principalmente por solos minerais, intemperizados, profundos e bem drenados do tipo Latossolo amarelo distrófico típico (IEPA, 2008; IBGE, 2004a).

Os aspectos climáticos são definidos pelo clima equatorial quente e úmido com relevantes índices pluviométricos. A concentração de chuvas se intensifica no período de janeiro a junho, meses nos quais são alcançados os mais elevados índices de precipitação pluviométrica, que podem chegar a 407 mm ao mês (IBGE, 2004b; IEPA, 2008; INMET, 2000).

A pesquisa localiza-se em uma área de influência urbana, onde a vegetação primária já foi bastante alterada e atualmente é caracterizada pela presença marcante de cerrado arbóreo e arbustivo, com transição para área de mata (IBGE, 2004c; IEPA, 2008; MENEZES; SOUZA, 2011).

3. MATERIAL E MÉTODOS

Após o reconhecimento da área delimitada como sítio arqueológico e o mapeamento das manchas lateríticas presentes em sua extensão, foi escolhido um marco inicial,

Downloaded from www.periodico.tchequimica.com

denominado ponto zero. Este marco inicial está localizado no centro da área já escavada por Saldanha e Cabral (2011), e serviu como referência para o cruzamento de duas transversais e coletas das amostras de solo.

A partir da marcação do ponto zero, localizado sob as coordenadas geográficas 0°00'29.480" S e 51°05'08.420" WGr, foi utilizada uma bússola para orientação dos pontos cardeais e posterior projeção das transversais com auxílio de uma trena de 50 m de comprimento.

As transversais foram projetadas perpendiculares entre si formando ângulos de 90°. A Transversal 1 (T1), traçada no sentido Norte-Sul, com 100 m de extensão, e a Transversal 2 (T2), no sentido Leste-Oeste, com 65 m de amplitude. Nas transversais, foram realizadas um total de 33 pontos de coleta, com intervalos de 5 m de distância, dos quais foram coletadas um quantitativo de 41 amostras de solo nas profundidades de 0-10 cm e 10-20 cm (Figura 2).

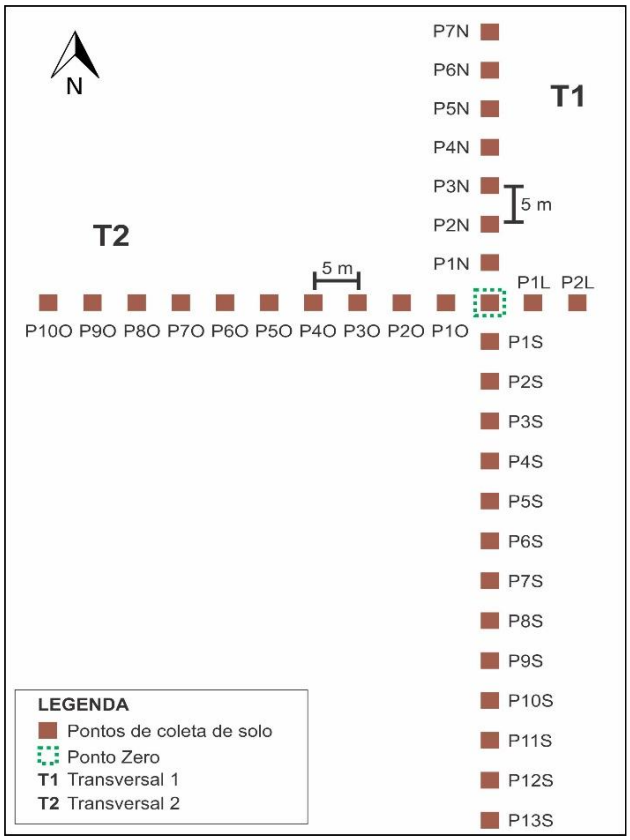

Figura 1. *Croqui esquemático da malha de sondagem e coleta de amostras de solo no sítio arqueológico AP-MA-05.*

Após as coletas as amostras foram preparadas para as análises laboratoriais sendo secas ao ar, destorroadas e peneiradas em malha de 2 mm formando a TFSA (Terra Fina Seca ao Ar). Os parâmetros químicos foram mensurados conforme os procedimentos metodológicos propostos por EMBRAPA (1997):

a) pH em água: Realizado através da medição eletroquímica da concentração efetiva de íons H^+ na solução do solo, por meio de potenciômetro com eletrodo combinado imerso em suspensão de 10g de solo diluído em 25 ml de água deionizada.

b) Matéria orgânica: Determinada por oxidação via úmida com dicromato de potássio em meio sulfúrico, empregando-se como fonte de energia o calor desprendido do ácido sulfúrico. O excesso de dicromato após a oxidação é titulado com solução padrão de sulfato ferroso amoniacal.

c) Fósforo disponível: A extração ocorreu com solução de Mehlich-1, relação solo/ extrator 1:10. O fósforo extraído foi determinado, através da leitura da intensidade da cor do complexo fosfomolíbdico por aparelho de espectrofotômetro produzido pela redução do molibdato com o ácido ascórbico, .

d) Sódio e Potássio trocáveis: A extração destes nutrientes foi realizada com solução Mehlich-1, seguida da determinação da concentração por espectroscopia de emissão de chama pelo equipamento fotômetro de chama. A determinação foi obtida pela medição da energia radiante emitida pelos elementos, individualmente, em chama.

e) Cálcio e Magnésio: Foram extraídos por solução de KCl a 1M e determinados através do equipamento de Espectrofotômetro de Absorção Atômica.

f) Alumínio: Este nutriente também foi extraído do solo por solução de KCl a 1M, e sua determinação realizada pelo método volumétrico, por titulação com hidróxido de sódio.

g) $H^+ + Al^{3+}$: A extração da acidez potencial foi alcançada pela solução de acetato de cálcio e baseada na propriedade tampão do sal devido à presença dos ânions acetato. A determinação foi feita através de titulação alcalimétrica do extrato.

4. RESULTADOS E DISCUSSÃO:

4.1 Matéria orgânica e pH

A matéria orgânica do solo (MOS) no sítio arqueológico apresentou teor máximo de 41,2 $g.dm^{-3}$ (Figura 3), sendo considerado um valor muito alto e consequentemente bom para os

Downloaded from www.periodico.tchequimica.com

solos, enquanto que o valor mínimo observado, bem como o teor de MOS na AD foram semelhantes (12,59 $g.kg^{-1}$) e considerados baixos e inadequados a manutenção das propriedades químicas e físicas do solo, concordando com Alvarez *et al.,* (1999) e Ribeiro (1999). Os valores médios de MOS, aos 0-10 cm, nas transversais foram de 21,69 $g.dm^{-3}$ na T1 e de 19,45 $g.dm^{-3}$ na T2, já na profundidade 10-20 cm da T1 foi de 18,04 $g.dm^{-3}$, valores bem mais elevados no sítio em comparação a AD, onde o teor de MOS foi de 12,59 $g.dm^{-3}$.

A manutenção das propriedades químicas através da MOS se dá por ela ser considerada uma fonte primária de nutrientes e o seu conteúdo é um dos principais indicadores de sustentabilidade e qualidade do solo. Além disso, a capacidade do solo em adsorver nutrientes, a diminuição da toxidez por alumínio e a estabilização do pH, são propriedades e processos cujo controle em solos tropicais fundamentalmente dependem da matéria orgânica (MADARI *et al.,* 2009).

Além disso, os resíduos orgânicos presentes nos solos contribuem na diminuição da sua densidade e criam poros de diâmetros grandes que favorecem a entrada de ar e a drenagem de água, melhorando a qualidade do solo, reduzindo a sua erodibilidade e consequentemente favorecendo as suas propriedades físicas (VASCONCELOS *et al.,* 2010; FRASER; CLEMENTE, 2008).

Os arqueoantrossolos são formados por um grande depósito estável de MOS, o que difere dos solos tipicamente tropicais que em função das altas temperaturas e elevados índices pluviométricos acabam se decompondo e os seus nutrientes são lixiviados mais facilmente. Em virtude dessa diferença, a MOS é de extrema importância para a identificação de sítios arqueológicos, pois ela se mantém nos solos mesmo em condições adversas, liberando nutrientes aos poucos, e mantendo seus bons níveis no solo (GLASER *et al.,* 2000).

O pH em água nos solos do sítio variou de 4,2 a 6,7 (Figura 3), apresentando uma grande variabilidade, com valores que são classificados como acidez muito elevada a baixa, ou seja, com solos muito ácidos e outros próximos a faixa de neutralidade. Os valores médios foram de 5,3 na profundidade de 0-10 cm em ambas as transversais e de 5,1 aos 10-20 cm, representando solos menos ácidos que os da AD que apresentou pH com valor de 4,9.

Falcão et al. (2009) ao pesquisar solos da camada superficial de 10 sítios com terra preta arqueológica (TPA), no Estado do Amazonas, verificou valores de pH com variação entre 4,32 e 6,61, possuindo um valor médio de 5,68, resultados semelhantes aos encontrados no sítio arqueológico estudado.

Os resultados desta pesquisa ratificam que os arqueoantrossolos do sítio AP-MA-05 apresentam maiores valores de pH, quando comparados com solos adjacentes, que são extremamente ácidos e em geral apresentam pH entre 4,0 e 5,0 (REIS *et al.,* 2009). Os valores mais baixos de pH nos solos naturais da região amazônica são causados pela elevada perda de bases trocáveis e consequente concentração de íons H^+, provocada pelo processo de intemperismo influenciado pelas altas temperaturas e longos períodos de precipitação (ALVAREZ *et al.,* 1999; FALCÃO *et al.,* 2009).

4.2 Macronutrientes diagnósticos em arqueoantrossolos

O cálcio disponível obteve teor máximo de 7,2 $cmol_c.dm^{-3}$ aos 0-10 cm da T1, sendo considerado um valor muito alto para solos tropicais e divergente de outras pesquisas como a realizada por Costa e Moura (2017) em solos identificados como Terra Mulata, presentes também no campus da UNIFAP, nos quais os valores de cálcio e magnésio somados apresentaram máxima de 4 $cmol_c.dm^{-3}$. E sendo muito distante dos dados obtidos por Melém Júnior (2003) na região de cerrado amapaense em solos sem interferência antrópica pretérita, onde os valores de Ca+Mg ficaram em torno de 0,36 $cmol_c.dm^{-3}$.

Os valores médios de cálcio a 0-10 cm foram de 2,6 $cmol_c.dm^{-3}$ na T1 e de 0,23 $cmol_c.dm^{-3}$ na T2. Na profundidade 10-20 o valor foi de 1,7 $cmol_c.dm^{-3}$ (Figura 4), já na AD o teor deste nutriente não foi detectado, o que mostra um enriquecimento de cálcio nos solos do sítio arqueológico AP-MA-05, em especial nas duas profundidades analisadas da T1.

Os níveis de cálcio no interior do sítio podem estar relacionados com a humificação pronunciada destes solos, o que favorece a atividade biológica, tornando o material orgânico menos solúvel e assim formando agregados mais estáveis, ou seja, causando sua menor lixiviação em função da grande afinidade com a superfície de troca do solo, observados também pelos altos teores de MOS no interior do sítio, concordando assim com Kern et al. (2015), Barros et al. (2012) e Lima et al. (2010).

Downloaded from www.periodico.tchequimica.com

Os teores de fósforo disponível variaram entre 1 e 13 mg.dm^{-3} (Figura 4), sendo o teor máximo classificado como um valor médio, entretanto, já considerado uma pequena anomalia por este nutriente na área, uma vez que Latossolos dificilmente apresentam esse valor sem algum tipo de interferência antrópica, normalmente apresentando valores de até 3 mg.dm^{-3} na região (KERN, 2009; RIBEIRO, 1999).

Os valores médios de fósforo na profundidade 0-10 cm foram de 4,1 mg.dm^{-3} na T1 e 2,1 mg.dm^{-3} na T2, já na profundidade 10-20 cm o valor foi de 2,66 mg.dm^{-3}. Na AD o teor de fósforo foi de 2 mg.dm^{-3}, revelando que os valores médios do sítio ainda são superiores ao da AD para este nutriente.

Em contrapartida aos altos resultados de MOS, pH e cálcio trocável no sítio, não foi observado o mesmo padrão para os teores de fósforo disponível, como encontrados em outros sítios da região Amazônica, com valores que chegam a alcançar 2.761 mg.dm^{-3}, como constatado por Pessoa Junior e Santana (2017) no sítio Santo Antônio localizado do município de Anori, Estado do Amazonas.

Contudo, valores baixos para fósforo e altos para cálcio trocável também foram observados por Campos et al. (2012) em dois perfis de solo de dois sítios com TPA no município de Manicoré-AM (máxima de 15,5 e 35,4 mg.dm^{-3} em superfície para cada perfil), por Pessoa Junior e Santana (2017) no sítio Balbina em Presidente Figueiredo, no mesmo Estado, com valor máximo de 17 mg.dm^{-3}, e por Silva et al. (2012) no sítio BJ8 em Bom Jesus-PA, com máxima de 20 mg.dm^{-3} do nutriente.

Os teores de fósforo identificados em arqueoantrossolos devem-se à ocupação humana pretérita, e seu enriquecimento se dá através do acúmulo e decomposição de matéria orgânica de origem animal, como restos de ossos, sangue e excrementos humanos. Por isso, o fósforo é um importante nutriente a ser analisado em solos de sítios arqueológicos, pois além de auxiliar na sua localização pode também ser utilizado para estimar o tamanho da população, duração e intensidade do assentamento. (KERN, 2009; RODRIGUES; COSTA, 2016; ROOSEVELT, 2013; SANTOS *et al.,* 2013).

Considerando-se a classificação do sítio AP-MA-05 como um sítio-cemitério com diversas urnas funerários e material arqueológico, além dos altos conteúdos de cálcio, é evidente sua riqueza em matéria orgânica animal, em especial ossos. No entanto, os baixos níveis de fósforo registrados na maior parte da área estudada sugerem a baixa influência do material das urnas funerárias aos solos mais superficiais, analisados neste estudo. Assim, é possível que o nutriente seja detectado em uma maior profundidade ou ainda ter formado compostos inorgânicos com baixa solubilidade com cátions como o ferro, alumínio ou cálcio, não sendo detectado em sua forma disponível, como os demais nutrientes investigados, conforme relatado por Lepsch (2002) e Silva (2007).

A forma de fósforo associado a compostos inorgânicos, pode estar também adsorvido ao material cerâmico abundante na área, como observados em outros trabalhos como o de Coelho et al. (1996) em fragmentos cerâmicos do sítio Manduquinha em Caxiuanã-PA e por Costa et al.(2004), em cerâmicas do sítio Cachoeira-Porteira, no município de Oriximiná, no mesmo Estado. Assim, há a necessidade de análises químicas totais, tanto do solo quanto dos fragmentos cerâmicos para confirmação desta hipótese.

Assim como o cálcio, o magnésio e o potássio também são cátions básicos que contribuem para os altos valores de CTC e para a soma de bases (SB) dos solos antropogênicos, entretanto sua abrangência espacial é mais restrita (KERN, 2009). Na área do sítio os teores de magnésio mais altos foram classificados como médios na T1, chegando a 0,7 $cmol_c.dm^{-3}$ e não sendo detectados em alguns pontos da T2. A média a 0-10 cm foi de 0,46 $cmol_c.dm^{-3}$ na T1, de 0,025 $cmol_c.dm^{-3}$ na T2 e de 0,39 na profundidade 10-20 cm. Na AD o valor de magnésio foi de 0,4 $cmol_c.dm^{-3}$, semelhante aos valores médios da T1.

O potássio trocável variou entre muito baixo (0,01 $cmol_c.dm^{-3}$) a níveis considerados como bons (0,2 $cmol_c.dm^{-3}$), segundo Ribeiro (1999), nas transversais. Os maiores teores deste nutriente foram observados em consonâncias aos pontos com maior destaque para cálcio e magnésio. A média de potássio na T1 foi de 0,048 $cmol_c.dm^{-3}$ a 0-10 cm e de 0,068 $cmol_c.dm^{-3}$ a 10-20 cm, já o valor médio da T2 foi igual ao da AD (0,02 $cmol_c.dm^{-3}$). Valores semelhantes foram observados por Silva *et al*. (2012), que constatou o teor máximo de 0,23 $cmol_c.dm^{-3}$ de potássio em solos superficiais classificados como TPA, no Estado do Pará.

Os níveis de alumínio trocável no sítio foram baixos ou fora dos limites de detecção. Os

Downloaded from www.periodico.tchequimica.com

valores médios foram de 0,42 $cmol_c.dm^{-3}$ na T1 e 1 $cmol_c.dm^{-3}$ na T2 a 0-10 cm e de 0,48 $cmol_c.dm^{-3}$ a 10-20 cm, tornando a maior parte dos solos com valores adequados para o nutriente, característica bastante incomum em solos tropicais. Na AD o alumínio apresentou concentração de 1,1 $cmol_c.dm^{-3}$, sendo considerado um valor alto e potencialmente prejudicial, além de estar acima da média dos valores observados no sítio.

Diferente dos cátions trocáveis discutidos anteriormente, o alumínio trocável no solo se torna satisfatório quando alcança valores inferiores a 0,51 $cmol_c.dm^{-3}$. Esse padrão se dá devido a sua concorrência com os demais nutrientes indispensáveis a nutrição vegetal (Ca, Mg e K) e por sua concentração muito elevada se tornar indesejável devido ao potencial de toxidez que este nutriente apresenta (PRIMAVESI, 2001; RIBEIRO *et al.,*1999).

Nas TPA normalmente é encontrada relação inversa e muito evidente do teor de alumínio com o de pH e cálcio (FALCÃO *et al.,* 2009). Ainda segundo estes autores, o valor máximo de alumínio encontrado para um conjunto de 100 amostras da camada superficial de solos de sítios arqueológicos pesquisados, ocorreu máxima de 1,60 $cmol_c.dm^{-3}$ de alumínio, média de 0,20 $cmol_c.dm^{-3}$ e valor mínimo de 0,01 $cmol_c.dm^{-3}$, resultados semelhantes aos do sítio AP-MA-05.

4.3 Parâmetros de fertilidade potencial em arqueoantrossolos

Os níveis de acidez potencial nas transversais estão dentro dos valores de referência de acordo com Ribeiro *et al*. (1999), no qual os níveis desta acidez acima de 5,01 $cmol_c.dm^{-}3$ são considerados bons para o solo, e inferiores de 2,5 $cmol_c.dm^{-3}$, tornam-se baixos. O menor valor encontrado no sítio foi de 2,5 $cmol_c.dm^{-3}$ na T1 e o valor máximo de 8,7 $cmol_c.dm^{-3}$ na mesma transversal, apresentando médias de 4,52 $cmol_c.dm^{-3}$ e 5,02 $cmol_c.dm^{-3}$ na T1 e T2, respectivamente, ambos superiores ao valor de 3,9 $cmol_c.dm^{-3}$ observado na AD, que foi considerado um valor médio.

Em relação aos parâmetros que estimam a fertilidade dos solos, além da MOS, acidez medida pelo pH em água e a acidez potencial, destacam-se também a Soma de Bases (SB), a Capacidade de Troca Catiônica (CTC), a Saturação por bases (V%) e a Saturação por alumínio (m%) (FALCÃO *et al.,* 2009; PRIMAVESI, 2001; RIBEIRO *et al.,* 1999).

Os valores de V% classificam o solo quanto a seu grau de fertilidade (Figura 5), sendo V> 50% solos eutróficos (férteis), logo, quanto maior este parâmetro no solo, maior a sua fertilidade (EMBRAPA, 2014, FALCÃO, 2009; RIBEIRO *et al.,* 1999). Nos solos do sítio foram observados valores de V% que chegaram a 84%, caracterizando uma alta fertilidade. Entretanto, a maior parte dos solos apresentou fertilidade média, sendo denominados de solos mesotróficos (média V=30%), enquanto que na AD o valor de V= 9%, sendo o solo classificado como distrófico.

No sítio, a SB variou entre 8 $cmol_c.dm^{-3}$ e 0,3 $cmol_c.dm^{-3}$, sendo o valor máximo observado na T1. Os valores médios foram de 3,14 $cmol_c.dm^{-3}$ e 2,32 $cmol_c.dm^{-3}$ para as profundidades 0-10 e 10-20 cm, respectivamente, da T1 e de 0,78 $cmol_c.dm^{-3}$ na T2.

A CTC teve média de 7,6 $cmol_c.dm^{-3}$ e 6,8 $cmol_c.dm^{-3}$, nos níveis 0-10 e 10-20, respectivamente na T1 e de 5,8 $cmol_c.dm^{-3}$ na T2. Já a m% obteve percentuais médios de 19,3% em 0-10 cm e 26% em 10-20 da T1 e 55,7% na T2. Resultados semelhantes aos deste trabalho foram observados por Silva et al. (2012) que encontraram em solos superficiais caracterizados como TPA no sítio BJ8 no Estado do Pará, valores máximos de CTC= 9,86 $cmol_c.dm^{-3}$; SB= 9,9 $cmol_c.dm^{-3}$ e V= 84%, caracterizando os solos como eutróficos.

Na AD, os valores de SB e CTC foram baixos (0,4 $cmol_c.dm^{-3}$ e 4,3 $cmol_c.dm^{-3}$, respectivamente). O solo apresenta um alto potencial a toxidez por alumínio, devido à alta saturação pelo nutriente (m%), assim como observado em alguns pontos na T2, onde os valores ultrapassaram a faixa adequada (m= 35%), chegando a máxima de 80% na T2 e 73% na AD, considerados percentuais muito altos e consequentemente prejudiciais aos cultivares.

A figura 6 mostra a grande variabilidade dos atributos químicos analisados nos solos do sítio arqueológico AP-MA-05, com seus respectivos valores máximos, mínimos e médios, visando traçar um perfil químico geral da área.

Quando calculado o coeficiente da correlação de Pearson para as 41 amostras das duas transversais do interior do sítio arqueológico, foi verificado valores de correlação fortes entre alguns dos parâmetros analisados, sendo positivas para pH com V, Ca e SB (r^2= +0,99; r^2= +0,88 e r^2= +0,86, respectivamente); para Ca com SB e V (r^2= +0,99 e r^2= +0,97,

respectivamente) e para SB com V (r^2= +0,97). As correlações fortes negativas foram observadas para pH com Al com V e m (r^2= -0,84; r^2= -0,83 e r^2= -0,82, respectivamente) e Mg e m (r^2= -0,82) (Tabela 1).

Ressalta-se que, apesar dos baixos conteúdos de fósforo no sítio arqueológico AP-MA-05, existe uma relação moderada positiva entre o mesmo e outros nutrientes como magnésio, cálcio e potássio, sendo os coeficientes desta relação iguais a r^2= +0,52; r^2= +0,51 e r^2= +0,50, respectivamente. Assim como há correlação positiva também com a Soma de bases (r^2= +0,51), sugerindo que estes nutrientes têm a mesma fonte (Tabela 1).

As concentrações dos parâmetros químicos no sítio arqueológico AP-MA-05 mostram uma maior distribuição de MOS, pH, cálcio, fósforo, SB, CTC, V% e os menores índices de m% na porção sul da transversal 1. Esta foi a zona de maior fertilidade dentro do sítio e consequentemente a que provavelmente apresentou maior influência por descarte de resíduos orgânicos por atividades antrópicas antigas. Em contrapartida, as áreas com menor concentração destes parâmetros, sugerem áreas mais limpas como caminhos e áreas de circulação em geral, com menor descarte de resíduos e, por conseguinte, menor fertilidade.

A organização hipotética apresentada na Figura 7 expõe uma visão geral da área do sítio estudada, mostrando as regiões com maior interferência humana pretérita através de maior descarte de resíduos orgânicos aos solos. O aumento da fertilidade dos solos ocorre no sentido sul do sítio, em espaços com edificações, como a área do prédio da Pró-Reitoria de Extensão e Ações Comunitárias (PROEAC), e consequentemente, para fora dos limites prévios estabelecidas por Machado (1997) e Saldanha e Cabral (2011).

Apesar das limitações desta distribuição espacial devido a necessidades da coleta de mais amostras de solo em uma malha regular e não apenas em duas transversais, este dado foi válido, tendo-se como comparação que a mesma distribuição foi proposta por Costa, Costa e Kern (2013) que utilizou malha regular de 60 x 120 m nos sítios arqueológicos TP1 e TP2, em Juruti, no Estado do Pará.

5. CONCLUSÕES

A amplitude entre os limites de pH mostrou a heterogeneidade química dos arqueoantrossolos, oriundas da influência das atividades humanas na área. Os valores mais elevados de pH foram identificados na porção sul do sítio, resultados condizentes com os altos teores de matéria orgânica, cálcio, magnésio e, no geral, a boa fertilidade destes solos na mesma região.

Os valores mínimos dos parâmetros químicos mensurados no sítio e semelhantes aos da área adjacente podem ser justificados pela grande variabilidade química existente em solos de sítios arqueológicos em função das atividades humanas pretéritas modificarem o ambiente, e consequentemente os solos, de maneira irregular.

O aumento da fertilidade ocorreu no sentido sul do sítio. Esta região apresentou também os maiores valores de nutrientes em comparação a área adjacente, com exceção do alumínio que foi maior na adjacência. Isto evidencia a área de deposição preferencial de resíduos, refletindo a dinâmica da ação antrópica no assentamento, pode ainda estar indicando uma possível área de habitação próxima ou sobreposta ao cemitério, como comumente observado em muitos sítios arqueológicos na região amazônica.

6. REFERÊNCIAS

1. ALVAREZ, V. H. et al. Interpretação dos resultados das análises de solos. Recomendação para o uso de corretivos e fertilizantes em Minas Gerais, v. 5, p. 25-32, 1999.

2. BARROS, K. R. M. et al. Fracionamento químico da matéria orgânica e caracterização física de Terra Preta de índio. Revista de Ciências Agrárias/ Amazonian Journal of Agricultural and Environmental Sciences, v. 55, n. 1, p. 44-51, 2012.

3. CAMPOS, M. C. C. et al. Caracterização física e química de terras pretas arqueológicas e de solos não antropogênicos na região de Manicoré, Amazonas. Revista Agro@mbiente On-line, v. 6, n. 2, p. 102-109, 2012.

4. COELHO, S. R. C. et al. Mineralogia e composição química dos fragmentos cerâmicos arqueológicos do sítio Manduquinha em Caxiuanã (Portel-Pa). SIMPÓSIO DE GEOLOGIA DA AMAZÔNIA,

Downloaded from www.periodico.tchequimica.com

v. 5, p. 234-237, 1996.

5. COSTA, M. L. et al. The ceramic artifacts in archaeological black earth (terra preta) from lower Amazon region, Brazil: Mineralogy. Acta Amazonica, v. 34, n. 2, p. 165-178, 2004.

6. COSTA, J. A.; COSTA, M. L. da; KERN, D. C. Analysis of the spatial distribution of geochemical signatures for the identification of prehistoric settlement patterns in ADE and TMA sites in the lower Amazon Basin. Journal of Archaeological Science, v. 40, n. 6, p. 2771-2782, 2013.

7. COSTA, J. A; MOURA, E. P. Uso e ocupação do solo no cerrado amapaense: a formação de antrossolos no campus da Universidade Federal do Amapá. In: BRITO, D. M. C; AVELAR, V. G. Geografia do Amapá em Perspectiva, v. 1. Macapá: Universidade Federal do Amapá, 2017. p. 84-95.

8. COSTA, M. L; KERN, D. C. Geochemical signatures of tropical soils with archaeological black earth in the Amazon, Brazil. Journal of Geochemical Exploration, v. 66, n. 1, p. 369-385, 1999.

9. EMPRESA BRASILEIRA DE PESQUISA AGROPECUÁRIA – EMBRAPA. Análises de solos. 2a ed. Rio de Janeiro: Embrapa Solos. Centro Nacional de Pesquisa de solos, 1997.

10. FALCÃO, N. P. S. et al. Fertilidade do solo de Terra Preta de Índio. TEIXEIRA, W. G; KERN, D. C; MADARI, B.E; LIMA, H. N & WOODS, W. I, orgs. As Terras Pretas de Índio da Amazônia - Sua caracterização e uso deste conhecimento na criação de novas áreas. Manaus, UFAM, p. 201-211, 2009.

11. FRASER, J. A.; CLEMENTE, C. R. Dark Earths and manioc cultivation in Central Amazonia: a window on pre-Columbian agricultural systems? Boletim do Museu Paraense Emilio Goeldi de Ciências Humanas, v. 3, p. 175-194, 2008.

12. GLASER, B. et al. Carbono negro em frações de densidade de solos antropogênicos da região amazônica brasileira. Geoquímica orgânica, v. 31, n. 7, p. 669-678, 2000.

13. HASTIK, R; GEITNER, C; NEUBURGER, M. Amazonian dark earths in bolivia? A soil study of anthropogenic ring ditches near baures (eastern llanos de mojos). Erdkunde, p. 137-149, 2013.

14. INSTITUTO BRASILEIRO DE GEOGRAFIA E ESTATÍSTICA – IBGE (Brasil). Mapa de pedologia do Estado do Amapá. Rio de Janeiro, 2004a. 1 Mapa. Escala 1: 750.000.

15. _____. Mapa de Clima do Brasil. Rio de Janeiro, 2004b. 1 Mapa. Escala 1: 5.000.000.

16. _____. Mapa de vegetação do Estado do Amapá. Rio de Janeiro, 2004c. 1 Mapa. Escala 1: 750.000.

17. INSTITUTO DE PESQUISAS CIENTÍFICAS E TECNOLÓGICAS DO ESTADO DO AMAPÁ - IEPA. Macrodiagnóstico do Estado do Amapá: primeira aproximação do ZEE. 3. ed. rev. ampl. Macapá: IEPA, 2008.

18. INSTITUTO NACIONAL DE METEOROLOGIA - INMET. Normais Climatológicas do Brasil: 1961-1990. Brasília: MAPA, 2000.

19. KAMPF, N. et al. Classificação das terras pretas de índio e outros solos antrópicos antigos. In: Teixeira, W.; Kern, D. Madari, B.; Lima, H. & Woods, W. As terras pretas de índio da Amazônia: sua caracterização e uso deste conhecimento na criação de novas áreas. p. 87-102. 2010.

20. KERN, D. C. Costa, J. A., da Silveira, M. I., de Oliveira, E. R., Frazão, F. J. L., Berredo, J. F., Kämpf, N. Pedo-Geochemical Signatures of Archeological Sites in the Tapirapé-Aquiri National Forest in Marabá, Amazonia, Brazil. Geoarchaeology, v. 30, n. 5, p. 430-451, 2015.

21. LEPSCH, I. P. Conservação dos solos. São Paulo: Caderno de textos, 2002.

22. LIMA, H. N. et al. Dinâmica da mobilização de elementos em solos da Amazônia submetidos à inundação. Acta Amazonica. v. 35, n. 3, p. 317–30, 2010.

23. MACHADO, A. Relatório do Salvamento Arqueológico do Sítio AP-MA-5: Campus Universitário Macapá-AP. Belém: Museu Paraense Emílio Goeldi, 1997.

24. MADARI, B. E. et al. Matéria orgânica dos solos antrópicos da Amazônia (Terra Preta de Índio): suas características e papel na sustentabilidade da fertilidade do solo. In: TEIXEIRA, W. G.; KERN, D. C.; MADARI, B. E.; LIMA, H. N.; WOODS, W. I. (Ed.). As Terras Pretas de Índio da Amazônia: sua caracterização e uso deste conhecimento na criação de novas áreas. Manaus: Embrapa Amazônia Ocidental, 2009. p. 172-188.

25. MELÉM JÚNIOR, N. J. et al. Caracterização dos cerrados do Amapá. Embrapa Amapá-Comunicado Técnico (INFOTECA-E), 2003.

Downloaded from www.periodico.tchequimica.com

26. MENEZES, C. R; SOUZA, G. K. C. Levantamento de Briófitas Bioindicadoras de Perturbação Ambiental do Campus Marco Zero do Equador da Universidade Federal do Amapá. Biota Amazônia, v. 1, n. 1, p. 63-73, 2011.

27. PARNELL, J. J; TERRY, R. E. Análise química do solo aplicada como ferramenta interpretativa para atividades humanas antigas em Piedras Negras, Guatemala. Journal of Archaeological Science, v. 29, n. 4, p. 379-404, 2002.

28. PESSOA JUNIOR, E. S. F; SANTANA, G. Uma abordagem sobre fósforo em Terra Preta Arqueológica. Scientia Amazonia. ISSN:2238.1910. v. 6, n. 1, 61-70, 2017.

29. PRIMAVESI, A. Manejo ecológico do solo: a agricultura em regiões tropicais. São Paulo: Nobel, 2001.

30. REIS, M. A. et al. Atributos físicos, químicos e biológicos de solo de cerrado sob diferentes sistemas de uso e manejo. Revista Brasileira de Ciência do Solo, v. 33, n. 1, 2009.

31. RIBEIRO, A. C. et al. Recomendações para o uso de corretivos e fertilizantes em Minas Gerais – 5ª Aproximação. Viçosa: MG, 1999. 359p.

32. RODRIGUES, S. F. S.; COSTA, M. L. Phosphorus in archeological ceramics as evidence of the use of pots for cooking food. Appl Clay Sci. v. 123, p. 224-31, 2016.

33. ROOSEVELT, A. C. The Amazon and the Anthropocene: 13,000 years of human influence in a tropical rainforest. Anthropocene. v. 4, p. 69–87, 2013.

34. SALDANHA, J. D. M.; CABRAL, M. P. Segundo relatório do Programa de Resgate Arqueológico no Campus Marco Zero da Universidade Federal do Amapá (UNIFAP), Macapá -AP. 2011.

35. SANTOS, L. A. C. et al. Caracterização de Terras Pretas Arqueológicas no Sul do Estado do Amazonas. Revista Brasileira de Ciência do Solo. v. 37. n. 6, p. 825–6, 2013.

36. SCHMIDT, M. J. A formação de Terra Preta: Análise de sedimentos e solos no contexto arqueológico. p. 121-176. In: Magalhães, M. P. (Org.) Amazônia Antropogênica. Belém: Museu Paraense Emílio Goeldi, 2016. 429 p.

37. SILVA, A. K. T. et al. Mineralogia e geoquímica de perfis de solo com Terra Preta Arqueológica do município de Bom Jesus do Tocantins, sudeste da Amazônia. Acta amazonica, v. 42, n. 4, 2012.

38. VASCONCELOS, R. F. B. et al. Estabilidade de agregados de um Latossolo Amarelo distrocoeso de tabuleiro costeiro sob diferentes aportes de resíduos orgânicos da cana-de-açúcar. Revista Brasileira de Ciência do Solo, v. 34, n. 2, 2010.

39. WOODS, W. Os solos e as ciências humanas: Interpretação do passado. In: TEIXEIRA, W. G.; KERN, D. C.; MADARI, B. E.; LIMA, H. N.; WOODS, W. I. (Ed.). As Terras Pretas de Índio da Amazônia: sua caracterização e uso deste conhecimento na criação de novas áreas. Manaus: Embrapa Amazônia Ocidental, 2009. p. 62-71.

Downloaded from www.periodico.tchequimica.com

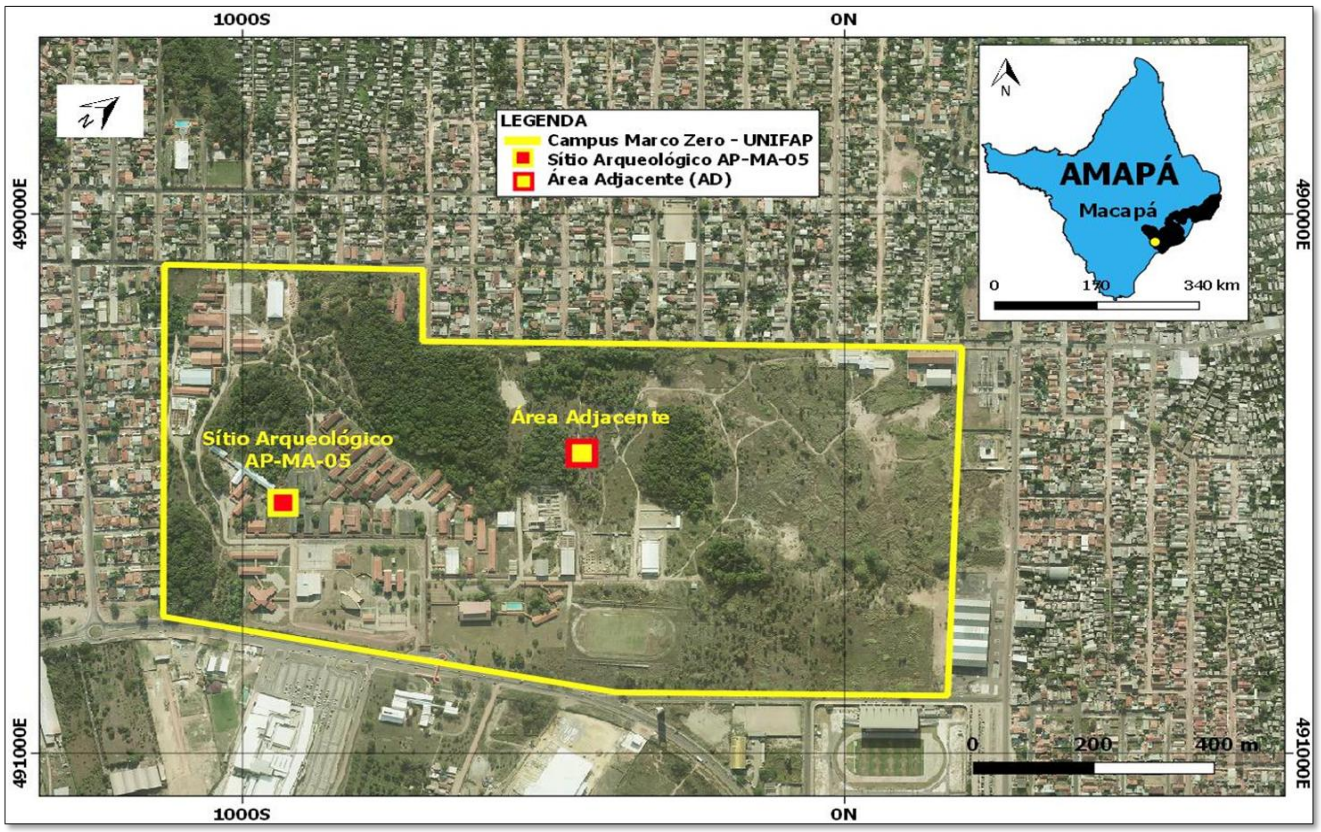

Figura 2. *Mapa de localização do campus Universitário Marco Zero da Universidade Federal do Amapá. Em destaque a Área do Sítio arqueológico AP-MA-05 e a sua Área adjacente.*

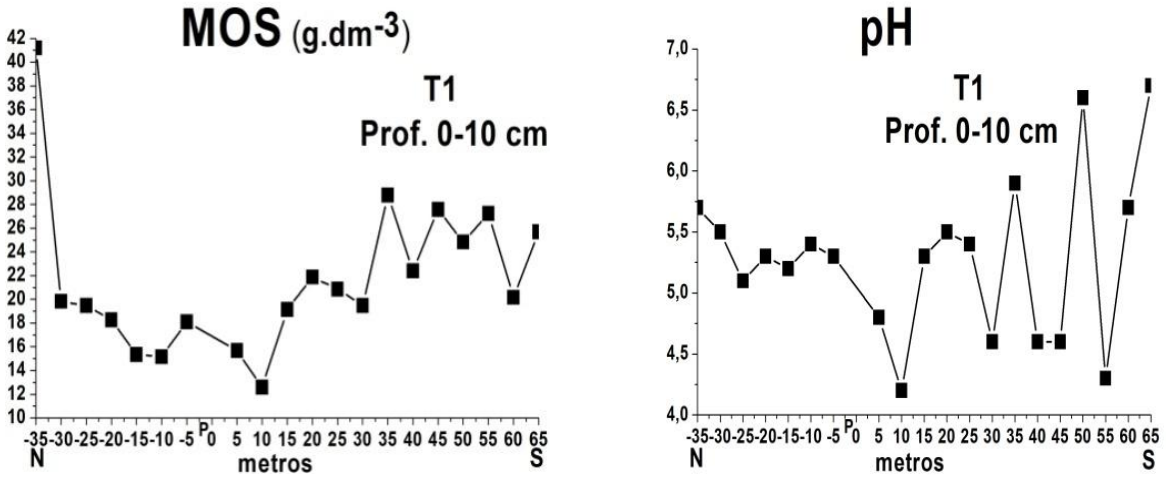

Figura 3. *Variabilidade de Matéria orgânica do solo (MOS) e pH na profundidade 0-10 cm da transversal T1 do sítio arqueológico AP-MA-05.*

Downloaded from www.periodico.tchequimica.com

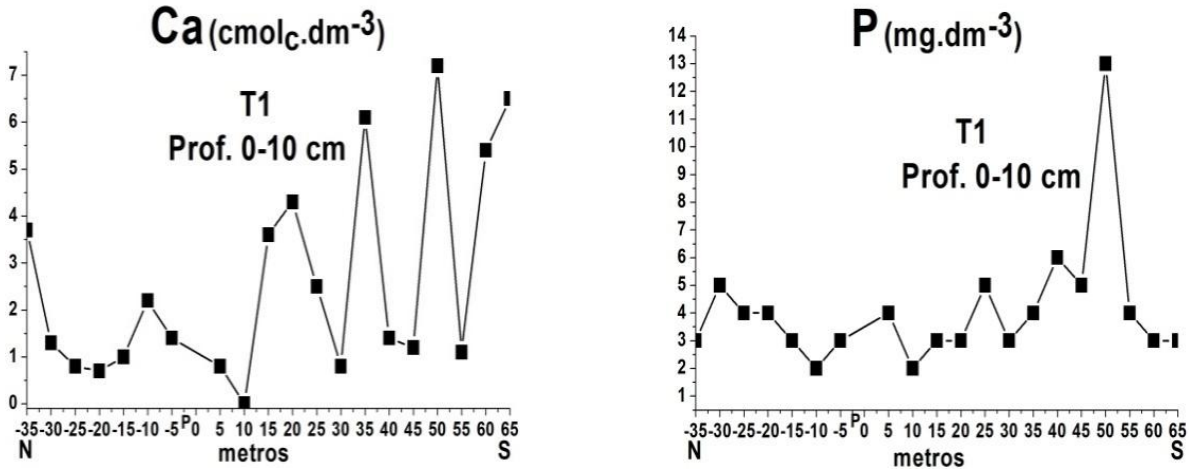

Figura 4. *Variabilidade de cálcio e fósforo na profundidade 0-10 cm da transversal T1 do sítio arqueológico AP-MA-05.*

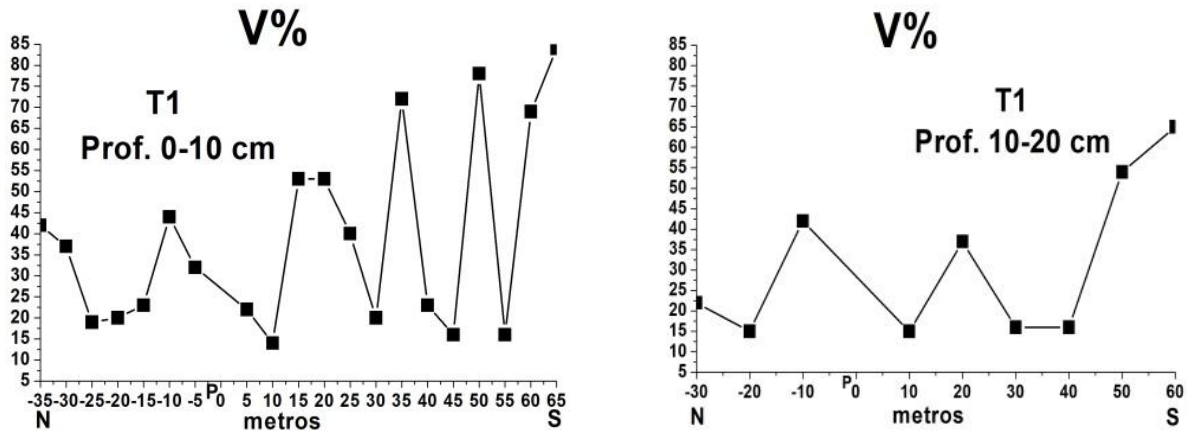

Figura 5. *Variabilidade de Saturação por Bases (V%) na profundidade 0-10 cm na transversal T1 no sítio arqueológico AP-MA-05.*

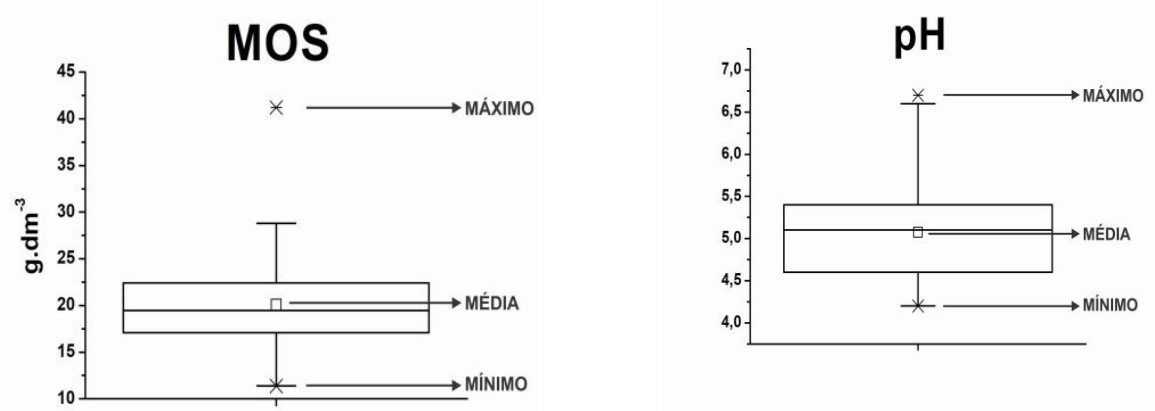

Downloaded from www.periodico.tchequimica.com

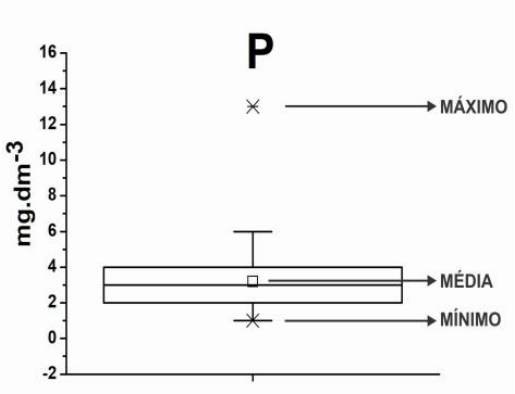

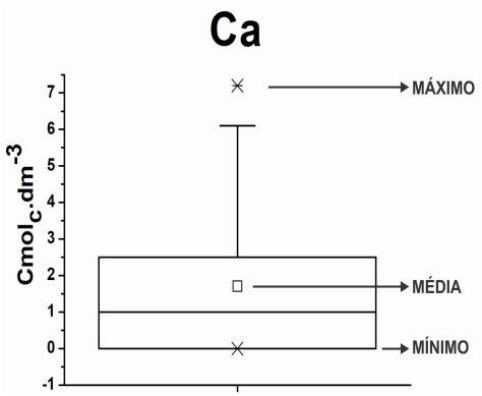

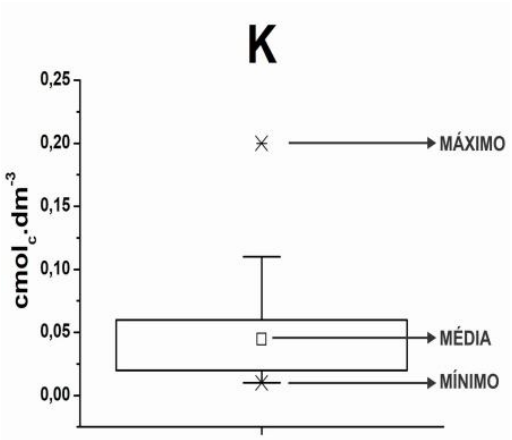

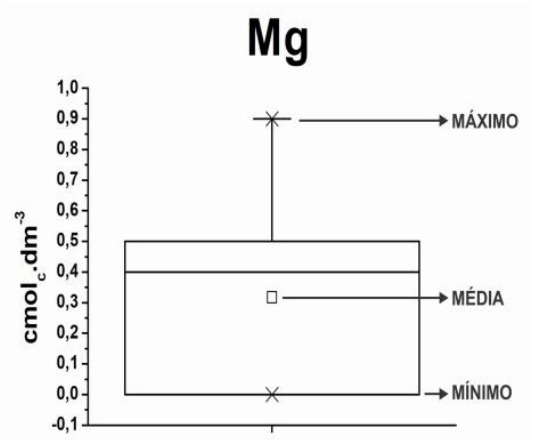

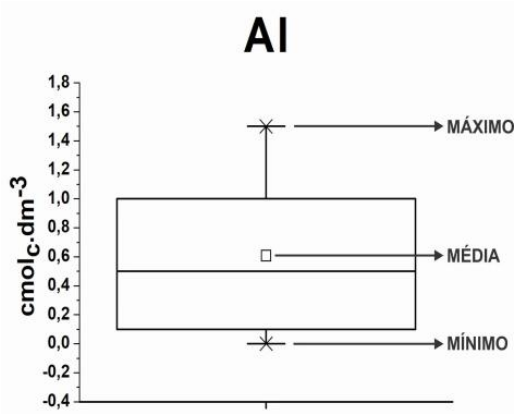

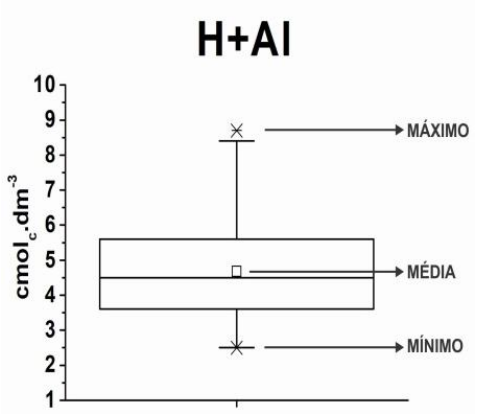

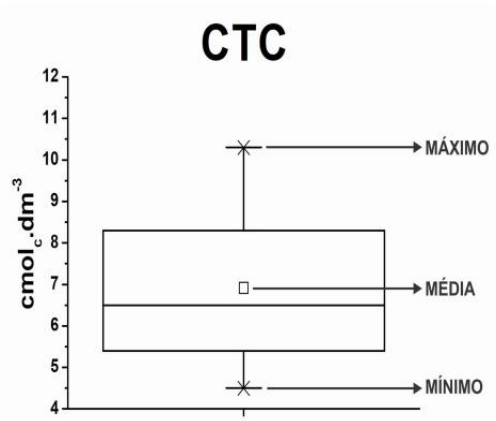

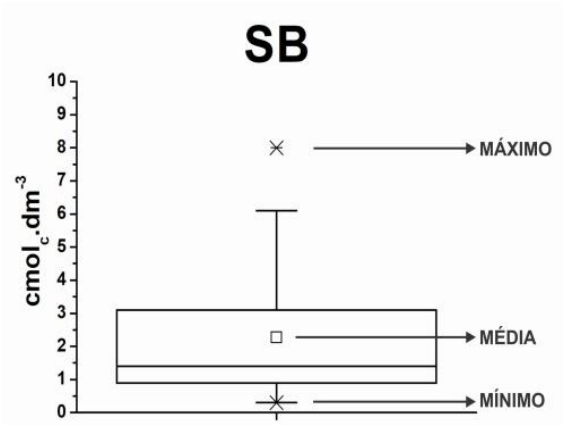

Downloaded from www.periodico.tchequimica.com

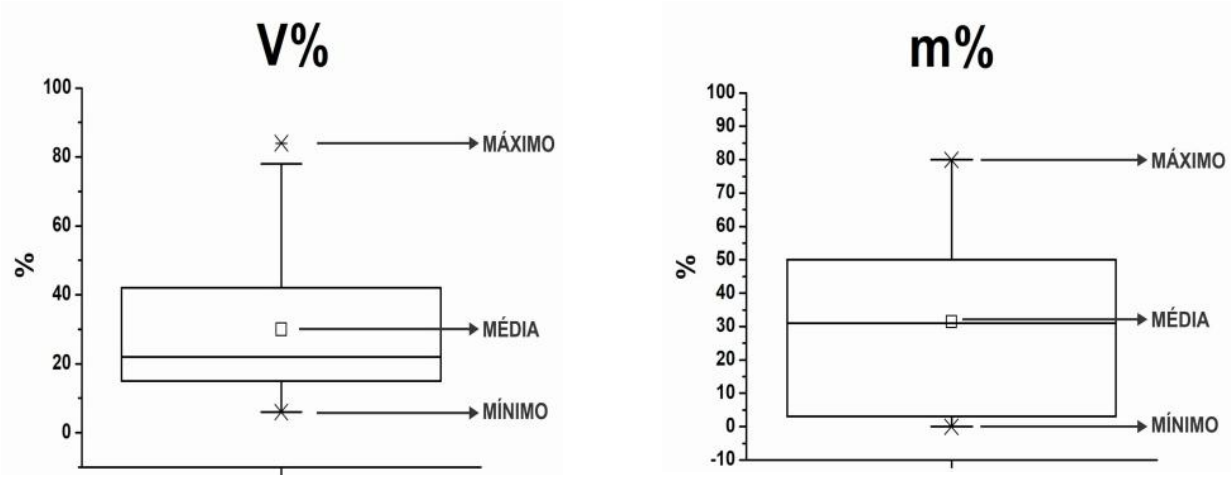

Figura 6. *Valores máximo, mínimo e médios dos parâmetros químicos do sítio arqueológico AP-MA-05 no campus da UNIFAP, em Macapá-AP.*

Tabela 1. *Matriz de correlação de Pearson (r^2) para os relacionamentos entre as propriedades químicas do solo (n = 41), a nível de 5% de significância.*

	pH	MO	P	K	Ca	Mg	Al	H + Al	SB	CTC
MO	0,26									
P	0,47	0,23								
K	0,38	0,14	0,50							
Ca	0,88	0,31	0,51	0,50						
Mg	0,67	0,22	0,52	0,44	0,79					
Al	-0,83	-0,04	-0,29	-0,34	-0,75	-0,70				
H + Al	-0,76	0,26	-0,13	-0,13	-0,56	-0,34	0,77			
SB	0,86	0,28	0,51	0,53	0,99	0,78	-0,74	-0,55		
CTC	0,34	0,55	0,48	0,50	0,68	0,62	-0,20	0,22	0,69	
V	0,92	0,18	0,44	0,44	0,97	0,80	-0,84	-0,69	0,97	0,54
m	-0,82	-0,17	-0,38	-0,39	-0,79	-0,82	0,95	0,60	-0,78	-0,39

Fonte: a autora (2018).

Downloaded from www.periodico.tchequimica.com

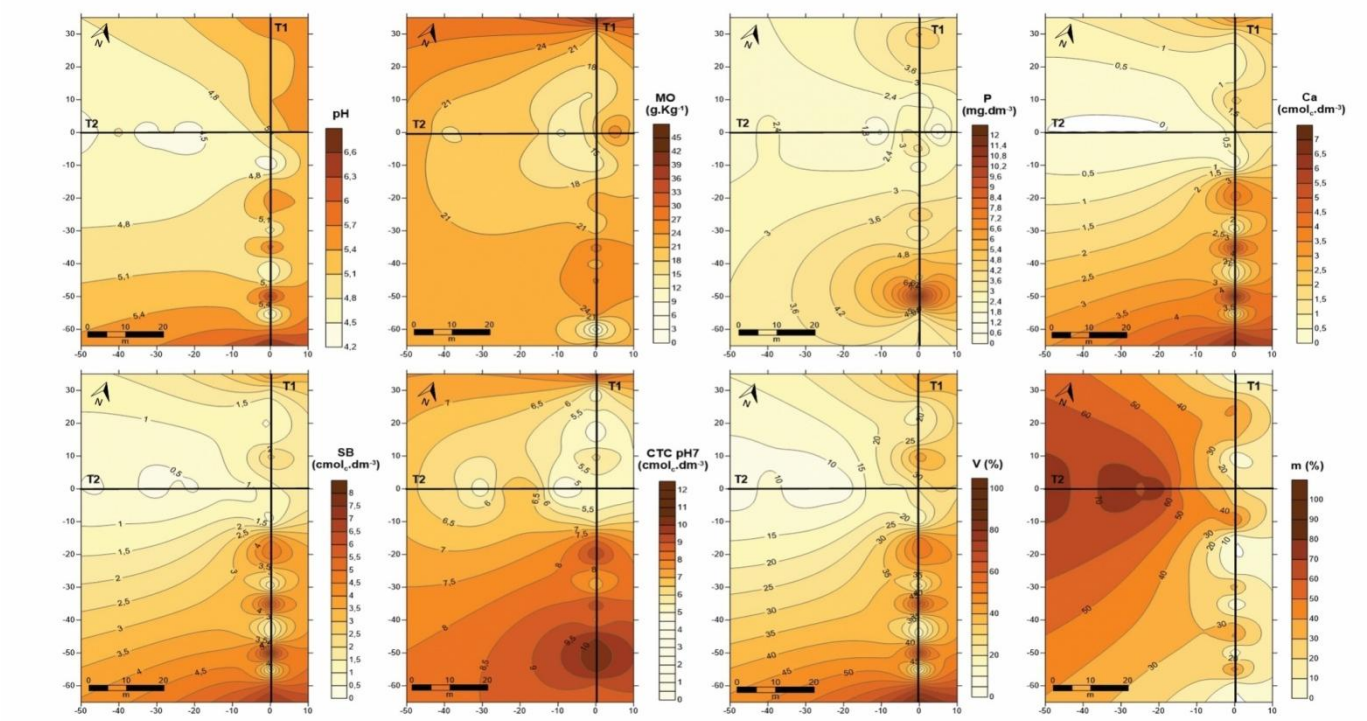

Figura 7. *Mapas de isovalor das concentrações dos parâmetros químicos pH, matéria orgânica, fósforo disponível, cálcio trocável, SB, CTC, V% e m%.*

Downloaded from www.periodico.tchequimica.com

PERIÓDICO TCHÊ QUÍMICA
ARTIGO ORIGINAL

CULTURA DE TECIDOS DE RINS DE RATOS PARA A AVALIAÇÃO DA TOXICIDADE DE ALGUNS CITOSTÁTICOS

TISSUE CULTURE OF MICE KIDNEYS FOR THE TOXICITY EVALUATION OF SOME CYTOSTATICS

ИСПОЛЬЗОВАНИЕ ТКАНЕВЫХ КУЛЬТУР ПОЧЕК МЫШЕЙ ДЛЯ ОЦЕНКИ ТОКСИЧНОСТИ НЕКОТОРЫХ ЦИТОСТАТИКОВ

PASHCHENKO, Vladimir Petrovich[1], NAZARENKO, Natalia Anatolievna[2] *, GROMOVA, Ludmila Evgenievna[3], PASHCHENKO, Galina Seraphimovna[4], NAZARENKO, Michail Yurievich[5];

[1] Northern State Medical University of the Ministry of Healthcare of the Russian Federation, Department of normal physiology

[2,3] Northern State Medical University of the Ministry of Healthcare of the Russian Federation, Department of Pharmacology

[4] Northern State Medical University of the Ministry of Healthcare of the Russian Federation, Department of Neurology and Neurosurgery

[5] Northern State Medical University of the Ministry of Healthcare of the Russian Federation, Department of Pediatric Dentistry

** Correspondence author*
e-mail: nasarenko_n_a@mail.ru

Received 06 June 2019; received in revised form 30 October 2019; accepted 18 November 2019

RESUMO

A justificativa para o presente estudo é explicada pelo alto risco de desenvolvimento de efeitos colaterais, incluindo nefrotóxicos, em pacientes que recebem o tratamento com citostáticos bleomicina, lastet e cisplatina para doenças oncológicas. O presente artigo enfoca a avaliação da toxicidade dos medicamentos mencionados. Foi utilizado o método de culturas de tecidos renais sem plasma em camundongos nos filtros perfurados de milípede. A identificação da toxicidade de diferentes doses dos fármacos foi realizada pela comparação das áreas das colônias cultivadas. Os autores apresentaram os dados de que a inibição do crescimento de culturas de tecidos renais (em 50%) exigiu um aumento de 4,3 vezes na dose de lastet em comparação com a bleomicina. A inibição do crescimento de colônias da cultura de tecidos com cisplatina em 85% foi registrada na dose do medicamento que correspondia a uma solução a 3%. Os materiais do artigo têm valor prático significativo, porque uma indicação racional dos citostáticos bleomicina, lastet e cisplatina em relação ao seu efeito nefrotóxico permitirá que os especialistas melhorem o resultado do tratamento e contribuam para a melhoria da qualidade de vida dos pacientes.

Palavras-chave: *cultura de tecidos, rim, rato, Lastet, Bleocina, Cisplatina, toxicidade.*

ABSTRACT

The rationale for the present study is explained by a high risk of the development of side effects, including nephrotoxic, in patients that receive the treatment with cytostatics bleocin, lastet, and cisplatin for oncologic diseases. The present article focuses on the evaluation of the toxicity of the mentioned drugs. The method of plasma-free renal tissue cultures in mice on the perforated millipore filters was used. The identification of the toxicity of different doses of the drugs was performed by the comparison of the areas of the grown colonies. The authors presented the data that the inhibition of the growth of renal tissue cultures (by 50%) required a 4.3-fold increase in the dose of lastet in comparison with bleocin. The inhibition of the tissue culture colony growth with cisplatin by 85% was registered in the dose of the drug that corresponded to a 3%

Downloaded from www.periodico.tchequimica.com

solution. The materials of the article have significant practical value because a rational indication of cytostatics bleocin, lastet, and cisplatin with regard to their nephrotoxic effect will allow the specialists to improve the treatment outcome and will contribute to the improvement of the quality of life of patients.

Keywords: *tissue culture, kidney, mouse, Lastet, Bleocin, Cisplatin, toxicity.*

АННОТАЦИЯ

Актуальность исследования обусловлена большим риском развития побочных эффектов в том числе нефротоксического действия при применении цитостатиков блеоцина, ластета и цисплатина у пациентов, страдающих онкологическими заболеваниями. В связи с этим, данная статья направлена на выявление токсичности данных препаратов. Одним из методов для исследования данной проблемы является метод бесплазменных тканевых культур почек мыши на поверхности перфорированных миллипоровых фильтров. Определение токсичности разных доз препаратов проводилось путём сопоставления площади выросших колоний. В статье представлены достоверные результаты, свидетельствующие, что ингибирование роста клеточной культуры почек (на 50%) требовало 4,3 кратного увеличения дозы ластета по сравнению с блеоцином. Угнетение численности тканевой культуры на 85% цисплатином регистрировалось в дозе препарата, соответствующего 3% раствору. Материалы статьи представляют важную практическую ценность, поскольку рациональное назначение цитостатиков блеоцина, ластета и цисплатина с учётом их нефротоксического действия позволят повысить результаты лечения и будут способствовать улучшению качества жизни пациентов.

Ключевые слова: *Тканевая культура, почки, мышь, ластет, блеоцин, цисплатин, токсичность.*

1. INTRODUCTION

One of the leading methods in the treatment of oncological diseases is chemotherapy. The drugs used for chemotherapy of tumors, which are represented by different classes of chemical compounds, exert an antiproliferative effect. Bleocin (bleomycin) is an antitumor antibiotic that is produced by *Streptomyces verticillus* fungi (Mashkovskiy, 2013). Primarily, it is effective in patients with squamous cancer of the skin, tumors of head and neck, esophagus, lungs, uterine cervix, vulva, kidney, testicle, and Hodgkin disease. According to the data on the pharmacokinetics of the drug, around 60-70% of the injected bleocin is excreted unchanged in the urine due to glomerular filtration. The concentration of the drug in plasma increases after the injection of high doses of bleocin to patients with impaired renal function. In clinical practice, the drug is indicated by different treatment schemes, primarily in the dose of 30-60 mg twice a week. Published studies indicate that there was experience of bleocin application in synchronous combined therapy, wherein along with the injection of antitumor drugs, in the doses that did not exceed single daily dose, directly in the body of the primary tumor or metastasis, radiographic fat-soluble contrast medium was used as a transporter and radiotherapy was performed along with it. This method sharply enhances the toxicity of antitumor drugs due to an increase in the concentration of free-radical compounds in the tumor that develops as a result of radiotherapy, which reduces the tumor size (Blank and Blank, 2018).

Cisplatin belongs to the pharmacological group of alkylating compounds (*cis*-diamminedichloridoplatinum) containing heavy metal (Mashkovskiy, 2013). It is often used in the combined chemotherapy for ovarian cancer, cancer of the uterine cervix, bladder, testicle, esophagus, squamous cancer of the head and neck, osteosarcoma, and neuroblastoma (Andreev *et al*., 2009; Smirnova *et al*.; 2018; Trushina *et al*., 2018). The drug is characterized by a high rate of distribution in biological fluids and tissues with the highest concentration in kidneys, liver, and prostate. The nephrotoxicity of the drug has a cumulative character. A single injection dose can be 100 mg/m^2.

Lastet (etoposide) is a semi-synthetic derivative of podophyllotoxin isolated from the root of perennial medicinal drug wild jalap *Podophyllum peltatum* L (Berberidaceae) (Gammerman *et al*., 1983; Yakovleva and Blinkova; 2002). The plant is poisonous and along with podophyltoxin, contains tropane alkaloids: hyoscyamine and scopolamine. The plant's common name is American mandragora that growth in Northern America.

It is indicated as a monotherapy and in combination with other antitumor drugs. It is effective in the treatment of small-cell lung cancer, testicle cancer, Hodgkin disease, lymphogranulomatosis, etc. The contraindications

Downloaded from www.periodico.tchequimica.com

to this drug include expressed impairments of renal and hepatic function. Lastet is indicated in 100 mg/m^2 doses, and the course duration is 4-5 days (Mashkovskiy, 2013).

The antitumor effect of bleocin, cisplatin, and lastet is primarily realized due to the inhibition of DNA synthesis of a tumor and healthy cells, including the cells of the excretory organs. The toxic effect of cytostatics is described in a number of scientific publications (Bezborodova *et al.*, 2013; Kolina and Bobkova, 2014; Hansen, 1990; Ozben *et al.,* 2007). Renal pathology varies from the mechanical impact of the tumor or metastasis on kidneys or urinary tract to paraneoplastic manifestations, such as nephritis, amyloidosis, and nephropathy induced by pharmaceutical agents. This pathology will be manifested by the increase in the concentration of creatinine, urea, uric acid, and other serum parameters. The enhancement of nephrotoxicity in cancer patients who receive combined chemotherapy with cisplatin is described in the study performed by Gozhenko *et al.* (2010). The authors performed a retrospective analysis of the medical histories of 100 patients (70 women and 30 men) aged 32 to 73 and revealed the increase in the incidence rate of renal pathologies, such as proteinuria, leukocyturia, erythrocyturia, etc. The successful outcome of chemotherapy was primarily determined by choice of the drugs that did not exert the nephrotoxic effect. One of the factors that reduce nephrotoxicity can be dose correction in regards to the level of creatinine in the serum (Dzhumabaeva and Birykova, 2015) or parallel indication of detoxicants. One of the promising examples of such therapy with the maintenance of expressed chemotherapeutic effect of lastet can be experimental study on Remaxol (succinic acid, N-methylglucamine, rhiboxinum, methionine, nicotinamide) (Bezborodova *et al*., 2013). The authors used mice tumor model of lymphatic leukemia P388 to show a decrease in the toxicity of lastet monotherapy that was injected at the dose of 100 mg/kg along with Remaxol, which was associated with an increase in the lifespan by 27.2%. At the same time, the effectiveness of the treatment depends on the localization of the tumor, stage of the tumor growth, development of metastasis, associated pathologies, etc. The correct evaluation of these parameters provides satisfactory long-term results of the indicated chemotherapy (Barsukov *et al*., 2015; Bychkov *et al.*, 2016; Zelenikhin *et al.,* 2016). However, in spite of the evident success of chemotherapy, an increase in the incidence rate of malignant neoplasms is observed, especially those that are associated with dangerous damage of kidneys.

For the evaluation of toxic peculiarities of pharmaceutical agents and the viability of cells and tissues, different methods are widely used, including the method of the evaluation of acute and chronic toxicity at the preclinical stage of pharmacological studies (Khabriev, 2005). Besides, the methods that involve cellular and tissue cultures are used (Pinaev and Bagdanova, 2008; Pinaev, 2008; Paschenko *et al.,* 2010; Alieva *et al.,* 2008a). In the studies on the evaluation of the toxicity of herbal composition “Phytomorozko” (Nazarenko *et al*., 2008b) and “herbal drugs” (Nazarenko *et al.,* 2008a), that exert frigoprotective effect and used for the treatment and prevention of freezing injuries, mice renal tissue culture was used as a study model (Alieva *et al.,* 2008b). The method of tissue culture was used for the evaluation of the safety of sodium fluoride in food products (Gromova *et al*., 2007, 2008) and drinking water (Paschenko, 2003). The utilization of tissue cultures for the evaluation of the toxicity of pharmaceutical agents is more feasible than cell cultures because the former preserve cellular associations that are observed in the organism (Paschenko, 2006; 2016). The processes that develop in the tissue culture have a lot in common with physiological mechanisms of tissue regeneration (Paschenko *et al.,* 2019). The growth of tissue culture (*in vitro*) is an integrative indicator of the condition of the whole organism (in vitro), its capacity to adapt to unfavorable environmental factors (Zaalkind and Tsypkin, 1971; Onischenko, 2004), including influence of toxic agents.

The aim of the present study was to evaluate the toxicity of cytostatics bleocin, lastet, and cisplatin that exerts the nephrotoxic effect on the renal tissue culture of mice.

The relevance of the study is explained by the fact that insufficient attention to the possible development of side effects in patients that receive antitumor therapy can reduce the favorable effect of the therapy and worsen the quality of life of patients.

2. MATERIALS AND METHODS

The tests were performed on white outbred male mice (18-20 g) that were kept in standard conditions of the vivarium (standard conditions according European Convention for the Protection of Vertebrate Animals used for Experimental and Other Scientific Purposes (msu.ru, 2019); confirming Protocol #01/04-19 date 24 April 2019 by Ethics committee of

Downloaded from www.periodico.tchequimica.com

Northern State Medical University of the Ministry of Healthcare of the Russian Federation). Renal tissue sampling was conducted during the decapitation of animals that were exposed to ether anesthesia. For the evaluation of the toxicity of antitumor drugs, the authors used the method of multiple plasma-free renal tissue cultures on the surface of perforated millipore filters, which allowed them to perform quantitative estimation of the degree of the toxic influence of the drugs on the cells of renal tissue of the laboratory animals (Paschenko, 1999; Alieva *et al.,* 2008a; Alper, 1980). The cultivation of the fragments of renal tissue was performed in test tubes in 1 ml of medium 199 with 5% embryonal serum. Preliminary, the kidneys taken from mice were separated from the capsule and divided into small fragments of tissue that were placed on the surface of perforated millipore filters (Millipore Corporation Belford MA 01730). Standard large filters were used for the preparation of small filters 7 mm in diameter. On the surface of each filter, 64 fragments of tissue (0.2±0.1 mm^2) were arranged randomly. Each test tube contained one filter with fragments of tissues. The studied drugs were diluted (several series of dilutions) and introduced directly to the nutrient medium in the test tube with filter for the period of cultivation (6 days). The incubation was performed in a microbiological water-cooled thermostat "SZ-1125 M" (ngpedia.ru, 2019) at 38°C. The stands with tubes were placed to a thermostat at 2-3° inclination. The cultures that grew on the surface of the filters were cleaned in a saline solution, fixed in Bouin's fixative, and hematoxylin-eosin stained (Gromova *et al.,* 2008; Paschenko *et al*., 2010). The filters were placed on microscope slides and covered with balsam and cover slides for further microscope investigation ("Biomed", (Biomed.ru, 2019) at x100 magnification.

For the evaluation of the areas of the grown cells colonies, the authors used statistical software ImageJ (Schneider *et al.,* 2012). The average size of the colonies around the tissue fragments varied within 0.30-0.05 mm^2. The graphs were drawn based on the conventional units of the size of cellular colonies defined by the software ImageJ (n=64. Conventional unit of 350,000 corresponded to 0.27 mm^2; 300,000 – 0.238 mm^2; 250 000 – 0.198 mm^2; 200,000 – 0.159 mm^2; 150,000 – 0.12 mm^2; 100,000 – 0.079 mm^2; 50,000 – 0.039 mm^2).

Statistical processing of the results was performed with Microsoft Excel and the software package Statistica 6. The parameters were compared with Student's t-test, the level of significance was $p<0.05$.

The evaluation of the toxicity of different doses of the drugs (inhibiting effect) was performed by the comparison of the areas of grown colonies and the areas of the colonies from the control test tubes that contained the same amount of nutrient medium but did not contain the studied drugs. Totally, 3 series of tests were performed.

The 1st series of tests included bleocin (15 mg flasks; "Hunnon Kayaku Co." Ltd, Japan). The drug was 2, 4, 8, and 16 times diluted in the Hanks' solution to obtain 50%; 25%; 12% and 6% solutions, respectively. The control probes were introduced the same volume of Hanks' solution. Thus, the content of bleocin in 1 ml of medium contained 0.0037 mg/ml; 0.00187 mg/ml; 0.00097 mg/ml and 0.00047 mg/ml, respectively.

The 2nd series of tests included lastet (5 ml flask with 100 mg of the active ingredient; "Hunnon Kayaku Co." Ltd, Japan). The test design and conditions of lastet cultivation were the same as for bleocin. The drug was 2, 4, 8 and 16 times diluted (50%; 25%; 12% and 6% solutions, respectively). Final content of the drug in 1 ml of medium corresponded to 0.0083 mg/ml; 0.0042 mg/ml; 0.0021 mg/ml and 0.00104 mg/ml.

The study of the toxicity of cisplatin (10 ml ampules with 10 mg of the active ingredient; "LENS-Pharm", Russia) showed that it had higher toxicity than bleocin and lastet. For this reason, the dynamics of the influence of cisplatin on renal cells was evaluated with more significant dilutions of the drug. The 3rd series of tests included 4, 6, 8, and 32 times dilutions of cisplatin in Hanks' solution, which corresponded to 25%; 12%; 6% and 3% solutions, respectively.

3. RESULTS AND DISCUSSION

The obtained results were presented in graphs (Fig. 1; 2). The tests showed that cytostatics bleocin and lastet cause dose-dependent inhibition of the quantity of renal tissue culture in mice (Fig. 1). The presented data show that the maximum statistically significant inhibition of the growth of renal tissue culture was observed after two-fold dilution (50% solution) of bleocin and lastet. A direct impact of lastet on the renal tissue culture was less toxic than bleocin. A similar effect of inhibition (without statistical significance) of the amount of cell culture was obtained with a higher dose of lastet (4.3 times) than bleocin, in particular, 0.0042 mg/ml of lastet and 0.00097 mg/ml of bleocin. It should be noted that a decrease in the concentration of these drugs in the medium led to the differences in their toxicity, except for 6% solutions of lastet and

Downloaded from www.periodico.tchequimica.com

bleocin, where the amount of cell culture remained similar (without statistical significance). In this dilution, the area of cells colonies exposed to bleocin was 279,120 relative conventional units (CU), which was lower than the control values by 12.8% (312,480 CU); the area of colonies exposed to lastet was equal to 270,500 CU, which was lower than the control values by 15.5%.

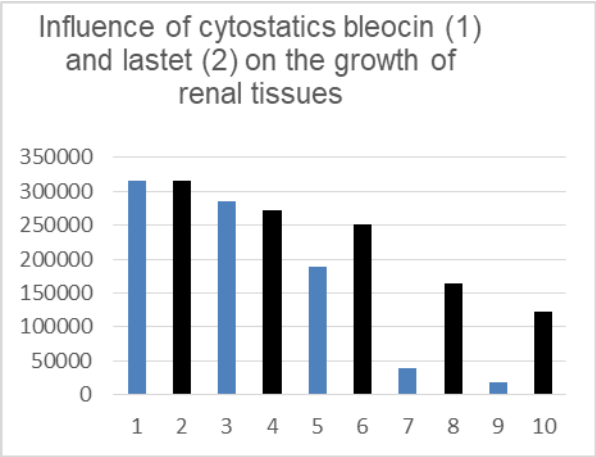

Figure 1. *The influence of bleocin* and lastet** on the growth of renal tissue in the dilution: 1-2 control; 3-4-(6%); 5-6-(12%); 7-8 (25%); 9-10 (50%) solutions. X – rows of studies; Y – quantitative content of cells in relative units*
*(Alieva *et al*., 2008b; Alper, 1980; Bezborodova *et al*., 2013; Gozhenko *et al.,* 2010; Gromova *et al*., 2007)
**(Alieva *et al.,* 2008a; Barsukov *et al.,* 2015; Bychkov *et al*., 2016; Gromova *et al*., 2008; Dzhumabaeva and Birykova, 2015)

Statistically significant inhibition of the renal cells population size in comparison with the control values in the series with bleocin was also registered in the samples №5 (12% solution) and №7 (25% solution), and in the series with lastet, it was registered only in the samples №8 (25% solution) and №10 (50% solution). There were no statistically significant differences registered in the samples №6 (12% solution) and №4 (6% solution) in comparison with the control samples.

The results of the test series with cisplatin showed that the studied drug exerts a high toxic effect (Fig. 2). In this test series, the area of the grown colonies in the control probe was equal to 230,000 CU. The drug inhibited the growth of cell culture in all the solutions with bleocin and lastet that were tested. In tests with the minimum dilution of the initial dose of cisplatin to 3% solution (32 times), the authors registered an expressed statistically significant decrease (by 85%) in the size of the renal cells population in comparison with the control values. In this sample, the area of the grown colonies corresponded to the size equal to 65,000 CU. In the sample with a 6% solution, the area of the grown cells colonies was even lower and was registered at the level of -10000 CU. Further, when the dose of the studied drug was raised to 12% and 25% solutions, the cell colonies count was not performed due to their absence.

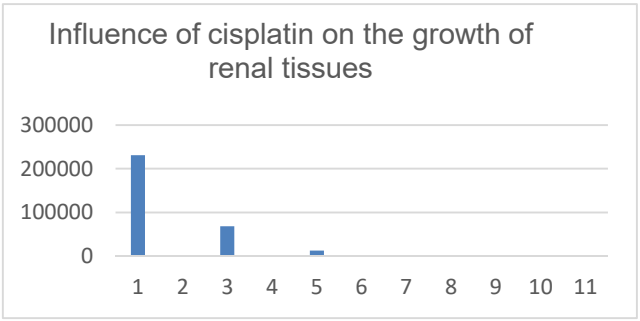

Figure 2. *The influence of cisplatin on the growth of renal tissues in the dilutions: 1 – control; 3-(3%); 5- (6%); 7-(12%); 9- (25%); 11- (50%) solutions. X – rows of studies; Y – quantitative content of cells in relative units*

The tests on the toxicity of bleocin and lastet by the method of renal tissue culture in mice allowed the authors to register the nephrotoxic effect of the mentioned cytostatics after direct contact with the culture in the respective doses. The extrapolation of the obtained results from animals to humans allows the authors to predict the development of a wider range of side effects in patients that receive bleocin than in those that receive lastet, which requires a more precise individual dosing in clinical practice. Especially, this is true in cases when bleocin or lastet are used in chemotherapies with high doses. Taking into account the factor of nephrotoxic effect, for the treatment of tumors of the same form and localization and a lack of contraindications, the therapy of choice would likely be lastet than bleocin. This conclusion fully agrees with a wide-known statement that plant-derived drugs (in this particular case, lastet) are less toxic for the organism than the synthesized ones. Although lastet is a synthesized derivative of natural podophylotoxin that exerts an antiproliferative effect on cancerous cells, it is toxic for the surrounding tissues only in high doses.

The analysis of the results of the test series with cisplatin showed its expressed toxicity. The only sample that allowed the authors

Downloaded from www.periodico.tchequimica.com

to perform a statistically significant comparative analysis of the results of the inhibition of the cell culture for all the tree drugs was the sample that was introduced the drugs as 6% solutions. In the samples with lower dilutions (12% and 25%), there was no technical possibility to evaluate the area of the grown population because of their complete absence. In the sample with the studied drugs in the doses that corresponded to 6% solution in the test series with bleocin, the area of the grown colonies was equal to 279,120 CU; lastet – 270,000 CU, and cisplatin - only 10,000 CU. A registered acute decrease in the size of mice renal cells culture colonies revealed a high toxic effect of cisplatin on renal tissue. The obtained result is highly predictable because cisplatin is a platinum-containing compound. This element exerts not only antiproliferative effect used in the treatment of oncologic diseases but also a high general toxic effect on the organism. As a rule, metal-containing compounds circulate in blood plasma for a long time, they are excreted via kidneys, get accumulated there, and harm renal function. This fact should be taken into account before the indication of metal-containing compounds to patients with renal pathology.

4. CONCLUSION

It can be concluded that the method of tissue culture with quantitative evaluation of the growth of tissues is a highly-sensitive method of the evaluation of the toxicity of antitumor drugs and provides more precise individual dosing of drugs used in chemotherapy in clinical practice. The use of mice renal tissues, that preserve intercellular associations, as a study model for the evaluation of the toxicity allowed the authors to provide a precise interpretation of the obtained study results in respect to the human organism and to confirm nephrotoxic effect in bleocin, lastet, and cisplatin, expressed in different degrees. The comparison of the areas of the grown colonies in the control samples and in the test series with different doses of the drugs (bleocin and lastet – 50%, 25%, 12% and 6% solutions; cisplatin – 25%, 12%, 6% and 3% solutions) allowed the authors to reveal the differences in the inhibiting influence of cytostatics. The test results did not reveal any difference in the renal cells colonies size after direct contact of the culture with bleocin and lastet in low doses (6% solutions). However, as the concentration of both drugs increased, the authors registered a statistically significant difference in the size of the grown colonies. Bleocin exerted a more expressed inhibiting effect than lastet on the renal culture. The highest nephrotoxicity was registered in cisplatin in all the possible dilutions. The obtained results agreed with the available published data and allowed the authors to provide additional proof of the nephrotoxicity in the studied cytostatics when they get in direct contact with the renal tissue.

1. For the inhibition of the growth of cells renal tissue culture in mice by 50%, the dose of lastet should be 4.3 times higher than the dose of bleocin.
2. The reduction of the size of the grown mice renal tissue colonies by 85% is registered after the dose of cisplatin that corresponds to 3% solution.

5. REFERENCES

1. Alieva A. A., Nazarenko N. A., Nazarenko M. Y., Kiseliova T. L. The influence of dexamethasone and herbal compositions on the markers of proliferation of cellular renal tissue in mice. *Cytology*, **2008a,** 50(9), 745.
2. Alieva A. A., Nazarenko N. A., Paschenko V. P., Kiseleva T. L. The study of the influence of herbal compositions on the growth of mice renal tissues. Collection of materials of 1st Russian Phytotherapeutical forum. Moscow, **2008b,** 162–164.
3. Alper T. Viability of cells exposed to low doses of radiation: theoretical and clinical aspects. VI Greev conference, Moscow, **1980.**
4. Andreev V. G., Mardynskiy Y. S., Baryshev V. V., Podlesnykh N. I., Pankratov V. A., Rozhnov V. A. Comparative characteristics of chemoradiotherapy in patients with nasopharyngeal cancer depending on the dose fractioning and methods of chemotherapy. *Siberian Oncologic Journal*, **2009,** 34(4), 12-17.
5. Barsukov Y. A., Tkachev S. I., Orel N. F., Aliev V.A. Gordeev S. S., Glebovskaya V.V., Timofeev Y.M., Atroschenko A. O., Ovchinnikova A.I., Nalbandin A.V. Successful treatment of squamous cancer of the rectum, Clinical observation. *Oncological coloproctology*, **2015,** 5(1), 54–60.
6. Bezborodova O. A., Nemtsova E. R., Venediktova Y. B., Yakubovskaya R. I., Aleksandrova L. N., Kovalenko A. L. Experimental study on Remaxol as a drug of supportive therapy in patients with tumors that undergo traditional and high-

Downloaded from www.periodico.tchequimica.com

dose chemotherapy. *Experimental and clinical pharmacology*, **2013**, 76(5), 18–22.
7. Biomed.ru. Monocular microscopes of the BIOMED, Description, **2019.** http://biomed.ru/info/item/2/
8. Blank M. A., Blank O. A. Synchronous combined therapy in oncology. *Oncology Issues*, **2018**, 64(4), 490–492.
9. Bychkov M. B., Bagrova S. G., Karpenko T. D. Stabilization of the disease as an important factor of the evaluation of the effectiveness of treatment and the prognosis of the survivability of cancer patients. *Russian oncologic journal*, **2016,** 21(1–2), 6–10.
10. Dzhumabaeva B. T., Birykova L. S. Nephrotoxicity of antitumor drugs, correction of their doses for patients with lymphoproliterative and oncological diseases associated with renal insufficiency. *Hematology and transfusiology*, **2015,** 60(4), 30–35.
11. Gammerman A. F., Kadaev G. N., Yatsenko-Khmelevskiy A. A. Medicinal plants. Reference book, 3rd edition revised and added. M.: Vusshaya Shkola, **1983.**
12. Gozhenko A. I., Moskalenko A. M., Steblovsliy V. V., Zhukov V. A. Nephrotoxicity of cisplatin in cancer patients. *Problems in Transport Medicine*, **2010,** 1(19), 81–86.
13. Gromova L. E., Nazarenko N. A., Pashenko V. P., Degteva G. N. Method of evaluation of toxicity of sodium fluoride: patent 2327988 RF, MPK G01N 33/48, C12N 5/06. №2006128302/15. Application dd 03.08.2006; published on 27.06.2008, **2008**.
14. Gromova L. E., Pashenko V. P., Degteva G. N., Nazarenko N. A. The method of primary tissue cultures for the evaluation and safety of sodium floride in food products. *Medicine of Labor and Industrial Ecology,* **2007**, 8, 39-41.
15. Hansen S. W. Autonomic neuropathy after treatment with cisplatin, vinblastine, and bleomycin for germ cell cancer. *BMJ*, **1990**, 300(6723), 511–512.
16. Khabriev R. U. Guidelines on experimental (preclinical) study of new pharmacological substances. Moscow: Medicine, **2005.**
17. Kolina I. B., Bobkova I. N. Renal disorders in patients with malignant neoplasms. *Clinician,* **2014,** 2, 7-14.
18. Mashkovskiy M. D. Pharmaceutical products: handbook for doctors, 16th edition, revised and added. Moscow: Novaya volna, **2013**.
19. Msu.ru. European Convention for the Protection of Vertebrate Animals used for Experimental and Other Scientific Purposes (Strasburg, March 18th, 1986). https://www.msu.ru/bioetika/doc/konv.doc.
20. Nazarenko N. A., Alieva A A., Kiseliova T. L., Nazarenko M. Y. Herbal composition for the prevention and treatment of freezing injuries: patent 2326684 RF, MPK A61K 36/738, A61P 17/02. № 2006137845/15; Application dd 26.10.2006; Published 20.06.2008, **2008a**.
21. Nazarenko N. A., Kiseliova T. L., Alieva A. A., Nazarenko M. Y., Karpeev A. A. Herbal composition “Phytomorozko” that exerts frigoprotective effect: patent 2336896 RF, MPK A61K 36/738, A61P 17/02. № 2006142403/15; Application dd 30.11.2006; published on. 27.10.2008, **2008b**.
22. Ngpedia.ru. Electric thermostat SZ-1125M Description, **2019.** https://www.ngpedia.ru/pg31511553qNvviy0005510577/
23. Onischenko N. A. Cellular technologies in modern medicine. *Pathologic Physiology and Experimental Therapy,* **2004**, 4, 2-11.
24. Ozben B., Kurt R., Oflaz H., Sezer M., Basaran M., Goren T., Umman S. Acute anterior myocardial infarction after chemotherapy for testicular seminoma in a young patient. *Clin. Appl. Thromb Hemost*, **2007**, 13 (4), 439–442.
25. Paschenko V. P. A device for the explantation of microfragments of tissues on a basecoat for cultivation. *Informational bulletin of cellular cultures SPb*, **1999**, 14, 56–57.
26. Paschenko V. P. Some peculiarities of the dynamics of the growth of primary tissue cultures in adult animals. *Cytology,* **2006**, 48(9), 787–788.
27. Paschenko V. P. The experience of utilization of tissue and cellular cultures in clinical practice. *Cellular cultures SPb,* **2016,** 32, 53–62.
28. Paschenko V. P., Balashov V. K., Sivkov A. N., Paschenko A. V. The method of primary tissue cultures for the evaluation of the quality of drinking water. *Human Ecology,* **2003**, 3, 27-29.
29. Paschenko V. P., Nazarenko N. A., Rekhacheva E. V., Paschenko A. V. The influence of aseptic stimulator Dorogova (ASD-2F). *Human ecology,* **2010**, 9, 22–26.

Downloaded from www.periodico.tchequimica.com

30. Paschenko V. P., Tikhonova E. V., Gudkov A. B. Quantitative peculiarities of renal tissue growth in animals of different age *in vitro*. *Journal of Medical-Biological Studies,* **2019**, 7(1), 16-23.
31. Pinaev G. P. Cell cultures in fundamental and applied studied. Methods of cells Cultivation. Saint Petersburg: Polytechnics University Press, **2008.**
32. Pinaev G. P., Bagdanova M. S. Methods of cells cultivation. Saint Petersburg: Polytechnics University Press, **2008**.
33. Schneider C. A., Rasband W. S., Eliceri K. W. NIH Image to ImageJ: 25 years of image analysis. *Nat. Methods*, **2012**, 9(7), 671–675.
34. Smirnova O. A., Bondarev N. E., Ulrikh E. F., Mikaya N. A., Petrova A.S., Abramov A. V., Ivantsov A. O., Gorodnova T.V., Nekrasova E. A., Lavrinovich O. E., Sidoruk A. A., Urmanteeva A. F., Berlev I. V. Elvaluation of the effectiveness of neoadjuvant dose-intensive platina-containing chemotherapy in the combined therapy of localaly spread uterine cervix cancer. *Tumors of Female Reproductive System*, **2018,** 46(4), 41-46**.**
35. Trushina O. V., Romanovskaya A. V., Khvorostukhina N. F., Balabanova E. S. Combined germ cells ovarian tumor in young girls. *Issues of Practical Pediatrics,* **2018**, 13(3), 56-60.
36. Yakovleva G. P., Blinkova K. F. Encyclopedic dictionary of medicinal plants and ingredients of animal origin. 2nd edition revised and added. Saint Petersburg: SpetsLit Press, **2002**.
37. Zaalkind S. Y., Tsypkin L. E. Some issues of differentiation and adaptation in cellular cultures. *Cytology,* **1971**, 13(5), 547-563.
38. Zelenikhin P. V., Makeeva A. V., Nchuen T. N., Sinage E. A., Ilyinskaya O. N. Combined influence of binase and bleomycin on the cells of human lung adenocarcinoma. *Biomedical chemistry*, **2016**, 62(3), 279–282.

Downloaded from www.periodico.tchequimica.com

PERIÓDICO TCHÊ QUÍMICA
ARTIGO ORIGINAL

ESTIMATIVA DE INCERTEZA PARA A MEDIÇÃO DA CONDUTIVIDADE ELETROLÍTICA POR MÉTODO SECUNDÁRIO USANDO CÉLULAS TIPO D

UNCERTAINTY ESTIMATION FOR THE MEASUREMENT OF ELECTROLYTIC CONDUCTIVITY BY SECONDARY METHOD USING CELL TYPE D

HINDAYANI, Ayu; ZUAS, Oman*; ELISHIAN, Christine; ARISTIAWAN, Yosi; HAMIM, Nuryatini

Chemical Metrology, Centre for Research and Human Resource Development (PUSRISBANG), National Standardization Agency of Indonesia (BSN) Kawasan PUSPIPTEK SNSU Building 420, Serpong 15314, Tangerang Selatan-Banten, Indonesia

** Correspondence author*
e-mail: oman@bsn.go.id; omanzuas.bsn@gmail.com

Received 22 June 2019; received in revised form 30 October 2019; accepted 18 November 2019

RESUMO

A medição da condutividade eletrolítica é um dos parâmetros importantes para avaliar a concentração de substâncias dissolvidas em uma solução e tem sido amplamente utilizada em vários campos da vida, ciência e tecnologia. Estava sendo usado para controle de processo e garantia de qualidade. A rastreabilidade dos resultados da medição é um requisito crucial para garantir a confiabilidade. O laboratório de eletroquímica - metrologia química da Indonésia começou a desenvolver um método secundário para medição de condutividade eletrolítica. O objetivo deste trabalho é fornecer uma cadeia de rastreabilidade para medição de condutividade eletrolítica na Indonésia por meio de material de referência secundário de cloreto de potássio (KCl) 1M. O material de referência secundário de KCl 1M pode ser usado como padrão para calibrar o medidor de condutividade, especialmente na análise da água do mar. O material de referência secundário que é desenvolvido tem um valor de condutividade eletrolítica de cerca de 111 mS/cm e foi medido usando o tipo de célula D de ZMK, Alemanha. Esta célula é feita de vidro com dois eletrodos de platinização no interior. A distância dos eletrodos é de 60 mm e o diâmetro do eletrodo é de 20 mm. A medição da incerteza foi estimada de acordo com a recomendação ISO GUM, identificando todas as fontes possíveis de incerteza no processo de medição da condutividade eletrolítica. O resultado mostrou que a incerteza expandida da medição de condutividade eletrolítica para KCl 1M por um método secundário usando o tipo de célula D foi de 0,33% (k = 2) para um nível de confiança de 95% com uma constante de célula e um desvio de temperatura das medições como as maiores fontes de incerteza, que contribuíram em 80% e 17%, respectivamente.

Palavras-chave: *rastreabilidade, constante celular, diagrama de causa e efeito*

ABSTRACT

Electrolytic conductivity measurement is one of the important parameters to evaluate the concentration of dissolved substances in a solution and has been widely used in various fields of life, science, and technology. It was being used for process control and quality assurance. The traceability of the measuring results is a crucial requirement to guarantee reliability. The electrochemistry laboratory - chemical metrology Indonesia has started to develop a secondary method for electrolytic conductivity measurement. The objective of this work is to provide a traceability chain for electrolytic conductivity measurement in Indonesia through secondary reference material of Potassium Chloride (KCl) 1 M. The secondary reference material of KCl 1 M can be used as a standard for calibrating the conductivity meter, especially in seawater analysis. The secondary reference material that is developed has an electrolytic conductivity value of about 111 mS/cm and was measured using cell type D from ZMK, Germany. This cell is made from glass with two platinization electrodes inside. The distance of the electrodes is 60 mm, and the diameter of the electrode is 20 mm. The uncertainty measurement was estimated according to the ISO GUM recommendation by identifying all possible uncertainty sources in the electrolytic conductivity measurement process. The result showed that the expanded uncertainty of electrolytic conductivity measurement for KCl 1 M by a secondary method using cell type D was 0.33% at k=2 for 95% confidence level with a repeatability of the measurements and cell constant as the biggest sources of uncertainty which contributed as 80% and 17%, respectively.

Keywords: *traceability, cell constant, cause and effect diagram*

Downloaded from www.periodico.tchequimica.com

1. INTRODUCTION

Electrolytic Conductivity (EC) is a measurand of the ionized substance in the solution (Isabel C. S. Fraga et al., 2008). EC is the most frequently measured in analytical measurement using conductivity meter, because of its low cost and easy to perform. The EC is indicated in several standards and test instruction as a control parameter for monitoring water purity and water quality in many fields such as pharmaceutical, semiconductor, powerplant, food industries, health care, environmental monitoring, and biotechnology (Orrù, 2014; S. Seitz et al., 2010). The result of EC measurement will affect decisions in the related field because it can directly related to product integrity, food safety, human health or environmental protection. In order to guarantee reliable and precise measurement results, the conductivity meter must be calibrated with traceable reference material (Freek Brinkmann et al., 2003).

The electrochemistry laboratory - chemical metrology Indonesia has developed an activity to prepare the traceable reference material of potassium chloride (KCl) 1 M. This EC value was determined by the secondary method using cell type D. Therefore, it is called as secondary reference material. According to OIML R56, KCl 1 M is a recommended standard solution for EC measurement with value 111 mS/cm at 25 °C (OIML, 1981). This standard solution can be used for calibrating the conductivity meter in monitoring quality of seawater with EC value about 50 mS/cm. (Breuel *et al.,* 2009). If the conductivity of the seawater is higher than 50 mS/cm, it indicates that more chemicals dissolved, including salts and heavy metals. The high concentrated substances in seawater will affect the fitness and survival of the organism and ecosystem (Miguel Cañedo-Argüelles et al., 2019; Staff, 2010).

The cell type D that used in the electrochemistry laboratory - chemical metrology Indonesia was purchased from ZMK, Germany. It is a glass tube with two platinization electrodes with a diameter of 20 mm and the distance of the two electrodes 60 mm. A cover plate of the cell was made from metal and had grips to set the cell into the thermostatic bath (Ulrich Breuel et al., 2008).

All measurements result, including the EC measurement of KCl 1 M is an estimation of the concentration of ionized substances in a liquid sample (Freek Brinkmann et al., 2003). It can not be known exactly how near the measured value with the true value. Many factors influence the EC measurement process. Therefore, uncertainty of measurement must be estimated. This paper will present the uncertainty estimation for the measurement of the EC by the secondary method using cell type D.

2. MATERIALS AND METHODS

All chemicals were analytical grade and used as received without any further purification. A certified reference material (CRM) of the primary standard solution with EC value 100 mS/cm at 25 °C (code CRM1714 batch 17101201JA, bottle 18) which purchased from DFM (Danish Metrology Institute-Denmark) was used to calculate the cell constant. A KCl with 99.5% purity was purchased from Sigma-Aldrich. Demineralized water 0.055 µs/cm was produced from Thermo Scientific Barnstead Smart2pure water purification system.

In this experiment, an analytical balance with accuracy 1 mg (PR5003 DualRange, Mettler Toledo Switzerland) was used and also the clean glassware, volumetric flask 2 L, and HDPE (High-Density Polypropylene) bottle 250 mL were used. For determination of the EC value of KCl 1 M, a cell type D was used. In addition to the cell, the measurement system also contains the following equipment (describe in Figure 1), such as precision thermostatic bath (water bath Proline PV36 and Chiller DLK25, Lauda Germany), temperature measuring device (MKT50, Anton Paar Germany) and precision LCR meter (8105G, GW-Instek Taiwan).

2.1. Preparation of secondary reference material solution

Secondary reference material was made from KCl 1 M. A certain amount of KCl (149.1 g) was dissolved with a few of demineralized water in the beaker glass. Then the solution was transferred into a clean volumetric flask (2 L) and the demineralized water was added until the mark etched on the neck of the flask. The procedure was similarly repeated until 7 times. Then the prepared KCl 1 M was transferred into 250 mL of HDPE bottles. This solution is called secondary reference material because the EC value was determined by secondary method.

2.2. The procedure of EC measurement

The EC measurements in these studies were carried out by the secondary method using cell type D. This cell has a conductivity measurement capability ranging from 20 to 100

Downloaded from www.periodico.tchequimica.com

mS/cm. Before used in the measurement, the cell must be rinsed with a small volume of the sample solution. The amount of 80 mL solution (KCl 1 M) was put into the cell type D. The cell was closed and placed in a thermostatic bath to maintain the temperature at 25 °C. When the temperature was stable, the resistance (R) measurements were measured in the frequencies (f) range from 120 until 480 using LCR meter. To evaluate the results, the data from R vs $\frac{1}{f}$ were interpolated by regression line ($y = mx + c$) where m is the slope and c is the intercept. The intercept is expected as the mean value of R. This value was used in the calculation of conductance using Eq. (3). After the measurements finished, the cell is emptied, and then rinsed with demineralized water for three times.

2.3. Procedure for determination the cell constant and conductivity value of KCl 1 M

EC (κ) is defined as the inversion of the resistance (R) multiplied by the cell constant (K_{cell}). The equation is described in Eq. (1) (Isabel Cristina Serta Fraga, 2013).

$$\kappa = K_{cell} \times \frac{1}{R} \quad \text{(Eq. 1)}$$

The cell in which the conductivity is measured has its cell constant. The cell constant is a function of the electrode areas, the distance between the electrodes and the electrical field pattern between the electrodes (Slovacek, 1998). It is influenced by geometrical factors, such as electrode distance and the active electrode surface. (Ulrich Breuel et al., 2009). The cell constant is defined in Eq. (2) (R. H Jameel et al., 2000).

$$K_{cell} = \frac{l}{A} \quad \text{(Eq. 2)}$$

where l is the effective length between the electrodes and A is the effective cross-sectional area. In the primary method, the cell constant was obtained through the physical dimensions of the cell geometry and the observed value of R is directly traceable to International System of Units (SI) (Freek Brinkmann et al., 2003). Any changes in the cell constants can be measured precisely by dimensional measurements. The measurement of conductivity using primary method has been widely developed during the last decade. But this system is not easy to handle. Therefore the secondary method can be used as an alternative measurement of conductivity (Ulrich Breuel et al., 2007).

In the secondary method, cell constant was determined using the primary standard solution that traceable to SI (Ulrich Breuel et al., 2007). In this case, CRM1714 from DFM was used as the standard reference solution with conductivity value 100 mS/cm. Consequently, the EC measurement of secondary method is traceable to DFM through CRM1714.

The resistance of primary standard solution (CRM1714) then converted into conductance (G). Conductance in Siemens (S) is reciprocal of the resistance (R) in ohm (Ω). The equation is described in Eq. (3) (Ulrich Breuel et al., 2007):

$$G = \frac{1}{R} \quad \text{(Eq. 3)}$$

Combination of the Eq. (1) and Eq. (2) produces an equation of the cell constant (K_{cell}), written as Eq. (4):

$$K_{cell} = \frac{\kappa}{G} \quad \text{(Eq. 4)}$$

where κ is the conductivity value of CRM1714 from the certificate. After the cell constant is known, this value can be used for calculation of the secondary reference material solution (KCl 1 M) by using Eq. (5):

$$\kappa = K_{cell} \times G \quad \text{(Eq. 5)}$$

2.4. Procedure for uncertainty estimation in EC measurement

A result measurement will be meaningless without the statement of measurement uncertainty because it represents the quality of a result measurement (Günther Meinrath and Spitzer, 2000; Vicki Barwick and Pricard, 2011). Similar to other experiments, EC measurement is affected by the measurement process.

The estimation process of measurement uncertainty is started by the specification of the measurand. Measurand is a particular quantity subject to be measured (JCGM, 2008). In this case, measurand is EC. Then all sources of uncertainty are identified and quantified. The final step is the calculation of the combined uncertainty (S. L. R Ellison and Williams, 2012).

All sources of uncertainty can be listed using a cause and effect diagram. It shows their relationship and indicates their influence on the uncertainty of the result (S. L. R Ellison and Williams, 2012). Figure 2 illustrates the cause and effect diagram for EC measurement using the secondary method. The procedure for uncertainty

Downloaded from www.periodico.tchequimica.com

estimation in EC measurement by the secondary method using cell type D is similar to the procedure for uncertainty estimation for measurement by a secondary method using cell type C (Nuryatini Hamim et al., 2019).

One of the uncertainty sources that contributes to the uncertainty is cell constant because it is an important factor of EC measurement. (SAS, 2004). Other factors that contribute to and influenced the EC measurement are LCR meter, temperature, carbon dioxide (CO_2) effect, and temperature coefficient (Tangpaisarnkul, 2017; Ulrich Breuel et al., 2009). The CO_2 from the air may form hydrogen carbonate ion (HCO_3^-) in the water and it will change the conductivity of the solution (SAS, 2004). Then, the temperature coefficient can influence the result of EC measurement because there is some correction of EC measurement at various temperatures for conductivity at a standard temperature (25 °C). It reflects the rate of conductance changes per degree of temperature (Smith, 1962).

3. RESULTS AND DISCUSSION

Every measurement cell of the EC system has its cell constant because the dimension of the two platinum electrodes is not the same, such as the distance between the electrodes and surface area of the electrodes. Different cell constants will be used in a different area of EC measurement. (Crison, 2004). The cell constant of the secondary method was determined using known standard solutions with traceable conductivity standards (Ulrich Breuel et al., 2009). In this study, CRM1714 from DFM was used to calculate the cell constant of the cell type D. Measurement results were tabulated in Table 1.

From the calculation, the cell constant of the cell type D is 1.5167 cm^{-1}. This value is then used to calculate the electrolytic conductivity value (κ) of secondary reference material solution (KCl 1 M). The measurement results for calculation K of KCl 1 M are tabulated in Table 2.

EC value for KCl 1 M from the calculation in Table 2 is 111.61 mS/cm. This value is in a good agreement with the conductivity values for KCl 1 M standard solution based on OIML R56 and CRM from ZMK using the same method (Breuel, 2018; OIML, 1981).

After the calculation of EC value for KCl 1 M, the uncertainty measurement can be calculated and quantified in order to involve assigning a statistical confidence level to the measurement result.

In general, the process in EC measurement is divided into two steps: determination of cell constant and measurement of the sample (John J. Barron and Ashton).

Therefore to estimate the uncertainty of EC measurement, firstly, the sources of the cell constant must be identified. A model equation for the determination of the cell constant follows the Eq. (6) (Tangpaisarnkul, 2017).

$$K_{cell} = \frac{\kappa+\delta_{drift}}{G+\delta_{extrapolation}} \times (1 + TK \times \Delta T) \qquad \text{(Eq.6)}$$

where κ is EC value of standard reference solution (CRM1714, DFM), TK is temperature coefficient of solution that found in the certificate with value is 1.77 %/°C at 25 °C (Snedden, 2017), ΔT is a temperature deviation of the measurements that consist of bath stability (T stab), bath homogeneity (T hom) and calibration of thermometer (T), and δ_{drift} is a drift of reading CRM1714 from LCR meter.

Drift is a source of uncertainty in measurement that should be included in the uncertainty budget (Hogan, 2019). Then, $\delta_{extrapolation}$ is extrapolated from the graph of R vs $\frac{1}{f}$.

Cause and effect diagram for determination the cell constant is described in Figure 3, and the uncertainty measurement budget for determination the cell constant of cell type D is tabulated in Table 3.

The result showed that κ of CRM1714 is the most significant contribution in the uncertainty budget of the cell constant measurement (93%) because the CRM1714 is used to calculate the cell constant of cell D which is an important factor of EC measurement (SAS, 2004). Besides that, the temperature deviation of the measurements (ΔT) becomes the second-largest contribution in the measurement of cell constant (4%). Since the measurements of EC is temperature dependence (Mäntynen *et al.*, 2011).

From the calculation, the expanded uncertainty (U) of determination the cell constant is 0.0020 at k=2 for 95% confidence level. Then, the uncertainty budget for determination of secondary reference material solution KCl 1 M is calculated using Eq (7). The budget uncertainty for determination of secondary reference material solution KCl 1 M is listed in Table 4. The value of CO_2 equilibrium, CO_2 sensitivity coefficient and CO_2 suppression factor were taken from the literature (Tangpaisarnkul, 2017). The results showed that the biggest contribution was resulted from the repeatability of measurement, which is 80%. It is because there are many factors that affect the measurement process and give the

Downloaded from www.periodico.tchequimica.com

difference measured value (Kedar A. Upasani and Patkar, 2015). The second-largest contributor is cell constant, which is 17%. Therefore it is recommended to check the cell constant regularly using standard reference solution, especially in platinization electrodes like cell type D, to minimize contamination on the electrode (SAS, 2004). From Table 4, expanded uncertainty (U) of the EC measurement for secondary reference material solution of KCl 1 M is 0.36 mS/cm or 0.33% at k=2 for 95% confidence level.

4. CONCLUSIONS

The electrochemistry laboratory - chemical metrology Indonesia has developed a secondary reference material for electrolytic conductivity (EC) measurement in the range of 20-100 mS/cm by a secondary method using cell type D. The expanded uncertainty was found to be 0.33% for the EC measurement of KCl 1 M.
These reference materials can be used to guarantee the quality of the EC measurement, establishing the traceability chain, and contributing to reduce the import of these reference materials.

5. ACKNOWLEDGMENTS

The authors gratefully acknowledged the Indonesian Institute for Science (LIPI) and PUI BSN for financially supporting this study.

6. REFERENCES

1. Barwick, Pricard, E., *Eurachem Guide: Terminology in Analytical Measurement - Introduction to VIM 3 First Edition,* **2011**.
2. Breuel, U., Werner, B., Spitzer, P., Jensen, H. D. *Experiences with novel developed secondary conductivity sensors within the German Calibration Service (DKD).* Paper presented at the 2007 NCSL International Workshop and Symposium, Braunschweigh, **2007**.
3. Breuel, U., Werner, B., Spitzer, P., Jensen, H. D. *Technical Papers,* **2008**, *3*, 64.
4. Breuel, U., Werner, B., Diana, J. *Chimia,* **2009**, *63*, 643.
5. Breuel, H. D. *Certificate of Analysis*: CRM for Electrolytic Conductivity 111.8 mS/cm. Germany: ZMK, **2018**.
6. Brinkmann, F., Dam, N. E., Deák, E., Durbiano. F., Ferrara. E., Fükö, J., Jensen. H. D., Máriássy. M., Shreiner, R. H., Spitzer, P., Sudmeier, U., Surdu. M., Vyskočil, L. *Accred Qual Assur,* **2003**, *8*, 346.
7. Cañedo-Argüelles, M., Kefford, B., Schäfer, R. *Philos Trans R Soc Lond B Biol Sci.,* **2019***, 374,* 1764.
8. Crison. *The conductivity cell-A little theory*, **2004**.
9. Ellison, S. L. R., Williams, A. Eurachem/CITAC Guide CG 4: Quantifying Uncertainty in Analytical Measurement, Third Edition, **2012**.
10. Fraga, I. C.S., Borges, P. P., Marques, B. S. R., Junior, W. B. S., Sobral, S. P., Ribeiro, C. M., Dias, J. C., Lopes, J. C., Cunha, V. S. *Simposio de Metrología, Mexico*, **2008**.
11. Fraga, I. C. S., Lopes, J. C., Sobral, S. P., Ribeiro, C. M. *Accred. Qual Assur,* **2013**, *18*, 99.
12. Hamim, N., Krismastuti, F. S. H., Hindayani, A., Aristiawan, Y. Paper presented at *The 5th International Symposium on Applied Chemistry,* Tangerang Selatan, **2019**.
13. Hogan, R. *8 sources of uncertainty in measurement for every uncertainty budget*, **2019**.
14. Jameel, R. H., Wu, Y. C., Pratt, K. W. *Primary Standards and Reference Materials for Electrolytic Conductivity*, NIST, **2000**.
15. JCGM. *Evaluation of measurement data- Guide to the expression of uncertainty in measurement,* **2008**.
16. Upasani, K. A., Patkar, S. *The International Journal Of Engineering And Science*, 4, 1, **2015**.
17. Mäntynen, M., Oy, P., *Working Report: Temperature Correction Coefficients of Electrical Conductivity and of Density Measurements for Saline Groundwater*, **2011**.
18. Meinrath, G., Spitzer, P. *Mikrochim. Acta,* **2000**, *135*, 155.
19. OIML R 56: *Standard solutions reproducing the conductivity of electrolyte*s, **1981**.
20. Orrù, E., *Traceability of electrolytic conductivity measurements for ultra pure water*. *Politecnico di Torino Porto Institutional Repository*, **2014**.
21. Radiometer Analytical SAS, *Conductivity Theory and Practice*, France, **2004**.
22. Seitz, S., Manzin, A., Jensen, H.D., Jakobsen, P.T., Spitzer, P. *Electrochimica Acta,* **2010***, 55*, 6323.

Downloaded from www.periodico.tchequimica.com

23. Slovacek, D. *Measurement of Conductivity*, Hach Company, **1998**.
24. Smith, S. H. *lymnology and oceanography*, **1962,** *7*, 330.
25. Snedden, A. C*ertificate of Analysis Certified Reference Material Reference Solution of Electrolytic Conductivity 100 mS/cm*, Denmark: DFM, **2017**.
26. Staff, F. *What is Conductivity,* **2010**. Retrieved 24/07/2019, from https://www.fondriest.com/news/what-is-conductivity.htm.
27. Tangpaisarnkul, N. *Uncertainty for secondary cell electrolytic conductivity measurement*, NIMT, **2017**.

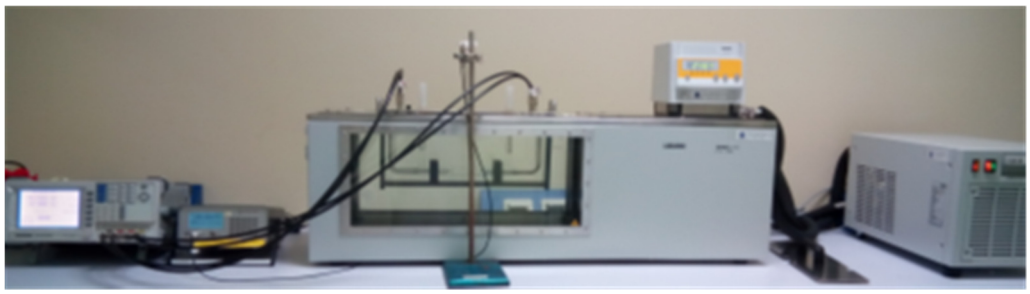

Figure 1. *The system of secondary EC measurement*

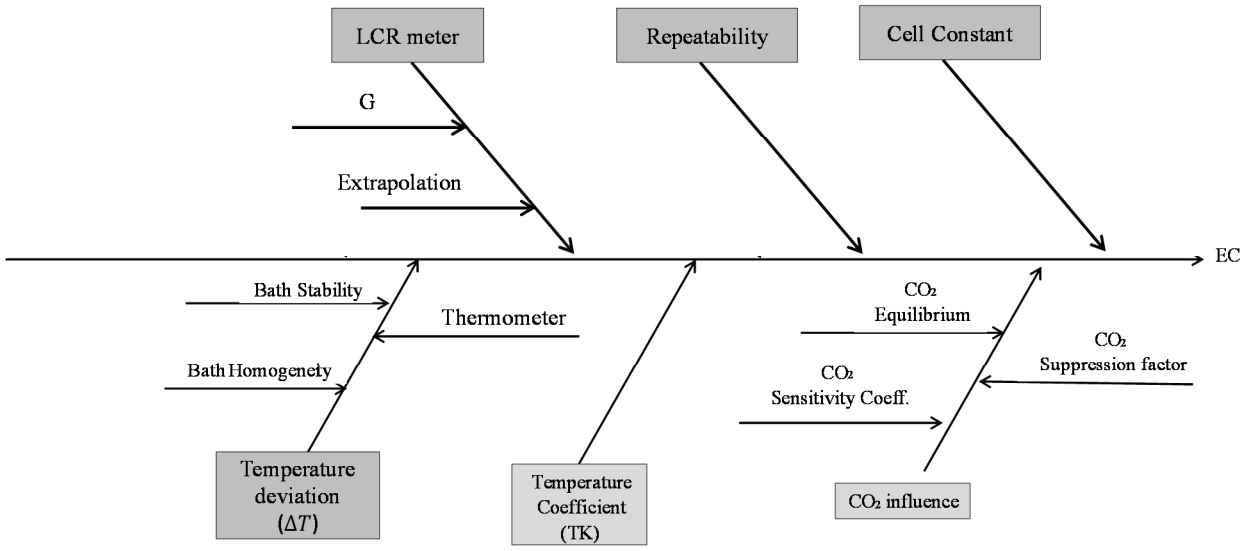

Figure 2. *Cause and effect diagram for EC measurement using a secondary method system (Tangpaisarnkul, 2017; Ulrich Breuel et al., 2007)*

Downloaded from www.periodico.tchequimica.com

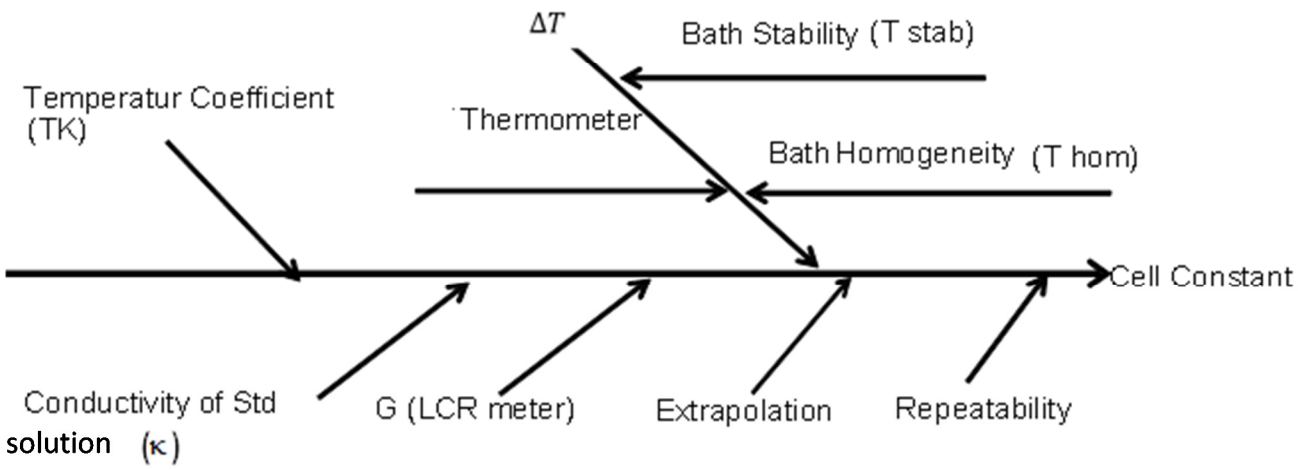

Figure 3. *Cause and effect diagram for the estimation uncertainty of determination the cell constant (Tangpaisarnkul, 2017; Ulrich Breuel et al., 2007)*

$$\kappa = \left(K_{cell} + \delta_{repeatability}\right)\left(G + \delta_{extrapolation}\right)\left(1 + TK \times \Delta T\right) + \frac{\delta_{CO_2 equilibrium} \times \delta_{CO_2\ sensitivity\ coefficient}}{\delta_{CO_2\ suppression\ factor}} \quad \text{(Eq. 7)}$$

Table 1*. Measurement result for the calculation of the cell constant*

f (Hz)	1/f (Hz^{-1})	Resistance (Ω)
120	0.0083	15.1788
130	0.0077	15.1779
140	0.0071	15.1771
150	0.0067	15.1764
160	0.0063	15.1759
170	0.0059	15.1754
200	0.0050	15.1741
210	0.0048	15.1737
330	0.0030	15.1715
360	0.0028	15.1707
480	0.0021	15.1696
Intercept value	(Ω)	15.1668
Conductance (G) using Eq. (3)	(S)	0.0659
	(mS)	65.9335
EC of CRM from certificate (κ)	(mS/cm)	100
Cell Constant (K_{cell}) using Eq. (4)	(cm^{-1})	1.5167

Downloaded from www.periodico.tchequimica.com

***Table 2**. Measurement results for the calculation κ of KCl 1 M*

f (Hz)	1/f (Hz^{-1})	Resistance (Ω)
120	0.0083	13.6012
130	0.0077	13.6002
140	0.0071	13.5995
150	0.0067	13.5988
160	0.0063	13.5982
170	0.0059	13.5976
200	0.0050	13.5963
210	0.0048	13.5959
330	0.0030	13.5938
360	0.0028	13.5930
480	0.0021	13.5922
Intercept value	(Ω)	13.5890
Conductance (G) using Eq. (3)	(S)	0.0736
	(mS)	73.5876
K_{cell} from Table 1	(cm^{-1})	1.5167
κ *of KCl 1 M* using Eq. (5)	(mS/cm)	111.61

***Table 3**. Uncertainty measurement budget for determination the cell constant of cell type D*

Sources (unit)	Value	Divisor	uncertainty	Sensitivity Coefficient (ci)	standard uncertainty (ui)	(ci x ui)²
$\kappa_{CRM1714}$ (mS/cm)	100	2	0.13	0.0152	0.0650	9.72E-07
G (mS)	65.933	2	0.0158	0.0230	0.0079	3.31E-08
Extrapolation (mS)	1	1	0.0002	0.0230	0.0002	1.28E-11
δ_{drift} (1/cm)	1	2.24	0.0006	0.0152	0.0003	1.69E-11
ΔT (K)	0.0037	2	0.0153	0.0268	0.0076	4.20E-08
TK (1/K)	0.0177	1.73	0.0009	0.0056	0.0005	8.06E-12
					sum of square	1.05E-06
					Combine Uncertainty (root of sum square)	0.0010
					Expanded uncertainty (U, k=2)	0.0020

Downloaded from www.periodico.tchequimica.com

***Table 4**. Budget uncertainty for determination of secondary reference material solution KCl 1 M*

Sources (unit)	Value	Divisor	uncertainty	Sensitivity Coefficient (ci)	standard uncertainty (ui)	(ci x ui)^2
K_{cell} (1/cm)	1.5167	2	0.0020	73.5927	0.0010	5.67E-03
G (mS)	73.588	2	0.0177	1.5168	0.0088	1.79E-04
Extrapolation (mS)	1	1	0.0001	1.5168	0.0001	3.32E-08
ΔT (K)	0.0023	2	0.0153	3.3483	0.0076	6.54E-04
TK (1/K)	0.030	1.73	0.0015	0.2585	0.0009	5.01E-08
Repeatability (mS/cm)	1	4.47	0.0099	73.5927	0.0022	2.67E-02
CO_2 equilibrium (ppm)	0	1.73	50	0.00002	28.8675	4.03E-07
CO_2 sens. Coeff. (mS/cm/ppm-vol)	0.0011	1.73	0.0005	0	0.0003	0
CO_2 suppression	50	1.73	10	0	5.7735	0
					sum of square	0.0032
					Combine Uncertainty (root of sum square)	0.1822
					Expanded uncertainty (U, k=2)	0.36
					%U	0.33

Downloaded from www.periodico.tchequimica.com

PERIÓDICO TCHÊ QUÍMICA
ARTIGO ORIGINAL

EFEITO DOS ADSORVENTES INTESTINAIS DE PECTINA/ MONTMORILLONITA EM PARÂMETROS BIOQUÍMICOS DO SANGUE DURANTE O TRATAMENTO CRÔNICO COM ÁCIDO ACETILSALICÍLICO

EFFECT OF PECTIN/MONTMORILLONITE INTESTINAL ADSORBENTS ON BLOOD BIOCHEMICAL PARAMETERS DURING CHRONIC TREATMENT WITH ACETYLSALICYLIC ACID

ВЛИЯНИЕ КИШЕЧНЫХ АДСОРБЕНТОВ НА ОСНОВЕ ПЕКТИН/МОНТМОРИЛЛОНИТА НА БИОХИМИЧЕСКИЕ ПАРАМЕТРЫ КРОВИ ПРИ ХРОНИЧЕСКОМ ЛЕЧЕНИИ АЦЕТИЛСАЛИЦИЛОВОЙ КИСЛОТОЙ

KAPYSHEVA, Unzira[1*]; BAKHTIYAROVA, Sholpan[2]; ZHAKSYMOV, Bolatbek[3]; SMAGULOVA, Zuchra[4]; TALGATOV, Eldar[5]

[1,2,3] Institute of Human and Animal Physiology, Laboratory of Ecological Physiology, Kazakhstan

[4] Institute of Human and Animal Physiology, Laboratory of Lymph Circulation, Kazakhstan

[5] Sokolskiy Institute of Fuel, Catalysis and Electrochemistry, Laboratory of Organocatalysis, Kazakhstan

** Correspondence author*
e-mail: kapysheva.ihap@bk.ru

Received 25 October 2019; received in revised form 21 November 2019; accepted 21 November 2019

RESUMO

O tratamento crônico com medicamentos anti-inflamatórios não esteroides, como o ácido acetilsalicílico, pode causar vários efeitos adversos e condições crônicas. Os adsorventes intestinais à base de materiais naturais são utilizados para prevenir ou tratar várias intoxicações. Neste estudo, foi descrita a desintoxicação e o efeito protetor de adsorventes intestinais compostos de pectina / montmorillonita em ratos que receberam altas doses de ácido acetilsalicílico. 60 ratos Wistar receberam 100 mg / kg de ácido acetilsalicílico sem ou juntamente com adsorventes intestinais compostos à base de montmorillonita e pectina a 5%, 10% e 20%. Após 16 dias de experimento, amostras de sangue foram coletadas para medir os perfis bioquímicos do sangue, incluindo níveis de proteína total, albumina, glicose, colesterol e enzimas hepáticas. Foram observadas mudanças significativas no perfil bioquímico do sangue e nos níveis de enzimas hepáticas em ratos que receberam ácido acetilsalicílico por 16 dias. A administração concomitante de ácido acetilsalicílico e adsorventes intestinais compostos à base de montmorillonita e pectina a 5%, 10% e 20% proporcionou um efeito protetor, julgado pela recuperação da bioquímica sanguínea e dos perfis de enzimas hepáticas para controlar os níveis. O adsorvente composto com pectina a 20% teve efeito máximo. Portanto, os adsorventes intestinais pectina / montmorillonita podem ser utilizados para diminuir a irritação gastrointestinal e os efeitos adversos de medicamentos, como o ácido acetilsalicílico.

Palavras-chave: *pectina, transorbente, inflamatório, anti-inflamatórios não esteroides.*

ABSTRACT

Chronic treatment with non-steroidal anti-inflammatory drugs such as acetylsalicylic acid may cause a number of adverse effects and chronic conditions. Intestinal adsorbents based on natural materials are used to prevent or treat various intoxications. In this study, it was described detoxification and protective effect of composite pectin/montmorillonite intestinal adsorbents in rats receiving high doses of acetylsalicylic acid. 60 Wistar rats received 100 mg/kg of acetylsalicylic acid without or together with composite intestinal adsorbents based on montmorillonite and 5%, 10%, and 20% pectin. After 16 days of the experiment, blood samples were collected to measure blood biochemistry profiles, including levels of total protein, albumin, glucose, cholesterol and liver enzymes. It was observed significant changes in blood biochemistry profile as well as in liver enzyme levels in rats receiving acetylsalicylic acid for 16 days. Concomitant administration of acetylsalicylic acid and composite intestinal adsorbents based on montmorillonite and 5%, 10%, and 20% pectin provided a protective effect as judged by recovery of blood biochemistry and liver enzyme profiles to control levels. The composite

Downloaded from www.periodico.tchequimica.com

adsorbent with 20% pectin had maximum effect. Therefore, pectin/montmorillonite intestinal adsorbents can be used to decrease gastrointestinal irritation and adverse effects of drugs, such as acetylsalicylic acid.

Keywords: *pectin, tagansorbent, inflammation, non-steriod anti-inflammatory drugs.*

АННОТАЦИЯ

Хроническое лечение нестероидными противовоспалительными препаратами, такими как ацетилсалициловая кислота, может вызвать ряд побочных эффектов и хронических состояний. Кишечные адсорбенты на основе натуральных материалов используются для профилактики или лечения различных интоксикаций. В этом исследовании мы описываем детоксикационный и защитный эффект кишечных адсорбентов пектина / монтмориллонита у крыс, получающих высокие дозы ацетилсалициловой кислоты. 60 крыс линии Вистар получали 100 мг / кг ацетилсалициловой кислоты без или вместе с кишечными композитными адсорбентами на основе монтмориллонита и 5%, 10% и 20% пектина. После 16 дней эксперимента отбирали образцы крови для измерения профилей биохимии крови, включая уровни общего белка, альбумина, глюкозы, холестерина и ферментов печени. Мы наблюдали значительные изменения в биохимическом профиле крови, а также в уровне ферментов печени у мышей, получавших ацетилсалициловую кислоту в течение 16 дней. Одновременное введение ацетилсалициловой кислоты и кишечных композитных адсорбентов на основе монтмориллонита и 5%, 10% и 20% пектина обеспечивало защитный эффект, судя по восстановлению биохимических показателей крови и профилей ферментов печени до контрольных уровней. Композитный адсорбент с 20% пектина имел максимальный эффект. Вывод: кишечные адсорбенты пектин/монтмориллонит могут быть использованы для уменьшения раздражения желудочно-кишечного тракта и побочных эффектов лекарств, таких как ацетилсалициловая кислота.

Ключевые слова: пектин, тагансорбент, воспалительные, нестероидные противовоспалительные препараты.

1. INTRODUCTION

Acetylsalicylic acid (ASA, aspirin) is a non-steroidal anti-inflammatory drug (NSAID) which acts through inhibition of prostaglandin synthesis. High-dose (more than 345 mg/day) ASA is used in clinical practice to treat fever, inflammation or pain. Chronic low-dose (75–325 mg/day) ASA therapy is a standard strategy to prevent the formation of blood clots and often used in patients after a heart attack or stroke (ATT Collaboration, 2009). Long-term treatment with NSAIDs often results in a chronic suppression of prostaglandin synthesis which leads to systemic and local adverse effects. Chronic ASA therapy often causes gastrointestinal symptoms (Iwamoto, 2013). According to the survey of patients treated with chronic low-dose ASA, 15% of patients suffered upper gastrointestinal (GI) symptoms, 70% being heartburn and/or eructation (Cayla, *et al.*, 2012). These symptoms are primarily caused by local epithelial reactions to ASA as this drug can potentially decrease the hydrophobic properties of epithelium and cause gastric mucosal damage. Additionally, ASA has a low pKa, which contributes to topical gastroduodenal damage (Sostres and Lanas, 2011). GI symptoms may occur due to inflammation-induced oxidative stress (Konturek *et al.*, 2010). Some patients treated with ASA have lower GI symptoms such as minor bleeds, which may cause iron deficiency anemia and protein loss (Fortun *et al.*, 2005). These symptoms can be reversed by a cessation of ASA treatment, however, the risk-benefit assessment demonstrates the benefit of chronic ASA treatment especially in preventing cardiovascular diseases.

There is a number of strategies to reduce the risk of adverse effects related to NSAID treatment. The choice of strategy depends on associated risk factors such as gastric ulcers and H. pylori infection, elderly age, and concomitant medications. One of such strategies is the replacement of ASA with similar drugs (e.g. clopidogrel). However, these drugs have similar adverse effects on mucosa (CAPRIE Steering Committee, 1996). Additionally, drugs such as omeprazole and famotidine can be used to prevent gastric damage (Sostres and Lanas, 2011). However, concomitant use of these drugs can be more expensive compared to ASA monotherapy. This can be unsuitable for patients in countries with low-income economies and/or undeveloped medical care system. Recent studies showed that melatonin and its precursor L-tryptophan may reduce mucosal damage in healthy volunteers, probably through their radical scavenging ability (Konturek *et al.*, 2010). The search for novel strategies to reduce the risk of

Downloaded from www.periodico.tchequimica.com

NSAID-related adverse effects continues.

Intestinal adsorbents are candidate protective agents that reduce GI mucosa damage. Adsorbents based on kaolin, diosmectite and other clay minerals are used in traditional and evidence-based medicine as a supportive aid in acute diarrhea treatment (Pérez-Gaxiola *et al.*, 2015; Zaid *et al.*, 1995). Clay minerals are known to adsorb heavy metal ions, bacteria and mycotoxins *in vitro* and *in vivo* (Drucker *et al.*, 1977; Kang *et al.*, 2016; Uddin, 2017; Wang *et al.*, 2017). Administration of diosmectite showed an anti-inflammatory effect in induced colitis in rats, probably due to its ability to adsorb luminal antigens, increase of colonic mucin levels and possibly directly modulates cytokine production by mucosal cells (González *et al.*, 2004). Furthermore, diosmectite improves intestinal barrier function in pigs (Hu *et al.*, 2013).

Clay minerals can be modified by organic polymers to produce composite adsorbents with desired sorption properties (Alcântara *et al.*, 2014). Previously, it had been synthesized and characterized pectin-montmorillonite composite intestinal adsorbent which has shown the detoxifying ability in rats after cobalt salts intoxication (Talgatov *et al.*, 2016). Tagansorbent is a sorbent based on unmodified montmorillonite from Tagansky deposit (Kazakhstan). It is a health supplement used topically or orally in patients with acute diarrhea, heartburn and bloating (Mukovozova, 2010; http://www.aptekar.kz). Pectins are plant polysaccharides and main components of plant cell walls. They are derived from fruit and vegetable pulp and used widely in food, biomedical, and pharmaceutical industry. In the colon, pectins act as prebiotic agents. They are fermented by bacteria into butyrate known to inhibit colon inflammation (Wicker *et al.*, 2014). Moreover, pectins reduce glucose and cholesterol levels in blood probably due to their reduced adsorption. Pectin administration was shown to increase the urinary excretion of toxic metals such as arsenic and cadmium. However, the mechanism remains unknown as pectin is not soluble in the GI tract and does not adsorb in blood (Eliaz *et al.*, 2006).

Naturally occurring materials may be promising components for the development of adsorbents with detoxification properties. Additionally, the use of locally sourced materials may decrease the cost of drugs and health supplements making them accessible to patients.

In this study, it was explored the effect of intestinal adsorbents based on apple pulp pectin and montmorillonite from Tagansky deposit (Kazakhstan) against adverse events related to ASA treatment.

2. MATERIALS AND METHODS

2.1. Animals

60 Wistar rats of 220±10 g body weight were randomized into 5 groups. GI inflammation was provoked by ASA administration per os. ASA was purchased from OAO “Borisovskiy zavod medicinskikh preparatov” (Belarus). ASA dose was determined experimentally as 100 mg/kg or 20 mg/day per animal. Rats were treated for 16 days.

All animals except control group received 0.5 ml ASA per os and suspension of pectin/montomorillonite intestinal adsorbents (Pc/TS) with 5%, 10%, and 20% pectin. Pc/TS dose was 28.6 mg/kg (daily dose 6.3 mg). Control animals received 0.5 ml of water per os. Groups were assigned as follows: Group 1 (control) (n=12); Group 2 (n=12) – ASA solution; Group 3 (n=12) – ASA + Pc (5%)/TS; Group 4 (n=12) – ASA + Pc (10%)/TS; Group 5 (n=12) – ASA + Pc (20%)/TS.

The study was performed in compliance with the decision of the local ethical committee (Abstract of meeting #4, Asfendiyarov Kazakh National Medical University, 09 Apr. 2018).

2.2. Preparation of composite intestinal adsorbents

Pectin was isolated from 'Golden delicious' apples. Apples were pulpified, the resulting pulp was dried at room temperature and milled. Pectin isolation and preparation of composite intestinal adsorbents were performed as described in (Talgatov *et al.*, 2016). Starting material was placed in a stainless steel reactor followed by the addition of citric acid solution (pH 1.4). The mixture was stirred continuously for 4 hours at 80°C. pH was corrected to 3.4 using sodium hydroxide solution. Pectin was precipitated by adding ethanol and separated using vacuum filtration. The precipitate was washed and air-dried in ambient conditions. To obtain solutions with 5%, 10%, 20% pectin was dissolved in water at 60°C and then added to montmorillonite (tagansorbent from Taganskiy deposit, Kazakhstan) suspension (1 g clay in 15 mL water). The solution was stirred for 2 h at ambient temperature and then kept in mother liquor for 16 h. Solids were washed with water

Downloaded from www.periodico.tchequimica.com

and air-dried.

2.3. Blood biochemistry and liver enzyme profiles

After 16 days of the experiment, blood samples were collected by decapitation. Fresh blood was stabilized with heparin (2-3 U/ml) and centrifuged at 1500 rpm for 15 min. Serum supernatant was collected and used for further analysis. Levels of total protein, albumin, glucose, cholesterol, alanine aminotransferase, aspartate aminotransferase, alkaline phosphatase was detected using A-25 automatic analyzer (BioSystems, Spain) and the respective reagent kits. Results were compared to the control group and group 2.

2.4. Statistical analysis

Statistical analysis was performed using Microsoft Excel. All data obtained from the experiment are expressed as mean ± standard deviation (SD). Differences between groups were calculated using unpaired Student's t-test and $p \leq 0.05$ were considered significant.

3. RESULTS AND DISCUSSION:

Blood samples from rats after 16 days of concomitant ASA and pectin/montmorillonite administration were analyzed. In the control group, total protein, albumin, glucose, and cholesterol serum levels were within the normal physiological range (Table 1). In contrast, we observed changes characteristic for inflammation processes in blood samples from animals receiving 20 mg/day ASA for 16 days. It is known that a decrease in total blood protein level and serum albumin levels are characteristic for liver and lower GI tract disorders (Danilova, 2003). Total protein and albumin levels in blood decreased by 10% and blood glucose and cholesterol levels increased by 18-20% and 10-11%, respectively.

The same parameters were studied in animals receiving ASA and composite intestinal adsorbents with various pectin concentrations. In animals receiving Pc/TS with 5% pectin (group 3), we observed a 4-5% decrease of total protein level and 3-4% increase of serum cholesterol level compared to control animals. However, these animals maintained elevated glucose level. Total protein levels, albumin, glucose and cholesterol levels in animals receiving Pc/TS with 10% pectin (group 4) were similar to the control group (Table 1). Correspondingly, animals receiving Pc/TS with 20% pectin (group 5) had biochemical profile similar to untreated animals. Interestingly, the mean cholesterol level in this group was significantly lower compared to the control group (Table 1).

Elevated levels of serum alanine aminotransferase (ALT), aspartate aminotransferase (AST), and alkaline phosphatase (AP) indicate increased hepatocyte membrane permeability and are considered is an indicator of acute liver damage (Danilova, 2003). Normally, ASA does not induce liver damage. However, it was sought to analyze ALT, AST, and AP levels in treated animals. In animals receiving only ASA (group 2), it was observed an increase of ALT levels by 20% and AST levels by 40-45% (Table 2). AP concentration increased 2.2-fold compared to control group.

In animals receiving Pc/TS with 5% pectin, ALT and AST levels were higher compared to the control group (4% and 9%, respectively). Administration of intestinal adsorbents did not change serum AP levels. After administration of intestinal adsorbents with 10% pectin (group 4), ALT and AST levels were restored to normal values, however, AP level was 25% higher compared to control (Table 2).

Animals receiving intestinal adsorbents with 20% pectin demonstrated maintenance of normal ALT and AST levels. Additionally, we found that the mean AP level of AP in this group was significantly lower compared to other groups (Table 2). This demonstrates an evident gastroprotective effect of pectin.

It was demonstrated that administration of high-dose ASA for 16 days leads to dramatic changes in biochemical and enzymatic profiles of treated animals. Total blood protein levels increased by 10%, serum liver enzyme levels (ALT, AST, and AP) increased by 20%, 40%, and 220% respectively. These changes are related to liver dysfunction which may also occur in patients chronically receiving high doses of ASA. In rats receiving ASA and pectin/montmorillonite adsorbents, we observed that the decrease of liver enzyme serum levels was in direct relationship to the increase of pectin concentrations. Therefore, pectin/montmorillonite intestinal adsorbents can be used to prevent drug-induced liver injury in patients receiving drugs which may cause liver damage.

Similarly to liver enzyme levels, a decrease of glucose and cholesterol levels in rats receiving ASA and Pc/Ts intestinal adsorbents was in direct relationship to the increase of pectin

Downloaded from www.periodico.tchequimica.com

concentrations. These findings corroborate the results of other studies showing lower cholesterol levels in subjects receiving pectin as a food supplement (Leclere *et al.*, 2013). Therefore, we assume that the components of the intestinal adsorbent used in this study retain their properties and function. Clay minerals are able to bind drug substances in vitro affecting drug release but not adsorption of the drug (Mináriková *et al.*, 2017; Djebbi *et al.*, 2018). Therefore we suggest that the composite mineral adsorbent acts through binding with ASA. Similar properties were shown for pectin (Bermúdez-Oria *et al.*, 2018). The pectin component of the composite intestinal adsorbent probably decreases ASA absorbability and correspondingly its systemic exposure and effect. However, it remains unknown whether the detoxification effects are more evident for pectin alone or as a component of the intestinal adsorbent. Moreover, there is a need in experiments accessing ASA pharmacokinetics after administration of individual components of the composite intestinal adsorbent.

Use of composite intestinal adsorbents as food supplements can be an effective strategy to reduce the rate of adverse effects during ASA treatment. This is particularly important as ASA and other non-steroidal anti-inflammatory drugs are one of the most prescribed medications particularly to elderly patients (Wongrakpanich *et al.*, 2018). Results of this study can be used to develop and more advanced intestinal adsorbents based on naturally occurring materials and investigate their mechanism of action.

4. CONCLUSIONS:

This study described the effect of composite pectin/montmorillonite intestinal adsorbents on blood biochemical parameters during chronic treatment with ASA. It was demonstrated that intestinal adsorbents with 20% pectin have maximum protective effect. Results of this study can be used to develop effective strategies to reduce adverse effects in patients receiving non-steroidal anti-inflammatory drugs and other medications.

5. ACKNOWLEDGMENTS:

The study was funded by grant AR 05131542 "The use of pachitin, obtained from various sources of plant materials, in compositions with natural montmorillonite of the Tagansky deposit in diseases of the digestive system", Science Committee of the Ministry of Education and Science of the Republic of Kazakhstan."

6. LIST OF ABBREVIATIONS:

ASA – acetylsalicylic acid; NSAID – non-steroidal anti-inflammatory drug; GI – gastrointestinal; Pc/TS – pectin/montmorillonite (Tagantsorbent) based intestinal adsorbent; ALT – alanine aminotransferase; AST – aspartate aminotransferase; AP – alkaline phosphatase.

7. REFERENCES:

1. Alcântara, A. C. S.; Darder, M.; Aranda, P.; Ruiz-Hitzky, E.; *Appl. Clay Sci.* **2014**, *96*, 2, doi:10.1016/j.clay.2014.02.018.
2. Antithrombotic Trialists' (ATT) Collaboration; Lancet **2009**, *373*, 1849, doi:10.1016/S0140-6736(09)60503-1.
3. Bermúdez-Oria, A.; Rodríguez-Gutiérrez, G.; Rodríguez-Juan, E.; González-Benjumea, A.; Fernández-Bolaños, J.; *Carbohydr. Polym.* **2018**, *197*, 260, doi:10.1016/j.carbpol.2018.05.089.
4. CAPRIE Steering Committee; *Lancet* **1996**, *348*, 1329, doi:10.1016/S0140-6736(96)09457-3.
5. Cayla, G.; Collet, J.-P.; Silvain, J.; Thiefin, G.; Woimant, F.; Montalescot, G. ; *Int. J. Cardiol.* **2012**, *156*, 69, doi:10.1016/j.ijcard.2010.10.027.
6. Danilova, L. A.; *Laboratory Blood and Urine Tests: Reference book*, 4th ed., Saint Petersburg: Salit Medkniga, **2003**.
7. Djebbi, M. A.; Boubakri, S.; Bouaziz, Z.; Elayachi, M. S.; Namour, P.; Jaffrezic-Renault, N.; Ben Haj Amara, A.; *Microporous Mesoporous Mater.* **2018**, *267*, 43. doi:10.1016/j.micromeso.2018.03.017.
8. Drucker, M. M.; Goldhar, J.; Ogra, P. L.; Neter, E.; *Infection* **1977**, *5*, 211, doi:10.1007/BF01640782.
9. Eliaz, I.; Hotchkiss, A. T.; Fishman, M. L.; Rode, D.; *Phytother. Res.* **2006**, *20*, 859, doi:10.1002/ptr.1953.
10. Fortun, P. J.; Hawkey, C. J.; *Curr. Opin. Gastroenterol.* **2005**, *21*, 169, doi: 10.1097/01.mog.0000153314.51198.58.

Downloaded from www.periodico.tchequimica.com

11. González, R.; Sánchez de Medina, F.; Martínez-Augustin, O.; Nieto, A.; Gálvez, J.; Risco, S.; Zarzuelo, A.; *Br. J. Pharmacol.* **2004**, *141*, 951, doi:10.1038/sj.bjp.0705710.
12. Hu, C.; Song, J.; Li, Y.; Luan, Z.; Zhu, K.; *Br. J. Nutr.* **2013**, *110*, 681, doi:10.1017/S0007114512005508.
13. Iwamoto, J.; *World J. Gastroenterol.* **2013**, *19*, 1673, doi:10.3748/wjg.v19.i11.1673.
14. Kang, F.; Ge, Y.; Hu, X.; Goikavi, C.; Waigi, M. G.; Gao, Y.; Ling, W.; *J. Hazard. Mater.* **2016**, *320*, 80, doi:10.1016/j.jhazmat.2016.08.006.
15. Konturek, P. C.; Konturek, S. J.; Celinski, K.; Slomka, M.; Cichoz-Lach, H.; Bielanski, W.; Reiter, R. J.; *J. Pineal Res.* **2010**, *48*, 318, doi:10.1111/j.1600-079X.2010.00755.x.
16. Leclere, L.; Cutsem, P. V.; Michiels, C.; *Front. Pharmacol.* **2013**, *4*, doi:10.3389/fphar.2013.00128.
17. Mináriková, M.; Fojtikova, V.; Vyskočilová, E.; Sedláček, J.; Šikut, M.; Borek-Dohalska, L.; Stiborová, M.; Martinkova, M.; *Environ. Toxicol. Pharmacol.* **2017**, *52*, 214, doi:10.1016/j.etap.2017.04.011.
18. Mukovozova, L. A.; Annals of Modern Clinical Science **2010**, *1*.
19. Pérez-Gaxiola, G.; Cuello-García, C. A. ; Pérez-Pico, V.; *Cochrane Database of Systematic Reviews* **2015**, 4, doi:10.1002/14651858.cd011526.
20. Sostres, C.; Lanas, A.; *Nat. Rev. Gastroenterol. Hepatol.* **2011**, *8*, 385, doi:10.1038/nrgastro.2011.97.
21. Talgatov, E. T.; Auezkhanova, A. S.; Kapysheva, U. N.; Bakhtiyrova, S. K.; Zharmagambetova, A. K.; *J. Inorg. Organomet. Polym. Mater.* **2016**, *26*, 1387, doi:10.1007/s10904-016-0422-7.
22. Uddin, M. K.; *Chem. Eng. J.* **2017**, *308*, 438, doi:10.1016/j.cej.2016.09.029.
23. Wang, M.; Maki, C. R.; Deng, Y.; Tian, Y.; Phillips, T. D.; *Chem. Res. Toxicol.* **2017**, *30*, 1694, doi:10.1021/acs.chemrestox.7b00154.
24. Wicker, L.; Kim, Y.; Kim, M.-J.; Thirkield, B.; Lin, Z.; Jung, J.; *Food Hydrocolloids* **2014**, *42*, 251, doi:10.1016/j.foodhyd.2014.01.002.
25. Wongrakpanich, S.; Wongrakpanich, A.; Melhado, K.; Rangaswami, J.; *Aging and Disease* **2018**, *9*, 143, doi:10.14336/AD.2017.0306.
26. Zaid, M.R.; Hasan, M.; Khan, A. A.; *Journal of Diarrhoeal Diseases Research* **1995**, *1*, 44.
27. http://www.aptekar.kz/catalog/drugs/bolezni-zheludochno-kishechnogo-trakta/kishechnye-adsorbenty/tagansorbent/, accessed November 2019.

Table 1. *Effect of composite intestinal adsorbents on blood total protein level, serum albumin level, glucose and cholesterol levels in rats after ASA and Pc/TS administration*

No.	Group	Parameter			
		Total protein (g/L)	**Albumin (g/L)**	**Glucose (mmol/L)**	**Cholesterol (mmol/L)**
1	Control	63.3±0.02	29.33±1.02	3.62±0.02	2.61±0.002
2	ASA	57.33±0.03*	25.74±1.42*	4.29±0.004*	2.84±0.004*
3	ASA + Pc (5%)/TS	60.99±0.04*	30.82±2.00*	4.45±0.002*	2.68±0.003*
4	ASA + Pc (10%)/TS	63.19±0.01*	29.90±1.29*	3.54±0.003*	2.51±0.005*
5	ASA + Pc (20%)/TS	63.55±0.01*	28.76±0.66*	3.55±0.003*	2.19±0.006*

* – $p \leq 0.05$ compared to group 1.

Downloaded from www.periodico.tchequimica.com

Table 2. *Effect of composite intestinal adsorbents on serum liver enzymes level in rats after ASA and Pc/TS administration*

No.	Group	Parameter		
		ALT (unit/L)	**AST (unit/L)**	**AP (unit/L)**
1	Control	63.3±0.02	29.33±1.02	3.62±0.02
2	ASA	57.33±0.03*	25.74±1.42*	4.29±0.004*
3	ASA + Pc (5%)/TS	60.99±0.04*	30.82±2.00*	4.45±0.002*
4	ASA + Pc (10%)/TS	63.19±0.01*	29.90±1.29*	3.54±0.003*
5	ASA + Pc (20%)/TS	63.55±0.01*	28.76±0.66*	3.55±0.003*

* – $p \leq 0.05$ compared to group 1.

Downloaded from www.periodico.tchequimica.com

PERIÓDICO TCHÊ QUÍMICA
ARTIGO ORIGINAL

INFLUÊNCIA DO USO DO ÓLEO DA *CARAPA GUIANENSIS* (ÓLEO DA ANDIROBA) COMPARADO COM FLUIDO DE CORTE COMERCIAL NO PROCESSO DE TORNEAMENTO DO AÇO ABNT 1045

INFLUENCE OF THE USE OF *CARAPA GUIANENSIS* OIL (ANDIROBA OIL) COMPARED WITH COMMERCIAL CUTTING FLUID IN THE TURNING PROCESS OF THE ABNT 1045 STEEL GRADES

BOTELHO, Tamires Isabela Mesquita[1*]; FIGUEIREDO, Gleidson Silva[1]; PRAXEDES Fernanda Malato[2]; TEIXEIRA, Jean Valdir Uchôa[2]; MONTEIRO, Elane Botelho[3];

[1] Universidade Federal do Pará, Faculdade de Engenharia Mecânica, Campus Belém, Belém – PA, Brasil

[2] Instituto Federal do Pará, Faculdade de Engenharia Materiais, Campus Belém, Belém – PA, Brasil

[3] Universidade do Vale do Taquari (UNIVATES), Programa de Pós-Graduação em Sistemas Ambientais Sustentáveis, Lajeado/RS – Brasil

* Autor correspondente
e-mail: tamiresisabela@yahoo.com.br

Received 19 July 2019; received in revised form 15 October 2019; accepted 13 November 2019

RESUMO

Os crescentes avanços tecnológicos obtidos tanto no desenvolvimento de novos materiais como de máquinas ferramenta aumentaram a demanda pelos processos de usinagem e aliado a isto o uso de fluidos de corte aumentou. Entretanto é necessário que os fluídos de corte possuam características que não agridam o ambiente ou o operador. Nos processos de usinagem os fluidos de corte, quando escolhidos e aplicados apropriadamente, podem refletir em benefícios durante o processo de fabricação. Este trabalho avaliou o desempenho de um fluido de corte comercial comparando-o com óleo vegetal extraído da carapa guianensis no processo de torneamento do aço abnt 1045. Manteve-se a velocidade de corte (vc), avanço da ferramenta (f) e a profundidade de corte (ap) e verificou-se a influência do uso de ambos a quais exerciam sobre o metal com as seguintes variáveis: análise do cavaco, acabamento superficial, temperatura de corte e desgaste da ferramenta. Foi observado que com a utilização do com óleo da andiroba gerou-se melhor cavaco para a segurança do operador, maiores temperaturas de corte na peça, maior desgaste da ferramenta e melhor acabamento superficial com diferença de 23%, comparado com fluido de corte comercial. Sendo assim o fluido à base da andiroba pela aplicação convencional comparado com o fluido de corte comercial demonstrou uma alternativa viável no processo de torneamento do aço abnt 1045, pelo fato de ser biodegradável e redução dos fluidos de corte derivados do petróleo.

Palavras-chave: *fluido de corte comercial, óleos vegetais, carapa guianensis, temperatura da peça, desgaste da ferramenta.*

ABSTRACT

The increasing technological advances obtained both in the development of new materials and of machine tools increased the demand for the machining processes and in addition, the use of increased cutting fluids. However, it's necessary to have characteristics that don't harm the environment and the operator. In machining processes, cutting fluids, when properly chosen and applied, may reflect benefits during the manufacturing process. This work evaluated the performance of a commercial cutting fluid by comparing it with vegetable oil extracted from carapa guianensis in the abnt 1045 steel turning process. The cutting speed (vc), tool feed (f) and depth (ap) and the influence of the use of both of them on the metal was verified with the following variables: chip analysis, surface finish, cutting temperature and tool wear. It was observed that with the use of andiroba oil, better chip was generated for the safety of the operator, higher cutting temperatures in the piece, higher tool wear and better surface finish with a difference of 23% compared to commercial cutting fluid. Thus, the fluid from andiroba based on the conventional application demonstrated a viable alternative in the turning process of abnt 1045 steel, because it's biodegradable and reduces petroleum-based cutting fluids.

Downloaded from www.periodico.tchequimica.com

Keywords: *commercial cutting fluid, vegetable oils, carapa guianensis, temperature of the part, tool wear.*

1. INTRODUÇÃO

A usinagem está presente na confecção dos mais variados produtos de diferentes ramos setoriais. É um processo de fabricação por remoção de cavacos. Sendo assim, todo processo em que há uma peça bruta que, após ser removido material em forma de cavaco de seu interior e exterior, formando uma peça com superfícies desejadas, detalhadas e acabadas de forma que satisfaça plenamente ao cliente, é considerado um processo de usinagem (Santos e Dias, 2010). Durante os processos de usinagem as ferramentas aquecem e sofrem altos desgastes que exigem trocas constantes de suas arestas de corte. Além disto, há o aquecimento das peças usinadas, o que pode provocar dois efeitos indesejáveis: alterações nas dimensões pretendidas e geração de tensões internas que podem comprometer a utilização das mesmas. Para minimizar os desgastes das ferramentas e o aquecimento das peças, vários recursos podem ser utilizados, entre os quais o emprego de um fluido de corte.

Com o aumento das atividades industriais e a evolução dos processos de usinagem, houve um acréscimo no consumo dos fluidos de corte, e também a necessidade dos fluidos serem mais eficientes. Surgiram então os fluidos de corte de extrema pressão (E.P.) que são óleos emulsionáveis, usados quando a lubrificação é um fator importante, isto é, em velocidades reduzidas de corte (onde o coeficiente de atrito é grande) e para usinagem de materiais mais duros. Nos dias de hoje, após constantes desenvolvimentos, surgiram óleos contendo cloro, associações de cloro e enxofre, fósforo enxofre e cloro (Diniz e Scandiffio, 2001).

O emprego de fluidos de corte melhora a eficiência dos processos de usinagem proporcionando: aumento da vida da ferramenta de corte, maior controle de tolerâncias dimensionais, melhoria no acabamento superficial da peça usinada, promove a redução nas forças de usinagem e amenização de vibrações (Rodrigues, 2005; Stemmer, 2005). O efeito do uso de fluidos de corte depende não somente das propriedades do fluido, mas também das condições de usinagem, ou seja, da ferramenta de corte, material peça e parâmetros de corte.

No entanto, apesar de todos os benefícios dos fluidos de corte, pesquisas ressaltam que sua aplicação cria severos impactos ambientais, como a poluição ou contaminação da água, do solo, e do ar, além de problemas para a saúde dos operadores. Neste cenário, tendências tecnológicas e de aplicação visam à redução, substituição ou à eliminação do uso dos fluidos de corte nos processos de usinagem (Vacaro, 2009; Souza, 2011; Lawal *et al*; 2012). Dentre os diversos tipos de fluidos de corte existentes, os fluidos de corte emulsionáveis, principalmente aqueles de base mineral, ainda são os mais utilizados nas indústrias metal-mecânica devido ao custo-benefício. Esses fluidos, dependendo da sua concentração, apresentam alto poder refrigerar a peça-ferramenta, fundamental para usinagem com altas rotações. Estudos realizados comparam fluidos sintéticos, semi-sintético, emulsionáveis e concluem que aqueles que utilizam emulsão são mais favoráveis que os demais para a propagação de microrganismos (Moore *et al.*, 2000; Veillete *et al.*, 2004).

Atualmente existe um crescente desenvolvimento de fluidos de corte com base em diversos óleos vegetais, por serem biodegradáveis e ambientalmente amigáveis. Alguns trabalhos como os óleos de milho, mamona, soja e recentemente a andiroba (Botelho *et al.,* 2019 e Grosse *et al.*, 2016). Com isso existe uma utilização e potencial como fluido de corte, nos processos de usinagem, no entanto segundo Gonçalves (2013) poucas pesquisas relatam estudos sobre a reologia e tribologia de óleos vegetais.

O aço ABNT 1045 é muito utilizado no setor metal-mecânica, possui características de boa usinabilidade, boa resistência mecânica, média soldabilidade e alta forjabilidade, sendo aplicado na fabricação de eixos e peças para indústria agrícola, automobilística, de máquinas e equipamentos em geral (Araújo, *et al*., 2015).

O objetivo deste trabalho é investigar a temperatura de corte, acabamento superficial, desgaste da ferramenta e análise do cavaco resultante em operação de torneamento do aço ABNT 1045, com velocidade de corte (vc), avanço da ferramenta (f) e a profundidade de corte (ap) iguais, comparando a influência do fluido de corte comercial com óleo vegetal extraído da *Carapa Guianensis*.

Downloaded from www.periodico.tchequimica.com

2. MATERIAIS E METÓDOS

2.1. Materiais

Para a realização da usinagem dos metais, foi utilizado um torno mecânico convencional, modelo Nardini NZ VS (figura 1). Foram utilizadas ferramentas bits de aço rápido 3/8 x 3” 12, com ângulos αo= 02°; $\gamma 0$ = 46°.

Figura 1. *Torno mecânico convencional*

Os materiais utilizados para a confecção dos corpos-de-prova foram 2 (duas) barras cilíndricas (tarugos) de 38mm de comprimento x 23mm de diâmetro de aço ABNT 1045 (Figura 2). Não foi feita nenhum tratamento térmico, sendo ensaiados em estado bruto, com dureza apresentada na Tabela 1. O fluido de corte utilizado foi o óleo emulsionável, fluido biodegradável elaborado a partir de aditivos de extrema pressão, aditivos (anti-ferruginosos), bactericidas, anti-espumantes e corantes, o fabricante recomenda a utilização pura ou diluída em água sendo a cada 1 litro para 19 litros de água.

O sistema utilizado para aplicação do fluido foi de forma convencional, métodos como este encontram-se na literatura (Biscione, 2010; Magri, 2015) que proporcionou uma vazão em torno de 757,23 mL/s. O fluido aplicado não foi diluído em água, pois segundo Muniz (2008), a estabilidade das emulsões de um fluido de corte pode ser afetada pela qualidade da água; esta deve ser isenta de impurezas, microorganismos e excesso de cloro. A dureza da água é uma propriedade de grande importância no preparo das emulsões.

Figura 2. *Corpo-de-prova do aço ABNT 1045.*

Tabela 1. *Dureza do aço ABNT 1045*

Aço ABNT	HB
1045	174 ± 0,5

2.1. Métodos

O fluido de corte, óleo da *carapa guianensis*, foi coletado de forma artesanal no município de Igarapé-Mirim (PA), sendo este material rejeito do processo de fabricação artesanal da região. O fluido foi aplicado na zona de corte via a técnica convencional por inundação (vazão de 630,93 ml/s) e na direção (sobrecabeça, como ilustrado na Figura 3).

A análise do pH foi realizada com pHmetro portátil digital da marca HI221. A viscosidade dinâmica da carapa guianensis utilizou-se um viscosímetro do fabricante Hake à temperatura de 40°C, uma vez que abaixo de 25°C o óleo permanece solidificado. Esta temperatura foi mantida constante durante o experimento utilizando um cilindro coaxial modelo VT-550, segundo a norma ASTM D 2770-4.

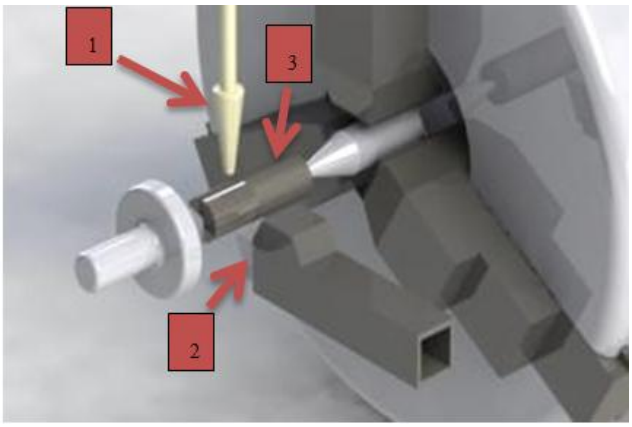

Figura 3. *Detalhe da montagem do sistema ferramenta-peça, com a seta 1 indicando o bocal, seta 2 a ferramenta de corte e a seta 3 a disposição da peça entre ponta.*

Downloaded from www.periodico.tchequimica.com

Foram definidos os seguintes parâmetros de corte como variáveis de entrada: velocidade de corte (Vc), avanço (f) e profundidade (ap), sendo obtida a Vc através da Equação (1).

$$Vc = \frac{\pi.d.n}{1000} \quad \text{(Eq. 1)}$$

Aplicada as condições de d = 23 mm e "n" igual à velocidade de rotação (m/mim), idênticas ás todas as operações de usinagem, tem-se, conforme Tabela 2.

Tabela 2. *Parâmetros de corte como variáveis de entrada.*

Vc (m/min)	f (mm/volta)	ap (mm/volta)
298	0,053	0,5

No processo de torneamento, após o primeiro e o último passe da usinagem de cada corpo-de-prova, foram coletados os cavacos resultantes, que foram analisados de acordo com a norma ISO 3685 para todas as amostras. Uma técnica de medição encontrada na literatura (Silva, Konno, *et.al.*, 2015) foi seguida. O termômetro infravermelho digital foi colocado de maneira que os pontos de corte sempre estivessem direcionados na zona do corte conforme mostra a Figura 4.a.

As aquisições dos dados foram possíveis através da interface do computador com o software de dados térmicos da termocâmera FLIR Tool®. Antes e após os processos de torneamento foi feita a captura das imagens para a identificação e análise visual do desgaste da ferramenta de corte. Para esta análise, utilizou-se o Microscópio Cooling Tech U200X (figura 4.b), com a ampliação do local especifico da ponta da ferramenta nas vistas superior e lateral (figura 4.c).

Por fim, após a usinagem dos corpos-de-prova foi realizada a análise do acabamento superficial de cada amostra em todas as condições citadas anteriormente, através do rugosímetro portátil digital modelo TR200 (figura 4.d). O parâmetro utilizado foi o desvio aritmético médio (Ra), cujo valor representa a média dos valores absolutos das coordenadas em relação á linha média no comprimento de amostragem (NBR ISO 4287, 2002).

3. RESULTADOS E DISCUSSÃO:

3.1. Viscosidade Dinâmica a 40°C e pH

O fluido de corte comercial utilizado no procedimento experimental possui a viscosidade cinemática de 2,2 Pa.s na temperatura de 20°. O valor de viscosidade dinâmica do óleo da *Carapa Guianesis* a 40°C, foi de 0,11 Pa.s (110 cP). Utilizando valores de densidade da literaturade 0,87 kg/m³ (Maia et al., 2014), estima-se que a viscosidade cinemática seja de 12,64 cSt.

Segundo Souza (2009), a viscosidade deve ser satisfatoriamente baixa para permitir uma boa movimentação do fluido e alta o suficiente para que ocorra uma boa aderência do fluido às superfícies da ferramenta, comportamento observado no óleo da andiroba. Ao satisfazer estes aspectos, o óleo de andiroba atua como lubrificante, reduzindo o atrito na interface peça-ferramenta. Como consequência, pode ocorrer uma redução das forças de corte e da rugosidade, este último analisado posteriormente. A elevada precisão de lubrificação torna-se uma vantagem do uso de fluidos de corte de base vegetal em relação os fluidos de cortes solúveis, independentes da condição de corte empregada (Gonçalves, 2013). Contudo, segundo Silva (2000), quanto menos viscoso for o fluido de corte melhor será a operação de usinagem.

O pH (potencial hidrogeniônico) é um indicativo da ação de microrganismos no fluido de corte devido a produção de subprodutos ácidos em seu metabolismo, além do consumo de emulgadores e agentes anticorrosivos. Como efeito, ocorre a redução do pH da emulsão e da proteção anticorrosiva (Boufleuer, 2004). O fluido de corte comercial utilizado possui pH 10,0, sendo este um valor ótimo de trabalho (Grub apud Runge e Duarte, 2013).

A análise de pH do óleo de andiroba revelou uma média de 2,3. Este valor se encontra abaixo dos valores encontrados na literatura. Melo da Silva et al. (2014) avaliaram parâmetros físico-químicos dos óleos de andiroba comercializados em 3 localidades, onde as médias de pH foram de 4,95 (supermercado), 5,80 (Bragança) e 5,83 (Ver-O-Peso). O pH encontrado para óleo de andiroba é significativamente mais ácido que o recomendado para os fluidos comerciais. Contudo, o pH ácido não é favorável ao crescimento de bactérias, os quais preferem

Downloaded from www.periodico.tchequimica.com

ambientes de neutralidade (6,5-7,5) (Grub apud Tortora, 2013), de forma que o crescimento de bactérias pode não ser favorecido. Deve-se ressaltar, no entanto, que elevada acidez não é desejável, pois contribui para os processos corrosivos (Maia *et al*., 2015).

3.2. Análises do Cavaco

A análise realizada nos cavacos resultantes no processo de usinagem do aço ABNT 1045 com aplicação do fluido de corte comercial e óleo da andiroba é mostrada na Tabela 2. Sua obtenção foi no decorrer de cada torneamento correspondente a cada condição e conforme a norma ISO 3685.

Observa-se que na condição com fluido de corte comercial o cavaco obtido é contínuo e helicoidal tipo arruela longo, isso acontece na usinagem de materiais dúcteis como aços, o metal cisalha na zona primária de cisalhamento com grandes deformações e permanece homogêneo, sem fragmentação mesmo de forma de fita externa não é possível observa nenhuma evidência clara de fratura ou trinca, esses fenômenos ocorrem para que uma nova superfície seja formada. Com o óleo da andiroba comportou-se como tubular emaranhada longo é um processo diferente do cavaco contínuo devido à diminuição da resistência mecânica do metal pelo aumento da temperatura (Machado, 2011).

3.3. Rugosidade

Na Figura 5 são mostrados os valores parâmetro Ra (μm), obtidos dos corpos de prova para as condições com o óleo da andiroba e com fluido de corte comercial do aço ABNT 1045.

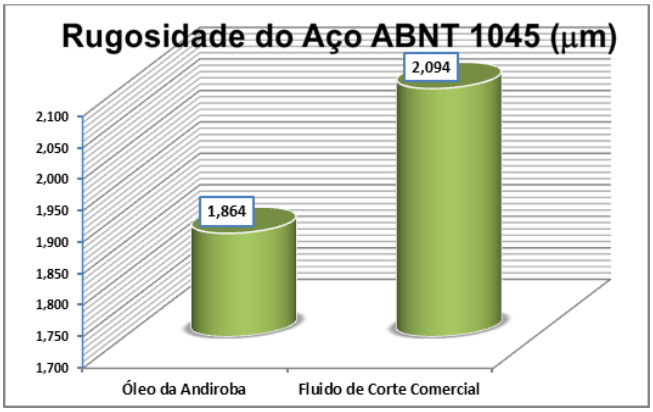

Figura 5. *Rugosidade da peça.*

Quanto aos valores de rugosidade, da Figura 5 observa-se que houve um melhor acabamento superficial com o uso do óleo da *Carapa Guinanesis* diminui 23% em relação ao fluido de corte comercial. A redução da rugosidade corrobora o bom desempenho do óleo de andiroba como lubrificante na viscosidade de trabalho encontrada.

Pesquisas vêm sendo realizadas para maior otimização dos processos de usinagem, para que se tenha uma melhor peça acabada, desta forma, irá agir de maneira direta ao desgaste da ferramenta. Botelho (2019) comparou a análise de acabamento superficial em aços ABNT 1020 e 1045 e apresentou comportamento semelhante com o uso do óleo da andiroba.

O desempenho do óleo do coco babaçu usado na técnica mínima quantidade de fluido – MQF, com diferentes vazões, durante o processo de usinagem o fresamento, apresentou menores resultados, ou seja, melhor acabamento superficial, comparado com o fluido de corte comercial, devido o atrito na interface cavaco-ferramenta (Araújo *et al*., 2013).

Um estudo da minimização do custo-benefício de usinagem por torneamento de aço ABNT 52100, aplica-se o método de superfície de resposta foi realizado por Mendes *et al*. (2007), considerando a vida da ferramenta e o acabamento superficial da peça. Seus resultados indicam que a diminuição do custo é obtida com as maiores rotações, ou seja, velocidades de corte utilizadas no seu experimento, com maiores taxas de remoção de material da peça usinada.

3.4. Temperatura da Peça

A temperatura de corte é um resultado da união dos seguintes parâmetros: Processo de torneamento, máquina ferramenta, ferramenta de corte, material e os diferentes fluídos de corte. A Figura 6 mostra a comparação das curvas de temperatura em função do tempo para as condições com o óleo da andiroba e com fluido de corte comercial.

Downloaded from www.periodico.tchequimica.com

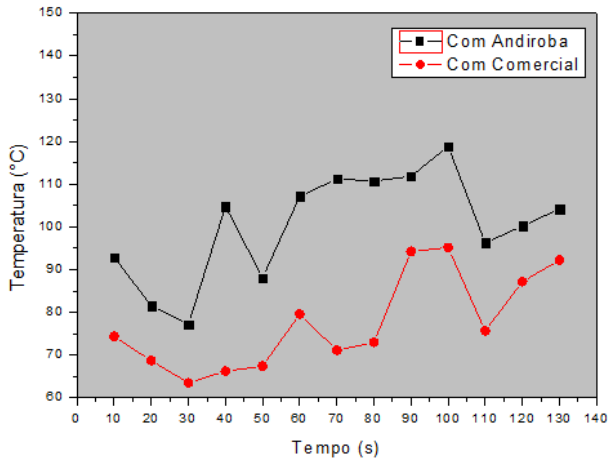

Figura 6. *Temperatura pelo tempo do aço ABNT 1045 com óleo da andiroba e com fluido de corte comercial.*

Segundo Diniz (2013) O aumento da temperatura está diretamente ligada com a velocidade de corte e consequentemente o conjunto ferramenta/peça, com a elevação da temperatura haverá alteração nas propriedades mecânica da ferramenta que diminuirá sua vida útil e reduzirá de maneira drástica sua produtividade, elevando o custo e tempo.

A redução da temperatura para o caso do uso de fluido de corte comercial é devido o fluido reduzir a área de contato na interface cavaco-ferramenta, diminuindo, dessa forma, a zona de aderência na superfície de saída do cavaco (Machado *et al*., 2009). Fluido de corte emusionável possui em sua composição aditivos de extrema pressão, aditivos (anti-ferruginosos), bactericidas, anti-espumantes e corantes, o que contribui para a diminuição da temperatura de corte no processo de torneamento. E a inconstância na curva de temperatura de corte no caso de utilização do fluido provavelmente deve-se ao sistema de aplicação utilizado (convencional).

Neste caso, devido à velocidade de corte estipulada e com o uso da *Carapa Guianesis*, houve um aumento na velocidade de escoamento do cavaco que conseqüentemente, ocasionou um aumento significativo da temperatura sobre a superfície de saída da ferramenta, fato também observado por Nouari *et al*. (2005) e Botelho *et al*. (2019).

Suarez *et al.* (2009) estudaram as temperaturas de usinagem que influencia no controle dimensional no processo de fabricação e no rugosidade final das peça. O aumento da temperatura somou-se ainda para diminuir as forças e a potência de usinagem. Sabe-se que a interface de contato entre a ferramenta-peça trabalho no processo de usinagem na superfície de flanco está sujeita a pressões elevadas e consequentemente a altas temperaturas (Tönshoff, 2004). Durante o processo de torneamento, observou-se que houve várias oscilações de temperatura para todas as condições. Tais resultados já são conhecidos da literatura (Guimarães, 2014; Haddag e Nouari, 2013).

3.5. Desgaste da Ferramenta

A seguir são apresentadas as imagens laterais e de topo, com seus respectivos desgastes e $VB_{Máx}$ das ferramentas utilizadas no processo experimental (figura 7).

O calor gerado durante a usinagem desses materiais é concentrado na região de corte, resultando em elevadas temperaturas nessa região, que aumentam os desgastes da ferramenta de corte por processo termicamente induzido, como difusão e a reação química entre a ferramenta e o material da peça (Shokrani *et al*. 2012). A usinagem com o óleo da andiroba apresenta maior desgaste da ferramenta de corte, para os parâmetros de corte definidos nesta pesquisa, isso se deve pela falta de aditivos, por ser um óleo vegetal puro comparado com o fluido de corte que obteve menor desgaste da ferramenta, ou seja, maior vida útil. Consequentemente, esses parâmetros irão refletir na baixa qualidade e alto custo de fabricação da peça (Korkut *et al.* 2003).

4. CONCLUSÕES:

Os resultados obtidos dos testes de torneamento, nas condições impostas pela metodologia do presente trabalho, possibilitaram as seguintes conclusões:

• O óleo da *carapa guianensis* apresentou valores para a análise da viscosidade dinâmica a 40°C de 0,11 Pa.s e o fluido de corte comercial a 20°C de 2,2 Pa.s. Para a análise de pH o resultado adquirido foi de 2,3 e 10, respectivamente para a andiroba e fluido comercial;

• Em relação ao estudo do cavaco, a condição com óleo da andiroba gera melhor segurança ao operador;

• Os valores de rugosidade média, Ra, a diferença de 23%, para o óleo da andiroba que obteve melhor acabamento superficial;

• A aplicação da andiroba proporcionou maiores temperaturas de corte na peça.

Downloaded from www.periodico.tchequimica.com

• Por fim, relacionado ao desgaste da ferramenta de corte, com o óleo da andiroba obteve maior VBmáx.

5. AGRADECIMENTOS:

Agradecemos a Base Naval de Val-de- Cans (BNVC), pelo espaço experimental, ao Instituto Federal Pará (IFPA), pelas análises e ao Conselho Nacional de Desenvolvimento Científico e Tecnológico (CNPq).

6. REFERÊNCIAS

1. ASTM D (**2004**), 2770-04: *Standard practice for calculating viscosity index from kinematic Viscosity at 40 and 100*. Annual Book of ASTM Standards, ASTM International, West Con-shohocken.
2. Araujo, A. S., Machado, A. R., Neves, T. E. S., Paiva, A. E., Rodrigues, J. R. P.; Esforços de usinagem e acabamento superficial no fresamento frontal do aço abnt 1045 com aplicação mqf do óleo refinado vegetal de coco babaçu. 7º Congresso brasileiro de engenharia de fabricação, Penedo, Rio de Janeiro, Brasil, 20-24 de maio de **2013**.
3. Araujo, A. S., Farias, F. P, Morais, L. O. Anais do 8º Congresso Brasileiro de Engenharia de Fabricação, **2015**.
4. Biscione, R. P. B. Dissertação (Mestrado) - Universidade Estadual Paulista, Faculdade de Bauru, **2010**.
5. Botelho, T. I. M, Monteiro Junior, P. L., DA Silva, M. A. S., Da Silva, R. B., Saldanha, A. Periódico Tchê Química, v. 31, p. 12, **2019**.
6. Boufleuer, N. T. Dissertação (mestrado) - Universidade Federal do Acre, Rio Branco, AC, Brasil, **2004**.
7. Diniz, A. E., Scandiffio, I. Anais do 1º Congresso Brasileiro de Engenharia de Fabricação, **2001**.
8. Diniz, A. E., Coppini, N. L. Tecnologia da Usinagem dos Materiais. 8 ed. Janeiro **2013**, p. 26.
9. Gonçalves, J.F.S. Proposição de método de desenvolvimento de fluido de corte de base vegetal. Tese de Doutorado, Instituto Tecnológico da Aeronáutica, São José dos Campos, São Paulo, Brasil, **2013**.
10. Grosse, T., Winter, M., Baron, S., Hoffmeister, H., Herrmann, C., Droder, K. CIRP Journal of Manufacturing Science and Technology. p. 89-98, **2016**.
11. Guimarães, C. B. Dissertação (mestrado), Universidade Federal do Pará, Pará, Brasil, **2014**.
12. Haddag, B., Nouari, M. Wear. 302, 1158–1170, **2013**.
13. Korkut, I; Kasap, M.;Ciftci, I; Seker, U. *Materials and Desing*. Turkey, v.25, p.303-305, out. **2003**.
14. Grub, A. M. Dissertação de Mestrado. Universidade Federal de Uberlândia, Uberlândia, MG. Brasil, **2013.**
15. ISO (**1993**) 3685: *Tool Life Testing with Single-Point Turning Tools*. ISO - International Organization for Standardization.
16. Lawal, S.A., Choudhudhury, I.A., Nukman, Y. J. Clean. Prod. 41, 210 e 221. **2013.**
17. Magri, A. XIX Colóquio de Usinagem, Anais em CD Rom, Artigo: 12. **2010.**
18. Machado, Á. R., Abrão, A. M., Coelho, R. T.; Da Silva, M. B. Teoria da Usinagem dos Materiais. 2.ed. São Paulo - SP: Editora Edgard Blucher, **2011**. 397p.
19. Machado, A.R.; Da Silva, M.B.; Coelho, R. T; Abrão, A. M. Teoria da Usinagem dos Materiais. 1ªed. São Paulo: Editora Blucher, **2009**.
20. Maia, D. J., Segre, N., Scatigno, A. G., Stella, M. B. Experimentação no Ensino de Química. P. 71-75, **2015**.
21. Melo da Silva, P. M, Da Silva, D. P, De Souza, E. C, Dos Silva, A. S, Muller, R. C. S. 54° Congresso Brasileiro de Quimica. Natal, Rio Grande o Norte, Brasil, 3 – 7 de outubro de **2014**.
22. Mendes, R. R. A, Paiva, A. P, Ferreira, J. R., 4º Congresso Brasileiro de Engenharia de Fabricação. Águas de São Pedro, SP, Brasil, 15-18 de abril de **2007**.
23. Moore, J.S., Christensen, M., Wilson, R.W., Wallace Jr.,R.J., Zhang, Y., Nash, D.R., Shelton, B. AIHAJ. USA, v. 61, n°2, p. 205-13, abr. **2000**
24. Muniz, C.A.S. Tese de Doutorado. Universidade federal do Rio Grande do Norte, RN, Natal, Brasil, **2008**.

Downloaded from www.periodico.tchequimica.com

25. NBR ISO (**2002**) 4287: Especificações geométricas do produto (GPS) - Rugosidade: Metódo do perfil - Termos, definições e parâmetros da rugosidade. NBR - Norma Brasileira. Interna-tional. ISO - Organization for Standardization
26. Nouari M., List G., Gehin D., Gomez B., Manaud J. *Wear behaviour of cemented carbide tools in dry machining of aluminum alloy*. França, **2005**.
27. Rodrigues, J. R. P. Revista Maquinas e Metais, v.476, pp.42-53, **2005**.
28. Santos, L. K; Dias, S. Estudo da viabilidade de modernização de um setor de usinagem de uma metalúrgica. <https://www.trabalhosfeitos.com/ensaios/Usinagem/43891630.html> Acessado em 01 de maio de 2016.
29. Shokrani, A.;Dhokia, V.; Newman, S.T.. International Journal of Machine Tools and Manufacture. United Kingdom, v.57, p. 83-101, Fev. **2012**.
30. Souza, A. J. de. Processos de fabricação por usinagem < http://en.lccv.ufal.br/wpcontent/uploads/sites/17/2015/04/ApostilaUsinagem_Parte1.pdf >. Acessado em 29 dez. 2015.
31. Souza, J. Dissertação (mestrado) - Instituto Tecnológico da Aeronáutica, São Paulo, SP, Brasil, **2009.**
32. Stemmer, C.E. Ferramentas de Corte I. Editora da UFSC, 6ª Edição, Florianópolis, **2005**.
33. Suarez, M. P., Costa, E.S., Machado, A.R., Abrão, A.M., V Congresso Brasileiro de Engenharia de Fabricação, Belo Horizonte, MG, Anais em CD Rom, Artigo: 011072262, 14-17 de Abril de **2009**.
34. Tönshoff, T., Ben Amor, R., Pereira, A. A., Boehs L. III Congresso Nacional de Engenharia Mecânica, Belém, PA, Brasil, 10-13 de agosto de **2004**.
35. VACARO, Tiago. Redução da utilização de fluidos de corte: uma abordagem ecológica na gestão de processos de usinagem.<https://www.ucs.br/ucs/pesquisa/jovenspesquisadores2009/trabalhos/poster/e_TiagoVacaro.pdf>. Acessado em 24 julho 2016.
36. Veillete, M., Thorne, P.S., Gordon, T.;Duchaine, C. *Six Month Tracking of Microbial Ghowth in a Metalworking Fluid After Sytem Cleaning and Recharging. Ann Occup Hyg*. Canadá, v. 48, n° 6, p. 541-546, Agosto. **2004**

Downloaded from www.periodico.tchequimica.com

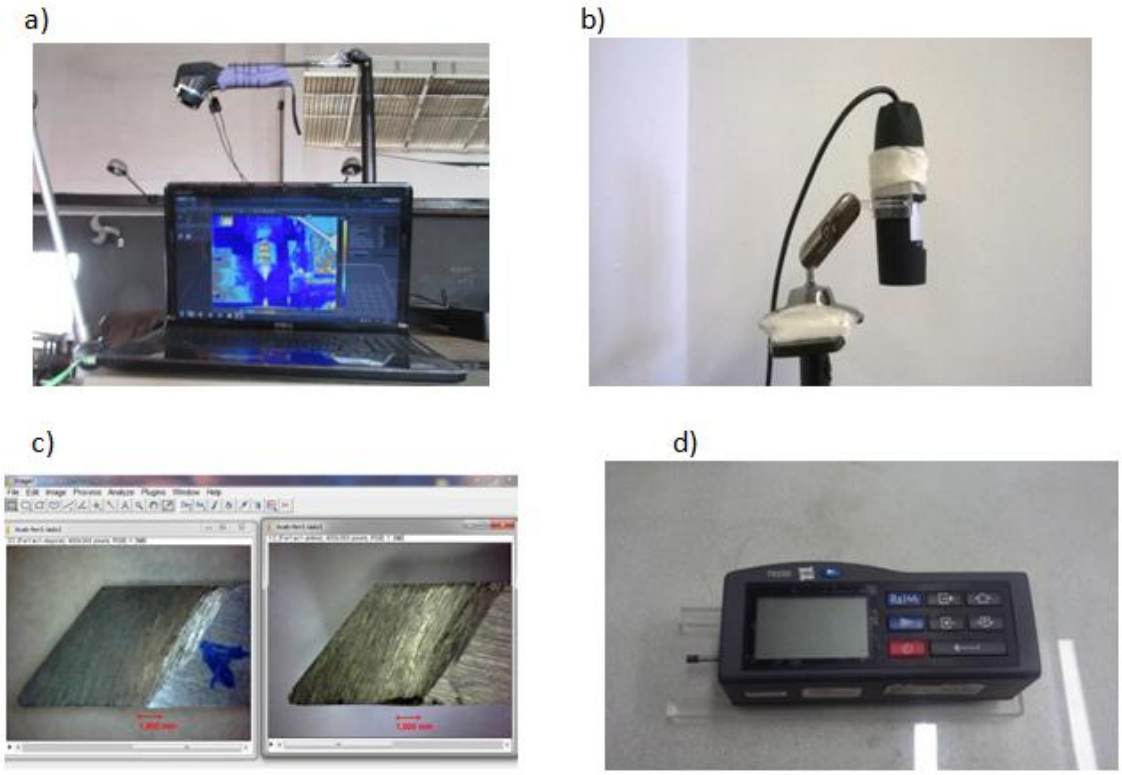

Figura 4. *a) Disposição do termômetro infravermelho em relação ao torno; b) microscópio cooling tech; c)vistas superior da ponta da ferramenta; d)rugosimetro digital.*

Tabela 2. *Cavaco gerado no torneamento, com fluido de corte comercial e óleo da andiroba.*

Fluido de Corte Comercial	Óleo da Andiroba
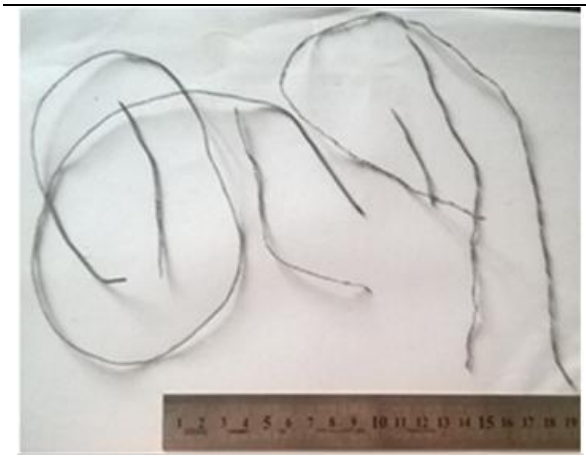	

Downloaded from www.periodico.tchequimica.com

PAGE CHARGES (1), DISCOUNTS (2), AND FREE PUBLICATION OPPORTUNITIES (3) FOR 2020

Authors are required to pay a publication fee in order to share in the costs of production. The fee will be asked if and when the article is accepted for publication. Once full payment has been made (PayPal only), the paper will be published at the Ahead of Print and scheduled for the next available issue. All waivers (as well as the publication fees requests) are applied to the accepted papers after successful peer-review only.

Please observe the flowchart below to understand how we work.

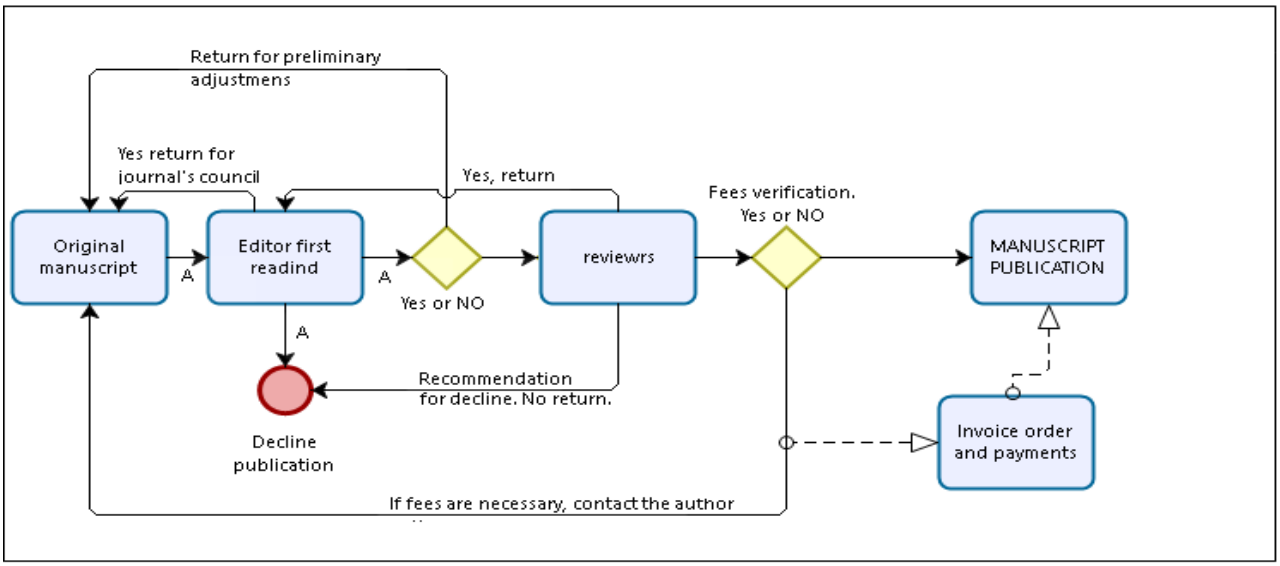

Move the mouse over the image.

1. Page charges prices:
*Brazilian authors, U$ 110
*Other countries income groups:
High income (or nuclear-capable countries) - U$ 300
Upper middle income U$ 250
Lower middle income U$ 120
Lower middle income (Heavily indebted poor countries (HIPC)) U$ 100
Low income U$ 100
Low income (Heavily indebted poor countries (HIPC)) U$ 80
(*) Classification according to the World Bank list of economies (June 2017)
** Optional page formatting fee + U$ 80. If you don't have time or the proper conditions to execute the formatting of your manuscript, we will find someone to do it for you.

2. Discounts
a) 50% discount for authors who support other journals from the team (Southern Brazilian Journal of Chemistry (this is a 100% free journal)), with 1 manuscript approved for publication;
b) 100% discount for authors who support other journals from the team (Southern Brazilian Journal of Chemistry (this is a 100% free journal)), with 2 manuscripts approved for publication;
c) Volume discount, if you are an author/collaborator of the journal, that has published with us 4 manuscripts (paid your full corresponded price), your fifth manuscript will be free of charge. Later the counting cycle restart.

3. Free publication
a) Young scientists publishing the first manuscript of their career with us. Requirements: Copy of the curriculum with no publications; maximum of 2 authors; join the author alliance program (free).
b) All personal related to the production of the journals, from Brazil and abroad;
c) Long-time collaborators. Authors that have beeing publishing with us over the last decade, for more than 4 times, will pay no fees. Thank you for working with us for all those years.
d) Paper considered by the Editors of high quality, priority, and relevance for the development of the society shall pay no fees. Note that this condition is a small recognition prize, not something that you may request. Thank you for your comprehension.

Downloaded from www.periodico.tchequimica.com

Preparation of Manuscripts

Preparation of Manuscripts

Please, observe the following points in preparing manuscripts. Papers not conforming closely to these instructions may be returned to their authors for appropriate revision or may be delayed in the review process.

Readability: Manuscripts should be written in clear, concise, and grammatically correct English (British or American English throughout). The editors can not undertake wholesale revisions of poorly written papers. Every paper must be free of unnecessary jargon and clearly readable by any specialist in the related field. The abstract should be written in an explanatory style that will be comprehensible also to readers who are not experts in the subject matter.

General format: The completed paper has to be written, preferably in Rich Text Format, either in an MS-Word (Ms-Word 2003 or MS-Word 2007) or in a Libre.Office (.odt) compatible file. Page size: A4, line spacing: single, font type: Arial. Please leave headers and footers unchanged, since it should be filled by the editors. Please check guidelines for accurate information based on all different categories (review articles, technical notes, etc.) available. A single file of the whole manuscript should then be submitted through TQJ's email. The Journal no longer accepts submissions in any other form.

The order of the material should be as follows: Title, Author(s), Abstract, Keywords, Main text (Introduction, Review of Literature, Definitions (if any), Materials and Methods, Results, Discussion), Acknowledgements (if any), References, Appendix (if any). This structure of the main text is not obligatory, but the paper must be logically presented. Footnotes should be avoided. The main text must be written with font size 11, justify. Within each main section, three levels of subheadings are available, and the titles must be bold, bold, and italic, italic, respectively.

The manuscript should contain the whole text, figures, tables, and explanations according to the followings (we suggest using the template file):

The first page of the material should be as follows:

Title: (both in Portuguese and English. The editors can provide the title in Portuguese for those who Portuguese is not the first language). It should be brief and informative. The title should reflect the most important aspects of the article, in a preferably concise form of not more than 100 characters and spaces. Font size 12, capital letters, center alignment.

By-line: Names (size 12, small capital) of the authors. No inclusion of scientific titles is necessary. In the case of two or more authors, place their names in the same row, separate them with a semicolon (;) and please indicate the corresponding author with * in superscript. The corresponding author should be the one submitting the article online and an e-mail given (only one e-mail) below the addresses of all authors. Authors from different institutions must be labeled with numbers in superscript after the names. Addresses of the authors, phone, and fax number, should also be given (size 10). The authors should be grouped by address.

Abstract: (both in Portuguese and English. The editors can provide the translation of the abstract to Portuguese for those who Portuguese is not the first language). Required for all manuscripts in which the problem, the principal results, and conclusions are summarized. The abstract must be self-explanatory, preferably typed in one paragraph, and limited to a minimum 250 words. It should not contain formulas, references or

Downloaded from www.periodico.tchequimica.com

abbreviations. The word ABSTRACT should be written in capital letters, arial, size 12, bold, left alignment. The abstract should be written font arial, size 10, justify.

Keywords: (both in Portuguese and English. The editors can provide the keywords in Portuguese for those who Portuguese is not the first language). Keywords should not exceed five, not including items appearing in the title. The keywords should be supplied indicating the scope of the paper. Size 10, italic, justify, only the word Keywords must be bold, left alignment.

The authors should include Abbreviations and Nomenclature listings when necessary.

The main text part of the material should be as follows: (

The words Introduction, Materials, and Methods, Results and Discussion, Conclusion, Acknowledgements, and References must be written in capital letters, arial, font size 12, left alignment, bold.

Introduction: The introduction must clearly state the problem, the reason for doing the work, the hypotheses or theoretical predictions under consideration, and the essential background. It should not contain equations or mathematical notation. A brief survey of the relevant literature so that a non-specialist reader could understand the significance of the presented results.

Materials and Methods: Provide sufficient details to permit repetition of the experimental work. The technical description of methods should be given when such methods are new.

Results and Discussion: Results should be presented concisely. Also, point out the significance of the results and place the results in the context of other work and theoretical background.

Conclusion: Summarize the data discussed in the Results and Discussion showing the relevance of the work and how different it is from others researches. Also, point out the benefits and improvements that can be observed in order to develop new science standards that can change something in the related field.

Acknowledgments: (if any) These should be placed in a separate paragraph at the end of the text, immediately before the list of references. It may include funding information too.

References: In the text, references should be cited in the Harvard style (Author, year). Alternatively, the author's surname may be integrated into the text, followed by the year of publication in parentheses. Cite only essential resources, avoid citing unpublished material. References to papers "in press" must mean that the article has been accepted for publication. At the end of the paper list references alphabetically by the last name of the first author. Please, list only those references that are cited in the text and prepare this list as an automatically numbered list. The word References with size 12, bold, capital letters, left alignment.

Guidelines for References

Journals

Journal abbreviations should be used, as defined by the Chemical Abstracts Service Source Index (see http://www.cas.org/sent.html). If the official short form can not be determined, and it is not obvious how to abbreviate the title, the full journal title should be given.

1. Varma, R. S.; Singh, A. P.; *J. Indian Chem. Soc.*, **1990**, 67, 518.

If the journal can not be easily accessed, its Chemical Abstracts number should be given, as follows:

Downloaded from www.periodico.tchequimica.com

2. Provstyanoi, M. V.; Logachev, E. V.; Kochergin, P. M.; Beilis, Y. *I.; Izv. Vyssh. Uchebn. Zadev.; Khim. Khim. Tekhnol.* **1976**, 19, 708. (CA 85:78051s).

If the article has a DOI number, but its complete reference is not given, the DOI number should be cited as follows:

3. Vidotti, M.; Silva, M. R.; Salvador, R. P.; de Torresi, S. I. C.; Dall'Antonia, L. H.; *Electrochimica Acta* (2007), doi:10.1016/j.electacta.2007.11.029.

It is recommended to give composite references instead of a list of separate references. The style of composite references is as follows:

4. Varela, H.; Torresi, R. M.; *J. Electrochem. Soc*. **2000**, 147, 665; Lemos, T. L. G.; Andrade, C. H. S.; Guimarães, A. M.; Wolter-Filho, W.; Braz-Filho, R.; *J. Braz. Chem. Soc*. **1996**, 7, 123; Ângelo, A. C. D.; de Souza, A.; Morgon, N. H.; Sambrano, J. R.; *Quim. Nova* **2001**, 24, 473.

Patents

Patents should be identified as follows (if possible, the Chemical Abstracts number should be given in parentheses):

5. Hashiba, I.; Ando, Y.; Kawakami, I.; Sakota, R.; Nagano, K.; Mori, T.; *Jpn. Kokai Tokkyo Koho 79 73,771* **1979**. (*CA 91:P193174v*)

6. Kadin, S.B.; *US pat. 4,730,004* **1988**. (*CA 110:P23729y*)

7. Eberlin, M. N.; Mendes, M. A.; Sparrapan, R.; Kotiaho, T. *Br PI 9.604.468-3*, **1999**.

Books

with editors

8. Regitz, M. *Multiple Bonds and Low Coordination in Phosphorus Chemistry*; Regitz, M.; Scherer, O. J., eds.; Georg Thieme Verlag: Stuttgart, 1990, cap. 2.

without editors

9. Cotton, F.A.: Wilkinson, G.; *Advanced Inorganic Chemistry*, 5th ed., Wiley: New York, 1988.

Computer programs (software)

10. Sheldrick, G. M.; *SHELXL-93; Program for Crystal Structure Refinement*; University of Göttingen, Germany, 1993.

Theses

11. Velandia, J. R.; *Ph.D. thesis*, Federal Rural University of Rio de Janeiro, Brazil, 1997.

Presentations at meetings

12. Ferreira, A. B; Brito, S. L.; Abstracts, *20th Annual Meeting of the Brazilian Chemical Society*, Poços de Caldas, Brazil, 1998.

Internet pages

13. http://www.sbq.org.br/jbcs, accessed June 2001.

Unpublished material

For articles accepted for publication: Magalhães, U. H.; *J. Braz. Chem. Soc.,* in press.

For articles submitted but not yet accepted: Magalhães, U. H.; *J. Braz. Chem. Soc*. submitted.

For unpublished articles or personal communications: Magalhães, U. H.; unpublished or Magalhães, U. H.; personal communication.

Unpublished results must only be cited with explicit permission from those who obtained them.

Whenever possible, authors should follow IUPAC recommendations (for all papers using chemical nomenclature) and use the International System of Units.

Figures: The number of figures (including graphs, diagrams, etc.) should not exceed 10 and should be submitted either in JPG or PNG formats. All photographs, graphs, and diagrams should be numbered consecutively (e.g., Figure 1) in the order in which they are referred in the text. The caption must appear below the figure (size 11, bold, italic) and should be sufficiently detailed to enable to understand apart from the text. Explanation of lettering and symbols should be given also in the caption and only exceptionally in the figures. Figures should be of good quality and preferably in black and white. (Color figures will appear in the downloadable files, but all papers will be printed in black and white.) Scanned figures should be at a resolution of 800 dpi/bitmap for line graphs. Diagrams containing chemical structures should be of high graphical quality and always be of the same size so that they can be uniformly reduced. Figures should have a maximum width of one Journal column (8.5 cm) to be inserted on body of the text so that they can be applied to the standards of the Journal. If the figures exceed 8.5 cm, they will be placed at the end of the article. In addition, authors may be requested to submit each figure also as an image file in one of the following formats: jpg or png. For figures, graphs, diagrams, tables, etc., identical to material already published in the literature, authors should seek permission for publication from the companies or scientific societies holding the copyrights and send it to the editors of TQ along with the final form of the manuscript.

Tables: Tables should be self-explanatory. They should be mentioned in the text, numbered consecutively (e.g., Table 1) and accompanied by title at the top (size 11, bold, italic). Please insert all the tables in the text. Do not enclose huge tables that can not be fit within the page margins.

Mathematical expressions: In general, minimize unusual typographical requirements, use solidus, built-up fractions. Avoid lengthy equations that will take several lines (possibly by defining terms of the equation in separate displays). For drawing equations, please use the Equation Editor of Word, if possible. Make subscripts and superscripts clear. Display only those mathematical expressions that must be numbered for later reference or that need to be emphasized. The number displayed equations consecutively throughout the paper. The numbers should be placed in parentheses to the right of the equation, e.g., (Eq. 1).

Supplementary material: Any Supplementary material (extra figures, tables, diagrams, etc.) should be placed at the end of the manuscript and clearly indicated as such. A single .pdf-document, including the supplementary material, should be submitted.

Editors, at any time of the editing process, may ask authors to split off part of the manuscript, presenting it as supplementary material.

Downloaded from www.periodico.tchequimica.com